



北京大学地球环境与生态系统塞罕坝实验站

河北塞罕坝森林生态系统定位研究站



成果资料汇编

2014 年 3 月 · 北京

北京大学地球环境与生态系统塞罕坝实验站 河北塞罕坝森林生态系统定位研究站

简介

北京大学地球环境与生态系统塞罕坝实验站(以下简称“塞罕坝实验站”)和河北塞罕坝森林生态系统定位研究站站址在河北省塞罕坝机械林场总场内,由北京大学与河北塞罕坝机械林场总场两个单位合作建立野外长期生态研究观测站,建站主体单位为北京大学。2005年7月由北京大学城市与环境学院生态学系负责具体筹建,基本建设全部由北京大学投资,国家林业局投入主要科研仪器,塞罕坝机械林场总场提供实验场地,以林地资产投入。

塞罕坝实验站站址占地1 ha,建筑面积约2650 m²,提供科研实验室和生活保障,可同时容纳80—100名学生实习,30多名科研人员。设有50—60人的中小型学术会议场所。设有约30 ha森林和草地野外样地,用于长期野外实验和观测的样方。

北京大学地球环境与生态系统塞罕坝实验站及其围边地区分布着森林、草原、荒漠、湿地和湖泊等多样的生态系统,是开展植被恢复与重建、荒漠化监测、全球气候变化、生态控制实验以及首都生态安全等方面生态研究与实验的理想场所。塞罕坝实验站具有科研、教学实习以及学术交流等三个主要功能。在科研方面,主要从事生态、大气、环境、地学等方面的研究工作。近期主要进行气候变化与生态系统响应、恢复生态学实验、生物多样性监测与保育、环境因子变化控制实验等;在教学实习方面,主要从事生态学、植物学、土壤学、地质地貌等学科的野外实习;在交流合作方面,同国内、外同行建立合作交流关系,将该站纳入国际有关环境、大气、生态等监测网络之中,并与当地政府或生产部门定期建立交流机制。

塞罕坝实验站通过野外长期定位观测、专题研究项目和大规模模拟实验研究手段,试图揭示在全球气候变化和人为活动影响下的生态系统格局、过程、功能及其变化机理;探索多源和多时空尺度生态系统功能、生态系统对全球气候变化的响应与适应的过程机理、生态系统能量转换与物质循环、生态系统管理与区域发展等生态学科问题。从而更好地理解人类生存与发展环境问题,进一步探索生态理论基础。实验站生态学研究方面主要包括:

- (1) 生态系统碳、氮和水等重要生命元素的循环
- (2) 生态系统的生产力
- (3) 生态系统的能量流动
- (4) 生物多样性维持机制和保护策略
- (5) 全球气候变化与生态系统的响应
- (6) 退化生态系统的恢复与重建
- (7) 人类活动对生态系统的影响
- (8) 环境质量与大气监测
- (9) 植被、生态学、土壤、生物、大气环境、地球化学、地质等多学科的教学。

实验站除开展科研、教学实习、学术交流以外,致于与当地的科研和生产实际相结合,为当地的社会发展和科技水平的提高做贡献。

目 录

发表主要论文	1
2014 年发表论文.....	1
Wang W., X. Zhang, N. Tao, D. Ao, W. Zeng, Y. Qian, and H. Zeng. 2014. Effects of litter types, microsite and root diameters on litter decomposition in <i>Pinus sylvestris</i> plantations of northern China. <i>Plant and Soil</i> , 374: 677-688. doi: 10.1007/s11104-013-1902-y	1
Yang Y., M. Zhao, X. Xu, Z. Sun, G. Yin, and S. Piao. 2014. Diurnal and Seasonal Change in Stem Respiration of <i>Larix principis-rupprechtii</i> Trees, Northern China. <i>PLoS ONE</i> , 9: e89294. doi: 10.1371/journal.pone.0089294.....	13
Ma Y., S. Piao, Z. Sun, X. Lin, T. Wang, C. Yue, and Y. Yang. 2014. Stand ages regulate the response of soil respiration to temperature in a <i>Larix principis-rupprechtii</i> plantation. <i>Agricultural and Forest Meteorology</i> , 184: 179-187. doi: http://dx.doi.org/10.1016/j.agrformet.2013.10.008	20
Du Z., W. Wang, W. Zeng, and H. Zeng. 2014. Nitrogen Deposition Enhances Carbon Sequestration by Plantations in Northern China. <i>PLoS ONE</i> , 9: e87975. doi: 10.1371/journal.pone.0087975	29
Zhang X., W. Wang, W. Chen, N. Zhang, and H. Zeng. 2014. Comparison of Seasonal Soil Microbial Process in Snow-Covered Temperate Ecosystems of Northern China. <i>PLoS ONE</i> , 9: e92985. doi: 10.1371/journal.pone.0092985	38
2013 年发表论文.....	48
Liu H., A. Park Williams, C.D. Allen, D. Guo, X. Wu, O.A. Anenkhonov, E. Liang, D.V. Sandanov, Y. Yin, Z. Qi, et al. 2013. Rapid warming accelerates tree growth decline in semi-arid forests of Inner Asia. <i>Global Change Biology</i> , 19: 2500-2510. doi: 10.1111/gcb.12217.....	48
Liu H. and S. Piao. 2013. Drought threatened semi-arid ecosystems in the Inner Asia. <i>Agricultural and Forest Meteorology</i> , 1-2: 178-179.	59
Wang W., W. Zeng, W. Chen, Y. Yang, and H. Zeng. 2013. Effects of Forest Age on Soil Autotrophic and Heterotrophic Respiration Differ between Evergreen and Deciduous Forests. <i>PLoS ONE</i> , 8: e80937.	61
Wang W., W. Zeng, W. Chen, H. Zeng, and J. Fang. 2013. Soil Respiration and Organic Carbon Dynamics with Grassland Conversions to Woodlands in Temperate China. <i>PLoS ONE</i> , 8: 10.1371/annotation/d1c26c59-62e8-4c8d-96f2-439ca922b14a.....	75
Liu G., Y. Yin, H. Liu, and Q. Hao. 2013. Quantifying Regional Vegetation Cover Variability in North China during the Holocene: Implications for Climate Feedback. <i>PLOS ONE</i> , 8: e71681.....	85
Ma Y., B. Zhu, Z. Sun, C. Zhao, Y. Yang, and S. Piao. 2013. The effects of simulated nitrogen deposition on extracellular enzyme activities of litter and soil among different-aged stands of larch. <i>Journal of Plant Ecology</i> doi: 10.1093/jpe/rtt028	94
Song Z., H. Liu, B. Li, and X. Yang. 2013. The production of phytolith-occluded carbon in China's forests: implications to biogeochemical carbon sequestration. <i>Global Change Biology</i> , 19: 2907-2915. doi: 10.1111/gcb.12275	104

Yin Y., H. Liu, G. Liu, Q. Hao, and H. Wang. 2013. Vegetation responses to mid-Holocene extreme drought events and subsequent long-term drought on the southeastern Inner Mongolian Plateau, China. <i>Agricultural and Forest Meteorology</i> , 178–179: 3-9. ..113	
2012 年发表论文.....	120
陈曦和刘鸿雁. 2012. 内蒙古草原区土壤碳密度(SOCD)和氮密度(TND)的影响因素分析. <i>北京大学学报(自然科学版)</i> , 48: 317-324.....	120
任艳林. 2012. 降水变化对樟子松人工林土壤无机氮和净氮矿化速率的影响. <i>北京大学学报(自然科学版)</i> , 48: 925-932.	128
任艳林. 2012. 1965—2011 年河北塞罕坝地区降水量变化规律的小波分析. <i>北京大学学报(自然科学版)</i> : 918-924.	136
任艳林和杜恩在. 2012. 降水变化对樟子松人工林土壤呼吸速率及其表观温度敏感性 Q10 的影响. <i>北京大学学报(自然科学版)</i> , 48: 933-941.....	143
2011 年发表论文.....	152
Zhao F., H. Liu, Y. Yin, G. Hu, and X. Wu. 2011. Vegetation succession prevents dry lake beds from becoming dust sources in the semi-arid steppe region of China. <i>Earth Surface Processes and Landforms</i> , 36: 864-871. doi: 10.1002/esp.2114.....	152
2010 年发表论文.....	160
Wang W., S. Peng, and J. Fang. 2010. Root respiration and its relation to nutrient contents in soil and root and EVI among 8 ecosystems, northern China. <i>Plant and Soil</i> , 333: 391-401. doi: 10.1007/s11104-010-0354-x.....	160
Wang W., S. Peng, T. Wang, and J. Fang. 2010. Winter soil CO ₂ efflux and its contribution to annual soil respiration in different ecosystems of a forest-steppe ecotone, north China. <i>Soil Biology and Biochemistry</i> , 42: 451-458. doi: http://dx.doi.org/10.1016/j.soilbio.2009.11.028	171
Wei W., C. Weile, and W. Shaopeng. 2010. Forest soil respiration and its heterotrophic and autotrophic components: Global patterns and responses to temperature and precipitation. <i>Soil Biology and Biochemistry</i> , 42: 1236-1244. doi: http://dx.doi.org/10.1016/j.soilbio.2010.04.013	179
Zhang Y. and H. Liu. 2010. How did climate drying reduce ecosystem carbon storage in the forest–steppe ecotone? A case study in Inner Mongolia, China. <i>Journal of Plant Research</i> , 123: 543-549. doi: 10.1007/s10265-010-0311-z	188
孙艳荣, 刘鸿雁, 范涛, 马利国和张铭杰. 2010. 河北坝上地区不同土地利用类型的土壤风蚀研究. <i>北京大学学报(自然科学版)</i> , 46: 649-654.....	195
2009 年发表论文.....	201
Wang W. and J. Fang. 2009. Soil respiration and human effects on global grasslands. <i>Global and Planetary Change</i> , 67: 20-28. doi: http://dx.doi.org/10.1016/j.gloplacha.2008.12.011	201
刘鸿雁和李宜垠. 2009. 半干旱区气候变化和人类活动的孢粉指示. <i>古生物学报</i> , 48: 211-221.	210
魏天凤, 任艳林, 曾辉和贺金生. 2009. 降水改变对樟子松人工林土壤微生物量碳及微生物商动态变化的影响. <i>北京大学学报(自然科学版)</i> , 45: 533-540.....	221
2008 年发表论文.....	229
Guo D., X. Xia M Fau - Wei, W. Wei X Fau - Chang, Y. Chang W Fau - Liu, Z. Liu Y Fau - Wang, and Z. Wang. 2008. Anatomical traits associated with absorption and	

mycorrhizal colonization are linked to root branch order in twenty-three Chinese temperate tree species. New Phytologist, 180: 673–683.....	229
2007 年发表论文.....	240
王妮, 汪涛, 彭书时和方精云. 2007. 冬季土壤呼吸:不可忽视的地气 CO ₂ 交换过程. 植物生态学报, 31: 394-402.	240
朱江玲, 刘鸿雁和王红亚. 2007. 河北坝上地区湖泊沉积物记录的中全新世干旱气候. 地理科学, 27: 380-384.	249
博士后出站报告和研究生、本科生毕业论文.....	265
博士后出站报告	254
河北省塞罕坝森林结构与生物量.....	254
塞罕坝地区主要树种树干呼吸速率的研究.....	328
博士论文	402
河北塞罕坝人工林主要碳循环过程对降水变化的响应.....	402
硕士论文	492
干旱极限条件下温带森林对气候变化的敏感性.....	492
内蒙古高原东南部荒漠化与风沙活动研究.....	628
北方农牧交错带关键地段退耕还林还草的生态效应.....	704
本科论文	732
400mm 等雨量线沿线森林群落的种类多样性及影响因子.....	732
森林—草原交错带草本植物分布格局及其与光照条件的关系.....	784
农牧交错带不同土地利用方式下的土壤风蚀与合理的植被恢复.....	856
塞罕坝樟子松人工林凋落物类型、土壤深度和根的径级对分解的影响以及碳氮动态研究.....	856
专题研究报告	901
七星湖和泰丰湖区植被概况.....	901
三道河口林场丘间盆地立地条件初步分析报告.....	905
教学实习报告(节选).....	908
塞罕坝野外生态学实习报告—群落特征与植被退化.....	908
不同植被类型植物根系对土壤的影响.....	916
林下与草原(草甸)草本植物多样性格局比较分析.....	923
沟谷阴坡林下土壤表层水分梯度的探究.....	930
大光顶子乌苏里风毛菊叶面积梯度格局分析.....	940
针叶林对草本层豆科植物种类多样性的影响.....	946
塞罕坝地区白桦林下草本层植物叶级影响因素分析.....	952
塞罕坝主要群落类型下草本层物种多样性研究.....	959

发表主要论文

2014 年发表论文

Effects of litter types, microsite and root diameters on litter decomposition in *Pinus sylvestris* plantations of northern China

Wei Wang · Xinyue Zhang · Na Tao · De Ao ·
Wenjing Zeng · Yuqi Qian · Hui Zeng

Received: 9 January 2013 / Accepted: 2 September 2013 / Published online: 28 September 2013
© Springer Science+Business Media Dordrecht 2013

Abstract

Background and aims Litter decomposition is a major process in the carbon (C) flow and nutrient cycling of terrestrial ecosystems, but the effects of litter type, microsite, and root diameter on decomposition are poorly understood.

Methods Litterbags were used to examine the decomposition rate of leaf litter and roots at three soil depths (5, 10 and 20 cm) over a 470-day period in *Pinus sylvestris* plantations in northern China.

Results Leaves and the finest roots decomposed more quickly at 5 cm depth and coarser roots (>1-mm) decomposed more quickly at 10 and 20 cm depth. Roots generally decomposed more quickly than leaf litter, except at 5 cm deep; leaves decomposed more quickly than the coarsest roots (>5-mm). Root decomposition was strongly influenced by root diameter. Leaves experienced net nitrogen (N) immobilization and coarse roots (>2-mm) experienced more N release than fine roots. Significant heterogeneity was seen in N release for fine-roots (<2-mm) with N immobilization occurring in smaller (0.5–2-mm) roots and N release in the finest roots (<0.5-mm).

Conclusions Soil depth of litter placement significantly influenced the relative contribution of the decomposition of leaves and roots of different diameters to carbon and nutrient cycling.

Keyword Decomposition · Litter placement
microsite · Litter type · Nitrogen dynamics ·
Root diameters · Plantations

Introduction

Decomposition of plant tissues in terrestrial ecosystems regulates the transfer of carbon (C) and nutrients to the soil, and represents an important source of carbon dioxide in the atmosphere (Aerts 1997; Silver and Miya 2001). Also, previous studies suggested that root-derived materials were transformed to stable fractions such as humin and humic acid to a greater extent compared with leaf litter (Bird et al. 2008; Mambelli et al. 2011). Climate and litter chemistry have been shown to be important drivers of decomposition (Adair et al. 2008; Cusack et al. 2009). However, the effects of climate controls on leaf litter decomposition may differ from those of root decomposition, because leaf litter generally decomposes on the soil surface where it is directly exposed to precipitation and subject to desiccation (Cusack et al. 2009). Although root tissue in the mineral soil is still exposed to climate (certain moisture and temperature conditions), it is probably less variable than the surface climate conditions (Silver and Miya 2001). Furthermore, the importance of litter chemistry may differ between

Responsible Editor: Alfonso Escudero.

W. Wang (✉) · X. Zhang · N. Tao · D. Ao · W. Zeng ·
Y. Qian

Department of Ecology, College of Urban and Environment
Science, Peking University,
Beijing 100871, China
e-mail: wangw@urban.pku.edu.cn

X. Zhang · N. Tao · H. Zeng
Shenzhen Graduate School, Peking University,
Shenzhen 518055, China

leaf and root litter during decomposition, because of the differences in the microbial decomposer communities on the surface vs. in the soil (Silver 1998; Chen et al. 2001) and because root tissue in the substrate commonly has higher levels of lignin and high C: N (nitrogen) ratios than commonly observed in leaf litter (Moretto and Distel 2003; Abiven et al. 2005). Thus, litter chemistry and the location where decomposition occurs (microsites) are often confounding factors when comparing leaf and root decomposition. However, few studies have assessed whether litter decomposes differently at different microsites (e.g. Gill and Burke 2002; Austin et al. 2009; Powers et al. 2009).

Aside from the chemical content of roots and various environmental factors, root diameter (which often indicates function) is another key factor that governs the decomposition and nutrient cycling of roots (Nambiar 1987), because it integrates both chemical and physical properties associated with root development (Fahey and Arthur 1994). For instance, nitrogen and phosphorus concentrations generally decrease with increasing root diameter (King et al. 2002). In most previous studies of root decomposition, all roots in a fine-root system with a diameter of less than 2 mm have been assumed to be physiologically identical units (Silver and Miya 2001). Recent studies have suggested this type of bulk fine roots are composed of a heterogeneous mixture of individual roots that vary in their longevity, chemistry, morphological characteristics and physiological functions (Guo et al. 2008; Valenzuela-Estrada et al. 2008). Moreover, the substantial heterogeneity among individual roots within a fine root pool may strongly influence their contribution to soil carbon and nutrient dynamics (Guo et al. 2004). However, few studies have focused on differences in decomposition of roots of different diameters that are within the ≤ 2 mm size class. Coarse roots (>2 -mm) act as conduits for nutrients and water, as storage sites for carbon and nutrients (Ludovici et al. 2002; Melin et al. 2009), and also provide physical anchorage (Knorr et al. 2005; Tobin and Nieuwenhuis 2007). In addition, the decomposition of coarse roots provides a slow delivery of C and nutrients to the soil and soil biota and may influence the long-term ecosystem productivity and CO₂ emissions from forests (Johnsen et al. 2005). However, few studies have paid much attention to coarse roots (>2 -mm).

Plantations are becoming a key component of the world's forest resources and playing an important role in the context of overall sustainable forest management.

Well-designed, multi-purpose plantations can reduce anthropogenic pressures on natural forests, restore some ecological services previously provided by natural forests and mitigate climate change through direct C sequestration (Paquette and Messier 2010). In China, plantations currently cover an area of 5.33×10^7 ha, accounting for 30 % of the total forest area of China and China has 29 % of the world's total plantations based on area. The Saihanba Forestry Center contains the largest area of plantation forests in China, with *Pinus sylvestris* var. *mongolica* (Mongolia pine) as the dominant species. Thus, studies on litter decomposition of the main tree species used in afforestation can provide a good opportunity to explore the patterns of C and N cycling in temperate plantation ecosystems.

We conducted a 470-day decomposition study in a *P. sylvestris* plantation to investigate the influences of litter microsite, litter type and root diameter on decomposition. First, we wanted to know how a litter microsite, such as depth in soil, influences decomposition. We predicted that litter decomposition will increase as depth increases; that is, for the same type of litter, decomposition will occur faster at 10 and 20 cm soil deep than surface 5 cm soil because conditions in deeper soil layer may be more favorable to decomposition. Second, we examined the effect of litter type and root-diameter on decomposition. We expected decomposition would occur faster for leaf litter than for roots, and that small roots would decompose faster than large roots; for example, we believe decomposition rates would be: very fine (<0.5 -mm diameter) roots $>$ fine to moderately fine roots (0.5–1-mm and 1–2-mm diameter) $>$ medium-sized to large roots (2–5-mm and >5 -mm diameter). Finally, we predicted that based on litter quality, small roots (<2 -mm) would release N, and leaf litter and coarse roots (>2 -mm) would immobilize N.

Materials and methods

Site description

The study area is situated at the Saihanba Forestry Center in Hebei Province, in northern China ($117^{\circ}12' - 117^{\circ}30'$ E, $42^{\circ}10' - 42^{\circ}50'$ N, 1,400 m a.s.l.). The semi-arid and semi-humid climate has a long, cold winter (November to March), and a short spring and summer. Annual mean air temperature and precipitation over the period from 1964 to 2004 were 1.4 °C and 450.1 mm,

respectively. The soils are predominantly sandy. Our study site lays within a typical forest-steppe ecotone in a temperate area of northern China. Primary forests were harvested by large-scale industrial logging in the late 1900s and have been replaced by secondary forests and plantations. This site contains the largest area of plantation forests in China, with *P. sylvestris* as the dominant species.

Decomposition experiment

P. sylvestris leaf litter was collected using litter traps and nylon mesh placed on the forest floor under the trees in the plantation in May 2010. Fresh roots were also collected from the top 30 cm of soil in the same *P. sylvestris* plantation. We opted to use fresh roots because they have not yet begun to decompose (Hobbie et al. 2010). The live roots were further divided into five size classes: <0.5-mm, 0.5–1-mm, 1–2-mm, 2–5-mm and >5-mm in diameter, and then air-dried them at room temperature to a constant mass.

We constructed litter bags using 20×20 cm nylon mesh bags. The litterbags had a 1-mm mesh top and a 48 µm mesh bottom (to reduce fragmentation losses) at 5 cm depth as designed in Gholz et al. (2000). Xiong et al. (2013) reported that within a 1-mm mesh, no significant effect of mesh size on decomposition rates was observed. Litter bags buried at depths of 10 and 20 cm were constructed completely of 48 µm mesh. Each leaf litterbag was filled with 4.50 g of air-dried mass and air-dried root samples of 0.70 g for <0.5 mm, 0.80 g for 0.5–1-mm, 1.00 g for 1–2-mm, 2.00 g for 2–5-mm and 2.20 g for >5-mm-diameter roots. Sub-samples of each material were used to develop air-dry to oven-dry (65 °C) conversions and were analyzed for initial tissue chemistry. Before the decomposition trial, ash content of root litter in each litterbag was determined using a subsample burnt at 550 °C for 4 h in a muffle furnace. The estimated ash content varied from 3 % to 10 %. This so-called “ash” consists of intrinsic minerals in the root samples and adhering soil particles that were not completely removed during root cleaning; the data were used to correct all root mass values.

The litterbags were re-buried with a small 45° angle slit in the top depths of 5, 10 and 20 cm in the soil at their original sites in June 2010. Four replicate litterbags were sequentially retrieved for each material in August 2010 (70 days), May 2011 (330 days), July 2011 (400 days) and October 2011 (470 days). At each

harvest date, leaf litter and roots were removed from bags, oven-dried at 65 °C to constant mass, weighed, ground and milled for tissue chemistry analyses.

Chemical analysis

Total carbon (C) concentration was determined by the dichromate oxidation method (Nelson et al. 1996). Total N concentration was determined by the Kjeldahl method (Bremner 1996). Four subsamples of each material were analyzed for C fractions using the method determined by Ryan et al. (1990). Fractions determined included extractives, acid-solubles (AS, mainly cellulose and hemicellulose), and acid-insolubles (AIF, mainly lignin and suberin). C fractions are presented on an ash-free dry mass basis. Ash content of each substrate used for the decomposition study was determined using a subsample burnt in a muffle furnace (500 °C for 4 h).

Environmental factors

Continuous measurements of soil temperature and water content at three soil depth (5, 10 and 20 cm) were recorded at 30-min intervals with EM-50 loggers (Decagon, Pulman, WA, USA). We used weather station data from actual study period at our study sites to calculate the Climate Decomposition Index (CDI), which incorporates the seasonality of rainfall and temperature in an integrated index to predict decomposition (Parton et al. 2007).

Statistical analyses

The model for constant potential mass loss (Olson 1963) was represented by the following single exponential model, $X/X_0 = e^{-kt}$, where X/X_0 is fractional mass remaining at time t , X is the mass remaining at time t , X_0 is the original mass, e is the base of natural logarithm, k is the decay constant, and t is the time. The proportion of initial N at each harvest date was calculated by multiplying the root N concentration by root mass and comparing it to the initial root N pool (Hobbie et al. 2010; Wang et al. 2010).

One-way ANOVA analysis was conducted to examine the differences of litter quality parameters, mass loss percentage and the decay constant (k -value) between leaf and root litter. Two-way ANOVA analysis was used to compare the differences in mass loss percentage using six litter types (leaf litter and five types of root litter

(<0.5 mm, 0.5–1-mm, 1–2-mm, 2–5-mm and >5-mm in diameter) and three microsites (top 5 cm, 10 cm and 20 cm soil depth) as the main factors. For the same litter type, one-way ANOVA was conducted to examine the effect of soil depth on the decomposition rate. When comparing root decomposition rates, we divided fine roots into three diameter classes (<0.5, 0.5–1 and 1–2 mm), and also compared <2-, 2–5- and >5-mm roots decomposition based on Silver and Miya (2001). Multiple linear regressions were conducted to explore the environmental and litter quality controls on litter decomposition rate. All analyses were performed using SPSS 17 with a significance level of $P < 0.05$ for all cases.

Results

Initial litter quality

Initial litter N concentrations were significantly higher in finest roots (<0.5-mm) than in leaves and in roots with diameters greater than 0.5-mm (Table 1). Leaf initial N concentration was lower than N in <0.5-mm and 0.5–1-mm roots, but did not differ significantly from larger roots. Root N concentration generally decreased with the diameter (Table 1). Initial litter phosphorus (P) concentrations were lower in leaves than in roots (Table 1). P concentrations of roots did not show clear patterns with the diameter (Table 1). Leaf litter had higher C: N and N: P ratios than roots (Table 1). The finest roots (<0.5-mm) had the lowest C: N and AIF: N ratios (Table 1). Root C: N and AIF: N ratios generally increased with diameter. But for the extractives, AS and AIF, no significant differences occurred among different litter types (Table 1).

Litter decomposition rates

Litter mass remaining decreased rapidly over time and later remained relatively stable (Fig. 1). During the entire experimental period (470 days), litter mass loss ranged from 8 to 27 % at 5 cm, 13 to 24 % at 10 cm and 12 to 28 % at 20 cm soil depth, respectively (Fig. 1). For the same soil depth, leaf litter generally decomposed more slowly than root litter, except at 5 cm deep, where leaf litter decomposed significantly slower than the finest roots (<0.5-mm), a similar rate as 0.5–2-mm roots, but faster than the coarse roots (>2-mm) (Fig. 1a). Root decomposition was strongly influenced by root diameter and the effect was dependent on soil depth (Fig. 1). At 5 cm of soil depth, the finest roots (<0.5-mm) decomposed most quickly and the coarsest roots (>5 mm) decomposed most slowly (Fig. 1a). But at 10 cm soil depth, no significant differences in decomposition rates occurred among fine-roots (<0.5, 0.5–1, 1–2-mm), and 2–5-mm roots decomposed more rapidly than <2-mm and >5-mm roots (Fig. 1b). At 20 cm soil depth, finer roots (<0.5-mm and 0.5–1-mm) decomposed more slowly than 1–2-mm and 2–5-mm roots, but did not significantly differ from the coarsest roots (>5-mm) (Fig. 1c). For the same litter type, the leaf litter decomposition rate decreased with soil depth, but the root decomposition rate varied with soil depth with the same pattern as occurred with leaves in finest root (<0.5-mm) and a contrasting pattern with more coarse roots (>1-mm) (Fig. 2). No significant difference occurred for 0.5–1-mm roots (Fig. 2). We observed significant effects of litter type, and interactions between soil depth and litter type on litter decomposition (Fig. 2). No significant effect of soil depth on litter decomposition was found when leaves and roots with different diameter were combined (Fig. 2). The decay constant k ranged from 0.11

Table 1 Initial litter chemistry of leaf and root tissues with different diameters used in decomposition experiments

Litter type	Extractives (%)	AS (%)	AIF (%)	N (mg/g)	P (mg/g)	C: N	N: P	AIF: N	AIF: AS
Leaf	18.64 ^a	48.01 ^a	33.35 ^a	4.82 ^a	0.19 ^a	118 ^d	25 ^c	69 ^b	0.76 ^a
Root <0.5 mm	10.59 ^a	56.27 ^a	33.13 ^a	10.48 ^c	0.56 ^c	33 ^a	19 ^b	32 ^a	0.59 ^a
Root 0.5–1 mm	7.49 ^a	49.69 ^a	42.81 ^a	7.69 ^b	0.49 ^c	67 ^b	16 ^{ab}	56 ^b	0.87 ^a
Root 1–2 mm	10.78 ^a	47.67 ^a	41.56 ^a	6.29 ^{ab}	0.40 ^b	85 ^{bc}	16 ^{ab}	67 ^b	1.03 ^a
Root 2–5 mm	12.53 ^a	51.23 ^a	36.22 ^a	6.39 ^{ab}	0.52 ^c	86 ^{bc}	12 ^a	58 ^b	0.72 ^a
Root >5 mm	9.71 ^a	56.30 ^a	33.99 ^a	5.97 ^{ab}	0.35 ^b	92 ^c	17 ^{ab}	62 ^b	0.61 ^a

Means ($N=4$ for each litter type) are indicated. Different superscripted letters in each column indicate significant differences among litter types ($P < 0.05$)

AS acid-solubles, AIF acid-insolubles, N nitrogen, P phosphorus, C carbon

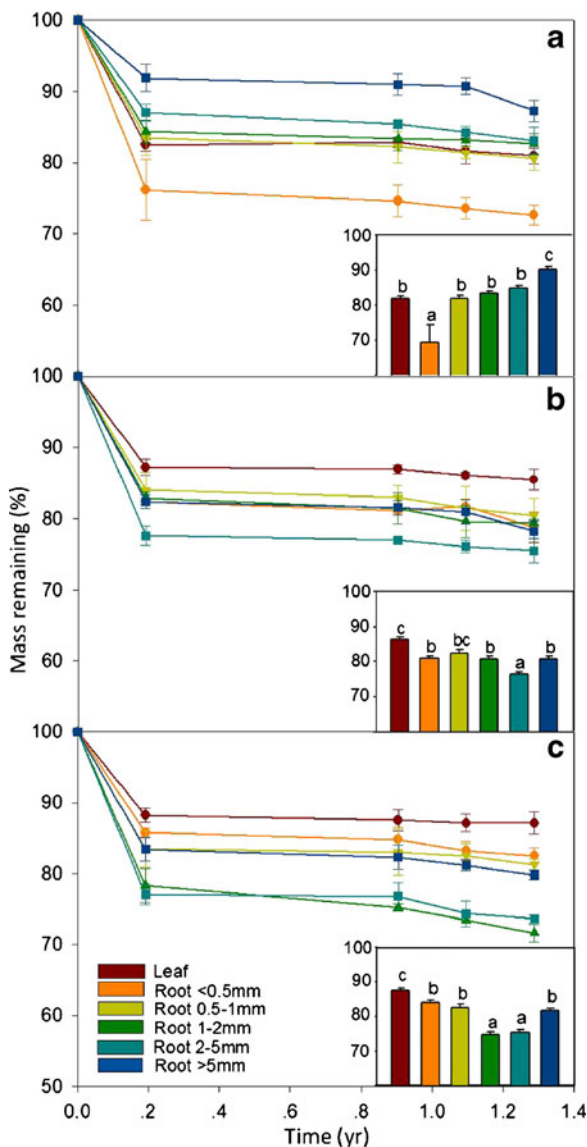


Fig. 1 Changes of mass remaining (%) with observation time in leaf litter and root decomposition at 5 cm (a), 10 cm (b) and 20 cm (c) soil depth, respectively. Inserted figure shows the effect of litter types on mass remaining (%) at each soil depth. Values with different letters are significantly different among different litter types at each soil depth ($P<0.05$)

to 0.16 year^{-1} in leaf litter and from 0.11 to 0.26 year^{-1} in root litter (Table 2).

During the entire experimental period, soil temperature ranged from 1.27 to 14.11°C (Fig. 3a) and soil water content ranged from 6 to 21% (Fig. 3b). The climate decomposition index (CDI) ranged from 0.04 to 0.94 (Fig. 3c). No significant relationship was found between soil temperature and the decay constant k (Fig. 4a) and

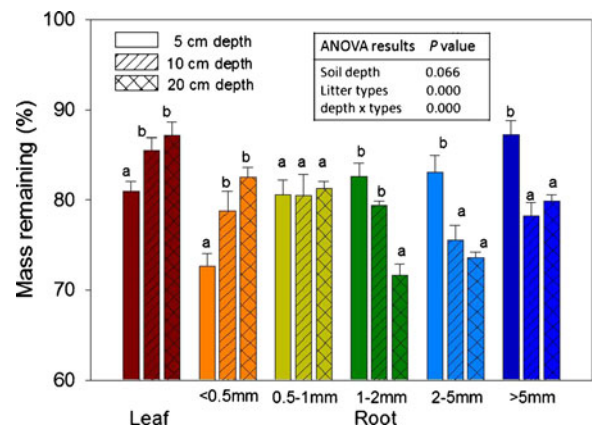


Fig. 2 Comparison of mass remaining (%) at different soil depths (5 cm, 10 cm and 20 cm) for the same litter types. Values with different letters are significantly different among soil depths ($P<0.05$). Inserted figure shows the effects of soil depth, litter types and the interaction between soil depth and litter types on the mass remaining (%)

between soil water content and the decay constant k (Fig. 4b). Initial litter phosphorus (P) content could explain 65% variation in the decomposition rate (Fig. 5).

Nitrogen release pattern vs. time

Leaf litter experienced net N immobilization (Fig. 6), whereas, root N release varied (Fig. 6). The finest roots ($<0.5\text{-mm}$) generally released N with an average of 16% of root N lost after 470 days decomposition (Fig. 6). In contrast, finer roots ($0.5\text{--}2\text{ mm}$) generally showed N immobilization (Fig. 6). Coarse roots ($>2\text{-mm}$) showed net N release with an average of 37% root N lost for $2\text{--}5\text{-mm}$ and 48% for $>5\text{-mm}$ diameter roots (Fig. 6). In leaf litter and fine roots ($<2\text{-mm}$), the C: N ratio generally showed a trend of first decreasing and then remaining relatively stable over time (Fig. 7). For coarse roots ($>2\text{-mm}$), the C: N ratio generally increased with time although there are small fluctuations (Fig. 7). Moreover, aside from the finest roots ($<0.5\text{-mm}$), initial root C: N ratios were negatively correlated with averaged nitrogen remaining (%) initial (Fig. 8).

Discussion

Leaf versus root decomposition

In our study site, litter mass remaining decreased rapidly during the first 2 months of the experiment and

Table 2 Decay constants (k) and the associated R^2 from regression equations of leaf litter and roots at depths of 5, 10 and 20 cm. Different superscripted lowercase letters in each column indicate significant differences of k -values among different litter

Litter types	k -values (5 cm)	R^2	k -values (10 cm)	R^2	k -values (20 cm)	R^2
Leaf	0.16 ^{b B}	0.95	0.12 ^{a A}	0.95	0.11 ^{a A}	0.97
Root <0.5 mm	0.19 ^{c B}	0.97	0.19 ^{b B}	0.95	0.15 ^{b A}	0.95
Root 0.5–1 mm	0.17 ^{b A}	0.96	0.17 ^{ab A}	0.95	0.16 ^{b A}	0.96
Root 1–2 mm	0.15 ^{ab A}	0.97	0.18 ^{b A}	0.96	0.26 ^{c B}	0.95
Root 2–5 mm	0.14 ^{ab A}	0.95	0.22 ^{b B}	0.96	0.24 ^{c B}	0.95
Root >5 mm	0.11 ^{a A}	0.88	0.19 ^{b B}	0.94	0.17 ^{b B}	0.95

types at the same soil depth; and different superscripted upper-case letters in each row indicate significant differences of k -values among different soil depths for the same litter type ($P < 0.05$)

later remained relatively stable (Fig. 1). The decay pattern was consistent with that of a previous leaf litter decomposition experiment, in which most of the litters

lost more than 20 % and some even lost more than 40 % of their initial mass (Mo et al. 2007). At the initial decomposition stage, the litters commonly have relative higher C compound concentrations in terms of more readily and moderately decomposable C (i.e., total nonstructural carbon and acid-hydrolysable fraction) (Hobbie et al. 2010; Sun et al. 2013b). The litter was placed out in June, the beginning of wet and warm season, so the high initial decay rate was probably due to higher moisture, higher temperature, increased microbial activity and potential impact of leaching of dissolved organic carbon (DOC) and dissolved organic nitrogen (DON). With the time increasing, DOC and DON rapidly decreased and thus relatively little change in mass losses occurred during the rest of the experiment. Decay constants ranged from 0.11 to 0.16 year⁻¹ in leaf litter, 0.15 to 0.19 year⁻¹ in <0.5-mm roots, 0.15 to 0.26 year⁻¹ in 0.5–2-mm roots, 0.14 to 0.24 year⁻¹ for 2–5-mm roots and 0.11 to 0.19 year⁻¹ in >5-mm roots in *P. sylvestris* (Table 2). Our rates of mass loss for both leaves and roots fell in the range reported for other temperate tree species (Gholz et al. 2000; Parton et al. 2007; Sun et al. 2013b).

In the few studies that have compared root and leaf litter decomposition rates simultaneously, there appears to be no consistent trend in decomposition rates. Roots have been reported to decompose faster (Seastedt et al. 1992; Hobbie 1996) or slower (Gorissen and Cotrufo 2000; Kemp et al. 2003; Majdi 2004) than leaves, or at a similar rate to leaf decomposition (Cusack et al. 2009). These divergences between leaves and roots in decomposition rates might be explained by the litter quality differences and decompositional environment between the two tissue types. To determine the effect of litter microsite on leaf and root decomposition, we established a factorial manipulation using both leaf and root litter at three soil depths in the *P. sylvestris* plantation. Inconsistent with our first

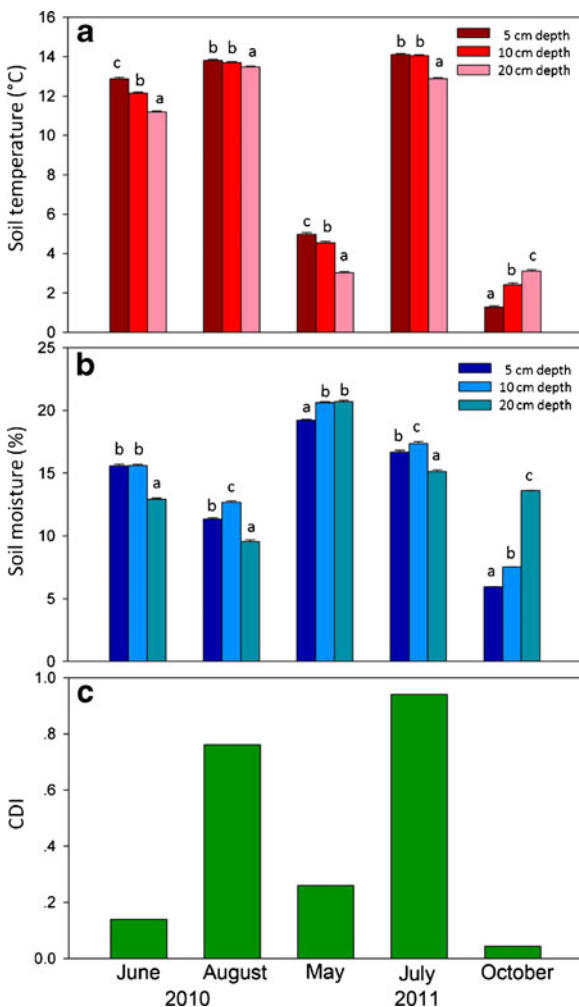


Fig. 3 Temporal dynamics of soil temperature, soil moisture, and climate decomposition index (CDI)

Fig. 4 Relationships between the decay constants (k -values) and soil temperature (a) and moisture (b)

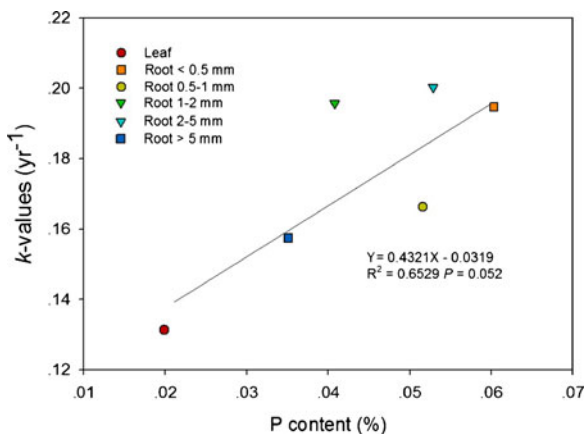
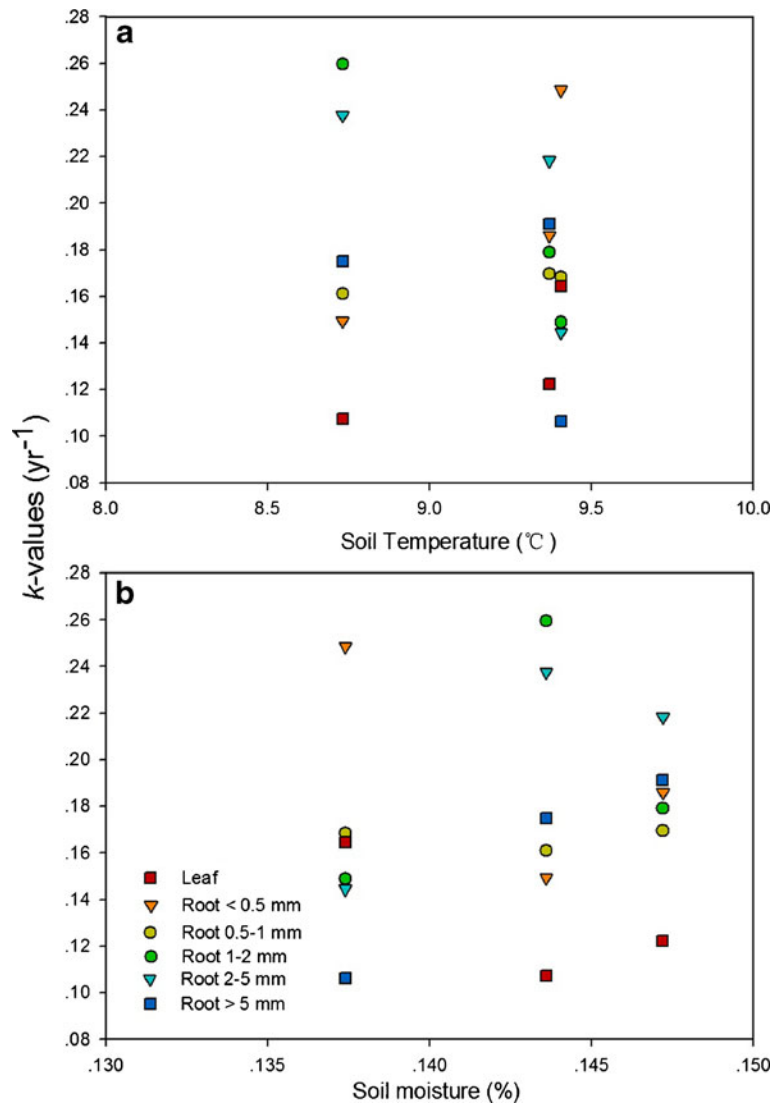


Fig. 5 Relationship between initial litter phosphorus (P) content and decay constants (k -values)

hypothesis, we found that leaves and the finest roots decomposed more quickly at 5 cm depth and coarser roots (>1-mm) decomposed more quickly at 10 and 20 cm depth (Fig. 2).

Our result was inconsistent with previous studies. For instance, Powers et al. (2009) studied decomposition of the same substrates both aboveground and in belowground soils and observed substrates decomposed faster belowground in drier forests. Nevertheless, they did not directly compare leaf *versus* root decomposition. In a mesocosm experiment, fine roots and leaves decomposed equally aboveground and roots decomposed significantly more slowly belowground (Austin et al. 2009). However, the mesocosm experiment may differ from the in-situ one used by our studies, thus leading to the different results.

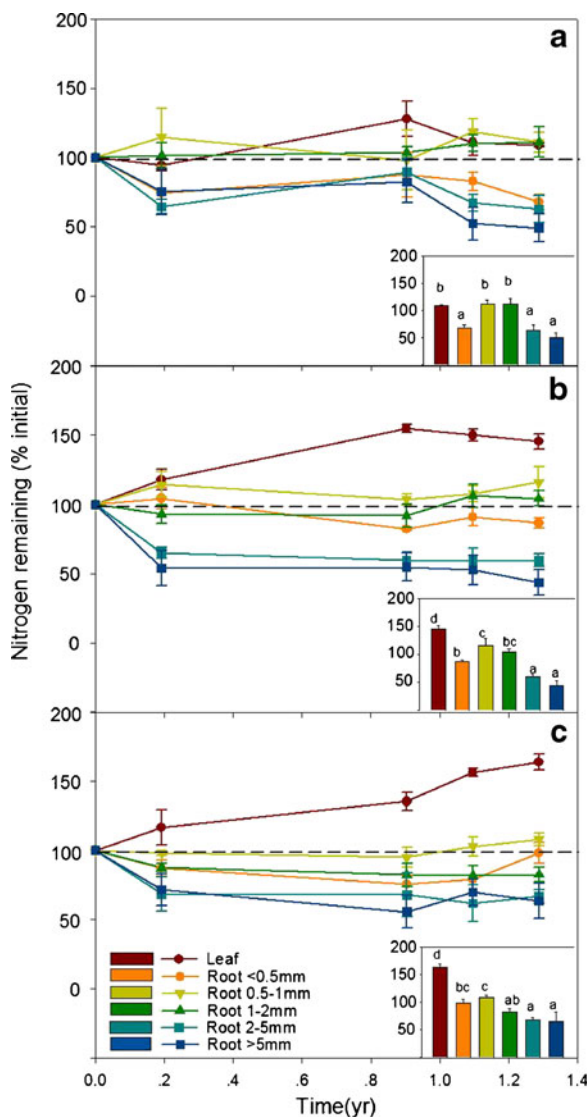


Fig. 6 Nitrogen remaining (% initial litter) vs. time for different litter types at 5 cm (a), 10 cm (b) and 20 cm (c) soil depth. Inserted figure shows the comparison of averaged nitrogen remaining (%) among different litter types

Although decomposition rates were significantly different at different soil depths, soil temperatures and levels of soil moisture (Fig. 3), no significant relationship was observed between either soil temperature or water content and the value of the decay constant k (Fig. 4). We suspected that the contrasting trends in decomposition rates between leaves, the finest roots and the coarser roots (>1 -mm) with soil depth (Fig. 2) may be caused by a type of “home-field advantage” of litter decomposition; that is leaf litter and the finer roots are distributed at or near the soil surface layer while coarser roots are

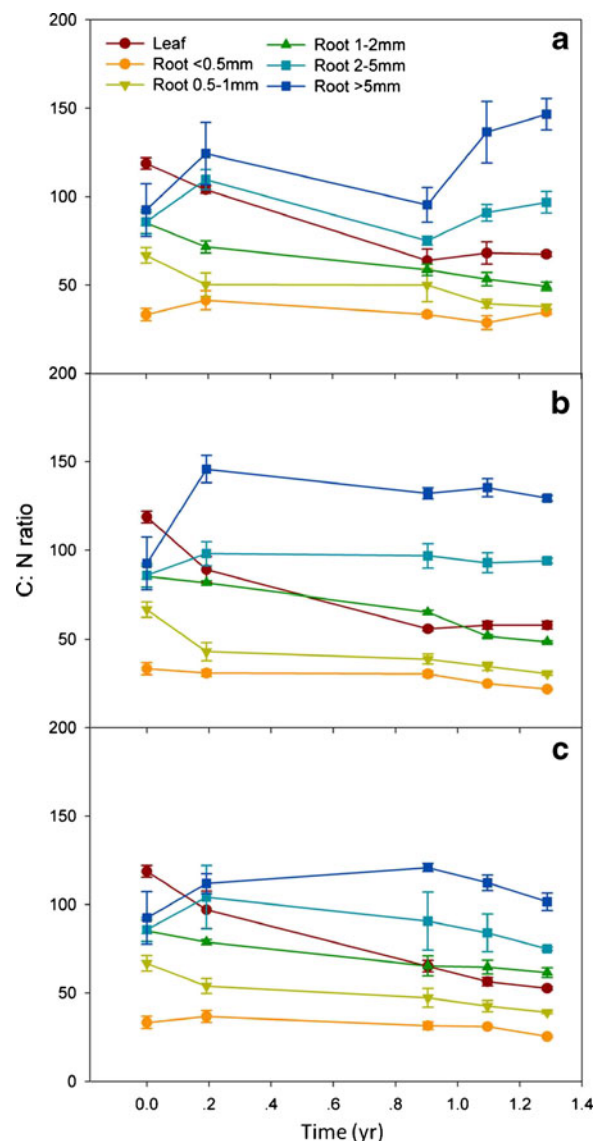


Fig. 7 Changes in the carbon to nitrogen (C:N) ratio vs. time for different litter types at 5 cm (a), 10 cm (b) and 20 cm (c) soil depth

typically distributed in deeper soil layers. Several leaf litter decay studies have indicated that plant litter often decomposes faster in the habitat from which it was derived (i.e. home) than when placed in foreign habitats (i.e. away), which has been called the home-field advantage of litter decomposition (Vivanco and Austin 2008; Ayres et al. 2009), although support for this idea has not been universal (John et al. 2011; Milcu and Manning 2011). However, the mechanisms involved in the effects of soil depth on leaf and root decomposition still needed further investigation.

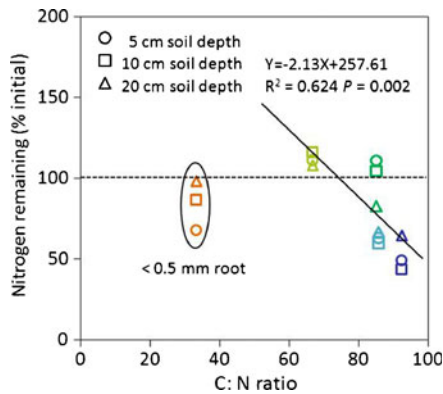


Fig. 8 Relationship between nitrogen remaining (% initial) and initial root carbon to nitrogen (C:N) ratio. The data from roots <0.5 mm were excluded. Different colors represent different root diameters roots (orange: 0.5–1 mm, green: 1–2 mm, blue: 2–5 mm, violet: >5 mm). Dashed line represents the initial residual nitrogen content

Previous studies have shown that simple chemical variables are commonly the best predictors of the decomposition rate when different litter types decompose in the same environment (Hobbie 2005; Santiago 2007; Hobbie et al. 2010; Birouste et al. 2012). In our study area, the general pattern of decomposition rate could be explained by initial litter P concentration (Fig. 5). Although N has been shown to be major limiting factor for plant growth in temperate ecosystems (Vitousek and Howarth 1991; Vitousek et al. 1994), we did not observe a significant correlation between decomposition rates and initial litter N concentration. Perhaps N was not the major limiting factor for litter decomposition in our study area.

Also, we observed that the root diameter effect on decomposition rate was strongly dependent on soil depths of litter placement (Fig. 1). To prevent the confounding effect of soil depth, we compared our data from a depth of 10 cm (the most commonly used in previous studies) with other similar studies. No significant differences in decomposition rates among fine roots (<0.5-mm, 0.5–1-mm and 1–2-mm diameter) (Fig. 1b) were observed, which was inconsistent with our second hypothesis. Our results were also inconsistent with some recent studies (Sun et al. 2013a, 2013b), indicating that the finest roots (<0.5-mm) decomposed at a slower rate than 0.5–2-mm roots. For example, <0.5-mm roots are believed to be physiologically more active than larger ones for a number of tree species (Joslin et al. 2006; Park et al. 2008; Fan and Guo 2010; Kramer et al. 2010; Prescott 2010; Burton et al. 2012). Initial litter carbon quality (Guo et al. 2004) and N

concentration (Berg and McClaugherty 2003) have been considered major factors influencing differences in decomposition rates between the very fine roots (<0.5-mm) and fine roots (0.5–2-mm). Lower AS and higher AIF concentrations were observed in <0.5-mm roots than 0.5–2-mm ones (Hättenschwiler and Jørgensen 2010; Hättenschwiler et al. 2011; Xiong et al. 2013). However, our data suggested that the concentration of AIF in <0.5-mm roots was not significantly different from that of 0.5–2-mm roots (Table 1). Although we found that the <0.5-mm roots had higher N concentrations than did the 0.5–2-mm roots (Table 1), the higher initial N concentrations did not result in significantly different decomposition rates. Therefore, we suspected that similar initial C quality (AIF and AS) (Table 1) may explain the similarity of the decomposition rates. Recently, Xiong et al. (2013) observed that decomposition rates did not differ significantly between root order classes in *Eucalyptus*, *Schima* and *Phellodendron*, corresponding to similar AIF concentrations between root order classes for these three species.

When the roots were divided into three diameter classes (<2-mm, 2–5-mm and >5-mm) (Silver and Miya 2001), 2–5-mm roots decomposed significantly faster than roots of other size classes (Fig. 1b). N-lignin complexes formed in N-rich fine roots (<2-mm) may be responsible for their slower decomposition rates when compared with 2–5-mm roots (Camiré et al. 1991). In addition, the slower decomposition of fine roots may be also caused by the ability of ectomycorrhizal fungi to retard root decomposition (Langley and Hungate 2003). Also, the discrepancy between decomposition rates of 2–5-mm and >5-mm roots might be lie in the fact that >5 mm-roots had lower P concentrations than did 2–5-mm roots (Table 1). It should be noted that even for the same litter type with the same litter quality, decomposition rates significantly differed with varying soil depth (Fig. 2). Thus, future research should consider the effect of soil depth to obtain a full understanding of the relative contribution of the decomposition of leaves and roots of different diameters to carbon and nutrient cycling.

N release dynamics

Roots and leaves that were produced and decomposed in the same site also differed in nutrient accumulation and release. It is commonly believed that net N immobilization and release in leaf litter were strongly controlled by initial N concentrations regardless of climate, other litter quality parameters, or site characteristics (Parton et al. 2007). When the initial leaf litter N concentration was less than

1 % and the average C: N ratio was less than 40, substantial net N release began (Parton et al. 2007) because at low C: N ratios (e.g., high N concentrations), decomposers meet their N requirements directly from the litter and at higher initial C: N ratios, net immobilization typically occurs as microbes access N exogenous to the litter and convert it to microbial biomass or exoenzymes (Frey et al. 2000). We observed leaf litter consistently immobilized N during the 470-day decomposition process (Fig. 6). The initial leaf litter N concentration averaged 0.48 % and C: N was 118 (Table 1). Patterns observed here were generally consistent with global trends (Parton et al. 2007) and patterns found in seven species decomposed in a Japanese subtropical forest (Xu and Hirata 2005) and five tropical forest types (Cusack et al. 2009).

Inconsistent with the pattern of leaf litter decomposition, we observed that coarse roots (>2-mm) with higher C: N ratios could release more N than fine roots (<2-mm) (Fig. 6). Our results therefore emphasized that coarse roots may contribute greatly to the nutrient release. Recent findings have also shown that fine roots may release limited amounts of N during the first several years of decomposition (Goebel et al. 2011; Olajuyigbe et al. 2012; Xiong et al. 2013). In our study site, fine roots (<2-mm) generally increased their relative N content during the entire experimental period, except that the finest roots (<0.5-mm) released very limited amounts of N (Fig. 6). These results were consistent with the recent studies, which showed that root N content declined more rapidly in very fine roots (<0.5-mm) than in 0.5–2-mm roots (Guo et al. 2004; Sun et al. 2013a, 2013b). However, our results were not consistent with the work showing that roots across all Long-term Inter-site Decomposition Experiment Team sites in North America released N linearly with mass loss, regardless of species or location (Parton et al. 2007). They believed that initial C: N ratios as high as 50 would allow the linear release of N during the initial phases of root decomposition (Parton et al. 2007). However, in our study, the finest roots (<0.5-mm) with C: N ratio <50 generally released N and lacked N immobilization; in contrast, 0.5–2-mm roots with C: N ratio >50 exhibited N immobilization (Fig. 4). Moreover, aside from the finest roots (<0.5-mm), initial root C: N ratios were negatively correlated with averaged nitrogen remaining (% initial) (Fig. 8). Therefore, other controlling factors existed aside from litter initial C: N ratio for driving nitrogen immobilization and release of N by the finest roots. Because N release during decay plays a fundamental role in net ecosystem production, further study is needed

related to the controls on net N release for roots with different diameters during decomposition; such research would greatly improve our ability to predict terrestrial C dynamics at global and regional scales.

Conclusions

Our findings showing that leaf litter generally decomposed more slowly than roots suggest that leaf litter may be an important contributor to soil organic matter in a *P. sylvestris* plantation. Soil depth has a significant effect on the decomposition rate for both leaves and roots. The general pattern of leaf and root decomposition was significantly affected by initial litter P concentration. Leaf litter and fine roots (<2-mm) immobilized N, but coarse roots (>2-mm) released N during the early stage of decomposition.

Acknowledgments This research was supported by the National Basic Research Program of China (2013CB956303 and 2010CB950600), projects of the National Natural Science Foundation of China (31222011, 31270363 and 31070428) and projects supported by the Foundation for Innovative Research Groups of the National Natural Science Foundation of China (31021001).

References

- Abiven S, Recous S, Reyes V, Oliver R (2005) Mineralisation of C and N from root, stem and leaf residues in soil and role and their biochemical quality. *Biol Fertil Soils* 42:119–128
- Adair EC, Parton WJ, Del Grosso SJ, Silver WL, Harmon ME, Hall SA, Burke IC, Hart SC (2008) Simple three-pool model accurately describes patterns of long-term litter decomposition in diverse climates. *Glob Chang Biol* 14:2636–2660
- Aerts R (1997) Climate, leaf litter chemistry and leaf litter decomposition in terrestrial ecosystems: a triangular relationship. *Oikos* 79:439–449
- Austin AT, Araujo PI, Leva PE (2009) Interaction of position, litter type, and water pulses on decomposition of grasses from the semiarid Patagonian steppe. *Ecology* 90:2642–2647
- Ayres E, Steltzer H, Simmons BL, Simpson RT, Steinweg JM, Wallenstein MD, Mellor N, Parton WJ, Moore JC, Wall DH (2009) Home-field advantage accelerates leaf litter decomposition in forests. *Soil Biol Biochem* 41:606–610
- Berg B, McClaugherty C (2003) Plant litter: decomposition, humus formation, carbon sequestration. Springer, Berlin
- Bird JA, Kleber M, Torn MS (2008) ¹³C and ¹⁵N stabilization dynamics in soil organic matter fractions during needle and fine root decomposition. *Org Geochem* 39:465–477

- Birouste M, Kazakou E, Blanchard A, Roumet C (2012) Plant traits and decomposition: are the relationships for roots comparable to those for leaves? *Ann Bot* 109:463–472
- Bremner JM (1996) Nitrogen-total. In: Sparks DL (ed) *Methods of soil analysis*. SSSA Book Ser, Madison, pp 1085–1122
- Burton AJ, Jarvey JC, Jarvi MP, Zak DR, Pregitzer KS (2012) Chronic N deposition alters root respiration–tissue N relationship in northern hardwood forests. *Glob Chang Biol* 18:258–266
- Camiré C, Côté B, Brulotte S (1991) Decomposition of roots of black alder and hybrid poplar in short-rotation plantings: nitrogen and lignin control. *Plant Soil* 138:123–132
- Chen H, Harmon ME, Griffiths RP (2001) Decomposition and nitrogen release from decomposing woody roots in coniferous forests of the Pacific Northwest: a chronosequence approach. *Can J For Res* 31:246–260
- Cusack DF, Chou WW, Yang WH, Harmon ME, Silver WL (2009) Controls on long-term root and leaf litter decomposition in neotropical forests. *Glob Chang Biol* 15:1339–1355
- Fahey TJ, Arthur MA (1994) Further studies of root decomposition following harvest of a northern hardwoods forest. *Forest Sci* 40:618–629
- Fan P, Guo D (2010) Slow decomposition of lower order roots: a key mechanism of root carbon and nutrient retention in the soil. *Oecologia* 163:509–515
- Frey S, Elliott E, Paustian K, Peterson G (2000) Fungal translocation as a mechanism for soil nitrogen inputs to surface residue decomposition in a no-tillage agroecosystem. *Soil Biol Biochem* 32:689–698
- Gholz HL, Wedin D, Smitherman SM, Harmon ME, Parton WJ (2000) Long-term dynamics of pine and hardwood litter in contrasting environments: toward a global model of decomposition. *Glob Chang Biol* 6:751–765
- Gill RA, Burke IC (2002) Influence of soil depth on the decomposition of *Bouteloua gracilis* roots in the shortgrass steppe. *Plant Soil* 241:233–242
- Goebel M, Hobbie SE, Bulaj B, Zadworny M, Archibald DD, Oleksyn J, Reich PB, Eissenstat DM (2011) Decomposition of the finest root branching orders: linking belowground dynamics to fine-root function and structure. *Ecol Monogr* 81:89–102
- Gorissen A, Cotrufo M (2000) Decomposition of leaf and root tissue of three perennial grass species grown at two levels of atmospheric CO₂ and N supply. *Plant Soil* 224:75–84
- Guo DL, Mitchell RJ, Hendricks JJ (2004) Fine root branch orders respond differentially to carbon source-sink manipulations in a longleaf pine forest. *Oecologia* 140:450–457
- Guo D, Xia M, Wei X, Chang W, Liu Y, Wang Z (2008) Anatomical traits associated with absorption and mycorrhizal colonization are linked to root branch order in twenty-three Chinese temperate tree species. *New Phytol* 180:673–683
- Hättenschwiler S, Coq S, Barantal S, Handa IT (2011) Leaf traits and decomposition in tropical rainforests: revisiting some commonly held views and towards a new hypothesis. *New Phytol* 189:950–965
- Hättenschwiler S, Jørgensen HB (2010) Carbon quality rather than stoichiometry controls litter decomposition in a tropical rain forest. *J Ecol* 98:754–763
- Hobbie SE (1996) Temperature and plant species control over litter decomposition in Alaskan tundra. *Ecol Monogr* 66:503–522
- Hobbie SE (2005) Contrasting effects of substrate and fertilizer nitrogen on the early stages of litter decomposition. *Ecosystems* 8:644–656
- Hobbie SE, Oleksyn J, Eissenstat DM, Reich PB (2010) Fine root decomposition rates do not mirror those of leaf litter among temperate tree species. *Oecologia* 162:505–513
- John MG, St. Orwin KH, Dickie IA (2011) No ‘home’ versus ‘away’ effects of decomposition found in a grassland-forest reciprocal litter transplant study. *Soil Biol Biochem* 43:1482–1489
- Johnsen K, Maier C, Kress L (2005) Quantifying root lateral distribution and turnover using pine trees with a distinct stable carbon isotope signature. *Funct Ecol* 19:81–87
- Joslin J, Gaudinski JB, Torn MS, Riley W, Hanson PJ (2006) Fine-root turnover patterns and their relationship to root diameter and soil depth in a ¹⁴C-labeled hardwood forest. *New Phytol* 172:523–535
- Kemp P, Reynolds J, Virginia R, Whitford W (2003) Decomposition of leaf and root litter of Chihuahuan desert shrubs: effects of three years of summer drought. *J Arid Environ* 53:21–39
- King JS, Albaugh TJ, Allen HL, Buford M, Strain BR, Dougherty P (2002) Below-ground carbon input to soil is controlled by nutrient availability and fine root dynamics in loblolly pine. *New Phytol* 154:389–398
- Knorr M, Frey S, Curtis P (2005) Nitrogen additions and litter decomposition: a meta-analysis. *Ecology* 86:3252–3257
- Kramer C, Trumbore S, Fröberg M, Cisneros Dozal LM, Zhang D, Xu X, Santos GM, Hanson PJ (2010) Recent (<4 year old) leaf litter is not a major source of microbial carbon in a temperate forest mineral soil. *Soil Biol Biochem* 42:1028–1037
- Langley JA, Hungate BA (2003) Mycorrhizal controls on belowground litter quality. *Ecology* 84:2302–2312
- Ludovici KH, Zarnoch SJ, Richter DD (2002) Modeling in-situ pine root decomposition using data from a 60-year chronosequence. *Can J For Res* 32:1675–1684
- Majdi H (2004) Root and needle litter decomposition responses to enhanced supplies of N and S in a Norway spruce forest in southwest Sweden. *Plant Biosystems* 138:225–230
- Mambelli S, Bird JA, Gleixner G, Dawson TE, Torn MS (2011) Relative contribution of foliar and fine root pine litter to the molecular composition of soil organic matter after in situ degradation. *Org Geochem* 42:1099–1108
- Melin Y, Petersson H, Nordfjell T (2009) Decomposition of stump and root systems of Norway spruce in Sweden—A modelling approach. *Forest Ecol Manag* 257:1445–1451
- Milcu A, Manning P (2011) All size classes of soil fauna and litter quality control the acceleration of litter decay in its home environment. *Oikos* 120:1366–1370
- Mo JM, Zhang W, Zhu WX, Fang YT, Li DJ, Zhao P (2007) Response of soil respiration to simulated N deposition in a disturbed and a rehabilitated tropical forest in southern China. *Plant Soil* 296:125–135
- Moretto AS, Distel RA (2003) Decomposition of and nutrient dynamics in leaf litter and roots of *Poa ligularis* and *Stipa gyneriodes*. *J Arid Environ* 55:503–514
- Nambiar EKS (1987) Do nutrients retranslocate from fine roots? *Can J For Res* 17:913–918
- Nelson DW, Sommers LE, Sparks D, Page A, Helmke P, Loeppert R, Soltanpour P, Tabatabai M, Johnston C, Sumner M (1996) Total carbon, organic carbon, and organic matter. *Methods of soil analysis Part 3-chemical methods*, pp 961–1010

- Olajuyigbe S, Tobin B, Hawkins M, Nieuwenhuis M (2012) The measurement of woody root decomposition using two methodologies in a Sitka spruce forest ecosystem. *Plant Soil* 360:77–91
- Olson JS (1963) Energy storage and the balance of producers and decomposers in ecological systems. *Ecology* 44:322–331
- Paquette A, Messier C (2010) The role of plantations in managing the world's forests in the Anthropocene. *Front Ecol Environ* 8:27–34
- Parton W, Silver WL, Burke IC, Grassens L, Harmon ME, Currie WS, King JY, Adair EC, Brandt LA, Hart SC (2007) Global-scale similarities in nitrogen release patterns during long-term decomposition. *Science* 315:361–364
- Park BB, Yanai RD, Fahey TJ, Bailey SW, Siccama TG, Shanley JB, Cleavitt NL (2008) Fine root dynamics and forest production across a calcium gradient in northern hardwood and conifer ecosystems. *Ecosystems* 11:325–341
- Powers JS, Montgomery RA, Adair EC, Brearley FQ, DeWalt SJ, Castanho CT, Chave J, Deinert E, Ganzhorn JU, Gilbert ME (2009) Decomposition in tropical forests: a pan-tropical study of the effects of litter type, litter placement and mesofaunal exclusion across a precipitation gradient. *J Ecol* 97:801–811
- Prescott CE (2010) Litter decomposition: what controls it and how can we alter it to sequester more carbon in forest soils? *Biogeochemistry* 101:133–149
- Ryan MG, Melillo JM, Ricca A (1990) A comparison of methods for determining proximate carbon fractions of forest litter. *Can J For Res* 20:166–171
- Santiago LS (2007) Extending the leaf economics spectrum to decomposition: evidence from a tropical forest. *Ecology* 88:1126–1131
- Seastedt TR, Parton WJ, Ojima DS (1992) Mass-loss and nitrogen dynamics of decaying litter of grasslands - the apparent low nitrogen immobilization potential of root detritus. *Can J Bot* 70:384–391
- Silver WL (1998) The potential effects of elevated CO₂ and climate change on tropical forest soils and biogeochemical cycling. *Climatic change* 39:337–361
- Silver WL, Miya RK (2001) Global patterns in root decomposition: comparisons of climate and litter quality effects. *Oecologia* 129:407–419
- Sun T, Mao ZJ, Dong LL, Hou LL, Song Y, Wang XW (2013a) Further evidence for slow decomposition of very fine roots using two methods: litterbags and intact cores. *Plant Soil* 366:633–646
- Sun T, Mao Z, Han Y (2013b) Slow decomposition of very fine roots and some factors controlling the process: a 4-year experiment in four temperate tree species. *Plant Soil*. doi:10.1007/s11104-013-1755-4
- Tobin B, Nieuwenhuis M (2007) Biomass expansion factors for Sitka spruce (*Picea sitchensis* (Bong.) Carr.) in Ireland. *Eur J For Res* 126:189–196
- Valenzuela-Estrada LR, Vera-Caraballo V, Ruth LE, Eissenstat DM (2008) Root anatomy, morphology, and longevity among root orders in *Vaccinium corymbosum* (Ericaceae). *Am J Bot* 95:1506–1514
- Vitousek P, Turner D, Parton W, Sanford R (1994) Litter decomposition on the Mauna Loa environmental matrix, Hawai'i: patterns, mechanisms, and models. *Ecology* 75:418–429
- Vitousek PM, Howarth RW (1991) Nitrogen limitation on land and in the sea: how can it occur? *Biogeochemistry* 13:87–115
- Vivanco L, Austin AT (2008) Tree species identity alters forest litter decomposition through long-term plant and soil interactions in Patagonia, Argentina. *J Ecol* 96:727–736
- Wang H, Liu S, Mo J (2010) Correlation between leaf litter and fine root decomposition among subtropical tree species. *Plant Soil* 335:289–298
- Xiong Y, Fan P, Fu S, Zeng H, Guo D (2013) Slow decomposition and limited nitrogen release by lower order roots in eight Chinese temperate and subtropical trees. *Plant Soil* 363:19–31
- Xu XN, Hirata EJ (2005) Decomposition patterns of leaf litter of seven common canopy species in a subtropical forest: N and P dynamics. *Plant Soil* 273:279–289

Diurnal and Seasonal Change in Stem Respiration of *Larix principis-rupprechtii* Trees, Northern China

Yan Yang¹, Miao Zhao¹, Xiangtao Xu^{1,2}, Zhenzhong Sun¹, Guodong Yin¹, Shilong Piao^{1*}

¹ Department of Ecology, College of Urban and Environmental Sciences, and Key Laboratory for Earth Surface Processes of the Ministry of Education, Peking University, Beijing, China, ² Department of Geosciences, Princeton University, Princeton, New Jersey, United States of America

Abstract

Stem respiration is a critical and uncertain component of ecosystem carbon cycle. Few studies reported diurnal change in stem respiration as well as its linkage with climate. In this study, we investigated the diurnal and seasonal change in stem respiration and its linkage with environmental factors, in larch plantations of northern China from 2010 to 2012. The stem respiration per unit surface area (R_s) showed clear diurnal cycles, ranging from 1.65 ± 0.10 to $2.69 \pm 0.15 \mu\text{mol m}^{-2} \text{s}^{-1}$, increased after 6:00, peaked at 15:00 and then decreased. Both stem temperature and air temperature show similar diurnal pattern, while the diurnal pattern of air relative humidity is just the opposite to R_s . Similar to the diurnal cycles, seasonal change in R_s followed the pattern of stem temperature. R_s increased from May ($1.28 \pm 0.07 \mu\text{mol m}^{-2} \text{s}^{-1}$) when the stem temperature was relatively low and peaked in July ($3.02 \pm 0.10 \mu\text{mol m}^{-2} \text{s}^{-1}$) when the stem temperature was also the highest. Further regression analyses show that R_s exponentially increases with increasing temperature, and the Q_{10} of R_s at mid daytime (1.97 ± 0.17 at 12:00 and 1.96 ± 0.10 at 15:00) is significantly lower than that of mid nighttime (2.60 ± 0.14 at 00:00 and 2.71 ± 0.25 at 03:00) Q_{10} . This result not only implies that R_s is more sensitive to night than day warming, but also highlights that temperature responses of R_s estimated by only daytime measurement can lead to underestimated stem respiration increase under global warming, especially considering that temperature increase is faster during nighttime.

Citation: Yang Y, Zhao M, Xu X, Sun Z, Yin G, et al. (2014) Diurnal and Seasonal Change in Stem Respiration of *Larix principis-rupprechtii* Trees, Northern China. PLoS ONE 9(2): e89294. doi:10.1371/journal.pone.0089294

Editor: Dafeng Hui, Tennessee State University, United States of America

Received: October 8, 2013; **Accepted:** January 17, 2014; **Published:** February 26, 2014

Copyright: © 2014 Yang et al. This is an open-access article distributed under the terms of the Creative Commons Attribution License, which permits unrestricted use, distribution, and reproduction in any medium, provided the original author and source are credited.

Funding: This study was funded by the National Natural Science Foundation of China (41171202 and 41125004). The funders had no role in study design, data collection and analysis, decision to publish, or preparation of the manuscript.

Competing Interests: The authors have declared that no competing interests exist.

* E-mail: slpiao@pku.edu.cn

Introduction

Rising atmospheric carbon dioxide (CO_2) is considered to have significant impacts on the climate system [1], which has triggered strong scientific interests in understanding the global carbon cycle. Forests play a key role in the global carbon cycle. They cover approximately one-third of the earth's land surface, and store about $861 \pm 66 \text{ Pg}$ of the total carbon [2]. Current terrestrial carbon sink has also been suggested to be mainly contributed by the forest sink [2]. Accordingly, accurate information on processes related to forest carbon cycle is essential to predict future evolution of the global carbon cycle and climate change. As a major pathway of carbon loss from terrestrial ecosystems, ecosystem respiration is critical to regulating forest ecosystem carbon fluxes and thus important to forest carbon balance. Ecosystem respiration is composed of two dominant fluxes, (i) soil respiration including heterotrophic respiration of decomposing microbes, respiration of plant roots and soil fauna, and (ii) above-ground respiration of plant woody tissues and leaves. Compared with soil respiration [3–5], our understanding of the linkage between above-ground respiration and climate is very limited [6,7].

As an important part of woody tissues, stem respiration contributes 9% of the total ecosystem respiration in boreal forest [8,9], 9% in dry Mediterranean forests [10], about 14% in Neotropical rainforests [11] and up to 21% in temperate forests [12]. Both environmental and biotic factors can influence stem respiration [13–20]. Among them, temperature is well known to

be a dominant environmental driver [6,9,21–23], and is often used to predict stem respiration [24–26]. Therefore, it is critical to accurately quantifying the temperature sensitivity of stem respiration, which may reduce the uncertainties in assessing the positive feedbacks between the carbon cycle and climate predicted by coupled carbon-climate models [27,28].

Temperature sensitivity of stem respiration is usually expressed in terms of Q_{10} (the rate of change in respiration resulting from a 10°C increase in temperature). Numerous studies on temperature sensitivity of stem respiration have been conducted across different forest types of the world and reported different Q_{10} values of stem respiration for different forests, varying from 1.00 to 6.40 [26,29–32]. It should be noted, however, that most of these previous studies estimated Q_{10} values based on the measurement of daytime stem respiration [33], and few studies measured diurnal change in stem respiration as well as its linkage with climate [34]. Since stem respiration is also influenced by other environmental and physiological processes [16,23,35–39], such as photosynthesis that occurs only during the daytime, it is possible that stem respiration responds to temperature changes in daytime and nighttime differently. Furthermore, both observations and model projection have showed that global warming is faster during the nighttime than that during the daytime [1]. Thus, understanding the possible differential responses of stem respiration to day and night warming will be helpful to improve the projection of future carbon cycle evolution as well as its feedback to climate.

In this study, we have conducted field measurement to investigate the diurnal and seasonal change in stem respiration and its linkage with environmental factors, in larch plantations of northern China since 2010. The primary object of this paper is to test the hypothesis that temperature sensitivity of stem respiration is different during daytime and nighttime.

Materials and Methods

Study Site and Experimental Design

This study was conducted at Saihanba ecological station ($42^{\circ}24.723'N$, $117^{\circ}14.844'E$, 1505 m a.s.l.) of Peking University, situated in Saihanba National Forest Park, Hebei Province (Fig. 1). Saihanba has a mean annual precipitation of approximately 450 mm, 70% of which occurs from June to August, and mean annual temperature of $-1.4^{\circ}C$ [40] with a long cold winter and a short growing season (May–September). The soils are predominantly sand. Soil bulk density is 1.47 g cm^{-3} , C:N ratio is 8.9 ± 0.3 , and soil pH (soil:water, 1:2.5) is 6.3 ± 0.2 [41].

The experiment was carried out in three $20 \times 20\text{ m}$ plots located within a 45-year-old larch plantation (*Larix principis-rupprechtii*). The topography of the plots is nearly flat and the stem density is $870 \pm 48\text{ stem}\cdot\text{ha}^{-1}$ with an average diameter at breast height (DBH) of $19.9 \pm 2.8\text{ cm}$ and an average height of $15.8 \pm 1.6\text{ m}$. Two larch trees were chosen randomly in each plot, and all together 6 trees were selected in the study area with an average DBH of $20 \pm 2\text{ cm}$ and an average height of $16 \pm 1.5\text{ m}$. Although the experiment plots and individuals were very homogeneous, it

should be reminded that the limited sample size (6 trees in total) might introduce biases originated from inter-individual differences and the effect of micro-topography. In this study, 3-hourly stem respiration measurements were made for a whole day, twice a month in growing season from 2010 to 2012, using a LI-6400-09 (Li-Cor, Lincoln, Nebraska, USA). In order to capture the CO_2 released by stems, a technique called horizontally oriented soil chamber (HOSC) [12,42] was exploited: the CO_2 chamber (9.9 cm in diameter) was connected to stem collars (10.1 cm in diameter), which completely enclosed a 10.1 cm segment of the tree stem at 1.3 m above ground and were fixed tightly onto the stems with nylon straps. To ensure an airtight seal between stem collars and stem surfaces, loose barks at two ends of the enclosed stem segment, which might leak air, were removed at first. Then the collars made of polyvinyl chloride (PVC) pipe were polished to fit the curvature of the stem surface. Finally the small gaps between the collars and stem surfaces were sealed completely with silicon sealant. Meanwhile, stem temperatures were measured with copper-constantan thermocouples at the depth of 5 mm from the stem surface with tree bark.

Data Analyses

To eliminate the influence of plant size, the measured stem respiration was firstly normalized by the surface area enclosed, which was calculated using the following equation [43]

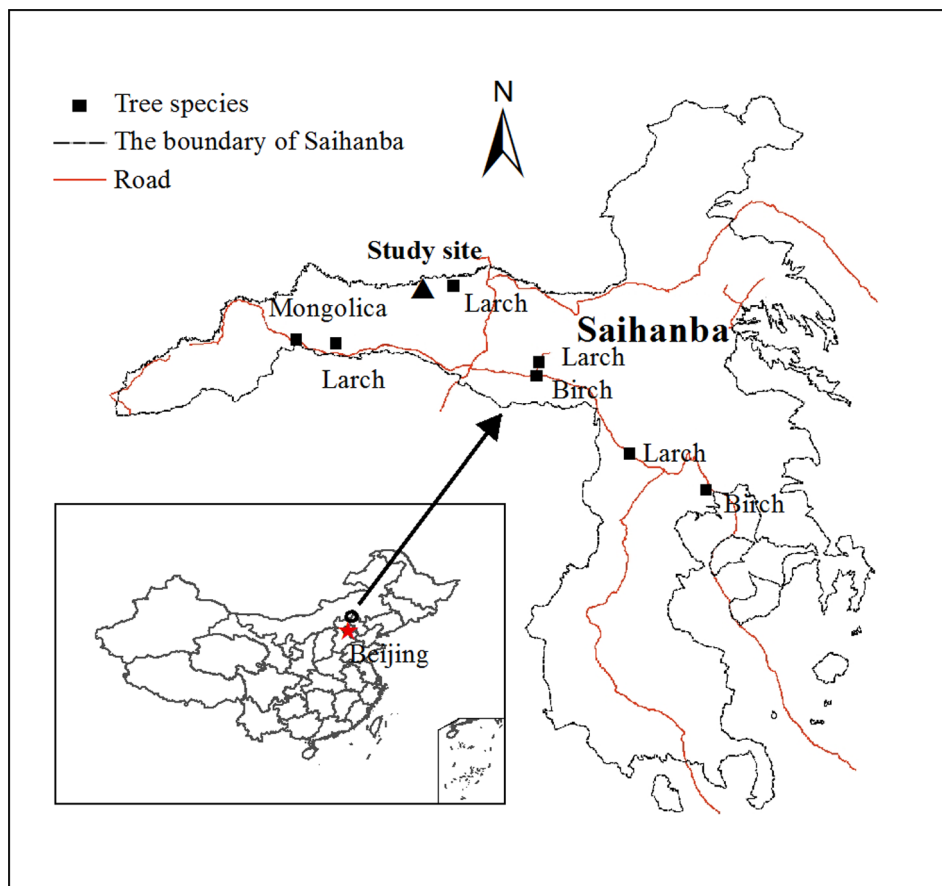


Figure 1. Location of study site in Saihanba National Forest Park, Hebei Province, China.

doi:10.1371/journal.pone.0089294.g001

$$A = \frac{\pi D_1 D_2}{4} \arcsin\left(\frac{D_1}{D_2}\right) \quad (1)$$

where A is the stem surface area enclosed by the collar (m^2), D_1 is the diameter of the chamber (m), D_2 is the diameter of the enclosed stem segment (m). Then the stem respiration per unit surface area R_S ($\mu\text{mol}\cdot\text{m}^{-2}\cdot\text{s}^{-1}$) should be the measurement results divided by the area A for each plant.

The relationship between stem respiration and corresponding stem temperature can be described by an exponential function

$$R_S = R_0 e^{\beta T} \quad (2)$$

where T is the measured stem temperature ($^{\circ}\text{C}$); R_S is the stem respiration per unit surface area ($\mu\text{mol}\cdot\text{m}^{-2}\cdot\text{s}^{-1}$) at temperature T ; R_0 is the potential stem respiration rate at 0°C and β is a fitting parameter, which indicates the temperature sensitivity of respiration [44]. The temperature sensitivity is often expressed by Q_{10} , which describes the proportional change in stem respiration rate for a 10°C increase in sapwood temperature). According to Eq.2, the Q_{10} values can be calculated as

$$Q_{10} = e^{10\beta} \quad (3)$$

For each plant individual, three-hourly R_0 and β were acquired by fitting stem respiration (R) and stem temperature (T) measured throughout the sampling period to Eq.2 and three-hourly Q_{10} values were calculated according to Eq.3. Then they are averaged for all six larch individuals. All the statistical analyses were performed in PASW statistic 18 (SPSS Inc., Chicago, IL, USA).

Results

Diurnal Variation

The measured stem respiration per unit surface area (R_S) and environmental factors showed clear diurnal cycles (Fig. 2), averaged over the whole sampling period. R_S , ranging from 1.65 ± 0.10 to $2.69 \pm 0.15 \mu\text{mol m}^{-2} \text{s}^{-1}$, increased after 6:00, peaked at 15:00 and then decreased. Both stem temperature and air temperature showed similar diurnal pattern. Nevertheless, stem temperature experienced a plateau after mid-day (12:00–15:00) and then decreased more quickly than R_S . As shown in Fig. 2A and C, the stem temperature values were comparable between 09:00 and 18:00 but the R_S value was much larger at 18:00. Air temperature had a similar fast afternoon decrease pattern as stem temperature did, but the amplitude of air temperature diurnal change (12.75°C) was larger than that of stem temperature (9.02°C). The diurnal pattern of air relative humidity was just the opposite to that of air temperature (Fig. 2B and D), ranging from $46.64 \pm 2.21\%$ at 12:00 to $89.45 \pm 2.13\%$ at 3:00.

Seasonal Variation

Figure 3 illustrated the seasonal changes of R_S , air relative humidity, stem temperature, and air temperature from May to September. Similar to the diurnal cycles, R_S followed the pattern of stem temperature (Fig. 3A and C). R_S increased from May ($1.28 \pm 0.07 \mu\text{mol m}^{-2} \text{s}^{-1}$) when the stem temperature was relatively low ($13.70 \pm 0.47^{\circ}\text{C}$) and peaked in July ($3.02 \pm 0.10 \mu\text{mol m}^{-2} \text{s}^{-1}$) when the stem temperature was also the highest ($17.73 \pm 0.30^{\circ}\text{C}$). Both of them decreased afterwards to the lowest point in September, with R_S as $1.19 \pm 0.05 \mu\text{mol}$

$\text{m}^{-2} \text{s}^{-1}$ and stem temperature as $9.13 \pm 0.56^{\circ}\text{C}$. It is also noteworthy that the R_S values did not differ very much between the start and the end of the growing season, while there was a significant gap between the stem temperature values (near 14°C in May but around 9°C in September). Similarly, the air temperature reached its peak value in June and July (Fig. 3D), and the minimum value occurred in September. Consistent with diurnal changes, seasonal maximum air temperatures were higher than maximum stem temperatures in June and July, meanwhile, seasonal minimum stem temperature was 8.80°C , lower than that of air temperature (9.13°C) in September. The seasonal pattern of air relative humidity was no longer the opposite to that of air temperature (Fig. 3B), which increased in early growing season, decreased a little in July, peaked in August and then dropped in September.

Diurnal Change in Q_{10}

To gain further understanding of how environmental factors influence stem respiration activity, the stem respiration rates and temperature measured in the sampling period were fitted to Eq.2 (Fig. 4A and B) and stem respiration rates were also linearly regressed against the air relative humidity (Fig. 4C). In general, R_S showed a good exponential relationship with both stem temperature (Fig. 4A, $R^2 = 0.47$, $P < 0.001$) and air temperature (Fig. 4B, $R^2 = 0.39$, $P < 0.001$). There was no good linear relationship between R_S and air relative humidity (Fig. 4C, $R^2 = 0.00$).

In order to investigate diurnal variations of temperature sensitivity of R_S , Q_{10} values were further calculated based on the seasonal variation in R_S for each time during one day. There was statistically significant difference between daytime (1.97 ± 0.17 at 12:00 and 1.96 ± 0.10 at 15:00) and nighttime (2.60 ± 0.14 at 00:00 and 2.71 ± 0.25 at 03:00) Q_{10} (Fig. 5). Q_{10} values in other time intervals fell in between and were not significantly different from each other.

Discussion

The magnitude of our R_S values (0.33 – $6.59 \mu\text{mol m}^{-2} \text{s}^{-1}$) is similar with previous studies on mature conifer forests. For example, Wang et al. [43] found that stem respiration rates in a 33-year-old larch forest varied from approximately $0.9 \mu\text{mol m}^{-2} \text{s}^{-1}$ to $6.6 \mu\text{mol m}^{-2} \text{s}^{-1}$ in June, 2001 and Acosta et al. [8] documented that the R_S range of a 22-year-old Norway spruce forest stand during the growing season from 1999 to 2002 was 0.34 – $6.52 \mu\text{mol m}^{-2} \text{s}^{-1}$. Meanwhile, the mean stem respiration ($2.15 \mu\text{mol m}^{-2} \text{s}^{-1}$) was lower than that of soil respiration rate ($3.22 \mu\text{mol m}^{-2} \text{s}^{-1}$) [41] at the same plot. Bolstad et al. [45] showed that the stem respiration was lower than the soil respiration which was typically more than 60% of total ecosystem respiration during the growing season while Clinton et al. [46] showed that the mean stem CO_2 efflux ($2.60 \pm 0.17 \mu\text{mol m}^{-1} \text{s}^{-2}$) was slightly higher than that of soil CO_2 efflux ($2.53 \pm 0.11 \mu\text{mol m}^{-1} \text{s}^{-2}$).

Stem respiration rates can respond to temperature changes and plant activities like photosynthesis, plant growth, etc. [47,48]. Our results show that variations of stem respiration rates in larch forests were largely influenced by diurnal and seasonal changes of stem temperature. During the study period, the maximum of the stem respiration occurred in the afternoon while the minimum occurred in the early morning within one day and stem respiration rates peaked in July in growing season, which is consistent with previous studies [9,18,23,31,42,49]. For example, Zha et al. [9] found that stem respiration of Scots pine peaked at around 16 h and was

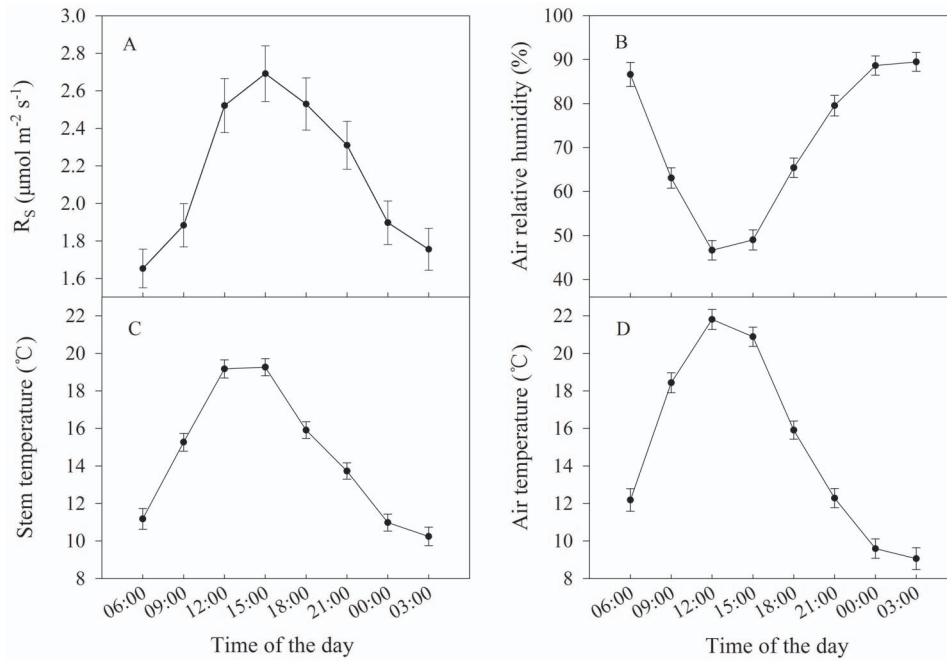


Figure 2. Diurnal changes in (A) stem respiration per unit surface area (R_S), (B) air relative humidity, (C) stem temperature and (D) air temperature. For each 3-hourly interval, measurements were averaged for the six sample trees in the whole growing season (May to Sep) from 2010 to 2012. The resulting standard errors are represented by the bars.
doi:10.1371/journal.pone.0089294.g002

highest in July. Acosta et al. [8] indicated that stem respiration of Norway spruce reached maximum between 13 h and 16 h and the highest rate occurred in June and July. Zhu et al. [23] suggested that stem respiration of *Schima superba* also followed a similar

diurnal pattern, reaching the highest in the afternoon and the lowest at about 8:00 in the early morning.

Nevertheless, stem temperature can't fully explain all of the variations of R_S [9]. In our study, the R_S values of afternoon (18:00) and late growing season (Aug) were higher than those in

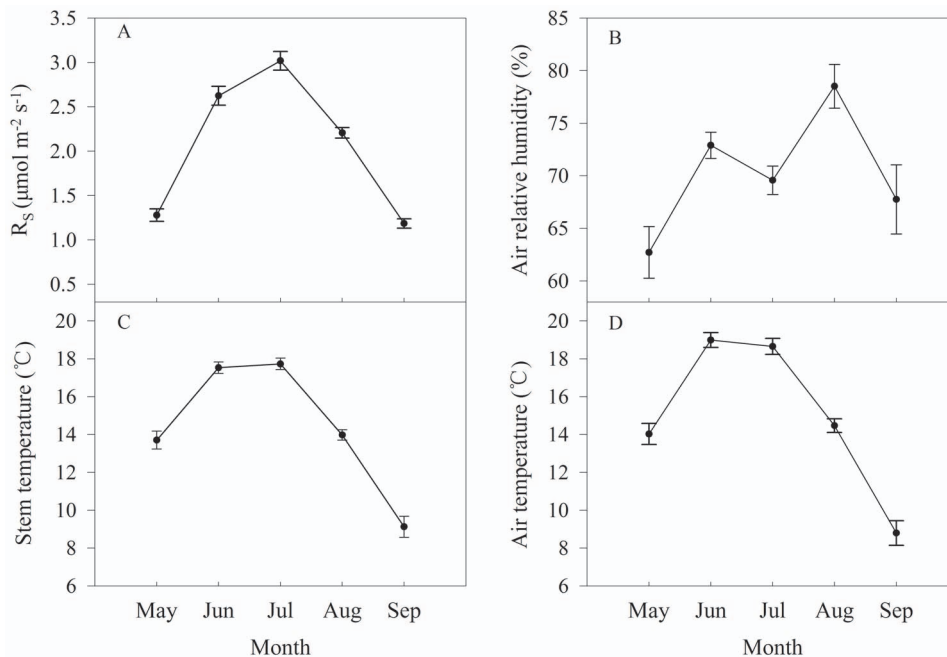


Figure 3. Seasonal changes in (A) stem respiration per unit surface area (R_S), (B) air relative humidity, (C) stem temperature and (D) air temperature. For each month, all the 3-hourly measurements were averaged for the six sample trees from 2010 to 2012. The resulting standard errors are represented by the bars.
doi:10.1371/journal.pone.0089294.g003

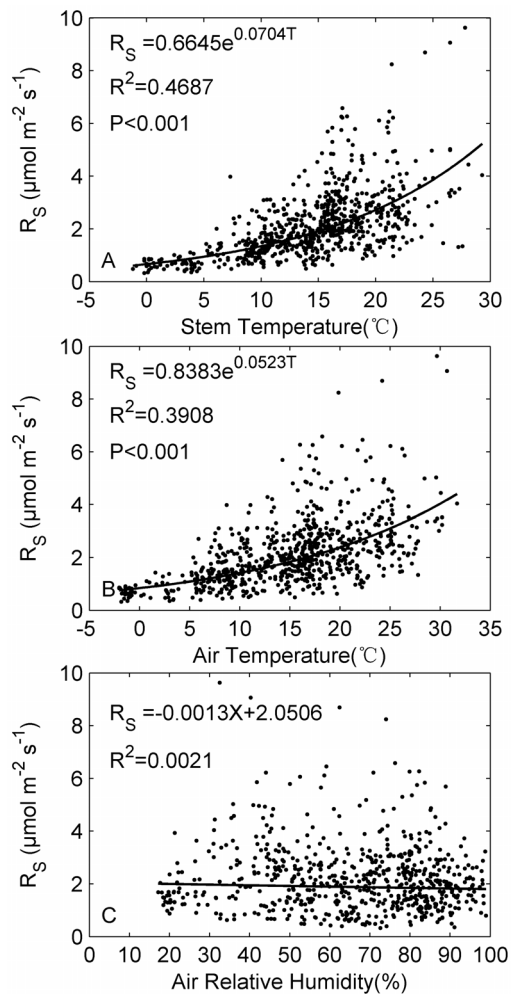


Figure 4. Relationship of the stem respiration per unit surface area (R_s) with (A) stem temperature, (B) air temperature and (C) air relative humidity.

doi:10.1371/journal.pone.0089294.g004

the morning (09:00) and early growing season (May) while the stem temperature were comparable (Fig. 2A and C, Fig. 3A and C). This phenomenon suggests that plant activities like photosynthesis and cambium activity probably play an important role in regulating stem respiration changes. Martin et al. [50] found that when temperature and transpiration are constant, R_s appears to be positively correlated with substrate supply. The diurnal change of respiratory substrate, supplied by photosynthesis, may also influence the respiration rates [48,51]. At seasonal scale, plant growth activities can't be ignored. The stem respiration mainly consists of maintenance respiration and growth respiration [52]. Maintenance respiration varies primarily with changes in temperature and is also reported to increase with relative growth rate [37,53]. Meanwhile, growth respiration is controlled by the timing and magnitude of plant growth [54]. That is to say, the stem respiration varies throughout the growing season, following not only the change of temperature, but also the change of phenology and environmental factors that control growth.

Accurate understanding of temperature response of respiration is critical in estimating global carbon balance and its response to current climate change. Our results show that Q_{10} values of R_s vary from 1.96 to 2.71, which are within the range reported by

previous studies [9,17,31,34,42,55,56]. In growing season average diurnal cycle, Q_{10} values were lowest in mid-day (12:00–15:00), which may be partly explained by the acclimation of respiration to rising temperature. Both theory and observations have suggested a decline temperature sensitivity of rates of respiratory CO_2 efflux from plants [52,57,58] and soils [5,59]. For example, Tjoelker et al. [57] reported that Q_{10} value of foliar respiration decline by 0.04 in response to 1°C increase in mean ambient temperature. In deed, highest stem temperature is observed during the mid-day. Another possible explanation of the suppressed temperature sensitivity of stem respiration in mid-day (12:00–15:00) may be midday depression of photosynthesis, particularly during summer with stem temperature approaching 30°C and air temperature above 30°C (Fig. 4A&B). High midday temperature is considered to be able to induce stomata closure and photosynthesis depression in water-limited regions by both observations (pine forest in Canary Islands) [60] and theoretical models. Reduced stomatal conductance and photosynthesis rates in midday during summer may further decline R_s , and thus influencing Q_{10} values derived from seasonal variation of R_s . Often in models [14,31,61], Q_{10} is set to be a constant value of 2, similar to the midday values and lower than the nighttime values from our study. This can lead to underestimated stem respiration increase under global warming, especially considering that temperature increase is faster during nighttime [1].

Vegetation activities have been shown to respond negatively to nighttime temperature increase in cold and mesic regions [65], probably due to increased carbon loss through respiration. Combined with stronger nighttime warming [1,62,63], our results imply that the carbon loss through respiration might increase more than former model projections [14,31,61], and might further cancel out the increased photosynthesis driven by daytime warming in those areas. In contrast, ecosystems in arid and semi-arid regions are thought to respond to night time temperature change in a more complex way [65]. A manipulative experiment study in a temperate steppe ecosystem in north China reported that daytime warming induced reduction in gross ecosystem productivity (GEP), and night-time warming stimulated photosynthesis and GEP in the following day because enhanced respiration drew down the leaf carbohydrates concentration [64]. With higher stem respiration sensitivity at night, the stimulation effect might be strengthened in the future, while it is also possible that the carbon loss through enhanced nighttime respiration goes up even faster and cancels out the stimulating effect. Thus, more experimental researches as well as modelling efforts are necessary to accurately quantify the temperature sensitivity of stem respiration and to better address its implications on future vegetation dynamics.

Conclusion

Temperature responses of rates of respiratory CO_2 efflux from plants and soils are generally modelled using exponential functions with a constant Q_{10} near 2.0, similar to the midday values and lower than the nighttime values from our study. This result has important implications for the predictions of forest responses to warming. Current carbon cycle models must consider diurnal change in temperature sensitivity of R_s to accurately predict ecosystem C cycling under climate warming. In the future, additional experiments with larger sample size need to be performed in other ecosystems in order to draw a more generalized conclusion and to further address detailed mechanisms responsible for diurnal change in Q_{10} of R_s .

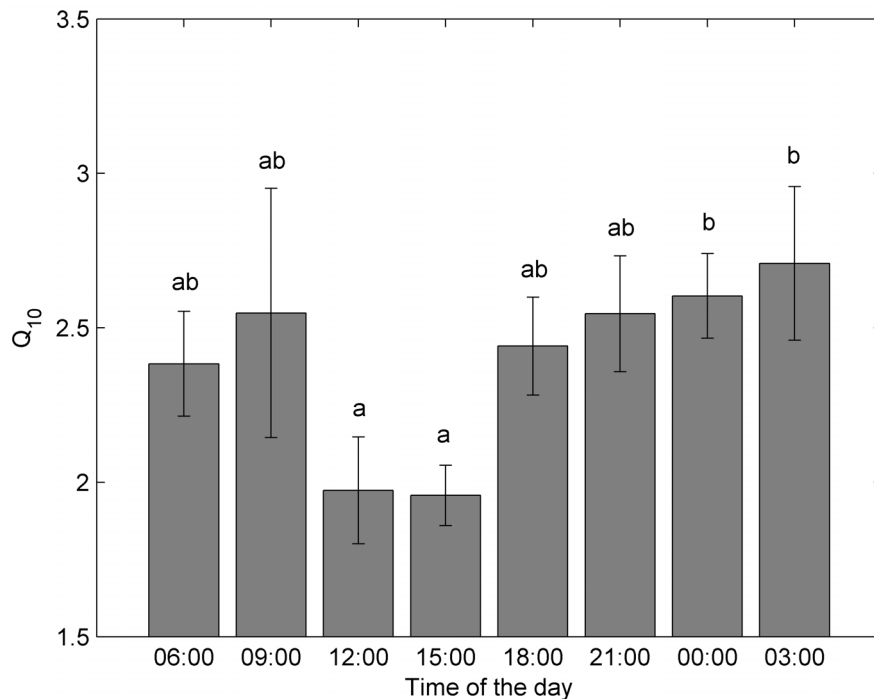


Figure 5. The diurnal variations of Q_{10} estimated based on the seasonal variation in R_s at different time during one day. Values not given a common letter are significantly different from each other at $P=0.05$. Bars represent the standard error. doi:10.1371/journal.pone.0089294.g005

Acknowledgments

We are grateful to all the technicians who assisted us in the field and lab for their hard work.

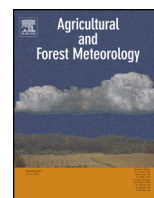
Author Contributions

Conceived and designed the experiments: SP YY. Performed the experiments: YY. Analyzed the data: YY MZ. Contributed reagents/materials/analysis tools: YY MZ. Wrote the paper: YY MZ XX ZS GY SP.

References

- IPCC, 2007 Climate Change (2007) The Physical Sciences Basis: Contribution of Working Group I to the Fourth Assessment Report of the Intergovernmental Panel on Climate Change. Cambridge: Cambridge University Press. pp. 235–337.
- Pan Y, Birdsey RA, Fang JY, Houghton R, Kauppi PE, et al. (2011) A Large and Persistent Carbon Sink in the World's Forests. *Science* 988: 988–993.
- Janssens IA, Kim P (2003) Large seasonal changes in Q_{10} of soil respiration in a beech. *Global Change Biol* 9: 911–918.
- Davidson EA, Janssens IA, Luo YQ (2006) On the variability of respiration in terrestrial ecosystems: moving beyond Q_{10} . *Global Change Biol* 12: 154–164.
- Peng SS, Piao SL, Wang T, Sun JY, Shen ZH (2009) Temperature sensitivity of soil respiration in different ecosystems in China. *Soil Biol Biochem* 41: 1008–1014.
- Paembonan SA, Hagihara A, Hozumi K (1991) Long-term measurement of CO_2 release from the aboveground parts of a hinoki forest tree in relation to air temperature. *Tree Physiol* 8: 399–405.
- Brito P, Soledad M, Morales D, Wieser G (2013) Assessment of ecosystem CO_2 efflux and its components in a *Pinus canariensis* forest at the treeline. *Soil Biol Biochem* 27: 999–1009.
- Acosta M, Pavelka M, Pokorný R, Janouš D, Marek MV (2008) Seasonal variation in CO_2 efflux of stems and branches of Norway spruce trees. *Ann Bot* 101: 469–477.
- Zha TS, Kellomaki S, Wang K, Aija R, Sini N (2004) Seasonal and Annual Stem Respiration of Scots Pine Trees under Boreal Conditions. *Ann Bot* 94: 889–896.
- Maseyk K, Grunzweig JM, Rotenmerg E, Yakir D (2008) Respiration acclimation contributes to high carbon-use efficiency in a seasonally dry pine forest. *Global Change Biol* 14: 1553–1567.
- Cavaleri MA, Oberbauer SF, Ryan MG (2008) Foliar and ecosystem respiration in an old-growth tropical rain forest. *Plant Cell Environ* 31: 473–483.
- Wang M, Guan DX, Han SJ, Wu JL (2010) Comparison of eddy covariance and chamber-based methods for measuring CO_2 flux in a temperate mixed forest. *Tree Physiol* 30: 149–63.
- Cerasoli S, McGuire MA, Faria J, Mourato M, Schmidt M, et al. (2009) CO_2 efflux, CO_2 concentration and photosynthetic refixation in stems of *Eucalyptus globulus* (Labill.). *J Exp Bot* 60: 99–105.
- Ryan MG (1991) Effects of Climate Change on Plant Respiration. *Ecol Soc Amer* 1: 157–167.
- Ryan MG, Hubbard RM, Clark DA, Sanford JRL (1994) Woody-Tissue Respiration for *Simarouba amara* and *Mimosa guianensis*, Two Tropical Wet Forest Trees with Different Growth Habits. *Oecologia* 100: 213–220.
- Ryan MG, Cavaleri MA, Almeida AC, Penchel R, Senock RS, et al. (2009) Wood CO_2 efflux and foliar respiration for *Eucalyptus* in Hawaii and Brazil. *Tree Physiol* 29: 1213–1222.
- Yang JY, Teskey RO, Wang CK (2012) Stem CO_2 efflux of ten species in temperate forests in Northeastern China. *Trees* 26: 1225–1235.
- Lavigne MB (1996) Comparing stem respiration and growth of jack pine provenances from northern and southern locations. *Tree Physiol* 16: 847–852.
- Hölttä T, Kolari P (2009) Interpretation of stem CO_2 efflux measurements. *Tree Physiol* 29: 1447–1456.
- Moore DJ, Gonzalez-Meler MA, Taneva L, Pippen JS, Kim HS, et al. (2008) The effect of carbon dioxide enrichment on apparent stem respiration from *Pinus taeda* L. is confounded by high levels of soil carbon dioxide. *Oecologia* 158: 1–10.
- Acosta M, Pokorný R, Janouš D, Marek M (2010) Stem respiration of Norway spruce trees under elevated CO_2 concentration. *Biologia Plantarum* 54: 773–776.
- Maier CA, Zarnoch SJ, Dougherty PM (1998) Effects of temperature and tissue nitrogen on dormant season stem and branch maintenance respiration in a young loblolly pine (*Pinus taeda*) plantation. *Tree Physiol* 18: 11–20.
- Zhu LW, Zhao P, Ni GY, Cao QP, Zhou CM, et al. (2012) Individual- and stand-level stem CO_2 efflux in a subtropical *Schima superba* plantation. *Biogeosciences* 9: 3729–3737.
- Bowman WP, Turnbull MH, Tissue DT, Whitehead D, Griffin KL (2008) Sapwood temperature gradients between lower stems and the crown do not influence estimates of stand-level stem CO_2 efflux. *Tree Physiol* 28: 1553–1559.

25. Stockfors J (2000) Temperature variations and distribution of living cells within tree stems: implications for stem respiration modeling and scale-up. *Tree Physiol* 20: 1057–1062.
26. Damesin C, Ceschial E, Goff NL, Ottorini J, Dufrenel E (2012) Stem and branch respiration estimations of at beech: the from stand level tree measurements to estimations at the stand level. *New Phytologist* 153: 159–172.
27. Cox PM, Betts RA, Jones CD, Spall SA, Totterdell IJ (2000) Acceleration of global warming due to carbon-cycle feedbacks in a coupled climate model. *Nature* 408: 184–187.
28. Friedlingstein P, Cox P, Betts R, Bopp L, von Bloh W, et al. (2006) Climate-Carbon Cycle Feedback Analysis: Results from the C 4 MIP Model Intercomparison. *J Climate* 19: 3337–3353.
29. McGuire MA, Cerasoli S, Teskey RO (2007) CO₂ fluxes and respiration of branch segments of sycamore (*Platanus occidentalis* L.) examined at different sap velocities, branch diameters, and temperatures. *J Exp Bot* 58: 2159–2168.
30. Kim MH, Nakane K, Lee JT, Bang HS, Na YE (2007) Stem/branch maintenance respiration of Japanese red pine stand. *Forest Ecol Manage* 243: 283–290.
31. Ryan MG, Gower ST, Hubbard RM, Waring RH, Gholz LH, et al. (1995) Woody Tissue Maintenance Respiration of Four Conifers in Contrasting Climates. *Oecologia* 101: 133–140.
32. Acosta M, Pavelka M, Tomášková I, Janous D (2011) Branch CO₂ efflux in vertical profile of Norway spruce tree. *Eur J Forest Res* 130: 649–656.
33. Liberloo M, Angelis PD, Ceulemans R (2008) Stem CO₂ efflux of a *Populus nigra* stand: effects of elevated CO₂, fertilization, and shoot size. *Biologia Plantarum* 52: 299–306.
34. Stockfors JAN, Linder S (1998) Effect of nitrogen on the seasonal course of growth and maintenance respiration in stems of Norway spruce trees. *Tree Physiol* 18: 155–166.
35. Saveyn A, Steppe K, McGuire AM, Lemeur R, Teskey RO (2008) Stem respiration and carbon dioxide efflux of young *Populus deltoides* trees in relation to temperature and xylem carbon dioxide concentration. *Oecologia* 154: 637–649.
36. Gruber A, Wieser G, Oberhuber W (2009) Intra-annual dynamics of stem CO₂ efflux in relation to cambial activity and xylem development in *Pinus cembra*. *Tree Physiol* 29: 641–649.
37. Lavigne MB, Ryan MG (1997) Growth and maintenance respiration rates of aspen, black spruce and jack pine stems at northern and southern BOREAS sites. *Tree Physiol* 17: 543–552.
38. Lavigne MB, Little CHA, Riding RT (2004) Changes in stem respiration rate during cambial reactivation can be used to refine estimates of growth and maintenance respiration. *New Phytologist* 162: 81–93.
39. Wittmann C, Pfanz H (2007) Temperature dependency of bark photosynthesis in beech (*Fagus sylvatica* L.) and birch (*Betula pendula* Roth.) trees. *J Exp Bot* 58: 4293–4306.
40. Ma YC, Zhu B, Sun ZZ, Zhao C, Yang Y, et al. (2013) The effects of simulated nitrogen deposition on extracellular enzyme activities of litter and soil among different-aged stands of larch. *J Plant Ecol* doi:10.1093/jpe/rtt028. 1–10.
41. Ma YC, Piao SL, Sun ZZ, Lin X, Wang T (2014) Stand ages regulate the response of soil respiration to temperature in a *Larix principis-rupprechtii* plantation. *Agricult Forest Meteorol* 184: 179–187.
42. Xu M, Debiase TA, Qi Y (2000) A simple technique to measure stem respiration using a horizontally oriented soil chamber. *Can J Forest Res* 30: 1555–1560.
43. Wang WJ, Yang FJ, Zu YG, Wang HM, Takagik K, et al. (2003) Stem respiration of a Larch (*Larix gmelini*) plantation in Northeast China. *Acta Botanica Sinica* 45: 1387–1397.
44. Boone RD, Nadelhoffer KJ, Canary JD (1998) Roots exert strong influence on the temperature sensitivity of soil respiration. *Nature* 396: 570–572.
45. Bolstad PV, Davis KJ, Martin J, Cook BD, Wang W (2004) Component and whole-system respiration fluxes in northern deciduous forests. *Tree Physiol* 24: 493–504.
46. Clinton BD, Maier CA, Ford CR, Mitchell RJ (2011) Transient changes in transpiration and stem and soil CO₂ efflux in longleaf pine (*Pinus palustris* Mill.) following fire-induced leaf area reduction. *Trees* 25: 997–1007.
47. Levy PE, Jarvis PG (1998) Stem CO₂ fluxes in two Sahelian shrub species (*Guiera senegalensis* and *Combretum micranthum*). *Funct Ecol* 12: 107–116.
48. Ryan MG, Hubbard RM, Pongracic S, Raison RJ, Mcmurtrie RE (1996) Foliage, fine-root, woody-tissue and stand respiration in *Pinus radiata* in relation to nitrogen status. *Tree Physiol* 16: 333–343.
49. Vose JM, Ryan MG (2002) Seasonal respiration of foliage, fine roots, and woody tissues in relation to growth, tissue N, and photosynthesis. *Global Change Biol* 8: 182–193.
50. Martin TA, Teskey R, Dougherty PM (1994) Movement of respiratory CO₂ in stems of loblolly pine (*Pinus taeda* L.) seedlings. *Tree Physiol* 14: 481–495.
51. Azcon-bieto J, Lambers H, Day DA (1983) Effect of Photosynthesis and Carbohydrate Status on Respiratory Rates and the Involvement of the Alternative Pathway in Leaf Respiration. *Plant Physiol* 72: 598–603.
52. Piao SL, Luyssaert S, Ciais P, Janssens IA, Chen AP, et al. (2010) Forest annual carbon cost: a global-scale analysis of autotrophic respiration. *Ecology* 91: 652–661.
53. Amthor JS (1989) Respiration and crop productivity. Springer-Verlag New York. 215 p.
54. Penning de Vries FWT, Brunsting AHM, van Laar HH (1974) Products, requirements and efficiency of biosynthesis: a quantitative approach. *J Theor Biol* 45: 339–377.
55. Ryan MG (1991) Effects of Climate Change on Plant Respiration. *Ecol Appl* 1: 157–167.
56. Carey EV, Callaway RM, Deluci EH (1997) Stem respiration of ponderosa pines grown in contrasting climates: implications for global climate change. *Oecologia* 111: 19–25.
57. Tjoelker MG, Oleksyn J, Reich PB (2001) Modelling respiration of vegetation: evidence for a general temperature-dependent Q₁₀. *Global Change Biol* 7: 223–230.
58. King AW, Gunderson CA, Post WM, Weston DJ, Wulschleger SD (2006) Plant respiration in a warmer world. *Science* 312: 536–537.
59. Davidson EA, Janssens IA (2006) Temperature sensitivity of soil carbon decomposition and feedbacks to climate change. *Nature* 440: 165–173.
60. Peters J, Morales D, Jimenez MS (2003) Gas exchange characteristics of *Pinus canariensis* needles in a forest stand on Tenerife, Canary Islands. *Trees* 17: 492–500.
61. Melillo JM, McGuire AD, Kicklighter DW, Moore B, Vorosmarty CJ, et al. (1993) Global climate change and terrestrial net primary production. *Nature* 363: 234–240.
62. Alward RD, Detling JK, Milchunas DG (1999) Grassland vegetation changes and nocturnal global warming. *Science* 283: 229–231.
63. Gou XH, Chen FH, Yang MX, Gordon J, Fang KY, et al. (2008) Asymmetric variability between maximum and minimum temperature in Northeastern Tibetan Plateau: Evidence from tree rings. *SCIENCE CHINA Earth Sciences* 51: 41–55.
64. Wan SQ, Xia JY, Liu WX, Niu SL (2009) Photosynthetic overcompensation under nocturnal warming enhances grassland carbon sequestration. *Ecology* 90: 2700–2710.
65. Peng SS, Piao SL, Ciais P, Myneni RB, Chen AP, et al. (2013) Asymmetric effects of daytime and night-time warming on Northern Hemisphere vegetation. *Nature* 501: 88–94.



Stand ages regulate the response of soil respiration to temperature in a *Larix principis-rupprechtii* plantation



Yuecun Ma^{a,1}, Shilong Piao^{a,*}, Zhenzhong Sun^a, Xin Lin^{b,c,d}, Tao Wang^d,
Chao Yue^d, Yan Yang^a

^a Department of Ecology, College of Urban and Environmental Sciences, and Key Laboratory for Earth Surface Processes of the Ministry of Education, Peking University, Beijing 100871, China

^b State Key Laboratory of Environmental Criteria and Risk Assessment, Chinese Research Academy of Environmental Sciences, Beijing 100012, China

^c College of Water Sciences, Beijing Normal University, Beijing 100875, China

^d Laboratoire des Sciences du Climat et de l'Environnement, CEA CNRS UVSQ, 91191 Gif sur Yvette, France

ARTICLE INFO

Article history:

Received 24 April 2013

Received in revised form 1 October 2013

Accepted 13 October 2013

Keywords:

Autotrophic respiration

Heterotrophic respiration

Soil respiration

Stand age

Temperature sensitivity of soil respiration

Larix principis-rupprechtii

ABSTRACT

Understanding the linkage of soil respiration and its sensitivity to temperature with forest structure including stand age is critical for accurately assessing the impact of afforestation on global carbon balance. In this study, we investigated the changes of soil respiration (R_S) and its components (soil heterotrophic (R_H) and autotrophic (R_A) respiration) in response to seasonal temperature change over three *Larix principis-rupprechtii* plantation stands (10-year-old sapling stand, 20-year-old young stand and 45-year-old mature stand) in North China. We found a significant seasonal variation of R_S , R_H and R_A ($P < 0.001$), and significant stand age effect on R_H ($P = 0.004$). Among the three age stands, sapling stand has the lowest R_H during the snow-free season, possibly due to the lowest soil organic carbon. All three stands show that R_S exponentially increases with increasing temperature, and the Q_{10} of R_H (from 2.69 to 3.03) is significantly lower than that of R_A (from 3.06 to 4.39). Furthermore, the Q_{10} of R_H is significantly dependent on stand age. The Q_{10} of R_H at mature stand (3.03 ± 0.09) was substantially higher than that at sapling stand (2.69 ± 0.08), highlighting the importance of stand age in regulating the response of soil respiration to temperature change. We also found that the transient turnover rate of soil organic carbon in sapling stand is significantly faster than those in young and mature stands ($P < 0.001$) due to the highest soil temperature at sapling stand. Such regulations of stand age on soil carbon cycling through abiotic factors must also be taken into account when investigating the effect of plantation on the global carbon cycle.

© 2013 Elsevier B.V. All rights reserved.

1. Introduction

Soil respiration (R_S) is the second largest carbon flux in most terrestrial ecosystems, approximately 50–90% of total ecosystem respiration (Longdoz et al., 2000; Schlesinger and Andrews, 2000). Globally, R_S is estimated to be 80–98 Pg C yr⁻¹ (Raich et al., 2002; Bond-Lamberty and Thomson, 2010), which is even higher than the cumulated industrial CO₂ emissions by fossil-fuel combustion over the last 10 years (Le Quéré et al., 2009). Furthermore, it has been estimated that global R_S has significantly increased by 0.1 Pg C yr⁻¹ over the last two decades (Bond-Lamberty and Thomson, 2010), and will continue to increase in the future and eventually induce an important positive feedback to climate change (Friedlingstein

et al., 2006). Thus, understanding the mechanisms that determine changes in R_S is important in global change research, and subsequently the center-piece of many studies (Reichstein et al., 2003; Davidson and Janssens, 2006; Sampson et al., 2007; Peng et al., 2009; Wang et al., 2010a).

Forests compose a major part of terrestrial ecosystems, occupying about 30% of the world's land area. The important role of forest in the global carbon cycle has motivated ecologists to investigate change in R_S and its driving factors. However, most previous studies focused on the effect of climate factors, such as temperature and precipitation, on R_S (e.g. Sampson et al., 2007; Bronson et al., 2008; Maseyk et al., 2008; Laganière et al., 2012; Schindlbacher et al., 2012), and less attention has been paid to examine the linkage of R_S and its components (soil heterotrophic (R_H) and autotrophic (R_A) respiration) with forest structure, particularly stand age. Accordingly, the effect of stand age on R_S is not parameterized in the most current carbon cycle models (e.g. LPJ, Sitch et al., 2003; ORCHIDEE, Krinner et al., 2005), which

* Corresponding author. Tel.: +86 10 6275 3298; fax: +86 10 6275 1179.

E-mail addresses: slpiao@pku.edu.cn, ShiLong.Piao@lscce.ips.fr (S. Piao).

¹ Deceased.

further limits the capacity to evaluate the role of plantations in the current global carbon balance. Based on a recent global forest resources assessment, the area of global plantation forest is about 1.408×10^8 ha, and about 30% is distributed in China (FAO, 2006).

Temperature exerts the dominant control over R_S in most forest ecosystems (Hanson et al., 2000). The Q_{10} value, the factor by which R_S is multiplied when temperature increases by 10 degrees, has been estimated to range from 1.81–3.05 (Wang et al., 2010a), depending on the environmental variables. In general, the Q_{10} spatially increases with the decrease in temperature, and with the increase in moisture across large spatial scales (Raich and Schlesinger, 1992; Bahn et al., 2008). A number of recent studies have revealed that the temperature sensitivity of R_S (particularly R_H) is also dependent on the substrate quality and availability (Curiel Yuste et al., 2004; Knorr et al., 2005; Conant et al., 2008; Gershenson et al., 2009; Wetterstedt et al., 2010; Subke and Bahn, 2010; Zhu and Cheng, 2011). Moreover, the quantity and quality of the aboveground and belowground detritus, as well as root activity can change with stand age (Bond-Lamberty et al., 2004; Salz et al., 2006). The findings of these studies beg the question: how temperature sensitivities of R_S vary with the forest age. Answering this question is critical to more accurately assessing the impacts of afforestation on global carbon balance.

In this study, we measured R_S and partitioned R_S into heterotrophic (R_H) and autotrophic respiration (R_A) from *Larix principis-rupprechtii* plantation in Northern China. We selected three age stands (10-, 20- and 45-year old) and measured R_S , R_H and R_A two times each month during the snow-free season in 2010, 2011 and 2012. The main objectives were to address (1) how do total soil respiration (R_S), heterotrophic respiration (R_H), and autotrophic respiration (R_A) change with stand age since the forest structure is significantly different, (2) how does the turnover rate of soil organic carbon vary with stand age and (3) does the temperature dependency of R_S , R_H , and R_A change with stand age?

2. Materials and methods

2.1. Site description

The study was performed at Saihanba ecological station ($42^\circ 24.723' N$, $117^\circ 14.844' E$, 1505 m a.s.l.) of Peking University, situated in Saihanba National Forest Park, Hebei Province. The climate is semi-humid, with a long, cold winter (November–March), and a short spring and summer. According to the long-term observation from Saihanba meteorological station during the period 1971–2010, the mean annual temperature was $-1.4^\circ C$ ($-21.8^\circ C$ in January and $16.2^\circ C$ in July), the mean annual precipitation was 450 mm, and the frost-free duration was 81 d. The well drained soils are predominantly sandy. Seasonal snowpack begins to appear in November, and snowmelt occurs in early April. In winter, snow accumulation is typically less than 30 cm in depth (Wang et al., 2010b). The topography is relatively flat.

2.2. Experimental design

In this study, we selected three different age stands, including a 10-year-old stand (Sapling stand), a 20-year-old stand (Young stand) and a 40-year-old stand (Mature stand) in August 2009. All three stands were dominated by *Larix principis-rupprechtii*, which was previously occupied by a stretch of primary forests that were harvested in large-scale industrial logging in the last century. The dominant species in the understory layer of each age stand are shown in Table 1. The distance between any two stands was not beyond 2 km, which avoided the differences in climate and soil type. Therefore, the differences in R_S and its components between

stands are predominantly caused by stand age. The basic characteristics of the three age stands are summarized in Table 1. All three age stands with the area of $100 m \times 100 m$ were fenced to minimize anthropogenic disturbance. In each age stand, $20 m \times 20 m$ plots were arranged with 3 replicates. There was more than 10 m buffer strip between the plots.

2.3. Soil carbon flux measurement

Soil respiration was measured using a Li-8100 soil CO_2 Flux system (LI-COR Inc., Lincoln, NE, USA) during the snow-free season from early May to late October in 2010, 2011 and 2012. The soil CO_2 efflux was calculated based on a linear increase in chamber CO_2 concentrations over time. Four polyvinyl chloride (PVC) collars (20 cm inside diameter, 11 cm height), determining R_S , were randomly placed and inserted 8 cm into the soil in each plot. Note that the litter layer depth can reach ~ 5 cm at the three age stands, which indicated that only the roots in the top 3 cm of soil were presumably injured (cut off) by mechanical insertion of 8 cm PVC soil collar. This was supposed not to have significant impacts on R_S . Four PVC deep collars (20 cm inside diameter, 50 cm height), determining R_H , were inserted 47 cm into the soil to cut the roots in each plot. Soil sampling by a hand auger (with a diameter of 4 cm) to 45-cm depth early in the experiment indicated that nearly no roots were present in soils deeper than 35 cm and the soil underneath it is predominantly sandy. We thus expected that soil insertion of 47 cm PVC soil collar severed nearly all the roots. In order to exclude respiration from the aboveground parts of plants, living plants inside the collars were eradicated by hand once a week and the removed plant material was left inside the collars. Soil collars were placed in the soil at least 24 h before measurements to avoid influence of soil disturbance and root injury on the measurements. Note that all PVC collars were left in the same locations throughout the snow-free period. Soil CO_2 effluxes were measured twice a month and five times during each measurement day (twice during night and three times during day). Respiration rates were calculated as means of three plots for each age stand. R_A was calculated as the difference between R_S and R_H .

2.4. Soil temperature and moisture

When respiration measurement was performed, soil temperature and moisture at the depth of 5 cm, were recorded automatically by LI-COR 8100 temperature (8100-201) and moisture (8100-204) probes near each collar. Furthermore, soil temperature and moisture at 5 cm depth was continuously recorded by EM50 (Decagon, USA) every 30 min during the snow-free period.

2.5. Net primary productivity

NPP was obtained as the annual increase in total woody biomass plus litter fall. The total woody biomass was estimated from the following equation:

$$\ln(\text{Total Biomass}) = 0.8016 \ln(D^2 H) + 4.8423 \quad (1)$$

where D and H were mean diameter at breast height and tree height. Tree height was measured with hypsometer.

2.6. Measurements of soil properties

In order to measure soil properties (total organic C, total N and pH values), soil was firstly air-dried and ground to pass through a 2-mm sieve. The concentration of total organic C and total N in the $0.5 M K_2SO_4$ extracts was determined with an auto-analyzer

Table 1Summary of three age stand properties of *Larix principis-rupprechtii* plantation in Saihanba, North China.

Stand (age)	Stem density (stems ha ⁻¹)	DBH (cm)	Height (m)	Soil bulk density (g cm ⁻³)	Soil texture (sand, silt, clay, %)	SOC (Mg ha ⁻¹)	Soil C:N	Understory species	Soil pH
Sapling (10 years)	2640 ± 157 ^b	2.4 ± 0.3 ^c	2.5 ± 0.2 ^c	1.47	54.2, 28.3, 17.5	39.5 ± 1.5 ^b	9.0 ± 0.2 ^b	<i>Potentilla acaulis</i> <i>Bromus inermis</i> <i>Vicia pseudo-orobus</i> <i>Bupleurum chinense</i>	6.7 ± 0.2 ^a
Young (25 years)	3160 ± 129 ^a	7.6 ± 0.1 ^b	7.8 ± 0.3 ^b	1.50	66.9, 20.0, 13.1	53.2 ± 5.1 ^a	9.7 ± 0.2 ^a	<i>Geum aleppicum</i> <i>Agrimonia pilosa</i>	6.4 ± 0.2 ^{ab}
Mature (45 years)	870 ± 48 ^c	19.9 ± 2.8 ^a	15.8 ± 1.6 ^a	1.47	74.0, 15.4, 10.6	47.9 ± 3.6 ^{ab}	8.9 ± 0.3 ^b	<i>Geum aleppicum</i> <i>Agrimonia pilosa</i> <i>Sanguisorba tenuifolia</i>	6.3 ± 0.2 ^b

Note: DBH is the diameter at breast height. All the stems in the plot were sampled to calculate DBH and stem density. SOC denotes soil organic carbon. pH is determined by soil/water ratio of 1:2.5. The values are the means ± standard error. Different letters (a, b, and c) within the same column mean significant differences between different age stands (one-way ANOVA, post hoc LSD test). All age stands are situated in a flat topography.

(Multi N/C 3100, AnalyticJena, UK), and soil pH was measured in 1:5 soil/water suspensions using a glass electrode.

2.7. Analysis

Soil respiration and the environmental factors were processed in EXCEL 97. The standard deviation (STD) was used to express spatial variability for three age stands. Two-way analysis of variance (ANOVA) was used to test the effect of sampling date and stand age on soil respiration ($P \leq 0.05$). The regression model was used to determine the relationship between R_S and soil temperature. R_S is often simulated by the Q_{10} function, with soil temperature as the driving variable (Curiel Yuste et al., 2004; Schindlbacher et al., 2009; Vicca et al., 2009).

$$F = \beta_0 Q_{10}^{((T-10)/10)} \quad (2)$$

where F is R_S rate ($\mu\text{mol m}^{-2} \text{s}^{-1}$), β_0 (basal rate) is the flux rate at 10 °C, Q_{10} represents the temperature sensitivity and T is the soil temperature (°C) at 5 cm depth. For each age stand, Eq. (2) is firstly fitted at each of the three plots and one-way ANOVA is then used to detect the differences in Q_{10} and β_0 across the three age stands ($P \leq 0.05$).

The snow-free season cumulated C efflux ($\text{gC m}^{-2} \text{yr}^{-1}$) was estimated based on parameters derived from Eq. (2).

$$\text{Cumulated C efflux} = 12 \times 1800 \times 10^{-6} \sum \beta_0 Q_{10}^{((T-10)/10)} \quad (3)$$

where 12 indicates the molecular weight of carbon, and 1800 is the constant value (unit: second) due to the fact that EM50 downloads soil temperature every 30 min.

Transient turnover time (reciprocal of transient turnover rate) of soil organic carbon was calculated as follows:

$$\text{Turnover time} = \frac{\text{SOM}}{\text{total } R_H} \quad (4)$$

where SOM indicates soil organic carbon (Mg C ha^{-1}) within the soil depth of 100 cm, and total R_H means the cumulative heterotrophic respiration during the snow-free period ($\text{Mg C ha}^{-1} \text{yr}^{-1}$). This transient SOM turnover time should be distinguished from the one computed at steady state (defined as zero partial derivative of SOM with respect to time), which may not be satisfied in this study. However, this transient SOM turnover time still provided us with proper insights into how rapidly the SOM recycles across different age classes in a transient state. We did not consider heterotrophic respiration during snow-covered period when calculating total R_H efflux. This neglected winter respiration may not significantly change the transient SOM turnover time. For example, Wang et al. (2010b) reported that the cumulative respiration during snow-covered time

period only accounted for ~7% of the total soil respiration in 42-year-old *Larix principis-rupprechtii*.

3. Results

3.1. Seasonal changes of soil respiration at different age stands

Statistically significant seasonal variations of R_S were observed in all three age stands ($P < 0.001$; Fig. 1a and Table 2). As shown in Fig. 1a, R_S first increased from early May to late July, and then decreased until late October in all three age stands. Such seasonal variations of R_S were strongly related to changes in soil temperature rather than changes in soil moisture. For example, soil temperature at the depth of 5 cm peaked in late July and was relatively low in the early and end of growing season (Fig. 1b), which was consistent with the change in R_S . In contrast, soil moisture showed a decreasing trend over time in all three age stands (Fig. 1c).

Further analyses showed that no significant effects of stand age or interaction of stand age and sampling date were found. However, differences of R_S among three age stands were observed in spring and autumn (Fig. 1a). In general, sapling stand had the largest R_S in spring, followed by mature stand and young stand, while R_S was the lowest at sapling stand in autumn. Although peak value of soil temperature for young and mature stand was comparable (Fig. 1b), peak value of R_S for young stand ($4.93 \pm 0.35 \mu\text{mol m}^{-2} \text{s}^{-1}$) was about 84% of that for mature stand ($5.85 \pm 0.25 \mu\text{mol m}^{-2} \text{s}^{-1}$). The peak value of R_S for sapling stand was $5.23 \pm 0.31 \mu\text{mol m}^{-2} \text{s}^{-1}$.

3.2. Seasonal changes in R_S components at different age stands

Seasonal patterns of R_H and R_A were similar to those of R_S in all three age stands (Fig. 2). Both R_H (Fig. 2a) and R_A (Fig. 2b) increased from early May to late July, but the relative increasing rate of R_A was faster than that of R_H (Fig. 2c), and thus the contribution of R_H to R_S ($R_H:R_S$ ratio) was substantially decreased from early May to early June. The smallest ratio of R_H vs. R_S was 0.56, 0.55 and 0.48 for mature, young and sapling stand, respectively.

Table 2

Results of two-way ANOVA on the effect of sampling date and stand age on total soil respiration (R_S), heterotrophic respiration (R_H), autotrophic respiration (R_A) and the contribution of R_H to R_S .

	F			P value		
	Date	Age	Date × Age	Date	Age	Date × Age
R_S	92.38	1.39	1.21	<0.001	0.26	0.27
R_H	62.9	5.98	2.15	<0.001	0.004	0.008
R_A	13.48	1.87	0.38	<0.001	0.16	0.99
$R_H:R_S$	8.62	2.78	1.55	<0.001	0.06	0.09

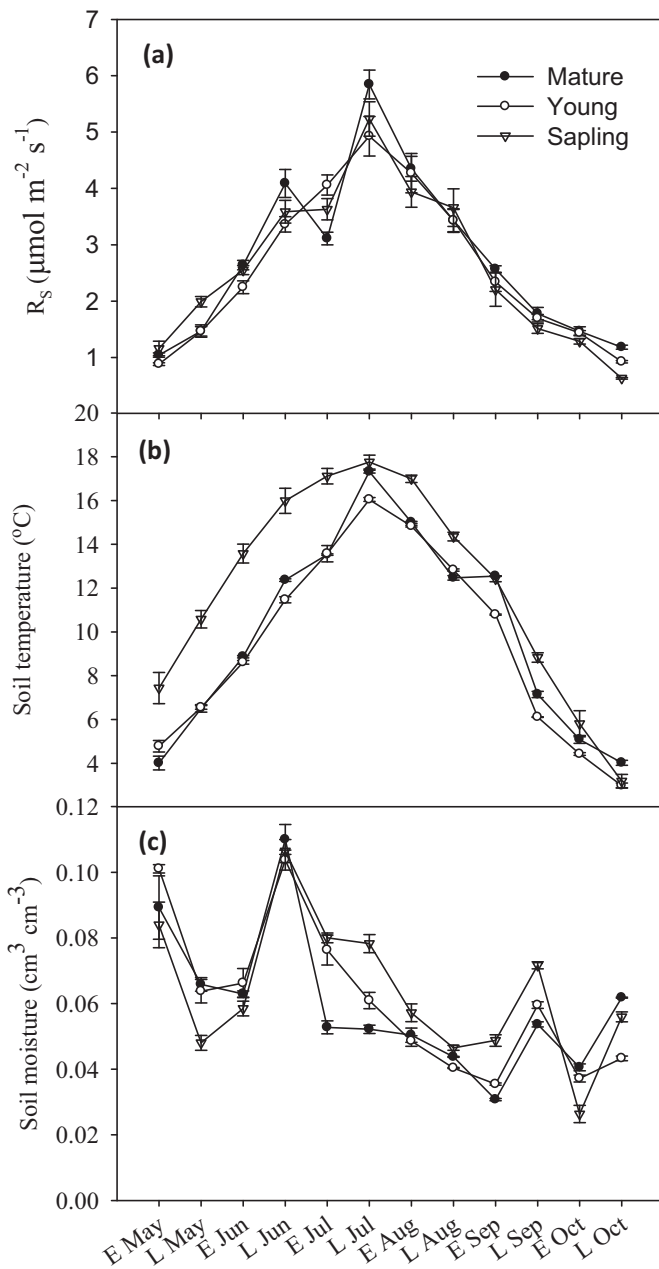


Fig. 1. Seasonal variation of (a) total soil respiration (R_S), (b) soil temperature and (c) soil moisture at three age stands across sampling date. The data were the averages of 2010, 2011 and 2012. The error bars mean standard errors ($n=3$). Mature, Young, and Sapling stand for 45-, 20- and 10-year-old stand, respectively. E and L stand for early and late, respectively.

Significant effects of stand age ($P=0.004$) and interaction of stand age and sampling date ($P=0.008$) on R_H was observed. The annual average R_H was 1.92 ± 0.19 , 1.76 ± 0.17 and $1.63 \pm 0.08 \mu\text{mol m}^{-2} \text{s}^{-1}$ for the mature, young and sapling stand, respectively. As shown in Fig. 2a, the mature stand had the highest growing season amplitude of R_H with the magnitude of $3.22 \mu\text{mol m}^{-2} \text{s}^{-1}$, while the young stand showed the lowest amplitude of $2.49 \mu\text{mol m}^{-2} \text{s}^{-1}$. The amplitude of R_H for the sapling stand was $2.82 \mu\text{mol m}^{-2} \text{s}^{-1}$. We also found marginal significant effects of stand age ($P=0.06$) and interaction of stand age and sampling date ($P=0.09$) on $R_H:R_S$ ratio. However, we did not find significant effect of stand age ($P=0.16$) or interactive effect of stand age and date ($P=0.99$) on R_A (Table 2).

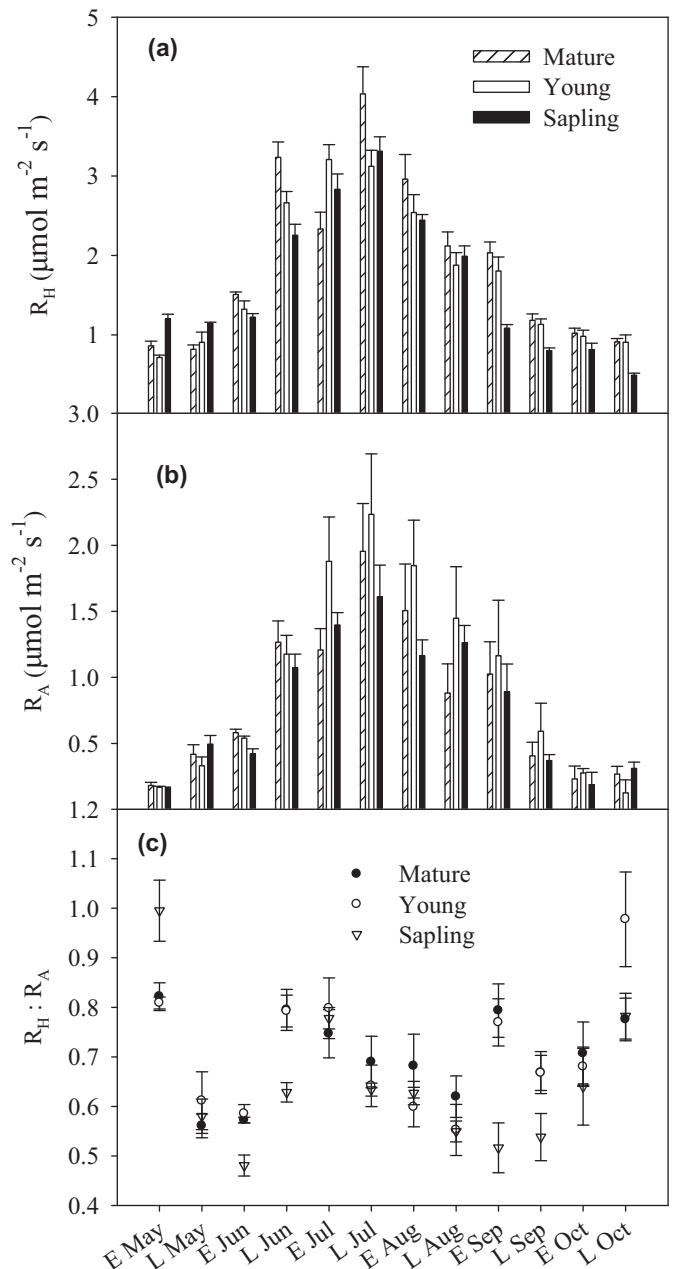


Fig. 2. Seasonal variation of (a) heterotrophic (R_H), (b) autotrophic (R_A) respiration and (c) their ratio for three age stands. The data were the averages of 2010, 2011 and 2012. The error bars mean standard errors ($n=3$). Mature, Young, and Sapling stand for 45-, 20- and 10-year-old stand, respectively. E and L stand for early and late, respectively.

3.3. Biotic factors at the three age stands

Fig. 3 illustrates the statistical comparison of microbial biomass carbon (C_{mic}) and C:N ratio across three age stands in both mineral soil and litter. A significant difference in C_{mic} was observed among three age stands in both mineral soil and litter (Fig. 3a and b). The C_{mic} at sapling stand was significantly higher than those at the other two age stands. For example, in mineral soil, C_{mic} of sapling stand was about $570 \pm 54 \text{ mg kg}^{-1}$, while the young and mature stand had values of 394 ± 27 and $283 \pm 56 \text{ mg kg}^{-1}$, respectively. For C:N ratio, the young stand had the highest C:N ratio in mineral soil (Fig. 3c). By contrast, in litter, the mature stand had the highest C:N ratio, which was followed by the young and sapling stands (Fig. 3d).

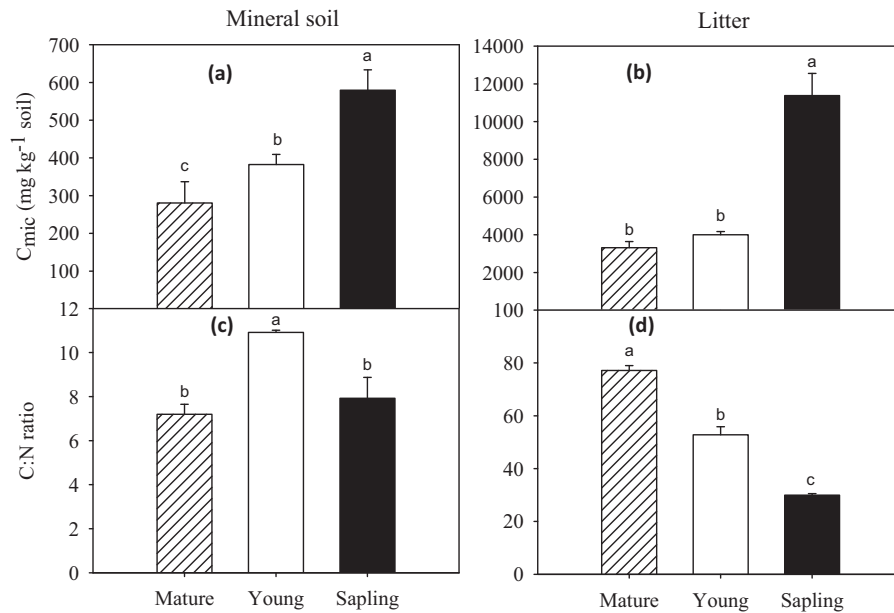


Fig. 3. Comparisons of microbial biomass carbon (a and b) and C:N ratio (c and d) among three age stands in mineral soil and litter layer. C_{mic} stands for microbial biomass carbon. The error bars mean standard errors. Different letters mean significant differences between different age stands (one-way ANOVA, post hoc LSD test).

For net primary productivity, the mature stand showed the lowest value, while the highest value appeared in the young stand (Fig. 4a). For litter mass, a significant difference was observed across different age stands. The young stand showed the highest value, while the lowest value occurred in the sapling stand (Fig. 4b).

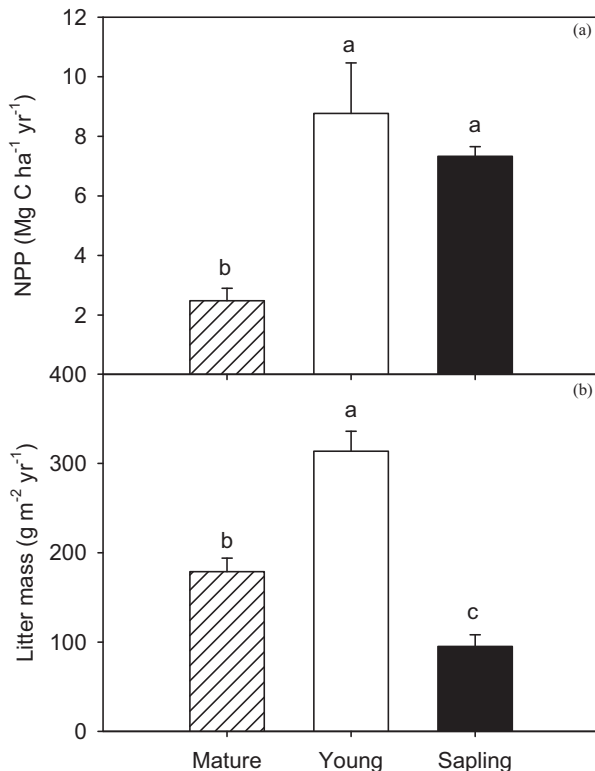


Fig. 4. The comparison of net primary productivity (NPP) (a) and litter mass (b) among three age stands. The error bars means standard errors ($n=3$). Different letters mean significant differences between different age stands (one-way ANOVA, post hoc LSD test).

3.4. Q_{10} at the three age stands

Fig. 5 illustrates the relationship of R_S , R_H , and R_A with the soil temperature at the depth of 5 cm in three age stands. Respiration exponentially increased with increasing temperature, with R^2 ranging from 0.34 to 0.68. Stand age impacted the Q_{10} . The sapling stand showed the lowest Q_{10} , with the Q_{10} value of 2.66 ± 0.08 for R_S , 2.69 ± 0.08 for R_H , and 3.06 ± 0.25 for R_A , lower than the Q_{10} values of corresponding respiration for the mature and young stands (Table 3). This was especially found in the sapling stand for the Q_{10} of R_A , which was significantly lower than the mature and young stands (Table 3). In addition, we found that Q_{10} values of R_H and R_A were significantly different (Fig. 5b and c). For example, the Q_{10} of R_H was about 3.03 ± 0.09 for the mature, 2.80 ± 0.11 for the young, and 2.69 ± 0.08 for the sapling stand, which is only 69%, 64%, and 88% of the corresponding Q_{10} values of R_A .

For the β_0 estimated by Eq. (2), or soil respiration at the reference temperature (10°C), the sapling stand showed the lowest β_0 value of R_S , R_H and R_A , while the highest value appeared in the young stand (Table 3). For the β_0 of R_S and R_H , they were significantly different among the three age stands (Table 3). The β_0 is the basal soil respiration, closely related to site conditions, history

Table 3

The parameters and statistics of soil respiration as the exponential function of soil temperature at three age stands. Parameter values are reported as means \pm SE. P values are for overall model fit. β_0 and Q_{10} are the regression coefficients of Eq. (2). R_S : total soil respiration; R_H : heterotrophic respiration; R_A : autotrophic respiration. Different letters (a and b) within the same column mean significant differences between different age stands (one-way ANOVA, post hoc LSD test).

		β_0	Q_{10}	R^2	P
R_S	Mature	2.236 ± 0.032^b	3.00 ± 0.09^a	0.654	<0.001
	Young	2.403 ± 0.040^b	2.83 ± 0.11^a	0.468	<0.001
	Sapling	1.759 ± 0.033^a	2.66 ± 0.08^a	0.600	<0.001
R_H	Mature	1.512 ± 0.024^b	3.03 ± 0.09^a	0.679	<0.001
	Young	1.616 ± 0.026^b	2.80 ± 0.11^a	0.534	<0.001
	Sapling	1.084 ± 0.022^a	2.69 ± 0.08^a	0.633	<0.001
R_A	Mature	0.684 ± 0.028^a	4.39 ± 0.40^b	0.423	<0.001
	Young	0.791 ± 0.003^a	4.35 ± 0.43^b	0.337	<0.001
	Sapling	0.572 ± 0.025^a	3.06 ± 0.25^a	0.364	<0.001

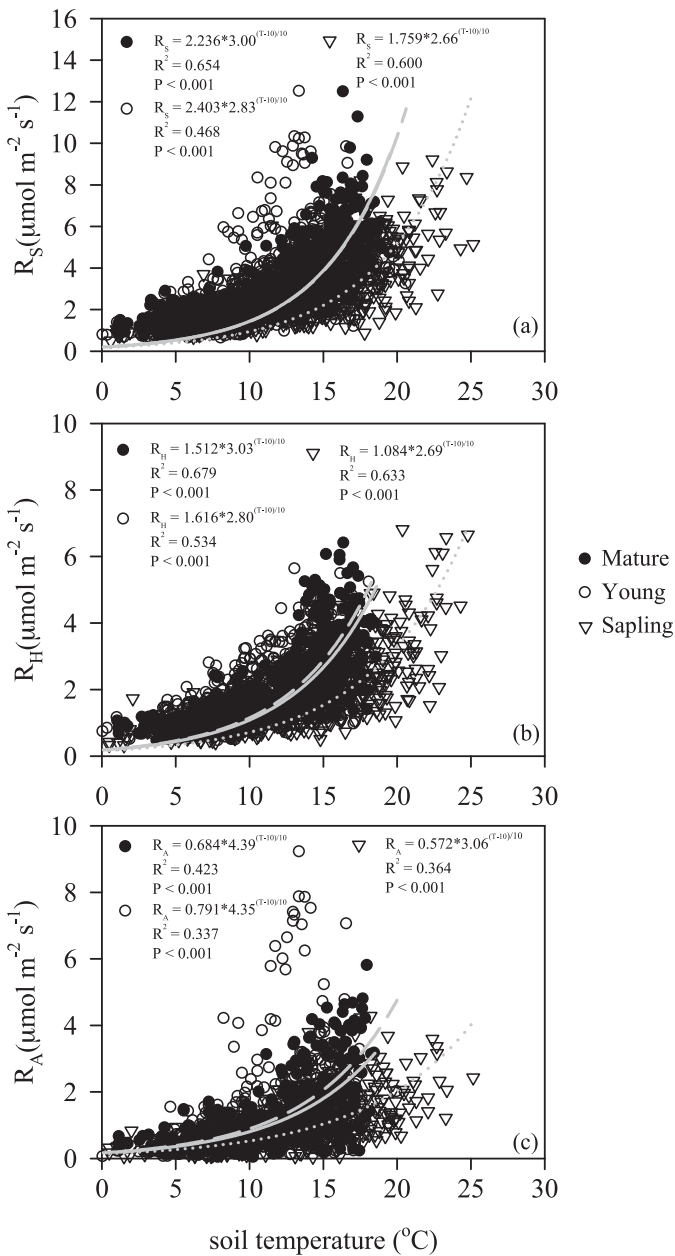


Fig. 5. The seasonal variation of total soil respiration (a), heterotrophic (b) and autotrophic (c) respiration against soil temperature at 5 cm depth for three age stands.

and characteristics. The observed difference in this quantity across different age stands could be related to their different soil organic carbon storages. For example, soil organic carbon in the top layer (0–10 cm) for mature, young and sapling stands were 47.9 ± 3.6 , 53.2 ± 5.1 and $39.5 \pm 1.5 \text{ Mg C ha}^{-1}$, respectively. While, other factors (e.g. nutrient availability, microbial community composition) not considered in this study can also contribute to the observed difference across three age stands. We should be informed that the difference in β_0 across age stands only reflected the difference in soil respiration rates calculated at the reference temperature (10°C in this study). If we investigated the differences in respiration rates across age stands over the entire temperature range, the residual analysis through removing the soil temperature effect according to Eq. (2) indicated that the residual respiration rates (R_s , R_H , and R_A) did not significantly differ among the three age stands (R_s : $P = 0.90$; R_H : $P = 0.98$ and R_A : $P = 0.08$).

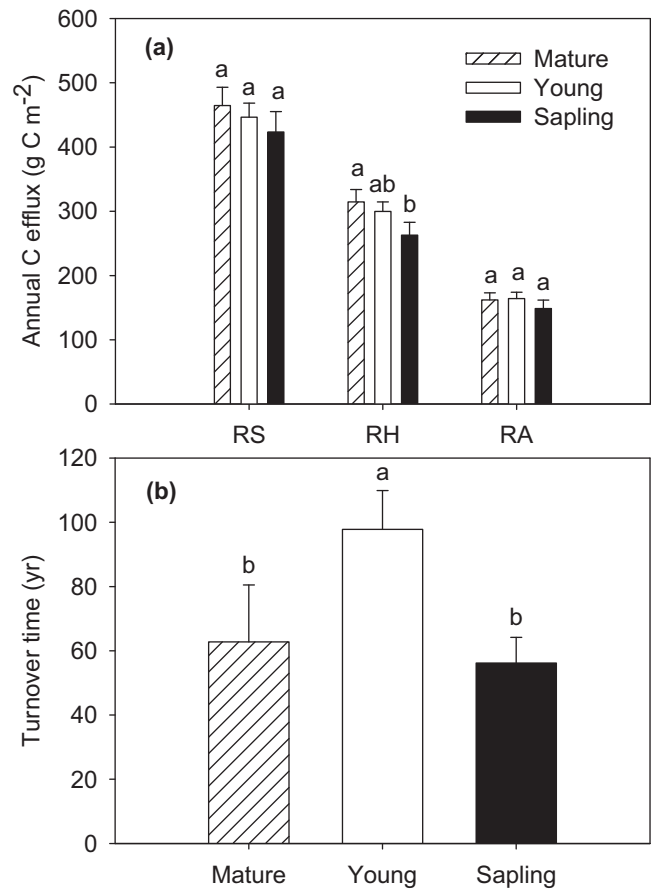


Fig. 6. Total annual C efflux (a) and turnover time (b) across three age stands. R_s , R_H and R_A stand for total soil respiration, heterotrophic and autotrophic respiration, respectively. Mature, Young, and Sapling stand for 45-, 20- and 10-year-old stand, respectively. Different letters mean significant differences between different age stands (one-way ANOVA, post hoc LSD test).

3.5. Transient turnover rates of soil organic carbon at the three age stands

In order to estimate transient turnover rates of soil organic carbon at the three age stands, cumulative soil respiration was calculated based on the exponential relationship between soil respiration and soil temperature derived in Fig. 5, and observed continuous soil temperature records during the snow-free season. We estimated that total R_H during the snow-free season was $315 \pm 19 \text{ g C m}^{-2}$ for the mature, $300 \pm 15 \text{ g C m}^{-2}$ for the young, and $263 \pm 20 \text{ g C m}^{-2}$ for the sapling stand (Fig. 6a), contributing 68%, 67%, 62% of total R_s of the mature ($465 \pm 28 \text{ g C m}^{-2}$), the young ($446 \pm 22 \text{ g C m}^{-2}$), and the sapling stand ($423 \pm 32 \text{ g C m}^{-2}$), respectively.

A significant difference in turnover time of SOC was observed among the three age stands ($P < 0.001$). The transient turnover rate of SOC at the sapling stand was faster than those at the other two stands (Fig. 6b). Transient turnover time of the sapling stand was about $56 \pm 8 \text{ yr}$, while the young and mature stands had turnover time of $98 \pm 12 \text{ yr}$ and $63 \pm 18 \text{ yr}$, respectively.

4. Discussion

4.1. Soil CO_2 efflux and the Q_{10} value

The strong link between soil respiration and temperature over seasonal course observed in this study is consistent with results

from individual *in situ* studies at most temperate and boreal forest ecosystems (Davidson et al., 1998; Janssens and Pilegaard, 2003; Ohashi and Gyokusen, 2007). We found that R_S exponentially increased with the increasing soil temperature at 5 cm depth by the Q_{10} of 2.7–3.0, which is within the range of the Q_{10} values reported by previous studies (Chen and Tian, 2005; Peng et al., 2009; Bond-Lamberty and Thomson, 2010; Wang et al., 2010a). A recent meta-analysis based on global soil respiration database showed that the Q_{10} varies from 1.9 to 5.7 (Bahn et al., 2010), depending on the depth of soil temperature measured (0 cm, 5 cm, 10 cm, 15 cm, and 20 cm) and climate conditions, such as mean annual temperature and precipitation (Chen and Tian, 2005; Peng et al., 2009; Wang et al., 2010a). In general, the Q_{10} increases with the depth of soil temperature measuring point (Pavelka et al., 2007; Graf et al., 2008), and is greater in cold, high-latitude ecosystems than in warm, temperate areas (Chen and Tian, 2005; Wang et al., 2010a).

Our results also showed that the Q_{10} is dependent on the component of soil respiration. The Q_{10} of R_A is about 1.1–1.6 times the Q_{10} of R_H , agreeing with previous studies (Lavigne et al., 2003; Gaumont-Guay et al., 2008) that showed root respiration had a higher Q_{10} value than soil heterotrophic respiration in temperate and boreal forests. This result also highlights the importance of root respiration in regulating the Q_{10} of R_S (Boone et al., 1998; Subke and Bahn, 2010). R_A is partitioned into two components: root growth or construction respiration (R_g) and maintenance respiration (R_m). R_g is generally controlled by allocation of recent photosynthates to roots, while R_m is tightly coupled with temperature theoretically (Enquist et al., 2007; Piao et al., 2010). Given that R_g is closely linked with plant photosynthesis (Högberg et al., 2001; Tang et al., 2005), and both photosynthesis and temperature have similar seasonal patterns, the effect of temperature change on R_A and eventually on R_S is generally enlarged (Wang et al., 2010a). In other words, the Q_{10} value estimated by the regression of seasonal change in observed R_A or R_S against contemporary seasonal changes in soil temperature is the apparent temperature sensitivity of soil respiration, rather than the ‘real’ temperature sensitivity of soil respiration (Curiel Yuste et al., 2004; Davidson and Janssens, 2006; Subke and Bahn, 2010).

A recent study suggested that when statistically removing the confounding effect of vegetation activity, the temperature sensitivity of soil respiration is about 1.5 (soil respiration increases 1.5 times when temperature increases by 10 degrees) (Wang et al., 2010a), which is comparable with the temperature sensitivity of ecosystem respiration (Mahecha et al., 2010). Using ecosystem respiration estimation across 60 FLUXNET sites, Mahecha et al. (2010) suggested that temperature sensitivity of ecosystem total respiration is about 1.4, and independent of mean annual temperature and biomes. Soil respiration measured by root exclusion method in this study, however, showed that the temperature sensitivity of soil heterotrophic respiration (the Q_{10} of R_H) is about 2.8, higher than the temperature sensitivity of both soil respiration (Wang et al., 2010a) and ecosystem respiration (Mahecha et al., 2010) at the global scale. Further studies are needed to accurately estimate the ‘real’ temperature sensitivity of soil respiration, which is critical for predicting future carbon cycle evolution as well as its feedback to climate change. Previous studies showed that the “real” Q_{10} could be approximated by its short-term (e.g. daily and weekly) value since the temperature had less interference with confounding factors over a relatively short time period (Vicca et al., 2009). However, in this study, 5 and 10 data points can only be available for each day and each month, respectively. Thus, the short-term Q_{10} values could not be robustly estimated based on this limited data size. We could combine more data from two or more months; however, the longer time period included in Q_{10} estimation, the larger the probability for confounding effects (Vicca et al., 2009). The reliability of this short-term Q_{10} in approximating intrinsic temperature

responses of respiration would then become reduced. This called for the necessity of applying automated soil respiration measurements in the future field study (Vargas et al., 2011).

4.2. Stand age effect on soil respiration and its components

Several studies suggested that the magnitude of carbon sink or source varies with the forest age (Law et al., 2003; Pregitzer and Euskirchen, 2004). In this study, we found significant effects of stand age on R_H . Among the three age stands, the sapling stand has the lowest R_H during the snow-free season, possibly related to the lowest soil organic carbon content. However, the transient turnover time of SOM for the sapling stand is faster than those of the other two stands. Several mechanisms can explain the relatively fast turnover rate for the sapling stand. Firstly, soil temperature at the sapling stand was highest among the three stands because of the direct exposure of soil surface to solar radiation (Scott et al., 1999). Soil temperatures at 5 cm depth were 9.91 ± 0.07 , 9.42 ± 0.06 and 12.00 ± 0.50 °C at mature, young and sapling stands, respectively in the present study. This suggests that such regulation of stand age on soil carbon cycling through the abiotic factors must be taken into account for investigating the effect of plantation on the global carbon cycle. Secondly, a large quantity of labile substrates input to the soil due to the dense understorey has fast turnover rate. These carbon inputs, primarily through root exudation and fine root turnover, are readily decomposable, leading to high microbial activity in the rhizosphere (Grayston et al., 1996; Phillips and Fahey, 2006). By contrast, the young stand with less dense understorey had relatively poor substrate quality in mineral soil and litter (Fig. 3c and d), which might contribute to the observed lowest transient turnover rate (Fig. 6b). Moreover, much larger carbon inputs to the soil (Fig. 4) can further increase the transient turnover time in the young stand. Thirdly, the soil disturbance when trees were planted on the former grassland might accelerate the decomposition of soil organic carbon (Jandl et al., 2007). Buchmann (2000) suggested that any soil disturbance will strongly enhance soil CO_2 efflux. Fourthly, the high microbial biomass (Fig. 3a and b) and enzyme activities might enhance the decomposition of SOC and litter at the sapling stand. The positive relationships were observed between soil respiration and the activities of two hydrolytic enzymes (BG and CB, Fig. 7), and our earlier work indicated that the activities of BG and CB were the highest at the sapling stand (Ma et al., in review).

Our results also showed the Q_{10} values of R_H at the mature and young stands were higher than that at the sapling stand, which might be attributed to the low substrate quality (Fig. 3c and d) and high litter mass (Fig. 4b) at the mature and young stands compared with those at the sapling stand. Several studies suggested that the decomposition of recalcitrant substrates is more temperature sensitive than the decomposition of labile substrates (Knorr et al., 2005; Fierer et al., 2005; Conant et al., 2008; Wetterstedt et al., 2010), although direct evidence is very limited (Fang et al., 2005, 2006; Reichstein et al., 2005). Furthermore, compared with the sapling stand, higher litter mass at the mature and young stands might have played a partial role in higher Q_{10} at the mature and young stands (Fig. 4), since substrate availability substantially impacted the temperature sensitivity of soil respiration (Davidson et al., 2006; Gershenson et al., 2009; Zhu and Cheng, 2011). In addition, given the highest soil temperature at the sapling stand, one can also suggest that the low Q_{10} value at the sapling stand is partly related to the acclimatization of soil respiration to higher soil temperature (Luo et al., 2001; Bradford et al., 2008), but further studies are needed to address this.

It should be noted that our results of the stand age effect on the Q_{10} value of R_H were inconsistent with the results of Tang et al. (2009), which reported that the Q_{10} value of R_S consistently and linearly decreased with stand age. This disagreement is not due

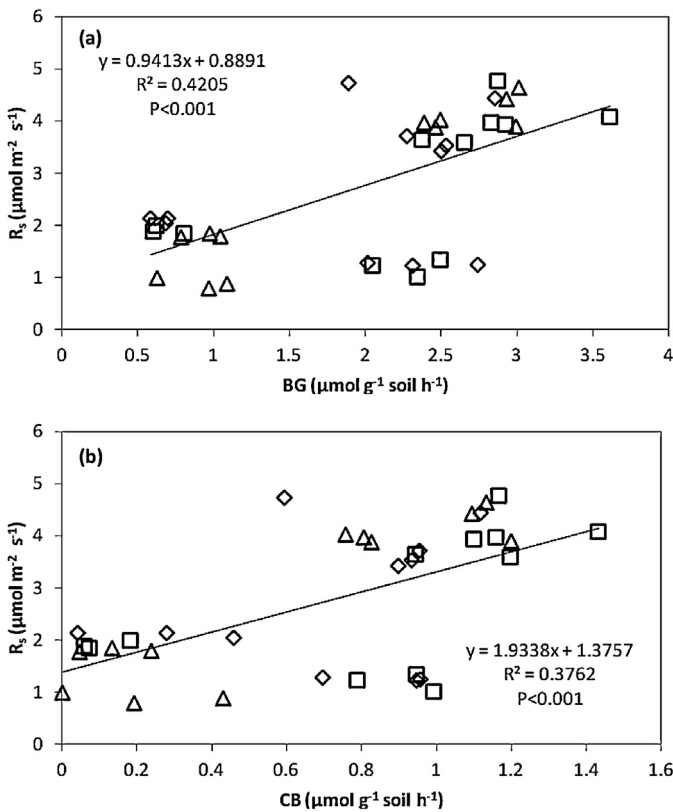


Fig. 7. The relationship between soil respiration and potential activities of β -glucosidase (a) and cellobiohydrolase (b). R_s means total soil respiration. BG and CB stand for β -glucosidase and cellobiohydrolase. The diamonds, cubes, and triangles stand for the data of mature, young and sapling stand, respectively.

to the different response of R_A , since the sapling stand also shows lower Q_{10} value of R_A and R_s than the mature and young stands, which is also consistent with the finding of previous studies (Clark et al., 2004; Yan et al., 2011). Clark et al. (2004) suggested that the Q_{10} value of R_s in older forests is higher than that of young forests. To help resolve this discrepancy and to more accurately quantify the effects of stand age on soil respiration and its temperature sensitivity in the global carbon cycle models, it is desirable to establish common protocols (e.g. sampling, measurements and reporting CO_2 fluxes) across a coordinated global network of sites.

5. Conclusions

The results presented in this study emphasized the importance of stand age in regulating soil respiration and its responses to temperature in *Larix principis-rupprechtii* plantation of Northern China. Such regulations of stand age on soil carbon cycling were manifested mainly by altering both abiotic (e.g. soil temperature) and biotic (e.g. soil organic carbon) factors. Thus, representing R_s (or its components R_H and R_A) as exponential functions of temperature without considering stand age impacts can over- or underestimate respiration, reducing the realism of carbon budget projections under future climate scenarios. Over the past four decades, China has been experiencing widespread forest plantations (or afforestation) (Piao et al., 2009), and the results presented here can be considered to provide guidance for constraining the uncertainty in model projections of climate impacts on Chinese ecosystem carbon balance. Moreover, our finding that a greater response of R_A than R_H across different age stands, which has not widely been reported by prior studies, can also contribute to soil carbon loss prediction in the future climate scenarios.

Finally, we should be informed that the temperature sensitivities of R_s (or R_H , R_A) derived from seasonal patterns across different age stands were not the real ones since they contained the seasonal changes in productivity and belowground carbon allocation. This might be overcome by calculating the temperature sensitivity over a relatively short time period (e.g. weekly) when the temperature has less interference with other confounding factors (e.g. site productivity). It thus calls for the deployment of automated soil respiration technique in the field, which could provide continuous measurements with a high time resolution (e.g. 30 min).

Acknowledgements

This study was funded by the National Natural Science Foundation of China (41171202 and 41125004) and National Youth Top-notch Talent Support Program in China. We are grateful to all the technicians who assisted us in the field and lab for their hard work.

References

- Bahn, M., Reichstein, M., Davidson, E.A., Grünzweig, J., Jung, M., Carbone, M.S., 2010. Soil respiration at mean annual temperature predicts annual total across vegetation types and biomes. *Biogeosciences* 7, 2147–2157.
- Bahn, M., Rodeghiero, M., Anderson-Dunn, M., Dore, S., Gimeno, C., Drosler, M., Williams, M., Ammann, C., Berninger, F., Flechard, C., Jones, S., Balzarolo, M., Kumar, S., Newesely, C., Priwitzer, T., Raschi, A., Siegwolf, R., Susiluoto, S., Tenhunen, J., Wohlfahrt, G., Cernusca, A., 2008. Soil respiration in European grasslands in relation to climate and assimilate supply. *Ecosystems* 11, 1352–1367.
- Bond-Lamberty, B., Thomson, A., 2010. Temperature-associated increases in the global soil respiration record. *Nature* 464, 579–584.
- Bond-Lamberty, B., Wang, C., Gower, S.T., 2004. Contribution of root respiration to soil surface CO_2 flux in a boreal black spruce chronosequence. *Tree Physiology* 24, 1387–1395.
- Boone, R.D., Nadelhoffer, K.J., Canary, J.D., Kaye, J.P., 1998. Roots exert a strong influence on the temperature sensitivity of soil respiration. *Nature* 396, 570–572.
- Bradford, M.A., Davies, C.A., Frey, S.D., Maddox, T.R., Melillo, J.M., Mohan, J.E., 2008. Thermal adaptation of soil microbial respiration to elevated temperature. *Ecology Letters* 11, 1316–1327.
- Bronson, D.R., Gower, S., Tanner, M., Linder, S., van Herk, I., 2008. Response of soil surface CO_2 flux in a boreal forest to ecosystem warming. *Global Change Biology* 14, 856–867.
- Buchmann, N., 2000. Biotic and abiotic factors controlling soil respiration rates in *Picea abies* stands. *Soil Biology and Biochemistry* 32, 1625–1635.
- Chen, H., Tian, H.Q., 2005. Does a general temperature-dependent Q_{10} model of soil respiration exist at biome and global scale? *Journal of Integrative Plant Biology* 47, 1288–1302.
- Clark, K.L., Gholz, H.L., Castro, M.S., 2004. Carbon dynamics along a chronosequence of slash pine plantations in north Florida. *Ecological Applications* 14 (4), 1154–1171.
- Conant, R.T., Drijber, R.A., Haddix, M.L., Parton, W.J., Paul, E.A., Plante, A.F., 2008. Sensitivity of organic matter decomposition to warming varies with its quality. *Global Change Biology* 14, 868–877.
- Curjel Yuste, J., Janssens, I.A., Carrara, A., Ceulemans, R., 2004. Annual Q_{10} of soil respiration reflects plant phenological patterns as well as temperature sensitivity. *Global Change Biology* 10, 161–169.
- Davidson, E.A., Belk, E., Boone, R.D., 1998. Soil water content and temperature as independent or confounded factors controlling soil respiration in a temperate mixed hardwood forest. *Global Change Biology* 4, 217–227.
- Davidson, E.A., Janssens, I.A., 2006. Temperature sensitivity of soil carbon decomposition and feedbacks to climate change. *Nature* 440, 165–173.
- Davidson, E.A., Janssens, I.A., Luo, Y.Q., 2006. On the variability of respiration in terrestrial ecosystem: moving beyond Q_{10} . *Global Change Biology* 12, 154–164.
- Enquist, B.J., Kerkhoff, A.J., Huxman, T., Economy, E.P., 2007. Adaptive differences in plant physiology and ecosystem paradoxes: insights from metabolic scaling theory. *Global Change Biology* 13, 591–609.
- Fang, C., Smith, P., Smith, J.U., 2006. Is resistant soil organic matter more sensitive to temperature than the labile organic matter? *Biogeosciences* 3, 65–68.
- Fang, C.M., Smith, P., Moncrieff, J.B., Smith, J.U., 2005. Similar response of labile and resistant soil organic matter pools to changes in temperature. *Nature* 433, 57–59.
- Fierer, N., Craine, J.M., Mclauchlan, K., Schimel, J.P., 2005. Litter quality and the temperature sensitivity of decomposition. *Ecology* 86 (2), 320–326.
- Food and Agricultural Organization, 2006. The Assessment of Global Forest Resources in 2005: Progress Towards Sustainable Forest Management. Food and Agricultural Organization of the United Nations, Rome, Italy.
- Friedlingstein, P., Cox, P., Betts, R., Bopp, L., von Bloh, W., Brovkin, V., 2006. Climate-carbon cycle feedback analysis: results from the C4MIP model inter-comparison. *Journal of Climate* 19, 3337–3343.

- Gaumont-Guay, D., Black, A., Barr, A.G., Jassal, R.S., Nesci, Z., 2008. Biophysical controls of rhizospheric and heterotrophic components of soil respiration in a boreal black spruce stand. *Tree Physiology* 28, 161–171.
- Gershenson, A., Bader, N.E., Cheng, W.X., 2009. Effects of substrate availability on the temperature sensitivity of soil organic matter decomposition. *Global Change Biology* 15, 176–183.
- Graf, A., Weihermüller, L., Huisman, J.A., Herbst, M., Bauer, J., Vereecken, H., 2008. Measurement depth effects on the apparent temperature sensitivity of soil respiration in field studies. *Biogeosciences* 5, 1175–1188.
- Grayston, S.J., Vaughan, D., Jones, D., 1996. Rhizosphere carbon flows in trees, in comparison with annual plants: the importance of root exudation and its impact on microbial activity and nutrient availability. *Applied Soil Ecology* 5, 29–56.
- Hanson, P.J., Edwards, N.T., Garten, C.T., Andrews, J.A., 2000. Separating root and soil microbial contributions to soil respiration: a review of methods and observations. *Biogeochemistry* 48, 115–146.
- Höglberg, P., Nordgren, A., Buchmann, N., Taylor, A.F.S., Ekblad, A., Höglberg, M.N., 2001. Large-scale forest girdling shows that current photosynthesis drives soil respiration. *Nature* 411, 789–792.
- Jandl, R., Lindner, M., Vesterdal, L., Bauwens, B., Baritz, R., Hagedorn, F., 2007. How strongly can forest management influence soil carbon sequestration? *Geoderma* 137, 253–268.
- Janssens, I.A., Pilegaard, K., 2003. Large seasonal changes in Q_{10} of soil respiration in a beech forest. *Global Change Biology* 9, 911–918.
- Knorr, W., Prentice, I.C., House, J.J., Holland, E.A., 2005. Long term sensitivity of soil carbon turnover to warming. *Nature* 433, 298–301.
- Krinner, G., Viovy, N., de Noblet-Ducoudré, N., Ogée, J., Polcher, J., Friedlingstein, P., 2005. A dynamic global vegetation model for studies of the coupled atmosphere–biosphere system. *Global Biogeochemistry Cycles* 19, GB1015, <http://dx.doi.org/10.1029/2003GB002199>.
- Laganière, J., Paré, D., Bergeron, Y., Chen, Y.H., 2012. The effect of boreal forest composition on soil respiration is mediated through variations in soil temperature and C quality. *Soil Biology and Biochemistry* 53, 18–27.
- Lavigne, M.B., Boutin, R., Foster, R.J., Goodine, G., Bernier, P.Y., Robitaille, G., 2003. Soil respiration responses to temperature are controlled more by roots than by decomposition in balsam fir ecosystem. *Canadian Journal of Forest Research* 33, 1744–1753.
- Law, B.E., Sun, O.J., Campbell, J., van Tuyl, S., Thornton, P.E., 2003. Changes in carbon storage and fluxes in a chronosequence of ponderosa pine. *Global Change Biology* 9, 510–524.
- Le Quéré, C., Raupach, M.R., Canadell, J.G., Marland, G., Bopp, L., Ciais, P., 2009. Trends in the sources and sinks of carbon dioxide. *Nature Geoscience* 2, 831–836.
- Longdoz, B., Yernaux, M., Aubinet, M., 2000. Soil CO₂ efflux measurements in a mixed forest: impact of chamber distances, spatial variability and seasonal evolution. *Global Change Biology* 6, 907–917.
- Luo, Y.Q., Wan, S.Q., Hui, D.F., Wallace, L.L., 2001. Acclimatization of soil respiration to warming in a tall grass prairie. *Nature* 413, 622–625.
- Mahecha, M.D., Reichstein, M., Carvalhais, N., Lasslop, G., Lange, H., Seneviratne, S.I., 2010. Global convergence in the temperature sensitivity of respiration at ecosystem level. *Science* 329, 838–841.
- Maseyk, K., Grünzweig, J.M., Rotenberg, E., Yakir, D., 2008. Respiration acclimation contributes to high carbon-use efficiency in a seasonally dry pine forest. *Global Change Biology* 14, 1553–1567.
- Ohashi, M., Gyokusen, K., 2007. Temporal change in spatial variability of soil respiration on a slope of Japanese cedar (*Cryptomeria japonica* D. Don) forest. *Soil Biology and Biochemistry* 39, 1130–1138.
- Pavelka, M., Acosta, M., Marek, M.V., Kutsch, W., Janous, D., 2007. Dependence of the Q_{10} values on the depth of the soil temperature measuring point. *Plant and Soil* 292, 171–179.
- Peng, S.S., Piao, S.L., Wang, T., Sun, J.Y., Shen, Z.H., 2009. Temperature sensitivity of soil respiration in different ecosystems in China. *Soil Biology and Biochemistry* 41, 1008–1014.
- Phillips, R.P., Fahey, T.J., 2006. Tree species and mycorrhizal associations influence the magnitude of rhizosphere effects. *Ecology* 87, 1302–1313.
- Piao, S.L., Fang, J.Y., Ciais, P., Peylin, P., Huang, Y., Sitch, S., Wang, T., 2009. The carbon balance of terrestrial ecosystems in China. *Nature* 458, 1009–1013.
- Piao, S.L., Luyssaert, S., Ciais, P., Janssens, I.A., Chen, A.P., Cao, C., 2010. Forest annual carbon cost: a global-scale analysis of autotrophic respiration. *Ecology* 91, 652–661.
- Pregitzer, K., Euskirchen, E., 2004. Carbon cycling and storage in world forests: biome patterns related to forest age. *Global Change Biology* 10, 2052–2077.
- Raich, J.W., Potter, C.S., Bhagawati, D., 2002. Interannual variability in global soil respiration, 1980–94. *Global Change Biology* 8, 800–812.
- Raich, J.W., Schlesinger, W.H., 1992. The global carbon dioxide flux in soil respiration and its relationship to vegetation and climate. *Tellus* 44(B), 81–89.
- Reichstein, M., Rey, A., Freibauer, A., Tenhunen, J., Valentini, R., Banza, J., Casals, P., Cheng, Y., Grünzweig, J.M., Irvine, J., Joffre, R., Law, B.E., Loustau, D., Miglietta, F., Oechel, W., Ourcival, J.-M., Pereira, J.S., Peressotti, A., Ponti, F., Qi, Y., Rambal, S., Rayment, M., Romanya, J., Rossi, F., Tedeschi, V., Tirone, G., Xu, M., Yakir, D., 2003. Modeling temporal and large-scale spatial variability of soil respiration from soil water availability, temperature and vegetation productivity indices. *Global Biogeochemical Cycles* 17, 1104, <http://dx.doi.org/10.1029/2003gb.002035>.
- Reichstein, M., Subke, J.A., Angeli, A.C., Tenhunen, J.D., 2005. Does the temperature sensitivity of decomposition of soil organic matter depend upon water content, soil horizon, or incubation time? *Global Change Biology* 11, 1754–1767.
- Salz, G., Byrne, K., Butterbach-Bahl, K., Kiese, R., Blujdea, V., Farrell, E.P., 2006. Stand age-related effects on soil respiration in a first rotation Sitka spruce chronosequence in central Ireland. *Global Change Biology* 12, 1007–1020.
- Sampson, D.A., Janssens, I.A., Yuste, J.C., Ceulemans, R., 2007. Basal rates of soil respiration are correlated with photosynthesis in a mixed temperate forest. *Global Change Biology* 13, 2008–2017.
- Schindlbacher, A., Zechmeister-Boltenstern, S., Jandl, R., 2009. Carbon losses due to soil warming: do autotrophic and heterotrophic soil respiration respond equally? *Global Change Biology* 15, 901–913.
- Schindlbacher, A., Wunderlich, S., Borken, W., Kitzler, B., Zechmeister-Boltenstern, S., Jandl, R., 2012. Soil respiration under climate change: prolonged summer drought offsets soil warming effects. *Global Change Biology* 18, 2270–2279.
- Schlesinger, W.H., Andrews, J.A., 2000. Soil respiration and the global carbon cycle. *Biogeochemistry* 48, 7–20.
- Scott, N.A., Tate, K.R., Ford-Robertson, J., 1999. Soil carbon storage in plantation forests and pastures: land-use change implications. *Tellus* 51B, 326–335.
- Sitch, S., Smith, B., Prentice, I.C., Arneeth, A., Bondeau, A., Cramer, W., Kaplan, J.O., Lewis, S., Lucht, W., Sykes, M.T., Thonicke, K., Venevsky, S., 2003. Evaluation of ecosystem dynamics, plant geography and terrestrial carbon cycling in the LPJ dynamic global vegetation model. *Global Change Biology* 9, 161–185.
- Subke, J.A., Bahn, M., 2010. On the “temperature sensitivity of soil respiration”: can we use the immeasurable to predict the unknown? *Soil Biology and Biochemistry* 42, 1653–1656.
- Tang, J.W., Baldocchi, D.D., Xu, L., 2005. Tree photosynthesis modulates soil respiration on a diurnal time scale. *Global Change Biology* 11, 1298–1304.
- Tang, J.W., Bolstad, P.V., Martin, J.G., 2009. Soil carbon fluxes and stocks in a Great Lakes forest chronosequence. *Global Change Biology* 15, 145–155.
- Vargas, R., Carbone, M.S., Reichstein, M., Baldocchi, D., 2011. Frontiers and challenges in soil respiration research: from measurements to model-data integration. *Biogeochemistry* 102, 1–13.
- Vicca, S., Janssens, I.A., Flessa, H., Fiedler, S., Jungkunst, H.F., 2009. Temperature dependence of greenhouse gas emissions from three hydromorphic soils at different groundwater levels. *Geobiology* 7, 465–476.
- Wang, X.H., Piao, S.L., Ciais, P., Janssens, I.A., Reichstein, M., Peng, S.S., 2010a. Are ecological gradients in seasonal Q_{10} of soil respiration explained by climate or by vegetation seasonality? *Soil Biology and Biochemistry* 42, 1728–1734.
- Wang, W., Peng, S.S., Wang, T., Fang, J.Y., 2010b. Winter soil CO₂ efflux and its contribution to annual soil respiration in different ecosystems of a forest-steppe ecotone, north China. *Soil Biology and Biochemistry* 42, 451–458.
- Wetterstedt, J.A.M., Persson, T., Ågren, G.I., 2010. Temperature sensitivity and substrate quality in soil organic matter decomposition: results of an incubation study with three substrates. *Global Change Biology* 16, 1806–1819.
- Yan, M., Zhang, X., Zhou, G., Gong, J., You, X., 2011. Temporal and spatial variation in soil respiration of poplar plantations at different developmental stages in Xinjiang, China. *Journal of Arid Environments* 75, 51–57.
- Zhu, B., Cheng, W.X., 2011. Rhizosphere priming effect increases the temperature sensitivity of soil organic matter decomposition. *Global Change Biology* 17, 2172–2183.

Nitrogen Deposition Enhances Carbon Sequestration by Plantations in Northern China

Zhihong Du^{1,2}, Wei Wang^{1*}, Wenjing Zeng¹, Hui Zeng²

1 Department of Ecology, College of Urban and Environmental Sciences, and Key Laboratory for Earth Surface Processes of the Ministry of Education, Peking University, Beijing, China, **2** Key Laboratory for Urban Habitat Environmental Science and Technology, Peking University Shenzhen Graduate School, Shenzhen, China

Abstract

Nitrogen (N) deposition and its ecological effects on forest ecosystems have received global attention. Plantations play an important role in mitigating climate change through assimilating atmospheric CO₂. However, the mechanisms by which increasing N additions affect net ecosystem production (NEP) of plantations remain poorly understood. A field experiment was initialized in May 2009, which incorporated additions of four rates of N (control (no N addition), low-N (5 g N m⁻² yr⁻¹), medium-N (10 g N m⁻² yr⁻¹), and high-N (15 g N m⁻² yr⁻¹)) at the Saihanba Forestry Center, Hebei Province, northern China, a locality that contains the largest area of plantations in China. Net primary production (NPP), soil respiration, and its autotrophic and heterotrophic components were measured. Plant tissue carbon (C) and N concentrations (including foliage, litter, and fine roots), microbial biomass, microbial community composition, extracellular enzyme activities, and soil pH were also measured. N addition significantly increased NPP, which was associated with increased litter N concentrations. Autotrophic respiration (AR) increased but heterotrophic respiration (HR) decreased in the high N compared with the medium N plots, although the HR in high and medium N plots did not significantly differ from that in the control. The increased AR may derive from mycorrhizal respiration and rhizospheric microbial respiration, not live root respiration, because fine root biomass and N concentrations showed no significant differences. Although the HR was significantly suppressed in the high-N plots, soil microbial biomass, composition, or activity of extracellular enzymes were not significantly changed. Reduced pH with fertilization also could not explain the pattern of HR. The reduction of HR may be related to altered microbial C use efficiency. NEP was significantly enhanced by N addition, from 149 to 426.6 g C m⁻² yr⁻¹. Short-term N addition may significantly enhance the role of plantations as an important C sink.

Citation: Du Z, Wang W, Zeng W, Zeng H (2014) Nitrogen Deposition Enhances Carbon Sequestration by Plantations in Northern China. PLoS ONE 9(2): e87975. doi:10.1371/journal.pone.0087975

Editor: Shuijin Hu, North Carolina State University, United States of America

Received: September 27, 2013; **Accepted:** January 2, 2014; **Published:** February 3, 2014

Copyright: © 2014 Du et al. This is an open-access article distributed under the terms of the Creative Commons Attribution License, which permits unrestricted use, distribution, and reproduction in any medium, provided the original author and source are credited.

Funding: This research was supported by the National Basic Research Program of China (No. 2010CB950600 and 2013CB956303), Projects of the National Natural Science Foundation of China (No. 31222011, 31270363, and 31070428), Projects of Innovative Research Groups of the National Natural Science Foundation of China (No. 31021001) and University Construction Projects from Central Authorities in Beijing. The funders had no role in study design, data collection and analysis, decision to publish, or preparation of the manuscript.

Competing Interests: The authors have declared that no competing interests exist.

* E-mail: wangw@urban.pku.edu.cn

Introduction

Terrestrial ecosystems sequester nearly 30% of anthropogenic carbon (C) emissions, offering the most effective, yet natural, means to mitigate climate change [1]. Nitrogen (N) is a major limiting nutrient to plant growth in most terrestrial ecosystems [2] and thus affects C sequestration in terrestrial ecosystems [3]. Human activity has led to a significant increase in N deposition owing to industrialization, agricultural practices, and the combustion of fossil fuels [4–6]. Numerous studies have shown that N deposition can increase net ecosystem production (NEP), as an indicator of ecosystem C sequestration [7–9]. However, the magnitude of the increased NEP following N addition varied greatly from 24.5 to 225 kg C per kg N [10–12]. Therefore, there is an urgent need to explore the mechanisms underlying this effect.

NEP is determined by the difference between net primary production (NPP) and soil heterotrophic respiration (HR). One important issue that needs addressing is how additional N affects the process of plant growth and thus enhances NPP. Many studies have attributed the increased tree growth to significantly higher foliar N concentrations in fertilized plots [8,13–15]. The increased

foliar N concentrations could improve biomass production through the following three pathways: by increasing the uptake of CO₂ [16–18], by increasing water-use efficiency of foliage via altering CO₂ assimilation and stomatal conductance [19], and by reducing the thermally dissipated light [20]. At the same time, N addition may also decrease leaf N resorption [21], and thus increase litter N concentrations. Consequently, more available N is released via decomposition to supply plant growth [22]. However, little research has been conducted to comprehensively analyze the mechanism of plant biomass growth caused by N addition.

How soil respiration (SR) responds to N addition is also relevant. SR consists of autotrophic respiration (AR, respiration by live roots, rhizospheric microorganism, and mycorrhizal fungi) and HR, which mainly originates from microbial decomposition of soil organic matter. With N addition, AR was either inhibited by decreasing the below-ground C allocation and fine root biomass of trees [23] or promoted by increasing the N concentration in fine roots [24–28]. At the same time, the enhanced tree growth caused by N addition is also likely to lead to more plant photosynthate being transported from above ground to below ground, thus increasing AR. HR is also commonly considered to be related to

microbial biomass and activity [29–31]. For instance, decreased HR was observed along with a consistent decrease in microbial biomass and extracellular enzyme activity [32]. Soil acidification caused by N deposition [33] is also a potential factor that could contribute to decreased HR. However, the inherent reasons concerning the responses of AR and HR to N addition are poorly understood.

Although there have been numerous studies investigating the effects of N deposition on ecosystem C sequestration [27,34,35], most of them focused on natural forests. Plantations are becoming a key component of world forest resources and play important roles in the context of overall sustainable forest management. Well-designed, multi-purpose plantations can reduce pressure on natural forests, restore some ecological services provided by natural forests, and mitigate climate changes through direct C sequestration [36]. However, there remain great uncertainties in the potential of plantations to sequester C [37]. Compared with natural forests, plantations appear to have lower NPP, root biomass, and soil microbial biomass [37]. Whether plantations have the same ecosystem C sequestration capacity as natural forests remains to be confirmed [38–40]. Among a few studies, increased ecosystem C sequestration with N deposition has been observed [41,42]. However the underlying mechanisms by which N increases the plant C accumulation and affects SR and its autotrophic and heterotrophic components are still poorly understood.

In China, the total plantation area reached 5.33×10^7 ha in 1998, accounting for 30% of the total forest area of China and 29% of the world's total plantation area [43]. C accumulation in China is mainly ascribable to its extensive afforestation efforts, as 80% of the observed increase in tree C stocks in China occurred on its 213,106 ha of plantations [43]. These reforestation and afforestation programs are considered to influence C storage in China. Thus, to assess the C sequestration capacity of plantations and optimize their role as C sinks, it is necessary to systematically explore ways in which N deposition affects C sequestration. Consequently, a 3-year field N addition experiment was conducted in the Saihanba Forestry Center, Hebei Province, northern China, which contains the largest area of plantations in China, with the dominant species being *Pinus sylvestris* var. *mongolica* (Mongolian pine). NPP, SR, and its autotrophic and heterotrophic components were measured. Relevant influential factors were also measured, including plant tissue C and N concentrations (foliage, litter, and fine roots), microbial biomass C, microbial community composition, potential extracellular enzyme activities (EEAs), and soil pH values. The study aimed to address three questions: (1) how does the N addition affect NPP? (2) What are the responses of SR and its autotrophic and heterotrophic components to N addition? (3) What is the effect of N addition on NEP? We hypothesized that: (1) N addition would increase NPP via increasing foliage or litter N concentrations; (2) AR would remain stable because of the contrasting effects from decreasing below-ground C allocation and fine root biomass and increased fine root N concentrations and photosynthate transport from above ground to below ground; HR would be reduced because of decreased microbial biomass, inhibited microbial activity, and reduced pH values; and (3) NEP would be enhanced because of the increasing NPP and decreased HR.

Materials and Methods

Ethics Statement

The administration of the Saihanba Forestry Center gave permission for the use of their plantation for our study site. We

confirm that the field studies did not involve endangered or protected species.

Site description

The study was conducted at the Saihanba Forestry Center in Hebei Province, northern China ($117^{\circ}12' - 117^{\circ}30'$ E, $42^{\circ}10' - 42^{\circ}50'$ N, 1400 m a.s.l.). The study area belongs to a typical forest-steppe ecotone of the temperate area. The climate is semi-arid and semi-humid, with a long and cold winter (November to March), and a short spring and summer. Annual mean air temperature and precipitation over the period from 1964 to 2004 were -1.4°C and 450.1 mm, respectively. The soils are predominantly sandy. The study site is located in the largest area of plantations in China, with the dominant species being *Pinus sylvestris* var. *mongolica*. The herbaceous layer is dominated by *Carex rigescens*, *Thalictrum aquilegifolium*, *Galium verum*, *Geum aleppicum*, *Artemisia tanacetifolia*, and *Agrimonia pilosa*.

Experimental treatments

The N addition experiment was initiated in May 2009. Urea solution was evenly sprayed once a month from May to September with the same dose each year. Four N addition treatments (in three replicates) were established, including a control (without N added), low N ($5 \text{ g N m}^{-2} \text{ yr}^{-1}$), medium N ($10 \text{ g N m}^{-2} \text{ yr}^{-1}$), and high N ($15 \text{ g N m}^{-2} \text{ yr}^{-1}$). Twelve plots, each of $20 \text{ m} \times 20 \text{ m}$ dimensions were established, each surrounded by a 10-m wide buffer strip. All plots and treatments were randomly laid out. During each application, the fertilizer was weighed, mixed with 10 L of water, and applied to each plot below the canopy using a backpack sprayer. The control plot received 10 L of water without N.

Field measurements

Biomass production and accumulation. An allometric method was used to estimate biomass production through establishing the relationship between component biomass (foliage, branches, stem, and roots) and diameter at breast height (DBH) and tree height (H) [44]. In July 2010, stems were cut at the soil surface in the area near our experimental plots. Total tree heights, length of live crown, DBH, and diameter at the base of the live crown were measured and recorded. All foliage on each live branch was collected and weighed. All live and dead branches from each canopy position were cut and weighed separately. The stems were cut into 1-m sections and weighed. Litter from each deforested tree was carefully collected and weighed. The entire root system of the sample trees was excavated using a combination of a pulley device and manual digging, and cleaned of adhering soil. The fresh mass of each component was determined to the nearest 1 g using an electronic balance. All of these procedures were conducted in the field immediately after the tree was felled. The total biomass was calculated as the sum of foliage, branch, litter, stem, and root biomass.

An allometric equation was established as:

$$\text{Biomass production (BP)} = a(D^2 H)^b (R^2 = 0.96, P < 0.01)$$

where H is the height of trees (m), D is DBH (cm), and a and b are regression constants ($b = 0.70$, $a = 107.01$). DBH was recorded on all living stems in each plot in July 2010 and July 2012. The height of each living tree was measured using a DME (Haglöf Vertex IV, Sweden). Because biomass production (BP) constitutes the largest fraction of NPP, BP is commonly used as a proxy for NPP [45–48]. It is important to note that NPP includes numerous

C-consuming processes such as plant growth, root exudation, and C allocation to symbionts [49]. The NPP in our study was thus underestimated. We used 50% as the C concentration in plant tissue [28]. The net primary production was calculated by the following equation:

$$NPP = (BP_{2012} - BP_{2010})/2,$$

where *NPP* is the net primary productivity ($\text{g C m}^{-2} \text{ yr}^{-1}$) and *BP* is the estimated biomass production ($\text{g C m}^{-2} \text{ yr}^{-1}$) in 2012 and 2010. The annual net ecosystem production (NEP, $\text{g C m}^{-2} \text{ yr}^{-1}$) was calculated as the annual NPP minus annual soil HR.

Fine root biomass. In July 2011 and 2012, five soil core samples were taken randomly using a 5.8-cm-diameter soil corer around the trees in each replicate plot, causing as little disturbance as possible to the surrounding soil. The roots were transported to the laboratory where they were washed free of soil, dried at 70°C, and weighed.

SR and its autotrophic and heterotrophic components. SR was measured using a Li-8100 soil CO₂ flux system (LI-COR Inc. Lincoln, NE, USA). Measurements were conducted at least once per month from May to October in 2011 and 2012. There were five subsamples (i.e., SR collars) in each plot. We used two kinds of soil collars in each plot to measure total SR and HR. A shallow surface collar (10 cm inside diameter, 6 cm height) that penetrated 3 cm into the soil was used to measure SR. The other kind of collar (10 cm inside diameter, 35 cm height), which was used for HR measurement, was inserted 30 cm into the soil with a 5-cm height above the soil surface. Because the majority of roots are found within the upper 30 cm of the soil profile in this forest (data not shown), these deeper collars should eliminate the majority of live roots and their contributions to respiration. All the polyvinyl chloride (PVC) collars were installed 6 months prior to the first measurements to minimize any disturbance of the soil environment. SR in the growing season was obtained from the monthly data directly measured in the field experiment using linear extrapolation methods. Winter SR was obtained from the data of Wang et al. (2010) [50] from the same study site.

Laboratory analyses

Plant chemical analyses. Five subsamples were collected in each plot for chemical analyses. Green foliage was sampled from vigorously growing trees in late July 2012 using a pole pruner and a steel ladder. Foliar litter was collected from litter traps. Fine root samples were selected after the soil was passed through a 2-mm sieve. All the green foliage, foliar litters, and fine roots were dried at 60°C to constant mass, and ground using an intermediate mill (0.5-mm mesh screen) to generate homogeneous samples for chemical analysis. The C and N concentrations were measured using an element analyzer (Vario EL III, Elementar, Hanau, Germany).

Soil chemical analyses. In July 2012, mineral soils were sampled at 0–10 cm depth from five random locations per plot using 5.8-cm-diameter soil corers. Once collected, the soils were immediately placed in a cooler and transported to the nearby laboratory (less than 30 min travel time per site). The cores from each plot were then combined and frozen for later processing. Within 24 h, frozen soils were allowed to thaw at room temperature. Plant litter in the upper layer, as well as all the coarse and fine roots, was carefully removed. The soils were then separated into four sub-samples for laboratory analysis, including pH, microbial biomass C and N, microbial community composition (PLFAs), and potential EEAs.

Air-dried soil had any roots removed, and was passed through a 2-mm sieve. Soil pH was determined using a 1:5 soil:water ratio with a pH meter (Model PHS-2; INESA Instrument, Shanghai, China).

MBC and MBN were measured using the chloroform fumigation extraction technique [51,52]. Two replicate samples, one unfumigated and one fumigated with alcohol-free CHCl₃ for 24 h, were pre-incubated at 25°C for 7 days and then extracted with 0.5 mol/L K₂SO₄ (1:2.5 w/v). The extracts were analyzed for total dissolved C and N using a total C analyzer (TOC-500; Shimadzu, Kyoto, Japan). The microbial biomass was calculated as the difference in extractable C and N between the fumigated and unfumigated soils. The efficiency factors used to calculate the respective MBC and MBN were $K_C = 0.379$ [52] and $K_N = 0.54$ [51].

Phospholipid fatty acids (PLFAs) analysis was used to assess microbial community composition. PLFAs were extracted and analyzed using a procedure described by [53]. Briefly, the soil was extracted in a single-phase mixture of chloroform: methanol: citrate buffer (1: 2: 0.8) [54]. After extraction, the lipids were separated into neutral lipids, glycolipids, and polar lipids (phospholipids) on a silicic acid column. The phospholipids were methylated and separated on a gas chromatograph equipped with a flame ionization detector. Peak areas were quantified by adding methyl nonadecanoate fatty acid (19:0) as the internal standard before the methylation step. Peaks were identified by chromatographic retention time and a standard qualitative mix in the range of C9–C30 using a microbial identification system (Microbial ID Inc., Newark, DE, USA). The fatty acid 18:2ω6, 9 was recognized as the fungal biomarker [55]. The sum of the following PLFAs was used as a measure of the bacterial biomass: i14:0, i15:0, a15:0, 15:0, i16:0, 10Me16:0, i17:0, a17:0, cy17:0, 17:0, br18, 10Me17:0, 18:1ω7, 10Me18:0, and cy19:0 [56].

Seven EEAs were measured, including five enzymes involving C metabolism (α -glucosidase (AG), β -1,4-glucosidase (BG), leucine aminopeptidase (LAP), β -D-cellobiosidase (CB), and xylosidase (XS)), one involving N metabolism (N-acetyl-glucosaminidase (NAG)), and one involving phosphorus (P) metabolism (acid phosphatase (AP)). The measurements were conducted following the method of Saiya-Cork et al. (2002) [57]. Briefly, sample suspensions were prepared by adding 2 g of fresh soil to 90 ml of 50 mmol/L, pH 6.0 acetate buffer and homogenizing for 1 min.

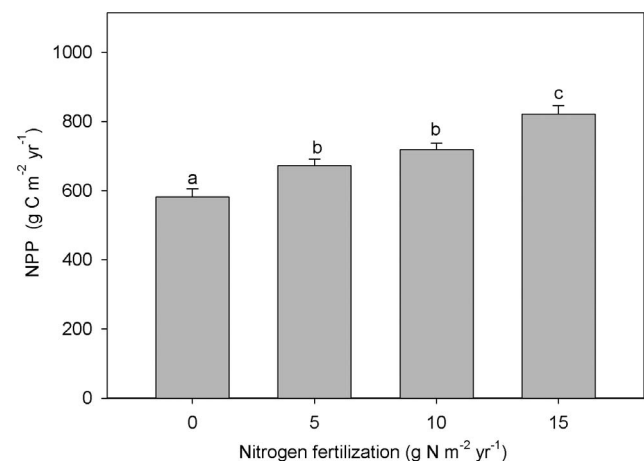


Figure 1. Average net primary productivity (NPP) in control and nitrogen (N) fertilized treatments. Significant differences among N treatments are indicated by different letters. doi:10.1371/journal.pone.0087975.g001

Continuously, 200- μ l suspensions were combined with the corresponding substrate in a 96-well microplate. There were six replicate wells per sample per assay. The micro-plates were incubated at 25°C for up to 3 h. Fluorescence was then measured using a microplate reader with 365-nm excitation and 450-nm emission filters (Tecan Infinite M200, Salzburg, Austria). Finally, the concentration was divided by incubation time and dry weight soil to estimate potential enzyme activity.

Statistical analysis

All statistical analyses were performed using SPSS statistical software (SPSS 18.0 for Windows; SPSS Inc., Chicago, IL, USA). One-way analysis of variance with Duncan's test was used to test the differences among the different N addition treatments in NPP, SR, and its AR and HR components, and in NEP, as well as plant and soil chemical parameters. Significant effects were determined

at $P < 0.05$ unless otherwise stated. Data was expressed as mean values \pm S.E. (standard error).

Results

Biomass production and accumulation

No significant differences were observed in DBH for both 2010 and 2012 among the different N addition treatments (Fig. S1a). However, in 2012, the tree height significantly increased with fertilization (Fig. S1b). The averaged NPP was 582.3 ± 22.8 g C m⁻² yr⁻¹ in the control plots. N addition increased NPP by 15.45%, 23.51%, and 41.21%, respectively, in the low-, medium-, and high-N plots (Fig. 1). Fine root biomass showed a decreasing trend with fertilization although no significant differences were observed (Fig. S2).

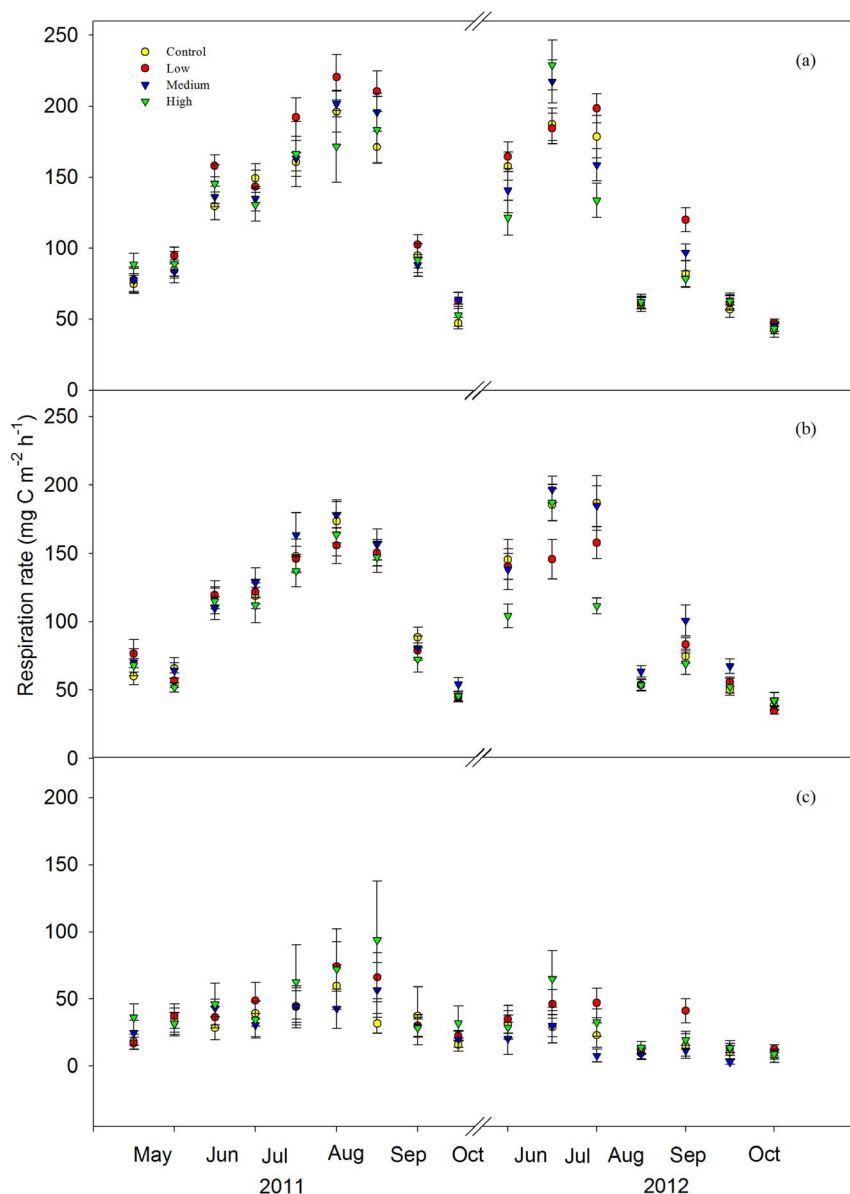


Figure 2. Soil respiration (a), heterotrophic respiration (b), and autotrophic respiration (c) in control (yellow circle), low-nitrogen (N) (red circle), medium-N (blue triangle), and high-N (green triangle) plots during the growing seasons of 2011 and 2012.

doi:10.1371/journal.pone.0087975.g002

SR and its autotrophic and heterotrophic components

Both total SR and HR followed a clear seasonal pattern with the highest rates in June–August and the lowest rates in spring and autumn for all the treatments (Fig. 2). SR was not significantly different among control and fertilized treatment plots in both 2011 ($P=0.43$) and 2012 ($P=0.36$) (Fig. 3a). There was no significant variance between the control and low-N treatment for AR and HR in both 2011 and 2012 ($P>0.05$) (Fig. 3b, Fig. 3c). With the fertilization gradient increasing, significantly higher AR (Fig. 3c) and lower HR (Fig. 3b) occurred in the high-N plots compared with the medium-N treatment in 2012.

Net ecosystem productivity (NEP)

With a decrease in HR and increased NPP, NEP significantly increased with fertilization, from 149 to 426.6 g C m⁻² yr⁻¹ (Fig. 4). The amount of C (kg) fixed by 1 kg N/ha N addition was in the range of 116.6–209.8 kg C per kg N/ha.

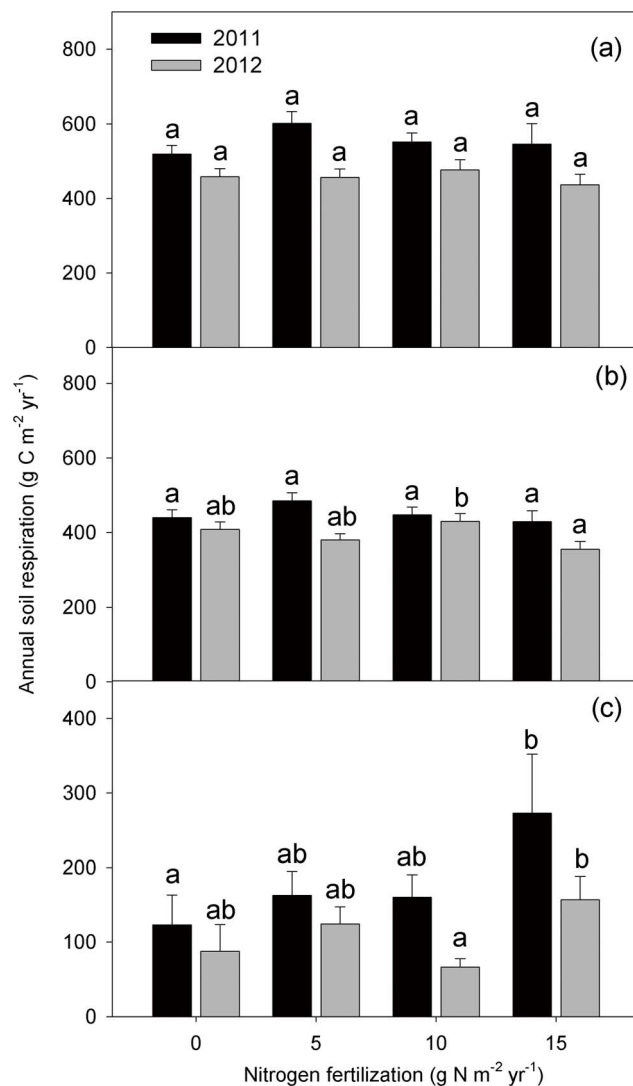


Figure 3. Comparison of annual soil respiration (a), autotrophic respiration (b), and heterotrophic respiration (c) among control, low-, medium-, and high-nitrogen (N) plots in 2011 (black) and 2012 (gray). Significant differences among N treatments are indicated by different letters. doi:10.1371/journal.pone.0087975.g003

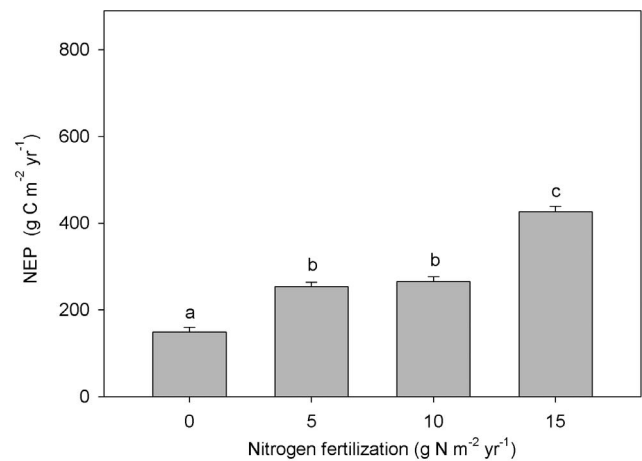


Figure 4. Net ecosystem productivity (NEP) in control and nitrogen (N) fertilized treatments. Significant differences among N treatments are indicated by different letters. doi:10.1371/journal.pone.0087975.g004

Plant chemical parameters

N addition significantly increased foliar N concentrations in the herbaceous layer (Fig. S3). However, N concentrations of the tree foliage showed no significant differences among the control and fertilization treatments (Fig. 5). C and N concentrations of foliar litter were significantly higher in the high-N and medium-N plots than in the control (Fig. 5). Fine root N concentrations showed no

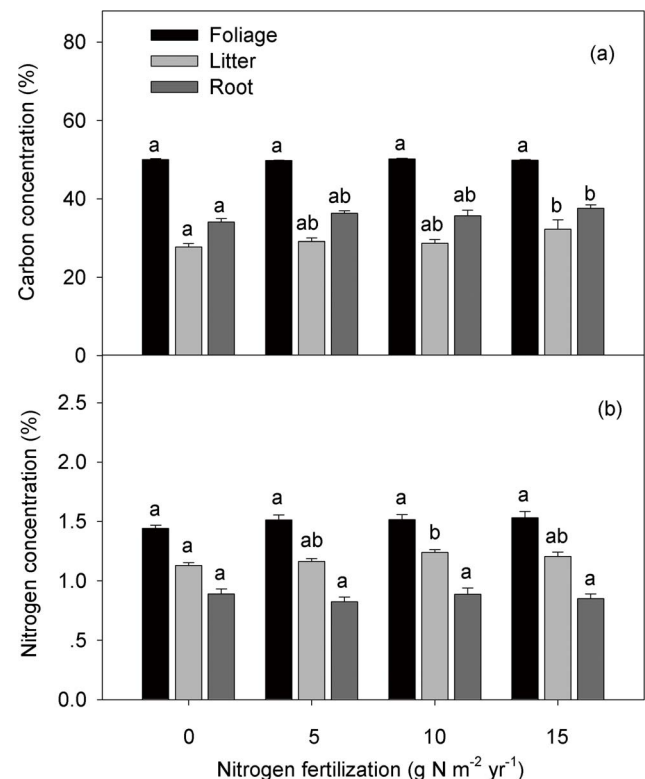


Figure 5. Carbon (a) and nitrogen (b) concentrations of foliage, litter, and fine roots in control and nitrogen (N) fertilized treatments. Significant differences among N treatments are indicated by different letters. doi:10.1371/journal.pone.0087975.g005

Table 1. Effects of nitrogen (N) addition on microbial biomass carbon (MBC), microbial biomass N (MBN), bacterial biomass (BB), and fungal biomass (FB).

Microbial properties	N treatment			
	Control	Low N	Medium N	High N
MBC	132.67±22.39 ^a	157.55±18.31 ^a	162.14±22.51 ^a	145.68±21.05 ^a
MBN	48.9±82.46 ^a	51.88±4.81 ^a	55.55±66.62 ^a	60.59±5.98 ^a
BB	17.0±1.52 ^a	18.94±2.73 ^a	16.19±2.53 ^a	12.91±1.58 ^a
FB	7.08±0.75 ^a	9.62±2.15 ^a	7.41±1.21 ^a	6.19±0.11 ^a

Data are expressed as mean ± S.E. (standard error). Different superscript letters indicated significant differences among N treatment plots ($P<0.05$).
doi:10.1371/journal.pone.0087975.t001

significant differences while fine root C concentrations increased by 10.28% in the high-N plots compared with the control (Fig. 5).

Soil chemical parameters

Soil pH significantly decreased with fertilization (Fig. S4). MBC and MBN were 132.67–145.68 mg C kg⁻¹ dry soil and 48.98–60.59 mg C kg⁻¹ dry soil, respectively. Although there were no significant differences among the control and fertilized treatments, MBC and MBN generally increased along the fertilization gradient (Table 1). Neither bacterial nor fungal biomass varied significantly with N addition (Table 1). The activities of all seven enzymes involving C, N, and P metabolism showed no significant differences between the control and fertilized plots (Fig. 6).

Discussion

Effects of N addition on NPP

N fertilization significantly increased NPP by 15.4–41.2% (Fig. 1) through the vertical growth of trees (Fig. S1). This maximum rate of increase of NPP is more than twice the average level of temperate forests (19.5%) [58]. The increased NPP could

not be related to fresh foliar N concentrations, because no significant differences occurred between the control and fertilized plots (Fig. 5). This is inconsistent with commonly observed increases in foliar N with N addition [59,13–15]. For instance, May et al. (2005) [15] found that foliar N concentrations averaged 11% higher in fertilization treatments than in the control in a mixed-deciduous forest. In this study, litter N concentrations significantly increased in the fertilized plots relative to the control ($P<0.05$) (Fig. 5b), suggesting a likely decrease in leaf N resorption by fertilization [15,60,61]. Litter with higher N concentration would be easily decomposed by microbes and release large amounts of available N for plant growth, thus potentially increasing forest productivity [62–65].

Foliage N concentrations of trees showed no significant differences among control and fertilized plots (Fig. 5), while foliage N concentrations in plants in the herbaceous layer significantly increased (Fig. S3). This may be because of differences in leaf shape. Compared with coniferous trees, the broad-leaved herbaceous plants may invest more N in foliage to produce enzymes and proteins associated with photosynthetic processes or increase their foliage area to improve photosynthesis. Increased

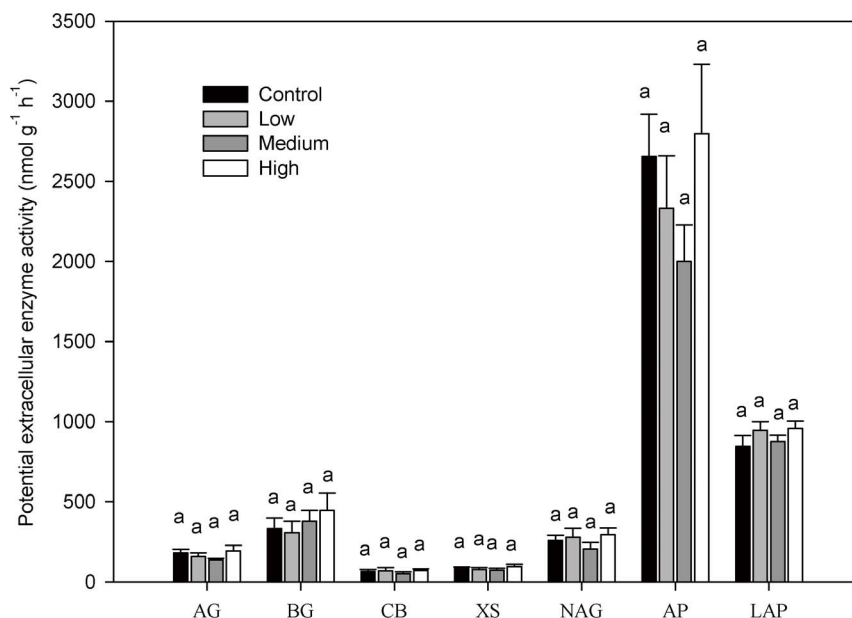


Figure 6. Potential extracellular enzyme activity at a soil depth of 0–10 cm in control and fertilized plots measured in 2012. Significant differences among nitrogen (N) treatments are indicated by different letters. AG = α -glucosidase; BG = β -1,4-glucosidase; CB = β -D-cellobiosidase; XS = xylosidase; NAG = N-acetyl-glucosaminidase; AP = acid phosphatase; LAP = leucine aminopeptidase.
doi:10.1371/journal.pone.0087975.g006

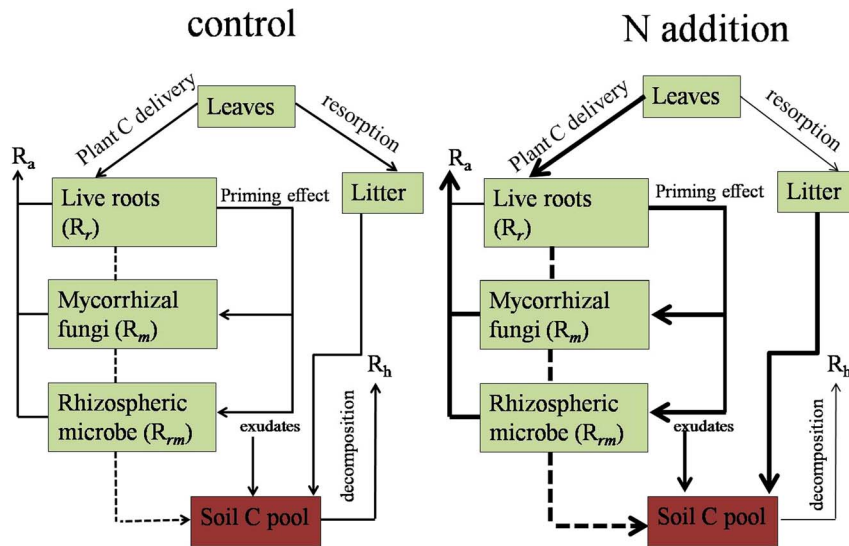


Figure 7. Carbon sequestration and its response to nitrogen (N) addition in plantations. R_a and R_h are autotrophic and heterotrophic respiration, respectively; R_r is live root respiration, R_m is respiration of mycorrhizal fungi, and R_{rm} is rhizospheric microbial respiration. Thick arrows represent the enhanced process and thin arrows represent the declined progress in the N addition treatment compared with the control. doi:10.1371/journal.pone.0087975.g007

foliage N concentrations following N addition have been commonly observed in previous studies of broadleaf species (i.e., *Acer rubrum*, *Liriodendron tulipifera*, *Prunus serotina*, *Acer saccharum*, and *Betula alleghaniensis*) [13–15]. Therefore, the nutrient use strategy of plants may be closely related to their foliage shape. Thus, foliage shape should be taken into consideration in the future when it comes to assessing the response of ecosystem C sequestration to N deposition.

SR and its autotrophic and heterotrophic components

No significant differences were observed in total SR among the control and fertilized treatments (Fig. 3a), which is inconsistent with a commonly reported reduction in SR following N addition [9,66–68]. Significantly higher AR in high-N plots than in the medium-N treatment was observed, although neither treatment showed any significant differences to the control (Fig. 3c). No significant differences in fine root biomass (Fig. S2) and N concentrations were observed among the different treatments (Fig. 5b), implying that live root respiration may not change with fertilization. Instead, fine root C concentrations significantly increased by 4.89%, 6.72%, and 10.28%, respectively, in the low-, medium-, and high-N addition foliage plots compared with the control treatment (Fig. 5a). This suggests an increased supply of photosynthetic products from above ground to below ground following N addition. Consequently, plant C may prime the growth and activity of mycorrhizal fungi [29] and rhizospheric microbes [23,69–72], thus promoting AR. However, fertilization may also suppress rhizospheric microbial respiration to a greater extent than that in the bulk soil because of the decreased C allocation to root symbionts and exudation [68]. Therefore, there is a need to distinguish different components of AR in the future to accurately explore the internal mechanism underlying the increased AR.

HR in the high-N treatment was significantly lower than that in the medium-N plot after 3 years' fertilization, although it did not significantly differ from the control and low-N plots (Fig. 3c). Decreased HR is believed to be mainly driven by a decreased microbial biomass [29,30] and depressed phenol oxidase activity (a

lignin-degrading enzyme) [31,73]. In contrast to most previous studies, we did not observe significant variation in the soil microbial biomass (Table 1), extracellular enzyme activity (Fig. 6), and microbial community composition (Table 1). Although soil pH was significantly lower in the high-N plots than in the control plots, it did not significantly differ from values in the medium- and low-N plots (Fig. S4). Hence, the decreased HR in the high-N plot could not be attributable to changes in the microbial biomass, extracellular enzyme activity, microbial community composition, or soil pH. The variation in HR may depend on the C-use efficiency of the decomposers (defined as the ratio of C employed in the new biomass relative to C consumed for respiration) [74]. When N availability is high, microbes may increase their efficiency leading to an efficient increase in biomass and a relatively low release of C to the atmosphere [75]. Because microbial biomass was measured only in July 2012, a greater frequency of measurement of microbial biomass should be conducted to better explore the reasons for the decrease in HR.

Effect of N fertilization on NEP

With the increasing NPP and decreasing HR, NEP greatly increased from the control to the high-N addition plots (149 versus 426.6 g C m⁻² yr⁻¹). NEP in our control plot fell within the published range for boreal forests (40–180 g C m⁻² yr⁻¹) [76]. The amount of C fixed per unit of added N fertilizer was in the range of 116.6–209.8 kg C/ha per kg N in this study, which is broadly similar to the range proposed by Magnani et al. (2008) (175–225 kg C per kg N) [11]. Thus, short-term N fertilization can greatly increase the NEP of plantations in northern China and enhance the role of plantations as an important C sink.

However, N fertilization may also induce alterations in the availability of other nutrients such as P, potassium, and calcium, because of the intrinsic stoichiometric constraints of plant growth. This could have an important influence on NEP. N deposition is also likely to be accompanied by other environmental changes including rising atmospheric CO₂ concentrations, global warming, and soil acidification and these changes will interact with N availability in complex ways. The complexity of these interacting

controls (i.e., temperature and nutrient availability) further restricts our ability to forecast future C sequestration capacities. In addition, we should be careful when extrapolating our results and mechanisms to systems with long-term N inputs. Finally, the stand age of plantations may also be a potentially influential factor in evaluating their sequestration capacity. This suggests a need for future studies in stands of various ages and incorporating long-term multi-factorial experiments.

Conclusion

This study has comprehensively analyzed the effects of N addition on biomass accumulation, SR, and its autotrophic and heterotrophic components in plantations of northern China. N addition might alter C sequestration capacity through the following possible pathways (Fig. 7): (1) increased litter N concentration because of decreased N resorption by foliage; (2) enhancement of the amount of photosynthetic products transported downward; (3) increased AR through the priming effect of plant C on rhizospheric microbial and mycorrhizal fungi activity; and (4) suppressed HR through increased microbial C use efficiency. Increasing N deposition is likely to stimulate NEP and slow the accumulation of atmospheric CO₂. In the context of global atmospheric N deposition, we highlighted that plantations might offer an important role to mitigate the future climate change.

References

- Le Quéré C, Raupach MR, Canadell JG, Marland G (2009) Trends in the sources and sinks of carbon dioxide. *Nature Geoscience* 2: 831–836.
- Vitousek PM, Cassman K, Cleveland C, Crews T, Field CB, et al. (2002) Towards an ecological understanding of biological nitrogen fixation. *Biogeochemistry* 57: 1–45.
- Thomas DC, Zak DR, Filley TR (2012) Chronic N deposition does not apparently alter the biochemical composition of forest floor and soil organic matter. *Soil Biology and Biochemistry* 54: 7–13.
- Vitousek PM, Aber JD, Howarth RW, Likens GE, Matson PA, et al. (1997) Human alteration of the global nitrogen cycle: sources and consequences. *Ecological Applications* 7: 737–750.
- Aber JD, Goodale CL, Ollinger SV, Smith ML, Magill AH, et al. (2003) Is nitrogen deposition altering the nitrogen status of northeastern forests? *BioScience* 53: 375–389.
- Galloway JN, Townsend AR, Erisman JW, Bekunda M, Cai Z, et al. (2008) Transformation of the nitrogen cycle: recent trends, questions, and potential solutions. *Science* 320: 889–892.
- Magnani F, Mencuccini M, Borghetti M, Berbigier P, Berninger F, et al. (2007) The human footprint in the carbon cycle of temperate and boreal forests. *Nature* 447: 849–851.
- Pregitzer KS, Burton AJ, Zak DR, Talhelm AF (2008) Simulated chronic nitrogen deposition increases carbon storage in Northern Temperate forests. *Global Change Biology* 14: 142–153.
- Janssens I, Dieleman W, Luyssaert S, Subke JA, Reichstein M, et al. (2010) Reduction of forest soil respiration in response to nitrogen deposition. *Nature Geoscience* 3: 315–322.
- de Vries W, Solberg S, Dobbervin M, Sterba H, Laubhahn D, et al. (2008) Ecologically implausible carbon response? *Nature* 451: E1–E3.
- Magnani F, Mencuccini M, Borghetti M, Berninger F, Delzon S, et al. (2008) Ecologically implausible carbon response? Reply. *Nature* 451: E3–E4.
- Liu L, Greaver TL (2009) A review of nitrogen enrichment effects on three biogenic GHGs: the CO₂ sink may be largely offset by stimulated N₂O and CH₄ emission. *Ecology letters* 12: 1103–1117.
- Boggs JL, McNulty SG, Gavazzi MJ, Myers JM (2005) Tree growth, foliar chemistry, and nitrogen cycling across a nitrogen deposition gradient in southern Appalachian deciduous forests. *Canadian Journal of Forest Research* 35: 1901–1913.
- Elvir JA, Rustad L, Wiersma GB, Fernandez I, White AS, et al. (2005) Eleven-year response of foliar chemistry to chronic nitrogen and sulfur additions at the Bear Brook Watershed in Maine. *Canadian Journal of Forest Research* 35: 1402–1410.
- May JD, Burdette SB, Gilliam FS, Adams MB (2005) Interspecific divergence in foliar nutrient dynamics and stem growth in a temperate forest in response to chronic nitrogen inputs. *Canadian Journal of Forest Research-Revue Canadienne De Recherche Forestiere* 35: 1023–1030.
- Aber JD, Nadelhoffer KJ, Steudler P, Melillo JM (1989) Nitrogen saturation in northern forest ecosystems. *Bioscience* 39: 378–286.
- Aber J, McDowell W, Nadelhoffer K, Magill A, Berntson G, et al. (1998) Nitrogen saturation in temperate forest ecosystems. *Bioscience* 48: 921–934.
- Driscoll CT, Lawrence GB, Bulger AJ, Butler TJ, Cronan CS, et al. (2001) Acidic deposition in the northeastern United States: sources and inputs, ecosystem effects, and management strategies. *Bioscience* 51: 180–198.
- Guerrieri R, Mencuccini M, Sheppard L, Saurer M, Perks M, et al. (2011) The legacy of enhanced N and S deposition as revealed by the combined analysis of $\delta^{13}\text{C}$, $\delta^{18}\text{O}$ and $\delta^{15}\text{N}$ in tree rings. *Global Change Biology* 17: 1946–1962.
- Tomaszewski T, Sievering H (2007) Canopy uptake of atmospheric N deposition at a conifer forest: Part II—response of chlorophyll fluorescence and gas exchange parameters. *Tellus B* 59: 493–501.
- van Heerwaarden LM, Toet S, Aerts R (2003) Nitrogen and phosphorus resorption efficiency and proficiency in six sub-arctic bog species after 4 years of nitrogen fertilization. *Journal of Ecology* 91: 1060–1070.
- Sullivan PF, Sommerkorn M, Rueth HM, Nadelhoffer KJ, Shaver GR, et al. (2007) Climate and species affect fine root production with long-term fertilization in acidic tussock tundra near Toolik Lake, Alaska. *Oecologia* 153: 643–652.
- Höberg MN, Briones MJ, Keel SG, Metcalfe DB, Campbell C, et al. (2010) Quantification of effects of season and nitrogen supply on tree below-ground carbon transfer to ectomycorrhizal fungi and other soil organisms in a boreal pine forest. *New Phytologist* 187: 485–493.
- Janssens IA, Crookshanks M, Taylor G, Ceulemans R (1998) Elevated atmospheric CO₂ increases fine root production, respiration, rhizosphere respiration and soil CO₂ efflux in Scots pine seedlings. *Global Change Biology* 4: 871–878.
- Pregitzer KS, Laskowski MJ, Burton AJ, Lessard VC, Zak DR (1998) Variation in sugar maple root respiration with root diameter and soil depth. *Tree Physiology* 18: 665–670.
- Jia SX, Wang ZQ, Li XP, Sun Y, Zhang XP, et al. (2010) N fertilization affects on soil respiration, microbial biomass and root respiration in *Larix gmelinii* and *Fraxinus mandshurica* plantations in China. *Plant and Soil* 333: 325–336.
- Burton AJ, Jarvey JC, Jarvi MP, Zak DR, Pregitzer KS (2011) Chronic N deposition alters root respiration-tissue N relationship in northern hardwood forests. *Global Change Biology* 18: 258–266.
- Tu LH, Hu TX, Zhang J, Li RH, Dai HZ, et al. (2011) Short-term simulated nitrogen deposition increases carbon sequestration in a *Pleioblastus amarus* plantation. *Plant and Soil* 340: 383–396.
- Craine JM, Morrow C, Fierer N (2007) Microbial nitrogen limitation increases decomposition. *Ecology* 88: 2105–2113.
- Fierer N, Lauber CL, Ramirez KS, Zaneveld J, Bradford MA, et al. (2011) Comparative metagenomic, phylogenetic and physiological analyses of soil microbial communities across nitrogen gradients. *The ISME journal* 6: 1007–1017.
- Zak DR, Pregitzer KS, Burton AJ, Edwards IP, Kellner H (2011) Microbial responses to a changing environment: implications for the future functioning of terrestrial ecosystems. *Fungal Ecology* 4: 386–395.

Supporting Information

Figure S1 Diameter at breast height (DBH) and height of trees with nitrogen (N) fertilization in 2010 (black) and 2012 (gray).

(TIF)

Figure S2 Fine root biomass among different nitrogen (N) fertilization gradients in 2012. Significant differences among N treatments are indicated by different letters.

(TIF)

Figure S3 Effects of nitrogen (N) addition on foliar N concentrations of herbaceous layer plants. Significant differences among N treatments are indicated by different letters.

(TIF)

Figure S4 Soil pH in control and nitrogen (N) treatments plots after 3 years fertilization. Significant differences among N treatments are indicated by different letters.

(TIF)

Author Contributions

Conceived and designed the experiments: WW. Performed the experiments: ZHD WJZ. Analyzed the data: ZHD. Contributed reagents/materials/analysis tools: HZ. Wrote the paper: ZHD.

32. Ramirez KS, Craine JM, Fierer N (2010) Nitrogen fertilization inhibits soil microbial respiration regardless of the form of nitrogen applied. *Soil Biology and Biochemistry* 42: 2336–2338.
33. Phoenix GK, Emmett BA, Britton AJ, Caporn SJ, Dise NB, et al. (2012) Impacts of atmospheric nitrogen deposition: responses of multiple plant and soil parameters across contrasting ecosystems in long-term field experiments. *Global Change Biology* 18: 1197–1215.
34. Hagedorn F, Kammer A, Schmidt MW, Goodale CL (2012) Nitrogen addition alters mineralization dynamics of ^{13}C -depleted leaf and twig litter and reduces leaching of older DOC from mineral soil. *Global Change Biology* 18: 1412–1427.
35. Hasselquist NJ, Metcalfe DB, Höglberg P (2012) Contrasting effects of low and high nitrogen additions on soil CO_2 flux components and ectomycorrhizal fungal sporocarp production in a boreal forest. *Global Change Biology* 18: 3596–3605.
36. Paquette A, Messier C (2010) The role of plantations in managing the world's forests in the Anthropocene. *Frontiers in Ecology and the Environment* 8: 27–34.
37. Liao C, Luo Y, Fang C, Li B (2010) Ecosystem carbon stock influenced by plantation practice: implications for planting forests as a measure of climate change mitigation. *Plos one* 5: e10867.
38. Harmon ME, Ferrell WK, Franklin JF (1990) Effects on carbon storage of conversion of old-growth forests to young forests. *Science* 247: 699–702.
39. Chen GS, Yang YS, Xie JS, Guo JF, Gao R, et al. (2005) Conversion of a natural broad-leaved evergreen forest into pure plantation forests in a subtropical area: effects on carbon storage. *Annals of forest science* 62: 659–668.
40. Yang YS, Guo J, Chen G, Xie J, Gao R, et al. (2005) Carbon and nitrogen pools in Chinese fir and evergreen broadleaved forests and changes associated with felling and burning in mid-subtropical China. *Forest Ecology and Management* 216: 216–226.
41. Hyvönen R, Ågren GI, Linder S, Persson T, Cotrufo MF, et al. (2007) The likely impact of elevated CO_2 , nitrogen deposition, increased temperature and management on carbon sequestration in temperate and boreal forest ecosystems: a literature review. *New Phytologist* 173: 463–480.
42. Zhao M, Xiang W, Tian D, Deng X, Huang Z, et al. (2013) Effects of Increased Nitrogen Deposition and Rotation Length on Long-Term Productivity of Cunninghamia lanceolata Plantation in Southern China. *Plos one* 8: e55376.
43. Fang J, Chen A, Peng C, Zhao S, Ci L (2001) Changes in forest biomass carbon storage in China between 1949 and 1998. *Science* 292: 2320–2322.
44. Wang C (2006) Biomass allometric equations for 10 co-occurring tree species in Chinese temperate forests. *Forest Ecology and Management* 222: 9–16.
45. Waring R, Landsberg J, Williams M (1998) Net primary production of forests: a constant fraction of gross primary production? *Tree Physiology* 18: 129–134.
46. DeLUCIA E, Drake JE, Thomas RB, Gonzalez-Meler M (2007) Forest carbon use efficiency: is respiration a constant fraction of gross primary production? *Global Change Biology* 13: 1157–1167.
47. Drake J, Davis S, Raetz L, DeLucia E (2011) Mechanisms of age-related changes in forest production: the influence of physiological and successional changes. *Global Change Biology* 17: 1522–1535.
48. Goulden ML, McMillan A, Winston G, Rocha A, Manies K, et al. (2011) Patterns of NPP, GPP, respiration, and NEP during boreal forest succession. *Global Change Biology* 17: 855–871.
49. Vicca S, Luyssaert S, Penuelas J, Campioli M, Chapin F, et al. (2012) Fertile forests produce biomass more efficiently. *Ecology letters* 15: 520–526.
50. Wang W, Peng S, Wang T, Fang J (2010) Winter soil CO_2 efflux and its contribution to annual soil respiration in different ecosystems of a forest-steppe ecotone, north China. *Soil Biology and Biochemistry* 42: 451–458.
51. Brookes P, Landman A, Pruden G, Jenkinson D (1985) Chloroform fumigation and the release of soil nitrogen: a rapid direct extraction method to measure microbial biomass nitrogen in soil. *Soil Biology and Biochemistry* 17: 837–842.
52. Vance E, Brookes P, Jenkinson D (1987) An extraction method for measuring soil microbial biomass C. *Soil Biology and Biochemistry* 19: 703–707.
53. Frostegard A, Tunlid A, Baath E (1993) Phospholipid fatty acid composition, biomass, and activity of microbial communities from two soil types experimentally exposed to different heavy metals. *Applied and Environmental Microbiology* 59: 3605–3617.
54. Bossio D, Scow K (1998) Impacts of carbon and flooding on soil microbial communities: phospholipid fatty acid profiles and substrate utilization patterns. *Microbial Ecology* 35: 265–278.
55. Zelles L (1997) Phospholipid fatty acid profiles in selected members of soil microbial communities. *Chemosphere* 35: 275–294.
56. Frostegard A, Baath E (1996) The use of phospholipid fatty acid analysis to estimate bacterial and fungal biomass in soil. *Biology and Fertility of Soils* 22: 59–65.
57. Saiya-Cork K, Sinsabaugh R, Zak D (2002) The effects of long term nitrogen deposition on extracellular enzyme activity in an *Acer saccharum* forest soil. *Soil Biology and Biochemistry* 34: 1309–1315.
58. LeBauer DS, Treseder KK (2008) Nitrogen limitation of net primary productivity in terrestrial ecosystems is globally distributed. *Ecology* 89: 371–379.
59. Reich PB, Tjoelker MG, Pregitzer KS, Wright JJ, Oleksyn J, et al. (2008) Scaling of respiration to nitrogen in leaves, stems and roots of higher land plants. *Ecology letters* 11: 793–801.
60. Li X, Hu Y, Han S, Liu Y, Zhang Y (2010) Litterfall and litter chemistry change over time in an old-growth temperate forest, northeastern China. *Annals of forest science* 67: 206.
61. Vergutz L, Manzoni S, Porporato A, Novais RF, Jackson RB (2012) Global resorption efficiencies and concentrations of carbon and nutrients in leaves of terrestrial plants. *Ecological Monographs* 82: 205–220.
62. Vitousek P (1982) Nutrient cycling and nutrient use efficiency. *American Naturalist* 119: 553–572.
63. Wieder WR, Cleveland CC, Townsend AR (2009) Controls over leaf litter decomposition in wet tropical forests. *Ecology* 90: 3333–3341.
64. Wood TE, Lawrence D, Clark DA, Chazdon RL (2009) Rain forest nutrient cycling and productivity in response to large-scale litter manipulation. *Ecology* 90: 109–121.
65. He H, Bleby TM, Veneklaas EJ, Lambers H (2011) Dinitrogen-fixing Acacia species from phosphorus-impooverished soils resorb leaf phosphorus efficiently. *Plant, cell and environment* 34: 2060–2070.
66. Bowden RD, Davidson E, Savage K, Arabia C, Steudler P (2004) Chronic nitrogen additions reduce total soil respiration and microbial respiration in temperate forest soils at the Harvard Forest. *Forest Ecology and Management* 196: 43–56.
67. Burton AJ, Pregitzer KS, Crawford JN, Zogg GP, Zak DR (2004) Simulated chronic NO_3^- deposition reduces soil respiration in northern hardwood forests. *Global Change Biology* 10: 1080–1091.
68. Phillips RP, Fahey TJ (2007) Fertilization effects on fineroot biomass, rhizosphere microbes and respiratory fluxes in hardwood forest soils. *New Phytologist* 176: 655–664.
69. De Nobili M, Contin M, Mondini C, Brookes P (2001) Soil microbial biomass is triggered into activity by trace amounts of substrate. *Soil Biology and Biochemistry* 33: 1163–1170.
70. Paterson E (2003) Importance of rhizodeposition in the coupling of plant and microbial productivity. *European Journal of Soil Science* 54: 741–750.
71. Marschner P, Crowley D, Yang CH (2004) Development of specific rhizosphere bacterial communities in relation to plant species, nutrition and soil type. *Plant and Soil* 261: 199–208.
72. Talbot JM, Allison SD, Treseder KK (2008) Decomposers in disguise: mycorrhizal fungi as regulators of soil C dynamics in ecosystems under global change. *Functional Ecology* 22: 955–963.
73. Edwards IP, Zak DR (2011) Fungal community composition and function after long-term exposure of northern forests to elevated atmospheric CO_2 and tropospheric O_3 . *Global Change Biology* 17: 2184–2195.
74. Del Giorgio PA, Cole JJ (1998) Bacterial growth efficiency in natural aquatic systems. *Annual Review of Ecology and Systematics* 21: 503–541.
75. Manzoni S, Taylor P, Richter A, Porporato A, Ågren GI (2012) Environmental and stoichiometric controls on microbial carbon-use efficiency in soils. *New Phytologist* 196: 79–91.
76. Bonan GB (2008) Forests and climate change: Forcings, feedbacks, and the climate benefits of forests. *Science* 320: 1444–1449.

Comparison of Seasonal Soil Microbial Process in Snow-Covered Temperate Ecosystems of Northern China

Xinyue Zhang^{1,2}, Wei Wang^{1*}, Weile Chen¹, Naili Zhang³, Hui Zeng²

1 Department of Ecology, College of Urban and Environmental Sciences and the Key Laboratory for Earth Surface Processes of the Ministry of Education, Peking University, Beijing, China, **2** Key Laboratory for Cyclic Economy, School of Urban Planning and Design, Shenzhen Graduate School, Peking University, Shenzhen, China, **3** State Key Laboratory of Vegetation and Environmental Change, Institute of Botany, Chinese Academy of Sciences, Beijing, China

Abstract

More than half of the earth's terrestrial surface currently experiences seasonal snow cover and soil frost. Winter compositional and functional investigations in soil microbial community are frequently conducted in alpine tundra and boreal forest ecosystems. However, little information on winter microbial biogeochemistry is known from seasonally snow-covered temperate ecosystems. As decomposer microbes may differ in their ability/strategy to efficiently use soil organic carbon (SOC) within different phases of the year, understanding seasonal microbial process will increase our knowledge of biogeochemical cycling from the aspect of decomposition rates and corresponding nutrient dynamics. In this study, we measured soil microbial biomass, community composition and potential SOC mineralization rates in winter and summer, from six temperate ecosystems in northern China. Our results showed a clear pattern of increased microbial biomass C to nitrogen (N) ratio in most winter soils. Concurrently, a shift in soil microbial community composition occurred with higher fungal to bacterial biomass ratio and gram negative (G-) to gram positive (G+) bacterial biomass ratio in winter than in summer. Furthermore, potential SOC mineralization rate was higher in winter than in summer. Our study demonstrated a distinct transition of microbial community structure and function from winter to summer in temperate snow-covered ecosystems. Microbial N immobilization in winter may not be the major contributor for plant growth in the following spring.

Citation: Zhang X, Wang W, Chen W, Zhang N, Zeng H (2014) Comparison of Seasonal Soil Microbial Process in Snow-Covered Temperate Ecosystems of Northern China. PLoS ONE 9(3): e92985. doi:10.1371/journal.pone.0092985

Editor: Jack Anthony Gilbert, Argonne National Laboratory, United States of America

Received: December 18, 2013; **Accepted:** February 27, 2014; **Published:** March 25, 2014

Copyright: © 2014 Zhang et al. This is an open-access article distributed under the terms of the Creative Commons Attribution License, which permits unrestricted use, distribution, and reproduction in any medium, provided the original author and source are credited.

Funding: This research was funded by grants from Projects of National Natural Science Foundation of China (31222011 and 31270363), National Basic Research Program of China (2010CB950604 and 2013CB956303), the Foundation for Innovative Research Groups of National Natural Science Foundation of China (31021001) and Construction Projects between Beijing City and the University in the Central Authorities. The funders had no role in study design, data collection and analysis, decision to publish, or preparation of the manuscript.

Competing Interests: The authors have declared that no competing interests exist.

* E-mail: wangw@urban.pku.edu.cn

Introduction

More than half of the earth's terrestrial surface currently experiences seasonal snow cover and soil frost [1,2]. In these ecosystems, some soil microorganisms are likely protected by the snowpack during winter. With adequate depth and density [3,4], the heat-insulation snowpack creates a relatively warmer habitat with liquid water films around soil particles [5,6]. Other soil microorganisms may develop their physiological adaption to survive the chilly environments [7]. Therefore, despite the freezing air temperature, winter catabolic processes of the soil microbial community, detected through biogenic CO₂ production, can still make a significant contribution to annual ecosystem fluxes across a wide variety of seasonally snow-covered ecosystems [8,9,10,11,12]. However, the influence of temporal variations in soil anabolic processes (i.e. microbial biomass accumulation) on annual N cycling is not well understood in these ecosystems [13,14,15].

Recent studies have reported peak microbial biomass C (MBC) and N (MBN) in late winter, followed by a quick decline when soil temperatures rise to 0°C at alpine and arctic sites [14,16,17,18]. An enlarged N pool was retained in the microbial biomass under the snowpack and subsequently released as a nutrient pulse when soils thawed, which may lead to an increase in N availability for plants at the start of the growing season [13,14,16,19]. The

microbial N immobilization observed during winter may play a crucial role in ecosystem function, since it could prevent dissolved N produced by fall litter degradation being lost from the ecosystem during a time when plants are mostly inactive [20]. Therefore, in these snow-covered ecosystems, N retained in the soil by microorganisms during winter may be vital for plant nutrient uptake in the following growing season [18,21,22,23,24,25].

Soil microbial community can adapt to changing environmental conditions on very short time scales [7], thus changes between summer and winter may be a key control on annual patterns of nutrient cycling and plant N uptake [26]. For instance, in the alpine tundra of Colorado, winter maximal microbial biomass corresponded with increased biomass in the soil fungal community [27,28]. Fungi was the primary decomposer of plant debris in the territorial ecosystems, as it could release a great number of extracellular enzymes that can digest a wide variety of substrates, even complex organic compound as lignin [29,30]. Besides, fungi can grow towards nutrient sources and force their hyphae into solid substrates [31], which help fungi to make use of any nutrient source presented in soils. Furthermore, fungi differ from bacteria in N concentrations and storage capabilities [26,32]. Based on above viewpoints, fungi dominance in winter may have profound effects on soil biogeochemical cycling in the subsequent growing season. In addition, different gram-staining groups of bacteria,

categorized by their cell wall composition, were also found to have various substrate preferences and survival strategies [33]. Therefore, the relative dominance of G- to G+ bacteria may differ between winter and summer. However, it remains poorly understood about the links between the seasonal variation of microbial biomass and the relative abundances of fungi and bacteria in snow-covered temperate areas.

As various decomposer microbes differ in their ability/strategy to efficiently use soil organic matter [34,35,36,37], shifts within the community composition may affect decomposition rates. SOC decomposition is the primary pathway where plant fixed CO₂ is released back into the atmosphere [38,39,40]. Along with frequently observed maximal microbial biomass in the winter of seasonally snow-covered ecosystems, the potential SOC mineralization rate (SOCMR, indicating intrinsic substrate use efficiency) may increase, releasing more CO₂ into the atmosphere when temperatures rise. However, winter potential SOCMR are seldom conducted [41,42].

Recent studies of winter soil microbial biogeochemical processes have mainly focused on alpine and tundra ecosystems. However, the wintertime conditions in snow-covered temperate areas could differ from those in alpine and tundra areas. In comparison with alpine and tundra, temperate ecosystems experience a shallower snowpack and shorter duration of snow cover [43,44], which may modify the extent of the N pool and the seasonal dynamics of its soil microbes. Moreover, temperate soil microbial communities are sensitive to climate changes, because the soil remains close to freezing throughout the winter [45], and small changes in winter temperatures may result in large changes in the amount and timing of snow cover [2]. More importantly, many temperate ecosystems are exposed to larger atmospheric N deposition as a result of increased emissions from industrial and agricultural activities [46]. Consequently, this may induce substantial changes in microbial N dynamics and ecosystem nutrient cycling. However, so far little investigation has been conducted on the winter biogeochemical process of soil microbes in temperate ecosystems [47]. Our study aims to explore the seasonal variation of microbial biomass, community composition and SOC mineralization in temperate ecosystems. The following three questions were addressed: (1) what is the C and N retention capacity of the winter soil microbial community in seasonally snow-covered temperate ecosystems? (2) Does microbial community composition shift from summer to winter? (3) What is the microbial function (organic matter decomposition), as indicated by potential SOCMR, in winter? To answer these questions, summer and winter soil samples were collected from the top 10 cm mineral soil in six seasonally snow-covered temperate ecosystems in northern China. The MBC and MBN, microbial community composition and mineralization rate of SOC were determined. We predicted (1) increased MBN immobilization because of relatively low quality substrates in winter (decreased root exudates and increased autumn litter input) may lead to microbial immobilization of N for growth [23,48]; (2) bacterial PLFAs to dominate in summer and fungal PLFAs in winter because fungi were commonly reported with a higher C to N ratio (targeting recalcitrant substrates in winter) compared with bacteria (targeting labile substrates in summer); and (3) a higher potential SOCMR in winter than summer because fungi were reported to produce more β -1,4-glucosidase (BG) enzyme (involved in C metabolism) than bacteria [49].

Materials and Methods

Ethics Statement

The administration of the Saihanba Forestry Center gave permission for this research at each study site. We confirm that the field studies did not involve endangered or protected species.

Site information

Our study sites were situated at the Saihanba Forestry Center in Hebei Province, North China (117°12'–117°30' E, 42°10'–42°50' N, 1400 m a.s.l.), which is a typical forest-steppe ecotone of a temperate area. The climate in this area is semi-arid and semi-humid, with a long and cold freezing period (November–March) and relatively short growing season. Annual mean air temperature and precipitation between 1964 and 2004 were -1.4°C and 450 mm, respectively. The soils in the region are dominated by aeolian sandy soil, together with meadow and swamp soil. Soil has low nutrient content with SOC content ranging from 0.71 to 2.65% and soil total nitrogen (STN) ranging from 0.08 to 0.26%, respectively (Table 1). Soil bulk density (SBD) ranged from 0.65 to 1.06 g cm⁻³; Soil pH varied from 5.8 to 6.5 and 6.0 to 6.6 in the summer and winter, respectively (Table 1). Soil moisture content was calculated on the gravimetric basis. Specifically, 10 g fresh soil samples were dried to a constant weight by an oven at a temperature of 105°C. All the soil and microbial properties were determined by the dry soil weight.

Primary forests were harvested via large scale industrial logging in the late 1900s and have been replaced by secondary forests and plantations. This site contains the largest area of plantation forests in China, the dominant species are *Pinus sylvestris* var. *mongolica* (Mongolia pine) and *Larix principis-rupprechtii* (Prince Rupprecht's larch). The Mongolia pine and larch herbaceous layers are similar, composed by *Radix Sanguisorbae*, *Thalictrum aquilegifolium* L., *Agrimonia pilosa* Ledeb., and *Carex stenophylla* Wahleub. The secondary forest mainly consists of *Betula platyphylla* (birch) with an herbaceous layer of *Agrimonia pilosa* Ledeband *Radix Sanguisorbae*. In addition, shrublands dominated by *Rosa bella* Rehd. et Wils (solitary rose) and *Malus baccata* (Siberian crabapple) and meadow grasslands are also very common. The solitary rose herbaceous layer consists of *Leymus chinensis*. The Siberian crabapple herbaceous layer is dominated by *Veronica linariifolia*, *Galium verum*, *Heteropappus hispidus*, *Trollius chinensis*, and *Bupleurum chinense*. The meadow grassland is zonal vegetation dominated by *L. chinensis*. Due to the sparse understory species of the forest sites and simple species composition of the grasslands and shrublands, we did not consider the potential impacts of vegetation diversity on microbial processes. The distribution of sampling sites was shown in Fig. 1, which was drawn by ArcMap (ArcGIS 10.0, Esri Inc., California, USA) with ancillary site information.

Study design and methods

Because of the significant effect of stand age on ecosystem C and N dynamics [50], we took forest age into consideration in the two coniferous plantation sites, namely Mongolia pine and Prince Rupprecht's larch. Three replicates were selected for each of three age classes (shown in Table 1) in Mongolia pine (sites P1, P2, and P3) and larch (sites L1, L2, and L3). We also selected three replicates for the birch stand (site BH), each of the two shrublands Siberian crabapple (site MA) and solitary rose (site RO) and one meadow grassland (site CG); 30 plot samples in total (Table 1). The area of each plot was 20 × 20 m. All sampling sites were less than 10 km away from each other (Fig. 1) to ensure similar climatic conditions.

Table 1. Site information and soil properties of the ten sampling sites.

Sites	Location	Domain species	SOC (%)	STN (%)	SBD (g cm ⁻³)	ST (°C)		pH	
						JUL.	JAN.	JUL.	JAN.
P1	42°24.707'N 117°14.071'E	<i>Pinus sylvestris</i>	0.71 ± 0.05	0.08 ± 0.01	0.98 ± 0.00	19.0	-7.3	6.45 ± 0.10	6.31 ± 0.08
P2	42°24.760'N 117°14.771'E	<i>Pinus sylvestris</i>	1.26 ± 0.09	0.12 ± 0.01	0.83 ± 0.05	14.7	-12.8	6.34 ± 0.05	6.36 ± 0.04
P3	42°25.079'N 117°15.974'E	<i>Pinus sylvestris</i>	1.10 ± 0.12	0.09 ± 0.01	0.85 ± 0.03	14.9	-8.1	6.31 ± 0.06	6.30 ± 0.07
L1	42°24.332'N 117°12.933'E	<i>Larix principis-rupprechtii</i>	0.94 ± 0.04	0.09 ± 0.00	1.06 ± 0.01	15.8	-9.4	6.30 ± 0.02	6.36 ± 0.01
L2	42°24.118'N 117°12.722'E	<i>Larix principis-rupprechtii</i>	0.95 ± 0.07	0.09 ± 0.01	0.88 ± 0.01	14.5	-9.7	5.94 ± 0.09	6.02 ± 0.09
L3	42°23.911'N 117°19.052'E	<i>Larix principis-rupprechtii</i>	1.88 ± 0.17	0.18 ± 0.02	0.74 ± 0.05	13.7	-7.2	5.78 ± 0.06	6.16 ± 0.04
BH	42°23.848'N 117°19.031'E	<i>Betula platyphylla</i>	2.65 ± 0.25	0.26 ± 0.04	0.65 ± 0.00	13.7	-7.8	5.92 ± 0.10	6.16 ± 0.04
MA	42°24.729'N 117°14.132'E	<i>Malus baccata</i>	2.10 ± 0.15	0.20 ± 0.01	0.72 ± 0.02	16.1	-7.3	6.39 ± 0.07	6.63 ± 0.06
RO	42°24.107'N 117°13.866'E	<i>Rosa bella</i>	1.22 ± 0.16	0.13 ± 0.02	0.73 ± 0.07	19.4	-11.2	6.20 ± 0.07	6.46 ± 0.06
CG	42°24.717'N 117°14.107'E	<i>Leymus chinensis</i>	1.00 ± 0.04	0.09 ± 0.00	0.88 ± 0.05	19.9	-11.7	6.28 ± 0.05	6.29 ± 0.09

Values are presented as mean ± standard errors. SOC = Soil Organic Carbon; STN = Soil total nitrogen; SBD = Soil Bulk Density; ST = Soil Temperature; JUL. = July; JAN. = January.

doi:10.1371/journal.pone.0092985.t001

All experiments were performed on upper 10 cm mineral soils at five random locations from each plot in July 2010 and January 2011. The two months we chose had the highest (July) and lowest (January) air temperature according to the local climate records of recent decade, representing two most stable seasons of the years, namely summer and winter. This approach has been commonly applied to investigate seasonal dynamics [18,28,51]. Under this circumstance, we assumed that the two single months can represent their respective seasons, and that changes over these

two seasons in the soil microbial community may be of greater magnitude than differences within the same season or from year to year [52]. In summer, soil was taken by 5.8-cm diameter soil cores, passed through a 2-mm sieve to remove plant litter and roots and homogenized. In winter, after the thickness of snow cover measured by a steel ruler, snows were swept away with a shovel before sampling. The snow thickness varied from 4–16 cm in different sampling sites (data not shown). After that, frozen soils were collected using axe or drill and the upper materials were cut

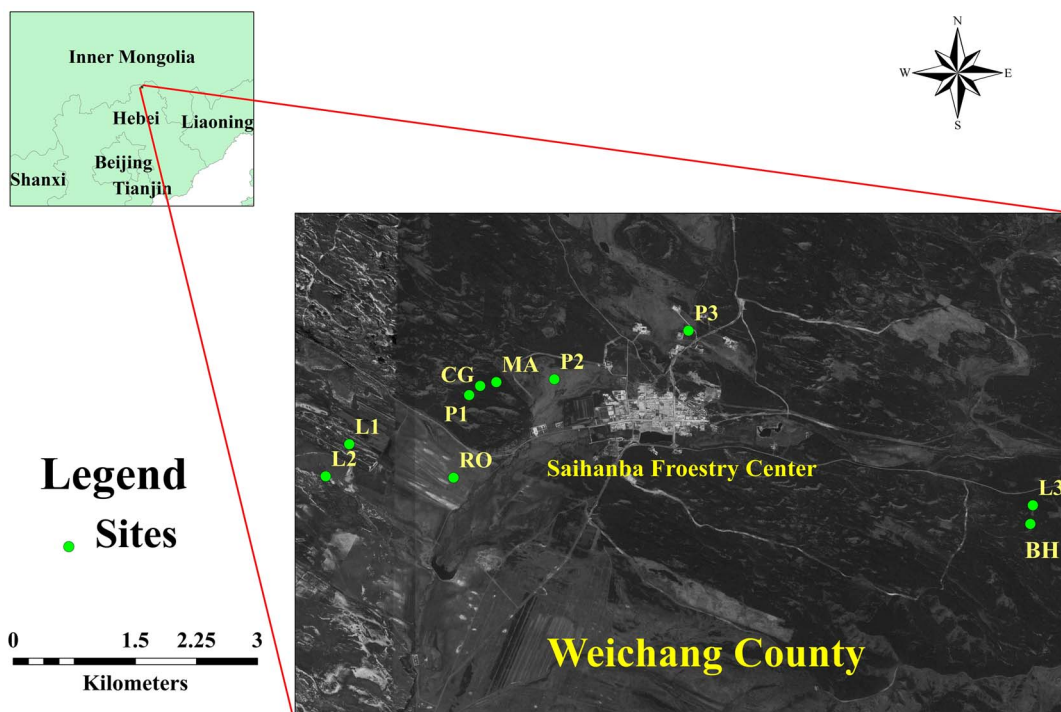


Figure 1. The distribution of sampling sites. P1 = ~15-year Mongolia pine; P2 = ~25-year Mongolia pine; P3 = ~35-year Mongolia pine; L1 = ~15-year Prince Rupprecht's larch; L2 = ~25-year larch; L3 = ~35-year larch; BH = Birch; MA = Siberian crabapple; RO = Solitary rose; CG = Meadow grassland.

doi:10.1371/journal.pone.0092985.g001

by knife. The processed soils were immediately transported to the laboratory (less than 30 min away) for subsequent analysis.

In situ continuous measurements of soil temperature were conducted at 30-min intervals with StowAway loggers (Onset Comp. Corp., Bourne, MA, USA) inserted into the soil at a depth of 5 cm. Extractable ammonium and nitrate nitrogen (NH_4^+ and NO_3^-) were measured simultaneously in 2 mol/L KCl solution (1:5 w/v) [53] using a Lachat Flow Injection Analyzer (Lachat Instruments, Milwaukee, WI). The amount of extractable ammonium and nitrate nitrogen were taken as total inorganic N. SOC was measured by the potassium dichromate oxidation method with ground air-dried soils [54] while STN was measured by Kjeldahl method [55]. Because of the minor variation of SOC and STN in our study sites over a year (data not shown), we only measured the values in summer time (July) and did not take the difference between summer and winter into consideration. Soil pH was determined using a pH meter (Denver, US) on a 1:1 (w/v) air-dried soil to distilled de-ionized water slurry.

MBN and MBN

MBC and MBN were measured by the chloroform fumigation extraction (CEF) method [56]. Two replicate samples, one unfumigated and one fumigated with alcohol-free CHCl_3 for 24 h and then extracted with 0.5 mol/L K_2SO_4 (1:2.5 w/v). MBC and MBN were calculated as the difference of C and N between fumigated and unfumigated soil extraction, which was estimated using the dichromate oxidation and titration method and Kjeldahl digestion, respectively. To avoid variations in CFE values due to the choice of conversion factor (corrects for the incomplete release and extraction of microbial biomass following CEF method), no conversion factor was used for fumigation efficiency as conducted by Edwards and Jefferies (2013) [18], since it could vary across different seasons as well as among different sampling sites [57]. Soil dissolved organic N (DON) was measured from the initial unfumigated extraction [18].

Phospholipid fatty acid (PLFA) analysis

PLFA analysis was used to determine the total microbial biomass and assess microbial community composition. In brief, PLFAs were extracted by a mixture of chloroform-methanol-phosphate buffer (1:2:0.8) [58]. Polar lipids in the initial soil extracts were separated from neutral and glycolipids by elution with 5 ml chloroform and 10 ml acetone followed by 5 ml methanol. The polar lipid fraction was used to perform mild alkaline methanolysis. The peak area of each resulting fatty acid methyl ester was recorded on the chromatogram for each sample before identification. Peaks were identified by chromatographic retention time and a standard qualitative mix that ranged from C9 to C30 using a microbial identification system (Microbial ID Inc., Newark, DE). The fatty acid 18:2 ω 6, 9 was recognized as the fungal biomarker [59]. Bacterial biomass was quantified as the sum of i14:0, i15:0, a15:0, 16:1 ω 9, 16:1 ω 7, i17:0, a17:0, cy17:0, 17:0, and cy19:0 [60]. G+ bacteria were marked by i15:0, a15:0, i16:0, a16:0, i17:0, and a17:0 [59]. The mono-unsaturated and cyclopropyl saturated peaks 16:1 ω 5, 16:1 ω 9, 17:1 ω 9, cy17:0, 18:1 ω 11, and cy19:0 were used as indicators for G- bacteria [59,61,62]. We also calculated the total lipids as an indicator of microbial biomass [63].

Potential SOCMR

We used a laboratory incubation experiment to measure the SOCMR through detection of CO_2 emission [41,64]. Approximately 25 g of fresh soil were placed into 250 ml glass gas tight jars and incubated at 25°C for 3 d. Respired CO_2 was captured by

a connecting vial with 5 ml 1 mol/L NaOH and determined by titration with 1 mol/L HCl. Potential SOCMR were expressed as the amount of CO_2 -C released per hour per gram soil dry weight. Because the winter soil temperature was below 0°C, it was unable to measure *in situ* mineralization activity using the laboratory incubation method. Thus, we conducted the potential SOCMR in winter using the same temperature as the summer (25°C, being the suitable condition for soil microbial growth in the field). Considering the condition for winter samples was quite different from the *in situ* environment, we indirectly estimated winter mineralization of SOC using the Q_{10} coefficient (increase in reaction rate per 10°C increase in temperature) obtained from our previous research in the same study sites [12].

$$\text{SOCMR}_{in-situ} = \text{SOCMR}_{25} / Q_{10}^{(25-T)/10} \quad (1)$$

Where $\text{SOCMR}_{in-situ}$ was the mineralization rate of SOC at an *in situ* temperature measured in winter, SOCMR_{25} was the mineralization rate of SOC at the room temperature of 25°C, and T was the winter soil temperature at 5 cm depth.

Statistical analysis

We used the averaged value of the subsamples in each plot to conduct statistical analysis. Statistical analyses were performed using SPSS (ver. 18.0, SPSS Inc., Chicago, IL, USA). Repeated measures analysis of variance (ANOVA) was used to determine the effects of seasons and dominate vegetation types on soil N concentrations, microbial biomass, microbial community composition and potential SOCMR. Besides, ANOVA was also used to determine the effect of stand age on above soil and microbial properties. Furthermore, simple correlation analysis was conducted to explore the relationships between microbial community related parameters and soil physical and chemical properties. In all cases, differences of $P < 0.05$ were regarded as statistically significant. Results were displayed as mean \pm standard error.

Besides, we analyzed the PLFAs data by principal components analysis (PCA) to determine whether the PLFA signatures of microbial community varied between summer and winter. PCA was performed on 21 different PLFAs identified from all the samples with concentration larger than 0.005 fraction (ratio of moles individual lipid to moles total lipid biomass) using R 3.0.1 (R Core Team, 2013). Statistical differences among PLFAs data were assessed using multi-response permutation procedures (MRPP) [65,66]. MRPP is a nonparametric procedure for testing the hypothesis of no differences between two or more pre-existing groups [67]. P value evaluated the significant differences due to chance, where A value described within-group homogeneity compared to random expectation [67]. An A value equal to 1 was found when all items within a group are identical; when heterogeneity within groups equaled expectation by chance $A = 0$.

In addition, inverse Simpson index was calculated to describe the microbial diversity obtained from PLFAs data in different seasons as well as in different sampling sites. We preferred this index to other measures of alpha-diversity because it is an indication of the richness in a community with uniform evenness that would have the same level of diversity.

Results

Soil physical and chemical properties

In July, soil temperature at 5-cm depth averaged 16.5°C, and decreased to -9.5°C in January across six ecosystems (Table 1).

Table 2. Soil inorganic nitrogen (NH_4^+ -N and NO_3^- -N) concentrations, microbial biomass carbon to nitrogen (MBC/N) ratio and fungi to bacteria biomass (F/B) ratio of the ten sampling sites.

Sites	NH_4^+ -N (mg kg ⁻¹)		NO_3^- -N (mg kg ⁻¹)		MBC/N		F/B	
	JUL.	JAN.	JUL.	JAN.	JUL.	JAN.	JUL.	JAN.
P1	1.48 ± 0.03	1.66 ± 0.21	0.04 ± 0.01	NT	15.90 ± 4.57	49.26 ± 5.18	0.024 ± 0.001	0.126 ± 0.011
P2	1.54 ± 0.00	1.92 ± 0.07	0.04 ± 0.00	NT	23.54 ± 5.07	41.58 ± 6.25	0.023 ± 0.002	0.136 ± 0.039
P3	1.60 ± 0.08	1.76 ± 0.08	0.02 ± 0.01	NT	30.68 ± 6.82	55.04 ± 5.31	0.033 ± 0.002	0.132 ± 0.011
L1	1.57 ± 0.04	1.69 ± 0.03	0.01 ± 0.00	NT	8.89 ± 2.49	31.48 ± 1.57	0.054 ± 0.013	0.115 ± 0.018
L2	1.61 ± 0.01	1.84 ± 0.06	0.01 ± 0.00	NT	35.36 ± 3.22	68.38 ± 16.33	0.083 ± 0.004	0.075 ± 0.003
L3	1.60 ± 0.03	1.78 ± 0.31	0.00 ± 0.00	NT	33.87 ± 8.95	47.83 ± 7.87	0.079 ± 0.003	0.097 ± 0.019
BH	1.73 ± 0.96	2.25 ± 0.03	0.02 ± 0.00	NT	15.34 ± 2.46	31.97 ± 4.28	0.056 ± 0.007	0.096 ± 0.006
MA	1.63 ± 0.08	2.23 ± 0.20	0.03 ± 0.01	NT	41.79 ± 13.95	33.74 ± 1.18	0.060 ± 0.004	0.076 ± 0.007
RO	1.73 ± 0.13	1.85 ± 0.10	0.06 ± 0.01	NT	9.70 ± 1.09	31.59 ± 7.83	0.073 ± 0.006	0.078 ± 0.004
CG	1.45 ± 0.03	1.67 ± 0.08	0.08 ± 0.01	NT	9.25 ± 3.72	33.69 ± 1.06	0.070 ± 0.008	0.066 ± 0.004

Values are presented as mean ± standard errors. NT = not detectable.
doi:10.1371/journal.pone.0092985.t002

Soil NH_4^+ -N and NO_3^- -N concentrations averaged 1.59 ± 0.02 mg kg⁻¹ and 0.03 ± 0.01 mg kg⁻¹ in July and 1.86 ± 0.05 mg kg⁻¹ and 0.02 ± 0.01 mg kg⁻¹ in January, respectively (Table 2). Although total soil inorganic nitrogen (NO_3^- -N + NH_4^+ -N) across all ecosystems was significantly higher in winter than in summer at a statistical level ($P < 0.001$), there was no large difference between them (1.88 ± 0.07 mg kg⁻¹ in winter vs. 1.63 ± 0.03 mg kg⁻¹ in summer) (Table 3; Fig. 2A; Table S1). DON was significantly higher in summer than in winter, with average value decreasing from 4.76 ± 0.52 mg kg⁻¹ in summer to 0.84 ± 0.06 mg kg⁻¹ in winter, respectively (Table 3; Fig. 2B; Table S1). Although DON significantly differed across different ecosystem types, no significant interaction between seasons and sampling sites was observed (Table 3; Fig. 2B).

Soil MBC and MBN

Across all the sampling sites, soil microbes showed a significantly higher MBC ($P < 0.001$) while lower MBN ($P = 0.015$) in winter than in summer (Table 3; Fig. 3). MBC consistently increased from 66.1 ± 7.4 mg kg⁻¹ in summer to 112.1 ± 8.5 mg kg⁻¹ in winter on average, except for site BH. MBN in most of the sites were lower in winter than in summer (4.5 ± 0.5 mg kg⁻¹ in summer vs. 3.3 ± 0.3 mg kg⁻¹ in winter) (Table S1). Both MBC and MBN varied significantly across different sites as well as in different seasons (Table 3). Besides, the interaction between seasons and sampling sites also showed significant effect on MBC but not MBN (Table 3). MBC significantly correlated with MBN in both summer ($R^2 = 0.27$, $P = 0.020$) and winter ($R^2 = 0.52$, $P < 0.001$). MBC to MBN (MBC/N) ratio varied from 9.25 ± 3.72 to 41.79 ± 13.95 in

summer, and 31.48 ± 1.57 to 68.38 ± 16.33 in winter (Table 2). The MBC/N ratio consistently increased from summer to winter across all the sampling sites, except for site MA, where a slight decrease was found (Table 2). Stand age exhibited no significant influence on MBC/N ratio for both summer and winter.

Microbial community composition

Microbial biomass indicated by total PLFAs showed no significant difference between summer and winter ($P = 0.509$), but varied significantly among different sampling sites ($P < 0.001$) (Table 3; Fig. 4; Table S1). In addition, microbial community composition shifted with higher fungal biomass abundance in winter (Table 3; Fig. 5A). The bacterial community biomass was not significantly different between summer and winter ($P = 0.802$) across all the sites, as well as the G+ bacterial community biomass ($P = 0.050$). However, G- bacterial biomass significantly increased in winter ($P < 0.001$; varying from 1.98 ± 0.35 nmol PLFAs g dry soil⁻¹ in summer to 3.66 ± 0.51 nmol PLFAs g dry soil⁻¹ in winter). Thus the G- to G+ bacterial biomass (G-/G+) ratio also exhibited a significant increase in winter (Fig. 5B; Table S1). In summer, fungal to bacterial biomass (F/B) ratio was negatively correlated with soil pH value ($R^2 = 0.43$, $P = 0.036$), whereas, in winter, F/B ratio was positively correlated with total microbial biomass indicated by PLFAs ($R^2 = 0.78$, $P = 0.001$) (Table 4). G-/G+ ratio was negatively correlated with soil temperature only in winter ($R^2 = 0.62$, $P = 0.007$) (Table 4).

Principle component analysis (PCA) also showed the differentiation in microbial community structure between seasons (Fig. 6). The first principle component axis (PC1) alone could explain as

Table 3. The repeated measure ANOVA results of soil and microbial properties tested in this study.

ANOVA results	IN	DON	MBC	MBN	MB	F/B	G-/G+	Potential SOCMR
Season	$P < 0.001$	$P < 0.001$	$P < 0.001$	$P = 0.015$	$P = 0.509$	$P < 0.001$	$P < 0.001$	$P < 0.001$
Sites	$P = 0.044$	$P = 0.032$	$P < 0.001$	$P = 0.002$	$P < 0.001$	$P = 0.509$	$P < 0.001$	$P < 0.001$
Interaction	$P = 0.297$	$P = 0.086$	$P = 0.048$	$P = 0.121$	$P = 0.390$	$P < 0.001$	$P < 0.001$	$P = 0.017$

IN = inorganic nitrogen; DON = dissolved organic nitrogen; MB = microbial biomass; G-/G+ = gram negative to positive bacteria biomass ratio; SOCMR = soil organic carbon mineralization rate.

doi:10.1371/journal.pone.0092985.t003

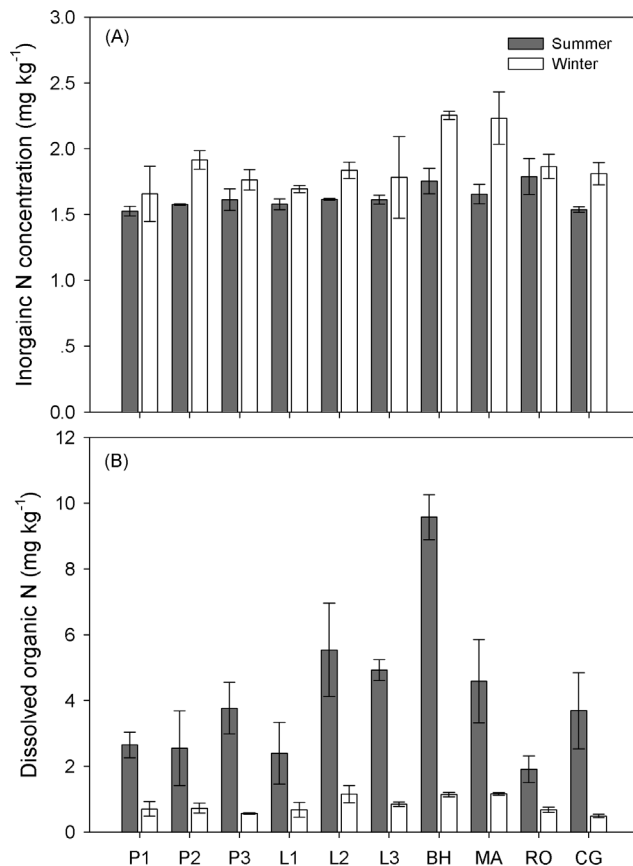


Figure 2. Inorganic nitrogen (N) (A) and dissolved organic N (B) across different sites in summer and winter. Results are presented as mean \pm standard error. Support information is presented in Table S1. doi:10.1371/journal.pone.0092985.g002

much as 96% of the variance in the PLFAs data. There was no evidence of difference in PLFAs data among different sampling sites (MRPP: $P = 0.693$, $A = 0$), however, significant difference of PLFAs was observed between summer and winter (MRPP: $P = 0.001$, $A = 0.56$). Microbial diversity was significantly lower in winter (4.76) than that in summer (8.59) indicated by inverse Simpson index ($P < 0.001$), and differed in each sampling site ($P < 0.001$). In all sampling sites, microbial diversity showed a decrease trend from summer to winter (Table S2). Stand age exerted no significant effect on microbial community composition or diversity.

Potential SOCMR

The C emission rate ranged from 5.31 ± 2.50 mg $\text{CO}_2\text{-C d}^{-1}$ g dry soil $^{-1}$ in summer to 63.22 ± 4.02 mg $\text{CO}_2\text{-C d}^{-1}$ g dry soil $^{-1}$ in winter under the same incubation temperature, showing a significantly higher potential SOCMR for winter microbes than summer ones (Table 3; Fig. 7; Table S1). However, when applied the Q_{10} value to model the *in situ* winter SOCMR, the average *in situ* mineralization rate was 0.26 mg $\text{CO}_2\text{-C d}^{-1}$ g dry soil $^{-1}$, quite lower than the averaged summer ones (12.57 mg $\text{CO}_2\text{-C d}^{-1}$ g dry soil $^{-1}$). No significant effect of stand age was observed on potential SOCMR for both summer and winter.

Discussion

Multiple studies in alpine and arctic tundra ecosystems have reported active microbial metabolism under snow-cover during

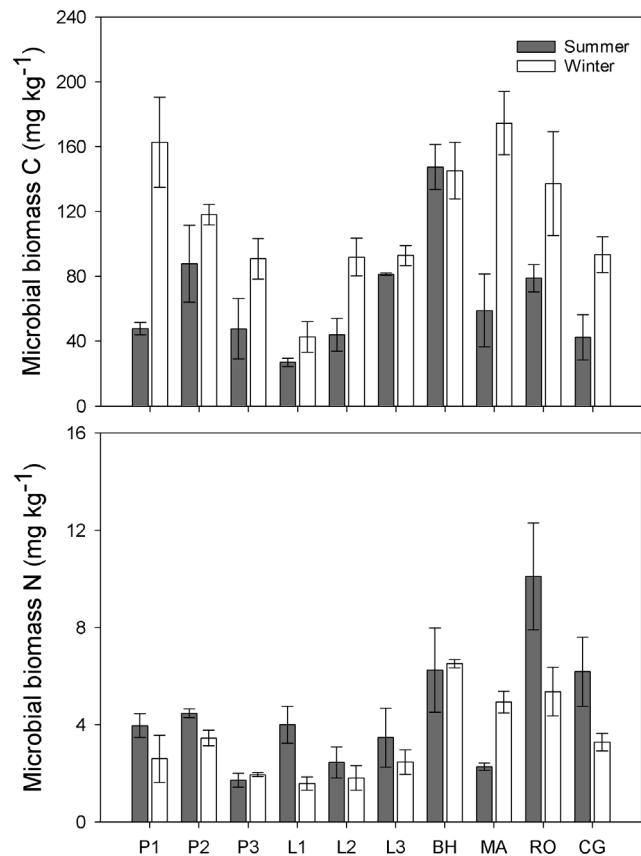


Figure 3. Microbial biomass carbon (C) (A) and nitrogen (N) (B) across different sites in summer and winter. Results are presented as mean \pm standard error. Support information is presented in Table S1. doi:10.1371/journal.pone.0092985.g003

winter [26,27,28,50,68,69]. However, until now little has been known about winter microbial biogeochemical processes in temperate areas. This study determined the soil microbial biomass, community composition and mineralization rate of SOC in a variety of seasonally snow-covered temperate ecosystems.

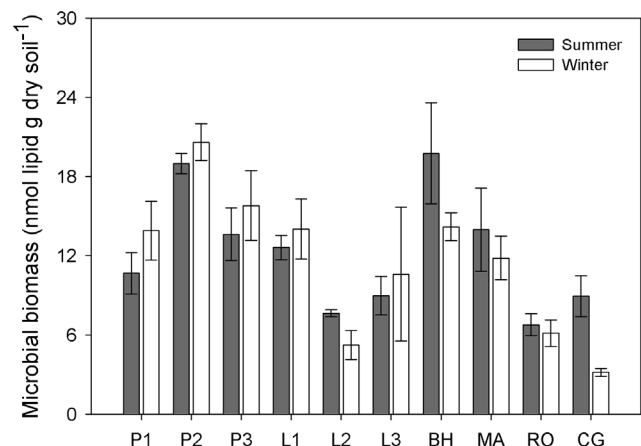


Figure 4. Total microbial biomass indicated by PLFAs across different sites in summer and winter. Results are presented as mean \pm standard error. Support information is presented in Table S1. doi:10.1371/journal.pone.0092985.g004

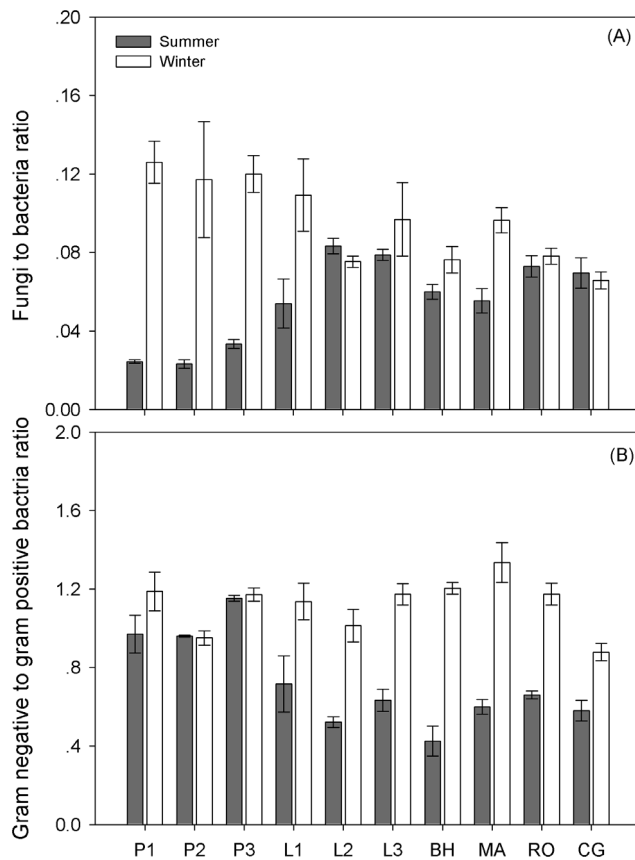


Figure 5. Soil fungal to bacterial PLFAs ratio (A) and gram negative to gram positive bacterial PLFAs ratio (B) across different sites in summer and winter. Results are presented as mean \pm standard error. Support information is presented in Table S1. doi:10.1371/journal.pone.0092985.g005

It was commonly thought that relatively low quality substrates may lead to microbial immobilization of N for growth [23,48]. Therefore, we expected increased MBN immobilization because of

decreased root exudates and increased autumn litter input in winter when plants were inactive. However, in our study area, there existed a clear pattern of increased MBC to MBN ratio in winter across almost all of the ecosystems, mainly through increased MBC (Fig. 3A) and reduced MBN (Fig. 3B). Non-increased microbial N pool in winter was unexpected and contrasted with the findings from alpine and tundra areas [26] and corresponding to a temperate beech forest soil [20]. Exception was only found in site MA, where MBN obviously increased from summer to winter (Fig. 3B). However, there was no soil or microbial properties measured in this study seemed to explain this exception. The lower levels of microbial N immobilization in our temperate winter soils indicate a smaller or no nitrogen pulse from winter soil microbes in the following spring. The discrepancy may be due to the differences of snow cover depth and duration. Across our studied sites, the snowpack was as thin as 4–16 cm and the duration of snow cover was short. Snowpack less than 30 cm depth could not effectively decouple soil temperatures from the atmosphere [70,71,72], and thus resulting in lower microbial N immobilization.

As total microbial PLFAs changed negligibly (Fig. 4), the microbial biomass was stable across different seasons. However, the increased fungal dominance seemed to partly explain the increased C and decreased N uptake. The positive relationship between fungal abundance and the MBC to MBN ratio has been observed in a previous global analysis [73]. Fungi were commonly reported with a higher C to N ratio (targeting recalcitrant substrates) compared with bacteria (targeting labile substrates) [74,75]. In summer, warmer temperature can increase root exudates (labile substrates) than in winter [76] and fresh plant litter input had a relatively lower C to N ratio. Therefore, we expected bacterial PLFAs to dominate. In contrast, in winter, a lot of leaf litter with a relative high C to N ratio accumulated on the soil floor and likely became a major substrate source for fungi. We did observe increased fungal PLFAs ($P < 0.001$), but no significant variation in bacterial PLFAs was found between summer and winter ($P = 0.809$). Because it is common for soil microbes to preferentially use simple organic compounds over complex polymers [77,78], winter substrate usage may be largely confined to microbial recycling of dead microbial cells and hyphae [79] or

Table 4. The correlation between soil properties (listed in the row) and microbial community parameters (listed in the line).

Correlation Matrix		MBC/N		MB		F/B		G-/G+	
		JUL.	JAN.	JUL.	JAN.	JUL.	JAN.	JUL.	JAN.
ST	R	-0.508	0.183	-0.508	0.134	-0.015	0.075	0.076	0.790**
	P	0.134	0.612	0.134	0.712	0.967	0.836	0.835	0.007
pH	R	0.138	-0.255	0.138	0.189	-0.665**	0.340	0.595	0.033
	P	0.704	0.477	0.704	0.601	0.036	0.337	0.070	0.928
SOC	R	0.515	-0.374	0.515	0.164	0.222	-0.234	-0.520	0.482
	P	0.128	0.287	0.128	0.651	0.537	0.516	0.123	0.158
STN	R	0.485	-0.408	0.485	0.145	0.226	-0.258	-0.551	0.507
	P	0.155	0.242	0.155	0.688	0.530	0.490	0.099	0.135
DON	R	0.406	0.170	0.406	-0.018	0.280	-0.340	-0.581	0.421
	P	0.244	0.639	0.244	0.961	0.433	0.336	0.078	0.225
IN	R	0.099	-0.380	0.099	0.094	0.363	-0.354	-0.448	0.361
	P	0.785	0.279	0.785	0.797	0.303	0.316	0.194	0.305

R = correlation coefficient; ** and * represents $P < 0.01$ and $P < 0.05$ respectively. doi:10.1371/journal.pone.0092985.t004

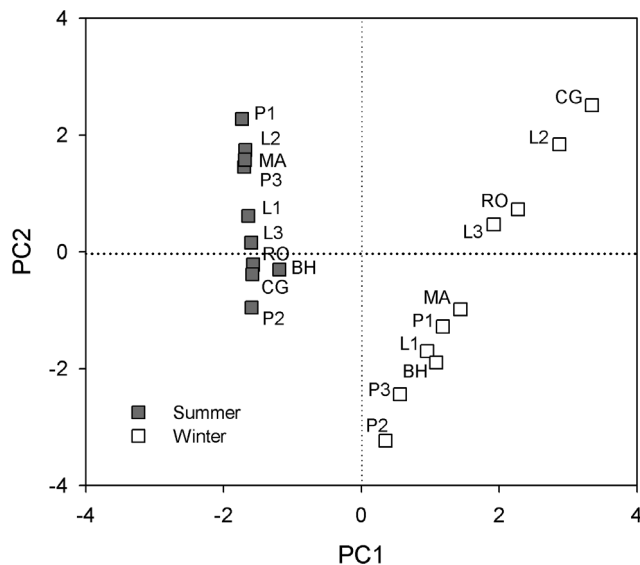


Figure 6. Principal component analysis (PCA) of PLFA signatures (mol percentages) from soil samples collected in summer and winter. PC1 and PC2 explained 96% and 2% variance of the PLFAs data, respectively.

doi:10.1371/journal.pone.0092985.g006

endogenous metabolism (the breakdown of living cell constituents/storage compounds for maintenance). Therefore, the dominance of fungi in winter may be largely due to their resistance to freeze-thawing events [80], and not to substrate preference. Fungal to bacterial PLFA ratios increased in winter across all sites (Fig. 5A). This result was consistent with those obtained in alpine and tundra ecosystems [27,28,50,69]. As seasonal shifts in microbial species composition may also occur at fine taxonomic scales [81], further research into the finer microbial community composition is warranted.

Although no significant variation occurred in the common bacterial PLFAs, we observed a significant increase of G- bacteria in cold environments ($P < 0.001$); in contrast, G+ bacterial PLFAs did not change under winter conditions ($P = 0.050$), which was consistent with previous observation in late winter tussock tundra soil [82]. G- bacteria can more easily access the soil aqueous phase

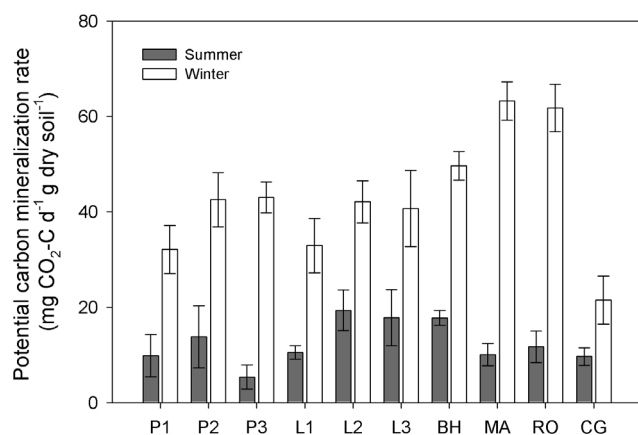


Figure 7. Potential carbon mineralization rates across different sites in summer and winter. Results are presented as mean \pm standard error. Support information is presented in Table S1.

doi:10.1371/journal.pone.0092985.g007

[33], thus the structure of the cell wall may help it to survive and grow in lower temperatures. Although G- bacteria seemed to take advantage over G+ at colder temperature, correlation analysis across different sampling sites showed that G- to G+ bacterial biomass ratio positively related to winter soil temperature (Table 4). Researches also suggested that G+ and G- bacteria differ in their patterns of substrate preference [83] with the former being dominant in soils with low substrate availability [60] and the latter in those with high availability of easily decomposable substrate [84]. Because the winter microbial substrate source was unknown, whether or not the increase in G- bacteria corresponds with the change of substrate preference across sites remains unclear.

A shift in microbial community composition along with fungal dominance in winter may subsequently change the enzyme production by the preference of different microbes and may ultimately influence the potential SOC mineralization rate. Fungi have been reported to produce more BG enzyme (involved in C metabolism) than bacteria [51]. As the BG enzyme was considered as an overall indicator of microbial activity [83,85], we expected a higher potential SOC MR in winter than summer. The result was consistent with our expectation, indicating without the temperature constraints substrate use efficiency was higher for winter microbes than the summer ones. However, *in situ* SOC MR was much lower in winter than in the summer. Although low winter temperature constrained the actual substrate mineralization rate, once temperature rise, the mineralization rate may experience a sharp increase, along with high C metabolism enzyme pool suggested by fungi dominance, and eventually leading to more CO_2 released back to atmosphere. The rapid increase of soil respiration from late winter to early spring has been observed in our previous field study conducted in the same ecosystems [12].

Conclusion

In summary, the trend of increased microbial C and decreased N uptake in winter dominate across all six seasonally snow-covered temperate ecosystems. Therefore, the N pool retained in the microbial biomass under the snowpack may not be major source for spring plant nutrient demand. The higher MBC to MBN ratio in winter was partly connected to the shift in microbial composition to fungal dominance in winter. Because there were significant differences in substrate use, nutrient limitation, and N storage capacity between fungi and bacteria, the changes in winter fungal to bacterial biomass ratios might substantially alter annual patterns of nitrogen cycling in seasonally snow-covered temperate ecosystems. Although *in situ* C mineralization was low due to the temperature constraints in winter, greater potential SOC MR indicated a higher intrinsic substrate use efficiency of winter microbes than summer ones. Our results suggested significant differences in microbial community structure and function between summer and winter. Considering the future changes in winter climate and N deposition in temperate areas, more detailed investigations of seasonal dynamics in soil microbial biomass, community structure and function including spring and autumn are urgently needed in the scenario of global changes.

Supporting Information

Table S1 Detailed summer (JUL.) and winter (JAN.) values of soil and microbial properties in Figure 2; 3; 4; 5B; 7. P1 = ~15-year Mongolia pine; P2 = ~25-year Mongolia pine; P3 = ~35-year Mongolia pine; L1 = ~15-year Prince Rupprecht's larch; L2 = ~25-year larch; L3 = ~35-year larch; BH = Birch; MA = Siberian crabapple; RO = Solitary rose; CG = Meadow grassland. DON = dissolved organic nitrogen,

MBC = microbial biomass carbon, MBN = microbial biomass nitrogen, MB = microbial biomass.
(DOCX)

Table S2 The inverse Simpson index of summer (JUL.) and winter (JAN.) PLFAs data in each sampling site.
(DOCX)

References

- Zhang T, Barry RG, Armstrong RL (2004) Application of satellite remote sensing techniques to frozen ground studies. *Polar Geography* 28: 63–196.
- Brooks PD, Grogan P, Templer PH, Groffman P, Öquist MG, et al. (2011) Carbon and nitrogen cycling in snow-covered environments. *Geography Compass* 5: 682–699.
- Aanderud ZT, Jones SE, Schoolmaster DRJ, Fierer N, Lennon JT (2013) Sensitivity of soil respiration and microbial communities to altered snowfall. *Soil Biology and Biochemistry* 57: 217–227.
- Robrock BJ, Heijboer A, Jassey VE, Hefting MM, Rouwenhorst TG, et al. (2013) Snow cover manipulation effects on microbial community structure and soil chemistry in a mountain bog. *Plant and soil* 369: 151–164.
- Romanovsky VE, Osterkamp TE (2000) Effects of unfrozen water on heat and mass transport processes in the active layer and permafrost. *Permafrost and Periglacial Processes* 11: 219–239.
- Price BP, Sowers T (2004) Temperature dependence of metabolic rates for microbial growth, maintenance, and survival. *Proceedings of the National Academy of Sciences* 101: 4631–4636.
- Schimel J, Balser TC, Wallenstein M (2007) Microbial stress-response physiology and its implications for ecosystem function. *Ecology* 88: 1386–1394.
- Brooks PD, Williams MW, Schmidt SK (1996) Microbial activity under alpine snowpacks, Niwot Ridge, Colorado. *Biogeochemistry* 3: 93–113.
- Grogan P, Jonasson S (2005) Temperature and substrate controls on intra-annual variation in ecosystem respiration in two sub-arctic vegetation-types. *Global Change Biology* 11: 465–475.
- Groffman PM, Hardy JP, Driscoll CT, Fahey TJ (2006) Snow depth, soil freezing, and fluxes of carbon dioxide, nitrous oxide and methane in a northern hardwood forest. *Global Change Biology* 12: 1748–1760.
- Monson RK, Lipson DL, Burns SP, Turnipseed AA, Delany AC, et al. (2006) Winter forest soil respiration controlled by climate and microbial community composition. *Nature* 439: 711–714.
- Wang W, Peng S, Wang T, Fang J (2010) Winter soil CO₂ efflux and its contribution to annual soil respiration in different ecosystems of a forest-steppe ecotone, north China. *Soil Biology and Biochemistry* 42: 451–458.
- Edwards KA, McCulloch J, Kershaw GP (2006) Soil microbial and nutrient dynamics in a wet Arctic sedge meadow in late winter and early spring. *Soil Biology and Biochemistry* 38: 2843–2851.
- Buckeridge KM, Jefferies RL (2007) Vegetation loss alters soil nitrogen dynamics in an Arctic salt marsh. *Journal of Ecology* 95: 283–293.
- Drott SH, Saparrman T, Nilsson MB, Schleucher J, Öquist MG (2010) Both catabolic and anabolic heterotrophic microbial activity proceed in frozen soils. *Proceedings of the National Academy of Sciences* 107: 21046–21051.
- Lipson DA, Schmidt SK, Monson RK (2000) Carbon availability and temperature control the post-snowmelt decline in alpine soil microbial biomass. *Soil Biology and Biochemistry* 32: 441–448.
- Larsen KS, Grogan P, Jonasson S, Michelsen A (2007) Respiration and microbial dynamics in two subarctic ecosystems during winter and spring thaw: effects of increased snow depth. *Arctic, Antarctic, and Alpine Research* 39: 268–276.
- Edwards KA, Jefferies RL (2013) Inter-annual and seasonal dynamics of soil microbial biomass and nutrients in wet and dry low-Arctic sedge meadows. *Soil Biology and Biochemistry* 57: 83–90.
- Weintraub MN, Schimel JP (2005) The seasonal dynamics of amino acids and other nutrients in Alaskan Arctic tundra soils. *Biogeochemistry* 73: 359–380.
- Kaiser C, Fuchslueger L, Koranda M, Gorfner M, Stange CF, et al. (2011) Plants control the seasonal dynamics of microbial N cycling in a beech forest soil by belowground C allocation. *Ecology* 92: 1036–1051.
- Nielsen CB, Groffman PM, Hamburg SP, Driscoll CT, Fahey TJ, et al. (2001) Freezing effects on carbon and nitrogen cycling in northern hardwood forest soils. *Soil Science Society of America Journal* 65: 1723–1730.
- Judd KE, Likens GE, Groffman PM (2007) High nitrate retention during winter in soils of the Hubbard Brook experimental forest. *Ecosystems* 10: 217–225.
- Buckeridge KM, Grogan P (2008) Deepened snow alters soil microbial nutrient limitations in arctic birch hummock tundra. *Applied Soil Ecology* 39: 210–222.
- Turner MM, Henry HAL (2010) Net nitrogen mineralization and leaching in response to warming and nitrogen deposition in a temperate old field: the importance of winter temperature. *Oecologia* 62: 227–236.
- Larsen KS, Michelsen A, Jonasson S, Beier C, Grogan P (2012) Nitrogen uptake during fall, winter and spring differs among plant functional groups in a subarctic heath ecosystem. *Ecosystems* 15: 929–939.
- Schmidt SK, Costello EK, Nemergut DR, Cleveland CC, Reed SC, et al. (2007) Biogeochemical consequences of rapid microbial turnover and seasonal succession in soil. *Ecology* 88: 1379–1385.
- Lipson DA, Schadt CW, Schmidt SK (2002) Changes in soil microbial community structure and function in an alpine dry meadow following spring snow melt. *Microbial Ecology* 43: 307–314.
- Schadt CW, Martin AP, Lipson DA, Schmidt SK (2003) Seasonal dynamics of previously unknown fungal lineages in tundra soils. *Science* 301: 1359–1361.
- Waldrop M, Balser T, Firestone M (2000) Linking microbial community composition to function in a tropical soil. *Soil Biology and Biochemistry* 32: 1837–1846.
- Sinsabaugh RL, Carreiro MM, Repert DA (2002) Allocation of extracellular enzymatic activity in relation to litter composition, N deposition, and mass loss. *Biogeochemistry* 60: 1–24.
- Walder F, Niemann H, Natarajan M, Lehmann MF, Boller T, et al. (2012) Mycorrhizal networks: common goods of plants shared under unequal terms of trade. *Plant physiology* 159: 789–797.
- Pokarzhevskii AD, van Straalen NM, Zabojev DP, Zaitsev AS (2003) Microbial links and element flows in nested detrital food-webs. *Pedobiologia* 47: 213–224.
- McMahon SK, Wallenstein MD, Schimel JP (2009) Microbial growth in Arctic tundra soil at -2°C . *Environmental Microbiology Reports* 1: 162–166.
- Balser TC, Wixon DL (2009) Investigating biological control over soil carbon temperature sensitivity. *Global Change Biology* 15: 2935–2949.
- Keiblinger KM, Hall EK, Wanek W, Szukics U, Hämmerle I, et al. (2010) The effect of resource quantity and resource stoichiometry on microbial carbon-use efficiency. *FEMS Microbiology Ecology* 73: 430–440.
- Lipson DA, Monson RK, Schmidt SK, Weintraub MN (2009) The trade-off between growth rate and yield in microbial communities and the consequences for under-snow soil respiration in a high elevation coniferous forest. *Biogeochemistry* 95: 23–35.
- Liptzin D, Silver WL (2009) Effects of carbon additions on iron reduction and phosphorus availability in a humid tropical forest soil. *Soil Biology and Biochemistry* 41: 1696–1702.
- Bond-Lamberty B, Thomson A (2010) Temperature-associated increases in the global soil respiration record. *Nature* 464: 579–582.
- Wang W, Chen W, Wang S (2010) Forest soil respiration and its heterotrophic and autotrophic components: Global patterns and responses to temperature and precipitation. *Soil Biology and Biochemistry* 42: 1236–1244.
- Zhou YM, Li MH, Cheng XB, Wang CG, Fan AN, et al. (2010) Soil respiration in relation to photosynthesis of quercus mongolica trees at elevated CO₂. *Plos one* 5:e15134.
- Yao H, Bowman D, Shi W (2011) Seasonal variations of soil microbial biomass and activity in warm-and cool-season turfgrass systems. *Soil Biology and Biochemistry* 43: 1536–1543.
- Baldrian P, Vetrovsky T, Cajthaml T, Dobíášová P, Petránková M, et al. (2013) Estimation of fungal biomass in forest litter and soil. *Fungal Ecology* 6: 1–11.
- Hayhoe K, Wake CP, Huntington TG, Luo L, Schwartz MD, et al. (2007) Past and future changes in climate and hydrological indicators in the US Northeast. *Climate Dynamics* 28: 381–407.
- Huntington TG, Richardson AD, McGuire KJ, Hayhoe K (2009) Climate and hydrological changes in the northeastern United States: recent trends and implications for forest and aquatic ecosystems. *Canadian Journal of Forest Research* 39: 199–212.
- Henry HAL (2008) Climate change and soil freezing dynamics: historical trends and projected changes. *Climatic Change* 87: 421–434.
- Galloway JN, Dentener FJ, Capone DG, Boyer EW, Howarth RW, et al. (2004) Nitrogen cycles: past, present, and future. *Biogeochemistry* 70: 153–226.
- Kreyling J (2010) Winter climate change: a critical factor for temperate vegetation performance. *Ecology* 91: 1939–1948.
- Pietikäinen J, Pettersson M, Bååth E (2005) Comparison of temperature effects on soil respiration and bacterial and fungal growth rates. *FEMS Microbiology Ecology* 52: 49–58.
- Kramer C, Gleixner G (2006) Variable use of plant- and soil-derived carbon by microorganisms in agricultural soils. *Soil Biology and Biochemistry* 38: 3267–3278.
- Yang Y, Luo Y, Finzi AC (2011) Carbon and nitrogen dynamics during forest stand development: a global synthesis. *New Phytologist* 190: 977–989.

Acknowledgments

We thanked two anonymous reviewers for their very constructive and valuable comments for its early version of our manuscript.

Author Contributions

Conceived and designed the experiments: WW. Performed the experiments: XZ WC. Analyzed the data: XZ NZ WC. Contributed reagents/materials/analysis tools: HZ. Wrote the paper: XZ WW.

51. Bjork RG, Bjorkman MP, Andersson MX, Klemedtsson L (2008) Temporal variation in soil microbial communities in Alpine tundra. *Soil Biology and Biochemistry* 40: 266–268.
52. Lipson DA, Schmidt SK (2004) Seasonal changes in an alpine soil bacterial community in the Colorado Rocky Mountains. *Applied and environmental microbiology* 70: 2867–2879.
53. Bradley RL, Fyles JW (1995) Growth of paper birch (*Betula papyrifera*) seedling increases soil available C and microbial acquisition of soil nutrients. *Soil Biology and Biochemistry* 27: 1565–1571.
54. Schumacher BA (2002) Methods for the determination of the total organic carbon (TOC) in soils and sediments. National ESD, ed. U.S. Environmental Protection Agency, Washington DC.
55. Ruzicka J (1983) Flow Injection Analysis – From Test Tube to Integrated Microconduits. *Analytical Chemistry* 55: 1040A–1053A.
56. Brookes PC, Landman A, Pruden G, Jenkinson DS (1985) Chloroform fumigation and the release of soil nitrogen- A rapid direct extraction method to measure microbial biomass nitrogen in soil. *Soil Biology and Biochemistry* 17: 837–842.
57. Ross DJ (1990) Estimation of soil microbial C by a fumigation-extraction method: influence of seasons, soils and calibration with the fumigation-incubation procedure. *Soil Biology and Biochemistry* 22: 295–300.
58. Bossio DA, Scow KM (1998) Impacts of carbon and flooding on soil microbial communities: phospholipid fatty acid profiles and substrate utilization patterns. *Microbial Ecology* 35: 265–278.
59. Zelles L (1997) Phospholipid fatty acid profiles in selected members of soil microbial communities. *Chemosphere* 35: 275–294.
60. Fierer N, Schimel JP, Holden PA (2003) Variations in microbial community composition through two soil depth profiles. *Soil Biology and Biochemistry* 35: 167–176.
61. Frostegård Å, Bååth E, Tunlio A (1993) Shifts in the structure of soil microbial communities in limed forests as revealed by phospholipid fatty acid analysis. *Soil Biology and Biochemistry* 25: 723–730.
62. Zogg GP, Zak DR, Ringelberg DB, White DC, MacDonald NW, et al. (1997) Compositional and functional shifts in microbial communities due to soil warming. *Soil Science Society of America Journal* 61: 475–481.
63. Gutknecht JL, Field CB, Balser TC (2012) Microbial communities and their responses to simulated global change fluctuate greatly over multiple years. *Global Change Biology* 18: 2256–2269.
64. Winkler JP, Cherry RS, Schlesinger WH (1996) The Q_{10} relationship of microbial respiration in a temperate forest soil. *Soil Biology and Biochemistry* 28: 1067–1072.
65. Anderson JPE (1982) Soil respiration, In *Methods of Soil Analysis, Part 2. Chemical and Microbiological Properties*. Soil Science Society of America, Madison: 831–871.
66. Mielke PW (1984) Meteorological applications of permutation techniques based on distance functions. In: Krishnaiah PR, Sen PK (eds) *Handbook of statistics, vol 4* New York/Elsevier Science Publishers
67. Mielke PW, Berry KJ (2001) *Permutation methods: a distance function approach*. Springer, Berlin Heidelberg New York.
68. Schimel JP, Bilbrough C, Welker JM (2004) Increased snow depth affects microbial activity and nitrogen mineralization in two Arctic tundra communities. *Soil Biology and Biochemistry* 36: 217–227.
69. Schimel JP, Weintraub MN (2003) The implications of exoenzyme activity on microbial carbon and nitrogen limitation in soil: a theoretical model. *Soil Biology and Biochemistry* 35: 549–563.
70. Mariko S, Nishimura N, Mo W (2000) Winter CO_2 flux from soil and snow surfaces in a cool-temperate deciduous forest, Japan. *Ecological Research* 15: 363–372.
71. Uchida M, Mo W, Nakatsubo T (2005) Microbial activity and litter decomposition under snow cover in a cool-temperate broad-leaved deciduous forest. *Agricultural and Forest Meteorology* 134: 102–109.
72. Schimel JP, Fahnstock J, Michaelson G (2006) Cold-season production of CO_2 in arctic soils: can laboratory and field estimates be reconciled through a simple modeling approach? *Arctic, Antarctic and Alpine Research* 38: 249–256.
73. Fierer N, Strickland MS, Liptzin D, Bradford MA, Cleveland CC (2009) Global patterns in belowground communities. *Ecology Letters* 12: 1238–1249.
74. Cleveland CC, Liptzin D (2007) C: N: P stoichiometry in soil: is there a “Redfield ratio” for the microbial biomass? *Biogeochemistry* 85: 235–252.
75. Rovira AD (1969) Plant root exudates. *The Botanical Review* 35: 35–57.
76. Strickland MS, Rousk J (2010) Considering fungal: bacterial dominance in soils—Methods, controls, and ecosystem implications. *Soil Biology and Biochemistry* 42: 1385–1395.
77. Cardon ZG, Hungate BA, Cambardella CA, Chapin III FS, Field CB, et al. (2001) Contrasting effects of elevated CO_2 on old and new soil pools. *Soil Biology and Biochemistry* 33: 365–373.
78. Liu LL, Kong JS, Booker FL, Giardina CP, Lee AH, et al. (2009) Enhanced litter input rather than changes in litter chemistry drive soil carbon and nitrogen cycles under elevated CO_2 : a microcosm study. *Global Change Biology* 15: 441–453.
79. Schimel JP, Mikán C (2005) Changing microbial substrate use in Arctic tundra soils through a freeze-thaw cycle. *Soil Biology and Biochemistry* 37: 1411–1418.
80. Hacı M, Rousk J, Ilstedt U, Öquist M, Bååth E, et al. (2011) Effects of soil frost on growth, composition and respiration of the soil microbial decomposer community. *Soil Biology and Biochemistry* 43: 2069–2077.
81. Wallenstein MD, McMahon S, Schimel J (2007) Bacterial and fungal community structure in Arctic tundra tussock and shrub soils. *FEMS Microbiology Ecology* 59: 428–435.
82. Wallenstein MD, McMahon SK, Schimel JP (2009) Seasonal variation in enzyme activities and temperature sensitivities in Arctic tundra soils. *Global Change Biology* 15: 1631–1639.
83. Schindlbacher A, Rodler A, Kuffner M, Kitzler B, Sessitsch A, et al. (2011) Experimental warming effects on the microbial community of a temperate mountain forest soil. *Soil Biology and Biochemistry* 43: 1417–1425.
84. Boer WD, Folman LB, Summerbell RC, Boddy L (2005) Living in a fungal world: impact of fungi on soil bacterial niche development. *FEMS microbiology reviews* 29: 795–811.
85. Sinsabaugh RL, Lauber CL, Weintraub MN, Ahmed B, Allison SD, et al. (2008) Stoichiometry of soil enzyme activity at global scale. *Ecology Letters* 11: 1252–1264.

2013 年发表论文

Rapid warming accelerates tree growth decline in semi-arid forests of Inner Asia

HONGYAN LIU*, A. PARK WILLIAMS†, CRAIG D. ALLEN‡, DALI GUO§, XIUCHEN WU*, OLEG A. ANENKHONOV¶, ERYUAN LIANG||, DENIS V. SANDANOV¶, YI YIN*, ZHAOHUAN QI* and NATALYA K. BADMAEVA¶

*College of Urban and Environmental Science and MOE Laboratory for Earth Surface Processes, Peking University, Beijing 100871, China, †Earth and Environmental Sciences Division, Los Alamos National Laboratory, MS-J495, Los Alamos, NM 87545, USA, ‡US Geological Survey, Jemez Mountains Field Station, Fort Collins Science Center, Los Alamos, NM 87544, USA, §Institute of Geographical Sciences and Natural Resources Research, Chinese Academy of Sciences, Beijing 100101 China, ¶Institute of General and Experimental Biology, Siberian Branch, Russian Academy of Sciences, Ulan Ude 670047, Russia, ||Institute of Tibetan Plateau Research, Chinese Academy of Sciences, Beijing 100085, China

Abstract

Forests around the world are subject to risk of high rates of tree growth decline and increased tree mortality from combinations of climate warming and drought, notably in semi-arid settings. Here, we assess how climate warming has affected tree growth in one of the world's most extensive zones of semi-arid forests, in Inner Asia, a region where lack of data limits our understanding of how climate change may impact forests. We show that pervasive tree growth declines since 1994 in Inner Asia have been confined to semi-arid forests, where growing season water stress has been rising due to warming-induced increases in atmospheric moisture demand. A causal link between increasing drought and declining growth at semi-arid sites is corroborated by correlation analyses comparing annual climate data to records of tree-ring widths. These ring-width records tend to be substantially more sensitive to drought variability at semi-arid sites than at semi-humid sites. Fire occurrence and insect/pathogen attacks have increased in tandem with the most recent (2007–2009) documented episode of tree mortality. If warming in Inner Asia continues, further increases in forest stress and tree mortality could be expected, potentially driving the eventual regional loss of current semi-arid forests.

Keywords: drought, forest die-off, Inner Asia, semi-arid, semi-humid, tree growth decline, tree ring

Received 15 February 2013 and accepted 26 March 2013

Introduction

Tree growth declines in semi-arid forests, whose carbon storage efficiency can be 60% higher than the global average for pine forests (Rotenberg & Yakir, 2010), could substantially reduce ecosystem carbon sequestration in the Earth's drylands (Schimel, 2010). On the other hand, extensive shifts from forests to desertified shrublands or grasslands in semi-arid regions (~17.7% of the Earth's total land surface area) could somewhat moderate climate warming effects by increasing the reflectivity of the earth's surface (Rotenberg & Yakir, 2010). Reduction of forest cover in semi-arid regions also increases emission and transport of soil dust (Breshears *et al.*, 2009; Wu *et al.*, 2012), redistributing aerosols and their radiative forcings (Kaufman *et al.*, 2002). If climate change results in widespread growth declines or even die-off of semi-arid forests, multiple

feedbacks would affect global ecosystems and climate (Adams *et al.*, 2010).

Semi-arid forests are seasonally or episodically under water stress and may be particularly vulnerable to even slight increases in water deficit, which can drive tree growth declines and increased mortality (Breshears *et al.*, 2005; Allen *et al.*, 2010; Williams *et al.*, 2010, 2013). Diverse recent work, ranging from greenhouse experiments (Adams *et al.*, 2009) and dendroclimatology modeling (Williams *et al.*, 2010, 2013) to regional-scale forest health monitoring (Carnicer *et al.*, 2011; Williams *et al.*, 2013) and global review of forest die-off (Allen *et al.*, 2010), shows that semi-arid forests could be particularly sensitive to warming-induced increases in atmospheric moisture demand. Yet, spatially extensive analyses of climate warming effects on tree growth declines are very limited (Peng *et al.*, 2011).

A large temperature gradient exists across the extensive semi-arid forests of Inner Asia, with temperate and boreal forests bordering steppes and the Gobi Desert, making this region potentially ideal for examining temperature-related patterns and trends in tree growth and

Correspondence: Hongyan Liu, tel. /fax +86 10 62759319, e-mail: lhy@urban.pku.edu.cn, Craig D. Allen, tel. +1 505 6723861 X 720, fax +1 505 6729607, e-mail: craig_allen@usgs.gov

mortality (Liu *et al.*, 2000; Savva *et al.*, 2003). Yet, we know relatively little about forest response to climate variability in this vast part of the world, which thus far has been represented by few dendroclimatological studies (e.g., Davi *et al.*, 2009, 2010; Liang *et al.*, 2009; Sidorova *et al.*, 2012). Importantly, parts of Inner Asia have warmed relatively rapidly in recent decades. Temperate and southern boreal regions in Asia have recently warmed faster than neighboring regions, particularly in the spring, and this warming pattern is projected to continue in coming decades (IPCC, 2007). Increasingly frequent and severe drought events also have been observed in northern and eastern Inner Asia in recent decades (Li *et al.*, 2009; Sheffield *et al.*, 2009). In addition, we and others (Kharuk *et al.*, 2013) have observed recent tree mortality in low-elevation temperate and southern boreal forest regions distributed close to the xeric treeline in Asia. We hypothesize that recent warming has caused reduced tree growth in relatively arid regions near the xeric treeline in Inner Asia. We sought to determine how drought and climate warming may have reduced tree growth and possibly amplified tree mortality across this broad region by collecting tree-ring width data from extensive portions of Inner Asia, including most parts of northern (east of $\sim 108^\circ\text{E}$) and northwestern (west of $\sim 108^\circ\text{E}$) China and southern Siberia in Russia (Fig. 1).

Materials and methods

Collection of tree-ring data

A total of 63 tree-ring width chronologies, representing 10 tree species, were utilized for this study (Table 1). Tree-ring cores were collected from 31 sites in three sub-regions: northwestern China, northern China, and southern Siberia to Mongolia in Inner Asia (Fig. 1). In northwestern China, we sampled the dominant tree species *Picea schrenkiana* Fisch. et C.A. Mey. on the northern slopes of the Tianshan Mountains from 2004 to 2006. In northern China, the dominant tree species *Pinus tabulaeformis* Carr. was sampled from the Inner Mongolian Plateau in 2004, and *Larix chinensis* Mill. and *Abies fargesii* Franch. were sampled from the Qinling Mountains in 2007. In southern Siberia of Russia, we sampled three dominant tree species (*Larix gmelinii* Rupr., *Larix sibirica* Ledeb., and *Pinus sylvestris* L.) in 2007 and 2008. In contrast to the selective coring used in many studies (e.g., Hogg *et al.*, 2008), we cored all tree individuals with d.b.h. >5 cm in a $25\text{ m} \times 25\text{ m}$ plot in each site. Only trees with age >70 years were used for further analysis for most sites, and age >60 years for three sites (87.24°E , 43.43°N ; 81.44°E , 44.47°N ; 104.88°E , 50.58°N) consisting of relatively younger trees.

In addition, we utilized raw tree-ring width chronologies from the International Tree-Ring Data Bank (<http://www.ncdc.noaa.gov/paleo/treering.html>): *Larix sibirica* Ledeb. from 10 sites in Mongolia and six sites in southern Siberia, and *Pinus sibirica* Du Tour from four sites in Mongolia. The other

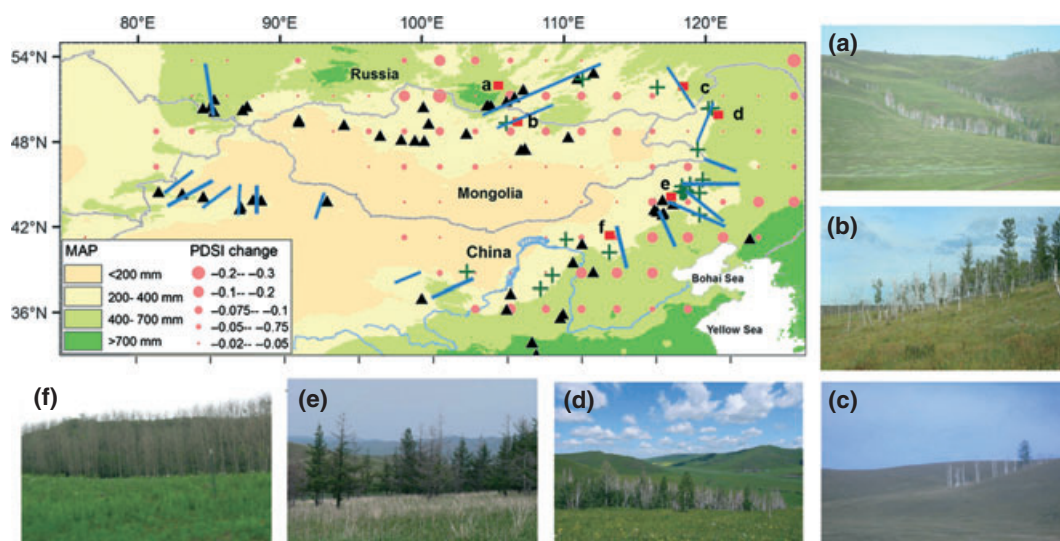


Fig. 1 Distribution of tree-ring sample plots (black triangles) and sites of forest die-off (green crosses) on a climate map of Inner Asia. Sites of significant decline ($P < 0.01$) in annual Palmer Drought Severity Index (PDSI) since 1951 calculated from the database by Dai *et al.* (2004) are also shown by filled red circles, with circle size representing PDSI change. Significant decline in PDSI occurred in northern China and southern Siberia-Mongolia, but not in northwestern China. In this map, field expedition transects as thick blue lines, and photo locations as red squares. Photos (a)–(d) show mortality of *Betula platyphylla* in mixed larch-birch forest stands; photo (e) illustrates mortality of *Larix gmelinii*, and photo (f) shows mortality of *Populus davidiana*.

Table 1 Site description of tree-ring data used in this study. NWC, SSM, and NC represent Northwest China, Southern Siberia-Mongolia, and North China, respectively

Longitude (°E)	Latitude (°N)	Elevation (m a.s.l.)	Sub-region	Semi-arid/semi-humid	Tree species	Amount of cores	Median core age (yr)	Mean sensitivity	EPS	Reference
107.78	33.92	3123	NC	Semi-humid	<i>Abies fargesii</i>	33	98	0.21	0.99	This study
107.79	33.91	3006	NC	Semi-humid	<i>Abies fargesii</i>	22	86	0.20	0.94	This study
107.79	33.91	2900	NC	Semi-humid	<i>Abies fargesii</i>	23	115	0.18	0.93	This study
108.08	33.08	2350	NC	Semi-humid	<i>Abies chensiensis</i>	50	250	0.16	NA	Ma <i>et al.</i> , 2001
107.77	33.94	3295	NC	Semi-humid	<i>Larix chinensis</i>	74	84	0.30	0.95	This study
107.78	33.93	3190	NC	Semi-humid	<i>Larix chinensis</i>	33	89	0.29	0.98	This study
107.79	33.92	3121	NC	Semi-humid	<i>Larix chinensis</i>	30	62	0.27	0.98	This study
117.05	42.99	1329	NC	Semi-arid	<i>Picea meyeri</i>	34	121	0.32	0.98	This study
106.27	37.32	2350	NC	Semi-arid	<i>Pinus tabulaeformis</i>	40	90	0.27	0.93	Wang <i>et al.</i> , 2009a
116.39	43.24	1363	NC	Semi-arid	<i>Pinus tabulaeformis</i>	43	132	0.46	0.99	This study
116.60	43.09	1331	NC	Semi-arid	<i>Pinus tabulaeformis</i>	27	134	0.48	0.99	This study
116.96	43.90	1285	NC	Semi-arid	<i>Pinus tabulaeformis</i>	27	79	0.37	0.98	This study
116.96	42.90	1250	NC	Semi-arid	<i>Pinus tabulaeformis</i>	22	71	0.34	0.98	This study
117.72	43.63	1197	NC	Semi-arid	<i>Pinus tabulaeformis</i>	31	93	0.55	0.99	This study
110.67	39.50	2050	NC	Semi-arid	<i>Pinus tabulaeformis</i>	20	214	0.34	NA	Shi <i>et al.</i> , 2007
111.29	40.80	1300	NC	Semi-arid	<i>Pinus tabulaeformis</i>	30	NA	0.34	NA	Liu & Ma, 1999
106.00	36.25	2150	NC	Semi-humid	<i>Pinus tabulaeformis</i>	26	98	0.37	0.87	Wang <i>et al.</i> , 2009b
112.08	38.83	2190	NC	Semi-humid	<i>Pinus tabulaeformis</i>	53	142	0.47	0.97	Yi <i>et al.</i> , 2006
109.78	35.65	1427	NC	Semi-humid	<i>Pinus tabulaeformis</i>	44	NA	0.30	0.90	Cai <i>et al.</i> , 2005
109.97	35.92	1370	NC	Semi-humid	<i>Pinus tabulaeformis</i>	46	NA	0.31	NA	Cai <i>et al.</i> , 2005
123.14	41.19	310	NC	Semi-humid	<i>Pinus tabulaeformis</i>	53	173	0.22	NA	Chen <i>et al.</i> , 2007
93.31	43.82	2600	NWC	Semi-arid	<i>Larix sibirica</i>	39	162	0.25	0.87	Wang <i>et al.</i> , 2007
93.34	43.82	2660	NWC	Semi-arid	<i>Larix sibirica</i>	41	156	0.23	0.97	Wang <i>et al.</i> , 2007
84.60	44.12	2135	NWC	Semi-arid	<i>Picea schrenkiana</i>	87	194	0.38	0.96	This study
84.61	44.13	1838	NWC	Semi-arid	<i>Picea schrenkiana</i>	23	90	0.47	0.98	This study
88.11	43.93	1740	NWC	Semi-arid	<i>Picea schrenkiana</i>	12	85	0.30	0.82	This study
88.67	43.89	1886	NWC	Semi-arid	<i>Picea schrenkiana</i>	84	80	0.55	0.99	This study
88.68	43.90	2005	NWC	Semi-arid	<i>Picea schrenkiana</i>	29	102	0.47	0.97	This study
83.13	44.35	1770	NWC	Semi-arid	<i>Picea schrenkiana</i>	47	86	0.44	0.99	This study
83.13	44.32	2200	NWC	Semi-humid	<i>Picea schrenkiana</i>	76	114	0.20	0.99	This study
87.18	43.28	2100	NWC	Semi-arid	<i>Picea schrenkiana</i>	12	99	0.47	0.99	This study
87.24	43.43	1532	NWC	Semi-arid	<i>Picea schrenkiana</i>	23	69	0.56	0.99	This study
81.44	44.47	2454	NWC	Semi-humid	<i>Picea schrenkiana</i>	16	70	0.43	0.93	This study
81.48	44.47	2000	NWC	Semi-arid	<i>Picea schrenkiana</i>	41	75	0.23	0.99	This study
98.66	37.04	3935	NWC	Semi-arid	<i>Sabina przewalskii</i>	50	407	0.19	0.95	Zhu <i>et al.</i> , 2008
110.98	52.49	1038	SSM	Semi-arid	<i>Larix gmelinii</i>	58	88	0.37	0.99	This study
112.10	52.89	991	SSM	Semi-arid	<i>Larix gmelinii</i>	110	109	0.31	0.99	This study
91.33	49.42	2000	SSM	Semi-arid	<i>Larix sibirica</i>	26	252	0.32	0.97	ITRDB mong007 ^c

Table 1 (continued)

Longitude (°E)	Latitude (°N)	Elevation (m a.s.l.)	Sub-region	Semi-arid/ semi-humid	Tree species	Amount of cores	Median core age (yr)	Mean sensitivity	EPS	Reference
97.07	48.46	1841	SSM	Semi-arid	<i>Larix sibirica</i>	28	280	0.36	0.98	ITRDB mong013 ^f
99.52	48.10	2060	SSM	Semi-arid	<i>Larix sibirica</i>	66	298	0.41	0.99	ITRDB mong015 ^e
100.17	48.09	1900	SSM	Semi-arid	<i>Larix sibirica</i>	36	338	0.39	0.99	ITRDB mong011 ^e
100.50	49.29	1800	SSM	Semi-arid	<i>Larix sibirica</i>	29	335	0.66	0.98	ITRDB mong014 ^e
107.27	47.54	1565	SSM	Semi-arid	<i>Larix sibirica</i>	42	128	0.36	0.98	ITRDB mong001 ^a
107.30	47.47	1415	SSM	Semi-arid	<i>Larix sibirica</i>	57	272	0.45	0.99	ITRDB mong006 ^b
91.34	49.55	2500	SSM	Semi-arid	<i>Larix sibirica</i>	38	334	0.34	0.97	ITRDB mong009 ^d
100.12	50.46	2300	SSM	Semi-arid	<i>Larix sibirica</i>	13	192	0.31	0.89	ITRDB mong001 ^a
103.14	48.59	1400	SSM	Semi-arid	<i>Larix sibirica</i>	27	312	0.50	0.97	ITRDB mong012 ^g
87.68	50.50	1950	SSM	Semi-arid	<i>Larix sibirica</i>	24	266	0.26	0.95	ITDRB rus133 ^c
87.38	50.25	2000	SSM	Semi-arid	<i>Larix sibirica</i>	30	243	0.26	0.96	ITDRB rus135 ^c
85.38	51.00	1450	SSM	Semi-humid	<i>Larix sibirica</i>	29	278	0.16	0.95	ITDRB rus129 ^c
84.59	50.39	1500	SSM	Semi-humid	<i>Larix sibirica</i>	30	219	0.32	0.95	ITDRB rus140 ^c
85.14	50.52	1400	SSM	Semi-humid	<i>Larix sibirica</i>	30	243	0.42	0.97	ITDRB rus130 ^c
85.37	50.15	1750	SSM	Semi-humid	<i>Larix sibirica</i>	24	339	0.29	0.96	ITDRB rus127 ^c
104.59	50.57	858	SSM	Semi-humid	<i>Larix sibirica</i>	46	77	0.41	0.98	This study
104.67	50.57	1035	SSM	Semi-humid	<i>Larix sibirica</i>	34	79	0.42	0.99	This study
104.88	50.58	876	SSM	Semi-humid	<i>Larix sibirica</i>	19	66	0.45	0.99	This study
94.53	49.22	2229	SSM	Semi-arid	<i>Pinus sibirica</i>	15	220	0.16	0.50	ITRDB mong008 ^d
98.56	48.18	2420	SSM	Semi-arid	<i>Pinus sibirica</i>	90	353	0.18	0.96	ITRDB mong003 ^a
107.00	47.46	1755	SSM	Semi-arid	<i>Pinus sibirica</i>	35	180	0.42	0.98	ITRDB mong002 ^a
110.33	48.34	1070	SSM	Semi-arid	<i>Pinus sibirica</i>	33	214	0.39	0.98	ITRDB mong005 ^b
107.16	51.70	950	SSM	Semi-arid	<i>Pinus sylvestris</i>	26	81	0.55	0.96	This study
106.55	51.17	834	SSM	Semi-arid	<i>Pinus sylvestris</i>	22	67	0.54	0.98	This study
105.98	50.87	920	SSM	Semi-arid	<i>Pinus sylvestris</i>	52	92	0.47	0.99	This study

Data contributors:

^aG.C. Jacoby, R. D'Arrigo, B.M. Buckley, N. Pederson.^bG.C. Jacoby, B.M. Buckley, N. Pederson.^cF. Schweingruber.^dG.C. Jacoby, R. D'Arrigo, N. Pederson.^eG. C. Jacoby, N. Davi, B. Nachin, O. Byambasuren.^fG. Jacoby, N. Davi, B. Nachin, N. Pederson.^gG. Jacoby, N. Davi, B. Nachin.

12 tree-ring chronologies were obtained from previous publications (Table 1).

The cross-dated tree-ring measurements were standardized to remove biological growth trends, as well as other low-frequency variation due to stand dynamics, using the ARSTAN program (Cook, 1985). Raw ring widths were detrended with either straight lines or negative exponential curves. If both of these curve types failed, a cubic smoothing spline with a 50% frequency-response cutoff of 55 years was applied. In addition, a data-adaptive power transformation was applied to stabilize the variance and mitigate non-normality in the series prior to detrending (details in Cook & Peters, 1997).

Ring-width index (*RWI*), an indicator of tree growth, was calculated as the difference between the power-transformed ring-width measurement and the value of the fitted curve. We also computed *RWI* records using the traditional ratio-method standardization, as a result of the division process (Cook & Peters, 1997), with our own samples and the archived raw ring-width data from ITRDB. The approaches show consistent trends and yielded an average *RWI* difference of 0.005 ± 0.04 for chronologies at semi-arid sites (defined at end of this section) and 0.012 ± 0.022 for chronologies at semi-humid sites. To retain potentially important trends eliminated during standardization, we also calculated Basal Area Increment (*BAI*) for the 31 sites collected by this study.

Mean ages of trees, length of the chronologies, number of samples from each site, common statistics such as Expressed Population Signal (*EPS*) and mean sensitivity are listed in Table 1. The *EPS*, a measure of chronology reliability, is generally above 0.84, a generally accepted level. Mean sensitivities range from 0.16 to 0.66. Mean ages of trees from semi-arid sites and those from semi-humid sites have no significant differences.

We classified the sites from which the 63 tree-ring chronologies come into two groups: semi-arid with a mean annual precipitation (*MAP*) range from 200 to 400 mm and semi-humid with a *MAP* range from 400 to 700 mm. These two sub-regions are consistent with semi-arid and dry sub-humid regions commonly accepted in desertification studies in Inner Asia based on aridity index (Millennium Ecosystem Assessment, 2005). *MAP* was derived using spatially interpolated estimates of monthly total precipitation during 1948–2006, developed by the Global Precipitation Climatology Centre (GPCC) (Rudolf *et al.*, 2005; Schneider *et al.*, 2011).

Calculation of the effects of drought on tree growth

Much of the influence of temperature on drought vulnerability of semi-arid forests is manifested through temperature's exponential influence on atmospheric moisture demand, defined as the vapor-pressure deficit (*VPD*: saturation vapor pressure minus actual vapor pressure) (e.g., Williams *et al.*, 2013). We used gridded (1° geographic resolution) daily data sets of maximum temperature (T_{\max}), mean specific humidity, and mean surface pressure developed by Sheffield *et al.* [(2006), hereafter referred to as Sheff2006] to estimate maximum daily vapor-pressure deficit (VPD_{\max}) for 1948–2008. Daily VPD_{\max} values were averaged to calculate monthly mean VPD_{\max} . Sheff2006 data are based on the NCEP/NCAR reanalysis (Kalnay *et al.*,

1996) and T_{\max} data are adjusted to match the CRU TS3.0 data set (Mitchell & Jones, 2005). For analysis of relationships between ring widths and prior year climate, we extended the monthly VPD_{\max} record back through 1947 using CRU TS3.0 T_{\max} data, calibrated to match the mean and variance of VPD_{\max} . We repeated these correlation analyses for potential evaporation (which is dictated by *VPD*, wind speed, and radiation) using Sheffield *et al.* (2012) estimates of monthly potential evaporation (*PET*). For trend analysis, we extended VPD_{\max} forward through 2012 using daily *VPD* data calculated with the MERRA reanalysis and adjusted to match the long-term mean and variance of Sheff2006 (Rienecker *et al.*, 2011). Monthly precipitation data come from the Global Precipitation Climatology Centre (GPCC) version 6 data set gridded at 0.5° geographic resolution (Rudolf *et al.*, 2005; Schneider *et al.*, 2011). We also repeated the correlation analyses using station data from the Global Historical Climate Network (<http://www.ncdc.noaa.gov/ghcnm/>), but only use the results to guide our interpretation of results obtained from analysis of gridded climate data because stations are varying distances from the sample sites and station data sets do not all cover the same years. To determine what time of year forests are most sensitive to drought-related climate variables, we tested correlation between *RWI* records and seasonal (3-month) precipitation totals and VPD_{\max} . For each *RWI* chronology, we calculated annual time series of seasonal precipitation total and average VPD_{\max} considering each 3-month time step beginning with January to March of the year prior to the growth year and extending through October to December of the current growth year (22 seasons total in a 24-month period).

Using knowledge gained from the seasonal correlation analysis, we identified the times of year when *RWI* chronologies tend to correlate strongest with precipitation total and VPD_{\max} . We evaluated how correlations during these times of year differ among populations growing at semi-arid vs. semi-humid sites using ANOVA analysis.

Trends of T_{\max} and VPD_{\max} at semi-arid and semi-humid sites in both the growing season (May to September) and the pre-growing season (October to April) were calculated for 1949–2012. For each group of sites and for each variable, we standardized each site's time series so all time series shared a common mean and variance equal to the average mean and variance of all sites in the group.

Delineation of tree mortality sites

We made empirical observations of recent tree mortality near many lower elevation xeric forest-grassland ecotones in Inner Asia, although this portion of the study was not designed to allow using these observations to rigorously determine the magnitude and extent of recent tree mortality across this large region. Sites of tree mortality were identified along field expedition routes. In southern Siberia-Mongolia and northern China, a total of 11 field expedition transects were established along regional precipitation gradients during 2000–2009. In northwestern China, 8 transects were established along elevation gradients because the forests are distributed on mountain slopes. Only uneven-aged forest stands with mortality of

dominant trees were recorded as tree mortality sites. Because tree mortality only occurred in patchy forests close to the xeric treeline where surrounded by more arid grasslands, patches with tree mortality area $>2500 \text{ m}^2$ were recorded as tree mortality sites, excluding fire-damaged forest patches. Historical records of tree mortality also were collected from reports and publications (Liang *et al.*, 2006).

Results

Spatial patterns of tree growth trend

Ring-width index (RWI) and Basal Area Increment (BAI) records are generally consistent within both semi-arid and semi-humid regions (Fig. 2). Interdecadal tree-growth variability differed markedly between semi-arid forests and semi-humid forests. Relative to the long-term mean, semi-arid forests of Inner Asia recorded low multi-year growth rates for periods in the

1920s and the late 1970s to early 1980s, with a particularly notable growth decline observed in the most recent period of analyses from 1994 to 2006 (Fig. 2a, b). In contrast, increasing tree growth rates were found for the most recent period in the semi-humid forests (Fig. 2c, d).

Relationship between tree growth and climate

The difference in growth variability between tree populations growing at semi-arid vs. semi-humid sites appears to be due to differing growth responses to moisture stress. Correlations between 1948 and 2006 ring-width index (RWI) and VPD_{\max} and precipitation differed between the semi-arid region and the semi-humid region (Fig. 3a, b). 79% of semi-arid RWI chronologies (vs. only 24% of semi-humid chronologies) correlate positively and significantly ($P < 0.05$) with total precipitation from March to June of the growth year and from June to September of the previous year. Similarly, 62% of semi-arid chronologies (and only 10% of semi-humid chronologies) correlate negatively and significantly with the average of VPD_{\max} from April to July of the growth year and from June to September of the previous year (Fig. 3c).

Notably, climate data for the more remote regions of northwest China, southern Russia, and northern Mongolia are relatively uncertain as indicated by relatively strong disagreement among various precipitation, temperature, and specific humidity data sets for those regions (Fig. S1). It is therefore probable that significant relationships between RWI and climate are more common and stronger than indicated by this analysis. In particular, wide variability among specific humidity data sets indicates that true correlations between RWI and VPD_{\max} are likely stronger than they appear here. Despite the relative inaccuracy of VPD data due to uncertain specific humidity data, correlations with VPD_{\max} still tend to be stronger than correlations with T_{\max} (Fig. S2), supporting the theory that atmospheric moisture demand is the primary mechanism by which high temperature influences drought-sensitive tree populations. Our determination that true correlations between RWI and climate may be substantially stronger than they appear in Fig. 3 is supported by a tendency for RWI records to correlate more strongly with raw station data (Global Historical Climate Network) than with the interpolated climate data sets used in this study, despite the nearest weather stations being up to 200 km away from some sample sites (results not shown). Correlations tended to improve most (by 0.05–0.1) for chronologies collected at semi-arid sites, suggesting that the true difference between climate responses at semi-arid vs. semi-humid sites is stronger than suggested by Fig. 3.

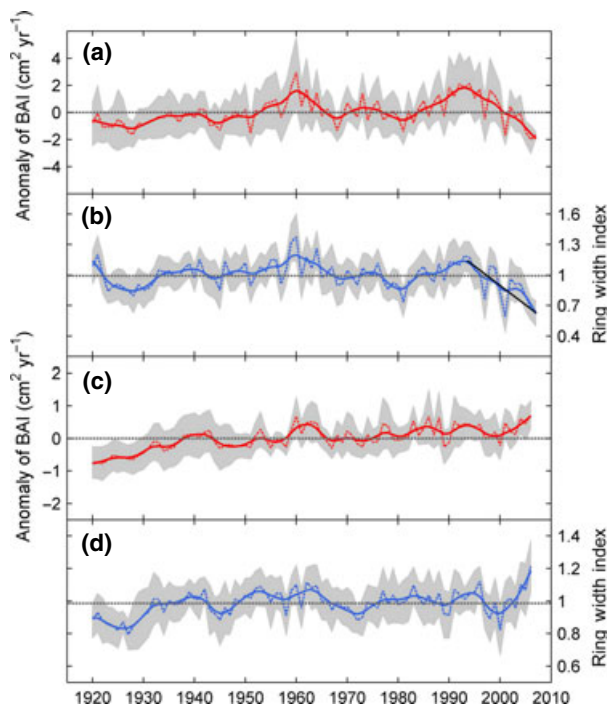


Fig. 2 Regional tree-ring chronologies of (a, c) basal-area increment (BAI) and (b, d) ring-width index (RWI) for 1920–2006. Semi-arid forests are represented in (a, b) where mean annual precipitation (MAP) is 200–400 mm ($n = 42$ for RWI and $n = 20$ for BAI); Semi-humid forests are represented in (c, d) where MAP is 400–700 mm ($n = 21$ for RWI and $n = 11$ for BAI). Thin dashed lines indicate annual values averaged across sites, bold solid lines indicate a five-year moving averages, and grey areas indicate inner-quartiles among sites. A significant negative trend in RWI trend of growth decline ($y = -0.025x + 50.38$, $P < 0.01$) since about 1994, determined by piecewise linear regression, is indicated by the black line in (b).

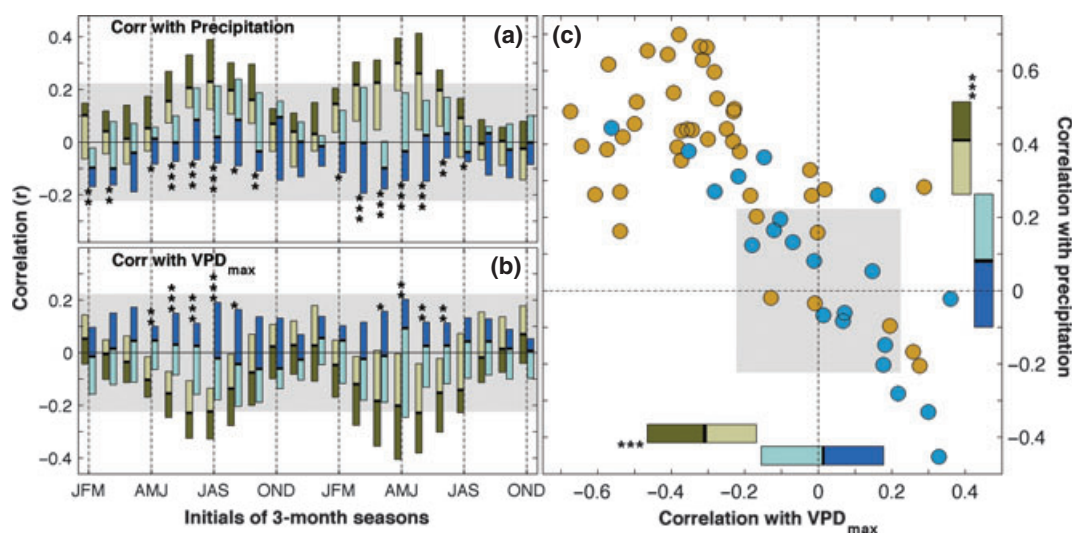


Fig. 3 Panels (a) and (b) show box plots of correlation coefficients of RWI with precipitation and mean maximum daily vapor-pressure deficit (VPD_{max}) during all 3-month periods in a 24-month window that begins in the January of the year before the growing season. Brown boxes represent populations at semi-arid sites. Blue boxes represent populations as semi-humid sites. Box plots show median and inner-quartile values. These plots show that drought in spring and summer of the growth year, and in summer of the previous year, influences growth at semi-arid sites. (c) Correlation between RWI and two climate variables related to drought: (*y*-axis) correlation with total precipitation from March to June of the growth year and from June to September of the preceding year; (*x*-axis) correlation with VPD_{max} from April to July of the growth year and June–September of the preceding year. Box plots parallel to axes in (c) are equivalent to those in (a) and (b). Gray areas in all panels bound correlation values insignificant at the 95% level. Significance was calculated assuming $N = 54$ (average number of overlapping years between RWI and climate during 1948–2006). Asterisks adjacent to box plots represent significant differences between correlation coefficients for semi-arid vs. semi-humid chronologies at 95% (one asterisk), 99% (two asterisks), and 99.9% (three asterisks) confidence levels.

Patterns of regional climatic warming and drying

Higher sensitivity to drought conditions at the semi-arid sites may be exacerbated by changing climate. Both pre-growing season and growing season warming rates of T_{max} have been higher in the semi-arid region than in the semi-humid region, and the semi-arid region has warmed significantly faster since 1949 in the pre-growing season than in the growing season (Fig. 4a, b). The warming rate has become especially rapid since the 1980s, particularly for the growing seasons (0.60 ± 0.26 °C/decade for the semi-humid region and 0.67 ± 0.27 °C/decade for the semi-arid region). VPD_{max} shows consistent trends with T_{max} for both the pre-growing and growing seasons as well as for both the semi-arid and semi-humid regions (Fig. 4c, d), particularly since the 1980s (0.93 ± 0.63 hPa/decade for the semi-arid region and 0.97 ± 0.42 hPa/decade for the semi-humid region).

Spatial patterns of tree mortality sites

We made empirical observations of recent tree mortality near many lower elevation xeric forest-grassland ecotones in Inner Asia (Fig. 1). Although our field

expeditions spanned 2000–2009, we only observed tree mortality attributable to drought stress in 2007–2009.

Discussion

In this study, tree-ring data demonstrate that tree growth at semi-arid forest sites throughout Inner Asia experience enhanced drought sensitivity relative to trees growing at semi-humid forest sites. This broad regional pattern has also been observed on a more local scale in Mongolia (Davi *et al.*, 2009, 2010). Results of the correlation analysis echo those from tree-ring studies of growth responses to climate variability in the southwestern United States, where ring-width records correlate negatively with drought intensity during the growing season as well as the months at the end of, and following, the previous growing season (Williams *et al.*, 2010, 2013).

The recent drought of the 1990s and 2000s, characterized by highly variable precipitation totals but significant warming (Fig. 4, Fig. S1), has resulted in large declines in radial growth rates at the semi-arid sites evaluated in this study. Without adequate moisture compensation through increased precipitation, the cor-

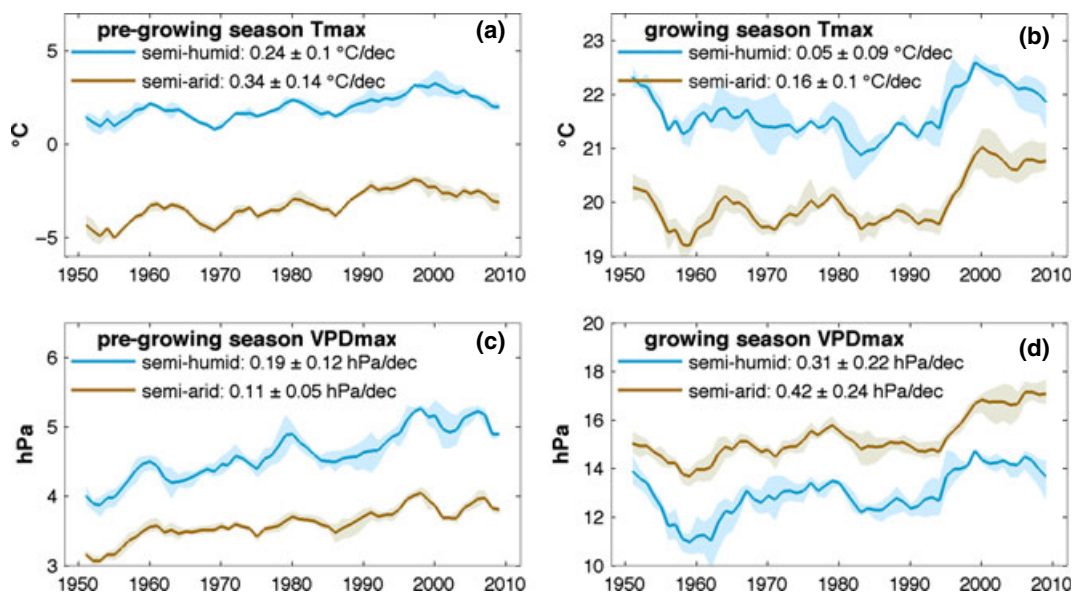


Fig. 4 (a) Pre-growing season (October to April) and (b) growing season (May to September) warming rates between 1949 and 2011 in the semi-arid and semi-humid regions. (c) Pre-growing season and (d) growing season increasing rate of vapor-pressure deficit (VPD_{max}) between 1949 and 2011 in the semi-arid and semi-humid regions. Brown and blue lines indicate 5-year moving averages for semi-humid and semi-arid sites, respectively. Shadows indicate inner-quartile ranges among site. Within each forest type, all sites' time series were standardized to share the average sites' mean and variance.

relation analysis summarized in Fig. 3 and the climate trends in Fig. 4 suggest that a ~ 1.5 °C increase in growing season temperature over 20 years was at least partially responsible for the declining trend observed in ring widths at semi-arid sites during the 1990s and 2000s (Fig. 2), as recently found for southwestern United States forests (Williams *et al.*, 2013).

Additionally, temperature and VPD have been steadily increasing during the pre-growing season in our study region since at least the 1940s (Fig. 4). Cambial cell division commences in early May in northern China (Liang *et al.*, 2009), whereas the ecologically significant shift in mean daily temperature from <0 °C to >0 °C occurs about a month earlier, in early April in northern China and late April in southern Siberia. While statistical relationships between RWI and VPD_{max} are most significant during the growing season (Fig. 3b), pre-growing season temperatures, independent of VPD, may become increasingly influential as temperatures increase beyond the historic range exhibited during the 20th century. In the past 60 years, warming has caused average daily T_{max} during the pre-growing season to rise above 0 °C at approximately 25% of the semi-arid sites considered in our study. Climate warming during the pre-growing season leads to reduced snowfall, earlier spring snowmelt, and earlier peak stream runoff, causing increasing frequency and severity of droughts during the subsequent growing season in middle to high latitudes (Pederson *et al.*,

2011). In China, this reduction in water availability at semi-arid sites appears to have been accompanied by an increase in annual actual evapotranspiration during 1960–2002, indicating increased PET (Gao *et al.*, 2007). In contrast, no change in annual actual evapotranspiration was found at semi-humid sites (Gao *et al.*, 2007). Sheffield *et al.* (2012) found that despite increases in VPD, PET appears to have decreased in parts of our study region due to declining wind speeds and solar radiation. We evaluated correlations between Sheffield *et al.* PET and our tree-ring records and found correlations to be substantially weaker for PET than for VPD_{max} or T_{max} (Fig. S3). Weak correlation with PET indicates that VPD has a disproportionately large impact on forests relative to its impact on estimated water balance according to a Penman-Monteith approach (as is also suggested by Williams *et al.*, 2013) or that Sheffield *et al.* PET calculations are less accurate than the Sheffield *et al.* VPD calculations.

Notably, significant tree growth declines may lead to or accompany significant increases in tree mortality and forest die-off (Peng *et al.*, 2011; Williams *et al.*, 2013). Indeed, historical forest die-off in Inner Asia was associated with tree growth declines in the 1920s in semi-arid northern China (Liang *et al.*, 2006). The period from the late 1970s to early 1980s also witnessed significant declines in tree growth – and during this period, high mortality rates of up to 45% were recorded in forest plantations in northern China (Xu, 1993).

Although documentation of more recent forest mortality is limited, historic correspondence between past tree mortality events and substantial declines in ring-width indices here and elsewhere (e.g., Peng *et al.*, 2011; Williams *et al.*, 2013) suggest that the recent ring-width declines at rapidly warming semi-arid sites may be associated with increased tree mortality in substantial portions of Inner Asia. This hypothesis is supported by recent documentation of similar patterns of growth and mortality in birch (*Betula*) trees at the forest-steppe boundary in the trans-Baikal region of southern Siberia by Kharuk *et al.* (2013), as well as the observations of tree mortality near lower elevation xeric forest-grassland ecotones that we made while conducting fieldwork in this region during 2007–2009 (Fig. 1). It is important to note, however, that our field observations of tree mortality were not designed to rigorously determine the magnitude, extent, or timing of recent tree mortality across this very large Inner Asia region, and it is possible that our pre-2007 fieldwork occurred before the onset of tree mortality along with those particular field expedition transects.

Rapid climate warming can have strong effects on multiple factors that drive tree growth declines and forest die-off, including fire, pathogens, and insects (Allen *et al.*, 2010; Dulamsuren *et al.*, 2010; McDowell *et al.*, 2011; Williams *et al.*, 2013). Fire frequency in summer has increased in northern China since 1980, particularly in Inner Mongolia, which has been attributed to the increased frequency of days with $T_{\max} > 12^{\circ}\text{C}$ (Zhao, 2007). In addition, the area of risk for pine caterpillar (*Dendrolimus spp.*) attack has increased since the 1950s, and since the 1980s the infestation center has moved north from southern China to Inner Mongolia, Hebei, and Shanxi in the southern part of the Inner Asian forest-steppe ecotone of northern China (Liu & Zhang, 1993; China Forestry Administration, 1982–2008). In the main region of semi-arid forests in northern China, the Great Hinggan Mountains region, insect and pathogen-affected forest areas have expanded since 1980, in contrast to a decrease on average over the whole of northern China (including semi-humid and semi-arid regions) (Fig. 5).

In summary, recent trends in Inner Asian forest growth are linked to mean annual precipitation (MAP) among at least the 63 tree populations evaluated in this study, with recent reductions in forest growth occurring at semi-arid sites receiving less than 400 mm of precipitation annually. Correlation analysis of relationships between tree-ring widths and climate data indicates that trees growing at semi-arid sites experience substantially enhanced sensitivity to drought-related variables such as growing season precipitation and atmospheric moisture demand relative to trees growing

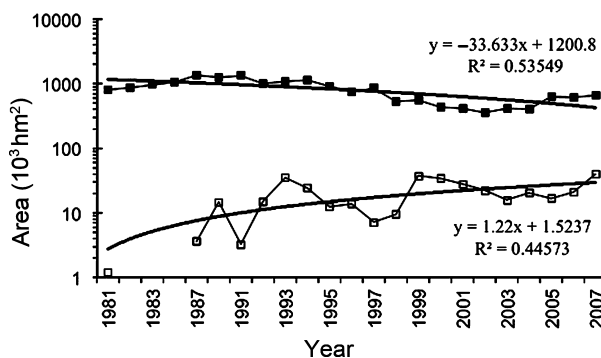


Fig. 5 Areal extent of forest pathogen attacks in the Great Hinggan Mountain region (empty squares), the dominant tract of semi-arid forest in northern China, relative to that in northern China (including semi-humid, semi-arid, and arid regions) as a whole (filled squares) (Data from China Forestry Administration, 1982–2008).

at semi-humid sites. Heightened sensitivity of semi-arid forests to drought, coupled with especially rapid warming in semi-arid zones of Inner Asia, suggests that semi-arid forests are becoming increasingly vulnerable to warming-induced forest growth declines and mortality. Indeed, tree-ring records indicate recent growth declines at many semi-arid sites across this region, and we have documented recent tree mortality near many lower elevation xeric forest-grassland ecotones in Inner Asia.

In our study, we find that tree growth rates have generally slowed at the semi-arid sites we studied. Because some of the sites we evaluated were selected specifically for drought sensitivity (the ITRDB sites), we cannot conclude that growth is decreasing throughout all semi-arid forests. At the very least, growth is declining within relatively drought-sensitive sub-sections of semi-arid forests, and the growth declines likely are due to intensified drought stress caused by warming-induced increases in atmospheric moisture demand. Continued warming-induced intensification of drought may be expected to not only impact trees at the driest sites but also cause trees at increasingly less xeric sites to become increasingly more vulnerable to drought-induced growth declines and even mortality, potentially driving the eventual conversion of these extensive semi-arid forests to grasslands, with a variety of associated feedbacks to the Earth system.

Acknowledgments

This study was supported by grants from the National Natural Science Foundation of China (NSFC 41071124, 40711120173 and 41011120251) and the Russian Foundation of Basic Research (RFBR 13-04-91180 and 10-04-91159); CDA was supported by the US Geological Survey Climate and Land Use

Change Program, and APW was supported by LANL-LDRD and DOE-BER. We thank Y. Guo, J. Ren, and S. He for their helps in tree-ring sampling, and J. Dai for providing the Liupan Mt. raw ring-width data. The authors stated no conflict of interest.

References

- Adams HD, Guardiola-Claramonte M, Barron-Gafford GA *et al.* (2009) Temperature sensitivity of drought-induced tree mortality portends increased regional die-off under global-change-type drought. *Proceedings of National Academy of Science of the United States of America*, **106**, 7063–7066.
- Adams HD, Macalady AK, Breshears DD *et al.* (2010) Forest mortality feedbacks to the earth system under global climate change. *Eos, Transaction, American Geophysical Union*, **91**, 153–154.
- Allen CD, Makalady AK, Chenchouni H *et al.* (2010) A global overview of drought and heat-induced tree mortality reveals emerging climate change risks for forests. *Forest Ecology and Management*, **259**, 660–684.
- Breshears DD, Cobb NS, Rich PM *et al.* (2005) Regional vegetation die-off in response to global-change-type drought. *Proceedings of National Academy of Science of the United States of America*, **102**, 15144–15148.
- Breshears DD, Whicker JJ, Zou CB *et al.* (2009) A conceptual framework for dryland aeolian sediment transport along the grassland–forest continuum: effects of woody plant canopy cover and disturbance. *Geomorphology*, **105**, 28–38.
- Cai Q, Liu Y, Yang Y *et al.* (2005) Dendrochronological tables and February–March precipitation records in Huanglong, Shaanxi Province, China. *Marine Geology and Quaternary Geology*, **25**, 133–139. (in Chinese with English abstract).
- Carnicer J, Coll M, Ninyerola M *et al.* (2011) Widespread crown condition decline, food web disruption, and amplified tree mortality with increased climate change-type drought. *Proceedings of National Academy of Science of the United States of America*, **108**, 1474–1478. Available at: <http://www.pnas.org/cgi/doi/10.1073/pnas.1010070108> (accessed 10 January 2011)
- Chen Z, Sun Y, He X *et al.* (2007) Chinese pine tree ring width chronology and its relations to climatic conditions in Qianshan Mountains. *Chinese Journal of Applied Ecology*, **18**, 2191–2201. (in Chinese with English abstract).
- China Forestry Administration (1982–2008) *China Forestry Yearbook (1981 to 2007)*. China Forestry Press, Beijing, China.
- Contributors to the International Tree-Ring Data Bank. IGBP PAGES/World Data Center for Paleoclimatology, NOAA/NCDC Paleoclimatology Program. Boulder, Colorado, USA. Available at: <http://www.ncdc.noaa.gov/paleo/treerings.html> (accessed 5 April 2012)
- Cook E (1985) *A Time Series Analysis Approach to Tree Ring Standardization (Dendrochronology, Forestry, Dendroclimatology, Autoregression Process)*. University of Arizona, Tucson, AZ, USA.
- Cook E, Peters K (1997) Calculating unbiased tree-ring indices for the study of climatic and environmental change. *Holocene*, **7**, 361–370.
- Dai AG, Tremberth KE, Qian T (2004) A global dataset of Palmer Drought Severity Index for 1870–2002: relationship with soil moisture and effects of surface warming. *Journal of Hydrometeorology*, **5**, 1117–1130.
- Davi NK, Jacoby GC, D'Arrigo RD *et al.* (2009) A tree-ring-based drought index reconstruction for far-western Mongolia: 1565–2004. *International Journal of Climatology*, **29**, 1508–1514.
- Davi NK, Jacoby GC, Fang K *et al.* (2010) Reconstructing drought variability for Mongolia based on a large-scale tree ring network: 1520–1993. *Journal of Geophysical Research*, **115**, D22103. doi: 10.1029/2010JD013907
- Dulamsuren C, Hauck M, Leuschner C (2010) Recent drought stress leads to growth reductions in *Larix sibirica* in the western Khentey, Mongolia. *Global Change Biology*, **16**, 3024–3035. doi: 10.1111/j.1365-2486.2009.02147.x
- Gao G, Chen D, Xu C *et al.* (2007) Trend of estimated actual evapotranspiration over China during 1960–2002. *Journal of Geophysical Research*, **112**, D11120. doi: 10.1029/2006JD008010
- Hogg EH, Brandt JP, Michaelian M (2008) Impacts of a regional drought on the productivity, dieback, and biomass of western Canadian aspen forests. *Canadian Journal of Forestry Research*, **38**, 1373–1384.
- IPCC (2007) *Climate Change 2007: The Physical Science Basis*. Contribution of Working Group I to the Fourth Assessment Report of the Intergovernmental Panel of Climate Change, IPCC, Geneva, Switzerland.
- Kalnay E, Kanamitsu M, Kistler R *et al.* (1996) The NCEP/NCAR 40-Year Reanalysis Project. *Bulletin of the American Meteorological Society*, **77**, 437–471.
- Kaufman YJ, Tanré D, Boucher O (2002) A satellite view of aerosols in the climate system. *Nature*, **419**, 215–223.
- Kharuk VI, Ranson KJ, Im ST, Oskorbin PA, Dvinskaya ML (2013) Climate induced birch mortality in Trans-Baikal Lake region, Siberia. *Forest Ecology and Management*, **289**, 385–392.
- Li JB, Cook ER, D'Arrigo R *et al.* (2009) Moisture variability across China and Mongolia: 1951–2005. *Climate Dynamics*, **32**, 1173–1186.
- Liang EY, Liu X, Yuan Y *et al.* (2006) The 1920S drought recorded by tree rings and historical documents in the semi-arid and arid areas of northern China. *Climate Change*, **79**, 403–432.
- Liang EY, Eckstein D, Shao X (2009) Seasonal cambial activity of relict Chinese pine at the northern limit of its natural distribution in north china – exploratory results. *IAWA Journal*, **30**, 371–378.
- Liu Y, Ma L (1999) Seasonal precipitation reconstruction during the last 376 years in Hohhot region using tree-ring width. *Chinese Science Bulletin*, **44**, 1986–1991.
- Liu K, Zhang XJ (1993) *Chronology and Events of Great Forest Disasters in China Vol. 7*, (ed. Ma Z), pp. 1007–1138. Ocean Press, Beijing, China.
- Liu H, Cui H, Pott R, Speier M (2000) Vegetation of the woodland-steppe ecotone in southeastern Inner Mongolia, China. *Journal of Vegetation Science*, **11**, 525–532.
- Ma L, Liu Y, An Z (2001) ENSO events recorded by tree-ring in Qinling Mountain Range. *Marine Geology and Quaternary Geology*, **21**, 93–98. (in Chinese with English abstract).
- McDowell NG, Beerling DJ, Breshears DD, Fisher RA, Raffa KF, Stitt M (2011) The interdependence of mechanisms underlying climate-driven vegetation mortality. *Trends in Ecology & Evolution*, **26**, 523–532.
- Millennium Ecosystem Assessment (2005) *Ecosystems and Human Well-being: Desertification Synthesis*. World Resources Institute, Washington, DC.
- Mitchell TD, Jones PD (2005) An improved method of constructing a database of monthly climate observations and associated high-resolution grids. *International Journal of Climatology*, **25**, 693–712.
- Pederson GT, Gray ST, Woodhouse CA *et al.* (2011) The unusual nature of recent snowpack declines in the North American Cordillera. *Science*, **333**, 332–335. doi: 10.1126/science.1201570
- Peng C, Ma Z, Lei X (2011) A drought-induced pervasive increase in tree mortality across Canada's boreal forests. *Nature Climate Change*, **1**, 467–471. doi: 10.1038/nclimate1293
- Rienecker NM, Suarez MJ, Gelaro R *et al.* (2011) MERRA – NASA's Modern-Era Retrospective analysis for Research and Applications. *Journal of Climate*, **24**, 3624–3648.
- Rotenberg E, Yakir D (2010) Contribution of semi-arid forests to the climate system. *Science*, **327**, 451–454.
- Rudolf B, Beck C, Grieser J, Schneider U (2005) *Global Precipitation Analysis Products*. Global Precipitation Climatology Centre (GPCC), DWD, Offenbach a. M., Germany, Internet publication, 1–8.
- Savva YV, Schweingruber FH, Vaganov EA, Milyutin LI (2003) Influence of climate changes on tree-ring characteristics of Scots pine provenances in southern Siberia (forest-steppe). *IAWA Journal*, **24**, 371–383.
- Schimel DS (2010) Drylands in the earth system. *Science*, **327**, 418–419.
- Schneider U, Becker A, Meyer-Christoffer A, Ziese M, Rudolf B (2011) *Global precipitation analysis products of the GPCC*. Global Precipitation Climatology Centre (GPCC), DWD, Offenbach a. M., Germany, Internet Publication, 1–13.
- Sheffield J, Goteti G, Wood EF (2006) Development of a 50-yr high-resolution global dataset of meteorological forcing for land surface modeling. *Journal of Climate*, **19**, 3088–3111.
- Sheffield J, Andreadis KM, Wood EF (2009) Global and continental drought in the second half of the twentieth century: severity-area-duration analysis and temporal variability of large-scale events. *Journal of Climate*, **22**, 1962–1981.
- Sheffield J, Wood EF, Roderick ML (2012) Little change in global drought over the past 60 years. *Nature*, **491**, 435–438.
- Shi J, Liu Y, Cai Q *et al.* (2007) Precipitation and its variations during the last 196 years in Helan Mountain reconstructed by tree-ring. *Marine Geology and Quaternary Geology*, **44**, 95–100. (in Chinese with English abstract).
- Sidorova OV, Saurer M, Myglan VS *et al.* (2012) A multi-proxy approach for revealing recent climatic changes in the Russian Altai. *Climate Dynamics*, **38**, 175–188.
- Wang J, Li J, Chen F *et al.* (2007) Variation of the dryness in the past 200 years derived from tree-ring width records in the East Tianshan Mountains. *Journal of Glaciology and Geocryology*, **29**, 209–216. (in Chinese with English abstract).
- Wang Y, Ma Y, Zheng Y (2009a) Response of tree-ring width of *Pinus tabulaeformis* to climate factors in Luoshan Mountains of Ningxia. *Journal of Desert Research*, **29**, 971–976.

- Wang M, Dai J, Bai J, Cui H (2009b) Humidity changes since 1900 in the Liupan Mountains using tree-ring width. *Journal of Palaeogeography*, **11**, 355–360. (in Chinese with English abstract).
- Williams AP, Allen CD, Millar CI *et al.* (2010) Forest responses to increasing aridity and warmth in the southwestern United States. *Proceedings of National Academy of Science of the United States of America*, **107**, 21289–21294.
- Williams AP, Allen CD, Macalady AK *et al.* (2013) Temperature as a potent driver of regional forest-drought stress and tree mortality. *Nature Climate Change*, **3**, 292–297. doi: 10.1038/NCLIMATE1693
- Wu J, Zhao L, Zheng Y, Lü A (2012) Regional differences in the relationship between climatic factors, vegetation, land surface conditions, and dust weather in China's Beijing-Tianjin Sand Source Region. *Natural Hazards*, **62**, 31–44.
- Xu GH (1993) *Remote Sensing Studies on Renewable Resources of the "Three North Shelter Forest Belt"*. Science Press, Beijing, (in Chinese).
- Yi L, Liu Y, Song H *et al.* (2006) Summer Temperaure Variations since 1676 AD in Luya Mountain, Shanxi Province of China, inferred from Tree Rings. *Journal of Glaciology and Geocryology*, **28**, 330–336. (in Chinese with English abstract).
- Zhao F (2007) Changes in the occurrence date of forest fires in the Inner Mongolia Daxing'anling forest region under global warming. *Scientia Silvae Sinica*, **45**, 166–172. (in Chinese with English Abstract).
- Zhu H, Zheng Y, Shao X *et al.* (2008) Millennial temperature reconstruction based on tree-ring width of Qilian Juniper from Wulan, Qinghai Province, China. *Chinese Science Bulletin*, **53**, 3914–3920.

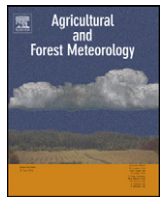
Supporting Information

Additional Supporting Information may be found in the online version of this article:

Figure S1. Various records of precipitation and T_{\max} in the study region. (a) mean annual precipitation Map of (dots) locations where tree-ring chronologies were collected. Brown and blue dots represent semi-arid and semi-humid sites, respectively.

Figure S2. Panels (a) and (b) show box plots of correlation coefficients of RWI with precipitation and daily maximum temperatures (T_{\max}) during all 3-month periods in a 24-month window that begins in the January of the year before that growing season.

Figure S3. Same as Fig. S2, but for potential evaporation (PET) from Sheffield *et al.* (2012).



Editorial

Drought threatened semi-arid ecosystems in the Inner Asia

The arid Gobi desert and its surrounding semi-arid forests and steppes in the Inner Asia, including most part of northern China, entire Mongolia and southern Siberia of Russia, constitute one of the largest drylands over the world. Ecosystems in this region are seasonally or episodically under water stress and can be particularly vulnerable to even a slight increase in water deficit. Over the past decades, Inner Asia experienced one of the planet's fastest warming, particularly in the spring, which is projected to continue in the coming decades (IPCC, 2007). Warming-induced water deficit reduces plant growth and contributes to the degradation of the semi-arid forest and grassland, which in return could change the northern hemispheric climate and environmental quality (Rotenberg and Yakir, 2010).

In this special issue, we seek to understand the climate change, its effect on both natural ecosystems, croplands in Inner Asia. To that end, a wide range of approaches, including field observation, remote sensing image interpretation, vegetation modeling, tree ring analysis, pollen analysis, were adopted. From the seven papers in this special issue, we can outline the climate trends, the effects of drought on forest, steppe, cropland ecosystems at different spatial, temporal scales.

1. Historical climate change and drought

At the millennial scale, the change from wet to dry was observed ever since ~4500 years before present in the southern part of the Inner Asia (Zhao et al., 2009). Lake sediment proxies from Anguli Nuur indicate there were three strong centennial scale drought events during 7000–6300 years before present (Yin et al., 2013). At centennial scale, historical streamflow of the Yeru River in the northcentral Mongolia reconstructed from tree-ring suggests that the 20th century was wetter than its two prior centuries, with strong heterogeneities across space and time (Pedersen, 2013). At the multi-decadal to centennial scales, a drying trend was found in the Northeast China and the southern Siberia (Dai, 2013). In north-central Mongolia, there were greater shifts in hydroclimate in the western breadbasket (the Selenge basin) than in its eastern portion (Pederson et al., 2013).

The increased drought stress can be caused by decreased precipitation and/or increased temperature. For instance, precipitation amount and seasonality as well as the frequency of heavy rainfall were the main causes for the drought in Inner Mongolia over the last three decades, which reduced ecosystem productivity (Peng et al., 2013). Similarly, temperature increase could also lead to more drought stress, particularly in spring (Mohammad et al., 2013). Interactions between changes in precipitation and air temperature

may enhance soil moisture stress and further reduce ecosystem productivity (Poulter et al., 2013).

2. Ecosystem responses to climate change

The responses of ecosystems to climate change are usually non-linear at both long- and short-term. For example, the changing dominance between forest and steppe may not linearly line up with the pace of the dominance shifts between wet and dry climates, possibly due to some strong buffering effect of non-climatic factors (Yin et al., 2013). Similarly, CO₂ fertilization effects might compensate for the negative effect of water stress at short time scale, which also implies a non-linear response of forest productivity to drought stress (Poulter et al., 2013).

Ecosystem responses to drought stress are also highly spatial heterogeneous. For instance, in Mongolia, annual tree ring growth increments are mainly limited by summer precipitation (June, July, August); but in northern China, spring precipitation (March, April, May) is more important (Poulter et al., 2013). In high altitudes or latitudes (>50°N), the impact of summer temperature becomes prominent (Mohammad et al., 2013).

In addition, semi-arid ecosystems in the Inner Asia are also highly sensitive to climate seasonality. For example, Poulter et al. (2013) found that ecosystem productivity increased in spring whereas decreased in summer. Computer simulation experiments show that re-allocating precipitation from other seasons to spring enhances annual NPP and net ecosystem production (NEP) (Peng et al., 2013). By contrast, re-allocating more precipitation to autumn decreases both annual NPP and NEP. Similarly, in consistency with the results of grassland field manipulation experiments the response of simulated NPP to the increase in the frequency of heavy rainfall days also vary a lot in different seasons (Peng et al., 2013).

3. Adaptation to future climate change

Human land use has been greatly changed in the Inner Asia during the last two decades. In China, the countrywide forestation has been implemented since 2000 (Yu et al., 2013). In contrary, Mongolia has recently entered a new agricultural era with large crop fields and center-pivot irrigation established across its “Breadbasket” in northcentral Mongolia during the last decade (Pederson et al., 2013).

Along with the continuous future warming, higher summer precipitation is also projected by IPCC climate models (Poulter et al., 2013). This change will favor agriculture activity and forestation in

this region. This kind of change, however, could be spatially and temporally heterogeneous. Future climate change in the Mongolia “breadbasket”, for example, is estimated to be wet for decades before becoming dry again (Pederson et al., 2013). In northern China, future drought stress would overwhelm the irrigation capacity of current supplies (Zhang et al., 2013). Because of the vulnerability of the arid and semi-arid ecosystems to climate change, it thus requires careful management strategies in agriculture and forest in this region to realize optimum ecosystem services such as sustainable runoff yield (Yu et al., 2013).

References

- Dai, A., 2013. Increasing drought under global warming in observations and models. *Nature Climate Change* 3, 52–58.
- IPCC, 2007. Climate Change 2007: The Physical Science Basis. Contribution of Working Group I to the Fourth Assessment Report of the Intergovernmental Panel of Climate Change. IPCC, Geneva, Switzerland.
- Mohammad, A., Wang, X., Xu, X., Peng, L., Zhang, X., Myneni, R.B., Piao, S., 2013. Drought and spring cooling induced recent decrease in vegetation growth in Inner Asia. *Agricultural and Forestry Meteorology* 178–179, 21–30.
- Pederson, N., Leland, C., Nachin, B., Hessel, A.E., Bell, A.R., Martin-Benito, D., Saladyga, T., Suran, B., Brown, P.M., Davia, N.K., 2013. Three centuries of shifting hydroclimatic regimes across the Mongolian Breadbasket. *Agricultural and Forestry Meteorology* 178–179, 10–20.
- Peng, S., Piao, S., Shen, Z., Ciais, P., Sui, Z., Chen, S., Bacour, C., Peylin, P., Chen, A., 2013. Precipitation amount, seasonality and frequency regulate carbon cycling of a semi-arid grassland ecosystem in Inner Mongolia, China: a modeling analysis. *Agricultural and Forestry Meteorology* 178–179, 46–55.
- Poulter, B., Pedersen, N., Liu, H., Zhu, Z., D'Arrigo, R., Ciais, P., Davi, N., Franke, D., Leland, C., Myneni, R.B., Piao, S., Wang, T., 2013. Recent trends in Inner Asian forest dynamics to temperature and precipitation indicate high sensitivity to climate change. *Agricultural and Forestry Meteorology* 178–179, 31–45.
- Rotenberg, E., Yakir, D., 2010. Contribution of semi-arid forests to the climate system. *Science* 5964, 451–454.
- Yin, Y., Liu, H., Liu, G., Hao, Q., Wang, H., 2013. Vegetation responses to mid-Holocene extreme drought events and subsequent long-term drought on the southeastern Inner Mongolian Plateau, China. *Agricultural and Forestry Meteorology* 178–179, 3–9.
- Yu, P., Wang, Y., Du, A., Guan, W., Feger, K.-H., Benell, M., Xiong, W., Xu, L., Zuo, H., 2013. The effect of site conditions on water yield reduction after forestation in dryland region, China. *Agricultural and Forestry Meteorology* 178–179, 66–74.
- Zhang, T., Simelton, E., Huang, Y., Shi, Y.A., 2013. Bayesian assessment of the current irrigation water supplies capacity under projected droughts for the 2030 in China. *Agricultural and Forestry Meteorology* 178–179, 56–65.
- Zhao, Y., Yu, Z., Chen, F., Zhang, J., Yang, B., 2009. Vegetation response to Holocene climate change in monsoon-influenced region of China. *Earth Science Reviews* 97, 242–256.

Hongyan Liu*

Shilong Piao

College of Urban and Environmental Sciences, Peking University, Beijing 100871, China

* Corresponding author.

E-mail address: lhy@urban.pku.edu.cn (H. Liu)

Available online 29 May 2013

Effects of Forest Age on Soil Autotrophic and Heterotrophic Respiration Differ between Evergreen and Deciduous Forests

Wei Wang^{1*}, Wenjing Zeng¹, Weile Chen¹, Yuanhe Yang³, Hui Zeng²

1 Department of Ecology, College of Urban and Environmental Sciences, and Key Laboratory for Earth Surface Processes of the Ministry of Education, Peking University, Beijing, China, **2** Shenzhen Graduate School, Key Laboratory for Urban Habitat Environmental Science and Technology, Peking University, Shenzhen, China, **3** Institute of Botany, The Chinese Academy of Sciences, Beijing, China

Abstract

We examined the effects of forest stand age on soil respiration (SR) including the heterotrophic respiration (HR) and autotrophic respiration (AR) of two forest types. We measured soil respiration and partitioned the HR and AR components across three age classes ~15, ~25, and ~35-year-old *Pinus sylvestris* var. *mongolica* (Mongolia pine) and *Larix principis-rupprechtii* (larch) in a forest-steppe ecotone, northern China (June 2006 to October 2009). We analyzed the relationship between seasonal dynamics of SR, HR, AR and soil temperature (ST), soil water content (SWC) and normalized difference vegetation index (NDVI, a plant greenness and net primary productivity indicator). Our results showed that ST and SWC were driving factors for the seasonal dynamics of SR rather than plant greenness, irrespective of stand age and forest type. For ~15-year-old stands, the seasonal dynamics of both AR and HR were dependent on ST. Higher Q_{10} of HR compared with AR occurred in larch. However, in Mongolia pine a similar Q_{10} occurred between HR and AR. With stand age, Q_{10} of both HR and AR increased in larch. For Mongolia pine, Q_{10} of HR increased with stand age, but AR showed no significant relationship with ST. As stand age increased, HR was correlated with SWC in Mongolia pine, but for larch AR correlated with SWC. The dependence of AR on NDVI occurred in ~35-year-old Mongolia pine. Our study demonstrated the importance of separating autotrophic and heterotrophic respiration components of SR when stimulating the response of soil carbon efflux to environmental changes. When estimating the response of autotrophic and heterotrophic respiration to environmental changes, the effect of forest type on age-related trends is required.

Citation: Wang W, Zeng W, Chen W, Yang Y, Zeng H (2013) Effects of Forest Age on Soil Autotrophic and Heterotrophic Respiration Differ between Evergreen and Deciduous Forests. PLoS ONE 8(11): e80937. doi:10.1371/journal.pone.0080937

Editor: Dafeng Hui, Tennessee State University, United States of America

Received: July 10, 2013; **Accepted:** October 7, 2013; **Published:** November 25, 2013

Copyright: © 2013 Wang et al. This is an open-access article distributed under the terms of the Creative Commons Attribution License, which permits unrestricted use, distribution, and reproduction in any medium, provided the original author and source are credited.

Funding: This research was supported by the National Basic Research Program of China (No. 2010CB950600 and 2013CB956303), the Projects of National Natural Science Foundation of China (No. 31222011, 31270363 and 31070428) and supported by the Foundation for Innovative Research Groups of the National Natural Science Foundation of China (No. 31021001). The funders had no role in study design, data collection and analysis, decision to publish, or preparation of the manuscript.

Competing Interests: The authors have declared that no competing interests exist.

* E-mail: wangw@urban.pku.edu.cn

Introduction

Forest soil respiration (SR) is the primary pathway where plant-fixed CO₂ is released into the atmosphere [1–3]. This occurs from the root activity and their associated mycorrhizal fungi (below-ground autotrophic respiration, AR) and from heterotrophic respiration (HR) [4,5]. Quantifying forest SR, AR and HR components and their environmental controls requires an accurate evaluation of the response of the terrestrial carbon balance to future climate changes [8–10], based on the large annual exchange of carbon between forest ecosystems and the atmosphere [6,7].

Forest age was reported to play an important role in determining the distribution of ecosystem carbon pools, fluxes and carbon sequestration [11–13]. Forest stands of various ages evolve with different abiotic and biotic environments that can differentially respond to environmental changes [14]. Older stands accumulate aboveground litter and root inputs, possibly decreasing HR and increasing AR [15]. Soil carbon dynamics may become more complex with increasing stand age [16]. For instance, the Great Lakes forest chronosequence showed that

changes in soil carbon stocks across different aged stands had different patterns, with old-growth stands accumulating carbon in the deep soil layers, but not surface soils [16]. Our limited knowledge in forest succession and carbon cycles has resulted in few large-scale ecosystem carbon models accounting for the change of forest metabolic rates with age [17]. To model the long-term forest carbon dynamics and its coupling with the climate system, we need to understand the response of forest ecosystems to the changing climate, including the role of stand age and the successional status on carbon dynamics [16].

Previous studies on the effect of stand age on forest carbon efflux focused on the measurements of total SR in a single forest type. Researchers have observed that total SR increased [18,19], decreased [15,20], was similar [21,22] or responded non-linearly [23,24] with forest age. However, the effect of forest age on SR may depend on the forest type [25]. For instance, deciduous forests are time-limited each year to photosynthesize and allocate carbon to storage and reproduction compared with evergreen forests [26]. These physiological and phenological differences between deciduous and evergreen forests [27] may modulate the SR response

across different aged stands to environmental changes. Additionally, AR and HR may respond differently to environmental changes [28]. AR is strongly influenced by photosynthetic activity compared with HR [28,29,30,31]. Therefore, the ratio of AR and HR (of total SR) will modulate the response of SR across different aged stands to environmental changes [32,33]. For instance, Jassal *et al.* (2012) observed that SR in younger stands (~21 years) was more responsive to soil temperature (ST) and soil water content (SWC) compared with older stands (~60 years) [34]. We measured SR and partitioned the HR and AR components across three age classes (~15, ~25, and ~35 years) for the evergreen species, *Pinus sylvestris* var. *mongolica* (Mongolia pine) and the deciduous species, *Larix principis-rupprechtii* (larch) from June 2006 to October 2009 in a forest-steppe ecotone, northern China. We analyzed the relationships between SR, HR, AR and ST, SWC and NDVI (normalized difference vegetation index, indicative of plant greenness and net primary productivity). Our objective was to determine if forest type modulated the seasonal dynamics of SR and the AR and HR components and their responses to ST, SWC and NDVI across different aged stands. We tested the following hypotheses: (1) ST, SWC and NDVI will have significant effects on the seasonal dynamics of SR across varied aged stands, irrespective of forest type. This was based on the findings that SR depended on ST, SWC [35,36] and primary productivity [29,37]; (2) HR is more sensitive to ST and SWC than AR, irrespective of forest type. AR is controlled by NDVI, depending on stand age and forest type. The dependence of AR on NDVI was expected to decrease with stand age, because of the perennial life cycle, long carbon transport pathways and high storage capacity in older trees. However, AR dependence on NDVI may increase from deciduous to evergreen forest because of the greater dependence on seasonal accumulation and consumption of stored carbon in deciduous rather than evergreen forest [38].

Materials and Methods

Ethics Statement

The administration of the Saihanba Forestry Center gave permission for this research at each study site. We confirm that the field studies did not involve endangered or protected species.

Site description

The study was conducted at Saihanba Forestry Center, Hebei Province, northern China (117°12'–117°30' E, 42°10'–42°50' N, 1400 m a.s.l.) adjacent to the Beijing-Tianjin region. Our study site lay within a typical forest-steppe ecotone in a temperate region. The climate is semi-arid, semi-humid, with long cold winters (November to March) and a short spring and summer. The annual mean air temperature and precipitation from 1964 to 2004 were -1.4°C and 450.1 mm, respectively. The soils are predominantly sandy, accompanied by meadow and marsh-type. The soil has low nutrient content with the organic carbon levels at 0.71–1.88% and total nitrogen at 0.08–0.19%. The bulk density ranged from 0.74 to 1.06 g cm^{-3} with litter and fine root biomass increasing with stand age (Table 1). Primary forests were harvested using large-scale industrial logging techniques in the late 1900s. This area has been threatened from sandstorm since the 1950s. Consequently, the China Forestry Administration proposed the establishment of a large plantation in Saihanba to ensure the environmental safety of the Beijing-Tianjin region. Saihanba forestry was established in 1962 with the plantation now 94,700 hm^2 , covering 76.8% of the area. This project has been the largest one in China with *P. sylvestris* var. *mongolica* (Mongolia pine) and *L. principis-rupprechtii* (larch) the most dominant species.

Table 1. Site characteristics of the six forest stands in this study.

Forest stands	Stand age (years)	Tree height (m)	DBH (cm)	Slope/aspect	Elevation (a.s.l.)	Soil texture	Tree density (stem ha^{-1})	SOC (%)	STN (%)	SBD (g cm^{-3})	LFB (g m^{-2})	FRB (g m^{-2})
<i>Larix principis-rupprechtii</i>	~15	3.34	3.1	0°/-	1582	Sandy soil	1900	0.94	0.09	1.06	1360	191
	~25	9.47	11.1	0°/-	1560	Sandy soil	2133	0.95	0.10	0.88	2207	198
	~35	15.67	21.4	0°/-	1500	Sandy soil	1825	1.88	0.18	0.74	3412	220
<i>Pinus sylvestris</i> var. <i>mongolica</i>	~15	2.70	4.3	1°/5	1509	Sandy soil	1800	0.71	0.08	0.98	1335	344
	~25	8.02	12.0	2°/5	1519	Sandy soil	2010	1.27	0.13	0.83	2798	483
	~35	14.70	20.7	1°/5	1502	Sandy soil	1760	1.60	0.19	0.85	2899	496

DBH = Diameter at Breast Height (1.3 m); NDVI = Normalized Difference Vegetation Index; SOC = Soil Organic Carbon; STN = Soil Total Nitrogen; SBD = Soil Bulk Density; LFB = Litter Floor Biomass; FRB = Fine Root Biomass. doi:10.1371/journal.pone.0080937.t001

Experimental design

To assess the effects of forest age on soil respiration (SR), autotrophic respiration (AR) and heterotrophic respiration (HR) across different forest types, we selected six stands with the same planting density (4995 stem/ha), including three age classes of Mongolia pine and larch. These were pure plantations established on former meadow grassland dominated by *Leymus chinensis*. In combination, these stands made up a chronosequence from 15 to 35 years old, with the oldest stand ready for intermediate cutting. Neither fertilization nor drainage works had been carried out since tree establishment in any of the stands. Moreover, the topography at all six stands is predominantly flat with a similar slope, position and elevation (Table 1). The selected Mongolia pine plantation has a stand area of 1.25 ha (15 years old), 5 ha (25 years old) and 10.14 ha (35 years old). The selected larch plantation had a stand area of 1.05 ha (15 years old), 3.67 ha (25 years old) and 5.11 ha (35 years old). The locations of the stands with different stand ages are shown in Figure 1. Detailed stand information is shown in Table 1. For each stand, three replicate plots were arranged in an area of 20 m×20 m. Five subsamples (i.e. SR collars) were randomly arranged in each plot. The distance between any two stands was ≤10 km, avoiding differences in climate and soil type. Stand age was obtained from forest management records and from core samples using an increment borer. Similar climate and soil properties among these stands create an ideal chronosequence to study age effects on soil carbon efflux.

Soil respiration (SR), soil temperature (ST) and water content (SWC)

SR was measured from June 2006 to October 2009 using a Li-8100 soil CO₂ flux system (LI-COR Inc., Lincoln, NE, USA). During the growing season, five polyvinyl chloride (PVC) collars (10 cm inside diameter, 6 cm height) were inserted 3 cm into the soil in each plot and left *in situ* throughout the study. The five PVC collars were placed in each plot, one in each of the four corners and the fifth in the middle. Live plants inside the collars were clipped at the soil surface 1 day before each measurement. SR was measured every 15–20 days. To minimize the daily variation in

SR and represent the daily mean, measurements were made between 0800 and 1100 h [39,40]. For each measurement, the respiration rate was calculated as the mean of three plots per stand. During winter, longer soil collars (determined by snow depth, commonly >30 cm) were inserted into the soil surface and stabilized for 24 h before the SR measurement [41,42]. The duration of winter at our site was 5 months from November to late March with near consistent, continuous mean daily soil temperature <0.5°C at 5 cm [43]. The Li-8100 soil CO₂ flux system was kept in an isolated/heated container to maintain the temperature above freezing. Winter SR was measured monthly except in February.

During respiration measurements, ST was recorded in each collar at 5 cm soil depth with the Li-8100 temperature probe. Continuous measurements of ST were recorded at 30-min intervals with StowAway loggers (Onset Comp. Corp., Bourne, MA, USA) inserted in the soil at each site. SWC at 0–10 cm was measured inside the collars using time domain reflectometry (Soil moisture Equipment Corp., Santa Barbara, CA, USA). No data for SWC were obtained during the winter because the probe could not be fully inserted into the frozen soil.

Harmonic analysis of time-series AVHRR normalized difference vegetation index (NDVI) dataset

NDVI is derived from the red: near-infrared reflectance ratio:

$$NDVI = \frac{(NIR - VIS)}{(NIR + VIS)} \quad (1)$$

where NIR and VIS represent the spectral reflectance measurements acquired in the near-infrared and visible (red) regions, respectively [44]. Due to their large areas, uniform distribution and sparse understory of both Mongolia pine and larch plantations, the NDVI of 16-Day L3Global 250 m product (MOD13 Q1) could well represent our plot measurements. We acquired the data from June 2006 to October 2009 using the website <https://wist.echo.nasa.gov/api>.

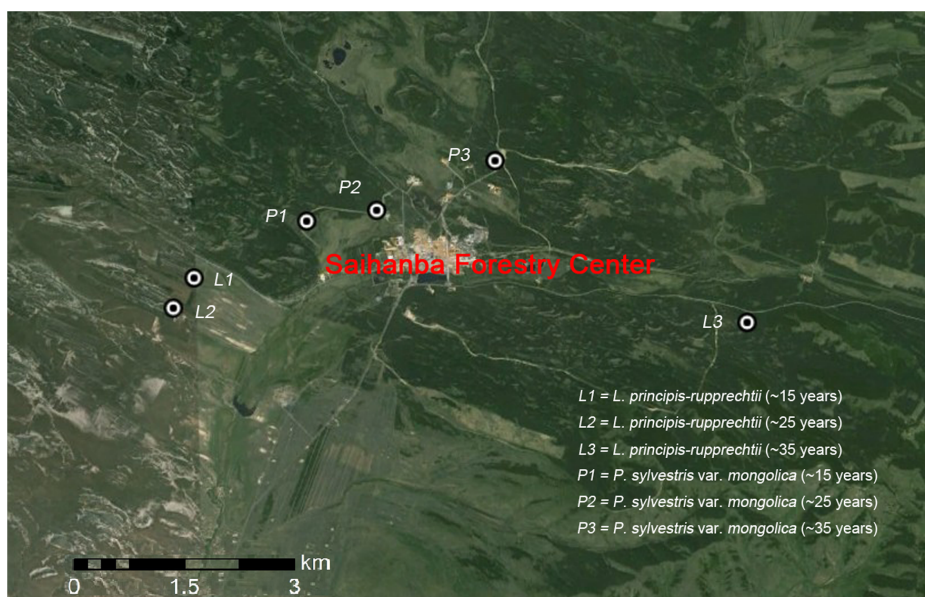


Figure 1. Location of sites showing different aged stands.
doi:10.1371/journal.pone.0080937.g001

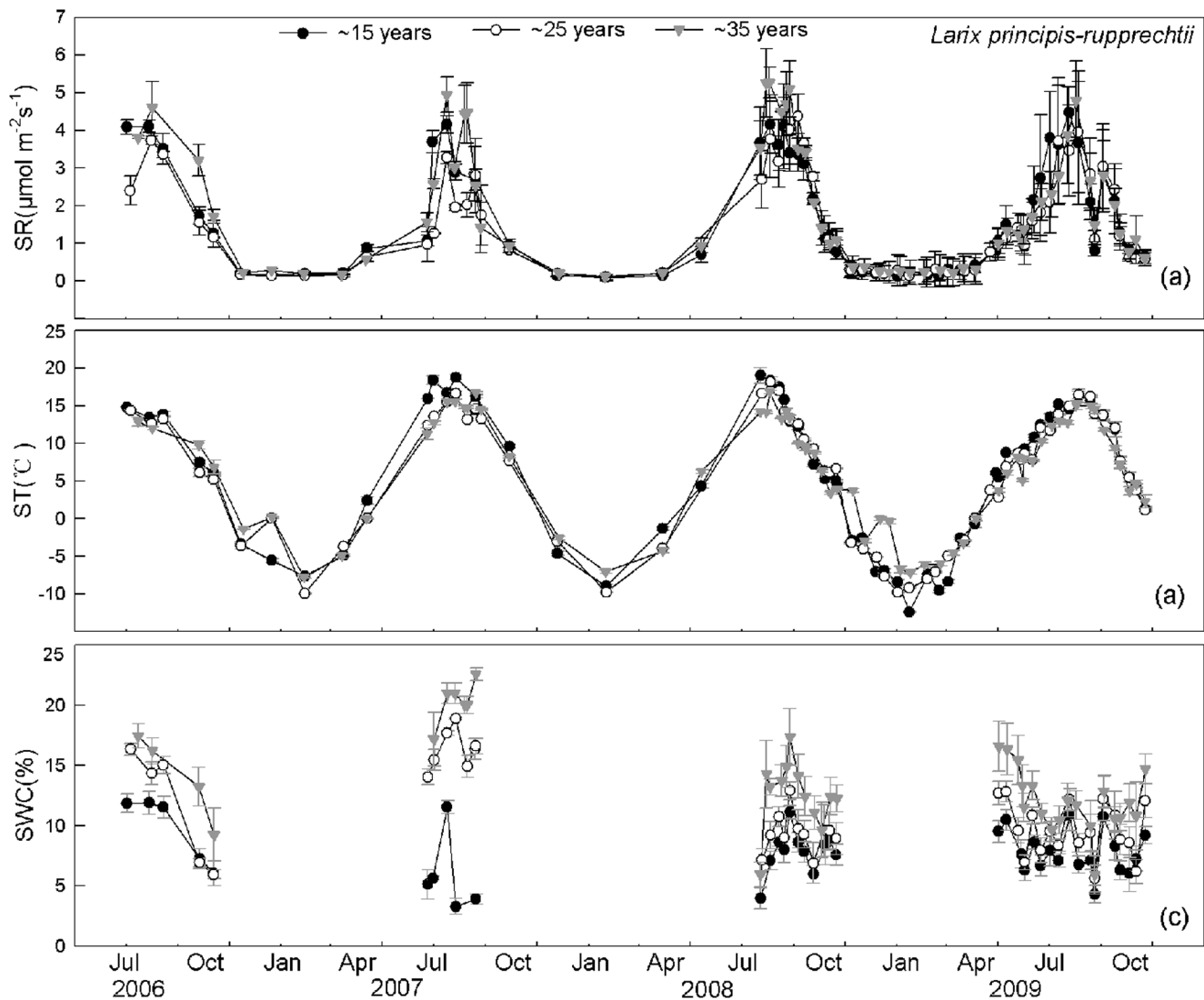


Figure 2. Seasonal changes of soil respiration (SR) and environmental factors across three stand ages of *Larix principis-rupprechtii*. SR (a), soil temperature at 5 cm depth (ST) (b) and soil water content at 10 cm depth (SWC) (c) are shown from June 2006 to October 2009. doi:10.1371/journal.pone.0080937.g002

Harmonic (Fourier) analysis was used to remove the excess noise remaining in the NDVI time-series from satellite-borne data sources and to obtain reasonably smooth continuous daily data [45]. The Fourier series analysis decomposes a signal into an infinite series of harmonic components. Each of these components is composed initially of a sine wave and a cosine wave of equal integer frequency. These two waves are then combined into a single cosine wave with a characteristic amplitude (size of the wave) and phase angle (offset of the wave) [46,47].

Heterotrophic respiration (HR) and autotrophic respiration (AR)

To detect the response of HR and AR to environmental changes, five additional soil collars per plot were placed with deep PVC collars (80 cm² and 70 cm deep) in October 2006. The 70-cm-long PVC collars isolated old plant roots, preventing new roots from growing inside the collars. This method has been successfully applied in various ecosystems to separate HR from the total SR [48–50].

To examine the transient response of dead root decomposition, we commenced the CO₂ efflux measurements above the PVC tubes immediately after installation. The interference of installation was eliminated after 1.5 years (from 2006) with the soil CO₂ efflux measured at the stands believed to represent HR. AR was calculated as the difference between SR and HR.

SR, its HR and AR components and their relationships with ST, SWC and NDVI

We examined the relationships between SR, HR, AR and ST by fitting exponential functions to the data from each stand using the following equation:

$$R = R_0 e^{\beta t} \quad (2)$$

where R is observed SR (plot-wide averages measured periodically throughout the year), t is the concurrent ST (5 cm depth), with R_0 being the basal respiration at temperature of 0°C and β the fitted parameters obtained using least squares nonlinear regression with

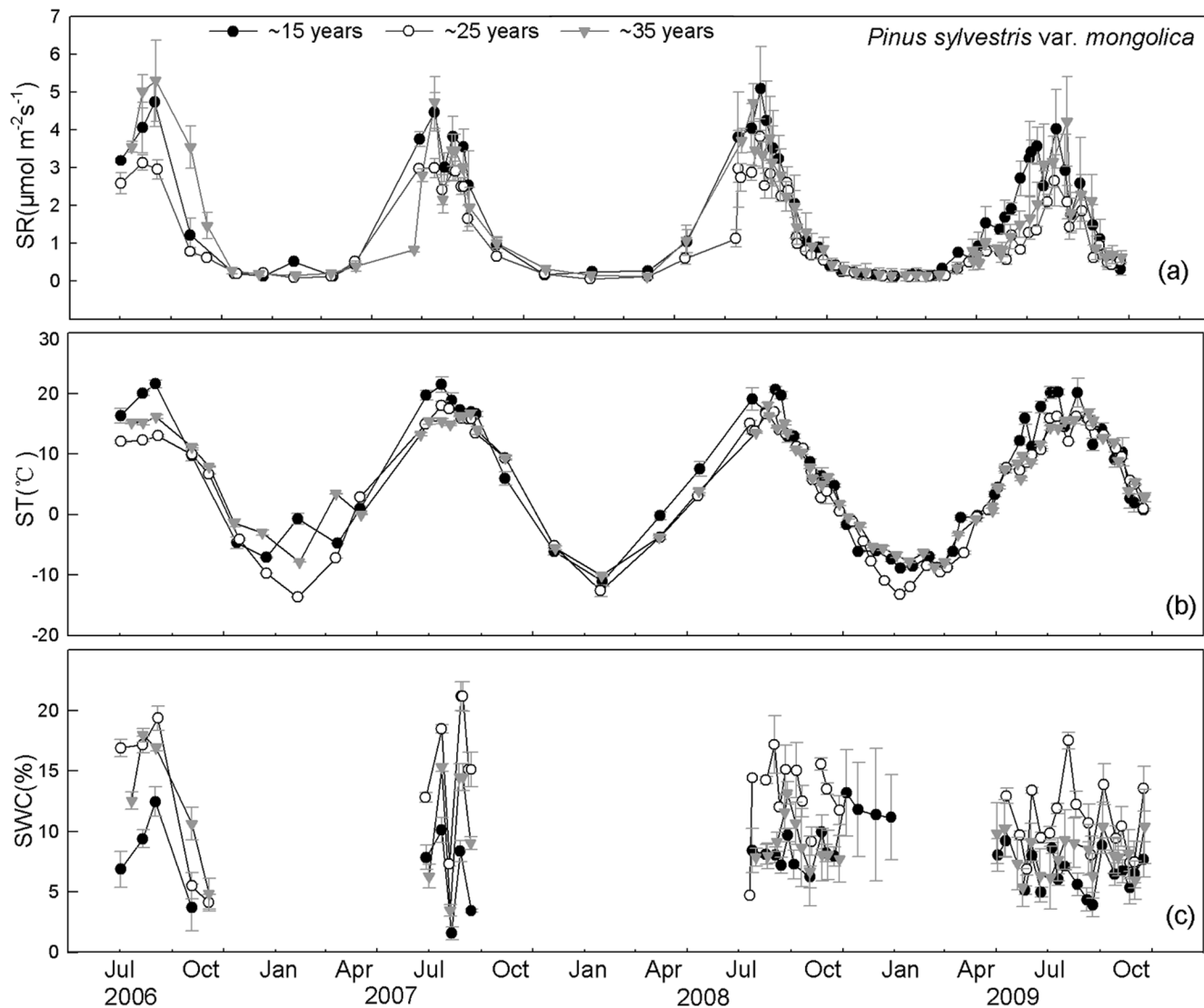


Figure 3. Seasonal changes of soil respiration (SR) and environmental factors across three stand ages of *Pinus sylvestris*. SR (a), soil temperature at 5 cm depth (ST) (b) and soil water content at 10 cm depth (SWC) (c) are shown from June 2006 to October 2009. doi:10.1371/journal.pone.0080937.g003

SigmaPlot V. 8.02. The β values were used to calculate apparent Q_{10} values, which describes the change in respiration rate over a 10°C increase in t using:

$$Q_{10} = e^{10\beta} \quad (3)$$

In addition, we calculated R_{15} , the respiration values at a reference temperature of 15°C (without stimulation introduced by photosynthetic activity and without water limitations) [51] according to equation 4, using a Q_{10} coefficient calculated from equation (3). To remove the effect of ST, we examined the relationships between R_{15} and SWC and NDVI.

$$R_{15} = RQ_{10}^{(15-T)/10} \quad (4)$$

where R_{15} is the respiration flux at a constant temperature of 15°C , R the measured respiration rate, Q_{10} from equation (3) and T the ST at a 5 cm depth.

Statistical analysis

To evaluate if SR, HR and AR significantly differed among different aged stands, forest type and measurement time, we used a three-way ANOVA. The relationships between SR, HR, AR and ST, SWC and NDVI were examined using regression analysis. All statistical analyses were performed with a significance level of 0.05 using SPSS (2009, ver. 18.0, SPSS Inc., Chicago, IL, USA).

Results

Seasonal dynamics of soil respiration (SR)

SR was significantly different among the different time measurements, irrespective of stand age and forest type (Table 2). SR was higher in summer and lower in winter, following the seasonal dynamics of ST, irrespective of stand age and forest type (Figs. 2, 3). Across different aged stands, the seasonal dynamics of SR were exponentially related to ST, possibly explaining the 88%–89% and 89%–95% variation in SR for larch and Mongolia pine, respectively (means for 4 years' measurements, Table 3). Apparent Q_{10} of SR across three stand ages ranged from 3.49–

Table 2. Results of the three-way ANOVA with soil respiration (SR), heterotrophic respiration (HR) and autotrophic respiration (AR) as the response variables respectively, and stand age (~15 years, ~25 years and ~35 years for SR, ~15 years and ~35 years for HR and AR), forest type (*Larix principis* vs. *Pinus sylvestris*) and measurement time (from June 2006 to October 2009 for SR, from August 2008 to August 2009 for HR and AR) as factors.

Factor	SR				HR				AR						
	d.f.	Type III SS	Mean square	F	P	d.f.	Type III SS	Mean square	F	P	d.f.	Type III SS	Mean square	F	P
stand age	2	11.872	5.936	2.975	0.052	1	0.351	0.351	0.426	0.516	1	0.418	0.418	1.258	0.266
forest type	1	0.423	0.423	0.212	0.646	1	0.774	0.774	0.94	0.336	1	5.047	5.047	15.192	<0.01
time	3	34.367	11.456	5.741	<0.01	1	3.469	3.469	4.211	<0.05	1	1.289	1.289	3.879	0.053
stand age × forest type	2	2.071	1.035	0.519	0.596	1	0.012	0.012	0.015	0.904	1	2.344	2.344	7.056	<0.01
stand age × time	6	4.808	0.801	0.402	0.878	1	1.202	1.202	1.459	0.231	1	0.338	0.338	1.017	0.317
forest type × time	3	3.716	1.239	0.621	0.602	1	0.064	0.064	0.078	0.781	1	1.336	1.336	4.021	<0.05
stand age × forest type × time	6	2.39	0.398	0.2	0.977	1	0.771	0.771	0.935	0.337	1	0.11	0.11	0.332	0.567

The data in ~25-year-old stands were absent because of the artificially damaged collars for separating AR and HR during the experiments.
doi:10.1371/journal.pone.0080937.t002

Table 3. Q_{10} of soil respiration (SR), basal respiration rate (R_0) and determination coefficient of exponential relationships between SR and soil temperature (ST), using $SR = R_0 \times e^{\beta T}$. L1, L2, L3 are ~15 years, ~25 years and ~35 years *Larix principis* stand, respectively.

	2006				2007				2008				2009				Mean values for 4 years			
	R ₀	β	Q ₁₀	R ²	R ₀	β	Q ₁₀	R ²	R ₀	β	Q ₁₀	R ²	R ₀	β	Q ₁₀	R ²	R ₀	β	Q ₁₀	R ²
L1	0.40	0.17	5.37	0.99	0.39	0.11	3.06	0.90	0.43	0.14	4.06	0.91	0.48	0.12	3.25	0.90	0.45	0.13	3.53	0.89
L2	0.29	0.18	6.30	0.87	0.37	0.12	3.22	0.91	0.49	0.14	3.97	0.94	0.50	0.11	3.10	0.90	0.45	0.13	3.49	0.88
L3	0.31	0.22	8.94	0.98	0.40	0.14	3.86	0.91	0.41	0.18	5.87	0.92	0.52	0.13	3.56	0.93	0.46	0.15	4.31	0.89
P1	0.35	0.13	3.49	1.00	0.38	0.12	3.35	0.97	0.50	0.12	3.25	0.94	0.42	0.11	3.10	0.95	0.43	0.12	3.19	0.95
P2	0.45	0.12	3.39	0.85	0.37	0.12	3.29	0.97	0.46	0.12	3.46	0.91	0.35	0.10	2.72	0.91	0.40	0.11	3.10	0.89
P3	0.36	0.17	5.53	0.98	0.38	0.12	3.39	0.85	0.50	0.14	3.94	0.94	0.39	0.12	3.35	0.94	0.42	0.13	3.67	0.90

P1, P2, P3 are ~15 years, ~25 years and ~35 years *Pinus sylvestris* stand, respectively.
doi:10.1371/journal.pone.0080937.t003

P1, P2, P3 are ~15 years, ~25 years and ~35 years *Pinus sylvestris* stand, respectively.

doi:10.1371/journal.pone.0080937.t003

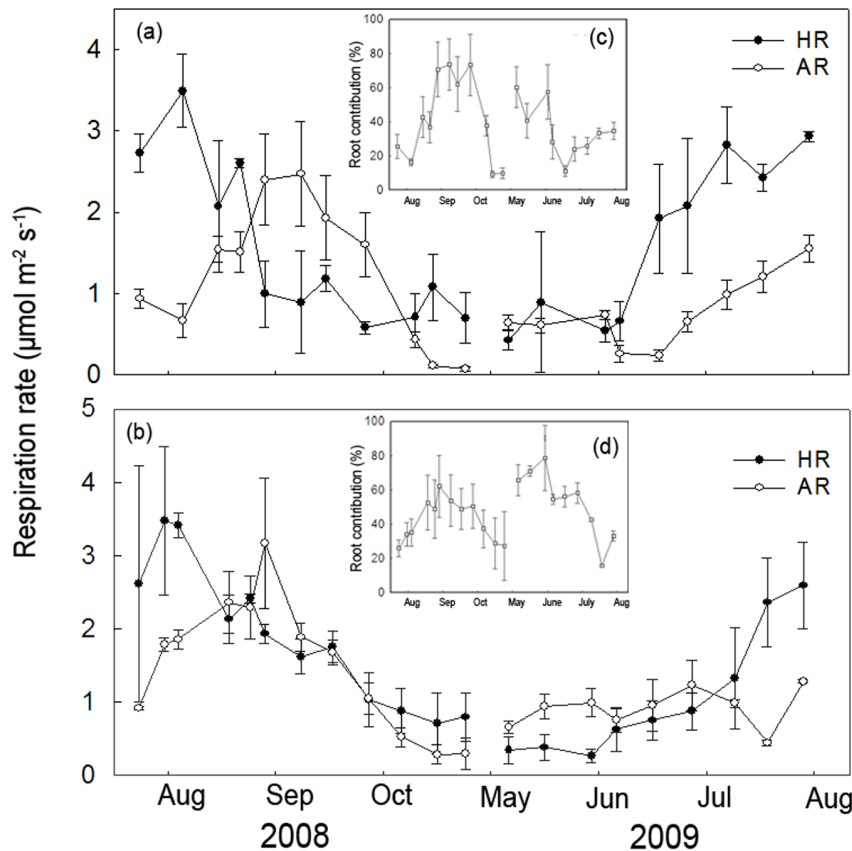


Figure 4. Seasonal changes in autotrophic and heterotrophic components of soil respiration (SR) for different aged stands of *Larix principis*. Autotrophic respiration (AR) and heterotrophic respiration (HR) in ~15-year-old (a) and ~35-year-old stands (b) are shown from August 2008 to August 2009. Seasonal changes in the contribution of AR to SR are shown in inserted figures for ~15-year-old (c) and ~35-year-old (d) stands. The data in the ~25-year-old stand were absent because of the artificially damaged collars for separating AR and HR during the experiments. doi:10.1371/journal.pone.0080937.g004

4.31 and 3.10–3.67 for larch and Mongolia pine, respectively (means of 4 years' measurements, Table 3). Apparent Q_{10} of ~35-year-old stand was significantly higher compared with ~15 and ~25-year-old stands, irrespective of forest type (Table 3). Soil basal respiration (R_0) was similar across three stand ages of both forest types (Table 3).

SR_{15} showed no significant relationship with NDVI, irrespective of forest age and type ($P > 0.05$ for all stands, Fig. S1). Conversely, a significant correlation was found between SR_{15} and SWC, which could explain the variation of 15%–26% and 10%–33% variation for larch and Mongolia pine, respectively (Fig. S2).

Seasonal dynamics of heterotrophic respiration (HR) and autotrophic respiration (AR)

HR was significantly different among different time measurements, irrespective of stand age and forest type (Table 2). The seasonal dynamics of HR were similar across different aged stands, showing higher values in summer and lower in spring and autumn (Figs. 4, 5). However, AR showed a more variable pattern. For larch, maximal AR occurred in early September with minimal values in late October, irrespective of stand age (Fig. 4a, 4b). The contribution of AR to total SR ranged from 9%–74% and 16%–79% (~15 and ~35-year-old-stands, respectively; Fig. 4c and d). HR, AR and the contribution of AR to total SR showed no significant differences between ~15 and ~35-year-old larch ($P > 0.05$ for all the comparisons, Table 2). For Mongolia pine,

AR peaked in early August and late August (~15 and ~35-year-old-stands, respectively), with minimum AR in late October for both stands (Fig. 5a, 5b). The contribution of AR to total SR ranged from 16%–63% (Fig. 5c) for ~15 and 8%–79% for ~35-year-old stands (Fig. 5d). AR and the contribution of AR to total SR was significantly lower in the ~35 compared with ~15-year-old stand (39% vs. 22%; $P < 0.05$). HR showed no significant differences between the two stands ($P > 0.05$, Table 2). AR was significantly different between the two forest types, with a significant interaction effect among forest type, stand age and measurement time (Table 2).

The seasonal dynamics of AR and HR were dependent on ST in the ~15-year-old stand, which could explain the 22% and 69% variation in AR and HR, respectively for larch (Fig. 6a–6d). Additionally, this could explain the 68% and 61% variation in AR and HR (respectively) for Mongolia pine (Fig. 7a–7d). We found a higher Q_{10} for HR compared with AR in larch (3.85 vs. 2.98). In contrast, Mongolia pine showed a similar Q_{10} for HR compared with AR (2.61 vs. 2.76). As the stand age increased, the Q_{10} of both HR (3.85, ~15-year-old vs. 5.07, ~35-year-old) and AR (2.98, ~15-year-old vs. 3.23, ~35 years) increased in larch (Fig. 5a, 5b). For Mongolia pine, the Q_{10} of HR increased (2.61, ~15-year-old vs. 2.71, ~35-year-old), but AR showed no significant relationship with ST in ~35-year-old stand (Fig. 7e). In ~15-year-old stand, neither HR nor AR was controlled by SWC, irrespective of forest type. As stand age increased, HR correlated with SWC in Mongolia pine (Fig. 7f). In contrast, larch AR was significantly

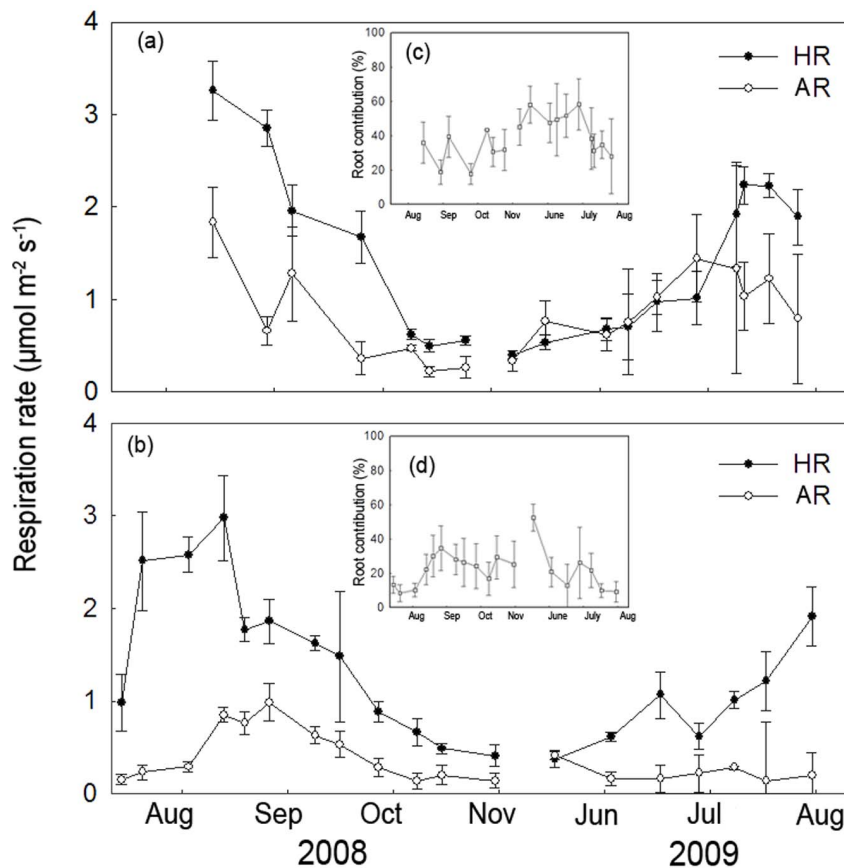


Figure 5. Seasonal changes in autotrophic and heterotrophic components of soil respiration (SR) for different aged stands of *Pinus sylvestris*. Autotrophic respiration (AR) and heterotrophic respiration (HR) in ~15-year-old (a) and ~35-year-old stands (b) are shown from August 2008 to August 2009. Seasonal changes in the contribution of AR to SR are shown in inserted figures for ~15-year-old (c) and ~35-year-old (d) stands. The data in the ~25-year-old stand were absent because of the artificially damaged collars for separating AR and HR during the experiments. doi:10.1371/journal.pone.0080937.g005

related with SWC ($P < 0.01$, Fig. 6g). The dependence of AR on NDVI only occurred in ~35-year-old Mongolia pine (Fig. 6d, 6h, Fig. 7d, 7h).

Discussion

Drivers of seasonal dynamics for soil respiration (SR)

We hypothesized (1) that ST, SWC and NDVI will impose significant effects on the seasonal dynamics of SR across different aged stands, irrespective of forest type. However, we found that the seasonal dynamics of SR were principally driven by ST and SWC, not by NDVI, across different aged stands, irrespective of forest type. Forest SR is closely related to gross primary productivity (GPP) and leaf area index (LAI) [52,53], suggesting a coupling between the CO_2 assimilation in the forest canopy and CO_2 released from the soil. NDVI has shown a close correlation with GPP [54,55] and LAI [56]. As a convenient proxy for productivity, NDVI was expected to be positively associated with AR because of the dependence on photosynthesis [52]. We expected a positive relationship between SR and NDVI based on the higher contribution of AR to SR (Figs. 4, 5). We found strong positive relationships between SR and NDVI (Fig. S3); however, these relationships disappeared when we used R_{15} for both forest types across three different aged stands (Fig. S1). These results imply that the correlation between SR and NDVI may occur because of the significant relationship between ST and NDVI (Fig.

S4). Our results emphasized the significance of ST and SWC on simulating total SR for both forest types across different aged stands. Our results were inconsistent with recent evidence showing that SR was closely related to canopy photosynthesis at various timescales [57,58]. The discrepancies may occur because NDVI measures integrated past photosynthetic activity rather than present photosynthetic activity [59]. In addition, differences may have occurred because the seasonal change in foliar photosynthetic capacity and NDVI are not necessarily coincidence [53]. Moreover, the temporal dynamics of SR were reported to lag behind those of NDVI [33,60], so our monthly SR measurements may not reflect the real relationship between these two variables. Therefore, high-frequency measurements should be conducted to explore the control of temporal dynamics in SR.

Drivers of seasonal dynamics of heterotrophic respiration (HR) and autotrophic respiration (AR)

In our second hypothesis, we expected greater sensitivity in HR to variation in ST compared with AR. However, we observed a mixed result. In ~15-year-old stand, we found a higher Q_{10} for HR compared with AR in larch and a similar Q_{10} for AR with HR in Mongolia pine (Fig. 6a, 7a). The lower Q_{10} of AR compared with HR in larch may be attributed to differing plant physiology and phenology in Mongolia pine. Deciduous trees are time-limited each year to photosynthesize, allocating more carbon for aboveground growth during summer when ST is highest [26].

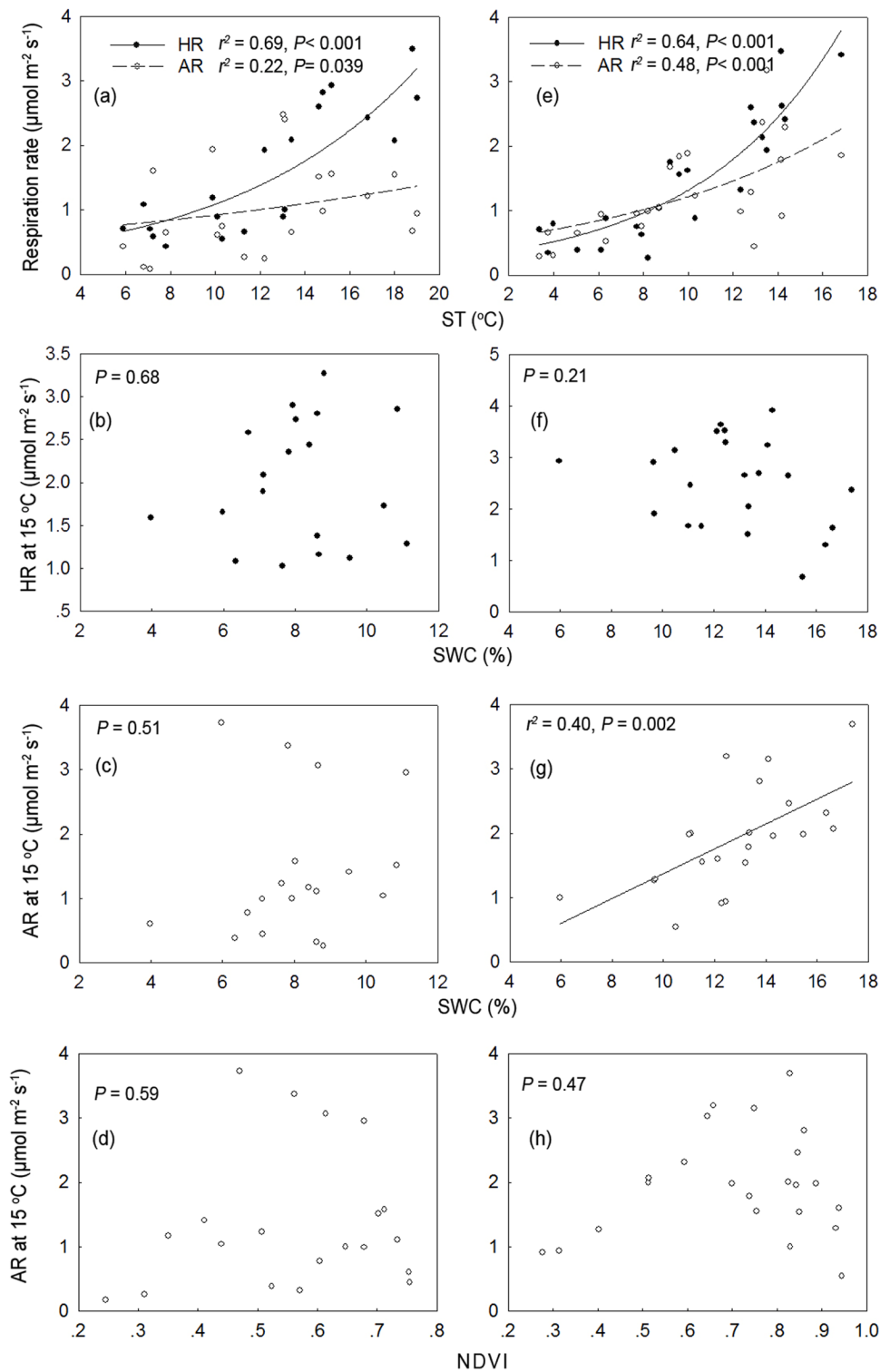


Figure 6. Relationships between autotrophic respiration (AR) and heterotrophic respiration (HR) and environmental factors across different aged stands of *Larix principis*. The relationships are shown between autotrophic respiration (AR) and heterotrophic respiration (HR) and soil temperature (ST) for ~15-year-old (a), ~35-year-old stands (e), between soil water content (SWC) and HR₁₅ for ~15-year-old (b), ~35-year-old stands (f), between SWC and AR₁₅ for ~15-year-old (c) and ~35-year-old stands (g), and between NDVI and AR₁₅ for ~15-year-old (d), and ~35-year-old (h) stands of *Larix principis*. The data in the ~25-year-old stand were absent because of the artificially damaged collars for separating AR and HR during the experiments.

doi:10.1371/journal.pone.0080937.g006

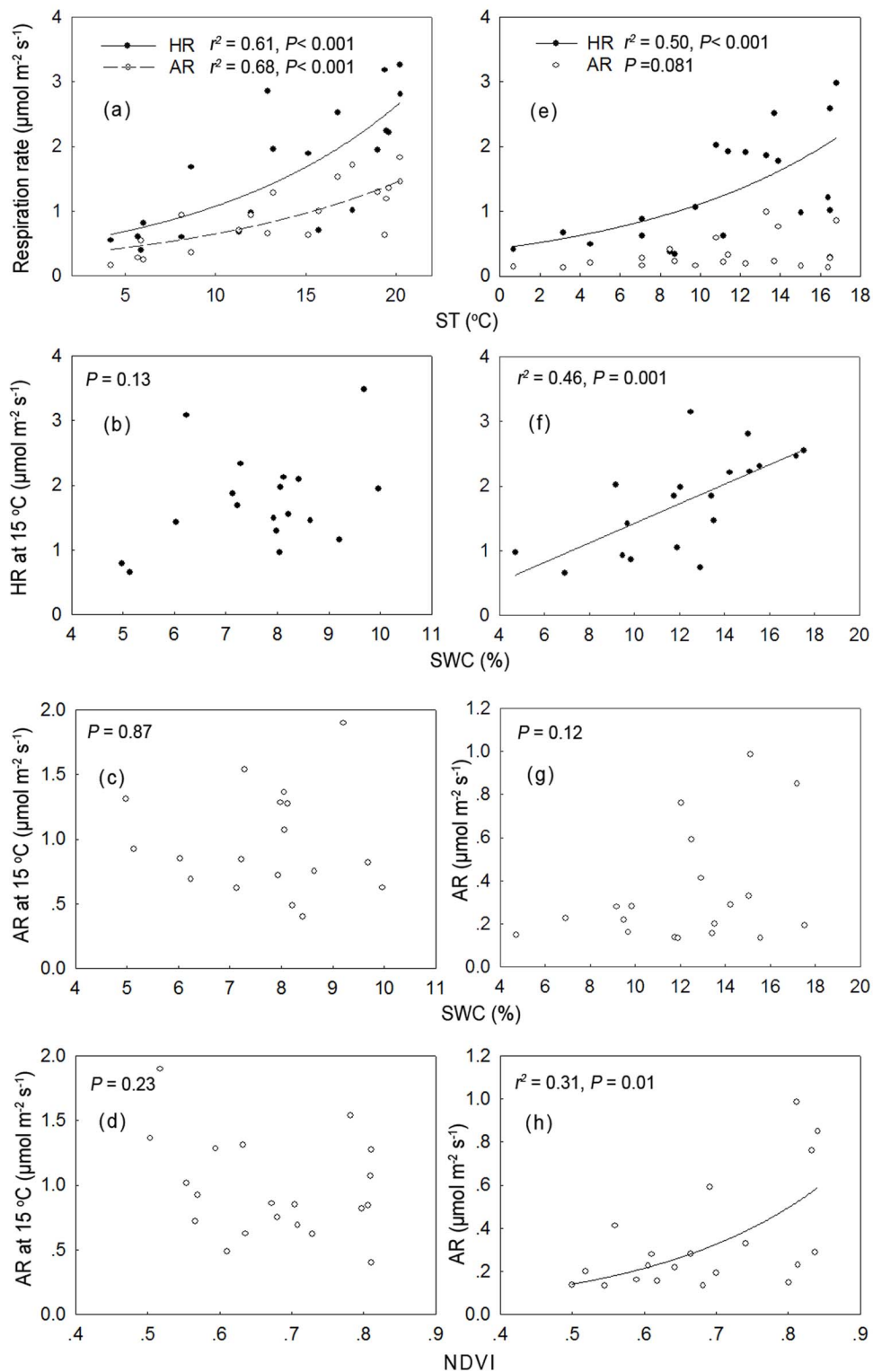


Figure 7. Relationships between autotrophic respiration (AR) and heterotrophic respiration (HR) and environmental factors across different aged stands of *Pinus sylvestris*. The relationships are shown between autotrophic respiration (AR) and heterotrophic respiration (HR) and soil temperature (ST) for ~15-year-old (a), ~35-year-old stands (e), between soil water content (SWC) and HR₁₅ for ~15 years (b) and ~35 years (f); between SWC and AR₁₅ for ~15-year-old (c) and ~35-year-old stands (g); between NDVI and AR₁₅ for ~15-year-old stand (d), and between NDVI and AR for ~35-year-old stands (h) of *Pinus sylvestris*. The data in the ~25-year-old stand were absent because of the artificially damaged collars for separating AR and HR during the experiments.

doi:10.1371/journal.pone.0080937.g007

Furthermore, peak root growth commonly occurs in spring and autumn for coniferous forests [61,62]. We observed the contribution of AR to total SR was higher in spring and autumn for larch. Therefore, the seasonal dynamics of AR in larch may be connected with those of root growth, resulting in lower Q_{10} of AR compared with HR. In contrast, Mongolia pine can photosynthesize year-round with little investment required in highly efficient photosynthetic activity. Consequently, the dynamics of AR in Mongolia pine stands may be associated with higher metabolic demand during leaf production [63]. We also found maximal AR in early summer in Mongolia pine (Fig. 5a), which was consistent with Lee *et al.* (2010), who observed maximal contribution of AR to total SR in summer for evergreen forest and in autumn for deciduous forest [64].

According to our second hypothesis, we expected that the seasonal dynamics of AR were more dependent on NDVI rather than HR. However, we found that AR was significantly affected by NDVI only in ~35-year-old Mongolia pine (Fig. 7h). We did not observe a significant relationship between AR and NDVI in larch, possibly because of greater carbon allocation in deciduous forest to storage and reproductive functions compared with evergreen forests [26]. The relationship between AR and NDVI in deciduous trees was more dependent on seasonal accumulation and consumption of stored C compared with evergreen trees [65]. The absence of a significant relationship in ~15-year-old Mongolia pine stand may be attributed to the soil water deficit, inducing a selection pressure favoring trees presenting high storage capability for reserve compounds to combat this stress [66,67]. Moreover, the carbon balance between growth and storage remained constant between age classes in evergreen forest [26]. Our results suggested that the correlation between AR and NDVI was dependent upon stand age, and this stand age-related effect was forest type-dependent.

We expected a higher dependence of HR on SWC compared with AR because AR was reported as less responsive to water variability compared with HR [68,69]. However, we found in ~15-year-old stand that neither HR nor AR was controlled by SWC, irrespective of forest type. This may occur because of the narrower variation in SWC in young forest characterized by high soil water evaporation [70]. With increased stand age, HR correlated with SWC in Mongolia pine (Fig. 7f). In contrast, larch AR was significantly related to SWC (Fig. 6g). Similar observations were reported by Lee *et al.* (2010), who found a significant correlation between AR and SWC in *Quercus*-dominated deciduous stand, not evergreen stands of *Abies holophylla*. One possible reason for this difference between Mongolia pine and larch in the dependence of AR and HR on SWC may be associated with reduced root longevity of deciduous tree species (<1 year) compared with evergreen species (<1–12 years) [71,72]. Higher turnover rates in deciduous tree roots may induce a rapid change in response to environmental fluctuations compared with evergreen trees. Therefore, our results suggest the response of AR and HR to SWC depended on stand age, with the effects of stand age dependent on forest type.

References

1. Bond-Lamberty B, Thomson A (2010) Temperature-associated increases in the global soil respiration record. *Nature* 464: 579–582.
2. Wang W, Chen W, Wang S (2010) Forest soil respiration and its heterotrophic and autotrophic components: Global patterns and responses to temperature and precipitation. *Soil Biology & Biochemistry* 42: 1236–1244.

Conclusions

In summary, we tested the effects of forest type on SR, AR and HR across different aged stands in the same location to prevent confounding from climatic and edaphic conditions. We observed that ST and SWC were significant factors controlling the seasonal dynamics of total SR, irrespective of forest age and type. However, the response of AR and HR to ST, SWC and NDVI differed across various aged stands, with the effects of stand age dependent on the forest type. These results suggest that in stimulating the response of forest carbon efflux to environmental changes, we should consider the effects of stand age and the influence of forest type on this age-related trend. Furthermore, our study emphasized considering the response of HR and AR to environmental changes separately when predicting the response of soil carbon efflux in different aged forests to global climate changes. Future research should attempt an in-depth understanding of the effects of more functional types on carbon efflux across different aged stands.

Acknowledgments

We thank two anonymous reviewers for their constructive suggestions on an early version of this manuscript.

Supporting Information

Figure S1 Relationships between soil respiration at 15°C (SR_{15}) and NDVI across different aged stands. The relationships are shown for ~15 (a), ~25 (b), ~35-year-old stands (c) of *Larix principis*, ~15 (d), ~25 (e), and ~35 year-old stands (f) of *Pinus sylvestris*. (TIF)

Figure S2 Relationships between soil respiration at 15°C (SR_{15}) and soil water content (SWC) across different aged stands. The relationships are shown for ~15 (a), ~25 (b) and ~35-year-old stands (c) of *Larix principis*, ~15 (d), ~25 (e) and ~35-year-old stands (f) of *Pinus sylvestris*. (TIF)

Figure S3 Relationships between soil respiration (SR) and NDVI across different aged stands. The relationships are shown for ~15 (a), ~25 (b) and ~35-year-old stands (c) of *Larix principis*, ~15 (d), ~25 (e) and ~35-year-old stands (f) of *Pinus sylvestris*. (TIF)

Figure S4 Relationships between ST (soil temperature at 5 cm depth) and NDVI for non-growing season (dotted line) and growing season (solid line). The relationships are shown for ~15 (a) and ~25-year-old stands (b) of *Larix principis*, ~15 (c), ~25 (d), and ~35-year-old stands (e) of *Pinus sylvestris*. The data of ~35-year-old stands *L. principis* were absent because of the damage of StowAway loggers inserted in the soil. (TIF)

Author Contributions

Conceived and designed the experiments: WW WC. Performed the experiments: WW WC. Analyzed the data: WW WZ WC. Contributed reagents/materials/analysis tools: WW YY HZ. Wrote the paper: WW WZ WC.

4. Hanson PJ, Edwards NT, Garten CT, Andrews JA (2000) Separating root and soil microbial contributions to soil respiration: A review of methods and observations. *Biogeochemistry* 48: 115–146.
5. Subke J-A, Inglima I, Corrufo MF (2006) Trends and methodological impacts in soil CO₂ efflux partitioning: A metaanalytical review. *Global Change Biology* 12: 921–943.
6. Bonan GB (2008) Forests and climate change: Forcings, feedbacks, and the climate benefits of forests. *Science* 320: 1444–1449.
7. Luyssaert S, Schulze ED, Boerner A, Knohl A, Hessenmoeller D, et al. (2008) Old-growth forests as global carbon sinks. *Nature* 455: 213–215.
8. Cox PM, Betts RA, Jones CD, Spall SA, Totterdell JJ (2000) Acceleration of global warming due to carbon-cycle feedbacks in a coupled climate model. *Nature* 408: 184–187.
9. Davidson EA, Janssens IA (2006) Temperature sensitivity of soil carbon decomposition and feedbacks to climate change. *Nature* 440: 165–173.
10. Mahecha MD, Reichstein M, Carvalhais N, Lasslop G, Lange H, et al. (2010) Global convergence in the temperature sensitivity of respiration at ecosystem level. *Science* 329: 838–840.
11. Pregitzer KS, Euskirchen ES (2004) Carbon cycling and storage in world forests: biome patterns related to forest age. *Global Change Biology* 10: 2052–2077.
12. Zhou G, Liu S, Li Z, Zhang D, Tang X, et al. (2006) Old-growth forests can accumulate carbon in soils. *Science* 314: 1417–1417.
13. Yang Y, Luo Y, Finzi AC (2011) Carbon and nitrogen dynamics during forest stand development: a global synthesis. *New Phytologist* 190: 977–989.
14. Hasselquist NJ, Allen MF, Santiago LS (2010) Water relations of evergreen and drought-deciduous trees along a seasonally dry tropical forest chronosequence. *Oecologia* 164: 881–890.
15. Saiz G, Byrne KA, Butterbach-Bahl K, Kiese R, Blujdeas V, et al. (2006) Stand age-related effects on soil respiration in a first rotation Sitka spruce chronosequence in central Ireland. *Global Change Biology* 12: 1007–1020.
16. Tang J, Bolstad PV, Martin JG (2009) Soil carbon fluxes and stocks in a Great Lakes forest chronosequence. *Global Change Biology* 15: 145–155.
17. Coomes DA, Holdaway RJ, Kobe RK, Lines ER, Allen RB (2012) A general integrative framework for modelling woody biomass production and carbon sequestration rates in forests. *Journal of Ecology* 100: 42–64.
18. Smith DR, Kaduk JD, Balzter H, Wooster MJ, Mottram GN, et al. (2010) Soil surface CO₂ flux increases with successional time in a fire scar chronosequence of Canadian boreal jack pine forest. *Biogeosciences* 7: 1375–1381.
19. Odum EP (1969) Strategy of ecosystem development. *Science* 164: 262–270.
20. Martin JG, Bolstad PV (2005) Annual soil respiration in broadleaf forests of northern Wisconsin: influence of moisture and site biological, chemical, and physical characteristics. *Biogeochemistry* 73: 149–182.
21. Pypker TG, Fredeen AL (2003) Below ground CO₂ efflux from cut blocks of varying ages in sub-boreal British Columbia. *Forest Ecology and Management* 172: 249–259.
22. Yermakov Z, Rothstein DE (2006) Changes in soil carbon and nitrogen cycling along a 72-year wildfire chronosequence in Michigan jack pine forests. *Oecologia* 149: 690–700.
23. Wang CK, Bond-Lamberty B, Gower ST (2002) Soil surface CO₂ flux in a boreal black spruce fire chronosequence. *Journal of Geophysical Research-Atmospheres* 108: DOI: 10.1029/2001JD000861.
24. Law BE, Sun OJ, Campbell J, Van Tuyl S, Thornton PE (2003) Changes in carbon storage and fluxes in a chronosequence of ponderosa pine. *Global Change Biology* 9: 510–524.
25. Campbell JL, Law BE (2005) Forest soil respiration across three climatically distinct chronosequences in Oregon. *Biogeochemistry* 73: 109–125.
26. Genet H, Breda N, Dufrene E (2010) Age-related variation in carbon allocation at tree and stand scales in beech (*Fagus sylvatica* L.) and sessile oak (*Quercus petraea* (Matt.) Liebl.) using a chronosequence approach. *Tree Physiology* 30: 177–192.
27. Falge E, Baldocchi D, Tenhunen J, Aubinet M, Bakwin P, et al. (2002) Seasonality of ecosystem respiration and gross primary production as derived from FLUXNET measurements. *Agricultural and Forest Meteorology* 113: 53–74.
28. Boone RD, Nadelhoffer KJ, Canary JD, Kaye JP (1998) Roots exert a strong influence on the temperature sensitivity of soil respiration. *Nature* 396: 570–572.
29. Hogberg P, Nordgren A, Buchmann N, Taylor AFS, Ekblad A, et al. (2001) Large-scale forest girdling shows that current photosynthesis drives soil respiration. *Nature* 411: 789–792.
30. Fang CM, Smith P, Moncrieff JB, Smith JU (2005) Similar response of labile and resistant soil organic matter pools to changes in temperature. *Nature* 433: 57–59.
31. Knorr W, Prentice IC, House JI, Holland EA (2005) Long-term sensitivity of soil carbon turnover to warming. *Nature* 433: 298–301.
32. Gong JR, Ge ZW, An R, Duan QW, You X, et al. (2012) Soil respiration in poplar plantations in northern China at different forest ages. *Plant and Soil* 360: 109–122.
33. Oishi AC, Palmroth S, Butnor JR, Johnsen KH, Oren R (2013) Spatial and temporal variability of soil CO₂ efflux in three proximate temperate forest ecosystems. *Agricultural and Forest Meteorology* 171: 256–269.
34. Jassal RS, Black TA, Nesic Z (2012) Biophysical controls of soil CO₂ efflux in two coastal Douglas-fir stands at different temporal scales. *Agricultural and Forest Meteorology* 153: 134–143.
35. Bond-Lamberty B, Wang CK, Gower ST (2004) A global relationship between the heterotrophic and autotrophic components of soil respiration? *Global Change Biology* 10: 1756–1766.
36. Gaumont-Guay D, Black TA, Griffis TJ, Barr AG, Morgenstern K, et al. (2006) Influence of temperature and drought on seasonal and interannual variations of soil, bole and ecosystem respiration in a boreal aspen stand. *Agricultural and Forest Meteorology* 140: 203–219.
37. Moyano FE, Kutsch WL, Rehmann C (2008) Soil respiration fluxes in relation to photosynthetic activity in broad-leaf and needle-leaf forest stands. *Agricultural and Forest Meteorology* 148: 135–143.
38. Kuzyakov Y, Gavrichkova O (2010) REVIEW: Time lag between photosynthesis and carbon dioxide efflux from soil: a review of mechanisms and controls. *Global Change Biology* 16: 3386–3406.
39. Pang X, Bao W, Zhu B, Cheng W (2013) Responses of soil respiration and its temperature sensitivity to thinning in a pine plantation. *Agricultural and Forest Meteorology* 171: 57–64.
40. Shi WY, Zhang JG, Yan MJ, Yamanaka N, Du S (2012) Seasonal and diurnal dynamics of soil respiration fluxes in two typical forests on the semiarid Loess Plateau of China: Temperature sensitivities of autotrophs and heterotrophs and analyses of integrated driving factors. *Soil Biology and Biochemistry* 52: 99–107.
41. Kurganova I, De Gerenyu VL, Rozanova L, Saponov D, Myakshina T, et al. (2003) Annual and seasonal CO₂ fluxes from Russian southern taiga soils. *Tellus Series B-Chemical and Physical Meteorology* 55: 338–344.
42. Elberling B (2007) Annual soil CO₂ effluxes in the High Arctic: The role of snow thickness and vegetation type. *Soil Biology & Biochemistry* 39: 646–654.
43. Grogan P, Jonasson S (2006) Ecosystem CO₂ production during winter in a Swedish subarctic region: the relative importance of climate and vegetation type. *Global Change Biology* 12: 1479–1495.
44. Gamon JA, Field CB, Goulden ML, Griffin KL, Hartley AE, et al. (1995) Relationships between NDVI, canopy structure, and photosynthesis in 3 Californian vegetation types. *Ecological Applications* 5: 28–41.
45. Jakubauskas ME, Legates DR, Kastens JH (2001) Harmonic analysis of time-series AVHRR NDVI data. *Photogrammetric Engineering and Remote Sensing* 67: 461–470.
46. Verhoef W, Menenti M, Azzali S (1996) A colour composite of NOAA-AVHRR-NDVI based on time series analysis (1981–1992). *International Journal of Remote Sensing* 17: 231–235.
47. Azzali S, Menenti M (2000) Mapping vegetation-soil-climate complexes in southern Africa using temporal Fourier analysis of NOAA-AVHRR NDVI data. *International Journal of Remote Sensing* 21: 973–996.
48. Vogel JG, Valentine DW (2005) Small root exclusion collars provide reasonable estimates of root respiration when measured during the growing season of installation. *Canadian Journal of Forest Research* 35: 2112–2117.
49. Wan SQ, Hui DF, Wallace L, Luo YQ (2005) Direct and indirect effects of experimental warming on ecosystem carbon processes in a tallgrass prairie. *Global Biogeochemical Cycles* 19: DOI:10.1029/2004GB002315.
50. Zhou X, Wan S, Luo Y (2007) Source components and interannual variability of soil CO₂ efflux under experimental warming and clipping in a grassland ecosystem. *Global Change Biology* 13: 761–775.
51. Migliavacca M, Reichstein M, Richardson AD, Colombo R, Sutton MA, et al. (2011) Semiempirical modeling of abiotic and biotic factors controlling ecosystem respiration across eddy covariance sites. *Global Change Biology* 17: 390–409.
52. Janssens IA, Lankreijer H, Matteucci G, Kowalski AS, Buchmann N, et al. (2001) Productivity overshadows temperature in determining soil and ecosystem respiration across European forests. *Global Change Biology* 7: 269–278.
53. Ide R, Oguma H (2010) Use of digital cameras for phenological observations. *Ecological Informatics* 5: 339–347.
54. Ahrends HE, Etzold S, Kutsch WL, Stoeckli R, Bruegger R, et al. (2009) Tree phenology and carbon dioxide fluxes: use of digital photography at for process-based interpretation the ecosystem scale. *Climate Research* 39: 261–274.
55. Richardson AD, Braswell BH, Hollinger DY, Jenkins JP, Ollinger SV (2009) Near-surface remote sensing of spatial and temporal variation in canopy phenology. *Ecological Applications* 19: 1417–1428.
56. Tagesson T, Ekland L, Lindroth A (2009) Applicability of leaf area index products for boreal regions of Sweden. *International Journal of Remote Sensing* 30: 5619–5632.
57. Ekblad A, Hogberg P (2001) Natural abundance of ¹³C in CO₂ respired from forest soils reveals speed of link between tree photosynthesis and root respiration. *Oecologia* 127: 305–308.
58. Liu Q, Edwards NT, Post WM, Gu L, Ledford J, et al. (2006) Temperature-independent diel variation in soil respiration observed from a temperate deciduous forest. *Global Change Biology* 12: 2136–2145.
59. Gamon JA, Field CB, Goulden ML, Griffin KL, Hartley AE, et al. (1995) Relationships between NDVI, canopy structure, and photosynthesis in 3 Californian vegetation types. *Ecological Applications* 5: 28–41.
60. Bond-Lamberty B, Bunn AG, Thomson AM (2012) Multi-year lags between forest browning and soil respiration at high Northern latitudes. *Plos one* 7: e50441.
61. Cisneros-Dozal LM, Trumbore S, Hanson PJ (2006) Partitioning sources of soil-respired CO₂ and their seasonal variation using a unique radiocarbon tracer. *Global Change Biology* 12: 194–204.
62. Scott-Denton LE, Rosenstiel TN, Monson RK (2006) Differential controls by climate and substrate over the heterotrophic and rhizospheric components of soil respiration. *Global Change Biology* 12: 205–216.
63. Liang N, Hirano T, Zheng ZM, Tang J, Fujinuma Y (2010) Soil CO₂ efflux of a larch forest in northern Japan. *Biogeosciences* 7: 3447–3457.

64. Lee N-y, Koo J-W, Noh NJ, Kim J, Son Y (2010) Seasonal variation in soil CO₂ efflux in evergreen coniferous and broad-leaved deciduous forests in a cool-temperate forest, central Korea. *Ecological Research* 25: 609–617.
65. Kuptz D, Matyssek R, Grams TEE (2011) Seasonal dynamics in the stable carbon isotope composition delta¹³C from non-leafy branch, trunk and coarse root CO₂ efflux of adult deciduous (*Fagus sylvatica*) and evergreen (*Picea abies*) trees. *Plant Cell and Environment* 34: 363–373.
66. Yordanov I, Velikova V, Tsonev T (2000) Plant responses to drought, acclimation, and stress tolerance. *Photosynthetica* 38: 171–186.
67. Chen G, Yang Y, Guo J, Xie J, Yang Z (2011) Relationships between carbon allocation and partitioning of soil respiration across world mature forests. *Plant Ecology* 212: 195–206.
68. Carbone MS, Winston GC, Trumbore SE (2008) Soil respiration in perennial grass and shrub ecosystems: Linking environmental controls with plant and microbial sources on seasonal and diel timescales. *Journal of Geophysical Research-Biogeosciences* 113: DOI: 10.1029/2007JG000611.
69. Muhr J, Borken W (2009) Delayed recovery of soil respiration after wetting of dry soil further reduces C losses from a Norway spruce forest soil. *Journal of Geophysical Research-Biogeosciences* 114: DOI: 10.1029/2009JG000998.
70. Drake P, Mendham D, White D, Ogden G, Dell B (2012) Water use and water-use efficiency of coppice and seedling *Eucalyptus globulus* Labill.: a comparison of stand-scale water balance components. *Plant and Soil* 350: 221–235.
71. Vogt KA, Grier CC, Vogt DJ (1986) Production, turnover, and nutrient dynamics of aboveground and belowground detritus of world forests. *Advances in Ecological Research* 15: 303–377.
72. Lyr H, Hoffman G (1967) Growth rates and growth periodicity of tree roots. *International Review of Forestry Research* 2: 181–236.

Copyright of PLoS ONE is the property of Public Library of Science and its content may not be copied or emailed to multiple sites or posted to a listserv without the copyright holder's express written permission. However, users may print, download, or email articles for individual use.

Soil Respiration and Organic Carbon Dynamics with Grassland Conversions to Woodlands in Temperate China

Wei Wang^{1*}, Wenjing Zeng^{1,2}, Weile Chen^{1,2}, Hui Zeng², Jingyun Fang¹

1 Department of Ecology, College of Urban and Environmental Sciences, and Key Laboratory for Earth Surface Processes of the Ministry of Education, Peking University, Beijing, China, **2** Key Laboratory for Urban Habitat Environmental Science and Technology, Peking University Shenzhen Graduate School Shenzhen, China

Abstract

Soils are the largest terrestrial carbon store and soil respiration is the second-largest flux in ecosystem carbon cycling. Across China's temperate region, climatic changes and human activities have frequently caused the transformation of grasslands to woodlands. However, the effect of this transition on soil respiration and soil organic carbon (SOC) dynamics remains uncertain in this area. In this study, we measured *in situ* soil respiration and SOC storage over a two-year period (Jan. 2007–Dec. 2008) from five characteristic vegetation types in a forest-steppe ecotone of temperate China, including grassland (GR), shrubland (SH), as well as in evergreen coniferous (EC), deciduous coniferous (DC) and deciduous broadleaved forest (DB), to evaluate the changes of soil respiration and SOC storage with grassland conversions to diverse types of woodlands. Annual soil respiration increased by 3%, 6%, 14%, and 22% after the conversion from GR to EC, SH, DC, and DB, respectively. The variation in soil respiration among different vegetation types could be well explained by SOC and soil total nitrogen content. Despite higher soil respiration in woodlands, SOC storage and residence time increased in the upper 20 cm of soil. Our results suggest that the differences in soil environmental conditions, especially soil substrate availability, influenced the level of annual soil respiration produced by different vegetation types. Moreover, shifts from grassland to woody plant dominance resulted in increased SOC storage. Given the widespread increase in woody plant abundance caused by climate change and large-scale afforestation programs, the soils are expected to accumulate and store increased amounts of organic carbon in temperate areas of China.

Citation: Wang W, Zeng W, Chen W, Zeng H, Fang J (2013) Soil Respiration and Organic Carbon Dynamics with Grassland Conversions to Woodlands in Temperate China. PLoS ONE 8(8): e71986. doi:10.1371/journal.pone.0071986

Editor: Han Y.H. Chen, Lakehead University, Canada

Received: March 22, 2013; **Accepted:** July 6, 2013; **Published:** August 23, 2013

Copyright: © 2013 Wang et al. This is an open-access article distributed under the terms of the Creative Commons Attribution License, which permits unrestricted use, distribution, and reproduction in any medium, provided the original author and source are credited.

Funding: This research was supported by the National Basic Research Program of China (No. 2012CB956303 and 2010CB950600), projects of the National Natural Science Foundation of China (31222011, 31270363 and 31070428), and projects supported by the Foundation for Innovative Research Groups of the National Natural Science Foundation of China (No. 31021001). The funders had no role in study design, data collection and analysis, decision to publish, or preparation of the manuscript.

Competing Interests: The authors have declared that no competing interests exist.

* E-mail: wangw@urban.pku.edu.cn

Introduction

Soils are the largest store of carbon in the biosphere [1], so small changes in soil organic carbon (SOC) storage will profoundly influence atmospheric CO₂ concentrations and potentially influence the global climate [2]. Moreover, soil respiration is the second largest flux of carbon between terrestrial ecosystems and the atmosphere [3]. Global changes have substantially impacted soil respiration and, in turn, SOC dynamics [4,5]. However, soils are the largest source of uncertainty in the terrestrial carbon balance [6].

Natural and anthropogenic-induced vegetation-type conversions are among the most important components of global changes [7]. The shifts between grasslands and plant communities dominated by woody vegetation are one of the most frequent occurring vegetation transition types [8,9,10,11,12]. For instance, deforestation is believed to be a major anthropogenic source of CO₂ to the atmosphere [13,14,15,16,17]. In contrast, large scale forest expansion and re-growth may be important sources for the missing carbon sink [18,19]. Vegetation-type conversions influence the balance of organic carbon in soil and hence may cause

changes in soil respiration [20,21]. Changes in vegetation-type are expected to have major effects on the terrestrial carbon balance [22].

Shifts in vegetation types may profoundly affect the dynamics of soil respiration and SOC by influencing soil microclimate and the production and transfer of aboveground photosynthate to belowground [23,24,25,26,27]. However, the direction of changes in the soil respiration and the consequent changes in organic carbon storage in soil within adjacent grass-woody vegetative transition is still controversial [28,29,30]. The inconsistencies may, to a large degree, be caused by the differences in the various locations and the types of transition occurring [31].

Because regional aspects of the global carbon cycle are drawing increasing scientific and political interest, there is a strong impetus to better understand how land use change effects China's carbon balance [32,33,34]. However, few reports on soil respiration and SOC dynamics are available. Furthermore, the currently available studies were mainly conducted in China's southern tropical and sub-tropical areas [35,36,37,38,39,40]. Nevertheless, the temperate areas of northern China are also experiencing frequent, diverse and continuous transitions in the vegetation types, which should

substantially affect SOC dynamics and soil respiration in this area. Since the 1970s, the Chinese government has implemented several ecological restoration projects, including the Three-North Shelterbelt Program covering 41% area of the country, across the temperate regions of China that receive less than 400 mm of precipitation annually. These reforestation and afforestation activities were believed to influence carbon cycling and carbon storage in this area [41,42]. In addition, the study of dynamics of organic carbon in soil shows the level of organic carbon in soil is relatively sensitive to increasing temperatures in the temperate climatic zone [43]. Therefore, evaluating how large-scale transitions of vegetation types influence soil respiration and consequent SOC storage is critical to calculating temperate China's carbon budget under the scenario of global change.

In this study, we quantify soil respiration and SOC dynamics from five adjacent grass-woody vegetation types in the temperate areas of northern China. We aimed to 1) measure annual soil respiration as well as SOC storage and residence time, and 2) explore the major drivers for the variations in soil respiration among different vegetation types. We hypothesized that 1) soil respiration as well as SOC storage and residence time were higher in woody vegetation types than in grasslands, and 2) vegetation-mediated change in soil microenvironments was a major driver for the variation of soil respiration.

Materials and Methods

Ethics Statement

The administration of the Saihanba Forestry Center gave permission for this research at each study site. We confirm that the field studies did not involve endangered or protected species.

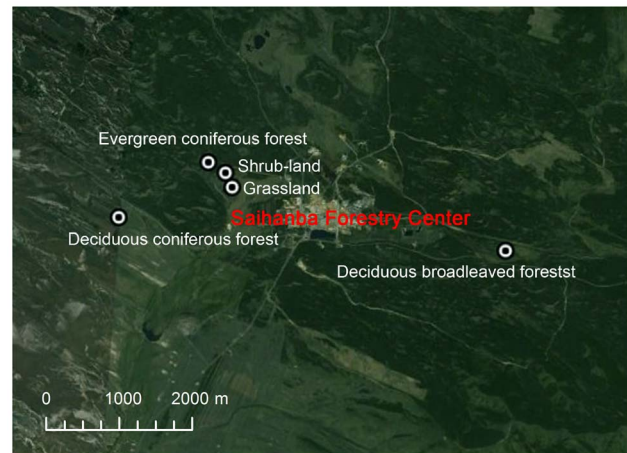


Figure 2. The location of five vegetation types in Saihanba Forestry Center.

doi:10.1371/journal.pone.0071986.g002

Site description and land-use history

The study was conducted at the Saihanba Forestry Center in Hebei Province and Inner Mongolia Autonomous Area, northern China (117°12'–117°30'E, 42°10'–42°50'N, 1,400 m a.s.l.). The study area has a semi-arid and semi-humid temperate climate and lies in a typical forest-steppe ecotone on predominately sandy soils with long and cold winters (November to March), and short springs and summers. Annual mean air temperature and precipitation from 1964 to 2004 were -1.4°C and 450.1 mm, respectively.

This area contains the largest of plantation forests in China, with evergreen *Pinus sylvestris* L. var. *mongolica* Litv. (Mongolia pine) and deciduous *Larix principis-rupprechtii* Mayr (larch) as dominant



Figure 1. Current land-use patterns at the study site. From a 1:1,000,000 scale map of the vegetation types of China [72].

doi:10.1371/journal.pone.0071986.g001

Table 1. Site characteristics and physical and chemical properties of topsoil (0–20 cm).

Site	Vegetation types	Domain species	NDVI	ST (°C)	SWC (%)	SOC (g m ⁻²)	STN (g m ⁻²)	Soil pH	SBD* (g cm ⁻³)
GR	grassland	<i>Leymus chinensis</i>	0.44 ^a	3.8 ^a	8.4 ^a	1476.7 ^a	136.5 ^a	6.28 ^a	0.92 ^a
SH	shrubland	<i>Rosa bella</i> Rehd. et Wils & <i>Malus baccata</i> *	0.38 ^b	3.4 ^a	12.6 ^b	1841.5 ^a	189.4 ^b	6.30 ^a	0.71 ^b
EC	~15 yr old evergreen coniferous plantation	<i>Pinus sylvestris</i> var. <i>mongolica</i>	0.55 ^c	3.2 ^a	7.3 ^a	2022.7 ^a	146.2 ^a	6.45 ^a	0.98 ^a
DC	~15 yr old deciduous coniferous plantation	<i>Larix principis-rupprechtii</i>	0.36 ^b	3.6 ^a	7.8 ^a	2993.9 ^b	172.8 ^a	6.30 ^a	1.06 ^a
DB	~45 yr old deciduous broadleaved forest	<i>Betula platyphylla</i>	0.51 ^d	1.7 ^b	19.7 ^c	2830.7 ^b	287.7 ^c	5.92 ^b	0.69 ^b

*SH contained two different dominant species in separate plots and the results of those plots were averaged in our study.

NDVI = Normalized Difference Vegetation Index, soil temperature = ST, SWC = soil water content, SOC = soil organic carbon, STN = soil total nitrogen, SBD = soil bulk density. Different lowercase letters indicated significant differences ($P < 0.05$).

doi:10.1371/journal.pone.0071986.t001

species; secondary deciduous forests mainly consist of *Betula platyphylla* Sukaczew (birch). In addition, shrublands dominated by *Rosa bella* Rehd. et Wils. (Solitary rose) and *Malus baccata* (L.) Borkh. (Siberian crabapple) and meadow grasslands are also very common (Fig. 1). The herbaceous layers of Mongolia pine and larch are similar, and are composed of *Sanguisorba officinalis* L. (Radix Sanguisorbae), *Thalictrum aquilegifolium* L., *Agrimonia pilosa* Ledeb. and *Carex stenophylla* Wahlenb., while the herbaceous layer of birch is made up of *Agrimonia pilosa* Ledeb. and Radix Sanguisorbae. The herbaceous layer of Siberian crabapple is dominated by *Veronica linariifolia* Pall. ex Link, *Galium verum* L., *Heteropappus hispidus* (Thunb.) Less., *Trollius chinensis* Bunge, and *Bupleurum chinense* DC. The herbaceous layer of Solitary rose

consists of *Leymus chinensis* (Trin.) Tzvelev. The meadow grassland is zonal vegetation dominated by *L. chinensis*.

The current land-cover pattern resulted from both natural and human-induced vegetation type transitions: from ~5900 to ~2900 ¹⁴C years BP, the original deciduous broadleaf forest (DB) were gradually replaced by evergreen coniferous forest (EC) and deciduous coniferous forest (DC) in those places when climate changed from humid to arid; after ~2900 ¹⁴C years BP, EC and DC shifted to grassland (GR) in some drier places [44]. In the late 1900 s, the remaining primary forests were harvested by large scale industrial logging and initially became grasslands, but more recently the grasslands have been replaced by secondary SH, DB and plantations of EC and DC. Furthermore, based on the trends for increasing temperature and precipitation in this area [45], together with the large-scale reforestation and afforestation policy of the Chinese government [42], the cover area of woody vegetation types is predicted to increase in the future.

Experimental plot design

The abundant vegetation types co-occurring in our study area provide an excellent opportunity to examine how ecological processes respond to changes in vegetation type. We selected five adjacent grass-woody vegetation types (Fig. 2) to study the influences of vegetation type transitions on biogeochemical processes. All sites for these vegetation types were less than 5 km apart to ensure each site had the same climatic and edaphic condition. Table 1 summarizes the characteristics and species composition of each vegetation type. Three replicates were designed for each of five vegetation types including: GR (*L. chinensis*), SH (*R. bella* & *M. baccata*), EC (~15 year old *P. sylvestris* var. *mongolica*), DC (~15 year old *L. principis-rupprechtii*), and DB

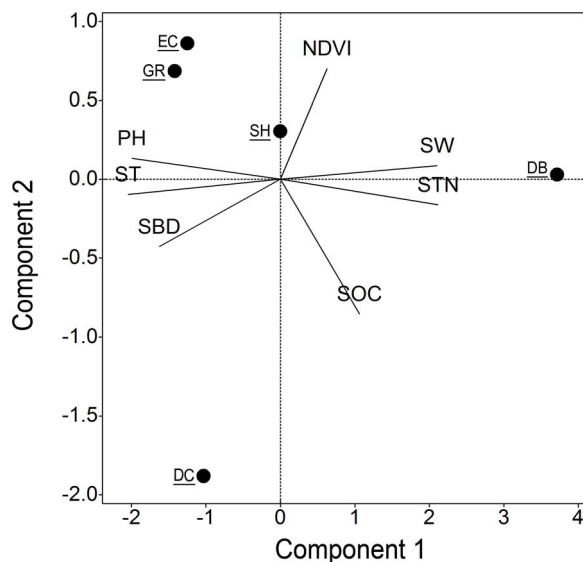


Figure 3. Principal component analysis of site properties. Score plot of five vegetation types during Principal Component Analysis of site properties, including normalized difference vegetation index (NDVI), soil temperature (ST), soil water content (SWC), soil organic carbon (SOC), soil total nitrogen (STN), soil pH, and soil bulk density (SBD). Habitats were grassland (GR), shrubland (SH), evergreen coniferous forest (EC), deciduous coniferous forest (DC), and deciduous broadleaved forest (DB). Seasonal dynamics of soil respiration

doi:10.1371/journal.pone.0071986.g003

Table 2. The proportion of variation explained from principal component analysis on the seven environmental variables.

Component	Eigenvalue	Proportion	Cumulative
1	4.61	0.66	0.66
2	1.21	0.17	0.83
3	1.01	0.15	0.98
4	0.16	0.02	1.00

doi:10.1371/journal.pone.0071986.t002

Table 3. The loading scores of traits on each component from principal component analysis on the seven environmental variables.

Variable	Component 1	Component 2	Component 3
NDVI	0.14	0.58	-0.71
ST	-0.44	-0.08	0.28
SWC	0.46	0.07	0.18
SOC	0.23	-0.71	-0.37
STN	0.46	-0.14	0.02
pH	-0.43	0.11	-0.10
SBD	-0.35	-0.35	-0.49

NDVI = normalized difference vegetation index, ST = soil temperature, SWC = soil water content, SOC = soil organic carbon, STN = soil total nitrogen, pH = soil pH, SBD = soil bulk density.

doi:10.1371/journal.pone.0071986.t003

(~45 year old *B. platyphylla*). Each 20 m×20 m plot was sampled with five subsamples (i.e. soil respiration measurement collars).

Soil respiration, soil temperature and moisture

Soil respiration (SR) was measured using a Li-8100 soil CO₂ flux system (LI-COR Inc. Lincoln, NE, USA) from Jan 2007 to Dec 2008. During the growing season (April to October), five polyvinyl chloride (PVC) collars (10 cm inside diameter, 6 cm height above the soil surface) were inserted 3 cm into the soil in each plot and were left in the same locations throughout the study period. These five PVC collars were placed in each plot, one in the center and one in each corner. Living plants inside the collars were clipped at the soil surface 1 day before each measurement to exclude the effect of aboveground vegetation. SR was measured every 10–15 days. Measurements were made between 08:00 and 11:00 am (based on our measurements of diurnal changes in SR, data not shown) to minimize the daily variation in SR and obtain mean daily SR. For each measurement, respiration rates were calculated as means of three plots for each stand. During winter (November to March), longer soil collars (determined by snow

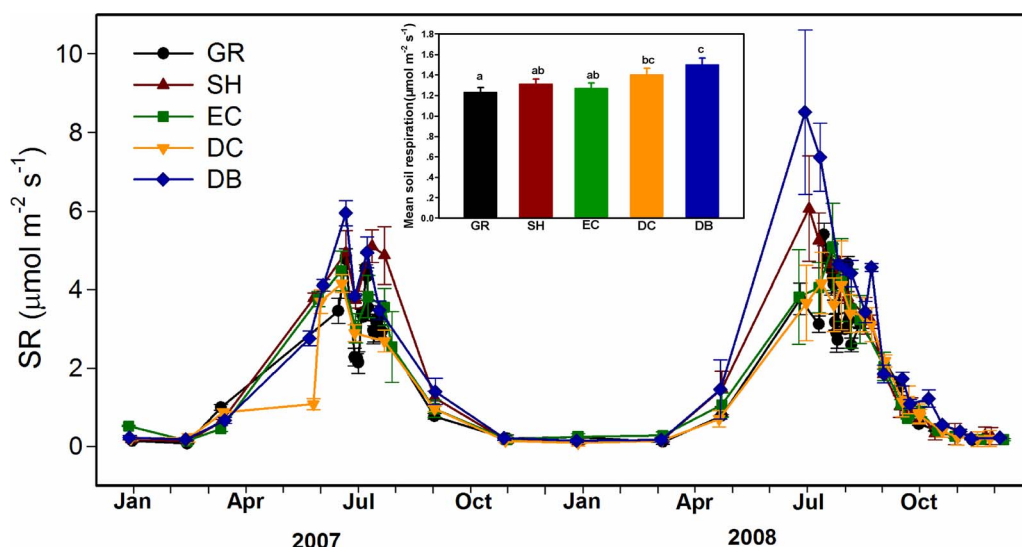
depth, less than 30 cm) were inserted into the soil surface and stabilized for 24 h before measurement of the winter SR [46,47]. The Li-8100 soil CO₂ flux system was kept in an isolated and heated container to keep its temperature above freezing point.

Soil temperature (ST) was recorded during respiration measurements near each collar at 5 cm soil depth with the LI-COR 8100 temperature probe. Continuous measurements of ST at 5 cm depth were recorded at 30-min intervals with StowAway loggers (Onset Comp. Corp., Bourne, MA, USA) inserted in the soil near one collar at each study site. Soil volumetric water content (SWC) at a depth of 0–10 cm was measured using time domain reflectometry (Soil Moisture Equipment Corp., Santa Barbara, CA, USA). SWC was only obtained during the growing season because the probe could not be fully inserted into the frozen soil in winter.

Soil sampling and measurements

Because the carbon stored in topsoil is the carbon pool that is most sensitive to land management practices [48,49], we sampled mineral soils at depths of 0–10 and 10–20 cm from five random locations per plot using 5.8-cm diameter soil cores during the summers of 2007 and 2008. Soil bulk density (SBD) of the two soil horizons was quantified in all soil surveys from the mass of the oven-dry soil (105°C) divided by the volume of the soil cores. Next, all plant materials were removed from fresh soil samples, and soil was passed through a 2-mm sieve. *In situ* root biomass per unit area was determined by the entire root biomass in the soil core divided by the cross section area of the core. Soil pH was determined from air-dried soil samples in distilled H₂O solution, with a pH meter (Model PHS-2, INESA Instrument, Shanghai, China). The SOC content and soil total nitrogen (STN) were determined from oven-dried soil samples with an elemental analyzer (Vario EL III Universal CHNOS Elemental Analyzer, Elementar, Hanau, Germany). The mass-based SOC and STN were converted into area-based with soil bulk density of each horizon (0–10 and 10–20 cm depth).

NDVI (Normalized Difference Vegetation Index) data

**Figure 4.** Seasonal dynamics of soil respiration (SR) among five adjacent vegetation types. Habitats are as listed in Fig. 2.

doi:10.1371/journal.pone.0071986.g004

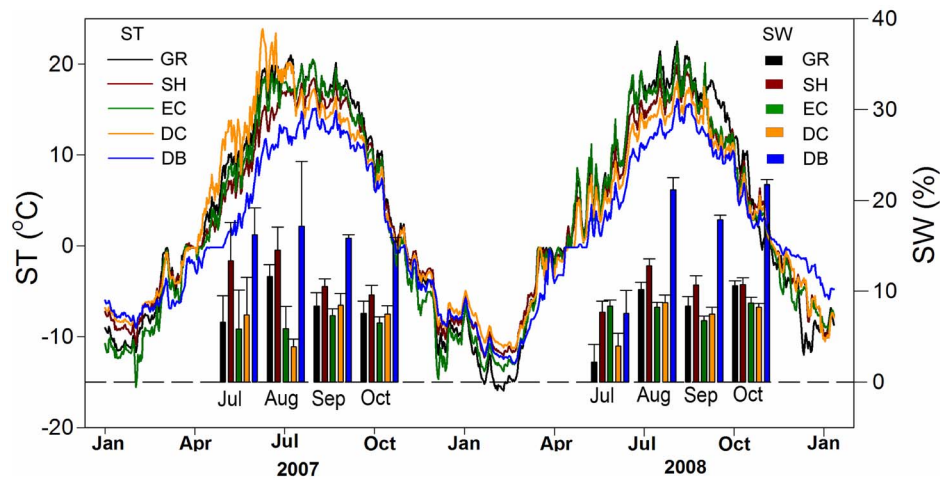


Figure 5. Seasonal dynamics of soil temperature and soil water content across five adjacent vegetation types. ST = soil temperature at 5 cm depth, SWC = soil water content at 10 cm depth. Habitats are as listed in Fig. 2.
doi:10.1371/journal.pone.0071986.g005

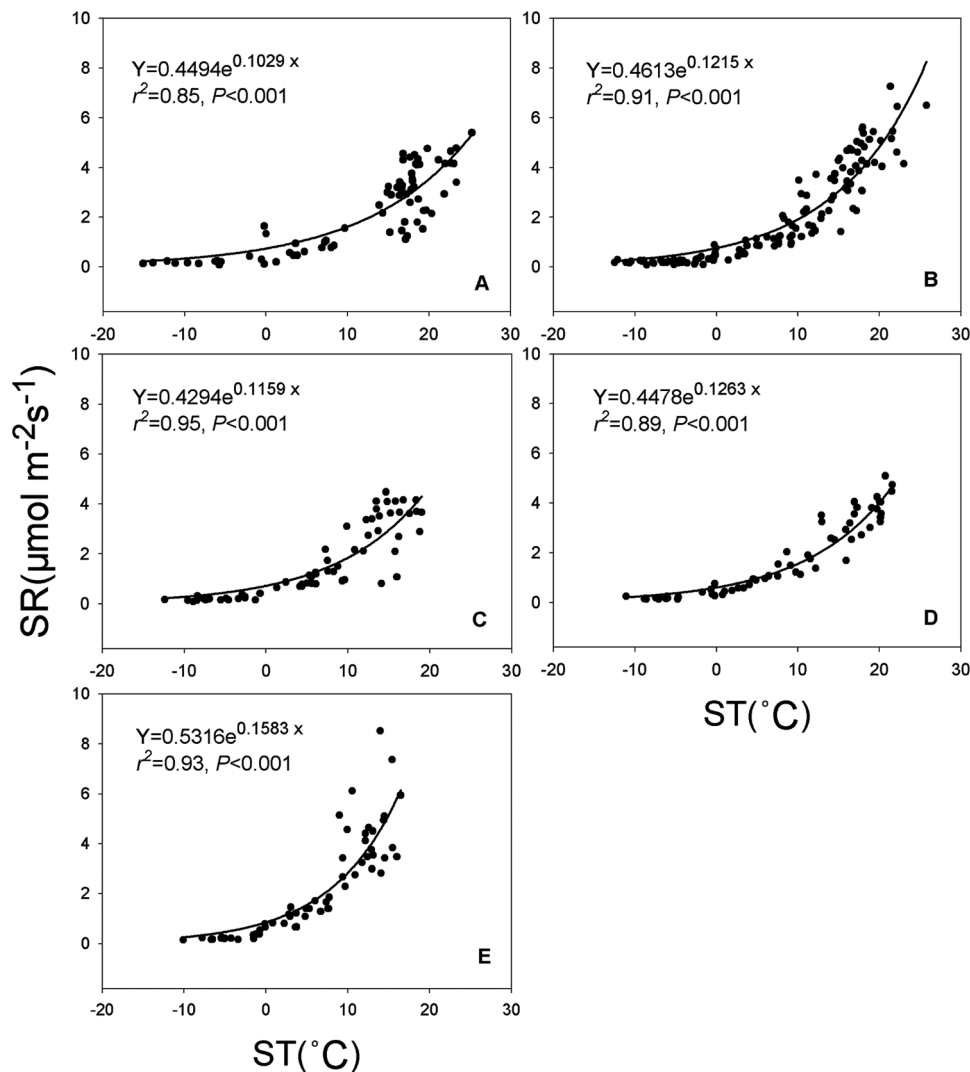


Figure 6. Relationships between the seasonal dynamics of soil respiration and soil temperature at 5 cm depth across habitats as listed in Fig. 2.
doi:10.1371/journal.pone.0071986.g006

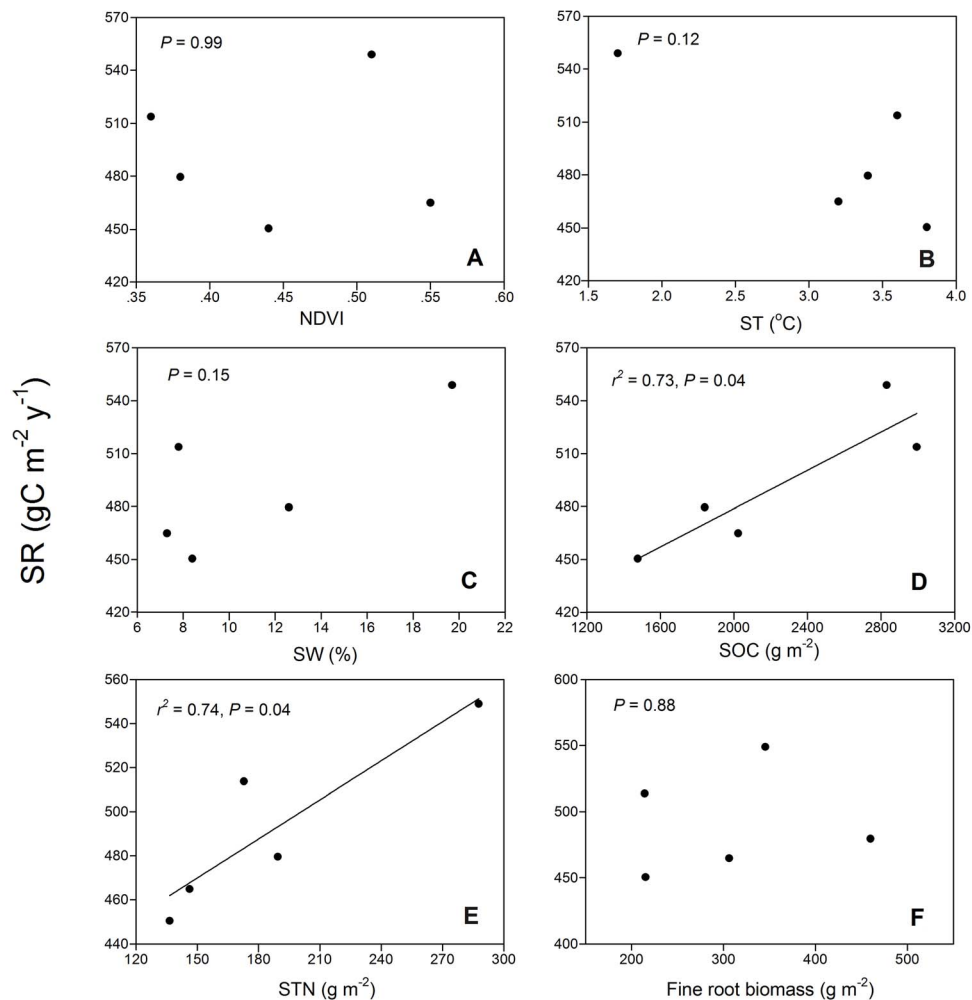


Figure 7. Relationships between annual soil respiration and NDVI (A), soil temperature at 5 cm depth (ST) (B), soil water content at 10 cm depth (SWC) (C), soil organic carbon (SOC) (D), soil total nitrogen (STN) (E) from the top 20 cm depth and fine root biomass at 0–30 cm depth (F) across the five adjacent vegetation types.

doi:10.1371/journal.pone.0071986.g007

NDVI is derived from the red: near-infrared reflectance ratio:

$$NDVI = \frac{(NIR - VIS)}{(NIR + VIS)}, \quad (1)$$

where NIR and VIS stand for the spectral reflectance measurements acquired in the near-infrared and visible (red) regions of the spectrum, respectively [50]. The NDVI depends on photosynthesis and is closely correlated to GPP [51,52]. We calculated the mean annual NDVI of each vegetation type from 2007–2008 to analyze the influence of aboveground carbon input on SR. Because the five vegetation types studied here covered large areas and had uniform distributions and sparse understories, NDVI of 16-Day L3Global 250 m product (MOD13 Q1) could well represent our plot measurements. We downloaded satellite data from our study period from <https://wist.echo.nasa.gov/api>. Harmonic (Fourier) analysis was used to remove the considerable noise remaining in the NDVI time series from satellite data to obtain reasonably smooth continuous data [53].

Statistical analysis

We examined the relationships between SR and ST by fitting exponential functions to the data from each vegetation type using the following equation:

$$SR = a \times e^{\beta \times ST}, \quad (2)$$

where SR is observed soil respiration (plot-wide averages measured periodically throughout the year), ST is the concurrently measured soil temperature (5 cm depth), with a and β being the fitted parameters obtained using least squares nonlinear regression with SigmaPlot V. 8.02.

Annual SR was estimated with the yearly period continuously measured ST and the exponential function between SR and ST for each vegetation type. The mean residence time of SOC was estimated for each vegetation type by dividing the mass of SOC in the top 20 cm of the soil profile by the heterotrophic respiration flux, which equals the total SR minus root respiration. Root respiration of each vegetation type was obtained based on the estimates from Wang *et al.* [54], who measured excised root respiration for all the five vegetation types we studied at the same sites during the same period.

Table 4. Annual soil respiration, contribution of root respiration to total soil respiration, and soil organic carbon residence time in the top 20 cm of soil.

Site	SR (g C m ⁻² yr ⁻¹)	Root respiration contribution* (%)	HR (g C m ⁻² yr ⁻¹)	SOC (g m ⁻²)	Residence time (yr)
GR	450.4 ^a	4.7	429.0	1476.7 ^a	3.4
SH	479.5 ^b	23.5	366.8	1841.5 ^a	5.0
EC	464.8 ^c	18.3	380.0	2022.7 ^a	5.3
DC	513.7 ^d	24.0	390.2	2993.9 ^b	7.7
DB	548.9 ^e	17.9	450.5	2830.7 ^b	6.3

*The estimates were derived from those of Wang *et al.* [54].

SR = annual soil respiration, HR = annual heterotrophic respiration, SOC = soil organic carbon, GR = grassland, SH = shrubland, EC = evergreen coniferous forest, DC = deciduous coniferous forest, DB = deciduous broadleaved forest. Different lowercase letters in mean SR and SOC indicated significant differences ($P < 0.05$).

doi:10.1371/journal.pone.0071986.t004

To analyze the environmental differences among vegetation types, principal component analysis (PCA) was performed on correlations among ST, SWC, NDVI, SOC, STN, soil pH and SBD, and the five vegetation types were ordered by their scores on the first two principal components. The relationships between annual SR and ST, SWC, NDVI, SOC, STN and live fine root biomass were examined by linear regression. The differences of SR among vegetation types were tested using one-way ANOVA. We used the averaged value of the five subsamples in each plot to

conduct statistical analysis. All statistical analyses were performed with a significance level of 0.05, using SPSS software (2009, ver. 18.0, SPSS Inc., Chicago, IL, USA).

Results

Microenvironment of different vegetation types

The annual average ST at 5 cm deep was not significantly different between grassland and woody vegetation types, with one exception (Table 1). The DB habitat had significantly lower ST at 5 cm deep and higher SWC at 10 cm deep. No significant differences in SWC occurred among GR, EC and DC habitats. The SH and DB habitats had lower soil bulk density than other vegetation types, but the DC forest and DB forest showed higher SOC content (Table 1, $P < 0.05$). Furthermore, STN content was highest in DB forest, and its pattern was consistent with that of SWC across different vegetation types. There is no significant difference in soil pH among all vegetation types (Table 1).

PCA identified three significant principle components (eigenvalue > 1) of variations (Fig. 3). The first two principle components explained 83% of the total variance in the dataset (Table 2, Table 3). The first principal component was mainly associated with the differences in ST, SWC, STN and soil pH across different vegetation types. The second and third principal components were correlated to SOC and NDVI, respectively. Among the four woody vegetation types, EC is the most similar environmentally to GR, followed by SH. However, DB and DC were the different from GR along the first and second principal component, respectively.

As expected, SR (Fig. 4) and ST (Fig. 5) were higher in summer and lower in winter (Fig. 4). The mean SR showed significant differences among five vegetation types, in the order of GR $<$ EC $<$ SH $<$ DC $<$ DB (Fig. 4). The seasonal dynamics of SR were exponentially related to ST across different vegetation types, which explained 85%, 91%, 95%, 89% and 93% of the variation in SR for GR, SH, EC, DC and DB, respectively (Fig. 6).

Annual soil respiration and soil organic carbon turnover

Annual SR was lower in GR than in the woody vegetation types (Table 4). The annual SR increased by 3% following the conversion from GR to EC, 6% to SH, 14% to DC, and 22% to DB. The variations in the annual SR among the five vegetation types were significantly correlated with SOC and STN, but not with ST, SWC, NDVI and fine root biomass (Fig. 7).

In contrast with the pattern of total SR, GR had higher annual heterotrophic respiration than SH, EC and DC, but lower than

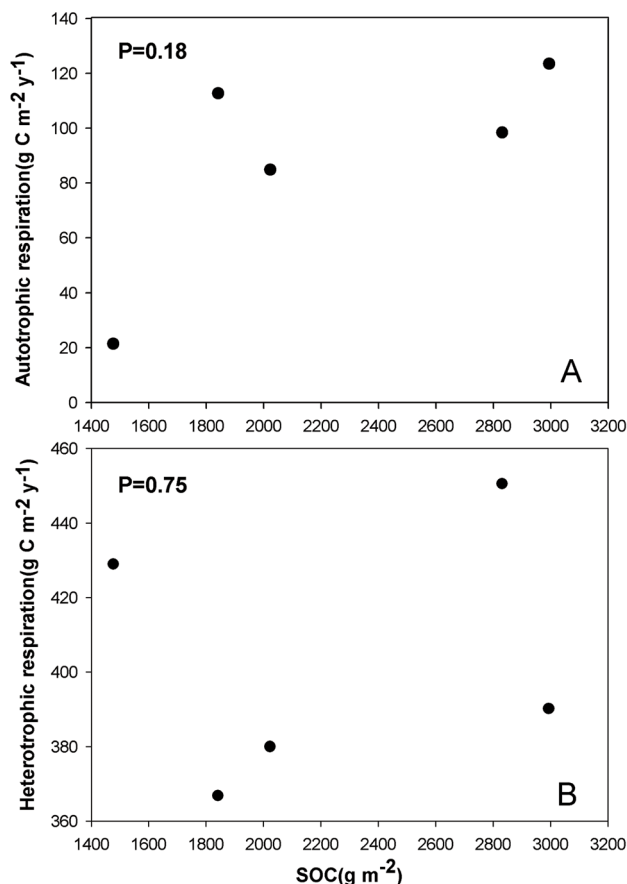


Figure 8. Relationships between heterotrophic respiration (A), autotrophic respiration (B) and soil organic carbon (SOC) across the five adjacent vegetation types.

doi:10.1371/journal.pone.0071986.g008

DB (Table 4). Because GR had a lower SOC content and higher heterotrophic respiration, the residence time of SOC in GR is shorter (3.4 yr), in comparison with the relatively longer time in woody vegetation types (5.0 yr in SH, 5.3 yr in EC, 6.3 yr in DB and 7.7 yr in DC, Table 4).

Discussion

Effects of vegetation types on soil respiration

Our estimates of annual SR ranged from 450.4 to 548.9 g C m⁻² yr⁻¹ (Table 4), which fell into the range reported in temperate areas [55,56]. Among the five vegetation types, GRs showed lower SR than woodlands, which contradicted with the conclusions made using a synthesis of global data that reported SR from various types of GRs was averaged about 20% greater than various types of forests [57]. Additionally, in a juniper woodland-grassland pair in Kansas (USA), SR from GRs was 38% higher than from woodlands [58]. Our findings therefore did not support earlier generalizations that state GRs tended to allocate large proportions of their photosynthate belowground, and this results in higher SR than occurs woodlands [58]. However, in a subalpine Australian ecosystem rates of respiration in woodland soils were twice more than those in nearby grassland soils, which is similar to our results [27].

Three factors, microclimate (ST and moisture), aboveground photosynthetic supply to roots and substrate availability have been known to be important controls on SR [57]. Our results suggested that SOC and STN were major contributing factors for the variations of SR among different vegetation types (Fig. 7). Heterotrophic respiration was the dominant component of total SR, ranging from 76% to 95% (Table 4). Therefore, we expected the correlation between SR and SOC was derived from the component of heterotrophic respiration, because heterotrophic respiration is a result of the mineralization of SOC that is stored in large stocks [59,60,61] while autotrophic respiration depends on fresh photosynthates [62]. However, we did not observe a correlation between HR and SOC (Fig. 8A). Moreover, we observed an increasing trend of root respiration with an increase in SOC (Fig. 8B) although statistical test was not significant. Therefore, root respiration may be the main driver of the differences in SR between the different vegetation types. The correlation between root respiration and SOC may be attributable to the fact that higher root respiration is connected to higher photosynthetic activity [63,64,65], which will increase the carbon input to soil and therefore SOC content. Therefore, accurate discrimination of root respiration and heterotrophic respiration from the total SR was critical for gaining an improved understanding of the driving factors of SR among different vegetation types. Our results thus indicate that when modeling SR across a temperate heterogeneous landscape, we should pay more attention to the differences in heterotrophic respiration and root respiration components among different vegetation types.

Effects of vegetation types on soil carbon storage and turnover

Reported changes of SOC storage varied widely with reported increases [28,30,66], no change [58] and decreases [67,68,69]

after grasslands were converted to woodlands. Our results showed that SOC storage was 92% higher in DB and 103% higher in DC compared with GR (Table 4), suggesting possible larger amounts of organic carbon are input to soil through litterfall and root turnover in woodlands than grassland. Moreover, grasslands have been reported to have stronger wind erosion than woodlands in our study area, which reduced the soil clay and silt content, possibly explaining the potential reductions of surface organic matter in our study area [70,71]. However, no significant increase was observed when EC and SH (Table 4) were compared with GR, possibly because of the small sample size and large spatial heterogeneity seen in SOC in this study.

In our study area, mean residence time of the near-surface SOC pool in woody communities exceeded that of GR (Table 4). Similarly, McCulley *et al.* [66] also observed that both SR and mean residence time of the near-surface SOC pool in wooded communities (11 years) exceeded that of GRs (6 years) in a subtropical ecosystem. However, in paired juniper woodland and C₄-dominated grassland sites, longer woodland topsoil residence time (33 years) was observed than in GRs (18 years) [58]. In addition, our estimates of SOC residence time were shorter than those of McCulley *et al.* [66] and Smith & Johnson [58], partly because of the differences in the estimates of heterotrophic respiration. In our study, heterotrophic respiration comprised a large portion of total SR (76% to 95%, Table 4), whereas, Smith & Johnson [58] assumed root respiration is 50% of SR and McCulley *et al.* [66] used three scenarios in which they assumed root respiration comprised 30%, 50%, or 70% of total SR.

Conclusion

In conclusion, by determining SR and SOC dynamics in five adjacent vegetation types (GR, SH, EC, DC and DB) in the temperate area of northern China, we identified an increase in both annual SR and residence time of SOC from grassland to woody vegetation types. The increase in annual SR was coupled with changes in soil substrate availability (SOC and STN). The increases in SR suggest an increase in landscape-scale carbon emissions occurred during both natural and anthropogenic transitions occurred from grassland to plant communities dominated by woody vegetation. However, the SOC pool storage and its residence time also increased, suggesting a larger increase in carbon input than in carbon loss from the surface soil layer, thus implying an accumulation of SOC during grassland conversion into woodlands in temperate China.

Acknowledgments

We thanked two anonymous reviewers for their very constructive and valuable comments for its early version of our manuscript.

Author Contributions

Conceived and designed the experiments: WW. Performed the experiments: WW. Analyzed the data: WW WC WZ. Contributed reagents/materials/analysis tools: HZ, JF. Wrote the paper: WW WZ WC.

References

1. Bond-Lamberty B, Thomson A (2010) Temperature-associated increases in the global soil respiration record. *Nature* 464: 579–582.
2. IPCC (2007) *Climate Change 2007: The Physical Science Basis*. Cambridge, UK: Contributions of Working Group I to the 4th Assessment Report of the Intergovernmental Panel on Climate Change.
3. Bahn M, Rodeghiero M, Anderson-Dunn M, Dore S, Gimeno C, et al. (2008) Soil respiration in European grasslands in relation to climate and assimilate supply. *Ecosystems* 11: 1352–1367.
4. Bond-Lamberty B, Bunn AG, Thomson AM (2012) Multi-year lags between forest browning and soil respiration at high northern latitudes. *PLoS one* 7: e50441.

5. Davidson EA, Janssens IA (2006) Temperature sensitivity of soil carbon decomposition and feedbacks to climate change. *Nature* 440: 165–173.
6. Piao SL, Fang JY, Ciais P, Peylin P, Huang Y, et al. (2009) The carbon balance of terrestrial ecosystems in China. *Nature* 458: 1009–1013.
7. Houghton RA (2010) How well do we know the flux of CO₂ from land-use change? *Tellus Series B-Chemical and Physical Meteorology* 62: 337–351.
8. Creamer CA, Filley TR, Boutton TW, Olenik S, Kantola IB (2011) Controls on soil carbon accumulation during woody plant encroachment: evidence from physical fractionation, soil respiration, and delta C-13 of respired CO₂. *Soil Biology & Biochemistry* 43: 1678–1687.
9. Eclesia RP, Jobbagy EG, Jackson RB, Biganzoli F, Pinciro G (2012) Shifts in soil organic carbon for plantation and pasture establishment in native forests and grasslands of South America. *Global Change Biology* 18: 3237–3251.
10. Eldridge DJ, Bowker MA, Maestre FT, Roger E, Reynolds JF, et al. (2011) Impacts of shrub encroachment on ecosystem structure and functioning: towards a global synthesis. *Ecology Letters* 14: 709–722.
11. Livesley SJ, Kiese R, Michle P, Weston CJ, Butterbach-Bahl K, et al. (2009) Soil-atmosphere exchange of greenhouse gases in a *Eucalyptus marginata* woodland, a clover-grass pasture, and *Pinus radiata* and *Eucalyptus globulus* plantations. *Global Change Biology* 15: 425–440.
12. Wheeler CW, Archer SR, Asner GP, McMurtry CR (2007) Climatic/edaphic controls on soil carbon/nitrogen response to shrub encroachment in desert grassland. *Ecological Applications* 17: 1911–1928.
13. Don A, Schumacher J, Freibauer A (2011) Impact of tropical land-use change on soil organic carbon stocks – a meta-analysis. *Global Change Biology* 17: 1658–1670.
14. Dutra Aguiar AP, Ometto JP, Nobre C, Lapola DM, Almeida C, et al. (2012) Modeling the spatial and temporal heterogeneity of deforestation-driven carbon emissions: the INPE-EM framework applied to the Brazilian Amazon. *Global Change Biology* 18: 3346–3366.
15. Saner P, Loh YY, Ong RC, Hector A (2012) Carbon stocks and fluxes in tropical lowland dipterocarp rainforests in Sabah, Malaysian Borneo. *PLoS one* 7: e29642.
16. Throp HL, Archer SR (2008) Shrub (*Prosopis velutina*) encroachment in a semidesert grassland: spatial-temporal changes in soil organic carbon and nitrogen pools. *Global Change Biology* 14: 2420–2431.
17. van der Werf GR, Morton DC, DeFries RS, Olivier JGJ, Kasibhatla PS, et al. (2009) CO₂ emissions from forest loss. *Nature Geoscience* 2: 829–829.
18. Paul KI, Polglase PJ, Nyakuengama JG, Khanna PK (2002) Change in soil carbon following afforestation. *Forest Ecology and Management* 168: 241–257.
19. Perez-Quezada JF, Bown HE, Fuentes JP, Alfaro FA, Franck N (2012) Effects of afforestation on soil respiration in an arid shrubland in Chile. *Journal of Arid Environments* 83: 45–53.
20. Poelplau C, Don A (2013) Sensitivity of soil organic carbon stocks and fractions to different land-use changes across Europe. *Geoderma* 192: 189–201.
21. Wiesmeier M, Spörlein P, Geuss U, Hangen E, Haug S, et al. (2012) Soil organic carbon stocks in southeast Germany (Bavaria) as affected by land use, soil type and sampling depth. *Global Change Biology* 18: 2233–2245.
22. Lai LM, Zhao XC, Jiang LH, Wang YJ, Luo LG, et al. (2012) Soil respiration in different agricultural and natural ecosystems in an arid region. *PLoS one* 7: e48011.
23. Arora VK, Boer GJ (2010) Uncertainties in the 20th century carbon budget associated with land use change. *Global Change Biology* 16: 3327–3348.
24. Browning DM, Archer SR, Asner GP, McClaran MP, Wessman CA (2008) Woody plants in grasslands: post-encroachment stand dynamics. *Ecological Applications* 18: 928–944.
25. Carbone MS, Winston GC, Trumbore SE (2008) Soil respiration in perennial grass and shrub ecosystems: linking environmental controls with plant and microbial sources on seasonal and diel timescales. *Journal of Geophysical Research-Biogeosciences* 113: G02022.
26. Gimeno TE, Escudero A, Delgado A, Valladares F (2012) Previous land use alters the effect of climate change and facilitation on expanding woodlands of Spanish Juniper. *Ecosystems* 15: 564–579.
27. Jenkins M, Adams MA (2010) Vegetation type determines heterotrophic respiration in subalpine Australian ecosystems. *Global Change Biology* 16: 209–219.
28. Boutton TW, Liao JD, Filley TR, Archer SR (2009) Belowground carbon storage and dynamics accompanying woody plant encroachment in a subtropical savanna. In: Lal R, Follett R, editors. *Soil Carbon Sequestration and the Greenhouse Effect*. Soil Science Society of America, Madison, WI. 181–205.
29. Marin-Spiotta E, Sharma S (2013) Carbon storage in successional and plantation forest soils: a tropical analysis. *Global Ecology and Biogeography* 22: 105–117.
30. McKinley DC, Blair JM (2008) Woody plant encroachment by *Juniperus virginiana* in a mesic native grassland promotes rapid carbon and nitrogen accrual. *Ecosystems* 11: 454–468.
31. Barger NN, Archer SR, Campbell JL, Huang CY, Morton JA, et al. (2011) Woody plant proliferation in North American drylands: a synthesis of impacts on ecosystem carbon balance. *Journal of Geophysical Research-Biogeosciences* 116: G00K07.
32. Houghton RA, Hackler JL (2003) Sources and sinks of carbon from land-use change in China. *Global Biogeochemical Cycles* doi:10.1029/2002GB001970.
33. Schimel DS, House JI, Hibbard KA, Bousquet P, Ciais P, et al. (2001) Recent patterns and mechanisms of carbon exchange by terrestrial ecosystems. *Nature* 414: 169–172.
34. Smith P, Davies CA, Ogle S, Zanchi G, Bellarby J, et al. (2012) Towards an integrated global framework to assess the impacts of land use and management change on soil carbon: current capability and future vision. *Global Change Biology* 18: 2089–2101.
35. Iqbal J, Hu R, Du L, Lan L, Shan L, et al. (2008) Differences in soil CO₂ flux between different land use types in mid-subtropical China. *Soil Biology & Biochemistry* 40: 2324–2333.
36. Li HM, Ma YX, Aide TM, Liu WJ (2008) Past, present and future land-use in Xishuangbanna, China and the implications for carbon dynamics. *Forest Ecology and Management* 255: 16–24.
37. Liu F, Wu XB, Bai E, Boutton TW, Archer SR (2011) Quantifying soil organic carbon in complex landscapes: an example of grassland undergoing encroachment of woody plants. *Global Change Biology* 17: 1119–1129.
38. Liu H, Zhao P, Lu P, Wang YS, Lin YB, et al. (2008) Greenhouse gas fluxes from soils of different land-use types in a hilly area of South China. *Agriculture Ecosystems & Environment* 124: 125–135.
39. Sheng H, Yang YS, Yang ZJ, Chen GS, Xie JS, et al. (2010) The dynamic response of soil respiration to land-use changes in subtropical China. *Global Change Biology* 16: 1107–1121.
40. Tang XL, Liu SG, Zhou GY, Zhang DQ, Zhou CY (2006) Soil-atmospheric exchange of CO₂, CH₄, and N₂O in three subtropical forest ecosystems in southern China. *Global Change Biology* 12: 546–560.
41. Berthrong ST, Jobbagy EG, Jackson RB (2009) A global meta-analysis of soil exchangeable cations, pH, carbon, and nitrogen with afforestation. *Ecological Applications* 19: 2228–2241.
42. Fang JY, Chen AP, Peng CH, Zhao SQ, Ci L (2001) Changes in forest biomass carbon storage in China between 1949 and 1998. *Science* 292: 2320–2322.
43. Henry HAL (2008) Climate change and soil freezing dynamics: historical trends and projected changes. *Climatic Change* 87: 421–434.
44. Zhang Y, Liu H (2010) How did climate drying reduce ecosystem carbon storage in the forest-steppe ecotone? A case study in Inner Mongolia, China. *Journal of Plant Research* 123: 543–549.
45. You L, Shen JG, Pei H (2002) Climatic changes in recent 50 years and forecast for the next 10–25 years in Inner Mongolia. *Meteorology of Inner Mongolia* 4: 14–18 (in Chinese).
46. Elberling B (2007) Annual soil CO₂ effluxes in the High Arctic: the role of snow thickness and vegetation type. *Soil Biology & Biochemistry* 39: 646–654.
47. Kurganova I, De Gerenyu VL, Rozanova L, Saponov D, Myakshina T, et al. (2003) Annual and seasonal CO₂ fluxes from Russian southern taiga soils. *Tellus Series B-Chemical and Physical Meteorology* 55: 338–344.
48. Kirschbaum MUF (2004) Soil respiration under prolonged soil warming: are rate reductions caused by acclimation or substrate loss? *Global Change Biology* 10: 1870–1877.
49. Leifeld J, Kogel-Knabner I (2005) Soil organic matter fractions as early indicators for carbon stock changes under different land-use? *Geoderma* 124: 143–155.
50. Gamon JA, Field CB, Goulden ML, Griffin KL, Hartley AE, et al. (1995) Relationships between NDVI, canopy structure, and photosynthesis in 3 Californian vegetation types. *Ecological Applications* 5: 28–41.
51. Ahrends HE, Etzold S, Kutsch WL, Stoeckli R, Bruegger R, et al. (2009) Tree phenology and carbon dioxide fluxes: use of digital photography at for process-based interpretation the ecosystem scale. *Climate Research* 39: 261–274.
52. Richardson AD, Braswell BH, Hollinger DY, Jenkins JP, Ollinger SV (2009) Near-surface remote sensing of spatial and temporal variation in canopy phenology. *Ecological Applications* 19: 1417–1428.
53. Jakubauskas ME, Legates DR, Kastens JH (2001) Harmonic analysis of time-series AVHRR NDVI data. *Photogrammetric Engineering and Remote Sensing* 67: 461–470.
54. Wang W, Peng SS, Fang JY (2010) Root respiration and its relation to nutrient contents in soil and root and EVI among 8 ecosystems, northern China. *Plant and Soil* 333: 391–401.
55. Raich JW, Schlesinger WH (1992) The global carbon-dioxide flux in soil respiration and its relationship to vegetation and climate. *Tellus Series B-Chemical and Physical Meteorology* 44: 81–99.
56. Wang W, Chen WL, Wang SP (2010) Forest soil respiration and its heterotrophic and autotrophic components: global patterns and responses to temperature and precipitation. *Soil Biology & Biochemistry* 42: 1236–1244.
57. Raich JW, Tufekcioglu A (2000) Vegetation and soil respiration: correlations and controls. *Biogeochemistry* 48: 71–90.
58. Smith DL, Johnson L (2004) Vegetation-mediated changes in microclimate reduce soil respiration as woodlands expand into grasslands. *Ecology* 85: 3348–3361.
59. Fang CM, Smith P, Moncrieff JB, Smith JU (2005) Similar response of labile and resistant soil organic matter pools to changes in temperature. *Nature* 433: 57–59.
60. Knorr W, Prentice IC, House JI, Holland EA (2005) Long-term sensitivity of soil carbon turnover to warming. *Nature* 433: 298–301.
61. Reichstein M, Falge E, Baldocchi D, Papale D, Aubinet M, et al. (2005) On the separation of net ecosystem exchange into assimilation and ecosystem respiration: review and improved algorithm. *Global Change Biology* 11: 1424–1439.

62. Höglberg P, Nordgren A, Buchmann N, Taylor AFS, Ekblad A, et al. (2001) Large-scale forest girdling shows that current photosynthesis drives soil respiration. *Nature* 411: 789–792.
63. Bahn M, Schmitt M, Siegwolf R, Richer A, Brüggemann N (2009) Does photosynthesis affect grassland soil-respired CO₂ and its carbon isotope composition on a diurnal timescale? *New Phytologist* 182: 451–460.
64. Höglberg P, Singh B, Löfvenius MO, Nordgren A (2009) Partitioning of soil respiration into its autotrophic and heterotrophic components by means of tree-girdling in old boreal spruce forest. *Forest Ecology & Management* 257: 1764–1767.
65. Schindlbacher A, Zechmeister-Boltenstern S, Jandl R (2009) Carbon losses due to soil warming: Do autotrophic and heterotrophic soil respiration respond equally? *Global Change Biology* 15: 901–913.
66. McCulley RL, Archer SR, Boutton TW, Hons FM, Zuberer DA (2004) Soil respiration and nutrient cycling in wooded communities developing in grassland. *Ecology* 85: 2804–2817.
67. Gill RA, Burke IC (1999) Ecosystem consequences of plant life form changes at three sites in the semiarid United States. *Oecologia* 121: 551–563.
68. Jackson RB, Banner JL, Jobbagy EG, Pockman WT, Wall DH (2002) Ecosystem carbon loss with woody plant invasion of grasslands. *Nature* 418: 623–626.
69. Wei XR, Shao MG, Fu XL, Horton R, Li Y, et al. (2009) Distribution of soil organic C, N and P in three adjacent land use patterns in the northern Loess Plateau, China. *Biogeochemistry* 96: 149–162.
70. Zhou RL, Li YQ, Zhao HL, Drake S (2008) Desertification effects on C and N content of sandy soils under grassland in Horqin, northern China. *Geoderma* 145: 370–375.
71. Zhang YK, Liu HY (2010) How did climate drying reduce ecosystem carbon storage in the forest-steppe ecotone? A case study in Inner Mongolia, China. *Journal of Plant Research* 123: 543–549.
72. Hou XY (2001) *Vegetation Atlas of China* (1: 1,000,000). Beijing, China: Science Press.

Quantifying Regional Vegetation Cover Variability in North China during the Holocene: Implications for Climate Feedback

Guo Liu, Yi Yin, Hongyan Liu*, Qian Hao

College of Urban and Environmental Sciences, Peking University, Beijing, China

Abstract

Validating model simulations of vegetation-climate feedback needs information not only on changes in past vegetation types as reconstructed by palynologists, but also on other proxies such as vegetation cover. We present here a quantitative regional vegetation cover reconstruction for North China during the Holocene. The reconstruction was based on 15 high-quality lake sediment profiles selected from 55 published sites in North China, along with their modern remote sensing vegetation index. We used the surface soil pollen percentage to build three pollen-vegetation cover transfer models, and used lake surface sediment pollen data to validate their accuracy. Our results showed that vegetation cover in North China increased slightly before its maximum at 6.5 cal ka BP and has since declined significantly. The vegetation decline since 6.5 cal ka BP has likely induced a regional albedo change and aerosol increase. Further comparison with paleoclimate and paleovegetation dynamics in South China reproduced the regional cooling effect of vegetation cover decline in North China modelled in previous work. Our discussion demonstrates that, instead of reconstructing vegetation type from a single site, reconstructing quantitative regional vegetation cover could offer a broader understanding of regional vegetation-climate feedback.

Citation: Liu G, Yin Y, Liu H, Hao Q (2013) Quantifying Regional Vegetation Cover Variability in North China during the Holocene: Implications for Climate Feedback. PLoS ONE 8(8): e71681. doi:10.1371/journal.pone.0071681

Editor: Dorian Q. Fuller, University College London, United Kingdom

Received: October 30, 2012; **Accepted:** July 2, 2013; **Published:** August 20, 2013

Copyright: © 2013 Liu et al. This is an open-access article distributed under the terms of the Creative Commons Attribution License, which permits unrestricted use, distribution, and reproduction in any medium, provided the original author and source are credited.

Funding: This study is granted by National Natural Science Foundation of China (NSFC, numbers 41071124, 31021001 and J1103406). The funders had no role in study design, data collection and analysis, decision to publish, or preparation of the manuscript.

Competing Interests: The authors have declared that no competing interests exist.

* E-mail: lhy@urban.pku.edu.cn

Introduction

The need for reducing uncertainty in global climate change predictions has highlighted the importance of integrating model evaluations, on-site and remote sensing monitoring, paleoecological investigation, and small-scale manipulative experiments [1], [2]. Paleoecological data, with their unique advantage in addressing earth system processes at large temporal scales and under extreme conditions, could offer unique insights in this respect [2], [3]. The application of paleoecological data in reconstructions, however, requires the conversion from geological proxies to time-series of reconstructed variables [4].

Vegetation type can be reliably interpreted from pollen records through palynological methods [5], [6], [7], but is hard to quantify and therefore difficult to compare with model simulations or remote sensing monitoring. Modern remote sensing techniques, on the other hand, have allowed the evaluation of vegetation through numerical characteristics that offer important information for model simulations [8], [9]. Using similar palynological methods, with remote sensing data as a modern analogue, vegetation in the past could be reconstructed in a different manner, avoiding a discrete and discontinuous vegetation type reconstruction while providing a detailed description of past vegetation that is comparable with model output. Although it remains uncommon, this approach to vegetation reconstruction has been successfully exploited in some former studies [10], [11], [12].

While paleoenvironmental reconstruction could provide evidence of ecological and climatological processes at large temporal scales, distinguishing variations due to regional trends from those due to local heterogeneity is difficult and thus interpretations are often restricted to being local-scale and case-specific when based on one single site [4], [13]. By combining data from multiple sites, vegetation reconstruction at a regional scale could provide a broader insight into regional scale earth system process: this has already been achieved in many data-rich regions such as Europe [6] and North America [14]. Published late-Quaternary pollen records from northern Asia have increased rapidly in number over the past several decades [15], [16], [17]; in North China, however, reliable pollen data sites with relatively high resolution remained scarce [10] until the collection of higher quality data in recent years (Tab. S1). In this study, we selected 15 sediment profiles with relatively high resolution and reliability from 55 published sites in North China (Table S1), and reconstructed the regional vegetation cover changes during the Holocene using a remote sensing vegetation index (NDVI, normalized difference vegetation index) as a modern analogue. This quantitative regional reconstruction provided an opportunity to examine millennial-scale regional vegetation-climate interaction, and supported the hypothesis of a cooling effect of vegetation decline [18], [19] [20] through comparison with previous model simulations [1].

Data and Methods

1. Pollen dataset

One major obstacle to past vegetation reconstruction is the deficiency of modern lake sediment analogues. Lake sediment profiles are widely used due to their ability to preserve signals of past environmental change; without these data, reconstructions are restricted to surface soil as the modern analogue for lake sediment profiles [21], [22], [23], with much uncertainty remaining with respect to the relationship between surface soil pollen and lake sediment pollen [24], [25]. In this study, both surface soil pollen data and lake surface sediment pollen data were utilized to render the reconstruction as reliable as possible: three simple pollen-NDVI transfer models were built from the modern surface soil pollen and modern NDVI, and were validated by the dataset from modern lake surface sediments. Finally, the most accurate transfer model was applied to the sediment profiles.

A total of 461 published surface-soil pollen records from across North China were collated in this study, collected in regions with mean annual precipitation ranging from 100 to 700 mm (Fig. 1). Over 60 pollen taxa were found in these records, of which *Pinus*, *Betula*, *Quercus*, *Artemisia* and *Chenopodiaceae* appeared most frequently; these taxa have already been identified as indicators of vegetation type in our study area [26], [27]. Redundancy analysis (RDA) with all the major taxa in the soil pollen (Fig. 2a in [35]) showed that these 5 taxa (especially *Pinus*, *Betula* and *Quercus*) could explain most of the geographical variation of the soil pollen dataset; in addition, comparing the R^2 of models constructed by these 5 most common taxa or by 18 common taxa showed that the difference (<0.05) is non-significant. While making use of more information from the pollen data, using more pollen types could at the same time increase the risk of model over-fitting, especially by artificial neural networks. In addition, models will be sensitive to taxa that only occur in few samples, which could introduce bias and uncertainty in the reconstruction. Therefore, the percentages of these five taxa were chosen as dependent variables to establish pollen-NDVI models. Lake surface sediments (upper 5 cm) of 27 perennial lakes with low human disturbance were collected and analysed, to validate the surface-soil pollen-NDVI models constructed by surface soil samples. The model with the highest accuracy was then applied to the selected sediment profiles.

To select the most appropriate data from the 55 available profiles in or near our study area, three criteria were used: 1, the profiles cannot be too far away from the 27 lakes with surface sediment pollen analysis data, to guarantee the effectiveness of the validation; 2, the profiles must cover the last 10 ka, to guarantee the same number of samples for every period; and 3, the profile must have a high temporal resolution, as the trend in vegetation cover largely depends on the time period selected, thus a higher temporal resolution will decrease the uncertainty in period selection. Among all the 55 profiles, 34 were close to the 27 lakes used in this study; among these 34 profiles, 29 had an average resolution higher than 500a; and among these 29 profiles, 15 covered the last 10 ka. Proportions of the five chosen taxa were digitised from these 15 profiles and the corresponding vegetation cover was then reconstructed (Fig. 1). We then resampled the 15 reconstructed vegetation cover time series to a resolution of 200a because different profiles cover different time periods, such that resampling to a finer resolution allowed better use of the data. Finally, the 15 profiles were averaged to yield the regional vegetation cover changes.

2. Modern NDVI distribution patterns

The GIMMS NDVI (normalized difference vegetation index) dataset [28], [29], [30], running from 1982 to 2006 with a spatial resolution of 8 km×8 km, was used to calculate the NDVI of each sampling site. The lakes in our sediment pollen dataset had an average diameter of less than 1 km and the local impact of lakes on albedo and vegetation was thus ignored at the scale of an NDVI pixel. We then calculated the average of the yearly maximum NDVI values from 1982 to 2006 for each site with both surface soil and lake surface sediment samples in our analysis. Distributions of averaged NDVI and mean annual precipitation, as well as vegetation types, are plotted in Fig. 1.

3. Pollen-NDVI transfer models

Three pollen-NDVI models were constructed using pollen records in surface soil and were verified by corresponding records in the lake surface sediment, with the most accurate model being used to reconstruct NDVI from the pollen spectrum in the sediment cores. Models of pollen-NDVI relationships were built using an artificial neural network (ANN), the modern analogue technique (MAT) and linear regression (LR). Then the lake surface sediment pollen and associated NDVI dataset were applied to these models to verify their accuracy.

Firstly, we constructed a model of the relationship between the pollen spectra and NDVI by applying an ANN, which is a very flexible nonlinear method that is able to precisely simulate complex mapping [31]. In our study, the ANN used the percentages of *Pinus*, *Betula*, *Quercus*, *Artemisia* and *Chenopodiaceae* of each sample as input variables and the corresponding NDVI as the target variable. After experimenting with different parameter matching configurations, we chose three hidden layers with node numbers of 8, 10, 10 and the activation functions *tansig*, *logsig*, *logsig* (in Matlab R2009b), respectively.

Next we applied MAT, which has been widely used in vegetation reconstruction with pollen data [32], using the squared chord distance (SCD) as the index of similarity [33], [34]:

$$SCD = \sum_{i=1}^n (\sqrt{x_i} - \sqrt{y_i})^2$$

where SCD is the squared chord distance between two multivariate samples X and Y , and x, y are the proportions of species i in samples X and Y . SCD values can range from 0 to n (number of species), with 0 indicating pollen spectra identical to those of the samples being compared. For each fossil record, five samples with the smallest SCD (with the sample itself excluded) were selected from the surface soil pollen dataset and the corresponding NDVI was reconstructed by the weighted-average:

$$NDVI_r = \frac{\sum_{i=1}^5 NDVI_i / SCD_i}{\sum_{i=1}^5 1 / SCD_i}$$

where $NDVI_r$ is the reconstructed NDVI, and $NDVI_i$ and SCD_i are the NDVI and squared chord distance of each sample.

The third method of reconstruction applied here was linear regression (LR). It can be assumed that for each taxon existing in a biome, every individual occupies a certain ratio of the area and contributes a corresponding value to the total NDVI; therefore, the relationship between total NDVI and the proportion of each taxon may have a linear component. LR has the significant advantage of being intuitive, with the respective parameters clearly showing the contribution of each taxon.

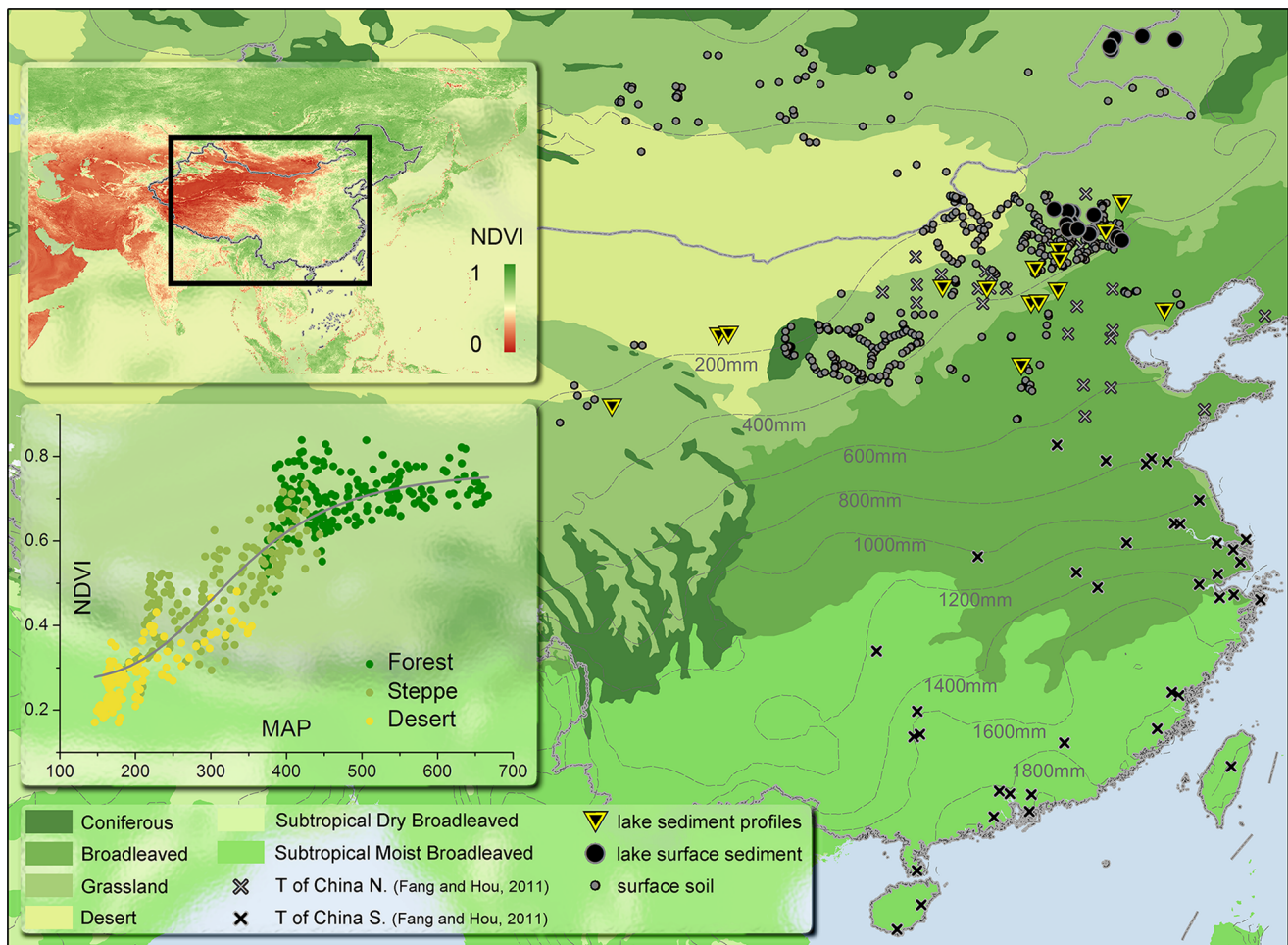


Figure 1. Sample locations and modern NDVI distribution. Modern NDVI data were acquired by averaging data for August from 1982–2006 of the GIMMS dataset. NDVI in South China is homogeneous at a high level, while that of North China varies widely with precipitation. Samples of NDVI-MAP relationships were randomly chosen from grid points with natural vegetation in our study area (North China) and fitted by a logistic curve. Sites with surface soil pollen, lake surface pollen and sediment profiles are distributed around the 400 mm isohyet; some sites with surface soil pollen samples are located in Mongolia, but in the same biome and precipitation regime. *T of China N.* and *T of China S.* indicate the paleotemperature records used in the temperature reconstruction of North China and South China [70], respectively. doi:10.1371/journal.pone.0071681.g001

These three models of pollen spectra and NDVI, built from our surface-pollen dataset, could have been evaluated by means of the adjusted correlation coefficient and residual error between the estimated NDVI and observed NDVI. A proper approach, however, has to extend its accuracy into the fossil sediment pollen record. Therefore, we used our sediment pollen dataset to test the reliability of extending the models into the sediment pollen record by calculating the correlation coefficient between the simulated NDVI and observed NDVI of lake surface sediment samples (Fig. 2b).

All the above calculations were performed with the Matlab R2009b software.

4. Statistical analysis of the reconstructed NDVI

To maximise accuracy of the results, the 15 sediment profiles were selected to occupy the same time range (11.5 cal. ka BP to present) and to have comparatively high resolution (200 yr or higher). Each profile was resampled to 200 years temporal resolution before reconstruction. The reconstruction thus produced 15 comparable time series ranging from 11.5 cal ka BP to present. The stalagmite $\delta^{18}\text{O}$ from a former study was sampled

from Dongge cave in the Pacific monsoon region of China as a proxy for precipitation in the monsoon region, and was linearly correlated with the reconstructed vegetation cover. Meanwhile, the coarse sand ($>63\ \mu\text{m}$) percentage from Anguli Nuur Lake in North China, located in the central-eastern region of our study area in the forest-steppe ecotone about 250 km northwest of Beijing, was used as an indicator of local soil coarsening, and was correlated with the reconstructed vegetation cover.

Results

The ANN yielded the highest accuracy in the pollen-NDVI transfer model and was therefore used in our vegetation cover reconstruction. Each of the three models (ANN, MAT and LR) performed well in establishing the relationship between surface soil pollen and NDVI, with adjusted R^2 values of 0.62, 0.49 and 0.41 ($P<0.01$), respectively. In the validation by lake surface sediment pollen, only ANN and LR continued to produce reliable results, with adjusted R^2 values of 0.56 and 0.47 ($p<0.01$), respectively. Therefore, only the reconstruction by ANN was used in the following analysis.

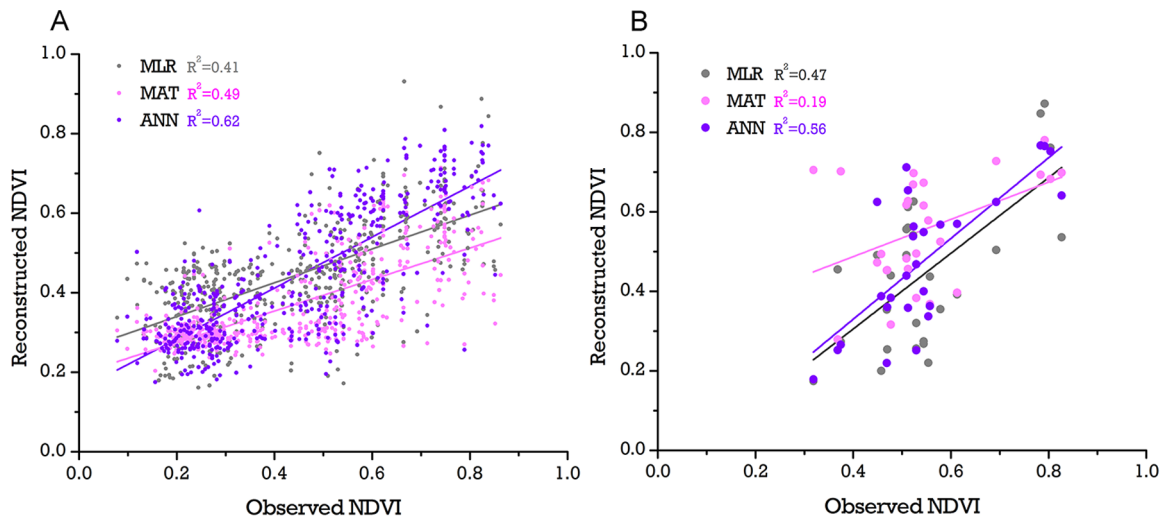


Figure 2. Result of model reconstruction and verification. In subplot A, LR, MAT and ANN all performed well in the model construction phase and passed the 0.01 significance level test; in subplot B, when verified by lake surface sediment pollen data, MAT failed to produce a reliable result. ANN was chosen for the reconstruction. All R^2 data are the adjusted R square. doi:10.1371/journal.pone.0071681.g002

Reconstruction results show that vegetation cover in North China increased slightly before its maximum at 6.5 cal. ka BP and has since declined significantly (Fig. 3). The Holocene can be divided into 3 periods according to the averaged results from 15 profiles with 200-year resolution, as follows. *Period III* (11.5–6.5 cal. ka BP): most profiles in this period were identified as forest in former studies; vegetation cover fluctuated greatly but showed an overall slight increase before reaching its maximum at 6.5 cal. ka BP. *Period II* (6.5–3 cal. ka BP): a greater number of profiles were identified as steppe or forest steppe in this period, regional vegetation cover declined significantly from 0.57 to approximately 0.46. *Period I* (3 cal. ka BP–present): most profiles were identified as steppe, but the decline in Period II ended and there was even a slight increase in the most recent 1 cal. ka BP. Although 15 profiles are not sufficient to map the distribution of vegetation cover, we calculated and plotted the mean reconstructed vegetation cover of each profile for 10–9, 7–6 and 2–1 cal. ka BP (Fig. 4) to indicate the state of each period. Upper and lower quartiles in each 200-yr period were also calculated, showing the difference within sub-regions with different levels of vegetation cover.

Discussion

1. Vegetation cover changes and their driving forces

The number of profiles adequate for regional vegetation reconstruction is directly related to the indicating area of lake sediment pollen and the vegetation heterogeneity in the studied area. Former studies conducted in small lakes with an assumption of neutral atmospheric conditions in regions dominated by forest generally showed that the source area of sediment pollen is within a radius of 1 km [35], [36], [37], [38]. With a source area of this scale, 15 profiles would be a poor representation of this region; however, in areas with a relatively open landscape, e.g. North China and the North American Central Plain, strong winds prevail through most of the year causing long distance transportation of dusts [39], which carry 20–1000 μm particles including pollen grains [40]. Combining surface soil pollen data and remote sensing data in a similar fashion to this study, research in eastern North America has yielded indicating areas with half-widths of 25–75 km [41]. Using a similar method, we have also calculated

the indicating area of surface soil pollen and lake surface sediment pollen (corresponding to the lake sediment profiles used in reconstruction) in our study area (Yin et al., unpublished manuscript) and identified an average indicating area much larger than that of traditional estimates (half-widths of 20 km for surface soil, and over 100 km for surface lake sediment).

Although we could not directly quantify the heterogeneity of paleo-vegetation cover in our study area from the 15 profiles, we were able to assess whether the variability in these profiles could cause uncertainties in our results, and we indirectly evaluated the uncertainty related to vegetation cover heterogeneity. As our conclusions were based on the trend in vegetation cover, the relative change in vegetation cover was more important than the actual value of reconstructed vegetation cover in our study. Despite the different magnitudes of variability, the upper quartile, the lower quartile and the average of the 15 sequences showed the same trends (Fig. 3), indicating that the difference between profiles has little influence on our conclusion. Thus we believe that the 15 profiles are representative of the geographical range they cover. However, as the 15 profiles did not include sediment from the Loess Plateau, which has markedly different vegetation, the reconstructed vegetation cover only includes the regions of North China outside of the plateau.

Average results from the 15 profiles showed that vegetation cover in North China increased slightly from 11 cal. ka BP and reached its maximum at 6.5 cal. ka BP, before decreasing significantly. Calculation of the upper and lower quartiles in each 200-year period revealed the range in levels of vegetation cover between different regions: accordingly, the overall trends in vegetation cover were mainly attributed to changes in regions with high vegetation cover (mostly forest), while regions with low vegetation cover (mostly grassland and desert) remained relatively stable. Our results coincide well with those of former studies of Holocene vegetation types in North China (Tab. S1): in *Period III*, when vegetation cover fluctuated greatly with a slight overall increase, the vegetation type was mainly forest; in *Period II*, vegetation cover declined significantly and changed from forest-dominated to grassland-dominated at most sites; in *Period I*, the decline of vegetation cover slowed and North China was dominated by grassland.

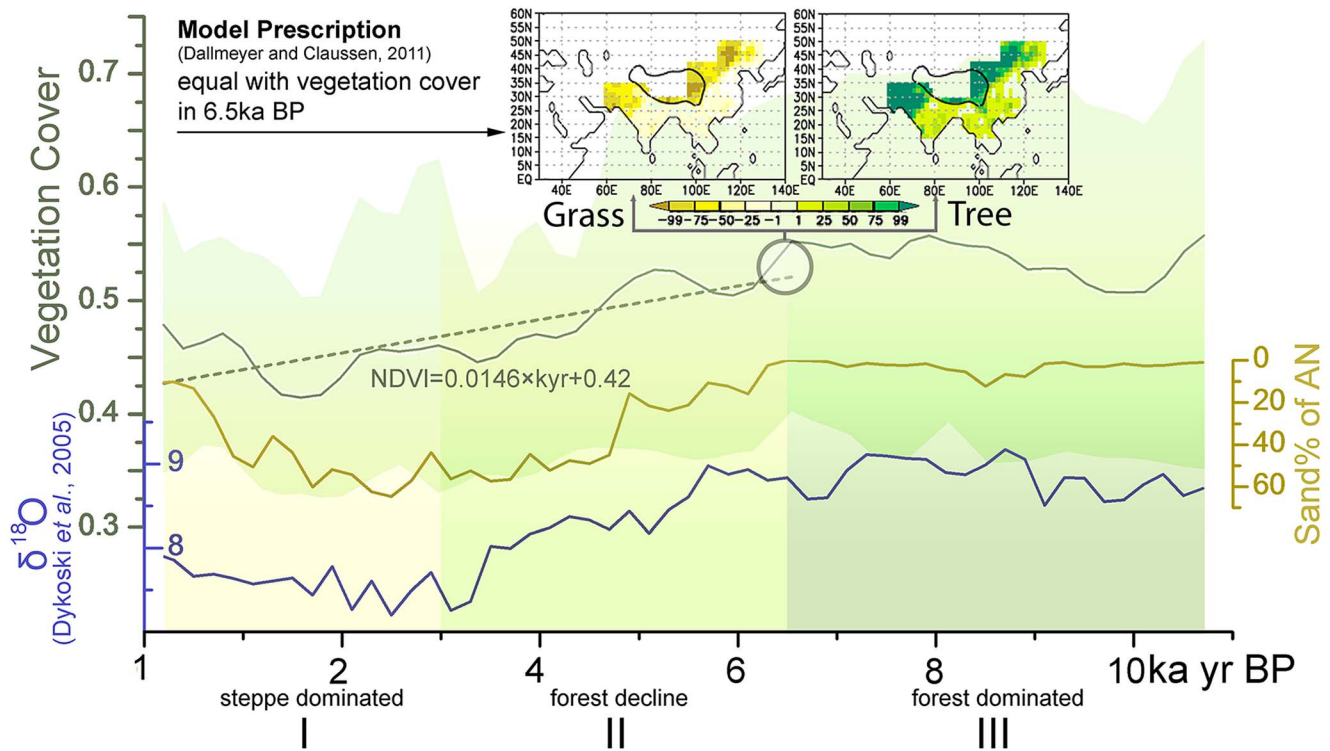


Figure 3. Mean reconstructed vegetation cover of each profile for 1–2, 6–7 and 9–10 ka BP. The circle diameters show the mean values of the reconstruction within 1 ka, while modern NDVI and modern MAP are plotted in the background. Because the heterogeneity between sites is much larger than the variation, the diameters of the circles were plotted according to the relative values compared to the mean value of the entire time series at each site.

doi:10.1371/journal.pone.0071681.g003

Regional reconstruction of vegetation cover provides an opportunity for studying regional driving forces of vegetation cover, and the partial correlation between reconstructed temperature and stalagmite $\delta^{18}\text{O}$ has revealed precipitation as the main driving factor of vegetation cover change. Precipitation in the Pacific monsoon regions of China during the Holocene could be indicated by the stalagmite $\delta^{18}\text{O}$ proxy from Dongge Cave [42], [43]. Linear regression shows that this proxy is significantly and negatively correlated with the reconstructed vegetation cover in North China ($R^2 = 0.701$, $P < 0.01$), indicating the influence of precipitation on vegetation (a lower $\delta^{18}\text{O}$ indicates higher precipitation). However, a potential risk of comparing the stalagmite $\delta^{18}\text{O}$ from Dongge Cave with results from our reconstruction is the uncertainty in the $\delta^{18}\text{O}$ interpretation. Although former studies have shown that $\delta^{18}\text{O}$ of stalagmites in the region of Dongge Cave can be interpreted reliably as an indicator of the overall precipitation at a continental scale [43], [44], it has been argued that $\delta^{18}\text{O}$ may also be influenced by temperature [45], [46]. Studies based on modern observations in North China, however, have shown that precipitation dominates vegetation growth while temperature only plays a minor role [47], [48], [49]. Thermal regulation of vegetation has been found in areas with vegetation decline due to warming-induced drought [48], [49], [50], which casts further doubt on the relationship between decreasing temperature and declining vegetation cover through the Holocene [51]. In addition, we conducted a model simulation using the ORCHIDEE dynamic global vegetation model (DGVM) to test the influence of precipitation and temperature on vegetation cover in this region, and have also found that precipitation strongly controls vegetation cover in

North China, while temperature has a relatively weak influence (Liu *et al.*, unpublished data).

2. Possible impacts of vegetation cover change

While vegetation cover is mainly controlled by precipitation, significant change on a regional scale could in return have impacts on regional climate. Among these impacts are the decrease in albedo and the increase of aerosol production. The degradation from forest to grassland or from grassland to desert is accompanied by an increase in albedo [52], [53]; in addition, NDVI, indicating vegetation cover change in our study, has a linear negative relationship with albedo [54], [55], and its reconstruction implies the albedo increase in *Period I*. A more significant mechanism contributing to albedo changes is related to the transformation between vegetation types. In the winter of higher latitudes, grassland is entirely covered by snow whereas forest can penetrate through snow cover and generally remains exposed. Therefore, the transformation from forest to grassland could significantly change the albedo of the land cover [56], [57]. This transformation has taken place in the past 6500 years in regions with high vegetation cover, corresponding to those regions which have been mainly attributed to the overall vegetation cover change owing to their position in the upper quartile of the reconstruction.

The other possible impact of vegetation cover decline is the increase in aerosol production: soil dust plays an important role in the production of aerosol, and could significantly alter the regional radiation balance [58], [59]. Soil coarsening or sandification, the main source of soil dust, could be indirectly inferred from the coarse sand percentage in sediment records. Vegetation cover decline may lead to soil sandification and an increase in wind

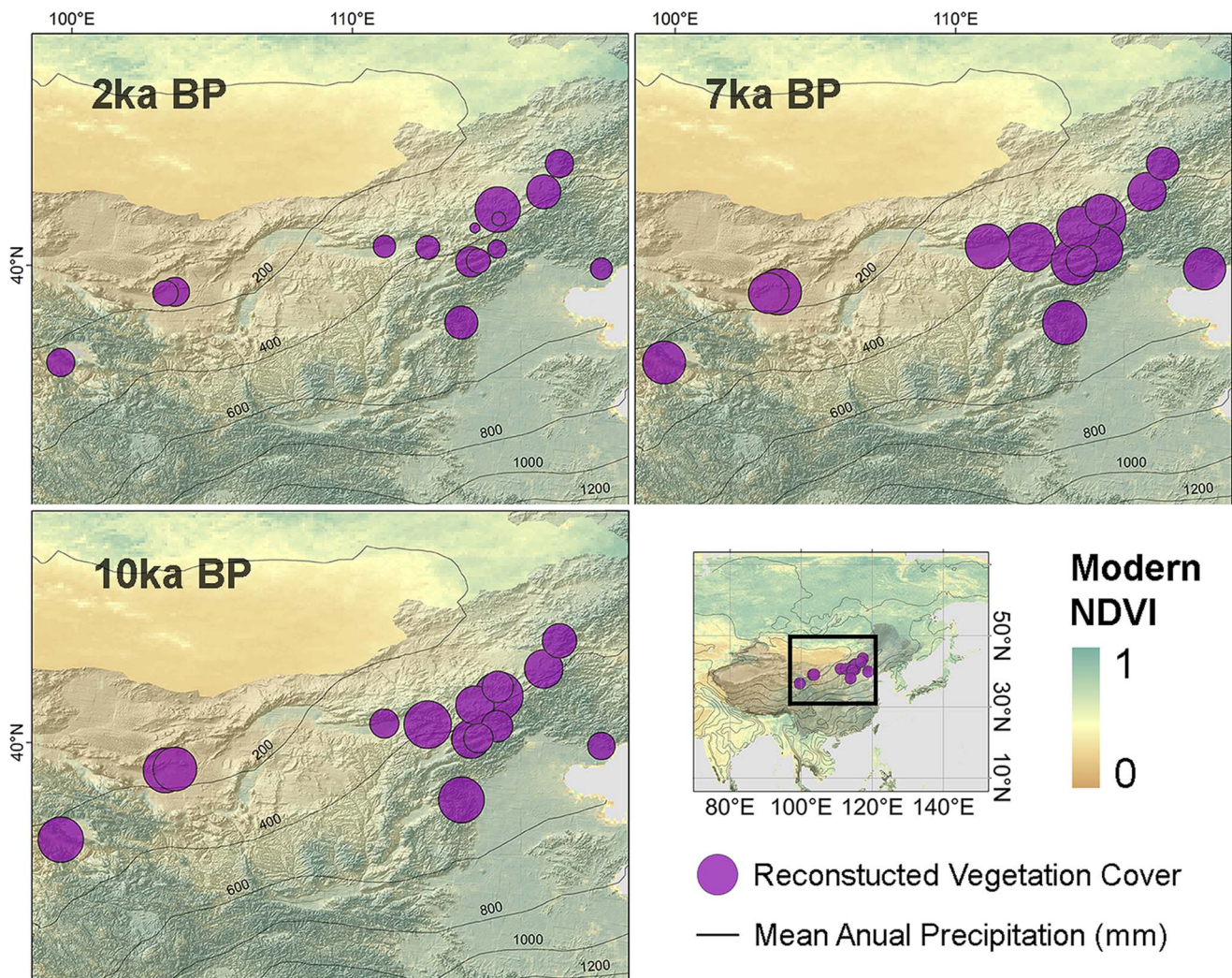


Figure 4. Reconstructed vegetation cover, related factors and prescribed values in previous studies. *Vegetation Cover* shows the reconstructed NDVI averaged from 15 sequences, with linear regression after 6.5 ka yr BP showing a decrease of 0.13. The light green area indicates the upper quartile and lower quartile of the 15 sequences, indicating that areas with higher NDVI experience larger fluctuations and were the major contributors to the vegetation decline in *Period II*. *Sand%* of AN shows the coarse sand ($>63 \mu\text{m}$) percentage in sediment cores from Anguli Nuur (inversely scaled). Stalagmite $\delta^{18}\text{O}$ of Dongge Cave (as $\delta^{18}\text{O}$, values are negative), coarse sand percentage of Anguli Nuur and reconstructed NDVI are significantly correlated with each other. Prescribed values in the model simulation by Dallmeyer and Claussen (2011) coincide with the vegetation cover at 6.5 cal ka BP as reconstructed here; the colour bar shows the percentage of grass/trees in comparison to the modern vegetation distribution. doi:10.1371/journal.pone.0071681.g004

velocity, both of which can contribute to a higher coarse sand percentage in lake sediments. Changes in wind velocity are attributed to the shift from forest to grassland, with a corresponding reduction in surface roughness [60], [61]. The vegetation type derived from this core has, however, shown the dominance of grassland since 5.0 cal. ka BP [62], while the coarse sand percentage has increased in tandem with the regional vegetation cover decline since then (except for a decrease in the past thousand years that coincides with the recovery of vegetation cover) (Fig. 4). A connection between coarse sand percentage and monsoon intensity has been reported throughout the last glacial maximum, but has mostly been observed at the larger temporal scale of the glacial-interglacial cycle and on plateaus such the Chinese Loess Plateau [63], [64]. The fluctuation of monsoon intensity during the Holocene was, however, much milder; in addition, the location of Anguli Nuur lake within a basin reduces its sensitivity to monsoon-controlled changes in wind velocity. A more likely

explanation is that the soil coarsening or sandification accompanied vegetation decline [65], [66], which can still be observed around Anguli Nuur Lake. Through the increase in dust transferred to the atmosphere, desertification could become a further source of aerosol [58], [59], [67]. The regional average vegetation cover is used in this study instead of that solely reconstructed from the sediment core of Anguli Nuur Lake due to the lower credibility of reconstruction from a single site. Although this coarse sand percentage is mainly a local indicator, the correlation reflects the relationship between regional vegetation cover decline and local soil sandification and implies the consequential increase of dust and aerosol.

Although the carbon emission accompanying the vegetation cover decline could have an impact at larger scales, both of the impacts discussed above suggest a cooling effect on regional climate (Fig. 5). Interactions between the regional vegetation-climate processes make it difficult to evaluate the overall effect of

these feedbacks; however, regional comparison of paleoenvironmental reconstructions could provide evidence for the overall response over a long period of time, disregarding the uncertainties in the mechanisms' details. While the vegetation cover has declined significantly in North China since 6.5 cal. ka BP, vegetation in South China has been relatively steady and constantly dominated by forest [68], and its NDVI has remained saturated even to modern times [48]. Comparison between the vegetation records and temperature records in these two regions could thus offer insight into the overall thermal feedback of forest. Moreover, the vegetation-climate interaction in these regions has been discussed through a model simulation in a previous study [1], whose result implied a cooling effect of vegetation cover decline in North China that can be compared to our reconstruction.

As prescribed in the model, approximately 70% forest was added and 60% steppe removed in our study area, while vegetation change was comparably small in South China [1]. This prescription change, according to the modern distribution of NDVI (Fig. 1), is equivalent to a change of 0.1–0.15 in the NDVI of North China. Our result showed that, within the past 10,000 years, the vegetation cover consistent with these prescribed conditions occurred at 6.5 cal. ka BP (0.13 higher than modern times in NDVI, Fig. 3). Modelling results have indicated that North China was 1–1.5 K warmer in the cold/dry season while South China was 0.25–0.5 K warmer in the cold/dry season [1]. These results can then be compared to reconstructed temperatures for this period. Reconstructed temperatures around 6.5 cal. ka BP from single sites have shown a more significant warming, specifically 1.7–2.6 K, 3.0 K and 3.0–4.0 K for North China, and 1.0 K, 1.7 K and 3.0–3.5 K for South China [69], with a similar north-south contrast. Recent synthetic reconstructions of temperature in these two regions agree better with the model simulation, in which the linear trend in the temperature time series shows that North China was 1.8 K warmer and that South China (Southeast China and Central East China in the original publication) was 0.4 K warmer at 6.5 cal ka BP [70].

Situated in the Pacific monsoon region, both North China and South China are controlled by the same monsoon system (referred to as the SE Asian Monsoon in previous studies) [71], [72], and have shared similar climate histories during the Holocene. The differences in their temperature changes could be attributed, at least partially, to the contrasting vegetation cover changes. An opposing view could be that the vegetation cover decline was a result of the temperate change. However, as discussed in *Section 4.1.*, warming generally intensifies the water deficit of vegetation in North China [73], [74]; therefore it is unlikely that the decrease in temperature could have led the decline in vegetation cover of North China. Although agreement between model simulation and

the mechanisms we have suggested cannot rigorously prove the causal-consequence relationship between vegetation cover and temperature, it strongly supports former modelling studies and clearly increase support for the existence of this feedback. While global warming due to greenhouse gas emissions is commonly regarded as a serious issue for the future, this cooling effect might partially compensate the decrease in carbon sinks and thus counteract the effects of global warming. Estimates of the intensity of this feedback are evidently critical for the precision of model simulations.

3. Prospective regional vegetation cover reconstruction

The importance of integrating models and paleoecology data, in both the process of constraining inverse modelling and in the structure adjustment in forward modelling, has been recognized with the development of mechanistic, comprehensive and complex structures in ecological models and with the rapid growth of data in paleoecology [3]. As many have argued before, the assimilation of proxy data into models has become important for the improvement of both palaeovegetation reconstructions and model simulations [75], [3]. As a result, while ecological models have been developed in preparation for the data assimilation application, palaeoclimate and palaeovegetation are being reconstructed in a manner that can be directly utilized by models [76], [77], [78], and intensive integration of paleoecological data and model simulations has recently been achieved [79], [80]. Reliable methodologies and a paradigm for single-site based vegetation type reconstructions has been developed and recognized, but the implications of such reconstructions are, however, often site-specific and locally-restricted, with results that are difficult to quantify. We have shown in this study that regional vegetation cover reconstruction, with the help of newly developed vegetation indices in remote sensing, could offer new insights in earth system models.

As a trial of this approach, we discuss the cooling effect of vegetation cover decline, which has been crucial not only because it might counteract the organic carbon release, but because it could also result in a regional overall cooling [19], [20]. This is in contrast to the long-held view that afforestation, which opposes the vegetation cover decline, can alleviate global warming [81], [82]. Previous observations, however, were conducted during comparatively short periods of time [19], [43], [83], which might be insufficient for a significant change in vegetation cover to take place. The long temporal scales in paleoecological studies are therefore valuable for the evaluation of similar processes. An ideal regional vegetation cover reconstruction would have a spatial resolution that could demonstrate the pattern of vegetation cover distribution, and could provide boundary conditions or driving

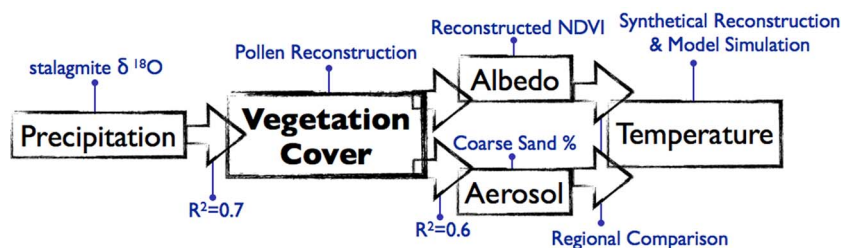


Figure 5. Mechanisms discussed in this study. Black boxes show the mechanisms discussed in the text, and are further explained by the blue annotations or the corresponding R^2 in the linear correlation. While vegetation cover in North China is mainly controlled by precipitation, its decline in the past 6500 years might have led to the changes in both land cover albedo and aerosol production, with a resulting regional cooling effect, as model simulations in previous studies and the regional comparison in this study have shown.

doi:10.1371/journal.pone.0071681.g005

parameters for model simulations. In North China, this could be achieved with the rapid accumulation of paleoecological data; however, at present, in this study the regional spatial pattern of vegetation cover could not be obtained reliably based on 15 profiles (which were selected out of 55 profiles in this region according to the quality control criteria) even if calibration with the modern vegetation cover pattern is taken into account. As a result, regional averaging was a compromise necessary in the comparison between results from the model and those from the reconstruction. Nevertheless, in view of the data-rich enterprise that palaeoecology has become, we here present a method of vegetation reconstruction that yields regional vegetation cover instead of vegetation type, and which is more suitable for addressing regional-scale questions and model-data comparison. Our discussion has demonstrated that this switch in the reconstruction objective could help in validating results from models, as well as in understanding the mechanisms underlying earth system process on a larger scale.

Conclusions

In this study we quantitatively reconstructed the Holocene vegetation cover changes in North China from multiple pollen records, using the modern NDVI as an index. The results shows that:

1. Vegetation cover in North China increased slightly after 11 cal. ka BP and reached its maximum at 6.5 cal ka BP, but has decreased significantly since then. This change was mainly attributed to vegetation dynamics in regions with a high vegetation cover, while regions with low vegetation cover changed relatively little.

References

1. Dallmeyer A, Claussen M (2011) The influence of land cover change in the Asian monsoon region on present-day and mid-Holocene climate. *Biogeosciences* 8: 1499–1519.
2. Reichstein M, Mahecha MD, Ciais P, Seneviratne SI, Blyth EM, et al. (2011) Elk-testing climate-carbon cycle models: a case for pattern-oriented system analysis. *iLEAPS Newsl.* 11, 14–21.
3. Peng C, Guiot J, Wu H, Jiang H, Luo Y (2011) Integrating models with data in ecology and palaeoecology: advances towards a model-data fusion approach. *Ecol. Lett.* 14, 522–536.
4. Tarasov PE, Guiot J, Cheddadi R, Andreev AA, Bezusko LG, et al. (1999) Climate in northern Eurasia 6000 years ago reconstructed from pollen data. *Earth Planet. Sci. Lett.* 171, 635–645.
5. Cheddadi R, Lamb H, Guiot J, Van Der Kaars S (1998) Holocene climatic change in Morocco: a quantitative reconstruction from pollen data. *Clim. Dyn.* 14, 883–890.
6. Parsons R, Prentice IC (1981) Statistical approaches to R-values and the pollen-vegetation relationship. *Rev. Palaeobot. Palynol.* 32, 127–152.
7. Prentice IC, Guiot J, Huntley B, Jolly D, Cheddadi R (1996) Reconstructing biomes from palaeoecological data: a general method and its application to European pollen data at 0 and 6 ka. *Clim. Dyn.* 12, 185–194.
8. Sugita S (1994) Pollen representation of vegetation in Quaternary sediments: theory and method in patchy vegetation. *J. Ecol.* 82, 881–897.
9. Sellers P, Meeson B, Hall F, Asrar G, Murphy R, et al. (1995) Remote sensing of the land surface for studies of global change: Models – algorithms – experiments. *Remote Sens. Environ.* 51, 3–26.
10. Field CB, Randerson JT, Malmström CM (1995) Global net primary production: combining ecology and remote sensing. *Remote Sens. Environ.* 51: 74–88.
11. Tarasov P, Williams JW, Andreev A, Nakagawa T, Bezrukova E, et al. (2007) Satellite- and pollen-based quantitative woody cover reconstructions for northern Asia: verification and application to late-Quaternary pollen data. *Earth Planet. Sci. Lett.* 264, 284–298.
12. Williams J, Shuman B (2008) Obtaining accurate and precise environmental reconstructions from the modern analog technique and North American surface pollen dataset. *Quat. Sci. Rev.* 27, 669–687.
13. Herzschuh U, Birks HJB, Ni J, Zhao Y, Liu H, et al. (2010) Holocene land-cover changes on the Tibetan Plateau. *The Holocene* 20, 91–104.
2. Vegetation cover decline in North China was mainly controlled by precipitation changes in the Pacific Monsoon region; this vegetation decline could have then induced local soil coarsening and a consequential increase in the production of aerosol.
3. One important implication of this result is its support of a thermal feedback of vegetation cover change as reported in former modelling studies, suggesting that the vegetation cover changes in North China could have had an overall cooling effect on this region during the late Holocene, owing to their alteration of albedo and aerosol production.
4. Combining multiple profiles and using modern vegetation indices as a modern analogue could yield a quantitative reconstruction of regional vegetation cover, which could be used in validating results from models as well as understanding ecological process on a larger scale. This advantage will become even more notable with the rapid accumulation of paleoecological data.

Supporting Information

Table S1 Site description of the 15 selected sediment profiles in North China. This table contains the references and basic information of the 15 profiles used for vegetation reconstruction in this study. (DOC)

Author Contributions

Conceived and designed the experiments: HL. Performed the experiments: GL YY. Analyzed the data: GL YY QH. Contributed reagents/materials/analysis tools: GL YY QH. Wrote the paper: GL HL.

- normalized difference vegetation index (NDVI), monthly 1981–2002. University of Maryland.
29. Tucker CJ, Pinzon JE, Brown ME, Slayback DA, Pak EW, et al. (2005) An extended AVHRR 8-km NDVI dataset compatible with MODIS and SPOT vegetation NDVI data. *Int. J. Remote Sens.* 26, 4485–4498.
 30. Pinzon J, Brown ME, Tucker CJ (2005) Satellite time series correction of orbital drift artifacts using empirical mode decomposition. Hilbert-Huang transform: introduction and applications.
 31. Chen S, Billings SA (1992) Neural networks for nonlinear dynamic system modelling and identification. *Intl. J. Control* 56, 319–346.
 32. Prell WL (1985) Stability of low-latitude sea-surface temperatures: an evaluation of the CLIMAP reconstruction with emphasis on the positive SST anomalies. Final report. Brown Univ., Providence, RI (USA). Dept. of Geological Sciences.
 33. Anderson P, Bartlein P, Brubaker L, Gajewski K, Ritchie J (1989) Modern analogues of late-Quaternary pollen spectra from the western interior of North America. *J. Biogeog.* 16, 573–596.
 34. Overpeck JT, Webb RS, Webb T (1992) Mapping eastern North American vegetation change of the past 18 ka: No-analogs and the future. *Geol.* 20, 1071–1074.
 35. Yin Y, Liu H, Liu Q, Hao Q, Wang H (2012) Vegetation responses to mid-Holocene extreme drought events and subsequent long-term drought on the southeastern Inner Mongolian Plateau, China. *Agricultural and Forest Meteorology*. E-pub ahead of print. doi:10.1016/j.agrformet.2012.10.005. In Press.
 36. Gaillard MJ, Sugita S, Bunting MJ, Middleton R, Broström A, et al. (2008) The use of modelling and simulation approach in reconstructing past landscapes from fossil pollen data: a review and results from the POLLANDCAL network. *Vegetation History and Archaeobotany*. 17, 419–443.
 37. Hellman S, Gaillard MJ, Bunting JM, Mazier F (2009) Estimating the relevant source area of pollen in the past cultural landscapes of southern Sweden – a forward modelling approach. *Review of Palaeobotany and Palynology*. 153, 259–271.
 38. Nielsen AB, Sugita S (2005) Estimating relevant source area of pollen for small Danish lakes around AD 1800. *The Holocene*. 15, 1006–1020.
 39. Wishart D (2004) The Great Plains Region, In: *Encyclopedia of the Great Plains*, Lincoln: University of Nebraska Press, xiii–xviii.
 40. Kellogg CA, Griffin DW (2006) Aerobiology and the global transport of desert dust. *Trends in ecology & evolution* 21, 638–644.
 41. Williams JW, Jackson ST (2003) Palynological and AVHRR observations of modern vegetational gradients in eastern North America. *The Holocene*. 13, 485–497.
 42. Yuan D, Cheng H, Edwards RL, Dykoski CA, Kelly MJ, et al. (2004) Timing, duration, and transitions of the last interglacial Asian monsoon. *Sci.* 304, 575–578.
 43. Dykoski CA, Edwards RL, Cheng H, Yuan D, Cai Y, et al. (2005) A high-resolution, absolute-dated Holocene and deglacial Asian monsoon record from Dongge Cave, China. *Earth Planet. Sci. Lett.* 233, 71–86.
 44. Hu C, Henderson GM, Huang J, Xie S, Sun Y, et al. (2008) Quantification of Holocene Asian monsoon rainfall from spatially separated cave records. *Earth Planet. Sci. Lett.* 266, 221–232.
 45. Wang YJ, Cheng H, Edwards RL, An Z, Wu J, et al. (2001) A high-resolution absolute-dated late Pleistocene monsoon record from Hulu Cave, China. *Sci.* 294, 2345–2348.
 46. McDermott F (2004) Palaeo-climate reconstruction from stable isotope variations in speleothems: a review. *Quat. Sci. Rev.* 23: 901–918.
 47. Wu X, Liu H, Ren J, He S, Zhang Y (2009) Water-dominated vegetation activity across biomes in mid-latitude eastern China. *Geophys. Res. Lett.* 36, L04402.
 48. Piao S, Mohammat A, Fang J, Cai Q, Feng J (2006) NDVI-based increase in growth of temperate grasslands and its responses to climate changes in China. *Glob. Environ. Change* 16, 340–348.
 49. Zou X, Zhai P, Zhang Q (2005) Variations in droughts over China: 1951–2003. *Geophys. Res. Lett.* 32: L04707.
 50. Li Z, Wang Y, Zhou Q, Wu J, Peng J, et al. (2008) Spatiotemporal variability of land surface moisture based on vegetation and temperature characteristics in Northern Shaanxi Loess Plateau, China. *J. Arid Environ.* 72: 974–985.
 51. Loarie SR, Lobell DB, Asner G.P., Field CB (2011) Land-Cover and Surface Water Change Drive Large Albedo Increases in South America. *Earth Interact.* 15, 1–16.
 52. Irvine PJ, Ridgwell A, Lunt DJ (2011) Climatic effects of surface albedo geoengineering. *J. Geophys. Res.* 116, D24112.
 53. Blok D, Schaepman-Strub G, Bartholomeus H, Heijmans MMD, Maximov TC, et al. (2011) The response of Arctic vegetation to the summer climate: relation between shrub cover, NDVI, surface albedo and temperature. *Environ. Res. Lett.* 6, 035502.
 54. Glenn E.P, Huete AR, Nagler PL, Nelson SG (2008) Relationship between remotely-sensed vegetation indices, canopy attributes and plant physiological processes: What vegetation indices can and cannot tell us about the landscape. *Sensors* 8, 2136–2160.
 55. Betts RA (2000) Offset of the potential carbon sink from boreal forestation by decreases in surface albedo. *Nat.* 408, 187–190.
 56. Lee X, Goulden ML, Hollinger DY, Barr A, Black TA, et al. (2011) Observed increase in local cooling effect of deforestation at higher latitudes. *Nat.* 479, 384–387.
 57. Lau K, Kim K (2007) Cooling of the Atlantic by Saharan dust. *Geophys. Res. Lett.* 34, L23811.
 58. Miller R, Tegen I (1998) Climate response to soil dust aerosols. *J. Clim.* 11, 3247–3267.
 59. Wolfe SA, Nickling WG (1993) The protective role of sparse vegetation in wind erosion. *Prog. Phys. Geogr.* 17, 50–68.
 60. Wieringa J (1986) Roughness-dependent geographical interpolation of surface wind speed averages. *Quart. J. R. Meteorol. Soc.* 112, 867–889.
 61. Yin Y, Liu H, He S, Zhao F, Zhu J, et al. (2011) Patterns of local and regional grain size distribution and their application to Holocene climate reconstruction in semi-arid Inner Mongolia, China. *Palaeogeogr., Palaeoclim., Palaeoecol.* 307, 168–176.
 62. Lu H, An Z (1998) Paleoclimatic significance of grain size of loess-palaeosol deposit in Chinese Loess Plateau. *Sci. in China Ser. D: Earth Sci.* 41, 626–631.
 63. Zhang Z, Zhao M, Lu H, Faiia AM (2003) Lower temperature as the main cause of C4 plant declines during the glacial periods on the Chinese Loess Plateau. *Earth Planet. Sci. Lett.* 214, 467–481.
 64. Glantz MH, Orlovsky N (1983) Desertification: A review of the concept. *Desert. Control Bull.* 9, 15–22.
 65. Frumkin A, Stein M (2004) The Sahara–East Mediterranean dust and climate connection revealed by strontium and uranium isotopes in a Jerusalem speleothem. *Earth Planet. Sci. Lett.* 217, 451–464.
 66. Tegen I, Harrison SP, Kohfeld K, Prentice IC, Coe M, et al. (2002) Impact of vegetation and preferential source areas on global dust aerosol: Results from a model study. *J. Geophys. Res.* 107, 4576.
 67. Zhao Y, Yu Z, Chen F, Zhang J, Yang B (2009) Vegetation response to Holocene climate change in monsoon-influenced region of China. *Earth Sci. Rev.* 97, 242–256.
 68. Herzschuh U (2006) Palaeo-moisture evolution in monsoonal Central Asia during the last 50,000 years. *Quat. Sci. Rev.* 25, 163–178.
 69. Wang S, Gong D (2000) Climate in China during the four special periods in Holocene. *Prog. Nat. Sci.* 10, 325–332.
 70. Fang X, Hou G (2011) Synthetically Reconstructed Holocene Temperature Change in China. *Scientia Geographica Sinica* 31, 385–393.
 71. Gao Y (1962) Some problems on East-Asia monsoon. Science Press, Beijing.
 72. Sun P, Yu Z, Liu S, Wei X, Wang J, et al. (2012) Climate change, growing season water deficit and vegetation activity along the north-south transect of Eastern China from 1982 through 2006. *Hydrol. Earth Syst. Sci. Discuss* 9, 6649–6688.
 73. Chuai X, Huang X, Wang W, Bao G (2012) NDVI, temperature and precipitation changes and their relationships with different vegetation types during 1998–2007 in Inner Mongolia, China. *Int. J. of Clim.*
 74. Widmann M, Goosse H, van der Schrier G, Schnur R, Barkmeijer J (2010) Using data assimilation to study extratropical Northern Hemisphere climate over the last millennium. *Clim. Past* 6, 627–644.
 75. Williams M, Richardson A, Reichstein M, Stoy P, Peylin P, et al. (2009) Improving land surface models with FLUXNET data. *Biogeosci.* 6, 1341–1359.
 76. Guiot J, Wu H, Garreta V, Hatté C, Magny M (2009) A few prospective ideas on climate reconstruction: from a statistical single proxy approach towards a multi-proxy and dynamical approach. *Clim. Past* 5, 571–583.
 77. Wu H, Guiot JEL, Peng C, Guo Z (2008) New coupled model used inversely for reconstructing past terrestrial carbon storage from pollen data: validation of model using modern data. *Glob. Change Biol.* 15, 82–96.
 78. Williams JW, Gonzales LM, Kaplan JO (2008) Leaf area index for northern and eastern North America at the Last Glacial Maximum: a data–model comparison. *Glob. Ecol. Biogeogr.* 17, 122–134.
 79. François L, Utescher T, Favre E, Henrot AJ, Warnant P, et al. (2011) Modelling Late Miocene vegetation in Europe: Results of the CARAIB model and comparison with palaeovegetation data. *Palaeogeogr., Palaeoclim., Palaeoecol.* 304, 359–378.
 80. Nakicenovic N, Inaba A, Messner S, Nilsson S, Nishimura Y, et al. (1993) Long-term strategies for mitigating global warming. *Energy* 18, 401–401.
 81. Ornstein L, Aleinov I, Rind D (2009) Irrigated afforestation of the Sahara and Australian Outback to end global warming. *Clim. Change* 97, 409–437.
 82. Rotenberg E, Yakir D (2010) Contribution of semi-arid forests to the climate system. *Sci.* 327, 451.
 83. Juang JY, Katul G, Siqueira M, Stoy P, Novick K (2007) Separating the effects of albedo from eco-physiological changes on surface temperature along a successional chronosequence in the southeastern United States. *Geophys. Res. Lett.* 34, L21408.

The effects of simulated nitrogen deposition on extracellular enzyme activities of litter and soil among different-aged stands of larch

Yuecun Ma^{1,†}, Biao Zhu², Zhenzhong Sun¹, Chuang Zhao¹, Yan Yang¹ and Shilong Piao^{1,*}

¹ College of Urban and Environmental Sciences, and Key Laboratory for Earth Surface Processes of the Ministry of Education, Peking University, Beijing 100871, China

² Earth Sciences Division, Lawrence Berkeley National Laboratory, Berkeley, CA 94720, USA

*Correspondence address. Department of Ecology, College of Urban and Environmental Science, Peking University, Beijing 100871, China. Tel/Fax: +86-010-62753298; E-mail: slpiao@pku.edu.cn

[†]Deceased.

Abstract

Aims

Nitrogen (N) addition could affect the rate of forest litter and soil organic matter decomposition by regulating extracellular enzyme activity (EEA). The impact of N addition on EEA may differ across different age stands with different organic matter quality. We were interested in whether the impact of N addition on EEA in litter and mineral soil during the growing season was dependent on stand age of a larch plantation in North China.

Methods

We added three levels of N (0, 20 and 50 kg N ha⁻¹ year⁻¹) in three age stands (11, 20 and 45 years old) of *Larix principis-rupprechtii* plantation in North China. We measured potential activities of β -1,4-glucosidase (BG), cellobiohydrolase (CB), β -1,4-N-acetylglucosaminidase (NAG) and phenol oxidase (PO) in litter (organic horizon) and mineral soil (0–10 cm) during the second growing season after N amendment. We also measured C and N concentrations, microbial biomass C and N, and KCl-extractable ammonium and nitrate in both litter and mineral soil.

Important Findings

We observed unimodal patterns of EEA during the growing season in all three stands, consistent with the seasonal variations of soil

temperature. Stand age had a strong effect on EEA in both litter and mineral soil, and this effect differed between litter and mineral soil as well as between different enzymes. N addition did not significantly affect the activities of BG or CB but significantly suppressed the activity of NAG in litter. We also found stand age-specific responses of PO activity to N addition in both litter and mineral soil. N addition suppressed PO activity of the high C:N ratio litters in 20- and 45-year-old stands but had no significant effect on PO activity of the low C:N ratio litter in 11-year-old stand. Moreover, N addition inhibited PO activity of the high C:N ratio soil in 20-year-old stand but had no significant impact on PO activity of the low C:N ratio soils in 11- and 45-year-old stands. Overall, stand age had a greater effect on EEA in litter and mineral soil compared to 2 years of N addition. Moreover, the effect of N addition on PO activity is stand age dependent, which may affect the long-term soil carbon storage in this forest.

Keywords: glucosidase, cellobiohydrolase, glucosaminidase, phenol oxidase, *Larix* plantation

Received: 17 April 2013, Revised: 20 May 2013, Accepted: 21 May 2013

INTRODUCTION

Nitrogen (N) deposition has been expected to increase in the future because of expansion of fossil fuel combustion, N fertilizer application and N-fixing crop cultivation (Galloway *et al.* 2008). It is estimated that global N deposition has

increased from 34 Tg N year⁻¹ in 1860 to 100 Tg N year⁻¹ by the end of the 20th century, and is projected to reach 200 Tg N year⁻¹ by 2050 (Galloway *et al.* 2004; Reay *et al.* 2008). This increase of N deposition will have significant impact on global carbon cycle and its feedback to climate change (Janssens *et al.* 2010; Liu and Greaver 2010; Reay *et al.* 2008).

The direct effect of N deposition was the increase of N availability in terrestrial ecosystems. Many studies have shown that N availability has significant effect on extracellular enzyme activity (EEA), which controls the decomposition rate of litter and soil organic matter (SOM) (Burns *et al.* 2013; Sinsabaugh 2010). Generally, extracellular enzymes responsible for the degradation of different fractions of litter or SOM were separated into two groups, namely hydrolytic enzymes, which are mainly responsible for the decomposition of labile organic matter to acquire nutrients for primary metabolism, and oxidative enzymes, which are responsible for the degradation of recalcitrant organic matter for co-metabolic acquisition of nutrients (Burns *et al.* 2013; Nannipieri *et al.* 2012). Previous studies have demonstrated that the activities of hydrolytic enzymes tend to increase with N addition, while the activities of oxidative enzymes are suppressed by N addition (Carreiro *et al.* 2000; DeForest *et al.* 2004; Saiya-Cork *et al.* 2002; but see Keeler *et al.* 2009).

However, the response of phenol oxidase activity to N addition varies with ecosystem-specific litter quality (Sinsabaugh 2010): it increases with N addition in ecosystems with high-quality plant litter (Saiya-Cork *et al.* 2002), but decreases with N addition in ecosystems with low-quality plant litter (Carreiro *et al.* 2000; Sinsabaugh *et al.* 2005; Waldrop *et al.* 2004b). For example, Carreiro *et al.* (2000) showed that N addition increased phenol oxidase activity in low-lignin dogwood litter, had little effect in moderate-lignin maple litter, but suppressed it in high-lignin oak litter. Waldrop *et al.* (2004b) and Sinsabaugh *et al.* (2005) reported that phenol oxidase activity was reduced in the black oak–white oak ecosystem (high C:N ratio of 133) by N addition, but was elevated in the sugar maple–basswood ecosystem (low C:N ratio of 80) by N addition.

All these divergent responses of phenol oxidase activity to N addition were observed in different ecosystems with different plant species and thus different litter qualities (e.g. Carreiro *et al.* 2000; Keeler *et al.* 2009; Sinsabaugh 2010; Sinsabaugh *et al.* 2005; Waldrop *et al.* 2004b). It is not clear whether plantations with the same dominant species but different stand age and litter quality (C:N ratio) also show divergent responses of phenol oxidase activity to N addition. A few studies have reported inconsistent patterns of EEAs in litter or mineral soil with stand age (e.g. Andersson *et al.* 2004; Gartner *et al.* 2012; Holden *et al.* 2013; Yuan and Yue 2012). In a boreal forest chronosequence after fire in Alaska, two recent studies reported that oxidative enzyme activities decreased with stand age (Gartner *et al.* 2012), while hydrolytic enzyme activities did not change significantly (Gartner *et al.* 2012) or showed increasing trend (Holden *et al.* 2013) with stand age. Moreover, Andersson *et al.* (2004) showed cellulose and chitinase activities did not change with stand age in two temperate forest chronosequences in Germany, while Yuan and Yue (2012) reported increase in hydrolytic enzyme activities with stand age in a Chinese pine plantation. Plantation accounts for a large portion of terrestrial ecosystem carbon sinks globally

(Pan *et al.* 2011) and in China particularly (Piao *et al.* 2009), and EEA plays an important role in regulating the decomposition of litter and SOM and thus soil carbon storage (Cusack *et al.* 2010; Waldrop *et al.* 2004a). Thus, understanding of the responses of EEA to N addition and stand age will benefit our projection of the responses of forest ecosystem carbon storage to future N deposition.

In this study, we measured the potential activities of four extracellular enzymes (β -1,4-glucosidase, BG; cellobiohydrolase, CB; β -1,4-N-acetyl-glucosaminidase, NAG and phenol oxidase, PO) in both litter and mineral soil of a *Larix principis-rupprechtii* plantation in North China. We selected three age stands (11, 20 and 45 years old), added three levels of N (0, 20 and 50 kg N ha⁻¹ year⁻¹) and measured enzyme activities in both litter (organic horizon) and mineral soil (0–10 cm A horizon) during the second growing season (June 12, July 10, August 10, October 22, 2011) after N addition. Our main objectives were to address (i) how EEAs in litter and mineral soil changed during the growing season, (ii) how EEAs in litter and mineral soil responded to stand age and N addition and (iii) whether the response of enzyme activities to N addition was dependent on stand age?

MATERIALS AND METHODS

Site description

The study was conducted at Saihanba ecological station (42°24.72'N, 117°14.84'E, 1505 m) of Peking University, situated in Saihanba National Forest Park, Hebei Province, China. The climate is semihumid, with a long cold winter (November–March) and a short spring and summer. According to the long-term observational record from a local weather station, the mean annual temperature is -1.4°C (-21.8°C in January and 16.2°C in July). The mean annual precipitation is 450 mm year⁻¹, 67.6% of which falls in the summer (June–August). The frost-free duration is 81 days. Ambient N deposition rate is currently 7 kg ha⁻¹ year⁻¹ at this site and will increase significantly in the next few decades (Liu *et al.* 2013; Reay *et al.* 2008). The well-drained soil is predominantly sandy (54–74% sand). Snowfall normally begins in November, and snowmelt occurs in early April. In winter, snow depth is typically less than 30 cm. The topography is relatively flat.

The study area belongs to a typical forest-steppe ecotone in the temperate areas of China. North China has been severely threatened by sand and dust storms since the 1950s. Consequently, China State Forestry Administration planted a large area of forests in Saihanba to reduce the impacts of sand and dust storms on the Beijing–Tianjin region. Saihanba plantation was established in 1962 and now covers 94 700 ha. It is the largest plantation in China with dominant species of *L. principis-rupprechtii* and *Pinus sylvestris* var. *mongolica*.

Experimental design

In this study, we selected three different age stands (sapling, young and mature) in August 2009. All three stands were

dominated by *L. principis-rupprechtii*. The distance between any two stands is less than 2 km in order to minimize the difference in climate and soil type and to ensure that differences between stands are predominantly caused by stand age. The trees in sapling (11 years old), young (20 years old) and mature (45 years old) stands were planted in 2000, 1991 and 1966 (thinned in 1989), respectively, according to the local management agency. The sapling stand has a species-rich understory because of the open canopy, including *Potentilla acaulis*, *Bromus inermis*, *Vicia pseudo-orobus* and *Bupleurum chinense*; the young stand has a sparse understory (mainly *Geum aleppicum* and *Agrimonia pilosa* in some forest gaps) due to high stem density and crown closure, while the mature stand has a moderately diverse understory because of the thinning in 1989, including *Geum aleppicum*, *Agrimonia pilosa* and *Sanguisorba tenuifolia*.

All three stands with the area of 100 × 100 m were fenced to reduce human disturbance since August 2009. In each stand, nine 20 × 20 m plots were set up with three plots for control (no N is added, ck), low N addition (20 kg N ha⁻¹ year⁻¹, 20N) and high N addition (50 kg N ha⁻¹ year⁻¹, 50N), respectively. Urea solution was applied on soil surface six times per year using backpack sprayers, from early May to early October since 2010. We applied urea instead of NH₄NO₃ because NH₄NO₃ is banned in China for security concerns. Although natural N deposition does not take place in the form of urea, but rather as ammonium and nitrate, previous studies suggested that the form of added N was not of major importance on microbial activity and decomposition (Berg and Matzner 1997; Fog 1988). The amount of water added to soil through N application was equivalent to 0.0625 mm rainfall, and the same amount of water was applied in control plots to avoid the additional water effect. Over 10 m buffer stripes were set up between the plots. The main characteristics of each stand are showed in Table 1.

Soil sampling and preparation

Samples were collected on June 12, July 10, August 10 and October 22, 2011. Litter samples were randomly sampled from six points (5 × 5 cm) in each plot, and mineral soil samples were collected with a hand auger (internal diameter 4 cm) to a depth of 10 cm from the six points where litter samples were collected. The samples were stored in a plastic bag inside an icebox and transported to laboratory immediately following collection. The six litter samples were mixed into a composite sample and then cut into 1 to 2 mm pieces. The six soil cores were also combined into one composite sample, which was handpicked to remove roots and then passed through a 2-mm sieve. One subsample was oven-dried (60°C for litter and 105°C for soil) and weighed to determine gravimetric soil moisture. Another subsample was kept refrigerated at 4°C for less than 4 days before measuring enzyme activity and microbial biomass (DeForest 2009). A third subsample was used to measure C and N concentration, microbial biomass C and N, and KCl-extractable ammonium and nitrate.

Table 1: forest structure and litter (organic horizon) and soil (0–10 cm A horizon) properties of the three age stands of *L. principis-rupprechtii* plantation in Saihanba, North China

Stand	Sapling	Young	Mature
Location (latitude, longitude)	42°23.3'N, 117°14.0'E	42°23.6'N, 117°14.1'E	42°23.9'N, 117°14.8'E
Stand age (year)	11	25	45
Stem density (stem ha ⁻¹)	2640 ± 157 b	3160 ± 129 a	870 ± 48 c
Diameter at breast height (cm)	2.4 ± 0.3 c	7.6 ± 0.1 b	19.9 ± 2.8 a
Average height (m)	2.5 ± 0.2 c	7.8 ± 0.3 b	15.8 ± 1.6 a
Basal area (m ² ha ⁻¹)	4.3 ± 0.7 a	39.1 ± 4.9 b	48.4 ± 3.8 a
Litter thickness (cm)	1–2	3–4	4–5
Litter C:N	29.9 ± 0.6 c	52.8 ± 3.1 b	77.2 ± 1.8 a
Soil bulk density (g cm ⁻³)	1.47	1.50	1.47
Soil texture (sand, silt, clay; %)	54.2, 28.3, 17.5	66.9, 20.0, 13.1	74.0, 15.4, 10.6
Soil C:N	9.0 ± 0.2 b	9.7 ± 0.2 a	8.9 ± 0.3 b
Soil organic carbon (Mg ha ⁻¹)	39.5 ± 1.5 b	53.2 ± 5.1 a	47.9 ± 3.6 ab
Soil NH ₄ ⁺ + NO ₃ ⁻ (mg kg ⁻¹ soil)	4.2 ± 0.9 b	6.9 ± 0.6 a	5.9 ± 1.3 a
Soil pH (soil:water, 1:2.5)	6.7 ± 0.2 a	6.4 ± 0.2 ab	6.3 ± 0.2 b

The values are the means ± standard error ($n = 3$). Different letters within the same row mean significant differences between different stands (one-way ANOVA, post hoc LSD test, $P < 0.05$).

Enzyme and chemical analysis

Litter and soil samples for each plot were assayed for the activities of BG, CB and NAG (hydrolytic enzymes that degrade cellulose, cellulose and chitin, respectively) using 200 μM methylumbelliferone (MUB)-labeled substrates, and for the activity of PO (oxidative enzyme that degrades lignin) using 25 mM L-3,4-dihydroxyphenylalanine (DOPA) as substrate, following published protocols (German et al. 2011; Saiya-Cork et al. 2002; Steinweg et al. 2012) with slight modifications. Sample suspensions were prepared by placing 1.0 g litter or 2.5 g soil when BG, CB and NAG were assayed and by placing 1.0 g litter or soil when PO was assayed in a 150-ml Nalgene bottle. Phosphate buffer (90 ml, pH 6.5) was added to the bottle and the resulting suspension was homogenized using a blender for approximately 1 min.

The hydrolytic enzymes were conducted in black 96-well microtiter plates. Here we used the standard curve (sample suspension + MUB standard of 0, 2.5, 5, 10, 25, 50, 100 μM; Steinweg et al. 2012) to determine the activities of BG, CB and NAG. Each litter or soil sample has a standard curve. We prepared standard plates by pipetting 200 μl of sample suspension and 50 μl of MUB standards into wells of standard plate. We also pipetted 200 μl sample suspension and 50 μl appropriate substrates into wells of substrate plate.

We placed the plates in an incubator at 25°C for 3 h. When the incubation was complete, we added 5 µl of 1.0 M NaOH solution to each well to terminate the reaction. Fluorescence was measured using a plate reader (BioTek, Synergy HT, USA) with excitation wavelength at 365 nm and emission wavelength at 450 nm. The activity of each enzyme was calculated based on the fluorescence data from the standard and substrate plates using a similar method described by Steinweg *et al.* (2012). The units were expressed as µmol g⁻¹ dry weight (DW) h⁻¹.

Phenol oxidase assays were conducted in clear 96-well microtiter plates. Sixteen replicate wells were used for enzyme activity assay, eight additional wells were used as negative substrate controls, and another eight wells served as negative sample controls. The assay wells received 200 µl aliquots of sample suspension and 50 µl of 25 mM DOPA substrate. The negative sample control wells contained 200 µl aliquots of sample suspension and 50 µl of phosphate buffer. The negative substrate control wells received 200 µl aliquots of phosphate buffer and 50 µl substrate. The plates were placed in an incubator at 25°C in the dark for 22 h. Activity was measured spectrophotometrically at 460 nm absorbance using a plate reader (BioTek). The activity of PO was expressed in units of µmol g⁻¹ DW h⁻¹.

C and N concentrations in litter and mineral soil were determined by an elemental analyzer (2400 II CHNS/O Elemental Analyzer, Perkin-Elmer, USA). The microbial biomass C and N was determined by chloroform fumigation extraction technique (Vance *et al.* 1987). The concentration of total organic C and total N in the 0.5 M K₂SO₄ extracts was measured by an autoanalyzer (Multi N/C 3100, AnalyticJena, UK). We also measured soil mineral N using 2 M KCl extraction (about 15 g soil and 50 ml solution) followed by measuring NH₄⁺ and NO₃⁻ concentration in the extracts on a Lachat QuikChem 8000 autoanalyzer.

Data analysis

For both litter and mineral soil, three-way ANOVA was used to determine the effects of date (June, July, August and October), stand age (sapling, young and mature) and N treatment (ambient, low N addition and high N addition) on enzyme activity (Table 2, Fig. 3) and microbial biomass (Table 3, Fig. 4). We chose significance level of 0.1 due to the known difficulty of observing significant changes in enzyme activities (Waldrop *et al.* 2004a) over a short period of time after N addition. All statistical analyses were done by SPSS 13.0 for Windows (SPSS Inc, USA).

RESULTS

Seasonal variation of enzyme activities

Soil temperature showed clear seasonal variations in all three stands. The temperature at 10-cm depth increased from 3–6°C in early May to 15–18°C in August and then decreased to 5°C in early November (Fig. 1). Moreover, soil temperature

Table 2: three-way ANOVA results (*P*-values) of EEAs in litter and mineral soil (0–10 cm) for samples collected from the three age stands of *L. principis-rupprechtii* plantation in Saihanba during the growing season of 2011 (July, August and October for litter; June, July, August and October for soil)

	Date	Age	N	Date × Age	Date × N	Age × N	Date × Age × N
Litter							
BG	<0.001	<0.001	0.713	0.001	0.789	0.503	0.334
CB	<0.001	<0.001	0.787	<0.001	0.832	0.992	0.973
NAG	<0.001	0.078	0.075	0.010	0.467	0.881	0.608
PO	0.401	<0.001	0.264	<0.001	0.527	0.178	0.370
Soil							
BG	<0.001	0.081	0.195	0.006	0.355	0.854	0.942
CB	<0.001	0.019	0.441	0.040	0.482	0.980	0.957
NAG	<0.001	0.160	0.269	0.278	0.152	0.898	0.879
PO	<0.001	0.283	0.496	0.021	0.869	0.052	0.345

Table 3: three-way ANOVA of C_{mic} and C_{mic}:N_{mic} in litter and mineral soil (0–10 cm) for samples collected from the three age stands of *L. principis-rupprechtii* plantation in Saihanba in 2011

	Date	Age	N	Date × Age	Date × N	Age × N	Date × Age × N
Litter							
C _{mic}	0.250	0.043	0.986	0.342	0.304	0.839	0.380
C _{mic} :N _{mic}	0.263	0.226	0.754	0.380	0.087	0.514	0.003
Soil							
C _{mic}	0.415	<0.001	0.203	0.847	0.549	0.467	0.931
C _{mic} :N _{mic}	0.007	0.759	0.149	0.002	0.812	0.330	0.641

C_{mic} and N_{mic} stand for microbial biomass carbon and microbial biomass nitrogen, respectively.

in sapling stand was 2–5°C warmer than that in young and mature stands from early May to late August.

Potential activities of the four extracellular enzymes in mineral soil showed clear unimodal patterns during the growing season (Fig. 2). For example, averaged across the three N treatments, soil PO activity in the mature stand increased from 0.468±0.018 µmol g⁻¹ DW h⁻¹ in June to its peak value of 0.837±0.018 µmol g⁻¹ DW h⁻¹ in July and then declined to 0.576±0.126 µmol g⁻¹ DW h⁻¹ in August and 0.189±0.018 µmol g⁻¹ DW h⁻¹ in October (Fig. 2). Similar patterns were also observed in young and sapling stands and in the other three enzymes (Fig. 2). In addition, sampling date also had significant effect on litter hydrolytic enzyme activity in all three stands (Table 2), but no clear seasonal pattern was observed because of only three sampling dates (data not shown).

Stand age effect on enzyme activities

There was a significant effect of stand age on litter enzyme activity (Table 2; *P* < 0.001 for BG, CB and PO; *P* < 0.10 for NAG). The activities of three hydrolytic enzymes were highest in sapling stand and lowest in young stand, while

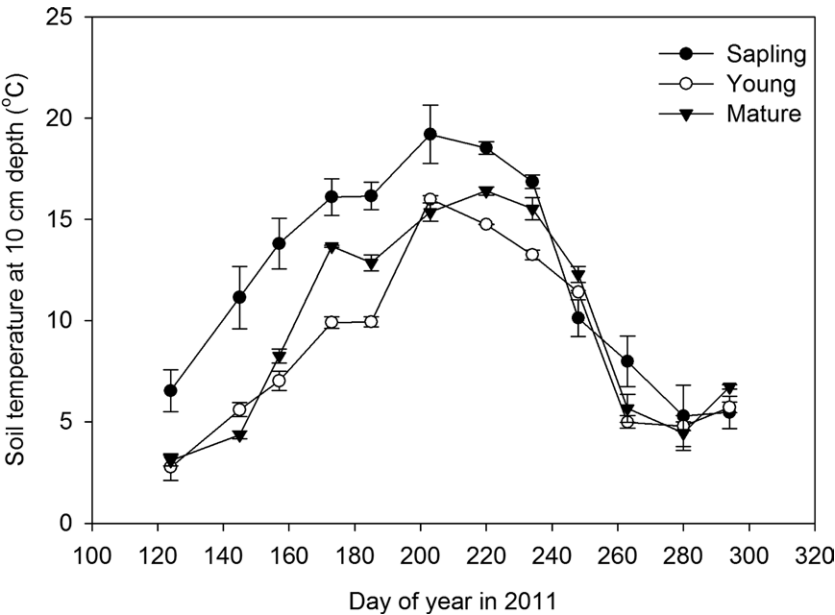


Figure 1: variation of soil temperature (mean \pm SE) at 10 cm depth at three age stands measured during the growing season of 2011.

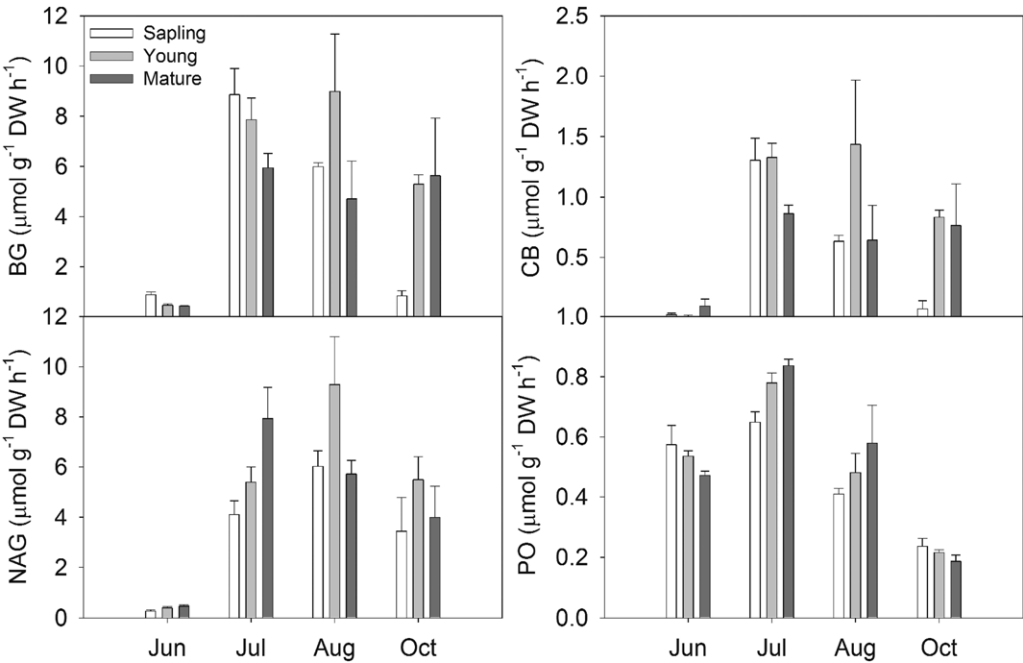


Figure 2: variation of enzyme activities (mean \pm SE) in mineral soil (0–10 cm) at three age stands during the growing season of 2011.

the activity of PO was highest in young stand and lowest in sapling stand (Fig. 3). Moreover, stand age had a significant effect on the activities of BG ($P < 0.10$) and CB ($P < 0.05$), but had no effect on the activities of NAG or PO in the mineral soil (Table 2). The activities of BG and CB in mineral soil were higher in young stand than those in sapling and mature stands, which was different with the pattern in litter (Fig. 3).

N addition effect on enzyme activities

N addition had no significant effect on the activities of BG and CB in litter and mineral soil, but reduced the activity of NAG in litter ($P < 0.10$; Table 2). High N addition ($+50 \text{ kg ha}^{-1} \text{ year}^{-1}$) suppressed NAG activity in litter by 74.5% and 65.5% in young ($P < 0.10$) and mature ($P < 0.01$) stands, respectively (Fig. 3). However, N addition did not affect NAG activity in mineral soil at the three age stands (Fig. 3).

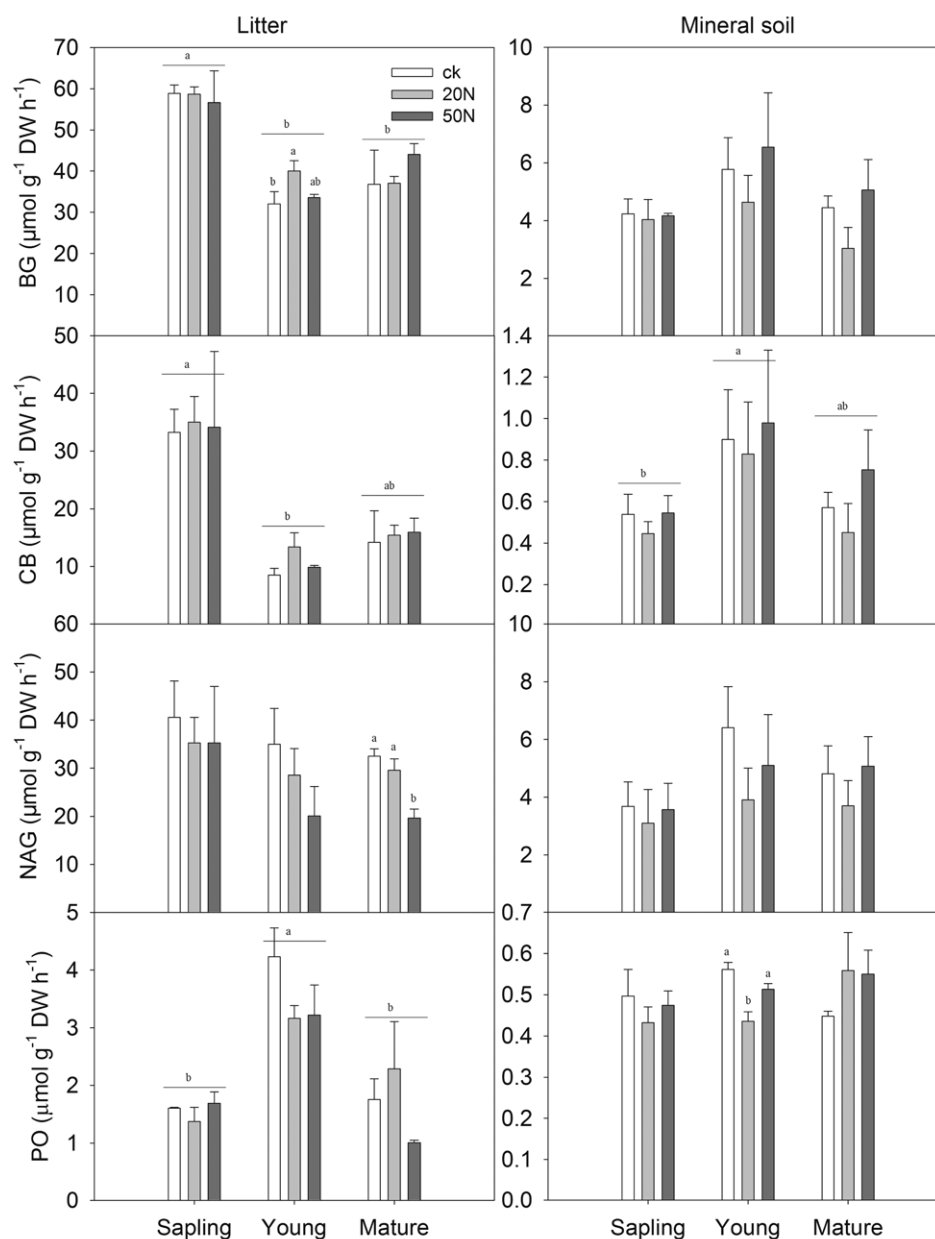


Figure 3: effects of stand age and N addition on enzyme activities (mean + SE) across all sampling dates in both litter and mineral soil. Different small letters mean significant differences between the two N addition treatments at $P < 0.05$ level, and different small letters above the lines mean significant differences between the two age stands at $P < 0.05$ level.

The responses of PO activity to N addition were divergent among the three age stands in both litter and mineral soil layer (Fig. 3). In litter layer, the activity of PO was inhibited in young ($P < 0.10$) and mature ($P < 0.10$) stands, but was not significantly affected in sapling stand by high N addition (Fig. 3). In mineral soil, however, the activity of PO was stimulated in mature stand ($P < 0.10$), but was suppressed in young stand ($P < 0.05$) by low N addition (Fig. 3). No significant effect of N addition was observed on the activity of PO in sapling stand.

Interaction of sampling date, stand age and N addition on enzyme activities

Three-way ANOVA results showed that no significant interactive effect of date, stand age and N addition was found on the three hydrolytic enzymes except for date \times stand age (Table 2). Significant interactions of date \times age ($P < 0.05$) were observed on the four enzymes in both litter and soil, except for NAG in soil. More importantly, a strong interaction of age \times N was observed for PO in soil ($P < 0.10$), and a weak interaction of age \times N was observed for PO in litter ($P > 0.10$; Table 2,

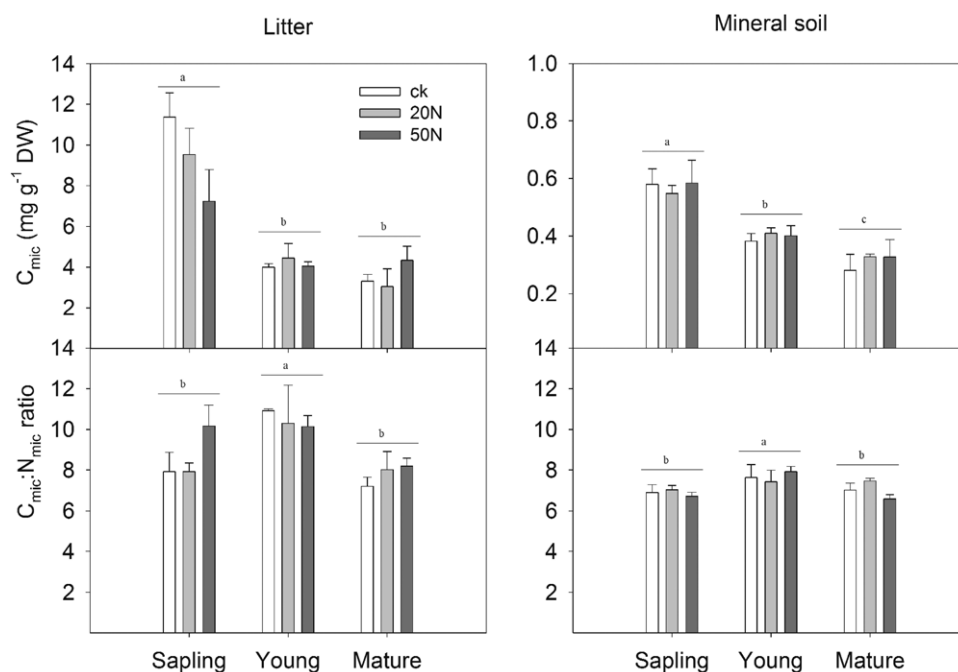


Figure 4: effect of stand age and N addition on C_{mic} and $C_{mic}:N_{mic}$ ratio (mean + SE) in both litter and mineral soil. C_{mic} and N_{mic} stand for microbial biomass carbon and microbial biomass nitrogen, respectively. Different small letters mean significant differences between the two N addition treatments at $P < 0.05$ level, and different small letters above the lines mean significant differences between the two age stands at $P < 0.05$ level.

Fig. 3). Moreover, there was no interaction of date \times N or date \times age \times N on the four enzymes in litter or mineral soil (Table 2).

DISCUSSION

Previous studies generally attributed the seasonal variations in microbial enzyme activity to the seasonal variations in soil temperature (Boerner et al. 2005) and substrate availability (Brzostek and Finzi 2011). We found a unimodal seasonal variation of enzyme activities in both litter and soil (Fig. 2), very similar to the seasonal variations of soil temperature (Fig. 1). This unimodal pattern was not consistent with some previous studies. Sinsabaugh et al. (2005) reported that soil PO activity peaked in spring and autumn rather than in summer, and Bell et al. (2010) showed that soil PO activity was much higher in spring than in summer and autumn. In addition, many studies did not find seasonal variations in enzyme activity, particularly for hydrolytic enzymes (Bell et al. 2010; Dick et al. 1988; Sinsabaugh et al. 2005). These different seasonal patterns of microbial enzyme activities among different studies may be due to different seasonal variations of soil temperature, substrate availability and microbial community structure at the study sites.

We observed higher enzyme activities in litter than in mineral soil in this study. The activities of PO in litter were 1.9–5.3, 4.9–7.5 and 2–17 times compared with the activities of PO in mineral soil for sapling, young and mature stands, respectively, which is consistent with the results in previous studies (e.g. Andersson et al. 2004; Olander and Vitousek 2000;

Saiya-Cork et al. 2002; Sinsabaugh et al. 2005). Olander and Vitousek (2000) demonstrated that NAG activity in litter was 81% higher than that in mineral soil in the Hawaiian Islands. Andersson et al. (2004) reported that the activities of NAG and CB in litter were 1.6 and 6.9 times, respectively, compared with the activities in mineral soil. This higher enzyme activity in litter layer can be attributed to the higher microbial activity in litter layer due to the large quantity of substrate (Andersson et al. 2004). In our study, the microbial biomass C in litter was 18.6, 9.5 and 10.8 times higher than that in mineral soil for sapling, young and mature stand, respectively (Fig. 4), which may explain the higher enzyme activity in the litter layer compared to the mineral soil (Fig. 3).

Stand age had strong impact on the four enzyme activities that we measured (Table 2, Fig. 3). However, the effect of stand age on hydrolytic enzyme activities in litter was different from that in mineral soil. In litter, the hydrolytic enzyme activities were highest in sapling stand. This could be attributed to the high-quality (low C:N ratio) litter input in sapling stand (Table 1) since the substrate induction was the main mechanism determining the extracellular enzyme production by soil microbial community (Allison and Vitousek 2005; Geisseler and Horwath 2009). Kourtev et al. (2002) and Hu et al. (2006) reported that soil enzyme activities changed significantly after different litters were added into soils. Furthermore, soil temperature in sapling stand was much higher than that in young and mature stands (Fig. 1), which may partly contribute to the higher enzyme activity at sapling stand. In mineral soil, however,

the activities of hydrolytic enzymes were highest in young stand (Fig. 3), which may be due to the higher mineral N ($\text{NH}_4^+ + \text{NO}_3^-$) in young stand ($6.9 \pm 0.6 \text{ mg kg}^{-1}$ soil) compared to sapling ($4.2 \pm 0.9 \text{ mg kg}^{-1}$ soil) and mature ($5.9 \pm 1.3 \text{ mg kg}^{-1}$ soil) stands.

We did not find a significant effect of N addition on BG and CB activities in either litter or mineral soil (Table 2, Fig. 3). Our result was not consistent with most previous studies, which demonstrated that the activities of BG and CB were significantly stimulated by N addition (Keeler *et al.* 2009; Sinsabaugh *et al.* 2005). As the sampling was conducted during the second year of N addition, the short treatment period may prevent us from detecting a statistically significant effect of N addition on the highly variable enzyme activity. The lack of a significant effect of N addition on soil microbial biomass (Table 3, Fig. 4) and soil respiration (Piao, unpublished data) is consistent with the explanation.

The NAG activity in litter was significantly suppressed by N addition (Table 2). The high N amendment ($50 \text{ kg N ha}^{-1} \text{ year}^{-1}$) strongly suppressed litter NAG activity in mature stand, but not in sapling and young stands (Fig. 3). As enzyme production is N- and energy-intensive, microbes should only produce enzymes at the expense of growth and metabolism if available nutrients are scarce (Allison and Vitousek 2005; Geisseler and Horwath 2009; Hernández and Hobbie 2010). Therefore, microbes will produce less NAG that converts chitin to inorganic N when there is a lot of freely available mineral N in the soil after N addition. The higher soil mineral N content in fertilization plots than in control plots (data not shown) seems to support this argument. Moreover, N addition has no effect on NAG activity in mineral soil in any of the stands (Fig. 3). In contrast to our results, few previous studies (Keeler *et al.* 2009) showed that the activity of NAG in litter and mineral soil was stimulated by N addition.

In litter layer, the enzyme activities are regulated by litter chemistry and substrate availability (Keeler *et al.* 2009; Kourtev *et al.* 2002). In this study, the effect of N addition on PO activity in litter varied with stand age. The activity of PO was suppressed by 32.5% and 23.6% by high N amendment in young and mature stands, respectively (Fig. 3), but was not significantly affected by N addition in sapling stand. It is likely that this age-specific response to N addition resulted from the variation of litter C:N ratio among the three stands (Fig. 4). These results were partly consistent with previous studies (Carreiro *et al.* 2000; Hu *et al.* 2006; Sinsabaugh *et al.* 2005), which found that N addition stimulated PO activity in litter with low C:N ratio, but suppressed PO activity in litter with high C:N ratio. One potential mechanism has been proposed to explain this divergent response. White-rot fungi are the main producer of PO in temperate forests with low-quality (high C:N ratio) litter (Sinsabaugh 2010) and are very sensitive to soil N availability (Edwards *et al.* 2011). In the young and mature stands with relatively high C:N ratio litter (53 and 77; Table 1), N addition may reduce

the abundance of white-rot fungi and thus suppress the PO activity (Carreiro *et al.* 2000; Fog 1988; Waldrop *et al.* 2004b). In the sapling stand with low C:N ratio litter (30; Table 1), however, the microbial community may have low abundance of white-rot fungi and retain much of the capacity to produce PO in response to N addition. As we do not have data of microbial community composition from these stands, the exact mechanisms behind the divergent responses of litter PO activity to N addition await further investigation.

In mineral soil, there was an interactive effect of stand age and N addition on PO activity ($P < 0.10$; Table 2). N addition inhibited PO activity in young stand, but not in sapling or mature stand (Fig. 3). This result was not consistent with previous studies (Saiya-Cork *et al.* 2002; Sinsabaugh *et al.* 2005), but was not surprising given the wide-range responses of soil PO activity to N amendment across different ecosystems (Sinsabaugh 2010). A recent synthesis found that N amendment tends to suppress soil PO activity in temperate and boreal forest ecosystems but does not strongly impact soil PO activity in grassland and agricultural systems (Sinsabaugh 2010). The divergent response of PO activity in mineral soil among different-aged stands observed in this study might be attributed to the difference in soil characteristics. Firstly, young stand had higher soil C:N ratio (9.7) compared to sapling (9.0) and mature (8.9) stands. The decomposition of the relatively lower quality (or higher C:N ratio) SOM in young stand may be suppressed by N addition, while the decomposition of relatively higher quality (or lower C:N ratio) SOM in sapling and mature stands shows neutral response to N addition (Sinsabaugh 2010). Secondly, the microbial biomass C:N ratio ($C_{\text{mic}}:N_{\text{mic}}$ ratio) in mineral soil was significantly higher in young stand (7.7) than in sapling (6.9) and mature (7.0) stands (Fig. 4). The significant negative relationship between PO activity and $C_{\text{mic}}:N_{\text{mic}}$ ratio in mineral soil (Fig. 5) suggests the stand age-specific response of soil PO activity to N addition may be partly due to the difference in microbial community

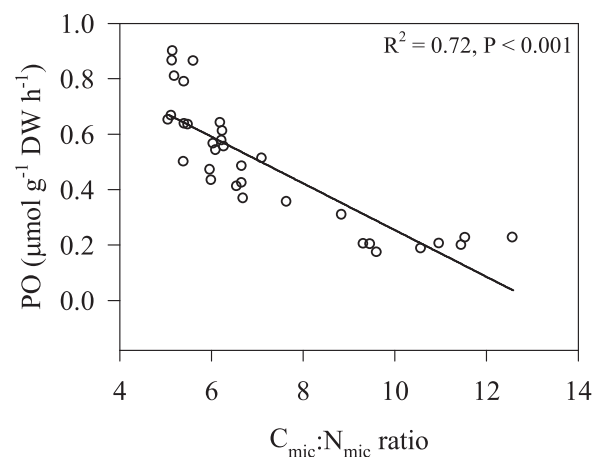


Figure 5: the relationship between microbial biomass C:N ratio ($C_{\text{mic}}:N_{\text{mic}}$ ratio) and PO activity in mineral soil across all treatments.

composition as indicated by the microbial biomass C:N ratio, although direct evidence for this hypothesis requires measurement of microbial community composition in the three age stands.

CONCLUSIONS

In summary, we found activities of the four hydrolytic and oxidative enzymes in litter and mineral soil of the *Larix* plantation showed clear seasonal patterns, likely due to changes in soil temperature and substrate availability. Microbial enzyme activities in both litter and mineral soil varied among the three age stands, which may be associated with differences in microclimate (soil temperature), substrate availability (litterfall amount and soil C stock) and quality (C:N ratio), and microbial community composition. Two years of N amendment had no significant impact on the activities of BG and CB, but suppressed the activity of NAG in litter. The phenol oxidase activity in both litter and mineral soil showed stand age-specific responses to N addition, which is generally consistent with the earlier finding that N addition suppresses PO activity in low-quality substrate but enhances or has neutral effect on PO activity in high-quality substrate. Overall, although the relatively short-term N amendment may prevent us from detecting significant effects on enzyme activities and the explicit mechanisms driving the observations await future study, we suggest that the impact of N deposition on organic matter decomposition and soil carbon storage may differ among plantations of different stand age that have the same dominant species but different soil characteristics. Stand age, among other factors, should be taken into account to better predict the impact of N deposition on ecosystem carbon and nutrient cycles.

FUNDING

National Natural Science Foundation of China (#41171202, 41125004).

ACKNOWLEDGEMENTS

We are grateful to all the technicians for their assistance in the field and lab. We also thank three anonymous reviewers for their helpful comments that improved the quality of this manuscript.

Conflict of interest statement. None declared.

REFERENCES

- Allison SD, Vitousek PM (2005) Responses of extracellular enzymes to simple and complex nutrient inputs. *Soil Biol Biochem* **37**:937–44.
- Andersson M, Kjoller A, Struwe S (2004) Microbial enzyme activities in leaf litter, humus and mineral soil layers of European forests. *Soil Biol Biochem* **36**:1527–37.
- Bell TH, Klironomos JN, Henry HAL (2010) Seasonal responses of extracellular enzyme activity and microbial biomass to warming and nitrogen addition. *Soil Sci Soc Am J* **74**:820–8.
- Berg B, Matzner E (1997) Effect of N deposition on decomposition of plant litter and soil organic matter in forest systems. *Environ Rev* **5**:1–25.
- Boerner REJ, Brinkman JA, Smith A (2005) Seasonal variations in enzyme activity and organic carbon in soil of a burned and unburned hardwood forest. *Soil Biol Biochem* **37**:1419–26.
- Brzostek ER, Finzi AC (2011) Substrate supply, fine roots, and temperature control proteolytic enzyme activity in temperate forest soils. *Ecology* **92**:892–902.
- Burns RG, DeForest JL, Marxsen J, et al. (2013) Soil enzymes in a changing environment: current knowledge and future directions. *Soil Biol Biochem* **58**:216–34.
- Carreiro MM, Sinsabaugh RL, Repert DA, et al. (2000) Microbial enzyme shifts explain litter decay response to simulated nitrogen deposition. *Ecology* **81**:2359–65.
- Cusack DE, Torn MS, McDowell WH, et al. (2010) The response of heterotrophic activity and carbon cycling to nitrogen additions and warming in two tropical soils. *Global Change Biol* **16**:2555–72.
- DeForest JL (2009) The influence of time, storage temperature, and substrate age on potential soil enzyme activity in acidic forest soils using MUB-linked substrates and L-DOPA. *Soil Biol Biochem* **41**:1180–6.
- DeForest JL, Zak DR, Pregitzer KS, et al. (2004). Atmospheric nitrate deposition, microbial community composition, and enzyme activity in northern hardwood forests. *Soil Sci Soc Am J* **68**:132–8.
- Dick RP, Rasmussen PE, Herle EA (1988) Influence of long term residue management on soil enzyme activities in relation to soil chemical properties of a wheat-fallow system. *Biol Fert Soils* **6**:158–64.
- Edwards IP, Zak DR, Kellner H, et al. (2011) Simulated atmospheric N deposition alters fungal community composition and suppresses ligninolytic gene expression in a Northern hardwood forest. *PLoS One* **6**:e20421.
- Fog K (1988) The effect of added nitrogen on the rate of decomposition or organic matter. *Biol Rev* **63**:433–63.
- Galloway JN, Townsend AR, Erismann JW, et al. (2008) Transformation of the nitrogen cycle: recent trends, questions, and potential solutions. *Science* **320**:889–92.
- Galloway JN, Dentener DG, Capone EW, et al. (2004) Nitrogen cycles: past, present, and future. *Biogeochemistry* **70**:153–226.
- Gartner TB, Treseder KK, Malcolm GM, et al. (2012) Extracellular enzyme activity in the mycorrhizospheres of a boreal forest chronosequence. *Pedobiologia* **55**:121–7.
- Geisseler D, Horwath W (2009) Relationship between carbon and nitrogen availability and extracellular enzyme activities in soil. *Pedobiologia* **53**:87–98.
- German DP, Weintraub MN, Grandy AS, et al. (2011) Optimization of hydrolytic and oxidative enzyme methods for ecosystem studies. *Soil Biol Biochem* **43**:1387–97.
- Hernández DL, Hobbie SE (2010) The effects of substrate composition, quantity, and diversity on microbial activity. *Plant Soil* **335**:397–411.
- Holden SR, Gutierrez A, Treseder KK (2013) Changes in soil fungal communities, extracellular enzyme activities, and litter decomposition along a fire chronosequence in Alaskan boreal forests. *Ecosystems* **16**:34–46.
- Hu YL, Wang SL, Zeng DH (2006) Effects of single Chinese fir and mixed leaf litters on soil chemical, microbial properties and soil enzyme activities. *Plant Soil* **282**:379–86.

- Janssens IA, Dieleman W, Luyssaert S, *et al.* (2010) Reduction of forest soil respiration in response to nitrogen deposition. *Nature Geoscience* **3**:315–22.
- Keeler BL, Hobbie SE, Kellogg LE (2009) Effects of long-term nitrogen addition on microbial enzyme activity in eight forested and grassland sites: implications for litter and soil organic matter decomposition. *Ecosystems* **12**:1–15.
- Kourtev PS, Ehrenfeld JG, Huang WZ (2002) Enzyme activities during litter decomposition of two exotic and two native plant species in hardwood forests of New Jersey. *Soil Biol Biochem* **34**:1207–18.
- Liu L, Greaver TL (2010) A global perspective on belowground carbon dynamics under nitrogen enrichment. *Ecol Lett* **13**:819–28.
- Liu XJ, Zhang Y, Han WX, *et al.* (2013) Enhanced nitrogen deposition in China. *Nature* **494**:459–62.
- Nannipieri P, Giagnoni L, Renella G, *et al.* (2012) Soil enzymology: classical and molecular approaches. *Biol Fert Soils* **48**:743–62.
- Olander L, Vitousek PM (2000) Regulation of soil phosphatase and chitinase activity by N and P availability. *Biogeochemistry* **49**:175–90.
- Pan Y, Birdsey RA, Fang J, *et al.* (2011) A large and persistent carbon sink in the world's forests. *Science* **333**:988–93.
- Piao SL, Fang JY, Ciais P, *et al.* (2009) The carbon balance of terrestrial ecosystems in China. *Nature* **458**:1009–14.
- Reay DS, Dentener F, Smith P, *et al.* (2008) Global nitrogen deposition and carbon sinks. *Nat Geosci* **1**:430–7.
- Saiya-Cork KR, Sinsabaugh RL, Zak DR (2002) The effects of long term nitrogen deposition on extracellular enzyme activity in an *Acer saccharum* forest soil. *Soil Biol Biochem* **34**:1309–15.
- Sinsabaugh RL (2010) Phenol oxidase, peroxidase and organic matter dynamics of soil. *Soil Biol Biochem* **42**:391–404.
- Sinsabaugh RL, Gallo ME, Lauber C, *et al.* (2005) Extracellular enzyme activities and soil organic matter dynamics for northern hardwood forests receiving simulated nitrogen deposition. *Biogeochemistry* **75**:201–15.
- Steinweg JM, Dukes JS, Wallenstein MD (2012) Modeling the effects of temperature and moisture on soil enzyme activity: linking laboratory assays to continuous field data. *Soil Biol Biochem* **55**:85–92.
- Vance ED, Brookes PC, Jenkinson DS (1987) An extraction method for measuring soil microbial biomass-C. *Soil Biol Biochem* **19**:703–7.
- Waldrop M, Zak DR, Sinsabaugh RL (2004a) Nitrogen deposition modifies soil carbon storage through changes in microbial enzymatic activity. *Ecol Appl* **14**:1172–77.
- Waldrop MP, Zak DR, Sinsabaugh RL (2004b) Microbial community response to nitrogen deposition in northern forest ecosystems. *Soil Biol Biochem* **36**:1443–51.
- Yuan BC, Yue DX (2012) Soil microbial and enzymatic activities across a chronosequence of Chinese pine plantation development on the loess plateau in China. *Pedosphere* **22**:1–12.

The production of phytolith-occluded carbon in China's forests: implications to biogeochemical carbon sequestration

ZHAOLIANG SONG*†‡§, HONGYAN LIU‡§, BEILEI LI† and XIAOMIN YANG†

*Zhejiang Provincial Key Laboratory of Carbon Cycling in Forest Ecosystems and Carbon Sequestration, Zhejiang Agricultural and Forestry University, Lin'an 311300, China, †School of Environment and Resources, Zhejiang Agricultural and Forestry University, Lin'an 311300, China, ‡College of Urban and Environmental Sciences, Peking University, Peking 100871, China, §Ministry of Education Laboratory for Earth Surface Processes, Peking University, Peking 100871, China

Abstract

The persistent terrestrial carbon sink regulates long-term climate change, but its size, location, and mechanisms remain uncertain. One of the most promising terrestrial biogeochemical carbon sequestration mechanisms is the occlusion of carbon within phytoliths, the silicified features that deposit within plant tissues. Using phytolith content–biogenic silica content transfer function obtained from our investigation, in combination with published silica content and aboveground net primary productivity (ANPP) data of leaf litter and herb layer in China's forests, we estimated the production of phytolith-occluded carbon (PhytOC) in China's forests. The present annual phytolith carbon sink in China's forests is $1.7 \pm 0.4 \text{ Tg CO}_2 \text{ yr}^{-1}$, 30% of which is contributed by bamboo because the production flux of PhytOC through tree leaf litter for bamboo is 3–80 times higher than that of other forest types. As a result of national and international bamboo afforestation and reforestation, the potential of phytolith carbon sink for China's forests and world's bamboo can reach 6.8 ± 1.5 and $27.0 \pm 6.1 \text{ Tg CO}_2 \text{ yr}^{-1}$, respectively. Forest management practices such as bamboo afforestation and reforestation may significantly enhance the long-term terrestrial carbon sink and contribute to mitigation of global climate warming.

Keywords: bamboo, biogeochemical carbon sequestration, carbon sink, China, forest, phytolith-occluded carbon (PhytOC)

Received 5 March 2013 and accepted 21 May 2013

Introduction

Terrestrial biogeochemical carbon sequestration is a long-term carbon sink and is fundamental to the long-term global carbon cycle (Scholes & Noble, 2001; Lackner, 2003; Parr *et al.*, 2010; Pan *et al.*, 2011; Song *et al.*, 2012a, b). One of the most promising biogeochemical carbon sequestration mechanisms is the occlusion of carbon within phytoliths, the silicified features which are deposited within plant tissues (Parr & Sullivan, 2005; Song *et al.*, 2012a, b). Phytolith-occluded carbon (PhytOC) is found in many plant species (Parr *et al.*, 2010; Parr & Sullivan, 2011; Zuo & Lü, 2011), is highly resistant to decomposition (Wilding, 1967; Mulholland & Prior, 1992; Parr & Sullivan, 2005), and may represent up to 82% of soil carbon (Parr & Sullivan, 2005) demonstrating the potential of phytoliths in the long-term biogeochemical sequestration of atmospheric CO_2 (Song *et al.*, 2012a).

Forest is one of the most widespread vegetation types worldwide, occupying more than one fifth of the

world's land surface. Despite lower leaf litter phytolith contents in most forests (except for bamboo, a phytolith accumulator), forest ecosystems may play a similar important role in the global terrestrial production of phytoliths with grasslands due to their similar large area but higher aboveground net primary productivity (ANPP) (Carnelli *et al.*, 2001; Blecker *et al.*, 2006). Forests may contribute at least 20% of the total terrestrial phytolith production rate (Blecker *et al.*, 2006; Song *et al.*, 2012a). However, large uncertainties still exist in estimates of forest phytolith production, and its contribution to global terrestrial phytolith production (Alexandre *et al.*, 1997; Meunier *et al.*, 1999; Carnelli *et al.*, 2001; Conley, 2002; Parr *et al.*, 2010). Moreover, to our best knowledge, the potential of forest phytoliths in the long-term biogeochemical sequestration of atmospheric CO_2 has not been quantified globally and even regionally.

China has $142.8 \times 10^6 \text{ hm}^2$ of forested land including $7.2 \times 10^6 \text{ hm}^2$ of bamboo forests (Zhou *et al.*, 2011), which are known to be particularly proficient PhytOC accumulators (Parr *et al.*, 2010). China's forests play an important role in the global carbon cycle (Fang *et al.*, 2001; Piao *et al.*, 2009; Pan *et al.*, 2011). However, the phytolith carbon sink in China's forests and its

Correspondence: Zhaoliang Song, tel. + 086-571-63740889, fax + 086-571-63740889, e-mail: songzhaoliang78@163.com; Hongyan Liu, e-mail: lhy@urban.pku.edu.cn

contribution from bamboo remain unknown. In this study, we examined the phytolith carbon sink in China's forests using data related to the phytolith content–biogenic silica content transfer function obtained from our investigation, in combination with data related to the PhytOC content in phytoliths, silica content, and ANPP for tree leaf litter and herb litter in China's forests.

Materials and methods

General characteristics of the forests

China's forests range from boreal forests in the north to tropical forests in the south. To gain a more complete knowledge of the phytolith carbon sink in China's forests, based on climatic conditions and physiology, we divided China's forests into eight broad forest types: cold-temperate and temperate coniferous (CTC) forest, subtropical and tropical coniferous (STC) forest, coniferous and broad-leaf mixed (CB) forest, deciduous broad- or small-leaf (DBS) forest, subtropical evergreen and deciduous broad-leaf (SEDB) forest, subtropical (sclerophyllous) evergreen broad-leaf (SEB) forest, tropical (T) forest, and subtropical and tropical bamboo (STB) forest (Table 1; Fig. 1). The ANPP, plant composition, and other characteristics vary greatly among the forest types (Table 1).

Phytolith content–silica content transfer function

Plant phytolith content can be estimated from plant silica content data. To construct the phytolith content–silica content transfer function for tree leaf litter, we collected mature leaf samples (three replicates) in forests of Inner Mongolia, Hebei, Zhejiang, and Hainan, China in August, 2011 and July, 2012 (Fig. 1). Table 2 shows which tree species were collected from each of the eight Chinese Forest types. Also, we sampled

typical herb species in each forest (Fig. 1; Table 3) to estimate the phytolith content in herb species and the contribution of the herb layer to the forest phytolith carbon sink. Each plant sample was made up of about 300 g of composite plant materials.

Plant samples were oven dried at 65 °C to a constant mass and cut into small pieces (<5 mm). They were ashed at 500 °C to remove organic matter, fused with Li-metaborate, dissolved in dilute nitric acid, and analyzed for silica content by inductively coupled plasma-optical emission spectroscopy (ICP-OES). The method used in this study for the isolation of plant phytoliths is a microwave digestion process followed by a Walkley–Black-type digestion to ensure extraneous organic materials in the samples were removed (Parr *et al.*, 2010). The phytolith isolates were then thoroughly dried at 75 °C for 24 h in a fan-forced oven and weighed to obtain plant phytolith content. The content of PhytOC was also determined (Parr *et al.*, 2010). In monitoring with standard samples (GSV-1 and GSS-5) and repetition analysis, the precision was better than 5% in phytolith and silica measurements, and better than 10% in PhytOC measurement.

The plant phytolith content–silica content transfer function was constructed with the regression analysis method based on the determined phytolith and silica contents of the samples (Fig. 2). Silica content could be converted into phytolith content using the following equation:

$$\text{Phytolith content (wt\%)} = 0.953 \times \text{silica content (wt\%)} \quad (1)$$

$$(R^2 = 0.96, P < 0.01)$$

Chemical data collection and phytolith content estimation

Chemical data related to silica content were obtained from published monographs (Hou, 1982; Chen *et al.*, 1997), papers (Li *et al.*, 2006; Ding *et al.*, 2008; Parr *et al.*, 2010) and our own determination. The mature leaves of tree species from eight forest types were used to estimate phytolith content with a conversion factor of 0.953 Eqn (1).

Table 1 Characteristics of the eight Chinese forest types

Forest type	Area (10 ⁶ hm ²)	MAP (mm)	MAT (°)	Tree species composition
CTC	24.14	400–600	–6~8	<i>Larix</i> spp., <i>Pinus</i> spp., <i>Picea</i> spp., <i>Abies</i> spp., <i>Platycladus orientalis</i>
STC	29.54	800–1600	8~20	<i>Pinus</i> spp., <i>Cunninghamia lanceolata</i> , <i>Cupressus</i> spp., <i>Abies</i> spp., <i>Picea</i> spp.
CB	4.68	500–1600	2~14	<i>Tilia amurensis</i> , <i>Acer mono</i> , <i>Pinus koraiensis</i>
DBS	42.40	500–1000	8~20	<i>Quercus</i> spp., <i>Tilia mongolica</i> , <i>Ulmus pumila</i> , <i>Betula</i> spp., <i>Populus</i> spp.
SEDB	12.48	800–1600	16~20	<i>Ulmaceae</i> , <i>Platycarya strobilacea</i> , <i>Cyclobalanopsis</i> spp., <i>Lithocarpus</i> spp., <i>Fagus</i> spp., <i>Tsuga</i> spp.
SEB	21.37	1000–1600	16~20	<i>Cyclobalanopsis</i> spp., <i>Castanopsis</i> spp., <i>Lithocarpus</i> spp., <i>Schima</i> spp., <i>Quercus aquifolioides</i>
T	0.95	1600–2000	21~26	<i>Burretiodendron hsienmu</i> , <i>Gironniera</i> spp., <i>Vatica astrotricha</i> , <i>Pometia tomentosa</i>
STB	7.20	1000–2000	14~26	<i>Phyllostachys</i> spp., <i>Sinocalamus offinis</i>

CTC, cold-temperate and temperate coniferous forest; TSC, tropical and subtropical coniferous forest; CB, coniferous and broad-leaf mixed forest; DBS, deciduous broad- or small-leaf forest; SEDB, subtropical evergreen and deciduous broad-leaf forest; SEB, subtropical (sclerophyllous) evergreen broad-leaf forest; T, tropical forest; and STB, subtropical and tropical bamboo forest.

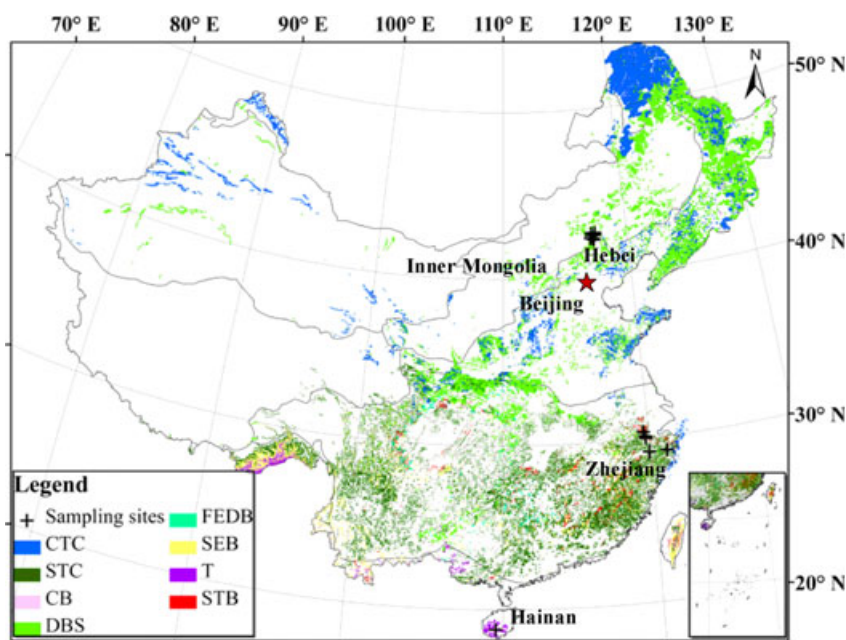


Fig. 1 Vegetation map of the eight Chinese forest types at a scale of 1 : 1000000 + indicates sampling site locations. Forests of CTC, CB, and DBS were sampled from Hebei and Neimeng. Forests of TSC, SEDB, SEB, and STB were sampled from Zhejiang. T forests were sampled from Hainan. For details of forest types, see Table 1.

Estimation of phytolith and PhytOC production

As the production of biogenic Si is primarily driven by plant Si concentration and ANPP of tree leaf litter and herb litter (Blecker *et al.*, 2006), the phytolith production flux of forest biomass can be estimated from data of the phytolith content and ANPP of the tree leaf litter and herb litter as

$$\text{Phytolith production flux} = \text{phytolith content} \times \text{ANPP} \quad (2)$$

where phytolith production flux is the phytolith production amount of a particular forest type through tree leaf litter and herb litter per area per year ($\text{kg hm}^{-2} \text{ yr}^{-1}$), phytolith content is the content of phytolith in mature tree leaves or above-ground herbs (wt%), and ANPP is the aboveground net primary productivity of the tree leaf litter and herb litter ($\text{t hm}^{-2} \text{ yr}^{-1}$). PhytOC production flux for tree leaf litter and herb litter can be estimated from data of phytolith production flux and PhytOC content of phytoliths as

$$\text{PhytOC production flux} = \text{Phytolith production flux} \times \text{PhytOC content} \times 44/12 \quad (3)$$

where PhytOC production flux is the PhytOC production amount of a particular forest type through tree leaf litter and herb litter per area per year ($\text{kg CO}_2 \text{ hm}^{-2} \text{ yr}^{-1}$), phytolith production flux is estimated from Eqn (2), PhytOC content is the content of PhytOC in phytoliths. According to our determination and published data (Parr *et al.*, 2010; Zuo & Lü, 2011), a median PhytOC content in phytoliths of 3% may be used in the PhytOC production flux calculation using Eqn (3). The PhytOC production rate can be estimated from data of PhytOC production flux and forest area as

$$\text{PhytOC production rate} = \text{PhytOC production flux} \times \text{area}/1000 \quad (4)$$

where PhytOC production rate is total PhytOC production of forest through tree leaf litter and herb litter ($\text{Tg CO}_2 \text{ yr}^{-1}$), PhytOC production flux is estimated from Eqn (3), and area is the area of forests (10^6 hm^2).

Results

Phytolith content in tree leaf and herb of China's forests

Phytolith content in mature leaves of trees varies greatly among plant species of the same forest type and among different forest types (0.05–12.45%, average 1.71%) (Tables 2 and 4). Generally, the phytolith content in STB forest (8.01–12.45%, average 10.52%) is 4–50 times higher than that of other forest types. The phytolith content of the herb layer for China's forests (average 4.12%) is generally lower than that of mature leaves for bamboo, but higher than that of other forests (Tables 3 and 4). The ANPP-weighted average phytolith content in tree leaves and herb of STB forest (10.07%) is 4–8.5 times higher than that of other forest types (Table 4).

Aboveground forest PhytOC production

The average production flux of PhytOC for the eight Chinese forest types through tree leaf litter and herb

Table 2 Content of phytolith in mature leaves of dominant tree species from the eight Chinese forest types

Forest type*	Species	Phytolith (%)		Data sources
		Mean	SE	
CTC	<i>Larix principis-rupprechtii</i>	1.43	0.27	This study
	<i>Pinus sylvestris</i> var. <i>mongolica</i>	0.47	0.04	This study
	<i>Larix sibirica</i>	1.87	0.52	1
	<i>Larix olgensis</i>	1.24		1
	<i>Pinus sibirica</i>	2.61		1
	<i>Picea jezoensis</i>	1.16		1
	<i>Picea crassifolia</i>	0.81	0.04	1
	<i>Abies nephrolepis</i>	0.50		1
	<i>Pinus densiflora</i>	0.45	0.08	1
	<i>Pinus tabulaeformis</i>	0.70	0.25	1; This study
	<i>Platycladus orientalis</i>	0.59		1
	Average	1.08	0.20	
STC	<i>Pinus massoniana</i>	0.15	0.10	1; This study
	<i>Pinus armandii</i>	0.26	0.10	1
	<i>Cunninghamia lanceolata</i>	0.19	0.10	1; This study
	<i>Cupressus funebris</i>	0.19	0.08	1; This study
	<i>Cupressus duclouxiana</i>	0.26	0.01	1
	<i>Pinus densata</i>	0.14		1
	<i>Picea asperata</i>	0.18		1
	<i>Picea purpurea</i>	0.18		1
	<i>Abies faxoniana</i>	0.23	0.03	1
	<i>Tsuga chinensis</i>	0.33		1
	Average	0.21	0.07	
CB	<i>Tilia amurensis</i>	0.48		1
	<i>Acer mono</i>	1.16		1
	<i>Lonicera maximoviczii</i>	0.48		1
	<i>Pinus koraiensis</i>	0.26		1
	Average	0.59	0.34	
DBS	<i>Quercus liaotungensis</i>	0.76		1
	<i>Quercus dentata</i>	2.27		1
	<i>Quercus acutissima</i>	0.58		1; This study
	<i>Tilia mongolica</i>	0.84		1
	<i>Ulmus pumila</i>	3.03		1
	<i>Betula platyphylla</i> var. <i>szechuanica</i>	0.34	0.12	1; This study
	<i>Populus davidiana</i>	0.74	0.12	1; This study
	<i>Populus euphratica</i>	0.54	0.32	1
	<i>Populus pruinosa</i>	0.71	0.09	1
	Average	1.09	0.24	
SEDB	<i>Pteroceltis tatarinowii</i>	3.85	1.27	1; This study
	<i>Celtis sinensis</i>	3.89	0.44	1
	<i>Ulmus parvifolia</i>	6.32	1.66	1
	<i>Pistacia chinensis</i>	0.23	0.08	1
	<i>Liquidambar formosana</i>	2.05	0.19	1
	<i>Quercus fabri</i>	1.45	0.52	1
	<i>Cyclobalanopsis glauca</i>	1.33	0.67	1; This study
	<i>Cyclobalanopsis oxylon</i> var. <i>fargesii</i>	0.36		1
	<i>Fagus longipetiolata</i>	1.43		1
	<i>Acer sinense</i>	1.92		1
SEB	Average	2.28	0.69	
	<i>Cyclobalanopsis glauca</i>	1.99	1.11	1; This study
	<i>Cyclobalanopsis glaucooides</i>	1.87	1.28	1
	<i>Castanopsis eyrei</i>	0.77	0.39	1; This study

Table 2 (continued)

Forest type*	Species	Phytolith (%)		Data sources
		Mean	SE	
T	<i>Castanopsis selerophylla</i>	0.33	0.18	1
	<i>Castanopsis carlesii</i>	0.93	0.31	1
	<i>Castanopsis tibetana</i>	0.28	0.17	1; This study
	<i>Castanopsis hystrix</i>	0.75	0.23	1
	<i>Quercus fabri</i>	1.42	0.42	1
	<i>Liquidambar formosana</i>	3.12	1.98	1
	<i>Schima superba</i>	0.17	0.05	1; This study
	<i>Quercus aquifolioides</i>	0.50		1
	Average	1.10	0.61	
	<i>Burretiodendron hsienmu</i>	0.12		1
	<i>Garcinia paucineris</i>	0.12		1
	<i>Ostodes paniculatus</i>	2.77		1
	<i>Cinnamomum calcarea</i>	0.18		1
	<i>Tarrietia parvifolia</i>	0.34		1
	<i>Gironniera subsequalis</i>	17.43		1
	<i>Albizia chinensis</i>	0.33		1
	<i>Cryptocarya</i> sp.	0.27		1
	<i>Liquidambar formosana</i>	1.63		1
	<i>Diospyros dumatorum</i>	0.15		1
	Average	2.34	2.21	
STB	<i>Phyllostachys heterocyclus</i>	10.18	1.26	This study; 1~5
	<i>Phyllostachys praecox</i>	10.71	1.88	This study
	<i>Phyllostachys propinqua</i>	9.11	0.64	This study; 4
	<i>Phyllostachys sulphurea</i>	12.43	1.59	This study
	<i>Phyllostachys bambusoides</i>	12.45	0.60	This study
	<i>Phyllostachys hsienuensis</i>	11.14	0.13	This study
	<i>Bambusa multiplex</i>	11.93	2.08	This study
	<i>Pseudosasa amabilis</i>	8.29	0.18	This study
	<i>Pseudosasa japonica</i>	10.95	0.31	This study
	<i>Shibataea chinensis</i>	10.48	0.52	This study
	<i>Racemobambos</i> sp.	8.01	0.27	4
	Average	10.52	0.86	

*For details of forest types, see Table 1. Data of 1~5 are from Hou (1982), Chen *et al.* (1997), Li *et al.* (2006), Ding *et al.* (2008), and Parr *et al.* (2010), respectively. Phytolith content data of Hou (1982), Chen *et al.* (1997), Li *et al.* (2006), and Ding *et al.* (2008) were estimated from silica content data with phytolith content–silica content transfer function. Phytolith content data of Parr *et al.* (2010) and this study were determined with microwave digestion method (Parr *et al.*, 2010).

litter is $13.6 \pm 3.1 \text{ kg CO}_2 \text{ hm}^{-2} \text{ yr}^{-1}$ (Table 4). The production flux of PhytOC through tree leaf litter for STB forest is 3–80 times higher than that of other forest types. The herb litter contributes about 27% of production flux of PhytOC for China's forests (Table 4).

The total rate of PhytOC production for the eight Chinese forest types through tree leaf litter and herb litter is $1.94 \pm 0.44 \text{ Tg CO}_2 \text{ yr}^{-1}$ ($1 \text{ Tg} = 10^{12} \text{ g}$) (Table 4). The average rate of PhytOC production through tree leaf litter is the highest in STB ($0.57 \text{ Tg CO}_2 \text{ yr}^{-1}$), followed by DBS ($0.23 \text{ Tg CO}_2 \text{ yr}^{-1}$), SEDB ($0.23 \text{ Tg CO}_2 \text{ yr}^{-1}$), and SEB ($0.20 \text{ Tg CO}_2 \text{ yr}^{-1}$); and the lowest in CTC ($0.11 \text{ Tg CO}_2 \text{ yr}^{-1}$), STC ($0.03 \text{ Tg CO}_2 \text{ yr}^{-1}$), T ($0.02 \text{ Tg CO}_2 \text{ yr}^{-1}$), and CB ($0.02 \text{ Tg CO}_2 \text{ yr}^{-1}$). The

PhytOC production rate for the eight Chinese forest types through the herb litter is $0.52 \pm 0.1 \text{ Tg CO}_2 \text{ yr}^{-1}$.

Discussion

Mechanisms of phytolith carbon sink

Relative to other forms of organic carbon, the PhytOC produced in terrestrial plants is very stable and can accumulate in soil for hundreds and thousands of years after plant decomposition (Fig. 3a and b) (Wilding, 1967; Mulholland & Prior, 1992; Parr & Sullivan, 2005). The role of PhytOC in soil total carbon (TC) accumulation increases significantly with carbon age as a result of the

Table 3 Content of phytolith in dominant understory herb species from the eight Chinese forest types

Forest type*	Species	Phytolith (%)		Forest type	Species	Phytolith (%)	
		Mean	SE			Mean	SE
CTC	<i>Carex lanceolata</i>	3.76	0.53	SEDB	<i>Poa sphondvodes</i>	3.72	1.15
	<i>Radix Sanguisorbae</i>	1.13	0.28		<i>Radix Sanguisorbae</i>	1.13	0.32
	<i>Chamaenerion angustifolium</i>	0.89	0.09		Average	1.92	0.40
	<i>Valeriana officinalis</i>	0.93	0.12		<i>Woodwardia maxima</i>	5.75	0.93
	<i>Artemisia eriopoda</i>	0.83	0.26		<i>Lophatherum gracile</i>	5.39	1.25
	<i>Alopecuruspratensis</i>	4.37	0.42		<i>Carex bodimieri</i>	3.74	0.72
	<i>Poa sphondvodes</i>	3.91	0.88		<i>Hicriopteris chinensis</i>	2.08	0.54
	<i>Artemisia tanacetifolia</i> Linn.	0.97	0.34		<i>Dryopteris atrata</i>	4.72	0.76
	Average	2.10	0.36		Average	4.34	0.84
STC	<i>Dicranopteris linearis</i>	3.23	0.12	SEB	<i>Dicranopteris pedata</i>	3.23	0.12
	<i>Rhizoma Cibotii</i>	7.84	1.14		<i>Lophatherum gracile</i>	5.52	1.09
	<i>Blechnum orientale</i> L.	4.38	0.91		<i>Miscan thus floridulus</i>	2.91	0.71
	<i>Dryopteris</i> spp.	4.72	0.76		<i>Hicriopteris glauca</i>	2.47	0.07
	<i>Pteridium aquilinum</i>	4.27	0.84		<i>Woodw ardia japonica</i> .	7.84	1.14
	<i>Miscan thus floridulus</i>	3.11	0.87		<i>Dryopteris atrata</i>	4.72	0.76
	<i>Ad iantum flabellulatum</i>	7.69	1.96		<i>Radix Sanguisorbae</i>	1.25	0.38
	<i>Lophatherum gracile</i>	5.04	1.13		<i>Ophiopogon japonicus</i>	3.79	0.93
	Average	5.03	0.97		Average	3.97	0.65
CB	<i>Carex bodimieri</i>	3.74	0.72	T	<i>Lophatherum gracile</i>	5.46	1.32
	<i>Carex lanceolata</i>	3.14	0.57		<i>Ophiopogon japonicus</i>	3.79	0.93
	<i>Dicranopteris linearis</i>	3.34	0.13		<i>Blechnum orientale</i>	4.38	0.98
	<i>Blechnum orientale</i> L.	4.12	0.45		<i>Microstegium vagans</i>	6.21	1.03
	<i>Ad iantum flabellulatum</i>	7.69	1.96		Average	4.96	1.06
	<i>Lophatherum gracile</i>	4.98	0.91		<i>Dryopteris atrata</i>	4.72	0.76
	<i>Artemisia tanacetifolia</i> Linn.	1.16	0.29		<i>Pteridium aquilinum</i>	4.25	1.01
	<i>Poa nemoralis</i> Linn.	3.61	1.07		<i>Carex brunnea</i> Thunb	1.97	1.27
	<i>Alopecuruspratensis</i>	4.37	0.42		<i>Woodwardia maxima</i>	5.38	1.53
DBS	Average	4.02	0.72	STB	<i>Miscan thus floridulus</i>	3.11	0.66
	<i>Carex lanceolata</i>	3.52	0.44		<i>Dicranopteris pedata</i>	3.23	0.12
	<i>Saussurea ussuriensis</i> Maxim.	0.60	0.11		<i>Lophatherum gracile</i>	5.08	1.49
	<i>Polygonum viviparum</i>	0.53	0.16		<i>Woodwardia japonic</i> .	7.84	1.14
	<i>Artemisia eriopoda</i>	0.83	0.29		<i>Arthraxon hispidus</i>	4.49	1.78
	<i>Vicia unijuga</i>	0.55	0.13		Average	4.45	1.08
	<i>Alopecuruspratensis</i>	4.49	0.57				

*For details of forest types, see Table 1. The sampling sites are shown in Fig. 1, and the phytolith content data are from this study.

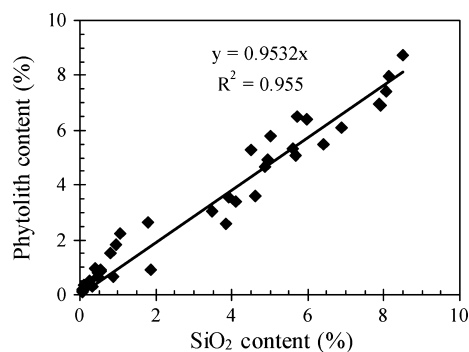


Fig. 2 The correlation of phytolith and SiO₂ in different plant species of forests. For details, see the Materials and Methods section.

PhytOC relative accumulation mechanism (Fig. 3b). The phytolith carbon sink of an ecosystem is the result of soil accumulation of PhytOC released from plant litters.

Estimation of phytolith carbon sink in China's Forests

Phytolith C sink in forests can be estimated from the production rate of PhytOC in forests and phytolith stability factor:

$$\text{Phytolith C sink} = \text{PhytOC production rate} \times \text{phytolith stability factor} \quad (5)$$

where phytolith C sink is the net phytolith C sink rate, PhytOC production rate is estimated from Eqn (4), and

Table 4 Estimated production of PhytOC in China's forests through tree leaf litter and herb litter

Forest type*	Area (10 ⁶ hm ²)	ANPP (t hm ⁻² yr ⁻¹)†	Phytolith content (%)‡		PhytOC production flux (kg CO ₂ hm ⁻² yr ⁻¹)		PhytOC production rate (Tg CO ₂ yr ⁻¹)	
			Mean	SE	Mean	SE	Mean	SE
Litter§								
CTC	24.14	3.98	1.08	0.20	4.75	0.88	0.11	0.02
STC	29.54	4.04	0.21	0.07	0.95	0.31	0.03	0.01
CB	4.68	5.35	0.59	0.34	3.49	2.00	0.02	0.01
DBS	42.40	4.59	1.09	0.24	5.50	1.21	0.23	0.05
SEDB	12.48	7.39	2.28	0.69	18.56	5.61	0.23	0.07
SEB	21.37	7.82	1.10	0.61	9.49	5.25	0.20	0.11
T	0.95	10.17	2.34	2.21	26.14	24.72	0.02	0.02
STB	7.20	6.82	10.52	0.86	78.93	6.45	0.57	0.05
Total	142.76	5.28	1.71	0.41	9.95	2.40	1.42	0.34
Herb								
CTC	24.14	1.21	2.10	0.36	2.79	0.48	0.07	0.01
STC	29.54	1.02	5.03	0.97	5.65	1.08	0.17	0.03
CB	4.68	1.25	4.02	0.72	5.52	1.00	0.03	0.00
DBS	42.40	1.44	1.92	0.40	3.04	0.63	0.13	0.03
SEDB	12.48	0.66	4.34	0.84	3.15	0.61	0.04	0.01
SEB	21.37	0.78	3.97	0.65	3.40	0.56	0.07	0.01
T	0.95	0.72	4.96	1.06	3.93	0.84	0.00	0.00
STB	7.20	0.55	4.45	1.08	2.69	0.66	0.02	0.00
Total	142.76	1.09	3.06	0.58	3.67	0.70	0.52	0.10
Litter + Herb								
CTC	24.14	5.19	1.32	0.24	7.54	1.36	0.18	0.03
STC	29.54	5.06	1.19	0.25	6.60	1.40	0.19	0.04
CB	4.68	6.60	1.24	0.41	9.01	3.00	0.04	0.01
DBS	42.40	6.03	1.29	0.28	8.55	1.84	0.36	0.08
SEDB	12.48	8.05	2.45	0.70	21.70	6.22	0.27	0.08
SEB	21.37	8.60	1.36	0.61	12.89	5.80	0.28	0.12
T	0.95	10.89	2.51	2.13	30.06	25.57	0.03	0.02
STB	7.20	7.37	10.07	0.88	81.63	7.11	0.59	0.05
Total	142.76	6.37	1.94	0.44	13.62	3.10	1.94	0.44

*For details of forest types, see Table 1.

†ANPP data of tree leaf litter are from Zhou *et al.* (2000), Ling *et al.* (2009), and Parr *et al.* (2010). ANPP of herb litter of China's forests are from Feng *et al.* (1999).

‡Phytolith content for tree leaf litter and herb of each forest in this table is the mean of each forest type listed in Table 2 and Table 3, respectively.

§The content of carbon occluded by phytolith used in the estimation of PhytOC production flux varies from 1 to 5%, with an average of 3% (Parr *et al.*, 2010; This study).

the stability factor of forest phytoliths is assumed to be 0.9 as most forest phytoliths are proved to be stable for thousands of years (Meunier *et al.*, 1999; Parr *et al.*, 2010).

The results indicate that the annual phytolith carbon sink in China's forests is 1.7 ± 0.4 Tg CO₂ yr⁻¹, approximately 5% of the average annual biomass carbon sink (35.1 Tg CO₂ yr⁻¹) in China's forests for the time period 1949–2007 (Fang *et al.*, 2001; Pan *et al.*, 2011). The relatively low phytolith carbon sink percentage of the total biomass carbon sink in China's forests is mainly a result of the rapid increase in forest biomass caused by the rapid national-scale afforestation and

reforestation for the time period 2000–2007 (Fang *et al.*, 2001; Pan *et al.*, 2011). About 30% of the phytolith carbon sink in China's forests comes from subtropical and tropical bamboo (STB) which occupies only 5% of the area for China's forests demonstrating the importance of bamboo in regulating forest phytolith carbon sink.

The role of bamboo in forest phytolith carbon sink enhancement: national and global perspectives

Although the total forest areas in many countries have decreased drastically, bamboo forests have increased at a rate of 3% annually, implying that bamboo is an

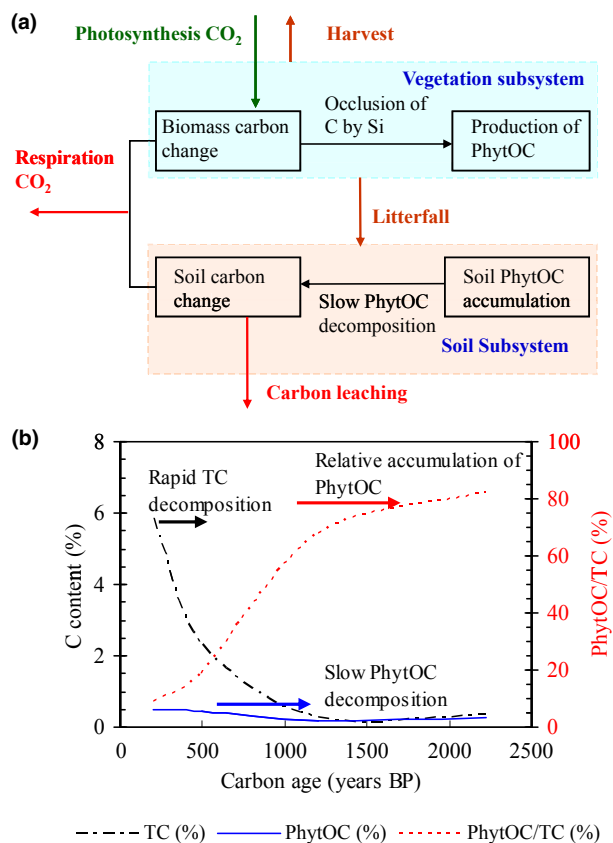


Fig. 3 Mechanisms of PhytOC formation and accumulation in terrestrial ecosystems. (a) Simplified processes of PhytOC formation and accumulation modified from Alexandre *et al.* (1997) and Piao *et al.* (2009). The production of PhytOC is a result of carbon occlusion by silicon in vegetation subsystems, whereas the relative accumulation of soil PhytOC is caused by high litter fall PhytOC input and slow PhytOC decomposition. (b) Changes of the role of PhytOC in soil TC accumulation with carbon age. The data are from Table 2 of Parr & Sullivan (2005). Relative accumulation of PhytOC is caused by rapid TC decomposition and relatively slow PhytOC decomposition over time.

increasingly significant carbon sink (Zhou *et al.*, 2011). The present total area of bamboo in China is $7.2 \times 10^6 \text{ hm}^2$ (Zhou *et al.*, 2011). The total area suitable for growing bamboo in China is at least $163 \times 10^6 \text{ hm}^2$, including $70 \times 10^6 \text{ hm}^2$ of forestry-priority land (Forestry Ministry of China, 1992). Currently, $43 \times 10^6 \text{ hm}^2$ of the forestry-priority land has already been covered by forests (Forestry Ministry of China, 2011), implying an additional $27 \times 10^6 \text{ hm}^2$ of forestry-priority land may be available for afforestation. Based on ecological and economic consideration (Zhou *et al.*, 2011), at least half of the land can be used for bamboo afforestation. It means that the total potential bamboo area in China can reach $20 \times 10^6 \text{ hm}^2$, approximately 13% of China's forests. Also, by selecting bamboo species with high

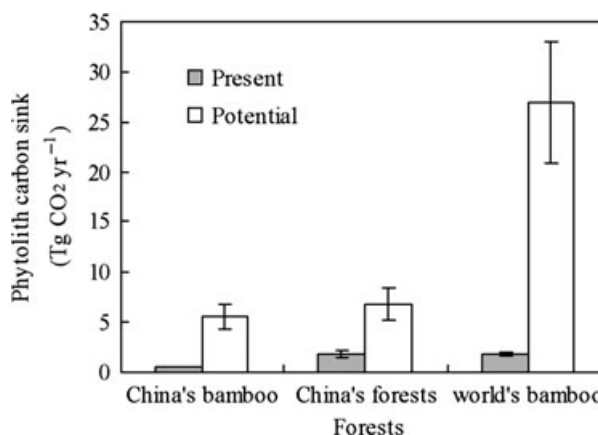


Fig. 4 The present and potential phytolith carbon sink in China's bamboo, China's forests, and world's bamboo. The present total rate of PhytOC production for China's bamboo and China's forests through tree leaf litter and herb litter is from Table 4. The potential of phytolith carbon sink for China's bamboo and China's forests is estimated by taking a median PhytOC production flux of bamboo ($300 \text{ kg CO}_2 \text{ hm}^{-2} \text{ yr}^{-1}$) (Parr *et al.*, 2010) and the present PhytOC production fluxes of other forests listed in Table 4. The present and potential total rate of phytolith carbon sink for the world's bamboo is extrapolated from that of China's bamboo. For details, see the text.

ANPP in the tree leaf litter and high PhytOC content, the PhytOC production flux of bamboo can reach $709 \text{ kg CO}_2 \text{ hm}^{-2} \text{ yr}^{-1}$ (Parr *et al.*, 2010). Relative to bamboo afforestation and reforestation, managing other forests to maximize PhytOC production flux is quite difficult because of their large area and low PhytOC production efficiency (Table 4). Taking a median PhytOC production flux of bamboo ($300 \text{ kg CO}_2 \text{ hm}^{-2} \text{ yr}^{-1}$) (Parr *et al.*, 2010) and present PhytOC production fluxes of other forests (Table 4), the potential of annual phytolith carbon sink for China's bamboo and China's forests (Fig. 4) can reach 5.6 ± 1.3 and $6.8 \pm 1.5 \text{ Tg CO}_2 \text{ yr}^{-1}$, respectively, equivalent to 16% and 19% of average annual biomass carbon sink in China's forests for the time period 1949–2007 (Fang *et al.*, 2001; Pan *et al.*, 2011).

Our results also have broad implications for global bamboo afforestation and reforestation as the area of the world's bamboo is $25 \times 10^6 \text{ hm}^2$ and may increase to $100 \times 10^6 \text{ hm}^2$ (approximately 3% of world's forests) in the following decades (Zhou, 1999; Zhou *et al.*, 2011). Taking a median PhytOC production flux of bamboo ($300 \text{ kg CO}_2 \text{ hm}^{-2} \text{ yr}^{-1}$) (Parr *et al.*, 2010), the annual phytolith carbon sink for the world's bamboo can reach $27.0 \pm 6.1 \text{ Tg CO}_2 \text{ yr}^{-1}$ (Fig. 4), a value slightly lower than that of world's grasslands (average $41.4 \text{ Tg CO}_2 \text{ yr}^{-1}$) reported by Song *et al.* (2012a).

In this study we have estimated the phytolith carbon sink in China's forests and demonstrated the role of

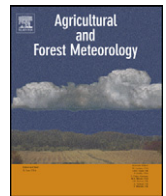
bamboo in national and global forest phytolith carbon sink enhancement. The annual phytolith carbon sink in China's forests is approximately $1.7 \pm 0.4 \text{ Tg CO}_2 \text{ yr}^{-1}$, 30% of which is contributed by bamboo. The potential of annual phytolith carbon sink for China's forests and world's bamboo in the following decades can reach 6.8 ± 1.5 and $27.0 \pm 6.1 \text{ Tg CO}_2 \text{ yr}^{-1}$, respectively. In the estimation of the forest phytolith carbon sink, we have ignored PhytOC input from fine root decomposition because of difficulties in sampling at a national scale and assumingly low phytolith content (Parr *et al.*, 2010). However, recent studies reveal that fine plant roots may also contain a certain amount of Si (Ding *et al.*, 2008) and are rapidly recycled (Gu *et al.*, 2011). Therefore, the phytolith carbon sink in this study may be underestimated. In spite of these uncertainties, we believe that bamboo afforestation/reforestation and other forest management practices designed to maximize forest PhytOC production may significantly enhance phytolith carbon sink and contribute to long-term terrestrial biogeochemical carbon sink.

Acknowledgements

We are grateful for support from the National Natural Science Foundation of China (Grant No. 41103042), the Zhejiang Province Key Science and Technology Innovation Team (No. 2010R50030), and the Opening Project of the Ministry of Education Laboratory for Earth Surface Processes, Peking University (201106). The authors have declared no conflict of interest.

References

- Alexandre A, Meunier JD, Colin F, Koud JM (1997) Plant impact on the biogeochemical cycle of silicon and related weathering processes. *Geochimica et Cosmochimica Acta*, **61**, 677–682.
- Blecker SW, McCulley RL, Chadwick OA, Kelly EF (2006) Biologic cycling of silica across a grassland bioclimate sequence. *Global Biogeochemical Cycles*, **20**, 1–11.
- Carnelli AL, Madella M, Theurillat J-P (2001) Biogenic silica production in selected alpine plant species and plant communities. *Annals of Botany*, **87**, 425–434.
- Chen L, Huang J, Yan C (1997) *Nutrient Cycles in Forest Ecosystems of China*, pp. 57–62. Meteorology Press of China, Beijing.
- Conley DJ (2002) Terrestrial ecosystems and the global biogeochemical silica cycle. *Global Biogeochemical Cycles*, **16**, 1–8.
- Ding TP, Zhou JX, Wan DF, Chen ZW, Wang CY, Zhang F (2008) Silicon isotope fractionation in bamboo and its significance to the biogeochemical cycle of silicon. *Geochimica et Cosmochimica Acta*, **72**, 1381–1395.
- Fang J, Chen A, Peng C, Zhao S, Ci L (2001) Changes in forest biomass carbon storage in China between 1949 and 1998. *Science*, **292**, 2320–2322.
- Feng Z, Wang X, Wu G (1999) *Biomass and Productivity of Forest Ecosystems in China*, pp. 1–231. Science Press, Beijing.
- Forestry Ministry of China (1992) *A Study on the Eco-economic Regional Planning and Development Strategies of China's Bamboo Forest*, pp. 53–70. China Forestry Publishing House, Beijing.
- Forestry Ministry of China (2011) *China Forestry Statistical Year Book 2010*, pp. 1–10. China Forestry Publishing House, Beijing.
- Gu J, Yu S, Sun Y, Wang Z, Guo D (2011) Influence of root structure on root survivorship: an analysis of 18 tree species using a minirhizotron method. *Ecological Research*, **26**, 755–762.
- Hou X (1982) *Vegetation Geography of China and Chemical Composition of its Dominant Plants*, pp. 188–243. Science Press, Beijing.
- Lackner KS (2003) A guide to CO₂ sequestration. *Science*, **300**, 1677–1678.
- Li Z, Lin P, He J, Yang Z, Lin Y (2006) Silicon's organic pool and biological cycle in moso bamboo community of Wuyishan Biosphere Reserve. *Journal of Zhejiang University Science B*, **7**, 849–857.
- Ling H, Chen G, Chen Z (2009) Controlling factors of litterfall in China's forests. *Journal of Subtropical Resources and Environment (In Chinese with English abstract)*, **4**, 66–71.
- Meunier JD, Colin F, Alarcon C (1999) Biogenic silica storage in soils. *Geology*, **27**, 835–838.
- Mulholland SC, Prior C (1992) Processing of phytoliths for radiocarbon dating by AMS. *The Phytolitharian Newsletter*, **7**, 7–9.
- Pan Y, Birdsey RA, Fang J *et al.* (2011) A large and persistent carbon sink in the world's forests. *Science*, **333**, 988–993.
- Parr JF, Sullivan LA (2005) Soil carbon sequestration in phytoliths. *Soil Biology and Biochemistry*, **37**, 117–124.
- Parr JF, Sullivan LA (2011) Phytolith occluded carbon and silica variability in wheat cultivars. *Plant and Soil*, **342**, 165–171.
- Parr JF, Sullivan LA, Chen B, Ye G (2010) Carbon bio-sequestration within the phytoliths of economic bamboo species. *Global Change Biology*, **16**, 2661–2667.
- Piao S, Fang J, Ciais P *et al.* (2009) The carbon balance of terrestrial ecosystems in China. *Nature*, **458**, 1008–1013.
- Scholes RJ, Noble IR (2001) Storing carbon on land. *Science*, **294**, 1012–1013.
- Song Z, Liu H, Si Y, Yin Y (2012a) The production of phytoliths in China's grasslands: implications to biogeochemical sequestration of atmospheric CO₂. *Global Change Biology*, **18**, 3647–3653.
- Song Z, Wang H, Strong PJ, Li Z, Jiang P (2012b) Plant impact on the coupled terrestrial biogeochemical cycles of silicon and carbon: implications for biogeochemical carbon sequestration. *Earth-Science Reviews*, **155**, 319–331.
- Wilding LP (1967) Radiocarbon dating of biogenetic opal. *Science*, **156**, 66–67.
- Zhou F (1999) Looking back to bamboo industry for the 20th century, looking forward bamboo industry for the 21st century. *Journal of Bamboo Research (In Chinese with English abstract)*, **18**, 1–5.
- Zhou Y, Yu Z, Zhao S (2000) Carbon storage and budget of major Chinese forest types. *Acta Phytocologica Sinica (In Chinese with English abstract)*, **24**, 518–522.
- Zhou G, Meng C, Jiang P, Xu Q *et al.* (2011) Review of carbon fixation in bamboo forests in China. *The Botanical Review*, **77**, 262–270.
- Zuo X, Lü H (2011) Carbon sequestration within millet phytoliths from dry-farming of crops in China. *Chinese Science Bulletin*, **56**, 3451–3456.



Vegetation responses to mid-Holocene extreme drought events and subsequent long-term drought on the southeastern Inner Mongolian Plateau, China

Yi Yin, Hongyan Liu*, Guo Liu, Qian Hao, Hongya Wang

College of Urban and Environmental Sciences and MOE Laboratory for Earth Surface Processes, Peking University, Beijing 100871, China

ARTICLE INFO

Article history:

Received 10 May 2012

Received in revised form 12 October 2012

Accepted 15 October 2012

Keywords:

Drought

Vegetation responses

Forest resilience

Semi-arid region

Soil coarsening

The Holocene

ABSTRACT

Ecological responses to climate change are strongly regulated by long-term processes, such as changes in species composition and carbon dynamics in soil; therefore, understanding and predicting these processes require long time scale studies. Based on high-resolution lake sediment records of the Angili Nuur Lake from the forest-steppe ecotone at the southeastern margin of the Asian Gobi, we found three pronounced drought events during the mid-Holocene (~7.0–6.3 ka BP, BP means “before present”, where present means 1950 and ka = 1000 years) and a subsequent gradual drying trend. During the extreme drought events, lake aquatic system showed strong desiccation and instant salty marsh expansion; whereas regional forest showed strong resilience. During the following long-term drying at millennial scale, broadleaf forest, coniferous forest and steppe successively dominated in this region, in 6.3–4.4 ka BP, 4.0–2.7 ka BP and since 2.7 ka BP, respectively; but the changing dominance between forest and steppe did not match the climate change rate as reconstructed in previous studies, suggesting a lagged and non-proportional change of vegetation type to the range of climate change. The resilience of forest implies a strong buffering effect of biotic and abiotic factors other than climate, probably explained by diverse micro-environments of this mountainous region that allowed forest to survive during the drought spells, and also by gradual soil coarsening that retarded soil field capacity change and nutrient loss. However, under accumulative drying trend, forest was in general replaced by steppe around 2.0 ka BP.

© 2012 Elsevier B.V. All rights reserved.

1. Introduction

In the context of recent global warming and drought intensifying (Solomon et al., 2008; Dai, 2011), the understanding of terrestrial ecosystem-climate interactions under rapid climate change is undoubtedly crucial to both scientific research and public (IPCC, 2007). Drought-related ecological degradation, including forest dieback (Breshears et al., 2005; Allen et al., 2010), grassland desertification (Schlesinger et al., 1990; Yang et al., 2005), wetland degradation and lake desiccation (Zhao et al., 2011; Lake, 2011) have been widely reported, especially in the semi-arid regions; however, these studies have mostly been restricted to annual to decadal scales, which might fail to cover the climate change range that current global change is likely to bring (Held, 2012). Moreover, the relative long lifespan of trees and long-term processes of forest regeneration and succession made it difficult to discuss vegetation responses to accumulative climate change on this relatively short time scale (Peng et al., 2011). Therefore, it is important to use palaeo-ecological records, where past droughts have been more severe and persistent than those of instrument-recorded his-

tory (Laird et al., 1996; Clark et al., 2002; Chen et al., 2003a, b; Cook et al., 2010; Nelson et al., 2011), to study vegetation responses to climate change over a longer time scale.

Forest and steppe exhibit mosaic distribution at the southern margin of the Asian Gobi desert and surrounding steppe region (Fig. 1), where lies the drought limit of temperate forest distribution range and water availability greatly controls vegetation growth (Walter and Breckle, 2002; Wu, 1980). Meanwhile, it is also the margin of Pacific monsoon influence, with highly fluctuated inter-annual precipitation associated with changing intensity of Pacific monsoon (Clift and Plumb, 2008). Vegetation dynamics in this region is hence sensitive to climate change, especially drought (Piao et al., 2003); but how vegetation type will respond to long-term climate change remains unclear due to complicated interactions among vegetation, climate and soil, including processes in carbon and nitrogen cycling, albedo and snow cover change, dust emission and transportation, as well as aerosol concentration change (Cox et al., 2000; Ridgwell and Watson, 2002; Rotenberg and Yakir, 2010).

A number of studies have reported the middle Holocene drought spells in these region (Chen et al., 2003a, b; Xiao et al., 2006, 2009; Chen et al., 2003a, b, 2008a), as well as soil development and sand accumulation cycles (Lu et al., 2005) and dust flux changes (Miao et al., 2007; An et al., 2011) during the Holocene. These drought

* Corresponding author.

E-mail address: lhy@urban.pku.edu.cn (H. Liu).

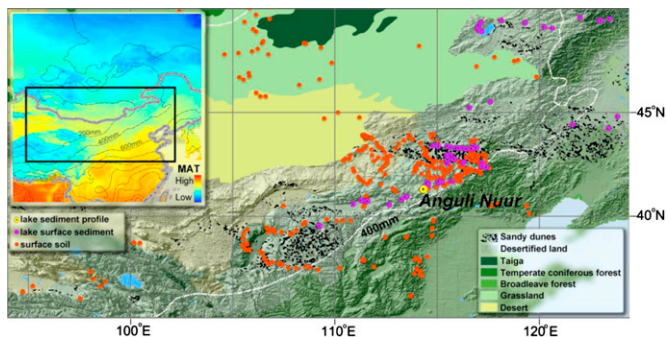


Fig. 1. Study area with sampling sites on a biome map with hills shaded; yellow circle represents sediment core site, *Anguli Nuur*; orange dots represent topsoil samples, including cited sites in the compiled database; purple dots represent paired lake surface sediment-surrounding topsoil sample sites. The inset in the upper left corner illustrates modern MAT (mean annual temperature, color) and MAP (mean annual precipitation, isolines).

spells provided us an opportunity to study a severe arid period and corresponding vegetation responses on a millennium time scale. However, these studies mainly worked on environment reconstruction, while vegetation responses to climate change are seldom discussed from the ecological point of view. In this study, based on well dated high-resolution lake sediment records, we found several extreme drought events in the mid-Holocene and subsequent long-term drought trend in the mid to late Holocene. Thus, we aimed at exploring following questions: (1) is this mid-Holocene drought only site-specific or of regional importance and what was the possible reason? (2) how vegetation responded to rapid extreme drought events and long-term drying trend, respectively? and (3) how other biotic or abiotic factors have influenced vegetation response to the mid-Holocene droughts?

2. Materials and methods

2.1. Data preparation and field sampling

Sediment cores retrieved from Anguli Nuur Lake ($\sim 41^{\circ}20'N$, $\sim 114^{\circ}20'E$; altitude, 1315 m.a.s.l.; mean annual precipitation (MAP), 380 mm; mean annual temperature (MAT), $3.1^{\circ}C$) were selected for analysis in this study (Fig. 1, yellow dot). This inland lake lies in the woodland-steppe ecotone of north China, at the southern border of the Asian Gobi, where is also the marginal area of the Pacific monsoon influence (Wu, 1980). The 1138 cm An-S core was drilled near the lowest position of the desiccated lake bed using a HZ-100Y drilling rig in 2005, and a second 1023 cm parallel supplementary core (An-A) was drilled in 2007 (Liu et al., 2010). The sediment cores were divided into 1 cm subsamples for further analysis.

Topsoil samples from 174 sites across the vegetation type gradient (desert, desert steppe, typical steppe, meadow steppe and forest) were collected for pollen analysis; in addition, a regional topsoil pollen database was established to expand the environmental range of topsoil pollen from Liu et al. (1999), Xu et al. (2007) and Gunin et al. (1999). In total, 461 topsoil pollen samples were used to analyze the relationship between surface pollen composition and vegetation (Fig. 1, orange dots).

Lake surface sediments from 45 natural lakes (Fig. 1, purple dots) covering a large annual precipitation range (from 100 to 800 mm) were sampled over water by a sediment sampler to grab the uppermost 5 cm; meanwhile, corresponding topsoil (uppermost 5 cm) of dominant vegetation types in the lake shore region were also sampled to validate the usage of topsoil pollen-vegetation relationships in sediments and to analyze the indicative chemical elements in the sediments. MAP and MAT of these 45 sample sites were

interpolated from those of meteorological stations in this region provided by the Chinese National Meteorological Center. Aridity was calculated as the inverse of the Thornthwaite humidity index (Thornthwaite, 1948).

2.2. Laboratory analysis

Next, sediment core samples (at 5 cm intervals) and all topsoil and lake surface samples were analyzed in the laboratory. The chronology of the sediment core was defined by integrated results of AMS ^{14}C dating and ^{210}Pb and ^{137}Cs activity analysis; all dates in this study were calibrated to calendar years (Fig. 3, left column, *Age-depth*, see details in Yin et al., 2011). Soluble salt and main ion contents were analyzed by the ion titration method. Chemical element components were analyzed by ARL ADVANT-XP X-ray Fluorescence Sequential Spectrometer (XRF). Grain size distributions were determined by *Malvern Mastersizer 2000* after standard pretreatment (Yin et al., 2011). Total organic carbon (TOC) and Total nitrogen (TN) were analyzed by colorimetric detection and high temperature oxidation (*Elementar Vario EL*), respectively, after removal of roots and other macro organic remains and grinding to pass through a 0.149 mm soil sieve. Pollen analysis, including three-step pretreatment with HCl, NaOH and coarse material sieving, an extraction procedure by centrifugal with heavy liquid solution (KI+HI+Zn) of specific gravity around 1.9, and an after-treatment with acetolysis and fine sieving were conducted for all sediment core, topsoil and lake surface samples. Approximately 300–400 terrestrial carpophyte pollen grains were counted and total pollen sum (not including aquatic plant, fern and algae) was used for pollen percentage calculation.

2.3. Statistical analysis

The main statistical techniques applied in this paper were Redundancy Analysis (RDA, Anderson and Willis, 2003), used for analyzing modern indexes–climate relationships, and Constrained Clustering (Bennett, 1996) for classifying profile pollen composition. These analyses were performed in R using the *vegan 2.0* and *rioja 0.7-3* packages.

3. Results

3.1. Indication of pollen taxon and chemical elements in the semi-arid region

Thirty-two families or genera of pollen grains were identified in total. RDA results for topsoil and lake surface pollen showed different clusters of pollen composition across vegetation types and illustrated the corresponding indication of labeled families/genera (Fig. 2a). The influences of environmental variables, including mean annual precipitation (MAP), mean annual temperature (MAT) and altitude (ALT) are statistically significant ($p < 0.005$), suggesting that differences in pollen composition effectively indicate environmental changes. Each pollen taxon showed similar characteristics when conducting RDA analysis in topsoil and lake surface pollen datasets separately, suggesting that the indication of topsoil and lake sediment pollen are generally in good agreement. Therefore, it is reasonable to use a topsoil pollen–climate relationship to interpret lake sediment pollen composition. In general, arboreal pollen indicates a humid environment, of which *Quercus* and *Carpinus* indicate warm conditions, while *Larix* and *Betula* indicate cool conditions; on the contrary, *Chenopodiaceae*, *Ephedra* and *Nitraria* are indicators of a dry climate.

RDA results of chemical elements showed that chemical element components in both soil and lake sediment differed across

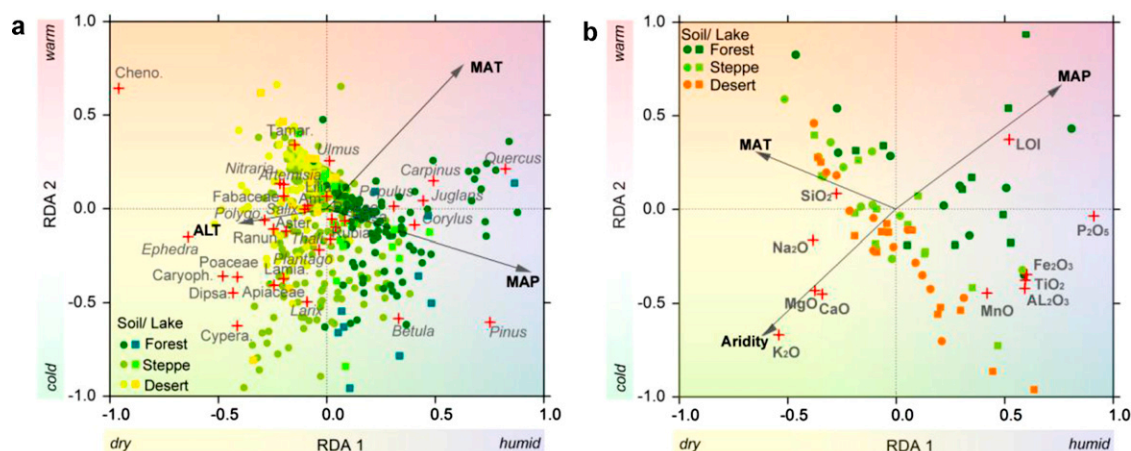


Fig. 2. RDA results of (a) pollen composition and (b) chemical element composition of soil and lake surface samples with environmental factors. Dots represent surface soil, squares represent lake sediments, while colors indicate different vegetation types. Red crosses represent the coordinates of pollen taxon or elements in the ordination axis. Black arrows represent environmental variable indication. Abbreviations of flora family: Cheno., Chenopodiaceae; Tamar., Tamaricaceae; Am., Amaranthaceae; Polygo., Polygonaceae; Aster., Asteraceae; Ranun., Ranunculaceae; Thali., Thalictrum; Lamia., Lamiaceae; Caryoph., Caryophyllaceae; Dipsa., Dipsacaceae; Cypera., Cyperaceae. (For interpretation of the references to color in this figure legend, the reader is referred to the web version of this article.)

vegetation types (Fig. 2b). The influences of environmental variables (MAP, MAT, Aridity) were statistically significant ($p < 0.005$), demonstrating that differences in chemical elements could effectively indicate ecological variance. Generally, K_2O , Na_2O , CaO , MgO indicate aridity, while P_2O_5 , Fe_2O_3 , TiO_2 , Al_2O_3 , MnO indicate humidity in our study region. Paired samples of lake sediment-surrounding soil in different vegetation groups showed similar characteristics in the RDA ranking, suggesting that sediment chemical characteristics could approximately indicate local soil features. The difference between soil and sediment was larger in humid regions than that in arid regions, owing to organic matter accumulation in the sediments.

3.2. Changes in physical and chemical properties of lake sediments during the Holocene

The most prominent change of all physical and chemical properties in the sediment was the abrupt shifts around 6.3–7.0 ka BP (Fig. 3, left panel – Lake Aquatic Ecosystem, indicated by red rectangle). Before 7.0 ka BP, dry to humid indicating element ratio (ER) of $(K + Na + Ca + Mg)$ to $(Fe + Mn)$ was generally low, with a slightly decreasing trend during the early Holocene (Fig. 3, left panel, red line), indicating transition from the termination of cold and dry ice age into a warmer and wetter phase. Soluble salt percentages slightly increased (Fig. 3, left panel, orange area), suggesting salt accumulation as more salt was transported in by water. Coarse sand percentages were generally low (Fig. 3, left panel, brown area, $>63 \mu m$ particles), indicating fine material input. The C/N ratio was high (Fig. 3, left panel, bright green line), with an increasing trend, implying terrestrial vegetation was flourishing.

During 7.0–6.3 ka BP, there was an abrupt increase in ER and soluble salt concentration. Three prominent drought events can be identified, with each drought period spanning several decades to over a hundred years. In the drought cycles, the C/N ratio was extremely low, accompanied with low values in both TOC and TN when compared with other periods, suggesting low lake aquatic productivity and small amounts of terrestrial organic material input during the drought events. Coarse sand percentages, however, did not increase simultaneously.

After 6.3 ka BP, coarse sand percentages increased sharply at first and have since increased steadily with high frequency fluctuations. The C/N ratio has decreased due to a faster decline of TOC than TN, suggesting intensive destruction of the lake's aquatic

ecosystem and reduced terrestrial biomass input. ER and soluble salts, however, did not show any evident trend, which is likely caused by less soluble salt input as climate drying and salt upward going with evaporation and subsequent erosion. In addition, the coarser sediment during this period might have resulted in lower mass percentages of soluble salts.

3.3. Changes in pollen assemblages of lake sediments during the Holocene

Numerical time constrained classification of 100-year averages for each pollen taxa of the whole profile suggested that the largest differences in pollen assemblages lay between recent 2000 years (Fig. 3, middle panel – Terrestrial Vegetation Ecosystem, Phase II, steppe dominance) and previous stages (Phase I, forest or forest-steppe dominance). The earlier stages was then divided into the early Holocene (Phase Ia) and the mid-Holocene (Phase Ib).

Phase Ia (11.4–9.6 ka BP) lay at the bottom of the whole profile. In the earliest stage, the arboreal pollen percentages were low, while the steppe pollen percentages were relatively high. Subsequently, there was a marked increase in both coniferous and broadleaf pollen and a decrease in *Artemisia* and *Chenopodiaceae* around 11 ka BP, suggesting rapid forest expansion and steppe retraction in the early Holocene. The percentage of each taxon was highly variable afterwards, suggesting dynamic and complicated interactions between vegetation and climate. The average of *Picea* and *Abies* percentages during this period was around 15%, with the peak value of the whole profile around 41%, suggesting a generally cool and humid environment.

Phase Ib.1 (9.6–6.9 ka BP) was dominated by high arboreal pollen percentages; both coniferous and broadleaf pollen were abundant with average value of 44% and 11%, respectively. Steppe components were lower than other stages, indicating forest dominance.

Phase Ib.2 (6.9–4.7 ka BP) had less arboreal but more steppe pollen. The percentages of coniferous and broadleaf tree pollen were slightly lower than those in the former and latter stages. During the mid-Holocene droughts (7.0–6.3 ka BP), the *Artemisia* pollen percentage increased markedly to 75%, together with sharp increases of *Nitraria* and *Ephedra*, which are indicators of local drought and salt tolerant vegetation. However, the regional terrestrial vegetation composition did not show directional change or dynamic replacement of forest by steppe, as relatively high percentages of forest persisted.

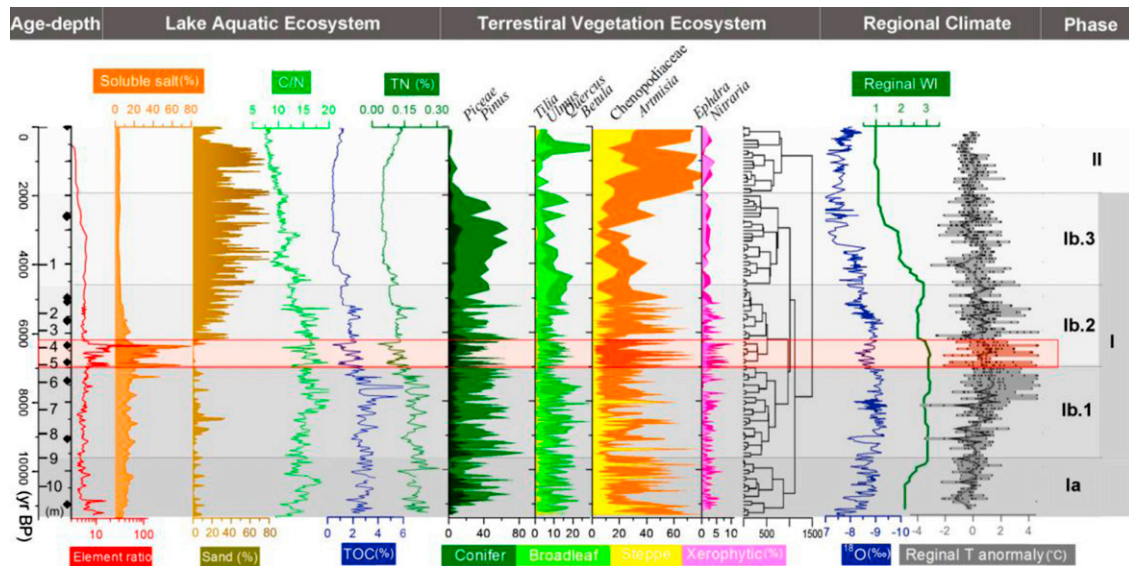


Fig. 3. An-S sediment proxies and comparison with regional climate change processes. From left to right: the first panel is the age-depth relationship from AMS ^{14}C dating (black diamonds); the second panel shows the local aquatic system indexes: element ratio of $(\text{K} + \text{Na} + \text{Ca} + \text{Mg})/(\text{Fe} + \text{Mn})$, soluble salt, sand percentages, TOC, TN and C/N; the middle panel shows the terrestrial vegetation indicator, namely the selected pollen compositions of coniferous, broadleaf, steppe and saline taxa; the right panel shows reconstructed regional climate proxies: Dongge ^{18}O isotope (Dykoski et al., 2005), temperate steppe wetness index (Zhao et al., 2009), and synthesized China temperature anomaly series (Fang and Hou, 2011).

Phase Ib.3 (4.7–2.0 ka BP) was a transitional period gradually from forest to steppe dominance. It was firstly dominated by broadleaf forest (around 4.7–4.0 ka BP) with the highest value of *Quercus* and *Tilia* of the whole Holocene; the broadleaf forest dominance was then replaced by coniferous forest (around 4.0–2.7 ka BP) and then by steppe vegetation (2.7–2 ka BP), when *Chenopodiaceae* and *Artemisia* pollen increased substantially, whereas coniferous and broadleaf pollen both decreased, indicating that more drought-resistant steppe and even desert elements had immigrated into this region.

Phase II (2.0 ka BP – present) was dominated by steppe vegetation with the highest average steppe pollen percentages and lowest arboreal pollen percentages during the whole Holocene. A sharp decrease of arboreal pollen and prominent increase of *Artemisia* and *Chenopodiaceae* pollen indicated extensive replacement of forest by steppe under cumulative drying in the lake catchment. Corresponding C/N ratio was also the lowest through the Holocene.

4. Discussion

4.1. Drought events and trends as regional phenomena

Our sediment sequence of the Anguli Nuur showed strong evidence for severe drought events in the mid-Holocene and a subsequent general drying trend. The studied lake lies in the marginal region of the Pacific monsoon influence, where the Pacific monsoon intensity strongly controls summer (annual) precipitation (Clift and Plumb, 2008). The lake basin occupies a shallow depression among small rolling basalt hills with no outlet, which emphasized the influence of evaporation on water table balance (Liu et al., in review). Meanwhile, there are no large geological movements since the Late Miocene (Zhai et al., 2006) and no large human population until recent 200 years (Deng, 2005). Thus changes in lake water balance are most possibly due to climatic change. Comparison of ecosystem proxies in Anguli Nuur with summer monsoon intensity as indicated by stalagmite $\delta^{18}\text{O}$ from Dongge cave in south China (Fig. 3, right panel – Regional Climate, blue line, after Dykoski et al., 2005) and regional synthesized temperature series of China reconstructed from multiple records (Fig. 3, right panel, gray dots,

after Fang and Hou, 2011) shows that the mid-Holocene drought (~7.0–6.3 ka BP) occurred during a period of high temperature and relatively weak summer monsoon intensity within a general strong phase of summer monsoon under the glacial-interglacial context. Therefore, the mid-Holocene drought in our study area, which was contemporaneous with the so called warm-wet Megathermal (Shi et al., 1992; An et al., 2000), was most likely caused by a high temperature-induced evaporation increase.

There are also other mid-Holocene dry spells reported in the semi-arid region of China by multiple proxies, for example, abrupt element and grain size distribution change of Yanhaizi (Chen et al., 2003a, b), rapid shift of grain size distribution in Dali Lake (Xiao et al., 2006, 2009) and sharp *Pediastrum* and Diatom concentration fluctuation in Bayanchagan Lake (Jiang et al., 2006). Although droughts at other sites were not shown as such severe desiccation as our case, it may be due to different environmental sensitivity of lake size and geophysical settings, which was supported by studies on different water area change rate of different lake size in this region under climate warming of recent decades (Liu et al., in review). Thus, we can infer that this mid-Holocene drought was not only site-specific in our study, but was widespread in this semi-arid area (Chen et al., 2003a, b, 2008a). Similar warm-drought events were also commonly found in semi-arid areas in North America (Nelson et al., 2011), the Mediterranean (Roberts et al., 2011) and Africa (Kropelin et al., 2008) during the mid-Holocene.

Drought/flood index and tree-ring records in recent 600 years also demonstrated that the dominant climate pattern in north-central China consisted of warm-dry and cold-wet alternations (Yi et al., 2012), implying that warming induced drought are of high possibility in the study area. The relationship between lake water surface area change based on remote sensing and climate change in recent 40 years also shows that fast warming is the most important factor causing lake shrinkage in this semi-arid steppe region (Liu et al., in review), which cautions us that warming induced drought and lake desiccation are very likely to be enhanced in the semi-arid region in the near future under rapid climate warming scenarios (Dai, 2011; Held, 2012).

In addition to the mid-Holocene drought events, our profile also showed an obvious drying trend after 5.0 ka BP, which

coincided well with other profiles in this semi-arid steppe region, e.g. reconstructed wetness index (WI) from multiple pollen profiles in temperate steppe region (Fig. 3, right panel, green line) after Zhao et al. (2009), and was possibly influenced by decreased summer monsoon intensity as indicated by stalagmite $\delta^{18}\text{O}$ from Dongge cave in south China (Dykoski et al., 2005) and Sanbao cave in central China (Wang et al., 2008). This widespread reduction in monsoon intensity has been widely discussed and generally accepted as driven by decreased summer insolation (Berger and Loutre, 1991; Wang et al., 2005, 2008). The stronger regional synchronization of this drying trend than that of the mid-Holocene drought suggests that longer-term droughts have more influence on regional climate pattern than short-term drought events.

4.2. Differentiated responses of local and regional vegetation to drought events

The lake aquatic system (hydrology and wetland vegetation) and regional terrestrial vegetation showed different sensitivities and resilience to the mid-Holocene drought events. Salt concentration, chemical components, TOC and TN, as indicators of lake aquatic system showed instant and marked responses to droughts, whereas terrestrial vegetation, as indicated by pollen assemblages, showed more progressive change. The dramatic changes in lake soluble salt concentration and sediment element components showed that the lake water has been greatly condensed and that the aquatic system underwent abrupt change (Fig. 3, left panel). These changes were very likely caused by evaporation greatly exceeding precipitation, when considering the geological background of this region as discussed above. Meanwhile, the C/N ratio has decreased continuously, with faster decrease in TOC than TN, suggesting that the productivity of the lake aquatic system and terrestrial organic matter input has greatly decreased (Woodward et al., 2012). Abrupt increases and subsequent sharp decreases in algae *Pediastrum* concentration (7.4–6.3 kyr BP) in the Bayanchagan Lake, which is only 120 km away from our study site, also support the inferred fast response of the lake aquatic system (Jiang et al., 2006).

In contrast to the lake system, regional vegetation indicated by our profile did not show such abrupt and directional trend of forest replacement by steppe during the mid-Holocene extreme drought events. During the drought spells, arboreal pollen decreased slightly, accompanied with an increase in the steppe species percentages and the local drought and saline tolerant species composition, *Ephedra* and *Nitraria*. When interpreting percentage data, the prominent increase of pollen taxa from relatively small patches with low productivity and inferior transportation could strongly indicate local vegetation responses (Minckley et al., 2012). This provides reliable evidence that, during the drought events the local saline vegetation expanded promptly, which is very similar to modern drought impacts on lakeshore wetlands (Zhao et al., 2011). However, after the drought events, unlike sand percentages and the C/N ratio, arboreal pollen percentages increased again very rapidly after the drought, showing the resilience of forest to drought impacts. A similar progressive vegetation pattern change was also found in other profiles in this region (Li et al., 2004; Jiang et al., 2006; Chen et al., 2008a; Zhao et al., 2009). Regional wetness index (WI) from synthesized pollen results did not show prominent decline during the drought events either (Fig. 3, right panel). In addition, sand percentages in the sediment was low during the drought events but increased afterwards, implying that the terrestrial vegetation cover might have sustained relatively high during this extreme drought event and higher vegetation coverage might have prevented soil from erosion (Munson et al., 2011). It also indicates that the terrestrial vegetation change might have lagged soil erosion and aeolian activity.

4.3. Forest resilience to fast climate change

Regional vegetation, mainly forest, showed strong resilience to drought disturbances in the mid-Holocene drought events, and quickly recovered in the following period, e.g. increase in broadleaf pollen in late Ib.2 (6.3–4.7 ka BP) and increase in coniferous pollen in Ib.3 (4.7–2.0 ka BP), during which period precipitation was relatively low as summer monsoon intensity generally declined (Fig. 3). Wetness Index (WI) of temperate steppe region also declined markedly since 4.7 ka BP; however, final replacement of forest by steppe in our study area did not occur until recent 2.0 ka BP. This lagged response of vegetation development implies that vegetation and climate condition may not always be in equilibrium (Webb, 1986) and other biotic or abiotic factors also strongly influence vegetation development except for climate changes (Davis, 1986). Modern studies suggest that vegetation responses to drought are directly affected by biotic factors (McDowell et al., 2008; Jackson et al., 2009; Scherrer et al., 2011), and additionally by soil moisture that is determined not only by precipitation, but also by topography resultant water redistribution, evapotranspiration and soil texture (Liu et al., 2008; Katul and Siqueira, 2010). In addition, wind erosion is severe in this semi-arid region, particularly during dry periods, strongly influencing vegetation growth and soil condition (Shi et al., 2004; Zhang et al., 2003). Therefore, the strong resilience of forest to drought stress in our study area is likely due to two processes: diverse micro-environment resulted from mountainous topography and lagged slow-process soil condition change.

Firstly, considering the effect of topographical heterogeneity, the woodland-steppe ecotone occupied in the rolling mountainous region (Fig. 1), where topographical settings have greatly redistributed precipitation, and also insolation intensity, evapotranspiration, as well as wind speed, and soil condition (Walter and Breckle, 2002). Forest patches existed nowadays under MAP of less than 400 mm on the northern steep slopes, where soil moisture could support forest survival (He et al., 2008). Thus under drought stress, when forest in some parts declined, there still could have been suitable microenvironment which allowed forest to survive and to reproduce; accordingly, when climate ameliorated, forest was then able to re-establish very rapidly, avoiding long-term dispersal or even extinction with active seed bank (Chen et al., 2008b; Tian et al., 2009; Svenning et al., 2008). These diverse niches provided by topographical heterogeneity permitted species to endure extreme climatic conditions, and recover when the climate become suitable again.

Secondly, considering the long-term soil process, sand percentages were low during the mid-Holocene drought events, however, increased markedly afterwards, implying that the terrestrial vegetation cover might have been relatively high during this extreme drought event and have thus alleviated soil erosion and aeolian activities (Munson et al., 2011). It also indicates that the slow process of soil erosion and resultant soil coarsening and nutrient loss might have retarded vegetation decline (Liu et al., 2008), and acted as a buffering effect. In return, soil condition of the late Holocene, with coarser texture and lower nutrients as suggested by grain size and partly by C/N, might have further caused vegetation deterioration as demonstrated by modern processes (Bakker et al., 2005; Li et al., 2009).

There has been wide debate regarding whether extant species have coped successfully with the extremely rapid climatic changes (Hof et al., 2011; Parducci et al., 2012), for example local temperature changes of up to 4°C per year near the end of the last glacial period (14.7 ka BP) in the Late Quaternary (Steffensen et al., 2008). These successes are perhaps due to the phenotypic variability of populations and their ability to survive in microclimatic pockets in a heterogeneous landscape (Botkin et al., 2007). However, many central European trees failed to survive the last glacial

maximum (LGM) (Svenning, 2003): the flat plain of west and central Europe, lacking refuge, may be a possible reason. In contrary, many tree species survived the LGM in Northern China; refuges were maintained across the range of forest distribution in both north and south during the LGM rather than that the species survived only in the south and subsequently dispersed northwards (Ren and Beug, 2002; Chen et al., 2008b; Tian et al., 2009). We thus came up with the hypothesis that topography and resultant micro-environment diversity are important for species' survival under rapid climate change by offering diverse micro-environment and buffering climate change. This hypothesis was primarily tested by the sediment results of the Anguli Nuur Lake, where vegetation over complicated regional topological settings was more resilient to the mid-Holocene drought, and the diverse topographical settings and soil conditions may have provided a buffering effect for vegetation change and allowed species to retreat or encroach according to environmental condition. However, it also needs to be stressed that, though forest may have strong resilience in mountainous areas, prominent forest dieback may also occur under cumulative drought effect, like the case after 2.0 ka BP. Soil coarsening induced by erosion may in return have accelerated vegetation decline as nutrient loss and soil field capacity decrease (Li et al., 2009). Therefore, forest patches in the forest-steppe ecotone, which is at the drought limits of forest survival, together with much coarsened soil texture, is likely to be more threatened by drought events in current patchy distribution than the mid-Holocene forest dominant condition.

5. Conclusions

From our study of palaeo-ecological records in the Anguli Nuur lake, we found severe drought events during the mid-Holocene Megathermal and subsequent gradual drying trend. These kinds of warm-induced droughts are likely to have regional significance and are of highly possibility to be enhanced in the semi-arid region under future rapid climate warming. Lake aquatic system and terrestrial forest vegetation showed different sensitivities in response to drought events: lake aquatic system and wetland vegetation showed profound changes instantly, whereas regional forest showed strong resilience. During the following long-term drying at millennial scale, broadleaf forest, coniferous forest and steppe successively dominated in this region, but the final replacement of forest by steppe did not match the climate change rate as reconstructed in previous studies, suggesting a lagged and non-proportional change of vegetation type to the range of climate change. This strong resilience of forest implied a strong buffering effect of other biotic and abiotic factors, probably including diverse micro-environments of this mountainous region that allowed forest to survive during the droughts, as well as gradual soil coarsening that retarded soil water carrying capacity change and nutrient loss. However, under accumulative drying trend, forest was eventually replaced by steppe in 2.0 ka BP.

Acknowledgments

This study was granted by National Natural Science Foundation of China (No. 41071124, 31021001, 41011120251). We thank Jian-gling Zhu and Ji Ren for their assistance in field work, and Dave Chandler for editing the text.

References

Allen, C., Macalady, A., Chenchouni, H., Bachelet, D., McDowell, N., Vennetier, M., Kitzberger, T., Rigling, A., Breshears, D., Hogg, E., 2010. A global overview of drought and heat-induced tree mortality reveals emerging climate change risks for forests. *For. Ecol. Manage.* 259, 660–684.

An, C.B., Zhao, J., Tao, S., Lv, Y., Dong, W., Li, H., Jin, M., Wang, Z., 2011. Dust variation recorded by lacustrine sediments from arid Central Asia since ~15 cal ka BP and its implication for atmospheric circulation. *Quat. Res.* 75, 566–573.

An, Z., Porter, S.C., Kutzbach, J.E., Wu, X., Wang, S., Liu, X., Li, X., Zhou, W., 2000. Asynchronous Holocene optimum of the East Asian monsoon. *Quat. Sci. Rev.* 19, 743–762.

Anderson, M.J., Willis, T.J., 2003. Canonical analysis of principal coordinates: a useful method of constrained ordination for ecology. *Ecology* 84, 511–525.

Bakker, M.M., Govers, G., Kosmas, C., Vanacker, C., Oost, K.V., Rounsevell, M., 2005. Soil erosion as a driver of land-use change. *Agric. Ecosyst. Environ.* 105, 467–481.

Bennett, K., 1996. Determination of the number of zones in a biostratigraphic sequence. *New Phytol.* 132, 155–170.

Berger, A., Loutre, M., 1991. Insolation values for the climate of the last 10 million years. *Quat. Sci. Rev.* 10, 297–317.

Botkin, D.B., Saxe, H., Araujo, M.B., Betts, R., Bradshaw, R.H.W., Cedhagen, T., Chesson, P., Dawson, T.P., Etterson, J.R., Faith, D.P., 2007. Forecasting the effects of global warming on biodiversity. *Bioscience* 57, 227–236.

Breshears, D., Cobb, N., Rich, P., Price, K., Allen, C., Balice, R., Romme, W., Kastens, J., Floyd, M., Belnap, J., 2005. Regional vegetation die-off in response to global-change-type drought. *Proc. Natl. Acad. Sci. U.S.A.* 102, 15144–15148.

Chen, C., Lan, H., Lou, J., Chen, Y., 2003a. The dry Holocene Megathermal in Inner Mongolia. *Palaeogeogr. Palaeoclimatol. Palaeoecol.* 193, 181–200.

Chen, F., Wu, W., Holmes, J., Madsen, D., Zhu, Y., Jin, M., Oviatt, C., 2003b. A mid-Holocene drought interval as evidenced by lake desiccation in the Alashan Plateau, Inner Mongolia China. *Chin. Sci. Bull.* 48, 1401–1410.

Chen, F., Yu, Z., Yang, M., Ito, E., Wang, S., Madsen, D., Huang, X., Zhao, Y., Sato, T., Birks, H., 2008a. Holocene moisture evolution in arid central Asia and its out-of-phase relationship with Asian monsoon history. *Quat. Sci. Rev.* 27, 351–364.

Chen, K., Abbott, R.J., Milne, R.I., Tian, X., Liu, J., 2008b. Phylogeography of *Pinus tabulaeformis* Carr. (Pinaceae), a dominant species of coniferous forest in northern China. *Mol. Ecol.* 17, 4276–4288.

Clark, J.S., Grimm, E.C., Donovan, J.J., Fritz, S.C., Engstrom, D.R., Almendinger, J.E., 2002. Drought cycles and landscape responses to past aridity on prairies of the northern great plains, USA. *Ecology* 83, 595–601.

Clift, P.D., Plumb, R.A., 2008. *The Asian Monsoon: Causes, History and Effects*. Cambridge University Press, Cambridge.

Cook, E.R., Anchukaitis, K.J., Buckley, B.M., D'Arrigo, R.D., Jacoby, G.C., Wright, W.E., 2010. Asian monsoon failure and megadrought during the last millennium. *Science* 328, 486–489.

Cox, P.M., Betts, R.A., Jones, C.D., Spall, S.A., Totterdell, I.J., 2000. Acceleration of global warming due to carbon-cycle feedbacks in a coupled climate model. *Nature* 408, 184–187.

Dai, A., 2011. Drought under global warming: a review. *Clim. Change* 2, 45–65.

Davis, M.B., 1986. Climatic instability, time lags and community disequilibrium. In: Diamond, J., Case, T.J. (Eds.), *Community Ecology*. Harper and Row Publisher.

Deng, H., 2005. From Natural to Cultural Landscape: Evolution of Man–Land Relationship in the Farming-pastoral Ecotone of North China from a Historical Geography Perspective. Commercial Press, Beijing (in Chinese).

Dykoski, C., Edwards, R., Cheng, H., Yuan, D., Cai, Y., Zhang, M., Lin, Y., Qing, J., An, Z., Revenaugh, J., 2005. A high-resolution, absolute-dated Holocene and deglacial Asian monsoon record from Dongge Cave, China. *Earth Planet. Sci. Lett.* 233, 71–86.

Fang, X., Hou, G., 2011. Synthetically reconstructed Holocene temperature change in China. *Sci. Geogr. Sin.* 31, 385–393 (in Chinese with English abstract).

Gunin, P.D., Vostokova, E.A., Dorofeyuk, N.I., Tarasov, P.E., Black, C.C., 1999. *Vegetation Dynamics of Mongolia*. Kluwer Academic Publishers.

He, S., Liu, H., Ren, J., Yin, Y., 2008. Landform–climate–vegetation patterns and countermeasures for vegetation rehabilitation of forest-steppe ecotone on southeastern Inner Mongolia plateau. *Sci. Geogr. Sin.* 28, 253–258 (in Chinese with English abstract).

Held, I., 2012. Climate science: constraints on the high end. *Nat. Geosci.* 5 (4), 236–237.

Hof, C., Levinsky, I., Araujo, M.B., Rahbek, C., 2011. Rethinking species' ability to cope with rapid climate change. *Glob. Change Biol.* 17, 2987–2990.

IPCC, 2007. *Climate Change 2007: Synthesis Report*. Contribution of Working Groups I, II and III to the Fourth Assessment Report of the Intergovernmental Panel on Climate Change. IPCC, Geneva, Switzerland.

Jackson, S.T., Betancourt, J.L., Booth, R.K., Gray, S.T., 2009. Ecology and the ratchet of events: Climate variability, niche dimensions, and species distributions. *Proc. Natl. Acad. Sci. U.S.A.* 106, 19685–19692.

Jiang, W., Guo, Z., Sun, X., Wu, H., Chu, G., Yuan, B., Hatté, C., Guiot, J., 2006. Reconstruction of climate and vegetation changes of Lake Bayanchagan (Inner Mongolia): Holocene variability of the East Asian monsoon. *Quat. Res.* 65, 411–420.

Katul, G.G., Siqueira, M.B., 2010. Biotic and abiotic factors act in coordination to amplify hydraulic redistribution and lift. *New Phytol.* 187, 3–6.

Kropelin, S., Verschuren, D., Lézine, A., Eggermont, H., Cocquyt, C., Francus, P., Cazet, J., Fagot, M., Rumes, B., Russell, J., 2008. Climate-driven ecosystem succession in the Sahara: the past 6000 years. *Science* 320, 765–768.

Laird, K.R., Fritz, S.C., Maasch, K.A., Cumming, B.F., 1996. Greater drought intensity and frequency before AD 1200 in the Northern Great Plains, USA. *Nature* 384, 552–554.

Lake, P.S., 2011. *Drought and Aquatic Ecosystems: Effects and Responses*. Wiley Blackwell.

- Li, J., Okin, G.S., Epstein, H.E., 2009. Effects of enhanced wind erosion on surface soil texture and characteristics of windblown sediments. *J. Geophys. Res.* 114, G02003.
- Li, X.Q., Zhou, J., Shen, J., Weng, C.Y., Zhao, H.L., Sun, Q.L., 2004. Vegetation history and climatic variations during the last 14 ka BP inferred from a pollen record at Daihai Lake, north-central China. *Rev. Palaeobot. Palynol.* 132, 195–205.
- Liu, H., Cui, H., Pott, R., Speier, M., 1999. The surface pollen of the woodland-steppe ecotone in southeastern Inner Mongolia, China. *Rev. Palaeobot. Palynol.* 105, 237–250.
- Liu, H., Yin, Y., Tian, Y., Ren, J., Wang, H., 2008. Climatic and anthropogenic controls of topsoil features in the semi-arid East Asian steppe. *Geophys. Res. Lett.* 35, L04401.
- Liu, H., Yin, Y., Zhu, J., Zhao, F., Wang, H., 2010. How did the forest respond to Holocene climate drying at the forest-steppe ecotone in northern China? *Quat. Int.* 227, 46–52.
- Liu, H., Piao, S., Yin, Y., Zhao, F., Zhang, Y., Long-term unusual climate warming in the semi-arid region of China threatens endangered cranes. *Sci. Rep.*, in review.
- Lu, H., Miao, X., Zhou, Y., Mason, J., Swinehart, J., Zhang, J., Zhou, L., Yi, S., 2005. Late quaternary aeolian activity in the Mu Us and Otindag dune fields (north China) and lagged response to insolation forcing. *Geophys. Res. Lett.* 32, L21716.
- McDowell, N., Pockman, W., Allen, C., Breshears, D., Cobb, N., Kolb, T., Plaut, J., Sperry, J., West, A., Williams, D., 2008. Mechanisms of plant survival and mortality during drought: why do some plants survive while others succumb to drought? *New Phytol.* 178, 719–739.
- Miao, X., Mason, J.A., Swinehart, J.B., Loope, D.B., Hanson, P.R., Goble, R.J., Liu, X., 2007. A 10,000 year record of dune activity, dust storms, and severe drought in the central Great Plains. *Geology* 35, 119–122.
- Minckley, T.A., Booth, R.K., Jackson, S.T., 2012. Response of arboreal pollen abundance to late-Holocene drought events in the Upper Midwest, USA. *Holocene* 22, 531–539.
- Munson, S.M., Belnap, J., Okin, G.S., 2011. Responses of wind erosion to climate-induced vegetation changes on the Colorado Plateau. *Proc. Natl. Acad. Sci. U.S.A.* 108, 3854–3859.
- Nelson, D.B., Abbott, M.B., Steinman, B., Polissar, P.J., Stansell, N.D., Ortiz, J.D., Rosenmeier, M.F., Finney, B.P., Riedel, J., 2011. Drought variability in the Pacific Northwest from a 6,000-yr lake sediment record. *Proc. Natl. Acad. Sci. U.S.A.* 108, 3870–3875.
- Parducci, L., Jørgensen, T., Tollefsrud, Elverland, E., Alm, T., Fontana, S.L., Bennett, K., Haile, J., Matetovici, I., Suyama, Y., 2012. Glacial survival of boreal trees in northern Scandinavia. *Science* 335, 1083–1086.
- Peng, C., Guiot, J., Wu, H., Jiang, H., Luo, Y., 2011. Integrating models with data in ecology and palaeoecology: advances towards a model–data fusion approach. *Ecol. Lett.* 14, 522–536.
- Piao, S., Fang, J., Zhou, L., Guo, Q., Henderson, M., Ji, W., Li, Y., Tao, S., 2003. Interannual variations of monthly and seasonal normalized difference vegetation index (NDVI) in China from 1982 to 1999. *J. Geophys. Res.* 108, 4401.
- Ren, G., Beug, H.J., 2002. Mapping Holocene pollen data and vegetation of China. *Quat. Sci. Rev.* 21, 1395–1422.
- Ridgwell, A.J., Watson, A.J., 2002. Feedback between aeolian dust, climate, and atmospheric CO₂ in glacial time. *Paleoceanography* 17, 1059–1069.
- Roberts, N., Brayshaw, D., Kuzucuoğlu, C., Perez, R., Sadori, L., 2011. The mid-Holocene climatic transition in the Mediterranean: causes and consequences. *Holocene* 21, 3–13.
- Rotenberg, E., Yakir, D., 2010. Contribution of semi-arid forests to the climate system. *Science* 327, 451–454.
- Scherrer, D., Bader, M.K.-F., Körner, C., 2011. Drought-sensitivity ranking of deciduous tree species based on thermal imaging of forest canopies. *Agric. For. Meteorol.* 151, 1632–1640.
- Schlesinger, W.H., Reynolds, J.F., Cunningham, G.L., Huenneke, L.F., Jarrell, W.M., Virginia, R.A., Whitford, W.G., 1990. Biological feedbacks in global desertification. *Science* 247, 1043–1048.
- Shi, P., Yan, P., Yuan, Y., Nearing, M.A., 2004. Wind erosion research in China: past, present and future. *Prog. Phys. Geogr.* 28, 366–385.
- Shi, Y., Kong, Z., Wang, S., Tang, L., Wang, F., Yao, S., Zhao, X., Zhang, P., Shi, S., 1992. Basic feature of climates and environments during the Holocene Megathermal in China. *Sci. China (Ser. B)* 35, 1300–1308.
- Solomon, S., Plattner, G.K., Knutti, R., Friedlingstein, P., 2008. Irreversible climate change due to carbon dioxide emissions. *Proc. Natl. Acad. Sci. U.S.A.* 106, 1704–1709.
- Steffensen, J.P., Andersen, K.K., Bigler, M., Clausen, H.B., Dahl-Jensen, D., Fischer, H., Goto-Azuma, K., Hansson, M., Johnsen, S.J., Jouzel, J., 2008. High-resolution Greenland ice core data show abrupt climate change happens in few years. *Science* 321, 680–684.
- Svenning, J.C., 2003. Deterministic Plio-Pleistocene extinctions in the European cool-temperate tree flora. *Ecol. Lett.* 6, 646–653.
- Svenning, J.C., Normand, S., Skov, F., 2008. Postglacial dispersal limitation of widespread forest plant species in nemoral Europe. *Ecography* 31, 316–326.
- Thornthwaite, C.W., 1948. An approach toward a rational classification of climate. *Geogr. Rev.* 38, 55–94.
- Tian, B., Liu, R., Wang, L., Qiu, Q., Chen, K., Liu, J., 2009. Phylogeographic analyses suggest that a deciduous species (*Ostryopsis davidiana* Decne., Betulaceae) survived in northern China during the Last Glacial Maximum. *J. Biogeogr.* 36, 2148–2155.
- Walter, H., Breckle, S.W., 2002. *Walter's Vegetation of the Earth: The Ecological Systems of the Geo-biosphere*. Springer Verlag.
- Wang, Y., Cheng, H., Edwards, R., He, Y., Kong, X., An, Z., Wu, J., Kelly, M., Dykoski, C., Li, X., 2005. The Holocene Asian monsoon: links to solar changes and North Atlantic climate. *Science* 308, 854–857.
- Wang, Y., Cheng, H., Edwards, R., Kong, X., Shao, X., Chen, S., Wu, J., Jiang, X., Wang, X., An, Z., 2008. Millennial- and orbital-scale changes in the East Asian monsoon over the past 224,000 years. *Nature* 451, 1090–1093.
- Webb, T., 1986. Is vegetation in equilibrium with climate? How to interpret late-Quaternary pollen data. *Plant Ecol.* 67, 75–91.
- Woodward, C., Potito, A., Beilman, D., 2012. Carbon and nitrogen stable isotope ratios in surface sediments from lakes of western Ireland: implications for inferring past lake productivity and nitrogen loading. *J. Paleolimnol.* 47, 167–184 (in Chinese).
- Wu, Z. (Ed.), 1980. *Vegetation of China*. Science Press, Beijing (in Chinese).
- Xiao, J., Chang, Z., Si, B., Qin, X., Itoh, S., Lomtatidze, Z., 2009. Partitioning of the grain-size components of Dali Lake core sediments: evidence for lake-level changes during the Holocene. *J. Paleolimnol.* 42, 249–260.
- Xiao, J., Wu, J., Si, B., Liang, W., Nakamura, T., Liu, B., Inouchi, Y., 2006. Holocene climate changes in the monsoon/arid transition reflected by carbon concentration in Daihai Lake of Inner Mongolia. *Holocene* 16, 551–560.
- Xu, Q., Li, Y., Yang, X., Zheng, Z., 2007. Quantitative relationship between pollen and vegetation in northern China. *Sci. China (Ser. B)* 50, 582–599.
- Yang, X., Zhang, K., Jia, B., Ci, L., 2005. Desertification assessment in China: an overview. *J. Arid Environ.* 63, 517–531.
- Yi, L., Yu, H., Ge, J., Lai, Z., Xu, X., Qin, L., Peng, S., 2012. Reconstructions of annual summer precipitation and temperature in north-central China since 1470 AD based on drought/flood index and tree-ring records. *Clim. Change* 110, 469–498.
- Yin, Y., Liu, H., He, S., Zhao, F., Zhu, J., Wang, H., Liu, G., Wu, X., 2011. Patterns of local and regional grain size distribution and their application to Holocene climate reconstruction in semi-arid Inner Mongolia, China. *Palaeogeogr. Palaeoclimatol. Palaeoecol.* 307, 168–176.
- Zhai, Q., Guo, Z., Li, Y., Li, R., 2006. Annually laminated lake sediments and environmental changes in Bashang Plateau, North China. *Palaeogeogr. Palaeoclimatol. Palaeoecol.* 241, 95–102.
- Zhang, X.Y., Gong, S., Zhao, T., Arimoto, R., Wang, Y., Zhou, Z., 2003. Sources of Asian dust and role of climate change versus desertification in Asian dust emission. *Geophys. Res. Lett.* 30, 2272.
- Zhao, F., Liu, H., Yin, Y., Hu, G., Wu, X., 2011. Vegetation succession prevents dry lake beds from becoming dust sources in the semi-arid steppe region of China. *Earth Surf. Proc. Landforms* 36, 864–871.
- Zhao, Y., Yu, Z., Chen, F., Zhang, J., Yang, B., 2009. Vegetation response to Holocene climate change in monsoon-influenced region of China. *Earth Sci. Rev.* 97, 242–256.

2012 年发表论文

内蒙古草原区土壤碳密度(SOCD)和氮密度(TND)的影响因素分析

陈曦 刘鸿雁[†]

北京大学城市与环境学院生态学系, 北京 100871; [†] 通信作者, E-mail: lhy@urban.pku.edu.cn

摘要 在内蒙古草原区选取 94 个样点, 涵盖耕地、退耕地、人工林和草原 4 种土地利用类型, 根据土壤质地将草原细分为沙质草原和非沙质草原。通过对这些样点土壤有机碳密度(SOCD)和全氮密度(TND)的研究, 发现在内蒙古草原区, SOCD 主要受到土壤质地的影响, 黏粒(<2 μm)、粉砂(2~16 μm)和细粉砂(16~63 μm)的含量越高, SOCD 越高。而 TND 同时受到土壤质地和土地利用类型的影响, 分布在非沙质土壤的草原具有最高的 TND。耕作不会导致 SOCD 显著降低, 但是会造成 TND 降低。人工林不能显著提高土壤养分含量, 相反, 由于人工林对养分和水分的需求很大, 可能导致土壤肥力的降低。此外, 草原区温度越高, 土壤养分越低, 这预示着在全球变暖的背景下, 这一地区的土壤可能成为重要的碳源。植被退化越严重, 土壤养分越低, 因此保护草原区的植被免受过度放牧的影响非常重要。

关键词 土壤有机碳密度(SOCD); 全氮密度(TND); 土地利用类型; 土壤质地; 植被退化

中图分类号 P935

Factors Affecting Soil Organic Carbon Density (SOCD) and Total Nitrogen Density (TND) in Inner Mongolian Steppe

CHEN Xi, LIU Hongyan[†]

Department of Ecology, College of Urban and Environmental Sciences, Peking University, Beijing 100871;

[†] Corresponding author, E-mail: lhy@urban.pku.edu.cn

Abstract The authors collected soil samples from 94 profiles in Inner Mongolia covering 4 land use types: cropland, abandoned cropland, artificial forest and steppe, in which steppe can be further classified into sandy steppe and non-sandy steppe. It is found that soil organic carbon density (SOCD) is affected by soil texture. It increases with the content of clay (<2 μm), fine silt (2–16 μm) and coarse silt (16–63 μm). However, total nitrogen density (TND) is affected both by soil texture and land use types. Non-sandy steppe has the highest TND. Cultivation leads to the decreasing of TND but not SOCD. The expected increase in SOCD of artificial forest does not realize. Since the requirement of soil nutrient and water is large, artificial forest may even cause strong negative effects on soil fertility and sustainability. It is also found that soil nutrient decreases when mean annual temperature (MAT) increases. Under global warming, the region may turn to an important carbon source. Soil nutrient decreases with vegetation degradation, so the protection of steppe vegetation from over grazing is very important.

Key words soil organic carbon density (SOCD); soil total nitrogen density (TND); land use types; soil texture; plant degradation

国家重点基础研究发展计划(2010CB950604)和国家自然科学基金(31021001)资助

收稿日期: 2011-04-02; 修回日期: 2011-05-05; 网络出版日期: 2011-06-07

网络出版地址: <http://www.cnki.net/kcms/detail/11.2442.N.20110607.1319.002.html>

对土壤有机碳(SOC)和全氮(TN)的研究对于探讨土壤质量和生态系统的固碳能力意义重大,同时也可以为碳、氮循环过程和储量的研究提供依据^[1]。土壤养分与土壤母质、土地利用和管理的历史以及气候因素都有重要的关系^[2-3]。研究土壤养分在空间上的变化与土壤质地、土地利用、植被等的关系对研究生态系统功能以及估计未来土地利用对土壤养分的影响具有重要的意义^[4]。

土壤质地对土壤养分有显著影响。土壤养分主要吸附在细颗粒物上,在不同土壤组分中,黏粒中 SOC 和 TN 含量最高,其次是粉砂,含量最少的是砂^[5]。土壤中的 SOC 和 TN 与黏粒和粉砂含量呈显著正相关关系,与砂含量呈显著负相关关系^[1,6]。

土地利用会影响土壤风蚀和植被覆盖,进而对土壤养分产生影响。一般认为农业活动会加速土壤风蚀^[7],导致细颗粒物流失和土壤粗化,进而导致 SOC 和 TN 的损失^[8-11]。但也有例外,在中国河西走廊的研究中,耕作增加了土壤黏粒含量和 SOC 含量^[6]。退耕还草通常会带来土壤养分的增加^[8-9]。但是由于养分主要吸附在细颗粒物上,如果土壤中的细颗粒物含量比较低,那么退耕还草也不一定提高土壤养分^[2]。过度放牧会导致植被退化和土壤风蚀增加,进而导致 SOC 和 TN 的损失^[12-14]。而随着禁牧年限增加,土壤黏粒组分和粉砂组分吸附的 SOC 和 TN 都显著升高^[5]。

内蒙古草原区从东北到西南,温度逐渐升高,降水逐渐增加,植被由温带草原变为草原到森林过渡带,最后变为森林^[15]。这一地区包括农、林、牧多种土地利用类型,在最近几十年经历了土地利用的巨大转变,早期为天然的草原被开垦为耕地,“三北防护林”工程的实施导致人工林面积快速扩大,最近实施的退耕还林还草产生了大量的退耕地^[16]。内蒙古草原区有多个沙地分布,天然的草原按照质地可以分为沙质草原和非沙质草原。这些草原都属于畜牧用地,其中一半以上受到过度放牧的威胁^[17],也由此具有了人为干扰的梯度,即从非退化或轻度退化草原到重度退化草原。

本文利用内蒙古草原区的环境梯度,通过两年的野外采样和室内试验,分析了内蒙古地区不同土地利用类型和土壤母质下土壤碳密度(SOCD)和氮密度(TND)的影响因素,拟合了草原的土壤养分与环境因子和植被退化的回归曲线。我们的结果可以为模拟区域养分循环提供数据基础,为未来的土地

利用转变提供指导依据。

1 研究方法

1.1 野外调查与采样

在研究区(42.26°—49.49°N, 112.05°—125.08°E)随机选取 94 个样点,包括 20 个耕地样点,14 个退耕地样点,18 个人工林样点,22 个沙质草原样点和 20 个非沙质草原样点(图 1)。样点海拔范围 135~1462 m,年均温度范围-1.0~7.0°C,年均降水范围 206~456 mm。

由于研究区土壤 A 层和 B 层主要在表层 30 cm,因此我们在每个采样点选取一个土壤剖面,深度 30 cm,每 5 cm 一层,共分 6 层,用直径 5 cm 的环刀由下向上,每层取一环刀土壤。对于草原样地,根据群落的异质性,选取 1~5 个 2 m × 2 m 的样方,进行群落调查,记录每个物种的丰富度、高度和盖度。

对每个草原样方,计算全部物种的重要值(IV):

$$IV = (\text{相对丰富度} + \text{相对高度} + \text{相对盖度})/3. \quad (1)$$

通过退化指示种的分析来研究人为干扰是非常可信的^[16,18-19]。例如,羊草(*Leymus chinensis*)草原是研究区内分布较为普遍的群落类型,由于受到人为干扰,样地内普遍出现冷蒿(*Artemisia frigida*),糙隐子草(*Cleistogenes squarrosa*),黄囊苔草(*Carex korshinskii*)和茵陈蒿(*Artemisia capillaris*),随人为干扰强度不同,这些物种都可能成为优势种^[19]。

根据物种对退化的指示程度,把全部物种分为 3 组:第一组是一年生植物,主要出现在严重退化的草原,如茵陈蒿;第二组是中度退化指示种,主要出现在中度退化的草原,如冷蒿、糙隐子草、黄囊苔草;第三组是非退化种,出现在轻度或没有退化的草原,如羊草。对第一组物种,重要值记为 IV_1 ,并给予系数 1/3,对第二组物种,重要值记为 IV_2 ,并给予系数 2/3,对第三组物种,重要值记为 IV_3 ,并给予系数 1。由此可以得到每个样地的人为干扰指数(HDI)^[16]:

$$HDI = 1/(IV_1 \cdot 1/3 + IV_2 \cdot 2/3 + IV_3). \quad (2)$$

1.2 土壤样品分析

取回的土壤样品烘干,称重。每个样品取 5 g,挑去石块和根,过 2 mm 筛,用激光粒度仪 Mastersizer 2000 进行粒度测试。土壤颗粒粒径可以分为 5 级:黏粒(< 2 μm)、细粉砂(2~16 μm)、粗粉砂(16~63 μm)、细砂(63~200 μm)和粗砂(200~2000 μm)。

另外,每个样品再取 1~2 g,挑去石块和根,研

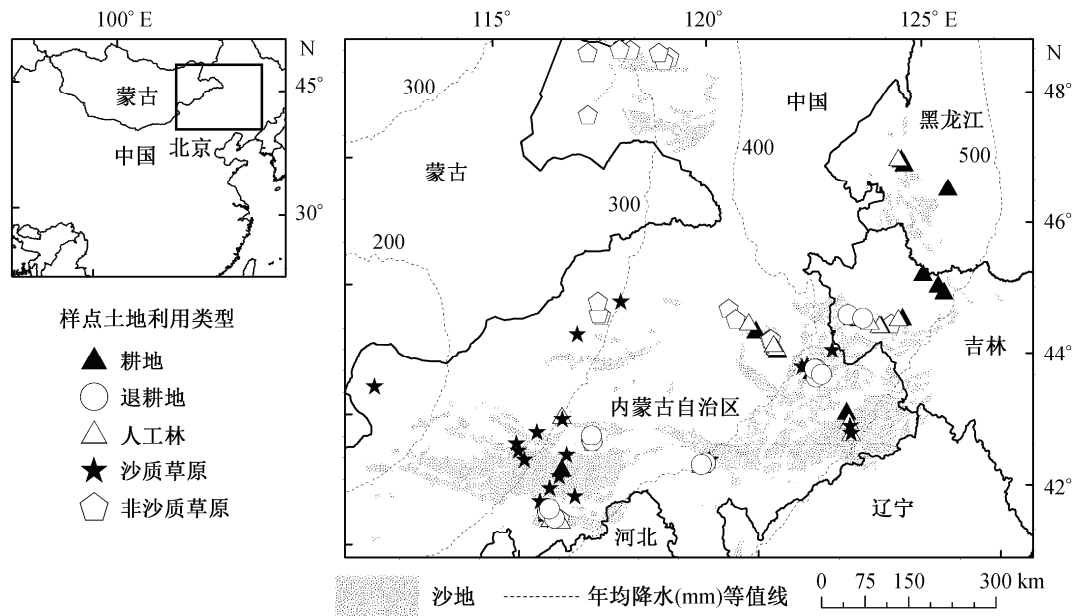


图 1 研究区取样点分布
Fig. 1 Sample sites distribution in the study area

磨并过 0.149 mm 土筛。由于在研究区, 相对于有机碳而言, 土壤表层 30 cm 中无机碳的含量非常低, 可以忽略^[20], 因此我们利用碳氮分析仪 Elementar Vario EL (德国) 测量土壤的有机碳(SOC)和总氮(TN)。由于碳密度(SOCD)和氮密度(TND)可以更直观地反映土壤养分情况, 因此我们选择 SOCD 和 TND 作为养分的主要指标。

对于每层的土壤 SOCD 和 TND, 计算公式为

$$\begin{cases} \text{SOCD}_i = \text{SOC}_i \cdot D_i, \\ \text{TND}_i = \text{TN}_i \cdot D_i, \end{cases} \quad (3)$$

i 为层数, $i = 1, 2, \dots, 6$; SOCD_i 和 TND_i 是第 i 层的 SOCD 和 TND, 单位为 mg/cm^3 ; SOC_i/TN_i 是第 i 层 SOC 和 TN 含量, 单位是 g/kg ; D_i 是第 i 层的容重, 单位为 g/cm^3 。

对于整个剖面总的 SOCD 和总的 TND, 计算公式为

$$\begin{cases} \text{SOCD} = \text{SOCD}_1 \cdot H_1/10 + \text{SOCD}_2 \cdot H_2/10 + \dots + \text{SOCD}_6 \cdot H_6/10, \\ \text{TND} = \text{TND}_1 \cdot H_1/10 + \text{TND}_2 \cdot H_2/10 + \dots + \text{TND}_6 \cdot H_6/10, \end{cases} \quad (4)$$

SOCD 和 TND 的单位是 t/hm^2 , H 表示土层深度, $H_1 = H_2 = \dots = H_6 = 5 \text{ cm}$ 。

1.3 气候指标

我们通过全国 670 个标准气象台站的数据^[21-22],

提取了样地所在经纬度的年平均温度(MAT)和年平均降水(MAP)。

1.4 统计分析

对所有土地利用类型的 SOCD 和 TND 与粒度之间, 以及草原区 SOCD 和 TND 与 MAT 和 MAP 之间采用线性回归进行拟合, 对草原区 SOCD 和 TND 与 HDI 之间采用负指数分布进行拟合。对于不同土地利用类型的粒度、SOCD 和 TND 之间的差异采用单向 ANOVA 进行分析, 并采用 Tukey's HSD test ($p = 0.05$) 进行显著性检验。统计分析利用 SPSS 19.0 软件完成, 作图在 OriginPro 8.0 中完成。

2 结果分析

2.1 不同土地利用类型和母质

对不同土地利用类型样地的粒度数据, 分别计算表层 5 cm 粒度的平均值和整个剖面粒度的平均值(图 2), 其中横坐标采用对数坐标。可以发现, 对所有利用类型, 粒度的分布均表现为双峰曲线。不同的土地利用类型和土壤母质下, 粒度有比较明显的差别, 且差异在表层和整个剖面相对一致。

不同土地利用类型和土壤质地下机械组成如表 1 所示。在表层 5 cm, 沙质草原的黏粒、细粉砂和粗粉砂的含量显著低于其他土壤, 粗砂含量显著高于其他土壤($p < 0.05$)。尽管不同利用类型的土壤质地差异并不显著, 但人工林的土壤质地相对较粗。

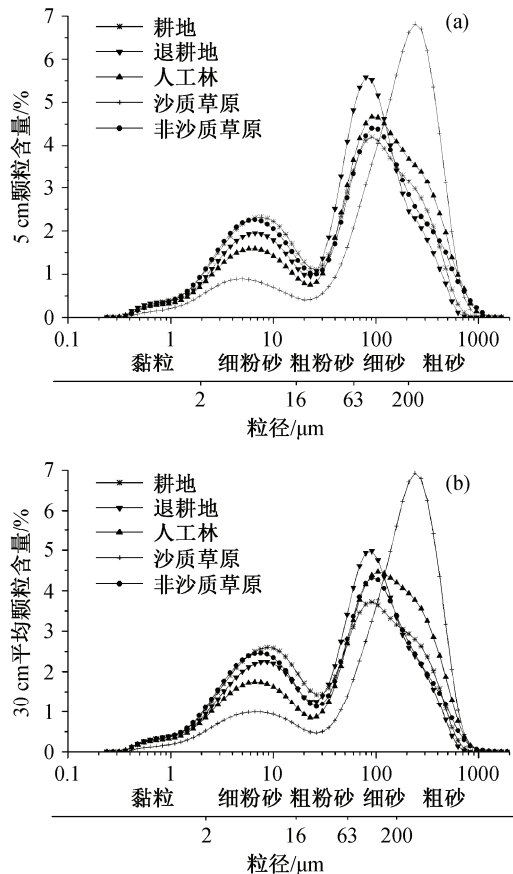


图 2 不同土地利用类型和土壤母质下表层 5 cm 和整个剖面(30 cm)平均粒度分布

Fig. 2 Grain size distribution of the top 5 cm and the whole profile's soil in different land use types and soil parent material

在 30 cm 剖面上来看, 沙质草原黏粒、细粉砂和粗粉砂的含量仍然显著低于其他土壤($p < 0.05$)。土地利用类型的差异变得显著, 人工林的黏粒含量显著低于其他草原, 细粉砂含量显著低于耕地、退耕地和非沙质草原($p < 0.05$), 而粗砂含量显著高于耕地、退耕地和人工林($p < 0.05$)。另外 3 种类型仅在细砂含量上差异显著, 耕地的细砂含量显著高于退耕地($p < 0.05$)。

2.2 不同土地利用类型和土壤母质下的 SOCD 和 TND

土壤母质对 SOCD 表现出决定性作用(图 3(a)和(c)), 土地利用类型的影响相对较小。在表层和整个剖面, 沙质草原的 SOCD 都显著低于耕地、退耕地和非沙质草原($p < 0.05$)。人工林的 SOCD 仅在表层显著低于耕地和非沙质草原, 在整个剖面上与其他 3 种类型差异不显著($p < 0.05$)。其他类型之间 SOCD 的差别均不显著。

土壤母质和土地利用共同影响土壤的 TND(图 3(b)和(d))。非沙质草原在表层和整个剖面的 TND 显著高于沙质草原, 同时也显著高于其他土地利用类型($p < 0.05$), 这体现了土壤母质和土地利用类型对 TND 的影响; 同时耕地表层的 TND 显著高于沙质草原($p < 0.05$)。

2.3 SOCD 和 TND 与土壤质地的关系

由于土壤质地对 SOCD 和 TND 影响显著, 我们

表 1 不同利用类型和土壤母质下表层(5 cm)和整个剖面(30 cm)粒度的差异比较

Table 1 Grain size distribution of the top 5 cm and the whole profile's soil in different land use types and soil parent material

类型	表层 5 cm 粒度/%				
	黏粒	细粉砂	粗粉砂	细砂	粗砂
耕地	4.47 ± 0.21^b	28.33 ± 2.56^b	16.78 ± 1.42^b	32.07 ± 2.90	18.34 ± 3.01^b
退耕地	4.34 ± 0.34^b	23.80 ± 2.63^b	19.48 ± 3.10^b	39.03 ± 2.26	13.35 ± 4.71^b
人工林	3.74 ± 0.42^b	19.74 ± 2.61^{ab}	14.66 ± 1.97^b	36.14 ± 2.68	25.71 ± 5.33^b
沙质草原	2.34 ± 0.43^a	11.96 ± 2.24^a	8.18 ± 1.27^a	34.32 ± 2.92	43.20 ± 5.19^a
非沙质草原	4.29 ± 0.35^b	27.81 ± 2.88^b	15.45 ± 1.58^b	33.07 ± 3.19	19.38 ± 4.42^b
类型	剖面 30 cm 平均粒度/%				
	黏粒	细粉砂	粗粉砂	细砂	粗砂
耕地	4.35 ± 0.12^{bc}	30.81 ± 1.09^c	18.71 ± 0.72^a	28.721 ± 1.14^a	17.41 ± 1.44^c
退耕地	4.25 ± 0.18^{bc}	26.85 ± 1.40^c	19.14 ± 1.10^a	35.69 ± 1.52^b	14.06 ± 1.88^c
人工林	3.82 ± 0.17^b	21.55 ± 1.11^b	14.19 ± 0.80^b	34.82 ± 1.05^b	25.61 ± 2.01^b
沙质草原	2.07 ± 0.15^a	12.54 ± 0.95^a	7.43 ± 0.55^a	32.47 ± 1.19^{ab}	45.49 ± 2.10^a
非沙质草原	4.48 ± 0.15^c	29.89 ± 1.09^c	16.78 ± 0.64^a	32.29 ± 1.17^{ab}	16.57 ± 1.49^c

说明: 数值是平均值 \pm 标准差。不同的字母(a, b, c)表示同一土壤颗粒组分(黏粒、细粉砂、粗粉砂、细砂、粗砂)在不同土地利用类型下, 数值之间具有显著差别($p < 0.05$)。ab 表示与 a 和 b 均没有显著差别; bc 表示与 b 和 c 没有显著差别, 与 a 有显著差别。

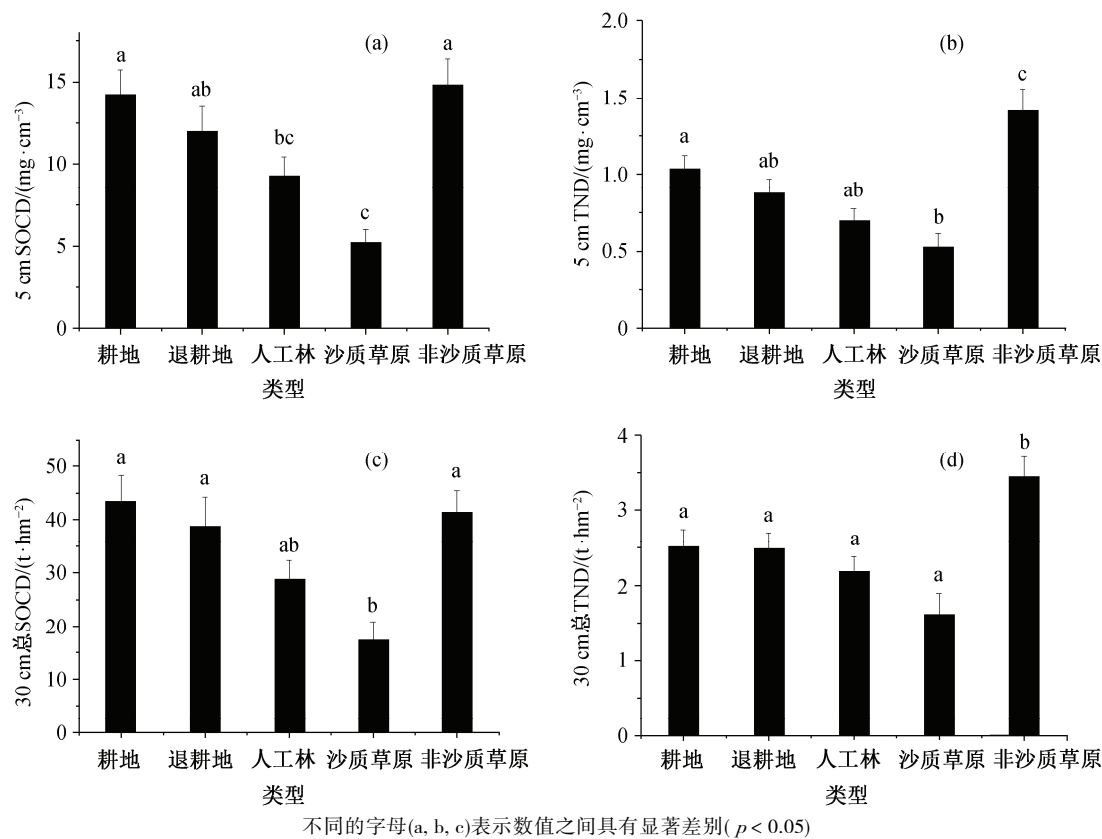


图 3 不同土地利用类型和土壤母质下层(5 cm)和整个剖面(30 cm)SOCD 和 TND 的差异

Fig. 3 Difference of the top 5 cm and the whole profile's SOCD and TND in different land use types and soil parent material

对全部样地计算了表层和整个剖面平均 SOCD 和 TND, 并分别与表层和整个剖面的平均粒度进行回归分析, 公式为 $SOCD/TND = a + by$ (y 为颗粒含量)。回归结果表明, 无论在表层还是整个剖面, SOCD 和 TND 都随着黏粒、细粉砂和粗粉砂含量升高而显著

升高 ($p < 0.001$), 随着粗砂比例的升高而显著降低 ($p < 0.001$), 与细砂的关系并不显著(表 2)。

2.4 草原 SOCD 和 TND 与环境因子及植被退化程度之间的关系

草原(包括沙质草原和非沙质草原)表层和整个

表 2 土壤质地与 SOCD 和 TND 的回归结果

Table 2 Regression of soil texture and SOCD, TND

颗粒	5 cm SOCD/(mg · cm ⁻³)			5 cm TND/(mg · cm ⁻³)		
	<i>a</i>	<i>b</i>	<i>R</i> ²	<i>a</i>	<i>b</i>	<i>R</i> ²
黏粒	3.365	2.052	0.311***	0.304	0.163	0.308***
细粉砂	3.396	0.351	0.468***	0.348	0.026	0.401***
粗粉砂	5.453	0.383	0.259***	0.558	0.024	0.164***
细砂	13.125	-0.063	0.015	1.035	-0.004	0.008
粗砂	15.090	-0.159	0.306***	1.209	-0.012	0.253***

颗粒	30 cm 总 SOCD/(t · hm ⁻²)			30 cm 总 TND/(t · hm ⁻²)		
	<i>a</i>	<i>b</i>	<i>R</i> ²	<i>a</i>	<i>b</i>	<i>R</i> ²
黏粒	3.259	8.161	0.460***	0.705	0.468	0.439***
细粉砂	6.657	1.132	0.496***	1.032	0.059	0.395***
粗粉砂	10.790	1.540	0.407***	1.431	0.068	0.232***
细砂	42.251	-0.271	0.025	2.728	-0.009	0.008
粗砂	48.032	-0.575	0.384***	3.198	-0.030	0.304***

说明: *** $p < 0.001$ 。公式为 $SOCD/TND = a + by$ (y 为颗粒百分含量)。

表 3 草原区 SOCD 和 TND 与环境因子的回归结果
Table 3 Regression of environmental factors and SOCD, TND

y	5 cm SOCD/(mg · cm ⁻³)			5 cm TND/(mg · cm ⁻³)		
	a	b	R^2	a	b	R^2
MAT/°C	12.992	-1.117	0.16**	1.225	-0.095	0.119**
MAP/mm	17.334	-0.023	0.03	1.676	-0.002	0.028

y	30 cm 总 SOCD/(t · hm ⁻²)			30 cm 总 TND/(t · hm ⁻²)		
	a	b	R^2	a	b	R^2
MAT/°C	38.882	-3.268	0.136**	3.358	-0.27	0.168**
MAP/mm	73.77	-0.129	0.097*	6.26	-0.011	0.12*

说明: * $p < 0.05$; ** $p < 0.01$ 。公式为 $\text{SOCD/TND} = a + by$ (y 为 MAT 或 MAP)。

剖面的平均 SOCD 和 TND 与 MAT 和 MAP 的线性回归关系如表 3 所示。从表 3 可以发现, 随着温度的升高, SOCD 和 TND 在表层和整个剖面都显著下降($p < 0.01$)。表层的 SOCD 和 TND 与 MAP 并不存在线性相关关系, 但是对整个剖面而言, 与 MAP 可用线性回归拟合, 且系数为负($p < 0.05$)。

草原的 SOCD 和 TND 与 HDI 之间可以用负指数函数拟合, 公式为 $\text{SOCD/TND} = ae^{bx}$ (x 为 HDI) (图 4)。随着 HDI 的增大, SOCD 和 TND 在表层和整个剖面都会减小, 且减小的幅度在开始非常迅速, 之后趋缓。这体现了人为干扰引起的草地退化对

SOCD 和 TND 的负面影响。

3 讨论

3.1 SOCD 主要受到土壤母质的影响

我们发现, SOCD 随着土壤中黏粒、细粉砂和粉砂含量的增加而增加, 这与前人的研究结果^[1,6]一致, 但是当把砂细分为细砂和粗砂后, SOCD 只随粗砂含量的增加而降低, 与细砂含量并没有显著的线性关系。

土壤母质表现出对 SOCD 的决定性作用, 土地利用类型的影响相对较小。无论是表层 5 cm 还是整

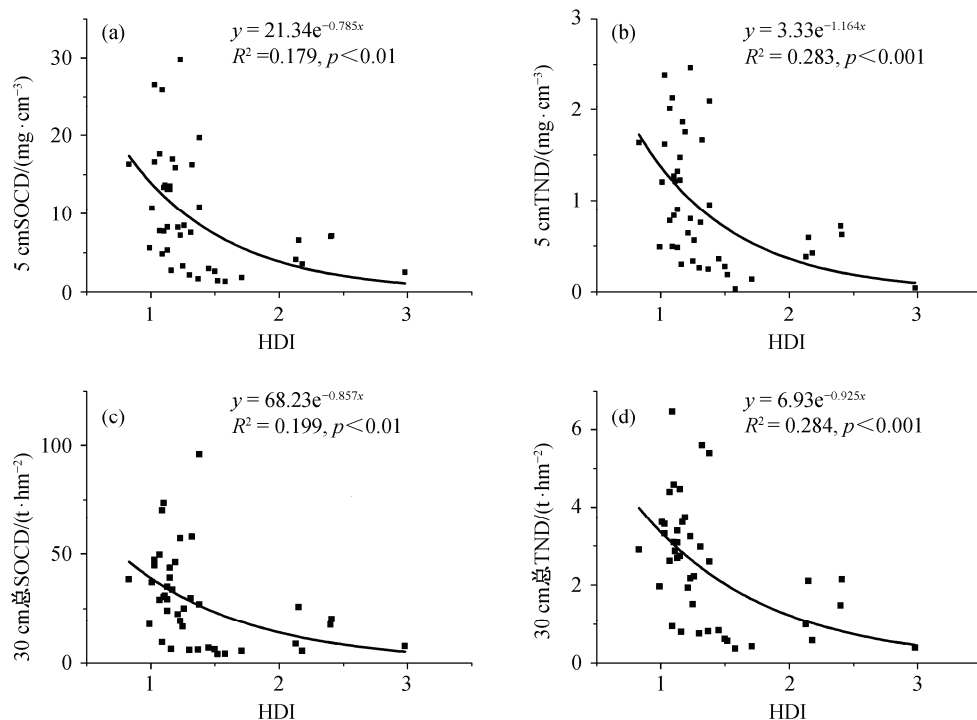


图 4 草原区 SOCD 和 TND 随 HDI 变化的趋势
Fig. 4 Relationship between HDI and SOCD, TND

个剖面,沙质草原都具有最低的细颗粒物含量(黏粒、细粉砂、粗粉砂)和最低的SOCD。与耕地、退耕地、人工林和其他草原相比,人工林的细颗粒物含量最低,同时人工林的SOCD也是最低的,这同样体现了土壤质地对SOCD的决定作用。另外3种土地利用类型之间,细颗粒物物质和SOCD均没有显著差别,说明土地利用类型对土壤SOCD的影响并不显著。不同植被退化程度下SOCD差异明显,表明人类干扰程度对草原区SOCD起决定作用。

农业活动并没有显著的降低土壤SOCD,这与以往的结果^[8-11]不同。人工林也没有对土壤养分和质地起到提升作用,这可能由于在研究区,水分是制约因子,而人工林对水分和养分的需求相对草地和耕地而言都要高,因此对土壤养分的可持续性可能带来负面的影响^[23]。因此,未来在研究区是否需要更多的人工林有待进一步的研究。

3.2 TND 受到土壤母质和土地利用类型的共同影响

我们发现,TND与SOCD和土壤质地的关系类似,随着土壤中黏粒、细粉砂和粉砂含量的增加而增加,只随粗砂含量的增加而降低,与细砂含量并没有显著的关系。

但是,与SOCD不同,土地利用和土壤母质共同影响土壤的TND。尽管相对耕地、退耕地和人工林而言,非沙质草原并不具有显著高的细颗粒物含量,但却在其表层和整个剖面都具有最高的TND,这体现出不同土地利用类型下TND的差别。同时考虑草原区非沙质草原和沙质草原,我们发现不同植被退化程度下TND差异明显,体现出人类干扰程度对草原区TND的决定作用。沙质草原尽管细颗粒物含量最低,TND和其他利用类型的差异却并不显著,这可能是由于人类影响导致耕地、退耕地和人工林TND的降低^[8-11]。由于非沙质草原具有最高的土壤TND,因此对非沙质草原的保护对维持土壤TND至关重要。

3.3 草原土壤养分还受到温度和植被退化的影响

在各种因素中,通常认为气候因素通过影响植被类型、生产力和凋落物的分解对土壤SOCD起着决定性的作用^[24]。在草原区,我们发现土壤SOCD和TND随MAT的升高显著降低($p<0.01$),与MAP的关系相对不密切。在区域尺度,由于MAT很低,

因而SOCD对MAT非常敏感^[25],相对于MAT而言,MAP对SOCD的影响较小^[26]。随着温度的增加,SOCD降低,因此在全球变暖的趋势下,内蒙古草原区土壤中的有机碳可能转化为CO₂大量释放到大气中,成为重要的碳源。

在草原区,草地退化会导致土壤养分的降低。我们发现HDI与土壤SOCD和TND具有负指数的关系,即随着人为干扰下植被的退化,土壤养分降低,且这种降低在退化初期表现得比较迅速,之后趋缓。在半干旱区,不恰当的放牧会导致土地退化,造成土壤沙化、养分丧失和植被退化^[9]。草原在荒漠化的初期养分迅速降低^[1,17],之后趋缓,而农田在荒漠化初期养分损失较小^[1]。由于非沙质草原具有最高的土壤TND和相对较高的SOCD,因此对于退化初期的草原进行保护对降低土壤养分损失具有至关重要的意义。

4 结论

通过在内蒙古草原区选取94个样点对SOCD和TND影响因素的研究,我们发现,土壤SOCD主要受到土壤母质的影响,黏粒、粉砂和细粉砂的含量越低,土壤SOCD越低。而土壤TND同时受到土壤母质和土地利用类型的影响,非沙质草原具有最高的土壤TND。耕作不会导致SOCD降低,但是会导致TND降低。人工林并不能提高土壤养分,反而可能对土壤存在负面影响。通过对草原区土壤养分与温度和植被退化分析,我们发现,随着年均温度的升高,草原区的土壤养分显著降低,因此在全球变暖的趋势下内蒙古草原区的土壤可能会变成重要的碳源。而草地退化会导致土壤养分降低,因此减少人为干扰导致的植被退化非常重要。

参考文献

- [1] Zhao H L, He Y H, Zhou R L, et al. Effects of desertification on soil organic C and N content in sandy farmland and grassland of Inner Mongolia. *Catena*, 2009, 77(3): 187-191
- [2] Don A, Scholten T, Schulze E D. Conversion of cropland into grassland: implications for soil organic-carbon stocks in two soils with different texture. *Journal of Plant Nutrition and Soil Science*, 2009, 172(1): 53-62
- [3] John B, Yamashita T, Ludwig B, et al. Storage of organic carbon in aggregate and density fractions of

- silty soils under different types of land use. *Geoderma*, 2005, 128: 63–79
- [4] Wang J, Fu B J, Qiu Y, et al. Soil nutrients in relation to land use and landscape position in the semi-arid small catchment on the Loess Plateau in China. *Journal of Arid Environments*, 2001, 48(4): 537–550
- [5] He N P, Wu L, Wang Y S, et al. Changes in carbon and nitrogen in soil particle-size fractions along a grassland restoration chronosequence in northern China. *Geoderma*, 2009, 150: 302–308
- [6] Li X G, Li F M, Rengel Z, et al. Cultivation effects on temporal changes of organic carbon and aggregate stability in desert soils of Hexi Corridor region in China. *Soil & Tillage Research*, 2006, 91: 22–29
- [7] Dong Z B, Wang X M, Liu L Y. Wind erosion in arid and semiarid China: an overview. *Journal of Soil and Water Conservation*, 2000, 55(4): 439–444
- [8] Guo Z B, Yan G J, Zhang R H, et al. Improvement of soil physical properties and aggregate-associated C, N, and P after cropland was converted to grassland in semiarid Loess Plateau. *Soil Science*, 2010, 175(2): 99–104
- [9] Hoshino A, Tamura K, Fujimaki H, et al. Effects of crop abandonment and grazing exclusion on available soil water and other soil properties in a semi-arid Mongolian grassland. *Soil & Tillage Research*, 2009, 105(2): 228–235
- [10] Wang X B, Oenema O, Hoogmoed W B, et al. Dust storm erosion and its impact on soil carbon and nitrogen losses in northern China. *Catena*, 2006, 66(3): 221–227
- [11] Wang Q, Zhang L, Li L, et al. Changes in carbon and nitrogen of chernozem soil along a cultivation chronosequence in a semi-arid grassland. *European Journal of Soil Science*, 2009, 60(6): 916–923
- [12] Diaz S, Lavorel S, McIntyre S, et al. Plant trait responses to grazing — a global synthesis. *Global Change Biology*, 2007, 13(2): 313–341
- [13] Li F R, Zhao W Z, Liu J L, et al. Degraded vegetation and wind erosion influence soil carbon, nitrogen and phosphorus accumulation in sandy grasslands. *Plant Soil*, 2009, 317: 79–92
- [14] Li J R, Okin G S O, Alvarez L, et al. Quantitative effects of vegetation cover on wind erosion and soil nutrient loss in a desert grassland of southern New Mexico, USA. *Biogeochemistry*, 2007, 85(3): 317–332
- [15] Liu H Y, Cui H T, Richard P, et al. Vegetation of the woodland-steppe transition at the southeastern edge of the Inner Mongolian Plateau. *Journal of Vegetation Science*, 2000, 11(4): 525–532
- [16] Liu H Y, Yin Y, Tian Y H, et al. Climatic and anthropogenic controls of topsoil features in the semi-arid East Asian steppe. *Geophysical Research letters*, 2008, 35(4): L04401, doi: 10.1029/2007GL032980
- [17] Zhou R L, Li Y Q, Zhao H L, et al. Desertification effects on C and N content of sandy soils under grassland in Horqin, northern China. *Geoderma*, 2008, 145: 370–375
- [18] 李博. 中国北方草地退化及其防治对策. *中国农业科学*, 1997, 30(6): 1–9
- [19] 黄永梅, 刘鸿雁, 崔海亭. 内蒙古高原东南缘森林草原过渡带景观的若干特征. *植物生态学报*, 2001, 25(3): 257–264
- [20] Zhang Y K, Liu H Y. How did climate drying reduce ecosystem carbon storage in the forest-steppe ecotone? A case study in Inner Mongolia, China. *Journal of Plant Research*, 2010, 123(4): 543–549
- [21] Piao S L, Fang J Y, Zhou L M, et al. Interannual variations of monthly and seasonal normalized difference vegetation index (NDVI) in China from 1982 to 1999. *Journal of Geophysical Research-Atmosphere*, 2003, 108 (D14): 4401, doi: 10.1029/2002JD002848
- [22] Piao S L, Fang J Y, Zhou L M, et al. Variations in satellite-derived phenology in China's temperate vegetation. *Global Change Biology*, 2006, 12(4): 672–685
- [23] Jackson R B, Jobbágy E G, Avissar R, et al. Trading water for carbon with biological carbon sequestration. *Science*, 2005, 310: 1944–1947
- [24] Alvarez R, Lavado R S. Climate, organic matter and clay content relationships in the Pampa and Chaco soils, Argentina. *Geoderma*, 1998, 83: 127–141
- [25] Wang S Q, Yu G R, Zhao Q J, et al. Spatial characteristics of soil organic carbon storage in China's croplands. *Pedosphere*, 2005, 15(4): 417–423
- [26] Wang D D, Shi X Z, Wang H J, et al. Scale effect of climate on soil organic carbon in the uplands of Northeast China. *Journal of Soils and Sediments*, 2010, 10(6): 1007–1017

降水变化对樟子松人工林土壤无机氮 和净氮矿化速率的影响

任艳林

北京大学城市与环境学院生态学系, 北京 100871; E-mail: ylrn@pku.edu.cn

摘要 在北京大学地球环境与生态系统塞罕坝实验站的樟子松(*Pinus sylvestris* var. *mongolica*)人工林内, 采用野外降水控制实验和顶盖埋管法, 在生长季内分 0~5, 5~10, 10~20 和 20~30 cm 4 层, 研究穿透雨增加或减少 30% 对土壤无机氮(铵态氮与硝态氮之和)及净氮矿化速率的影响。结果表明, 樟子松人工林地下 0~30 cm 无机氮含量为 6.70 ± 2.31 mg/kg, 其中铵态氮 5.59 ± 1.78 mg/kg, 硝态氮 1.11 ± 0.77 mg/kg。不同土壤深度的无机氮含量无显著差异, 3 种穿透雨处理间的土壤铵态氮和无机氮含量无显著差异, 增雨处理的硝态氮含量显著低于对照。0~30 cm 的土壤净氮矿化速率为 -0.24 ($-6.65 \sim 10.24$) mg/(kg·30d)。穿透雨处理和土壤深度对净氮矿化速率无显著影响, 0~5 cm 的净硝化速率和净氮矿化速率显著高于其余 3 层, 增雨和减雨处理的净硝化速率和净氮矿化速率显著高于对照。研究结果说明降水变化对土壤铵态氮及氨化作用的影响弱于对硝态氮及硝化作用的影响, 这有助于更准确地评估降水变化对人工林生态系统服务功能和氮素生物地球化学循环过程的影响。

关键词 土壤氮有效性; 氮矿化; 降水变化; 土壤深度; 控制实验; 塞罕坝地区

中图分类号 X171

Effects of Precipitation Change on Inorganic Nitrogen and Net Nitrogen Mineralization Rate at a Plantation of Mongolian Pine

REN Yanlin

Department of Ecology, College of Urban and Environmental Sciences, Peking University, Beijing 100871; E-mail: ylrn@pku.edu.cn

Abstract The contents of inorganic Nitrogen (N) and rates of soil N mineralization at soil depths of 0–5, 5–10, 10–20 and 20–30 cm were measured by a field manipulative experiment of $\pm 30\%$ throughfall and closed-top tube incubation method in a *Pinus sylvestris* var. *mongolica* plantation at PKU-SOGES, China. The results show that the contents of inorganic N, $\text{NH}_4^+\text{-N}$, and $\text{NO}_3^-\text{-N}$ at the soil depths of 0–30 cm are 6.70 ± 2.31 , 5.59 ± 1.78 , 1.11 ± 0.77 mg/kg, respectively. There is no significant difference among inorganic N contents of different soil depths and throughfall treatments but the $\text{NO}_3^-\text{-N}$ of $+30\%$ is lower than that of control. Net N mineralization rates of 0–30 cm was -0.24 (-6.65 to 10.24) mg/(kg·30d). Throughfall treatments and soil depths have no significant effects on net ammonification rates. According to the net nitrification rates and net N mineralization rates, both of them at 0–5 cm are significantly higher than those at other soil depths, and treatments of $\pm 30\%$ throughfall are higher than the control. In a word, both the $\pm 30\%$ throughfall treatments decrease inorganic N, and increase net N mineralization rates. The results also indicate that impacts of precipitation change on soil $\text{NH}_4^+\text{-N}$ and ammonification are weaker than those on $\text{NO}_3^-\text{-N}$ and nitrification. This study will contribute to assessment of precipitation changes on plantation ecosystem service and N biogeochemical cycle.

Key words soil nitrogen availability; nitrogen mineralization; precipitation change; soil depth; manipulative experiment; Saihanba

氮是植物生长所需的大量营养元素之一,但自然生态系统中普遍存在着氮限制^[1]。绝大部分(>99%)的土壤氮来源于植物、动物和微生物残体,微生物分解这些生物残体时,在胞外酶的作用下,不溶性有机氮被转化为可溶性有机氮,然后通过微生物裂解以铵态氮形式释放到土壤中(氨化作用, ammonification),最后由硝化细菌转化为硝态氮(硝化作用, nitrification),变成植物可利用的各种形式。净矿化作用(net mineralization)是在特定时间内,无机氮进入土壤溶液的净积累。当可溶性有机氮不能满足微生物分解者对氮的需求时,它们也会从土壤溶液中吸收额外的无机氮。通过微生物的吸收和化学固定从可利用氮汇中去除无机氮的这一过程就被称为固持作用(immobilization)^[2]。土壤氮有效性通常是指无机氮(铵态氮和硝态氮)的供应速率和限制性^[3],主要由氮矿化-固持过程控制,通常以净氮矿化速率作为评价指标^[4]。

可溶性有机氮与微生物 C:N 比是直接控制土壤氮矿化作用的生物因子,土壤温度与水分是直接影响土壤净氮矿化速率的重要环境因子^[2]。在野外条件下,土壤层的水分变化可能比生物因素对氮矿化的调节更为重要。目前国内多数研究都是通过实验室培养、单纯调控土壤水分的方式来比较不同土壤水分状况对氮矿化作用的影响^[5-9],通过野外大型控制实验改变自然降水、进行原位培养来研究不同土壤深度土壤无机氮和氮矿化作用的工作还很少^[10]。

2007 年 IPCC 第 4 次评估报告指出,未来的降水格局变化具有不确定性^[11]。降水改变会直接影响土壤的水分状况,从而对土壤氮素有效性与氮矿化作用产生影响。降水改变还会通过影响土壤无机氮的输入过程(如凋落物的数量与质量、细根周转、微生物残体数量等)、无机氮的输出过程(如植物对有效氮的吸收利用、微生物对无机氮的固持作用、硝态氮的淋溶速率等)和氮循环调控因素(如氮矿化速率)^[2]来影响土壤氮有效性,进而影响植物对土壤氮素的利用效率,最终影响陆地生态系统的生产力^[4]和生物多样性。河北塞罕坝地区处于我国北方半干旱半湿润气候区的森林-草原过渡带,是气候变化的敏感区,主要土壤类型为风沙土,降水和土壤养分是影响当地植被分布与生长的重要因子。本研究采用野外降水控制实验的方法,主要从土壤无机氮

及其组分含量、净氮矿化速率两个方面分析降水增加或减少对不同深度森林土壤氮循环关键过程的影响,对于预测降水变化对人工林生态系统服务功能和氮素生物地球化学循环过程的影响具有重要意义。

1 研究区概况与方法

1.1 研究区自然概况

塞罕坝地区位于河北省承德市围场满族蒙古族自治县北部,包括坝上和接坝地区两部分,是内蒙古高原、大兴安岭山系与冀北山地交汇之处,也是内蒙古浑善达克沙地的东南边缘。气候区划属半干旱半湿润气候区,处于暖温带向温带的过渡带。冬季漫长而寒冷;春秋季较短,干燥多风;夏季不明显,气候凉爽。无霜期短,平均 60 天左右,昼夜温差大,年平均气温 -1.4°C 。降水以降雨为主,降雪为辅,降水量偏少,多集中在 6—9 月,年平均降水量 454.2 mm,最大年降水量 636.0 mm,最小年降水量 258.0 mm,年均降水日数 134 天。年平均蒸发量为 1244.4 mm。年均 6 级(强风)以上大风日 76 天,以西风或西北风为主。积雪长达 7 个月,最大冻土深 168 cm^[12-13]。坝上地区以风沙土为主,兼有草甸土和沼泽土,主要成土母质为风积物、残积物、堆积物及冲积物等^[12]。

塞罕坝地区位于我国境内 3 条全球变化样带的交汇处^[14],是全球变化研究的关键区域。作为森林-草原过渡带,这一地区对气候变化比较敏感,是气候变化的良好指示体。特殊的地理位置、复杂的自然条件使塞罕坝地区具有独特的生态学意义,是进行大规模气候控制实验、探讨全球变化生态响应的理想区域。

1.2 研究地点概况

降水控制实验样地位于北京大学地球环境与生态系统塞罕坝实验站西侧的樟子松(*Pinus sylvestris* var. *mongolica*)人工林内。海拔 1531 m,地理坐标为 $42^{\circ}25'\text{N}$, $117^{\circ}15'\text{E}$,位于阳面缓坡中上部。样地东侧距林缘 100 m,南侧距林缘 20 m。土壤类型为风沙土,乔木平均胸径约 12 cm,平均树高约 9 m,林下灌木稀少,草本层以披针叶苔草 (*Carex lanceolata*)、腺毛委陵菜 (*Potentilla longifolia*)、地榆 (*Sanguisorba officinalis*)、瓣蕊唐松草 (*Thalictrum petaloideum*)等为主。样地选址综合考虑了林分密度、地形均匀度和电力供应。

1.3 降水控制实验设计

降水控制实验样地占地 1 hm², 采取正交试验设计, 设置了 9 个 20 m × 20 m 的样方。包括 3 种穿透雨处理: 1) 自然穿透雨量(对照); 2) 穿透雨减少 30%(减雨 30%), 用覆盖地表面积 30%的薄膜水槽转移走该样方 30%的穿透雨量(图1); 3) 穿透雨增加 30%(增雨 30%), 把减雨样方转移来的 30%穿透雨用固定在地表的喷灌系统增加到该样方, 从而实现穿透雨的有效截流与转移。每种处理 3 个重复, 水平方向上 3 个不同的处理为一组, 各样方间距 10 m 作为缓冲带。

在每个穿透雨减少样方中, 12 条离地 1.5 m 并用镀锌管支撑呈一定倾斜角度的 0.5 m × 20 m (覆盖地表 30%)无色透明塑料薄膜水槽将穿透雨汇集到 2000 L 的黑色 PE 卧式水箱中, 水罐中的浮球阀开关可以自动控制系统, 当水位到达预定高度, 自动将雨水喷灌到相应的穿透雨增加样方中, 实现穿透雨的有效截流与转移。这种控制方式只改变降水量不改变降水频率。

各样方的土壤体积含水量监测采用 DT50 数据采集器(Dataaker Pty Ltd, Rowville, Australia)和 Trime-IT 土壤水分传感器(IMKO GmbH, Ettlingen, Germany)组成的 AZ-DT 土壤水分自动监测系统(澳作生态仪器有限公司, 北京), 每小时采集并记录土壤体积含水量数据, 土壤水分传感器垂直埋设深度为 10 cm, 水平埋设深度分别为 20 cm 和 40 cm。土壤温度用埋在地下 10 cm 处的 StowAway TidBiT 袖珍温度记录仪(Onset Computer Corporation, Pocasset, USA)每小时自动测量并记录土壤温度数据。各土壤深度不同穿透雨处理的土壤体积含水量(SVWC)有显著差异 ($p < 0.001$, 图 2(a), (b)和(c)), 增雨 30% > 对照 > 减雨 30%; 土壤温度为增雨 30% < 对照 < 减雨 30% (图 2(d))。

1.4 野外培养、采样与测定

土壤氮矿化采取野外顶盖培养法(closed-top tube incubations), 该方法能较好地反映土壤氮的实际矿化速率^[15]。主要分为培养前采样、野外培养、培养后采样、浸提过滤和仪器分析 5 步。

用电钻在长度 35 cm 内径 40 mm 的 PVC 管管口 1 cm 处的管壁四周垂直方向上打直径 4 mm 的小孔 4 个, 可保证气体交换, 也便于取出 PVC 管。每月在各样方中按照 S 形布点埋入 8 根管, 9 个样方共

72 根管; 共设 3 次重复, 分别于 2007 年 6 月、7 月、8 月埋入, 7 月、8 月、9 月取出。埋管时保留地表凋落物, 直接用橡胶锤把 PVC 管垂直砸入土中 32 cm (多余的 2 cm 可保证土芯能够完整取出), 地面上露出 3 cm 用通气但不漏水的保鲜膜封口, 以避免雨水对管内硝态氮的淋溶, 并注意让小孔露在外面。同时, 在各管旁用土钻分 4 层采集相同深度的土壤样品作为培养前背景值。背景值样品也用于土壤无机氮及其组分研究。

在培养 1 个月后取出 PVC 管, 将其中的土芯推出后分成 0~5, 5~10, 10~20 和 20~30 cm 共 4 段, 分别装入编号的封口袋, 每个样方中同层样品混合作为一个样品, 9 个样方共 4 层、36 个培养后样品。土壤样品用有冰种的保温箱带回实验室后, 在冰箱中 4℃保存。

在实验室内, 直接在封口袋中将样品混合均匀后用四分法取其中 1/4 土壤样品, 称量约 20 g 新鲜土壤样品, 105℃烘干 24 小时至恒重后计算得出土壤重量含水量。将剩余土壤样品过 2 mm 筛后, 称取约 22 g 样品放入编号的 200 mL 方形塑料瓶中。量取 100 mL 2 mol/L KCl 溶液倒入方形瓶内, 用封口膜密封后在摇床上震荡 1 小时, 将上清液经覆盖慢速定性滤纸的漏斗过滤后, 把滤出液放入 100 mL 小塑料瓶中, 用封口膜密封后, -18℃冷冻保存。

将浸提液自然解冻后, 用 10 mL 注射器吸取 5 mL 浸提液, 经 0.4 mm 水系膜过滤后, 用 FIAstar 5000 流动注射分析仪(FOSS, Denmark)测定浸提液中的铵态氮和硝态氮。

1.5 数据处理与统计分析

流动注射分析仪测定的浸提液浓度单位是 mg/L, 乘以浸提液体积(0.1 L)后分别得到浸提液中铵态氮和硝态氮的总量, 然后除以用于浸提的土壤干重, 即为以干土计的浓度(mg/kg), 其中, 土壤干重=用于浸提的筛后土壤鲜重×(1-筛后重量含水量), 无机氮为铵态氮与硝态氮二者之和。

根据培养前后土壤铵态氮、硝态氮含量之差, 分别计算土壤氮素的净氨化速率、净硝化速率和净氮矿化速率, 单位均为 mg/(kg·30d)。

$$\text{净氨化速率} = (\text{培养后铵态氮} - \text{培养前铵态氮}) / \text{培养天数} \times 30,$$

$$\text{净硝化速率} = (\text{培养后硝态氮} - \text{培养前硝态氮}) / \text{培养天数} \times 30,$$



图 1 穿透雨减少样方

Fig. 1 Throughfall displacement plot

净氮矿化速率=(培养后无机氮-培养前无机氮)/
培养天数×30。

对以上各指标进行线性混合效应模型(linear mixed effects model)方差分析^[16], 把穿透雨处理和土壤深度作为固定效应(fixed effects), 把月份和重复作为随机效应(random effect), 并用 Tukey HSD (honest significant difference) 检验对均值进行了多重比较。统计分析绘图均在 R 软件(Version 2.14.0, R Foundation for Statistical Computing, Vienna, Austria)中进行^[17]。

2 结果与讨论

2.1 穿透雨处理和土壤深度对土壤无机氮的影响

在自然生态系统中, 土壤中的无机氮主要来源于微生物对可溶性有机氮(dissolved organic nitrogen, DON)的裂解和转化, 以铵态氮和硝态氮的形式存在, 这都是植物可以直接吸收利用的氮素。当微生物生长存在碳限制时, 它会使用可溶性有机氮中的碳架来支持其生长与维持的能量需要, 同时释放铵盐到土壤中。在硝化细菌作用下, 部分或全部的铵盐会先变为亚硝酸盐, 再变成硝酸盐, 硝酸盐相对容易移动和被植物利用^[2]。生态系统土壤中的无机氮除了被植物利用、微生物固持, 一部分会通过氨挥发和反硝化作用变成气体扩散到大气中, 还有一部分会因为降水淋溶作用向下迁移, 远离植物根系可利用的土壤, 渗透到地下水中, 从而离开生态系统。

樟子松人工林地下 0~30 cm 土壤无机氮及其组成的平均浓度为铵态氮 5.59 ± 1.78 mg/kg, 硝态氮 1.11 ± 0.77 mg/kg, 无机氮 6.70 ± 2.31 mg/kg, 铵态氮浓度显著高于硝态氮。与章古台地区的樟子松林生

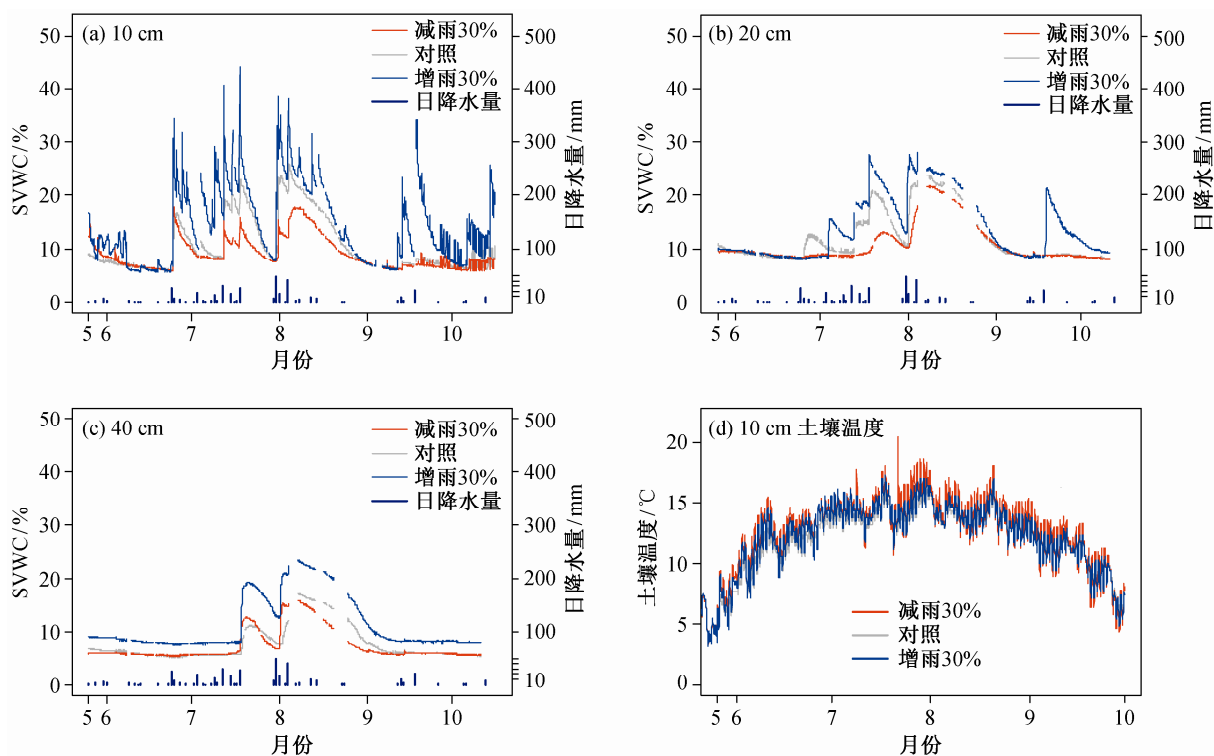


图 2 穿透雨处理对不同深度土壤体积含水量((a)~(c))和地下 10 cm 土壤温度(d)的效应

Fig. 2 Effects of throughfall treatment on soil volumetric water content at different soil depth ((a)~(c)) and 10 cm soil temperature (d)

态系统 0~15 cm 土壤(铵态氮 3.86 mg/kg, 硝态氮 1.89 mg/kg, 无机氮 5.76 mg/kg)^[18]相比, 塞罕坝樟子松人工林的土壤无机氮含量, 主要是铵态氮含量略高。与内蒙锡林河流域草甸草原生态系统 0~15 cm 土壤(铵态氮 2.16 mg/kg, 硝态氮 5.72mg/kg)^[19]相比较, 塞罕坝樟子松人工林的土壤铵态氮含量高, 硝态氮含量偏低, 无机氮含量略低。这可能与樟子松林土壤类型主要为风沙土, 硝态氮更容易被淋溶有关。

通过对培养前铵态氮、硝态氮和无机氮背景值的线性混合模型方差分析, 发现穿透雨处理对铵态氮无显著影响, 而对硝态氮却有显著影响(表 1)。由于铵态氮占无机氮总量的 80%以上(表 2), 总体上穿透雨处理对无机氮无显著影响。增雨处理土壤硝态氮显著低于对照, 减雨处理与对照及增雨的硝态氮含量统计上均无显著差别(表 2), 可能原因如下: 1) 因为铵态氮比较容易吸附在土壤中的矿物或带负电的有机物表面^[2], 不易随水分向下迁移, 所以相对稳定, 而增雨处理加强了对硝态氮的淋溶作用, 使其显著低于对照; 2) 由于硝态氮比铵态氮更容易被植物利用、微生物固持, 而且增雨处理显著地增加了土壤水分, 因此土壤中的硝态氮含量低于铵态氮,

增雨处理硝态氮含量显著下降。邓东周^[10]在辽宁章古台的樟子松幼树人工林降水控制实验中也发现在干旱半干旱地区土壤中存在类似的“水氮有效性的不同步性”现象。巴塔哥尼亚半干旱草原的遮雨实验结果表明, 降雨量增加导致的氮淋溶、微生物活性和植物吸收的增加造成了土壤无机氮含量的降低^[20]。美国橡树岭国家实验室在田纳西州东部落叶阔叶林穿透雨转移实验中用张力渗透仪和树脂渗透仪测定了土壤溶液中的离子浓度, 结果表明, 穿透雨处理对铵态氮和硝态氮含量均无显著差异($p>0.10$), 这与他们的假设“随着土壤水分含量增加离子浓度下降”有所不同, 但也没有找到合理的解释^[21]。

土壤深度及其与穿透雨的交互作用对铵态氮、硝态氮和无机氮均无显著影响(表1)。数值上随着土壤深度增加, 铵态氮、硝态氮、无机氮含量逐渐下降, 但 Tukey HSD 均值多重比较表明, 各土层间的无机氮含量并无显著差异($p>0.05$, 表 2)。这可能是因为 0~30 cm 土壤是细根分布最多、微生物最活跃的层次, 通过细根分解向土壤输入的氮可能大于叶^[22-23], 无机氮输入相对均衡, 因此氮有效性的差别也较小。

表 1 穿透雨处理与土壤深度对樟子松人工林土壤无机氮影响的混合模型方差分析

Table 1 Linear Mixed Model ANOVA of effects of throughfall treatments and soil depth on soil mineral nitrogen in a Mongolian pine plantation

差异来源	df	铵态氮		硝态氮		无机氮	
		<i>F</i>	<i>p</i>	<i>F</i>	<i>p</i>	<i>F</i>	<i>p</i>
穿透雨处理	2	0.542	0.584	4.618	0.012	0.898	0.411
土壤深度	3	2.000	0.119	2.391	0.073	2.463	0.067
穿透雨处理×土壤深度	6	0.135	0.991	1.023	0.415	0.348	0.909

表 2 樟子松人工林不同土壤深度与穿透雨处理的土壤无机氮

Table 2 Soil mineral nitrogen of different throughfall treatments and soil depth in a Mongolian pine plantation

因素	水平	铵态氮/(mg·kg ⁻¹)	硝态氮/(mg·kg ⁻¹)	无机氮/(mg·kg ⁻¹)
穿透雨处理	减雨 30%	5.34 ± 1.06 ^a	1.14 ± 0.63 ^{ab}	6.48 ± 1.54 ^a
	对照	5.77 ± 1.96 ^a	1.36 ± 0.94 ^a	7.12 ± 2.53 ^a
	增雨 30%	5.67 ± 2.15 ^a	0.83 ± 0.63 ^b	6.50 ± 2.69 ^a
土壤深度	0~5 cm	6.22 ± 2.03 ^a	1.29 ± 0.83 ^a	7.51 ± 2.60 ^a
	5~10 cm	5.75 ± 1.67 ^a	1.30 ± 0.99 ^a	7.05 ± 2.23 ^a
	10~20 cm	5.26 ± 1.85 ^a	0.93 ± 0.68 ^a	6.18 ± 2.41 ^a
	20~30 cm	5.15 ± 1.40 ^a	0.91 ± 0.44 ^a	6.06 ± 1.70 ^a
平均值		5.59 ± 1.78	1.11 ± 0.77	6.70 ± 2.31

说明: 表中数据为平均值±标准差。小写字母 a 和 b 为 Tukey HSD 多重比较结果, 不同字母表示同一因素不同水平的均值间有显著差异($p<0.05$), 字母顺序按均值由大到小排列。

在土壤瘠薄的生态系统, 无机氮可能只是有效氮中很少的一部分, 对可溶性有机氮的研究将有助于全面了解生态系统土壤氮有效性及氮循环的特征。

2.2 穿透雨处理对土壤氮矿化的影响

塞罕坝樟子松人工林 0~30 cm 的土壤净氨化速率为 -0.4 ($-4.74 \sim 5.28$) $\text{mg}/(\text{kg} \cdot 30\text{d})$, 其中 0~5 cm 平均净氨化速率为 0.55 ± 2.48 $\text{mg}/(\text{kg} \cdot 30\text{d})$, 5~30 cm 的净氨化速率均为负值。混合模型方差分析结果表明, 穿透雨处理和土壤深度及其交互作用对净氨化速率均无显著影响($p>0.05$, 表 3)。Tukey HSD 均值多重比较结果表明不同处理间和不同土壤深度间的净氨化速率统计上均无显著差异(表 4)。

樟子松人工林 0~30 cm 的土壤净硝化速率为 0.16 ($-4.17 \sim 5.26$) $\text{mg}/(\text{kg} \cdot 30\text{d})$ 。穿透雨处理与土壤深度对净硝化速率均有显著差异($p<0.001$, $p=0.002$), 二者的交互作用无显著差异($p=0.483$)(表 3)。Tukey HSD 多重比较结果表明, 减雨处理与增雨处理的净硝化速率无显著差异($p=0.758$), 二者都显著高于对照($p=0.001$, $p=0.008$)(表 4)。相同土壤深度各穿透雨处理的净硝化速率均无显著差异($p>0.05$)。不同土壤深度的净硝化速率 0~5 cm $>$ 10~20

cm $>$ 20~30 cm $>$ 5~10 cm, 其中, 0~5 cm 分别与其余 3 层有显著差异($p=0.023$, 0.014 , 0.003), 后者之间无显著差异($p>0.05$)。具体而言, 这些差异主要是由于增雨 0~5 cm 和减雨处理 0~5 cm 显著高于对照各土层的净硝化速率($p<0.05$), 增雨 0~5 cm 净硝化速率为 1.60 ($-0.32 \sim 5.26$), 减雨 0~5 cm 净硝化速率为 1.11 ($-1.26 \sim 3.87$) $\text{mg}/(\text{kg} \cdot 30\text{d})$ 。

樟子松人工林 0~30 cm 的土壤净氮矿化速率为 -0.24 ($-6.65 \sim 10.24$) $\text{mg}/(\text{kg} \cdot 30\text{d})$ 。穿透雨处理与土壤深度对净氮矿化速率均有显著影响($p=0.004$, $p=0.007$), 二者的交互作用无显著影响($p=0.522$)(表 3)。不同穿透雨处理的净氮矿化速率为增雨 $>$ 减雨 $>$ 对照, 其中, 增雨与减雨处理无显著差异, 二者均显著高于对照(表 4)。不同土壤深度的净氮矿化速率 0~5 cm $>$ 20~30 cm $>$ 10~20 cm $>$ 5~10 cm, 其中, 0~5 cm 为 1.43 ± 3.59 $\text{mg}/(\text{kg} \cdot 30\text{d})$, 5~30 cm 的净氮矿化速率均为负值, 0~5 cm 显著高于其余 3 层, 后者之间无显著差异(表 4)。Tukey HSD 多重比较表明, 主要差异来源是增雨处理 0~5 cm 的净氮矿化速率显著高于对照 5~10 cm ($p=0.002$)和 20~30 cm ($p=0.013$), 以及减雨处理 0~5 cm 高于对照 5~10 cm ($p=0.07$), 而增雨和减雨处理 0~5 cm 的净氮矿化速

表 3 穿透雨处理与土壤深度对樟子松人工林土壤氮矿化影响的混合模型方差分析

Table 3 Mixed Model ANOVA of effects of throughfall treatments and soil depth on soil N mineralization in a Mongolian pine plantation

差异来源	df	净氨化速率		净硝化速率		净氮矿化速率	
		<i>F</i>	<i>p</i>	<i>F</i>	<i>p</i>	<i>F</i>	<i>p</i>
穿透雨处理	2	2.182	0.118	10.378	<0.001	5.813	0.004
土壤深度	3	2.310	0.081	5.211	0.002	4.266	0.007
穿透雨处理 \times 土壤深度	6	0.603	0.727	0.922	0.483	0.868	0.522

表 4 樟子松人工林不同土壤深度和穿透雨处理的氮矿化速率

Table 4 Soil N mineralization rates of different soil depth and throughfall treatments in a Mongolian pine plantation

因素	水平	净氨化速率/ ($\text{mg} \cdot \text{kg}^{-1} \cdot 30 \text{ d}^{-1}$)	净硝化速率/ ($\text{mg} \cdot \text{kg}^{-1} \cdot 30 \text{ d}^{-1}$)	净氮矿化速率/ ($\text{mg} \cdot \text{kg}^{-1} \cdot 30 \text{ d}^{-1}$)
穿透雨处理	减雨 30%	-0.12 ± 1.68^a	0.40 ± 1.02^a	0.28 ± 2.36^a
	对照	-1.04 ± 1.95^a	-0.52 ± 1.06^b	-1.55 ± 2.26^b
	增雨 30%	-0.05 ± 2.92^a	0.60 ± 1.40^a	0.55 ± 3.96^a
土壤深度	0~5 cm	0.55 ± 2.48^a	0.88 ± 1.67^a	1.43 ± 3.59^a
	5~10 cm	-0.81 ± 2.25^a	-0.19 ± 1.41^b	-1.00 ± 3.13^b
	10~20 cm	-0.84 ± 2.01^a	0.00 ± 0.59^b	-0.83 ± 2.32^b
	20~30 cm	-0.51 ± 2.16^a	-0.05 ± 0.83^b	-0.56 ± 2.66^b
平均值		-0.40 ± 2.28	0.16 ± 1.26	-0.24 ± 3.09

说明: 表中数据为平均值 \pm 标准差。小写字母 a 和 b 为 Tukey HSD 多重比较结果, 不同字母表示同一因素不同水平的均值间有显著差异($p<0.05$), 字母顺序按均值由大到小排列。

率无显著差异。

顶盖埋管法利用 PVC 管切断了植物的根系, 导致土壤中的铵态氮和硝态氮无法被植物生长所利用; 顶端用保鲜膜封口又避免了降水淋溶, 当然也可能存在少量土壤水分蒸发凝结后对表土产生的淋溶。3 种处理的净氮化速率为负值意味着通过微生物的铵态氮是净吸收, 铵态氮可能被氮限制的微生物固持或被硝化细菌转化为硝态氮。这也意味着樟子松林土壤中的微生物生长可能不存在碳限制, 即微生物无须使用来自可溶性有机氮中的碳架来支持其生长和呼吸作用, 也就不会释放铵态氮到土壤溶液中^[2]。0~5 cm 净氮化速率为正值可能是因为该层土壤水分含量较高(图 2), 土壤微生物数量最多、对碳的竞争最激烈, 导致碳限制的出现, 转而利用可溶性有机氮中的碳来支持其生长, 产生铵态氮的净释放。

硝化作用主要是自养硝化细菌这类专性好氧微生物, 使用从 NH_4^+ 或 NO_2^- 氧化过程中获得的能量来固定和还原 CO_2 , 合成组织结构与新陈代谢所需碳化合物的过程^[2]。增雨处理和减雨处理的净硝化速率为正值意味着硝态氮的净释放, 对照的净硝化速率为负值意味着硝态氮的净吸收, 微生物的固持作用最强。由于样地土壤中的硝酸盐含量较低, 不符合反硝化作用高硝酸盐浓度的条件, 所以发生反硝化作用的概率较低。铵态氮可利用性和氧气浓度是影响硝化作用的直接因素^[2], 虽然 3 种处理土壤中的铵态氮含量并无显著差异(表 2), 但是土壤水分的适度增加, 有利于铵态氮向硝化细菌渗透, 增加铵态氮的可利用性。硝化细菌的活动对温度很敏感, 温度适度增加有利于硝化细菌的活动。与对照相比, 增雨处理的土壤水分含量较高, 减雨处理的土壤温度较高(图 2), 有利于增强硝化细菌的活性, 提高硝化作用速率。

净矿化作用是在特定时间内, 无机氮进入土壤溶液的净积累。当微生物生长更强烈地受到碳限制, 而不是氮限制时, 会发生净矿化作用, 而净固持则发生于氮限制的微生物群落中^[2]。与其他研究相比, 本研究的净氮矿化速率均值偏低^[5-10,18-19], 除了因生态系统、土壤类型与季节变化产生的差别, 由于氮矿化速率通常会随着土壤深度增加而降低^[24-25], 所以土壤深度不同也可能导致结果产生差异。塞罕坝樟子松人工林的净氮矿化速率平均值为负值, 发生了净固持, 说明当地土壤微生物群落的活动可能

受氮限制, 而非碳限制。在贫瘠生态系统中, 低速率的净氮矿化作用也说明, 此途径可能只是自然发生的有效氮通量的一小部分^[2]。而且净氮矿化速率把植物根系及菌根真菌排除在净矿化作用分析之外, 可能低估了根系存在情况下的矿化氮的量^[2,26], 应当使用可以更真实地反映氮矿化作用的指标与方法。

增雨和减雨 0~5 cm 净氮矿化速率为正值, 而不同深度土壤无机氮含量之间又无显著差异(表 2), 说明碳限制对该层微生物群落的影响更大。土壤水分和温度直接影响着土壤氮矿化过程和无机氮的形式及含量^[2], 可能是影响氮矿化作用最重要的因子, 而且土壤温度的影响重于土壤水分, 二者还具有正交互作用^[27-28]。林下穿透雨处理改变了土壤水分和温度, 增雨处理土壤水分显著高于对照和减雨, 减雨处理的土壤温度又略高于对照和增雨(图 2), 这都可能让土壤微生物种类、数量及活性发生变化^[29], 从而导致增雨和减雨处理的净氮矿化速率都高于对照。

3 结论

塞罕坝樟子松人工林土壤无机氮及氮矿化作用对穿透雨增加或减少 30% 的初期响应表明, 未来降水格局变化对生态系统土壤氮有效性及氮矿化作用的影响是复杂的, 降水减少会使土壤水分减少、温度升高, 降水增加会使土壤水分增加、温度降低, 从而导致土壤硝态氮含量降低、净氮矿化速率提高。降水变化对土壤铵态氮及氨化作用的影响弱于对硝态氮及硝化作用的影响。

参考文献

- [1] Vitousek P M, Howarth R W. Nitrogen limitation on land and in the sea: how can it occur?. *Biogeochemistry*, 1991, 13(2): 87-115
- [2] Chapin F S, Matson P A, Mooney H A. 陆地生态系统生态学原理. 李博, 赵斌, 彭容豪, 等, 译. 北京: 高等教育出版社, 2005: 168-183
- [3] Chapin F S, Vitousek P M, van Cleve K. The nature of nutrient limitation in plant-communities. *American Naturalist*, 1986, 127(1): 48-58
- [4] Reich P B, Grigal D F, Aber J D, et al. Nitrogen mineralization and productivity in 50 hardwood and conifer stands on diverse soils. *Ecology*, 1997, 78(2): 335-347

- [5] 周才平, 欧阳华. 温度和湿度对长白山两种林型下土壤氮矿化的影响. 应用生态学报, 2001, 12(4): 505–508
- [6] 周才平, 欧阳华. 温度和湿度对暖温带落叶阔叶林土壤氮矿化的影响. 植物生态学报, 2001, 25(2): 204–209
- [7] 王常慧, 邢雪荣, 韩兴国. 温度和湿度对我国内蒙古羊草草原土壤净氮矿化的影响. 生态学报, 2004, 24(11): 2472–2476
- [8] Chen F, Zeng D, Singh A N, et al. Effects of soil moisture and soil depth on nitrogen mineralization process under Mongolian pine plantations in Zhanggutai sandy land, P. R. China. *Journal of Forestry Research*, 2005, 16(2): 101–104
- [9] 陈伏生, 余烟, 甘露, 等. 温度、水分和森林演替对中亚热带丘陵红壤氮素矿化影响的模拟实验. 应用生态学报, 2009, 20(7): 1529–1535
- [10] 邓东周. 降雨量变化对科尔沁沙地东南部樟子松人工林主要生态过程的影响[D]. 沈阳: 中国科学院沈阳应用生态研究所, 2009: 59
- [11] IPCC. WGI fourth assessment report. climate change 2007: the physical science basis. Geneva: Intergovernmental Panel on Climate Change, 2007
- [12] 黄金祥, 李信, 钱进源. 塞罕坝植物志. 北京: 中国科学技术出版社, 1996: 1
- [13] 郑成洋. 河北省塞罕坝森林结构与生物量[R]. 北京: 北京大学, 2005: 3
- [14] 张新时, 杨奠安. 中国全球变化样带的设置与研究. 第四纪研究, 1995, 15(1): 43–52, 99–100
- [15] 陈伏生, 曾德慧, 范志平, 等. 沙地不同树种人工林土壤氮素矿化过程及其有效性. 生态学报, 2006, 26(2): 343–347
- [16] Bates D, Maechler M, Bolker B. lme4: Linear mixed-effects models using S4 classes, 2011, R package version 0.999375-42 [CP/OL]. <http://CRAN.R-project.org/package=lme4>
- [17] R Development Core Team. R: a language and environment for statistical computing. Vienna: R Foundation for Statistical Computing, 2011: ISBN 3-900051-07-0. <http://www.R-project.org/>
- [18] 陈伏生, 曾德慧, 范志平, 等. 章古台沙地樟子松人工林土壤有效氮的研究. 北京林业大学学报, 2005, 27(3): 6–11
- [19] 王其兵, 李凌浩, 白永飞, 等. 气候变化对草甸草原土壤氮素矿化作用影响的实验研究. 植物生态学报, 2000, 24(6): 687–692
- [20] Yahdjian L, Sala O, Austin A T. Differential controls of water input on litter decomposition and nitrogen dynamics in the Patagonian steppe. *Ecosystems*, 2006, 9(1): 128–141
- [21] Johnson D W, Hanson P J, Todd D E. Nutrient availability and cycling // Hanson P J, Wullschlegel S D. North American temperate deciduous forest responses to changing precipitation regimes. New York: Springer-Verlag, 2003: 396–414
- [22] Langley J A, Hungate B A. Mycorrhizal controls on belowground litter quality. *Ecology*, 2003, 84: 2303–2312
- [23] 郭大立, 范萍萍. 关于氮有效性影响细根生产量和周转率的四个假说. 应用生态学报, 2007, 18(10): 2354–2360
- [24] Federer C A. Nitrogen mineralization and nitrification: depth variation in four New England forest soils. *Soil Science Society of America Journal*, 1983, 47: 1008–1014
- [25] Hadas A, Feigin A, Feigenbaum S, et al. Nitrogen mineralization in the field at various soil depths. *Journal of Soil Science*, 1989, 40: 131–137
- [26] Stark J M. Nutrient transformation // Sala O E, Jackson R B, Mooney H A, et al. Methods in ecosystem ecology. New York: Springer-Verlag, 2000: 215–234
- [27] Puri G, Ashman M R. Relationship between soil microbial biomass and gross N mineralization. *Soil Biology & Biochemistry*, 1998, 30(2): 251–256
- [28] 李贵才, 韩兴国, 黄建辉, 等. 森林生态系统土壤氮矿化影响因素研究进展. 生态学报, 2001, 21(7): 1187–1195
- [29] 魏天凤, 任艳林, 曾辉, 等. 降水改变对樟子松人工林土壤微生物量碳及微生物商动态变化的影响. 北京大学学报: 自然科学版, 2009, 45(3): 533–540

1965—2011 年河北塞罕坝地区降水量 变化规律的小波分析

任艳林

北京大学城市与环境学院生态学系, 北京 100871; E-mail: ylrn@pku.edu.cn

摘要 采用 Morlet 复小波函数对河北省塞罕坝地区 1965—2011 年降水变化规律进行了小波分析, 揭示了塞罕坝地区降水变化的多时间尺度特征。结果表明, 47 年来该地区月降水量、年降水量与生长季降水量距平值变化主要表现在两种尺度上: 一种是 4 年左右的年际尺度振荡, 这是经过高频滤波后的年际变化中的低频部分; 另一种是 18 年左右时间尺度的年代际振荡。由于塞罕坝地区生长季降水平均占年降水量的 83.1%, 通常二者的变化趋势相同, 但也不完全一致。由典型尺度小波系数过程线图可预测, 2012—2015 年塞罕坝地区的降水量仍然偏多, 但距平值会减少。

关键词 降水量; 多时间尺度; 小波分析; Morlet 小波; 塞罕坝地区
中图分类号 P467

Wavelet Analysis of Precipitation Fluctuation at Saihanba in Hebei Province from 1965 to 2011

REN Yanlin

Department of Ecology, College of Urban and Environmental Sciences, Peking University, Beijing 100871; E-mail: ylrn@pku.edu.cn

Abstract The author used Morlet complex wavelet analysis to analyze the precipitation fluctuation from 1965 to 2011 at Saihanba in Hebei Province and to reveal the multi-time scale feature of precipitation pattern. It shows that the anomalies of monthly precipitation, growing season precipitation (May to September) and annual precipitation in the last 47 years vary at two time-scales: one is 4 years of inter-annual oscillation, which is the low-frequency part of the inter-annual fluctuation after high-frequency filtering; and the other is about 18 years of decadal oscillation. The growing season precipitation of Saihanba accounts for 83.1 percent of the annual precipitation, thus both of them often show the same trends but with some exceptions. The wavelet coefficient curve under the scale of 18 years indicates that precipitation will keep higher than mean annual precipitation with decreased anomalies in 2012–2015.

Key words precipitation; multi-time scale; wavelet analysis; Morlet wavelet; Saihanba

河北省塞罕坝地区地处我国暖温带半湿润气候和半干旱气候的过渡带、森林植被和草原植被的过渡带, 降水是影响这一地区植物生长的主要限制因子。研究该地区过去的降水变化规律对于在这里进行降水控制实验和气候变化研究具有重要意义。

小波分析(wavelet analysis)是一种信号的时间

尺度分析方法, 其核心是小波变换(wavelet transform), 具有多分辨率分析的特点, 在时域和频域都具有表征信号局部特征的能力, 可以对信号进行多尺度细化分析, 得到各个频率随时间的变化特征和不同频率之间的关系, 因而优于传统的傅立叶(Fourier)分析^[1]。

国家重点基础研究发展计划(2010CB950602)和北京大学 985 工程二期资助
收稿日期: 2012-03-09; 修回日期: 2012-04-06; 网络出版日期: 2012-10-23
网络出版地址: <http://www.cnki.net/kcms/detail/11.2442.N.20121023.1745.003.html>

对于降水等气候因子的变化而言,并不存在真正意义上的周期性,而是在时域中存在多时间尺度的嵌套结构和局部化特征,即使是加窗的傅立叶分析也无法分析此类特征。因为小波变换在时域和频域中都具有良好的局部化特性,还可以检测气候变化突变点,进行多尺度趋势预测,所以它是分析降水等气候因子变化的必要工具。近年来,国外学者将小波分析应用于降水、气温、径流及海洋等各类研究,国内研究人员也应用小波分析对各地区的降水和气温等气候因子进行了一些探讨^[2-11],并得出当地的多尺度气候变化规律。

在降水时间序列中包含多种时间尺度的连续周期变化,因此本文采用 Morlet 复小波作为基函数进行一维连续小波变换,对塞罕坝地区近 50 年来的降水时间序列进行时频局部化分析,揭示其在不同时间尺度上的变化规律和突变特征。

1 研究区概况与方法

1.1 塞罕坝地区气候概况

塞罕坝地区属半干旱半湿润气候区,处于暖温带向温带的过渡带。冬季漫长而寒冷;春秋季较短,干燥多风;夏季不明显,气候凉爽。无霜期短,平均 60 天左右。昼夜温差大,年平均气温 -1.2°C ,1 月平均气温 -21.8°C ,7 月平均气温 16.2°C 。极端最低温度 -43.2°C ,极端最高温度 33.4°C ,日平均气温 $\geq 0^{\circ}\text{C}$ 的年积温为 2072.80°C , $\geq 5^{\circ}\text{C}$ 的年积温为 1984.00°C , $\geq 10^{\circ}\text{C}$ 的年积温为 1663.5°C 。降水以降雨为主,降雪为辅,降水量偏少,多集中在 6—9 月,多年平均降水量 454.2 mm ,最大年降水量 636.0 mm ,最小年降水量 258.0 mm ,年均降水日数 134 天。年均日照 2367.8 h ,日照率 58%。年均相对湿度 74.4%。年平均蒸发量 1244.4 mm 。年均 6 级(强风)以上大风日 76 天,以西风或西北风为主。积雪长达 7 个月,最大冻土深 168 cm ^[12-13]。

1.2 小波分析方法

小波分析是近 20 年来迅速成熟起来的具有良好时域和频域局部分析性质的数学分支,来源于伸缩和平移方法,基本原理是用一族函数去表示或逼近一个信号或函数,其核心内容是小波变换。小波变换就是通过“小波”(wavelet)与待分析函数“相乘”(内积),以达到分解原函数的目的。小波变换是把某一被称为基本小波(也称母小波, mother wavelet)

的函数 $\psi(t)$ 位移 τ 后,再在不同尺度 a 下与待分析函数 $f(t)$ 作内积:

$$C(a, \tau) = \frac{1}{\sqrt{a}} \int_{-\infty}^{\infty} f(t) \psi\left(\frac{t-\tau}{a}\right) dt, a > 0, \quad (1)$$

a 为尺度因子, τ 为平移因子, C 为小波系数。 $\psi(t)$ 为平方可积函数,即 $\psi(t) \in L^2(R)$ 。经过基本小波与待分析函数作内积之后,可分解得到不同尺度下的小波系数。这一过程就是小波变换。小波系数模、小波系数实部及小波系数位相是小波变换得到的 3 个最重要的变量。小波系数模的大小表示特征时间尺度信号的强弱。通过小波分析可以得到时间序列在任一时刻的频率及其在时间-频率上的变化特征。

本文采用 Morlet 小波(Morlet wavelet)函数对塞罕坝地区的降水量进行研究。Morlet 小波是一种单频复正弦调制高斯波,具有很好的时域和频域局部性,常用于复数信号的分解和时频分析。由于 Morlet 小波的实部本身也是一个对称的小波函数,小波系数的实部可以表示不同特征时间尺度信号在不同时间的强弱和位相两方面的信息。Morlet 小波没有尺度函数,其小波函数如下:

$$\psi(t) = e^{-\frac{t^2}{2}} e^{i\omega_0 t}, \omega \geq 5. \quad (2)$$

1.3 数据准备与处理

降水观测数据来源于《河北省塞罕坝机械林场 1960—2011 年气候因素汇编》,因 1962—1964 年缺测严重,仅分析 1965—2011 年逐月降水量、年降水量以及生长季(5—9 月)降水量变化规律,47 年共 564 个月。首先,计算所有月份的多年平均降水量,用月降水量减去该月多年平均降水量后构成各月份的降水距平序列,这也可以滤去一年自然周期的影响。对年降水量和生长季降水量数据也进行同样的处理。为了减小两端边界效应的影响,在降水数据的两端分别向外增加数据^[2],在距平资料的两端进行对称性延伸 1 倍长度资料(对称延伸法),方法如下。

设原数据系列为 $f(1), f(2), \dots, f(n)$,

向前延伸 n 点 $f(-i) = f(i+1), i = 0, 1, \dots, n-1$,

向后延伸 n 点 $f(i+n) = f(n+1-i), i = 1, \dots, n$ 。

对降水量距平序列数据做标准化处理后,用 Morlet 复小波进行一维连续小波变换得到相应的小波系数,小波变换后仅保留原资料序列时段内的小

波系数。在计算小波系数时,延伸后的降水距平序列均采用 2^n 的模式,年降水量、生长季降水量尺度参数最小值为 2 年,最大值设为 $32(2^5)$ 年;逐月降水量尺度参数最小值为 2 个月,最大值设为 $512(2^9)$ 个月。输出得到复数小波系数,用其模部的平方插值后绘成小波系数模平方等值线图(小波能量图)。

为了判断各降水距平序列的主要周期,进行小波方差检验($\alpha=0.05$),并绘制小波方差图。小波方差 $\text{Var}(a)$ 反映了波动的能量随尺度的分布,可以确定降水时间序列中各种尺度扰动的相对强度,对应峰值处的尺度称为该序列的主要时间尺度,即主周期^[1]。小波方差是小波变换系数模部的平方在时间域上对 τ 的积分,其计算公式为

$$\text{Var}(a) = \int_{-\infty}^{\infty} |C(a, \tau)|^2 d\tau. \quad (3)$$

数据分析与绘图在 MATLAB 7.0 中完成。

2 结果与讨论

2.1 月降水量距平值变化特征

在塞罕坝地区 1965—2011 年逐月降水量距平值变化图(图 1(a))中,1990 年 7 月出现最大值 132 mm,2000 年 7 月出现最小值 -101.8 mm,而且月降水距平值出现峰值或谷值的月份通常是在 7 月或 8 月,这是因为塞罕坝地区降水主要集中在 6—8 月,夏季的降水变化更加明显。

由 1965—2011 年塞罕坝地区月降水量距平值小波变换模平方等值线图可以看出,月降水量距平值在小波变化域中的波动能量曲面上有众多能量聚集中心。从模平方极值的大小看,2~4 个月尺度上能量变化强度大、频率高,月降水量在此尺度上频繁剧烈地波动,进行着枯丰交替。此外,在中心(222, 2010)处,月降水量在小波变化域中的波动能量很强,几乎影响到整个时域,波动能量影响尺度的范围是 128~512 个月。在 16 和 50 个月的时间尺度上,也分布着若干能量聚集中心。这说明,月降水量距平在整个时间域中,主要存在以 2010 年左右为振荡中心,以 222 个月(准 18 年)为尺度中心的波动变化;同时辅以 1972 年和 1990 年左右为振荡中心,以 50 个月(准 4 年)左右为尺度中心的波动变化。以上这些周期的波动,代表着月降水量距平值波动变化的本质特性,主导其在整个时域内的变化。

按照式(3)计算各降水距平序列的小波方差,并由此来确定各序列中的主要周期。月降水量距平序

列的主要周期约为 16 个月、4 年和 18 年左右(图 1(c)),在一年内还有 3 个月、4 个月、6 个月等显著的小周期。

2.2 年降水量距平值变化特征

1965—2011 年塞罕坝地区年降水量平均值为 453.0 mm,年降水量距平见图 2(a),由图中可知年降水量总体呈增加趋势,20 世纪 60 年代末到 80 年代末降水较少,1990 年后有较大的增加,2000 年后降水基本在多年平均值上下波动。年降水量距平的最小值为 1971 年的 -191.1 mm,最大值为 1991 年的 186.1 mm。

在 1965—2011 年塞罕坝地区年降水量小波变换模平方等值线图(图 2(b))中,从模平方极值的大小看,能量最集中的中心有 3 个,它们的中心点分别是(4, 1972), (4, 1990)和(18, 2010)。

在中心(18, 2010)处,年降水量波动能量强,在小波变化时频域中影响范围最广,几乎涉及整个时域,这与月降水量模平方等值线图中观察到的结果一致。波动能量影响尺度的范围是 14~32 年,尺度中心在 18 年左右。

在中心(4, 1990)处,波动能量的强度与中心(18, 2010)相同,影响时域范围是 1980—2007 年,在此范围波动能量变化梯度基本一致,时域上振荡中心在 1990 年左右,而波动能量影响尺度的范围是 2~6 年,尺度中心在 4 年左右。

在中心(4, 1972)处,年降水量在小波变化域中的波动能量最强,强集中影响范围 1965—1978 年,振荡中心在 1972 年左右,而波动能量影响尺度的范围也是大约 2~6 年,尺度中心在 4 年左右。

这 3 个能量聚集中心导致 4 年和 18 年成为年降水量距平变化的主要周期,年降水量显著的周期还有 2 年和 6 年(图(2(c)))。

2.3 生长季降水量距平值变化特征

1965—2011 年塞罕坝地区生长季降水量平均值为 377.6 mm,生长季降水量占年降水量的平均值为 83.1%。20 世纪 60 年代末到 80 年代末生长季降水总体较少,70 年代初生长季降水波动较大,90 年代降水量先增加后减少,2000 年后降水继续呈现减少趋势,其中最小距平值为 1971 年 -176.1 mm,最大值为 1973 年 164.1 mm(图 3(a))。

塞罕坝地区气候比较寒冷,植物的生长季通常从 5 月中旬开始,持续到 9 月中旬结束,生长季降水对植物生长很重要。生长季降水占全年降水量的

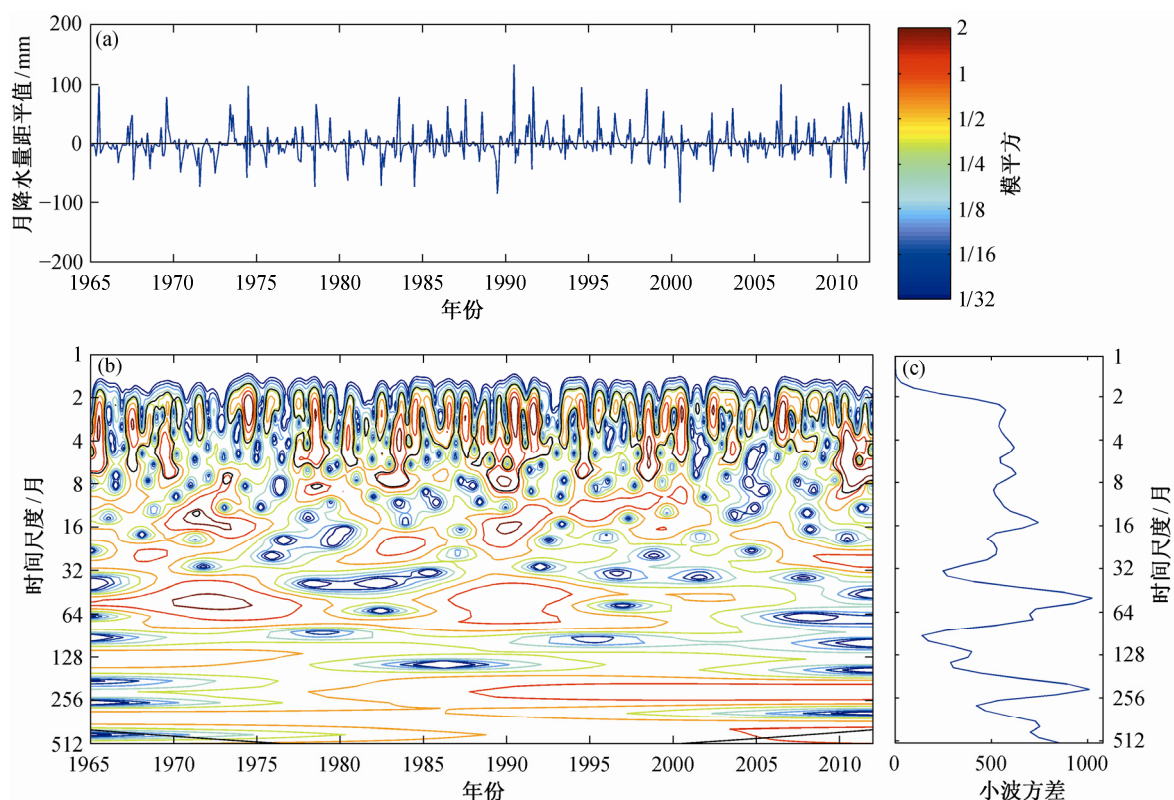


图 1 1965—2011 年塞罕坝地区月降水量距平序列(a)、小波变换模平方等值线图(b)及小波方差图(c)
Fig. 1 Monthly precipitation anomaly fluctuation (a), wavelet power spectrum (b) and global wavelet variance (c) at Saihanba from 1965 to 2011

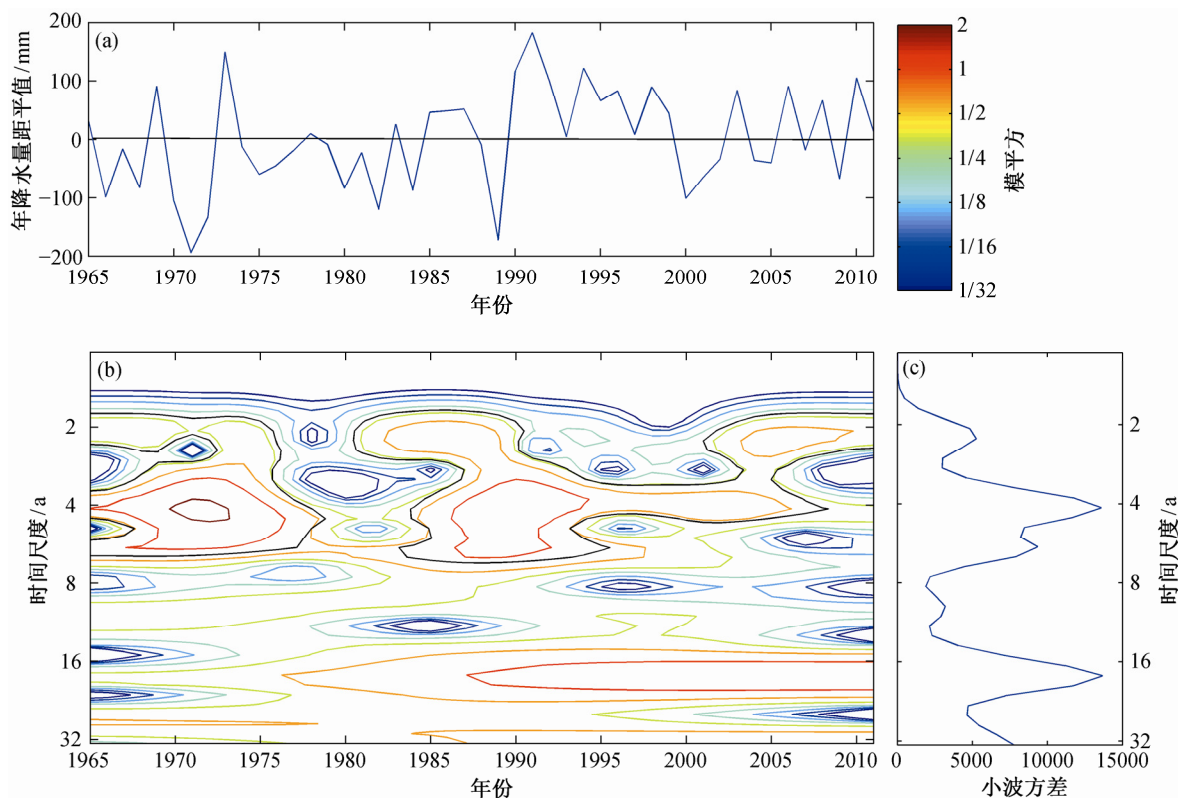


图 2 1965—2011 年塞罕坝地区年降水量距平序列(a)、小波变换模平方等值线图(b)及小波方差图(c)
Fig. 2 Annual precipitation anomaly fluctuation (a), wavelet power spectrum (b) and global wavelet variance (c) at Saihanba from 1965 to 2011

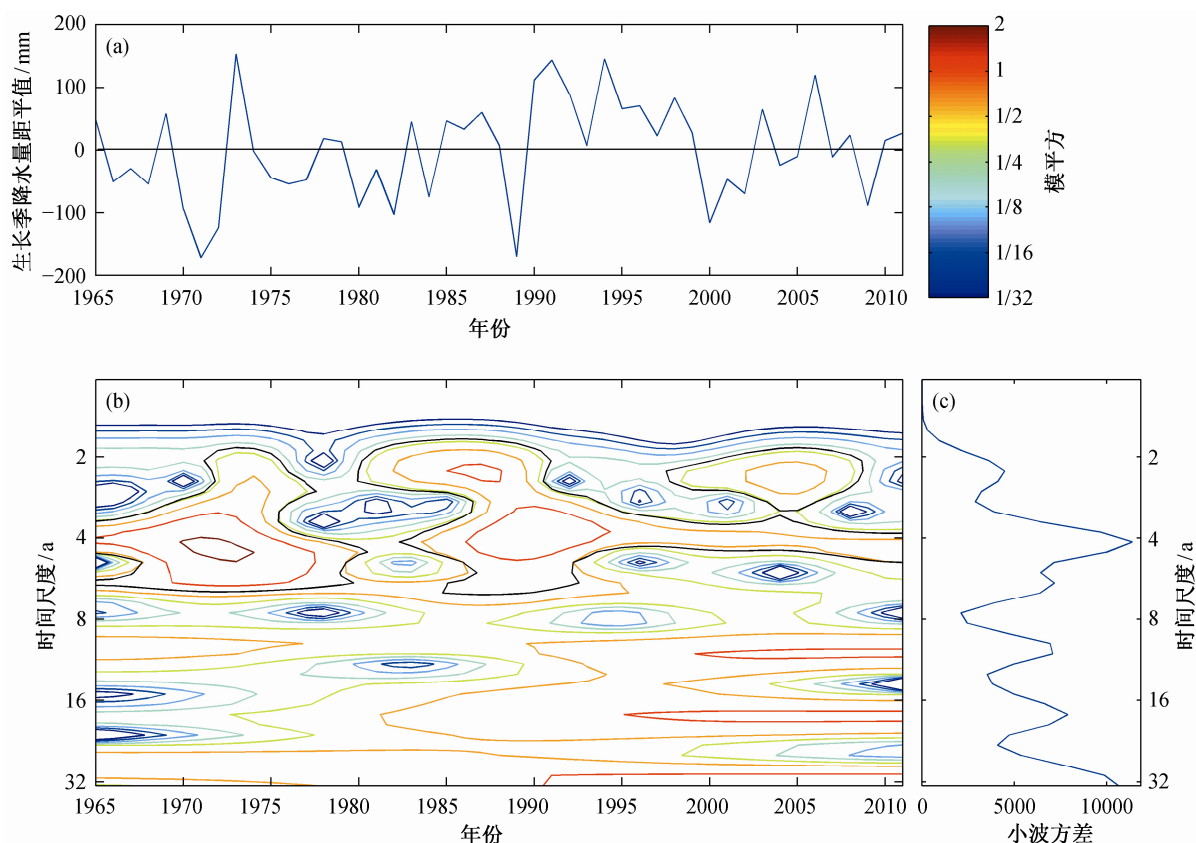


图 3 1965—2011 年塞罕坝地区生长季降水量距平序列(a)、小波变换模平方等值线图(b)及小波方差图(c)
Fig. 3 Growing season precipitation anomaly fluctuation (a), wavelet power spectrum (b) and global wavelet variance (c) at Saihanba from 1965 to 2011

70.3%~92.3%，生长季降水增加的年份，其降水量占全年降水量的百分比不一定大，反之亦然。如 1991 年生长季降水量距平值为 158.0 mm，生长季降水占全年降水的 86%，而 2001 年生长季降水距平值为 -48.8 mm，生长季降水占年降水的 90%。

由 1965—2011 年塞罕坝地区 5—9 月生长季降水量小波变换模平方等值线图(图3(b))可知，生长季降水量距平在小波时频域中波动能量最集中的中心多于年降水量，除了(4, 1972)，(4, 1990)和(18, 2010)，还有波动能量较弱的(2, 1987)，(2, 2005)和(10, 2010)，这也是生长季降水量主要周期多于年降水量的原因。除了包含年降水量的主要周期，生长季降水量距平序列还有 10 年和准 32 年的周期，其中，2, 4 和 6 年为小波方差检验显著的周期(图 3(c))。

2.4 降水量距平序列典型尺度的过程线及趋势预测

根据小波方差值的大小，可以确定 1965—2011 年塞罕坝地区月降水量、年降水量距平序列的第一

主周期为 4 年，第二主周期为 18 年，月降水量还存在 16 个月的主周期。李春强等^[9]采用 Morlet 小波函数对 1965—2005 年河北省降水量进行了小波分析，发现存在 4, 8 和 18 年这 3 个主周期。1965—2011 年塞罕坝地区生长季降水量距平序列的第一主周期为 4 年，第二主周期为 10 年，第三主周期为 8 年，生长季降水主导年降水量变化。许月卿等^[1]采用墨西哥帽小波函数对 1955—2000 年河北平原的年降水与各季节降水进行小波变换后发现，年降水与季节降水均存在 8~12 年尺度的周期特征，在 4~6 年左右的时间尺度上周期特征也比较明显，夏季降水主导年降水量变化。

典型尺度(主周期)的过程线可以揭示降水量变化的突变特征，也可以体现小波变换的多尺度分析与预测功能。使用典型尺度下各降水距平小波系数实部序列作图(图 4)，观察小波系数变化的突变特征，并预测其变化趋势。在图 4 中可以清楚地观察到，在 4 年和 18 年的尺度上，月降水量、年降水量

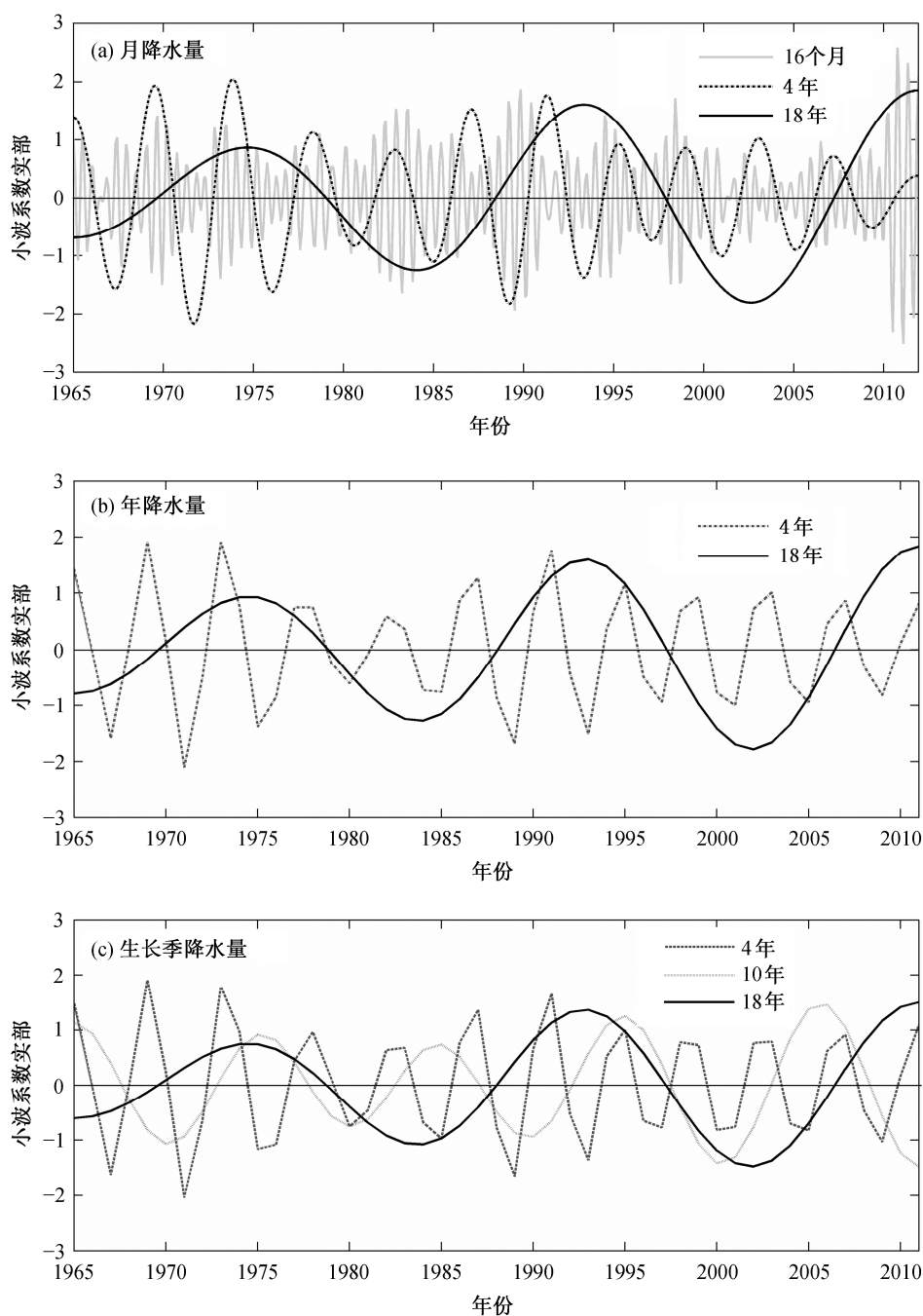


图 4 1965—2011 年塞罕坝降水量距平序列典型尺度小波系数实部变化过程线图

Fig. 4 Real part of precipitation anomaly wavelet transform coefficients under typical scales at Saihanba from 1965 to 2011

和生长季降水量的频率与位相大体一致, 生长季降水量振荡的幅度略小于月降水量与年降水量。在 18 年左右的年代际尺度上, 降水量呈现少—多—少—多—少—多的 3 个枯丰交替周期。在 4 年左右的年际尺度上有 11 个多—少—多的小周期。在 16 个月的时间尺度上, 月降水量变化的幅度与 4 年尺度上

比较接近, 但并不完全一致, 小尺度的变化比大尺度更复杂。

2011 年是月降水量和年降水量在 4 年和 18 年尺度上变化的峰值, 前一个降水量距平为零的拐点在 2007 年左右。由小波系数在 18 年主周期的变化趋势可预测, 2012 年后塞罕坝地区的生长季降水

量和年降水量开始同时减少,但总体上还是处于丰水期,降水量高于常年,年降水量低于常年的拐点大约会出现在 2015 年左右,2016—2025 年降水量将会偏少。

3 结论

1) 塞罕坝地区月降水量、年降水量和生长季降水量变化都存在多尺度特征,由这 3 个降水距平序列的小波分析得到的信息既有联系,又有区别,互相补充。其联系体现在 18 年的年代际时间尺度上,月降水量、年降水量和生长季降水量变化均呈少—多—少—多—少—多 3 个枯丰交替周期;在 4 年的年际时间尺度上,呈 11 个多—少—多的循环交替。区别在于,生长季降水量距平的主要尺度多于年降水量,月降水量在 2 年内的尺度上变化频繁,表现出降水量的季节变化与小尺度变化细节,体现了降水量变化的多尺度嵌套特征。

2) 在小波变化时频域上,塞罕坝地区年降水量和生长季降水量距平值均存在(4, 1972), (4, 1990)和(18, 2010) 3 个能量聚集中心,这主导着整个时频域上降水量的变化特征。

3) 由于塞罕坝地区生长季降水量平均占年降水量的 83.1%,二者的变化趋势大体相同,但由于变化第二主周期不同,生长季降水量与年降水量变化趋势并不完全一致。由小波系数实部典型尺度过程线图可预测,2012 年后生长季降水量和年降水量距平会同时减少,向多年平均值回归,年降水量低于常年的拐点大约会出现在 2015 年。

4) 小波分析可对气候值序列进行多时间尺度分析,不仅能够研究和预测气候的宏观变化,而且能对气候变化的精微结构进行分析,是气候变化分析的有力工具。

参考文献

- [1] 许月卿,李双成,蔡运龙. 基于小波分析的河北平原降水变化规律研究. 中国科学: D 辑, 2004, 34(12): 1176–1183
- [2] 邓自旺,林振山,周晓兰. 西安市近 50 年来气候变化多时间尺度分析. 高原气象, 1997(1): 81–93
- [3] 吴慧,陈小丽. 海南省四十年来气候变化的多时间尺度分析. 热带气象学报, 2003, 19(2): 213–218
- [4] 牛存稳,张利平,夏军. 华北地区降水量的小波分析. 干旱区地理, 2004, 27(1): 66–70
- [5] 严华生,万云霞,邓自旺,等. 用正交小波分析近百年来中国降水气候变化. 大气科学, 2004, 28(1): 151–157
- [6] 毕云,许利. 用一维 Morlet 小波变换对降水作诊断分析. 内蒙古气象, 2000(4): 26–28
- [7] 陈仁升,康尔泗,张济世. 小波变换在河西地区水文和气候周期变化分析中的应用. 地球科学进展, 2001, 16(3): 339–345
- [8] 路云阁,李双成,蔡运龙. 近 40 年气候变化及其空间分异的多尺度研究: 以内蒙古自治区为例. 地理科学, 2004, 24(4): 432–438
- [9] 李春强,杜毅光,李保国. 1965—2005 年河北省降水量变化的小波分析. 地理科学进展, 2010, 29(11): 1340–1344
- [10] 张军涛,李哲,郑度. 温度与降水变化的小波分析及其环境效应解释: 以东北农牧交错区为例. 地理研究, 2002, 21(1): 54–60
- [11] 邵晓梅,许月卿,严昌荣. 黄河流域降水序列变化的小波分析. 北京大学学报: 自然科学版, 2006, 42(4): 503–509
- [12] 黄金祥,李信,钱进源. 塞罕坝植物志. 北京: 中国科学技术出版社, 1996: 1
- [13] 郑成洋. 河北省塞罕坝森林结构与生物量[R]. 北京: 北京大学, 2005: 3

降水变化对樟子松人工林土壤呼吸速率及其表观温度敏感性 Q_{10} 的影响

任艳林[†] 杜恩在

北京大学城市与环境学院生态学系, 北京 100871; [†] E-mail: ylren@pku.edu.cn

摘要 为了研究降水变化对土壤呼吸及其温度敏感性的影响, 在北京大学地球环境与生态系统塞罕坝实验站的樟子松(*Pinus sylvestris* var. *mongolica*)人工林中进行了降水控制实验, 用减雨 30%、增雨 30% 和对照 3 种穿透雨处理来模拟长期的降水变化情景。重复测量方差分析结果表明, 3 种穿透雨处理总体上对生长季土壤呼吸速率及其表观温度敏感性 Q_{10} 无显著影响($p>0.05$)。配对 t 检验多重比较结果则显示, 土壤呼吸速率平均值大小为对照<减雨 30%<增雨 30%, 增雨处理的土壤呼吸速率显著高于对照 ($p<0.001$), 对照和减雨处理之间无显著差异($p>0.05$); 土壤呼吸表观 Q_{10} 平均值大小为减雨 30%<对照<增雨 30%, 随着降水量增加, 表观 Q_{10} 逐渐增大, 但处理间差异在统计上并不显著($p>0.05$)。研究结果意味着降水量减少 30% 可能对森林土壤呼吸的限制较小, 而降水量增加 30% 则可能显著地增加土壤呼吸 CO_2 释放量。

关键词 土壤呼吸速率; 表观 Q_{10} ; 降水变化; 控制实验; 塞罕坝

中图分类号 X171

Effects of Precipitation Change on Soil Respiration Rate and Apparent Q_{10} of Temperature Sensitivity in a Mongolian Pine Plantation

REN Yanlin[†], DU Enzai

Department of Ecology, College of Urban and Environmental Sciences, Peking University, Beijing 100871; [†] E-mail: ylren@pku.edu.cn

Abstract A chronic field manipulative experiment of $\pm 30\%$ throughfall (+30%, -30%, and control, respectively) in a Mongolian pine plantation was carried out to detect the responses of forest soil respiration and its temperature sensitivity to precipitation change at PKU-SOGES, China. Results of repeated measures ANOVA indicate that there is no statistically significant effect of three throughfall treatments on soil respiration rates and apparent Q_{10} generally ($p>0.05$). Multiple comparisons of paired t -test show that the soil respiration rates of +30% is statistically higher than that of the control ($p<0.001$), and the latter is not different from -30% statistically ($p>0.05$). The order of apparent temperature sensitivity of soil respiration for three throughfall treatments is -30% < control < +30% ($p>0.05$), which has a weak increasing trend along with increased precipitation. The results imply that the impact of chronic precipitation decrease of 30% on forest soil respiration may be rather limited, but the precipitation increase of 30% will stimulate soil CO_2 efflux dramatically.

Key words soil respiration rate; apparent Q_{10} ; precipitation change; manipulative experiment; Saihanba

在全球气候变化背景下, 大气环流和水循环在气候变暖的驱动下发生了显著变化, 对全球和区域尺度的降水格局产生了深刻的影响, 引起降水量、

降水季节分配和降水强度的改变^[1-2]。降水变化主要通过改变土壤水分来影响生态系统的功能与过程。森林生态系统是最大的陆地碳库^[3], 其碳循环

过程的变化对全球气候系统具有重要的调控作用。区域降水变化可能会对森林生态系统碳循环过程及其通量产生直接影响。模型预测结果显示, 21 世纪中国降水变化趋势呈现南北分异, 北方地区降水将显著减少, 中部、东部以及南方地区夏季降水将显著增加, 而冬季降水增加不明显^[4]。2007 年 IPCC 第 4 次评估报告则预测中国北方温带地区本世纪降水量有 5%~20% 的小幅增加, 而且未来干旱、洪涝等极端气候事件发生的频率也会增加^[2]。不同的模型对于北方地区未来降水格局变化预测的结果不同, 正是由于这种不确定的存在, 非常有必要同时进行降水减少和降水增加两种情景的模拟, 来研究未来降水变化对森林生态系统碳循环的影响。

土壤呼吸(soil respiration)是土壤微生物、动物和植物的地下部分(根和根茎)产生 CO_2 的过程^[5]。土壤呼吸是陆地上仅次于光合作用的第二大碳通量^[6], 占全球陆地生态系统总呼吸的 60%~90%^[7]。由于土壤呼吸释放碳的速率远高于人类活动释放碳的速率, 因此土壤呼吸的微小变化能显著地改变大气 CO_2 的平衡^[8], 在调控区域和全球尺度的碳循环上起着关键作用。

土壤温度和水分是影响土壤呼吸的重要环境因子。土壤呼吸对温度变化的响应通常采用 Q_{10} 来表示, 即温度每升高 10°C , 土壤呼吸速率所增加的倍数^[9]。在生物化学水平上, Q_{10} 的测量值通常在 2 左右, 即: 温度每升高 10°C , 呼吸速率就增长一倍。估算的土壤呼吸 Q_{10} 因地理位置和生态系统类型的不同而相差很大, 从略大于 1 (低敏感性) 直到大于 10 (高敏感性)^[5]。土壤水分通过影响底物或氧气的扩散来调控土壤呼吸速率^[10] 和土壤呼吸温度敏感性^[11]。土壤水分和温度对 CO_2 和 O_2 扩散的复杂交互作用以及根和微生物活性, 都可能导致土壤 CO_2 通量的温度敏感性对水分有效性产生不同的响应^[5]。

降水对生态系统地下生物化学过程具有重要的调控作用, 会直接影响土壤呼吸。短期内, 单次的降水事件可能会因降水取代土壤孔隙中的空气, 使之从土壤中迅速排出, 或使微生物活动增强或数量增加而强烈地激发土壤呼吸, 也可能因为土壤孔隙中过多的水分影响 CO_2 扩散而产生阻滞效应^[12]。为了研究长期降水变化会对土壤呼吸产生什么影响, 国外研究者利用降水控制实验进行了不同情景的模拟。在美国大平原南部草地的控制实验中, 增雨促进了干旱季节的土壤 CO_2 通量, 但不同的水分添加

量对土壤呼吸的影响不同^[13]。在 Kanza 高草草原, 自然降雨量减少 70% 时, 季节平均土壤呼吸速率降低了 8%; 改变降水时间, 土壤呼吸速率降低 13%; 而在这两种改变同时发生时, 土壤呼吸速率降低 20%^[14]。以上这些研究多是在草地生态系统进行的, 有关降水变化对森林土壤呼吸的影响研究还很少。在哈佛森林(温带落叶阔叶林)进行的生长季遮雨极端干旱模拟实验中, 遮雨处理明显降低了土壤呼吸速率和累积量^[15]。而在美国橡树岭国家实验室温带落叶阔叶林穿透雨转移实验中, 增加或减少 33% 穿透雨对森林土壤呼吸没有显著影响^[16]。

长期的降水变化会对森林生态系统土壤呼吸产生何种影响? 是降水增加导致土壤呼吸增加、降水减少土壤呼吸减少, 还是森林生态系统比较稳定, 土壤呼吸对长期的降水变化不敏感? 土壤水分是影响土壤呼吸温度敏感性的主要因素^[17], 土壤呼吸速率和土壤呼吸表观温度敏感性 Q_{10} 对降水变化的响应方式是否会有所不同? 为了回答这些问题, 我们在河北塞罕坝地区樟子松(*Pinus sylvestris* var. *mongolica*) 人工林中进行了增加和减少 30% 穿透雨的降水控制实验, 来检验长期降水变化对森林土壤呼吸的影响。了解森林土壤呼吸及其温度敏感性对降水变化的响应, 对于预测在全球变暖背景下的降水格局变化对陆地生态系统碳收支的影响, 具有重要的意义。

1 研究区概况与方法

1.1 研究区概况

塞罕坝地区位于河北省承德市围场满族蒙古族自治县北部, 包括坝上和接坝地区两部分, 是内蒙古高原、大兴安岭山系与冀北山地交汇之处, 也是内蒙古浑善达克沙地的东南边缘。气候区划属半干旱半湿润气候区, 处于暖温带向温带的过渡带。冬季漫长而寒冷; 春秋季较短, 干燥多风; 夏季不明显, 气候凉爽。无霜期短, 平均 60 天左右, 昼夜温差大, 年平均气温 -1.4°C 。降水以降雨为主, 降雪为辅, 降水量偏少, 多集中在 6—9 月, 年平均降水量 454.2 mm, 最大年降水量 636.0 mm, 最小年降水量 258.0 mm, 年均降水日数 134 天。年平均蒸发量为 1244.4 mm。年均 6 级(强风)以上大风日 76 天, 以西风或西北风为主。积雪长达 7 个月, 最大冻土深 168 cm^[18-19]。坝上地区以风沙土为主, 兼有草甸土和沼泽土, 主要成土母质为风积物、残积物、堆积

物及冲积物等^[18]。

塞罕坝地区位于我国境内 3 条全球变化样带的交汇处^[20], 是全球变化研究的关键区域。作为森林-草原过渡带, 这一地区对气候变化敏感, 是气候变化的良好指示体。特殊的地理位置、复杂的自然条件使塞罕坝地区具有独特的生态学意义, 是进行大规模气候控制实验、探讨全球变化生态响应的理想区域。

1.2 研究地点概况

降水控制实验样地位于北京大学地球环境与生态系统塞罕坝实验站西侧的樟子松人工林内。海拔 1531 m, 地理坐标为 42°25'N, 117°15'E, 位于阳面缓坡中上部。样地东侧距林缘 100 m, 南侧距林缘 20 m。土壤类型为风沙土, 乔木平均胸径约 12 cm, 平均树高约 9 m, 林下灌木稀少, 草本层以披针叶苔草 (*Carex lanceolata*)、腺毛委陵菜 (*Potentilla longifolia*)、地榆 (*Sanguisorba officinalis*)、瓣蕊唐松草 (*Thalictrum petaloideum*) 等为主。样地选址综合考虑了林分密度、地形均匀度和电力供应。

1.3 降水控制实验设计

降水控制实验样地占地 1 hm², 采取正交试验设计, 设置了 9 个 20 m×20 m 的样方。包括 3 种穿透雨处理: 1) 自然穿透雨量(对照); 2) 穿透雨减少 30% (减雨 30%), 用覆盖地表面积 30% 的薄膜水槽转移走该样方 30% 的穿透雨量(图 1(a)); 3) 穿透雨增加 30% (增雨 30%), 把减雨样方转移来的 30% 穿透雨用固定在地表的喷灌系统增加到该样方, 从而实现穿透雨的有效截流与转移。每种处理 3 个重复, 水平方向上 3 个不同的处理为一组, 各样方间距 10 m 作为缓冲带。

在每个减雨样方中, 12 条离地 1.5 m 并用镀锌管支撑呈一定倾斜角度的 0.5 m×20 m (覆盖地表 30%) 无色透明塑料薄膜水槽将穿透雨汇集到 2000 L 的黑色 PE 卧式水箱中(图 1(b)), 水罐中的浮球阀开关可以自动控制喷灌系统, 当水位到达预定高度, 自动将雨水喷灌到相应的增雨样方中, 实现穿透雨的有效截流与转移。这种控制方式只改变降水量不改变降水频率。

1.4 生长季土壤呼吸速率测定及表观 Q_{10} 估算

土壤呼吸速率测定采用 LI-8100 开路式土壤碳通量测量系统(LI-COR Inc., Lincon, NE, USA)。测定环(soil collar)是内径 10 cm, 高度 5 cm, 一端磨尖 PVC 管。每个样方中布置 5 个测定环。在首次测量前一天, 选择地表无植物生长的地方(人工林林下草本植物盖度较低), 将测定环用橡皮锤和木条砸到需要测定的位置, 使测定环上沿水平, 距地表约 2~3 cm, 为防止插入时对土壤的干扰, 稳定 1 天后进行测定。

从 6 月到 9 月, 每两周测一次土壤呼吸。用钢卷尺测量测定环内侧地表至环顶的距离, 间隔 90° 在 4 个方向上测量测定环高出土壤表面的距离 (collar offset), 求平均值后输入 PDA。用 LI-8100 测量土壤 CO₂ 通量, 每个测定环上重复测量 3 次取平均值作为当次测量值。在仪器测量前, 把 LI-8100 配套的热传感器或探针式温度计插入土中 10 cm, 在数据稳定后, 记录土壤温度数据。在仪器测量过程中, 用 Field Scout TDR 100 土壤水分速测仪(Spectrum Technologies, Plainfield, IL, USA)间隔 120°, 在测定环周边 3 个不同位置上测定 10 cm 处土壤体积含



图 1 穿透雨减少样方

Fig. 1 Throughfall displacement plot

水量并记录。

基于 3 个生长季内对土壤呼吸的原位测定, 我们把各个样方的所有土壤呼吸速率 SR 及其测量时相应的 10 cm 土壤温度 T 代入 van't Hoff 指数方程, 计算其参数 a 和 b :

$$SR = ae^{bT}, \quad (1)$$

土壤呼吸表观温度敏感性 Q_{10} 可通过以下公式计算得到:

$$Q_{10} = e^{10b}. \quad (2)$$

1.5 统计分析

用每个样方 5 个测定环的土壤呼吸速率平均值作为该样方当次测量的土壤呼吸速率, 3 个生长季内共 126 条土壤呼吸速率数据(14 次测定 \times 9 个样方)。因原始数据不符合正态分布, 采用非参数方差分析方法 Kruskal-Wallis 秩和检验(Kruskal-Wallis rank sum test)与箱线图(box plot)来比较 3 种穿透雨处理的土壤呼吸速率的差异。在对原始数据取自然对数进行正态化处理后, 用重复测量方差分析(repeated measures ANOVA)来分析穿透雨处理和测定日期对生长季土壤呼吸速率的影响。其中, 以样方作为研究对象, 穿透雨处理作为组间效应, 测定日期及其与穿透雨处理的交互作用作为组内效应。选择适用于重复测量数据多重比较的 Bonferroni 校正配对 t 检验(paired t -test)来比较不同处理土壤呼吸速率时间序列两两之间的差异, 以减少犯 I 类错误的概率。对每种处理地下 10 cm 土壤体积含水量和土壤温度时间序列也进行了配对 t 检验。用单因素方差分析比较穿透雨对土壤呼吸表观温度敏感性 Q_{10} 的影响。用 Tukey HSD (honest significant difference)检验对 Q_{10} 均值进行多重比较。统计显著性检验水平均为 $\alpha=0.05$ 。统计分析与绘图在 R 软件 (Version 2.14.0, R Foundation for Statistical Computing, Vienna, Austria)中进行^[21]。

2 结果

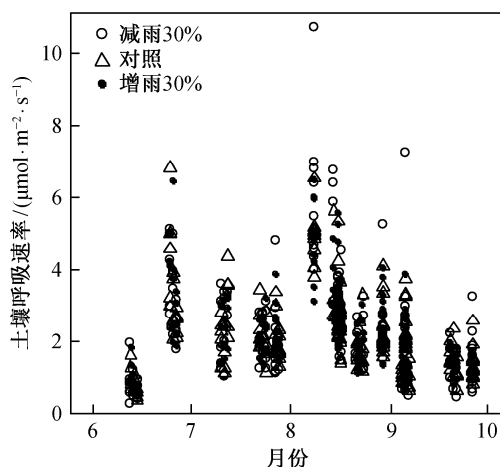
2.1 生长季土壤呼吸对降水变化的响应

2006—2008 年生长季土壤呼吸速率的定期连续测定结果显示, 塞罕坝樟子松人工林生长季的土壤呼吸速率正如我们所预期的模式, 随着季节变化基本呈现单峰的形态(图 2)。这可能是因为塞罕坝气候具有雨热同期的特点, 生长季降水占年降水量的 80%以上。

在图 2 中, 减雨处理的土壤呼吸速率似乎较高,

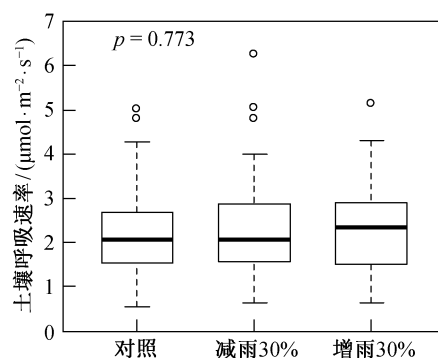
最大值也出现在减雨处理 8 月份, 那么减雨处理的土壤呼吸速率是否高于其他处理? 我们用箱线图直观地对比了 3 种穿透雨处理生长季土壤呼吸速率的差异(图 3)。由图 3 可知, 虽然减雨处理的离群值高于对照和增雨, 但是增雨处理的土壤呼吸速率总体来说数值较高, 该处理的中位数(2.340 $\mu\text{mol}/(\text{m}^2\cdot\text{s})$) 高于对照 (2.065 $\mu\text{mol}/(\text{m}^2\cdot\text{s})$) 和减雨处理 (2.050 $\mu\text{mol}/(\text{m}^2\cdot\text{s})$), 而 Kruskal-Wallis 秩和检验结果却表明, 3 种处理间并无显著差异($p=0.773$)。

箱线图仅显示了各处理土壤呼吸速率测定值总



数据点为 2006—2008 年 3 种穿透雨处理所有的土壤呼吸速率测定值

图 2 2006—2008 年生长季土壤呼吸速率的季节动态格局
Fig. 2 Seasonal pattern of growing seasons soil respiration rates for the combined dataset from 2006 to 2008



每个箱体的 5 条横线自上而下分别为该处理土壤呼吸速率的最大值、上四分位数、中位数、下四分位数和最小值。圆圈为离群值。 p 值为 Kruskal-Wallis 秩和检验显著性检验结果

图 3 2006—2008 年生长季 3 种穿透雨处理的土壤呼吸速率对比箱线图

Fig. 3 Box plot of growing season soil respiration rates of throughfall treatments from 2006 to 2008

体的分布情况, Kruskal-Wallis 检验说明的也只是 3 种处理所有测定值的比较结果, 由于土壤呼吸存在明显的季节动态变化, 同一处理不同测定日期的差异也较大(图 2), 那么对于各测定日期的土壤呼吸速率穿透雨处理的效应又会如何? 我们对每个样方生长季土壤呼吸速率平均值的自然对数时间序列进行了重复测量方差分析(表 1)。结果表明, 穿透雨处理对土壤呼吸速率总体上无显著影响 ($p=0.295$), 测定日期对土壤呼吸速率有显著影响 ($p<0.001$), 二者的交互作用无显著影响 ($p=0.997$)。

虽然重复测量方差分析结果也表明 3 种穿透雨处理对土壤呼吸速率统计上无显著影响(表 1), 但是由于土壤呼吸速率季节变化大, 而处理间差异相对较小, 为了具体比较不同穿透雨处理土壤呼吸速率对降水变化响应的差异, 我们对各处理的生长季土壤呼吸速率平均值时间序列两两之间进行了配对 t 检验(表 2)。

3 种穿透雨处理土壤呼吸速率的平均值 \pm 标准差分别为: 减雨处理 $2.324\pm1.175\text{ }\mu\text{mol}/(\text{m}^2\cdot\text{s})$, 对照 $2.221\pm0.941\text{ }\mu\text{mol}/(\text{m}^2\cdot\text{s})$, 增雨处理 $2.343\pm0.954\text{ }\mu\text{mol}/(\text{m}^2\cdot\text{s})$ 。配对 t 检验多重比较的结果表明, 增雨处理土壤呼吸速率的平均值显著高于对照($p=0.0005$), 减雨与对照、减雨与增雨的土壤呼吸速率无显著差异 ($p>0.05$)。在 3 种处理土壤呼吸速率平

均值的季节动态图中也可以观察到这样的规律(图 4(a)), 增雨处理土壤呼吸速率的平均值在多数测定日期都高于减雨和对照, 而减雨和对照的曲线经常重合在一起。

对土壤体积含水量和土壤温度的配对 t 检验结果也表明, 10 cm 土壤体积含水量大小正如我们所预期的一样, 增雨 30% $>$ 对照 $>$ 减雨 30% (图 4(b))($p<0.05$); 3 种处理的 10 cm 土壤温度无显著差异($p>0.05$), 但减雨处理的温度平均值略高于对照和增雨(图 4(c))。在图 4 中也可以观察到 2006 年 8 月 9 日的土壤呼吸速率、土壤体积含水量和土壤温度都高于其他测定日期, 这次测定的贡献可能是导致季节动态图(图2)中 8 月份出现土壤呼吸速率峰值的主要因素。

2.2 土壤呼吸温度敏感性对降水变化的响应

降水控制实验样地的土壤呼吸表观温度敏感性 Q_{10} 平均值 \pm 标准差为 2.315 ± 0.293 , 变幅为 1.908 ~ 2.668。穿透雨处理显著地改变了样地的土壤水分, 为了研究樟子松人工林土壤呼吸温度敏感性对土壤水分改变的响应, 我们分析了 3 种穿透雨处理的土壤呼吸表观 Q_{10} 。对各样方表观 Q_{10} 的单因素方差分析结果表明(表 3), 穿透雨处理对土壤呼吸表观 Q_{10}

表 1 穿透雨处理与测定日期对土壤呼吸速率影响的重复测量方差分析表
Table 1 Repeated measures ANOVA of effects of throughfall treatments and determination dates on soil respiration rates

方差来源		自由度	平方和	均方和	<i>F</i>	<i>p</i>
组间效应	穿透雨处理	2	0.075	0.037	1.505	0.295
	残差	6	0.149	0.025		

组内效应	测定日期	13	25.447	1.958	56.902	<0.001
	处理 \times 测定日期	26	0.327	0.013	0.366	0.997
	残差	78	2.683	0.034		

说明: 重复测量方差分析所用数据为经过自然对数变换正态化后的土壤呼吸速率。

表 2 3 种穿透雨处理土壤呼吸速率的配对 t 检验统计值表
Table 2 Paired t -test among soil respiration rates of three throughfall treatments

处理间比较	自由度	差值	差值的 95%置信区间	<i>t</i>	<i>p</i>
减雨 30%与对照	13	0.103	-0.066~0.271	1.318	0.210
减雨 30%与增雨 30%	13	-0.019	-0.208~0.169	-0.221	0.829
增雨 30%与对照	13	0.122	0.065~0.179	4.611	0.0005

说明: 土壤呼吸速率单位为 $\mu\text{mol}/(\text{m}^2\cdot\text{s})$ 。

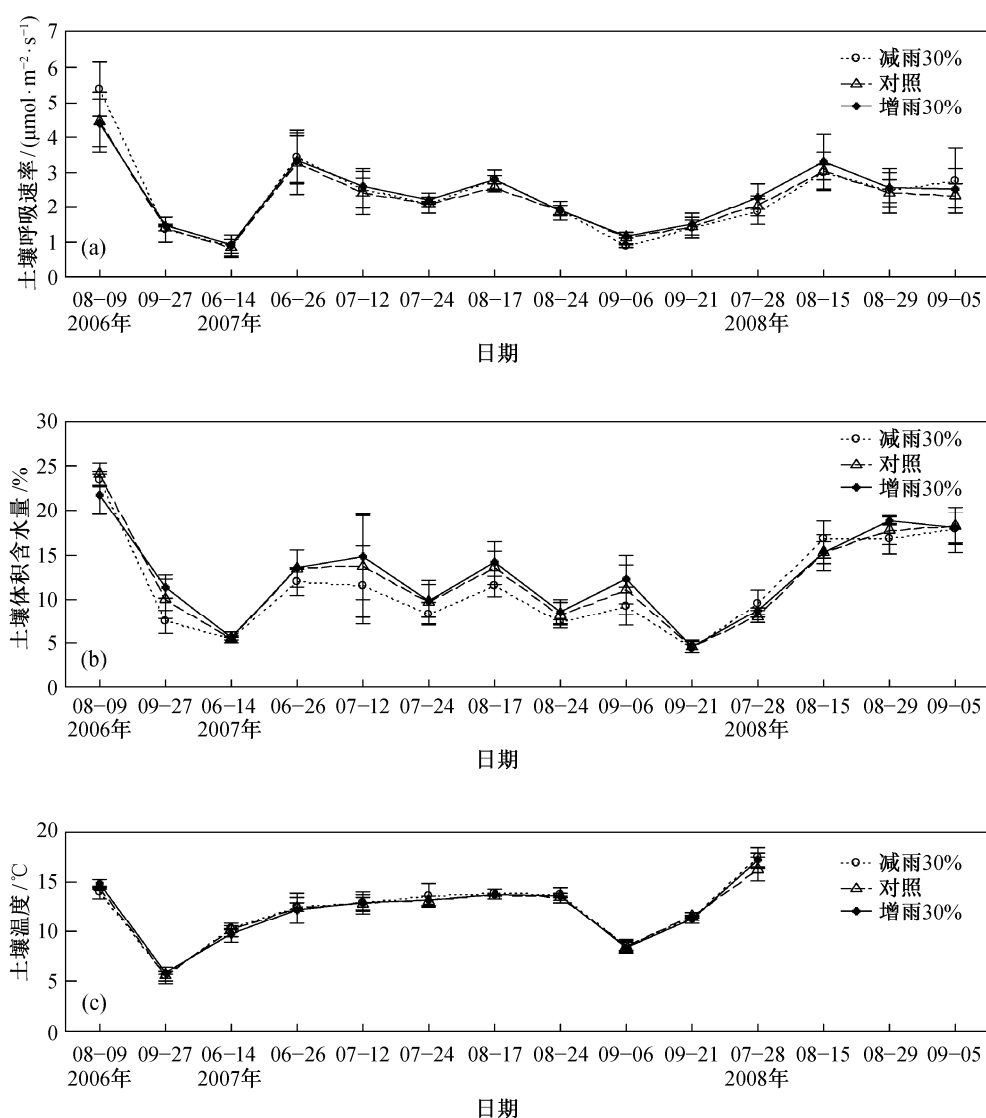


图 4 2006—2008 年生长季的土壤呼吸速率(a), 地下 10 cm 土壤体积含水量(b)和土壤温度(c)
Fig. 4 Soil respiration rates (a), soil volumetric water content (b) and soil temperature (c) at 10 cm depth in growing seasons from 2006 to 2008

统计上无显著影响($p=0.844$)。但由 Tukey HSD 多重比较可发现, 表观 Q_{10} 的平均值大小为减雨 30% < 对照 < 增雨 30% ($p>0.05$), 随着降水量增加, 表观 Q_{10} 有逐渐增大的微弱趋势(图 5)。

表 3 穿透雨处理对土壤呼吸表观 Q_{10} 效应的单因素方差分析表

Table 3 One way ANOVA of throughfall treatment effects on apparent Q_{10} of soil respiration

方差来源	自由度	平方和	均方和	F	p
穿透雨处理	2	0.038	0.019	0.175	0.844
残差	6	0.648	0.108		

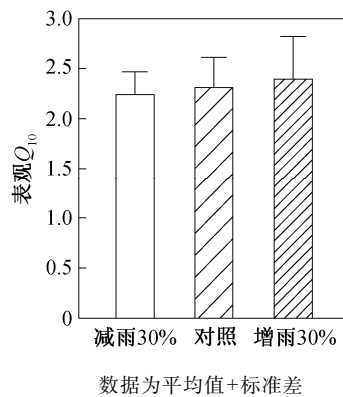


图 5 3 种穿透雨处理的土壤呼吸表观 Q_{10}
Fig. 5 Apparent Q_{10} of soil respirations among three throughfall treatments

3 讨论

3.1 降水变化对生长季土壤呼吸速率的影响

降水变化首先会显著地改变土壤水分。通常认为土壤呼吸与土壤水分之间的关系是: 土壤 CO_2 通量在干燥条件下较低, 在中等土壤水分水平时最大, 当含水量很高、厌氧条件占优势导致好氧微生物的活性受到抑制时又下降; 最适的含水量是接近田间持水量, 这时大孔隙空间大部分充满空气, 利于氧气扩散, 小孔隙空间大部分充满水, 利于可溶性底物的扩散^[5]。一些室内研究的结果表明, 在最适土壤含水量时土壤呼吸速率最大, 很多野外测量的结果则表明土壤水分只有在最低和最高的情况下才会抑制 CO_2 通量^[13,22]。在本研究中, 增雨处理的土壤含水量虽然高于对照和减雨, 但通常还未达到田间持水量, 因此对土壤呼吸始终具有促进作用。减雨处理的土壤体积含水量虽然最低, 但可能也未到足以限制土壤呼吸的程度。此外, 由于土壤水分与土壤温度存在交互作用, 同样的热量进入不同含水量的土壤时, 含水量较低的土壤温度相对较高。减雨处理的土壤体积含水量较低, 但土壤温度略高 ($p > 0.05$), 这也可能是它的土壤呼吸速率没有如预期的那样低于对照, 而是与对照无显著差异。

土壤呼吸组分对降水变化的敏感性不同, 异养呼吸比自养呼吸更为敏感, 这是由于植物根系和微生物对不同深度土壤水分的响应不同导致的。在美国哈佛森林的生长季遮雨极端干旱模拟实验中, 遮雨处理明显降低了土壤呼吸速率和累积量, Borken 等^[15]认为这主要归因于土壤异养呼吸的减少。在降水控制实验中, 2007 年生长季也研究了土壤微生物量碳与土壤有机碳的比值, 该比值可以作为土壤微生物数量的表征, 而且可以部分消除由土壤有机质异质性引起的差异。虽然重复测量方差分析结果表明总体上穿透雨增加和减少 30% 对土壤微生物量碳与土壤有机碳的比值的影响统计上并不显著 ($p = 0.193$), 但除了 5 月, 该比值在其他月份都呈现增雨 30% > 对照 > 减雨 30% 的规律^[23]。这说明随着降水量增加, 土壤微生物的数量有所增加, 虽然增加的幅度还不足以达到统计显著性, 但也可能导致异养呼吸随之增加。

哈佛森林控制实验中在林下用 5 m × 5 m 的遮雨棚完全移除穿透雨来模拟生长季极端干旱情景, 这明显地降低了土壤呼吸速率^[15]。而在 Walker

Branch 落叶阔叶林的穿透雨转移实验中, 增加或减少 33% 穿透雨对森林的土壤呼吸没有显著影响^[16]。这也说明, 我们的降水控制实验模拟的 30% 的穿透雨改变量可能比较温和, 虽然这更接近于自然降水格局长期的变化, 但减少 30% 穿透雨量对土壤呼吸的抑制作用可能还不够, 不足以引起生长季土壤呼吸速率的响应。

3.2 降水变化对土壤呼吸温度敏感性的影响

由于土壤水分与温度的相互作用, 土壤水分处理也会影响土壤呼吸温度敏感性^[5]。土壤水分通过影响底物或氧气的扩散来调控土壤呼吸速率^[10]和土壤呼吸温度敏感性^[11]。在干旱条件下, 土壤水分是土壤呼吸季节和年际变化的主要驱动因子, 土壤呼吸对温度的响应也受到土壤水分的限制^[24]。在北美高草原的一项研究中发现, 干湿交替的时间延长时, 土壤 CO_2 通量对土壤含水量比对土壤温度更敏感^[25]。在排水良好的土壤中, 土壤水分的降低会限制微生物对底物的利用, 导致土壤呼吸温度敏感性的降低^[4,26]。在本研究中, 随着降水量增加, 土壤呼吸表观 Q_{10} 有逐渐增大的微弱趋势, 这与以上研究结果一致。我们的研究结果也意味着在全球变暖的背景下, 如果降水量增加, 可能会导致生态系统土壤呼吸温度敏感性也相应增加, 这种增加可能会抵消掉一部分由于土壤呼吸对温度升高的适应性而导致的温度敏感性降低, 使得土壤呼吸在未来气候变化情景下变化的不确定性增加。

此外, 由 van't Hoff 指数模型得到的表观 Q_{10} 值是单一的, 用来预测土壤呼吸时会在高温时高估, 低温时低估土壤呼吸^[27], 既不能反映土壤呼吸温度敏感性随着温度升高而降低的适应性特征, 也不能反映土壤水分对土壤呼吸温度敏感性的影响。而在模拟和预测生态系统与气候系统的相互作用时, 又常常使用一个不变的 Q_{10} 值, 这都会导致模拟和预测的精度降低^[28]。如果在模型中考虑土壤呼吸 Q_{10} 的温度适应性和土壤水分或降水量对 Q_{10} 的影响, 将有利于提高这些模型的精度, 更准确地预测生态系统碳收支的变化。

4 结论与展望

3 种穿透雨处理(减雨 30%、增雨 30%、对照)对塞罕坝樟子松人工林生长季土壤呼吸速率和土壤呼吸表观温度敏感性 Q_{10} 总体上无统计显著效应。

由于土壤水分与土壤温度的交互作用, 生长季土壤呼吸速率和土壤呼吸温度敏感性对降水变化的响应方式有所不同。3 种穿透雨处理的生长季土壤呼吸速率平均值大小为对照<减雨 30%<增雨 30%, 其中, 增雨 30% 的土壤呼吸速率显著高于对照和减雨 30%; 土壤呼吸表观温度敏感性 Q_{10} 平均值大小为减雨 30%<对照<增雨 30%, 随着降水量增加, 表观 Q_{10} 有逐渐增大的微弱趋势。

就未来降水格局变化而言, 降水量减少 30% 可能对森林土壤呼吸的限制较小, 而降水量增加 30% 则可能显著地增加土壤呼吸(尤其是异养呼吸) CO_2 释放量, 从而导致森林净生态系统生产力(NEP)降低。在全球变暖的背景下, 如果降水量增加, 森林土壤呼吸温度敏感性也可能随之增加, 土壤呼吸和气候变暖之间的正反馈作用也会因降水量增加而加强, 对森林生态系统碳循环产生深刻影响。

我们通常在降水 24 小时后的晴天测定土壤呼吸速率, 刻意避开降水事件发生 24 小时内土壤呼吸的高峰期, 但这也可能会低估土壤呼吸 CO_2 释放量。可以采用系统采样的方法, 按照确定的时间间隔而不是靠主观判断是否适合测量来进行测定, 并在工作量安排可行的范围内, 适当增加测量频率来减小误差。此外, 我们的降水控制实验只进行了 3 个生长季, 而且未具体区分土壤呼吸不同组分对降水变化响应的差异, 今后可以针对长期降水变化对森林生态系统土壤自养呼吸与异养呼吸的影响做进一步研究。

参考文献

- [1] Houghton J T, Ding Y, Griggs D J, et al. Climate change 2001: the scientific basis. Cambridge: Cambridge University Press, 2001
- [2] IPCC. WGI fourth assessment report. Climate change 2007: the physical science basis. Geneva: Intergovernmental Panel on Climate Change, 2007
- [3] Dixon R K, Brown S, Houghton R A, et al. Carbon pools and flux of global forest ecosystems. *Science*, 1994, 263: 185–190
- [4] Xu Y L, Huang X Y, Zhang Y, et al. Statistical analyses of climate change scenarios over China in the 21st century. *Advances in Climate Change Research*, 2006, 2(Suppl 1): 50–53
- [5] Luo Y, Zhou X H. 土壤呼吸与环境. 姜丽芬, 曲来叶, 周玉梅, 等, 译. 北京: 高等教育出版社, 2007
- [6] Raich J W, Potter C S. Global patterns of carbon-dioxide emissions from soils. *Global Biogeochemical Cycles*, 1995, 9(1): 23–36
- [7] Schimel D S, House J I, Hibbard K A, et al. Recent patterns and mechanisms of carbon exchange by terrestrial ecosystems. *Nature*, 2001, 414: 169–172
- [8] 崔骁勇, 陈四清, 陈佐忠. 大针茅典型草原土壤 CO_2 排放规律的研究. *应用生态学报*, 2000, 11(3): 390–394
- [9] 方精云. 全球生态学: 气候变化与生态响应. 北京: 高等教育出版社, 2000
- [10] Linn D M, Doran J W. Effects of water-filled pore space on carbon dioxide and nitrous oxide production in tilled and nontilled soils. *Soil Science Society of America Journal*, 1984, 48: 1267–1272
- [11] Gaumont-Guay D, Black T A, Griffis T J, et al. Influence of temperature and drought on seasonal and interannual variations of soil, bole and ecosystem respiration in a boreal aspen stand. *Agricultural and Forest Meteorology*, 2006, 140: 203–219
- [12] 陈全胜, 李凌浩, 韩兴国, 等. 水分对土壤呼吸的影响及机理. *生态学报*, 2003, 23(5): 972–978
- [13] Liu X Z, Wan S Q, Su B, et al. Response of soil CO_2 efflux to water manipulation in a tallgrass prairie ecosystem. *Plant and Soil*, 2002, 240(2): 213–223
- [14] Harper C W, Blair J M, Fay P A, et al. Increased rainfall variability and reduced rainfall amount decreases soil CO_2 flux in a grassland ecosystem. *Global Change Biology*, 2005, 11: 322–334
- [15] Borken W, Savage K, Davidson E A, et al. Effects of experimental drought on soil respiration and radiocarbon efflux from a temperate forest soil. *Global Change Biology*, 2006, 12(2): 177–193

- [16] Hanson P J, O'Neill E G, Chambers M L S, et al. Soil respiration and litter decomposition // Hanson P J, Wullschlegel S D. North American temperate deciduous forest responses to changing precipitation regimes. New York: Springer, 2003: 163–189
- [17] Xu M, Qi Y. Spatial and seasonal variations of Q_{10} determined by soil respiration measurements at a Sierra Nevada forest. *Global Biogeochemical Cycles*, 2001, 15(3): 687–696
- [18] 黄金祥, 李信, 钱进源. 塞罕坝植物志. 北京: 中国科学技术出版社, 1996
- [19] 郑成洋. 河北省塞罕坝森林结构与生物量[R]. 北京: 北京大学, 2005
- [20] 张新时, 杨奠安. 中国全球变化样带的设置与研究. 第四纪研究, 1995(1): 43–52, 99–100
- [21] R Development Core Team. R: a language and environment for statistical computing. R Foundation for Statistical Computing, Vienna, Austria. 2011, ISBN 3-900051-07-0. <http://www.R-project.org/>
- [22] Xu M, Qi Y. Soil-surface CO_2 efflux and its spatial and temporal variations in a young ponderosa pine plantation in northern California. *Global Change Biology*, 2001, 7: 667–677
- [23] 魏天凤, 任艳林, 曾辉, 等. 降水改变对樟子松人工林土壤微生物量碳及微生物商动态变化的影响. 北京大学学报: 自然科学版, 2009, 45(3): 533–540
- [24] Asensio D, Penuelas J, Llusia J, et al. Interannual and interseasonal Soil CO_2 efflux and VOC exchange rates in a Mediterranean holm oak forest in response to experimental drought. *Soil Biology & Biochemistry*, 2007, 39(10): 2471–2484
- [25] Bremer D J, Ham J M, Owensby C E, et al. Responses of soil respiration to clipping and grazing in a tallgrass prairie. *Journal of Environmental Quality*, 1998, 27(6): 1539–1548
- [26] Davidson E A, Janssens I A. Temperature sensitivity of soil carbon decomposition and feedbacks to climate change. *Nature*, 2006, 440: 165–173
- [27] Lloyd J, Taylor J A. On the temperature dependence of soil respiration. *Functional Ecology*, 1994, 8: 315–323
- [28] 方精云, 王妮. 作为地下过程的土壤呼吸: 我们理解了多少?. 植物生态学报, 2007, 31(3): 345–347

2011 年发表论文

Vegetation succession prevents dry lake beds from becoming dust sources in the semi-arid steppe region of China

Fengjun Zhao, Hongyan Liu*, Yi Yin, Guozheng Hu and Xiuchen Wu

College of Urban and Environmental Sciences and MOE Laboratory for Earth Surface Processes, Peking University, Beijing, P.R. China

Received 14 July 2010; Revised 21 October 2010; Accepted 30 October 2010

*Correspondence to: Hongyan Liu, College of Urban and Environmental Sciences and MOE Laboratory for Earth Surface Processes, Peking University, Beijing, 100871, P.R. China. E-mail: lhy@urban.pku.edu.cn

ESPL

Earth Surface Processes and Landforms

ABSTRACT: East Asian dust storms have become increasingly intense over the last two decades, and the arid inland regions of northern China have been recognized as the main dust source areas. Numerous lakes in this region have recently become desiccated, leaving large areas of bare ground prone to becoming potential dust sources. Vegetation cover characteristics and vegetation succession following lake desiccation remain unclear. Here we chose eight inland dry lakes, one outflow lake and one river on the southeast edge of the Inner Mongolian Plateau to investigate vegetation patterns along transects from lake bed to lake shore, and determine the relationships between vegetation patterns and environmental factors. The results show that dry lake bed soils do indeed have high contents of fine particles. Also, soil salt content is the most critical control on vegetation succession on desiccated lake beds, and vegetation is unlikely to colonize areas with soil salt content $\geq 5\%$. Soil texture additionally influenced vegetation patterns by affecting soil salt content. The likely vegetation succession on dry lake beds is *Nitraria tangutorum* community > *Suaeda corniculata* and *Suaeda glauca* communities > *Achnatherum splendens* and *Elymus sibiricus* communities, and finally *Carex duriuscula* community as the probable climax. When vegetation is at the later stages of succession, for example with *Achnatherum splendens* communities, *Elymus sibiricus* communities and *Carex duriuscula* communities, soil may be protected from wind erosion because of their high vegetation cover and high proportion of perennials. We suggest grazing should be avoided around lake shores, especially in *Achnatherum splendens* communities, because high vegetation cover and biomass not only protect soil from erosion, but also promote the deposition of fine particles blown from upwind regions. Copyright © 2010 John Wiley & Sons, Ltd.

KEYWORDS: dust storms; vegetation succession; wind erosion; soil salt content

Introduction

East Asian dust storms have become increasingly intense over the last two decades (Cyranoski, 2003). They are generated over dry/semi-dry areas by strong winds near cold fronts (Gao *et al.*, 2000; Husar *et al.*, 2001) and transport dust to northern, eastern and south-eastern China (e.g. Lin, 2001; Murayama *et al.*, 2001), across Korea and Japan (e.g. Chun *et al.*, 2001; Kanayama *et al.*, 2002a, 2002b), to the north Pacific Ocean (e.g. Chadwick *et al.*, 1999; Pettke *et al.*, 2000), North America (e.g. Tratt *et al.*, 2001; Husar *et al.*, 2001), and occasionally even to Greenland and Europe (e.g. Bory *et al.*, 2002; Grousset *et al.*, 2003). East Asian dust storms increase atmospheric aerosol loads, which cool the climate in downwind areas (Kaufman *et al.*, 2002), alter nutrient cycling in the Pacific Ocean (Bishop *et al.*, 2002), and have an impact on air quality and human health as far away as North America (Griffin *et al.*, 2001).

The arid inland regions of northern China have been recognized as the main dust source area for Asian dust emissions (e.g. Darmenova *et al.* 2005; Washington *et al.*, 2003). In this region, land cover types generally considered as contributing most of this dust are sand deserts (e.g. Zhang *et al.*, 1997), sandy lands (huge area of vegetation-covered sandy dunes, e.g. Zhang *et al.*, 2008) and Gobis (e.g. Sun *et al.*, 2000), which usually refers to stony deserts extending from southern Mongolia to northern China (Zhang *et al.*, 2008). However, degraded grassland, abandoned farmland (Yang *et al.*, 2008), and in particular dry lake beds, are recognized as important dust sources in recent studies (Yue *et al.*, 2004; Zhang *et al.*, 2008). Dry lake beds can provide much smaller particles (e.g. $<10\ \mu\text{m}$) during wind erosion than sand deserts and Gobis, but are effectively 'point sources' when compared with deserts (Yue *et al.*, 2004; Yang *et al.*, 2008). The fine lake bed particles are the main material involved in long-distance transport and can therefore affect the continental and even global climate (Wang *et al.*, 2005; Littmann,

1991). Whether dry lake beds become dust sources, however, depends on their vegetation cover (Yang *et al.*, 2008; Hoffmann *et al.*, 2008; Ravi *et al.*, 2010).

Prior to the 1990s, the Inner Mongolian Plateau in northern China held a wide distribution of lakes, of which about 90% were salt lakes (60–67%) or brackish lakes (32–26%) (Zheng *et al.*, 1992). Due to climatic warming, most of these lakes have dried up in recent years, leaving large areas of dry lake beds. Grasslands of the Inner Mongolian region are natural deposition areas for sand and dust carried by storms from upwind source areas (Li *et al.*, 2004; Wang *et al.*, 2000). Prompt development of vegetation cover following desiccation may prevent dry lake beds from becoming dust source areas. It is unclear how, following lake desiccation, vegetation cover and vegetation succession affect dust emissions from the dry regions of China (Yue *et al.*, 2004; Yang *et al.*, 2008).

Here, we chose the southeast edge of the Inner Mongolian Plateau as a study area for investigating changes in vegetation patterns from lake bed to lake shore, and the relationship between vegetation patterns and environmental factors. To understand more clearly how dry lake beds evolve into dust source areas, we have addressed the following questions: (1) how will vegetation succeed in desiccated lake beds; (2) how do soil salt content and sand content change during vegetation succession; and (3) how do changes in soil content contribute to vegetation succession? At the same time, we have attempted to determine which species or vegetation patterns are stable and most able to establish on dry lake beds, to direct regional vegetation restoration and dust emission reduction.

Material and Methods

Study area

The study was carried out on the south-eastern edge of the Inner Mongolian Plateau [41–42°N, 114–116°E, 1300–1800 m above seal level (a.s.l.)] in China (Figure 1). The region is located at the transition from a continental semi-humid climate to a semi-arid climate, and lies in the marginal area of Pacific monsoon influence characterized by long cold winters and warm wet summers. The mean annual temperature is around 2.5°C and diurnal temperature variations are large. The mean annual precipitation is about 370 mm, falling mainly in summer. The mean annual wind speed ranges from 3.4 to 4.3 m s⁻¹. Gales with wind speeds ≥ 17.2 m s⁻¹ occur on 60–80 days per year, mainly in spring and winter. The most widespread vegetation type is dry steppe, with *Stipa grandis*, *Stipa krylovii* and *Leymus chinensis* as dominant species (Liu *et al.*, 2006), while meadow, swamp and halophytic vegetation occur mainly in low-lying areas such as lake shores.

The study area used to include a number of lakes and marshes, covering an area of up to 400 km² and with a water storage of 3.8×10^8 m³ (Wang, 2000), however, things have changed since the late 1960s and severely since late 1990s (Li, 2007). Satellite images show that most of these inland lakes are now dry in all seasons, and the scattering of outflow rivers and lakes in the eastern part of the study area are now suffering insufficient water supply.

Methods

Field investigation

To represent different hydrological conditions, eight dry inland lakes were selected for vegetation surveying: Haxiatu Nuur (HXT, ~4 km²), East Ulan Nuur (DWL, ~7 km²), Jiuliancheng

Nuur (JLC, ~10 km²), Bai Nuur (Bai, ~2 km²), Xiaoyan Nuur (XY, ~1.5 km²), Dayan Nuur (DY, ~3 km²), Alamiao Nuur (ALM, ~1 km²) and Anguli Nuur (AGL, ~45 km²). One outflow lake (Hulun Nuur, ~8 km²) and one river (Shandian River) were selected for comparative studies (Figure 1). Only the lake bed of Haxiatu Nuur was covered by sparse vegetation and this was considered as a vegetation-covered lake bed; the other seven dry lake beds with almost no vegetation were considered as bare lake beds.

Locations of the 11 sites (two on the shores of Shandian River and one by each lake) are shown in Figure 1. At each site, a transect was established roughly perpendicular to the lake shore and across different vegetation zones. The first plot of each transect was located on the dry lake bed or close to the water's edge, and subsequent plots were located within each vegetation zone. From visual inspection of vegetation patterns in the field, four or five plots were set for each transect. Plant features, including the abundance, cover and height of each species, as well as land form features, were recorded in a total of 51 plots 2 m × 2 m. In addition, soil cores were taken for each plot to a depth of 50 cm or to the full soil depth for soils shallower than 50 cm. Soil samples were taken for every 10 cm using a 7 cm diameter auger. As there is one plot which only has 40 cm soil depth and another plot only 20 cm soil depth, a total of 251 soil samples was collected. The samples were air-dried, crushed and sieved using a 2-mm mesh (Ortiz *et al.* 1995).

Measurements of soil chemical properties

Total salt content for each sample was determined following a 1 : 5 dilution in deionized water and measurement by an EC200 salinometer (produced by Lovibond Tintometer Ltd, Germany). Total dissolved solid (TDS) was used as an indicator of salt content. The soil total organic carbon (TOC) was measured by the Walkley–Black procedure (Nelson and Sommers, 1996). The grain size distribution was measured in the liquid phase using a Malvern Mastersizer 2000 laser grain-size analyzer after chemical procedures to remove organic material, carbonate, and clay minerals (Konert and Vandenberghe, 1997).

Statistical analysis

Plant communities were identified using two-way indicator species analysis (TWINSpan) (Hill, 1979). The relationships between vegetation types and environmental characteristics were examined using canonical correspondence analysis (CCA) (McCune and Mefford, 1997; Ter Braak, 1986) and quantile regression (Cade and Noon, 2003). Differences between the environmental characteristics for each plant community and each dominant species, and relationships between plant species and environmental factors were assessed using one-way analysis of variance (ANOVA). TWINSpan and CCA were carried out using PC-ORD v.3.17 (MjM Software, Gleneden Beach, OR, USA), quantile regression was performed using R2.6.2, and one-way ANOVA was performed with Microsoft Excel.

Results

Environmental factors

Lake bed soils were found to be finer than steppe soils in the study area. The fraction of particles with grain size ≤ 0.05 mm reached 80% in most of the investigated dry lake beds, compared with only 40% in the surrounding steppe (Figure 2). The very fine (≤ 0.01 mm) particle fraction was about 40% in dry lake beds, but only 20% in the surrounding steppe.

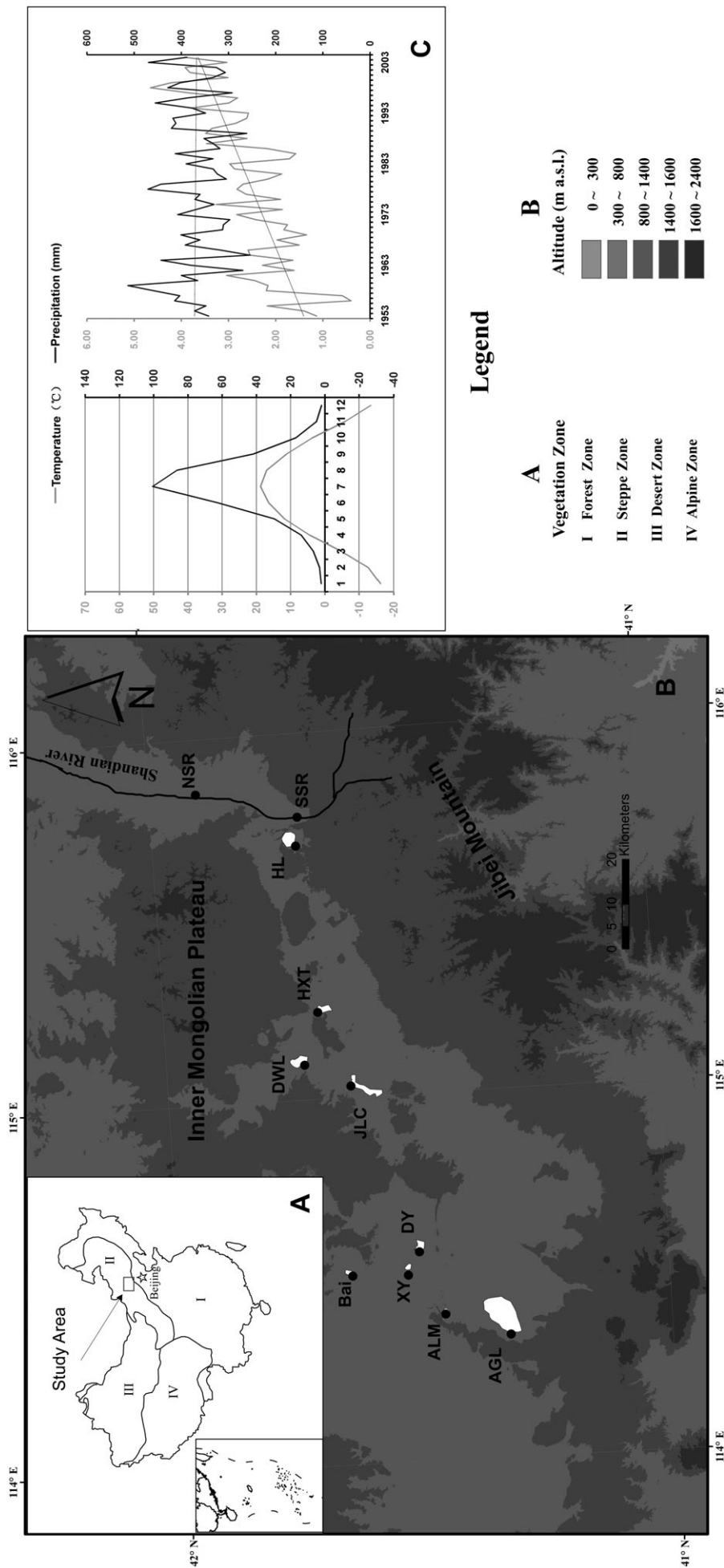


Figure 1. (a) Location of the study area in China. The star shows Beijing. (b) Map of study area and location of sample sites. The black line is the Shandian River and white polygons with black edge are lakes. Abbreviated lake names: AGL = Anguli Nuur, ALM = Alamiao Nuur, Bai = Bai Nuur, DWL = East Ulan Nuur, DY = Dayan Nuur, HXT = Haxiatu Nuur, JLC = Jilianchen Nuur, NSR = north Shandian River, SSR = south Shandian River, XY = Xiaoyan Nuur. (c) Monthly temperature and precipitation, and MAT and MAP trends from 1953 to 2003. The grey lines are temperature and the black lines are precipitation.

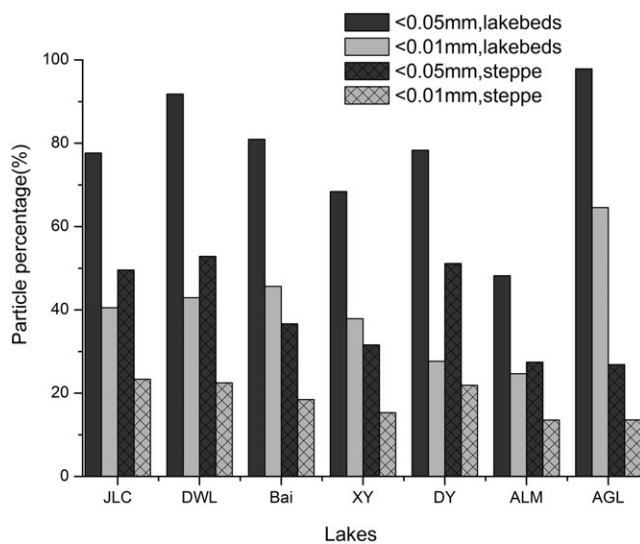


Figure 2. Dust content (%) of dry lake beds and steppe soil. The columns without grid lines are lake beds while columns with grid lines are the surrounding steppe. The dark grey columns show the content of particles <0.05mm while the light grey columns show the content of particles <0.01mm. Lake names follow those in Fig. 1.

Only the soil salt content showed significant differences between lake beds and lake shores (Table I). Lake beds always had higher soil salt content than lake shores, while no significant differences were found between lake beds and lake shores in terms of soil sand content and TOC. Both soil salt content and TOC showed significant negative correlations with soil sand content, but there was no significant correlation between soil salt content and TOC (Table II).

Plant community classification and descriptions

Across the 51 plots, a total of 59 species were recorded, of which 40 had cover values of $\geq 1\%$ in at least one plot and were thus included in the classification. The resulting classification distinguished seven plant community types as indicated by their dominants (Table I): the *Elymus sibiricus* community ($n = 7$), *Achnatherum splendens* community ($n = 10$), *Carex duriuscula* community ($n = 13$), *Chenopodium acuminatum* community ($n = 3$), *Suaeda corniculata* community ($n = 3$), *Suaeda glauca* community ($n = 4$) and *Nitraria tangutorum* community ($n = 4$). TWINSpan identified two main categories of plant communities at the first division level. The first category included the *Elymus sibiricus* community, *Achnatherum splendens* community, *Carex duriuscula* community and *Chenopodium acuminatum* community, and was mainly distributed along riverbanks or far from salt lake shores. The second category included the *Suaeda corniculata* community, *Suaeda glauca* community and *Nitraria tangutorum* and mainly appeared at or near salt lake shores.

Species richnesses of the *Suaeda glauca* and *Nitraria tangutorum* communities were significantly lower than those of the other plant communities ($p < 0.01$). Only the vegetation cover of the *Nitraria tangutorum* community was significantly smaller ($p < 0.05$) than that of other plant communities. The three plant community traits (biomass, vegetation cover and species richness) considered in this study had significant correlations with each other (Table II). However, among the three plant community traits, only aboveground plant community biomass was significantly distinguishable between the seven community types (Table I). Community biomass of the plant communities in

Table I. Plant community types, features and soil conditions.

Plant community (indicated by dominant species)	Distribution ^a	Species richness (number m ⁻²) (mean \pm SE) ^b	Vegetation cover (%) (mean \pm SE) ^b	Biomass (g m ⁻²) (mean \pm SE) ^b	Salt content (%) (mean \pm SE) ^b	TOC (%) (mean \pm SE) ^b	Sand (≥ 0.063 mm, %) (mean \pm SE) ^b
<i>Elymus sibiricus</i> + <i>Carex duriuscula</i> + <i>Iris pallasii</i> var <i>chinensis</i>	At riverbanks or far away from lake shores (7)	3.3 \pm 1.1a	58.6 \pm 9.0a	29.9 \pm 17.5a	0.32 \pm 0.22a	3.0 \pm 1.9a	48.4 \pm 23.6a
<i>Achnatherum splendens</i> + <i>Elymus sibiricus</i> + <i>Carex duriuscula</i>	At riverbanks or far away from lake shores (10)	3.3 \pm 1.2a	65 \pm 15.2a	85.6 \pm 76.1b	0.29 \pm 0.30a	1.3 \pm 0.8b	46.5 \pm 19.7a
<i>Carex duriuscula</i> + <i>Puccinellia macranthera</i> + <i>Potentilla anserina</i>	At riverbanks or far away from lake shores (13)	2.6 \pm 1.1a	61.4 \pm 18.5a	24.0 \pm 9.2c	0.37 \pm 0.29a	1.0 \pm 0.8b	60.0 \pm 23.7a
<i>Chenopodium acuminatum</i> + <i>Artemisia capillaris</i> + <i>Suaeda glauca</i>	Near lake shores (3)	2.7 \pm 0.6a	50 \pm 8.7a	78.2 \pm 51.6d	0.68 \pm 0.12a	1.1 \pm 0.3b	61.6 \pm 3.7b
<i>Suaeda corniculata</i> + <i>Puccinellia macranthera</i> + <i>Chenopodium acuminatum</i>	At or near lake shores (3)	1.1 \pm 0.3a	38.3 \pm 16.1a	18.5 \pm 9.8e	1.14 \pm 0.84b	1.4 \pm 1.0b	26.4 \pm 11.4a
<i>Suaeda glauca</i> + <i>Suaeda corniculata</i>	At lake shores(4)	0.5 \pm 0.2b	63.8 \pm 13.8a	31.3 \pm 29.6e	1.49 \pm 0.80b	1.0 \pm 0.7b	51.3 \pm 24.4a
<i>Nitraria tangutorum</i> + <i>Kalidium cuspidatum</i>	At lake shores(4)	0.6 \pm 0.1b	67.5 \pm 2.9b	38.0 \pm 15.1e	2.00 \pm 0.87b	2.8 \pm 0.9b	34.9 \pm 31.5a
None	Lake beds(7)	0	0	0	3.59 \pm 1.94b	1.4 \pm 0.7b	20.0 \pm 15.6a

a – Value in parenthesis gives the number of sites.

b – Values with different letters are significantly different between different sites ($p < 0.05$).

Table II. Correlations between plant community traits and environmental factors.

	Salt (%)	TOC	Sand (≥ 0.063 mm, %)	Vegetation cover (%)	Biomass (g m ⁻²)	Species richness (number m ⁻²)
Salt (%)	1					
TOC	-0.003	1				
Sand (≥ 0.063 mm, %)	-0.527**	-0.443**	1			
Vegetation cover (%)	-0.639**	0.054	0.401**	1		
Biomass (g m ⁻²)	-0.279*	0.009	0.068	0.475**	1	
Species richness (number m ⁻²)	-0.639**	0.479**	0.188	0.564**	0.330*	1

* Correlation is significant at the 0.05 level (two-tailed).

** Correlation is significant at the 0.01 level (two-tailed).

the second category was significantly less than that of plant communities in the first category.

Relationship between plant communities and environmental factors

The total soil salt contents of plant communities were significantly different between the two groups (Table I), showing that plant communities in the second category live in more saline soils. There was no significant difference in soil TOC among the seven plant community types, except for the soils of the *Elymus sibiricus* community, which had relatively higher TOC ($p < 0.05$). The *Chenopodium acuminatum* community may live on relatively more sandy soil, whereas soils of other plant community types showed no significant difference in sand content.

Soil salt content had a strong negative correlation (-0.969) with the first CCA axis (Figure 3a). Plant communities in the two categories were clearly distinguished on the first axis, whereas plant communities in the second categories were found in more saline environments. Clay/sand ratio and topsoil TOC showed some degree of positive correlation with the second axis, with values more than 0.75. The eigenvalues of the first and second axes were 0.686 and 0.307, respectively, and the first two CCA axes explained 99% of the variance in environmental factors.

Soil salt content showed significant negative correlation with all three plant community traits (Table II). TOC only showed significant correlation with species richness, but did show a weak relationship with biomass and vegetation cover. Sand content was only significantly correlated with vegetation cover.

Spatial variation of vegetation types in relation to the environmental factors

Variation in aboveground biomass with soil salt content Aboveground biomass varied greatly under low soil salt content conditions, even in the same plant community type, but was less variable and generally low under high soil salt content conditions (Figure 3b). Plant communities in the first category were generally distributed in soil with salt content $< 1\%$, while plant communities in the second category were mostly distributed in soil with salt content between 1% and 3%. 90th, 95th and 99th quantile regressions showed that the highest aboveground biomass was reduced remarkably with rising soil salt content (Figure 3b). When the soil salt content exceeded $\sim 5\%$, as was observed in three of the seven dry lake beds (East Ulan Nuur, DWL; Jiulianchen Nuur, JLC; Anguli Nuur, AGL; in Figure 3b), the community aboveground biomass was zero. The other four dry lake beds had relatively low soil salt content.

Variation in aboveground biomass with soil sand content Plant communities were distributed across a wide range of sand contents (Figure 3c), and sand content showed no significant correlation with aboveground biomass (Table II). No clear fit was found in the 90th, 95th or 99th quantile regression (not shown in the figure).

Aboveground biomass distributions with soil salt content and sand content

Aboveground community biomass was influenced by both salt and sand contents, as shown in Figure 3d where both the 90th and 95th quantile regressions show a clear negative trend. When the soil salt content increased, the upper sand content threshold for vegetation growth decreased. Linear regression for the *Carex duriuscula* community (dotted line in Figure 3d) showed a good fit ($R^2 = 0.7681$, $p < 0.001$), with sand content decreasing sharply as salt content increased (Fig. 3d). A similar trend was found in the *Suaeda corniculata* and *Nitraria tangutorum* communities. The *Elymus sibiricus* and *Achnatherum splendens* communities were mainly found in low salt content conditions, and across a wide range of sand contents. The *Chenopodium acuminatum* community was distributed in a relatively small range of conditions, whereas the *Suaeda glauca*-community seemed to be distributed across a wide range of both salt and sand contents.

Discussion

The desiccated lakes in our study area are potential dust sources. Particles with sizes < 0.01 mm can be transported over several thousands kilometers by light storms (wind speed up to 6 m s^{-1}) (Yang *et al.*, 2008), and may become major contributors to continental or even global climate change (Wang *et al.*, 2005; Littmann, 1991). In our study area, the grain size ≤ 0.05 mm fraction in the top sediments of most of the dry lake beds was about 80%, double that of the 40% found in the surrounding steppe communities. The fraction of particles available for long distance transport (grain sizes ≤ 0.01 mm) was 40%, again double that of the surrounding steppe communities. The Mongolian cyclone makes this area exposed to severe wind erosion (Darmenova *et al.* 2005; Washington *et al.*, 2003), so that vegetation colonization is the best choice for minimizing dust emission.

Vegetation conditions can influence the processes of dust emission and dust deposition (Hoffmann *et al.*, 2008), and the different vegetation succession stages may have different relationships with wind erosion. Our study shows that the vegetation succession order on salty lake beds may be *Nitraria tangutorum* community $>$ *Suaeda corniculata* and *Suaeda glauca* communities $>$ *Achnatherum splendens* and *Elymus sibiricus* communities, and finally *Carex duriuscula* commu-

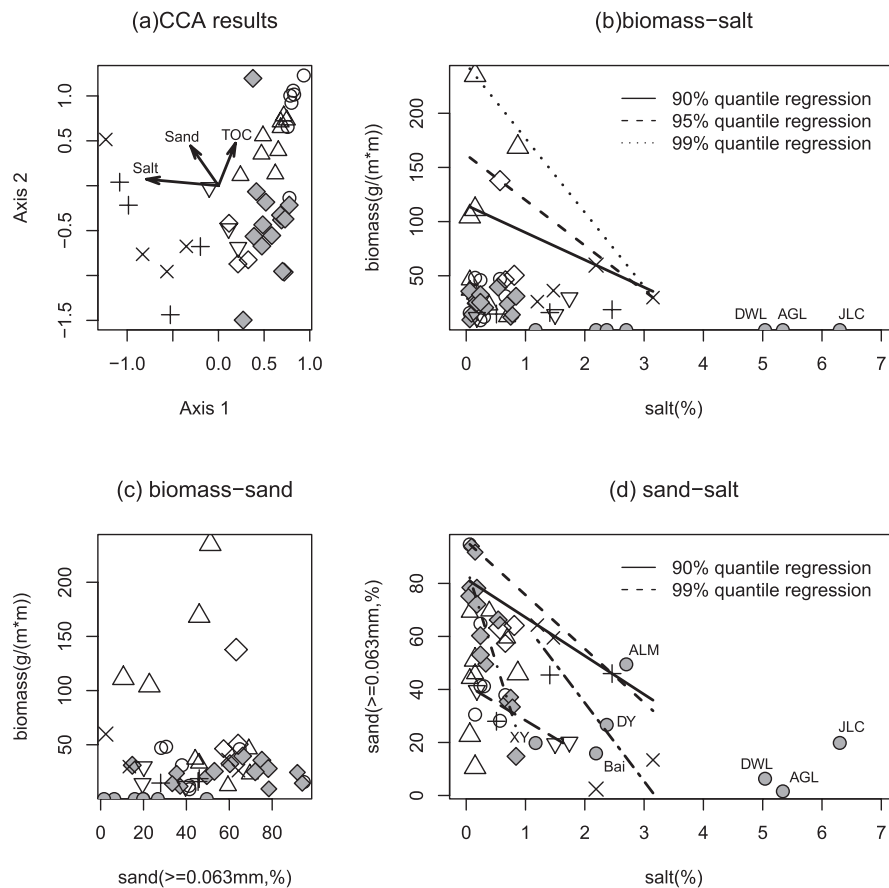


Figure 3. (a) CCA results. (b) Relationship between biomass and soil salt content. The 90th quantile regression equation is $y = 115 - 25x$. The 95th quantile regression equation is $y = 162 - 42x$. The 99th quantile regression equation is $y = 245 - 68x$. When $x \geq 5$ (%), all the three equations equal zero. (c) Relationship between biomass and sand content. The 90th, 95th and 99th quantile regressions do not yield a good fit (not shown). (d) Relationship between sand content and salt content. The 90th quantile regression equation is $y = 82 - 14.5x$. The 99th quantile regression equation is $y = 96 - 20x$. In Figs. 3a, 3b, 3c and 3d, plant communities are shown in different symbols, with the *Elymus sibiricus* community in open circle, the *Carex duriuscula* community in filled diamond, the *Achnatherum splendens* community in open triangle, the *Chenopodium acuminatum* community in open diamond, the *Suaeda glauca* community in plus, the *Suaeda corniculata* community in reversed open triangle, and the *Nitraria tangutorum* community in cross. Dry lake beds are shown as filled circle. In Fig. 3d, linear regressions for the *Carex duriuscula* community, the *Suaeda corniculata* community and *Nitraria tangutorum* community are showed by dotdash line, longdash line and twodash line, separately. Lake names follow those in Fig. 1.

nity as the probable climax, as indicated by the current vegetation zonation from lake bed to lake shore (Figure 4). Dry bare lake beds are easily eroded by wind to become dust source areas. The vegetation characteristics of pioneer communities such as the *Nitraria tangutorum* and *Suaeda corniculata* communities generally provide little soil protection, so that areas colonized by these communities remain as dust source areas. However, the intermediate stages of succession, dominated by *Suaeda glauca* communities and *Achnatherum splendens* communities, may play an important role in protecting soil from wind erosion. This is demonstrated by the relatively low sand content at this point in the succession (Figure 4), especially for the *Achnatherum splendens* communities, which always have high biomass. The subsequent stages with *Elymus sibiricus* communities and *Carex duriuscula* communities always have good vegetation cover and high proportion of perennials well-suited to protecting the soil from wind erosion.

Soil salt content was the most critical control on vegetation succession on desiccated lake beds. When the soil salt content was low, other factors such as TOC had an increased influence and led to large variations in aboveground biomass, whereas when the soil salt content was so high that it became the limiting factor, the aboveground biomass remained low and showed less variation. Saline stress is a common phenomenon

around the world, and it is estimated that >6% of the world's land and 30% of the world's irrigated areas already suffer from salinity problems (Unesco Water Portal, 2007). Our study showed that the highest aboveground biomass decreased markedly with increasing soil salt content, and that the lake beds of East Ulan Nuur, Jiuliancheng Nuur and Anguli Nuur had salt contents that were too high ($\geq 5\%$) to allow plant growth. If dry lake beds have relatively low soil salt content, some halophytes may colonize those lake beds when other environmental factors are not severe, especially dominant species in communities in the second category, such as *Suaeda corniculata*, *Suaeda glauca* and *Nitraria tangutorum*. The Haxiatu Nuur, Bai Nuur, Xiaoyan Nuur, Dayan Nuur and Alamiao Nuur lake beds belong to this type and the Haxiatu Nuur has already been covered by sparse *Suaeda corniculata* community.

Soil texture influenced vegetation pattern by affecting soil salt content. While sand content had no significant direct relationship with aboveground biomass in our study area (Table II), vegetation growth on high sand content soils was only observed at low salt content. When the soil salt content increased, the upper threshold of sand content for vegetation growth decreased. Salt is closely associated with clay particles (Williams and Hoey, 1987), and shortly after lake desiccation, the very fine clay particles at the surface easily retain saline

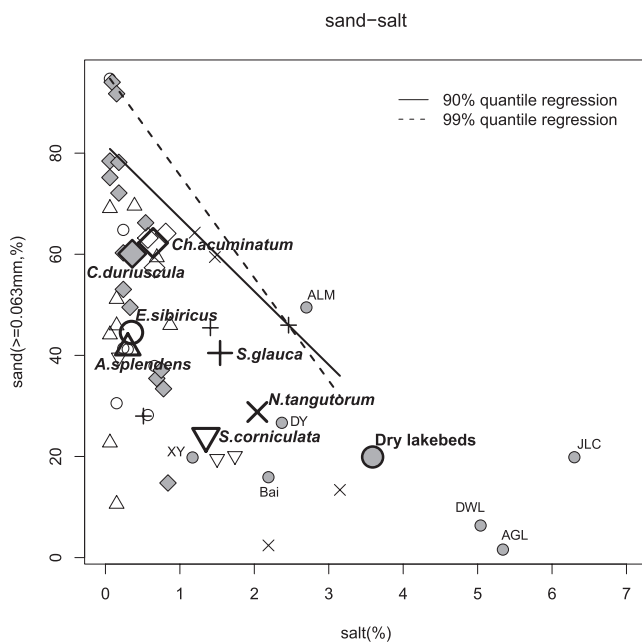


Figure 4. Sand and salt content of each plot. A possible plant community succession can be observed with changes in sand and salt contents in the soil. Symbols follow Fig. 3. Bold larger symbols are weighted averages of each plant community type. The bold larger open circle is the weighted average of the seven dry lake beds. Lake names follow those of Fig. 1.

materials. However, these particles are removed by the wind, with the result that soil salt content is reduced and sand content increases as desertification progresses. Once soil salt is sufficiently reduced (say, <5%), vegetation can begin to colonize the lake bed and start controlling the interaction between wind erosion, soil salt content and soil texture. In this way, wind erosion may act as driver of vegetation succession. The first colonizers might be *Nitraria tangutorum* communities, as they showed great adaptation to high salt stress (Figure 4). *Suaeda corniculata* and *Suaeda glauca* communities follow, growing in relatively less salty soil, and the latter may grow on soil with relatively high sand content. As the fine clay particles with saline material continue to be blown away, soil salt content keeps decreasing and sand content continues rising, and eventually *Achnatherum splendens* communities and *Elymus sibiricus* communities may become established. Finally, as salinity is further reduced the *Carex duriuscula* communities become established, and may be the climax communities. Those lake beds with relatively high sand content and therefore low salt content may skip the first stages of succession and start with *Suaeda glauca* communities or even *Achnatherum splendens* communities, and so on. Of course this succession model is ideal and it works only if there are no other special influencing factors or other mechanisms in place that would cause salt accumulation over time, for example saline groundwater with shallow water tables (Runyan and D'Odorico, 2010).

Our study also provides insights into regional vegetation conservation. *Chenopodium acuminatum* dominated communities in our study area grow in high sand content and relatively saline conditions, similar to the conditions that might be caused by exploitive human activities such as livestock grazing. These activities can therefore lead to new stable equilibria (e.g. Weetman *et al.*, 1990; Laycock, 1991), suggesting that human activities may have severe influences on vegetation succession and vegetation characteristics. The *Achnatherum splendens* community in our study region not only

had high biomass, but also had relatively high vegetation cover and species richness. As an intermediate stage, the sand content in *Achnatherum splendens* communities was quite low, indicating that this plant community type may enhance clay deposition, and protect soil from wind erosion. The same function of *Achnatherum splendens* was shown by Fan *et al.* (2006). We therefore suggest that grazing should be avoided in *Achnatherum splendens* communities.

Conclusions

From our study of soil conditions and vegetation changes from the lake bed to the lake shore, we conclude that the desiccated lakes in the study area are potential dust sources because of their high content of fine particles. Vegetation colonization is the best means of preventing dust release. Soil salt content is the most critical control on vegetation succession on desiccated lake beds and can prevent recolonization when soil salt content exceeds 5%. Soil texture influenced vegetation patterns due to its effect on soil salt content.

The general vegetation succession order on salty lake beds in this region may be *Nitraria tangutorum* community > *Suaeda corniculata* and *Suaeda glauca* communities > *Achnatherum splendens* and *Elymus sibiricus* communities, and finally the *Carex duriuscula* community as the probable climax. Dry lake beds that are bare or with vegetation at early stages of succession may become dust sources. When vegetation is in the later stages of succession, such as *Achnatherum splendens* community, *Elymus sibiricus* community and *Carex duriuscula* community (especially *Achnatherum splendens* community), soil may be protected from wind erosion owing to the high vegetation cover and density as indicated by the high aboveground biomass of these communities. We therefore suggest that grazing should be avoided in *Achnatherum splendens* communities.

Acknowledgments—This work was supported by the Beijing Municipal Natural Science Foundation (No. 6072015) and National Natural Science Foundation of China (No. 40771208). The authors would like to thank Yuke Zhang and Yunxiang Su for assisting with fieldwork and Weijie Miao for the laboratory work. The authors also thank Ji Ren and Siyuan He for their constructive comments and Dave Chandler for text editing.

References

- Bishop JKB, Davis RE, Sherman JT. 2002. Robotic observations of dust storm enhancement of carbon biomass in the North Pacific. *Science* **298**: 817–882.
- Bory AJ, Biscaye PE, Svensson A, Grousset FE. 2002. Seasonal variability in the origin of recent atmospheric mineral dust at North GRIP, Greenland. *Earth and Planetary Science Letters* **190**: 123–134.
- Cade BS, Noon BR. 2003. A gentle introduction to quantile regression for ecologists. *Frontiers in Ecology and the Environment* **1**(8): 412–420.
- Chadwick OA, Derry LA, Vitousek PM, Huebert BJ, Hedin LO. 1999. Changing sources of nutrients during four million years of ecosystem development. *Nature* **397**: 491–497.
- Chun Y, Kim J, Choi JC, Boo KO, Oh SN, Lee M. 2001. Characteristic number size distribution of aerosol during Asian dust period in Korea. *Atmospheric Environment* **35**: 2715–2721.
- Cyranoski D. 2003. China plans clean sweep on dust storms. *Nature* **421**: 101.
- Darmenova K, Sokolik IN, Darmenov A. 2005. Characterization of East Asian dust outbreaks in the spring of 2001 using groundbased and satellite data. *Journal of Geophysical Research* **110**(D2): D02204.

- Fan WB, Lei Y, Muo L, Zheng YK, Cheng B, Liu LY. 2006. Studies on improving microclimate of desert by *A. Splendens*. *Journal of Shihezi University (Natural Science)* **24**(2): 213–216 (in Chinese with English Abstract).
- Gao QX, Li LJ, Zhang YG, Hu M. 2000. Studies on the springtime dust storm of China. *China Environmental Science* **20**(6): 495–500 (in Chinese with English Abstract).
- Griffin DW, Kellogg CA, Shinn EA. 2001. Dust in the wind: long range transport of dust in the atmosphere and its implications for global public and ecosystem health. *Global Change & Human Health* **2**(1): 20–33.
- Grousset F, Ginoux P, Bory A, Biscaye PF. 2003. Case study of a Chinese dust plume reaching the French Alps. *Geophysical Research Letters* **30**: 10–11.
- Hill MO. 1979. *TWINSPAN – A Fortran Program for Arranging Multivariate Data in an Ordered Two-way 314 Table by Classification of the Individuals and Attributes*. Cornell University: Ithaca, NY.
- Hoffmann C, Funk R, Wieland R, Li Y, Sommer M. 2008. Effects of grazing and topography on dust flux and deposition in the Xilingele grassland, Inner Mongolia. *Journal of Arid Environments* **72**: 792–807.
- Husar RB, Tratt DM, Schichtel BA, Falke SR, Li F, Jaffe D, Gasso S, Gill T, Laulainen NS, Lu F, Reheis MC, Chun Y, Westphal D, Holben BN, Gueymard C, McKendry I, Kuring N, Feldman GC, McClain C, Frouin RJ, Merrill J, DuBois D, Vignola F, Murayama T, Nickovic S, Wilson WE, Sassen K, Sugimoto N, Malm WC. 2001. The Asian dust events of April 1998. *Journal of Geophysical Research* **106**: 18317–18330.
- Kanayama S, Yabuki S, Yanagisawa F, Motoyama R. 2002a. The chemical and strontium isotope composition of atmospheric aerosols over Japan: the contribution of long range-transported Asian dust (Kosa). *Atmospheric Environment* **36**: 5159–5175.
- Kanayama S, Yabuki S, Yanagisawa F, Abe O. 2002b. Geochemical features and source characterization from Sr isotopes of 'Kosa' particles in Red Snow that fell on Yamagata prefecture, NE Japan in January and March, 2001. *Journal of Arid Land Studies* **11**: 291–300.
- Kaufman YJ, Tanre D, Boucher O. 2002. A satellite view of aerosols in the climate system. *Nature* **419**: 215–223.
- Konert M, Vandenberghe J. 1997. Comparison of laser grain size analysis with pipette and sieve analysis: a solution for the underestimation of the clay fraction. *Sedimentology* **44**: 523–535.
- Laycock WA. 1991. Stable states and thresholds of range condition on North American rangelands: a viewpoint. *Journal of Range Management* **44**: 427–433.
- Li FR, Zhao LY, Zhang H, Zhang TH, Shirato Y. 2004. Wind erosion and airborne dust deposition in farmland during spring in the Horqin Sandy Land of eastern Inner Mongolia, China. *Soil and Tillage Research* **75**: 121–130.
- Li SJ. 2007. Changes in lakes of China. *Forest & Humankind (China)* **7**: 12–25 (in Chinese).
- Lin TH. 2001. Long-range transport of yellow sand to Taiwan in Spring 2000: observed evidence and simulation. *Atmospheric Environment* **35**: 5873–5882.
- Littmann T. 1991. Dust storm frequency in Asia: climatic control and variability. *International Journal of Climatology* **11**: 393–412.
- Liu HY, Wang Y, Tian YH, Zhu JL, Wang HY. 2006. Climatic and anthropogenic control of surface pollen assemblages in East Asian steppes. *Review of Palaeobotany and Palynology* **138**: 281–289.
- McCune B, Mefford MJ. 1997. *Multivariate Analysis of Ecological Data*. MjM Software Design: Gleneden Beach, OR.
- Murayama T, Sugimoto N, Uno I, Kinoshita K, Aoki K, Hagiwara N, Liu ZY, Matsui I, Sakai T, Shibata T, Arao K, Sohn BJ, Won JG, Yoon SC, Li T, Zhou J, Hu HL, Abo M, Iokibe K, Koga R, Iwasaka Y. 2001. Ground-based network observation of Asian dust events of April 1998 in East Asia. *Journal of Geophysical Research* **106**: 18345–18359.
- Nelson DW, Sommers LE. 1996. Total carbon, organic carbon, and organic matter. In *Methods of Soil Analysis, Part 2*, 2nd ed., Page AL, et al. (eds). American Society of Agronomy: Madison, WI; 961–1010.
- Ortiz R, Álvarez-Rogel J, Alcaraz AF. 1995. Soil–vegetation relationships in two coastal salt marshes in southeastern Spain. *Arid Soil Research and Rehabilitation* **9**: 481–493.
- Pettke T, Halliday AN, Hall CM, Rea DK. 2000. Dust production and deposition in Asian and the North Pacific Ocean over the past 12 Myr. *Earth and Planetary Science Letters* **178**: 397–413.
- Ravi S, Breshears DD, Huxman TE, D'Odorico P. 2010. Land degradation in drylands: interactions among hydrologic–aeolian erosion and vegetation dynamics. *Geomorphology* **116**: 236–245.
- Runyan CW, D'Odorico P. 2010. Ecohydrological feedbacks between salt accumulation and vegetation dynamics: the role of vegetation–groundwater interactions. *Water Resource Research*. DOI: 10.1029/2010WR009464
- Sun JM, Liu TS, Lei ZF. 2000. Source of heavy dust fall in Beijing, China on April 16, 1998. *Geophysical Research Letters* **27**(14): 2105–2108.
- Ter Braak CJF. 1986. Canonical correspondence analysis: a new eigenvector technique for multivariate direct gradient analysis. *Ecology* **67**: 1167–1179.
- Tratt DM, Frouin RJ, Westphal DL. 2001. April 1998 Asian dust event: a southern California perspective. *Journal of Geophysical Research* **106**: 18371–18379.
- Unesco Water Portal. 2007. <http://www.unesco.org/water>. [25 October 2007].
- Washington R, Todd M, Middleton NJ, Goudie AS. 2003. Dust-storm source areas determined by the total ozone monitoring spectrometer and surface observations. *Annals of the Association of American Geographers* **93**(2): 297–313.
- Wang HL. 2000. *Taipusi Banner Chronicle*. Inner Mongolia Culture Press: Hailar (China); 83 (in Chinese).
- Wang SG, Wang JY, Zhou ZJ, Shang KZ. 2005. Regional characteristics of three kinds of dust storm events in China. *Atmospheric Environment* **39**: 509–520.
- Wang YF, Chen ZZ, Huang DH, Han JM. 2000. Temporal variation in dust deposition in Xilin River Basin. *Acta Phytocologica Sinica* **24**(4): 459–462 (in Chinese with English Abstract).
- Weetman GF, Fournier R, Schnorbus Panozzo E, Barker J. 1990. Post-burn nitrogen and phosphorus availability of deep humus soils in coastal British Columbia cedar/hemlock forests and the use of fertilization and salal eradication to restore productivity. In *Sustained Productivity of Forest Soils*, Gessel SP, Lacate DS, Weetman GF, Powers RF (eds), Proceedings of the 7th North American Forest Soils Conference. Faculty of Forestry, University of British Columbia: Vancouver; 451–499.
- Williams BG, Hoey D. 1987. The use of electromagnetic induction to detect the spatial variability of the salt and clay contents of soils. *Australian Journal of Soil Research* **25**: 21–27.
- Yang LR, Yue LP, Li ZP. 2008. The influence of dry lakebeds, degraded sandy grasslands and abandoned farmland in the arid inland of northern China on the grain size distribution of East Asian aeolian dust. *Environmental Geology* **53**: 1767–1775.
- Yue LP, Yang LR, Li ZP, Wang M, Zhang WJ, Nie HG. 2004. Grain-size distribution of the sediments of dry lake-bed in the northwest of China and sand–dust weather in the East Asia. *Acta Sedimentologica Sinica* **22**(2): 325–331 (in Chinese with English Abstract).
- Zhang BL, Tsunekawa A, Tsubo M. 2008. Contributions of sandy lands and stony deserts to long-distance dust emission in China and Mongolia during 2000–2006. *Global and Planetary Change* **60**: 487–504.
- Zhang XY, Arimoto R, An ZS. 1997. Dust emission from Chinese desert sources linked to variations in atmospheric circulation. *Journal of Geophysical Research* **102**(D23): 28041–28047.
- Zheng XY, et al. 1992. *Salt Lakes in Inner Mongolia*. Science Press: Beijing; 41–43 (in Chinese).

2010 年发表论文

Root respiration and its relation to nutrient contents in soil and root and EVI among 8 ecosystems, northern China

Wei Wang · Shushi Peng · Jingyun Fang

Received: 5 November 2009 / Accepted: 11 March 2010 / Published online: 27 March 2010
© Springer Science+Business Media B.V. 2010

Abstract Root respiration is a critical and uncertain component of ecosystem carbon budgets. We assessed whether variation in root respiration at a reference temperature were associated with that of root and soil nutrient contents and enhanced vegetation index (EVI) among 8 ecosystems, including three forests, two shrublands, two meadow grasslands, and one meadow in a forest-steppe ecotone in northern China. Mass specific root respiration was positively related to root nitrogen content when data from all the different classes of root diameter were pooled. Area specific root respiration increased with soil available nitrogen through increasing fine root biomass. Beside the effect of soil or root nutrient contents, mass specific respiration of fine roots followed EVI patterns, suggesting that root respiration was strongly dependent on photosynthesis. A simple respiration–EVI relationship may provide a convenient way to

estimate root respiration and has potential applications in quantitative spatial extrapolation.

Keywords Enhanced vegetation index · Root nitrogen · Root respiration · Scaling relationships · Soil available nitrogen

Introduction

Respiration is a critical component of ecosystem and global carbon (C) budgets (Cox et al. 2000; King et al. 2006), and a trait that influences metabolic fitness (Walters and Reich 2000; Wright et al. 2004). Root respiration (RR) represents a major source of CO₂ loss from plants (Rodeghiero and Cescatti 2006; Subke et al. 2006). Between 8 and 52% of CO₂ fixed by photosynthesis is released back into the atmosphere by RR (Lambers et al. 1998). Therefore, it is important to understand and characterize variation in RR as a fundamental aspect of plant ecology and physiology, and also as an important factor in the science of global change (Reich et al. 2008).

Root nitrogen (RN) content is believed to be a key determinant of RR (Comas and Eissenstat 2004; Atkinson et al. 2007). Most regional and global scale models predict RR directly from RN (Cox et al. 2000; Sitch et al. 2003). Leaf respiration (R) and nitrogen (N) content are consistently coupled among species and communities worldwide (Reich et al. 1997; Wright et al. 2004). However, the idea of a general

Electronic supplementary material The online version of this article (doi:10.1007/s11104-010-0354-x) contains supplementary material, which is available to authorized users.

Responsible Editor: Tjeerd Bouma.

W. Wang (✉) · S. Peng · J. Fang
Department of Ecology,
College of Urban and Environmental Sciences,
and Key Laboratory for Earth Surface Processes
of the Ministry of Education, Peking University,
Beijing 100871, China
e-mail: wangw@urban.pku.edu.cn

RR–RN relation has less experimental data to support it, as studies have been conducted only on individual forests (Pregitzer et al. 1998; Maier and Kress 2000; Vose and Ryan 2002; Drake et al. 2008) or grasslands (Bahn et al. 2006; Atkinson et al. 2007). Recently, strong R–N scaling relationships were reported for different organs of terrestrial plants (Reich et al. 2008). However, it is poorly understood whether a general RR–RN relationship exists among different ecosystems. Furthermore, the effects of root C and phosphorus (P) on RR have rarely been reported.

At the ecosystem level, RR depends on change in mass specific respiration rate and root biomass. Soil nutrient contents may affect RR through changing RN content (Zogg et al. 1996; Burton et al. 2000) and root biomass (Verburg et al. 2004). Mass specific root respiration is expected to increase with greater soil nutrient availability (Craine and Wedin 2002; Jones et al. 2005). Root biomass is commonly believed to inversely relate to nutrient availability (Haynes and Gower 1995; Phillips and Fahey 2007). Several field studies have shown that in general, fertile soil negatively affects soil respiratory activity (Bowden et al. 2004; Giardina et al. 2004; Ammann et al. 2007). However, the effects of soil nutrient contents on RR were seldom determined (Olsson et al. 2005).

In addition to nutrient contents in soil and root, RR is dependent on photosynthetic substrate supply (Högberg et al. 2008; Moyano et al. 2008; Bahn et al. 2009; Högberg et al. 2009; Schindlbacher et al. 2009). Enhanced vegetation index (EVI), one of the NASA's MODIS (Moderate Resolution Imaging Spectroradiometer) satellite products, is a surrogate for gross primary productivity (GPP) over a range of biomes (Rahman et al. 2005; Huete et al. 2006; Sims et al. 2006). Therefore, EVI is likely to positively correlate with RR due to the dependence of RR on photosynthesis (Heinemeyer et al. 2007; Högberg et al. 2009). Consequently, it would be simpler and more direct to result in a truly continuous output of RR at spatial resolution from satellite data. However, it remains unclear to what extent the changes in RR can be estimated from EVI alone.

In this study, we used a Li-8100 soil CO₂ Flux system to measure RR, and used EVI satellite data and chemical composition analyses of soil and root nutrient as covariates. We also estimated the contribution of RR to soil respiration (SR) in 8 ecosystems, including three forests, two shrublands, two meadow

grasslands and one meadow in a forest-steppe ecotone in northern China. We tried to address the following questions: (i) to what extent do variations in root C, N, and P contents affect RR among different ecosystems? (ii) are soil C, N and P contents associated with variation in RR? (iii) do the variations in RR respond positively to that of EVI? Our specific hypotheses were that: (i) proportional scaling of RN to RR represents a fundamental biological relationship (Reich et al. 2008), and hence a general RR–RN relationship exists among different ecosystems; (ii) RR changes with variation in soil nutrient content (Noguchi and Terashima 2006); (iii) RR increases with EVI due to its dependence on assimilate supply (Högberg et al. 2001; Kuzyakov and Cheng 2001).

Materials and methods

Site description

The study area was situated at the Saihanba Forestry Center in Hebei Province, northern China (117°12'–117°30' E, 42°10'–42°50' N, 1400 m a.s.l.). The climate is semi-arid and semi-humid, with a long, cold winter (November to March), and a short spring and summer. Annual mean air temperature and precipitation over the period from 1964 to 2004 were −1.4°C and 450.1 mm, respectively. The soils are predominantly sandy.

Our study site lay within a typical forest-steppe ecotone in a temperate area of northern China. Primary forests were harvested via large-scale industrial logging in the late 1900s and have been replaced by secondary forests and plantations. This site contains the largest area of plantation forests in China, with dominant species of *Pinus sylvestris* var. *mongolica* (Mongolia pine) and *Larix principis-rupprechtii* (Prince Rupprecht's larch). The secondary forest mainly consists of *Betula platyphylla* (birch). In addition, shrublands dominated by *Rosa bella* Rehd. et Wils (Solitary rose) and *Malus baccata* (Siberian crabapple), meadow grasslands, and meadows are also very common. The herbaceous layer of Siberian crabapple is dominated by *Veronica linariifolia*, *Galium verum*, *Heteropappus hispidus*, *Trollius chinensis*, and *Bupleurum chinense*. The herbaceous layer of Solitary rose consists of *Leymus chinensis*. The meadow grassland is an zonal vegetation domi-

nated by *L. chinensis* and the meadow is an non-zonal vegetation, forming in a surface runoff collection of low-lying land with moderate moisture conditions. The meadow includes rich grass species such as *Saussurea iodostegia*, *Dianthus chinensis*, *Adenophora elata*, *Angelica dahurica*, *Geranium sibiricum*, and *Sanguisorba officinalis*.

Mass specific respiration (R_m) of roots

We selected 21 independent forest plots arranged as three replicates for each of three age classes (~15, ~25, and ~35 years) in Mongolia pine and Prince Rupprecht's larch plantations, and three replicates for birch stand (~46 years). An additional 15 independent plots from other ecosystems were selected including three replicates for each of two shrublands, two meadow grasslands, and one meadow. The area of each plot was 20 m×20 m. The different ecosystems were less than 10 km away from each other to ensure similar climatic conditions.

During the summer (from June to August) of 2007 and 2008, root respiration (RR) was measured on excised roots at 0–30 cm soil depth from 4 to 6 random locations per plot using 5 cm diameter soil cores. Soil cores were transported to a nearby laboratory (less than 30 min travel time per site), and then the cores from each plot were composited. Roots were washed from soil cores with water over a 1.3 mm mesh size screen and separated into fine (<2 mm diameter), medium (2–5 mm diameter) and coarse size classes (>5 mm diameter). Live and dead roots were distinguished by eye based on color and consistency (Wang et al. 2009). Excess water was blotted from the root samples, and 5 g (fresh weight) root samples were placed into a self-made aluminum chamber (volume: 471 cm³) with a base of 10 cm diameter. We measured RR by determining the increase of CO₂ concentration with the time at a standard temperature (20±0.4°C) and atmospheric CO₂ concentration (366±13 μmol mol⁻¹) using the chamber attached to a Li-8100 soil CO₂ Flux system (LI-COR Inc., Lincoln, NE, USA). Because fine roots can hardly be excised without damaging them, time must pass for the stress induced respiration to subside, and to allow time for the diffusion rates and production rates of CO₂ to come back to equilibrium. To test if excision of roots could alter RR with the time through the effects of wounding or substrate depletion, we measured RR of the samples from each

site repeatedly over a period of 10–12 h in 2007, starting measurements immediately after sampling and washing. Our results showed that excision of roots need 15–30 min to come back to equilibrium and does not significantly affect RR within 6–8 h when root samples were kept moist during measurement of respiration (data not shown).

Q₁₀ of RR was measured by varying chamber temperatures with an external water bath that circulated water through the base of the chamber (Bahn et al. 2006). Separate root samples were measured at 5, 20 and 35°C, respectively, and they were kept moist during measurement of respiration. Root samples were allowed to equilibrate to each measurement temperature for at least 1 h, after which time CO₂ concentration was monitored. All measurements were taken when the rate of CO₂ efflux had stabilized, typically within 10 min of enclosing the roots in the chamber. Three measurements per chamber were averaged per temperature. On the basis of the measured data, exponential functions were established to describe the relationships between RR and measurement temperature (T):

$$RR = a \times e^{\beta T} \quad (1)$$

The Q₁₀ of RR was calculated as:

$$Q_{10} = e^{10 \times \beta} \quad (2)$$

Following respiration measurements, root mass was determined after oven-drying (65°C, 24 h) to calculate R_m (nmol g⁻¹ s⁻¹) of roots.

Area specific respiration (R_a) of roots

R_a of roots at a reference temperature of 20°C were estimated by multiplying R_m by their respective root biomasses at 0–30 cm soil depth. Root biomass was measured in five subsamples per plot using 5 cm diameter soil cores. Roots were picked by hand, dried and weighed. R_T (R_a of roots at in situ soil temperature) was estimated as:

$$R_T = R_{20} [\exp(\ln(Q_{10})(T - 20))/10] \quad (3)$$

Where R_{20} is R_a of roots at a reference temperature of 20°C; T is soil temperature at a depth of 5 cm. The contribution of RR to SR (RC) was calculated as:

$$RC = R_T / SR \quad (4)$$

Soil and root carbon (C), nitrogen (N) and phosphorus (P) contents

After respiration measurements, C and N contents of dried and ground root samples were measured using a CHN elemental analyzer (Carlo Erba NA 1500 N.C., CE Elantech, Lakewood, N.J.). Root P content was determined colorimetrically after digestion with a mixture of HNO_3 , HClO_4 , and H_2SO_4 (3:1:1; v/v) by the phosphovanadate method (Hanson 1950).

Soil samples were collected in August 2008 using 10 cm deep by 5.4 cm diameter soil cores. The five samples were collected in the central part of each plot, one in each of the four corners, and the fifth in the middle. These samples were transported in coolers to nearby laboratories and the cores from a plot were composited. They were air dried, roots were removed, and soil was passed through a 2 mm mesh size sieve. Soil total C and N were determined using a CHN elemental analyzer (Carlo Erba NA 1500 N.C., CE Elantech, Lakewood, N.J.). Extractable ammonium- and nitrate-N were measured simultaneously in 1 M KCl extracts using a Lachat Flow Injection Analyzer (Bradley and Fyles 1995). Soil P was determined by the phosphovanadate method (Hanson 1950).

Enhanced vegetation index (EVI)

EVI, as a surrogate for GPP, is less sensitive to soil and atmospheric effects than the normalized difference vegetation index (NDVI) and remains sensitive to increases in canopy density beyond the point where NDVI becomes saturated (Xiao et al. 2005). EVI is a composite property of canopy structure, leaf area, and canopy chlorophyll content, taking the form:

$$EVI = G \times \frac{\rho_{nir} - \rho_{red}}{\rho_{nir} + (C_1 \times \rho_{red} - C_2 \times \rho_{blue}) + L} \quad (5)$$

Where ρ_{nir} , ρ_{red} , ρ_{blue} are partially atmospherically corrected surface reflectances, using near infrared, red and blue bands, L is the canopy background adjustment ($L=1$), C_1 and C_2 are coefficients of the aerosol resistance term that uses the 500 m blue band (458–479 nm) of MODIS to correct for aerosol influences in the red band ($C_1=6$ and $C_2=7.5$), and G is a gain factor ($G=2.5$) (Sims et al. 2006).

Because of their large areas and uniform distribution, we selected Mongolia pine and Prince Rupprecht's larch plantations for comparisons with the EVI of 16-Day L3

Global 250 m product (MOD13 Q₁) (<https://wist.echo.nasa.gov/api>) during summer of 2007 and 2008. A 16-day composite interval was proved adequate to smooth out short-term variation in atmospheric properties and registration errors while offering sufficient resolution to capture trends over the growing season (Wardlow et al. 2007).

Soil respiration (SR)

SR was measured once every 2 weeks using an LI-8100 soil CO_2 flux system in the summer of 2007 and 2008. In each plot, five polyvinyl chloride (PVC) collars (10 cm inside diameter, 6 cm height) were inserted 3 cm into the soil, and were left in the same locations throughout the study. The five PVC collars were placed in the central part of each plot, one in each of the four corners, and the fifth in the middle. Living plants inside the collars were clipped at the soil surface 1 day before each measurement. In order to minimize daily variation in SR and represent the average daily SR, measurements were made between 08:00 and 11:00 h (based on our measurements of diurnal changes in soil respiration for each ecosystem, data not shown). In each measurement, respiration rates were calculated as means of three plots. Soil temperature was recorded during respiration measurements near each collar at 5 cm soil depth with a LI-COR 8100 temperature probe.

Statistical analyses

One-way ANOVA was used to evaluate whether root chemistry, soil nutrient contents, and root respiration rates differed significantly among different ecosystems. The relationships among the nutrients for soils and roots and RR were examined using standardized major axis (SMA) estimation (Falster et al. 2006; Warton et al. 2006). All statistical analyses were performed with a significance level of 0.05 using StatView 5.0 (SAS Institute, Inc., Cary, NC, USA).

Results

RR and its relationships with root C, N and P contents

Among the eight ecosystems, mass specific respiration (R_m) of fine roots (<2 mm diameter) at a

reference temperature of 20°C ranged from 0.98 to 3.81 nmol g⁻¹ s⁻¹ (Fig. 1a). In both years, similar patterns with higher rates were observed in 12-year-old Prince Rupprecht's larch, and with lower rates in meadow grasslands. Within the same ecosystem, R_m generally decreased with increasing root diameter (Fig. 1a). The Q_{10} (between 5 and 35°C) of fine root respiration ranged from 1.56 to 2.17, showing no significant variation among the different ecosystems (Fig. 1b).

Root C contents generally increased with root diameter across all ecosystems (Supplement Fig. S1a); In contrast, there was an inverse relationship between RN and diameter (Supplement Fig. S1b). Root P contents ranged from 0.033 to 0.171%, showing no significant change with diameter (Supplement Fig. S1c).

Pooling all the data across three root diameter classes, root N and P contents and R_m were well correlated (Fig. 2). Furthermore, multiple stepwise regression analyses showed that RN was the major controlling factor in determining the variation in R_m . The variation in RN explained 22% of variation in R_m . However, there was no significant relationship found when the R_m of each size class was analyzed separately.

Area specific root respiration (R_a) at a reference temperature of 20°C showed large variation from 0.18 to 1.27 $\mu\text{mol m}^{-2} \text{s}^{-1}$ (Fig. 3). Across all ecosystems, fine roots made up the largest portion of the 0–30 cm

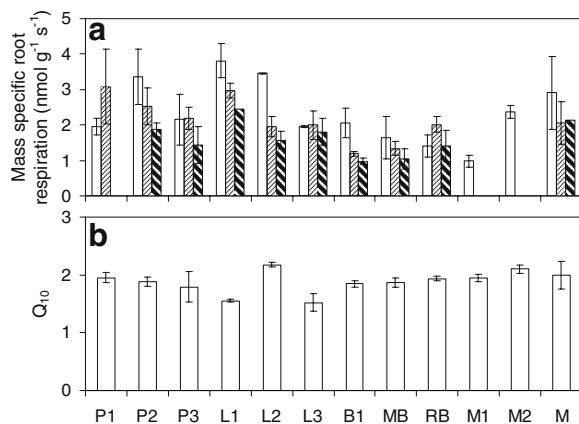


Fig. 1 **a** Mass specific root respiration at 20°C (nmol g⁻¹ s⁻¹) and **b** Q_{10} (between 5 and 35°C) of fine roots (means \pm S.D.) across 8 ecosystems. P1, P2, P3 are 12-, 23-, and 39-year-old *P. sylvestris*; L1, L2, L3 are 12-, 22-, and 42-year old *L. principis-rupprechtii*; B1, MB, RB, M1, M2 and M are 46-year-old *B. platyphylla*, *M. baccata*, *R. bella*; meadow grassland 1, meadow grassland 2 and meadow

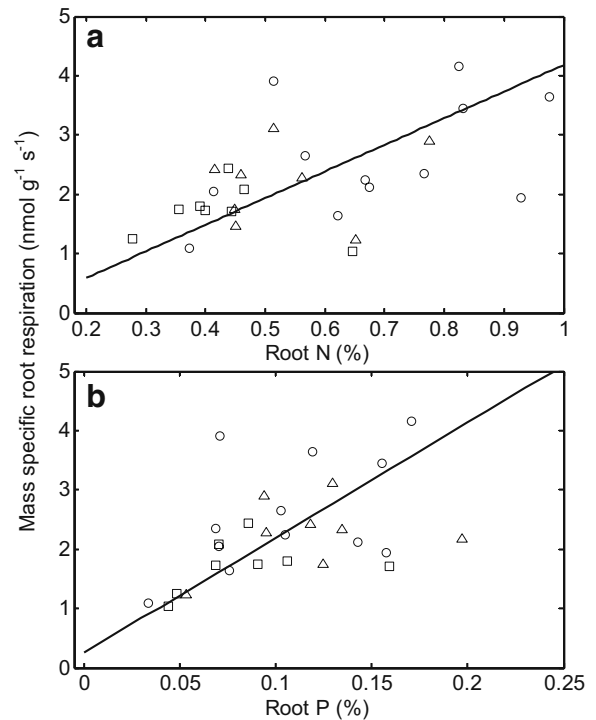


Fig. 2 Relationships between mass specific root respiration at 20°C (nmol g⁻¹ s⁻¹) and **a** root N content (%) ($Y=4.49 X-0.31$; $R^2=0.22$; $P=0.007$) and **b** root P content (%) ($Y=8.55 X+0.25$; $R^2=0.18$; $P=0.007$) pooling all the data from roots with diameters of 0–2 mm (open circle), 2–5 mm (open triangle) and >5 mm (open square) in 2008

root biomass (Table 1). In general, fine roots accounted for the largest proportion of R_a (51–100%).

Variation in RR in relation to soil C, N and P contents

Soil organic carbon (SOC) and soil total nitrogen (STN) at 0–30 cm depth showed significant variation, ranging from 1.02 to 7.88% and from 0.06 to 0.30% (Supplement Fig. S2a, S2b), respectively. Soil available N ranged from 5.29 to 18.9 mg kg⁻¹ (Supplement Fig. S2c), contributing 0.45–1.45% to STN. Soil total phosphate (STP) averaged 0.01% with little variation among 8 ecosystems (Supplement Fig. S2d). R_m was not significantly related to SOC, STN, STP, or soil available N ($P>0.05$ for all comparisons). Soil available N was correlated with R_a of fine root (Fig. 4a), because fine root biomass at 0–30 cm depth was positively related to soil available N (Fig. 4b). There was no significant relationship between R_m of fine roots and soil available N (Fig. 4c).

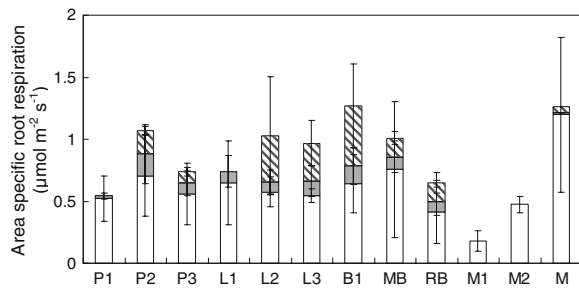


Fig. 3 Contribution of different root size classes to area specific root respiration at a reference temperature of 20°C. Values are means \pm S.D. for roots with diameters of 0–2 mm (white); 2–5 mm (gray) and >5 mm (right diagonal). P1, P2, P3 are 12-, 23-, and 39-year-old *P. sylvestris*; L1, L2, L3 are 12-, 22-, and 42-year old *L. principis-rupprechtii*; B1, MB, RB, M1, M2 and M are 46-year-old *B. platyphylla*, *M. baccata*, *R. bella*; meadow grassland 1, meadow grassland 2 and meadow

RR in relation to enhanced vegetation index (EVI)

In the plantations of both Mongolia pine and Prince Rupprecht's larch, R_m of fine roots in 2008 was generally higher than that in 2007. This corresponded to the dynamics of EVI (Fig. 5). The R_m was higher in Prince Rupprecht's larch than in Mongolia pine, which was similar to the changes in EVI. Variation in EVI explained 45% of that in R_m of fine root (Fig. 5). No significant relationship occurred between coarse root respiration and EVI ($P > 0.05$).

Table 1 Mean, standard deviation (S.D.), standard error (S.E.) and coefficient of variation (C.V.) of root biomass across 0–2 mm, 2–5 mm and >5 mm diameters in different ecosystems. P1, P2, P3 are 12-, 23-, and 39-year-old *P. sylvestris*; L1, L2,

	0–2 mm diameter				2–5 mm diameter				0–2 mm diameter			
	Mean (g m ⁻²)	S.D.	S.E.	C.V.	Mean (g m ⁻²)	S.D.	S.E.	C.V.	Mean (g m ⁻²)	S.D.	S.E.	C.V.
P1	306.17	122.47	35.35	0.40	15.25	27.64	7.98	1.81	19.61	51.14	14.76	2.61
P2	379.55	100.83	29.11	0.27	118.55	81.51	23.53	0.69	96.26	149.33	43.11	1.55
P3	276.04	129.02	37.25	0.47	65.91	58.39	16.86	0.89	65.82	126.12	36.41	1.92
L1	214.29	64.91	24.53	0.30	33.12	55.53	20.99	1.68				
L2	191.65	48.63	14.04	0.25	85.05	45.38	13.10	0.53	145.12	250.23	79.13	1.72
L3	217.30	53.69	17.90	0.25	90.34	83.35	27.78	0.92	233.84	275.67	97.46	1.18
B1	345.47	120.42	38.08	0.35	198.91	125.84	39.79	0.63	267.23	282.04	99.72	1.06
MB	556.20	203.36	76.86	0.37	129.51	143.88	54.38	1.11	149.58	353.80	133.72	2.37
RB	363.34	192.52	64.17	0.53	75.81	69.49	23.16	0.92	121.48	96.13	32.04	0.79
M1	215.26	68.52	20.66	0.32								
M2	190.58	56.44	16.29	0.30								
M	450.10	78.52	55.52	0.17	24.29	23.77	16.81	0.98				

Contribution of RR to SR

SR ranged from 2.89 $\mu\text{mol m}^{-2} \text{s}^{-1}$ in 23-year-old Mongolia pine to 6.68 $\mu\text{mol m}^{-2} \text{s}^{-1}$ in meadow (Fig. 6b). The contribution of RR to SR varied from 5 to 37% (Fig. 6a), indicating that heterotrophic respiration dominated SR. In both years, similar trends were observed with higher values in 23-year-old Mongolia pine and 22-year-old Prince Rupprecht's larch, and lower values in meadow grasslands.

Discussion

The effect of experimental setup on RR estimates

We estimated RR among 8 ecosystems using excised root method. This method is relatively simple, cheap and could be widely used across different ecosystems (Bahn et al. 2006; Drake et al. 2008; Tjoelker et al. 2008). However, there are still some limitations about this method, possibly resulting in a bias to the estimates for RR. First, the disturbance of root soil interface through excision resulted in the absence of normal rhizosphere processes. Mycorrhizal fungi has been recently observed to be a major component of SR and may dominate root respiration (Heinemeyer et al. 2007; Moyano et al. 2007; Höglberg et al. 2009).

L3 are 12-, 22-, and 42-year old *L. principis-rupprechtii*; B1, MB, RB, M1, M2 and M are 46-year-old *B. platyphylla*, *M. baccata*, *R. bella*; meadow grassland 1, meadow grassland 2 and meadow

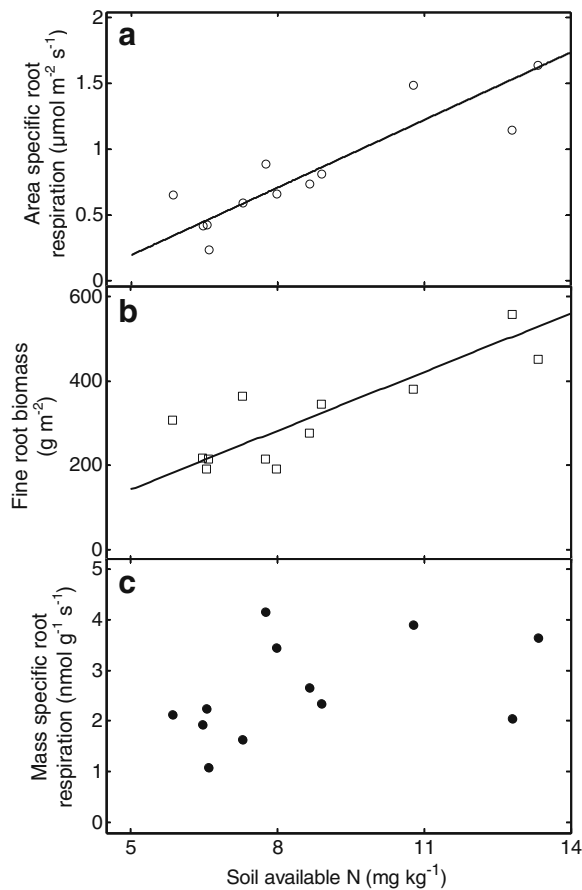


Fig. 4 Relationship between soil available N (mg kg^{-1}) and **a** area specific respiration of fine roots ($\mu\text{mol m}^{-2} \text{s}^{-1}$) ($Y=0.17 X-0.66$; $R^2=0.76$, $P=0.000$); **b** fine root biomass (g m^{-2}) ($Y=46.17 X-121.47$; $R^2=0.64$, $P=0.001$) and **c** mass specific root respiration ($\text{nmol g}^{-1} \text{s}^{-1}$)

Second, one chronic problem is the underestimation of fine root biomass. Some of the fine root biomass less than 0.5 mm in diameter was difficult to recover from the soil. Therefore, this scaled-up respiration measurements, using excised (mycorrhizal-deprived) roots, may underestimate RR. However, the potential underestimation of RR would not alter our major conclusions drawn from the data, as it would have been consistent across all sites.

How does RN content affect R_m of roots among different ecosystems?

In our study, there was no significant R_m –RN relationship when coarse root or fine root data were analyzed separately. Tjoelker et al. (2005) showed a

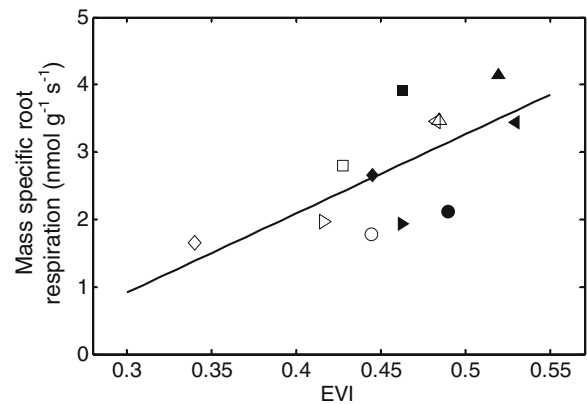


Fig. 5 Relationship between mass specific respiration of fine roots ($\text{nmol g}^{-1} \text{s}^{-1}$) and enhanced vegetation index (EVI) ($Y=0.0012 X-2.5326$, $R^2=0.45$, $P=0.013$). Open and solid symbols indicate values in 2007 and 2008, respectively. Circle, square, diamond, triangle, left triangle, and right triangle indicate 12-, 23-, and 39-year-old *P. sylvestris*, and 12-, 22-, and 42-year-old *L. principis-rupprechtii*, respectively

large scatter in the R_m –RN relationship for fine roots of a range of herbaceous C_3 species. In a *Pinus strobus* ecosystem, fine root respiration was not related to RN (Vose and Ryan 2002). However, Burton et al. (2002) reported a strong R_m –RN correlation ($R^2>0.81$) in ten forested sites across North America. The discrepancies may result from

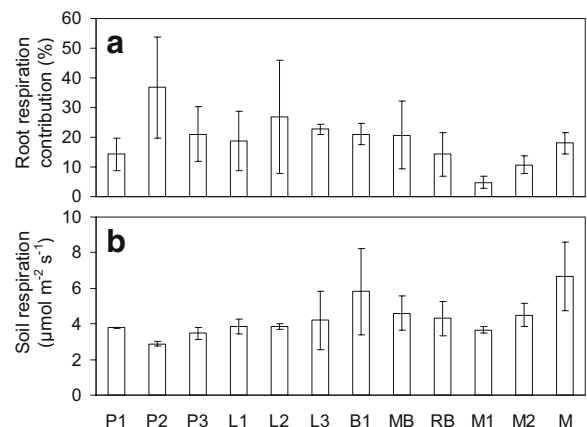


Fig. 6 **a** Contribution of root respiration to soil respiration (%) and **b** soil respiration ($\mu\text{mol m}^{-2} \text{s}^{-1}$) in different ecosystems. P1, P2, P3 are 12-, 23-, and 39-year-old *P. sylvestris*, respectively; L1, L2, L3 are 12-, 22-, and 42-year old *L. principis-rupprechtii*, respectively; B1, MB, RB, M1, M2 and M are 46-year-old *B. platyphylla*, *M. baccata*, *R. bella*; meadow grassland 1, meadow grassland 2 and meadow, respectively

the range of RN within each studied system. In our study, for instance, there was a narrow range of fine RN across the eight ecosystems (0.38–0.98%) (Supplement Fig. S1b). However, after pooling the data obtained from both coarse and fine roots to increase the range in RN contents, as suggested by Pregitzer et al. (1998), a significant relationship was detected (Fig. 2). Similar observations were also reported by Desrochers et al. (2002) in an aspen (*Populus tremuloides*) stand and among 11 temperate mountain grasslands (Bahn et al. 2006).

In the present study, the slope (4.49) of the R_m –RN relationship (Fig. 2) was higher than the reported values for global terrestrial plants (1.57–2.24; Reich et al. 2008) and for 11 temperate mountain grasslands (1.50–3.02; Bahn et al. 2006). Our data further confirmed that although fine RN contents in our study area were lower than global means (1.1–1.17%, Jackson et al. 1997; Gordon and Jackson 2000), R_m of fine roots at either forest or grassland sites (Fig. 1) lay within the ranges reported for forests (1.8–10.4 nmol g⁻¹ s⁻¹, Burton et al. 2008) or temperate C₃ grasslands (1.0–2.6 nmol g⁻¹ s⁻¹, Bahn et al. 2006). The variation in RN could only explain 22% of variation in R_m (Fig. 2). This is far below those for global terrestrial plants (57–72%; Reich et al. 2008), for individual forests (65–70%; Pregitzer et al. 1998; Desrochers et al. 2002) or for temperate grasslands (60%; Bahn et al. 2006). Therefore, our results suggest that the factors aside from RN may have important effects on R_m . Such factors may include nutrient supply (Lambers et al. 1995; Tjoelker et al. 2008) and photosynthesis (Boone et al. 1998; Moyano et al. 2008). Although RN content have a significant overall effect on R_m , different species may show marked variability in their use of RN for R_m . Thus, care should be taken when interpolating global patterns to estimate R_m from RN content at individual sites.

Are variation in RR associated with variation in soil nutrient contents?

According to our assumption, R_m is greater at sites with greater N availability (Ryan et al. 1996; Zogg et al. 1996; Burton et al. 2002), because RN is greater (Zogg et al. 1996). However, we did not observe significant relationships between R_m and soil C, N or P contents. As well, soil C, N and P contents were not related to root C, N and P contents. Therefore, our results suggest

that soil nutrient status had little effect on variation in R_m and root chemistry across different ecosystems. These findings are consistent with some recently published data; for instance, Drake et al. (2008) reported that nitrogen availability was not related to R_m in a loblolly pine (*Pinus taeda* L) forest exposed to elevated CO₂ and N fertilization. In modal communities of north-temperate tree species, King et al. (2005) reported only small changes in root chemical composition in response to increased soil resource availability.

Interestingly, we found that fine root biomass increased with soil available N, resulting in an increase of R_a of roots (Fig. 4). In the linear relationship between root biomass and soil available N, two data points were vital, including meadow and Siberian crabapple sites. If we excluded these two data, no significant trend was found ($P > 0.05$). The two sites had higher fine root biomass than other ecosystems (Table 1). At the same time, they belong to non-zonal vegetations in our study area, forming in a surface runoff collection of low-lying land with moderate moisture conditions and fertile soil conditions. In addition to these two sites, other ecosystems with lower fine root biomass are very infertile with the soils predominantly sandy. Therefore, our results based on a natural gradient of N availability across different species may reflect genetic adaptation of each species to the range of site conditions where it normally occurs (Burton et al. 2000), rather than N availability.

Our results were different from the most previous experiments studying a single tree species (or forest type) across a range of N availabilities (Olsson et al. 2005; Phillips and Fahey 2007), which explored a short-term response of root biomass to N availability (Burton et al. 2000). This short response was partly connected with plant developmental stages (Butnor et al. 2003), site fertility conditions (Bloom et al. 1985; Chapin et al. 1986; Ostertag 2001; Treseder and Vitousek 2001), and plant life history strategy (King et al. 2005) in the investigated systems. All of these factors may explain the reported various responses of root biomass across different N availability (Maier and Kress 2000; Retzlaff et al. 2001; King et al. 2005; Phillips and Fahey 2007).

Do variation in RR respond to variation in EVI?

In our study, EVI was generally higher for Prince Rupprecht's larch than for Mongolia pine (Fig. 5).

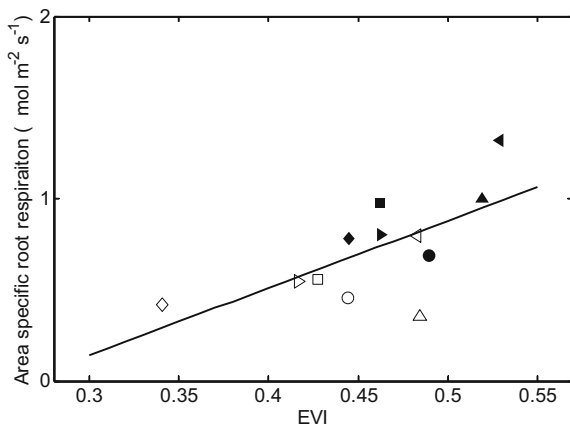


Fig. 7 Relationship between area specific roots respiration ($\mu\text{mol m}^{-2} \text{s}^{-1}$) at ambient soil temperature and enhanced vegetation index (EVI) ($Y=0.0004 X-0.961$; $R^2=0.43$, $P=0.02$). Open and solid symbols indicate values in 2007 and 2008, respectively. Circle, square, diamond, triangle, left triangle, and right triangle indicate 12-, 23-, and 39-year-old *P. sylvestris*, and 12-, 22-, and 42-year-old *L. principis-rupprechtii*, respectively

Higher EVI for deciduous species may maximize carbon gain during the growing season (Kohout and Read 2006). This trend of EVI corresponded with the change in R_m of fine root (Fig. 5), suggesting that more photo synthetically active plants have higher R_m . Carbohydrates generated by photosynthesis, such as sugar, are reported to be transported at high rates from leaves to roots, where they are then lost via root respiration (Kuzakov and Cheng 2001). Such an influx of sugar would likely stimulate RR because of substrate limitation during summer (Drake et al. 2008).

We also observed a significant relationship between R_a of roots at ambient soil temperature (called ecosystem root respiration) and EVI ($P=0.02$; Fig. 7). However, there is one datapoint vital for driving this positive relationship. If we excluded closed left triangle point (22-year-old *L. principis-rupprechtii*), this trend was insignificant ($P=0.08$). Therefore, the relationship between ecosystem root respiration and EVI remains to be further investigated. Future work is needed to explore the implications of in-situ ecosystem root respiration and EVI coupling because this scaled-up respiration measurements has some limitations in the estimates of ecosystem root respiration. The reason may be due to the large spatial variation of root biomass within each ecosystem. In our study, the

coefficient of variation (CV) of fine root biomass ranged from 25% to 47% (Table 1); for coarse roots, CV were much higher, ranging from 53% to 181% within 2–5 mm in diameter and 118% to 261% within >5 mm in diameter (Table 1). Therefore, the spatial variation of root biomass within an ecosystem may result in a bias in the estimates of area based root respiration.

To our knowledge, no other studies have investigated the link between R_m of roots and EVI. The relationship between R_m and EVI (Fig. 5) implies that a significant fraction of RR can be modeled simply as a fraction of canopy greenness during the peak growing season. Currently, separation of SR into its heterotrophic and autotrophic components remains the greatest challenge in experimental validation of common process-based models for assessing C balance (Battaglia et al. 2004). There is a very wide range of reported values for RR (Hanson et al. 2000). A considerable proportion of this variability results from the variety of measurement techniques used (Marsden et al. 2008). Therefore, EVI has potential as a convenient way to estimate RR. Furthermore, integration of R_m and EVI could be used for quantitative spatial extrapolation when evaluating regional or global carbon balances.

Conclusions

Our results have shown that a significant relationship between RN content and R_m of roots only occurred when pooling all data across different root diameter classes, suggesting that care should be taken when interpolating global patterns to estimate R_m from RN content at individual sites. Fine root respiration generally made up the largest portion of area specific respiration (R_a) and showed similar Q_{10} values across different ecosystems. Soil available N contents imposed positive effect on fine root biomass, and thus increasing R_a of fine roots. The positive relationship between R_m of fine roots and enhanced vegetation index (EVI) may provide a convenient way for estimating root respiration and for quantitative spatial extrapolation when evaluating regional or global carbon balances.

Acknowledgments This work was supported by the National Natural Science Foundation of China (Project Nos. 30870408, 30670342, and 90711002). We thank Z. F. Liu for his help with data analyses.

References

- Ammann C, Flechard CR, Leifeld J, Neftell A, Fuhrer J (2007) The carbon budget of newly established temperate grassland depends on management intensity. *Agric Ecosyst Environ* 121:5–20
- Atkinson LJ, Hellicar MA, Fitter AH, Atkin OK (2007) Impacts of temperature on the relationship between respiration and nitrogen concentration in roots: an analysis of scaling relationships, Q_{10} values and thermal acclimation ratios. *New Phytol* 173:110–120
- Bahn M, Knapp M, Garajova Z, Pfahringer N, Cernusca A (2006) Root respiration in temperate mountain grasslands differing in land use. *Global Change Biol* 12:995–1006
- Bahn M, Schmitt M, Siegwolf R, Richer A, Brüggemann N (2009) Does photosynthesis affect grassland soil-respired CO_2 and its carbon isotope composition on a diurnal timescale? *New Phytol* 182:451–460
- Battaglia M, Sands P, White D, Mummery D (2004) Cabala: a linked carbon, water and nitrogen model of forest growth for silvicultural decision support. *Forest Ecol Manag* 193:251–282
- Bloom AJ, Chapin FS III, Mooney HA (1985) Resource limitation in plants—an economic analogy. *Annu Rev Ecol Syst* 16:363–393
- Boone RD, Nadelhoffer KJ, Canary JD, Kaye JP (1998) Roots exert a strong influence on the temperature sensitivity of soil respiration. *Nature* 396:570–572
- Bowden RD, Davidson E, Savage K, Arabia C, Steudler P (2004) Chronic nitrogen additions reduce total soil respiration and microbial respiration in temperate forest soils at the Harvard forest. *Forest Ecol Manag* 196:43–56
- Bradley RL, Fyles JW (1995) Growth of paper birch (*Betula papyrifera*) seedling increases soil available C and microbial acquisition of soil nutrients. *Soil Biol Biochem* 27:1565–1571
- Burton AJ, Pregitzer KS, Hendrick RL (2000) Relationships between fine root dynamics and nitrogen availability in Michigan northern hardwood forest. *Oecologia* 125:389–399
- Burton AJ, Pregitzer KS, Ruess RW, Hendrick RL, Allen MF (2002) Root respiration in North American forest: effects of nitrogen concentration and temperature across biomes. *Oecologia* 131:559–568
- Burton AJ, Melilo JM, Frey SD (2008) Adjustments of forest ecosystem root respiration as temperature warms. *J Integr Plant Biol* 50:1467–1483
- Butnor JR, Johnsen KH, Oren R, Katul GG (2003) Reduction of forest floor respiration by fertilization on both carbon dioxide enriched and reference 17-year-old loblolly pine stands. *Global Change Biol* 9:849–861
- Chapin FS III, Vitousek PM, Cleve KV (1986) The nature of nutrient limitation in plant communities. *Am Nat* 127:48–58
- Comas LH, Eissenstat DM (2004) Linking fine root traits to maximum potential growth rate among 11 mature temperate tree species. *Funct Ecol* 18:388–397
- Cox PM, Betts RA, Jones CD, Spall SA, Totterdell IJ (2000) Acceleration of global warming due to carbon-cycle feedbacks in a coupled climate model. *Nature* 408:184–187
- Craine FM, Wedin DA (2002) Determinants of growing season soil CO_2 flux in a Minnesota grassland. *Biogeochemistry* 59:303–313
- Desrochers A, Landhausser SM, Lieffers VJ (2002) Coarse and fine respiration in aspen *Populus tremuloides*. *Tree Physiol* 22:725–732
- Drake JE, Stoy PC, Jackson RB, Delucia EH (2008) Fine-root respiration in a loblolly pine (*Pinus taeda* L) forest exposed to elevated CO_2 and N fertilization. *Plant Cell Environ* 31:1663–1672
- Falster DS, Warton DI, Wright IJ (2006) SMATR: standardized major axis tests and routines, ver2.0. <http://www.bio.mq.edu.au/ecology/SMATR/>
- Giardina GP, Binkley D, Ryan MG, Fownes JH, Senock RS (2004) Belowground carbon cycling in a humid tropical forest decreases with fertilization. *Oecologia* 139:545–550
- Gordon WS, Jackson RB (2000) Nutrient concentration in fine roots. *Ecology* 81:275–280
- Hanson WC (1950) The photometric determination of phosphorus in fertilizers using the phosphovanado-molybdate complex. *J Sci Food Agric* 1:172–173
- Hanson PJ, Edwards NT, Garten CT, Andrews JA (2000) Separating root and soil microbial contributions to soil respiration: a review of methods and observations. *Biogeochemistry* 48:115–146
- Haynes BE, Gower ST (1995) Belowground carbon allocation in unfertilized and fertilized plantations in northern Wisconsin. *Tree Physiol* 15:317–325
- Heinemeyer A, Hartley IP, Evans SP, Carreira JA, Fuente DL, Ineson P (2007) Forest soil CO_2 flux: uncovering the contribution and environmental responses of ectomycorrhizas. *Global Change Biol* 13:1786–1797
- Högberg P, Nordgren A, Buchmann N, Taylor AFS, Ekblad A, Höglberg MN, Nyberg G, Ottosson-Lofvenius M, Read DJ (2001) Large-scale forest girdling shows that current photosynthesis drives soil respiration. *Nature* 411:789–792
- Högberg P, Höglberg MN, Göttlicher SG et al (2008) High temporal resolution tracing of photosynthate carbon from the tree canopy to forest soil microorganisms. *New Phytol* 177:220–228
- Högberg P, Singh B, Löfvenius MO, Nordgren A (2009) Partitioning of soil respiration into its autotrophic and heterotrophic components by means of tree-girdling in old boreal spruce forest. *Forest Ecol Manag* 257:1764–1767
- Huete AR, Didan K, Shimabukuro YE, Ratana P, Saleska SR, Hutrya LR, Yang WZ, Remani RR, Myneni R (2006) Amazon rainforest green-up with sunlight in dry season. *Geophys Res Lett* 33:L06405. doi:10.1029/2005GL025583
- Jackson RB, Mooney HA, Schulze ED (1997) A global budget for fine roots biomass, surface area and nutrient contents. *Proc Natl Acad Sci USA* 94:7362–7366
- Jones SK, Rees RM, Skiba UM, Ball BC (2005) Greenhouse gas emissions from a managed grassland. *Global Planet Change* 47:201–211
- King JS, Pregitzer KS, Zak DR, Holmes WE, Schmidt K (2005) Fine root chemistry and decomposition in model communities of north-temperate tree species show little response to elevated atmospheric CO_2 and varying soil resource availability. *Oecologia* 146:318–328
- King AW, Gunderson CA, Post WM, Weston DJ, Wullschlegel SD (2006) Plant respiration in a warmer world. *Science* 312:536–537

- Kohout M, Read J (2006) Instantaneous photosynthetic responses to temperature of deciduous and evergreen *Nothofagus* species. *Aust J Bot* 54:249–259
- Kuzyakov Y, Cheng W (2001) Photosynthesis controls of rhizosphere respiration and organic matter decomposition. *Soil Biol Biochem* 33:1915–1925
- Lambers H, Nagel OW, Jeroen JGM, van Arendonk J (1995) The control of biomass partitioning in plants from “favorable” and “stressful” environments: a role for gibberellins and cytokinins. *Bulg J Plant Physiol* 21:24–32
- Lambers H, Chapin FS, Pons TL (1998) Plant physiological ecology. Springer-Verlag, New York
- Maier CA, Kress LW (2000) Soil CO₂ evolution and root respiration in 11 year-old loblolly pine (*Pinus taeda*) plantations as affected by moisture and nutrient availability. *Can J For Res* 30:347–359
- Marsden C, Nouvellon Y, Bou ATM, Saint-Andre L, Jourdan C, Kinana A, Epron D (2008) Two independent estimations of stand-level root respiration on clonal *Eucalyptus* stands in Congo: up scaling of direct measurements on roots *versus* the trenched-plot technique. *New Phytol* 177:676–687
- Moyano FE, Kutsch WL, Schulze ED (2007) Response of mycorrhizal, rhizosphere and soil basal respiration to temperature and photosynthesis in a barley field. *Soil Biol Biochem* 39:843–853
- Moyano FE, Kutsch WL, Rebmann C (2008) Soil respiration fluxes in relation to photosynthetic activity in broad-leaf and needle-leaf forest stands. *Agric For Meteorol* 148:135–143
- Noguchi K, Terashima I (2006) Responses of spinach leaf mitochondria to low N availability. *Plant Cell Environ* 29:710–719
- Olsson P, Linder S, Giesler R, Högborg P (2005) Fertilization of boreal forest reduces both autotrophic and heterotrophic soil respiration. *Global Change Biol* 11:1745–1753. doi:10.1111/j.1365-2486.2005.01033.x
- Ostertag R (2001) Effects of nitrogen and phosphorous availability on fine-root dynamics in Hawaiian Montane Forests. *Ecology* 82:485–499
- Phillips RP, Fahey TJ (2007) Fertilization effects on fine root biomass, rhizosphere microbes and respiratory fluxes in hardwood forest soils. *New Phytol* 176:655–664
- Pregitzer KS, Laskowski MJ, Burton AJ, Lessard VC, Zak DR (1998) Variation in sugar maple root respiration with root diameter and soil depth. *Tree Physiol* 18:665–670
- Rahman AF, Sims DA, Cordova VD, El-Masri BZ (2005) Potential of MODIS EVI and surface temperature for directly estimating per-pixel ecosystem C fluxes. *Geophys Res Lett* 32:L19404. doi:10.1029/2005GL024127
- Reich PB, Walters MB, Ellsworth DS (1997) From tropics to tundra: global convergence in plant functioning. *Proc Natl Acad Sci USA* 94:13730–13734
- Reich PB, Tjoelker MG, Pregitzer KS, Wright IJ, Oleksyn J, Machado JL (2008) Scaling of respiration to nitrogen in leaves, stems and roots of higher land plants. *Ecol Lett* 11:793–801
- Retzlaff WA, Handest JA, O’Malley DM, McKeand SE, Topa MA (2001) Whole-tree biomass and carbon allocation of juvenile trees of loblolly pine (*Pinus taeda*): influence of genetics and fertilization. *Can J For Res* 31:960–970
- Rodeghiero M, Cescatti A (2006) Indirect partitioning of soil respiration in a series of evergreen forest ecosystems. *Plant Soil* 284:7–22
- Ryan MG, Hubbard RM, Pongracic S, Raison RJ, Mcmurtrie RE (1996) Foliage, fine-root, woody-tissue and stand respiration in *Pinus radiata* in relation to nitrogen status. *Tree Physiol* 16:333–343
- Schindlbacher A, Zechmeister-Boltenstern S, Jandl R (2009) Carbon losses due to soil warming: Do autotrophic and heterotrophic soil respiration respond equally? *Global Change Biol* 15:901–913
- Sims DA, Rahman AF, Cordova VD et al (2006) On the use of MODIS EVI to assess gross primary productivity of North American ecosystems. *J Geophys Res* 111:G04015. doi:10.1029/2006JG000162
- Sitch S, Smith B, Prentice IC et al (2003) Evaluation of ecosystem dynamics, plant geography and terrestrial carbon cycling in the LPJ dynamic global vegetation model. *Global Change Biol* 9:161–185
- Subke J, Ingleima I, Cotrufo MF (2006) Trends and methodological impacts in soil CO₂ efflux partitioning: a meta-analytical review. *Global Change Biol* 12:921–943
- Tjoelker MG, Craine JM, Wedin D, Reich PB, Tilman D (2005) Linking leaf and root trait syndromes among 39 grassland and savannah species. *New Phytol* 167:493–508
- Tjoelker MG, Oleksyn J, Reich PB, Zytowski R (2008) Coupling of respiration, nitrogen, and sugars underlies convergent temperature acclimation in *Pinus banksiana* across wide-ranging sites and populations. *Global Change Biol* 14:782–797
- Treseder K, Vitousek PM (2001) Effects of soil nutrient availability on investment in acquisition of N and P in Hawaiian rain forest. *Ecology* 82:946–954
- Verburg PSJ, Arnone JA, Obrist D, Schorran DE, Evans R, Leroux-swarthout D, Johnson DW, Luo Y, Coleman JS (2004) Net ecosystem exchange in two experimental grassland ecosystems. *Global Change Biol* 10:498–508
- Vose JM, Ryan MG (2002) Seasonal respiration of foliage, fine roots, and woody tissues in relation to growth, tissue N, and photosynthesis. *Global Change Biol* 8:182–193
- Walters MB, Reich PB (2000) Trade-offs in low-light CO₂ exchange: a component of variation in shade tolerance among cold temperate tree seedlings. *Funct Ecol* 14:155–165
- Wang W, Feng J, Oikawa T (2009) Contribution of root and microbial respiration to soil CO₂ efflux and their environmental controls in a humid temperate grassland of Japan. *Pedosphere* 19:31–39
- Wardlow BD, Egbert SL, Kastens JH (2007) Analysis of time-series MODIS 250 m vegetation index data for crop classification in the U.S. Central Great Plains. *Remote Sens Environ* 108:290–310
- Warton DI, Wright DS, Westoby M (2006) Bivariate line-fitting methods for allometry. *Biol Rev* 81:259–291
- Wright IJ, Reich PB, Westoby M, Ackerly DD, Baruch Z, Bongers F, Cavender-Bares J, Chapin T, Cornelissen JHC, Diemer M et al (2004) The worldwide leaf economics spectrum. *Nature* 428:821–827
- Xiao XM, Zhang QY, Saleska S, Hutyra L, Camargo PD, Wofsy S, Frolking S, Boles S, Keller M, Moore B III (2005) Satellite-based modeling of gross primary production in a seasonally moist tropical evergreen forest. *Remote Sens Environ* 94:105–122
- Zogg GP, Zak DR, Burton AJ, Pregitzer KS (1996) Fine root respiration in northern hardwood forests in relation to temperature and nitrogen availability. *Tree Physiol* 16:719–725



Winter soil CO₂ efflux and its contribution to annual soil respiration in different ecosystems of a forest-steppe ecotone, north China

Wang Wei*, Peng Shushi, Wang Tao, Fang Jingyun

Department of Ecology, College of Urban and Environmental Sciences, and Key Laboratory for Earth Surface Processes of the Ministry of Education, Peking University, Beijing 100871, China

ARTICLE INFO

Article history:

Received 26 June 2009

Received in revised form

15 November 2009

Accepted 24 November 2009

Available online 5 December 2009

Keywords:

Mid-latitude ecosystems

Soil organic carbon

SR₁₀

Q₁₀

Winter soil CO₂ efflux

ABSTRACT

Most soil respiration measurements are conducted during the growing season. In tundra and boreal forest ecosystems, cumulative winter soil CO₂ fluxes are reported to be a significant component of their annual carbon budgets. However, little information on winter soil CO₂ efflux is known from mid-latitude ecosystems. Therefore, comparing measurements of soil respiration taken annually versus during the growing season will improve the accuracy of ecosystem carbon budgets and the response of soil CO₂ efflux to climate changes. In this study we measured winter soil CO₂ efflux and its contribution to annual soil respiration for seven ecosystems (three forests: *Pinus sylvestris* var. *mongolica* plantation, *Larix principis-rupprechtii* plantation and *Betula platyphylla* forest; two shrubs: *Rosa bella* and *Malus baccata*; and two meadow grasslands) in a forest-steppe ecotone, north China. Overall mean winter and growing season soil CO₂ effluxes were 0.15–0.26 μmol m⁻² s⁻¹ and 2.65–4.61 μmol m⁻² s⁻¹, respectively, with significant differences in the growing season among the different ecosystems. Annual Q₁₀ (increased soil respiration rate per 10 °C increase in temperature) was generally higher than the growing season Q₁₀. Soil water content accounted for 84% of the variations in growing season Q₁₀ and soil temperature range explained 88% of the variation in annual Q₁₀. Soil organic carbon density to 30 cm depth was a good surrogate for SR₁₀ (basal soil respiration at a reference temperature of 10 °C). Annual soil CO₂ efflux ranged from 394.76 g C m⁻² to 973.18 g C m⁻² using observed ecosystem-specific response equations between soil respiration and soil temperature. Estimates ranged from 424.90 g C m⁻² to 784.73 g C m⁻² by interpolating measured soil respiration between sampling dates for every day of the year and then computing the sum to obtain the annual value. The contributions of winter soil CO₂ efflux to annual soil respiration were 3.48–7.30% and 4.92–7.83% using interpolated and modeled methods, respectively. Our results indicate that in mid-latitude ecosystems, soil CO₂ efflux continues throughout the winter and winter soil respiration is an important component of annual CO₂ efflux.

© 2009 Elsevier Ltd. All rights reserved.

1. Introduction

Soil respiration is the primary pathway by which CO₂ fixed by plants returns to the atmosphere (Chapin et al., 1996). Most soil respiration measurements are conducted during the growing season, in part because of the difficulty in measuring CO₂ efflux under snow but also reflecting the assumption that microbial activity in frozen or snow-covered soils is negligible (Fahnestock et al., 1998).

However, the published data has convincingly demonstrated that soil microbial activity in the field occurs at freezing temperatures (Schmidt and Lipson, 2004; Nobrega and Grogan, 2007; Panikov and Sizova, 2007) and soil could release CO₂ when incubated in the laboratory at freezing temperatures down to –39 °C (Panikov et al., 2006). Therefore, comparing measurements of soil respiration taken

annually versus during the growing season is important for accurately estimating annual carbon budgets, modeling the effects of climate changes on soil carbon storage and release to the atmosphere (Chapin et al., 1996), and calculating belowground carbon allocation by plants (Giardina and Ryan, 2000).

In arctic and boreal ecosystems, significant rates of CO₂ emission from snow-covered soils have been reported (Groffman et al., 2006; Ludwig et al., 2006; Schimel et al., 2006; Miller et al., 2007). Respiratory losses during winter may offset a major portion of the carbon fixed during the growing season and could be critical in determining annual carbon cycling (Monson, 2005; Monson et al., 2006; Nobrega and Grogan, 2007). For example, the inclusion of wintertime losses of CO₂ into annual carbon budgets could increase the annual carbon efflux of arctic tundra ecosystems by 17% and change some ecosystems from net annual sinks to net sources of CO₂ to the atmosphere (Fahnestock et al., 1999). Annual carbon sequestration is overestimated by 72% in deciduous forests and

* Corresponding author. Tel.: +86 10 62767922; fax: +86 10 62756560.

E-mail address: wangw@urban.pku.edu.cn (W. Wang).

111% in coniferous forests when winter CO₂ fluxes are not included (Brooks et al., 2004).

Compared with arctic and boreal ecosystems, mid-latitude ecosystems are dominated by a shorter winter season and are typically snow-covered for less than half a year. These mid-latitude ecosystems are believed to be major sources of the terrestrial carbon sink in the northern hemisphere (Schimel et al., 2001). However, the carbon loss from mid-latitude soils during the winter and the contribution of winter soil respiration to total annual soil carbon efflux are seldom determined (Mariko et al., 2000; Uchida et al., 2005).

The global surface temperature is predicted to increase by 1.8–4.0 °C over the next century (IPCC, 2007). The response of soil CO₂ efflux to global warming is sensitive to slight changes in the relationship between soil respiration and soil temperature (Davidson et al., 2006). Q₁₀ (known as the increase in respiration rate per 10° increase in temperature) is commonly used to express the relationship between soil respiration and temperature (Kirschbaum, 2006). Most estimates of the Q₁₀ are based on measurements during the growing season, without considering soil CO₂ efflux in winter. Q₁₀ values range between 60 and 200 below 0 °C, while the maximum Q₁₀ above 0 °C is 9 (Mikan et al., 2002). Thus, there is a need for *in situ* measurement of soil respiration in winter to improve our understanding of the temperature sensitivity and mechanisms of soil respiration.

We conducted field experiments in seven ecosystems (three forests: *Pinus sylvestris* var. *mongolica* plantation, *Larix principis-rupprechtii* plantation and *Betula platyphylla* forest; two shrubs: *Rosa bella* and *Malus baccata*; and two meadow grasslands) in a forest-steppe ecotone, north China from June 2006 to October 2007. Our major objectives were (1) to determine the magnitude of winter soil CO₂ efflux and its contribution to total annual soil efflux for the different ecosystems; and (2) to quantify environmental controls of soil respiration, including soil temperature, water content and soil organic carbon density.

2. Materials and methods

2.1. Field sites

The study area was situated in the Saihanba Forestry Center in Hebei Province, north China (117°12′–117°30′E, 42°10′–42°50′N, 1400 m a.s.l.). The climate is semi-arid and semi-humid, with a long, cold winter (November–March), and a short spring and summer. The annual mean air temperature and precipitation over the period 1964–2004 are –1.4 °C and 450.1 mm, respectively. Seasonal snow cover begins to develop in November and snowmelt occurs in early April. In winter, snow accumulation is typically less than 30 cm in depth. The soils are predominantly sandy.

The study area belongs to a typical forest-steppe ecotone in the temperate areas of China. The primary forest has been harvested in large-scale industrial logging since the last century and replaced by secondary forests and plantations. This area contains the largest area of plantations in China, with dominant species of *P. sylvestris* var. *mongolica* and *L. principis-rupprechtii*. The secondary forest mainly consisted of *B. platyphylla*. Our study was conducted in two plantations of *P. sylvestris* var. *mongolica* and *L. principis-rupprechtii*, a secondary forest of *B. platyphylla*, two shrubs of *M. baccata* and *R. bella*, and two meadow grasslands, representing characteristic local ecosystem types. The herbaceous layer of *M. baccata* is dominated by *Veronica linariifolia*, *Galium verum*, *Heteropappus hispidus*, *Trollius chinensis* and *Bupleurum chinense*. The herbaceous layer of *R. bella* consisted of *Leymus chinensis*. Two meadow grasslands were selected with meadow grassland 1 dominated by *L. chinensis* and meadow grassland 2 with rich grass species such as *Saussurea iodostegia*, *Dianthus chinensis*, *Adenophora elata*, *Angelica dahurica*, *Geranium sibiricum*, *T. chinensis*, *Delphinium grandiflorum*, and *Sanguisorba officinalis*.

2.2. Soil CO₂ efflux measurements

We selected 9 independent forest plots arranged as three replicates for each forest type including 39-year-old *P. sylvestris* var. *mongolica*, 42-year-old *L. principis-rupprechtii* and 46-year-old *B. platyphylla* forest. An additional 12 independent plots from other ecosystem types were selected including three replicates for each of the *M. baccata*, *R. bella*, and two meadow grasslands. The area of each plot was 20 m × 20 m, with 5 subsamples (i.e. soil respiration collars) in each plot. The different ecosystems were less than 10 km away from each other to ensure similar climatic conditions.

Soil respiration was measured using a Li-8100 soil CO₂ Flux system (LI-COR Inc., Lincoln, NE, USA) from June 2006 to October 2007. The soil CO₂ efflux was calculated on the basis of a linear increase in chamber CO₂ concentrations over time.

During the growing season, five polyvinyl chloride (PVC) collars (10.2 cm inside diameter, 6 cm height) were inserted 3 cm into the soil in each plot, and left in the same locations throughout the study. The five PVC collars were placed in the central part of each plot, one in each of the four corners, and the fifth in the middle. Living plants inside the soil collars were clipped at the soil surface 1 day before each measurement of soil respiration. Soil CO₂ effluxes were measured every 15–20 days. In order to minimize daily variation in soil respiration and represent the average daily soil CO₂ efflux, measurements were made between 08:00 and 11:00 h (based on our measurements of diurnal changes in soil respiration, data not shown). In each measurement, respiration rates were calculated as means of three plots for each ecosystem.

During the winter, longer soil collars (determined by snow depth) were inserted into the soil surface and stabilized for 24 h before measurement of the winter soil CO₂ efflux (Kurganova et al., 2003; Elberling, 2007). The winter length in the study site was 5 months from November to March that was almost consistent with the continuous periods with <0.5 °C of mean daily soil temperature at 5 cm depth defined by Grogan and Jonasson (2006). The Li-8100 soil CO₂ Flux system was kept in an isolated and heated container to keep its temperature above freezing point. Soil CO₂ effluxes were measured once a month except for February.

2.3. Soil temperature and water content measurements

Soil temperature was recorded during respiration measurements near each collar at 5 cm soil depth with the LI-COR 8100 temperature probe. Continuous measurements of soil temperature at 5 cm depth were recorded at 30-min intervals with StowAway loggers (Onset Comp. Corp., Bourne, MA, USA) inserted in the soil near one collar at each study site.

Soil volumetric water content at a depth of 0–10 cm was measured using time domain reflectometry (Soilmoisture Equipment Corp., Santa Barbara, California). Since the absolute soil water content of different soil types depends on texture and stone content (Reichstein et al., 2003), relative water content values were computed by normalizing daily values of absolute soil water content with respect to the maximum value recorded at the site. No data of soil volumetric water content was obtained during the winter because the probe could not be fully inserted into the frozen soil.

2.4. The dependence of soil respiration on soil temperature and water content

On the basis of the measured data, exponential and polynomial functions were established to describe the relationship between soil respiration and soil temperature and between soil respiration and soil water content:

$$SR = a \times e^{\beta t} \quad (1)$$

$$SR = \chi M^2 + \delta M + \varepsilon \quad (2)$$

where SR, t , and M are soil respiration, temperature, and water content, respectively and a , β , χ , δ and ε are constant coefficients.

The temperature sensitivity (Q_{10}) of soil respiration was calculated as $Q_{10} = \exp(10 \times \beta)$. On the basis of year-round and growing season data, we calculated annual Q_{10} , SR_{10} (defined as the basal soil respiration rate at a reference temperature of 10 °C) and growing season Q_{10} and SR_{10} values.

A third equation was established by combining Equations (1) and (2) to describe the interactive effects of soil temperature and water content on soil respiration (Wan and Luo, 2003):

$$SR = a \times e^{\beta t} \frac{\chi M^2 + \delta M + \varepsilon}{\chi M_0^2 + \delta M_0^2 + \varepsilon} \quad (3)$$

where M_0^2 is the soil water content when soil respiration rate reaches the maximum.

2.5. Soil organic carbon density (SOCD)

Soil cores (5 cm diameter, 0–30 cm depth with a 10 cm sampling interval) from each ecosystem were collected in August 2006 (the peak plant growth period). Samples were air dried, roots removed and passed through a 2 mm sieve. Soil organic carbon (SOC) was measured using the dichromate oxidation method (Nelson and Sommers, 1982).

Soil bulk density was determined at each layer using soil cores of known volume and used to calculate the SOCD of each soil layer. Total SOCD to 30 cm was calculated by summing the SOCD in each soil layer.

2.6. Scaling for annual and winter soil CO₂ efflux

Soil CO₂ efflux over one year was calculated by integrating CO₂ effluxes for the period from 1 November 2006 to 31 October 2007 using the observed ecosystem-specific response equation between soil respiration and soil temperature (Equation (1)).

A further estimate of annual and winter soil respiration for each ecosystem was obtained by interpolating measured soil respiration between sampling dates for every day of the year and then computing the sum to obtain the annual or winter values (Frank and Dugas, 2001; Sims and Bradford, 2001) as follows:

$$SR = \sum F_{m,k} \Delta t_k \quad (4)$$

Where SR is soil respiration, $\Delta t_k = (t_k - t_{k-1})$, $\{t_0, t_1, t_2, \dots\}$ is the time sequence of field measurements across the season, and $F_{m,k}$ is

the average CO₂ efflux over the interval (t_{k-1} , t_k) recorded by the Li-8100 CO₂ system.

2.7. Statistical analysis

Kolmogorov–Smirnov statistics showed that all the data sets measured are normally distributed ($P > 0.05$). In order to reduce the dependence between samples that were measured at the same experimental core through time, we used the differences between measured value of each ecosystem and mean value of all ecosystem at each measurement to conduct one-way ANOVA for evaluating whether soil temperature, water content and soil respiration significantly differed among different ecosystems. Relationships between SR, Q_{10} and soil temperatures, water content, and soil characteristics were explored by linear regression and reported only when significant ($P < 0.05$). All statistical analyses were performed with a significance level of 0.05 with StatView 5.0 (SAS Institute, Inc., Cary, NC, USA).

3. Results

3.1. The magnitude of winter soil CO₂ efflux and its relationship with temperature

Mean winter soil CO₂ efflux ranged from 0.148 to 0.26 $\mu\text{mol m}^{-2} \text{s}^{-1}$ among different ecosystems (Table 1), which was 3.77–7.27% of the growing season efflux. No significant differences were found in winter soil CO₂ efflux among different ecosystems ($P > 0.05$ for all the comparisons). During the growing season, soil CO₂ efflux differed significantly among different ecosystems ($P < 0.05$ for all the comparisons), with a higher soil respiration rate in the meadow grassland 2 than in other ecosystems ($P < 0.05$ for all the treatments). For the forest ecosystems, *B. platyphylla* had a higher soil CO₂ efflux than *P. sylvestris* var. *mongolica* and *L. principis-rupprechtii* ($P < 0.05$ for all the treatments). This variation in the growing season soil respiration among different ecosystems was significantly correlated with SOCD (Supplement Fig. 1). Soil temperature or water content could not significantly affect the variation in the growing season soil respiration among different ecosystems.

Soil temperature at 5 cm depth was generally at a minimum in January, and reached a maximum in mid summer (Fig. 1), responding to changes in air temperature (data not shown). Mean winter soil temperatures in forests and shrubs (−5.71 °C and −5.34 °C) were significantly higher than those in two meadow grasslands (−7.35 °C and −7.05 °C) (Supplement Fig. 2, $P < 0.05$ for all the comparisons). No obvious relationship occurred between winter soil CO₂ efflux and soil temperature. However, when combining the April data (early spring) with the winter soil efflux, a significant increased trend was found between soil respiration and temperature (Fig. 2).

Table 1
Winter soil CO₂ efflux and its contribution to annual soil CO₂ efflux for different ecosystems.

Ecosystem types	Mean and range of winter CO ₂ efflux (WCE) ($\mu\text{mol m}^{-2} \text{s}^{-1}$)	Mean and range of growing season CO ₂ efflux ($\mu\text{mol m}^{-2} \text{s}^{-1}$)	Estimated WSE (g C m^{-2})		Annual soil respiration (g C m^{-2})		WCE/annual soil respiration (%)	
			Interpolated	Modeled	Interpolated	Modeled	Interpolated	Modeled
Forests								
<i>P. sylvestris</i> (39 years)	0.205(0.15–0.28)	2.82(0.38–5.03)	31.64	21.62	453.26	439.52	6.98	4.92
<i>L. principis</i> (42 years)	0.205(0.17–0.26)	3.03(0.58–5.78)	31.80	35.49	435.59	—	7.30	—
<i>B. platyphylla</i> (46 years)	0.26 (0.16–0.37)	3.98(0.65–6.81)	39.96	41.41	575.86	565.33	6.94	7.32
Shrubs								
<i>M. baccata</i>	0.168(0.11–0.20)	3.39(0.77–6.97)	26.05	31.73	620.75	405.37	4.20	7.83
<i>R. bella</i>	0.190(0.14–0.31)	3.68(0.92–6.45)	29.19	36.47	653.22	640.74	4.47	5.69
Meadow grassland 1	0.148(0.05–0.21)	2.65(0.61–4.77)	17.75	27.00	424.90	394.76	4.18	6.84
Meadow grassland 2	0.174(0.04–0.30)	4.61(0.41–8.24)	27.33	50.33	784.73	973.18	3.48	5.17

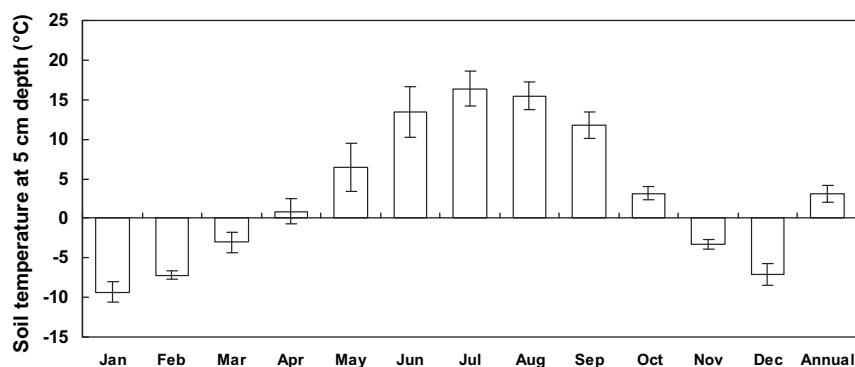


Fig. 1. Temporal changes of soil temperature at 5 cm depth in a forest-steppe ecotone, north China.

3.2. Comparison of Q_{10} and SR_{10} taken annually versus during the growing season

An exponential regression of observed soil CO_2 effluxes versus soil temperature (Fig. 3) showed that annual Q_{10} values (3.10–4.69) were generally higher than those for the growing season (2.77–5.23) (Fig. 4a). Annual SR_{10} (1.03 – $3.50 \mu mol m^{-2} s^{-1}$) were generally similar to those during the growing season (1.13 – $3.54 \mu mol m^{-2} s^{-1}$) (Fig. 4b).

Soil water content explained 84% of the variation in the growing season Q_{10} (Fig. 5a) and soil temperature range explained 88% of the variation in the annual Q_{10} values (Fig. 5b) among different ecosystems. For a constant soil temperature of $10^\circ C$, differences in soil respiration rates taken annually and during the growing season could be explained by SOCD to 30 cm depth among different ecosystems (Fig. 6).

3.3. Dependence of soil CO_2 efflux on soil temperature and water content

Over the whole year, soil respiration rates increased exponentially with soil temperature for all of the 7 different ecosystems (Fig. 3, Supplement Table 1). Soil temperature alone explained 86–94% of the annual temporal changes in soil respiration (Supplement Table 1). During the growing season, soil temperature explained 52–90% of the variation in soil respiration (Supplement Table 1).

A polynomial function provided the best fit for the relationship between soil CO_2 efflux and soil water content (Supplement Fig. 3). Soil water content alone explained 54–80% of the variation in soil respiration (Supplement Fig. 3). The combined use of soil

temperature and soil water content functions could only explain 34–81% of the variation in soil respiration (Supplement Table 1), indicating that the inclusion of soil water content function did not improve the explanation of soil CO_2 efflux compared with the regressions based on the soil temperature only.

Soil temperature was the main determinant of temporal changes in soil respiration for each ecosystem and was a good surrogate for estimating annual soil respiration. The temporal dynamics of soil CO_2 efflux followed the distinct seasonal pattern of soil temperature for all ecosystems, being high during summer and low in winter (Supplement Fig. 4). The model using an exponential relationship between soil respiration and soil temperature at 5 cm depth simulated the seasonal variation of soil respiration very well, but underestimated or overestimated the values during the summer (Supplement Fig. 4).

3.4. Contribution of winter soil respiration to annual soil efflux

The modeled annual soil CO_2 effluxes (394.76 – $973.18 g C m^{-2}$) were higher or lower than interpolated values (435.59 – $784.73 g C m^{-2}$), depending on the ecosystem types (Fig. 7b). For meadow grassland 2, the modeled value was 24% higher than the interpolated value. For other vegetation types, the modeled values were similar or lower than the interpolated values. For example, in *M. baccata*, the interpolated value was 35% higher than the modeled value.

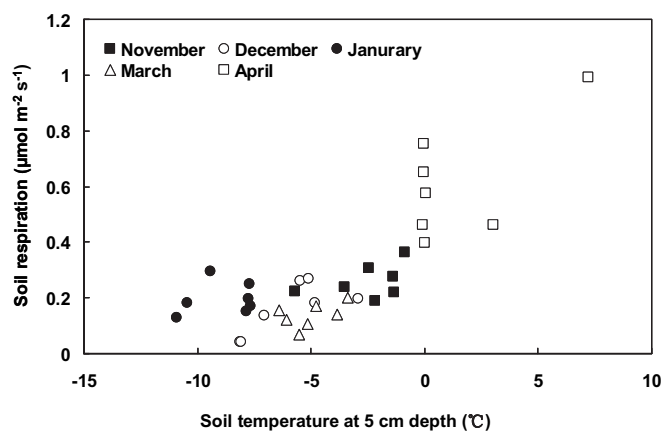
The modeled winter CO_2 effluxes (21.62 – $50.33 g C m^{-2}$) were typically 12–85% higher than those estimated by linear interpolation (17.75 – $39.96 g C m^{-2}$, Fig. 7a), except for *P. sylvestris*, which was 32% lower than the interpolated value. The contributions of winter soil CO_2 efflux to annual soil efflux were 3.48–7.30% and 4.92–7.83% using the interpolated and modeled methods, respectively (Table 1).

4. Discussion

4.1. The magnitude of winter soil CO_2 efflux and its Q_{10}

Our measured values of mean winter soil CO_2 efflux (0.148 – $0.26 \mu mol m^{-2} s^{-1}$) for different ecosystems (Table 1) are consistent with the modeled values of Raich and Potter (1995). According to their model, in ecosystems with distinct dry seasons, soil respiration rates during winters with mean air temperatures from -15 to $-5^\circ C$ were generally below $0.263 \mu mol m^{-2} s^{-1}$.

Meadow grassland measurements (0.04 – $0.30 \mu mol m^{-2} s^{-1}$) fell within the reported values (0.025 – $1.55 \mu mol m^{-2} s^{-1}$) (Sommerfeld et al., 1993; Frank et al., 2002). For instance, in a semi-arid northern mixed-grass prairie in North Dakota, Frank et al. (2002) found averaged winter respiration rate was $0.48 \mu mol m^{-2} s^{-1}$.



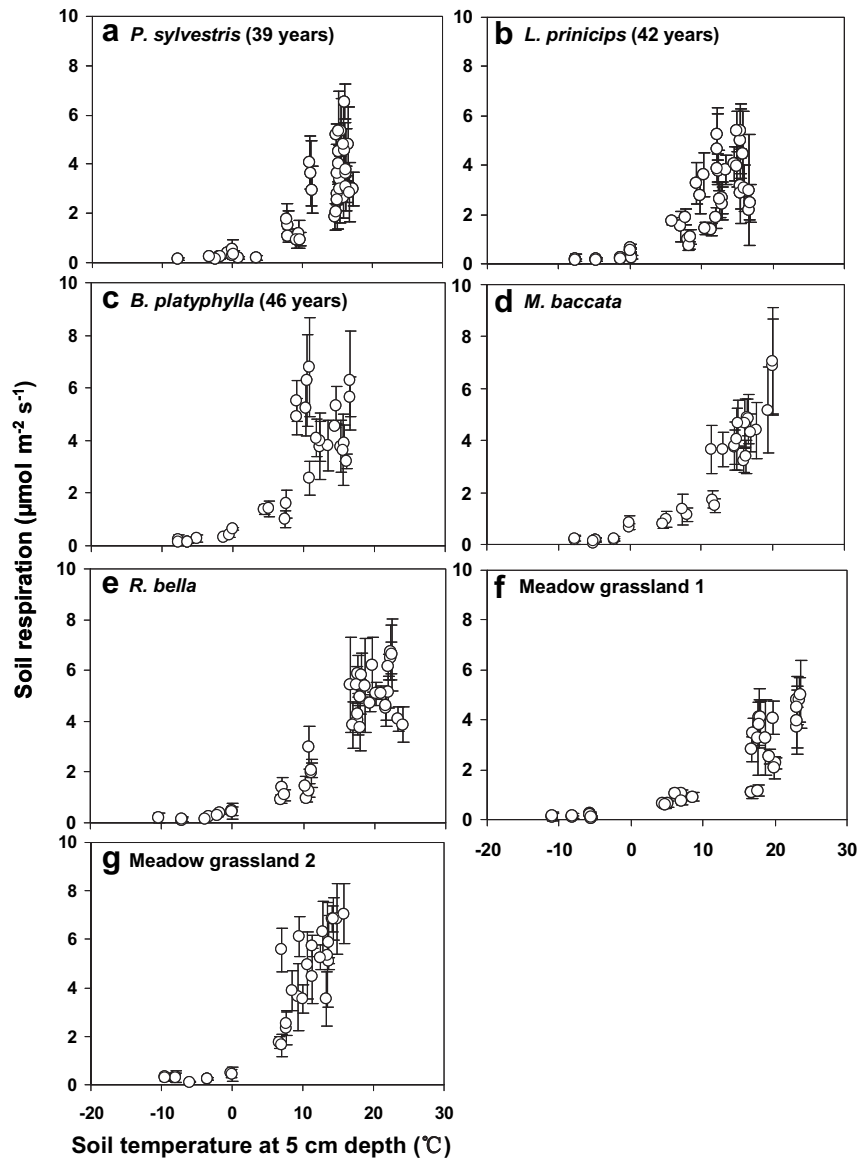


Fig. 3. Responses of soil respiration to soil temperature at 5 cm depth from June 2006 to October 2007 for different ecosystems in a forest-steppe ecotone, north China. Error bars are standard deviation of the measured values.

For the forests and shrubs, our estimates in winter soil CO_2 effluxes ($0.168\text{--}0.26 \mu\text{mol m}^{-2} \text{s}^{-1}$) were similar to those ($0.11\text{--}0.28 \mu\text{mol m}^{-2} \text{s}^{-1}$) reported by Elberling (2007) for three dominating types of vegetation (Dryas, Cassiope, and Salix) at Svalbard with soil

temperature ranging from -9.1 to -3.3°C . However, our estimates were lower than most of the reported values in tundra and boreal ecosystems (McDowell et al., 2000; Hubbard et al., 2005; Suzuki et al., 2006). For example, soil CO_2 efflux during the winter averaged

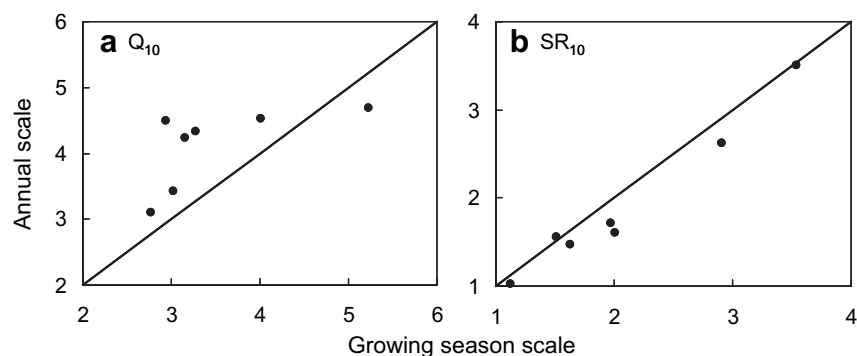


Fig. 4. Comparison of Q_{10} and SR_{10} taken annually versus during the growing season for different ecosystems in a forest-steppe ecotone, north China.

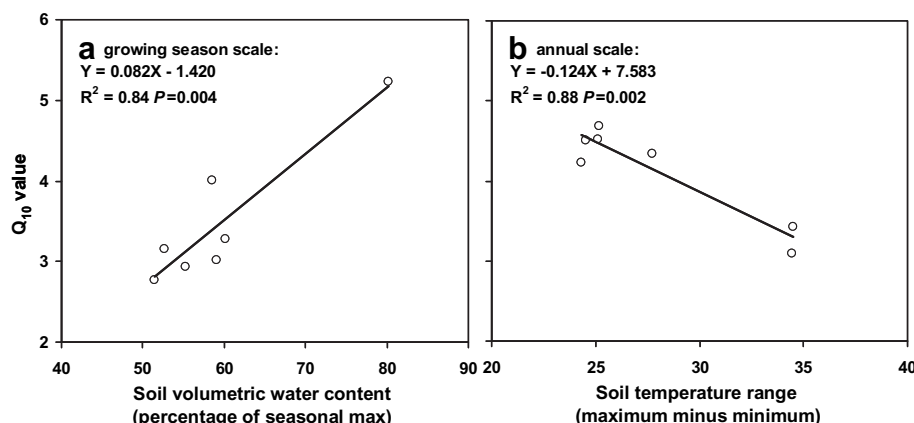


Fig. 5. Relationships (a) between soil volumetric water content at 0–10 cm depth and growing season Q_{10} and (b) between soil temperature range at 5 cm depth and annual Q_{10} .

$0.34 \mu\text{mol m}^{-2} \text{s}^{-1}$ in subalpine forests (Hubbard et al., 2005) and $0.37 \mu\text{mol m}^{-2} \text{s}^{-1}$ in a deciduous broad-leaved forest in Japan (Suzuki et al., 2006). Much higher rates were found in a mixed conifer forest in Washington State ($0.67 \mu\text{mol m}^{-2} \text{s}^{-1}$, McDowell et al., 2000), in an Austrian mountain forest ($0.64 \mu\text{mol m}^{-2} \text{s}^{-1}$, Schindlbacher et al., 2007) and in an Engelmann spruce forest in Wyoming ($0.52 \mu\text{mol m}^{-2} \text{s}^{-1}$, Sommerfeld et al., 1996).

The differences of winter soil CO_2 efflux among different sites may be mainly connected with the subsurface temperature influenced by thickness and duration of snow cover (Elberling, 2007). In our study area, the snow cover was thin ranging from 7 to 22 cm among different ecosystems and the duration of snow cover was short for all the ecosystems except *B. platyphylla*, which remained consistently snow-covered until early April. The snow cover less than 30 cm depth could not effectively decouple soil temperatures from the atmosphere (Mariko et al., 2000; Uchida et al., 2005; Schimel et al., 2006), resulting in lower soil temperatures and respiration rates.

Although soil temperature was a key environmental factor controlling seasonal trends of soil respiration, there was no direct relationship between soil temperature and winter soil CO_2 efflux. Winter soil temperature showed distinct temporal changes (Supplement Fig. 2), but no significant temporal changes occurred in winter soil CO_2 efflux (Fig. 2). Our results indicate that a critical threshold of soil temperature may exist for active respiration, below which a lack of free water limits contemporaneous heterotrophic contributions to winter CO_2 loss (Schimel and Clein, 1996; Brooks et al., 1997).

The unfrozen water content of soils below 0°C was reported to decline as an exponential or power function of temperature (Romanovsky and Osterkamp, 2000).

We observed a rapid increase of soil CO_2 efflux by a factor of 2–14 from late winter to early spring (April) (Fig. 2) among different ecosystems. This rapid increase of CO_2 release from winter to early spring has also been found in other forests (Hubbard et al., 2005; Schindlbacher et al., 2007) and tundra ecosystems (Zimov et al., 1996; Oechel et al., 1997; Brooks et al., 1997). This pattern of soil efflux most likely reflects abiotic conditions that are conducive to microbial and root respiration at the end of winter such as warmer soil temperatures and greater availability of unfrozen water (Ostroumov and Sievert, 1996) and root growth (Hanson et al., 2003).

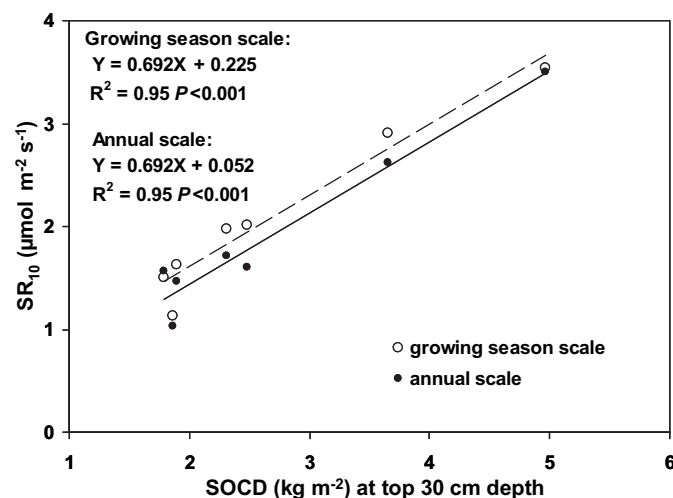


Fig. 6. Relationship between SR_{10} and SOCD to 30 cm depth.

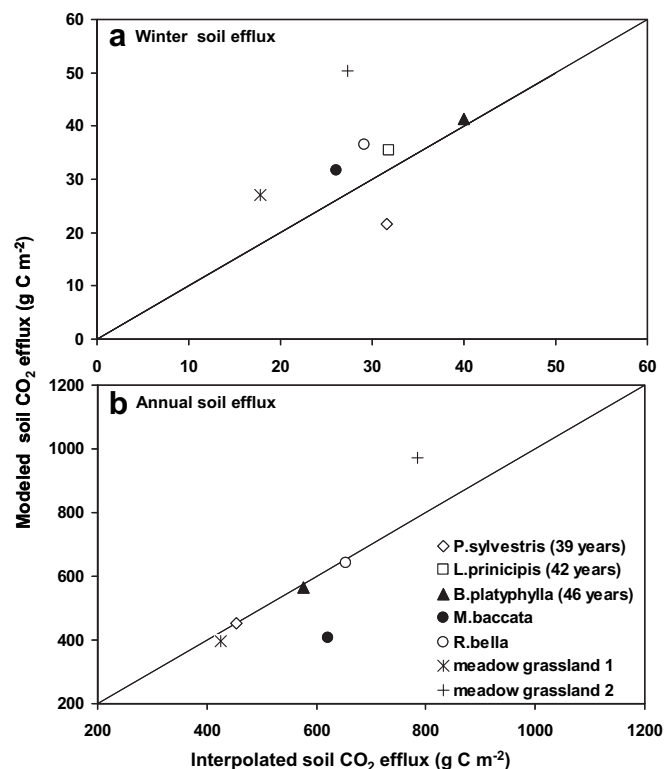


Fig. 7. Comparison of interpolated soil effluxes and modeled ones for (a) winter soil efflux and (b) annual soil efflux from different ecosystems. The former was estimated by linear interpolation based on periodic measurements and the latter was estimated by exponential relationship between soil respiration and soil temperature. Solid line is the 1:1 line.

4.2. Comparison of Q_{10} and SR_{10} taken annually versus during the growing season

Annual and growing season Q_{10} values ranged from 3.10 to 4.69 and from 2.77 to 5.23, respectively, which are well within the range (2.0–6.3) reported for other temperate ecosystems (Kirschbaum, 1995; Davidson et al., 1998; Saiz et al., 2006; Wang et al., 2006). Higher annual than the growing season Q_{10} values were also observed by Elberling (2007). Q_{10} values were negatively correlated with soil temperature range (Fig. 5b), indicating that a reduction in Q_{10} with temperature range may be attributed to direct physiological acclimation of the roots or microorganisms to the changing soil temperature regime (Atkin and Tjoelker, 2003). Although soil temperature range is the main controlling factor throughout the entire year, the variations in Q_{10} might reflect confounding effects of temperature sensitivity and seasonal changes in physiological activities induced by root phenology, microbial biomass, and other factors (Curiel Yuste et al., 2004). Where temperature and substrate supply positively vary together naturally, the apparent Q_{10} is likely to be elevated, reflecting both the true temperature sensitivity of respiration and the seasonality of substrate supply (Davidson et al., 2006).

During the growing season, soil water content was a major factor accounting for the differences in Q_{10} values among different ecosystems (Fig. 5a). A strong dependence of Q_{10} values on soil water content has been observed in many ecosystems (Xu and Qi, 2001a,b; Reichstein et al., 2002; Widén, 2002; Harper et al., 2005). For instance, Reichstein et al. (2002) reported a reduction of Q_{10} for soil respiration from about 2.5 to 1 with increasing drought severity in three Mediterranean evergreen stands and Wang et al. (2006) found that Q_{10} values tended to increase with soil water content before reaching a threshold and then declining. The lower temperature sensitivity of soil respiration observed during dry conditions may largely be a result of substrate limitation caused by limited diffusion of solutes in thin soil water films.

Annual and growing season SR_{10} values varied from 1.03 to 3.50 $\mu\text{mol m}^{-2} \text{s}^{-1}$ and from 1.13 to 3.54 $\mu\text{mol m}^{-2} \text{s}^{-1}$, respectively. These values are similar to those reported for other temperate soils (0.7–4.9 $\mu\text{mol m}^{-2} \text{s}^{-1}$) (Raich and Schlesinger, 1992; Davidson et al., 1998; Janssens and Pilegaard, 2003). Both annual and seasonal SR_{10} were positively correlated with SOCD to 30 cm depth (Fig. 6), indicating that a change in the supply of substrate for heterotrophic respiration may be responsible for most of the observed variation in SR_{10} among the different ecosystems when soil temperature is held constant.

4.3. The contribution of winter soil respiration to annual soil CO_2 efflux

Our estimates in the contribution of winter soil respiration to annual soil CO_2 efflux (3.48–7.30% and 4.92–7.83% using the interpolated and modeled methods, respectively) were lower than the reported values (8–50%) from alpine and high-latitude ecosystems (Mariko et al., 2000; Kurganova et al., 2003; Vogel and Valentine, 2005; Schindlbacher et al., 2007). For instance, by including the winter respiratory losses, the measurements of soil CO_2 efflux during the winter increased estimates of net annual carbon loss in the Arctic by an average of 17% (Fahnestock et al., 1999) and by 14–30% in the High Arctic (Elberling, 2007); 10–15% in cool-temperate deciduous forest, Japan (Mariko et al., 2000; Mo et al., 2005) and 50% in Siberia (Zimov et al., 1996). The lower contribution of winter soil CO_2 efflux to annual soil respiration in our study area may be attributable to a thinner snow cover inducing lower soil temperatures and a shorter wintertime length.

5. Conclusions

Mean winter soil CO_2 efflux ranged from 0.15 to 0.26 $\mu\text{mol m}^{-2} \text{s}^{-1}$ among different ecosystems. This is consistent with the modeled

estimates of soil respiration rates during the winter with mean air temperatures from -15 to -5 °C in ecosystems with distinct dry seasons being generally below 0.263 $\mu\text{mol m}^{-2} \text{s}^{-1}$ (Raich and Potter, 1995). The differences in soil respiration rates among different ecosystems occurred during the growing season. The factors influencing Q_{10} values differed when taken annually versus during the growing season. Growing season Q_{10} values increased with soil water content and annual Q_{10} values decreased with soil temperature range. When soil temperature was held constant, SOCD to 30 cm depth was a good surrogate for SR_{10} . The contribution of winter soil respiration to the annual soil efflux ranged from 3.48–7.30% to 4.92–7.83% among different ecosystems using interpolated and modeled methods, respectively, which is lower than the reported values (8–50%) in alpine and high-latitude ecosystems (Vogel and Valentine, 2005; Schindlbacher et al., 2007).

Acknowledgments

This work was supported by the Projects of National Natural Science Foundation of China.

Appendix. Supplementary material

Supplementary data associated with this article can be found in the online version at doi:10.1016/j.soilbio.2009.11.028.

References

- Atkin, O.K., Tjoelker, M.G., 2003. Thermal acclimation and the dynamic response of plant respiration to temperature. *Trends in Plant Science* 8, 343–351.
- Brooks, P.D., Mcknight, D., Elder, K., 2004. Carbon limitation of soil respiration under winter snowpacks: potential feedbacks between growing season and winter carbon fluxes. *Global Change Biology* 11, 231–238.
- Brooks, P.D., Schmidt, S.K., Williams, M.W., 1997. Winter production of CO_2 and N_2O from alpine tundra: environmental controls and relationship to inter-system C and N fluxes. *Oecologia* 110, 403–413.
- Chapin, F.S., Zimov, S.A., Shaver, G.R., 1996. CO_2 fluctuation at high latitudes. *Nature* 383, 585–586.
- Curiel Yuste, J., Janssens, I.A., Carrara, A., Ceulemans, R., 2004. Annual Q_{10} of soil respiration reflects plant phenological patterns as well as temperature sensitivity. *Global Change Biology* 10, 161–169.
- Davidson, E.A., Belk, E., Boone, R.D., 1998. Soil water content and temperature as independent or confounded factors controlling soil respiration in a temperate mixed hardwood forest. *Global Change Biology* 4, 217–227.
- Davidson, E.A., Janssens, I.A., Luo, Y., 2006. On the variability of respiration in terrestrial ecosystems: moving beyond Q_{10} . *Global Change Biology* 12, 154–164.
- Elberling, B., 2007. Annual soil CO_2 effluxes in the High Arctic: the role of snow thickness and vegetation type. *Soil Biology and Biochemistry* 39, 646–654.
- Fahnestock, J.T., Jones, M.H., Brooks, P.D., 1998. Winter and early spring CO_2 efflux from tundra communities of Northern Alaska. *Journal of Geophysical Research – Atmospheres* 103, 29023–29027.
- Fahnestock, J.T., Jones, M.H., Welker, J.M., 1999. Wintertime CO_2 efflux from arctic soils: implications for annual carbon budgets. *Global Biogeochemical Cycles* 13, 775–779.
- Frank, A.B., Dugas, W.A., 2001. Carbon dioxide fluxes over a northern, semi-arid, mixed-grass prairie. *Agricultural and Forest Meteorology* 108, 317–326.
- Frank, A.B., Liebig, M.A., Hanson, J.D., 2002. Soil carbon dioxide fluxes in northern semiarid grassland. *Soil Biology and Biochemistry* 34, 1235–1241.
- Giardina, C.P., Ryan, M.G., 2000. Evidence that decomposition rates of organic carbon in mineral soil do not vary with temperature. *Nature* 404, 858–861.
- Groffman, P.M., Hardy, J.P., Driscoll, C.T., Fahey, T.J., 2006. Snow depth, soil freezing, and fluxes of carbon dioxide, nitrous oxide and methane in a northern hardwood forest. *Global Change Biology* 12, 1748–1760. doi:10.1111/j.1365-2486.2006.01194.x.
- Grogan, P., Jonasson, S., 2006. Ecosystem CO_2 production during winter in a Swedish subarctic region: the relative importance of climate and vegetation type. *Global Change Biology* 12, 1479–1495.
- Hanson, P.J., O'Neill, E.G., Chambers, M.L.S., Riggs, J.S., Joslin, J.D., Wolfe, M.H., 2003. Soil respiration and litter decomposition. In: Hanson, P.J., Wullschlegel, S.D. (Eds.), *North American Temperate Deciduous Forest Responses to Changing Precipitation Regimes*. Springer-Verlag, New York, pp. 163–189.
- Harper, C.W., Blair, J.M., Fay, P.A., Knapp, A.K., Carlisle, J.D., 2005. Increased rainfall variability and reduced rainfall amount decreases soil CO_2 efflux in a grassland ecosystem. *Global Change Biology* 11, 322–334.
- Hubbard, R.M., Ryan, M.G., Elder, K., Rhoades, C.C., 2005. Seasonal patterns in soil surface CO_2 flux under snow cover in 50 and 300 year old subalpine forest. *Biogeochemistry* 73, 93–107.

- IPCC, 2007. Summary for policy makers. In: Solomon, S., Qin, D., Manning, M., Chen, Z., Marquis, M., Avery, K.B., Tignor, M., Miller, H.L. (Eds.), *Climate Change 2007: the Physical Science Basis. Contribution of Working Group I to the Fourth Assessment Report of the Intergovernmental Panel on Climate Change*. Cambridge University Press, Cambridge, United Kingdom and New York, NY, pp. 1–18.
- Janssens, I.A., Pilegaard, K., 2003. Large seasonal changes in Q_{10} respiration in a beech forest. *Global Change Biology* 9, 911–918.
- Kirschbaum, M.U.F., 1995. The temperature dependence of soil organic matter decomposition and the effect of global warming on soil organic C storage. *Soil Biology and Biochemistry* 27, 753–760.
- Kirschbaum, M.U.F., 2006. The temperature dependence of organic-matter decomposition—still a topic of debate. *Soil Biology and Biochemistry* 38, 2510–2518.
- Kurganova, I., De Gerenyu, V.L., Rozanova, L., 2003. Annual and seasonal CO_2 fluxes from Russian southern taiga soils. *Tellus* 55B, 338–344.
- Ludwig, B., Teepe, R., de Gerenyu, V.L., Flessa, H., 2006. CO_2 and N_2O emissions from gleyic soils in the Russian tundra and a German forest during freeze–thaw periods – a microcosm study. *Soil Biology and Biochemistry* 38, 3516–3519.
- Mariko, S., Nishimura, N., Mo, W., 2000. Winter CO_2 flux from soil and snow surfaces in a cool-temperate deciduous forest, Japan. *Ecological Research* 15, 363–372.
- McDowell, N.G., Marshall, J.D., Hooker, T.D., 2000. Estimating CO_2 flux from snowpacks at three sites in the Rocky Mountains. *Tree Physiology* 20, 745–753.
- Mikan, C.J., Schimel, J.P., Doyle, A.P., 2002. Temperature controls of microbial respiration in arctic tundra soils above and below freezing. *Soil Biology and Biochemistry* 34, 1785–1795.
- Miller, A.E., Schimel, J.P., Sickman, J.O., Meixner, T., Doyle, A.P., Melack, J.M., 2007. Mineralization responses at near-zero temperatures in three alpine soils. *Biogeochemistry* 84, 233–245.
- Mo, W.H., Lee, M.S., Uchida, M., Inatomi, M., Saigusa, N., Mariko, S., Koizumi, H., 2005. Seasonal and annual variations in soil respiration in a cool-temperate deciduous broad-leaved forest in Japan. *Agricultural and Forest Meteorology* 134, 81–94.
- Monson, R.K., 2005. Climatic influences on net ecosystem CO_2 exchange during the transition from wintertime carbon source to springtime carbon sink in a high-elevation, subalpine forest. *Oecologia* 146, 130–147.
- Monson, R.K., Lipson, D.L., Burns, S.P., Turnipseed, A.A., Delany, A.C., Williams, M.W., Schmidt, S.K., 2006. Winter forest soil respiration controlled by climate and microbial community composition. *Nature* 439, 711–714.
- Nelson, D.W., Sommers, L.E., 1982. Total carbon, organic carbon and organic matter. In: Page, A.L. (Ed.), *Methods of Soil Analysis Part 1*, second ed. ASA, Madison, pp. 539–577.
- Nobrega, S., Grogan, P., 2007. Deeper snow enhances winter respiration from both plant-associated and bulk soil carbon pools in Birch Hummock tundra. *Ecosystems* 10, 419–431.
- Oechel, W.C., Vourlitis, G., Hastings, S.J., 1997. Cold season CO_2 emission from arctic soils. *Global Biogeochemical Cycles* 11, 163–172.
- Ostroumov, V.E., Siegert, C., 1996. Exobiological aspects of mass transfer in micro-zones of permafrost deposits. *Advances in Space Research* 18, 79–86.
- Panikov, N.S., Sizova, M.V., 2007. Growth kinetics of microorganisms isolated from Alaskan soil and permafrost in solid media frozen down to $-35\text{ }^{\circ}\text{C}$. *FEMS Microbial Ecology* 59, 500–512.
- Panikov, N.S., Flanagan, P.W., Oechel, W.C., Mastepanov, M.A., Christensen, T.R., 2006. Microbial activity in soils frozen to below $-39\text{ }^{\circ}\text{C}$. *Soil Biology and Biochemistry* 38, 785–794.
- Raich, J.W., Schlesinger, W.H., 1992. The global carbon dioxide flux in soil respiration and its relationship to vegetation and climate. *Tellus* 44B, 81–99.
- Raich, J.W., Potter, C.S., 1995. Global patterns of carbon dioxide emissions from soils. *Global Biogeochemical Cycles* 9, 23–36.
- Reichstein, M., Rey, A., Freibauer, A., Tenhunen, J., Valentini, R., Banza, J., Casals, P., Cheng, Y., Gruenzweig, J.M., Irvine, J., Joffre, R., Law, B.E., Loustau, D., Miglietta, F., Oechel, W., Ourcival, J.-M., Pereira, J.S., Peressotti, A., Ponti, F., Qi, Y., Rambal, S., Rayment, M., Romanya, J., Rossi, F., Tedeschi, V., Tirone, G., Xu, M., Yakir, D., 2003. Modeling temporal and large-scale spatial variability of soil respiration from soil water availability, temperature and vegetation productivity indices. *Global Biogeochemical Cycles* 17, 1104–1118.
- Reichstein, M., Tenhunen, J.D., Rouspard, O., Ourcival, J.M., Rambal, S., Miglietta, F., Peressotti, A., Pecchiari, M., Tirone, G., Valentini, R., 2002. Severe drought effects on ecosystem CO_2 and H_2O fluxes at three Mediterranean evergreen sites: revision of current hypotheses? *Global Change Biology* 8, 999–1017.
- Romanovsky, V.E., Osterkamp, T.E., 2000. Effects of unfrozen water on heat and mass transport processes in the active layer and permafrost. *Permafrost and Periglacial Processes* 11, 219–239.
- Saiz, G., Byrne, K.A., Butterbach-Bahl, K., Kiese, R., Blujdea, V., Farrell, E.P., 2006. Stand age-related effects on soil respiration in a first rotation Sitka spruce chronosequence in central Ireland. *Global Change Biology* 12, 1007–1020. doi:10.1111/j.1365-2486.2006.01145.x.
- Schimel, J.P., Clein, J.S., 1996. Microbial response to freeze–thaw cycles in tundra and taiga soils. *Soil Biology and Biochemistry* 28, 1061–1066.
- Schimel, D.S., House, J.I., Hibbard, K.A., 2001. Recent patterns and mechanisms of carbon exchange by terrestrial ecosystems. *Nature* 414, 169–172.
- Schimel, J.P., Fahnestock, J., Michaelson, G., 2006. Cold-season production of CO_2 in arctic soils: can laboratory and field estimates be reconciled through a simple modeling approach? *Arctic, Antarctic and Alpine Research* 38, 249–256.
- Schindlbacher, A., Zechmeister-Boltenstern, S., Glatzel, G., Jandl, R., 2007. Winter soil respiration from an Austrian mountain forest. *Agricultural and Forest Meteorology* 146, 205–215.
- Schmidt, S.K., Lipson, D.A., 2004. Microbial growth under the snow: implications for nutrient and allelochemical availability in temperate soils. *Plant and Soil* 259, 1–7.
- Sims, P.L., Bradford, J.A., 2001. Carbon dioxide fluxes in a southern plains prairie. *Agricultural and Forest Meteorology* 109, 117–134.
- Sommerfeld, R.A., Mosier, A.R., Musselman, R.C., 1993. CO_2 , CH_4 and N_2O flux through a Wyoming snowpack and implications for global budgets. *Nature* 361, 140–142.
- Sommerfeld, R.A., Massman, W.J., Musselman, R.C., 1996. Diffusional flux of CO_2 through snow: spatial and temporal variability among alpine–subalpine sites. *Global Biogeochemical Cycles* 10, 473–482.
- Suzuki, S., Ishizuka, S., Kitamura, K., 2006. Continuous estimation of winter carbon dioxide efflux from the snow surface in a deciduous broadleaf forest. *Journal of Geophysical Research – Atmospheres* 111 (D17). doi:10.1029/2005JD006595 Art. No. D17101.
- Uchida, M., Mo, W., Nakatsubo, T., 2005. Microbial activity and litter decomposition under snow cover in a cool-temperate broad-leaved deciduous forest. *Agricultural and Forest Meteorology* 134, 102–109.
- Vogel, J.G., Valentine, D.W., 2005. Small root exclusion collars provide reasonable estimates of root respiration when measured during the growing season of installation. *Canadian Journal of Forest Research* 35, 2112–2117.
- Wan, S.Q., Luo, Y.Q., 2003. Substrate regulation of soil respiration in a tallgrass prairie: results of a clipping and shading experiment. *Global Biogeochemical Cycles* 17, 1054. doi:10.1029/2002GB001971.
- Wang, C.K., Yang, J.Y., Zhang, Q.Z., 2006. Soil respiration in six temperate forests in China. *Global Change Biology* 12, 1–12. doi:10.1111/j.1365-2486.2006.01234.x.
- Widén, B., 2002. Seasonal variation in forest-floor CO_2 exchange in a Swedish coniferous forest. *Agricultural and Forest Meteorology* 111, 283–297.
- Xu, M., Qi, Y., 2001a. Spatial and seasonal variations of Q_{10} determined by soil respiration measurements at a Sierra Nevada forest. *Global Biogeochemical Cycles* 15, 687–696.
- Xu, M., Qi, Y., 2001b. Soil-surface CO_2 efflux and its spatial and temporal variations in a young ponderosa pine plantation in northern California. *Global Change Biology* 7, 667–677.
- Zimov, S.A., Davidov, S.P., Voropaev, Y.V., 1996. Siberian CO_2 efflux in winter as a CO_2 source and cause of seasonality in atmospheric CO_2 . *Climate Change* 33, 111–112.



Forest soil respiration and its heterotrophic and autotrophic components: Global patterns and responses to temperature and precipitation

Wang Wei*, Chen Weile, Wang Shaopeng

Department of Ecology, College of Urban and Environmental Sciences, and Key Laboratory for Earth Surface Processes of the Ministry of Education, Peking University, Beijing 100871, China

ARTICLE INFO

Article history:

Received 3 January 2010

Received in revised form

15 April 2010

Accepted 18 April 2010

Available online 5 May 2010

Keywords:

Autotrophic respiration

Heterotrophic respiration

Mean annual precipitation

Mean annual temperature

Non-linear responses

ABSTRACT

Quantifying global patterns of forest soil respiration (SR), its components of heterotrophic respiration (HR) and belowground autotrophic respiration (AR), and their responses to temperature and precipitation are vital to accurately evaluate responses of the terrestrial carbon balance to future climate change. There is great uncertainty associated with responses of SR to climate change, concerning the differences in climatic controls and apparent Q_{10} (the factor by which respiration increases for a 10 °C increase in temperature) over HR and AR. Here, we examine available information on SR, HR, AR, the contribution of HR to SR (HR/SR), and Q_{10} of SR and its components from a diverse global database of forest ecosystems. The goals were to test how SR and its two components (AR and HR) respond to temperature and precipitation changes, and to test the differences in apparent Q_{10} between AR and HR. SR increased linearly with mean annual temperature (MAT), but responded non-linearly to mean annual precipitation (MAP) in naturally-regenerated forests. For every 1 °C increase in MAT, overall emissions from SR increased by 24.6 g C m⁻² yr⁻¹. When MAP was less than 813 mm, every 100 mm increase in MAP led to a release of 75.3 g C m⁻² yr⁻¹, but the increase rate declined to 20.3 g C m⁻² yr⁻¹ when MAP was greater than 813 mm. MAT explained less variation in AR than that in HR. The overall emissions in AR and HR for every 1 °C increase in MAT, increased by 12.9 and 16.1 g C m⁻² yr⁻¹, respectively. The AR emissions for every 100 mm increase in MAP, increased by 44.5 g C m⁻² yr⁻¹ when MAP less than 1000 mm. However, above the threshold, AR emissions stayed relatively constant. HR increased linearly by 15.0 g C m⁻² yr⁻¹ with every 100 mm increased in MAP. The Q_{10} value of SR increased with increasing depth at which soil temperature was measured up to 10 cm and was negatively correlated with HR/SR. Our synthesis suggests AR and HR differ in their responses to temperature and precipitation change. We also emphasized the importance of information on soil temperature measurement depth when applying field estimation of Q_{10} values into current terrestrial ecosystem models. Q_{10} values derived from field SR measurements including AR, will likely overestimate the temperature response of HR on a future warmer earth.

© 2010 Elsevier Ltd. All rights reserved.

1. Introduction

Forest soil respiration (SR) is the primary pathway by which plant-fixed CO₂ is released back to the atmosphere (Högberg and Read, 2006; Gaumont-Guay et al., 2009), arising from the activity from roots and their associated mycorrhizal fungi (belowground autotrophic respiration, AR) and of heterotrophic respiration (HR) (Hanson et al., 2000; Subke et al., 2006). Because of large annual fluxes of carbon between forest ecosystems and the atmosphere (Bonan, 2008; Luyssaert et al., 2008), these ecosystems are likely to influence the global carbon balance in response to projected climate

change (Dixon et al., 1994; Grace and Rayment, 2000; Savage et al., 2008). The net effect of climate change on an ecosystem carbon budget depends on the impact of changes in climatic parameters on photosynthesis and respiration (Schulze et al., 2000; Campbell et al., 2007). While our knowledge of the assimilatory component of the carbon balance (photosynthesis) and its response to climate change is well known (Melliolo et al., 1993; Litton and Giardina, 2008), there are considerable gaps in our understanding of the responses of SR to climate change (Trumbore, 2006; Davidson et al., 2006).

Mean annual temperature (MAT) is predicted to rise by 1.8–4.0 °C, and precipitation frequency and intensity are predicted to change at both regional and global scales over the next century (IPCC, 2007). At the global scale, SR is linearly correlated with MAT and mean annual precipitation (MAP) (Raich and Schlesinger, 1992; Schimel et al., 2001; Raich et al., 2002; Schuur, 2003). However,

* Corresponding author. Tel.: +86 10 62767922; fax: +86 10 62756560.
E-mail address: wangw@urban.pku.edu.cn (W. Wei).

most ecological processes respond non-linearly to environmental changes (Briske et al., 2006; Sasaki et al., 2008). For example, Luyssaert et al. (2007) found that canopy photosynthesis (gross primary production; GPP) initially increased linearly with MAP, but the response saturated at 1500 mm MAP. SR has been found to be strongly related to aboveground plant processes (Högberg et al., 2001) and thus may respond non-linearly to climate change. Furthermore, AR and HR may respond differently to changing temperature and moisture (Boone et al., 1998). However, little is known about the general pattern of SR and its two components for global forests.

Another important uncertainty in predicting ecosystem carbon cycling within the context of climate change is the sensitivity of SR and its two components to temperature (Cox et al., 2000; Luo et al., 2001; Baath and Wallander, 2003; Reichstein et al., 2003; Davidson and Janssens, 2006). There are two measures for temperature sensitivity, including intrinsic temperature sensitivity and apparent temperature sensitivity (Davidson and Janssens, 2006). The former is the theoretic sensitivity determined by molecular structure, while the latter is the observed temperature sensitivity determined by both molecular structure and environmental constraints caused by heterogeneous soil properties. Hereafter, the temperature sensitivity in this study is stated for apparent temperature sensitivity. AR utilizes fresh photosynthates (Högberg et al., 2001), while HR derives from the mineralization of soil organic matter which is stored in large stocks (Fang et al., 2005; Knorr et al., 2005; Reichstein et al., 2005). However, most simulation models of regional and global carbon cycles use a single, fixed, Q_{10} coefficient (defined as the increase in respiration rate per 10 °C increase in temperature) to express this temperature sensitivity (Kirschbaum, 2006). Eventual differences in the temperature sensitivities of AR and HR may compromise modeling results of future soil C dynamics and atmospheric CO₂ concentrations (Zhou et al., 2009). Despite a growing body of information on SR (Hibbard et al., 2005; Bond-Lamberty and Thomson, 2010), the information on apparent Q_{10} of AR and HR is highly controversial (Boone et al., 1998; Epron et al., 1999; Giardina and Ryan, 2000; Rey et al., 2002; Baath and Wallander, 2003; Lavigne et al., 2003; Bhupinderpal-Singh et al., 2003; Schindlbacher et al., 2008).

In the past two decades, numerous studies on SR have been conducted across different forest types of the world, and some global databases have been established (Raich and Schlesinger, 1992; Hanson et al., 2000; Bond-Lamberty et al., 2004; Luyssaert et al., 2007; Bond-Lamberty and Thomson, 2010). However, information from these databases needs to be synthesized to address some of the remaining uncertainties. We assembled a new comprehensive global database, which included SR, HR, AR, HR/SR, and Q_{10} of SR, as well as ancillary site information, such as climate and vegetation types (Supplement Table 1). This new data set enabled us to test (1) how SR and its two components (AR and HR) respond to temperature and precipitation changes and (2) the differences in apparent Q_{10} between AR and HR.

2. Material and methods

We collected data related to forest SR, HR and AR from published databases such as the ones of Raich and Schlesinger (1992), Hanson et al. (2000), Bond-Lamberty et al. (2004), Lee et al. (2006), Subke et al. (2006), Luyssaert et al. (2007) and many published papers in English and Chinese, from additional studies of forest sites that were not included in these earlier syntheses (Supplement Table 1). For annual SR data, we only used estimates with one or more years of direct field measurements. We excluded data from forest sites that had been burned or fertilized and sites used for climate change experiments (increased temperature, precipitation, or CO₂ concentration). AR herein represents the combination of root respiration,

respiration of their mycorrhizal fungi, and respiration of rhizosphere microorganisms (Högberg and Read, 2006). HR or AR data derived mostly from the data set of Hanson et al. (2000), Bond-Lamberty et al. (2004) and Luyssaert et al. (2007), and the measurement methods are also described in Supplement Table 1.

We separated naturally-regenerated forests from plantations because no significant relationship was found between SR and MAT or MAP for plantations (Supplement Fig. 1; $P > 0.05$), unlike for naturally-regenerated sites. We therefore used information only from naturally-regenerated sites in the study of climatic control on SR. In naturally-regenerated forests, each study site was classified by four forest types: deciduous broadleaf forest (DBF), evergreen broadleaf forest (EBF), evergreen needleleaf forest (ENF) and needle and broadleaf mixed forest (MF).

MAT and MAP for each study site were extracted from literatures. A global climate database was used to estimate climate data for sites where original climate data were unavailable (Hijmans et al., 2005). Among all of climate data in our database, the observed vs. inferred values were 222 vs. 103 for MAT and 221 vs. 104 for MAP. In order to test the accuracy of inferred climate data using global climate database, we used the latitude and longitude information of the observed sites to infer their MAT and MAP. Through comparing the inferred values with the observed ones, we found that MAT could be simulated well, and MAP was slightly less than its observed ones (Fig. 1). Sites from our data set span a wide gradient of forest types and climates (MAT: −5–27 °C; MAP: 270–4250 mm, Supplement Table 1).

When available, Q_{10} of SR was summarized from every paper, as well as from Peng et al. (2009) (Chinese Q_{10} data set) and Hashimoto (2005) (Japanese Q_{10} data set). It is worth pointing out that the temperature sensitivity reported in the studies we use for our analysis is the apparent temperature sensitivity. The methods used to determine Q_{10} of SR are critical, with larger values occurring in laboratory incubation studies than in soil warming experiments or in field observations (Gu et al., 2004). To avoid method-induced bias, we only selected Q_{10} data from *in situ* field studies calculated by the van't Hoff equation ($SR = a \times e^{\beta T}$; $Q_{10} = e^{10\beta}$) (Van't Hoff, 1898), which provides a measure of apparent temperature sensitivity (Reichstein et al., 2003; Davidson and Janssens, 2006; Kirschbaum, 2006).

Within these constraints, we obtained 321 data sets from 174 publications available for analysis. Of these, 294 data sets from 161 publications contained the estimates for annual SR, 124 data sets contained AR (or HR) estimates from 69 publications, 185 data sets contained Q_{10} of SR from 69 publications and 13 data sets contained Q_{10} of HR and AR from 8 publications (Supplement Table 1). Geographic distribution of the sites contained in the database is shown in Fig. 2.

In order to test whether measurement depth of soil temperature influences the estimation of Q_{10} values, we compared Q_{10} values calculated by the soil temperature at five different depths (ST₀ (soil surface temperature), ST₅ (soil temperature at 5 cm), ST₁₀ (soil temperature at 10 cm), ST₁₅ (soil temperature at 15 cm), and ST₂₀ (soil temperature at 20 cm)) for the same site. Paired *t*-test was used to compare the Q_{10} values among different measurement depths. In addition, we tested the role of forest types on Q_{10} at 5 cm soil depth because most studies reported Q_{10} values calculated from ST₅, to remove the effect of measurement depth bias. One-way ANOVA was used to evaluate whether Q_{10} values significantly differed among forest types.

To characterize the responses of SR, AR, and HR to climate change, we analyzed the data using a bent-cable form of a piecewise-regression model (Toms and Lesperance, 2003), to identify critical thresholds for climate changes. The piecewise-regression is a “broken-stick” model, where two or more lines are joined at

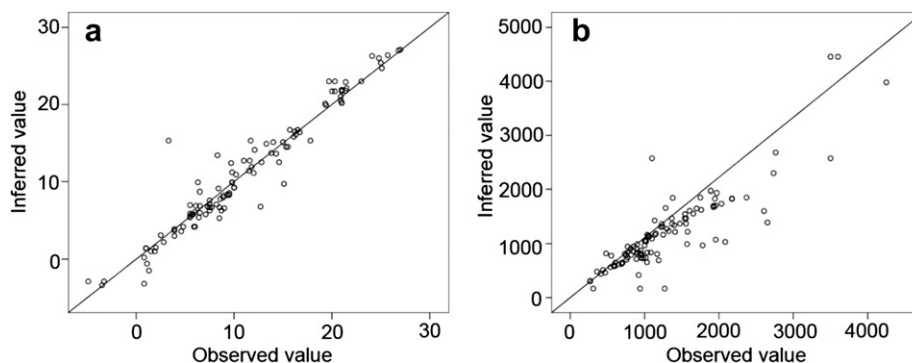


Fig. 1. Comparison of MAT (a) and MAP (b) between observed values and inferred ones from global climate database. Linear regression equations between observed and inferred values were $Y = 1.02X - 0.216$ for MAT ($R^2 = 0.94$, $P < 0.001$) and $Y = 0.886X + 49.7$ ($R^2 = 0.77$, $P < 0.001$). MAT = Mean Annual Temperature; MAP = Mean Annual Precipitation.

unknown point(s), called breakpoint(s), representing the threshold (s) (Toms and Lesperance, 2003). When the slopes before and after the breakpoint were significantly different, piecewise-regression models were used; otherwise, a simple linear regression model was adopted. Generally, the piecewise-regression method attempts to detect one or more potential breakpoints and fits linear trends before and after each breakpoint. The optimal solutions for the model are the breakpoints and phase slopes that minimize the residual sum of squares. In our calculations, restriction was made because our data points clustered in the median of MAT or MAP, so we assumed that only one breakpoint existed in each series, to avoid breakpoints occurring at the ends of the regression curve.

To test the differences of apparent Q_{10} between AR and HR, the relationships between HR, AR, HR/SR and the magnitude of the warming response (Q_{10} of SR at 5 cm soil depth) were examined using linear regression. All statistical analyses were performed with a significance level of 0.05 with R software (version 2.4.1).

3. Results and discussions

3.1. SR and its climatic controls

Observed SR in naturally-regenerated forests ranged from 220 to 2560 $\text{g C m}^{-2} \text{yr}^{-1}$. These data derived mostly from boreal and temperate areas (Fig. 2), which were well represented. However, there were very few measurements from tropical area; the lack of measurements in this area represented a major deficiency in estimating global forest SR. Therefore, despite an abundance of SR data, global coverage is poor. Raich and Schlesinger (1992) reported that SR averaged 322, 662 and 1092 $\text{g C m}^{-2} \text{yr}^{-1}$ for boreal, temperate and tropical forests, which were significantly lower than our estimates of 521, 900 and 1489 $\text{g C m}^{-2} \text{yr}^{-1}$ for boreal, temperate and tropical forests, respectively. This discrepancy may be due to the method used. In earlier studies, SR was mainly measured by alkaline absorption method. This method was shown to underestimate

SR (Janssens et al., 2001; Kabwe et al., 2002). SR was higher in EBF ($1189.4 \pm 79.8 \text{ g C m}^{-2} \text{yr}^{-1}$ (mean \pm SE)), and lower in ENF ($650.4 \pm 37.4 \text{ g C m}^{-2} \text{yr}^{-1}$ (mean \pm SE)). Overall SR increased linearly with MAT (Fig. 3). For every 1°C increase in MAT, overall emissions from SR increased by $24.6 \text{ g C m}^{-2} \text{yr}^{-1}$. This was similar to the mean increase rate for global vegetation ($25.6 \text{ g C m}^{-2} \text{yr}^{-1}$) (Raich and Schlesinger, 1992) and higher than that of global grasslands ($16.5 \text{ g C m}^{-2} \text{yr}^{-1}$) (Wang and Fang, 2009). Within four forest types, this linear positive relationship still existed (Fig. 4).

Unlike to MAT, SR responded non-linearly to MAP with a breakpoint of 813 mm (Fig. 5). Below the threshold, for every 100 mm increase in MAP, additional $75.3 \text{ g C m}^{-2} \text{yr}^{-1}$ was released. However, once that threshold was exceeded, the increase rate declined to $20.3 \text{ g C m}^{-2} \text{yr}^{-1}$ (Fig. 5). For global vegetation, Raich and Schlesinger (1992) reported that SR increased linearly with MAP, and showed that for every 100 mm increase in MAP, SR released additional $40 \text{ g C m}^{-2} \text{yr}^{-1}$. The different response of SR to MAP was mainly due to the difference in regression method used. The simple linear model used by Raich and Schlesinger (1992) is a special case of piecewise-regression model, in which the values for the two slopes are identical. When a simple linear regression was used through our results, SR released additional $27 \text{ g C m}^{-2} \text{yr}^{-1}$ for every 100 mm increase in MAP. Our estimate was below to that of global vegetation (Raich and Schlesinger, 1992).

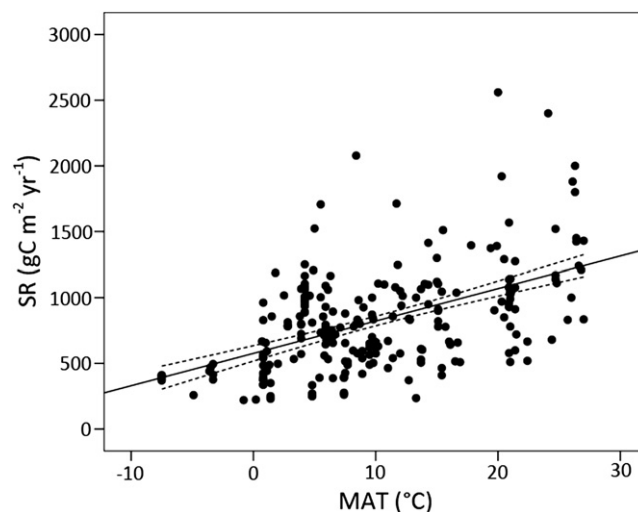


Fig. 3. SR correlates linearly with MAT in naturally-regenerated forests ($Y = 576 + 24.6X$; $R^2 = 0.26$, $P < 0.001$). SR = Soil Respiration. MAT = Mean Annual Temperature. Dash lines showed 95% confidence intervals.



Fig. 2. Geographic distribution of the sites contained in the database.

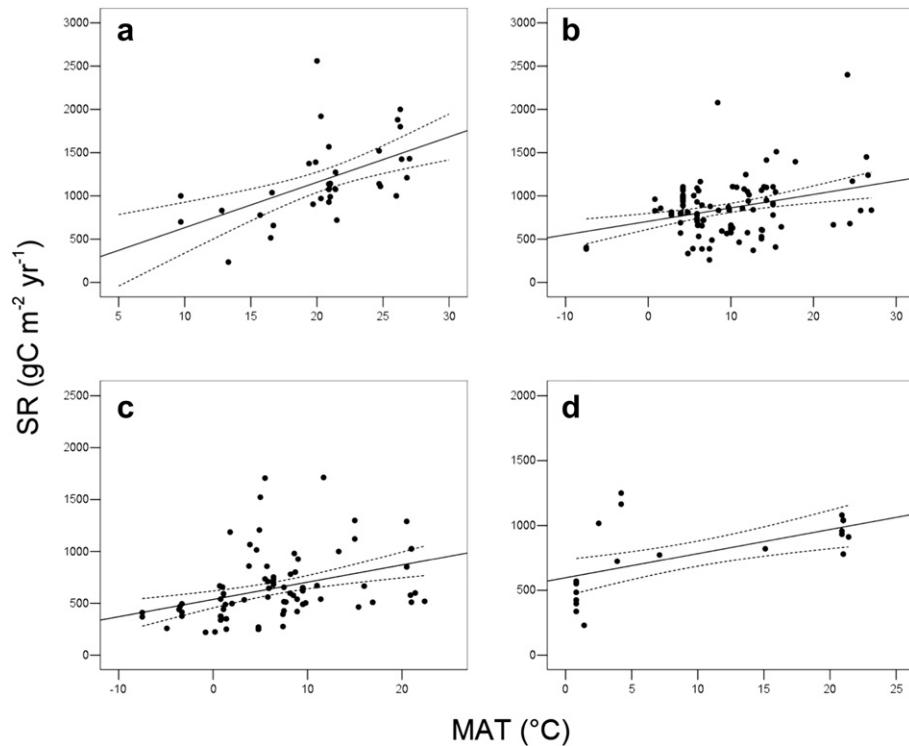


Fig. 4. SR correlates linearly with MAT within evergreen broadleaf forest (EBF) (a: $Y = 109 + 52.4 X$; $R^2 = 0.28$, $P = 0.001$), deciduous broadleaf forest (DBF) (b: $Y = 706 + 15.5 X$; $R^2 = 0.10$, $P = 0.002$), evergreen needleleaf forest (ENF) (c: $Y = 537 + 16.6 X$; $R^2 = 0.13$, $P < 0.001$) and needle and broadleaf mixed forest (MF) (d: $Y = 597 + 18.6 X$; $R^2 = 0.34$, $P = 0.008$). MAT = Mean Annual temperature. SR = Soil Respiration. Dash lines showed 95% confidence intervals.

Different forest types differed in their responses to MAP (Fig. 6). SR increased linearly with MAP, when below the thresholds of 1800 mm, 1113 mm and 813 mm for EBF, ENF and MF, respectively; every 100 mm increase in MAP, additional emissions were released by 79, 62, 140 $\text{g C m}^{-2} \text{yr}^{-1}$ for EBF, ENF, MF, respectively. However,

when above these thresholds, SR kept relatively constant (Fig. 6). In DBF, SR increased linearly by $14.6 \text{ g C m}^{-2} \text{yr}^{-1}$ with 100 mm increased in MAP.

3.2. Climatic control over HR and AR

On a global scale, both HR and AR were positively and linearly correlated with MAT (Fig. 7a, c). MAT explained 29% and 12% of the variation in HR and AR, respectively, indicating that AR was less influenced by MAT than HR. Two possible mechanisms could account for the fact that AR had a lower dependence on temperature. First, AR has been reported to be more dependent on photosynthesis than on temperature (Högberg et al., 2001; Bhupinderpal-Singh et al., 2003; Edwards et al., 2004; Heinemeyer et al., 2007). Root respiration (Luo et al., 2001; Hartley et al., 2007a) and root-associated respiration of ectomycorrhizal (Malcolm et al., 2008) and arbuscular mycorrhizal fungi (Heinemeyer et al., 2006) were reported to be relatively insensitive to temperature when compared with the temperature sensitivity of HR. This higher dependence on photosynthetic substrate supply may therefore reduce the dependence of AR on temperature (Kirschbaum, 2006). When we pooled the values for DBF and ENF with relatively sufficient observation numbers, we confirmed that MAT explained less variation in AR than HR (Table 1), especially in DBF. In addition, physiology and phenology of trees may play important roles in determining the amount of roots active at particular times of the year (Lenton and Huntingford, 2003). For example, AR was found to peak in spring, coinciding not only with high temperatures but also with leaf flush, and to peak again in autumn prior to litterfall (Dickmann et al., 1996).

AR and HR also responded differently to MAP. HR increased linearly with MAP (Fig. 7d). AR responded non-linearly to MAP with the threshold of 1000 mm. Before the threshold, AR increase by

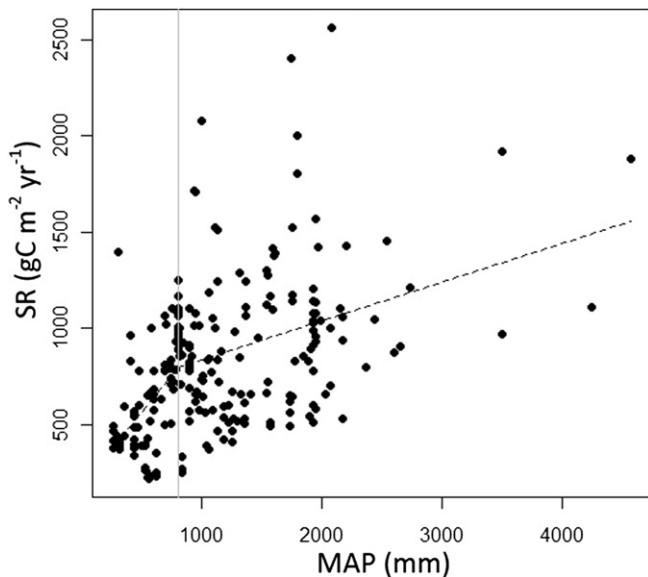


Fig. 5. Response of SR to MAP in naturally-regenerated forests. The breakpoint occurred at 813 mm MAP ($P = 0.003$) with 95% confidence interval between 640 mm and 1106 mm ($R^2 = 0.26$, $P < 0.001$). Before the breakpoint, slope = 0.753, $P < 0.001$; after the breakpoint, slope = 0.203, $P < 0.001$. SR = Soil Respiration, MAP = Mean Annual Precipitation.

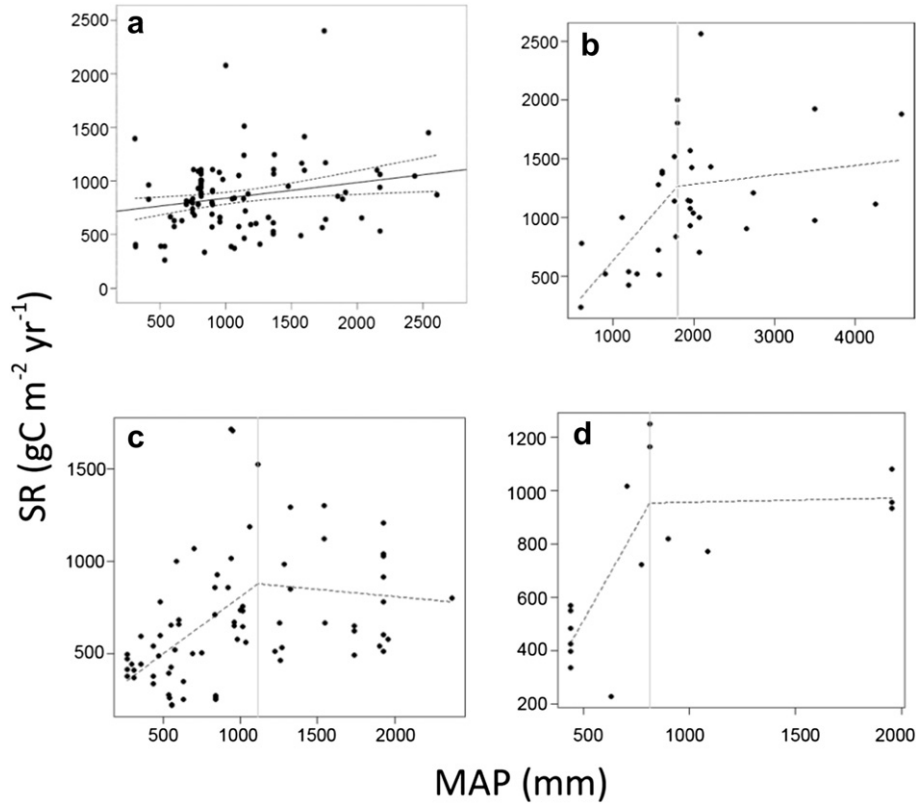


Fig. 6. Response of SR to MAP within deciduous broadleaf forest (DBF) (a: $Y = 693 + 0.146 X$; $R^2 = 0.34$, $P = 0.026$), evergreen broadleaf forest (EBF) (b: breakpoint = 1800 mm, $P = 0.02$, $R^2 = 0.34$; when MAP < 1800 mm, slope = 0.79, $P < 0.05$; when MAP > 1800 mm, slope = 0.08, $P > 0.05$), evergreen needleleaf forest (ENF) (c: breakpoint = 1113 mm, $P = 0.004$, $R^2 = 0.26$; when MAP < 1113 mm, slope = 0.62, $P < 0.05$; when MAP > 1113 mm, slope = -0.08, $P > 0.05$) and needle and broadleaf mixed forest (MF) (d: breakpoint = 813 mm, $P = 0.006$, $R^2 = 0.64$; when MAP < 813 mm, slope = 1.40, $P < 0.05$; when MAP > 813 mm, slope = 0.02, $P > 0.05$). MAT = Mean Annual Temperature. SR = Soil Respiration. Dash lines (a) showed 95% confidence intervals.

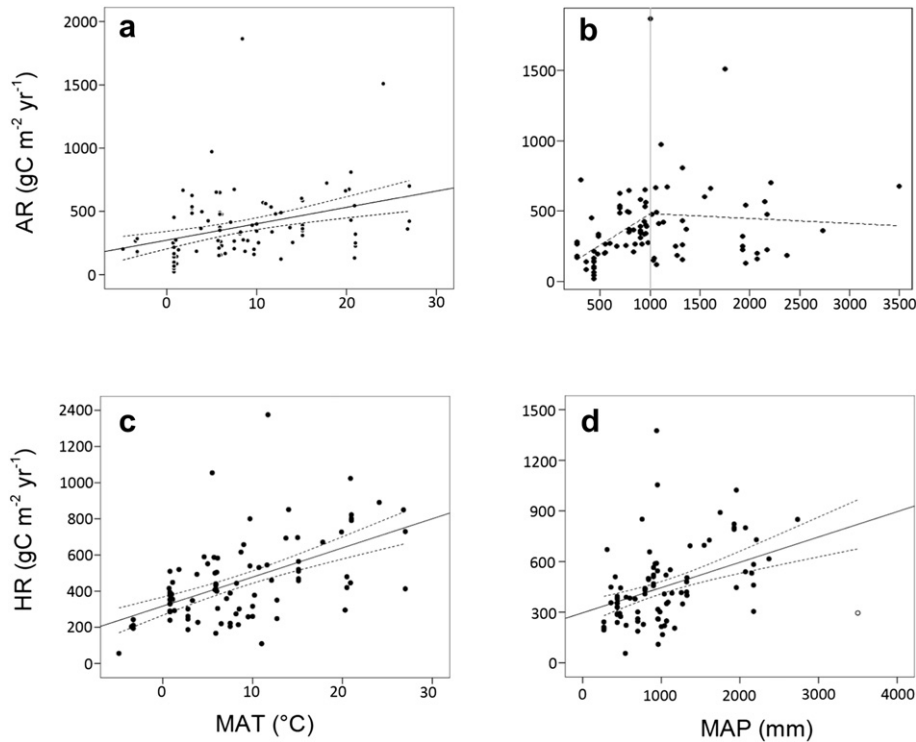


Fig. 7. AR responded linearly to MAT (a: $Y = 273 + 12.9 X$; $R^2 = 0.12$, $P = 0.001$). AR responded non-linearly to MAP. The breakpoint occurred in 1000 mm MAP with 95% confidence intervals between 580 mm and 1655 mm ($P = 0.004$, $R^2 = 0.15$); when MAP < 1000 mm, slope = 0.445, $P < 0.05$; when MAP > 1000 mm, slope = -0.035, $P > 0.05$; HR responded linearly to both MAT (c: $Y = 317 + 16.1 X$; $R^2 = 0.29$, $P < 0.001$) and MAP (d: $Y = 296 + 0.15 X$; $R^2 = 0.17$, $P < 0.001$). MAT = Mean Annual Temperature; MAP = Mean Annual Precipitation; HR = Heterotrophic Respiration; AR = Autotrophic Respiration. Dash lines in linear regression showed 95% confidence intervals.

Table 1

Correlation between MAT (mean annual temperature) and AR (autotrophic respiration) and between MAT and HR (heterotrophic respiration) in deciduous broadleaf forest (DBF) and evergreen needleleaf forest (ENF).

	N	AR		HR	
		R ²	P	R ²	P
DBF	37	0.03	0.31	0.28	0.001
ENF	39	0.12	0.03	0.17	0.01

Note: N = sample size.

44.5 g C m⁻² yr⁻¹ for every 100 mm increased MAP. After the threshold, AR kept relatively constant (Fig. 7b). The difference may be connected with the strong dependence of AR on plant activity (Högberg et al., 2001, 2009; Liu et al., 2006; Moyano et al., 2008). Increased precipitation may be coupled with increased cloudiness (Sellers et al., 1997; Luyssaert et al., 2007), which in turn may decrease solar radiation at the forest canopy below photosynthetic light saturation. This would indirectly lead to a decline in AR.

3.3. Q₁₀ of SR and its control

3.3.1. Effect of measurement depth and forest types

Observed Q₁₀ values of SR varied from 0.98 to 6.27 (Supplement Table 1). The modal Q₁₀ values ranged from 2.5 to 3.0 with an overall arithmetic mean of 2.67 (Fig. 8). Our averaged estimate was slightly higher than that of global grasslands (2.13) (Wang and Fang, 2009) and that of global vegetation (2.4) (Raich and Schlesinger, 1992). Averaged Q₁₀ values derived from air temperature and soil temperature at 0, 5, 10, 15, and 20 cm depths were (Mean ± SE) 1.43 ± 0.09, 2.00 ± 0.11, 2.55 ± 0.10, 3.01 ± 0.08, 3.16 ± 0.54, and 3.78 ± 0.76, respectively. As expected, Q₁₀ increased with measurement depth because soil temperature fluctuates less in deeper soil. This was however only apparent in the top 10 cm soil (P < 0.05), whereas no difference occurred below 10 cm depth (P < 0.05; Fig. 9). The latter may be attributable to the attenuation and phase shift of temperature fluctuations with increasing depth (Davidson et al., 1998). At deeper depths below 10 cm, amplitudes in soil temperatures do not significantly change in response to changes in soil depth (Xu and Qi, 2001; Graf et al., 2008). Similar patterns were previously observed in several field studies with multiple temperature measurement depths within the same site (Borken et al., 2002; Wang et al., 2006; Pavelka et al., 2007). The same effect was also identified in model simulations by Hashimoto and Komatsu (2006) and was demonstrated with synthetically-

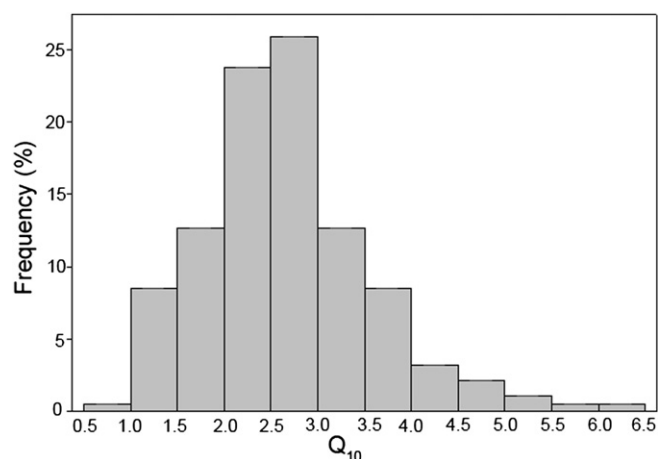


Fig. 8. Frequency distribution of Q₁₀ values for *in situ* soil respiration as reported in the literatures.

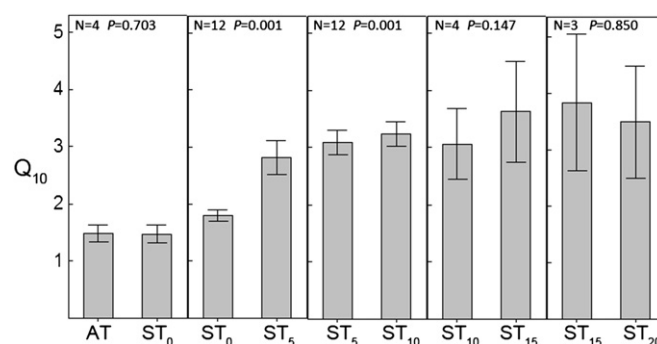


Fig. 9. Comparisons of apparent temperature sensitivity of soil respiration (Q₁₀) estimated by air temperature (AT) and soil temperature at different depths (soil surface temperature (ST₀), soil temperature at 5 cm (ST₅), soil temperature at 10 cm (ST₁₀), soil temperature at 15 cm (ST₁₅), and soil temperature at 20 cm (ST₂₀)). Paired t-test was used to compare the differences in the Q₁₀ values. N is the number of samples used in the paired t-test. The error bar denotes the stand error (SE) of Q₁₀ at any given depth of measured soil temperature.

derived data by Reichstein and Beer (2008). Therefore, the strong dependence in Q₁₀ of SR on measurement depth highlights the importance of information on soil temperature measurement depth when applying field estimation of Q₁₀ values into current terrestrial ecosystem models.

Q₁₀ values at a soil depth of 5 cm were as follows (Mean ± SE): EBF: 1.98 ± 0.12, DBF: 2.79 ± 0.14, ENF: 3.00 ± 0.21, MF: 2.66 ± 0.41, respectively. No significant difference existed among DBF, ENF and MF (P > 0.05) and between EBF and MF (P > 0.05). Q₁₀ of EBF was significantly lower than that of DBF and ENF (P = 0.002 and 0.006, respectively) (Fig. 10).

3.3.2. Effect of HR/SR

Raich and Schlesinger (1992) presumed HR to be 70% of SR. However, our results showed the reported HR/SR varied within a wide range from 10.3% to 94% (Supplement Table 1), with significant lower values in DBF than other types (Fig. 11). The outlier in DBF derived from an oak forest with humid climate in north-western of France and HR was calculated through carbon balance method. The outlier when included or excluded did not significantly change the results of comparison. The differences among different forest types partly reflected diversity of the studied types

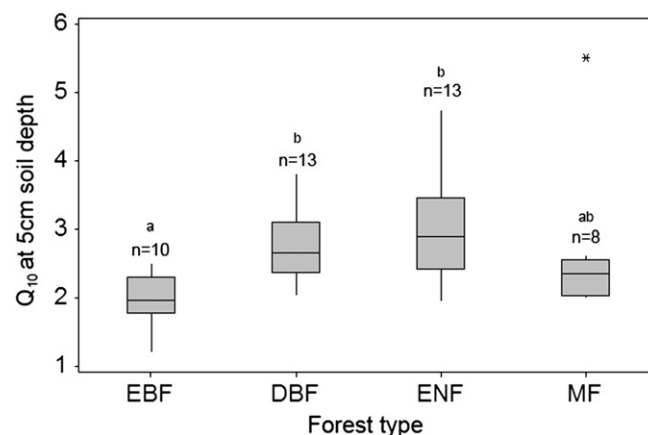


Fig. 10. Box-plot of Q₁₀ values at 5 cm soil depth for different forest types including deciduous broadleaf forest (DBF), evergreen broadleaf forest (EBF), evergreen needleleaf forest (ENF) and needle and broadleaf mixed forest (MF). 'n' indicates sample size, different lowercase letters indicate significant differences (One-way ANOVA, P < 0.05), and * indicates outliers.

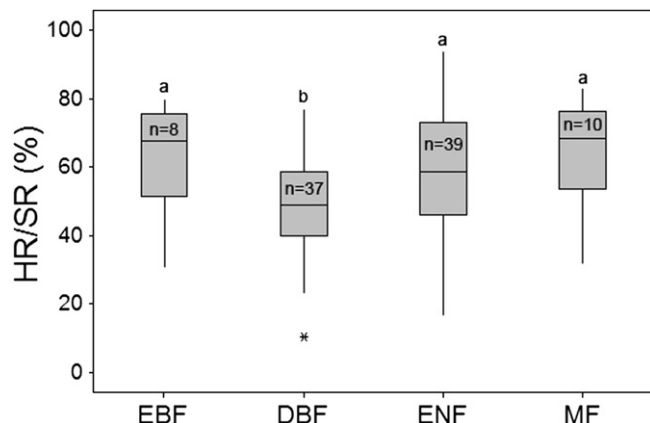


Fig. 11. Comparisons of HR/SR among deciduous broadleaf forest (DBF), evergreen broadleaf forest (EBF), evergreen needleleaf forest (ENF) and needle and broadleaf mixed forest (MF). 'n' indicates sample size, different lowercase letters indicate significant differences (One-way ANOVA, $P < 0.05$), and * indicates outliers. HR = Heterotrophic Respiration; SR = Soil Respiration.

of soils and ecosystems, however, a considerable proportion of it probably originates from the variety of measurement techniques used (Hanson et al., 2000; Kuzyakov, 2006; Subke et al., 2006; Marsden et al., 2008).

No significant relationship occurred between HR and Q_{10} of SR at 5 cm soil depth (Fig. 12b). There was a significant positive relationship between AR and Q_{10} of SR (Fig. 12a), however this relationship was largely dependent on the far right two data points. Therefore, the relationship between AR and Q_{10} still requires further investigation. A significant negative correlation was found between HR/SR and Q_{10} of SR (Fig. 12c). Among all the 18 data points for the analysis, 4 data points derived from the estimates of modeling (Luyssaert et al., 2007). When these modeled values were excluded or included, no significant effect occurred on this negative relationship ($P > 0.05$). Our results indicated that a higher contribution of AR to SR would produce higher Q_{10} of SR. Based on the negative relationship when all the data pooled, Q_{10} values of AR and HR were 3.92 ± 0.38 (HR/SR = 0) and 1.66 ± 0.29 (HR/SR = 1), respectively, suggesting apparent Q_{10} of AR were higher than that of HR. Similarly, apparent Q_{10} of AR measured in the field were significantly higher than that of HR (3.40 ± 0.32 (Mean \pm SE; $n = 13$) vs. 2.42 ± 0.15 (Mean \pm SE; $n = 13$)) (Supplement Table 1). Greater phenological seasonality of AR than that of HR (Boone et al., 1998; Widen & Majdi, 2001; Tierney et al., 2003) could partly account for its higher Q_{10} . For instance, apparent temperature sensitivities would be inflated if data from springtime root growing periods were included (Hanson et al., 2003). Furthermore, changes in substrate supply from photosynthesis could also largely be overlooked, resulting in additional overestimation of the temperature sensitivity of AR (Bhupinderpal-Singh et al., 2003; Davidson and Janssens, 2006). Thus, Q_{10} values derived from field measurements, including AR, could overestimate the response of heterotrophic SR to temperature changes on a future warmer earth (Borken et al., 2002).

However, there has been considerable debate on whether AR or HR is more sensitive to long-term temperature changes. For instance, Baath and Wallander (2003) showed that there were no differences in the temperature relationship between root-associated and non-root-associated organisms in a model system. A similar conclusion was also drawn by Schindlbacher et al. (2008) by warming the top soil of a mature coniferous forest stand on control and trenched plots within 24 h by 10°C at 1 cm soil depth. However, Hartley et al. (2007b) investigated the response of belowground

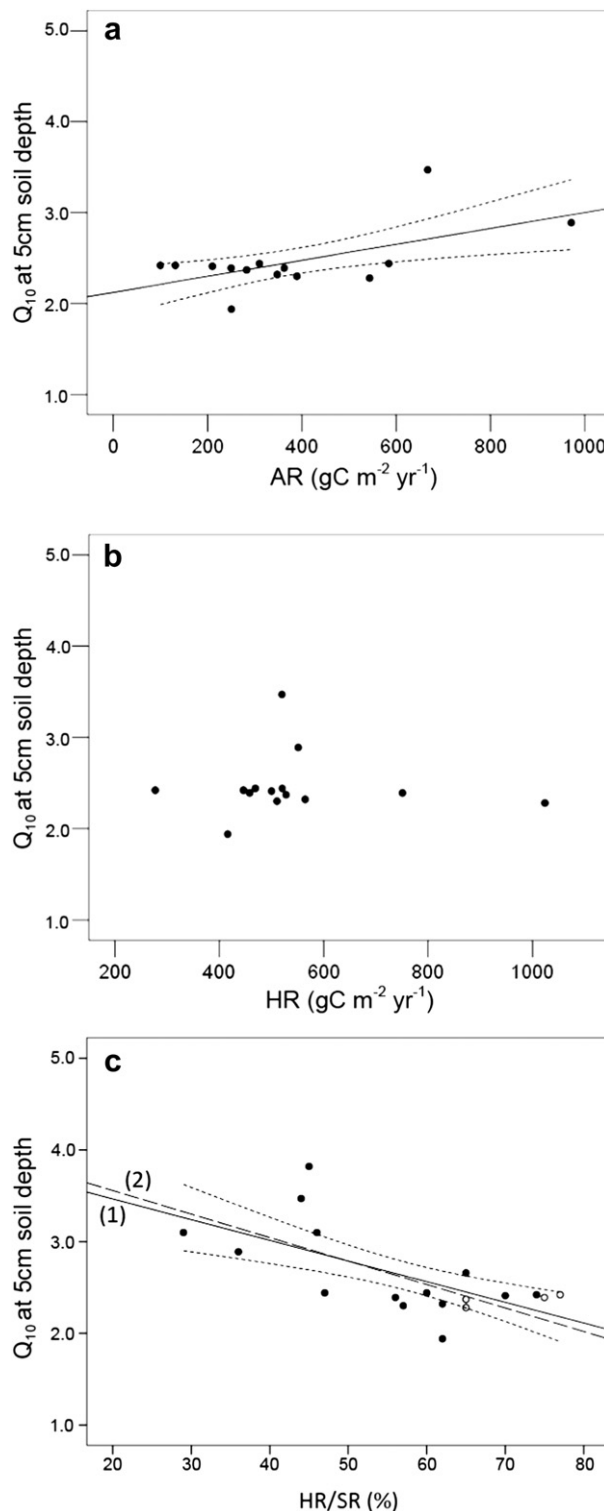


Fig. 12. Q_{10} at 5 cm soil depth was positively correlated with AR (a, $Y = 2.12 + 0.001 X$, $R^2 = 0.35$, $P = 0.026$) and uncorrelated with HR (b, $P = 0.908$). Q_{10} at 5 cm soil depth was negatively correlated with HR/SR (c). The regression equations were $Y = 3.92 - 2.26 X$ (1) for modeled data included ($R^2 = 0.43$, $P = 0.003$) and $Y = 4.01 - 2.56 X$ (2) when modeled data excluded ($R^2 = 0.42$, $P = 0.013$). Based on equation (1), we inferred Q_{10} of AR to be 3.92 ± 0.38 (Mean \pm SE, HR/SR = 0) and Q_{10} of HR to be 1.66 ± 0.29 (Mean \pm SE, HR/SR = 1). '●' shows measured data and '○' shows modeled data. Dash lines shows 95% confidence intervals. SR = Soil Respiration; HR = Heterotrophic Respiration; AR = Autotrophic Respiration.

respiration to soil warming by 3 °C above ambient in bare soil plots and plots planted with wheat and maize. They found that as the growing season progressed, HR is more temperature sensitive than AR. According to Hartley et al. (2007b), the higher Q_{10} for HR than for AR in their study was probably explained by the difference in the dependence on photosynthate supply between AR and HR.

The collected Q_{10} values in our analysis were calculated from a sequence of measurements taken over a period of time during which seasonal changes of the temperature occurred. This apparent Q_{10} may reflect the effects of plant phenological patterns (Curiel Yuste et al., 2004), desiccation stress, substrate production and allocation, and etc (Davidson and Janssens, 2006), as well as temperature sensitivity. When predicting the effects of long-term temperature changes, it is important to differentiate between the direct effect of temperature and other conditions (e.g. light), co-varying with temperature over the year (Baath and Wallander, 2003; Schindlbacher et al., 2008). The existing controversies highlight the importance of determining the intrinsic temperature response of SR in future studies. Some recent studies have made good attempts by making short-term temperate responses (Vicca et al., 2009; Curiel Yuste et al., 2010). For instance, using intact soil cores from an oak savanna ecosystem, Curiel Yuste et al. (2010) applied short-term temperature cycles to study temperature sensitivity of SR. This short-term Q_{10} is less likely to comprise confounding effects and is in general a better approximation of the intrinsic temperature response of a process (Vicca et al., 2009). Further evaluations of the feedback intensity between soil carbon efflux and global warming can thus not be satisfactorily predicted if we do not understand patterns of intrinsic temperature sensitivity.

4. Conclusions

Our results pointed to global patterns of SR, AR, HR and HR/SR in forests across a broad scale gradient of MAT and MAP. In addition, we analyzed the changes in Q_{10} of SR with measurement depth, forest types, HR, AR and HR/SR. Our results have great implications to modeling efforts and ecosystem-level C cycling studies. (i) Different responses of AR to temperature and precipitation from HR demonstrate the importance of using separate functions for modeling the responses of AR and HR to climatic variables as well as substrate supply. (ii) Strong dependence in Q_{10} of SR on measurement depth highlights the importance of information on soil temperature measurement depth when applying field estimation in Q_{10} values into current terrestrial ecosystem models. (iii) Q_{10} of SR positively correlated with AR/SR, suggesting apparent Q_{10} values derived from field measurements including AR may overestimate the temperature sensitivity of heterotrophic SR on a future warmer earth.

Acknowledgments

We appreciated all the people who contributed themselves to the database. We thanked Dr. Niu K C for his helps in data analysis and three anonymous reviewers for their very constructive and valuable comments for its early version of our manuscript. This work was supported by the Projects of National Natural Science Foundation of China (30870408, 30670342, and 90711002) and an A₃ Foresight Program.

Appendix. Supplementary data

Supplementary data associated with this article can be found, in the online version, at doi:10.1016/j.soilbio.2010.04.013.

References

- Baath, E., Wallander, H., 2003. Soil and rhizosphere microorganism have the same Q_{10} for respiration in a model system. *Global Change Biology* 9, 1788–1791.
- Bhupinderpal-Singh, Nordgren A., Ottosson Löfvenius, M., Högborg, M.N., Mellander, P.E., Högborg, P., 2003. Tree root and soil heterotrophic respiration as revealed by girdling of boreal Scots pine forest: extending observations beyond the first year. *Soil Biology and Biochemistry* 27, 753–760.
- Bonan, G.B., 2008. Forests and climate change: forcings, feedbacks, and the climate benefits of forest. *Science* 320, 1444–1449.
- Bond-Lamberty, B., Thomson, A., 2010. A global database of soil respiration data. *Biogeosciences Discuss* 7, 1321–1344.
- Bond-Lamberty, B., Wang, C.K., Gower, S.T., 2004. A global relationship between the heterotrophic and autotrophic components of soil respiration. *Global Change Biology* 10, 1756–1766.
- Boone, R.D., Nadelhoffer, K.J., Canary, J.D., Kaye, J.P., 1998. Roots exert a strong influence on the temperature sensitivity of soil respiration. *Nature* 396, 570–572.
- Briske, D.D., Fuhlendorf, S.D., Smeins, F.E., 2006. A unified framework for assessment and application of ecological thresholds. *Rangeland Ecology and Management* 59, 225–236.
- Borken, W., Xu, Y.J., Davidson, E.A., Beese, F., 2002. Site and temporal variation of soil respiration in European beech, Norway spruce, and Scots pine forests. *Global Change Biology* 8, 1205–1216.
- Campbell, C., Atkinson, L., Zaragoza-Castells, J., Lundmark, M., Atkin, O., Hurry, V., 2007. Acclimation of photosynthesis and respiration is asynchronous in response to changes in temperature regardless of plant functional group. *New Phytologist* 176, 375–389.
- Cox, P.M., Betts, R.A., Jones, C.D., Spall, S.A., Totterdell, I.J., 2000. Acceleration of global warming due to carbon-cycle feedbacks in a coupled climate model. *Nature* 408, 184–187.
- Curiel Yuste, J., Janssens, I.A., Carrara, A., Ceulemans, R., 2004. Annual Q_{10} of soil respiration reflects plant phenological patterns as well as temperature sensitivity. *Global Change Biology* 10, 161–169.
- Curiel Yuste, J., Ma, S., Baldocchi, D.D., 2010. Plant-soil interactions and acclimation to temperature of microbial-mediated soil respiration may affect predictions of soil CO₂ efflux. *Biogeochemistry*. doi:10.1007/s10533-009-9381-1.
- Davidson, E.A., Janssens, I.A., 2006. Temperature sensitivity of soil carbon decomposition and feedbacks to climate change. *Nature* 440, 165–173.
- Davidson, E.A., Belk, E., Boone, R.D., 1998. Soil water content and temperature as independent or confound factors controlling soil respiration in a temperate mixed hardwood forest. *Global Change Biology* 4, 217–227.
- Davidson, E.A., Janssens, I.A., Luo, Y.Q., 2006. On the variability of respiration in terrestrial ecosystems: moving beyond Q_{10} . *Global Change Biology* 12, 154–164.
- Dickmann, D.I., Nguyen, P.V., Pregitzer, K.S., 1996. Effects of irrigation and coppicing on aboveground growth, physiology, and fine-root dynamics of two field-grown hybrid poplar clones. *Forest Ecology and Management* 80, 163–174.
- Dixon, R.K., Brown, S., Houghton, R.A., Solomon, A.M., Trexler, M.C., Wisniewski, J., 1994. Carbon pools and flux of global forest ecosystems. *Science* 263, 185–190.
- Edwards, E.J., Benham, D.G., Marland, L.A., Fitter, A.H., 2004. Root respiration is determined by radiation flux in a temperate grassland community. *Global Change Biology* 10, 209–227.
- Epron, D., Farque, L., Lucot, E., Badot, P.M., 1999. Soil CO₂ efflux in a beech forest: the contribution of root respiration. *Annals of Forest Science* 56, 289–295.
- Fang, C.M., Smith, P., Moncrieff, J.B., Smith, J.U., 2005. Similar response of labile and resistant soil organic matter pools to changes in temperature. *Nature* 433, 57–59.
- Gaumont-Guay, D., Black, T.A., McCaughy, H., Barr, A.G., Krishnan, P., Jassal, R.S., Nesic, Z., 2009. Soil CO₂ efflux in contrasting boreal deciduous and coniferous stands and its contribution to the ecosystem carbon balance. *Global Change Biology* 15, 1302–1319.
- Giardina, C.P., Ryan, M.G., 2000. Evidence that decomposition rates of organic carbon in mineral soil do not vary with temperature. *Nature* 404, 858–861.
- Grace, J., Rayment, M., 2000. Respiration in the balance. *Nature* 404, 819–820.
- Graf, A., Weihermüller, L., Huisman, J.A., Herbst, M., Bauer, J., Vereecken, H., 2008. Measurement depth effects on the apparent temperature sensitivity of soil respiration in field studies. *Biogeosciences Discussions* 5, 1867–1898.
- Gu, L., Post, W.M., King, A.W., 2004. Fast labile carbon turnover obscures sensitivity of heterotrophic respiration from soil to temperature: a model analysis. *Global Biogeochemical Cycles* 18, 1022–1032.
- Hanson, P.J., Edwards, N.T., Garten, C.T., Andrews, J.A., 2000. Separating root and soil microbial contributions to soil respiration: a review of methods and observations. *Biogeochemistry* 48, 115–146.
- Hanson, P.J., O'Neill, E.G., Chambers, M.L.S., Rigg, J.S., Joslin, J.D., Wolfe, M.H., 2003. Soil respiration and litter decomposition. In: Hanson, P.J., Wullschlegel, S.D. (Eds.), *North American Temperate Deciduous Forest Responses to Changing Precipitation Regimes*. Springer-Verlag, New York, pp. 163–189.
- Hartley, I.P., Heinemeyer, A., Ineson, P., 2007a. Effects of three years of soil warming and shading on the rate of soil respiration: substrate availability and not thermal acclimation mediates observed response. *Global Change Biology* 13, 1761–1770.
- Hartley, I.P., Heinemeyer, A., Evans, S.P., Ineson, P., 2007b. The effect of soil warming on bulk soil vs. rhizosphere respiration. *Global Change Biology* 13, 2654–2667.
- Hashimoto, S., Komatsu, H., 2006. Relationships between soil CO₂ concentration and CO₂ production, temperature, water content, and gas diffusivity: implications for field studies through sensitivity analyses. *Journal of Forest Research* 11, 41–50.

- Hashimoto, S., 2005. Q_{10} values of soil respiration in Japanese forests. *Journal of Forest Research* 10, 409–413.
- Heinemeyer, A., Ineson, P., Ostle, N., Fitter, A.H., 2006. Respiration of the external mycelium in the arbuscular mycorrhizal symbiosis shows strong dependence on recent photosynthates and acclimation to temperature. *New Phytologist* 171, 159–170.
- Heinemeyer, A., Hartley, I.P., Evans, S.P., Carreira, J.A., Fuente, D.L., Ineson, P., 2007. Forest soil CO_2 flux: uncovering the contribution and environmental responses of ectomycorrhizas. *Global Change Biology* 13, 1786–1797.
- Hibbard, K.A., Law, B.E., Sulzman, J., 2005. An analysis of soil respiration across northern hemisphere temperate ecosystems. *Biogeochemistry* 73, 29–70.
- Hijmans, R.J., Cameron, S.E., Parra, J.L., Jones, P.G., Jarvis, A., 2005. Very high resolution interpolated climate surfaces for global land areas. *International Journal of Climatology* 25, 1965–1978.
- Högberg, P., Read, D.J., 2006. Towards a more plant physiological perspective on soil ecology. *Trends in Ecology and Evolution* 21, 548–554.
- Högberg, P., Nordgren, A., Buchmann, N., Taylor, A.F.S., Ekblad, A., Högberg, M.N., Nyberg, G., Ottosson-Lofvenius, M., Read, D.J., 2001. Large-scale forest girdling shows that current photosynthesis drives soil respiration. *Nature* 411, 789–792.
- Högberg, P., Singh, B., Löfvenius, M.O., Nordgren, A., 2009. Partitioning of soil respiration into its autotrophic and heterotrophic components by means of tree-girdling in old boreal spruce forest. *Tropical Ecology and Management* 257, 1764–1767.
- IPCC, 2007. Summary for policy makers. In: Solomon, S., Qin, D., Manning, M., Chen, Z., Marquis, M., Avery, K.B., Tignor, M., Miller, H.L. (Eds.), *Climate Change 2007: the Physical Science Basis. Contribution of Working Group I to the Fourth Assessment Report of the Intergovernmental Panel on Climate Change*. Cambridge University Press, Cambridge, United Kingdom and New York, NY, pp. 1–18.
- Janssens, I.A., Lankreijer, H., Matteucci, G., Kowalski, A.S., Buchmann, N., Epron, D., Pilegaard, K., Kutsch, W., Longdoz, B., Grunwald, T., Montagnani, L., Dore, S., Reimann, C., Moors, E.J., Grelle, A., Rannik, U., Morgenstern, K., Oltchev, S., Clement, R., Gudmundsson, J., Minerbi, S., Berbigier, P., Ibrom, A., Moncrieff, J., Aubinet, M., Bernhofer, C., Jensen, N.O., Vesala, T., Granier, A., Schulze, E.D., Lindroth, A., Dolman, A.J., Jarvis, P.G., Ceulemans, R., Valentini, R., 2001. Productivity overshadows temperature in determining soil and ecosystem respiration across European forests. *Global Change Biology* 7, 269–278.
- Kabwe, L.K., Hendry, M.J., Wilson, G.W., Lawrence, J.R., 2002. Quantifying CO_2 fluxes from soil surfaces to the atmosphere. *Journal of Hydrology* 260, 1–14.
- Kirschbaum, M.U.F., 2006. The temperature dependence of organic-matter decomposition—still a topic of debate. *Soil Biology and Biochemistry* 38, 2510–2518.
- Knorr, W., Prentice, I.C., House, J.I., Holland, E.A., 2005. Long-term sensitivity of soil carbon turnover to warming. *Nature* 433, 298–300.
- Kuzyakov, Y., 2006. Sources of CO_2 efflux from soil and review of partitioning methods. *Soil Biology and Biochemistry* 38, 425–448.
- Lavigne, M.B., Boutin, R., Foster, R.J., Goodine, G., Bernier, P.Y., Robitaille, G., 2003. Soil respiration responses to temperature are controlled more by roots than by decomposition in balsam fir ecosystems. *Canadian Journal of Forest Research* 33, 1744–1753.
- Lee, M.S., Mo, W.H., Koizumi, H., 2006. Soil respiration of forest ecosystems in Japan and global implications. *Ecological Research* 21, 828–839.
- Lenton, T.M., Huntingford, C., 2003. Global terrestrial carbon storage and uncertainties in its temperature sensitivity examined with a simple model. *Global Change Biology* 9, 1333–1352.
- Litton, C.M., Giardina, C.P., 2008. Below-ground carbon flux and partitioning: global patterns and response to temperature. *Functional Ecology* 22, 941–954.
- Liu, Q., Edwards, N.T., Post, W.M., Gu, L., Ledford, J., Lenhart, S., 2006. Temperature-independent diel variation in soil respiration observed from a temperate deciduous forest. *Global Change Biology* 12, 2136–2145.
- Luo, Y.Q., Wan, S.Q., Hui, D.F., Wallace, L.L., 2001. Acclimatization of soil respiration to warming in a tall grass prairie. *Nature* 413, 622–625.
- Luyssaert, S., Inglima, I., Jung, M., Richardson, A.D., Reichstein, M., Papale, D., Piao, S.L., Schulze, E.D., Wingate, L., Matteucci, G., Aragao, L., Aubinet, M., Beer, C., Bernhofer, C., Black, K.G., Bonal, D., Bonnefond, J.M., Chambers, J., Ciais, P., Cook, B., Davis, K.J., Dolman, A.J., Gielen, B., Goulden, M., Grace, J., Granier, A., Grelle, A., Griffis, T., Grunwald, T., Guidolotti, G., Hanson, P.J., Harding, R., Hollinger, D.Y., Hutry, L.R., Kolar, P., Kruijt, B., Kutsch, W., Lagergren, F., Laurila, T., 2007. CO_2 balance of boreal, temperate, and tropical forests derived from a global database. *Global Change Biology* 13, 2509–2537.
- Luyssaert, S., Schulze, E.D., Börner, A., Knohl, A., Hessenmöller, D., Law, B.E., Ciais, P., Grace, J., 2008. Old-growth forests as global carbon sinks. *Nature* 455, 213–215.
- Malcolm, G.M., López-Gutiérrez, J.C., Koide, R.T., Eissenstat, D.M., 2008. Acclimation to temperature and temperature sensitivity of metabolism by ectomycorrhizal fungi. *Global Change Biology* 14, 1169–1180.
- Marsden, C., Nouvellon, Y., Bou, A.T.M., Saint-Andre, L., Jourdan, C., Kinana, A., Epron, D., 2008. Two independent estimations of stand-level root respiration on clonal Eucalyptus stands in Congo: up scaling of direct measurements on roots versus the trenching-plot technique. *New Phytologist* 177, 676–687.
- Mellilo, J.M., McGuire, A.D., Kicklighter, D.W., Moore, B.I., Vorosmarty, C.J., Schloss, A.L., 1993. Global climate change and terrestrial net primary production. *Nature* 363, 234–240.
- Moyano, F.E., Kutsch, W.L., Reibmann, C., 2008. Soil respiration fluxes in relation to photosynthetic activity in broad-leaf and needle-leaf forest stands. *Agricultural and Forest Meteorology* 148, 135–143.
- Pavelka, M., Acosta, M., Marek, M.V., Kutsch, W., Janous, D., 2007. Dependence of the Q_{10} values on the depth of the soil temperature measuring point. *Plant and Soil* 292, 171–179.
- Peng, S.S., Piao, S.L., Wang, T., Sun, J.Y., Shen, Z.H., 2009. Temperature sensitivity of soil respiration in different ecosystems in China. *Soil Biology and Biochemistry* 41, 1008–1014.
- Raich, J.W., Schlesinger, W.H., 1992. The global carbon dioxide flux in soil respiration and its relationship to vegetation and climate. *Tellus* 44B, 81–99.
- Raich, J.W., Potter, C.S., Bhagawati, D., 2002. Interannual variability in global soil respiration, 1980–1994. *Global Change Biology* 8, 800–812.
- Reichstein, M., Beer, C., 2008. Soil respiration across scales: the importance of a model-data integration framework for data interpretation. *Journal of Plant Nutrition and Soil Science* 171, 1–11.
- Reichstein, M., Rey, A., Freibauer, A., Tenhunen, J., Valentini, R., Banza, J., Casals, P., Cheng, Y.F., Grünzweig, J.M., Irvine, J., Joffre, R., Law, B.E., Loustau, D., Miglietta, F., Oechel, W., Ourcival, J.M., Pereira, J.S., Peressotti, A., Ponti, F., Qi, Y., Rambal, S., Rayment, M., Romanya, J., Rossi, F., Tedeschi, V., Tirone, G., Xu, M., Yakir, D., 2003. Modeling temporal and large-scale spatial variability of soil respiration from soil water availability, temperature and vegetation productivity indices. *Global Biogeochemical Cycles* 4, 1104. doi:10.1029/2003GB002035.
- Reichstein, M., Kätterer, T., Andrén, O., Ciais, P., Schulze, E.D., Cramer, W., Papale, D., Valentini, R., 2005. Does the temperature sensitivity of decomposition vary with soil organic matter quality? *Biogeosciences Discussions* 2, 737–747.
- Rey, A., Pegoraro, E., Tedeschi, V., Parri, I.D., Jarvis, P.G., Valentini, R., 2002. Annual variation in soil respiration and its components in a coppice oak forest in Central Italy. *Global Change Biology* 8, 851–866.
- Sasaki, T., Okayasu, T., Jamsran, U., Takeuchi, K., 2008. Threshold changes in vegetation along a grazing gradient in Mongolian rangelands. *Journal of Ecology* 96, 145–154.
- Savage, K., Davidson, E.A., Richardson, A.D., 2008. A conceptual and practical approach to data quality and analysis procedures for high-frequency soil respiration measurement. *Functional Ecology* 22, 1000–1007.
- Schimel, D.S., House, J.I., Hibbard, K.A., Bousquet, P., Ciais, P., Peylin, P., Braswell, B.H., Apps, M.J., Baker, D., Bondeau, A., Canadell, J., Churkina, G., Cramer, W., Denning, A.S., Field, C.B., Friedlingstein, P., Goodale, C., Heimann, M., Houghton, R.A., Melillo, J.M., Moore, B., Muriyarso, D., Noble, I., Pacala, S.W., Raupach, M.R., Rayner, P.J., Scholes, R.J., Steffen, W.L., Wirth, C., 2001. Recent patterns and mechanisms of carbon exchange by terrestrial ecosystems. *Nature* 414, 169–172.
- Schindlbacher, A., Zechmeister-Boltenstern, S., Kitzler, B., Jandl, R., 2008. Experimental forest soil warming: response of autotrophic and heterotrophic soil respiration to a short-term 10 °C temperature rise. *Plant and Soil* 303, 323–330.
- Schulze, E.D., Wirth, C., Heimann, M., 2000. Managing forests after Kyoto. *Science* 289, 2058–2059.
- Schuur, E.A.G., 2003. Productivity and global change revisited: the sensitivity of tropical forest growth to precipitation. *Ecology* 84, 1165–1170.
- Sellers, P.J., Dickinson, R.E., Randall, D.A., Betts, A.K., Hall, F.G., Berry, J.A., Collatz, G.J., Denning, A.S., Mooney, H.A., Nobre, C.A., Sato, N., Field, C.B., Henderson-Sellers, A., 1997. Modeling the exchanges of energy, water, and carbon between continents and the atmosphere. *Science* 275, 502–509.
- Subke, J.A., Inglima, I., Cotrufo, F., 2006. Trends and methodological impacts in soil CO_2 efflux partitioning: a metaanalytical review. *Global Change Biology* 12, 921–943.
- Tierney, G.L., Fahey, T.J., Groffman, P.M., Hardy, J.P., Fitzhugh, R.D., Driscoll, C.T., Yavitt, J.B., 2003. Environmental control of fine root dynamics in a northern hardwood forest. *Global Change Biology* 9, 670–679.
- Toms, J.D., Lesperance, M.L., 2003. Piecewise regression: a tool for identifying ecological thresholds. *Ecology* 84, 2034–2041.
- Trumbore, S.E., 2006. Carbon respired by terrestrial ecosystems—recent progress and challenges. *Global Change Biology* 12, 141–153.
- Van't Hoff, J.H., 1898. Chemical dynamics. In: *Lectures on Theoretical and Physical Chemistry*. Edward Arnold, London, pp. 224–229.
- Vicca, S., Janssens, I.A., Flessa, H., Fiedler, S., Jungkunst, H.F., 2009. Temperature dependence of greenhouse gas emissions from three hydromorphic soils at different groundwater levels. *Geobiology* 7, 465–476.
- Wang, W., Fang, J.Y., 2009. Soil respiration and human effects on global grasslands. *Global and Planetary Change* 67, 20–28.
- Wang, C.K., Yang, J.Y., Zhang, Q.Z., 2006. Soil respiration in six temperate forests in China. *Global Change Biology* 12, 2103–2114.
- Widen, B., Majdi, H., 2001. Soil CO_2 efflux and root respiration at three sites in a mixed pine and spruce forest: seasonal and diurnal variation. *Canadian Journal of Forest Research* 31, 786–796.
- Xu, M., Qi, Y., 2001. Spatial and seasonal variations of Q_{10} determined by soil respiration measurements at a Sierra Nevada forest. *Global Biogeochemical Cycles* 15, 687–696.
- Zhou, T., Phi, P., Hui, D., Luo, Y., 2009. Global pattern of temperature sensitivity of soil heterotrophic respiration (Q_{10}) and its implications for carbon-climate feedbacks. *Journal of Geophysical Research* 114, G02016. doi:10.1029/2008JG000850.

How did climate drying reduce ecosystem carbon storage in the forest–steppe ecotone? A case study in Inner Mongolia, China

Yuke Zhang · Hongyan Liu

Received: 7 August 2009 / Accepted: 13 December 2009 / Published online: 20 February 2010
© The Botanical Society of Japan and Springer 2010

Abstract The projected recession of forests in the forest–steppe ecotone under projected climate drying would restrict the carbon sink function of terrestrial ecosystems. Previous studies have shown that the forest–steppe ecotone in the southeastern Inner Mongolia Plateau originally resulted from climate drying and vegetation shifts during the mid- to late-Holocene, but the interrelated processes of changing soil carbon storage and vegetation and soil shifts remain unclear. A total of 44 forest soil profiles and 40 steppe soil profiles were excavated to determine soil carbon storage in deciduous broadleaf forests (DBF), coniferous forests (CF) and steppe (ST) in this area. Carbon density was estimated to be 106.51 t/hm² (DBF), 73.20 t/hm² (CF), and 28.14 t/hm² (ST) for these ecosystems. Soil organic carbon (SOC) content was negatively correlated with sand content ($R = -0.879$, $P < 0.01$, $n = 42$), and positively correlated with silt ($R = 0.881$, $P < 0.01$, $n = 42$) and clay ($R = 0.858$, $P < 0.01$, $n = 42$) content. Consistent trends between fractions of coarse sand and a proxy index of relative aridity in sediment sequences from two palaeo-lakes further imply that climate drying reduced SOC through coarsening of the soil texture in the forest–steppe ecotone. Changes in carbon storage caused by climate drying can be divided into two stages: (1) carbon storage of the ecosystem was reduced to 68.7%, mostly by soil coarsening when DBF were replaced by CF at $\sim 5,900$ ¹⁴C years before present (BP); and (2) carbon storage was reduced to 26.4%, mostly by vegetation shifts when CF were replaced by ST at $\sim 2,900$ ¹⁴C years BP.

Keywords Carbon density · Forest–steppe ecotone · Soil organic carbon · Soil texture · Holocene

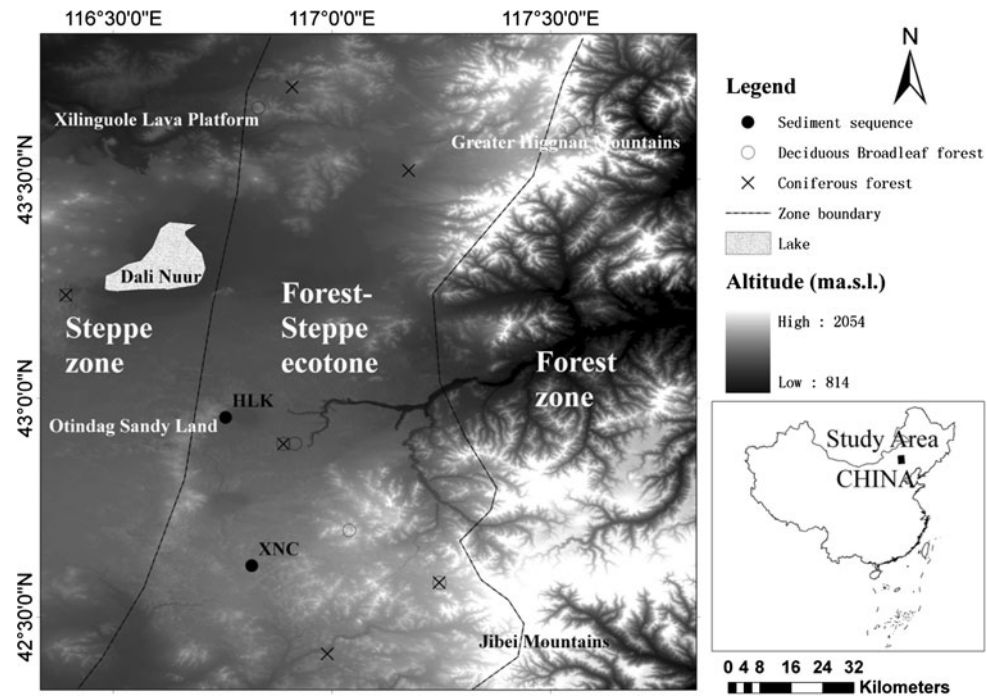
Introduction

By 2080, climate change will lead to a loss of forest vegetation in many formerly forested areas of the world, and the loss of carbon from declining forests will effectively eliminate the global terrestrial carbon sink (White et al. 1999). Temperate forest biomes contain approximately 10% of global soil carbon storage; therefore, any changes in their distribution could have significant impacts on terrestrial carbon budgets (Rasmussen et al. 2006). There are still important gaps in knowledge regarding the recession of temperate forests and its potential impact on carbon budgets.

Ecotones are expected to be especially sensitive to environmental change because they are the boundaries between biomes or communities occurring at distinctive locations along environmental gradients (Gosz 1991). For example, in the 1950s in northern New Mexico, USA, the ecotone between semiarid ponderosa pine forests and pinon-juniper woodlands shifted extensively (2 km or more) and rapidly (<5 years) because of increased mortality of ponderosa pine in response to a severe drought. The shift has persisted for 40 years. Forest patches within the shift zone became much more fragmented and soil erosion greatly accelerated (Allen and Breshears 1998). It is clear that the dynamic responses of soil and vegetation to climate change are interrelated. Decreased vegetation cover will enhance soil erosion and soil erosion will accelerate vegetation degradation. Thus, a scientific question arises, how climate drying force vegetation and soil degradation and further lead to the loss of carbon storage in ecosystems? Research into the dynamics of carbon storage

Y. Zhang · H. Liu (✉)
Department of Ecology, College of Urban and Environmental
Sciences and MOE Laboratory for Earth Surface Processes,
Peking University, 100871 Beijing, People's Republic of China
e-mail: lhy@urban.pku.edu.cn

Fig. 1 Map of the study area with location of sampling sites



patterns in the forest–steppe ecotone will help to improve our understanding of how terrestrial ecosystems respond to climate change, and allow us to project the potential carbon storage loss caused by forest recession in future climate change.

The forest–steppe ecotone in the southeastern Inner Mongolia Plateau lies between temperate broad-leaved forest and steppe. It is regarded as a sensitive monitor of regional environmental change (Wang and Feng 1991). The current forest–steppe ecotone resulted from forest recession during the Holocene, as documented by regional-scale palaeoecological studies (Zhao et al. 2009). By combining temporal and spatial patterns of the forest–steppe ecotone, we aimed to reconstruct the processes of carbon loss forced by climate drying and to distinguish the roles of soil degradation and vegetation shift in terms of their contribution to carbon sink function dynamics of the enormous forest–steppe ecotone in Inner Asia.

Study area and methods

Study area

The study area (42°20′–43°50′N, 116°20′–117°50′E) displays great variation in its geomorphologic features. The Xilinguole Lava Platform is situated in the north. The Otindag Sandy Land dominates the western part of the study area. The Greater Hinggan Mountains to the northeast and the Jibei Mountains to the south and southeast border the

Inner Mongolian Plateau in the study area (Liu et al. 2000; Fig. 1).

Climate in the study area is transitional from a temperate semi-humid monsoon climate to a semi-arid continental one. The mean annual temperature is 0–4°C without an obvious spatial gradient. The mean annual precipitation (MAP) is 350–450 mm, decreasing from the southeast to northwest; and along this precipitation gradient, vegetation zones gradually shift from the forest zone through the forest–steppe ecotone to a temperate steppe zone. The forest–steppe landscape of the area is characterized by islands of forest patches embedded in the steppe. Forest patches are found only on shady slopes of hills or mountains, which become smaller with decreasing MAP and disappear entirely in the steppe zone (Liu et al. 2000).

The soil types of the study area are diversified owing to the precipitation gradient and the geomorphologic patterns (Liu et al. 2000). From the Jibei Mountains in the southeast to the Xilinguole Lava Platform in the northwest, the soil types change from brown soil, grey forest soil, light chernozem to chestnut soil. Sandy soils are prevalent on the Otindag Sandy Land. Other azonal soil types appear locally, for example, subalpine meadow soil (Anon 1988, 1989).

Methods

In order to illuminate changes in carbon storage within the ecosystem, we compared the carbon storage patterns in three vegetation types: deciduous broadleaf forest (DBF), coniferous forest (CF) and steppe (ST). Carbon pools in

ecosystems were divided into soil, litter and vegetation. Soil organic carbon (SOC) was measured in field studies and the carbon content in vegetation and litter of the three vegetation types was obtained from previously published research.

AMS ^{14}C -dated sediment sequences from two palaeo-lakes in the study area, Hao-Lu-Ku (HLK, $42^{\circ}57.38'\text{N}$, $116^{\circ}45.42'\text{E}$, 1295 m a.s.l.) and Xiao-Niu-Chang (XNC, $42^{\circ}37.05'\text{N}$, $116^{\circ}49.02'\text{E}$, 1460 m a.s.l.), were used to reconstruct the Holocene history of climate change and vegetation development (Liu et al. 2002). By comparing vegetation history and carbon components of different vegetation types, the process of regional carbon storage dynamics was reconstructed.

Soil samples

Three sample plots were established in each of the four dominant forest types, *Betula platyphylla* forest, *Populus davidiana* forest, *Pinus tabulaeformis* forest and *Picea meyeri* forest. Four soil profiles were dug in August and September of 2007 in each plot close to a relatively intact forest patch on a shady slope, and soil profiles for steppe were located in steppe on the opposite sunny slope. As the *Betula platyphylla* forest and *Pinus tabulaeformis* forest were mixed on the same slope at one site and on two adjacent slopes at another site, we collected a total of 44 forest soil profiles and 40 steppe soil profiles. In most profiles, the A-horizon and B-horizon were restricted to the upper 30 cm. Soil samples were taken from the depths of 0–10, 10–20 and 20–30 cm. Samples were air-dried at room temperature before laboratory measurement. Measured items included soil particle proportion, bulk density and SOC concentration. Grain sizes of soil samples of the depth 0–10 and 10–30 cm from 11 forest sites and 10 steppe sites (total of 42 samples) were analyzed using a Master Size 2000 Laser Grain Size Analyzer. According to international soil fraction classification standards, soil grains were divided into four size fractions: clay (<0.002 mm), silt (0.002–0.02 mm), sand (0.02–2 mm) and gravel (>2 mm) (Lu 1999). Samples for chemical analyses were passed through a 0.149 mm soil sieve. Owing to an exceptionally low inorganic carbon concentration in the total carbon, a Perkin Elmer Model 2400 II CHN elemental analyzer was used to measure the SOC.

Soil organic carbon density (SOCD) in the upper 30 cm was calculated by Eq. 1:

$$\text{SOCD} = \sum_{i=1}^n H_i B_i O_i \quad (1)$$

where H_i is the thickness of layer i , which is 10 cm in this study, B_i , the bulk density of layer i , O_i the organic carbon concentration of layer i , i the number of soil depth, $n = 3$.

Lake sediments

^{14}C radio carbon dating was used to determine the age of different samples from different sediment strata. Grain-size percentages and content of six mineral elements, including K_2O , Na_2O , CaO , MgO , Fe_2O_3 , and MnO were measured. The content ratio of ($\text{K}_2\text{O} + \text{Na}_2\text{O} + \text{CaO} + \text{MgO}$) to ($\text{Fe}_2\text{O}_3 + \text{MnO}$) was used as a relative aridity index for climate dryness with a greater value indicating drier climate (Liu et al. 2002). Diagrams of pollen concentration were reported in Liu et al. (2002). In this study, pollen in lake sediments was classified into four types: herbs, deciduous broadleaf tree, coniferous tree, and shrub to show the Holocene vegetation shift.

Statistical analysis

Student's t test (performed with Microsoft Excel 2007) was used to evaluate whether different vegetation types have significant difference in soil texture.

Results

Patterns of regional soil carbon storage in the forest–steppe ecotone

Soil organic carbon densities in the deciduous broadleaf forest, coniferous forest and steppe were 52.91, 18.60 and 24.10 t/hm², respectively. Soil carbon storage under the deciduous broadleaf forest was 2.8 times as large as the coniferous forest and 2.2 times as large as the steppe. These differences were associated with the soil textures in different vegetation types: the silt content in CF soil was significantly lower than the silt content in DBF (Fig. 2). The range of soil textures in DBF and ST was large, indicating that these ecosystems are supported by a wide-range of soil textures. However, the range of soil textures for CF was small, indicating that conifers are more adaptive to coarse soil, but less competitive with broadleaf trees in fine soil. Conifers grow mainly on sandy soil in the study area.

Relationships between soil texture and SOC

Soil organic carbon content was correlated negatively with sand content ($R = -0.879$, $P < 0.01$, $n = 42$) and positively with silt ($R = 0.881$, $P < 0.01$, $n = 42$) and clay ($R = 0.858$, $P < 0.01$, $n = 42$) content (Fig. 3).

Changes in coarse sand percentage and the aridity index in sediment sequences

Coarse sand percentage and the index of relative aridity in sediment sequences are shown in Fig. 4 (the aridity index

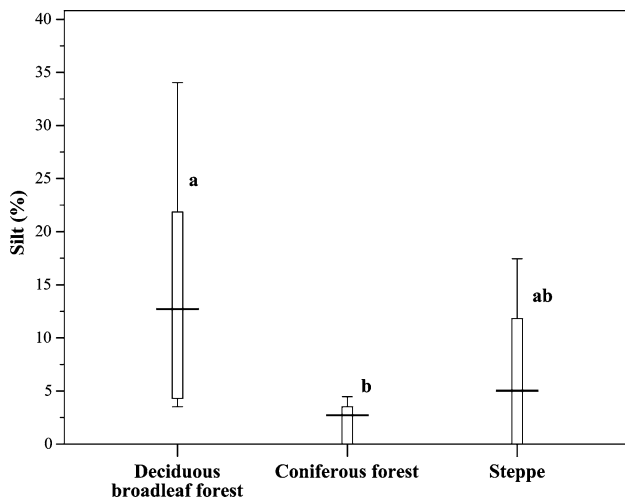


Fig. 2 Silt content in top soil (0–10 cm) in different types of vegetation. *a, b* Significantly different at $P < 0.05$; *ab* not significantly different from *a* or *b*. Since there is no silt in some plots of both coniferous forest (CF) and steppe (ST), their first quartile and minimum value are 0

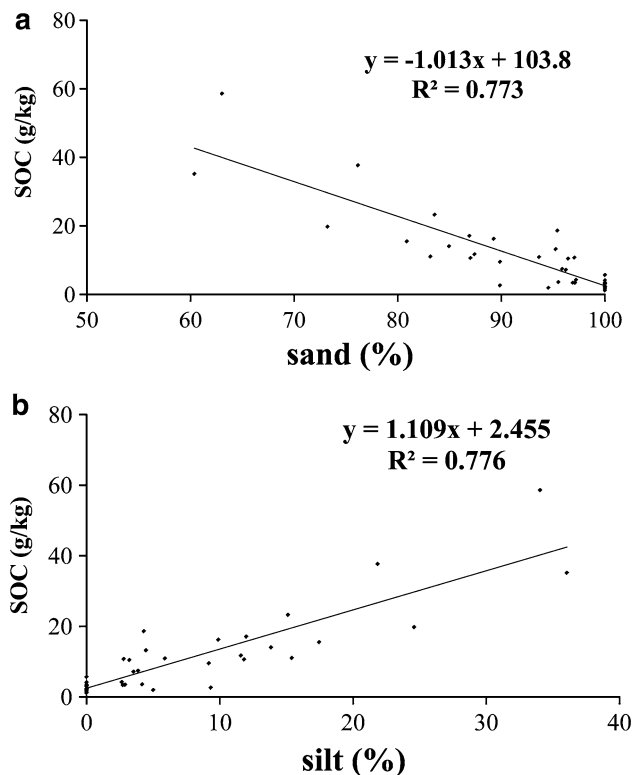


Fig. 3 Relationship between soil organic carbon (SOC) content and **a** sand content, and **b** silt content

was multiplied by 10). The aridity index in HLK and XNC both began to rise at $\sim 5,900$ ^{14}C years before present (BP). Coarse sand percentages in both sequences show similar trends. Before 5,900 ^{14}C years BP, the coarse sand percentages in HLK and XNC were 0.13–3.15 and 1.46–22.06%. These increase to 7.11–18.23 and 8.96–35.33%

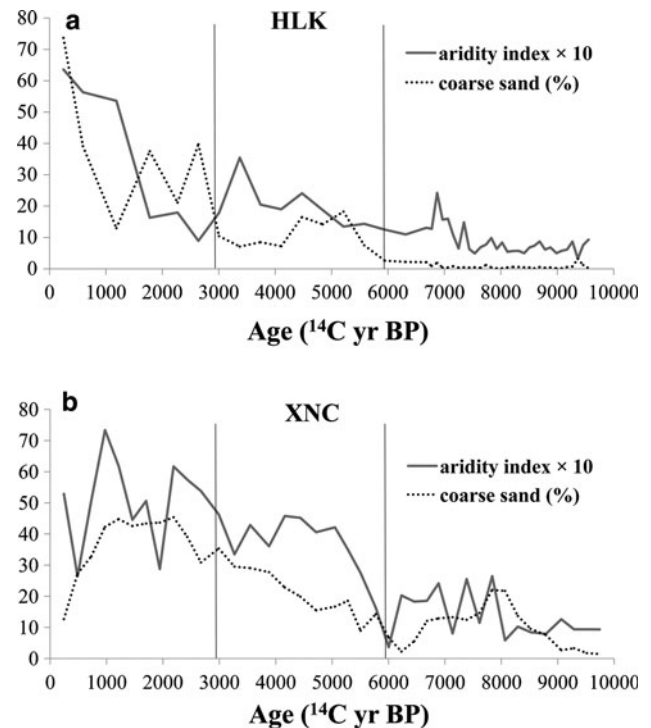


Fig. 4 Dynamics of relative aridity index and coarse sand percentages in the two sediment sequences from two palaeo-lakes, **a** HLK (Hao-Lu-Ku); **b** XNC (Xiao-Niu-Chang)

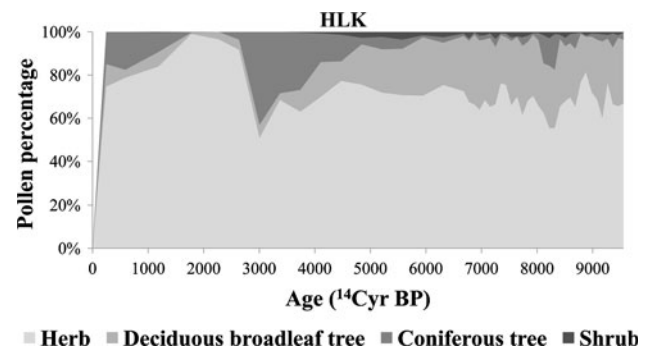


Fig. 5 Percentages of four pollen groups during the Holocene in HLK (Hao-Lu-Ku)

from $\sim 5,900$ to $\sim 2,900$ ^{14}C years BP, and then to 12.98–73.66 and 12.68–45.37% after $\sim 2,900$ ^{14}C years BP. Consistency between the tendencies of coarse sand percentages and the aridity index exists for both lakes, indicating a similar history of climate drying and sediment coarsening despite local differences between the two lakes (Fig. 4).

Pollen assemblages and Palaeovegetation shift

From 61.5 cm to the top of the sequence of XNC, pollen concentration is exceptionally low and percentages were not calculated. Therefore, only pollen percentages in the

HLK sequence were presented to show shifts of vegetation among ST, DBF, CF, and scrub. It was found that DBF were replaced by CF beginning $\sim 5,900$ ^{14}C years BP. CF began to recede and ST began to encroach into forests since $\sim 2,900$ ^{14}C years BP (Fig. 5).

Discussion

The relationship between sediment sequence and modern patterns of vegetation and soil

There was high correlation between SOC and silt content and high negative correlation between SOC and sand content in the study area, which serves as the basis for the Holocene SOC dynamics represented by the coarse sand fraction in the lake sediment. Significant correlation of soil texture and SOC has also been shown in other works (Guo et al. 2004; Wang et al. 2003). Because the high surface area of the fine silt and clay fractions enhances formation of organo-mineral complexes that protect carbon from microbial oxidation (Grigal and Berguson 1998), organic matter decomposes more rapidly in sandy soil than in clay (Sorensen 1983). Therefore, soil texture can be used as an indicator of SOC given the absence of historical SOC data.

Wind erosion can reduce clay and silt, leading to coarse soil texture (Hennessy et al. 1986), and reductions in organic matter and nutrient content (Zhou et al. 2008; Zhao et al. 2006). Coarse sand in sediment sequences derives mainly from wind-driven sedimentation with a higher percentage of coarse sand, indicating stronger wind erosion (Liu et al. 2002) as well as a coarser soil texture in the study area. Based on the high correlation between soil texture and SOC, we determined that more coarse sand in sediment sequences means less SOC in the soil.

Different chemical elements are concentrated in soil under different climate conditions. When the soils are eroded and transported into lakes, the contents of chemical elements in the sediment can be used to indicate climatic changes (Liu et al. 2002). K, Na, Ca, and Mg are concentrated when the climate is dry, whereas Fe and Mn are rich in sediments when the climate is wet (Guan 1992). Therefore, a relative aridity index based on the ratio of the above two groups of chemical elements is considered reliable.

Good correlation exists between coarse sand percentages and the relative aridity index in our study area, which might be accounted for by the following factors: (1) the forest–steppe ecotone is sensitive to climate change, and thus, vegetation grew well and provided protection for the top soil in relatively humid periods; whereas in arid periods, low vegetation coverage made the soil more vulnerable to wind erosion; and (2) the Mongolian

Table 1 Carbon density (t/hm^2) in different ecosystems in the study area

	Vegetation	Litter	Soil	Total
Deciduous broadleaf forest	47.75 ^a	5.85 ^a	52.91	106.51
Coniferous forest	43.26 ^a	11.34 ^a	18.60	73.20
Steppe	3.44 ^b	0.60 ^c	24.10	28.14

^a Zhou et al. (2000)

^b Ma et al. (2006)

^c Estimated value. Few previous studies have related to carbon density of litter in steppe (ST), which was estimated to be $30\text{--}400$ $\text{g C}/\text{m}^2$ ($0.30\text{--}4.00$ t/hm^2), and generally higher than that of aboveground biomass (Li and Chen 1998). Considering that the carbon density in aboveground biomass was 0.51 t/hm^2 (Ma et al. 2006), we estimated the carbon density of ST litter was 0.60 t/hm^2 , slightly higher than the aboveground value

anticyclone, a system of strong, frequent winds that can easily erode soil associated with uncovered ground surfaces in winter and spring.

Dynamics of soil carbon pool and regional carbon storage

Changes in the aridity index and pollen assemblage clearly show that vegetation shifts driven by climate drying can be divided into two stages: (1) from $\sim 5,900$ to $\sim 2,900$ ^{14}C years BP, the original DBF were gradually replaced by CF when the climate changed from humid to arid; and (2) after $\sim 2,900$ ^{14}C years BP, CF shifted to ST when the climate became drier. Previous studies also indicate that DBF was dominated by oak and birch, whereas CF was dominated by pine (Liu et al. 2002). Among these three vegetation types, DBF has the strongest ability to protect soil from wind erosion owing to the high vegetation cover, whereas ST has the weakest ability to conserve soil. Vegetation cover of the CF is lower than the DBF (as indicated by field observation) and its ability to conserve soil is moderate. Therefore, carbon storage in this area was determined to have experienced a decline as vegetation shifted as a result of climate drying.

Ecosystem carbon storage patterns are presented in Table 1. Vegetation and litter carbon density data were obtained from previous publications. In the study area, the growth of forests is limited by water availability (Liu et al. 2000), so the carbon stored in vegetation and litter are likely lower than the values shown in Table 1. The vegetation carbon density of DBF and CF are similar and more than 12 times that of ST.

Soil organic carbon decreases when DBF shifts to ST, which can be confirmed by soil coarsening in sediment sequences. The SOC in the present ST is higher than in the CF, although sediment sequences indicate a historical decrease in SOC when CF was replaced by ST. Reviewing

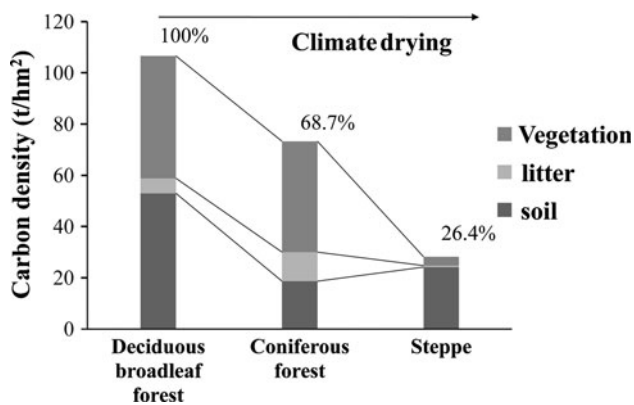


Fig. 6 Sketch map showing processes of ecosystem carbon loss forced by climate drying during the Holocene

the patterns of the three vegetation types, we can see that both the DBF and the CF are unable to grow on sunny slopes despite high organic matter content in the soil, leaving this habitat solely occupied by ST. Conifers are less competitive with broadleaf trees in fine soil inside the ecotone, so they grow mainly on coarse soil with lower SOC, resulting in less SOC for CF than for ST. However, pine forests grew on both shady and sunny slopes when the climate was not as dry as present (Liu et al. 2002) and, therefore, SOC in the CF was higher than in the ST.

Climate drying leads to carbon storage loss in both the biomass and soil pool. When DBF were replaced by CF under climate drying, the carbon storage in vegetation and soil was reduced by 9.4 and 64.9%, respectively, and was increased in litter by 93.9%. The total carbon budget in the ecosystem was reduced by 31.3%, so the carbon storage loss in this period was represented mostly by the loss of SOC (Table 1). If the climate continues to become dryer, CF dominated by pine will decrease in this area and, as a result, ST will expand. The loss of carbon storage resulted mostly from the shifting of vegetation, where the carbon storage was reduced by 92.1%, and the total loss of carbon storage in ecosystem was reduced by 61.6%. Compared with the DBF, carbon storage was reduced to 68.7% in the CF, and finally to 26.4% in the ST (Fig. 6).

Our results are in accord with the conclusion that when forest shifts to grassland, most of the aboveground biomass carbon in ecosystem will be lost, whereas soil can be either a carbon sink or a source (Chen and Tian 2007).

Conclusions

A significant correlation between soil texture and SOC was found for the forest–steppe ecotone in Inner Mongolia, China. Climate drying leads to reduction in SOC through coarsening of the soil texture in the forest–steppe ecotone.

As the climate transitioned from humid to arid, the loss of carbon storage was summarized as a two step process: in the first step, when DBF was replaced by CF at ~5,900 ^{14}C years BP, carbon storage of the ecosystem reduced to 68.7%, mostly owing to soil coarsening; in the second step, CF dominated by pine were replaced by ST at ~2,900 ^{14}C years BP, and carbon storage reduced to 26.4%, mostly through vegetation biomass reduction.

Acknowledgments This study was financed by National Natural Science Foundation Project (No. 40771208). We also thank Siyuan He for assistance with laboratory work and Guozheng Hu for drawing the figures.

References

- Allen CD, Breshears DD (1998) Drought-induced shift of a forest–woodland ecotone: rapid landscape response to climate variation. *Proc Natl Acad Sci USA* 95(25):14839–14842
- Anon (1988) Serial maps of resources of Inner Mongolia (in Chinese). Science Press, Beijing
- Anon (1989) Forest of Inner Mongolia (in Chinese). China Forestry Publishing House, Beijing
- Chen GS, Tian HQ (2007) Land use/cover change effects on carbon cycling in terrestrial ecosystems (in Chinese). *J Plant Ecol* 31:189–204
- Gosz JR (1991) Gradient analysis of ecological change in time and space-implications for forest management. *Ecol Appl* 2:248–261
- Grigal DF, Berguson WE (1998) Soil carbon changes associated with short-rotation systems. *Biomass Bioenergy* 14:371–377
- Guan YZ (1992) The element, clay mineral and depositional environment in Horqin Sand Land (in Chinese with English abstract). *J Desert Res (China)* 12:9–15
- Guo R, Wang XK, Liu K, Yang F (2004) Carbon and nitrogen pool in forest soil under *Pinus sylvestris* var. *mongolica* (in Chinese with English abstract). *Soil* 36:192–196
- Hennessy JT, Kies B, Gibbens RP, Tromble JM (1986) Soil sorting by 45 years of wind erosion on a southern New-Mexico range. *Soil Sci Soc Am J* 50:391–394
- Li LH, Chen ZZ (1998) The global carbon cycle in grassland ecosystems and its responses to global change. I. Carbon flow compartment model, inputs and storage (in Chinese with English abstract). *Chin Bull Bot* 15:14–22
- Liu HY, Cui HT, Pott R, Speier M (2000) Vegetation of the woodland-steppe transition at the southeastern edge of the Inner Mongolia Plateau. *J Veg Sci* 11:525–532
- Liu HY, Xu LH, Cui HT (2002) Holocene history of desertification along the woodland-steppe border in northern China. *Q Res* 57:259–270
- Lu RK (1999) Chemical analysis technique of soil in agriculture (in Chinese). China Agriculture Science and Technology Press, Beijing
- Ma WH, Han M, Lin X, Ren YL, Wang ZH, Fang JY (2006) Carbon storage in vegetation of grasslands in Inner Mongolia (in Chinese with English abstract). *J Arid Land Resour Environ* 20:192–195
- Rasmussen C, Southard RJ, Horwath WR (2006) Mineral control of organic carbon mineralization in a range of temperate conifer forest soils. *Glob Change Biol* 12:834–847
- Sorensen LH (1983) Size and persistence of the microbial biomass formed during the humification of glucose, hemicellulose, cellulose, and straw in soils containing different amounts of clay. *Plant Soil* 75:121–130

- Wang S, Feng M (1991) Environmental change and its relation with the weakening of the summer monsoon in Daihai, Inner Mongolia. *Sci China Ser B* 21:759–768
- Wang HJ, Li XW, Shi XZ (2003) Distribution of soil nutrient under different land use and relationship between soil nutrient and soil granule composition (in Chinese with English abstract). *J Soil Water Conserv* 17:44–50
- White A, Cannell MGR, Friend AD (1999) Climate change impacts on ecosystems and the terrestrial carbon sink: a new assessment. *Glob Environ Change* 9:s21–s30
- Zhao HL, Yi XY, Zhou RL, Zhao XY, Zhang TH, Drake S (2006) Wind erosion and sand accumulation effects on soil properties in Horqin Sandy Farmland, Inner Mongolia. *Catena* 65:71–79
- Zhao Y, Yu ZC, Chen FH (2009) Spatial and temporal patterns of Holocene vegetation and climate changes in arid and semi-arid China. *Q Int* 194:6–18
- Zhou YR, Yu ZL, Zhao SD (2000) Carbon storage and budget of major Chinese forest types (in Chinese with English abstract). *Acta Phytoecol Sin* 24:518–522
- Zhou RL, Li YQ, Zhao HL, Drake S (2008) Desertification effects on C and N content of sandy soils under grassland in Horqin, northern China. *Geoderma* 145:370–375

河北坝上地区不同土地利用类型的土壤风蚀研究

孙艳荣^{1,†} 刘鸿雁² 范涛¹ 马利国¹ 张铭杰²

1. 北华航天工业学院材料工程系,廊坊 065000; 2. 北京大学城市与环境学院,北京 100871;

† E-mail: sunyanrong@pku.edu.cn

摘要 通过¹³⁷Cs示踪和土壤粒度分析,着重探讨了河北坝上地区土地利用与土壤风蚀的关系,揭示了不同土地利用类型的侵蚀强度为沙质丘陵草原>耕地>退耕还草地>人工林>石质丘陵草原,提出了对研究区保持石质丘陵草原现状、保护原有人工林等植被恢复的建议。

关键词 土壤风蚀;土地利用;农牧交错带;粒度分析

中图分类号 S151

Soil Wind Erosion under Different Land Use Types in Bashang of Hebei Province

SUN Yanrong^{1,†}, LIU Hongyan², FAN Tao¹, MA Liguang¹, ZHANG Mingjie²

1. Department of Materials Engineering, North China Institute of Aerospace Engineering, Langfang, 065000;

2. School of Urban and Environmental Sciences, Peking University, Beijing, 100871; † E-mail: sunyanrong@pku.edu.cn

Abstract By the trace of ¹³⁷Cs and soil granularity analysis, the relationship between land-use and soil wind erosion was investigated in Bashang of Hebei Province. The results indicate that the land use types with erosion intensity, from the higher to the lower, are sandy hilly grassland > cultivated land > grassland converted from cultivated land > artificial forest > gravel hill grassland. Hence, to recover the vegetation, the gravel hilly grassland in this region should be reserved and the original vegetation in it should be protected.

Key words soil wind erosion; land use; agriculture-pasture transition zone; granularity analysis

河北坝上地区地处我国北方农牧交错带,是近50年来土地利用变化最为明显的地区之一^[1]。该地区生态脆弱,对于人类的干预反应敏感,过度的人为利用已经造成了突出的生态问题^[2]。土地利用的变化必然带来生态系统服务的变化,有关研究表明,河北坝上地区的植被退化与北京地区的沙尘天气关系密切^[3]。尽管对这一地区的土壤风蚀有少量的研究^[1,4],但在土地利用与土壤风蚀、植被和土壤特征与土壤风蚀等方面的研究仍然较少,尤其是将植被覆盖减少土壤风蚀作为一种生态系统服务仍

然缺少研究。由于土地利用变化与土壤风蚀之间的关系缺少实测结果,也就难以为未来的植被恢复和生态建设提供较为合理的依据。本文通过¹³⁷Cs示踪与土壤粒度分析相结合,探讨了这一研究区域不同土地利用类型的土壤风蚀情况,为制定切实可行的植被恢复对策提供依据。

¹³⁷Cs是20世纪50—70年代原子弹爆炸产生的放射性尘埃,降落到地表后,被土壤黏粒和有机物强烈吸附,基本不被植物吸收和淋溶流失,半衰期为30.17 a,是研究土壤侵蚀^[5]和泥沙沉积^[6]的一种良

好的示踪源。通过测定不同土壤类型及不同层次的 ^{137}Cs 含量,并与背景值相比较,可以确定土壤侵蚀率,探讨土壤侵蚀规律。近几十年来, ^{137}Cs 法在全球土壤侵蚀研究中取得了显著的成就,但以往的 ^{137}Cs 法应用主要集中在水蚀方面,很少涉及风蚀问题^[7],直到20世纪90年代才逐渐被用在土壤风蚀的研究领域^[8]。

国内,严平等^[9-10]和濮励杰等^[11]最早尝试将 ^{137}Cs 法作为土壤风蚀的研究手段。严平等^[9-10]选择青海共和盆地作为研究区,探讨了 ^{137}Cs 的区域和剖面分布特征,确定了区域 ^{137}Cs 背景值,并将 ^{137}Cs 深度分布划分为正常剖面、沉积剖面、侵蚀剖面 and 人为扰动剖面4种类型。濮励杰等^[11]以新疆库勒勒地区为例,运用 ^{137}Cs 示踪分析法对我国西部风蚀地区土壤侵蚀的强度与区域分布进行了研究,探讨了不同土地利用类型与土地退化之间的相关关系及空间特征。赵焯等^[12]测定了滦河源区土壤样品 ^{137}Cs 的比活度,发现自然栗钙土以及被风蚀土壤剖面中 ^{137}Cs 比活度随深度呈指数递减式分布,其最大渗透深度可达约30 cm。胡云锋等^[13]以内蒙古太仆寺旗为研究区,发现不同土地利用类型/土地覆盖等级的 ^{137}Cs 剖面分布特征差异明显:在低覆盖草地和中覆盖草地土壤剖面中, ^{137}Cs 活度分布形态为负指数分布;在高覆盖草地土壤剖面中, ^{137}Cs 活度分布形态在剖面上部为单峰状,单峰后继续为负指数分布;在耕地剖面中, ^{137}Cs 集中在犁底层以上,且均匀分布。刘纪远等^[14-15]在蒙古高原也开展了一定的研究工作,张素红等^[16]还用 ^{137}Cs 示踪法研究了海南岛滨海地区风沙活动特征,发现海南岛 ^{137}Cs 水平普遍偏低,主要原因是 ^{137}Cs 沉积量有限。

在 ^{137}Cs 示踪用于土壤风蚀的研究中, ^{137}Cs 活度与土壤粒度的关系多有报道。文献[7]指出, ^{137}Cs 在土壤中主要被黏粒、极细沙(<0.01 mm)所吸附。赵焯等对滦河源区栗钙土风蚀的研究表明不同粒径土壤颗粒中 ^{137}Cs 的比活度与粒径关系密切^[12],并进一步结合风积层中土壤颗粒参数如土壤风蚀相对强度指数重建滦河源区过去区域的土壤风蚀过程^[17]。

1 研究区域及研究方法

1.1 研究区概况

如图1所示,研究区域主体部分为位于内蒙古

高原东南部的浑善达克沙地和河北坝上地区,在行政区划上包括河北省张家口地区的张北、康保等县以及承德市的丰宁、围场两县的坝上部分,地理坐标为114—117°E,41—43°N。取样点选择在内蒙古高原东南缘围场坝上、丰宁坝上、沽源坝上3条样带,主体部分海拔为1100~1400 m。西部为浑善达克沙地,由多条东西走向的沙带组成。东南和南部为冀北山地。气候条件为温带大陆性半湿润气候向半干旱气候逐渐过渡,年降水量在200~450 mm之间,为季风气候影响的尾间区(marginal area)。地表类型包括人工林、沙质丘陵草地、石质丘陵草地、退耕还草地、退耕撂荒地、耕地、黄土、退化草原等^[2]。

1.2 ^{137}Cs 示踪分析

^{137}Cs 背景值是指特定地区保存下来的 ^{137}Cs 沉降总量,即未受扰动、非蚀非积条件下的沉积总量,其分布函数一般呈负指数形式,如式(1)所示:

$$C = A_1 \cdot e^{-h/T_1}, \quad (1)$$

上式中 C 是特定土层样品中 ^{137}Cs 的活度(Bq/kg), h 为土层深度(cm), A_1 和 T_1 是与土壤性状相关的常数^[12]。由于 ^{137}Cs 的迁移只受土壤颗粒物理运动控制,对比不同样地土壤剖面 ^{137}Cs 活度相比区域背景值的损失变化可以有效判断土壤风蚀状况。

本研究样品采集于2005年7月,选择沙质丘陵草地、人工林、耕地、石质丘陵草地和退耕还草地等5种不同土地利用类型样地作为研究对象,选择未受人为活动干扰的尚海林白桦林拟作为区域标准样。除尚海林白桦林选取一个采样点外,其他每种

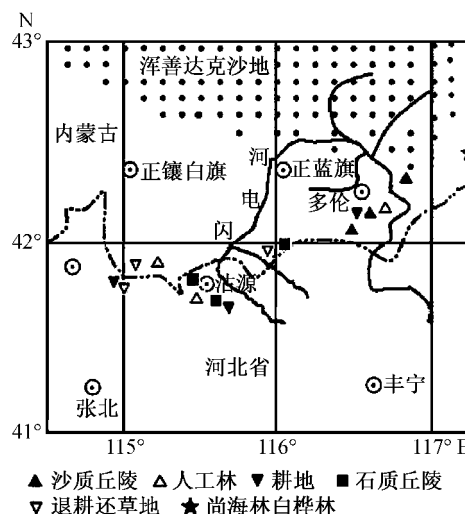


图1 研究区采样点分布图

Fig. 1 Sketch map of sample sites distribution in the study area

样地各选择 3 个采样点, 共计 16 个采样点, 采样点分布见图 1。每个采样点挖取一个土壤剖面, 深度在 30 cm 以上, 用直径 5 cm 的环刀自 30 cm 深处由下至上依次分层取样。每个样点取 6 层土壤样品。样品经烘干后, 称重、研磨过筛(孔径为 1.0 mm), 剔除大颗粒及草根, 每个样品挑出 30 g, 在核工业北京化工冶金研究院分析测试中心用高纯锗 γ 谱仪进行测试, 测试仪器为美国坎培拉公司(ORTEC)生产的高纯锗(Ge)探测器, ^{137}Cs 含量用其 661.6 keV γ 射线的全峰面积计算。

1.3 土壤粒度分析

粒度分析是土壤风蚀常用的研究方法^[18]。将上述 ^{137}Cs 测试所用的样品分别进行土壤粒度分析。每个样品挑出 5 g, 在北京大学城市与环境学院地表过程分析与模拟教育部重点实验室用激光粒度仪 Mastersizer 2000 进行测试。技术参数为 0.02 ~ 2000 μm 、1000 次/s 扫描速度、高灵敏亚微米区测量性能。

2 结果和讨论

2.1 不同土地利用类型的 ^{137}Cs 分布分析

每种样地 ^{137}Cs 活度取所选采样点测试结果的平均值, 结果见表 1。根据表 1 绘制了不同土地利用类型样地 ^{137}Cs 活度随土壤深度的变化曲线, 如图 2。已有研究者把 ^{137}Cs 深度分布划分为正常剖面、沉积剖面、侵蚀剖面 and 人为扰动剖面^[9]。由图 2 可知, 尚海林白桦林 ^{137}Cs 主要集中分布于 0 ~ 10 cm 的表层, 其分布曲线接近负指数形式。进一步将尚海林白桦林分层 ^{137}Cs 活度按式(1)拟合, 不难得出 $T_1 = 8.80$, $A_1 = 0.41$, 相关系数 $R = 0.89$, 相关性比较高。通常未受人为扰动、无侵蚀也无堆积的土壤呈现正常剖面, 其分布函数一般表现为负指数形式, 具

有正常剖面特征的样地类型可作为区域标准样选用。可见, 在历史上未经历任何形式的侵蚀或堆积的尚海林白桦林土壤剖面能够反映该区域 ^{137}Cs 原始沉积, 其总量能够代表 ^{137}Cs 背景值, 符合作为区域标准样的相关要求。

图 2 反映了各样地土壤剖面的 ^{137}Cs 深度分布特征。耕地、人工林、退耕还草地均呈现出受到一定人为扰动的剖面分布, 尤其是耕地样品 ^{137}Cs 活度分布较为均匀, 这是由于人为耕作而产生的 ^{137}Cs 混和作用而使得耕地土壤呈现出典型的人为扰动剖面。石质丘陵草原表现为受到一定侵蚀的剖面分布, 而沙质丘陵草原则为明显的侵蚀-沉积剖面。究其原因, 沙质丘陵草原表层 ^{137}Cs 活度较低, 而在其下层, ^{137}Cs 活度显著增大, 出现了明显的堆积形态, 严平等^[9]在青海共和盆地对流动沙丘的研究也得到了类似的侵蚀-沉积剖面分布, 这与历史上各时期不同的土壤侵蚀和堆积行为有关。根据图 3, 沙质丘陵草原土壤中细颗粒含量随土壤深度的变化呈现出与 ^{137}Cs 活度近似的变化趋势, 可见沙质丘陵下层出现了细颗粒的堆积, 导致 ^{137}Cs 活度较大; 而其表层受到侵蚀, 细颗粒含量相对较少, ^{137}Cs 活度也相对降低。因此, 沙质丘陵草原历史上经历过不同方式和程度的 ^{137}Cs 再分配过程是侵蚀-沉积剖面形成的根本原因。

进一步分析图 2, 与区域标准样尚海林白桦林相比, 研究区域中各种样地表层(0 ~ 10 cm)都存在着严重的土壤风蚀。通过比较 ^{137}Cs 活度大小可直观判断其侵蚀状况: 0 ~ 5 cm 层为沙质丘陵草原 > 退耕还草地 > 耕地 > 人工林 > 石质丘陵草原; 5 ~ 10 cm 层为沙质丘陵草原 \approx 退耕还草地 > 人工林 \approx 耕地 \approx 石质丘陵草原。比较而言, 0 ~ 5 cm 表层的风蚀更为显著, 而且 3 种受人为扰动影响的样地中人工林的风蚀程度最轻。总体来说, 沙质丘陵草原土

表 1 不同土地利用类型样地分层 ^{137}Cs 活度
Table 1 ^{137}Cs content in different depth of the soil in different land use types

样地类型	^{137}Cs 活度 / ($\text{Bq} \cdot \text{kg}^{-1}$)					
	0 ~ 0.05 m	0.05 ~ 0.10 m	0.10 ~ 0.15 m	0.15 ~ 0.20 m	0.20 ~ 0.25 m	0.25 ~ 0.30 m
沙质丘陵	0.044(0.002)	0.076(0.030)	0.118(0.018)	0.121(0.016)	0.112(0.068)	0.181(0.153)
人工林	0.114(0.039)	0.093(0.024)	0.085(0.024)	0.077(0.032)	0.075(0.031)	0.055(0.026)
耕地	0.101(0.007)	0.103(0.007)	0.092(0.006)	0.080(0.024)	0.077(0.027)	0.067(0.026)
石质丘陵	0.139(0.051)	0.105(0.057)	0.061(0.024)	0.055(0.028)	0.047(0.024)	0.020(0.003)
退耕还草地	0.083(0.020)	0.067(0.023)	0.074(0.022)	0.042(0.005)	0.034(0.011)	0.035(0.013)
尚海林白桦林	0.367	0.146	0.048	0.028	0.015	0.030

说明: 括号中数字为标准差 s 。

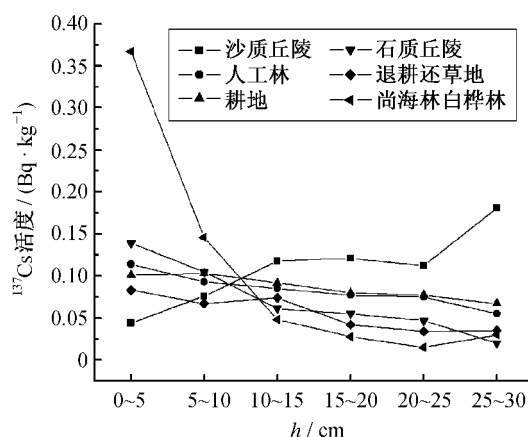


图 2 不同土地利用类型样地¹³⁷Cs 活度与土壤深度的关系

Fig. 2 Depth distribution of ¹³⁷Cs in the soil of different land use types

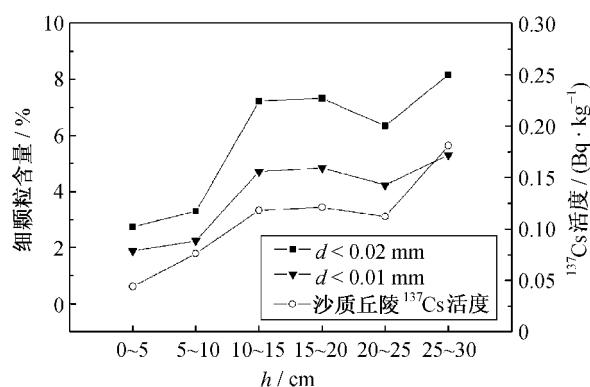


图 3 沙质丘陵草原¹³⁷Cs 活度及细颗粒含量随土壤深度的变化趋势

Fig. 3 ¹³⁷Cs and fine particle content varying with soil depth of sandy hilly grassland

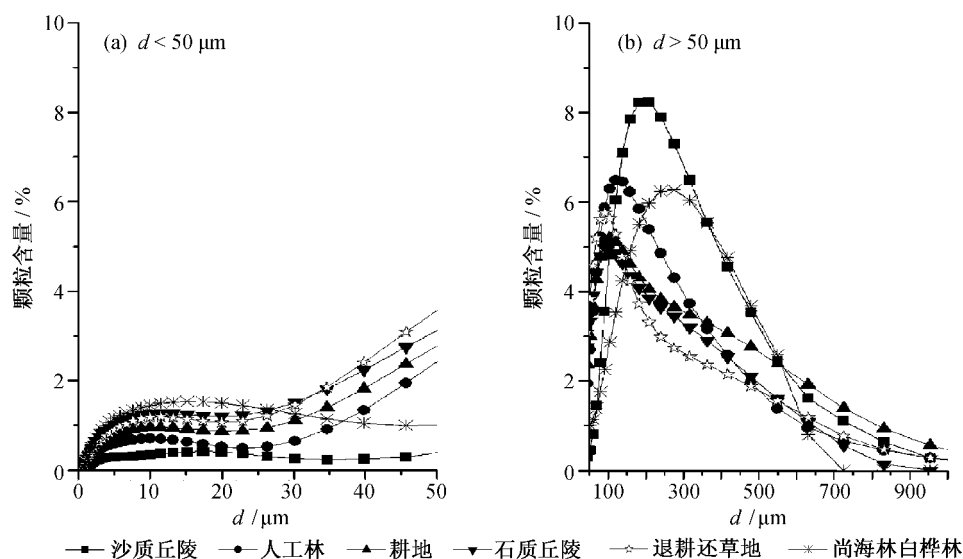


图 4 不同土地利用类型样地粒度分布比较

Fig. 4 Granularity distribution of the soil in different land use types

壤侵蚀程度最严重,石质丘陵草原侵蚀程度最弱,其他 3 种样地侵蚀状况居中。人工林、耕地和退耕还草地由于在历史上都存在一定的人为扰动因素,通过表层¹³⁷Cs 活度大小难以对比其侵蚀情况,尚需要进一步采用土壤粒度分析来确认其侵蚀状况大小。

2.2 不同土地利用类型的土壤粒度分布分析

将不同土地利用类型样地分层粒度数据加和平均后可分析对比各种不同土壤类型粒度分布之间的相互关系,如图 4 所示。为了清晰地表示不同样地粒径 $d < 50 \mu\text{m}$ 细粒部分的分布情况,我们放大了粒径 $0 \sim 50 \mu\text{m}$ 部分的横坐标(图 4(a))。区域标准样尚海林白桦林的土壤粒度分布均匀,接近于正态分布,侵蚀和堆积都不明显。沙质丘陵的粒度在几种样地里最大而且峰值最高,这是长期风力侵蚀的结果。石质丘陵草原峰尖部分位于较低的粒度范围,因为裸露岩石的保护,细粒物质得到了一定的保留。耕地由于人为活动的影响,土壤中细粒物质较多且分布比较均匀。耕地转化为退耕还草地后,土壤明显出现了堆积过程,细粒物质含量最为丰富,且积聚程度较高,这说明多年生草本植物覆盖已经起到了改善土壤的作用。人工林的土壤粒度含量相对于耕地、退耕还草地以及石质丘陵草原等颗粒物质虽然较粗,但分布比较平滑,其特殊的林地背景,以及较高的草本覆盖度使其防风固沙功能较强,故粒度分布较为均匀。

叶笃正等^[3]指出沙尘颗粒集中在 $0.002 \sim$

0.063 mm之间。陈静生等^[19]通过北京至内蒙古集宁一线21个地点的系统采样,也得出绝大多数地点的降尘中小于0.05 mm粒径部分占绝对优势的结论。盛学斌等^[20]1989年8月—1993年9月在坝上康保县照阳河乡三义村进行的风蚀沙化实验表明,被风蚀扬走的主要是0.05 mm以下的细粒物质。故选取粒径 $d < 0.05$ mm的细颗粒含量作为重要的划分标准来判断土壤风蚀情况^[21]。

图5给出了不同土地利用类型样地细颗粒($d < 0.05$ mm)含量随土壤深度的变化情况。根据图5,区域标准样尚海林白桦林粒度分布均匀无明显的风蚀和堆积情况。石质丘陵草原风蚀程度最轻,所含细粒物质较多,这是风蚀过后黏土类物质遗留在石质颗粒中的结果。人工林表层拥有大量的细粒物质沉积,说明人工林已经起到防风固沙作用。耕地由于人为影响有少量侵蚀,而且由于耕作的混和作用各深度细粒物质分布较为均匀。退耕还草后土壤的质地得到了一定程度的改善,表现为细粒物质增多。沙质丘陵草原细粒物质较少,毫无疑问地处于强烈的风蚀过程中。通过各样地细粒物质尤其是表层细粒物质的比较,我们认为人工林、退耕还草地的风蚀程度要弱于耕地。

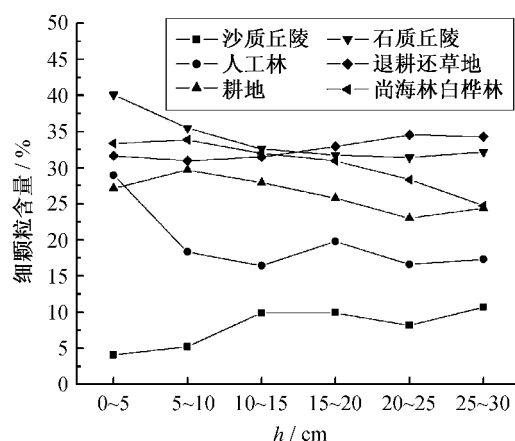


图5 不同土地利用类型样地细颗粒($d < 0.05$ mm)含量随土壤深度的变化情况

Fig. 5 Fine particle content ($d < 0.05$ mm) varying with the soil depth of the soil in different land use types

3 结论

本文由¹³⁷Cs示踪分析方法得出了研究区域各种不同土地利用类型的土壤风蚀状况,再根据其相关的土壤粒度的性质对各种土地利用类型的土壤风蚀状况进行判断和分析。

根据¹³⁷Cs分析方法可得出研究区域的不同土地利用类型中沙质丘陵草原土壤侵蚀程度最严重,石质丘陵草原侵蚀程度最弱,耕地、退耕还草地和人工林侵蚀状况居中,人工林的受侵蚀程度要弱于耕地和退耕还草地。

根据土壤粒度的分析得出沙质丘陵草原处于强烈的风蚀过程中,而石质丘陵草原风蚀程度最轻。退耕还草地较耕地的土壤质地得到一定的改善,人工林已经体现出一定的防风固沙作用,两者受侵蚀程度要弱于耕地。

综合¹³⁷Cs示踪与土壤粒度分析,可得出不同土地利用类型土壤侵蚀强度的顺序为:沙质丘陵草原 > 耕地 > 退耕还草地 > 人工林 > 石质丘陵草原。

因此,在河北坝上地区防治沙漠化的过程中无论是退耕还草还是种植人工林都可以在一定程度上减缓土壤风蚀的作用,应该保护现有的人工林使之不遭受破坏,因为这些土地利用类型有大量的细颗粒物质的沉降,一旦破坏就有可能成为受风蚀最为严重的沙源。同时在植树种草的区位选择上要科学论证所改造的原土地利用类型,本研究区域石质丘陵受土壤风蚀影响比人工林和退耕还草地更为轻微,所以不应该在该地区对石质丘陵草原进行人工植树造林的工作。

参考文献

- [1] 王石英,蔡强国,吴淑安. 中国北方农牧交错区研究展望. 水土保持研究, 2004, 11(4): 138-142
- [2] 田育红. 内蒙古高原东南部荒漠化与风沙活动研究[D]. 北京: 北京大学, 2003
- [3] 叶笃正,丑纪范,刘纪远,等. 关于我国华北沙尘天气的成因与治理对策. 地理学报, 2000, 55(5): 513-520
- [4] 海春兴,周心澄,李晓佳. 河北坝上不同土地利用方式下土壤表层水分变化对风蚀的影响. 水土保持学报, 2005, 19(2): 29-32
- [5] 曾海鳌,吴敬禄,林琳. ¹³⁷Cs示踪法研究太湖流域土壤侵蚀分布与总量. 海洋地质与第四纪地质, 2008, 28(2): 79-84
- [6] 张信宝,温仲明,冯明义,等. 应用¹³⁷Cs示踪技术破译黄土丘陵区小流域坝库沉积赋存的产沙记录. 中国科学: D辑, 2007, 37(3): 405-410
- [7] 严平,张信宝. ¹³⁷Cs法在风沙过程研究中的应用前景. 中国沙漠, 1998, 18(2): 182-187
- [8] 王宇飞,濮励杰. ¹³⁷Cs应用于我国土壤侵蚀研究评述. 南京大学学报: 自然科学版, 2002, 38(6): 803-

- 812
- [9] 严平,董光荣,张信宝,等. 青海共和盆地土壤风蚀的 ^{137}Cs 法研究(I): ^{137}Cs 分布特征. 中国沙漠, 2003, 23(3): 268-274
- [10] 严平,董光荣,张信宝,等. 青海共和盆地土壤风蚀的 ^{137}Cs 法研究(II): ^{137}Cs 背景值与风蚀速率测定. 中国沙漠, 2003, 23(4): 391-397
- [11] 濮励杰,包浩生,彭补拙,等. ^{137}Cs 应用于我国西部风蚀地区土地退化的初步研究: 以新疆库尔勒地区为例. 土壤学报, 1998, 35(4): 441-449
- [12] 赵烨,岳建华,徐翠华,等. ^{137}Cs 示踪技术在滦河源区栗钙土风蚀速率估算中的应用. 环境科学学报, 2005, 25(4): 562-566
- [13] 胡云锋,刘纪远,庄大方,等. 风蚀土壤剖面 ^{137}Cs 的分布及侵蚀速率的估算. 科学通报, 2005, 50(9): 933-937
- [14] 刘纪远,齐永青,师华定,等. 蒙古高原塔里亚特—锡林郭勒样带土壤风蚀速率的 ^{137}Cs 示踪分析. 科学通报, 2007, 52(23): 2785-2791
- [15] 齐永青,刘纪远,师华定,等. 蒙古高原北部典型草原区土壤风蚀的 ^{137}Cs 示踪法研究. 科学通报, 2008, 53(9): 1070-1076
- [16] 张素红,严平,李森. 海南岛滨海沙地风沙活动的 ^{137}Cs 示踪初步研究. 中国沙漠, 2007, 27(6): 932-935
- [17] 张平,陈志凡,赵烨,等. 运用 ^{137}Cs 示踪技术重建近30年滦河源区土壤风蚀变化过程. 北京师范大学学报: 自然科学版, 2008, 44(6): 635-639
- [18] 胡云锋,刘纪远,庄大方,等. 不同土地利用/土地覆盖下土壤粒径分布的分维特征. 土壤学报, 2005, 42(2): 336-339
- [19] 陈静生,邓宝山,贾振邦. 关于“外来尘”对北京大气质量影响的研究. 中国环境科学, 1984, 4(1): 10-17
- [20] 盛学斌,刘云霞,孙建中. 农牧交错带土壤及某些表生植被特性变异与荒漠化的相关性: 以冀北康保县为例. 应用生态学报, 2002, 13(7): 909-910
- [21] 刘鸿雁,田育红,丁登. 内蒙古浑善达克沙地和河北坝上地区不同地表覆盖类型对北京沙尘天气物源的贡献. 科学通报, 2003, 48(11): 1229-1232

*

*

*

*

*

简 讯

北京大学朱玉贤教授课题组在棉纤维伸长机制方面取得进展

北京大学生命科学学院蛋白质工程及植物基因工程国家重点实验室朱玉贤教授课题组通过比较野生型和无长绒、无短绒突变体棉花胚珠的蛋白质组学数据发现,核苷糖合成途径在棉纤维快速伸长期最显著上调,而植物激素乙烯可能通过促进植物细胞初生壁中果胶的生物合成来调控纤维等具有线性伸长机制的细胞生长。这是他们继2006年发现乙烯在棉花纤维细胞伸长过程中的主导作用,2007年发现超长链脂肪酸位于乙烯信号上游,在转录水平调控乙烯生物合成,从而影响棉纤维伸长后,有关棉花等线性伸长细胞生长发育机制研究中的又一重要贡献。

(摘自北京大学新闻网 2010-06-17)

2009 年发表论文



Soil respiration and human effects on global grasslands

Wei Wang^{*}, Jingyun Fang

Department of Ecology, College of Environmental Science, and Key Laboratory for Earth Surface Processes of the Ministry of Education, Peking University, Beijing 100871, China

ARTICLE INFO

Article history:

Accepted 8 February 2008

Available online 3 January 2009

Keywords:

grassland ecosystem
soil respiration
 Q_{10} value
turnover rate
grazing
fertilization

ABSTRACT

Grasslands comprise approximately 40% of the earth's land area (excluding areas of permanent ice cover) and play a critical role in the global carbon cycle. In this paper, by reviewing literature, we quantify annual soil CO_2 efflux, contribution of root respiration to total soil respiration, apparent temperature sensitivity of soil respiration (indicated by Q_{10}), and turnover rates of soil organic carbon (SOC). We discuss effects of human activities (grazing, land-use changes, and fertilization) on soil respiration rates of global natural grasslands. The soil CO_2 efflux from temperate and tropical natural grasslands is $389.8 \pm 45.5 \text{ g C m}^{-2} \text{ yr}^{-1}$ and $601.3 \pm 45.6 \text{ g C m}^{-2} \text{ yr}^{-1}$ (mean \pm S.E.), respectively. The contribution of root respiration to total soil respiration averages 36%, ranging from 8% to 64%. Annual soil CO_2 efflux increases with temperature and precipitation, but increased precipitation can cause a decrease in soil respiration rate in rainy regions. Mean turnover rates of SOC are 71 years in temperate grasslands and 15 years in tropical grasslands. The average Q_{10} value is 2.13, with 2.23 for temperate grasslands and 1.94 for tropical grasslands. Human activities significantly affect soil respiration but the extent varies among sites.

© 2008 Elsevier B.V. All rights reserved.

1. Introduction

Soil respiration is the primary pathway for CO_2 fixed by plants returning to the atmosphere (Högberg and Read, 2006). It releases carbon (C) in the magnitude of 68 to 80 petagrams ($\text{Pg} = 10^{15} \text{ g}$) (Raich and Schlesinger, 1992; Raich et al., 2002) to the atmosphere each year, which is more than 10 times that of fossil fuel burning (Schlesinger, 1997). Due to the magnitude of the soil-to-atmosphere CO_2 efflux and the large pool of potentially mineralizable C in soils, any increases in soil CO_2 efflux in response to environmental changes have the potential to exacerbate increasing atmosphere CO_2 levels and to provide a positive feedback to global warming (Rustad et al., 2000).

Grasslands comprise approximately 40% of the earth's land area (excluding areas of permanent ice cover) (White et al., 2000) and play a critical role in the global carbon cycle. However, the size and distribution of CO_2 sources or sinks of the global grassland ecosystems remain uncertain (Ojima et al., 1993; Baldocchi et al., 2001; Soussana and Lüscher, 2007). The accurate estimation of soil respiration is of great importance in resolving these uncertainties, but is poorly understood (Grace and Rayment, 2000; Valentini et al., 2000; Ryan and Law, 2005).

Soil respiration in grasslands consists mainly of respiration from roots and associated mycorrhizal fungi and microbial respiration. With regard to the CO_2 -driven greenhouse effect, only microbial respiration contributes to changes in atmospheric CO_2 concentration. The contribution of root respiration, as well as root-induced changes in the turnover

of soil organic carbon (SOC) (Kuzakov, 2002a,b; Cheng et al., 2005), obscures the real role of soil respiration in global warming. Moreover, microbial and root respiration respond differently to changing temperature (Boone et al., 1998). Therefore, quantifying the contributions of these two major components to total soil respiration is critical to accurately estimate the carbon balance of an ecosystem, and to better understand how soil respiration responds to global changes.

The global average surface temperature increased by 0.6°C and rainfall increased by 0.5–1% every 10 years during the 20th century (IPCC, 2001). The response of soil CO_2 efflux to global warming is sensitive to slight changes in the relationship between soil temperature and soil respiration (Davidson and Janssens, 2006). Most simulation models of regional and global carbon cycles use a single, fixed Q_{10} coefficient (defined as the increase in respiration rate per 10°C increase in temperature) to express the relationship between soil respiration and temperature (Kirschbaum, 2006). However, Q_{10} varies among ecosystems and across temperature ranges. Therefore, clarifying the Q_{10} changes should be a high priority for modeling studies of the carbon cycle.

Human activities are significantly modifying biogeochemical cycles in many ways. For example, land use and management changes have been widely recognized as key drivers of global C dynamics (Houghton et al., 1999). They can induce changes in the structure or species composition of plant communities, soil chemical and physical properties, soil microclimate and ground climate (Raich and Schlesinger, 1992), and thus affect soil respiration rates.

In the past two decades, a number of studies on soil respiration have been conducted across the different grassland types of the world. These studies make it possible to analyze soil respiration in global grasslands.

^{*} Corresponding author. Department of Ecology, College of Urban and Environmental Sciences, Peking University, 100871 China. Tel.: +86 10 62767922; fax +86 10 62752287.
E-mail address: wangw@urban.pku.edu.cn (W. Wang).

Table 1Annual soil CO₂ efflux (g C m⁻² yr⁻¹) in natural grasslands of the world. DC= dynamic chamber method; AA=alkaline absorption method.

No.	Grassland type	Latitude	Longitude	Soil respiration	Method	References
<i>Temperate grassland</i>						
1	Matador grassland, Saskatchewan	50°36' N	107°45' W	187	AA	De Jong et al. (1974)
2	Matador grassland, Saskatchewan	50°36' N	107°45' W	132	AA	Warembourg and Paul (1977)
3	<i>Alopecurus</i> meadow, Czechoslovakia	48°40' N	16°55' E	830 ^a	AA	Tesarova and Gloser (1976)
4	<i>Festuca</i> meadow, Czechoslovakia	48°40' N	16°55' E	600 ^a	AA	Tesarova and Gloser (1976)
5	Short-grass prairie	40°49' N	104°46' W	230	AA	Coleman et al. (1976)
6	Tallgrass prairie	38°50' N	92°02' W	488	AA	Buyanovsky et al. (1987)
7	Tallgrass prairie	38°50' N	92°02' W	457	DC	Kucera and Kirkham (1971)
8	Tallgrass prairie, Oklahoma	36°57' N	96°33' W	662	AA	Risser et al. (1981)
9	Successional grassland, S. Carolina	33°30' N	81°40' W	389	AA	Coleman (1973)
10	<i>Leymus chinensis</i> steppe, Inner Mongolia, China (ungrazed)	43°26' N	115°32' E	285.1	AA	Li et al. (2000)
11	<i>Leymus chinensis</i> steppe, Inner Mongolia, China (grazed)	43°26' N	115°32' E	271.3	AA	Li et al. (2000)
12	<i>Stipa grandis</i> steppe, Inner Mongolia, China (ungrazed)	43°26' N	115°32' E	150.27	AA	Cui et al. (2000)
13	<i>Stipa grandis</i> steppe, Inner Mongolia, China (grazed)	43°26' N	115°32' E	52.1	AA	Cui et al. (2000)
14	Typical steppe, Inner Mongolia, China	43°26' N	115°32' E	390	AA	Wang et al. (2004)
15	<i>Leymus chinensis</i> steppe, Inner Mongolia, China	44° 39' N	115° 32' E	374.97	DC	Qi et al. (2006, 2007)
16	<i>Stipa krylovii</i> steppe, Inner Mongolia, China	44° 39' N	115° 32' E	128.43	DC	Qi et al. (2006, 2007)
17	<i>Leymus chinensis</i> steppe, northeast China	44° 45' N	123° 45' E	360.61	AA	Wang et al. (2007)
18	<i>Puccinellia tenuiflora</i> steppe, northeast China	44° 45' N	123° 45' E	239.5	AA	Wang et al. (2007)
19	Semi-arid steppe community, Inner Mongolia, China	43°26' N	115°32' E	189.25	AA	Zhang et al. (2003)
20	Alpine meadow, Tibetan Plateau, China	37°32' N	101°15' E	556.36	DC	Cao et al. (2004)
21	Tallgrass prairie, Temple, TX, USA	31°06' N	97°20' W	327.28	DC	Bremer et al. (1998)
22	California grassland, USA	37°24' N	122°14' W	323	DC	Luo et al. (1996)
23	Tallgrass prairie, Eastern Kansas, USA	39° N	96° W	858.40	DC	Smith and Johnson (2004)
24	Humid grassland, Atlantic Canada	NA	NA	456	DC	Kellman et al. (2007)
25	<i>Lolium perenne</i> grassland, Scotland	55°53' N	3°26' W	302.59	DC	Jones et al. (2005)
26	Mixed-grass prairie, Mandan, ND, USA	46°46' N	100°55' W	220.91	DC	Frank et al. (2002)
27	Fenced <i>Leymus chinensis</i> steppe, Inner Mongolia, China	43°55' N	116°31' W	123.09	DC	Jia et al. (2007)
28	Native prairie, Temple, TX	31°06' N	97°20' W	650	DC	Dugas et al. (1999)
29	Northern semiarid grassland, North Dakota USA	46°46' N	100°55' W	1000	DC	Frank et al. (2006)
30	Semi-arid typical steppe, Inner Mongolia, China	43°30' N	117°06' E	112	AA	Zou et al. (2007)
31	<i>Stipa baicalensis</i> steppe, Inner Mongolia, China	43°26' N	115°32' E	355.43	DC	Qi et al. (2006, 2007)
32	Swathgrass (<i>Panicum virgatum</i> L.) grassland, USA	44°10' N	96°41' W	128.73	DC	Lee et al. (2007)
33	Tallgrass prairie, Oklahoma, USA	34°59' N	97°31' W	1004	DC	Zhou et al. (2006)
<i>Tropical grassland</i>						
1	Mixed grassland, India	29°58' N	76°51' E	470	AA	Gupta and Singh (1981)
2	<i>Themeda</i> grassland, India	23°11' N	75°43' E	690	AA	Upadhyaya et al. (1981)
3	<i>Iseilema</i> grassland, India	23°11' N	75°43' E	640	AA	Upadhyaya and Singh (1981)
4	<i>Sehima</i> grassland, India	23°11' N	75°43' E	900	AA	Upadhyaya et al. (1981)
5	<i>Dichanthium</i> grassland, India	23°11' N	75°43' E	615	AA	Upadhyaya et al. (1981)
6	Mixed grassland, India	20°30' N	84°01' E	568	AA	Behera and Pati (1986)
7	Semi-arid woodland, Australia	19°38' S	146°50' E	380	AA	Holt et al. (1990)
8	<i>Eucalyptus</i> woodland, Australia	14°36' S	132°12' E	600 ^b	AA	Bridge et al. (1983)
9	Lamto savanna, Ivory coast	6°13' N	5°02' W	800	AA	Lamotte (1975)
10	Oak grass savanna, California	38°43' N	120°96' W	488	DC	Tang and Baldocchi (2005)
11	Woodland, Central Rio Grande Plain	27°40' N	98°12' W	745	DC	McCulley et al. (2004)
12	Remnant grasslands, Central Rio Grande Plain	27°40' N	98°12' W	611	DC	McCulley et al. (2004)
13	Semi-arid grasslands, Madurai, Southern India	10°00' N	78°10' E	309.6	DC	Sundaravalli and Paliwal (2000)

NA=not available.

^a Estimated from figure in text.^b Total for wet season only.

In this paper, we summarize relevant literature and provide estimates of annual soil CO₂ efflux, the ratio of root respiration to total soil respiration, and Q₁₀ values for soil respiration. These are used to evaluate relationships between soil respiration and the main climatic factors, and to provide the newest estimates of these parameters for global grasslands. We also discuss the human effects on soil CO₂ efflux focusing on grazing, land-use changes and fertilization.

2. Data collection

We made every effort to collect publications related to soil respiration of grasslands, such as Raich and Schlesinger (1992), Raich and Tufekcioglu (2000), Hanson et al. (2000), and many others cited in the ISI Web of Science database. Unpublished data were not used in this analysis.

For the data of annual soil CO₂ efflux, we only used those with one or more years of measurements. For the analysis of the relationship between soil respiration and climatic variables, we only used the data

from natural grasslands and excluded those from managed grasslands (e.g. burning, clipping, and fertilization) and sites used for climate changes experiments (e.g. increased temperature or CO₂ concentration).

With these constraints, we obtained 118 data sets available for the analysis of soil respiration of global grasslands. Of these, 46 were for annual soil CO₂ efflux (Table 1), 31 for the contribution of root respiration to total soil respiration (Table 2), and 41 for Q₁₀ values of soil respiration (Table 3).

In Tables 1–3, each study site is classified by vegetation type. Mean annual air temperature and annual precipitation for each study site were recorded. For the sites where the climatic data were unavailable, they were estimated using a global climate database (www.worldclim.org).

3. Soil respiration in global grasslands

Annual soil CO₂ efflux varied widely within and between temperate and tropical grasslands (Table 1). The annual soil CO₂ efflux averaged 389.8 ± 45.5 g C m⁻² yr⁻¹ and 601.3 ± 45.6 g C m⁻² yr⁻¹ (mean ± S.E.)

Table 2

Published estimates of the root contributions to total soil respiration (RC) by vegetation type and experimental approach. Time intervals are also provided (d=1 day or less, w=week or weeks, m=monthly or seasonal, and a=annual).

Ecosystem	Method ^a	Step	RC	References
Tropical grassland	Clip	m	0.53	Robertson et al. (1995)
	R exc.	a	0.47	Robertson et al. (1995)
	M bal.	a	0.59	Trumbore et al. (1995)
	R reg.	a	0.58	Gupta and Singh (1981)
	R reg.	a	0.64	Upadhyaya and Singh (1981)
	S comp.	a	0.41	Tang and Baldocchi (2005)
Temperate grassland	Clip	a	0.48	Wan and Luo (2003)
	Clip	w	0.19	Craine et al. (1999)
	Clip	m	0.42	Silvola et al. (1996)
	Shade	w	0.39	Craine et al. (1999)
	R exc.	d	0.4	Craine et al. (1999)
	R reg.	d	0.34	Herman (1977)
	R exc.	d	0.25	Herman and Kucera (1975)
	R exc.	d	0.17	Kirkham (1971)
	I- ¹⁴ C	a	0.1	Dörr and Münnich (1987)
	Mod.	a	0.41	Kutsch et al. (2001)
	R reg.	a	0.28	Buyanovsky et al. (1987)
	R reg.	m	0.37	Kucera and Kirkham (1971)
	R exc.	m	0.38	Yoneda and Okata (1987)
	R exc.	m	0.39	Yazaki et al. (2004)
	R reg.	m	0.4	Wang et al. (2005a)
	R reg.	m	0.44	Wang and Guo (2006)
	R reg.	m	0.25	Li et al. (2002)
	R reg.	m	0.56	Wang et al. (2006)
	M bal.	a	0.15	Coleman (1973)
	Cint.	m	0.08	Coleman (1973)
	I- ¹⁴ C	a	0.1	Dörr and Münnich (1987)
	R reg.	m	0.5	Cui et al. (2000)
	R reg.	m	0.37	Jia et al. (2006)
	I- ¹⁴ C	m	0.19	Warembourg and Paul (1973)
	Clip	m	0.5	Byrne and Kiely (2006)

^a R exc.=Root exclusion, M bal.=Mass balance; I-¹⁴C=Isotopic labeling approaches with indicated isotope ¹⁴C, Mod=Modeling, R reg.=Root mass regression, C int.=Component integration, S. com=Site comparison between under tree stands and open stands.

for temperate and tropical grasslands, respectively. The large variations may be due to the differences in soil microclimate and structure, the quantity and quality of detritus supplied to the soil, and the overall rates of root respiration among sites (Raich and Potter, 1995). Raich and Schlesinger (1992) estimated an average annual soil CO₂ efflux of $442 \pm 78 \text{ g C m}^{-2} \text{ yr}^{-1}$ ($n=9$) and $629 \pm 53 \text{ g C m}^{-2} \text{ yr}^{-1}$ ($n=9$) for temperate and tropical grasslands, respectively. Our estimates were lower than theirs, especially for the temperate grasslands. The difference probably arose from the methods used for the measurement of soil respiration. In earlier studies, soil respiration was mainly measured by the alkaline absorption method. This method was shown to underestimate soil respiration (Janssens et al., 2000; Kabwe et al., 2002). However, on an annual basis, there did not seem to be a significant difference between the alkaline absorption (AA) method and the dynamic chamber (DC) method (Yim et al., 2002). Therefore, the differences in the estimates of soil respiration for global grasslands may be due to reasons, for example, the numbers of study sites, other than the method.

The total amount of annual soil respiration of the global grasslands can be simply estimated by multiplying the land area of temperate and tropical grasslands by their mean annual soil respiration. Grasslands are one of the most widespread vegetation types worldwide, covering 15 million km² in the tropics and a further 9 million km² in temperate regions (Lieth, 1978). As a result, annual soil CO₂ efflux averages $12.53 \text{ Pg C yr}^{-1}$ globally, with $3.51 \text{ Pg C yr}^{-1}$ in temperate grasslands and $9.02 \text{ Pg C yr}^{-1}$ in tropical grasslands.

Most of the present study sites for soil respiration in grasslands (Table 1) are located between 30° and 60° latitude, and thus temperate regions are very well represented. The tropics cover about one-third of the global land area, contain a great diversity of biomes, and include regions with very high rates of soil respiration. However, there are very few measurements of soil respiration from tropical grasslands,

although Raich and Schlesinger (1992) have pointed out that tropical regions should be priorities for future research. Therefore, insufficient data in tropical areas may influence the accurate estimation of global soil CO₂ efflux in grassland ecosystems.

4. Contribution of root respiration to total soil respiration

Published data (Table 2) indicate that root respiration accounts for as little as 8% to greater than 64% of total soil respiration depending on community types, methods and season. The modal root contribution to total soil respiration (RC) lies in a range from 30% to 50% with an overall mean of 36% (Fig. 1). Hanson et al. (2000) used 50 studies in the literature to estimate RC for global soils. In their studies, 37 were for forests and 14 for grasslands or crop systems. They concluded that the modal RC ranged from 40% to 50% with an overall mean of 48%, of which RC for forest and nonforest vegetation averaged 48.6% and 36.7%, respectively.

Much of the variability in RC may be associated with the methods used (Kuzyakov and Larionova, 2005; Kuzyakov, 2006), developmental stages of plants (Fu et al., 2002), nutrient availability (Bradley and Fyles, 1996), photosynthetically active radiation and N content (Kuzyakov and Cheng, 2001), soil moisture (Flanagan et al., 2002), and temperature (Buchmann, 2000). The variability was also related to the time scales (i.e. days, weeks, months, or a year). Data in the present study suggested that RC was 29%, 29%, 38% and 38%, for the daily, weekly, monthly and annual scale, respectively, showing that RC increased with time (Table 2).

Most of the measurements (Table 2) were conducted during the growing season; and very few in winter. Much lower RC was observed during the dormant seasons (Rochette and Flanagan, 1997). Root respiration is dependent on short-term changes in the supply of carbohydrates from plant shoots (Högberg et al., 2001) and is also controlled by morphological and internal metabolic changes (Johnson-Flanagan and Owens, 1986). Therefore, long-term measurements throughout an annual cycle are needed for accurately estimating the carbon balance of grasslands.

5. Climatic controls on soil respiration

Temperature and precipitation are considered to be the most important factors in determining spatial variations of soil respiration (Xu and Qi, 2001; Schimel et al., 2001). On a global scale, soil respiration rates correlated significantly with mean annual air temperature (Fig. 2a), suggesting that temperature-induced increases in soil CO₂ efflux have the potential to exacerbate increasing atmospheric CO₂ levels, providing a positive feedback to global warming. On the other hand, soil respiration increased with annual precipitation, but increased precipitation resulted in decreased soil respiration in rainy regions (Fig. 2b), probably due to limited aerobic respiration. Our analysis suggests that the temperature-derived increase in soil respiration rate may be partly offset by the effect of precipitation in rainy regions. Thus, precipitation potentially provides a negative feedback to greenhouse effects in such rainy areas.

6. Apparent temperature sensitivity of soil respiration

The Q_{10} values vary greatly from 0.9 to 4.6 (Table 3). The modal Q_{10} values ranged from 1.5 to 2.0 with an overall mean of 2.13 (Fig. 3). The Q_{10} value averaged 2.23 and 1.94 in temperate and tropical grasslands, respectively. Our estimate was lower than previous estimates for global vegetation (2.4) (Raich and Schlesinger, 1992) and for forest ecosystems (2.74) (Wang et al., 2005b). Therefore, a single, fixed Q_{10} coefficient for modeling the relationship between soil respiration and temperature can bias estimates of the carbon budget for a specific ecosystem type.

Several factors account for the variability in the Q_{10} value. Firstly, the temperature itself substantially affects the Q_{10} value; it is higher at lower

Table 3
Temperature sensitivity (Q_{10}) of soil respiration in natural temperate and tropical grasslands.

No.	Grassland type	Latitude	Longitude	Q_{10}	Measurement temperature	References
<i>Temperate grassland</i>						
1	<i>Filifolium sibiricum</i> and mixed herbaceous	43°30'N	116°49'E	1.53	–5–25	Chen et al. (2003)
2	Wet mixed grasses	43°37'N	116°41'E	1.75	–5–25	Chen et al. (2003)
3	<i>Artemisia frigida</i> and <i>potentilla acaulis</i>	43°37'N	116°41'E	1.47	–5–25	Chen et al. (2003)
4	<i>Leymus chinensis</i>	43°48'N	116°34'E	1.78	–5–25	Chen et al. (2003)
5	<i>Achnatherum splendens</i>	43°49'N	116°31'E	1.66	–5–25	Chen et al. (2003)
6	<i>Artemisia frigida</i> and <i>Cleistogenes squarrosa</i>	43°54'N	116°18'E	1.63	–5–25	Chen et al. (2003)
7	Dune <i>caragana microphylla</i>	43°54'N	116°06'E	1.52	–5–25	Chen et al. (2003)
8	<i>Leymus chinensis</i>	43°56'N	115°47'E	1.69	–5–25	Chen et al. (2003)
9	<i>Caragana stenophylla</i>	43°56'N	115°29'E	1.62	–5–25	Chen et al. (2003)
10	<i>Stipa grandis</i> and <i>cleistogenes squarrosa</i>	43°57'N	115°11'E	1.62	–5–25	Chen et al. (2003)
11	Tallgrass prairie	40°49'N	104°46'W	3.95	0.7–6.3	Rustad et al. (2001)
12	<i>Leymus chinensis</i> community, Meadow steppe	44°45'N	123°45'E	2.16	5–28	Wang et al. (2007)
13	<i>Puccinellia tenuiflora</i> community Meadow steppe	44°45'N	123°45'E	2.36	5–28	Wang et al. (2007)
14	Alpine meadow (heavy grazed)	37°32'N	101°15'E	2.75	10–20	Cao et al. (2004)
15	Alpine meadow (light grazed)	37°32'N	101°15'E	3.22	10–20	Cao et al. (2004)
16	Mountain grassland	47°30'N	11°32'W	2	14–21	Bahn et al. (2006)
17	Tallgrass prairie	48°50'N	10°02'W	2	10–30	Kucera and Kirkham (1971)
18	<i>Leymus chinensis</i> and <i>stipa grandis</i> grassland	43°26'N	115°32'E	2.5	–5–25	Li et al. (2000)
19	Tallgrass prairie	35°2'N	97°4'W	1.93	5–30	Wan and Luo (2003)
20	Tallgrass prairie	35°12'N	135°24'W	2.70	2–35	Luo et al. (2001)
21	Tallgrass prairie	39°N	101°15'E	2.4	0–25	Smith and Johnson (2004)
22	Tallgrass prairie (world's oldest prairie, 65 years)	43°2'N	89°26'W	2.62	–2–25	Kucharik et al. (2006)
23	Tallgrass prairie (adjacent prairie remnant)	43°2'N	89°26'W	2.9	–2–25	Kucharik et al. (2006)
24	Humid grassland	NA	NA	2.47	3–23	Kellman et al. (2007)
25	Tallgrass prairie	31°06'N	97°20'W	2.4	5–30	Mielnick and Dugas (2000)
26	Switchgrass (<i>Panicum virgatum</i> L.) grassland	44°10'N	96°41'W	2.7	–5–25	Lee et al. (2007)
27	Northern semiarid grasslands	46°46'N	100°55'W	2.7	10–25	Frank et al. (2002)
28	Konza Prairie	39°05'N	96°35'W	2.22	15–35	Harper et al. (2005)
29	Tallgrass prairie	39°59'N	97°31'W	2.51	5–35	Zhou et al. (2006)
<i>Tropical grasslands</i>						
1	Tropical forest and pasture (Costa Rica)	10°41'N	85°29'W	1.4–4.6	20–40	Holland et al. (2000)
2	Tropical forests and pasture (Hawaii)	19°45'N	155°15'W	1.4–2.0	20–40	Holland et al. (2000)
3	Subtropical pasture and woodland (Texas)	27°40'N	98°12'W	0.9–2.9	20–40	Holland et al. (2000)
4	Tropical forest and pasture (Brazil)	2°59'N	47°31'W	1.6–3.1	20–40	Holland et al. (2000)
5	Oak–grass savanna (open area site)	38°43'N	120°97'W	1.1	2–35	Tang and Baldocchi (2005)
6	Oak–grass savanna (under tree site)	38°43'N	120°97'W	1.23	2–35	Tang and Baldocchi (2005)
7	Oak–grass savanna	38°43'N	120°97'W	1.17 ^a	26–48	Tang et al. (2003)
8	Oak–grass savanna	38°43'N	120°97'W	1.27 ^b	26–48	Tang et al. (2003)
9	Oak–grass savanna	38°43'N	120°97'W	1.54 ^c	26–48	Tang et al. (2003)
10	Oak–grass woodland	38°24'N	120°57'W	2.51 ^d	2–18	Xu and Baldocchi (2004)
11	Oak–grass woodland	38°24'N	120°57'W	2.2 ^e	10–20	Xu and Baldocchi (2004)
12	Oak–grass woodland	38°24'N	120°57'W	2.1 ^f	15–35	Xu and Baldocchi (2004)

^{a, b, c} Estimated from the relationship between soil respiration and soil temperature at 2 cm, 8 cm, and 16 cm depth, respectively. ^{d, e, f} Estimated during late senescence, non-growing season and winter, respectively. NA=Not available.

than at higher temperatures (Kirschbaum, 1995; Luo et al., 2001; Fang et al., 2005). Most of the present studies (Table 3) were conducted during the growing season, whereas little research has been done in the non-growing season (e.g., winter). The Q_{10} values ranged between 60 and 200 below 0 °C, while the maximum Q_{10} above 0 °C was reported to be 9 (Mikan et al., 2002). Thus, there is an absolute need for *in situ* measurements of soil respiration in winter to improve our understanding of its temperature sensitivity and its mechanisms.

Secondly, the methods used are critical to the magnitude of the Q_{10} value. Larger values are obtained from laboratory incubations than from soil warming experiments and field observations *in situ* using differences in seasonal temperatures (Trumbore et al., 1996; Gu et al., 2004). According to Davidson and Janssens (2006), temperature sensitivity of soil respiration includes two measures; apparent and intrinsic sensitivity. The former refers to the values measured *in situ* and includes the effects of other environmental factors (e.g., mineralogy, clay content, aggregation, or soil water content) as well as temperature, and the latter indicates only temperature-induced sensitivity. The data used in this study were primarily based on the measurements under field conditions and provide a measure of apparent sensitivity. In this way, these data *in situ* dampened or obscured intrinsic temperature sensitivity (Kirschbaum, 2006; Davidson and Janssens, 2006).

Finally, components (root and microbial respiration) of soil respiration are also responsible for the variability of the Q_{10} value. Root respiration has its own temperature dependence, but over periods of more than a few hours, acclimation can take place so that root respiration becomes relatively insensitive to temperature, compared with microbial respiration (Luo et al., 2001; Hartley et al., 2007). The seasonal pattern of root respiration and its relationship with temperature are also affected by plant phenological factors such

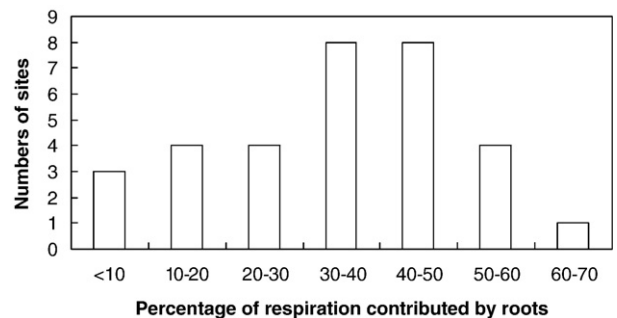


Fig. 1. Root contribution to soil respiration for grassland sites.

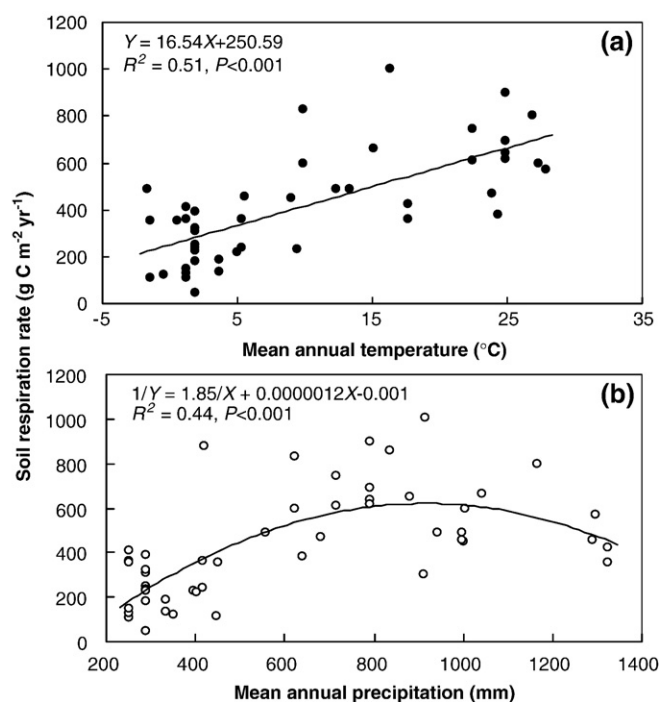


Fig. 2. Relationship between soil respiration and (a) mean annual air temperature and (b) annual precipitation.

as the seasonality of root growth and death (Lenton and Huntingford, 2003). However, few studies have been conducted that separate the temperature sensitivity of root and microbial respiration from total soil respiration.

In summary, three high research priorities should be (1) winter CO₂ efflux from soils and its temperature sensitivity; (2) discrimination between intrinsic and apparent temperature sensitivity; and (3) partitioning of temperature sensitivity between the two components of total soil respiration.

7. Soil carbon turnover

Soil respiration rate can be used to calculate the mean residence or turnover time of the soil organic carbon (SOC), based on the estimated RC. The remaining portion is thus from the decomposition of soil organic matter, representing the true turnover of SOC. The turnover time can be measured from carbon stocks and microbial respiration rate, and hence it is 71 years for temperate grasslands, and 15 years for tropical grasslands (Table 4). Raich and Schlesinger (1992) estimated an average turnover time of 61 years in temperate grasslands, and 10 years in tropical grasslands, based on an assumption of 30% RC. In this present study, the mean RC was 32% for temperate grasslands and

Table 4

Estimated turnover time of soil organic carbon (SOC) based on mean carbon stocks (Schlesinger, 1984) and mean soil respiration rates (SR), and contribution of root respiration to total soil respiration (RC) (in this paper).

Grassland type	SOC (kg m ⁻²)	SR (g C m ⁻² yr ⁻¹)	RC (%)	Turnover (yr)
Temperate grasslands	18.9	389.80	32	71
Tropical grasslands	4.2	601.28	54	15

54% for tropical grasslands, and larger than the value estimated by Raich and Schlesinger (1992). The larger heterotrophic respiration rate estimated by Raich and Schlesinger (1992) led to a smaller estimate of the turnover time for global grasslands.

8. Human effects on soil respiration rates

8.1. Grazing

Grasslands may currently support grazing pressures 10 times higher than those experienced in their natural state before livestock were introduced (Oesterheld et al., 1992). Grazing alters the diversity of different taxa (Bradgett and Wardle, 2003), the size and composition of carbon and nutrient pools (Bremer et al., 1998; Wilsey et al., 2002), the quantities and composition of soil microorganisms, and physical and chemical properties of soil (Lal, 2001). Grazing therefore potentially influences the CO₂ efflux from soils. According to Ojima et al. (1993), the carbon loss from temperate grasslands would be about 6.95 Pg in the next 50 years if the present grazing intensity increased by 30% to 50%.

Table 5 shows that grazing generally causes a reduction in soil respiration rate. For example, Cao et al. (2004) reported that soil CO₂ efflux at the lightly grazed site was almost double that of the heavily grazed site during the growing season in an alpine meadow on the Tibetan Plateau. In the Amazon River basin, overgrazing decreased the annual soil CO₂ efflux by 33% (Davidson et al., 2000). However, grazing increased soil CO₂ efflux in a semi-arid mixed-grass prairie (Frank et al., 2002) and in a shortgrass steppe in Colorado (LeCain et al., 2002). The controversy may be associated with study site, climate, community types, physical and chemical properties of the soil, grazing history and soil management practices, but current knowledge cannot explain the mechanisms of these grazing effects.

Besides, grassland responses to grazing have different time scales, from minutes to centuries (Brown and Allen, 1989). It is well known that short-term effects (within a growing season) of grazing are mostly associated with physiological responses of plants. However, little information is available for the mid-term (from years to decades) and long-term impacts (centuries to millennia), which are primarily

Table 5

Comparison of annual soil respiration rates (g C m⁻² yr⁻¹) in grazed vs. ungrazed grasslands.

Grassland type, location	Management	Soil respiration	References
Tallgrass prairie, Kansas USA	Ungrazed	367.36	Bremer et al. (1998)
	Simulated grazing	305.45	
<i>Stipa grandis</i> steppe, Inner Mongolia, China	Fenced	151	Cui et al. (2000)
	Grazed	52	
Humid pastures, Eastern Amazonia	Active pastures	1500	Davidson et al. (2000)
	Degraded pastures	1000	
Alpine meadow, Tibetan Plateau, China	Light grazing	556	Cao et al. (2004)
	Heavy grazing	417	
Tallgrass prairie, Manhattan K S	Ungrazed	1900	Owensby et al. (2006)
	Grazed	1588	
Semi-arid steppe, Inner Mongolia, China	Primary protected	157	Zou et al. (2007)
	Moderately protected	112	
	Highly degraded	57	

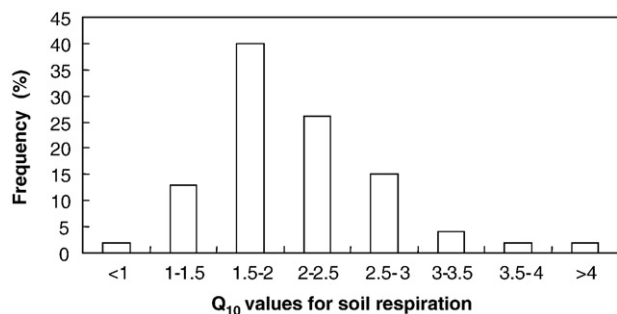


Fig. 3. Q₁₀ values for total *in situ* soil respiration rates as reported in the literature.

Table 6
Effect of land-use changes on annual soil respiration rates ($\text{g C m}^{-2} \text{ yr}^{-1}$) for grasslands.

Grassland type, location	Management	Soil respiration	References
Tallgrass native prairie, Temple, USA	Conversion of grassland to cropland	Native prairie: 650 Bermudagrass: 450 Sorghum: 60	Dugas et al. (1999)
Riparian buffers, Iowa, USA	Conversion of grassland to forest or cropland	Grassland: 1185 Forest: 1140 Cropland: 750	Tufekcioglu et al. (2001)
<i>Stipa baicalensis</i> steppe, Inner Mongolia, China	Conversion of grassland to cropland	Grassland: 355.5 Cropland: 261.6	Qi et al. (2006, 2007)
Northern semi-arid grassland, Mandan, USA	Conversion of grassland to cropland	Grassland: 1000 Wheat-fallow: 700 Continuous wheat: 600	Frank et al. (2006)
Subtropical grassland, Central Rio Grande Plains, USA	Conversion of grassland to woodland	Grassland: 611 Woodland: 745	McCulley et al. (2004)
Pasture, Nova Scotia, Canada	Conversion of pasture to forest	Pasture: 456 Forest: 271	Kellman et al. (2007)
Tropical pastures, Brazilian Amazon, Brazil	Conversion of tropical forest to pasture	Forest: 137 Pasture: 205	Fernandes et al. (2002)

coupled with changes in soil properties and biogeochemical cycles of ecosystems (Ferraro and Oesterheld, 2002). Therefore, caution should be applied when short-term observations are extended to long-term ecological responses, because short-, mid- and long-term responses of soil respiration to grazing are not necessarily consistent (Hyvönen et al., 1998). For example, no differences in soil respiration were found between high and low grazing sites in a semi-natural, species-rich pasture at Theix, France, in which had been subjected to grazing for 14 years (Klumpp et al., 2007).

8.2. Land-use changes

Land-use changes are considered to be the most dominant component of global change in terms of impacts on terrestrial ecosystems, as they profoundly alter land cover and biogeochemical cycles. They affect nitrogen availability (Zeller et al., 2000), species composition (Tasser et al., 1999), leaf and canopy photosynthesis (Wohlfahrt et al., 2005), root biomass and the partitioning of biomass to fine and coarse roots (Tasser et al., 2005), and thus can potentially alter soil respiration (Bahn et al., 2006; Huang et al., 2007).

Cultivation disturbs soil aggregates, usually improves soil aeration and moisture, and exposes native soil organic matter to microbial decomposition (Six et al., 2002). It can also change the distribution of fresh carbon at depth, and thus result in a stimulation of loss of the ancient buried carbon (Fontaine et al., 2007). In the short term, therefore, soil respiration is generally stimulated by cultivation disturbance. For example, soil CO_2 efflux from wheat is greater than that from the native grassland in Missouri (Buyanovsky et al., 1987). However, long-term cultivation usually decreases soil respiration rates over time (Table 6) due to depleted substrates for microbial decomposition.

The conversion from grasslands to forests can lead to an alteration of soil respiration rates, depending on the conditions (Table 6). For example, the transformation from grasslands to woodlands led to a 22% increase in soil respiration rates in subtropical grasslands, whereas in a pasture of Canada, the conversion of pasture to forests decreased soil respiration rates by 41% (Table 6).

Merino et al. (2004) studied the effects of soil management and land-use changes on soils of three adjacent plots of cropland, pasture and oak forest, and found that the CO_2 release from soils followed the order of pasture > forest > cropland. However, McCulley et al. (2007) found that soil respiration in woody communities was higher than that in grasslands in a subtropical savanna parkland in the Rio Grande Plains of southern Texas, USA. The differences in soil respiration among different ecosystems reflected the differences in environmen-

tal conditions (mainly soil moisture contents and temperature), input of organic residues, soil microbial biomass and, in the case of the forest site, acidification. All of these factors influence soil organic contents, microbial activities and root densities.

Effects of land use changes on soil CO_2 efflux have rarely been investigated, and virtually nothing is known about how they influence components of grassland soil respiration. Therefore, the effects of land use changes on components of soil respiration should be priorities for future research.

8.3. Fertilization

Land management has significant immediate effects on soil CO_2 efflux. In grazed temperate grasslands, fertilization is one of the major practices of land management. Fertilization generally increases C, N, and P contents of soils, changes soil chemical element composition, affects easily-decomposed soil organic carbon contents and root biomass, and thus affects the decomposition of soil microorganisms and root respiration (Verburg et al., 2004).

Fertilization also affects soil respiration by changing the structure of soil microbial communities. In a North American upland pasture, fungi dominated decomposition pathways in semi-natural, unfertilized soils, whereas in fertilized soils the fungal community was repressed (Bardgett et al., 1993). Similarly, Lovell et al. (1995) showed that the application of fertilizer to grassland favored bacterial communities, and the number of culturable bacteria was more than four times higher in long-term fertilized grassland than in the adjacent unfertilized grassland.

The effects of fertilization on soil respiration are dependent on nutrient availability. Withholding fertilizer from fertile grassland did not show any effects on microbial biomass (Sarathchandra et al., 1988), whereas in less fertile upland grassland soil microbial biomass decreased when fertilizer inputs were reduced (Bardgett and Lee-mans, 1995). The fertilization effect also differs with the time scales (Luo and Zhou, 2006; Ammann et al., 2007). Liu et al. (2007) and Stark and Kytöviita (2006) observed that nitrogen fertilization did not significantly change soil microbial biomass or activities during a growing season. However, they had decreased under long-term nitrogen fertilization due to recalcitrant and toxic compounds of the fertilization (Wallenstein et al., 2006).

Fertilization generally enhances soil respiration (Table 7), mainly through an increase in the decomposition of soil organic matter and in fine-root biomass (Mosier et al., 1991; Reich et al., 2001; Craine and Wedin, 2002; Verburg et al., 2004). For example, soil respiration rates from the plots receiving manure were 1.6 times larger than those from control plots, and 1.7 times larger compared with inorganic treatments (Jones et al., 2005). However, nitrogen fertilization depressed soil CO_2 efflux in a native grassland in Saskatchewan, Canada (De Jong et al., 1974) and in a newly established temperate grassland in Oensingen, Switzerland (Ammann et al., 2007), due to decreased carbon allocation to roots.

Table 7
Effect of fertilization on annual soil respiration rates ($\text{g C m}^{-2} \text{ yr}^{-1}$) for grasslands.

Grassland type, location	Management	Soil respiration	References
Experimental grassland, Kansas, USA	Unfertilized	287	Verburg et al. (2004)
	Fertilized	469	
Managed grassland, Scotland	Control	304	Jones et al. (2005)
	Fertilized ($\text{NH}_4\text{NO}_3\text{-N}$)	303	
	Fertilized (Urea)	352	
	Fertilized (Sludge pellets)	402	
	Fertilized (Cattle slurry)	411	
	Fertilized (Poultry manure)	470	
Managed grassland, South Dakota, USA	Unfertilized	129	Lee et al. (2007)
	Fertilized ($\text{NH}_4\text{NO}_3\text{-N}$)	133	
	Fertilized (Manure-N)	193	

In fact, the effect of fertilization on soil respiration rates is a trade-off between increased organic matter decomposition and plant productivity and decreased relative carbon allocation to roots (Waring and Schlesinger, 1985). Therefore, the fertilization effect may vary among sites, soils, vegetation types and time scales (Chapin et al., 1986).

9. Concluding remarks

Our analysis suggests that annual soil CO₂ efflux averages 12.53 Pg C yr⁻¹ for global grasslands, with 3.51 Pg C yr⁻¹ in temperate grasslands and 9.02 Pg C yr⁻¹ in tropical grasslands. The contribution of root respiration to total soil respiration averaged 32% and 54% for temperate and tropical grasslands, respectively. The average Q₁₀ value (2.13) of soil respiration for global grasslands was slightly lower than that of global vegetation (2.4) (Raich and Schlesinger, 1992), but the estimate of the turnover rates was higher than their estimate. Temperature-induced increases in soil respiration rates may be partly offset by the effect of precipitation in rainy regions, and thus, precipitation potentially provides a negative feedback to greenhouse effects in rainy areas. The human effects on soil respiration rates vary among sites, but are poorly documented.

Acknowledgements

This work was supported by the Projects of National Natural Science Foundation of China (30870408, 30670342 and 90711002). We thank Z H Wang for his help with data analysis.

References

- Ammann, C., Flechard, C.R., Leifeld, J., Neftell, A., Fuhrer, J., 2007. The carbon budget of newly established temperate grassland depends on management intensity. *Agriculture, Ecosystems and Environment* 121, 5–20.
- Bahn, M., Knapp, M., Garajova, Z., Pfahrringer, N., Cernusca, A., 2006. Root respiration in temperate mountain grasslands differing in land use. *Global Change Biology* 12, 995–1006.
- Baldocchi, D., Falge, E., Gu, L., Olson, R., Hollinger, D., Running, S., Anthoni, P., Bernhofer, Ch., Davis, K., Evans, R., Fuentes, J., Goldstein, A., Katul, G., Law, B., Lee, X., Malhi, Y., Meyers, T., Munger, W., Oechel, W., Paw, U.K.T., Peilgaard, K., Schmid, H.P., Valentini, R., Verma, S., Vesala, T., Wilson, K., Wofsy, S., 2001. FLUXNET: a new tool to study the temporal and spatial variability of ecosystem-scale carbon dioxide, water vapor, and energy flux densities. *Bulletin of the American Meteorological Society* 82, 2415–2434.
- Bardgett, R.D., Leemans, D.K., 1995. The short-term effects of cessation of fertilizer applications, liming and grazing on microbial biomass and activity in a reseeded upland grassland soil. *Biology and Fertility of Soils* 19, 148–154.
- Bardgett, R.D., Frankland, J.C., Whittaker, J.B., 1993. The effects of agricultural management on the soil biota of some upland grasslands. *Agriculture, Ecosystems and Environment* 45, 25–45.
- Behner, N., Pati, D.P., 1986. Carbon budget of a protected tropical grassland with reference to primary production and total soil respiration. *Review of Ecology, Biology and Soil* 23, 167–181.
- Boone, R.D., Nadelhoffer, K.J., Canary, J.D., Kaye, J.P., 1998. Roots exert a strong influence on the temperature sensitivity of soil respiration. *Nature* 396, 570–572.
- Bradgett, R.D., Wardle, D.A., 2003. Herbivore-mediated links between aboveground and belowground communities. *Ecology* 84, 2258–2268.
- Bradley, R.L., Fyles, J.W., 1996. Interactions between tree seedling roots and humus forms in the control of soil C and N cycling. *Biology and Fertility of Soils* 23, 70–79.
- Bremer, D.J., Ham, J.M., Owensby, C.E., Knapp, A.K., 1998. Responses of soil respiration to clipping and grazing in a tallgrass prairie. *Journal of Environmental Quality* 27, 1539–1548.
- Bridge, B.J., Mott, J.J., Hartigan, R.J., 1983. The formation of degraded areas in the dry savanna woodlands of northern Australia. *Australian Journal of Soil Research* 21, 91–104.
- Brown, B.J., Allen, T.F.H., 1989. The importance of scale in evaluating herbivory impacts. *Oikos* 54, 189–194.
- Buchmann, N., 2000. Biotic and abiotic factors controlling soil respiration rates in *Picea abies* stands. *Soil Biology and Biochemistry* 32, 1625–1635.
- Buyanovsky, G.A., Kucera, C.L., Wagner, G.H., 1987. Comparative analysis of carbon dynamics in native and cultivated ecosystems. *Ecology* 68, 2023–2031.
- Byrne, K.A., Kiely, G., 2006. Partitioning of respiration in an intensively managed grassland. *Plant and Soil* 282, 281–289.
- Cao, G.M., Tang, Y.H., Mo, W.H., Wang, Y.S., Li, Y.N., Zhao, X.Q., 2004. Grazing intensity alters soil respiration in an alpine meadow on the Tibetan plateau. *Soil Biology and Biochemistry* 36, 237–243.
- Chapin, F.S., Vitousek, P.M., Van Cleve, K., 1986. The nature of nutrient limitation in plant communities. *The American Naturalist* 127, 48–58.
- Chen, Q.S., Li, L.H., Han, X.G., Yan, Z.D., Wang, Y.F., Zhang, Y., Yuan, Z.Y., Tang, F., 2003. Responses of soil respiration to temperature in eleven communities in Xilingol Grassland, Inner Mongolia. *Acta Phytocologica Sinica* 27, 441–447 (in Chinese).
- Cheng, W., Fu, S., Susfalk, R.B., Mitchell, R.J., 2005. Measuring tree root respiration using ¹³C natural abundance: rooting medium matters. *New Phytologist* 167, 297–307.
- Coleman, D.C., 1973. Soil carbon balance in a successional grassland. *Oikos* 24, 195–199.
- Coleman, D.C., Andrews, R., Ellis, J.E., Singh, J.S., 1976. Energy flow and partitioning in selected managed and natural ecosystems. *Agro-Ecosystems* 3, 45–54.
- Craine, F.M., Wedin, D.A., 2002. Determinants of growing season soil CO₂ flux in a Minnesota grassland. *Biogeochemistry* 59, 303–313.
- Craine, J.M., Wedin, D.A., Chapin III, F.S., 1999. Predominance of ecophysiological controls on soil CO₂ flux in a Minnesota grassland. *Plant and Soil* 207, 77–86.
- Cui, X.Y., Chen, S.Q., Chen, Z.Z., 2000. CO₂ release from typical *Stipa grandis* grassland soil. *Chinese Journal of Applied Ecology* 11, 390–394 (in Chinese).
- Davidson, E.A., Janssens, I.A., 2006. Temperature sensitivity of soil carbon decomposition and feedbacks to climate change. *Nature* 440, 165–173.
- Davidson, E.A., Verchot, L.V., Cattaneo, J.H., Ackerman, I.L., Carvalho, J.E.M., 2000. Effects of soil water content on soil respiration in forests and cattle pastures of eastern Amazonia. *Biogeochemistry* 48, 53–69.
- De Jong, Schappert, H.J.V., MacDonald, K.B., 1974. Carbon dioxide evolution from virgin and cultivated soil as affected by management practices and climate. *Canadian Journal of Soil Science* 54, 199–307.
- Dörr, H., Münnich, K.O., 1987. Annual variation in soil respiration in selected areas of the temperate zone. *Tellus* 38B, 114–121.
- Dugas, W.A., Heuer, M.L., Mayeux, H.S., 1999. Carbon dioxide fluxes over bermudagrass, native prairie, and sorghum. *Agricultural and Forest Meteorology* 93, 121–139.
- Fang, C., Smith, P., Moncrieff, J.B., Smith, J.U., 2005. Similar response of labile and resistant soil organic matter pools to changes in temperature. *Nature* 433, 57–59.
- Fernandes, S.A.P., Bernoux, M., Cerri, C.C., Feigl, B.J., Piccolo, M.C., 2002. Seasonal variation of soil chemical properties and CO₂ and CH₄ fluxes in unfertilized and P-fertilized pastures in an Ultisol of the Brazilian Amazon. *Geoderma* 107, 227–241.
- Ferraro, D., Oosterheld, M., 2002. Effect of defoliation on grass growth. A quantitative review. *Oikos* 98, 125–133.
- Flanagan, L.B., Weaver, L.A., Carlson, P.J., 2002. Seasonal and interannual variation in carbon dioxide exchange and carbon balance in a northern temperate grassland. *Global Change Biology* 8, 599–615.
- Fontaine, S., Barot, S., Barré, P., Bdioui, N., Mary, B., Rumpel, C., 2007. Stability of organic carbon in deep soil layers controlled by fresh carbon supply. *Nature* 450, 277–280.
- Frank, A.B., Liebig, M.A., Hanson, J.D., 2002. Soil carbon dioxide fluxes in northern semiarid grasslands. *Soil Biology and Biochemistry* 34, 1235–1241.
- Frank, A.B., Liebig, M.A., Tanaka, D.L., 2006. Management effects on soil CO₂ efflux in northern semiarid grassland and cropland. *Soil and Tillage Research* 89, 78–85.
- Fu, S.L., Cheng, W., Susfalk, R., 2002. Rhizosphere respiration varies with plant species and phenology: a greenhouse pot experiment. *Plant and Soil* 239, 133–140.
- Grace, J., Rayment, M., 2000. Respiration in the balance. *Nature* 404, 819–820.
- Gu, L., Post, W.M., King, A.W., 2004. Fast labile carbon turnover obscures sensitivity of heterotrophic respiration from soil to temperature: a model analysis. *Global Biogeochemical Cycles* 18, 1022–1032.
- Gupta, S.R., Singh, J.S., 1981. Soil respiration in a tropical grassland. *Soil Biology and Biochemistry* 13, 261–268.
- Hanson, P.J., Edwards, N.T., Garten, C.T., Andrews, J.A., 2000. Separating root and soil microbial contributions to soil respiration: a review of methods and observations. *Biogeochemistry* 48, 115–146.
- Harper, C.W., Blair, J.M., Fay, P.A., Knapp, A.K., Carlisle, J.D., 2005. Increased rainfall variability and reduced rainfall amount decreases soil CO₂ flux in a grassland ecosystem. *Global Change Biology* 11, 322–334.
- Hartley, I.P., Heinemeyer, A., Evans, S.P., Ineson, P., 2007. The effect of soil warming on bulk soil vs. rhizosphere respiration. *Global Change Biology* 13, 2654–2667. doi:10.1111/j.1365-2486.2007.01454x.
- Herman, P., 1977. Root contribution to 'total soil respiration' in a Tallgrass Prairie. *The American Midland Naturalist* 98, 227–232.
- Herman, R.P., Kucera, C.L., 1975. Vegetation management and microbial function in a tallgrass prairie. *Iowa State Journal of Research* 50, 255–260.
- Högberg, P., Read, D.J., 2006. Towards a more plant physiological perspective on soil ecology. *Trends in Ecology and Evolution* 21, 548–554.
- Högberg, P., Nordgren, A., Buchmann, N., Taylor, A.F.S., Ekblad, A., Högberg, M.N., Nyberg, G., Ottosson-Lofvenius, M., Read, D.J., 2001. Large-scale forest girdling shows that current photosynthesis drives soil respiration. *Nature* 407, 789–792.
- Holland, E.A., Neff, J.C., Townsend, A.R., McKeown, B., 2000. Uncertainties in the temperature sensitivities of decomposition in tropical/subtropical ecosystems: implications of models. *Global Biogeochemical Cycles* 14, 1137–1151.
- Holt, J.A., Hodgen, M.J., Lamb, D., 1990. Soil respiration in the seasonally dry tropics near Townsville, North Queensland. *Australian Journal of Soil Research* 28, 737–745.
- Houghton, R.A., Hackler, J.L., Lawrence, K.T., 1999. The U.S. carbon budget: contributions from land-use change. *Science* 285, 574–578.
- Huang, M., Ji, J.J., Li, K.R., Liu, Y.F., Yang, F.T., Tao, B., 2007. The ecosystem carbon accumulation after conversion of grasslands to pine plantations in subtropical red soil of South China. *Tellus* 59B, 439–448.
- Hyvönen, R., Agren, G.I., Bosatta, E., 1998. Predicting long-term soil carbon storage from short-term information. *Soil Science Society of America Journal* 6, 1000–1005.
- IPCC, 2001. In: Houghton, J.T., Ding, Y., Griggs, D.J., Noguer, M., van der Linden, P.J., Dai, X., Maskell, K., Johnson, C.A. (Eds.), *Climate Change 2001: The Scientific Basis. Contribution of Working Group I to the Third Assessment Report of the Intergovernmental Panel on Climate Change*. Cambridge University Press, Cambridge, UK.
- Janssens, I.A., Kowalski, A.S., Longdoz, B., Ceulemans, R., 2000. Assessing forest soil CO₂ efflux: an *in situ* comparison of four techniques. *Tree Physiology* 20, 23–32.

- Jia, B.R., Zhou, G.S., Wang, F.Y., Wang, Y.H., Yuan, W.P., Zhou, L., 2006. Partitioning root and microbial contributions to soil respiration in *Leymus chinensis* populations. *Soil Biology and Biochemistry* 38, 653–660.
- Jia, B.R., Zhou, G.S., Yuan, W.P., 2007. Modeling and coupling of soil respiration and soil water content in fenced *Leymus chinensis* steppe, Inner Mongolia. *Ecological Modelling* 201, 157–162.
- Johnson-Flanagan, A.M., Owens, J.N., 1986. Root respiration in white spruce (*Picea glauca* [Moench] Voss) seedlings in relation to morphology and environment. *Plant Physiology* 81, 21–25.
- Jones, S.K., Rees, R.M., Skiba, U.M., Ball, B.C., 2005. Greenhouse gas emissions from a managed grassland. *Global and Planetary Change* 47, 201–211.
- Kabwe, L.K., Hendry, M.J., Wilson, G.W., Lawrence, J.R., 2002. Quantifying CO₂ fluxes from soil surfaces to the atmosphere. *Journal of Hydrology* 260, 1–14.
- Kellman, L., Beltrami, H., Risk, D., 2007. Changes in seasonal soil respiration with pasture conversion to forest in Atlantic Canada. *Biogeochemistry* 82, 101–109.
- Kirkham, D.R., 1971. Relations of dead plant materials in a Missouri tallgrass prairie. Ph.D. Dissertation, University of Missouri, Columbia. 159p.
- Kirschbaum, M.U.F., 1995. The temperature dependence of soil organic matter decomposition, and the effect of global warming on soil organic C storage. *Soil Biology and Biochemistry* 27, 753–760.
- Kirschbaum, M.U.F., 2006. The temperature dependence of organic-matter decomposition—still a topic of debate. *Soil Biology and Biochemistry* 38, 2510–2518.
- Klumpp, K., Soussana, J.F., Falcimagne, R., 2007. Effects of past and current disturbance on carbon cycling in grassland mesocosms. *Agriculture, Ecosystems and Environment* 121, 59–73.
- Kucera, C.L., Kirkham, D.R., 1971. Soil respiration studies in tallgrass prairie in Missouri. *Ecology* 52, 912–915.
- Kucharik, C.J., Fayram, N.J., Cahill, K.N., 2006. A paired study of prairie carbon stocks, fluxes, and phenology: comparing the world's oldest prairie restoration with an adjacent remnant. *Global Change Biology* 12, 122–139.
- Kutsch, W.L., Eschenbach, C., Dilly, O., Middelhoff, U., Steinborn, W., Vanselow, R., Weisheit, K., Wötzel, J., Kappen, L., 2001. The carbon cycle of contrasting landscape elements of the Bornhöved Lake district. In: Tenhunen, J.D., Lenz, R., Hantschel, R. (Eds.), *Ecosystem Approaches to Landscape Management in Central Europe*. Ecological Studies, vol. 147, pp. 75–95.
- Kuzyakov, Y., 2002a. Review: factors affecting rhizosphere priming effects. *Journal of Plant Nutrition and Soil Science* 165, 382–396.
- Kuzyakov, Y., 2002b. Separating microbial respiration of exudates from root respiration in non-sterile soils: a comparison of four methods. *Soil Biology and Biochemistry* 34, 1619–1629.
- Kuzyakov, Y., 2006. Sources of CO₂ efflux from soil and review of partitioning methods. *Soil Biology and Biochemistry* 38, 425–448.
- Kuzyakov, Y., Cheng, W., 2001. Photosynthesis controls of rhizosphere respiration and organic matter decomposition. *Soil Biology and Biochemistry* 33, 1915–1925.
- Kuzyakov, Y., Larionova, A.A., 2005. Root and rhizomicrobial respiration: a review of approaches to estimate respiration by autotrophic and heterotrophic organisms in soil. *Journal of Plant Nutrition and Soil Science* 168, 503–520.
- Lal, R., 2001. The physical quality of soil on grazing lands and its effect on sequestering carbon. In: Follet, R.F., Kimble, J.M., Lal, R. (Eds.), *The Potential of U.S. Grazing Lands to Sequester Carbon and Mitigate the Greenhouse Effect*. Lewis Publishers, New York, pp. 249–266.
- Lamotte, M., 1975. The structure and function of a tropical savanna. In: Golley, F.B., Medina, E. (Eds.), *Tropical Ecological Systems: Trends in Terrestrial and Aquatic Research*. New York/New York, Springer-Verlag, pp. 179–222.
- LeCain, D.R., Morgan, J.A., Schuman, G.E., Reeder, J.D., Hart, R.H., 2002. Carbon exchange and species composition of grazed pastures and exclosures in the shortgrass steppe of Colorado. *Agriculture, Ecosystems and Environment* 93, 421–435.
- Lee, D.K., Doolittle, J.J., Owens, V.N., 2007. Soil carbon dioxide fluxes in established switchgrass land managed for biomass production. *Soil Biology and Biochemistry* 39, 178–186.
- Lenton, T.M., Huntingford, C., 2003. Global terrestrial carbon storage and uncertainties in its temperature sensitivity examined with a simple model. *Global Change Biology* 9, 1333–1352.
- Li, L.H., Wang, Q.B., Bai, Y.F., Zhou, G.S., Xing, X.R., 2000. Soil respiration of a *Leymus chinensis* grassland stand in the Xilin River Basin as affected by over-grazing and climate. *Acta Phytocologica Sinica* 24, 680–686 (in Chinese).
- Li, L.H., Han, X.G., Wang, Q.B., Chen, Q.S., Zhang, Y., Yang, J., Bai, W.M., Song, S.H., Xing, X.R., Zhang, S.M., 2002. Separating root and soil microbial contributions to total soil respiration in a grazed grassland in the Xilin River Basin. *Acta Phytocologica Sinica* 26, 29–32 (in Chinese).
- Lieth, H., 1978. Patterns of Primary Productivity in the Biosphere. Hutchinson Ross, Stroudsburg.
- Liu, W.X., Xu, W.H., Han, Y., Wang, C.H., Wan, S.Q., 2007. Responses of microbial biomass and respiration of soil to topography, burning, and nitrogen fertilization in a temperate steppe. *Biology and Fertility of Soils* 44, 259–268.
- Lovell, R.D., Jarvis, S.C., Bardgett, R.D., 1995. Soil microbial bio-mass and activity in long-term grassland: effects of management changes. *Soil Biology and Biochemistry* 27, 969–975.
- Luo, Y.Q., Zhou, X.H., 2006. Soil respiration and the environment. Academic Press/Elsevier, San Diego, USA.
- Luo, Y.Q., Jackson, R.B., Field, C.B., 1996. Elevated CO₂ increases belowground respiration in California grasslands. *Oecologia* 108, 130–137.
- Luo, Y., Wan, S., Hui, D., Wallace, L., 2001. Acclimatization of soil respiration to warming in a tall grass prairie. *Nature* 413, 622–625.
- McCulley, R.L., Archer, S.R., Boutton, T.W., Hons, F.M., Zuberer, D.A., 2004. Soil respiration and nutrient cycling in wooded communities and developing in grassland. *Ecology* 85, 2804–2817.
- McCulley, R.L., Boutton, T.W., Archer, S.R., 2007. Soil respiration in a subtropical savanna parkland: Response to water additions. *Soil Science Society of America Journal* 71, 820–828.
- Merino, A., Pérez-Batlón, P., Macías, F., 2004. Responses of soil organic matter and greenhouse gas fluxes to soil management and land use changes in a humid temperate region of southern Europe. *Soil Biology and Biochemistry* 36, 917–925.
- Mielnick, P.C., Dugas, W.A., 2000. Soil CO₂ flux in a tallgrass prairie. *Soil Biology and Biochemistry* 32, 221–228.
- Mikan, C., Schimel, D., Doyle, A., 2002. Temperature controls of microbial respiration above and below freezing in Arctic tundra soils. *Soil Biology and Biochemistry* 34, 1785–1795.
- Mosier, A.R., Schimel, D., Valentine, D., Bronson, K., Parton, W., 1991. Methane and nitrous oxide fluxes in native, fertilized and cultivated grasslands. *Nature* 350, 330–332.
- Oosterheld, M., Sala, O.E., McNaughton, S.J., 1992. Effect of animal husbandry on herbivore-carrying capacity at a regional scale. *Nature* 356, 234–236.
- Ojima, D.S., Dirks, B.O.M., Glenn, E.P., Owensby, C.E., Scurlock, J.O., 1993. Assessment of C budget for grasslands and drylands of the world. *Water, Air, and Soil Pollution* 70, 95–109.
- Owensby, C.E., Ham, J.M., Auen, L.M., 2006. Fluxes of CO₂ from grazed and ungrazed tallgrass prairie. *Rangeland Ecology and Management* 59, 111–127.
- Qi, Y.C., Dong, Y.S., Manfred, D., Geng, Y.B., Liu, L.X., Liu, X.R., 2006. Comparison of CO₂ effluxes and their driving factors between two temperate steppes in Inner Mongolia, China. *Advances in atmospheric sciences* 23, 726–736.
- Qi, Y.C., Dong, Y.S., Liu, J.Y., Domroes, M., Geng, Y.B., Liu, L.X., Liu, X.R., Yang, X.H., 2007. Effect of the conversion of grassland to spring wheat field on the CO₂ emission characteristics in Inner Mongolia, China. *Soil and Tillage Research* 94, 310–320.
- Raich, J.W., Potter, C.S., 1995. Global patterns of carbon-dioxide emissions from soils. *Global Biogeochemical Cycles* 9, 23–36.
- Raich, J.W., Schlesinger, W.H., 1992. The global carbon dioxide flux in soil respiration and its relationship to vegetation and climate. *Tellus* 44B, 81–99.
- Raich, J.W., Tufekcioglu, A., 2000. Vegetation and soil respiration: correlations and controls. *Biogeochemistry* 48, 71–90.
- Raich, J.W., Potter, C.S., Bhagawati, D., 2002. Interannual variability in global soil respiration, 1980–94. *Global Change Biology* 8, 800–812.
- Reich, P.B., Knops, J., Tilman, D., Craine, J., Ellsworth, D., Tjoelker, M., Lee, T., Wedin, D., Naeem, S., Bahaeddin, D., Hendrey, G., Jose, S., Wrage, K., Goth, J., Bengtson, W., 2001. Plant diversity enhances ecosystem responses to elevated CO₂ and nitrogen deposition. *Nature* 411, 809–824.
- Risser, P.G., Birney, E.C., Blocker, H.D., May, S.W., Parton, W.J., Wiens, J.A., 1981. *The True Prairie Ecosystem*. Hutchinson Ross Publication Company, Stroudsburg/Pennsylvania.
- Robertson, F.A., Myers, R.J.K., Saffigna, P.G., 1995. Respiration from soil and litter in a sown perennial grass pasture. *Australian Journal of Soil Research* 33, 167–178.
- Rochette, P., Flanagan, L.B., 1997. Quantifying rhizosphere respiration in a corn crop under field conditions. *Soil Science Society of America Journal* 61, 466–474.
- Rustad, L.E., Huntington, T.G., Boone, R.D., 2000. Controls on soil respiration: implications for climate change. *Biogeochemistry* 48, 1–6.
- Rustad, L.E., Campbell, J.L., Marion, G.M., Norby, R.J., Mitchell, M., Hartley, A., Cornelissen, J., Gurevitch, J., GCTE-NEWS, 2001. A meta-analysis of the response of soil respiration, net nitrogen mineralization, and aboveground plant growth to experimental ecosystem warming. *Oecologia* 126, 543–562.
- Ryan, M.G., Law, B.E., 2005. Interpreting, measuring, and modeling soil respiration. *Biogeochemistry* 73, 3–27.
- Sarathchandra, S.U., Perrott, K.W., Boase, M.R., Waller, J.E., 1988. Seasonal changes and the effects of fertiliser on some chemical, biochemical and microbiological characteristics of high-producing pastoral soil. *Biology and Fertility of Soils* 6, 328–335.
- Schimel, D.S., House, J.I., Hibbard, K.A., Bousquet, P., Ciais, P., Peylin, P., Braswell, B.H., Apps, M.J., Baker, D., Bondeau, A., Canadell, J., Churkina, G., Cramer, W., Denning, A.S., Field, C.B., Friedlingstein, P., Goodale, C., Heimann, M., Houghton, R.A., Melillo, J.M., Moore, B., Muriyarso, D., Noble, I., Pacala, S.W., Raupach, M.R., Rayner, P.J., Scholes, R.J., Steffen, W.L., Wirth, C., 2001. Recent patterns and mechanisms of carbon exchange by terrestrial ecosystems. *Nature* 414, 169–172.
- Schlesinger, W.H., 1984. Soil organic matter: a source of atmospheric CO₂. In: Woodwell, G.M. (Ed.), *The Role of Terrestrial Vegetation in the Global Carbon Cycle: Measurement by Remote Sensing*. John Wiley and Sons, Chichester/U.K., pp. 111–127.
- Schlesinger, W.H., 1997. *Biogeochemistry, an Analysis of Global Change*, 2nd ed. Academy, San Diego, California.
- Silvola, J., Alm, J., Ahlholm, U., Nykänen, H., Martikainen, P.J., 1996. The contribution of plant roots to CO₂ fluxes from organic soils. *Biology and Fertility of Soils* 23, 126–131.
- Six, J., Conant, R.T., Paul, E.A., Paustian, K., 2002. Stabilization mechanisms of soil organic matter: implications for C-saturation of soils. *Plant and Soil* 241, 155–176.
- Smith, D.L., Johnson, L., 2004. Vegetation-mediated changes in microclimate reduce soil respiration as woodlands expand into grasslands. *Ecology* 85, 3348–3361.
- Soussana, J.F., Lüscher, A., 2007. Temperate grasslands and global atmospheric change: a review. *Grass and Forage Science* 62, 127–134.
- Stark, S., Kytöviita, M., 2006. Simulated grazer effects on microbial respiration in a subarctic meadow: implications for nutrient competition between plants and soil microorganisms. *Agriculture, Ecosystems & Environment*. *Applied Soil Ecology* 31, 20–31.
- Sundaravalli, M., Paliwal, K., 2000. Primary production and soil carbon dioxide emission in the semi-arid grazing lands of Madurai, India. *Tropical Grasslands* 34, 14–20.
- Tang, J.W., Baldocchi, D.D., 2005. Spatial-temporal variation in soil respiration in an oak-grass savanna ecosystem in California and its partitioning into autotrophic and heterotrophic components. *Biogeochemistry* 73, 183–207.

- Tang, J.W., Baldocchi, D.D., Qi, Y., Xu, L.K., 2003. Assessing soil CO₂ efflux using continuous measurements of CO₂ profiles in soils with small solid-state sensors. *Agricultural and Forest Meteorology* 118, 207–220.
- Tasser, E., Prock, S., Mulser, J., 1999. The impact of land-use on vegetation along the Eastern Alpine transect. In: Cernusca, A., Tappeiner, U., Bayfield, N. (Eds.), *Land-use Changes in European Mountain Ecosystems*. Blackwell Wissenschaft, Berlin, pp. 235–246.
- Tasser, E., Tappeiner, U., Cernusca, A., 2005. Ecological effects of land use changes in the European Alps. In: Huber, U.M., Bugmann, H.K.M., Reasoner, M.A. (Eds.), *Global Change and Mountain Regions—a State of Knowledge Overview*. Springer, Dordrecht, pp. 413–425.
- Tesarova, M., Gloser, J., 1976. Total CO₂ output from alluvial soils with two types of grassland communities. *Pedobiologia* 16, 364–372.
- Trumbore, S.E., Davidson, E.A., de Camargo, P.B., Nepstad, D.C., Martinelli, L.A., 1995. Belowground cycling of carbon in forest and pastures of Eastern Amazonia. *Global Biogeochemical Cycles* 9, 515–528.
- Trumbore, S.E., Chadwick, O.A., Amundson, R., 1996. Rapid exchange between soil carbon and atmospheric carbon dioxide driven by temperature change. *Science* 272, 393–396.
- Tufekcioglu, A., Raich, J.W., Isenhardt, T.M., Schultz, R.C., 2001. Soil respiration within riparian buffers and adjacent crop fields. *Plant and Soil* 229, 117–124.
- Upadhyaya, S.D., Singh, V., 1981. Microbial turnover of organic matter in a tropical grassland soil. *Pedobiologia* 21, 100–109.
- Upadhyaya, S.D., Siddiqui, S.A., Singh, V.P., 1981. Seasonal variation in soil respiration of certain tropical grassland communities. *Tropical Ecology* 22, 157–161.
- Valentini, R., Matteucci, G., Dolman, A.J., Schulze, E.-D., Rebmann, C., Moors, E.J., Granier, A., Gross, P., Jensen, N.O., Pilegaard, K., Lindroth, A., Grelle, A., Bernhofer, C., Grunwald, T., Aubinet, M., Ceulemans, R., Kowalski, A.S., Vesala, T., Rannik, U., Berbigier, P., Loustau, D., Guomundsson, J., Thorgeirsson, H., Ibrom, A., Morgenstern, K., Clement, R., Moncrieff, J., Montagnani, L., Minerbi, S., Jarvis, P.G., 2000. Respiration as the main determinant of carbon balance in European forests. *Nature* 404, 861–865.
- Verburg, P.S.J., Arnone, J.A., Obrist, D., Schorran, D.E., Evans, R., Leroux-swarthout, D., Johnson, D.W., Luo, Y., Coleman, J.S., 2004. Net ecosystem exchange in two experimental grassland ecosystems. *Global Change Biology* 10, 498–508.
- Wallenstein, M.D., McNulty, S., Fernandez, I.J., Boggs, J., Schlesinger, W.H., 2006. Nitrogen fertilization decreases forest soil fungal and bacterial biomass in three long-term experiments. *Forest Ecology and Management* 222, 459–468.
- Wan, S., Luo, Y., 2003. Substrate regulation of soil respiration in a tallgrass prairie: results of a clipping and shading experiment. *Global Biogeochemical Cycles* 17, 1–12.
- Wang, W., Guo, J.X., 2006. The contribution of root respiration to soil CO₂ efflux in *Puccinellia tenuiflora* dominated community in a semi-arid meadow steppe. *Chinese Science Bulletin* 51, 697–703.
- Wang, G.C., Du, R., Kong, Q.X., Lü, D.R., 2004. Experimental study on soil respiration in temperate grassland in China. *Chinese Science Bulletin* 49, 642–646.
- Wang, W., Ohse, K., Liu, J.J., Mo, W.H., Oikawa, T., 2005a. Contribution of root respiration to soil respiration in a C₃/C₄ mixed grassland. *Journal of Biosciences* 30, 507–514.
- Wang, W.J., Wang, H.M., Zhu, Y.G., Li, X.Y., Koike, T., 2005b. Characteristics of root, stem and soil respiration Q₁₀ temperature coefficients in forest ecosystems. *Acta Phytocologica Sinica* 29, 680–691 (in Chinese).
- Wang, W., Guo, J.X., Feng, J., Oikawa, T., 2006. Contribution of root respiration to total soil respiration in a *Leymus chinensis* grassland of northeast China. *Journal of Integrative Plant Biology* 48, 409–414.
- Wang, W., Guo, J.X., Oikawa, T., 2007. Contribution of root to soil respiration and carbon balance in disturbed and undisturbed grassland communities, northeast China. *Journal of Biosciences* 32, 375–384.
- Warembourg, F.R., Paul, E.A., 1973. The use of ¹⁴CO₂ canopy techniques for measuring carbon transfer through the plant–soil system. *Plant and Soil* 38, 331–345.
- Warembourg, F.R., Paul, E.A., 1977. Seasonal transfers of assimilated ¹⁴C in grassland: Plant production and turnover, soil and plant respiration. *Soil Biology and Biochemistry* 9, 295–301.
- Waring, R.H., Schlesinger, W.H., 1985. *Forest Ecosystems: Concepts and Management*. Academic Press, Incorporation, Orlando/Florida.
- White, R., Murray, S., Rohweder, M., 2000. *Pilot Analysis of Global Ecosystems (PAGE): Grassland Ecosystems*. World Resources Institute, Washington, DC.
- Wilsey, B.J., Parent, G., Roulet, N.T., Moore, T.R., Potvin, C., 2002. Tropical pasture carbon cycling, relationships between C source/sink strength, above-ground biomass and grazing. *Ecology Letters* 5, 367–376.
- Wohlfahrt, G., Anfang, C., Bahn, M., Haslwanter, A., Newesely, C., Schmitt, M., Drösler, M., Pfadenhauer, J., Cernusca, A., 2005. Quantifying ecosystem respiration of a mountain meadow using eddy covariance, chambers and modeling. *Agricultural and Forest Meteorology* 128, 141–162.
- Xu, L.K., Baldocchi, D.D., 2004. Seasonal variation in carbon dioxide exchange over a Mediterranean annual grassland in California. *Agricultural and Forest Meteorology* 123, 79–96.
- Xu, M., Qi, Y., 2001. Spatial and seasonal variations of Q₁₀ determined by soil respiration measurements at a Sierra Nevada forest. *Global Biogeochemical Cycles* 15, 687–696.
- Yazaki, Y., Mariko, S., Koizumi, H., 2004. Carbon dynamics and budget in a *Miscanthus sinensis* grassland in Japan. *Ecological Research* 19, 511–520.
- Yim, M.H., Joo, S.J., Nakane, K., 2002. Comparison of field methods for measuring soil respiration; a static alkali absorption method and two dynamic closed chamber methods. *Forest Ecology and Management* 170, 189–197.
- Yoneda, T., Okata, H., 1987. An assessment of root respiration in a *Solidago altissima* community. *Natural Science and Applied Science* 36, 147–158.
- Zeller, V., Bahn, M., Aichner, M., Tappeiner, U., 2000. Impact of land-use change on nitrogen mineralization in the Southern Alps. *Biology and Fertility of Soils* 31, 441–448.
- Zhang, Y., Li, L.H., Wang, Y.F., Tang, F., Chen, Q.S., Yang, J., Yuan, Y.Z., Dong, Y.S., 2003. Comparison of soil respiration in two grass-dominated communities in the Xilin River Basin: correlations and controls. *Acta Botanica Sinica* 45, 1024–1029.
- Zhou, X.H., Sherry, R.A., An, Y., Wallace, L.L., Luo, Y.Q., 2006. Main and interactive effects of warming, clipping, and doubled precipitation on soil CO₂ efflux in a grassland ecosystem. *Global Biogeochemical Cycles* 20, GB1003. doi:10.1029/2005GB002526.
- Zou, C.J., Wang, K.Y., Wang, T.H., Xu, W.D., 2007. Overgrazing and soil carbon dynamics in eastern Inner Mongolia of China. *Ecological Research* 22, 135–142.

半干旱区气候变化和人类活动的孢粉指示*

刘鸿雁 李宜垠

(北京大学城市与环境学院, 北京 100871)

提要 中国半干旱区是季风气候影响的边缘地区, 气候波动性明显, 文明的演化表现为农牧业交替, 而当前的土地利用则表现为农牧交错。用孢粉学证据复原这一地区复杂的气候变化和人类活动历史的前提是区分不同孢粉类群的指示意义, 并提出在景观和区域尺度上复原植被演化历史的模式。本文通过中国半干旱区不同地点沉积剖面的对比分析, 结合表土花粉和现代植被地理研究, 从孢粉来源的角度对以上科学问题进行了探讨, 结果表明: 1) 桦属、蔷薇科、石竹科和白刺属的花粉最能反映降水量和湿度变化; 云杉和冷杉属花粉是温度变化的良好指示体; 藜科、蒿属、菊科等的花粉含量与气候和人类活动均有密切的关系; 禾本科植物的峰值, 在低人为干扰和高人为干扰的情况下都有出现, 其花粉含量较多地反映了人类活动的影响; 车前属植物主要出现在低湿地点, 低的车前属花粉含量(5%以内)在半干旱区对气候干湿变化的指示意义更明显; 高的榛属花粉含量(10%以上)更多地指示森林破坏之后的灌丛化。2) 藜科植物常在干涸湖泊周边形成盐化草甸, 可以导致沉积物中藜科花粉含量的富集。3) 地形条件导致了森林-草原交错带林草植被的镶嵌分布, 森林一般分布在陡阴坡, 由于温度升高导致蒸发加强, 区域气候变暖湿可能使得阴坡更湿而阳坡更旱, 从而出现更喜湿的乔木与更耐旱的草本植物共存。

关键词 孢粉指示体 气候变化 人类干扰 半干旱区

1 前言

中国半干旱区是季风气候影响的边缘地区, 年降水量为 150–400mm 且波动明显, 是气候变化的敏感区域(Jin *et al.*, 2004)。这一地区的植被为温带和暖温带草原, 与此毗邻的半湿润区的植被则为落叶阔叶林, 二者之间形成或宽或窄的森林-草原过渡带(也称交错带), 在土地利用上表现为农牧相交错。气候变化、人类活动与植被动态之间复杂的相互关系在森林-草原交错带体现得最为充分, 也是当前科学研究关注的热点(Mills *et al.*, 2006)。

在中国半干旱区分布着科尔沁、浑善达克和毛乌素等多处沙地, 植被退化和土地沙化是这一地区最主要的生态危害, 被称为我国的生态危急带(赵松乔, 1991)。沙化不仅影响到当地, 还通过沙尘传输等影响到下风向地区。因此, 这一地区全新世植被动态, 特别是气候变化和人类活动在植被演化中的相对作用, 对我国制订气候变化和荒漠化防治对策, 如退耕还林还草的方案, 有非常重要的指导意义。

半干旱区全新世以来林草格局及其对气候变化的响应方式, 一直是第四纪生态学研究的重要目标, 但也存在很多的争论。针对黄土高原北部地区是否在历史时期曾经被森林广泛覆盖所产生的争论, Lü 等(2003)将现代地形-植被关系引入分析, 指出历史时期森林曾分布在沟谷和石质山地, 较好地解释了气候变化和人类活动对这一地区植被动态的影响。

前人在运用孢粉证据复原中国半干旱区全新世植被动态方面做了大量的工作, 早期主要有《东北平原第四纪自然环境形成与演化》基金课题组(1990)对西辽河流域的研究以及北京师范大学的研究人员对中国北方农牧交错带全新世环境演变的研究(周廷儒、张兰生, 1992)。近十余年来, 为了更准确地运用沉积物孢粉证据复原古植被, 表土和表层沉积物的花粉研究倍受重视, 如王奉瑜等(1996)、Liu 等(1999)、李宜垠等(2000)以及李月丛等(2004)开展了较为系统的研究。花粉-气候响应面(Sun *et al.*, 1996)、花粉-气候转化函数(Song *et al.*, 1997; Liu *et al.*, 2002a)以及孢粉-植被判别分析(Liu *et al.*,

2001) 等定量手段也得到了应用。一些研究工作集中分析了我国半干旱区不同局部的植被和气候演化, 在内蒙古高原中部的调角海子(宋长青等, 1996; 杨志荣等, 1997)、察素齐(Wang *et al.*, 1999) 和岱海(许清海等, 2004; Xiao *et al.*, 2004)、浑善达克沙地东南部(如 Liu *et al.*, 2002b) 和南缘(Jiang *et al.*, 2006)、科尔沁沙地南缘(任国玉, 1999) 等地取得了一批高分辨率的孢粉资料。植硅体证据和孢粉证据的结合更好地反映了草原植被的动态(Huang *et al.*, 2005)。从总体上看, 前人的研究工作仍然侧重在植被对气候变化的响应方面。

在人类活动对植被动态的影响方面, 半干旱区的不同地点有着显著不同的人类活动历史。西辽河流域是我国农业文明的发祥地之一, 早在 8 000 多年前就已经出现了原始的农业。黄土高原的北部地区也有长期的人类活动历史, 这一地区沉积物中的孢粉组合同时反映了气候变化和人类活动的综合影响。而阴山以北、大兴安岭以东的内蒙古高原面上却少有农业文明遗迹的发现, 人类开垦的历史仅仅 100 余年, 因此沉积物中的孢粉组合更多地反映了气候变化影响下的自然植被动态。

Li 等(2006) 将孢粉证据和考古记录相结合, 探讨了科尔沁沙地一带距今 5 400 年以来植被动态与文化发展之间的关系, 指出人类活动对这一地区植被动态产生了重要的影响; 任国玉(1999) 也利用乔木、藜科、蒿属三类花粉的相对变化推断科尔沁沙地南部近 3 000 年来的植被退化主要由人为活动引起。浑善达克沙地及其周边地区地处内蒙古高原面上, 大规模人类活动的历史较短。崔海亭和王文江(2003) 根据元代古籍中的景观与物候信息, 复原了 13—14 世纪浑善达克沙地南缘的自然景观, 发现该地区元代的景观与现代基本一致。张宝秀(1997) 根据文献证实, 浑善达克沙地南缘大规模聚落的形成始于清代后期。尽管近百年来强烈的人为活动导致了大范围的植被退化, 但气候变化依然是区域尺度植被动态的主要驱动因子。因此, 地处半干旱区的科尔沁沙地周边及浑善达克沙地周边地区的比较研究, 可为区分气候变化和人类活动在植被动态中的作用提供好的素材。

本文拟从不同气候格局和人类干扰状况条件下植被、表土花粉和沉积物孢粉组合的比较, 系统分析孢粉指标对于半干旱区气候变化和人类活动的指示意义, 为准确恢复半干旱区气候变化、人类活动和植被演化的历史提供依据。

2 研究区域概况

本文研究区包括内蒙古高原东、中部以及相邻的东北平原西部、大兴安岭山地、冀北山地的部分地区。内蒙古高原的平均海拔在 1 200 m 左右, 而相邻的东北平原(含西辽河平原) 海拔总体上在 300 m 以下, 大兴安岭山地和冀北山地的海拔总体上在 300—2 000 m 之间。

研究区年降水量在西北—东南方向上存在显著的梯度(插图 1), 而温度梯度主要为南北向(西北师范学院地理系, 1984)。

研究区的植被随降水量的减少由草甸草原过渡到荒漠草原: 1) 草甸草原: 主要分布在大兴安岭山地和冀北山地, 以贝加尔针茅(*Stipa baicalensis*) 和线叶菊(*Filifolium sibiricum*) 为优势种, 杂类草丰富。在景观格局上表现为森林和草原的交错分布, 通常森林分布在陡阴坡。2) 典型草原: 在内蒙古高原中东部广泛分布。在受人类干扰影响较小的地区, 优势种为克氏针茅(*S. krylovii*) 和大针茅(*S. grandis*)。3) 荒漠草原: 在内蒙古高原的中西部分布, 优势种为戈壁针茅(*S. gobica*)、沙生针茅(*S. glareosa*)。一些荒漠灌木种类, 琵琶柴(*Reaumuria soongorica*) 等, 也进入到本植被带。

在半干旱区的东南和南部边缘存在不同程度的开垦, 形成了或宽或窄的农牧交错带。草原植被存在不同程度的过度放牧。

3 研究方法

3.1 野外取样

野外样地调查采用全球定位系统(GPS) 进行定位。在研究区内不同的地表覆盖类型下选取具有代表性的样点 177 个。所有取样点位置见插图 1。

野外植被调查运用样方法, 依据植被的差异性和退化状况做样方 1—3 个, 共做样方 249 个。样方面积为: 草原 2 m × 2 m, 灌丛 4 m × 4 m。每个样方记录各物种的多度或丛数、盖度、高度、物候相。记录内容还有每个样方的生境特征, 包括海拔、坡度、坡向、地表覆盖物、土壤类型及厚度、湿度状况和土地利用状况。

在样方调查的过程中同时采集表土花粉样品, 在样方内不同部位采集表土 2 cm 以上部分, 对沙质 21 化草原采样深度偏厚, 采样量约为 500 克。

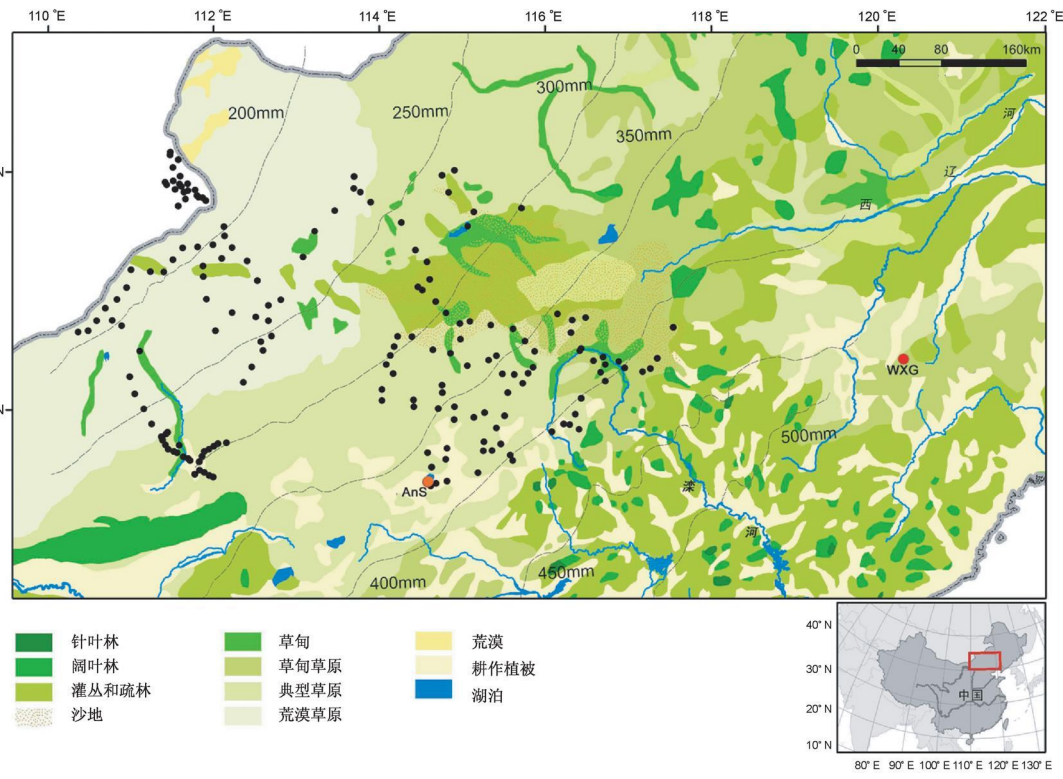


插图 1 研究区气候、植被格局以及取样地点分布

Climate and vegetation patterns of the study region and location of sampled sites

黑色圆点表示本文中用到的表土花粉取样地点, 红色圆点表示本文中用到的沉积物剖面。

Black and white dots indicate sampled sites for surface pollen and sediment core used in this paper respectively.

沉积物剖面的对比分析采用作者以前完成的各剖面 (Liu *et al.*, 2002a, b; Li *et al.*, 2006; Liu *et al.*, in submission)。

3.2 实验室分析

表土花粉样品处理采用重液浮选法, 具体步骤如下: 1) 用 KI+ HI+ Zn 粒配置重液, 比重为 1.8—1.9g/ml; 2) 表土花粉样品加水和 HCl 若干, 边加热边搅拌以打散结块直至煮沸, 然后过滤; 3) 滤液离心后加重液浮选两遍; 4) 将含有花粉的重液加水稀释, 静置分离; 5) 在花粉底样中加入硫酸和乙酸酐 1: 9 的混合液, 反应 5—10 分钟, 洗净后离心并转移入小试管中; 6) 制片。

花粉鉴定工作在 Olympus 光学显微镜下进行, 多数样品鉴定到属, 部分鉴定到科。花粉统计每个样品一般在 500 粒以上, 部分样品 250 粒以上, 每个样品至少观察 5 片 (18mm × 18mm)。对于观察 25 片花粉数仍小于 250 粒的舍弃。共有 147 个有效样品。

3.3 数据处理

3.3.1 表土花粉数据处理

每个样品在进行花粉统计后分别进行花粉百分含量和指示性孢粉比值的计算。

花粉百分含量是用每类植物花粉数除以该样品的花粉数总和。

3.3.2 植被数据处理

1) 指示种植物分类: 对于内蒙古高原主要草原草场来说, 在持续自由放牧下均趋同于冷蒿 (*Artemisia frigida*) 草原; 当放牧压力过大时, 冷蒿进一步退化为星毛委陵菜 (*Potentilla acaulis*), 然后就是一年生植物甚至裸地 (李永宏, 1994; 李博, 1997)。李博 (1997) 研究了我国北方草甸草原及典型草原的退化演替情况, 得到各个阶段植被指示情况, 结果表明原始类型的建群种有羊草 (*Leymus chinensis*)、贝加尔针茅、大针茅等, 并伴生一些较为中生的优良牧草; 当放牧强度增加, 草地开始退化时, 这些植物逐渐减少; 至重度退化阶段, 这些种大部分消失。与此同时, 原生群落的一些伴生成分, 如糙隐子草 (*Cleistogenes squarrosa*)、冷蒿、百里香 (*Thymus serpyllum*)、麻花头 (*Serratula centauroidus*)、狗娃花 (*Heteropappus hispidus*)、阿尔泰狗娃花 (*H. 212taicus*)、星毛委陵菜等则随放牧程度的增加而增

加,甚至代替原来的优势植物而成为建群种。在荒漠草原中,当放牧强度增加,草原开始退化时,无芒隐子草(*Cleistogenes songorica*)、银灰旋花(*Convolvulus amarii*)、栉叶蒿(*Neopallasia pectinata*)、骆驼蓬(*Peganum harmala*)逐渐增加,最后甚至成为优势种。

本文基于不同牧压强度下群落的种类组成分析,将样地中出现的共 287 种植物分为三大类。第一类为一、二年生植物,主要指示严重退化的草地,这一类共 80 种;第二类为出现在放牧区、盐碱化草地和流动沙地的多年生植物,主要指示中等退化的草地,这一类共 38 种;第三类为除第二类植物外的多年生植物,主要指示退化轻微或尚未退化的草地,这一类共 168 种。在实际运用中,只要区分出第一、二类,其余均可以归为第三类。

2) 重要值计算: 根据以下公式:

$$\text{重要值} = \frac{\text{相对多度} + \text{相对盖度} + \text{相对高度}}{3}$$

相对多度为该植物的多度除以样地所有植物的多度和。相对盖度和相对高度的计算方法与相对多度的计算方法相同。高度均以营养枝高度为标准。

3) 退化指数计算: 依据植物的重要值和指示种分类,计算出每个样地的植被退化指数。具体方法是: 把样地中记录到的所有植物种分成三类,然后对这三种类型分别赋予权重如下: 一、二年生植物种 1, 中等退化程度指示种 2/3, 轻度退化和无退化指示种 1/3, 则某一样地的植被退化指数就等于每一种类型的重要值乘以该类型所赋予的权重的和, 计算公式如下:

$$\text{植被退化指数} = 1 / (A_1 \times 1/3 + A_2 \times 2/3 + A_3)$$

其中 A_1 、 A_2 、 A_3 分别代表三种类型植物的重要值。

植被退化指数考虑了样地中植物的组成、不同种的多度、盖度、高度等, 因此是比较全面的, 能够较好地指示植被退化状况。退化指数的数值介于 1 到 3 之间, 数值越大表示退化程度越高。放牧程度很轻的样地中, 退化指数接近 1。耕地中主要是一年生杂草, 退化指数的计算结果接近 3。

由于气候变化引起的植被退化是区域性的, 主要表现为植被生产力的变化以及群落优势种类的更替, 而本文中不同退化程度的指示种是依据不同放牧程度下的植物群落种类组成而确定的。虽然降水量较少的地区一年生植物比例偏高, 但减少 100mm

降水量导致一年生植物比例仅增加 6%, 与每公顷多放牧 5 只羊的左右相当(任佑, 2007), 可以忽略。因此, 以上计算出的植被退化指数同样反映了人类干扰程度, 也可以表示人类干扰指数(Human disturbance index, HDI)。

3.4 多元统计

本文采用二歧指示种分类(TWINSPAN)对样地进行划分, 孢粉类群作为划分的指示种(Hill, 1979)。根据样地所在地的气候和植被特点进一步分析各孢粉类群的气候指示意义。

4 结果

4.1 基于孢粉类群的植物群落种类组成随人类干扰强度的变化

插图 2 表示不同人类干扰强度下主要的植物科属(结合孢粉类群的划分)在群落中的重要值以及植物物种多样性的变化, 从图中看出主要的植物类群可以分成 5 类:

禾本科(Gramineae): 禾本科植物的峰值在低人为干扰和高人为干扰的情况下都有出现。尽管拟合系数偏低, 但达到 $p < 0.01$ 的显著性水平。在接近自然状态的草原中, 通常以禾本科的针茅属(*Stipa*)植物占优势。而在高人类干扰的农田中, 狗尾草(*Setaria viridis*)、止血马唐(*Digitaria ischaemum*)等植物占据优势。

藜科(Chenopodiaceae)和菊科(Compositae): 在中等偏强人类干扰指数下, 藜科植物重要值高, 主要反映在高强度放牧的草原中, 常见藜科种类包括藜(*Chenopodium album*)、刺藜(*C. aristatum*)、滨藜(*Atriplex patens*)、猪毛菜(*Salsola collina*)、地肤(*Kochia scoparia*)等, 常见的菊科种类包括阿尔泰狗娃花等。而在农田中, 这两个科的植物重要值开始下降。

莎草科(Cyperaceae)和车前科(Plantaginaceae): 主要出现在湿度条件较好的草甸草原中, 这类草原抗干扰能力强。

蒿属: 在不同人为干扰强度下均有出现, 但以中低干扰强度为主。在高强度人为干扰下常出现的种类有猪毛蒿(*Artemisia scoparia*)、茵陈蒿(*A. capillaris*)、黄蒿(*A. annua*)等。

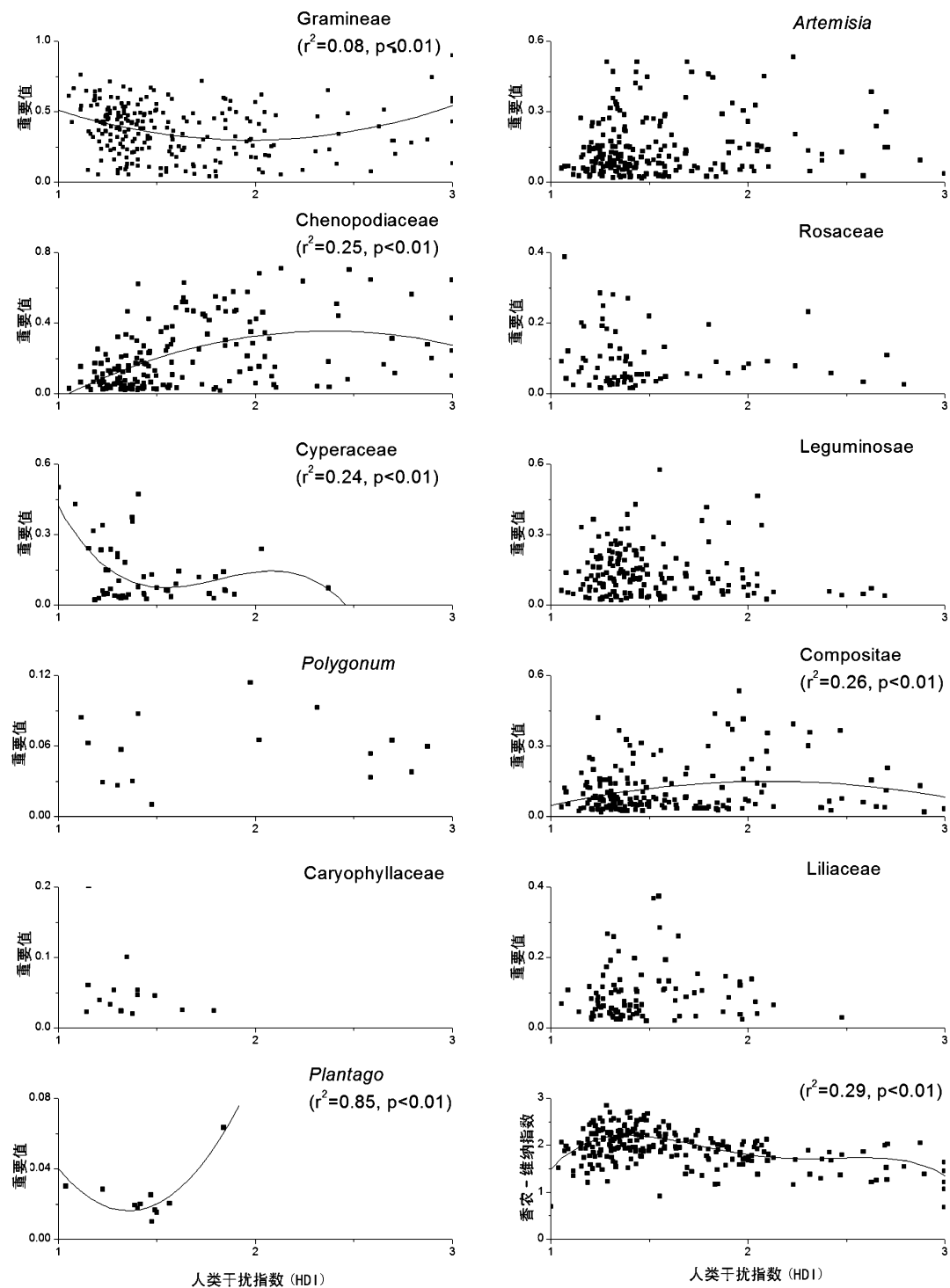


插图 2 不同人类干扰强度下植物群落主要科属的重要值和多样性的变化

Changes of importance value and richness of main families and genera in plant communities under different degrees of human disturbance

蔷薇科 (Rosaceae)、豆科 (Leguminosae)、蓼科 (Polygonaceae)、石竹科 (Caryophyllaceae)、百合科 (Liliaceae): 这类双子叶植物抗干扰能力低, 仅仅出现在人类干扰强度较低的地区。

植物物种多样性: 总体上, 在人类干扰程度约为 1.2 时, 植物群落的种类多样性(用Shannon Wiener

指数表示) 最高, 高强度的人类活动明显降低了群落的种类多样性。

4. 2 表土花粉空间分布及其对气候变化和人类活动的指示

4. 2. 1 不同植被带的孢粉组合特征

由插图 3 可以看出蒿属、藜科、松属(*Pinus*)、桦属(*Betula*)花粉随着植被带的变化都有很好的趋势性。

1) 荒漠草原带: 藜科花粉占优势, 含量为 65%; 蒿属花粉含量在 25% 以下; 禾本科花粉含量仅占 2.8%; 乔木花粉, 如松属和桦属花粉含量均在 3% 以下。花粉组合为藜-蒿型。

2) 典型草原带: 蒿属花粉占优势, 含量达 50%; 藜科花粉含量占 40%; 禾本科花粉含量 5.8%; 松属和桦属花粉含量均不足 1%。花粉组合为蒿-藜型。

3) 草甸草原带: 蒿属花粉占绝对优势, 含量为

75%; 藜科的花粉含量占 13.5%; 禾本科花粉含量占 6.3%; 桦属花粉含量占 2.6%; 松属花粉含量占 0.8%。花粉组合为蒿型。

4) 落叶阔叶林带: 以桦属(37%)和松属(25%)花粉占优势; 蒿属花粉含量在 20% 以下; 藜科和禾本科花粉含量均在 5% 以下。花粉组合为桦-松-蒿型。

4. 2. 2 表土中主要花粉类群的指示意义

基于各样地表土中花粉的百分含量组成, 运用 TWINSpan 对样地进行分类, 结果如插图 4 所示。共将 147 个样地分为 6 类。

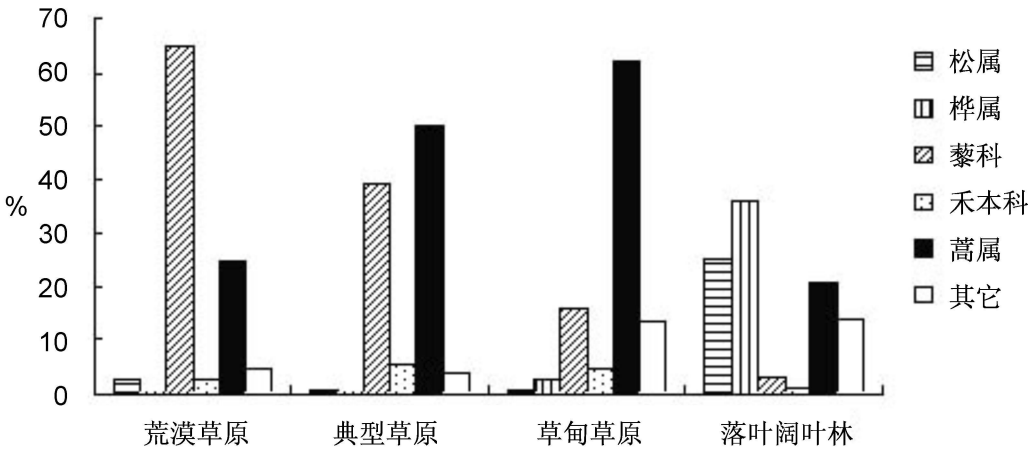


插图 3 主要的表土花粉类型随植被带的变化规律

Percentages of main pollen taxa in different vegetation zones

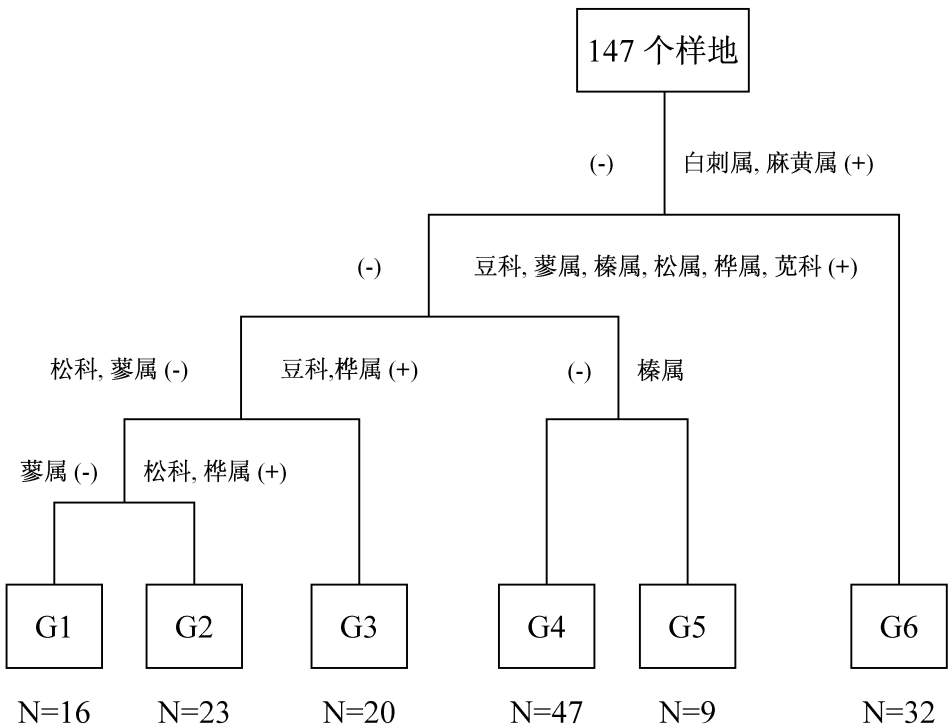


插图 4 表土花粉样地的 TWINSpan 分类, + 表示出现, - 表示不出现

TWINSpan classification of surface pollen samples with + for presence and - for absence

第一级分类的指示种为白刺属(*Nitraria*)和麻黄属(*Ephedra*),这两种花粉所对应的植物均为干旱区的植物类型,第一级分类主要将干旱区与非干旱区分开。

第二级分类指示种为豆科、蓼属、松属、桦属、苋科(*Amaranthaceae*)、榛属(*Corylus*),此级分类主要是将半干旱区与半湿润区分开。不再区分干旱区。

第三级分类是在第二级的基础上再分别对半干旱区和半湿润区进行细分,共分为5类。松属和桦属花粉的出现指示半湿润区的森林群落,榛属的出现指示森林遭受破坏后形成的灌丛群落。

4.3 基于沉积物分析的孢粉指示研究

对比内蒙古高原的 AnS 剖面($41^{\circ}18' - 24' N$, $114^{\circ}20' - 27' E$, 1 324 m a. s. l.)和西辽河平原南缘的 WXG 剖面($119^{\circ}55' E$, $42^{\circ}04' N$, 751 m a. s. l.),发现二者的孢粉组合及其变化存在如下不同(插图5):1) AnS 剖面出现云杉/冷杉(*Picea/Abies*)花粉,而 WXG 剖面没出现;2) AnS 剖面榛属/虎榛子属(*Corylus/Ostryopsis*)花粉含量在5%以内,而 WXG 剖面这两类花粉含量通常在10%以上,最高达50%;3) WXG 剖面一直出现杂草花粉,如葎草属(*Humulus*),而 AnS 剖面不出现。

云杉属和冷杉属都属于喜冷湿的植物种类,由于 AnS 剖面所在地为内蒙古高原的高原面上,海拔1 324m,而 WXG 剖面地处西辽河平原边缘丘陵,海拔751m,两地虽然处于大致相近的降水范围,但由于海拔差异引起的温度条件差异明显。因此,可以认为在半干旱区,云杉和冷杉属的花粉含量可以指示温度条件的变化。

在暖温带落叶阔叶林带和森林-草原交错带,榛属和虎榛子属植物是普遍出现的林下灌木,在森林因自然和人为因素退却后,形成以这两个属的植物占优势的灌丛植被。WXG 异常高的榛花粉含量可能代表人类活动对森林植被的破坏。从插图5b可以看出,榛属和虎榛子属的峰值对应农业文明的繁盛,而谷值对应牧业文明主导的时期,进一步证实了二者花粉含量对半干旱区人类活动的指示意义。

由于禾本科、蒿属、藜科花粉对人类活动和气候变化的双重指示意义,它们很难作为人类活动的稳定指示体。从插图5也可以看出, WXG 剖面禾本科花粉含量虽然出现了15%以上的峰值,但总体上并不比 AnS 剖面高。葎草属是一种常见的伴人植物,主要分布在居民点附近。WXG 剖面高的葎草

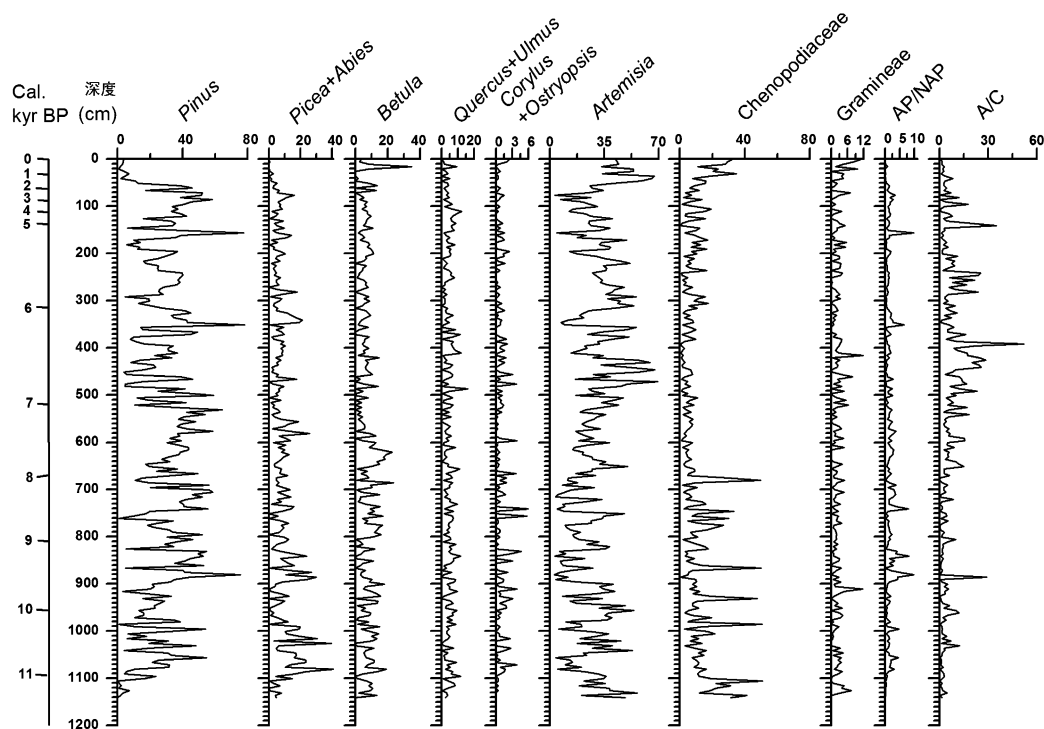
属花粉含量也说明了高强度的人类定居,特别是近2 300年以来。

5 讨论

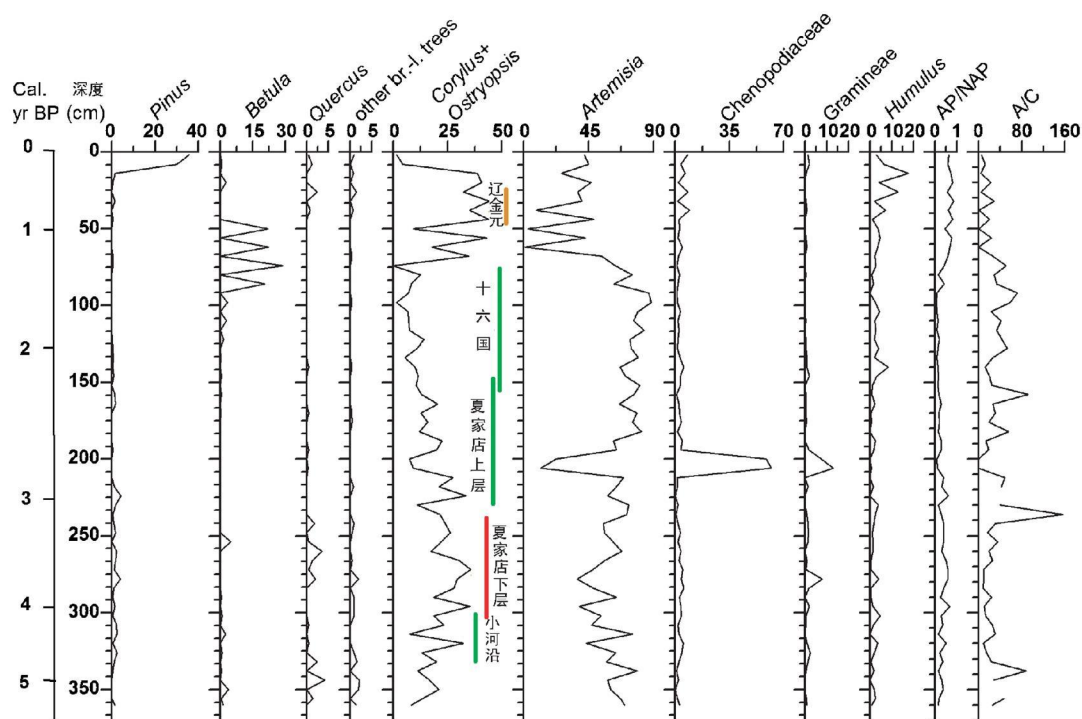
5.1 半干旱区孢粉来源与指示意义

本文的研究结果表明,半干旱区的植物群落组成以禾本科、蒿属、藜科、蔷薇科、豆科、菊科(除蒿属以外)和莎草科为主,而表土花粉中以蒿属、藜科和禾本科占据优势,说明这一地区的孢粉来源以本区域的植物为主。草甸草原带(森林-草原交错带)广泛分布的双子叶植物(杂类草),如蔷薇科、豆科、菊科(除蒿属以外)、莎草科,孢粉产量低,且主要集中在干扰程度低的样地中。与草本植物花粉相比,木本植物花粉产量很低,在缺少森林分布的典型草原带和荒漠草原带以外源花粉为主。

前人对内蒙古高原中部表土花粉的 CCA 排序分析表明,蔷薇科、桦木科、白刺属的花粉含量与年降水量的关系最为密切,与温度和降水相关的干燥度变化直接引起石竹科花粉含量的变化;禾本科花粉含量受到人类活动的强烈影响,藜科、蒿属、榛属、豆科的花粉含量同时受到气候变化和人类活动的影响。这一结果与不同气候和人类干扰格局下植物种类组成的结果有较好的一致性(Liu *et al.*, 2006)。李宜垠等总结了草原植被中人类活动的孢粉指示,特别提出禾本科含量的增加指示了人类活动的增强(Li *et al.*, 2008),与本文中植被调查和表土花粉分析结果吻合,这种变化主要是由开垦引起。任国玉等(1999)认为藜科花粉含量的增加与强烈人为活动的关系密切,但本文结果表明藜科花粉对气候干旱化和人类活动增强有着双重的指示意义。车前属植物具有很强的耐践踏能力,其花粉通常作为耐人类干扰的指示类群。本文结果证实,车前属植物在喜湿的草甸草原带普遍存在,与人类干扰强度无显著的对应关系。事实上,在浑善达克沙地边缘的好鲁库剖面中,车前属花粉在全新世大部分时期普遍存在,含量一般在3%以内(Liu *et al.*, 2002b),由此说明,低的车前属花粉含量(5%以内)可能更多地与气候条件关系密切,而高的车前属花粉含量才能反映半干旱区人类活动的影响。同样,榛属/虎榛子属不同的花粉含量指示意义可能不同,从本文中 AnS 和 WXG 两个剖面的比较来看,5%以内的榛属/虎榛子属花粉含量可能指示气候变化,而10%以上的榛属/虎榛子属花粉含量指示人类活动对森林的破坏。



(a) AnS 剖面



(b) WXG 剖面

插图 5 不同人类干扰强度下的孢粉谱对比

Comparison of pollen spectra under different degrees of human disturbance

WXG 剖面中不同的文化时期在图上用不同颜色表示: 绿色表示牧业文明占优势, 红色表示农业文明占优势, 棕色表示农牧共存。

Colored bars in (b) show different culture stages: green for pastoralism prevailed, red for agriculture prevailed, and brown for coexistence of both.

由于本文的研究区主要在半干旱区南部, 森林草原交错带(草甸草原带)的范围有限, 对个别孢粉类型的指示意义可能存在局限。如本文的结果表明, 石竹科植物主要分布在草甸草原带, 事实上在半干旱区北段温度较低的地区, 耐寒的石竹科卷耳属(*Cerastium*)植物在过渡放牧地点也较多出现, 需要在实际应用中加以区分。

5.2 地形与半干旱区植被格局和气候条件的复原

在孢粉谱的解读中, 区分出区域、景观和局部不同层次的孢粉类型, 对重建呈镶嵌分布的植被格局具有重要意义(Li *et al.*, 2008)。半干旱区的植被还包括水体和低湿地的沼泽植被以及周边的草甸植被, 它们与草原镶嵌分布。在草原带还分布有面积广阔的沙生植被。以前对于半干旱区表土花粉的研究较多侧重地带性分布的草原植被, 而进入湖泊沉积物的孢粉往往包括草甸和沼泽的孢粉类型。对内蒙古高原边缘的安固里淖湖盆研究发现, 湖内沉积物中的藜科花粉含量要明显高于坡面(即表土)的藜科花粉含量, 与湖泊干涸后碱蓬为优势种的盐生草甸植被繁盛有关。同样, 受到局地藜科花粉的影响, 湖内沉积物中 A/C (*Artemisia/Chenopodiaceae*) 比值会低于周围的表土花粉组合中的 A/C 值, 湖内沉积物的 A/C 平均值为 1.43, 而坡面上的 A/C 平均值为 2.5(Liu *et al.*, 2008)。所以如果用沉积物中的 A/C 值来恢复古气候和古植被, 应该乘上一个校正系数。

野外样方调查发现, 在森林草原过渡带内, 山地落叶阔叶林多分布在陡阴坡, 草原植被一般分布在阳坡、缓阴坡和平地(Liu *et al.*, 1999)。这种植被格局与林草生长所需的水分多少关系密切。从研究区太阳直接辐射量来看, 森林分布的陡阴坡(坡度 25° — 39°)接受的太阳直接辐射量年平均照度约为 56.0 — 75.7 W/m^2 , 而 10° 的阳坡可接受的太阳直接辐射量年平均照度可达 131.7 W/m^2 , 几乎为陡阴坡的两倍, 计算结果表明陡阴坡年蒸发量为 338.6 — 448.7 mm , 而 10° 的阳坡年蒸发量为 999.2 mm , 且阳坡的蒸发量随着坡度增加而增加, 这样陡阴坡土壤有效水分可以支持树木生存而阳坡出现草原植被(何思源等, 2008)。同时, 山体可能会形成阴影区, 影响太阳的有效辐射, 减少阴坡的有效辐射量, 在坡度和缓时, 太阳光线也大多只能达到阴坡的下部。

可以认为, 在同等降水量的情况下, 阴阳坡的分异导致了森林-草原过渡带森林和草原植被的空间

分异。由于半干旱区地处季风气候的尾间区, 东南季风的增强会导致温度和降水同时增加, 温度的增加可能导致蒸发量的增加, 而这种蒸发量的变化在阳坡更加明显, 这样可能会出现阳坡变干而阴坡变湿的情况, 进而导致更耐旱的草原种类与更喜湿的森林植物种类(如暖温带南段的植物种类)共存。植被的这种变化可能导致孢粉谱中更喜湿和更耐旱的类群同时出现, 需要在对孢粉谱的气候指示意义进行分析时加以注意。

6 结 论

本文从不同气候条件和人类干扰下的植物群落种类组成、表土花粉组合探讨了不同孢粉类群对气候和人类活动的指示意义。桦属、蔷薇科、石竹科和白刺属的花粉最能反映降水量和气候的干湿变化。藜科、蒿属、菊科等的花粉含量与气候和人类活动均有密切的关系。禾本科植物的峰值在低人为干扰和高人为干扰的情况下都有出现, 其孢粉含量更多地反映了人类干扰的程度。车前属植物主要出现在低湿地点, 其较低(5%以内)的花粉含量在半干旱区对气候干湿变化的指示意义更明显。较高(10%以上)的榛属花粉更多地指示了森林破坏之后的灌丛化。半干旱区的植被存在复杂的空间格局, 在草原带, 存在草原和低湿地草甸沼泽的镶嵌分布, 可能导致盐化草甸中的藜科花粉被大量带入沉积物中; 在森林草原交错带, 阴阳坡由于蒸发量不同而导致了森林和草原在不同的地形条件下分布, 东南季风加强导致的区域气候暖湿化可能使得阳坡更干而阴坡更湿润。在利用沉积物孢粉组合复原半干旱区的植被和气候动态时, 必须从区域植被组合动态的角度来认识。

参 考 文 献 (References)

- Cui Hai ting (崔海亭), Wang Weng jiang (王文江), 2003. Landscape and phenology of the upper reaches of the Luanhe River in the Yuan Dynasty. *Acta Geographica Sinica*(地理学报), 58(1): 101—108(in Chinese with English abstract).
- Department of Geography, Northwest Teacher's College(西北师范学院地理系), 1984. *Atlas of Physical Geography of China*. Beijing: Map Press. 1—252.
- He Si yuan (何思源), Liu Hong yan (刘鸿雁), Ren Ji (任 佶), Yin Yi (印 轶), 2008. Landform climate vegetation patterns and countermeasures for vegetation rehabilitation of forest steppe ecotone on Southeastern Inner Mongolia Plateau. *Scientia Geographica Sinica*(地理科学), 28(2): 253—258(in Chinese with

- English abstract).
- Hill M O, 1979. TWINSPAN—A Fortran program for arranging multivariate data in a ordered two way table by classification of the individuals and attributes. New York: Cornell University, Ithaca. 1—90.
- Huang F, Lisa K, Xiong S F, Huang F B, 2005. Holocene grassland vegetation, climate and human impact in central eastern Inner Mongolia. *Science in China Series D-Earth Sciences*, **48**(7): 1025—1039.
- Jiang W Y, Guo Z T, Sun X J, Wu H B, Chu G Q, Yuan B Y, Hatté C, Guiot J, 2006. Reconstruction of climate and vegetation changes of Lake Bayanchagan (Inner Mongolia): Holocene variability of the East Asian monsoon. *Quaternary Research*, **65**(3): 411—420.
- Jin H L, Su Z Z, Sun L Y, Sun Z, Zhang H, Jin L Y, 2004. Holocene climatic change in Hunshandake Desert. *Chinese Science Bulletin*, **49**(16): 1730—1735.
- Li Bo (李博), 1997. Grassland degradation and measurements in northern China. *Scientia Agricultura Sinica*(*中国农业科学*), **30**(6): 1—9(in Chinese with English abstract).
- Li Yuecong(李月丛), Xu Qinghai(许清海), Yang Xiaolan(阳小兰), 2004. Distribution and source of pollens and spores in surface sediments of Daihai Lake, Inner Mongolia. *Journal of Palaeogeography*(*古地学报*), **6**(3): 317—329(in Chinese with English abstract).
- Li Yonghong(李永宏), 1994. Research on the grazing degradation model of the main steppe rangelands in Inner Mongolia and some considerations for the establishment of a computerized range land monitoring system. *Acta Phytocologica Sinica*(*植物生态学报*), **18**(1): 68—79(in Chinese with English abstract).
- Li Y Y, Zhou L P, Cui H T, 2008. Pollen indicators of human activity. *Chinese Science Bulletin*, **53**(9): 1281—1283.
- Li Y Y, Willis K J, Zhou L P, Cui H T, 2006. The impact of ancient civilization on the northeastern Chinese landscape: palaeoecological evidence from the Western Liaohe River Basin, Inner Mongolia. *The Holocene*, **16**(8): 1109—1121.
- Liu H Y, Cui H T, Pott R, Speier M, 1999. Surface pollen of the woodland steppe ecotone in southeastern Inner Mongolia, China. *Review of Palaeobotany and Palynology*, **105**(3-4): 237—250.
- Liu H Y, Cui H T, Huang Y M, 2001. Detecting Holocene movements of the woodland steppe ecotone in northern China using discriminant analysis. *Journal of Quaternary Science*, **16**(3): 237—244.
- Liu H Y, Xu L H, Tian Y H, Cui H T, 2002a. Temporal spatial variations of Holocene precipitation at the marginal area of the eastern Asia monsoon influences from pollen evidence. *Acta Botanica Sinica*, **44**(7): 864—871.
- Liu H Y, Xu L H, Cui H T, 2002b. Holocene history of desertification along the woodland steppe border in northern China. *Quaternary Research*, **57**: 259—270.
- Liu H Y, Wang Y, Yang S, Wen Y J, Wang H Y, 2006. Climatic and anthropogenic control of surface pollen assemblages in East Asian steppe. *Review of Palynology and Palaeobotany*, **138**: 1730—1735.
- Liu H Y, Wei F L, Liu K, Zhu J L, 2008. Determinants of pollen dispersal in the East Asian steppe at different spatial scales. *Review of Palaeobotany and Palynology*, **149**(3-4): 219—228.
- Liu H Y, Li Y Y, Zhu J L, Wang H Y, Yin Y, Zhao F J, Mo D W. Precipitation driven 8 000 year discontinuous agriculture development in semiarid northern China. *Quaternary Science Review*(in submission).
- Lü H Y, Liu D S, Guo Z T, 2003. Natural vegetation of geological and historical periods in Loess Plateau. *Chinese Science Bulletin*, **48**(5): 411—416.
- Mills A J, Rogers K H, Stalmans M, Witkowski E T, 2006. A framework for exploring the determinants of savanna and grassland distribution. *Bioscience*, **56**(7): 579—589.
- Ren Guoyu(任国玉), 1999. Vegetation development and human activities during the last 3 000 years in Korqin Sandy Land. *Scientia Geographica Sinica*(*地理科学*), **19**(1): 42—48(in Chinese with English abstract).
- Ren Ji(任佶), 2008. Quantitative estimation of the effects on grassland degradation by climate change and grazing in Inner Mongolia. Beijing: Master's thesis of Peking University. 1—112(in Chinese with English abstract).
- Research Team of "Formation and development of Quaternary environment in western Northeast Plain"(《东北平原西部第四纪自然环境形成与演化》基金课题组), 1990. Formation and Development of Quaternary Environment in Western Northeast Plain, China. Harbin: Harbin Map Press. 1—257.
- Song Changqing(宋长青), Wang Fengyu(王奉瑜), Sun Xiangjun(孙湘君), 1996. Indicator of Holocene palaeovegetation dynamics in DJ core, Daqingshan Mountain, Inner Mongolia. *Acta Botanica Sinica*(*植物学报*), **38**(7): 568—575(in Chinese with English abstract).
- Song C Q, Lu H Y, Sun X J, 1997. Establishment and application of transfer functions of the pollen climatic factors in northern China. *Chinese Science Bulletin*, **42**(20): 2182—2186.
- Sun X J, Wang F Y, Song C Q, 1996. Pollen climate response surfaces of selected taxa from Northern China. *Science in China, Ser. D*, **39**(5): 486—493.
- Wang Fengyu(王奉瑜), Song Changqing(宋长青), Sun Xiangjun(孙湘君), 1996. Studies on surface pollen in central Inner Mongolia. *Acta Botanica Sinica*(*植物学报*), **38**(11): 902—909(in Chinese with English abstract).
- Wang F Y, Song C Q, Sun X J, 1999. Palynological records of palaeovegetation change during Holocene at North Tumd Plain in Inner Mongolia, China. *Chinese Geographical Science*, **9**(1): 87—91.
- Xiao J L, Xu Q H, Nakamura T, Yang X L, Liang W D, Inouchi Y, 2004. Holocene vegetation variation in the Daihai Lake region of north central China: a direct indication of the Asian monsoon climatic history. *Quaternary Science Review*, **23**: 1669—1679.
- Xu Qinghai(许清海), Xiao Jurle(肖举乐), Nakamura T, 2004.

Climate Changes of Daihai Basin during the Past 1 500 from a Pollen Record. *Quaternary Science(China)* (第四纪研究), **24** (3): 341—347(in Chinese with English abstract).

Yang Zhirong(杨志荣), Shi Pei jun(史培军), Fang Xiu qi(方修琦), 1997. Vegetation and environment development in Diaojiaohaizi area, Daqingshan Mountain. *Acta Phytocologica Sinica* (植物生态学报), **21**(6): 551—563 (in Chinese with English abstract).

Zhang Bao xiu(张宝秀), 1997. Relationship between land development and environment degradation in southeastern Inner Mongolia Plateau. *Geography and Land Research(地理学与国土研究)*, **13**(3): 16—22(in Chinese with English abstract).

Zhao Song qiao(赵松乔), 1991. Semi arid region in eastern and middle Inner Mongolia: environmental dynamics in a critical zone. *Arid Land Resource and Environment(干旱区资源与环境)*, **5** (2): 1—9(in Chinese with English abstract).

Zhou Ting ru(周廷儒), Zhang Lan sheng(张兰生), 1992. Holocene Environmental Change and Prediction in the Agro-pastoral Transitional Zone of China. Beijing: Geological Press. 1—146 (in Chinese).

POLLEN INDICATORS OF CLIMATE CHANGE AND HUMAN ACTIVITIES IN THE SEMI-ARID REGION

LIU Hong-yan and LI Yi-yin

(College of Urban and Environmental Sciences, Peking University, Beijing 100871)

Key words Pollen indicator, climate change, human disturbance, semi-arid region

Abstract

Climate fluctuates strongly in the semi arid region in China, which is also the marginal area of Pacific monsoon influences. This area was one of the cradles for agriculture civilization in China, but agricultural development was interrupted several times. The modern landscape is characterized by an agro-pastoral transition. Even inside the steppe landscape, lowland meadow and fens frequently occur to form a vegetation mosaic with zonal steppe. Finding pollen indicator for landscape or even regional scale vegetation changes is thus crucial to the reconstruction of regional environmental history. From comparison among sediment sequences, together with surface pollen and modern vegetation studies, we found that: 1) *Betula*, Rosaceae, Caryophyllaceae and *Nitraria* pollen are good indicators of precipitation and humidity changes; *Picea* and *Abies* pollens indicate temperature changes. Both climate pattern and human disturbance affect the percentages of Chenopodiaceae,

Artemisia, Compositae pollen. High values of Gramineae species appear under both low and high human disturbances and its pollen percentage reflects more anthropogenic influence than climatic influence. Low percentage (< 5%) of *Plantago* pollen indicates humidity changes because of presence of *Plantago* species at lowland meadow and meadow steppe; High percentage (> 10%) in *Corylus/Ostryopsis* pollen reflects a clearance of forest in the forest-steppe zone. 2) Chenopodiaceae species frequently and densely occur on lakeshore when water table goes down, which leads to a higher percentage in Chenopodiaceae pollen in lake sediments than in soil surface. 3) A mosaic of forest and steppe patches forms due to topographic differentiation, with forest occurring on steep shady slope. A drier sunny slope and a wetter shady slope might occur, due to more evapotranspiration on sunny slope caused by increased temperature, when climate become warmer and wetter. This might lead to a co-existence of more wet-type forest species with more drought-tolerant steppe species.

降水改变对樟子松人工林土壤微生物量碳及微生物商动态变化的影响

魏天凤¹ 任艳林² 曾辉¹ 贺金生^{2,†}

1. 北京大学深圳研究生院环境与城市学院,深圳 518055;2. 北京大学城市与环境学院生态学系,北京 100871;
†通讯作者,E-mail: jshe@pku.edu.cn

摘要 在北京大学地球环境与生态系统塞罕坝实验站樟子松(*Pinus sylvestris* var. *mongolica*)人工林内设置降水控制实验,研究地下生态系统过程的两个重要指标土壤微生物量碳和微生物商对穿透雨增加或减少 30% 的响应。在 2007 年 5 月到 9 月的生长季,土壤微生物量碳和微生物商平均值分别为 260.7 mg/kg 和 1.84%,二者随土壤深度增加呈下降趋势。总体上,穿透雨增加或减少 30% 对土壤微生物量碳和微生物商的生长季内平均值影响不显著,但穿透雨减少 30% 的土壤微生物量碳及微生物商的变幅较大,变化范围分别为 243.1 ~ 354.3 mg/kg 和 1.43% ~ 2.16%,5 月最高,7 月最低,表明生长季内穿透雨减少将导致土壤微生物活动的较大波动,从而可能改变地下碳过程的季节变化规律。

关键词 碳循环;生态系统地下过程;穿透雨;塞罕坝;樟子松人工林

中图分类号 S718

Effects of Throughfall Manipulation on the Dynamics of Soil Microbial Biomass Carbon and Microbial Quotient in a *Pinus sylvestris* var. *mongolica* Plantation

WEI Tianfeng¹, REN Yanlin², ZENG Hui¹, HE Jinsheng^{2,†}

1. School of Environment and Urban Studies, Shenzhen Graduate School, Peking University, Shenzhen 518055;
2. Department of Ecology, College of Urban and Environmental Sciences, Peking University, Beijing 100871;
† Corresponding Author, E-mail: jshe@pku.edu.cn

Abstract A field experiment manipulating throughfall was constructed in a *Pinus sylvestris* var. *mongolica* plantation at PKU-SOGES. This study investigated the response of two indicators of belowground ecosystem processes, soil microbial biomass carbon and microbial quotient, to $\pm 30\%$ throughfall amount. During the growing season from May to September, 2007, soil microbial biomass carbon (260.7 mg/kg) and microbial quotient (1.84%) decreased with soil depth. Generally, the effects of $\pm 30\%$ throughfall amount on the means of soil microbial biomass carbon and soil microbial quotient in the growing season were not significant. Interestingly, the dynamics were much clear for the -30% throughfall treatment, with soil microbial biomass ranged from 243.1 mg/kg to 354.3 mg/kg and microbial quotient from 1.43% to 2.16%, and the highest value was in May and the lowest was in July. This indicates that the decrease of precipitation in a growing season may lead to a stronger fluctuation in soil microbial activity, thus alter the dynamics of belowground carbon cycle processes.

Key words carbon cycles; ecosystem belowground process; throughfall; Saihanba; *Pinus sylvestris* var. *mongolica* plantation

国家重点基础研究发展计划项目(2002CB412502)和国家自然科学基金(90411004)资助

收稿日期:2008-05-26;修回日期:2008-06-17

未来全球气候变化情景下,全球或局部地区的降水格局(降水量、降水强度及降水的季节分配)将发生改变^[1]。例如,1900—2005年,北半球中高纬度(30—85°N)降水量增加了6%~8%^[1]。从我国来看,1960—2000年,虽然总的降水量只增加了2%,但降水频率减少了10%,降水强度明显增加^[2]。降水格局改变引起的土壤水分变化将直接影响植物和土壤微生物对水分的利用,并间接影响到陆地生态系统功能与过程^[3],这已成为全球变化研究的重要内容之一。

自20世纪90年代以来,一些研究机构开始进行大型野外降水控制实验来评估降水格局改变对生态系统的影响过程。这些研究包括草原和森林生态系统的物种组成、植被生产力以及土壤呼吸等对降水格局改变的响应^[4-7]。但最近很多研究都强调土壤微生物在降水改变条件下,通过影响土壤养分的矿化作用,从而影响生态系统的功能^[8]。随着我国全国范围的植树造林活动的开展,未来人工林生态系统将在全国森林中占有较大比重。这些人工林生态系统对未来的气候变化如何响应,将关系到人工林的生态系统服务功能,特别是碳汇功能。

土壤微生物是生态系统分解者亚系统中的主要组成部分,可以调控养分循环、能量流动,并最终影响植被与生态系统生产力^[9]。土壤微生物量碳作为土壤活性有机碳的一部分,只占土壤总有机碳的1%~3%,但其周转时间较快,对外界环境变化较敏感,因此可以作为土壤总有机质变化的早期预测指标^[10]。土壤微生物量碳和微生物商作为生态系统地下过程的两个重要指标,在研究生态系统对降水响应过程中,具有重要作用。

樟子松是一种耐干旱、耐寒冷、耐瘠薄的树种,在我国遏制土壤荒漠化进程中起到重要作用,也是河北省塞罕坝机械林场的主要造林树种之一。过去对樟子松人工林的研究大多关注植被生产力、土壤肥力和固沙能力等,而对这种营养匮乏的生态系统与气候变化之间的关系则鲜有研究。河北坝上樟子松人工林分布在对气候变化敏感的森林草原交错区,降水改变引起的土壤水分变化可能对樟子松人工林生态系统有重要影响。因此,本研究的具体目的为:1)揭示樟子松人工林土壤微生物量碳与微生物商随土壤剖面的垂直变化特征;2)分析土壤微生物量碳与微生物商在生长季内的动态变化;3)比较穿透雨增加和减少30%对人工林土壤微生物

量碳与微生物商的影响。

1 材料与方法

1.1 样地概况

本研究在北京大学地球环境与生态系统实验站西侧的樟子松人工林降水控制实验样地内进行(图1)。该样地位于河北省围场县塞罕坝机械林场境内,海拔约1531 m,地理坐标为42°25′N,117°15′E。塞罕坝地区位于内蒙古高原东南缘,地处森林草原交错带,属于半干旱半湿润气候区。冬季漫长而寒冷,春季较短,夏季不明显;年平均气温-1.2℃,1月平均气温-21.8℃,7月平均气温16.2℃,年平均降雨量437.8 mm。样地土壤类型为风沙土,主要植被类型为24年生樟子松林,乔木胸径平均为12 cm,树高平均为9 m。林下灌木稀少,草本层以披针叶苔草(*Carex lanceolata*)、腺毛委陵菜(*Potentilla longifolia*)、地榆(*Sanguisorba officinalis*)、瓣蕊唐松草(*Thalictrum petaloideum*)为主。

1.2 实验设计及降水控制效果

实验样地占地1 hm²,设置了9个20 m×20 m的样方,包括以下3种处理方式。

- 1) 对照:保持自然穿透雨量。
- 2) 穿透雨减少30%:用覆盖地表面积30%的薄膜水槽转移走该样地30%的穿透雨量。
- 3) 穿透雨增加30%:把相应穿透雨减少样地转移来的30%穿透雨量用固定在地表的自动喷灌系统增加到该样地。

每种处理包括3个重复样方,各样方间距10 m作为缓冲带。在每个穿透雨减少样方中,12条离地1.5 m,用镀锌管支撑呈一定倾斜角度的0.5 m×20 m(覆盖地表30%)无色透明塑料薄膜水槽将穿



图1 降水控制实验设施

Fig. 1 Throughfall manipulation system

透雨汇集到 2000 L 的黑色树脂水罐中,在雨水到达水罐中预先设置的水位后自动控制系统启动,将雨水喷灌到相应的穿透雨增加样地中,实现穿透雨的有效截流与转移。在对照、穿透雨增加的样方中,覆盖地表 30 % 的无色透明塑料薄膜水槽均匀打孔,让降水自然穿透薄膜,使林下光照和穿透雨减少样方保持一致。根据坝上地区的气候特点,降水控制实验主要对生长季的穿透雨进行转移与再分配。冬季撤掉降雨设施是国际惯例,目的是不改变冬季积雪对土壤的保温作用。本实验设施于 2006 年 6 月建成并开始运转,同年 10 月将塑料薄膜撤掉,并于 2007 年 5 月初重新安装,继续观测至 2007 年 10 月。本研究自 2007 年 5 月生长季开始一直持续观测到 2007 年晚秋 9 月。

降水控制实验对土壤含水量的处理效果明显(表 1,图 2(a)),除 2007 年 5 月外,穿透雨增加 30 %,土壤含水量的平均值最高;穿透雨减少 30 %,土壤含水量的平均值最低。处理间的显著差异主要体现在 7、8、9 月。3 种穿透雨处理样地地下 10 cm 处的土壤日均温在生长季内有显著差异 ($P = 0.033$) (表 1),穿透雨减少 30 % 的土壤温度略高 ($P = 0.009$) (表 1,图 2(b))。这种情况也同样出现在其他

降水控制实验研究中^[4-5]。从土壤特性和群落特征来看,土壤容重、土壤总有机碳、林分密度以及林下草本植物群落地上生物量的处理间差异总体上都不显著 ($P > 0.05$)。但多重比较结果表明(表 1),穿透雨减少 30 % 的土壤总有机碳高于对照处理 ($P = 0.040$),这主要是由土壤背景值异质性引起的。

1.3 采样与分析

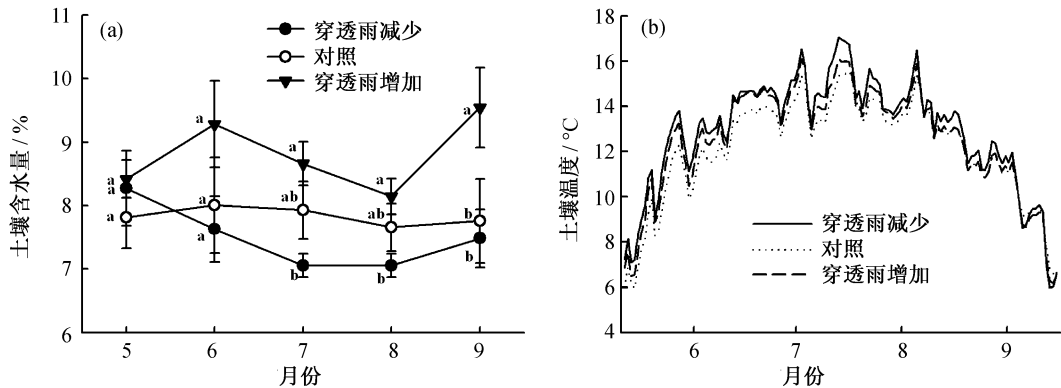
土壤样品分 5 次于 2007 年 5 月 26 日、6 月 26 日、7 月 24 日、8 月 22 日和 9 月 20 日采集。首次采样时在每个样地内随机选取 5 个 1 m × 1 m 的小样方,去除采样点地表枯落物后,用内径 5 cm 的土钻分 4 层(0 ~ 5, 5 ~ 10, 10 ~ 20 和 20 ~ 30 cm)钻取土芯样品,将 5 个小样方中的样品同层混匀后作为该样地的样品。随后的 4 次采样都在首次采样划定的小样方内。采回的土样立即通过 2 mm 筛,一部分在冰箱中 4 °C 保存以分析土壤微生物量碳,另一部分在室温下风干,过 1 mm 和 0.25 mm 筛,供土壤总有机碳分析使用。

土壤微生物量碳采用氯仿熏蒸 - K_2SO_4 浸提法测量^[11-12]。浸提液中的有机碳采用总有机碳分析仪(Multi N/C 3100, Analytik jena AG, Germany)测定。以熏蒸土样与未熏蒸土样提取的有机碳差值除以浸

表 1 3 种处理样地基本情况的比较
Table 1 Comparisons of different throughfall treatments

处理	土壤含水量/ %	土壤温度/	土壤容重 /(g cm ⁻³)	土壤总有机碳 /(g kg ⁻¹)	林分密度 /(株 hm ⁻²)	地上生物量 /(g m ⁻²)
穿透雨减少 30 %	7.50 ^a	12.88 ^a	1.32 ^a	17.06 ^a	3300 ^a	17.77 ^a
对照	7.83 ^b	12.09 ^b	1.36 ^a	12.59 ^b	4100 ^a	18.26 ^a
穿透雨增加 30 %	8.81 ^c	12.49 ^{ab}	1.35 ^a	13.32 ^{ab}	3400 ^a	23.28 ^a

说明:土壤含水量为采样期的平均值,土壤温度为 2007 年 5 月 26 日—9 月 30 日的日均温平均值,地上生物量为林下草本植物群落的地上生物量。列中不同小写字母上角标表示处理间平均值差异显著 ($P < 0.05$)。



图中数据点为平均值 ± 标准误差;不同小写字母表示同一月份内不同处理的平均值差异显著 ($P < 0.05$)。土壤含水量为每次采样时测定的土壤质量含水量,土壤温度为地下 10 cm 土壤日均温

图 2 降水控制实验对土壤含水量(a)和地下 10 cm 土壤温度(b)的效应

Fig. 2 The effects of throughfall manipulation on soil water content (a) and - 10 cm soil temperature (b)

提有效转换系数 k_{ec} , k_{ec} 取值 $0.37^{[12-13]}$, 计算土壤微生物量碳。土壤总有机碳采用 $K_2Cr_2O_7-H_2SO_4$ 氧化法, 土壤质量含水量采用差量法测量, 土壤容重用环刀法测定, 每小时的土壤温度用埋在地下 10 cm 处 StowAway TidBiT 袖珍温度记录仪 (Onset Computer Corporation, Pocasset, USA) 自动监测。

1.4 数据处理

数据经 Microsoft Excel 整理后, 主要采用 SPSS 13.0 进行统计分析。采用重复测定方差法 (repeated measures of ANOVA) 比较多种因素如穿透雨增加和减少 30 % 的处理、月份、土壤深度及其交互作用对土壤微生物量碳和微生物商的影响; 对不同处理、月份、土壤深度的土壤微生物量碳和微生物商进行多重比较时采用 Fisher's LSD 法 (Fisher's least significant difference) 进行检验。在所有分析中, 如果 $P < 0.05$ 则认为结果显著。绘图软件采用 SigmaPlot 10.0。

2 结果与讨论

2.1 土壤微生物量碳、微生物商及其垂直分布

樟子松人工林地下 0 ~ 30 cm 的土壤微生物量碳的平均值为 260.7 mg/kg (表 2)。与 Zhang 等^[14] 在半干旱地区栎树林对土壤微生物量碳的研究 (100 ~ 300 mg/kg) 接近。土壤微生物量碳变幅为 51.0 ~ 646.0 mg/kg, 与半干旱地区针叶林土壤微生物量碳的变幅 (142.4 ~ 729.5 mg/kg)^[15] 以及中亚热带地区不同林地 0 ~ 30 cm 土壤微生物量碳的变幅 (95.6 ~ 680.2 mg/kg)^[16] 接近。

微生物商是土壤微生物量碳与土壤总有机碳的比值, 可以解释为底物碳的可利用度或被微生物固

定的总有机碳的比例^[17]。樟子松人工林地下 0 ~ 30 cm 土壤微生物商变幅为 0.78 % ~ 4.12 %, 平均值为 1.84 %。Bauhus 等^[18] 报道不同林地的土壤微生物商变幅为 0.53 % ~ 2.41 %, 姜培坤^[16] 所研究的林地 0 ~ 30 cm 土壤微生物商的变幅为 0.90 % ~ 2.51 %。土壤异质性和穿透雨改变处理可能是导致本研究与上述研究相比微生物商变幅较大的原因。

土壤微生物量碳随土壤深度的增加有下降的趋势 (表 2), 这与以前的研究^[16,19] 一致, 这种递减现象可能与土壤容重密切相关 (图 3(a))。样地土壤中的有机质主要集中在表层, 底层土壤容重较大, 导致土壤微生物量碳较低。同样, 微生物商随土壤深度增加而下降的趋势与姜培坤^[16]、Castellazzi 等^[20] 的研究一致, 也说明土壤表层积累的土壤微生物量碳较多。

2.2 穿透雨增加或减少 30 % 对土壤微生物量碳及微生物商的影响

由于和土壤深度相关的交互作用对土壤微生物量碳及微生物商的影响都不显著 (表 3), 以下综合所有土壤层次的数据进行分析。重复测定方差分析结果表明, 穿透雨增加或减少 30 % 对土壤微生物量碳的影响不显著 ($P = 0.067$) (表 3); 而多重比较结果则显示, 穿透雨减少 30 % 的土壤微生物量碳高于对照 ($P = 0.029$) (图 4(a))。同样, 穿透雨增加或减少 30 % 对微生物商的影响也不显著 ($P = 0.193$) (表 3, 图 4(b))。穿透雨增加或减少 30 % 和月份两种因素的交互作用对土壤微生物量碳及微生物商的影响显著 ($P = 0.001$, $P = 0.002$) (表 3)。5 月穿透雨减少 30 % 的土壤微生物量碳较高, 9 月穿透雨减少 30 % 的微生物商较低 (图 5)。

表 2 土壤微生物量碳及微生物商的垂直分布
Table 2 Vertical distribution of soil microbial biomass carbon and microbial quotient

变量	土壤深度/cm	穿透雨处理		
		穿透雨减少 30 %	对照	穿透雨增加 30 %
土壤微生物量碳/(mg kg ⁻¹)	0 ~ 5	424.1 (37.1) ^a	353.6 (25.0) ^a	371.3 (20.4) ^a
	5 ~ 10	289.6 (24.9) ^b	228.2 (17.5) ^b	276.8 (13.4) ^b
	10 ~ 20	238.6 (16.6) ^c	186.2 (13.3) ^c	218.7 (12.1) ^{bc}
	20 ~ 30	198.4 (14.3) ^d	145.9 (11.6) ^d	196.9 (12.2) ^c
		2.38 (0.21) ^a	2.52 (0.13) ^a	2.35 (0.16) ^a
微生物商/ %	5 ~ 10	1.62 (0.10) ^b	1.75 (0.09) ^b	2.18 (0.10) ^a
	10 ~ 20	1.51 (0.10) ^b	1.70 (0.10) ^{bc}	1.67 (0.09) ^b
	20 ~ 30	1.33 (0.09) ^c	1.41 (0.11) ^c	1.64 (0.08) ^b

说明: 表中数据为 2007 年 5 月到 9 月的平均值 (标准误差)。微生物商为土壤微生物量碳与土壤总有机碳的比值。列中不同小写字母上角标说明同一处理不同土壤深度的平均值之间存在显著差异 ($P < 0.05$)。

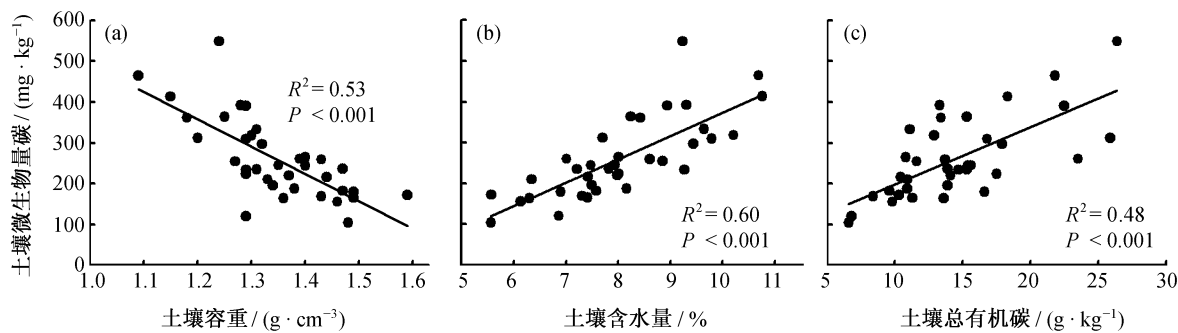


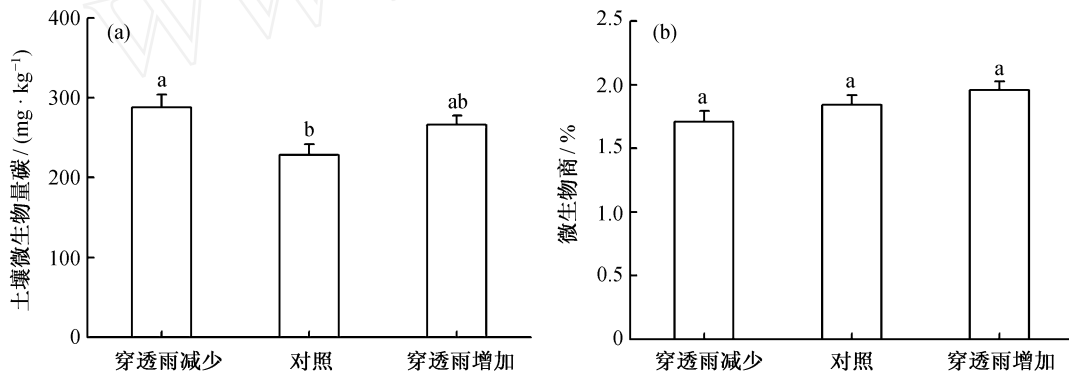
图 3 土壤微生物量碳与土壤容重(a)、土壤含水量(b)、土壤总有机碳(c)的关系

Fig. 3 Relationships of soil microbial biomass carbon with soil bulk density (a) , soil water content (b) , and soil total organic carbon (c)

表 3 穿透雨增加或减少 30 %对土壤微生物量碳和微生物商影响效应的重复测定方差分析

Table 3 Repeated measures of ANOVA for the effects of ± 30 % throughfall on soil microbial biomass carbon and microbial quotient

差异来源	土壤微生物量碳			微生物商		
	自由度	F 值	P 值	自由度	F 值	P 值
组内效应						
月份	4	3.269	0.015	4	2.762	0.032
月份 ×处理	8	3.567	0.001	8	3.356	0.002
月份 ×深度	12	1.375	0.191	12	1.431	0.165
月份 ×处理 ×深度	24	0.960	0.524	24	1.100	0.359
组间效应						
处理	2	3.032	0.067	2	1.763	0.193
深度	3	14.594	0.000	3	15.003	0.000
处理 ×深度	6	0.153	0.987	6	0.067	0.675



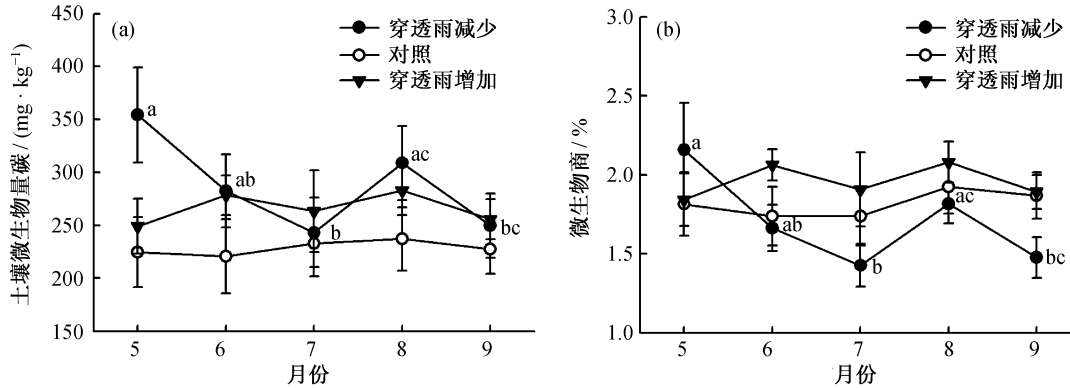
图中数据为平均值 + 标准误差。不同的小写字母表示多重比较中不同穿透雨处理的平均值差异显著 ($P < 0.05$)

图 4 穿透雨增加或减少 30 %对土壤微生物量碳 (a) 及微生物商 (b) 的影响

Fig. 4 Effects of ± 30 % throughfall on soil microbial biomass carbon (a) and microbial quotient (b)

总体来说,增加和减少 30 %穿透雨量的处理对坝上樟子松人工林 2007 年生长季内的土壤微生物量碳的平均值影响不显著。增加 30 %的穿透雨量没有导致土壤微生物量碳的显著变化,这与半干旱地区柞树林生态系统中的研究结果相似^[14]。在该研究中,添加水分后的几小时到几天内,土壤微生物量碳显著下降,但随后几个月内添加水分与对照之间并没有显著差别。Illeris 等^[21]则发现生长季内增加一倍降水会导致极地半干旱荒漠生态系统土壤

微生物量碳增加。本研究结果可能主要是以下原因引起的。第一,与其他研究相比,本研究在未改变降水频率的情况下将穿透雨增加和减少 30 %的处理强度较低。虽然土壤微生物量碳与土壤含水量之间具有显著的正相关关系(图 3(b)),但所测定的土壤含水量为每次采样时的瞬时值,而土壤微生物量碳对穿透雨改变处理的响应可能还受到季节性温度、养分动态的干扰。第二,由于所测定的土壤微生物量是微生物细胞质中的含量,反映的是整体微生物



图中数据为平均值 \pm 标准误差。不同小写字母表示穿透雨减少 30% 处理不同月份间的平均值差异显著 ($P < 0.05$)

图 5 穿透雨增加或减少 30% 对土壤微生物量碳(a)及微生物商(b)动态变化的影响

Fig. 5 Effects of $\pm 30\%$ throughfall on dynamics of soil microbial biomass carbon (a) and microbial quotient (b)

量,并没有将休眠的以及非活跃态的同活跃态的微生物量区分开^[22-23],很可能只是土壤中处于活跃态的土壤微生物发生了变化,但这部分变化不足以引起穿透雨增加 30% 与对照处理间的差异。第三,植物通过根系输送到土壤中的碳是限制土壤中微生物量碳含量的重要因素之一^[24-25]。在降水增加减少 33% 的长期控制实验中(5 年),水分改变并没有对落叶松林的细根生产力产生显著影响^[26],因此降水改变对土壤环境的影响较为复杂,较小幅度的改变并不能直接影响到土壤微生物的活动,土壤中养分的浓度、碳周转速率等因素对土壤微生物的影响可能更重要。第四,土壤微生物量碳对水分改变的响应存在滞后效应,但本研究观察时间较短。穿透雨增加 30% 的土壤微生物量碳平均值比对照处理的平均值高 16.2%,说明穿透雨增加对土壤微生物量碳具有潜在影响,但穿透雨量改变的程度以及观察时间的长短可能是决定这种影响是否显著的重要因素之一。

虽然总体上穿透雨增加或减少 30% 对土壤微生物量碳平均值没有显著影响,但多重比较结果表明,穿透雨减少 30% 处理的土壤微生物量碳高于对照,这与其他研究不一致。例如 Jensen 等^[8]的研究表明完全移除降水会减少欧石楠(*Erica carnea*)灌丛土壤微生物量碳,Salamanca 等^[27]则发现降水量减少 50% 并没有对落叶阔叶林地表土壤微生物量碳产生显著影响。本研究结果可能主要与土壤异质性导致穿透雨减少 30% 的样地土壤总有机碳背景值较高有关。由于土壤微生物依赖土壤有机质以及可利用的活性有机碳维持自身生长,土壤微生物量的大小还主要取决于有机质的多少^[28],土壤微生物量碳和

土壤总有机碳之间显著的相关关系也能说明这一点($P < 0.001$) (图 3(c))。另外,穿透雨减少 30% 的土壤微生物量碳较高的情况只出现在 5 月,自 2007 年 5 月初降水控制实验开始至第一次采样期间无降雨,3 种处理间的土壤含水量并没有显著差异(图 2(a)),因此 5 月的情况并不是由土壤水分的改变引起的,很可能是 5 月末土壤的冻融作用刺激了微生物活动^[29-30],促进了碳源供应充足的穿透雨减少 30% 的土壤微生物的生长。其次,土壤温度也是影响微生物量碳的因素之一^[28]。本研究中穿透雨减少 30% 的土壤温度显著高于对照,因此,也可能是减少 30% 的穿透雨量通过改变了土壤温度对土壤微生物产生了间接影响。

微生物商是个比值,与土壤微生物量碳不同,它能够消除由土壤有机质异质性引起的问题。穿透雨增加或减少 30% 对微生物商的总体影响也不显著(图 4(b))。2007 年 9 月穿透雨减少 30% 的微生物商显著低于对照和穿透雨增加 30%,采样前 48 小时内曾有明显的降水过程,说明在有降水补充后,穿透雨减少短期内可能会抑制土壤微生物获得土壤中可利用的碳。但 9 月各处理间的土壤微生物量碳并没有显著差异,这也部分印证了穿透雨减少 30% 样地土壤总有机碳背景值较高的因素可能掩盖了土壤微生物量碳对穿透雨增加或减少 30% 的响应。

2.3 土壤微生物量碳和微生物商对降水改变的响应

就不同处理的动态变化而言,在 2007 年生长季中,穿透雨减少 30% 的土壤微生物量碳及微生物商比穿透雨增加 30% 和对照的波动更大(图 5),其平均值的变幅分别为 243.1 ~ 354.3 mg/kg 和 1.43 % ~

2.16%,而对照为220.6~237.0 mg/kg和1.74%~1.92%,穿透雨增加30%为249.1~282.9 mg/kg和1.84%~2.08%。重复测定方差分析表明,穿透雨减少30%的土壤微生物量碳和微生物商在生长季初期的5月最高,生长季旺期的7月最低,8月显著升高,9月又再次下降(图5)。

穿透雨减少30%的土壤微生物量碳的动态变化与次生栎林和火炬松人工林^[31]以及半干旱地区栎树林中的研究结果相似^[14]。虽然土壤微生物量碳与土壤含水量呈正相关(图3(b)),但其动态变化与土壤含水量变化并不完全一致(图2(a),图5(a))。Wardle^[28]指出,土壤水分、土壤温度以及植物根系生产力的相互作用及其相对重要性决定了土壤微生物量的动态变化。对照和穿透雨增加30%的土壤微生物量碳和微生物商没有显著的动态变化,可能是该生长季的土壤水分动态不足以影响对照处理的土壤微生物活动,而水分条件相对较好的穿透雨增加30%的处理则可能掩盖了土壤微生物量碳及微生物商的动态变化。穿透雨减少30%的土壤微生物量碳及微生物商的波动更大(图5),这也说明生长季内穿透雨减少将导致土壤微生物活动的较大波动。半干旱生态系统内,分散的降水事件对干旱土壤的淋湿过程会刺激土壤微生物的活动,引起土壤微生物量碳的动态变化^[32]。因此,生长季降水量减少、土壤干旱程度增加很可能会导致土壤微生物量的波动加剧。

3 结论

樟子松人工林的土壤微生物量碳平均值为260.7 mg/kg,变幅51.0~646.0 mg/kg;微生物商平均值为1.84%,变幅0.78%~4.12%,二者都随土壤深度的增加呈下降趋势。总体上看,穿透雨增加或减少30%对土壤微生物量碳及微生物商的平均值影响不显著。穿透雨减少30%的土壤微生物量碳及微生物商的波动幅度大于对照和穿透雨增加30%。土壤微生物量及其动态变化受多种因素影响,需要较长时间的进一步研究。

参考文献

- [1] IPCC. WGI Fourth Assessment Report. Climate Change 2007: The physical science basis. Geneva: Intergovernmental Panel on Climate Change, 2007
- [2] Liu B H, Xu M, Henderson M, et al. Observed trends of

- precipitation amount, frequency, and intensity in China, 1960-2000. *Journal of Geophysical Research*, 2005, 110, D08103, doi: 10. 1029/2004JD004864
- [3] Weltzin J F, Loik M E, Schwinning S, et al. Assessing the response of terrestrial ecosystems to potential changes in precipitation. *BioScience*, 2003, 53(10): 941-952
- [4] Fay P A, Carlisle J D, Knapp A K, et al. Altering rainfall timing and quantity in a mesic grassland ecosystem: Design and performance of rainfall manipulation shelters. *Ecosystems*, 2000, 3(3): 308-319
- [5] Hanson P J, Wullschlegel S D. North American temperate deciduous forest responses to changing precipitation regimes. New York: Springer-Verlag, 2003: 15
- [6] Harper C W, Blair J M, Fay P A, et al. Increased rainfall variability and reduced rainfall amount decreases soil CO₂ flux in a grassland ecosystem. *Global Change Biology*, 2005, 11(12): 322-334
- [7] Knapp A K, Fay P A, Blair J M, et al. Rainfall variability, carbon cycling and plant species diversity in a mesic grassland. *Science*, 2002, 298: 2202-2205
- [8] Jensen K D, Beier C, Michelsen A, et al. Effects of experimental drought on microbial processes in two temperate heathlands at contrasting water conditions. *Applied Soil Ecology*, 2003, 24(2): 165-176
- [9] Wardle D A. Controls of temporal variability of the soil microbial biomass: A global-scale synthesis. *Soil Biology & Biochemistry*, 1998, 30(13): 1627-1637
- [10] 何友军,王清奎,汪思龙,等. 杉木人工林土壤微生物生物量碳氮特征及其与土壤养分的关系. *应用生态学报*, 2006, 17(12): 2292-2296
- [11] Wu J, Joergensen R G, Pommerening B, et al. Measurement of soil microbial biomass C by fumigation-extraction —An automated procedure. *Soil Biology & Biochemistry*, 1990, 22(8): 1167-1169
- [12] Vance E D, Brookes P C, Jenkinson D S. An extraction method for measuring soil microbial biomass C. *Soil Biology & Biochemistry*, 1987, 19(6): 703-707
- [13] Sparling G P, Feltham C W, Reynolds J, et al. Estimation of soil microbial C by a fumigation-extraction method: Use on soils of high organic matter content, and a reassessment of the k_{ec} -factor. *Soil Biology & Biochemistry*, 1990, 22: 301-307
- [14] Zhang Q S, Zak J C. Effects of water and nitrogen amendment on soil microbial biomass and fine root production in a semi-arid environment in west Texas. *Soil Biology & Biochemistry*, 1998, 30(1): 39-45
- [15] Bastida F, Moreno J L, Hernández T, et al. The long-term

- effects of the management of a forest soil on its carbon content, microbial biomass and activity under a semi-arid climate. *Applied Soil Ecology*, 2007, 37(1-2): 53-62
- [16] 姜培坤. 不同林分下土壤活性有机碳库研究. *林业科学*, 2005, 41(1): 10-13
- [17] Anderson T H, Domsch K H. Ratio of microbial biomass carbon to total organic carbon in arable soils. *Soil Biology & Biochemistry*, 1989, 21(4): 471-479
- [18] Bauhus J, Par D, C t L. Effects of tree species, stand age and soil type on soil microbial biomass and its activity in a southern boreal forest. *Soil Biology & Biochemistry*, 1998, 30(8): 1077-1089
- [19] Blume E, Bischoff M, Reichert J M, et al. Surface and subsurface microbial biomass, community structure and metabolic activity as a function of soil depth and season. *Applied Soil Ecology*, 2002, 20(3): 171-181
- [20] Castellazzi M S, Brookes P C, Jenkinson D S. Distribution of microbial biomass down soil profiles under regenerating woodland. *Soil Biology & Biochemistry*, 2004, 36(9): 1485-1489
- [21] Illeris L, Michelsen A, Jonasson S. Soil plus root respiration and microbial biomass following water, nitrogen and phosphorus application at a high arctic semi desert. *Biogeochemistry*, 2003, 65(1): 15-29
- [22] Zak D R, Ringelberg D B, Pregitzer K S, et al. Soil microbial communities beneath *Populus grandidentata* grown under elevated atmospheric CO₂. *Ecological Applications*, 1996, 6(1): 257-262
- [23] Teesier L, Gregorich E G, Topp E. Spatial variability of soil microbial biomass measured by the fumigation extraction method, and k_{EC} as affected by depth and manure application. *Soil Biology & Biochemistry*, 1998, 30(10-11): 1369-1377
- [24] Anderson T H, Domsch K H. Maintenance of carbon requirements of actively-metabolizing microbial populations under in situ conditions. *Soil Biology & Biochemistry*, 1985, 17(2): 197-203
- [25] Bardgett R D, Bowman W D, Kaufmann R, et al. A temporal approach to linking aboveground and belowground ecology. *Trends in Ecology & Evolution*, 2005, 20(11): 634-641
- [26] Joslin J D, Wolfe M H, Hanson P J. Effects of altered water regimes on forest root systems. *New Phytologist*, 2000, 147(1): 117-129
- [27] Salamanca E F, Kaneko N, Katagiri S. Rainfall manipulation effects on litter decomposition and the microbial biomass of the forest floor. *Applied Soil Ecology*, 2003, 22(3): 271-281
- [28] Waddle D A. A comparative assessment of factors which influence microbial biomass carbon and nitrogen in soil. *Biological Reviews*, 1992, 67(3): 321-358
- [29] Deluca T H, Keeney D R. Soluble carbon and nitrogen pools of prairie and cultivated soils: Seasonal variation. *Soil Science Society of America Journal*, 1994, 58: 835-840
- [30] Edwards K A, Mcculloch J, Kershaw G P, et al. Soil microbial and nutrient dynamics in a wet Arctic sedge meadow in late winter and early spring. *Soil Biology & Biochemistry*, 2006, 38(9): 2843-2851
- [31] 王国兵, 阮宏华, 唐燕飞, 等. 北亚热带次生栎林与火炬松人工林土壤微生物生物量碳的季节动态. *应用生态学报*, 2008, 19(1): 37-42
- [32] Huxman T E, Snyder K A, Tissue D, et al. Precipitation pulses and carbon fluxes in semiarid and arid ecosystems. *Oecologia*, 2004, 141(2): 254-268

2008 年发表论文

Anatomical traits associated with absorption and mycorrhizal colonization are linked to root branch order in twenty-three Chinese temperate tree species

Dali Guo^{1,3}, Mengxue Xia¹, Xing Wei², Wenjing Chang³, Ying Liu² and Zhengquan Wang²

¹Department of Ecology, College of Urban and Environmental Sciences, Peking University, Beijing 100871, China; ²School of Forestry, Northeast Forestry University, Harbin 150040, China; ³Shenzhen Graduate School, Peking University, Shenzhen 518055, China

Summary

Author for correspondence:

D. L. Guo

Tel/Fax: +86 10 62753063

Email: dlguo@urban.pku.edu.cn

Received: 9 April 2008

Accepted: 29 May 2008

- Different portions of tree root systems play distinct functional roles, yet precisely how to distinguish roots of different functions within the branching fine-root system is unclear.
- Here, anatomy and mycorrhizal colonization was examined by branch order in 23 Chinese temperate tree species of both angiosperms and gymnosperms forming ectomycorrhizal and arbuscular–mycorrhizal associations.
- Different branch orders showed marked differences in anatomy. First-order roots exhibited primary development with an intact cortex, a high mycorrhizal colonization rate and a low stele proportion, thus serving absorptive functions. Second and third orders had both primary and secondary development. Fourth and higher orders showed mostly secondary development with no cortex or mycorrhizal colonization, and thus have limited role in absorption. Based on anatomical traits, it was estimated that c. 75% of the fine-root length was absorptive, and 68% was mycorrhizal, averaged across species.
- These results showed that: order predicted differences in root anatomy in a relatively consistent manner across species; anatomical traits associated with absorption and mycorrhizal colonization occurred mainly in the first three orders; the single diameter class approach may have overestimated absorptive root length by 25% in temperate forests.

Key words: anatomy, arbuscular mycorrhizas, ectomycorrhizas, fine roots, root architecture, root diameter, root function, root length.

New Phytologist (2008) **180**: 673–683

© The Authors (2008). Journal compilation © *New Phytologist* (2008)

doi: 10.1111/j.1469-8137.2008.02573.x

Introduction

In mature trees, woody roots extend 10 m or more from the tree trunk to support the shoot system, and to explore a large volume of soil, whereas small nonwoody roots arising from the woody root framework provide a large surface area and intimate contact with soil to ensure effective resource acquisition (Pregitzer, 2002; Robinson *et al.*, 2003). Multiple root functions are performed simultaneously by different portions of the root system (Robinson *et al.*, 2003).

The recognition of the functional differentiation in the tree root system has led to the efforts of separating roots with

different functions. For example, roots with the primary function of resource acquisition needed be defined so that root uptake could be better understood (Jackson *et al.*, 1997). From an ecosystem perspective, it is necessary to distinguish the rapidly cycling portion within the root system (McClagherty *et al.*, 1982; Jackson *et al.*, 1997; Joslin *et al.*, 2006). Consequently the entire root system was divided into different parts and, often more conveniently, into two parts (Jackson *et al.*, 1997). One is termed fine roots (e.g. all roots < 2 mm diameter), which are considered to be nonwoody, ephemeral absorptive roots, another is termed coarse roots (e.g. all roots > 2 mm diameter), or the perennial roots serving

mainly transport, anchorage, and storage functions (Pregitzer, 2002).

Research in the past decade, however, has begun to question the validity of such a simple division between fine and coarse roots, and the view that all roots of a given size class function in the same way (Majdi *et al.*, 2001; Wells & Eissenstat, 2001; Pregitzer *et al.*, 2002; Wells *et al.*, 2002; Joslin *et al.*, 2006; Guo *et al.*, 2008a,b). Increasing evidence suggests that tree fine roots are complex branching structures composed of a large number of individual root segments differing in morphology, chemistry, and physiology (Pregitzer *et al.*, 1998, 2002; Majdi *et al.*, 2001; Wells *et al.*, 2002; Guo *et al.*, 2004). Moreover, these functionally distinct root segments may be grouped according to their position on the branching root system such that the most distal root tips (or first-order roots) are thinner, richer in nitrogen and have higher respiration rates than more basal roots, implying that they are more active in nutrient uptake (Pregitzer *et al.*, 1998, 2002; Pregitzer, 2002). In addition, the majority of the root length was found to concentrate on the distal branches consisting of first- and second-order roots, suggesting that these lower roots provide most of the root surface for resource uptake whereas higher orders may serve mainly transport functions (Pregitzer *et al.*, 2002). Branching order of individual roots seems important for understanding root functions in the fine root systems of trees.

However, no study so far has determined whether branch order effectively distinguishes roots with absorptive capacity in the entire root system. This task is challenging because root functions, such as resource uptake, are difficult to measure directly (Lucash *et al.*, 2007). A common method, measuring nutrient uptake on excised roots, is questionable because excision significantly alters nutrient uptake processes, especially the energy-intensive processes such as nitrate uptake, leading to errors in uptake estimates (Bloom & Caldwell, 1988; Volder *et al.*, 2005; Lucash *et al.*, 2007). Another method, the intact root method, avoids root excision, but measures uptake of the entire root branching system, and thus can not quantify the differences in uptake capacity among individual roots differing in branching position, chemistry and physiology (Pregitzer *et al.*, 2002; Hishi, 2007).

Indirect methods, particularly anatomical methods, may be useful because anatomy and physiology are tightly linked (Esau, 1977; McKenzie & Peterson, 1995a,b; Eissenstat & Achor, 1999; Hishi, 2007). In trees, root systems can be separated into the root segments with primary development and those that undergo secondary development and eventually become structural portion of the root system (Esau, 1977; Peterson *et al.*, 1999; Pregitzer *et al.*, 2002). It is generally considered that roots with primary development have a living cortex and mycorrhizal association and are mainly responsible for water and nutrient absorption (Esau, 1977; Peterson *et al.*, 1999; Brundrett, 2002). Losing cortex greatly curtails root uptake capacity because of the loss of absorptive surface area and preclusion of mycorrhizal colonization (Enstone *et al.*,

2001; Brundrett, 2002; Wells & Eissenstat, 2003; Kumar *et al.*, 2007).

By contrast, roots that undergo secondary development may have limited capacity for uptake. When secondary growth occurs, pericycle forms cork cambium, which produces cork tissue with hydrophobic suberized cells and eventually develops into a continuous cork layer. This cork layer serves as a barrier to water and nutrient absorption (Peterson *et al.*, 1999; Taylor & Peterson, 2000) so that a root with a continuous cork layer may lack absorptivity (Wells & Eissenstat, 2003; Hishi, 2007). Moreover, development of secondary xylem increases root transport capacity (Kumar *et al.*, 2007). Therefore, secondary development may represent a major shift of root function from absorption to transport (Wells & Eissenstat, 2003; Hishi, 2007). It appears that the anatomical features reveal critical differences in resource uptake, mycorrhizal colonization, and transport capacity among individual roots.

In this study, we attempted to distinguish roots of different functions by examining anatomical features of different branch orders in the branching fine root systems of 23 Chinese temperate tree species differing in taxonomic rank (angiosperms vs gymnosperms) and mycorrhizal type (ectomycorrhizas (EM), and arbuscular mycorrhizas (AM)). We predicted that root anatomy associated with resource absorption and transport would vary consistently with root branch order despite the wide differences in root diameter among species.

Materials and Methods

Study site and species selection

The study sites were located in four different temperate regions of China. These four sites represented four points on a national-scale sampling of root architecture of Chinese tree species. Our main sampling site (Site 1) was located in Maoershan research station (45°21'–45°25'N, 127°30'–127°34'E) of Northeast Forestry University, in Heilongjiang, China. This site had a continental temperate monsoon climate with mean January, July and annual temperatures of –19.6°C, 20.9°C, and 2.8°C, respectively. The mean annual precipitation was 723 mm, with 477 mm distributed from June to August (Zhou, 1994). Soils were Hap-Boric Luvisols (Gong *et al.*, 1999) with high organic matter, and were well drained.

At this site, three forest types were chosen for root sampling in mid August of 2007. From a naturally regenerated secondary deciduous hardwood forest *c.* 50 yr old (Site 1a) four AM angiosperm species, five EM angiosperm species and six angiosperm species capable of supporting both AM and/or EM were sampled. Two EM gymnosperms were sampled from a pine plantation *c.* 40 yr old (Site 1b) and a deciduous EM conifer was sampled from a larch plantation *c.* 50 yr old (Site 1c). All species sampled were listed in Table 1. All trees sampled had an age of 20–50 yr.

Table 1 Taxonomic list, species abbreviation, dominant mycorrhizal (MYC) type and sampling site of the 23 tree species in this study

	Abbreviation	MYC type ^a	Site ^b
Gymnosperm			
Pinaceae			
<i>Larix gmelinii</i>	Lagm	EM	Site 1c
<i>Pinus sylvestris</i>	Pisy	EM	Site 1b
var. <i>mongolica</i>			
<i>Pinus koraiensis</i>	Piko	EM	Site 1b
<i>Pinus tabulaeformis</i>	Pita	EM	Site 3
Angiosperm			
Aceraceae			
<i>Acer davidii</i>	Acda	AM	Site 1a
<i>Acer ginnala</i>	Acgi	AM & EM	Site 1a
<i>Acer ukurunduense</i>	Acuk	AM & EM	Site 1a
Betulaceae			
<i>Alnus mandshurica</i>	Alma	AM & EM	Site 1a
<i>Alnus hirsute</i>	Alhi	AM & EM	Site 1a
<i>Betula platyphylla</i>	Bepl	EM	Site 1a
<i>Betula costata</i>	Beco	EM	Site 1a
Cornaceae			
<i>Cornus officinalis</i>	Coof	AM & EM	Site 4
Fagaceae			
<i>Quercus acutissima</i>	Quac	EM	Site 1a
<i>Quercus dentate</i>	Qude	EM	Site 1a
<i>Quercus mongolica</i>	Qumo	EM	Site 1a
Juglandaceae			
<i>Juglans mandshurica</i>	Juma	AM	Site 1a
Oleaceae			
<i>Fraxinus mandschurica</i>	Frma	AM	Site 1a
<i>Fraxinus rhynchophylla</i>	Frrh	AM	Site 2
<i>Syringa pekinensis</i>	Sype	AM & EM	Site 2
Rutaceae			
<i>Phellodendron amurense</i>	Pham	AM	Site 1a
Tiliaceae			
<i>Tilia mandshurica</i>	Tima	AM	Site 2
Ulmaceae			
<i>Ulmus laciniata</i>	Ulla	AM & EM	Site 1a
<i>Ulmus japonica</i>	Ulja	AM & EM	Site 1a

^aAM, arbuscular mycorrhizas; EM, ectomycorrhizas.^bSee detailed site information in the Materials and Methods section.

To complement the root sampling at site 1, species sampled earlier at three other sites (Sites 2, 3 and 4) were included. At Site 2, three angiosperm species were sampled in late July 2006, including two AM species and one AM and EM species from a naturally regenerated forest c. 50 yr old. This site was located in Baihua Mountain of Northwest Beijing (39°49'–39°53'N, 115°30'–115°38'E). The site had a warm-temperature continental climate with mean January, July, and annual temperatures of –7.1°C, 18.3°C and 4.8°C and mean annual precipitation of 595 mm with > 75% distributed from June to August (Land Environmental Protection Department of Beijing Municipal Planning Committee, 1988). Soils were Haplic Luvisols (Gong *et al.*, 1999) with high organic matter and were well drained.

At Site 3, an EM gymnosperm from naturally regenerated forest c. 80 yr old (Table 1) was sampled in early July 2006.

This site was located in the Guandishan Pangquangou Nature Reserve in the middle range of LuLiang Mountain in Shanxi Province (37°20'–38°20'N, 110°18'–111°18'E), with mean January, July and annual temperatures of –7.7°C, 23.5°C and 8.8°C, respectively. The mean annual precipitation was 400–600 mm with 65% mm occurring from July to September. Soils were Haplic Luvisols (Gong *et al.*, 1999) with medium organic matter content, and were well drained.

At Site 4, an AM and EM angiosperm from planted trees c. 20 yr old (Table 1) was sampled in early July 2006. The sampling location for Coof was at the southern part of Taihang Mountain in Shanxi Province (35°52'–37°20'N, 110°24'–111°45'E), with mean January, July and annual temperatures of –4.6°C, 21°C, and 9.9°C, respectively. The mean annual precipitation was 670 mm with 47% mm distributed from June to August. Soils were Haplic Luvisols (Gong *et al.*, 1999) with medium organic matter content, and were well drained.

Root excavation and preliminary processing

For each species, three root samples (one sample from each of the three chosen trees) were collected from 0–20 cm of soil following three steps. A 1 × 1 m plot was first identified within a 2-m distance of the tree stem. A specially constructed fork (with three teeth, each 20 cm long and 1 cm diameter, and having a pointed tip) was then used to loosen the soil in the sampling area. Root branches were followed to the tree stem and cut from the main lateral woody roots. When necessary, more plots were established to ensure that each root sample contained at least eight intact distal root branches including more than five orders.

Once collected, each root sample was divided into two subsamples: one was gently washed in deionized water and immediately fixed in Formalin-Aceto-Alcohol (FAA) solution (90 ml 50% ethanol, 5 ml 100% glacial acetic acid, 5 ml 37% methanol); the other was immediately put on ice and transported to the laboratory within 4 h and frozen for dissection and morphological analysis at a later date.

Anatomical assessments

More than 15 root branches of each species fixed in FAA solution were dissected into different orders as described in Fitter (1982, 1987), Berntson (1997), and Pregitzer *et al.* (2002) with the most distal root tips labeled as first order. Our order designation strictly followed Strahler's stream ordering system (described in detail by Pregitzer *et al.*, 2002). We therefore did not differentiate between the finest first-order roots located at distal ends of a well-branched fine root system and the root tips of pioneer roots (often of larger diameters) that are rapidly developing and may be destined to become higher-order roots (Wells & Eissenstat, 2003).

For each species, 20 segments were randomly chosen per order for first to third order, and fifteen segments per order for

fourth and fifth order. The sample size differed among branch orders because of the limited number of high-order roots obtained in the field sampling for some species. In total, 2070 individual root segments across 23 species were dissected for anatomical analysis.

After the dissection, individual root segments were stained with safranin-fast green, dehydrated in a set of alcohol solutions, embedded in paraffin, and sections 8 µm thick were prepared (de Neergaard *et al.*, 2000). These sections were measured for anatomical features, and photographed under a compound microscope (BH1; Olympus). For each root segment, three cross-sections were chosen. For root segments < 1 cm long, three sections near the root base were chosen. For root segments > 1 cm long, three sections evenly distributed between 1 cm from root tip (for the first-order roots) or the branching point (for higher-order roots) to root base were chosen.

For each root cross-section, root diameter, cortex thickness, and stele diameter were measured to the nearest 1 µm, and the presence of mycorrhizal colonization, secondary xylem (SX) and continuous cork layer (CCL) were recorded (see the Supporting Information, Fig. S1). For root diameter, cortex thickness, and stele diameter of each root segment, the average values of the three sections were calculated. In addition, the ratio of stele diameter to root diameter (or stele : root diameter ratio) was calculated to indicate the proportion of root diameter devoted for resource transport. For mycorrhizal colonization and features of secondary development (SX and CCL), their appearance on any of the three sections was regarded as the presence on the entire root segment. For AM, appearance of coils (or arbuscules) was accepted as evidence of colonization (Brundrett, 2004; Vierheilig *et al.*, 2005). For EM, fungal sheath and/or Hartig net in sections were considered evidence for colonization (de Neergaard *et al.*, 2000).

Morphological analyses

More than five intact root branches for each species were dissected for morphology as described in Pregitzer *et al.* (2002). The length of relatively short root segments were measured using a 40× stereomicroscope with an ocular micrometer (± 0.025 mm), while the length of relatively long root sections (e.g. fourth- and fifth-order roots) was assessed using a measuring tape to the nearest 0.5 mm (Guo *et al.*, 2004). The total root length for the first five orders was calculated for each species.

Data analysis

Root diameter, cortex thickness, stele diameter, stele : root diameter ratio were rank-transformed to satisfy the assumption of normality (Zar, 1999). Differences in these variables among root order, diameter class (0.25-mm intervals), and species were analysed by a mixed-level ($5 \times 11 \times 23$) three-way

factorial ANOVA with Tukey's HSD for unequal sample size. The Spearman's rank correlation coefficients were calculated for order, diameter class of 0.25-mm intervals, root diameter, cortex thickness, stele diameter, stele : root diameter ratio, mycorrhizal colonization presence, SX presence and CCL presence.

Stepwise discrimination analysis was conducted to examine the groupings of species based on morphological and anatomical traits of first-order roots. Root traits used in the analysis included mean root diameter, mean cortex thickness, mean stele diameter, and mean stele : root diameter ratio of each species. In each step one variable was selected on the basis of its significance.

The proportion of the total root length with uptake capacity (i.e. no CCL) and mycorrhizal colonization was calculated as the ratio of the cumulative absorptive or mycorrhizal root length to the total root length of the first five orders. All statistical analyses were performed using SPSS software (2001, ver. 13.0, SPSS Inc., Chicago, IL, USA).

Results

Variations in root traits by branch order

Across all species, root diameter, cortex thickness, stele diameter, and stele : root diameter ratio (i.e. the ratio of stele diameter to root diameter) differed by branch order (all *P* values < 0.01) (see the Supporting Information, Table S1). In addition, root diameter, stele diameter, and stele : root diameter ratio differed significantly between each order, whereas cortex thickness did not show significant differences between first and second order but did among other orders (see the Supporting Information, Table S2).

Branch order and root traits correlated strongly but the direction of correlation differed by root trait. Correlation was positive and strong between order and stele diameter ($r = 0.862$), stele : root diameter ratio ($r = 0.833$), SX presence ($r = 0.802$), CCL presence ($r = 0.792$) and root diameter ($r = 0.613$), but was negative and strong between order and mycorrhizal colonization ($r = -0.733$) and cortex thickness ($r = -0.597$) (Table 2). Similar patterns were found across species of the same mycorrhizal type and taxonomy rank, or within each species (detailed results not shown).

The species differed in their relationship between order and various root traits. Average diameter generally increased with order, but the specific patterns differed among species (Fig. 1): diameter showed no significant differences in at least three consecutive orders and then increased dramatically in the higher orders in 13 species; diameter was constant across five orders in two species (i.e. *Acer ukurunduense* and *Betula costata*); and diameter increased steadily across five branch orders in eight species.

Stele diameter increased gradually with order in most species and significant differences frequently were found between the

Table 2 Spearman's rank correlation coefficient matrix for order, diameter class, root diameter, cortex thickness, stele diameter, stele : root diameter ratio, mycorrhizal (MYC) colonization presence, secondary xylem (SX) presence and continuous cork layer (CCL) presence across 2070 root segments from 23 tree species

	Order	Diameter class	Root diameter	Cortex thickness	Stele diameter	Stele : root diameter ratio	MYC presence	SX presence
Diameter class	0.615**							
Root diameter	0.613**	0.951**						
Cortex thickness	−0.597**	−0.156*	−0.166*					
Stele diameter	0.862**	0.794**	0.828**	−0.458**				
Stele : root diameter ratio	0.833**	0.464**	0.741**	−0.742**	0.862**			
MYC presence	−0.733**	−0.392**	−0.399**	0.615**	−0.664**	−0.718**		
SX presence	0.802**	0.374**	0.375**	−0.731**	0.717**	0.806**	−0.807**	
CCL presence	0.792**	0.378**	0.383**	−0.771**	0.717**	0.812**	−0.845**	0.934**

**, *, Correlation was significant at $P = 0.01$ and $P = 0.05$, respectively.

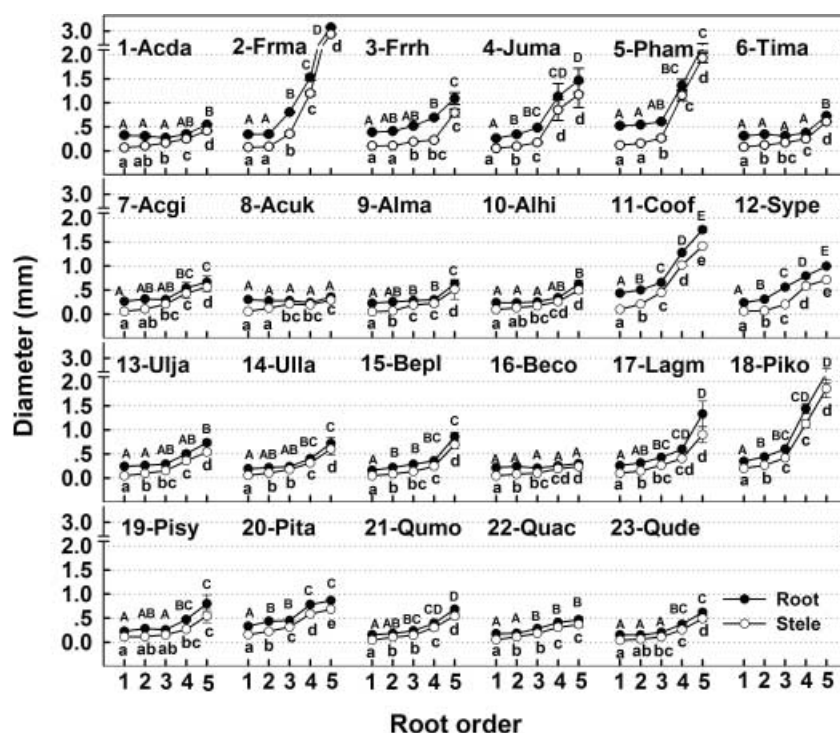


Fig. 1 Root diameter and stele diameter by branch order in 23 Chinese temperate tree species. Arbuscular mycorrhizal (AM) species, 1–6; AM and ectomycorrhizas (EM), 7–14; EM species, 15–23. See Table 1 for species abbreviations. Error bars represent 1 SE of the mean. Upper case letters that differ within a species indicate significant ($P < 0.05$) differences in root diameter among root orders, whereas lower case letters that differ within a species indicate significant ($P < 0.05$) differences in stele diameter among root orders.

successive orders (Fig. 1). Even in species whose root diameter remained constant in the first four or five orders, the stele diameter increased steadily and significantly with order, as in *Acer davidii*, *Acer ukurunduense*, *Alnus hirsuta*, *Betula costata*, *Tilia mandshurica*, and *Ulmus japonica* (Fig. 1).

Stele : root diameter ratio increased dramatically in the first three or four orders, but leveled off in higher orders in most species (Fig. 2). The magnitude of increase became much smaller from fourth to fifth order in 12 species, and from third to fourth order in eight species. The exceptions were *T. mandshurica*, *Quercus dentate*, and *Pinus koraiensis* whose stele : root diameter ratio increased constantly (almost linearly) with root order (Fig. 2). Overall, the greatest increase in

stele : root diameter ratio occurred most frequently between second and third order, or third and fourth order (Fig. 2).

Cortex thickness was either stable (fourteen species) or increased (seven species) in lower orders in most species. Cortex disappeared at a certain higher order, primarily at fourth order (18 species) (Fig. 3).

Mycorrhizal colonization was confined primarily to the first three orders (Table 3). Colonization rate generally declined with order in the first three orders. First order had the highest colonization rate, reaching 100% in eight out of nine EM species, six out of eight AM and EM species, and two out of six AM species. In comparison, third order had a colonization rate $< 50\%$ in 15 species with five species devoid of colonization.

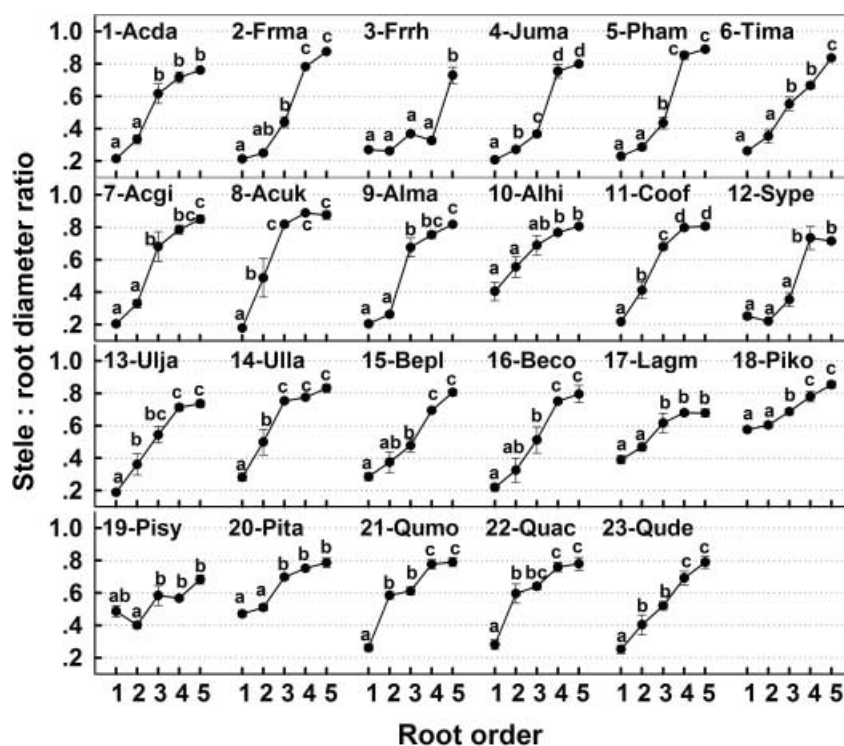


Fig. 2 Stele : root diameter ratio by branch order in 23 Chinese temperate tree species. Arbuscular mycorrhizal (AM) species, 1–6; AM and ectomycorrhizas (EM), 7–14; EM species, 15–23. See Table 1 for species abbreviations. Error bars represent 1 SE. Lower case letters that differ within a species indicate significant ($P < 0.05$) differences among root orders.

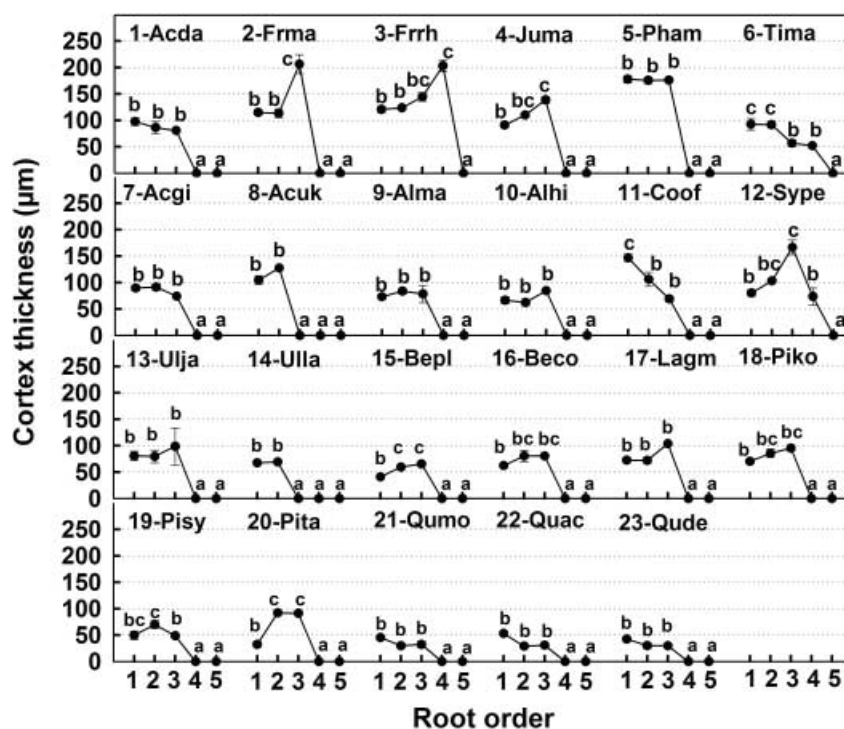


Fig. 3 Cortex thickness by branch order in 23 Chinese temperate species. Arbuscular mycorrhizal (AM) species, 1–6; AM and ectomycorrhizas (EM), 7–14; EM species, 15–23. See Table 1 for species abbreviations. Error bars represent 1 SE of the mean. Lower case letters that differ within a species indicate significant ($P < 0.05$) differences among root orders.

No mycorrhizal colonization was found in fourth and higher orders, with the only exception of *Fraxinus rhynchophylla* (Table 3).

Secondary development, as indicated by the presence of both SX and CCL occurred primarily in the fourth and higher

orders (Table 3). Secondary development did not occur in the first order roots of any species except *A. hirsuta*, and occurred in a portion of second- and third-order roots: 17–71% of second-order roots in eight species, 7–88% of third-order roots in 14 species, and all third order roots in five species

Table 3 Mycorrhizal colonization and secondary development of different root orders in 23 tree species

	Order 1			Order 2			Order 3			Order 4			Order 5		
	MC	SX	CCL	MC	SX	CCL	MC	SX	CCL	MC	SX	CCL	MC	SX	CCL
AM															
<i>Acer davidii</i>	+			++++			+	■	○		■	●		■	●
<i>Fraxinus mandschurica</i>	+			++			+	□	○		■	●		■	●
<i>Fraxinus rhynchophylla</i>	++++			++++			++++			++++				■	●
<i>Juglans Mandshurica</i>	+			+			+	□			■	●		■	●
<i>Phellodendron amurense</i>	+++			++++			+++	□	○		■	●		■	●
<i>Tilia mandshurica</i>	++++			++++				■	●		■	●		■	●
AM and EM															
<i>Acer ginnala</i>	++++			++++			+	□	○		■	●		■	●
<i>Acer ukurunduense</i>	++++			+	□	○		■	●		■	●		■	●
<i>Alnus mandshurica</i>	++++			++++			+	□	○		■	●		■	●
<i>Alnus hirsuta</i>	+++	□	○	+	□	○	+	□	○		■	●		■	●
<i>Cornus officinalis</i>	++++			++	□	○		■	●		■	●		■	●
<i>Ulmus laciniata</i>	++++			+	□	○		■	●		■	●		■	●
<i>Ulmus japonica</i>	++++			+++	□	○	+	□	○		■	●		■	●
<i>Syringa pekinensis</i>	+++			++++			++	□			■	●		■	●
EM															
<i>Betula costata</i>	++++			+++	□	○	+	□	○		■	●		■	●
<i>Betula platyphylla</i>	++++			++	□	○	++	■	○		■	●		■	●
<i>Larix gmelinii</i>	++++			++++			+	□	○		■	●		■	●
<i>Pinus koraiensis</i>	++++			++++			++++				■	●		■	●
<i>Pinus sylvestris</i> var. <i>mongolica</i>	++++			++++			++	□	○		■	●		■	●
<i>Pinus tabulaeformis</i>	++++			++++			+++	□	○		■	●		■	●
<i>Quercus acutissima</i>	+++			++	□	○	+	□	○		■	●		■	●
<i>Quercus dentata</i>	++++			++++			+++	□	○		■	●		■	●
<i>Quercus mongolica</i>	++++			+++				■	●		■	●		■	●

AM, arbuscular mycorrhizas; EM, ectomycorrhizas; MC, mycorrhizal colonization; SX, secondary xylem; CCL, continuous cork layer.

□, A portion of root segments observed had secondary xylem; ■, 100% roots observed had secondary xylem.

○, A portion of root segments observed had continuous cork layers; ●, 100% roots observed had secondary xylem.

+, ++, +++, +++++, colonization rates of 1–49%, 50–75%, 76–99%, and 100%, respectively.

Blanks mean that mycorrhizal colonization, secondary xylem, or cork layer were not observed in any root segments.

(*A. ukurunduense*, *Cornus officinalis*, *T. mandshurica*, *Ulmus laciniata* and *Quercus mongolica*). Secondary development occurred in all individual roots of fourth and fifth order in all but one species (i.e. *F. rhynchophylla*, Table 3).

Variations in root traits by diameter and diameter class

Root diameter, stele diameter, stele : root diameter ratio differed significantly by diameter class of 0.25-mm intervals whereas cortex thickness did not differ significantly (Table S1). In addition, Tukey's HSD tests found no significant differences in stele : root diameter ratio and cortex thickness among first three diameter classes (i.e. 0–0.25 mm, 0.25–0.5 mm and 0.5–0.75 mm, Table S2).

Across 23 species, significant correlations were found between diameter and most root traits. However, these correlations were weaker than those between root order and the same root traits (Table 2), and the same pattern was found across species of the same mycorrhizal type and taxonomy rank, or within each species (detailed results not shown).

Variations in root traits by mycorrhizal type and taxonomy rank

Stele : root diameter ratio and root diameter were the two key variables to separate all species into four groups along two function axes ($P < 0.05$, Fig. 4). Function 1 was mainly related to stele : root diameter ratio and distinguished angiosperms from gymnosperms, whereas function 2 was mainly related to root diameter and distinguished different mycorrhizal types in angiosperm species (Fig. 4). The discrimination rate was 74% with six mistakes out of 23 training samples, resulted from the incorrect categorization between AM and EM angiosperms and other angiosperms (Fig. 4).

Root length with uptake capacity and mycorrhizal colonization

A large proportion of the root length in the first five orders had root anatomical features associated with resource acquisition (e.g. large proportion of root cortex, low stele : root diameter ratio, no continuous cork layer) and mycorrhizal fungal

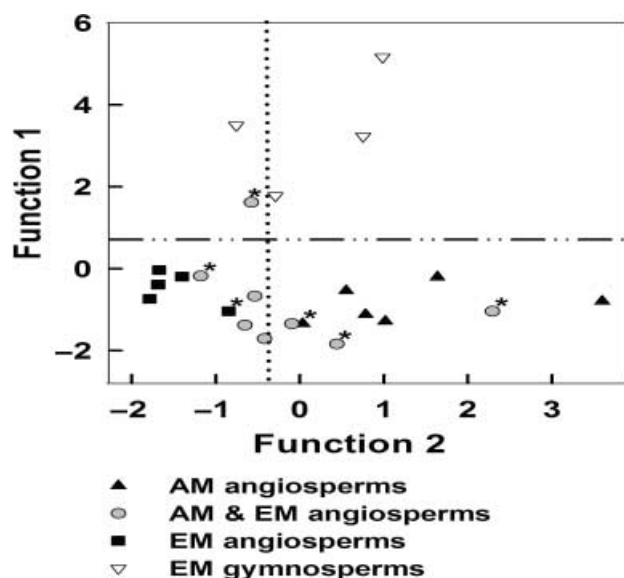


Fig. 4 Localization of 23 species of four groups defined by two discriminant functions. Function 1 was mainly related to stele : root diameter ratio; function 2 was mainly related to root diameter. AM, arbuscular mycorrhizal; EM, ectomycorrhizal. *, Species were categorized mistakenly by the discriminant analysis.

appearance. Averaged across species, the potentially absorptive length accounted for 75% of the total root length, ranging from 43% in *A. hirsuta* to 96% in *F. rhynchophylla* and *Syringa pекinensis*. Mycorrhizal length accounted for 68% of total root length, averaged across species, with a range of 22% in *Juglans mandshurica* to 96% in *F. rhynchophylla* (detailed results not shown).

Discussion

Anatomical features and functional roles of different branch orders

Anatomical traits differed significantly by root branch order within each species sampled in this study. As order increased, root diameter (Fig. 1), stele diameter (Fig. 1), stele : root diameter ratio (used to indicate transport capacity here) (Fig. 2) and the degree of secondary development such as presence of SX and CCL increased significantly (Table 3), whereas cortex thickness (Fig. 3) and mycorrhizal colonization rate declined significantly (Table 3).

Changes in root anatomy by branch order suggest that root segments of different branch order play different roles in root functioning. Based on the existence of the cortex, stele : root diameter ratio, mycorrhizal colonization rate, and CCL presence rate, five branch orders may be separated into two groups: roots with the primary function of resource uptake and roots serving functions other than absorption (Figs 1–3, Table 3). First-order roots had an intact cortex, a high mycorrhizal colonization rate, a low stele : root diameter ratio, and

showed no signs of secondary growth in all but one species, thus representing absorptive roots. By contrast, fourth- and higher-order roots had SX and CCL in all individual roots across all species except *F. rhynchophylla* (which lacked CCL in the fourth order). Moreover, the roots of these two orders had no cortex and mycorrhizal occurrence in all species, but a high stele : root diameter ratio. Therefore, they may have limited uptake capacity and primarily serve functions such as transport, anchorage, and storage. Second and third order showed some signs of secondary development, according to species (Table 3). Overall, the distal two or three orders seem to be the ones that are responsible for resource uptake in most species.

We recognized that anatomical traits, although tightly linked to root functions, are not direct measures of them. Therefore, our conclusions about functional roles of different branch orders need be validated by direct measures of root uptake and transport capacity in future studies. Nonetheless, the findings of this study represent a significant step forward in understanding the relationship between root form and root function.

The anatomical differences among branch orders found in this study might explain the systematic variations in root chemistry and lifespan with increasing order (Pregitzer *et al.*, 2002; Guo *et al.*, 2004, 2008a), and the role of different root orders in ecosystem C and nutrient cycling (Guo *et al.*, 2008b). Our results showed that first-order roots comprised mostly cortical cells (Figs 1–3). Cortical cells generally have high metabolic rate and require higher concentrations of nitrogen and phosphorus to support their physiological activity (Lux *et al.*, 2004). Thus, it is hardly surprising to find the highest concentrations of nitrogen (Pregitzer *et al.*, 2002; Guo *et al.*, 2004) and respiration rates (Pregitzer *et al.*, 1998; D.L. Guo, unpublished) in first-order roots. In addition, cortical cells are easily damaged or lost under stress (Brundrett, 2002; Wells & Eissenstat, 2003; Soukup *et al.*, 2004), which renders first-order roots the most ephemeral of all orders. Their short lifespan, combined with their considerable biomass, make the first-order roots the biggest contributor to root turnover among all branch orders (Guo *et al.*, 2008a,b). By contrast, fourth and fifth order were mainly composed of secondary vascular tissues which are known to have low physiological activity because of the large proportion of dead cells (Pregitzer *et al.*, 2002), and thus require low concentrations of nitrogen (Guo *et al.*, 2004), and probably have low respiration rates. Moreover, the well-developed cork layer and secondary xylem can protect roots from environmental stresses and herbivore pressure (Brundrett, 2002), ensuring high-order roots long life spans, and thus, low turnover rates (Wells & Eissenstat, 2003; Guo *et al.*, 2008a,b).

Our results also revealed which roots in the tree fine-root systems might be colonized by mycorrhizal fungi. Mycorrhizal colonization was found in the first to third order in 18 species, but was absent in the fourth and fifth orders in all species except *F. rhynchophylla* (Table 3). Our results confirm the general view that first-order roots are preferentially colonized

(Pregitzer, 2002), but show that at least two more branch orders can be colonized (Fig. 3, Table 3). Therefore, quantifying mycorrhizas in roots must go beyond first-order root tips.

Moreover, we found that mycorrhizal colonization rate was generally higher in EM than AM species (Table 3). In particular, first-order root tips had 100% colonization rate in all but one EM but not in AM species (Table 3), supporting the notion that EM species rely heavily on mycorrhizal fungi for resource uptake (Read & Perez-Moreno, 2003; Chapman *et al.*, 2006).

The correspondence between root anatomy and branch order suggest that branch order can be used as a tool to separate roots of different functions. However, our results also support the possibility that several orders might form a functional module as proposed by Pregitzer *et al.* (2002) because first two or three order roots were similar in anatomy. We noted that the number of branch orders that were confined to primary development differed markedly by species (Table 3) so that the functional module, if exists, may have different architecture in different species. Future studies linking root anatomy, physiology, and demography on the branching fine root systems may better resolve the precise definition of functional root modules in trees.

Diameter classes and anatomical features

Our results support the proposition that a single diameter class cannot be used to define functional root module (or 'fine roots' in the traditional sense) across multiple species (see Pregitzer, 2002) because the diameter of the same branch order varied markedly across species (Fig. 1). Given the relatively consistent linkage between order and anatomy across species (i.e. first-order roots had primary development in all but one species, and fourth-order roots had secondary development in all but one species, Table 3), wide variations in diameter of the same order make a single diameter class unreliable in comparing roots of same functions across species (Fig. 1). For example, *Phellodendron amurense* had a first-order root diameter of > 0.5 mm, which is similar to the fifth order root diameter in *A. davidii*, *A. ukurunduense*, *B. costata*, and *Quercus acutissima* (Fig. 1).

Even within species, root diameter (a continuous variable) or diameter class fails as a reliable tool for root functional classification because in some species diameter was relatively constant yet root anatomy clearly changed. For example, diameter did not change significantly in the first four or five orders in *A. davidii*, *A. ukurunduense*, *A. hirsuta*, *B. costata*, *T. mandshurica*, and *U. japonica* (Fig. 1), but shifts of root anatomy occurred as order increased (Table 3). Therefore, in these species, diameter obscures critical changes such as the loss of cortex and mycorrhizal colonization, and the appearance of SX and CCL as order increased. The generally weak correlation between diameter (or diameter classes of 0.25 mm intervals) and root anatomical indices (Table 2) supports the notion that diameter was an inferior predictor of root anatomical change than branch order.

Anatomical differences by taxonomic rank and mycorrhizal type

Stele : root diameter ratio of first-order roots was the primary trait distinguishing gymnosperms from angiosperms (Fig. 4). Gymnosperms had higher stele : root diameter ratios (Figs 2 and 4), and thus a higher stele and lower cortex proportion than angiosperms, which probably reflects the inherent differences between these two groups. The gymnosperms studied here are all conifers, which are known to have xeromorphic foliage that reduces water loss (Richardson & Berlyn, 2002). The greater stele proportion in first-order roots of these conifers may also be a xeromorphic feature that facilitates water uptake and transport. Another explanation is that tracheids in conifers have lower conductivity than vessels in angiosperms so that more of them are needed by conifers to achieve a transport capacity comparable to that of angiosperms (Sperry *et al.*, 2006). Notably, the difference in stele : root diameter ratio between gymnosperms and angiosperms disappeared in the fourth- and higher-order roots (Fig. 2).

By contrast, the diameter of first-order roots was the major trait separating different mycorrhizal types in angiosperm species. The AM angiosperms had greater diameter and cortex area than EM and AM & EM angiosperms (Figs 1–3), which probably reflects the advantage of AM fungi in roots that have greater cortex area (Brundrett, 2002).

Root length with uptake capacity and mycorrhizal colonization

Our study provided estimates of the absorptive and mycorrhizal length proportions in the first five orders based on anatomical evidence. Averaged across species, the absorptive length accounted for 75%, and the mycorrhizal length for 68% of the total root length in the first five orders. Even though these estimates were based on one-time sampling, a limited number of species and indirect methods, they represent an improvement from the total absorptive root length estimates based solely on 0–2 mm diameter class, which considered all fine root length as being equally absorptive (Jackson *et al.*, 1997). Assuming that the total fine root length for the 0–2 mm diameter class included only the first five orders (a conservative assumption, as indicated by our data showing that 18 out of 23 species contained at least five orders within the < 1.5 mm diameter class, Fig. 1), the absorptive length estimated based on root anatomy would be 25% less than the estimates based on diameter class in temperate forests.

Conclusions

For the past several decades, roots have been one of the least understood components of plant functioning and ecosystem material cycling, largely owing to the inability of linking root structure and function (Wells & Eissenstat, 2001; Pregitzer

et al., 2002; Withington *et al.*, 2006). Our results showed that branch order relatively consistently predicted anatomical changes in the branching fine root system across 23 temperate tree species. Therefore, branch order may serve as a useful tool to distinguish the roots that are confined to primary development, and are mainly absorptive and mycorrhizal, from the roots that have lost their cortex and undergone secondary development, and thus perform mainly transport, anchorage and storage functions. Specifically, we showed that first two orders were primarily absorptive and mycorrhizal roots, and that shifts of root function from uptake to transport appeared to occur at the third or fourth order in most species.

The correspondence between root anatomy and branch order reported here, along with the growing appreciation that distal two or three branch orders have much shorter life spans than higher orders (Withington *et al.*, 2006; Guo *et al.*, 2008 a,b) show that these smallest distal roots (possibly as modular units) play a disproportionately important role in resource acquisition and ecosystem carbon and nutrient flux. Future studies linking anatomy, demography and physiology on the branching fine root network should lead to a better understanding of functional modules in plant root systems.

Acknowledgements

We thank Youzhi Han, Jinliang Liu and Wei Shi for assistance in the field and laboratory, and Drs Dave Eissenstat, Harbin Li, Kurt Pregitzer and an anonymous reviewer for valuable comments. The funding for this research was provided by Natural Science Foundation of China (NSFC Grants 90511002 and 30130160).

References

- Berntson GM. 1997. Topological scaling and plant root system architecture: developmental and functional hierarchies. *New Phytologist* 135: 621–634.
- Bloom AJ, Caldwell RM. 1988. Root excision decreases nutrient absorption and gas fluxes. *Plant Physiology* 87: 794–796.
- Brundrett MC. 2002. Coevolution of roots and mycorrhizas of land plants. *New Phytologist* 154: 275–304.
- Brundrett MC. 2004. Diversity and classification of mycorrhizal associations. *Biological Reviews* 78: 473–495.
- Chapman SK, Langley JA, Hart SC, Koch GW. 2006. Plants actively control nitrogen cycling: uncorking the microbial bottleneck. *New Phytologist* 169: 27–34.
- Eissenstat DM, Achor DS. 1999. Anatomical characteristics of roots of citrus rootstocks that vary in specific root length. *New Phytologist* 141: 309–321.
- Enstone DE, Peterson CA, Hallgren SW. 2001. Anatomy of seedling tap roots of loblolly pine (*Pinus taeda* L.). *Trees – Structure and Function* 15: 98–111.
- Esau K. 1977. *Anatomy of seed plants*, 2nd edn. New York, NY, USA: Wiley, 215–255.
- Fitter AH. 1982. Morphometric analysis of root systems: application of the technique and influence of soil fertility on root system development in two herbaceous species. *Plant, Cell & Environment* 5: 313–322.
- Fitter AH. 1987. An architectural approach to the comparative ecology of plant root systems. *New Phytologist* 106: 61–77.
- Gong ZT, Chen ZC, Luo GB, Zhang GL, Zhao WJ. 1999. Soil reference with Chinese soil taxonomy. *Soils* 31: 57–63 (in Chinese).
- Guo DL, Li H, Mitchell RJ, Han WX, Hendricks JJ, Fahey TJ, Hendrick RL. 2008a. Heterogeneity by root branch order: exploring the discrepancy in root longevity and turnover estimates between Minirhizotron and C isotope methods. *New Phytologist* 177: 443–456.
- Guo DL, Mitchell RJ, Hendricks JJ. 2004. Fine root branch orders respond differentially to carbon source-sink manipulations in a longleaf pine forest. *Oecologia* 140: 450–457.
- Guo DL, Mitchell RJ, Withington JM, Fan PP, Hendricks JJ. 2008b. Endogenous and exogenous controls of root lifespan, mortality and nitrogen flux in a longleaf pine forest: root branch order predominates. *Journal of Ecology* 96: 737–745.
- Hishi T. 2007. Heterogeneity of individual roots within the fine root architecture: causal links between physiological and ecosystem functions. *Journal of Forest Research* 12: 126–133.
- Jackson RB, Mooney HA, Schulze ED. 1997. A global budget for fine root biomass, surface area, and nutrient contents. *Proceedings of the National Academy of Sciences, USA* 94: 7362–7366.
- Joslin JD, Gaudinski JB, Torn MS, Riley WJ, Hanson PJ. 2006. Fine-root turnover patterns and their relationship to root diameter and soil depth in a ¹⁴C-labeled hardwood forest. *New Phytologist* 172: 523–535.
- Kumar P, Hallgren SW, Enstone DE, Peterson CA. 2007. Root anatomy of *Pinus taeda* L. seasonal and environmental effects on development in seedlings. *Trees-Structure and Function* 21: 693–706.
- Land Environmental Protection Department of Beijing Municipal Planning Committee. 1988. *Land and resources of Beijing*. Beijing, China: Beijing Science and Technology Press, 117–120 (in Chinese).
- Lucash MS, Eissenstat DM, Joslin JD, McFarlane KJ, Yanai RD. 2007. Estimating nutrient uptake by mature tree roots under field conditions: challenges and opportunities. *Trees – Structure and Function* 21: 593–603.
- Lux A, Luxova M, Abe J, Morita S. 2004. Root cortex: structural and functional variability and responses to environmental stress. *Root Research* 13: 117–131.
- Majdi H, Damm E, Nylund JE. 2001. Longevity of mycorrhizal roots depends on branching order and nutrient variability. *New Phytologist* 150: 195–202.
- McClagherty CA, Aber JD, Melillo JM. 1982. The role of fine roots in the organic matter and nitrogen budgets of two forested ecosystems. *Ecology* 63: 1481–1490.
- McKenzie BE, Peterson CA. 1995a. Root browning in *Pinus banksiana* Lamb. and *Eucalyptus Pilularis* Sm. 1. Anatomy and permeability of the white and tannin zones. *Botanica Acta* 108: 127–137.
- McKenzie BE, Peterson CA. 1995b. Root browning in *Pinus banksiana* Lamb. and *Eucalyptus Pilularis* Sm. 2. Anatomy and permeability of the white and tannin zones. *Botanica Acta* 108: 138–143.
- de Neergaard E, Lyshede OB, Gahoonia TS, Care D, Hooker JE. 2000. Anatomy and histology of roots and root-soil boundary. In: Smit AL, Bengough AG, Engels C, Noordwijk M, Pellerin S, Geijn SC, eds. *Root Methods: A Handbook*. Berlin, Germany: Springer-Verlag, 33–74.
- Peterson CA, Enstone DE, Taylor JH. 1999. Pine root structure and its potential significance for root function. *Plant and Soil* 217: 205–213.
- Pregitzer KS. 2002. The fine roots of trees – a new perspective. *New Phytologist* 156: 267–270.
- Pregitzer KS, Deforest JL, Burton AJ, Allen MF, Ruess RW, Hendrick RL. 2002. Fine root architecture of nine North American trees. *Ecological Monographs* 72: 293–309.
- Pregitzer KS, Laskowski MJ, Burton AJ, Lessard VC, Zak DR. 1998. Variation in sugar maple root respiration with root diameter and soil depth. *Tree Physiology* 18: 665–670.
- Read DJ, Perez-Moreno J. 2003. Mycorrhizas and nutrient cycling in ecosystems – a journey towards relevance? *New Phytologist* 157: 475–492.

- Richardson A, Berlyn GP. 2002. Changes in foliar spectral reflectance and chlorophyll fluorescence of four temperate species following branch cutting. *Tree Physiology* 22: 499–506.
- Robinson D, Hodge A, Fitter AH. 2003. Constraints on the form and function of root systems. In: de Kroon H, Visser EJW, eds. *Root ecology. Ecological studies*, Vol. 168. Berlin, Germany: Springer-Verlag, 7–18.
- Soukup A, Mala J, Hrubcova M, Kalal J, Votrubova O, Cvikrova M. 2004. Differences in anatomical structure and lignin content of roots of pedunculate oak and wild cherry-tree plantlets during acclimation. *Biologia Plantarum* 48: 481–489.
- Sperry JS, Hacke UG, Pittermann J. 2006. Size and function in conifer tracheids and angiosperm vessels. *American Journal of Botany* 93: 1490–1500.
- Taylor JH, Peterson PA. 2000. Morphometric analysis of *Pinus banksiana* Lamb. root anatomy during a 3-month field study. *Trees-Structure and Function* 14: 239–247.
- Vierheilig H, Schweiger P, Brundrett M. 2005. An overview of methods for the detection and observation of arbuscular mycorrhizal fungi in roots. *Physiologia Plantarum* 125: 393–404.
- Volder A, Smart DR, Bloom AJ, Eissenstat DM. 2005. Rapid decline in nitrate uptake and respiration with age in fine lateral roots of grape: implications for root efficiency and competitive effectiveness. *New Phytologist* 165: 493–502.
- Wells CE, Eissenstat DM. 2001. Marked differences in survivorship among apple roots of different diameters. *Ecology* 82: 882–892.
- Wells CE, Eissenstat DM. 2003. Beyond the roots of young seedlings: the influence of age and order on fine root physiology. *Journal of Plant Growth Regulation* 21: 324–334.
- Wells CE, Glenn DM, Eissenstat DM. 2002. Changes in the risk of fine-root mortality with age: a case study in peach, *Prunus persica* (Rosaceae). *American Journal of Botany* 89: 79–87.
- Withington JM, Reich PB, Oleksyn J, Eissenstat DM. 2006. Comparisons of structure and life span in roots and leaves among temperate trees. *Ecological Monographs* 76: 381–397.
- Zar JH. 1999. *Biostatistical analysis*, 4th edn. Upper saddle River, NJ, USA: Prentice Hall, 178–206.
- Zhou XF. 1994. *Long-term research on China's forest ecosystems*. Harbin, China: Northeast Forestry University Press, 213–221 (in Chinese).

Supporting Information

Additional supporting information may be found in the online version of this article.

Fig. S1 Light micrograph of root cross-sections.

Table S1 Results of mixed-level three-way factorial ANOVA

Table S2 Root diameter, cortex thickness, stele diameter, and stele : root ratio by order and diameter class of 0.25-mm intervals

Please note: Wiley-Blackwell are not responsible for the content or functionality of any supporting information supplied by the authors. Any queries (other than missing material) should be directed to the journal at *New Phytologist* Central Office.



About New Phytologist

- *New Phytologist* is owned by a non-profit-making **charitable trust** dedicated to the promotion of plant science, facilitating projects from symposia to open access for our Tansley reviews. Complete information is available at www.newphytologist.org.
- Regular papers, Letters, Research reviews, Rapid reports and both Modelling/Theory and Methods papers are encouraged. We are committed to rapid processing, from online submission through to publication 'as-ready' via *Early View* – our average submission to decision time is just 29 days. Online-only colour is **free**, and essential print colour costs will be met if necessary. We also provide 25 offprints as well as a PDF for each article.
- For online summaries and ToC alerts, go to the website and click on 'Journal online'. You can take out a **personal subscription** to the journal for a fraction of the institutional price. Rates start at £135 in Europe/\$251 in the USA & Canada for the online edition (click on 'Subscribe' at the website).
- If you have any questions, do get in touch with Central Office (newphytol@lancaster.ac.uk; tel +44 1524 594691) or, for a local contact in North America, the US Office (newphytol@ornl.gov; tel +1 865 576 5261).

2007 年发表论文

冬季土壤呼吸:不可忽视的地气 CO₂ 交换过程

王 妮 汪 涛 彭书时 方精云

(北京大学环境学院生态学系,北京 100871)

摘 要 冬季土壤呼吸是生态系统释放 CO₂ 的极为重要的组成部分,并显著地影响着碳收支。然而,过去绝大多数工作集中在生长季节土壤呼吸的测定,对年土壤呼吸量的估算大多基于冬季土壤呼吸为零的假设。目前为数不多的研究集中在极地苔原和亚高山,其它植被类型的研究只有零星报道。极地苔原和森林冬季土壤呼吸速率分别为 0.002 ~ 1.359 和 0.22 ~ 0.67 $\mu\text{mol C m}^{-2} \cdot \text{s}^{-1}$;土壤呼吸的 CO₂ 释放量分别为 0.55 ~ 26.37 和 22.4 ~ 152.0 g C m^{-2} ,是地气 CO₂ 交换过程中不可忽视的环节。雪是土壤呼吸过程的重要调节者,积雪厚度和覆盖时间的长短均会影响土壤呼吸的强弱;水分的可获取性是重要的限制因素;对于维持活跃的土壤呼吸有一个关键的土壤温度临界值(-7 ~ -5 °C),低于这个值会因自由水的缺乏而抑制异养微生物的呼吸。如果存在绝缘的积雪层,可溶性碳底物在自由水存在的情况下可控制异养微生物的活力。该文对冬季土壤呼吸的重要性、研究方法、土壤呼吸强度及其影响机制等进行了综述,并讨论了冬季土壤呼吸研究中存在的问题及未来研究方向。

关键词 冬季土壤呼吸 碳收支 雪 冻原 森林

REVIEW OF WINTER CO₂ EFFLUX FROM SOILS: A KEY PROCESS OF CO₂ EXCHANGE BETWEEN SOIL AND ATMOSPHERE

WANG Wei, WANG Tao, PENG Shu-Shi, and FANG Jing-Yun

Department of Ecology, College of Environmental Sciences, Key Laboratory for Earth Surface Processes of Ministry of Education, Peking University, Beijing 100871, China

Abstract Winter CO₂ efflux from soils is a significant component of annual carbon budgets and can greatly determine carbon balance of ecosystems. However, present estimates of annual soil respiration are mostly based on measurements taken during the growing season and assume that microbial respiration in frozen or snow-covered soils is negligible. We analyze methods used, magnitude of winter soil respiration, and influencing factors. There are very few measurements of winter soil respiration except in tundra and alpine ecosystems. Winter CO₂ efflux from soils ranged from 0.002 to 1.359 $\mu\text{mol C m}^{-2} \cdot \text{s}^{-1}$ and 0.22 to 0.67 $\mu\text{mol C m}^{-2} \cdot \text{s}^{-1}$ in tundra and forest ecosystems, respectively. No direct relationship between soil temperature and winter CO₂ efflux from soils was found, but there is a critical threshold for active respiration, typically between -7 and -5 °C, below which lack of free water limits microbial contributions to winter soil respiration. The depth, timing and duration of snow cover greatly influence the magnitude of winter CO₂ efflux from soils, with water availability an important limiting factor. If insulating snowpack is present, carbon availability also controls heterotrophic activity. We discuss current problems and future research needs.

Key words winter soil respiration, carbon sequestration, snow, tundra, forest

土壤呼吸是植物固定的碳以 CO₂ 形式返回到大气中的主要途径,是陆地生态系统碳循环的重要环节。理解土壤呼吸的季节动态对于估算生态系统的碳收支,模拟气候变化对土壤碳固存和 CO₂ 向大气释放的影响(Chapin *et al.*, 1996)及估算植物的地下碳分配(Gardina & Ryan, 2002)均具有重要的意义。

过去绝大多数工作集中在生长季节土壤呼吸的测定,对年土壤呼吸量的估算大多基于冬季土壤呼

吸为零的假设(Fahnestock *et al.*, 1998)。然而,近10年来的研究表明,冬季土壤呼吸占年土壤呼吸量的14% ~ 30%(Jones, 1999)。由于积雪能够防止土壤冻结,维持了微生物较高的活力(Decker *et al.*, 2003; Schmidt & Lipson, 2004; Brooks *et al.*, 2004; Goffman *et al.*, 2001, 2006; Monson *et al.*, 2006b)。冬季土壤呼吸释放的 CO₂ 是区域碳收支非常重要的组成部分(Mast *et al.*, 1998; Mariko *et al.*, 2000;

Welker *et al.*, 2000; Wickland *et al.*, 2001; Uchida *et al.*, 2005; Schimel *et al.*, 2006), 并显著地影响着生态系统的碳平衡 (Hubbard *et al.*, 2005; Monson, 2005)。

随着全球变暖, 尤其是冬季增温和雪覆盖的减少, 冬季土壤呼吸对区域和全球碳循环的贡献显得更为重要。在过去的 100 年里, 全球平均地表温度升高了 0.6 °C, 降水每 10 年增加 0.5 % ~ 1 %, 雪覆盖减少了 10 % (Houghton *et al.*, 2001; IPCC, 2001)。如在美国和欧洲西部的山地, 冬季积雪大范围减少 (Latenser & Schneebeli, 2003; Mote *et al.*, 2005)。积雪的减少导致土壤呼吸速率降低 (Monson *et al.*, 2006b), 提高了土壤碳固存的潜力。

全球气候变化还通过改变土壤呼吸对温度的敏感性来影响冬季土壤呼吸。区域和全球碳循环模型通常都采用一个单一和固定的 Q_{10} 来描述土壤呼吸和温度之间的关系 (Fung *et al.*, 1987; Kicklighter, 1994)。然而, 目前已有的 Q_{10} 的估算大多基于生长季节野外观测或室内培养的结果 (Lloyd & Taylor, 1994; Rustad & Fernandez, 1998), 没有考虑冬季土壤呼吸对温度的敏感性。研究表明, 土壤呼吸的 Q_{10} 值在寒冷条件下可高达 60 ~ 200, 而零上温度时 Q_{10} 最大值仅为 9 (Mikan *et al.*, 2002)。

因此, 冬季土壤呼吸的研究对于精确测定生态系统的碳收支和土壤碳固存及其对温室效应的贡献、改善区域和全球的碳循环模型、预测生态系统对全球变化的响应及其相互作用具有重要意义。本文从冬季土壤呼吸的测定方法、土壤呼吸强度及其影响因素 3 个方面进行了综述, 并讨论了冬季土壤呼吸研究中存在的问题及未来研究方向。

1 冬季土壤呼吸速率的测定方法

冬季土壤呼吸的测定主要包括两种方法, 一种是通过扩散模型 (Sommerfeld *et al.*, 1993; Massman *et al.*, 1995; Brooks *et al.*, 1997) 进行间接估算, 另一种是通过动态气室法进行直接测量 (Winston *et al.*, 1995; Kurganova *et al.*, 2003)。McDowell 等 (2000) 比较了这两种方法, 认为第一种方法最为可信。目前, 通过扩散模型的方法被普遍认为是国际标准方法。

1.1 土壤和雪表面 CO₂ 浓度梯度的扩散模型

1.1.1 Fick 定律及其 3 种表达式

目前共有 3 种模型表达式, 均是在 Fick 定律的基础上进行不断改进的。对于一定温度和压力下的

一维定态扩散, 假定稳定状态, 并忽略水分运动的影响, CO₂ 和大气之间的扩散模型可以用 Fick 第一定律来表示 (de Jong & Schappert, 1971; Cerling, 1984; Collin & Rasmuson, 1988):

$$F = - D_e \frac{dC(x)}{dx} \quad (1)$$

其中, D_e 为扩散系数, C 为深度为 x 的 CO₂ 浓度。土壤中 CO₂ 扩散速率和化学反应共同决定 CO₂ 浓度梯度, 可通过 Fick 第二定律来描述 (Cerling, 1984)。

$$\frac{\partial^2 C}{\partial x^2} = \frac{R}{D_e} \quad (2)$$

其中, R 为单位体积土壤的净消耗速率 (或生产速率, 如果 R 为负值)。该模型的前提条件是 D_e 和 R 不随深度而改变。土壤中测定的 CO₂ 浓度可近似等于 $\frac{\partial^2 C}{\partial x^2}$ 。已知 D_e 就可以求得土壤剖面任意点的 R 值。

该模型的优点在于参数少, 操作简便。缺点在于没有考虑到雪的特性, 例如雪的密度、阻力和通气性等对土壤呼吸的影响。

Sommerfeld 等 (1993) 对上述模型进行了改进:

$$J_g = D_g \frac{d[g]}{dz} f \quad (3)$$

其中, J_g 为土壤呼吸, D_g 为扩散系数, $\frac{d[g]}{dz}$ 为 CO₂ 浓度的垂直梯度, t 为阻力系数, f 为通气性。该模型的缺点在于没有校正温度和大气压对 CO₂ 摩尔体积的影响。

Massman 等 (1995) 对上述模型进一步改进:

$$J_g = f t D \frac{P_0}{RT_0} \left(\frac{T}{T_0} \right)^{0.81} \frac{d[g]}{dz} \quad (4)$$

其中, $\frac{P_0}{RT_0}$ 为 CO₂ 在 STP 下的分子密度 (44.63 mol m⁻³)。该模型表达式是目前最为理想的估算冬季土壤呼吸的方法。

1.1.2 模型参数的获取

尽管扩散模型被认为是广为接受的国际标准方法, 但模型中参数的获取还存在极大的不确定性。模型中参数的准确性是决定冬季土壤呼吸估算的关键所在。

1.1.2.1 CO₂ 浓度

CO₂ 浓度的测定通常采取挖雪壕沟 (Snowpits) 的方法 (Sommerfeld *et al.*, 1993)。首先挖雪壕沟, 在雪与土壤界面放置直径为 4.2 cm、长为 5 cm 的 PVC 管, 两头用 200 目的筛网封住, 并连接内径为 0.32

cm 的塑料管的一端,塑料管的另一端用夹子夹上并固定于树上(离地面 2 m)。土壤-雪界面之间的 CO₂ 浓度及雪表面的大气 CO₂ 浓度通过移走一定体积的空气,采用红外气体分析仪(Brooks *et al.*, 1999; Welker *et al.*, 2000)或利用注射器抽取样品,带回实验室采用气象色谱法测定(Brooks *et al.*, 1997)。

1.1.2.2 其它参数

CO₂ 的扩散系数通常采用常值 0.129 cm²·s⁻¹ (Fahnestock *et al.*, 1999)。雪的密度通过每 10 cm 雪层密度的平均值求得。绝大多数研究通过密度来推导通气性(*f*)。通气性目前有 3 种不同的算法:

- (1) $f = 1 / \text{冰的密度}$ (Brooks *et al.*, 1997);
- (2) $f = (1 - \text{雪的密度}) / \text{冰的密度}$ (Welker *et al.*, 2000)
- (3) $f = 1 - (\text{雪的密度} / \text{冰的密度})$ (Hubbard *et al.*, 2005)

通过实际测定得到的通气性和通过密度推导得到的结果的可比性目前还不清楚,需进一步研究以提高测量的准确性。阻力系数是一个耗时且难以估测的参数(Winston *et al.*, 1995; Massman *et al.*, 1997),目前或是作为通气性的函数(Brooks *et al.*, 1997; McDowell *et al.*, 2000),或者假定它是一个常量 0.35 (Sommerfeld *et al.*, 1996; Welker *et al.*, 2000),或者直接测定(Winston *et al.*, 1995; Massman *et al.*, 1997)进行估算。直接测定和作为通气性函数在相似的深度和密度剖面下获得的数值分别为 0.75 ~ 0.94 (Massman *et al.*, 1997)和 0.84 ~ 0.92 (Hubbard *et al.*, 2005)。此外,雪的厚度空间变异非常大,准确的测量对于精确估算土壤呼吸速率也是非常关键的。

1.2 动态气室法

采用较长的土壤环(视雪的厚度而定)预先插入土壤,稳定一段时间后,直接采用土壤呼吸仪进行测量(Winston *et al.*, 1995; Kurganova *et al.*, 2003)。该方法比较适用于雪层较薄(<30 cm)时土壤呼吸速率的测定。优点在于简便、快速、参数少、数据的不确定性小。缺点在于仪器较为昂贵,低温下使用土壤呼吸仪进行直接测定较不稳定,超过仪器的工作范围便不能使用。

2 冬季土壤呼吸速率的大小

目前有关冬季土壤呼吸的研究主要集中在极地苔原(Zimov *et al.*, 1996; Brooks *et al.*, 1997; Fahnestock *et al.*, 1998, 1999; Welker *et al.*, 2000;

Wickland *et al.*, 2001; Schimel & Mikan, 2005; Grogan & Jonasson, 2006; Elberling, 2007),对于森林的研究较少,主要集中在亚高山(Sommerfeld *et al.*, 1993, 1996; Winston *et al.*, 1995; Kurganova *et al.*, 2003; Wang *et al.*, 2003)。其它生态系统类型冬季土壤呼吸的研究偶见报道。

2.1 极地苔原

不同群落类型土壤呼吸速率变化很大。如高山带下部 9 种群落土壤呼吸速率为 0.002 ~ 1.359 μmol C·m⁻²·s⁻¹ (表 1),高山带上部 3 种群落为 0.11 ~ 0.28 μmol C·m⁻²·s⁻¹ (Elberling, 2007)。Jones (1999) 估算了美国阿拉斯加 4 种群落,其 11 月土壤呼吸速率平均为 0.05 ~ 0.14 μmol C·m⁻²·s⁻¹, 4 月平均为 0.02 ~ 0.05 μmol C·m⁻²·s⁻¹。

极地苔原冬季土壤呼吸释放的 CO₂ 是年碳收支非常重要的组成部分,并显著地影响生态系统的源汇功能(Hubbard *et al.*, 2005; Monson, 2005)。如高山带下部 9 种群落冬季 CO₂ 排放量为 0.55 ~ 26.37 g C·m⁻² (平均为 12.30 g C·m⁻²),将冬季(11 月 ~ 翌年 4 月)释放量纳入年释放量可提高 CO₂ 释放量的 17%,使某些生态系统从净碳库转变为碳源。高山带上部 3 种群落冬季 CO₂ 排放量为 14.42 ~ 45.6 g C·m⁻²,占年土壤呼吸的 14% ~ 30% (Elberling, 2007)。潮湿的苔原和草甸苔原冬季平均 CO₂ 排放量高达 120 和 60 g C·m⁻² (Schimel *et al.*, 2006)。

2.2 森林

目前对森林的测定仅见几则报道。与极地苔原相比,森林具有较高的土壤呼吸速率。已有研究表明:森林土壤呼吸速率为 0.22 ~ 0.67 μmol C·m⁻²·s⁻¹ (Sommerfeld *et al.*, 1996; McDowell *et al.*, 2000; Hubbard *et al.*, 2005; Suzuki *et al.*, 2006)。如 Hubbard 等(2005)报道了 300 年和 50 年亚高山土壤呼吸速率平均为 0.22 μmol C·m⁻²·s⁻¹ (12 月和翌年 1 月),5 月升至 0.61 μmol C·m⁻²·s⁻¹,平均为 0.35 和 0.31 μmol C·m⁻²·s⁻¹。华盛顿州一个混生针叶林土壤呼吸速率可高达 0.67 μmol C·m⁻²·s⁻¹ (McDowell *et al.*, 2000)。Sommerfeld 等(1996)估算,美国怀俄明云杉(*Picea asperata*)林土壤呼吸速率平均为 0.52 μmol C·m⁻²·s⁻¹。Suzuki 等(2006)估算,日本一个落叶阔叶林土壤呼吸平均为 (0.37 ± 0.26) μmol C·m⁻²·s⁻¹。

已有研究表明:森林冬季土壤呼吸的 CO₂ 排放量平均为 94.9 g C·m⁻² (表 2)。最小值出现在日本一个寒温带落叶阔叶林,为 22.4 g C·m⁻²,占年释

放量的 15 % (Mariko *et al.* , 2000) , 最大值出现在美国科罗拉多州的针叶林 (Monson *et al.* ,2002) ,为 145 g C · m⁻² 。针叶林冬季土壤呼吸为 40 ~ 145 g C · m⁻² ,平均为 89.1 g C · m⁻² ,变异系数达 43 % ;落叶林为 22 ~ 152 g C · m⁻² ,平均为 103.3 g C · m⁻² ,变异系数达 46 % 。

森林冬季土壤呼吸也是区域碳收支非常重要的组成部分。如日本的落叶阔叶林冬季土壤呼吸占冬季生态系统呼吸的 35 % ~ 48 % 、年生态系统呼吸的 7 % ~ 10 % (Suzuki *et al.* ,2006) 。不考虑冬季土壤呼吸导致落叶林和针叶林净生态系统交换量 (*NEE*) 则分别高估 48 % (- 244 vs. - 165 g C · m⁻²) 和 90 % (- 167 vs. - 79 g C · m⁻²) (Brooks *et al.* , 2004) 。亚高山冬季土壤呼吸相当于森林年总初级生产力

(*GPP*) 的 8 % (Hubbard *et al.* , 2005) ~ 25 % (Sommerfeld *et al.* , 1993) 、净初级生产力 (*NPP*) 的 80 % (Ryan & Waring ,1992) 。西伯利亚针叶林雪覆盖下土壤 CO₂ 释放量占年总初级生产力的 60 % (Zimov *et al.* , 1993) 。

3 冬季土壤呼吸的影响因素

3.1 雪

冬季北半球近 50 % 的陆地生态系统被雪覆盖 (Sommerfeld *et al.* , 1993) 。雪是土壤过程的重要调节者 ,持续的雪覆盖能有效地隔离土壤与大气 ,起着绝缘体的作用 ,通常能够防止土壤冻结 ,为生物过程提供有效的水分 (Marchand , 1987 ; Jones , 1999) 。Bertrand等 (1994) 在成熟的糖槭 (*Acer saccharum*) 林

表 1 季节性积雪的极地苔原不同群落冬季土壤呼吸排放量 (Fahnestock *et al.* , 1999)
Table 1 Average net winter CO₂ efflux from soils of Arctic tundra communities (Fahnestock *et al.* , 1999)

群落类型 Tundra community type	平均土壤呼吸速率 Mean CO ₂ efflux (μmol C · m ⁻² · s ⁻¹)	变化范围 Seasonal range of measurements (μmol C · m ⁻² · s ⁻¹)	样本数 Number of samples	冬季 CO ₂ 排放量 Estimated winter CO ₂ efflux rates (g C · m ⁻²)
草丛 (酸性) Tussock (Acidic)	0.68	0.002 ~ 1.360	352	20.95
河岸 (河柳) Riparian (Riverside willow)	0.05	0.006 ~ 0.420	180	12.82
湿生莎草 Wet sedge	0.05	0.020 ~ 0.830	150	12.19
自然河道 Natural drifts	0.11	0.003 ~ 0.520	119	26.37
石南灌丛 Dry heath	0.05	0.002 ~ 1.210	92	9.46
水道 Water track	0.16	0.066 ~ 0.749	30	21.65
草丛 (非酸性) Tussock (Nonacidic)	0.01	0.007 ~ 0.082	20	2.10
湿生矮灌丛 Moist dwarf shrub	0.02	0.019 ~ 0.088	20	0.55
干扰/ 再生植被 Disturbed/ Revegetated	0.03	0.010 ~ 0.186	20	4.55
平均 Average	0.11	0.002 ~ 1.359		12.30

表 2 已发表的季节性积雪森林生态系统冬季土壤呼吸的年释放量 (g C · m⁻²)
Table 2 Reported values of winter CO₂ efflux (g C · m⁻²) from seasonally snow-covered forests

地点 Location	生态系统类型 Ecosystem types	冬季 CO ₂ 排放量 Winter CO ₂ efflux
美国科罗拉多州 Colorado , USA	针叶林 Coniferous	143、145 (Monson <i>et al.</i> , 2002)
芬兰 Finland	针叶林 Coniferous	60 ~ 90 (Suni <i>et al.</i> , 2003)
美国科罗拉多州 Colorado , USA	针叶林 Coniferous	45 (Brooks <i>et al.</i> , 1999)
美国怀俄明州 Wyoming , Gees , USA	针叶林 Coniferous	110 (Sommerfeld <i>et al.</i> , 1993)
加拿大 Canada	针叶林 Coniferous	40 ~ 55 (Winston <i>et al.</i> , 1997)
美国科罗拉多州 Colorado , USA	针叶林 Coniferous	71 (Hubbard <i>et al.</i> , 2005)
美国爱达荷州 Idaho , USA	针叶林 Coniferous	132 (McDowell <i>et al.</i> , 2000)
加拿大 Canada	落叶林 Deciduous	89 ~ 132 (Lafleur <i>et al.</i> , 2003)
美国科罗拉多州 Colorado , USA	落叶林 Deciduous	81 (Brooks <i>et al.</i> , 1999)
美国怀俄明州 Wyoming , Gees , USA	落叶林 Deciduous	152 (Sommerfeld <i>et al.</i> , 1993)
日本岐阜县 Gifu Prefecture , Japan	落叶林 Deciduous	22.4 (Mariko <i>et al.</i> , 2000)

中发现,30 cm 的积雪厚度能够防止根冻结和死亡。Decker 等(2003)在 Vermont 北部森林也发现了同样的现象,即积雪深度超过 30 cm 能有效地起到保温层的作用,而浅的暂时性的积雪不能形成一个良好的保温层。使用人工去除覆盖雪的研究进一步证明了雪在冬季生物地理化学循环中的热绝缘作用(Groffman *et al.*, 2001; Fitzhugh, 2003; Decker *et al.*, 2003)。雪厚度(Brooks *et al.*, 1997)以及绝缘效应(Oechel *et al.*, 1997)也是影响不同群落土壤呼吸速率的重要原因。

覆盖雪的减少可加大土壤温度的日变化、增加冻融循环的次数(Decker *et al.*, 2003)、影响根的死亡率以及土壤颗粒体的稳定性和营养物的损失(Lehrsch *et al.*, 1991; Stottlemeyer & Toczydlowski, 1991; Ron Vaz *et al.*, 1994)。雪还影响气体、水分和溶解物的交换,是春季雪融化时营养物输出的主要调节者(Rascher *et al.*, 1987; Williams & Melack, 1991; Stottlemeyer & Toczydlowski, 1996, 1999)。Monson 等(2006a)在一个山地森林的研究表明:冬季土壤呼吸对积雪厚度的变化非常敏感,雪覆盖的减少导致了土壤呼吸速率的降低,这表明:在全球变暖的气候条件下,由于雪厚度的变化可能改变森林的生物地理化学过程,从而改变土壤呼吸速率和碳固存率。但 Jones(1999)对美国阿拉斯加极地苔原的研究表明:积雪厚度与土壤呼吸速率没有直接的关系,而可能受其它机制的影响。

积雪的时间长短也影响土壤呼吸的大小。高山苔原/冻土不连续的雪覆盖和严寒冰冻后连续长时间积雪的情况下,冬季土壤呼吸量分别为 $0.3 \text{ g C} \cdot \text{m}^{-2}$ 和 $125.7 \text{ g C} \cdot \text{m}^{-2}$,积雪覆盖的冬季土壤微生物活力可以矿化 1% ~ 25% 的地上净初级生产力(Brooks *et al.*, 1997)。Fahnestock 等(1998)测定了阿拉斯加北部苔原冬季和早春的土壤呼吸速率,发现更早的更深的积雪有利于土壤微生物免于冬季低温的影响,土壤呼吸速率高于更晚的更浅积雪的群落。

3.2 土壤温度和含水量

土壤温度和含水量被认为是决定土壤呼吸季节动态的最主要因素(Raich & Schlesinger, 1992; Irvine & Law, 2002; Melillo *et al.*, 2002; Conant *et al.*, 2004)。然而,近年来的研究表明,限制寒冷气候下的生命活动的因素是水分的可获取性,而不是温度(Mazur, 1980; Evans *et al.*, 1989; Kennedy, 1993; Osterkamp & Romanovsky, 1997; Fisk *et al.*, 1998)。在

土壤温度高于 -5°C 条件下,可以检测到微生物的活力(Clein & Schimel, 1995)和土壤中自由水的存在(Measures, 1975; Brooks *et al.*, 1997)。还有的研究表明, -10°C 仍能检测到非冻结的土壤水分和土壤呼吸(Clein & Schimel, 1995; Brooks *et al.*, 1997; Fahnestock *et al.*, 1998),甚至在 -39°C 时,土壤仍能释放出 CO_2 (Panikov *et al.*, 2006)。所有这些研究结果都表明,冬季土壤呼吸可能不受温度限制,而是受温度以外的其它因素控制的。尽管土壤温度和冬季土壤呼吸之间可能没有直接关系,但是对于维持活跃的呼吸来说,有一个关键的土壤温度临界值,一般认为它在 -7°C ~ -5°C 之间,低于这个温度会由于自由水的缺乏而抑制异养微生物的呼吸(Schimel & Clein, 1996; Brooks *et al.*, 1997)。

3.3 土壤微生物活力与可溶性碳

冬季土壤呼吸主要来自异养微生物的呼吸。气候的变异性驱动了积雪厚度、存留时间和冬季土壤温度、自由水以及异养微生物活力之间的关系。在积雪的冬季,土壤微生物含量非常高(Brooks *et al.*, 1998; Lipson *et al.*, 1999, 2002)。真菌和细菌(Brooks *et al.*, 1996; Lipson *et al.*, 2002)的生物量在积雪覆盖的土壤中甚至比在夏季还要高。冬季土壤微生物对枯枝落叶的分解通常占年物质损失的 40% ~ 60% (Taylor & Jones, 1990)。它还通过改变植物枯枝落叶的化学组成(Schmidt & Lipson, 2004)影响土壤呼吸速率的大小。

如果存在绝缘的积雪层,异养微生物的活力还受到可溶性碳的影响(Brooks *et al.*, 1997)。可溶性碳底物在自由水存在的情况下可控制异养生物的活力(Nadelhoffer *et al.*, 1991; Schimel & Clein, 1996; Brooks *et al.*, 1997),从而影响土壤呼吸速率的大小。

4 问题与展望

4.1 非极地苔原冬季土壤呼吸的研究十分匮乏

由于高纬度地区生态系统对全球变暖的敏感性和特殊性,目前绝大多数冬季土壤呼吸的测定都是在极地苔原和高山生态系统中开展的(Chapin *et al.*, 1996; Zimov *et al.*, 1996; Brooks *et al.*, 1997; Fahnestock *et al.*, 1998, 1999; Oechel *et al.*, 2000; Welker *et al.*, 2000; Wickland *et al.*, 2001; Schimel & Mikan, 2005; Grogan & Jonasson, 2006; Elberling, 2007),而对于非极地苔原生态系统的研究十分匮乏。譬如,对含有陆地生态系统地上碳贮量的 80%

和地下碳贮量的 40 % 的森林生态系统 (Dixon *et al.*, 1994) 的研究极少, 对占陆地植被面积的 32 %、碳贮量的 23 % 的草地 (Adams *et al.*, 1990; White *et al.*, 2000) 几乎未见报道。因此, 急需开展这些生态系统冬季土壤呼吸的测定。

4.2 冬季土壤呼吸测定方法的改进是降低土壤呼吸估算不确定性的关键

尽管目前已经发展了测定冬季土壤呼吸速率的国际通用方法(扩散模型方法), 但该方法的准确性在很大程度上取决于模型参数的取值, 尤其是雪的通气性和阻力参数。通过直接测定或间接估算得到的数值差距很大, 因此, 未来急需开展模型参数的校正, 以降低估算的不确定性。

4.3 冬季土壤呼吸的调控机制有待研究

研究土壤呼吸及其影响机制对于正确认识和理解陆地生态系统碳循环过程, 合理和客观地评价生态系统的碳平衡至关重要。迄今为止, 对冬季土壤呼吸的影响机制研究甚少, 尚未取得一致的结论, 主要体现在以下 4 个方面。

4.3.1 冬季土壤呼吸的时间动态

冬季土壤呼吸呈现明显的时间动态, 即晚冬高, 春季冰雪融化时低 (Hirano, 2005; Monson *et al.*, 2006b), 这种季节变化的原因尚不清楚。部分学者认为与冻融事件有关 (Brooks *et al.*, 1998)。冻融可导致微生物损伤, 影响可利用底物的水平 (Meyer *et al.*, 1975; Mazur, 1980)。还有的学者认为, 呼吸速率在晚冬的迅速增加是由于微生物对融雪的强烈反应和对土壤温度极高的敏感性 (Monson *et al.*, 2006b)。Lipson 等 (2002) 研究认为, 可溶性碳可能是主要的限制因素。在积雪条件下, 可溶性碳比较充足, 可以满足在零度左右的微生物活力, 但当土壤温度升高后, 代谢增加, 土壤可溶性碳难以满足呼吸的需要。但这种机制尚不清楚, 大多研究停留在假说阶段。尽管在极地苔原和高山开展了一些研究, 但结论不同, 甚至相反。

4.3.2 不同群落类型冬季土壤呼吸速率的差异

不同群落类型冬季土壤呼吸速率具有明显的差异, 但其影响机制尚不清楚。影响苔原群落冬季土壤呼吸速率大小的可能机制在于: 1) 雪被厚度、CO₂ 积累和扩散速率 (Brooks *et al.*, 1997); 2) 雪对土壤温度的绝缘效应 (Oechel *et al.*, 1997) 和相关联的非冻结自由水的可获取性 (Osterkamp & Romanovsky, 1997); 3) 地形和植被 (Evans *et al.*, 1989; Sommerfeld *et al.*, 1993) 以及它们对雪分布和积累模式的影响;

4) 微生物呼吸底物可获取性 (Nadelhoffer *et al.*, 1991)。

4.3.3 冬季土壤呼吸所涉及的关键生态学过程

冬季土壤呼吸所涉及的关键生态学过程尚不清楚, 现有研究绝大多数停留在假说阶段, 亟待验证。例如, 夏季和冬季微生物可能对温度的响应机制不同。冬季微生物对夏季微生物可以存活的温度非常敏感。在冬季, 土壤微生物可以在零度以下进行呼吸, 而在夏季, 土壤呼吸在零度以下很难检测出来。冬季微生物和夏季微生物不同的特性是由于优势种的转变 (Lipson *et al.*, 1999), 还是由于相对稳定的微生物物种的生理适应所致, 仍是一个未知数。

4.3.4 冬季土壤呼吸的温度敏感性

冬季土壤呼吸的温度敏感性在很大程度上决定全球变暖对生态系统 CO₂ 收支的影响, 然而, 目前极少研究涉及土壤呼吸在冬季低温下的温度敏感性。因此, 未来急需开展土壤呼吸及其相关环境因子在全年的测量, 以揭示影响冬季土壤呼吸时空动态的机制。研究土壤呼吸对低温的敏感性以及相关的关键生态过程将是今后该领域研究的重点。

参 考 文 献

- Adams JM, Faure H, Faurendard L (1990). Increases in terrestrial carbon storage from the last glacial maximum to the present. *Nature*, 348, 711 - 714.
- Bertrand A, Robitaille G, Nadeau P (1994). Effects of soil freezing and drought stress on abscisic acid content of sugar maple sap and leaves. *Tree Physiology*, 14, 413 - 425.
- Brooks PD, Campbell DH, Tonnessen KA, Heuer K (1999). Natural variability in N export from headwater catchments: snow cover controls on ecosystem N retention. *Hydrological Processes*, 13, 2191 - 2201.
- Brooks PD, McKnight D, Elder K (2004). Carbon limitation of soil respiration under winter snowpacks: potential feedbacks between growing season and winter carbon fluxes. *Global Change Biology*, 11, 231 - 238.
- Brooks PD, Schmidt SK, Williams MW (1997). Winter production of CO₂ and N₂O from alpine tundra: environmental controls and relationship to inter-system C and N fluxes. *Oecologia*, 110, 403 - 413.
- Brooks PD, Williams MW, Schmidt SK (1996). Microbial activity under alpine snowpacks, Niwot Ridge, Colorado. *Biogeochemistry*, 32, 93 - 113.
- Brooks PD, Williams MW, Schmidt SK (1998). Inorganic N and microbial biomass dynamics before and during spring snowmelt. *Biogeochemistry*, 43, 1 - 15.
- Cerling TE (1984). The stable isotopic composition of modern soil carbonate and its relationship to climate. *Earth and Planetary*

- Science Letters*, 71, 229 - 240.
- Chapin FS, Zimov SA, Shaver GR (1996). CO₂ fluctuation at high latitudes. *Nature*, 383, 585 - 586.
- Clein JS, Schimel JP (1995). Microbial activity of tundra and taiga soils at sub-zero temperatures. *Soil Biology Biochemistry*, 27, 1231 - 1234.
- Collin M, Rasmuson A (1988). A comparison of gas diffusivity models for unsaturated porous media. *Soil Science Society of American Journal*, 53, 1559 - 1565.
- Conant RT, Dalla-Betta P, Klopatek CC (2004). Controls on soil respiration in semiarid soils. *Soil Biology Biochemistry*, 36, 945 - 951.
- de Jong E, Schappert HJV (1971). Calculating of soil respiration and activity from CO₂ profiles in the soil. *Soil Science*, 113, 328 - 333.
- Decker KL, Wang D, Waite C (2003). Snow removal and ambient air temperature effects on forest soil temperatures in northern Vermont. *Soil Science Society of American Journal*, 67, 1234 - 1242.
- Dixon RK, Brown S, Houghton RA (1994). Carbon pools and flux of global forest ecosystems. *Science*, 263, 185 - 190.
- Elberling B (2007). Annual soil CO₂ effluxes in the High Arctic: the role of snow thickness and vegetation type. *Soil Biology Biochemistry*, 39, 646 - 654.
- Evans BM, Walker DA, Benson CS (1989). Spatial interrelationships between terrain, snow distribution and vegetation patterns at an arctic foothills site in Alaska. *Holarctic Ecology*, 12, 270 - 278.
- Fahnestock JT, Jones MH, Brooks PD (1998). Winter and early spring CO₂ efflux from tundra communities of northern Alaska. *Journal of Geophysical Research Atmosphere*, 103, 29023 - 29027.
- Fahnestock JT, Jones MH, Welker JM (1999). Wintertime CO₂ efflux from arctic soils: implications for annual carbon budgets. *Global Biogeochemistry Cycle*, 13, 775 - 779.
- Fisk MC, Schmidt SK, Seastedt TR (1998). Topographic patterns of above- and belowground production and nitrogen cycling in alpine tundra. *Ecology*, 79, 2253 - 2266.
- Fitzhugh RD (2003). Soil freezing and the acid-base chemistry of soil solutions in a northern hardwood forest. *Soil Science Society of American Journal*, 67, 1897 - 1908.
- Fung IY, Tucker CJ, Prentice KC (1987). Application of advanced very high resolution vegetation index to study atmosphere-biosphere exchange of CO₂. *Journal of Geophysical Research*, 92, 299 - 301.
- Gardina CP, Ryan MG (2002). Total belowground carbon allocation in a fast-growing *Eucalyptus* plantation estimated using a carbon balance approach. *Ecosystems*, 5, 487 - 499.
- Goffman PM, Driscoll CT, Fahey TJ (2001). Colder soils in a warmer world: a snow manipulation study in a northern hardwood forest ecosystem. *Biogeochemistry*, 56, 135 - 150.
- Goffman PM, Hardy JP, Driscoll CD (2006). Snow depth, soil freezing, and fluxes of carbon dioxide, nitrous oxide and methane in a northern hardwood forest. *Global Change Biology*, 12, 1748 - 1760.
- Grogan P, Jonasson S (2006). Ecosystem CO₂ production during winter in a Swedish subarctic region: the relative importance of climate and vegetation type. *Global Change Biology*, 12, 1479 - 1495.
- Hirano T (2005). Seasonal and diurnal variations in topsoil and subsoil respiration under snowpack in a temperate deciduous forest. *Global Biogeochemistry Cycles*, 19, CB2011, doi:10.1029/2004CB002259.
- Houghton JT, Ding Y, Griggs DJ (2001). *Climate Change 2001: the Scientific Basis. Contribution of Working Group I to the Third Assessment Report of the Intergovernmental Panel on Climate Change (IPCC)*. Cambridge University Press, Cambridge, England.
- Hubbard RM, Ryan MG, Elder K, Rhoades CC (2005). Seasonal patterns in soil surface CO₂ flux under snow cover in 50 and 300 year old subalpine forest. *Biogeochemistry*, 73, 93 - 107.
- IPCC (Intergovernmental Panel on Climate Change) (2001). *Climate Change 2001: the Scientific Basis. Technical Summary*. Cambridge University Press, Cambridge, England.
- Irvine J, Law BE (2002). Contrasting soil respiration in young and old-growth ponderosa pine forests. *Global Change Biology*, 8, 1183 - 1194.
- Jones HG (1999). The ecology of snow-covered systems: a brief overview of nutrient cycling and life in the cold. *Hydrological Processes*, 13, 2135 - 2147.
- Kennedy AD (1993). Water as a limiting factor in the antarctic terrestrial environment. *Arctic Alpine Research*, 25, 308 - 315.
- Kicklighter DW (1994). Aspects of spatial and temporal aggregation in estimating regional carbon dioxide fluxes from temperate forest soils. *Journal of Geophysical Research*, 99, 1303 - 1315.
- Kurganova I, de Gerenyu VL, Rozanova L, Sapronov D, Myakshina T, Kudeyarov V (2003). Annual and seasonal CO₂ fluxes from Russian southern taiga soils. *Tellus*, 55B, 338 - 344.
- Lafleur PM, Roulet NT, Bubier JL (2003). Interannual variability in the peatland-atmosphere carbon dioxide exchange at an ombrotrophic bog. *Global Biogeochemistry Cycles*, 17, 1036, doi: 10.1029/2002CB001983
- Latenser M, Schneebeli M (2003). Long-term snow climate trends of the Swiss Alps (1931 ~ 99). *International Journal of Climatology*, 23, 733 - 750.
- Lehrsch GA, Sojka RE, Carter DL (1991). Freezing effects on aggregate stability affected by texture, mineralogy, and organic matter. *Soil Science Society of America Journal*, 55, 1401 - 1406.
- Lipson DA, Schadt CW, Schmidt SK (2002). Changes in microbial community structure and function following snowmelt in an alpine soil. *Microbial Ecology*, 43, 307 - 314.

- Lipson DA, Schmidt SK, Monson RK (1999). Links between microbial population dynamics and nitrogen availability in an alpine ecosystem. *Ecology*, 80, 1623 - 1631.
- Lloyd J, Taylor JA (1994). On the temperature dependence of soil respiration. *Functional Ecology*, 8, 315 - 323.
- Marchand PJ (1987). *Life in the Cold: an Introduction to Winter Ecology*. University Press of New England, Hanover, NH, USA.
- Mariko S, Nishimura N, Mo W (2000). Winter CO₂ flux from soil and snow surfaces in a cool-temperate deciduous forest. *Japan Ecological Research*, 15, 363 - 372.
- Massman WJ, Sommerfeld RA, Mosier AR (1997). A model investigation of turbulence-driven pressure-pumping effects on the rate of diffusion of CO₂, N₂O, and CH₄ through layered snowpacks. *Journal of Geophysical Research Atmosphere*, 102, 18851 - 18863.
- Massman WJ, Sommerfeld RA, Zeller K (1995). CO₂ flux through a Wyoming seasonal snowpack: diffusional and pressure pumping effects. In: Hudnell L, Rochelle S eds. *Biogeochemistry of Snow-Covered Catchments*. International Association of Hydrological Sciences, Wallingford, UK, 71 - 79.
- Mast MA, Wickland KP, Striegl RT (1998). Winter fluxes of CO₂ and CH₄ from subalpine soils in Rocky Mountain National Park, Colorado. *Global Biogeochemistry Cycles*, 12, 607 - 620.
- Mazur P (1980). Limits to life at low temperatures and at reduced water contents and water activities. *Origins of Life*, 10, 137 - 159.
- McDowell NG, Marshall JD, Hooker TD (2000). Estimating CO₂ flux from snowpacks at three sites in the Rocky Mountains. *Tree Physiology*, 20, 745 - 753.
- Measures J (1975). Role of amino acids in osmoregulation of non-halophilic bacteria. *Nature*, 257, 398 - 400.
- Melillo JM, Steudler PA, Aber JD (2002). Soil warming and carbon cycle feedbacks to the climate system. *Science*, 298, 2173 - 2176.
- Meyer ED, Sinclair NA, Nagy B (1975). Comparison of the survival and metabolic activity of psychrophilic and mesophilic yeasts subjected to freeze-thaw stress. *Applied Microbiology*, 29, 739 - 744.
- Mikan C, Schimel J, Doyle A (2002). Temperature controls of microbial respiration above and below freezing in Arctic tundra soils. *Soil Biology Biochemistry*, 34, 1785 - 1795.
- Monson RK (2005). Climatic influences on net ecosystem CO₂ exchange during the transition from wintertime carbon source to springtime carbon sink in a high-elevation, subalpine forest. *Oecologia*, 146, 130 - 147.
- Monson RK, Burns SP, Williams MW (2006a). The contribution of beneath-snow soil respiration to total ecosystem respiration in a high-elevation, subalpine forest. *Global Biogeochemistry Cycles*, 20, CB3030, doi:10.1029/2005GB002684.
- Monson RK, Turnipseed AA, Sparks JP (2002). Carbon sequestration in a high-elevation, subalpine forest. *Global Change Biology*, 8, 459 - 478.
- Monson RK, Lipson DL, Burns SP (2006b). Winter forest soil respiration controlled by climate and microbial community composition. *Nature*, 439, 711 - 714.
- Mote PW, Hamlet AF, Clark MP (2005). Declining mountain snow pack in western North America. *Bulletin of the American Meteorological Society*, 86, 39 - 49.
- Nadelhoffer KJ, Giblin AE, Shaver GR (1991). Effects of temperature and substrate quality on element mineralization in six arctic soils. *Ecology*, 72, 242 - 253.
- Osterkamp TE, Romanovsky VE (1997). Freezing of the active layer on the coastal plain of the Alaskan Arctic. *Permafrost and Periglacial Process*, 8, 23 - 33.
- Oechel WC, Vourlitis G, Hastings SJ (1997). Cold season CO₂ emission from arctic soils. *Global Biogeochemistry Cycles*, 11, 163 - 172.
- Oechel WC, Vourlitis CL, Hastings SJ (2000). Acclimation of ecosystem CO₂ exchange in the Alaskan Arctic in response to decadal climate warming. *Nature*, 406, 978 - 981.
- Panikov NS, Flanagan PW, Oechel WC (2006). Microbial activity in soils frozen to below - 39 °C. *Soil Biology Biochemistry*, 38, 785 - 794.
- Raich JW, Schlesinger WH (1992). The global carbon dioxide flux in soil respiration and its relationship to vegetation and climate. *Tellus*, 44B, 81 - 99.
- Rascher CM, Driscoll CT, Peters NE (1987). Concentration and flux of solutes from snow and forest floor during snowmelt in the west-central Adirondack region of New York. *Biogeochemistry*, 3, 209 - 224.
- Ron Vaz MD, Edwards AC, Shand CA (1994). Changes in the chemistry of soil solution and acetic-acid extractable P following different types of freeze/thaw episodes. *European Journal of Soil Science*, 45, 353 - 359.
- Rustad LE, Fernandez JJ (1998). Experimental soil warming effects on CO₂ and CH₄ flux from a low elevation spruce-fir forest soil in Maine, USA. *Global Change Biology*, 4, 597 - 605.
- Ryan MG, Waring RH (1992). Maintenance respiration and stand development in a subalpine lodgepole pine forest. *Ecology*, 73, 2100 - 2108.
- Schimel JP, Klein JS (1996). Microbial response to freeze-thaw cycles in tundra and taiga soils. *Soil Biology Biochemistry*, 28, 1061 - 1066.
- Schimel JP, Fahnstock J, Michaelson G (2006). Cold-season production of CO₂ in arctic soils: can laboratory and field estimates be reconciled through a simple modeling approach? *Arctic Antarctic Alpine Research*, 38, 249 - 256.
- Schmidt SK, Lipson DA (2004). Microbial growth under the snow: implications for nutrient and allelochemical availability in temperate soils. *Plant and Soil*, 259, 1 - 7.
- Schimel JP, Mikan C (2005). Changing microbial substrate use in Arctic tundra soils through a freeze-thaw cycle. *Soil Biology Biochemistry*, 37, 1011 - 1021.

- chemistry, 37, 1411 - 1418.
- Sommerfeld RA, Massman WJ, Musselman RC (1996). Diffusional flux of CO₂ through snow: spatial and temporal variability among alpine-subalpine sites. *Global Biogeochemical Cycles*, 10, 473 - 482.
- Sommerfeld RA, Mosier AR, Musselman RC (1993). CO₂, CH₄ and N₂O flux through a Wyoming snowpack and implications for global budgets. *Nature*, 361, 140 - 142.
- Stottlemeyer R, Toczydlowski D (1991). Stream chemistry and hydrologic pathways during snowmelt in a small watershed adjacent Lake Superior. *Biogeochemistry*, 13, 177 - 197.
- Stottlemeyer R, Toczydlowski D (1996). Precipitation, snowpack, stream-water ion chemistry, and flux in a northern Michigan watershed, 1982 - 1991. *Canadian Journal of Fisheries and Aquatic Sciences*, 53, 2659 - 2672.
- Stottlemeyer R, Toczydlowski D (1999). Seasonal changes in precipitation, snowpack, snowmelt, soil water and streamwater chemistry, northern Michigan. *Hydrological Processes*, 13, 2215 - 2232.
- Suni T, Berninger F, Markkanen T (2003). Interannual variability and timing of growing-season CO₂ exchange in a boreal forest. *Journal of Geophysical Research*, 108, 2312 - 2318.
- Suzuki S, Ishizuka S, Kitamura K (2006). Continuous estimation of winter carbon dioxide efflux from the snow surface in a deciduous broadleaf forest. *Journal of Geophysical Research*, 111, D17101, doi:10.1029/2005JD006595.
- Taylor BR, Jones HG (1990). Litter decomposition under snow cover in a balsam fir forest. *Canadian Journal of Botany*, 68, 112 - 120.
- Uchida M, Mo W, Nakatsubo T (2005). Microbial activity and litter decomposition under snow cover in a cool-temperate broad-leaved deciduous forest. *Agricultural and Forest Meteorology*, 134, 102 - 109.
- Wang CK, Bond-Lamberty B, Gower ST (2003). Soil surface CO₂ flux in a boreal black spruce fire chronosequence. *Journal of Geophysical Research*, 108, 8224, doi:10.1029/2001JD000861.
- Welker JM, Fahnestock JT, Jones MH (2000). Annual CO₂ flux in dry and moist Arctic tundra: field responses to increases in summer temperatures and winter snow depth. *Climatic Change*, 44, 139 - 150.
- White R, Murray S, Rohweder M (2000). *Pilot Analysis of Global Ecosystems (PAGE): Grassland Ecosystems*. World Resources Institute, Washington, DC.
- Wickland KP, Striegl RG, Mast MA (2001). Carbon gas exchange at a southern Rocky Mountain wetland, 1996 - 1998. *Global Biogeochemistry Cycles*, 15, 321 - 335.
- Williams MW, Melack JM (1991). Solute chemistry of snowmelt and runoff in an alpine basin, Sierra Nevada. *Water Resource Research*, 27, 1575 - 1588.
- Winston GC, Stephens BB, Sundquist ET, Hardy JP, Davis RE (1995). Seasonal variability in gas transport through snow in a boreal forest. In: Tonnessen K, Williams MW, Trantor M eds. *Biogeochemistry of Seasonally Snow-Covered Catchments*. International Association of Hydrological Sciences, Wallingford, UK, 61 - 70.
- Winston GC, Sundquist ET, Stephens BB (1997). Winter CO₂ fluxes in a boreal forest. *Journal of Geophysical Research*, 102, 28795 - 28804.
- Zimov SA, Davidov SP, Voropaev YV (1996). Siberian CO₂ efflux in winter as a CO₂ source and cause of seasonality in atmospheric CO₂. *Climatic Change*, 33, 111 - 120.
- Zimov SA, Zimova GM, Davidov SP (1993). Winter biotic activity and production of CO₂ in Siberian soils: a factor in the greenhouse effect. *Journal of Geophysical Research*, 98, 5017 - 5023.

责任编辑: 姜联合 王 葳

河北坝上地区湖泊沉积物记录的全全新世干旱气候

朱江玲, 刘鸿雁, 王红亚

(北京大学环境学院地表过程分析与模拟教育部重点实验室, 北京 100871)

摘要: 根据位于典型草原带的河北坝上地区白诺尔及毗邻的内蒙古乌兰诺尔湖泊沉积物的 K、Na、Ca、Mg 等化学元素组成、总有机碳 (TOC) 与氧同位素 ($\delta^{18}\text{O}$) 的分析, 以 $(\text{K} + \text{Na} + \text{Ca} + \text{Mg}) / (\text{Fe} + \text{Mn})$ 值指示干旱度, $\delta^{18}\text{O}$ 值指示夏季风的强弱, TOC 值指示湖区植被状况, 探讨了该地区 ^{14}C 测年 9.8~5.3 ka B.P. 以来的气候变化与环境变迁。结果表明: 两个剖面所记录的气候变化趋势相近, ^{14}C 测年 7.0~5.7 ka B.P. 为偏干期。反映夏季风强弱的氧同位素指标与干旱程度的变化没有明显的对应关系, 说明夏季风引起的降水量变化不是气候干湿变化的主要影响因素, 温度升高导致的蒸发加强可能对气候干旱化的影响更加明显。

关键词: 干旱气候; 全新世; 夏季风; 坝上地区

中图分类号: P532 **文献标识码:** A **文章编号:** 1000-0690(2007)03-0380-05

中国半干旱区地处季风气候的尾间区, 年降水量 150~350 mm, 且波动明显, 是气候变化的敏感区域。中国半干旱区的植被为温带和暖温带草原。相对于森林植被来说, 草原植被对气候的变化比较敏感, 植被退化和土地沙化是这一地区最主要的生态危害。对中国半干旱区全新世景观演化的系统研究有助于回答季风气候的演化机制、荒漠化发生发展机制等前沿性理论问题, 对中国制定气候变化和荒漠化防治对策有重要的指导意义。

对全新世大暖期的气候状况, 中国东部季风区的证据表明多为湿润气候^[1~4], 而在干旱区则检测到了明显的干旱过程^[5~8]。对于半干旱区, 目前有一些研究工作提及了中全新世存在暖干气候, 但主要依赖孢粉和粒度的证据, 缺少更可靠的代用气候资料^[9~13]。本文选取来自半干旱区典型草原带的河北坝上及毗邻地区内陆湖泊白诺尔、乌兰诺尔两个剖面, 拟通过多种代用气候资料分析中全新世时期研究区的气候变化过程, 并通过与前人工作的对比, 对半干旱区全新世气候旱化过程进行探讨。

康保县以及毗邻的内蒙古太仆寺旗 (图 1), 二者相距约 45 km, 以距离两个取样点均较近的康保气象站为例, 多年平均气温为 1.2℃, 多年平均降水量为 346.7 mm, 存在明显的年际波动。自然植被为典型草原。研究区地处北京的上风向, 为环北京生态圈的一部分。坝上地区处于全国北部 11 个省区的万里风沙线上, 土地沙化是这一地区存在的突出的生态环境问题, 由于紧邻北京外围, 其生态环境的变化直接影响到北京的生态安全, 这一地区的气候变化、植被演化和荒漠化过程近年来倍受关注^[14]。

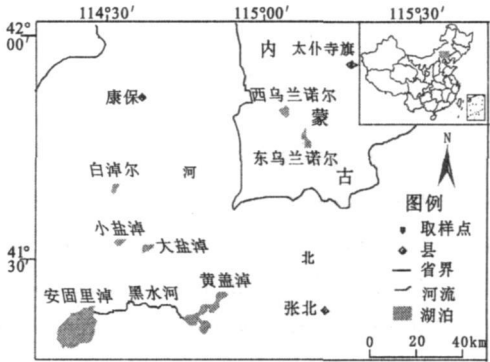


图 1 研究区位置图

Fig 1 Location of the study area

1 研究区与研究方法

白诺尔和乌兰诺尔分别位于河北坝上地区的

收稿日期: 2005-12-13 修订日期: 2006-02-11

基金项目: 国家自然科学基金项目 (编号: 40171097) 资助。

作者简介: 朱江玲 (1981-), 女, 河北石家庄人, 硕士研究生, 主要研究方向为植被生态学与第四纪生态学。E-mail: jiangling_zhu@pku.edu.cn

通讯联系人: 刘鸿雁 (1968-), 男, 教授, 主要从事第四纪生态学与植被生态学方面的研究工作。E-mail: lhy@urban.pku.edu.cn

乌兰诺尔与白诺尔属于内陆湖泊, 其面积分别为 70 km² 与 40 km² 左右。主要靠降水补给, 水量的损失主要取决于蒸发量。2002年在乌兰诺尔与白诺尔分别采得长度为 244 cm, 215 cm 的沉积柱样。两地 2002年前有水, 2002年干涸。室内以 4 cm 为间隔取样封口保存, 乌兰诺尔剖面得到 62 个样品, 白诺尔剖面得到 54 个样品。碳酸钙中氧同位素由中国科学院地质与地球物理研究所岩石圈构造演化国家重点实验室测试, 质谱仪型号 MAT252。元素分析由北京大学地球化学实验室完成, 使用美国制造的等离子发射光谱仪, 型号为 JA 900Q。

2 AMS¹⁴C 年代测定

由北京大学 AMS 实验室进行年龄测定, 其中, 119 cm 处用提取的孢粉测年, 其它年代样均为沉积物中提取的腐殖酸, 测年结果如表 1。图 2 看出, 两个湖泊的沉积速率分别在 7 600 a B. P. 和 9 300 a B. P. 以后大致保持恒定, 推断其属于连续沉积, 没有出现间断性干涸。由此可推断整个剖面的沉积年龄。两湖泊接近地面的沉积速率都较低, 考虑为连续沉积, 因此推断都在 5 400~ 5 300 a B. P. 左右干涸, 且是气候变干的结果。

表 1 AMS¹⁴C 测年结果
Table 1 Result of AMS¹⁴C dating

样品号	深度 (cm)	测年结果 (a B. P.)
BA 03203(白诺尔)	119	9290±80
BA 03393(白诺尔)	205	9700±40
BA 03394(白诺尔)	163	9360±40
BA 03395(白诺尔)	81	8440±60
BA 03396(白诺尔)	3	5490±40
BA 03397(乌兰诺尔)	234	7770±40
BA 03398(乌兰诺尔)	190	7670±40
BA 03399(乌兰诺尔)	158	7250±40
BA 03400(乌兰诺尔)	5	5350±40

3 代用气候指标之间的关系及环境解释

湖泊沉积物中总有机碳含量 (TOC) 是恢复古气候的重要指标^[15], 黄麒等利用 TOC 指标探讨了柴达木盆地察尔汗盐湖古气候波动^[16], 并证实了有机碳含量作为气候变化的可行性。姜加明等结合 TOC 含量、碳酸盐含量与沉积物粒度等指标解释了安固里淖沉积物记录的气候环境变迁^[17], 25 获得了较好的效果^[25 26]。

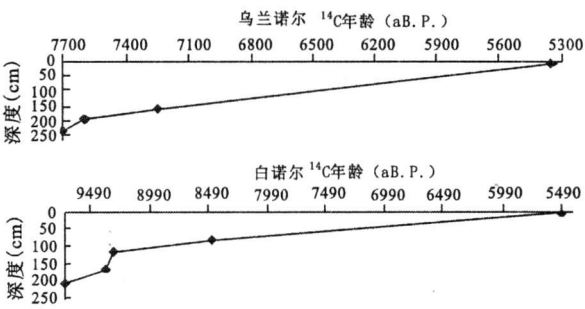


图 2 乌兰诺尔、白诺尔年代 - 深度关系
Fig. 2 Age-depth relationships in Ulan Nuur and Bai Nuur

且其所研究湖泊与本文研究区性质相近, 因此, 可采用 TOC 作为恢复研究区古气候的重要指标。研究区湖泊中水生植被不发育, 沉积物中的总有机碳含量 (TOC) 主要来源于陆生植物碎屑, 气候越适宜, 植被生长状况越好, TOC 值越高。虽然降水量的增加会导致有机碳的稀释, 但研究区蒸发量很大, 对稀释过程具有补偿作用。因此可以作为集水区植被生长状况的间接指标, 其值越高, 代表环境越适宜。

卫克勤等认为湖水 $\delta^{18}\text{O}$ 组成变化主要受到湖泊汇水区气温、湿度和雨水同位素组成三者的影响^[18]。对于半干旱区的内陆封闭湖泊来说, 由于主要靠降水补给, 因此, 雨水同位素的影响最大。通常状况下, 雨水同位素的组成与温度成正比, 即温度效应^[19]。但是, 季风气候使得雨水同位素的影响在某种程度上不符合温度效应^[20], 即温度越高, 同位素含量越低。顾炎武认为湖水 $\delta^{18}\text{O}$ 值与大气相对湿度为负相关^[21], 因此, 总体上说, $\delta^{18}\text{O}$ 值越高越说明气候干冷, 可以用来指示夏季风的强弱。研究区湖泊为内陆封闭湖泊, 因此认为沉积物 $\delta^{18}\text{O}$ 值指示夏季风强度的变化。

湖泊沉积物中的化学元素含量变化主要受到气温、降水的影响, 因此其化学组成往往可以作为气候变化的代用指标^[22~24]。Fe Mn 等元素在湿润条件下, 活性大, 迁移能力强, 趋于集中; 反之在干冷条件下, 其活性降低, 趋于分散。Ca Mg K Na 在干旱条件下, 趋于集中, 湿润条件下分散。(K + Na + Ca + Mg) / (Fe + Mn) 值可以作为干旱程度的代用指标^[25], 此值越大, 气候越干旱, 反之越湿润。该比值在毗邻本研究区的河北安固里淖以及同属于草原带的内蒙古科尔沁沙地全新世气候恢复中 25 获得了较好的效果^[25 26]。

4 结 果

根据以上解释模式, 分别讨论乌兰诺尔剖面与白诺尔剖面沉积物分析结果所反映的环境演变过程。

4.1 乌兰诺尔剖面 (图 3)

阶段 W1 时间范围为 ^{14}C 年 7.7~7.1 ka B. P. (根据图 2 插值得出, 下同)。干旱指数、TOC 与 $\delta^{18}\text{O}$ 值在这一阶段波动较大。总体来说, 干旱指数和 TOC 呈现出一定程度的反相位关系。

阶段 W2 时间范围为 ^{14}C 年 7.1~6.1 ka B. P.。干旱指数呈增加的趋势而 TOC 呈减小的趋势, 反映夏季风强弱 $\delta^{18}\text{O}$ 值也呈逐渐减小的趋势, 说明降水量在增加之中。

阶段 W3 时间范围为 ^{14}C 年 6.1~5.4 ka B. P.。虽然干旱指数总体上较高, 但呈下降趋势, 特别是在 ^{14}C 年 5.9 ka B. P. 以后下降趋势明显。TOC 总体上较低, 但 ^{14}C 年 5.7 ka B. P. 以后呈波动增加的趋势。 $\delta^{18}\text{O}$ 值总体上较高, 说明这一阶段降水量偏低。

阶段 W4 时间范围为 ^{14}C 年 5.4~5.3 ka B. P.。干旱程度增加, TOC 显著降低, $\delta^{18}\text{O}$ 值的增加也反映了夏季风带来的降水减少, 可能是湖泊干涸的原因。

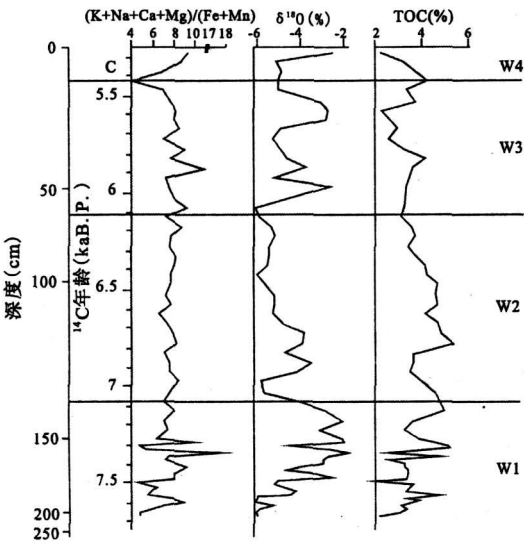


图 3 乌兰诺尔剖面代用气候指标的变化
Fig 3 Diagram of climatic proxies in Ulan Nuur

4.2 白诺尔剖面 (图 4)

阶段 B1 时间范围为 ^{14}C 年 9.8~9.0 ka B. P. (根据图 2 插值得出)。三个气候指标波动大。干

旱指数和 $\delta^{18}\text{O}$ 值呈减小的趋势, 而 TOC 的变化趋势不明显。

阶段 B2 时间范围为 ^{14}C 年 9.0~7.0 ka B. P.。干旱指数较为平稳, 总体上较低, 反映气候较为湿润。TOC 总体呈下降的趋势。 $\delta^{18}\text{O}$ 值在 ^{14}C 年 7.8 ka B. P. 以后开始呈明显下降趋势, 说明夏季风带来的降水量增加。

阶段 B3 时间范围为 ^{14}C 年 7.0~5.8 ka B. P.。 $\delta^{18}\text{O}$ 值呈明显下降趋势, 反映夏季风带来的降水继续增加, 但干旱指数呈上升趋势。 TOC 反映的植被退化趋势也非常明显。

阶段 B4 时间范围为 ^{14}C 年 5.8~5.5 ka B. P.。三个指标的变化趋势均不明显。

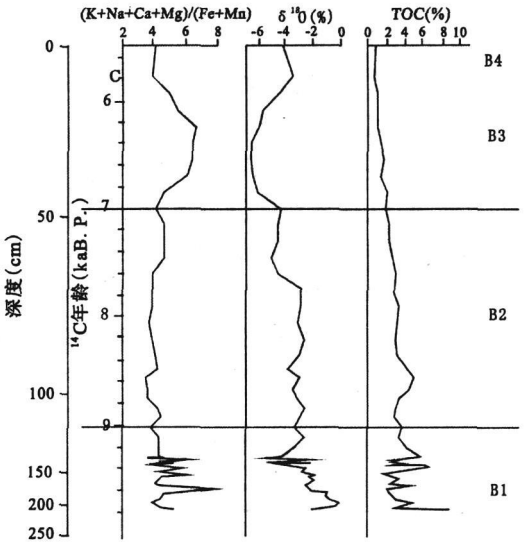


图 4 白诺尔剖面代用气候指标的变化
Fig 4 Diagram of climatic proxies in Bai Nuur

5 中全新世干旱气候讨论

对比白诺尔与乌兰诺尔 $\delta^{18}\text{O}$ 值的变化曲线可以看出, 其总体趋势几乎相同, 可认为两个剖面所记录的夏季风变化相近。同样, 其干旱指数 $(\text{K} + \text{Ca} + \text{Na} + \text{Mg}) / (\text{Fe} + \text{Mn})$ 值变化的总体趋势也近似, 总体上 ^{14}C 年 7.0~5.7 ka B. P. 干旱指数较高, 气候偏干。

已有的对半干旱区气候变化的研究, 一些研究认为中全新世气候是湿润的, 如河北坝上安固里淖的沉积记录表明全新世中期湖面最高, 气候湿润^[27]; 岱海孢粉分析的结果也指示了暖湿气候^[28]。而另一些研究则认为, 全新世中期确有干旱 25 事件发生, 如内蒙古中部地区的察素齐剖面记录^[14] C

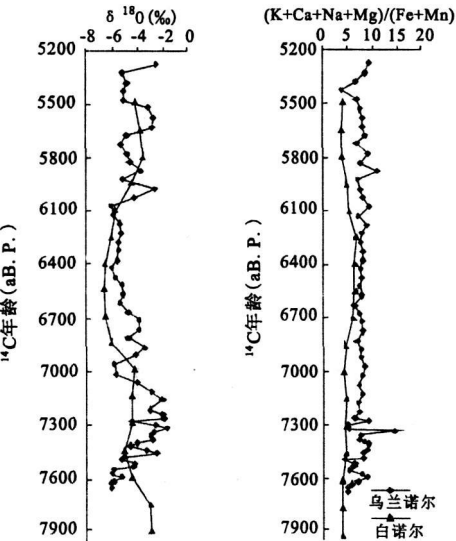


图 5 乌兰诺尔、白诺尔 $\delta^{18}O$ 值、

$(K + Na + Ca + Mg) / (Fe + Mn)$ 值变化曲线

Fig 5 Diagram of $\delta^{18}O$ and $(K + Na + Ca + Mg) / (Fe + Mn)$ in Bai Nuur and U lan Nuur

年 7.4~6 ka B. P. 气候温和偏干旱^[11],但是具体的时间有差异。Wang et al 在研究内蒙古中部达里诺尔地区气候变化时发现,¹⁴C 年约 60 ka B. P. 气候开始变干^[29]。内蒙古大青山地区钻孔研究发现¹⁴C 年 63 ka B. P. 为大暖期转折点,此后气候开始向暖干变化,植被退化为疏林草原和森林草原^[10 30],而此时的沙漠-黄土过渡带也为暖干气候^[31]。本文的结果进一步说明了中全新世半干旱区偏干气候的存在。尽管半干旱区中全新世干旱事件的发生具有空间、时间上的差异,但是其区域性还是较为明显的,这与同期东部季风区的湿润气候是不同的^[1~4 32]。

值得注意的是,本研究中两个沉积剖面 $\delta^{18}O$ 所反映的夏季风强弱变化与气候干旱程度的变化不存在一致的关系。在¹⁴C 年 7.0~5.7 ka B. P. 这一阶段,二者存在反相位的关系,也就是说,夏季风增强导致降水强度增加,但气候干旱程度反而增加。干旱程度不仅与降水有关,而且与温度升高引起的蒸发增加有关,是蒸发与降水差值的函数。Chen et al 对毛乌素沙地的研究表明,蒸发与降水的差值随着温度升高而急剧上升,也就是说,虽然降水量增加,但温度升高导致的蒸发增加仍然使湿度条件降低^[33]。在季风尾闾区,虽然全新世大暖期夏季风增强带来了降水的增加,但增加的量在季风尾闾区是非常有限的,不足以抵消高温带来的蒸

发量的增加,这也是地处季风气候尾闾区的半干旱区全新世气候变化过程与湿润区不同的地方。

6 结 论

本文通过位于典型草原带的两个湖泊沉积剖面的研究,得出以下初步结论:

- 1) $(K + Na + Ca + Mg) / (Fe + Mn)$ 值能较好地指示干旱程度的变化,与前人研究相符。
- 2) 两个剖面所记录的气候变化趋势相近。白诺尔与乌兰诺尔地区¹⁴C 年 7.0~5.7 ka B. P. 为偏干期,并在 5.3 ka B. P. 左右干涸。
- 3) 夏季风强弱变化不是研究区气候干旱程度变化的原因,高温带来的蒸发量的增加对气候干旱具有重要作用。

参考文献:

[1] ShiY F, KongZ C, WangSM, et al. Mid-Holocene climates and environment in China[J]. Global and Planetary Change, 1993, 7: 219- 233.

[2] Sangheon Y, Yoshike S, Zhao Q H, et al. Vegetation and climate changes in the Changjiang (Yangtze River) Delta, China, during the past 13 000 years inferred from pollen records[J]. Quaternary Science Reviews 2003 22 1501- 1509.

[3] Zheng Z, LiQ Y. Vegetation, Climate, and Sea Level in the past 55 000years Hanjiang Delta Southeastern China[J]. Quaternary Research, 2000, 53 330- 340.

[4] 杨永兴,王世岩. 8.0 ka B. P. 以来三江平原北部沼泽发育和古环境演变研究[J]. 地理科学, 2003 23(1): 32~ 38.

[5] 莫多闻,李 非,李水城,等. 甘肃葫芦河流域中全新世环境演化及其对人类活动的影响[J]. 地理学报, 1996, 51(1): 59~ 69

[6] 王红亚,汪美华,谢 强,等. 泥河湾盆地东部中全新世晚期的干/冷事件与中全新世湿润状况的结束[J]. 地理科学, 2002, 22(5): 557~ 562.

[7] 张虎才,马玉贞,李吉均,等. 腾格里沙漠南缘全新世古气候变化初步研究[J]. 科学通报, 1998 43(12): 1252~ 1258

[8] 陈发虎,吴 薇,朱 艳,等. 阿拉善高原中全新世干旱事件的湖泊记录研究[J]. 科学通报, 2004 49(1): 1~ 9

[9] 翟秋敏,邱维理,李容全,等. 内蒙古安固里淖-泊江海子全新世中晚期湖泊沉积及其气候意义[J]. 古地理学报, 2000, 2(2): 84~ 91

[10] 杨志荣. 内蒙古大青山调角海子地区全新世气候与环境重建研究[J]. 生态学报, 2001, 21(4): 538~ 543.

[11] 王琰璋,宋长青,程全国,等. 利用花粉-气候响应面恢复察素齐泥炭剖面全新世古气候的尝试[J]. 植物学报, 1998, 40 (11): 1067~ 1074

[12] 许清海,阳小兰,杨振京,等. 孢粉分析定量重建燕山地区 5 000 年来的气候变化[J]. 地理科学, 2004 24(3): 339~

345

[13] 钟 巍,熊黑钢,王立国,等. 塔里木盆地南缘策勒绿洲近 4 000年来的环境变化 [J]. 地理科学, 2004, **24**(6): 687~ 692

[14] 孙建中,杨明华,盛学斌,等. 河北坝上地区脆弱生态环境特征 [J]. 中国沙漠, 1994 **14**(4): 37~ 46

[15] 王 建,黄巧华,柏春广,等. 2 5 Ma以来柴达木盆地的气候干湿变化特征及其原因 [J]. 地理科学, 2002 **22**(1): 34~ 38.

[16] 黄 麒,陈克造. 七十三万年来柴达木盆地察尔汗盐湖古气候波动的形式 [J]. 第四纪研究, 1990 (3): 205~ 212.

[17] 姜加明,吴敬禄,沈 吉. 安固里淖沉积物记录的气候环境变迁 [J]. 地理科学, 2004 **24**(3): 346~ 351.

[18] 卫克勤,林瑞芬. 内陆封闭湖泊自生碳酸盐氧同位素剖面的古气候意义 [J]. 地球化学, 1995 **24**(3): 215~ 224.

[19] Dansgaard W. Stable isotopes in precipitation [J]. Tellus, 1964 **16**(4): 436~ 468.

[20] 卫克勤,林瑞芬. 论季风气候对我国雨水同位素组成的影响 [J]. 地球化学, 1994 **23**(1): 33~ 40

[21] 顾兆炎. 黄土 - 古土壤序列碳酸盐同位素组成与古气候变化 [J]. 科学通报, 1991, **36**(10): 767~ 770.

[22] Sekar B, G Rajagopalan and A Bhattacharyya. Chemical analysis and ¹⁴C dating of a sediment core from Tsokar lake, Ladakh and its implication on climatic change[J]. Current Science, 1994, **67**(1): 36~ 38

[23] 王国平,刘景双,翟正丽. 沼泽沉积剖面特征元素比值及其环境意义——盐碱化指标及气候干湿变化 [J]. 地理科学, 2005 **25**(3): 335~ 339.

[24] 王国平,刘景双. 向海湿地元素地球化学特征与高分辨沉积记录 [J]. 地理科学, 2003 **23**(2): 208~ 212.

[25] 关有志. 科尔沁沙地的元素、粘土矿物和沉积环境 [J]. 中国沙漠, 1992, **12**(1): 9~ 15

[26] 翟秋敏,郭志永. 坝上高原安固里淖全新世沉积地球化学特征与环境变化 [J]. 古地理学报, 2002 **4**(4): 55~ 60.

[27] 邱维理,翟秋敏,扈海波. 安固里淖全新世湖面变化及其环境意义 [J]. 北京师范大学学报 (然科学版), 1999, **35**(4): 542~ 548

[28] Xiao J, Xu Q H, Nakamura T, et al. Holocene vegetation variation in the Dahuai Lake region of north-central China: a direct indication of the Asian monsoon climatic history[J]. Quaternary Science Review, 2004 **23** 1669~ 1679.

[29] Wang H Y, Liu H Y, Liu Y H, et al. Mineral magnetism of lacustrine sediments and Holocene paleoenvironmental changes in DaliNor area, southeast InnerMongolia Plateau, China[J]. Paleogeography, Paleoclimatology, Paleoecology, 2004 **208** 175~ 193

[30] Song C Q, Wang F Y. Paleovegetational reconstruction through high resolution pollen analysis of Diaojiao Lake in Daqingshan Mts., middle part of InnerMongolia, North China[J]. Scientia Geologica Sinica, 1995, (1): 215~ 222.

[31] 李小明,周卫建,安芷生,等. 沙漠 /黄土过渡带 13 ka B. P. 以来季风演化的古植被记录 [J]. 植物学报, 2000, **42**(8): 868~ 872.

[32] 王苏民,吉 磊,薛 滨,等. 东南季风区及青藏高原东部湖泊沉积研究与古环境重建 [J]. 第四纪研究, 1995 **3** 243~ 248.

[33] Chen C T, Lan H C, Lou J Y, et al. The dry Holocene Megathermal in InnerMongolia[J]. Paleogeography, Paleoclimatology, Paleoecology, 2003, **193** 181~ 200.

M id-Holocene Dry Climate Recorded by Lacustrine Sediments in Bashang Region of Hebei Province

ZHU Jiang-Ling, LU Hong-Yan, WANG Hong-Ya

(College of Environmental Sciences and MOE Laboratory of Earth Surface Processes and Simulation, Peking University, Beijing 100871)

Abstract Based on the analyses of chemical elements (K, Na, Ca, Mg, etc.), total organic content (TOC) and oxygen isotope ($\delta^{18}\text{O}$) of two lacustrine sediment sequences from Bashang area of Hebei Province and its surrounding (K + Ca + Na + Mg) / (Fe + Mn) was demonstrated to well indicate aridity change. $\delta^{18}\text{O}$ and TOC were adopted as proxies of intensity of summer monsoon and vegetation cover respectively. Climatic changes of this area during 9.8~5.3 ka B. P. were reconstructed. It is shown that climate changes of both sequences were quite similar and an arid stage from 7.0~5.7 ka B. P. was detected. However, the intensity of summer monsoon did not necessary correspond with the changes of aridity, implying that precipitation brought by summer monsoon in the study area was not the major factor of aridity change. On the other hand, evapotranspiration in the marginal area of Pacific monsoon, also called summer monsoon, was deterministic to the climatic aridity.

Key words arid climate, the Mid-Holocene, summer monsoon, Bashang area, Hebei Province

博士后出站报告和研究生、本科生毕业论文

博士后出站报告

类号_____

密级_____

U D C _____

编号_____



北京大学

博士后研究工作报告

河北省塞罕坝森林结构与生物量

郑 成 洋

工作完成日期 _____ 2004.1—2005.12

报告提交日期 _____ 2005.12

2005 年 12 月

河北省塞罕坝森林结构与生物量

Forest Composition and Biomass of Saihanba,
Hebei Province, China

博士后姓名: 郑成洋

设站单位: 环境学院

流动站名称
(一级学科): 环境科学与工程

专业名称
(二级学科): 自然地理学

研究方向: 植被生态

合作导师: 江家驹 方精云 教授

工作完成日期 2004 年 1 月—2005 年 12 月

报告提交日期 2005 年 12 月



北京大学环境学院 (北京)

2005 年 12 月

摘 要

本报告利用植物样方和林班调查数据,研究了河北省塞罕坝机械林场总场的森林结构和生物量。为了研究不同森林类型群落结构及生长特征,调查了7个1 ha典型森林样方,采用胸径偏斜度(skew)分析不同取样面积与胸径的关系,并用胸径CV空间差异解释与偏斜度变化特征的关系。同时,为了准确森林资源清查中蓄积量及其变化的估算,采用空间代替时间方法和GLM模型方法估算森林生物量及其动态变化。通过研究得出以下主要结论:

(1) 塞罕坝机械林场总场土地利用类型以人工林为主,森林占总面积76.7%。森林组成以落叶松为主,占总面积38.7%,其次是白桦林,占总面积15.1%;落叶松林是主要的商品林,大多数白桦林为公益林。落叶松径级与树高有很好关系,各林龄段均有一定比例,其中以21~35年林龄占绝大多数。白桦林多为天然更生次生林,20年林龄以上,树高和胸径变化缓慢。樟子松林龄比较小,单位面积个体数多,径级比较小,近一时期来大量营林的物种的结果。蒙古栎、云杉、油松、山杨等其它森林占比例相对较小,占总面积6.2%,占总蓄积量4.1%。

(2) 塞罕坝针叶林群落(落叶松林、樟子松林、云杉林、油松林等)的胸径与树高关系显著,但落叶阔叶林(白桦林、蒙古栎林)关系不显著。通过树高影响因子相关分析结果表明:树高除了林龄关系密切外,不同森林类型与各因子相关性有较大的差异。通过建立GLM模型分析,分析结果也表明,除了林龄有较高解释率以外,其它各因子如郁密度、森林利用类型、土壤、盖度、土地经营类型和坡度解释率有很大差别。用胸径与各因子分析的结果,也有相类似情形,除了林龄为主要影响因子外,其它各因子解释率明显较高。

(3) 用7个ha样方数据分析结果表明:落叶松和樟子松样方数量径级分布,呈明显正态分布;白桦林三个样方个体数量径级分布型差异比较大。用八种方法计算胸径偏斜度的变化,表明按对角10×10m,20m×20m,30m×30m...增加面积方式,得出4个方向的偏斜度,变化差别很大,很难正确评估群落胸径变化。按每一次增加10m×10m方式计算,得出四种不同方向的计算结果,在相对均一植物群落中,最终偏斜度趋于稳定;分析结果也表明塞罕坝森林群落结构中,森林群落取样面积在2000m²以上,偏斜度趋于稳定,说明取样在2000m²情况下,用胸径计算蓄积量及生物量与实际偏差很小。影响偏斜度波动与群落生长特征有关,也与环境梯度变化有关。

(4) 采用森林资源小班清查详细资料,并用空间代替时间以及GLM模型方法计算森林蓄积量及其生长率,并用BEF方法转换成生物量,计算结果:塞罕坝林场森林蓄积总量为 $4.9 \times 10^6 \text{ m}^3$,平均每年增长蓄积量为 $1.8 \times 10^5 \text{ m}^3$;森林总生物量为6.5 Tg。森林类型生物量由大到小分别是落叶松、白桦林、樟子松、混交林、蒙古栎、山杨、云杉和油松。

(5) 用林龄、森林类型、树高/年龄、郁密度、土壤类型、土壤深度、坡度、土地经营类型和森林利用类型等变量与各森林类型蓄积量建立GLM模型表明:森林类型、林龄对蓄积量影响解释率最高,其它各因素与蓄积量有很好的相关性,但不同森林类型解释率有差别。

关键词: 森林结构, 蓄积量, 生物量, 生长变化, 塞罕坝

目 录

第一章 绪 论	1
1.1 概况	1
1.2 研究进展	1
1.3 本研究的科学问题	2
第二章 研究区概况	3
2.1 地理位置	3
2.2 自然条件	3
2.2.1 气候	3
2.2.2 地质地貌	3
2.2.3 土壤	4
2.2.4 水文	4
2.3 植物资源	4
2.3.1 植被的历史演变	4
2.3.2 森林—草原交错带植物过渡性特点	5
2.3.3 植物组成	5
2.3.4 特有植物	8
2.4 动物资源	8
2.5 土地利用	8
第三章 研究方法	9
3.1 资料来源	9
3.2 数据分析	10
3.2.1 森林蓄积量和生长量估算	10
3.2.2 样方数据分析	10
第四章 气候特征	12
4.1 气温	13
4.2 降水	15
4.3 风	16
4.4 日照	16
第五章 主要森林结构和生长特征	17
5.1 土地利用	17
5.1.1 森林经营类型	17
5.1.2 不同行政单元的森林类型	18
5.2 森林类型	18
5.2.1 落叶松林	19
5.2.2 白桦林	20
5.2.3 樟子松林	21
5.2.4 蒙古栎林	21
5.2.5 其它森林类型	22
5.3 森林生长特征	23
5.3.1 年龄结构	23
5.3.2 树高与胸径的关系	23

5.4 主要森林类型的径级分布..... 25

5.4.1 样方径级 25

5.4.2 径级数量分布 25

5.4.3 径级分布与取样面积 26

第六章 森林蓄积量和生物量 34

6.1 森林蓄积量 34

6.1.1 总森林蓄积量 34

6.1.2 不同森林类型的蓄积量 34

6.2 森林蓄积量的变化..... 36

6.3 不同森林类型蓄积量的变化..... 38

6.3.1 落叶松蓄积量的变化 38

6.3.2 白桦林蓄积量的变化 39

6.3.3 樟子松蓄积量的变化 40

6.3.4 蒙古栎蓄积量的变化 41

6.3.5 其它森林类型蓄积量的变化 42

6.4 森林生物量及其变化..... 43

6.4.1 地上总生物量 43

6.4.2 主要森林类型生物量的变化 45

第七章 结 论 48

参考文献 52

附录 河北省塞罕坝高等植物名录 55

第一章 绪 论

1.1 概况

塞罕坝又名“坝上”，蒙语即“美丽的高岭”，地处华北平原和内蒙古高原交接地带，海拔陡然升高，成阶梯状，属冀北高原的一部分。位于河北省北部围场满族蒙古族自治县境内，与内蒙古自治区赤峰市克什克腾旗以及锡林郭勒盟多伦县接壤，北面是平均海拔 1400 m 以上的坝上高原，南面是地势较低的燕山山脉余脉。距北京 460 km，距旅游名城承德市 240 km。这里山峦起伏、气候温和、雨量充沛、河流纵横。塞罕坝野生资源丰富，植被类型多样，有草原、森林、荒漠、湿地和湖泊，是我国温带地区十分典型的农牧交错带。

324 年前（公元 1681 年）清朝康熙帝选中包括现今塞罕坝机械林场在内设置皇家猎苑—木兰围场，共 72 围，以木栅、柳条边为界，设 40 座巡逻哨所，巡边保护，禁止平民百姓进入皇家禁地。历史记载，这里森林茂密，古木参天，禽兽繁集。从坝下的落叶阔叶林到坝上的森林草原景观，植被十分完好。自乾隆以后，国势渐衰，于同治元年和光绪二十七年宣布围场开禁后，经过几次大规模的砍伐和开荒垦种，原始森林荡然无存，野生动物种群几乎绝迹。

二十世纪 50 年代末京津地区受到日益严重风沙侵袭，国家林业局（原林业部）提出在河北省塞罕坝建设一个大型国营林场，作为京津风沙源治理区，并制定了“以造为主，造育并举，综合经营，永续利用”的经营方针。1962 年正式成立塞罕坝机械林场，开始大面积恢复植被计划，经营总面积 94,700 hm²。经过 43 年的艰苦奋斗，营造落叶松为主的人工林 100 多万亩，森林覆盖率达 76.8%，林木总蓄积 6.9×10⁶ m³。目前已成为我国最大人工林种植基地，主要由落叶松、樟子松、云杉、白桦、山杨等优势树种组成的万顷林海，有效地阻滞了我国浑善达克沙地南侵，成为京津唐绿色保护屏障。同时，对改善当地水资源和气候条件方面发挥了巨大作用。

1.2 研究进展

该地区近代植物及其区系的研究真正始于建国后，以往的研究主要集中在植物物种组成、区系、气候条件变迁和历史演变等，并绝大多数以森林—草原过渡带这一特征为研究主线。刘濂（1965）在植被调查的基础上把该地区划定为森林草原区；黄永梅等（2001）研究结果认为森林-草原过渡带的界线明显，过渡带植物物种递变规律显著。

1989-1994 年，河北省林业厅组织有关专家对该地区的植物进行了大规模、系统地调查采集（黄金祥等，1996a），同时对该地区的植物区系进行总结和报道（黄金祥等，1994，黄金祥等，1996b，王庆锁等，2005）。该过渡带的植物区系成分以北温带成分为主（王庆锁，2005），植物区系具有明显的过渡性，森林-草原过渡带植物多样性高，特别在森林草甸区物种多样性最高（王庆锁，2000）；研究结果认为在森林草甸区不仅物种丰富，而且森林景观斑块多（王庆锁，2004）。塞罕坝植物物种多样性高并有显著差异，主要是由于坝缘山地海拔迅速抬升，导致降水和温度迅速变化，以落叶阔叶林地理分布为例，它并没有处于落叶阔叶林气候分布边缘，主要是由于地形剧烈变化所导致的（黄永梅等，2001）。

该区域植被历史演变也有较深入的研究，Liu *et al.* (2002a, 2002b) 和靳鹤龄等（2004）利用 C¹⁴ 年代测定方法，重建全新世气候变迁与植被变化关系，并认为森林—草原过渡带的变迁除了

人为因素影响外, 气候变化的变迁是导致植被景观的变化主要因素。由于该地区历史悠久, 有大量文史资料和诗文描述这一地区的自然景观, 崔海亭和王文江 (2003) 用自然地理学和生态学的方法, 根据元代古籍中的景观与物候信息复原了 13 ~ 14 世纪滦河上游及其邻近地区的自然景观, 认为元代的植被景观与现代基本一致。

以往的研究资料来看, 塞罕坝机械林场大面积种植人工林后, 有关森林群落结构和生长特征、森林生物量的研究很少。

1.3 本研究的科学问题

森林—草原过渡带是一种十分特殊的生态系统, 1962 年在该地区成立大型国有机械林场—河北省塞罕坝机械林场, 目的是通过“三北防护林工程”建设, 在环北京生态圈形成绿色保护屏障, 塞罕坝机械林场的建设是该生态保护圈的一个重要组成部分。通过 40 多年来的不断种植大面积的人工林, 该地区生态系统结构与功能以及生态景观发生很大变化。如何正确决策林场的生产和经营活动显得十分重要, 一个大型国有林场十分关心问题是需要找到一种客观估算森林的蓄积量和生长量, 以便合理安排担负双重生态意义的塞罕坝机械林场的生产经营活动。该林场地处森林—草原交错带, 坝上和坝下气候条件和立地条件差异很大, 导致不同或相同森林类型生长量差异较大, 必须找到一种合理估算森林生长量的方法。因此, 如何正确、科学地估算现存森林蓄积量和森林增长量成为本研究的科学问题。以往森林经营一般先采用资源清查的方法, 即每隔 4-5 年进行一次大规模资源清查, 这种调查方法往往投入大量的人力和物力, 但估算结果由于没有区分不同森林类型生长情况, 忽视不同林龄森林增长规律, 并且前后资源清查抽样的不一致性和调查人员差异, 导致估算上误差很大, 影响生产经营活动, 难以正确预测森林资源增长情况。

上世纪 80 年代以来, 我国加大对生态环境整治工作力度。1979—1985 年实施了“三北”防护林体系建设; 1986 年开始实施京津周围绿化工程; 1992 年全国防沙治沙工程正式启动; 1996 年坝上生态建设工程实施。为了评估这些工程的实施成效, 需要对种植人工林进行深入的研究, 这不仅有助于评价我国重大生态工程的生态效益, 还为生产实践提供有力科学依据。

第二章 研究区概况

2.1 地理位置

研究区域设在以河北省塞罕坝机械林场总场，该区域位于河北省围场满族蒙古族自治县北部 (图 2-1)，地理位置 $42^{\circ}10' - 50' N$ ， $117^{\circ}12' - 30' E$ 。面积 $94,700 \text{ km}^2$ 。1962 年正式成立塞罕坝机械林场总场，总场划分为六个林场：北曼店林场、大唤起林场、千层板林场、三道河口林场、三乡林场和阴河林场。

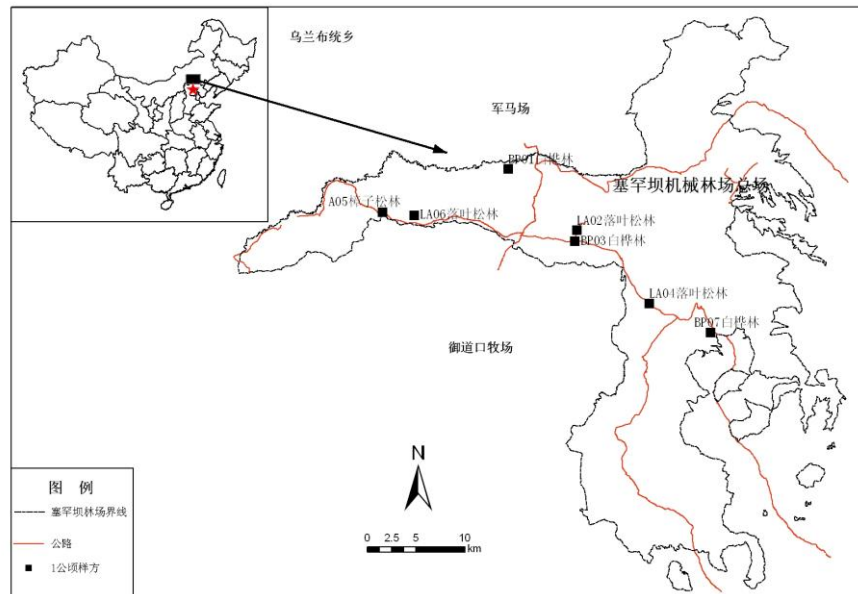


图 2-1 研究区域

2.2 自然条件

2.2.1 气候

塞罕坝地处暖温带向温带的过渡地带，半湿润气候向半干旱气候过渡。由于地势高，冬季长而寒冷，春季短，夏季不明显；日较差大，无霜期短，多大风。根据塞罕坝机械林场气象站 40 年的观测记录，年平均气温 -1.2°C ，1 月平均气温 -21.8°C ，7 月平均气温 16.2°C ，极端高温 33.4°C ，极端低温 -43.2°C ； $\geq 5^{\circ}\text{C}$ 积温 1957.5°C ， $\geq 10^{\circ}\text{C}$ 积温 1645.2°C ， $\geq 15^{\circ}\text{C}$ 积温 866.4°C ；平均降雨量 450.1 mm ，平均无霜期仅 60.8 天，平均年日照时数 2558.4 小时，相对湿度 69.5%，最大冻土深 168 cm，年平均大风天数 74.6 天。

2.2.2 地质地貌

塞罕坝是内蒙古高原、大兴安岭山系与冀北山地交汇处，也是内蒙古浑善达克沙地的东南边缘。属阴山—燕山纬向隆起带的一部分，冀北纬向隆起带自元古代以来长期上升隆起，发育有不同高度的夷平面，一级夷平面形成约在早第三纪末至晚第三世纪初，高度 1500-2000 m；二级夷平面形成于第三纪末至第四纪，海拔 1000-1300 m；随后经过数次的地壳运动的影响，尤其是燕山运动，形成一系列复杂断裂带；新生代喜马拉雅运动又使该地区断裂带加剧，并沿着

断裂带伴随玄武岩喷流。塞罕坝地区位于燕山山地向内蒙古高原的过渡地区，分北部坝上和南部坝下两部分。坝上为高原，属于内蒙古高原的东南缘，海拔 1300-1500 m，包括丘陵和波状高原，相对高度 80-150 m，也有沙丘和沙垄，相对高度<50 m；坝下属冀北山地，属于燕山山脉，海拔 1000-1900 m，山峰起伏大，山体陡峭。

2.2.3 土壤

根据河北省土壤分布带，塞罕坝土壤类型属于灰色森林与黑土带 (刘濂主编, 1996)。由于塞罕坝气候梯度明显，地貌类型多样，在塞罕坝及周边地区分布的土壤类型有灰色森林土、黑钙土、淡黑钙土、棕壤、暗栗钙土、亚高山草甸土和风沙土 (赤峰市土壤普查办公室, 1989; 内蒙古草场资源遥感应用考察队, 1988)，但塞罕坝林场土壤类型以风沙土占绝大多数。

2.2.4 水文

塞罕坝是潮河、滦河、辽河、大凌河四大河流的发源地和主要集水区。其中潮河、滦河是京津唐两大水源一密云水库和潘家口水库的主要河流，潮河水系占密云水库年入库水量的 56.7%，滦河水系占潘家口水库年入库水量的 93.4%。水源保护是塞罕坝机械林场的重要任务之一。

2.3 植物资源

按中国植被带划分，塞罕坝地区处于我国暖温带落叶阔叶林向温带草原的过渡带，即森林带和草原带交错区，以森林和草原两种植被镶嵌共存为特色。该地区的植被带是冀北山地落叶阔叶林的北部边缘，温带草原的南缘。坝下为冀北山地天然次生林，主要有白桦 (*Betula platyphylla*) 林、山杨 (*Populus davidiana*) 林、华北落叶松 (*Larix principis-rupprechtii*) 林、白杆 (*Picea meyeri*) 林、蒙古栎 (*Quercus mongolica*) 林，油松 (*Pinus tabulaeformis*) 林等。坝上植物群落类型包括白桦林、棘皮桦 (*Betula dahurica*) 林、落叶松林、油松林，除了森林植被外，还有草甸和草甸草原，如贝加尔针茅 (*Stipa baicalensis*) 草原、羊草 (*Leymus chinensis*) 草原和线叶菊 (*Filifolium sibiricum*) 草原，以及在低湿地和水体周边分布沼泽植被。

2.3.1 植被的历史演变

河北坝上地区植被演变与气候变迁有密切关系，植被的演化主要是一个自然过程 (Liu *et al.*, 2002b, 何钢和刘鸿雁, 2004)。我国的森林-草原交错带大致呈东北-西南向分布，它的形成要追溯到地质时期新生代第三纪末期。由于喜马拉雅造山运动，青藏高原隆起，改变了世界大气环流形式，我国北方地区气候转为干旱，草原开始形成，不过那时的植被仍以森林为主。我国的森林-草原形成于第四纪更新世，在此期间出现了几次冰期，起源于西伯利亚冷湿气候的云杉迁移到这里，冰期过后，温度上升，云杉逐渐退缩，但也有一部分保留下来，像白音敖包的沙地云杉 (*Picea mongolica*) 林。由于河北北部没有受到冰川的影响，起源于劳亚古陆第三纪热带的蒙古栎 (*Quercus mongolica*) 保存下来 (李博等, 1980; 中国科学院内蒙古宁夏综合考察队, 1985; 邹厚远等, 1994; 崔海亭等, 1997)。第四纪古生态研究也表明，该地区的气候变迁大致经历 10000 ~ 8000 年前的寒冷湿润期，8000 ~ 5900 年前温暖湿润期，5900 ~ 2900 年前温暖干燥期，和 2900 前 ~ 至今寒冷干燥期，这一气候变迁伴随着风沙活动大约始于 6000 年前 (崔海亭等, 1997); 晚更新世时，浑善达克沙地开始形成并逐渐向东扩展 (李智佩等, 2002)，在全新世早

期, 该地区的气候条件与现代长白山附近的气候条件类似, 是一种冷湿的气候 (崔海亭等, 1997), 随着降水量的下降, 喜暖湿的落叶阔叶树如栎 (*Quercus*) 等, 逐渐从这一地区退出, 局部针叶林和草原逐渐成为主要植被景观。由于沙地良好的土壤水分条件, 油松 (*Pinus tabulaeformis*) 林得以在沙地存在, 但总体上覆盖度较低。降水量的减少和低的植被盖度又为风沙活动创造了条件。晚全新世以来, 随着降水量的进一步减少和植被覆盖度的进一步降低, 这一地区的沙化呈进一步增强的趋势 (Liu *et al.*, 2002b)。

直到清代前中期, 这一区域的开垦活动仍然较弱 (张宝秀, 1997)。崔海亭等 (2003) 根据元代古籍中的景观和物候信息复原了这一地区 13 ~ 14 世纪的自然景观, 认为当时的景观结构与现代基本一致, 特别是浑善达克沙地的范围与现代几乎没有大的差别, 14 世纪时以固定沙地为主, 景观面貌与现代大体相同 (崔海亭和王文, 2003)。直至 1 个世纪以前, 河北坝上和内蒙古浑善达克沙地仍然是水草肥美的草原。但随着人为活动的加强, 近年来的生态状况与 100 年前, 甚至 50 年前相比已经严重退化。

2.3.2 森林—草原交错带植物过渡性特点

我国森林—草原交混带北起内蒙古东北额尔古纳河边缘的吉拉林, 沿着大兴安岭西麓向西南方向延伸, 经河北坝上高原、山西大同盆地、陕西黄土高原, 到甘肃渭源一带结束 (刘濂, 1965, 吴征镒, 1980)。由于塞罕坝地处蒙古高原、大兴安岭山系与燕山山脉余脉交汇处, 植物分布具有明显的过渡性。在中国植物区系区划上, 是我国东北区、蒙古高原区和华北区系交汇处。代表性植物区系成分属于冀北山地森林和内蒙草甸草原, 其中蒙古高原草原区系植物物种成份占 70% 以上。代表草原区系的植物成份的代表属有蒿属 (*Artemisia*)、鸢尾属 (*Iris*)、针茅属 (*Stipa*)、冰草属 (*Agropyron*)、葱属 (*Allium*)、拂子茅属 (*Calamagrostis*) 等共 38 种。除了禾草类外, 还有灌木物种如小叶锦鸡儿 (*Caragana microphylla*)、百里香 (*Thymus mongolicus*) 等。兴安—蒙古成份如大针茅 (*stipa grandis*)、柴胡 (*Bupleurum sp.*)、线叶菊 (*Filifolium sibiricum*) 等, 以及欧亚—北美草原成分如冷蒿 (*Artemisia frigida*)、草 (*Koeleria cristata*)。塞罕坝地势高, 气温低, 蒸发量小, 有效雨量较多, 气候比较湿润, 相对水热条件较为优越, 从 1962 年成立塞罕坝机械林场后, 种植大面积落叶松、樟子松和云杉林, 以及坝上的大部分阴坡自然更新成白桦林和坝下较低海拔山坡地发育成蒙古栎林, 成为塞罕坝主要的森林景观。除了大面积人工森林外, 还有保留部分草甸—草原景观, 植物种类有贝加尔针茅 (*Stipa baicalensis*)、线叶菊 (*Filifolium sibiricum*)、拂子茅 (*Calamagrostis epigeios*)、沙生冰草 (*Agropyron desertorum*)、赖草 (*Leymus secalinus*)、无芒雀麦 (*Bromus inermis*)、草、直立黄芪 (*Astragalus adsurgens*)、短穗看麦娘 (*Alopecurus brachystachyus*) 等。

2.3.3 植物组成

根据以往塞罕坝植物调查数据 (路端正等, 1996, 黄金祥等, 1996a) 和我们近两年来样方调查植物标本数据统计, 塞罕坝记录维管束植物有 80 科 311 属 622 种 (含变种和亚种, 但不计栽培种), 其中蕨类植物 6 科 10 属 16 种; 裸子植物 2 科 5 属 12 种; 被子植物 72 科 296 属 634 种。统计结果如表 2-1。

表 2-1 塞罕坝维管束植物统计

类型	科	属	种
蕨类植物	6	10	16
裸子植物	2	5	12
被子植物	72	296	634
其中： 双子叶植物	62	233	497
单子叶植物	10	63	137
合 计	80	311	662

该地区主要的乔木物种有白桦、黑桦 (*Betula dahurica*)、山杨 (*Populus davidiana*)、蒙古栎 (*Quercus mongolica*)、华北落叶松 (*Larix principis-rupprechtii*)、白杆 (*Picea meyeri*)、油松 (*Pinus tabulaeformis*)、华北五角枫 (*Acer truncatum*)、山荆子 (*Malus baccata*)、花楸 (*Sorbus pohuashanensis*)等。

主要灌木物种有东陵八仙花 (*Hydrangea bretschneideri*)、兰靛果忍冬 (*Lonicera coerulea* var. *edulis*)、华北忍冬 (*L. tatarinowii*)、金花忍冬 (*L. chrysantha*)、蒙古荚蒾 (*Viburnum mongolicum*)、毛榛 (*Corylus mandshurica*)、平榛 (*C. heterophylla*)、锦带花 (*Weigela florida*)、京山梅花 (*Philadelphus pekinensis*)、大叶小蘗 (*Berberis amurensis*)、小花溲疏 (*Deutzia parviflora*)、接骨木 (*Sambucus williamsii*)、山刺玫 (*Rosa davidii*)、稠李 (*Prunus padus*)、毛山茱萸 (*Cornus brtschneideri*)等。草原灌木植物种有：山竹岩黄芪 (*Hedysarum fruticosum*)、百里香 (*Thymus mongolicus*)、冷蒿 (*Artemisia frigida*) 等。

主要草本物种有披针叶苔草 (*Carex lanceolata*)、贝加尔针茅、克氏针茅 (*Stipa klylovii*)、羊草 (*Leymus chinensis*)、线叶菊 (*Filifoliumsibiricum*)、细叶韭 (*Allium tenuissimum*)、星毛委陵菜 (*Potentilla acaulis*)、白花黄芪 (*Astragalus galactites*)、北柴胡 (*Bupleurum chinense*)、瓦松 (*Orostachysfimbriatus*)、沙蓬 (*Agriophyllum squarrosum*)、软毛虫实 (*Corispermum puberulum*)、臭草 (*Melica turczaninowiana*)、口外糙苏 (*Phlomis jeholensis*)、种阜草 (*Moehringia lateriflora*)、细茎鸢尾 (*Iris ruthenica*)、七瓣莲 (*Trientalis europaea*)、七筋姑 (*Clintonia udensis*)、尖唇鸟巢兰 (*Neottia acuminata*)、华北对叶兰 (*Listera puberula*)、沼兰 (*Malaxis monophyllos*)、二叶舌唇兰 (*Platanthora chlorantha*)、假香野豌豆 (*Vicia pseudo-orobus*)、玉竹 (*Polygonatum odoratum*)、舞鹤草 (*Maianthemum bifolium*) 等。

塞罕坝植物物种数最多的前十个科分别是菊科、禾本科、蔷薇科、豆科、莎草科、毛茛科、唇形科、杨柳科、石竹科、玄参科，其中菊科排列第一为 90 种，其次是禾本科 70 种，其他各科物种数详见表 2-2。

表 2-2 塞罕坝植物物种数前十个科属、种数

科	属数	种数
菊科	37	90
禾本科	35	70
蔷薇科	17	50
豆科	15	38
莎草科	6	31
毛茛科	14	27
唇形科	13	24
杨柳科	2	24
石竹科	9	19
玄参科	9	19

塞罕坝单科单属植物有 23 种 (表 2-3); 单科少种共 34 种, 其中 1 科 1 属 2 种有 22 种, 1 科 2 属 1 种 12 种。

表 2-3 单科单属植物物种

序号	中 名	学 名	科	属
1	蕨	<i>Pteridium aquilinum</i> var. <i>latiusculum</i>	蕨科	蕨属
2	心岩蕨	<i>Woodsia subcordata</i>	岩蕨科	岩蕨属
3	急折百蕊草	<i>Thesium refractum</i>	檀香科	百蕊草属
4	反枝苋	<i>Amaranthus retroflexus</i>	苋科	苋属
5	马齿苋	<i>Portulaca oleracea</i>	马齿苋科	马齿苋属
6	大叶小檗	<i>Berberis amurensis</i>	小檗科	小檗属
7	蝙蝠葛	<i>Menispermum dauricum</i>	防己科	蝙蝠葛属
8	五味子	<i>Schisandra chinensis</i>	木兰科	五味子属
9	白鲜	<i>Dictamnus dasycarpus</i>	芸香科	白鲜属
10	水马齿	<i>Callitriche stagnalis</i>	水马齿科	水马齿属
11	卫矛	<i>Euonymus alatus</i>	卫矛科	卫矛属
12	华北五角枫	<i>Acer truncatum</i>	槭树科	槭属
13	水金凤	<i>Impatiens noli-tangere</i>	凤仙花科	凤仙花属
14	沙棘	<i>Hippophae rhamnoides</i>	胡颓子科	沙棘属
15	鹿蹄草	<i>Pyrola calliantha</i>	鹿蹄草科	鹿蹄草属
16	二色补血草	<i>Limonium bicolor</i>	白花丹科	补血草属
17	中华花荵	<i>Polemonium coeruleum</i> var. <i>chinense</i>	花荵科	花荵属
18	旋蒴苣苔	<i>Boea hygrometrica</i>	苦苣苔科	旋蒴苣苔属
19	华北蓝盆花	<i>Scabiosa tschiliensis</i>	川续断科	蓝盆花属
20	水烛	<i>Typha angustifolia</i>	香蒲科	香蒲属
21	水麦冬	<i>Triglochin palustre</i>	水麦冬科	水麦冬属

22	浮萍	<i>Lemna minor</i>	浮萍科	浮萍属
23	穿龙薯蓣	<i>Dioscorea nipponica</i>	薯蓣科	薯蓣属

2.3.4 特有植物

根据《河北植物志》资料统计，塞罕坝属于河北特有植物共有 5 种，隶属于 4 科 4 属。分别是雾灵香花芥 (*Hesperis oreophila*)、口外糙苏 (*Phlomis jeholensis*)、多歧沙参 (*Adenophora wawreana*)、雾灵沙参 (*Adenophora wulingshanica*)、柔软早熟禾 (*Poa leptota*)。

2.4 动物资源

据统计，塞罕坝共记录陆生野生动物 152 种(亚种)，隶属于 21 目 51 科。其中两栖纲 1 目 3 科 4 种；爬行纲 1 目 3 科 4 种；鸟纲 14 目 33 科 118 种；哺乳纲 5 目 12 科 26 种。塞罕坝共有国家重点保护动物 47 种，其中鸟类 39 种，兽类 7 种，鱼类 1 种。《濒危野生动植物种国际贸易公约》保护种 30 种，中澳候鸟保护协定种 12 种，日中候鸟保护协定种 61 种。

2.5 土地利用

塞罕坝机械林场主要营林为主，主要土地利用类型为人工林。除了人工林外，在各分场仍然少量农业用地，部分的防火林带春夏季种植庄稼，秋季收成后作为防火林隔离带。同时，在全场范围内仍然保存部分的天然林或天然更新植被；也有一些立地条件较差，仍然保留荒山荒地

第三章 研究方法

3.1 资料来源

(1) 野外调查数据

样方数据来源于 2005 年塞罕坝不同森林植被类型样方调查。选择占森林总面积 84.4% 代表性塞罕坝森林类型：落叶松、樟子松和白桦。分别设置 7 个 100 m×100 m 样方，其中落叶松林 3 个、白桦林 3 个及樟子松 1 个。样方设置方法：根据森林面积和地形条件限制，在满足 100 m×100 m 样方大小条件下，森林周围必须是一定面积的缓冲带，尽量选择森林结构相对均匀，人为干扰少。每一样方划分成 10 m×10 m 的小样方，每一小样方的边界四个角用 Φ2×10 cm PVC 管为界桩，按从左到右方向逐行调查每一 10 m×10 m 小样方内的乔木胸径和树高。在每一乔木测量胸径处作醒目标记，并逐一对乔木进行编号。样方的设置情况见表 3-1。

表 3-1 7 个 1ha 植物调查样方基本情况

样地 编号	群落类型	面积 (m ²)	经度 (°E)	纬度 (°N)	海拔 (m)	坡度 (°)	坡向	坡位	地理位置
BP01	白桦林	200×50	117°14'00"	42°27'52"	1536	24.5	N	中部	泰丰湖
LA02	人工落叶松林	100×100	117°19'06"	42°24'27"	1609	2			尚海林
BP03	白桦林	100×100	117°18'58"	42°23'52"	1610	23	N	中下坡	尚海林对面
LA04	人工落叶松林	100×100	117°24'30"	42°20'23"	1668	8	W	中坡	月亮湖
A05	人工樟子松林	100×100	117°04'36"	42°25'30"	1461	8	S	中下坡	菜木山
LA06	人工落叶松林	100×100	117°06'58"	42°25'19"	1463				菜木山
BP07	白桦林	200×50	117°29'03"	42°18'46"	1488	25	N		83 号作业区

每 1 ha 样方划分为 100 个 10 m×10 m 的小样方，小样方采用逐行逐序统一编号，调查顺序按编号进行逐一调查。

(2) 小班调查数据

2002 ~ 2003 年在河北省林业局和塞罕坝机械林场组织下，以河北省林业规划设计院为主要技术力量，开展塞罕坝机械林场详细的森林资源调查，该调查抽调 80 人技术人员，历时 2 年。对塞罕坝机械林场的森林植被进行详细的林业小班调查。

本研究利用上述的野外调查数据和塞罕坝机械林场总场森林资源小班调查数据，分析塞罕坝机械林场森林蓄积量及其变化。

(3) 植物分布调查数据

以北京大学地球环境与生态系统实验站为研究基地，开展塞罕坝植物分布本底调查。根据不同植被类型，作植物群落样方，采集植被标本，记录样方内植物物种的分布。

1989 ~ 1994 年由河北省林业局（原省林业厅）组织有关专家对塞罕坝机械林场的植物进行了全面调查。结合该调查数据，分析塞罕坝植物分布及区系，对塞罕坝机械林场植物分布进行补充和修订，并编制塞罕坝植物名录。

(4) 气象观测数据

塞罕坝机械林场气象站于 1960 年开始观测, 其间 1962 ~ 1963 年由于当时条件的限制数据不全外, 1964 年后气象观测数据十分完全。利用该气象数据分析了塞罕坝机械林场气候变化情况, 为进一步深入理解塞罕坝森林生态系统提供参考。

3.2 数据分析

3.2.1 森林蓄积量和生长量估算

植物生长量计算方法很多, 针对不同类型植被类型有不同的方法。在研究草地和灌丛时, 常用收割法研究生长量; 在测量森林类型时, 常用森林资源清查方法如作解析木、测量胸径和树高等。

森林蓄积量的估算常用方法是森林资源清查, 在一定时期 (通常五年) 重复调查一次, 二次比较就得出森林蓄积量的变化。这种估算方法由于二次取样空间、时间尺度上差异, 也由于取样频度和均匀性不一致, 导致较大误差。

空间代替时间方法估算法: 由于森林资源清查详细记录了调查小班林龄, 用空间代替时间方法将逐一计算出不同时间尺度的各类型森林小班面积, 建立林龄与蓄积的关系, 计算出各森林类型的蓄积量。

森林生长模型估算法: 由于森林生长受各种环境条件控制, 不是单因子的简单作用, 而是水热条、环境梯度综合的结果, 主要包括温度、降水、土壤、坡度、起源等, 用这些综合环境因子建立不同森林类型生长模型, 提高森林生长量估算精度。

3.2.2 样方数据分析

塞罕坝机械林场以人工森林群落为主, 为了研究不同类型森林群落结构及生长特征, 选择有代表性森林群落, 作 7 个 1 ha 森林样方。样方数据重点分析了在不同取样面积与胸径变化规律。取样面积增大方法: (1) 按样方四个对角不同方向 (图 3-1) 增加面积, 面积增加大小为 10 m×10 m, 20 m×20 m, 30 m×30 m..., 四个方向如图 3-1 i)、ii)、iii)、iv)所示。(2) 以 10 m×10 m 小样方面积逐一递增方法, 采用四种, a) 顺序从下到上; b) 顺序从上到下; c) 逐一从下到上; d) 逐一从上到下 (图 3-1)。每一样方按八种不同方式计算胸径偏斜度。

胸径偏斜度 (skew) 计算: 偏斜度反映以平均值为中心的分布的不对称程度。正偏斜度表示不对称部分的分布更趋向正值。负偏斜度表示不对称部分的分布更趋向负值。计算公式如下:

$$\text{偏斜度的计算公式: } \frac{n}{(n-1)(n-2)} \sum \left(\frac{x_i - \bar{x}}{s} \right)^3 \quad \text{公式(1)}$$

胸径变化程度可能用变异系数 CV 表示, 计算各小样方内胸径 CV 变化, 在 ArcGIS 支持建立空间分布关系。CV 计算公式如下:

$$\text{CV 计算公式: } \text{CV} = \text{标准差} / \text{平均值} \quad \text{公式(2)}$$

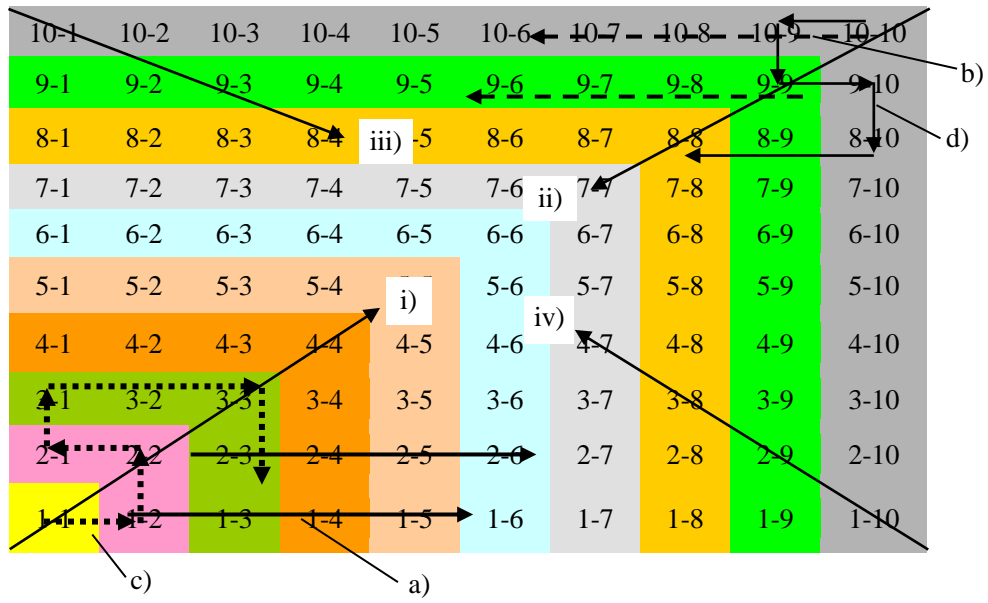


图 3-1 径级 skew 分布的样方面积扩大示意图

第四章 气候特征

塞罕坝地区属于暖温带向温带的过渡带，是我国受太平洋季风气候影响的北限。由于塞罕坝海拔迅速升高，在季风气候的影响下，形成了气温低（年平均温在-2.7℃ ~ -0.5℃之间），降水量高的气候特点。

塞罕坝 40 年来气候数据记录表明（表 4-1），1 月平均气温最低（-21.9℃），7 月平均气温最高（16.1℃）；降水集中在 5~9 月，其中以 7 月最高（122.9 mm），蒸发量主要在 4~9 月，其中 5 月达到蒸发量的最高值（233.0 mm），大风天气集中在 3~5 月和 10~12 月。

塞罕坝生态气候图（图 4-1）可以看出，塞罕坝年平均气温低，月平均温度只有 4~9 月在零度以上，而降水集中在 6~9 月。

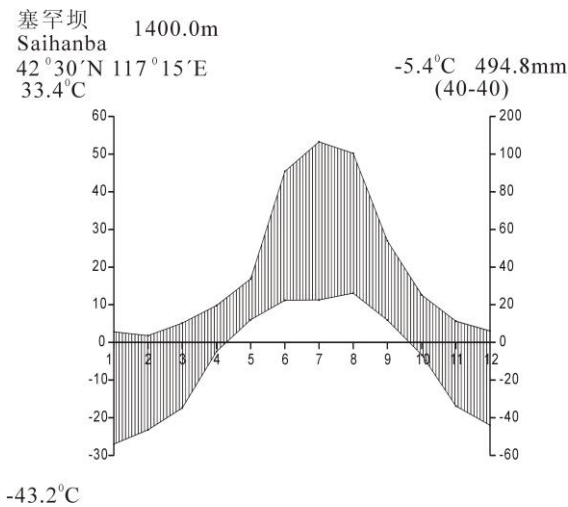


图 4-1 塞罕坝生态气候图

表 4-1 塞罕坝月平均气候基本情况

月份	平均气温 (℃)	降水量 (mm)	相对湿度 %	平均日照时数 (hr)	平均蒸发量 (mm)	平均大风天数 (d)
1	-21.9	4.1	79.3	188.9	16.2	4.8
2	-18.1	5.2	75.5	191.0	29.3	5.2
3	-9.3	10.6	65.2	229.7	72.4	7.8
4	1.5	16.4	53.2	223.4	156.2	10.8
5	8.9	36.8	51.1	245.6	233.0	10.5
6	13.5	71.4	65.4	222.7	198.1	5.1
7	16.1	122.9	76.8	209.7	171.0	3.1
8	14.6	99.7	78.5	215.6	150.3	2.0
9	8.1	48.9	71.5	219.9	129.4	4.0
10	0.2	23.1	68.7	220.9	95.6	6.1
11	-10.0	9.80	72.9	185.2	43.2	6.2
12	-18.4	4.7	79.2	173.4	19.1	5.5

4-2 塞罕坝 30 年(1970 ~ 2000 年)来气候变化相关性分析

相关系数 (r)	气温	降水	蒸发量	日照	大风日数
1 月	-0.04	0.20	0.56**	0.03	-0.35*
2 月	0.23	-0.13	0.36	0.09	-0.23
3 月	0.38*	-0.07	0.30	-0.20	-0.15
4 月	0.06	0.28	-0.09	0.04	-0.11
5 月	-0.15	0.10	-0.49**	0.05	-0.30
6 月	-0.05	0.29	-0.17	0.11	-0.04
7 月	0.30	0.23	0.09	0.07	-0.10
8 月	0.03	0.18	-0.08	0.02	-0.50**
9 月	0.22	0.11	-0.27	0.10	-0.08
10 月	-0.02	0.00	-0.51	-0.03	0.05
11 月	-0.01	0.23	-0.05	-0.01	-0.27
12 月	0.20	0.31	0.32	0.28	-0.19
年平均气温	0.34				
年极端最高气温	0.29				
年极端最低气温	0.24				
年降水量		0.42*			
年降水日数		0.50**			
年蒸发总量			-0.18		
最大月蒸发量			-0.43*		
年日照总时数				0.17	
年大风日数					-0.36*

* $P < 0.05$, ** $P < 0.01$

4.1 气温

图 4-2 为 1970 ~ 2000 年的年平均气温变化趋势图。从图中可以看出逐年平均气温变化, 1970 ~ 1985 年间年平均气温变化幅度大, 气温升中有降; 至 1985 年平均气温达到最低年。1985 ~ 2000 年气温变化幅度降低, 各年平均气温最低值 -1.5°C 以上, 这与全球气候变暖相一致。

从图 4-2 可以看出, 年平均气温有上升趋势 ($R^2=0.11$), 但相关分析不显著, 可用线性回归方程表示: $y=0.0237x-48.283$ ($R=0.34$)。年极端最高气温和极端最低气温的变化均略有所上升 ($R^2_{\max}=0.084$,

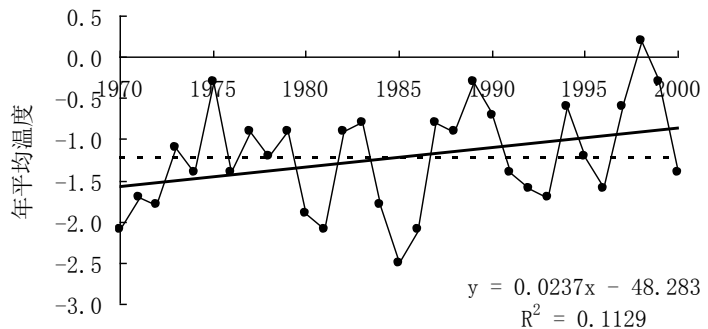


图 4-2 塞罕坝 1970-2000 年平均温度

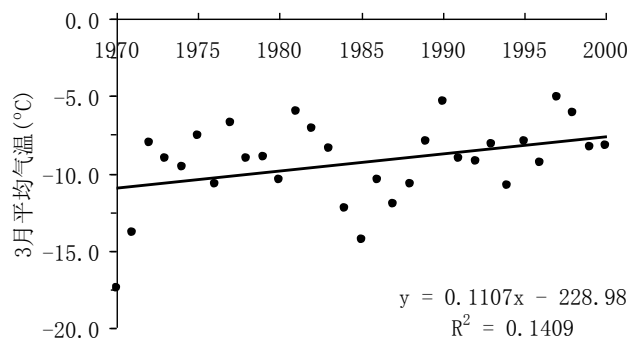


图 4-3 塞罕坝 1970-2000 年 3 月平均气温变化趋势

$R^2_{\min}=0.058$), 但二者均不显著。

各月气温变化差异较大(表 4-2), 其中 3 月气温变化较显著, 相关性分析表明有显著上升趋势($R=0.38, P<0.05$, 图 4-3), 2、4 月份气温变化也为正相关, 但不显著。7~9 月气温变化为正相关, 其中以 7 月和 9 月更为明显, 这使得植物生长期延长。10、11、1 月气温变化较为缓和或略微下降。为进一步研究植物生长季的气温变化, 还分析了 5~9 月极端温度变化 (表 4-3), 结果表明 5~9 月最高极端温度均正相关, 其中以 9 月为显著正相关 ($R=0.53, P<0.05$)。极端最低温度规律不明显, 5、7 月为负相关, 8 月为正相关。

表 4-3 塞罕坝 1970~2000 年 5~9 月极端最高气温、极端最低气温变化相关分析

R	5 月	6 月	7 月	8 月	9 月
极端最高气温	0.04	0.17	0.34	0.25	0.53*
极端最低气温	-0.20	0.02	-0.15	0.14	-0.02

统计结果表明 1960~2002 年 4~10 月 $\geq 5.0^{\circ}\text{C}$ 、 $\geq 10.0^{\circ}\text{C}$ 、 $\geq 15.0^{\circ}\text{C}$ 积温变化明显。 $\geq 5.0^{\circ}\text{C}$ 积温在 4~10 月为负相关; $\geq 10.0^{\circ}\text{C}$ 温度除了 9 月份外, 在其它月份均为负相关; $\geq 15.0^{\circ}\text{C}$ 积温除了在 4 月、9 月正相关外, 在其它月份均负相关 (表 4-4)。虽然年平均气温有增加趋势, 但 5~9 月的积温变化并不明显, $\geq 15^{\circ}\text{C}$ 积温分别在 4 月和 9 月为正相关, 说明植物生长的季初始高温天气增多, 生长季结束日期推迟。在生长季的 6~8 月降雨量增加(表 4-6), 平均气温并没有明显变化。相关分析结果表明有效积温与年日照时数有显著负相关, 与降水正相关, 但不显著 (表 4-5)。

表 4-4 塞罕坝 30 年来 5~9 月最高、最低气温变化相关分析

相关性	$\geq 5^{\circ}\text{C}$	$R_{\geq 5^{\circ}\text{C}}$	$\geq 10^{\circ}\text{C}$	$R_{\geq 10^{\circ}\text{C}}$	$\geq 15^{\circ}\text{C}$	$R_{\geq 15^{\circ}\text{C}}$
分析	平均积温		平均积温		平均积温	
4 月	64.8	-0.07	18.7	-0.17	1.2	0.22
5 月	261.6	-0.28	168.7	-0.16	47.0	-0.34
6 月	407.8	-0.04	375.4	-0.10	171.8	-0.08
7 月	509.5	0.02	507.5	-0.01	391.0	0.01
8 月	455.1	-0.15	446.0	-0.15	242.9	-0.15
9 月	222.6	-0.05	127.1	0.11	15.6	0.26
10 月	39.6	-0.25	5.2	-0.19	0.0	-
合 计	1960.9	-0.20	1648.1	-0.14	869.6	-0.10

表 4-5 塞罕坝 30 年来 5~9 月最高、最低气温变化相关分析

相关性	年气温	$\geq 5^{\circ}\text{C}$ 积温	年降水量	年日照时数	年蒸发量
$\geq 5^{\circ}\text{C}$ 积温	0.53**				
年降水	0.00	-0.17			
年日照	-0.05	-0.44*	0.38		
年蒸发量	0.52**	0.42*	-0.42*	0.07	
年大风日数	-0.16	-0.08	-0.08	0.41*	0.40*

4.2 降水

用塞罕坝气象站的观测资料分析 30 年来降雨量的变化, 求算每 5 年际的降水相对变化率, 公式如下:

$$R_i = (x_i - \bar{x}) / \bar{x}$$

式中 R_i 为降水相对变率, x_i 为 5 年均值, \bar{x} 为 1970 ~ 2000 年均值, 结果如表 4-6。

表 4-6 1971 ~ 2000 年塞罕坝降雨量年际变化率

年 代	X_i	R_i	%
1971-75	403.1	-0.109	-10.9
1976-80	423.8	-0.063	-6.3
1981-85	421.5	-0.068	-6.8
1986-90	460.1	0.017	1.7
1991-95	548	0.212	21.2
1996-2000	477.9	0.057	5.7
\bar{x}	452.2		

从表 4-6 可见, 该地区 30 年来降水量变化明显, 总体上呈增加趋势。虽然 1973 年出现高降水年 (603.1 mm), 但 1971 ~ 75 年降水量仍然保持低降水量。随后降水量以偏低的水平持续了 10 年; 从上世纪 80 年代中期, 降水量开始明显增加, 至 90 年代增加幅度更大, 其中 1991 ~ 95 年相对降水变化率达 21.2%, 这与 1991 年出现的近 30 年来最大降水量 (636.0mm), 以及 1992、1994、1995 年出现的降水量超过 500.0 mm 有关。

从图 4-4 中可以得出, 1971 ~ 85 年降水量偏低, 只在 1973 年降雨量大大超过其平均水平; 1985 年后降水量明显增加, 只在 1989 年降水量远低于平均值, 仅为 280.2 mm, 其它年份高低于平均值。

30 年降水量变化的相关分析也表明, 年降水量显著正相关 ($R=0.42$, $P<0.05$), 日降水日数明显增多 ($R=0.50$, $P<0.001$)。

蒸发量受气温、风力和太阳辐射等因素的综合影响。塞罕坝 30 年来蒸发量变化趋势特点是: 在 12 月 ~ 翌年 3 月蒸发量有增长趋势, 尤其是 1 月增加显著, 其它月份变化不显著。4 月至 11 月各月蒸发量多为负相关, 其中 5 月蒸发量明显负相关 ($R=-0.49$, $P<0.001$, 图 4-5), 可能与气温和大风天气增多有关, 其它各月年际变化略有下降, 可能与该地区种植大面积人

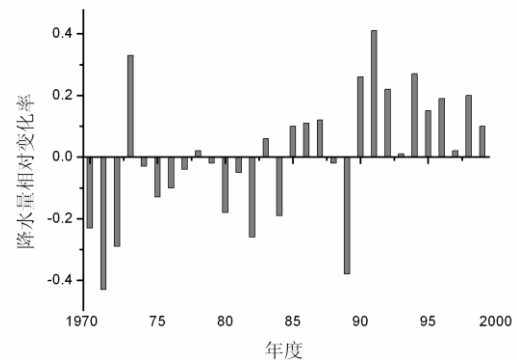


图 4-4 塞罕坝 1970-2000 年标准化距平降水量的年际变化

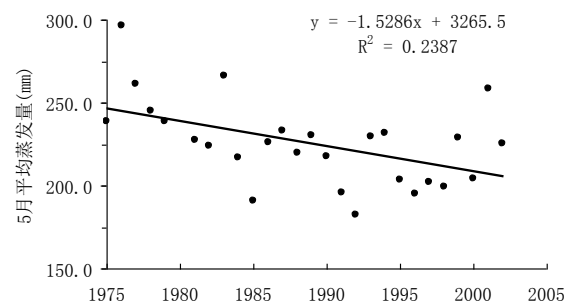


图 4-5 塞罕坝 1975-2002 年蒸发量的年际变化

工林，改善了当时气候条件有关。

4.3 风

本区地处内蒙古高原南缘，海拔高，为典型的大陆型气候，风多风大，持续时间长。各季主要受蒙古高压控制，出现稳定的西北风和偏西风(刘全友, 1994)。塞罕坝机械林场气象站观测资料显示，大风日¹全年频率平均为 18.6% (6.0% - 32.6%)，年平均大风日为 67.8 日，最多年份为 119 天 (1966 年)，最低为 22 天(1991 年)。1960 ~ 2002 年近 42 年大风日数标准化的年际变化统计如图 4-6。从该地区大风日变化情况来看，大风日各月均多见，春、夏季交替 3~5 月最为多见，而以 7~9 月大风日数最少 (图 4-7)。

从年际变化来看，1960’s 到 1980’s 中期是大风频数高发期，绝大多数在平均线以上 (图 4-6)；1985 ~ 92 年出现连续 7 年大风日数在平均线以下，1994 ~ 96 大风日数回升到平均线以上，但从 1997 ~ 2002 年大风日数相对减少。不同月份分析表明，30 年来塞罕坝大风天气日数相对减少，有 1 月、8 月大风天数显著负相关($R_{1月}=-0.35$, $R_{8月}=-0.50$, $P<0.001$)。虽然大风日数相对减少，但资料统计表明大风日强度加强，日持续时间长。

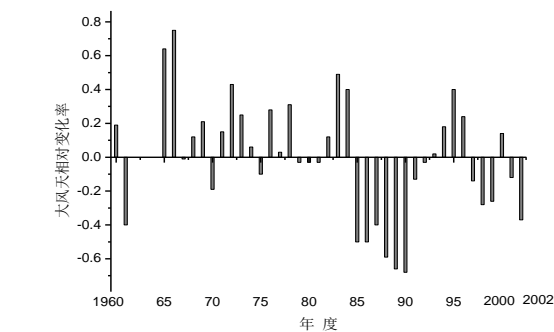


图 4-6 塞罕坝 1970-2000 年距平大风日数的年际变化

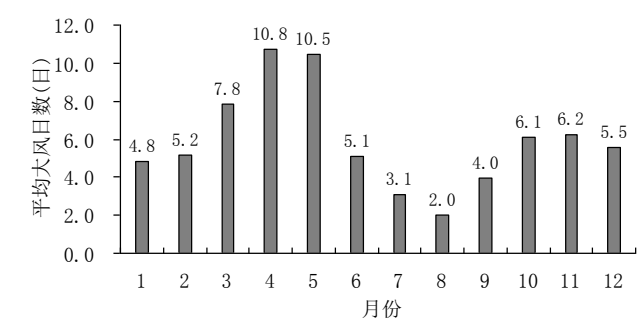


图 4-7 塞罕坝月平均大风日数

4.4 日照

塞罕坝月平均日照时数 210.5 小时，平均总日照时数 2526.0 小时。各月日照时数差异如图 4-8，其中 12 月平均日照时数最低 (173.4 hr)，5 月最高 (245.6 hr)。3、4、5、6 月明显高于平均水平，7、8 月由于多云或降水天气多，日照时数较低。30 年来日照时数无明显变化趋势 (表 4-2)。

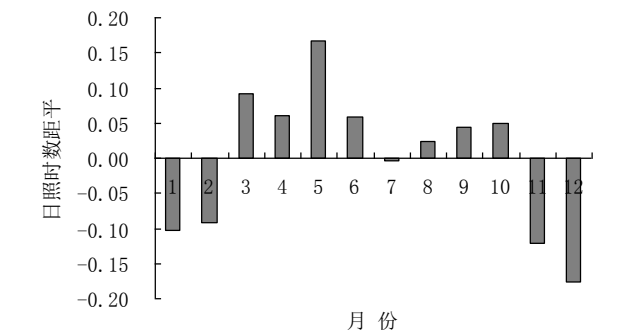


图 4-8 塞罕坝不同月份距平日照时数变化

¹ 大风指风速≥1.7 米/秒，或大风≥7 级时，规定为一个大风日。

第五章 主要森林结构和生长特征

5.1 土地利用

塞罕坝机械林场主要土地利用类型有：森林、荒地、湿地和水体、农田、草地、灌木林、防火带以及基础设施。森林面积最大，共有72,605.7 hm²，占总面积的 76.7%；其次是荒地，该类型主要是瘠薄山地或荒山荒地，总场下设的各林场均有分布，以阴河林场分布最多；湿地主要在低洼的河谷两侧以及水泡两测，水体为零星的小型湖泊；草地在林场范围内已保存不多，绝大草地转变为人工林，仅存总面积的 1.4%；灌木林面积比较小，只占 1.2%。

表 5-1 塞罕坝机械林场土地利用类型

土地类型新	小班面积 (hm ²)	%
森林	72,605.7	76.7
荒地	10,860.0	11.5
湿地和水体	5,565.5	5.9
农田	1,747.3	1.8
草地	1,368.3	1.4
灌木林	1,174.5	1.2
防火带	844.1	0.9
基础设施	509.2	0.5
合 计	94,674.6	

5.1.1 森林经营类型

按土地经营类型上划上，可分为商品林和公益林，少量防护林和特用林等，各类型面积和蓄积量见图 5-1。公益林面积占 46.6% (43926.8 hm²) 大于商品林面积 (28,478.0 hm²，占 30.1%)，但商品林蓄积 (3,793,327.0 hm²，55.1%) 多于公益林蓄积 (3,040,226.0 hm²，44.1%)。商品林主要是落叶松林，占总蓄积的 94.1%，占总商品林的面积 91.5%；公益林主要是白桦林、落叶松林、樟子松林，分别占面积的 31.5%、28.1%、16.2%，蓄积量分别占 31.3%、42.1%t 和 9.6% (表 5-2)。

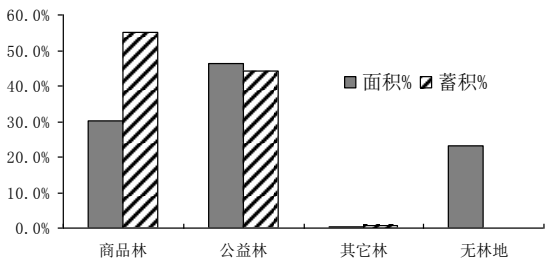


图 5-1 土地经营类型的面积和蓄积量

表 5-2 公益林面积和蓄积

优势树种	公益林		商品林	
	面积(hm ²)	%	蓄积量(m ³ /hm ²)	%
白桦林	13,858.6	31.5	952,071.0	31.3
落叶松林	12,349.9	28.1	1,278,885.0	42.1
樟子松林	7,104.9	16.2	291,212.0	9.6
蒙古栎林	3,649.2	8.3	120,937.0	4.0
混交林	3,700.8	8.4	281,685.0	9.3
山杨林	1,030.0	2.3	63,467.0	2.1
其它林	2,233.4	5.1	51,969.0	1.7

5.1.2 不同行政单元的森林类型

按行政管理单元划分，塞罕坝机械林场总场可分为北曼店、大唤起、千层板、三乡和阴河林场，各林场的商品林和公益林面积如图 5-2。商品林面积以北曼店、大唤起林场多于其它各林场，北曼店、大唤起、阴河林场商品林的森林蓄积多于其它林场。三道河口现已成立自然保护区，森林类型已转化为公益林；公益林面积以北曼店面积最少，其它各林场均占一定比例，以千层板林场公益林面积最大、其次是大唤起和三道河口。塞罕坝机械林场总场森林营林管理和经营方针上，已从单纯森林生产经营转变为多种经营，大力发展旅游产业，林业生产经营并举的措施，促进林业发展建设。

5.2 森林类型

塞罕坝林场的植被类型主要有：针叶林、落叶阔叶林、针阔混交林、灌丛、草甸草原、湿生植被和水生植被等，但以森林植被为主，占总面积的 76.7% (表 5-1)。

森林类型的优势树种分别有：白桦、落叶松、樟子松、蒙古栎、山杨、云杉、山杏、油松、榆树和柳树。塞罕坝机械林场总场以大面积工人林为主，森林类型相对比较单一。按森林优势树种划分，落叶松林面积最大 38,670.84 hm²，占面积的 38.7%，其次是桦木林，面积 15,072.4 hm²，占 15.1%，樟子松面积 7,536.1 hm²，占 7.5%。蒙古栎主要分布在低海拔、坡度较大的山坡，均为天然林或天然次生林，其它森林类型的面积比较小，只占 3.6%。

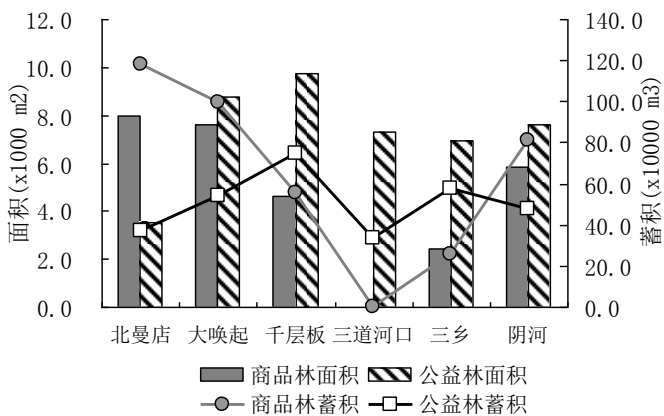


图 5-2 各林场森林面积和蓄积量

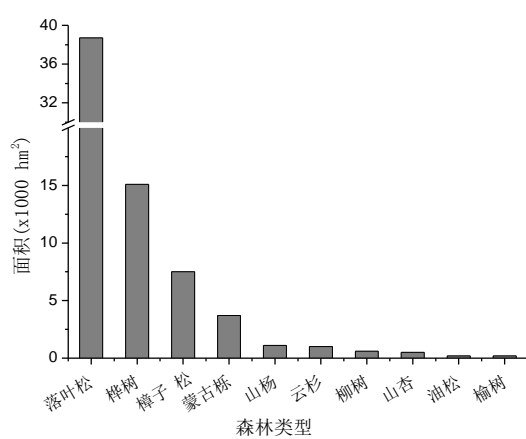


图 5-3 森林类型面积

5.2.1 落叶松林

塞罕坝原始的落叶松林为华北落叶松 (*Larix principis-rupprechtii*)，是该地区原始森林的建群种，分布海拔 1500 ~ 1900 m，但到解放初期，由于人为砍伐，森林已全部破坏，只剩下极少数量。1962 年成立塞罕坝机械林场总场后，开始大面积营林，但由于当时土地沙化严重，表层土壤水分极低，曾尝试多种营林树种，但成活率十分低下。后经过长期不断努力，采取各种有效措施，以落叶松林为主要人工种植树种。种植

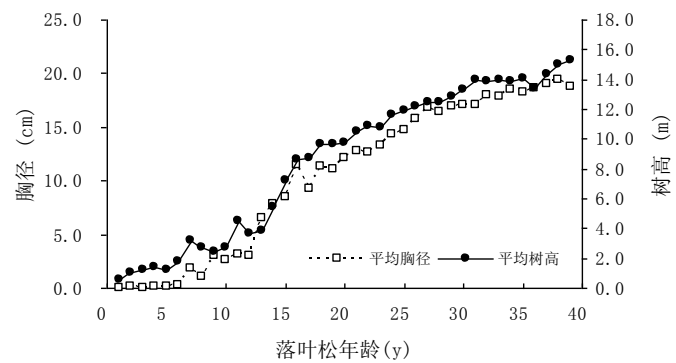


图 5-4 落叶松不同年龄径级与树高的关系

的落叶松种类主要是华北落叶松 (*Larix principis-rupprechtii*)、兴安落叶松 (*L. dahurica*)，少量的日本落叶松 (*L. kaempferi*)、黄花落叶松 (*L. olgensis*)、西伯利亚落叶松 (*L. sibirica*)，但绝大多数为华北落叶松，部分为从东北引种兴安落叶松。

塞罕坝落叶松大多为工人种植纯林，少数与樟子松、白桦组成混交林。落叶松为强阳性树种，主要分布在中上坡位，一般种植在平坦的坝顶或坡地。林层单一，林下灌木和草本稀少，常见的灌木物种有：忍冬(*Lonicera sp.*)、蔷薇(*Rosa sp.*)、茶藨子(*Ribes sp.*)等；主要草本有苔草(*Carex sp.*)、歪头菜(*Vicia unijuga*)、委陵菜(*Potentilla sp.*)、高山露珠草(*Circaea alpina*)、舞鹤草(*Maianthemum bifolium*)、风毛菊(*Saussurea sp.*)等。

经调查数据统计，落叶松森林面积为 38,670.8 hm²，占总面积 38.7%，森林蓄积量为 4,887,207.0 m³，占总蓄积量的 70.9%。落叶松林平均森林最大树高 23.0 m，平均森林最大胸径 28.5 cm。林龄在 21 ~ 35 年之间占绝大多数，占总面积的 70.8%，占总蓄积量的 86.3% (表 5-3)。落叶松的林龄与平均树高、平均胸径有较好的关系 (图 5-4)，落叶松林 0 ~ 15 年生长缓慢，15 ~ 35 年生长加速，35 年后生长减缓。

表 5-3 塞罕坝林落叶松不同林龄的生长情况

林龄 (年)	斑块数 (块)	小班面积 (hm ²)	蓄积量 (m ³)	平均树高 (m)	最大树高 (m)	平均胸径 (cm)	最大胸径 (cm)	密度 (株/hm ²)	平均斑块 面积	平均蓄积量 (m ³)
0-5	185	3,100.4	1,073.0	0.9	9.6	0.1	4.0	2994	16.8	0.3
5-10	177	2,764.0	1,744.0	2.6	17.0	1.7	17.1	3117	15.6	0.6
11-15	63	677.7	19,819.0	4.9	12.1	5.8	14.8	2782	10.8	29.2
16-20	169	2,532.4	227,504.0	9.3	16.5	11.0	19.9	1634	15.0	89.8
21-25	511	7,113.0	973,114.0	11.1	15.5	13.6	24.4	1472	13.9	136.8
26-30	747	12,959.0	2,021,560.0	12.7	23.0	16.5	22.0	1084	17.3	156.0
31-35	440	7,490.6	1,264,489.0	13.9	21.2	17.9	26.3	957	17.0	168.8
36-40	108	1,822.4	335,022.0	14.2	19.5	18.3	25.3	997	16.9	183.8
41-45	12	200.0	41,124.0	16.1	19.5	20.9	28.5	855	16.7	205.6
>45	2	11.3	1,758.0	20.6	22.0	18.6	21.1	683	5.7	155.6

5.2.2 白桦林

白桦林喜湿润，在塞罕坝大片纯林多见于山地阴坡，均为天然次生林或天然更新林。塞罕坝白桦纯林是河北的集中分布区（刘濂主编，1996）。桦树林主要有白桦和黑桦组成，前者主要分布在海拔较高的坝上，黑桦分布在海拔较低的坝下，但两者常常交叉分布；此外，还有分布有硕桦 (*Betula costata*)、沙生桦 (*Betula gmelinii*)、赛黑桦 (*Betula schmidtii*)。伴生树种有：山杨 (*Populus davidiana*)、华北五角槭 (*Acer truncatum*)、蒙古栎 (*Quercus mongolica*)、中国黄花柳 (*Salix sinica*)和谷柳 (*S. taraikensis*)等，林下灌木主要有榛 (*Corylus sp.*)、胡枝子 (*Lespedeza bicolor*)、悬钩子 (*Rubus sp.*)、绣线菊 (*Spiraea sp.*)、忍冬 (*Lonicera sp.*)、荚蒾 (*Viburnum sp.*) 等。草本层主要有蕨类、苔草类、柴胡 (*Bupleurum sp.*)、风毛菊、柳兰 (*Chamaenerion angustifolium*)、野豌豆 (*Vicia sp.*)。坝上白桦林主要以纯林为主，散生少量的山杨或云杉；坝下白桦林常与山杨、蒙古栎组成共建群落。

白桦林面积为 94,674.6 hm²，占总面积的 15.9%，森林蓄积量为 1,086,851.0 m³。本区白桦林年龄在 15 ~ 40 年占绝大多数，50 年林龄以上很少，最大森林平均胸径为 20.4 cm，最大森林平均树高为 19.6 m (表 5-4)。0 ~ 10 年的白桦林生长十分迅速，胸径和树高均增长很快，10 年后生长胸径与树高生长减缓 (图 5-5)。坝上桦树林喜生长阴坡，阳坡无乎没有分布，低偏湿的生境也分布少量的桦树，但生长径级均较小。

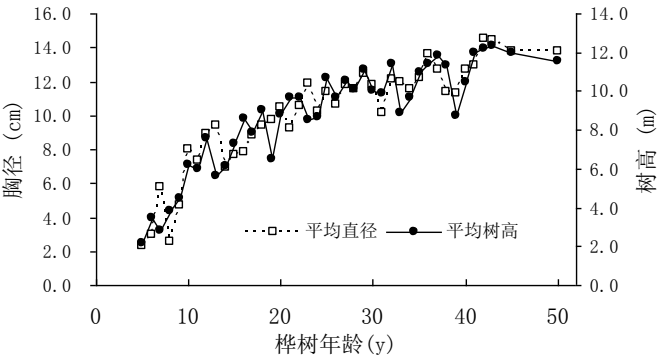


图 5-5 桦树林不同年龄径级与树高的关系

表 5-4 塞罕坝林白桦林不同林龄的生长情况

林龄 (年)	斑块数 (块)	小班面积 (hm ²)	蓄积量 (m ³)	平均树高 (m)	最大树高 (m)	平均胸径 (cm)	最大胸径 (cm)	密度 (株/hm ²)	平均斑块 面积	平均蓄积量 (m ³)
0-5	8	91.0	87.0	2.1	3.5	8.3	14.4	1321.1	11.4	1.0
5-10	17	208.5	7,211.0	4.2	12.0	4.8	11.6	3582.8	12.3	34.6
11-15	47	776.6	35,942.0	6.5	12.0	8.1	12.6	2495.6	16.5	46.3
16-20	152	1,984.4	122,759.0	8.2	14.0	9.3	17.7	2058.6	13.1	61.9
21-25	151	2,058.6	128,681.0	9.4	14.5	10.7	18.7	1535.0	13.6	62.5
26-30	287	3,936.2	303,727.0	10.3	15.0	11.7	20.3	1521.6	13.7	77.2
31-35	190	2,611.5	204,493.0	10.2	17.5	11.6	18.8	1557.0	13.7	78.3
36-40	138	1,913.8	150,904.0	10.7	17.0	12.3	18.2	1349.6	13.9	78.9
41-45	54	841.7	72,758.0	12.1	19.6	13.9	20.4	1416.8	15.6	86.4
46-50	28	514.7	47,234.0	12.1	18.0	12.0	19.1	1342.7	18.4	91.8
>50	5	135.4	13,055.0	9.6	11.5	13.9	17.3	1048.3	27.1	96.4

5.2.3 樟子松林

樟子松 (*Pinus sylvestris* var. *mongolica*) 是强阳性、耐干旱常绿针叶树种。在落叶松种植不易成活的林地能较好的生长。樟子松郁密度高，林下灌木和草本较少，林下灌木物种主要有：忍冬、胡枝子、悬钩子等，草本主要物种有：苔草、鸢尾(*Iris sp.*)、委陵菜等。

塞罕坝机械林场大面积营造樟子松林时间比较晚，林龄为 10 ~ 20 年占大多数。樟子松面积为 7,536.1 hm²，占总面积的 8.0%，总蓄积量为 329,688.0 m³，占总蓄积量的 4.8% (表 5-5)。从图 5-6 可以看出，在 25 年以下，林龄与树高和胸径有很好的关系，但在 25 年以上，由于立地条件差异，樟子松后期生长的差异比较大。

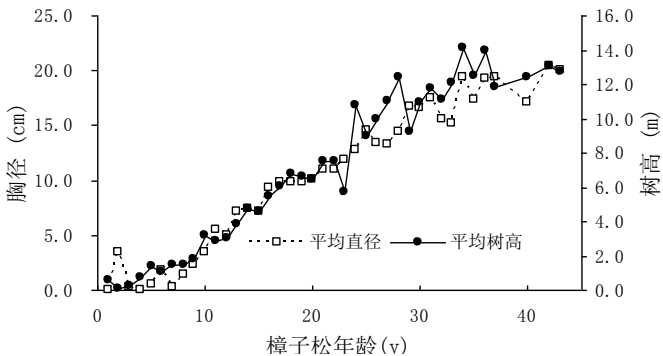


图 5-6 樟子松林不同年龄径级与树高的关系

表 5-5 塞罕坝林樟子松林不同林龄的生长情况

林龄 (年)	斑块数 (块)	小班面积 (hm ²)	蓄积量 (m ³)	平均树高 (m)	最大树高 (m)	平均胸径 (cm)	最大胸径 (cm)	密度 (株/hm ²)	平均斑块 面积	平均蓄积量 (m ³)
0-5	83	965.3	2,020.0	0.6	9.0	0.8	30.9	2682.6	11.6	2.1
5-10	97	1,368.4	1,901.0	1.8	15.0	1.8	16.9	2211.0	14.1	1.4
11-15	100	1,327.7	21,290.0	3.8	9.0	6.4	10.9	1903.8	13.3	16.0
16-20	157	2,723.6	180,127.0	6.3	11.7	9.8	15.8	1867.9	17.3	66.1
21-25	40	467.5	33,359.0	8.1	12.0	12.2	18.2	1747.1	11.7	71.4
26-30	28	291.4	31,072.0	10.7	21.4	14.9	18.7	1148.8	10.4	106.6
31-35	20	232.5	32,361.0	12.3	15.5	17.0	20.0	1167.8	11.6	139.2
36-40	9	98.6	17,541.0	12.0	14.2	18.6	23.0	1163.5	11.0	177.9
>40	5	61.1	10,017.0	10.4	15.6	16.3	23.1	1362.5	12.2	163.9

5.2.4 蒙古栎林

蒙古栎属于落叶阔叶林，是河北省地带性植被类型。蒙古栎林是栎林中比较耐寒的森林类型，也是栎类中分布最靠北的种类，构成乔木层的阔叶树在冬季全部落叶，林下灌木也是冬季落叶的种类，草本植物到了冬季其地上部分枯死或以种子越冬。塞罕坝的蒙古栎均为天然次生林或天然更新林，分布在较低海拔 (1300 ~ 1600 m) 的坝下沟谷山坡，林相不整齐，伴生黑桦、白桦、

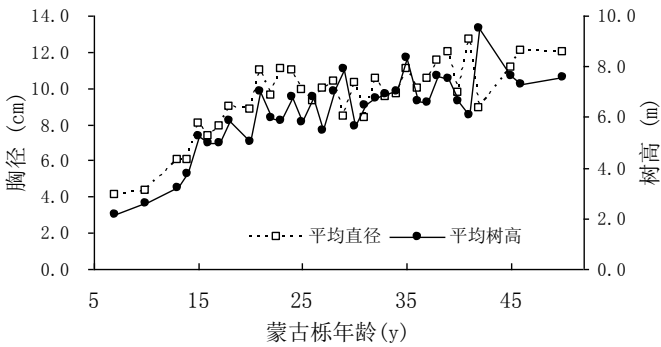


图 5-7 蒙古栎林不同年龄径级与树高的关系

山杨、华北五角槭等。林下灌木层和草本层物种比较丰富，灌木物种主要有：榛类、绣线菊、照山白 (*Rhododendron micranthum*)、迎山红 (*R. mucronulatum*)、丁香 (*Syringa sp.*)、鼠李 (*Rhamnus davurica*)、胡枝子、忍冬。草本物种主要有：龙芽草 (*Agrimonia pilosa*)、委陵菜、柴胡、歪头菜、口外糙苏 (*Phlomis jeholensis*)、玉竹 (*Polygonatum odoratum*)、苔草等。

该类森林面积比较少，只有 3671.7 hm²，占总面积 3.9%，蓄积量也比较少，有 121,337.0 m³，占总蓄积量的 1.8%。由于蒙古栎乔木层高度较低，森林平均最大树高为 17.0 m，森林平均最大胸径为 17.0 cm (表 5-6)。由于蒙古栎生长生境立地条件差异显著，林龄与树高和胸径关系差异性较大 (图 5-7)。

表 5-6 塞罕坝林蒙古栎林不同林龄的生长情况

林龄 (年)	斑块数 (块)	小班面积 (hm ²)	蓄积量 (m ³)	平均树高 (m)	最大树高 (m)	平均胸径 (cm)	最大胸径 (cm)	密度 (株/hm ²)	平均斑块 面积	平均蓄积量 (m ³)
0-5	3	50.8	-	1.1	1.6	0.0	0.0	2137.5	16.9	0.0
5-10	15	203.3	632.0	2.0	4.0	2.1	12.4	1424.2	13.6	3.1
11-15	22	256.9	3,928.0	3.7	8.0	5.0	11.3	814.3	11.7	15.3
16-20	40	444.3	9,661.0	5.2	8.5	8.3	13.6	3244.0	11.1	21.7
21-25	44	481.7	16,838.0	6.3	13.5	10.5	16.0	1113.9	10.9	35.0
26-30	60	757.4	23,373.0	6.6	10.0	9.7	17.0	1505.1	12.6	30.9
31-35	34	520.8	23,000.0	7.1	17.0	9.8	16.4	2022.9	15.3	44.2
36-40	42	554.7	23,804.0	7.0	13.8	10.8	16.4	1508.7	13.2	42.9
41-45	15	250.8	13,299.0	7.7	11.5	10.9	16.3	1365.8	16.7	53.0
>45	10	151	6,802.0	7.4	12.0	12.0	15.0	960.9	15.1	45.0

5.2.5 其它森林类型

1) 山杨林：山杨主要分布在坝下山地，常与白桦林混生。海拔较高的坝上山杨少量伴生在白桦林中，山场所占比例很少，面积有 1075.5 hm²，仅占总面积的 1.1%，蓄积量 67,470.0 m³，占总蓄积量的 1.0%。林龄以 20 ~ 30 年为主。

2) 云杉林：云杉、冷杉为生态幅度较窄的冷湿气候的指示种 (崔海亭等, 1997)。云杉林主要分布在北曼店海拔较高区域，分布海拔在 1700 ~ 1800 m。云杉林也是近几年来开始人工种植，林龄较大的云杉常散生在白桦、落叶松林内。云杉林面积有 986.2 hm²，占总积的 1.0%，大部分为幼龄树，蓄积小，为 50,297.0 m³。

3) 油松：塞罕坝主要分布在大唤起、黄花沟、样板沟、得胜沟及第三乡等，三道河口有少量树林较大，散生在落叶松林中。大部分油松为人工种植，分布在阳坡或半阳坡，海拔 1400 ~ 1700 m。人工油松林纯林化程度高，偶有黑桦、蒙古栎伴生。人工种植的油松大多分布海拔较低的坡地。树龄为 25 ~ 50 年居多，油松林面积为 224.7 hm²，占 0.2%，蓄积量较少 (28,979.0 m³)，占总蓄积量的 0.4%。

5.3 森林生长特征

5.3.1 年龄结构

塞罕坝机械林场森林年龄结构以 21 ~ 30 年最多，其次是 31 ~ 40 年，分别占蓄积 52.6% 和 30.5%，占面积 40.7% 和 21.9%；41 ~ 50 年森林主要为天然林；1 ~ 10 年和 11 ~ 20 年未成林各占一定比例（图 5-8）。塞罕坝机械林场在经营过程中，对密度高的人工林进行间伐生产；对 35 ~ 45 林龄的落叶松或樟子松进行采伐，同时不断种植新的人工林。

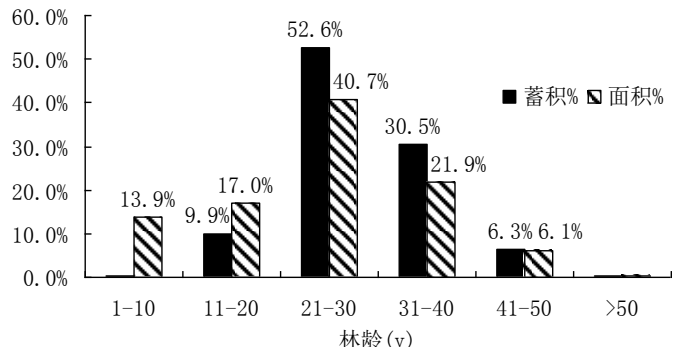


图 5-8 不同林龄面积与树蓄积量

5.3.2 树高与胸径的关系

从图 5-9 可以看出，落叶松、樟子松、云杉和油松的胸径与树高良好关系，这些森林类型均属于为针叶林，直立主干，并且由于人工种植，立地条件相对比较好，生长比较均匀；而落叶阔叶林中白桦林和蒙古栎林，为天然次生林，立地条件差异大，主干多分叉，平均树高低于针叶树种，白桦和蒙古栎等落叶阔叶林生长到 10 年以后，树高增加缓慢，表现为树高与胸径关系不明显。

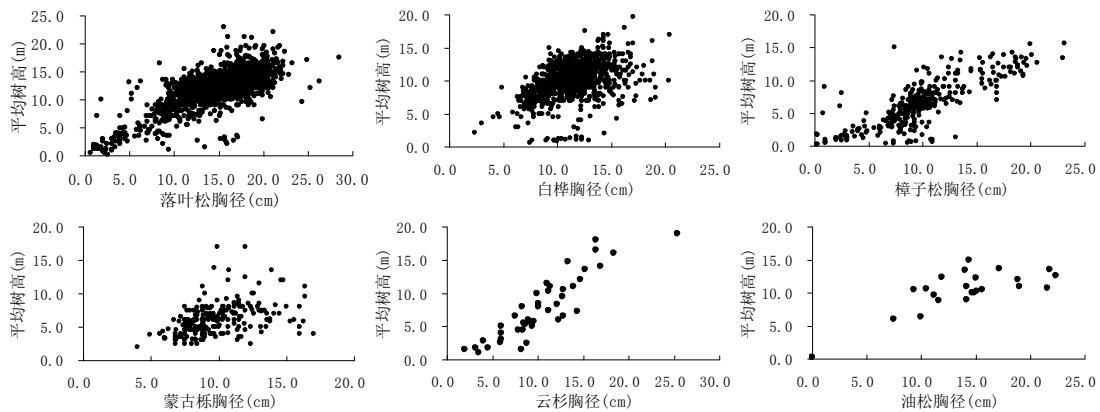


图 5-9 不同森林类型与树高的关系

树高和胸径受到各种环境因素的影响。用“树高-(林龄+郁密度+森林利用类型+土壤类型+土壤深度+森林起源+盖度+土地经营类型+坡度)”建立 GLM 模型，分析结果如表 5-7。树高主要决于林龄，但塞罕坝三个主要类型对林龄的解释率有很大区别，分别为 41.53%，14.30% 和 60.20%。落叶松是速生，受其它因素影响大；樟子松是强抗贫瘠树种，生长比落叶松慢，大多种植在立地条件比较差的地块，林龄对树高影响最大；白桦为天然次生群落，林型比较低矮，生长到 10 年后树高变化不大，因此在塞罕坝三个主要森林类型中林龄因素解释率最低。落叶松

和白桦除了林龄因素外，其它各因子对树高影响均有一定影响；但樟子除了土壤类型外，其它因素几乎没有相关性。

表 5-7 基于 GLM 模型的树高影响因子分析

相关因子	落叶松			白 桦			樟子松		
	自由度	%SS	P	自由度	%SS	P	自由度	%SS	P
林龄	1	41.53	<0.001	1	14.30	<0.001	1	60.20	<0.001
郁密度	1	0.25	<0.001	1	0.01	0.71	1	0.19	0.18
森林利用类型	3	2.47	<0.001	3	2.52	<0.001	2	0.04	0.84
土壤类型	2	0.94	<0.001	2	0.50	0.04	2	1.91	<0.001
土壤深度	1	0.05	0.17	1	1.23	<0.001	1	0.60	0.02
森林起源	2	0.61	<0.001	2	0.11	0.48	2	0.03	0.86
盖度	1	0.30	<0.001	1	0.29	0.05	1	0.13	0.26
土地经营类型	2	0.34	<0.001	1	1.03	<0.001	2	0.08	0.70
坡度	1	0.49	<0.001	1	1.04	<0.001	1	0.46	0.04
残差	1925	53.00		1030	78.97		339	36.37	

胸径是森林群落另一个重要生长特征，胸径差异最主要的决定因素是森林类型和林龄。为了进一步分析胸径与各因子之间的关系，用“胸径-(林龄+郁密度+森林利用类型+土壤类型+土壤深度+森林起源+盖度+土地经营类型+坡度)”建立 GLM 模型，结果见表 5-8。胸径与林龄关系解释率分别为 45.81%，20.55%和 50.30%；与树高情况相似，白桦胸径与林龄关系解释率最低，但与密度相关性强，解释率达 21.79%。落叶松胸径与郁密度关系也十分密切，但与樟子松关系不明显，这一结果显得十分重要，在营林过程中，落叶松郁密度要严格控制，才能达到最大生产量，而樟子松没有这一要求。

土壤类型主要与土壤水分密切联系，但不论是树高、胸径与土壤类型或土壤深度关系均不密切，解释率都比较低，主要是因为塞罕坝土壤绝大多数为沙土或沙壤土，土壤质地、深度差异不大。森林经营类型和森林利用类型直接反映到森林管理，森林起源反映天然林与人工区别，幸均不同程度与树高、胸径直接相关。盖度是只是反映小班林地占有比例，郁密度才是反映森林密度，相关分析结果表明，盖度与树高、胸径关系不密切。

表 5-8 基于 GLM 模型的胸径影响因子分析

相关因子	落叶松			白 桦			樟子松		
	自由度	%SS	P	自由度	%SS	P	自由度	%SS	P
林龄	1	45.81	<0.001	1	20.55	<0.001	1	50.30	<0.001
郁密度	1	12.18	<0.001	1	21.79	<0.001	1	0.79	0.01
森林利用类型	3	2.22	<0.001	3	2.64	<0.001	2	2.61	<0.001
土壤类型	2	1.33	<0.001	2	0.27	0.07	2	0.51	0.12
土壤深度	1	0.16	<0.001	1	0.01	0.68	1	0.05	0.52
森林起源	2	1.90	<0.001	2	0.01	0.87	2	0.03	0.87
盖度	1	0.18	<0.001	1	0.06	0.28	1	0.09	0.37
土地经营类型	1	0.32	<0.001	1	0.08	0.22	2	6.40	<0.001
坡度	1	0.09	0.02	1	1.20	<0.001	1	0.32	0.10
残差	1920	35.81		1030	53.38		325	38.89	

5.4 主要森林类型的径级分布

5.4.1 样方径级

以 7 个 1 ha 样方数据，分析塞罕坝主要森林类型的径级分布，这 7 个样方的类型分别是：落叶松样方 3 个，白桦样方 3 个和樟子松样方 1 个。样方 1 和样方 3 为坝上纯白桦林，林龄相对大，样方 7 为坝下白桦林，混生许多山杨；样方 2 和样方 6 为坝上缓坡坡底落叶松林，样方 4 为坝顶平坡落叶松林。落叶松在塞罕坝林场生长良好，其平均胸径大于白桦和樟子松林。落叶松平均胸径在 20 cm 左右，白桦平均胸径在 10 cm 左右，樟子松在胸径在 10 cm 左右。统计各样方的株数，样方 7 白桦林和样方 5 樟子松林最多；落叶松 3 个样方数量相对较少，以样方 4 在坝顶落叶松立株数略多一些。

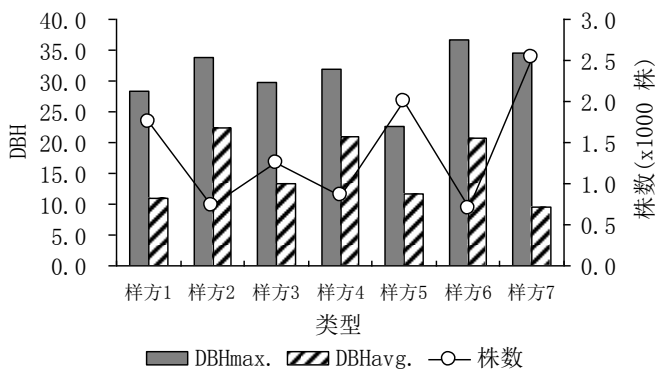


图 5-10 不同森林类型胸径与株数

表 5-9 7 个 1ha 样方基本情况表

样方编号	群落类型	面 积 (m ²)	种数	株数	DBHmax. (cm)	DBHavg. (cm)	TBA (m ² /ha)
BP01	白桦林	200*50	4	1750	28.4	11.0	19.28
BP03	白桦林	100*100	6	1248	29.8	13.4	20.25
BP07	白桦林	200*50	9	2544	34.5	9.4	20.71
LA02	人工落叶松林	100*100	1	727	33.9	22.4	29.09
LA04	人工落叶松林	100*100	3	865	31.8	20.9	30.41
LA06	人工落叶松林	100*100	2	699	36.7	20.8	24.42
A05	人工樟子松林	100*100	1	1993	22.7	11.7	22.66

5.4.2 径级数量分布

径级随着取样面积大小的变化规律是评价森林群落生长特征、演替阶段、环境梯度变化的综合指标。一般森林发育过程中，森林径级分布在演替阶段的初期为正态分布，到了演替阶段的后期，径级由正态分布转为偏指数下降分布。在植物群落研究过程中，一般采用样方取样法，取样的大小和取样位置的不同，常常导致结果的偏差。通过不同森林类型径级分布的研究，能有效地解释群落生长特征与环境梯度的变化的关系，并可以进一步了解空间分布的异质性。

对每个 1 ha 样方按 8 种不同方向，研究径级偏斜度 (skew)。8 个不同方向分别是：a) 左上；b) 右下；c) 左下；d) 右上；i) 从顺序从下到上；ii) 顺序从上向下；iii) 逐一从下到上；iv) 逐一从上到下 (图 3-1)。在求算径级偏斜度 (skew) 同时，计算径级变异系数(CV)。

图 5-11 为 7 个样方径级数量分布图, 白桦 BP01 和 BP03 样方径级分布模式相似, 与 BP07 样方差别比较大。BP01 和 BP03 白桦林林龄大, 处于演替后期, 小径级个体株数小, 尤其是 BP07 为小径级个体明显下降, 与 BP01、BP03 相比, BP07 白桦林处于演替的早期, 呈现明显的正态分布, 但白桦 3 个样方大径级数目却十分接近。

落叶松 LA02、LA04、LA06 径级数量分布模型相似, 均为正态分布。LA04 和 LA06 径级偏小, LA02 径级大于 LA04 和 LA06。3 个样方林龄比较一致, 但立地条件有差异, LA02 为水分条件最好, LA06 水分条件偏低, 而 A04 生长在坝顶, 海拔最高。樟子松为 A05 林龄小, 个体数多, 平均径级小, 径级分布明显的正态分布。

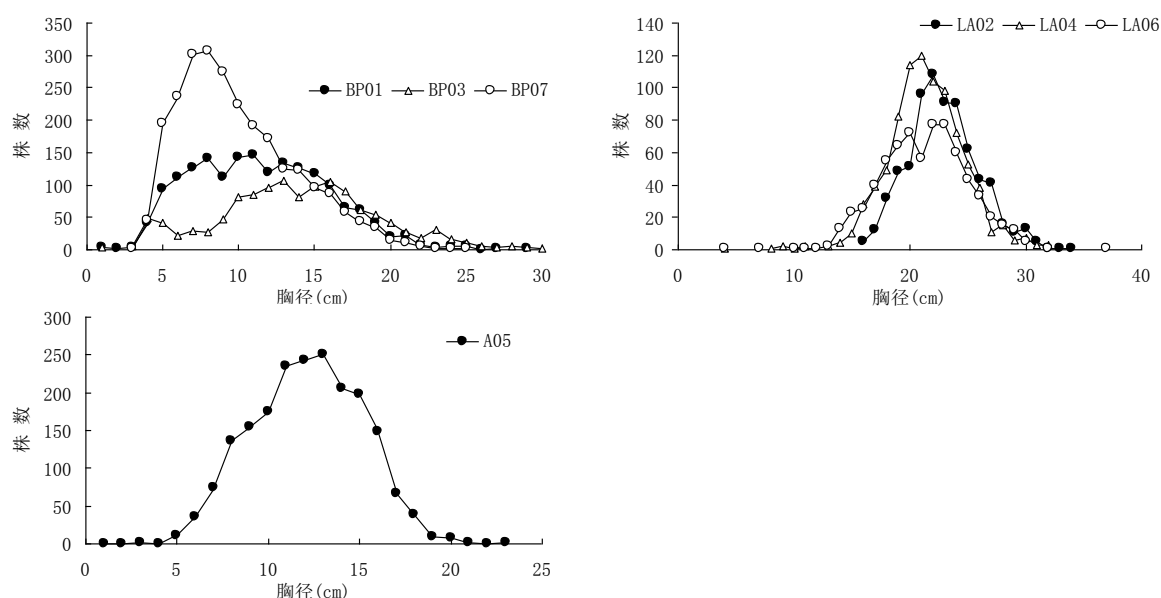


图 5-11 样方径级数量分布

5.4.3 径级分布与取样面积

径级分布的差异与取样面积有很大关系, 如果森林分布比较均一, 径级偏斜度 (skew) 会随着取样面积的增加而趋于稳定; 如果森林生长受环境异质条件如地形、土壤、坡度等强烈影响, 植物生长变异性增加, 会直接反映到径级偏斜度的变化上。森林样方调查时, 径级偏斜度是决定设置样方面积大小的一个重要指标。偏斜度随着取样面积的变化计算, 往往以对角方式扩大, 如 $10\text{ m} \times 10\text{ m}$, $20\text{ m} \times 20\text{ m}$, $30\text{ m} \times 30\text{ m}$..., 这种面积扩大方法计算出偏斜度由于取样面积增加幅度大, 偏斜度变化波动大, 难于反映出变化规律。如果用随机小样方组合的方法, 计算量过大, 难于对 1 ha 以上样方进行计算。6 个 1 ha 样方采用 8 种不同面积计算方式, 得出图 5-12 至 5-18。

6 个样方计算结果表明, 对角面积增加方法, 不论是那一方向, 结果差别都很大, 各偏差值波动不稳定。逐一面积增加法, 4 种方式总是有一种方式计算出偏斜度 (除样方 LA04 外) 趋于稳定。以 iii) 和 iv) 两种方式计算出结果更有效。

(1) 落叶松林径级变化

若用对角线 $10\text{ m} \times 10\text{ m}$, $20\text{ m} \times 20\text{ m}$, $30\text{ m} \times 30\text{ m}$... 扩大面积方式计算胸径偏斜度, 落叶松样方 LA02、LA04、LA06 计算结果差异很大, 很难反应胸径变化, 由于对角线扩大面积方式, 增加面积过

多, 计算结果点数太小, 难于正确反应胸径大小的变化。

以面积 10 m^2 递增方法, 采用 4 种不同方式增加面积方法, 计算胸径偏斜度。计算结果显示落叶松样方 LA02 径级分布变化, 不论是那一种方向, 随着面积的增大偏斜度 (skew) 都趋于稳定, 而且共同特征是面积在 2000 m^2 以上, 胸径偏斜度趋于稳定, 这说明该森林类型正确估算蓄积量的变化, 若取样在 2000 m^2 以上, 估算结果误差非常小。

落叶松样方 LA06 胸径偏斜度用 i) 顺序从下到上和 iii) 逐一从下到上, 结果表明偏斜度波动比较大, 其主要原因第 4 行 (4-1 ~ 4-10) 样方个体数少 (图 5-14 直方图), 另外, 在 3000 m^2 处遇到 DBH 最小值, 偏斜度下降到最低点; 而在 8000 m^2 处遇到 DBH 最大值, 偏斜度突然上升。但用 ii) 顺序从下到上和 iv) 逐一从上到下, 两个方向计算 DBH 偏斜度却是比较平稳, 主要是: ii) 和 iv) 方向计算时, 在 1600 m^2 处出现 DBH 最大值, 一直影响到所有样方计算结束; 而 iv) 方向计算, 逐一通过第 4 行样方, 大大抵消偏斜度的变化。

落叶松 LA04 不论用那种方向增加面积, 偏斜度变化都呈现不稳定波动 (图 5-13), LA04 样方胸径分布很不均一。从图 5-13 每 $10\text{ m} \times 10\text{ m}$ CV 变化可以看出, 如第 1 样方行与第 4 样方行胸径分布差别很大; 同样第 8 样方行与第 10 样方行差别很大。由于塞罕坝人工林总体上胸径变化比较均匀, 样方面积增大到 3000 m^2 以上偏斜度变化趋于比较平稳, 但在 LA04 样方中跳跃式变化, 主要原因是样方中小径级云杉的存在。在样方 6-7 样方中, 有一株胸径 3.6 cm 的白杆; 在小样方 9-1 中有二株胸径为 8.0 cm 和 10.7 cm 的白杆和一株胸径 7.1 的落叶松。如果把这一株数小、胸径差异的个体去除, 偏斜度变化在 4000 m^2 以上趋于平稳 (图 5-13 i)。

(2) 白桦林径级变化

白桦共有三个样地, 由于白桦林 BP01 样方编号顺序与其它两个样方不一致, 因此未参与径级分析。与落叶松林相比, 白桦林径级有两个特点: (a) 白桦分布在阴坡, 坡度较大, 大样方植物个体的径级差异受地形影响大; (b) 白桦林在样方内植物个体胸径差别大, 从 $2.0 \sim 30.0$ 均有分布。BP03 和 BP07 样方径级变化均随着面积增加而趋于平稳, 但是两个样方增加面积大小和表现方式有一定区别。在 BP03 样方不同方法计算偏斜度时, 采用 i) 方向计算要到 6000 m^2 以上, 径级偏斜度变化才趋于稳定变化; 而采用 ii)、iii) 和 iv) 三种方向计算均在 2000 m^2 以上就趋于稳定, 这种变化是由于地形变化引起的 (图 5-16 v), 很明显在平坡的地形条件下胸径差异性小; 在陡坡的地形条件下, 胸径差异性大。

白桦 BP07 样方在坝下, 植物个体数多, 从 5-17v 可以看出, CV 空间分布相对比较均一, 样方胸径偏斜度在 2000 m^2 以上, 趋于稳定, 但 iv) 从逐一从上到下方向计算偏斜度, 由于样方顶部, 差异比较大, 在 $0 \sim 7000\text{ m}^2$ 范围之内, 偏斜度波动比较大。

(3) 樟子松径级变化

樟子松 A05 样方典型特点个体数量多, 胸径从大小比较均匀分布 (图 5-11), 每一小样方变化的差异主要是由于个体数量与胸径不均匀引起的, 如 5-5 小样方植物个体只有 8 棵, 数远小于平均个体数量 20 棵, 而且胸径从 $7.3 \sim 19.4\text{ cm}$ 。樟子松径级偏斜度按 i)、iii) 方向计算波动较小, 但 ii)、iv) 方向计算波动比较大, 主要是由于该植物群落空间变化不均一形成, 但总体没有跳跃式变化, 说明群落胸径变化仍然比较均一。因此, 在计算径级偏斜度变化时, 应从不同方向计算进行比较, 才能真正反映群落生长特征。

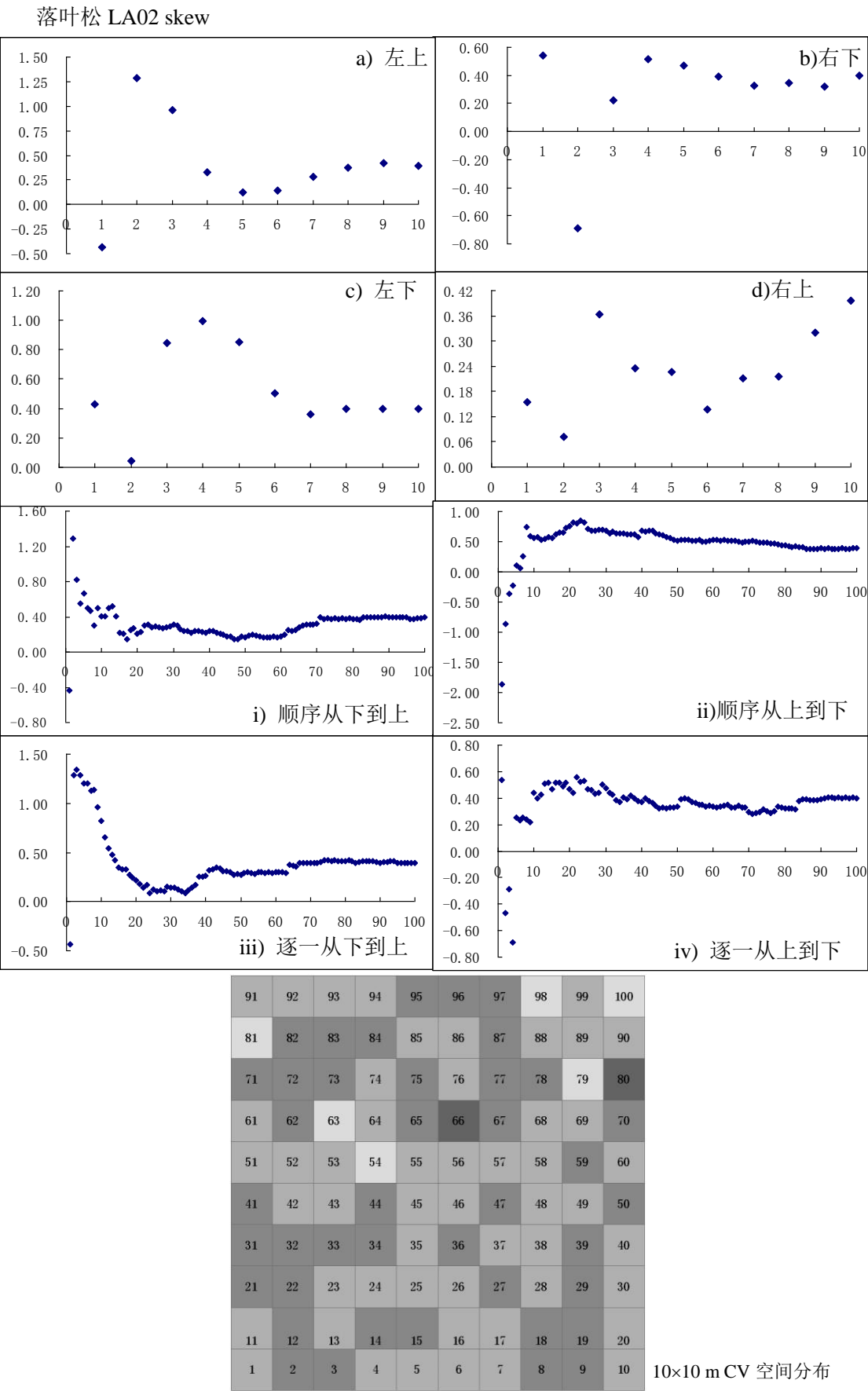


图 5-12 落叶松 LA02 胸径偏度分布图

落叶松 LA04 skew

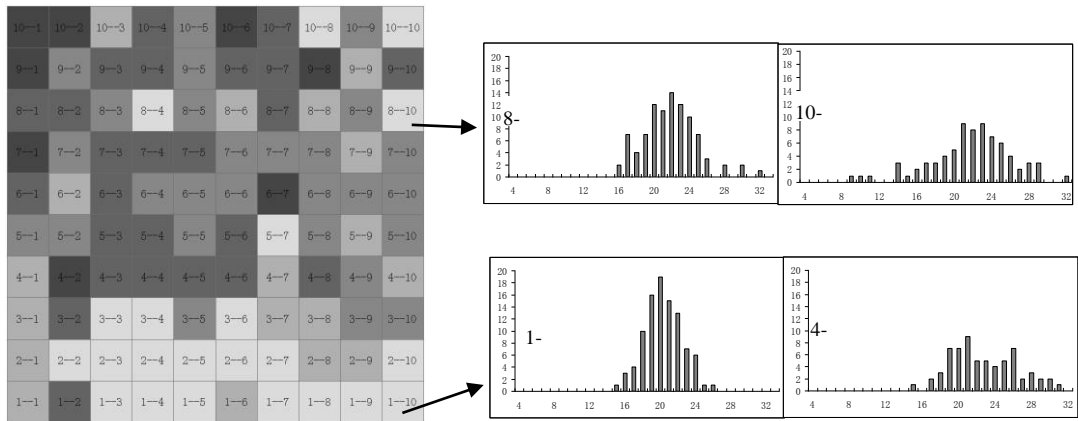
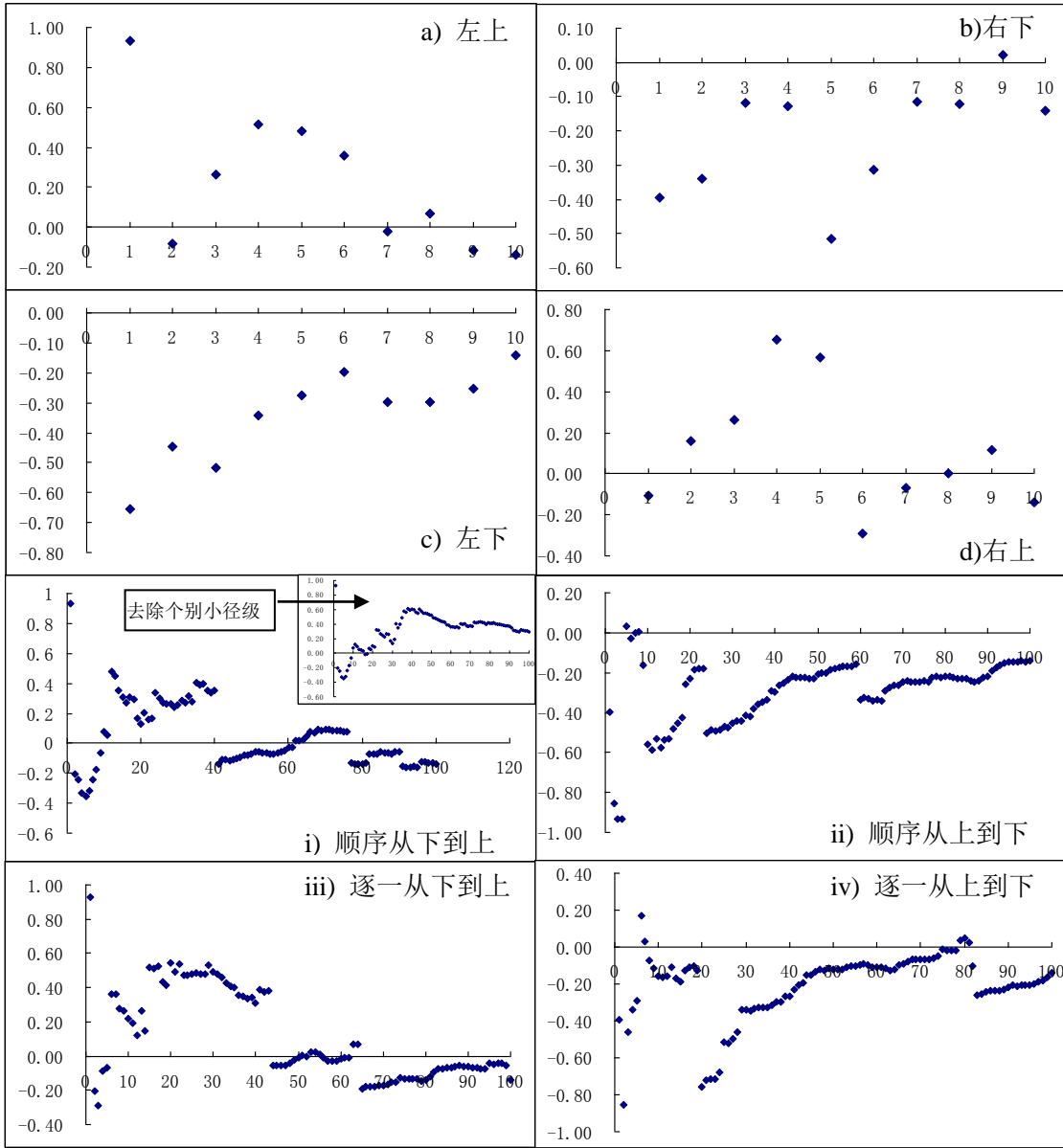


图 5-13 落叶松 LA04 胸径偏度分布图

落叶松 LA06 skew

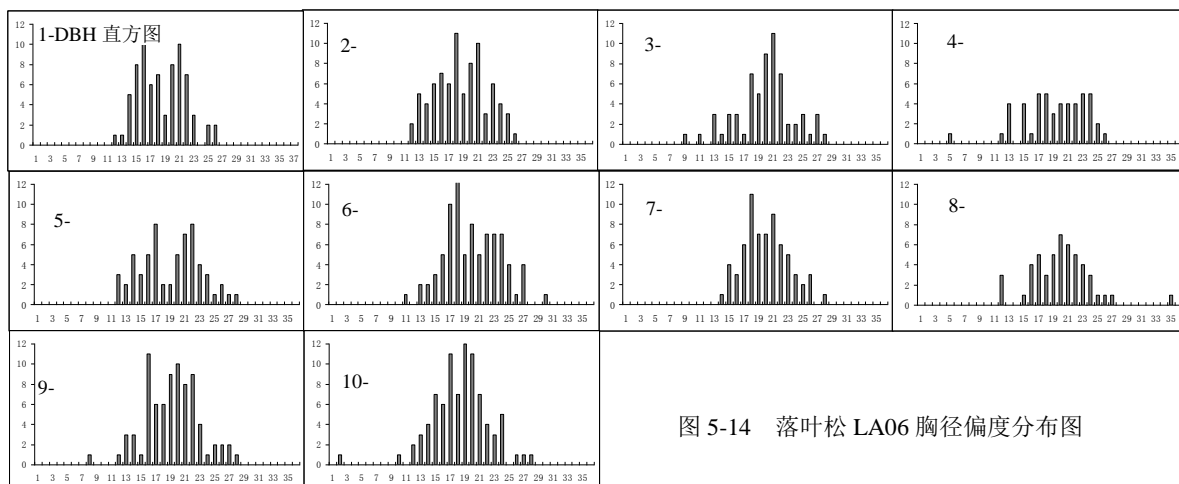
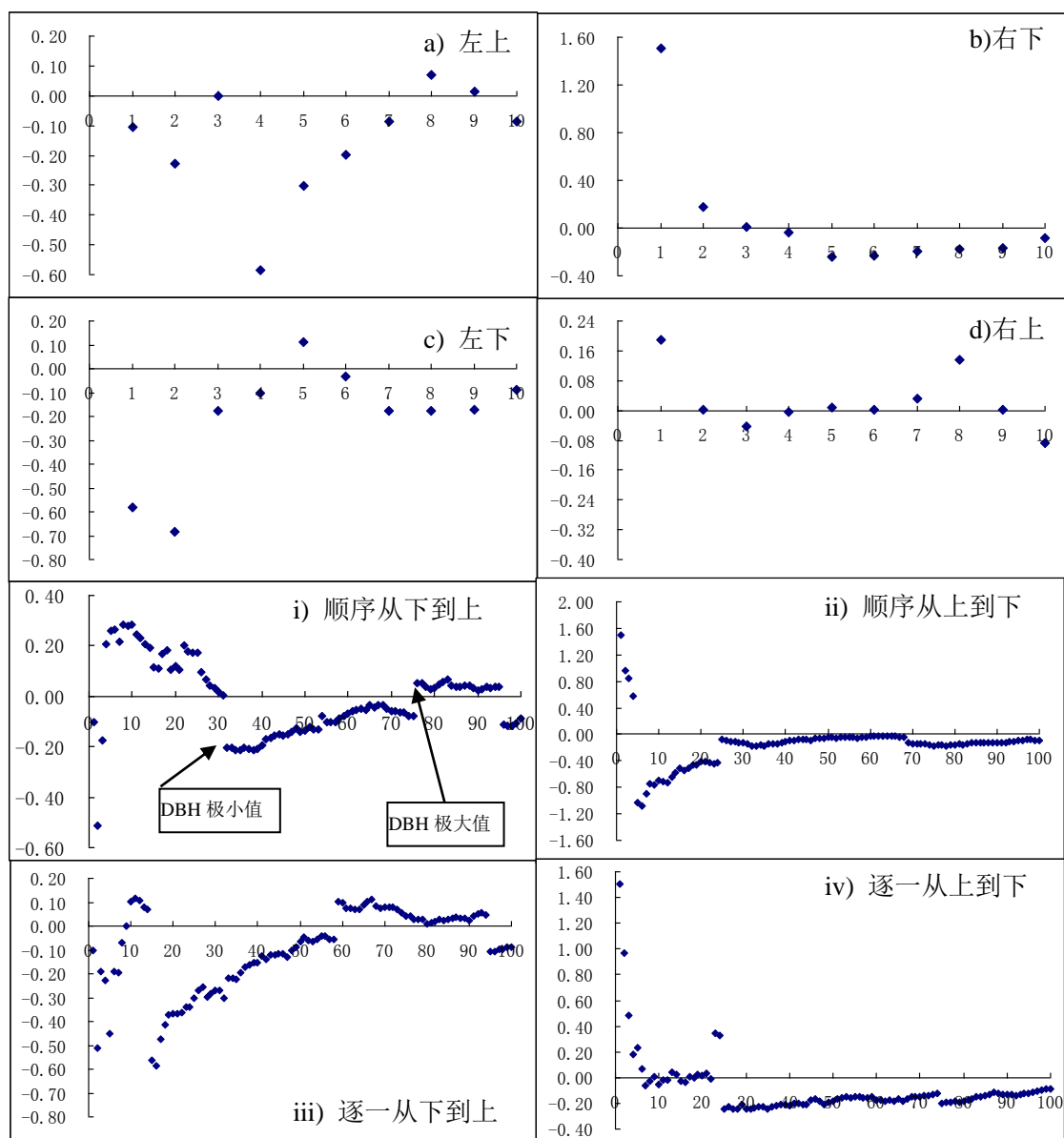


图 5-14 落叶松 LA06 胸径偏度分布图

白桦 BP03 skew

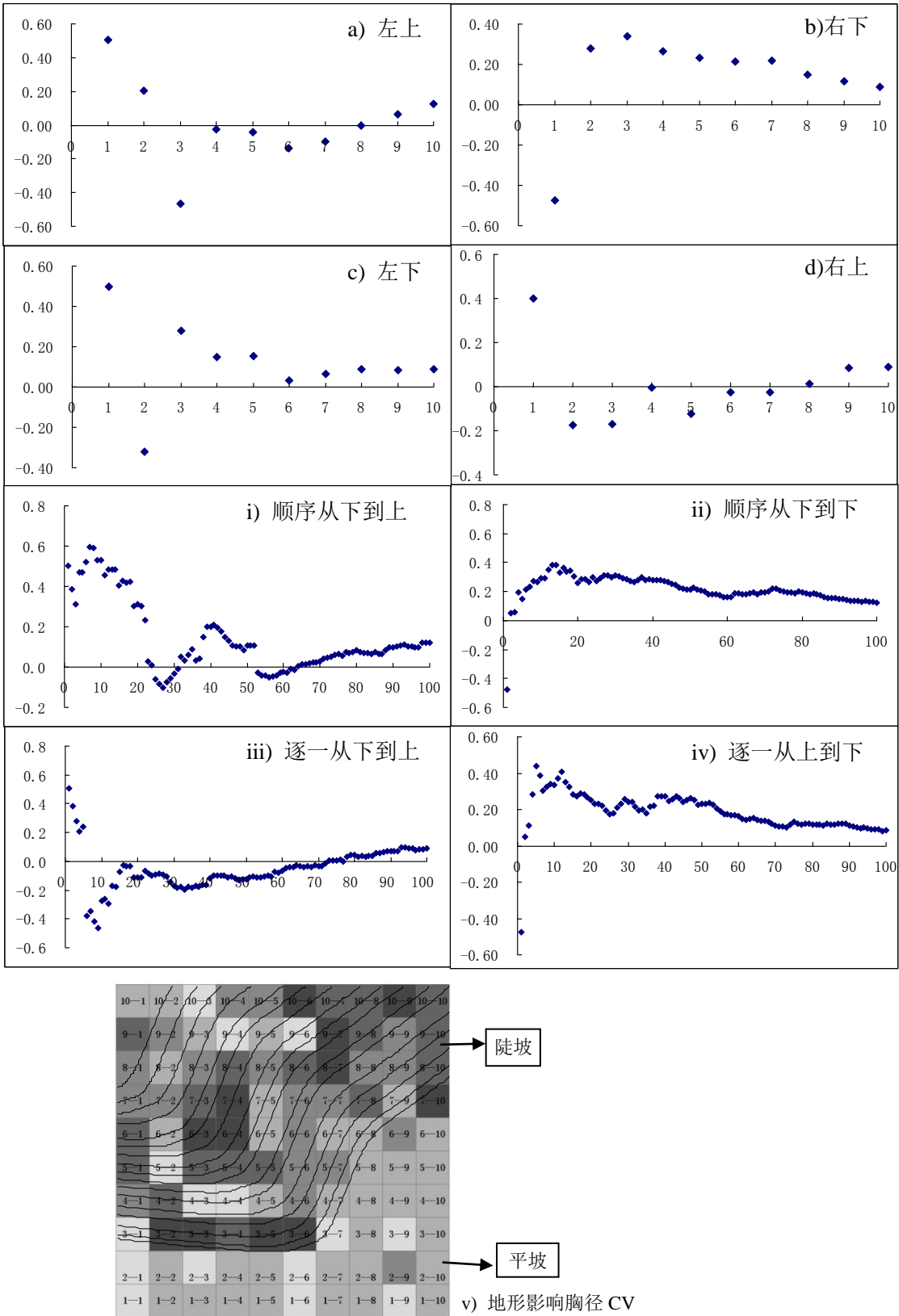


图 5-16 白桦 BP03 胸径偏度分布图

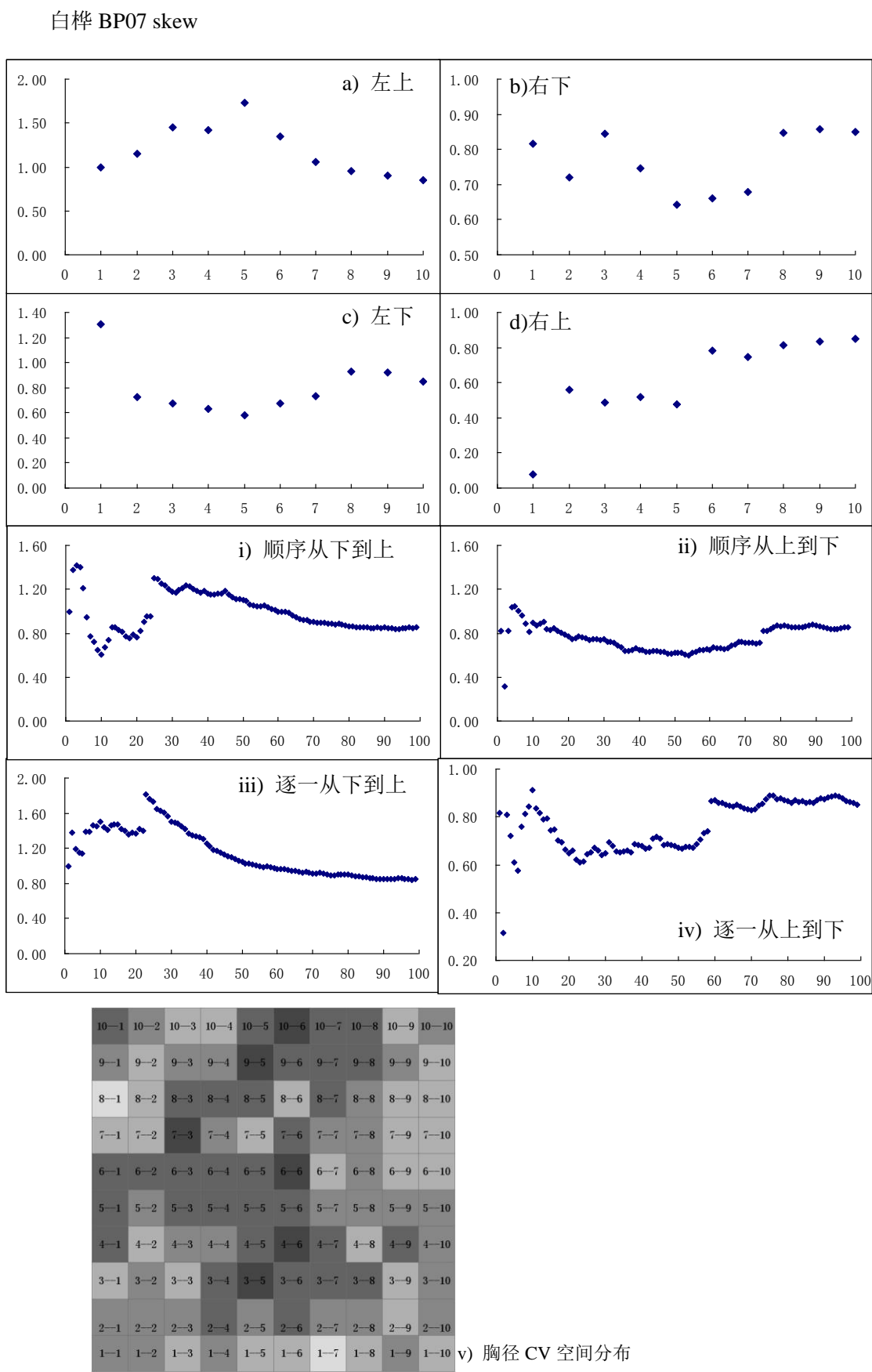


图 5-17 白桦 BP07 胸径偏度分布图

樟子松 LA05 skew

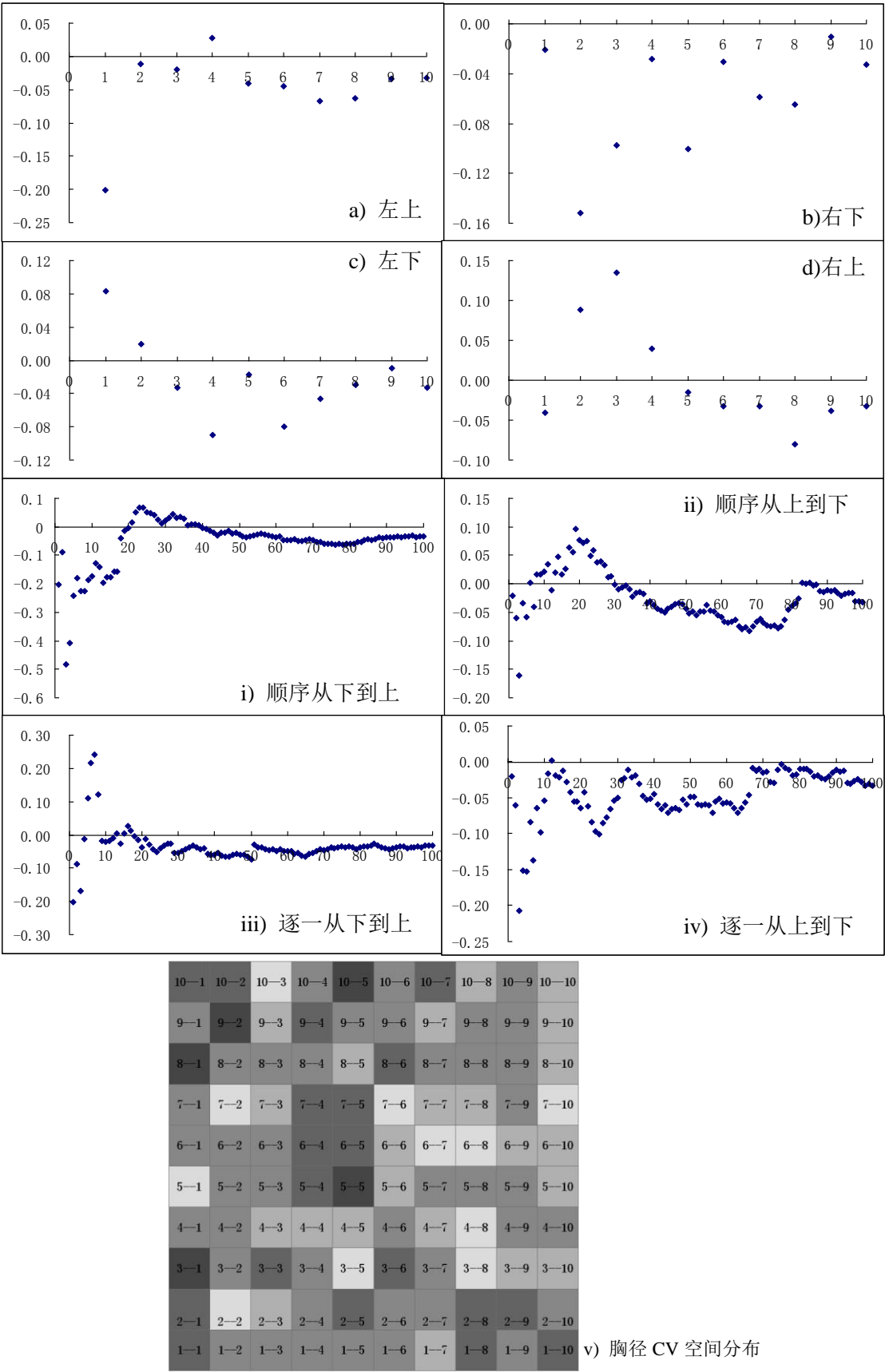


图 5-18 樟子松 A05 胸径偏度分布图

第六章 森林蓄积量和生物量

6.1 森林蓄积量

6.1.1 总森林蓄积量

根据 2003 年塞罕坝机械林场总场 6936 个小班调查资料统计，塞罕坝林场总蓄积量为 6,888,999.0 m³。其中以落叶松蓄积量最多 4,887,207.0 m³，占 70.9%；其次是桦树、樟子松蓄积量分别占 15.8%和 4.8%，其它森林类型的蓄积量占总蓄积量的 8.4% (表 6-1)。

表 6-1 塞罕坝机械林场总场现存总蓄积量

森林类型	面 积 (hm ²)	蓄 积 (m ³)	蓄 积 %
落叶松林	38,670.8	4,887,207.0	70.9
白桦林	15,072.4	1,086,851.0	15.8
樟子松林	7,536.1	329,688.0	4.8
混交林	3,858.2	306,111.0	4.4
蒙古栎林	3,671.7	121,337.0	1.8
山杨林	1,075.5	67,470.0	1.0
云杉林	986.2	50,297.0	0.7
油松林	224.7	28,979.0	0.4
其它	23,579.0	11,059.0	0.2
合 计	94,674.6	6,888,999.0	

6.1.2 不同森林类型的蓄积量

不同森林类型的蓄积量有很大差别，而且同一森林类型不同年龄的蓄积量也有很大的差异。不同年龄的蓄积量反映了不同时期人工种植的数量与经营现状。

(1) 落叶松

绝大多数的落叶松是在 1975 年前后种植，不同年龄的蓄积量分布如图 6-1。15 ~ 40 龄占 98.9%，面积占 83.1%。1 ~ 10 年林龄的落叶松面积占总面积的 14.0%。由于林场有计划采伐落叶松商品，采伐后重新种植，低林龄落叶松占一定比例，目前落叶松林龄结构的比较合理，但落叶松在全林场所占比例过大，森林过于单纯，生态系统比较脆弱，抵抗病虫害能力比较差。在生产过程中，对新种植的落叶松需要重新考虑不同商品林的比例。

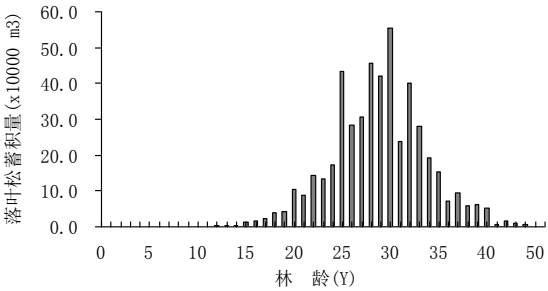


图 6-1 落叶松不同年龄蓄积量

(2) 白桦

白桦不同林龄的蓄积分布见图 6-2。白桦不同龄分布比较分散，但仍以 30 林龄最多，1963

年成立林场后,白桦林作为水源涵养和风沙保护林而保留下来,只有个别小班进行过的采伐,绝大多数白桦林通过自然更新发育而成白桦林。白桦林在塞罕坝机械林场生长良好,由于阴阳坡热量和水分配上的差异,几乎所有的白桦林分布在阴坡山坡,多见于 15~40°坡地。为加强当地生态环境的保护,目前 91.9%白桦林划为公益林。

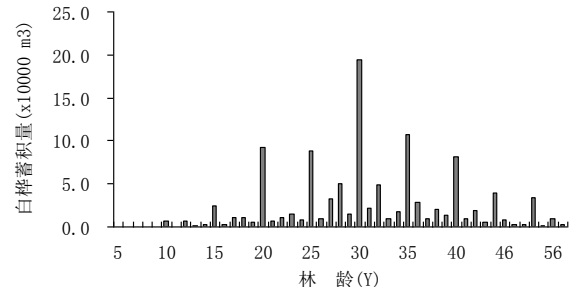


图 6-2 白桦不同年龄蓄积量

(3) 樟子松林

塞罕坝机械林场的樟子松林蓄积主要集中在 15~25 林龄,占 67.5%,25~43 林龄占较少比例(图 6-4 a)。近年来塞罕坝机械林场总场为了改善单一的落叶松纯林森林结构,扩大樟子松营林面积,进一步改善森林结构,也将一些土地类型相对贫瘠的土地种植樟子松,面积 0~15 年幼樟子松林大面积扩大(占总樟子松 48.6%)。0~15 年林龄的樟子松面积平稳增加(图 6-4 b)。

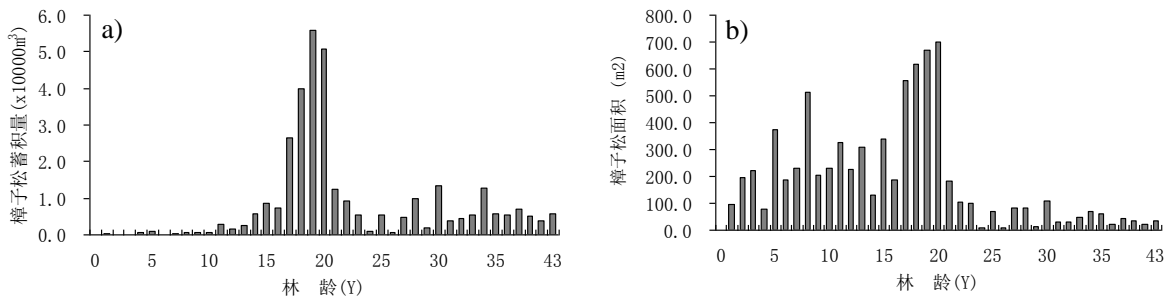


图 6-4 樟子松不同年龄蓄积量和不同年龄的面积

(4) 其它森林类型

除了上述 3 个主要森林以外,其它森林类型蓄积量与面积大小如图 6-5。蒙古栎、山杨、云杉、油松均形成较大面积森林群落,但山杨、云杉、油松均为人工林;榆树残存在个别林缘,单株树林较大,幼树很小,更新能力较差。山丁子为主要林下混生树种,呈灌木状,成林很少,偶有林窗或林缘自然更生生长成片山丁子。沙棘为人工种植的经济林,除此外,还种植山杏、榛等经济林。塞罕坝为商品林为主,果食等经济林很少,只有占总面积的 0.67%。塞罕坝除森林类型以外,还有面积 1747.3 hm² 农业用地,占土地总面积 1.85%,用于种植土豆和莜面等。

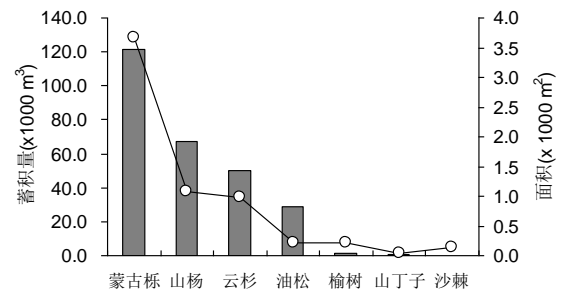


图 6-5 其它不同森林类型蓄积量与面积

6.2 森林蓄积量的变化

森林生长十分重要的指标是蓄积量的变化，尤其对塞罕坝大型国有林场种植大面积的人工林，不仅需要掌握森林蓄积量的变化，而且要掌握不同森林类型蓄积量增长规律，这样才能合理安排林业生产。从生态系统功能作用上，蓄积量的变化直接关系到陆地碳循环变化，大面积种植人工林后，森林地上、地下和土壤碳循环发生了很大的变化，如何正确估算碳的变化，需要解决的首要问题是正确估算蓄积量的变化。蓄积动态变化常常需要花费大量的人力、物力的进行实际测量。在林业生产过程中，往往只能获得某一时间的调查数据；即使可获得不同时期的数据，数据详细程度差别很大，时间跨度不一，难于计算动态变化。我们尝试用同一时期详细林业小班调查资料，用空间代替时间方法，建立不同立地条件的生长模式，推算塞罕坝森林蓄积的变化。

用林业森林调查数据，各小班数据包涵各种生态环境因子的数据，这些环境因子与植物生长直接相关。这些环境因子包括：土壤类型、土壤深度、坡度、坡向、土地利用类型、森林类型、森林起源；与蓄积量相关的森林群落变量有：林龄、平均树高、郁密度、盖度、胸径等。用这些环境变量共同作用，影响森林蓄积量的变化，经过建立 GLM (General linear Model) 模型，推算蓄积量的时间变化。

采用单位面积的蓄积量与林龄、森林类型、土壤深度、土壤类型、坡度、盖度、林地类型、经营类型建立多元线性模型 (GLM)。模型各参数表 6-1 及模型解释率表 6-2。

表 6-1 蓄积量 GLM 模型参数表

变 量		GLM 模型参数	标准差	t-值	P	显著性
截距		-63.48	10.10	-6.29	<0.001	***
林龄		3.53	0.09	38.37	<0.001	***
森林类型	落叶松	31.90	3.93	8.11	<0.001	***
	蒙古栎	-14.20	2.76	-5.14	<0.001	***
	油松	28.46	8.10	3.52	<0.001	***
	针阔混	16.08	3.46	4.65	<0.001	***
	樟子松	13.93	4.43	3.14	<0.001	**
	硬阔杂	26.21	9.72	2.70	0.01	**
	山杨	-9.28	4.21	-2.21	0.03	*
	榆树	-16.04	15.35	-1.05	0.30	
	云杉	-6.23	7.00	-0.89	0.37	
平均树高/林龄		13.25	0.60	22.13	<0.001	***
盖度		-0.23	0.02	-12.05	<0.001	***
土壤类型	沙壤	-13.55	1.30	-10.40	<0.001	***
	沙土	-30.68	2.47	-12.43	<0.001	***
土壤深度		0.24	0.05	4.73	<0.001	***
坡度		-0.35	0.07	-4.87	<0.001	***
林地起源	人工	17.11	3.15	5.44	<0.001	***
	天然	-6.03	2.91	-2.07	0.04	*

林地类型	疏林地	-50.80	5.69	-8.93	<0.001	***
	未成林	43.12	26.57	1.62	0.10	
经营类型	公益林	6.97	8.10	0.86	0.39	
	商品林	23.42	8.18	2.86	<0.001	**
	用材林	30.98	11.37	2.73	<0.001	**

$R^2=0.6561$, $P<0.001$

表 6-2 蓄积量 GLM 模型各参数的解释率

	自由度	F 值	P	%SS
林龄	1	1286.28	<0.001	11.06
森林类型	9	549.98	<0.001	42.55
树高/年龄	1	683.41	<0.001	5.87
郁密度	1	149.70	<0.001	1.29
土壤类型	2	133.70	<0.001	2.30
土壤深度	1	38.51	<0.001	0.33
坡度	1	40.24	<0.001	0.35
森林起源	2	24.30	<0.001	0.42
土地经营类型	2	42.30	<0.001	0.73
森林利用类型	3	35.37	<0.001	0.91
残 差	3978			34.20

所建立的 GLM 模型与各参数关系均十分显著 ($R=0.810$, $P<0.001$)。GLM 蓄积量模型中, 森林类型是蓄积量差异主要来源, 解释率最高为 42.55%; 其次是林龄, 解释率 11.05%; 另外树高/年龄、土壤类型和郁密度解释相对比较高, 其它因素如坡度、森林起源、土地经营类型、森林利用类型等解释比较低。该模型各参数对蓄积量影响与当地实际情况直接相关, 并非一般规律, 如土壤深度, 塞罕坝土壤类型主要以沙土、沙壤、沙质, 差异性小, 土壤深度也未见明显差异。土壤类型的差异主要反映在土壤水分上。

森林蓄积量的变化如下:

检查各小班蓄积量剔除明显异常值, 计算小班不同林龄森林蓄积量的平均值, 根据林龄推算不同时期森林面积, 得出不同时期蓄积量的变化, 蓄积量的变化见图 6-6a。用这种方法计算的蓄积量会由于不同年龄平均蓄积量小班个数的差异, 不能得到正确的估算结果, 因此出现蓄积量在时序上下波动的情况, 这种波动与实际并不吻合; 另外, 这种估算方法, 由于没有考虑立地条件的差异, 假设各种立地条件蓄积量一致, 因此, 用空间代替时间方法, 在计算上有一定的误差。

GLM 蓄积量模型充分考虑了不同环境因素, 用多元线性拟合和矩阵运算法, 将各小班的环境梯度变化与蓄积量建立多元线性模型, 并用时间为变量, 计算出不同时间序列的蓄积量变化, 结果如图 6-6a, 这种方法计算结果与实际蓄积量比较接近。模型不仅计算蓄积量总量, 通过拟合逐一计算所有小班蓄积量的变化, 各小班蓄积量计算结果与小班实际调查数据进行相关分析, 结果表明, 相关性十分显著 ($R=0.932$, $P<0.001$, 图 6-6b)。

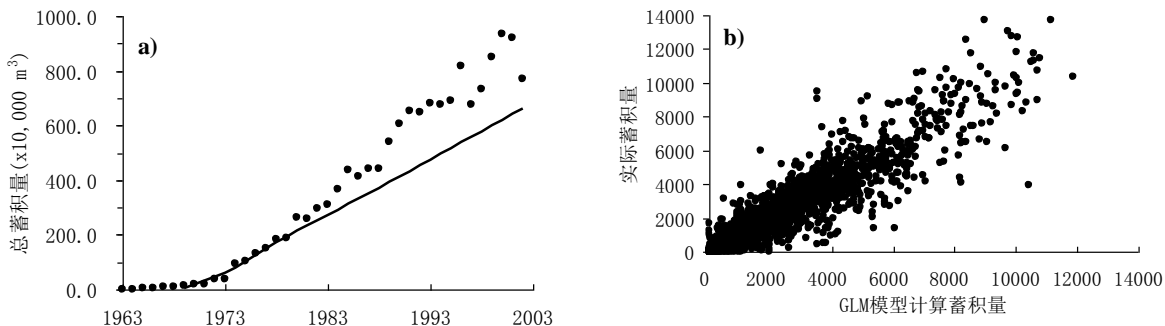


图 6-6 小班调查蓄积与 GLM 模型计算的蓄积量年度变化

6.3 不同森林类型蓄积量的变化

6.3.1 落叶松蓄积量的变化

塞罕坝落叶松面积最大，共有 2336 个小班，小班林龄分布不均，10 ~ 20 林龄和 35 林龄小班个数最少，这两段小班平均记录个数为 16 个；以 11、13、14 林龄的小班个数最少，分别只有 8、7、9 个小班，其它不同林龄小班数量比较多。计算不同林龄平均蓄积量时，各林龄均有一定数量，计算各林龄平均蓄积量的结果较为可靠 (图 6-7)。

总蓄积量变化并非总是呈线性的，落叶松 15 ~ 30 年林龄平均蓄积量增加快于 0-15 龄和 30 林龄以后。落叶松 30 林龄后，蓄积量增加明显缓慢。落叶松蓄积总量变化与不同林龄蓄积量变化模式十分接近，1960 ~ 1970 年蓄积量很少，只有 8075.7 m^3 ，1970 ~ 1985 年经过蓄积量快速增长期，到 1985 年达到 31898.4 m^3 ，增长了 74.7%。落叶松蓄积量变化十分快速，从 1960 年的 211.3 m^3 ，到 2003 年蓄积量为 38665.9 m^3 。平均每年增长 915.6 m^3 。

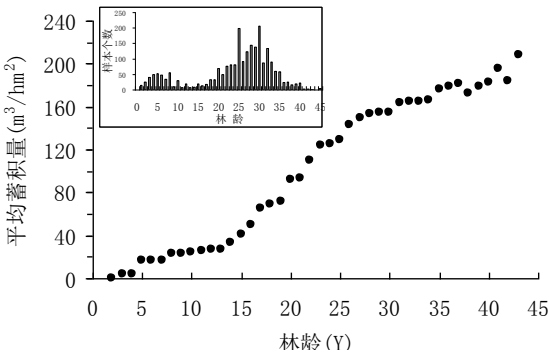


图 6-7 落叶松不同林龄蓄积量变化

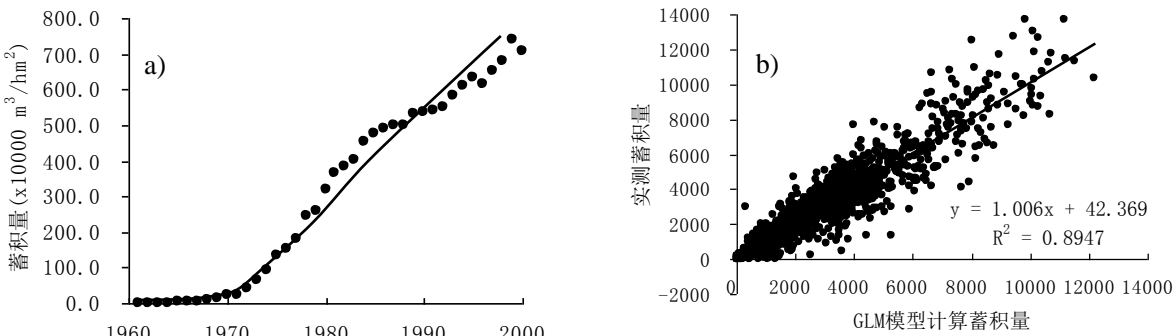


图 6-8 落叶松蓄积量变化及其模型拟合

为了增加 GLM 模型合理性,单独提取落叶松数据建立蓄积量与林龄、树高/林龄、郁密度、土壤类型、土壤深度、坡度、林地起源、土地利用类型、森林分类经营类型的关系模型。模型各参数的解释率如表 6-3。

表 6-3 落叶松蓄积量 GLM 模型各参数的解释率

参 数	自由度	<i>F</i> 值	<i>P</i>	%SS
林龄	1	1050.20	<0.001	26.68
树高/林龄	1	414.90	<0.001	10.54
郁密度	1	180.03	<0.001	4.57
土壤类型	2	109.38	<0.001	5.56
土壤深度	1	12.98	<0.001	0.33
坡度	1	19.65	<0.001	0.50
森林起源	2	18.04	<0.001	0.92
土地经营类型	2	20.44	<0.001	1.04
森林利用类型	3	9.93	<0.001	0.76
残差	1933			49.11

$R^2=0.5089$, $P<0.001$

从表 6-3 中看出,模型各参数都显著相关,但解释率不同。模型以林龄、树高/年龄参数解释率最高,其次是郁密度和土壤类型,其它各参数解释均较低。

GLM 模型是一个多元线性模型,模型计算结果蓄积量是一直线上升(图 6-8a),但落叶松的增长并非线性关系,这是 GLM 模型仍然不能解决的问题。但 GLM 模型能十分客观地反映各参数与蓄积量变化的关系(表 6-3);模型对各小班蓄积量的变化计算,能够较准确的落叶松蓄积量的变化(图 6-8b, $R=0.9459$, $P<0.001$),对最终总量的计算准确率达 97.7%。因此, GLM 模型能够重建蓄积量与时间变化的关系。

6.3.2 白桦林蓄积量的变化

白桦林不同林龄的蓄积量变化差异较大(图 6-9)。通过林场有效的保护,绝大多数白桦林已列入公益林,不再进行砍伐,而作为天然保护林。白桦最大林龄为 60 年,15 年林龄以下和 45 年林龄以上的白桦林很少,白桦林林龄在不同立地条件蓄积量差别较大,很难用林龄平均方法准确估算其该时间段内的蓄积量变化。蓄积量模型计算方法在白桦林显得更有必要。

从小班数据分析,白桦林 0~10 林龄蓄积量很低,10 年林龄后迅速上升,这很可能是由于低林龄的白桦林很少,过高或过低估计这一段林龄的白桦林;同样情况出现在 35 林龄以上的白桦林,35~45 年林龄的白桦林蓄积量比 30-35 年林龄的蓄积量更低,这与实际蓄积量偏差较大,结果会导致对总体蓄积量偏低的估算。

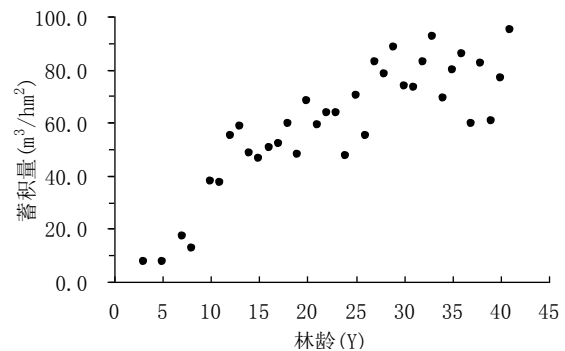


图 6-9 白桦不同林龄蓄积量变化

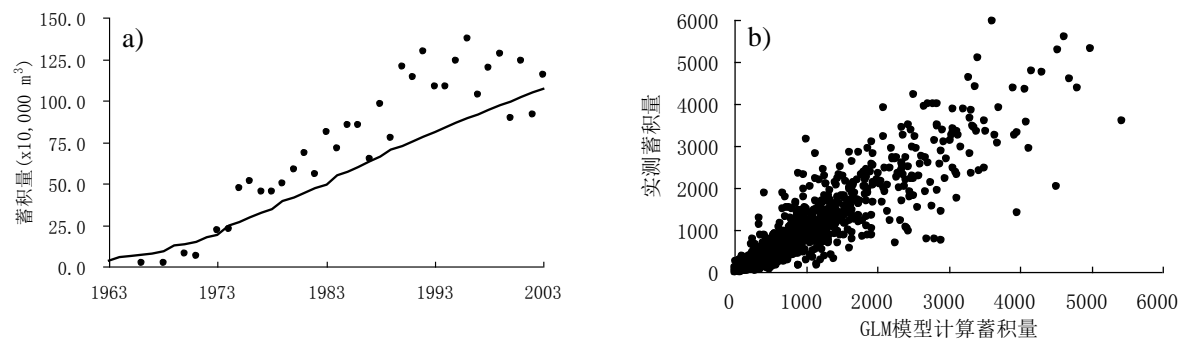


图 6-10 白桦蓄积量变化及其模型拟合

白桦林蓄积量的 GLM 模型参数如表 6-4 所示。白桦林的林龄、树高/林龄两个参数值远低于落叶松，白桦林蓄积量更易受人为活动的影响，不同立地条件对白桦林影响大，坡度、土壤类型、土壤深度、郁密度参数对白桦蓄积量影响不显著。

表 6-4 白桦蓄积量 GLM 模型各参数的解释率

参数	自由度	<i>F</i> 值	<i>P</i>	%SS
林龄	1	106.68	<0.001	7.42
树高/林龄	1	107.31	<0.001	7.46
土地经营类型	1	53.67	<0.001	3.73
森林利用类型	3	31.48	<0.001	6.57
森林起源	2	10.46	<0.001	1.45
坡度	1	2.88	0.09	0.20
土壤类型	2	4.60	0.01	0.64
土壤深度	1	3.06	0.08	0.21
郁密度	1	1.50	0.22	0.10
残差	1038			72.20

$R^2=0.278$, $P<0.001$

白桦林现存蓄积总量为 15072.4 m³，以不同年龄平均白桦林推算 1960 年白桦蓄积量为 1491.8 m³，增长了 13580.6 m³，每年平均增长 323.3 m³。用模型拟合方法计算白桦林蓄积量与平均方法计算的蓄积量如图 6-10a，图中可以看出，模型拟合计算白桦林蓄积量低于平均值计算的蓄积量。从图 6-10b 可以看出，用模型计算各小班的蓄积量与小班实际蓄积关系点较离散，表明实际调查与估算值偏差比较大。

6.3.3 樟子松蓄积量的变化

从图 6-11 可得出，樟子松林龄偏小，0 ~ 20 林龄的占绝大多数，20 年林龄以上小班数量少。30 年林龄以下樟子松蓄积量生长规律比较明显；30 年林龄以上，蓄积量变化差异较大。

樟子松 0 ~ 10 年林龄蓄积量增加十分缓慢，比落叶松林和白桦林要慢许多；10 ~ 30 年蓄积量增加十分迅速，30 年林龄以上蓄积量差

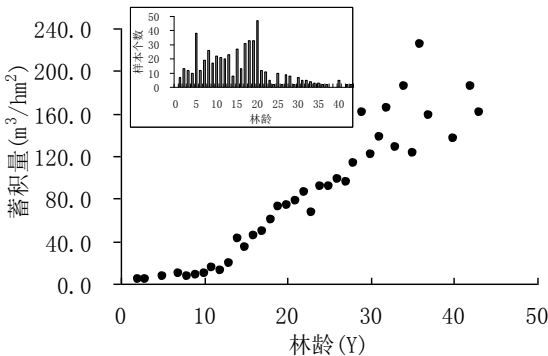


图 6-11 樟子松不同林龄蓄积量变化

别比较大,但总体上增加快速。这种生长规律与樟子松适应生长环境有关,樟子松人工种植后,幼树不断适应环境,伴有大量侧枝生长,改善其生长环境,增加土壤养分和水分,经过较长时间的适应,樟子松生长迅速提高。

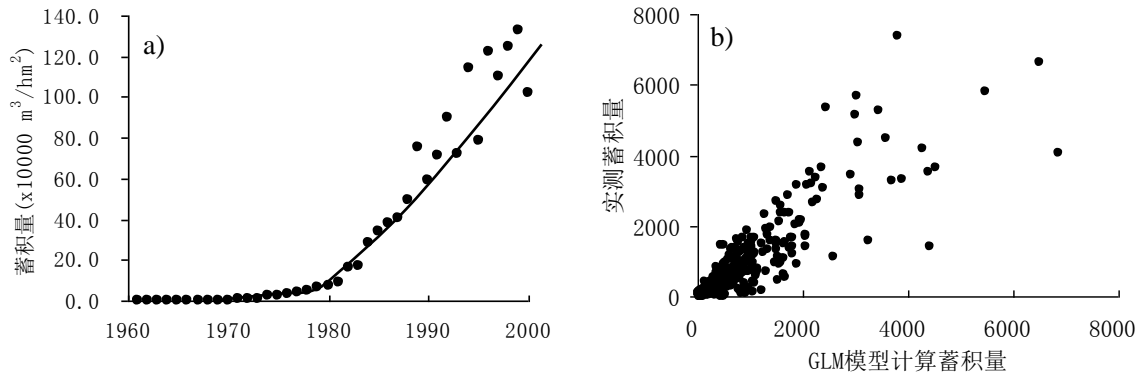


图 6-12 樟子松蓄积量变化及其模型拟合

用蓄积量 GLM 模型计算得出解释率主要由林龄因素引起,解释率高达 56.68%。除了树高/林龄和土地经营类型相关外,其它参数影响相关性不显著。模型计算结果表明,樟子松林龄偏小,幼林蓄积量很小;高林龄蓄积量偏差比较大,各点分布与拟合线有一定偏差。

表 6-4 樟子松蓄积量 GLM 模型各参数的解释率

参数	自由度	F 值	P	%SS
林龄	1	526.45	<0.001	56.68
树高/林龄	1	33.53	<0.001	3.61
土地经营类型	1	23.80	<0.001	2.56
森林利用类型	2	0.30	0.74	0.06
林龄	2	0.20	0.82	0.04
土壤类型	2	1.74	0.18	0.37
土壤深度	1	0.61	0.43	0.07
森林起源	2	0.05	0.95	0.01
坡度	1	0.84	0.36	0.09
残 差	339			36.50

$R^2=0.635$, $P<0.001$

6.3.4 蒙古栎蓄积量的变化

由于不同林龄的蒙古栎蓄积量差异非常大 (图 6-13a),用不同林龄平均值估算蓄积量对结果可能会引起很大的偏差 (图 6-13b)。造成不同林龄蓄积量的差异主要是由于: 1) 立地条件差异造成蒙古栎林生长的差异; 2) 人为干扰影响,择伐降低蓄积量; 3) 蓄积调查估算偏差,蒙古栎树形及枝下高差异大,在计算蓄积量需要准确的抽样。按小班蓄积量得出蓄积量为 121,337.0 m^3 。因此,要准确估算蒙古栎的蓄积量,需要对小班资料进行进一步的调查,划分不同类型,重新建胸径与蓄积量的关系。

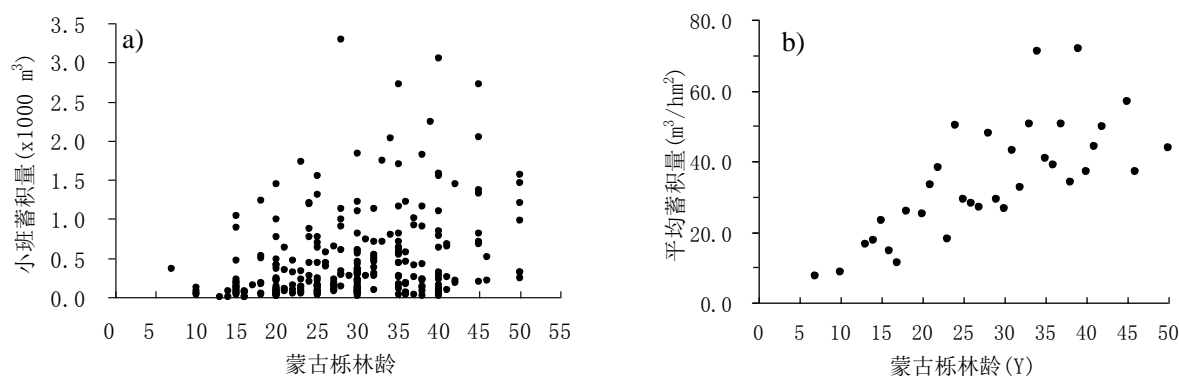


图 6-13 蒙古栎蓄积量变化及其模型拟合

6.3.5 其它森林类型蓄积量的变化

塞罕坝除了以上四个主要森林类型外，还有混交林、山杨、云杉和油松。混交林蓄积量比较大，依据混交优势物种的不同，可划分为：落叶松+樟子松，落叶松+白桦，落叶松+油松，樟子松+白桦、樟子松+油松，白桦+山杨。总蓄积量达 281,685.0 m³，占森林总蓄积量的 9.3%。混交林主要成份仍然是落叶松，有些小班是落叶松占绝对优势，混交林共是小班 240 个，其中 22、25、30 林龄小班数量最多；林龄与小班蓄积相关性分析显著($R=0.221$, $P<0.01$)。用空间代替时间方法，计算出蓄积量变化如图 6-14。混交林计算结果有些年份偏低，个别年份如 1997、1998 年估算过高，但整体趋势明显。

山杨人工种植面积较少，共有 94 个小班，平均小班面积 11.4 hm²；总蓄积量为 67,470.0 m³，平均小班蓄积量为 717.8 m³/小班，单位面积蓄积量 62.7 m³/hm²。山杨林主要分布在低海拔的坝下，坝上没有纯林分布，只少量与白桦林混交。不同时期蓄积量计算结果如图 6-14，山杨林估算波动比较大，不同林龄蓄积量集中在 10、15、20、30 林龄，可能与估算年龄有关。因此，估算其蓄积量最好按 5 年林龄间隔计算。

云杉林人工林主要种植在海拔较高的坝上，共有 81 个小班，其中有 47 个小班为 0~10 幼林，面积为 517.6 hm²，成林共有 34 个小班，总蓄积量为 50,297.0 m³，由于缺乏 1993~2000 年小班林龄数据，该时间段内蓄积量变化无法用平均蓄积量方式进行计算。建立蓄积量增长模型，数据偏少，需要进一步收集数据。

油松总蓄积量 28,979.0 m³，共只有 26 个林班，年龄均在 15 龄以上，最大林龄为 48 年。由 15~48 林龄平均蓄积量差别大，用空间代替时间方法计算平均蓄积量数据缺，推算结果不理想。需要对油松森林资源进一步调查与追踪。

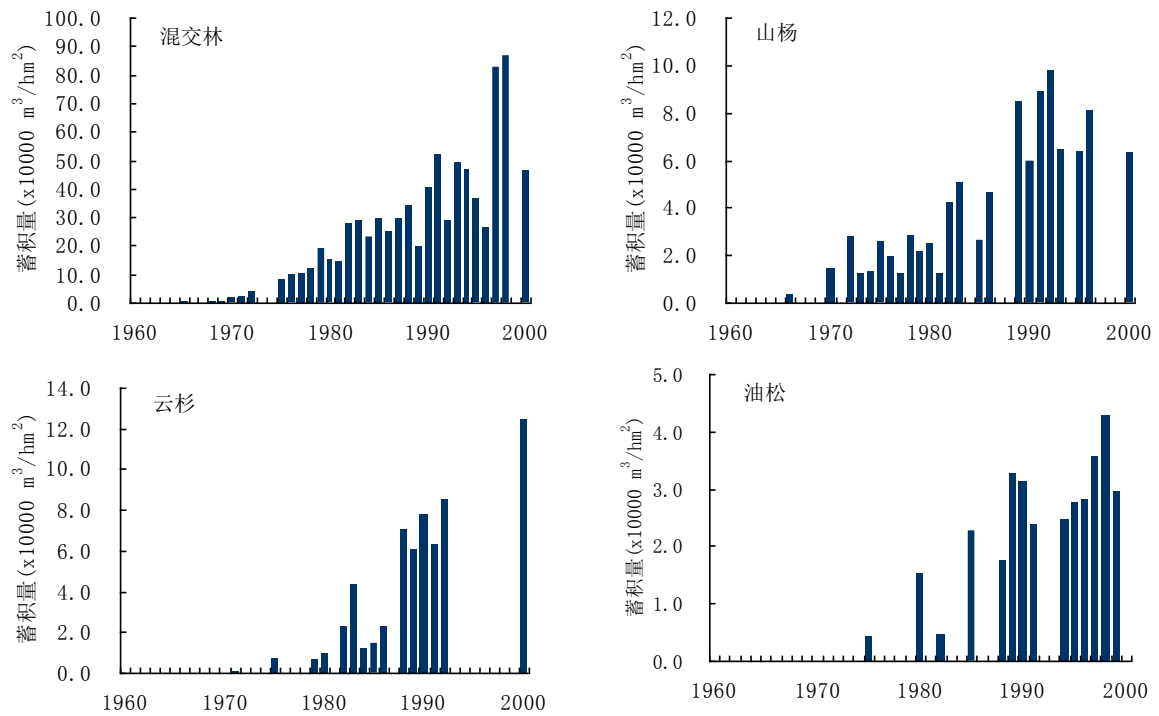


图 6-14 混交林、山杨、云杉和油松蓄积量变化

6.4 森林生物量及其变化

6.4.1 地上总生物量

史料记载，从清朝皇家猎苑开围至解放初期，植被已严重退化，绝大部分土地已沙化。1960年代中期开始大面积植树造林，经过 40 多年来持续不断营林，在沙化的土地上种植万顷森林，生物量发生巨大变化，塞罕坝林场是我国北方温带区生物量变化最突出的例子。营造大面积森林，大大改善当地生态环境，增加生态系统碳储量。生物量是衡量碳储量变化一个重要指标，现存生物量可以通过 BEF (Biomass Expansion Factor) 换算 (Fang *et al*, 2001)，建立蓄积量和生物量关系，较准确地估算了塞罕坝林场的生物量及其变化。

蓄积量与生物量可以表达为： $BEF=a+b/x$ ，其中： x 为森林蓄积量， a 、 b 为常数，不同森林类型常数不同。引用 Fang *et al* (2001) BEF 参数，计算各森林类型蓄积量与生物量的关系。BEF 相关常数见表 6-5。

表 6-5 蓄积量与生物量 BEF 换算系数*				
编 号	森 林 类 型		a	b
			(Mg m-3)	(Mg)
1	冷杉、云杉林	<i>Abies and picea</i>	0.4642	47.4990
2	白桦林	<i>Betula</i>	1.0687	10.2370
3	落叶栎林	<i>Deciduous oaks</i>	1.1453	8.5473
4	落叶松林	<i>Larix</i>	0.6096	33.8060
5	针阔混交林	<i>Mixed conifer and deciduous forests</i>	0.8136	18.4660
6	樟子松林	<i>P. sylvestris</i> var. <i>mongolica</i>	1.0945	2.0040
7	油松林	<i>P. tabulaeformis</i>	0.7554	5.0928
8	山杨林	<i>Populus</i>	0.4754	30.6034

* 资料来源：Jingyun Fang, 2001.

经过 BEF 换算公式，得出塞罕坝林场总生物量 6,529,084.8 Mg，其中落叶松生物量 4,028,010.2 Mg，占 61.7%。桦树、樟子松生物量分别占 20.1%和 5.7%，各森林类型详细生物量如表 6-6。

优势树种	面 积 (hm ²)	生物量 Mg	生物量 %
落叶松	38,670.8	4,028,010.2	61.7
桦树	15,072.4	1,311,492.0	20.1
樟子松	7,536.1	371,627.6	5.7
混交林	3,858.2	312,275.4	4.8
蒙古栎	3,671.7	168,109.3	2.6
山杨	1,075.5	64,392.4	1.0
云杉	986.2	45,829.1	0.7
油松	224.7	23,035.1	0.4
其它	23,579.0	204,313.6	3.1
合 计	94,674.6	6,529,084.8	

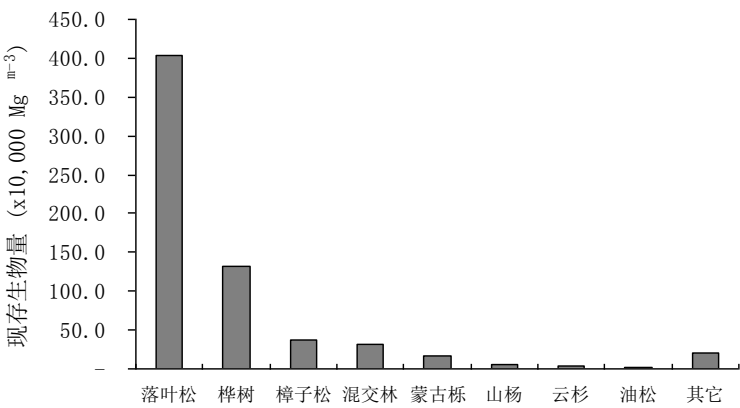


图 6-15 塞罕坝不同森林类型生物量

塞罕坝生物量以落叶松最多，其它类型森林由多到少，依次是白桦林、樟子松、混交林、蒙古栎、山杨、云杉和油松。落叶松面积最大，营林时间最长，大部分林龄在 30 ~ 40 年左右；白桦林为天然次生，不仅有较大面积的纯林，也混生在不同森林群落中；樟子松近 10 几年来才开始大面积种植，种植面积不断扩大；山杨、云杉、油松面积比较少，近期生物量不会有很大的变化。

用空间代替时间方法，计算出各类型森林生物量，落叶松生物量变化与 GLM 模型拟合有一定的偏差，GLM 模型拟合是直线上升过程，但用空间代替时间方法计算结果：1970 ~ 1980 年间增长为直线上升，但 1990 ~ 2000 年增和明显缓慢，这一增长模式可能与落叶松增长实际比较吻合，GLM 模型模拟其生物量时间变化，仍然有一些偏差，需要对落叶松生长进一步的检查和野外调查。图 6-18 白桦林从 1965 ~ 1990 年增长十分迅速，但有些年份的生物量计算结果偏低。1990 年后，白桦林生物量却下降，根据塞罕坝机械林场总场生产记录统计 1990 年白桦林没有生产活动，显然这种下降趋势与实际不相符合。从 1975 ~ 1995 年樟子松总生物量迅速上升，有些年份可能估算偏高，有些年份变化估算可能偏低；到 1995 年后，由于缺乏小班调查数据，未能正确估算。对蒙古栎总生物量估算时，各年份变化计算结查差别大，采用空间代替时间方法，可能无法正确反应总体生物量的变化。山杨、云杉和油松由于缺乏不同林龄的数据，无法估算不同年份的生物量；而且大多数林龄数据少，相关年份的平均数可能也存在偏差。

6.4.2 主要森林类型生物量的变化

(1) 落叶松林

塞罕坝林场森林类型中落叶松生物量最大，用 GLM 模型计算蓄积量变化时，实际蓄积量与模型蓄积量关系十分接近。用 BEF 换算生物量，结果如图 6-16。模型计算结果可以用简单的公式表示： $y=114306x-2E+8$ 。该模型未考虑生产经营对生物量的影响，另外，对长时间尺度生物量变化还需要对模型作进一步调整。

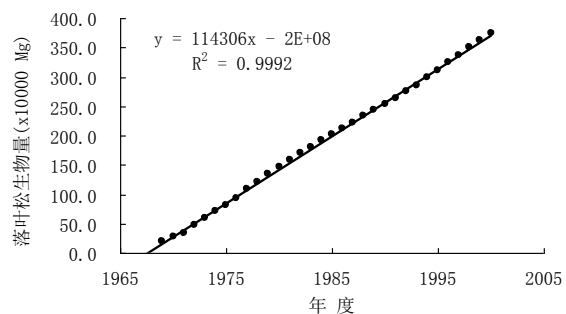


图 6-16 落叶松 GLM 模型生物量估算

落叶松生物量年平均增长 11.7×10^4 Mg/年，仅地上部分就固定 5.3×10^4 Mg C。若计地下生物量、土壤 C 库等的增长，估计超过该生物量二倍，目前缺乏地下和土壤生物量，需要进一步收集野外数据才能准确估算。

(2) 白桦林

白桦林生物量仅次于落叶松，总生物量为 1,311,492.0 Mg。由于立地条件的差异，小班内平均蓄积量差别大，用 GLM 模型计算白桦林各小班蓄积量有一定的偏差，但年总蓄积量估算十分准确。计算白桦林生物量用 GLM 模型

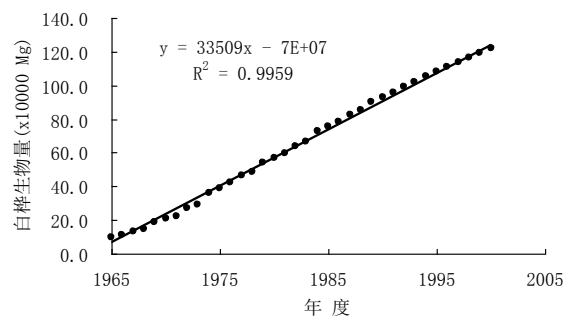


图 6-16 白桦 GLM 模型生物量估算

计算，其结果可用简单公式表示： $y=33509x-7E+7$ 。

白桦林平均生物量增长为 3.2×10^4 Mg/年，该生物量的增长约只有落叶松 1/4 左右。可见塞罕坝机械林场总场白桦生物量占仍然占十分重的地位。

(3) 樟子松

樟子松生物量相对较小，总计 371,627.6 Mg，只占总生物量的 5.7%。樟子松的平均年增长 2.4×10^4 Mg/年，与白桦林相比，樟子松增长平均生物量略小，但樟子松增长率大(图 6-17)。

塞罕坝机械林场总场的樟子松绝大部分处于幼林或生长期，该阶段樟子松枝杆比例大，通过 BEF 的蓄积量估算生物量时可能会造成樟子松生物量偏小。需要进一步建立不同林龄樟子松的生物量的关系。

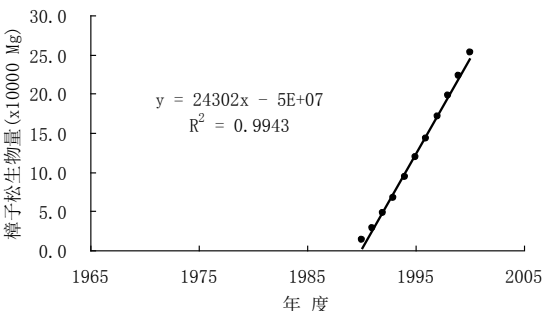


图 6-17 樟子松 GLM 模型生物量估算

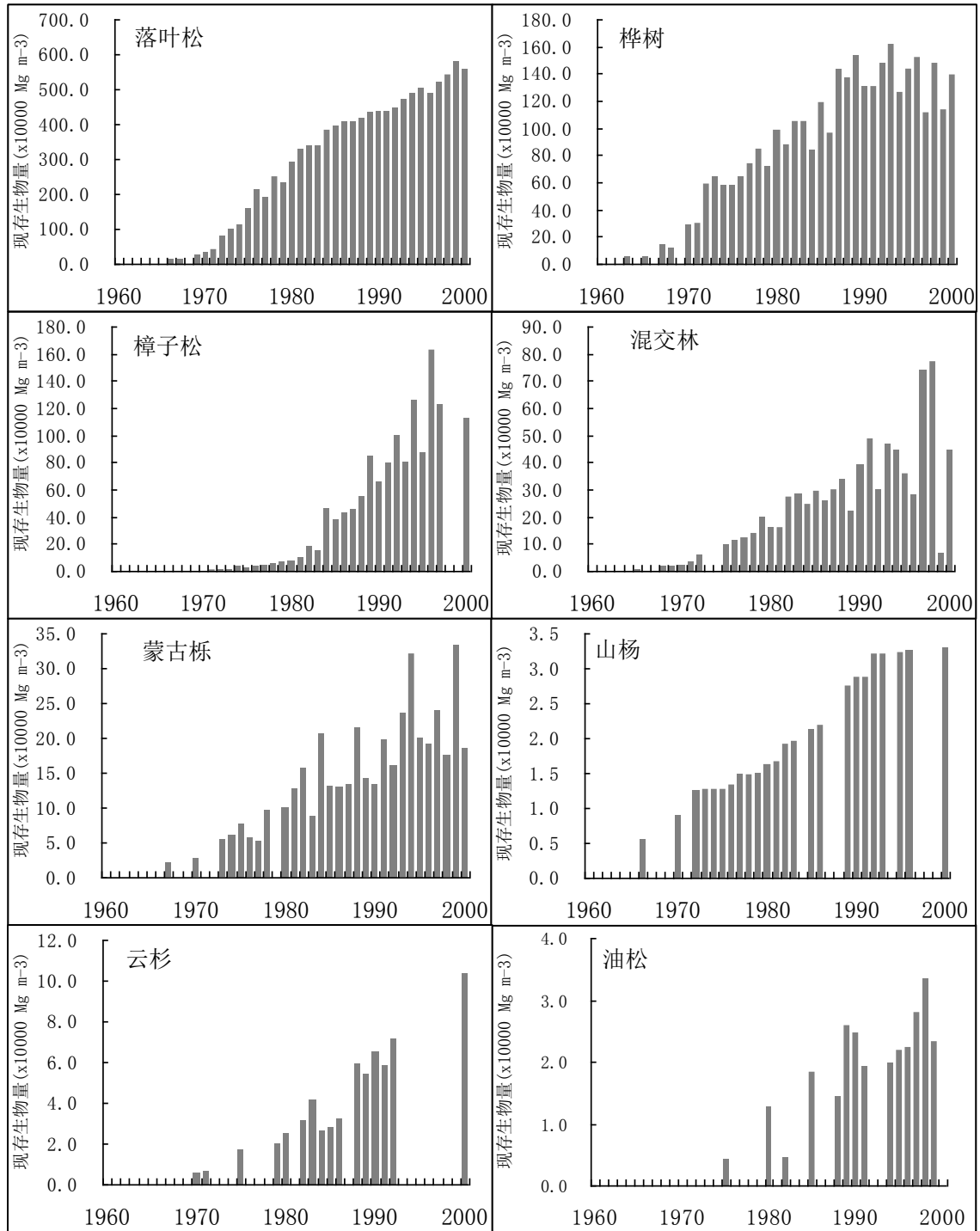


图 6-18 樟子松 GLM 模型生物量估算

第七章 结 论

本报告在分析样方数据和林班数据基础上,研究了河北省塞罕坝机械林场总场的森林植物群落的组成和生长结构,森林蓄积量、生物量及其变化,主要结论如下:

- (1) 塞罕坝记录维管束植物有 80 科 311 属 622 种(含变种和亚种,但不计栽培种),其中蕨类植物 6 科 10 属 16 种;裸子植物 2 科 5 属 12 种;被子植物 72 科 296 属 634 种。植物物种数最多的前十个科分别是菊科、禾本科、蔷薇科、豆科、莎草科、毛茛科、唇形科、杨柳科、石竹科、玄参科。单科单属植物有 23 种。河北特有植物有 5 种。
- (2) 分析塞罕坝 40 年气候数据,表明平均气温有上升趋势 ($R=0.34$),但相关分析不显著;各月气温变化差异大,其中 3 月气温变化最显著;5 ~ 9 月最高极端温度均正相关,其中以 9 月为显著正相关 ($R=0.53$, $P<0.05$)。极端最低温度规律不明显,5、7 月为负相关,8 月为正相关; $\geq 5.0^{\circ}\text{C}$ 积温 4 ~ 10 月变化负相关,虽然年平均气温有增加的趋势,但 5 ~ 9 月积温变化并不明显。降水量从 60 年代以来,年降水量显著正相关 ($R=0.42$, $P<0.05$),日降水日数明显增多 ($R=0.50$, $P<0.001$),70 年代至 90 年代降水偏少,90 年代后到今,降水量明显增加。
- (3) 塞罕坝机械林场总场土地利用类型以人工林为主,森林占总面积 76.7%。森林组成以落叶松为主,占总面积 38.7%,其次是白桦林,占 15.1%;落叶松林是主要的商品林,大多数白桦林为公益林。落叶松径级与树高有很好关系,各林龄段均有一定比例,其中以 21 ~ 35 年林龄占绝大多数。白桦林为天然更生次生林居多,林龄 20 年以后,树高和胸径变化缓慢。塞罕坝机械林场总场樟子松林龄比较小,单位面积个体数多,径级比较小。
- (4) 塞罕坝森林群落特征:针叶林(落叶松林、樟子松林、云杉林、油松林等)的胸径与树高关系显著,但落叶阔叶林(白桦林、蒙古栎林)关系不显著。通过树高影响因子相关分析结果表明:树高除了林龄关系密切外,不同森林类型与各因子相关性有较大的差异。通过建立 GLM 模型分析,分析结果表明与郁密度、森林利用类型、土壤、盖度、土地经营类型和坡度有不同程度的相关。胸径大小变化分析结果,也有相类似情形,但除了林龄为主要影响因子外,其它各因子解释率明显比较高。
- (5) 径级分布是植物群落另一个重要特征,变化规律受演替阶段、环境梯度影响。用 7 个 1 ha 样方数据分析结果表明:落叶松和樟子松样方数量径级分布,呈明显正态分布;白桦林三个样方个体数量径级分布型差异比较大。偏斜度(skew)是径级分布变化另一种有效表达方法,用八种方法计算胸径偏斜度的变化,表明按对角 $10\times 10\text{m}$, $20\text{m}\times 20\text{m}$, $30\text{m}\times 30\text{m}$...增加面积方式,得出 4 个方向的偏斜度,变化差别很大,很难正确评估群落胸径变化。按每一次增加 $10\text{m}\times 10\text{m}$ 方式计算,得出四种不同方向的计算结果,在相对均一植物群落中,最终偏斜度趋于稳定;分析也表明塞罕坝森林群落结构中,森林群落取样面积在 2000m^2 以上,偏斜度趋于稳定,说明取样在 2000m^2 情况下,测量的胸径计算蓄积量及生物量,与实际偏差很小。胸径偏斜度差异与

群落生长阶段有关,也受环境梯度变化影响,其中地形是引起塞罕坝机械林场总场胸径的森林胸径偏斜度变化重要因素。三个落叶松样方是胸径偏斜度变化的典型例子,而白桦林更重要是反映与环境梯度的变化;而樟子松样方则突出反映生长阶段从大到小径级均存在情况下,偏斜度的变化情况。

- (6) 本文通过小班调查资料,有效地估算了塞罕坝各类型森林的蓄积量,并用空间代替时间以及 GLM 模型方法计算其蓄积量的变化。塞罕坝森林类型中以落叶松蓄积量最多,占 70.9%,其次是白桦林,占 15.8%。各森林类型蓄积量在不同林龄段差异很大,落叶松 25 ~ 35 林龄占比例最大,而白桦林 20 ~ 45 林龄占比例大,樟子松则在 15 ~ 20 林龄占多数。塞罕坝林场森林蓄积总量为 $4.9 \times 10^6 \text{ m}^3$,平均每年增长蓄积量为 $1.8 \times 10^5 \text{ m}^3$ 。用林龄、森林类型、树高/年龄、郁密度、土壤类型、土壤深度、坡度、土地经营类型和森林利用类型与蓄积量建立 GLM 关系,表明森林类型、林龄对蓄积解释率最高,其它各因素与蓄积量很好的相关性。用 GLM 模型计算出各小班蓄积量与小班实际蓄积量有很好的相关性。
- (7) 分别对各主要森林类型建立 GLM 模型,与蓄积量紧密相关的林龄在各森林类型中解释率差别很大,以白桦最低,樟子松最高;其它各因子解释率也很不相同。樟子松林耐干旱、耐瘠薄的物种, GLM 模型各除了林龄外,其它各参数解释率均比较低得到充分的反映。塞罕坝各森林主要类型蓄积量变化并非线性,对各类型森林用平均蓄积量计算蓄积量与 GLM 模型计算蓄积量相比,落叶松林在生长中期 (15 ~ 25 年) 过程有明显的差异;白桦林平均蓄积量偏差比较大,推算总数十分吻合,但对不同小班计算却有一定偏差。
- (8) 用 BEF 方法推算塞罕坝森林生物量,森林总生物量为 $6.5 \times 10^6 \text{ Mg}$ 。森林生物量由大到小分别是落叶松、白桦林、樟子松、混交林、蒙古栎、山杨、云杉和油松。

致 谢

感谢我的合作导师方精云教授不论是在我的博士学习阶段还是在博士后学习阶段，他对我那种无私的关爱，使我终身难忘。他对科研工作永不停息的追求，永远向上的心，深深感召了我，使我真正领悟科研道路上的艰难旅程。我的点滴进步都是方老师言传身教分不开，

领悟到先生对植被生态研究真知灼见，对学术问题的敏锐洞察力和深邃的视野。他那严谨、求实的科学态度、渊博的学识，对科学的不懈追求和永不知疲倦的工作激情，诲人不倦的治学态度，永远铭记我心，终身受益。本研究论文更是在方老师悉心指导下完成的，从论文的选题，整体思路，内容框架，到最后定稿，无不倾注着方老师的心血和教诲。在此表示由衷感谢。

感谢陈昌笃教授和崔海亭教授，帮助我加深理解生态学理论体系，开拓新思路，调整知识结构，并且在论文内容补充和调整上的精心指导。

感谢黄润华教授、沈泽昊副教授、曾辉副教授、刘鸿雁副教授、贺金生副教授和吉成均老师，他们对我的论文提出了许许多多有价值的建设性意见。特别感谢沈泽昊老师对论文初稿的仔细审阅和修改；与他同行的那个难于忘怀的南迦巴瓦野外考察之旅，加深我对山地生态研究的理解。

感谢刘初铤高级工程师鉴定植物标本，细致地介绍武夷山自然保护区的植被类型全貌，指导野外调查样方路线设计，无私奉献他在武夷山植物研究中一生积累的宝贵经验，提供了十分有价值的调查资料，并参加了猪母岗东南坡植物样方调查。

感谢刘增力同学在武夷山植被样方调查期间与我并肩在野外度过的日日夜夜，所收集的详实的野外资料成为本文的基石。野外样方调查还得到福建武夷山自然保护区曾发旭、徐志坤、林建丽；福建将石自然保护区谢少和；以及武夷山市桐木村吴新兴和大安村丁国书等人的帮助。调查还得到何建源和方燕鸿在生活和工作上的配合和鼓励，在此一并致谢。

在我赶写论文最紧张的一段日子里，感谢师弟王志恒同学帮助分析地形数据，王襄平同学帮助植被分类，唐志尧同学帮助解决植被生态有关问题，朱彪和吴晓莆同学帮助分析植物群落结构数据，朴世龙同学帮助解决地形分析 GIS 技术和 DEM 数据制作。另外，我要特别感谢师妹谭琨、金丽佳、郭允允、彭博、李书舒、王瑾芳和师弟周萌、周睿等十分辛苦地数字化武夷山地形图。王志恒、王襄平、唐志尧、朱彪、杨元合、冯建孟、韩文轩等同学帮助校对文稿，感谢 Dan Flynn 修改英文摘要。没有他们热诚的帮助，论文将不可能如期完成。感谢所有生态研究组同学帮助、关心和支持，难以忘记他们在 seminar 上提出诸多宝贵建议，对我论文的完成起到了很大的促进作用，难于一一列举，在此致以我最诚挚谢意。

感谢福建武夷山国家级自然保护区管理局为我提供博士学习氛围，感谢国家林业局 GEF 项目资助，让我顺利完成学业。

三年多来的博士求学生活即将画上句号，希望把我的深深的谢意传达给所有热情支持、关心、帮助过我的人们。特别感谢我的妻子陈家玉，无时无刻给我关心和支持，并认真地理顺论文的文字。内心深处奶奶永恒的关爱，是我奋发向上和克服困难的动力和源泉。父母的养育和勉励是我顺利完成论文的基础。

参考文献

- 程云霄, 李忠孝. 1989. 兴安落叶松三个主要林型森林生物量的初步研究. 内蒙古林业调查设计, 7: 29-39.
- 崔海亭, 刘鸿雁, 腰希申. 1997. 浑善达克沙地古云杉木材的发现及其古生态学意义. 中国科学(D), 27: 457-461.
- 崔海亭, 王文, 2003. 从生态学角度复原元代滦河上游的景观和物候. 地理学报 58: 101-108.
- 丁宝永, 刘世荣, 蔡体久. 1990. 落叶松人工林群落生物生产力的研究. 植物生态学与地植物学学报, 14: 226-236.
- 方精云, 陈安平. 2001. 中国森林植被碳库的动态变化及其意义. 植物学报, 43: 967-973.
- 冯林, 杨玉琪. 1981. 内蒙古地区油松、白桦、山杨生物量研究. 内蒙古林学院学报, 3: 1-17.
- 冯林, 杨玉琪. 1985. 兴安落叶松原始林三种林型生物产量的研究. 林业科学, 21: 86-92.
- 冯宗炜, 王效科, 吴刚. 1999. 中国森林生态系统的生物量和生产力. 北京: 科学出版社.
- 何钢, 刘鸿雁, 2004. 河北坝上地区及浑善达克沙地植被演化及其与风沙活动关系. 北京大学学报(自然科学版), 40: 669-675.
- 黄金祥, 冯天杰, 王建中, 钱进源, 胡永富, 倪志云. 1994. 塞罕坝植物区系新分类群与河北新分布 I. 河北农业大学学报, 17:11-18.
- 黄金祥, 李信, 钱进源. 1996. 塞罕坝植物志. 北京: 中国科学技术出版社.
- 黄金祥, 王建中, 冯天杰, 钱进源, 胡永富, 张向忠, 赵亚民. 1996b. 塞罕坝植物区系新分类群与河北新分布 II. 河北农业大学学报, 19:92-96.
- 黄永梅, 刘鸿雁, 崔海亭, 2001. 内蒙古高原东南缘森林草原过渡带景观的若干特征. 植物生态学报, 25: 257-264.
- 靳鹤龄, 苏志珠, 孙良英, 孙忠, 张洪, 靳立亚, 2004. 浑善达克沙地全新世气候变化. 科学通报, 49(15): 1532-1536.
- 李博, 孙鸿良, 曾涸弟. 1980. 呼伦贝尔牧区草场植被资源及其利用方向的探讨. 自然资源 2:30-36.
- 李智佩, 张维吉, 王岷, 聂浩刚和岳乐平. 2002. 中国北方东部沙质荒漠化的地学观. 西北地质, 35:7-22.
- 刘国华, 傅伯杰, 方精云. 2000. 中国森林碳动态及其对全球碳平衡的贡献. 生态学报, 20: 733-740.
- 刘濂, 1965. 河北省坝上草原植被概况. 植物生态学与地植物学丛刊, 3: 307-316.
- 刘濂主编, 1996. 河北植被. 北京: 科学出版社.
- 刘全友. 1994. 河北省坝上地区气候与沙化关系的研究. 环境科学进展 2:47-57.
- 刘世荣, 柴一新, 蔡体久, 彭长辉. 1990. 兴安落叶松人工群落生物量与净初级生产力的研究. 东北林业大学学报, 18: 40-46.
- 刘志刚, 马钦彦, 潘向丽. 1994. 兴安落叶松天然林生物量及生产力的研究. 植物生态学报, 18: 328-337.
- 路端正, 王庆锁和罗菊春. 1996. 河北植物增补. 北京林业大学学报 18:88-90.
- 王庆锁, 2004. 河北北部和内蒙古东部森林-草原交错带森林景观格局初步研究. 生态学杂志, 23 (3): 11-15.
- 王庆锁, 冯宗炜, 2000. 河北北部、内蒙古东部森林-草原交错带生物多样性研究. 植物生态学报, 24(2): 141-146.

- 王庆锁, 李玉中, 路端正, 罗菊春, 冯宗炜. 2005. 河北省塞罕坝地区种子植物区系的过渡性分析. 生态学杂志, 2005, 24 (5) : 473-477.
- 吴刚, 冯宗炜. 1994. 中国油松林群落特征及生物量的研究. 生态学报, 14: 416-422.
- 吴征镒. 1980. 中国植被北京: 科学出版社.
- 张宝秀. 1997. 内蒙古高原东南缘土地开发与环境退化关系论析. 地理学与国土研究 13:16-22.
- 张成林, 周晓峰. 1991. 天然次生白桦林生物量的研究. 见: 周晓峰主编. 森林生态系统定位研究(第一集), 428-435. 哈尔滨: 东北林业大学出版社.
- 中国科学院内蒙古宁夏综合考察队. 1985. 内蒙古植被. 科学出版社, 北京.
- 邹厚远, 李玲和刘克俭. 1994. 黄土高原植被及其合理利用与保护. 见: 姜恕和陈昌笃. 植被生态学研究. 北京: 科学出版社, 146-153.
- Brown S. 2002. Measuring carbon in forests: current status and future challenges. Environmental Pollution, 116: 363-372.
- Fang JY, Piao SL, Field CB, Pan YD, Guo QH, Zhou LM, Peng CH, Tao S. 2003. Increasing net primary production in China from 1982 to 1999. Frontiers in Ecology and the Environment, 1: 293-297.
- Fang JY, Wang GG, Liu GH, Xu SL. 1998. Forest biomass of China: An estimate based on the biomass-volume relationship. Ecological Applications, 8: 1084-1091.
- Fang JY, Wang ZM. 2001. Forest biomass estimation at regional and global levels, with special reference to China's forest biomass. Ecological Research, 16: 587-592.
- Fang, JY, Chen AP, Peng CH, Zhao SQ and Ci LJ. 2001. Changes in forest biomass carbon storage in China between 1949 and 1998. Science, **292**:2320-2322.
- Jiang H, Apps MJ, Zhang YL, Peng CH, Woodard PM. 1999a. Modelling the spatial pattern of net primary productivity in Chinese forests. Ecological Modelling, 122: 275-288.
- Jiang H, Peng CH, Apps MJ, Zhang YL, Woodard PM, Wang ZM. 1999b. Modelling the net primary productivity of temperate forest ecosystems in China with a GAP model. Ecological Modelling, 122: 225-238.
- Li KR, Wang SQ, Cao MK. 2004. Vegetation and soil carbon storage in China. Science in China (Series D), 47: 49-57.
- Liu HY, Xu LH, and Cui HT, 2002. Holocene History of Desertification along the Woodland-Steppe Border in Northern China. Quaternary Research, 57: 259 - 270
- Liu, HY, Cui HT, Tian YH and Xu LH. 2002a. Temporal- Spatial Variances of Holocene Precipitation at the Marginal Area of the East Asian Monsoon Influences from Pollen Evidence. Acta Botanica Sinica 44:864-871.
- Liu, HY, Xu LH and Cui HT. 2002b. Holocene History of Desertification along the Woodland-Steppe Border in Northern China. Quaternary Research 57:259-270.
- Myneni RB, Dong J, Tucker CJ, Kaufmann RK, Kauppi PE, Liski J, Zhou L, Alexeyev V, Hughes MK. 2001. A large carbon sink in the woody biomass of Northern forests. Proceeding of the National Academy of Sciences of the United States of America, 98: 14784-14789
- Ni J. 2003. Net primary productivity in forests of China: scaling-up of national inventory data and comparison with model predictions. Forest Ecology and Management, 176: 485-495.
- Pan YD, Luo TX, Birdsey R, Hom J, Melillo JM. 2004. New estimate of carbon storage and

- sequestration in China's forests: effects of age-class and method on inventory-based carbon estimation. *Climatic Change*, 67: 211-236.
- Shvidenco A, Nilsson S. 2002. Dynamics of Russian forests and the carbon budget in 1961-1998: an assessment based on long-term forest inventory data. *Climatic Change*, 55: 5-37.
- Wang SQ, Zhou CH, Liu JY, Tian HQ, Li KR, Yang XM. 2002a. Carbon storage in northeast China as estimated from vegetation and soil inventories. *Environmental Pollution*, 116 (Supp.): S157-S165.
- Zhao M, Zhou GS. 2005. Estimation of biomass and net primary productivity of major planted forests in China based on forest inventory data. *Forest Ecology and Management*, 207: 295-313.
- Zhou GS, Wang YH, Jiang YL, Yang ZY. 2002. Estimating biomass and net primary production from forest inventory data: a case study of China's *Larix* forests. *Forest Ecology and Management*, 169: 149-157.

附录 河北省塞罕坝高等植物名录

序号	科中名	科学名	属中名	属学名	种中名	种学名
1	卷柏科	Selaginellaceae	卷柏属	<i>Selaginella</i>	圆枝卷柏	<i>Selaginella sanguinolenta</i>
2					旱生卷柏	<i>S. stauntoniana</i>
3	木贼科	Equisetaceae	木贼属	<i>Hippochaete</i>	问荆	<i>Hippochaete arvense</i>
4					木贼	<i>H. hiemale</i>
5					草问荆	<i>H. pratense</i>
6					节节草	<i>H. ramosissimum</i>
7					林下木贼	<i>H. sylvaticum</i>
8	蕨科	Pteridiaceae	蕨属	<i>Pteridium</i>	蕨	<i>Pteridium aquilinum</i> var. <i>latiusculum</i>
9	蹄盖蕨科	Athyriaceae	短肠蕨属	<i>Allantodia</i>	黑鳞短肠蕨	<i>Allantodia crenata</i>
10			蹄盖蕨属	<i>Athyrium</i>	多齿蹄盖蕨	<i>Athyrium multidentatum</i>
11					中华蹄盖蕨	<i>A. sinense</i>
12			冷蕨属	<i>Cystopteris</i>	冷蕨	<i>Cystopteris fragilis</i>
13			羽节蕨属	<i>Gymnocarpium</i>	欧洲羽节蕨	<i>Gymnocarpium dryopteris</i>
14	球子蕨科	Onocleaceae	荚果蕨属	<i>Matteuccia</i>	荚果蕨	<i>Matteuccia struthiopteris</i>
15			球子蕨属	<i>Onoclea</i>	球子蕨	<i>Onoclea interrupta</i>
16	岩蕨科	Woodsiaceae	岩蕨属	<i>Woodsia</i>	心岩蕨	<i>Woodsia subcordata</i>
17	松科	Pinaceae	油杉属	<i>Keteleeria</i>	兴安落叶松	<i>Larix dahurica</i>
18			落叶松属	<i>Larix</i>	日本落叶松	<i>Larix kaempferi</i>
19					黄花落叶松	<i>L. olgensis</i>
20					华北落叶松	<i>L. principis-rupprechtii</i>
21					西伯利亚落叶松	<i>L. sibirica</i>
22			云杉属	<i>Picea</i>	白杆	<i>Picea meyeri</i>
23			松属	<i>Pinus</i>	红松	<i>Pinus koraiensis</i>
24					樟子松	<i>P. sylvestris</i> var. <i>mongolica</i>
25					油松	<i>P. tabulaeformis</i>
26					黑皮油松	<i>P. tabulaeformis</i> var. <i>mukdensis</i>
27	柏科	Cupressaceae	圆柏属	<i>Sabina</i>	圆柏	<i>Sabina chinensis</i>
28					兴安圆柏	<i>S. davurica</i>
29	杨柳科	Salicaceae	杨属	<i>Populus</i>	北京杨	<i>Populus beijingensis</i>
30					中东杨	<i>P. berolinensis</i>
31					青杨	<i>P. cathayana</i>
32					山杨	<i>P. davidiana</i>
33					小青杨	<i>P. pseudo-simonii</i>
34					小叶杨	<i>P. simonii</i>
35			柳属	<i>Salix</i>	垂柳	<i>Salix babylonica</i>
36					密齿柳	<i>S. characta</i>
37					乌柳	<i>S. cheilophila</i>
38					崖柳	<i>S. floderusii</i>
39					黄柳	<i>S. gordejewii</i>
40					兴安柳	<i>S. hsinganica</i>

41					沙杞柳	<i>S. kochiana</i>
42					小穗柳	<i>S. microstachya</i>
43					越桔柳	<i>S. myrtilloides</i>
44					五蕊柳	<i>S. pentandra</i>
45					北沙柳	<i>S. psammophila</i>
46					大黄柳	<i>S. raddeana</i>
47					粉枝柳	<i>S. rorida</i>
48					细叶沼柳	<i>S. rosmarinifolia</i>
49					中国黄花柳	<i>S. sinica</i>
50					谷柳	<i>S. taraikensis</i>
51					三蕊柳	<i>S. triandra</i>
52					细叶蒿柳	<i>S. viminalis</i> var. <i>angustifolia</i>
53	桦木科	Betulaceae	桦木属	<i>Betula</i>	硕桦	<i>Betula costata</i>
54					黑桦	<i>B. dahurica</i>
55					沙生桦	<i>B. gmelinii</i>
56					白桦	<i>B. platyphylla</i>
57					赛黑桦	<i>B. schmidtii</i>
58			榛属	<i>Corylus</i>	榛	<i>Corylus heterophylla</i>
59					毛榛	<i>C. mandshurica</i>
60			虎榛子属	<i>Ostryopsis</i>	虎榛子	<i>Ostryopsis davidiana</i>
61	壳斗科	Fagaceae	栎属	<i>Quercus</i>	辽东栎	<i>Quercus liaotungensis</i>
62					蒙古栎	<i>Q. mongolica</i>
63	榆科	Ulmaceae	榆属	<i>Ulmus</i>	旱榆	<i>Ulmus glaucescens</i>
64					裂叶榆	<i>U. laciniata</i>
65					大果榆	<i>U. macrocarpa</i>
66					榆	<i>U. pumila</i>
67	桑科	Moraceae	大麻属	<i>Cannabis</i>	大麻	<i>Cannabis sativa</i>
68			葎草属	<i>Humulus</i>	葎草	<i>Humulus scandens</i>
69	荨麻科	Urticaceae	墙草属	<i>Parietaria</i>	墙草	<i>Parietaria micrantha</i>
70			荨麻属	<i>Urtica</i>	狭叶荨麻	<i>Urtica angustifolia</i>
71					麻叶荨麻	<i>U. cannabina</i>
72	檀香科	Santalaceae	百蕊草属	<i>Thesium</i>	急折百蕊草	<i>Thesium refractum</i>
73	蓼科	Polygonaceae	荞麦属	<i>Fagopyrum</i>	苦荞麦	<i>Fagopyrum tataricum</i>
74			蓼属	<i>Polygonum</i>	两栖蓼	<i>Polygonum amphibium</i>
75					篇蓄	<i>P. aviculare</i>
76					拳蓼	<i>P. bistorta</i>
77					卷茎蓼	<i>P. convolvulus</i>
78					叉分蓼	<i>P. divaricatum</i>
79					水蓼	<i>P. hydropiper</i>
80					酸模叶蓼	<i>P. lapathifolium</i>
81					箭叶蓼	<i>P. sieboldii</i>
82					珠芽蓼	<i>P. viviparum</i>
83					高山蓼	<i>P. alpinum</i>
84					习见蓼	<i>P. plebeium</i>

85					齿翅蓼	<i>P. dentato-alatum</i>
86			大黄属	<i>Rheum</i>	波叶大黄	<i>Rheum franzenbachii</i>
87			酸模属	<i>Rumex</i>	酸模	<i>Rumex acetosa</i>
88					巴天酸模	<i>R. patientia</i>
89					毛脉酸模	<i>R. gmelini</i>
90	藜科	Chenopodiaceae	沙蓬属	<i>Agriophyllum</i>	沙蓬	<i>Agriophyllum squarrosum</i>
91			轴藜属	<i>Axyris</i>	轴藜	<i>Axyris amaranthoides</i>
92			藜属	<i>Chenopodium</i>	尖头叶藜	<i>Chenopodium acuminatum</i>
93					藜	<i>C. album</i>
94					刺藜	<i>C. aristatum</i>
95					菊叶香藜	<i>C. foetidum</i>
96					灰绿藜	<i>C. glaucum</i>
97					杂配藜	<i>C. hybridum</i>
98			虫实属	<i>Corispermum</i>	烛台虫实	<i>Corispermum candelabrum</i>
99					兴安虫实	<i>C. chinganicum</i>
100			地肤属	<i>Kochia</i>	碱地肤	<i>Kochia scoparia</i> var. <i>sieversiana</i>
101			猪毛菜属	<i>Salsola</i>	猪毛菜	<i>Salsola collina</i>
102					刺沙蓬	<i>S. ruthenica</i>
103					细叶猪毛菜	<i>S. ruthenica</i> var. <i>filifolia</i>
104	苋科	Amaranthaceae	苋属	<i>Amaranthus</i>	反枝苋	<i>Amaranthus retroflexus</i>
105	马齿苋科	Portulacaceae	马齿苋属	<i>Portulaca</i>	马齿苋	<i>Portulaca oleracea</i>
106	石竹科	Caryophyllaceae	蚤缀属	<i>Arenaria</i>	灯心草蚤缀	<i>Arenaria juncea</i>
107					毛梗蚤缀	<i>A. capillaris</i>
108			卷耳属	<i>Cerastium</i>	卷耳	<i>Cerastium arvense</i>
109					簇生卷耳	<i>C. caespitosum</i>
110					细叶卷耳	<i>C. arvense</i> var. <i>angustifolium</i>
111			石竹属	<i>Dianthus</i>	石竹	<i>Dianthus chinensis</i>
112					簇茎石竹	<i>D. repens</i>
113					瞿麦	<i>D. superbus</i>
114			石头花属	<i>Gypsophila</i>	北丝石竹	<i>Gypsophila davruica</i>
115			剪秋罗属	<i>Lychnis</i>	浅裂剪秋罗	<i>Lychnis cognata</i>
116			女娄菜属	<i>Melandrium</i>	女娄菜	<i>Melandrium apricum</i>
117			种阜草属	<i>Moehringia</i>	种阜草	<i>Moehringia lateriflora</i>
118			蝇子草属	<i>Silene</i>	绳子草	<i>Silene fortunei</i>
119					匍生绳子草	<i>S. repens</i>
120					旱麦瓶草	<i>S. jensisensis</i>
121			繁缕属	<i>Stellaria</i>	异色繁缕	<i>Stellaria discolor</i>
122					内曲繁缕	<i>S. infracta</i>
123					绿花繁缕	<i>S. cherleriae</i>
124					沼繁缕	<i>S. palustris</i>
125	毛茛科	Ranunculaceae	乌头属	<i>Aconitum</i>	细叶黄乌头	<i>Aconitum barbatum</i>
126					华北乌头	<i>A. soongaricum</i> var. <i>angustius</i>
127			银莲花属	<i>Anemone</i>	银莲花	<i>Anemone cathayensis</i>
128					大花银莲花	<i>A. silvestris</i>

129			耧斗菜属	<i>Aquilegia</i>	华北耧斗菜	<i>Aquilegia yabeana</i>
130			水毛茛属	<i>Batrachium</i>	水毛茛	<i>Batrachium bungei</i>
131			驴蹄草属	<i>Caltha</i>	驴蹄草	<i>Caltha palustris</i>
132			升麻属	<i>Cimicifuga</i>	兴安升麻	<i>Cimicifuga dahurica</i>
133			铁线莲属	<i>Clematis</i>	短尾铁线莲	<i>Clematis brevicaudata</i>
134					棉团铁线莲	<i>C. hexapetala</i>
135					长瓣铁线莲	<i>C. macropetala</i>
136			翠雀属	<i>Delphinium</i>	翠雀	<i>Delphinium grandiflorum</i>
137			碱毛茛属	<i>Halerpestes</i>	水葫芦苗	<i>Halerpestes cymbalaria</i>
138			芍药属	<i>Paeonia</i>	草芍药	<i>Paeonia obovata</i>
139					白花山芍药	<i>P. japonica</i>
140			白头翁属	<i>Pulsatilla</i>	细叶白头翁	<i>Pulsatilla turczaninovii</i>
141			毛茛属	<i>Ranunculus</i>	毛茛	<i>Ranunculus japonicus</i>
142					石龙芮	<i>R. sceleratus</i>
143			唐松草属	<i>Thalictrum</i>	唐松草	<i>Thalictrum aquilegifolium</i> var. <i>sibiricum</i>
144					贝加尔唐松草	<i>T. baicalense</i>
145					瓣蕊唐松草	<i>T. petaloideum</i>
146					狭裂瓣蕊唐松草	<i>T. petaloideum</i> var. <i>supradecompositum</i>
147					长柄唐松草	<i>T. przewalskii</i>
148					箭头唐松草	<i>T. simplex</i>
149					展枝唐松草	<i>T. squarrosus</i>
150			金莲花属	<i>Trollius</i>	宽瓣金莲花	<i>Trollius asiaticus</i>
151					金莲花	<i>T. chinensis</i>
152	小檗科	Berberidaceae	小檗属	<i>Berberis</i>	大叶小檗	<i>berberis amurensis</i>
153	防己科	Menispermaceae	蝙蝠葛属	<i>Menispermum</i>	蝙蝠葛	<i>Menispermum dauricum</i>
154	木兰科	Magnoliaceae	五味子属	<i>Schisandra</i>	五味子	<i>Schisandra chinensis</i>
155	罂粟科	Papaveraceae	紫堇属	<i>Corydalis</i>	齿瓣延胡索	<i>Corydalis remota</i>
156			角茴香属	<i>Hypecoum</i>	节裂角茴香	<i>Hypecoum leptocarpum</i>
157			罂粟属	<i>Papaver</i>	山罂粟	<i>Papaver nudicaule</i> subsp. <i>rubro-aurantiacum</i> var. <i>chinense</i>
158	十字花科	Cruciferae	庭芥属	<i>Alyssum</i>	北方庭芥	<i>Alyssum lenense</i>
159			南芥属	<i>Arabis</i>	垂果南芥	<i>Arabis pendula</i>
160			芥属	<i>Capsella</i>	芥	<i>Capsella bursa-pastoris</i>
161			播娘蒿属	<i>Descurainia</i>	播娘蒿	<i>Descurainia sophia</i>
162			花旗杆属	<i>Dontostemon</i>	花旗杆	<i>Dontostemon dentatus</i>
163					小花花旗杆	<i>D. micranthus</i>
164			葶苈属	<i>Draba</i>	葶苈	<i>Draba nemorosa</i>
165					光果葶苈	<i>D. nemorosa</i> var. <i>leiocarpa</i>
166			芝麻菜属	<i>Eruca</i>	芝麻菜	<i>Eruca sativa</i>
167			糖芥属	<i>Erysimum</i>	糖芥	<i>Erysimum bungei</i>
168					小花糖芥	<i>E. cheiranthoides</i>
169					华北糖芥	<i>E. macilentum</i>

170			香花芥属 <i>Hesperis</i>	雾灵香花芥	<i>Hesperis oreophila</i>
171			独行菜属 <i>Lepidium</i>	独行菜	<i>Lepidium apetalum</i>
172			蔊菜属 <i>Rorippa</i>	沼生蔊菜	<i>Rorippa islandica</i>
173			蔊属 <i>Thlaspi</i>	蔊(遏蓝菜)	<i>Thlaspi arevense</i>
174				山蔊(遏蓝菜)	<i>T. thlaspidioides</i>
175	景天科	Crassulaceae	瓦松属 <i>Orostachys</i>	钝叶瓦松	<i>Orostachys malacophyllus</i>
176			红景天属 <i>Rhodiola</i>	小丛红景天	<i>Rhodiola dumulosa</i>
177			景天属 <i>Sedum</i>	费菜	<i>Sedum aizoon</i>
178				景天	<i>S. erythrostictum</i>
179				堪察加景天	<i>S. kamtschaticum</i>
180				华北景天	<i>S. tatarinowii</i>
181	虎耳草科	Saxifragaceae	落新妇属 <i>Astilbe</i>	落新妇	<i>Astilbe chinensis</i>
182			溲疏属 <i>Deutzia</i>	小花溲疏	<i>Deutzia parviflora</i>
183			绣球属 <i>Hydrangea</i>	东陵绣球	<i>Hydrangea bretschneideri</i>
184			梅花草属 <i>Parnassia</i>	细叉梅花草	<i>Parnassia oreophila</i>
185				梅花草	<i>P. palustris</i>
186			山梅花属 <i>Philadelphus</i>	太平花	<i>Philadelphus pekinensis</i>
187			茶藨子属 <i>Ribes</i>	楔叶茶藨	<i>Ribes diacanthum</i>
188				围场茶藨	<i>R. diacanthum</i> f. <i>weichangensis</i>
189				光枝楔叶茶藨	<i>R. diacanthum</i> f. <i>inermis</i>
190				簇花茶藨	<i>R. fasciculatum</i>
191				山麻子藨	<i>R. manschuricum</i>
192				美丽茶藨	<i>R. pulchellum</i>
193	蔷薇科	Rosaceae	龙芽草属 <i>Agrimonia</i>	龙芽草	<i>Agrimonia pilosa</i>
194			地蔷薇属 <i>Chamaerhodos</i>	地蔷薇	<i>Chamaerhodos erecta</i>
195			栒子属 <i>Cotoneaster</i>	灰栒子	<i>Cotoneaster acutifolius</i>
196				全缘栒子	<i>C. integerrimus</i>
197				黑果栒子	<i>C. melanocarpus</i>
198				毛叶水栒子	<i>C. submultiflorus</i>
199			山楂属 <i>Crataegus</i>	光叶山楂	<i>Crataegus dahurica</i>
200				光萼山楂	<i>C. laevicalyx</i>
201				毛山楂	<i>C. maximowiczii</i>
202				辽宁山楂	<i>C. sanguinea</i>
203			蚊子草属 <i>Filipendula</i>	蚊子草	<i>Filipendula palmata</i>
204			草莓属 <i>Fragaria</i>	东方草莓	<i>Fragaria orientalis</i>
205				野草莓	<i>F. vesca</i>
206			路边青属 <i>Geum</i>	路边青	<i>Geum aleppicum</i>
207			苹果属 <i>Malus</i>	山荆子	<i>Malus baccata</i>
208				苹果	<i>M. pumila</i>
209				海棠花	<i>M. spectabilis</i>
210			委陵菜属 <i>Potentilla</i>	星毛委陵菜	<i>Potentilla acaulis</i>
211				蕨麻	<i>P. anserina</i>
212				白萼委陵菜	<i>P. betonicifolia</i>
213				二裂委陵菜	<i>P. bifurca</i>

214				委陵菜	<i>P. chinensis</i>	
215				大萼委陵菜	<i>P. conferta</i>	
216				狼牙委陵菜	<i>P. cryptotaeniae</i>	
217				匍枝委陵菜	<i>P. flagellaris</i>	
218				莓叶委陵菜	<i>P. fragarioides</i>	
219				三叶委陵菜	<i>P. freyniana</i>	
220				金露梅	<i>P. fruticosa</i>	
221				银露梅	<i>P. glabra</i>	
222				沼委陵菜	<i>P. palustris</i>	
223				多裂委陵菜	<i>P. multifida</i>	
224				匍匐委陵菜	<i>P. reptans</i>	
225				朝天委陵菜	<i>P. supina</i>	
226				菊叶委陵菜	<i>P. tanacetifolia</i>	
227				轮叶委陵菜	<i>P. verticillaris</i>	
228				密枝委陵菜	<i>P. virgata</i>	
229		李属	<i>Prunus</i>	山杏	<i>Prunus sibirica</i>	
230				稠李	<i>P. padus</i>	
231		梨属	<i>Pyrus</i>	秋子梨	<i>Pyrus ussuriensis</i>	
232		蔷薇属	<i>Rosa</i>	美蔷薇	<i>Rosa bella</i>	
233				山刺玫	<i>R. davurica</i>	
234		悬钩子属	<i>Rubus</i>	复盆子	<i>Rubus idaeus</i>	
235				石生悬钩子	<i>R. saxatilis</i>	
236		地榆属	<i>Sanguisorba</i>	地榆	<i>Sanguisorba officinalis</i>	
237		珍珠梅属	<i>Sorbaria</i>	华北珍珠梅	<i>Sorbaria kirilowii</i>	
238		花楸属	<i>Sorbus</i>	花楸树	<i>Sorbus pohuashanensis</i>	
239		绣线菊属	<i>Spiraea</i>	耧斗菜叶绣线菊	<i>Spiraea aquilegifolia</i>	
240				绣球绣线菊	<i>S. blumei</i>	
241				土庄绣线菊	<i>S. pubescens</i>	
242				绣线菊	<i>S. salicifolia</i>	
243	豆科	Leguminosae	黄芪属	<i>Astragalus</i>	直立黄芪	<i>Astragalus adsurgens</i>
244					达乌里黄芪	<i>A. dahuricus</i>
245					草木樨状黄芪	<i>A. melilotoides</i>
246					内蒙黄芪	<i>A. mongholicus</i>
247					白花黄芪	<i>A. galactites</i>
248			锦鸡儿属	<i>Caragana</i>	小叶锦鸡儿	<i>Caragana microphylla</i>
249			米口袋属	<i>Gueldenstaedtia</i>	稀花米口袋	<i>Gueldenstaedtia pauciflora</i>
250			岩黄耆属	<i>Hedysarum</i>	山岩黄耆	<i>Hedysarum alpinum</i>
251					蒙古岩黄耆	<i>H. mongolicum</i>
252					拟蚕豆岩黄耆	<i>H. vicioides</i>
253			鸡眼草属	<i>Kummerowia</i>	长萼鸡眼草	<i>Kummerowia stipulacea</i>
254			香豌豆属	<i>Lathyrus</i>	矮香豌豆	<i>Lathyrus humilis</i>
255					山黧豆	<i>L. quinquenervius</i>
256			胡枝子属	<i>Lespedeza</i>	胡枝子	<i>Lespedeza bicolor</i>
257					达乌里胡枝子	<i>L. davurica</i>

258			苜蓿属	<i>Medicago</i>	天蓝苜蓿	<i>Medicago lupulina</i>
259			草木樨属	<i>Melilotus</i>	黄香草木樨	<i>Melilotus officinalis</i>
260			棘豆属	<i>Oxytropis</i>	硬毛棘豆	<i>Oxytropis hirta</i>
261					狐尾藻棘豆	<i>O. myriophylla</i>
262					黄毛棘豆	<i>O. ochrantha</i>
263					砂珍棘豆	<i>O. psammocharis</i>
264					球花棘豆	<i>O. strobilacea</i>
265					缘毛棘豆	<i>O. ciliata</i>
266					蓝花棘豆	<i>O. caerulea</i>
267					大花棘豆	<i>O. grandiflora</i>
268			槐属	<i>Sophora</i>	苦参	<i>Sophora flavescens</i>
269			黄华属	<i>Thermopsis</i>	披针叶黄华	<i>Thermopsis lanceolata</i>
270			车轴草属	<i>Trifolium</i>	野火球	<i>Trifolium lupinaster</i>
271			胡卢巴属	<i>Trigonella</i>	花苜蓿	<i>Trigonella ruthenica</i>
272			野豌豆属	<i>Vicia</i>	山野豌豆	<i>Vicia amoena</i>
273					三齿蓼野豌豆	<i>V. bungei</i>
274					广布野豌豆	<i>V. cracca</i>
275					假香野豌豆	<i>V. pseudo-orobus</i>
276					四籽野豌豆	<i>V. tetrasperma</i>
277					歪头菜	<i>V. unijuga</i>
278					北野豌豆	<i>V. ramuliflora</i>
279					柳叶野豌豆	<i>V. venosa</i>
280					长柔毛野豌豆	<i>V. villosa</i>
281	牛儿苗科	Geraniaceae	老鹳草属	<i>Geranium</i>	粗根老鹳草	<i>Geranium dahuricum</i>
282					毛蕊老鹳草	<i>G. eriostemon</i>
283					草原老鹳草	<i>G. pratense</i>
284					鼠掌老鹳草	<i>G. sibiricum</i>
285					大花老鹳草	<i>G. transbaicalicum</i>
286					突节老鹳草	<i>G. japonicum</i>
287	亚麻科	Linaceae	亚麻属	<i>Linum</i>	亚麻	<i>Linum usitatissimum</i>
288					宿根亚麻	<i>L. perenne</i>
289	芸香科	Rutaceae	白鲜属	<i>Dictamnus</i>	白鲜	<i>Dictamnus dasycarpus</i>
290	大戟科	Euphorbiaceae	大戟属	<i>Euphorbia</i>	锥花大戟	<i>Euphorbia savaryi</i>
291			叶底珠属	<i>Securinega</i>	叶底珠	<i>Securinega suffruticosa</i>
292	水马齿科	Callitrichaceae	水马齿属	<i>Callitriche</i>	水马齿	<i>Callitriche stagnalis</i>
293	卫矛科	Celastraceae	卫矛属	<i>Euonymus</i>	卫矛	<i>Euonymus alatus</i>
294	槭树科	Aceraceae	槭属	<i>Acer</i>	元宝槭	<i>Acer truncatum</i>
295	凤仙花科	Balsaminaceae	凤仙花属	<i>Impatiens</i>	水金凤	<i>Impatiens noli-tangere</i>
296	鼠李科	Rhamnaceae	鼠李属	<i>Rhamnus</i>	鼠李	<i>Rhamnus davurica</i>
297					东北鼠李	<i>R. var. manshurica</i>
298					乌苏里鼠李	<i>R. ussuriensis</i>
299	椴树科	Tiliaceae	椴树属	<i>Tilia</i>	辽椴	<i>Tilia mandshurica</i>
300					蒙椴	<i>T. mongolica</i>
301	锦葵科	Malvaceae	蜀葵属	<i>Althaea</i>	蜀葵	<i>Althaea rosea</i>

302			锦葵属	<i>Malva</i>	锦葵	<i>Malva sinensis</i>
303					北野葵	<i>M. mohileviensis</i>
304	藤黄科	Guttiferae	金丝桃属	<i>Hypericum</i>	黄海棠	<i>Hypericum ascyron</i>
305					赶山鞭	<i>H. attenuatum</i>
306	堇菜科	Violaceae	堇菜属	<i>Viola</i>	鸡腿堇菜	<i>Viola acuminata</i>
307					双花堇菜	<i>V. biflora</i>
308					球果堇菜	<i>V. collina</i>
309					掌叶堇菜	<i>V. dactyloides</i>
310					斑叶堇菜	<i>V. variegata</i>
311					阴地堇菜	<i>V. yezoensis</i>
312	瑞香科	Thymelaeaceae	栗麻属	<i>Diarthron</i>	草瑞香	<i>Diarthron linifolium</i>
313			狼毒属	<i>Stellera</i>	狼毒	<i>Stellera chamaejasme</i>
314	胡颓子科	Elaeagnaceae	沙棘属	<i>Hippophae</i>	沙棘	<i>Hippophae rhamnoides</i>
315	柳叶菜科	Onagraceae	柳兰属	<i>Chamaenerion</i>	柳兰	<i>Chamaenerion angustifolium</i>
316			露珠草属	<i>Circaea</i>	高山露珠草	<i>Circaea alpina</i>
317			柳叶菜属	<i>Epilobium</i>	多枝柳叶菜	<i>Epilobium fastigiato-ramosum</i>
318	五加科	Araliaceae	五加属	<i>Acanthopanax</i>	刺五加	<i>Acanthopanax senticosus</i>
319					无梗五加	<i>A. sessiliflorus</i>
320	伞形科	Umbelliferae	当归属	<i>Angelica</i>	长鞘当归	<i>Angelica cartilagino-marginata</i>
321			柴胡属	<i>Bupleurum</i>	北柴胡	<i>Bupleurum chinense</i>
322					红柴胡	<i>B. scorzonrifolium</i>
323					兴安柴胡	<i>B. sibiricum</i>
324					黑柴胡	<i>B. smithii</i>
325			毒芹属	<i>Cicuta</i>	毒芹	<i>Cicuta virosa</i>
326			独活属	<i>Heracleum</i>	短毛独活	<i>Heracleum moellendorffii</i>
327			藁本属	<i>Ligusticum</i>	岩茴香	<i>Ligusticum tachiroei</i>
328			前胡属	<i>Peucedanum</i>	刺尖前胡	<i>Peucedanum elegans</i>
329					石防风	<i>P. terebinthaceum</i>
330			棱子芹属	<i>Pleurospermum</i>	棱子芹	<i>Pleurospermum camtschaticum</i>
331			防风属	<i>Saposhnikovia</i>	防风	<i>Saposhnikovia divaricata</i>
332			迷果芹属	<i>Sphallerocarpus</i>	迷果芹	<i>Sphallerocarpus gracilis</i>
333	山茱萸科	Cornaceae	楝木属	<i>Swida</i>	红瑞木	<i>Swida alba</i>
334					沙楝	<i>S. bretschneideri</i>
335	鹿蹄草科	Pyrolaceae	鹿蹄草属	<i>Pyrola</i>	鹿蹄草	<i>Pyrola calliantha</i>
336	杜鹃花科	Ericaceae	杜鹃花属	<i>Rhododendron</i>	照山白	<i>Rhododendron micranthum</i>
337					迎红杜鹃	<i>R. mucronulatum</i>
338	报春花科	Primulaceae	点地梅属	<i>Androsace</i>	北点地梅	<i>Androsace septentrionalis</i>
339			假报春属	<i>Cortusa</i>	假报春	<i>Cortusa matthioli</i>
340			海乳草属	<i>Glaux</i>	海乳草	<i>Glaux maritima</i>
341			珍珠菜属	<i>Lysimachia</i>	虎尾草	<i>Lysimachia barystachys</i>
342					黄连花	<i>L. davurica</i>
343			报春花属	<i>Primula</i>	箭报春	<i>Primula fistulosa</i>
344					胭脂花	<i>P. maximowiczii</i>
345					黄花胭脂花	<i>P. flaviflora</i>

346	白花丹科	Plumbaginaceae	补血草属	<i>Limonium</i>	二色补血草	<i>Limonium bicolor</i>	
347	木犀科	Oleaceae	桤属	<i>Fraxinus</i>	水曲柳	<i>Fraxinus mandschurica</i>	
348			丁香属	<i>Syringa</i>	暴马丁香	<i>Syringa reticulata</i>	var.
349					红丁香	<i>S. villosa</i>	
350	龙胆科	Gentianaceae	龙胆属	<i>Gentiana</i>	达乌里秦艽	<i>Gentiana dahurica</i>	
351					秦艽	<i>G. macrophylla</i>	
352					鳞叶龙胆	<i>G. squarrosa</i>	
353			花锚属	<i>Halenia</i>	花锚	<i>Halenia sibirica</i>	
354	旋花科	Convolvulaceae	旋花属	<i>Convolvulus</i>	田旋花	<i>Convolvulus arvensis</i>	
355			菟丝子属	<i>Cuscuta</i>	菟丝子	<i>Cuscuta chinensis</i>	
356	花荵科	Polemoniaceae	花荵属	<i>Polemonium</i>	中华花荵	<i>Polemonium coeruleum</i>	var.
357	紫草科	Boraginaceae	琉璃草属	<i>Cynoglossum</i>	大果琉璃草	<i>Cynoglossum divaricatum</i>	
358			鹤虱属	<i>Lappula</i>	鹤虱	<i>Lappula myosotis</i>	
359			狼紫草属	<i>Lycopsis</i>	狼紫草	<i>Lycopsis orientalis</i>	
360			滨紫草属	<i>Mertensia</i>	长筒滨紫草	<i>Mertensia davurica</i>	
361			勿忘草属	<i>Myosotis</i>	湿地勿忘草	<i>Myosotis caespitosa</i>	
362	唇形科	Labiatae	筋骨草属	<i>Ajuga</i>	白苞筋骨草	<i>Ajuga lupulina</i>	
363			青兰属	<i>Dracocephalum</i>	光萼青兰	<i>Dracocephalum argunense</i>	
364					毛建草	<i>D. rigidulum</i>	
365					青兰	<i>D. ruyschiana</i>	
366			香薷属	<i>Elsholtzia</i>	香薷	<i>Elsholtzia ciliata</i>	
367					密花香薷	<i>E. densa</i>	
368			鼬瓣花属	<i>Galeopsis</i>	鼬瓣花	<i>Galeopsis bifida</i>	
369			益母草属	<i>Leonurus</i>	鋤菜	<i>Leonurus pseudomacranthus</i>	
370					细叶益母草	<i>L. sibiricus</i>	
371			薄荷属	<i>Mentha</i>	薄荷	<i>Mentha haplocalyx</i>	
372			荆芥属	<i>Nepeta</i>	康藏荆芥	<i>Nepeta prattii</i>	
373			糙苏属	<i>Phlomis</i>	口外糙苏	<i>Phlomis jeholensis</i>	
374			香茶菜属	<i>Rabdosia</i>	内折香茶菜	<i>Rabdosia inflexa</i>	
375					毛叶香茶菜	<i>R. japonica</i>	
376			裂叶荆芥属	<i>Schizonepeta</i>	多裂叶荆芥	<i>Schizonepeta multifida</i>	
377					长柱多裂叶荆芥	<i>S. multifida</i> var. <i>longostyla</i>	
378					裂叶荆芥	<i>S. tenuifolia</i>	
379			黄芩属	<i>Scutellaria</i>	黄芩	<i>Scutellaria baicalensis</i>	
380					京黄芩	<i>S. pekinensis</i>	
381					狭叶黄芩	<i>S. regeliana</i>	
382					并头黄芩	<i>S. scordifolia</i>	
383			水苏属	<i>Stachys</i>	毛水苏	<i>Stachys baicalensis</i>	
384			百里香属	<i>Thymus</i>	百里香	<i>Thymus mongolicus</i>	
385					地椒	<i>T. quinquecostatus</i>	
386	茄科	Solanaceae	天仙子属	<i>Hyoscyamus</i>	天仙子	<i>Hyoscyamus niger</i>	

387			枸杞属	<i>Lycium</i>	枸杞	<i>Lycium chinense</i>
388	玄参科	Scrophulariaceae	小米草属	<i>Euphrasia</i>	小米草	<i>Euphrasia pectinata</i>
389					芒小米草	<i>E. pectinata</i> ssp. <i>Simplex</i>
390			柳穿鱼属	<i>Linaria</i>	柳穿鱼	<i>Linaria vulgaris</i>
391			山罗花属	<i>Melampyrum</i>	山罗花	<i>Melampyrum roseum</i>
392			疗齿草属	<i>Odontites</i>	疗齿草	<i>Odontites serotina</i>
393			马先蒿属	<i>Pedicularis</i>	返顾马先蒿	<i>Pedicularis resupinata</i>
394					红色马先蒿	<i>P. rubens</i>
395					穗花马先蒿	<i>P. spicata</i>
396					红纹马先蒿	<i>P. striata</i>
397					秀丽马先蒿	<i>P. venusta</i>
398					轮叶马先蒿	<i>P. verticillata</i>
399			鼻花属	<i>Rhinanthus</i>	鼻花	<i>Rhinanthus glaber</i>
400			阴行草属	<i>Siphonostegia</i>	阴行草	<i>Siphonostegia chinensis</i>
401			婆婆纳属	<i>Veronica</i>	大婆婆纳	<i>Veronica dahurica</i>
402					白婆婆纳	<i>V. incana</i>
403					细叶婆婆纳	<i>V. linariifolia</i>
404					兔儿尾苗	<i>V. longifolia</i>
405					水苦荬	<i>V. undulata</i>
406			腹水草属	<i>Veronicastrum</i>	草本威灵仙	<i>Veronicastrum sibiricum</i>
407	列当科	Orobanchaceae	列当属	<i>Orobanche</i>	列当	<i>Orobanche coerulescens</i>
408					黄花列当	<i>O. pycnostachya</i>
409	苦苣苔科	Gesneriaceae	旋蒴苣苔属	<i>Boea</i>	旋蒴苣苔	<i>Boea hygrometrica</i>
410	车前科	Plantaginaceae	车前属	<i>Plantago</i>	车前	<i>Plantago asiatica</i>
411					平车前	<i>P. depressa</i>
412	茜草科	Rubiaceae	拉拉藤属	<i>Galium</i>	北方拉拉藤	<i>Galium boreale</i>
413					线叶拉拉藤	<i>G. linearifolium</i>
414					篷子菜	<i>G. verum</i>
415			茜草属	<i>Rubia</i>	茜草	<i>Rubia cordifolia</i>
416	忍冬科	Caprifoliaceae	忍冬属	<i>Lonicera</i>	蓝果忍冬	<i>Lonicera caerulea</i>
417					金花忍冬	<i>L. chrysantha</i>
418					北京忍冬	<i>L. elisae</i>
419					华北忍冬	<i>L. tatarinowii</i>
420			接骨木属	<i>Sambucus</i>	接骨木	<i>Sambucus williamsii</i>
421			荚蒾属	<i>Viburnum</i>	修枝荚蒾	<i>Viburnum burejaeticum</i>
422					鸡树条荚蒾	<i>V. sargentii</i>
423			锦带花属	<i>Weigela</i>	锦带花	<i>Weigela florida</i>
424	败酱科	Valerianaceae	败酱属	<i>Patrinia</i>	岩败酱	<i>Patrinia rupestris</i>
425					败酱	<i>P. scabiosaefolia</i>
426			缬草属	<i>Valeriana</i>	缬草	<i>Valeriana officinalis</i>
427	川续断科	Dipsacaceae	蓝盆花属	<i>Scabiosa</i>	华北蓝盆花	<i>Scabiosa tschiliensis</i>
428	桔梗科	Campanulaceae	沙参属	<i>Adenophora</i>	狭叶沙参	<i>Adenophora gmelinii</i>
429					柳叶沙参	<i>A. gmelinii</i> var. <i>coronopifolia</i>

430				石沙参	<i>A. polyantha</i>	
431				长柱沙参	<i>A. stenanthina</i>	
432				轮叶沙参	<i>A. tetraphylla</i>	
433				多歧沙参	<i>A. wawreana</i>	
434				雾灵沙参	<i>A. wulingshanica</i>	
435		风铃草属	<i>Campanula</i>	紫斑风铃草	<i>Campanula punctatata</i>	
436	菊科	Compositae	蓍属	<i>Achillea</i>	高山蓍	<i>Achillea alpina</i>
437				亚洲蓍	<i>A. asiatica</i>	
438			蒿属	<i>Artemisia</i>	青蒿	<i>Artemisia apiacea</i>
439				艾蒿	<i>A. argyi</i>	
440				山蒿	<i>A. brachyloba</i>	
441				茵陈蒿	<i>A. capillaris</i>	
442				变蒿	<i>A. commutata</i>	
443				龙蒿	<i>A. dracunculus</i>	
444				南牡蒿	<i>A. eriopoda</i>	
445				冷蒿	<i>A. frigida</i>	
446				细裂叶莲蒿	<i>A. gmelinii</i>	
447				柳叶蒿	<i>A. integrifolia</i>	
448				牡蒿	<i>A. japonica</i>	
449				野艾蒿	<i>A. lavandulaefolia</i>	
450				蒙古蒿	<i>A. mongolica</i>	
451				黑蒿	<i>A. palustris</i>	
452				猪毛蒿	<i>A. scoparia</i>	
453				萎蒿	<i>A. selengensis</i>	
454				大籽蒿	<i>A. sieversiana</i>	
455				宽叶山蒿	<i>A. stolonifera</i>	
456				线叶蒿	<i>A. subulata</i>	
457				裂叶蒿	<i>A. tanacetifolia</i>	
458		紫菀属	<i>Aster</i>	高山紫菀	<i>Aster alpinus</i>	
459				紫菀	<i>A. tataricus</i>	
460		苍术属	<i>Atractylodes</i>	苍术	<i>Atractylodes lancea</i>	
461		鬼针属	<i>Bidens</i>	狼把草	<i>Bidens tripartita</i>	
462		蟹甲草属	<i>Cacalia</i>	山尖子	<i>Cacalia hastata</i>	
463		翠菊属	<i>Callistephus</i>	翠菊	<i>Callistephus chinensis</i>	
464		飞廉属	<i>Carduus</i>	丝毛飞廉	<i>Carduus crispus</i>	
465		蓟属	<i>Cirsium</i>	莲座蓟	<i>Cirsium esculentum</i>	
466				魁蓟	<i>C. leo</i>	
467				烟管蓟	<i>C. pendulum</i>	
468				刺儿菜	<i>C. setosum</i>	
469				绒背蓟	<i>C. vlassovianum</i>	
470		白酒草属	<i>Conyza</i>	小蓬草	<i>Conyza canadensis</i>	
471		菊属	<i>Dendranthema</i>	小红菊	<i>Dendranthema chaneltii</i>	
472				紫花野菊	<i>D. zawadskii</i>	
473		蓝刺头属	<i>Echinops</i>	驴欺口	<i>Echinops latifolius</i>	

474	飞蓬属	<i>Erigeron</i>	飞蓬	<i>Erigeron acer</i>
475	线叶菊属	<i>Filifolium</i>	线叶菊	<i>Filifolium sibiricum</i>
476	狗娃花属	<i>Heteropappus</i>	阿尔泰狗娃花	<i>Heteropappus altaicus</i>
477			狗娃花	<i>H. hispidus</i>
478			砂狗娃花	<i>H. meyerendorffii</i>
479	山柳菊属	<i>Hieracium</i>	山柳菊	<i>Hieracium umbellatum</i>
480			宽叶山柳菊	<i>H. coreanum</i>
481	旋覆花属	<i>Inula</i>	欧亚旋覆花	<i>Inula britannica</i>
482	苦菜属	<i>Ixeris</i>	山苦荬	<i>Ixeris chinensis</i>
483			抱茎苦荬菜	<i>I. sonchifolia</i>
484	莴苣属	<i>Lactuca</i>	山莴苣	<i>Lactuca indica</i>
485			山莴苣	<i>L. indica</i> var. <i>dentata</i>
486			北山莴苣	<i>L. sibirica</i>
487			蒙山莴苣	<i>L. tatarica</i>
488	大丁草属	<i>Leibnitzia</i>	大丁草	<i>Leibnitzia anandria</i>
489	火绒草属	<i>Leontopodium</i>	火绒草	<i>Leontopodium leontopodioides</i>
490			长叶火绒草	<i>L. longifolium</i>
491	橐吾属	<i>Ligularia</i>	蹄叶橐吾	<i>Ligularia fischeri</i>
492			全缘橐吾	<i>L. mongolica</i>
493	毛连菜属	<i>Picris</i>	毛连菜	<i>Picris hieracioides</i> ssp. <i>japonica</i>
494	盘果菊属	<i>Prenanthes</i>	大叶盘果菊	<i>Prenanthes macrophylla</i>
495	风毛菊属	<i>Saussurea</i>	草地风毛菊	<i>Saussurea amara</i>
496			龙江风毛菊	<i>S. amurensis</i>
497			北风毛菊	<i>S. discolor</i>
498			紫苞风毛菊	<i>S. indostegia</i>
499			风毛菊	<i>S. japonica</i>
500			翼茎风毛菊	<i>S. japonica</i> var. <i>alata</i>
501			小花风毛菊	<i>S. parviflora</i>
502			亚卷苞风毛菊	<i>S. parasclerolepis</i>
503			美花风毛菊	<i>S. pulchella</i>
504			折苞风毛菊	<i>S. recurvata</i>
505			柳叶风毛菊	<i>S. salicifolia</i>
506			卷苞风毛菊	<i>S. sclerolepis</i>
507			乌苏里风毛菊	<i>S. ussuriensis</i>
508	鸦葱属	<i>Scorzonera</i>	笔管草	<i>Scorzonera albicaulis</i>
509	千里光属	<i>Senecio</i>	红轮千里光	<i>Senecio flammeus</i>
510			狗舌草	<i>S. kirilowii</i>
511			林荫千里光	<i>S. nemorensis</i>
512	狗舌草属	<i>tephroseris</i>	湿生狗舌草	<i>tephroseris palustris</i>
513	麻花头属	<i>Serratula</i>	麻花头	<i>Serratula centauroides</i>
514			伪泥胡菜	<i>S. coronata</i>
515			多花麻花头	<i>S. polycephala</i>
516	一枝黄花属	<i>Solidago</i>	钝苞一枝黄花	<i>Solidago pacifica</i>

517			苦苣菜属 <i>Sonchus</i>	苦苣菜	<i>Sonchus brachyotus</i>
518			漏芦属 <i>Stemmacantha</i>	漏芦	<i>Stemmacantha uniflora</i>
519			山牛蒡属 <i>Synurus</i>	山牛蒡	<i>Synurus deltoides</i>
520			蒲公英属 <i>Taraxacum</i>	红梗蒲公英	<i>Taraxacum erythropodium</i>
521				蒲公英	<i>T. monogolicum</i>
522				异苞蒲公英	<i>T. heterolepis</i>
523			女菀属 <i>Turczaninovia</i>	女菀	<i>Turczaninovia fastigiata</i>
524			苍耳属 <i>Xanthium</i>	苍耳	<i>Xanthium sibiricum</i>
525			黄鹌菜属 <i>Youngia</i>	细叶黄鹌菜	<i>Youngia tenuifolia</i>
526	香蒲科	Typhaceae	香蒲属 <i>Typha</i>	水烛	<i>Typha angustifolia</i>
527	芝菜科	Scheuchzeriaceae	水麦冬属 <i>Triglochin</i>	水麦冬	<i>Triglochin palustre</i>
528	禾本科	Gramineae	芨芨草属 <i>Achnatherum</i>	远东芨芨草	<i>Achnatherum extremiorientale</i>
529				羽茅	<i>A. sibiricum</i>
530				芨芨草	<i>A. splendens</i>
531			冰草属 <i>Agropyron</i>	冰草	<i>Agropyron cristatum</i>
532				沙生冰草	<i>A. desertorum</i>
533				沙芦草	<i>A. mongolicum</i>
534				毛沙生冰草	<i>A. mongolicum</i> f. <i>desertorum</i>
535			剪股颖属 <i>Agrostis</i>	华北剪股颖	<i>Agrostis clavata</i>
536				巨序剪股颖	<i>A. gigantea</i>
537				芒剪股颖	<i>A. trinii</i>
538			看麦娘属 <i>Alopecurus</i>	看麦娘	<i>Alopecurus aequalis</i>
539				短穗看麦娘	<i>A. brachystachyus</i>
540			野古草属 <i>Arundinella</i>	毛秆野古草	<i>Arundinella hirta</i>
541			蔺草属 <i>Beckmannia</i>	蔺草	<i>Beckmannia syzigachne</i>
542			短柄草属 <i>Brachypodium</i>	兴安短柄草	<i>Brachypodium pinnatum</i>
543			雀麦属 <i>Bromus</i>	无芒雀麦	<i>Bromus inermis</i>
544				短枝雀麦	<i>B. inermis</i> var. <i>malzevii</i>
545				缘毛雀麦	<i>B. ciliatus</i>
546			拂子茅属 <i>Calamagrostis</i>	拂子茅	<i>Calamagrostis epigeios</i>
547				大拂子茅	<i>C. macrolepis</i>
548				假苇拂子茅	<i>C. pseudophragmites</i>
549				忽略拂子茅	<i>C. neglecta</i>
550			细柄草属 <i>Capillipedium</i>	细柄草	<i>Capillipedium parviflorum</i>
551			隐子草属 <i>Cleistogenes</i>	中华隐子草	<i>Cleistogenes chinensis</i>
552			野青茅属 <i>Deyeuxia</i>	野青茅	<i>Deyeuxia arundinacea</i>
553				大叶章	<i>D. langsдорffii</i>
554			马唐属 <i>Digitaria</i>	马唐	<i>Digitaria sanguinalis</i>
555			稗属 <i>Echinochloa</i>	稗	<i>Echinochloa crusgali</i>
556			披碱草属 <i>Elymus</i>	圆柱披碱草	<i>Elymus cylindricus</i>
557				肥披碱草	<i>E. excelsus</i>
558				老芒麦	<i>E. sibiricus</i>
559				麦草	<i>E. tangutorum</i>

560		画眉草属	<i>Eragrostis</i>	小画眉草	<i>Eragrostis minor</i>	
561		羊茅属	<i>Festuca</i>	紫羊茅	<i>Festuca rubra</i>	
562		甜茅属	<i>Glyceria</i>	水甜茅	<i>Glyceria aquatica</i>	
563		异燕麦属	<i>Helictotrichon</i>	异燕麦	<i>Helictotrichon schellianum</i>	
564		茅香属	<i>Hierochloe</i>	茅香	<i>Hierochloe odorata</i>	
565		大麦属	<i>Hordeum</i>	短芒大麦草	<i>Hordeum brevisubulatum</i>	
566		草属	<i>Koeleria</i>	草	<i>Koeleria cristata</i>	
567		赖草属	<i>Leymus</i>	羊草	<i>Leymus chinensis</i>	
568				赖草	<i>secalinus</i>	
569		臭草属	<i>Melica</i>	大臭草	<i>Melica turczaninoviana</i>	
570		狼尾草属	<i>Pennisetum</i>	白草	<i>Pennisetum centrasiaticum</i>	
571		藨草属	<i>Phalaris</i>	藨草	<i>Phalaris arundinacea</i>	
572		芦苇属	<i>Phragmites</i>	芦苇	<i>Phragmites communis</i>	
573				热河芦苇	<i>P. jeholensis</i>	
574		早熟禾属	<i>Poa</i>	细叶早熟禾	<i>Poa angustifolia</i>	
575				极地早熟禾	<i>P. arctica</i>	
576				光盘早熟禾	<i>P. elanata</i>	
577				柔软早熟禾	<i>P. lepta</i>	
578				长颖早熟禾	<i>P. longiglumis</i>	
579				林地早熟禾	<i>P. nemoralis</i>	
580				草地早熟禾	<i>P. pratensis</i>	
581				假泽早熟禾	<i>P. pseudo-palustris</i>	
582				西伯利亚早熟禾	<i>P. sibirica</i>	
583		棒头草属	<i>Polypogon</i>	棒头草	<i>Polypogon fugax</i>	
584				长芒棒头草	<i>P. monspeliensis</i>	
585		碱茅属	<i>Puccinellia</i>	碱茅	<i>Puccinellia distans</i>	
586		鹅观草属	<i>Roegneria</i>	直穗鹅观草	<i>Roegneria turczaninovii</i>	
587				百花山鹅观草	<i>R. turczaninovii</i> var. <i>pohuashanensis</i>	
588		狗尾草属	<i>Setaria</i>	狗尾草	<i>Setaria viridis</i>	
589				紫狗尾草	<i>S. viridis</i> var. <i>purourascens</i>	
590				金狗尾草	<i>S. lutescens</i>	
591		大油芒属	<i>Spodiopogon</i>	大油芒	<i>Spodiopogon sibiricus</i>	
592		针茅属	<i>Stipa</i>	西北针茅	<i>Stipa sareptana</i> var. <i>krylovii</i>	
593				大针茅	<i>S. grandis</i>	
594		三毛草属	<i>Trisetum</i>	西伯利亚三毛草	<i>Trisetum sibiricum</i>	
595		早熟禾属	<i>Poa</i>	堇色早熟禾	<i>Poa ianthina</i>	
596				蒙古早熟禾	<i>P. mongolica</i>	
597				硬质早熟禾	<i>P. sphondylodes</i>	
598		针茅属	<i>Stipa</i>	狼针草	<i>Stipa baicalensis</i>	
599	莎草科	Cyperaceae	扁穗草属	华扁穗草	<i>Blysmus sinocompressus</i>	
600				节秆扁穗草	<i>B. sinocompressus</i> var. <i>nodosus</i>	
601			苔草属	灰脉苔草	<i>Carex appendiculata</i>	
602				义齿苔草	<i>C. gotoi</i>	

603					点叶苔草	<i>C. hancockiana</i>
604					矮丛苔草	<i>C. humilis</i> var. <i>nana</i>
605					黄囊苔草	<i>C. korshinskii</i>
606					多花苔草	<i>C. karoï</i>
607					披针苔草	<i>C. lanceolata</i>
608					尖嘴苔草	<i>C. leiorhyncha</i>
609					直穗苔草	<i>C. orthostachys</i>
610					大穗苔草	<i>C. rhynchophysa</i>
611					白颖苔草	<i>C. rigescens</i>
612					沙地苔草	<i>C. satsumensis</i>
613					亚柄苔草	<i>C. subpediformis</i>
614					陌上营	<i>C. thunbergii</i>
615			荸荠属	<i>Eleocharis</i>	中间型荸荠	<i>Eleocharis intersita</i>
616					大基荸荠	<i>E. kamtschatica</i>
617			羊胡子草属	<i>Eriophorum</i>	白毛羊胡子草	<i>Eriophorum vaginatum</i>
618			蔗草属	<i>Scirpus</i>	蔗草	<i>Scirpus triqueter</i>
619					水葱	<i>S. validus</i>
620			断节莎属	<i>Torulinium</i>	渐狭早熟禾	<i>Poa attenuata</i>
621			扁穗草属	<i>Blysmus</i>	蒙古扁穗草	<i>Blysmus rufus</i>
622			苔草属	<i>Carex</i>	圆穗苔草	<i>Carex angarae</i>
623					白山苔草	<i>C. conescens</i>
624					麻根苔草	<i>C. arnellii</i>
625					扁囊苔草	<i>C. coriophora</i>
626					异鳞苔草	<i>C. heterolepis</i>
627					大穗苔草	<i>C. rhynchophysa</i>
628					宽叶苔草	<i>C. siderosticta</i>
629					柄苔草	<i>C. moliissima</i>
630	浮萍科	Lemnaceae	浮萍属	<i>Lemna</i>	浮萍	<i>Lemna minor</i>
631	灯心草科	Juncaceae	灯心草属	<i>Juncus</i>	小灯心草	<i>Juncus bufonius</i>
632					细灯心草	<i>J. gracillimus</i>
633					小花灯心草	<i>J. lampocarpus</i>
634					竹节灯心草	<i>J. turczaninowii</i>
635			地杨梅属	<i>Luzula</i>	淡花地杨梅	<i>Luzula pallescens</i>
636	百合科	Liliaceae	葱属	<i>Allium</i>	长梗韭	<i>Allium neriniflorum</i>
637					山韭	<i>A. senescens</i>
638					细叶韭	<i>A. tenuissimum</i>
639					葱	<i>A. victoralis</i>
640			天门冬属	<i>Asparagus</i>	兴安天门冬	<i>Asparagus dauricus</i>
641			铃兰属	<i>Convallaria</i>	铃兰	<i>Convallaria majalis</i>
642			贝母属	<i>Fritillaria</i>	轮叶贝母	<i>Fritillaria maximowiczii</i>
643			萱草属	<i>Hemerocallis</i>	小黄花菜	<i>Hemerocallis minor</i>
644			百合属	<i>Lilium</i>	渥丹	<i>Lilium concolor</i>
645					山丹	<i>L. pumilum</i>

646			舞鹤草属	<i>Maianthemum</i>	舞鹤草	<i>Maianthemum bifolium</i>
647			重楼属	<i>Paris</i>	北重楼	<i>Paris verticillata</i>
648			黄精属	<i>Polygonatum</i>	小玉竹	<i>Polygonatum humile</i>
649					玉竹	<i>P. odoratum</i>
650			藜芦属	<i>Veratrum</i>	毛穗藜芦	<i>Veratrum maackii</i>
651					藜芦	<i>V. nigrum</i>
652	薯蓣科	Dioscoreaceae	薯蓣属	<i>Dioscorea</i>	穿龙薯蓣	<i>Dioscorea nipponica</i>
653	鸢尾科	Iridaceae	射干属	<i>Belamcanda</i>	射干	<i>Belamcanda chinensis</i>
654			鸢尾属	<i>Iris</i>	紫苞鸢尾	<i>Iris ruthenica</i>
655					细叶鸢尾	<i>I. tenuifolia</i>
656					白花马蔺	<i>I. lactea</i>
657					囊花鸢尾	<i>I. ventricosa</i>
658	兰科	Orchidaceae	杓兰属	<i>Cypripedium</i>	大花杓兰	<i>Cypripedium macranthum</i>
659			手参属	<i>Gymnadenia</i>	手参	<i>Gymnadenia conopsea</i>
660			鸟巢兰属	<i>Neottia</i>	尖唇鸟巢兰	<i>Neottia acuminata</i>
661			兜被兰属	<i>Neottianthe</i>	二叶兜被兰	<i>Neottianthe cucullata</i>
662			舌唇兰属	<i>Platanthera</i>	二叶舌唇兰	<i>Platanthera chlorantha</i>
663			蜻蜓兰属	<i>Tulotis</i>	小花蜻蜓兰	<i>Tulotis ussuriensis</i>
664			沼兰属	<i>Malaxis</i>	沼兰	<i>Malaxis monophyllos</i>

资料来源:

- (1) 2004-2005 年植物样方调查和生态学生学实习调查资料;
- (2) 黄金祥, 李信, 钱进源, 1996. 塞罕坝植物志. 北京: 中国科学技术出版社;
- (3) 黄金祥, 冯天杰, 王建中, 钱进源, 胡永富, 倪志云. 1994. 塞罕坝植物区系新分类群与河北新分布 I. 河北农业大学学报, 17:11-18;
- (4) 黄金祥, 王建中, 冯天杰, 钱进源, 胡永富, 张向忠, 赵亚民. 1996b. 塞罕坝植物区系新分类群与河北新分布 II. 河北农业大学学报, 19:92-96.

分类号_____

密级_____

U D C_____

编号_____

北 京 大 学
博 士 后 研 究 工 作 报 告

塞罕坝地区主要树种树干呼吸速率的研究

杨 艳

工作完成日期 2012 年 4 月-2014 年 3 月

报告提交日期 2014 年 3 月

北 京 大 学 （北京）

2014 年 3 月

塞罕坝地区主要树种树干呼吸速率的研究

Stem respiration rate of main species in Saihanba, Northern China

博士后姓名	<u>杨艳</u>
合作导师	<u>朴世龙, 要茂盛</u>
流动站（一级学科）名称	<u>环境科学</u>
专 业（二级学科）名称	<u>环境科学</u>

研究工作起始时间：	2012 年 4 月
研究工作期满时间：	2014 年 3 月

北京大学环境学院（北京）

摘 要

树干呼吸速率是森林生态系统碳循环的一个重要组成部分。目前对树干呼吸速率的日变化、不同树种的树干呼吸速率随林龄的变化规律及其对全球变化（如温度，大气氮沉降）的响应的研究比较少。

本文在我国最大的人工林种植基地-塞罕坝机械林场,对三个主要树种（白桦、樟子松和华北落叶松）的树干呼吸速率进行研究。主要结论如下：

（1）对于不同林龄，不同树种，树干呼吸速率与树干温度的关系存在三种形式：指数、二次曲线和关系不显著。

（2）树干呼吸速率的树干温度测定范围和树干呼吸酶的最适宜温度对树干呼吸速率与树干温度关系具有一定的影响。

（3）不同树种，树干呼吸速率随林龄的变化趋势有所不同。白桦和樟子松的树干呼吸速率随林龄的增加而增大，华北落叶松的树干呼吸速率随林龄增加而减小。

（4）白桦和樟子松的树干呼吸速率随着林龄的增加而增大，可能与树干边材面积的增长量密切相关。华北落叶松的树干呼吸速率随着林龄的增加而减小，可能是受控于树干温度和树干氮含量的变化。

（5）树干呼吸速率的 Q_{10} 值具有日变化规律，白天的 Q_{10} 值（12:00-15:00）显著的低于夜间的 Q_{10} 值（00:00-03:00）。

(6) 华北落叶松的树干呼吸速率随着施氮浓度的增加而增加。树干胸径生长量和树干氮含量对施氮的响应不显著。针叶的氮含量随着施氮浓度的增加而增大。

Abstract

Stem respiration is a critical and uncertain component of ecosystem carbon cycle. Few studies reported diurnal change in stem respiration, stem respiration changing with stand age as well as its linkage with climate.

In this study, we investigated the stem respiration and its linkage with environmental factors for three dominant tree species (*Betula platyphylla*, *Pinus sylvestris* var. *mongolica*, and *Larix principis-rupprechtii*) in Saihanba, the largest plantation in China from 2010 to 2012. The main conclusions are as follows

(1) We found three types of relationships between stem respiration and stem temperature, namely exponential, quadratic, and no relationship, depending on the specific species-age combination.

(2) The measurement temperature range in relation to the optimum temperature, and many other species-specific factors such as seasonal changes in substrate supply from photosynthesis and the time of CO₂ diffusion from respiring cells to the stem surface, may have contributed to the apparent relationships between stem respiration and stem temperature observed in this study.

(3) Tree size or stand age has significant impact on stem respiration. The trend of stem respiration changing with stand age were species-specific.

(4) The stem respiration of *B. platyphylla* and *P. sylvestris* var. *mongolica* increased with stand age or tree size, likely driven by the increase in growth respiration as indicated by the increase in sapwood area increment, while the stem respiration of *L. principis-rupprechtii* decreased with stand age or tree size, possible due to the decrease in maintenance respiration as a result of the decrease in stem temperature and N concentration.

(5) Q_{10} of stem respiration showed diurnal pattern and the Q_{10} of stem respiration at mid daytime (1.97 ± 0.17 at 12:00 and 1.96 ± 0.10 at 15:00) was significantly lower than that of mid nighttime (2.60 ± 0.14 at 00:00 and 2.71 ± 0.25 at 03:00) Q_{10} for *L. principis-rupprechtii*.

(6) Stem respiration increased with adding nitrogen content increased for *L. principis-rupprechtii*. Nitrogen content of stem and DBH growth did not respond to N fertilization. Nitrogen content of needle increased with increasing adding nitrogen content.

目 录

第 1 章 前 言	1
1.1 研究背景	1
1.1.1 人工林的重要碳汇作用	1
1.1.2 氮沉降对森林生态系统的影响	2
1.2 理论基础与国内外研究进展	6
1.2.1 树干呼吸速率	6
1.2.2 树干呼吸速率的测定方法	6
1.2.3 树干呼吸速率的影响因素	7
1.3 研究意义	12
第2章 研究区域概况与研究方法	13
2.1 研究区域自然地理概况	13
2.1.1 研究区域概况	13
2.1.2 地质与地貌	14
2.1.3 气候	15
2.1.4 植被群落	15
2.2 研究方法	17
2.2.1 样地设置与实验设计	17
2.2.2 树干呼吸速率的测定	18
2.2.3 土壤温、湿度的测定	19
2.2.4 树干呼吸速率的计算	19
2.3 数据统计分析	21
第 3 章 树干呼吸速率与林龄	22
3.1 树干呼吸速率的季节变化	23
3.2 温度对树干呼吸速率的影响	25
3.3 树干呼吸速率与林龄	29
3.4 结论	31

第 4 章 树干呼吸速率的温度敏感度	33
4.1 树干呼吸速率的日变化	34
4.2 Q_{10} 的日变化	36
4.3 结论	39
第 5 章 施氮对树干呼吸速率的影响	40
5.1 驱动因子的确定	41
5.2 树干呼吸速率的日变化	42
5.3 树干呼吸速率的季节变化	44
5.4 外加氮对树干呼吸速率的影响	46
5.5 结论	48
第 6 章 结 论	50
参考文献	51
致谢	61
发表文章	63
个人简历	64
永久通讯地址	65

图表目录

序 号	内 容	页 码
图 1.1	全球氮沉降空间分布图	4
图 1.2	树干呼吸、树干生长量与树干温度的变化	11
图 1.3	树干呼吸与树干内活细胞数量	11
图 2.1	研究区域地理位置	14
图 2.2	45 年华北落叶松林样地	18
图 3.1	树干呼吸速率和树干温度的季节变化	24
表 3.1	树干呼吸速率与树种、林龄和时间的三因素 方差分析结果	25
图 3.2	三个不同林龄不同树种的树干呼吸速率与树 干温度的关系	26
表 3.2	建立树干呼吸速率与树干温度和胸径的关系 模型	27
图 3.3	三个不同树种的树干呼吸速率的树干呼吸速 率、树干温度、生长季边材面积增长量和树 干氮含量随林龄的变化规律	30
图 4.1	树干呼吸速率，树干温度，空气温度及空气 相对湿度的日变化	34
图 4.2	树干呼吸速率与树干温度、空气温度和空气 相对湿度之间的关系	36
图 4.3	树干呼吸速率的 Q_{10} 值的日变化	37
图 5.1	树干温度和不同深度的土壤温度和土壤含水 量对树干呼吸速率变化的解释率	41
图 5.2	不同月份树干呼吸速率、土壤含水量和土壤 温度的日变化	42
表 5.1	不同森林树干呼吸日变化规律	43
图 5.3	树干呼吸速率，不同深度的土壤温度和土壤 含水量的季节变化	44
表 5.2	不同森林类型的树干呼吸季节变化规律	45
图 5.4	不同施氮浓度的树干呼吸速率、胸径增长量， 树干氮含量和针叶氮含量	46

第 1 章 前 言

1.1 研究背景

1.1.1 人工林的重要碳汇作用

作为大气中二氧化碳的重要源和汇，陆地生态系统是全球碳循环过程中极其重要的一种 (Canadell, 2000)，是一个植被-土壤-岩石-大气碳库相互作用的复杂系统，也是维持自然界平衡和发展的重要系统之一 (陶波, 2001)。对陆地碳循环系统的研究，将为更好预测大气二氧化碳浓度及变化提供重要依据 (Chen, 2003)。在全球碳循环计划 (Global Carbon Project, GCP)、国际地圈生物圈计划 (International Geosphere-Biosphere Programme, IGBP)、世界气候研究计划 (World Climate Research Programme, WCRP) 以及全球环境变化国际人文因素计划 (International Human Dimensions Programme on Global Environmental Change, IHDP) 等多个重大的碳循环研究计划中，陆地碳循环系统都是重要的研究内容，是进行大尺度碳通量研究的有效方法。目前，作为碳源和碳汇的陆地生态系统的时空格局尚还不太清楚，Schindler (1993) 认为：在 20 世纪 80 年代陆地生态系统基本是平衡的，而在 90 年代是一个碳汇；Tans (1998) 认为：陆地植被对目前碳源和碳汇的贡献不大；而 Schimel (1995, 2000) 的研究表明：陆地生态系统则是碳汇；政府间气候变化专门委员会 (IPCC, 2007) 的评估报告指出，目前全球碳循环研究中最大的不确定性主要来自陆地生态系统 (陶波, 2001)。

陆地生态系统包括：森林生态系统、农田生态系统、草地生态系统以及湿地生态系统等，不同生态系统有较大差异 Houghton (1993)。森林和草原是陆地生态系统的主体，在维护区域生态环境中起着重要作用 (Moraes, 1995; Post, 1982; Sedjo, 1993)。森林植被具有分布广，吸收量大的特点，在陆地生态系统中占有主体地位，在各种生态系统的交互作用中起着重要的“缓冲器”和“阀门”的作用。方精云等人 (方精云, 2001) 利用 1949 年至 1998 年间 7 次森林资源清查资料，结合使用森林生物量实测资料，推算了我国 50 年来森林碳库和平均碳密度的变化，结果表明，70 年代中期以前，主要由于森林砍伐等人为作用，中国森林碳库和碳密度都是减少的，碳储量减少了 0.62PgC ($\text{Pg}=10^{15}\text{g}$)。之后，呈上升趋势。在最近的 20 多年中，森林碳库由 70 年代末期的 4.38 PgC 增加到 1998 年的 4.75 PgC，共增加了 0.37 PgC。由此可见，中国森林碳汇主要来自人工林的贡献。为了控制和缓解大气中 CO_2 浓度升高导致的全球变暖，“京都议定书”鼓励各国通过人工造林，增加陆地生态系统碳吸收量来抵消部分 CO_2 排放。中国是世界人工林面积最多的国家，约占世界人工林面积的 1/4。对中国人工林生态系统碳循环和的研究是十分重要的。因此，对我国人工林植被碳库的研究具有重要意义。

1.1.2 氮沉降对森林生态系统的影响

全球环境变化中除了二氧化碳浓度升高外，另一个新近出现而又令人担忧的是氮沉降。氮沉降是一个具有综合性和概括性的名词，是指大气中的含氮化合物，通过降水或在重力吸附作用下沉降到地表的过程。

大气中氮含量大约占其总体积的78%，但是由于氮氮三键的键能很大，导致可供生物体利用的活性氮量很低。在自然状态下，氮固定主要通过物理作用（高能固氮）和生物作用（生物固氮）完成。近百年来，由于化石燃料使用，化肥工业及农业的快速发展，人类活动极大的增加了自然界的活性氮。世界各地大气氮沉降的通量与氮排放量呈线性关系（Bartnick, 1989），在某些地区氮素的人为排放已超过自然排放量而居主导地位（Apsimon, 1987）。例如，由于人为活动的结果，北半球大面积的陆地的氮沉降日益增加。西欧降水中的氮超过美国大陆的5倍还多（樊后保, 2002）。20世纪50年代至80年代，北欧和西欧雨水中的 NO_3^- 平均浓度明显增加，而 NH_4^+ 平均浓度在大多数地区有所上升，在少数地区则变化趋势不明显（Rodhe, 1986）。与此同时，随着中国经济和社会的发展，我国已成为全球三大氮沉降集中区（分别为欧洲、美国和中国）之一（Reay et al., 2008）。我国一些地区高氮沉降量的问题也凸显出来，如广东鼎湖山国家级自然保护区，1989-1990年和1998-1999年的降水氮沉降分别为35.57和38.4 $\text{kg N hm}^{-2} \text{ a}^{-1}$ （周国逸, 2001；刘世荣, 1992），与欧洲高氮沉降量地区相当。随着我国社会经济、工农业的进一步发展，氮沉降量可能还会继续升高，我国氮沉降的目前状况和未来的发展趋势已引起了人们的高度关注。

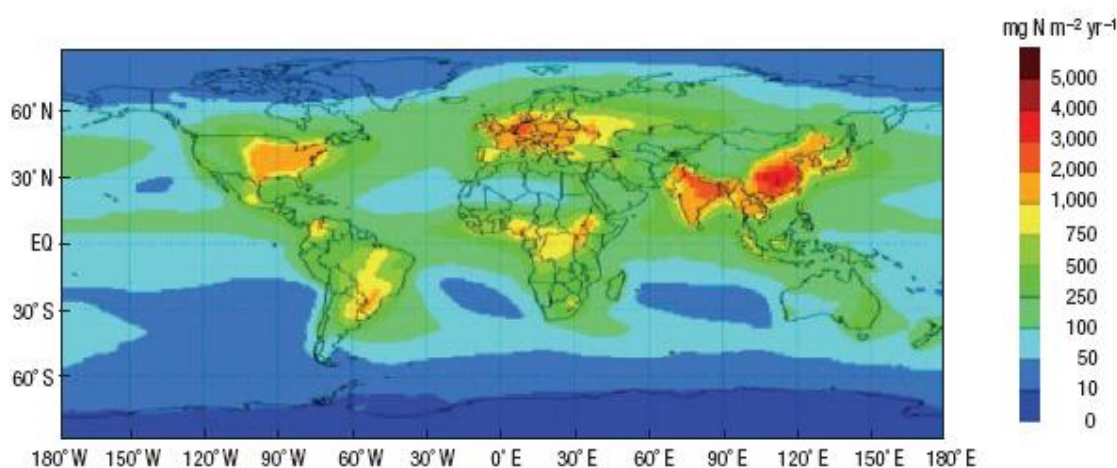


图 1.1 全球氮沉降空间分布图 (Reay et al., 2008)

因氮沉降而引起的大气组成变化及对森林生态系统结构与功能的影响受到越来越多科学家的关注 (Urennfelt, 1986; Högerg, 2006)。李德军等人 (李德军, 2003) 从6个方面描述了氮沉降对森林植物的影响: (1) 在一定量范围内的氮沉降有利于植物的光合作用, 但过量后则会引起植物的光合速率下降; (2) 当植物生长受氮限制时, 在一定程度上的氮沉降增加植物生产力, 但当氮过量后, 氮沉降则使植物的生产力下降; (3) 过量的氮沉降导致植物体各种营养元素含量的比例失衡; (4) 氮沉降会改变植物的形态结构, 集中表现为根/冠比减小; (5) 氮沉降会增加植物对天然胁迫如干旱、病虫害和风的敏感性, 减少其抵御能力; (6) 氮沉降会改变植物组成和降低森林植物的多样性。周薇等人 (周薇, 2010; 张维娜, 2009; Matson, 2002) 也综述了氮沉降对森林生态系统的土壤、植物光合作用、植物营养状况、植物抗逆性和生物多样性的影响。氮素是植物生长不可或缺的营养元素, 但过量的氮素会对森林生态系统产生负面影响, 如植物光合作用减弱, 降低生态系统多样性, 土壤酸化和有

机质溶出等。因此，在氮沉降全球化的环境背景下，研究和预测我国氮沉降对森林生态系统的影响及其反馈，对于制定合理的经济发展战略、引导有效的经济活动和制定我国森林资源和环境管理计划以及提高我国在全球变化研究中的地位均具有重要理论和实践意义。

大气氮沉降对森林生态系统碳循环具有怎样的影响呢？要回答这个问题，我们首先需要弄清楚大气氮沉降怎样影响着植物光合作用、植物自养呼吸作用、以及土壤微生物和动物的异养呼吸作用，这三个过程是决定陆地生态系统碳汇功能即生态系统净生产力的关键。氮是限制大多数陆地植物光合作用的主要因子，因此不少研究结果表明，叶片氮含量与光合速率之间存在很强的相关性（Aber, 1998）氮沉降引起叶片氮含量增加，其结果使植物的净光合速率增加（Aber, 1998）但是，过量的氮沉降则会降低光合速率。氮沉降对植物光合作用影响主要是通过改变叶片中与光合作用有关的酶的浓度和活性。在一定范围内，氮沉降增加引起Rubisco的浓度和活性及叶绿素含量增加，从而光合速率增加（Nakaji, 2001, 2002），但是，过量的氮沉降会引起植物体内营养失衡，而营养失衡对光合作用不利。如Nakaji（2001, 2002）发现生长在最高氮处理水平下的日本赤松幼苗针叶中Rubisco的浓度和活性及叶绿素含量降低与针叶中P含量的减少和Mn含量的增加明显相关，这类幼苗针叶中的N/P和Mn/Mg比值升高。对于植物的自养呼吸而言，其速率与植物体的N含量有着显著的正线性关系（Scheaberg et al., 1997; Reich et al., 2006），因此氮沉降通常导致植物自养呼吸的增加。树干是森林木质组织的重要组成部分

分，对森林总自养呼吸的影响巨大，其贡献率因不同森林类型而不同；从寒带森林的9%到温带森林的42% (Acosta et al., 2008, Wang et al., 2010, Ryan et al., 1996)。因此，树干呼吸是森林生态系统碳收支平衡的重要组成部分，对其进行准确的测定准确有助于准确估算森林生态系统的碳，对我国北方森林生态系统的碳预算具有重要作用。

1.2 理论基础与国内外研究进展

1.2.1 树干呼吸速率

在树干或粗枝中，多数呼吸作用发生在新的韧皮部和木质部临近层。虽然活的辐射细胞和轴向薄壁细胞也吸收氧气，但由于该类型的细胞数量较少，所以其呼吸总量较低。在一项实验中研究发现心材吸收了少量的氧气，这可能是由于坏死组织氧化有机化合物所致，而不是由于呼吸作用。因为心材块不管煮与不煮，都能吸收同样多的氧气 (Goodwin and goddard, 1940)。

从树干细胞呼吸出的 CO_2 或者扩散到大气中，或者溶解到树干液流中。所以从树干内部和外部测到的 CO_2 通量值并不一致的 (Teskey and McGuire, 2002; Aubrey and Teskey, 2009)，但由于扩散大气中的 CO_2 和溶解到树干液流中的 CO_2 是很难分开的 (Teskey and McGuire, 2002; Aubrey and Teskey, 2009)，而且，木质部液流运输的 CO_2 只占很小的一部分 (Maier and Clinton, 2006; Teskey and McGuire, 2002, 2007)，所以，我们通常用树干外部测量的树干通量来代替树干呼吸速率。

1.2.2 树干呼吸速率的测定方法

Johansson (1933) 于二十世纪前半叶就开始了树干呼吸的研究，随后许多学者也开始了树干呼吸速率的研究工作。所使用的方法大多数是离体测定碱液吸收法。此种方法的优势是能分别测定树干的的不同部位（木质部、韧皮部和形成层薄壁细胞等）的树干呼吸数量，并可根据实验的特定要求（例如不同温度环境）进行树干呼吸速率的研究，但受伤的组织可能会影响到树干呼吸速率的准确度。

随着树干呼吸速率研究的进一步开展和仪器设备的引入，树干呼吸速率的研究有离体转入活体研究。起初，活体测定采用的是密闭方法，在树干上建一个密闭气室，通过测定室内 CO_2 浓度变化来计算其通量。后来，为了方便测定工作的进行，采用了开路系统。在树干胸高附近的一段树干（40-50cm），套上一个密闭的盒子，通过测定器进出口 CO_2 的浓度差来估算树干呼吸通量。它的优点是操作简单，同一样本可以进行重复或连续的测定，进一步提高了数据的可靠性。目前，大多数研究使用的是美国（Li-Cor 6400）便携式光合仪的土壤呼吸室。在树干的不同高度和不同方向安装PVC环(根据树干直径的大小,选择不同尺寸的PVC环，直径过大或过小需使用变口径的轴承)，与土壤呼吸室相连接用于树干呼吸速率的测定。其优点是操作简捷，测定数据准确。但如果测定环境湿度过大或温度过低，可能会影响到仪器的正常工作状态。

1.2.3 树干呼吸速率的影响因素

树干呼吸是一个复杂的生物学过程，不仅受温度、湿度、大气 CO_2 浓度，土壤养分等环境因素的影响 (Liberloo et al., 2008; Moore et al., 2008), 而且还与树木年龄、径阶和树种等遗传特征有关(Lavigne and Ryan 1997; Pruyn et al., 2003, Kim et al., 2007)。

(1) 温度

温度是影响树干呼吸的最主要环境因子，树干温度可以解释约 60-70% 的不同树种树干呼吸的季节变化(Maier et al., 1998; Wieser and Bahn, 2004; Yang et al., 2011)。大多数研究表明，树干呼吸速率随着温度的升高而呈指数增加，其原因可能存在三方面：(1) 呼吸速率是酶促反应，酶活一般随着温度升高而增大，呼吸速率随着温度的升高而增大；(2) 根据 Fick 法则，随着温度升高 CO_2 释放系数增加，进而提高 CO_2 通量；(3) 根据 Henry 法则，树干液流中 CO_2 溶解度减低，气态 CO_2 增加，加大了树干释 CO_2 量。但不同林龄的不同树种，对温度的响应也各不相同。在其它内在和外在因素的影响下，树干呼吸速率与温度的关系曲线，更是难以确定。

树干呼吸对温度的敏感度通常用温度系数 (Q_{10}) 来表示，指温度每改变 10°C 树干呼吸速率的增加倍数(杨金艳等, 2009)。温度系数 (Q_{10}) 是提高模型预测全球气候变暖对森林生态系统碳循环影响的准确度的关键，因为 Q_{10} 是大多数生态系统模型的重要参数，一般过程模型都认为 Q_{10} 值是一个常数 ($Q_{10}=2$)。然而，在以往的研究中发现，不同物种之间的

Q_{10} 值变化范围1.0-4.4 之间且不同树种的树干呼吸的温度系数 Q_{10} 随着温度, 生长季节及径阶的变化具有不同的变化趋势 (Acosta and Brossaud, 2001; Ceschia et al., 2002; Edwards and Hanson, 1996; Lavigne, 1996; Maunoury et al., 2007; Ryan et al., 2009; Wang et al., 2008; Wieser and Bahn, 2004; Y Xu et al., 2001)。Larcher (1983) 研究表明植物 Q_{10} 值随着温度的升高而降低, 即: 当温度在25-30℃之间是, Q_{10} 小于1.5, 当温度为5-25℃时, Q_{10} 约为2.0, 当温度低于5℃, Q_{10} 为3.0。而McGuire等人(2007)对 *Platanus occidentalis* L.的树枝呼吸的研究表明, 5-20℃时的 Q_{10} 约为2.0低于20-35℃时的 Q_{10} 值 (3.19)。还有一些研究表明树干呼吸的温度系数随着径阶的增大而减小, 而Acosta 等人(2008)对 *Picea abies* 的 Q_{10} 研究表明树干的 Q_{10} 值在2.20-2.32, 而树枝的 Q_{10} 值为2.03-2.25。此外, 也有一些研究表明生长季树干呼吸对温度的敏感度大于非生长季(Gruber et al., 2009)。但Lavigne (1996) 对*Pinus banksiana*的研究结果是生长季的 Q_{10} 值小于非生长季的 Q_{10} 值。由此可见, Q_{10} 值还有待于进一步的研究。

(2) 林龄

林龄是影响树干呼吸的一个重要因子(Chambers et al. 2004; Kim et al. 2007; Robertson et al. 2010; Yang et al. 2012a)。一般而言, 林木的树干呼吸速率随着林龄的增加而减小。Ryan 等 (2009) 研究表明, *Eucalyptus Saligma* 树干呼吸速率随着林龄的增大而减小。肖复明等 (2005) 对湖南杉木人工林的树干呼吸速率的研究也得到了一致的变化规律 (树干呼吸速率13年生杉木>17年生杉木>20年生杉木)。姜丽芬等 (2003) 对东北地

区兴安落叶松的研究表明幼龄兴安落叶松的树干呼吸速率明显高于成熟林木的树干呼吸速率（两者最大相差2倍多）。

但也有一些研究表明，树干呼吸速率随着林龄的增加而增大。Pruyn等（2002）对俄勒冈吉尔克里斯特的喀斯喀特山脉东侧的美国黄松（*Pinus Ponderosa*）进行研究，发现200年生林木树干的单位表面积树干呼吸速率大于50年生和15年生林木。Xu等（2012）研究表明*Quercus Rubra*的树干呼吸速率随着林龄的增加而增加。王淼等（2005）对长白山地区红松的研究发现树干呼吸速率随着林木径阶的增加而增大。在不同研究中，树干呼吸速率与林木林龄（径阶）之间的关系各不相同。

（3）氮浓度

氮是蛋白质和核酸的重要组分，同时是植物需求量最大的矿质元素。充足的氮肥供应可以使植物保持高水平的氨基酸和蛋白质合成促进植物的生长。由于树木生理代谢增强，生长活动加快，构造自身物质的活动加强，树干生长呼吸也相应增加。

呼吸作用根据其功能不同可分为生长呼吸和维持呼吸（Amthor et al., 1989, 2000; Ryan et al., 1991）。生长呼吸是用于提供合成新组织代谢的能量，所以生长呼吸主要与生长量密切相关，且与树干生长量呈线性正相关（Havranek, 1981; Lavigne et al., 2004; Ryan et al., 1994）（如图 1）。Gruber 等人（2009）利用树干径向变化记录仪，对阿尔卑斯山的瑞士五叶松树干生长量的研究发现，树干生长量不仅与管胞的数量紧密相关（如图 2），

还与生长季活细胞的数量和形成层的活动密切相关。维持呼吸是指保持或维持活细胞正常生命活动的代谢(Ceschia et al., 2002; Penning de Vries, 1975)。蛋白质转换是一种维持过程，它消耗了绝大多数的呼吸底物(Ryan, 1991; Amorth, 1984) 因此，任何可以改变组织中氮含量的变化(例如，大气氮沉降的增加, Aber et al., 1989; Hungate et al., 1997) 都会引起维持呼吸速率的变化。大多数研究表明，组织中的 N 浓度高，维持呼吸也随之增加，例如欧洲赤松 (*Pinus sylvestris*, Zha et al., 2002)、枫香 (*Liquidambar styraciflua*, Tissue et al., 2002)、美洲黑杨 (*Populus deltoids*, Griffin et al., 2002)、白栎 (*Quercus alba*)、北美红栎 (*Q. rubra*) 和红糖槭 (*Acer rubrum*, Lee et al., 2005)。维持呼吸变化是 GPP 转化为 NPP 效率变化的最可能原因，而且大多数碳平衡模型研究中，也都在利用维持呼吸值计算净生产力 (Hölttä et al., 2009)。准确判断氮沉降对树

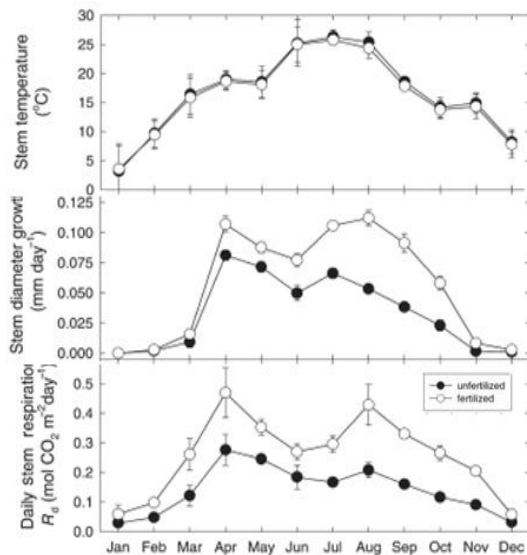


图1.2 树干呼吸、树干生长量与树干温度的变化
(Maier 2001)

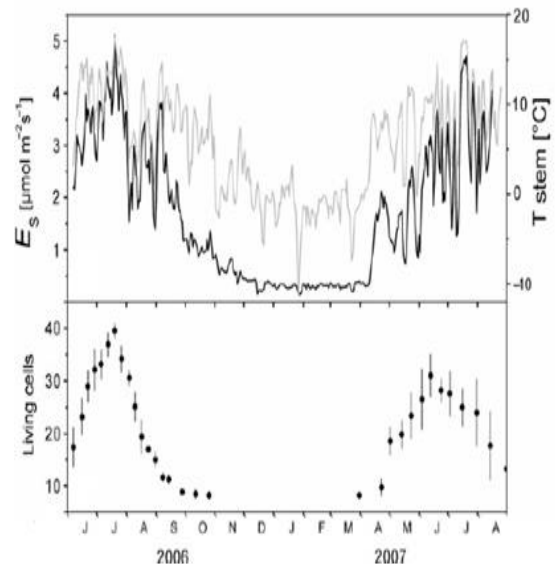


图1.3 树干呼吸与树干内活细胞数量
(Gruber et al. 2009)

干维持呼吸的影响，对利用模型准确估算森林生态系统碳收支平衡具有

重要意义。Magnani 等人(2007)通过对涡度相关法技术获得的碳通量数据和大气氮沉降数据的分析, 提出大气氮沉降主要决定着温带和北方森林生态系统的碳汇大小的空间分布(图 3), 随着每 1 g N 的氮沉降的增加, 森林生态系统碳储量将增加 200 g C。然而,, 也有一些研究却认为, 氮沉降将导致森林生态系统氮饱和(Cao et al., 2008), 由此可见, 不同的氮沉降速率, 对不同地区的森林碳循环会有不同的影响。目前, 我国已成为全球三大氮沉降集中区(分别为欧洲、美国和中国)之一(Reay et al., 2008), 而且氮沉降的速度还在逐年上升(鲁显楷等, 2008)。瑞典研究人员发现, 小剂量的多次增氮肥能够比较好的模拟自然过程(Ingestad et al., 1981)。在过去的 30 年里, 国内外已进行了大量的林地施肥试验。据报道, 施肥对林木生长的促进作用一般为 30%-50%, 最高达 500%。施肥能导致林木将较大比例的碳分配给树干(McMurtrie et al., 1990)。因此, 利用人工施氮模拟大气氮沉降的方法, 对树干呼吸进行研究具有重要意义。

1.3 研究意义

全球森林约占地球陆地面积的1/3, 森林生物量约为整个陆地生态系统的90%, 净生产量约占陆地生态系统的70%。森林在全球碳循环中起着重要作用。我国是世界上人工林面积最多的国家, 塞罕坝机械林场是我国最大的人工林种植基地, 对该林场的主要种植树种樟子松、华北落叶松和主要天然林白桦进行研究, 对我国的陆地生态系统碳汇功能的研究具有重要意义。近年来, 全球气候变化及其对陆地生态系统的影响受到人们的高度重视, 其中, 因大气氮沉降而引起的生态系统结构和功能的

变化也受到越来越多的科学家的关注。中国已成为世界三大沉降区之一，然而氮沉降对森林生态系统的影响还处于起步阶段，有关氮沉降对树干呼吸及土壤呼吸的研究更是很少。因此，本研究将为全球变化提供新的信息，不仅有利于正确评价树干呼吸对我国北方森林生态系统碳循环的影响，还有助于更加正确的发展我国北方人工林生态系统碳循环模式，为推测森林生态系统碳收支状况在全球变化进程中的可能表现提供可够数据。

第2章 研究区域概况与研究方法

2.1 研究区域自然地理概况

2.1.1 研究区域概况

塞罕坝系满汉结合语，意为“美丽的高岭”。塞罕坝位于河北围场满族蒙古族自治县北部，内蒙古浑善达克沙地南缘，系内蒙古高原与大兴安岭余脉、阴山余脉交接处，海拔 1 018-1 940 米，区域地理经纬度坐标为北纬 42°02′~42°36′ 东经 116°32′~ 117°14′（如图 2.1）。塞罕坝机械林场是清朝著名的皇家猎苑——“木兰围场”的重要组成部分，距北京 396 公里，距承德 168 公里，是华北地区重要的人工林基地，集生态公益林建设、商品林经营、自然保护和森林旅游于一体。

由于无霜期短，适生树种较少。优势的天然植物群落类型包括蒙古栎林（*Quercus mongolica*）、棘皮桦林（*Betula utilis*）、白桦林（*B. platyphylla*）、山杨林（*Populus davidiana*）、油松（*Pinus tabulaeformis*）林、贝加尔针茅（*Stipa baicalensis*）草原和羊草（*Leymus chinensis*）草原。林场于上世纪 60 年代开始种植大面积人工林，主要包括华北落叶松（*Larix principis-rupprechtii*）林和樟子松（*Pinus sylvestris* var. *mongolica*）林，现已发展成为我国最大人工林种植基地，是我国三北防护林体系的一部分。华北落叶松（*Larix principis-rupprechtii*）和樟子松（*Pinus sylvestris* var. *mongolica*）是该林场的主要树种。林分总面积 53 207.7hm²，落叶松

30 673.6hm²，占 57.6%，其中落叶松人工林 30 393.3hm²。全场活立木总蓄积 2 543 572m³，落叶松 1 552 659m³，占 61%；桦树 627 652m³，占 24.7%，全场林木资产总值 42 亿元。

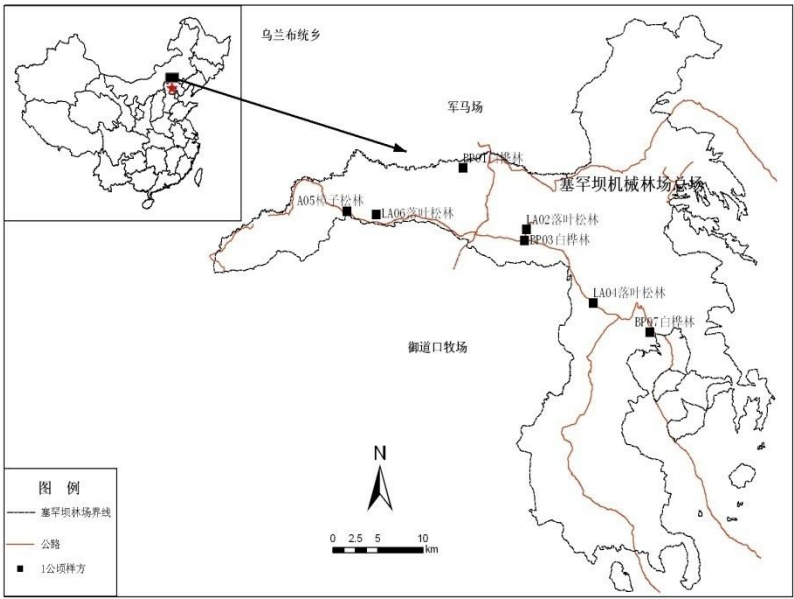


图 2.1 研究区域地理位置

2.1.2 地质与地貌

塞罕坝地区地质上属于内蒙古台背斜。其褶皱以宝元栈向斜为主，断裂带以北西向与北东向断裂交叉并生为特点。塞罕坝地区地貌上界于两个一级单元即（内蒙古）熔岩高原和（冀北）山地之间，主要是高原台地。地形大体上可分为熔岩高原丘陵地形和熔岩高原丘陵平原两种类型。作为内蒙古高原的一部分，本区一直处于缓慢的上升阶段，目前，上升趋势仍未停止。整个地势分坝上、坝下两大类。坝上东部曼甸，向下割为深谷，坡度较大。西部周沙地，呈山状起伏，坡度一般在15°以下。坝

下是阴山山脉与大兴安岭余脉的交接地带，具有山高坡陡的特点。境内最高点位于东北部的大光顶子峰，海拔为1 940m，最低点位于南端，海拔为1 018m。本区的地形地貌组合为高原-波状丘陵-漫滩-接坝山地。

2.1.3 气候

塞罕坝机械林场位于河北省最北部，按照温度带区划，地处中温带，临近暖温带北界；按照气候类型区划，地处温带大陆性气候与温带季风气候交错带。按照林场气象站 50 多年的实际观测划分，本区气候寒冷，冬长、春秋短、夏季不明显，属半干旱向半湿润过渡、寒温带向中温带过渡、大陆性季风型山地气候。无霜期 67~128 天，年平均日照 2367.8h，日照率为 58%，年均降水量 380~560 mm，最大年降水量 636.0mm，最小年降水量 258.0mm，6-8 月降水量占年降水量的 67.6%。年均蒸发潜力为 1388mm，是降水量的 2.6 倍。年均相对湿度为 74.4%。多风是本地区气候的特点之一，年均 6 级以上的大风 68 天，最多年份达 114 天，最少年份 48 天。

2.1.4 植被群落

塞罕坝机械林场湿地资源十分丰富，且具有独特的保护和观赏价值。尤其在海拔1 500米左右的塞罕坝湿地，属于独特的高寒河源湿地类型，植物群落非常丰富，有水生植物群落、沼泽植物群落、草甸植物群落，还有森林植物群落和草原植物群落，具有完整的水生生态序列，集森林、草原、草甸、沼泽和水体为一体。

森林植物群落：森林中常见的灌木有近10种，包括蔷薇科的山丁子、稠李、土庄绣线菊、刺梅蔷薇和美蔷薇、辽西山楂，忍冬科的金银木。常见草本植物有56种，分布广泛的有莎草科的矮紫苞鸢尾，禾本科的野青茅，菊科的小红菊、乌苏里风茅菊，毛茛科的东亚唐松草、展枝唐松草，蔷薇科的龙牙草、莓叶委陵菜、菊叶委陵菜、地榆，豆科的歪头菜、山野豌豆，蓼科的拳参、珠芽蓼，芍药科的白芍，花忍科的花忍，景天科的土三七，大戟科的京大戟，败酱科的缬草，百合科的二叶舞鹤草、藜芦、小玉竹、铃兰等。

草原植物群落：在草原植物群落中，广泛出现耐旱的禾本科贝加尔针茅。初步统计，共出现草本植物45种，较常出现的除禾本科和莎草科的种类外，还有蔷薇科的高二裂委陵菜、腺毛委陵菜，豆科的狐尾藻棘豆，瑞香科的狼毒，唇形科的荆芥，茜草科的蓬子菜、伞形科的北柴胡，百合科的小黄花菜、山丹，禾本科的无芒雀麦、细叶鸢尾。林缘的草原植被中双子叶植物种类丰富，和森林非常靠近。

草甸植物群落：以灰脉苔草占优势的沼泽化草甸，形成塔头、双子叶，植物种类丰富，初步统计共出现47种植物，较常见分布的还有毛茛科的驴蹄草、金莲花、毛茛、低矮华北乌头、翠雀，豆科的岩黄芪、广布野豌豆、柳叶野豌豆，蔷薇科的柳叶绣线菊、蚊子草、地榆，蓼科的珠芽蓼、毛脉酸模，玄参科的返顾马头蒿，伞形科的迷果芹、骨缘当归、辽藁木，败酱科的缬草，菊科的紫苞凤毛菊、裂叶蒿、柳叶蒿、肾叶橐吾，禾本科的硬质早熟禾。

沼泽植物群落：主要由沼生植物组成，包括禾本科和莎草科的种类以及大量的双子叶植物。七星湖、泰丰湖及其周边地区保存了非常完整的水生生态序列。这一序列包括沉水植物、浮水植物、挺水植物、湿生植物、中生植物和旱生植物。这种生态序列只有在森林—草原过渡带才有出现。七星湖周边的假鼠妇草属于假鼠妇草沼泽，主要以禾本科和莎草科植物为主，常见禾本科种类有假鼠妇草、假稻等，常见的莎草科种类包括灰脉苔草、柄苔草和红穗苔草等。在七星湖水体中主要以浮水植物占优势，而在泰丰湖水体中主要以沉水植物占优势。

2.2 研究方法

2.2.1 样地设置与实验设计

本实验选择白桦、樟子松和华北落叶松作为研究对象，每个树种分别选择三个不同林龄的林地三个。在不同树种的树干呼吸速率与林龄关系的研究中，在每个样地中，分别选择胸径大致相同，生长正常的林木 6 棵，在 2012 年 5 月-9 月，每个月进行 2-3 次的树干呼吸速率的测定。在生长季开始（5 月）和生长季末期（9 月），分别进行了树干胸径的测量。并在 9 月末采集一定量树干边材，用于树干氮含量的测定。

氮沉降对树干呼吸速率影响研究实验设计如下：

样地设计：本实验选取面积均为 100m×100m 的 45 年的华北落叶松人工林样地（如图 2.3）。参照欧洲 NITREX 项目和北美 Harvard Forest

等类似研究的设计，样地分别设置 9 个氮处理样方，每个样方面积为 20m×20m，相邻样方间留有 10m 宽的隔离带，以防止相互干扰。每个样方选择 2 棵树，2010-2012 年 5-9 月每月进行两次连续 24 小时的测定，每 3 小时测定一次。

施氮处理：根据本地区的氮沉降背景值($7 \text{ kg N hm}^{-2} \text{ yr}^{-1}$) (宋玲2008)，



图 2.2 45 年华北落叶松林样地

参考国际上同类研究的氮处理强度和频度 (Pregitzer et al. 2008)。每个林龄的样地分别进行3个处理 (0、20和50 $\text{kg N hm}^{-2} \text{ yr}^{-1}$ ，后文分别简称为对照组、20kg施氮组和50kg施氮组)，每个处理均设3个重复。在生长季 (5月-10月) 的每月月初，根据氮处理水平，以背式喷雾器人工来回均匀喷洒林下的方式进行人工施肥。由于硝酸铵在国内被禁用，因此，本研究中氮肥采用尿素。为了保证氮素与土壤层有充足的时间接触，参考天气预报来安排施肥日期，以确保施氮后第二天无雨。

2.2.2 树干呼吸速率的测定

利用 Li-Cor 6400 便携式光合仪的土壤呼吸室进行树干呼吸的测定。根据胸径的大小分别用直径为 4.4cm 和 10.1cm，长 5cm 的 PVC 管，其中管的一端按照树木的实际形状进行切割以保证在安装时 collar 环能够与

树干表面充分接触，管的另一端进行垂直切割即可，所有切割处要用细砂纸充分打磨，并且将需要安装 collar 环处的疏松的树皮剥除，这样可以保证树干和 collar 环的弯曲段相对光滑。然后用 100% 的硅胶将 collar 环连接在相应的树干处，待硅胶充分凝固后方可进行树干呼吸的测定。为了尽量避免其他因素对树干呼吸测定值的影响，我们将尽可能减少树皮的移除量和硅胶的使用量以及采用尽可能薄的 PVC 管，所有的 collar 环将安装在树干 1.3m 处 (Xu 2000; Maier 2001)。由于土壤呼吸室的直径为 9.9cm，可以直接用于胸径较大林木的树干呼吸的测定，胸径较小林木的 collar 环直径较小，两者需用自制的轴承进行连接。

2.2.3 土壤温、湿度的测定

采用 EM50 进行华北落叶松 45 年林生长季期间土壤温度和水分含量的测定。EM50 具有 5 个通道，对华北落叶松林三个施氮处理，生长季分别进行 5cm, 10cm, 30cm, 50cm 和 100cm 的土壤温度和湿度的测定。每 30min 记录一次数据。

2.2.4 树干呼吸速率的计算

为计算树干呼吸速率，我们需要测定 collar 环覆盖的树干面积，由于树干是一个圆柱体，所以我们使用以下公式计算其面积：

$$A = \frac{\pi D_1 D_2}{4} \arcsin \left(\frac{D_1}{D_2} \right) \quad (\text{式 2.1})$$

式中：A — collar 环覆盖的树干表面积；

D_1 — collar环的直径;

D_2 — collar环所在处树干的直径。

我们用指数函数拟合树干呼吸速率与树干温度的关系

$$R_{st} = \alpha \times e^{\beta T} \quad (\text{式 2.2})$$

式中: R_{st} — 树干呼吸速率 ($\mu\text{mol} \cdot \text{m}^{-2} \text{s}^{-1}$);

T — 树干温度 ($^{\circ}\text{C}$);

α — 常数, 表示 0°C 的树干呼吸速率;

β — 常数, 可反映温度的敏感度。

树干呼吸对温度的敏感度, 通常用 Q_{10} 来表示,

$$Q_{10} = e^{10\beta} \quad (\text{式 2.3})$$

生长季内边材面积的增长量, 我们用下面公式进行计算:

$$\Delta A = \frac{\pi(D_3^2 - D_4^2)}{4} \quad (\text{式 2.4})$$

式中: ΔA — 边材面积增长量

D_3 — 九月所测胸高处的树干直径

D_4 — 五月所测胸高处的树干直径

在2012年的九月, 我们还对每棵测定林木进行了树芯取样, 用于树干氮含量的测定, 所用仪器是元素分析仪 (2400 II CHNS/O 元素分

析仪， 美国）

2.3 数据统计分析

数据处理中使用EXCEL2007进行数据整理， Sigma plot 用于图形制作。用PASW 18（SPSS 公司， 美国）进行数据的统计分析。

在树干呼吸速率与林龄关系研究中， 我们首先计算了每棵树的树干呼吸速率和树干温度的月均值， 再根据月均值计算整个生长季（五月-九月）的树干呼吸速率与树干温度的均值。同时， 计算了整个生长季树干边材面积的增长量和生长季末树干的氮含量。

我们对树干呼吸速率与树干温度的关系分别建立指数模型

（ $E_s = ae^{bT_s}$ ）和二次曲线模型（ $E_s = a + bT_s + cT_s^2$ ）。为了更好的探讨两者之间的关系， 我们又在模型中添加了DBH（胸径）因子。为了建立线性关系， 我们首先建立对树干呼吸速率进行了对数转化（Yang et al. 2012a）， 回归模型如下：

$$\ln(E_s) = a + bT_s + cDBH \quad (\text{式 } 2.5)$$

利用方差分析法计算树干呼吸速率的月均值在不同时间， 不同林龄的不同树种之间的差异性， 同时分析了在每个树种中， 林龄对生长季内树干呼吸速率与树干温度关系， 树干氮含量， 边材面积增长量的影响。显著性水平选择为 $P < 0.05$ 。

第3章 树干呼吸速率与林龄

树干呼吸速率是一个复杂的生物学过程，不仅受非生物因素（例如，温度）还受生物因素（例如，林龄或径阶）的影响（Amthor 2000; Ma *et al.* 2007; Teskey *et al.* 2008; Yang *et al.* 2012a）。温度是影响树干呼吸速率的重要环境因素之一。它是模型中用于估算林木整体总的呼吸速率的重要参数（Damesin *et al.* 2002; Zha *et al.* 2004; Bowman *et al.* 2008; Zhu *et al.* 2012）。然而，对于不同的树种，树干呼吸速率与树干温度的关系并不一致。大多数研究表明树干呼吸速率与树干温度具有显性的指数相关性，树干温度对树干呼吸速率的变化具有较高的解释率（Edwards and Hanson 1996; Xu *et al.* 2000; Zha *et al.* 2004; Yang *et al.* 2012a）。例如，在东北地区的10温带树种的树干温度可以反映树干呼吸速率变化的35-66%（Yang *et al.* 2012a）。但是，也有研究表明，树干呼吸速率与树干温度之间的关系并不显著（Lavigne *et al.* 1996; Teskey and McGuire 2002; Saveyn *et al.* 2007; Zach *et al.* 2010）。可见，树干呼吸速率与树干温度的指数相关性，并不适用于所有的树种。

温度主要通过对呼吸酶活性的影响而影响了树干呼吸速率（Amthor 2000）。不同树种的呼吸酶的最适宜温度各不相同，而且随着外界环境的变化，呼吸酶的最适宜温度也会有所不同。在外界环境相同的情况下，在较低的温度范围内，树干呼吸速率一般随着温度的升高而增加，当达到最适宜温度以后，树干呼吸速率会随着温度的升高而降低。因此，在

一个完整的温度范围内，树干呼吸速率与树干温度之间的关系应该呈现一个很好的二次曲线关系。因此，测定的温度范围和最适宜温度也会影响到树干呼吸速率与树干温度之间的关系曲线形状。

除了温度，林龄或径阶也是影响树干呼吸速率的重要因素（Chambers *et al.* 2004; Kim *et al.* 2007; Robertson *et al.* 2010; Yang *et al.* 2012a）。例如，Ryan等（2009）研究表明桉树的树干呼吸速率随着林龄增加而降低，而Xu等（2012）对红栎树的进行研究发现，木质组织的呼吸速率随着林龄的增加而增大。但前人大多数都只针对同一树种进行研究。本研究对塞罕坝地区三个主要树种白桦、樟子松和华北落叶松的树干呼吸速率与温度和林龄（径阶）的关系进行了研究。

3.1 树干呼吸速率的季节变化

三个树种的树干呼吸速率均具有显著的季节变化规律（ $P < 0.001$ ，图 3.1，表 3.1）。树干呼吸速率的最大值出现在七月或者八月，而最小值出现在五月或九月。白桦、樟子松和华北落叶松的树干呼吸速率的最大值分别是 4.92 ， 2.39 和 $6.16 \mu\text{mol m}^{-2} \text{s}^{-1}$ ；而三个树种的树干呼吸速率的最小值分别是 0.55 ， 0.47 和 $1.39 \mu\text{mol m}^{-2} \text{s}^{-1}$ 。整个生长季（五月-九月）的树干呼吸速率的均值，华北落叶松（ $3.60 \mu\text{mol m}^{-2} \text{s}^{-1}$ ）明显高于白桦（ $2.25 \mu\text{mol m}^{-2} \text{s}^{-1}$ ）和樟子松（ $1.60 \mu\text{mol m}^{-2} \text{s}^{-1}$ ）。与树干呼吸速率不同，三个树种的树干温度均不具有显著的季节变化规律（见图 3.1d-f）。

树干呼吸速率的季节动态可能与树木木质部形成层生理活动能力的

变化有密切关系，树木形成层活动具有明显的季节变化(Catesson, 1980)。在 5 月树干细胞开始分裂化时，树干呼吸速率较小；6 月随着细胞的分裂

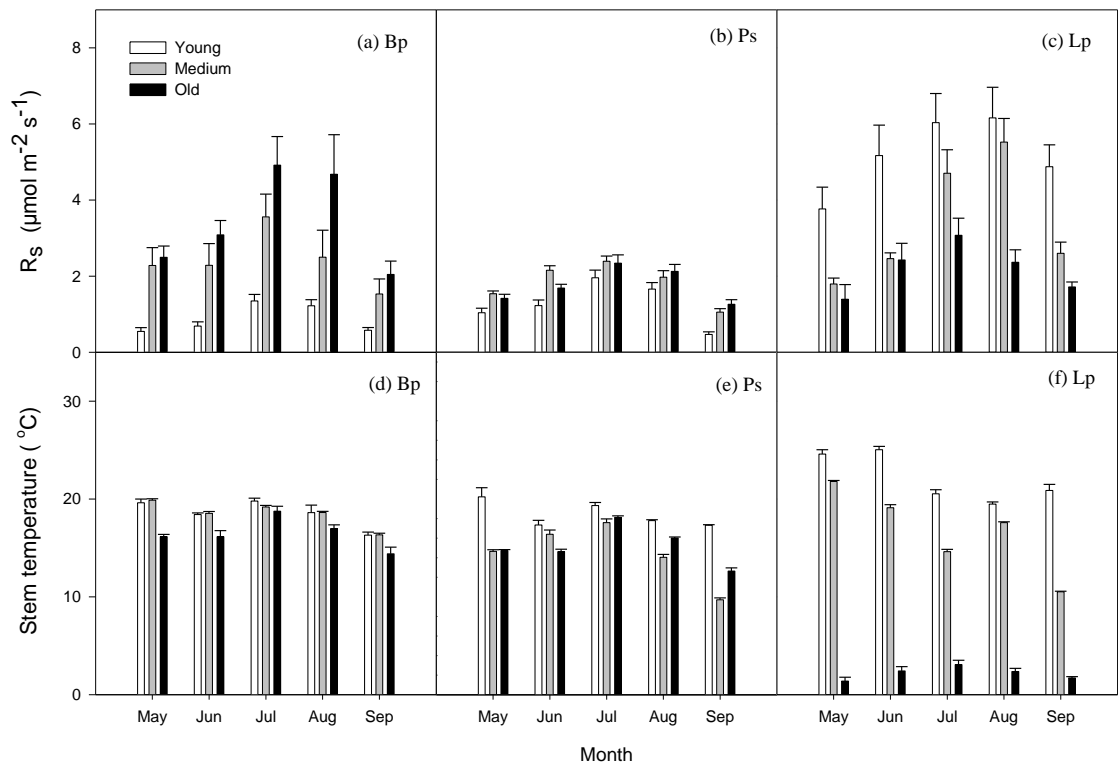


图 3.1 树干呼吸速率和树干温度的季节变化

注：Rs 表示树干呼吸速率，Bp 表示白桦树，Ps 代表樟子松；Lp 代表华北落叶松；误差线表示标准误 (n=6)

和体积的增大，树干呼吸速率在逐渐增大；7 月筛管和薄壁细胞数量增加，树干呼吸速率达到峰值；8 月细胞壁增厚，开始沉积，细胞分裂和生长的速度在减少，树干呼吸速率也随之降低；9 月所有细胞都非常有规律的开始在径向排列，树干呼吸速率较快的降低。树干呼吸的季节变化与形成层的活动是否紧密相关，还需进一步研究。

也有研究表明，呼吸速率的季节变化反映了冷暖对生长周期的影响，以及温度对呼吸速率的直接影响。湖南会同杉木人工林的树干呼吸在1-3

月维持在较低值，3-7月随着树木生长和气温的升高，树干呼吸呈上升趋势，7月达到最大值，8-12月呈逐渐递减的趋势（肖复明等，2005）。长白山地区红松林树干呼吸速率有类似的变化规律（王淼等，2005），即6月树木新叶长出前，树干呼吸速率变化趋于平稳，随后呈直线上升态势，8月初达到峰值，然后迅速降低。东北地区兴安落叶松生长季的树干呼吸从5月开始，树干呼吸逐渐增强，7月达到最大值，尔后逐渐减弱（Wang et al., 2003）。

表 3.1 树干呼吸速率与树种、林龄和时间的三因素方差分析结果

	自由度	<i>F</i> -值	<i>P</i> -值
树种	2	87.0	<0.001
林龄	2	0.3	0.718
时间	4	27.3	<0.001
树种×林龄	4	56.4	<0.001
树种×时间	8	2.2	0.028
Age ×时间	8	0.4	0.915
树种×林龄×时间	16	1.8	0.032

3.2 温度对树干呼吸速率的影响

温度一直被公认为是影响树干呼吸速率的最重要环境驱动因子之一（Paembonan *et al.* 1991; Maier *et al.* 1998; Zha *et al.* 2004; Zhu *et al.* 2012）。大多数研究以表明树干呼吸速率随着树干温度的升高而呈指数上升（Ryan *et al.* 1995; McGuire *et al.* 2007; Saveyn *et al.* 2008a; Yang *et al.* 2012a）。在此研究中（见图3.2），三个不同林龄的不同树种，树干呼吸速率与树干温度的关系呈现三种情况：指数关系、二次曲线关系和关系不

显著。其中林龄较大的白桦与林龄中等和林龄较大的樟子松，树干呼

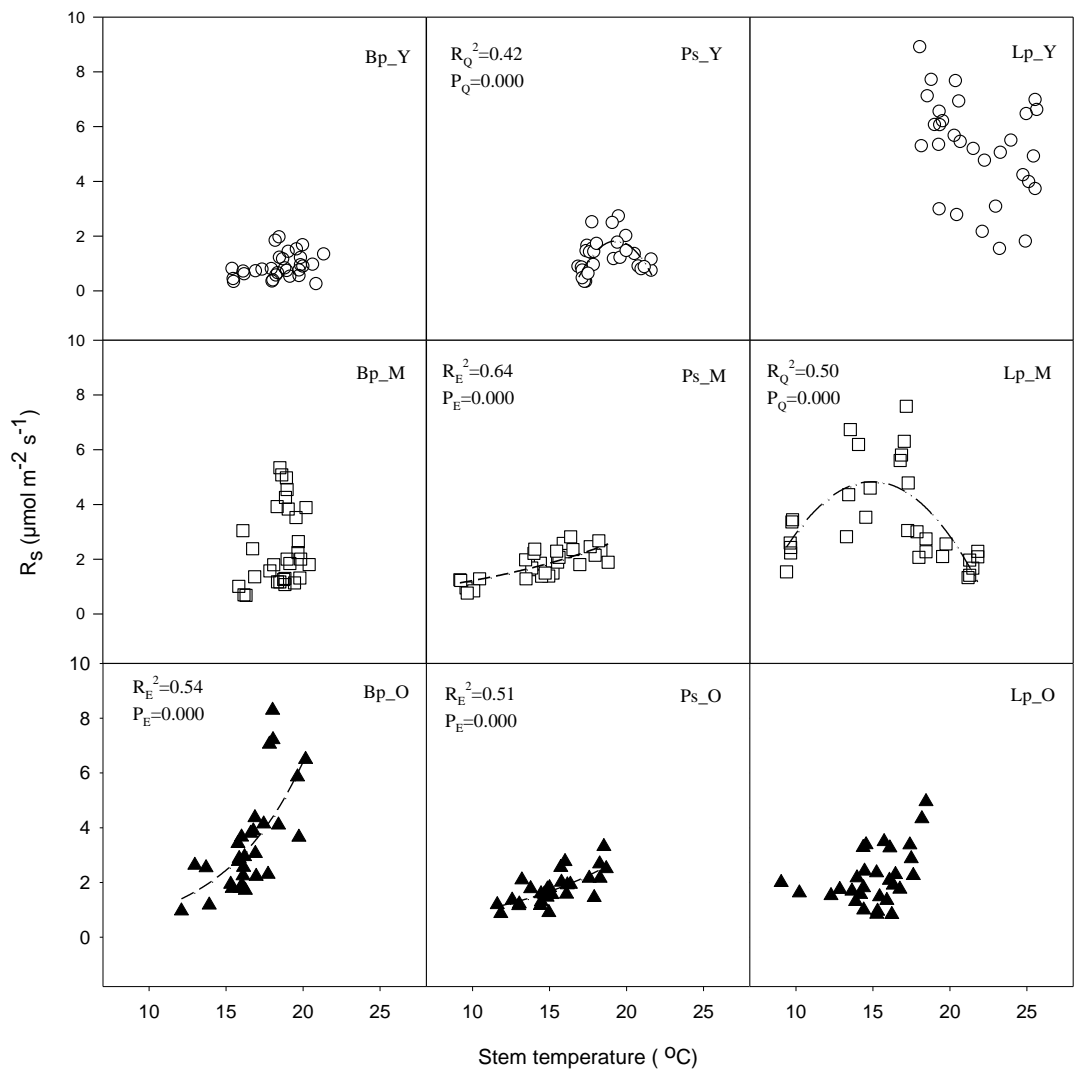


图3.2 三个不同林龄不同树种的树干呼吸速率与树干温度的关系

注：下小标E表示指数关系 ($R_s = \exp(a + b T_s)$)，Q表示二次曲线关系 ($R_s = a + b T_s + c T_s^2$)。Bp, Ps和Lp分别表示白桦，樟子松和华北落叶松。Y, M和O分别表示林龄较小，林龄中等和林龄较大。

吸速率与树干温度具有显著的指数关系；林龄较小的樟子松和林龄中等的华北落叶松，树干呼吸速率与树干温度呈现显著的二次曲线关系；而其它林龄的树种的树干呼吸速率与树干温度的关系并不显著。当我们将树干呼吸速率与树干温度和胸径（DBH）进行多维回归分析，结果表明，白桦和樟子松的树干呼吸速率与树干温度具有显著的相关性，而华北落

叶松的树干呼吸速率与树干温度的关系并不显著（见表 3.2）。

表 3.2 建立树干呼吸速率与树干温度和胸径的关系模型

树种	<i>N</i>	<i>a</i>	<i>b</i>	<i>c</i>	<i>R</i> ²	<i>P</i>
白桦	90	-4.083	0.192	0.081	0.59	<0.001
樟子松	90	-0.959	0.049	0.030	0.21	<0.001
华北落叶松	90	1.698		-0.051	0.35	<0.001

注：为了建立线性关系，现将树干呼吸速率取对数，然后进行回归分析
 $(\ln(E_s) = a + b T_s + c DBH)$ 。

树干呼吸速率与树干温度的指数关系或者二次曲线关系之间的一个潜在机制可能与树干呼吸速率的最适宜温度和测定树干呼吸的温度范围有关。当测定树干呼吸速率的树干温度范围低于最适宜温度时，树干呼吸速率会随着树干温度的升高而呈指数上升（Amthor 2000; Teskey *et al.* 2008）。很多研究（e.g. Ryan *et al.* 1995; Xu *et al.* 2000; Zha *et al.* 2003; Acosta *et al.* 2008; Wang *et al.* 2008; Zach *et al.* 2010; Yang *et al.* 2012a）已发现树干呼吸速率与树干温度具有很好的指数关系，进行测定时，树干温度的范围是在0-30°C之间，大多数的测定温度是在0-20°C之间。同样我们也观察到，当测定温度在10-20°C之间时，林龄较大的白桦树与林龄中等和林龄较大的樟子松的树干呼吸速率与树干温度具有显著的指数相关。

但是，当测定温度范围包含最适宜温度时，树干呼吸速率应先随着温度的升高而增大，当达到最适宜温度以后，树干呼吸速率将随着温度的升高而降低，在整个温度范围内，呈现一个很好的二次曲线关系，例

如此研究中的林龄较小的樟子松和林龄中等的华北落叶松，两者的树干呼吸速率的最适宜温度在16-18°C（见图3.2）。与指数关系相比，树干呼吸速率与树干温度的二次曲线关系的报道很少。由于大多数研究（特别是温带地区），树干呼吸速率的测定温度范围都是低于树干呼吸酶活性的最适宜温度，很难发现两者之间的完整的关系曲线。同时，其它因素对树干呼吸的影响也值得我们关注，例如，可氧化底物的供应，树干的生长和树干的氮含量等。不管怎样，树干呼吸速率的最适宜温度与测定的温度范围对树干呼吸速率与树干温度关系的影响在本研究中是可见的。

除了树干呼吸速率与树干温度呈现指数和二次曲线关系外，我们还发现有些林龄的树种的树干呼吸速率与树干温度的关系并不显著，与前人的研究相一致（例如 Teskey and McGuire 2002; Bowman *et al.* 2005; Saveyn *et al.* 2008b; Zach *et al.* 2010），可能是其它因素影响的结果。例如树干呼吸所必需的呼吸底物来自与光合作用，具有季节性的变化规律（Martin *et al.* 1994; Moore *et al.* 2008）。Maier 等(2010)研究表明，校正温度的树干呼吸速率与松属树干中可溶性糖和淀粉浓度呈显著线性相关；Wertin和Teskey（2008）发现由于大气CO₂浓度和光辐射变化所导致的冠层光合作用的变化对杨树苗的树干呼吸速率的变化具有一定的影响。生长呼吸主要取决于呼吸底物的供应，并不完全依赖于温度（Amthor 2000），这也可能是导致树干呼吸速率与树干温度关系不显著的一个重要原因。此外，树干内部呼吸细胞所产生的CO₂扩散到树干表面需要一定的时间，可能是导致树干呼吸速率与树干温度关系不显著的另一重要原因。一些研究表

明, 树干呼吸速率可能与滞后的树干温度显著相关 (Teskey and McGuire 2002; Bosc *et al.* 2003; Saveyn *et al.* 2007)。滞后的时间与边材的体积含水量, 树皮的厚度, 胸径的大小和树木的种类等密切相关 (Ryan *et al.* 1995; Wang *et al.* 2003; Acosta *et al.* 2008; Teskey *et al.* 2008; Yang *et al.* 2012a)。

3.3 树干呼吸速率与林龄

林龄 (或径阶) 是影响树干呼吸速率的重要生物因素之一 (Ma *et al.* 2007; Teskey *et al.* 2008; Yang *et al.* 2012a)。前人研究表明, 有些树种树干呼吸速率随着林龄的增加而增大 (Cavaleri *et al.* 2006; Yang *et al.* 2012a); 有些随着林龄的增加而减小 (Kim *et al.* 2007; Ryan *et al.* 2009); 有些并没有显著的变化 (Robertson *et al.* 2010)。

在本研究中, 华北落叶松的生长季树干呼吸速率均值随着林龄 (胸径) 的增加而减小, 而白桦和樟子松的树干呼吸速率随着林龄 (胸径) 的增加而增大 (见图 3.3a)。而且, 树干呼吸速率与树干温度和胸径的回归模型比只使用树干温度预测树干呼吸速率的解释率要高好, 华北落叶松的树干胸径变化对树干呼吸速率的解释率要高于树干温度对树干呼吸速率的解释率 (见表 3.2)。三个树种的树干呼吸速率具有显著的差异 (见表 3.1)。结果显示, 华北落叶松的树干呼吸速率最大, 其次是白桦和樟子松 (图 3.1, 3.3)。

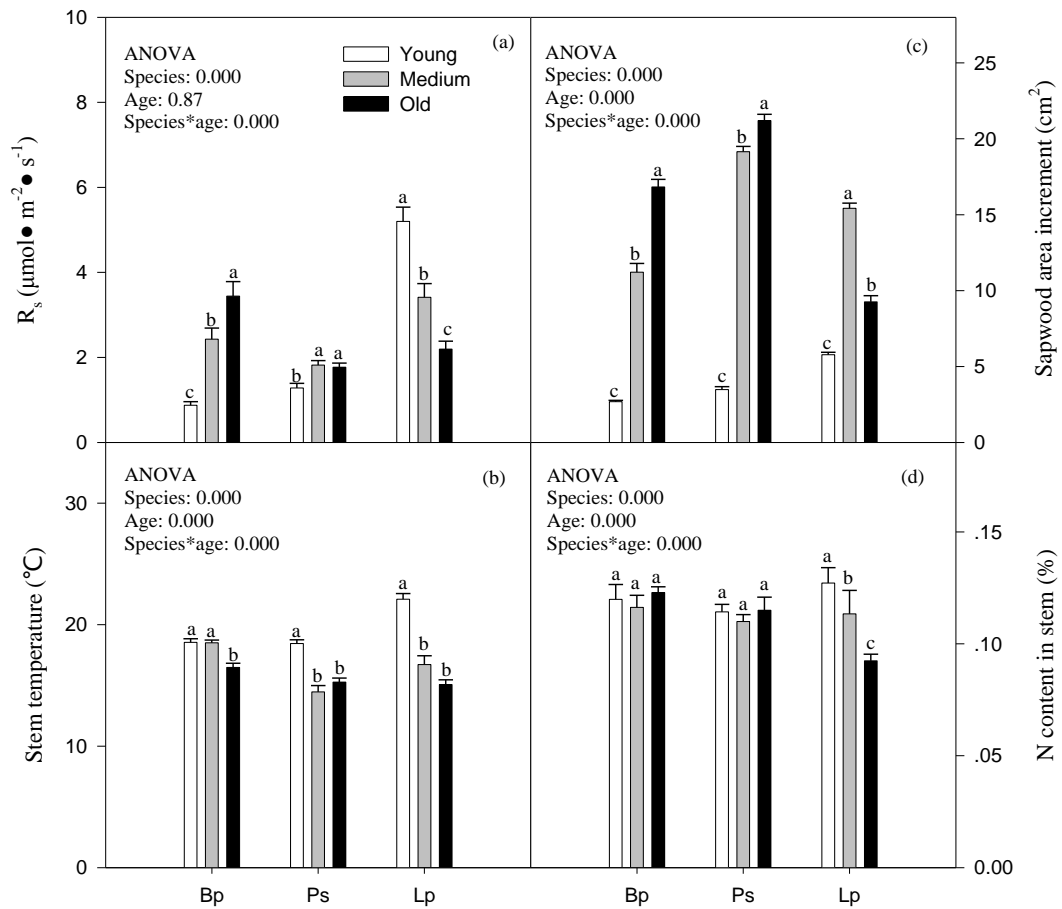


图 3.3 三个不同树种的树干呼吸速率的树干呼吸速率 (a)、树干温度 (b)、生长季边材面积增长量 (c) 和树干氮含量 (d) 随林龄的变化规律

白桦和樟子松的树干呼吸速率随着林龄的增加而增大与树干边材面积增量随着林龄的增加而增加相一致。而白桦和樟子松的树干温度均随着林龄的增加而降低，树干氮含量在不同林龄间没有显著的差异（见图 3.3）。可能是由于树干生长比较快，树干呼吸速率中的生长呼吸占主导地位，从而降低了维持呼吸对树干呼吸速率的影响。前人也有研究表明，树干呼吸速率对着树干生长量的增加而增加。例如， Moore 等（2008）发现 *P.taeda* 树干直径的年生长量可以解释树干呼吸速率变化的 42-74%；Vose 和 Ryan（2002）也报道了树干直径的年生长量可以解释 *P. strobus*

的树干呼吸速率变化的 43%。

华北落叶松的树干呼吸速率随着林龄的增加而减小；这与树干温度和树干氮含量随林龄的变化相一致。树干边材面积的增长量随着林龄增加先增大后减小。温度和树干氮含量都是影响树干维持呼吸的重要因素，对于华北落叶松，树干维持呼吸可能在树干呼吸速率随林龄变化中起着重要作用。很多研究也表明，树干呼吸速率与树干温度（Ryan *et al.* 1995; Acosta *et al.* 2008; Yang *et al.* 2012a）和树干氮含量（Maier 2001; Vose and Ryan 2002; Reich *et al.* 2008）呈正相关。因此，华北落叶松的树干呼吸速率随林龄的变化主要是由于维持呼吸随着树干温度和树干含量变化所决定的。

3.4 结论

（1）本研究表明，对于不同林龄，不同树种，树干呼吸速率与树干温度的关系存在三种形式：指数、二次曲线和关系不显著。

（2）测定树干呼吸速率的树干温度范围和树干呼吸酶的最适宜温度都对两者之间关系具有一定的影响。此外，光合作用所提供的树干呼吸底物及树干呼吸细胞所产生的 CO_2 向树干表面的扩散速度，都会影响到树干呼吸速率与树干温度的关系。

（3）不同树种，树干呼吸速率随林龄的变化趋势有所不同，可能与不同树种树干呼吸速率的主要控制因素不同。

(4) 白桦和樟子松的树干呼吸速率随着林龄的增加而增大，可能与树干边材面积的增长量密切相关。

(5) 华北落叶松的树干呼吸速率随着林龄的增加而减小，可能是受控于树干温度和树干氮含量的变化。

第4章 树干呼吸速率的温度敏感度

温度是影响树干呼吸速率的重要环境驱动因子 (Acosta et al., 2010; Paembonan et al., 1991; Maier et al., 1998; Zha et al., 2004; Zhu et al., 2012), 在许多模型中被用于树干呼吸速率的预测 (Bowen et al., 2008; Stockfors, 2000; Damesin et al., 2002)。因此, 提高树干呼吸速率的温度敏感度的准确度, 有助于森林生态系统碳循环的预测, 使碳-气候耦合模型估算森林生态系统对气候变化的反映更加接近实际 (Cox et al., 2000; Friedlingstein et al., 2006)。

树干呼吸速率的温度敏感度通常用温度系数 Q_{10} 表示, 指温度每升高 10°C, 树干呼吸速率增加的倍数 (杨金艳等, 2009)。然而, 在不同地带的不同森林类型得到的树干呼吸速率的 Q_{10} 值在 1.0-6.4 之间 (McGuire et al., 2007, Damesin et al., 2002, Kim et al., 2007; Ryan et al., 1995; Wang et al., 2003; Acosta et al., 2011), 各不相同。然而, 大多数 Q_{10} 的计算是基于白天的测定数据 (Liberloo et al., 2008), 只有部分研究测定了树干呼吸速率的日变化 (Storkfors et al., 1998)。除了温度, 其它环境因素和林木的生理过程对树干呼吸速率也具有一定的影响 (Ryan et al., 2009; Saveyn et al., 2008; Zhu et al., 2012; Gruber et al., 2009; Lavigne and Ryan, 1997; Lavigne et al., 2004; Wittmann and Pfan, 2007), 例如, 光合作用只发生在白天, 它可能会影响到树干呼吸速率在白天和夜晚对温度敏感度的不同。此外, 实验和模型数据均表明, 全球变暖, 夜间的升高温度要大于

白天 (IPCC, 2007)。因此, 探讨白天和夜晚树干呼吸速率对温度敏感度的不同, 有助于更好地预测森林生态系统的碳预算及其对气候的响应。

4.1 树干呼吸速率的日变化

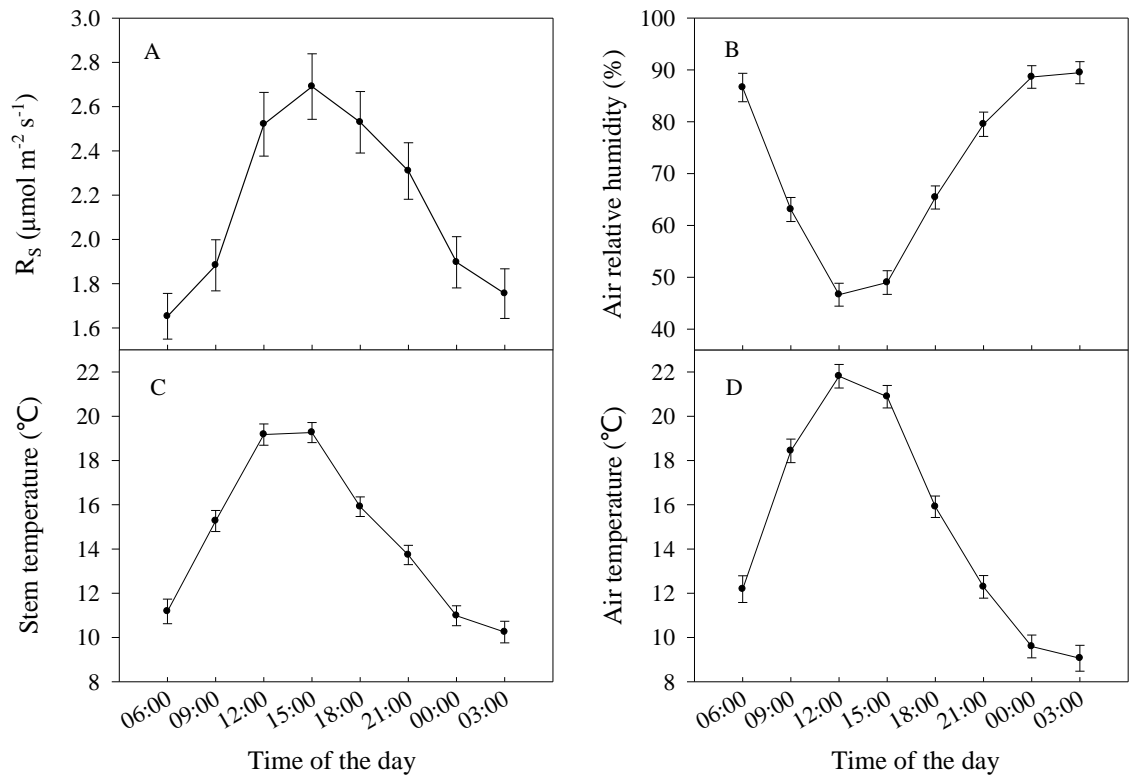


图 4.1 树干呼吸速率, 树干温度, 空气温度及空气相对湿度的日变化

由图 4.1 可见, 树干呼吸速率、树干温度和空气温度均具有显著的日变化规律。树干呼吸速率为 $1.65 \pm 0.10 - 2.69 \pm 0.15 \mu\text{mol m}^{-2} \text{s}^{-1}$, 树干呼吸速率从 6:00 起开始逐渐上升, 到 15:00 达到峰值, 然后逐渐下降。树干温度和空气温度具有相似的日变化规律。但空气日变化幅度 (12.75°C) 明显大于树干温度的日变化幅度 (9.05°C)。由图 4.1a 和 4.1c, 还显示, 在 9:00-18:00, 树干呼吸速率比树干温度的变化幅度大; 树干温

度在午后 12:00-15:00 出现最大值后，下降的速度比树干呼吸速率下降的速度快。空气相对湿度的日变化规律与空气温度相反，最大值（ $89.45 \pm 2.13\%$ ）出现在 3:00，最小值（ $46.64 \pm 2.21\%$ ）在 12:00。

本研究的树干呼吸速率测定值（ $0.33-6.59 \mu\text{mol m}^{-2}\text{s}^{-1}$ ）与前人测定的成熟针叶林的树干呼吸速率相似。例如，Wang 等（2003）研究表明，33 年的落叶松的在 2001 年六月的树干呼吸速率在 $0.9-6.6 \mu\text{mol m}^{-2}\text{s}^{-1}$ 之间。Acosta 等（2008）在 1999 年-2002 年对 22 年云杉的树干呼吸速率进行测定，结果表明树干呼吸速率的变化范围是 $0.34-6.52 \mu\text{mol m}^{-2}\text{s}^{-1}$ 。

在本实验研究中，树干呼吸速率的最大值出现在午后，最小值出现在凌晨，这与前人的研究结果相一致。例如，Zha 等（2004）发现欧洲赤松的树干呼吸速率日变化的最大出现在 16:00 左右；Acosta 等（2008）表明云杉树干呼吸速率的最大值出现在 13:00-16:00 之间；Zhu 等（2012）暗示木荷的树干呼吸速率具有相似的日变化规律，最大值出现在下午。在本研究中，树干温度也是影响树干呼吸速率日变化的一个重要因素。但树干温度并不能完全解释树干呼吸速率的日变化（Zha et al. 2004）。例如，在本研究中，树干呼吸速率在午后 18:00 明显大于上午 9:00 左右，但两个时间段的树干温度基本一致。这表明树干呼吸速率也会受到林木生理活动的等因素的影响，例如光合作用，林木的生长等（Levy and Jarvis, 1998; Ryan et al. 1996; Kozlowski and Pallardy, 1997; Thornley and Cannell, 2000）。Martin 等（1994）发现，但温度和蒸腾作用不变的情况下，树干呼吸速率会随着呼吸底物的增加而增大。呼吸底物来源于光合作用，所

以，光合作用也可能是影响树干呼吸速率日变化的一个重要因素。

4.2 Q_{10} 的日变化

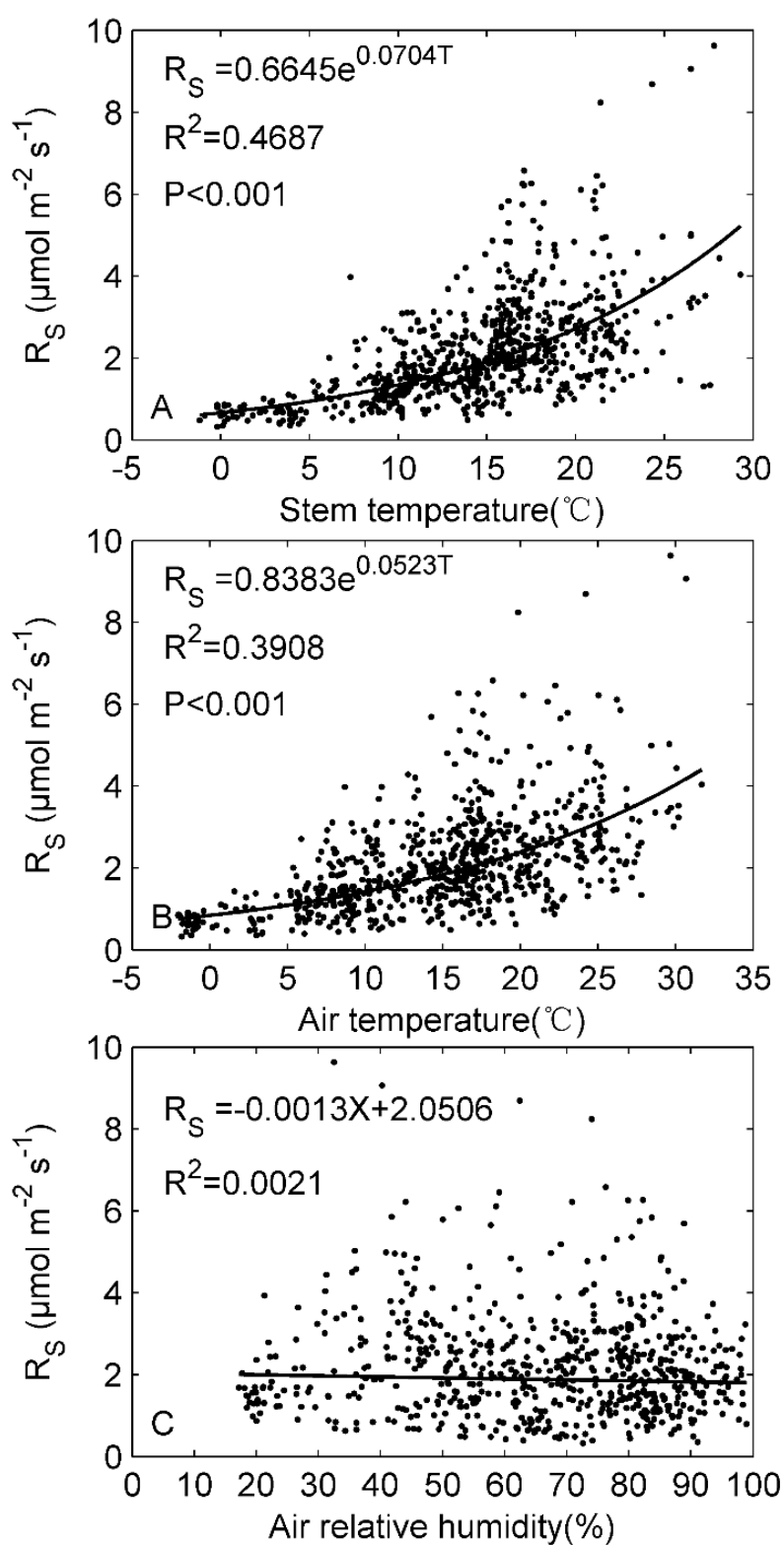


图 4.2 树干呼吸速率与树干温度、空气温度和空气相对湿度之间的关系

为了进一步探讨树干呼吸的生理机制，利用式 2.2，我们对树干呼吸

速率与树干温度和大气温度进行了回归分析，并探讨了树干呼吸速率与空气相对湿度的线性关系。结果表明，树干呼吸速率与树干温度($R^2=0.47$, $P<0.001$)和空气温度 ($R^2=0.39$, $P<0.001$) 都具有显著的指数相关性；而树干呼吸速率与空气相对湿度的相关性并不显著 ($R^2=0.00$)。

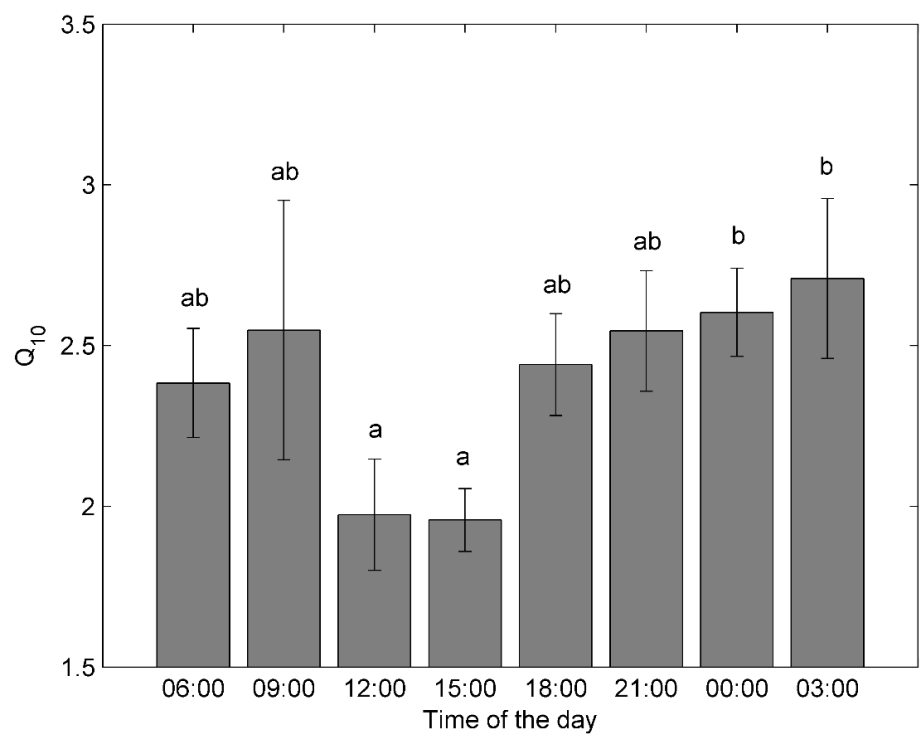


图 4.3 树干呼吸速率的 Q_{10} 值的日变化

利用式 2.3，我们进行了温度敏感度 Q_{10} 值的计算。准确理解树干温度的敏感度对全球碳平衡的计算和了解树干呼吸对气候变化的响应都具有重要的意义。为了对树干呼吸速率的温度敏感性的日变化进行研究，利用整个生长季的日变化数据数据，计算了生长季 Q_{10} 值的日变化。我们计算的树干呼吸速率的 Q_{10} 值是在 1.96-2.71 之间，在前人研究结果的范围之内(Ryan, 1990; Ryan et al., 1995; Carey et al., 1997; Stockfors and Linder,

1998; Xu et al., 2000; Zha et al., 2004; Yang et al. 2012)。生长季的 Q_{10} 值的日变化规律是，最小 Q_{10} 值出现在午后 12:00-15:00。而且，白天的 Q_{10} 值（12:00 是 1.97 ± 0.17 ；15:00 为 1.96 ± 0.10 ）夜晚的 Q_{10} 值（00:00 是 2.60 ± 0.14 ；03:00 为 2.71 ± 0.25 ）具有显著差异性。其它时间段的 Q_{10} 值介于两者之间，与其它时间段的差异性不显著。

Q_{10} 最小值出现在午后（12:00-15:00），部分原因可能是由于树干呼吸对高温度的驯化。理论和实测数据都表明，全球变暖会导致植物（Tjoelker et al., 2001; King et al., 2006; Piao et al., 2010）和土壤呼吸速率（Davidson and Janssens 2006; Peng et al., 2009）的温度敏感性的降低。例如 Tjoelker 等（2001）报道，大气温度每升高 1°C ，叶呼吸的 Q_{10} 值会减小 0.04。的确，在本研究中，树干温度的最大值是在 12:00-15:00 之间。另一个抑制树干呼吸速率中午温度敏感度的原因可能是由于中午光合作用的午休造成的，特别是夏季当树干温度超过 30 度。观测数据和理论模型都表明中午的高温使叶片气孔关闭，在水分限制区域，光合作用受到抑制（Peters et al. 2003）。减小的气孔导度和光合速率的可能会进一步影响到树干呼吸速率，从而影响了树干呼吸速率对温度的敏感度。

近来很多研究表明，全球变暖具有不对称增温的特点，即全球夜间的增温速度大于白天（Alward et al. 1999; Gou et al. 2008; Peng et al. 2013）。这也会促使树干呼吸速率的温度敏感度白天比晚上低。全球变暖的不对称增温和 Q_{10} 值的日变化会导致树干呼吸速率在夜间比在白天的变化幅度更大。这与 Wan 等（2009）的多维控制实验相一致，即夜间增

温叶呼吸和根呼吸速率的增加明显大于白天增温。因此，我们的研究结果表明，在树干呼吸速率的预测中，要考虑树干呼吸速率的温度敏感度在白天和夜间的差异。

4.3 结论

（1）树干呼吸速率与树干温度的变化趋势相一致，具有显著的日变化规律。

（2）树干呼吸速率的 Q_{10} 值具有日变化规律，白天的 Q_{10} 值（12:00-15:00）显著的低于夜间的 Q_{10} 值（00:00-03:00）。

第5章 施氮对树干呼吸速率的影响

氮是植物需求量最大的矿物质元素（李新鹏和童依平，2007）。近几十年来，由于人类活动诸如人口增长、矿物燃料燃烧、含氮化肥的生产和使用、畜牧业的大规模发展等，向大气中排放的含氮化合物越来越多，导致大气氮沉降成比例增加（Wright and Rasmussen 1998）。并且，随着经济发展的全球化，氮沉降问题也呈现出全球化趋势。目前，我国已成为继欧、美之后的第三大氮沉降集中区之一(Mo et al. 2004)。从1961年至2000年，我国活性氮的排放从 $1.4 \times 10^7 \text{ t a}^{-1}$ 升至 $6.8 \times 10^7 \text{ t a}^{-1}$ ，预计在2030年将上升至 $1.05 \times 10^8 \text{ t a}^{-1}$ (Zhang et al. 2002)，而且，随着社会经济的进一步发展，氮沉降量可能会继续增加，预计2050年将会达到 195 Tg a^{-1} (Galloway et al. 2004)。不断加剧的全球氮沉降对森林生态系统碳循环和碳吸存产生了深刻的影响（王汝南等，2011）。树干呼吸是森林生态系统碳循环的一个重要组成部分。外加氮是模拟大气氮沉降的一种重要方法。Will 等（2006）发现施加氮肥使树干生物量增加，并提高了树干的氮含量。Maier (2001) 通过三年的施氮实验研究表明，施氮的10年生火炬松的树干氮含量和树干生长速率明显大于对照组。我国模拟大气氮沉降对陆地生态系统的研究开始于二十世纪九十年代(Liu et al., 2011)，但大部分研究集中于农田和草地生态系统。我国是世界上最大人工林种植基地，模拟大气氮沉降对我国人工林树干呼吸速率影响的研究，对预测森林生态碳平衡对全球变化响应的研究具有重要的意义。

5.1 驱动因子的确定

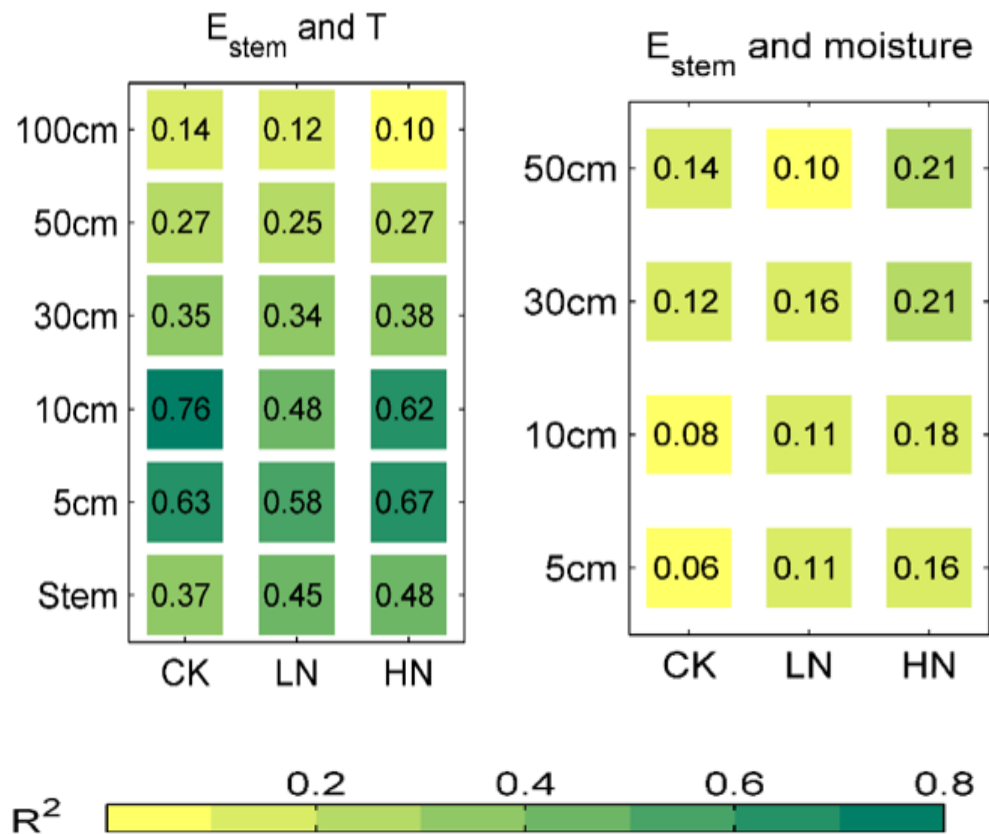


图 5.1 树干温度和不同深度的土壤温度和土壤含水量对树干呼吸速率变化的解释率

温度是影响树干呼吸速率的重要环境因素之一。树干温度可以解释约60-70%的不同树种树干呼吸的季节变化(Maier et al., 1998; Wieser and Bahn, 2004; Yang et al., 2011)。在本研究中，树干温度可解释37-48%树干呼吸速率的季节变化，而5cm土壤温度对树干呼吸速率变化的解释率为58-67%，10cm土壤温度对树干呼吸速率变化的解释率为48-76%（见图5.1）。Stahld等（2011）对热带森林进行研究，发现表层土壤含水量比树干温度能够更好的解释树干呼吸速率的季节变化。但在本研究中我们发现树干呼吸速率的季节变化与表层土壤含水量的相关性不显著小，而与

表层土壤温度相关性非常显著，且比树干温度能够更好的解释树干呼吸速率的季节变化（见图5.1）。可见，土壤温度与树干呼吸速率可能会具有很好的日变化和季节性变化规律。

5.2 树干呼吸速率的日变化

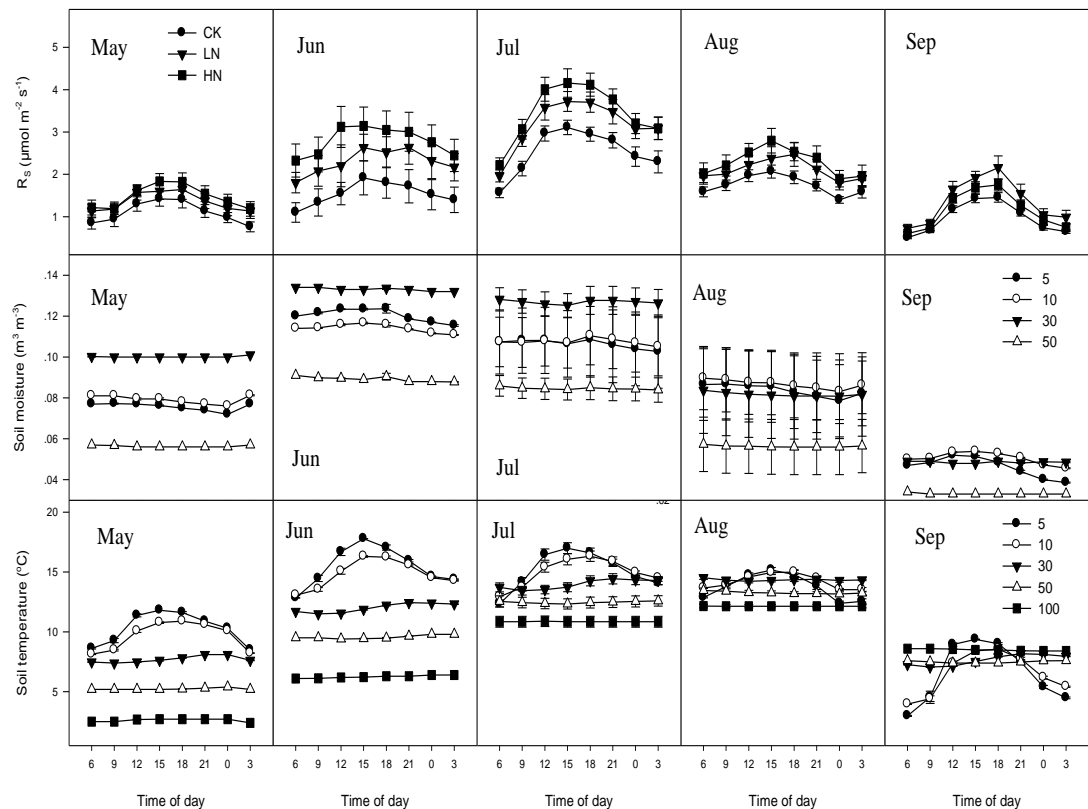


图5.2 不同月份树干呼吸速率、土壤含水量和土壤温度的日变化

图中，CK表示对照组，LN表示低氮组，HN表示高氮组。5，10，30，50和100分别表示土壤的深度。

如图5.2所示，生长季的树干呼吸速率的日变化均呈单峰型曲线，从早晨开始树干呼吸速率逐渐升高，到下午达到峰值，然后又逐渐减小。生长季内树干呼吸速率的日变化，具有相似的变化趋势在午后12:00 - 15:00左右达到峰值，凌晨3:00 - 6:00左右达到谷值。但每个月的变化幅度并不一致，六月份的变化范围最大 ($4.19 \mu\text{mol} \cdot \text{m}^{-2} \cdot \text{s}^{-1}$)，九月份的变化范

围最小 ($0.96\mu\text{mol}\cdot\text{m}^{-2}\cdot\text{s}^{-1}$)，研究发现，树干呼吸速率的变化范围的大小随着所测当天的大气温度的变化范围的大小而变化（如图3-3）。

不同树种树干呼吸速率的日变化规律相似，但出现最大呼吸速率的时间却有所不同如表 5.1。树干呼吸速率的日变化是否主要有环境因素所决定，尚还不确定。一些研究认为，树干呼吸速率的日变化主要由树干温度的变化所决定（Lavigne et al., 1996; Xu et al., 2000）。另一些研究表明，温度的不同不能完全解释树干呼吸速率的日变化（例如，Negisi, 1972;1978），形成层的活动和生物化学过程都会引起树干呼吸速率的变化。（Kozlowski and Pallardy, 1997; Thornley and Cannell, 2000）。他们认为，上午树干温度可能是树干呼吸速率的一个限制因素，到了下午，土壤和大气中的水分减少会使木质部中水分缺乏，因此，它们可能会与温度成为树干呼吸速率的共同限制因素。在本研究中，树干呼吸速率的变化与大气相对湿度的变化呈负相关。在树干呼吸速率较大时，大气相对湿度都很小，但其是否是树干呼吸的限制因素，还有待于进一步研究。

表 5.1 不同森林树干呼吸日变化规律

树种 Tree species	直径 Diameter(cm)	树龄 Tree age	测定时间	最大呼吸 出现时间	数据来源
杉木 <i>Cunninghamialanceolata</i>	-	20	0:00-24:00	12:00-16:00; 22:00-24:00	肖复明 等, 2005
兴安落叶松 <i>Larixgmelinii</i>	18-20	33	6:00-18:00	12:00,16:00	Wang et al., 2003
红松 <i>Pinuskoraiensis</i>	-		0:00-24:00	16:00-20:00	王淼等, 2005
美国枫香 <i>Liquidambar styraciflua</i>	-	14.3	0:00-24:00	15:00	Mcguire and Teskey, 2004
欧洲赤松 <i>Pinussyvestris</i>	-	50	0:00-24:00	16:00	Zha et

美国枫香 <i>Liquidambar styraciflua</i>	14.3	15	0:00-24:00	23:00	al., 2004 Edwards et al., 2002
马尾松 <i>Pinus massoniana</i> Lamb	25.7	28	0:00-24:00	15:00	Yang et al., 2011

5.3 树干呼吸速率的季节变化

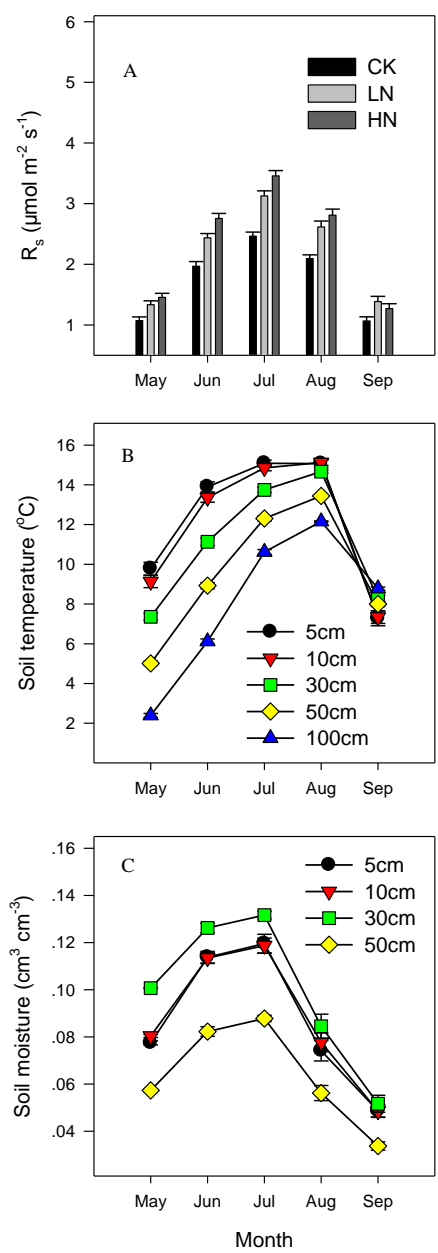


图 5.3 树干呼吸速率 (A)，不同深度的土壤温度 (B) 和土壤含水量 (C) 的季节变化

树干呼吸速率、土壤温度和土壤含水量具有显著的季节变化趋势。树干呼吸速率从五月（ $1.07\text{-}1.45\mu\text{mol m}^{-2} \text{s}^{-1}$ ）开始逐渐上升，到七月（ $2.46\text{-}3.46\mu\text{mol m}^{-2} \text{s}^{-1}$ ）达到最大值，然后呈逐渐下降趋势（九月为 $1.07\text{-}1.39\mu\text{mol m}^{-2} \text{s}^{-1}$ ）。土壤温度从五月开始逐渐上升到七八月份达到峰值，然后急剧下降。在五月-八月，土壤温度随着土壤深度的增加而逐渐减小，但在九月，各层土壤温度基本相同。土壤含水量也是从五月开始逐渐增加到七月达到最大值，然后开始迅速下降。在五月-七月，30cm 深度的土壤含水量最大，其次是表层（5-10cm），50cm 以下的土壤含水量较小。树干呼吸速率的变化趋势与土壤温度和含水量的变化趋势相似。但五月和九月树干呼吸速率基本相等，而五月的表层土

壤温度比九月约高2℃，五月的表层土壤含水量约是九月的两倍。可见，土壤温度和含水量并不是树干呼吸速率的完全决定因子。不同树种都有类似的季节变化（见表5.1）。美国田纳西州东部地区美国枫香的树干呼吸从4月开始增加，8、9月达到最大值，尔后逐渐降低，11月达到最低值（Edwards et al.，2002）。欧洲白桦（Matyssek et al.，2002）日本山毛榉（Gansert et al.，2002）的树干呼吸最小值出现在1、2月，之后随着温度的上升而增加，8月达到峰值，此后随着温度的降低而减少，至翌年1、2月达到最小值。

表5.2 不同森林类型的树干呼吸季节变化规律^[马玉娥等 2007]

树种 Tree species	直径 Diameter (cm)	树龄 Tree age	测定时间 Time of measurement	呼吸最大 约 Month of maximum respiration	呼吸最小 月 Month of minimum respiration	文献来源 Data sources
兴安落叶松 <i>Larix gmelinii</i>	16.4	31	5-10月 May-Oct	7	-	Jiang et al., 2003
兴安落叶松 <i>L. gmelinii</i>	10.2	17	5-10月 May-Oct	8	-	Jiang et al., 2003
兴安落叶松 <i>L. gmelinii</i>	18-20	33	1-12月 Jan-Dec	7	-	Wang et al., 2003
红松 <i>Pinus koraiensis</i>	25, 45, 65		5-9月 May-Sept	8	-	王淼等, 2005
杉木 <i>Cunninghamia lanceolata</i>	-	20, 17	1-12月 Jan-Dec	7	1	肖复明等, 2005
美国枫香 <i>Liquidambar styraciflua</i>	14.3	15	1-12月 Jan-Dec	7或8	1	Edwards et al., 2002
欧洲赤松 <i>Pinus sylvestris</i>	-	50	1-12月 Jan-Dec	7	-	Zha et al., 2004
欧洲山毛榉 <i>Fagus sylvatica</i>	-	25-35	4-11月 Apr-Nov	6或7	-	Ceschia et al., 2002
欧洲白桦 <i>Betula pendula</i>	-		6-10月 Jun-Oct	8	-	Matyssek et al., 2002
火炬松 <i>Pinus taeda</i>	10.92	12	1-12月 Jan-Dec	5	-	Maier et al., 2004

挪威云杉	-	14	5-9月	7	-	Janous et al., 2000
<i>Piceaabies</i>			May-Sept			
花旗松	-	60-112	4-12月	5	11	Pruyn et al.,
<i>Pseudotsugamenziesii</i>			Apr-Dec			2002
瑞士五针松	-	95	10-翌年12月	6	12	Wieser&Bahn,2004
<i>Pinuscembra</i>			Oct-next Dec			
美国红枫	40-75	21-52	2-10月	6	-	Edwards & Hanson
<i>Acer rubrum</i>			Feb-Oct			1995
白栎	40-75	20-65	2-10月	6或7	-	Edwards & Hanson
<i>Quercus alba</i>			Feb-Oct			1995
橡栎	40-75	21-62	2-10月	6或7	-	Edwards & Hanson
<i>Q. prinus</i>			Feb-Oct			1995
桦木	16,38,86	85	7-翌年11月	8	2	Cansert et al., 2002
<i>B.ermanii</i>						
日本山毛榉	50,75	130,140	7-翌年11月	8	2	Cansert et al., 2002
<i>F.crenata</i>						

5.4 外加氮对树干呼吸速率的影响

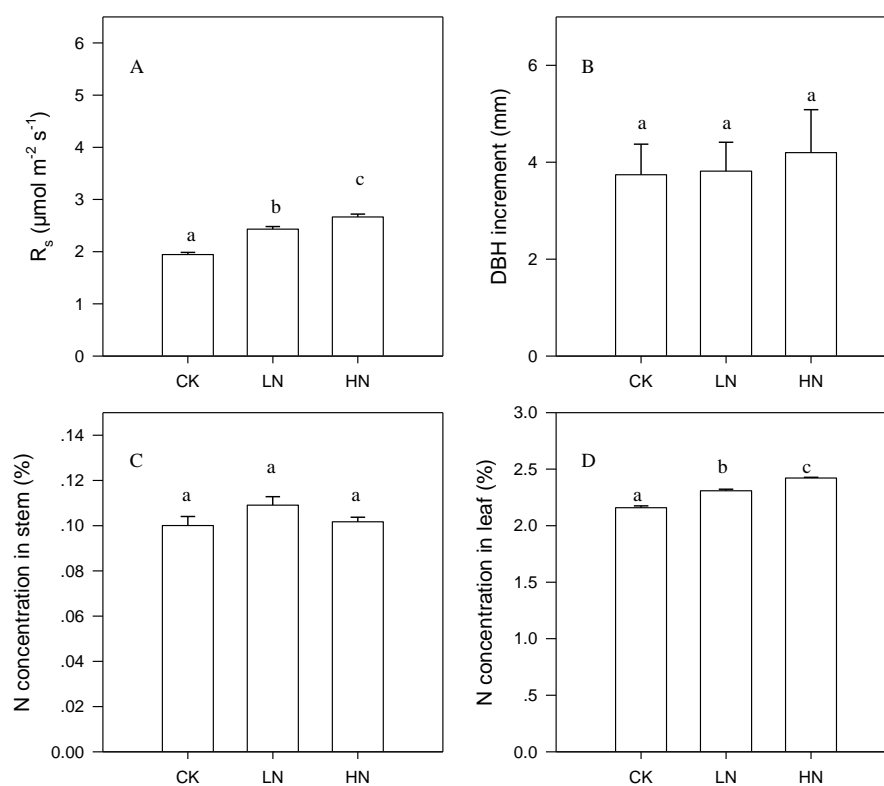


图5.4 不同施氮浓度的树干呼吸速率 (A)、胸径增长量 (B), 树干氮含量 (C) 和针叶氮含量 (D)

由图5.4可知，不同施氮浓度的树干呼吸速率具有显著的差异性 ($P<0.001$)，且随着施氮浓度的增加，树干呼吸速率逐渐增大。胸径生长量和树干氮含量在不同施氮处理，没有显著的差异性。但针叶的氮含量随着施氮浓度的增加而增大。针叶的氮含量以光合作用呈正相关，因此，氮含量较高的针叶，可能会提供较多的呼吸底物。

树干呼吸速率按照其结构功能不同可分为生长呼吸和维持呼吸。生长呼吸主要用于林木生长的能量消耗，而维持呼吸与树干的氮含量密切相关。本研究中树干呼吸随施氮浓度增加而增加，但反映生长呼吸的树干胸径生长量与反映维持呼吸的树干氮含量两个参数对施氮都没有显著响应，反而是反映提供呼吸底物的参数针叶氮含量出现相同趋势的变化。可见，在本研究中呼吸底物的供给对树干呼吸速率具有一定的影响。

5.5 结论

- (1) 树干呼吸速率具有显著的日变化和季节性变化规律。
- (2) 树干呼吸速率随着施氮浓度的增加而增加。
- (3) 外加氮对树干胸径生长量和树干氮含量影响不显著。
- (4) 针叶的氮含量随着施氮浓度的增加而增大。

第6章 结 论

(1) 对于不同林龄，不同树种，树干呼吸速率与树干温度的关系存在三种形式：指数、二次曲线和关系不显著。

(2) 树干呼吸速率的树干温度测定范围和树干呼吸酶的最适宜温度对树干呼吸速率与树干温度关系具有一定的影响。

(3) 不同树种，树干呼吸速率随林龄的变化趋势有所不同。白桦和樟子松的树干呼吸速率随林龄的增加而增大，华北落叶松的树干呼吸速率随林龄增加而减小。

(4) 白桦和樟子松的树干呼吸速率随着林龄的增加而增大，可能与树干边材面积的增长量密切相关。华北落叶松的树干呼吸速率随着林龄的增加而减小，可能是受控于树干温度和树干氮含量的变化。

(5) 树干呼吸速率的 Q_{10} 值具有日变化规律，白天的 Q_{10} 值（12:00-15:00）显著的低于夜间的 Q_{10} 值（00:00-03:00）。

(6) 华北落叶松的树干呼吸速率随着施氮浓度的增加而增加。树干胸径生长量和树干氮含量对施氮的响应不显著。针叶的氮含量随着施氮浓度的增加而增大。

参考文献:

1. Aber J D, McDowell W, Nadelhoffer K J, et al (1998). Nitrogen saturation in Northern forest ecosystems, hypotheses revisited. *Bioscience* **48**:921-934.
2. Acosta M, Brossaud J (2001) Stem and branch respiration in a Norway spruce forest stand. *Journal of Forest Science* **47**:136-140.
3. Acosta M, Pavelka M, Pokorný R, Janouš D, Marek M V (2008) Seasonal variation in CO₂ efflux of stems and branches of Norway spruce trees. *Annals of Botany* **101**:469-477.
4. Acosta M, Pokorný R, Janouš D, Marek MV (2010) Stem respiration of Norway spruce trees under elevated CO₂ concentration. *Biologia Plantarum* **54**:773-776.
5. Acosta M, Pavelka M, Tomášková I, Janous D, (2011) Branch CO₂ efflux in vertical profile of Norway spruce tree. *European Journal of Forest Research* **130(4)**:649-656.
6. Alward R D, Detling J K, Milchunas D G (1999) Grassland vegetation changes and nocturnal global warming. *Science* **283**: 229-231.
7. Amthor J S (1984) The role of the maintenance respiration in plant growth. *Plant cell Environment* **7**: 561-569.
8. Amthor J S (2000) The McCree–de Wit–Penning de Vries–Thornley respiration paradigms: 30 years later. *Ann Bot* **86**:1-20.
9. Apsimon H, Kruse M, Bell J N B (1987). Ammonia emissions and their role in acid deposition. *Atmos. Environ* **21**:1939-1946.
10. Amthor J S (1989). Respiration and crop productivity. Springer-Verlag New York, 215.
11. Azcon-bieto J, Lambers H, Day D A, (1983). Effect of Photosynthesis and Carbohydrate Status on Respiratory Rates and the Involvement of the Alternative Pathway in Leaf Respiration. *Plant Physiology* **72**:598-603.
12. Bartnick J, Alcamo J (1989) Caeculating nitrogen deposition in Europe. *Water Air Soil Pollut* **47**:101-123.
13. Bolstad P V, Davis K J, Martin J, et al. (2004) Component and whole-system respiration fluxes in northern deciduous forests. *Tree Physiol* **24**:493-504.
14. Boone R D, Nadelhoffer K J, Canary J D, (1998). Roots exert strong influence on the temperature sensitivity of soil respiration. *Nature* **396**, 570-572.
15. Bosc A, Grandcourt A D, Loustau D (2003) Variability of stem and branch maintenance respiration in a *Pinus pinaster* tree. *Tree Physiol* **23**:227-236.
16. Bowman W P, Barbour M M, Turnbull M H, et al. (2005) Sap flow rates and sapwood density are critical factors in within- and between-tree variation in CO₂ efflux from stems of mature *Dacrydium cupressinum* trees. *New Phytol* **167**:815-828
17. Bowman W P, Turnbull M H, Tissue D T, et al. (2008) Sapwood temperature gradients between lower stems and the crown do not influence estimates of stand-level stem CO₂ efflux. *Tree Physiol* **28**:1553-1559.
18. Brito P, Morales D, Wieser G, Jiménez M S (2010) Spatial and seasonal variations in stem CO₂ efflux of *Pinus canariensis* at their upper distribution limit. *Trees-Structure and Function* **24**:523-531.
19. Brito P, Soledad M, Morales D, Wieser G, (2013) Assessment of ecosystem CO₂ efflux and its components in a *Pinus canariensis* forest at the treeline. *Soil Biology and*

Biochemistry **35**:999-1009.

20. Carey E V, DeLucia E H, Ball J T (1996) Stem maintenance and construction respiration in *Pinus ponderosa* grown in different concentrations of atmospheric CO₂. *Tree Physiol* **16**:125-130.
21. Carey E V, Callaway RM, Delucia E H, (1997) Stem respiration of ponderosa pines grown in contrasting climates: implications for global climate change. *Oecologia* **111**: 19-25.
22. Cao B, Dang Q L, Yu X G, Zhang S R (2008) Effects of [CO₂] and nitrogen on morphological and biomass traits of white birch (*Betula papyrifera*) seedlings. *Forest Ecology and Management* **254**:217-224.
23. Catesson A M (1980). The vascular cambium. In: Little CHA ed. Control of Shoots Growth in Trees. International Union of Forestry Research Organisations Workshop Proceeding Mari , Forest Respiration Centre. Fredericton, NB, Canada. 12-40.
24. Cavaleri M A, Oberbauer S F, Ryan M G (2006) Wood CO₂ efflux in a primary tropical rain forest. *Global Change Biol* **12**:2442-2458.
25. Cavaleri M A, Oberbauer S F, Ryan M G, (2008) Foliar and ecosystem respiration in an old-growth tropical rain forest. *Plant Cell Environ* **31**:473-483.
26. Ceschia É, Damesin C, Lebaube S, Pontailier J Y, Dufrêne É (2002) Spatial and seasonal variations in stem respiration of beech trees (*Fagus sylvatica*). *Annals of Forest Science* **59**:801-812.
27. Cerasoli S, McGuire M A, Faria J, Mourato M, et al (2009) CO₂ efflux, CO₂ concentration and photosynthetic refixation in stems of *Eucalyptus globulus* (Labill.). *Journal of Experimental Botany* **60**:99-105.
28. Chambers J Q, Tribuzy E S, Toledo L C, et al. (2004) Respiration from a tropical forest ecosystem: partitioning of sources and low carbon use efficiency. *Ecol Appl* **14**:S72-S88.
29. Chen Q B, Shen L X. The role of pesticides and the importance of safety assessment[C]//Jiang Shu Ren. Proceedings of international symposium on pesticide and environmental safety. Beijing:China Agriculture University Press, 2003:83-91
30. Clinton B D, Maier C A, Ford C R, et al (2011) Transient changes in transpiration and stem and soil CO₂ efflux in longleaf pine (*Pinus palustris* Mill.) following fire-induced leaf area reduction. *Trees* **25**:997-1007.
31. Cox P M, Betts R A, Jones C D, et al (2000) Acceleration of global warming due to carbon-cycle feedbacks in a coupled climate model. *Nature* **408**: 184-187.
32. Davidson E A, Janssens I A, (2006) Temperature sensitivity of soil carbon decomposition and feedbacks to climate change. *Nature* **440**:165-173.
33. Davidson E A, Janssens I A, Luo Y Q , (2006) On the variability of respiration in terrestrial ecosystems: moving beyond Q₁₀. *Global Change Biology* **12**:154-164.
34. Damesin C, Ceschia E, Le Goff N, et al (2002) Stem and branch respiration of beech: from tree measurements to estimations at the stand level. *New Phytol* **153**:159-172.
35. Dhakhwa G B, Campbell C L (1998) Potential effects of differential day-night warming in global climate change on crop production. *Climate Change* **40**: 647-667.
36. Dixon R K, Brown S, Houghton R A, et al. (1994) Carbon pools and flux of global forest ecosystem. *Science* **263**:185-190.

37. Edwards N T, Hanson P J (1996) Stem respiration in a closed-canopy upland oak forest. *Tree Physiology* **16**:433-439.
38. Edwards N T, Tsehaplinski T J, Norby R J (2002). Stem respiration increases in CO₂-enriched sweetgum trees. *New Phytologist* **155**:239-248.
39. Edoardo D, Amilcare P, Ignacio R, (2004) Coupled Dynamics of Photosynthesis, Transpiration, and Soil Water Balance. Part I: Upscaling from Hourly to Daily Level. *Journal of Hydrometeorology* **5**: 546-558.
40. Fang J Y, Chen A P, Peng C H, et al (2001). Changes in forest biomass carbon storage in China between 1949 and 1998. *Science* **292**: 2320-2322.
41. Friedlingstein P, Cox P, Betts R, (2006) Climate-Carbon Cycle Feedback Analysis: Results from the C4 MIP Model Intercomparison. *Journal of Climate* **19**:3337-3353.
42. Gamert D, Baekes K, Yodaitaka K (2002). Seasonal variation of branch respiration of a treeline forming deciduous broad-leaved tree species on Mt. Fuji, Japan. *Flora* **197**:186-202.
43. Galloway JN, Dentener FJ, Capone DG, et al. Nitrogen cycles: past, present and future[J]. *Biogeochemistry*, 2004, 70, 153-226.
44. Gifford R M. (2003) Plant respiration in productivity models: Conceptualization, representation and issues for global terrestrial carbon-cycle research. *Funct. Plant Biol* **30**:171-186
- Griffin K L, Turnbull M, Murthy R (2002) Canopy position affects the temperature response of leaf respiration in *Populus deltoids*. *New Phytol* **32**: 609-619.
45. Gruber A, Wieser G, Oberhuber W (2009) Intra-annual dynamics of stem CO₂ efflux in relation to cambial activity and xylem development in *Pinus cembra*. *Tree Physiology* **29**:641-649.
46. Gou X H, Chen F H, Yang M X, et al (2008) Asymmetric variability between maximum and minimum temperature in Northeastern Tibetan Plateau: Evidence from tree rings. *Science in China Series D: Earth Sciences* **51**: 41-55.
47. Hölttä T, Kolari P (2009) Interpretation of stem CO₂ efflux measurements. *Tree Physiology* **29**:1447-1456.
48. Houghton R A (1993). Is carbon accumulating in the northern temperate zones, *Global Biogeochemical Cycle* **7**(3):611-617.
49. Höger P, Fan H B, Quist M, et al (2006). Tree growth and soil acidification in response to 30 years of experimental nitrogen loading on boreal forest. *Global Change Biology* **12**:489-499.
50. Ingestad T, Aronsson A, Agren G I (1981) Nutrient flux density model of mineral nutrition in conifer ecosystems. *Studia Frestalia Suecica* **160**:61-71.
51. IPCC, 2007. Climate Change 2007: The Physical Sciences Basis: Contribution of Working Group I to the Fourth Assessment Report of the Intergovernmental Panel on Climate Change. Cambridge University Press.
52. IPCC. IPCC Climate Change 2007: Mitigation of Climate Change. Working Group III Contribution to the Fourth Assessment Report of the IPCC 2007. UK: Cambridge University Press.
53. Janssens I A, Kim P, (2003) Large seasonal changes in Q₁₀ of soil respiration in a beech. *Global Change Biology* **9**: 911-918.

54. Jiang L F, Shi F C, Zu Y G, Wang wJ, Koike T (2003). Study on stem respiration of *Larix gmelinii* of different ages and its relationship to environmental factors. *Bulletin of Botanical Research* **23**: 296-301.
55. Kim M H, Nakane K, Lee J T, et al (2007) Stem/branch maintenance respiration of Japanese red pine stand. *Forest Ecology Management* **243**:283-290.
56. King A W, Gunderson C A, Post W M, et al (2006) Atmosphere: Plant respiration in a warmer world. *Science* **312**:536-537.
57. Kinerson R S (1975) Relationships between plant surface area and respiration in loblolly pine. *J. Appl. Ecol* **12**:965-971.
58. Kuptz D, Matyssek R, Granms T E E (2011) Seasonal dynamics in the stable carbon isotope composition ($\delta^{13}\text{C}$) from non-leafy branch, trunk and coarse root CO_2 efflux of adult deciduous (*Fagus sylvatica*) and evergreen (*Picea abies*) trees. *Plant, Cell and Environment* **34**:363-373.
59. Kozlowski T T, Pallardy S G. (1997) Physiology of woody plants (2ed). New York: Academic Press, 411P.
60. Kozlowski T T (1992) The physiological ecology of forest stands. In (W.J. Nierenberg, ed.) Encyclopedia of Environmental Biology, Vol.3, pp. 81-91. Academic Press, San Diego.
61. Landsberg J J (1986). Physiological Ecology of Forest Production. Academic Press, New York.
62. Lavigne M B, Franklin S E, Hunt E R Jr. (1996) Estimating stem maintenance respiration rates of dissimilar balsam fir stands. *Tree Physiology* **3**: 225-233.
63. Lavigne M B, Franklin S E, Hunt E R (1996) Estimating stem maintenance respiration rates of dissimilar balsam fir stands. *Tree Physiol* **16**:687-695.
64. Lavigne M B (1996) Comparing stem respiration and growth of jack pine provenances from northern and southern locations. *Tree Physiology* **16**:847-852.
65. Lavigne M B, Ryan M G (1997) Growth and maintenance respiration rates of aspen, black spruce and jack pine stem at northern and southern BOREAS sites. *Tree Physiology* **17**:543-551.
66. Lavigne M B, Little C H A, Riding R T (2004) Changes in stem respiration rate during cambial reactivation can be used to refine estimates of growth and maintenance respiration. *New Phytologist* **162**:81-93.
67. Lee S H, Chung G C, (2005) Sensitivity of root system to low temperature appears to be associated with the root hydraulic properties through aquaporin activity, *Sci. Hortic* **105**:1-11.
68. Levy P E, Jarvis P G, (1998) Stem CO_2 fluxes in two Sahelian shrub species (*Guiera senegalensis* and *Combretum micranthum*). *Functional Ecology* **12**: 107-116.
69. Liberloo M, De Angelis P, Ceulemans R (2008) Stem CO_2 efflux of a *Populus nigra* stand: effects of elevated CO_2 , fertilization, and shoot size. *Biologia Plantarum* **52**:299-306.
70. Ma Y C, Piao S L, Sun Z Z, (2013). Stand ages regulate the response of soil respiration to temperature in a *Larix principis-rupprechtii* plantation. Agricultural and Forest Meteorology. In press.
71. Ma Y C, Zhu B, Sun Z Z, et al (2013) The effects of simulated nitrogen deposition on

- extracellular enzyme activities of litter and soil among different-aged stands of larch. *J Plant Ecol* doi:10.1093/jpe/rtt028.
72. Magill A H, Aber J D, Hendricks J J, et al (1997). Biogeochemical response of forest ecosystems to simulated chronic nitrogen deposition. *Ecol Appl* **7**(2): 402-415.
 73. Maier C A, Johnsen K H, Clinton B D, et al (2010) Relationships between stem CO₂ efflux, substrate supply, and growth in young loblolly pine trees. *New Phytol* **185**:502-513.
 74. Maier C A, Zarnoch S J, Dougherty P M (1998) Effects of temperature and tissue nitrogen on dormant season stem and branch maintenance respiration in a young loblolly pine (*Pinus taeda*) plantation. *Tree Physiol* **18**:11-20
 - Maseyk K, Grunzweig J M, Rotenmerg E (2008) Respiration acclimation contributes to high carbon-use efficiency in a seasonally dry pine forest. *Global Change Biology* **14**: 1553-1567.
 75. Martin T A, Teskey R O, Dougherty P M (1994) Movement of respiratory CO₂ in stems of loblolly pine (*Pinus taeda*) seedlings. *Tree Physiol* **14**:481-495.
 76. Maier C A, Clinton B D (2006) Relationship between stem CO₂ efflux, stem sap velocity and xylem CO₂ concentration in young loblolly pine trees. *Plant, Cell and Environment* **29**:1471-1483.
 77. Maier C A 2001. Stem growth and respiration in loblolly pine plantations differing in soil resource availability. *Tree Physiol* **21**: 1183-1193.
 78. Maunoury F, Berveiller D, Lelarge C, et al (2007) Seasonal, daily and diurnal variations in the stable carbon isotope composition of carbon dioxide respired by tree trunks in a deciduous oak forest. *Oecologia* **151**:268-279.
 79. McGuire M A, Teskey R O, (2004) Estimating stem respiration in trees by a mass balance approach that accounts for internal and external fluxes of CO₂. *Tree Physiology* **24**: 571-578.
 80. McGuire M A, Cerasoli S, Teskey R O (2007) CO₂ fluxes and respiration of branch segments of sycamore (*Platanus occidentalis* L.) examined at different sap velocities, branch diameters, and temperatures. *Journal of Experimental Botany* **58**:2159-2168.
 81. McMurtrie R E, Rook D A, Kelliher F M (1990) Modelling the yield of *Pinus radiata* on a site limited by water and nitrogen. *Forest Ecology and Management* **30**:381-413.
 82. Maier C A, Albaugh T J, Allen H L, (2004). Respiratory Carbon use and carbon storage in mid-rotation loblolly pine (*Pinus taeda* L.) plantation: the effect of site resources on the stand carbon balance. *Global Change Biology* **10**: 1335-1350.
 83. Matyssek R, Gunthardt-Goerg M S, Maurer S, Christ R (2002). Tissue structure and respiration of stems of *Betula pendula* under contrasting ozone exposure and nutrition. *Trees* **16**:375-385.
 84. Melillo J M, McGuire A D, Kicklighter D W, et al (1993) Global climate change and terrestrial net primary production. *Nature* **363**:234-240.
 85. Mo J M, Xue J H, Fang Y T (2004) Litter decomposition and its responses to simulated N deposition for the major plants of Dinghushan forests in subtropical China *Acta Ecologica Sinica*, **24** (7): 1413-1420.
 86. Moore D J, Gonzalez-Meler M A, Taneva L, et al (2008) The effect of carbon dioxide enrichment on apparent stem respiration from *Pinus taeda* L. is confounded by high levels of soil carbon dioxide. *Oecologia* **158**:1-10.

87. Moraes J L. (1995) Carbon stocks of the brazilian amazonbasin. *Soil Science Society of America Journal* **59**(1): 244-247.
88. Nakaji T, M Fukami, Y Dokiya, et al (2001) Effects of high nitrogen load on growth,photosynthesis and nutritrient status of Cryptomeria japonica and Pinus densiflora seedlings. *Trees* **15**:453-461.
89. Nakaji T,Takenaga S, Kuroha M, et al (2002) Photosynthetic response of Pinus densiflora seedlings to high nitrogen load. *Enviornmental Science* **9**(4):269-282.
90. Negisi K. (1972) Diurnal fluctuation of CO₂ release from the bark of a standing Magnolia obovata tree. *J Jap For Soc* **54**: 257-263.
91. Negisi K. (1978) Daytime depression in bark respiration and radial shrinkage in stem of a standing young Pinus densiflora tree. *J Jap For Soc* **60**: 380-382.
92. Paembonan S A, Hagihara A, Hozumi K (1991) Long-term measurement of CO₂ release from the aboveground parts of a hinoki forest tree in relation to air temperature. *Tree Physiol* **8**:399-405.
93. Pan Y D, Birdsey R A, Fang J Y, et al (2011) A large and persistent carbon sink in the world's forests. *Science* **333**:988-993.
94. Piao S L, Fang J Y, Ciais P, (2009) The carbon balance of terrestrial ecosystems in China. *Nature* **458**:1009-1013.
95. Piao S L, Luyssaert S, Ciais P, et al (2010) Forest annual carbon cost: a global-scale analysis of autotrophic respiration. *Ecology* **91**:652-661.
96. Poorter H, Niklas K J, Reich P B, et al. (2012) Tansley review: Biomass allocation to leaves, stems and roots: meta-analyses of interspecific variation and environmental control. *New Phytol* **193**:30-50.
97. Peng S S, Piao S L, Ciais P, et al (2013) Asymmetric effects of daytime and night-time warming on Northern Hemisphere vegetation. *Nature* **501**: 88-94.
98. Peng S S, Piao S L, Wang T, et al (2009) Temperature sensitivity of soil respiration in different ecosystems in China. *Soil Biology and Biochemistry* **41**: 1008-1014.
99. Penning de Vries F W T, Brunsting A H M, van Laar H H, (1974) Products, requirements and efficiency of biosynthesis: a quantitative approach. *Journal of Theoretical Biology* **45**: 339-377.
100. Peters J, Morales D, Jimenez M S, (2003) Gas exchange characteristics of Pinus canariensis needles in a forest stand on Tenerife, Canary Islands. *Trees* **17**: 492-500.
101. Post W M. (1982) Carbon pools and word life zones. *Nature* **298**(8):156-159.
102. Pruyn M L, Garmer B L, Harmon M E (2002). Within-stem variation of respiration in Pseudotsuga menzesii(Douglas-fir)trees. *New Phytologist* **154**:359-372.
103. Pruyn M L, Harmon M E, Gartner B L (2003) Stem respiratory potential in six softwood and four hardwood tree species in the central cascades of Oregon. *Oecologia* **137**:10-21.
104. Reay D S, Dentener F, Smith P, et al (2008) Global nitrogen deposition and carbon sinks. *Nature Geoscience* **1**: 430-437.
105. Reich P B, Tjoelker M G, Machado J L, et al.(2006) Universal scaling of respiratory metabolism, size and nitrogen in plants. *Nature* **439**: 457-461.
106. Reich P B, Tjoelker M G, Pregitzer K G, et al. (2008) Scaling of respiration to nitrogen in leaves, stems and roots of higher land plants. *Ecol Lett* **11**:793-801.

107. Rodhe H, Rood M J (1986) Temporal evolution of nitrogen compounds in Swedish precipitation since 1955. *Nature* **321**: 762-764.
108. Rosenzweig C, Tubiello F N (1996) Effects of changes in minimum and maximum temperature on wheat yields in the central US—a simulation study. *Agricultural and Forest Meteorology* **80**: 215-230.
109. Robertson A L, Malhi Y, Farfan-Amezquita F, et al. (2010) Stem respiration in tropical forests along an elevation gradient in the Amazon and Andes. *Global Change Biol* **16**:3193-3204.
110. Ryan M G (1988). Growth and maintenance respiration in stems of *Pinus contorta* and *Picea engelmannii*. *Canadian Journal of Forest Research* **20**:48-57.
111. Ryan M G (1991) Effect of climate change on plant respiration. *Ecologica Applications* **1**:157-167.
112. Ryan M G, Linder S, Vose J M, Hubbard R M (1994) Dark respiration of pines. *Ecological Bulletins* **43**:50-63.
113. Ryan M G, Hubbard R M, Clark D A et al (1994). Woody-Tissue Respiration for *Simarouba amara* and *Minquartia guianensis*, Two Tropical Wet Forest Trees with Different Growth Habits. *Oecologia* **100**: 213-220.
114. Ryan M G, Gower S T, Hubbard R M, et al. (1995) Woody tissue maintenance respiration of four conifers in contrasting climates. *Oecologia* **101**:133-140.
115. Ryan M G, Hubbard R M, Pongracic S, et al (1996) Foliage, fine-root, woody-tissue and stand respiration in *Pinus radiata* in relation to nutrient status. *Tree Physiology* **16**:333-343.
116. Ryan M G, Cavaleri M A, Almeida A C, et al (2009) Wood CO₂ efflux and foliar respiration for *Eucalyptus* in Hawaii and Brazil. *Tree Physiology* **29**:1213-1222.
117. Saveyn A, Steppe K, Lemeur R (2007) Drought and the diurnal patterns of stem CO₂ efflux and xylem CO₂ concentration in young oak (*Quercus robur*). *Tree Physiol* **27**:365–374.
118. Saveyn A, Steppe K, Lemeur R (2008) Report on non-temperature related variations in CO₂ efflux rates from young tree stems in the dormant season. *Trees* **22**:165-174.
119. Saveyn A, Steppe K, McGuire M A, et al. (2008) Stem respiration and carbon dioxide efflux of young *Populus deltoids* trees in relation to temperature and xylem carbon dioxide concentration. *Oecologia* **154**:637-649.
120. Schindler D W, Bailey S E (1993). The biosphere as an increasing sink for atmospheric carbon: estimates from increased nitrogen deposition. *Global Biogeochemical Cycles* **7**(4): 717-733.
121. Schimel D S (1995) Terrestrial ecosystems and the carbon cycle. *Glob Change Biology* **1**: 77-91.
122. Schimel D S, Melillo J, Tian H, et al (2000) Contribution of increasing CO₂ and climate to carbon storage by ecosystems in the United States. *Science* **287**(5460): 2004-2006.
123. Sedjo R A (1993) The Carbon cycle and global forest ecosystem. *Water, Air and Soil Pollution* **70**(1-4):295-307.
124. Skeffington R A, Wilson E J (1988) Excess nitrogen deposition: Issues for

- consideration. *Environ . Pollut.* **54**: 159-184.
125. Sprugel D G and Benecke U (1991). Measuring woody-tissue respiration and photosynthesis. In *Techniques and Approaches in Forest Tree Ecophysiology*(J.P. Lassoie and T.M.Hinckley, eds.),pp.329-355.CRC Press, Boca Raton, Florida.
 126. Stahl C, Burban B, Goret JY, Bona D (2011)Seasonal variations in stem CO₂ efflux in the Neotropicalrainforest of French Guiana. *Annals of Forest Science* **68**:771-782.
 127. Stockfors J A N, Linder S, (1998) Effect of nitrogen on the seasonal course of growth and maintenance respiration in stems of Norway spruce trees. *Tree Physiology* **18**: 155-166.
 128. Tans P, White J W C(2000). In balance, with a little help from the plants. *Science*, 1998, 281 (5374): 183184. Stockfors, J., Temperature variations and distribution of living cells within tree stems: implications for stem respiration modeling and scale-up. *Tree Physiology* **20**:1057-1062.
 129. Teskey R O, McGuire M A (2002) Carbon dioxide transport in xylem causes errors in estimation of rates of respiration in stems and branches of trees. *Plant, Cell and Environment* **25**:1571-1577.
 130. Teskey R O, McGuire M A (2007) Measurement of stem respiration of sycamore (*Platanus occidentalis* L.) trees involves internal and external fluxes of CO₂ and possible transport of CO₂ from roots. *Plant, Cell and Environment* **30**:570-579.
 131. Teskey RO, Saveyn A, Steppe K, et al. (2008) Tansley review: Origin, fate and significance of CO₂ in tree stems. *New Phytol* **177**:17-32.
 132. Thornley J H M, Cannell M G R (2000) Modelling the components of plant respiration: representation and realism. *Annals of Botany* **85**:55-67.
 133. Tissue D T, Lewis J D, Wullscheleger S D, et al (2002). Leaf respiration at different canopy positions in sweetgum (*Liquidambar styraciflua*) grown in ambient and elevated concentrations of carbon dioxide in the field. *Tree Physiol.* **22**:1157-1166.
 134. Tjoelker M G, Oleksyn J, Reich P B (2001) Modelling respiration of vegetation: evidence for a general temperature-dependent Q₁₀. *Global Change Biology* **7**: 223-230.
 135. Urennfeldt Y. Hultberg H (1986). Effect of nitrogen deposition on the acidification of terrestrial and aquatic ecosystems. *Water Air Soil Pollution* **30**:945-963.
 136. Vose J M, Ryan M G (2002) Seasonal respiration of foliage, fine roots and woody tissues in relation to growth, tissue N, and photosynthesis. *Global Change Biol* **8**:182-93.
 137. Wan S Q, Xia J Y, Liu W X, Niu S L (2009) Photosynthetic overcompensation under nocturnal warming enhances grassland carbon sequestration. *Ecology* **90**: 2700-2710.
 138. Wang W J, Yang F J, Zu Y G, et al (2003). Stem respiration of a larch (*Larix gmelini*) plantation in Northeast China. *Acta Botanica Sinica* **45**:1387-1397.
 139. Wang M, Wu Y X, Wu J L (2008) Stem respiration of dominant tree species in broad-leaved Korean pine mixed forest in Changbai Mountains. *Chinese J Appl Ecol* **19**:956-960.
 140. Wang M, Guan D X, Han S J, Wu J L (2010) Comparison of eddy covariance and

- chamber-based methods for measuring CO₂ flux in a temperate mixed forest. *Tree Physiology* **30**:149-163.
141. Wang W, Zeng W J, Chen W L, et al (2013) Soil respiration and organic carbon dynamics with grassland conversions to woodlands in temperate China. *PLoS One* **8**:e71986. doi:10.1371/journal.pone.0071986
 142. Wertin T M, Teskey R O (2008) Close coupling of whole-plant respiration to net photosynthesis and carbohydrates. *Tree Physiol* **28**:1831–1840.
 143. Wieser G, Bahn M (2004) Seasonal and spatial variation of woody tissue respiration in a *Pinus cembra* tree at the alpine timberline in the central Austrian Alps. *Trees-Structure and Function* **18**:576-580.
 144. Wittmann C, Pfanz H (2007) Temperature dependency of bark photosynthesis in beech (*Fagus sylvatica* L.) and birch (*Betula pendula* Roth.) trees. *Journal of Experimental Botany* **58**:4293-4306.
 145. Wright R F, Roelofs J G M, Bredemeier M, et al (1995) NITREX: responses of coniferous forest ecosystems to experimentally changed deposition of nitrogen. *Forest Ecology and Management* **71**:163-169.
 146. Wright R F, Rasmussen L (1998). Introduction to the NITREX and EXMAN projects. *Forest Ecology and Management* **101**: 1-7.
 147. Xu C Y, Turnbull M H, Tissue D T, et al. (2012) Age-related decline of stand biomass accumulation is primarily due to mortality and not to reduction in NPP associated with individual Tree Physiol, tree growth or stand structure in a *Quercus*-dominated forest. *J Ecol* **100**:428–440.
 148. Xu M, DeBiase T A, Qi Y (2000) A simple technique to measure stem respiration using a horizontally oriented soil chamber. *Can J Forest Res* **30**: 1555-1560.
 149. Yang J Y, Teskey R O, Wang C K (2012) Stem CO₂ efflux of ten species in temperate forests in Northeastern China. *Trees* **26**:1225-1235.
 150. Yang Q P, Xu M, Chi Y G, et al. (2012) Temporal and spatial variations of stem CO₂ efflux of three species in subtropical China. *J Plant Ecol* **5**:229-237.
 151. Yang Q P, Xu M, Chi Y G, (2011) Temporal and spatial variations of stem CO₂ efflux of three species in subtropical China. *Journal of Plant Ecology* **23**:1-9.
 152. Zach A, Horna V, Leuschner C (2010) Diverging temperature response of tree stem CO₂ release under dry and wet season condition in tropical montane moist forest. *Trees* **24**:285-296.
 153. Zha T S, Kellomäki S, Wang KY (2003) Seasonal variation in respiration of 1-year-old shoots of Scots pine exposed to elevated carbon dioxide and temperature for 4 years. *Ann Bot* **92**:89-96.
 154. Zha T S, Wang K Y, Ryyppö A, et al (2002) Needle dark respiration in relation to within-crown position in Scots pine trees grown in long-term elevation of CO₂ concentration and temperature. *New Phytol* **156**:33-41.
 155. Zha T, Kellomäki S, Wang KY, Ryyppö A, Niinistö S (2004) Seasonal and annual stem respiration of Scots pine trees under boreal conditions. *Annals of Botany* **94**:889-896.
 156. Zheng X, Fu C, Xu X, et al (2002) The Asian nitrogen case study. *Ambio* **31**:79-87.

157. Zhu L W, Zhao P, Ni G Y, et al (2012) Individual- and stand-level stem CO₂ efflux in a subtropical *Schima superba* plantation. *Biogeosciences* **9**:3729-3737.
158. 方精云, 陈安平 (2001)。中国森林植被碳库的动态变化及其意义. *植物学报*, **43** (9) : 967-973.
159. 方运霆, 莫江明, 周国逸, 薛璟花 (2005), 鼎湖山主要森林类型植物胸径生长队氮沉降增加的初期响应. *热带亚热带植物学报* **13** (3) : 198-204.
160. 樊后保 (2002) 酸雨与森林衰退关系研究综述. *福建林学院学报* **23**(1): 88-92.
161. 李德军, 莫江明, 方运霆, 彭少麟 (2003). 氮沉降对森林植物的影响. *生态学报*, **23** (9) : 1891-1900.
162. 刘世荣 (1992). 兴安落叶松人工林生态系统营养元素生物地球化学循环特征. *生态学杂志* **11**: 1-6.
163. 鲁显楷, 莫江明, 董少峰 (2008) 氮沉降对森林生物多样性的影响. *生态学报* **28**: 5532-5548.
164. 马玉娥, 项文化, 雷丕锋 (2007). 林木树干呼吸变化及其影响因素研究进展. *植物生态学报* **31**(3): 403-412
165. 陶波, 葛全胜, 李克让, (2001). 陆地生态系统碳循环研究进展. *地理研究* **20**(5): 564-574.
166. 伍光和, 田连恕, 胡双熙, 等, 自然地理学 (第三版). 北京: 高等教育出版社, 2000
167. 肖复明, 汪思龙, 杜天真, (2005). 湖南会同林区杉木人工林呼吸量测定, *生态学报* **25**(10): 141-145
168. 张维娜, 廖周瑜 (2009) 氮沉降增加对森林植物影响的研究进展, *环境科学导刊*, **28** (3) : 21-24.
169. 严玉平, 沙丽清, 曹敏 (2008), 西双版纳热带季节雨林优势树种树干呼吸特征. *植物生态学报* **32**(1): 231-236.
170. 杨金艳, 杨阔, 王传宽(2009) 生物环境因子对树干呼吸时空变异的影响. *应用与环境生物学报* **15**: 880-887.
171. 周国逸, 闫俊华 (2001). 鼎湖区域大气降水特征和物质元素输入对森林生态系统存在和发育的影响. *生态学报* **21**(12): 2002-2012.
172. 王淼, 姬兰柱, 李秋荣, (2005). 长白山地区红松树干呼吸的研究[J]. *应用生态学报* **16**(1): 7-13.
173. 王汝南, 蔺兆兰, 王春梅 (2011). 氮沉降对森林土壤碳收支机制的影响. *生态环境学报* **20**(3): 576-582.

致 谢

本论文是在国家自然科学基金（41040008）“塞罕坝地区华北落叶松（*Larix principis-rupprechtii*）人工林碳循环对模拟氮沉降的响应”项目的资助下完成的，非常感谢国家自然科学基金委的资助。

近四年来，朴世龙老师渊博的知识、开阔的视野、对科学一丝不苟的严谨作风，宽厚、诚恳待人的品格和对学生的关怀深深地影响着我。朴老师不仅教会了我更多的知识，而且教会了我应该如何做人！他的一言一行时刻影响着我，使我终身难忘，他的品行也将影响我的一生。

两年来，一直在坝上进行野外实验，非常感谢赛罕坝机械林场为我们提供的样地和北京大学生态实验站为我们实验顺利进行所提供的条件及在坝上李大爷和郑成洋老师给予我的帮助！也非常感谢在野外实验工作中给予我很大帮助的马月存、孙振中、赵闯、赵淼，孙凯、胡国铮、徐晓天、马承恩、陈伟乐、王嘉慧、曾文静和张馨月等同学！特别感谢馨月在实验方面给予我的特别帮助！

在野外的意外受伤，让我感受到了生命的脆弱，也感受到了集体的温暖。非常感谢大家对我的帮助！非常感谢我们党支部崔海亭、王妮、刘鸿雁、金冬梅和徐敏云老师给予我经济上的捐助！感谢学院和学校博管办给予我经济上的捐助！因为此事，也为杨荣祥、李珊、刘鸿雁，徐岩、朴世龙、王华老师和学校的人事处，工伤科和财务处等部门带来了很多的额外的工作，在此我深表歉意，同时，也非常感谢

各位老师为我所做的一切！我会永远深记各位老师的帮助！谢谢大家！

感谢在校内的学习生活中，崔海亭、方精云、王妮、刘鸿雁、郭大立、沈泽昊、吉成均、贺金生、唐志尧、朱江玲、沈海花、赵雪梅和于凤等各位老师的帮助！特别感谢我的导师朴世龙老师在各个方面给予我的大力帮助！感谢赵淼、赵红芳、李溪然、杨慧、李跃、丛楠、梁爽、南慧娟、林欣、彭书时、王旭辉、曾振中、谷玉兵、彭立新、殷国栋、刘晔、印轶、赵峰君、吴秀臣、孙振中、赵闯、张原、谭建光、孙岩、黄萌甜、宋宏权和赵志强等同学的帮助！特别感谢和我在一个房间工作的宋宏权和赵志强！让我们的房间充满了和谐和生机！同时也非常感谢北京大学的老师和同学为我们创建的良好学习和生活环境！

特别感谢我的家人对我学习的理解和大力支持，使我能够全心投入学习，顺利完成学业！同时，在报告撰写过程中引用了很多专家、学者的研究成果，在此一并表示感谢！

发表文章:

1. **Yan Yang**, Miao Zhao, Zhenzhong Sun, Shilong Piao. Diurnal and seasonal change in stem respiration of *Larix principis-rupprechtii* trees, northern China, *PloS one*, 2014, (Accepted)(SCI-2 区, IF: 4.411).
2. **Yan Yang**, Biao Zhu, Miao Zhao, Guodong Yin, Xiran Li. Stem CO₂ efflux of three species in relation to stem temperature and tree size in North China. *Journal of Plant Ecology (UK)*, 2014, (Under review).
3. **Yan Yang**, Biao Zhu, Miao Zhao, Guodong Yin, Xiran Li. Nitrogen effects on stem respiration of larch plantation in north China. *Agricultural and Forest Meteorology*, 2014, (Under review, SCI-1 区, IF: 3.228)
4. Anwar Mohammat, Xuhui Wang, Xiangtao Xu, Liqing Peng, **Yan Yang**, Xinping Zhang, Ranga B. Myneni, Shilong Piao. Drought and spring cooling induced recent decrease in vegetation growth in Inner Asia. *Agricultural and Forest Meteorology*, 2013, 178-179: 21-30. (SCI-1 区, IF: 3.228)
5. Yuecun Ma, Biao Zhu, Zhenzhong Sun, Chuang Zhao, **Yan Yang**, Shilong Piao. The effects of simulated nitrogen deposition on extracellular enzyme activities of litter and soil among different-aged stands of larch. *Journal of Plant Ecology*, 2013, 4:1-10.
6. Yuecun Ma , Shilong Piao, Zhenzhong Sun, Xin Lin, Tao Wang, Chao Yue, **Yan Yang**. Stand ages regulate the response of soil respiration to temperature in a *Larix principis-rupprechtii* plantation. *Agricultural and Forest Meteorology*, 2014, 184:179-187. (SCI-1 区, IF: 3.228)

个人简历

杨艳，女，1978 年生。2001 年毕业于黑龙江科技大学资源与环境工程学院。2001 年任江苏省淮海工学院化工学院教师，主要讲授化工原理、工业企业管理和无机工艺学等课程。2004-2007 年在中国地质大学（北京）海洋学院攻读硕士学位。之后进入中国地质大学（北京）地球科学与资源学院攻读博士学位，探讨盐亭县地方病食管癌与环境地球化学的关系。博士期间，得到国家留学基金委的资助，于 2008 年 9 月-2009 年 9 月，赴英国爱丁堡大学地球科学学院学习一年。利用 GEOS-Chem 模型对全球二十二个地区大气中二氧化碳浓度变化的影响等问题进行了分析。2010 年 3 月至今，在北京大学城市与环境学院，做博士后，主要进行大气氮沉降对森林生态系统碳循环影响的研究。

永久通讯地址

电话: 13718052379

Email: yan2013yang@163.com

博士论文



北京大学

博士研究生学位论文

题目：河北塞罕坝人工林主要碳循环过程对降水变化的响应

姓 名：任艳林

学 号：10413810

院 系：城市与环境学院

专 业：自然地理学

研究方向：全球气候变化

导师姓名：方精云教授 贺金生教授

二〇一二年六月

版权声明

任何收存和保管本论文各种版本的单位和个人，未经本论文作者同意，不得将本论文转借他人，亦不得随意复制、抄录、拍照或以任何方式传播。否则，引起有碍作者著作权之问题，将可能承担法律责任。



河北塞罕坝人工林主要碳循环过程对降水变化的响应

摘 要

降水格局变化作为全球气候变化的一部分,可能会直接影响陆地生态系统碳循环。为了探讨森林生态系统对未来降水格局变化的响应,我们在位于森林—草原过渡带与半干旱半湿润气候区的河北塞罕坝地区进行了降水控制实验,用增加和减少 30% 穿透雨来模拟自然降水变化,研究降水改变对樟子松(*Pinus sylvestris* var. *mongolica*)—落叶松(*Larix* spp.)人工混交林生态系统碳循环主要过程的影响。主要结果如下:

1. 降水减少保存了土壤养分,降水增加降低了土壤养分含量但提高了可利用性。因降水淋溶作用和养分可利用性增强,增雨处理土壤硝态氮显著降低;减雨处理土壤中保有的可溶性有机碳高于对照和增雨。穿透雨处理对净氨化速率无显著影响,增雨和减雨处理的净硝化速率和净氮矿化速率显著高于对照。穿透雨增加或减少 30% 对 0-30cm 土壤微生物生物量碳及其与土壤总有机碳的比值、铵态氮和无机氮(铵态氮与硝态氮之和)含量没有显著影响。当地土壤贫瘠,微生物活动主要受氮限制,而非碳限制。

2. 植物生长对降水变化的响应存在但统计上不显著,降水减少对植物生长的影响大于降水增加。不同树种与径级的乔木胸径年增长率、群落乔木层胸高断面积年增长率和生物量年增长率都有不显著的随着降水量增加而增加的趋势。年增长率比年增长量更适合作为评价植物生长对控制实验处理响应的指标。群落净初级生产力对降水变化的响应不明显,降水减少对群落净初级生产力的影响大于降水增加。

3. 土壤呼吸对降水变化的响应比较灵敏,降水增加对土壤呼吸的影响大于降水减少。增雨 30% 显著增加了土壤呼吸速率和土壤年呼吸量,减雨 30% 对土壤呼吸速率和土壤年呼吸量统计上无显著影响。穿透雨处理对土壤呼吸的表观温度敏感性(Q_{10})影响不显著,但随着降水量增加,土壤呼吸的表观温度敏感性增加。我们提出的基于土壤温度与水分因素的土壤呼吸速率预测模型 $\ln R = a + b T \times VWC$ 比传统的 van't Hoff 指数方程具有更好的预测性。

4. 增加或减少 30% 穿透雨对人工林净生态系统生产力统计上无显著影响。但由于生态系统净初级生产力和土壤异养呼吸对降水格局变化的响应方式与程度不同,在净初级生产力无显著变化的情况下,生态系统碳收支对降水变化的响应取决于土壤异养呼吸。

关键词: 植物生长, 土壤呼吸, 净初级生产力, 净生态系统生产力, 降水控制实验

Responses of Main Carbon Cycle Processes of Plantation Ecosystem to Precipitation Change at Saihanba, Hebei Province, China

Yanlin Ren

(Ecology)

Directed by Prof. Jingyun Fang & Jinsheng He

As a part of global climate change, precipitation pattern change impacts terrestrial ecosystem carbon cycle directly. A chronic field manipulative experiment of $\pm 30\%$ throughfall ($+30\%$, -30% , respectively) in a mixed plantation of mongolian pine and larch was carried out to detect the response of forest ecosystem to precipitation changes at PKU-SOGES, Saihanba, Hebei Province, China. A package of indicators were measured to study the main ecosystem carbon cycle processes to precipitation changes. The main results are as follows:

1. The soil of -30% contains more nutrients, and soil of $+30\%$ keeps less nutrients but improves availability. Soil of -30% maintains more water-soluble carbon, and that of $+30\%$ has lower NO_3^- -N content due to heavier leaching and improvement of nutrient availability to roots and soil microbes. Both $\pm 30\%$ treatments have no significant effects on net ammonification rate, but the net nitrification rates of $\pm 30\%$ are higher than the control. The throughfall treatments have no significant effects on contents of soil microbial biomass carbon and its ratio to soil organic carbon, NH_4^+ -N and inorganic nitrogen (NH_4^+ -N and NO_3^- -N) at the soil depth of 0-30 cm. The local soil microbial community tolerated N limits rather than C limits.
2. The responses of plant growth to precipitation change are insignificant, and the response to -30% is greater than that to $+30\%$. The annual increment rates of diameter at breast height, basal area and biomass of trees increase along with increasing precipitation. No significant responses to the throughfall treatments were observed for the community NPP, but the response to -30% is greater than that to $+30\%$.
3. Both soil respiration rates and annual soil CO_2 efflux are sensitive to throughfall treatments with a significant increasing in $+30\%$ treatments. The apparent Q_{10} does not response significantly with a decreasing trend as the soil water content declines. We developed a model ($\ln R = a + b T \times \text{VWC}$) to predict the soil respiration rates with 10cm soil temperature (T) and soil volumetric water content (VWC) which is more effective than the van't Hoff model.
4. Throughfall treatments have no significant effects on net ecosystem productivity. The carbon budget of forest ecosystem is determined by soil heterotrophic respiration (R_h) rather than NPP due to their different sensitivities to precipitation changes.

Key words: plant growth, soil respiration, NPP, NEP, precipitation manipulative experiment

目 录

摘 要.....	I
Abstract.....	II
目 录.....	III
图目录.....	V
表目录.....	VI
第一章 前言.....	1
1.1 全球气候变化与降水格局变化.....	1
1.2 降水变化对森林生态系统碳循环主要过程的影响.....	1
1.2.1 降水变化对森林净初级生产力的影响.....	2
1.2.2 降水变化对森林土壤呼吸的影响.....	3
1.2.3 降水变化对森林净生态系统生产力的影响.....	5
1.2.4 森林生态系统碳循环对降水变化的响应机制.....	5
1.3 降水控制实验研究进展.....	7
1.4 研究目的和创新点.....	8
第二章 研究区概况与研究方法.....	11
2.1 研究区概况.....	11
2.1.1 自然概况.....	11
2.1.2 气候变化.....	13
2.2 研究方法.....	17
2.2.1 降水控制实验样地概况.....	17
2.2.2 实验设计.....	17
2.2.3 降水控制实验设施.....	18
2.2.4 测量指标与方法.....	20
2.2.5 数据统计分析.....	27
第三章 降水变化对土壤理化性质的影响.....	29
3.1 降水变化对土壤水分的影响.....	29
3.2 降水变化对土壤温度的影响.....	31
3.3 降水变化对土壤活性有机碳的影响.....	32
3.3.1 微生物量碳及其与土壤总有机碳的比值.....	32
3.3.2 水溶性有机碳.....	35
3.4 降水变化对土壤无机氮及氮矿化的影响.....	35
3.4.1 降水变化对土壤无机氮的影响.....	35
3.4.2 降水变化对土壤净氮矿化速率的影响.....	37
3.5 小结.....	39
第四章 植物生长对降水变化的响应.....	41
4.1 乔木径向生长对降水变化的响应.....	41

4.1.1	数据处理与统计分析	41
4.1.2	降水控制实验样地乔木层群落结构特征.....	42
4.1.3	不同树种与径级乔木胸径年增长率对降水变化的响应.....	42
4.1.4	乔木胸高断面面积生长对降水变化的响应.....	45
4.2	乔木生物量与群落净初级生产力对降水变化的响应.....	47
4.2.1	数据处理与统计分析	47
4.2.2	乔木生物量和净初级生产力对降水变化的响应.....	49
4.2.3	群落净初级生产力对降水变化的响应.....	53
4.3	降水变化对植物生长的影响.....	55
4.4	小结	56
第五章	土壤呼吸对降水变化的响应.....	57
5.1	生长季土壤呼吸对降水变化的响应.....	57
5.1.1	土壤呼吸的季节动态与空间格局	57
5.1.2	生长季土壤呼吸对降水变化的响应	58
5.2	土壤呼吸温度敏感性对降水变化的响应.....	59
5.3	基于土壤温度和水分因素的土壤呼吸速率预测模型.....	60
5.4	土壤年呼吸量对降水变化的响应.....	63
5.5	降水变化对土壤呼吸及其温度敏感性的影响.....	64
5.6	小结	66
第六章	净生态系统生产力对降水变化的响应.....	67
6.1	净生态系统生产力对降水变化的响应.....	67
6.2	净初级生产力与土壤呼吸对降水变化的响应及其对净生态系统生产力的影响	69
6.3	小结	70
第七章	结论与展望.....	71
7.1	主要结论	71
7.1.1	降水减少保存了土壤养分，降水增加降低了土壤养分含量但提高了可利用性	71
7.1.2	植物生长对降水变化的响应存在但不显著.....	71
7.1.3	土壤呼吸速率和土壤年呼吸量对降水增加响应显著，表观温度敏感性响应不显著 ..	72
7.1.4	净生态系统生产力对降水变化的响应取决于土壤异养呼吸的变化.....	72
7.2	研究展望	72
7.2.1	加强森林生态系统对降水变化响应的长期定位研究.....	72
7.2.2	进行森林生态系统多因子控制实验	72
7.2.3	区分土壤自养呼吸和异养呼吸对降水变化的响应.....	73
7.2.4	加强土壤养分循环对降水变化响应的研究.....	73
	参考文献.....	75
	致 谢.....	82
	北京大学学位论文原创性声明和使用授权说明.....	85

图目录

图 1-1 降水变化对森林生态系统碳循环过程的影响概念框架	6
图 2-1 研究区与降水控制实验样地位置	11
图 2-2 1960~2010 年塞罕坝地区年均温、年最高温与年最低温变化图	14
图 2-3 1960~2011 年塞罕坝地区年降水量与 5~9 月生长季降水量变化图	14
图 2-4 1960~2010 年塞罕坝地区年蒸发量变化图	15
图 2-5 2006~2008 年塞罕坝月降水量与年降水量	15
图 2-6 1965~2011 年塞罕坝降水量距平序列典型尺度过程线图	16
图 2-7 降水控制实验样地设计及减雨样方	18
图 2-8 微喷头布置图	19
图 2-9 AZ-DT 土壤水分监测系统	20
图 3-1 2007 年 5 月~10 月地下 10CM、20CM、40CM、80CM 土壤体积含水量与日降水量	29
图 3-2 2006 年 8 月~2007 年 10 月地下 10CM 土壤体积含水量与日降水量	30
图 3-3 2007 年 6 月~10 月每周手测地下 10CM 土壤体积含水量	30
图 3-4 2008 年 0-10CM 土壤体积含水量	30
图 3-5 2006~2007 年地下 10 厘米土壤温度变化	31
图 3-6 2006~2007 年地下 10 厘米土壤温度变化(土壤呼吸测定数据)	31
图 3-7 土壤微生物量碳与土壤容重(A)、土壤含水量(B)、土壤总有机碳(C)的关系	32
图 3-8 穿透雨处理对土壤微生物量碳(A)及其与土壤总有机碳比值(B)的影响	34
图 3-9 穿透雨处理对土壤微生物量碳(A)及其与土壤总有机碳比值(B)动态变化的影响	34
图 4-1 2006 年和 2007 年各穿透雨处理样地乔木胸径与树高对比(平均值+标准差)	42
图 4-2 不同穿透雨处理各树种与径级乔木胸径年增长率对比(平均值+标准差)	43
图 4-3 各树种与径级的乔木胸径年增长率对增雨或减雨 30% 响应值的比较	43
图 4-4 不同穿透雨处理各树种与径级乔木胸径年增长率(%)的 TUKEY HSD 均值多重比较图	44
图 4-5 不同处理的胸高断面积及其年增长率(率)(平均值+标准差)	46
图 4-6 不同穿透雨处理胸高断面积的 TUKEY HSD 均值多重比较图	46
图 4-7 群落乔木层胸高断面积年增长率(BAAI)和年增长率(BAAIR)对增雨或减雨 30% 的响应值	47
图 4-8 2006 年和 2007 年乔木根、干、枝、叶生物量	49
图 4-9 不同穿透雨处理乔木生物量年增长率与 NPP 的 TUKEY HSD 均值多重比较图	50
图 4-10 不同穿透雨处理的乔木各组分生物量增长率和 NPP(平均值+标准差)	52
图 4-11 乔木生物量年增长率和 NPP 对增加或减少 30% 穿透雨的响应值	52
图 4-12 不同穿透雨处理群落净初级生产力及其组分的 TUKEY HSD 均值多重比较图	54
图 4-13 不同穿透雨处理的群落净初级生产力及其组分(平均值+标准差)	54
图 4-14 群落净初级生产力及其组分对增雨或减雨 30% 的响应值	55
图 5-1 土壤呼吸的季节动态(A)与空间格局(B)	58
图 5-2 2006~2008 年土壤呼吸速率(A)、地下 10CM 土壤体积含水量(B)和土壤温度(C)变化图	59
图 5-3 土壤自养呼吸、异养呼吸和总呼吸的 TUKEY HSD 多重比较图	64
图 6-1 各样方的群落净初级生产力 NPP、土壤异养呼吸 R_h 与净生态系统生产力 NEP	67
图 6-2 各穿透雨处理净生态系统生产力均值的 TUKEY HSD 多重比较图	68
图 6-3 不同穿透雨处理的生态系统碳收支	68

表目录

表 2-1 2006~2008 年塞罕坝地区年降水量与生长季降水量 (单位: MM).....	15
表 2-2 野外测量指标与样品采集.....	21
表 2-3 实验室样品分析指标与方法.....	21
表 3-1 不同穿透雨处理的土壤活性有机碳.....	32
表 3-2 降水变化对土壤微生物量碳及其与土壤总有机碳比值影响的重复测量方差分析.....	33
表 3-3 穿透雨处理对土壤水溶性有机碳影响的重复测量方差分析.....	35
表 3-4 不同土壤深度与穿透雨处理的土壤无机氮.....	36
表 3-5 穿透雨处理与土壤深度对土壤无机氮影响的混合模型方差分析.....	37
表 3-6 不同土壤深度和穿透雨处理的氮矿化速率.....	37
表 3-7 穿透雨处理与土壤深度对土壤氮矿化影响的混合模型方差分析.....	38
表 4-1 降水控制实验样地各样方树种及径级的乔木株数统计 (单位: 株).....	42
表 4-2 穿透雨处理对不同树种与径级乔木胸径年增长率影响的单因素方差分析表.....	43
表 4-3 穿透雨处理间各树种与径级乔木胸径年增长率均值的TUKEY HSD多重比较.....	44
表 4-4 穿透雨处理对群落乔木胸高断面积及其年生长量(率)的单因素方差分析.....	45
表 4-5 穿透雨处理间群落乔木胸高断面积均值的TUKEY HSD多重比较.....	45
表 4-6 落叶松和樟子松相关生长方程.....	48
表 4-7 穿透雨处理对群落乔木生长的单因素方差分析.....	50
表 4-8 不同穿透雨处理群落乔木生物量年增长率与NPP的TUKEY HSD多重比较.....	51
表 4-9 穿透雨处理对群落净初级生产力及其组分影响的单因素方差分析.....	53
表 4-10 不同穿透雨处理间群落净初级生产力及其组分的TUKEY HSD多重比较.....	53
表 5-1 穿透雨处理与测定日期对土壤呼吸速率影响的双因素重复测量方差分析表.....	58
表 5-2 不同穿透雨处理生长季土壤呼吸速率的配对T检验统计值表.....	58
表 5-3 各样方土壤呼吸的表观温度敏感性(Q_{10}).....	60
表 5-4 穿透雨处理对土壤呼吸的表观温度敏感性(Q_{10})效应的单因素方差分析表.....	60
表 5-5 穿透雨处理间土壤呼吸表观 Q_{10} 均值的TUKEY HSD多重比较.....	60
表 5-6 $\ln R = A + BVWC$ 拟合参数及显著性检验.....	61
表 5-7 $\ln R = A + BT + CVWC + DT \times VWC$ 拟合参数及显著性检验.....	61
表 5-8 $\ln R = A + BT + CT \times VWC$ 拟合参数及显著性检验.....	61
表 5-9 $\ln R = A + BVWC + CT \times VWC$ 拟合参数及显著性检验.....	62
表 5-10 $\ln R = A + BT \times VWC$ 拟合参数及显著性检验.....	62
表 5-11 各样方的土壤自养呼吸、异养呼吸与总呼吸.....	63
表 5-12 穿透雨处理对土壤自养呼吸、异养呼吸和总呼吸的单因素方差分析.....	64
表 5-13 穿透雨处理间土壤自养呼吸、异养呼吸和总呼吸的TUKEY HSD多重比较.....	64
表 6-1 穿透雨处理对净生态系统生产力影响的单因素方差分析表.....	68
表 6-2 穿透雨处理间净生态系统生产力均值的TUKEY HSD多重比较表.....	68

第一章 前言

1.1 全球气候变化与降水格局变化

工业革命以来, 人类活动(尤其是化石燃料的燃烧)增加了大气中 CO_2 等温室气体的浓度, 导致全球气候变暖。大气环流和水循环在气候变暖驱动下发生了显著变化, 对全球和区域尺度上的降水格局产生了深刻影响, 引起了降水量、降水季节分配和降水强度的改变(Houghton et al., 2001; IPCC, 2007)。在气候变暖的背景下, 20 世纪初以来, 全球陆地表面降水量已经增加了 2% (Jones & Hulme, 1996; Hulme et al., 1998)。1900 ~ 2005 年, 北半球中高纬度 ($30 \sim 85^\circ\text{N}$) 降水量增加了 6 ~ 8% (IPCC, 2007)。据模型预测, 21 世纪全球降水将增加 7% 左右, 但在不同区域存在很大的异质性(Easterling et al., 2000)。

1960 ~ 2000 年, 中国的总降水量增加了 2%, 但降水频率减少了 10%, 降水强度明显增加(Liu et al., 2005)。降水变化趋势因区域而异, 总体而言, 西北地区和南方地区降水呈增加趋势, 而北方地区降水则呈显著减少趋势(Qian & Zhu, 2011; Qian & Qin, 2008)。1960 ~ 2009 年, 中国干旱事件频发区主要分布在西南地区、黄河流域、北方以及东北地区的西南部, 其中, 北方地区和黄河上游干旱发生频率显著高于其他地区; 除长江上游地区以外, 中国干旱事件发生频率整体呈上升趋势(Qian et al., 2011)。模型预测结果显示, 21 世纪中国降水变化趋势呈现南北分异, 北方地区降水将显著减少, 中部、东部以及南方地区夏季降水将显著增加而冬季降水增加不明显(Xu et al., 2006)。IPCC(2007)报告则预测中国北方温带地区本世纪降水量有 5 ~ 20% 的小幅增加, 而且未来干旱、洪涝等极端气候事件发生的频率也会增加。不同的模型对于北方地区未来的降水格局变化预测的结果不同, 正是由于这种不确定的存在, 非常有必要同时进行降水减少和降水增加两种情景的模拟研究。

1.2 降水变化对森林生态系统碳循环主要过程的影响

降水变化主要通过改变土壤水分来影响生态系统过程。关于生态系统对降水变化响应的研究方法主要有以下四种: 长时间序列的生态系统特性和降水过程观察分析、短期的水分控制实验、降水梯度上的多点比较分析和模型模拟分析降水效应(Weltzin et al., 2003)。森林生态系统具有重要的生态服务功能, 全球和区域尺度的降水变化会对森林生态系统结构和分布及其内在生态过程产生重要影响, 例如物候期提前或推迟、植被生产力增加或者减少、凋落物分解和温室气体排放变化、水循环和养分循环变化、群落结构组成和生物多样性变化、树木死亡和衰退、以及植被地理分布变化等(Billings et al., 2000; Hanson & Weltzin, 2000; Hughes, 2000; Johnson et al., 2000; Schuur, 2003; Weltzin et al., 2003; Wullschleger & Hanson, 2006; Allen et al., 2010; Bonebrake &

Mastrandrea, 2010; Wyckoff & Bowers, 2010; DeSantis et al., 2011; Ni, 2011)。此外, 降水变化会与全球变化因子(如 CO_2 浓度增加、温度升高和氮沉降增加)相互作用来影响生态系统过程的响应(Johnson et al., 2000; Smith et al., 2000; Boisvenue & Running, 2006)。森林生态系统是最大的陆地碳库(Dixon et al., 1994), 其碳循环过程的变化对全球气候系统具有重要的调控作用。区域降水变化会对森林生态系统碳循环过程及其通量产生直接影响, 以下将分三个方面综述有关降水变化对森林生态系统净初级生产力、土壤呼吸及其组分和净生态系统生产力影响的国内外研究进展, 并分别讨论其响应机制。

1.2.1 降水变化对森林净初级生产力的影响

总初级生产力(Gross primary productivity, GPP)是指单位时间内生物(主要是绿色植物)通过光合作用途径所固定的有机碳量, 又称总第一性生产力。GPP 决定了进入陆地生态系统的初始物质和能量。净初级生产力(Net primary productivity, NPP)表示植被所固定的有机碳中扣除本身呼吸消耗的部分, 这一部分用于植被的生长和生殖, 也称净第一性生产力。NPP 反映了植物固定和转化光合产物的效率, 也决定了可供异养生物(包括各种动物和人)利用的物质和能量。净生态系统生产力(Net ecosystem productivity, NEP)指净初级生产力中减去异养生物呼吸消耗(土壤异养呼吸)光合产物之后的部分。NEP 表示大气 CO_2 进入生态系统的净光合产量, 它的大小受制于多种环境因子, 尤其是大气 CO_2 浓度和气候条件(方精云等, 2001)。GPP、NPP、NEP 三者的关系如下:

$$\text{NPP} = \text{GPP} - R_a \quad (1-1)$$

$$\text{NEP} = (\text{GPP} - R_a) - R_h = \text{NPP} - R_h \quad (1-2)$$

其中, R_a 为自养生物本身呼吸所消耗的同化产物; R_h 为异养生物呼吸消耗量(土壤异养呼吸)。

植物生长形成的有机碳主要有两种流向, 大部分以凋落物的形式进入地表、成为土壤有机质的一部分(从较长的时间尺度看, 它们又通过土壤呼吸而释放到大气中)或以凋落物分解的形式回到大气; 另一部分则构成植物的生物量。生物量是指单位面积上活有机体的干物质重量(方精云等, 2001)。已有研究表明, 土壤异养呼吸(R_h)是陆地生态系统 NEP 的决定因素(Valentini et al., 2000; Grace & Rayment, 2000)。

植被净初级生产力受降水限制的区域在全球分布广泛(Boisvenue & Running, 2006)。一般而言, 降水增加会促进森林生长从而增加净初级生产力, 而降水减少引起的干旱则会降低森林的净初级生产力。美国长期生态研究网络((US Long Term Ecological Research Network, LTER) 22 个森林站点的长期监测结果显示, 地上净初级生产力与年降水量之间存在显著正相关(Knapp & Smith, 2001)。Zhao & Running (2010)研究发现, 2000~2009 年区域性干旱显著降低了南半球 NPP, 在全球尺度上, 干旱使 NPP 降低了 0.55 Pg C 。Ma et al. (2012)研究发现, 干旱引起的水分胁迫减少了

加拿大西部的北方森林生物量碳汇。干旱区的生态系统 NPP 与土壤水分可利用性显著正相关,降水增加将显著增加 NPP(Loik et al., 2004)。热带森林生态系统生产力对降水变化的响应尚存在较大争议, Schuur(2003)在综合全球热带森林最新 NPP 调查数据分析后发现, 热带森林 NPP 和年降水之间存在很强的相关性, 说明气候湿润的热带森林 NPP 对降水变化响应也是敏感的。

1.2.2 降水变化对森林土壤呼吸的影响

土壤呼吸(Soil respiration)是土壤微生物、动物和植物的地下部分产生 CO_2 的过程(Hanson et al., 2000; Luo & Zhou, 2007)。土壤呼吸可分为土壤自养呼吸(Soil autotrophic respiration)和土壤异养呼吸(Soil heterotrophic respiration)两部分。前者主要包括根和共生真菌的呼吸, 后者主要包括分解凋落物和土壤有机质的土壤微生物的异养呼吸以及含碳物质的化学氧化作用。通常用未经扰动的土壤表面的 CO_2 释放速率(Soil CO_2 efflux rate)作为土壤呼吸速率。土壤呼吸是陆地上仅次于光合作用的第二大碳通量(Raich & Potter, 1995), 占全球陆地生态系统总呼吸的 60 ~ 90%(Schimel et al., 2001)。同时, 土壤呼吸释放碳的速率要远高于人类活动释放碳的速率, 因此土壤呼吸的微小变化能显著地改变大气中 CO_2 的平衡, 它在调控区域和全球尺度的碳循环上起着关键作用。土壤呼吸作为生态系统碳循环的一个主要组成部分, 与生态系统生产力的许多组分都有联系, 与土壤中的营养过程(如分解作用和矿化作用)也密切相关。在全球变化的背景下, 了解降水变化对土壤呼吸的影响机理, 对于估计和预测未来全球变化的方向、理解陆地生态系统的碳汇源功能, 都有很重要的理论和实践意义(邓东周, 2009)。

全球变暖会显著地刺激土壤呼吸, 导致更多 CO_2 释放到大气中, 从而在气候系统与全球碳循环之间形成了正反馈, 使两者都被加强。土壤呼吸对温度变化的响应通常采用表观温度敏感性(Q_{10})来表示, 即温度每升高 10°C , 土壤呼吸速率所增加的倍数(方精云, 2000)。在生物化学水平上, Q_{10} 的测量值通常在 2 左右, 即温度每升高 10°C , 呼吸速率就增长一倍。估算的土壤呼吸 Q_{10} 因地理位置和生态系统类型的不同相差很大, 从略大于 1(低敏感性)直到大于 10(高敏感性)(Luo & Zhou, 2007)。目前大多数关于气候变化和全球碳循环之间的反馈关系和大小的研究, 都是基于一个固定的 Q_{10} 值(如 2.0), 模型模拟的结果均表明气候变暖与全球碳循环之间存在着较强的正反馈效应, 由于土壤呼吸的温度 z 敏感性在调控全球碳循环中的关键作用, 因此近些年来对它进行了广泛的实验和模型研究(Luo & Zhou, 2007)。

土壤水分是除温度外影响土壤呼吸的另一重要因子。土壤水分通过影响底物或氧气的扩散来调控土壤呼吸速率(Linn & Doran, 1984)和土壤呼吸的温度敏感性(Gaumont-Guay et al., 2006)。通常认为土壤呼吸与土壤水分之间的关系是: 土壤呼吸在干燥条件下较低, 在中等土壤水分水平时最大, 当含水量很高、厌氧条件占优势导致好氧微生物的活性受到抑制时又下降。最适的含水量

通常是接近田间持水量,这时大孔隙空间大部分充满空气,利于氧气扩散,小孔隙空间大部分充满水,利于可溶性底物的扩散(Luo & Zhou, 2007)。实验室的研究指出在最适土壤含水量时土壤呼吸速率最大,很多野外测量的结果则显示土壤水分只有在最低和最高的情况下才会抑制 CO_2 通量(Liu et al., 2002; Xu et al., 2004)。

研究表明,降水增加会促进土壤呼吸,而干旱则显著降低土壤呼吸(Gaumont-Guay et al., 2006; Borken et al., 2006; Asensio et al., 2007; Misson et al., 2010)。在干旱处理条件下,土壤水分是土壤呼吸季节和年际变化的主要驱动因子,土壤呼吸对温度的响应也受到土壤水分的限制(Asensio et al., 2007)。土壤呼吸组分对降水变化的敏感性不同,异养呼吸要比自养呼吸更为敏感,这是由于植物根系和微生物对土壤水分及其分布的响应不同导致的。例如,干旱导致土壤呼吸降低主要归因于土壤异养呼吸的减少(Borken et al., 2006),这是因为干旱发生时虽然表层根系受到抑制,但深层根系生物量和水分吸收增加,因而根系呼吸变化不大(Borken et al., 1999)。降水数量、频率和强度的变化对旱生生态系统的土壤呼吸影响最大。研究发现,干燥土壤的土壤呼吸在雨后会猛增到一个很高的值,然后随着土壤变干而逐渐下降,降雨引起的土壤呼吸增加与降雨前土壤呼吸速率成反比(Xu et al., 2004)。在美国大平原南部草地上进行的控制实验中,加水促进了干旱季节的土壤呼吸,但不同的水分添加量对土壤呼吸的影响不同(Liu et al., 2002)。Borken et al. (2006)在温带落叶混交林进行的生长季遮雨实验中,遮雨处理明显降低了土壤呼吸速率和累积量。美国橡树岭国家实验室在田纳西州温带落叶阔叶林的穿透雨转移实验中发现,增加或减少 33% 穿透雨对森林的土壤呼吸没有显著影响,穿透雨处理对凋落物的质量与分解速率的影响也不显著(Hanson et al., 2003)。

降水减少通常导致土壤呼吸下降,同样,两次降水之间水分亏缺的时间延长、植物和微生物的水分胁迫加重,也会降低土壤二氧化碳通量(Bremer et al., 1998)。延长的夏季干旱期会减少 O 层土壤的异养呼吸,进而引起森林土壤总有机碳的积累(Borken et al., 2006)。在 Kanza 草原,自然降雨量减少 70% 时,季节平均土壤呼吸速率降低了 8%,改变降水时间,土壤呼吸速率降低 13%,而在这两种改变同时发生时,土壤呼吸降低 20%(Harper et al., 2005)。

由于自然和人为干扰常常会造成多个因子同时改变,有可能对土壤呼吸作用产生复杂的交互作用。两个或多个变量复杂的交互作用一般不能从单因子影响的方向和大小来预测。因此,进行多因子的控制实验来检验多个因子对土壤呼吸的交互作用很重要(Beier, 2004; Norby & Luo, 2004)。Zhou et al. (2006)在北美高草草原上进行了两个实验:一个是长期的 2°C 增温和刈割,另一个是短期的 4.4°C 增温和降水加倍,来研究增温、刈割和降雨量加倍这三个因子对土壤呼吸及其温度敏感性的主效应和交互作用。增温和降雨加倍的主效应是显著的,但除了“增温 \times 刈割”对土

壤呼吸及其温度敏感性具有显著的交互作用外,其他因子间的交互作用都不具有统计学上的显著性。

由于土壤水分与温度的相互作用,水分处理也会影响土壤呼吸的温度敏感性。在高草草原的一项研究中发现,干燥循环的时间延长时,土壤二氧化碳通量对土壤含水量比对土壤温度更敏感(Bremer et al., 1998)。降雨的变异性加大会降低 Q_{10} , 因为改变降雨频率的处理中,更频繁地出现土壤含水量过低与过高的情况(Harper et al., 2005)。土壤呼吸的温度敏感性随年份及生态系统的其他特性而异。 Q_{10} 在湿润年份较低,而在干旱年份较高(Dörr & Münnich, 1987; Luo & Zhou, 2007)。但也有一些研究发现 Q_{10} 在排水良好的地点比在湿润的地点更低(Davidson et al., 1998; Xu & Qi, 2001; Reichstein et al., 2003)。Davidson et al. (1998)将 Q_{10} 的不同响应归因于不同地点所特有的湿度条件和降雨在一年中的分布。土壤水分和温度对 CO_2/O_2 扩散的复杂交互作用以及根和微生物活性都可能导致土壤 CO_2 通量的温度敏感性对水分的有效性产生不同的响应(Luo & Zhou, 2007)。

1.2.3 降水变化对森林净生态系统生产力的影响

森林净生态系统生产力(NEP)对降水变化的响应取决于生态系统生产力和呼吸组分的综合响应结果。例如,加拿大北方森林的研究结果表明,干旱同时降低了北方森林的生产力和呼吸组分,由于呼吸响应更为敏感,因此生态系统净生态系统生产力显著降低(Grant et al., 2006; Kljun et al., 2007)。目前关于降水变化对森林生态系统 NEP 影响的实验研究结果仍然非常少,有待进一步研究。

1.2.4 森林生态系统碳循环对降水变化的响应机制

降水变化主要通过改变土壤水分含量、土壤养分可利用性、光照可利用性和生长季长度等对森林生态系统碳循环过程产生影响(图 1-1)。土壤含水量的变化受降水量和降水频率的直接驱动,同时受土壤水分蒸散速率、植物蒸发速率以及土壤水分水平和垂直运移等因素影响(Weltzin et al., 2003)。土壤含水量变化可以改变土壤物理结构、养分可获取性及土壤氮矿化,进而影响植物生长和微生物异养呼吸过程(Emmett et al., 2004; Sardans & Penuelas, 2007)。同时,降雨格局改变对全年光照强度产生影响,也会在一定程度上影响植物光合作用,尤其是热带雨林地区这一影响更为明显。

森林生态系统净初级生产力受降水变化驱动的机制主要表现在光合作用强度和生长季长度两方面。生长季是温带和北方森林净初级生产力的决定因素之一,降水变化会影响植物物候期和生长季长度(Kimball et al., 2004; Misson et al., 2011),从而影响光合作用年初级生产量。初级生产力强度对降水变化的响应主要表现在以下两个方面:(1)水分和养分可利用性、叶片气孔导度对 CO_2 供应的调节以及光照强度的变化等对光合生产强度产生影响;(2)水分变化引起竞争和适应改

变从而使群落结构和物种组成发生变化, 最终改变群落光合生产特征。不同物种对降水变化的响应程度和适应能力不同(Pasho et al., 2011; Hoffmann et al., 2011), 因而降水变化会影响植物对水分的竞争, 进而引起群落组成的变化。DeSantis et.al. (2011)对北美中部森林—草原过渡带的研究表明, 干旱会导致森林群落由阔叶树占优势的林型向针叶树占优势的林型转变。此外, 干旱会引起树木死亡增加(Allen et al., 2010; Michaelian et al., 2011), 也会降低森林生产力。

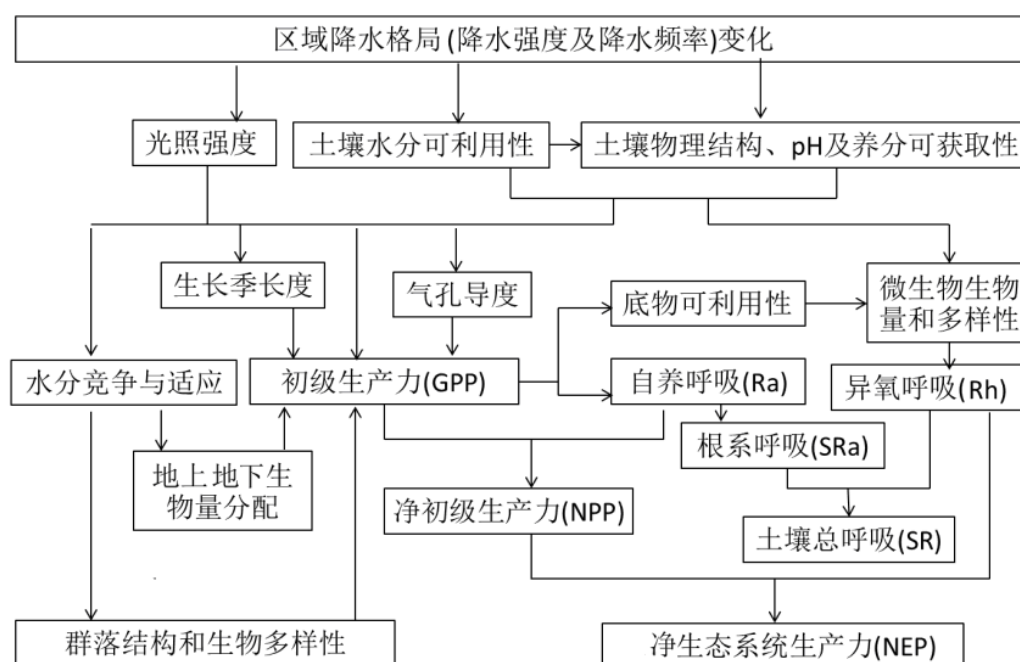


图 1-1 降水变化对森林生态系统碳循环过程的影响概念框架

降水变化对土壤呼吸的影响主要包括土壤呼吸理化条件以及底物供应两方面。适宜的土壤含水量和土壤 pH 值、养分可利用性是根系活动和土壤微生物生长的基本条件。底物供应是土壤呼吸的另一重要条件(Hogberg et al., 2001), 降水变化通过改变凋落物产量、地下生产力及根系空间分布, 改变了底物供应对土壤呼吸的驱动(Misson et al., 2010)。此外, 降水变化引起群落物种组成和结构的变化, 使得凋落物的理化性质、产量和时间以及地下生物量分配都随之变化, 间接对土壤呼吸及其组分产生重要影响(Hanson et al., 2000)。此外, 由于不同树种对水分利用能力的不同(Hölscher et al., 2005), 物种组成的变化会对群落蒸腾特性产生变化, 从而影响土壤水分及土壤生物过程如土壤呼吸。

森林 NEP 对降水变化的响应取决于生产力和呼吸响应的差异。若 NPP 对降水变化的响应比土壤异养呼吸更为敏感, 那么随着降水增加 NEP 会增加; 反之, 若土壤异养呼吸对降水变化响应更为敏感, 那么随着降水增加 NEP 将会减少。以往的研究表明, 生态系统呼吸比生产力对降

水变化更为敏感(Kljun et al., 2006), 这可能是因为土壤呼吸主要受土壤表层的水分影响而生产力则是受树木根系所能吸收的不同深度的水分的总量影响的(Reichstein et al., 2002)。

1.3 降水控制实验研究进展

生态系统对全球变化的响应与适应性研究是当今全球变化与生态学研究科学前沿, 而控制实验则是研究全球气候变化对生态系统影响的重要手段之一。Jentsch et al. (2007)对近年来有关实验模拟气候变化影响的文献进行了分类分析, 他们发现在 364 篇原创性研究论文中, 关于实验模拟气候变化对植物影响的研究从 1990s 后开始迅速增多, 1996 年后稳定于一个较高水平, 这些模拟气候变化的研究主要集中在模拟温度和 CO_2 浓度升高两个方面, 其中, 利用 FACE(Free-air CO_2 Enrichment, 自由 CO_2 气体施肥实验)等技术对 CO_2 浓度变化后果的研究已经取得了许多成就(方精云, 2000; 蒋高明等, 1997)。降水是生态系统净初级生产力的主要控制因素之一, 降水变化作为全球变化的重要组成部分必然会对陆地生态系统分布格局和生产力必将产生深刻影响, 而有关研究却相对较少(Jentsch et al., 2007; 邓东周, 2009)。

前人研究多数是利用定点长期监测的数据, 在区域尺度上沿降水梯度或综合不同生态系统来研究降水变化对生态系统的影响。Knapp & Smith(2001)利用美国 LTER 11 个样地的数据研究得出, 生态系统 ANPP 与年均降水量有显著相关关系, 但他们的研究也认为 ANPP 年际变化与降水量的年际变化没有关系。而 Fang et al. (2001)利用高分辨率遥感数据对中国的植被变化与降水变化的关系进行了研究, 指出中国的情况与 Knapp & Smith(2001)的发现相反。这种不确定性说明需要用更好的方法来研究降水变化对生态系统的影响。

野外降水控制实验可就同一地点不同降水模式对生态系统的影响进行深入研究。以前的野外降水实验多是通过人工灌溉来实现。自 1990s 以来, 国外一些研究机构开始进行大型野外降水控制实验, 用遮雨棚和自然降雨灌溉设施来改变降雨量, 研究降水量、降水季节分配及降水频率变化在塑造荒漠、疏林草地、高草草原、落叶阔叶林等生态系统过程中的作用, 以阐明降水—土壤—植物间可以指示生态系统对降水格局变化响应的许多复杂而相互交织的关系(Fay et al., 2000; Weltzin & McPherson, 2000; Hanson et al., 2001; Knapp et al., 2002; Harper et al., 2005)。其中, 大多数研究都是针对草地或灌丛生态系统的。从 1993 年开始, 美国橡树岭国家实验室在田纳西州东部的温带落叶阔叶林中开始了穿透雨转移实验(Throughfall displacement experiment, TDE), 在林下用集水槽和和 PVC 管转移、滴灌的方式, 研究穿透雨变化对生态系统的影响(Hanson et al., 1998)。后来, 他们又在林下搭建遮雨棚、开展了小规模极端干旱控制实验, 研究完全去除穿透雨和树干茎流后生态系统的变化。哈佛森林也用林下搭建遮雨棚的方式进行了极端干旱模拟实验, 来研究干旱对温带落叶阔叶林生态系统的影响(Borken et al., 2006)。美国的降水与生态系统变化研究网

络(The Precipitation and Ecosystem Change Research Network, PrecipNet, <http://precipnet.ucsc.edu>)为进行降水变化的生态系统响应研究的研究者们提供了一个交流和合作的平台,对于评估未来降水格局变化对陆地生态系统结构与功能的影响具有很大的促进作用。

国内以前的降雨控制实验大多以盆栽草本植物或树木幼苗为研究对象,通过人工灌溉产生不同降雨量处理来研究植物的生理生态特性(肖春旺, 2001; 寇详明, 2007)。盆栽实验虽然能准确便捷地控制水量,但得到的结果很难演绎推广到生态系统中。

2004年,中国科学院植物所以内蒙古多伦草地生态系统为研究对象,开始通过多因子田间控制实验研究,探讨我国北方草地生态系统结构与功能及关键生态学过程对温度升高、降雨变化(Niu et al., 2008)和人类干扰等因子的响应机制,这是我国目前运转时间最长、科研成果最多的一项野外生态控制实验。

但对于森林生态系统,由于野外模拟不同降水量的难度较大,所以相关研究很少。中国科学院长白山森林生态系统定位站在野外水泥池中以红松和蒙古栎幼苗为研究对象,进行了降雨量增减30%的模拟实验。2007~2008年,在我们的降水控制实验进行的同一时期,中国科学院沈阳应用生态学研究所在辽宁大青沟实验站樟子松(*Pinus sylvestris* var. *mongolica*)人工林中用冠层顶部遮雨棚的方式对平均树高约1.9m的10年生樟子松人工林进行了降水控制实验(邓东周, 2009)。但这两个实验都是针对幼苗或幼树,不能完全代表森林生态系统,后者更侧重对植物生理方面的研究。中国科学院自2011年1月启动了“天然森林和草地土壤固碳功能与固碳潜力研究”项目,开始在鼎湖山亚热带季风常绿阔叶林、秦岭北亚热带落叶常绿阔叶混交林、长白山温带针阔混交林中进行包括加氮和穿透雨增加和减少30%处理的多因子控制实验,实验结果还未见报道。

综上所述,国内外针对森林生态系统、在野外原位模拟降水变化、从群落和生态系统尺度上研究降水变化对生态系统影响的研究还很少见。

1.4 研究目的和创新点

最近的研究表明,气候变化尤其是降水变化使得北半球的碳汇能力有所减弱(Angert et al., 2005; Stephens et al., 2007; Ma et al., 2012),但尚缺乏降水控制实验结果的证实。目前关于森林生态系统(尤其是水分限制地区的森林生态系统)碳循环对降水变化响应的系统性实验研究仍然比较缺乏,中国森林生态系统碳循环对降水变化响应的实验研究结果几乎仍是空白。森林生态系统生产力和土壤呼吸过程对降水变化的响应是否一致?降水减少或增加是否会相应地抑制或者促进森林生态系统碳吸收?这些问题亟待控制实验结果的证实。

半干旱区的生态系统过程对降水变化的响应极为敏感(Allen & Breshears, 1998),河北塞罕坝地区属于中国北方半干旱半湿润气候区,位于我国境内三条全球变化样带的交汇处(张新时&杨奠

安, 1995), 是全球变化研究的关键区域(刘鸿雁, 1998)。研究区内森林与草甸、草原镶嵌共存, 是典型的森林—草原过渡带, 特殊的地理位置和生态意义让塞罕坝成为进行降水控制实验、探讨降水格局变化生态响应的理想平台。为了探讨半干旱半湿润地区人工林生态系统对降水格局变化的响应, 本研究通过降水控制实验设施在野外模拟增加或减少 30% 穿透雨, 研究塞罕坝樟子松—落叶松人工混交林生态系统碳循环主要过程对降水变化的响应, 并对其机制进行探讨。我们的研究也可在大尺度上评估降水格局变化对陆地生态系统的影响提供一定科学依据。

第二章 研究区概况与研究方法

2.1 研究区概况

2.1.1 自然概况

降水控制实验样地位于河北省塞罕坝机械林场总场千层板林场。塞罕坝机械林场地处北纬 $42^{\circ}10' \sim 42^{\circ}50'$ 、东经 $117^{\circ}12' \sim 117^{\circ}30'$ ，海拔 1010 ~ 1939.9 m，位于河北省围场满族蒙古族自治县北部，北部隔河与内蒙古自治区赤峰市克什克腾旗、锡林郭勒盟多伦县接壤，南部、东部分别与承德市御道口牧场和围场县的五乡一镇相邻，与北京市直线距离约为 283 km。

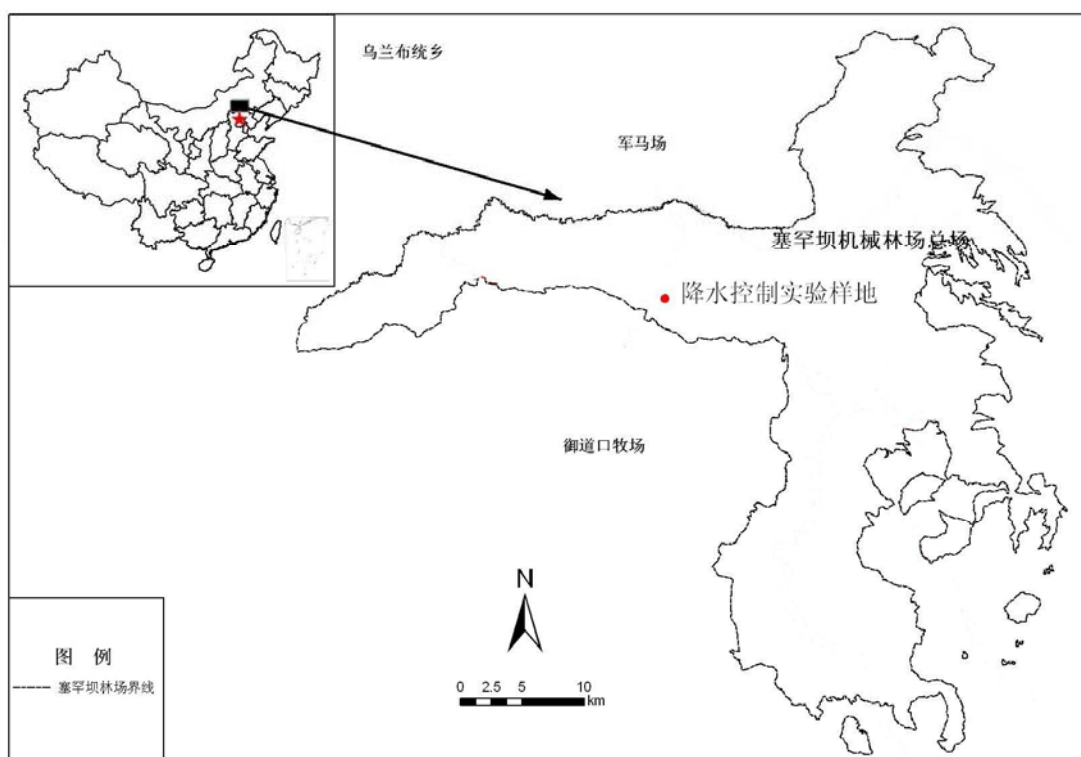


图 2-1 研究区与降水控制实验样地位置

塞罕坝机械林场于 1962 年 2 月由原国家林业部建场，1969 年归属河北省林业局(厅)管理，目前已成为我国最大的人工林种植基地，总场又划分为六个林场：北曼甸林场、大唤起林场、千层板林场、三道河口林场、三乡林场和阴河林场。塞罕坝机械林场总经营面积 9.39×10^4 ha，有林地面积 7.47×10^4 ha，森林覆盖率 80%，林木总蓄积量 1.012×10^7 m³，平均年增长量 6.2×10^5 m³。其中，人工林占有林地面积的 74.6%，天然次生林占有林地面积的 25.4%。按森林优势树种划分，落叶松(*Larix* spp.)人工林面积最大，占森林总面积的 38.7%，樟子松人工林占森林总面积的 7.5% (黄金祥等，1996)。

塞罕坝地区还是全球变化研究的关键区域。作为森林—草原过渡带，这一地区对气候变化敏

感,是气候变化的良好指示体。我国境内有三条全球变化样带,分别是 NECT(中国东北温带森林—草原样带)、CENT1(中国东部森林生态系统样带)和 CENT2(北温带森林—草原—荒漠生态系统样带)(张新时&杨莫安, 1995)。塞罕坝地区正位于这三条样带的交汇处,特殊的地理位置、复杂的自然条件使塞罕坝具有独特的生态学意义,是进行大规模控制实验、探讨全球变化生态响应的理想区域。

(1) 地貌

塞罕坝是内蒙古高原、大兴安岭山系与冀北山地交汇之处,也是内蒙古浑善达克沙地的东南边缘。地跨两个地貌单元,即坝上与接坝山区。坝上属内蒙古高原东南缘,既有高原的一般特征,沙丘起伏、地势开阔、山体浑圆,又有湖淖谷甸较多的特点。海拔 1500m 以上,至高点大光顶子为 1939.9m。接坝山区系阴山山脉与大兴安岭余脉的交汇地带,海拔 1300~1700m。北坡作为内蒙古高原的接合部相对低缓,南面相对高度较高,略显陡峭(黄金祥等, 1996)。

(2) 气候

本地区属半干旱半湿润气候区,处于暖温带与温带的过渡带,冬季漫长而寒冷;春秋季较短,干燥多风;夏季不明显,气候凉爽。无霜期短,约 60 天左右,昼夜温差大,年平均气温 -1.4°C , 1 月平均气温 -21.8°C , 7 月平均气温 16.2°C ; 极端最低温度 -43.2°C , 极端最高温度 33.4°C , 日平均气温 $\geq 0^{\circ}\text{C}$ 的年积温为 2072.8°C , $\geq 5^{\circ}\text{C}$ 的年积温为 1984°C , $\geq 10^{\circ}\text{C}$ 的年积温为 1663.5°C ; 降水以降雨为主、降雪为辅,降水量偏少,多集中在 6-9 月,年平均降水量 454.2mm,最大年降水量 636.0mm,最小年降水量 258.0mm,年均降水日数 134 天;年均日照 2367.8h,日照率为 58%;年均相对湿度为 74.4%;年均蒸发量为 1244.4mm;年均六级以上大风日 76 天,积雪长达 7 个月,最大冻土深 168cm(郑成洋, 2005; 黄金祥等, 1996)。该地区是我国受太平洋季风气候影响的北限,由于海拔迅速升高,在季风气候的影响下,形成了气温低、降水量高的气候特点。

(3) 土壤

根据河北省土壤水平分布带划分,塞罕坝土壤类型应属于灰色森林土与黑土带(刘濂, 1996)。但由于塞罕坝地区气候梯度明显、地貌类型多样,因此当地土壤又可细分为棕壤、草甸土、沼泽土、灰色森林土、黑土、风沙土六大土类。棕壤为在暖温带落叶阔叶林条件下形成的土壤,主要分布在东部坝缘山地;草甸土为直接受地下水季节性浸润、在草甸植被下发育而成的半水成土类,多分布于河流两岸及水泡子周围;沼泽土一般分布于沼泽和滞水洼地;灰色森林土是在寒温性湿润森林草原植被下发育的土壤,集中分布在马蹄坑、烟子窑一带;黑土类土壤为半湿润寒温气候型草原、草甸上形成的土壤;风沙土为干旱多风条件下发育在风积母质上的土壤。总体来说,坝上地区以风沙土为主,兼有草甸土和沼泽土,主要成土母质为风积物、残积物、堆积物及冲积物

等(黄金祥等, 1996)。

(4)水文

塞罕坝是滦河与辽河的发源地和主要集水区。其中, 滦河水系占京津唐水源地之一——潘家口水库年入库水量的 93.4%。水源地保护是塞罕坝机械林场的重要任务之一。

(5)植被概况

塞罕坝地区在清朝光绪二十七年(1909 年)前曾为“皇家猎苑”禁地, 是森林茂密、水草肥美之地。清朝末年开围放垦后, 逐渐增加的人类活动, 尤其是战争期间的掠夺性砍伐, 导致塞罕坝的原始森林到解放初期时已破坏殆尽, 只剩下零星残存的华北落叶松(*Larix principis-rupprechtii*)林和大量伐根。在塞罕坝机械林场建立后, 林业工人在原采伐迹地上营造了大量的落叶松林、白杆(*Picea meyeri*)、油松(*Pinus tabulaeformis*)和樟子松林, 恢复了昔日的壮观林海(黄金祥等, 1996)。

塞罕坝地区处于我国暖温带落叶阔叶林向温带草原的过渡带(森林—草原过渡带), 以森林和草原两种植被镶嵌共存为特色。坝下为冀北山地天然次生林, 主要有白桦(*Betula platyphylla*)林、山杨(*Populus davidiana*)林、华北落叶松林、白杆林、蒙古栎(*Quercus mongolica*)林、油松林等。坝上植物群落类型包括落叶松林、油松林、白桦林、棘皮桦(*Betula dahurica*)林, 还有草甸和草甸草原, 以及在低湿地和水体周边分布的沼泽植被(郑成洋, 2005)。

落叶松林是塞罕坝主要的人工林类型。落叶松喜光, 耐严寒, 耐干旱, 浅根性, 生长较快, 是东北和华北地区森林更新与造林的主要树种。塞罕坝地区的落叶松人工林大多为纯林, 少数与樟子松、白桦组成混交林, 主要分布在中上坡位, 一般种植在平坦的坝顶或坡地。林层单一, 林下灌木和草本稀少。

樟子松作为欧洲赤松(*Pinus sylvestris*)在远东的一个地理变种, 继承了欧洲赤松适应各种生境的能力, 是“三北”防护林和治沙工程的主要造林树种。在我国, 樟子松天然分布于湿润半湿润地区的大兴安岭、呼伦贝尔草原红花尔基和海拉尔一带。樟子松是强阳性、耐干旱的常绿针叶树种, 对土壤的要求不严格, 能在山脊、向阳坡地及较干旱的沙地、砂砾地上生长, 是坝上重要的造林树种, 在落叶松不易成活的立地条件下也长势良好。樟子松林郁密度高, 林下灌木和草本较少。塞罕坝机械林场大面积营造樟子松林起步时间比较晚, 大多营造于 1980~1995 年, 面积为 7 536.1 ha, 主要包括樟子松纯林和樟子松—落叶松人工混交林两种林型。樟子松作为改善塞罕坝人工林树种构成的重要树种, 其作用正日益受到重视。

2.1.2 气候变化

(1) 1960~2011 年年均温、年降水量与年蒸发量的变化

塞罕坝机械林场气象站距离降水控制实验样地约 500 m, 我们利用该站 1960~2011 年的气象

数据分析了塞罕坝地区的气候变化情况。我们发现,当地的年均温与最低温均无显著变化趋势($P > 0.05$),年最高温有显著的增加趋势($R^2 = 0.16, P = 0.002$, 图 2-2)。年降水量与 5~9 月生长季降水量随年份增加有统计上不显著的增加趋势($P > 0.05$, 图 2-3)。年蒸发量呈明显的下降趋势($R^2 = 0.38, P < 0.001$, 图 2-4),这可能与当地人工林生长改善小气候、降低风速有关,年大风日数的年代平均值已由 1960s 的 86 天减少为 2000s 的 39 天。蒸发量下降,土壤的水分可利用性也会得到改善。

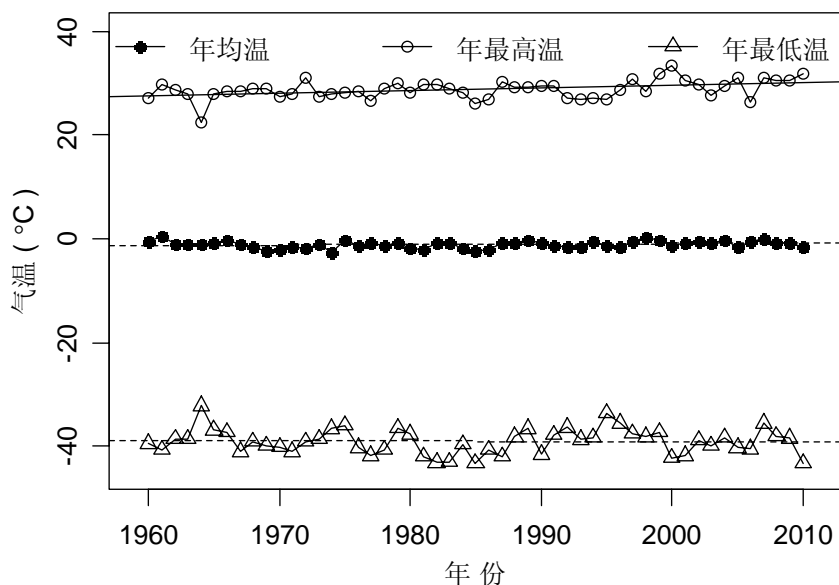


图 2-2 1960 ~ 2010 年塞罕坝地区年均温、年最高温与年最低温变化图

注: 图中虚线表示线性关系不显著($P > 0.05$)。

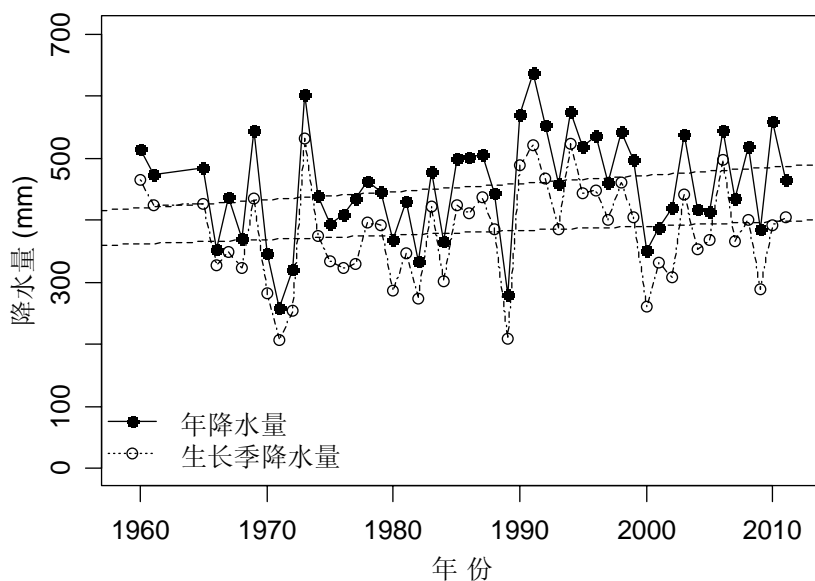


图 2-3 1960 ~ 2011 年塞罕坝地区年降水量与 5 ~ 9 月生长季降水量变化图

注: 图中虚线表示线性关系不显著($P > 0.05$)。

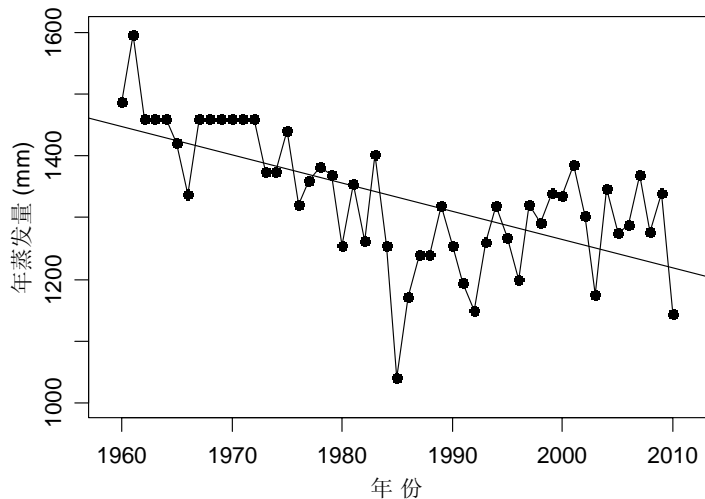


图 2-4 1960 ~ 2010 年塞罕坝地区年蒸发量变化图

(2) 2006 ~ 2008 年塞罕坝降水量情况

2006 ~ 2008 年塞罕坝地区年降水量与生长季降水量总体来说与多年平均值比较接近(图 2-3), 2006 年的生长季降水量、年降水量以及二者之比略高于常年, 2007 年的降水量与多年平均值持平, 2008 年也接近于多年平均值(表 2-1)。2006 年 8 月 7 日出现了三年中的最大日降水量 84.5mm, 导致其月降水量偏高(图 2-5)。2007 年与 2008 年的最大日降水量分别为 48.2mm 和 51.7mm。

表 2-1 2006 ~ 2008 年塞罕坝地区年降水量与生长季降水量 (单位: mm)

年份	年降水量	生长季 降水量	年降水量 距平值	生长季降水量 距平值	生长季/年降水量
2006	544.1	497.7	91.1	120.1	91%
2007	434.9	366.6	-18.1	-11.0	84%
2008	519.2	401.5	66.2	23.9	77%
多年平均值	454.7	380.3			83%
多年最大值	636	531.2	183.0	153.6	92%
多年最小值	258.8	206.4	-194.2	-171.2	70%

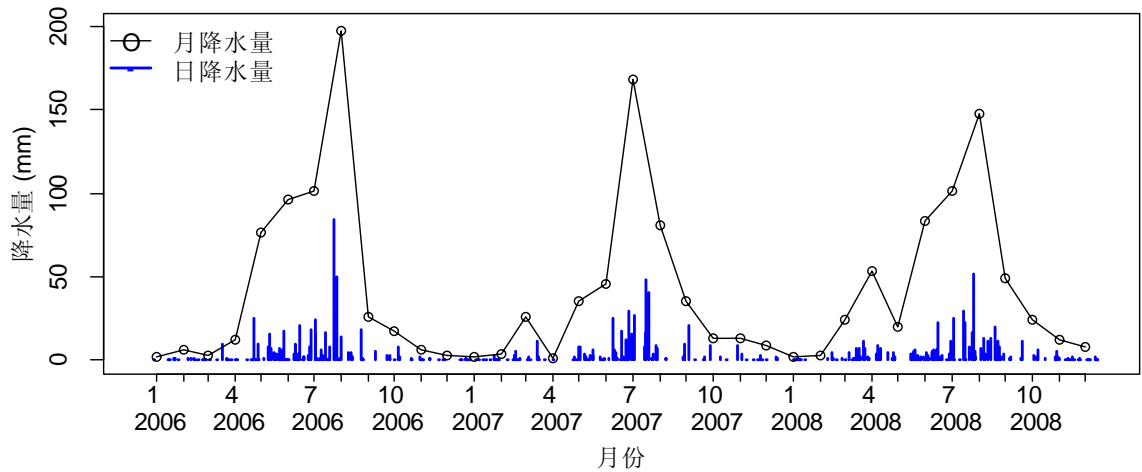


图 2-5 2006 ~ 2008 年塞罕坝月降水量与年降水量

(3) 1965 ~ 2011 年塞罕坝降水量变化规律的小波分析

揭示塞罕坝地区过去的降水变化规律对于在这里进行降水控制实验和气候变化研究具有重要的意义。我们采用 Morlet 复小波函数,对塞罕坝地区 1965 ~ 2011 年月降水量、5 ~ 9 月生长季降水量以及年降水量距平值(与相应多年平均值之差)时间序列数据进行了一维连续变换小波分析,发现塞罕坝地区降水变化存在多时间尺度嵌套的特征。47 年来该地区的月降水量、年降水量与生长季降水量距平值的变化主要表现在两种尺度上:一种是 4 年左右的年际尺度振荡,这是经过高频滤波后的年际变化中的低频部分,另一种就是 18 年左右时间尺度的年代际振荡。由于塞罕坝地区生长季降水平均占年降水量的 83.1%,通常二者的变化趋势相同,但也不完全一致。月降水量变化的主周期为 16 个月、4 年和 18 年,年降水量变化的主周期为 4 年和 18 年,生长季降水量变化的主周期为 4 年、10 年和 18 年。

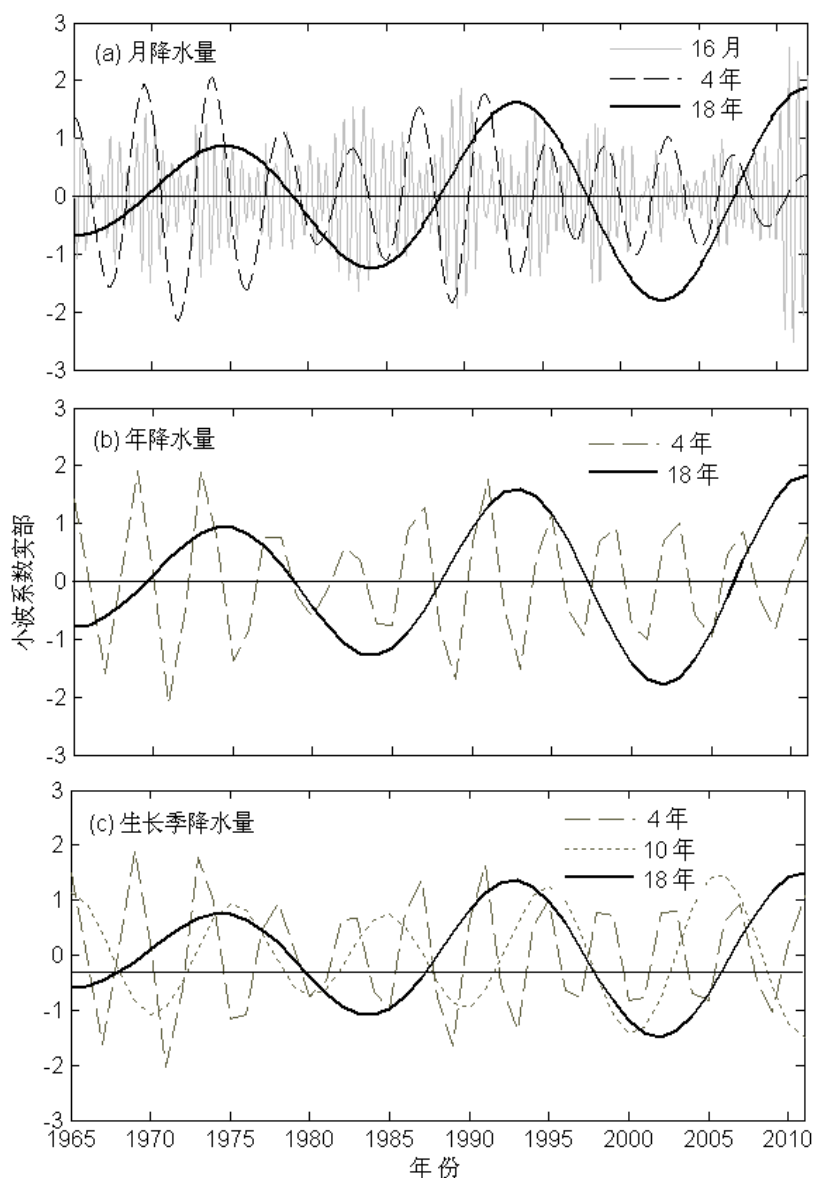


图 2-6 1965 ~ 2011 年塞罕坝降水量距平序列典型尺度过程线图

典型尺度(主周期)的过程线可以揭示降水量变化的突变特征,也可以体现小波变换的多尺度分析与预测功能。我们用典型尺度下各降水距平小波系数实部序列作图,观察小波系数变化的突变特征,并预测其变化趋势。由典型尺度小波系数过程线图(图 2-6)可知,在 4 年和 18 年尺度上,月降水量、年降水量和生长季降水量距平值的频率与位相大体一致,生长季降水量振荡的幅度略小于月降水量与年降水量。2007 年左右是一个降水量距平为零的拐点,降水控制实验进行的 2006~2008 年的降水量与生长季降水量与常年接近。由小波系数在 18 年主周期的变化趋势可预测(图 2-6b),2012 年后塞罕坝地区的生长季降水量和年降水量开始同时减少,但总体上还是处于丰水期,降水量高于常年,年降水量低于常年的拐点大约会出现在 2015 年左右,2016~2025 年降水量将会偏少。在 18 年左右的年代际尺度上,降水量呈现三个枯丰交替,但是振荡幅度逐渐增大(图 2-6b),这说明未来降水量年际变化幅度可能会增大,降水量变化的不确定性也会相应增加,因此非常有必要同时进行降水增加和降水减少两种降水变化情景的模拟。

2.2 研究方法

2.2.1 降水控制实验样地概况

降水控制实验样地位于北京大学地球环境与生态系统塞罕坝实验站西侧的樟子松—落叶松人工混交林内。海拔 1 531 m,地理坐标为 42°25' N, 117°15' E,位于阳面缓坡中上部,东侧距林缘 100 m,南侧距林缘 20 m。土壤类型为风沙土,乔木平均胸径约 12 cm,平均树高约 9 m,林下灌木稀少,草本层以披针叶苔草(*Carex lanceolata*)、腺毛委陵菜(*Potentilla longifolia*)、地榆(*Sanguisorba officinalis*)、瓣蕊唐松草(*Thalictrum petaloideum*)等为主。样地选址综合考虑了林分密度、地形均匀度和电力供应。

2.2.2 实验设计¹

降水控制实验样地占地 1 ha,采取正交试验设计,设置了 9 个 20 m × 20 m 的样地(图 2-7a)。包括 3 种穿透雨处理:(1)对照(Control),保持自然穿透雨量;(2)减雨(Dry),减少 30%穿透雨量,用覆盖地表面积 30%的薄膜水槽转移走该样地 30%的穿透雨量(图 2-7b);(3)增雨(Wet),增加 30%穿透雨量,把相应穿透雨减少样地转移来的 30%穿透雨用固定在地表的喷灌系统增加到该样地,从而实现穿透雨的有效截流与转移。每种处理 3 个重复,水平方向上三个不同的处理为一组,各样地间距 10 m 作为缓冲带。

¹ 本文作者从 2005 年开始参与了降水控制实验样地选址、实验方案设计与施工、仪器购买全过程。



图 2-7 降水控制实验样地设计及减雨样方

2.2.3 降水控制实验设施

降水控制实验设施由北京大学生态学系与北京农博科公司(承建单位)共同完成, 分为穿透雨收集系统、自动控制系统、喷灌系统和 AZ-DT 土壤水分监测系统四部分, 其中, AZ-DT 土壤水分监测系统由北京澳作生态仪器有限公司开发、组装。实验方案设计、购置仪器及前期外围设施施工于 2005 年和 2006 年初进行, 实验设施于 2006 年 6 月落成并开始运转。每年 10 月将塑料薄膜水槽撤掉, 并于次年 5 月初重新安装。共运行了 2006~2008 年三个生长季, 后因水分监测系统遭遇雷灾损坏导致实验未能按预期长期进行下去。

(1) 穿透雨收集系统

在每个减雨样方中, 设有 12 条宽度 0.50 m、长度 20 m 无色透明塑料薄膜水槽(图 2-7b), 共覆盖地表面积的 30%。水槽上沿平均离地 1.5 m, 既减少了对地表植被的干扰, 又方便在样地内工作。这些塑料薄膜为温室专用加厚透光塑料, 呈 U 型用蓝色卡箍固定在由黑色卡簧连接的镀锌钢管支撑架上。水槽自东向西呈一定倾斜角度, 利用重力作用保证雨水可以顺畅地流到西端直径 150 mm 的 PVC 圆形漏斗中。薄膜剪出直径略小于地漏进水口的圆洞, 并用地漏过滤盖压实, 然后用螺丝把地漏盖固定在地漏上, 过滤盖可以将凋落物过滤阻挡在漏斗表面。地漏底部连接着一段直径 75 mm 的 PVC 管, 便于把地漏拧在 PVC 集水管的 PVC 三通上。集水管与集水罐相连, 由总长度大于 20m、直径 110 mm 的 PVC 管和 12 个直径 110 mm 的 PVC 三通组成。雨水通过集水管后最终汇聚到放置在该样方西南角的 2 000 L 黑色不透光 PE 卧式集水罐(LT-2000L, 浙江慈溪爱迪威塑胶工业有限公司)中, 不透光的黑色可以有效减少罐中藻类繁殖。集水罐进水口处用 100 目的纱袋过滤水中细小杂质, 工作人员定期检查清理过滤物。

(2) 自动控制系统

自动控制系统由电柜、与其相连的浮球阀和电缆线组成。从集水罐进水口放入浮球阀, 调整电缆线长度, 使之刚好离开桶底, 并将电线固定在桶外。随着罐中水位上升, 浮球阀的一端逐渐

浮起；在水面到达预先设置的高水位后，浮球阀中开关吸合连通电路，集水罐旁电柜中的喷灌控制系统启动；水面降到桶底时，浮球阀开关断开，切断电路，喷灌自动停止。当然，也可以手动控制喷灌。

(3) 喷灌系统

喷灌系统由离心泵、过滤器、水表、黑色 PE 输水管和微喷头组成。雨水从集水罐出来经水泵加压后经过分压阀，分压阀连接的 PPR 管可将部分水返回罐中。然后，雨水经过过滤器精细滤网的第三次过滤后流经水表，水表会记录下有效的喷灌水量，最后通过 1' PE 输水干管送到增雨样地。干管位于增雨样地的一侧，连接着 6 条长约 20 m 的 6" 支管，每条支管上有 6 个间距约 3.5 m、喷射直径 4 m 的微喷头，将雨水均匀地喷灌到增雨样地中(图 2-8)。

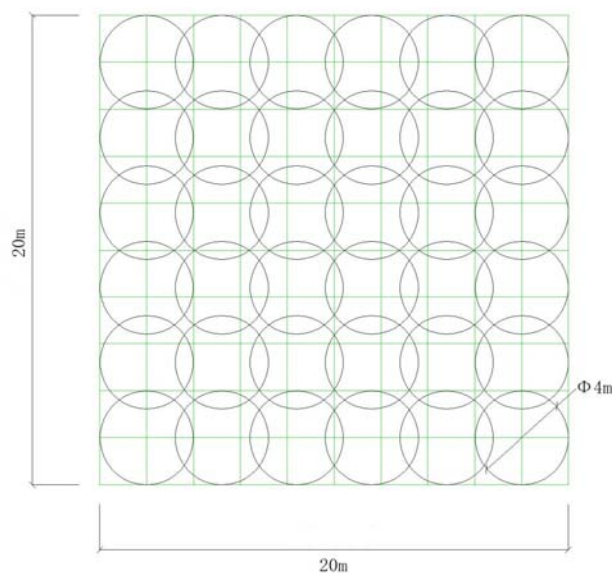


图 2-8 微喷头布置图

(4) AZ-DT 土壤水分监测系统

AZ-DT 土壤水分测定系统由 1 台 DT50 多通道数据采集器(Datataker Pty Ltd, Rowville, Australia)、1 个电源分配器、9 个 TRIME-IT 传感器(IMKO GmbH, Ettlingen, Germany)、1 块 12V 蓄电池、1 套交流电源(交流开关, 开关电源, 充放电控制器)、1 个防水机箱组成(图 2-9)。

在 DT50 数据采集器上, 插有一张数据存储卡, 容量为 1M 字节, 可用一根 RS232 数据通讯线与电脑连接。加电后, 系统会自动运行预装载的程序, 按既定的采样间隔将数据记录在存储卡和内存里。换电池或意外断电使系统停机后, 重新加电系统会自动运行, 无需人工干预。

TRIME-IT 传感器采用的是 TDR 原理(Time Domain Reflectometry, 时域反射原理), 根据探测器发出的电磁波在不同介电常数物质中的传输时间的不同, 计算出被测物的体积含水量, 能够使用水平或垂直方式进行埋设。



图 2-9 AZ-DT 土壤水分监测系统

为了保障数据安全，样地配置了 ECO A 和 ECO B(图 2-9)两套土壤水分监测系统，其中，ECO A 为蓄电池供电的数据采集器系统，ECO B 为交流电与蓄电池供电的数据采集器系统。

2006 年在每个样方放置了两个水分传感器，土壤体积含水量数据采样间隔设置为 1 小时。在综合考虑土壤水分监测层次的特征、传感器数量及数据线长度的基础上，2007 年在每个样方 A 点设置一个传感器，将余下的 9 个传感器分三组水平安装在中坡的增雨、减雨和对照样地西南角 5 m×5 m 处，对 10 cm、20 cm、40 cm、80 cm 四个不同深度进行土壤水分监测，采样记录时间间隔为 1 小时。

2.2.4 测量指标与方法²

为了全面系统地研究降水格局变化对人工林生态系统碳循环主要过程的影响，我们选择了以下指标进行野外测量与样品采集(表 2-2)，相应的样品分析指标与方法见表 2-3。

² 本文作者于 2006 年和 2007 年 5 月~10 月驻守野外，负责降水控制实验设施运行与几乎全部指标的野外观测采样和室内实验测定，2006 年 8~10 月的土壤呼吸速率由硕士研究生汪涛测定，2007 年土壤活性有机碳室内实验由硕士研究生魏天凤完成；2008 年各项指标由博士研究生杜恩在完成。

表 2-2 野外测量指标与样品采集

指 标	方 法	工具/仪器	时 间
10 cm 土壤水分	TDR	AZ-DT 土壤水分监测系统; TRIME-HD, TDR 100	5-9 月
10 cm 土壤温度	热电偶法	StowAway TidBiT	5-9 月
乔木径向生长、树高	每木检尺	卷尺、测高尺	5 月、9 月
固定样方草本及灌木物种多样性	群落调查	样方框、卷尺、相机	8 月 19 日
草地上生物量	收割法	样方框	8 月 20 日
凋落物量与凋落物现存量	样方框法	纱框	5-9 月
土壤呼吸速率	IRGA	LI-8100	5-9 月
土壤活性有机碳	土钻法	土钻	5-9 月
土壤无机氮及净氮矿化速率	野外培养法	土钻、PVC 管等	6-9 月
土壤总有机碳	土钻法	土钻	9 月
土壤容重	环刀法	铁锹、环刀、剖面刀	9 月

表 2-3 实验室样品分析指标与方法

项 目	指标/分析项目	方法/仪器
草本植物生物量	地上生物量	烘干法/烘箱、电子天平
0-100 cm 土壤容重	容重、砾石含量	烘干法/烘箱、电子天平
0-30 cm 土壤活性有机碳	土壤微生物量碳	氯仿熏蒸浸提法、TOC 分析仪
	水溶性有机碳	水浸提法
土壤总有机碳		重铬酸钾氧化外加热法
土壤重量含水量		质量法/烘箱、电子天平
0-30 cm 土壤氮矿化	NO_3^- -N, NH_4^+ -N	流动注射分析仪

(1) 土壤体积含水量

土壤体积含水量是指土壤中水分占有的体积和土壤总体积的比值。用于降水控制实验背景值监测和大部分数据分析，文中的土壤水分数据如未特别指明均为土壤体积含水量，主要通过定点自动监测和样线法手工测量两种途径获得。此外，每次测土壤呼吸时也会测量相应的土壤体积含水量数值。土壤水分自动监测数据采集时间间隔为 1 小时。

样线法：在每个样地西北角和东南角对角线上拉一条红色细绳，并用编号的电工胶带标签将对角线平分为 10 段，每个样地共计 11 个监测点。每周用 Field Scout TDR 100 土壤水分速测仪 (Spectrum Technologies, Plainfield, IL, USA) 或 TRIME-HD 手持式土壤水分读数表 (IMKO GmbH, Ettlingen, Germany)，沿各对角线上的 11 个监测点测量一次。测量时要注意让传感器的两个探针平行垂直插入土中。

(2) 土壤重量含水量

土壤重量含水量是指土壤中水分的重量与相应固相物质重量的比值。在本研究中主要用于土

壤活性有机碳和土壤氮矿化分析。土壤重量含水量用烘干称重法测定,这是唯一可以直接测量土壤水分方法,也是目前国际上的标准方法。将新鲜土壤样品后装入铝盒(烘干重量 M_0)后称重 M_1 ,在 105 °C 的烘箱内将土样烘干 24 小时至恒重后,称量铝盒与土样总重量 M_2 。计算公式如下:

$$\text{土壤重量含水量} = (M_1 - M_2) / (M_2 - M_0) \times 100 \% \quad (2-1)$$

(3) 土壤温度

地下 10 cm 土壤温度通过自动监测与手测两种途径获得。每个样地 A、B 两点各放置 1 个 StowAway TidBiT 袖珍温度记录仪(Onset Computer Corporation, Pocasset, USA)自动监测土壤温度,共计 18 个。用土钻取出深度 10 cm 的土芯,将温度记录仪正面朝下水平放入,用土芯和凋落物盖住温度记录仪,将标签露在地表,便于查找。在生长季结束后,将温度记录仪从土壤中取出并清理后,LED 灯闪烁说明工作状态正常,与计算机相连后读取数据。StowAway TidbiT 袖珍温度记录仪小巧可靠,非常适合野外使用,唯一的缺点是埋入地下后不容易找到,一定要在地面做好标记。每次测量土壤呼吸时用热传感器或金属探针温度计测量地下 10 cm 的土壤温度。

(4) 土壤活性有机碳

我们选取了土壤微生物生物量碳(Microbial biomass carbon, 简称为微生物量碳)和水溶性有机碳作为土壤活性有机碳的指标。首次采样时在每个样地内随机选取 5 个 1 m×1 m 的小样方,去除采样点地表枯落物后,用内径 5 cm 的土钻分 4 层(0-5 cm、5-10 cm、10-20 cm、20-30 cm)钻取土芯样品,将 5 个小样方中的样品同层混匀后作为该样地的样品。每次采样共 36 个样品(9 样地 4 层)。随后的 4 次采样都在首次采样划定的小样方内。采出的土壤样品放入写有编号和采样时间的 10 号封口袋,用放有冰种的保温箱运回实验室,放在 4 °C 的冰箱内保存。采样频率为每 4 周一次。用四分法取其中的 1/2(0-5 cm、5-10 cm)或 1/4(10-20 cm、20-30 cm)。用精度 0.0001 g 的天平称取约 20g 筛前的新鲜土壤样品放入编号的 4 号封口袋中,以测定过筛前土壤重量含水量。将剩余土壤样品中的石块和凋落物、根系等杂物从样品中挑出后过 2 mm 筛。用精度 0.01 g 的天平称取其中约 200 g 样品放入编号的 7 号封口袋中,在 4 °C 冰箱中保存以分析土壤微生物量碳和水溶性有机碳;其余部分也放入编号的 7 号封口袋中,在室温下风干,过 1 mm 和 0.25 mm 筛,供土壤总有机碳分析使用(一年测定一次即可)。

土壤微生物量碳采用氯仿熏蒸浸提法测定(Chloroform fumigation-extraction method, FE) (Brookes et al., 1985; Vance et al., 1987a)。从每个土壤样品中用精度 0.0001 g 的天平称取一份 20 g 的样品 105 °C 烘干后测定筛后土壤重量含水量,再称量 2 份 10 g 土壤样品,将一份放入 250 ml 塑料瓶中,另一份放在真空干燥器内的玻璃瓶中,两份土壤都放在 25 °C 的保温箱内进行培养 7 天。用量筒称取 50 ml 0.5 mol L⁻¹ 的硫酸钾溶液,倒入塑料瓶内,在摇床上震荡 1 个小时,密封

后放到离心机中以 2000 r/min 的速度离心析出上清液，将上清液经覆盖慢速滤纸的漏斗过滤后，放入 25 ml 小塑料瓶中-18 °C 冷冻保存以测定总有机碳。将装有另一份 10 g 土壤样品的玻璃瓶中放到 25 °C 真空干燥器内，干燥器内放入无酒精氯仿，干燥器底部有多张用去离子水浸湿的滤纸，用真空泵抽出干燥器内空气，密封并在黑暗条件下保存 24 h。24 h 后打开真空干燥器，将无酒精氯仿和滤纸取出，再进行多次抽气，将残留在干燥器内和土壤中的氯仿气体抽出。然后再进行浸提过滤以测定总有机碳。浸提液总有机碳用 Multi N/C 3100 总有机碳分析仪 (Analytik Jena AG, Jena, Germany) 测定。将浸提液有机碳转换为微生物量碳使用的系数 K_{EC} 为 0.37 (Vance et al., 1987a)，计算方法为：

$$\text{土壤微生物量碳} = (\text{熏蒸的土壤总有机碳} - \text{未熏蒸的土壤总有机碳}) / K_{EC} \quad (2-2)$$

水溶性有机碳的浸提过程与土壤微生物量碳的浸提过程相似，主要区别是用 50 ml 去离子水溶解 10 g 土壤，滤出液放到 25 ml 小瓶中-18 °C 冷冻保存。浸提液中的有机碳用总有机碳分析仪测定。

(5) 土壤总有机碳

土壤总有机碳采用重铬酸钾—硫酸加热氧化法测定 (GB9834—88)。

称取风干过 100 目筛的土壤样品 0.2 ~ 0.4 g 放入硬质试管中，先加 5 ml 0.8 mol L⁻¹ 的重铬酸钾溶液，再加 5 ml 浓硫酸来氧化土壤总有机碳。在试管口放一个小漏斗，将其插入铁丝笼固定后放进 180 °C 预热的油浴锅内，控制油浴温度在 170 ~ 180 °C，使其沸腾 5 min。取出试管冷却后，将试管内和漏斗上的溶液用蒸馏水冲洗入 250 ml 锥形瓶，加邻苯氨基苯甲酸指示剂 3 ~ 5 滴，最后用 0.5 mol L⁻¹ 硫酸亚铁滴定，当溶液由棕红色变成蓝绿色时即为滴定终点，根据反应消耗的重铬酸钾量计算出有机碳含量。

(6) 土壤容重

土壤容重采用环刀法进行测定。在每个样方中随机选一点，通常在已采过土样的点附近，分 0-5 cm、5-10 cm、10-20 cm、20-30 cm、30-50 cm、50-70 cm 和 70-100 cm 七层采样。9 个样方共 63 个样品。把环刀装在土钻中采样，将环刀小心取出后，用剖面刀小心地将环刀两面的土壤样品削平，将环刀中的土壤倒入编号的封口袋中。带回实验室后在阴凉通风处风干，注意在袋口上覆盖报纸以避免灰尘污染。将风干后的样品倒在 10 号封口袋拆开做成的塑料布上，用擀面杖轻轻碾压，压过的土样过 2 mm 筛，将筛出的石子称重以测定土壤砾石含量，并将过筛后的样品放到已称重的铝盒中，在 105 °C 烘箱中烘干 48 h。用电子天平称量样品干重并计算土壤容重 (g cm⁻³)。

(7) 土壤铵态氮、硝态氮与净氮矿化速率

我们采取野外顶盖培养法 (Closed-Top Tube Incubations) 来研究土壤氮矿化，该方法能较好地

反映土壤有机氮的实际矿化速率(陈伏生等, 2006)。

用电钻在长度 35cm、内径 40 mm 的 PVC 管管口 1 cm 处的管壁四周垂直方向上打直径 4 mm 的小孔 4 个(用于保证气体交换和取出 PVC 管), 并在 3 cm 处用记号笔做标记。每月在样地中按照 S 形布置 8 管, 9 个样地共 72 管; 同时在各管旁用土钻采集相同深度(0-5 cm、5-10 cm、10-20 cm、20-30 cm)的土壤作为背景值, 各样地同层样品放入编号的 10 号封口袋, 9 个样地每次共 36 个背景值样品。用有冰种的保温箱带回实验室后在冰箱中 4℃ 保存。无须去除地表凋落物, 直接用橡胶锤把 PVC 管垂直砸入土中, 直到 3 cm 标记处与管外的土壤表面齐平(实际埋入土中 30 cm), 地面上露出 3 cm(易封口, 易拔出)。将 PVC 管口用通气但不漏水的保鲜膜和电工胶带封住(避免降水氮沉降及雨水对管内氮素的淋溶)。共设 3 次重复, 分别于 6 月、7 月、8 月埋入, 在培养 1 个月后取出。

把直径 4 mm 的钢丝用钳子弯成拉长的 Ω 形, 将略微上翘的钢丝两端插入 PVC 管上端相对的小孔中, 将另一根 PVC 管穿过钢丝的 Ω 弯, 把 PVC 管小心地提出地面。把一根长度为 40 cm 的 PVC 六分管(外径略小于 40 mm)的一端用电工胶带封口, 以封口端为原点、在 5-15-25-30-35 cm 处分别划线标记。用此管自上而下将土柱推出培养管: 推到 5 cm 刻度时将管口外多余的 2 cm 土柱用裁纸刀切到旁边塑料布上, 将土芯推到 15 cm 刻度时的样品直接盛入编号的 10 号封口袋作为 20-30 cm 的样品, 将土芯推到 25 cm 刻度时的样品为 10-20 cm 的样品, 将土芯推到 30 cm 刻度时为 5-10 cm 的样品, 将土芯推到 35 cm 刻度时的样品为 0-5 cm 的样品, 注意不要把地表凋落物推入袋中, 分别装入编号的封口袋, 每个样地 8 管中同一层的样品混合作为一个样品, 9 个样地共 4 层、36 个野外培养样品。放入有冰种的保温箱带回实验室后在冰箱中 4℃ 保存。将 PVC 管清理并再次砸入土中培养一个月。

打开封口袋, 然后让袋中充气后用手攥紧一端, 将袋中样品混合均匀; 用四分法取其中 1/4 土壤样品。用精度 0.0001 g 的天平称取约 20 g 未过筛的新鲜土壤样品放入编号的封口袋中, 用来测定筛前土壤重量含水量。将剩余的土壤样品中的石块和植物凋落物、根系等杂物从样品中挑出后过 2 mm 筛。用精度 0.01 g 的天平称取约 200 g, 在 4 °C 冰箱中保存。

在采样后 24 h 内从每个土壤样品中用精度 0.0001 g 的天平称取一份 20 g 的样品测定筛后土壤重量含水量, 再称量一份 22 g 左右的土壤样品放入编号的 200 ml 塑料瓶中。其余过筛的土壤样品在室温下风干后供其他指标分析使用。用量筒称取 100 ml 2 mol L⁻¹ KCl 溶液倒入塑料瓶内, 密封后在摇床上震荡 1 h, 然后将上清液经覆盖慢速滤纸的漏斗过滤, 将滤出液放入 100 ml 小塑料瓶中, 用封口膜密封后-18 °C 冷冻保存。分别将称重后的筛前和筛后土壤重量含水量样品装入已称重编号的铝盒中, 在 105 °C 下烘干 24 小时后称重, 用差量法计算得出土壤重量含水量。

将冷冻的浸提液解冻后,用 10 ml 注射器吸取 5 ml 浸提液,经 0.4 mm 水系膜过滤后用封口膜密封在 5 ml 的离心管中, -18 °C 冷冻保存。用 FIAstar 5000 流动注射分析仪(FOSS, Denmark)测定浸提液中的铵态氮和硝态氮。

流动注射分析仪测定的浸提液浓度单位是 mg L^{-1} , 乘以浸提液体积(0.1 L)后分别得到浸提液中铵态氮和硝态氮的总量, 然后除以用于浸提的土壤干重即为以干土计的浓度(mg kg^{-1}), 其中:

$$\text{土壤干重} = \text{用于浸提的筛后土壤鲜重} \times (1 - \text{筛后重量含水量}) \quad (2-3)$$

无机氮为铵态氮与硝态氮二者之和。

根据培养前后土壤铵态氮、硝态氮含量之差, 分别计算土壤氮素的净氨化速率、净硝化速率和净氮矿化速率, 单位均为 $\text{mg kg}^{-1} 30\text{d}^{-1}$ 。

$$\text{净氨化速率} = (\text{培养前铵态氮} - \text{培养后铵态氮}) / \text{培养天数} \times 30 \quad (2-4)$$

$$\text{净硝化速率} = (\text{培养前硝态氮} - \text{培养后硝态氮}) / \text{培养天数} \times 30$$

$$\text{净氮矿化速率} = (\text{培养前无机氮} - \text{培养后无机氮}) / \text{培养天数} \times 30$$

(8) 乔木胸径与树高

在每年生长季开始与结束时进行每木检尺并计算乔木胸径, 在每个样方中随机选择樟子松和落叶松各 5 株准确测量树高。在每株乔木离地垂直距离 1.3 m 处用钉子把红色铝制树牌钉在树上, 保证树牌上沿距地面 1.3 m。将卷尺沿树牌上沿水平环绕一周, 使卷尺重叠处与树牌上沿重合, 读数并记录周长(CBH), 根据周长求胸径(DBH)。1.3 m 以下分枝的乔木作为两株独立的乔木分别测量。如果分枝距离太近以致无法用卷尺环绕测量时, 可用游标卡尺直接在红色树牌上沿处测胸径, 并在记录表中注明是胸径数据。

首次测量树高时, 在每个样方中随机选择樟子松与落叶松各 5 株, 用伸缩测高尺准确测量树高(m)。一人将测高尺沿树干垂直向上拉伸, 另一人从远处观察, 当测高尺顶端与树顶齐平时, 读数并记录树高。用这些乔木的胸径和树高建立异速生长回归方程, 估算出其余乔木的树高。

(9) 草本植物地上生物量

每个样方内布置 5 个 $1\text{ m} \times 1\text{ m}$ 的小样方, 共 45 个小样方; 每年都要重新布置不重复的小样方, 并在图上标记位置。每年 8 月 20 日刈割小样方内地表以上草本植物。在每个样地内用卷尺、样方绳和竹篾围 5 个 $1\text{ m} \times 1\text{ m}$ 的小样方。用剪刀贴地面剪去样方内所有草本植物, 装在编号的档案袋中, 封口。档案袋上记录小样方编号、采样时间、小样方总盖度(%)。采回样品后在阳光下曝晒风干后, 放到烘箱中 $60\text{ }^{\circ}\text{C}$ 烘干 48 h。用精度为 0.01g 的电子天平称重。

(10) 生长季土壤呼吸速率和表观 Q_{10}

土壤呼吸速率测定采用 LI-8100 开路式土壤碳通量测量系统(LI-COR Inc., Lincon, NE, USA)。

为了保证推算结果的正确, 测量室内外的浓度梯度、气压、土壤温湿度应该相似, 并且每次测量时间限制在 0.5 ~ 3 min 之间, 以保证测量室中 CO₂ 浓度变化尽可能小。

测定环(soil collars)是内径 10cm、高度 5cm、一端磨尖的 PVC 管。在首次测量前一天, 将测定环用橡皮锤和木条砸到需要测定的位置, 使测定环上沿水平、距地表约 2-3cm, 为防止插入时对土壤的干扰, 稳定 1 天后进行测定。每个样地中布置 5 个测定环, 其中, 每个样方上方的 2 个要装在塑料薄膜水槽投影内, 中间和下方的 3 个在塑料薄膜水槽外。水槽投影面积占样方面积的 30%, 因此需用 5 个测定环测量值的加权平均值作为当天测量的样方土壤呼吸值。

从 6 月到 9 月, 每两周测一次土壤呼吸。用钢卷尺测量测定环内侧地表至环顶的距离, 间隔 90° 在四个方向上测量测定环高出土壤表面的距离(collar offset), 求平均值后输入 PDA。用 LI-8100 开路式土壤碳通量测量系统在每个测定环上测量土壤 CO₂ 通量, 每个测定环上重复测量三次。在仪器测量前把 LI-8100 配套的热传感器或探针式温度计插入土中 10 cm, 在数据稳定后, 记录土壤温度数据。在仪器测量过程中, 用 Field Scout TDR 100 土壤水分速测仪间隔 120 度、在 Collar 周围的三个不同位置上测定 10cm 处土壤体积含水量并记录。

基于三个生长季内对土壤呼吸的原位测定, 我们把土壤呼吸速率 R 和 10cm 土壤温度 T 代入 van't Hoff 指数方程(Van't Hoff, 1898; Luo & Zhou, 2007)计算其参数 a 和 b :

$$R = ae^{bT} \quad (2-5)$$

土壤呼吸的表观温度敏感性指标 Q_{10} 可通过以下公式计算得到:

$$Q_{10} = e^{10b} \quad (2-6)$$

用一年的地下 10cm 土壤温度 T 与土壤体积含水量(volumetric water content, VWC)时间序列数据, 分别代入我们开发的土壤温度与水分交互作用土壤呼吸预测新模型计算各时间点的土壤呼吸速率, 乘以相应的时间间隔后求和即为土壤呼吸 CO₂ 年通量。模型如下:

$$\ln R = a + b T \times VWC \quad (2-7)$$

(11) 凋落物量与现存凋落物量

在每块样方中测定土壤呼吸和草本植物生物量的小样方附近设置 3 个 1×1 m² 的小样方(共 27 个小样方), 将铁丝和尼龙网(70 目)制成的面积为 1×1m² 的样方框放置于样方内, 四角支撑离地约 30cm。每月收集凋落物, 分开针叶和小枝及杂物, 分别称其风干重和烘干重(80℃)。每两到三月收集样方内的大的落枝, 称鲜重, 然后称取部分样品烘干称重, 据此计算落枝的干重。在上述 27 个小样方测定凋落物量之前, 把小样方内的凋落物全部取回样品袋, 分选枝叶及杂物分别称风干重及烘干重, 作为现存凋落物量。

2.2.5 数据统计分析

作为野外定位控制实验，很多指标都需要重复测量，所以我们用重复测量方差分析(Repeated measure of ANOVA)或混合模型(Linear Mixed Effects Model)方差分析(Bates et al., 2011)来分析不同穿透雨处理对重复测量指标的影响。其中，穿透雨处理和土壤深度作为组间效应或固定效应(fixed effect)，月份(日期)和重复作为组内效应或随机效应(random effect)。用经过 Bonferroni 校正的配对 t 检验(paired t test)来比较不同处理时间序列的差异，可以减少犯 I 类错误的概率。用单因素方差分析比较穿透雨对非重复测量数据的影响。用 Tukey HSD(Honest Significant Difference)检验对均值进行多重比较。统计分析与绘图均在 R(version 2.14.0, R Foundation for Statistical Computing, Vienna, Austria)中进行(R Development Core Team, 2011)。文中统计显著性检验水平均为 $\alpha = 0.05$ 。

第三章 降水变化对土壤理化性质的影响

3.1 降水变化对土壤水分的影响

在2006年生长季,我们连续监测了每个样方地下10cm的土壤体积含水量;2007年又分10cm、20cm、40cm和80cm四种土壤深度监测了不同层次土壤体积含水量的变化,每周采用样线法测量了地下10cm的土壤体积含水量;2008年因雷灾(塞罕坝的雷灾比较严重)导致土壤水分监测系统损坏,所以定期用土钻取土测定0-10cm的重量含水量,然后用土壤容重换算为体积含水量。

方差分析和配对t检验的结果表明,穿透雨处理对土壤体积含水量的影响是显著的($P < 0.001$),10cm、20cm和40cm土壤体积含水量增雨 > 对照 > 减雨(图3-1, 3-2, 3-3),80cm处的土壤体积含水量对照 > 减雨 > 增雨(图3-1d)。2008年8次手测数据配对t检验的结果表明,三种处理在水槽下方和水槽外测定的土壤体积含水量均有显著差异($P < 0.05$),每个样方5个测量点取平均值作为样方土壤水分后,增雨与对照有显著差异($P = 0.04$),增雨与减雨、减雨与对照却无显著差异($P > 0.05$)。

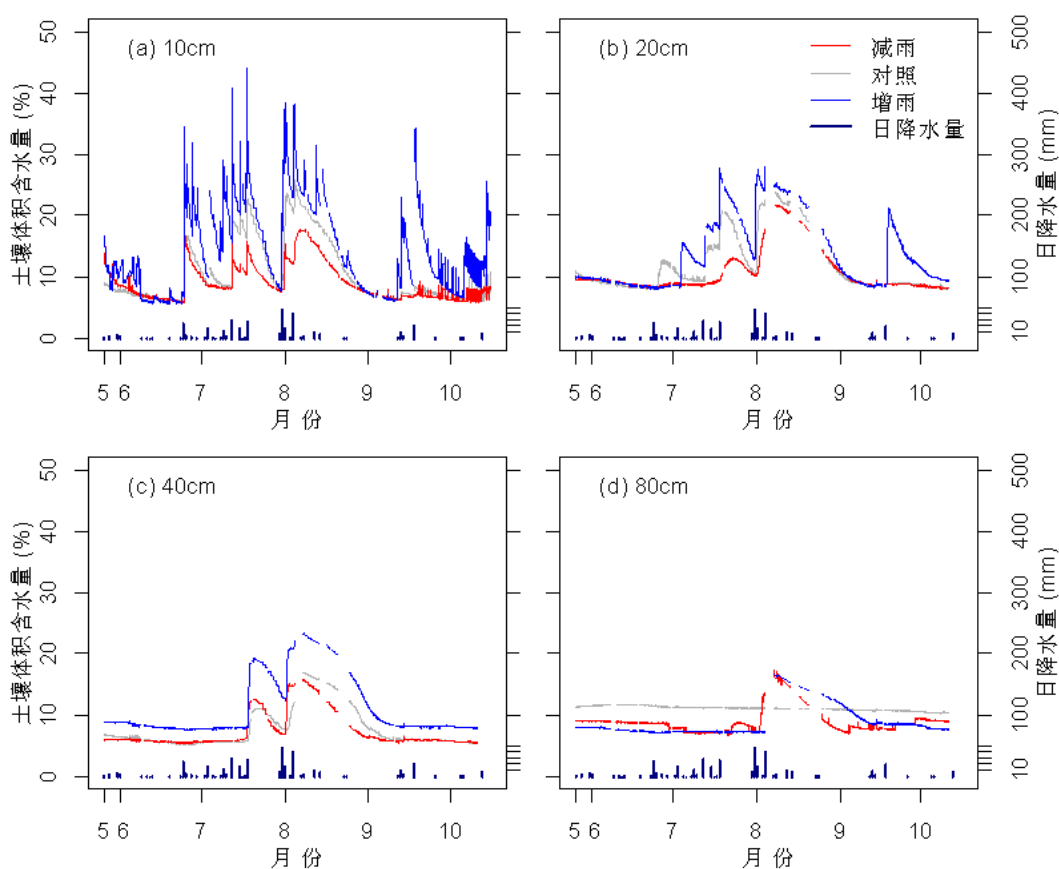


图 3-1 2007 年 5 月~10 月地下 10cm、20cm、40cm、80cm 土壤体积含水量与日降水量

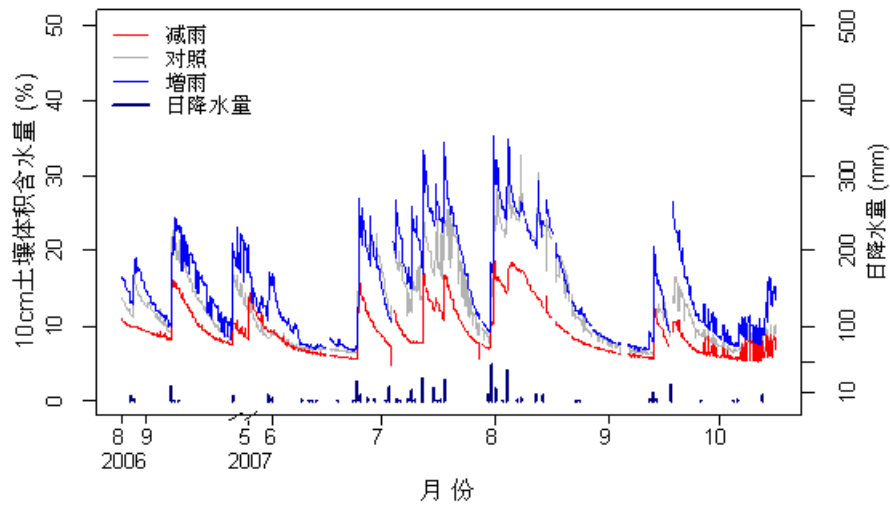


图 3-2 2006 年 8 月 ~ 2007 年 10 月地下 10cm 土壤体积含水量与日降水量

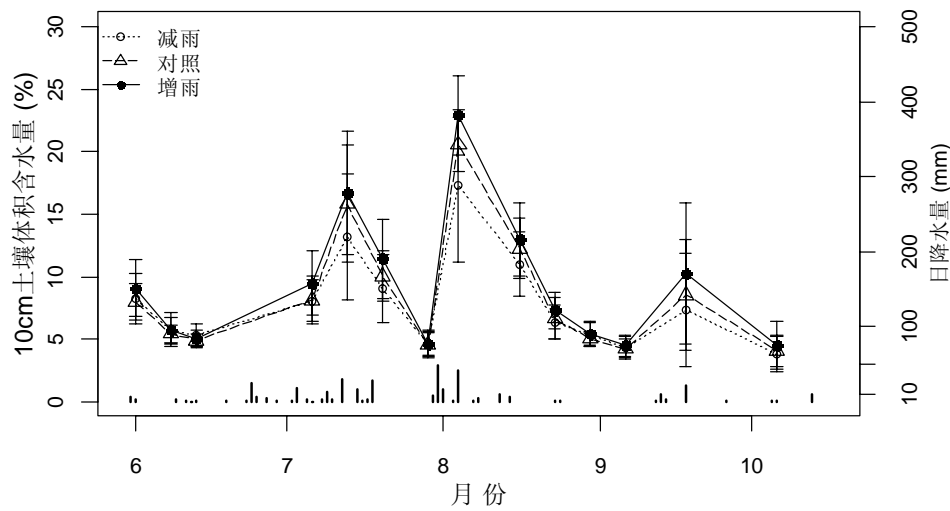


图 3-3 2007 年 6 月 ~ 10 月每周手测地下 10cm 土壤体积含水量

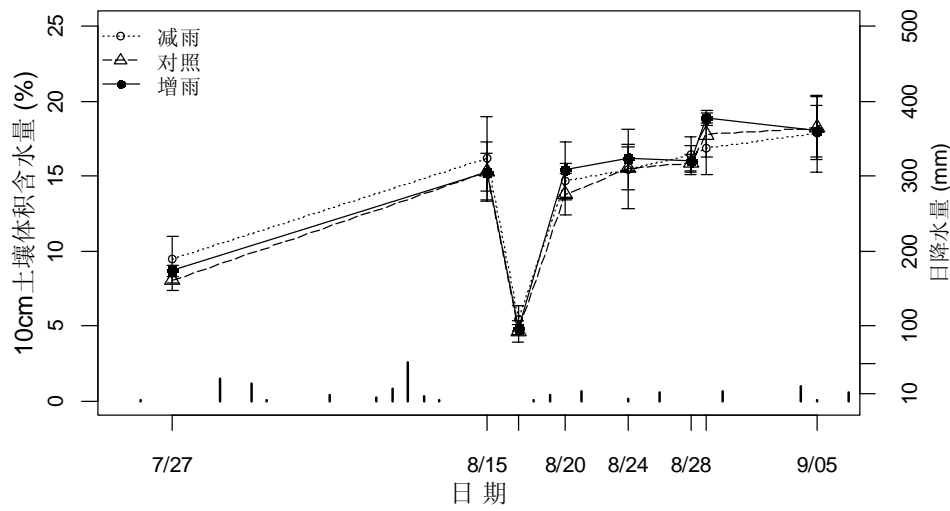


图 3-4 2008 年 0-10cm 土壤体积含水量

注：图中数据点为平均值±标准差，土壤体积含水量数据由重量含水量与土壤容重计算得到。

3.2 降水变化对土壤温度的影响

我们对样地土壤温度的时间序列数据进行了配对 t 检验, 结果表明 2006 年和 2007 年三种处理的土壤温度统计上均无显著差异, 但减雨处理的温度略高于增雨和对照。我们还比较了 2006 ~ 2008 年土壤呼吸测定时的温度, 发现三种处理间也无显著差异($P > 0.05$)。这与美国橡树岭国家实验室在田纳西州 Walker Branch 落叶阔叶林穿透雨转移实验中观察到的结果是一致的(Hanson et al., 1998)。

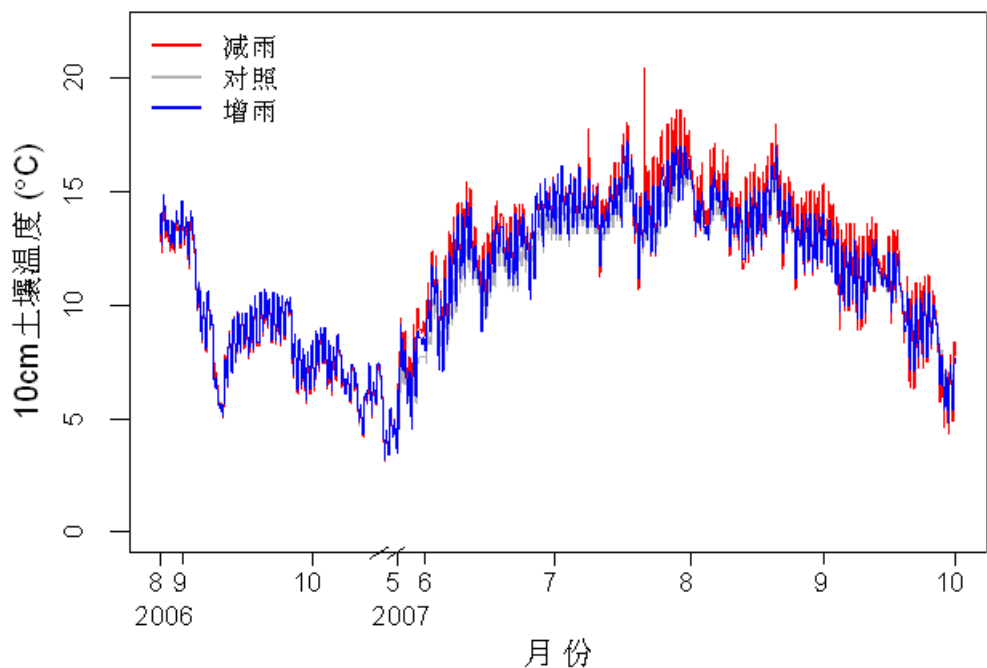


图 3-5 2006 ~ 2007 年地下 10 厘米土壤温度变化

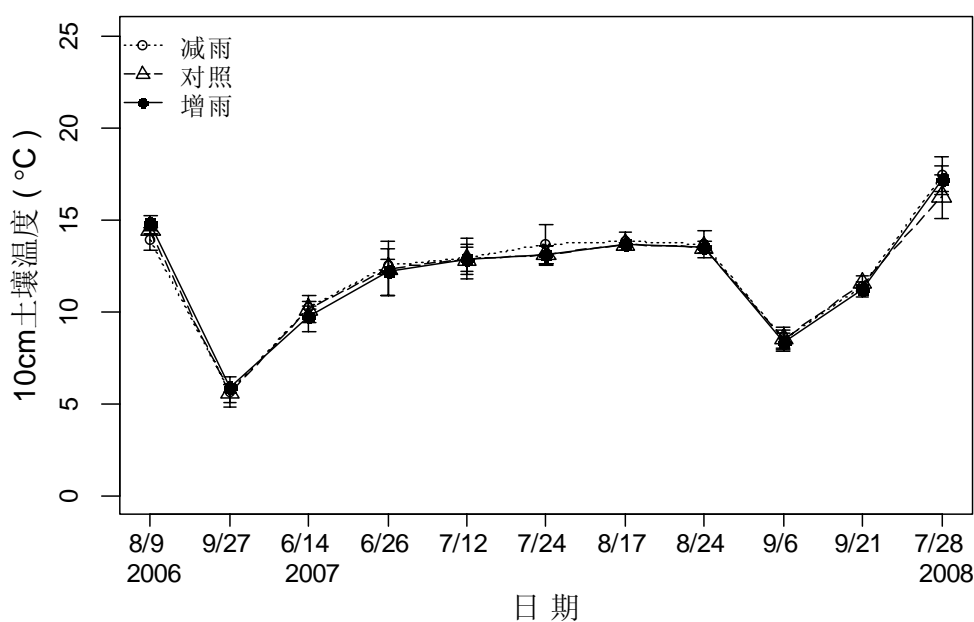


图 3-6 2006 ~ 2007 年地下 10 厘米土壤温度变化(土壤呼吸测定数据)

3.3 降水变化对土壤活性有机碳的影响³

3.3.1 微生物量碳及其与土壤总有机碳的比值

2007年5~9月的研究表明,樟子松—落叶松人工混交林土壤微生物量碳的平均值为260.7 mg kg⁻¹, 变幅为51.0~646.0 mg kg⁻¹, 最大值出现在减雨处理的0-5cm土层, 最小值出现在对照的20-30 cm土层。三种处理的土壤微生物量碳平均值分别为增雨处理265.9 mg kg⁻¹、对照228.5 mg kg⁻¹、减雨处理287.7 mg kg⁻¹。土壤微生物量碳随土壤深度的增加呈显著下降趋势(表3-1)。在10-20 cm土层内, 减雨处理的土壤微生物量碳平均值显著高于对照; 在20-30 cm土层内, 减雨和增雨处理的土壤微生物量碳都显著高于对照(表3-1)。

表 3-1 不同穿透雨处理的土壤活性有机碳

土壤活性有机碳	土壤深度 (cm)	穿透雨处理		
		减雨 30%	对照	增雨 30%
土壤微生物量碳 (mg kg ⁻¹)	0-5	424.1 ± 143.7	353.6 ± 96.8	371.3 ± 79.0
	5-10	289.6 ± 96.4	228.2 ± 67.8	276.8 ± 51.9
	10-20	238.6 ± 64.3	186.2 ± 51.5	218.7 ± 46.9
	20-30	198.4 ± 55.4	145.9 ± 44.9	196.9 ± 47.3
土壤微生物量碳/ 土壤总有机碳(%)	0-5	2.38 ± 0.81	2.52 ± 0.50	2.35 ± 0.62
	5-10	1.62 ± 0.39	1.75 ± 0.35	2.18 ± 0.39
	10-20	1.51 ± 0.39	1.7 ± 0.39	1.67 ± 0.35
	20-30	1.33 ± 0.35	1.41 ± 0.43	1.64 ± 0.31
水溶性有机碳 (mg kg ⁻¹)	0-5	88.32 ± 51.67	59.52 ± 21.88	49.46 ± 6.00
	5-10	70.68 ± 46.59	42.1 ± 11.27	40.71 ± 6.16
	10-20	56.95 ± 34.86	39.98 ± 6.55	39.03 ± 3.10
	20-30	46.28 ± 8.64	41.03 ± 8.25	38.25 ± 5.19

注: 表中数据为2007年5月到9月的平均值±标准差。

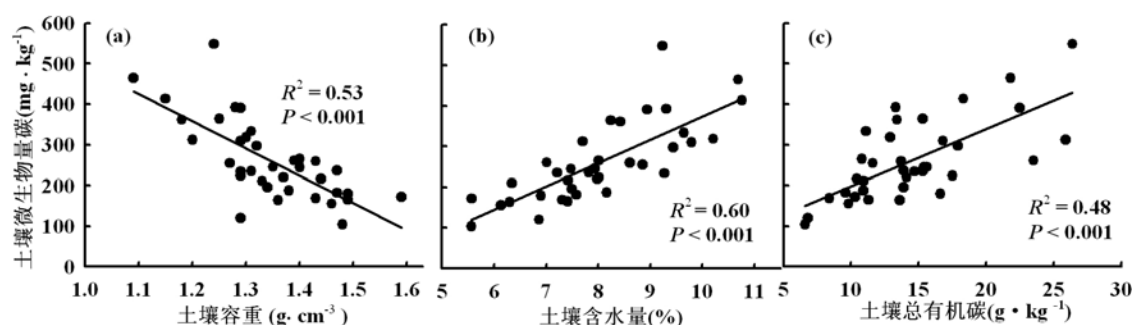


图 3-7 土壤微生物量碳与土壤容重(a)、土壤含水量(b)、土壤总有机碳(c)的关系

土壤微生物量碳随土壤深度增加而下降, 这种递减现象与土壤容重密切相关(图3-7a)。样地土壤中的有机质主要集中在0-10 cm, 10 cm以下土壤容重较高, 土壤微生物量碳减少。土壤微生物

³ 土壤活性有机碳实验是降水控制实验的一部分, 主要由硕士研究生魏天凤完成。本文作者因需长期驻守野外, 未能亲自在实验室测定土壤活性有机碳与土壤总有机碳指标, 但参与了该指标的实验设计、野外采样、样品前处理、结果分析等过程。

物量碳也与土壤水分(图 3-7b)、土壤总有机碳(图 3-7c)显著正相关。

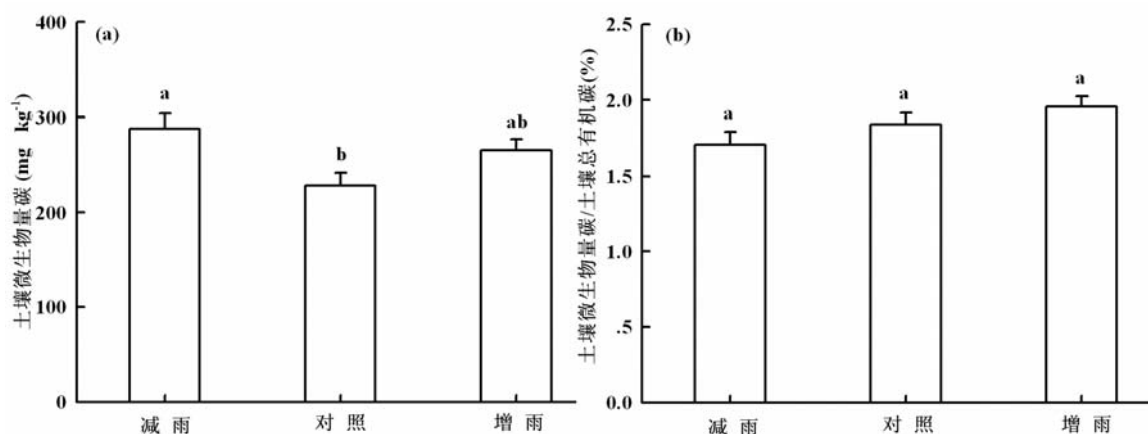
土壤微生物量碳与土壤总有机碳的比值是被微生物固定的总有机碳的比例,可以反映底物对土壤微生物区系供应有效养分的能力,若可利用碳的浓度低,此比值也随之降低(Brookes, 1995)。土壤微生物量碳与土壤总有机碳的比值能够消除土壤有机质的异质性引起的问题。樟子松—落叶松人工混交林地下0-30cm土壤微生物量碳与土壤总有机碳比值的平均值为1.84%,变幅为0.78~4.12%,三种处理平均值分别为增雨1.96%、对照1.84%、减雨1.71%。土壤微生物量碳与土壤总有机碳的比值随土层深度增加也呈现明显的下降趋势。就不同处理同一土壤深度而言,只有5-10cm土层的土壤微生物量碳与土壤总有机碳的比值增雨处理显著高于减雨和对照,这可能是因为该层根系分布较多,根系分泌物为微生物生长提供了营养来源。

重复测量方差分析结果表明,穿透雨增加或减少 30%对土壤微生物量碳的影响不显著($P = 0.067$)(表 3-2);而多重比较结果则显示,穿透雨减少 30%的土壤微生物量碳高于对照($P = 0.029$)(图 3-8a)。同样,穿透雨增加或减少 30%对土壤微生物量碳与土壤总有机碳比值的影响也不显著($P = 0.193$)(表 3-2, 图 3-8b)。穿透雨增加或减少 30%和月份两种因素的交互作用对土壤微生物量碳及其与土壤总有机碳比值的影响显著($P = 0.001$, $P = 0.002$)(表 3-2)。5 月穿透雨减少 30%的土壤微生物量碳较高,9 月穿透雨减少 30%的土壤微生物量碳与土壤总有机碳的比值较低(图 3-9)。

表 3-2 降水变化对土壤微生物量碳及其与土壤总有机碳比值影响的重复测量方差分析

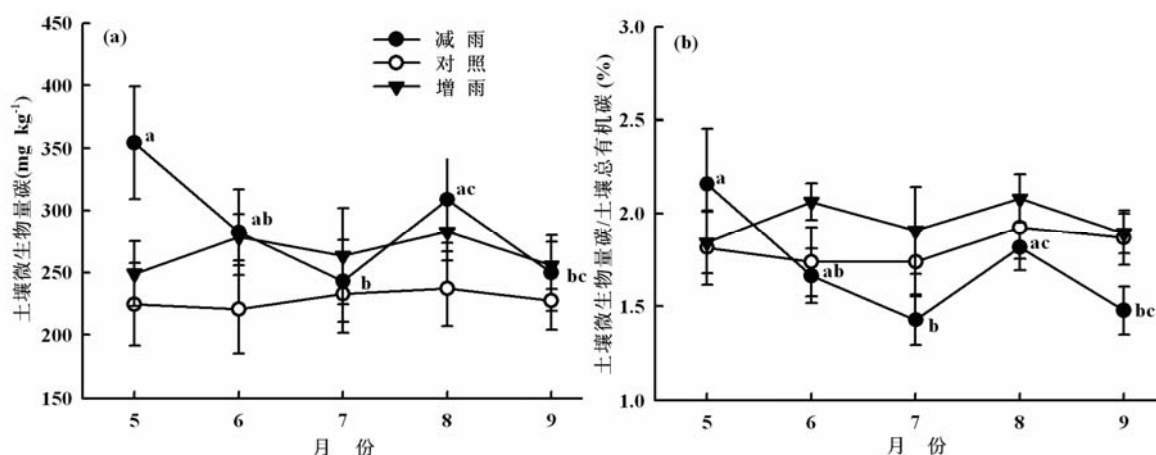
差异来源	土壤微生物量碳			土壤微生物量碳/土壤总有机碳		
	自由度	F	P	自由度	F	P
组内效应						
月份	4	3.269	0.015	4	2.762	0.032
月份×处理	8	3.567	0.001	8	3.356	0.002
月份×深度	12	1.375	0.191	12	1.431	0.165
月份×处理×深度	24	0.960	0.524	24	1.100	0.359
组间效应						
处理	2	3.032	0.067	2	1.763	0.193
深度	3	14.594	0.000	3	15.003	0.000
处理×深度	6	0.153	0.987	6	0.067	0.675

穿透雨增加和减少30%的处理对樟子松—落叶松人工混交林生长季土壤微生物量碳影响不显著($P=0.067$)。在半干旱地区森林生态系统的水分添加实验中,灌溉后的几小时到几天内,土壤微生物量碳显著下降,但随后几个月内添加水处理与对照之间并没有显著差别(Zhang & Zak, 1998)。而在一些极端降水控制实验中,生长季内增加一倍降水会导致极地半干旱沙漠生态系统土壤微生物量碳增加(Illieris et al., 2003),完全移除降水会减少欧石楠(*Erica carnea*)灌丛土壤微生物量碳(Jensen et al., 2003)。



图中数据为平均值+标准误, $n = 15$ 。不同小写字母表示不同穿透雨处理的平均值差异显著 ($P < 0.05$)。

图 3-8 穿透雨处理对土壤微生物量碳(a)及其与土壤总有机碳比值(b)的影响



图中数据点为平均值±标准误。不同小写字母表示减雨处理不同月份间的平均值差异显著 ($P < 0.05$)。

图 3-9 穿透雨处理对土壤微生物量碳(a)及其与土壤总有机碳比值(b)动态变化的影响

降水变化对土壤微生物量碳无显著影响的可能原因如下：第一，与这些极端降水控制研究相比，本研究在未改变降水频率的情况下将穿透雨增加和减少30%的处理强度较低，也更接近于自然降水变化的特征。第二，由于所测定的土壤微生物量碳并没有将休眠和非活跃态的微生物量与活跃态的微生物量区分开 (Zak et al., 1996; Teesier et al., 1998)，因此很可能只是土壤中处于活跃态的土壤微生物发生了变化，而这部分微生物的数量变化还不足以观察到穿透雨处理与对照的差异。第三，由于微生物依赖土壤有机质以及可利用的活性有机碳来维持自身生长，土壤微生物量的大小还取决于土壤有机质的多少 (Wardle, 1992)，土壤微生物量碳和土壤总有机碳之间显著的相关关系也能说明这一点 ($P < 0.001$, 图3-7c)。水分改变可能对土壤环境的影响较为复杂，可能还受土壤中营养物的浓度、碳周转速率等因素的交互影响。

穿透雨处理对微生物量碳与土壤总有机碳比值的影响统计上也不显著 ($P = 0.193$)，这说明水分条件的改变总体上没有影响土壤微生物对有机底物的利用效率。但是除了5月，该比值在其他月份都呈现增雨30% > 对照 > 减雨30%的规律 (图3-9b)。

3.3.2 水溶性有机碳

樟子松—落叶松人工混交林土壤水溶性有机碳的变幅为 27.0 ~ 231.5 mg kg⁻¹，平均值为 51.0 mg kg⁻¹。三种穿透雨处理的土壤水溶性有机碳平均值分别为增雨 41.3 mg kg⁻¹、对照 45.7 mg kg⁻¹、减雨 65.6 mg kg⁻¹。减雨处理的土壤水溶性有机碳值高于其他两种处理，土壤表层尤为明显(表 3-1)。

重复测量方差分析结果表明(表 3-3)，穿透雨处理对生长季内土壤水溶性有机碳有显著影响($P = 0.002$)。多重比较结果显示，减雨处理的土壤水溶性有机碳高于对照($P = 0.013$)和增雨($P = 0.002$)，比后两者分别高 43.5%和 58.9%。穿透雨处理和时间两种因素的交互作用对土壤水溶性有机碳有一定影响，统计上接近于显著($P = 0.055$ ，表 3-3)。

表 3-3 穿透雨处理对土壤水溶性有机碳影响的重复测量方差分析

差异来源	自由度	F	<i>P</i>
组内效应			
时间	4	2.902	0.025
时间 × 处理	8	1.979	0.055
时间 × 深度	12	0.438	0.945
时间 × 处理 × 深度	24	0.383	0.994
组间效应			
处理	2	7.659	0.002
深度	3	4.798	0.008
处理 × 深度	6	0.268	0.947

Borken et al. (1999)对挪威云杉人工林进行了穿透雨截流实验，发现穿透雨减少对水溶性有机碳的年淋溶速率没有显著影响。Park & Matzner(2003)在落叶林表层土壤增加一倍降水后，发现降水增加导致地表Oi层沥出液中可溶性有机质的浓度显著下降，但却对Oa层可溶性有机质浓度没有显著影响。Kalbitz et al. (2007)的研究表明，长期的降水增加会导致水溶性有机碳浓度降低，这种浓度降低可能是因为Oe/Oa层潜在的可溶性有机质被耗尽。

3.4 降水变化对土壤无机氮及氮矿化的影响

3.4.1 降水变化对土壤无机氮的影响

在自然生态系统中，土壤中的无机氮以铵态氮和硝态氮的形式存在，主要来源于微生物对可溶性有机氮(dissolved organic nitrogen, DON)的裂解和转化，是植物可以直接吸收利用的氮素。当微生物生长存在碳限制时，它会使用可溶性有机氮中的碳架来支持其生长与维持的能量需要，同时释放铵盐到土壤中。在硝化细菌作用下，部分或全部的铵盐会先变为亚硝酸盐，再变成硝酸盐，硝酸盐相对容易移动和被植物利用(Chapin et al., 2005)。生态系统土壤中的无机氮除了被植物利

用、微生物固持，一部分会通过氨挥发和反硝化作用变成气体扩散到大气中，还有一部分会因为降水淋溶作用向下迁移远离植物根系可利用的土壤、渗透到地下水中，从而离开生态系统。

2007 年 6~9 月的研究表明，塞罕坝樟子松—落叶松人工混交林 0-30 cm 土壤无机氮及其组分的平均浓度为铵态氮 $5.59 \pm 1.78 \text{ mg kg}^{-1}$ 、硝态氮 $1.11 \pm 0.77 \text{ mg kg}^{-1}$ 、无机氮 $6.70 \pm 2.31 \text{ mg kg}^{-1}$ (表 3-4)，铵态氮浓度显著高于硝态氮。与章古台地区的樟子松林生态系统 0-15 cm 土壤(铵态氮 3.86 mg kg^{-1} 、硝态氮 1.89 mg kg^{-1} 、无机氮 5.76 mg kg^{-1})相比(陈伏生等, 2005)，塞罕坝樟子松—落叶松人工混交林的土壤无机氮含量，主要是铵态氮含量略高。与内蒙锡林河流域草甸草原生态系统 0-15 cm 土壤(铵态氮 2.16 mg kg^{-1} 、硝态氮 5.72 mg kg^{-1})相比(王其兵等, 2000)，塞罕坝樟子松—落叶松人工混交林的土壤铵态氮含量高，硝态氮含量偏低，无机氮含量略低。这可能与樟子松林土壤类型为风沙土，硝态氮更容易被淋溶有关。

表 3-4 不同土壤深度与穿透雨处理的土壤无机氮

因素	水平	铵态氮(mg kg^{-1})	硝态氮(mg kg^{-1})	无机氮(mg kg^{-1})
穿透雨处理	减雨 30%	$5.34 \pm 1.06 \text{ a}$	$1.14 \pm 0.63 \text{ ab}$	$6.48 \pm 1.54 \text{ a}$
	对照	$5.77 \pm 1.96 \text{ a}$	$1.36 \pm 0.94 \text{ a}$	$7.12 \pm 2.53 \text{ a}$
	增雨 30%	$5.67 \pm 2.15 \text{ a}$	$0.83 \pm 0.63 \text{ b}$	$6.50 \pm 2.69 \text{ a}$
土壤深度	0-5 cm	$6.22 \pm 2.03 \text{ a}$	$1.29 \pm 0.83 \text{ a}$	$7.51 \pm 2.60 \text{ a}$
	5-10 cm	$5.75 \pm 1.67 \text{ a}$	$1.30 \pm 0.99 \text{ a}$	$7.05 \pm 2.23 \text{ a}$
	10-20 cm	$5.26 \pm 1.85 \text{ a}$	$0.93 \pm 0.68 \text{ a}$	$6.18 \pm 2.41 \text{ a}$
	20-30 cm	$5.15 \pm 1.40 \text{ a}$	$0.91 \pm 0.44 \text{ a}$	$6.06 \pm 1.70 \text{ a}$
平均值		5.59 ± 1.78	1.11 ± 0.77	6.70 ± 2.31

注：表中数据为平均值 \pm 标准差。小写字母为 Tukey HSD 多重比较结果，不同字母表示同一因素不同水平的均值间有显著差异($P < 0.05$)，字母顺序按均值由大到小排列。

通过对培养前铵态氮、硝态氮和无机氮背景值的线性混合模型方差分析，我们发现穿透雨处理对铵态氮无显著影响，而对硝态氮却有显著影响(表 3-5)。增雨处理硝态氮显著低于对照，减雨处理与对照及增雨的硝态氮含量统计上均无显著差别(表 3-4)，这可能是因为铵态氮比较容易吸附在土壤中的矿物或带负电的有机物表面(Chapin et al., 2005)，不易随水分向下迁移，所以相对稳定，而增雨处理加强了对硝态氮的淋溶作用，使其显著低于对照。由于铵态氮占无机氮总量的 80%以上(表 3-4)，总体上穿透雨处理对无机氮无显著影响。

表 3-5 穿透雨处理与土壤深度对土壤无机氮影响的混合模型方差分析

差异来源	自由度	铵态氮		硝态氮		无机氮	
		F	P	F	P	F	P
穿透雨处理	2	0.542	0.584	4.618	0.012	0.898	0.411
土壤深度	3	2.000	0.119	2.391	0.073	2.463	0.067
穿透雨处理×土壤深度	6	0.135	0.991	1.023	0.415	0.348	0.909

土壤深度及其与穿透雨的交互作用对铵态氮、硝态氮和无机氮均无显著影响(表 3-5)。数值上随着土壤深度增加, 铵态氮、硝态氮、无机氮含量逐渐下降, 但 Tukey HSD 均值多重比较表明, 各土层的无机氮含量并无显著差异($P > 0.05$, 表 5-5)。这可能是因为 0-30 cm 土壤中细根分布最多、微生物最活跃, 通过细根分解向土壤输入的氮可能大于叶片凋落物 (Langley & Hungate, 2003; 郭大立&范萍萍, 2007), 无机氮输入相对均衡, 因此氮有效性的差别也较小。

3.4.2 降水变化对土壤净氮矿化速率的影响

塞罕坝樟子松—落叶松人工混交林 0-30 cm 的土壤净氮化速率为 $-0.4(-4.74 \sim 5.28) \text{ mg kg}^{-1} 30\text{d}^{-1}$, 其中 0-5 cm 平均净氮化速率为 $0.55 \pm 2.48 \text{ mg kg}^{-1} 30\text{d}^{-1}$, 5-30 cm 的净氮化速率均为负值(表 3-6)。混合模型方差分析结果表明, 穿透雨处理和土壤深度及其交互作用对净氮化速率均无显著影响($P > 0.05$, 表 3-7)。Tukey HSD 均值多重比较结果表明不同处理和不同土壤深度的净氮化速率统计上均无显著差异(表 3-6)。

表 3-6 不同土壤深度和穿透雨处理的氮矿化速率

因素	水平	净氮化速率 ($\text{mg kg}^{-1} 30\text{d}^{-1}$)	净硝化速率 ($\text{mg kg}^{-1} 30\text{d}^{-1}$)	净氮矿化速率 ($\text{mg kg}^{-1} 30\text{d}^{-1}$)
穿透雨处理	减雨 30%	$-0.12 \pm 1.68 \text{ a}$	$0.40 \pm 1.02 \text{ a}$	$0.28 \pm 2.36 \text{ a}$
	对照	$-1.04 \pm 1.95 \text{ a}$	$-0.52 \pm 1.06 \text{ b}$	$-1.55 \pm 2.26 \text{ b}$
	增雨 30%	$-0.05 \pm 2.92 \text{ a}$	$0.60 \pm 1.40 \text{ a}$	$0.55 \pm 3.96 \text{ a}$
土壤深度	0-5 cm	$0.55 \pm 2.48 \text{ a}$	$0.88 \pm 1.67 \text{ a}$	$1.43 \pm 3.59 \text{ a}$
	5-10 cm	$-0.81 \pm 2.25 \text{ a}$	$-0.19 \pm 1.41 \text{ b}$	$-1.00 \pm 3.13 \text{ b}$
	10-20 cm	$-0.84 \pm 2.01 \text{ a}$	$0.00 \pm 0.59 \text{ b}$	$-0.83 \pm 2.32 \text{ b}$
	20-30 cm	$-0.51 \pm 2.16 \text{ a}$	$-0.05 \pm 0.83 \text{ b}$	$-0.56 \pm 2.66 \text{ b}$
平均值		-0.40 ± 2.28	0.16 ± 1.26	-0.24 ± 3.09

注: 表中数据为平均值 \pm 标准差。小写字母为 Tukey HSD 多重比较结果, 不同字母表示同一因素不同水平的均值间有显著差异($P < 0.05$), 字母顺序按均值由大到小排列。

樟子松—落叶松人工混交林 0-30 cm 土壤净硝化速率为 $0.16(-4.17 \sim 5.26) \text{ mg kg}^{-1} 30\text{d}^{-1}$ 。穿透雨处理与土壤深度对净硝化速率均有显著差异($P < 0.001$, $P = 0.002$), 二者的交互作用无显著差异($P = 0.483$)(表 3-7)。Tukey HSD 多重比较结果表明, 减雨处理与增雨处理的净硝化速率无显著差异($P = 0.758$), 二者都显著高于对照($P = 0.001$, $P = 0.008$)(表 3-6)。相同土壤深度各处理的净

硝化速率均无显著差异($P > 0.05$)。不同土壤深度的净硝化速率 $0-5\text{ cm} > 10-20\text{ cm} > 20-30\text{ cm} > 5-10\text{ cm}$, 其中, $0-5\text{ cm}$ 分别与其他三层有显著差异($P = 0.023, 0.014, 0.003$), 后者之间无显著差异($P > 0.05$)。具体而言, 这些差异主要是由增雨 $0-5\text{ cm}$ 和减雨处理 $0-5\text{ cm}$ 显著高于对照各土层的净硝化速率($P < 0.05$), 增雨 $0-5\text{ cm}$ 净硝化速率为 $1.60(-0.32 \sim 5.26)\text{ mg kg}^{-1} 30\text{d}^{-1}$, 减雨 $0-5\text{ cm}$ 净硝化速率为 $1.11(-1.26 \sim 3.87)\text{ mg kg}^{-1} 30\text{d}^{-1}$ 。

表 3-7 穿透雨处理与土壤深度对土壤氮矿化影响的混合模型方差分析

差异来源	自由度	净氨化速率		净硝化速率		净氮矿化速率	
		F	P	F	P	F	P
穿透雨处理	2	2.182	0.118	10.378	< 0.001	5.813	0.004
土壤深度	3	2.310	0.081	5.211	0.002	4.266	0.007
穿透雨处理 \times 土壤深度	6	0.603	0.727	0.922	0.483	0.868	0.522

樟子松—落叶松人工混交林 $0-30\text{ cm}$ 的土壤净氮矿化速率为 $-0.24(-6.65 \sim 10.24)\text{ mg kg}^{-1} 30\text{d}^{-1}$ 。穿透雨处理与土壤深度对净氮矿化速率均有显著差异($P = 0.004, P = 0.007$), 二者的交互作用无显著差异($P = 0.522$)(表 3-7)。不同穿透雨处理的净氮矿化速率为增雨 $>$ 减雨 $>$ 对照, 其中, 增雨与减雨处理无显著差异, 二者均显著高于对照(表 3-6)。不同土壤深度的净氮矿化速率 $0-5\text{ cm} > 20-30\text{ cm} > 10-20\text{ cm} > 5-10\text{ cm}$, 其中, $0-5\text{ cm}$ 为 $1.43 \pm 3.59\text{ mg kg}^{-1} 30\text{d}^{-1}$, $5-30\text{ cm}$ 的净氮矿化速率均为负值, $0-5\text{ cm}$ 显著高于其余三层, 后者之间无显著差异(表 3-6)。Tukey HSD 多重比较表明, 主要差异来源是增雨处理 $0-5\text{ cm}$ 的净氮矿化速率显著高于对照 $5-10\text{ cm}$ ($P = 0.002$)、 $20-30\text{ cm}$ ($P = 0.013$), 和减雨处理 $0-5\text{ cm}$ 高于对照 $5-10\text{ cm}$ ($P = 0.07$), 增雨和减雨处理 $0-5\text{ cm}$ 的净氮矿化速率无显著差异。

顶盖埋管法利用 PVC 管切断了植物的根系, 导致土壤中的铵态氮和硝态氮无法被植物生长所利用; 顶端用保鲜膜封口又避免了降水淋溶, 当然也可能存在少量土壤水分蒸发凝结后对表土产生的淋溶。三种处理的净氨化速率为负值说明通过微生物的铵是净吸收, 铵态氮可能被氮限制的微生物固持或被硝化细菌转化为硝态氮; 这也意味着樟子松林土壤中的微生物生长可能不存在碳限制, 即微生物无须使用来自可溶性有机氮中的碳架来支持其生长和呼吸作用, 也就不会释放铵态氮到土壤溶液中(Chapin et al., 2005)。 $0-5\text{ cm}$ 净氨化速率为正值可能是因为该层土壤水分含量较高, 土壤微生物数量最多、对碳的竞争最激烈, 导致碳限制的出现, 转而利用可溶性有机氮中的碳来支持其生长, 产生铵态氮的净释放。

硝化作用主要是自养硝化细菌这类专性好氧微生物, 使用从 NH_4^+ 或 NO_2^- 氧化过程中获得的能量来固定和还原 CO_2 、合成组织结构与新陈代谢所需碳化合物的过程(Chapin et al., 2005)。增雨

处理和减雨处理的净硝化速率为正值意味着硝态氮的净释放, 对照的净硝化速率为负值意味着硝态氮的净吸收, 微生物的固持作用最强。由于样地土壤中的硝酸盐含量较低, 不符合反硝化作用高硝酸盐浓度的条件, 所以发生反硝化作用的概率较低。铵态氮可利用性和氧气浓度是影响硝化作用的直接因素(Chapin et al., 2005), 虽然三种处理土壤中的铵态氮含量并无显著差异(表 3-4), 但是土壤水分的适度增加, 有利于铵态氮向硝化细菌渗透、增加铵态氮的可利用性。硝化细菌的活动对温度很敏感, 温度适度增加有利于硝化细菌的活动。与对照相比, 增雨处理的土壤水分含量较高、减雨处理的土壤温度略高, 有利于增强硝化细菌的活性, 提高硝化作用速率。

净氮矿化作用是在特定时间内, 无机氮进入土壤溶液的净积累。当微生物生长更强烈地受到碳限制, 而不是氮限制时, 会发生净氮矿化作用, 而净固持则发生于氮限制的微生物群落中(Chapin et al., 2005)。与其他研究相比, 本研究的净氮矿化速率均值偏低(周才平&欧阳华, 2001a; 周才平&欧阳华, 2001b; 王常慧等, 2004; 陈伏生等, 2005; 陈伏生等, 2006; 陈伏生等, 2009; 王其兵等, 2000), 除了因生态系统、土壤类型与季节变化产生的差别, 由于净氮矿化速率通常会随着土壤深度增加而降低(Federer, 1983; Hadas et al., 1989), 所以土壤深度不同也可能导致结果产生差异。塞罕坝樟子松—落叶松人工混交林的净氮矿化速率平均值为负值、发生了净固持, 说明当地的土壤微生物活动受氮限制, 而非碳限制。在贫瘠生态系统中, 低速率的净氮矿化作用也说明此途径可能只是自然发生的有效氮通量的一小部分(Chapin et al., 2005)。

增雨和减雨 0-5 cm 净氮矿化速率为正值(表 3-4), 说明该层的微生物群落受碳限制更强烈。土壤水分和温度直接影响着土壤氮矿化过程和无机氮的形式及含量(Chapin et al., 2005), 可能是影响氮矿化作用最重要的因子, 而且土壤温度的影响重于土壤水分, 二者还具有正交互作用(Puri & Ashman, 1998)。林下穿透雨处理显著地改变了土壤水分和温度, 增雨处理土壤水分显著高于对照和减雨, 减雨处理的土壤温度又略高于对照和增雨, 这可能是导致增雨和减雨处理的净氮矿化速率都高于对照的主要原因。

3.5 小结

穿透雨增加和减少 30% 显著地改变了塞罕坝樟子松—落叶松人工混交林的土壤体积含水量, 10cm、20cm 和 40cm 土壤体积含水量增雨 > 对照 > 减雨, 80cm 处的土壤体积含水量对照 > 减雨 > 增雨。三种处理的土壤温度统计上均无显著差异, 但减雨处理的温度略高于增雨和对照。

穿透雨处理对 0-30cm 土壤微生物量碳及其与土壤总有机碳的比值无显著影响, 对土壤水溶性有机碳有显著影响, 减雨处理的水溶性有机碳显著高于对照和增雨。三种穿透雨处理的土壤铵态氮和无机氮含量无显著差异, 增雨处理的硝态氮含量显著低于对照。降水变化对土壤铵态氮及

氨化作用的影响弱于对硝态氮及硝化作用的影响。穿透雨处理对净氨化速率无显著影响，增雨和减雨处理的净硝化速率和净氮矿化速率均显著高于对照。

塞罕坝樟子松—落叶松人工混交林土壤活性有机碳、无机氮及氮矿化作用对降水变化的初期响应表明，未来降水格局变化对森林土壤及土壤微生物活动的影响是复杂的，降水减少会导致土壤水分减少、温度升高，降水增加会导致土壤水分增加、温度降低，这都可能让土壤微生物种类、数量及活性发生变化，从而改变土壤的养分状态与可利用性。我们对土壤活性有机碳、无机氮的综合研究也表明，塞罕坝地区的土壤相对比较瘠薄，氮素对当地土壤微生物群落的限制大于碳限制。

第四章 植物生长对降水变化的响应

不同的降水、温度与土壤等环境因素的组合塑造了现在地球上植被类型的基本分布，在较长时间尺度上，降水变化对植被的影响是确定的。但是，在气候变暖的背景下，降水格局变化在中小时间尺度会对植物生长产生什么样的影响？国外研究者采用气候控制实验的方法进行了降水情景模拟。美国橡树岭国家实验室在田纳西州东部的温带落叶阔叶混交林中进行了增加或减少33%穿透雨量的穿透雨转移实验，结果发现，1994~2005年样地内胸径大于20cm的乔木胸高断面面积年增长率没有对穿透雨处理产生显著的响应，甚至应该会对降水变化比较敏感的幼苗和幼树也没有如预期的那样对处理产生显著响应⁴。他们的研究结果似乎与降水增加促进植物生长、降水减少抑制植物生长的规律不完全一致。在位于森林—草原过渡带和半干旱半湿润气候区的塞罕坝地区，人工林中的植物是否会对生长季降水的变化产生较快的反馈？不同树种和不同径级的乔木、乔木与草本植物、乔木个体生长与群落生产力是否会对降水变化产生响应？响应的特点是否有所不同？为了回答这些问题，我们在塞罕坝的樟子松—落叶松人工混交林进行了增加和减少30%穿透雨的降水控制实验，所选指标包括个体水平的乔木胸径年增长率、群落乔木层的胸高断面面积年增长率与乔木生物量年增长率(乔木净初级生产力)及年增长率，和群落水平的净初级生产力，试图从植物群落的不同层次全面研究中小时间尺度的降水变化对植物生长的影响，比较不同类型植物对降水变化响应方式的异同。

4.1 乔木径向生长对降水变化的响应

4.1.1 数据处理与统计分析

我们根据2006年和2007年生长季结束后每木检尺的胸径计算得到每株乔木胸径年增长率(Annual increment rate, AIR)，计算公式如下：

$$\text{AIR}(\%) = (\text{DBH}_{2007} - \text{DBH}_{2006}) / \text{DBH}_{2006} \times 100\% \quad (4-1)$$

分别统计每个样方所有乔木、不同树种(樟子松、落叶松)、不同径级(0-10cm、10-20cm、20-30cm)的胸径年增长率的平均值。由三个重复样方的平均胸径年增长率求得每种处理的平均值，分别用增雨和减雨处理的平均值减去对照的胸径年增长率平均值，将此差值作为胸径年增长率响应值。其他指标的响应值计算方法也与此相同。

用每株乔木的胸径计算得到胸高断面面积(Basal area, BA)，然后将每个样方内的乔木胸高断面

⁴ 研究结果来自2006年9月Paul Hanson在中国科学院植物所做的报告 Precipitation Change Responses of an Upland Oak Forest and Their Relationship to Future Multi-Factor Environmental Change Scenarios。

积之和作为该样方的乔木胸高断面积(单位: $\text{m}^2 \text{ha}^{-1}$), 用每个样方 2006 年与 2007 年的胸高断面积数据计算胸高断面积年增长量(Basal area increment, BAI)和胸高断面积年增长率(Basal area increment rate, BAIR), 计算方程如下:

$$\text{BAI}(\text{m}^2 \text{ha}^{-1}) = \text{BA}_{2007} - \text{BA}_{2006} \quad (4-2)$$

$$\text{BAIR}(\%) = \text{BAI} / \text{BA}_{2006} \times 100\% \quad (4-3)$$

对以上各指标进行单因素方差分析, 并用 Tukey HSD 检验对其均值进行多重比较。

4.1.2 降水控制实验样地乔木层群落结构特征

降水控制实验样地人工林为 23 年生樟子松—落叶松人工混交林(2007 年), 林分比较均匀, 以樟子松为主, 混交少量落叶松, 各样方及整个样地的乔木树种及径级组成情况见表 4-1, 除了对照 3 样方的落叶松株数较多、密度较大, 其他样方的乔木林分结构都相似。样地乔木平均树高 8.9m, 平均胸径为 11.5cm(图 4-1), 其中樟子松平均胸径 11.3cm, 落叶松平均胸径 12.2cm。

表 4-1 降水控制实验样地各样方树种及径级的乔木株数统计 (单位: 株)

处理	重复	树种		径 级			乔木
		樟子松	落叶松	0-10cm	10-20cm	20-30cm	
减雨 30%	1	117	24	48	90	3	141
	2	112	11	40	82	1	123
	3	91	38	45	79	5	129
对照	1	129	9	46	90	2	138
	2	138	8	58	86	2	146
	3	110	97	120	87	0	207
增雨 30%	1	133	5	42	96	0	138
	2	146	2	53	95	0	148
	3	71	48	53	60	6	119
样地合计		1047	242	505	765	19	1289

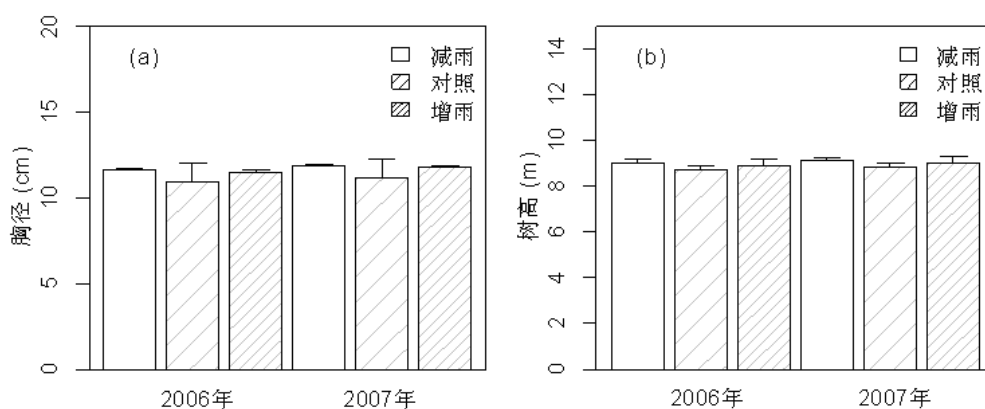


图 4-1 2006 年和 2007 年各穿透雨处理样地乔木胸径与树高对比(平均值+标准差)

4.1.3 不同树种与径级乔木胸径年增长率对降水变化的响应

穿透雨处理对不同树种与径级乔木胸径年增长率的单因素方差分析表明, 处理对各树种、各

径级的乔木胸径年增长率均无显著影响($P > 0.05$, 表 4-2)。为了进一步观察各类乔木的胸径年增长率是否存在差异, 我们进行了 Tukey HSD 多重比较, 显著性检验结果与方差分析结果一致($P > 0.05$, 表 4-3, 图 4-2)。我们似乎已经可以断言增加或减少 30% 穿透雨对人工林乔木径向生长毫无影响。但是当我们比较增雨和减雨处理胸径年增长率的响应值(处理与对照的差值)时, 有趣的现象出现了。

表 4-2 穿透雨处理对不同树种与径级乔木胸径年增长率影响的单因素方差分析表

乔木类型	自由度	平方和	均方和	F	P
落叶松	2	0.000442	0.000221	0.646	0.557
樟子松	2	0.000072	0.000036	1.932	0.225
0-10cm	2	0.000002	0.000001	0.012	0.988
10-20cm	2	0.000045	0.000022	0.757	0.509
20-30cm	2	0.000340	0.000170	0.198	0.83
乔木	2	0.000036	0.000018	1.499	0.297

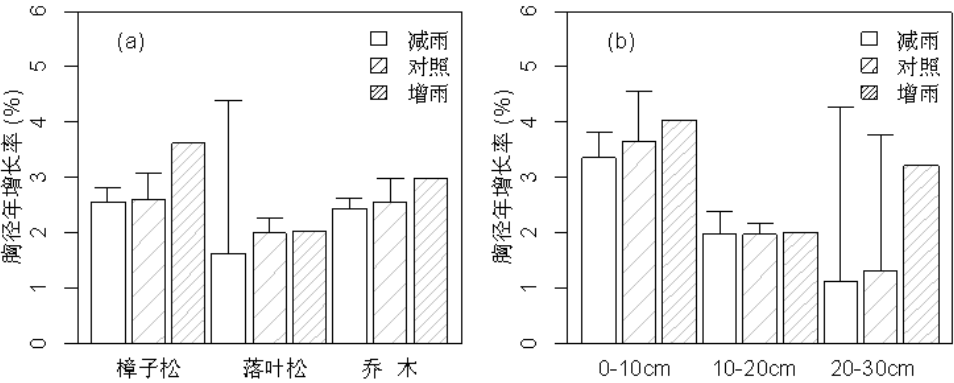


图 4-2 不同穿透雨处理各树种与径级乔木胸径年增长率对比(平均值+标准差)

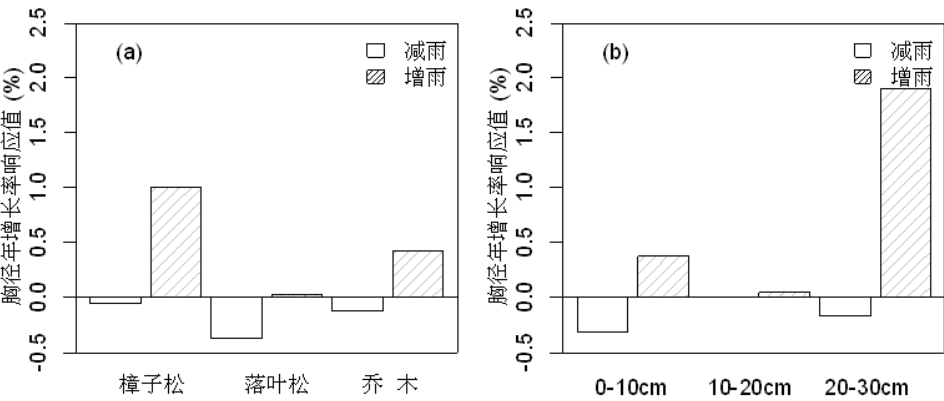


图 4-3 各树种与径级的乔木胸径年增长率对增雨或减雨 30% 响应值的比较

减雨处理各树种与径级的响应值都为负值，而增雨处理各树种与径级的响应值都为正值(图 4-3)，其中，减雨处理中的落叶松、胸径 0-10cm 对减雨的响应略大，而增雨处理中的樟子松、胸径 20-30cm 的乔木对增雨的响应较大(图 4-3)。于是我们又反观多重比较的结果，减雨和增雨对乔木胸径年增长率的影响确实存在，减雨与对照差值的均值和 95%置信区间相对于 0 都向左偏，增雨与对照、增雨与减雨差值的均值和 95%置信区间都向右偏(图 4-4)。

表 4-3 穿透雨处理间各树种与径级乔木胸径年增长率的 Tukey HSD 多重比较

类别	比较	差值	95%置信区间下限	95%置信区间上限	<i>P</i>
落叶松	减雨-对照	-1.068	-5.703	3.567	0.768
	增雨-对照	0.630	-4.005	5.265	0.910
	增雨-减雨	1.698	-2.937	6.333	0.535
樟子松	减雨-对照	0.077	-1.005	1.160	0.974
	增雨-对照	0.636	-0.447	1.719	0.247
	增雨-减雨	0.558	-0.525	1.641	0.323
乔木	减雨-对照	-0.306	-1.169	0.557	0.554
	增雨-对照	0.175	-0.688	1.038	0.814
	增雨-减雨	0.481	-0.382	1.344	0.277
0-10cm	减雨-对照	-0.099	-2.112	1.915	0.988
	增雨-对照	-0.035	-2.049	1.978	0.998
	增雨-减雨	0.063	-1.950	2.077	0.995
10-20cm	减雨-对照	-0.401	-1.760	0.959	0.657
	增雨-对照	0.119	-1.240	1.479	0.961
	增雨-减雨	0.520	-0.839	1.880	0.509
20-30cm	减雨-对照	-0.167	-11.325	10.990	0.998
	增雨-对照	1.908	-13.061	16.878	0.862
	增雨-减雨	2.076	-12.038	16.189	0.823

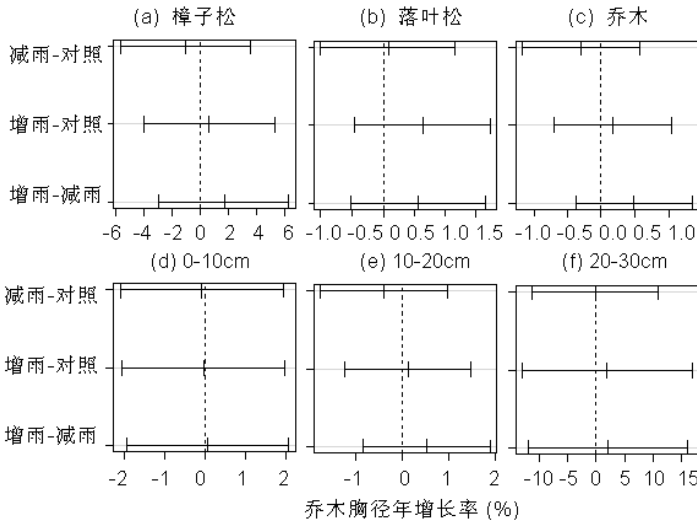


图 4-4 不同穿透雨处理各树种与径级乔木胸径年增长率(%)的 Tukey HSD 均值多重比较图

x 轴为处理平均值的差值，横线上的三条竖线从左到右分别是差值的 95%置信区间下限、平均值和置信区间上限。

4.1.4 乔木胸高断面积生长对降水变化的响应

在个体水平的乔木径向生长中观察到的穿透雨处理间普遍但统计不显著的差异，在每个样方群落水平的胸高断面积增长中是否会被放大？因为穿透雨处理改变的水分通量是基于整个样方的，所以我们又分析了穿透雨处理对样方群落乔木层胸高断面积及其年增长量的影响。单因素方差分析表明，穿透雨处理对 2006 年和 2007 年的胸高断面积、胸高断面积年增长量及年增长率均无显著影响 ($P > 0.05$, 表 4-4, 图 4-5)。由 Tukey HSD 多重比较结果可知(表 4-5, 图 4-6), 2006 年和 2007 年增雨和减雨处理的平均胸高断面积都略低于对照 ($P > 0.05$, 图 4-6a, 4-6b)。胸高断面积年增长量增雨与对照相当, 减雨低于对照(图 4-6c, 图 4-5), 但统计上差异也不显著 ($P = 0.556$)。而在胸高断面积年增长率中, 我们发现了和胸径年增长率相似的规律(图 4-5d, 图 4-7), 减雨 $<$ 对照 $<$ 增雨, 但是这些差异在统计上仍然不够显著 ($P > 0.05$)。

表 4-4 穿透雨处理对群落乔木胸高断面积及其年增长量(率)的单因素方差分析

变量	自由度	平方和	均方和	F	P
BA2006	2	15.77	7.883	1.21	0.362
BA2007	2	17.24	8.618	1.054	0.405
BAAI	2	0.3357	0.1678	0.924	0.447
BAAIR	2	2.143	1.0716	1.45	0.306

注：BA 为胸高断面积，BAAI 为胸高断面积年增长量，BAAIR 为胸高断面积年增长率。

表 4-5 穿透雨处理间群落乔木胸高断面积均值的 Tukey HSD 多重比较

变量	比较	差值	95%置信区间下限	95%置信区间上限	P
BA2006	减雨-对照	-2.528	-8.924	3.867	0.489
	增雨-对照	-3.022	-9.417	3.374	0.377
	增雨-减雨	-0.493	-6.889	5.902	0.970
BA2007	减雨-对照	-2.906	-10.071	4.259	0.473
	增雨-对照	-2.964	-10.129	4.201	0.460
	增雨-减雨	-0.058	-7.223	7.107	1.000
BAAI	减雨-对照	-0.378	-1.446	0.690	0.556
	增雨-对照	0.058	-1.010	1.125	0.985
	增雨-减雨	0.435	-0.632	1.503	0.469
BAAIR	减雨-对照	-0.639	-2.793	1.515	0.654
	增雨-对照	0.555	-1.598	2.709	0.722
	增雨-减雨	1.194	-0.960	3.348	0.280

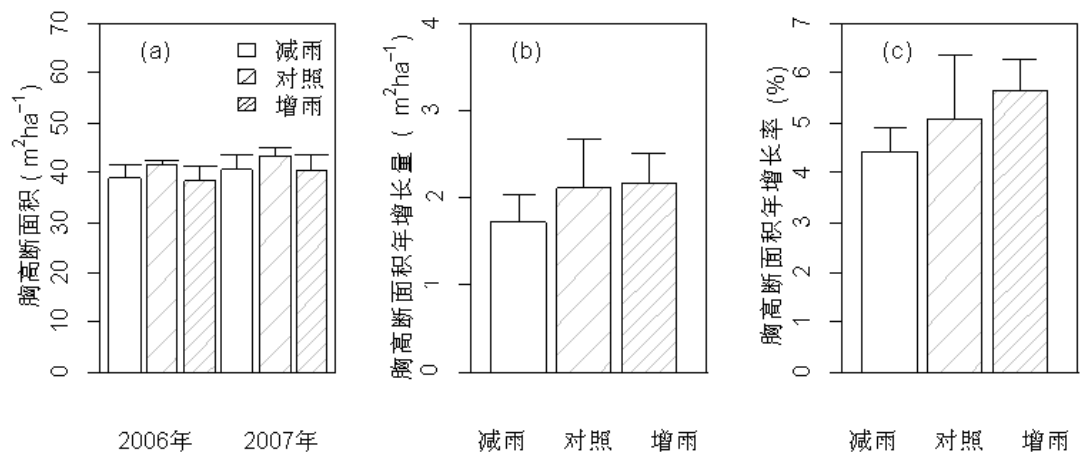


图 4-5 不同处理的胸高断面积及其年增长量(率)(平均值+标准差)

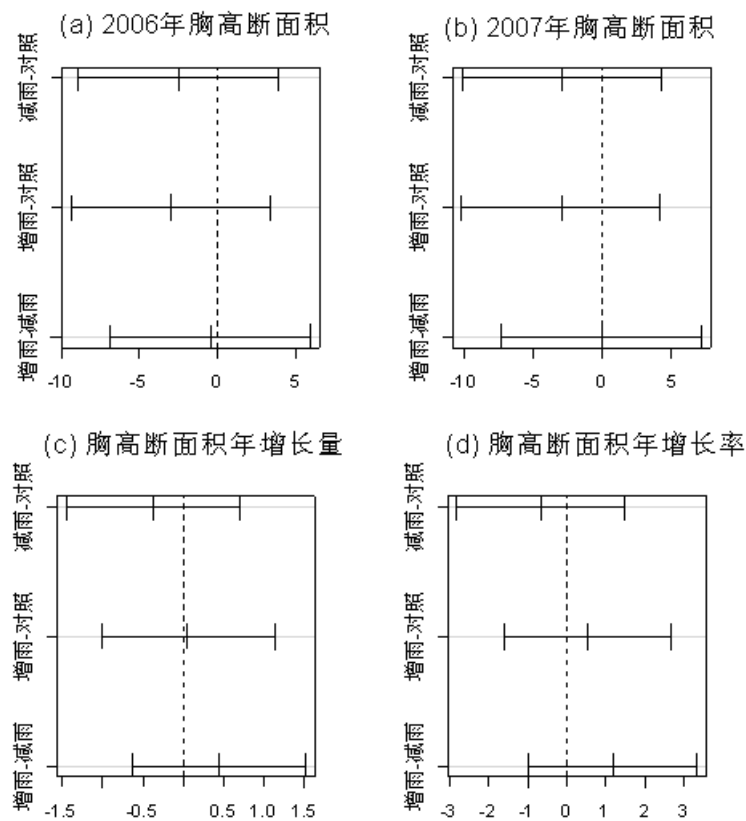


图 4-6 不同穿透雨处理胸高断面积的 Tukey HSD 均值多重比较图

x 轴为处理平均值的差值，横线上的三条竖线从左到右分别是差值的 95%置信区间下限、平均值和置信区间上限。

2006 年和 2007 年的胸高断面积及其年增长量单位是 $\text{m}^2 \text{ha}^{-1}$ ，胸高断面积年增长率(%)。

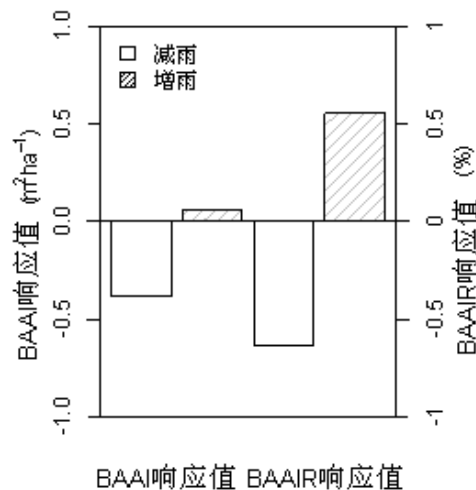


图 4-7 群落乔木层胸高断面积年增长率(BAAI)和年增长率(BAAIR)对增雨或减雨 30%的响应值

4.2 乔木生物量与群落净初级生产力对降水变化的响应

穿透雨处理对乔木个体和群落乔木层胸高断面积的效应均有统计上不显著的随着降水量增加、植物生长增加的趋势。如果从群落水平上综合考虑乔木、草本植物的地上及地下生物量，又会出现什么样的规律呢？乔木层是否会因包括了树高生长与植物根系生长而使处理间的差异放大？为了验证这个想法，我们分别估算了各样方的乔木和群落生物量，并计算得到植物净初级生产力(NPP)，其中包括地上净初级生产力(ANPP)和地下净初级生产力(BNPP)。

4.2.1 数据处理与统计分析

(1) 建立异速生长方程估算树高

我们根据每木检尺的胸径(DBH)数据与 90 株准确测高的乔木树高(H)数据(每个样方樟子松与落叶松各 5 株)，建立了异速生长方程来估算出样地内所有乔木的树高：

落叶松: $H = 3.5794 \times DBH^{0.437}$ (4-4)

樟子松: $H = 2.5608 \times DBH^{0.5055}$ (4-5)

(2) 用相关生长方程估算乔木各部分的生物量

我们采用了 2007 年岳超、郭兆迪等在塞罕坝人工林中用标准解析木方法建立的樟子松和落叶松相关生长方程⁵。具体方法如下：

选取了 0-10yr、10-20yr、20-30yr 和 30-40yr 四个林龄组的落叶松和樟子松人工纯林，对于 30-40yr 林龄组，选取了 6 个重复样地，其他林龄组选取了 3 个重复样地。在每个样地选取 2-3 株具有代表性的标准木。标准木伐倒后，将树冠等分为上、中、下三部分，取下每部分的活枝和死枝并分别称鲜重。对于活枝，在上、中、下每一部分各取两个枝，将其叶子剥下，并将枝分解

⁵ 岳超，郭兆迪等. 我国北方森林草原生态过渡带人工针叶林生物量及其分配动态(拟定题目)(未发表).

为粗枝(直径>1cm)和细枝(直径<1cm),分别称取粗枝、细枝和叶的鲜重,以获取上、中、下各部分中粗枝、细枝和叶所占比例,然后采集 200-500g 粗枝、细枝和叶的样品并称其鲜重,在实验室内将样品在 70℃下烘干至恒重测其干重,获取每部分粗枝、细枝和叶的水分含量,将整个树冠各部分的鲜重数据换算为干重。

对于树干,根据树干的长度,按照每 1m、2m 或 4m 一段将树干截为若干段,在每一段头部取长度约 5cm 的圆盘一个,测定圆盘的鲜重,并在实验室内 70℃下烘干至恒重,计算各圆盘的水分含量,并将对应树干鲜重换算为干重,然后相加得到整个树干的干重。

根系生物量的获取采用挖掘法。将根按照直径 < 0.2cm、0.2-0.5cm、0.5-2cm、2-5cm 和>5cm 以及根桩进行分级,分别测各级根的总鲜重并采集部分样品测定其水分含量,最后计算得出各级根的干重,相加得到整个根系的干重。

根据所获得的解析木干、枝、叶、根的干重数据和对应的胸径、树高数据,建立相关生长方程。我们选取了其中树龄>10yr 的樟子松和落叶松相关生长方程参数(表 4-6),方程形式如下:

$$B = a(DBH^2 H)^b \quad (4-6)$$

其中, B 为生物量, DBH 为胸径, H 为树高。

表 4-6 落叶松和樟子松相关生长方程

项目	a	b	R ²	P	样本量	备注
落叶松(>10 yr)						
干	0.039	0.888	0.99	<0.01	52	胸径范围(cm): 1.8 ~ 31.0; 树高范围(m):2.6 ~ 20.4
枝	0.047	0.705	0.90	<0.01	51	
叶	0.075	0.404	0.58	<0.01	51	
根	0.012	0.873	0.95	<0.01	50	
合计	0.122	0.807	0.98	<0.01	50	
樟子松(>10 yr)						
干	0.065	0.793	0.99	<0.01	21	胸径范围(cm): 2.1 ~ 26.6; 树高范围(m):1.3 ~ 15.6
枝	0.052	0.679	0.86	<0.01	21	
叶	0.139	0.457	0.53	<0.01	21	
根	0.023	0.750	0.94	<0.01	21	
合计	0.251	0.696	0.96	<0.01	21	

根据相关生长方程,我们用实测的胸径数据和估算的树高数据分别推算出了 2006 年和 2007 年样地内每株樟子松与落叶松的干、枝、叶、根的生物量,将样方内所有乔木的干、枝、叶生物量之和作为样方乔木地上生物量,根生物量作为样方乔木地下生物量,二者之和为乔木总生物量(biomass, B),并将单位换算成以干重计的 kg ha⁻¹。按照以下方程计算乔木生物量年增长率(biomass annual increment rate, BAIR):

$$\text{BAIR}(\%) = (\text{B}_{2007} - \text{B}_{2006}) / \text{B}_{2006} \times 100\%$$

(4-7)

(3) 计算净初级生产力

将以干重计的乔木生物量乘以系数 0.5 换算成以 C 计(kg C ha^{-1})，用 2007 年秋季各样方的乔木地上生物量、地下生物量及总生物量分别减去 2006 年秋季相应的数值，作为乔木地上净初级生产力、地下净初级生产力及净初级生产力($\text{kg C ha}^{-1} \text{ yr}^{-1}$)。将草本地上生物量乘以 2(设根冠比为 1)作为草本植物净初级生产力，与乔木净初级生产力相加即为群落净初级生产力(NPP)。我们未使用根钻法采集的根系生物量作为地下生物量，因为根钻法可能会低估森林植物根系生物量。

(4) 统计分析

用单因素方差分析分析穿透雨处理对各指标的影响，用 Tukey HSD 法对均值进行多重比较。

4.2.2 乔木生物量和净初级生产力对降水变化的响应

由于各样地的乔木密度和树种组成的差异，2006 年和 2007 年的乔木生物量都是对照 > 减雨 > 增雨(图 4-8)，根(地下生物量)、干、枝、叶分别占总生物量的 15.1%、57.5%、19.0%、8.4%。

在对乔木生物量年增长率和 NPP 分成干、枝、叶、根等组分进行分析对比后，我们发现了在乔木胸径和胸高断面面积生长中同样的现象。单因素方差分析表明，穿透雨处理对生物量年增长率及 NPP(生物量的年增长量)无显著影响($P > 0.05$, 表 6-7)。

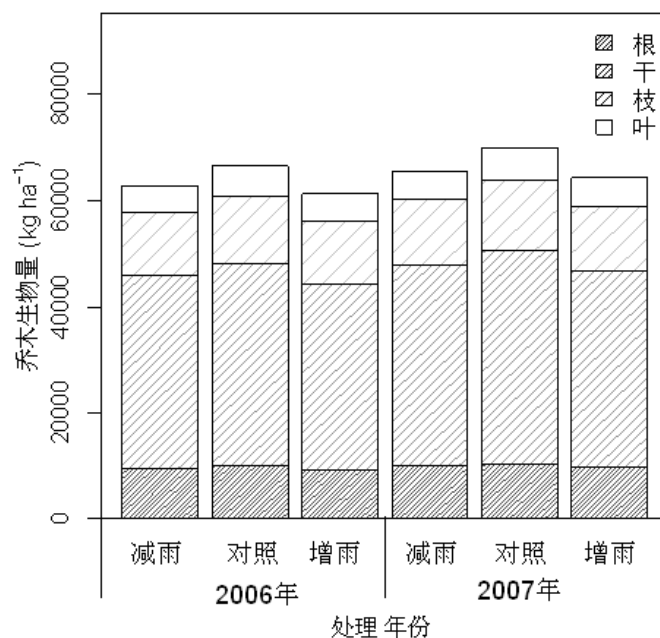


图 4-8 2006 年和 2007 年乔木根、干、枝、叶生物量

表 4-7 穿透雨处理对群落乔木生长的单因素方差分析

指标	组分	自由度	平方和	均方和	F	P
2006 年乔木生物量	干	2	12722729	6361364	0.501	0.629
	枝	2	2526218	1263109	1.276	0.345
	叶	2	743604	371802	0.384	0.697
	根	2	988410	494205	0.394	0.690
	总生物量	2	45675768	22837884	0.837	0.478
2007 年乔木生物量	干	2	13601668	6800834	0.417	0.677
	枝	2	2788184	1394092	1.107	0.390
	叶	2	781560	390780	0.379	0.700
	根	2	1071957	535979	0.339	0.725
	总生物量	2	50064967	25032484	0.699	0.533
乔木生物量年增长率(%)	干	2	2.389	1.195	0.968	0.432
	枝	2	1.564	0.7819	1.234	0.356
	叶	2	0.580	0.290	3.358	0.105
	根	2	2.179	1.089	0.844	0.475
	总生物量	2	1.923	0.962	0.985	0.427
乔木 NPP	干	2	297943	148972	0.463	0.650
	枝	2	27032	13516	0.693	0.536
	叶	2	2195	1098	0.853	0.472
	ANPP(干+枝+叶)	2	564286	282143	0.559	0.599
	BNPP(根)	2	20072	10036	0.393	0.691
	NPP	2	796067	398033	0.528	0.615

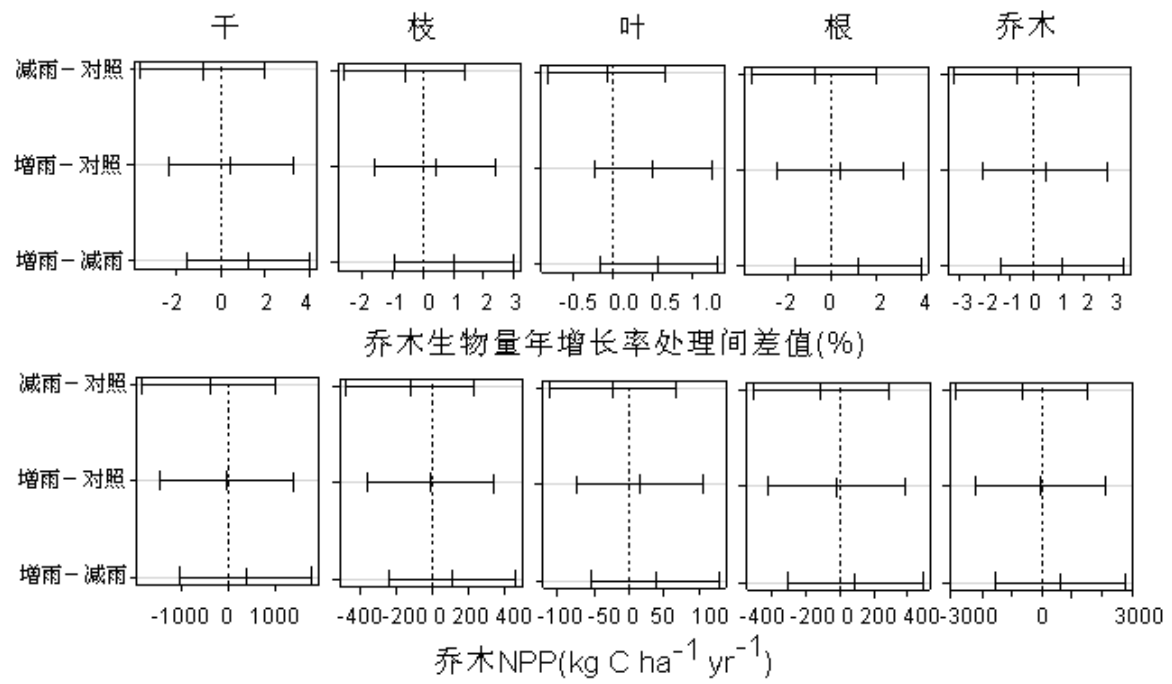


图 4-9 不同穿透雨处理乔木生物量年增长率与 NPP 的 Tukey HSD 均值多重比较图

x 轴为处理平均值的差值，横线上的三条竖线从左到右分别是差值的 95%置信区间下限、平均值和置信区间上限。

表 4-8 不同穿透雨处理群落乔木生物量年增长率与 NPP 的 Tukey HSD 多重比较

变量	组分	比较	差值	95%置信 区间下限	95%置信 区间上限	<i>P</i>
乔木生物量年增长率 (%)	干	减雨-对照	-0.784	-3.566	1.999	0.680
		增雨-对照	0.465	-2.317	3.248	0.868
		增雨-减雨	1.249	-1.534	4.031	0.409
	枝	减雨-对照	-0.605	-2.599	1.390	0.643
		增雨-对照	0.410	-1.584	2.405	0.809
		增雨-减雨	1.015	-0.980	3.009	0.331
	叶	减雨-对照	-0.072	-0.808	0.664	0.952
		增雨-对照	0.499	-0.237	1.235	0.175
		增雨-减雨	0.571	-0.165	1.307	0.119
	根	减雨-对照	-0.779	-3.626	2.067	0.694
		增雨-对照	0.406	-2.440	3.253	0.901
		增雨-减雨	1.186	-1.661	4.032	0.456
	总生物量	减雨-对照	-0.685	-3.160	1.790	0.689
		增雨-对照	0.438	-2.037	2.914	0.854
		增雨-减雨	1.123	-1.352	3.599	0.402
乔木 NPP (kg C ha ⁻¹ yr ⁻¹)	干	减雨-对照	-401.545	-1821.906	1018.815	0.678
		增雨-对照	-33.313	-1453.673	1387.048	0.997
		增雨-减雨	368.232	-1052.128	1788.593	0.719
	枝	减雨-对照	-122.583	-472.490	227.324	0.562
		增雨-对照	-13.902	-363.809	336.005	0.992
		增雨-减雨	108.682	-241.225	458.588	0.630
	叶	减雨-对照	-21.826	-111.690	68.037	0.747
		增雨-对照	16.297	-73.566	106.161	0.847
		增雨-减雨	38.124	-51.740	127.987	0.445
	ANPP	减雨-对照	-545.955	-2325.503	1233.593	0.637
		增雨-对照	-30.917	-1810.466	1748.631	0.998
		增雨-减雨	515.037	-1264.511	2294.586	0.667
	BNPP	减雨-对照	-107.875	-508.459	292.709	0.702
		增雨-对照	-17.766	-418.350	382.818	0.990
		增雨-减雨	90.109	-310.475	490.693	0.778
	NPP	减雨-对照	-653.830	-2829.237	1521.577	0.647
		增雨-对照	-48.683	-2224.090	2126.724	0.997
		增雨-减雨	605.147	-1570.260	2780.554	0.686

由 Tukey HSD 多重比较结果可知(图 4-9, 表 4-8), 各组分生物量年增长率和 NPP 处理间均无显著差异($P > 0.05$)。增雨处理的生物量年增长率略高于对照和减雨, 各组分生物量年增长率对处理的响应方式略有差异。从增雨或减雨与对照生物量年增长率差值的绝对值来看(表 4-8), 增雨处理对叶生物量年增长率的影响略大于减雨处理, 减雨处理对根、干、枝生物量生长率影响略大于增雨, 总体来说减雨对生物量的影响略大于增雨(图 4-9)。除了叶 NPP 略大一些, 增雨与对照的 NPP 几乎相同, 减雨处理的 NPP 都低于对照(图 4-9)。

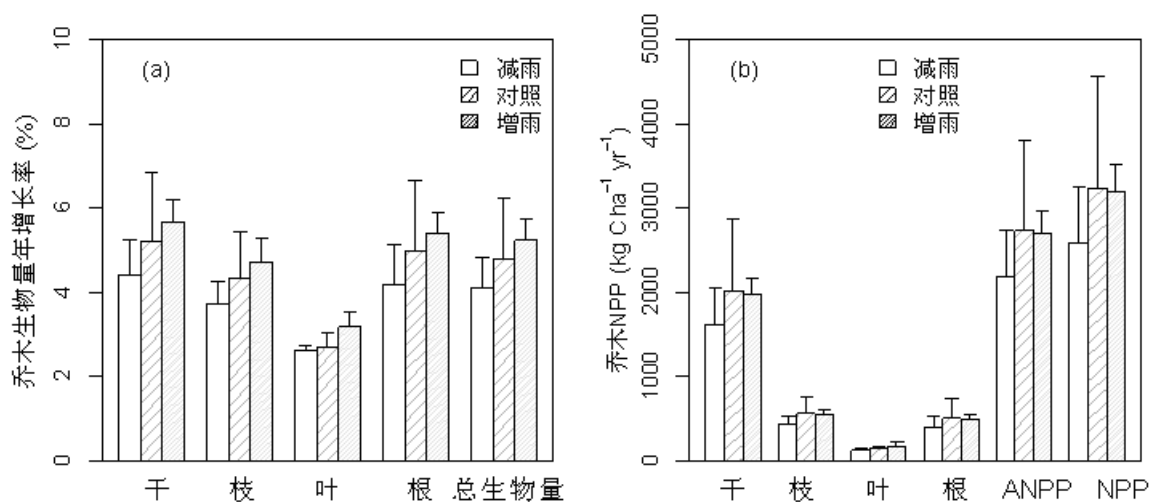


图 4-10 不同穿透雨处理的乔木各组分生物量增长率和 NPP(平均值+标准差)

在分析乔木生物量年增长率时，我们发现了和胸径及胸高断面积年增长率相似的规律(图 4-10a, 图 4-11a)，乔木干、枝、叶、根及总生物量的年增长率都呈现减雨<对照<增雨的趋势，但这些差异在统计上还是不够显著 ($P > 0.05$)。叶的生物量年增长率最低，NPP 也最低。大部分的 NPP 都分配到了树干(图 4-10b)，地下 NPP 平均占总 NPP 的 15.6%，干、枝、叶 NPP 分别占总 NPP 的 62.1%、17.2%和 5.1%，与生物量的地上地下分配大体一致，树干分配到的 NPP 份额大于其占总生物量的比例，而叶分配到的 NPP 份额低于其占总生物量的比例。

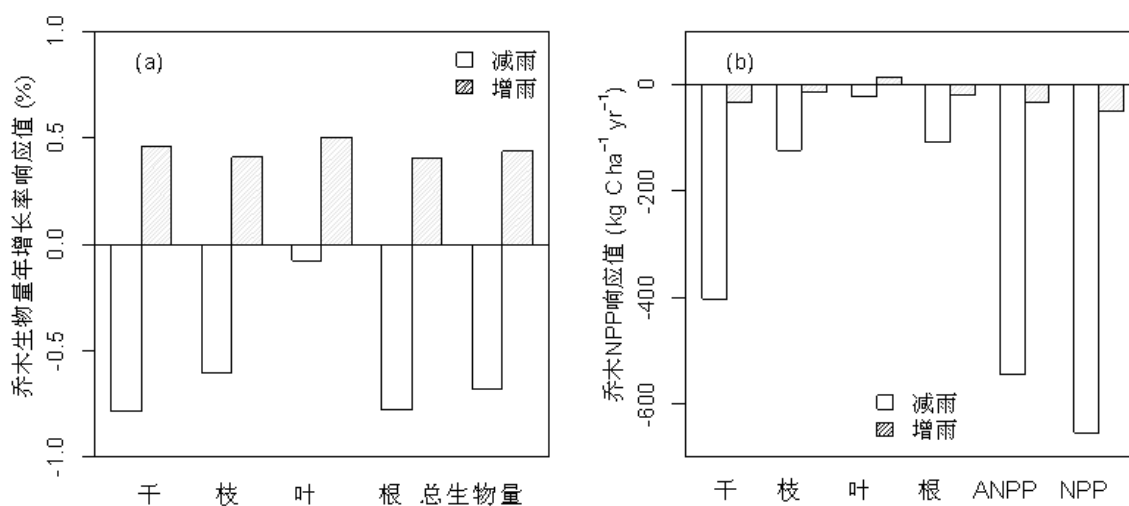


图 4-11 乔木生物量年增长率和 NPP 对增加或减少 30%穿透雨的响应值

乔木生物量年增长率和 NPP 对穿透雨处理的响应值规律不同。减雨处理降低了乔木的生物量年增长率，增雨处理提高了乔木的生物量年增长率。干、枝、根、叶生物量年增长率对增雨处理的响应值都比较接近，而叶生物量年增长率对减雨处理的响应值低于对其他器官的影响(图 4-11a)。由于对照的生物量高于减雨和增雨样地，除了增雨处理增加了叶 NPP，两种处理 NPP 的响应值均为负值，减雨处理 NPP 响应值的绝对值都远大于增雨，减雨样地的总生物量高于增雨，

但生物量的年增长率(NPP)却远低于增雨,除了样地本身树种组成与密度的差异外,这也可以说明降水减少对乔木 NPP 的影响可能更大(图 4-11b)。

4.2.3 群落净初级生产力对降水变化的响应

最后,我们在群落水平综合考虑了分配到凋落物中的 NPP 和草本植物 NPP,把它们与乔木 NPP 之和作为群落净初级生产力。单因素方差分析表明,穿透雨处理对乔木、草本植物及群落 NPP 无显著影响,对凋落物 NPP 有显著影响($P = 0.019$, 表 4-9)。Tukey HSD 多重比较发现,凋落物 NPP 中减雨与对照之间的显著差异是主要的差异来源($P = 0.015$, 表 4-10, 图 4-12b),增雨处理的凋落物也低于对照。这可能与对照样地中落叶松较多有关,但也不能否认穿透雨处理对凋落物的影响。草本植物应该会比乔木对降水变化的反馈更敏感,由多重比较结果我们发现增雨处理的草本植物 NPP 高于对照($P > 0.05$),而减雨处理与对照的均值无差别,这说明增雨对草本植物生长的促进作用比减雨的限制作用更明显(表 4-10, 图 4-12c)。

表 4-9 穿透雨处理对群落净初级生产力及其组分影响的单因素方差分析

净初级生产力	自由度	平方和	均方和	F	P
乔木	2	796067	398033	0.528	0.615
凋落物	2	1067234	533617	8.310	0.019
草本植物	2	22309	11155	0.348	0.720
群落	2	3723136	1861568	2.309	0.180

表 4-10 不同穿透雨处理间群落净初级生产力及其组分的 Tukey HSD 多重比较

净初级生产力	处理间比较	差值	95%置信区间下限	95%置信区间上限	P
乔木	减雨-对照	-653.830	-2829.237	1521.577	0.647
	增雨-对照	-48.683	-2224.090	2126.724	0.997
	增雨-减雨	605.147	-1570.260	2780.554	0.686
凋落物	减雨-对照	-843.333	-1478.179	-208.488	0.015
	增雨-对照	-407.222	-1042.068	227.624	0.201
	增雨-减雨	436.111	-198.735	1070.957	0.168
草本植物	减雨-对照	-9.800	-458.414	438.814	0.998
	增雨-对照	100.373	-348.240	548.987	0.780
	增雨-减雨	110.173	-338.440	558.787	0.743
群落	减雨-对照	-1506.964	-3756.174	742.247	0.180
	增雨-对照	-355.532	-2604.743	1893.679	0.881
	增雨-减雨	1151.431	-1097.779	3400.642	0.327

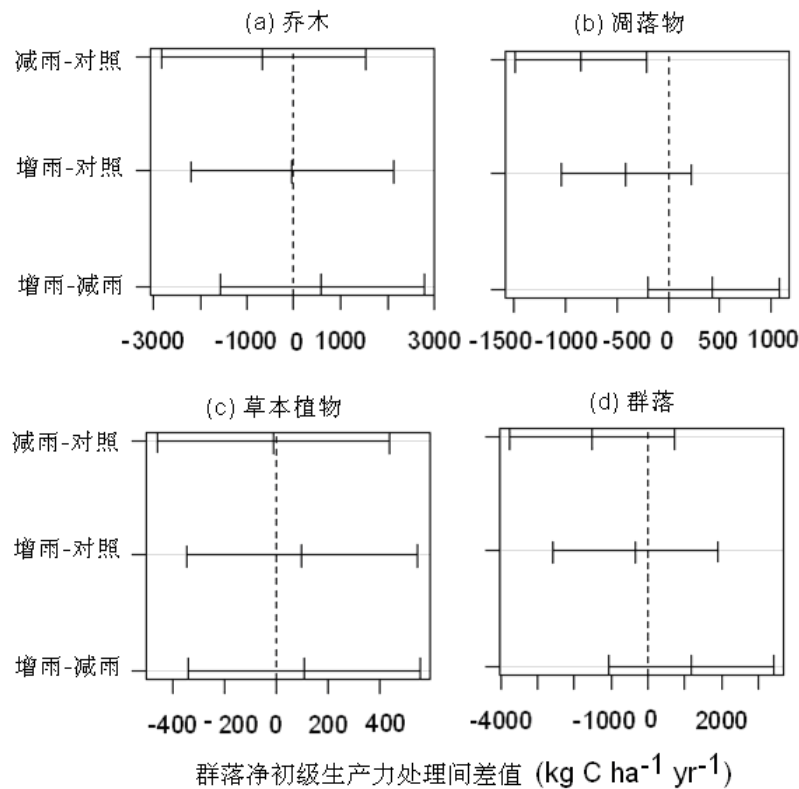


图 4-12 不同穿透雨处理群落净初级生产力及其组分的 Tukey HSD 均值多重比较图

x 轴为处理平均值的差值，横线上的三条竖线从左到右分别是差值的 95%置信区间下限、平均值和置信区间上限。

在比较不同穿透雨处理的群落 NPP 及其组分后，我们发现对照的乔木 NPP 及凋落物 NPP 均高于增雨和减雨，这可能与对照 3 样方中的落叶松株数多、密度大有关；草本植物 NPP 处理间差异表现出不一样的特征，虽然这种差异在统计上并不显著，但是也可以观察到增雨处理的草本植物 NPP 高于对照和减雨(图 4-13)。在群落净初级生产力及其组分对增雨和减雨 30% 的响应值图中，可以更清楚地看到这种差别(图 4-14)。群落净初级生产力对增雨和减雨的响应值均为负值，但是减雨处理的绝对值更大。

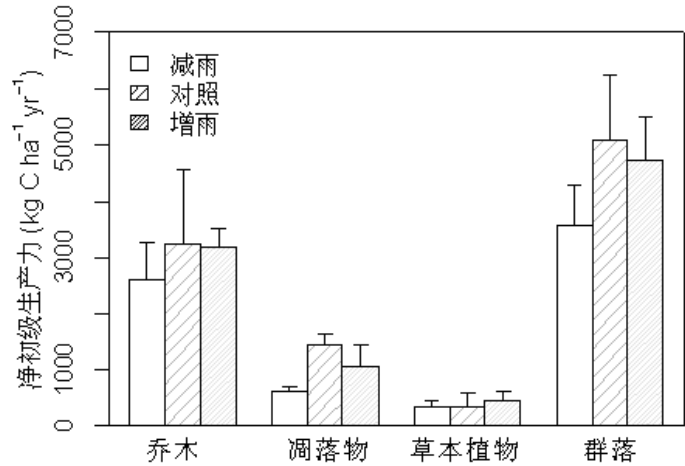


图 4-13 不同穿透雨处理的群落净初级生产力及其组分(平均值+标准差)

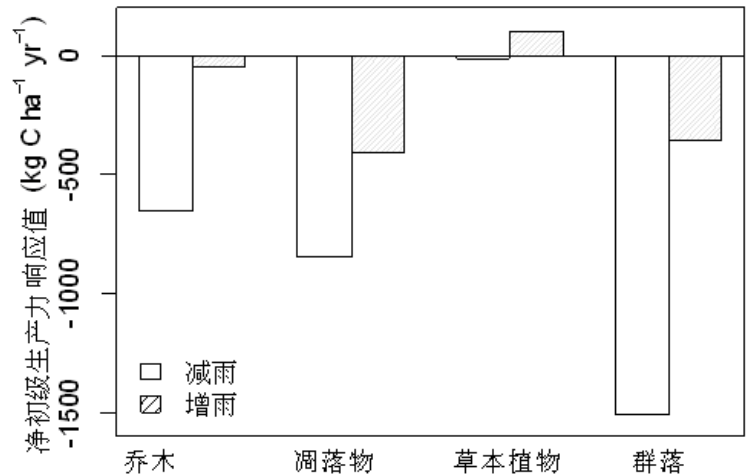


图 4-14 群落净初级生产力及其组分对增雨或减雨 30% 的响应值

4.3 降水变化对植物生长的影响

从个体水平的乔木胸径到群落水平的胸高断面积、乔木生物量和净初级生产力，我们研究了穿透雨处理对植物生长的影响。总体上，增加和减少 30% 穿透雨对樟子松—落叶松人工混交林乔木和草本植物生长统计上无显著影响。但在年增长率的对比中，都存在一致但统计不显著的趋势，即随着降水量增加，乔木胸径年增长率、群落乔木层胸高断面积年增长率和乔木生物量年增长率也在增加。而在考察群落乔木层净初级生产力和群落净初级生产力时，这种规律消失了，这可能是由于净初级生产力是生物量在一年周期内的增加量，与初始生物量的大小有关，年增长率比年增长量更适合作为评价植物生长对控制实验处理响应的指标。

樟子松—落叶松人工混交林乔木生长对穿透雨处理的初期响应和美国橡树岭国家实验室在田纳西州东部温带落叶阔叶混交林中进行的增加或减少 33% 的穿透雨转移实验结果一致⁶。在比较了 1994~2005 年样地乔木和幼树的胸高断面积年增长量后，他们发现胸径大于 20cm 的乔木胸高断面积年增长量没有对穿透雨处理产生显著的响应，除了减雨处理看起来一直相对较低，增雨和对照的胸高断面积年增长量之间的关系并不确定，各个年份穿透雨处理间也没有在本研究中乔木胸高断面积年增长率中存在的减雨 < 对照 < 增雨的一致规律。他们还发现植物生长的年际差异与年降水量的相关关系很微弱；木材密度没有因处理或年际干旱而发生显著变化；幼苗和幼树也没有如预期的那样对处理产生显著的响应。由此推测乔木没有对干旱发生响应可能与其生长物候期在大多数年份中都于干旱出现的时间不重叠，树木生长旺期出现在 4~5 月，而干旱一般发生于 8 月(Halson et al., 2001)。由于改变冬季降雪可能会改变其对土壤的保温作用，产生更复杂的

⁶ 研究结果来自 2006 年 9 月 Paul Hanson 在中国科学院植物所做的报告 Precipitation Change Responses of an Upland Oak Forest and Their Relationship to Future Multi-Factor Environmental Change Scenarios。

影响,而且塞罕坝 5-9 月的降水量平均占年降水量的 83%,所以我们的控制实验选择在生长季进行。在春季植物生长初期,由于融雪滋润土壤,而且气温较低,土壤水分蒸发量较少,所以土壤的水分状况相对较好,可能不会对植物生长产生限制作用。由于人工林树龄基本一致,林下无幼树,仅在草本层发现少量高度不超过 5 厘米的幼苗,所以我们无法比较穿透雨处理对幼苗定居、幼树生长的影响。在比较穿透雨处理对乔木和草本植物NPP的影响时,虽然穿透雨处理对二者统计上均无显著影响($P > 0.05$),但我们还是可以发现草本植物对穿透雨处理(尤其是生长季增雨)的响应更灵敏一些。对于群落NPP而言,由于草本植物NPP所占比例很小,所以穿透雨处理对群落NPP几乎无影响。

此外,虽然人工林与天然林相比,林分已经比较均匀,但还是不能排除由于各处理林分密度、径级分布和树种组成等因素的差异对研究结果的影响。

4.4 小结

我们从个体水平的乔木径向生长到群落水平的乔木层胸高断面积、乔木生物量和群落净初级生产力等不同层次,全面分析了降水变化对植物生长的影响。总体上,增加和减少 30%穿透雨对樟子松—落叶松人工混交林的乔木和草本植物生长统计上无显著影响,但是不同树种与径级的乔木胸径年增长率、群落乔木层胸高断面积年增长率和生物量年增长率都有不显著的随着降水量增加而增加的趋势。年增长率的变化表明,虽然穿透雨处理的影响在统计上不显著,但这种影响还是确实存在的。年增长率比年增长量更适合作为评价植物生长对控制实验处理响应的指标。

第五章 土壤呼吸对降水变化的响应

降水对地下生物化学过程具有重要的调控作用，会直接影响土壤呼吸。短期内单次的降水事件可能会因降水取代土壤孔隙中的空气使之从土壤中迅速排出、使微生物活动增强、数量增加而强烈地激发土壤呼吸，也可能因为土壤孔隙中过多的水分影响 CO_2 扩散而产生阻滞效应(陈全胜等, 2003)。但是长期的降水变化究竟会将对土壤呼吸产生什么影响？国外研究者用降水控制实验进行了不同降水情景的模拟与研究。在美国大平原南部的草地控制实验中，加水促进了干旱季节的土壤呼吸，但不同的水分添加量对土壤呼吸的影响不同(Liu et al., 2002)。在 Kanza 高草草原，自然降雨量减少 70% 季节平均土壤呼吸速率降低了 8%，改变降水频率后土壤呼吸速率降低 13%，而在这两种改变同时发生时，土壤呼吸降低 20%(Harper et al., 2005)。这些研究大多以草地生态系统为研究对象，有关降水变化对森林土壤呼吸的影响还很少。在温带落叶阔叶林进行的生长季遮雨实验中，遮雨处理明显降低了土壤呼吸速率和累积量(Borken et al., 2006)。美国橡树岭国家实验室研究人员在田纳西州东部温带落叶阔叶林穿透雨转移实验中发现，增加或减少 33% 穿透雨对森林的土壤呼吸没有显著影响(Hanson et al., 2003)。降水变化会对森林生态系统土壤呼吸产生何种影响？是降水增加导致土壤呼吸增加、降水减少土壤呼吸减少，还是森林生态系统比较稳定、土壤呼吸对降水变化不敏感？生长季土壤呼吸速率与土壤年呼吸量对降水变化的响应是否会有所不同？我们在处于半干旱半湿润气候区的塞罕坝樟子松—落叶松人工混交林中进行了增加和减少 30% 穿透雨的降水控制实验，来检验长期降水变化对森林土壤呼吸的影响。

5.1 生长季土壤呼吸对降水变化的响应

5.1.1 土壤呼吸的季节动态与空间格局

2006 ~ 2008 年生长季的连续测定结果显示，塞罕坝樟子松—落叶松人工混交林的土壤呼吸速率正如我们所预期的模式，随着季节变化呈现单峰的形态(图 5-1a)。土壤呼吸速率出现最大值的时间大约在 8 月中旬温度较高但降水量大的时候，这可能是因为塞罕坝气候具有雨热同期的特点，生长季降水占年降水量的 80% 以上，也可能是因为土壤水分含量对土壤呼吸的影响大于土壤温度的影响。从样地中每个测定环土壤呼吸速率平均值的分布格局直观图来看，上坡位三个样方的土壤呼吸速率平均值似乎略小(图 5-1b)，单因素重复测量方差分析表明，坡位对土壤呼吸速率并无显著影响($P = 0.239$ ，图 5-1b)。

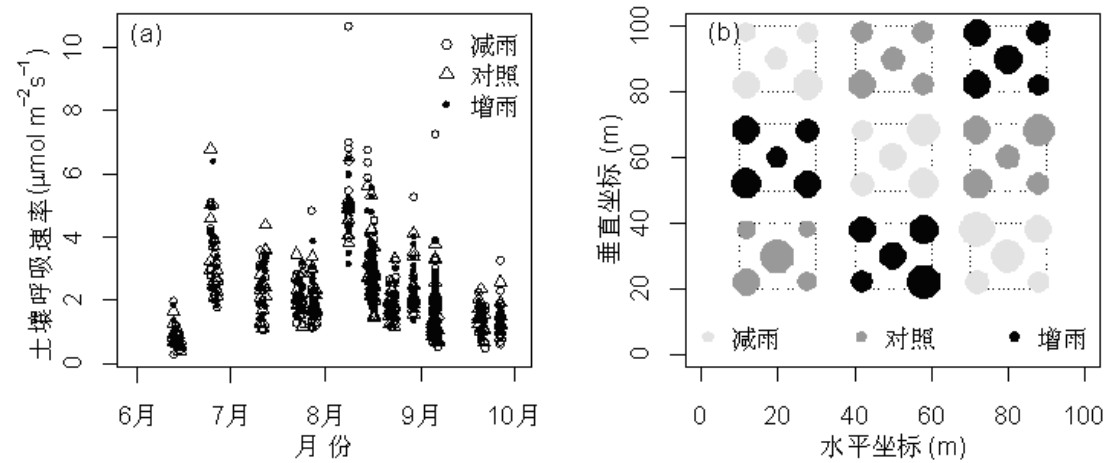


图 5-1 土壤呼吸的季节动态(a)与空间格局(b)

(a)中数据点为 2006~2008 年三种处理所有的土壤呼吸速率测定值。(b)中圆点位置为土壤呼吸测定环在降水控制实验样地中的坐标，直径为每个测定环整个生长季中土壤呼吸的平均值，浅灰、深灰、黑色分别代表减雨、对照、增雨三种处理，每个图例圆点直径的大小表示 $1 \mu\text{mol m}^{-2} \text{s}^{-1}$ ；图中虚线表示样方边界，每个样方 5 个测定环里上面的 2 个在薄膜水槽下方，其余 3 个在水槽外。

5.1.2 生长季土壤呼吸对降水变化的响应

我们对每个样方的生长季土壤呼吸速率平均值进行了穿透雨处理与测定日期的双因素重复测量方差分析(表 5-1)，结果表明，穿透雨处理对土壤呼吸速率无显著影响($P = 0.295$)，测定日期对土壤呼吸速率有显著影响($P < 0.001$)，二者的交互作用无显著影响($P = 0.997$)。

表 5-1 穿透雨处理与测定日期对土壤呼吸速率影响的双因素重复测量方差分析表

差异来源	自由度	平方和	均方和	F	P
组间效应					
穿透雨处理	2	0.075	0.037	1.505	0.295
残差	6	0.149	0.025		
组内效应					
测定日期	13	25.447	1.958	56.902	< 0.001
处理×测定日期	26	0.327	0.013	0.366	0.997
残差	78	2.683	0.034		

注：重复测量方差分析所用数据为经自然对数变换正态化处理后的土壤呼吸速率。

表 5-2 不同穿透雨处理生长季土壤呼吸速率的配对 t 检验统计值表

处理间比较	自由度	差值	差值的 95%置信区间	t	P
减雨 对 对照	13	0.103	-0.066 0.271	1.318	0.210
减雨 对 增雨	13	-0.019	-0.208 0.169	-0.221	0.829
增雨 对 对照	13	0.122	0.065 0.179	4.611	0.0005

注：土壤呼吸速率单位为 $\mu\text{mol m}^{-2} \text{s}^{-1}$

然后, 我们还对各处理生长季土壤呼吸速率平均值的时间序列做配对 t 检验来进行多重比较(表 5-2)。三种处理土壤呼吸速率平均值大小为增雨 > 减雨 > 对照, 增雨处理土壤呼吸的平均值显著高于对照($P = 0.0005$), 减雨与对照、减雨与增雨的土壤呼吸无显著差异($P > 0.05$), 这在土壤呼吸速率的季节动态图中也能观察到(图 5-2a)。增雨处理土壤呼吸速率的平均值在多数测定日期都高于减雨和对照, 而减雨和对照的曲线经常重合在一起。土壤体积分含水量的处理间差异则相对比较稳定(图 5-2b), 也如我们所预期的一样, 增雨 > 对照 > 减雨($P < 0.05$)。10cm 土壤温度三种处理间无显著差异($P > 0.05$), 但减雨处理的温度平均值略高于对照和增雨(图 5-2c)。

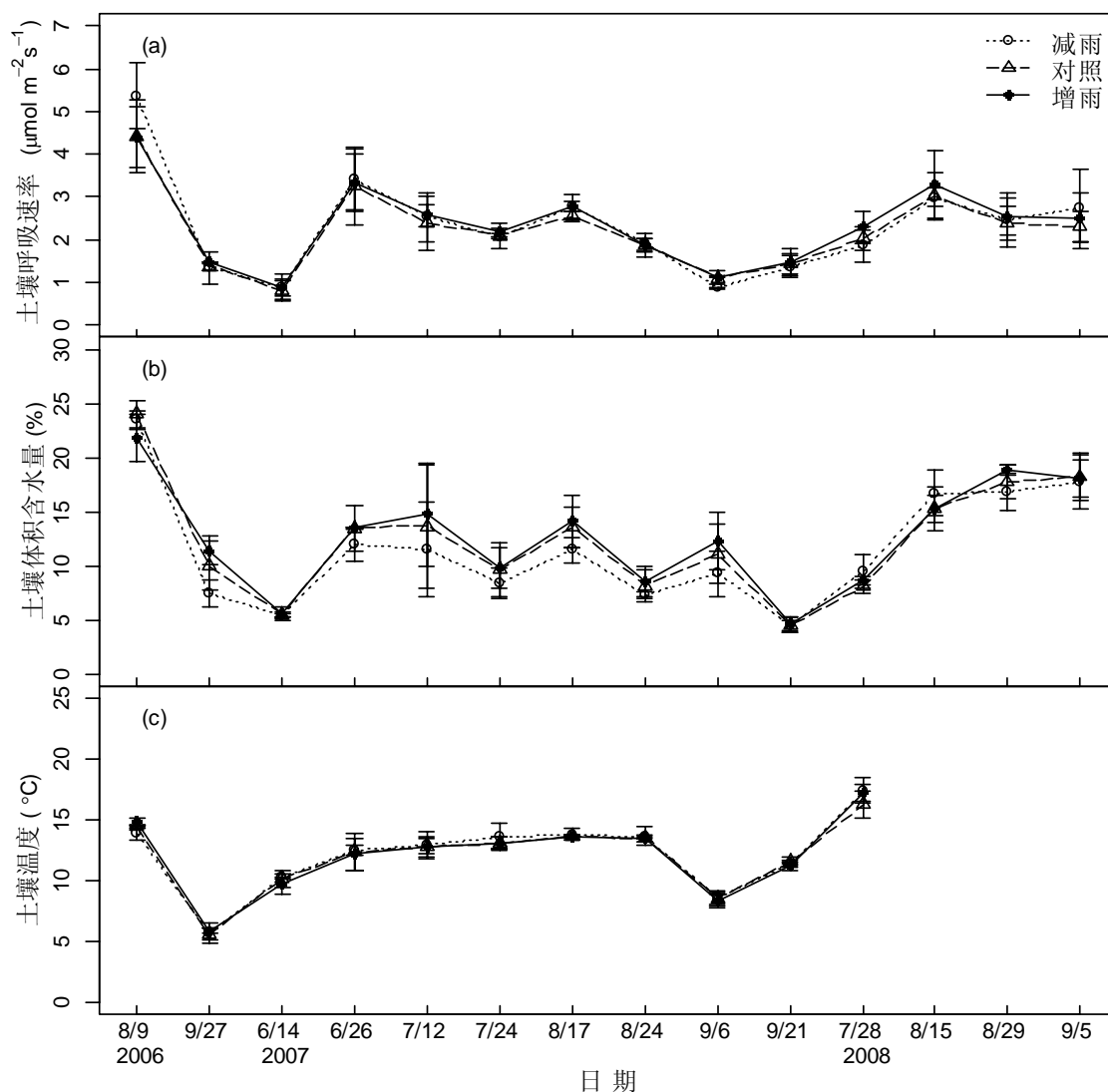


图 5-2 2006 ~ 2008 年土壤呼吸速率(a)、地下 10cm 土壤体积分含水量(b)和土壤温度(c)变化图

5.2 土壤呼吸温度敏感性对降水变化的响应

穿透雨处理显著地改变了样地的土壤水分, 为了研究樟子松-落叶松人工混交林土壤呼吸温度敏感性对土壤水分改变的响应, 我们把每个样方所有的土壤呼吸测定值 R 和测定时的土壤温度 T 用 Van't Hoff 指数方程 $R = ae^{bT}$ (van't Hoff, 1898) 拟合, 得到参数 a 和 b 的估计值, 并用参数 b

计算出土壤呼吸的表观温度敏感性指标 $Q_{10} = e^{10b}$, 各样方的表观 Q_{10} 见表 5-3。降水控制实验样地的土壤呼吸表观 Q_{10} 为 2.315 ± 0.293 (平均值 \pm 标准差), 变幅为 1.908 ~ 2.668。由表中指数方程拟合时的 R^2 和 P 值, 可以看出此方程单纯用土壤温度并不能很好地预测样地的土壤呼吸。

表 5-3 各样方土壤呼吸的表观温度敏感性(Q_{10})

处理	重复	a	b	R^2	P	表观 Q_{10}
减雨	1	-0.155	0.069	0.195	0.174	1.994
	2	-0.458	0.089	0.142	0.138	2.439
	3	-0.481	0.082	0.119	0.175	2.281
对照	1	-0.213	0.070	0.221	0.082	2.023
	2	-0.252	0.082	0.124	0.155	2.276
	3	-0.665	0.097	0.184	0.120	2.631
增雨	1	-0.089	0.065	0.176	0.110	1.908
	2	-0.467	0.096	0.276	0.056	2.613
	3	-0.533	0.098	0.268	0.072	2.668

对各样方表观 Q_{10} 值的单因素方差分析结果表明(表 5-4), 穿透雨处理对表观 Q_{10} 无显著影响 ($P = 0.844$)。但由 Tukey HSD 多重比较结果可以发现(表 5-5), 表观 Q_{10} 的均值为减雨 < 对照 < 增雨, 随着降水量增加, 表观 Q_{10} 有逐渐增大的微弱趋势。

表 5-4 穿透雨处理对土壤呼吸的表观温度敏感性(Q_{10})效应的单因素方差分析表

	自由度	平方和	均方和	F	P
穿透雨处理	2	0.0377	0.01885	0.175	0.844
残差	6	0.6476	0.10793		

表 5-5 穿透雨处理间土壤呼吸表观 Q_{10} 均值的 Tukey HSD 多重比较

处理比较	差值	95%置信区间下限	95%置信区间上限	P
减雨-对照	-0.072	-0.895	0.751	0.961
增雨-对照	0.086	-0.737	0.909	0.945
增雨-减雨	0.158	-0.665	0.981	0.830

5.3 基于土壤温度和水分因素的土壤呼吸速率预测模型

穿透雨处理显著地改变了样地的土壤水分, 也对土壤温度产生了影响, 这都可能会影响植物根呼吸和微生物呼吸, 从而影响土壤总呼吸。那么土壤温度和水分与土壤呼吸速率的关系到底如何? 从表 5-3 也可以看到只用温度拟合的模型 $\ln R = a + bT$ 并不能很好地预测土壤呼吸速率($R^2 < 0.3$), 于是我们用另外 5 种包括 10cm 土壤体积含水量(volumetric water content, VWC)在内的指数方程对各样方的土壤呼吸速率进行了拟合(表 5-6, 表 5-7, 表 5-8, 表 5-9, 表 5-10), 以期找到更适合预测土壤呼吸速率的模型, 并观察土壤水分与温度对土壤呼吸的影响方式与大小。

表 5-6 $\ln R = a + bVWC$ 拟合参数及显著性检验

样 方	a	VWC			R ²	F	P
		b	P				
对照 1	-0.200	0.076	< 0.001	***	0.813	44.510	< 0.001
对照 2	-0.282	0.079	< 0.001	***	0.734	28.650	< 0.001
对照 3	-0.689	0.147	0.018	*	0.467	8.882	0.018
减雨 1	-0.238	0.083	< 0.001	***	0.735	28.800	< 0.001
减雨 2	-0.500	0.109	< 0.001	***	0.824	47.670	< 0.001
减雨 3	-1.255	0.242	< 0.001	***	0.781	33.100	< 0.001
增雨 1	-0.093	0.065	< 0.001	***	0.753	31.460	< 0.001
增雨 2	-0.370	0.088	0.005	**	0.562	13.830	0.005
增雨 3	-0.539	0.133	0.012	*	0.509	10.330	0.012

显著性水平: $P < 0.001$, ***; $0.001 \leq P < 0.01$, **; $0.01 \leq P < 0.05$, *; $0.05 \leq P < 0.1$, .

表 5-7 $\ln R = a + bT + c VWC + d T \times VWC$ 拟合参数及显著性检验

样 方	a	T		VWC		VWC×T		R^2	F	P
		b	P	c	P	d	P			
对照 1	-0.69	0.05	0.28	0.07	0.24	0	1.00	0.94	53.75	<0.001
对照 2	-2.29	0.16	0.09	0.20	0.07	-0.01	0.22	0.83	17.39	<0.001
对照 3	-8.66	0.67	0.004	**	1.02	0.003	**	0.90	27.70	<0.001
减雨 1	-4.34	0.33	0.02	*	0.49	0.014	*	0.85	20.63	<0.001
减雨 2	-2.11	0.13	0.17	0.25	0.12	-0.01	0.32	0.86	21.49	<0.001
减雨 3	-5.94	0.39	0.14	0.86	0.07	-0.05	0.15	0.81	13.86	<0.001
增雨 1	-0.78	0.06	0.11	0.07	0.08	-0.0003	0.92	0.96	73.93	<0.001
增雨 2	-1.77	0.12	0.31	0.14	0.33	-0.005	0.64	0.69	8.47	0.01
增雨 3	-4.77	0.38	0.008	**	0.47	0.007	**	0.93	41.59	<0.001

显著性水平: $P < 0.001$, ***; $0.001 \leq P < 0.01$, **; $0.01 \leq P < 0.05$, *; $0.05 \leq P < 0.1$, .

表 5-8 $\ln R = a + bT + c T \times VWC$ 拟合参数及显著性检验

样 方	a	T		T×VWC		R^2	F	P
		b	P	c	P			
对照 1	-0.017	-0.002	0.851	0.005	<0.001	***	0.936	<0.001
对照 2	-0.039	-0.006	0.863	0.005	0.001	**	0.757	0.001
对照 3	-0.547	0.001	0.977	0.011	0.020	*	0.594	0.018
减雨 1	0.220	-0.027	0.476	0.006	0.003	**	0.680	0.004
减雨 2	-0.152	-0.014	0.649	0.007	<0.001	***	0.822	<0.001
减雨 3	0.175	-0.103	0.104	0.018	0.004	**	0.706	0.006
增雨 1	0.026	-0.002	0.900	0.005	<0.001	***	0.940	<0.001
增雨 2	-0.265	0.011	0.769	0.005	0.007	**	0.687	0.004
增雨 3	-0.433	-0.005	0.880	0.011	0.003	**	0.781	0.002

显著性水平: $P < 0.001$, ***; $0.001 \leq P < 0.01$, **; $0.01 \leq P < 0.05$, *; $0.05 \leq P < 0.1$, .

表 5-9 $\ln R = a + bVWC + c T \times VWC$ 拟合参数及显著性检验

样方	a	VWC		T×VWC			R ²	F	P
		b	P	c	P				
对照 1	-0.071	0.010	0.581	0.004	0.002	**	0.938	76.310	<0.001
对照 2	-0.188	0.027	0.460	0.004	0.151		0.773	17.990	0.001
对照 3	-0.620	0.028	0.715	0.009	0.095	.	0.602	7.817	0.016
减雨 1	-0.186	0.058	0.238	0.002	0.555		0.716	13.600	0.003
减雨 2	-0.405	0.048	0.349	0.004	0.222		0.837	26.720	<0.001
减雨 3	-1.185	0.206	0.047	*	0.002		0.758	15.110	0.003
增雨 1	-0.017	0.008	0.518	0.004	0.001	***	0.943	83.440	<0.001
增雨 2	-0.183	0.003	0.955	0.006	0.068	.	0.684	11.800	0.004
增雨 3	-0.563	0.026	0.551	0.009	0.011	*	0.792	18.120	0.002

显著性水平: $P < 0.001$, ***; $0.001 \leq P < 0.01$, **; $0.01 \leq P < 0.05$, *; $0.05 \leq P < 0.1$, .

表 5-10 $\ln R = a + b T \times VWC$ 拟合参数及显著性检验

样方	a	T×VWC			R ²	F	P
		b	P				
对照 1	-0.039	0.005	<0.001	***	0.942	164.500	<0.001
对照 2	-0.093	0.005	<0.001	***	0.783	37.020	<0.001
对照 3	-0.536	0.011	0.003	**	0.645	17.340	0.003
减雨 1	-0.009	0.005	0.001	***	0.696	23.900	0.001
减雨 2	-0.287	0.007	<0.001	***	0.838	52.520	<0.001
减雨 3	-0.492	0.011	0.004	**	0.614	15.330	0.004
增雨 1	0.012	0.005	<0.001	***	0.946	177.100	<0.001
增雨 2	-0.172	0.006	0.001	***	0.719	26.530	0.001
增雨 3	-0.470	0.011	<0.001	***	0.808	38.790	<0.001

显著性水平: $P < 0.001$, ***; $0.001 \leq P < 0.01$, **; $0.01 \leq P < 0.05$, *; $0.05 \leq P < 0.1$, .

在各种模型中, 土壤水分的主效应都与土壤呼吸速率正相关。只考虑土壤水分对土壤呼吸的效应时, 土壤水分与温度成显著的正相关关系($P < 0.02$, 表 5-6); 当同时考虑土壤温度、土壤水分及二者的交互作用时, 土壤温度和土壤水分的主效应与土壤呼吸正相关, 而交互作用的效应为负 (表 5-7); 当考虑土壤温度及其与土壤水分的交互作用时, 交互作用与土壤呼吸成显著正相关, 而土壤温度主效应与土壤呼吸的负相关关系均不显著(表 5-8); 当同时考虑土壤水分及其与土壤温度的交互作用时, 土壤水分与土壤呼吸的正相关关系不显著, 而交互作用与土壤呼吸的正相关作用比较显著(表 5-9); 最后, 当只考虑土壤温度与土壤水分的交互作用时, 它与土壤呼吸的正相关关系极其显著($P < 0.004$, 表 5-10)。

经过筛选, 我们选择了表 5-10 中只考虑土壤温度与土壤水分交互作用对土壤呼吸影响的模型 $\ln R = a + b T \times VWC$, 该模型 R^2 均值为 0.777, 变幅为 0.614 ~ 0.946, F 检验的 P 值小于 0.004, 而且形式简单, 预测效果好。在用不同方程进行拟合的过程中, 开始我们只是发现土壤温度对土

壤呼吸的解释率远低于土壤体积含水量(表 5-3, 表 5-6), 后来我们逐渐发现土壤体积含水量与土壤温度二者的交互作用才是引起这种差异的主要原因。因此, 在考虑土壤温度和水分对土壤呼吸的影响作用时, 应着重分析二者的交互作用对土壤呼吸的影响, 而不应只从土壤温度或土壤水分某一方面考虑。由于土壤呼吸速率对土壤水分的响应曲线呈单峰形(Luo & Zhou, 2007), 我们的模型适用于土壤体积含水量区间低于田间持水量、土壤呼吸未受到土壤水分含量抑制的情况。

5.4 土壤年呼吸量对降水变化的响应

利用预测模型 $\ln R = a + b T \times VWC$, 结合样方的土壤温度与土壤水分连续监测数据(非生长季使用同一组土壤温度及水分背景值监测数据), 计算了每个样方在土壤温度时间序列各时间点上的土壤呼吸速率, 然后乘以相应的时间间隔, 求和得到了各样方的土壤年呼吸量, 并按照樟子松—落叶松人工混交林中降水控制实验样地旁用壕沟法(trenching)测定的土壤自养呼吸(根呼吸)占总呼吸的比例 22%(王妮, 2007), 将土壤年呼吸量(土壤总呼吸)分成了自养呼吸和异养呼吸(表 5-11)。

表 5-11 各样方的土壤自养呼吸、异养呼吸与总呼吸

样 方	自养呼吸 (kg C ha ⁻¹ yr ⁻¹)	异养呼吸 (kg C ha ⁻¹ yr ⁻¹)	土壤总呼吸 (kg C ha ⁻¹ yr ⁻¹)
对照 1	970.728	3432.847	4412.400
对照 2	1025.641	3627.038	4662.002
对照 3	794.634	2810.116	3611.974
减雨 1	797.346	2819.704	3624.298
减雨 2	900.113	3183.127	4091.423
减雨 3	822.143	2907.397	3737.014
增雨 1	1441.745	5098.536	6553.388
增雨 2	1316.574	4655.885	5984.428
增雨 3	1437.255	5082.657	6532.978

单因素方差分析表明, 穿透雨处理对土壤自养呼吸、异养呼吸与总呼吸的影响非常显著($P = 0.0005$) (表 5-12)。Tukey HSD 多重比较结果显示, 穿透雨处理对土壤年呼吸量影响的差异来源主要是增雨处理(表 5-13, 图 5-3), 增雨处理的土壤年呼吸量均值显著高于减雨($P = 0.0005$), 也显著高于对照($P = 0.0014$), 减雨略低于对照, 但二者之间的差异不显著($P = 0.5$)。这也印证了我们先前在建立土壤呼吸速率与土壤温度和水分模型过程中发现的土壤水分对土壤呼吸的影响大于土壤温度的现象。增雨处理和对照的土壤水分都显著高于减雨($P < 0.05$), 虽然减雨处理的土壤温度不显著地高于增雨和对照, 但由于土壤水分比温度对土壤呼吸的影响更大, 导致增雨和对照的土壤呼吸均大于减雨。降水增加会显著地增加土壤年呼吸量, 而降水减少对土壤年呼吸量的影响不显著, 这与土壤呼吸速率时间序列配对 t 检验的结果一致。

表 5-12 穿透雨处理对土壤自养呼吸、异养呼吸和总呼吸的单因素方差分析

变量	差异来源	自由度	平方和	均方和	F	P
土壤自养呼吸	穿透雨处理	2	539485	269743	35.99	0.0005 ***
	残差	6	44965	7494		
土壤异呼吸	穿透雨处理	2	6746732	3373366	35.99	0.0005 ***
	残差	6	562328	93721		
土壤总呼吸	穿透雨处理	2	11146390	5573195	35.99	0.0005 ***
	残差	6	929032	154839		

显著性水平: $P < 0.001$, ***

表 5-13 穿透雨处理间土壤自养呼吸、异养呼吸和总呼吸的 Tukey HSD 多重比较

变量	处理比较	差值	95%置信区间下限	95%置信区间上限	P
土壤自养呼吸	减雨-对照	-90.467	-307.343	126.409	0.4552
	增雨-对照	468.191	251.315	685.066	0.0014
	增雨-减雨	558.658	341.782	775.534	0.0005
土壤异养呼吸	减雨-对照	-319.925	-1086.876	447.027	0.4552
	增雨-对照	1655.692	888.741	2422.644	0.0014
	增雨-减雨	1975.617	1208.666	2742.568	0.0005
土壤总呼吸	减雨-对照	-411.214	-1397.013	574.584	0.4552
	增雨-对照	2128.139	1142.341	3113.938	0.0014
	增雨-减雨	2539.354	1553.555	3525.152	0.0005

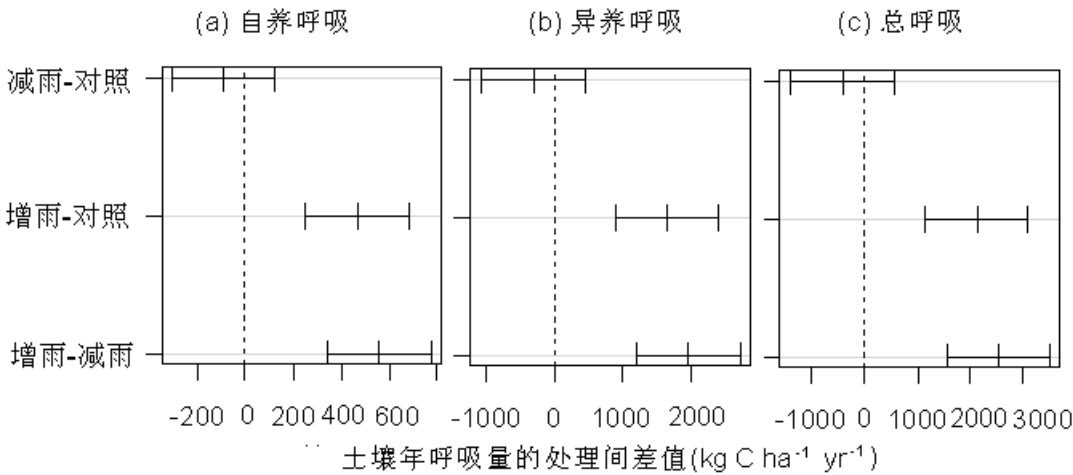


图 5-3 土壤自养呼吸、异养呼吸和总呼吸的 Tukey HSD 多重比较图

5.5 降水变化对土壤呼吸及其温度敏感性的影响

通常认为土壤呼吸与土壤水分之间的关系是：在干燥条件下，由于胞外酶及呼吸底物扩散和微生物移动的减少，土壤呼吸较低；当含水量很高、厌氧条件占优势时，好氧微生物的活性受到抑制、导致土壤呼吸下降；最适合的土壤含水量接近于田间持水量，这时大孔隙空间充满空气，利于氧气扩散，小孔隙空间充满水，利于可溶性底物的扩散(Luo & Zhou, 2007)，土壤呼吸速率最大。实验室研究指出，在最适土壤含水量时的土壤呼吸速率最大，很多野外测量的结果则表明土

壤水分只有在最低和最高的情况下才会抑制土壤呼吸(Liu et al., 2002; Xu et al., 2004)。加水会促进干旱季节的土壤呼吸,但不同的水分添加量对土壤呼吸的影响不同(Liu et al., 2002)。在本研究中,增雨处理的土壤含水量虽然高于对照和减雨,但通常情况下还未达到田间持水量,因此对土壤呼吸始终具有促进作用。减雨处理的土壤体积含水量虽然最低,但可能也未低到足以限制土壤呼吸的程度,因此,减雨处理的土壤呼吸与对照无显著差异。

土壤水分是影响土壤呼吸温度敏感性的主要因素(Xu & Qi, 2001)。土壤水分通过影响底物或氧气的扩散来调控土壤呼吸速率(Linn & Doran, 1984)和土壤呼吸温度敏感性(Gaumont-Guay et al., 2006)。在排水良好的土壤中,土壤水分降低会限制微生物对底物的利用,导致土壤呼吸温度敏感性降低(Davidson et al., 2006; Xu & Qi, 2001)。在本研究中,虽然穿透雨处理间的表观 Q_{10} 统计上无显著差异,但其平均值为增雨 > 对照 > 减雨,这与其他研究的结果一致,土壤水分降低导致土壤呼吸温度敏感性也降低。

我们的研究发现,增雨 30%显著地增加了土壤呼吸速率(配对 t 检验 $P < 0.05$)和土壤年呼吸量,但减雨 30%对土壤呼吸速率和土壤年呼吸量的影响不显著。在温带落叶阔叶林的穿透雨转移实验中,增加或减少 33%穿透雨对森林土壤呼吸无显著影响(Hanson et al., 2003)。在哈佛森林的生长季极端干旱模拟实验中,林下 $5\text{m} \times 5\text{m}$ 的遮雨棚明显地降低了土壤呼吸速率和累积量(Borken et al., 2006)。这也说明,我们的降水控制实验模拟的 30%的穿透雨改变量比较小,虽然可能更接近于自然降水格局长期的变化,但减少 30%穿透雨对土壤呼吸的抑制作用可能还不够,不足以引起生长季土壤呼吸速率和土壤年呼吸量的响应。当然,这也可能与减雨处理样地土壤温度略高、土壤中可溶性有机碳及硝态氮含量较高有关。比较和区分根系呼吸与土壤微生物呼吸对降水变化的响应方式会有助于解释这种结果。

单次降水事件会对旱生生态系统的土壤呼吸产生很大影响,干燥土壤的土壤呼吸在雨后会猛增到一个很高的值,然后随着土壤变干而逐渐下降(Xu et al., 2004)。虽然我们通常在降水 24h 后测定土壤呼吸,但也很难完全避免降水事件对单次土壤呼吸测定的影响。但是,如果刻意避开降水后 24h 土壤呼吸的高峰期,又会低估了土壤 CO_2 释放量。因此,也许用土壤温度和水分时间序列预测土壤年呼吸量可以比较客观地反映和评价土壤呼吸,或者也可以采用系统采样、按照确定的时间间隔而不是靠主观判断是否适合测定,并适当增加测定频率来减少因测定时间带来的误差。

由我们提出基于土壤温度和水分因素的土壤呼吸速率预测模型的过程可知,二者的交互作用对土壤呼吸的影响比其中任一因子更显著。在生态系统中,由于自然和人为干扰常常会造成多个因子同时改变,有可能对土壤呼吸产生复杂的交互作用。两个或多个变量复杂的交互作用一般不

能从单因子影响的方向和大小来预测(Luo & Zhou, 2007)。因此, 进行多因子控制实验来检验多个环境因子对土壤呼吸的交互作用很重要(Beier, 2004; Norby & Luo, 2004)。

5.6 小结

在塞罕坝人工林降水控制实验中, 生长季土壤呼吸速率和土壤年呼吸量对穿透雨增加 30%产生了显著的响应, 穿透雨减少 30%对生长季土壤呼吸速率和土壤年呼吸量统计上无显著影响。不同穿透雨处理的土壤呼吸速率平均值大小顺序为增雨 > 减雨 > 对照, 而土壤年呼吸量的平均值顺序为增雨 > 对照 > 减雨。

降水控制实验样地土壤呼吸的表观温度敏感性(Q_{10})为 2.315 ± 0.293 (平均值 \pm 标准差), 变幅为 1.908 ~ 2.668。穿透雨处理对表观 Q_{10} 统计上无显著影响, 其平均值增雨 > 对照 > 减雨, 随着降水量减少, 土壤呼吸的温度敏感性降低。

我们提出的基于土壤温度与水分因素的土壤呼吸速率预测模型 $\ln R = a + b T \times VWC$ 比传统的 van't Hoff 指数方程 $R = ae^{bT}$ 具有更好的预测性。

第六章 净生态系统生产力对降水变化的响应

我们研究了以土壤活性有机碳和土壤无机氮为表征的土壤理化性质，以乔木胸径年增长率、群落乔木层胸高断面积年增长率、乔木生物量年增长率及净初级生产力、群落净初级生产力为指标的植物生长，和土壤呼吸及其表观温度敏感性(Q_{10})对穿透雨增加或减少 30%的不同响应。对于樟子松—落叶松人工混交林生态系统，生长季降水变化是否会对净生态系统生产力产生影响？降水增加或减少会如何影响生态系统碳收支？为了回答这些问题，我们分析了降水变化对净生态系统生产力及其组分的影响。

6.1 净生态系统生产力对降水变化的响应

通常用群落净初级生产力(NPP)与土壤异养呼吸(R_h)之差，作为净生态系统生产力(NEP)，它是生态系统碳收支的重要指标。

在图 6-1 中可以清楚地观察到，对照的净生态系统生产力总体高于减雨和增雨处理，而且增雨处理中有两个样方的净生态系统生产力还是负值(图 6-1c)。那么增加或减少 30%穿透雨的处理是否对净生态系统生产力产生了显著的影响？

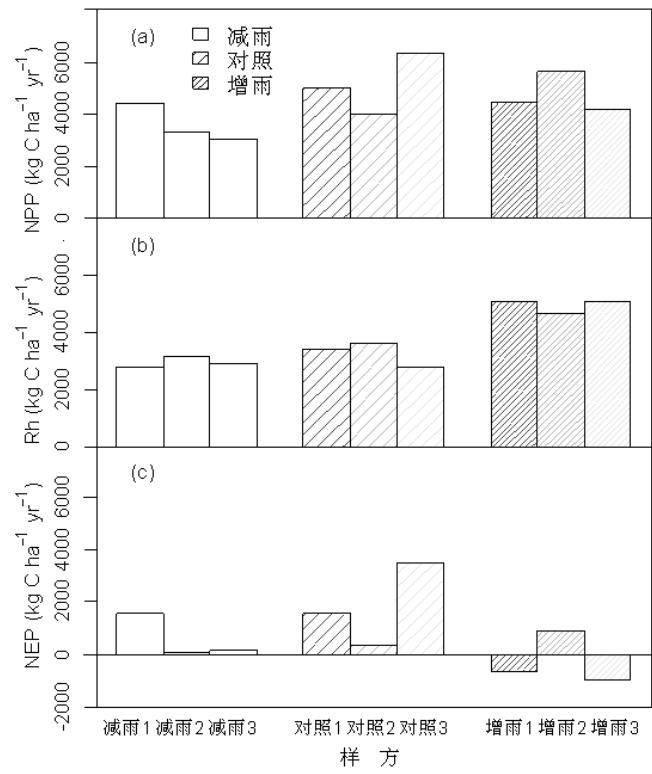


图 6-1 各样方的群落净初级生产力 NPP、土壤异养呼吸 R_h 与净生态系统生产力 NEP

单因素方差分析结果表明, 增加或减少 30% 穿透雨对人工林生态系统 NEP 无显著影响($P = 0.193$, 表 6-2)。由 Tukey HSD 均值多重比较图表可知, NEP 的均值大小为增雨 < 减雨 < 对照, 但三者之间都没有显著的差异($P > 0.05$, 表 6-2, 图 6-2)。

表 6-1 穿透雨处理对净生态系统生产力影响的单因素方差分析表

差异来源	自由度	平方和	均方和	F	P
穿透雨处理	2	6133367	3066684	2.195	0.193
残差	6	8384252	1397375		

表 6-2 穿透雨处理间净生态系统生产力均值的 Tukey HSD 多重比较表

处理比较	差值	95%置信区间下限	95%置信区间上限	P
减雨-对照	-1187.039	-4148.494	1774.416	0.480
增雨-对照	-2011.225	-4972.679	950.230	0.174
增雨-减雨	-824.186	-3785.640	2137.269	0.686

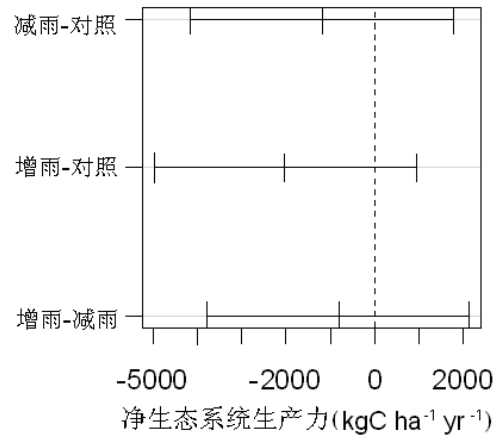


图 6-2 各穿透雨处理净生态系统生产力均值的 Tukey HSD 多重比较图

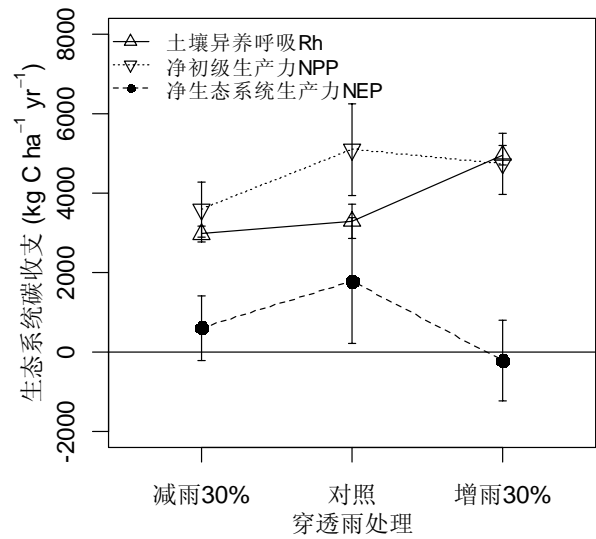


图 6-3 不同穿透雨处理的生态系统碳收支

6.2 净初级生产力与土壤呼吸对降水变化的响应及其对净生态系统生产力的影响

虽然穿透雨处理总体上对净生态系统生产力的影响不显著($P > 0.05$),但是净生态系统生产力还是对穿透雨处理产生了响应。这主要是由于群落净初级生产力和土壤呼吸对降水变化响应的方式和敏感程度不同造成的。就群落净初级生产力而言,可能是因为对照样地本身的初始生物量总量高于增雨和减雨,导致其净初级生产力最高,而群落净初级生产力对穿透雨处理的响应又不显著($P > 0.05$),本该是一条随着降水增加而向上的趋势线因此而被折成了中间高两边低、增雨一端略高于减雨的折线。当然,这也可能是因为净初级生产力对减雨处理的响应大于增雨,所以减雨处理的净初级生产力低于对照,而增雨处理的净初级生产力又没有如预期的那样高于对照,最终呈现出净初级生产力对照 > 增雨 > 减雨的状态(图 6-3)。

土壤呼吸则不然,它对穿透雨处理的响应更敏感($P < 0.05$)。增雨处理显著地增加了土壤年呼吸量及土壤异养呼吸,导致其生态系统 CO_2 排放量增加。减雨处理的土壤呼吸本该低于对照,但可能是因为土壤水分还没低到足以显著限制土壤呼吸的程度,再加上减雨处理土壤温度略高于对照和增雨($P > 0.05$),土壤中的水溶性有机碳和硝态氮含量显著高于增雨处理($P < 0.05$),土壤水分、温度、养分的共同作用导致本该明显下降的趋势有所矫正,甚至与对照接近持平。就这样,一条本该随着降水增加而增加的趋势线被减雨处理从较低的一端抬了起来,呈现出增雨土壤呼吸显著高于对照和减雨,而减雨和对照无显著差异的状态(图 6-3)。

预期中随着降水量增加而上升的两条平行趋势线,因净初级生产力和土壤异养呼吸对增雨和减雨响应的程度和方式不同,变成了近似平行四边形的形式(图 6-3)。因为减雨处理的净初级生产力最低、土壤呼吸与对照相当;对照净初级生产力本来就最高,土壤呼吸保持原来的状态;增雨处理净初级生产力没有如预期那样增加,但土壤异养呼吸却最高。三者综合的结果就是让作为净初级生产力与土壤异养呼吸差值的净生态系统生产力随着降水量增加呈现出中间高、两边低的趋势。年际尺度的降水增加和减少都可能会将降低净生态系统生产力,削弱森林生态系统的碳汇能力(Angert et al., 2005; Stephens et al., 2007; Ma et al., 2012)。

总之,植被净初级生产力对降水变化的响应不显著,而土壤异养呼吸对降水变化的响应相对敏感。在年际尺度上,降水增加或减少都不会显著改变生态系统净初级生产力。降水增加会显著增加土壤水分,同时降低土壤温度,由于土壤水分对土壤呼吸的影响显著高于土壤温度,因此降水增加会显著地增加土壤异养呼吸;降水减少虽然减少了土壤水分,但也许只有极端干旱出现时才会对土壤异养呼吸产生限制作用,而同时降水减少却可能会提高土壤温度,保存土壤中易淋溶的水溶性有机碳和硝态氮,在土壤温度、水分和养分的共同作用下,年际尺度上的降水减少对土壤异养呼吸的影响会折衷一下,表现为与现状无显著差异。因此,降水变化对生态系统碳收支的

影响，主要决定于土壤异养呼吸对不同降水格局的响应。

Cao & Woodward(1998)曾用模型模拟了气候变化对净生态系统生产力的影响，他们认为全球的 NEP 会随着大气 CO₂ 浓度和降水量增加而增加，随着温度上升而减少。在我们的研究中，人工林生态系统对不同降水格局变化短期响应的结果是，降水量增加对生态系统净初级生产力的影响不显著，但显著地增加了土壤异养呼吸，导致 NEP 反而下降，土壤异养呼吸是 NEP 对降水变化响应的关键因素。这与 Valentini et al. (2000)、Grace & Rayment(2000)等的观点是一致的，他们也认为土壤异养呼吸(R_h)是陆地生态系统 NEP 的决定因素。

6.3 小结

塞罕坝樟子松—落叶松人工混交林生态系统净初级生产力对降水变化的响应不显著，而土壤异养呼吸对降水变化的响应比较敏感。生态系统净初级生产力对降水减少的响应相对比较明显，而土壤异养呼吸则对降水增加的响应更灵敏。增加和减少 30% 穿透雨量对作为生态系统碳收支指标的净生态系统生产力统计上无显著影响。但由于净初级生产力和土壤异养呼吸对降水格局变化的响应方式与程度不同，在净初级生产力无显著变化的情况下，净生态系统生产力对降水变化的响应取决于土壤异养呼吸。

第七章 结论与展望

7.1 主要结论

为了探讨森林生态系统对未来降水格局变化的响应,我们在位于森林—草原植被过渡带、半干旱半湿润气候区的河北塞罕坝地区进行了人工林降水控制实验,用增加和减少 30% 穿透雨来模拟自然降水变化,并系统选取了多种指标,从地下生态过程到地上部分植物生长、从微生物到生态系统、从瞬时值测量到全年通量估算,研究了降水变化对樟子松—落叶松人工混交林生态系统碳循环主要过程的影响。主要结论如下:

7.1.1 降水减少保存了土壤养分,降水增加降低了土壤养分含量但提高了可利用性

穿透雨增加和减少 30% 显著地改变了样地土壤体积含水量,土壤体积含水量增雨 > 对照 > 减雨。三种处理的土壤温度统计上均无显著差异,但减雨处理的土壤温度略高于增雨和对照。穿透雨处理对 0-30cm 土壤微生物量碳及其与土壤总有机碳的比值、铵态氮和无机氮(铵态氮与硝态氮之和)无显著影响。穿透雨处理对土壤水溶性有机碳和硝态氮有显著影响。增雨处理水溶性有机碳和硝态氮都显著降低,这可能是因为降水淋溶作用加剧,也可能因为土壤水分含量高导致植物根系和微生物对土壤养分的利用增加。减雨处理土壤中保有的水溶性有机碳高于对照和增雨。降水变化对土壤铵态氮及氨化作用的影响弱于对硝态氮及硝化作用的影响。穿透雨处理对净氨化速率无显著影响,由于温度和水分的变化,增雨和减雨处理的净硝化速率和净氮矿化速率显著高于对照。

塞罕坝樟子松—落叶松人工混交林土壤活性有机碳、无机氮及氮矿化作用对降水变化的初期响应表明,未来降水格局变化对生态系统土壤及土壤微生物活动的影响是复杂的,降水减少会使土壤水分减少、土壤温度升高,降水增加会使土壤水分增加、土壤温度降低,这都可能让土壤微生物的种类、数量及活性发生变化,从而改变土壤养分的状态与可利用性。我们对土壤活性有机碳、无机氮的综合研究也表明,塞罕坝地区的土壤比较瘠薄,土壤微生物群落受氮限制,而非碳限制。

7.1.2 植物生长对降水变化的响应存在但不显著

增加和减少 30% 穿透雨对樟子松—落叶松人工混交林的乔木和草本植物生长统计上无显著影响,但是不同树种与径级的乔木胸径年增长率、群落乔木层胸高断面积年增长率和生物量年增长率都有不显著的随着降水量增加而增加的趋势。年增长率的变化表明,虽然穿透雨处理的影响在统计上不显著,但这种影响是确实存在的,年增长率比年增长量更适合作为评价植物生长对控制实验处理响应的指标。森林生态系统对降水格局变化反馈的显著性可能需要更长时间的积累。

7.1.3 土壤呼吸速率和土壤年呼吸量对降水增加响应显著，表观温度敏感性响应不显著

在塞罕坝人工林降水控制实验中，土壤呼吸速率和土壤年呼吸量对增加 30% 穿透雨产生了显著的响应，而减少 30% 穿透雨对土壤呼吸速率和土壤年呼吸量统计上无显著影响。不同穿透雨处理的土壤呼吸速率平均值大小顺序为增雨 > 减雨 > 对照，土壤年呼吸量的平均值顺序为增雨 > 对照 > 减雨。

降水控制实验样地土壤呼吸的表观温度敏感性(Q_{10})为 2.315 ± 0.293 (平均值 \pm 标准差)，变幅为 1.908 ~ 2.668。穿透雨处理对表观 Q_{10} 统计上无显著影响，其平均值增雨 > 对照 > 减雨，随着降水量减少，土壤呼吸温度敏感性降低。

基于土壤温度与水分因素的土壤呼吸速率预测模型 $\ln R = a + b T \times VWC$ 比传统的 van't Hoff 指数方程 $R = ae^{bT}$ 预测效果更好。配对 t 检验比重复测量方差分析更适合分析时间序列数据。

7.1.4 净生态系统生产力对降水变化的响应取决于土壤异养呼吸的变化

樟子松—落叶松人工混交林生态系统净初级生产力对降水变化的响应不显著，而土壤呼吸对降水变化的响应比较敏感。生态系统净初级生产力对降水减少的响应相对比较明显，而土壤异养呼吸则对降水增加的响应更灵敏。在本研究中，增加或减少 30% 穿透雨量对作为生态系统碳收支指标的净生态系统生产力统计上无显著影响。但由于净初级生产力和土壤异养呼吸对降水格局变化的响应方式与程度不同，在净初级生产力无显著变化的情况下，净生态系统生产力对降水变化的响应取决于土壤异养呼吸。

7.2 研究展望

7.2.1 加强森林生态系统对降水变化响应的长期定位研究

我们在河北塞罕坝地区进行了为期三年的降水控制实验，从地上到地下测量了生态系统的很多指标，其中包括工作量很大但出于论文整体性考虑未在此使用的内生长法测定细根生产力和土钻法采集的根系生物量数据。虽然后来降水控制实验因为各种主客观条件(监测系统意外损坏无法修复)未能按计划长期进行下去，但在结果分析过程中，我们越来越发现长期定位监测对于研究气候变化的生态系统响应的重要性，土壤温度与水分等背景值的长期连续监测对于估算土壤年呼吸量等具有重要意义。

7.2.2 进行森林生态系统多因子控制实验

关于草地生态系统多因子控制实验的报道已经很多，方法也比较成熟，但森林生态系统的多因子控制实验还较少，由于气候变化会引起土壤水分、温度、养分可利用性同时发生变化，多因子控制实验有助于更全面地理解、更准确地预测森林生态系统对气候变化的响应。

7.2.3 区分土壤自养呼吸和异养呼吸对降水变化的响应

由于本实验最初设计为多年长期控制实验，出于样地保护等考虑，未用壕沟法来区分土壤自养呼吸和异养呼吸，虽然邻近样地进行了相关测定，但这也是我们研究中的一个遗憾。由于植物根系和土壤微生物对土壤水分变化响应的方式不同，土壤自养呼吸与异养呼吸对降水变化的响应可能也会有所不同，这对于准确预测净生态系统生产力对降水变化的响应具有重要意义。

7.2.4 加强土壤养分循环对降水变化响应的研究

我们的研究初步表明，降水变化确实会对土壤养分产生显著的影响，但是由于未能考虑土壤可溶性有机氮、植物凋落物分解与土壤有机碳矿化等指标与过程，未能全面评价降水变化对土壤碳氮循环的影响。今后应加强研究土壤碳氮循环各主要过程与指标，综合植物生长、土壤呼吸等生态系统主要碳循环过程，用地上地下关联的方法来系统地研究气候变化的生态响应。

参考文献

- 陈伏生, 余燧, 甘露等. 2009. 温度、水分和森林演替对中亚热带丘陵红壤氮素矿化影响的模拟实验. 应用生态学报, 20 (7): 1529-1535.
- 陈伏生, 曾德慧, Singh A N 等. 2005. 不同土壤层次和土壤水分对章古台樟子松固沙林土壤 N 矿化过程的影响. 林业研究(英文版), 16 (2): 101-104.
- 陈伏生, 曾德慧, 范志平等. 2005. 章古台沙地樟子松人工林土壤有效氮的研究. 北京林业大学学报, 27 (3): 6-11.
- 陈伏生, 曾德慧, 范志平等. 2006. 沙地不同树种人工林土壤氮素矿化过程及其有效性. 生态学报, 26 (2): 343 - 347.
- 陈全胜, 李凌浩, 韩兴国等. 2003. 水分对土壤呼吸的影响及机理. 生态学报, 23 (5): 972-978.
- 邓东周. 2009. 降雨量变化对科尔沁沙地东南部樟子松人工林主要生态过程的影响. 博士学位论文. 沈阳: 中国科学院沈阳应用生态研究所.
- 方精云, 柯金虎, 唐志尧等. 2001. 生物生产力的“4P”概念、估算及其相互关系. 植物生态学报, 25 (4): 414-419.
- 方精云. 2000. 全球生态学: 气候变化与生态响应. 北京: 高等教育出版社.
- 黄金祥, 李信, 钱进源. 1996. 塞罕坝植物志. 北京: 中国科学技术出版社: 1.
- 黄永梅, 刘鸿雁, 崔海亭. 2001. 内蒙古高原东南缘森林草原过渡带景观的若干特征. 植物生态学报, 25 (3): 257-264.
- 寇祥明, 杨利民, 韩梅等. 2007. 不同施水量对五叶地锦幼苗生长及抗性生理的影响. 干旱区资源与环境, (03): 139-143.
- 李贵才, 韩兴国, 黄建辉等. 2001. 森林生态系统土壤氮矿化影响因素研究进展. 生态学报, 21 (7): 1187-1195.
- 刘鸿雁. 1998. 内蒙古高原东南缘森林—草原过渡带景观及其演化的生态学研究. 北京: 北京大学.
- 刘濂主编, 1996. 河北植被. 北京: 科学出版社: 38.
- 王常慧, 邢雪荣, 韩兴国. 2004. 温度和湿度对我国内蒙古羊草草原土壤净氮矿化的影响. 生态学报, 24 (11): 2472-2476.
- 王其兵, 李凌浩, 白永飞等. 2000. 气候变化对草甸草原土壤氮素矿化作用影响的实验研究. 植物生态学报, 24 (6): 687 - 692.
- 王妮. 2007. 我国北方坝上地区不同植被类型土壤呼吸及其影响机制的研究. 博士后出站报告. 北京: 北京大学.
- 肖春旺, 周广胜, 赵景柱. 2001. 不同水分条件对毛乌素沙地油蒿幼苗生长和形态的影响. 生态学报, (12): 2136-2140.
- 张新时, 杨奠安. 1995. 中国全球变化样带的设置与研究. 第四纪研究, (01): 43-52, 99-100.
- 郑成洋. 2005. 河北省塞罕坝森林结构与生物量. 博士后出站报告. 北京: 北京大学: 3.
- 周才平, 欧阳华. 2001a. 温度和湿度对长白山两种林型下土壤氮矿化的影响. 应用生态学报, 12 (4): 505-508.
- 周才平, 欧阳华. 2001b. 温度和湿度对暖温带落叶阔叶林土壤氮矿化的影响. 植物生态学报, 25 (2): 204-209.
- Allen C D, Breshears D D. 1998. Drought-induced shift of a forest-woodland ecotone: Rapid landscape response to climate variation. Proceedings of the National Academy of Sciences of the United States of America, 95 (25): 14839-14842.

- Allen C D, Macalady A K, Chenchouni H, et al. 2010. A global overview of drought and heat-induced tree mortality reveals emerging climate change risks for forests. *Forest Ecology and Management*, 259 (4): 660-684.
- Angert A, Biraud S, Bonfils C, et al. 2005. Drier summers cancel out the CO₂ uptake enhancement induced by warmer springs. *Proceedings of the National Academy of Sciences of the United States of America*, 102 (31): 10823-10827.
- Asensio D, Penuelas J, Llusia J, et al. 2007. Interannual and interseasonal Soil CO₂ efflux and VOC exchange rates in a Mediterranean holm oak forest in response to experimental drought. *Soil Biology & Biochemistry*, 39 (10): 2471-2484.
- Austin A T, Sala O E. 2002. Carbon and nitrogen dynamics across a natural precipitation gradient in Patagonia, Argentina. *Journal of Vegetation Science*, 13 (3): 351-360.
- Austin A T, Vitousek P M. 1998. Nutrient dynamics on a precipitation gradient in Hawai'i. *Oecologia*, 113 (4): 519-529.
- Bai W, Wan S, Niu S, et al. 2010. Increased temperature and precipitation interact to affect root production, mortality, and turnover in a temperate steppe: implications for ecosystem C cycling. *Global Change Biology*, 16 (4): 1306-1316.
- Bates C, Maechler M, Bolker B. 2011. lme4: Linear mixed-effects models using S4 classes. R package version 0.999375-42. <http://CRAN.R-project.org/package=lme4>
- Beier C. 2004. Climate change and ecosystem function - full-scale manipulations of CO₂ and temperature. *New Phytologist*, 162 (2): 243-245.
- Billings S A, Richter D D, Yarie J. 2000. Sensitivity of soil methane fluxes to reduced precipitation in boreal forest soils. *Soil Biology & Biochemistry*, 32 (10): 1431-1441.
- Boisvenue C, Running S W. 2006. Impacts of climate change on natural forest productivity - evidence since the middle of the 20th century. *Global Change Biology*, 12 (5): 862-882.
- Bonebrake T C, Mastrandrea M D. 2010. Tolerance adaptation and precipitation changes complicate latitudinal patterns of climate change impacts. *Proceedings of the National Academy of Sciences of the United States of America*, 107 (28): 12581-12586.
- Borken W, Savage K, Davidson E A, et al. 2006. Effects of experimental drought on soil respiration and radiocarbon efflux from a temperate forest soil. *Global Change Biology*, 12 (2): 177-193.
- Borken W, Xu Y J, Brumme R, et al. 1999. A climate change scenario for carbon dioxide and dissolved organic carbon fluxes from a temperate forest soil: Drought and rewetting effects. *Soil Science Society of America Journal*, 63 (6): 1848-1855.
- Bremer D J, Ham J M, Owensby C E, et al. 1998. Responses of soil respiration to clipping and grazing in a tallgrass prairie. *Journal of Environmental Quality*, 27 (6): 1539-1548.
- Brookes P C, Landman A, Pruden G, et al. 1985. Chloroform fumigation and the release of soil nitrogen: a rapid direct extraction method to measure microbial biomass nitrogen in soil. *Soil Biology and Biochemistry*, 17: 837-842.
- Brookes P C. 1995. The use of microbial parameters in monitoring soil pollution by heavy metals. *Biology and Fertility of Soil*, 19: 269-279.
- Cao M, Woodward F I. 1998. Dynamic responses of terrestrial ecosystem carbon cycling to global climate change. *Nature*, 393: 249-252.
- Chapin F S III, Ruess R W. 2001. The roots of the matter. *Nature*, 411: 749-752.
- Chapin F S, Matson P A, Mooney H A. 2005. 李博等译. 陆地生态系统生态学原理. 北京: 高等教育出版社: 168-183.
- Davidson E A, Belk E, Boone R D. 1998. Soil water content and temperature as independent or

- confounded factors controlling soil respiration in a temperate mixed hardwood forest. *Global Change Biology*, 4 (2): 217-227.
- Davidson E A, Janssens I A. 2006. Temperature sensitivity of soil carbon decomposition and feedbacks to climate change. *Nature*, 440: 165-173.
- DeSantis R D, Hallgren S W, Stahle D W. 2011. Drought and fire suppression lead to rapid forest composition change in a forest-prairie ecotone. *Forest Ecology and Management*, 261 (11): 1833-1840.
- Dixon R K, Brown S, Houghton R A, et al. 1994. Carbon pools and flux of global forest ecosystems. *Science*, 263 (5144): 185-190.
- Dörr H, Münnich K O. 1987. Annual variation in soil respiration in selected areas of the temperate zone. *Tellus*, 39B, 114-121.
- Easterling D R, Meehl G A, Parmesan C, et al. 2000. Climate extremes: Observations, modeling, and impacts. *Science*, 289 (5487): 2068-2074.
- Emmett B A, Beier C, Estiarte M, et al. 2004. The response of soil processes to climate change: Results from manipulation studies of shrublands across an environmental gradient. *Ecosystems*, 7 (6): 625-637.
- Fang J Y, Piao S L, Tang Z Y, et al. 2001. Interannual variability in net primary production and precipitation. *Science*, 293: 1723.
- Fay P A, Carlisle J D, Knapp A K, Blair J M, Collins S L. 2000. Altering rainfall timing and quantity in a mesic grassland ecosystem: Design and performance of rainfall manipulation shelters. *Ecosystems*, 3: 308-319.
- Federer C A. 1983. Nitrogen mineralization and nitrification: depth variation in four New England forest soils. *Soil Science Society of America Journal*, 47: 1008-1014.
- Gaumont-Guay D, Black T A, Griffis T J, et al. 2006. Influence of temperature and drought on seasonal and interannual variations of soil, bole and ecosystem respiration in a boreal aspen stand. *Agricultural and Forest Meteorology*, 140 (1-4): 203-219.
- Grace J, Rayment M. 2000. Respiration in the balance. *Nature*, 404 (6780): 819-820.
- Grant R F, Black T A, Gaumont-Guay D, et al. 2006. Net ecosystem productivity of boreal aspen forests under drought and climate change: Mathematical modelling with Ecosys. *Agricultural and Forest Meteorology*, 140 (1-4): 152-170.
- Hadas A, Feigin A, Feigenbaum S, et al. 1989. Nitrogen mineralization in the field at various soil depths. *Journal of Soil Science*, 40: 131-137.
- Hanson P J, Todd D E, Harter K M. 1995. The Walker Branch Throughfall Displacement Experiment: An overview, field performance data, and initial growth responses. *Bulletin of the Ecological Society of America*, 76 (2 Suppl. Part 2): 109.
- Hanson P J, Todd D E, Huston M A, et al. 1998. Description and field performance of the Walker Branch Throughfall Displacement Experiment: 1993-1996. ORNL Technical Memorandum 13586. O. R. N. Laboratory. Oak Ridge, Tenn., USA.
- Hanson P J, Weltzin J F. 2000. Drought disturbance from climate change: response of United States forests. *Science of the Total Environment*, 262 (3): 205-220.
- Hanson P J, Edwards N T, Garten C T, et al. 2000. Separating root and soil microbial contributions to soil respiration: A review of methods and observations. *Biogeochemistry*, 48 (1): 115-146.
- Hanson P J, O'Neill E G, Chambers M L S, et al. 2003. Soil respiration and litter decomposition. In: Hanson P J, Wullschlegel S D. *North American temperate deciduous forest responses to changing precipitation regimes*. New York: Springer: 163-189.

- Hanson P J, Todd D E, Amthor J S. 2001. A six-year study of sapling and large-tree growth and mortality responses to natural and induced variability in precipitation and throughfall. *Tree Physiology*, 21 (6): 345-358.
- Harper C W, Blair J M, Fay P A, Knapp A K, Carlisle J D. 2005. Increased rainfall variability and reduced rainfall amount decreases soil CO₂ flux in a grassland ecosystem. *Global Change Biology*, 11: 322 - 334.
- Hoffmann W A, Marchin R M, Abit P, et al. 2011. Hydraulic failure and tree dieback are associated with high wood density in a temperate forest under extreme drought. *Global Change Biology*, 17 (8): 2731-2742.
- Hogberg P, Nordgren A, Buchmann N, et al. 2001. Large-scale forest girdling shows that current photosynthesis drives soil respiration. *Nature*, 411 (6839): 789-792.
- Hölscher D, Koch O, Korn S, et al. 2005. Sap flux of five co-occurring tree species in a temperate broad-leaved forest during seasonal soil drought. *Trees-Structure and Function*, 19 (6): 628-637.
- Hooper D U, Johnson L. 1999. Nitrogen limitation in dryland ecosystems: Responses to geographical and temporal variation in precipitation. *Biogeochemistry*, 46 (1-3): 247-293.
- Houghton J T, Ding Y, Griggs D J, et al. 2001. *Climate change 2001: The scientific basis*. Cambridge, Cambridge University Press.
- Hughes L. 2000. Biological consequences of global warming: is the signal already apparent? *Trends in Ecology & Evolution*, 15 (2): 56-61.
- Hulme M, Osborn T J, Johns T C. 1998. Precipitation sensitivity to global warming: Comparison of observations with HadCM2 simulations. *Geophysical Research Letters*, 25: 3379-3382.
- Illeris L, Michelsen A, Jonasson S. 2003. Soil plus root respiration and microbial biomass following water, nitrogen and phosphorus application at a high arctic semi desert. *Biogeochemistry*, 65: 15 - 29.
- IPCC. 2001. *Climate change 2001: Synthesis report, third assessment report of the Intergovernmental Panel on Climate Change*, Cambridge Univ. Press, New York.
- IPCC. 2007. *WGI Fourth Assessment Report. Climate Change 2007: The physical science basis*. Geneva: Intergovernmental Panel on Climate Change.
- Jamieson N, Monaghan R, Barraclough D. 1999. Seasonal trends of gross N mineralization in a natural calcareous grassland. *Global Change Biology*, 5 (4): 423-431.
- Jensen K D, Beier C, Michelsen A, et al. 2003. Effects of experimental drought on microbial processes in two temperate heathlands at contrasting water conditions. *Applied Soil Ecology*, 24: 165-176.
- Jentsch A, Kreyling J, Beierkuhnlein C. 2007. A new generation of climate-change experiments: events, not trends. *Frontiers in Ecology and the Environment*, 5 (7): 365-374.
- Johnson D W, Susfalk R B, Gholz H L, et al. 2000. Simulated effects of temperature and precipitation change in several forest ecosystems. *Journal of Hydrology*, 235 (3-4): 183-204.
- Jones P D, Hulme M. 1996. Calculating regional climatic time series for temperature and precipitation: methods and illustrations. *International Journal of Climatology*, 16: 361-377.
- Kalbitz K, Meyer A, Yang R, et al. 2007. Response of dissolved organic matter in the forest floor to long-term manipulation of litter and throughfall inputs. *Biogeochemistry*, 86: 301-318.
- Kimball J S, McDonald K C, Running S W, et al. 2004. Satellite radar remote sensing of seasonal growing seasons for boreal and subalpine evergreen forests. *Remote Sensing of Environment*, 90 (2): 243-258.
- Kljun N, Black T A, Griffis T J, et al. 2006. Response of net ecosystem productivity of three boreal forest stands to drought. *Ecosystems*, 9 (7): 1128-1144.

- Knapp A K, Smith M D. 2001. Variation among biomes in temporal dynamics of aboveground primary production. *Science*, 291 (5503): 481-484.
- Knapp A K, Fay P A, Blair J M, et al. Rainfall variability, carbon cycling and plant species diversity in a mesic grassland. *Science*. 2002, 298: 2202-2205.
- Linn D M, Doran J W. 1984. Effects of water-filled pore space on carbon dioxide and nitrous oxide production in tilled and nontilled soils. *Soil Science Society of America Journal*, 48: 1267-1272.
- Liu B H, Xu M, Henderson M, et al. 2005. Observed trends of precipitation amount, frequency, and intensity in China, 1960-2000. *Journal of Geophysical Research-Atmospheres*, 110, D08103, doi:10.1029/2004JD004864..
- Liu H Y, Cui H T, Tian Y H, et al. 2002. Temporal- spatial variances of Holocene precipitation at the marginal area of the East Asian monsoon influences from pollen evidence. *Acta Botanica Sinica* 44:864-871.
- Liu X Z, Wan S Q, Su B, et al. 2002. Response of soil CO₂ efflux to water manipulation in a tallgrass prairie ecosystem. *Plant and Soil*, 240 (2): 213-223.
- Luo Y, Zhou X H. 2007. 姜丽芬等译. 土壤呼吸与环境. 北京: 高等教育出版社.
- Ma Z, Peng C, Zhu Q, et al. 2012. Regional drought-induced reduction in the biomass carbon sink of Canada's boreal forests. *Proceedings of the National Academy of Sciences of the United States of America*, 109 (7): 2423-2427.
- Michaelian M, Hogg E H, Hall R J, et al. 2011. Massive mortality of aspen following severe drought along the southern edge of the Canadian boreal forest. *Global Change Biology*, 17 (6): 2084-2094.
- Misson L, Degueldre D, Collin C, et al. 2011. Phenological responses to extreme droughts in a Mediterranean forest. *Global Change Biology*, 17 (2): 1036-1048.
- Misson L, Rocheteau A, Rambal S, et al. 2010. Functional changes in the control of carbon fluxes after 3 years of increased drought in a Mediterranean evergreen forest? *Global Change Biology*, 16 (9): 2461-2475.
- Ni J. 2011. Impacts of climate change on Chinese ecosystems: key vulnerable regions and potential thresholds. *Regional Environmental Change*, 11: S49-S64.
- Niu S L, Wu M Y, Han Y, et al. 2008. Water-mediated responses of ecosystem carbon fluxes to climatic change in a temperate steppe. *New Phytologist*, 117: 209-219
- Norby R J, Luo Y Q. 2004. Evaluating ecosystem responses to rising atmospheric CO₂ and global warming in a multi-factor world. *New Phytologist*, 162 (2): 281-293.
- Park J H, Matzner E. 2003. Controls on the release of dissolved organic carbon and nitrogen from a deciduous forest floor investigated by manipulations of aboveground litterinputs and water flux. *Biogeochemistry*, 66: 265-286.
- Pasho E, Julio Camarero J, de Luis M, et al. 2011. Impacts of drought at different time scales on forest growth across a wide climatic gradient in north-eastern Spain. *Agricultural and Forest Meteorology*, 151 (12): 1800-1811.
- Puri G, Ashman M R. 1998. Relationship between soil microbial biomass and gross N mineralisation. *Soil Biology, Biochemistry*, 30 (2): 251-256
- Qian W H, Qin A. 2008. Precipitation division and climate shift in China from 1960 to 2000. *Theoretical and Applied Climatology*, 93 (1-2): 1-17.
- Qian W, Shan X, Zhu Y. 2011. Ranking regional drought events in China for 1960-2009. *Advances in Atmospheric Sciences*, 28 (2): 310-321.
- R Development Core Team. 2011. R: A language and environment for statistical computing. R Foundation for Statistical Computing, Vienna, Austria. ISBN 3-900051-07-0, URL

- <http://www.R-project.org/>
- Raich J W, Potter C S. 1995. Global patterns of carbon-dioxide emissions from soils. *Global Biogeochemical Cycles*, 9 (1): 23-36.
- Randerson J T, Chapin F S, Harden J W, et al. 2002. Net ecosystem production: A comprehensive measure of net carbon accumulation by ecosystems. *Ecological Applications*, 12 (4): 937-947.
- Reichstein M, Rey A, Freibauer A, et al. 2003. Modeling temporal and large-scale spatial variability of soil respiration from soil water availability, temperature and vegetation productivity indices. *Global Biogeochemical Cycles*, 17 (4): 1104. DOI: 10.1029/2003GB002035.
- Sardans J, Penuelas J. 2007. Drought changes phosphorus and potassium accumulation patterns in an evergreen Mediterranean forest. *Functional Ecology*, 21 (2): 191-201.
- Schimel D S, House J I, Hibbard K A, et al. 2001. Recent patterns and mechanisms of carbon exchange by terrestrial ecosystems. *Nature*, 414 (6860): 169-172.
- Schlesinger W H, Reynolds J F, Cunningham G L, et al. 1990. Biological feedbacks in global desertification. *Science*, 247 (4946): 1043-1048.
- Schuur E A G. 2003. Productivity and global climate revisited: The sensitivity of tropical forest growth to precipitation. *Ecology*, 84 (5): 1165-1170.
- Sierra J. 1997. Temperature and soil moisture dependence of N mineralization in intact soil cores. *Soil Biology and Biochemistry*, 29 (9-10): 1557-1563.
- Smith S D, Huxman T E, Zitzer S F, et al. 2000. Elevated CO₂ increases productivity and invasive species success in an arid ecosystem. *Nature*, 408 (6808): 79-82.
- Stephens B B, Gurney K R, Tans P P, et al. 2007. Weak northern and strong tropical land carbon uptake from vertical profiles of atmospheric CO₂. *Science*, 316 (5832): 1732-1735.
- Teesier, L, Gregorich E G, Topp E. 1998. Spatial variability of soil microbial biomass measured by the fumigation extraction method, and k_{EC} as affected by depth and manure application. *Soil Biology and Biochemistry* 30: 1369-1377.
- Valentini R, Matteucci G, Dolman A J, et al. 2000. Respiration as the main determinant of carbon balance in European forests. *Nature*, 404 (6780): 861-865.
- Vance E D, Brookes P C, Jenkinson D S. 1987a. An extraction method for measuring soil microbial biomass C. *Soil Biology and Biochemistry*, 19: 703-707.
- Vance E D, Brookes P C, Jenkinson D. 1987b. Microbial biomass measurements in forest soils: the use of the chloroform fumigation-incubation technique in strongly acid soils. *Soil Biology and Biochemistry*, 19: 697-702.
- van't Hoff J H. 1884. *Études de dynamique chimique (Studies of Chemical dynamics)*. Amsterdam: Frederik Muller.
- Vitousek P M. 1994. Beyond global warming: Ecology and global change. *Ecology*, 75: 1861-1876.
- Wardle D A, Bardgett R D, Klironomos J N, et al. 2004. Ecological linkages between aboveground and belowground biota. *Science*, 304 (5677): 1629-1633.
- Wardle D A. 1992. A comparative assessment of factors which influence microbial biomass carbon and nitrogen levels in soil. *Biology Reviews*, 67: 321-358.
- Weihong Q, Yafen Z. 2001. Climate change in China from 1880 to 1998 and its impact on the environmental condition. *Climatic Change*, 50 (4): 419-444.
- Weltzin J F, Loik M E, Schwinning S, et al. 2003. Assessing the response of terrestrial ecosystems to potential changes in precipitation. *Bioscience*, 53 (10): 941-952.
- Weltzin J F, McPherson G R. 2000. Implications of precipitation redistribution for shifts in temperate savanna ecotones. *Ecology*, 81: 1902-1913.

- Weltzin JF, Loik ME, Schwinning S, et al. 2003. Assessing the response of terrestrial ecosystems to potential changes in precipitation. *Bioscience*, 53: 941-952.
- Wullschleger S D, Hanson P J. 2006. Sensitivity of canopy transpiration to altered precipitation in an upland oak forest: evidence from a long-term field manipulation study. *Global Change Biology*, 12 (1): 97-109.
- Wyckoff P H, Bowers R. 2010. Response of the prairie-forest border to climate change: impacts of increasing drought may be mitigated by increasing CO₂. *Journal of Ecology*, 98 (1): 197-208.
- Xu L K, Baldocchi D D, Tang J W. 2004. How soil moisture, rain pulses, and growth alter the response of ecosystem respiration to temperature. *Global Biogeochemical Cycles*, 18 (4): GB4002, DOI: 10.1029/2004GB002281.
- Xu M, Qi Y. 2001a. Soil-surface CO₂ efflux and its spatial and temporal variations in a young ponderosa pine plantation in northern California. *Global Change Biology*, 7: 667-677.
- Xu M, Qi Y. 2001b. Spatial and seasonal variations of Q₁₀ determined by soil respiration measurements at a Sierra Nevadan forest. *Global Biogeochemical cycles*. 15(3): 687-696.
- Xu Y L, Huang X Y, Zhang Y, et al. 2006. Statistical analyses of climate change scenarios over China in the 21st century. *Advances in Climate Change Research*, 2 (Suppl 1): 50-53.
- Zak D R, Ringelberg D B, Pregitzer K S, et al. 1996. Soil microbial communities beneath *populus grandidentata* grown under elevated atmospheric CO₂. *Ecological Applications* 6: 257-262.
- Zhang, Q S, Zak J C.1998. Effects of water and nitrogen amendment on soil microbial biomass and fine root production in a semi-arid environment in west Texas. *Soil Biology and Biochemistry*, 30: 39-45.
- Zhao M, Running S W. 2010. Drought-induced reduction in global terrestrial net primary production from 2000 through 2009. *Science*, 329 (5994): DOI: 10.1126/science.1199544.
- Zhou X H, Sherry R A, An Y, et al. 2006. Main and interactive effects of warming, clipping, and doubled precipitation on soil CO₂ efflux in a grassland ecosystem. *Global Biogeochemical Cycles*, 20 (1): GB1003. DOI: 10.1029/2005GB002526.

致 谢

转眼间，在北大已经整整八年了。在延期的四年中，曾经无数次想象要在学位论文致谢中说的话，但却担心自己没有这样的机会。在老师、同学和家人的鼓励与帮助下，我终于要迎来博士毕业的日子了，也终于可以正式地对那些在我博士期间给予帮助的人表达我的谢意了。

首先，我要感谢我的导师方精云老师。方老师为人方正严谨，生活简单环保，工作勤奋热情，学术视野广阔，他的人品和学术造诣是我一生学习的楷模。2008年初，我发现自己意外怀孕后非常焦虑，方老师宽容与支持的态度让我可以安心地迎接宝宝的到来。后来，我又因为育儿一再延期，方老师始终都很理解并鼓励我继续完成学业。宝宝健康快乐地成长，我也能顺利地完成学业，这与方老师的关心与帮助是分不开的。

贺金生老师是指导我做降水控制实验的导师。贺老师学术思维活跃、对待科学研究热情又严谨，他的一些工作方法对我的影响很大(如文献阅读与管理、数据汇总与统计)。在降水控制实验从设计到运行的过程中，贺老师的指导与信任是我工作的重要动力。我们投入了大量时间、精力与科研经费的降水控制实验结果至今未能在国际学术期刊上发表，对此我感到非常抱歉，这也是我继续努力的方向。

郑成洋老师在我进行降水控制实验的过程中给予了很多帮助，他的灿烂微笑和热情无私始终让我心怀感激。从搭车往返于坝上和北京、来回搬运沉重的仪器与样品、订做样地围栏、订购样地施工材料、提供方便的实验与食宿条件、为获得降水控制实验需要的坝上气候数据多次奔走，到针对降水控制实验提出宝贵建议、共享研究资料，我需要感谢郑老师的地方真是太多太多。

王妮老师对我来说亦师亦友，与王老师在坝上一起工作和生活的日子让我至今难忘。王老师总是不停地提出新的科学问题、不断地为自己提出新的挑战，她积极阳光的工作与生活态度让我受益良多。非常感谢王老师在我测定土壤呼吸与数据分析、写作过程中给予的悉心指导与帮助，也非常感谢她对我的论文提出的诸多宝贵意见，这让我可以不断地完善自己的研究。

吉成均老师曾在野外出差、室内实验和样品管理方面给我提供了很多便利与帮助，特别是在我既没信心、又很茫然、不知如何能够顺利毕业时，吉老师能够设身处地为我考虑，他的督促、鼓励与建议让我终于拨开迷雾、找到了前进的方向。

郭大立老师在降水控制实验氮矿化及细根生产力等指标测定方面给予了耐心具体的指导，刘鸿雁老师教我认识了许多坝上的植物，还帮我鉴定了样地的植物标本，跟随你们在坝上实习是我全面认识坝上植被的最好机会。我还要感谢沈泽昊老师、朴世龙老师、唐志尧老师和朱江玲老师，

大家的鼓励和帮助让我在北大的时光增添了更多温暖的人情味儿。

生态学系老教授陈昌笃先生、崔海亭先生和黄润华先生的学术造诣、社会责任感和乐观的生活态度都让我非常景仰，非常有幸能够在北大聆听你们的教诲。

我最想感谢的同学是师弟杜恩在。2008 年，在我因怀孕无法亲赴坝上做实验的时候，是他挺身而出、接手了降水控制实验的维持与运行。在面对各种困难的情况下，他出色地完成了多项指标的测定。在我撰写毕业论文的时候，杜恩在同学在论文结构和数据分析方面都提供了宝贵的建议，让我在几乎想要放弃的情况下重振精神、克服困难，最终完成了毕业论文，也终于体验到了科学发现的乐趣。虽然论文内容还不够完善，但这对我来说已经像一个奇迹。见证了杜恩在同学这几年在学术方面的快速成长后，我相信他会继续不断进步、成为一名优秀的青年科研工作者。

魏天凤同学负责了降水控制实验中土壤活性有机碳的测定，汪涛同学在 2006 年 8~10 月帮忙测定了土壤呼吸，彭书时同学在我测定土壤呼吸日动态时给予了大力支持，岳超同学和郭兆迪同学提供了他们辛苦工作获得的樟子松与落叶松相关生长方程，和他们一起在坝上工作与生活的日子有苦趣，更有乐趣。感谢王襄平博士、王永慧同学和王少鹏同学在统计方面的建议。

北京农博科公司的韩建宁工程师在降水控制实验方案设计和施工运行过程中起到了重要的作用，帮助我们想法变成现实；澳作仪器有限公司的高工和史大伟工程师在仪器调试、维修方面给予了专业支持。塞罕坝机械林场气象站的李宝华站长和马玉华工程师为我们提供了坝上的多年平均气象数据和重要的日降水数据，2006 年我住在气象站的时候，马工在生活方面对我也很关心。坝上定位站工地的各位工程师和工人师傅为我的实验和生活提供了很多帮助与便利，他们的智慧和开朗也丰富了我的人生阅历。感谢现在还在坝上定位站工作的李大爷，他像长辈一样的关心、像孩子一样的笑容常常令我感动。我还要感谢那些在野外工作中先后给予诸多帮助的科研辅助人员，他们是秦海、孔令民、马永唐、门跃坡、宋永利、王常丽、马静、郭海艳、王健美、王立波、庄俭、电工范利国、司机姜新龙、王诚等，还有一些甚至都不知道姓名的师傅。没有他们的帮助，仅凭我一己之力是不可能完成大量样品的野外采样和前处理工作的。还有那些在坝上生活的当地人，你们的善意和微笑让我在异乡获得了归属感。

感谢五位匿名审稿人对我的研究工作的肯定和提出的宝贵意见，感谢你们帮助我完善学位论文。虽然我试图把自己新获得的科研发现的快乐传递给读者、增加学术论文可读性的尝试未能通过你们的最终检验，但我还是非常感谢你们作为学术把关人的严谨态度。

最后，我要感谢我的家人。我的父母公婆在生活方面给予我们许多帮助，在学业上也不断地鼓励我，我的丈夫一如既往地支持我完成学业。三岁半的女儿呦呦是我最终能够完成学业的重要动力，这也是为了有始有终地完成一件事情给她看，让她长大以后不要轻言放弃、相信自己会创

造“奇迹”。

需要感谢的人很多很多，千言万语汇成一句话：谢谢所有给予我帮助的师长、同学和家人！


任艳林

2012年6月7日于燕园

北京大学学位论文原创性声明和使用授权说明

原创性声明

本人郑重声明：所呈交的学位论文，是本人在导师的指导下，独立进行研究工作所取得的成果。除文中已经注明引用的内容外，本论文不含任何其他个人或集体已经发表或撰写过的作品或成果。对本文的研究做出重要贡献的个人和集体，均已在文中以明确方式标明。本声明的法律结果由本人承担。

论文作者签名： 日期：2012 年 5 月 31 日

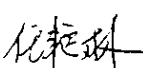

学位论文使用授权说明

(必须装订在提交学校图书馆的印刷本)

本人完全了解北京大学关于收集、保存、使用学位论文的规定，即：

- 按照学校要求提交学位论文的印刷本和电子版本；
- 学校有权保存学位论文的印刷本和电子版，并提供目录检索与阅览服务，在校园网上提供服务；
- 学校可以采用影印、缩印、数字化或其它复制手段保存论文；
- 因某种特殊原因需要延迟发布学位论文电子版，授权学校 ☐ 一年 / ☐ 两年 / ☒ 三年以后，在校园网上全文发布。

(保密论文在解密后遵守此规定)

论文作者签名： 导师签名：

日期：2012 年 5 月 31 日



硕士论文

北京大学

硕士研究生学位论文

题目： 干旱极限条件下温带森林
对气候变化的敏感性

姓 名： 何思源

学 号： 10613101

院 系： 城市与环境学院

专 业： 生态学

研究方向： 植被生态学

导 师： 刘 鸿 雁 教授

二〇〇九年六月

版权声明

任何收存和保管本论文各种版本的单位和个人，未经本论文作者同意，不得将本论文转借他人，亦不得随意复制、抄录、拍照或以任何方式传播。否则，引起有碍作者著作权之问题，将可能承担法律责任。

论文摘要

由于气候的干旱化，全球许多地区出现的森林的衰退。在温带森林分布的干旱极限，森林与草原交错分布，植被格局和动态对水分过程非常敏感。量化这种敏感性对于认识森林植被响应气候干旱化的机理以及模拟未来气候变化背景下森林的动态具有非常重要的意义。

本文分别从温带落叶阔叶林干旱林线树木个体、森林草原交错带森林群落以及温带森林和草原生物群区三个水平入手，探讨植物功能类型和生态系统对水分的时空变化的响应，试图揭示森林分布和生长对气候变化的敏感性，预测干旱林线未来可能的动态。

在个体水平上，干旱极限下树木高生长受到水分限制，不与径向增长同步进行，树高与水分利用效率（WUE）的关系表明矮化是为维持蒸腾需求并满足光合同化产物分配，达到水分有效利用。由于决定 WUE 的光合速率和蒸腾速率分别受到土壤湿度和空气湿度的影响，干旱林线形成的背景是区域水热组合。

在群落水平上，降水和植被类型影响土壤粒径，进而影响土壤水分的时空格局，决定了干旱林线的林草格局。阔叶林下细的土壤质地条件对水分的吸持和砂质土壤的水力特征有利于提高水分有效性。阔叶林下土壤水分的季节波动反映了森林生长前期土壤储水的主要作用。

在生物群区尺度上，森林和草原 NDVI 对季节性气候因子具有时空响应，用 LPJ-DGVM 动态植被模型模拟的森林分布格局和生产力对不同气候变化趋势下季节性气候因子的响应敏感性，以及对极端干旱的程度、频率和持续时间的响应特征结果表明，森林覆盖度和年净第一性生产力对生长前、中期气温和降水响应敏感，敏感性在气候暖干化方向，气候变化趋势剧烈以及气候变化程度大时更强，在降水和气温波动 50% 以上时敏感性趋同。当出现持续的干旱时，季节性干旱程度越大，植被生产力越低，夏季干旱的影响最严重；连季干旱的对生产力的影响大于单季干旱；干旱频率和持续时间主要对后期生产力的恢复产生影响，频率低、持续时间短的干旱事件后生产力恢复能力强，但这种恢复力会随时间而衰减。

论文关键词：干旱极限 森林-草原交错带 植被敏感性 植被动态
水分利用效率（WUE） 土壤含水量

Sensitivity of Temperate Forest to Climate Change in Its Drought Limit

He Siyuan (Ecology)

Directed by Professor Liu Hongyan

Temperate forest decline has already been seen in some areas globally due primarily to climate aridity. Forest and steppe exhibit mosaic distribution at the drought limit of temperate forest distribution range, where the vegetation pattern and dynamics are sensitive to hydrologic process. It is of great significance to quantify the sensitivity so as to realize the mechanism of forest vegetation responding to climate aridity and to simulate forest dynamics under climate change conditions.

This thesis combines research in three levels, individual, plant community and biome, to analyze the response of plant functional type (PFT) and ecosystems to spatial and temporal change of water resource, so as to reveal the sensitivity of both the forest distribution and productivity to climate change, and to predict the future dynamics of xeric tree line.

In individual level, height growth is not proportioned to radial increment in drought limit. The relationship between WUE and tree height indicates that dwarfing is an adaption to balance transpiration requirement and photosynthate allocation to root and shoot. Because the component of WUE is photosynthesis rate and transpiration rate, which are mostly affected by soil moisture and air humidity respectively, the final control of forest drought limit is the combination of precipitation and temperature which defines the microclimate.

In community level, soil particle size is affected by precipitation and vegetation type which further modifies soil water content to form the forest-steppe pattern. The water holding capacity of finer particle and the hydraulic character of sandy soil improve water availability under broadleaved forest. Temporally soil water storage in early growing season is important to forest growth.

In biome level, seasonal and growing season NDVI of forest and steppe shows different response to seasonal precipitation and temperature. Modeled forest coverage and productivity are sensitive to precipitation and temperature in early and mid growing season, more sensitive when climate oscillation is stronger, has an aridity tendency, or coupled with rapid climate change. When the seasonal oscillation of precipitation and temperature are higher than 50% they incline to have convergent impact on forest growth. Simulations of consecutive seasonal drought show that the severity of drought affects productivity in progress of drought, while the frequency and duration of drought affect the recovery from drought.

Keywords: drought limit; forest-steppe ecotone; vegetation sensitivity; vegetation dynamics; water use efficiency (WUE); soil water content;

目 录

第一章 前言.....	1
1.1 干旱极限森林生长及对环境变化的敏感性.....	1
1.1.1 干旱极限下森林生长和干旱林线的提出.....	1
1.1.2 干旱极限森林生长的敏感性及其量化.....	2
1.2 森林旱极驱动因子及气候干旱指标.....	3
1.2.1 降水作为森林旱极的驱动因子.....	3
1.2.2 土壤水分作为森林旱极的驱动因子.....	5
1.2.3 非生长季降水作为森林旱极的驱动因子.....	6
1.2.4 水分以外的因素作为森林旱极的驱动因子.....	8
1.2.5 气候干旱的定义及其量化指标.....	9
1.3 森林旱极的响应特征和动态模拟.....	10
1.3.1 植被生长和生产力的响应.....	10
1.3.2 生态系统过程的响应.....	12
1.3.3 植被分布和种类组成的响应.....	12
1.3.4 生态系统格局和过程的动态模拟.....	14
1.4 中国林草过渡带研究进展.....	17
1.5 研究内容和技术路线.....	19
1.5.1 研究内容.....	19
1.5.2 技术路线.....	20
第二章 研究区和研究方法.....	21
2.1 研究区概况及选择依据.....	21
2.1.1 研究区自然概况.....	21
2.1.2 研究区选择依据.....	22
2.2 研究方法.....	23
2.2.1 树木生长和生理数据分析.....	23
2.2.2 森林草原交错带土壤采样设计和处理.....	25
2.2.3 气象台站数据.....	27
2.2.4 遥感数据.....	28
2.2.5 动态模型结构.....	29
第三章 树木对干旱的生理适应及林线形成机制.....	35
3.1 干旱极限森林生长特征.....	35
3.2 树木对干旱的生理适应性.....	36
3.2.1 水分利用效率与树高的关系.....	36
3.2.2 理想干旱林线形成机制.....	37
3.3 小结.....	38

第四章 群落水平上林草交错带土壤水分.....	39
4.1 交错带 1982-2004 年气候变化.....	39
4.2 森林草原交错带土壤水分的时空差异.....	40
4.2.1 土壤水的空间分布特征.....	40
4.2.2 森林草原交错带土壤水的时间特征.....	44
4.3 土壤机械组成对水分的影响.....	48
4.3.1 区域内采样点粒度分布特征.....	48
4.3.2 土壤机械组成与土壤含水量.....	53
4.4 小结.....	58
第五章 生物群区水平温带森林动态的决定因子.....	59
5.1 基于 NDVI 分析的森林与草原对过去 21 年气候变化的响应.....	59
5.1.1 春季 NDVI 对春季气候响应的时空格局.....	59
5.1.2 夏季 NDVI 对夏季气候响应的时空格局.....	63
5.1.3 秋季 NDVI 对秋季气候响应的时空格局.....	66
5.1.4 生长季植被 NDVI 对气候综合响应的时空格局.....	69
5.2 基于模型模拟的森林生长对气候的响应.....	72
5.2.1 LPJ 模型植被格局模拟结果的验证.....	72
5.2.2 植被生长对气候年际变化的响应.....	74
5.3 不同气候变化情景下的森林生长状况.....	77
5.3.1 植被覆盖和生产力的敏感性分析.....	77
5.3.2 森林动态对于干旱程度和时间特征的响应.....	84
5.3.3 实际气候数据下的干旱分析.....	93
5.4 小结: 中国林草交错带未来动态及其意义.....	95
第六章 讨论.....	97
6.1 干旱极限条件下树木个体的水分利用策略.....	97
6.2 森林群落水分利用策略和干旱林线的形成.....	100
6.2.1 干旱林线森林对土壤质地的适应和改造.....	100
6.2.2 干旱林线森林对土壤水分的利用.....	100
6.3 温带落叶阔叶林对气候变化的敏感性和潜在危机.....	102
6.3.1 森林对气候变化的敏感性.....	102
6.3.2 干旱对森林生长的影响.....	104
6.4 研究的不确定性分析.....	106
6.4.1 实验数据的不确定性和改进.....	106
6.4.2 模型结果的可靠性分析.....	106
第七章 结论.....	109
参考文献.....	110
附录.....	127

第一章 前言

1.1 干旱极限森林生长及对环境变化的敏感性

1.1.1 干旱极限下森林生长和干旱林线的提出

森林草原交错带以森林和草原两种植被共存为特色，在落叶阔叶林和温带草原之间的交错带，植被格局以落叶阔叶林和草甸、草原的大型镶嵌体为特征。气候愈湿润，落叶阔叶林占优势，草原呈分散的岛状分布。当气候愈干旱，情况就相反，接近草原带，只有岛状森林分布在大片的草原上（Walter, 1985）。

干旱气候是限制树木分布的一个重要因子，不同降水和气温组合下的干旱极限森林分布格局不尽相同。热带稀树草原表现为随着干旱程度增加，树木盖度降低，形成一个宽阔的疏林草原景观。在欧亚大陆温带地区，森林片段与草原片段共存，形成森林草原。

温带落叶阔叶林具有明显的季相变化，特别是基于温度的物候过程。从春季积雪融化开始到林冠闭合再到落叶，完成一个完整的生长季。在落叶阔叶林带内同时存在水分控制，在北美表现为由郁闭栎林（oak forest）逐渐过渡到具有林下草本层的开阔林地（woodland）再到树木散生的稀树草原（savanna）。我国典型暖温带落叶阔叶林带年降水量约 600-900mm，冬、春季降水分别占全年降水的 3-7%和 10-40%，夏季降水最丰富，占全年降水的 60-70%，通常 10 月至来年 4 月干燥，5 月至 9 月湿润，土壤含水量变化具有季节性。分布北界的森林净第一性生产力（NPP, Net Primary Productivity, 下同）积累出现在 5 月至 9 月，最大 NPP 出现在 7 月末至 8 月中，NPP 高值出现在 6 月至 8 月（Yuan *et al.*, 2006）。

降水量是决定森林生长的首要因子，在晋西北黄土高原森林草原交错带，森林利用了小地形对土壤水分的影响，在沟谷中生长，但是由东南向西北随着降水量减少，沟谷中森林也逐渐减少；内蒙古东南缘的森林草原交错带从森林带到森林草原交错带，森林斑块依次变小，森林覆盖率降低，景观破碎化程度变高。交错带森林多出现在低山和高大沙丘的阴坡，斑块小，外界干扰大，树高低（王庆锁, 2004），阴坡温度较低，相对湿度较高，土壤蒸发量小，春季解冻迟，利于树木生长（赵文智和宝音, 1994）。温带落叶阔叶林对养分要求相对较低，一般不会耗尽土壤元素库（Duvigneaud & Denaeyer-de-Smet, 1970），因而水分是首要因素。水分亏缺影响植被蒸腾，导致叶片气孔闭合从而影响光合作用。在温带森林草原

交错带，森林生长不缺乏二氧化碳，也有足够的生长季，因此水分尤为重要。

全球范围内的研究认为，养分是湿润区限制 NPP 分配的因子，而干旱地区水分是限制 NPP 分配的因子。因此有人提出“低海拔树线”(Kimmins, 2005)一词区别于高山林线，也可以称为“干旱林线”，“大陆林线”，是森林让位于草原的界线。本研究中干旱林线是指温带落叶阔叶林让位于温带草原的过渡带，即温带落叶阔叶林分布的干旱极限(旱极)。有人指出，旱极存在于郁闭森林(closed forest)和森林草原(woodlands or forest steppe)之间，在旱极(xeric forest limits)存活的树木其旱极由气候干旱决定(Calos & Matyas, 2008)。

1.1.2 干旱极限森林生长的敏感性及其量化

森林草原交错带的形成和发展是一个动态平衡过程，受地质地貌、气候以及人为干扰的综合影响，其格局、结构乃至生产力在时间和空间上出现明显波动。对其结构、功能和动态特征的研究长期以来一直为科学界所关注(House *et al.*, 2003)。特别是近年来随着计算机技术的发展，传统的群落调查逐渐辅助以新的研究手段，如遥感技术、地理信息系统分析和动态植被模型等，都为探究森林草原交错带形成机理注入了新的活力。

中国的森林草原交错带处于欧亚大陆森林草原过渡带的东南缘，是森林分布的干旱极限，与草原带相连的森林植被类型丰富(吴征镒, 1980; 侯学煜, 1988)，由于处于太平洋季风影响的边缘区域，对气候变化敏感，是研究中国全球变化的关键区域。

当前，植被对气候变化响应的敏感性分析是揭示植被动态的驱动力的重要方法，许多植被对气候响应的研究都采用相关分析等手段，试图寻找不同时段的因素对植被生长的驱动。然而，真正意义上的敏感性分析应当控制其他因素的变化，分析单一自变量变化一定比率时因变量的变化率，因此，除了在模型分析中采用标准意义上的敏感性分析外，许多相关分析表示的敏感性缺乏机理分析(李晓兵和史培军, 2000; 齐述华等, 2004)。

干旱极限下森林对什么环境因子响应敏感，采用什么指标表征森林生长状况，是探究森林生长对环境因子变化的响应的关键。针对干旱极限下不同影响因子对森林生长的影响主要可以根据不同尺度提出 3 组影响因子：

气候主导作用。降水控制着森林最大盖度，降水的量级、频率、持续时间和季节分配决定了根系对水分的利用时机，降水不足或时间不利，导致光合同化作用不能正常进行以增加生物量。气温叠加在降水之上，影响水分的有效性，形成森林分布的一定区域。

土壤水分胁迫作用。气候主导的森林分布区内，土壤水分有效性决定植被根区水分有效性，土壤水分缺乏与高蒸发需求导致木质部导管和根际空穴化，影响水分运输并使植物脱水，或因气孔关闭中止光合作用导致缺乏代谢所需碳水化合物（McDowell *et al.*, 2008）。

干扰因子作用。放牧、火、动物啃食嫩叶等在半干旱区影响树木的种子传播、立木更新和种内竞争。

除了干扰因素外，森林在个体、群落和生物群区（biome）水平上对环境因子的响应都表现在对水分有效性的响应上，气候因子连同它所影响的土壤水分是对森林生长影响最明显的因子。

1.2 森林旱极驱动因子及气候干旱指标

1.2.1 降水作为森林旱极的驱动因子

干旱林线处于半干旱区，该地区年降水量不大但变率较强（Noy-Meir, 1973），对植被生产力和种类组成产生重要的影响（Bates *et al.*, 2006）。降水的频率和季节分配在土壤水分有效性中起主要作用。降水对植被水分利用至关重要，一般认为在年蒸散量超过年降水量的地区植被生产力与降水总量直接相关（Rosenzweig, 1968; Chong *et al.*, 1993），在水分限制地区，NPP 与水分在根区的有效性也表现出近似的线性关系（De Michele *et al.*, 2008）。

由于降水是半干旱区最重要的非生物因子，大量关于半干旱区的研究集中在降水格局与植被分布的关系，如地中海地区、北美和南美西海岸，非洲热带和副热带干旱半干旱区等（eg: Sarris *et al.*, 2007; Cowling & Campbell, 1980; Kraaij & Milton, 2005）。特别是北美温带草原、稀树草原以及非洲热带稀树草原地区（eg: Weltzin *et al.*, 2000; Sankaran *et al.*, 2005）。长期以来，对于降水量是否是森林分布的决定因素以及降水量究竟在多大程度上决定森林的分布一直存在争议。Sankaran 等（2005）通过对非洲地区 854 个地点的研究，试图提出一个统一的解释模式（图 1.1），认为 MAP（年均降水量）小于 650mm 的地点木本的最大覆盖率受到 MAP 的控制，并随之增减而增减，可以认为这些干旱-半干旱地区在水分控制下的木本和草本共生是稳定系统，火、草食动物和土壤性质在 MAP 控制所达到的覆盖率上界内共同作用减少木本覆盖率；而 MAP 高于 650mm 的地点，热带稀树草原被认为是不稳定系统，MAP 已经足以使林冠达到郁闭。

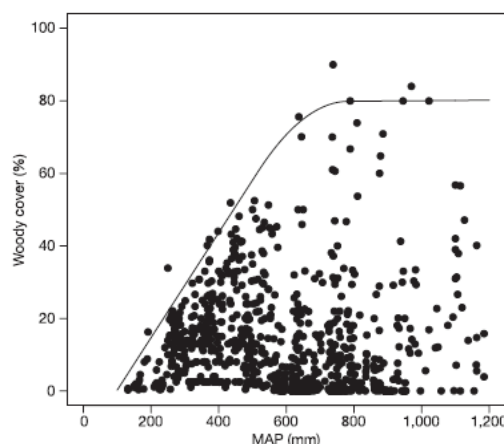


图 1.1 非洲萨瓦纳木本盖度的变化与年均降水量的关系（引自 Sankaran *et al.*, 2005）

水分利用效率（Water Use Efficiency, WUE，下同）涉及到一定水分条件下植被的生长和生产力情况，越来越多的研究在水分限制地区开展，原因在于气候变化下生产力提高背后的水分消耗（carbon assimilation to water loss）代价不容忽视。半干旱区森林生长极限的 WUE 关系到其生存和对未来气候变化的应对。植物 WUE 随降水量的变化而变化，从而影响到树草竞争，最后影响到林草比例。一些研究工作也发现树木 WUE 随着降水量减少而减少，而草本植物的平均 WUE 随降水量减少而增大（Caylor & Shugart, 2004）。在各种植被类型的干旱极限下，生态系统降水利用效率（RUE, ANPP/Rain）趋同（Huxman, 2004）。

由于降水对后续的土壤水分再分配起主导作用，对降水格局研究始终保持着旺盛活力，主要探究大气环流驱动下的降水格局时空变化（Ropelewski & Halpert, 1986; Wilby, 2002），及其在空间上形成的独立区域和类型（Domroes *et al.*, 1998; Munot, 2000; Bartzokas, 2003）。这些研究可以明确区域基本气候特征，为预测降水的变动趋势提供支持。

降水在年内季节分配影响不同功能型植被的生长，主要以 C3 和 C4 植物或者木本与草本的根系分布等差别为依据。冬季降水被认为更可能渗透至土壤深层，而夏季降水可能在入渗前就已经蒸发（Schwinning *et al.*, 2003）。

在年际尺度上植被活动不但对年降水总量变动响应，而且与降水年内频率（frequency）、量级（size）和持续时间（duration）等关系密切，因此研究的热点开始从降水的年内总量或生长季的降水量向降水的频率、量级和持续时间等转移（Fang *et al.*, 2005）。全球陆地降水自 20 世纪以来上升了 2%，并具有明显的区域差异（Bates *et al.*, 2006）。过去 50 年中国年均降水减少，降水日数减少但极端降水事件增加（Zhai *et al.*, 1999）。在中国北方交错带，日降水极端情况增多，到 2000 年为止，降水日数量下降而强度上升，单次持续时间长的降水减少，长

期干旱增多 (Gong *et al.*, 2004)。降水作为概率事件直接影响生态系统, 所以时空变化研究比年、季平均研究更重要, 还要考虑滞后效应 (Weltzin *et al.*, 2003)。这些因素不是单一作用, 而是与前期的土壤含水量、植物功能型和物候等密切相关。在半干旱生态系统下进行的降水控制实验已经表明, 降水的强度和间隔强烈影响水分入渗, 长降水间隔促进水分向土壤下层入渗, 通过稳定的下层供水减小表层波动, 但降水间隔可能对 ANPP 影响不大 (Fay *et al.*, 2008)。

尽管全球范围内干旱和半干旱区植被变化已经有了较为详细的记录 (Archer *et al.*, 2001), 但是在进行降水控制实验时仍存在问题 (Weltzin *et al.*, 2003):

1. 长时期降水和群落变化的观测在干旱区开展较好, 但其相关性结果由于存在与降水共变的干扰因素而不可靠;
2. 短期土壤湿度控制实验很难控制实际降水, 在小块实验地受外因干扰多;
3. 水分-生态模型对根系分布、土壤分层和根区深度的模型化不令人满意;
4. 缺乏对落叶林和针叶疏林的研究。

1.2.2 土壤水分作为森林旱极的驱动因子

土壤湿度是综合了气候、土壤和植被的水分平衡以及水分平衡动态对植被影响的关键变量 (Rodriguez-Iturbe *et al.*, 2001), 比降水更能解释植被生活状况。在干湿交接的过渡地带, 土壤湿度和降水具有耦合性质 (Koster *et al.*, 2004), 并在半干旱地区比降水更好的说明了森林水分利用 (Bonilla *et al.*, 2002)。Joffre (1993) 等对伊比利亚半岛地中海林下草本和开阔草原土壤水分平衡的研究表明, 年降水量不能代表夏季干旱程度, 土壤储水量在林下和草原显著不同, 最大值出现在年降水量最大的林下; Reynolds & Kemp (2000) 用生态系统模型探索了长时间尺度不同功能组群落的蒸发蒸腾状况, 发现土壤蒸发比降水变率小; Paruelo (2000) 等发现在巴塔哥尼亚西北部沿降水梯度土壤水分变率比年降水变率小。

植物可利用的水分直接来源于土壤, 不同功能型植物根系分布对土壤水分的利用是植被生理和土壤湿度最紧密的结合点 (Porporato *et al.*, 2001), 植物内部水分胁迫与土壤湿度相关性强 (Branson *et al.*, 1976)。土壤水分状况可用于解释季节性降水对植被的响应。增加的冬季降水有利于增强水分向土壤深层补给, 满足深根系物种的需要 (Bates *et al.*, 2006)。一般认为树木相对于草本在湿度梯度上占据湿润段 (Porporato *et al.*, 2003)。还有研究认为群落对降水格局变动的响应直接来源于土壤水分有效性。因此, 土壤湿度是水分平衡动态的重要反映, 是土壤蒸发和植被蒸腾的基础。在降水季节分配一定的前提下, 土壤湿度受到环境

内蒸发散条件的影响 (Welker *et al.*, 1991)。对世界上三个典型的受水分制约的半干旱区的研究表明, 较高的蒸散率导致土壤湿度迅速下降, 浅根系植物需要很高的水分利用效率来利用短暂的土壤水分。

在林草动态方面针对土壤水分的垂直分配和水平动态以及与植被的关系提出过多种假说, 包括广为人知的两层根系分层模型 (Two-Layer Model), 该模型提出土壤水分的垂直分层减小了木本和草本间的竞争。针对该模型的验证有支持 (e.g., Knoop and Walker, 1985; Sala *et al.*, 1989; Fargione & Tilman, 2005) 也有怀疑 (Franco & Nobel, 1990; Le Roux, 1995)。Schwinning & Ehleringer (2001) 用不同生活型植被对模型检验发现植物在不同的生长阶段会同时利用两个层位的水分, 哪一层更重要取决于生活型本身和每一层性水分的时效性。树木初期根系也在浅层, 有主根, 在没有养分限制的条件下达达到下层后, 叶面积迅速增大以阴蔽下层植被, 减弱对水分和养分的竞争, 树木下层根系吸水后会导致表层根富水, 可以蒸发到干燥的表层从而促进浅根系植被吸水 (Kimmins, 2005)。最近有人综合以往的植被-土壤-水分模型提出以水分功能划分土壤水分为上层生长水分库和下层维持水分库 (Ryel *et al.*, 2008), 但不具有普适性, 也缺乏验证。一些植被动态模型中的土壤或根系分层仍缺乏理论依据, 根系生物量不能代表根系的生理作用, 没有区分吸收养分的细根和起固定作用的粗根。

近年来使用的稳定同位素示踪法可以更细致的揭示植被生长时的水分来源。由于不同来源的水分同位素组成各异, 而植物根系在吸收水分时并不存在特定偏好, 所以该方法可以追踪水分的季节来源。Weltzin & McPerson (1997) 在北美温带稀树草原提出不同龄级的乔木和草本植物利用不同层位的土壤水分; 沿着美国夏季季风降水梯度, 犹他松 (*Pinus edulis*) 和犹他桧柏 (*Juniperus osteosperma*) 使用较大比例的季风降水而栎林 (*Quercus gambelii*) 即使在夏季充沛降水时也只用深层土壤水; 在蒙古东北部地区, 在水分供应充足的条件下, 兴安落叶松 (*Larix gmelinii*) 主要利用浅层土壤水; 而在水分短缺时, 可利用深层土壤水 (Li *et al.*, 2007); 在毛乌素沙地, 本地种沙地柏 (*Sabina vulgaris*) 和引进种旱柳 (*Salix matsudana*) 使用较深的土壤水分和地下水, 而沙地油蒿 (*Artemisia ordosica*) 只使用浅层土壤水。

1.2.3 非生长季降水作为森林旱极的驱动因子

对植被生长的研究往往集中于生长季植被动态和影响因子, 忽略了非生长季环境因子的复杂性和与来年植物生长的关系 (Nemoto *et al.*, 2006)。季节性积雪是广大温带地区的特色, 特别是在东亚季风区, 冬季降水以降雪的形式降落, 与

典型的高温多雨的夏季气候截然不同。

季节性土壤冻结是温带季风地区的常见现象，在温带落叶阔叶林分布区，降雪对土壤冻结以至来年解冻后的土壤水分具有一定的影响。由于冻结深度与积雪深度反向变化，所以缺乏积雪或者积雪积累迟缓，就会带来更深更久的土壤冻结（Stadler *et al.*, 1996; Shanley & Chalmers, 1999）。冻结层强烈影响融雪下渗量和时间，因此冻结深度和持续时间会影响冬季和早春土壤水分的运移。冻结改变土壤水力特征，限制冬季寒冷时水分入渗，在融化过程后增加土壤孔隙度，创造更多大孔隙和土壤干裂（Nakayama & Watanabe, 2004）。冻结也改变融雪时的水流动态和养分循环（Rascher *et al.* 1987; Williams & Melack, 1991; Stottlemyer & Toczydlowski 1996; Brooks *et al.* 1999）。对全球变暖的模拟中包括由冬季温度下降引起降雪量减小，导致土壤温度低，冻结深，开春土壤湿度比全年其他时候小，下渗量与对照组下渗量比值也下降（Hardy *et al.*, 2001）。

植被结构和地形影响近地面风场，影响降雪沉积导致冬季降水再分配，带来空间上积雪分布的差异性并影响融水传输。在温带森林内，积雪量不仅影响冬季土壤温度和季节性冻结状况，而且影响来年温度回升时土壤水分的蒸发和下渗（Mellander *et al.*, 2004）。较深的积雪通过减少雪和土壤间的温度梯度减轻过冬的土壤干燥（Pomeroy & Brun, 2001），积雪（>1m）还可以帮助从底层未冻结土壤层向上传导热使表层冻结层回暖（Yukiyoshi *et al.*, 2008）。落叶阔叶林林地积雪春季融化后，融水几乎全部渗入枯枝落叶层，温带落叶阔叶林中发育良好的森林几乎利用了全部收入的降雪。积雪融化时间如果持续很长，有利于保持土壤水分交换延续到夏季。不过尽管积雪融水补充了土壤水分，但是延续到夏季的雪盖似乎并未影响森林生长（Marks *et al.*, 2005），移走积雪后的土壤在春季时土壤湿度比正常土壤低，但是到夏季这种区别就消失了（Hardy *et al.*, 2001）。

积雪也是地表能量平衡的主要影响因子。积雪影响反照度引起的能量变化在来年积雪消融时明显。在积雪消融前后，净辐射和感热通量迅速上升（Nemoto *et al.*, 2006）。已有证据表明，以冬季增温为标志的气候变暖加剧了春季干旱（袁婧薇和倪健, 2007），土壤冻结深度和冻结持续时间也由于气候变暖而改变（e.g., Cutforth *et al.*, 2004; Fraunfeld *et al.*, 2004; Hirota *et al.*, 2006），并且影响到生物地球化学过程（Mitchell *et al.*, 1996; Brooks *et al.*, 1998; Groffman *et al.*, 1999）。森林林冠层通过减小湍流输送减少融雪所需能量，增加长波辐射，减小短波辐射，所以雪盖在林下存在更久，减轻了生长季的潜在蒸散需求（Marks *et al.*, 2005）。

1.2.4 水分以外的因素作为森林旱极的驱动因子

积温作为重要的物候指标反映了温度对植被初始生长的作用。Piao 等人 (2006) 对中国北方植被物候对气候变化的响应时发现, 生长季前两个月 (3 月和 4 月) 的累积温度显著地影响森林生长。但用积温来预测植物的分布是不准确的, 它忽视了温周期的复杂性、植物成熟时的温度变化、不同植物种之间以及不同生态型之间的差异以及高温期间日照长度的变化 (Kimmins, 2005)。Zhang (2004) 的研究认为在北美和欧亚中高纬度地区, 森林主导湿润生态系统, 它对纬度和温度的依赖性强于相对干旱的灌丛和草原。模型模拟表明地中海气候区夏季温度升高带来干旱, 影响森林生长 (Battles *et al.*, 2008)。除了影响植被初始生长时间和速率, 温度也会通过影响光合作用速率而影响生物量积累, 同时也会引起蒸腾速率的变化。如果水分供给充足, 温度升高时植被有能力适应上升的蒸腾速率。由于森林植被往往会经历比草原更高的蒸腾速率变化, 许多地区, 降水的区域性升高可能并不能满足林冠的蒸腾需求 (Kirschbaum, 2000), 因此温度对于森林生长的促进或限制作用必须结合降水的变动情况。不过, 也有研究表明 CO_2 浓度升高对温度升高引起的干旱具有一定的缓冲作用, 如在北美东南的温带森林, 树木在升高的 CO_2 环境中会降低蒸散, 减轻干旱的影响。但是如果土壤水势减小到 -0.5MPa , 这种作用就不明显了, 表明了水分限制仍然存在 (Warren *et al.*, 2007)。

森林干旱极限地区温度主要通过影响土壤水分平衡起作用, 也是降水再分配的影响因子之一。

此外, 微域条件对土壤水分有着至关重要的作用。地形强烈影响森林分布, 是山地丘陵植被空间分异的主要自然约束因子, 通过海拔、坡度和坡向对决定植被生境的其他要素分异 (土壤、小气候、水文) 产生影响 (林超和李昌文, 1985)。海拔主要结合风向和风速影响降水的形成, 坡度和坡向主要对降水进行重分配, 以缓解年际降水量的波动。Dulamsuren (2005) 等在蒙古的研究发现, 肯特山森林草原交错带的各植物生态类群分别占据水分条件不同的坡位和坡向, 草地、灌丛和森林都是斑块状分布; Singh (1998) 等的研究表明半干旱草原植被覆盖度在在土壤湿度最大的坡中最好; Bai (2004) 等在不列颠哥伦比亚森林草原过渡带的研究发现开阔草地出现在南坡, 并有乔木入侵的现象, 但这种现象由于陡坡水分不良而减少; 郁闭森林在北坡出现, 并且开阔林地向郁闭林地的转化多出现在北坡。风速在有些半干旱地区是不可忽略的影响因子。高风速增加了水分亏缺的倾向性, 影响蒸发情况。

在欧洲和北美的一些温带森林生态系统中, 啃食(herbivores)和放牧(grazing)作为生态系统管理手段长期以来用于生产和自然保护。放牧会引起森林土壤的紧实和板结, 通过限制根系发展, 减少水分、养分有效性和土壤通气性而影响幼树的生长和成熟林地的生产力 (Broersma *et al.*, 2000)。在草原地带放牧会引起草原退化, 草本植物盖度减少, 枯落物减少, 使得可燃物减少, 从而导致火的频率和强度减小 (Humphrey & Mehrhoff, 1958a), 促进了幼树生长 (Fisher *et al.*, 1987) 引起森林扩张。人们认为火在温带落叶阔叶林中具有重要作用, 但并不像其他生态系统, 如北美针叶林系统中那样易燃。在北美, 火频率下降导致岩栎 (*Quercus montana*) 密度上升 (Hoss *et al.*, 2008)。对于森林群落演替早期到中期的栎林而言, 高草草原过分频繁的施火或森林过度低频的施火都抑制了栎林的生存, 而低强度的地表火 (surface fire) 是维持栎树更新的必要条件 (Abrams, 1992)。

此外, 土壤条件也是影响森林生长的条件之一。土壤理化条件影响树木根系生长, 通气性差、机械性紧实、化学胶结 (铁或钙磐)、地下水位高、有毒化学物质以及低土壤温度等均可将根系活动限制在浅层表土中 (Kimmins, 2005)。土壤质地影响土壤的持水和供水能力。有机层和矿质土壤层影响着生物地球化学循环对养分的供给。土壤在水分循环和地球化学循环中的重要地位决定了其对森林植被影响的多样性和复杂性。因此, 森林向其他植被的转变可以由土壤性质的变化引起, 同时也影响着土壤条件。

1.2.5 气候干旱的定义及其量化指标

温带森林草原交错带是落叶阔叶林生长的干旱极限, 也是典型的半干旱区。气候干旱是一个地区由固定的因素形成的常年水分短缺情况。由于森林生长极限往往是气候干旱引起的, 但区域降水变化本身并不足以引起土壤水分短缺, 气候干旱化应当是区域降水和温度协同作用的产物, 降水减小与温度升高带来的暖干气候是气候干旱化最明显的趋势, 但是在一些地区, 降水波动远远没有温度变化趋势明显, 因此降水波动不能完全代表气候干旱化, 在研究森林干旱极限生长状况时, 气候干旱化也必须考虑温度因素。

干燥度用来反映气候干燥程度, 也称为干旱指数, 在地理学和生态学研究中长期应用, 并成为全球变化研究中经常涉及到的气候指标之一, 尤其是在气候变化和干旱化、荒漠化等研究中。中外学者自 1900 年以来提出了许多计算干燥度的方法, 简单的以降水 and 气温的比值建立经验公式, 复杂的则通过计算潜在蒸散量与降水的比值反映时空水分的收入和支出。

最直接的干燥度计算是以多年平均降水量 (precipitation, P) 为标准, 不考虑

水分支出,无法说明水分盈亏。根据潜在蒸散的定义(Penman, 1948)计算的潜在蒸散量(PE)与降水量(P)比值即干燥度(K)具有多种不同的计算方法,其中的 Thornthwaite 方法(Thornthwaite, 1948)进一步根据月平均降水量与潜在蒸散的差值进行土壤水分平衡的计算。该方法的湿度气候类型划分比较合理,在气候分区中应用较多,适于逐月的资料;Holdrige 也是一个通过温度来获得可能蒸散量的方法,引入年生物温度进行计算。最简单的气候干燥度计算方法利用温度与降水计算干燥度,即平均降水量和平均温度值;利用积温计算干燥度的方法有两种,一种是以日温度大于或等于 10℃的年积温计算的 Selianinov 干燥度计算方法;另一种是以月平均气温高于 5℃的年积温计算的 Kira 干湿指数;特别是 Kira 的计算方法简便,与植被的对应性好。另外还有辐射计算的 Budyko 干燥度。这 5 类计算方法主要还是应用于大尺度的植被区划和气候区划,其中 Kira 指数考虑了东亚季风气候区,整体而言对我国植被的划分具有较好的指示作用,特别是对东北林区。但是从应用性来看,在具有明显的季节性气候变化的地区,干燥度指标计算的气候年均值无法反映季节间和年际间的气候波动,并且缺乏对季风气候下植被不同物候时期干燥度对植被生长、盖度和生物量影响的探究,特别是特定时间的气候因子对植被生长的关键时期的指示作用。

近年来常用的 Palmer 干旱指数基于月空气温度和降水,并考虑了地面湿度(Dai, 1998)。干旱的形成和发展是土壤水分亏缺缓慢积累的结果,Palmer 干旱指数反映了干旱程度(卫捷等, 2003),是为处理半干旱和干旱气候区的干旱问题设计的,那里的降水是当地唯一或主要水分来源(Doesken, *et al.*, 1991)。不过在目前可获取的数据中该指数空间分辨率较低,在大尺度范围内适用。

1.3 森林旱极的响应特征和动态模拟

1.3.1 植被生长的和生产力的响应

受到各种因素制约的森林生长状况可以由不同来源的替代指标表征。除了实际测定生产力、生物量等方法,叶面积指数(leaf area index)因为与森林生物量、能量循环和森林生产力密切相关经常被作为替代指标(Bolstad *et al.*, 2001),在大尺度经常以遥感影像提取的森林覆盖类型(forest cover type)和叶面积指数用于生态过程模型估计生产力(Franklin, 2001),轮宽显示的径向生长也可以代表当年生长季生物量的增加,并与 NDVI 在半干旱区相互印证(Liang *et al.*, 2005)。

不同的驱动因子会影响森林生长的各个方面,在不同尺度上,森林生长的不

同方面对驱动因子变化进行响应。在个体水平上,控制实验可以考察叶片光合速率、蒸腾速率对空气湿度、土壤湿度等因子的响应;在群落水平上,可以考察森林覆盖、生产力等对降水、气温和土壤水分等的响应;在生物群区水平上,长期动态植被观测和模拟是考察森林动态的重要手段。

植被指数被广泛用于生物群区水平的研究。干旱极限下的森林动态始终是关注的热点。植被生长对水分的响应一方面印证了水分对干旱极限下植被的制约作用,可以作为良好的模型检测。另一方面,可以为寻找干旱极限下其他协同作用因子提供线索。归一化植被指数(Normalized Different Vegetation Index, NDVI)可以综合反应植被分布和生长(Chen *et al.*, 2004),与绿叶密度高度相关,代表了光合能力和生产力状况(Jupp *et al.* 2007),并被认为是地上生物量的代表。NDVI 时间序列在过去 20 年中一直被用来评估植被条件的变化和它们对气候变化的依赖(Tucker *et al.*, 2001; Xiao & Moody, 2004)。

在半干旱区,NDVI 与降水之间具有显著相关关系(Tucker & Sellers, 1986; Reed *et al.*, 1994; Yang *et al.*, 1998; Li *et al.*, 2004; Budde *et al.*, 2004)。Scanlon 等(2005)在非洲南部 Kalahari 样带(IGBP)中树/草交错带发现,在一致的沙土背景下,树木密度高度依赖长期平均湿季降雨。两-三个月前的降水是影响植被生长的主要因素(e.g., Nicholson, 1990; Davenport & Nicholson, 1993; Karabulut, 2003; Nezhlin *et al.*, 2005)。NDVI 对降水的响应在不同生长阶段不同,在生长季中晚期响应最慢,在“湿度敏感期”相关性最强(Lei & Peters, 2004)。但是 NDVI 所反映的植被生长对降水的响应不是无限的,降水和其他影响因素如温度都可能影响这种关系。Nicholson(1990)对东非和萨赫勒地区的研究表明,年降水量在 200-1200mm 的地区降水波动和 NDVI 在季节性和年际时间尺度上很吻合,但是 NDVI 在高降水区不太有代表性。对此作者给出两种解释:当降水量高于阈值时,已不再是植被生长的限制因子和/或 NDVI 不是一个植被生长的良好指示;还有一种可能是当植被密度很高时,NDVI 已经不能充分代表光合作用情况,因而也就丧失了表征生物量的意义。

NDVI 所代表的植被生长在半干旱地区并不单一代表对降水的响应,因为温度变化引起的蒸散发在整个水分平衡中起重要作用。Rikie(2001)在西伯利亚、蒙古和中国进行的研究发现,即使降水量很高,温度超过一定阈值也会限制 NDVI 值,月均温 18℃是一个降水无限制时的温度限制(西伯利亚);7 月降水最大且温度达到 18℃的地方植被可能达到最大 NDVI 值;向北受到温度限制,向南受到降水限制。气候变化干湿冷暖都会对陆地生态系统造成影响,因此在探究森林生长极限的限制因子时必须明确干旱的气候意义,正确地予以表征。

1.3.2 生态系统过程的响应

气候变化对树木种群动态的影响可以是间接的,如影响火和虫灾爆发,也可以是直接的,如树木建群和死亡率。在全球变化的背景下,有必要将传统的局地空间尺度生态学与区域尺度的气候变化联系起来,反映生态系统对大尺度区域气候控制的响应 (Villalba & Veblen, 1998)。

植物生理和生物地球化学方面的研究始于植物生长与资源有效性的数量关系,于上世纪 60 年代在国际生物圈计划 (IBP) 中开展。Walter (1962, 1968) 在《世界植被》中将传统的植物地理原则与新兴的植被生产结合起来,而 Lieth (1975) 通过分析 IBP 数据的统计关系建立了由气候数据计算净初级生产力的著名的 Miami 模型。Schulze (1982) 总结了碳、水和养分对于决定 PFT 分布的限制作用并强调了资源竞争成功与生存限制同等重要。从生物物理和生物化学角度看,气候变化可以引起林冠高度、生物量和叶面积指数以及碳氮在陆地植被中循环的变化。

目前所关注的“Trading Water for Carbon”,强调了植被生长中的积累与消耗,成为成功模拟植被真实生长过程并对水分限制进行评估的关键,在半干旱系统尤为重要。Gerten (2007) 在探讨未来气候变化下植被生态系统的水分限制性时发现土壤湿度不是植被实际水分利用限制的表征,特别是在温度主导或温度和降水协同作用地区。并肯定了 CO_2 对水分利用的益处,指出如果缺乏, L_{TA} (以气孔通导度衡量的水分限制指标) 值将由正转负,表明水分限制出现。模拟表明,在未来水热都增加的情景下,半干旱生态系统会经历更强的干旱,但是没有土壤湿度表征得严重 (如中亚), L_{TA} 在温带地区值中等,冬季高而夏季低。在模拟中强调区域性差异性。Leipprand (2006) 模拟了 CO_2 倍增后全球生态系统水分平衡,分蒸腾、截留蒸腾、土壤蒸发、径流和土壤湿度进行全球和区域分析,发现干旱和湿润地区由于植被生理和结构不同导致不同的水分平衡状况。Gerten (2008) 等人关注 NPP 对降水变化的不同反应。发现响应不仅在地点间有差异,在同一地点一年内也存在差异。NPP 变化的幅度基本上由生态系统水分限制决定,以大气蒸散和土壤水分供给的比率决定,干旱地区或干旱时段这种响应更明显。NPP 对降水倍增、减半和季节变化的响应比年降水量一定时的频率和强度变化更大。

1.3.3 植被分布和种类组成的响应

陆地植被对气候在不同时空尺度上响应。在全球尺度上,气候带来的物种进

化和迁移可能需要上百万年；在区域尺度上，植被在演替、竞争和再生产的变化历经多年甚至几个世纪；在局地尺度上，植物生理过程的变化如呼吸率，在几小时到几个季节间变动。从生物地理角度看，气候变化可以改变陆地植被的分布、结构和组成。

在全球变暖的大背景下，中国增暖的总体趋势是北方大南方小，其中东北西部及内蒙古的东部增温幅度最大，增温率达到 $0.5^{\circ}\text{C}/10\text{a}$ ；从季节分布看，冬季增温最明显。中国降水变化的总趋势为东部减少，西部增加（马柱国和任小波, 2006）。在北方，降水减少的大变率区域对应东亚夏季风的北部边缘，这些地区降水的多少主要决定于夏季降水量的变化。同时，土壤显著干化的地区正好位于中国北方的过渡带区域，即使少量的降水减少也能造成深层土壤的干化（马柱国和符淙斌, 2006）。研究表明，植被对降水增加和温度升高呈正响应。在美国，降水和湿度增加促进了植物生长（Nemani, *et al.*, 2002）。在全球其他大陆都发现的木本入侵在一定程度上源于气候变化，主要表现在降水的年际波动影响的雨季和旱季长度以及降水的季节分配，反映了一种阔叶林不断扩张的趋势。在中国利用表土孢粉重建的生物群区与现代的潜在自然植被有较好的对应性，与现代相比，全新世中期较强的夏季季风下的暖冬、较长的生长季节和更多的降水对应下的森林-灌丛-草原界线和森林-荒漠界线的西推揭示了森林对水分和温度的正响应（陈瑜和倪健, 2008）。对中国植被动态的模拟表明，高纬度升温后，夏季温暖期影响增强，针叶林向北扩张，这与大部分研究结果一致：温度升高对北方森林生物区的影响更大（IPCC 2007a）。

虽然气候变暖在以温度为生长限制的高纬地区的影响明显，但在中纬度地区，特别是那里分布的半干旱地区植被对温度升高的响应由于同时存在水分限制的影响比高纬地区更为复杂。尽管一般认为，在大陆尺度上植被生长和生产力对降水的响应弱于对温度的响应，但这只是因为与地表温度变化相比降水变化甚小（Zhou, 2002），因此，具体到区域尺度或更小尺度的半干旱区（非洲、澳大利亚和南美），植被对降水比对温度响应更为敏感（Myneni *et al.*, 1996）值得重视。也正是基于此，Neilson（1995）提出：干旱区和半干旱区水分平衡的限制决定植被格局对大气变暖的响应。

Yu（2003）对亚洲中部的研究发现，在 1982 到 1990 年间， 50°N 以北的泰加林，包括草甸草原在春季变绿提前，然而在荒漠草原却推后，所以春季增温在干旱和半干旱区会引起水分胁迫。在广大的欧亚温带森林草原交错带，由于气候变暖干化，并未见报道阔叶林向草原推进，反而由于受到土壤水分的限制可能引起森林衰退（decline）。降水限制地区降水减少的同时温度升高会进一步影响植被

响应。对东北亚气候和植被分布的研究中表明,在受到温带季风气候影响的地区,雪被太少很可能引起春季和初夏的区域性干旱,从而限制依赖于降水的物种的分布 (Krestov *et al.*, 2007)。积雪可以在地表积存到深冬,之后在春季干旱时提供土壤水分 (Ellis *et al.*, 2001),内蒙古东南缘落叶阔叶林干旱极限也是东亚季风影响的尾闾区,水分胁迫强,冬季和早春变暖很可能会延迟春季回绿。从地表湿润指数看,该区域在近 50 年来显著地干旱化 (符淙斌和马柱国, 2008),坝上高原 60-90 年代平均增温达 1℃ 以上 (刘芳园等, 2008)。

与植被功能型的分布变化相比,个体物种对气候变化的响应更难以预测,因为群落内每个物种对气候表现出独特的反应并且对气候的不同方面反应程度不同 (Davis, 1981)。所以有必要依据对资源供给波动的不同反应来定义植被功能型组,从而预测环境变化对功能组的影响 (e.g., Chapin *et al.*, 1993)。对美国东南部松林和栎林在干旱胁迫下的生长表明,栎林比松林更为适应干旱从而可能引起气候变化下美国东南森林物种组成的变化 (Klos *et al.*, 2009)。有些物种和植物群落更容易受到全球变暖的影响,第一个就是生物群区交错区的边缘树木种群 (peripheral populations of trees in ecotones) (Krauchi & Xu, 1996)。在各种空间尺度上 (from coarser to finer) 对生活在降雨梯度旱极、阳坡、干旱山脊或浅层土壤上的树木的预测都表明,这些树木更容易死亡。年际生长波动很大的树木以及对气候高度敏感的树木的死亡风险也比较大 (Suarez *et al.*, 2004)。

1.3.4 生态系统格局和过程的动态模拟

模型是科学研究的主要辅助手段,包括概念模型,统计模型和机理模型。概念模型不能做预测,统计模型不可外推,机理模型是当前发展较快的模拟手段。系统学上,模拟的对象应该有可辨识的边界和内部的一致性,边界要达到足以容纳生态过程。在全球生态系统研究中,机理模型具有尺度问题,带来模型通用性和精确性的平衡。机理模型需要大量的参数率定 (calibration) 和检验 (validation)。

生态模型包括种群动态模型 (Population Dynamic Model, PDMs), 演替模型 (Succession Model, SM) 和生态系统模型 (Ecosystem Model, EM)。生态系统模型包括: (1) 陆地表面模型 SVAT (Soil-Vegetation-Atmosphere Transfer Model), 基于彭曼公式、达西定律等,多用于气候研究,模拟土壤-植被-大气系统中能量、水分和动量 (momentum) 平衡; (2) 生物地球化学模型 BGC (Biogeochemistry Models), 以气候、土壤条件、植被类型等为输入变量,碳、水和营养物质循环为输出变量,包括 Biome-BGC, CENTURY 以及 TEM 等,一般以给定的植被类型为基础,不能预测变化,如果对模型进行验证,一般是对一个明显的变量进行

模拟, 再将结果与实际结果比较, 或模型间横向比较; (3) 生物地理模型 BGMs (Biogeography Models), 包括 Biome 系列, 含有水分和温度参数的 Doly (Woodward, 1987), 含有土壤分层和树草间的水分竞争的 MAPSS (Neilson, 1995), 多为静态描述。

在生物物理模型方面, GCM 包括了对控制能量、水汽和动量在大气和地表的交换的因子的模拟, 以此为目的 GCM 也被称陆地表面表面方案 (land surface scheme) 或土壤-植被-大气传输模型 (SVATs)。GCM 需要包括根系深度、土壤孔隙度、地表反照度、地表粗糙度、植被分盖度和地表传导度等植被特征数据, 精确地模拟陆地和自由对流层的通量交换还需要界定明确的行星边界 (planetary boundary layer, PBL)。首个清晰描述植被的 GCM 陆面模型是 SiB (Sellers *et al.*, 1986) 以及 BATS (Dickinson *et al.*, 1993)。之后的模型进一步强调了 CO₂ 与水汽在气孔通导度影响下的交换 (Collatz *et al.*, 1991)。在 GCM 的基础上发展了用于 GCM 耦合的 DGVMs IBIS (Foley *et al.* 1996) 和 TRIFFID (Cox, 2001)。Foley *et al.* (1998) 和 Delire *et al.* (2002) 首先发展了完整耦合到大气 GCM 的 DGVM, Gallimore 和其他人员完成了向海洋-大气 GCM 的完整物理耦合。

最早被广泛应用生物地球化学模型是陆地生态系统模型 (TEM) (Melillo *et al.*, 1993), 用来估算给定生态系统分布基础上的 NPP。其他 TEM 还包括 Century (Parton *et al.*, 1993), BGC (Running & Gower, 1991), BIOME-BGC (Running & Hunt, 1993) CASA (Field *et al.*, 1995), G'DAY (Comins & McMurtrie, 1993), CARAIB (Warnant *et al.*, 1994), DOLY (Woodward *et al.*, 1995) 和 BETHY (Knorr, 2000; Knorr & Heimann, 2001)。近期的生物地球化学模型大都采用 Farquhar 等人 (1980) 建立的光合作用模块。这种模式的核心是光合作用由叶片内部细胞间 CO₂ 分压决定的, 使过程模拟中 CO₂ 的作用得以明确定义。早期全球生物圈模型 (TEM) 仍得到广泛应用。此外, BIOME 的后继版本 (Haxeltine & Prentice, 1996a; b; Kaplan *et al.*, 2003) 结合了平衡态的生物地理模型和生物地球化学模型, 可以通过模拟不同功能型在生存限制内的 NPP, 来预测它们的地理分布, 从而在早期的平衡生物地理模型中加入基于资源竞争导致的独特分布, 并在机理上引入 CO₂ 的作用 (Cowling, 1999; Harrison & Prentice, 2003)。

在植物地理方面, 最早的预测性模型可以追溯到 Köppen (1931) 提出的世界气候分区, 他试图将生物群区的分布与气候的季节性相匹配。之后 Holdridge (1947) 提出了基于年际气候统计的生命地带分类系统, 在此基础上 Emanuel 等人 (1985) 首次制作了气候驱动的全球潜在自然植被图, 并首次实现了以通用环流模型 (GCM) 模拟温室气体情形下的全球气候植被。之后 Whittaker (1975)

及其他人提出气候与生物群区分类系统。尽管 Raunkiaer (1909,1913,1934) 早就提出了植被分布的控制因素理论,但是以上分类系统都没有清楚的立足于该理论。他提出不同类型的植被其分布依赖于在恶劣气候下的生存方式,即我们今天熟知的植物功能型 (plant functional types-PFT)。基于该理论, Box (1981) 首次完成了气候驱动下的全球 PFT 分布的数字模型, Woodward (1987) 首次完成了基于过程的全球生物群区分布模型,模型根据实验数据提出了限制木本植物生存的寒冷耐受性以及基于水分有效性的叶面积指数 (Specht, 1972)。Woodward 的工作继续向前推进得以形成平衡生物地理模型 BIOME (Prentice *et al.* 1992) 和 MAPSS (Neilson *et al.* 1992; Neilsen & Marks, 1994; Neilson, 1995)。

传统的生态学研究 (Sernander, 1936; Watt, 1947; Sprugel, 1976) 为描述植被动态提供了基础。在实践中应用最成功的是“林窗模型”,对个体树木定居、生长和死亡的模拟,最初由 Botkin *et al.* (1972) 在研究美国 Hubbard Brook 森林演替中提出,称为 JABOWA 模型, Shugart (1984) 对其作了改进,提出了 FOREST 林窗动态模型,并对其生态学意义进行了讨论,主要用于阿巴拉契亚山落叶林。后来的学者又发表了一系列林窗模型 (Leemans & Prentice, 1989; Prentice & Leemans, 1990; Pacala *et al.*, 1993; Prentice *et al.*, 1993; Fulton & Prentice, 1997; Bugmann & Cramer, 1998; Smith *et al.* 2001), 并将其推广到了非森林植被动态模拟上,如 Prentice *et al.* (1987)。这些模型借助传统生态学所建立的关系,将个体物种环境因子参数化,通过运算大量个体的随机行为来模拟群落动态。但是随着发展,林窗模型包含的变量越来越多,并且其参数多适用于特定研究区,将其上推到区域尺度甚至全球尺度需要进行相当大的简化。

在传统的生态模型的基础上,动态全球植被模型 (Dynamic Global Vegetation Models, DGVM) 在过去的 10-15 年中得到了长足发展。最初的四个研究大组包括:植物地理,植物生理和生物地球化学,植被动态以及生物物理,关注点主要在于模拟在没有人类干扰的情况下的生物过程和相互作用,之后又将研究点扩展到包括人类干预 (农业、城市化和森林管理) 下的植被过程。目前应用广泛的 DGVM 包括 LPJ, ORCHIDEE 和 SDGVM 等 (eg: Hickler *et al.*, 2009; Piao *et al.*, 2008; Bond *et al.*, 2005)。

Lund-Potsdam-Jena (LPJ) 是一个生物地理与生物地球化学循环耦合的非平衡模型,包括了基于过程的陆地植被动态模拟和陆地-大气碳水循环。详细的 LPJ 介绍在 (Sitch *et al.* 2003) 中。LPJ 明确的考虑了生态系统关键过程,包括植被生长、死亡、碳分配和资源竞争,具有中等复杂性,在全球尺度的研究中被广泛应用。它的特点包括:(1) 基于过程,地表/大气的耦合模式建立在早期平衡态

生物地理学模型 (Haxeltine *et al.*, 1996; Haxeltine & Prentice, 1996a) 的基础上。

(2) 明确引入植被动态的主要过程, 包括天然火的影响, 生长和竞争, 在林窗模型中广泛使用的统计学过程, 也被调整以适用大尺度模拟。其景观尺度的模型版本 (GUESS) 使用相同的地表/大气耦合模式, 但区域和全球尺度的模型进行了相应调整 (Smith *et al.*, 2001)。(3) 运用现有的气候数据和生态研究数据对模型进行了全面深入的评估。

交错带独特的性质使得对其进行生态学研究意义重大: 它是植物物种对环境梯度响应的指示剂; 是物种多样性的汇; 是气候变化的指示剂; 是物种、物质和能量空间通量的调节剂 (Malanson, 1997)。因此, 使用合适的植被动态模型全面模拟生态系统在不同气候条件下的可能变化对于预测未来意义重大。

1.4 中国林草过渡带研究进展

国内的研究工作主要集中在森林草原交错带的植被格局方面, 早期的研究工作确定了森林草原交错带的植被性质 (侯学煜和马溶之, 1956; 钱崇澍, 1957; 中国科学院自然区划工作委员会, 1959; 刘慎谔等, 1959; 侯学煜, 1960, 1964; 中国科学院内蒙古宁夏综合考察队, 1985), 对森林草原交错带的范围也进行了确定, 尤其对河北坝上高原 (刘濂, 1965, 1981)、内蒙古呼伦贝尔草原 (李博等, 1980)、松辽平原 (李博等, 1980)、内蒙古锡林郭勒河流域 (李博等, 1988)、黄土高原 (朱士诚, 1983; 邹厚远等, 1980, 1994) 的森林草原交错带的范围进行了比较准确的确定。崔海亭和雍世鹏 (1986) 将大兴安岭南段中、低山和赤峰市西南部山地划为山地森林草原区。侯学煜 (1988) 明确指出森林草原不是一条“接触线”, 而是一个植被带, 并在温带草原区和暖温带草原区中划分森林草原带。近年来, 一些研究工作探讨了森林草原交错带内部的植被格局, 如郭庆华等 (1999) 利用 NOAA AVHRR 影像得出的 NDVI 数据, 对内蒙古高原东南缘及其以西地区森林、森林草原、草原等的分布进行了划分, 发现了它们具有较好的空间分异。黄永梅等 (2001) 利用群落特征和遥感资料划分森林草原过渡带与森林带以及草原带的界线, 并对过渡带内部的景观异质性及其形成机制做了进一步的研究。王庆锁 (2004) 对森林草原交错带的植被类型、分布规律、第一性生产力、环境条件、人为影响进行了系统总结, 对交错带云杉林群落特征也进行了比较全面的研究。

在森林草原交错带环境条件对植被的影响方面有不少工作。张军涛 (2001)、李栋梁 (2002)、赵哈林 (2003) 对农牧交错带植被动态与环境变化的研究证实

水分条件是决定植被空间分布格局的主导因素。影响我国森林草原交错带土壤水分的环境因子非常复杂,土壤质地是重要因子。张信宝等(1998)分析了半干旱区不同岩土组成的坡地土壤水分特征及对植被类型的影响,表明岩土组成是影响半干旱区植被类型的关键环境因子,质地细的土壤降水入渗浅,地面蒸发耗水分多,土壤水分环境较差,适合草本植物生长,反之,质地粗的土壤条件适合木本植物生长。甘超华等(2005)对河北坝上地区的降水时空分布和对土壤水分状况的影响的分析得到土壤水分多年亏缺而丰年可补充的地方为森林草原过渡带,土壤水分经常亏缺且降水难以补充的地方为草原带。赵文智(1996)在河北坝上分析了过渡带阴坡华北落叶松林地、沙地华北落叶松人工林地、沙地沙棘林地、沙地草场、平滩草地的土壤水分物理参数、机械组成和土壤水分状况,表明田间持水量、毛管持水量、最大持水量与土壤 0.05mm-0.01mm、0.01mm-0.001mm 两个粒级颗粒含量显著正相关,与 0.50mm-0.25mm 粒级呈负相关。

在自然植被为森林草原交错分布的黄土高原地区,目前已经开展了一系列土壤水分格局和植被格局关系的测定,一些研究工作中发现人工植被下土壤中出现干层(李裕元, 2001; 王力, 2005)。陈洪松(2005)等指出,黄土高原地区深层土壤干燥化(土壤干层)是人工林草植被过度耗水导致土壤水分负平衡的结果。胡良军(2004)对黄土高原天然草地土壤的分析表明土壤水分在垂直方向上存在速变层和积累层,前者受水热条件变化的影响强烈,其土壤水分含量随降水的有无而具有较大的波动性,后者则主要由上层补充,变化缓慢;在水平方向上受到坡位、坡度和坡向的影响。

近年来,利用树轮重建气候并分析在干旱胁迫下树木径向生长状况得到了一些结果。Liang(2008)等发现旱极油松的生长受到当年和前一年生长季月降水和空气相对湿度的限制。极端气候干旱会对自然植被造成明显影响(Liang *et al.*, 2006)。树轮研究所采用的气候敏感性分析可以深入到每个月的气象条件考察树木径向生长的响应,但是往往缺乏超越相关分析的机理性研究,并且在阔叶树样品的采集上有局限性。

目前,大部分植被动态模拟是在全国尺度上进行的。赵茂盛(2002)用改进的 MAPASS 模型应用大气环流模式 HadCM2 对未来气候变化的预测模拟了我国未来潜在植被的可能变化,在考虑了东亚季风气候的前提下,模拟结果表明温带落叶阔叶林带由于对水分利用效率敏感,但仍然有扩大面积的趋势。模拟降水和温度都上升的中国植被变化可以看到温带落叶阔叶林北部向草原转化(Weng & Zhou, 2006)。梁妙玲(2006)应用 LPJ 模型对全国植被分布的气候影响的模拟表明,从 1961 年 2000 年 20 年间隔图上看,青藏高原西北、内蒙古、东北、华

北森林区域减小, 草原面积增加, 呈向东南方向扩张的趋势, 90 年代以来尤其明显。从气候对 NPP 的影响看, 降水在干旱半干旱区和湿润区影响都很显著, 但温度仅在干旱半干旱区影响显著。

迄今为止, 对森林草原交错带植被格局的机理研究仍然没有系统地开展, 不能从环境条件格局对植被空间格局进行合理的解释, 对整个森林生长状况缺乏必要的监测和预测。作为温带落叶阔叶林生长干旱极限的内蒙古森林草原交错带, 抛开地形带来的水分分配差异, 森林生长的限制仍然应当表现为不同水热结合下树木对水分的利用能力。树木对气候季节性和年际波动的敏感性是决定树木生长、覆盖度变化乃至森林推进或退后等动态的关键所在。干旱极限的森林需要放在整个森林和草原分布区域内方能显示出在气候变化条件下植被敏感性的高低。

因此, 在进行森林草原交错带研究时要关注群落水平上典型的地形分异导致的同样降水条件下林草水分利用分异, 因为土壤水分含量高或低并不表明潜在水分条件好, 而是作为水分平衡动态的一环表明在持续的蒸散发过程中, 土壤水分能够维持森林生长; 同时更应当关注森林干旱极限在整个森林区域和草原区域内处于怎样的敏感地位, 在不同的水热条件下其动态会发生怎样的改变, 从而在消除局地条件影响的情况下理清干旱极限森林对气候变化响应的机理。

1.5 研究内容和技术路线

1.5.1 研究内容

森林与草原分布格局的本质是气候因素差异, 特别是降水量。探讨森林生长对气候变化的响应敏感性并预测其可能的动态, 是在生物群区尺度上淡化土壤、地形等影响群落分布的局地因子的作用, 从植被分布格局的水热组合本质出发, 考虑温带落叶阔叶林和温带草原分布的气候背景, 由此探究干旱林线的动态。这种尺度的跨越需要在探究干旱极限下树木个体的生长特性, 交错带森林群落水分利用情况的基础上进行。因此, 本文拟在已有工作的基础上, 运用野外观测描述、文献整理、取样分析、气象数据和遥感数据集成以及选择具有生态系统环境指示效应的指标, 在个体生长、群落分布和水分关系的基础上, 运用动态全球植被模型 (DGVM) 对落叶阔叶林和草原两个生物群区进行模型模拟, 探究森林干旱极限植被的敏感性, 并回答以下科学问题:

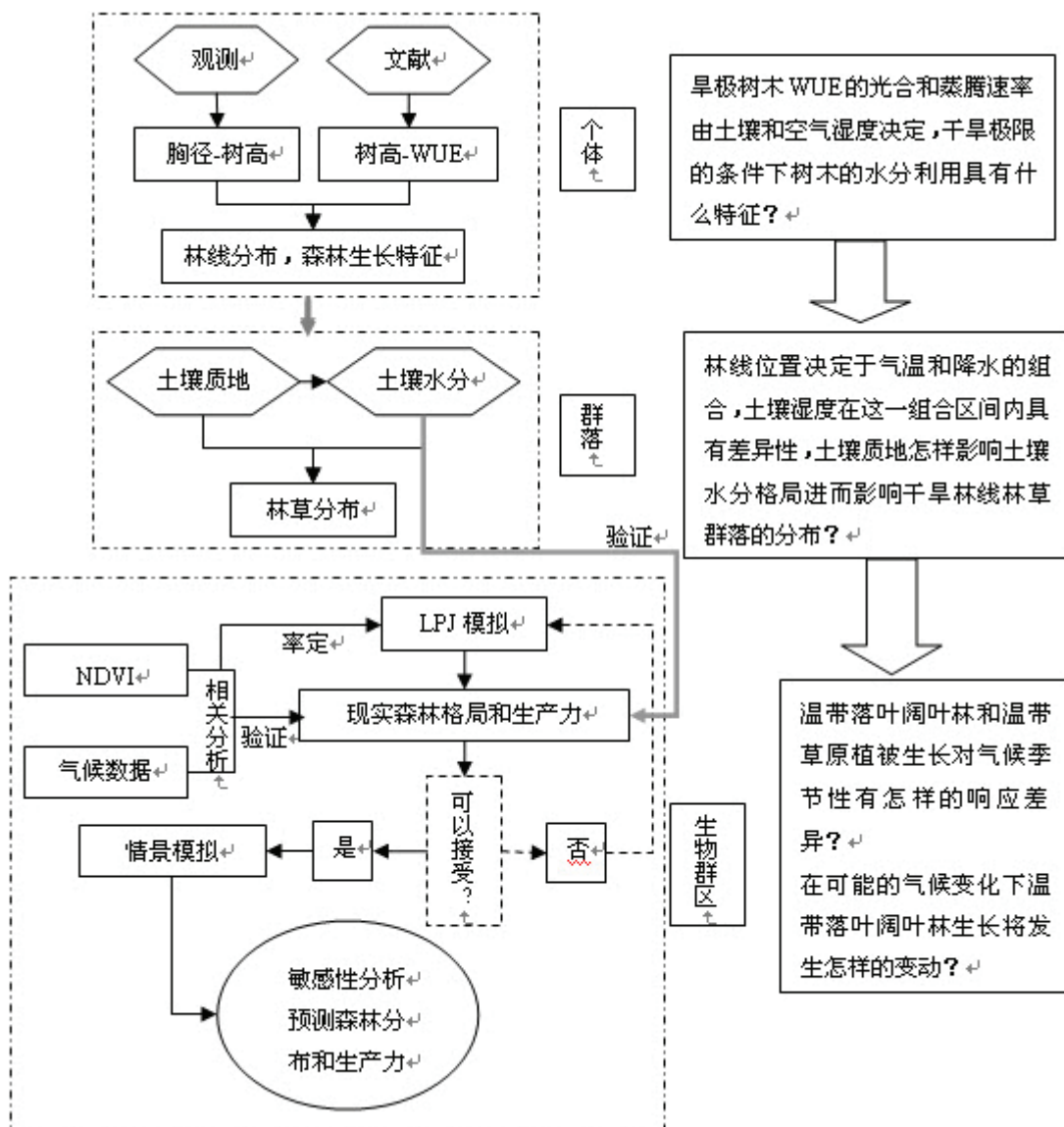
1. 干旱极限的条件下树木的水分利用具有什么特征?
2. 土壤质地怎样影响土壤水分格局进而影响干旱林线林草群落的分布?

3. 温带落叶阔叶林和温带草原植被生长对气候的季节变化和年际波动格局有怎样的响应差异？
4. 在可能的气候变化情景下温带落叶阔叶林的生长和分布将发生怎样的变动？

相应的研究内容包括以下几个方面：

1. 干旱极限树木生长特征和可能的影响因素；
2. 土壤水分剖面特征和季节变化对森林群落类型和分布的影响；
3. 落叶阔叶林生产力和分布对气候季节变化和年际波动的敏感性；
4. 未来气候变化情景下森林旱极林草植被的命运。

1.5.2 技术路线



第二章 研究区和研究方法

2.1 研究区概况及选择依据

2.1.1 研究区自然概况

植被对气候变化响应的生物群区为根据中国 1:400 万植被类型图的温带落叶阔叶林和温带草原区（图 2.1），去除农业植被。

本文还选择内蒙古高原东南缘森林草原交错带作为群落水平的研究区，经纬度范围为 116°20′-117°50′E，41°55′-42°35′N，是内蒙古高原、大兴安岭山地南延部分以及冀北山地交界处（图 2.2）。研究区自然地理背景具有明显的过渡性。气候属于温带半湿润季风气候与半干旱大陆性气候的过渡带（表 2.1）。总体上说坝下温度偏高，坝缘山地和大兴安岭南段山地温度偏低，内蒙古高原内部温度差异较小。年降水量 350-450mm，具有明显的 SE-NW 向梯度（图 2.2）。夏季 6-8 月的降水量占全年降水量的 60%-70%。

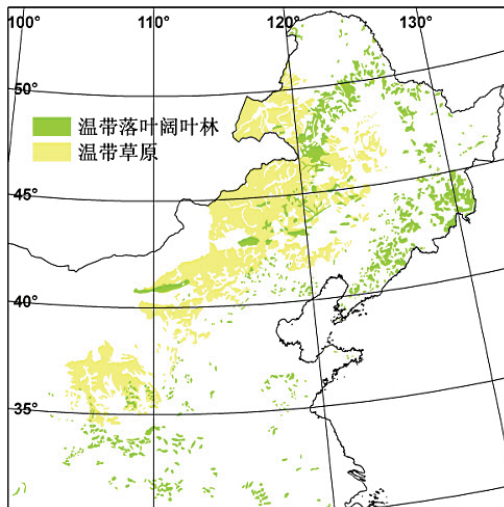


图 2.1 植被分布图

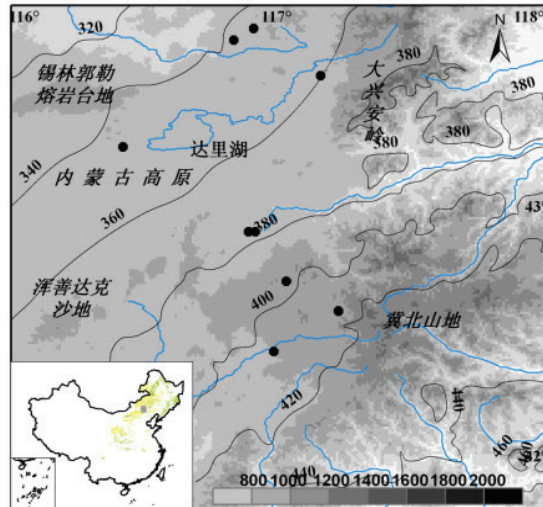


图 2.2 森林草原交错带研究区（示采样点）

表 2.1 森林草原交错带及其周围气候指标（据王庆锁，2004）

地点	围场	多伦	塞罕坝	锡林浩特
北纬	41°56′	42°11′	42°24′	43°57′
东经	117°45′	116°28′	117°15′	116°04′
海拔(m)	842.3	1244.4	1504.0	989.5
植被区域	森林带	森林草原交错带	森林草原交错带	草原带
1 月均温(℃)	-12.2	-18.1	-21.2	-19.8
7 月均温(℃)	20.8	18.7	17.3	20.8
年降水量(mm)	454.7	384.2	437.8	294.9

研究区处于暖温带落叶阔叶林向温带草原过渡的地带,植物区系组成呈明显的过渡性。从冀北山地向内蒙古高原过渡,东亚成分逐渐减少而达乌里-蒙古成分增多(中国科学院内蒙古宁夏综合考察队,1985)。阔叶林主要分布在海拔1300-1800m之间,坝缘山地和大兴安岭南缘最多,64%在阴坡和半阴坡(何思源等,2008)。过渡带内以白桦(*Betula platyphylla*)林和山杨(*Populus davidiana*)林为主,多分布在低山和高大丘陵的陡阴坡,白桦林主要在海拔1100-1750m分布,山杨林主要在1450m以下分布。蒙古栎(*Quercus mongolica*)林和棘皮桦(*Betula davurica*)林呈零星分布,蒙古栎林在海拔1400m以下的阴坡和阳坡均可出现,在阳坡出现草原化,在阴坡、半阴坡与白桦、山杨共生(黄永梅,2001)。天然针叶林主要是油松(*Pinus tabulaeformis*)、白扦(*Picea meyeri*)和华北落叶松(*Larix principis-rupprechtii*)。油松主要分布在海拔1400-1700m的阳坡或半阳坡,白扦林主要分布在沙地以及海拔1700-1800m的阴坡或半阴坡,落叶松分布在海拔1500-1900m的地段,为地带性森林。

2.1.2 研究区选择依据

本文选择植物个体,群落和生物群区三个水平进行研究,是因为温带落叶阔叶林分布的干旱极限在区域尺度上表现为温带落叶阔叶林和温带草原的交错带,在局地尺度上则表现为地形影响下的森林和草原斑块交错分布。

森林草原交错带的森林区域作为温带落叶阔叶林带的一部分,其生长必然受到制约整个森林植被带分布和生长的水热条件限制,与草原具有不同的功能类型组成,对季节性气候变化产生与草原不完全相同的响应,表现出从生理机制到生态系统的差异性反馈。在区域尺度上研究森林和草原,有助于宏观把握这两种生态系统对季节性气候变化的反馈差异,具体分析水热条件对于植被生长的作用,区分两者相同和不同的影响因子,把握森林生长的气候驱动因子。

从交错带本身来看,作为森林生长的干旱极限及东亚季风的尾闾区,气候波动和相应的植被反馈比植被核心区更为复杂,一方面植被动态具有鲜明的季节特征,另一方面森林生长受到干旱制约。清晰的植被格局有利于对比林草生长状况,存在值得探究的植被-土壤水分反馈的局地现象,但是缺乏系统的土壤水分资料和土壤质地分析。

因此,将区域尺度林草气候驱动因子对比和交错带植被生长的水分反馈结合,可以避免由于地形分异引起的交错带林草分异过于局地化的表现而掩盖树木生存和生长的气候驱动因子,有助于了解森林在干旱极限下的生存机理和在气候变化下的森林动态。

2.2 研究方法

研究数据包括植物个体，群落和生物群区三方面的基础数据：

个体：样方调查的乔木层冠幅、高度和胸径，植被水分利用效率数据；

群落：土壤剖面调查资料，实验室分析的土壤水分、田间持水量和粒度数据。冬季雪被厚度，土壤冻结深度和枯落物厚度；

生物群区：数字化 1:400 万中国植被图，全国气象台站气温和降水量月值资料，1982-2003 年全球 NDVI 月值资料。

2.2.1 树木生长和生理数据分析

利用 1995、1996 年野外植被样方调查数据，提取油松林、山杨林、白桦林和蒙古栎林样地树木胸径和树高记录建立树高和胸径的相关生长关系，并根据采样点经纬度提取该点多年平均降水量作为参考指标。

统计对植物生长季日平均水分利用效率（Water Use Efficiency, WUE）的测定记录，建立乔木高度、灌木高度与 WUE 的关系，经筛选后得到乔木数据 40 个，灌木数据 39 个，种名见表 2.2，可能出现同一地点多个树种或同一树种不同高度的测定。文献中有明确地理坐标的如图 2.3。利用 Excel 2003 进行相关分析。

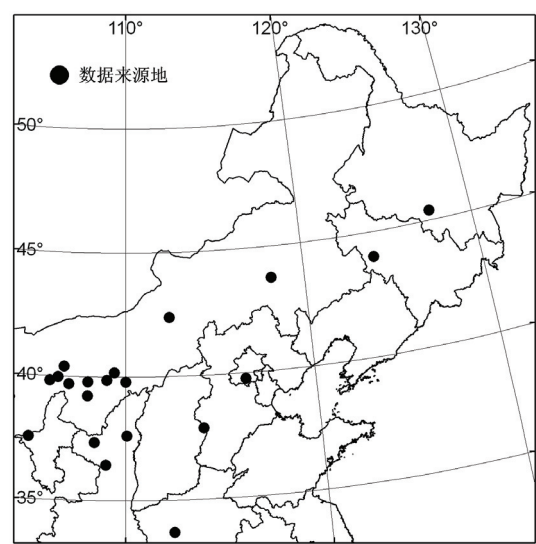


图 2.3 WUE 数据点分布图

表 2.2 测定树种和数据来源

物种		来源
栾树	<i>Rekoelreuteria paniculata</i>	吕爱霞等, 2005
刺楸	<i>Kalopanax septemlobus</i>	
黄连木	<i>Pistacia chinensis</i>	
玉兰	<i>Magnolia denudate</i>	王颖等, 2006
紫叶李	<i>Prunus cerasifera</i>	谭瑶等, 2007
悬铃木	<i>Platanus hispanica</i>	何春霞等, 2008
刺槐	<i>Robinia pseudoacacia</i>	
白蜡	<i>Fraxinus chinensis</i>	
银杏	<i>Ginkgo biloba</i>	
红松	<i>Pinus koraiensis</i>	霍宏和王传宽, 2007
胡杨	<i>Populus euphratica</i>	刘建平, 2004
灰叶胡杨	<i>P.pruinosa</i>	
辽东栎	<i>Quercus liaotungensis</i>	严昌荣等, 2001
核桃楸	<i>Juglans mandshurica</i>	周海光和土小宁, 2008
大叶白蜡	<i>F. rhynchophylla</i>	
小叶杨	<i>P. simonii</i>	
旱柳	<i>Salix matsudana</i>	牛书丽等, 2003
臭椿	<i>Alianthus altissima</i>	梁月等, 2008
侧柏	<i>Platyciadus orientalis</i>	田晶会等, 2005
红栎	<i>Quercus rubra</i>	Gazal & Kubiske, 2003
樱桃皮栎	<i>Q. pagoda</i>	
柠条	<i>Caragana korshinskii</i>	苏培玺等, 2005
霸王	<i>Zygophyllum xanthoxylum</i>	周海光和土小宁, 2008
白刺	<i>Nitraria tangutorum</i>	李清河等, 2006; 2008
北京丁香	<i>Syringa pekinensis</i>	严昌荣等, 2001
山杏	<i>P. armniaca</i>	周海光和土小宁, 2008
荆条	<i>Vitex negundo</i>	
北沙柳	<i>S. psammophila</i>	牛书丽等, 2003;
黄柳	<i>S. gordejvii</i>	蒋高明和何维明, 1999
小叶锦鸡儿	<i>Caragana microphylla</i>	
枸杞	<i>Lycium chinense</i>	
金花忍冬	<i>Lonicera chrysantha</i>	
紫穗槐	<i>Amorpha fruticosa</i>	
兴安胡枝子	<i>Lespedeza davurica</i>	蒋高明和何维明, 1999
油蒿	<i>Artemisia ordosica</i>	李清河等, 2006; 2008
蒙古岩黄耆	<i>Hedysarum fruticosum</i> var.	张翠霞等, 2007
花棒	<i>H.scoparium</i>	
牛心朴子	<i>Cynanchum komarovii</i>	
节节草	<i>Equisetum ramosissimum</i>	
乌柳	<i>S. cheilophila</i>	
小穗柳	<i>S. microstachya</i>	
甘草	<i>Glycyrrhiza uralensis</i>	
小花溲疏	<i>Deutzia parviflora</i>	周海光和土小宁, 2008
山桃	<i>Prunus davidiana</i>	
欧洲丁香	<i>Syringa vulgaris</i>	
连翘	<i>Forsythia suspense</i>	
楝棠	<i>Kerria japonica</i>	王颖等, 2006
甘蒙怪柳	<i>Tamarix austromongolica</i>	李清河等, 2006; 2008
沙冬青	<i>Ammopiptanthus mongolicus</i>	苏培玺等, 2005
梭梭	<i>Haloxylon ammodendron</i>	

2.2.2 森林草原交错带土壤采样设计和处理

2.2.2.1 生长季不同树种下土壤样品采集

交错带内白桦林和山杨林为广泛分布的落叶阔叶林，油松林处于分布北界，白扦是孑遗种，生活在沙地上。对以上 4 个树种按年降水量梯度（1961-1990 均值）从相对湿润到相对干旱（表 2.3，图 2.2）各选 3 个地点（有重叠）：白桦林、山杨林和白扦林采样点森林均分布在阴坡，阳坡为草原，油松林在三道河口分布在阳坡，阴坡为密灌。采样时间为 2006 年 7、8、9 月，2007 年 5、7 月，2008 年 7 月。每个采样点阴坡和阳坡各三个土壤剖面（2006 年两个），以 20 厘米为间隔，自下而上用环刀取 70、50、30、10 厘米层位（2008 年 7 月样品以 10 厘米为间隔）土壤样品一环刀，立即装入塑封袋，当天称量新鲜土重。

表 2.3 生长季分树种采样信息

森林	地点	经度	纬度	降水(mm)	森林	地点	经度	纬度	降水(mm)
白桦	白扦坑对面	117.25	42.58	410.9	油松	三道河口	114.99	42.42	404.5
	源水头	114.89	42.90	374.1		源水头	114.89	42.90	374.1
	干其纳尔斯	114.39	42.24	344.4		干其纳尔斯	114.39	42.24	344.4
山杨	松树井子	117.04	42.70	398.8	白扦	白扦坑	117.25	42.58	410.9
	好鲁库	114.92	42.90	377.4		白音敖包	117.18	42.52	360.1
	草原站	114.83	42.66	344.1		草原站	114.91	42.71	344.7

源水头：阴坡油松和白桦交错分布；

2.2.2.2 白桦林下土壤样品采集

白桦林作为次生天然林代表，在研究区乃至整个交错带内广泛分布，按照年降水量梯度（表 2.4）在 2008 年 7 月采样，每个采样点阴坡和阳坡各三个剖面，以 10 厘米为间隔自下而上取得 70、60、50、40、30、20、10 厘米层位土壤样品。

表 2.4 白桦林土壤取样信息

地点	经度	纬度	降水量(mm)	地点	经度	纬度	降水量(mm)
大唤起*	117.42	42.15	429.1	宝日格斯台	118.92	44.99	370.2
尚海林*	117.31	42.40	423.6	阿尔昆	119.82	45.32	390.5
白扦坑对面	117.25	42.57	411.3	阿尔山	119.98	47.16	393.1
将军泡子*	117.04	42.58	402.6	杜拉尔	119.69	47.34	373.5
巴林右旗荣升	118.25	44.36	366.0	罕达盖	119.47	47.45	362.3
罕山保护区	118.74	44.19	398.2	姑子庙	120.69	50.40	367.4
高力罕	118.35	44.85	355.2	小乌尔根	120.48	50.38	358.8
太本	118.64	44.57	372.6	额尔古纳	120.23	50.35	351.1

*2008 年 10 月后采样

2.2.2.3 非生长季土壤样品采集

采样主要考虑森林代表性和树种一致性，选择油松（三道河口）、山杨（松树井子）和白桦（白扞坑对面）保证森林代表性，大唤起、尚海林和将军泡子保证白桦林树种一致性。采样时间为 2008 年 10 月、11 月以及 2009 年 1 月。

2.2.2.4 土壤样品处理

用烘干法测定土壤水分含量，在百分之一精度天平上称量新鲜土壤重量（ m_1 ），将土壤风干后放入铝盒内，在 $105^{\circ}\text{C}\pm 2^{\circ}\text{C}$ 的恒温干燥箱内烘至恒重，在百分之一精度天平上称量烘干土壤重量（ m_2 ），测定土壤质量水分含量（ W_m ）。

$$W_m = \frac{m_1 - m_2}{m_2} \times 100\%$$

使用英国出产的 Mastersizer2000 激光粒度仪测定 2007 年 7 月土壤样品的粒度。首先进行试样，将土壤内残留根系和大于 2mm 的非土壤机械组成成分剔除。根据测量时遮光度在 10-20%的要求称量合适的样品量，使用对角线称量法使样品均匀混合。一般来说粒径越大所需样品量越大，研究区内样品砂质含量较大，样品量在 1.0-5.0g 间。称量后对样品进行前处理使原始样品分散成单颗粒。分别加入浓度 10%的双氧水（ H_2O_2 ）和浓度 10%的盐酸（ HCl ）除去有机质和钙质，调节溶液 pH 值为 6-7，加入 0.05mol/L 的六偏磷酸钠（ $(\text{NaPO}_3)_6$ ）分散剂，在 6 小时内测样，测样时使用超声波器对样品进行轰击，击碎胶结的微小颗粒。

2.2.2.5 土壤水分特征曲线拟合

使用 Rawls（1982）的经验公式对-1500~-10kPa 之间的土壤水势与体积含水量进行拟合，大于-10kPa 的土壤一般为饱和土壤，在研究区内几乎不存在。

表 2.5 水分特征曲线拟合参数

土壤吸水压力(KPa)	等式
> 1500 to 10	$\Psi = A \Theta^B$ $A = \exp[a + b(\%C) + c(\%S)^2 + d(\%S)^2(\%C)] 100.0$ $B = e + f(\%C)^2 + g(\%S)^2(\%C)$
系数	
$a = -4.396$ $b = -0.0715$ $c = -4.880 \times 10^{-4}$ $d = -4.285 \times 10^{-5}$	
$e = -3.140$ $f = -2.22 \times 10^{-3}$ $g = -3.484 \times 10^{-5}$	
定义	
$\Psi =$ 水势, kPa	$(\%S) =$ 沙砾含量 (e.g., 40.0)
$\Theta =$ 体积含水率, m^3/m^3	$(\%C) =$ 黏粒含量 (e.g., 30.0)

2.2.3 气象台站数据

2.2.3.1 交错带气象数据处理

提取代表森林带、森林-草原交错带和草原带气候的围场、多伦和锡林浩特气象台站 1982-2004 年降水和气温月值，全年划分为生长季（5-9 月），非生长季（10-4 月），四季为春（3-5 月），夏（6-8 月），秋（9-11 月），冬（12-2 月）。计算各季节、生长季、非生长季和全年降水和气温时间序列和变异系数（cv）：

$$\text{变异系数 (cv)} = \frac{\text{均值}}{\text{标准差}}$$

2.2.3.2 植被区域气象数据处理

将全国基准气象台站坐标矢量化为点文件，用中国植被图中温带落叶阔叶林和温带草原多边形文件（附录）提取植被区内气象台站 384 个（图 2.4）。

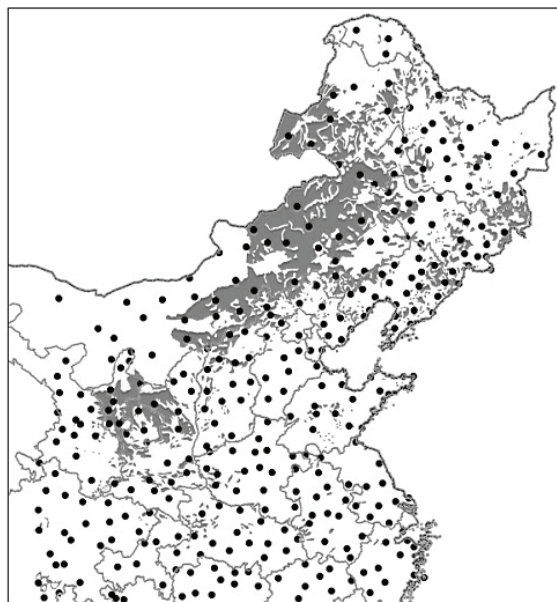


图 2.4 气象台站分布（灰色部分为植被区域）

计算气象台站 1983-2003 年逐年季节降水和温度值，在 Arcgis 9.3 中插值，利用中国植被图温带落叶阔叶林和温带草原点文件（point）在逐年气候插值图上提取植被点 1983-2003 年季节降水及温度。植被图在编制时每个点文件对应一个多边形文件（polygen），该多边形表示完整的植被斑块，每一点的信息代表这个植被斑块的信息，森林斑块 615 个，草原斑块 305 个。利用 Excel 2003 和 SPSS 16 进行相关和线性回归分析，用 R 软件进行非线性分位回归（quantile regression）。

2.2.4 遥感数据

2.2.4.1 NDVI 数据来源和应用原因

归一化植被指数 (NDVI) 综合反映植被分布和生长 (Chen *et al.*, 2004), 与绿叶密度相关性高, 代表光合能力和生产力状况 (Jupp *et al.* 2007), 是地上生物量的代表 (Tucker & Stellers, 1986), 其空间分辨率可以与气象台站降水数据匹配。NDVI 时间序列在过去 20 年中一直被用来评估植被条件的变化和它们对气候变化的依赖 (Tucker *et al.*, 2001; Xiao & Moody, 2004)。其局限性在于在植被高覆盖区存在 NDVI 饱和, 以及没有考虑树冠背景对植被指数的影响等。在半干旱区研究中还需要考虑土壤背景的影响, 这一影响在进行时间序列研究时在固定的测定区域内可以消除 (Peters & Eve, 1995; Peters *et al.*, 1997)。

NDVI 使用可见光上段和近红外光谱谱宽内的反射系数进行计算:

$$NDVI = \frac{a_{NIR} - a_{VIS}}{a_{NIR} + a_{VIS}}$$

NOAA/AVHRR 数据空间分辨率为 1km, 但可以免费得到全球尺度上每日的连续影像, 使用的光谱范围是近红外 (0.72-1.10 μ m), 红光 (0.58-0.68 μ m)。根据上述公式, NDVI 数值从-1.0 到+1.0。正值 (NIR>RED) 表明绿色植被表面, 数据增高表明植被增加。负值表明非植被表面, 如水体、冰面或积雪。

本文采用的 NDVI 数据是 GIMMS (Global Inventory Monitoring and Modeling Studies) 工作组对 1981 年 7 月至 2003 年 12 月间的 NOAA/AVHRR 数据加工处理后提供的, 时间分辨率为 15 天, 图像空间分辨率为 8km \times 8km。该 NDVI 数据集校正了传感器的改变、传感器灵敏度随时间变化、卫星轨道的漂移和太阳高度角等因素对数据质量的影响, 消除了 ElChichon 火山和菲律宾 Pinatubo 火山爆发导致的大气中气溶胶对数据质量的影响。因此, GIMMS-NDVI 数据更好地保证了数据质量, 在全球及区域大尺度植被活动变化研究中广泛使用 (Myneni *et al.*, 2001; Tucker *et al.*, 2001; Zhou *et al.*, 2001; Fang *et al.*, 2003; Piao *et al.*, 2003)。

2.2.4.2 NDVI 数据处理

计算春季 (4-5 月)、夏季 (6-8 月)、秋季 (9-11 月) 月均 NDVI 以及生长季 (4-11 月) 平均 NDVI, 利用中国植被图中温带落叶阔叶林和温带草原点文件提取各植被点 1983-2003 年春季、夏季和秋季月均 NDVI 值。

2.2.5 动态模型结构

2.2.5.1 模型结构和模拟区域

LPJ 模型是在 BIOME 系列模型基础上发展起来的，它在同一个模式框架中联合了机理性的陆地植被动态、碳和水循环，主要包括通过冠层导度以及光合与水分平衡过程之间反馈的快速过程和生态系统水平上的慢速过程（包括植被资源竞争和生产、植物组织周转、生长、出生和死亡、土壤和凋落物碳周转以及干扰相）的密切耦合。根据生理、形态、物候和干扰响应属性及一些生物气候限制因子，模型中定义了 10 种植物功能型（以下简称 PFT），其中 8 种木本 PFT（热带两种，温带三种，寒带三种），2 种草本 PFT（C₃ 和 C₄ 光合作途径）。LPJ 模型是通过输入月平均的气候数据（降水，气温，云量），土壤质地和 CO₂ 浓度作为驱动的，输出数据为日潜在蒸散发量和月土壤温度，进而计算夏绿型植被的叶片物候的季节进程。采用 BIOME3 对于光合作用和水分平衡的设计，通过每日的计算更新每种 PFT 的 GPP，从中减去因维持和生长的呼吸消耗以及通过凋落物进入土壤的生物量。剩下的生物量按照相关生长关系分配到植物的各个器官。种群密度基于定居和死亡率以年为单位进行更新。枯落物和土壤有机物（SOM）分解以季节温度和土壤水分驱动。每天的生产力，累加得到每月的生物量以及产生的碳通量等。通过汇总每个 PFT 的输出值，可以得到整个象元的输出值。

平均功能型个体（average individual of a PFT）是模型模拟的最小单元，它是单个像元中的特定 PFT，其生理动态由一系列参数和限制因子调节。限制生长在气候数据的 20 年平均值超过限度时触发。每一种 PFT 都有一系列的变量来定义平均个体的特点。例如对于木本 PFT，对平均个体定义了冠幅面积（m²）和四个组织碳库（gC）：叶、边材、心材和细根，并定义了四种转换规则确定生物量在组织库中的迁移规则。对于草本 PFT 的定义比较简单，比如种群密度被指定为 1，只有叶和细根的生物量而不存在边材和心材。

LPJ 模型的空间分辨率为 0.5°，根据中国植被图提取的温带落叶阔叶林在全球的模拟单元中提取中国温带落叶阔叶林模拟点 547 个（图 2.5）。

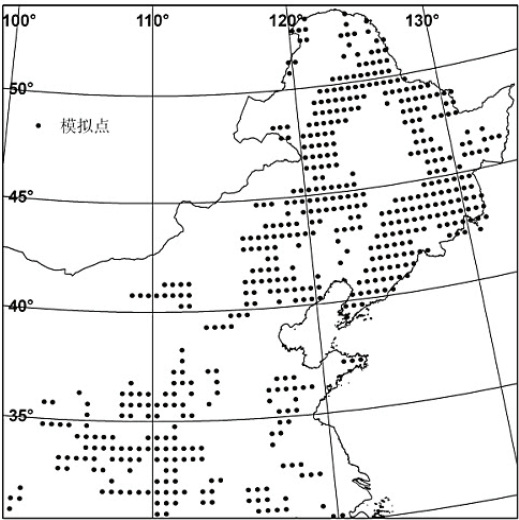


图 2.5 模型模拟单元分布

2.2.5.2 模型的修改和参数修订

由于需要模拟自然植被的动态，对植被模型中的土地利用模块进行关闭，使得输出的 PFT 分盖度均为自然植被对应值。

由于模型运行区域主要是中国部分，针对中国植被的特殊性和研究目的，需要得到比较符合实际气候条件约束的潜在植被，因此对 LPJ 划分的 PFT 中的相关参数进行必要的修改（表 2.6）。

根据翁恩生和周广胜（2005）对我国植物功能型的划分中对各植物功能型环境限定因子和优势等级的划分，分类体系中的“温带常绿树种”根据习惯将其改称为“亚热带常绿树种”，由此确定的 GDD_{min} （℃，minimum degree-day sum, 5℃ 以上积温）为 3300（LPJ 原为 1200），温带草原为 900（-），热带草地为 4000（-）。

表 2.6 我国几种植物功能型的生物气候指标的划分（引自孙艳玲等, 2007）

植物功能型 (PFT)	$T_{c,min}/^{\circ}C$	$T_{c,max}/^{\circ}C$	植物功能型 (PFT)	$T_{c,min}/^{\circ}C$	$T_{c,max}/^{\circ}C$
热带季雨林、雨林树	12.0 (15.5)	—	北方针叶树	— (-32.5)	-27.0 (-2.0)
温带常绿针叶树	-2.0	22.0	北方夏绿阔叶树	—	-17.0 (-2.0)
温带常绿阔叶树	0.0 (3.0)	13.5 (18.8)	温带草本	—	-6.0 (15.5)
温带夏绿阔叶树	-17.0	0.0 (15.5)			

$T_{c,min}/^{\circ}C$ ：最冷月最低温度 $T_{c,max}/^{\circ}C$ ：最冷月最高温度 括号内为修改前参数

Jackson（1996）根据 250 个根系研究对不同植物功能型组的根系-土壤深度关系进行了总结，提出了根系分布的渐进方程（asymptptic equation）： $Y = 1 - \beta^d$ ，d 为土壤深度，Y 为根系从表层到深度 d 的分布比例，以此纠正模型表层根系分布比例参数（表 2.7）。

表 2.7 表层 50cm 根系生物量比例

植物功能型	β	Y (d=50cm)
北方森林树种 (boreal forest)	0.943	0.95
温带针叶树 (temperate coniferous)	0.976	0.70
温带落叶树 (temperate deciduous)	0.966	0.82
温带草本 (temperate grassland)	0.943	0.95
热带落叶树 (tropical deciduous)	0.961	0.86
热带常绿树 (tropical evergreen)	0.962	0.86
热带萨瓦那 (tropical savanna)	0.972	0.76

2.2.5.3 情景设定

1、气候渐变

情景 1：设定降水和温度对照组气候数据为 1961-1990 年的气候均值，该气候状况在未来 103 年内不发生变化；情景分别为春、夏、秋、冬季各月降水±各月标准差，春、夏、秋季各月均温±各月标准差。以上 16 种情景内其他月份降水和气温与对照组一样保持 30 年均值，气候状况持续 103 年。

1901-2003 年大气 CO₂ 浓度来自 Carbon Cycle Model Linkage Project (Sitch *et al.*, 2003)。2010-2100 年的情景数据，采用政府间气候变化专门委员会 (IPCC) 第四次评估报告 (AR4) 排放情景特别报告 (SRES) 中的 B1 (图 2.6)，由 IMAGE 气候变化综合评估模型 (Integrated Assessment Models) 计算，是 CO₂ 增多最缓慢的情景。SRES 中的 CO₂ 浓度预测是由两个不同的碳循环模型 ISAM 和 BERN 计算的 (IPCC, 2001)，本研究采用 ISAM 的参考值 (reference case)，这组值定义在气候敏感度 2.5℃，其陆地吸收值参考了包括 LPJ 模型在内的中尺度模型的反馈。由于数据是 10 年值，这里将其插值到每一年内。CO₂ 浓度序列中空心圆为 1958-2007 年现代大气 CO₂ 浓度观测年均值 (夏威夷 Mauna Loa)，空心三角为 SRES 报告中 B1 情景值。

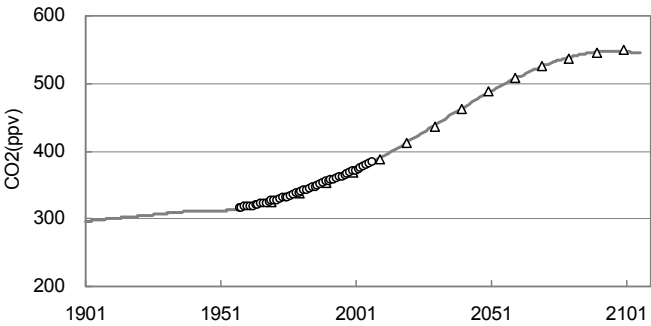


图 2.6 CO₂ 浓度变化趋势

情景 2, 3: 因为研究区较小, 而一般的预测数据时间分辨率为 20 年以上, 本文未采用 SRES 预测, 而利用数学方法进行外推, 组成两组分别基于前 103 年气候状况 (情景 2) 和 1983 年以来气候状况 (情景 3) 的对照数据, 在此基础上, 分别将春、夏、秋、冬降水和春、夏、秋温度升降 50% 进行敏感性分析。对情景 2 的夏季降水减少和温度上升设定 10%-80%, 间隔 10% 的变化进行敏感性分析。模型输入的 CRU 气候数据表明温带落叶阔叶林区域的年降水量在 60 年代和 80 年代都发生过明显的变化, 而 80 年代以来是我国北方夏季降水急剧减少而增温持续的时代 (黄荣辉等, 1999; 张晶晶等, 2006)。

由于气象数据的外推本身具有混沌性, 数学计算的总体思路是将线性回归和随机扰动相结合, 在线性回归效果过于粗糙时用分段线性回归 (情景 3)。考虑到程序处理的时间代价以及气候本身的区域性特征, 对模拟点的气候数据进行聚类 (cluster) 处理, 算出该类的平均值进行线性回归, 得到结果后再根据前期真实气候数据按照聚类簇和月份分配平均值, 聚类算法参考 “Affinity Propagation” (Frey *et al.*, 2007), 其特点是自动确定合适的聚类个数而不需用户指定。

为了生成与模拟点对应的用于聚类算法的点集, 对每个点计算其前 103 (21) 年内相应季节的降水量 (均温), 这样就得到一个三维空间中的点集。对该点集进行聚类, 最终得到 9 个聚类簇, 分别对它们所对应的 103 (21) 年数据进行线性回归可得到未来气候数据。考虑到问题规模, 用于预测的数据取的是每个聚类簇所对应的 10 年平均值, 预测结果是以后 103 年中每年的年平均值, 为了把它们转化为每个点所对应的月份值, 首先我们计算前 103 (21) 年中, 每个观测点对应的年平均值与它所在聚类簇平均值的差, 假设该值是稳定的, 计算后 103 年中某一年 (设为第 k 年) 中, 第 m 个观测点的年平均值时, 只需用计算出的聚类簇平均值加上上面算出的差值即可。利用类似的办法, 可以把每一点对应的年平均值转化为对应的按月份计算的数值。

为了更加逼真地模拟自然界中的气候变化, 程序对上面生成的基础数据进行一定的随机扰动。这里所使用的随机数生成器与 LPJ 模型中降水随机分配所用的相同。首先, 程序设置一个浮动范围上界 u , 再生成一个 $[-1, 1]$ 内的均匀随机数 x , 用 $u \cdot x \cdot v$ 作为初始值 v 的实际改变量, 然后用 v 加上该扰动量即可。程序中还需注意到不能导致数据越界, 如降水变成负的, 温度低于绝对零度等。采用的修正方案是如扰动后的值不合理则温度取绝对零度, 降水取 0。

2、模拟干旱:

根据月降水距平百分率设计不同季节不同程度的干旱情景, 反映了温带落叶阔叶林地区可能出现的极端干旱情况, 距平百分率的计算方法如下:

$$P_a = \frac{P - \bar{P}}{\bar{P}} \times 100\%$$

P_a 为月平均降水量(mm), \bar{P} 为 30 年气候平均值 (1961-1990)。

对我国 160 个气象台站数据进行的 1951-2000 年 PDSI 修正指数研究表明, 华北地区春夏旱涝具有连续性, 干旱具有 3 个月持续性, 并且干旱年份一般在 2 年以上。降水距平表示的干旱程度与 PDSI 修正指数的相关性强, 因为 PDSI 抓住了降水是干旱最重要的决定因素, 同时 PDSI 判断的干旱情况持续性更强, 研究发现已经出现的三次干旱持续时间分别为 1980-1984 (5 年), 1986-1989 (4 年) 和 1998-2000 (3 年), 因此在干旱情景的设计中, 采用季节性 3 个月连续干旱设计, 分别为春 (3-5 月), 夏 (6-8 月), 秋 (9-11 月), 冬 (12-2 月)。根据连续三个月的月降水距平百分比评价的干旱情况规定, 距平值为 -25%~-50% 为偏旱, -50%~-80% 为干旱。干旱持续月份, 正常年份和干旱年份设定如下表, 其中 5 年连续干旱后 5 年正常年份时干旱程度分为偏旱和干旱两种, 其余程度都为干旱。两季和三季连续干旱设定时都按照 5 年旱 5 年正常。如第二行第二列“春夏秋冬”代表 8 种干旱模拟情况, 干旱出现任何季节都持续 5 年后正常 5 年, 干旱程度是偏旱和干旱两种; 第三行第二列“春夏”代表 2 种情况, 分别是春季、夏季单季干旱持续 4 年后正常 1 年。

表 2.8 干旱情景模拟

干旱期 \ 间隔期	5	3	1
5	春、夏、秋、冬	春、夏	春、夏
4			春、夏
3			春、夏

2.2.5.4 敏感性分析

一般来说, 敏感性分析是指一个计算机模型参数的变化情况怎样影响由模型产生的结果。模型结果可能对输入数据、模型模拟的物理或化学过程以及数字精度敏感。Saltell (2000) 在 “What is sensitivity analysis?” 中将其定义为研究模型输出量的变化 (variation) (数值或其他形式) 怎样被分摊 (apportion) 到 (定性或定量) 不同的变化来源中, 这些来源是指输入或因子, 包括了输入变量, 模型参数, 模型结构, 假设和规格 (specifications)。

在本文中, 敏感性分析用来进行表征植被覆盖和生长的模型输出变量 FPC 和 NPP 对输入的气候数据变化的反馈程度, 也即气候因子的影响效应。FPC 和 NPP 分别代表叶投影盖度和年净第一性生产力, 是模型的输出变量 (output

variables, y), 逐月降水和温度在分析中经过季节整合, 是模型输入参数 (input parameters, x), 输出变量对于输入参数的敏感性(或参数 x 对变量 y 的影响) $\Delta y/\Delta x$ 用来计算输出变量变化相对于输入参数变化的比率 (变化以%为单位), 用于解释敏感性数值, 可以认为比率为负值意味着参数值增大时变量减小, 反之亦然。比率的绝对值 ($|\Delta y|/|\Delta x|$) 反映了参数对输出变量的影响性大小, 参数影响程度以大于 0.2 为强效应 (strong), 0.1-0.2 为中等强度效应 (medium), 小于 0.1 为弱效应 (Tatarinov & Cienciala, 2006)。

第三章 树木对干旱的生理适应及林线形成机制

3.1 干旱极限森林生长特征

在欧亚大陆温带森林草原交错带，落叶阔叶林的生长极限是由水分控制的干旱极限，接近干旱极限，森林格局和形态会发生明显的变化，郁闭的林冠可能稀疏化，林斑的规模可能会减小，但这两种现象往往受到地形因素的影响，局地效应较强。干旱极限下更为明显的现象是树木的矮化，即树木高生长与径向生长不同步，高相对生长缓慢乃至停滞。孤立的评价树木的高矮没有意义，因此，判断高生长和径向生长的相对情况才能反映干旱极限下树木生长状况的改变。

油松和山杨是温带森林草原交错带干旱极限树种，图 3.1 表明油松在不同降水量下高生长和径向生长的关系。敖伦那尔斯和干其那尔斯降水量在 350mm 以下，随着径向增粗，高生长无明显变化，基本上在 4-8m 之间波动；而在降水量 400mm 以上的坝下三道河口和第三乡，高生长与径向增粗同步。图 3.2 表明山杨在不同降水量下高生长和径向生长的关系。在降水量约 390mm 以下的旧庙西山和黄芩塔拉，树高和胸径无明显相关生长关系，而在降水量 400mm 以上的后两个地点，高生长与径向增粗同步进行。

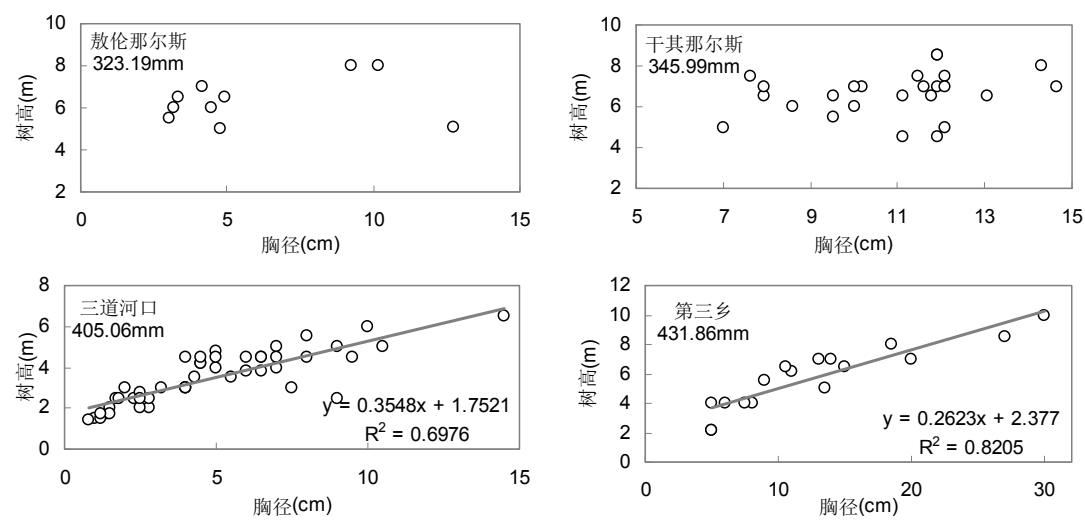


图 3.1 油松树高-胸径关系

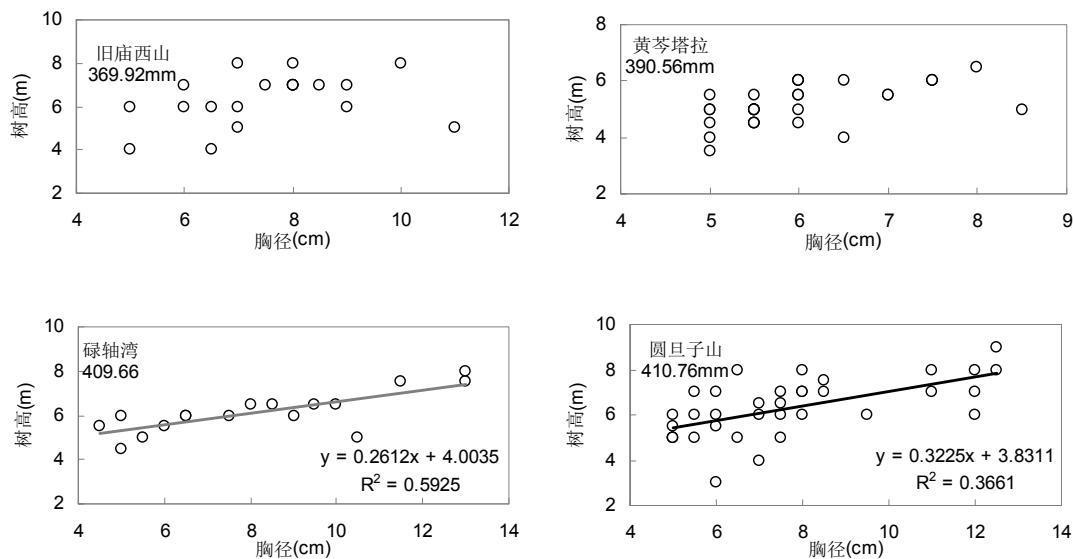


图 3.2 山杨树高-胸径关系

森林草原交错带次生天然林主要类型是山杨林和白桦林，前者比后者分布更接近草原带；蒙古栎作为落叶阔叶林核心区树种，不在干旱极限下大量分布。因此，这两个树种没有表现出干旱极限和非极限明显的树高-胸径生长关系的差别。

对于交错带树木生长的同化作用而言，CO₂ 不是限制因子，叶温也不是限制因子（Helliker & Richter, 2008），高生长缓慢乃至停滞的最大限制因子是水分，特别是土壤水分的缺乏影响树木有效的进行水分运输以满足蒸腾作用。

3.2 树木对干旱的生理适应性

3.2.1 水分利用效率与树高的关系

木本植物高度与生长季日平均水分利用效率（WUE）具有如图 3.3 的关系，WUE 是光合速率与蒸腾速率的比值，用以判断同化作用与水分消耗的相对关系。

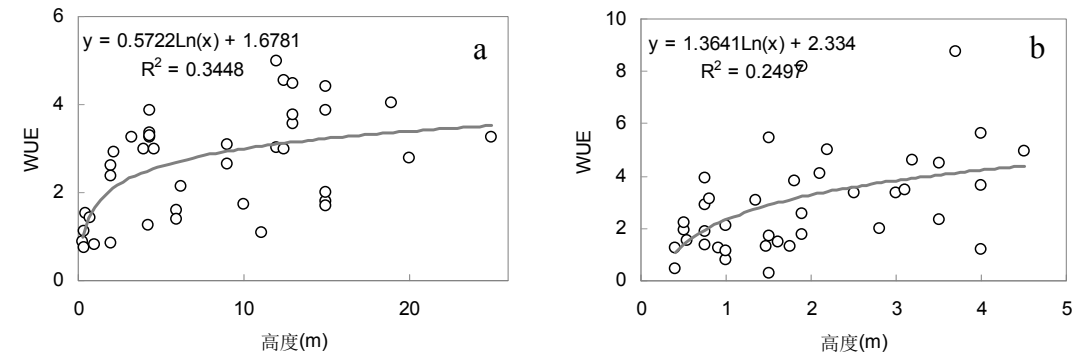


图 3.3 木本高度与 WUE 的关系 乔木(a) 灌木(b)

随着乔木高度增加,水分利用效率提高,在一定高度范围内关系明显,但 WUE 增高趋势不是无限的。WUE 随高度升高而增大的趋势在灌木中也存在,但是在草本植物中不明显。

根据乔木高度与 WUE 的关系,我们可以提出对生长限制的一种解释:在温带森林干旱极限下树木的矮化表现为高生长不随径向生长同步进行,树木最终被草本植物取代;从水分利用的角度来看,是由于树木需要高的 WUE 产生足够的同化产物维持高生长;然而在干旱极限条件下树木无法实现较高的 WUE,因为此时为了维持树木的蒸腾需求需要加大光合速率产生更多的地下组分以满足水分吸收需求,这对于水分缺乏地区的植被是不经济的;所以干旱极限下树木倾向于低矮化以维持一定的 WUE,但当 WUE 随着树高降到一定阈值以下(树高极低值设定为 2m),此时的高度已不足以称其为树木,从而被其他功能型所取代。

WUE 与树高的关系所反映的干旱极限下的生长限制是从植被水分利用的角度提出的。在进行干旱条件下植被生理生态研究时往往单纯考虑土壤水分供给并以此定义干旱,其实是没有意义的。水分的有效性在任何地方都会显示出一个很宽的幅度(埃塞林顿, 1989),即使在荒漠这样土壤水分供给极低的地区,仍然存在灌木。干旱条件应该对应于植被的水分利用能力,树木在荒漠地区的供水条件下不能充分利用水分,而荒漠灌丛则可以得到足够的水分,因此荒漠对树木而言具有干旱限制。

3.2.2 理想干旱林线形成机制

树木的生长是同化产物分配的结果,在水分制约的条件下,树木难以以较高的 WUE 来维持高生长:一方面高生长提出了更高的蒸腾要求,必然导致同化产物向根系分配以利于吸收根的生长;另一方面光合速率本身受到水分制约,即使蒸腾速率也下降,光合产物也可能会因为要满足根系生长而无法实现高生长。

相对于草本植物柔软富有弹性的叶片,乔木和灌木的叶子比较坚硬,细胞储水容量低,更容易受到水分胁迫,而且乔木中水分移动始于树冠顶端部分枝的前端,拉动起自根部到树干基部的水柱,因此水分运输与高度密切相关;另一方面,乔木不如草本植物进入冠层的光照充足,光合效率较低。

由 WUE-树木高生长推测的生长限制模式可知,树木生长的关键过程主要是光合作用和蒸腾作用的平衡,两者共同的控制因素主要是大气湿度和土壤湿度,表现在对气孔开闭的影响上(Jones, 1998)。任何大气湿度和土壤湿度条件其本质是时间和空间上的降水和温度的组合,不但成为气候区划和植被分区的依据,

也衍生出各种指标和指数作为植被生长条件优劣的判断,特别是反映水分和温度综合特征的干燥度。

因此,树木维持高生长的 WUE 是由一定的降水和温度通过维持光合作用和蒸腾作用的平衡来达到同化产物的分配而实现的。归根结底,水热结合在植被区域上的影响是植被生理活动进行的前提,因此,在理想状态下温带森林向干旱极限靠近时应表现为树高不断降低,最后森林与草原边界呈一条界线鲜明的分界。

3.3 小结

根据树木 WUE 与高度以及温带森林干旱极限下树木生长状况提出了干旱极限的树木生长限制是一种基于水分利用的生理适应,干旱极限下树木倾向于低矮化以维持一定的 WUE 以达到蒸腾需求和光合产物地上地下分配的平衡。树木维持高生长的 WUE 是由土壤湿度和空气湿度通过维持光合作用和蒸腾作用的平衡,来达到同化产物的分配而实现的。推至区域尺度,土壤湿度和空气湿度都是在一定的降水和气温的组合内出现的,是植被生理活动进行的重要因素,因此,在理想状态下,水平面温带森林向干旱极限靠近时应表现为树高不断降低,最后森林与草原边界呈一条界线鲜明的分界。然而,现实的森林草原交错带并不具有截然的界线,这是由于森林分布在降水和气温的组合区间内受到群落可以利用的土壤水分的影响,出现了现实的森林和草原交错分布的格局。

第四章 群落水平上林草交错带土壤水分

4.1 交错带 1982-2004 年气候变化

根据森林带（围场）、森林草原交错带（多伦）以及草原带（锡林浩特）三个台站 1982-2004 年降水资料分析，年降水量、生长季和非生长季降水量均是森林带最多，但没有显著趋势（图 4.1）。非生长季降水比率基本相同，约为 12%，主要为降雪。森林带非生长季降水波动较大，变异系数达到 0.55，交错带为 0.38，草原带较和缓，为 0.28。较大的波动可能是更为重要的生长制约因子。交错带生长季降水较稳定，变异系数为 0.18，森林带为 0.22，草原带达到 0.33。对于交错带来说，冬季降水变率大，夏季降水稳定，降水没有明显趋势性。

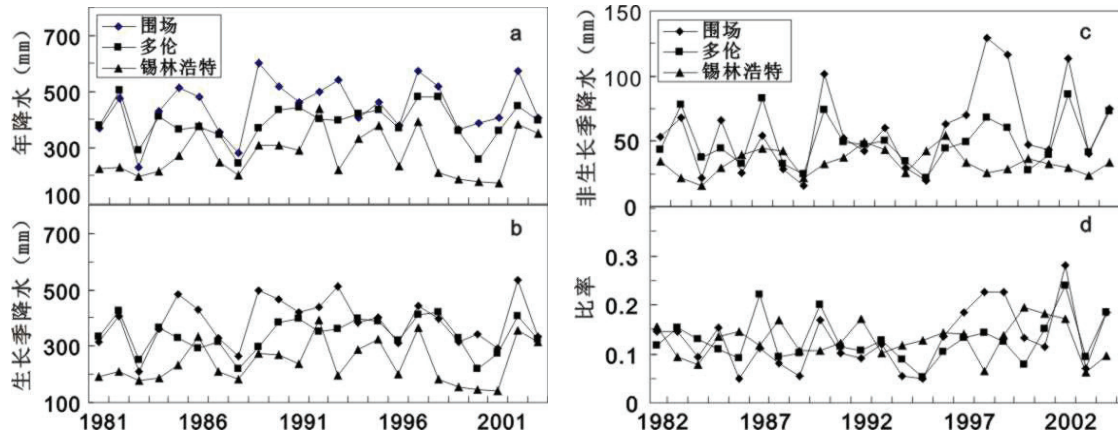


图 4.1 年降水量(a) 非生长季降水量(b) 生长季降水量(c) 非生长季降水量比率(d)

三个植被带年平均气温、非生长季、生长季及各季节气温呈上升趋势（图 4.2），不过 2001 年以来非生长季和夏季气温呈明显的下降趋势。交错带生长季和非生长季气温升高显著，春季增温最显著（ $R=0.56$, $p<0.01$ ），冬季次之（ $R=0.51$, $p<0.01$ ）。冬、春同时增温对积雪、冻土具有复杂的影响。生长季前的高温会加剧开阔地冻土的融化和土壤蒸发，引起水分亏缺。变异系数反映了气温波动程度，年均温和非生长季气温波动较大，主要来源于春季和秋季气温波动，两者是影响植被返青和生长季持续时长的关键因素；生长季和夏季气温波动小，冬季气温波动程度中等。春季和秋季植被带气温波动差异相对较大，森林带波动小，交错带次之，草原带最大。

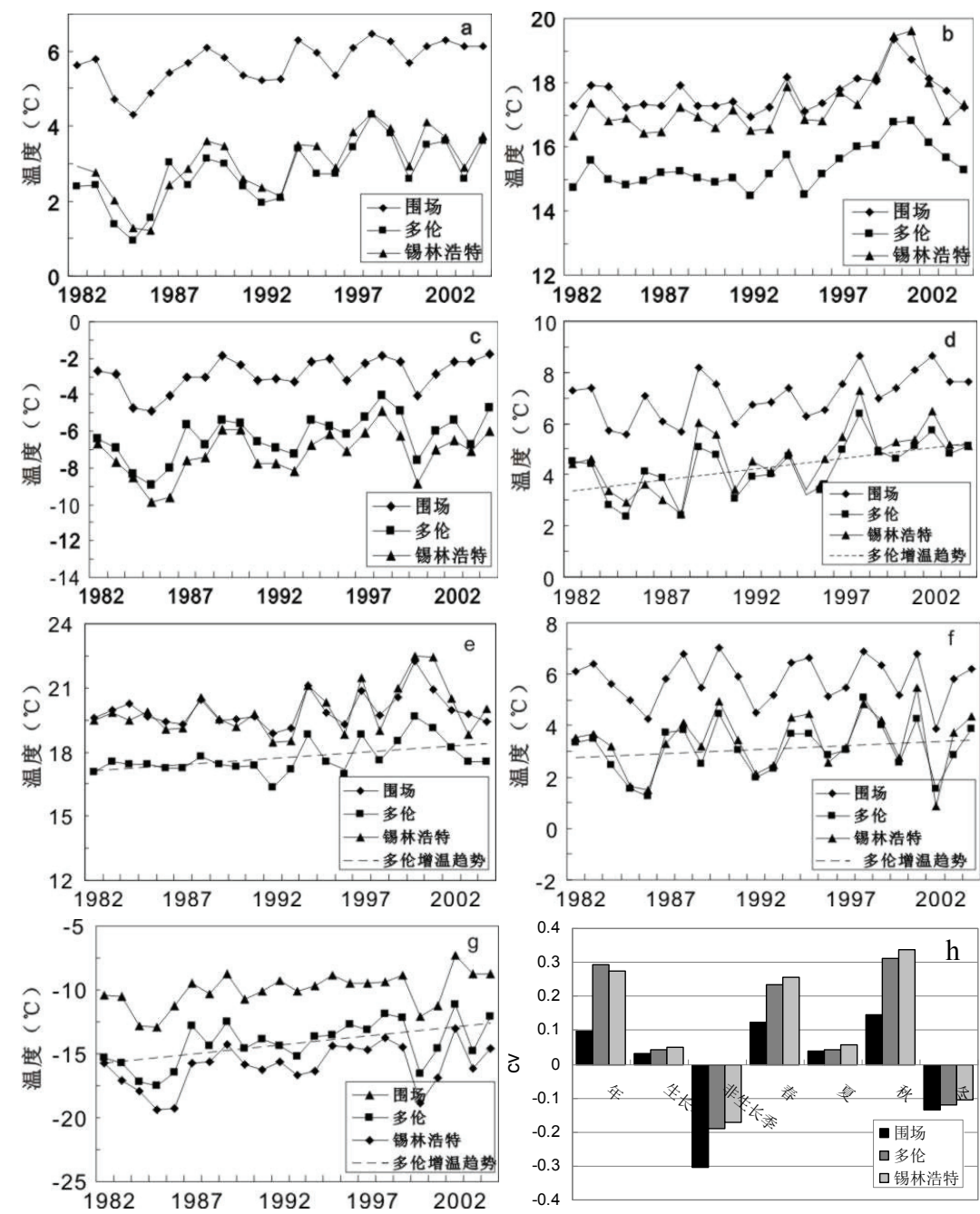


图 4.2 年均温(a) 生长季均温(b) 非生长季均温(c) 春季月均温(d)
夏季月均温(e) 秋季月均温(f) 冬季月均温(g) 变异系数(h)

4.2 森林草原交错带土壤水分的时空差异

4.2.1 土壤水分的空间分布特征

4.2.1.1 不同森林土壤水分与降水梯度的关系

降水是控制干旱极限森林生长的首要因素，沿降水梯度，土壤剖面水分总体

状况与降水量具有一定的关系。2006-2008 年三组 7 月的数据表明，白桦林和山杨林下土壤湿度与降水梯度一致，白桦林和油松林下二者则没有明显关系，表明阔叶林的生长和土壤发育可能与降水量密切相关，而针叶林对局地土壤状况的适应性更强。

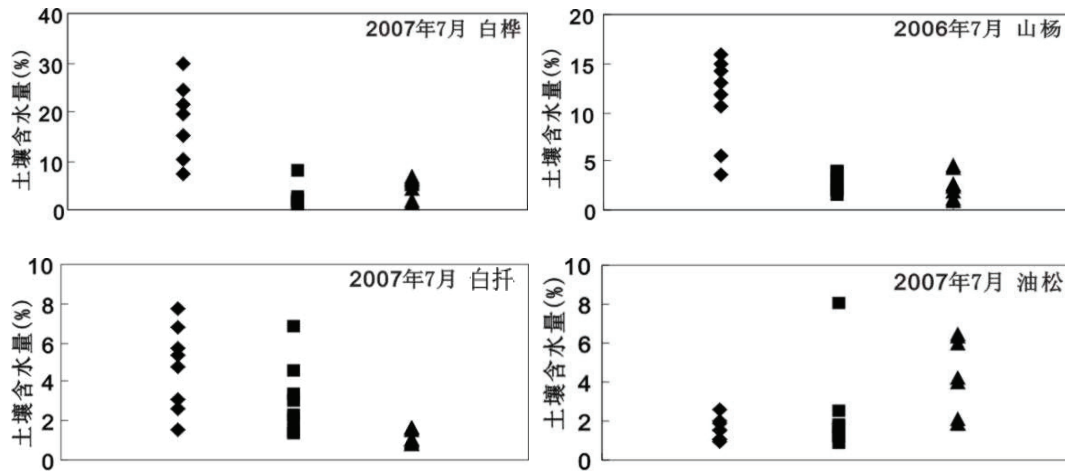


图 4.3 土壤含水量与降水梯度

4.2.1.2 气候综合因素对土壤水分的影响

以 14 个地点的白桦林和相应草原的年降水量和土壤含水量进行分析发现，由于采样点扩展到北纬 50° ，10cm 层土壤含水量与降水量不再是单一的正相关关系（图 4.4）。在纬度梯度上，高纬地区尽管降水量低，但由于温度也低，土壤水分仍可以维持较高值。在年降水量小于 380mm 的采样点中土壤含水量高值都出现在额尔古纳、小乌尔根和姑子庙（空心圆）三个地点，纬度都在北纬 50° 以北。如果将北纬 50° 以上的地点去掉，降水量与剖面表层土壤含水量的关系就较为密切了 ($R=0.55$)。

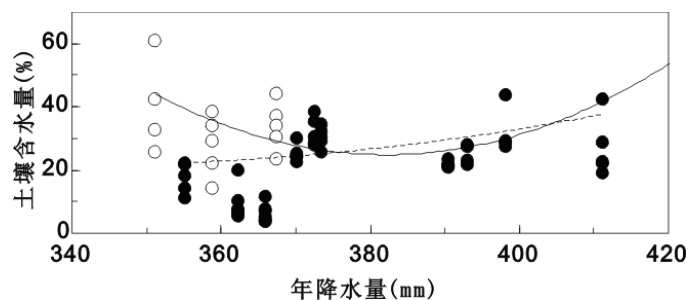


图 4.4 降水梯度下的白桦林土壤含水量

降水量与剖面土壤含水量在纬度梯度上表现为降水量从低纬到高纬波动式递减，而阴坡森林和阳坡草原剖面的土壤含水量波动式上升，并且阳坡上升更快（图 4.5a）。因此，随着纬度升高，阴坡和阳坡土壤含水量差距逐渐减小（图 4.5c），

表明地形对水分进行重分配时,在纬度较低蒸发受到温度影响大的区域带来阴阳坡较大的差异,而在高纬度这种差异由于温度对蒸发的调节而减弱,阴阳坡土壤含水量差异随着纬度增高而减小在表层土壤表现更为明显(图 4.5d)。表层土壤水分的蒸发受到温度的控制,在高纬地区温度降低,表层土壤蒸发减少,特别是减少了阳坡的土壤蒸发,从而缩小了阴阳坡土壤水分差距(图 4.5d)。

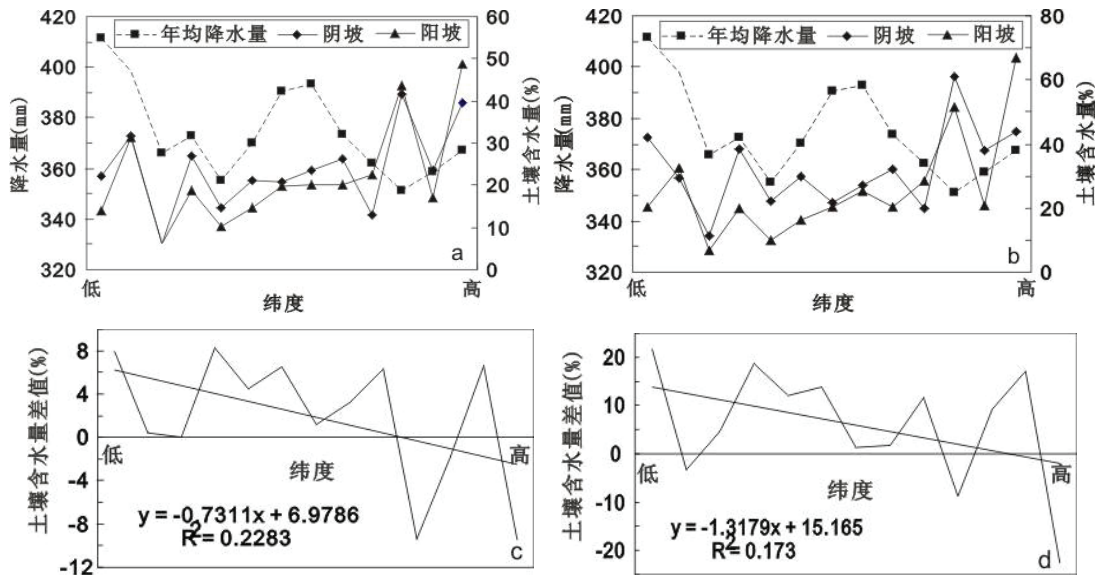


图 4.5 白桦林土壤含水量的纬度梯度和阴阳坡差值 剖面平均(a,c) 表层土壤(b,d)

4.2.1.3 土壤水分剖面分布和坡向差异

由于土壤水分存在时间变化,本文以生长季(2008 年 7 月)和非生长季(2008 年 10 月)土壤水分剖面垂直分布为例,说明不同类型的森林和草原土壤水分剖面垂直变化规律。在 7 月,受到植被水分利用及土壤水分蒸散影响的土壤水分在剖面上垂直下降,阴坡和阳坡的总体趋势一致(图 4.6a),但在区域内受到土壤质地和植被影响各层土壤含水量波动较大(图 4.6b)。阴坡表层(10cm)土壤含水量大于阳坡($P < 0.01$),波动程度小于阳坡,表层以下阴坡土壤水分不显著的高于阳坡,表明阴坡表层可以储水并下渗。土壤含水量从表层到 40cm 明显下降,在更深层逐渐平缓,阴阳坡土壤水分差异减小,水分变异系数在阳坡持续下降,而在阴坡上升,表明区域内阴坡下层土壤水分变动情况在生长季比较复杂,树种间的变化很大,而草原由于群落组成差别小,波动较小。7 月作为植被耗水时期并没有出现根系集中区含水率偏低的情况。

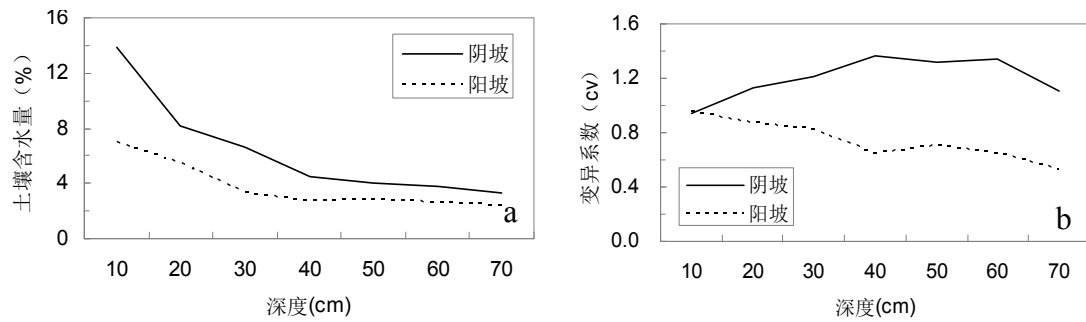


图 4.6 生长季垂直剖面土壤含水量(a) 变异系数(b)

10 月土壤水分剖面变化规律与 7 月类似, 阴坡和阳坡在整个剖面上仍表现出由表层向深层递减的趋势 (图 4.7)。由于采样点不完全一致, 绝对数值不具有可比性。此时森林和阳坡的灌丛或草原都已经停止生长。

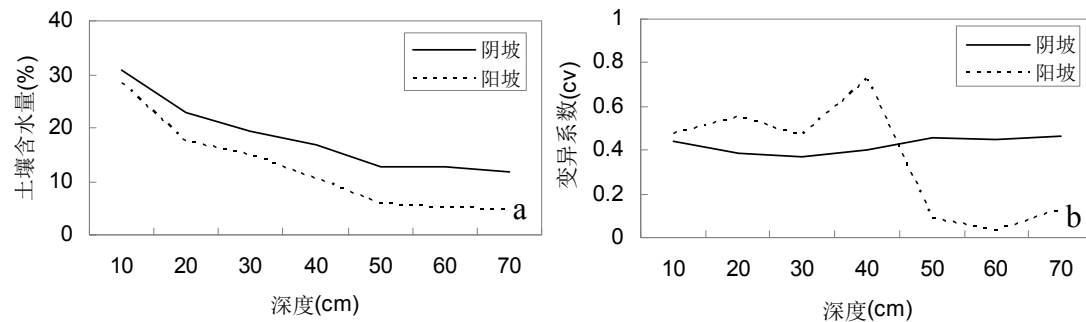


图 4.7 非生长季垂直剖面土壤含水量(a) 变异系数(b)

由于土壤水分受到实时降水影响, 单年单月土壤含水量阴阳坡差异较大, 因此根据取样的一致性, 用 2006 年 7、8、9 月和 2007 年 5 月和 7 月数据共同分析阴坡森林和阳坡草原土壤水分差异 (表 4.1)。均值是森林在三个采样点 5 个月土壤水分的平均值, 代表区域内这种森林生长季土壤水分状况。土壤水分反映的是降水扣除蒸散发后的平衡状态, 从表中可知, 总体而言阴坡白桦林和山杨林林下土壤水分条件比阳坡草原好, 但区域波动稍大, 随着深度加深, 含水量波动性减小, 区域深层土壤含水量较为一致; 油松林没有明显的坡向含水量分异, 因为区域内油松在阳坡可以生长, 阴坡与森林分布不一致, 阳坡水分甚至高于阴坡, 但区域内土壤水分波动很大; 白桦林也没有明显水分坡向分异, 因为沙地白桦生长环境均一, 阴阳坡土壤机械组成相似, 水分波动较大。由于落叶阔叶林林下和对应阳坡草原的成土情况差异较大, 阴坡和阳坡土壤水分差异可以持续到较深的土层并保持森林土壤水分始终大于草原, 而阴阳坡土壤质地相对均一的针叶林, 阴坡和阳坡水分差异不明显。

表 4.1 森林与草原垂直剖面土壤含水量（黑体示显著差异, $p<0.05$ ）

森林类型 坡向/深度(cm)	白桦		山杨		油松		白桦	
	均值	cv	均值	cv	均值	cv	均值	cv
阴坡 10	9.19%	0.09	10.43%	0.06	3.1%	0.48	5.9%	0.57
阳坡 10	7.35%	0.06	7.02%	0.05	4.1%	0.62	5.0%	0.56
阴坡 30	7.55%	0.08	7.74%	0.05	1.7%	0.52	2.6%	0.46
阳坡 30	4.95%	0.04	5.39%	0.04	3.7%	1.00	3.3%	0.98
阴坡 50	6.26%	0.07	6.15%	0.04	1.9%	0.80	2.1%	0.58
阳坡 50	4.82%	0.04	3.62%	0.02	3.3%	0.73	2.6%	0.55
阴坡 70	4.69%	0.05	7.08%	0.08	1.5%	0.58	2.2%	0.48
阳坡 70	4.04%	0.02	3.65%	0.02	3.8%	0.99	3.2%	0.79

4. 2. 2 森林草原交错带土壤水分的时间变化

4. 2. 2. 1 土壤水分变动的时间趋势

取 2006 年 7 月、8 月和 2007 年 7 月的土壤水分平均状况作为生长旺盛期代表，与 5 月（生长前期）和 9 月（生长后期）土壤水分状况做对比（图 4.8）。结果表明，阔叶林土壤含水量在生长前期>生长旺盛期>生长末期（白桦林 $p<0.05$ ，山杨林 $p<0.01$ ）。针叶林表现出不同的状况：油松土壤含水量在生长末期>生长旺盛期>生长前期（ $p<0.05$ ），而白桦土壤含水量在整个生长季没有规律性。这个结果表明，白桦的生境特殊而且均一，在不同的降水条件下砂质土壤调节水分处于相对稳定状态。油松生境地表缺乏枯落物层，并且有的分布在阳坡，冻土春季开化时蒸发强，生长前期水分少；阔叶林有枯落物层和雪盖，一方面土壤冻结浅，另一方面保水性强，开春融水蒸发少，下渗多。

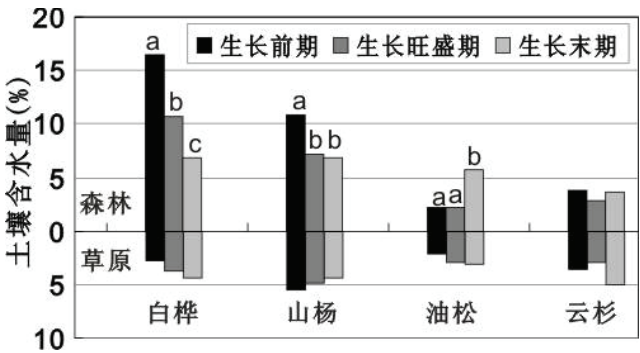


图 4.8 不同生长时期土壤含水量

草原土壤水分不像森林具有明显的季节性，基本上表现为生长前期水分小于生长末期（山杨林对应的草原除外）。可能由于冬季土壤冻结强烈，2008 年 10 月时草原土壤冻结已经开始冻结到表层以下 15cm，大风带来的降雪重分配导致

地表积雪只维持在一些稍高大的地上干枯部分。4、5 月平均风速可达 4-6m/s, 最大达到 30-35m/s, 大风和强烈的辐射带来较强的蒸发, 所以生长前期土壤水分较差; 而在生长末期植被耗水减轻, 土壤水分有所恢复。

4.2.2.2 田间持水量与土壤水分波动

比较 2006 年到 2008 年每年 7 月在同一采样点采集的土壤样品含水量可知 (图 4.9), 土壤含水量具有一定的稳定性, 相同地点土壤含水量在同一时段没有大的波动 ($p>0.1$), 因此, 可以用正常年份多点土壤水分数值粗略估计区域内土壤水分状况。因此, 以采样点为单位, 以 07 年 5 月、7 月和 06 年 9 月分别代表的生长前期, 旺盛期和末期的 10cm 和 30cm 土壤含水量与田间持水量做对比。

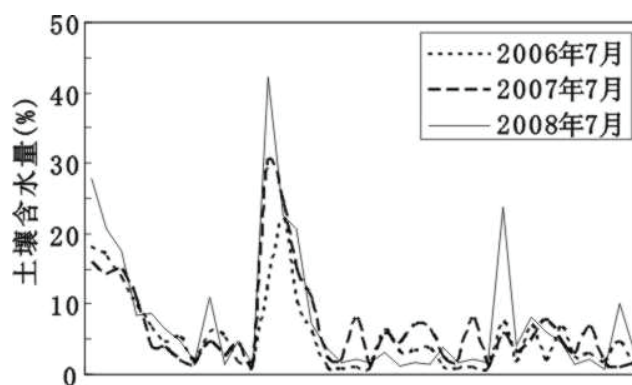


图 4.9 多年土壤含水量比较

田间持水量是土壤水分的基础, 不同植被在不同生长期的土壤含水量与田间持水量有关。从时段来看, 生长前期 (5 月) 和生长末期 (9 月) 的土壤含水量与田间持水量呈显著的正相关 ($p<0.01$), 表明春季融雪后生长伊始和进入生长末期时土壤水分由于植被利用减少, 含量比较平稳。生长前期土壤含水量与田间持水量相关性更强, 在阴阳坡相关性一致, 表明生长前期可能因为植被活动尚不旺盛, 土壤水分来源于上年留存的水分和补充的融雪, 更接近土壤的良好水分状态。这种关系在不同树种间存在差异, 土壤含水量在白桦和山杨林采样点比油松和白桤更趋向于与田间持水量一致。生长旺盛期土壤含水量波动大, 土壤含水量与田间持水量相关性弱。

从各树种各地点土壤相对含水量 (实际含水量/田间持水量) 可以看出 (图 4.10), 除个别点受到降水影响呈过饱和外, 各时段相对含水量均小于 100%。一般认为, 相对含水量在 70%-100% 时植被水分利用情况最好, 所以研究区内大部分地区土壤含水量不理想。从生长三个时期的相对含水量来看, 区域内 7 月相对含水量并不比 5 月和 9 月差, 表明生长旺期的土壤水分有所补充。

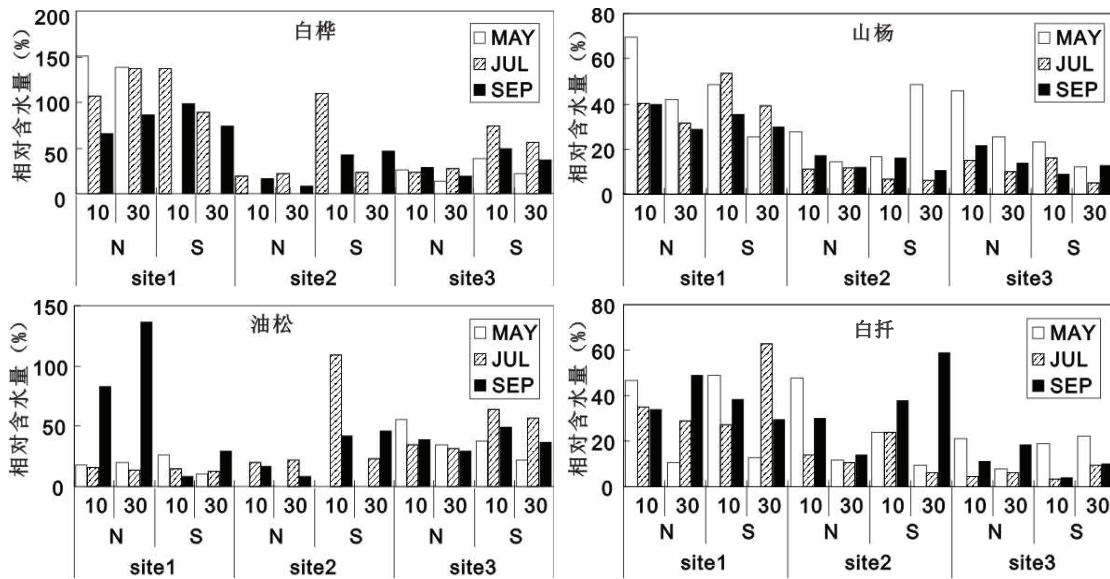


图 4.10 土壤相对含水量 N 为森林所在阴坡 S 为草原所在阳坡

相对含水量在不同时期具有一定的坡向分异。在 5 月份（图 4.11a），山杨林在表层 10cm 和 30cm 都表现为林下相对含水量高，白桦林和油松林数据不足，白桦林也具有类似趋势，表明生长前期的水分补充在阴坡比在阳坡好。

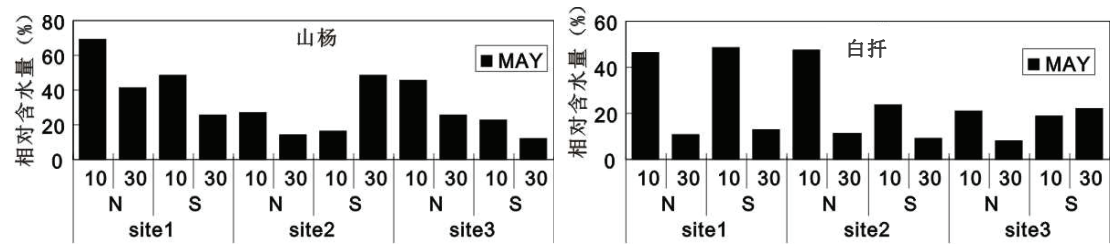


图 4.11a 生长前期土壤相对含水量坡向分异

7 月份（图 4.11b）植被活动旺盛，土壤相对含水量变化复杂。林下 10cm 土壤相对含水量低于草原（山杨林 site2 和白桦林 site1 除外），生长旺盛期森林蒸散发强于草原，研究表明交错带阳坡土壤蒸发量远大于阴坡，因此阳坡很可能无法承受森林的蒸腾失水。

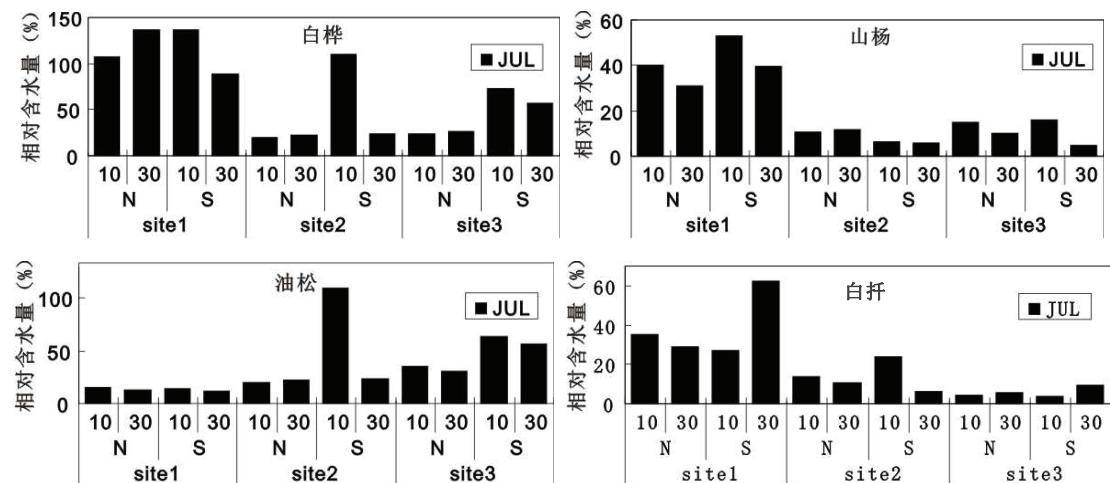


图 4.11b 生长旺盛期土壤相对含水量坡向分异

9 月份（图 4.11c）10cm 层相对含水量除山杨林外，其余森林至少在两个地点表现出林下较阳坡低，表明生长季末期森林耗水和阳坡草原耗水后的土壤水分状况。30cm 层阔叶林林下、油松和对应的阳坡相比，土壤相对含水量接近或林下稍低，但是白桦林没有明显规律。

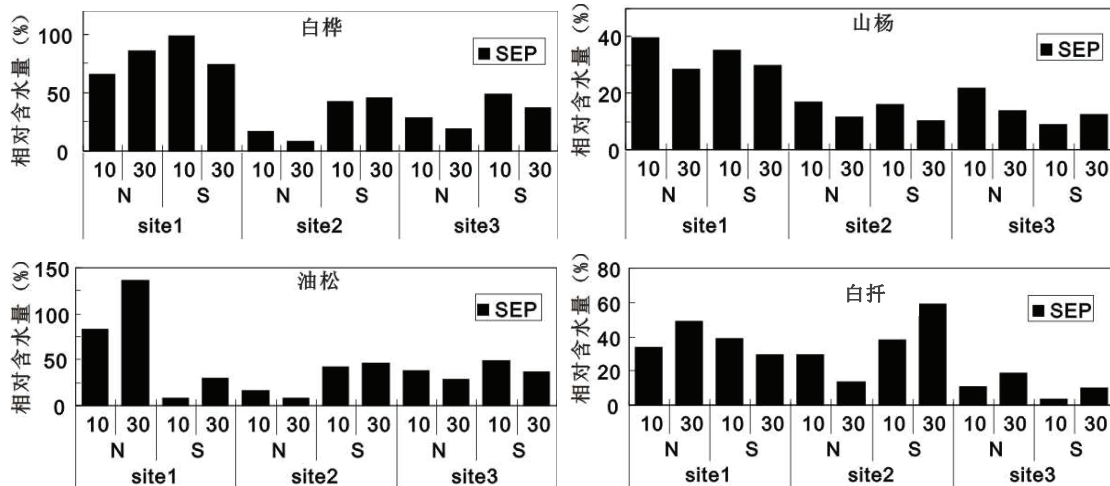


图 4.11c 生长末期土壤相对含水量坡向分异

综上所述，田间持水量作为反映土壤湿度潜力的指标，结合实际含水量可以看出区域内土壤水分普遍不足。生长前期林下相对含水量高，生长旺盛期和末期低，可能对于森林生长是限制。各个时期不同类型森林林下和草原土壤含水量波动情况不同，在生长旺盛期最为偏离田间持水量，在生长前期与田间持水量最为一致。总体而言，在生长前期，林下土壤水分条件较好，在生长旺盛期，林下土壤含水量相对较低。生长末期与生长时期的土壤水分消耗和供给有关，林下一般会低于草原。所以对于森林生长而言，生长季前期的土壤含水量十分重要。

4.2.2.3 非生长季土壤水分动态

植被由生长季进入生长停滞时，土壤含水量出现变化。以生长前期（5 月），生长旺盛期（7-8 月）、生长末期（9 月）和生长停滞期（10、11、1 月）的土壤水分状况做一比较，地点为白桦坑对面白桦林和松树井子山杨林（图 4.12a）以及相应的草原土壤（图 4.12b）。

白桦林 10 月土壤含水量比 9 月显著回升 ($p<0.01$)，进入 11 月后趋于稳定。山杨土壤含水量稳定期比白桦推后，进入 11 月后土壤含水量回升。10 月的土壤水分状况影响着冬季土壤水分的储量，此时研究区内森林土壤一般还没有冻结，已经出现了降雪的积累。

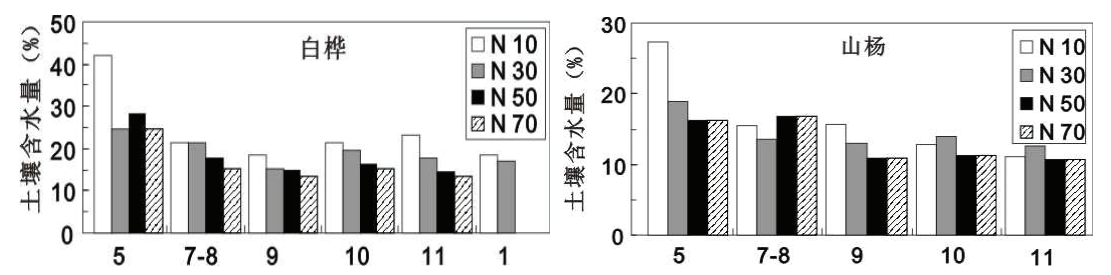


图 4.12a 非生长季森林土壤含水量

对应的草原在生长停滞开始后土壤水分保持稳定。山杨林对应的草原 10 月土壤含水量略有回升 ($p<0.05$)。在 10 月，草原降雪积累远薄于林下，并且土壤已经开始冻结，固化的土壤水分不如林下仍为液态的水分活跃。

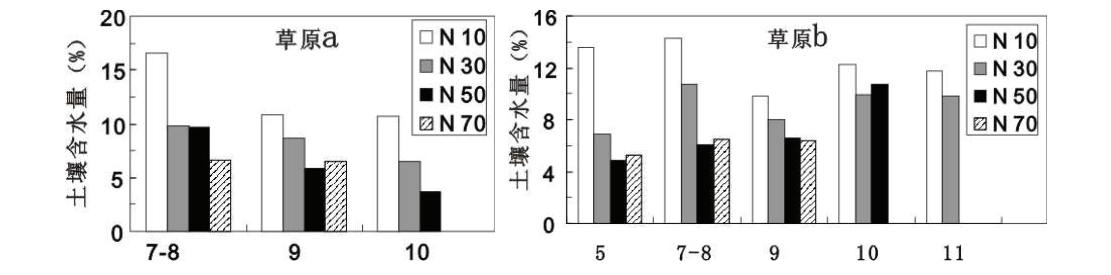


图 4.12b 非生长季草原土壤含水量

进入 11 月份后，森林林下土壤也开始冻结，一般而言，土壤冻结深度与降雪积累厚度相关，简略估测后可以建立以下关系（图 4.13）：

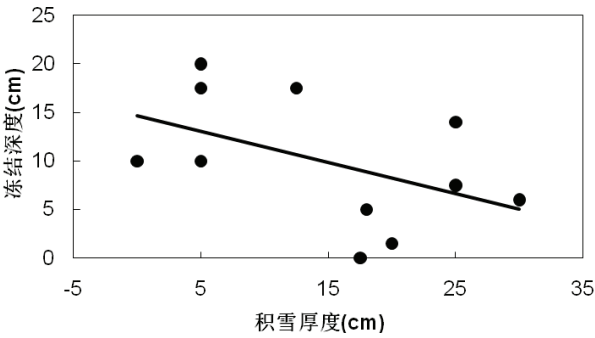


图 4.13 11 月土壤冻结深度与积雪厚度的关系

4.3 土壤机械组成对水分的影响

4.3.1 区域内采样点粒度分布特征

4.3.1.1 森林和草原土壤粒度分布特征

区域内土壤粒度分布具有单峰和双峰两种形态（图 4.14），但同一采样点对应坡向土壤粒度分布形式一致（a-b, c-d），各层位分布形式也一致。粒度分布为

双峰形式的都是在落叶阔叶林样点，次峰出现 10 到 30 μm 的粉粒级。

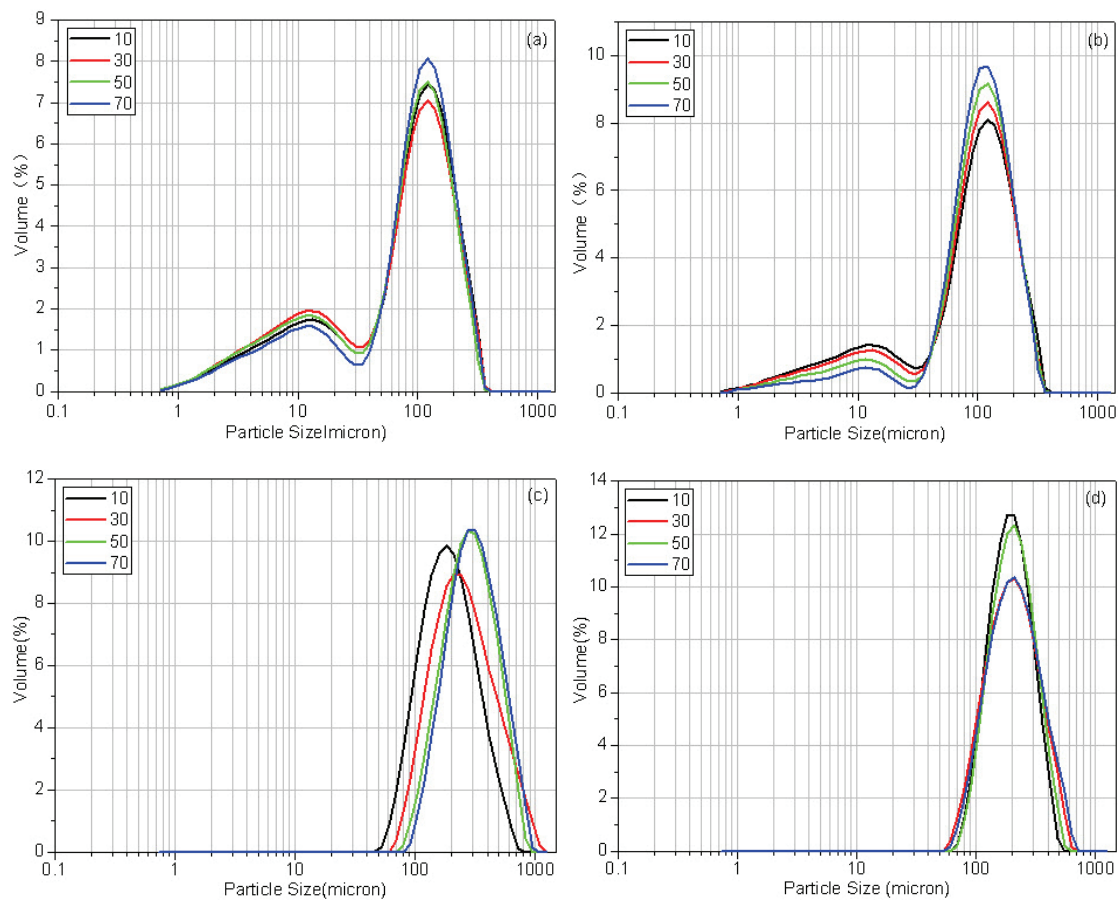


图 4.14 粒度分布曲线形态 松树井子山杨(a) 松树井子草原(b) 白桦坑白桦(a) 白桦坑草原(d)

研究区内土壤平均粒径在垂直剖面自上而下增加（图 4.15），剖面平均粒径表现为阔叶林<草原<针叶林。平均粒径无法反映植被生长土壤环境的细微区别，这一点必须通过细致划分粒径组 come 来分析。区域内土壤平均粒径变幅很大，表明该地区除了受到降水制约外，土壤对于水分再分配十分重要，与植被关系密切。

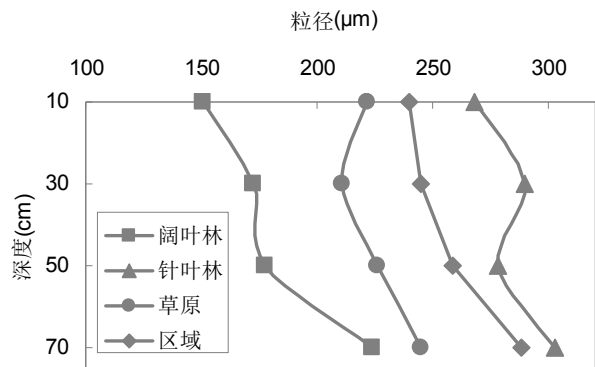


图 4.15 垂直剖面平均粒径

下表显示了每一树种所在的阴坡土壤沿着降水梯度分布下的各层土壤平均粒径（ μm ）。降水对表层土壤的作用较为明显，沿着降水梯度，针叶林和阔叶林

在表层 10cm 附近土壤平均粒径增大，不过针叶林在土壤形成过程中土壤粒径的差别远远没有阔叶林那样明显，成土过程作为一个长期的过程，针叶林和阔叶林的成土机制中植被的作用很可能强度不同。

表 4.2 降水梯度下森林植被土壤分层平均粒径

森林植被	地点	10	30	50	70
油松	三道河口*	252.236	248.435	236.191	250.899
	源水头	319.218	321.17	294.212	378.97
	甘其纳尔斯	311.578	280.709	316.818	N/A
白扦	白扦坑	229.428	319.357	334.831	362.248
	白音敖包	289.193	288.399	260.455	285.79
	草原站	299.450	301.788	281.783	395.163
山杨	松树井子	107.304	101.296	100.502	109.843
	好鲁库	155.617	217.364	207.586	246.053
	草原站	253.987	286.293	307.752	315.742
白桦	白扦坑对面	86.396	85.781	94.565	N/A
	源水头	319.218	321.17	294.212	378.97
	甘其纳尔斯	329.075	478.415	557.419	567.248

* 油松林在阳坡

4.3.3.2 植被土壤机械组成差别

在分析平均粒径的基础上，对土壤机械组成采用粒径分级方式进行进一步分析，首先采用国际土壤质地分类标准进行分类，计算每一粒级土壤颗粒所占体积百分比。分类标准为：砂粒：0.02-2mm，粉砂：0.002-0.02mm，黏土：<0.002mm（20-2000 μm ，2-20 μm ，<2 μm ）。部分结果如图 4.3 所示。

图 4.16a 表明整个研究区域内土壤为明显砂质土，砂砾含量达到 94.41%，粉砂和黏土含量分别为 4.13%和 0.46%。砂砾含量到黏土含量的变异系数逐渐增大，从 0.09 到大于 1，表明砂砾含量的区域均一性明显，粉砂质颗粒含量随地点变动很大，区域内基本上没有黏土成分。区域内阴坡和阳坡三种粒径含量均有显著差别，阳坡的砂砾含量显著大于阴坡（ $p<0.01$ ），而粉砂和黏土阴坡显著大于阳坡（ $p<0.01$ ）。阴坡和阳坡三种粒径含量的变化趋势和波动情况与区域整体趋势一致，阳坡比阴坡的变异系数稍小。

图 4.16b 表明区域内随着剖面深度加深，砂粒比例上升，粉砂和黏土比例下降，砂粒含量变异性逐渐减小，表明深层成土作用弱，与砂性母质构成越来越接近。这种随深度变化的颗粒组成变化在阴坡和阳坡与区域趋势一致（图略），在各层位上，阳坡的颗粒组成变异系数都小于阴坡，表明每一层位阳坡的土壤发育由于类似的植被背景和土壤母质具有相似性。

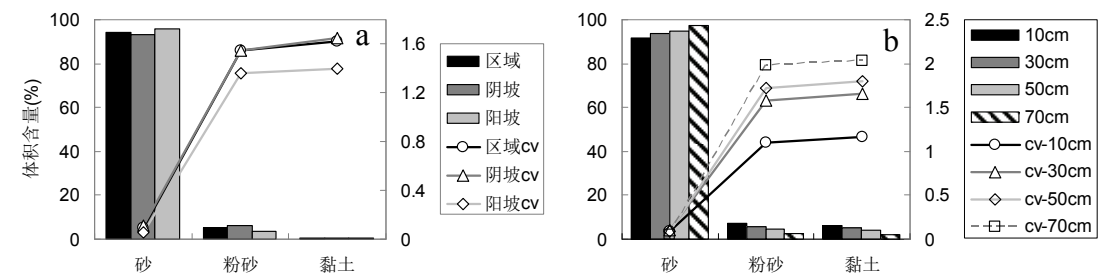


图 4.16 土壤三级粒径组成 位置比较(a) 层位比较(b)

原假设阴坡各层粒度不小于阳坡的成对样本 t 检验单侧检验 p 值标识如表 4.3 所示，由于黏土含量很低，在各层位上没有可比性；70cm 处成土作用在林下和草原都很微弱，p 值很大，阴阳坡没有差异，其他层位两坡向砂粒和粉砂含量存在差异，粉砂含量在 50cm 差别显著，表明由于阴坡 50cm 有生长良好的阔叶林，成土作用较强。

表 4.3 阴阳坡层位粒度差异显著值 p（黑体 p<0.1）

层位	砂	粉砂	黏土
10cm	0.071	0.069	0.106
30cm	0.076	0.073	0.104
50cm	0.043	0.041	0.110
70cm	0.469	0.472	0.431
区域内	<0.01	<0.01	<0.01

综上所述，区域内土壤黏土含量极低，粉粒含量可能对土壤水分和养分的作用更为重要，同时，区域砂质土壤内砂砾含量按照以上标准在各个地点没有明显区别，需要知道是否不同粒级的砂砾对土壤质地的影响不同，因此，对砂砾和粉砂部分做进一步的分析。采用美国农业部 1952 年土壤粒级划分标准：≥2mm 为石砾；2-1mm 为极粗砂；1-0.5mm 为粗砂；0.5-0.25mm 为中砂；0.25-0.1mm 为细砂；0.1-0.05mm 为极细砂；0.05-0.002mm 为粉粒；≤0.002mm 为黏粒。根据研究需要重分成 5 组：>0.5mm 为粗砂及以上（下为粗砂）；0.5-0.25mm 为中砂；0.25-0.1mm 为细砂；.1-0.05mm 为极细砂；<0.05mm 为粉粒及以下（下为粉粒）。

图 4.17a 表明，整个研究区内中砂和细砂含量最大，变异很小，是土壤粒径的主要组成部分，粒径由粗到细变异系数呈 U 形，粗粒和细粒部分变异性强。阴坡和阳坡两个地形部位土壤颗粒粒级组成类似，不同粒级含量的变化趋势和变异性趋势与整个区域一致。阴坡和阳坡的显著差异在细砂、极细砂和粉粒的含量上：阳坡具有更多的砂质，阴坡具有更多的粉粒以下级颗粒，这种趋势与上文三级土壤分类一致。各个粒级含量变异系数都是阴坡比阳坡大，可见阴坡由于多种

植被类型不同的影响，土壤质地存在差异。阴、阳坡粗砂和中砂的含量没有显著区别，表明这不是影响植被生长和土壤水分等其他因素的关键。

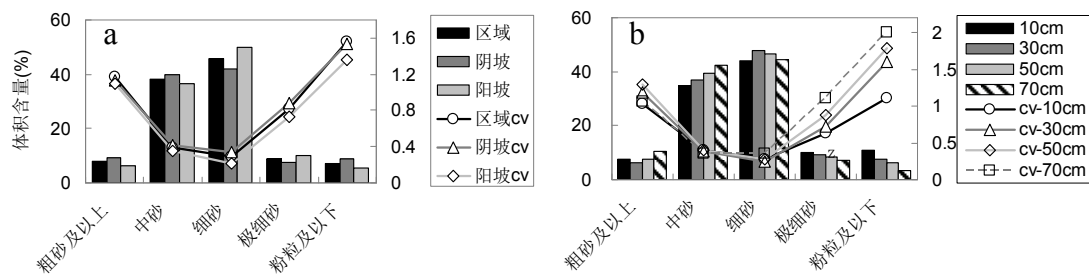


图 4.17 砂含量细分后土壤各粒级含量 位置比较(a) 层位比较(b)

从区域土壤分层情况看（图 4.17b），粗砂和中砂含量随深度增加，极细砂和粉粒减少，40 厘米左右可能存在分界，上层细粒增多，下层粗粒增多，细砂含量大致相同。粗砂、极细砂和粉粒在 10cm 的变异最小，表明表层既反映了背景又是细颗粒稳定集中的地方。

从分层阴阳坡对比看，10cm 阴坡粉粒明显多于阳坡 ($p=0.07$)，粗砂少于阳坡 ($p=0.15$)；30cm 阴坡在粗砂多于阳坡，细砂和极细砂比较少，但粉粒稍多 ($p=0.07$)，可见 30cm 左右阴坡土壤没有 10cm 细。50cm 的砂粒含量在阴坡和阳坡几乎不存在差异，粉粒以下粒级的含量阴坡多于阳坡但变异大，极细砂阳坡多 ($p=0.09$)；70cm 阴坡粗砂增多，中砂也比较多 ($p=0.08$)，细砂 ($p=0.08$) 和极细砂都少，粉粒以下稍多 ($p=0.11$)，说明到 70cm 已经不存在阴阳坡的差异了。

由此可见，在砂质土壤背景下，区域内土壤各粒级中比例最大的是中砂和细砂，两者含量在阴坡和阳坡差别不大，极细砂和细砂含量在阳坡高，粉粒含量在阴坡高。所有样点各粒级含量与平均粒径最相关的是粗砂和极细砂，相关系数达到 0.882 和 -0.757，而所有粒级含量的相关性都在 0.001 水平上显著。平均粒径从细砂开始与该粒级含量呈负相关，表明粗砂和中砂使得土壤机械组成偏粗而细砂以下使土壤出现较细的趋势，因此在砂质土壤发育过程中更粗的颗粒如果能被逐渐分散成至少细砂级的颗粒，都可以土壤质地逐渐变细。

4.3.3.3 典型森林土壤机械组成

研究区土壤发育受地形和植被影响存在差异性，考虑到同一剖面各层发育的一致性和表层土壤发育的代表性，以四种森林各一个样点 10cm 层土壤进行对比，可以对交错带植被-土壤关系的复杂性有更直观的了解。机械组成显示阔叶林林下土壤粗砂、中砂含量少，细砂以下粒级颗粒含量高，针叶林粗极细砂以下含量少（图 4.18a），表明阔叶林林下的成土作用带来了更多的细颗粒，这对于土壤水

分保持意义重大。阔叶林表土粒度具有双峰分布，主峰与针叶林的单峰相比靠左，峰值低，次峰在粉粒级附近，是机械组成偏细的原因（图 4.18b）。

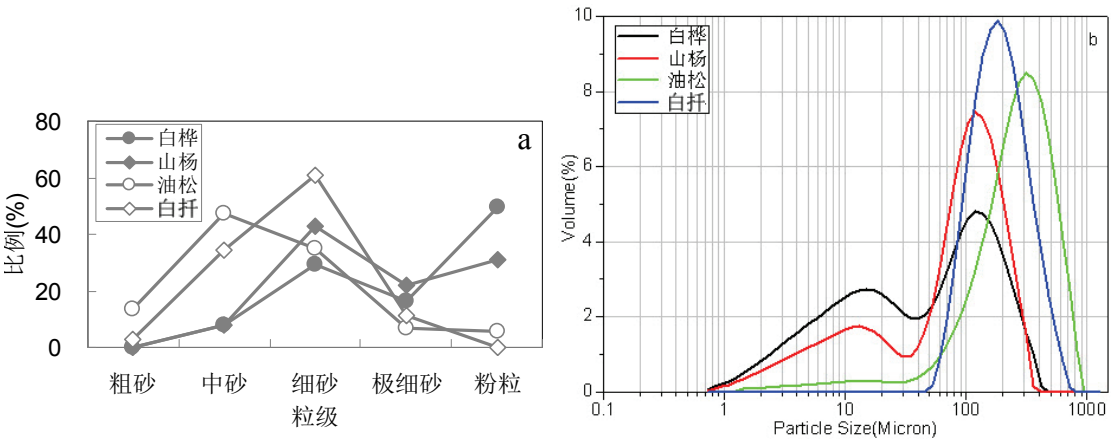


图 4.18 森林土壤机械组成与粒度分布 各粒级含量(a) 粒度分布(b)

森林和对应草原 10cm 土壤机械组成对比表明，白桦林和山杨林对土壤性状的变化比草原强，粉粒比例增加；油松和白扦林下与对应草原差别不大(图 4.19)。

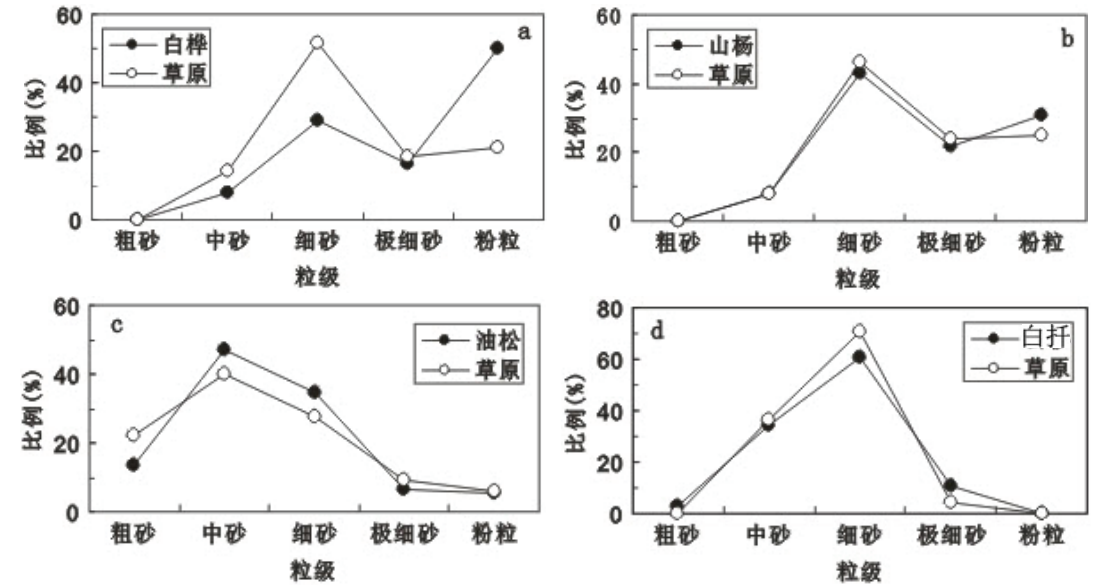


图 4.19 森林和草原土壤机械组成

4. 3. 2 土壤机械组成与土壤含水量

4. 3. 2. 1 土壤机械组成与田间持水量

土壤含水量与土壤机械组成有关，研究表明，表层土壤（5cm）含水量与土壤含砂量负相关（何思源等，2008）。本文进一步分析 10cm 和 30cm 层田间持水量与土壤机械组成的关系。

由土壤机械组成分析可知区域内土壤具有砂质的一致性和其他粒级含量的差异性。研究表明，土壤田间持水量与粉粒以下粒级的颗粒含量关系最大，其次

是中砂含量（表 4.4）。粉粒以下粒级的颗粒含量越大，田间持水量越大，中砂含量越大，田间持水量越小。

阴坡具有显著相关性的是极细砂、粉粒以下、中砂和粗砂含量，极细砂颗粒含量的增多在阴坡预示着成土作用的进一步进行。阳坡仅有粉粒以下颗粒含量对田间持水量具有显著地正向影响，由于阳坡土壤细粒比例低，机械组成更不均一，田间持水量对其敏感性高。

从层位上看，10cm 和 30cm 层极细砂作用不显著，30cm 层粉粒含量对田间持水量的作用更明显，粗砂含量有显著负作用。

阴坡 10cm 土壤机械组成的影响大而显著，特别是中砂和粉粒含量，表明阴坡表层成土作用在植被影响下十分强烈，阳坡表层虽然没有显著相关关系，但粉粒含量影响很大。阳坡 30cm 层粉粒含量与田间持水量显著正相关。由此可见，阴坡表层森林土壤机械组成相对均一，粗粒和细粒含量分别减少和增加田间持水量；阳坡粉粒含量少，田间持水量对此含量更敏感。

表 4.4 土壤机械组成与田间持水量关系

粒级 粒径(mm)	粗砂以上 >0.5	中砂 0.25-0.5	细砂 0.1-0.25	极细砂 0.05-0.1	粉粒以下 <0.05
区域	-0.215	-0.386 ^c	-0.205	0.312 ^b	0.538 ^c
阴坡	-0.488 ^b	-0.516 ^b	-0.239	0.554 ^c	0.553 ^c
阳坡	-0.101	-0.234	-0.144	0.106	0.480 ^a
10cm	-0.268	-0.395 ^a	-0.155	0.340	0.522 ^b
30cm	-0.383 ^a	-0.378 ^a	-0.267	0.287	0.544 ^c
阴坡 10	-0.609 ^b	-0.777 ^c	-0.250	0.584 ^b	0.901 ^c
阳坡 10	-0.127	-0.208	-0.044	0.145	0.344
阴坡 30	-0.325	-0.473	-0.110	0.542 ^a	0.503 ^a
阳坡 30	-0.361	-0.288	-0.174	0.112	0.629 ^b

a: $p<0.05$, b: $p<0.01$, c: $p<0.001$

用四种森林类型采样点土壤样本的平均粒径与田间持水量做相关，结果表明由于油松林和白扦林土壤整体组成偏粗，田间持水量具有均一性，相比机械组成更为复杂的山杨林和白桦林，平均粒径与田间持水量的关系不那么密切。而对阔叶林而言，平均粒径越大，田间持水量越小，表明发育良好的林下土壤细粒物质对于田间持水量的贡献很大。

表 4.5 平均粒径与田间持水量关系

森林类型	油松林	白扦林	山杨林	白桦林
平均粒径均值	274.8	274.3	192.7	254.3
R	-0.370	0.374	-0.602*	-0.719*

* $p<0.05$

4.3.2.2 土壤容重与土壤水分含量

土壤容重是土壤的一个基本物理形状,对土壤水分入渗和持水能力有很大的影响。自然条件下土壤容重由于受到成土母质、成土过程、气候、生物作用等,是一个高度变异的复合体,研究区内明显的地形分异和不同的植被类型必然导致不同的土壤容重,反映潜在的不同持水能力。研究区矿质土壤层较薄,在上层30cm以10cm为间距测定土壤容重。

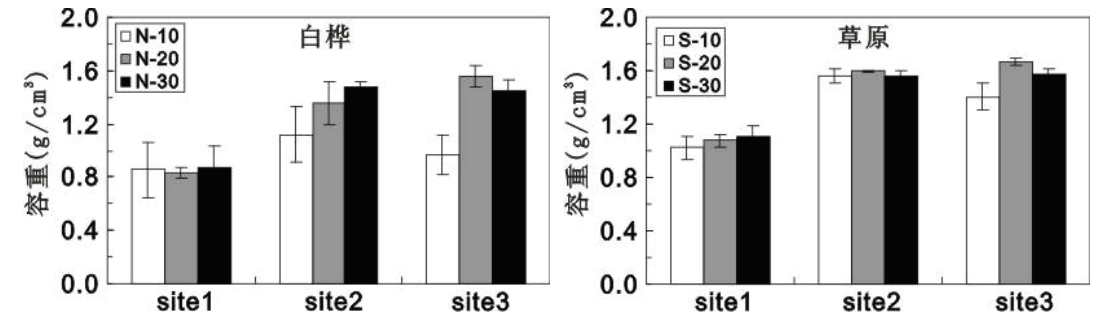
研究区土壤容重较大,并随深度增加而增加,10cm、20cm和30cm均值分别为1.17,1.32和1.35g/cm³,变异系数减小。林下和草原土壤容重变动和波动趋势与区域整体一致,森林各层容重均值都小于草原相应层位(p<0.001),但变异系数较大,表明区域内草原土壤容重更为均一,成土情况较森林简单。方差分析(ANOVA)表明,林下和草原土壤不同层位的容重差异是显著的(森林:p=0.001,草原:p=0.018)。

降水梯度和坡向都对土壤容重有影响,坡向反映了植被类型差异,对容重的影响显著,降水梯度对容重的影响显著性弱,两者没有交互影响(表4.6)。

表4.6 植被和降水对土壤容重的方差分析结果

方差来源	平方和	自由度	均方	F统计量	显著系数
坡向(A)	1.148	1	1.148	34.668	0.026
降水(B)	1.060	2	.530	14.070	0.059
交互作用(AB)	.066	2	.033	.728	0.484
误差(W)	8.106	179	.045		

气候对成土的作用在研究区内主要体现在降水上,土壤容重在阔叶林下和相应的草原具有一定的梯度性(图4.20),随着降水量减少(从site1到site3),土壤容重增大,而且林下比草原更为明显,表明降水和植被共同影响对土壤发育。在油松林和白桦林没有发现降水梯度的影响,各层容重在降水梯度下没有一致的趋势。



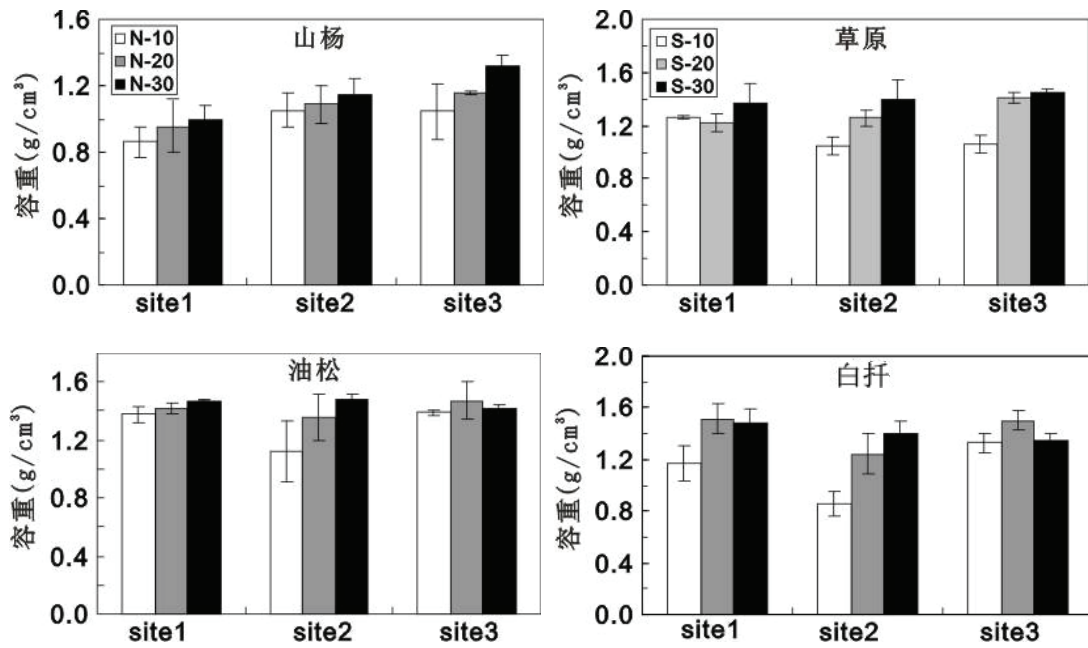


图 4.20 降水梯度下的容重变化

一般来说,土壤有机质含量高结构好的容重低。白桦和山杨林林下土壤容重比相应的阳坡草原或灌丛的土壤容重小(图 4.21a, b, $p < 0.01$),而白桦林在林下和草原没有显著的差异(图 4.21d),油松作为喜阳树种,在三道河口生长在阳坡,阴坡灌丛土壤容重小于林下(图 4.21c)。总体而言,针叶林本身对沙地土壤较为适应而改变较少,从土壤容重上几乎看不出对土壤形状的改良,而阔叶林则对土壤物理性状有明显的改善。

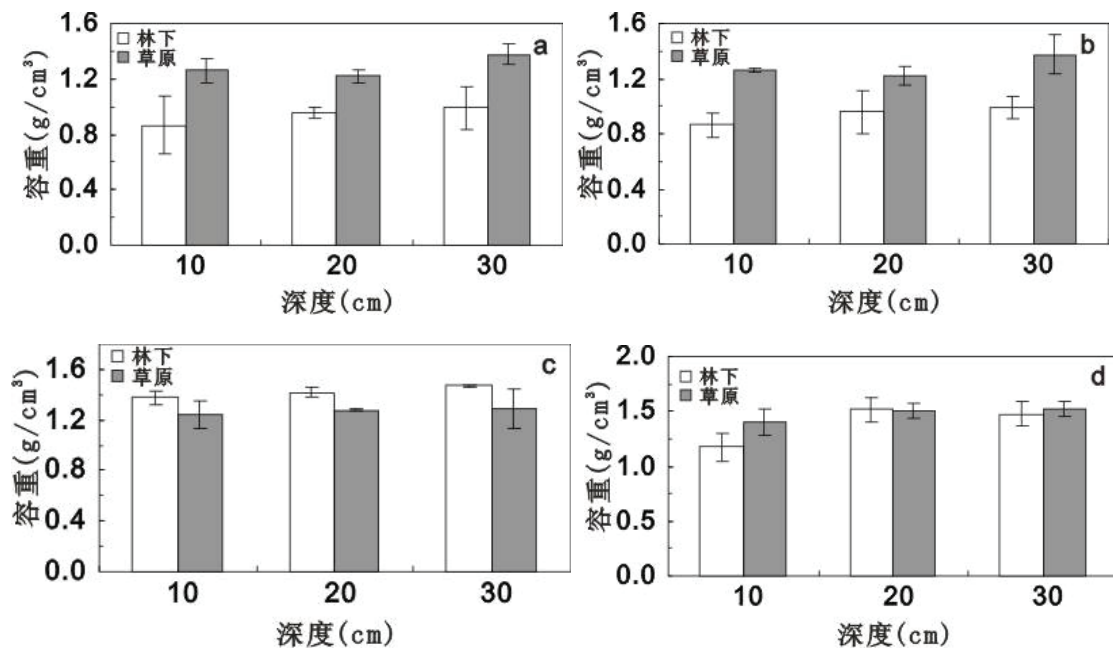


图 4.21 植被类型对容重的影响 白桦林(a) 山杨林(b) 油松林(c) 白桦林(d)

4.3.2.3 土壤机械组成推算的水分特征曲线

由于土壤机械组成存在差异，土壤水分的有效性并不能单以土壤含水量评估。粗质土壤绝大部分有效水吸持在 100kPa 吸力之下，植被根系对水分的吸力约为 1500kPa，如果在某一含水量条件下土壤对水分的吸附力小于该临界值，植物就可以吸收利用水分，否则就属于无法吸收利用的无效水。因此，用土壤粒径推算土壤水分特征曲线，可以反映土壤含水量与该含水量时土壤水所受的吸引力，从而判断一定的土壤含水量下水分的有效性。

经过计算的表层 10cm 土壤水分特征曲线如下图（-10kPa 以下的非饱和土），分别选择植被类型为油松林、白桦林和山杨林的三个地点（图 4.22）。从图中可以明显看出，土壤机械组成不同，水分特征曲线也存在较大差异。

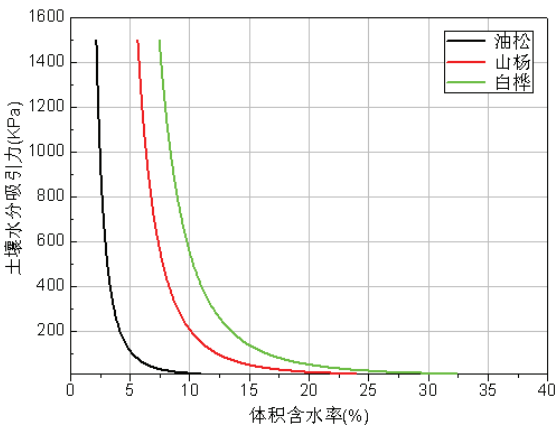


图 4.22 土壤水分特征曲线

下表给出了主要的土壤物理参数：

表 4.7 土壤物理参数			
参数	三道河口	松树井子	白杆坑对面
容重 (g/cm ³)	1.2	0.9	0.9
含水量 (质量%)	2	14.8	29.9
含水量 (体积%)	2.4	14.22	17.94
中值粒径 (μm)	190.747	98.947	52.235

对应到图中，油松林表层土壤水分吸力约为 1130kPa，白桦林仅为 80kPa，山杨林约为 60kPa。所以油松林所在地点表层土壤尽管含水量很低，但仍在有效水范围内。

4.4 小结

本章就森林-草原交错带土壤水分的空间分布和季节波动进行了分析，并详细分析了影响土壤质地的土壤机械组成。研究表明，在局地尺度上，土壤粒度分布在森林和草原区别很大，平均粒径与气候有关，同时又影响到土壤水分，进而影响到林草格局。空间上土壤水分反映了与降水梯度的一致性，但在高纬地区由于叠加了气温的影响而更加复杂。土壤水分的季节波动反映了森林和草原对水分利用的不同程度，是一种消耗后的状态。因此，尽管土壤质地和水分充分反映了森林草原交错带森林群落的生长环境，但是具有区域的局限性，只能反映某时间点或时间段森林群落局地分布对水分有效性的响应，无法进行长时期动态的植被生长与气候响应研究。

第五章 生物群区水平温带森林动态的决定因子

5.1 基于 NDVI 分析的森林与草原对过去 21 年气候变化的响应

5.1.1 春季 NDVI 对春季气候响应的时空格局

春季（4-5 月）是生长的上升阶段（rising phase），达到一定积温后的绿化（greening）已是周知的事实。初始生长期的水资源包括融雪和春季降水。冬季降水一般以降雪的形式下落，积存在地表并在春季温度回升时融化下渗。

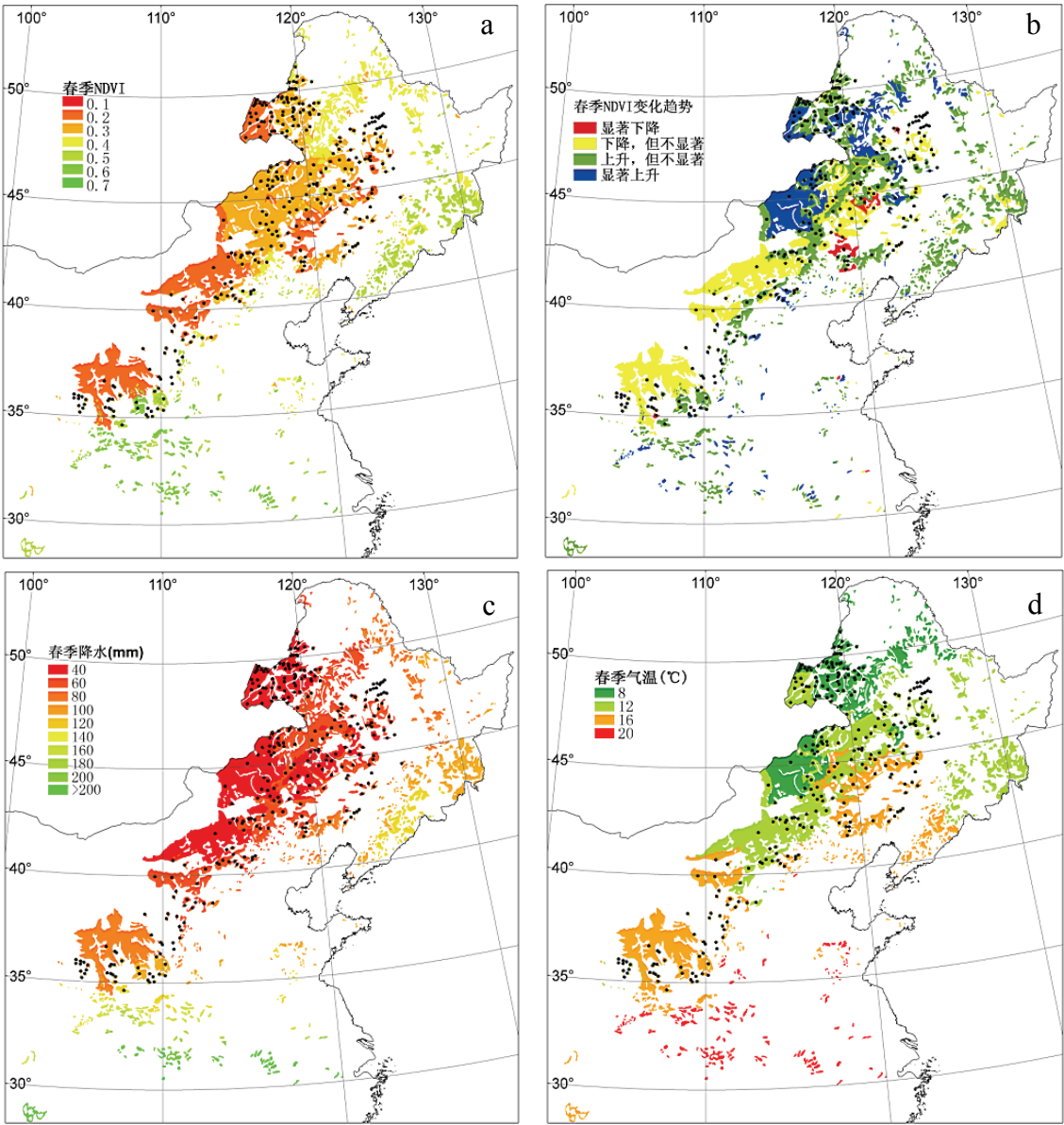


图 5.1 春季 NDVI 分布、变化趋势以及气候因子分布（点所在斑块为温带草原）

温带落叶阔叶林和温带草原春季 NDVI、冬季降水、春季降水和春季气温具

有一定的时空分布。森林春季 NDVI 分布反映了热量影响下由南向北绿化开始的早晚，草原斑块分布相对集中，纬度趋势弱，整体小于森林（图 5.1a）。森林 21 年来春季 NDVI 基本处于上升趋势，草原西南部为不显著的下降，东北部上升（图 5.1b）。森林春季降水自南向北减少，草原春季降水自西南向东北递减（图 5.1c），冬季降水类似；春季气温与纬度相关，自南向北减小（图 5.1d）。

研究区域内森林和草原春季 NDVI 对冬春降水响应不同。森林春季 NDVI 随冬春降水增大逐渐达到稳定（图 5.2a,b），分别在春季降水量 220mm 左右以及冬季降水量 120mm，相关系数分别为 0.66 和 0.52 ($p < 0.0001$)。草原 NDVI 在达到一定降水量后迅速上升（图 5.2c,d）。

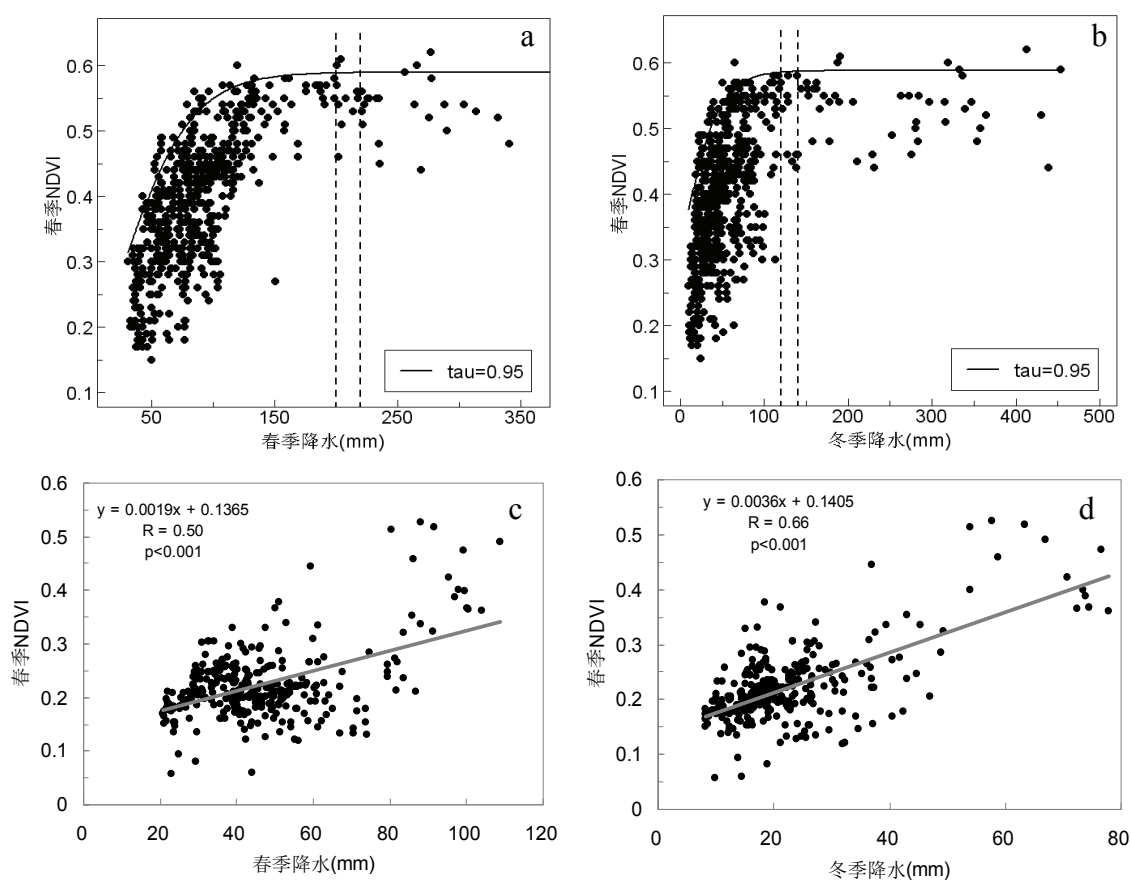


图 5.2 春季 NDVI 与春冬降水量的关系 森林(a, b) 草原(c, d)

森林和草原春季 NDVI 与春季月均温显著正相关（图 5.3），相关系数分别为 0.56 和 0.20 ($p < 0.01$)，森林响应更强。

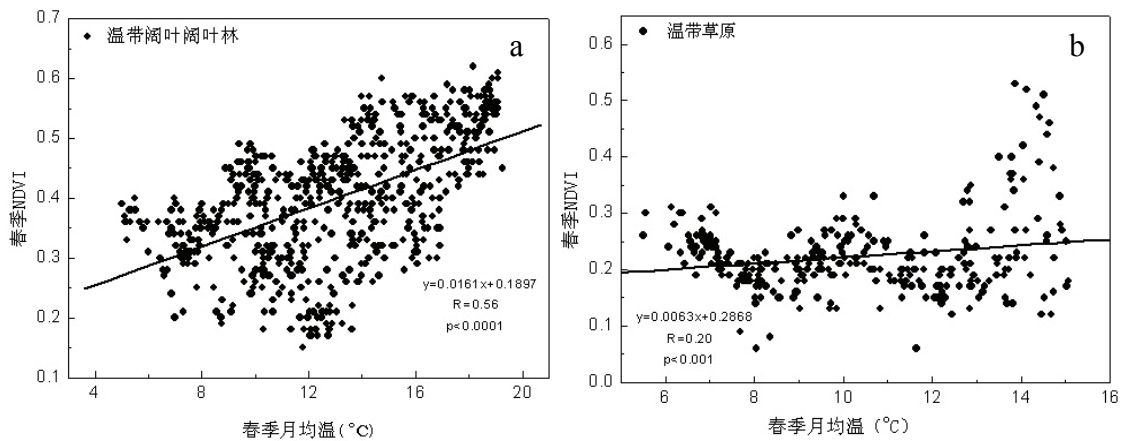


图 5.3 春季 NDVI 与春季月均温的关系 森林(a) 草原(b)

在年际变化上,森林冬季降水略有上升,春季降水波动下降(图 5.4),NDVI 显著地上升 ($p < 0.05$),并与冬春降水显著正相关(图 5.4a,b)。草原冬春降水都不显著地下降,NDVI 不显著地上升,并与春季降水显著正相关,与冬季降水不显著地正相关性(图 5.4c,d)。

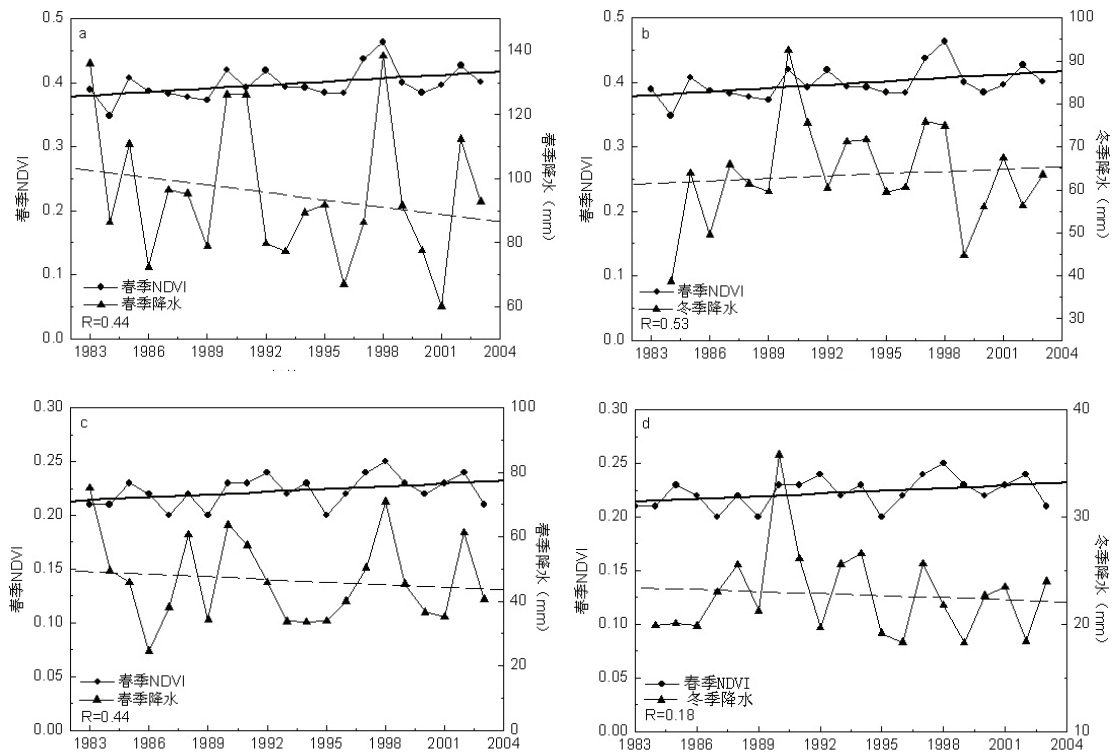


图 5.4 春季 NDVI 和春冬降水量的时间序列 森林(a, b) 草原(c, d)

森林和草原春季月均温逐年波动显著上升,春季 NDVI 与春季月均温显著正相关(图 5.5)。

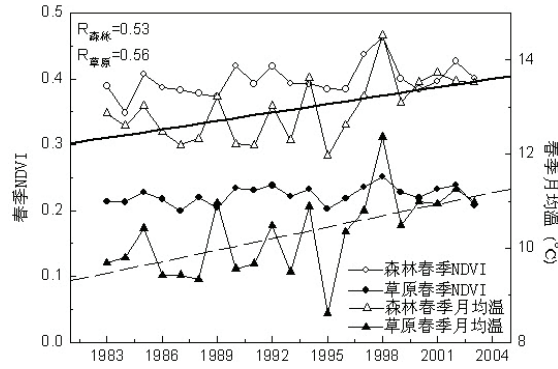


图 5.5 春季 NDVI 和春季月均温的时间序列

气候平均状况影响 NDVI 对气候年际变化的响应敏感性。森林和草原春季 NDVI 对春季温度年际变化的正反馈程度随着植被所在地多年平均春季温度的升高而显著减小，在平均气温过高时负反馈的可能性增大（图 5.6a,b, $p < 0.01$ ）。同时，气候年际变化趋势也影响 NDVI 响应的敏感性。春季月均温明显上升的地区 NDVI 的正反馈强，冬季降水明显减少的地区 NDVI 的正反馈弱，春季降水明显减少的森林地区 NDVI 的正反馈弱，草原则没有明显规律。

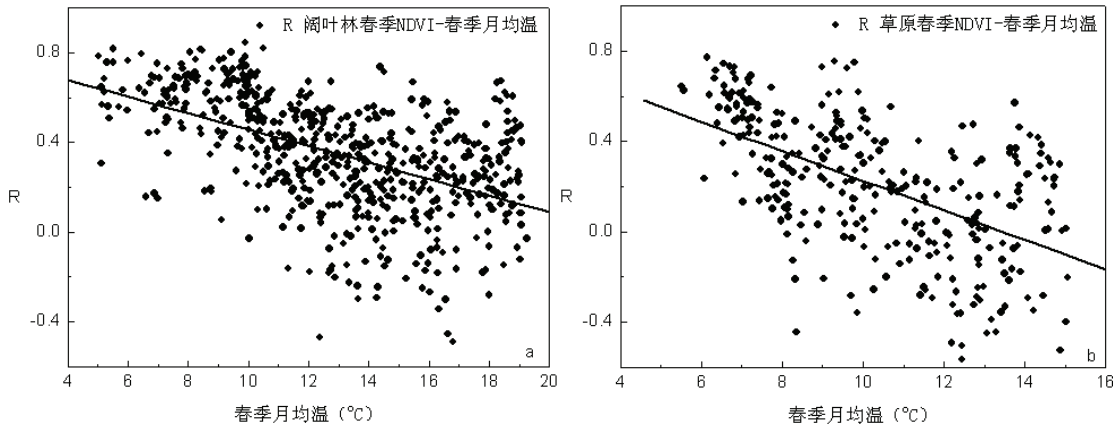


图 5.6 多年平均春季月均温对时序响应的影响 森林(a) 草原(b)

春季空间上水热同期促进森林和草原生长，尽管 NDVI 年际波动趋势与春季降水不一致，但森林和草原 NDVI 与冬春降水呈正相关，与春季温度呈正相关，并由于波动趋势一致相关性更强。冬春降水对春季森林生长的促进作用具有饱和性而对草原具有一种积累到某个降水量后的快速增加性。可见，森林在降水较少的干旱极限春季 NDVI 远离饱和值 (0.6)，如果降水增加，春季生产力可能提高。春季气温对森林和草原 NDVI 都具有显著地促进作用，气温高的地方生长季开始早，并且对森林的促进作用更显著。这表明空间上森林生长初期更多的受到温度的影响。相比之下，春冬降水对春季草原生长的影响更大，表明草原是受到降水控制的植被功能型，这在前人研究中已经得到证实 (Gu *et al.*, 2007)。结合相关

系数，气候年际波动表现为春季变暖对森林和草原春季生长的促进作用很大，春冬降水促进森林生长，春季降水促进草原生长。由于不同类型的草原对冬季降水的反馈并不一致（李晓兵等, 2000），冬季降水对草原影响不显著，但这种促进因素在年际上不容忽视。春季降水在森林和草原区都在下降，春季 NDVI 在森林和草原的上升更多的得益于春季温度上升。

5.1.2 夏季 NDVI 对夏季气候响应的时空格局

夏季（6-8 月）水热组合强烈的影响着植被生长，NDVI 均值反映了生长旺盛期的植被动态。

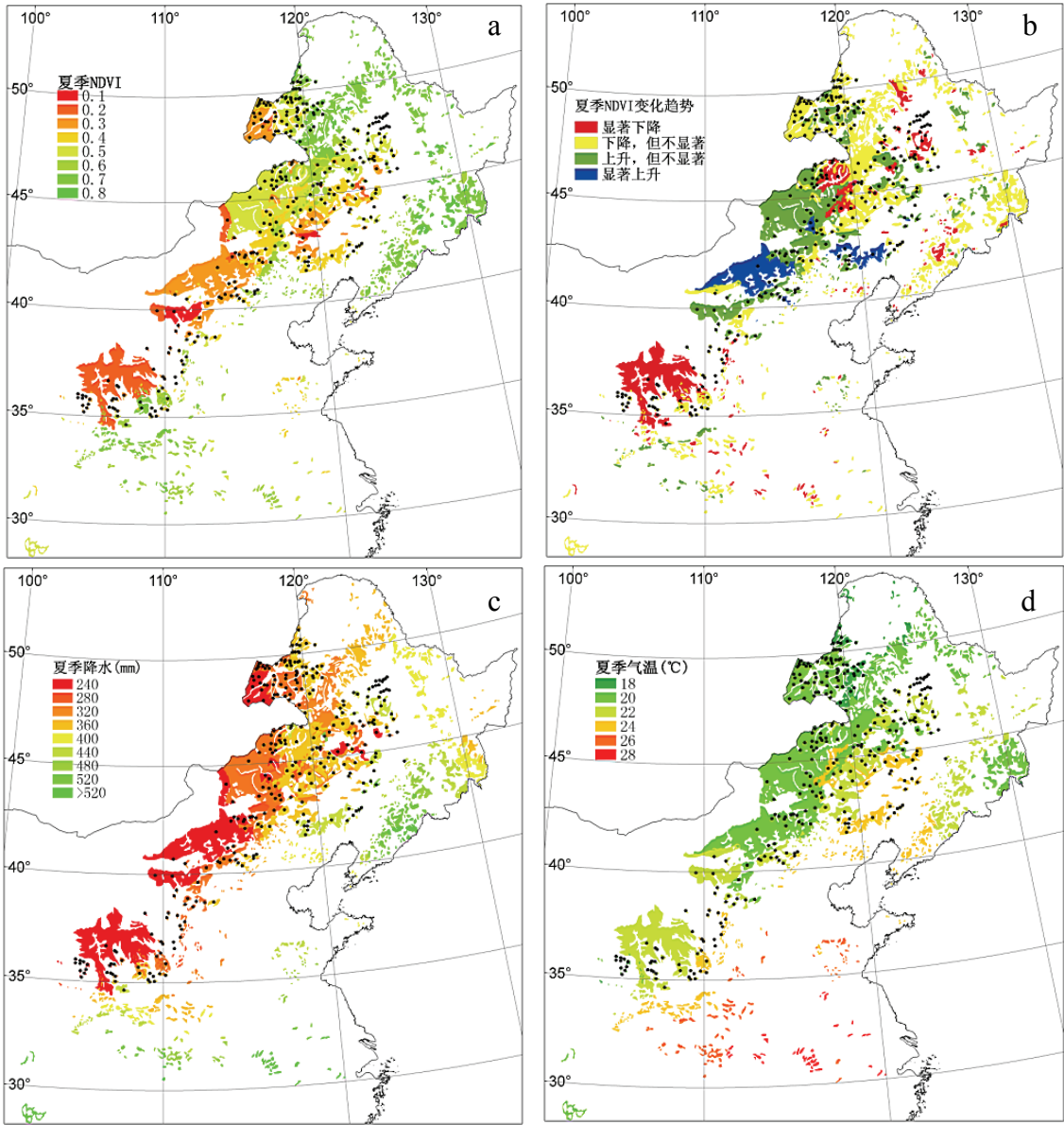


图 5.7 夏季 NDVI 分布格局、变化趋势和气候因子分布

温带落叶阔叶林和温带草原夏季 NDVI 均值、降水和月均温具有一定的空间

分布特征。森林夏季 NDVI 普遍较高，但在交错带有比较明显的低值，草原夏季 NDVI 在东北部高（图 5.7a）。森林夏季 NDVI 主要呈下降趋势，在南部有不显著的上升，草原南部和北部主要呈下降趋势，中部偏南为显著上升，偏北为不显著地上升（图 5.7b）。夏季降水在森林分布区具有明显的东南-西北递减趋势，在草原东北部降水较高（图 5.7c）。夏季月均温梯度小，具有纬向变化（图 5.7d）。

研究区域内森林夏季 NDVI 在降水量 400mm 左右达到饱和，经历一个平稳过程，在降水量达到 550mm 后 NDVI 会下降（图 5.8a）；草原 NDVI 与夏季降水量显著正相关，在降水量 300mm 左右达到极值，基本没有平稳过程 NDVI 值就会下降（图 5.8b）。夏季 NDVI 与夏季月均温显著负相关（图 5.8c,d），相关系数分别为-0.32 和-0.23（ $p<0.01$ ），森林响应更强。

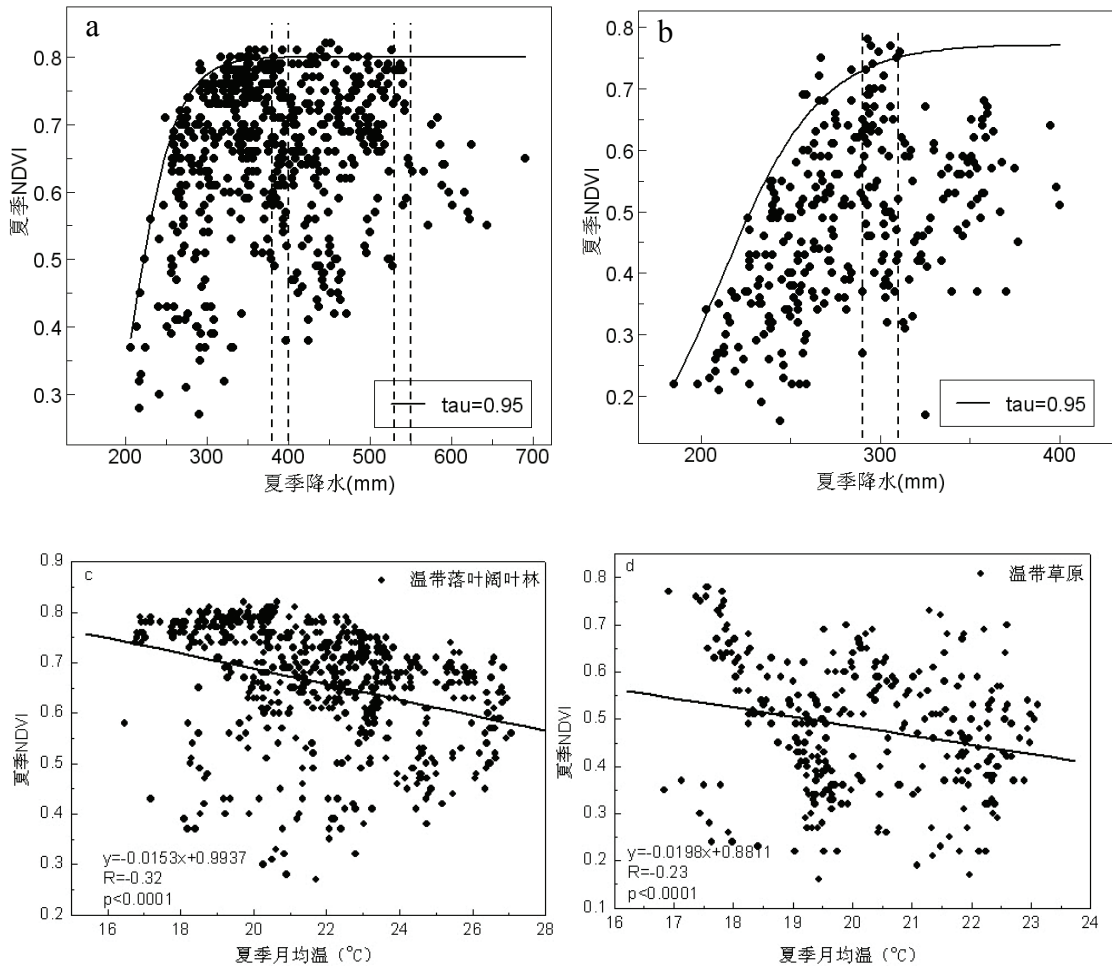


图 5.8 夏季 NDVI 与夏季降水量和气温的关系 森林(a, c) 草原(b, d)

在年际变化上，森林和草原夏季降水下降，森林夏季 NDVI 显著减小，草原夏季 NDVI 不显著地减小，都对夏季降水正相关，森林区域不显著（图 5.9a,b）。森林和草原夏季月均温显著上升，夏季 NDVI 则与温度不显著地负相关(图 5.9c)。

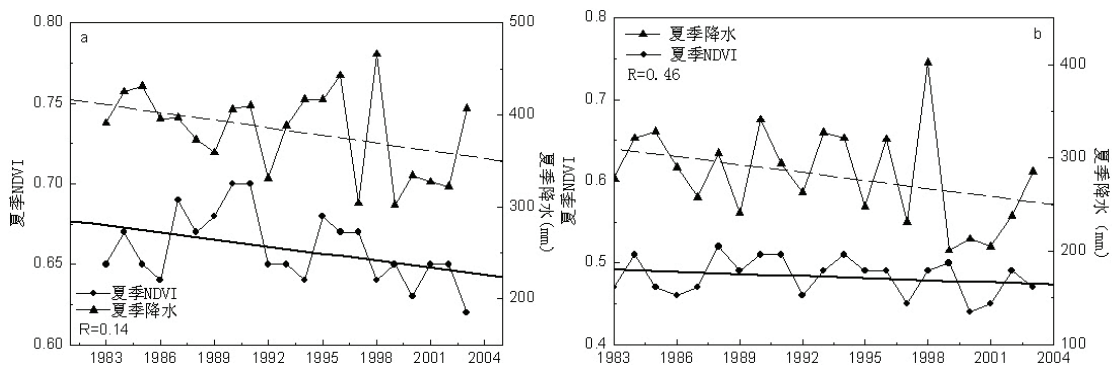


图 5.9 夏季 NDVI 和夏季降水的时间序列 森林(a) 草原(b)

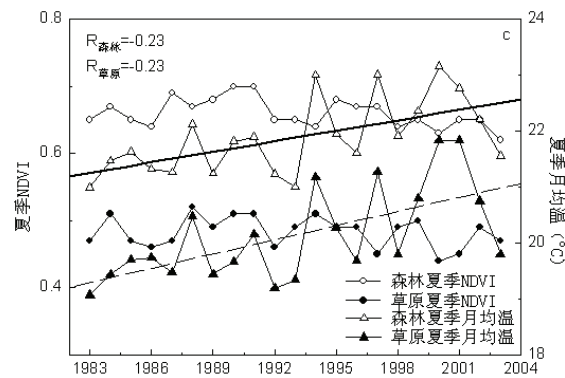
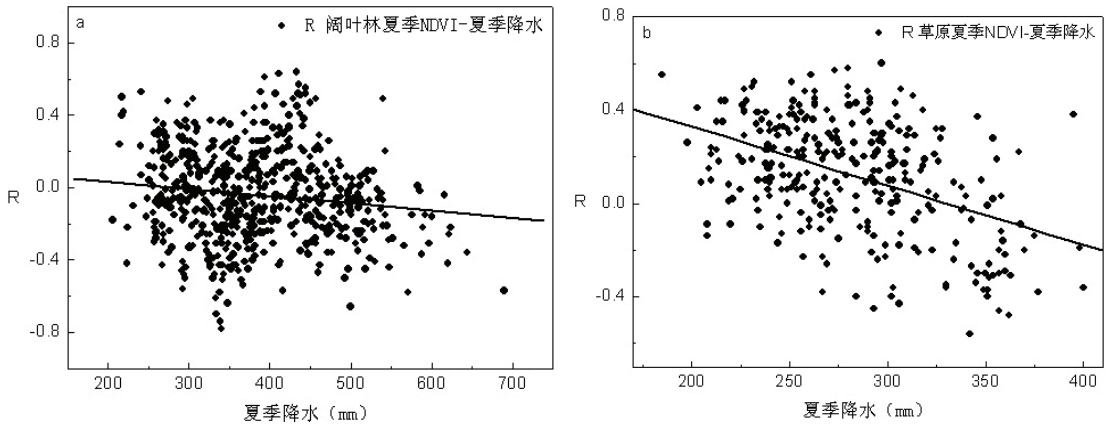


图 5.9 夏季 NDVI 和夏季月均温的时间序列(c)

夏季气候平均状况影响 NDVI 对气候年际变化的响应敏感性,对草原影响更明显。森林和草原夏季 NDVI 对夏季降水的正反馈程度随植被所在地多年平均夏季降水量增大而减小, (图 5.10a,b, $p<0.01$)。草原夏季 NDVI 对夏季月均温的负反馈随植被所在地多年平均夏季月均温增大而增大 (图 5.10d, $p<0.01$), 但森林在夏季月均温大于约 22°C 后, 夏季 NDVI 对夏季月均温的负反馈减弱 (图 5.10c, $p<0.01$)。同时, 气候年际变化趋势也影响响应敏感性。夏季降水明显减少的草原地区 NDVI 对降水正反馈强, 夏季气温明显升高的森林区域负反馈强。



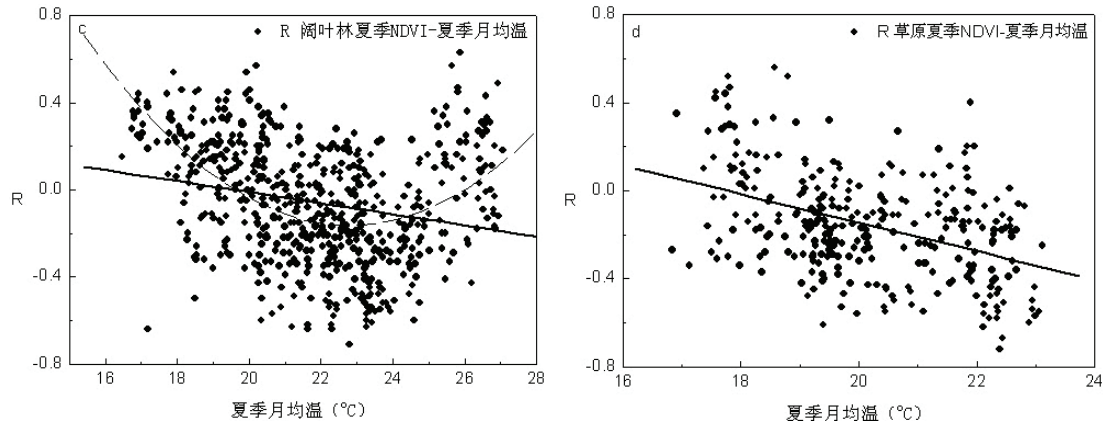
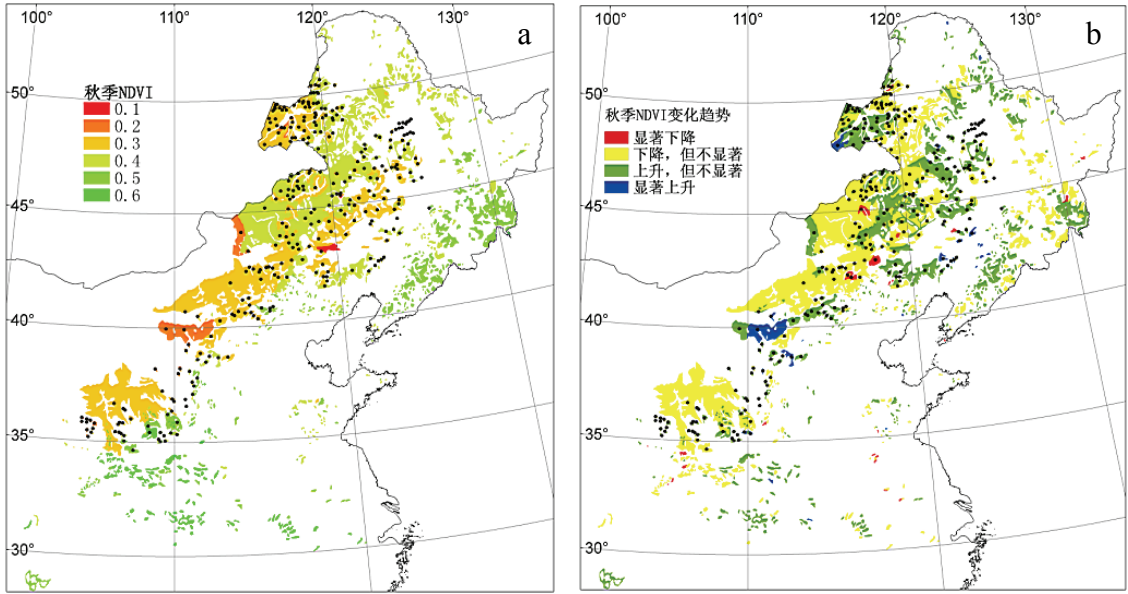


图 5.10 多年平均夏季气候因子对时序响应的影响 森林(a, c) 草原(b, d)

研究区内森林 NDVI 对降水的响应具有饱和性，降水对草原促进作用更强。尽管一般认为生长旺季水热同期有利于植被生长，但夏季气温对夏季森林和草原生长却存在抑制作用。结合相关系数，气候年际波动表现为夏季降水对草原生长促进作用很大，对森林生长有一定促进作用，夏季气温升高对森林和草原生长都具有一定的抑制作用。

5.1.3 秋季 NDVI 对秋季气候响应的时空格局

秋季是生长的衰退阶段（falling phase），是温带落叶阔叶林的落叶季节，影响整个生长季长度和生物量。秋季 NDVI 反映了落叶实际的森林覆盖和生产力情况，对气候的响应可以帮助发现水热作用在落叶期的特征。



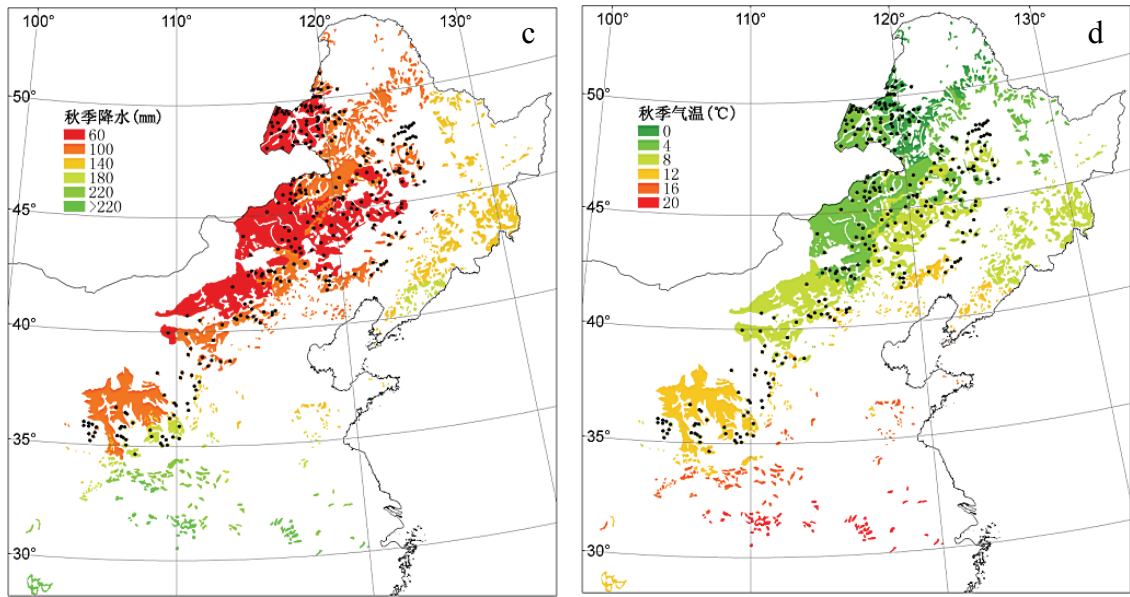
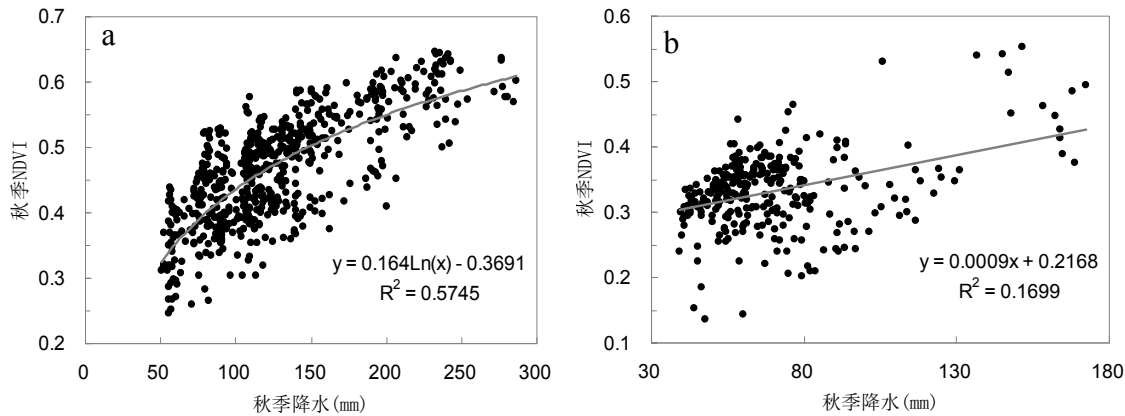


图 5.11 秋季 NDVI 分布格局、变化趋势和气候因子分布

温带落叶阔叶林和温带草原秋季 NDVI 均值、降水和月均温具有一定的空间分布特征。森林秋季 NDVI 由南向北递减，在交错带较低，东北部草原区高（图 5.11a）。森林秋季 NDVI 在交错带呈下降趋势，南部区域和东北主要呈上升趋势，草原秋季 NDVI 主要呈下降趋势（图 5.11b）。秋季降水在森林分布区具有明显南-北和东南-西北递减趋势，在草原分布区，秋季降水在西南较高（图 5.11c）；秋季月均温具有明显的纬向变化（图 5.11d）。

区域植被生长的气候响应在森林和草原地区具有差异性。森林和草原秋季 NDVI 与秋季降水显著正相关（图 5.12a,b），相关系数分别为 0.75 和 0.41 ($p<0.01$)，但草原秋季降水量在西南区域明显偏高，在整个区域不连续，在 100mm 以下时 NDVI 对降水的响应不显著。森林和草原秋季 NDVI 与秋季月均温显著正相关（图 5.12c,d），相关系数分别为 0.63 和 0.16 ($p<0.01$)。



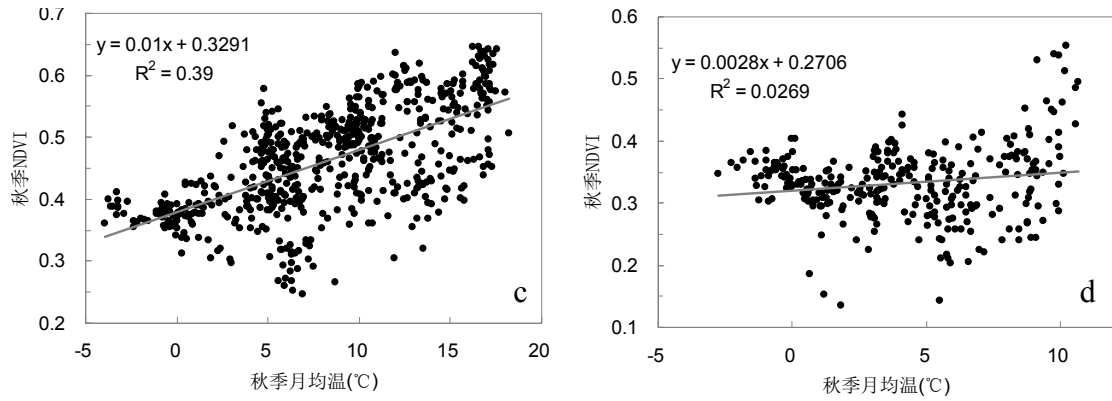


图 5.12 秋季 NDVI 与秋季降水 and 气温的关系 森林(a, c) 草原(b, d)

在年际变化上, 森林和草原秋季降水在下降, 但秋季 NDVI 在森林和草原没有明显趋势性 (图 5.13a,b)。NDVI 与降水不显著地负相关。森林和草原秋季月均温在上升, 森林区域上升更快 (图 5.14a,b), 秋季 NDVI 与气温显著正相关 ($p < 0.05$)。

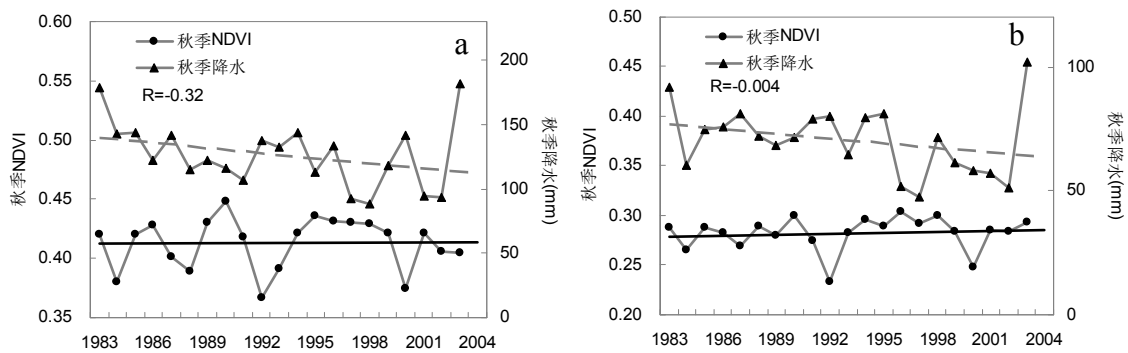


图 5.13 秋季 NDVI 与秋季降水的时间序列 森林(a) 草原(b)

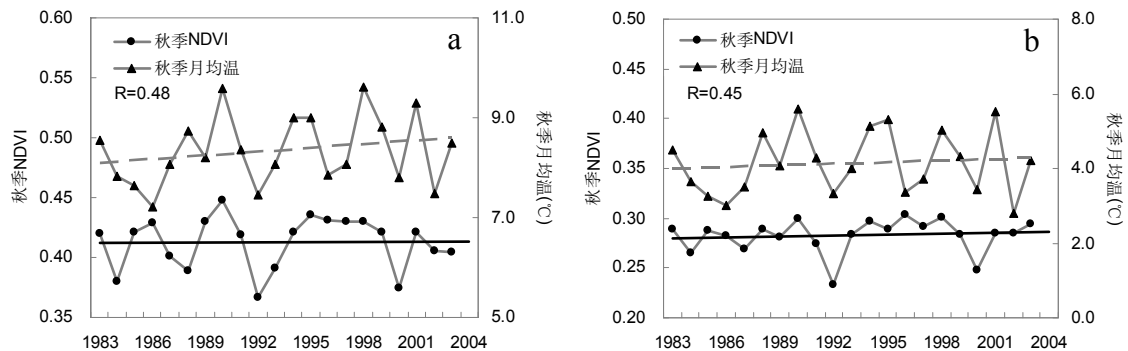


图 5.14 秋季 NDVI 与秋季月均温的时间序列 森林(a) 草原(b)

秋季气候平均状况影响 NDVI 对气候年际变化的响应敏感性。秋季 NDVI 对气温的正反馈程度随森林所在地多年平均秋季月均温升高而减小 (图 5.15, $p < 0.05$)。同时, 气候年际变化趋势也影响响应敏感性。秋季降水量明显下降的森林和草原地区, NDVI 负反馈强。秋季月均温明显上升的地区森林 NDVI 正反馈减小, 草原地区正反馈增强。

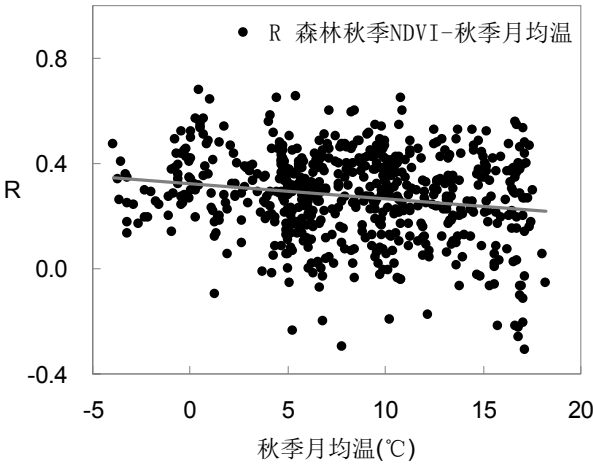


图 5.15 多年平均秋季月均温对时序响应的影响

研究区内秋季水热组合促进森林和草原生长，但对草原影响较弱，这可能 NDVI 所反映的植被叶面积情况有关，在落叶期（leaf senescence periods）NDVI 对叶面积指数很敏感（Wang *et al.*, 2005），森林落叶对叶面积指数影响更明显。秋季气候年际波动呈现暖干化，结合相关系数，秋季降水 and 气温协同维持森林秋季 NDVI，冷湿与暖干对森林 NDVI 的作用相似。秋季变暖对草原秋季生长具有促进作用。

5.1.4 生长季植被 NDVI 对气候综合响应的时空格局

季节 NDVI 与季节降水量和气温的区域相关性显示了空间植被格局的水热影响因子，年际相关性表明森林和草原两种不同植被类型 NDVI 对气候因子的响应机制。生长季平均 NDVI 含有完整生长周期内各季节气候因子的作用结果，以多元回归统计分析形成森林和草原空间格局的气候因子的作用（表 5.1），给出简单相关系数（0 order）和偏相关系数（Partial），后者表明单个因子在剔除共变因子情况下对生长季 NDVI 的影响。

表 5.1 生长季平均 NDVI 对季节性气候因子空间分布的响应

		降水				气温		
	R	春	夏	秋	冬	春	夏	秋
森林	0 order	0.453 ^b	0.391 ^b	0.551 ^b	0.288 ^b	0.219 ^b	0.190 ^b	0.237 ^b
	Partial	-0.017	0.189 ^b	0.419 ^b	-0.099 ^a	0.172 ^b	-0.092 ^a	-0.239 ^b
草原	0 order	0.118 ^a	0.449 ^b	0.273 ^b	0.316 ^b	-0.112	-0.065	-0.148 ^a
	Partial	-0.230 ^b	0.429 ^b	0.156 ^b	0.168 ^b	0.054	-0.212 ^b	-0.010

a:p<0.05,b:p<0.01

气候因子在时空尺度上是综合起作用的，不同气候因子之间的交互作用对植

被生长的实际影响与单季分析时的简单相关系数所揭示的响应关系可能不同。

偏相关分析表明,森林区域内上述气候因子单独作用时除春季降水外,对森林生长都具有显著影响:夏秋降水和春季气温促进了生长,冬季降水和夏秋气温抑制了植被生长,但是这只是在其他气候因素不变的条件下植被生长对单一气候因素变化的响应,冬季降水和夏季气温抑制作用显著性低($p < 0.05$),并且结合简单相关系数分析就会发现这些抑制因子在其他气候因子也变化的同时,其抑制作用实际上并没有表现出来,反而都成为植被生长的促进因子。冬春降水主要影响春季植被发芽展叶等,不同物种对具体降水量的响应存在差异,因此偏相关系数负值,显著性水平不同;夏季气温在达到一定值后对森林生长影响不大,反而可能引起水分不足,所以偏相关系数为负。这一方面说明气候因子存在协同作用,另一方面说明当气候异常变化打破了协同作用后,这些抑制性可能被表现出来。同时,单季气候因子对整个生长季的影响可能存在更明显的时滞效应。总体而言,森林区域上水热协同作用促进了森林生长,春夏降水简单相关系数低于秋季并不是两者的作用小,而是在空间上存在降水饱和作用,冬季降水对来年的生产力也存在促进,但是作用小而不稳定,夏秋气温对植被生长存在潜在的抑制作用,在夏季高温会引起的干旱影响光合同化作用,在秋季高温则可能引起森林提前落叶。

综合分析两种相关系数会发现,草原地区降水条件的影响大于气温条件。在气候因子共同作用下,夏季和冬季降水的影响大而显著。夏季气温的潜在抑制作用显著,但在其他气候条件共变时不明显,此时秋季气温抑制着草原生产力。

由于时间序列较短,气候因素影响的显著性水平低(表 5.2)。气候因子在时程上的变化趋势不同,前面分析表明,森林和草原区域的各季降水都在缓慢下降,而气温在显著上升。在这样的气候变化背景下,森林生长季平均 NDVI 对气候年际波动的实际响应(偏相关系数)与简单相关系数结果类似。春、夏、冬降水促进森林生长,秋季降水多的年份会因为影响地表辐射从而降温或降低光合作用;尽管春季 NDVI 对春季气温的年际波动正反馈,但春夏气温偏高时生长季 NDVI 减小,秋季气温促进生长季 NDVI,延长叶片进行光合作用的时间。草原春夏降水作用显著,秋季气温也具有促进作用,但秋冬降水都对生长季 NDVI 有一定的抑制作用,春季气温同样抑制生长季 NDVI。这表明,在目前的气候格局下,春夏降水仍然是促进草原生长的主导因子。

表 5.2 生长季 NDVI 对季节性气候因子年际波动的响应

		降水				气温		
R		春	夏	秋	冬	春	夏	秋
森林	0 order	0.485^a	0.198	-0.624^b	0.627^b	-0.105	0.006	0.443^a
	Partial	0.092	0.236	-0.684^b	0.521	-0.199	-0.171	0.068
草原	0 order	0.526^a	0.559^a	-0.044	0.344	-0.022	-0.095	0.491^a
	Partial	0.360	0.472	-0.271	-0.141	-0.206	0.049	0.462

a:p<0.05,b:p<0.01

综合上述单季植被与气候因子分析，气候因子的空间分布和年际变化对植被 NDVI 的影响存在不一致，季节气候因子对该季节 NDVI 的影响与其对整个生长季平均 NDVI 的影响不尽相同，植被生长对气候的反馈与气候因子的多年平均状况以及研究起点时间的气候状况关系密切。在整个生长季中季节性气候因子的作用可能出现差异，这些出现差异的因子可能是更为复杂的影响因子。对于森林而言，空间驱动因子差异主要是在冬季降水和秋季气温，而年际驱动因子只有春季气温有差异。综合森林生长的时空反馈可知，森林生长季平均 NDVI 的格局是由降水和气温共同决定的，夏秋降水多，冬季降水少，春季气温高，夏秋气温低的森林地区生长季平均 NDVI 大。冬季降水虽然出现抑制作用时，但由于冬季降水的影响持续时程短，仅对春季 NDVI 有一定作用。秋季气温抑制森林生长季 NDVI 是因为其他共变的气候因子作用被剔除后气温对生长季的延长可能转为引起暖干。森林生长季平均 NDVI 的年际波动受到冬、春、夏降水和秋季气温的正向促进作用，而受到秋季降水和春夏气温的抑制作用，考虑到单季 NDVI 变化，生长季 NDVI 变化没有太大的趋势性，而未来的变化则要看植被生长对气候因子变化的敏感性，才能确定促进和抑制作用的净效应。

5.2 基于模型模拟的森林生长对气候变化的响应

5.2.1 LPJ 模型植被格局模拟结果的验证

经过模型修改和参数调整,模拟的 547 个单元中,根据每个点最大 FPC(叶面积投影盖度)确定的植物功能型(PFT)可以确定有 409 个模拟单元为 LPJ 模型中设定的温带落叶阔叶林和北方落叶阔叶林(图 5.16),这些格点位置在数字化 1:400 万中国植被图中被划定为温带落叶阔叶林,模型的模拟准确率达到 75%。模型的偏差主要出现在 50°以北的部分点模拟为北方常绿针叶林,110°以东,30°-35°之间零星温带常绿阔叶林和温带常绿针叶林。

经过参数修正后 LPJ-DGVM 在中国温带落叶阔叶林区上层(50cm)土壤相对湿度的 103 年均值、2003 年结果与实测数据(30cm)对比(图 5.17),冬季偏低,可能由于实测地区土壤冻结保有固态水;生长季早期偏高,生长季内稍低,但在趋势上一致,其中可能存在土壤层差异的缘故。模型结果在生长季早期偏高,在区域模拟(Local scale)中俄罗斯的模拟单元上也存在这种现象(Sitch *et al.*, 2003)。

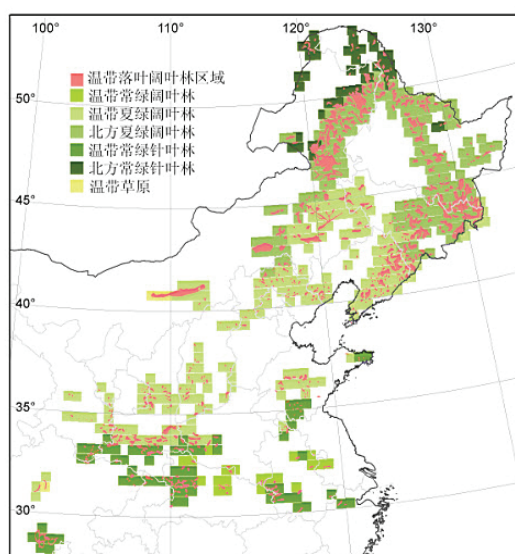


图 5.16 LPJ 模拟的现实植被格局

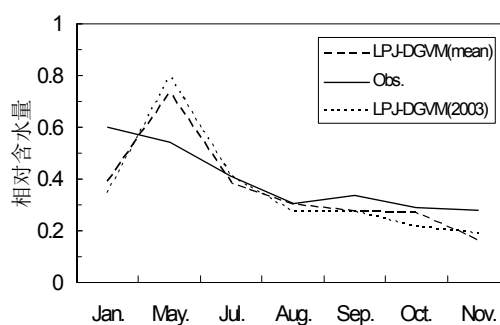


图 5.17 模拟结果与实测土壤相对湿度对比

将温带阔叶阔叶林区域内年 NPP 和 FPC 平均值与生长季 NDVI 平均值(1983-2003)进行比较(图 5.18),NPP 年际变化与生长季 NDVI 年际变化相关系数为 0.38 ($p < 0.1$),在趋势上是一致的,比 FPC 与 NDVI 的相关关系强。

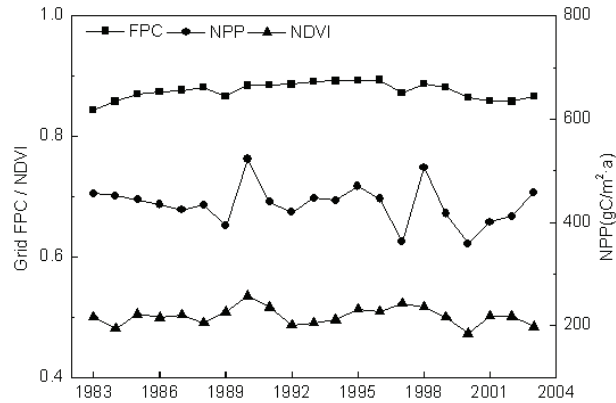


图 5.18 模拟 FPC、NPP 和生长季 NDVI 的年际波动

格点模拟的植被类型根据每个点最大 FPC 确定,表明每个格点还存在其他植被类型。温带落叶阔叶林的干旱极限附近模拟得到的植被类型主要是森林,其次是温带草原。图 5.19 以 117.25° , 41.75° 和 117.25° , 42.75° 两个格点说明不同功能型植被 FPC 与年降水量的关系。森林与草原 FPC 变化趋势相反,年降水量在 1960 年左右发生了趋势变化,由显著增加转为减少或基本不变,导致森林植被覆盖的下降或下降后的维持和缓慢上升。

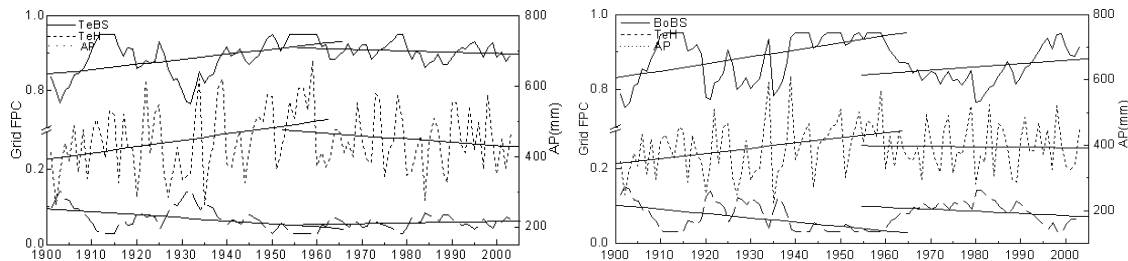


图 5.19 不同功能型植被 FPC 与年降水量变化趋势

模拟结果表明,反映植被生长平均状况的指标 FPC 和 NPP 对气候空间格局的响应在区域内具有一致性(表 5.3),在空间上 NPP 对降水的响应强, FPC 对气温的响应强。

表 5.3 研究区植被生长与不同季节降水和气温之间的偏相关性

R Partial	降水				气温		
	春	夏	秋	冬	春	夏	秋
FPC	0.034	0.207^b	-0.096	-0.117 ^a	-0.143^b	-0.031	0.192^b
NPP	0.133^b	0.337^b	0.020	-0.064	-0.119^a	-0.067	0.102^a

a: $p < 0.05$,b: $p < 0.01$

取 1983-2003 年气候和年 NPP 做同样分析,与 5.1.4 节结果对比。由于存在气候数据来源的不同、区域大小差异,以及 NDVI 表征的植被生产与模型运算的净第一性生产力本身的差异,在春季降水、春季和秋季气温方面存在响应方向的差

异，但这三个方面均有 NPP 或者 NDVI 的响应不够显著。

表 5.4 研究区 NDVI 和模拟 NPP 与不同季节降水和气温之间的偏相关性

R Partial	降水				气温		
	春	夏	秋	冬	春	夏	秋
NPP	0.107^a	0.269^b	0.036	-0.018	-0.049	-0.061	0.037
NDVI	-0.017	0.189^b	0.419^b	-0.099^a	0.172^b	-0.092^a	-0.239^b

a: $p<0.05$,b: $p<0.01$

5.2.2 植被生长对气候年际变化的响应

整个区域平均植被动态和气候年际变化在 1901 年以来（103 年）中存在某些趋势性，但是与 1983 年（21 年）以来的变化趋势存在差异（表 5.5），正相关表示上升趋势，负相关表示下降趋势 1983 年以来春、夏季降水明显减少，气温明显上升，区域内春、夏、秋都呈现暖干化。

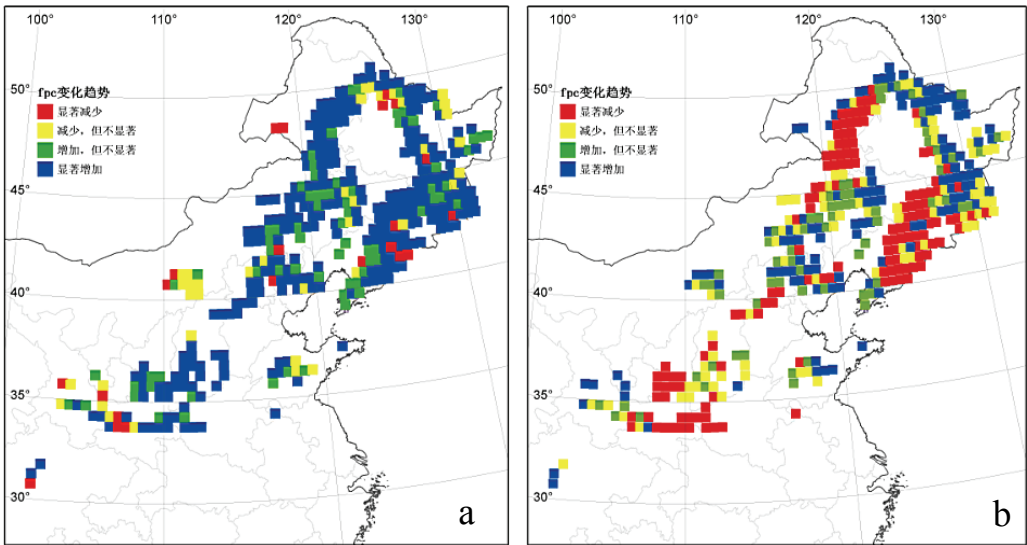
表 5.5 植被年际动态和气候变化趋势

R	植被生长		降水				气温				
	FPC	NPP	春	夏	秋	冬	年	春	夏	秋	年
103	0.75^b	0.64^b	0.01	0.11	-0.11	-0.07	0.05	0.33^b	-0.27^b	0.14	0.42^b
21	0.12	-0.25	-0.22	-0.33	-0.12	0.00	-0.29	0.30	0.38	0.08	0.48^a

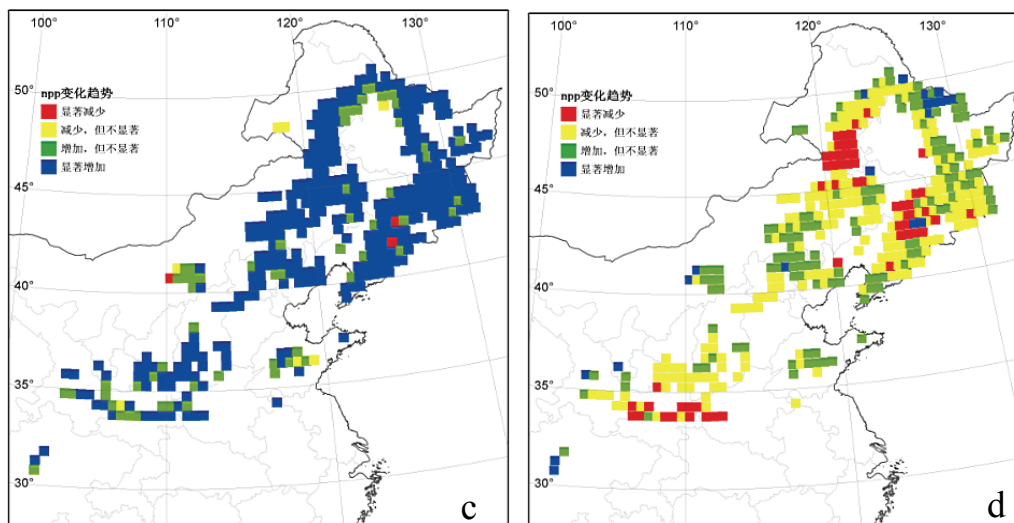
a: $p<0.05$,b: $p<0.01$

比较百年来和 21 年来植被生长年际变化和主要的季节性气候变化趋势，1901 年以来呈增加（减少）的区域（左），最近可能出现趋势的逆转或显著性减弱（右）。

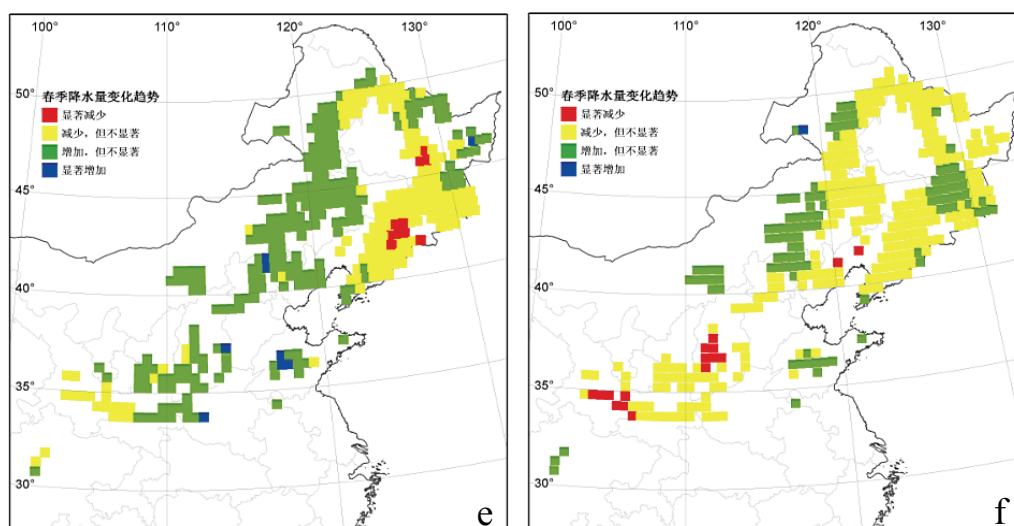
50%的区域 FPC 由增加变为减少，38%维持增加趋势（图 5.20a-b）。



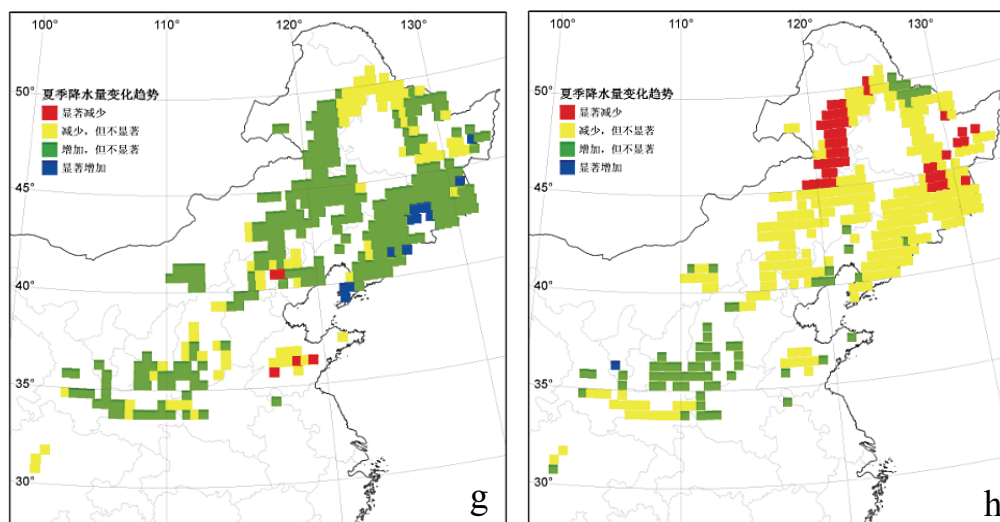
63%的区域 NPP 由增加变为减少，34%维持增加的趋势。维持增加的区域主要在东北部（图 5.20c-d）。



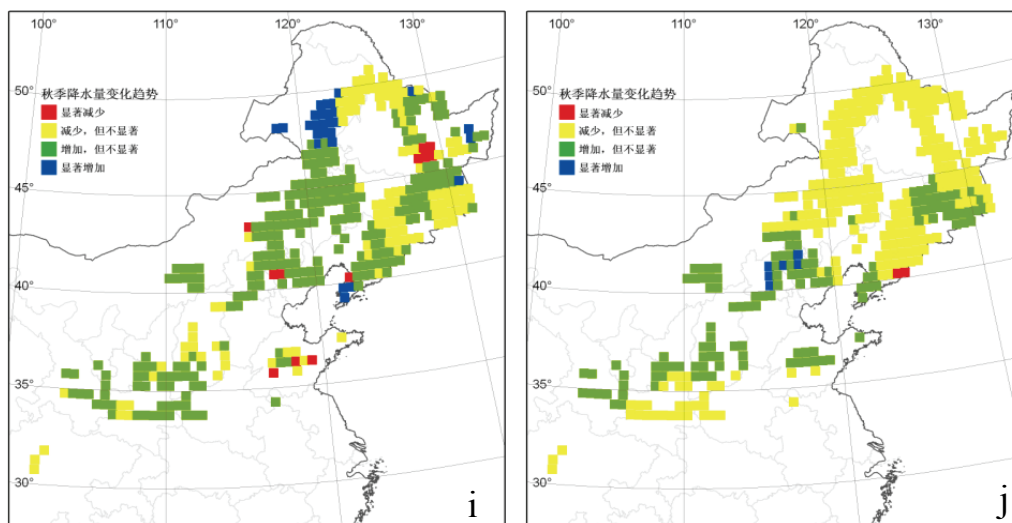
40%的区域春季降水由增加变为减小, 52%没有趋势变化, 变为减少趋势的主要是在北纬 42° 至 45° 之间以及 35° 附近 (图 5.20e-f)。



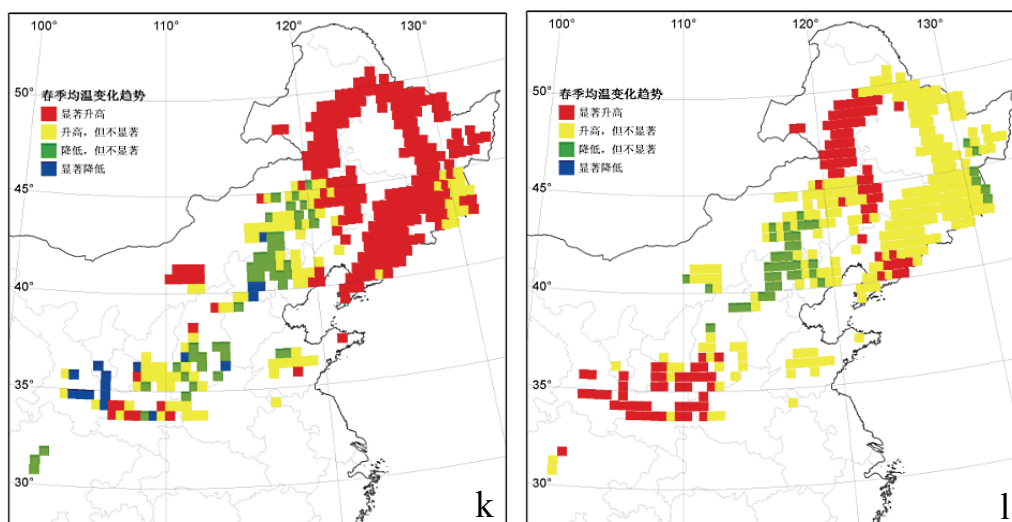
65%的区域夏季降水由增加变为减小, 变化主要在北部地区 (图 5.20g-h)。



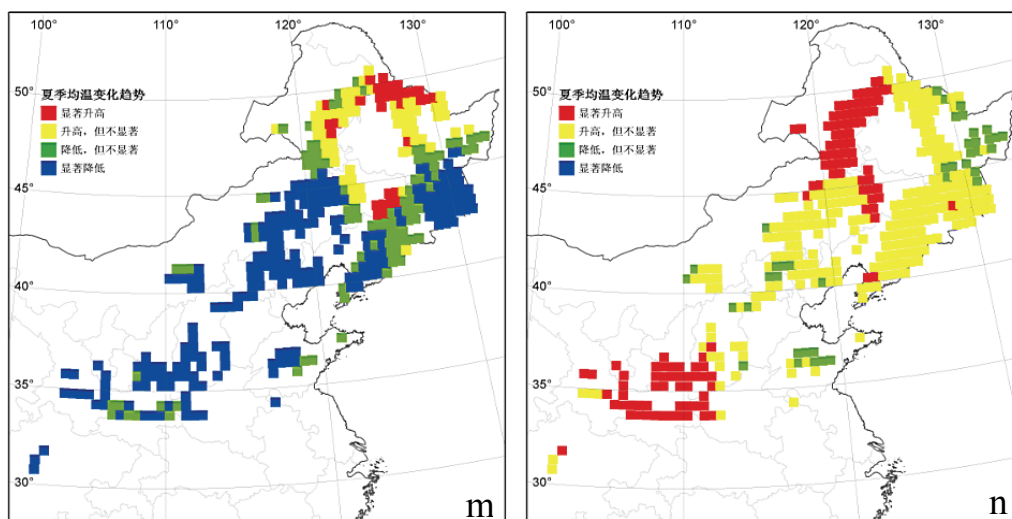
44%的区域秋季降水由增加变为减少，主要出现在南部和东北部（图 5.20i-j）。



11%的区域春季变成增温趋势，大部分区域原有升温趋势减缓（图 5.20k-l）。



69%的区域夏季由降温趋势变为升温趋势，整个植被区域基本都呈升温趋势（图 5.20m-n）。



21%的区域由秋季降温变为升温，而 36%由升温变为降温。变为升温的地区主要在南部，降温地区在东北部（图 5.20o-p）。

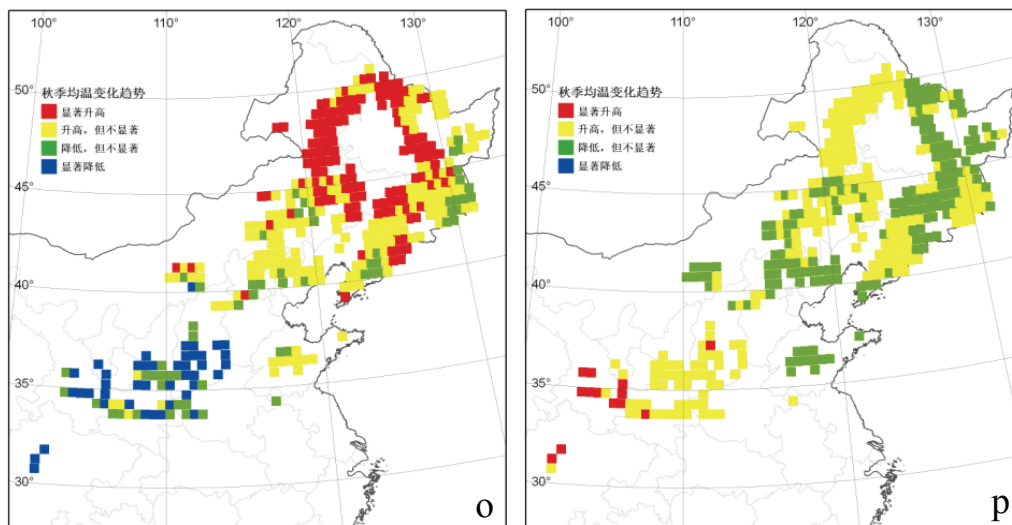


图 5.20 植被生长和气候变化趋势的区域分布

由此可见，最近 21 年植被生长的限制主要来源于春季和夏季降水量的减少以及夏季均温的升高，秋冬季气候影响小。

植被生长对气候变化的响应在不同时段也具有不同的程度（表 5.6）。两个时间序列中植被生长对某些气候因子出现了方向相反的响应，是由于气候本身在不同时间段的波动趋势所致。FPC 对气候年际变化响应弱于 NPP 的响应，综合来看，各个因子在 21 年来影响增强，但秋冬季气候影响仍不显著。

表 5.6 植被生长对气候年际变化的响应的偏相关系数

R Partial	降水				气温		
	春	夏	秋	冬	春	夏	秋
FPC(103)	0.061	0.100	0.016	0.020	0.305^b	-0.379^b	0.015
FPC(21)	0.071	0.184	0.151	0.011	-0.343	-0.176	0.223
NPP(103)	0.408^b	0.524^b	0.015	0.067	0.398^b	-0.590^b	0.235^a
NPP(21)	0.777^b	0.848^b	0.070	-0.369	-0.099	-0.900^b	0.806^b

a: $p<0.05$,b: $p<0.01$

5.3 不同气候变化情景下的森林生长状况

5.3.1 植被覆盖和生产力的敏感性分析

季节性气候变化代码如下，如 P1，P2 指春季降水相对对照组增减，在情景 1（S1）中增减一个标准差，情景 2、3（S2，S3）中增减 50%。NPP 单位均为 $\text{gC}/\text{m}^2\cdot\text{a}$ 。

表 5.7 敏感性分析情景编号

气候	降水				气温				干旱	
季节	春	夏	秋	冬	春	夏	秋	春	夏	
代码	P1 P2	P3 P4	P5 P6	P7 P8	T1 T2	T3 T4	T5 T6	A1	A2	
S1	±sd	±sd	±sd	±sd	±sd	±sd	±sd	P2+T1	P4+T3	
S2、3	±50%	±50%	±50%	±50%	±50%	±50%	±50%	P2+T1	P4+T3	

情景 1 中 CO_2 浓度缓慢上升，每年气候条件一致，然而 FPC 和 NPP 对照组表现出明显的趋势差异性（图 5.21a）：FPC 轻微波动，而 NPP 在前 50 年内波动上升。FPC 年际变异系数仅为 0.008，而 NPP 为 0.05。这种波动趋势在各个季节气候变化模拟也是一致的（图 5.21b,c）。在夏季降水减少（P4）和夏季干旱（A2）中 FPC 前 50 年出现了很大偏离，与 NPP 趋势类似。

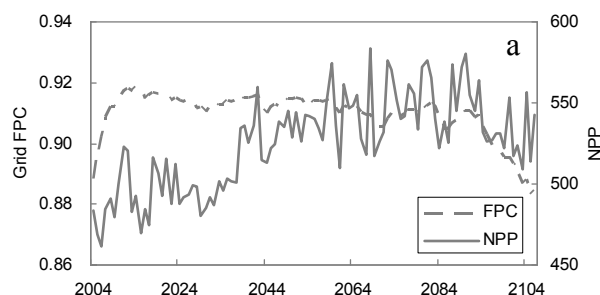


图 5.21a 对照组 FPC 和 NPP 变化趋势

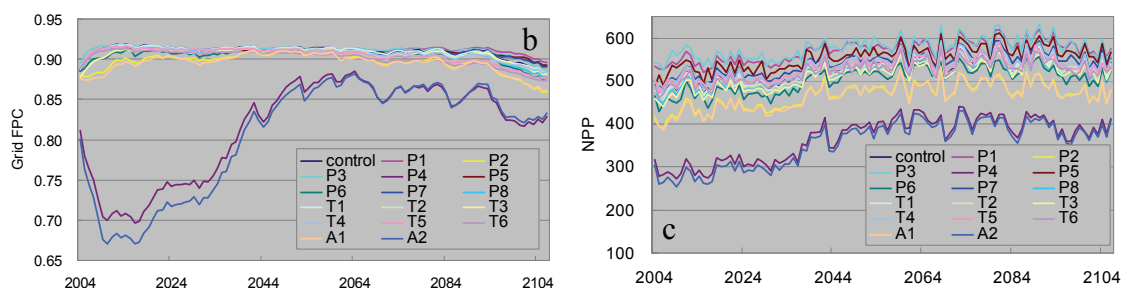


图 5.21 FPC(b)和 NPP(c)不同情景年际波动

情景 1 中的季节性气候变动是加减多年平均（1961-1990）气候状况的标准差，由此引起了 FPC 和 NPP 在模拟的温带落叶阔叶林范围内不同的变化率（图 5.21d）。FPC 与 NPP 的变化方向基本一致，但变化率远小于 NPP，基本都在 1% 以下，只有春、夏降水减少（P2, P4）以及干旱（A1, A2）时变化率比较大。在平均气候状况基础上进行季节性变动表明，各季降水对 NPP 都具有促进作用，春夏降水增减标准差引起 NPP 变化率绝对值大于 5%，秋冬降水不明显；季节性温度变化中夏季气温的升降一个标准差对 NPP 影响最大，气温升高会引起 NPP 下降，而春秋气温升降一个标准差虽然对 NPP 影响不大，但这两季在气温升高一个标准差时对 NPP 具有促进作用，表明平均状况下的春秋气温没有成为植被生长抑制因子，其

有限度的上升可以通过延长生长季促进生长。春夏干旱的模拟（A1, A2）表明降水减少和温度升高的组合抑制植被生长。同时，植被生长对气候变化的不同方向的响应程度不同，在季节性降水减少和气温升高时变化率更大。

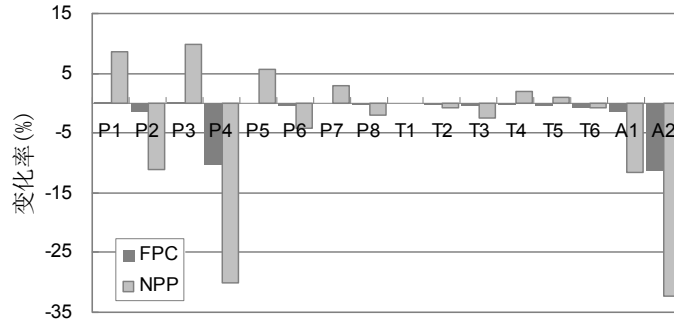


图 5.21d 不同情景 FPC 和 NPP 变化率

情景 2 中未来气候变化具有一定的趋势性，即对照组基于 1901 年以来百年气候变化趋势（图 5.22）进行气候输入的计算。1901 年以来气候表现为春、夏降水微弱上升，秋、冬季降水微弱下降，春季温度显著上升，夏季温度显著下降，秋季气温平稳上升。在这种情况下，植被类型分布会发生一定的变化（图 5.24）。与 1901 年以来实际气候相比轻微的干旱化，主要表现在在东北部出现温带草原。

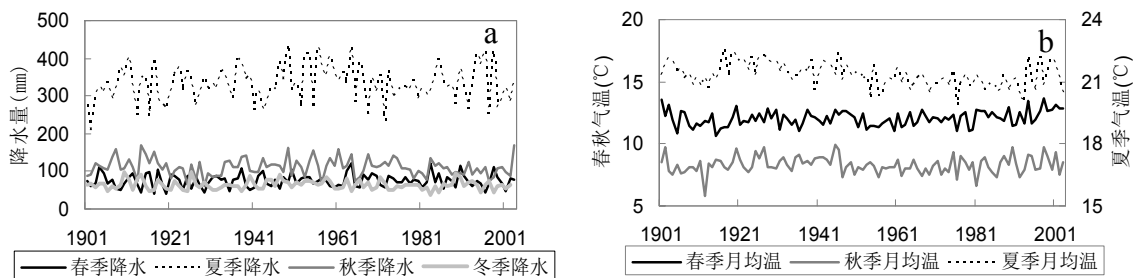


图 5.22 季节性降水(a)和气温(b)年际波动

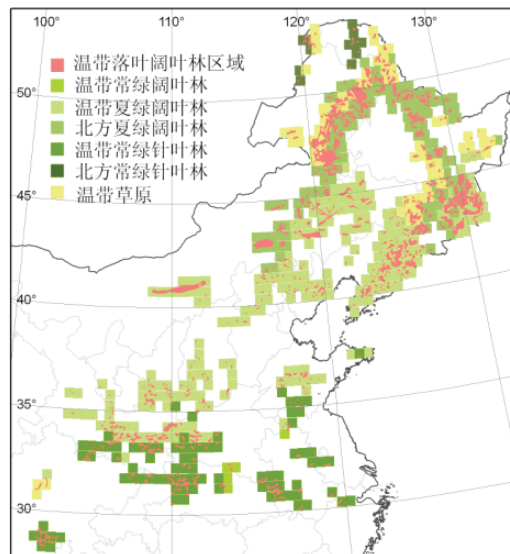


图 5.23 基于 103 气候变化趋势模拟的未来 103 年植被格局

依照 1901 年以来的气候变化趋势, FPC 和 NPP 年际波动趋势一致(图 5.24a), NPP 波动较大, cv 为 0.06, FPC 为 0.01。在夏季温度升高 50% (T3)、夏季降水减少 50%(P4)以及两者组合(A2)模拟时 FPC 和 NPP 偏离对照组很大(图 5.24b,c)。

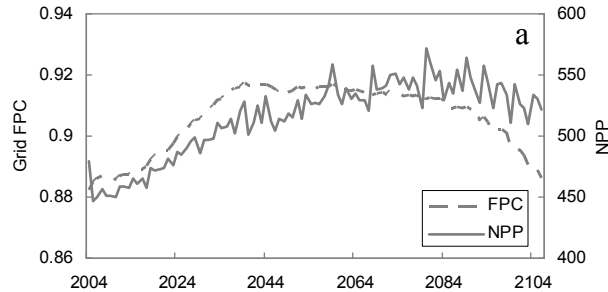


图 5.24a 对照组 FPC 和 NPP 变化趋势

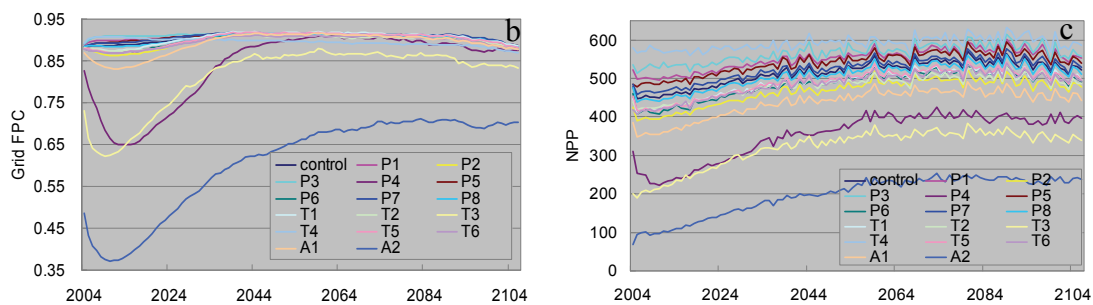


图 5.24 FPC(b)和 NPP(c)不同情景年际波动

敏感性分析中参数影响程度以大于 0.2 为强效应 (strong), 大于 0.1-0.2 为中等强度效应 (medium), 小于 0.1 为弱效应。根据这个标准, FPC 和 NPP 对不同季节的气候变动和方向具有不同的响应敏感性 (图 5.24d)。

FPC 对气候变化的响应敏感性远弱于 NPP, 仅对夏季降水减少 (P4) 和夏季气温升高 (T3) 具有中等程度和强的敏感性。春季降水对 NPP 有中等强度效应, 降水减少时 NPP 响应更敏感; 夏季降水对 NPP 具有中等强度效应, 在夏季降水减少时 NPP 响应敏感性达到强效应; 秋季降水对 NPP 刚达到中等强效应, 降水减少时响应更敏感; 冬季降水对 NPP 为弱的正效应; 夏季温度对 NPP 具有强负效应, 在升温时 NPP 的响应更敏感; 春、秋季温度对 NPP 具有中等强度效应, 春季稍强。在这种气候趋势下, 春秋两季升温与降温 NPP 都在下降, 说明两者在对照组的运行趋势处于一种适宜状态。

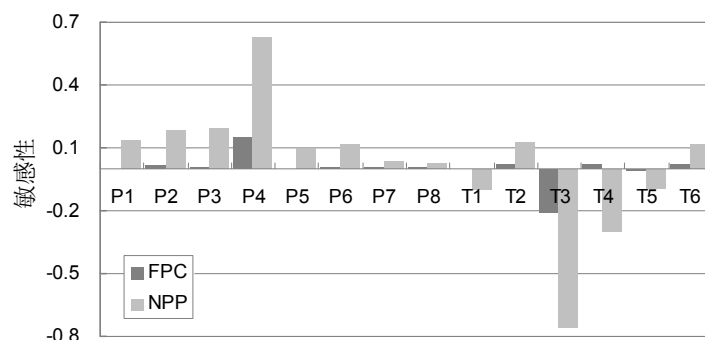


图 5.24d 不同情景 FPC 和 NPP 的气候响应敏感性

情景 3 中未来气候变化也具有一定的趋势性，即对照组根据基于 1983 年以来的 21 年气候变化趋势（图 5.25a,b）进行气候输入的计算。最近气候趋势表现为春、夏、秋降水减少，冬季降水增加，春、夏、秋温度上升，并在植被格局上出现明显变化（图 5.26），温带草原大面积取代落叶阔叶林。

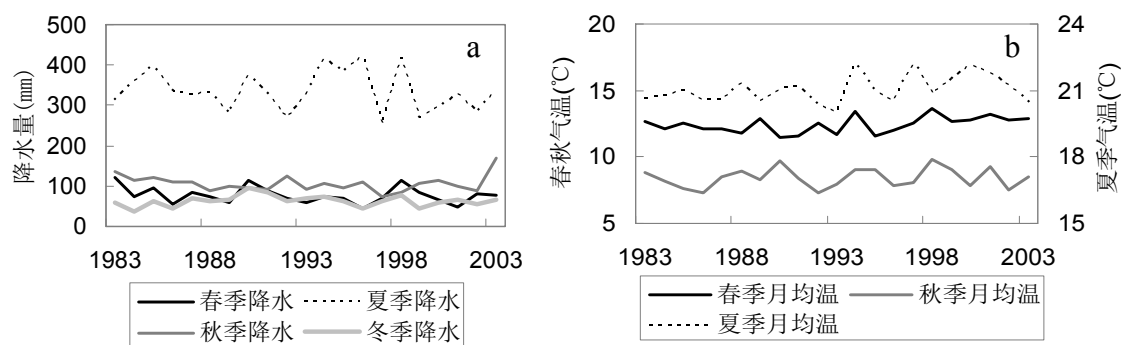


图 5.25 季节性降水(a)和气温(b)年际波动

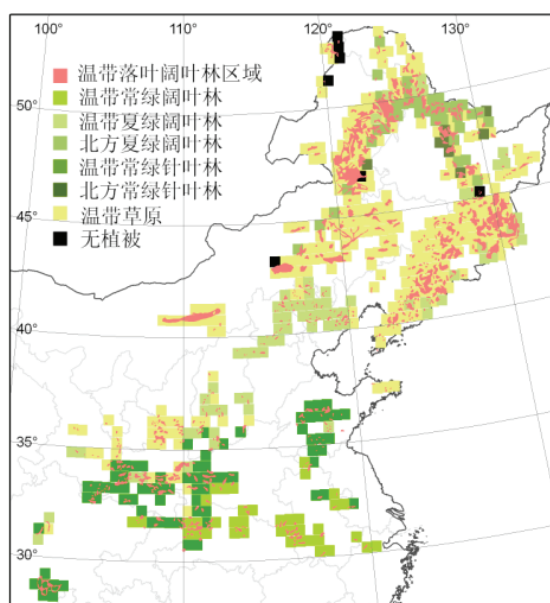


图 5.26 基于 21 气候变化趋势模拟的未来 103 年植被格局

在未来 100 年气候具有 1983 年以来趋势的情况下，FPC 和 NPP 在时序上的

趋势一致（图 5.27a），但 NPP 波动稍大，变异系数为 0.37，大于 FPC 的 0.28。在夏季温度升高 50%（T3），夏季降水减少 50%（P4）以及两者组合（A2）模拟时 FPC 和 NPP 偏离对照组很大（图 5.27b,c）。

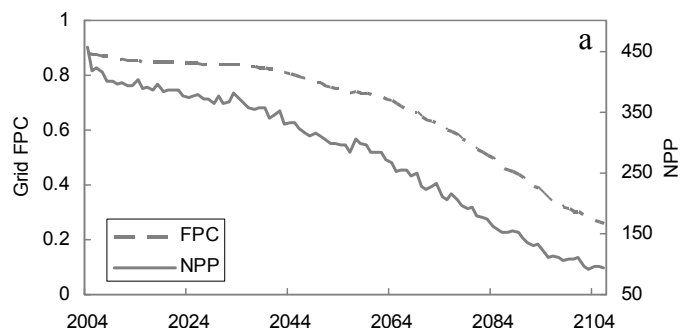


图 5.27a 对照组 FPC 和 NPP 变化趋势

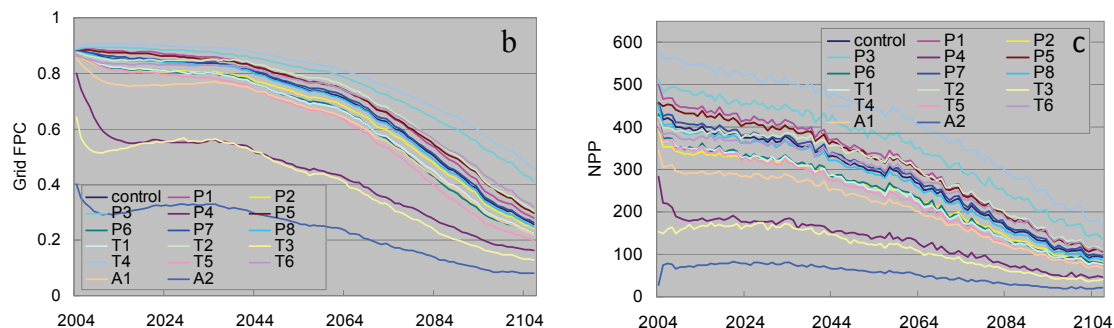


图 5.27 FPC(b)和 NPP(c)不同情景年际波动

从敏感性分析看（图 5.27d），在情景 3 的气候趋势下，FPC 对气候响应的敏感性提高，除了夏季降水减少（P4）和夏季气温升高（T3）达到强效应外，夏季降水增加（P3）、秋季降水减少（P8）、春秋气温上升（T1，T5）以及夏季气温降低（T4）都对 FPC 产生了中等强度效应。NPP 的敏感性也都有所提高，春、夏、秋季降水对 NPP 有强正效应，降水减少时 NPP 响应更敏感，特别是对夏季降水。冬季降水对 NPP 为弱的正效应。春、夏、秋季气温对 NPP 具有强负效应，其中夏季气温波动始终是强效应，春季气温下降的作用为中等强度效应，而秋季气温下降时为弱效应，总体表现为气温升高时植被响应更敏感。

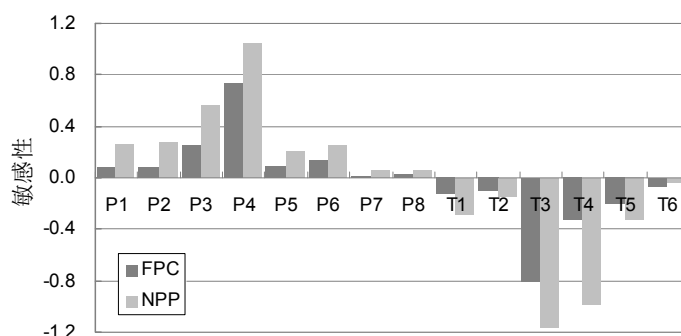


图 5.27d 不同情景 FPC 和 NPP 的气候响应敏感性

FPC 和 NPP 对气候变化的响应敏感性与气候的波动程度有关。以森林生长的关键时段为例，在基于 103 年的气候变化基础上设定夏季降水和气温分别降低和升高 10%-80%，以 10%为间隔，可以发现植被生长情况的组间变化和与对照组比较得到的敏感性分析具有一定的规律。结果中敏感性取绝对值，表示降水（温度）减少（升高）1%时，温带落叶阔叶林区域平均 FPC 和 NPP 降低的百分比，NPP 对照组取值 1，其他结果取相对于对照组的值。

与前文分析一致，降水和温度对植被覆盖（FPC）的影响效应整体小于对植被生产力的影响效应（图 5.28a）。单就这里分析的夏季气候而言，降水（温度）在减（增）50%以上时才能对 FPC 产生强效应，而在 10%的变化就可以对 NPP 产生强效应。植被的响应敏感性，亦即气候的影响效应，随着季节性降水和温度偏离正常程度的增大而增强。降水（温度）每减少（上升）10%，带来的植被 FPC 和 NPP 的下降越来越多（图 5.28b, c）。降水下降 20%与 10%相比，NPP 只减少了 5%，而降水下降 80%与 70%相比，NPP 减少达到 35%（图 5.28c），表明气候变化越大，单位变化对植被生长的影响越强。降水和温度对 FPC 的影响效应差别小于两者对 NPP 的影响效应差别。同样程度的变化，夏季气温比夏季降水的影响程度大，然而随着变化加剧到 50%以上时，气候因子的影响程度趋同（图 5.28a）。

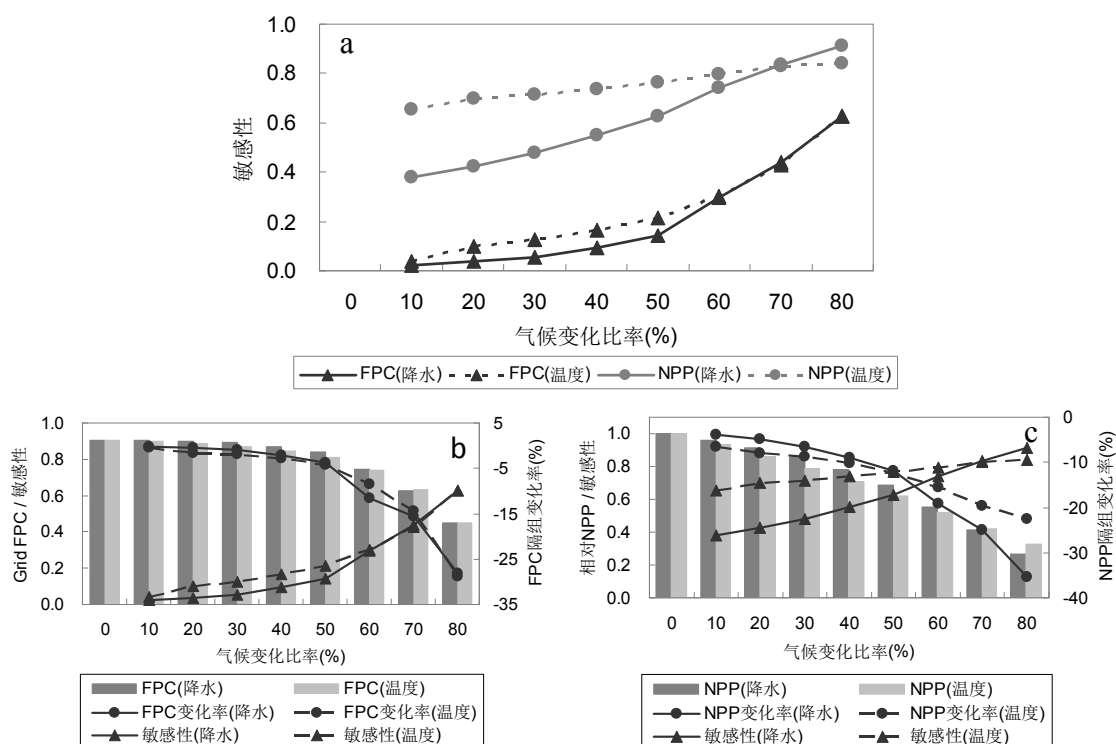


图 5.28 不同夏季气候因子变化程度与敏感性分析 敏感性(a) FPC 分析(b) NPP 分析(c)

从以上分析可以得到以下结论：

1. 在气候不发生年际变化时，植被覆盖（FPC）和生产力（NPP）仍会发生

波动，这可能是由于月内降水的日分配在某些生长的关键时期不同所致，同时，NPP 比较稳定的上升受到大气 CO₂ 升高的影响。

2. NPP 对气候变化的响应比 FPC 更为敏感，无论是在气候平稳（情景 1）还是存在趋势性时（情景 2、3）。
3. 温带落叶阔叶林对气候季节性变化具有不同的响应敏感性，并在气候暖干化波动时更为敏感；对夏季温度和夏季降水最敏感，其次是春季降水和春季温度，再次为秋季降水和温度，对冬季降水敏感性较弱。温度和降水变化率在 50% 以上时，生产力响应敏感性趋同。
4. 不同的气候变化趋势下，植被的响应敏感性不同。基于百年气候和缓变化的未来气候下植被响应敏感性较弱，而基于最近 20 余年气候明显变化的未来气候下植被响应敏感性很强；不同的气候变化程度，植被的响应敏感性不同。随着气候变化程度加大，气候对植被生长影响加强。

以上的气候变化仍是气候的逐年变化，不涉及气候的极端波动，所以从植被覆盖和生产力的时间序列上看没有剧烈的波动。

5.3.2 森林动态对干旱程度和时间特征的响应

森林植被覆盖和生产力对干旱的响应具有一致性，干旱的影响来自降水距平百分比代表的干旱程度，干旱出现的季节，干旱出现的频率以及干旱持续的时间。

模型输入使用的 CRU 数据（图 5.29）与修正的 PDSI 数据指出的干旱时段基本相符，干旱时段分别为 1980-1984，1986-1989，1998-2000，所以对照组采用 CRU 数据不偏离气象数据的研究结果。

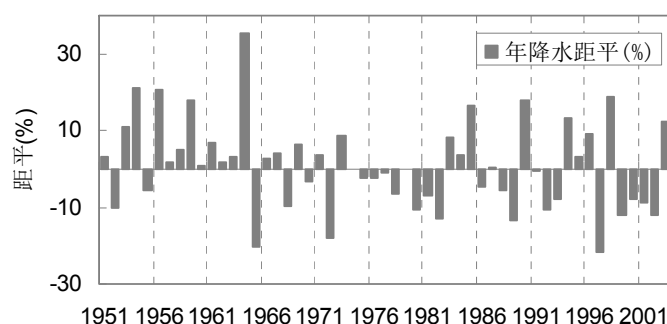


图 5.29 1951-2001 年的年降水距平值

从干旱程度看，FPC 和 NPP 季节性干旱时都是旱比偏旱更小 ($p < 0.001$)。与对照组相比，NPP 受到的影响都是显著的 ($p < 0.001$)，连续 5 年干旱的平均 NPP 在不同干旱程度时不同（图 5.30），这与模型在 103 年的真实气候下运行得到的 NPP 与降水的正相关性一致。

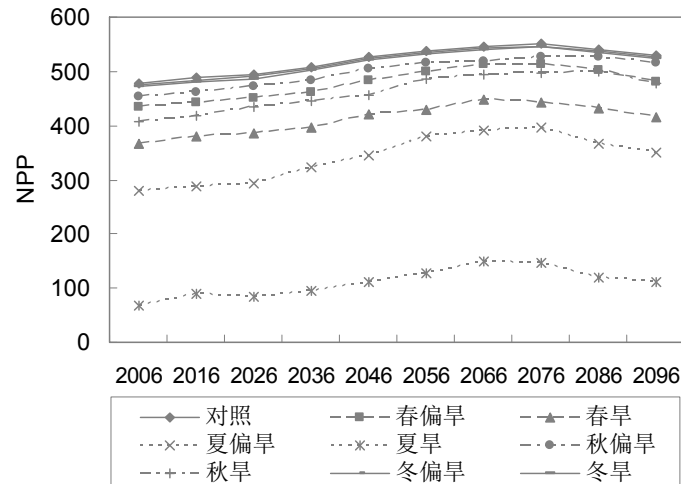


图 5.30 不同季节及干旱程度的干旱时期生产力

从季节影响看，夏季干旱影响最大，冬季干旱影响最小（表 5.8）。每次季节性干旱后的正常年份里 NPP 逐渐恢复，但其恢复程度在不同季节和干旱程度上有所差别。综合来看，越严重的干旱其正常年份恢复的程度也越大（图 5.31a），恢复比例逐渐下降，夏季旱后恢复的平均比例最大（表 5.8）。干旱后的正常年份植被生产力与没有受到干旱扰动的对照组相比，不同季节和干旱程度也存在差别。各季节偏旱时都基本可恢复到正常，但旱时除春季外都不能恢复，特别是夏旱后 NPP 远远不能恢复到未受扰动时的状态（表 5.8），然而这种恢复程度在时间进程上并不是一成不变的，在早期的干旱事件后，正常年份的 NPP 往往小于未受到干旱影响时的 NPP，随后恢复程度逐渐加强甚至可以完全恢复，但如果干旱事件持续不断进行，这种恢复力又会减小（图 5.31b）。

表 5.8 干旱程度和季节对 NPP 的影响

季节和干旱程度	春偏旱	春旱	夏偏旱	夏旱	秋偏旱	秋旱	冬偏旱	冬旱
NPP 减少(%)	8.01	20.89	34.61	78.91	4.31	11.35	0.61	1.18
正常年恢复(%)	11.69	31.62	57.08	268.63	6.11	15.21	2.53	2.95
恢复程度(%)	0.72	2.06	0.35	-24.78	0.06	-0.45	-0.09	-0.25

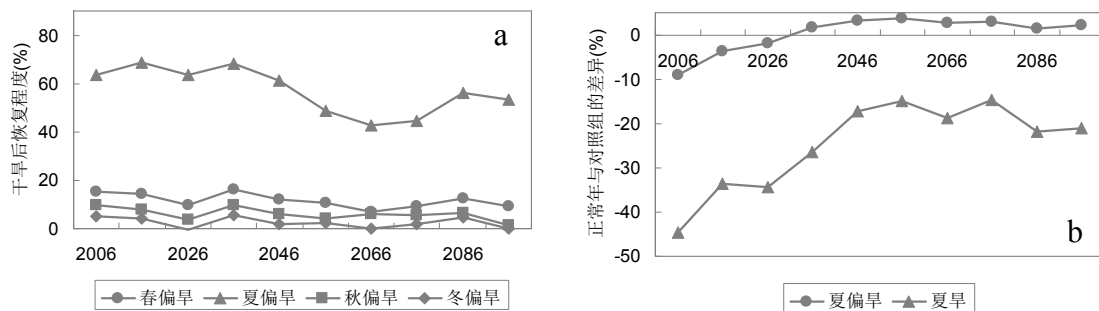


图 5.31 干旱后正常年份生产力的恢复比例(a) 干旱后正常年份与未受扰动年份生产力差异(b)

由于春季和夏季干旱在北方常见，所以着重分析春夏两个季节干旱程度为旱的干旱事件频率和持续时间对植被生产力的影响。

干旱出现频率是干旱特征的组成部分，春季和夏季干旱持续时间都为 5 年，正常年份分别为 1 年、3 年和 5 年。干旱时期的平均生产力在春旱和夏旱的 4 组间都没有显著差异，两两组间也没有差异，表明季节性干旱持续时间一样时，干旱对减少生产力的作用相似。

但是干旱频率对干旱后生产力的恢复有影响。对比春季 4 组干旱后的正常年份的生产力恢复程度可以发现，随着干旱事件出现频率降低，生产力的恢复程度逐渐上升，分别为 28.1%，30.3%和 31.6%。尽管单因素方差分析（ANOVA）表明干旱频率在组间没有显著差异，但是最小频率和最大频率的差异显著（ $p < 0.1$ ），说明随着干旱事件出现频率的减小，干旱后生产力的恢复程度是逐渐增强的。随着干旱事件进程，干旱事件后生产力的恢复程度却在逐渐减小，并且频率小的恢复程度减小更快（图 5.32a）。

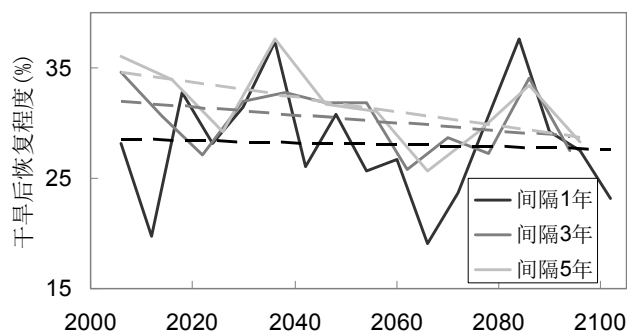


图 5.32a 不同频率春季干旱后生产力恢复程度 图中虚线表示拟合的趋势性，下同

如果干旱出现在夏季，则随着干旱事件出现频率降低，由于夏季干旱对生产力的抑制作用大于春季，干旱结束后的生产力恢复程度大于春季，也表现出逐渐上升的趋势，分别为 1.6，2.1，2.6 倍。ANOVA 分析表明干旱频率在组间有显著差异（ $p < 0.001$ ），在两两组间也都存在显著差异（ $p < 0.05$ ）。同样在时间进程上存在生产力恢复程度的减小（图 5.32b），并且与同样频率的春季干旱相比，夏季干旱后生产力的恢复程度减小的更快。

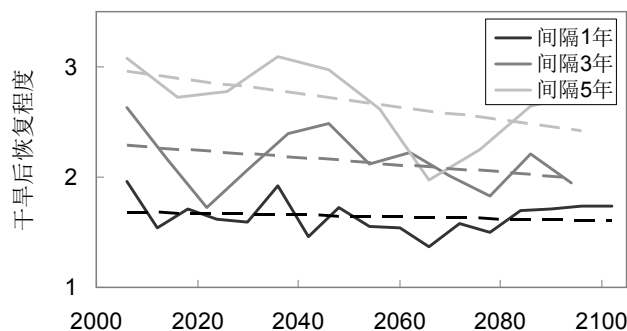


图 5.32b 不同频率夏季干旱后生产力恢复程度

受到干旱扰动后的正常年份平均生产力与没有受到扰动的对照组相应年份的平均生产力相比, 春旱后恢复程度相当强, 在研究设定的干旱频率下平均恢复程度都可以达到对照组的生产力, 并且随着干旱事件出现频率降低, 恢复后的生产力与未受扰动时的差异减小, 分别为 4.0%, 2.3%和 2.0%, ANOVA 检验表明组间差异明显 ($p<0.02$), 并且差异主要来源于最大频率干旱 (正常年份 1 年) 与最小频率 (正常年份 5 年)、次小频率 (正常年份 3 年), $p<0.01$, 表明恢复期长的生态系统会逐渐平稳到未受干扰时的状态。与季节性干旱对生产力的影响相同, 干旱频率影响下的恢复程度在时间进程上也存在变化, 恢复程度逐渐加强到完全恢复甚至有所增加, 但如果干旱事件持续不断进行, 这种恢复力又会减小(图 5.32c)。

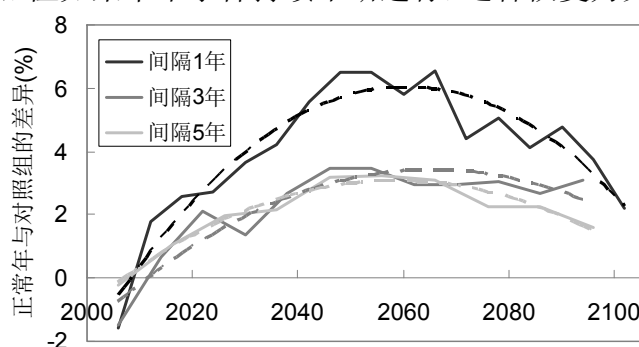


图 5.32c 春季干旱后正常年份与未受扰动年份生产力差异

当干旱出现在夏季, 干旱时期生产力下降程度可以达到春季干旱的近 4 倍, 正常年份生产力的恢复力没有春旱后强, 与没有受到扰动的对照组相应年份的生产力相比, 在研究设定的干旱频率下无法恢复到对照组的生产力。随着干旱事件出现频率降低, 恢复后的生产力越来越接近对照组的生产力, 差别分别为-38.1%, -29.7%和-24.8%。ANOVA 检验表明组间差异明显 ($p<0.05$), 差异来源与不同频率的春季干旱一样, 显著性稍低 ($p<0.1$)。与春季干旱相比, 最大频率的夏季干旱后在时程上的恢复过程在百年内尚未达到恢复程度的最大值 (图 5.32d)。

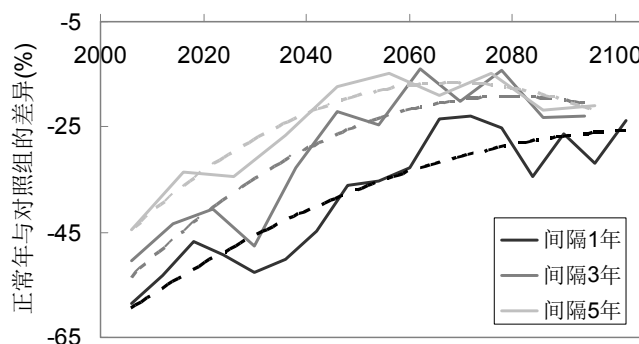


图 5.32d 夏季干旱后正常年份与未受扰动年份生产力差异

干旱持续时间也是干旱事件的重要特征, 在干旱频率一样的情况下, 不同的干旱持续时间影响着植被动态。设定的春季和夏季正常年份为 2 年, 干旱持续时

间分别为 5 年、4 年和 3 年。尽管干旱持续时间不同，但干旱时期的平均生产力在春旱和夏旱的 3 组间都没有显著差异，两两组间也没有差异。

干旱持续时间对其后生产力的恢复有影响。对比春季 3 组干旱后的正常年份的生产力恢复程度可以发现，随着一次干旱事件持续时间缩短，生产力的恢复程度逐渐上升，分别为 29.1%，29.1%和 30.2%，不过这种差异与干旱频率不同造成的差异相比，在组间没有显著差异。随着干旱事件不断发生，干旱后生产力的恢复程度却在逐渐减小，并且持续时间短的恢复程度减小更快（图 5.33a），这与干旱频率时表现出一致的规律。

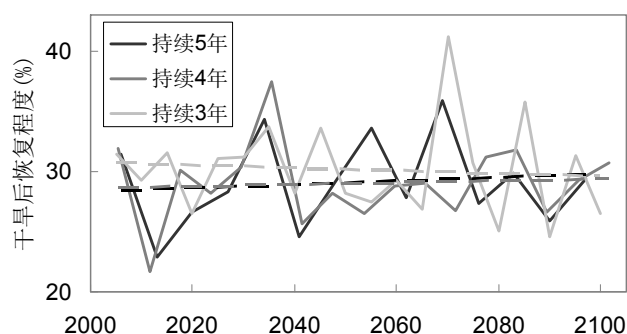


图 5.33a 不同时长春季干旱后生产力恢复程度

干旱出现在夏季时，干旱后的生产力恢复程度大于春季，随着干旱持续时间的减小，生产力恢复程度同样也表现出逐渐上升的趋势，分别为 1.9，1.9 和 2.0 倍，不过差异也不显著。同样在时间进程上存在生产力恢复程度的下降（图 5.33b），并且同等持续时间的夏季干旱后生产力恢复程度在进程上减小更快。

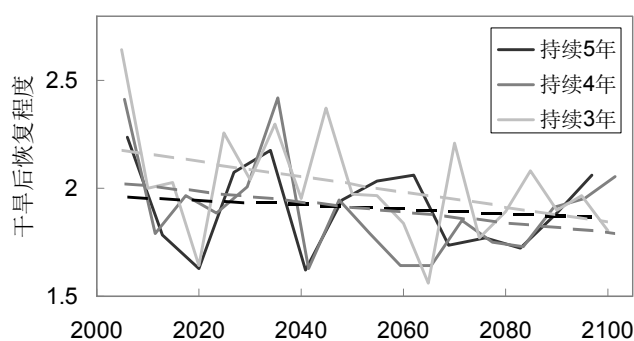


图 5.33b 不同时长夏季干旱后生产力恢复程度

与对干旱频率的研究结果相似，受到干旱扰动后的正常年份平均生产力与没有受到扰动的对照组相应年份的平均生产力相比，春旱后恢复程度是相当强的，在研究设定的干旱持续时间后平均恢复程度都可以达到对照组的生产力，并且随着干旱持续时间减小，恢复后的生产力与未受扰动时的差异减小，多年平均分别为 3.1%，2.4%和 2.3%，但同样未发现显著的组间差异。干旱持续时间影响下的恢复程度在时间进程上存在变化，到 2050 年左右，恢复程度逐渐加强到完全恢复

甚至有所增加,但如果干旱事件持续不断进行,这种恢复力又会减小(图 5.33c)。

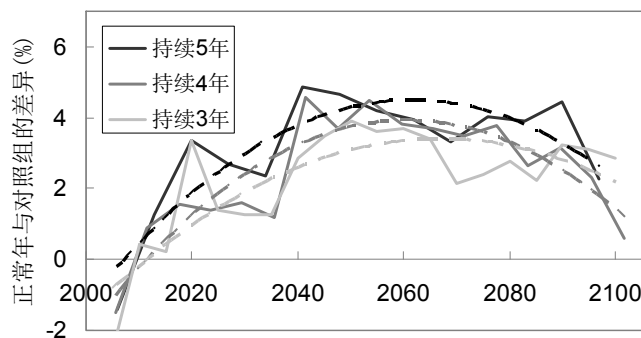


图 5.33c 春季干旱后正常年份与未受扰动年份生产力差异

夏旱后正常年份生产力的恢复力没有春旱强,与没有受到扰动的对照组响应年份的生产力相比,在研究设定的干旱频率下无法恢复到对照组的生产力。随着干旱持续时间缩短,恢复后的生产力越来越接近对照组的生产力,差别分别为-32.1%, -30.5%和-27.9%,但不显著。与不同持续时间的春季干旱相比,持续时间最长的夏季干旱后的恢复过程在百年内尚未达到恢复程度的最大值(图 5.33d)。

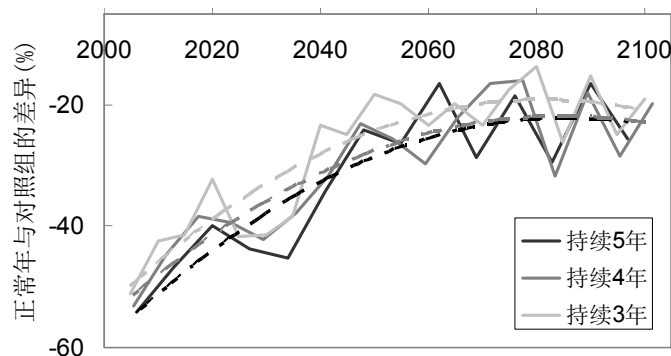


图 5.33d 夏季干旱后正常年份与未受扰动年份生产力差异

干旱持续时间没有干旱频率对干旱后生产力恢复影响大,是因为在干旱后,生产力的恢复是逐年进行的(图 5.34),时间段没有特殊性。图中为夏季干旱模拟,干旱年份其生产力下降程度大致相同,但间隔两年的恢复尚未完成就又进入了干旱,因此频率大的干旱恢复时间短,恢复能力有限。

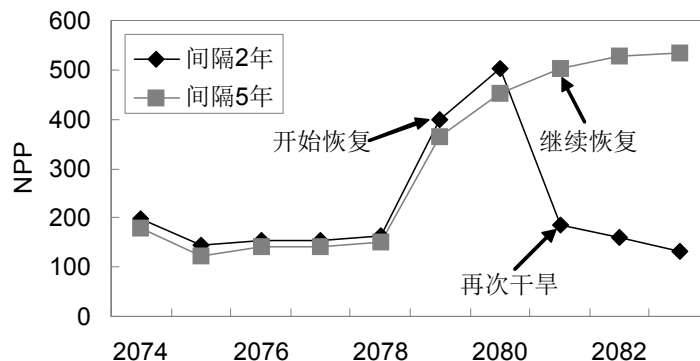


图 5.34 不同频率的干旱后生产力恢复

干旱事件频率和持续时间的综合作用影响了干旱程度，从而对植被动态有不同的影响。在上述不同干旱频率和持续时间的组合内进行针对干旱事件频率和持续时间的双因素方差分析，包括干旱时期的平均生产力，干旱后的生产力恢复程度以及恢复生产力与未受到干旱扰动时的生产力的差异。

对干旱时期生产力的双因素方差分析表明，干旱事件频率、干旱持续时间以及两者的交互对生产力没有显著的影响 ($p>0.05$)，干旱时期的平均生产力水平相近，春季和夏季干旱都如此。

干旱后生产力恢复程度在春季干旱和夏季干旱中不同。干旱事件频率、干旱持续时间和两者的交互对春季干旱后生产力的恢复程度没有显著影响 ($p>0.05$)，但干旱频率和持续时间对夏季干旱后生产力的恢复影响十分显著 ($p>0.001$)。LSD 法 (least significant difference method) 进行的均值两两比较表明，干旱持续时间对干旱后生产力恢复的影响在 3 年与 4 年，4 年与 5 年间显著。

干旱后正常年份恢复的生产力与未受到扰动的生产力差异受到干旱频率的显著影响，在春季 ($p=0.008$) 比夏季 ($p=0.017$) 更为显著。LSD 分析表明，干旱间隔 1 年与间隔 3 年和 5 年之间的扰动与未扰动情形的生产力差异存在显著差别。

从以上分析中可以得到以下结论：

1. 以连续三个月降水距平百分率表征的干旱程度可以反映森林覆盖和生产力的变动，表现为降水距平百分率越大（干旱越严重），植被生产力越低。
2. 同样程度的干旱发生在不同季节对生产力有不同程度的影响，从大到小分别为夏季、春季和秋季。冬季干旱对生产力几乎没有任何影响。
3. 相比春季干旱，夏秋干旱后生产力不易恢复。春季干旱后往往可以恢复到未受到扰动的生产力水平，甚至可以超过。
4. 干旱事件出现的频率对干旱时期的平均生产力没有显著影响，但对其后生产力的恢复有影响，并且在夏季干旱中更为明显。随着干旱事件出现频率降低，生产力的恢复程度逐渐上升，在持续不断的干旱事件进程中，干旱后生产力的恢复程度逐渐减小，干旱事件频率小的恢复程度减小更快。与同样频率的春季干旱相比，夏季干旱后生产力的恢复程度减小的更快。
5. 干旱事件持续时间对干旱时期的平均生产力没有显著影响，对其后生产力的恢复影响弱于干旱事件频率的影响，随着干旱事件持续时间减少，生产力的恢复程度逐渐上升，在持续不断的干旱事件进程中，干旱后生产力的恢复程度逐渐减小，干旱持续时间短的恢复程度减小更快。与同样历程的春季干旱相比，夏季干旱后生产力的恢复程度减小得更快。
6. 受到干旱扰动后的正常年份平均生产力与没有受到扰动的对照组相应年

份的平均生产力相比,春旱后恢复程度大于夏旱后恢复程度。干旱事件频率小、恢复期长的生态系统会逐渐接近到未受干扰时的状态,但随着干旱事件持续不断进行,与正常状态的差异可能转而增加,最小的差异在夏季干旱时程上出现得晚于春季干旱,表明夏季干旱恢复更慢。干旱事件的持续时间与干旱频率具有相同的影响,但显著性弱。

实际气候记录表明干旱并不一定仅仅出现在一个季节,而是在年内和年际间具有连续性。以干旱时间为5年之后正常时间为5年进行季节性连续干旱的模拟表明,季节性连续干旱比单季干旱对NPP的影响程度更大,并涉及到跨年度的影响(图5.35a)。图中清晰地表明,夏旱叠加另一季干旱会对生产力造成近乎彻底的打击,平均生产力下降可达94.2%,远大于单季干旱时的影响程度,而秋冬连旱与秋季干旱对生产力的影响没有差别($p>0.1$),延续到冬季的干旱对下一年的生产力影响也不显著($p>0.1$)。冬春连旱主要影响下一年生产力,与春季干旱相比,生产力平均下降程度相差无几($p>0.05$)。再次表明夏季干旱的影响最为显著而冬季干旱对本年和下一年的生产力的影响微弱。如果年内或年际干旱持续的季数更长,那么对生产力的影响就更大,仍然表现出夏季、春季、秋季和冬季影响依次递减的规律(图5.35b)。

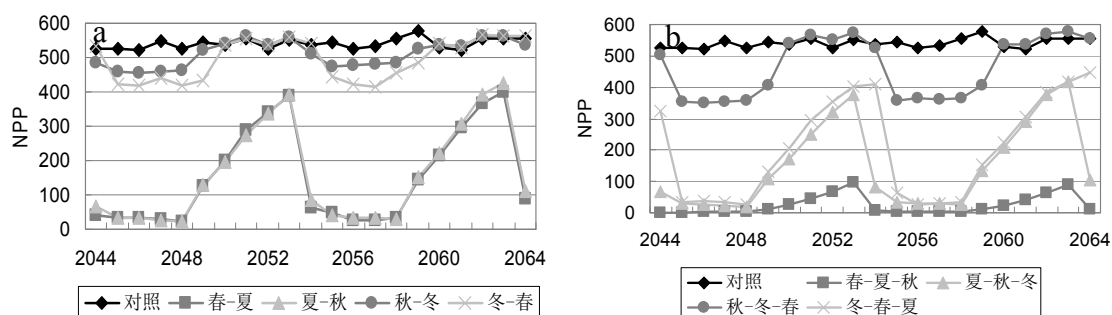


图 5.35 季节性连旱时 NPP 的年际波动 两季(a) 三季(b)

年内不同季节的干旱组合对生产力的影响也存在差异,一季干旱与其他三季的不同组合明确的反映了季节性干旱对生产力的影响程度大小。含有春季、秋季和冬季的两季干旱组合表明春夏干旱的影响最强,三种组合差异显著(图5.36a,b,d);含有夏季的组合表明夏季干旱在连季干旱中具有主导作用,生产力急剧降低,逐渐恢复(图5.36c)。

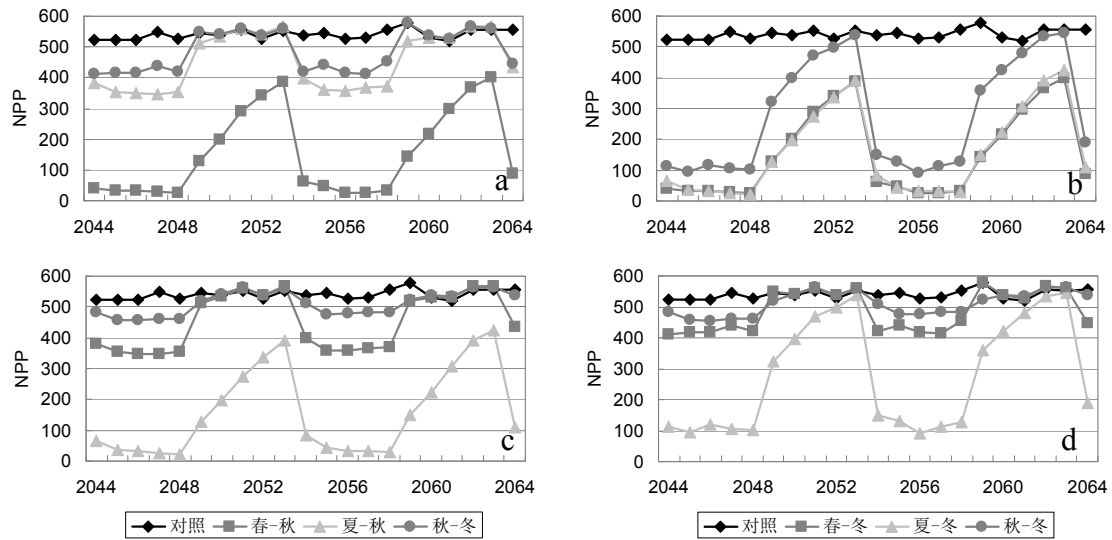


图 5.36 季节性干旱组合的 NPP 年际波动 春季组合(a) 夏季组合(b) 秋季组合(c) 冬季组合(d)

NPP 动态反映了现有温带落叶阔叶林在极端的干旱气候条件下的变化，而每个格点最大 FPC 所代表的植被类型动态则反映了主导植被类型的变化和植被界线的推移。从 NPP 和 FPC 对气候的响应可知，NPP 对气候变化响应更敏感，而 FPC 变化不是该种植被类型的主导性变化，因此 FPC 所表示的植被分布在一定程度上也受到干旱程度、干旱出现的季节、干旱事件出现的频率和持续时间的影响，但在空间上变化可能不剧烈。各种干旱情形的模拟都表明，干旱时增加的温带草原由温带落叶阔叶林转化而来，反映了一种林草交错的潜在格局。

干旱对植被主导类型有明显的影响，以持续 5 年的夏季干旱模拟结果与以 30 年平均气候状态运行的模型结果相比较，落叶阔叶林区域（最大 FPC 确定的主导植被类型）减少 38.8%，温带落叶阔叶林北部和北方落叶阔叶林南部向温带草原转化，北纬 40° 以北的森林干旱极限一带尤为明显（图 5.37a,b）。

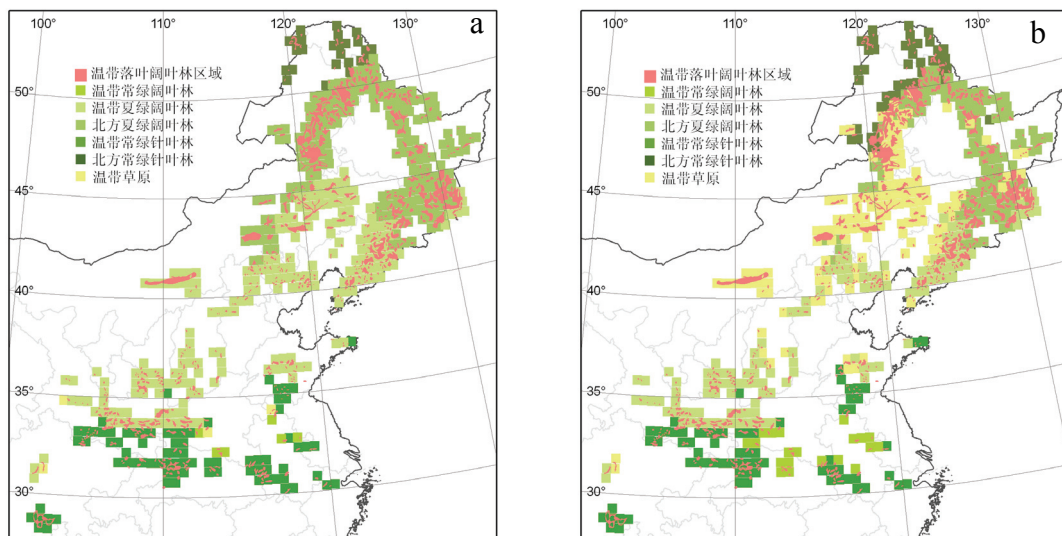


图 5.37 模拟植被格局 平均气候状态(a), 夏季 5 年旱 5 年正常(b)

干旱出现的季节对 FPC 的影响存在明显的差别, 同样程度的干旱, 在春、秋出现对 FPC 确定的植被格局几乎没有影响 (图 5.38), 与夏季干旱 (图 5.37b) 相比差别显而易见。

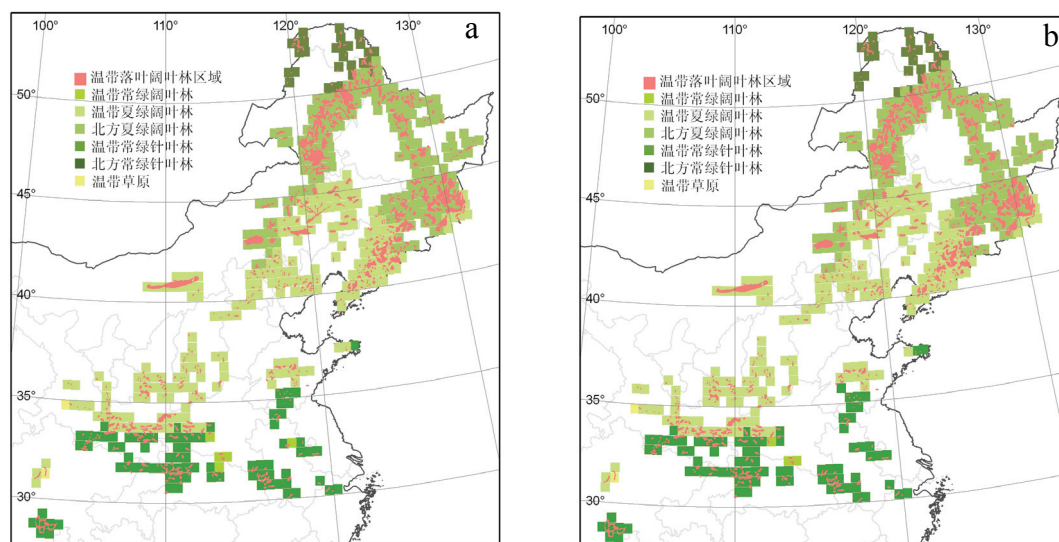


图 5.38 模拟植被格局 春季 5 年旱 5 年正常(a), 秋季 5 年旱 5 年正常(b)

干旱事件出现的频率对 FPC 确定的植被类型有影响, 但并没有出现随着干旱事件频率增加植被类型始终向某一方向演进。夏旱时间 5 年, 正常时间为 5 年, 3 年和 1 年的模型结果表明随着干旱频率增大, 落叶阔叶林区域减少率在最大干旱频率时为 36.3%, 在频率减小为 3 年一次后森林减少率降低为 33.3%, 但在频率为 5 年一次时减少率又增大为 38.8%, 没有明显的趋势性。干旱持续时间对 FPC 确定的植被类型有影响, 在持续时间为由 3 年增大到 4 年后, 阔叶林减少率由 29.8% 增大到 33.7%。在干旱持续达到 5 年时, 落叶阔叶林减少率又减小到 30.2%。

5.3.3 实际气候数据下的干旱分析

由于现有的植被生产力数据无法达到足够的时间长度, 因此使用模型模拟得到净第一性生产力数据配合 CRU1901-2003 年气候数据分析实际暖干气候对生产力的影响。以春夏降水量相对 1961-1990 年均值距平百分率小于 -25% 确定干年, 以春夏月均温距平大于 0.5°C 确定暖年。降水干旱指标是确定的, 气温干旱指标具有尝试性。虽然没有分析秋冬气候, 但作为生产力影响最大的季节, 春季和夏季气候对生产力的影响是决定性的。

由以上标准判断的春季和夏季偏干年份的 NPP 如图 5.39a, 不包括同时偏暖的年份。在落叶阔叶林区春季偏干的年份多于夏季, 说明这里可能春季降水的异常更常见。夏季偏干年份的生产力均值为 292.1gC/m^2 , 小于春季偏干年份的生产

力均值 316.7gC/m^2 ，可能由于春季偏干时生产力并不都是低值（NPP 均值为 351.5gC/m^2 ）。实际气候远远没有情景设定的干旱那样有规律，频率和时序时间都不定，但仍表现出夏季偏干的影响更强，因此在规律的干旱模拟下得到的敏感性等在一定程度上是可信的。

由上述标准判断的春季和夏季偏暖年份的 NPP 如图 5.39b，不包括同时偏干的年份。夏季偏暖的年份要多于春季偏暖的年份，同时偏暖的季节持续性比较强。不考虑持续两季的偏暖，夏季一季偏暖年份的平均生产力为 319.0gC/m^2 ，显著地小于春季一季偏暖年份平均值 380.9gC/m^2 ，表明夏季偏暖的影响更强。

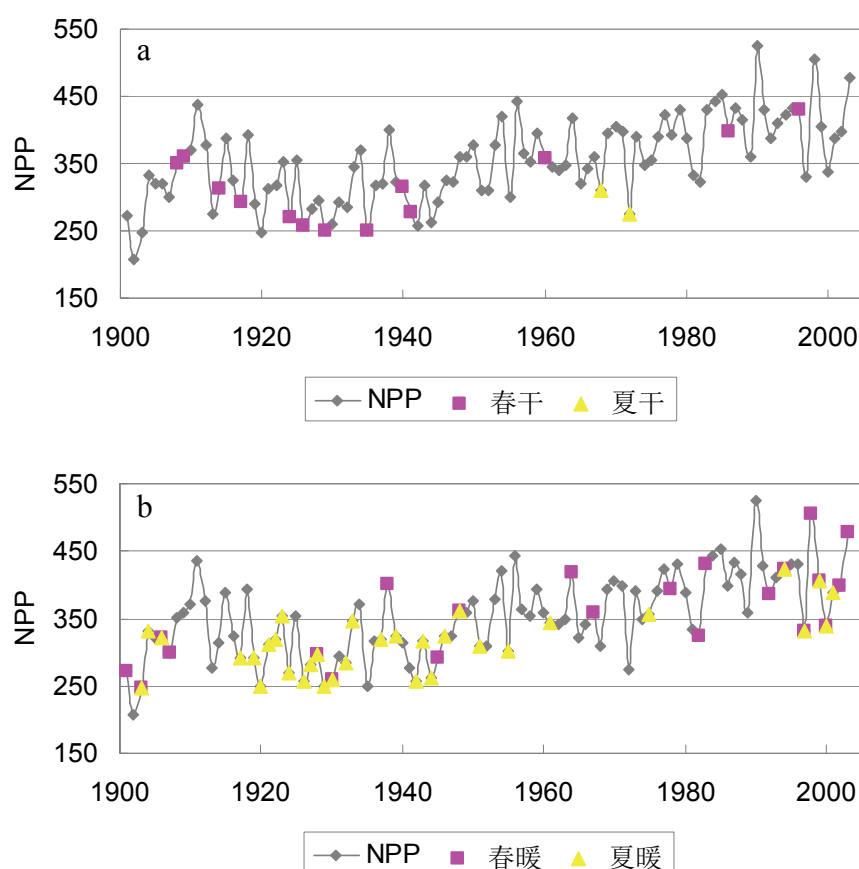


图 5.39 季节性偏暖 and 偏干时期的生产力状况 偏干(a) 偏暖(b)

降水 and 气温究竟哪个对生产力的影响更大其实是难以判断的，以上偏干与偏暖两个标准只能表明偏干和偏暖在不同季节间的影响。在不同频率和持续时间的干旱模拟中没有用气温的变动作为依据，也是由于气温对干旱的影响复杂，并且没有一个定量的标准。在实际气候中存在暖干的叠加（图 5.40），有春干夏暖但没有春暖夏干。夏季暖干时出现了 NPP 的最低值（1902 年）。在 NPP 前十个最低值中，有一半出现时季节性气候是暖干型的，一个是两季气候偏暖（1903 年），其余是春季偏干或夏季偏暖的单独影响。这支持了敏感性分析中设定的干旱情形

(A1, A2) 是气候暖干的叠加, 比仅有偏暖或偏干气候对生产力影响更大。综合分析降水和气温的影响 (图 5.41) 发现, 其实季节性暖干在 100 多年来始终是伴随出现的, 但是前半叶偏干的情况多于后半叶, 而偏暖的情况少于后半叶, 这意味着可能越来越多的暖干化是温度升高引起的。不过, 这并不影响模型以降水距平为依据对干旱的模拟。在前后半叶 NPP 的对比中可以发现, 同样程度的暖干似乎对 NPP 的抑制作用在减弱, 这可能是由于大气 CO_2 浓度的持续上升的补偿作用, 不过这种补偿作用是有限的。

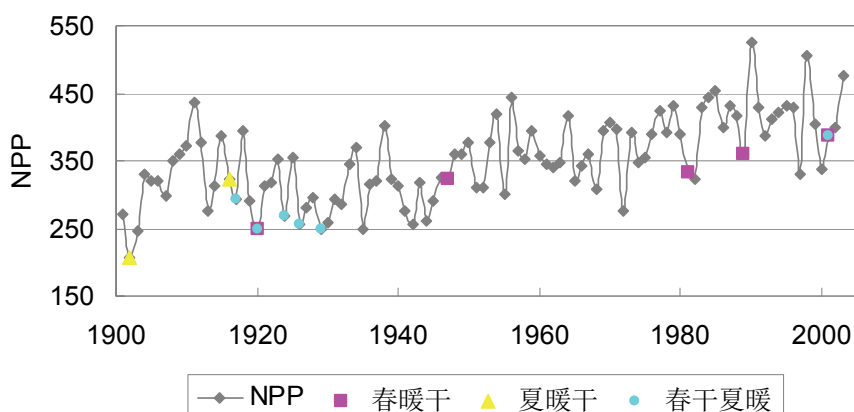


图 5.40 暖干气候叠加影响的 NPP

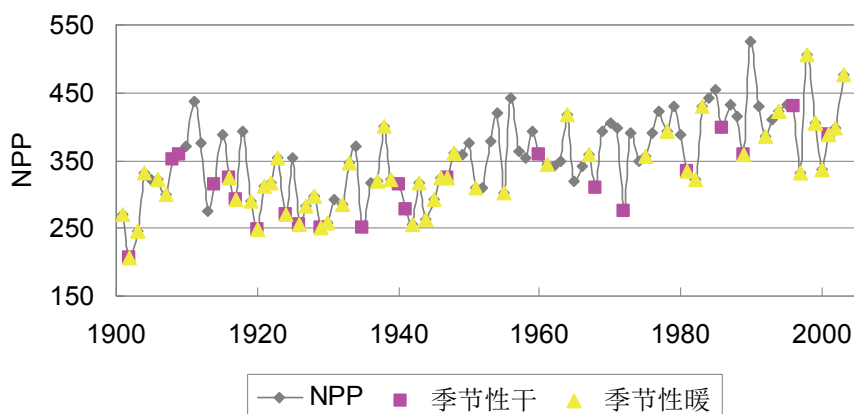


图 5.41 季节性降水和气温影响下的 NPP 年际变化

5.4 小结：中国林草交错带未来动态及其意义

中国温带森林草原交错带是温带落叶阔叶林生长的干旱极限, 局地研究发现这里存在明显的树木生长限制状况, 在区域研究上发现季节性气候因子的综合作用显著地影响着植被生长。在未来气候变化下, 特别是季节性气候的暖干化背景下, 气温的升高会对植被生长带来更多的抑制作用。

不考虑森林草原交错带特殊的局地地形和特征和土壤性质差异,气候变化仍然会对森林分布格局和生产力造成影响。从模型得到的植被生长的敏感性以及干旱的影响作用来看,森林生产力比森林覆盖对气候的响应更为敏感,并且在气候暖干化时森林生长的响应更敏感。因此,林草过渡带的森林可能会经历高生长停滞——生产力下降——森林被草原取代,这从气候暖干化(图 5.28)和夏季干旱模拟(图 5.39b)的植被格局图中可以明显看出。目前,森林分布的干旱极限下存在山杨林的成片死亡,虽然没有定量的研究结果,但这是调查中最靠近草原带的森林,树木密集矮小,生产力很低,很可能首先受到干旱的胁迫,导致水分供应不足,抑制了光合同化产物的形成,或者叠加虫害等足以引起死亡的灾害爆发(McDowell *et al.*, 2008)。森林生产力的降低和森林分布面积的减少,将对整个森林生态系统碳平衡造成一定的影响,阔叶林向针叶林乃至草原的转变也将带来土壤性质的缓慢变化,从而对土壤碳库产生影响(Zhang *et al.*, 2009, in submission)。这种植被功能型的转变和连同发生的生态系统功能的变化将不限于本文的局地研究区,而是在交错带一线都有可能发生。

森林草原交错带的未来动态除了具有生态学意义外,也与当前和未来的植被建设以及经济发展相关。交错带森林可能出现的退却和草原面积扩大对植被建设工程中乔、灌、草搭配,树种的选择以及栽种位置提出新的要求,需要以动态的眼光看待进行的生态工程是否具有长期的生态作用。同时,植被分布和生产力的变动也需要周边行政区的农牧生产方式随之变化,将植被建设与农牧生产结合,减轻气候变化造成的生态系统服务可能恶化的影响。

第六章 讨论

6.1 干旱极限条件下树木个体的水分利用策略

树木个体的生长不可避免的受到气温、降水和土壤水分的共同影响，为进行光合作用和蒸腾作用提供了条件。树木生长归根结底是一个水分利用有效性问题。植被在干旱条件下死亡被归结于水分不足引起的气孔关闭对光合作用的抑制以及水分不足以运输形成的导管或根区空穴化 (McDowell *et al.*, 2009)。

我们认为，树木在高生长进行的同时会对光合速率要求更高以达到同化产物对根系的分配来满足增加的蒸腾需求，也就是说高增长必然需要根系增长的支持，这就涉及到根冠比 (R:S)、同化产物分配 (allocation) 和根系生长问题。关于全球植被根冠比、同化产物分配和根系生长的研究为解释干旱极限树木生长限制提供了某些依据。研究表明，温带森林倾向于高的根冠比 (Mokany *et al.*, 2006)，因此树木在高生长的同时，必须增加更多的根生长量；根据根冠比的水分有效性假说，根冠比随水分有效性增加而减小，并由根冠比与降水的关系得到初步支持 (Mokany *et al.*, 2006)。因此，在正常环境中根冠比可以维持，甚至由于地上部分的同化分配高而表现为随地上部分生物量增加而减小；但在干旱条件下，根生物量的增加是根同化产物用于产生根毛以增加根的导水性 (蒋高明, 2004)，同化产物向根系分配增加，根冠比变大，而付出的代价恰恰是高生长的缺乏。可见，生长限制模式中干旱环境下高 WUE 不可能性就是由于光合产物无法满足充分的向地上分配维持高增长并向地下分配满足更大的蒸腾吸水需求。

那么根冠比和树高究竟是怎样的关系呢？树木长高必然带来更高的蒸腾需求，干旱条件下的水分不足以维持蒸腾拉力，需要根系增长增多以满足吸收要求。在这个前提下我们来看具体的分析：

树木高度增高意味着地上生物量 (S) 高，为了满足 S 增高，地下器官 (R) 也要增多（一方面是细根增多满足蒸腾耗水，一方面是粗根增多满足支撑要求），只是由于增高程度差别，R:S 整体可能降低，这是环境可以维持的情况；如果环境恶化，可能引起 R:S 升高 (R:S 水分有效性假说)，但如果由于光合速率 (P) 达不到光合产物足以维持 R 生长，树木不会倾向于高生长，树木自然就矮小化。树木倾向于高生长付出的代价有移植栽种实验进行验证发现，美洲黑杨 (*Populus deltoids*) 在移植到草原上后死亡的可能源于阔叶林对水的高需求以及光合产物太多的向茎 (stem) 分配 (Wilson, 1993)。将以上的论述模式化：

假定水分条件良好时存在一个 $R:S$;

水分条件恶化, 则 R 变大, S 变大或维持, $R:S$ 变大, 树高增加或维持;

水分条件更好, 则 S 变大, R 维持, $R:S$ 减小, 树高增加;

尽管生物量的比值 ($R:S$) 并不能代表 $TBCF:ANPP$ (地上净初级生产力:总地下碳通量), 比如, 根系生物量大并不一定是总地下碳通量大 (Litton *et al.*, 2007), 因为后者主要源于细根的周转, 前者包括了支持性的粗根, 但我们在生长限制模式中认为光合产物的地下分配不足同时包括了吸取资源的细根和支持的粗根, 在这个概念上存量和增量的来源一致。对森林生态系统中光合产物分配的研究中并未发现优先性 (priority), 但是向叶分配的比例较为稳定, 向茎和地下部分分配更容易在资源限制下分别表现出降低和升高 (Litton *et al.*, 2007)。水分有效性在森林生态系统中改变了光合产物在各部分的配给 (partition, % of GPP), 尽管并非所有的研究都一致, 大部分研究表明水分有效性的降低增加了光合产物在根部的配给 ($TBCF/GPP$), 表明增量配给受到了资源限制的影响。

在世界范围内从生产力 (productivity) 角度看, 低矮的植被占据着生产力相对较弱的生境。Tilman (1988) 总结了 6 种生产力植被梯度, 包括 Whittaker (1975) 指出的水分梯度 (moisture gradient), 即由美国西北沙漠灌丛——干草地——矮草草原——高草草原——栎树稀树草原——栎树-山核桃林——糖枫林——鹅掌楸-椴树林。在这种梯度上, 最富有生产力的生境被高大的闭合林冠并具有高的叶面积指数 (LAI) 的森林占据。因此, 在欧亚大陆温带阔叶林的干旱极限上观察到树木的矮小化也是与北美大陆的植被梯度类似的。同时, Tilman (1988) 指出, 高大植物比矮小植物需要更多的支持 (Greenhill, 1881; MacMahon, 1973), 也必须向地下支持组织分配更多的同化产物。基于以上观点, 缺乏足够高的 WUE 也难以满足同化产物向支持根 (粗根) 的分配。在一个广泛的生产力梯度上, 光合产物向根配给 ($TBCF/GPP$) 也随着生产力上升而下降 (Litton *et al.*, 2007)。

一个不争的事实是自然界存在枝干 (shoot) 规模和活性与根系 (root) 规模和活性的功能性平衡。在对根系生长的研究时必然要将其分为木质化、寿命长的粗根和快速周转的细根。当干旱被根感知后向茎传递信息, 并在那里开始进行碳利用和分配的调整。Gholz 等 (1990) 证实叶生长受限是树木对水分胁迫的主要反馈, 因此茎的碳汇活动下降而碳向根系分配 (Ericsson *et al.*, 1996)。从根系生长所需的同化产物在植物体内的运输来看, 长叶和长根时叶片运输光合产物的方向相反, 所以在落叶阔叶林和针叶林中长叶和根的时段具有异相性 (out of phase) (Dickson, 1989)。在生长季, 向上和向下运输是循环的, 先是叶部大量的碳汇

集,在全叶展开后向低端的茎部和和根部运输,并且不用于枝条生长和维持的光合产物才会向下输送到主茎,主要向下输送到低端茎和根部 (Dickson, 1989)。尽管树木可以储存碳水化合物供叶生长,但是新的细根的生长依赖于当前的 (current) 光合作用产物 (van den Driessche, 1987; Lippu, 1998), 新陈代谢活跃的细根寿命几乎完全与糖汇 (carbohydrate sink) 的强度有关 (Andersen, 2003)。

鉴于气孔是控制二氧化碳和水汽的关键通道,气孔导度的变化必然引起碳吸收和水蒸腾消耗的重新平衡,包括碳向根部的分配 (Cannell & Dewar, 1994)。自然选择可以以一种最佳的气孔状态使 WUE 在每日范围内最大化 (Cowan & Farquhar, 1977), 其中包括在茎与根之间的最佳碳分配假说 (Givnish, 1986a)。尽管这个假说充分考虑了气孔行为、叶水势、根部通导性等因素,并预期在空气干燥,对水分吸收抗性大或者叶肉阻碍二氧化碳传输时更多的碳向根部分配 (图 6.1), 但仍然没有将气体交换与养分和水分吸收的碳消耗结合 (Givnish, 1986a)。

树木在高生长时不仅需要更多的根系加强水分通导,同时地上部分也要配合产生更多的传到通导,因此边材横切面积与叶面积的正相关关系支持了管道假说 (pipe-model theory) (Shinozaki *et al.*, 1964), 该假说认为单位叶面积需要单位管道从根部导水。将管道假说与碳分配结合起来, Valentine (1985) 提出树木总是需要一定量的吸收根 (feeder roots) 来支持单位叶。Mäkelä (1986) 也成功的将管道模型与碳在地上/地下的功能性平衡相结合, 两人的模式都表明随着树高增大, 边材的生长消耗必须付出长叶和长根的代价, 从而导致高增量减缓乃至死亡 (图 6.2, 不同线形代表不同胸径欧洲赤松 (*Pinus sylvestris*))。这个理论也间接证明我们提出的模型中碳向根系分配不足的原因部分来源于同时向地上茎部导水组织 (韧皮部) 分配。

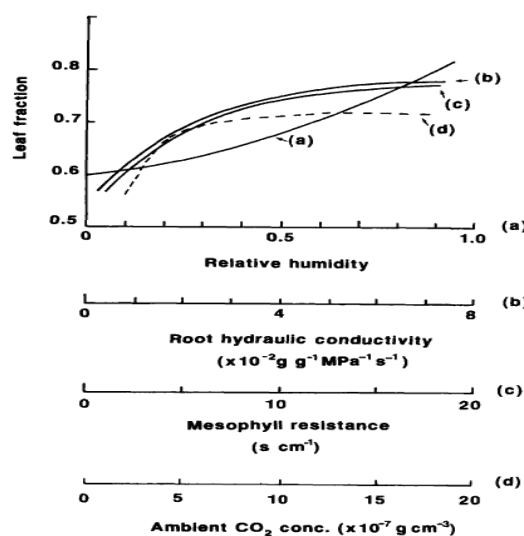


图 6.1 Givnish 假说验证 (引自 Cannell & Dewar, 1994)

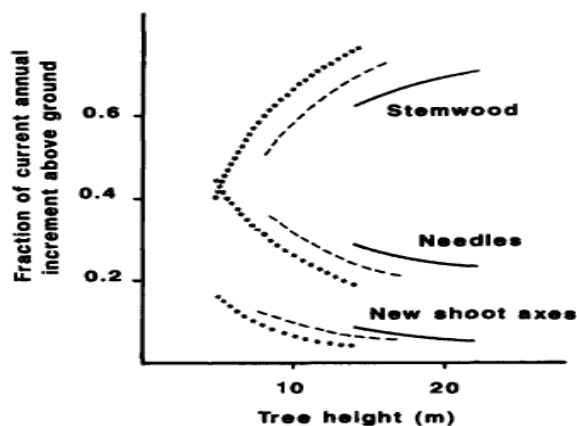


图 6.2 pipe-model 的验证 (来源同图 6.1)

6.2 森林群落水分利用策略和干旱林线的形成

6.2.1 干旱林线森林对土壤质地的适应和改造

尽管在整个温带落叶阔叶林区域上植被都会受到干旱的影响,表现出一致的气候响应,但在森林草原交错带响应会更敏感。温带森林草原交错带的阔叶林是温带落叶阔叶林的分布北界,也是分布的干旱极限。广大的落叶阔叶林生长所受到的水热条件限制在这里更为局地化,更需要小生境的调控,特别是土壤有效水分的利用以维持森林的生长,形成了干旱林线的实际格局(何思源等, 2008)。

在温带落叶阔叶林干旱极限下的土壤质地往往被认为对维持森林的生存意义重大,主要是考虑砂质土壤微弱的毛管作用减小了水分蒸发,更多的水分下渗到树木根系可以达到的深度。这个解释更适合于对如浑善达克沙地榆树疏林等沙地景观的解释,特别是对于沙地生长的一些特定树种(Zou *et al.*, 2000)。对森林-草原交错带土壤机械组成的分析结果更倾向于认为落叶阔叶林与土壤发育的协同作用促进了林木的维持。

同一地点的森林和草原群落土壤粒度分布曲线具有相似性,表明阴阳坡很可能经历过相同植被类型导致的类似成土过程,但由于植被类型的分异,植被影响的程度也产生了分异。这可能表明在气候变干时森林在阳坡退出了与草本的竞争,维持在阴坡相对有利的水分环境并对不利的土壤条件加以改造以更好的利用土壤资源,逐渐形成当前的干旱林线格局。水分与植被之间的非线性作用可能是形成半干旱区植被异质性格局的内在机制(Meinders & Breemen, 2005)。

森林在土壤形成中最重要的就是促进细颗粒物质的产生,维持更高的保水性。干旱极限下森林群落一方面不断地改善土壤性状,增加持水能力强的细颗粒物质比例,这一点在表层更为突出,另一方面从水分有效性来说,砂质土壤尽管持水性差,但其对水分的吸附力小,更容易被根系吸取。因此,温带落叶阔叶林干旱极限下依托地形对水分的调控而生存的森林,在对土壤性状的改造上也在向一个土壤水分最佳状态调整,不断地提高细颗粒物质来增加对水分的保有,同时在土壤水分含量低时依赖于砂质土壤较低的水分吸附力进行水分吸收。

6.2.2 干旱林线森林对土壤水分的利用

尽管实际林线受到土壤性质的深刻影响,但多年平均降水量反映的常年的干湿状况仍然是决定土壤水分含量的主导因子。从土壤水分含量垂直剖面变化看,研究区内 40cm 以上的土壤是水分变化相对活跃的层位,在此之下土壤水分变动

趋于平稳,这与根系分布有关,已有研究发现生长季温带落叶阔叶林土壤水分活跃层为上层(0-50cm)(Tuzinsky, 2005)。对全球陆地生态系统根系分布研究表明,温带落叶阔叶林有82%的根系集中在上层(0-50cm)(Jackson *et al.*, 1996),另一份关于细根(fine root, $d \leq 2\text{mm}$)的研究也表明81%的细根集中在上层(Jackson *et al.*, 1997)。阴坡阔叶林下土壤水分的平均状况明显优于相应草原,这与其粒径组成和相应的容重分析都是一致的,只有在平均降水量最大的白桦和山杨采样点才有可能出现容重小于1的情况,这是在一般森林土壤中常常出现的(马雪华, 1993)。相比之下,针叶林与其对应草原的水分差异在层位上不明显,在容重上也没有反映出来,这表明针叶林更为适应倾向于干旱的生境(Bugmann, 1995; 何思源, 2008),在砂质土壤上生长不完全像阔叶林那样依靠不断地对土壤进行改良,而是依靠长期进化的适应性或其他方式,如沙地林下共生的苔藓对于维持森林土壤水分意义重大(崔海亭, 个人通讯)。

阔叶林下土壤水分含量时间变化趋势明显,生长季前期林下相对含水量高,生长旺盛期和末期林下相对含水量反而低于草原。这意味着春季土壤水分的储备对于阔叶林生长至关重要,尽管生长旺盛的7、8月份降水丰沛,但土壤水分含量远离田间持水量,并且在到生长季末期时一直处于消耗状态,直到进入休眠期后,林下土壤水分稍有回升,并开始有降雪积累。生长季土壤水分波动状况涉及到整个土壤水分平衡状态,在世界其他温带落叶阔叶林中也有类似研究(Tuzinsky, 2005):在栎林生长季初期,土壤水分以毛管水形式上升,水分有效性强;而后随着蒸散发增强,土壤水分供给降低。如果在生长季遇到干旱,则很可能出现土壤水分的持续下降,当达到永久萎蔫点后,根系由于土壤水吸力增大而难以吸水,从而减弱了蒸腾和光合同化过程。这种干旱现象可能在林线持续存在,导致高生长的缓慢和停滞。

温带森林草原交错带的东北一线尽管也与内蒙古东南缘一样显示了地形对降水的重分配作用,但降水不是唯一的主导因子,向东北部延伸,降水量大约在350mm到370mm之间,在 45° 以上地区较低的温度得以维持土壤水分保持一个相对较高的值,显示了实际林线受到了区域气候的影响。因此,干旱林线下森林生长受到水分条件的制约,在有限的降水条件下,森林占据了地形上有利于土壤水分保存的位置,逐渐适应于砂质土壤的弱毛管蒸发,并不断改变土壤粒度以提高保水性。生长前期的土壤水分提供了森林生长的保障,生长季土壤水分的耗用在休眠期开始后慢慢得以补充。在降水与温度的双重作用下,落叶阔叶林北界可以到达 50° 。

6.3 温带落叶阔叶林对气候变化的敏感性和潜在危机

6.3.1 森林对气候变化的敏感性

森林生产力对气候变化不同方向的敏感性不同,对季节性降水减少和气温升高更为敏感,即气候暖干化时森林生产力的恶化程度要大于气候冷湿化时生产力的上升程度。同时,敏感性越强的气候因子这种生产力反馈的差异越大。这表明,温带森林的最大生产力是有限的。从实测研究和模型得到的温带落叶阔叶林净第一性生产力来看,我国温带落叶阔叶林 NPP 的实测数据为 $250-700\text{gC/m}^2\cdot\text{a}$ (刘世荣等, 1993),而各种模型模拟值为 $142-850\text{gC/m}^2\cdot\text{a}$ (周广胜和张新时, 1996; 孙睿和朱启江, 2000; 朴世龙等, 2001; 李高飞和任海, 2004),其均值一般都在 $600\text{gC/m}^2\cdot\text{a}$ 以下。在温带落叶阔叶林 NPP 减小的同时,模型中格网 FPC 确定的主导植被类型可能发生变化。已经有研究提到木本的死亡损失比树木生长积累发生得更快 (Allen, 2006),并且伴随着明确而持续的生态学影响,如对其他干扰过程(如火,侵蚀)的反馈以及对碳的埋存(sequestration)能力下降(IUFRO, 2009)。

夏季温度和夏季降水是最为敏感的影响因子,其次是春季降水和温度,再次是秋季降水和温度,冬季降水的敏感性很弱。这一结果凸显了我国温带季风气候特征。夏季气候条件最大程度的决定了植被生产力和植被覆盖,并且生产力对夏季温度变动始终是负反馈的,很难得到夏季温度的提高会促进生产力这一推论(IUFRO, 2009),并且现在已经提出这样的看法,即温带森林分布的半干旱到半湿润气候区的偏干地区由于会经历更频繁的干旱,从而导致初级生产力(primary productivity)在未来呈减少趋势。IPCC2007c[p.12-13]提出,目前在温带区域经历生产力快速增加的森林区域在未来会由于气候更为干旱化而转变为生产力下降,从而在将来某个未知时点出现整体生产力下降(Lucht *et al.*, 2006; Schaphoff *et al.*, 2006; Scholze *et al.*, 2006; Canadell *et al.*, 2007; Fischlin *et al.*, 2007; Raupach *et al.*, 2007),这种现象将极有可能在已经被定性为易受干旱胁迫的温带森林中凸显,包括美国西部,中国北方,欧洲南部,地中海地区和澳大利亚。我国温带落叶阔叶林区域处于这类地区偏干并且将持续干旱的地区。可能经历的春夏降水减少和气温上升无疑会加强干旱趋势(表 8.3)。在实际气候条件下,华北地区春旱发生也比较频繁,模型模拟的森林生产力对春季降水敏感,表明温带落叶阔叶林仍处于春旱多发地带,春季降水有利于增加土壤湿度,促进生长。由于春季是植被生长伊始,气温影响植被初始展叶(Welp *et al.*, 2007)。在情景 1 气候在平均状态下平稳运行时,春季和秋季气温升高一个标准差会引起生产力的微小上升,

但在春秋季气温逐渐上升的情景中,气温大幅度上升(50%)则会引起生产力的下降。春季林冠成长时期的干旱可能对碳平衡产生持续的影响(Noormets *et al.*, 2008),在北方生态系统中,春季变暖可以增加森林生产力(Arain *et al.*, 2002)。在一项对北方落叶阔叶林(白杨和柳树)净生态系统交换(NEE)对春季气温上升的敏感性研究中发现,春季温度升高20%,NEE上升88%(Welp *et al.*, 2007 seasonal drought3)。不过,温带落叶林阔叶林可能没有北方生态系统受到的温度限制强烈,因此才会对春季升温的响应更多的取决于气候变化的趋势(情景1-3)和升温的程度(50%为例)。森林生产力对秋季降水的反馈敏感性远小于夏季,可能是因为我国秋季降水的集中区域在35°N以南,北部降水大多小于250mm,同时气温相对偏低(谌芸和施能, 2003),对促进生产力作用有限。但这种中等强度正效应表明,在森林地区降水增加对生产力的促进作用大于减少地表辐射和温度而缩短生长周期的作用。在实际气候经历大范围秋季升温时,降水增加在一定程度上可以促进植被生长,所以春、秋季气温的稳定和小幅上升对维持森林生产力更有利。冬季降雪对森林NPP的影响效应微弱,但仍然保持正效应,这与春季融水量对土壤水分的影响有关。

植被生长对气候变化的反馈敏感性受到气候变化趋势本身的影响。我国气候变化预估中在CO₂中等排放水平下预计表面气温在21世纪的100年内将达到0.3~0.5℃/10a的增温趋势(丁一汇等, 2007),CRU数据显示温带落叶阔叶林带1983年以来的年均温增速为0.46℃/10a,1901年以来的趋势为0.08℃/10a,根据气候自然变化幅度0.05~0.1℃/10a(瞿章等, 1991),1983年以来的气候变化已经不属于气候的自然波动,情景3更为接近可能的气候变化。在趋势性气候变化时叠加季节性极端气候变化(本文中增减50%的气温或降水),提供了极端气候事件的可能影响,如1901年以来夏季气温变化趋势为-0.05℃/10a,1983年以来为0.36℃/10a,在这两种气候趋势下对夏季均温进行增减,明显的反映出更迅速的气候变化趋势下季节性气候波动会造成植被生产力更大的变化率。这表明,森林处于持续干旱化的环境时抵御干旱的能力会更低。同时,即使在和缓的气候变化下,偏离正常气候程度越大,对生产力造成的影响越大,敏感性并不是不变的,而是随着气候恶化愈加敏感。

因此,气候干旱化叠加气候极端事件对森林生长的影响可能会对当前森林格局造成较大的改变。气候暖干带来的森林覆盖降低可能会引起成片森林的破碎化,从而使得森林更容易受到周期性气候灾害的影响。在亚马逊,斑块状森林容易受到ENSO带来的干旱影响,导致树木死亡率提高,特别是在森林边缘区(Laurance & Williamson, 2001)。木本植被在其寿命时程内将要经历的气候变化

可能会增加死亡率和枯梢(die back),后者可能因为其他自然和人为原因而加剧。森林枯梢和衰退在世界各个拥有森林的大陆内已经成为了普遍现象(Allen, 2006): 1) 2002 年以来从美国西南阿拉斯加到亚利桑那犹他松(*Pinus edulis*)的片段性枯梢; 2) 亚马逊盆地的干旱影响; 3) 葡萄牙、西班牙和法国地中海山区松属(*Pinus*)和栎属(*Quercus*)一些种的枯梢; 4) 近年来蒙古北部低山森林-草原交错带欧洲赤松(*Pinus sylvestris*)枯梢; 5) 澳大利亚桉树(*Eucalypt*)枯梢; 6) 西非荒漠草原(Sahel)森林物种的枯梢。在我国内蒙古温带森林草原交错带低山丘陵上也出现了山杨(*Populus davidiana*)的干枯乃至死亡。一两次季节性干旱有可能引发一系列可以导致枯梢、改变火险概率或大型的害虫爆发(e.g. Hanson & Weltzin, 2000),从而导致温带森林生态系统由碳汇变为碳源。从长期气候变化看,温带森林生产力由于干旱限制在下一个世纪会减少,森林衰退和枯梢期将在全球变暖的趋势下更频繁的出现(Bréda *et al.*, 2006)。

6.3.2 干旱对森林生长的影响

我国北方地区干旱出现的季节性、年内持续时间和年际持续时间比较有规律,为进行干旱模拟提供了依据。气候变化通过改变自然干扰的频率(frequency)、强度(intensity)、持续时间(duration)和产生时间(timing)来影响森林(Dale *et al.*, 2001),并且有关于东亚落叶阔叶林的研究表明,干旱对NPP的影响与土壤水分胁迫比与气温更为密切(Hwang *et al.*, 2008)。在以降水距平设定的干旱模拟结果表明,干旱越严重,植被生产力越低,表明二氧化碳的同化在降水严重的减少的情况下更低。模型没有出现森林停止更新,但严重的干旱目前已经引起了美国犹他松的死亡(Breshears *et al.*, 2005)。同样程度的干旱,出现在夏季对生产力影响最大,其次是春季和秋季。不同季节树木生长处于不同的物候期,所以不同时期的干旱对植被生长的影响有差别。有研究表明,春季干旱主要抑制林冠生长和峰值叶面积形成,夏季干旱通过减少碳利用效率影响植物的碳状态(Ciais *et al.*, 2005),秋季干旱可能加速落叶,缩短生长季(Goulden *et al.*, 1996; Flanagan *et al.*, 2002),从而减少季节性的总第一性生产力积累。本文在极端干旱情景的模拟中没有考虑温度升高的影响,仅仅从水分亏缺的角度进行模拟,结果表明,由水分主导的干旱对碳利用效率的影响大于对同化器官形成不足的影响,而后者又大于秋季提前结束生长季的影响。夏季干旱之所以对植被生产力的影响最大,是因为我国温带落叶阔叶林处于东亚季风区,夏季风带来的丰沛降水配合较高的气温,是森林生长的最佳时期,但如果降水量减少,夏季高温导致的干旱

对植被生长就由促进转为抑制。对中国东部近 500 年来的极端干旱事件研究表明, 这些极端干旱事件都经历了一个夏季降水显著减少的过程(约 50%或以上), 这与本文的模拟设定一致。同时, 这些极端干旱都在中国北方首先出现然后向南扩展, 并且这种夏季降水的减少一般都由夏季季风的减弱和西太平洋副热带高压的异常西迁北上引起 (Shen *et al.*, 2007)。尽管生产力的骤然降低往往会由林火带来, 但在模型模拟中始终没有出现火烧。

模型结果进一步表明, 干旱事件的频率和持续时间对干旱时期的生产力平均状况影响不大, 这表明干旱达到一定持续时间和频率后的危害性相似。频率和持续时间对干旱的生产力恢复影响明显, 这种生产力的恢复既表现在由干旱到正常年份的恢复, 也表现在这种受到干旱扰动后的恢复与没有受到扰动时的正常生产力的差异。两者生产力的恢复都表现为随着干旱频率降低、持续时间缩短恢复程度越大, 并且干旱事件的频率比持续时间对后续生产力的恢复影响更显著。这表明干旱频率和持续时间作为干旱重要的性质, 决定了干旱的影响程度, 并为干旱后的恢复提供了应对依据。对于更依赖水分的草原植被而言, 干旱的频率和持续时间在决定气候对生物组成的影响的重要性早已有了认识 (Cook & Sims, 1975), 但在温带季风气候的森林生态系统中尚不多见。在对地中海植被的研究中发现, 严重的干旱后森林仍然具有一系列的光合保护机制来保有潜在的光合器官功能性, 从而在干旱结束后迅速恢复光合活性 (Gallé *et al.*, 2007)。同时, 如果干旱是不断出现的现象, 那么干旱后生产力的恢复程度并不是一成不变的, 相对于干旱时期的生产力, 旱后生产力的恢复程度会逐渐减小, 表明长期出现的干旱并不利于植被生产力的恢复; 相对于未受干扰的生产力, 受到干扰后恢复的生产力先逐渐接近前者, 但随后又慢慢远离前者, 表明植被受到胁迫后其恢复能力是有限的。这种恢复能力在时间上的变化表明干旱的影响具有持续性。对地中海植被干旱后恢复力的研究表明, 反复出现的干旱将通过减少存活植物再生而造成恢复力的持续性丧失 (Lloret *et al.*, 2004)。生产力的变化仅仅反映了一个侧面 (Birdsey *et al.*, 2008), 生态系统结构、物种组成和功能也可能由于某些物种或大小的树木死亡而发生改变 (Hanson & Weltzin, 2000; Breshears *et al.*, 2005), 模型无法确切的模拟出树种差异, 而不同树种对干旱的敏感性不同 (Ogaya *et al.*, 2003)。

6.4 研究的不确定性分析

6.4.1 植被和环境因子指标的不确定性和可能改进

土壤含水量受气候条件影响很大,在生长旺盛期采样,研究区降水比较频繁,在降水期间和降水后一段时间土壤含水量会出现明显的饱和,尽管分析表明各个地点的土壤含水量相对大小年际上没有差别,但个别异常值可能对分析造成较大的影响。此外,选择进行采样的地点每个树种只有 3 个,刚刚达到统计分析的要求,在数量上是否满足对环境的代表性可能存在问题。土壤含水量观测需要长期进行,并针对研究区干旱林线根据依据地形位置进行采样点设计,这需要进行永久样地的设置,并配合以长期的气象观测。然而,目前的研究条件难以满足多个固定样地长期连续的土壤水分观测。

本研究在使用归一化植被指数 (NDVI) 进行分析主要考虑了 NDVI 对植被覆盖和生物量的代表作用。在进行分析时,各个季节和生长季的研究空间范围一致,有助于消除土壤背景的影响,NDVI 月均值采用 MVC (Maximum Vegetation Composition) 方法,目的在于消除大气和云的影响。NDVI 的空间分辨率可以与气象台站的降水数据相匹配,并表现出对气候因子的显著响应,表明它可以在一定程度上代表植被生长状况,显示不同季节和物候期的植被生长特征。然而,NDVI 毕竟是一个“标准化”的指标,所做的信息提取具有即时性,与气象观测记录的时间不完全一致,因此,以 NDVI 分析植被生长对气候变化的响应可能存在时间的错位。同时,植被动态在某些关键时段以季节为单位进行分析不够精细,使用的 NDVI 的时间分辨率无法满足对植被生长的关键时期的动态观测。也是由于 NDVI 的即时性,除植被信息外的其他信息,如土壤背景、地表枯落物等的影响会对探究 NDVI 的真实气候响应有干扰。尽管如此,在目前的研究中,NDVI 作为分析植被动态和检验植被模型的重要指标仍然具有不可替代的作用。

6.4.2 模型结果的可靠性分析

为了探究森林生长对未来可能气候变化的响应敏感性,本文从两个方面在 LPJ 模型中进行了植被生长模拟,分别是气候趋势性变化和极端干旱,并且在趋势性变化中选择了平均值稳定序列、百年来气候趋势和 21 年来气候趋势三个情景;在极端干旱波动变化中设定了干旱程度、频率和持续时间。LPJ 模型对生物量的模拟比较成熟,但由于在植被功能型 (PFT) 生理和物候等参数的设定上我国存在偏差,对此进行了纠正,并考虑了根系分布的合理性。模型中存在的降

水随机发生器以及其他不可知的因素对模型结果可能具有影响,经验证,对同一套数据进行 5 次模型运行后,对区域 NPP 均值的时间序列分析没有发现显著差异, LSD 检验也没有发现组间差异,因此,模型的任何一次运行都是可以接受的。

模拟得到的基于格点最大 FPC 的植被类型图表明,LPJ 模型对模型植被功能型的准确度较高,对于我国而言,尽管区分了温带落叶阔叶林南北两部分,但其位置基本正确。这种本质上对潜在植被的模拟,与中国植被图确定的实际植被吻合度也可以接受,具有现实意义,在此基础上进行植被动态模拟可以在一定程度上预计植被的未来变动。

利用实际气候模拟得到的落叶阔叶林区域年 NPP 在趋势上与生长季 NDVI 的趋势一致,但是反映植被盖度的 FPC 与 NDVI 的波动一致性弱,一方面说明 NDVI 被用于代表生物量的可靠性,另一方面较为稳定的 FPC 在一定程度上反映了植被在气候的有限波动下仍可以维持其主导植被类型。模型强调植物生理过程,模拟的 NPP 包含了生产力的累积,而 NDVI 只是植被即时信息的提取,并受到土壤等背景因子的影响。

由于用来进行验证的 NDVI 序列只有 20 多年,而模拟的基本时长可以达到 100 年,气候的趋势性必然会发生变化。对我国夏季降水的年代际变化研究表明(黄荣辉等, 1999),华北地区 50 年代降水偏多, 60 年代转为偏少, 80 年代继续加剧。CRU 数据也表明温带落叶阔叶林区域的年降水量在 60 年代和 80 年代都发生过明显变化,因此分析 1983-2003 年序列是有意义的。百年来和 20 多年来气候变化的相反趋势主要表现在春夏降水和夏季温度上,引起了 NPP 由正转负的趋势,从空间分布看,这种趋势的扭转是普遍存在的。从短期年际波动看(表 6.1),除了秋冬降水, NPP 对各个因子的响应方向与 NDVI 一致,表明生长季 NDVI 均值和模拟得到的 NPP 在植被生长前期和中期对气候的响应具有可比性。模型模拟的生产力对气候年际变化的响应总体而言比 NDVI 对气候的响应更敏感。模型对生物量的模拟是根据设定好的统计关系,通过输入日降水、气温、云量以及 CO₂ 数据计算不同物候时期 PFT 的碳平衡的,因此对生物量的模拟是直接针对植物体本身的,并且具有积累性。

表 6.1 NDVI 与模型 NPP 对季节性气候年际波动的反馈

指标	春季降水	夏季降水	秋季降水	冬季降水	春季气温	夏季气温	秋季气温
NPP	0.777^b	0.848^b	0.070	-0.369	-0.099	-0.900^b	0.806^b
NDVI	0.092	0.236	-0.684 ^a	0.521	-0.198	-0.171	0.068

气候平均状况下模型的运行结果显示了 NPP 具有上升趋势。鉴于 NPP 对气

候波动的敏感性,模型对降水数据的运用是由月份数据随机化到日,这在某些物候的关键时期可能会带来植被生长的差异。大气 CO_2 浓度缓慢平稳上升会增加森林生态系统 NPP (Melillo *et al.*, 1993) 并促进树木生物量积累。但还有研究表明 CO_2 激发的生长随着时间和树苗年龄增大而减小 (Bazzaz *et al.*, 1993; Norby *et al.*, 1995; Lee & Jarvis, 1995)。鉴于技术条件,很少能够开展对天然林长期 CO_2 浓度升高的观测。Körner 等 (2005) 在瑞士森林进行了为期 4 年的 CO_2 升高的研究,模拟浓度达到 530ppm,利用树轮分析发现树种间存在较大的响应差异,尽管主要树种刚生长到其寿命的一半,并且只有最大规模的 2/3 大,生长应该很有活性,但并没有显示出持续的生长,在落叶林生物量中没有固定更多的碳。模型结果中 FPC 的波动很小,变异系数 (cv) 仅有 0.02,反映了盖度所代表的森林生长状况基本上处于饱和,并受制于模型设定的最大建群率 (Sitch *et al.*, 2003)。而 NPP 呈现平稳上升然后缓慢下降一方面表明如果没有气候条件的变异,大气 CO_2 浓度的升高可以在至少 60 年内促进森林生物量的积累,但这种促进作用会减弱。LPJ 模型内树木的更新是基于个体的,并将新树苗的产生与生物量的增加联系起来,同时只确定一个年龄层级,因此无法判断这种 NPP 对 CO_2 的正反馈是由于幼树增加,还是由于光合作用增强。

模型考虑了详尽的生理过程,但由于 LPJ 是一个全球尺度的植被动态模型,无论是设定的参数还是本研究中修正的一些参数,它们都还不能完全反映研究区的真实状况,包括土壤物理性质、植被根系分布以及干旱极限下高增长和径向增长的不同步性,这增加了模型结果的不确定性。

第七章 结论

本文从树木个体、森林群落和温带落叶阔叶林生物群区三个水平探究了干旱极限条件下树木和森林的水分利用及其影响因子，量化了植被动态对气候变化响应的敏感性，模拟了温带森林对未来不同干旱情景的响应，主要得到以下结论：

1. 树木在干旱极限下表现为高生长缓慢或停滞；随着树木高度增加，WUE 增加；从水分有效利用角度看，干旱条件下树木倾向于降低树高维持蒸腾作用和光合产物地上地下分配的平衡。
2. 土壤水分的时空格局决定了旱极下林草交错带的植被格局；高降水和细的土壤质地条件下的森林群落土壤含水量高，但季节性波动性强，在生旺盛期和末期表层含水量一般低于草原，在生长前期高于草原，生长前期水分的储存利于维持森林后续需求；砂质土壤的水力特征提高了水分有效性；阔叶林下土壤水分的季节波动反映了森林前期土壤储水的主要作用。
3. 温带落叶阔叶林 NPP 比 FPC 对气候变化响应更敏感；FPC 和 NPP 对生长前、中期气温和降水响应敏感；敏感性在季节性气候暖干化方向、气候变化趋势剧烈以及气候变化程度大时更强，在降水和气温波动 50%以上时响应敏感性则趋同。
4. 当出现持续的干旱时，季节性干旱程度越大，森林生产力越低，夏季干旱的影响最大；连季干旱的对生产力的影响大于单季干旱；干旱频率和持续时间主要对后期生产力的恢复产生影响，频率低、持续时间短干旱事件后森林生产力恢复能力强，但这种恢复力会随时间而衰减。

参考文献

1. 埃塞林顿. 1989. 环境和植物生态学. 北京: 科学出版社.
2. 陈洪松, 劭明安, 王克林. 2005. 黄土区深层土壤干燥化与土壤水分循环特征. 生态学报, 25(10): 2491-2498.
3. 陈瑜, 倪健. 2008. 利用孢粉记录定量重建大尺度古植被格局. 植物生态学报, 32(5): 1201-1212.
4. 崔海亭, 雍世鹏. 1986. 大兴安岭南段植被空间结构遥感分析. 内蒙古草场资源遥感应应用研究. 呼和浩特: 内蒙古大学出版社.
5. 丁一汇, 任国玉, 赵宗慈等. 2007. 中国气候变化的检测及预估. 沙漠与绿洲气象, 1(1): 16-18.
6. 甘超华, 马礼, 南秋菊. 2005. 基于水资源的坝上植被生态恢复建设. 干旱区资源与环境, 19(4): 39-42.
7. 郭庆华, 喻红. 1999. 北方森林草原生态过渡带的遥感研究. 北京大学学报(自然科学版), 35(4): 550-557.
8. 何思源, 刘鸿雁, 任佶等. 2008. 内蒙古高原东南部森林-草原交错带的地形-气候-植被格局和植被恢复对策. 地理科学, 28(2): 253-258.
9. 侯学煜. 1960. 中国植被. 北京: 人民教育出版社.
10. 侯学煜. 1960. 中国植被. 北京: 人民教育出版社.
11. 侯学煜. 1964. 论中国植被分区的原则、依据和系统单位. 植物生态学与地植物学丛刊, 2(2): 153-179.
12. 侯学煜. 1988. 中国自然地理·植物地理(下册). 北京: 科学出版社.
13. 胡良军, 劭明安, 杨文治. 2004. 黄土高原土壤水分的空间分异及其与林草布局的关系. 草业学报, 13(6): 14-20.
14. 黄荣辉, 徐予红, 周连童. 1999. 我国夏季降水的年代际变化及华北干旱化趋势. 高原气象, 18(4): 466-476.
15. 黄永梅, 刘鸿雁, 崔海亭. 2001. 内蒙古东南缘森林草原过渡带景观的若干特征. 植物生态学报, 25(3): 257-264.
16. 蒋高明. 2004. 植物生理生态学. 北京: 高等教育出版社.
17. 李博, 孙鸿良, 曾泗弟等. 1980. 呼伦贝尔牧区草场植被资源及其利用方向的探讨. 自然资源, 2(4): 30~36.
18. 李博, 壅世鹏, 李忠厚. 1988. 锡林河流域植被及其利用. 见: 草原生态系统研究(第3集). 中国科学院内蒙古草原生态系统定位站编. 北京: 科学出版社. pp84-183.
19. 李栋梁, 吕兰芝. 2002. 中国农牧交错带的气候特征与演变. 中国沙漠, 22(5): 483-488.
20. 李高飞, 任海. 2004. 中国不同气候带各类型森林的生物量和净第一性生产力. 热带地理, 24(4): 306-310.
21. 李晓兵, 史培军. 2000. 中国典型植被类型 NDVI 动态变化与气温、降水变化的敏感性分析. 植物生态学报, 24(3): 379-382.
22. 李晓兵, 王瑛, 李克让. 2000. NDVI 对降水季节性和年际变化的敏感性. 地理学报, 55(Supplement): 82-89.
23. 李裕元, 劭明安. 1996. 黄土高原气候变迁、植被演替与土壤干层的形成. 干旱区资源

- 与环境, 15(1): 72-77.
24. 梁妙玲, 谢正辉. 2006. 我国对植被分布和净初级生产力影响的数值模拟. 气候与环境研究, 11(5): 582-592.
25. 林超, 李昌文. 阴阳坡在山地地理研究中的意义. 地理学报, 1985, 40(1): 20-28.
26. 刘芳园, 肖嗣荣, 张可慧等. 2008. 河北省干旱化初探. 气候与环境研究, 13(3): 309-317.
27. 刘濂. 1965. 河北省坝上草原植被概况. 植物生态学与地植物学丛刊, 3(2): 30-316
28. 刘濂. 1981. 关于河北境内森林草原的划分. 植物生态学与地植物学丛刊, 5(4): 308-312.
29. 刘慎谔, 冯宗炜, 赵大昌. 1959. 关于中国植被区划的若干问题. 植物学报, 8(2): 87-105.
30. 刘世荣, 徐德应, 王兵. 1993. 气候变化对中国森林生产力的影响. 林业科学研究, 6(6): 634-642.
31. 马柱国, 符淙斌. 2006. 1951-200 年中国北方干旱化的基本事实. 科学通报, 51(20): 2429-2439.
32. 马柱国, 任小波. 2007. 1951-2006 年中国区域干旱化特征. 气候变化研究进展, 3(4): 195-201.
33. 齐述华, 王长耀, 牛铮等. 2004. 利用 NDVI 时间序列数据分析植被长势对气候因子的响应. 地理科学进展, 23(3): 91-99.
34. 瞿章等. 1991. 近几十年来北半球 30hPa 气温、中国气温和 O₃ 含量的演变趋势. 气候变化与环境问题全国学术讨论会论文汇编, 中国科学技术协会编.
35. 孙睿, 朱启疆. 2000. 中国陆地植被净第一性生产力及季节变化研究. 地理学报, 55(1): 36-45.
36. 孙艳玲, 延晓冬, 谢德体等. 2007. 应用动态植被模型 LPJ 模拟中国植被变化研究. 西南大学学报, 29(11): 88-91.
37. 王庆锁. 2004. 河北北部\内蒙古东部森林草原交错带植被和生物多样性的研究. 北京: 气象出版社.
38. 翁恩生, 周广胜. 2005. 用于全球变化研究的中国植被功能型划分. 植物生态学报, 29(1): 81-97.
39. 吴征镒(主编). 1980. 中国植被. 北京: 科学出版社.
40. 袁婧薇, 倪健. 2007. 中国气候变化的植物信号和生态证据. 干旱区地理, 30(4): 465-473.
41. 张晶晶, 陈爽, 赵昕奕. 2006. 近 50 年中国气温变化的区域差异及其与全球气候变化的联系. 干旱区资源与环境, 20(4): 2-6.
42. 张军涛, 李哲. 2001. 东北农牧交错区水分条件及其对植被分布的影响. 地理科学, 21(4): 297-300.
43. 张信宝, 安芷生, 陈玉德. 1998. 半干旱区植被恢复与岩土性质. 地理学报, 53(B12): 134-140.
44. 赵哈林, 赵学勇, 张铜会等. 2002. 北方农牧交错带的地理界定及其生态问题. 地球科学进展, 17(5): 739-747.
45. 赵茂盛, Neilson RP, 延晓冬等. 气候变化对中国植被可能影响的模拟. 地理学报, 57(1): 28-38.
46. 赵文智, 宝音. 1994. 河北坝上疏缓丘陵华北落叶松人工林生长特性研究. 中国沙漠, 14(4): 66-71.
47. 赵文智. 1996. 河北坝上半干旱/半湿润过渡带土壤水分状况研究. 中国沙漠, 16(2): 105-111.

48. 中国科学院内蒙古宁夏综合考察队. 1985. 内蒙古植被. 北京: 科学出版社.
49. 中国科学院自然区划工作委员会. 1959. 中国植被区划(初稿). 北京: 科学出版社.
50. 周广胜, 张新时. 1996. 全球气候变化的中国自然植被的净第一性生产力研究. 植物生态学报, 20(1): 11-19.
51. 朱士诚. 1983. 陕北黄土高原上森林草原的范围. 植物生态学与地植物学丛刊, 7(2): 122-131.
52. 邹厚远, 李玲, 刘克俭. 1994. 黄土高原植被及其合理利用与保护. 见: 植被生态研究. 姜恕, 陈昌笃编. 北京: 科学出版社. pp146-153.
53. 邹厚远, 梁一民, 孙建亭. 1980. 陕北黄土区植被区划的初步研究. 植物学报, 22(4): 399-401.
54. Abrams MD 1990. Where has all the White Oak gone? *BioScience*, 53(10): 927-939.
55. Allen CD. 2006. Climate-induced forest dieback: an emergent global phenomenon? USGS Jemez Mountains Field Station, Los Alamos NM, 87544.
56. Andersen CP 2003. Source-sink balance and carbon allocation below ground in plants exposed to ozone. *New Phytologist*, 157(2): 213-228.
57. Arain MA, Black TA, Barr AG *et al.* 2002. Effects of seasonal and interannual climate change variability on net ecosystem productivity of boreal deciduous and conifer forests. *Canadian Journal of Forest Research* 32, 878-891.
58. Archer S, Boutton TW, Hibbard KA 2001. Trees in grasslands: biogeochemical consequences of woody plant expansion. In: *Global Biogeochemical Cycles in the Climate System* (eds Schulze E-D, Harrison SP, Heimann M, Holland EA, Lloyd J, Prentice IC, Shimel D), Academic Press, San Diego.
59. Bai YG, Broersma K, Thompson D *et al.* 2004. Landscape-level dynamics of grassland-forest transitions in British Columbia. *Journal of Range Management*, 57(1): 66-75.
60. Bartzokas A, Lolis CJ, Metaxas DA 2003. A study on the intra-annual variation and the spatial distribution of precipitation amount and duration over Greece on a 10 day basis. *International Journal of Climatology*, 23(2): 207-222.
61. Bates JD, Svejcar T *et al.* 2006. The effects of precipitation timing on sagebrush steppe vegetation. *Journal of Arid Environments*, 64(4): 670-697.
62. Battles JJ, Robards T, Das A *et al.* 2008. Climate change impacts on forest growth and tree mortality: a data-driven modeling study in the mixed conifer forest of the Sierra Nevada, California. *Climate Change*, 87(Suppl1): S193-S213.
63. Bazzaz FA, Miao SL. 1993. Successional status, seed size, and responses of tree seedlings to CO₂, light, and nutrients. *Ecology*, 74(1): 104-112.
64. Birdsey RA, Dahm CN, Heath LS *et al.* 2008. Land Resources: Forest and Arid Lands. In: *The Effects of Climate Change on Agriculture, Land Resources, Water Resources, and Biodiversity*. Synthesis and Assessment Product 4.3 U.S. pp83, Climate Change Science Program, Washington, DC.
65. Bolstad P, Vose J, McNulty S. 2001. Forest productivity, leaf area, and terrain in southern Appalachian deciduous forests. *Forest Science*, 47(3): 287-330.
66. Bond WJ, Woodward FI, Midgley GF. 2005. The global distribution of ecosystems in a world without fire. *New Phytologist*, 165(2): 525-537.

67. Bonilla CA, Bonomelli C, Urrutia G 2002. Spatial and temporal distribution of precipitation and soil water content at three forest sites of VIII Region of Chile. *Agricultura Técnica*, 62(4): 541-554.
68. Botkin DB, Janak JF Wallis JR 1972. Some ecological consequences of a computer model of forest growth. *Journal of Ecology*, 60(3):849-872.
69. Box EO 1981. Predicting physiognomic vegetation types with climate variables. *Plant Ecology*, 45(2): 127-139.
70. Branson FA, Miller RF, McQueen IS 1976. Moisture relationships in twelve Northern Desert shrub communities near Grand Junction, Colorado. *Ecology*, 57(6): 1104-1124.
71. Bréda N, Roland H, Granier A *et al.* 2006. Temperate forest trees and stands under severe drought: a review of ecophysiological responses, adaptation processes and long-term consequences. *Ann. For. Sci.*, 63, 625-644.
72. Breshears DD, Cobb NS, Rich PM. 2005. Regional vegetation die-off in response to global-change-type drought. *PNAS*, 102(42): 15144-15148.
73. Briggs JM, Knapp A, Archer S *et al.* 2006. Shrub encroachment across North America: a multi-site synthesis of patterns, mechanisms, and consequences. 91st Ecological Society of America Annual Meeting, August 6-11, 2006, Memphis, Tennessee. pp.99.
74. Broersma K, Krzic M, Newman RF *et al.* 2000. Effects of grazing on soil compaction and water infiltration in forest plantations in the Interior of British Columbia. In: *Proceedings, From science to management and back: a science forum for southern interior ecosystems of British Columbia* (eds Hollstedt C, Sutherland K, Innes T), Southern Interior Forest Extension and Research Partnership, Kamloops, B.C., pp. 89-92.
75. Brooks PD, Campbell DH, Tonnessen KH *et al.* 1999. Natural variability in N export from headwater catchments: Snow cover controls on ecosystem N retention. *Hydrological Processes*, 13(14-15): 2191-2201.
76. Brooks PD, Williams WM, Schmidt SK 1998. Inorganic nitrogen and microbial biomass dynamics before and during spring snowmelt. *Biogeochemistry*, 43(1): 1-15.
77. Budde ME, Tappan G *et al.* 2004. Assessing land cover performance in Senegal, West Africa using 1-km integrated NDVI and local variance analysis. *Journal of Arid Environments*, 59(3): 481-498.
78. Bugmann H, Cramer W 1998. Improving the behavior of forest gap models along drought gradients. *Forest Ecology and Management*, 103(2-3): 247-263.
79. Bugmann H, Solomon AM. 1995. The use of a European forest model in North America: A study of ecosystem response to climate gradients. *Journal of Biogeography*, 22(2-3): 477-484.
80. Canadell JG, Pataki DE, Gifford R *et al.* 2007. Saturation of the terrestrial carbon sink. In: *Terrestrial ecosystems in a changing world* (eds Canadell JG, Pataki DE and Pitelka LF), pp.59-78, Springer-Verlag, Berlin.
81. Cannell MGR, Dewar RC 1994. Carbon allocation in trees: a review of concepts for modeling. In: *Advances in Ecological Research*, 25 (eds Begon, Fitter AH), pp. 83-87, 88-90. Academic Press, London, UK.
82. Caylor KK, Shugart HH 2004. Simulated productivity of heterogeneous patches in Southern

- African savanna landscapes using a canopy productivity model. *Landscape Ecology*, 19(4): 401-415.
83. Chapin FS, Rincon E, Huante P 1993. Environmental responses of plants and ecosystems as predictors of the impact of global change. *Journal of Bioscience*, 18(4): 515-524.
84. Chen ZM, Babiker IS, Chen ZX *et al.* 2004. Estimation of interannual variation in productivity of global vegetation using NDVI data. *International Journal of Remote Sensing*, 25(16): 3139-3159.
85. Chong DS, Mougin E, Gastellu-Etchegorry JP 1993. Relating the global vegetation index to net primary productivity and actual evapotranspiration over Africa. *International Journal of Remote Sensing*, 14(8): 1517-1546.
86. Ciais P, Reichstein M, Viory N *et al.* 2005. Europe-wide reduction in primary productivity caused by the heat and drought in 2003. *Nature*, 437: 529-533.
87. Collatz GJ, Ball JT, Grivet C *et al.* 1991. Physiological and environmental regulation of stomatal conductance, photosynthesis and transpiration: a model that includes a laminar boundary layer. *Agricultural and Forest Meteorology*, 54(2-4):107-136.
88. Comins HN, McMurtrie RE 1993. Long-term response of nutrient limited forests to CO₂-enrichment; equilibrium behavior of plant-soil models. *Ecological Applications*, 3(4): 666-681.
89. Cook CW and Sims PL. 1975. Drought and its relationship to dynamics of primary productivity and production of grazing animals. In: *Proceedings, Evaluation and Mapping of Tropical African Rangelands*. pp163-168, Addis Ababa, Ethiopia.
90. Cowan IR, Farquhar GD 1977. Stomatal function in relation to leaf metabolism and environment. *Symposia of the Society for Experimental Biology*, 31: 471-505.
91. Cowling RM, Campbell BM. 1980. Convergence in vegetation structure in the Mediterranean communities of California, Chile and South Africa. *Plant Ecology*, 43(3): 1573-5052.
92. Cowling SA 1999. Simulated effects of low atmospheric CO₂ on structure and composition of North American vegetation at the Last Glacial Maximum. *Global Ecology and Biogeography*, 8(2): 81-93.
93. Cox PM. 2000. Description of the TRIFFID dynamic global vegetation model. Hadley Centre Technical Note, No. 24, Met Office, Bracknell, UK, pp16.
94. Cutforth H, O'Brien EG, Tuchelt J *et al.* 2004. Long-term changes in the frost-free season on the Canadian prairies. *Canadian Journal of Plant Science*, 84(4): 1085-1091.
95. Dale VH, Joyce LA, McNulty S *et al.* 2001. Climate change and forest disturbances. *BioScience*, 51(9): 723-734.
96. Davenport ML, Nicholson SE 1993. On the relation between rainfall and the Normalized Difference Vegetation Index for diverse vegetation types in East Africa. *International Journal of Remote Sensing*, 14(12): 2369-2389.
97. Davis MB 1981. Quaternary history and the stability of forest communities. In: *Forest succession: concepts and applications* (eds West DC, Shugart HH, Botkin DB), pp132-153, New York: Springer-Verlag.
98. De Michele C, Vezzoli R *et al.* 2008. A minimal model of soil water-vegetation interactions forced by stochastic rainfall in water-limited ecosystems. *Ecological Modelling*, 212(3-4):

- 397-407.
99. Delire C, Levis S, Bonan G *et al.* 2002. Comparison of the climate simulated by the CCM₃ coupled to two different land-surface models. *Climate Dynamics*, 19: 657-669.
100. Dickinson RE, Henderson-Sellers A, Kennedy PJ 1993. Biosphere-Atmosphere Transfer Scheme (BATS) Version 1e as coupled to the NCAR Community Climate Model, University Corporation for Atmospheric Research, Boulder, CO., pp 69.
101. Dickson RE 1989. Carbon and nitrogen allocation in trees. *Annales des sciences forestières*, 46(Supl.): 631-647.
102. Domroes M, Kaviani M *et al.* 1998. An Analysis of Regional and Intra-annual Precipitation Variability over Iran using Multivariate Statistical Methods. *Theoretical and Applied Climatology*, 61(3): 151-159.
103. Dulamsuren C, Welk E, Jager E J *et al.* 2005. Range-habitat relationships of vascular plant species at the taiga forest-steppe borderline in the western Khentey Mountains, northern Mongolia. *Flora*, 200(4): 376-397.
104. Duvalignaud P, Denaeyer-De-Smet, S 1970. Biological cycling of minerals in temperate zone forests. In: *Analysis of temperate forest ecosystems* (eds Reichle DE), pp.199-205, Springer-Verlag, New York.
105. Ellis J, Price P, Boone R *et al.* 2001. Integrated assessment of climate change affects on steppe vegetation in Mongolia and Inner Mongolia. In: *Fundamental Issues Affecting Sustainability of the Mongolian Steppe* (eds Chuluun T, Ojima, D), Ulaan Baatar, Mongolia: Mongolian Academy of Science.
106. Emanuel WR, Shugart HH, Stevenson MP 1985. Climatic change and the broad-scale distribution of terrestrial ecosystem complexes. *Climatic Change*, 7(1): 29-43.
107. Ericsson T, Rytter L, Vapaavuori E 1996. Physiology of carbon allocation in trees. *Biomass and Bioenergy*, 11(2/3): 115-127.
108. Fang J, Piao S, Field C *et al.* 2003. Increasing net primary production in China from 1982 to 1999. *Frontier in Ecology and Environment*, 1 (6): 293-297.
109. Fang J, Piao S, Zhou L *et al.* 2005. Precipitation pattern alter growth of temperate vegetation. *Geophysical Research Letters*, 32: L21411, doi: 10.1029/2005GL024231.
110. Fargione J, Tilman D 2005. Niche differences in phenology and rooting depth promote coexistence with a dominant C4 bunchgrass. *Oecologia*, 143(4): 1432-1939.
111. Farquhar GD, van Caemmerer S, Berry JA 1980. A biochemical model of photosynthetic CO₂ assimilation in leaves of C₃ species. *Planta*, 149(1): 78-90.
112. Fay PA., Kaufman DM, Jesse B *et al.* 2008. Changes in grassland ecosystem function due to extreme rainfall events: implications for responses to climate change. *Global Change Biology*, 14(7): 1600-1608.
113. Field CB, Randerson JT, Malmström CM 1995. Global net primary production: combining ecology and remote sensing. *Remote Sensing of Environment*, 51: 74-88.
114. Fischlin A, Midgley GF, Price JT *et al.* 2007. Ecosystems, their properties, goods and services. In: *Climate change 2007: Impacts, adaptation and vulnerability. Contribution of Working Group II to the Fourth Assessment Report of the Intergovernmental Panel of Climate Change (IPCC)* (eds Parry ML, Canziani OF, Palutikof JP. *et al.*), pp. 211-272, Cambridge

- University Press, Cambridge, UK.
115. Fisher RF, Jenkins MJ, Fisher WF 1987. Fire and the prairie-forest mosaic of Devils Tower National Monument. *American Midland Naturalist*, 117(2): 250-257.
116. Flanagan LB, Wever LA, Carlson PJ. 2002. Seasonal and interannual variation in carbon dioxide exchange and carbon balance in a northern temperate grassland. *Global Change Biology*, 8: 599-615.
117. Foley JA, Levis S, Prentice IC *et al.* 1998. Coupling dynamic models of climate and vegetation. *Global Change Biology*, 4: 561-579.
118. Foley JA, Prentice IC, Ramankutty N *et al.* 1996. An integrated biosphere model of land surface progresses, terrestrial carbon balance, and vegetation dynamics. *Global Biogeochemical Cycles*, 10:603-628.
119. Franco AC, Nobel PS 1990. Influence of root distribution and growth on predicted water uptake and interspecific competition. *Oecologia*, 82(2): 151-157.
120. Franklin SE. 2001. Modeling forest net primary productivity with reduced uncertainty by remote sensing of cover type and leaf area index. In: *Spatial uncertainty in ecology: implication for remote sensing and GIS applications* (eds. Hunsaker CT, Goodchild MF, Friedl MA *et al.*), pp 284, Springer Science & Business, New York.
121. Frauenfeld OW, Zhang T, Barry RG 2004. Interdecadal changes in seasonal freeze and thaw depths in Russia. *Journal of Geophysical Research*, 109: D05101, doi:10.1029/2003JD004245.
122. Frey BJ and Dueck D. 2007. Clustering by passing messages between data points. *Science*, 315, 972-976.
123. Fulton MR, Prentice IC 1997. Edaphic controls on the boreonemoral forest mosaic. *Oikos*, 78(2): 291-298.
124. Gallé A, Haldimann P, Feller U. 2007. Photosynthetic performance and water relations in young pubescent oak (*Quercus pubescens*) trees during drought stress and recovery. *New Phytologist*, 174: 799-810.
125. Gerten D, Luo Y, Le Maire G *et al.* 2008. Modelled effects of precipitation on ecosystem carbon and water dynamics in different climatic zones. *Global Change Biology*, 14(10): 2365-2379.
126. Gerten D, Schaphoff S, Lucht W 2007. Potential future changes in water limitations of the terrestrial biosphere. *Climatic Change*, 80(3-4): 277-299.
127. Gholz HL, Ewel KC, Teskey RO 1990. Water and forest productivity. *Forest Ecology And Management*, 30, 1-18.
128. Givnish TJ 1986a. On the use of optimality argument. In: *On the Economy of Plant Form and Function* (ed. Givnish TJ), pp. 3-9. Cambridge University Press, Cambridge.
129. Gong DY, Shi PJ, Wang JA 2004. Daily precipitation changes in the semi-arid region over northern China. *Journal of Arid Environments*, 59(4): 771-784.
130. Goulden ML, Munger JW, Fan SM *et al.* 1996. Exchange of carbon dioxide by a deciduous forest: response to interannual climate variability. *Science*, 271: 1576-1578.
131. Greenhill G 1881. Determination of the greatest height consistent with stability that a vertical pole or mast given proportion can grow. *Proceedings of Cambridge Philosophical Society*,

- 4(1881), 65-73.
132. Gu Z, Chen J, Shi P *et al.* 2007. Correlation analysis of Normalized Different Vegetation Index (NDVI) difference series and climate variables in the Xilingole steppe, China from 1983 to 1999. *Frontiers of Biology in China*, 2(2): 218-228.
133. Hanson PJ and Weltzin JF. 2000. Drought disturbance from climate change: response of United States forests. *The Science of the Total Environment*, 262(3): 205-220.
134. Hardy JP, Groffman PM, Fitzhugh RD *et al.* 2001. Snow depth manipulation and its influence on soil frost and water dynamics in a northern hardwood forest. *Biogeochemistry*, 56(2): 151-174.
135. Harrison SP, Prentice IC 2003. Climate and CO₂ controls on global vegetation distribution at the last glacial maximum: analysis based on palaeovegetation data, biome modeling and palaeoclimate simulations. *Global Change Biology*, 9(7): 983-1004.
136. Haxeltine A, Prentice IC 1996a. BIOME3: an equilibrium terrestrial biosphere model based on ecophysiological constraints, resource availability, and competition among plant functional types. *Global Biogeochemical Cycles*, 10(4): 693-709.
137. Haxeltine A, Prentice IC 1996b. A general model for the light use efficiency of primary production. *Functional Ecology*, 10(5): 551-561.
138. Haxeltine A, Prentice IC, Cresswell ID 1996. A coupled carbon and water flux model to predict vegetation structure. *Journal of Vegetation Science*, 7(5): 651-666.
139. Helliker BR, Richter SL 2008. Subtropical to boreal convergence of tree-leaf temperatures. *Nature*, 454, 511-514.
140. Hickler T, Fronzek S, Araújo M *et al.* 2009. An ecosystem model-based estimate of changes in water availability differs from water proxies that are commonly used in species distribution models. *Global Ecology and Biogeography*, 18(3): 304-313.
141. Holdridge LR 1967. Life-zone ecology reviewed. Tropical science center, San Jose. Costa Rica: 206.
142. Horita T, Iwata Y, Hayashi M *et al.* 2006. Decreasing soil-frost depth and its relation to climate change in Tokachi, Hokkaido, Japan. *Journal of the Meteorological Society of Japan*, 84(4): 821-833.
143. Hoss JA, Lafon CW, Grissino-Mayer HD *et al.* 2008. Fire history of a temperate forest with an endemic fire-dependent herb. *Physical Geography*, 29(5): 424-441.
144. House JI, Archer S, Breshears DD *et al.* 2003. Conundrums in mixed woody-herbaceous plant systems. *Journal of Biogeography*, 30: 1763-1777.
145. Humphrey RR, Mehrhoff LA 1958. Vegetation changes on a Southern Arizona grassland range. *Ecology*, 39(4): 720-726.
146. Huxman TE, Smith MD, Fay PA *et al.* 2004. Convergence across biomes to a common rain-use efficiency. *Nature*, 429: 651-654.
147. Hwang T, Kang S, Kim J *et al.* 2008. Evaluating drought effect on MODIS Gross Primary Production (GPP) with an eco-hydrological model in the mountainous forest, East Asia. *Global Change Biology*, 14, 1037-1056.
148. Jackson RB, Canadell J, Ehleringer JR *et al.* 1996. A global analysis of root distributions for terrestrial biomes. *Oecologia*, 108: 389-411.

149. Jackson RB, Mooney HA, Schulze E-D. 1997. A global budget for fine root biomass, surface area, and nutrient contents. *PNAS*, 94(14): 7362-7366.
150. Joffre R, Rambal S 1993. How tree cover influences the water balance of Mediterranean rangelands. *Ecology*, 74(2): 570-582.
151. Jones HG. 1998. Stomatal control of photosynthesis and transpiration. *Journal of Experimental Botany*, 49(Special Issue): 387-398.
152. Jupp TE, Weedon GP, Los SO *et al.* 2007. Feedbacks between vegetation and precipitation inferred from remote sensing. *Geophysical Research Abstracts*, 9(06809).
153. Kaplan JO, Bigelow NH, Prentice IC *et al.* 2003. Climate change and arctic ecosystems II: Modeling, paleodata-model comparisons, and future projections. *Journal of Geophysical Research*, 108(D09), 8171, doi: 8110.1029/2002JD002559.
154. Karabulut M 2003. An examination of relationships between vegetation and rainfall using Maximum Value Composite AVHRR-NDVI data. *Turkish Journal of Botany*, 27: 93-101.
155. Kimmmins JP 2005. *Forest Ecology. A Foundation for Sustainable Forest Management and Environmental Ethics in Forestry*. 3rd Edition, Pearson Education, Inc, Prentice Hall.
156. Kirschbaum MU 2000. Forest growth and species distribution in a changing climate. *Tree Physiology*, 20(5-6): 309-322.
157. Klos RJ, Wang GG, Bauerle WL *et al.* 2009. Drought impact on forest growth and mortality in the southeast USA: an analysis using Forest Health and Monitoring data. *Ecological Applications*, 19(3): 699-708.
158. Knoop, W.T., Walker, H. 1985. Interactions of woody and herbaceous vegetation in a Southern African savanna. *Journal of Ecology*, 73(1): 235-253.
159. Knorr W 2000. Annual and interannual CO₂ exchanges of the terrestrial biosphere: process-based simulations and uncertainties. *Global Ecology and Biogeography*, 9(3):225-252.
160. Knorr W, Heimann M 2001. Uncertainties in global terrestrial biosphere modeling. Part II: global constraints for a process-based vegetation model. *Global Biogeochemical Cycles*, 15(1): 227-246.
161. Köppen W 1931. *Grundriss der Klimakunde*. Walter de Gruyter, Berlin.
162. Körner C, Asshoff R, Bignucolo, O *et al.* 2005. Carbon flux and growth in mature deciduous forest trees exposed to elevated CO₂. *Science*, 309, 1360-1362.
163. Koster RD, Dirmeyer PA, Guo Z *et al.* 2004. Regions of strong coupling between soil moisture and precipitation. *Science*, 205(5687): 1138-1140.
164. Krauchi N, Xu D 1996. Climate change effects on forests. In: *Caring for the forest: Research in a changing world* (eds Korpilahti E, Mikkela H, Salonen T), Congress Report, Volume II, pp 34-45.
165. Krestov PV, Nakamura Y 2007. Climatic controls of forest vegetation distribution in Northeast Asia. *Bericht der Reinhold-Tuexen-Gesellschaft*, 19: 131-145.
166. Laurance W and Williamson GB. 2001. Positive feedbacks among forest fragmentation, drought, and climate change in the Amazon. *Conservation Biology*, 15(6): 1529-1535.
167. Le Roux X, Mordet P 1995. Leaf and canopy CO₂ assimilation in a West African humid savanna during the early growing season. *Journal of Tropical Ecology*, 11(4): 529-545.

168. Lee HSJ, Jarvis PG. 1995. Trees differ from crops and from each other in their responses to increases in CO₂ concentration. *Journal of Biogeography*, 22: 323-330.
169. Leemans R, Prentice IC 1989. FORSKA, a general forest succession model. *Meddelande från Västbiologiska Institutionen*, Uppsala.
170. Lei J, Peters AJ 2004 A spatial regression procedure for evaluating the relationship between AVHRR-NDVI and climate in the northern Great Plains. *International Journal of Remote Sensing*, 25(2): 297-311.
171. Leipprand A, Gerten D 2006. Global effects of doubled atmospheric CO₂ content on evapotranspiration, soil moisture and runoff under potential natural vegetation. *Hydrological Sciences*, 51(1): 171-185.
172. Li J, Lewis J *et al.* 2004. Evaluation of land performance in Senegal using multi-temporal NDVI and rainfall series. *Journal of Arid Environments*, 59(3): 463-480.
173. Li S, Romero-Silto H, Tsujimura M *et al.* 2007. Plant water sources in the cold semiarid ecosystem of the upper Kherlen River catchment in Mongolia: A stable isotope approach. *Journal of Hydrology*, 333(1): 109-117.
174. Liang E, Eckstein D, Liu H 2008. Climate-growth relationships of relict *Pinus tabulaeformis* at the northern limit of its natural distribution in northern China. *Journal of Vegetation Science*. 19: 393-406.
175. Liang E, Liu X, Yuan Y *et al.* 2006. The 1920s drought recorded by tree rings and historical documents in the semi-arid and arid areas of Northern China. *Climatic Change*, 79(3-4): 403-432.
176. Liang E, Shao X, He J. 2005. Relationships between tree growth and NDVI of grassland in the semi-arid grassland of north China. *Remote Sensing*, 26(13): 2901-2908.
177. Lieth H 1975. Modeling the Primary Productivity of the World. In: *Primary Productivity of the Biosphere* (eds Lieth H, Whittaker RH), Berlin: Springer-Verlag.
178. Lippu J 1998. Redistribution of ¹⁴C-labelled reserve carbon in *Pinus sylvestris* seedlings during shoot elongation. *Silva Fennica*, 32: 3-10.
179. Litton CM, Raich JW, Ryan MG 2007. Carbon allocation in forest ecosystem. *Global Change Biology*, 13(10): 2089-2109.
180. Lloret F, Siscart D and Dalmses C. 2004. Canopy recovery after drought dieback in holm-oak Mediterranean forest of Catalonia (NE Spain). *Global Change Biology*, 10: 2092-2099.
181. Lucht W, Schaphoff S, Erbrecht T. *et al.* 2006. Terrestrial vegetation redistribution and carbon balance under climate change. *Carbon Balance Manage*, 1(6): 1-7.
182. Mäkelä A 1986. Implications of the pipe model theory on dry matter partitioning and height growth of trees. *Journal of Theoretical Biology*, 123:103-120.
183. Malanson GP 1997. Effects of feedbacks and seed rain on ecotone patterns. *Landscape Ecology*, 12(1): 27-38.
184. Marks D, Pomeroy J, Winstral A 2005. Interaction between snow cover and climate, topography and vegetation in semi-arid mountain catchments. *Eos Trans, AGU*, 86(52), Fall Meet, Suppl., Abstract C21A-1072.
185. Martin PH. 1996. Climate change, water stress, and fast forest response: a sensitivity study. *Climatic Change*, 34: 223-230.

186. McLendon T, Hubbard PJ, Martin DW 2008. Partitioning the use of precipitation- and groundwater-derived moisture by vegetation in an arid ecosystem in California. *Journal of Arid Environments*, 72(6): 986-1001.
187. McMahon TA 1973. Size and shape in biology: elastic criteria impose limits on biological proportions, and consequently on metabolic rates. *Science*, 179:1201-1204.
188. Meinders M and van Breemen N. Formation of soil-vegetation patterns. In: *Ecosystem function in heterogeneous landscapes* (eds: Gary Lovett, Clive G. Jones, Monica G. Turner *et al.*). Birkhauser.
189. Melillo JM, McGuire AD, Kicklighter EW *et al.* 1993. Global climate change and terrestrial net primary production. *Nature*, 363, 234-240.
190. Melillo, J.M, McGuire, A.D, Kicklighter, D.W. *et al.* 1993. Global climate change and terrestrial net primary production. *Nature*, 363: 234-240.
191. Mellander P, Bishop K, Lundmark T 2004. The influence of soil temperature on transpiration: a plot scale manipulation in a young Scots pine stand. *Forest Ecology and Management*, 195(1-20): 15-28.
192. Mitchell MJ, Driscoll CT, Kahl JS *et al.* 1996. Climate control of nitrate loss from forested watersheds in the northeast United States, *Environmental Science Technology*, 30(8): 2609-2612.
193. Mokany K, Raison RJ, Prokushkin AS 2006. Critical analysis of root: shoot ratios in terrestrial biomes. *Global Change Biology*, 12(1): 84-96.
194. Munot AA, Kothawale DR 2000. Intra-seasonal, inter-annual and decadal scale variability in summer monsoon rainfall over India. *International Journal of Climatology*, 20(11): 1387-1400.
195. Myneni RB, Dong J, Tucker CJ *et al.* 2001. A large carbon sink in the woody biomass of northern forests. *Proceedings of the National Academy of Sciences*, 98(26): 14784-14789.
196. Myneni RB, Los SO, Tucker CJ 1996. Satellite-based identification of linked vegetation index and sea surface temperature anomaly areas from 1982-1990 for Africa, Australia and South America. *Geophysical Research Letters*, 23(7): 729-732.
197. Nakayama T, Watanabe M 2004. Simulation of spring snowmelt by considering effect of local topography on snow cover and freezing/thawing soil layer in Kushiro Mire. *Eos Trans. AGU*, 85(47), Fall Meet. Suppl., Abstract H11F-0359.
198. Neilson RP 1995. A model for predicting continental scale vegetation distribution and water balance. *Ecological Applications*, 5(2): 362-385.
199. Neilson RP 1995. A model for predicting continental-scale vegetation distribution and water balance. *Ecological Application*, 5(2): 362-385.
200. Neilson RP, King GA, Koerper G 1992. Toward a rule based biome model. *Landscape Ecology*, 7(1): 27-43.
201. Neilson RP, Marks D 1994. A global perspective of regional vegetation and hydrologic sensitivities and risks from climatic change. *Journal of Vegetation Science*, 5(5): 715-730.
202. Nemani R, White M, Thomton P *et al.*, 2002. Recent trends in hydrological balance have enhanced the terrestrial carbon sink in the United States. *Geophysical Research Letters*, 29(10), 1468, doi: 10.1029/2002GL014867.

203. Nemoto M, Shinoda M, Nakano T 2006. Impact of snow and vegetation activity on surface energy balance in Mongolian grassland. *Eos Trans. AGU*, 87(52), Fall Meet. Suppl., Abstract A41B-0028.
204. Nezlin NP, Kostianoy AG, Li B 2005. Inter-annual variability and interaction of remote-sensed vegetation index and atmospheric precipitation in the Aral Sea region. *Journal of Arid Environments*, 62(4): 677-700.
205. Nicholson S E, Davenport M L, Malo AR 1990. A comparison of the vegetation response to rainfall in the Sahel and East Africa, using normalized difference vegetation index from NOAA AVHRR. *Climatic Change*, 17(2-3): 209-241.
206. Noormets A, McNulty SG, DeForest JL *et al.* 2008. Drought during canopy development has lasting effect on annual carbon balance in a deciduous temperate forest. *New Phytologist*, 179(3): 818-828.
207. Norby RJ, Wullschleger SD, Gunderson CA *et al.* 1995. Increased growth efficiency of *Quercus alba* trees in a CO₂-enriched atmosphere. *New Phytologist*, 131: 91-97.
208. Noy-Meir I 1973. Desert ecosystems: environment and producers. *Annual Review of Ecology and Systematics*, 4: 25-51. (doi: 10.1146/annurev.es.04.110173.000325) .
209. Ogaya R, Peñuelas J, Martínez-Vilalta J *et al.* 2007. Effect of drought on diameter increment of *Quercus ilex*, *Phillyrea latifolia*, and *Arbutus unedo* in a holm oak forest of NE Spain. *Forest Ecology and Management*, 180, 175-184.
210. Pacala SW, Canham CD, Saponara J, *et al.* 1993. Forest models defined by field measurements: I. The design of a northeastern forest simulator. *Canadian Journal of Forest Research*, 23: 1980–1998.
211. Parton WJ, Scurlock JMO, Ojima DS, *et al.* 1993. Observations and modeling of biomass and soil organic matter dynamics for the grassland biome worldwide. *Global Biogeochemical Cycles*, 7(4): 785–809.
212. Paruelo JM, Sala OE, Beltrán AB 2000. Long-term dynamics of water and carbon in semi-arid ecosystems: a gradient analysis in the Patagonian steppe. *Plant Ecology*, 150(1-2): 133-143.
213. Peters AJ, Eve MD 1995. Satellite monitoring of desert plant community response to moisture availability. *Environmental Monitoring and Assessment*, 37(1): 273-287.
214. Peters AJ, Eve MD, Holt EH *et al.* 1997. Analysis of Desert Plant Community Growth Patterns with High Temporal Resolution Satellite Spectra. *The Journal of Applied Ecology*, 34(2): 418-432.
215. Piao S, Fang J, Zhou L *et al.* 2003. Interannual variations of monthly and seasonal NDVI in China from 1982 to 1999. *Journal of Geophysical Research*, 108(D14): 4401, doi:10.1029/2002JD002848.
216. Piao S, Fang J, Zhou L *et al.* 2006. Variations in satellite-derived phenology in China's temperate vegetation. *Global Change Biology*, 12(4): 672-685.
217. Piao S, Fang J, Zhou L *et al.* 2007. Changes in biomass carbon stocks in China's grasslands between 1982 and 1999. *Global Biogeochemical Cycles*, 21: GB2002, doi:10.1029/2005GB002634.
218. Piao S, Ciais P, Friedlingstein P *et al.* 2008. Net carbon dioxide losses of northern ecosystems

- in response to autumn warming. *Nature*, 451, 49-52.
219. Pomeroy JW, Brun E 2001. Physical properties of snow. In: *Snow Ecology: An Interdisciplinary Examination of Snow-Covered Ecosystems* (eds Jones HG *et al*), pp. 45-118, Cambridge University Press, New York.
 220. Porporato A, Laio F, Ridolfi L *et al*. 2003. Soil moisture and plant stress dynamics along the Kalahari precipitation gradient. *Journal of Geophysical Research*, 108(D3): 4127-4134.
 221. Porporato A, Laio F, Ridolfi L *et al*. 2001. Plants in water-controlled ecosystems: active role in hydrologic processes and response to water stress: III. Vegetation water stress. *Advances in Water Resources*, 24(7): 725-744.
 222. Prentice IC, Cramer W, Harrison SP *et al*. 1992. A global biome model based on plant physiology and dominance, soil properties and climate. *Journal of Biogeography*, 19(2):117-134.
 223. Prentice IC, Leemans R 1990. Pattern and process and the dynamics of forest structure: a simulation approach. *Journal of Ecology*, 78(2): 340-355.
 224. Prentice IC, Sykes MT, Cramer W 1993. A simulation model for the transient effects of climate change on forest landscapes. *Ecological Modeling*, 65(1-2): 51-70.
 225. Prentice IC, van Tongeren O, de Smidt JT 1987. Simulation of heathland vegetation dynamics. *Journal of Ecology*, 75(1): 203-219.
 226. Rascher CM, Driscoll CT, Peters NE 1987. Concentration and flux of solutes from snow and forest floor during snowmelt in the West-Central Adirondack region of New York. *Biogeochemistry*, 3(1-3): 209-224.
 227. Raunkiær C 1909. Formationsundersøgelse og formationstatistik. *Bot. Tidsskr.* 30:20-80.
 228. Raunkiær C 1913. Formationsstatistiske Undersøgelser paa Skagens Odde. *Botanisk Tidsskrift. Dansk Botanisk Forening* 33:197-243.
 229. Raunkiær C 1934. The life-forms of plants and statistical plant geography. Clarendon Press, Oxford.
 230. Raupach MR, Marland G, Ciais P *et al*. 2007. Global and regional drivers of accelerating CO₂ emissions. *PNAS*, 104(24): 10288-10293.
 231. Rawls WJ, Brakensiek DL, Saxton KE 1982. Estimation of soil water properties. *Transactions of ASAE*, 25:1316-1320.
 232. Reed BC, Brown JF *et al*. 1994. Measuring Phenological Variability from Satellite Imagery. *Journal of Vegetation Science*, 5(5): 703-714.
 233. Reynolds JF, Kemp PR, Tenbunen JD 2000. Effects of long-term rainfall variability on evapotranspiration and soil water distribution in the Chihuahuan Desert: A modeling analysis. *Plant Ecology*, 150(1-2): 145-159.
 234. Rodriguez-Iturbe I, Porporato A, Laio F *et al*. 2001. Plants in water-controlled ecosystems: active role in hydrologic processes and response to water stress: I. Scope and general outline. *Advance in Water Resources*, 24(7): 695-705.
 235. Ropelewski CF, Halpert MS 1986. North American Precipitation and Temperature Patterns Associated with the El Niño/Southern Oscillation (ENSO). *Monthly Weather Review*, 114(12): 2352-2362.
 236. Rosenzweig ML 1968. Net primary productivity of terrestrial communities: prediction from

- climatological data. *The American Naturalist*, 102(923): 67-74.
237. Running SW, Gower ST 1991. FOREST-BGC, a general model of forest ecosystem processes for regional applications. II. Dynamic carbon allocation and nitrogen budgets. *Tree Physiology*, 9: 147-160.
238. Running SW, Hunt ER 1993. Generalization of a forest ecosystem process model for other biomes, BIOME-BGC, and an application for global-scale models. Scaling processes between leaf and landscape levels. In: *Scaling Physiological Processes: Leaf to Globe* (eds Ehleringer JR, Field CB), San Diego: Academic Press.
239. Ryel RJ, Ivans CY, Peek MS *et al.* 2008. Functional differences in soil water pools: a new perspective on plant water use in water-limited ecosystems. In: *Progress in Botany*, 69 (eds Lüttge U, Beyschlag W, Murata J), pp. 397-422, Springer, New York.
240. Sala OE, Golluscio RA, Lauenroth WK *et al.* 1989. Resource partitioning between shrubs and grasses in the Patagonian steppe. *Oecologia*, 49: 101-110.
241. Saltelli A. What is sensitivity analysis? 2000. In: *Sensitivity Analysis* (eds Saltelli A, Chan K, Scott EM), Wiley, New York.
242. Sankaran M, Hanan NP, Scholes RJ *et al.* 2005. Determinants of woody cover in African savannas. *Nature*, 438(8): 845-849.
243. Sarris D, Christodoulakis D, Körner C. 2007. Recent decline in precipitation and tree growth in the eastern Mediterranean. *Global Change Biology*, 13(6): 1187-1200.
244. Scanlon TM, Caylor KK *et al.* 2005. Dynamic response of grass cover to rainfall variability: implications for the function and persistence of savanna ecosystems. *Advances in Water Resources*, 28(3): 291-302.
245. Schaphoff S, Lucht W, Gerten D. *et al.* 2006. Terrestrial biosphere carbon storage under alternative climate projections. *Climate Change*, 74(1-3): 97-122.
246. Scholze M, Knorr W, Arnell NW *et al.* 2006. A climate change risk analysis for world ecosystems. *PNAS*, 103(35): 13116-13120.
247. Schulze ED 1982. Plant life forms and their carbon, water and nutrient relations Encyclopedia of Plant Physiology. Berlin Heidelberg: Springer-Verlag.
248. Schwinning S, Starr BI, Ehleringer JR 2003. Dominant cold desert plants do not partition warm season precipitation by event size. *Oecologia*, 136(2): 252-260.
249. Schwinning S, Ehleringer JR 2001. Water use trade-offs and optimal adaptations to pulse-driven arid ecosystems. *Journal of Ecology*, 89(3): 464-480.
250. Sellers PJ, Mintz Y, Sud YC *et al.* 1986. A simple biosphere model (SiB) for use within general circulation models. *Journal of the Atmospheric Sciences*, 43(6):505-531.
251. Sernander R 1936. The primitive forest of Granskär and Fiby. *Acta Phytogeogr. Suec.* 8.
252. Shanley JB, Chalmers A 1999. The effect of frozen soil on snowmelt runoff at Sleepers River, Vermont. *Hydrological Processes*, 13(12-13): 1843-1857.
253. Shen C, Wang W, Hao Z *et al.* 2007. Exceptional drought events over eastern China during the last five centuries. *Climate Change*, 85: 453-471.
254. Shinozaki K, Yoda K, Hozumi K *et al.* 1964. A quantitative analysis of plant form-the pipe model theory. I. Basic analysis. *Japanese Journal of Ecology*, 14: 97-105.
255. Shugart HH 1984. A Theory of Forest Dynamics. New York: Springer.

256. Singh JS, Milchunas DG, Lauenroth W K 1998. Soil water dynamics and vegetation patterns in a semiarid grassland. *Plant Ecology*, 134(1): 77-89.
257. Sitch S, Smith B, Prentice IC *et al.* 2003. Evaluation of ecosystem dynamics, plant geography and terrestrial carbon cycling in the LPJ dynamic global vegetation model. *Global Change Biology*, 9: 161-185.
258. Smith B, Prentice IC, Sykes MT 2001. Representation of vegetation dynamics in the modeling of terrestrial ecosystems: comparing two contrasting approaches within European climate space. *Global Ecology and Biogeography*, 10(6): 621-637.
259. Specht RL 1972. Water use by perennial evergreen plant communities in Australia and Papua New Guinea. *Australian Journal of Botany*, 20(3): 273-299.
260. Sprugel DG 1976. Dynamic structure of wave-generated *Abies balsamea* forests in the northeastern United States. *Journal of Ecology*, 64(3): 889-911.
261. Stadler D, Wunderli H, Auckenthaler A *et al.* 1998. Measurement of frost-induced snowmelt runoff in a forest soil. *Hydrological Processes*, 10(10): 1293-1304.
262. Stottlemeyer R, Toczydlowski D. 1996. Precipitation, snowpack, stream-water ion chemistry, and flux in a northern Michigan watershed, 1982-1991. *Canadian Journal of Fisheries and Aquatic Sciences*, 53(12): 2659-2672.
263. Suarez ML, Ghermandi L, Kitzberger T 2004. Standard Paper: Factors predisposing episodic drought-induced tree mortality in *Nothofagus*-site, climatic sensitivity and growth trends. *Journal of Ecology*, 92(6): 954-966.
264. Suzuki R, Nomaki T, Yasunari T 2001. Spatial distribution and its seasonality of satellite-derived vegetation index (NDVI) and climate in Siberia. *International Journal of Climatology*, 21(11): 1321-1335.
265. Tatarinov FA and Cienciala E. 2006. Application of BIOME-BGC model to managed forests: 1. Sensitivity analysis. *Forest Ecology and Management*, 237(1-3): 267-279.
266. Tilman D 1988. Plant strategies and the dynamics and structure of plant communities, pp. 153, Princeton: Princeton University Press.
267. Tucker CJ, Sellers PJ 1986. Satellite remote sensing of primary production. *International Journal of Remote Sensing*, 7(11): 1395-1416.
268. Tucker CJ, Slayback DA, Pinzon JE *et al.* 2001. Higher northern latitude normalized difference vegetation index and growing season trends from 1982 to 1999. *International Journal of Biometeorology*, 45(4): 184-190.
269. Tuzinský L. 2005. Temporal dynamics of soil water in oak forest stand of Southern Slovakia. *Ekológia*, 24(3): 304-313.
270. Valentine HT 1985. Tree-growth models: derivations employing the pipe-model theory. *Journal of Theoretical Biology*, 117, 579-585.
271. van den Driessche R 1987. Importance of current photosynthate to new root growth in planted conifer seedlings. *Canadian Journal of Forest Research*, 17: 776-782.
272. Villalba R, Veblen T 1998. Influence of large-scale climatic variability on episodic tree mortality in Northern Patagonia. *Ecology*, 79(8):2624-2640.
273. Walter H 1962. Die Vegetation der Erde in ökophysiologischer Betrachtung-Die tropischen und subtropischen Zonen, Band 1. VEB Gustav Fischer Verlag, Jena.

274. Walter H 1968. Die Vegetation der Erde in ökophysiologischer Betrachtung-Die gemässigten und arktischen Zonen, Band 2. VEB Gustav Fischer Verlag, Jena.
275. Walter H 1985. Vegetation of the earth and ecological system of geo-biosphere. Berlin; New York: Springer-Verlag.
276. Wang Q, Adiku S, Tenhunen J. *et al.* 2005. On the relationship of NDVI with leaf area index in a deciduous forest site. *Remote Sensing of Environment*, 94(2): 244-255.
277. Warnant P, François L, Strivay D *et al.* 1994. CARAIB: a global model of terrestrial biological productivity. *Global Biogeochemical Cycles*, 8(3): 255-270.
278. Warren JM, Norby RJ, Wullschlegel SD 2007. Do extreme climatic events drive ecosystem water flux under elevated CO₂ in a temperate forest? *Eos Trans. AGU*, 88(52): Fall Meet. Suppl., Abstract GC13A-0928.
279. Welker JM, McClelland S, Weaver T 1991. Soil water retention after natural and simulated rainfall on a temperate grassland. *Theoretical and Applied Climatology*, 44(3): 229-237.
280. Welp LR, Randerson JT and Liu HP. 2007. The sensitivity of carbon fluxes to spring warming and summer drought depends on plant functional type in boreal forest ecosystems. *Agriculture and Forest Meteorology*, 147: 172-185.
281. Weltzin JF and McPherson GR. 2000. Implication of precipitation redistribution for shifts in temperate savanna ecotones. *Ecology*, 81(7): 1902-1913.
282. Weltzin JF, Loik ME, Schwinning S *et al.* 2003. Assessing the response of terrestrial ecosystems to potential changes in precipitation. *Bioscience*, 53(10): 941-952.
283. Weltzin JF, McPherson GR 1997. Spatial and temporal soil moisture resource partitioning by trees and grasses in a temperate savanna, Arizona, USA. *Oecologia*, 112(2):156-164.
284. Weng E, Zhou G 2006. Modeling distribution changes of vegetation in China under future climate change. *Environmental Modeling and Assessment*, 11(1): 45-58.
285. Whittaker RH 1975. Communities and ecosystems, 2nd edition. Macmillan, New York.
286. Wilby RL, Conway D, Jones PD 2002. Prospects for downscaling seasonal precipitation variability using conditioned weather generator parameters. *Hydrological Processes*, 16(6): 1215-1234.
287. Williams MW, Melack JM 1991. Solute chemistry of snowmelt and runoff in an alpine basin, Sierra Nevada. *Water Resource Research*, 27(7): 1575-1588.
288. Willson SD 1993. Belowground competition in forest and prairie. *Oikos*, 68(1): 146-150.
289. Woodward FI, Smith TM, Emanuel WR 1995. A global land primary productivity and phytogeography model. *Global Biogeochemical Cycles*, 9(4): 471-490.
290. Woodward FI, Williams BG 1987. Climate and plant distribution at global and local scales. *Vegetation*, 69(1-3): 189-197.
291. Xiao J, Moody A 2004. Trends in vegetation activity and their climatic correlates: China 1982 to 1998. *International Journal of Remote Sensing*, 25(24): 5669-5689.
292. Yang L, Wylie BK *et al.* 1998. An Analysis of Relationships among Climate Forcing and Time-Integrated NDVI of Grasslands over the U.S. Northern and Central Great Plains. *Remote Sensing of Environment*, 65(1): 25-37.
293. Yu F, Price KP, Ellis J *et al.* 2003. Response of seasonal vegetation development to climatic variations in eastern central Asia. *Remote Sensing of Environment*, 87(1): 42-54.

294. Yuan J, Niu Z, Wang C 2006. Vegetation NPP distribution based on MODIS data and CASA Model-a case study of Northern Hebei Province. *Chinese Geographical Science*, 16(4): 334-341.
295. Yuki Yoshi I, Hayashi M, Hirota T 2008. Comparison of snowmelt infiltration under different soil freezing conditions influenced by snow cover. *Vadose Zone Journal*, 7(1): 79-86.
296. Zhai P, Sun A, Ren F *et al.* 1999. Changes of climate extremes in China. *Climatic Change*, 42(1): 203-218.
297. Zhang X, Friedl MA, Schaff CB *et al.* 2004. Climate controls on vegetation phenological patterns in northern mid- and high latitudes inferred from MODIS data. *Global Change Biology*, 10(7): 1133-1145.
298. Zhou L, Kaufmann RK, Tian Y *et al.*, 2002. Relation between interannual variations in satellite measures of northern forest greenness and climate between 1982 and 1999. *Journal of Geophysical Research*, 108(D1): 4004, doi:10.1029/2002JD002510.
299. Zhou LM, Tucker CJ, Kaufmann RK *et al.* 2001. Variations in northern vegetation activity inferred from satellite data of vegetation index during 1981 to 1999. *Journal of Geophysical Research*, 106(D17): 20069-20083.
300. Zou C, Han S, Zhang J *et al.* 2000. Characteristics and dynamics of sandy natural forests in sandy forest-steppe ecotone in the northern area of China. *Journal of Forestry Research*, 11(3): 161-166.

附 录

数字化 1:400 万中国植被图植被类型编码:

编号	植被类型
1208017	落叶栎林
1208018	椴、榆、桦杂木林
1208019	石灰岩榆科树种、黄连木杂木林
1209020	桦、杨林
1210021	榆树疏林结合沙生灌丛
1533065	线叶菊草原
1533066	羊草草原
1533067	贝加尔针茅草原
1533068	白羊草、黄背草草原
1534069	大针茅、克氏针茅草原
1534070	克氏针茅、糙隐子草草原
1534071	本氏针茅、短花针茅草原

后 记

终于要离开，没有留恋。

论文就此打住，三年的硕士生活宣告结束，在学术和学术以外的道路上反复挣扎，最后终于发现，其实无论怎样，只要过的是充实的生活，只要还有抓得住的新鲜，只要还能不断成长，人生就还有精彩。

我失望过，也许还在失望中，我痛苦过，也许痛苦并没有过去，在这神秘莫测的大自然面前，我终究是个忙碌的行者，哪怕再仔细的钻研寻觅，收获的仍旧是不确定，我对一切充满了怀疑，甚至不再相信进化论。我深深地恐慌生态学变成了管中窥豹的观测和高深的数学游戏的集合，无论是在热烈的阳光下呼吸青草的芬芳，还是在过膝的雪地上彳亍，无论是在电脑前手臂酸痛的玩弄一堆一堆的数字，还是静静的看着模型一年一年的转过，我都无法自信满满的说出一句“相信我，它就是这个样子！”在永远搞不定的不确定中我丧失了自信，失去了方向，然而我的个性告诉我，走下去，哪怕永远没有尽头，身边还有风景。

于我而言，七年的北大生活是对照鲜明的两段。前段青涩活泼，后段成熟压抑，理想到现实的转换没有让我猝不及防，但让我无可奈何。可以经得起森林里真正的狂风暴雨，却扛不住周遭的世态炎凉。幸而我还有些尚可触碰的温暖，幸而我还有些暂可停靠的码头，在与焦虑的斗争中还有心力将一切做完，做好。在兴奋的时候将我唤醒，在沮丧的时候催我前行，对你们，我永远的心怀感激。

感谢我的导师刘鸿雁教授，从指导我的本科论文到如今我的硕士论文完成，您对我比我自己还有信心。您治学严谨，思维敏捷，待人诚恳，无论在学术上还是人生的道路上都为我树立了楷模。您包容了我的愚钝与任性，对我的选择做出最大的支持。我带着没有 SCI 的遗憾离开，只能用一生铭记您的谆谆教诲。

感谢方精云老师，在您的课堂上我对宏观生态学有了深刻的认识，您的勤勉治学孜孜不倦让这个领域不断地出现惊喜。感谢朴世龙老师，您治学的严谨精深和对模型运用的游刃有余让我折服，您的开朗幽默让我在与您为邻的日子里倍感轻松。感谢郭大立老师，数次野外实习和考察的同行，您让我了解到治学的艰辛和坚持不懈的可贵。感谢生态学系的曾辉老师，沈泽昊老师，吉成均老师，唐志尧老师，郑成洋老师，王娓老师，朱江玲师姐，印婧婧师姐，你们的关心和帮助让我在前行的道路上倍受鼓舞。

感谢我的同门兄弟姐妹们。感谢任佶师兄从我大四起在知识和技术上给予我莫大的帮助，在离校后的日子里尽力的解答我所有的问题。感谢张语克师弟与我在野外患难与共，寒冬的冰雪，宰人的黑车，生态站里热乎乎的面条，没有你

同行，我不可能完成采样。感谢老吴总是热心的帮我解决遇到的困难，你的乐观和能力是我学习的榜样。感谢小印在野外帮我处理样品至凌晨，你在异国他乡的时候还为我鼓励加油。感谢烽君，陈曦，胡国铮，你们在我论文最困难的日子里分担了我的痛苦。

感谢逸夫二楼 3650，它从旧到新，尽管依然狭小拥挤，却酝酿了我们的学术理想，荡漾了我们的喜怒哀乐，它有种任何办公室都没有的独特气质，让我感到温暖安定，感谢这其中的每一个成员，我的同门们，还有梁军、李鹏。

感谢与我三年同行的办公室友兼宿舍舍友李果，我们互相鼓励，让枯燥的研究僧生活朝气蓬勃。感谢室友吴漪，你的开朗乐观为我们小小的宿舍增添了快乐。

感谢与我相伴七年的兄弟姐妹们，李惊、陈默、小赵、新平、王乐……，你们一如既往的相信我，支持我，我们互相扶持，在这个青春常驻的校园里留下了最绚丽的回忆。

感谢为我的论文提供各种数据的机构、网站、论坛和为我的实验创造条件的老师和同学们，没有你们，论文只是空中楼阁。

感谢在这三年里为我制造困难，为我提供机会的机构和人们，你们让我认清了社会现实，接触了世间百态，磨练了毅力，展现了实力。从稚气未脱的 2007，与祖国共同经历了悲喜交加的 2008，我在 2009 对未来信心百倍。

感谢我的男友，你的独特思维给了我无数思想上的启发。

大恩不言谢。双鬓渐白的父母永远是我坚强的后盾，你们的爱，女儿无以为报，唯有以快乐向上度过每一日，不再为你们平添忧愁。

愿姥爷在天之灵可以知晓，我研究生后两年的生活忙碌充实，始终奋斗不息。

别了，我深深爱恋的北大！

何思源 2009 年 5 月 31 日于 45 楼

北京大学学位论文原创性声明和使用授权说明

原创性声明

本人郑重声明： 所呈交的学位论文，是本人在导师的指导下，独立进行研究工作所取得的成果。除文中已经注明引用的内容外，本论文不含任何其他个人或集体已经发表或撰写过的作品或成果。对本文的研究做出重要贡献的个人和集体，均已在文中以明确方式标明。本声明的法律结果由本人承担。

论文作者签名： 日期： 年 月 日

学位论文使用授权说明

（必须装订在提交学校图书馆的印刷本）

本人完全了解北京大学关于收集、保存、使用学位论文的规定，即：

- 按照学校要求提交学位论文的印刷本和电子版本；
- 学校有权保存学位论文的印刷本和电子版，并提供目录检索与阅览服务，在校园网上提供服务；
- 学校可以采用影印、缩印、数字化或其它复制手段保存论文；
- 因某种特殊原因需要延迟发布学位论文电子版，授权学校 ☐ 一年 / ☐ 两年 / ☐ 三年以后，在校园网上全文发布。

（保密论文在解密后遵守此规定）

论文作者签名： 导师签名：

日期： 年 月 日

北京大学硕士学位论文

内蒙古高原东南部荒漠化与风沙活动研究

Studies on desertification and aeolian activities in southeastern Inner Mongolia Plateau

姓 名 : 田 育 红

学 号 : 10015087

系 别 : 环境学院

专 业 : 环境科学

研究方向 : 植被生态学

指导老师 : 刘 鸿 雁

二零零三年六月

任何收存和保管本论文各种版本的单位和个人，未经本论文作者授权，不得对本论文进行复制、修改、发行、出租、改变等有碍作者著作权益之行为，否则，将可能承担法律责任。

北京大学研究生院
2003 年 6 月 6 日

摘要

荒漠化是我国面临的重大生态问题。本文以内蒙古高原东南部及其周边地区为例研究区,通过野外调查、实验室分析和遥感影像解译相结合的手段,探讨研究区植被退化和土壤退化的关系,建立了适合于研究区的荒漠化评价指标体系,分析了研究区荒漠化的空间格局。在此基础上,分析了气候波动和人为活动对植被动态的驱动作用,探讨了沙尘暴发生时的植被和气候条件。全文包括以下五个方面的内容:

1. 研究区植被退化状况

利用 TWINSpan 分类和 DCA 排序对野外调查获取的植被数据和土样数据进行分析,得到不同退化机制下不同地表覆盖类型的植被退化程度分级。结果表明,利用草地退化指示种建立的植被退化指数能很好地反映不同类型草原的退化状况;不同地表覆盖类型的植被退化指数与总草本盖度之间并无直接的关系,即植被退化指数高的地方总草本盖度不一定就低;而多年生植物盖度占总盖度的比例较高的类型,其植被退化指数相对较低。

2. 研究区荒漠化程度评估

利用 DCA 排序法,通过野外调查得到的植被和土壤数据分析研究区荒漠化现状,并对沙地草原和非沙地草原两种类型分别建立荒漠化程度评价模型。结果表明,沙地草原和非沙地草原的退化机理不同,沙地草原的退化表现为土壤中粗颗粒含量的增加,草群高度降低;非沙地草原的退化表现为土壤中粗颗粒含量增加,土壤有机质含量下降,一、二年生植物和退化指示种的含量增加。无论是非沙地草原还是沙地草原,物种多样性都不随荒漠化程度的加深而逐渐减少。

3. 研究区荒漠化的空间格局

利用 MODIS 遥感影像进行研究区景观格局解译,得到景观格局图,在此基础上提取出典型草原亚区、荒漠化草原亚区和沙地疏林灌丛草原亚区。通过 MODIS 影像不同波段组合进行运算,得出研究区荒漠化程度分布图,并对研究区不同区(亚区)荒漠化程度的空间格局进行了分析。

4. 研究区植被动态及其驱动因子的分析

对研究区 1980~2000 年来植被覆盖(NDVI)、气候和人为活动的动态研究表明,在对 NDVI_{max-min} 和 NDVI_{max} 的作用中,大部分区(亚区)气候因素的作用要大于人为因素的,尤其是 0cm 地温的作用;在对 NDVI_{spring} 的作用中,大部分区域(农区除外)气候因子的作用占绝对优势,尤其是 1 月份气温均值和 1 月份气候湿润指数的作用。在大部分区(亚区)中,多数年份气候因子对 NDVI 旬值的影响都是气温>0cm 地温>降水。

5. 荒漠化与风沙活动的关系

利用沙尘暴资料对研究区 50 年来的沙尘暴活动情况进行分析,并结合野外调查资料研究不同地表覆盖类型对北京沙尘活动的贡献,然后利用 NDVI、气候和人为活动资料对近年来沙尘暴发生次数和强度的驱动因子进行分析。结果表明石质丘陵典型草原、石质丘陵荒漠草原和农田对北京沙尘天气物源贡献较大。1980~2000 年来 NDVI 和气候因子对沙尘暴发生次数的影响都不太显著。沙尘暴发生相对强度在不同区(亚区)的影响因子不同,其中降水的作用要相对较强。

关键词: 植被退化, 荒漠化, 沙尘暴, 气候波动, 内蒙古高原

Abstract

Desertification is one of the greatest ecological problems in China. Southeastern part of Inner Mongolia Plateau and its surroundings is selected to study desertification and its links to sandy stormy weather in this paper. Based on field investigation, laboratory works and interpretation of remotely sensed image, links between vegetation and soil degradations were discussed, and also the spatial pattern of desertification was analyzed after established desertification assessment models. Driving of climatic oscillation and human activities in vegetation dynamics and the vegetation and climate conditions in sandy storm outbreaks were also discussed. The entire paper contains five parts:

1. Vegetation degradation status

With TWINSpan classification and DCA ordination, the vegetation data and soil sample data obtained from field investigation were analyzed and different vegetation degradation classes in different degradation mechanisms were achieved. It is demonstrated that the Vegetation Degradation Index constructed by grassland degradation indicator species can well reflect the degradation of different types of grasslands; there is no direct relation between Vegetation Degradation Index and total grass cover in different land cover types, i.e. where Vegetation Degradation Index is low may be not low in total grass cover; there is no direct relation between Vegetation Degradation Index and total grass cover in different land cover types, i.e. where Vegetation Degradation Index is low may be not low in total grass cover; while for the types with high proportion of perennial cover in total grass cover has a relative low Vegetation Degradation Index.

2. Desertification degree assessment

With DCA ordination, desertification degree in the study area is analyzed through the vegetation and soil data obtained from field investigation and desertification assessment models were constructed for none-sandlot grassland and sandlot grassland respectively. It is demonstrated that the degradation mechanisms of none-sandlot grassland and sandlot grassland are different: the degradation of sandlot grassland appears to be the increase of fine particle percent in the soil and decrease of grass height; the degradation of none-sandlot grassland performs to be the increase of the fine particle in the soil and decrease of TOC in the soil and the increase of the percentage of therophytes and degradation indicator species; for both none-sandlot grassland and sandlot grassland, the species diversity will not decrease gradually with the deepening of desertification.

3. Spatial pattern of desertification in research region

Map of spatial pattern is obtained from MODIS remotely sensed image. Ranges of typical steppe sub-region, desert steppe sub-region and sandy land open forest and shrubby steppe sub-region were obtained. The map of desertification degree was

obtained through calculation of different channel of MODIS image. Spatial pattern of desertification in different sub-region was discussed.

4. The relationship of vegetation dynamic and its drive factors

Multi-variable analyses of links among vegetation cover (NDVI), climate and human activities demonstrated that, in the contribution to the dynamic of NDVI_{max-min} and NDVI_{max}, climate factors overweigh human activity factors in most regions, especially the contribution of the 0 cm ground surface temperature; in the contribution to the dynamic of NDVI_{spring}, climate factors are also the exceeding one except for agriculture region, especially the mean temperature of January and the wetness index of January. In most years, the sequence of climate factors contribution to NDVI always is temperature, the earth surface temperature and precipitation.

5. The relationship of desertification and Aeolian activity

Dust storm frequencies and intensities during fifty years were discussed. Contributions of different vegetation cover types in the study area to the sand stormy weather in Beijing were analyzed by using field investigation data and dust storm data. Driving factors of sand storm frequencies and intensities were linked to NDVI and climatic conditions by multi-variable analysis. It is demonstrating that, from all the land cover types, stony hill typical steppe and stony hill desert steppe the have the highest ability of release dusts for the sand stormy weather in Beijing. The effects of NDVI and climatic conditions are not significant to sand storm frequencies from 1980 to 2000. As for the relative intensities of dust storms in different regions, the effects of precipitation are remarkable.

Keywords : Vegetation degradation, Desertification, Sandy storm, Climate oscillation, Inner Mongolia Plateau

目 录

摘 要.....	i
ABSTRACT.....	ii
第一章 引言.....	1
1.1 荒漠化研究的现状与意义.....	1
1.2 荒漠化评价指标体系的研究.....	3
1.3 荒漠化与沙尘暴.....	4
1.4 本研究的内容与目标.....	5
第二章 研究区概况.....	8
2.1 研究区自然地理概况.....	8
2.2 研究区人类活动与土地利用.....	11
2.3 区域选择的意义.....	11
第三章 研究方法.....	13
3.1 野外调查.....	13
3.2 植物群落分析.....	13
3.3 土壤分析.....	15
3.4 遥感影象分析.....	15
3.5 气候资料的获取和处理.....	16
第四章 区域植被退化分析.....	17
4.1 研究区植被退化现状.....	17
4.2 研究区植被退化程度的数量分析.....	18
4.3 小结.....	20
第五章 荒漠化评估的指标体系.....	21
5.1 指标选取.....	21
5.2 荒漠化评价指标体系的建立.....	22
5.3 讨论.....	29
5.4 小结.....	30
第六章 研究区荒漠化的空间格局.....	31
6.1 MODIS 影像数据.....	31
6.2 信息提取.....	31
6.3 结果分析.....	33
6.4 小结.....	34
第七章 研究区及周边地区 1984~2000 年气候、植被与人为活动动	

态.....	38
7.1 植被动态.....	38
7.2 1981~2000 年气候的变化.....	42
7.3 人为活动的变化.....	44
7.4 植被变化的驱动因子.....	46
7.5 讨论.....	51
7.6 小结.....	51
第八章 荒漠化与风沙活动的关系.....	52
8.1 沙尘暴地理分布与季节、年际变化.....	52
8.2 不同地表覆盖类型对北京沙尘暴物源的贡献.....	54
8.3 气候波动以及人为活动对沙尘暴的贡献.....	57
8.4 小结.....	58
第九章 结论与讨论.....	60
9.1 结论.....	60
9.2 研究区的荒漠化防治对策探讨.....	60
参考文献.....	62
附录 : 样方植物名录.....	65
致谢.....	69

第一章 引言

1.1 荒漠化研究的现状与意义

荒漠化是全人类共同关注的生态问题,也是生态学研究的重点领域,是目前危及人类生存的重大生态问题和自然灾害之一。荒漠化是由下列原因共同作用造成的:(1)超过土地资源自然负荷程度的人为干扰和破坏活动;(2)资源系统内部的生态脆弱性和较低的可持续发展能力;(3)严重的自然灾害,如旱灾、雪灾使生态系统变得更加脆弱。荒漠化发展的结果是使土地资源变为沙漠、戈壁、石漠、壤漠、盐漠等丧失生物生产力和生态功能的土地。一般把荒漠化程度分为轻度、中度、重度和极度四个退化等级(Dregne, 1992)。

1.1.1 世界荒漠化研究概况

早在1949年,法国学者奥布列维尔就提出了“荒漠化”这一术语。二十世纪六十年代末七十年代初,西非出现的特大干旱加重了这一地区的荒漠化程度,使一些国家的经济受到很大威胁,为此,联合国于1975年出台了3337号决议,提出“向荒漠化进行斗争”的口号,并于1977年8月的联合国荒漠化会议上正式确定了荒漠化是一个世界公认的环境问题。根据1993年召开的两次荒漠化国际公约会议的资料,荒漠化影响全球大约100多个国家9亿的人口和36亿ha的土地,占世界陆地面积的1/4(朱震达,1994)。

在1982年和1984年的两次国际荒漠化会议之后,国际上做了大量的实际工作,使荒漠化的内容更为明确,具体包括:(1)把荒漠化的研究和治理与整个干旱、半干旱地区生态系统的合理利用与管理密切结合起来;(2)把荒漠化的成因、过程、监测与评估密切地结合起来;(3)把荒漠化的研究和防治重点放在预防及制止其蔓延方面,同时特别注重生态环境脆弱带的研究。

长期以来,对于“荒漠化”这一术语存在不同的理解,在中国一度被称为“沙漠化”。1990年2月联合国环境署在内罗毕举行荒漠化评估会议,总结了1977年来荒漠化的发展显著和趋势,提出了一个新的定义,即“荒漠化是包括气候变异和人类活动在内的种种因素造成的干旱、半干旱和亚湿润干旱地区的土地退化”(UNEP, 1994)。荒漠化新定义不仅是理论上的飞跃,而且有利于实践上的应用,“世界荒漠化地图集”的编辑出版就是一个实例,这个图集不仅从宏观上提供了因荒漠化而造成退化土地的形成、分布规律,同时也反映了人口密度与荒漠化关系,明显地说明了土地退化程度严重的地区并不是在人口稀少的七大沙质荒漠化地区,而是在人口密度中等(25~100人/km²),有土地生产潜力的脆弱生态地区,这些地区一旦人为干扰超过了生态系统的承载能力,就会发生沙漠化(朱震达,1994)。

1.1.2 我国荒漠化研究动向和现状

中国是受到荒漠化威胁的主要国家之一。中国荒漠化主要包括4种类型,即沙质荒漠化(沙漠化)、水土流失、土壤盐渍化和冻融荒漠化,其中沙漠化是干旱、半干旱区荒漠化的

主要类型。由于荒漠化定义的变更,对于我国荒漠化的面积说法不一(董光荣,2002)。就沙漠化土地而言,中国防治荒漠化协调小组办公室提出的中国沙漠化土地面积为 160.7 万 Km^2 ,其中包括了第四纪形成的大部分原生沙漠。国家林业局朱俊风等(1999)计算的中国沙漠化土地面积为 48.8 万 Km^2 ,仅考虑了人类历史时期由于自然和社会因素作业形成的类似沙漠景观的土地。

我国的荒漠化研究工作注重理论与实践相结合,研究与治理并举。就其内容而言可追溯到二十世纪三、四十年代的水土保持和土壤盐渍化的研究。1959 年中国科学院治沙队成立,开展了大规模的沙漠考察研究工作,同时对农田和草场沙化进行了调查,并在西北六省沙区建立定点治沙试验站。自 1977 年联合国荒漠化会议以来,我国有关的科研机构和生产部门对这一问题也逐渐重视起来,重点开展了中国北方沙质荒漠化的研究,包括:(1)中国北方干旱、半干旱及部分半湿润地区的土地沙漠化发生发展过程、类型和特点的研究,特别是对脆弱生态环境下及人类活动频繁地区的研究;(2)对沙漠化的成因、危害程度等进行多专题的研究;(3)选择沙漠化严重危害的地区建立不同自然条件下不同类型的沙漠化治理的试验示范基地。近年来的研究重点主要围绕全国沙漠化发生过程、趋势监测和沙漠化土地整治宏观战略,也有多个大型综合性课题涉及到荒漠化的发生机制,取得了一系列初步的成果。

从二十世纪五十年代以来中国加大对荒漠化治理的力度,采取了一系列有效举措,取得一定成绩。中科院兰州沙漠所曾在不同类型的沙漠化(风沙化)地区建立了 9 个整治试验站(点),探讨了整治模式和配套技术,建立了显示效益的示范样板区,以此推动沙漠化的治理,取得了重大的社会、生态和经济效益。同时,中国科学院的其它相关研究所、林业部门也相继建立了试验站和治沙林场,共同开展了“三北”地区沙漠化区域整治工作及相关研究,取得了显著的区域生态效益。有关资料表明,我国北方地区约有 10% 的沙漠面积得到初步治理,有 12% 的沙漠化土地已经开始逆转,但总体上治理速度还是跟不上沙化的速度,形势依然非常严峻(李福兴,1996;朱震达,1994)。

1.1.3 荒漠化研究中存在的问题

综观国内外荒漠化研究的现状,以下三个方面的问题仍然没有得到很好的解决:

1. 荒漠化概念确定较晚,荒漠化评价指标体系还未完全确定,影响对荒漠化面积和程度的评价。

虽然早在 1949 年就有人提出“荒漠化”这个名词,但荒漠化的含义一直都没确定。在二十世纪中期,国外对荒漠化有过很多的定义,但都不过是对沙漠化发展的不同表述(Middleton et al.,1997)。荒漠化最终确定的定义是在 1994 年,联合国环境规划署把荒漠化定义为“包括气候变异和人类活动在内的种种因素造成的干旱、半干旱和亚湿润干旱地区的土地退化”,这一定义作为荒漠化公约签署的定义。在国内,也长期将“荒漠化”与“沙漠化”混淆。对于“沙漠化”,也存在不同的理解,有人将现有沙地都归为沙漠化土地,有人则将沙漠化理解为现有沙漠的扩大。有人将自然过程形成的沙地归为荒漠化土地,有人则侧重考虑人为活动形成的土地退化。UNEP 的定义使有关研究人员的认识开始逐渐得到统一。

在我国,荒漠化研究是一个相对比较新的学科,许多方面的理论和技术有待于进一步完善和发展,而作为荒漠化评价和监测的荒漠化指标体系更是非常不完善,荒漠化类型的划分、荒漠化土地的分类、分布和面积众说纷纭,很难实现区域和国际间监测数据的连接和对比。目前在荒漠化评价体系方面主要存在以下几个方面的不足:(1)荒漠化指标评价体系各有侧重,缺乏可比性;(2)评价标准不一,缺乏有说服力的科学证据;(3)不同的荒漠化评价体系建立在不同的尺度上,难以推广;(4)评价指标多注重于地表形态变化,对荒漠化的生态

学过程,即土地系统结构和功能退化的描述不够;(5)主要针对风蚀荒漠化类型,而对其他类型的评价指标涉及较少。

2. 自然和人为因素在荒漠化加重过程中所起的作用不清楚,影响治理荒漠化合理对策的制定

目前学术界对荒漠化成因争议颇多(董光荣,1998)。以风力作用形成的沙质荒漠化(简称沙漠化)为例,有的学者认为,沙漠化是气候干旱的产物,而多种尺度的干旱是全球或半球气候变化的结果(方修琦,1990),另一些学者认为,导致沙漠化的诸多因子中干旱气候仅起到诱发和促进作用,人为因素才是决定性的,沙漠化是人类实践的产物(Dregne,1984;朱震达,王涛,1992),更多学者认为,沙漠化是气候干旱和人类活动两者共同作用的结果,但时间和空间尺度不同两者的作用程度存在差异(董光荣等,1990,1993; Menshing et al., 1985; 巴巴耶夫,1987)。关于现代荒漠化的研究结果也表明:如果人类活动尚未超过自然系统的负荷限度,即使在具有荒漠化发生潜在条件的地区,天然植被会通过自然调节,维持生态系统的相对平衡,且具有较高的产出率,环境不会产生急剧的退化现象,但一旦人类活动过度,使得荒漠化发生的潜在因素就会被激活,从而引起荒漠化,因此人为因素是现代荒漠化过程的直接原因。

一些专家估计,自然变化引起的荒漠化土地仅占13%,其余87%都是人为原因引起的。人类活动对荒漠化的影响包括两个方面的内容,一是不合理的土地利用环境。二是高人口增长率和急剧的城市化(刘爱民等,1997)。在对我国荒漠化成因进行调查分析时发现,由于不适当耕作或过度农垦而引起的荒漠化土地占全国荒漠化土地总面积的25.4%,过度放牧造成的荒漠化土地占28.3%,樵采引起的荒漠化土地面积占31.8%,水资源利用不当造成的荒漠化土地占8.3%,以工矿交通城市建设破坏植被为主造成的荒漠化土地占0.7%。可见人为因素是土地荒漠化的重要原因(李慧卿等,2000)。

3. 荒漠化与风沙活动等方面生态问题的关系缺少研究

沙尘暴是荒漠化的一个重要生态效应之一,近年来沙尘暴的频繁发生越来越受到政府和人们的关注,但对于沙尘暴的研究目前多见于驱动沙尘暴的物理过程的研究,关于荒漠化与沙尘暴发生的关系方面的研究目前仍然较少。对沙尘暴的发生与沙尘源区不同地表覆盖类型下的植被退化、土壤退化之间的联系的研究几乎没有。由于以上原因,很难从控制严重荒漠化地区的人为破坏活动的角度来遏制沙尘暴的进一步加剧,因此也很难提出具有科学依据的治理措施。

1.2 荒漠化评价指标体系的研究

1.2.1 荒漠化评价指标体系的研究进展

无论是研究荒漠化的动态过程还是研究沙化机理都需要建立一个可行的监测指标体系,最早的评价体系是1984年FAO、UNEP和UNESCO提出的荒漠化分类分级体系,但这种体系非常的复杂,于是就出现了以此标准为基础的多个简化体系,应用最广泛的是以人为作用下的土壤退化为基础的绝对退化评价。另外还有以地表景观和植被盖度为指标的评价方法等(UNEP,1992a,1992b)。我国目前较多研究工作仍然侧重与荒漠化评价指标体系的理论探

讨(孙武, 1999; Zhang et al., 2002), 建议的评价指标往往面面俱到, 包含了植被、土壤、地貌等诸多方面, 如高尚武等(1998)根据植被盖度(G)、裸沙占地百分比(S)和土壤质地(T)三个因子给出了沙质荒漠化的现状监测评价指标体系, 将沙质荒漠化分为轻度、中度、重度和极度四类, 给出了每一类上述三项指标的权重范围, 由于缺少地面研究的支持, 权重范围的给定往往比较主观。刘刚才等(1999)在对金沙江干热河谷的土地荒漠化进行指标评价体系的研究中通过地貌(包括切割密度、坡度)、土壤(包括土壤厚度和土壤有机质)和植被(包括植被指数)等多因子的比较和取舍, 确定了采用土层厚度和总有机碳(TOC)这两个指标评价这一地区的荒漠化程度。类似的区域工作目前仍然较少。

1.2.2 荒漠化评价指标选择的原则

目前, 有不少研究工作探讨了荒漠化评价指标选取的原则(孙武等, 2000; 刘淑珍等, 2000; 范建容, 2002; 贾宝全, 2001)。综合前人的研究工作, 可以认为, 荒漠化指标选取应该遵循以下几点原则:(1)区域分异原则: 要想建立一个统一的标准, 必须要求气候因子对该区域的影响是一致的;(2)相似退化机理原则: 在气候因子影响一致的情况下, 要求人为和自然的干扰方式也相似, 亦即退化机理相似;(3)主导因子原则, 不同的土壤质地和地貌类型下, 影响荒漠化的因子的重要性不同, 要根据实际情况具体选择主导的指标因子(4)信息量集中原则: 最后所用的荒漠化评价指标要有代表性, 要尽可能多地反映能够指示荒漠化程度的植被信息、土壤信息和人为干扰信息等。(5)基线原则: 选取尚未退化的土地作为荒漠化退化程度的客观基线, 以此标准来确定其他评价单元的退化程度。总之, 根据区域特点提出合理的、操作性强的、同时又能在不同区域间进行比较的指标体系仍然是今后的努力目标。

1.3 荒漠化与沙尘暴

1.3.1 沙尘暴的定义和研究进展

沙尘暴是指强风把地面大量沙尘卷扬空中, 使空气特别混浊, 水平能见度低于 1km 的一种危害性极大的自然灾害性天气现象。沙尘暴主要发生于位于北半球的中纬度地带, 其来源区均位于干旱、半干旱地区, 全球最大的沙尘暴源区为撒哈拉沙漠及其南部和亚洲中纬度干旱区(吴国雄, 1979; Zhang et al., 1998)。

沙尘暴的影响有正、反两个方面。一方面, 沙尘暴使人类的居住地、周围环境、健康状况、甚至生命财产等都受到很大的威胁和伤害; 另一方面, 也有研究表明, 沙尘暴能够中和酸雨, 减缓温室效应的影响, 给海洋生物带来丰富的有机质(Bishop, 2002)。

二十世纪九十年代以前的研究重点为撒哈拉沙漠和亚洲中西部沙漠向大陆及海洋的输送问题, 侧重沙尘暴的气象过程。九十年代后的研究开始系统化, 主要从沙尘暴的天气气候学特征、分析预报、遥感监测、沙尘暴的成分分析、数值模拟、灾害预防等方面进行深入探讨(胡金明等, 1999)。但探讨不同的地表植被覆盖状况对沙尘释放的影响研究仍然较少。

1.3.2 沙尘暴爆发的原因及其与荒漠化的关系

沙尘暴作为一种高强度风沙灾害,并不是在所有有风的地方都能发生,只有那些气候干旱、植被稀疏的地区,才有可能发生沙尘暴。沙尘暴的形成及其大小,直接取决于风力、气温、降水及与其相关的土壤表层状况。它的发生必须具备三个基本条件:沙源、大风、低层大气层结构不稳,而这三者主要与脆弱的自然生态环境、一定的天气系统过程、独特的地貌结构有关(胡金明等,1999)。沙尘微粒的消长直接和地面的植被覆盖状况和土壤状况有关系。人为活动毁坏了大面积的森林和草地,导致植被覆盖率下降,植被对土壤的保护作用减弱,为沙尘暴的发生提供沙源的可能性增加。因此,荒漠化为沙尘暴的发生提供了更多的物源,而沙尘暴的发生则进一步恶化了沙尘源区的荒漠化程度,带走了富含营养的土壤细颗粒,使得植物更难生存,进而导致气候进一步恶化。由此可知,荒漠化与沙尘暴的相互作用形成一个恶性循环,必须从根本上找出它们之间关系的内在机理以及引起这种生态恶化的根源,才能制订出有效的措施来防止荒漠化和沙尘暴。目前,有较多的研究工作试图通过沙尘暴的时空分布与气候及植被因子的统计分析来推断沙尘暴爆发与植被和气候条件的关系(顾卫等,2002),然而,只能得出较为笼统的结论,如植被覆盖率下降,则沙尘暴日数增加。

1.3.3 北京等地沙尘天气的物源与上风向沙尘释放

近年来北京地区爆发的强沙尘暴引起了科学界和政府的广泛关注。北京处于东亚沙尘暴多发区域($35^{\circ} \sim 45^{\circ} \text{N}$)的下风方向,是亚洲沙尘气溶胶向近中国海及西北太平洋输送的主要通道,因此对北京地区开展有关沙尘暴的研究对于海上沙尘传输等有重要的意义。

前人研究明确指出浑善达克沙地边缘是北京地区沙尘暴的主要物源区(张仁健,2000;Liu H et al.,2000)。叶笃正等将沙尘暴途径地区沙化土地进一步划分了沙化发展区、潜在沙化区和非沙化区,认为沙化发展区是沙尘的主要源地,然而没有根据土壤和植被的性质对起沙机理进行进一步探讨(叶笃正等,2000)。目前对于沙尘暴物源的研究大致有两种途径,一是从遥感影像判断,如李令军等(2001)利用卫星云图得出,在浑善达克沙地的西部和南部存在两条东西向沙尘点源群;二是通过沙尘暴理化性质的分析,如张仁健等(2000)通过沙尘暴爆发期间气溶胶理化性质的分析得出沙尘暴期间来自远方的大粒子占了很大比重。然而,即使通过以上手段探知沙尘暴的源区,仍然无法从机理上回答以下问题,究竟何种地表覆盖类型对沙尘暴的物源贡献大?沙尘暴是土地荒漠化程度的重要指标,回答以上问题则是荒漠化防治的关键,也就是说防沙治沙工作才能够对症下药。

1.4 本研究的内容与目标

本文以河北坝上地区、内蒙古浑善达克沙地及其周边地区为例研究区,通过野外调查、实验室分析和遥感影像解译相结合的手段,探讨研究区植被退化和土壤退化的关系,建立比较完善的荒漠化评价指标体系,分析荒漠化的空间格局。在此基础上,通过收集研究区1984~2000年间的气候、人为活动、归一化植被指数(NDVI)和沙尘暴资料,分析沙尘暴发生时的植被条件,进而探讨气候波动和人为活动变化对植被退化和沙尘暴发生的贡献。

本文的目标主要有以下几个方面:

1. 研究区的植被退化和荒漠化评估的指标体系和方法

根据植物群落的种类组成计算植被退化指数来指示植被退化程度,通过土壤有机质和机

械组成分析来确定土壤的退化程度,通过多元统计方法分析研究区植被退化与土壤退化的关系,进而确定研究区荒漠化评价的指标体系;

2. 研究区荒漠化空间格局

利用分辨率为 $250 \times 250\text{m}$ 的 MODIS 影像进行研究区植被分类,得到区域植被和土地利用格局;根据前面得到的荒漠化评价指标,通过遥感影像的处理,得到研究区荒漠化程度分布图;

3. 植被对气候波动和人为活动的响应

在不同的植被和土地利用格局类型内选择有代表性的地点,利用分辨率为 $8 \times 8\text{km}$ 的 NOAA/AVHRR 影像,获取各类型 1984~2000 年归一化植被指数 (NDVI) 的变化过程;从统计年鉴获得代表性地点相应时段内的人为活动状况,通过多元统计分析,探讨气候波动和人为活动对植被变化的影响;

4. 不同地表覆盖对沙尘暴的贡献

根据植被调查记录和土壤分析结果,探讨不同的地表覆盖类型下沙尘释放的能力;根据 1984~2000 年的沙尘暴记录和气候资料,探讨不同类型的植被覆盖动态与沙尘暴次数和强度动态之间的关系,进而分析荒漠化与沙尘暴之间的联系;

5. 研究区荒漠化防治对策

根据研究区荒漠化现状,植被退化与风沙活动的关系,提出研究区防治荒漠化和减缓沙尘暴的切实可行的对策。

全文的技术路线如图 1.1 所示。

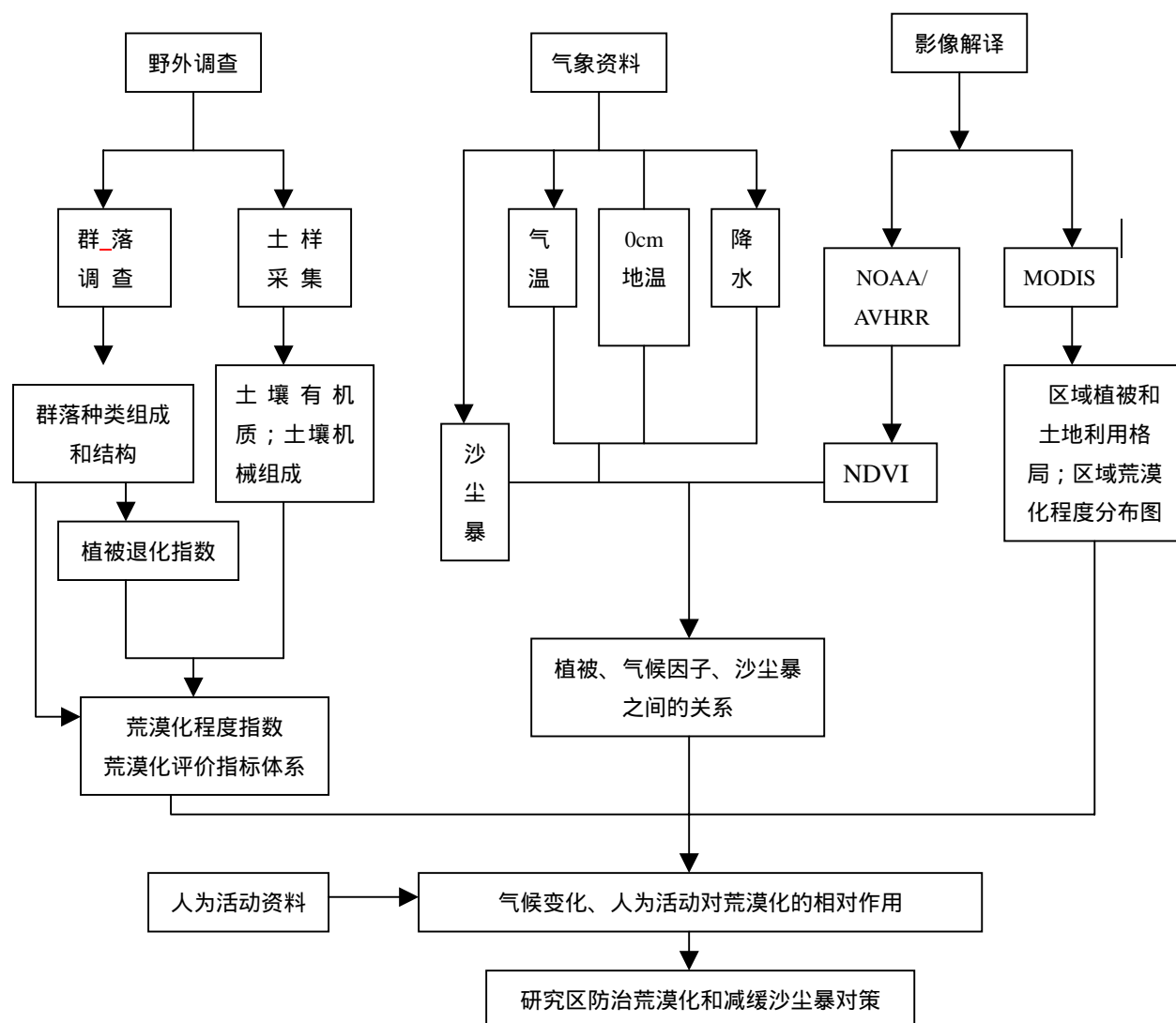


图 1.1 论文技术路线图

第二章 研究区概况

2.1 研究区自然地理概况

2.1.1 地理位置

研究区主体部分为位于内蒙古高原东南部的浑善达克沙地和河北坝上地区，海拔在 1100~1500m 左右。在行政区划上包括内蒙古自治区锡林郭勒盟的所有旗县，乌兰察布盟的化德和商都等县，河北省张家口地区的张北、沽源、康保等县以及承德市的丰宁、围场两县的坝上部分。为了分析风沙活动的规律，研究区还涉及到下风向的北京、天津和河北北部的其它县市。研究区的地理坐标为 E 112~119°，N 39~45° (图 2.1)。

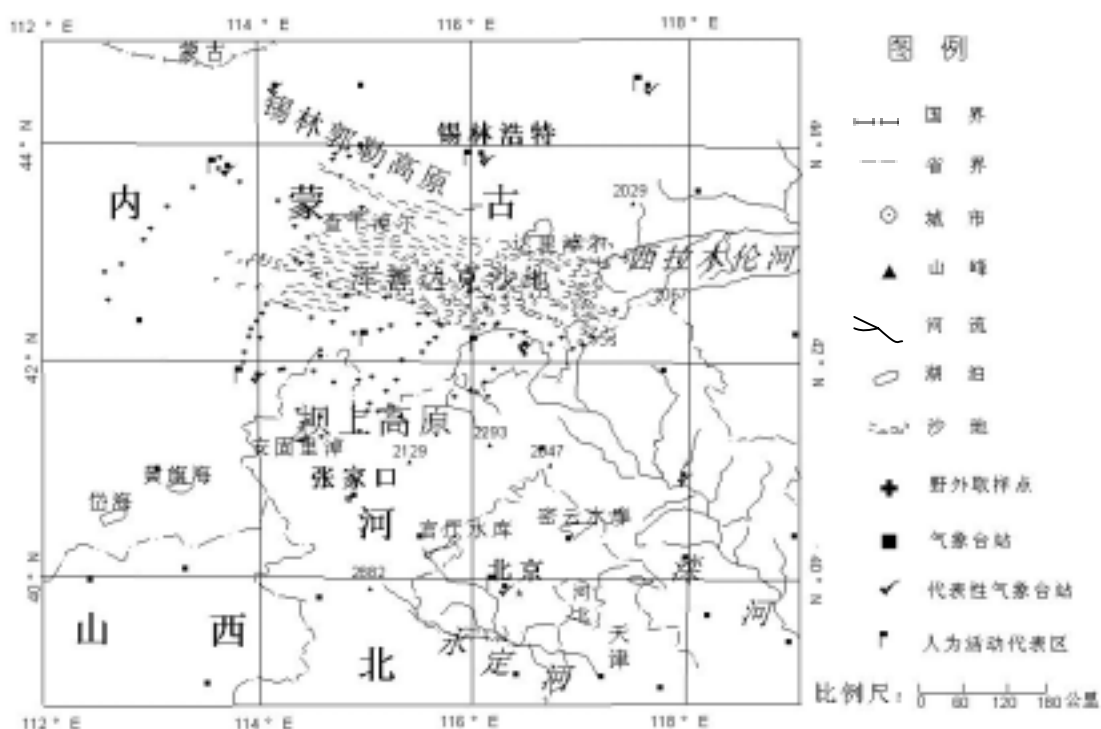


图 2.1 研究区区域图

2.1.2 地质、地貌

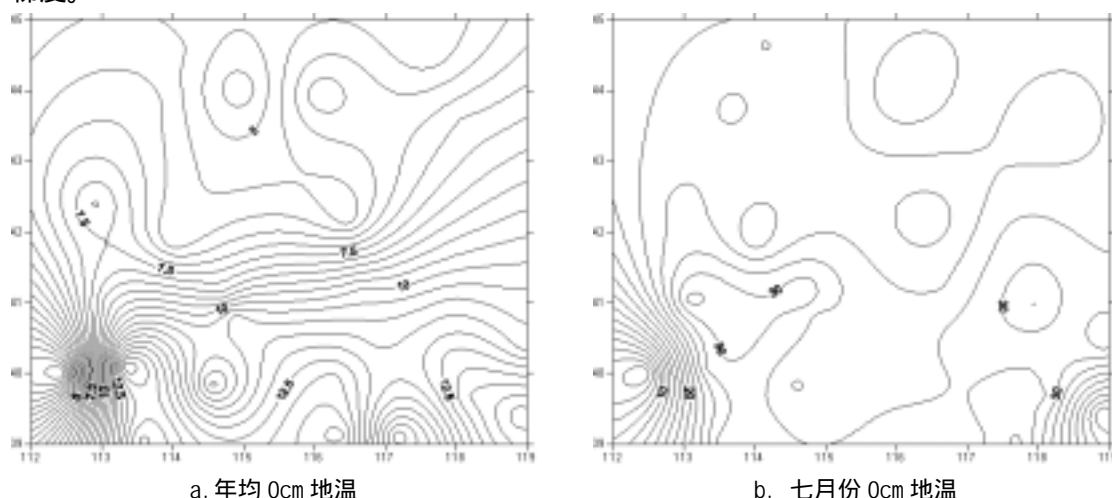
研究区的东南和南部为冀北山地，沟谷海拔在 500~700m 之间，向北和西北方向的内蒙古高原海拔则复又缓缓下降，内蒙古高原的边缘部分与冀北山地交界的部分称为“坝上高原”。在坝缘部分，山地海拔迅速上升到 1400~1700m，最高海拔在 2000m 以上。

研究区地貌类型复杂多样。中部为浑善达克沙地，核心部分为东西向条带状的沙垄，边缘部分为覆沙丘陵。北部为锡林郭勒高原，以波状高平原地貌为代表，有大面积火山活动形成的火山锥和熔岩台地。西北部为苏尼特盆地。南部坝上高原部分以波状高原为主，有阴山余脉形成的低缓丘陵。在高原面上，有众多湖泊出现，较大的有达里淖尔、查干淖尔和安古里淖等。

2.1.3 气候

研究区的气候条件为温带大陆性半湿润气候向半干旱气候逐渐过渡。主体部分海拔高，气温低，年降水量在 200~450mm 之间，为季风气候影响的尾闾区（marginal area）。浑善达克沙地与内蒙古其他地区的沙地有所不同，其气候特点是夏季温凉，降水较多，冬季寒冷干燥，热量自东向西递增，风大沙多。研究区中的草原区部分全年 8 级以上的起风时日高达 60~80 天，形成了沙尘暴的动力基础，研究区也被认为是华北等地沙尘天气的重要物源区之一（叶笃正，2000）。

利用研究区和周边地区的 30 个气象台站（站点位置见图 2.1）1980~2000 年多年平均气候资料，对研究区的气温、降水和 0cm 地温进行克里格（Krig）插值，得出主要气候指标的空间分布规律（图 2.2）。可以看出：研究区的年均气温和年均 0cm 地温存在明显的由南向北的梯度，受地形条件的影响，坝缘部分温度变化的幅度较高原内部和坝下部分剧烈。一月份的平均气温和平均 0cm 地温存在类似的规律，而七月份相应气候指标的变化则不具有明显的梯度，反映了气候指标空间格局的季节差异。年降水量则存在明显的由东南向西北方向的梯度。



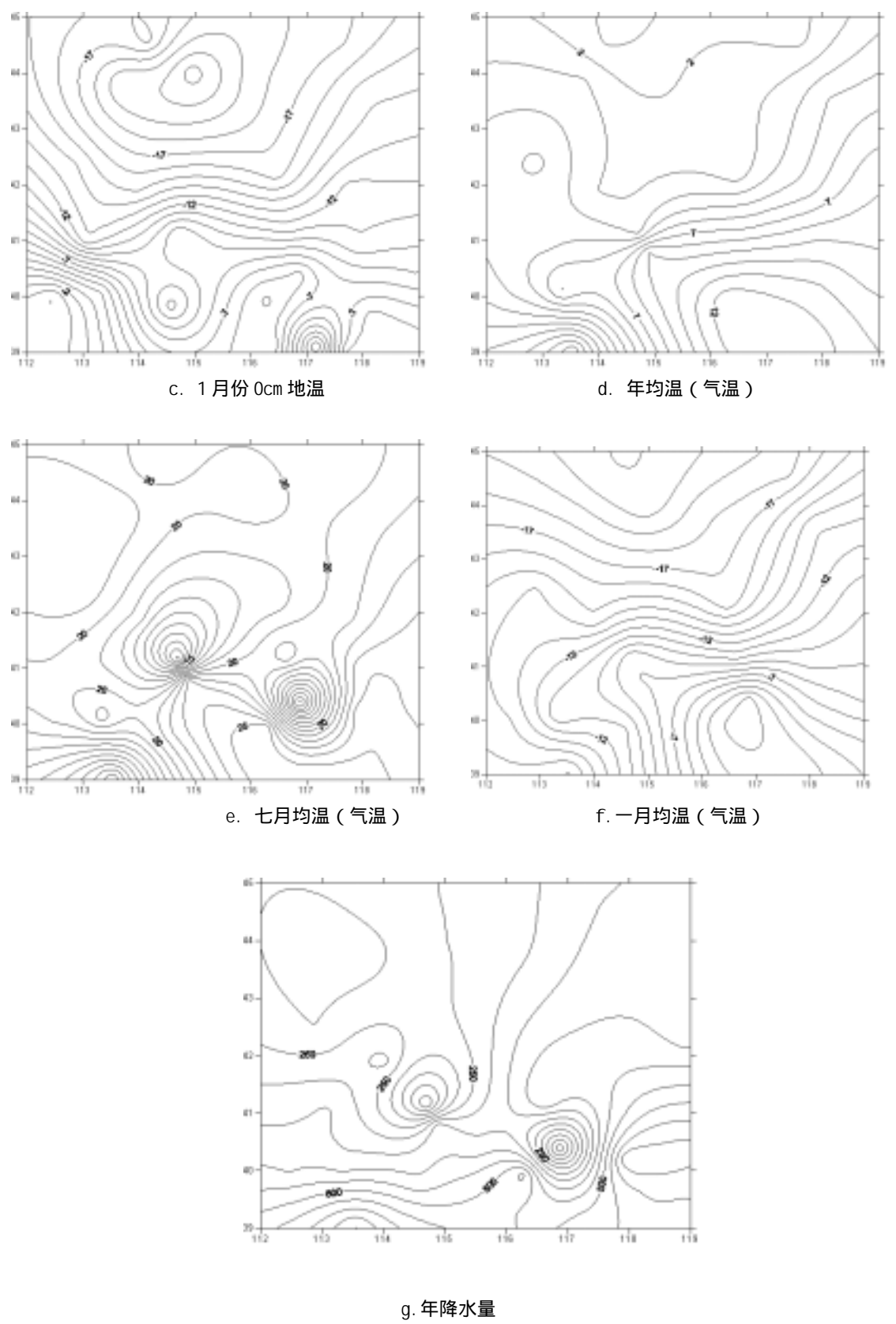


图 2.2 研究区主要气候指标分布图 (其中 X、Y 轴分别为经、纬度)

图中气温和 0cm 地温的单位是 ，降水的单位是 mm

2.1.4 植被和土壤

土壤和植被格局反映了气候条件和地貌特征的空间分异。冀北山地的植被以落叶阔叶林和落叶阔叶灌丛为主,相应的土壤类型为褐土和棕壤。坝上高原东部为草甸草原,土壤为黑钙土。坝上高原西部和锡林郭勒高原则以典型草原植被和栗钙土为主。浑善达克沙地西部为沙地小叶锦鸡儿灌丛草原,东部为榆树疏林草原,土壤为风沙土。在西北部的苏尼特盆地,植被为荒漠化草原,土壤为棕钙土。在高原内部低地处常发育有草甸、盐化草甸与沼泽、盐碱地,相应的土壤类型为草甸土、沼泽土和盐碱土。

2.2 研究区人类活动与土地利用

研究区历史上华北、蒙古、东北三大地区经济文化的汇合点,自古以来就是多民族争夺、交流、融合的农牧交错地带,区域开发过程复杂、多变,尤其是十七世纪中叶以来,区域开发速度快、强度大,使这里的生态环境发生了显著的变化。区域的开发和人类活动历史可以分为以下几个阶段:(1)明代以前的农牧交错开发时期,又分为先秦原始开拓阶段、秦西汉初步开发阶段、东汉至五代游牧为主阶段、辽金农业为主开发阶段和元明农牧转换阶段,其特征是数次农牧交错或农牧并存交错分布;(2)清代围场、行宫、晃庄为主全面开发时期,又包括全面开发时期和后期农业缓慢发展与清末围场放垦阶段;(3)民国区域经济曲折发展阶段,民国前期,由于北洋军阀实行移民实边政策,奖励垦辟蒙荒,坝上多伦-沽源一线东南舒缓丘陵草原区又有大量汉人移入开垦,出现了大批农业聚落,蒙族人进一步北移,大部分地区成为半农半牧或农业区(张宝秀,1997)。

整个研究区的土地利用格局表现为南农北牧,河北坝上地区以及内蒙古多伦县、太仆寺旗、化德县、正蓝旗南部、正镶白旗南部、镶黄旗局部则表现为农牧交错。由南往北,耕地所占的比例逐渐减小。由于地处季风气候尾部区,降水量的波动性明显,这一农牧交错带生态上脆弱,对于人类的干预反应敏感,过度的人为利用已经造成了突出的生态问题。

2.3 区域选择的意义

选择内蒙古浑善达克沙地及其周边地区以及河北坝上地区作为研究区具有重要的理论和实践意义。

首先,从北京经河北坝上至浑善达克沙地,降水量逐渐降低,土地利用方式也由以农为主、到农牧交错,再到以牧为主。从北京到浑善达克沙地腹地不仅有着从半湿润到半干旱的气候梯度,也有从森林到森林草原、进而到草原的植被梯度,还有从土地利用方式的明显差异和利用强度的梯度,因此,是研究植被退化和土地利用/土地覆盖变化的理想的区域性样带。通过样带综合分析,不仅可以揭示浑善达克沙地和河北坝上地区生态脆弱性的控制因子,还可以更好地分析这一地区植被退化与当地及下风向的北京地区沙尘天气之间的联系。

其次,河北坝上紧邻首都外围,内蒙古浑善达克沙地是距离北京最近的沙地,它们地处北京的上风向,土地沙化是这一地区存在的突出的生态环境问题,并直接影响到北京的生态安全。这一地区的景观演化过程,尤其是荒漠化过程,与北京地区沙尘天气关系密切,是近年来倍受关注的研究地区和研究领域。

最后,这一地区是京津以至整个华北地区的生态屏障,是环首都生态圈的重要组成部分,

也是当前生态建设的重点区域,本研究的成果可以为制定因地制宜的和切实可行的荒漠化防治对策提供理论依据。

第三章 研究方法

3.1 野外调查

采用全球定位系统 (GPS) 定位, 在研究区内不同的地表覆盖类型下选取具有代表性的地点 120 个 (图 2.1)。在每一个取样点, 采取样方法 (Mueller-Dombois and Ellenburg, 1974) 进行植被调查, 依据植被的差异性和退化状况做样方 1~3 个, 共做样方 137 个。每个样方记录各物种的多度、盖度高度、物候相, 并记录其生境特征, 包括海拔、坡度、坡向、地表覆盖物、土壤类型及厚度、湿度状况和土地利用状况。根据不同地点植被的差异性, 在其中 125 个样方中采集表土 (0~5cm) 样品, 在样方内不同部位采集后均匀混合, 采样量为 500g 左右。其中非沙地草原上采集土样 64 个, 沙地草原上采集 21 个, 其它类型采集 40 个。

3.2 植物群落分析

3.2.1 植被数量分析

在本研究中, 采用 TWINSpan 对样方资料进行分类, 然后运用 DCA 排序分析植物群落与环境因子及人为活动之间的关系, 使用的软件为 Windows 版的 PCord。采用的数据为样方内不同种类的重要值矩阵。

重要值的计算根据以下公式:

$$\text{重要值} = \frac{\text{相对多度} + \text{相对盖度} + \text{相对高度}}{3}$$

在计算过程中, 首先对德氏多度进行量化, 相对高度的取值统一以营养枝高度为标准。

此外, 本文还采用 DCA 分析荒漠化程度, 原始数据为以荒漠化程度评价指标因子的值建立的矩阵。

文中群落内植物种类多样性的计算采用香农 - 威纳指数 (Shannon-Wiener Index) 来表示, 其计算公式为:

$$H' = - \sum P_i \log_2 P_i$$

其中 H' 为香农 - 威纳指数, i 代表样本中的物种数, P_i 为各个物种的重要值。

3.2.2 指示种分析

1. 草原退化的指示种概况

能够描述特定生境特征的植物种称为植物指示种, 将植物指示种作为研究草地退化的指标是评价草地荒漠化的一种重要方法, 其研究历史也比较悠久。每一种植物最繁盛的环境总是与其它种有很大差异, 因此可以把具有严格生存条件要求的植物种作为特定的单个因素或

因素组的指示种。指示种的概念在生态学上具有很大的价值,被广泛应用于土地分类、农业、放牧和森林中。近年来,植物指示的概念则广泛应用于为各种不同的农业目的而进行的土地适宜性的决策分析中(Devaraj, 1999)。

草原草场的放牧指示植物可进一步分为正的或负的、定性的和定量的指示植物,这些不同的指示植物类型与非指示植物,构成不同的放牧生态种组。

对于内蒙古高原主要草原草场来说,在持续自由放牧下均趋同于冷蒿(*Artemisia frigida*)草原,冷蒿是最可靠的定量放牧指示植物,但同时又是优良牧草和草原退化的阻击者;当放牧压力过大时,冷蒿进一步退化为星毛委陵菜(*Potentilla acaulis*),然后就是一年生植物甚至裸地(李永宏, 1994; 李博, 1997)。李博(1997)研究了我国北方草甸草原及典型草原的退化演替情况,得到各个阶段植被指示情况,结果表明原始类型的建群种有羊草(*Leymus chinensis*)、贝加尔针茅(*Stipa baicalensis*)、大针茅(*Stipa grandis*)等,并伴生一些较为中生的优良牧草;当放牧强度增加,草地开始退化时,这些植物逐渐减少,至重度退化阶段,这些种大部分消失。与此同时,原生群落的一些伴生成分,如糙隐子草(*Cleistogenes squarrosa*)、冷蒿、百里香(*Thymus serpyllum*)、麻花头(*Serratula centauroides*)、狗娃花(*Heteropappus hispidus*)、星毛委陵菜等则随放牧程度的增加而增加,甚至代替原来的优势植物而成为建群种。以小针茅(*Stipa gobica*, *S. klementz*, *S. breviflora*)为建群种的荒漠草原,当放牧强度增加,草原开始退化时,无芒隐子草(*Cleistogenes songorica*)、银灰旋花(*Convolvulus amanii*)、栉叶蒿(*Neopallasia pectinata*)、骆驼蓬(*Peganum harmala*)逐渐增加,最后取代小针茅而成为优势种。但在不同自然地带和不同群落类型中,退化指示植物是不同的,只有在充分了解各草地类型演替规律的基础上,才可利用指示种来推断草地退化程度。

由此可知,在草地退化的研究中指示种是比较可靠的一种指示植被退化的方式;而百里香、麻花头、糙隐子草、狼毒(*Stellera chamaejasme*)、冷蒿等草地退化指示的植物都可以代表植被退化的状况,可以把这些植物当作植被退化指示植物,当然在不同的植被类型下选择的指示种也有不同。

2. 植物种分类

本文在前人总结的基础上,通过对植物不同习性的分析,把总的植物种分为三大类,其中第一类为一、两年生植物,主要出现于退化严重的草地,第三类由除了第二类植物外的多年生植物组成,代表退化轻微或者尚未退化的草地。第二类由放牧退化指示种、盐碱化指示种以及流动沙地指示种等组成,主要出现于退化程度介于第一类和第三类之间的草地,代表性物种见表 3.1,详细名录见附录。

表 3.1：中等退化程度指示种（第二类植物）

	放牧退化指示种		沙生和固沙植物以及指示沙质特征的植物	耐盐植物
典型草原带	星毛委陵菜、黄囊苔草	糙隐子草、冷蒿、狼毒、高二裂委陵菜	叉分蓼、变蒿(柔毛蒿)、麻花头、砂引草、蜆菊、冰草、差不嘎蒿、狭叶锦鸡儿、小叶锦鸡儿、百里香	芨芨草、马蔺、匍根骆驼蓬
草甸草原带	阿尔泰狗娃花			
荒漠草原带	匍根骆驼蓬、多根葱、阿氏旋花			
沙地(喜沙植物)	沙蒿、沙柳、沙生冰草、沙竹			

3.2.3 退化指数的计算

依据植物的重要值和指示种分类,计算出每个样地的植被退化指数。具体方法是:对样地中记录到的所有植物种按照上文所述分成三类,然后对这三种类型分别赋予权重如下:一、二年生植物种 1/3,中等退化程度指示种 2/3,轻度退化和无退化指示种 1,则某一样地的植被退化指数就等于每一种类型的重要值乘以该类型所赋予的权重的和,计算公式如下:

$$\text{植被退化指数} = 1 / (A_1 * 1/3 + A_2 * 2/3 + A_3)$$

其中 A_1 , A_2 , A_3 分别代表三种类型植物的重要值。

植被退化指数考虑了样地中植物的组成、不同种的多度、盖度、高度等,因此是比较全面的,能够较好地指示植被退化状况。植被退化指数越大,说明植被的退化程度越高。

3.3 土壤分析

将土壤样品充分混合,去除植物根系,然后送到中国科学院地理科学与自然资源研究所,使用英国产 Mastersize2000 激光粒度仪对每个土壤样品进行了粒度分析。测定结果将土壤粒度分为以下等级: >1.0mm, 1~0.5 mm, 0.5~0.25 mm, 0.25~0.10 mm, 0.10~0.063 mm, 0.063~0.05 mm, 0.05~0.04 mm, 0.04~0.03 mm, 0.03~0.02 mm, 0.02~0.01 mm, 0.01~0.005 mm, 0.005~0.002 mm, 0.002~0.001 mm, <0.001 mm。然后根据粒级划分标准,将土壤机械组成划分为砾石(>1mm)、砂(0.063~1mm)、粉砂(0.002~0.063mm)和黏土(<0.002mm)。土壤有机质分析采用电热板加热-重铬酸钾容量法,有机质含量以占土壤干重的百分比来表示。

将研究区的地表覆盖类型划分为石质丘陵草甸草原、石质丘陵典型草原、熔岩台地典型草原、熔岩台地草甸草原、沙地榆树疏林草原、沙地小叶锦鸡儿灌丛草原、现有耕地、撂荒和退耕地、人工林、低湿地草甸和湖滨草甸。对于不同的地表覆盖类型,将得到的土壤有机质和粒度数据与前面提到的植被退化指数进行多元统计分析。在进行荒漠化程度评价分析时将沙地榆树疏林草原和沙地小叶锦鸡儿灌丛草原合并为沙地草原,把石质丘陵草甸草原、石质丘陵典型草原、石质丘陵荒漠草原以及熔岩台地典型草原合并为非沙地草原。

3.4 遥感影像分析

3.4.1 应用 NOAA/AVHRR 遥感影像进行植被指数 NDVI 分析

NOAA/AVHRR 气象卫星影像在大尺度植被分类及其变化研究方面具有其他影像不可替代的作用,它能够提供地表覆盖的概貌,可以作为建立地表覆盖数据库的基础,也可以提供有关植被的许多特征信息,如季节性信息,植被光合能力的信息等。NOAA 影像还具有时间和空间上的连续性和长期性、时间分辨率高(每日覆盖全球)、价格低廉等优点,是极有价值的区域和全球植被研究的数据源(李晓兵,1999)。

从美国 NASA 网站获取了 1981~2000 年的 NDVI 数字影像,具有完整年份能够利用的数据为 14 年,其中 1981 年上半年、1982 年全年、1983 年 9 月份、1992 年和 1993 年全年、1994 年 10、11、12 月份的数据缺失。数据的处理方法是先将研究区分为草甸草原、典型草原、

荒漠草原、森林、农田、农田和典型草原混合植被、沙地小叶锦鸡儿灌丛草原和沙地疏林灌丛草原等植被类型,然后根据中国植被图等对每个类型分别选取具有代表性的样区(0.5 经度 \times 0.5 纬度),利用二次开发程序提取这些样区内各像元的 NDVI 值,计算每个样区的均值,作为各植被类型的 NDVI 值。

3.4.2 运用 MODIS 影像进行区域地表覆盖和荒漠化空间格局分析

Terra/EOS 星上搭载的中分辨率成像光谱仪(MODIS)使用户能够有机会同时获得 36 个覆盖可见光、近红外和远红外波段的百米量级的遥感资料,从而为把大气-陆地-海洋作为一个整体来综合探讨地区环境演化变迁的内在科学规律提供了新的数据来源。MODIS 在对地观测过程中,每秒可同时获得 6.1 兆比特的来自大气、海洋和陆地表面信息,每日或每两日可获取一次全球观测数据。文中利用能够代表植被信息的空间分辨率为 $250 \times 250\text{m}$ 的 MODIS 1, 2 波段(其中第一波段为红外可见光波段,第二波段为近红外可见光波段)进行植被分类,利用能够区分腐殖土的波段 26/3 的组合以及能够区分沙土和黏土的 5、6 波段进行荒漠化程度景观格局分析。

从中国农科院规划所遥感中心获得 2001 年 7 月 19 日和 8 月 15 日的两幅 MODIS 1B 影像,对影像进行几何精校正、辐射校正和地理坐标配准,然后根据它的波段与 TM 波段的对应情况,选择植被分类最佳的波段组合进行地表覆盖的格局分析。然后根据荒漠化评价所选取的指标,选取能够代表这些指标的相应波段的影像进行合成,得出研究区荒漠化的空间格局。

3.5 气候资料的获取和处理

从中国气象局气象数据中心获得研究区及周边地区 30 个主要气象台站连续 1980~2000 年的气候资料,包括旬平均地温、旬平均气温、旬平均降水、旬平均风速、风向、沙尘暴爆发日的能见度以及沙尘暴爆发频率等项目。

从中国沙尘暴数据库获得以上每个植被类型样区内或样区旁代表性气象台站的 1980~2000 年的沙尘暴数据,并将不同地表覆盖类型的 NDVI 的动态与沙尘暴发生的强度和频率进行多元统计分析。

第四章 区域植被退化分析

草地植被退化是荒漠化的重要表现,探讨草地植被退化对于荒漠化的防治和生物多样性的保护都具有重要意义。本章通过分析研究区的植被状况,借助植物指示种指示当地的植被退化情况,得出该地区植被退化的现状并预测未来变化的趋势,从而为改善该地区的生态环境,提供理论依据。

4.1 研究区植被退化现状

结合植被类型和地貌类型,将研究区的地表覆盖划成为低湿地草甸、湖滨草甸、耕地、退耕地或撂荒地、人工林、石质丘陵草甸草原、石质丘陵典型草原、石质丘陵荒漠化草原、熔岩台地典型草原、沙地小叶锦鸡儿灌丛草原、沙地榆树疏林草原共 11 类。每种类型的植被退化指数(用 DEG 表示)、草本层平均高度(HIG)、草本层总盖度(COV)、多年生植物平均盖度占总草本盖度的比例(PER)和多样性指数 Shannon-Wiener 指数(H')等特征如表 4.1 所示。

表 4.1 不同类型的多样性指数、植被退化指数的计算结果

植被类型	样地数	项目	DEG	HIG	COV	PER	H'
低湿地草甸	8	均值	1.42	12.44	63.69	0.50	0.42
		方差	0.33	9.18	21.75	0.33	1.94
耕地	10	均值	1.97	11.60	32.75	0.24	1.59
		方差	0.52	5.23	20.33	0.24	0.25
湖滨草甸	5	均值	1.31	17.31	40.40	0.59	1.95
		方差	0.11	7.63	23.05	0.44	0.56
人工林	6	均值	1.54	13.31	33.90	0.21	2.16
		方差	0.26	4.15	13.72	0.49	0.28
熔岩台地典型草原	5	均值	1.49	11.37	23.40	0.19	1.66
		方差	0.25	4.99	11.96	0.34	0.21
沙地小叶锦鸡儿灌丛草原	11	均值	1.66	21.92	46.64	0.06	1.94
沙地榆树疏林草原	11	均值	1.62	22.59	36.85	0.34	1.57
		方差	0.55	17.57	20.79	0.84	0.41
石质丘陵草甸草原	6	均值	1.46	12.89	52.92	0.44	2.13
		方差	0.17	8.94	13.60	1.31	0.52
石质丘陵典型草原	52	均值	1.51	9.95	34.06	0.29	2.32
		方差	0.36	4.56	13.74	0.64	2.04
石质丘陵荒漠化草原	6	均值	1.34	8.65	27.58	0.39	2.32
退耕地	7	均值	2.18	27.09	48.21	0.10	1.82
		方差	0.60	6.13	15.53	0.12	0.36

从表 4.1 可以看出,低湿地草甸、石质丘陵草甸草原和湖滨草甸的植物总平均盖度、多年生植物平均盖度占总盖度的比例都较其它类型偏高,植被退化指数很低,可以判断这些类型的植被退化程度相对较轻;撂荒地或退耕地的植被退化指数很高,虽然总盖度比较高,但多年生植物盖度占总草本盖度的比例却非常低,所以它的植被退化指数相对较高,植被的退

化程度也高，沙地小叶锦鸡儿灌丛草原也有类似的规律。这些符合实际情况，因此也可以认为通过植物的指示意义得出的植被退化指数是可靠的，可以用来进行植被退化程度的分析。

从表 4.1 可以得出不同类型不同指标的从小到大排列顺序表（表 4.2），其中从上到下为相应指标下各类型由小到大的排列顺序。

表 4.2 不同类型各指标的大小排列顺序表

由小到 大次序	DEG	COV	PER	H'
1	湖滨草甸	熔岩台地典型草原	沙地小叶锦鸡儿灌丛	沙地榆树疏林草原
2	石质丘陵荒漠化草原	石质丘陵荒漠化草原	退耕地	耕地
3	低湿地草甸	耕地	熔岩台地典型草原	熔岩台地典型草原
4	石质丘陵草甸草原	人工林	人工林	退耕地
5	熔岩台地典型草原	石质丘陵典型草原	耕地	低湿地草甸
6	石质丘陵典型草原	沙地榆树疏林草原	石质丘陵典型草原	沙地小叶锦鸡儿灌丛
7	人工林	湖滨草甸	沙地榆树疏林草原	湖滨草甸
8	沙地榆树疏林草原	沙地小叶锦鸡儿灌丛	石质丘陵荒漠化草原	石质丘陵草甸草原
9	沙地小叶锦鸡儿灌丛	退耕地	石质丘陵草甸草原	人工林
10	耕地	石质丘陵草甸草原	低湿地草甸	石质丘陵典型草原
11	退耕地	低湿地草甸	湖滨草甸	石质丘陵荒漠草原

从表 4.2 可以看出，不同类型的植被退化指数与总草本盖度之间并无直接的关系，即植被退化指数高的地方总草本盖度不一定就低，而多年生草本盖度占总盖度比例与植被退化指数之间则存在着相对较为有规律的关系，即除个别类型外，多年生植物盖度占总盖度的比例较高的类型，其植被退化指数相对较低。

4.2 研究区植被退化程度的数量分析

4.2.1 TWINSpan 分类

TWINSpan 的分类结果将所有 125 个样地按照指示种分为 8 类，序号依次是 G1、G2、G3、G4、G5、G6、G7、G8，其中 G1 类代表了低湿地草甸和湖滨草甸，指示种为草甸和盐碱地的代表性物种，如盐地碱蓬(*Suaeda salsa*)，蒲公英 (*Taraxacum mongolicum*)；G2 代表多年生草本植物盖度占总盖度的比例相对较低的样地；G3 代表草本层总盖度和土壤 TOC 都较低的样地；G4 代表人为干扰比较严重的样地如人工林、耕地等；G7 代表所有因子都处于中等的样地；G8 这一类型代表草本层总盖度和土壤 TOC 都较低的草原地带的样地；G5 代表沙地小叶锦鸡儿灌丛草原，该类型中的样地，植被总盖度较低，其中小叶锦鸡儿是该类型的指示种；G6 草本层覆盖中等的退耕地，益母草 (*Leonurus japonicus*)、刺儿菜(*Cirsium segetum*)等都是该类型的代表性植物。

从 TWINSpan 结果的二歧图中可以看出，低湿地和湖滨草甸的指示种为代表其生境特征的物种，如盐地碱蓬，蒲公英和芨芨草。而其它类型的指示性物种绝大部分都是一、二年生植物，如刺儿菜、猪毛菜(*Salsola collina*)、猪毛蒿(*Artemisia scoparia*)、益母草、肥披碱草(*Elymus excelsus*)、扁蓄 (*Polygonum aviculare*)、狗尾草 (*Setaria viridis*)，和植被退化指示种，如糙隐子草、黄囊苔草、碱蓬、冷蒿、小叶锦鸡儿等，另外还有一些非退化草原代表种，如克氏针茅(*Stipa krylovii*)、贝加尔针茅等，进一步说明这一分类结果在能够较好反映草原植被的不同退化程度。

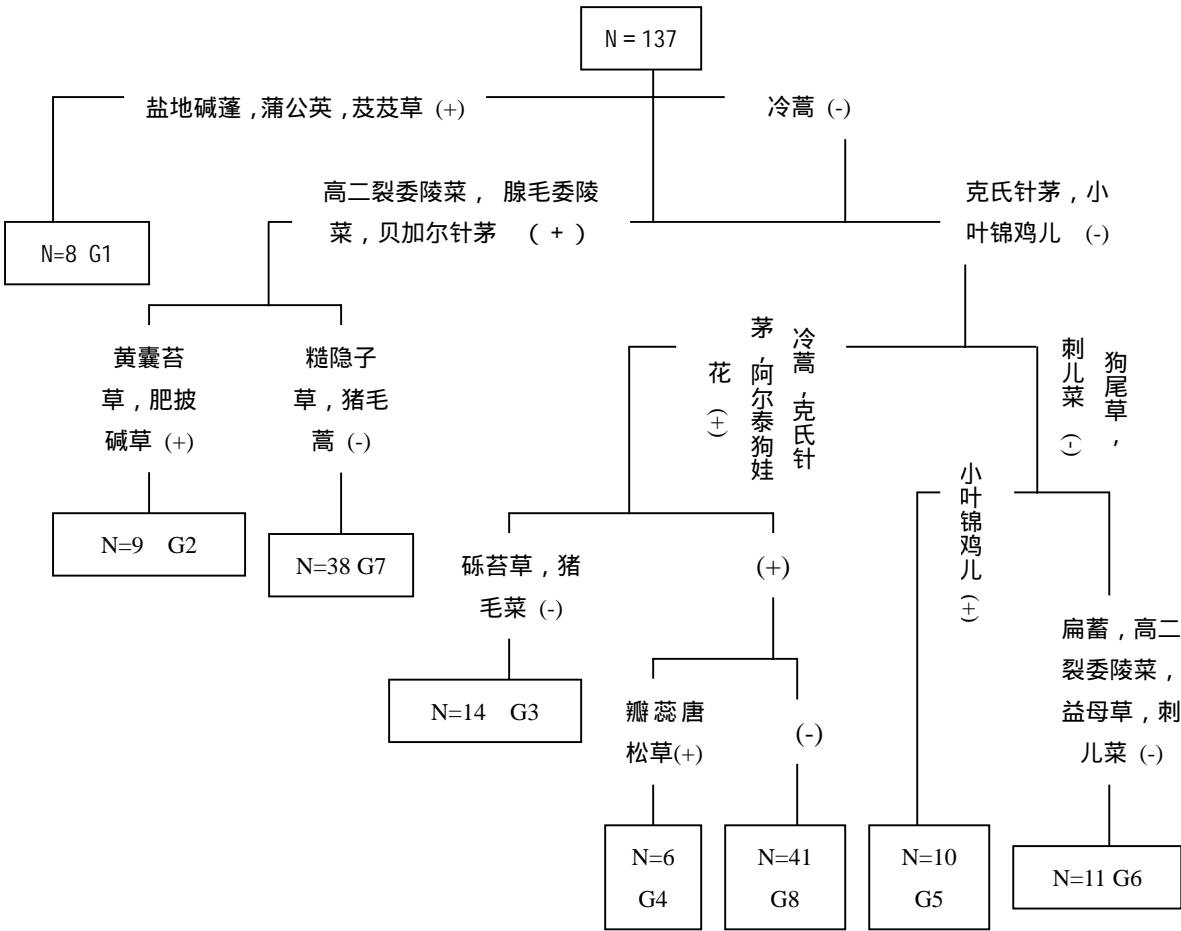


图 4.1：TWINSpan 分类结果

4.2.2 DCA 排序

对所有样地进行DCA排序，结果如图4.2所示。三个排序轴与各个植被和土壤指标的关系如表4.3所示，这些指标包括植被退化指数（DEG），土壤有机质含量（TOC）和土壤的机械组成粗颗粒砂的含量等土壤特征。表4.3反映了三个指标与DCA的三个排序轴的关系，样本数为125个。从表中可以看出，第一个轴AX₁与土壤有机质（TOC）之间为显著的正相关关系，第二轴AX₂则与DEG有显著的负相关关系。而一般认为荒漠化程度越重，TOC含量就越低，DEG的值就越高，SAD的含量就越高，因此DCA排序的前两个轴AX₁、AX₂都反映了荒漠化发展程度下降的趋势。

表4.3：DCA排序轴与各指标之间的相关系数			
	TOC	DEG	SAD
AX ₁	0.278**	0.052	-0.062
AX ₂	0.177*	-0.455**	-0.019

其中*表示显著水平在95-99%之间，较显著相关；**表示显著水平高于99%，明显显著相关。

综合分析图4.1，图4.2和野外调查结果，可以看出，低湿地和湖滨草甸（G1）、沙地草原（G5）、退耕地（G6）、草甸草原、典型草原和荒漠草原的混合类型（G2、G3、G7）很容易与其他类型区分，而人工林和耕地（G4）与草甸草原、典型草原和荒漠草原的混合类型（G3、

G8)混合在了一起。前面提到,DCA排序的两个轴均反映了荒漠化程度的下降趋势,而且DCA排序往往第一轴所占的信息量最大,其次是第二轴。从第一轴可以看出在所有类型中G1的退化程度最轻低,其次是G2,然后是G5、G6和G7并列,退化程度最重的是G3、G4和G8,在第二轴上可以区分出G5、G6和G7以及G3、G4和G8,即G6的退化程度大于G7和G5,G5的退化程度大于G7,G3的退化程度大于G8,G8的退化程度大于G4,因此可知在整个研究区退化程度由轻到重依次是 $G1 < G2 < G7 < G5 < G6 < G4 < G8 < G3$,其中退化机制相近的草甸草原、典型草原和荒漠草原混合类型G2、G3、G7、G8的退化程度由轻到重依次是 $G2 < G7 < G8 < G3$ 。

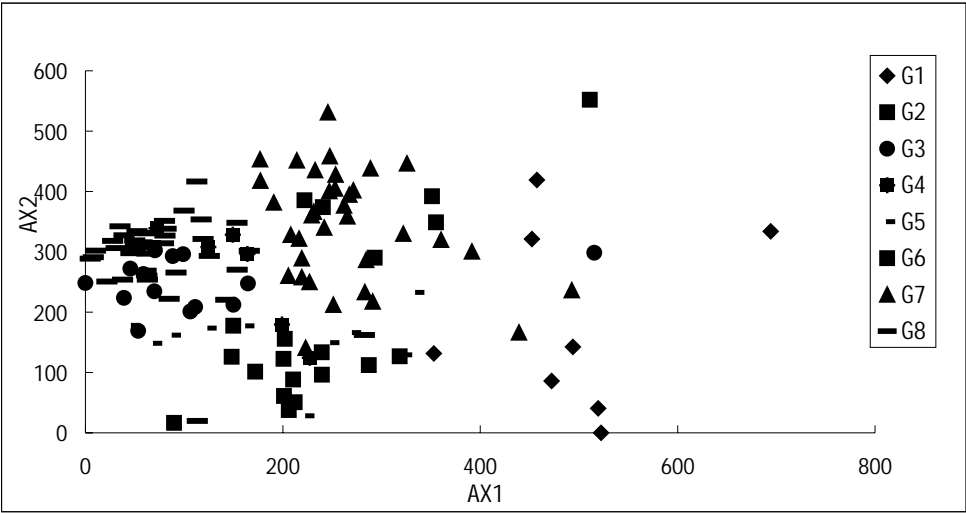


图 4.2 DCA 排序结果

4.3. 小结

- 1. 通过植物退化指示得出的植被退化指数符合实际情况，因此是真实可靠的，可以用作研究区不同地表覆盖类型的植被退化程度研究。由 TWI SNPAN 分类和 DCA 排序得出的区域植被退化程度分析很好地反映了不同植被退化机制下的植被退化状况。
- 2. 不同类型的植被退化指数与总草本盖度之间并无直接的关系，而与多年生草本盖度占总盖度比例关系密切，多年生植物盖度占总盖度的比例较高的类型，其植被退化指数总体上相对较低。

第五章 荒漠化评估的指标体系

荒漠化评价是目前荒漠化研究领域的一个重要问题,是干旱、半干旱区生态监测的一个主要任务。前人的研究结果大都给出了一个指标评价的范围(刘朝霞,1996;高尚武等,1998;王小丹等,2002),但对指标选取和指标范围确定的依据缺少讨论,因此主观性强。本文在前人工作的基础上,利用植被生态学上常用的 DCA 排序法,通过野外调查得到的植被和土壤数据来探讨研究区荒漠化现状,对沙地草原和非沙地草原分别建立荒漠化程度指数方程,该指数既包括植被退化方面的因子,又包括土壤退化方面的因子。最后根据该指数与植被因子和土壤因子之间的关系,对沙地草原和非沙地草原分别建立荒漠化程度评价模型。

5.1 指标选取

为了更准确地反映不同地表覆盖类型的荒漠化程度,进而对每个类型建立一个较为完善的荒漠化指标体系,我们选取植被和土壤两方面的多个指标作为分析荒漠化指标评价体系的因子,其中植被方面的指标包括植被退化指数(DEG)(代表种类组成)、样地总盖度(COV)、多年生植物盖度在总盖度中所占的比例(PER)以及草本层高度(HIG);土壤方面的因子包括砾石含量(GRV)、砂含量(SAD)、砂/黏土(S/C)和土壤有机质含量(TOC)。因子之间的相关系数如表 5.1 所示。为了简便起见,表中用数字来代替各种植被类型。

表 5.1 指标因子之间的相关性								
	DEG	HIG	TOC	COV	PER	GRV	SAD	S/C
DEG								
HIG								
TOC								
COV		2*; 4**	3**					
PER	-1*; -2*; -3**	2**						
GRV				-3**				
SAD	-1* ;		-3**					
S/C				-3**		2**	1*; 3*	

其中：1. 草甸（样本数：13）；2. 沙地草原（样本数：21）；3. 非沙地草原（样本数：69）；4. 退耕地（样本数：7）

*表示显著水平在 95 ~ 99%之间，较显著相关；**表示显著水平高于 99%，明显显著相关。“ - ”代表负相关。

从表 5.1 可以看出：

（1）从总体上看，植被类型不同，因子间的相关性差异很大。沙地草原（第 2 类）和非沙地草原（第 3 类）这两个类型中具有明显相关和较强相关性的因子对数较多，因子之间的关系较为紧密，而退耕地（第 4 类）中因子之间的相关性不明显。在所有具有显著相关或较强相关的因子中，相对较多的类型里植被退化指数与多年生植物盖度占总盖度比例之间的联系、平均高度与总盖度之间的联系以及 TOC 与总盖度之间的联系都比较密切。

（2）草甸植被 DEG 与 PER 以及 SAD 之间呈现较强的负相关关系；沙地草原 DEG 与 PER 之间呈现强烈的负相关关系，而 HIG 与 PER 之间以及 GRV 与 S/C 之间有强烈的正相关关系，此外，HIG 与 COV 之间的关系也较显著；非沙地草原中因子之间联系最密切，其中 DEG 与 PER

之间、TOC 与 SAD 之间、COV 与 GRV 和 S/C 之间均呈现强烈的负相关关系，而 TOC 与 COV 之间则表现出显著的正相关关系；退耕地上仅有 HIG 与 COV 之间为强烈的正相关关系。

5.2 荒漠化评价指标体系的建立

5.2.1 荒漠化指标体系建立的依据

内蒙古自治区有关部门针对当地不同草地类型（包括草甸草原，典型草原，荒漠草原）的天然草地的退化制定出只限于本地使用的地方标准（内蒙古自治区地方标准，1999）。退化等级的划分主要是依据草群中优势种和退化指示植物的种类、数量以及它们在草群总产量中所占的比例。根据前文所获得的研究区不同地表覆盖类型植被退化和土壤退化的关系，结合此标准，可以得出本研究区非沙地草原和沙地草原的理论退化模式如下：

1. 非沙地草原：理论上当草原退化时 DEG 增大，HIG 降低，PER 和 COV 降低，退化指示植物及一二年生植物大量出现，土壤中砂含量（SAD）、砾石含量（GRV）以及砂/黏土（S/C）增加。具体退化程度评价依据如下：

轻度荒漠化：草群结构和外貌无明显变化，TOC 含量相对较高，群落中原有优势种仍占据优势，以多年生植物为主，植被退化指数低。

中度荒漠化：草群结构和外貌发生明显的变化，原有优势种衰退，出现阿氏旋花、狼毒、阿尔泰狗娃花、星毛委陵菜等中度退化指示植物，植被退化指数中等。

重度荒漠化：草群中原有的建群植物和优势植物严重消退，草群发生根本性的改变，植被退化指数较高。退化指示植物狼毒、星毛委陵菜等和一年生植物大量出现，土壤表面覆沙严重，有较多砾石出现。

极度荒漠化：草群已失去原有构造，只有少量的一年生植物或者退化指示植物，植被覆盖度严重下降，植物种类显著减少，甚至只剩下零星几株草本植物，土壤颗粒变粗，沙化程度严重，有发展为沙地的趋势。

2. 沙地草原：沙地土壤粗颗粒含量相对于其他类型来说要高，理论上该类型退化时，地表的沙粒粗化，土壤腐殖质减少至消失，具有代表性的沙生植物大量出现继而减少至地表裸露，沙丘形成并由固定半固定沙丘演化为流动沙丘，HIG 变化不确定，GRV 增大，SAD 增大，S/C 增大，植被覆盖 COV 下降。由于植被的覆盖度本来就不高，所以 TOC 的变化不能确定。由于该类型相对来说植被要稀少，生长的大部分是一些耐沙、喜沙植物，所以评价荒漠化程度时最先要考虑的是植被组成和植被覆盖以及土壤粗颗粒含量的情况，而草本层平均高度和土壤有机质的变化则不是很确定。具体评价依据如下：

轻度荒漠化：植被覆盖度较高，土壤中腐殖质较多，可形成一定的土壤腐殖质层，一些在草原上常见的物种出现，物种多样性较丰富，TOC 较高，植被退化指数较低，土壤颗粒比较细；

中度荒漠化：地表土壤粗化，土壤中有一定的腐殖质含量，植被覆盖较高，出现部分小叶锦鸡儿灌丛，植被以中等退化指示种（如冷蒿，星毛委陵菜，麻花头，狼毒，隐子草，阿尔泰狗娃花）以及一年生植物为主，植被退化指数较大；

重度荒漠化：以固定半固定沙丘为主，植被大部分全为小叶锦鸡儿和其他沙生植物（如沙竹，沙蒿，沙蓬，沙葱），有零星草原生种；

极度荒漠化：以流动沙丘为主，地表全部裸露或有零星植物，如小叶锦鸡儿、沙竹等沙生植物出现。

5.2.2 不同类型荒漠化程度指数方程的建立

将前述 8 个因子的数据作为 DCA 排序的矩阵值 ,通过 DCA 分析将所有 8 个评价指标的信息集中到前三个轴上 ,然后把每个轴的特征值作为相应轴的权重 ,再根据每个轴代表的荒漠化程度趋势的意义列出荒漠化程度指数方程 ,根据这一方程对每个类型的样地进行荒漠化程度的分类 ,并给出不同退化程度下 8 个指标评价因子的均值。

根据草原退化的机理 ,对沙地草原(包括沙地榆树疏林灌丛草原和沙地小叶锦鸡儿灌丛草原)和非沙地草原(包括草甸草原、典型草原和荒漠草原三类)两种类型进行荒漠化评价分析 ,根据8个选中的用来评价荒漠化程度的指标因子对沙地草原和非沙地草原进行 TWINSpan分类和DCA排序。

1 沙地草原

样本数为21个。

(1) DCA排序

通过DCA排序 ,把8个因子的信息集中到前三个轴上 ,得到三个轴的排序值 ,然后将这三个轴的排序值与8个因子做相关分析 ,结果如下 :

表5.2 : 沙地草原DCA排序的三个轴与指标因子之间的相关系数

	AX ₁	AX ₂	AX ₃
HIG	-0.541**	0.434*	-0.030
TOC	-0.282	-0.559**	0.568**
DEG	-0.301	-0.619**	-0.773**
COV	-0.236	0.017	0.377
PER	0.140	0.759**	0.265
GRV	0.817**	0.142	0.433
SAD	0.043	0.277	-0.580**
S/C	0.877**	0.344	0.376

其中*表示显著水平在95-99%之间 ,较显著相关 ;**表示显著水平高于99% ,明显显著相关。

根据前面所述 ,沙地草原退化时平均高度和土壤有机质 TOC 的变化往往不是很显著 ,具有显著变化的是反映物种组成的植被退化指数(DEG) 多年生草本盖度占总草本盖度的比例 (PER) 砾石含量 (GRV) 砂含量 (SAD) 和砂/黏土 (S/C) 的值等 ,理论上说 ,沙地草原退化到一定程度后植被总盖度 COV 和多年生草本植物盖度占总盖度的比例下降 ,植被退化指数 (DEG) 增加 ,土壤砂含量 (SAD) 增加。从表 5.2 可以看出 , DCA 的三个排序轴与指标因子之间的关系都比较密切 ,其中 AX1 代表了草本层平均高度的下降以及土壤粗颗粒砾石 GRV 和砂/黏土 S/C 的增加了趋势 ,AX2 代表了草本层平均盖度和多年生草本盖度占草本层总盖度比例增加以及植被退化指数下降的趋势 ,第三轴代表了土壤 TOC 的增加以及植被退化指数 DEG 和土壤砂含量下降的趋势 ,因此第一轴反映了样地荒漠化程度增加的趋势 ,而第二轴和第三轴反映了样地荒漠化程度的降低趋势。

将这三个轴的数据分别与 8 个荒漠化评价因子做线性逐步回归分析 ,得到方程如表 5.3。 $F_{0.01}(7.21) = 4.9$,回归分析的 F 值均大于 $F_{0.01}(7.21)$,通过检验。

表 5.3 沙地草原 DCA 排序的前三个轴与指标因子之间的关系

线性逐步回归方程	R ²	F 值	检验情况
AX ₁ =50.979+0.01282*S/C-1.091*HIG+4.903*GRV +26.9*PER-16.939*TOC+0.152*COV	0.995	457.058	通过
AX ₂ =135.957+61.666*PER-44.407-24.289*DEG+0.343*COV	0.947	71.647	通过
AX ₃ =72.160-24.098*DEG+2.971*GRV+30.107*TOC+38.093*PER +0.525*COV-0.52*HIG+0.004075*S/C	0.991	205.947	通过

由上述各排序轴的方程可知，各方程的回归系数都非常高，回归拟合较好。各个因子之前的正负号代表了因子对该轴的贡献趋势，正值代表正的贡献率，负值代表负的贡献率，前面分析知道 AX₁ 轴代表荒漠化程度增加的趋势，其它两轴反映荒漠化程度的减少趋势，而每个因子前的正负号也一般反映了这种趋势，比如第一轴 AX₁ 代表荒漠化程度的正向发展，在它的方程中，S/C、GRV 这些代表荒漠化正向发展的因子（即理论上该因子数值越大表示荒漠化程度越严重）前面的系数都为正值；TOC、HIG 这些反映荒漠化逆向发展的因子（即理论上该因子越大表示荒漠化程度越轻）前面的系数都为负值；PER、COV 这些因子与 AX₁ 的相关性并不显著，对方程的贡献却很小。

（2）荒漠化程度指数方程的建立

从前面的分析可以知道，由 DCA 排序得出的三个轴可以代表 8 个荒漠化评价因子来反映样地的荒漠化程度，结合每个轴的特征值，就可以根据下列方程得到每个样地的荒漠化程度指数(用 DI 来表示)：

$$DI = (+/-)a_1*AX_1 + (-) a_2*AX_2 + (-) a_3*AX_3$$

(5-1)

其中 Y 表示每个样地的荒漠化程度指数，a₁、a₂、a₃ 分别代表相应轴的特征值，AX₁、AX₂、AX₃ 表示每个样地的三个轴的值，而 a₁、a₂、a₃ 前面的正负号要根据每个轴所代表的荒漠化程度的趋势来确定，即若该轴代表的是荒漠化程度的加重趋势，其符号就为正，否则为负。只要符合该方程建立的条件即由 DCA 排序或者主成分分析得到的三个轴代表荒漠化程度的趋势，就可以用这个方程来进行荒漠化程度指数的计算。

由此可以得到沙地草原上的荒漠化指数方程为：

$$DI = 0.2245947868*AX_1 - 0.1246720850*AX_2 - 0.0406823345*AX_3$$

(5-2)

荒漠化指数越高，说明样地的退化程度就越高。

荒漠化程度指数集中了 8 个荒漠化评价因子的信息，因此是比较可靠的反映荒漠化程度的指标。利用荒漠化程度指数方程求得各个样地的荒漠化指数，并对其进行分类，分类时以荒漠化程度指数为主体，参考野外实地调查资料以及前面所总结的不同类型荒漠化程度评价特征，最后将沙地的 21 个样地分为以下四类，表中同时列出了不同类型的香农 - 维纳多样性指数。

表 5.4：沙地草原不同荒漠化程度下指标因子的数据组合

荒漠化程度	轻度	中度	重度	极度
包含样地	2, 18	11-2, 13, 14, 14-2, 58, 59, 61. 74	1, 3, 13-2, 24-2, 62, 97	19, 71, 72, 73, 63, 70
荒漠化程度指数范围	< -15	-5 ~ -15	0 ~ -5	> 0
H' 均值	1.84	1.791118	1.70109	1.865978
H' 方差	0.268701	0.457483	0.399033	0.604772

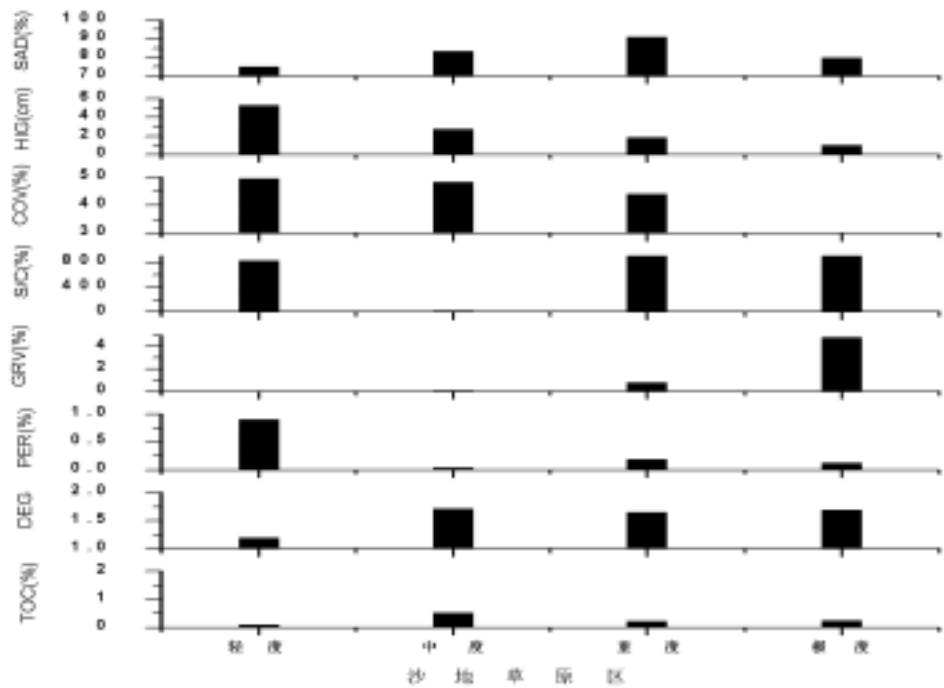


图 5.1 沙地草原区不同荒漠化程度下指标因子间的比较分析（图中数据为均值）

从图 5.1 中可以看出，随着荒漠化程度的增加，GRV、S/C 都有增加的趋势，PER、COV、HIG 都呈下降的趋势，符合理论推断，但值得注意的是土壤有机质（TOC）和植被退化指数（DEG）在沙地草原中随着荒漠化程度加重的变化趋势一致，均表现为中度>重度>极度>轻度，说明由于沙地植被覆盖率相对较低，很多喜沙植物都属于重度退化指示种，因此沙地的荒漠化程度评价中 TOC 和 DEG 的变化规律不大，并不是随着荒漠化程度的增加，土壤有机质含量（TOC）降低而植被退化指数（DEG）上升，而是在中度退化时它们的值最高。

（3）. 不同荒漠化程度下多样性的分析

从表 5.4 的数据可以看出，并不是荒漠化程度越重，物种的多样性越低。随着荒漠化程度增加，沙地草原上物种多样性的变化是极度退化>轻度退化>中度退化>重度退化，退化程度最严重的地区，其物种多样性指数却最高，因此，荒漠化的发展程度不能单单依赖地表植被的物种多样性来分析，还要结合土壤、地貌等方面的因素来探讨。

2 非沙地草原

 样本数 64 个。

（1）DCA 排序

 分析方法同上。

 由前面的分析得知，非沙地草原退化时一般草本层的平均高度降低，土壤有机质含量（TOC）减少，植被退化指数（DEG）增大，多年生草本盖度占总草本盖度增大，土壤砾石（GRV）和砂（SAD）和砂 / 黏土（S/C）增加，而总草本盖度（COV）的变化不确定。从表 5.5 可以看出，DCA 排序后的第一轴与 TOC、COV 显著负相关，与 SAD、GRV 显著正相关，因此可以说这一轴代表荒漠化程度的增加趋势，第二轴与植被退化指数显著负相关，与多年生草本盖度占总草本盖度的比例显著正相关，所以该轴代表荒漠化程度的下降趋势，第三轴与 TOC、COV

以及 PER 显著负相关，与植被退化指数 DEG 显著正相关，与 SAD 呈较显著正相关关系，因此该轴代表荒漠化程度的增加趋势。

表 5.5 非沙地草原 DCA 排序的前三个轴与指标因子之间的相关系数

	AX ₁	AX ₂	AX ₃
HIG	0.063	0.088	-0.026
TOC	-0.746**	0.047	-0.383**
DEG	-0.195	-0.451**	0.533**
COV	-0.626**	-0.476**	-0.304*
PER	0.316*	0.671**	-0.696**
GRV	0.684**	0.279*	0.238
SAD	0.403**	-0.070	0.300*
S/C	0.063	0.088	-0.026

其中*表示显著水平在95-99%之间，较显著相关；**表示显著水平高于99%，明显显著相关。

将由 DCA 方法获得的三个排序轴的值与 8 个荒漠化评价指标因子做线性逐步回归，得到方程如表 5.6 所示。 $F_{0.01}(7.64) = 2.95$ ，回归分析的 F 值均大于 $F_{0.01}(7.64)$ ，通过检验。

表 5.6 非沙地草原 DCA 排序轴与指标因子之间的关系

线性逐步回归方程	R ²	F 检验	检验情况
AX ₁ =43.575-20.458*TOC+34.046*PER+2.592*GRV-0.333*COV +0.236*SAD-0.00357*S/C+0.454*HIG+3.509*DEG	0.985	328.118	通过
AX ₂ =52.914+0.01503*S/C+45.139*PER+1.602*GRV+11.587*TOC -0.472*COV-8.787*DEG	0.984	435.344	通过
AX ₃ =48.334-67.382*PER+0.01357*S/C-8.541*TOC+1.171*GRV +8.39*DEG-0.208*COV+0.118*SAD+0.224*HIG	0.985	333.985	通过

上表中方程的回归系数都在 0.98 以上，估计的标准误差也非常小，说明方程的拟合是可行的。和沙地草原上因子与轴之间的关系所反映的规律一样，从 AX₁、AX₂、AX₃ 的方程也可以看出，非沙地草原中绝大多数因子前的系数都基本与三个轴所代表的荒漠化程度趋势一致，即 AX₁ 和 AX₃ 反映荒漠化程度越来越严重的趋势，AX₂ 反映荒漠化程度越来越轻的趋势；而且 AX₁ 反映的趋势主要受 TOC、COV、GRV 和 PER 影响，AX₂ 反映的趋势主要受 DEG、COV、PER 和 GRV 影响，AX₃ 反映的趋势主要受 TOC、DEG、PER 和 COV、SAD 的影响。

（2）荒漠化程度指数的建立

依据前面的荒漠化程度指数方程 5 - 1，可以得到非沙地草原这一类型下的荒漠化指数方程：

DI = 0.1050725505* AX₁- 0.0740316138 * AX₂ + 0.0446734354 * AX₃ （5 - 3）

将该方程代入各个样地的数据中，求得的样地分类如表 5.7 所示。

表 5.7：草原不同荒漠化程度下指标因子的数值组合

荒漠化程度	轻度	中度	重度	极度
包含样地数	16, 67-1, 100-1, 101, 96, 99-1	10, 64, 17, 21, 76, 92-1, 27, 25, 95-2, 98, 84, 22, 66, 69, 10, 48, 94-1	29-2, 65, 81, 89, 8, 83, 56, 26, 44, 36, 28, 9, 80, 51, 23, 78, 75, 85, 34, 52, 36-3, 11, 45-1, 82, 20-3, 20-2	37-2, 35, 45-2, 79, 54, 53, 50, 57, 16-2, 77, 55, 91-1, 47, 42, 46
荒漠化指数范围	< 0	(0, 4)	(4, 7)	> 7
H ' 均值	2.007421	2.166887	2.682288	2.116323
H ' 方差	0.44061	0.409689	2.869623	0.242946

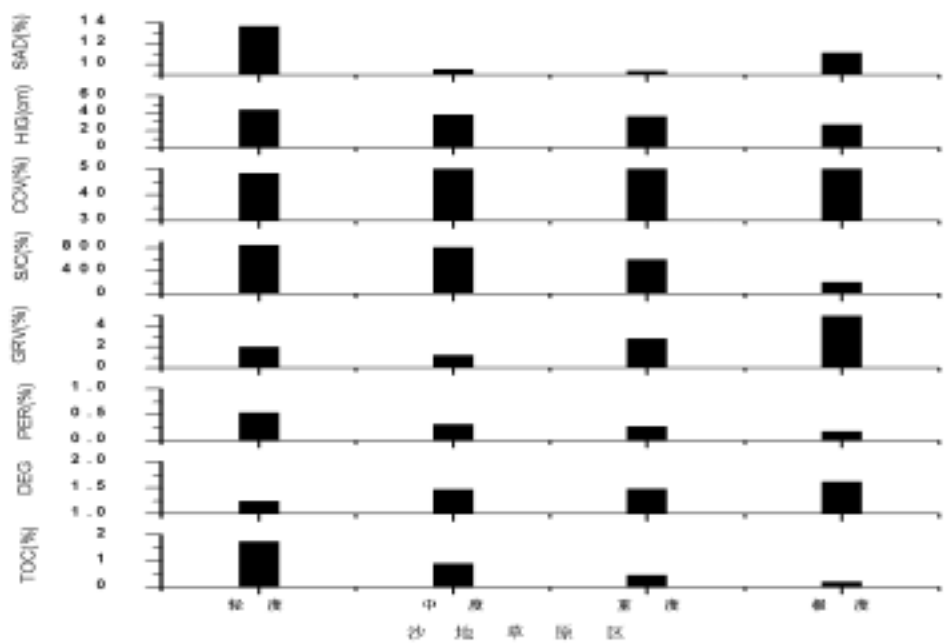


图 5.2 非沙地草原区不同荒漠化程度下指标因子间的比较分析（图中数据为均值）

随着荒漠化程度的增加，8 个指标因子的变化趋势如图 5.2 所示。从图中可以看出，随着荒漠化程度的增加，DEG、SAD 逐渐增加，TOC、PER、COV 逐渐下降，与理论上的推测一致，值得注意的是砾石的含量在草原轻度退化时的值要略高于中度退化时的值，随后随着荒漠化程度的加重，砾石含量才进一步增加；另外草本层平均高度也不是随着荒漠化程度的增加而逐渐减少的，极度退化的草原上草本层平均高度的值要高于中度和重度退化的草原；而且随着荒漠化程度的增加，土壤砂与黏土的比值 S/C 反而呈下降的趋势，说明随着荒漠化程度的增大，黏土的含量逐渐上升，并且上升的幅度要大于砾石的增加幅度。

（3）不同荒漠化程度下物种多样性的变化

从表 5.7 中得知，非沙地草原和沙地草原上物种多样性的变化一样，都不是随着荒漠化程度的加重而逐渐减少的，而是重度退化>中度退化>极度退化>轻度退化，进一步证明了仅靠物种多样性来分析样地退化程度的片面性。

5.2.3 不同类型下荒漠化指标体系模型的建立

1 荒漠化程度对指标因子的响应

表 5.8 是荒漠化评价指标因子与荒漠化程度指数之间的相关系数表，用 DI 来表示荒漠化程度指数：

从表 5.8 可以看出：

（1）对于非沙地草原，在总体上荒漠化程度指数 DI 与指标因子之间的关系要比单个荒漠化程度下 DI 与指标因子的关系密切的多。其中 SAD、GRV 与荒漠化程度之间有明显的正相关关系，而 TOC 与荒漠化程度之间有明显的负相关关系，另外 DEG 增加表示荒漠化程度也增加，而 COV、PER 则在一定程度上代表荒漠化程度的减弱趋势；轻度荒漠化条件下，S/C 对

荒漠化程度的加重起着重要的作用，TOC 的增加则有利于荒漠化程度的减弱；重度荒漠化条件下，只有 TOC 和 DEG 两个因子与荒漠化程度的关系分别具有较为明显的负相关关系和正相关关系；极度荒漠化条件下只有 GRV 对荒漠化程度起到很明显的促进作用，即 GRV 越高，DI 的值就越大。

（2）与非沙地草原相比，沙地草原上荒漠化程度指数与所选的指标因子之间的关系要弱的多。整体上来说，HIG 与 DI 有非常显著的负相关关系，而 GRV 和 S/C 数值的增加，则大大加重了荒漠化的程度；由于样本数不足，轻度荒漠化与指标因子之间的关系就不再分析；中度荒漠化条件下，仅有 PER 和 GRV 对 DI 的影响较为显著，并且都是负相关的关系；重度和极度荒漠化条件下没有指标因子与 DI 存在密切的关系，但在重度荒漠化条件下，TOC 对荒漠化发展趋势的促进作用和 PER 对荒漠化发展程度的抑制作用都不容忽视，而在极度荒漠化条件下，GRV 和 S/C 对荒漠化程度的促进作用不容忽略。

表 5.8 指标因子与荒漠化程度指数之间的相关系数表

DI		N	HIG	TOC	DEG	COV	PER	GRV	SAD	S/C	H'
非沙地草原	所有	64	-0.032	-0.801* *	0.263*	-0.392 *	-0.331*	0.51**	0.486* *	-0.064	-0.005
	轻度	6	0.248	-0.878*	-0.355	-0.474	.0259	0.064	0.071	0.932**	-0.661
	中度	17	0.259	-0.807*	-0.167	-0.464	0.528*	0.010	0.349	0.359	-0.166
	重度	26	0.242	-0.494*	0.393*	0.105	-0.337	-0.172	0.039	0.205	-0.16
	极度	15	-0.121	-0.386	-0.092	-0.331	0.103	0.86**	-0.241	-0.213	0.008
沙地草原	所有	22	-0.691**	-0.103	0.096	-0.328	-0.39	0.719**	-0.052	0.638**	0.174
	轻度	2									
	中度	8	0.692	-0.075	-0.088	-0.059	-0.804*	-0.801*	-0.081	-0.379	0.648
	重度	6	0.376	0.703	0.237	0.571	-0.73	0.33	-0.604	0.208	0.473
	极度	6	-0.52	0.05	-0.506	-0.055	0.265	0.747	0.066	0.749	0.458

其中 N 表示物种数，DEG 表示植被退化指数，HIG 表示草本层平均高度，TOC 表示土壤有机质含量，COV 表示草本层总盖度，PER 表示多年生草本植物盖度占总盖度的百分比，GRV 表示砾石含量，SAD 表示砂含量，S/C 表示土壤粗粒组成砂/黏土，H' 表示香农 - 威纳指数。

2 荒漠化程度指标体系模型的建立

利用线性逐步回归分析得到不同类型下的荒漠化程度评价模型如表 5.9 所示，均通过检验。

表 5.9 不同类型下荒漠化程度评价模型关系

类型	线性逐步回归模型	R ²	F 值	检验情况
非沙地草原	DI = 3.682-3.415*TOC-2.887*PER-0.000787*S/C+0.22*GRV+0.0238 5*SAD+1.22*DEG	0.985	237.012	通过*
沙地草原	DI=-0.442+1.565*GRV-0.274*HIG	0.883	31.97	通过**

* F>F_{0.01}(7.21)=4.9；** F>F_{0.01}(7.64)=2.95。

从模型拟合的 R² 可以看出，这两个类型的方程都拟合的非常好。而且进入方程的因子也都是在前面的相关系数分析中与 DI 有非常密切或者较为密切的因子。

5.3 讨论

5.3.1 不同地貌类型下不同退化程度下植被退化与土壤退化的关系

植被退化可以定义为植被退化指数 DEG 增大,植被盖度尤其是多年生植被盖度所占比例降低,植被的平均高度降低,物种多样性减少等因素的综合;土壤退化可以定义为土壤有机质 TOC 下降、土壤粗化即土壤砂、黏土 (S/C) 增加、砾石 GRV 和砂 SAD 增加等的组合。一般情况下荒漠化程度越严重,植被退化和土壤退化的程度也越严重,但不同地貌和土壤类型下,这种关系也各有不同。下面对沙地和非沙地草原两种类型进行分析。通过将沙地和非沙地草原不同退化程度 8 个指标因子的均值进行排序,得到沙地和非沙地草原上不同植被因子的荒漠化程度排序表如下,数值由小到大依次为序号 1、2、3、4。

表 5.10 不同类型不同荒漠化程度下指标因子的大小比较

类型	荒漠化程度	HIG	TOC	DEG	COV	PER	GRV	SAD	S/C	H'
沙地	轻度	4	1	1	4	4	1	1	2	1
	中度	3	4	4	2	1	2	3	1	3
	重度	2	2	2	3	3	3	4	3	2
	极度	1	3	3	1	2	4	2	4	4
非沙地草原	轻度	4	4	1	4	4	2	1	4	1
	中度	2	3	2	3	3	1	2	3	3
	重度	1	2	3	2	2	3	3	2	4
	极度	3	1	4	1	1	4	4	1	2

从表 5.10 可以看出,非沙地草原上因子随着荒漠化程度的加重而而导致的各因子的变化趋势要比沙地草原上更明显,并且植被退化与土壤退化之间的关系也密切得多。

沙地草原上随着荒漠化程度的增加,HIG 逐渐减小,COV、PER 有减小趋势,TOC、DEG、GRV、SAD 和 S/C 有增大趋势,其中 TOC 和 DEG 在中度退化时数值最大。多样性指数 H' 的趋势不明显。非沙地草原上随着荒漠化程度的增加,DEG、SAD 逐渐增大,PER、COV、TOC 逐渐减小,虽然 HIG 和 GRV 有些异常,但整体趋势也是分别增大和减小的;从植被退化与土壤退化的关系上分析就是随着 COV 和 PER 以及 HIG 的减小,土壤的有机质 TOC 也逐渐减小,粗颗粒 GRV、SAD 逐渐增大,而 S/C 逐渐减小,多样性指数 H' 的趋势不明显。

5.3.2 对于荒漠化评价指标体系和方法的改进

针对目前荒漠化评价中存在的不足,根据前文中总结的荒漠化评价的几个原则,在本研究中采取了一下措施,是评价体系和方法更科学,同时可操作性更强。这些措施包括:1) 根据野外调查和的 1:100 万中国植被图对研究区进行严格的植被和地表覆盖类型划分;2) 选取所有可以获取的评价指标(主要是植被和土壤方面的因子);3) 由于每一个植被类型的退化机制不同,针对每一个类型给出一个荒漠化程度指数,并给出一个在各个类型下都适用的统一的荒漠化程度指数,并尽可能从生态学过程的角度来阐述研究区的荒漠化状况。

5.4 小结

1. 将评价指标作为排序的因子,利用 DCA 排序法建立起来的荒漠化程度指数,进而通过逐步回归方法,得出荒漠化程度评价模型:沙地草原荒漠化程度 $DI = -0.442 + 1.565 \cdot GRV - 0.274 \cdot HIG$,非沙地草原荒漠化程度 $DI = 3.682 - 3.415 \cdot TOC - 2.887 \cdot PER - 0.000787 \cdot S/C + 0.22 \cdot GRV + 0.2385 \cdot SAD + 1.22 \cdot DEG$,以上回归均通过 F 检验。

2. 沙地草原上随着荒漠化程度的加重,GRV、S/C 有增加的趋势,PER、COV、HIG 有下降的趋势;非沙地草原上随着荒漠化程度的增加,DEG、SAD 逐渐增加,TOC、PER、COV 逐渐下降,这些都符合理论推测。说明本文建立的评价模型符合实际,能够在研究区内推广应用。

3. 无论是非沙地草原还是沙地草原,物种多样性都不随荒漠化程度的增加而逐渐减少,因此在进行荒漠化评价时,物种多样性不能作为评价指标。

第六章 研究区荒漠化的空间格局

区域荒漠化格局是因地制宜开展荒漠化防治工作的关键。本章拟根据第五章建立的荒漠化评价指标体系,从遥感影像获得不同地表覆盖类型下反映荒漠化程度的主要指标的空间格局,进而通过影像运算得出研究区荒漠化的空间格局。

6.1 MODIS 影像数据

MODIS 影像在区域荒漠化评价中的可行性分析 MODIS 影像是目前比较新颖和先进的获取大区域地表信息的遥感数据,它较之气象卫星数据和陆地卫星数据的优势可以概况为如下几点(熊利亚等,2002):(1) MODIS 具有较高的光谱分辨率,共分为 36 个波段,远多于 NOAA/AVHRR 的 5 个波段和 TM 的 7 个波段,地面分辨率分别为 250m(1~2 波段),500m(3~7 波段),1000m(8~36 波段),高于 NOAA/AVHRR(1.1km),1~2 天可以覆盖全球一次。(2) MODIS 数据在存储格式上采用 HDF-EOS(Hierarchical Data Format)数据格式,各通道输出的量化等级为 12 比特,温度分辨率可达 0.03 度,比 NOAA/AVHRR 的 10 比特精度提高 4 倍。(3) MODIS 首次使用了复杂的可见光通道星上校准技术,使长期观测的稳定度得到保障。由于具有较宽的光谱范围和空间覆盖以及随时间变化的资料连续覆盖,MODIS 比较适合于大区域地表信息特征,如植被和土壤特征的分析。本文选取 MODIS 影像作为区域景观类型划分和荒漠化程度空间格局的数据源,主要出于以下几个方面的考虑:(1)研究区属于的范围为 700km×600km 尺度范围,利用 TM 影像需要多景影像的拼接,工作量大,费用高,而利用 1km*1km 的 NOAA/AVHRR 则空间分辨率较低,精度难以符合要求,MODIS 影像成像面积大,减少了数据处理容量,空间分辨率可达 250m,因此对于研究区景观类型的划分比较适合;(2) MODIS 的植物吸收段 CH1(0.62~0.67 μm)和植物发射段 CH2(0.841~0.876 μm)分别对应 NOAA/AVHRR 的第一波段和第二波段,利用这两个波段计算归一化植被指数 $NDVI = (CH2 - CH1) / (CH2 + CH1)$ 可以很好地获取研究区地面覆盖情况(唐俊梅等,2002),同时,空间分辨率也比较高。由于利用 MODIS 的 NDVI 数据进行植被分类目前国内还鲜有成果,处于摸索阶段,很难对该方法进行客观评价,分类结果精度有待进一步探讨。

6.2 信息提取

将获取的 2002 年 7 月 9 日和 8 月 15 日两景影像,经过几何纠正和地理校正后,得到的影像投影是双标准纬线等积圆锥投影(China Albers),椭球体为 KRASOVSKY,坐标系为 Beijing 1954。经过投影转换把原投影转化为 Geographic(Lat/Lon)投影,截取研究区范围。

6.2.1 波段选择,

研究中所用到的波段有 1,2,3,4,5,6,17,18,19,26。波段 1、2 为红外、近红外波段,主要用来进行 NDVI 计算。波段 4 为叶绿素的主要反射波段,可以反映植被分布范围和生长密度;17、18、19 为近红外波段,植物在这些近红外波段的光谱特性与在红外

波段（1）的光谱特性的对比很敏感，可以对植被进行观测，所以可以将波段 17、18、19 进行融合，最大可能地获取植被信息，然后与波段 1 做比较；另外黏土在波段 5、6 具有强吸收性，而沙土在波段 5、6 则具有强反射性，所以可以用波段 5、6 的不同组合方式来区分土壤中砂含量，而 26 波段与 3 波段的比值则能清楚地表达土壤中腐殖质的状况，通过 3、5、6、26 几个波段的组合可以区分土壤类型，并为判断研究区的荒漠化程度进而建立荒漠化程度分布图提供必要依据（曲辉，2002）。

表 6.1 研究中所选用波段的特征及其与 TM、AVHRR 的对应关系

波段	波段范围 μm	对应光谱	光谱辐射率	空间分辨率	TM 波段	AVHRR 波段	用途	分析结果
1	0.620-0.670	红	21.8	250m		1	计算 NDVI，植被类型	
2	0.841-0.876	近红外	24.7	250m	4	2	解译解译	
4	0.545-0.565	绿	29.0	500m	2		用于对植被信息的观测，为解译提供依据	得到研究区景观类型图
17	0.890-0.920	近红外	10.0	1km		2		
18	0.931 - 0.91	近红外	3.6	1km		2	同 4	
19	0.915 - 0.965	近红外	15.0	1km		2		
5	1.230-1.250	近红外	5.4	500m			由波段 5、6 的组合（5 + 6）可以获得砂含量分布	与 NDVI 分布图结合得到区域荒漠化程度分布图
6	1.628-1.652		7.3	500m	5			
3	0.459-0.479	蓝/青	35.3	500m	1		由波段 3、26 的组合（26/3）可以获得土壤腐殖质的分布格局	
26	1.360-1.390	近红外	6.0	1km				

6.2.2 影像解译

1. 研究区景观格局图的解译

为了更好地反映大尺度的植被梯度和植被格局，进行植被景观解译时选取的研究范围为 E112~119 °，N39~45 °。将 7 月 9 日和 8 月 15 日两景影像的 NDVI 值数字图进行最大值计算，得到少云干扰并且能最大程度获取植被信息的 NDVI 值数字合成图，利用该图作为影像解译的底图，再将 4、17、18、19 波段等按不同方案合成为判别植被类型提供依据；将解译后的影像在 Erdas 下进行滤波处理，然后在 Photoshop 下将分类不合适的像元进行修正，得到的分类图是包含水体、农田、森林、灌丛、典型草原、草甸草原、荒漠草原以及建成区的区域景观分类图（图 6.1）。

2. 研究区荒漠化程度分类图解译

在第五章中分析得出荒漠化程度主要与土壤砂含量、地表植被覆盖以及土壤 TOC 含量有关，并且荒漠化程度与土壤砂含量成正比，与地表植被覆盖程度成反比，与土壤 TOC 成反比，因此可以利用反映这三个方面信息的波段的运算进行研究区荒漠化程度分类。前面已经提到 5、6 波段的组合可以反映土壤中的砂含量，26、3 波段的组合可以反映土壤腐殖质含量，而 1、2 波段的组合可以得到植被覆盖状况。根据以上关系，将波段组合（5 + 6）作为研究区砂含量分布灰度图，波段组合 26/3 作为研究区土壤 TOC 含量即腐殖土分布的灰度图，将景观格局解译中所用到的 NDVI 作为地表植被覆盖分布的灰度图，将这三幅图经过归一化处理后按照 TOC*植被盖度/砂的方式进行组合，即波段之间以公式(26/3)*NDVI/(5+6)的形式组合，运算结果得到荒漠化程度分布灰度图，作为荒漠化分类底图，在该图基础上进行荒漠化程度分类，其中组合后的图像灰度值越高表面荒漠化程度越低。

6.3 结果分析

1．研究区景观格局

通过上述各步骤的分析，得到区域的景观格局图（图 6.1）。由于沙地位于典型草原之中，并延伸至草甸草原的边缘，所以把它以线条的形式覆盖于典型草原上。

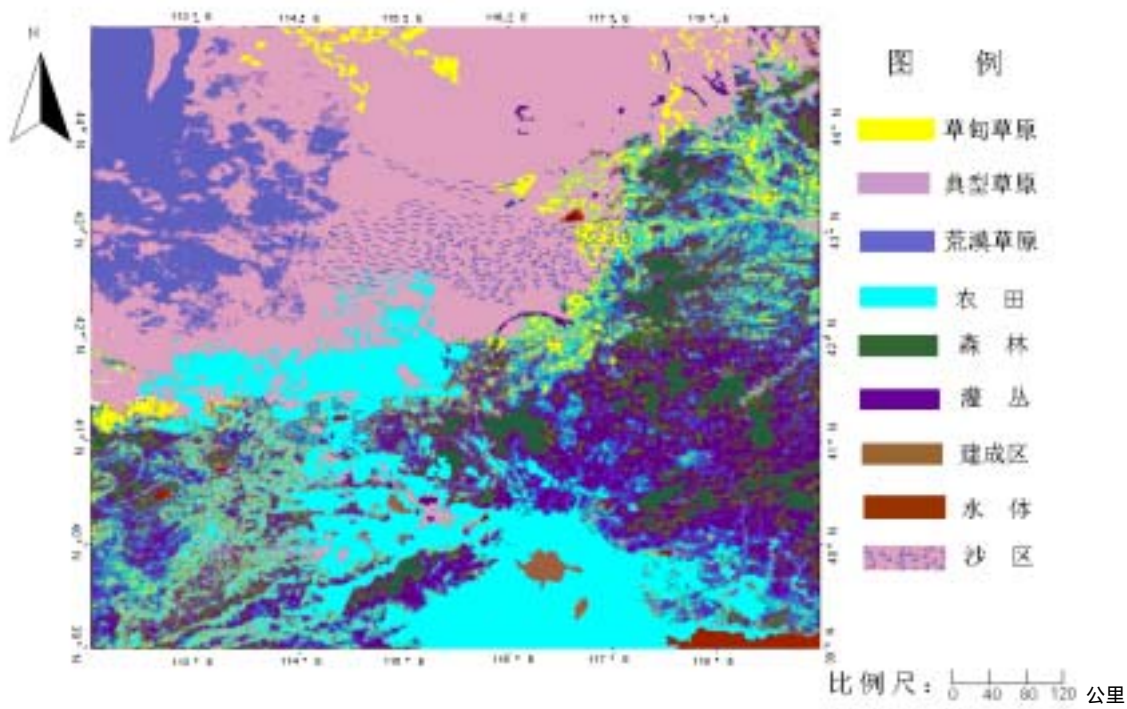


图 6.1 研究区景观格局

从图 6.1 可以看出，研究区的景观格局非常清晰，各类型之间界限明显。根据不同地点优势的景观类型，结合不同地点的土地利用方式，可以区分出牧区（包括荒漠草原亚区、典型草原亚区、草甸草原亚区、山地疏林和灌丛草原亚区）、林区（森林与灌丛混合）、农牧交错区、农区。其中荒漠草原亚区位于研究区的西北部，经纬度范围为 E112~114.54°，N42.045~45°，典型草原亚区主要位于研究区的中北部，范围较广。草甸草原亚区包括坝上高原的东部和大兴安岭的西麓，面积较小。农牧交错区表现为典型草原与农田的交错分布，主要为坝上高原的西部。研究区中的林区指冀北山地、燕山山地等，以森林和灌丛植被占优势，沟谷中有农田分布。农区则指华北平原的北部。

2．研究区荒漠化程度分布

由于荒漠化程度的评价与荒漠化发生机理有关，因此对研究区内典型草原亚区、荒漠草原亚区以及沙地疏林草原亚区和沙地灌丛草原亚区（二者合并为沙地草原亚区）分别进行评价。草甸草原带荒漠化程度低，且与森林带处于逐渐过渡之中，不再进行分析。农区和农牧交错区的荒漠化程度的影响因子比较复杂，在此不做探讨。

根据图 6.1 的各景观类型的分布，在研究区内截取典型草原亚区（不含沙地部分）、荒漠化草原亚区和沙地疏林灌丛草原亚区分别进行荒漠化程度评价和分析。对每种亚区给出腐

殖土分布图、NDVI 分布图和砂含量分布图三张灰度图以及荒漠化程度分类图,其中腐殖含量分布图中,亮度越大,表示土壤中所含的腐殖质含量越高;NDVI 分布图中,亮度越大,表示 NDVI 值越高;砂含量分布图中,亮度越大,表示土壤中砂含量越高。利用这三幅图分别来代表区域土壤的有机质 TOC 含量、砂含量和地表植被覆盖程度,利用表达式(腐殖质含量*NDVI/砂含量)来表示区域的荒漠化程度,运算后得到的影像中像元的灰度值越高,荒漠化程度越低,并将荒漠化程度划分为四个等级,即得到各亚区荒漠化程度分布图。

(1) 典型草原亚区

从图 6.2~6.6 可以看出典型草原亚区腐殖土中等,在接近草甸草原带和荒漠草原带的地方土壤腐殖质含量较低,NDVI 的分布则是由西向东依次增大,这是因为接近荒漠草原带植被覆盖较低,而接近草甸草原带和森林的地方植被覆盖较高,符合研究区由西向东植被覆盖依次增大的规律。砂含量的分布与 NDVI 的分布相反,由西向东依次减小,由此得出典型草原亚区的荒漠化程度由西向东逐渐降低(图 6.6)。

(2) 荒漠化草原亚区

从图 6.7~6.11 可以看出,土壤的腐殖质在西南部较高,由此向东北部依次降低,植被覆盖则是西南较低,北部和东部较高,砂含量的分布规律也比较明显,西南部最高,东南部较低,北部接近蒙古国的地方最低,由此得出的荒漠草原带区域荒漠化分布为西北部和中部地区较低,向东南和北部荒漠化程度依次升高,北部靠近蒙古国的地方最高(见图 6.11)。

(3) 沙地疏林和灌丛草原亚区

从图 6.12~6.16 可以看出,沙地土壤腐殖质含量中部地区稍微高于周围地区,植被覆盖则是由西向东逐渐增加,砂含量的分布与植被覆盖的分别相反,因此荒漠化程度中部较轻而边缘地区较高(图 6.16)。

综合上述分析可知,在整个进行荒漠化程度分析的区域,典型草原亚区西北部 and 荒漠化草原亚区北部之间的过渡区荒漠化程度最高,沙地靠与草甸草原亚区接壤处及荒漠草原亚区的西北部荒漠化程度最低,荒漠草原带与沙地相连接的地方荒漠化程度相对较高,可能与风沙活动有关。

6.4 小结

1. 典型草原亚区的荒漠化程度由西向东依次减小;荒漠化草原亚区的荒漠化程度分布为西部的下半部分和中部地区较低,向东南和北部荒漠化程度依次升高,北部靠近蒙古国的地方最高;沙地荒漠化程度总体上为中部偏低而边缘偏高。

2. 典型草原亚区西北部 and 荒漠化草原亚区北部的过渡区为荒漠化程度最高的地方,沙地与草甸草原接壤处以及荒漠化草原亚区的西北部荒漠化程度最低,荒漠化草原亚区与沙地接壤处荒漠化程度相对较高。

3. 利用 MODIS 影像的各个波段进行运算后分析荒漠化程度的空间格局不仅在方法上可行,结论与实际也比较符合。

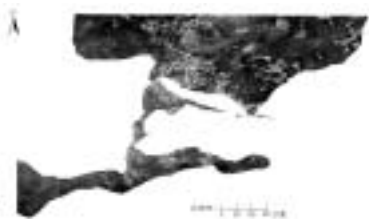


图 6.2 典型草原亚区土壤腐殖质
含量分布图



图 6.3 典型草原亚区 NDVI
分布图



图 6.4 典型草原亚区土壤砂含
量分布图

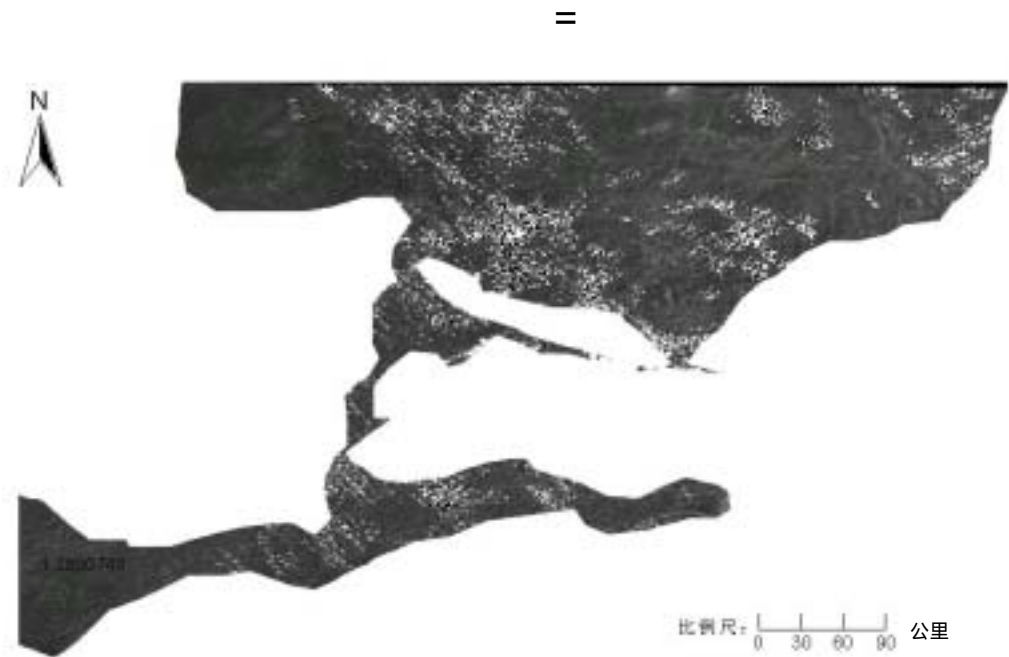


图 6.5 典型草原亚区荒漠化程度灰度图

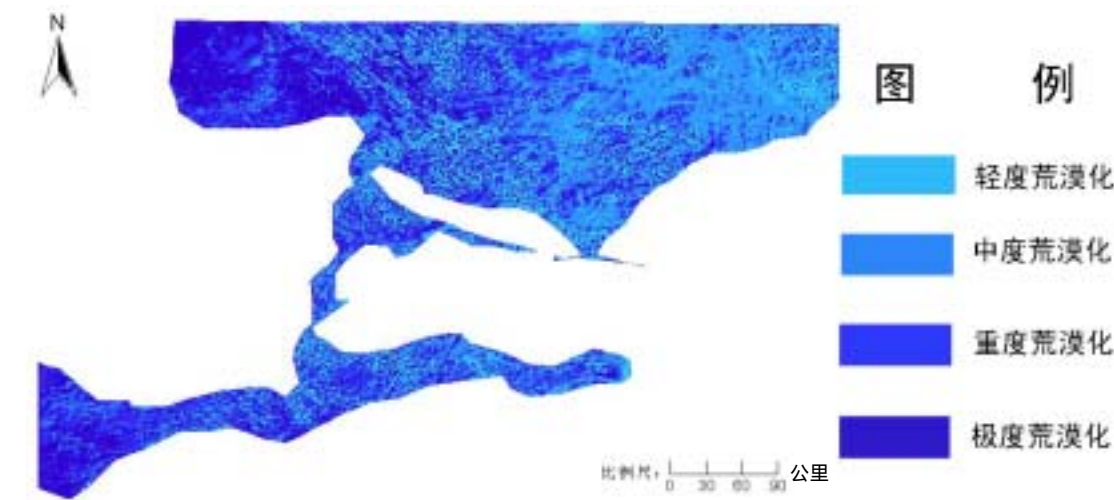


图 6.6 典型草原亚区荒漠化程度分级图



图 6.7 荒漠草原亚区土壤腐殖土含量分布图

×



图 6.8 荒漠化草原亚区 NDVI 分布图

÷



图 6.9 荒漠化草原亚区土壤砂含量分布图

=

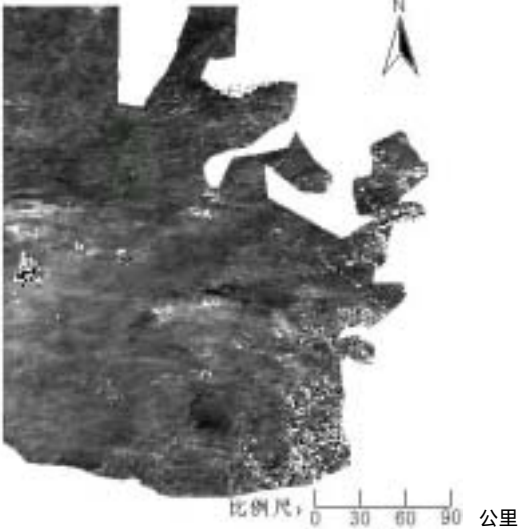


图 6.10：荒漠化草原亚区荒漠化程度灰度图

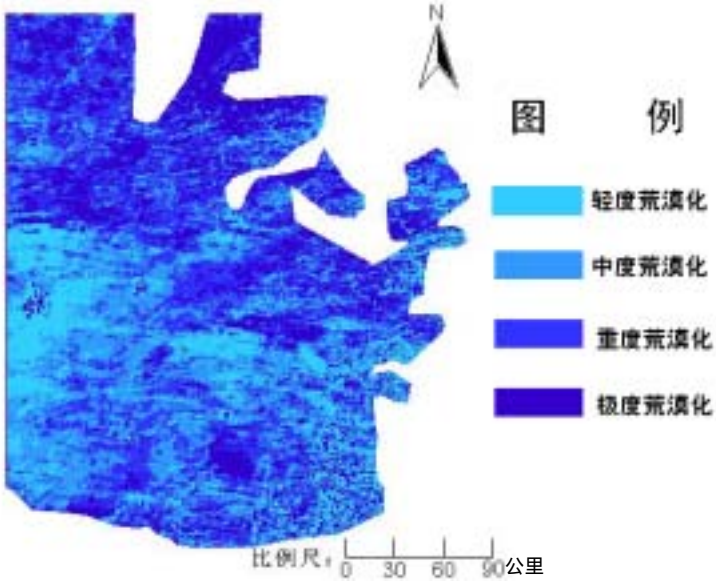


图 6.11：荒漠化草原亚区荒漠化程度分级图



图 6.12 沙地土壤腐殖质含量分布图



图 6.13 沙地 NDVI 分布图



图 6.14 沙地土壤砂含量分布图

=

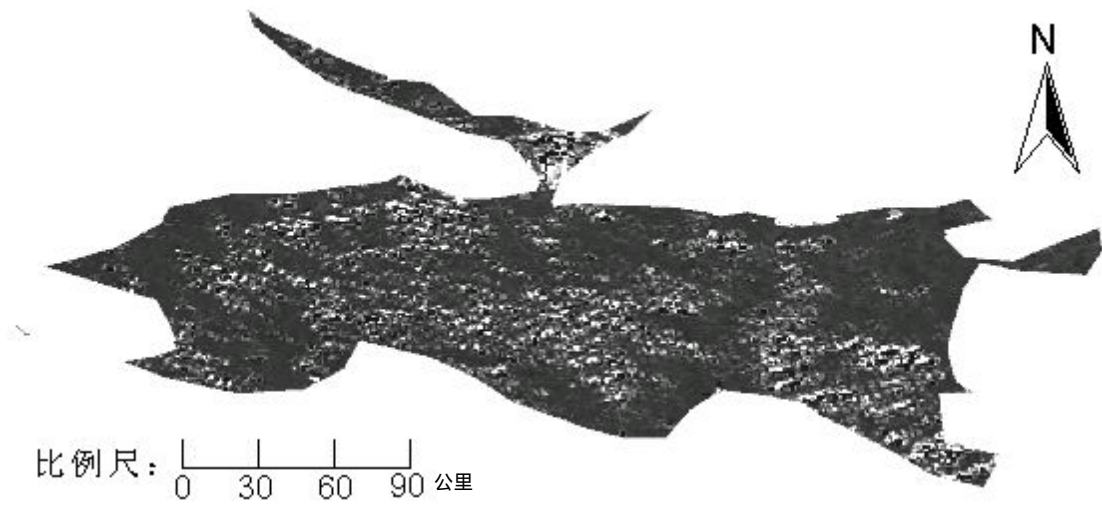


图 6.15：沙地荒漠化程度灰度图

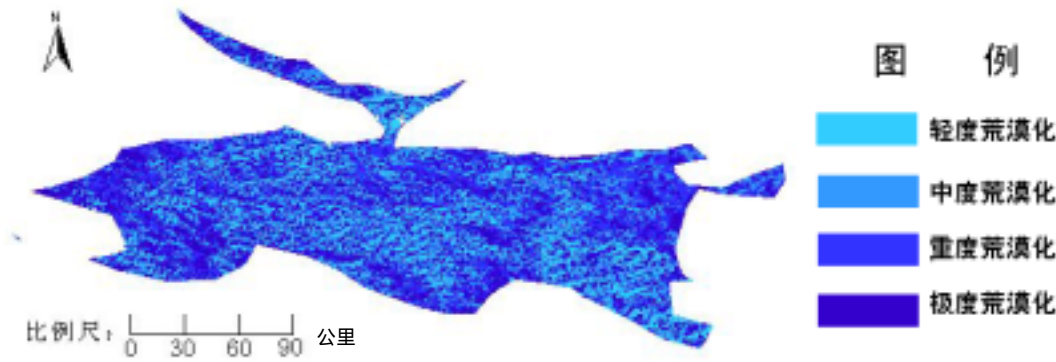


图 6.16：沙地荒漠化程度分级图

第七章 研究区及周边地区 1984~2000 年植被动态及其驱动因子

区域植被动态受气候变化和土地利用双重因素的驱动。根据研究区及周边地区土地利用方式,可以将研究区及周边地区划分为农区、林区、农牧交错区和牧区。在牧区根据植被特点的进一步差异可以划分为草甸草原为主的牧区、典型草原为主的牧区、沙地榆树疏林草原为主的牧区、沙地小叶锦鸡儿灌丛草原为主的牧区和荒漠化草原为主的牧区五个亚区。每一区(亚区)内选择有代表性的台站,分析台站记录的气候动态,以及台站附近植被指数和人为活动的动态变化,探讨气候变化和人为活动对植被动态的驱动作用。各区(亚区)的植被特点、土地利用方式和代表性台站如表 7.1 所示。

表 7.1 各区(亚区)植被特点及代表性地点

代号	土地利用分区	植被特点	气候变化分析代表性气象台站	人为活动因子分析代表性地区
I	农区	耕作植被为主	北京	北京
II	林区	森林和灌丛植被为主	承德	无
III	农牧交错区	兼有耕作植被和典型草原	化德	化德
IV1	牧区	草甸草原为主	西乌珠穆沁旗	西乌珠穆沁旗
IV2	牧区	典型草原为主	锡林浩特	锡林浩特
IV3	牧区	沙地榆树疏林草原为主	多伦	正蓝旗
IV4	牧区	沙地小叶锦鸡儿灌丛草原为主	那仁宝力格	正镶白旗
IV5	牧区	荒漠化草原为主	苏尼特左旗	苏尼特左旗

7.1 植被动态

根据一年中植物生长的规律以及一年中 NDVI 的动态变化,将一年中 NDVI 最大值和最小值之差定义为该年 NDVI 的变化量,并且用一年中 NDVI 的最大值(利用每年的 NDVI 旬值影像进行最大值运算来得到)来表示该年植被生长最好的状态;另外选取每年的 3、4、5 月份为春季的 NDVI 状况,利用 IDRISI 软件将 3、4、5 月份中每月各旬的 NDVI 值进行最大值合成,得到该月的 NDVI 最大值,然后以这三个月的数据构造一个三维列向量,计算该列向量的模,用求得的结果代表当年春季的植被状况,即 NDVI_{spring}(顾卫等,2002)。所采用的 NDVI 数据是 1984~1991 和 1995~2000 年共 14 年的旬值数字影像。由于 NDVI 数字影像的质量问题,计算 2000 年 NDVI 最大值时仅用了前 11 个月的,计算最小值时去掉了 11 月中下旬和 12 月,1984 年的 10 月前两旬、11 月和 12 月前两旬也被略去。

7.1.1 不同区(亚区) NDVI_{max} 的年际变动

利用 Idri si 软件计算一年中 NDVI 的最大值,即 NDVI_{max}。图 7.1 为 1984~2000 年各区(亚区) NDVI_{max} 的变化趋势。

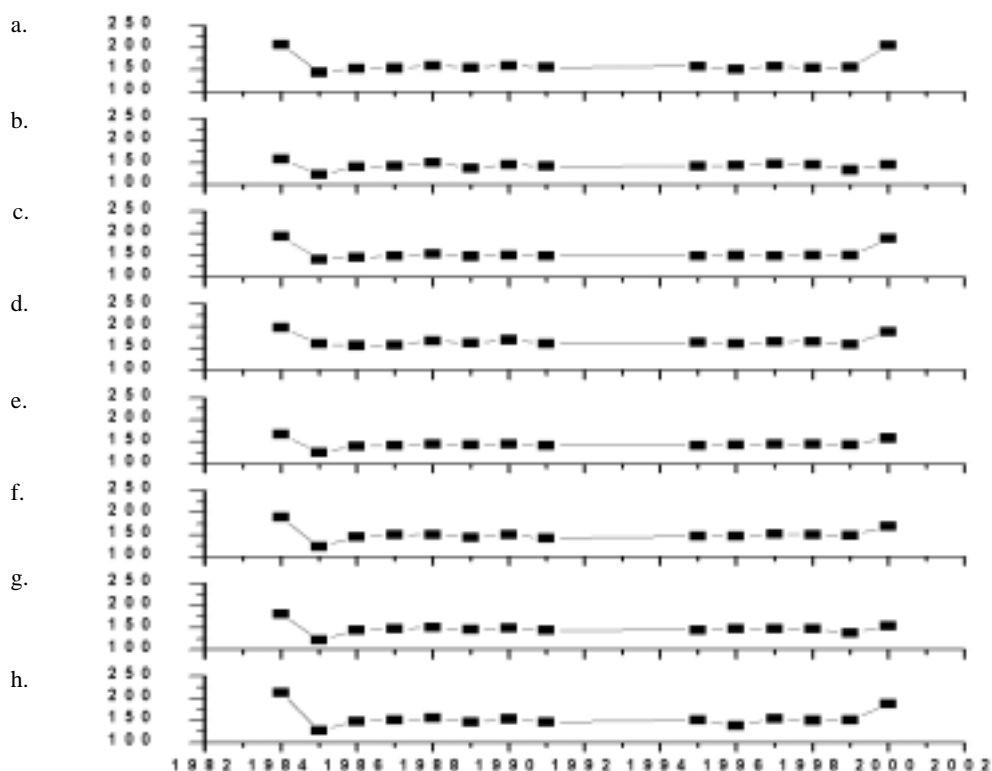


图 7.1 1984~2000 年各区 (亚区) 的 NDVI_{max} 的变化趋势

图中 a. 林区; b. 牧区荒漠草原亚区; c. 农牧交错区; d. 农区; e. 牧区沙地小叶锦鸡儿灌丛草原亚区; f. 牧区沙地榆树疏林草原亚区; g. 牧区典型草原亚区; h. 牧区草甸草原亚区。纵轴为 NDVI 值, 无量纲, 横轴为年份

从图 7.1 可以看出:

(1) 从年际动态看, 1984 年所有区 (亚区) 的 NDVI_{max} 都较其它年份偏高, 1985 年 NDVI_{max} 迅速下降, 有可能是数据本身存在误差。但从农区的变化可以发现, 这种影响还是比较低的。1985~1988 年所有区 (亚区) 的 NDVI_{max} 都逐渐上升 (农区 1985 年 NDVI_{max} 比 1986 年的要稍高), 1989 年和 1990 年所有区 (亚区) 分别出现一个波谷和一个波峰, 1991 年又下降。2000 年较 1999 年各区 (亚区) NDVI_{max} 均有增加。

(2) 从不同区域的比较来看, 除了 1984 年, 农区的 NDVI_{max} 比其它区域都要高, 甚至超过林区。林区的 NDVI_{max} 则在几乎所有年份里居于第二位。牧区草甸草原亚区在大部分年份都位居第三、第四位。而牧区典型草原亚区大部分年份中 (1996 年除外) 植被的最好状态不及牧区草甸草原亚区。在大部分年份里, 牧区沙地小叶锦鸡儿灌丛草原亚区是所有区 (亚区) NDVI_{max} 最低的; 而牧区沙地榆树疏林草原亚区的 NDVI_{max} 则明显优于牧区沙地小叶锦鸡儿灌丛草原亚区, 除了 1989 年、1991 年和 1996 年外, 它的最佳状态甚至要好于牧区典型草原亚区的。牧区荒漠化草原亚区的 NDVI_{max} 也比较低, 很多年份仅比牧区沙地小叶锦鸡儿灌丛草原亚区稍好, 1984 年、1989 年、1991 年和 1999 年其植被指数比其它类型的均低;

7.1.2 不同区（亚区）下 NDVI max-min 的年际变动

各区（亚区）NDVI max-min 的变化趋势如图 7.2 所示。

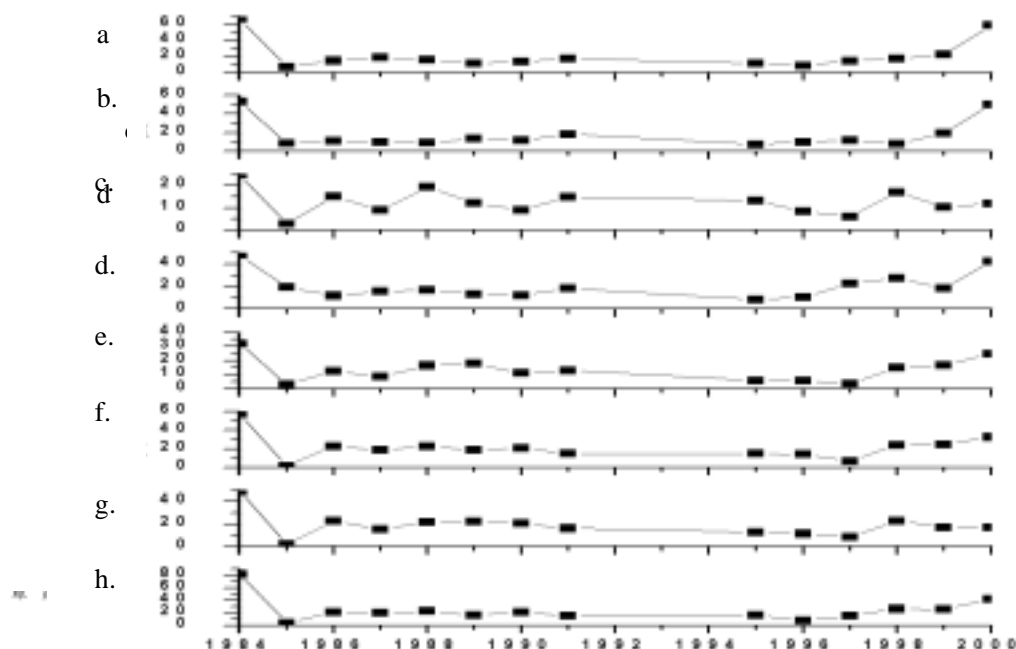


图 7.2 1984~2000 年各区(亚区)NDVI max-min 的变化趋势

图中 a~h 的含义以及横轴和纵轴的含义均同图 7.1

从图 7.2 可以看出：

(1) 和 NDVI 的年最大值一样，所有类型的 NDVI 年变化量在 1984 年出现最大值，可能为系统误差。其它时期 1996 年的年变化幅度较低，而 1998、1999 年 NDVI 的年变化幅度又开始增大。

(2) 在所有类型中，1984、1988、1990、1995 和 1999 年牧区草甸草原亚区的 NDVI 年变化量最大，1985 年、1991 年、1997 和 1998 年，农区的 NDVI 年变化量最大。1986~1997 年间牧区草甸草原亚区、牧区典型草原亚区和牧区沙地榆树疏林草原亚区的 NDVI 变化量降低趋势显著，尤其是牧区典型草原亚区，除了 1987 年比 1988 年稍低外，其它这些年份几乎是直线下降，而另外三个区（亚区）则在下降的过程中有所波动。牧区小叶锦鸡儿灌丛草原亚区在 1986~1997 年间的下降趋势不太明显，年际波动稍大。林区的变化与其它区（亚区）不同，年际波动较小，NDVI 变化量只在 1985 年、1989 年和 1996 年出现波谷。

7.1.3 不同区（亚区）下春季 NDVI spring 的年际变化动态

在计算春季 NDVI 值时用了 1983~1991 年和 1994~2000 年总共 16 年的数据。首先在 Idrisi 支持下对每年的三、四、五月份的 NDVI 分别做最大值计算，得出这三个月的 NDVI，分别用 $NDVI_3$ 、 $NDVI_4$ 和 $NDVI_5$ 表示，然后根据 $NDVI_{spring} = \sqrt{((NDVI_3^2 + NDVI_4^2 + NDVI_5^2)/3)}$ ，所得到的结果反映春季 NDVI 值的综合状况。

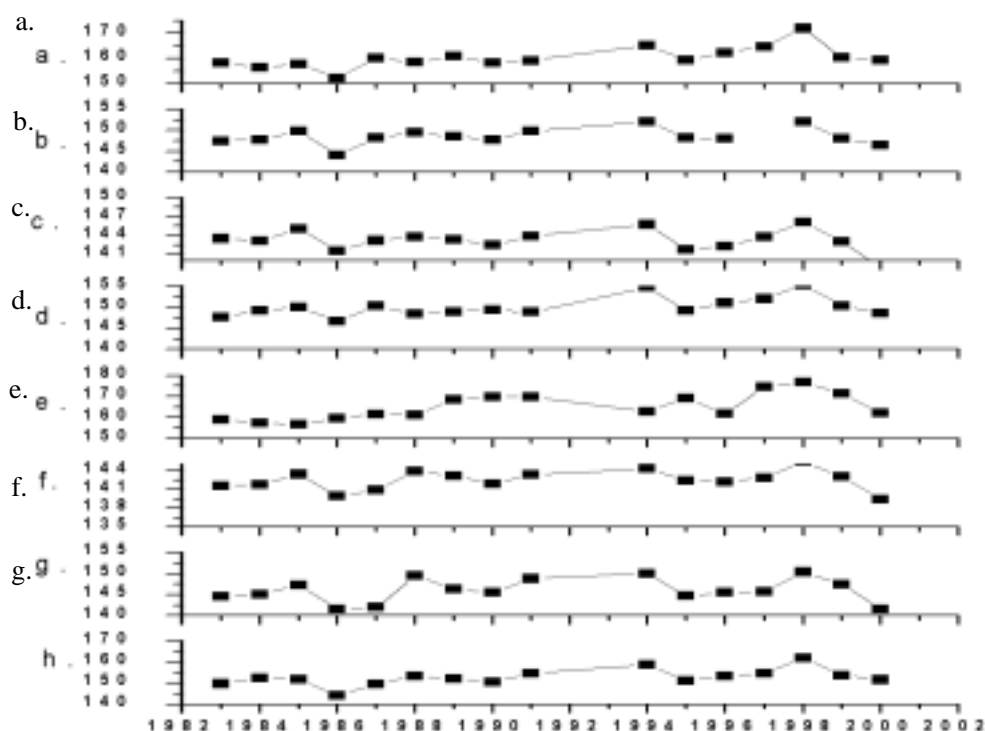


图 7.3 1983~2000 年各区（亚区）NDVI spring 的变化趋势

图中 a~h 的含义以及横轴和纵轴含义均同图 7.1

从图 7.3 可以看出：

（1）牧区草甸草原亚区：春季植被的长势整体上呈波动型，几乎每隔一年都有一个峰谷的波动，总趋势有所上升，1986 年为其最低点，1994 年 NDVI spring 值出现一个波峰，1995 年~1998 年该值持续上升，1998 年达到所有年份的最大值，后有所下降；

（2）牧区典型草原亚区和牧区荒漠草原亚区：这两个类型 NDVI spring 的变化趋势基本相同，1981~1985 年 NDVI spring 持续下降，然后在 1986 年、1989 年、1992 年出现波峰，从 1995 年到 1998 年 NDVI spring 持续上升，后又稍有下降；

（3）农区：与其它区（亚区）完全不同，1992 年以前 NDVI spring 波动较大，其中 1987 年出现最大值，1991 年 NDVI spring 的最小值，1992 年到 2000 年 NDVI spring 变化不明显；

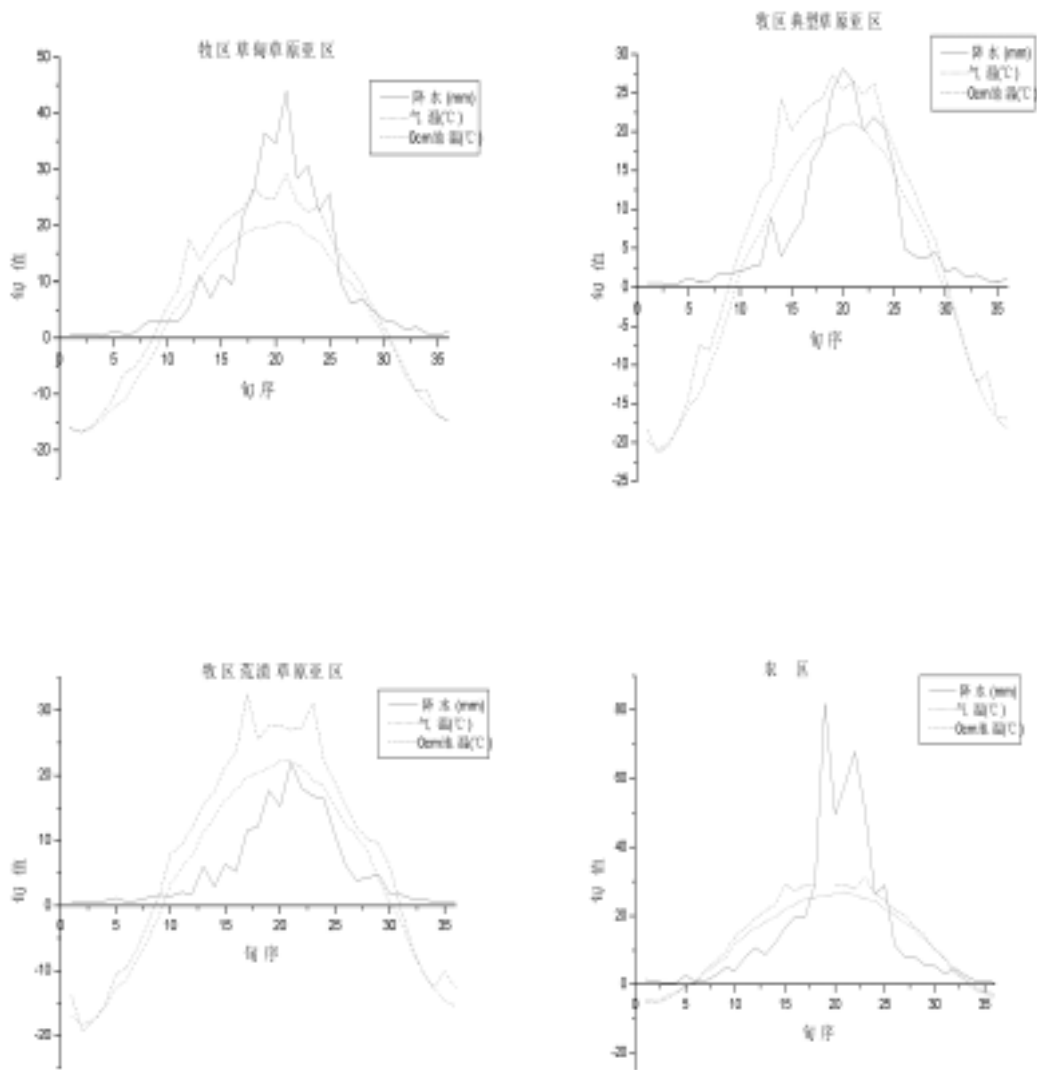
（4）牧区沙地小叶锦鸡儿灌丛草原亚区和沙地榆树疏林灌丛草原牧区：这两个类型的变化趋势也非常相近，1980 年到 1985 年 NDVI spring 一直处于下降的趋势，1986 年出现小的波峰，1989 年和 1990 年再出现两个小的波峰，1994 年出现大的波峰，1995 年后呈波动中上升的趋势；

（5）农牧交错区：1980 - 1985 年 NDVI spring 持续下降，1986 年出现一个小的峰值，1986 ~ 1995 年又出现持续下降的趋势，1995 年后 NDVI spring 开始出现大的波动。

（6）林区：林区的 NDVI spring 变化趋势在 1986 年前和农区和牧区一样，1986 年后林区的波动比较大。

7.2 1981~2000 年气候的变化

图 7.4 为不同区(亚区)代表性地点 0cm 地温、气温和降水的 1981~2000 年的各旬均值。



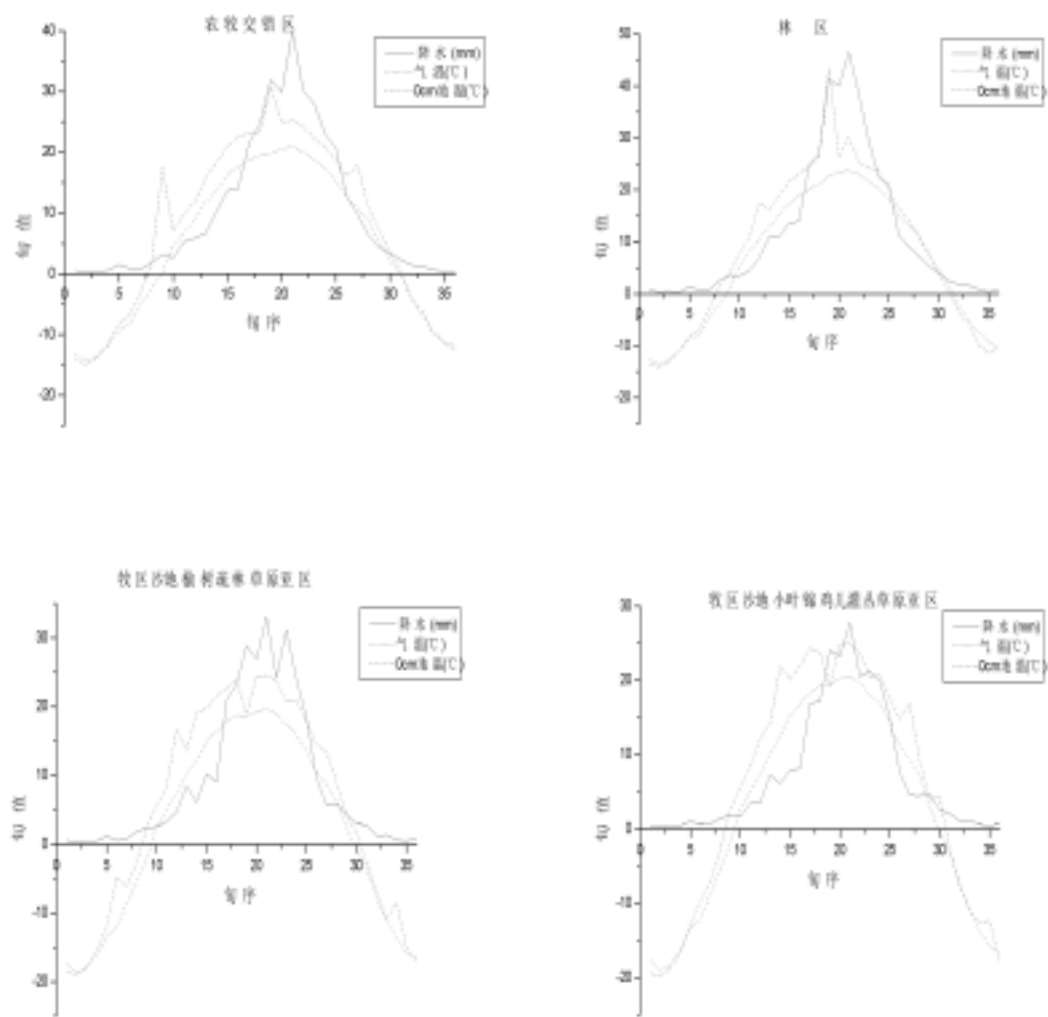


图 7.4：不同区(亚区)代表性地点 0cm 地温、气温和降水的 1981~2000 年的季节变化

从图 7.4 可以看出：

(1) 11、12、1、2、3 月 5 个月中所有区(亚区)的 0cm 地温均低于 0℃，而 7 月本是 0cm 地温最高的时候，但牧区沙地小叶锦鸡儿灌木草原亚区，牧区榆树疏林草原亚区的 0cm 地温则低于 6 月份和 8 月份的。林区和农区的 0cm 地温在各个时期都要比别的类型高。此外，牧区草甸草原亚区 4 月下旬、农牧交错区 3 月下旬等的 0cm 地温都出现较高的波峰，其它类型的气温季节变化都基本遵循和 0cm 地温相同的规律，其中农区在所有区域中全年的气温都是最高的。各区(亚区)同一时期降水的变化要比 0cm 地温和气温的变化大，并且旬间的波动也较大，其中牧区草甸草原亚区、农区和林区的 7、8 月份降水量都比较高，而其它区(亚区)的几乎所有旬的降水量都处于 30mm 以下。农区的降水量在 7 月下旬出现一个波谷，这与其它类型的变化稍有不同。

(2) 在高桑和瓦尔特的生态气候图解方法中，月降水量低于月均温的 2 倍为干旱期，低于月均温的 3 倍为相对干旱期，据此推断，旬均气温高于旬降水量时代表气候相对干旱，而旬均气温低于旬降水量时代表气候相对湿润，由此可以得到不同区(亚区)一年内气候相对干旱的时间范围(表 7.2)。

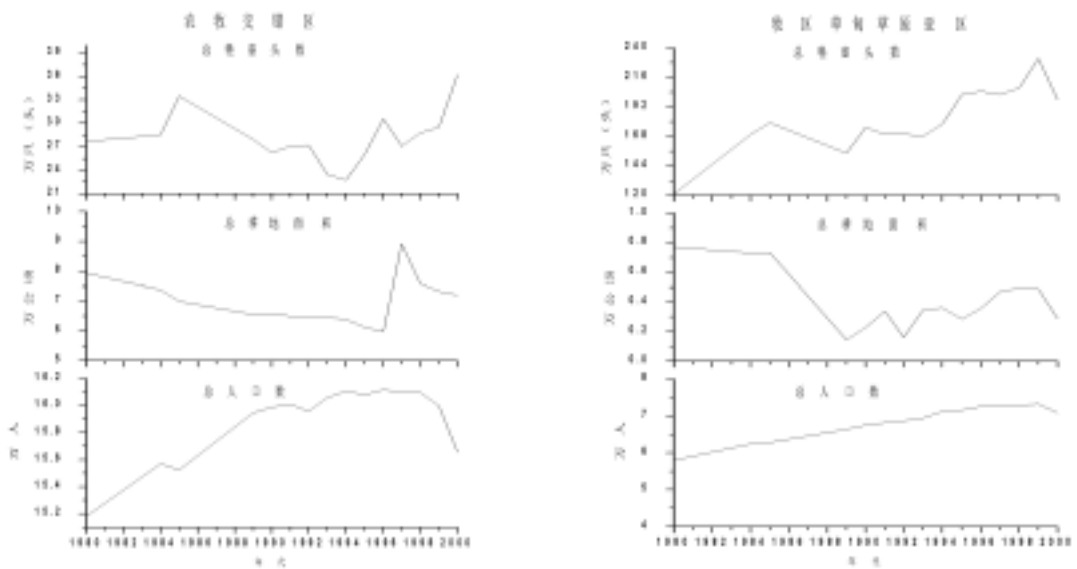
表 7.2 不同区（亚区）干旱时间范围

区域	干旱旬期	干旱持续时间（旬数）
牧区草甸草原亚区	11 ~ 13, 26 ~ 28	6
牧区典型草原亚区	10 ~ 18, 22, 26 ~ 31	16
牧区荒漠草原亚区	10 ~ 28	19
牧区沙地榆树疏林草原亚区	11 ~ 16, 26 ~ 28	9
牧区小叶锦鸡儿灌丛草原亚区	10 ~ 18, 26 ~ 28	12
农区	7 ~ 17, 26 ~ 31	17
农牧交错区	10 ~ 16, 27 ~ 29	10
林区	10 ~ 16, 26 ~ 30	11

从表 7.2 中可以看出，4 月、5 月、6 月上旬以及 9 月中旬、下旬和 10 月上旬为研究区普遍干旱的时期。其中牧区荒漠草原亚区早期时间最长，从 3 月上旬开始直到 10 月上旬。值得注意的是，农区的相对干旱的时间也较长，高于大部分牧区和农牧交错区，与这一地区春季和秋季气温偏高，而降水量集中在七、八两月有关。

7.3 人为活动的变化

为了与前面的植被变化和气候变化相结合，对各区（亚区）选择有代表性的行政区域，分别为农区（选取北京）、牧区草甸草原亚区（选取西乌珠穆沁旗）、牧区典型草原亚区（选取锡林浩特）、牧区荒漠草原亚区（选取苏尼特左旗）、农牧交错区（选取化德）和牧区沙地榆树疏林草原亚区（选取正蓝旗）和牧区沙地小叶锦鸡儿灌丛草原亚区（选取正镶白旗），统计与人类活动有关的指标的年际变化。利用 1980~2001 年（包括 1980、1984、1985、1989、1990~2001 年）的内蒙古统计年鉴和北京统计年鉴得到研究区不同区（亚区）的总人口数（农区以北京的农业人口为基础）、总耕地面积数和总牲畜头数的年际变化（组图 7.6）。北京则包括 1980~2001 年连续的资料。



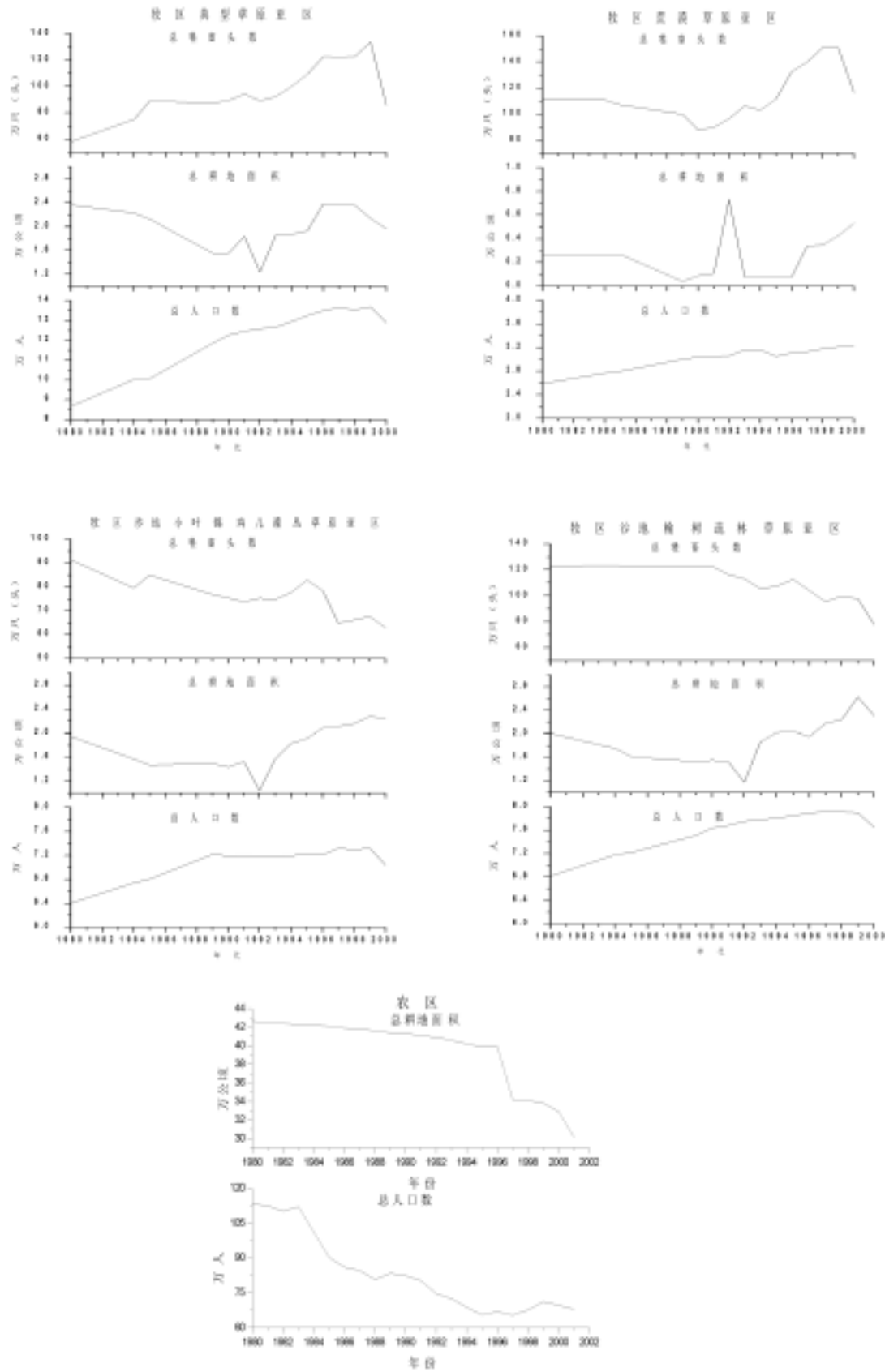


图 7.5 : 1980~2000(2001)年不同区(亚区)代表性地点人为活动因子的变化

从图 7.5 可以看出,牧区和农牧交错区的人口总体上呈逐渐上升趋势,除牧区荒漠草原亚区(苏尼特左旗)外,总人口数都在 2000 年略有下降。大部分区域总耕地面积在 1992 年前持续下降的,后上升。农牧交错区和非沙地草原牧区的大部分区域总牲畜头数在 1999 年前逐渐上升,1999 年后有所下降,沙地草原牧区则呈逐渐下降的趋势。农区的变化和前面的类型不同,由于城市化的影响,其农业人口数和总耕地面积逐年下降。

7.4 植被变化的驱动因子

7.4.1 气候因素和人为因素与 NDVIspring 以及 NDVI max、NDVI max-min 之间的关系

不同的气候因子对 NDVI 的不同指标影响不同,为了尽可能地反映气候条件对 NDVI 的作用,针对不同的 NDVI 指标选取不同的气候因子进行分析。根据植被-气候关系推断,能够对 NDVI max 产生较大影响的气候因子可能有一月、七月和全年气温均温,一月、七月和全年 0cm 地温均温和年降水量;能够对 NDVIspring 产生较大影响的气候因子可能有一月气温和 0cm 地温均温,上年七月气温和 0cm 地温均温,上年全年气温均值和 0cm 地温均值以及春季和上年全年降水量,能够对 NDVI max-min 产生作用的气候因子可能有一月、七月和全年气温均温,一月、七月和全年 0cm 地温均温,当年最热月(七月)和最冷月(一月)气温和 0cm 地温的温差、年降水量以及夏季和春季降水量差值。其中春季的范围为三、四、五月份,夏季的范围六、七、八月份的季度。人为因素则选取能够代表人为活动影响情况的总人口数、总耕地面积和总牲畜头数,将 NDVI 的各项指标与相应的气候因子指标以及人为活动因子指标进行相关分析,得到相关系数如表 7.3。本文中用旬降水量与旬均气温的比值来表示该旬的湿润指数,将它与相应的 NDVI 旬值进行相关分析,在对 NDVI max 进行分析时,选取了一月份各旬的湿润指数均值和七月份各旬湿润指数的均值,在对 NDVIspring 进行分析时选取了三、四、五月份各旬湿润指数的均值,结果见表 7.3。

表 7.3 各区(亚区) NDVI max-min、NDVI max、NDVIspring 与不同气候因子的相关系数

		NDVI max-min							
		牧区草 甸草原 亚区	牧区典 型草原 亚区	牧区荒 漠草原 亚区	农区	农牧交 错区	牧区沙 地榆树 疏林草 原亚区	牧区沙地 小叶锦鸡 儿灌丛草 原亚区	林区
0cm 地 温	一月均温	-0.396	0.074	0.133	-0.678*	-0.236	-0.124	-0.027	-0.612*
	七月均温	0.862**	0.54*	0.313	-0.079	-0.112	-0.156	-0.312	0.527
	最冷月最热 月温差	0.855**	0.288	0.016	-0.067	-0.084	-0.075	-0.263	0.599*
	年均温	0.611*	-0.05	0.015	-0.03	0.278	-0.175	-0.114	0.769**
气 温	一月均温	-0.35	-0.046	0.022	-0.588*	-0.41	-0.227	-0.204	-0.484
	七月均温	0.229	-0.12	-0.06	-0.042	0.257	0.169	0.112	0.068
	最冷月最热 月温差	0.364	-0.041	-0.048	-0.036	0.464	0.224	0.173	0.209
	年均温	0.035	-0.01	-0.092	-0.048	-0.131	0.107	-0.006	-0.106

降水	夏季降水量 与春季降水量 差值	-0.087	0.098	0.167	-0.179	-0.432	-0.21	-0.034	-0.262
	年降水量	-0.029	-0.003	0.219	-0.253	-0.452	-0.305	-0.28	-0.394
	总人口数	-0.336	-0.372	-0.188	0.06	-0.644*	-0.342	-0.379	
	总耕地面积	0.358	-0.065	0.015	0.259	0.18	0.125	-0.007	
	总牲畜头数	-0.136	-0.426	-0.039		0.43	-0.021	-0.249	
NDVI max									
		牧区草 甸草原 亚区	牧区典 型草原 亚区	牧区荒 漠草原 亚区	农区	农牧交 错区	牧区沙 地榆树 疏林草 原亚区	牧区沙地 小叶锦鸡 儿灌丛草 原亚区	林区
0cm	一月均温	-0.417	-0.125	-0.121	-0.706*	-0.202	-0.11	-0.039	-0.609*
地温	七月均温	0.805**	0.702**	0.231	-0.001	-0.031	0.076	-0.034	0.554*
	年均温	0.579*	-0.011	-0.333	0.047	0.37	0.003	0.032	0.769**
气温	一月均温	-0.371	-0.106	-0.219	-0.572*	-0.408	-0.265	-0.317	-0.436
	七月均温	0.285	0.109	0.189	-0.131	0.352	0.253	0.229	0.175
	年均温	0.064	0.076	0.087	-0.135	-0.008	0.17	0.118	-0.136
降水	夏季降水量	-0.098	0.017	0.26	-0.172	-0.339	-0.203	-0.102	-0.312
	年降水量	-0.156	-0.064	0.228	-0.21	-0.402	-0.366	-0.25	-0.428
	一月湿润指数均值	0.458	0.25	0.201	0.446	0.655*	0.285	0.435	0.536
	七月湿润指数均值	-0.162	-0.205	-0.046	-0.214	-0.527	0.169	-0.412	-0.554*
	全年湿润指数均值	0.085	-0.443	-0.042	0.002	-0.151	0.112	-0.195	-0.181
	总人口数	-0.253	-0.191	0.024	0.015	-0.571*	-0.182	-0.227	
	总耕地面积	0.209	0.072	0.007	0.297	0.17	0.208	0.184	
	总牲畜头数	-0.138	-0.37	0.001		0.376	-0.205	-0.338	
NDVI spring									
		牧区草 甸草原 亚区	牧区典 型草原 亚区	牧区荒 漠草原 亚区	农区	农牧交 错区	牧区沙 地榆树 疏林草 原亚区	牧区沙地 小叶锦鸡 儿灌丛草 原亚区	林区
0cm	一月均温	0.309	0.019	-0.283	0.211	0.085	0.635**	0.491	0.152
地温	上年七月 均温	-0.07	0.171	0.103	-0.418	0.069	0.21	-0.19	-0.328
	上年年均温	0.335	0.026	-0.419	-0.417	-0.011	0.176	-0.243	-0.149
气温	一月均温	0.185	0.605*	0.516*	0.29	-0.007	0.478	0.562*	0.119
	上年七月均 温	0.366	0.094	0.141	0.289	-0.222	0.118	-0.144	0.314
	上年年均温	0.428	0.27	0.182	0.493	-0.497	0.144	-0.179	0.306
降水	上年冬季降 水量	0.045	-0.009	0.086	0.496	0.157	-0.162	-0.261	-0.395
	春季降水量	0.483	0.334	0.289	-0.069	0.3	0.592*	0.396	0.485
	上年年降水 量	0.164	0.295	0.026	0.18	-0.116	0.017	-0.219	0.035
	三、四、五月 湿润指数均值	0.099	0.248	0.268	0.245	0.14	0.416	0.31	0.237
	一月湿润指数	0.344	0.488	-0.53*	-0.121	-0.348	-0.566*	-0.614*	-0.199

上 年	总人口数	0.314	-0.118	-0.259	0.629*	0.347	-0.05	-0.271
	总耕地面积	-0.064	0.011	-0.111	-0.699*	0.326	-0.402	-0.371
	总牲畜头数	0.145	-0.287	-0.242		-0.117	-0.061	-0.002
当 年	总人口数	0.444	0.101	0.035	0.572*	0.488	0.221	0.081
	总耕地面积	0.141	0.075	-0.277	-0.612*	0.243	-0.023	-0.249
	总牲畜头数	0.226	0.306	0.22		-0.373	0.107	0.213

表中带**的表示因子之间的相关性很强,显著水平高于 0.01,用黑斜体表示;带*的表示因子之间相关性较强,显著水平介于 0.01~0.05 之间,用黑体表示;没有带*的表示因子之间的相关性较不明显,显著水平低于 0.05,其中相关系数绝对值越大,表示因子间相关性越强。

从表 7.3 可以看出气候因子和人为活动与 NDVI 各个指标的关系如下:

(1) 从气候因子对 NDVI_{max} 和 NDVI_{max-min} 的作用上看,0cm 地温在大部分区(亚区)都起着很重要的作用,其它气候因子的作用则相对较弱。气候因子对春季 NDVI 的作用与其对其它两个 NDVI 指标的影响不同。0cm 地温的指标中仅有一月份的 0cm 地温均值在牧区沙地榆树疏林草原亚区对 NDVI_{spring} 起着非常显著的作用,而一月份气温均值在牧区典型草原亚区、牧区荒漠草原亚区和牧区小叶锦鸡儿灌丛草原亚区对 NDVI_{spring} 均起着较为显著的作用。春季降水量对牧区沙地榆树疏林草原亚区的影响明显,其它降水指标与 NDVI 指标之间的相关性均较低。由此说明,在气候因子对 NDVI 不同指标的影响方面,研究区不同的地表覆盖类型下的 NDVI 指标均受到温度条件的明显影响,降水量的影响仅限于沙地榆树疏林草原,原因在于榆树的生长与沙地特殊的水分供应有关(Liu et al., 2000)。

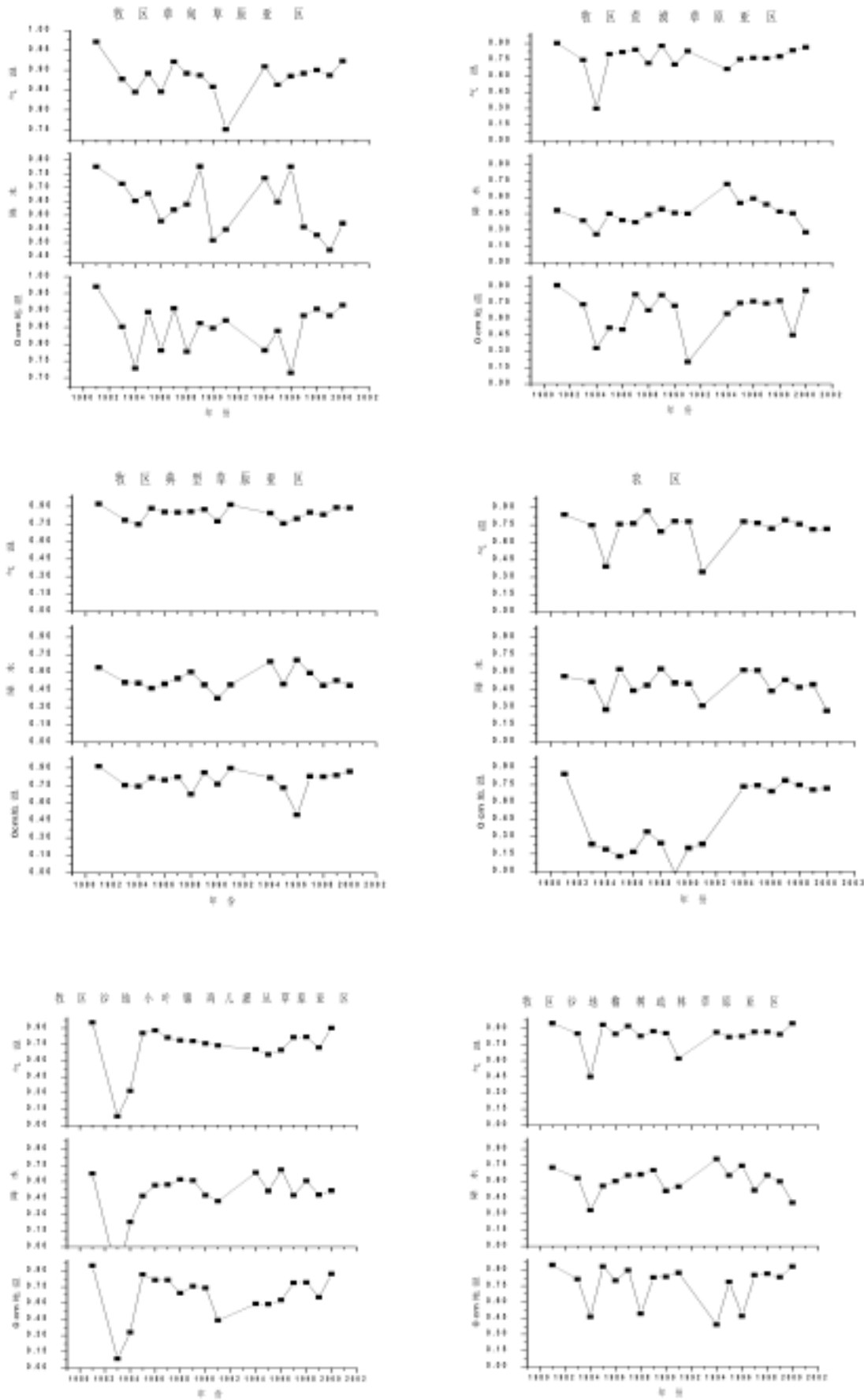
(2) 无论是上一年还是当年,所选择的三个人为活动指标在大部分区域对 NDVI 的影响均不明显,理论上,牧区的植被覆盖动态与总牲畜头数关系密切,但在本研究中发现,总牲畜头数对 NDVI 各个指标的作用均不显著,由此可知,研究区的植被覆盖动态主要还是受到气候因子的影响。除此之外,在农区总人口数和总耕地面积与春季 NDVI 的关系分别为较为显著的正相关和负相关,不同的是前者的作用为正,后者的作用为负,与理论上的并不相符,这是因为农区的代表区域北京的情况比较复杂,减少的耕地可能转化成绿地,也可能转化为城镇,另外大棚种菜也影响了 NDVI 对地表植被覆盖的反映,而集约式的农业也使得人口数的减少不能直接地作用于地表的植被覆盖上,因此,北京农区人为活动的变化不能准确反映地表植被覆盖的变化;在农牧交错区总人口数与 NDVI_{max} 以及 NDVI_{max-min} 有较为显著的负相关性,而与春季 NDVI 的关系则不明显。

(3) 从气候因子的干湿条件对 NDVI 的作用上看,各项湿润指数对 NDVI 的影响并不大,仅在个别区域内起作用。其中全年的湿润指数对全年的 NDVI 最大值几乎不起作用,一月份的湿润指数仅在农牧交错区与 NDVI_{max} 有较为显著的正相关,七月份的湿润指数也仅在林区与 NDVI_{max} 有较为显著的负相关,而在整个区域内春季的湿润指数对春季的 NDVI 几乎不起作用。相比较而言,一月份的湿润指数对 NDVI_{spring} 的作用要比春季的湿润指数大的多,并且在牧区荒漠草原亚区、牧区榆树疏林草原亚区和牧区小叶锦鸡儿灌丛草原亚区其负面作用都比较显著。

(4) 从显著性水平上可以看出,在对 NDVI_{max-min} 和 NDVI_{max} 的作用中,大部分区域气候因素的作用要大于人为因素的,尤其是 0cm 地温的作用。在对 NDVI_{spring} 的作用中,大部分区域(农区除外)气候因子的作用占绝对优势,尤其是一月份气温均值和一月份气候湿润指数的作用。

7.4.2 NDVI 旬值对气温、地温和降水年际波动的响应

对每一年各旬的 NDVI 旬值与相应旬期的气温均值、0cm 地温均值和旬降水量做相关分析,得到不同类型每一年 NDVI 值与气候因子之间的相关系数,相关系数的年趋势图如图 7.6 所示。



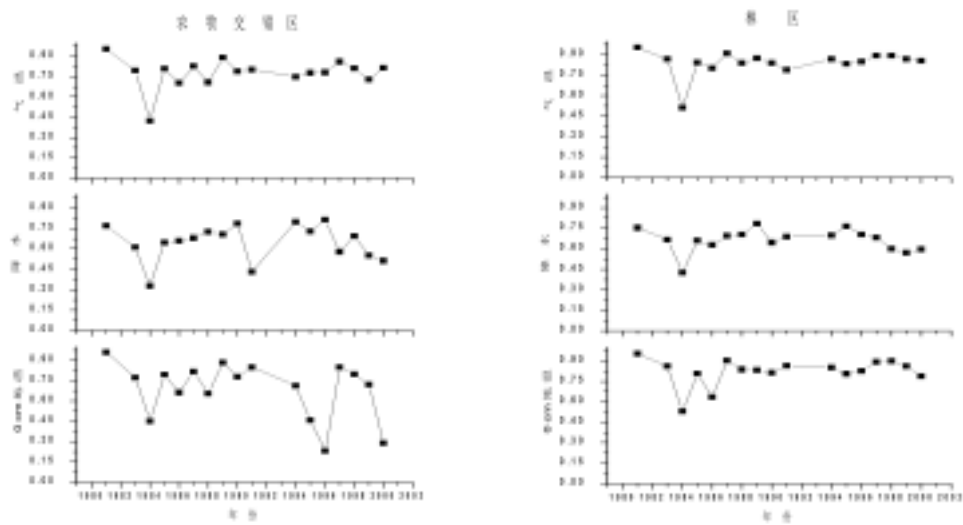


图 7.6：1980~2000 年 NDVI 对气候因子年际变化的响应
纵轴为相关系数

从图 7.6 中可以看出：（1）NDVI 旬值与相应的气候因子旬值之间存在着非常密切的相关关系，尤其是牧区草甸草原亚区和牧区典型草原亚区地带，NDVI 旬值与各个气候因子旬值之间的相关系数都很高，其它类型下也只有个别时期 NDVI 值与气候因子之间的关系较差。（2）在大部分区（亚区）中，多数年份对 NDVI 影响都是气温>0cm 地温>降水，而且 0cm 地温对 NDVI 的作用趋势总是和气温对 NDVI 的作用趋势相一致，所不同的是 0cm 地温的年际波动要大一些，另外除了牧区草甸草原亚区和牧区典型草原亚区两个类型，其它类型气候因子对 NDVI 的作用在 1984 年都出现较低值。

7.4.3 NDVI 旬值对干湿条件年际波动的响应

降水量与气温的组合所反映的干湿条件的变化是本区植被空间分布格局的决定性因子，探讨 NDVI 旬值对干湿条件年际波动的相应对分析植被空间格局的成因及其对未来气候变化的响应具有十分重要的意义。不同区（亚区）1981~2000 年各旬 NDVI 旬值的多年平均状况与相应旬期的多年平均湿润指数之间的相关系数如表 7.4 所示。

表 7.4 不同区（亚区）NDVI 旬值与相应旬湿润指数的相关系数	
区域	相关系数
牧区草甸草原亚区	0.581*
牧区典型草原亚区	0.523*
牧区荒漠草原亚区	0.492*
牧区沙地榆树疏林草原亚区	0.522*
牧区小叶锦鸡儿灌丛草原亚区	0.319
农区	0.527*
农牧交错区	0.242
林区	0.583*

表中带**的表示因子之间的相关性很强，显著水平高于 0.01，用黑斜体表示；带*的表示因子之间相关性较强，显著水平介于 0.01~0.05 之间，用黑体表示。

从表 7.4 中可以看出，除了牧区沙地小叶锦鸡儿灌丛草原亚区和农牧交错区外，其它区

(亚区)的 NDVI 值与湿润指数之间均有较为显著的正相关关系,说明湿度条件的年际波动也是植被年际动态的决定性因子之一。在牧区小叶锦鸡儿灌丛草原亚区和农牧交错区,湿度条件的影响不明显,原因有待进一步探讨。

7.5 讨论

利用 NDVI 来进行中国植被动态与气候变化之间的关系分析目前已经有较多的研究成果,然而大部分是针对全国尺度的植被动态及其驱动因子(李晓兵等,1999;李本纲等,2000;陈云浩等,2001)。前人的研究大都集中在气温或者降水的单个因子分析或者两个因子作用的比较方面以及气候变化所造成的植被覆盖区域分异方面(李晓兵等,2000),利用多个气候因子并结合人为活动的变化进行气候和人为因素对 NDVI 动态变化的影响分析方面的研究成果目前仍然较少。

前人的研究工作大都得出气温对 NDVI 动态的作用要大于降水的作用,如李本纲等(2000)对全国 160 个气象站点的 1983 年~1992 年连续 10a 的 NDVI 数据与气象观测资料进行的相关分析表明,结果表明中国大部分区域下气温对植被的作用要大于降水的,龚道溢等(2002)对北半球春季 NDVI 与气温的相关分析中也表明,春季的 NDVI 与气温具有非常显著的相关性,这与本文的结果是一致的。本文针对中尺度的植被动态的驱动因子进行分析,与大尺度的结果有较好的一致性,可能与本研究区明显的气候梯度有关。在中国干旱、半干旱区,湿度条件对植被的空间格局起着决定性作用,前人的工作中较多考虑温度和降水的影响,而对湿度条件的作用缺少探讨。本文的结果表明,湿度条件的波动也是 NDVI 年际动态的驱动因子之一。由于湿度条件是温度和降水的综合,湿度条件与其它因子的相对作用有待进一步探讨。

7.6 小结

1. 在气候因子对 NDVI_{max-min} 和 NDVI_{max} 的作用中,0cm 地温各项指标所起的作用要比其它气候因子大,而且在几乎所有区(亚区)中,1 月份 0cm 地温均温的作用基本上是负面的,其它 0cm 地温指标所起的作用都是促进性的;在气候因子对 NDVI_{spring} 的作用中,气温和降水指标的作用则相对有所增强,尤其是 1 月份的气温和春季的降水量。

2. 在人为活动对 NDVI 的作用中,在不同区(亚区)人为活动的影响基本都不显著,其中总人口数始终是影响最大的因子。

3. 从显著性水平上可以看出,在对 NDVI_{max-min} 和 NDVI_{max} 的作用中,大部分区域气候因素的作用要大于人为因素的,尤其是 0cm 地温的作用;在对 NDVI_{spring} 的作用中,大部分区域(农区除外)气候因子的作用占绝对优势,尤其是 1 月份气温均值和 1 月份气候湿润指数的作用。

4. 在大部分区(亚区)中,多数年份气候因子对 NDVI 旬值影响都是气温>0cm 地温>降水。

第八章 荒漠化与风沙活动的关系

8.1 沙尘暴地理分布与季节、年际变化

根据第七章中的分区，对每个区（亚区）从获得的研究区 30 个气象台站中选出一个代表性的气象台站，将每个台站每年所发生的沙尘暴日数累积，求得逐年沙尘暴爆发日数。值得说明的是，这里的沙尘暴日数统计不包括扬沙和浮尘天气的日数。

8.1.1 50 年不同区域沙尘暴发生趋势

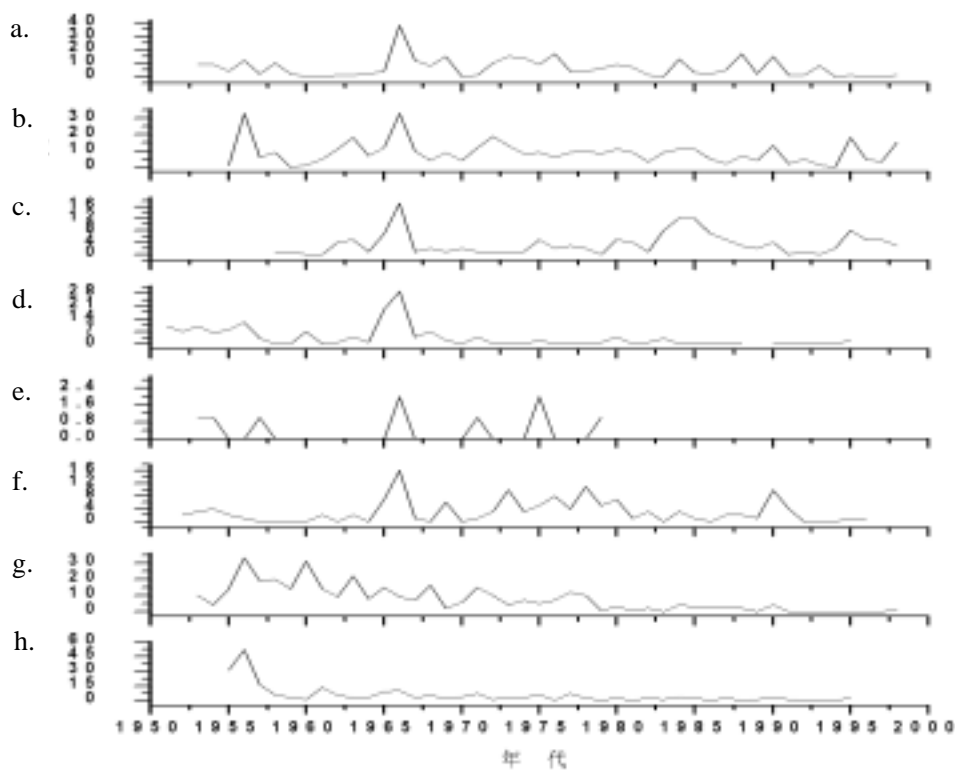


图 8.1 不同类型 50 年来风沙发生日数

图中 a. 农牧交错区；b. 牧区荒漠化草原亚区；c. 牧区沙地小叶锦鸡儿灌丛草原亚区；d. 农区；e. 林区；f. 牧区沙地榆树疏林草原亚区；g. 牧区典型草原亚区；h. 牧区草甸草原亚区。纵轴为沙尘暴日数

从图 8.1 可以看出，1966 年是研究区沙尘暴的高发年，有些区域该年沙尘暴的发生次数远远高于其他年份。50 年来，牧区草甸草原亚区、牧区典型草原亚区和北京周围的农区沙尘暴的发生次数有明显下降的趋势；牧区荒漠化草原亚区和牧区沙地小叶锦鸡儿灌丛草原亚区沙尘暴的发生近年来有所增加；牧区沙地榆树疏林草原亚区沙尘暴的发生只在近几年才有所降低；冀北山地森林和灌丛为主的地区由于地理位置、地形和地表覆盖的影响，沙尘暴

发生的次数和日数均少于其它区（亚区）。

8.1.2 不同年代沙尘暴的动态分析

利用 1950~2000 年的沙尘暴资料，对不同时期不同区域的沙尘暴发生次数进行比较分析，结果见如表 8.1 所示。

表 8.1 不同区域沙尘暴的动态变化

区（亚区）	代表性台站	50 年代	60 年代	70 年代	80 年代	90 年代
牧区草甸草原亚区	西乌珠穆沁旗	109	57	31	15	3
牧区典型草原亚区	锡林浩特	131	108	74	22	2
牧区沙地榆树疏林草原亚区	多伦	3	34	57	23	7
林区	承德	1	2	4	0	0
农区	北京	30	67	14	7	4
牧区沙地小叶锦鸡儿灌丛草原亚区	那仁宝力格	2	40	21	58	24
牧区荒漠化草原亚区	苏尼特左旗	50	113	105	74	49
农牧交错区	化德	30	81	89	65	16

从表 8.1 可以看出：

（1）从沙尘暴的地理分布上看：二十世纪六十年代和七十年代沙尘暴的地理分布规律比较相似，八十年代和九十年代沙尘暴的地理分布规律比较相似。其中牧区典型草原亚区和牧区草甸草原亚区在五十年代爆发的沙尘暴日数最多，以后各年趋于减少，直到九十年代的 10 年期间沙尘暴分别发生 2、3 次；牧区荒漠化草原亚区在六十年代沙尘暴爆发次数最高，达到 57 次，以后沙尘暴发生的次数逐渐减少，九十年代基本上和五十年代持平；农牧交错区和牧区沙地榆树疏林草原亚区五十年代发生的沙尘暴次数较低，六十年代、七十年代陡然增加，八十年代开始下降，九十年代达到最低；北京周围的农区不同年间沙尘暴的发生次数与石质丘陵荒漠化草原的相似，六十年代最多，后急剧减少，九十年代仅发生了 4 次；牧区沙地小叶锦鸡儿灌丛草原亚区沙尘暴发生次数与前面几个区域稍有不同，八十年代为其沙尘暴发生的高峰期，六十年代和七十年代逐渐下降，九十年代又增加，五十年代是其沙尘暴发生次数最少的 10 年；在整个研究区域中冀北山地以森林和灌丛为主的地区沙尘暴发生的次数最少，前 30 年间总共发生沙尘暴 7 次，八十年代、九十年代无任何记录。

（2）从沙尘暴发生次数的规律上看：二十世纪五十年代牧区典型草原亚区和牧区草甸草原亚区发生的沙尘暴最多，此后下降明显，从五十年代的总次数超过 10 次到九十年代的总次数不到 5 次；六十年代以后年份牧区荒漠化草原亚区发生的沙尘暴次数占据首位；农牧交错区发生的沙尘暴次数在六十年代开始跃居第二位和第三位；牧区小叶锦鸡儿灌丛草原亚区在五十、六十、七十年代沙尘暴发生的次数还不十分明显，八十年代达到 58 次，成为研究区当时沙尘暴发生最多的地带，九十年代有所下降，为 24 次；总之，不同区域五十年来沙尘暴的发生次数均呈下降趋势，除个别区域（如牧区沙地小叶锦鸡儿灌丛草原亚区和牧区沙地榆树疏林草原亚区）外，九十年代是沙尘暴爆发次数最少的 10 年。

8.2 不同地表覆盖类型对北京沙尘天气物源的贡献

根据地貌、植被和土地利用,可以将地处北京上风向的浑善达克沙地及周边地区以及河北坝上地区的地表覆盖划分为以下 9 个类型:(1)沙地榆树疏林灌丛草原(包括固定沙地和流动沙地);(2)沙地小叶锦鸡儿灌丛草原(半固定沙地);(3)石质丘陵草甸草原;(4)石质丘陵典型草原;(5)石质丘陵荒漠化草原;(6)耕地(含撂荒地);(7)人工林;(8)低湿地草甸;(9)湖滨草甸。

8.2.1 不同地表覆盖类型下的植被和土壤性状

1. 沙地榆树疏林草原和沙地小叶锦鸡儿灌丛草原:草本层以草原成分为主。根据退化程度的不同,可以分为固定、半固定沙地和流动沙地。土壤类型为风沙土,无明显的剖面结构。

2. 石质丘陵典型草原:分布于河北坝上地区西部,地带性植被以克氏针茅占据优势,草本层盖度 20~40%。随着放牧活动的增加,覆盖程度降低。土壤类型为栗钙土,在坡中和坡顶土层薄,石块含量高。在坡脚有黄土覆盖处土层较厚。

3. 石质丘陵草甸草原:分布于河北坝上地区东部,地带性植被以贝加尔针茅占据优势,草本层盖度达 40~60%。土壤类型为黑钙土。

4. 农田(含撂荒地)/退耕地:主要分布于丘间低地和缓坡,种植莜麦等作物。退耕或者撂荒以后,田间出现大量一年生植物。

5. 人工林:主要为杨树林,属于“三北”防护林的一部分。在局部地区有人工落叶松林。

6. 石质丘陵荒漠化草原:分布于二连浩特周围,地带性植被为戈壁针茅,草本层植被盖度在 20%左右,石块含量高,很大地方达到 50%以上,土壤类型为棕钙土。

7. 湖泊和低湿地草甸:在这一区域有数量众多的湖泊和低湿地。在湖岸和低湿地以草甸为主,随着湖水退缩,一些盐生灌木进入湖滨草甸中。

8.2.2 沙尘天气的物源来自于不同地表覆盖的可能性

一些研究工作探讨了北京地区沙尘天气的粒径组成。从 2000 年 4 月北京特大沙尘天气的粒径组成来看,主要以 0.01mm 以下的粉沙和黏土为主,占 84.24%(庄国顺等,2001)。盛学斌等(2002)发表的 1989 年 8 月~1993 年 9 月在坝上康保县照阳河乡三义村进行的风蚀沙化实验也表明,被风蚀扬走的主要是 0.05mm 以下的细颗粒物。叶笃正等(2000)也指出沙尘颗粒集中在 0.002~0.063mm 之间。陈静生等(1984)通过北京至内蒙古集宁一线 21 个地点的系统采样,也得出绝大多数地点的降尘以<0.05mm 粒径部分占绝对优势的结论。

表 8.2 为研究区不同地表覆盖类型表土粒径的累计百分比组成。按照粒径 0.05mm 以下的物质含量排序,依次为低湿地草甸>石质丘陵荒漠化草原>石质丘陵草甸草原>人工林>湖滨草甸>石质丘陵典型草原=固定沙地>农田>半固定沙地>流动沙地。粒径<0.01mm 的物质含量也有类似的规律。可以认为,从单位面积提供物源的可能性来说,流动沙地、半固定沙地对北京沙尘天气物源的贡献极为有限。低湿地草甸、石质丘陵荒漠化草原、石质丘陵草甸草原、人工林等均具备为北京沙尘天气提供较多物源的能力。

表 8.2 不同地表覆盖类型表土粒径的累计百分比

地表覆盖类型	土壤粒径	
	<0.05mm	<0.01mm
沙地榆树疏林草原	6.2(9.3)	1.9(3.4)
其中：流动沙地	1.1(0.6)	0.5(0.5)
其中：固定沙地	16.6(11.1)	5.9(4.3)
沙地小叶锦鸡儿灌丛草原（半固定沙地）	13.19(6.66)	4.02(3.19)
石质丘陵荒漠化草原	16.8(7.55)	7.8(9.65)
石质丘陵典型草原	16.6(10.6)	4.1(3.3)
石质丘陵草甸草原	31.4(13.4)	8.1(4.8)
农田（含退耕/撂荒地）	8.0(5.1)	2.4(3.7)
人工林	22.6(13.7)	9.0(5.9)
低湿地草甸	40.1(13.3)	15.9(7.3)
湖滨草甸	17.5(6.0)	3.1(1.5)

* 括号内为方差

8.2.3 不同地表覆盖类型的固沙能力

具备了细颗粒物并非表明具有起沙的可能。地表植被状况对起沙具有决定性作用。如果地表植被覆盖度高，草群高度大，即使细颗粒物含量高，起沙的可能性仍然较低。然而，沙尘天气的发生集中在春季，此时地表植被没有返青，植被对地表的固定作用取决于植物根系和枯枝的作用，在这方面，多年生植物明显优于一年生植物。不同地表覆盖类型中多年生植物的盖度及草本植物总盖度如表 8.3 所示。

表 8.3 不同地表覆盖类型的植被盖度（%）和草群高度（cm）

地表覆盖类型	样本数	草本植物总盖度	多年生草本植物盖度	一年生草本植物盖度	草群高度
沙地榆树疏林草原	11	33.3(30.6)*	23.1(12.5)	10.2(18.2)	23.2(18.5)
其中：流动沙地	7	30.8(15.9)	16.2(13.5)	14.7(14.5)	18(12.3)
其中：固定沙地	4	32.5(29.3)	31.0(30.1)	1.5(2.5)	27.4(20.7)
沙地小叶锦鸡儿灌丛草原（半固定沙地）	15	36.96(2.25)	14.71(3.49)	22.25(3.3)	20.43(12.5)
石质丘陵荒漠化草原	6	27.58(2.8)	25.58(5.2)	2.0(1.8)	8.65(2.0)
石质丘陵典型草原	17	33.4(8.9)	20.4(11.9)	13.1(12.0)	8.4(3.5)
石质丘陵草甸草原	6	43.3(16.9)	40.1(16.5)	3.2(3.9)	13(8.9)
农田（含退耕/撂荒地）	4	55(13.2)	0.7(0.6)	54.3(13.1)	20.2(14.3)
人工林	4	30(13.2)	14.8(21.5)	15.2(14.8)	12.3(4.5)
低湿地草甸	7	65(8.7)	58.8(18.1)	6.2(13.3)	9.4(7.7)
湖滨草甸	4	45(26.4)	44.2(23.5)	0.8(0.9)	17.1(8.8)

*括号内为方差

从表 8.3 中可以看出，不同地表覆盖类型草本植物总盖度的顺序为：低湿地草甸>农田>湖滨草甸>石质丘陵草甸草原>半固定沙地>石质丘陵典型草原>固定沙地>流动沙地>人工林>石质丘陵荒漠化草原；多年生草本植物盖度的顺序为：低湿地草甸>湖滨草甸>石质丘陵草甸草原>固定沙地>石质丘陵荒漠化草原>石质丘陵典型草原>流动沙地>人工林>半固定沙地>农田；草群高度的顺序为：固定沙地>耕地>半固定沙地>流动沙地>湖滨草甸>人工林>石质丘陵草甸草原>低湿地草甸>石质丘陵荒漠化草原>石质丘陵典型草原。综合考虑以上三个方面的影响，低湿地草甸、湖滨草甸和固定沙地的植被对起沙有较好的阻止作用，而人工林、流动沙地和石质丘陵典型草原的作用则要弱得多。

结合表 8.2 和表 8.3 可以认为，虽然低湿地草甸、湖滨草甸和石质丘陵草甸草原这三种土地覆盖类型中细颗粒物含量高，但其多年生草本植物盖度均在 40% 以上，在同等气象条件下，单位面积的沙尘释放能力小。固定沙地中多年生草本植物的盖度达到 31%，虽然

其中 $<0.05\text{mm}$ 的物质占 17.8%，单位面积的沙尘释放能力偏低。半固定沙地上草本层的总盖度比较高，但大部分是一年生植物，而且土壤中粗颗粒含量较高，因此它对固沙的作用不大，反而可能是沙尘源之一。石质丘陵典型草原单位面积内的沙尘物源量较高，且在人为活动的影响下，植被出现不同程度的退化，多年生草本植物的盖度只有 20.4%，草群高度也低。在浑善达克沙地和河北坝上地区，这类地表覆盖的面积大，可以推断这一类型地表覆盖单位面积的释放能力强。石质丘陵荒漠化草原的总草本盖度虽然比较低，而且细颗粒物质含量较高，起沙能力也偏高。本农田撂荒或退耕以后，出现大量的一年生杂草，总盖度较高，草群高度也大，对地表植被有一定的固定能力。农田中 $<0.05\text{mm}$ 的物质占 8%，如果春季耕翻，在强风作用下，仍有一定的释放能力。流动沙地中虽然多年生草本植物的盖度仅为 16.2%，但其中细颗粒物质含量很低，可以推断对北京沙尘天气物源的贡献较小。人工林的作用主要是防风，林下草本植物的固沙能力弱，是当前防护林建设中需要考虑的问题。

8.2.4 荒漠化的发生发展与沙尘天气的关系

沙尘天气与荒漠和荒漠化关系密切。从本文结果可以看出，在提供沙尘天气物源方面，可以将地表覆盖类型归纳为 3 大类：（1）过去沙尘天气物源：如流动沙地、半固定沙地，细颗粒物质含量低，原因在于过去的风沙活动将其中大部分的细颗粒物质吹走，土壤出现粗化；（2）当前沙尘天气物源：石质丘陵典型草原处于退化之中，有一定的细颗粒物质，沙尘被吹扬的可能性大。石质丘陵荒漠化草原由于植被覆盖低，且细颗粒物质含量偏高，起沙的可能性也较高。正在耕作的土地具有一定含量的细颗粒物质，春季耕翻加大了被吹扬的可能性，但耕地撂荒和退耕以后，一年生草本植物大量出现，植被盖度大，草群高度也大，对起沙过程有一定的抑止作用。（3）潜在沙尘天气物源：低湿地草甸、湖滨草甸、石质丘陵草甸草原和固定沙地多年生草本植物覆盖高，细颗粒物质含量也高，在未来植被遭受破坏时可能成为沙尘天气的潜在物源。值得指出的是沙尘天气的出现不仅与地表覆盖有关，也与气候条件有非常密切的关系，以上划分只是说明了不同地表覆盖类型单位面积内提供物源的可能性。此外，粗颗粒物质虽然不能远距离传输，但在强风作用下出现近距离搬运，对当地造成了不良影响，如出现流动沙丘向前推移等。

荒漠化的发生发展是自然和人为因素共同作用下的结果。在气候变化的影响下，这一地区的荒漠化和风沙活动可以追溯到 5900 ^{14}C yr BP (Liu et al., 2002)。根据文献记载北京地区自公元 440 年就有强沙尘天气，强沙尘暴一般发生在干旱时期（陈广庭，2002）。一般认为，近 50 年来北京地区沙尘天气的频率总体上减少，但近年来强沙尘天气的出现频率较以往高（叶笃正，2000）。除了沙尘天气途径地区近年来气候持续干旱外，超强度的人为活动是主要原因。从表 2 可以看出，石质丘陵典型草原中一年生植物的比例大大高于石质丘陵草甸草原，除了典型草原的抗干扰能力低以外，农牧交错带高强度的放牧也是非常重要的因素。

8.3 气候波动以及人为活动对沙尘暴的贡献

8.3.1 不同区（亚区）不同月份下沙尘暴发生次数的影响因子

从 1980~2000 年来的沙尘暴资料中选取不同区（亚区）沙尘暴发生月份，统计相同月份的沙尘暴发生次数及相应的沙尘暴发生时所在旬的 NDVI 值和气候因子气温均值、0cm 地

温均值以及当月降水总量，求出 1980~2000 年间不同月份沙尘暴发生次数与 NDVI 和气候因子之间的相关系数见表 8.4，其中降水为月降水总量，气温和 0cm 地温为月均温。

表 8.4 不同类型下不同月份沙尘暴发生次数与 NDVI、气象因子之间的相关系数

类型	沙尘暴发生月份(次数)	NDVI	降水	气温	0cm 地温
牧区荒漠草原亚区	2(1), 3(3), 4(22), 5(9), 6(4), 7(2), 8(8), 11(2)	-0.314	-0.136	0.195	0.198
农牧交错区	1(2), 2(2), 3(6), 4(18), 5(11), 6(3)	-0.094	0.007	0.423	0.419
牧区草甸草原亚区	3(1), 4(4), 5(6), 7(1), 11(1)	-0.362	-0.191	0.14	0.132
牧区典型草原亚区	3(1), 4(6), 5(2), 6(4), 8(1), 11(2)	-0.362	-0.405	0.172	0.203
牧区沙地榆树疏林草原亚区	1(1), 3(4), 4(10), 5(3)	0.116	0.106	0.483	0.522
林区	1(2), 3(1), 4(2), 5(1)	0.576	-0.506	-0.431	-0.433
农区	3(1), 4(6), 5(2), 6(3), 7(2)	-0.147	-0.196	-0.047	0.052

从表 8.4 中可以看出，春季是发生沙尘暴的旺季，几乎所有区域的沙尘暴都集中于 3、4、5 月份，而 4 月份是除林区外的其他类型发生沙尘暴次数最多的月份，除了 3、4、5 月份外，1、2、6、7、8、11 月份都有地区发生沙尘暴，尤其是 1 月和 6 月不止一个区域发生沙尘暴，而且次数也较多。20 年来牧区荒漠化草原亚区发生沙尘暴次数最多，而且出现沙尘暴的月份也最多，农牧交错区次之，林区最少，农区次少；另外沙尘暴发生次数与 NDVI 和气候因子之间的关系不同类型下有所不同，NDVI 和气候因子对沙尘暴发生次数的影响都不太显著，在大部分区(亚区)下 NDVI 和降水的值越大，沙尘暴发生次数就越低，气温的值越高，沙尘暴发生次数就越多，而 0cm 地温对沙尘暴的作用则不同区域有所不同，其中林区 NDVI 和气候因子对沙尘暴发生次数的影响较大。在牧区荒漠化草原亚区沙尘暴发生次数受地表植被覆盖程度的影响较大，在农牧交错区以及牧区沙地榆树疏林草原亚区受气温和 0cm 地温的影响较大，在牧区典型草原亚区和林区受 NDVI 值和降水的影响较大，在牧区草甸草原亚区上述所有因子都对沙尘暴发生次数有一定的作用，在农区上述所有因子都基本不起作用。

8.3.2 1980~2000 年各区(亚区)沙尘暴发生强度的影响因子

1980~1999 年不同区(亚区)能见度/风速(表示沙尘暴发生的相对强度，其中能见度/风速越大，沙尘暴的相对强度就越小)与 NDVI、降水、气温和 0cm 地温之间的关系见表 8.5，其中 NDVI 用的是沙尘暴发生时所在的旬值，气温、0cm 地温为旬均值，降水为旬降水总量，能见度/风速为每次发生沙尘暴时能见度与风速的比值，去掉没有发生沙尘暴和 NDVI 数值不全的旬期。

表 8.5 20 年来各区(亚区)能见度/风速与植被、气候因子之间的相关系数

类型	样本数(沙尘暴发生总次数)	NDVI	降水	气温	0cm 地温
牧区荒漠化草原亚	45	-0.054	0.581**	0.355*	0.258

区					
农牧交错区	43	0.405**	0.388*	0.385*	0.384*
牧区草甸草原亚区	13	0.679*	0.626*	0.169	0.614*
牧区典型草原亚区	16	0.339	0.335	0.292	0.272
牧区沙地榆树疏林草原亚区	18	0.168	0.533*	0.215	0.206
林区	6	-0.196	0.499*	0.012	-0.084
农区	14	-0.038	0.224	0.052	0.107

其中*表示显著水平在95-99%之间,较显著相关;**表示显著水平高于99%,明显显著相关。

从表 8.5 中可以看出,几乎所有区域 NDVI 和气候因子(气温、降水和 0cm 地温)与能见度/风速的相关系数是正相关的,即 NDVI、气温、降水和 0cm 地温越大,沙尘暴发生强度越小。其中牧区荒漠化草原亚区降水对能见度/风速有非常显著的影响,也是对其影响最大的因子,其次是气温;农牧交错区 NDVI 对沙尘暴发生强度有非常显著的作用,而降水、气温和 0cm 地温对沙尘暴发生强度则有较为明显的影响;牧区草甸草原亚区对沙尘暴发生强度有较为显著影响的是 NDVI、降水和 0cm 地温;牧区典型草原亚区各因子对沙尘暴发生的相对强度影响都是不显著的,其中影响最大的是 NDVI;牧区沙地榆树疏林草原亚区只有降水对沙尘暴发生强度影响较为显著;林区没有因子对沙尘暴发生相对强度影响显著,其中降水对其影响最大;农区没有因子对沙尘暴发生相对强度起到很大的作用。

8.4 小结

1. 50 年来,牧区草甸草原亚区、牧区典型草原亚区和北京周围的农区沙尘暴的发生次数有明显下降的趋势;牧区荒漠化草原亚区和牧区沙地小叶锦鸡儿灌丛草原亚区沙尘暴的发生近年来有所增加;牧区沙地榆树疏林草原亚区沙尘暴的发生只在近几年才有所降低;林区则极少有沙尘暴发生。其中二十世纪五十年代、六十年代,牧区草甸草原亚区、牧区典型草原亚区发生的沙尘暴次数最多,此后牧区荒漠化草原亚区发生的沙尘暴次数开始居于首位。

2. 从沙尘源的角度看,研究区的地表覆盖类型可以划分为三类:(1)过去沙尘暴物源:沙地疏林灌丛草原中的流动沙地和固定沙地以及半固定沙地(沙地小叶锦鸡儿灌丛草原)等地表覆盖类型;(2)当前沙尘暴物源:石质丘陵荒漠化草原和石质丘陵典型草原以及耕地(含撂荒地);(3)潜在沙尘暴物源:低湿地草甸、湖滨草甸、石质丘陵草甸草原和沙地疏林灌丛草原中的固定沙地。

3. 不同月份下沙尘暴发生强度主要受降水的影响,沙尘暴发生次数主要受地表植被覆盖程度的影响,各个区(亚区)这种影响又有所不同。

4. 1980~2000 年来沙尘暴发生强度在不同区(亚区)的影响因子不同,其中降水的作用要相对强一些,而且在农牧交错区、牧区荒漠化草原亚区和牧区草甸草原亚区沙尘暴发生强度较容易受到 NDVI 和气候因子的影响,在农区和牧区典型草原亚区 NDVI 和气候因子几乎不起作用。

第九章 结论与讨论

9.1 结论

本文以河北坝上地区、内蒙古浑善达克沙地及其周边地区为研究区,对这一地区荒漠化的现状与评价、空间格局、成因及其与风沙活动的关系进行了详细研究,可以得出以下结论:

1. 利用草地退化指示种建立的植被退化指数能很好地反映不同类型草原的退化状况。不同类型的植被退化指数与总草本盖度之间并无直接的关系,即植被退化指数高的地方总草本盖度不一定就低;而多年生植物盖度占总盖度的比例较高的类型,其植被退化指数相对较低。

2. 对沙地草原和非沙地草原分别建立了上荒漠化程度指标体系模型。模型的对比分析表明,沙地草原和非沙地草原的退化机理不同,沙地草原的退化表现为土壤中粗颗粒含量的增加,草群高度降低;非沙地草原的退化表现为土壤中粗颗粒含量增加,土壤有机质含量下降,一、二年生植物和退化指示种的含量增加。

3. 无论是非沙地草原还是沙地草原,物种多样性都不随荒漠化程度的加重而逐渐减少。

4. 在气候因子对 NDVI max-min 和 NDVI max 的作用中,0cm 地温各项指标所起的作用要比其它气候因子大;在气候因子对 NDVI spring 的作用中,气温和降水指标的作用则相对有所增强,尤其是 1 月份气温和春季降水量。大部分区域气候因素的作用要大于人为因素。在大部分区(亚区)中,多数年份气候因子对 NDVI 旬值影响都是气温>0cm 地温>降水。

5. 通过 MODIS 影像分析得出的研究区荒漠化程度分布图表明,典型草原带西北部和荒漠草原带北部的过渡区为荒漠化程度最高的地方,沙地与草甸草原接壤处以及荒漠草原亚区的西北部荒漠化程度最低,荒漠草原亚区与沙地接壤处荒漠化程度相对较高。

6. 对不同地表覆盖类型沙尘释放与北京沙尘天气关系的分析表明:作为荒漠化结果的流动沙地只是作为过去沙尘天气的物源,当前单位面积沙尘释放的能力低,而正处于荒漠化过程中的大面积的石质丘陵典型草原在同样的气候条件下单位面积内具有较高的释放能力。农田如果春季耕翻,则具有一定的沙尘释放能力,而退耕/撂荒地上出现大量的一年生草本植物,对起沙过程有一定的抑制作用。固定沙地、石质丘陵草甸草原、低湿地草甸等由于多年生草本植物的覆盖率高,单位面积内沙尘释放的能力低。未来气候变化引起的沙丘活化以及湖泊和低湿地变干则可能使它们成为沙尘天气的潜在物源。

8. 1980~2000 年 NDVI 和气候因子对沙尘暴发生次数的影响都不太显著;来沙尘暴发生相对强度在不同区(亚区)的影响因子不同,其中降水的作用要相对强一些,而且在农牧交错区、牧区荒漠草原亚区和牧区草甸草原亚区沙尘暴发生相对强度较容易受到 NDVI 和气候因子的影响,在农区和牧区典型草原亚区 NDVI 和气候因子几乎不起作用。

9.2 研究区的荒漠化防治对策探讨

根据本文的结果,研究区荒漠化防治对策的制订需要考虑以下因素:

1. 研究区地表覆盖类型多样,不同的地表覆盖类型荒漠化的发生机制不同,为此,在荒漠化防治对策的制定方面,需要充分考虑不同地表覆盖类型的差异性。本文结果表明,典

型草原的植被退化程度已非常明显,荒漠草原的植被也有一定的退化,采取适当措施如禁牧、减少放牧量等的措施还是很必要的;农田对沙尘暴的贡献不可忽视,退耕还草的措施需要加大力度;撂荒地和退耕地还需要继续围栏禁牧;人工林在一定程度上起到一些保护作用,但不可滥栽,要因地制宜;山地草甸和低湿地草甸的植被退化程度还不太明显,当务之急是防止水体变干。

2. 为了防止风沙而建立的人工防护林体系实践证明已起到一定的作用,人工林主要围绕村庄、农田而建,一定程度上保护了人和庄稼的安全。但人工林耗水量大,林下草本植物的生长明显受到限制,减弱了人工林对风蚀的防护作用。适地造林、适地种草仍然是今后生态建设的关键。

3. 气候变化对研究区的植被动态起着决定性的作用。而研究区由于地处季风气候尾间区,气候的波动性明显。根据气候条件确定研究区的人口承载水平是制订区域发展政策的关键。

4. 在植被恢复的同时,加强对现有植被的保护,避免由于人为破坏造成新的土地沙化也是一个重要的任务。研究区内石质丘陵草甸草原的破坏程度较轻,应该加强保护,而不是盲目地去植树。

参考文献：

- Bishop J. K. B., Davis R. E., Sherman J. T., 2002. Robotic observations of dust storm enhancement of carbon biomass in the North Pacific. *Nature*, **298**: 817-820
- Ding D. S., Bao H. S., Ma Y. L., 1998. Progress in the study of desertification in China. *Progress in Physical Geography*, **22**(4): 521-527
- Dregne H., 1984. Desertification-present and future. *International Journal for Development Technology*, (2): 255-259
- Liu H. Y., Cui H. T., Pott R., Speier M., 2000. Vegetation of the woodland-steppe ecotone in southeastern Inner Mongolia, China. *Journal of Vegetation Science*, **11**(4): 525-532
- Liu H. Y., Xu L. H., Cui H. T., 2002. Holocene history of desertification along the woodland-steppe border in northern China. *Quaternary Research*, **57**: 259-270
- Menshing H., Ibrahim E., 1985. Note toward the desertifications and geographical analysis of the problem of desertification in and around arid lands. *Scientific Reviews on Arid Zone Research*, **3**: 105-114
- Middleton N., Thomas D. S. G., 1997. World Atlas of Desertification. Arnold, London.
- Devaraj P., 1999. Plant Indicators Principles and Concepts, *Ecology. Environment. & Conservation*. **5**(2): 137-140
- Zhang K. B., Yang X. H., 2002. Desertification Assessment Indicator System in China. *Forestry Studies in China*. **4**(1): 44-48
- Zhou M., 1994. Effects of two dust storms on solar radiation in the Beijing-Tianjin area. *Geophysical Research Letters*, **21**(24): 2697-2700
- UNEP. 1992a. Status of desertification and implementation of the United Nations plan of action to combat desertification. Report of the Executive Director, United Nations Environment Programme, Nairobi
- UNEP. 1992b. World Atlas of desertification. Edward Arnold, London
- Zhang X. Y., Arimoto R., Zhu G. H., et al. 1998. Concentration, size-distribution and deposition of mineral aerosol over Chinese desert regions. *Tellus*, **50B**(4): 317-330
- 巴巴耶夫, A., 1987. 沙漠化和自然保护问题. 地理译报, **3**: 37-40
- 陈静生, 邓宝山, 贾振邦, 1984. 关于“外来尘”对北京大气质量影响的研究. 中国环境科学, **4**(1): 10-17
- 陈广庭, 2002. 北京强冷沙尘暴与周围生态环境的变化. 中国沙漠, **22**(3): 210-213
- 陈云浩, 李晓兵, 史培军, 2001. 1983~1992年中国陆地 NDVI 变化的气候因子驱动分析. 植物生态学报. **25**(6): 716-720
- Dregne, H. E., 1992. 全球荒漠化土地的分布及其整治费用. 世界沙漠研究, **93**(1): 1-12
- 董光荣, 高尚玉, 金炯等, 1993. 青海共和盆地土地沙漠化与防治途径. 北京: 科学出版社. 142-165
- 董光荣, 靳鹤龄, 陈惠忠, 张春来, 1998. 中国北方半干旱和半湿润地区沙漠化的成因. 第四纪研究, (2): 136-144
- 董光荣, 金炯, 申建友等, 1990. 晚更新世初以来我国陆生生态系统的沙漠化过程及其成因. 见: 刘东生主编, 黄土. 第四纪地质. 全球变化(第二集). 北京: 科学出版社. 91-101

- 董光荣, 2002. 沙漠与沙漠化, 见: 王绍武, 董光荣主编, 中国西部环境演变评估(第一卷). 北京: 科学出版社. 104~118
- 范建容, 刘淑珍, 钟祥浩, 李勇, 2002. 金沙江干热河谷土地荒漠化评价方法研究. 地理科学, 22(2): 243~248
- 方修琦, 1987. 陕北鄂尔多斯地区降水变化与沙漠化. 北京师范大学学报(自然科学版), (1): 90~95
- 高尚武, 王葆芳, 朱灵益, 王君厚, 张玉贵, 1998. 中国沙质荒漠化土地监测评价指标体系. 林业科学, 34(2): 1~10
- 龚道溢, 史培军, 何学兆, 2002. 北半球春季植被 NDVI 对温度变化响应的区域差异. 地理学报, 57(5): 505~514
- 顾卫, 蔡雪鹏, 谢锋, 李彰俊, 2002. 吴学宏植被覆盖与沙尘暴日数分布关系的探讨 - 以内蒙古中西部地区为例. 地球科学进展, 17(2): 273~277
- 胡金明, 崔海亭, 唐志尧, 1999. 中国沙尘暴时空特征及人类活动对其发展趋势的影响. 自然灾害学报, 8(4): 49~56
- 黄永梅, 刘鸿雁, 崔海亭, 2001. 内蒙古高原东南缘森林草原过渡带景观的若干特征. 植物生态学报, 25(3): 257~264
- 贾宝全, 慈龙骏, 高志海等, 2001. 绿洲荒漠化及其评价指标体系的初步探讨, 干旱区研究, 18(2): 19~24
- 李本纲, 陶澍, 2000. AVHRR NDVI 与气候因子的相关分析. 生态学报, 20(5): 898~902
- 李博, 1997. 中国北方草地退化及其防治对策. 中国农业科学, 30(6): 1~9
- 李福兴, 1996. 全球荒漠化现状和我国荒漠化研究的动向. 水土保持研究, 3(4): 103~110
- 李慧卿, 李慧勇, 2000. 干旱与荒漠化. 世界林业研究, 3(4): 79~80
- 刘刚才, 刘淑珍, 1999. 金沙江干热河谷区土地荒漠化程度的土壤评判指标确定. 土壤学报, 36(4): 559~563
- 李令军, 高庆生, 2001. 2000 年北京沙尘暴源地解析. 环境科学研究, 14(2): 1~4
- 张仁健, 2000. 2000 年春季北京特大沙尘暴物理化学特性的分析. 气候与环境研究, 5(3): 258~265
- 李晓兵, 史培军, 1999. 基于 NOAA/AVHRR 数据的中国主要植被类型 NDVI 变化规律研究. 植物学报, 41(3): 314~324
- 李晓兵, 王瑛, 李克让, 2000. NDVI 对降水季节性和年际变化的敏感性. 地理学报, 55(增刊): 82~89
- 李永宏, 1994. 内蒙古草原草场放牧退化模式研究及退化监测专家系统雏议. 植物生态学报, 18(1): 68~79
- 刘爱民, 慈龙骏, 1997. 现代荒漠化过程中人为影响的系统分析 - 以内蒙古自治区乌审旗现代荒漠化过程为例, 自然资源学报, 12(3): 211~218
- 刘淑珍, 柴宗新, 范建容, 2000. 中国土地荒漠化分类系统探讨. 中国沙漠, 20(1): 35~39
- 刘毅, 周明煜, 1998. 北京及近中国海春季沙尘气溶胶浓度变化规律的研究. 环境科学学报, 19(6): 642~647
- 刘朝霞, 李钢铁, 李玉灵, 1996. 用聚类分析法进行毛乌素风蚀荒漠化强度分级 - 以乌审旗为例. 内蒙古林学院学报(自然科学版), 18(1): 27~33
- 内蒙古自治区地方标准, 1999. 内蒙古自治区天然草地退化标准, 内蒙古草业, (2): 61~62
- 朴世龙, 方精云, 2001. 最近 18 年来中国植被覆盖的动态变化. 21(4): 294~302
- 邱新法, 曾燕, 缪启龙, 2001. 我国沙尘暴的时空分布规律及其源地和移动路径. 地理学报, 56(3): 316~322

- 曲辉, 陈圣波, 2002. 中分辨率成像光谱仪 (MODIS) 数据在地学中的应用前景. 世界地质, 21(6): 176-180
- 任振球, 1990. 全球变化. 北京: 科学出版社. 193-214
- 盛学斌, 刘云霞, 孙建中, 2002. 农牧交错带土壤及某些表生植被特性变异与荒漠化的相关性——以冀北康保县为例. 应用生态学报, 13(7): 909-910
- 孙武, 李保生, 1999. 荒漠化分类分级理论的初步探讨. 地理研究, 18(3): 225-230
- 孙武, 南忠仁, 李保生等, 2000. 荒漠化指标体系设计原则. 自然资源学报, 15(2): 160-163
- 唐俊梅, 张树文, 2002. 基于 MODIS 数据的宏观土地利用/土地覆盖监测研究. 遥感技术与应用, 17(2): 104-107
- 王小丹, 钟祥浩, 范建容, 2002. 荒漠化评价的物元可拓识别方法. 山地学报, 20(5): 636-640
- 叶笃正, 丑纪范, 刘纪远等, 2000. 关于我国华北沙尘天气的成因及治理对策. 地理学报, 55(5): 513-521
- 吴国雄, 1979. 甘肃省“4.22”特大沙尘暴分析. 气象学报, 37(4): 26
- 熊利亚, 李海萍, 庄大方, 2002. 应用 MODIS 数据研究沙尘信息定量化方法探讨. 地理科学进展, 21(4): 327-333
- 杨东贞, 房秀梅, 李兴生, 1998. 我国北方沙尘暴变化趋势的分析. 应用气象学报, 9(3): 352-358
- 杨东贞, 王超, 温玉璞等, 1995. 1990 年春季两次沙尘暴特征分析. 应用气象学报, 6(1): 18-26
- 张宝秀, 1997. 内蒙古高原东南缘土地开发与环境退化关系论析. 地理学与国土研究, 13(3): 16-22
- 张仁健, 2000. 2000 年春季北京特大沙尘暴物理化学特性的分析. 气候与环境研究, 5(3): 258-265
- 朱震达, 1994. 土地荒漠化问题研究现状和展望. 地理研究, 13(1): 104-113
- 朱震达, 1994. 中国荒漠化问题研究的现状和展望. 地理学报, 49(增刊): 650-659
- 朱震达, 王涛, 1992. 中国沙漠化研究的理论与实践. 第四纪研究, 2: 97-106
- 朱俊风, 朱震达, 1999. 中国沙漠化防治. 北京: 中国林业出版社. 113-118
- 庄国顺, 郭敬华, 袁蕙等, 2001. 2000 年我国沙尘暴的组成、来源、粒径分布及其对全球环境的影响. 科学通报, 46(3): 191-196

附录：样方中出现的植物名录

(**表示中等退化指示植物, *表示严重退化指示植物)

A

**阿尔泰狗娃花 *Heteropappus altaicus*
 **阿氏旋花 *Convolvulus ammannii*
 矮锦鸡儿 *Caragana pygmaea*

B

白草 *Pennisetum flaccidum*
 白刺 *Nitraria tangutorum*
 白花碎米荠 *Cardamine leucantha*
 白莲蒿 *Artemisia sacrorum*
 **百里香 *Thymus serpyllum*
 瓣蕊唐松草 *Thalictrum petaloideum*
 北柴胡 *Bupleurum chinense*
 *北点地梅 *Androsace septentrionalis*
 北方拉拉藤 *Galium boreale*
 北方沙参 *Adenophora borealis*
 *北京黄芩
 贝加尔唐松草 *Thalictrum baicalense*
 贝加尔针茅 *Stipa baicalensis*
 笔管草 *Scorzonera albicaulis*
 *扁蓄 *Polygonum aviculare*
 扁蓿豆 *Pocockia ruthenica*
 扁茎黄芪 *Astragalus complanatus*
 变蒿 (柔毛蒿) *Artemisia pubescens*
 **冰草 *Agropyron cristatum*
 并头黄芩 *Scutellaria scordifolia*
 *滨藜 *Atriplex patens*

C

*苍耳 *Xanthium sibiricum*
 糙叶黄芪 *Astragalus scaberrius*
 糙苏 *Phlomis umbrosa*
 **糙隐子草 *Cleistogenes squarrosa*
 *草木樨 *Melilotus suaveolens*
 *草木樨状黄芪 *Astragalus melilotoides*
 草原丝石竹 *Gypsophila davurica*
 草芸香 *Haplophyllum dauricum*
 叉分蓼 *Polygonum divaricatum*

**差不嘎蒿 *Artemisia halodendron*
 柴胡 (北柴胡) *Bupleurum chinense*
 长叶百蕊草 *Thesium longifolium*
 长叶火绒草 *Leontopodium longifolium*
 *朝天委陵菜 *Potentilla supina*
 **车前 *Plantago asiatica*
 *虫实 *Corispermum L.*
 串铃草 *Phlomis mongolica*
 刺儿菜 *Cirsium segetum*
 *刺藜 *Chenopodium aristatum*
 *刺沙蓬 *Salsola pestifer*
 丛生隐子草 *Cleistogenes caespitosa*
 粗根鸢尾 *Iris tigridia*
 *粗壮女娄 *Melandrium firmum*
 寸草苔 *Carex duriuscula*

D

达乌里胡枝子 *Lespedeza davurica*
 达乌里黄芪 *Astragalus dahuricus*
 达乌里龙胆 *Gentiana dahurica*
 达乌里苳芭 *Cymbaria dahurica*
 *大籽蒿 *Artemisia sieversiana*
 等齿委陵菜 *Potentilla simulatrix*
 *地锦 *Euphorbia humifusa*
 *地梢瓜 *Cynanchum thesioides*
 *地蔷薇 (直立地蔷薇) *Chamaerhodos erecta*
 地榆 *Sanguisorba officinalis*
 *东北茵陈蒿 (猪毛蒿) *Artemisia scoparia*
 冬青叶兔唇蒿 *Lagochilus ilicifolius*
 *独行菜 *Rorippa indica*
 *断穗狗尾草 *Setaria arenaria*
 **多根葱 *Allium polyrhizum*
 多叶棘豆 *Ostryopsis myriophylla*
 *打碗花 *Calystegia hederacea*

E

二色补血草 *Limonium bicolor*

F

防风 *Saposhnikovia divaricata*

*飞廉 *Carduus crispus*

*肥披碱草 *Elymus excelsus*

*锋芒草 *Tragus racemosus*

拂子茅 *Calamagrostis epigejos*

G

甘草 *Glycyrrhiza uralensis*

杠柳 *Periploca sepium*

**高二裂委陵菜 *Potentilla bifurca* var. *major*

狗舌草 *Senecio campestris*

*狗尾草 *Setaria viridis*

冠芒草 *Enneapogon borealis*

H

旱麦瓶草 *Silene jensisensis*

*鹤虱 *Lappula myosotis*

*虎尾草 *Chloris virgata*

*华北驼绒藜 *Ceratoides intramongolica*

黄花菜 *Emmercallis citrina*

**黄囊苔草 *Carex korshinskii*

黄芩 *Scutellaria baicalensis*

*黄花蒿 *Artemisia annua*

灰叶黄芪 *Astragalus discolor*

J

芨芨草 *Achnatherum splendens*

*蒺藜 *Tribulus terrestris*

*戟叶蓼 *Polygonum thunbergii*

*加拿大飞蓬 *Conyza canadensis*

*尖头叶藜 *Chenopodium acuminatum*

尖叶铁扫帚 *Lespedeza hedysaroides*

剪刀股 (西伯利亚蓼) *Polygonum sibiricum*

*碱蓬 *Suaeda glauca*

*角果碱蓬 *Suaeda liaotungensis*

*芥菜 *Brassica juncea*

堇菜 *Viola verecunda*

菊叶委陵菜 *Potentilla tanacetifolia*

苣荬菜 *Sonchus arvensis*

瞿麦 *Dianthus superbus*

卷叶唐松草 *Thalictrum petaloides* var. *supradecompositum*

K

克氏针茅 *Stipa krylovii*

*苦苣菜 *Ixeris denticulata*

*魁薊 *Cirsium leo*

L

**狼毒 *Stellera chamaejasme*

老鹳草 *Geranium wilfordii*

**冷蒿 *Artemisia frigida*

*藜 *Chenopodium album*

砾苔草 *Carex stenophylloides*

裂叶蒿 *Artemisia laciniata*

裂叶堇菜 *Viola dissecta*

龙须菜 *Asparagus schoberioides*

楼斗叶绣线菊 *Spiraea aquilegifolia*

芦苇 *Phragmites communis*

驴耳风毛菊 *Saussurea amara*

M

**麻花头 *Serratula centauroides*

麻黄 *Ephedra sinica*

麻叶荨麻 *Urtica cannabina*

*马唐 *Digitaria Heist.*

猫眼草 *Euphorbia fischeriana*

毛茛 *Ranunculus japonicus*

毛蕊老鹳草 *Geranium eriostemon*

茅根 *Imperata cylindrica*

*蒙古冰草(沙芦草) *Agropyron mongolicum*

*蒙古虫实 *Corispermum mongolicum*

*蒙古葶苈 *Draba mongolica*

蒙古蕨 *Caryopteris mongolica*

米口袋 *Geldenstaedtia verna*

膜荚黄芪 *Astragalus memdranaceus*

*木地肤 *Kochia prostrata*

P

蓬子菜 *Galium verum*

披碱草 *Elymus dahuricus*

**披针叶黄华 *Thermopsis lanceolata*

琵琶柴 *Reaumaria soongorica*

**匍根骆驼蓬 *Peganum nigellastrum*
匍枝委陵菜 *Potentilla flagellaris*
蒲公英 *Taraxacum mongolicum*

Q

洽草 *Koeleria cristata*
茜草 *Rubia cordifolia*
曲枝天门冬 *Allium trichophyllum*
全缘恂子 *Cotoneaster integerrimus*
*雀麦 *Bromus japonicus*

R

日阴菅苔草 *Carex pediformis*

S

三出叶委陵菜 *Potentilla betonicaefolia*
三芒草 *Aristida adscensionis*
沙参 *Adenophora elata*
**沙蒿 *Artemisia desertorum*
**沙柳 *Salix psammophylla*
*沙蓬 *Agriophyllum pungens*
**沙生冰草 *Agropyron cristatum*
**沙珍珠豆 *Ostryopsis gracillima*
**沙竹 *Psammochloa villosa*
**砂韭 *Allium bidentatum*
*砂蓝刺头 *Echinops gmelini*
**砂引草 *Messerschmidia sibirica*
山莴苣 *Lagedium sibiricum*
山岩黄芪 *Hedysarum fruticosum*
山野豌豆 *Vicia amoena*
*绳虫实 *Corispermum declinatum*
鼠掌老鹳草 *Geranium sibiricum*
双花黄堇菜 *Viola biflora*
*水棘针 *Amethystea coerulea*
丝叶鸦葱 *Scorzonera curvata*
宿根亚麻 *Linum perenne*

T

苔草 *Carex dispalata*
田旋花 *Convolvulus arvensis*
*铁杆蒿 (白莲蒿) *Artemisia gmelinii*
*驼绒藜 *Ceratoides latens*

W

歪头菜 *Vicia unijuga*
**蜆菊 *Olgaea lomonosowii*
蚊子草 *Filipendula palmata*
问荆 *Equisetum arvense*
乌苏里风毛菊 *Saussurea ussuriensis*
*无芒雀麦 *Bromus inermis*
无芒隐子草 *Cleistogenes songorica*
*雾冰藜 *Bassia dasyphylla*

X

*西伯利亚滨藜 *Atriplex sibirica*
西伯利亚早熟禾 *Poa sibirica*
细茎鸢尾 (山马蔺) *Iris ruthenica*
细叶扁蓿豆 *Melilotoides ruthenica*
细叶委陵菜 *Potentilla multifida*
*细叶益母草 *Leonurus sibiricus*
**狭叶锦鸡儿 *Cragana stenophylla*
线叶菊 *Filifolium sibiricum*
腺毛委陵菜 *Potentilla longifolia*
小根蒜 *Allium macrostemon*
小果白刺 *Nitraria sibirica*
*小果虫实
小红菊 *Dendranthema chanetii*
**小叶锦鸡儿 *Caragana microphylla*
*小画眉草 *Eragrostis minor*
兴安天门冬 *Asparagus davuricus*
**星毛委陵菜 *Potentilla acaulis*
雪白委陵菜 *Potentilla nivea*

Y

鸦葱 *Scorzonera austriaca*
岩青兰 *Dracocephalum rupestre*
*盐地碱蓬 *Suaeda salsa*
盐穗木 *Halostachys caspica*
羊草 *Leymus chinensis*
羊茅 *Festuca ovina*
野艾蒿 *Artemisia lavandulaefolia*
野韭 *Allium ramosum*
*野亚麻 *Linum steuroides*
*页蒿 *Carum carvi*
*野滨藜 *Atriplex fera*(L.)
*益母草 *Leonurus japonicus*
硬毛棘豆 *Ostryopsis hirta*
*硬质早熟禾 *Poa sphondylodes*

羽茅 *Achnatherum sibiricum*
圆叶牵牛 *Pharbitis purpurea*
远志 *Polygala tenuifolia*

Z

*杂配轴藜 *Axyris hybrida*
展枝唐松草 *Thalictrum Squarrosum*
知母 *Anemarrhena asphodeloides*
直穗鹅观草 *Roegneria turczaninovi*
中麻黄 *Ephedra intermedia*
种阜草 *Moehringia lateriflora*
*轴藜 *Axyris amaranthoides*
皱叶鸦葱 *Scorzonera sinensis*
珠芽蓼 *Polygonum viviparum*
*猪毛菜 *Salsola collina*
*烛台虫实 *Corispermum candelabrum*

致 谢

论文交稿之际，感觉非常的愉快，多少次的泪水和汗水，多少人的鼓励和支持，换来这一结晶。回首三年紧张而又充实的求学生涯，感慨万千，身边许多人的关怀和帮助让我难以表达心中的感激，我非常荣幸能和他们有这样一段快乐难忘的时光。

首先，我要特别感谢我的导师刘鸿雁副教授，三年中，刘老师无论是在学习、工作还是在生活上，都给了我莫大的关心和帮助，对于我的很多过失，都给予了很多宽容和指正。从论文的框架设计、思路构建到内容和文字的修正，都凝聚着刘老师的智慧和心血。刘老师对科学研究严谨务实的态度以及广阔的思维让我毕生难忘。

再次，感谢崔海亭教授，是崔教授带我走进遥感这一领域，并对我粗心的解译进行了严格的批评指正，在论文的写作过程中，无论植物指示种的选择还是研究区景观类型的划分，崔教授都给予了很多帮助。

感谢方精云教授、曾辉副教授、贺金生副教授、沈泽昊副教授，无论是在学习上、工作上还是生活上，各位老师都给了我很大的支持、鼓励和帮助，对我各方面的不足都提出了很多有益的建议。

感谢黄润华教授，从生活上给予了我很多关怀和批评指正。

感谢师兄朴世龙，三年中从工作、学习和生活上，朴师兄都给予了我很大的关心和帮助，尤其在论文气象数据和 NDVI 数据处理上，给我提供了很多建议和实质性的支持；感谢师姐赵淑清在遥感解译和分析方面给我解决了很多技术难题；感谢师弟纪中奎帮助我很快掌握了几种很重要的软件，使我能够在较短时间内完成论文写作；感谢师妹丁登在土壤数据的前期处理和分析上给我提供了很多帮助；感谢师姐徐丽宏、张玲，师妹邢秋如以及教研室里各位师兄、师弟、师姐、师妹在生活上和工作上给了我巨大的支持和帮助。

感谢中国农业科学院的同行无偿提供 MODIS 遥感影像两景的数据；感谢国家气象局资料中心提供气象资料。

感谢我的父母和周围关心我支持我的朋友们，他们的关爱、呵护和无私奉献是我人生中最宝贵的财富，帮助我在以后的路上不怕失败，更加勇敢地往前行。

感谢你们，让我在生活上走向逐渐成熟，工作上学会如何去做研究。前路漫漫，任重而道远，你们的无限关怀和帮助将支持我披荆斩棘，走向更美好的未来。我也衷心祝福你们前途光明、事业辉煌。我终不会辜负你们的期望，若干年后我会呈上一份完美的答卷。

田育红

2003 年 6 月

北 京 大 学 学 位 论 文 原 创 性 声 明

本人郑重声明：所呈交的学位论文，是本人在导师的指导下，独立进行研究工作所取得的成果。除文中已经注明引用的内容外，本论文不含任何其它个人或集体已经发表或撰写过的作品成果。对本文的研究做出重要贡献的个人和集体，均已在文中以明确方式标明。本人完全意识到本声明的法律结果由本人承担。

学位论文作者签名： 田育红

日期：2003 年 6 月 10 日



北京大学

本科生毕业论文

题目：北方农牧交错带关键地段

退耕还林还草的生态效应

姓名：杨树

学号：00015063

院系：环境学院

专业：环境科学

指导教师：刘鸿雁 副教授

二 四年五月

摘要

北方农牧交错带的退耕还林草工程是正在实施的改善我国生态状况的重大生态建设举措。本文在野外调查和观测的基础上,利用定量分析手段,选择北方农牧交错带关键地段的内蒙古四子王旗和山西浑源开展研究,对退耕还林还草的生态效应进行初步分析和探讨,主要侧重在以下几个方面:(1)采用双向指示种分析(TWINSPAN)和除趋势对应分析(DCA)方法对四子王旗植物群落进行了分类和排序,并分析植被变化与退耕年限关系;(2)通过土壤砂、粉砂、粘土含量,土壤 TOC 与总氮百分比的分析说明不同退耕还林还草模式下土壤性状变化;(3)计算 Shannon-Wiener 指数说明退耕还林还草对物种多样性的影响;(4)进行风沙观测实验解释不同土地利用类型中地表覆盖对风沙的阻碍作用。

通过以上的分析可以得出以下结论:

1. 人为控制了苜蓿、沙打旺的种植周期的退耕还草工程对土壤起到了固氮的作用,虽然对土壤性质改良没有显著效果,但却使得退耕还草后植物群落完全不同于自然群落植被的演替过程,退耕年限达到 6 年后严重退化指示植物消失,退耕还草效用体现出来。

2. 退耕还林与退耕还草均起到了阻沙作用。物种多样性与土壤有机质含量、土壤氮含量等方面的结果表明,退耕还林的成效优于退耕还草。但退耕还草在降低土壤砂含量方面效果相对明显。

3. 退耕还林还草所带来的植被物种多样性变化与土壤性状变化存在正相关关系,说明土壤性状的改良对物种多样性的增加有明显作用。

关键词: 农牧交错带, 退耕还林还草, 生态效应

Abstract

The project of “Restoring woodlands and grasslands from croplands” in the farming-pastoral transitional zone in Northern China is one of the most important issues of the improvement of China’s ecological situation. In this study, with field investigation and observation, quantitative methods are employed to analyze the ecological effects on restoring woodlands and grasslands from croplands in the farming-pastoral transitional zone in Northern China. It focuses on the following aspects: (1) On the basis of TWINSpan and DCA, the ordination and the classification of the plant communities in Siziwang Banner are obtained. Links between different plant community types and restoring years are also discussed. (2) The relationship between the soil features and different modes of restoring woodlands and grasslands from croplands is indicated by the analysis of the contents of sand, silt, clay and the percentage of Total Organic Carbon (TOC) and Total Nitrogen (TN) in soil. (3) Changes of plant species diversity with different restoring years are demonstrated by calculating the Shannon-Wiener Index. (4) An aeolian movement observation experiment is carried out to illuminate the effect of preventing sand and dust from releasing in different land use types.

Following conclusions are drawn in this study:

1. The artificial periodical planting of *Medicago sativa* etc. leguminous crops is of nitrogen fixation, and the effects of restoring woodlands and grasslands from croplands are obvious 6 years after the project was put in practice.
2. Restoring woodlands and restoring grasslands are both beneficial to preventing sands and dust from releasing. Restoring woodlands is more effective than restoring grasslands when species diversity and improvements of soil properties are considered, and restoring grasslands is more effective than restoring woodlands with an eye to the sand content in the soil.
3. The plant species diversity in plant communities is well correlated to TOC in soil, which demonstrates the improvement of soil features lead to the increase of species diversity.

Key words: farming-pastoral transitional zone, restoring woodlands and grasslands from croplands, ecological effects

目录

第一章 前言.....	1
1.1 研究意义.....	1
1.2 研究现状.....	1
1.3 本研究的内容与技术路线.....	2
第二章 研究区概况.....	4
2.1 北方农牧交错带的地理界定和空间分布.....	4
2.2 北方农牧交错带的自然地理概况.....	4
2.3 研究区的典型性和代表性.....	5
第三章 研究方法.....	7
3.1 野外调查.....	7
3.2 实验室分析.....	7
3.3 数据处理.....	8
3.4 地表起沙观测.....	9
第四章 不同退耕还草年限下植被和土壤性状变化.....	11
4.1 退耕还草年限与植被变化分析.....	11
4.2 土壤性状的变化.....	14
第五章 不同植被恢复模式下植被与土壤性状变化的比较.....	15
5.1 植物群落类型的变化.....	15
5.2 群落内物种多样性的变化.....	17
5.3 退耕还林与退耕还草模式下土壤性状变化.....	18
5.4 不同退耕还林还草模式下地表起沙的观测结果.....	21
第六章 讨论与结论.....	22
6.1 植被恢复与土壤恢复的关系分析.....	22
6.2 结论.....	22
参考文献.....	23
致谢.....	24

第一章 前言

1.1 研究意义

人类为了生存将自然生态系统改造为城镇和农田,原有的生态系统结构及功能退化,甚至丧失了生产力。环境污染、植被破坏、土地退化、水资源短缺、气候变化、生物多样性丧失等增加了对自然生态系统的胁迫。20世纪80年代,恢复生态学(restoring ecology)应运而生(Bradshaw and Chadwick, 1980)。据估计,由于人类对土地的开发导致了全球 $50 \times 10^8 \text{ hm}^2$ 以上土地退化,使全球43%的陆地植被生态系统的服务功能受到了影响(任海等, 2001)。

贫困往往出现在自然恢复力最低、环境破坏最为严重的地区。而对压力和冲击的低恢复能力意味着任何外部事件,都可能使穷人采取使环境进一步退化的行为。我国西部地区的自然生态状况处于令人十分担忧的境地。其总体特征表现是:恶化严重,退化明显,稳定性差,脆弱性强,各项生态指标的优化程度水平较低。其具体的表现形式是:植被稀少、水土流失严重、荒漠化发展加剧,污染强烈,严重削弱了可持续发展的各项基础。目前,全国水土流失面积360多万 km^2 ,西部地区约占80%;全国沙化土地面积已达174万 km^2 ,占国土面积的18.2%,而且大都在西部地区(彭少麟等, 2001)。造成我国水土流失和土地沙化的重要原因是毁林毁草开荒,陡坡耕种。

西部地区是我国大江大河的源头和重要的生态屏障,从生态环境治理入手,全面推进西部大开发,既是推进西部经济与社会发展的根本,也是保证国家生态安全和可持续发展的关键所在,对于世纪中国的发展具有重要意义。退耕还林草工程正是实施西部大开发的切入点和根本所在。

1.2 研究现状

中国北方农牧交错带一直是中国全球变化研究所关注的区域。在气候变化、土地利用和土地覆盖变化、生态脆弱性的成因以及生态治理对策方面取得了较多的成果,然而,有关基础研究仍然很薄弱,特别是在生态恢复与重建、生产力、景观格局变化等前沿理论问题方面(程序, 1999)。“荒漠化是指包括气候变异和人为活动在内的种种因素造成的干旱、半干旱和亚湿润干旱地区的土地退化”,具体包括土壤理化性质的改变、植被覆盖率的下降、生产力的降低、生物多样性的丧失等(UNEP, 1994)。这些变化意味着生态系统服务功能的退化

甚至丧失 (Scheffer et al., 2001)。以荒漠化治理为目标的退耕还林还草可以理解为通过合理配置土地利用方式和土地覆盖类型,促进生态系统服务功能的改善。

在地处北方农牧交错带中部的内蒙古乌盟一带,退耕还林还草有十余年的历史。然而,迄今为止,对退耕还林还草的生态效应只有零星的研究,且主要集中在土壤性质变化方面(苏永中等, 2002; 韩永伟等, 2003; 盛学斌, 2003)。由于基础研究薄弱,在退耕还林还草的具体实施方面,目前普遍存在一定的盲目性,何处还林、何处还草、林草如何配置等,仍然值得探讨。在北方农牧交错带东段的科尔沁沙地一带,对退化生态系统的植被恢复机制有一定的研究基础,特别是在人工固沙植物群落的冗余结构与补偿效应方面取得了进展(姜凤歧等, 2002),对探讨生态系统服务功能的改善机制有一定的指导意义。研究表明,气候变化和土地利用、覆盖的变化是我国北方农牧交错带风沙活动的主要驱动因素(史培军等, 2001)。通过北方农牧交错带关键地段退耕还林还草生态效应研究,可以为制定正确的退耕还林还草政策以及合理开展生态效益补偿提供理论基础。

1.3 本研究的内容与技术路线

本研究从野外样方调查出发,结合实验室工作研究植被与土壤性质的变化,力求在植被演替模式、退耕还林和退耕还草的生态效应比较等方面提出原创性结论。技术路线设计如图 1.1 所示。

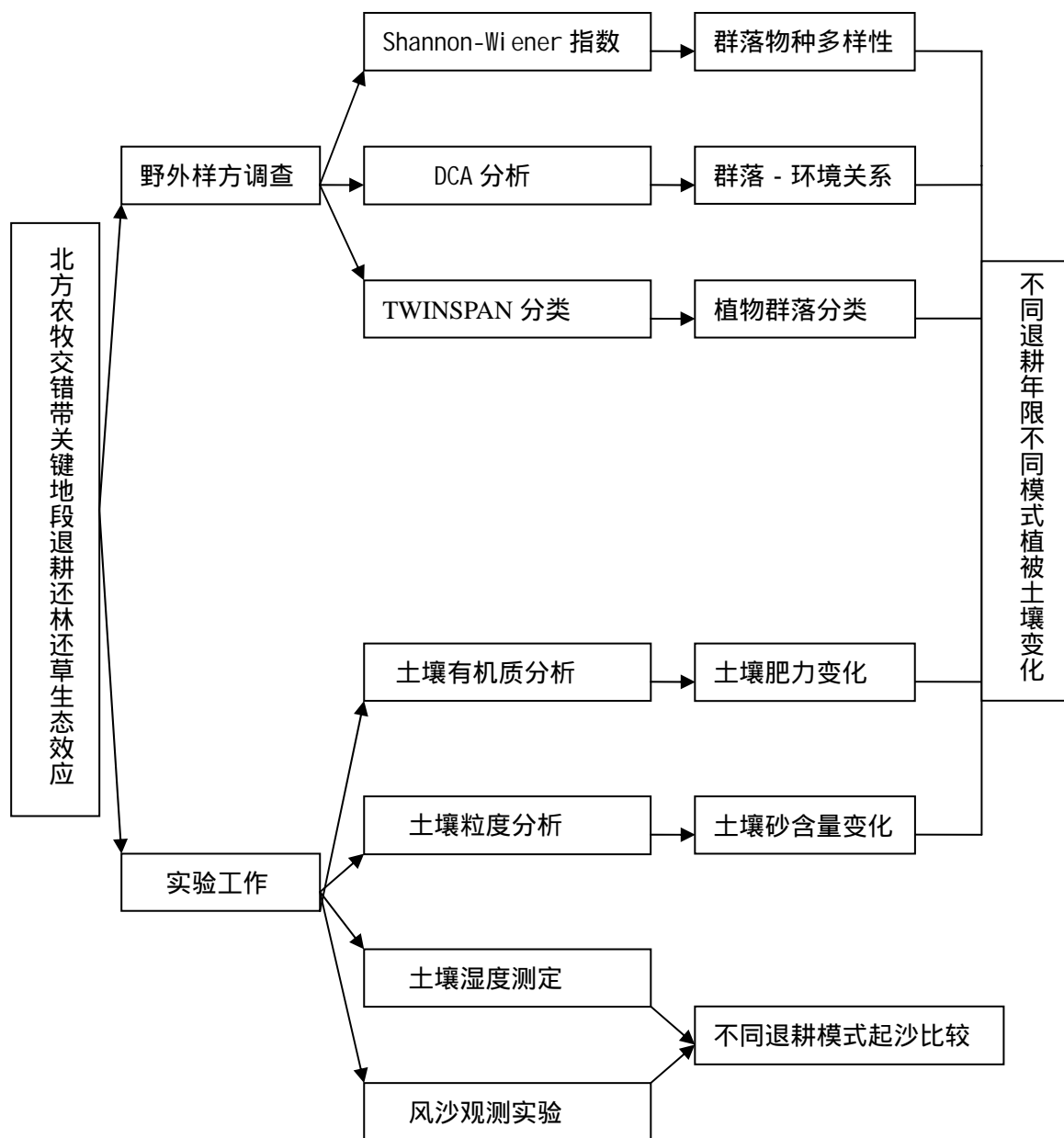


图 1.1 本文技术路线图

Figure 1.1 A framework of this study

第二章 研究区概况

2.1 北方农牧交错带的地理界定和空间分布

关于北方农牧交错带的分布和界定,目前国内已有一些研究报导,但认识不尽相同。如李世奎等(1988)指出,沿着年降水量400mm左右等值线走向的内蒙古高原东南缘和黄土高原北部,是我国近代农牧史上半农半牧交错地带,它位于北部牧区和南部农区之间,把我东部季风农业区与西北干旱、半干旱牧业区分开。王静爱等(1999)认为,中国北方农牧交错带是指我国东北、华北农区与天然草地牧区分隔的生态过渡带,即年平均降水250-500mm的半干旱地区,跨越内蒙古、辽宁、河北、山西、陕西、宁夏等8个省。刘良梧等(1998)认为,中国北方农牧交错带,北起大兴安岭西麓的内蒙古呼伦贝尔,向西南延展,经内蒙古、河北北部、山西北部,直至鄂尔多斯、陕西北部,它是季风气候与大陆性气候,湿润区与干旱区,农区与牧区的过渡地带。

本文参考赵哈林(2002)的看法,将我国北方农牧交错带界定于降水量300-450mm,降水年变率15%-30%,干燥度1.0-2.0范围内,其走向北起大兴安岭西麓的内蒙古呼伦贝尔盟,向南至内蒙古通辽市和赤峰市,再沿长城经河北北部、山西北部 and 内蒙古中南部向西南延展,直至陕西北部、甘肃东北部和宁夏南部的交接地带。东南界为黑龙江的龙江、安达和肇州,吉林的乾安和长岭,辽宁的康平、阜新、建平,河北的平泉、丰宁、怀来,山西的浑源、宁武、五寨,陕西神木、榆林、靖边、甘肃环县,宁夏同心;其西界和北界为内蒙古的陈巴尔虎旗、乌兰浩特、林西、多伦、托克托、鄂托克和宁夏盐池。地理坐标最北为 $49^{\circ}36'N$,最东 $124^{\circ}42'E$,最西 $105^{\circ}45'E$,最南 $36^{\circ}01'N$ 。整个农牧交错带呈带状分布,其东段较宽,最宽处为科尔沁沙地和松嫩沙地,宽度可达300km以上;西段较窄,为毛乌素沙地和黄土风沙区,宽为100-150km;中段为内蒙古锡盟南三旗和河北北部地区,宽200km左右。其行政区划涉及9个省106个旗(县市),总面积 654564km^2 。

2.2 北方农牧交错带的自然地理概况

我国北方农牧交错带大致沿400mm降水等值线两侧分布。降水主要集中于6-8月,占全年降水量的60%-70%,1-3月降水量不足全年降水量的10%。年际间降水变化很大,大部分旗县丰雨年份降水量可达500-600mm,干旱年份则低于250mm,甚至不足100mm。年蒸发量1600-2500mm(赵哈林,2002)。

由于南北跨越 10 多个纬度,区内温度和生长季长短差异很大。如东段科尔沁沙地年均温 $3-7^{\circ}\text{C}$, 10 年积温 $2200-3200^{\circ}\text{C}$, 无霜期 100-140 天;中段的河北坝上地区,虽纬度较低(40°N 左右),但由于海拔较高,年均温仅为 $0-1^{\circ}\text{C}$, 10 年积温只有 $1400-1800^{\circ}\text{C}$, 无霜期 100-120 天;西段毛乌素沙地年均温 $6.0-9.0^{\circ}\text{C}$, 10 年积温为 $2500-3500^{\circ}\text{C}$, 无霜期 130-160 天。该区年均风速 $3.0-3.8\text{m/s}$, 全年 5m/s 起沙风日数约 30-100 天, 8 级大风日数 20-80 天。风季主要发生于每年的 3-6 月,此时地表裸露,表土干燥疏松,是风蚀沙化最易发生的时期(赵哈林, 2002)。

区内地貌类型差异很大。最北端为呼伦贝尔高原,海拔 650-750m,向南至科尔沁沙地,为东北平原与内蒙古高原的过渡地带,海拔 200-700m,向西至河北坝上为内蒙古高原的南缘,海拔 1300-1800m;西部毛乌素沙地地处鄂尔多斯高原,海拔 1400-1500m。土壤类型按地表物质组成大致分为两个类型区,即风沙土覆盖区和黄土覆盖区。其中呼伦贝尔、科尔沁、浑善达克、毛乌素等沙地多为风沙土覆盖,其土壤贫瘠、含沙量高,松散易流动。其余主要为黄土覆盖,其结构疏松,孔隙裂隙多,垂直节理发育,地形破碎,沟壑纵横。另外,还有零星棕钙土和栗钙土分布(赵哈林等, 2002)。

2.3 研究区的典型性和代表性

本文选择农牧交错带中段的内蒙古四子王旗和山西省浑源县进行研究(如图 2.1)。隶属典型草原与荒漠草原的过渡带的内蒙古四子王旗是北方农牧交错带中段的农区北界,生态问题突出。该旗地处乌兰察布盟西北部、阴山北麓风蚀沙化区,是内蒙古自治区乌兰察布盟最大的以牧为主、农牧结合的旗县。全旗历年平均降水量为 150-300 毫米,无霜期不足 110 天,农区属于典型的旱作农业区,牧区一大部分为荒漠化草原。80 年代以来,该旗有 2576 万亩土地不同程度的退化沙化,退化沙化面积已占到该旗总面积的 67%。

1994 年开始,四子王旗开始大面积退耕种树种草。1996 年以前退耕还草模式中采用 10 米草带 1 米柠条带交替种植,后来经过探索逐步调整为 6 米草带 1 米柠条带,直至 2000 年退耕还草模式基本确定为 4 米草带 1 米柠条带。退耕还草以五年为周期种植苜蓿、沙打旺,退耕还林种植榆树和小叶杨,截止到 2002 年该旗累计退耕种树种草 207 万亩。

山西省浑源作为农牧交错带的南缘,2002 年开始退耕,主要种植苜蓿和一些杏树。有耕地、翻耕地、退耕还林地、退耕还草地、天然草地等不同的土地利用类型进行对比研究。

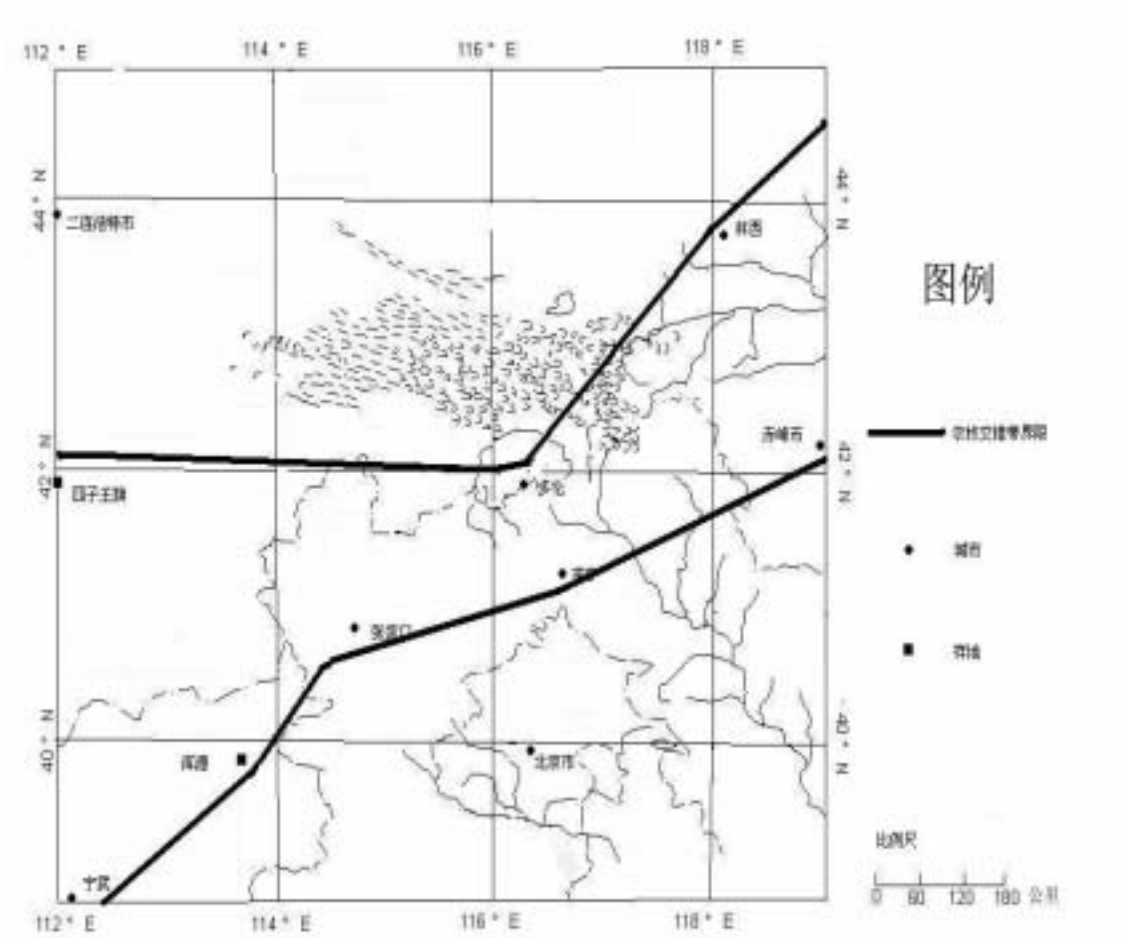


图 2.1 研究区区域示意图

Figure 2.1 A sketch map of the study area

第三章 研究方法

3.1 野外调查

1. 群落调查：

在内蒙古四子王旗研究区内不同的地表覆盖类型下选取具有代表性的地点 53 个。样方规格为灌丛 4×4 米，草甸 2×2 米。每个样方根据全球定位系统（GPS）记录经纬度、海拔以及土地利用状况，并测量记录各物种的名称高度、德氏多度、盖度。

2. 土壤取样：

在每一个取样点，应用梅花型九点取样方法采集表土（0-5cm）样品充分混合并收集，采样量约为 200g。

3.2 实验室分析

1. 土壤粒度分析：

- A. 将土壤样品过筛滤去直径大于 2 毫米的砾石部分，去除植物根系，并用四分法称取 0.75 克左右放入烧杯；
- B. 将样品浸湿后，加入 1:3 的 H_2O_2 10ml 于烧杯中，去出土壤中有机质；
- C. 待有机质全部反应去除后，加热溶液至沸腾去除过量 H_2O_2 ；
- D. 像烧杯中加入过量 HCl（10ml 浓度为 1:3 的 HCl），之后加入去离子水至 150ml，加热至沸腾去除白云石。静置 24 小时后，抛去清液。加入去离子水至 200ml，静置 24 小时后再抛去清液，重复此步骤，直到 200ml 悬浮液呈弱酸性（PH 值 6-7）；
- E. 抽去清液，加入 0.05N 六偏磷酸钠 10ml，再加去离子水至 200ml 后，加热至沸腾持续 5 分钟；
- F. 使用 Malvern2000 激光粒度仪对每个土壤样品进行了粒度分析，测定结果以样品含量小于指定粒径体积百分比输出，将土壤粒度分为以下等级： $<2mm$ ， $<1mm$ ， $<0.5mm$ ， $<0.2mm$ ， $<0.1mm$ ， $<0.063mm$ ， $<0.05mm$ ， $<0.04mm$ ， $<0.03mm$ ， $<0.02mm$ ， $<0.01mm$ ， $<0.005mm$ ， $<0.002mm$ ， $<0.001mm$ 。然后根据粒级划分标准，将土壤机械组成划分为砾石（ $>1mm$ ）、砂（ $0.063-1mm$ ）、粉砂（ $0.002-0.063mm$ ）和黏土（ $<0.002mm$ ）。

2. 土壤有机质分析

将土壤样品充分混合,去除植物根系,然后送到中国科学院地理科学研究所,进行土壤总有机碳和总氮分析。土壤有机质分析采用电热板加热-重铬酸钾容量法,有机质含量以占土壤干重的百分比来表示。

3.3 数据处理

在本研究中,采用 TWINSpan 对样方资料进行二歧分类,然后运用 DCA 排序分析植物群落与环境因子关系,使用的软件为康奈尔生态程序 (Cornell Ecological Program) 的相关程序。采用的数据为样方内不同种类的重要值矩阵。重要值的计算根据以下公式:

$$\text{重要值} = \frac{\text{相对多度} + \text{相对盖度} + \text{相对高度}}{3}$$

在计算过程中,首先对德氏多度进行量化,采取的指标为 Cop3=100、Cop2=75、Cop1=50、Sp=20、Sol=5、Un=1,相对高度的取值统一以营养枝高度为标准。

群落内植物种类多样性的计算采用香农-威纳指数 (Shannon-Wiener Index) 来表示,其计算公式为:

$$H' = - \sum P_i \ln P_i$$

其中 H' 为香农-威纳指数, i 代表样本中的物种数, P_i 为各个物种的重要值。

1. 植物群落分类

TWINSpan 是康奈尔生态程序中的一个等级分类程序,为 U. O. Hill (1979) 所发展。它是对原来的指示种分析的改进,可称为“二元指示种分析”(Two-way Indicator Species Analysis)或“二歧排序分析”(Dichotomized Ordination Analysis)。它通过 RA (Reciprocal Averaging) 相互平均法排序找出有指示意义的种,采用类似于 Braun-Blanquet 表格排列的方式对样方进行分划分类。其最重要的特征是首先构成一个样方的分类,以此分类来得到一个根据种的生态适宜性的种的分类,再用这两个分类一起来得到一个二元的表格,表现出种的群体生态关系。

本文运用 TWINSpan 工具,对四子王旗记录的不同退耕年限的 53 个样方进行群落分析,并试图分析不同群落类型之间的演替关系。

2. 植物群落-环境因子的关系

DCA (Detrended Correspondence Analysis) 无倾向对应分析是对 RA 的实质性改进。其第一轴即 RA 的第一轴,但对以后的轴进行了调整。它避免了 RA 的两个重要问题,即由于

其第二轴对第一轴的二次项依赖性而经常出现的拱形或马蹄形问题，以及在轴终端的压缩。本文根据 DCA 排序的结果，分析不同环境条件和退耕年限对植物群落分异的影响。

3.4 地表起沙观测

在山西浑源县西留乡进行。观测点设于一个 SE 向的坡上，坡度为 10° 。天然草地、耕地、退耕还林地、退耕还草地依次分布于坡顶与坡脚约 3km 的范围内。

将 $170\text{mm} \times 120\text{mm}$ 塑料自封袋置于容积 750ml 的小口瓶中，封口外翻用皮筋绑紧。同样 5 只塑料瓶间隔 25cm 缚于长约 1.5m 的木杆，制成仿楔型集沙器（图 3.1）。在天然草地、耕地（含翻耕地和未翻耕地）、退耕还林地、退耕还草地 5 种土地利用类型中各放置 5 个仿楔型集沙器。取样周期为一周，每次取样将小口瓶中自封袋取出称重以计算观测周期内起沙量，并于小口瓶补充新的自封袋。每种土地利用类型同时取土样测量土壤湿度，以比较不同土地类型的土壤湿度对起沙影响效果。

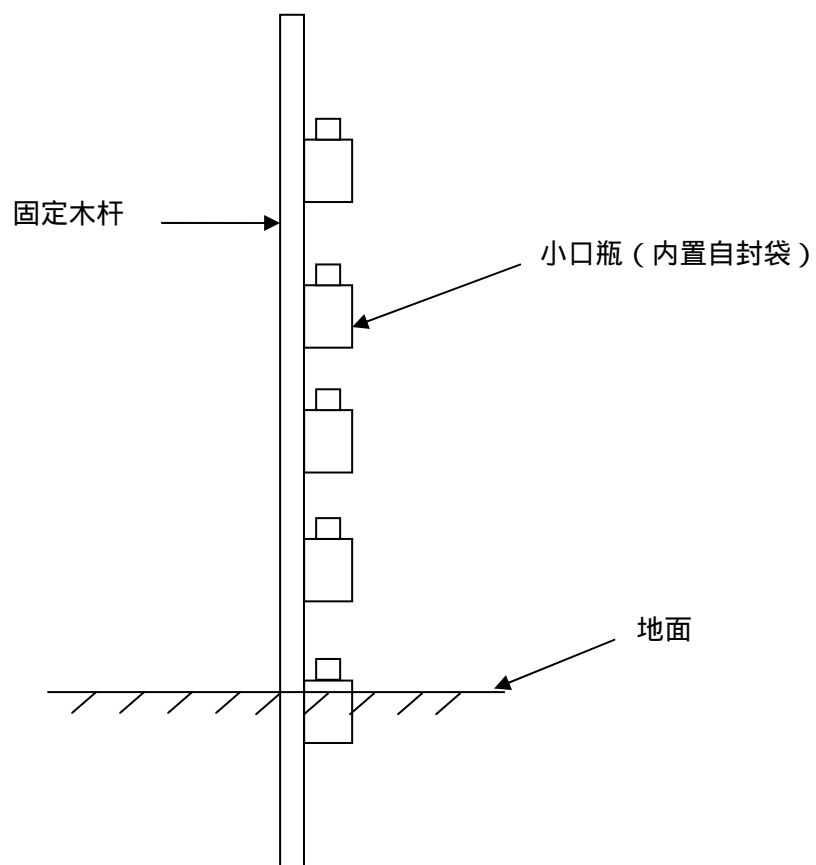


图 3.1 仿楔型集沙器示意图

Figure 3.1 Sketch map of wedge-shaped sand collector

第四章 不同退耕还草年限下植被和土壤性状变化

4.1 退耕还草年限与植被变化分析

1. 群落的 TWINSAN 分类

对四子王旗 53 个样方进行分类，分类结果如图 4.1 所示：

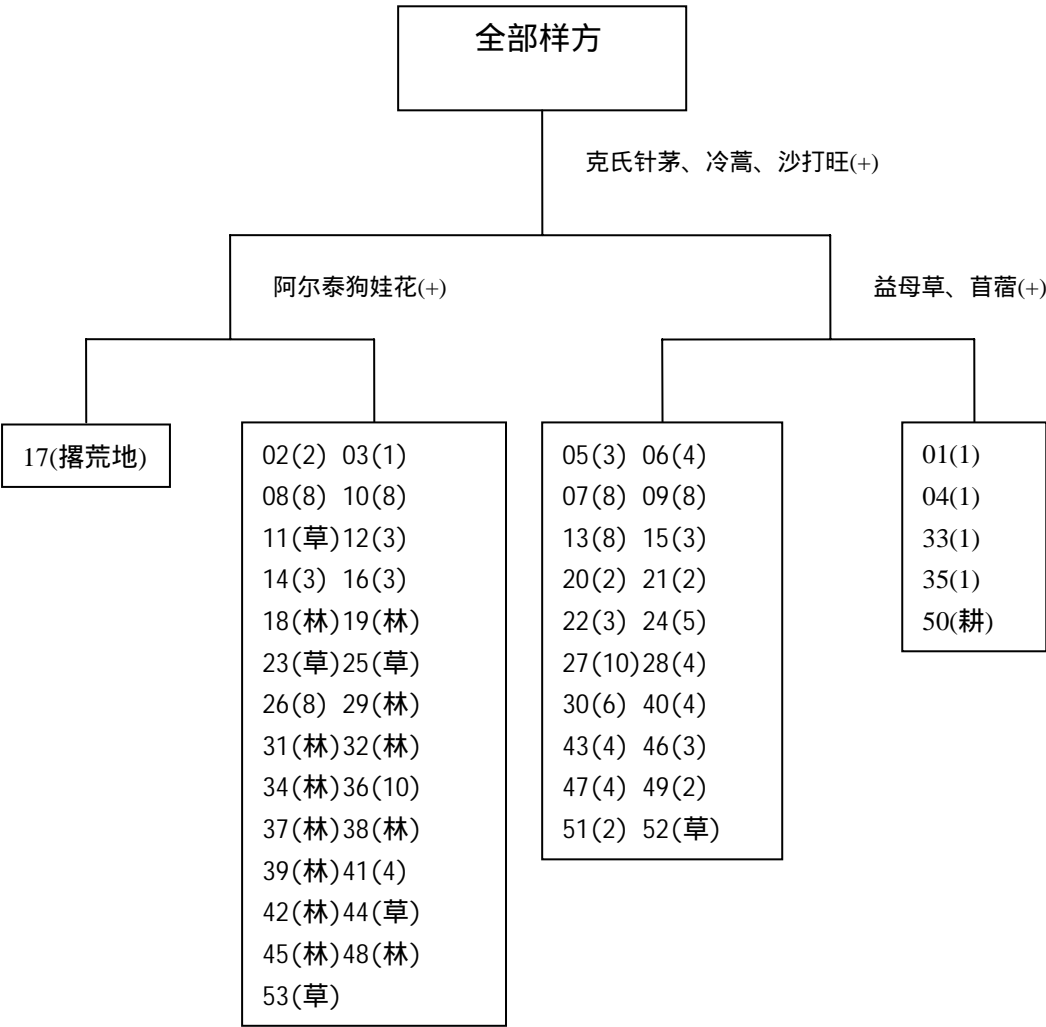


图 4.1 四子王旗样方群落 TWINSAN 分类图

Figure 4.1 TWINSAN classification of sample plots in Siziwang Banner

图中括号外数字为样方序号，括号内数字或文字为退耕年限或土地利用描述

从 TWINSAN 的分类结果来看，四子王旗样方群落可以划分为三个级别。第一级别以克氏针茅（*Stipa krylovii*）、沙打旺（*Astragalus adsurgens*）和中等退化指示植物冷蒿

(*Artemisia frigida*) 为指示种划分出来。第二级别中以中等退化指示植物阿尔泰狗娃花将撂荒地与退耕还林地和退耕还草地加以区分,严重退化指示种益母草(*Leonurus japonicus*) 和人类活动指示种苜蓿(*Medicago sativa*) 将退耕年限不同的样方区别出来。

2. 植物群落 DCA 排序

四子王旗退耕还林还草样地 DCA 排序结果见图 4.2 :

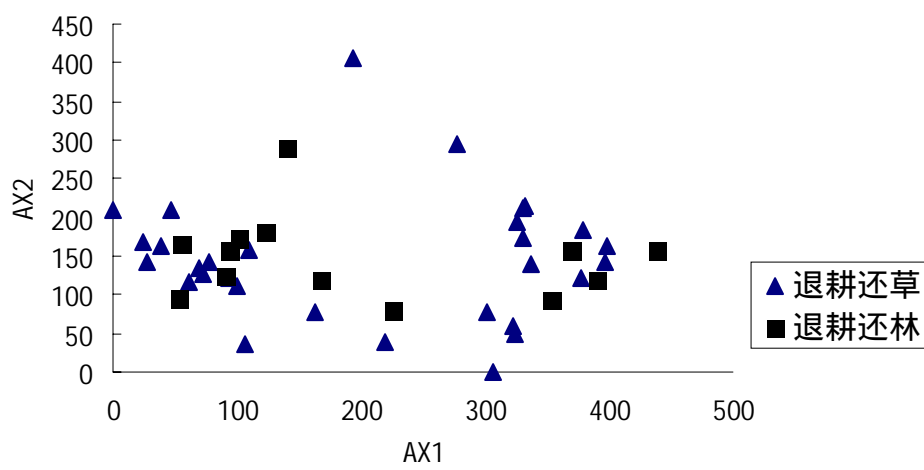


图 4.2 四子王旗样方群落 DCA 排序图

Figure 4.2 DCA Ordination of samples in Siziwangqi

图中退耕还草 DCA 排序结果在两轴的分化并不明显，以两个排序轴数值分别对退耕还草样方进行趋势线拟合，结果如下：

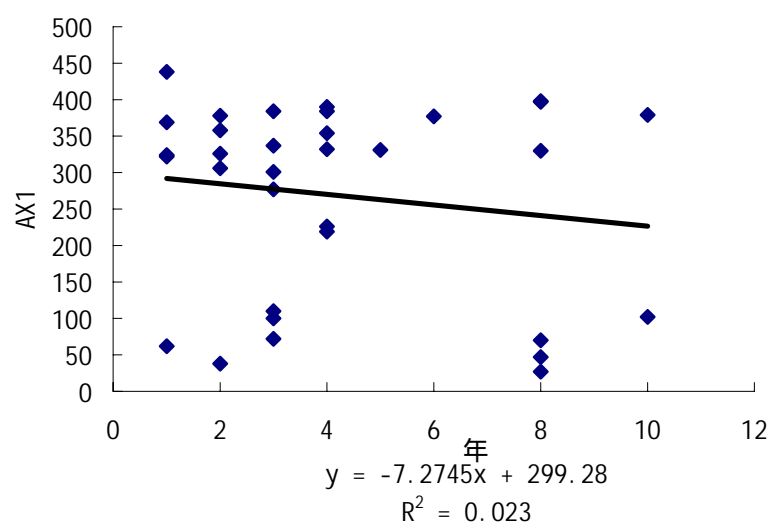


图 4.3 四子王旗退耕还草年限-AX1 轴图

Figure 4.3 AX1 value along years of restoring

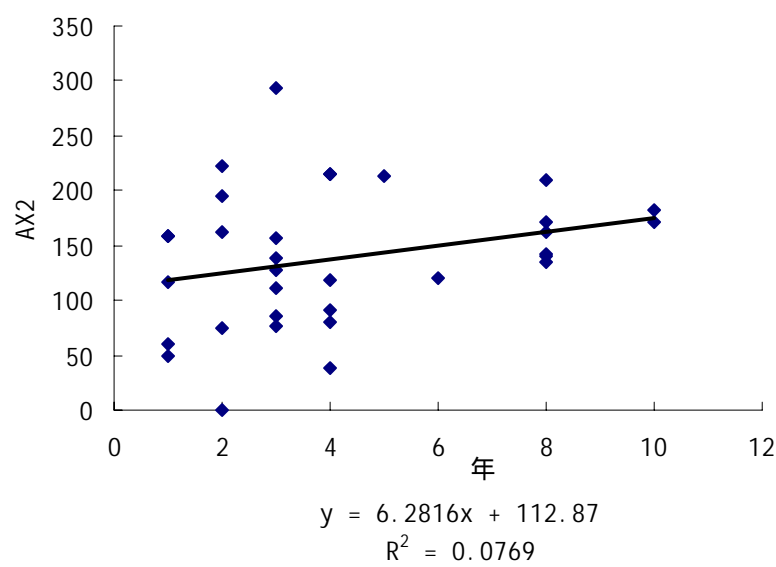


图 4.4 四子王旗退耕还草年限-AX2 轴图

Figure 4.4 AX2 value along years of restoring

由结果不难看出四子王旗样方群落 DCA 排序结果两轴与退耕年限几无相关关系。完全不同于自然群落植被的演替过程，原因在于研究区的退耕还草工程中人为控制了苜蓿、沙打旺的种植周期。

4.2 土壤性状的变化

研究区不同退耕还草年限下土壤 TOC 含量与退耕年限关系如图 4.5 所示

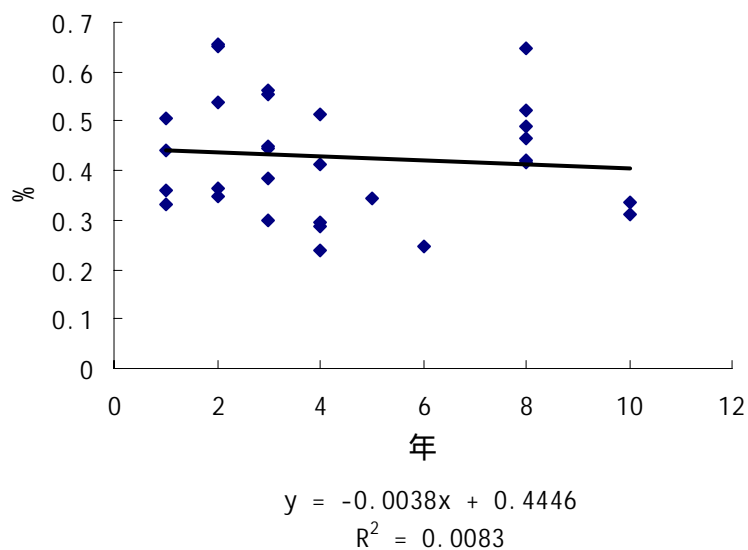


图 4.5 四子王旗退耕还草年限-土壤 TOC 图

Figure 4.5 TOC along Years of Restoring

从图 4.5 可以看出,土壤 TOC 百分比与退耕年限几无相关关系,人为种植作物对土壤性质改良没有显著效果。

第五章 不同植被恢复模式下植被与土壤性状变化的比较

5.1 植物群落类型的变化

将退耕还林还草样方中出现的 85 个物种和该样方退耕年限列表表示 (表 5.1)。

表 5.1 不同退耕年限样方中出现物种

Table 5.1 Species in sample plots of different restoring years

严重退化指示植物\退耕年限	1	2	3	4	6	8	10	20*
狗尾草 <i>Setaria viridis</i>	+	+	+	+	+	+	+	+
苦苣菜 <i>Ixeris denticulata</i>	+	+	+	+	+	+	+	+
田旋花 <i>Convolvulus arvensis</i>	+	+	+	+	+	+		
茵陈蒿 <i>A. capillaris</i>	+	+	+	+			+	+
苍耳 <i>Xanthium sibiricum</i>	+	+	+	+				+
蒙古冰草 <i>Agropyron mongolicum</i>	+	+	+			+		+
刺穗藜 <i>Chenopodium aristatum</i> L.	+	+	+	+				
益母草 <i>Leonurus japonicus</i>	+	+	+	+				
鹤虱 <i>Lappula myosotis</i>	+	+		+				+
页蒿 <i>Carum carvi</i>		+		+			+	+
藜 <i>Chenopodium album</i>	+			+				+
太阳花 <i>Polygonum capitatum</i>		+	+		+			
平车前 <i>Plantago depressa</i>						+	+	+
黄蒿 <i>Artemisia annua</i>	+			+				
刺沙蓬 <i>Salsola pestifer</i>			+			+		
地蔷薇 <i>Chamaerhodos erecta</i>							+	+
硬质早熟禾 <i>Poa sphondylodes</i>							+	+
扁蓄 <i>Polygonum aviculare</i>	+							
滨藜 <i>Atriplex patens</i>	+							
草木樨 <i>Melilotus suaveolens</i>	+							
打碗花 <i>Calystegia hederacea</i>	+							
大籽蒿 <i>A. sieversiana</i>				+				
鬼针草 <i>Bidens bipinnata</i>						+		
大画眉草 <i>Eragrostis cilianensis</i>								+
野亚麻 <i>Linum steuroides</i>								+
退化指示植物\退耕年限	1	2	3	4	6	8	10	20
阿尔泰狗娃花 <i>Heteropappus altaicus</i>	+	+	+	+	+	+	+	+
猪毛菜 <i>Salsola collina</i>	+	+	+	+	+	+	+	+
冷蒿 <i>Artemisia frigida</i>	+	+	+	+	+	+		+
变蒿 <i>Artemisia pubescens</i>	+	+	+	+		+	+	+
糙隐子草 <i>Cleistogenes squarrosa</i>	+	+	+	+		+	+	+
猪毛蒿 <i>Artemisia scoparia</i>	+	+	+			+	+	+
赖草 <i>L. secalinus</i>		+		+	+	+		+
沙生冰草 <i>Agropyron cristatum</i>			+	+		+	+	+
高二裂委陵菜 <i>Potentilla bifurca</i> var.		+	+	+				+

小叶锦鸡儿 <i>Caragana microphylla</i>	+	+				+		
阿氏旋花 <i>Convolvulus ammannii</i>		+	+			+		
百里香 <i>Thymus serpyllum</i>			+			+		+
麻花头 <i>Serratula centaurooides</i>	+		+					
刺儿菜 <i>Cirsium segetum</i>	+			+				
马蔺 <i>Iris ensata</i>							+	+
硬阿魏 <i>Ferula bungeana</i> Kitag.							+	+
蝟菊 <i>Olgaea lomonosowii</i>			+					
轮叶委陵菜 <i>P. verticilaris</i>						+		
沙珍棘豆 <i>Ostryopsis gracillima</i>								+
非退化指示植物\退耕年限	1	2	3	4	6	8	10	20
糙叶黄芪 <i>Astragalus scaberimus</i>	+	+	+	+		+	+	+
克氏针茅 <i>Stipa krylovii</i>	+	+	+	+		+	+	+
扁蓿豆 <i>Pocockia ruthenica</i>		+	+	+		+	+	+
蒙古韭 <i>Allium mongolicum</i>	+	+	+			+		+
草地风毛菊 <i>Saussurea amara</i>	+		+	+		+	+	
扁茎黄芪 <i>Astragalus complanatus</i>		+		+		+	+	+
蒲公英 <i>Taraxacum mongolicum</i>			+	+	+		+	+
冬青叶兔唇花 <i>Lagochilus ilicifolius</i>	+	+	+			+		
香青兰 <i>Dracocephalum moldavica</i>	+		+	+				+
苁蓉 <i>Cistanche deserticola</i>			+	+			+	+
羊草 <i>Leymus chinensis</i>		+	+				+	
大苞鸢尾 <i>Iris bungei</i> Maxim.			+			+		+
狗舌草 <i>Senecio campestris</i>	+		+					
达乌里苘蓓 <i>Cymbaria dahurica</i>	+					+		
苣荬菜 <i>Sonchus arvensis</i>		+		+				
菊叶委陵菜 <i>Potentilla tanacetifolia</i>						+		+
北芸香 <i>Haplophyllum dauricum</i>		+						
戈壁天门冬 <i>Asparagus gobicus</i>		+						
细叶远志 <i>Polygala tenuifolia</i> Willd.			+					
东亚唐松草 <i>Thalictrum minus</i>								+
旱麦瓶草 <i>Silene jenssenensis</i>								+
披针叶黄华 <i>Thermopsis lanceolata</i>					+			
黄芩 <i>Scutellaria baicalensis</i>								+
堇色早熟禾 <i>Poa annua</i>								+
鳞萼棘豆 <i>Oxytropis squamulosa</i>								+
柳穿鱼 <i>Linaria vulgaris</i>						+		
轮叶棘豆 <i>Oxytropis chiliophylla</i>								+
米口袋 <i>Geldendstaedtia verna</i>								+
乳浆大戟 <i>Euphorbia esula</i>								+
山莴苣 <i>Lagidium sibiricum</i>				+				
头状丝石竹 <i>Gypsophila oldhamiana</i> Miq.						+		
无芒隐子草 <i>Cleistogenes songorica</i>						+		
狭叶米口袋 <i>Geldendstaedtia stenocephala</i>						+		

斜茎黄芪 <i>Astragalus adsargens</i>							+	
野艾蒿 <i>Artemisia lavandulaefolia</i>								+
早熟禾 <i>P. annua</i>								+
人为种植植物\退耕年限	1	2	3	4	6	8	10	20
苜蓿 <i>Medicago sativa</i>	+	+	+	+	+	+	+	+
沙打旺 <i>Astragalus adsurgens</i>	+	+	+	+	+	+	+	
白花草木樨 <i>Melilotus albus</i>	+	+	+	+	+	+	+	
黄花草木樨 <i>Melilotus officinalis</i>	+		+	+		+		
柠条 <i>Caragana korshinskii</i>			+	+		+		

*退耕还林年限以 20 表示

从表 5.1 可以清晰地看出 ,退耕年限达到 6 年的样方中严重退化指示植物刺穗藜、鹤虱、黄蒿、益母草已经消失了 ,在一定程度上显示了土地退化的恢复。狗尾草、猪毛蒿、阿尔泰狗娃花三物种在所有退耕年限样方中均有出现 ,构成了草本植物的主体 ,苜蓿、沙打旺作为灌木的优势种出现是人为种植作物的结果。在退耕还林地中 ,大量的多年生草本植物出现 ,如东亚唐松草、鳞萼棘豆、米口袋、乳浆大戟、野艾蒿、早熟禾、旱麦瓶草、黄芩、董色早熟禾。由于退耕还林地中一直没有禁牧 ,一年生的严重退化指示植物也较多出现。

5 . 2 群落内物种多样性的变化

分别计算退耕还林与退耕还草样地的 Shannon-Wi ener 指数 ,见表 5.2。

表 5.2 所有样地物种的香农-威纳指数

Table 5.2 Shannon-Wi ener Index of species in all sample plots

编 号	退耕 年限	Shannon-Wi ener 指数	编 号	退耕 年限	Shannon-Wi ener 指数	编 号	退耕 年限	Shannon-Wi ener 指数
1	1	1.6357	46	3	1.5601	36	10	2.6319
2	1	2.6405	6	4	2.1792	11	20*	2.0210
4	1	1.3656	28	4	2.1917	18	20	1.9309
33	1	1.6865	40	4	1.6267	19	20	1.9387
35	1	1.9635	41	4	2.1128	29	20	1.8428
3	2	2.3110	43	4	1.4559	31	20	2.0890
20	2	1.6377	47	4	1.2297	32	20	2.3747
21	2	2.3042	24	5	1.7597	34	20	1.9544
49	2	1.7444	30	6	1.5992	37	20	1.9285
51	2	1.7092	7	8	1.3989	38	20	2.7131
5	3	2.0092	8	8	2.3497	39	20	2.3191
12	3	2.2132	9	8	1.6854	42	20	2.2600
14	3	2.2036	10	8	2.2481	45	20	2.1530
15	3	1.7741	13	8	2.1192	48	20	2.3100
16	3	2.2428	26	8	2.1331			
22	3	2.0435	27	10	1.5369			

*退耕还林年限以 20 表示

对不同退耕年限样地做均值标准差分析，得出以下结果：

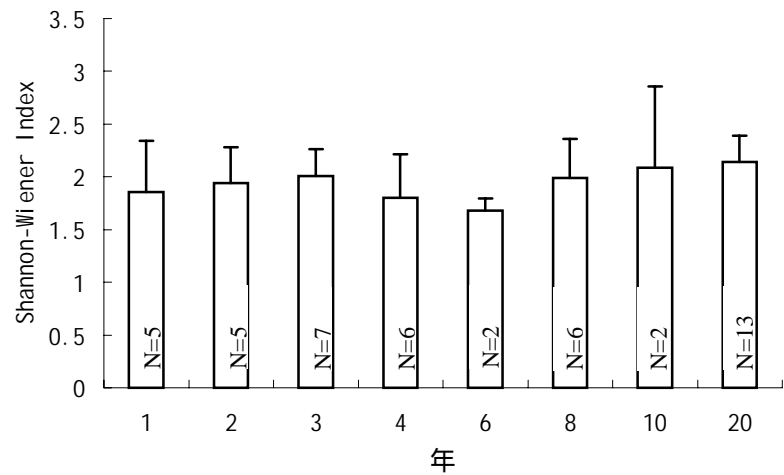


图 5.1 香农-威纳指数均值标准差图

Fig. 5.1 Shannon-Wiener Index Average and standard deviation

由图 5.1 中看出还林还草样方比较起来，虽然 Shannon-Wiener 指数均值波动不大，但仍然可以看出还林样方的 Shannon-Wiener 指数最高，从物种多样性角度考虑，退耕还林的成效优于退耕还草。

5.3 退耕还林与退耕还草模式下土壤性状变化

1. 退耕还林与退耕还草对土壤砂、粉砂和黏土含量的影响

对不同退耕年限样地的土壤做均值方标准差分析，得出以下结果（图 5.2、5.3、5.4）。

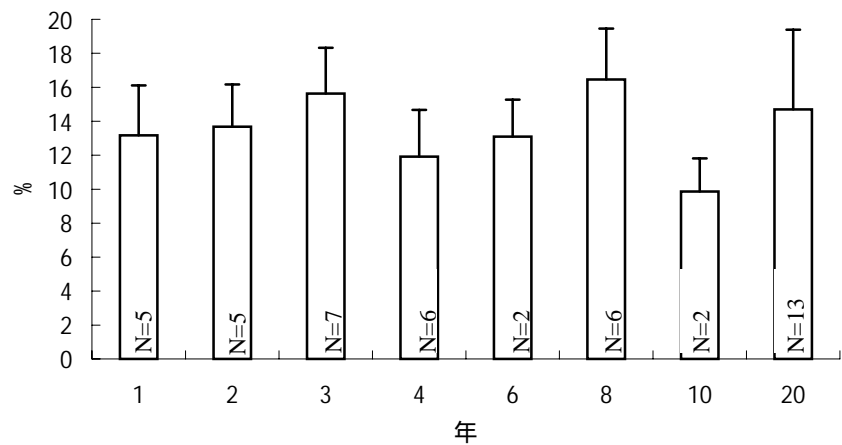


图 5.2 土壤砂含量均值标准差图

Figure5.2 Average and standard deviation of soil sand content

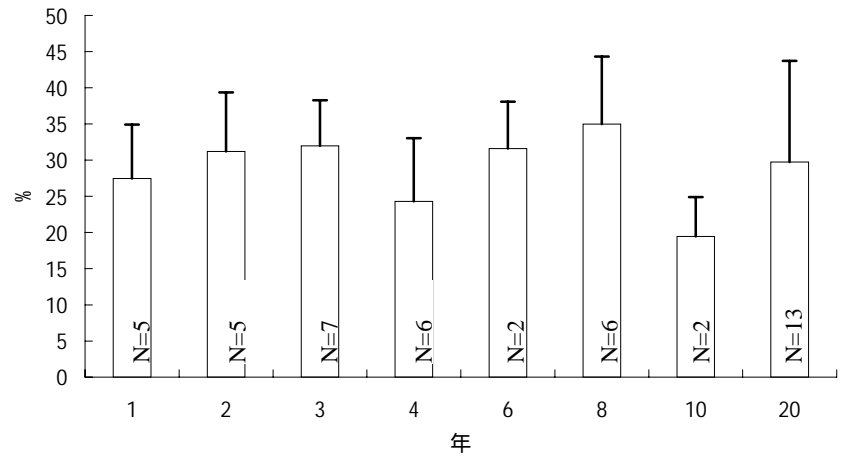


图 5.3 土壤粉砂含量均值标准差图

Fig. 5.3 .Average and standard deviation of soil silt content

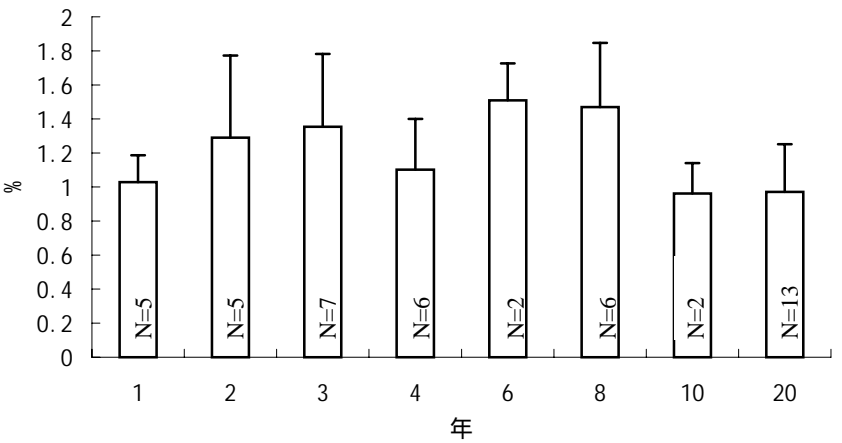


图 5.4 土壤黏土含量均值标准差图

Figure 5.4 Average and standard deviation of soil clay content

砂含量的降低是退耕还林还草生态效应的重要体现。从图 5.2、5.3、5.4 中可以看出不同年限退耕还草对土壤砂（0.063-1mm）、粉砂（0.002-0.063mm）和黏土（<0.002mm）含量的影响是有波动的，然而退耕还林与退耕还草相比没有能带来土壤砂含量的显著下降，由于退耕还林的效果至少需要 20 年时间才能得到明显体现，如果仅从均值以及时间方面考虑的话，显然退耕还草防沙效用要好于退耕还林。

此外，从图 5.2、5.3、5.4 中可以看出由于人为以五年为周期种植作物翻耕土地导致土壤中砂、粉砂和黏土含量以五年为周期变化，每五年出现最低值。

2. 土壤 TOC 与总氮含量分析

土壤有机质分析结果如表 5.2 所示：

表 5.2 土壤 TOC 与氮含量百分比

Table 5.2 Percentage of TOC and Nitrogen

编 号	退耕 年限	TOC(%)	全氮(%)	碳氮 比值	编 号	退耕 年限	TOC(%)	全氮(%)	碳氮 比值
1	1	0.44	0.058	7.521	7	8	0.464	0.053	8.672

2	1	0.506	0.063	8.006	8	8	0.488	0.069	7.082
33	1	0.331	0.048	6.824	9	8	0.416	0.067	6.172
35	1	0.361	0.05	7.234	10	8	0.648	0.087	7.456
3	2	0.654	0.085	7.649	13	8	0.523	0.072	7.233
20	2	0.348	0.046	7.598	26	8	0.422	0.057	7.442
21	2	0.653	0.077	8.447	27	10	0.31	0.042	7.451
49	2	0.366	0.06	6.151	36	10	0.337	0.051	6.607
51	2	0.537	0.078	6.875	11	20	0.414	0.061	6.775
12	3	0.561	0.074	7.53	18	20	0.195	0.037	5.227
14	3	0.555	0.087	6.35	19	20	0.428	0.063	6.815
15	3	0.446	0.063	7.056	29	20	0.436	0.063	6.942
16	3	0.301	0.043	7.049	31	20	0.638	0.065	9.845
22	3	0.451	0.056	8.024	32	20	0.477	0.056	8.503
46	3	0.384	0.049	7.773	34	20	0.413	0.062	6.715
28	4	0.24	0.041	5.783	37	20	0.33	0.045	7.3
40	4	0.414	0.051	8.198	38	20	0.754	0.091	8.313
41	4	0.514	0.06	8.509	39	20	1.418	0.166	8.542
43	4	0.287	0.053	5.405	42	20	0.658	0.077	8.567
47	4	0.295	0.04	7.449	45	20	0.289	0.04	7.261
24	6	0.342	0.052	6.621	48	20	0.406	0.056	7.25
30	6	0.246	0.037	6.684					

对不同退耕年限样地做均值方标准差分析，得出以下结果：

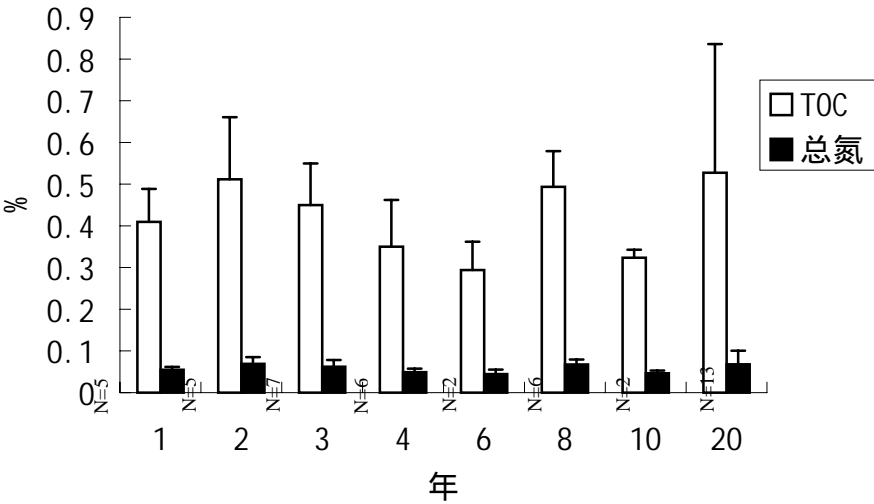


图 5.5 土壤 TOC 与氮含量均值标准差图

Table 5.5 TOC and Nitrogen Average and standard deviation

土壤 TOC 是土壤性状改良程度的有效指示，从图 5.5 中可以看出受到人为以五年为周期种植作物翻耕土地的影响，退耕还草对土壤性状的改良波动很大，相对来讲退耕还林对土壤改良效果优于还草。

土壤的氮含量则指示了人工施肥对土壤的影响，从图 5.5 中可以看出，已经退耕不再施肥的土壤氮含量没有任何下降趋势，说明人为种植苜蓿等豆科植物对土壤起到了固氮的作用。

5 . 4 不同退耕还林还草模式下地表起沙的观测结果

在长达 2 个月的山西浑源地表覆盖与风蚀的关系观测工作中，仅于 2004 年 3 月 21 日观测到 1 次沙尘暴天气，降沙量计算如表 5.3 所示。

表 5.6 不同土地类型起沙结果

Table 5.3 The sand quantity result of different land use types

耕地类型\起沙质量（克）	1 号瓶*	2 号瓶	3 号瓶	4 号瓶	5 号瓶	平均质量
翻耕地	2.58	2.73	2.56	-	2.71	2.64
耕地	2.36	2.73	2.28	2.69	2.59	2.53
退耕还林地	2.43	2.21	2.2	2.35	2.32	2.3
退耕还草	—	—	2.23	—	2.31	2.27
天然草地	2.38	2.63	2.21	2.37	2.25	2.37

*1 - 5 号瓶分别为离地面 5cm 处的 5 个平行样，在离地面的其它高度没有接收到沙尘，—表示数据缺失

从表 5.6 可以看出，退耕后不同土地利用类型在同一次沙尘天气中起沙量是有区别的。翻耕地由于土质疏松所以起沙量多余其他土地类型，退耕还林还草地对阻沙起到了一定效用。

第六章 讨论与结论

6.1 植被恢复与土壤恢复的关系分析

在第四章不同退耕还草年限下和第五章不同植被恢复模式下植被和土壤性状的分析基础上,本章探讨植被变化与土壤变化关系,对相同退耕年限样方土壤 TOC 与 Shannon-Wiener 指数作相关分析,结果如图 6.1 所示。

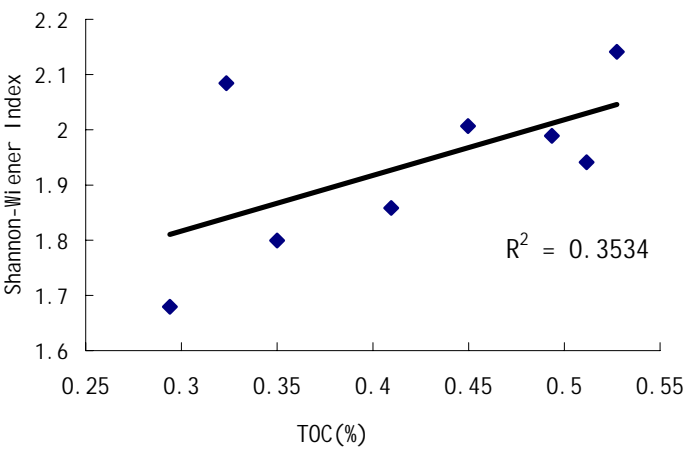


图 6.1 相同退耕年限样方土壤 TOC 与 Shannon-Wiener 指数

Fig. 6.1 Relationships between TOC and Shannon-Wiener Index in the same year of restoring

从图 6.1 中可以看出相同退耕年限样方土壤 TOC 与 Shannon-Wiener 指数呈正相关趋势, R^2 达到 0.35, 说明土壤性状的改良对物种多样性的增加有明显作用。

6.2 结论

- 通过本研究可以得到一下初步结论：
- 1. 人为控制了苜蓿、沙打旺的种植周期的退耕还草工程对土壤起到了固氮的作用，虽然对土壤性质改良没有显著效果,但却使得退耕还草后植物群落完全不同于自然群落植被的演替过程，退耕年限达到 6 年后严重退化指示植物消失，退耕还草效用体现出来。
 - 2. 退耕还林与退耕还草均起到了阻沙作用。物种多样性与土壤有机质含量、土壤氮含量等方面的结果表明，退耕还林的成效优于退耕还草。但退耕还草在降低土壤砂含量方面效果相对明显。
 - 3. 退耕还林还草所带来的植被物种多样性变化与土壤性状变化存在正相关关系，说明土壤性状的改良对物种多样性的增加有明显作用。

参考文献

- Bradshaw, AD and Chadwick MJ, 1980, The restoration of Land. Oxford, Blackwell.
- Sheffer, M, Carpenter S, Foley, JA, Folke, C, Walker, B, 2001, Catastrophic shifts in ecosystems, *Nature*, 413: 591-596
- UNEP. 1994, United Nations convention to combat desertification in those countries experiencing serious drought and or desertification, particularly in Africa. Geneva: United Nations Environment Programme for the Convention to Combat Desertification (CCD), Interim Secretariat for the CCD.71.
- 程序, 1999, 农牧交错带研究中的现代生态学前沿问题, *资源科学*, 21(5)。
- 韩永伟, 2002, 农牧交错带退耕还草对土壤物理性状的影响, *草地学报*, 10(2)。
- 姜凤岐, 曹成有, 曾德慧, 2002, 科尔沁沙地生态系统退化与恢复, 中国林业出版社。
- 李世奎, 王石立, 1988 中国北部半干旱地区农牧气候界线探讨, 中国干旱半干旱地区自然资源研究, 中国自然资源协会等编, 科学出版社。
- 刘良梧, 周建民, 刘多森 1998 农牧交错带不同利用方式下草原土壤的变化, *土壤*, (5): 225-229
- 任海, 彭少麟, 2001, 恢复生态学导论, 科学出版社。
- 盛学斌, 刘云霞, 孙建中, 2002, 农牧交错带土壤及某些表生植被特性变异与荒漠化的相关性——以冀北康保县为例, *应用生态学报*, 13(7): 909-910。
- 史培军, 严平, 袁艺, 2001, *第四纪研究*, 21(1)。
- 苏永中, 2002, 退化沙质草地开垦和封育对土壤理化性状的影响, *水土保持*, 16(4)。
- 孙武, 李保生, 1999, 荒漠化分类分级理论的初步探讨, *地理研究*, 18(3): 225-230。
- 王静爱, 徐霞, 刘培芳 1999 中国北方农牧交错带土地利用与人口负荷研究, *资源科学*, 21(5): 19-24。
- 赵哈林, 赵学勇, 张铜会, 周瑞莲, 2002, 北方农牧交错带的地理界定及其生态问题, *地球科学进展* 17(5)。
- 赵哈林, 周瑞莲, 张铜会, 赵学勇, 2003, 我国北方农牧交错带的草地植被类型、特征及其生态问题, *中国草地*, 25(3)。

致谢

本论文是在刘鸿雁老师的指导下完成的。从我进入北京大学生态系第一天起，刘老师无微不至的关怀伴我走过了本科学习的最后两年时光，这是我茫茫人生中最有收获的两年。刘老师精湛的专业理论、严谨的治学态度、敏锐的思维视野和独特的研究思路是我终身学习和追求的治学境界！两年来，导师带给我的不仅仅是知识，更有做人、做学问的原则和态度，我对有这样的导师深感荣幸，在此向导师致以衷心的感谢和最诚挚的敬意！

在学习和论文期间，我得到了许多老师和朋友的无私帮助，我的工作和成果是在他们的共同参与下完成的。在此我要感谢资源与环境学地理系王红亚老师在生产实习中的指导，马军老师和中科院地球所的杨京蓉老师在土壤实验中的教诲，生态学系沈泽昊老师在软件使用上的讲解，我还要感谢师姐邢秋如、朱江玲、师兄纪中奎，以及我宿舍同学还有和我一起野外实习的温雨金、王同学的帮助，我的学习片断都永远留下了他们的影子。

最后，向百忙中抽出宝贵时间对本论文进行评审的各位老师致以最深切的敬意，感谢你们辛勤的评阅和闪烁着真知灼见的指教！

再次谢谢你们，所有关心、支持和帮助过我的老师和同学们！

本科论文



北京大学

本科生毕业论文

400mm等雨量线沿线森林群落的种类多样性及影响因子

Plant species diversity of forests along the 400 mm annual
precipitation isopleth and its affecting factors

姓 名： 曹 善 平

学 号： 00313072

院 系： 环境学院

专 业： 生态 学

导 师： 刘鸿雁 教授

二零零七年六月

摘要

生物多样性的空间格局及影响因子是生物多样性研究的热点问题,以往的研究较多沿环境梯度进行,或在一些热点地区进行区域尺度的生物多样性研究。虽然有大量研究集中在森林-草原交错带进行,然而由于影响生物多样性的环境因子复杂多样且彼此相互作用,影响生物多样性的空间格局的因子往往难以确定。

在 400mm 等雨量线附近,森林处于生长的干旱极限,植被类型表现为森林和草原的过渡,植物区系兼有森林和草原的成分。由于降水量接近,有助于分析其他因素对于多样性格局的影响。本研究通过沿 400mm 等雨量线进行不同纬度不同地点的实地调查,总结植物种类多样性的空间格局,并通过多元统计分析的方法,解释影响多样性格局的因子。

结果显示,400mm 等雨量线森林群落草本植物多样性具有明显的地理梯度,1 月均温、年均温和坡度与多样性指数、丰富度指数显著相关,是显著影响多样性格局的环境因子,同时近 50 年降水波动状况对多样性格局也具有显著影响。

关键词: 400mm 等雨量线, 物种多样性, 空间格局, 环境因子, 降水波动

Abstract

The spatial pattern of biodiversity and its controlling factors are key issues of ecological study. Traditional researches are mostly based on environmental gradients, or regional-scaled located in hotspots. Although there are a lot of researches carried out in forest-steppe ecotone, the controlling factors of biodiversity spatial pattern are uncertain due to the complexity of environmental factors and their interrelationship.

Forest finds it dry extreme on 400 mm annual precipitation isopleths. Vegetation types are found to be transitional from forest to steppe, and biome is constituted by both forest and steppe composition. Since precipitation is close in quantity, the other possible influences on biodiversity are easily understood. This study is based on surveys of different sites on different latitudes. It summarizes the spatial pattern of species diversity, and explains the controlling factors.

The results show a significant gradient on longitude and latitude, as well as mean temperature of January, mean annual temperature, slope, and correlation with diversity indices, abundance indices. Those are all environmental factors that contribute to the formation of biodiversity spatial pattern. Also, the fluctuation in precipitation in the past 50 years significantly influences the diversity pattern.

Key Words: 400 mm annual precipitation isopleths, species diversity, spatial pattern, environmental factor, Precipitation fluctuation

目 录

摘 要.....	I
ABSTRACT	II
第一章 前言.....	1
1. 1 科学问题.....	1
1. 2 研究进展	1
1.2.1 不同植被类型的植物多样性格局及成因	1
1.2.2 林冠层对于林下植物多样性格局的影响	3
1.2.3 地形条件对植物多样性格局的影响	3
1. 3 本文内容框架	4
第二章 研究区域概况.....	5
2.1 研究区自然状况	5
2.2 研究区选择依据	6
第三章 研究方法.....	6
3.1 野外调查取样	6
3.2 气象台站气候数据处理	8
3.3 数据分析	11
3.3.1 林下草本植物重要值.....	11
3.3.2 物种丰富度指数.....	11
3.3.3 α 多样性指数.....	11
3.3.4 种面积曲线.....	12
3.3.5 相关分析.....	12
第四章 结果.....	12
4.1 野外调查结果	12
4.1.1 研究区地形格局.....	12
4.1.2 植被群落类型	14
4.1.3 林下植物科属划分	16
4.2 林下植物分布空间格局	17
4.2.1 林下草本植物分布空间格局	17
4.2.2 林下灌木分布空间格局	17
4.3 林下草本植物种类多样性空间格局	19
4.4 气象台站气候资料回归结果	24
4.4.1 23 个点气候因子数据	24
4.4.2 23 个地点近 50 年降水量年际变化	26
4.5 多样性影响因子分析	26
4.5.1 环境因子.....	26
4.5.2 近 50 年降水波动影响	28
第五章 讨论.....	29
5.1 400mm 等雨量线林下草本植物种类多样性空间格局特征	29

5.2 400mm 等雨量线林下草本植物种类多样性空间格局影响因子	29
5.3 人为活动对多样性的影响	30
第六章 结论.....	31
附录 1 林下草本植物名录	34
附录 2 林下灌木植物名录	42
附录 3 林下草本植物分布格局	44

第一章 前言

1. 1 科学问题

由于影响生物多样性的环境因子复杂多样且彼此相互作用,影响生物多样性空间格局的因子往往难以确定。在 400mm 等雨量线附近,森林处于生长的干旱极限,植被类型表现为森林和草原的过渡,植物区系兼有森林和草原的成分。由于降水量接近,有助于分析其他因素对于多样性格局的影响。在降水量近似的情况下,热量条件与种类多样性是否存在正比关系 (Evans et al,2005)? 另一方面,中国 400mm 等降雨量线附近的近 50 年以来降水量的波动明显,是否对森林植物种类多样性存在明显影响甚至有决定性作用也未得到证实。本文试图根据中国 400mm 等雨量线东段的调查结果,探讨干旱极限附近森林植物多样性格局的影响因子。

1. 2 研究进展

1.2.1 不同植被类型的植物多样性格局及成因

生物多样性的空间格局及影响因子是生物多样性研究的热点问题。较多的研究沿环境梯度进行,如海拔梯度。但单一的地形梯度往往包括温度和水分的不同组合,给认识生态因子的相互作用带来困难。

区域尺度生物多样性及其影响因子往往在一些热点地区进行,如热带雨林。南美洲亚马逊流域的林分和功能有着两个明显的梯度变化,一个与土壤肥力的主要梯度相吻合,一个与干季长度变化梯度相吻合。并且种子质量的大小可能是决定优势种分布的因素,而不是根系对土壤的适应 (Steege, et al., 2006)。这一地区植物种类多样性的复杂成因给进一步的环境解释带来一定的困难。不同学者从不同角度出发得到 4 种经常被用来解释森林高物种多样性的机制:生态位分布、取食压力、生活史负相关和随机竞争。热带森林植物沿微环境梯度的非随机空间分布表明其生态位分化很明显,并对其多样性起重要作用。动物的取食降低母树周围同种幼苗的生长率和存活率,为其他物种存活提供了机会。生活史负相关使得热带森林的许多植物能够共存。冠层植物的抑制使得随机性在林下植物的建立过程中起决定作用 (项华均等, 2004)。

乔木结构多样性丰富时草本植物多样性丰富 (Leniere et al., 2006)。北美内华达山脉混交针叶林林下草本植物丰富度与直接辐射负相关 (North et al., 2005)。也有学者认为林下植被种类组成与乔木胸高处年龄为 50 年时的树高以及一些气候、土壤变量有关 (Chen et al., 2004)。林下植物丰富度与多样性的增加可能是由于种子库的存在, 且在干扰程度和生物量中等的时候丰富度最高 (Weiher, 2003, Leniere et al., 2006)。

物种丰富度大尺度格局与环境可利用能量有关联, 但至少有两种解释这种格局的机理被提出。Evans & Gaston (2005) 企图验证“高环境能量导致高进化速率”这一假设的前提, 包括高能量增加突变几率, 突变几率限制新种产生的几率, 过去的环境能量和现在的环境能量有很强的相关性, 物种形成速率和物种丰富度的相关性并不因为物种的形成而被减弱。经过对这些前提的验证, Evans & Gaston 认为, 高环境能量导致高进化速率这一机制的不确定因素过多。

常绿季雨林和常绿阔叶林共有 6 个主要群落类型, 常绿季雨林群落内各层多样性指数和均匀度指数顺序为灌木层> 乔木层> 草本层, 常绿阔叶林群落内各层多样性指数和均匀度指数顺序为乔木层> 灌木层> 草本层; 常绿季雨林和常绿阔叶林乔木、灌木层物种多样性比较中, 常绿季雨林< 常绿阔叶林, 草本层比较中, 常绿季雨林> 常绿阔叶林; 常绿季雨林和常绿阔叶林都具有亚热带向热带过渡的明显特征。过度的人类干扰将导致植物物种多样性降低 (张荣京等, 2005)。

王庆锁 (2004) 对森林草原交错带的植被类型、分布规律、第一性生产力、环境条件、人为影响进行了系统的总结, 对交错带植物多样性进行了比较全面的研究。不同尺度不同类型的生态交错带均显示出较高的生物多样性 (王庆锁等, 1997)。森林草原交错带植物群落多样性在森林群落和草原群落表现不同, 森林群落从森林带到草原带依次降低, 草原群落则表现出在森林草原交错带植物多样性高, 尤其是森林草甸。从森林带到森林-草原交错带, 森林斑块变小、森林景观破碎化程度提高。森林-草原交错带森林景观的形成是气候变化和现代气候、地形、火灾和人类活动综合作用的结果 (王庆锁等, 2000; 2004)。

在相同的地点(较小尺度), 物种丰富度及多样性指数也有差异, 有时还具有很大的差异, 呈现空间异质性分布的特征; 因为影响这些多样性指数的环境因子更加复杂, 不仅受经度、纬度和海拔的影响, 也受地形、群落的年龄、干扰史等多种生态因子影响 (于顺利等, 2004)。

1.2.2 林冠层对于林下植物多样性格局的影响

影响森林下草本层的因素有地形、土壤养分和水分条件、气候因子、直接辐射、乔木冠幅等。林下草本植物依次受光照、土壤水分、杀虫剂、木本凋落物的影响，顺序从大到小排列（Harrington et al., 1999）。

王伯荪等（2001）对海南岛四大林区的热带山地玉林群落物种多样性的分析表明，林区间即大尺度的范围内变化：乔木层和草本层物种多样性变化与灌木层和层间植物变化趋势相反，层间植物和乔木层在物种多样性的空间波动比灌木层和草本层有较高的稳定性，各层植物多样性在海拔梯度上表现出不同的变化趋势，各层的物种多样性在不同坡向上也表现出不同的特征。

各森林景观类型乔木层物种丰富度均较低，灌木层和草本层物种丰富度较高，大部分景观类型的物种丰富度均表现出：草本层> 灌木层> 乔木层的特点；各森林景观类型的 Simpson 指数和 Shannon-Wiener 指数同物种丰富度具有相似的规律（白顺江等，2006）。林下植物丰富度与多样性的增加可能是由于种子库的存在，且在干扰程度和生物量中等的时候丰富度最高（Weiher, 2003, Leniere et al., 2006）。

低海拔带上的山地雨林各指数值在群落不同层次中均表现为草本层> 灌木层> 乔木层，而物种丰富度在不同层次中无一定变化规律；高海拔带上山地雨林的物种丰富度和多样性指数表现为乔木层> 灌木层> 草本层，而均匀度指数在不同层次中则无一定变化趋势。高海拔带上的山地雨林乔木层和灌木层的物种丰富度、多样性和均匀度指数均明显高于低海拔带上的山地雨林，这是由于前者所处生境较为优越。沿着海拔梯度，群落乔木层的物种丰富度、多样性和均匀度指数均在中等海拔高度地带达到最高值（李宗善等，2004）。

1.2.3 地形条件对植物多样性格局的影响

通过数字高程模型与野外调查的结合发现，在加拿大温带混交林中，坡向、坡度是决定林下物种丰富度、均匀度、多样性的首要因素（Chipman et al., 2002）。

海拔梯度是山地制约植物群落分布的主要因子，而坡向和坡度则起着次要作用。对物种多样性的分析表明，物种总数、木本植物物种多样性和草本植物物种多样性在南北坡具有不同的海拔梯度格局。物种总数在南坡呈现单峰分布格局，在北坡分布趋势不明显。木本植物物种多样性在南北坡具有相似的分布格局；在低海拔沿海海拔梯度变化不明显，而在高海拔则随海拔上升而急剧下降；草本植物物种多样性在南北坡沿海海拔梯度变化规律不明显（唐志

尧等, 2004a, b)。地形与土壤、光照等直接生境因子对植被格局解释量之和相当。但在不同尺度上, 地形特征都是解释能力最强的一组生境变量 (沈泽昊, 2000), 在牯牛降和小五台山等地得到了证实 (刘增力等, 2004; 沈泽昊等, 2007)。多样性指数随着生境异质性的变化而产生较大的差异。群落多样性指数随地形差异而表现出南坡> 北坡、坡底> 坡中> 坡顶的变化趋势。海拔梯度与多样性指数的线性关系不很明显, 但仍有随海拔升高而下降的倾向 (彭闪江等, 2003)。物种多样性和丰富度在越接近坡底部位越大, 可能是由于土壤水分和养分的增加 (Chipman et al., 2002)。

一般认为, 森林-草原交错带具有较高的植物种类多样性, 以往的解释仅仅局限于森林和草原种类的汇集。然而对生境异质性与种类多样性的关系仍然缺少研究。

1. 3 本文内容框架

本文选择我国 400mm 等雨量线东段作为研究区。这一地区是东亚季风影响的尾闾区, 植物受到的干旱胁迫明显。本研究通过不同纬度多个地点的实地调查, 总结植物种类多样性的空间格局, 并通过多元统计分析的方法, 解释影响多样性格局的因子。

第二章 研究区域概况

2.1 研究区自然状况

研究区主体处于我国暖温带落叶阔叶林与温带草原的过渡地带，行政区划上包括宁夏、陕西、山西、河北、内蒙古，经纬度范围为 $35^{\circ}\text{N}\sim 45^{\circ}\text{N}$ ， $105^{\circ}\text{E}\sim 120^{\circ}\text{E}$ ，海拔变化范围为 $800\sim 2500\text{m}$ 左右，地貌类型丰富，包括黄土高原、内蒙古高原东部边缘、冀北山地以及大兴安岭山地南延部分等。

研究区主体自然地理背景具有明显的过渡性。气候属于温带半湿润季风气候与半干旱大陆性气候的过渡带，年均温 $2\sim 12^{\circ}\text{C}$ ，NW-SE 向梯度明显；1 月均温 $-20\sim -4^{\circ}\text{C}$ ，以 N-S 向梯度为主，稍具 W-E 向梯度；7 月均温变化不大，为 $21\sim 24^{\circ}\text{C}$ ，梯度变化略同 1 月均温，但变化趋势不如前者明显；年降水量 $300\sim 500\text{mm}$ ，具有明显的 NW-SE 向梯度，降水集中在夏季，6~8 月份的降水量占全年降水量的 60%~70%。从大范围整体来看，研究区水分分配基本平衡，东南（或东）部降水丰富且热量较高，西北（或西）部降水较少且热量条件差。（图 2.2 a、b、c、d）。

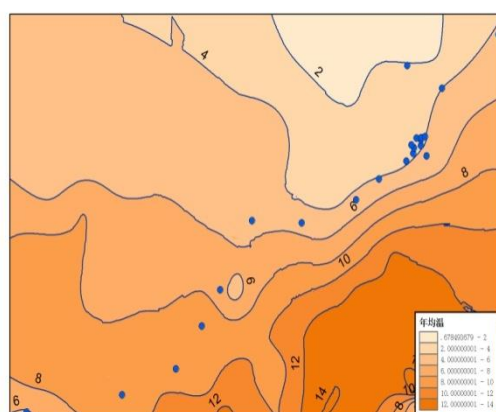


图 2.2a 研究区年均温格局图

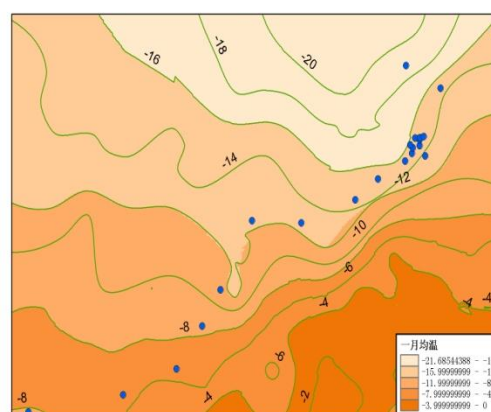


图 2.2b 研究区 1 月均温格局图

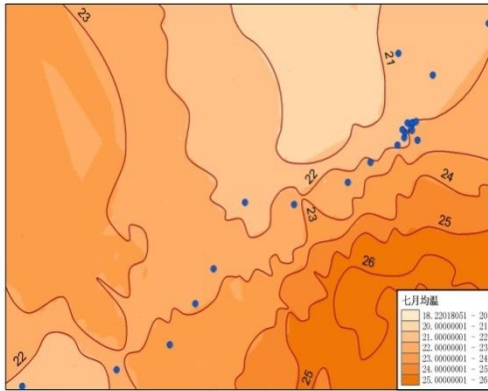


图 2.2c 研究区 7 月均温格局图

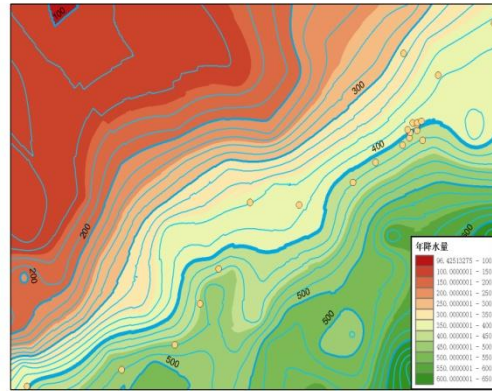


图 2.2d 研究区年降水量格局图

研究区处于暖温带落叶阔叶林向温带草原过渡的地带，植物区系组成呈明显的过渡性，从东向西，表现为东亚成分逐渐减少而达乌里-蒙古成分增多（中国科学院内蒙古宁夏综合考察队，1984）。过渡带内，森里草原物种汇集，植物种类多样性较高。（王庆锁，1997）

2.2 研究区选择依据

本文基于暖温带落叶阔叶林-温带草原过渡带，选择我国 400mm 等雨量线东段开展研究，主要基于以下原因：

- （1）研究区处于暖温带落叶阔叶林与温带草原的过渡带，森林和草原物种汇集明显，森林植物种类多样性较高，有利于研究森林草原过渡带森林植物多样性格局。
- （2）研究区位于东亚季风影响的尾部区，植物受到的干旱胁迫明显。通过控制水分因子的影响，有利于分析其他环境因子对森林草原过渡带森林植物多样性格局的影响。
- （3）研究区经纬范围跨度大，地貌类型丰富，植物生长环境不尽相同，有利于分析生境异质性与种类多样性的关系。

第三章 研究方法

3.1 野外调查取样

通过查阅内蒙植物志、河北植物志、山西植物志、陕西植物志以及宁夏植物志等判断沿

400mm 等雨量线附近那里分布有天然林, 包括白桦林、山杨林以及蒙古栎林等, 然后在 2006 年 7、8 两月进行实地调查。根据实际情况, 共选择 23 个地点进行了野外植物样方调查, 分布宁夏、陕西、山西、河北和内蒙古五个省份 (图 3.1)。

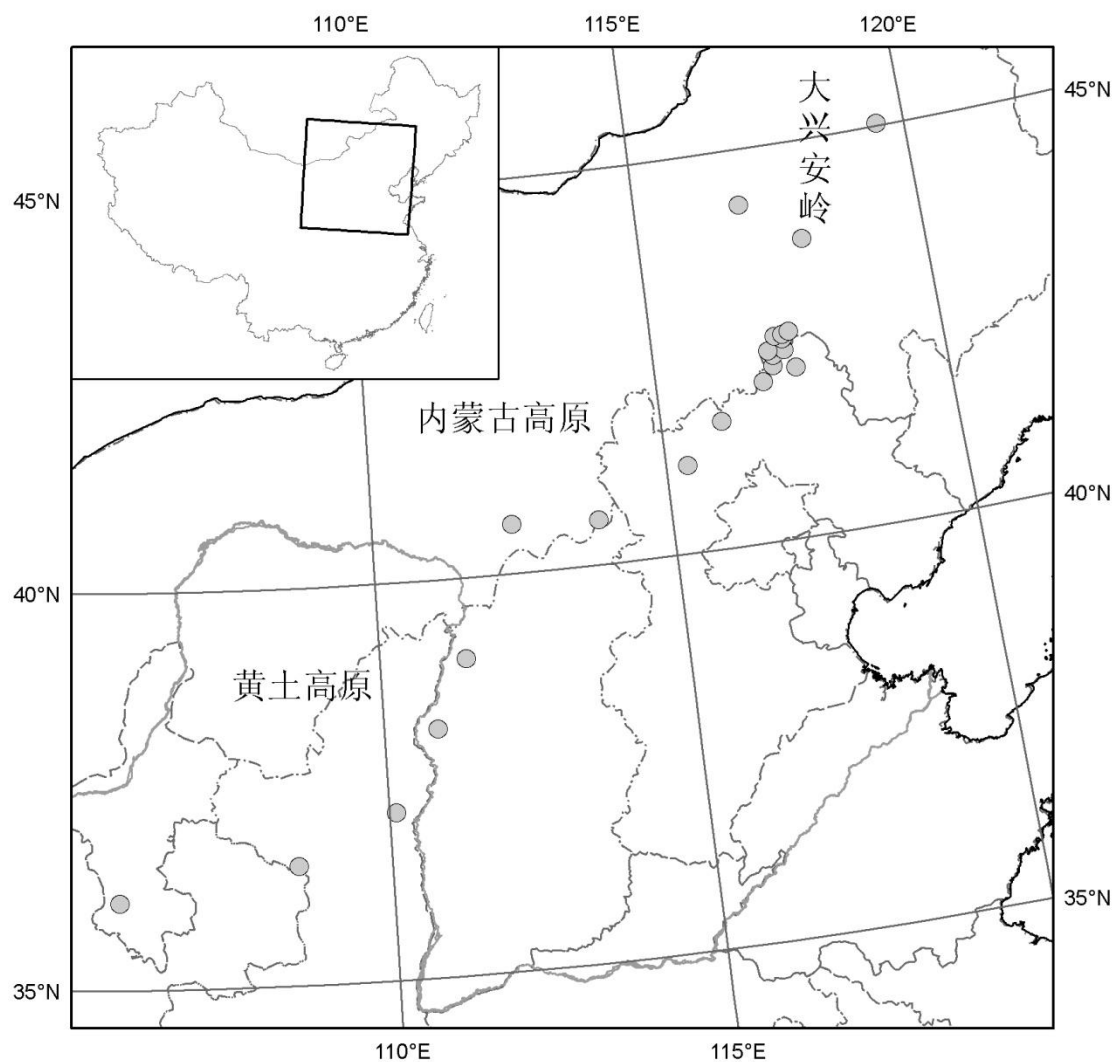


图 3.1 取样点示意图

根据每个地点的实际情况, 在阴坡林下设置 10m×10m 的大样方, 每个大样方内按梅花形设置 5 个 2m×2m 的小样方, 根据各地的不同情况, 样方设置情况有所差异, 共设置 42 个大样方, 186 个小样方, 设置结果如表 3.1:

表 3.1 样地设置情况

西吉火石寨	36.09	105.76	2353	白桦林	2	10
志丹麻台林场	36.50	108.54	1416	白桦林	1	5

清涧	37.11	110.11	935	青杨	1	5
临县紫金山	38.12	110.86	1550	蒙古栎	2	10
河曲赵家沟	38.98	110.40	1560	山杨	2	10
兴和苏木山	40.56	113.78	1891	白桦	1	5
凉城蛮汗山	40.62	112.33	1610	白桦	2	10
崇礼狮子沟	41.11	115.37	1567	白桦	1	5
半坝	41.61	116.03	1612	白桦	1	5
丰宁大滩	41.61	116.03	1610	白桦	2	10
多伦	42.03	116.83	1551	白桦	1	5
围场塞罕坝 1	42.15	117.42	810	棘皮桦	4	12
围场塞罕坝 2	42.22	117.03	1340	白桦	1	5
围场塞罕坝 3	42.34	117.05	1342	山杨-白桦	1	5
围场塞罕坝 4	42.40	117.25	1550	白桦	4	20
围场塞罕坝 5	42.41	116.98	1380	白桦	4	12
围场塞罕坝 6	42.53	117.25	1588	白桦	1	5
围场塞罕坝 7	42.58	117.12	1500	白桦	4	12
围场塞罕坝 8	42.59	117.26	1574	白桦	1	5
围场塞罕坝 9	42.62	117.38	1604	白桦	1	5
林西宝地	43.76	117.87	1388	棘皮桦-白桦	1	5
巴林左旗石棚沟	44.30	116.85	941	棘皮桦	2	10
阿旗罕山林场	45.03	119.52	1027	白桦	2	10

注：塞罕坝 1、塞罕坝 5、塞罕坝 7 三个地点每个大样方内设置 3 个小样方

对于每个样方，利用 GPS、罗盘记录经纬度、海拔高度、坡向和坡度，人类活动干扰情况等生境条件的特征，以及样方内所有植物种类的数量特征。阴坡森林群落分乔木层、立木更新、灌木层、草本层分别进行记载，其中乔木层和立木更新以大样方为单元，灌木层和草本层以小样方为单元。乔木层，测量胸径、基径、并估测高度、冠幅、总的郁闭度；立木更新，根据高度划分龄级，根据龄级记载不同幼苗和幼树的数量，定性描述其分布状况；灌木层和草本层，记载种名、多度或丛数、盖度、高度以及物候相。

3.2 气象台站气候数据处理

收集研究区及周边地区 81 个气象台站（纬度跨度为 $36^{\circ}\text{N}\sim 46^{\circ}\text{N}$ ，经度跨度为 $105^{\circ}\text{E}\sim 120^{\circ}\text{E}$ ）的温度和降水数据进行运算，包括累年各月均温、年均温、年均降水量，以及近 50 年来各年降水量。为显示方便，表只罗列出台站纬度、经度、海拔、年均温、年降水量和数值年限（累年资料）（表 3.2）。

表 3.2 气象台站数据

台站名	纬度($^{\circ}$)	经度($^{\circ}$)	海拔(m)	年均降水量	年均温度	数值年限
-----	------------------	------------------	-------	-------	------	------

				(mm)	(℃)	
西吉	35.97	105.72	1916.5	397.7	5.5	1971-2000
固原	36.00	106.27	1753.0	435.2	6.4	1971-2000
长治	36.05	113.07	991.8	533.9	9.9	1986-2000
安阳	36.05	114.40	62.9	556.9	14.1	1971-2000
临汾	36.07	111.50	449.5	468.5	12.6	1971-2000
沂源	36.18	118.15	305.1	668.2	12.2	1971-2000
莘县	36.23	115.67	37.8	526.2	13.2	1987-2000
泰山	36.25	117.10	1533.7	1042.7	5.6	1971-2000
海原	36.57	105.65	1854.2	367.3	7.3	1971-2000
环县	36.58	107.30	1255.6	407.6	8.9	1971-2000
延安	36.60	109.50	958.5	510.7	9.9	1971-2000
济南	36.60	117.05	170.3	672.8	14.7	1971-2000
隰县	36.70	110.95	1052.7	493.7	9.3	1971-2000
潍坊	36.75	119.18	22.2	588.3	12.5	1971-2000
吴旗	36.92	108.17	1331.4	446	8.0	1971-2000
同心	36.97	105.90	1339.3	267.9	9.1	1971-2000
介休	37.03	111.92	743.9	454.8	10.6	1971-2000
榆社	37.07	112.98	1041.4	535.1	8.8	1971-2000
邢台	37.07	114.50	77.3	493.4	13.9	1971-2000
南宫	37.37	115.38	27.4	477.3	13.2	1971-2000
东营	37.43	118.67	6.0	559.3	13.1	1971-2000
中宁	37.48	105.68	1183.4	202.1	9.5	1971-2000
惠民	37.48	117.53	11.7	568.6	12.6	1971-2000
绥德	37.50	110.22	929.7	428.7	9.9	1971-2000
离石	37.50	111.10	950.8	461.5	9.1	1971-2000
中卫	37.53	105.18	1225.7	178.3	8.7	1971-2000
定边	37.58	107.58	1360.3	318.9	8.8	1989-2000
太原	37.78	112.55	778.3	431.1	10.0	1971-2000
盐池	37.80	107.38	1349.3	273.5	8.3	1971-2000
阳泉	37.85	113.55	741.9	515.9	11.3	1971-2000
横山	37.93	109.23	1111.0	348.3	8.9	1971-2000
石家庄	38.00	114.42	81.0	517.1	13.4	1971-2000
饶阳	38.23	115.73	19.0	513.9	12.5	1971-2000
榆林	38.27	109.78	1157.0	365.7	8.3	1971-2000
黄骅	38.37	117.35	6.6	567.8	12.5	1971-1991
兴县	38.47	111.13	1012.6	470	8.8	1971-2000
银川	38.48	106.22	1111.4	186.3	9.0	1971-2000
原平	38.73	112.72	828.2	417.1	9.0	1971-2000
陶乐	38.80	106.70	1101.6	166.9	8.6	1971-2000
阿拉善左旗	38.83	105.67	1561.4	207.2	8.2	1971-2000
保定	38.85	115.52	17.2	512.6	12.9	1971-2000
五寨	38.92	111.82	1401.0	453.9	5.0	1971-2000

天津塘沽	39.05	117.72	4.8	566.5	12.6	1971-2000
天津	39.08	117.07	2.5	544.3	12.7	1971-2000
鄂托克旗	39.10	107.98	1380.3	264.5	7.1	1971-2000
霸州	39.12	116.38	9.0	507	12.2	1971-1984
惠农	39.22	106.77	1092.5	167.6	8.8	1971-2000
河曲	39.38	111.15	861.5	385.5	8.0	1971-2000
乐亭	39.43	118.88	10.5	607	10.6	1971-2000
吉兰泰	39.78	105.75	1031.8	106.1	9.1	1971-2000
北京	39.80	116.47	31.3	571.8	12.3	1971-2000
东胜	39.83	109.98	1461.9	381.2	6.2	1971-2000
蔚县	39.83	114.57	909.5	407	7.0	1971-2000
秦皇岛	39.85	119.52	2.4	634.2	11.0	1971-2000
大同	40.10	113.33	1067.2	371.6	7.0	1971-2000
包头	40.67	109.85	1067.2	297.6	7.2	1971-2000
巴彦淖尔盟	40.75	107.42	1039.3	145.7	8.1	1971-2000
承德	40.98	117.95	385.9	512	9.1	1971-2000
乌兰察布	41.03	113.07	1419.3	363.9	4.3	1971-2000
张北	41.15	114.70	1393.3	392.5	3.2	1971-2000
丰宁	41.22	116.63	661.2	457	6.8	1971-2000
建平县	41.38	119.70	422.0	455.6	8.4	1971-1994
海力素	41.40	106.40	1509.6	126.8	5.2	1971-2000
四子王旗	41.53	111.68	1490.1	315.5	3.5	1971-2000
海流图	41.57	108.52	1288.0	199.8	5.3	1971-2000
达茂旗	41.70	110.43	1376.6	256	4.2	1971-2000
化德	41.90	114.00	1482.7	320.6	2.8	1971-2000
围场	41.93	117.75	842.8	444.6	5.3	1971-2000
多伦	42.18	116.47	1245.4	386.5	2.4	1971-2000
赤峰	42.27	118.93	568.0	371.1	7.5	1971-2000
朱日和	42.40	112.90	1150.8	210.7	5.1	1971-2000
满都拉	42.53	110.13	1225.2	170.4	5.3	1971-2000
林西	43.60	118.07	799.5	384.9	4.8	1971-2000
二连浩特	43.65	111.97	964.7	142.3	4.0	1971-2000
苏尼特左旗	43.87	113.63	1036.7	185.3	3.1	1971-2000
锡林浩特	43.95	116.12	1003.0	286.6	2.6	1971-2000
巴林左旗	43.98	119.40	486.2	390.2	5.3	1971-2000
阿巴嘎旗	44.02	114.95	1126.1	249.5	1.4	1971-2000
西乌珠穆沁旗	44.58	117.60	995.9	345.9	1.6	1971-2000
那仁宝力格	44.62	114.15	1181.6	237.4	0.7	1971-2000
东乌珠穆沁旗	45.52	116.97	838.9	258.7	1.4	1971-2000

以各月均温、年均温、各年降水量和年均降水量为因变量，以纬度、经度、海拔作为自变量作多元线性回归，得到温度和降水与纬度、经度、海拔的关系：

$$Tm=a0+a1*lat+a2*long+a3*alt$$

$$P_n = b_0 + b_1 \cdot \text{lat} + b_2 \cdot \text{long} + b_3 \cdot \text{alt}$$

T_m 为各月均温和年均温度 (°C), P_n 为各年降水量和年均降水量 (mm), 系数分别为温度和降水量随纬度、经度、海拔的变化率, 得到 p 值用以判断置信度。通过回归方程计算 23 个地点的各月均温、年均温、各年降水量和年均降水量。

根据 23 个地点各月均温计算各地点的温暖指数和寒冷指数, 其公式分别为 (刘春迎, 1999):

$$\begin{aligned} \text{温暖指数 } WI &= \sum_{i=1}^n (t_i - 5) \\ \text{寒冷指数 } CI &= -\sum_{j=1}^m (5 - t_j) \end{aligned}$$

其中 t_i 为平均温度 5°C 以上的第 i 个月的平均温度, n 为月平均气温 > 5°C 的月数; t_j 为平均温度 5°C 以下的第 j 个月的平均温度, m 为月平均气温 < 5°C 的月数, WI 和 CI 的单位都是 °C 月。

用离差系数 (CV 值) 表示 23 个地点 50 年来降水波动状况, 其公式为:

$$C_v = \frac{\sigma}{\bar{x}} = \frac{1}{\bar{x}} \sqrt{\frac{\sum (x_i - \bar{x})^2}{n}}$$

其中 σ 为 50 年降水量的均方差, \bar{x} 为 50 年降水量的均值。

3.3 数据分析

3.3.1 林下草本植物重要值

草本植物的重要值: $IV_{sh} = (\text{相对多度} + \text{相对盖度} + \text{相对频度}) / 3$

3.3.2 物种丰富度指数

Margalef 指数 $D = (S - 1) / \ln N$

其中, S 为样方中的物种数目, N 为样方中所有物种的个体数之和 (张金屯, 2004)。

3.3.3 α 多样性指数

S

Shannon-Wiener 指数 $H = -\sum_{i=1}^s p_i \log_2 p_i$

其中，s 是群落中种的数目，pi 表示属于第 i 个物种的个体数占群落中总个体数的比值（介于 0 和 1 之间）。因为 pi 总是<1，取对数后<0，所以公式前面加上负号。H 指数因满足相同种数情况下，种间个体数越均匀，指数越高的条件，所以出包含物种丰富度的信息外，还反映了物种的均匀度（张金屯，2004）。

3.3.4 种面积曲线

Arrhenius（1921）模型 $\lg S = c + z \lg A$

其中，S 表示物种数（物种的丰富度），A 表示研究地的面积，参数 c 对应于单位面积中出现的物种数，参数 z 与使用的面积单位无关，代表随着面积的改变物种数改变的速率，被认为是空间异质性的一种度量（克里施纳默西，2006；张金屯，2004）

3.3.5 相关分析

为进行种类多样性的影响因子分析，本研究中将各 100 平方米大样方的丰富度指数、α 多样性指数以及种面积曲线斜率分别与环境因子（包括经纬度、海拔高度、1 月均温、7 月均温、年均温、温暖指数、寒冷指数、坡度以及坡向）在 SPSS 中进行相关分析。

第四章 结果

4.1 野外调查结果

4.1.1 研究区地形格局

42 个大样方对应 23 个取样地点，根据纬度从南至北依次编号为 s1～s42，每个大样方记载的地形因子包括海拔高度、坡度和坡向，分布如表 4.1：

表 4.1 42 个大样方地形格局

样方编号	纬度（°）	经度（°）	海拔（m）	坡度（°）	坡向 N-E°
s1	36.09	105.76	2353	25	20

s2	36.09	105.76	2353	25	20
s3	36.50	108.54	1416	15	15
s4	37.11	110.11	935	35	20
s5	38.12	110.86	1550	30	35
s6	38.12	110.86	1550	30	35
s7	38.98	111.40	1560	8	55
s8	38.98	111.40	1560	15	5
s9	40.56	113.78	1891	15	30
s10	40.62	112.33	1610	5	345
s11	40.62	112.33	1610	5	345
s12	41.11	115.37	1567	25	8
s13	41.61	116.03	1612	10	45
s14	41.61	116.03	1610	12	0
s15	41.61	116.03	1610	10	45
s16	42.03	116.83	1551	18	300
s17	42.15	117.42	810	22	28
s18	42.15	117.42	810	22	28
s19	42.15	117.42	810	22	28
s20	42.15	117.42	810	22	28
s21	42.22	117.03	1340	25	355
s22	42.34	117.05	1342	5	20
s23	42.40	117.25	1550	24	0
s24	42.40	117.25	1550	24	0
s25	42.40	117.25	1550	24	0
s26	42.40	117.25	1550	24	0
s27	42.41	116.98	1380	30	30
s28	42.41	116.98	1380	30	30
s29	42.41	116.98	1380	30	30
s30	42.41	116.98	1380	30	30
s31	42.53	117.25	1588	22	12
s32	42.58	117.12	1500	20	5
s33	42.58	117.12	1500	20	5
s34	42.58	117.12	1500	20	5
s35	42.58	117.12	1500	20	5
s36	42.59	117.26	1574	38	25
s37	42.62	117.38	1604	17	25
s38	43.76	117.87	1388	25	35
s39	44.30	116.85	941	32	350
s40	44.30	116.85	941	32	350
s41	45.03	119.52	1027	10	50
s42	45.03	119.52	1027	10	50

从表 4.1 中可以看出，42 个大样方所在位置的海拔高度最低 810m，最高 2353m，平均海拔 1500 左右，海拔在 1300~1699m 的样方数占总样方数的 79%；坡度最小 5°，最大 38°，

坡度在 20° ~29° 的样方数占总样方数的 43%；坡向在阴坡（NE0° ~45° 和 NE315° ~360° ）的样方数占总样方数的 91%，另有部分在半阴坡（NE45° ~135° ），还有一个在半阳坡（NE300° ）。42 个大样方海拔高度、坡度和坡向的分布比例分别如图 4.1a、b、c。

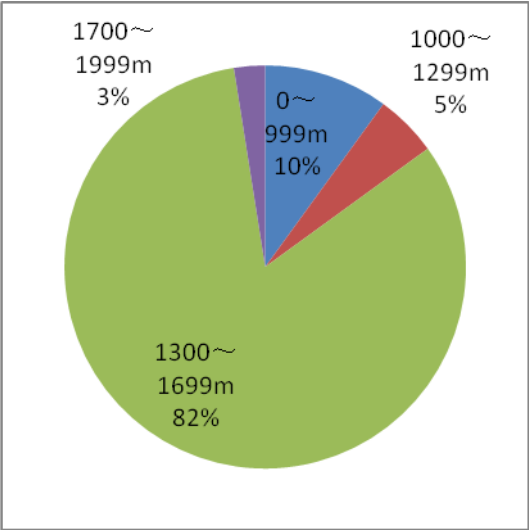


图 4.1a 42 个大样方不同海拔高度百分比

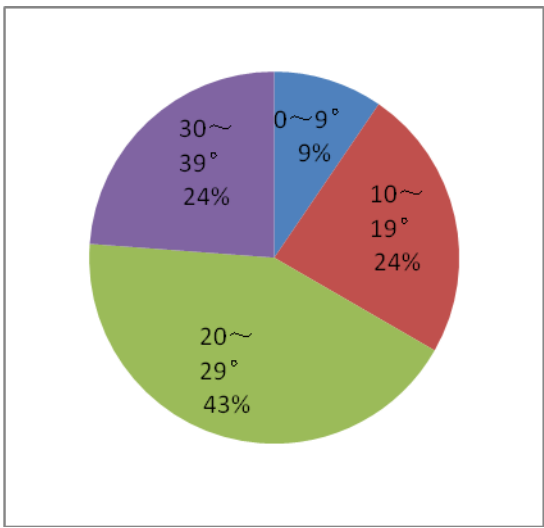


图 4.1b 42 个大样方不同坡度百分比

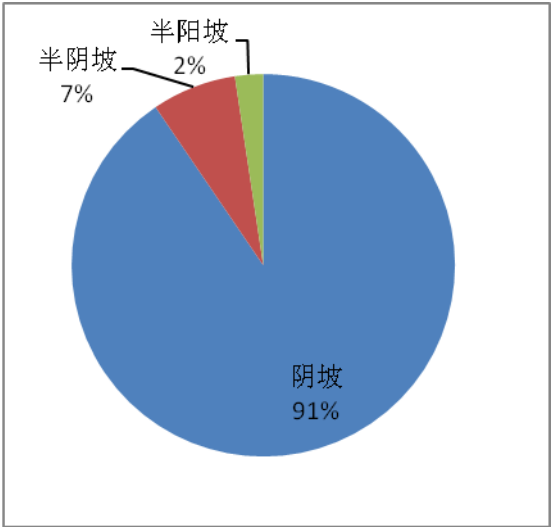


图 4.1c 42 个大样方不同坡向百分比

4.1.2 植被群落类型

42 个大样方各层的优势种如表 4.2 所示。

表 4.2 42 个大样方各层的优势种

样方编号	乔木类型	灌木类型	草本层重要值前两位
s1	白桦	中国黄花柳	蕨、野草莓
s2	白桦	中国黄花柳	莓叶委陵菜、直穗鹅观草

s3	白桦	绒毛绣线菊	披针叶苔草、玉竹
s4	青杨	尖叶胡枝子	苜蓿、黄囊苔草
s5	蒙古栎	绒毛绣线菊	披针叶苔草、野青茅
s6	蒙古栎	绒毛绣线菊	披针叶苔草、野青茅
s7	山杨	绒毛绣线菊	铁杆蒿、小红菊
s8	山杨	绒毛绣线菊	披针叶苔草、狭叶山野豌豆
s9	白桦	毛叶水栒子	披针叶苔草、糙苏
s10	白桦	绒毛绣线菊	披针叶苔草、龙芽草
s11	白桦	绒毛绣线菊	披针叶苔草、龙芽草
s12	白桦	美蔷薇	披针叶苔草、东北堇菜
s13	白桦	美蔷薇	披针叶苔草、林生银莲花
s14	白桦	绒毛绣线菊	黄囊苔草、地榆
s15	白桦	绒毛绣线菊	披针叶苔草、野青茅
s16	白桦	绒毛绣线菊	披针叶苔草、地榆
s17	棘皮桦	二色胡枝子	披针叶苔草、乌苏里风毛菊
s18	棘皮桦	平榛	披针叶苔草、大瓣铁线莲
s19	棘皮桦	平榛	乌苏里风毛菊、披针叶苔草
s20	棘皮桦	平榛	石生悬钩子、披针叶苔草
s21	白桦	绒毛绣线菊	披针叶苔草、硬质早熟禾
s22	山杨	美蔷薇	披针叶苔草、地榆
s23	白桦	虎榛子	披针叶苔草、乌苏里风毛菊
s24	白桦	栒子	披针叶苔草、大瓣铁线莲
s25	白桦	栒子	披针叶苔草、鹿蹄草
s26	白桦	栒子	乌苏里风毛菊、短尾铁线莲
s27	白桦		乌苏里风毛菊、披针叶苔草
s28	白桦	美蔷薇	披针叶苔草、乌苏里风毛菊
s29	白桦	金露梅	披针叶苔草、地榆
s30	白桦	美蔷薇	乌苏里风毛菊、地榆
s31	白桦	美蔷薇	黄囊苔草、乌苏里风毛菊

s32	白桦	稠李	披针叶苔草、贝加尔唐松草
s33	白桦	美蔷薇	披针叶苔草、乌苏里风毛菊
s34	白桦	虎榛子	披针叶苔草、种阜草
s35	白桦	山丁子	林地早熟禾、披针叶苔草
s36	白桦	绒毛绣线菊	东北堇菜、老鹳草
s37	白桦	山刺玫	柳兰、披针叶苔草
s38	棘皮桦	虎榛子	披针叶苔草、山马蔺
s39	棘皮桦	照山白	披针叶苔草、山马蔺
s40	棘皮桦	照山白	披针叶苔草、铁杆蒿
s41	白桦	绒毛绣线菊	玉竹、披针叶苔草
s42	白桦	绒毛绣线菊	披针叶苔草、野艾蒿

4.1.3 林下植物科属划分

样地调查结果共记录林下草本 374 个种，其中确定到种（Species）的有 334 个，只确定到属（Genus）的有 10 个，另有 30 个标本丢失（草本名录见附录 1）。344 个物种分布在 42 个科，154 个属，其中有 10 个科出现种数最多，均超过了 10 种（表 4.3）。

表 4.3 种数超过 10 的科

科	科拉丁名	种数
菊科	<i>Compositae</i>	76
豆科	<i>Leguminosae</i>	28
毛茛科	<i>Ranunculaceae</i>	27
禾本科	<i>Gramineae</i>	25
桔梗科	<i>Campanulaceae</i>	19
堇菜科	<i>Violaceae</i>	17
蔷薇科	<i>Rosaceae</i>	17
百合科	<i>Liliaceae</i>	15
伞形科	<i>Umbelliferae</i>	15
唇形科	<i>Labiatae</i>	13

林下灌木共有 48 个种，其中有 46 个确定到种，另有 2 个标本丢失（灌木名录见附录 2）。

4.2 林下植物分布空间格局

研究区纬度范围为 35° N~45° N，故以 40° N 为界，将研究区划分为南北两部分，出现在南部的共有 5 个取样地点，包括宁夏、陕西和山西的取样点；出现北部的共有 18 个取样地点，包括内蒙古和河北的取样点。以南北分异划分阴坡林下植物分布的空间格局。

4.2.1 林下草本植物分布空间格局

选择确定到种的 334 个草本物种做南北分布空间格局（附录 3），共有 167 个种仅出现在北部，85 个种仅出现在南部，另 82 个种南北均有分布，南北分异较为明显（图 4.2）。

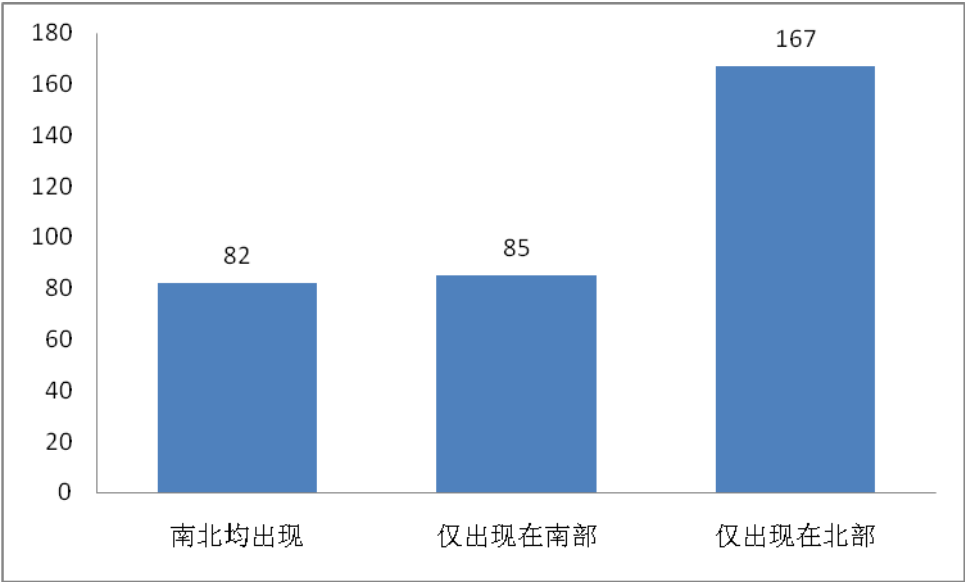


图 4.2 草本物种南北分布空间格局

4.2.2 林下灌木分布空间格局

选择确定到种的 46 个灌木物种做南北分布空间格局（表 4.5），共有 12 个种仅出现在北部，25 个种仅出现在南部，另 9 个种南北均有分布，南北分异明显（图 4.3）。

表 4.5 灌木南北分布格局

南北均出现	仅出现南部	仅出现北部
二色胡枝子	茶藨子	茶条槭
虎榛子	稠李	葱皮忍冬
黄花忍冬	大叶小檗	尖叶胡枝子

卷边柳	东北鼠李	蒙古莢蒾
毛叶水栒子	冻叶鼠李	蒙古栒子
绒毛绣线菊	黑果栒子	拧条锦鸡儿
山刺玫	胡枝子	牛奶子
山丁子	花楸	山荆子
小檗	华北忍冬	水栒子
	花茶藨子	小叶鼠李
	黄花柳	中国黄花柳
	灰栒子	准噶尔栒子
	金露梅	
	金银木	
	蓝靛果忍冬	
	毛山楂	
	美蔷薇	
	平榛	
	沙棘	
	山杏	
	山杨	
	水杨梅	
	栒子	
	银露梅	
	照山白	

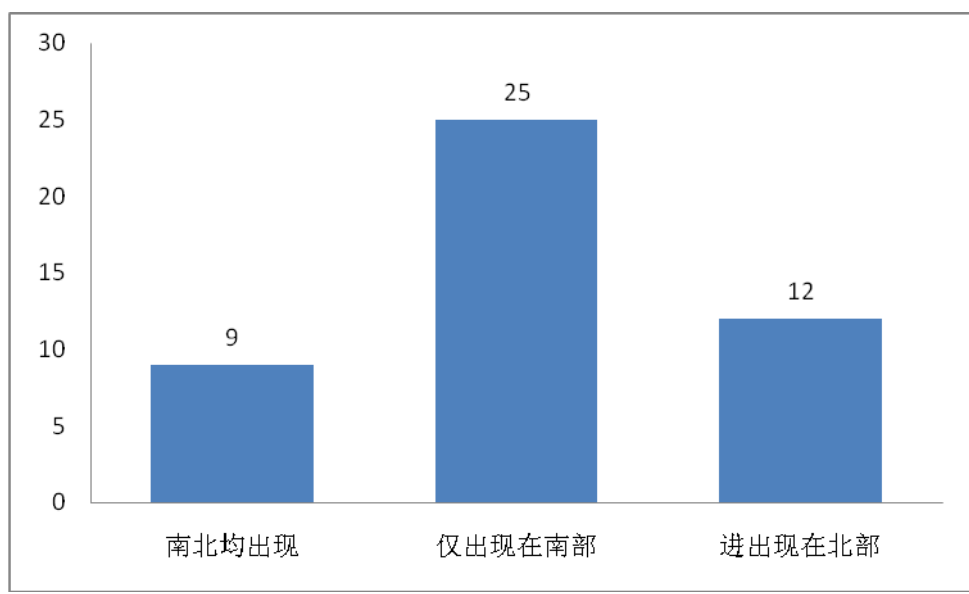


图 4.3 灌木物种南北分布空间格局

4.3 林下草本植物种类多样性空间格局

42 个大样方的草本多样性指数（H）、丰富度指数（D）以及种面积曲线斜率（z）如表 4.6 所示：

表 4.6 42 个大样方多样性指数（H）、丰富度指数（D）和种面积曲线斜率（z）

样方编号	H	D	z
s1	4.984	8.246	0.693
s2	4.864	6.679	0.522
s3	3.488	3.495	0.650
s4	4.343	4.505	0.242
s5	2.781	2.267	0.408
s6	3.404	2.937	0.371
s7	5.500	7.610	0.499
s8	4.839	5.277	0.429

s9	4.820	5.403	0.252
s10	5.440	7.895	0.326
s11	5.415	6.895	0.326
s12	4.445	4.410	0.424
s13	4.712	4.740	0.506
s14	4.615	4.527	0.288
s15	4.315	4.508	0.435
s16	4.976	5.463	0.402
s17	4.309	4.244	0.494
s18	5.020	6.003	0.665
s19	4.907	6.938	0.431
s20	5.111	6.510	0.513
s21	4.885	6.982	0.605
s22	3.907	3.977	0.540
s23	3.822	3.642	0.361
s24	4.285	4.026	0.358
s25	4.345	5.288	0.266
s26	3.866	3.747	0.416
s27	4.208	4.275	0.567
s28	4.426	4.933	0.422
s29	4.146	4.452	0.293
s30	4.094	4.131	0.629
s31	4.312	4.510	0.355
s32	4.024	3.549	0.203
s33	4.128	4.378	0.547
s34	4.059	5.423	0.674
s35	4.025	3.521	0.683
s36	3.780	3.346	0.257
s37	4.952	6.221	0.570

s38	4.246	3.723	0.578
s39	3.908	3.352	0.501
s40	3.905	3.556	0.461
s41	3.959	3.424	0.270
s42	4.311	4.169	0.383

以纬度为横轴做多样性指数的散点分布图如下（图 4.4），从图中可以看出，多样性指数大体随纬度升高而降低，但趋势并不明显，尤其是出现在陕西志丹、清涧和山西临县紫金山三个地点的 4 个大样方的多样性指数较为远离趋势线，而从另一层面来说，这 4 个样方的多样性指数也极大的影响了趋势线的拟合。

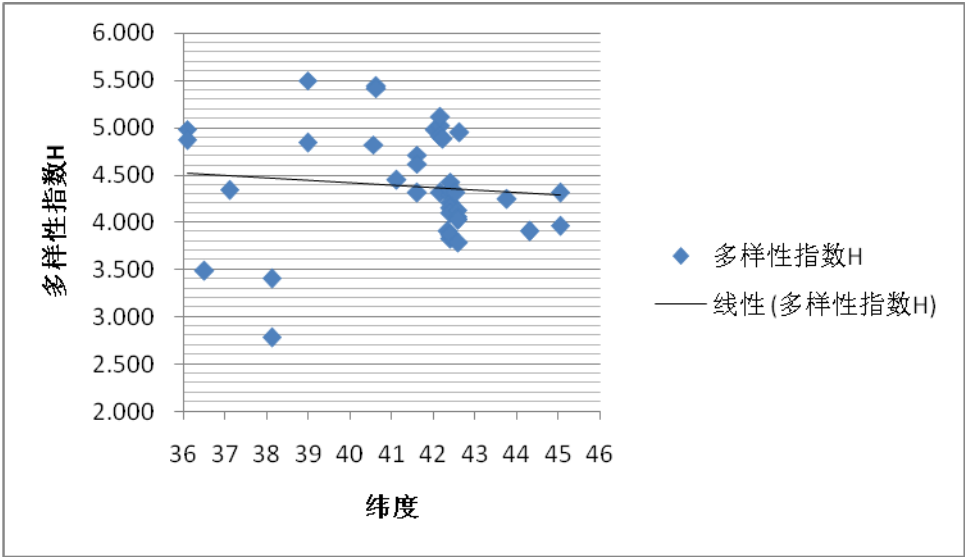


图 4.4 42 个大样方多样性指数散点图

根据野外实际调查结果，志丹麻台林场主要为人工种植的油松林，人为活动干扰明显，仅分布极少片状白桦林，故野外调查时也仅仅做了一个大样方；清涧为青杨林，没有明显的乔木生长分异，出现在取样点的乔木大小相差不多，疑似为人工林；紫金山为蒙古栎林，灌丛化十分明显，所作两个大样方内，每个小样方的灌木盖度均达 50% 以上。由于该三个地点明显区别与其他取样地点，故在去除掉该三个地点的 4 个样方数据之后，重新做多样性指数沿纬度分布的散点图（图 4.5），发现变化趋势明显，多样性指数呈现明显的随纬度升高而降低的变化趋势。

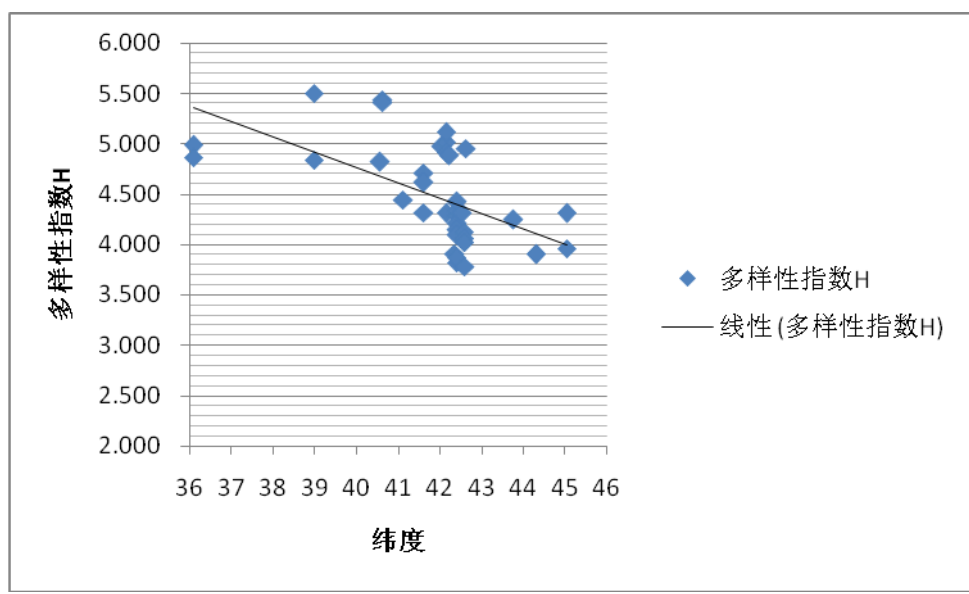


图 4.5 38 个大样方多样性指数散点图

以纬度为横轴做丰富度指数的散点图如下（图 4.6），其结果和多样性指数散点图类型，但稍微有明显的变化趋势。根据前文所述原因，去除掉陕西志丹、清涧和山西临县紫金山三个地点的 4 个样方数据之后，重新做散点图（图 4.7），发现其随纬度变化趋势明显增强，即随纬度升高丰富度指数呈明显降低趋势。

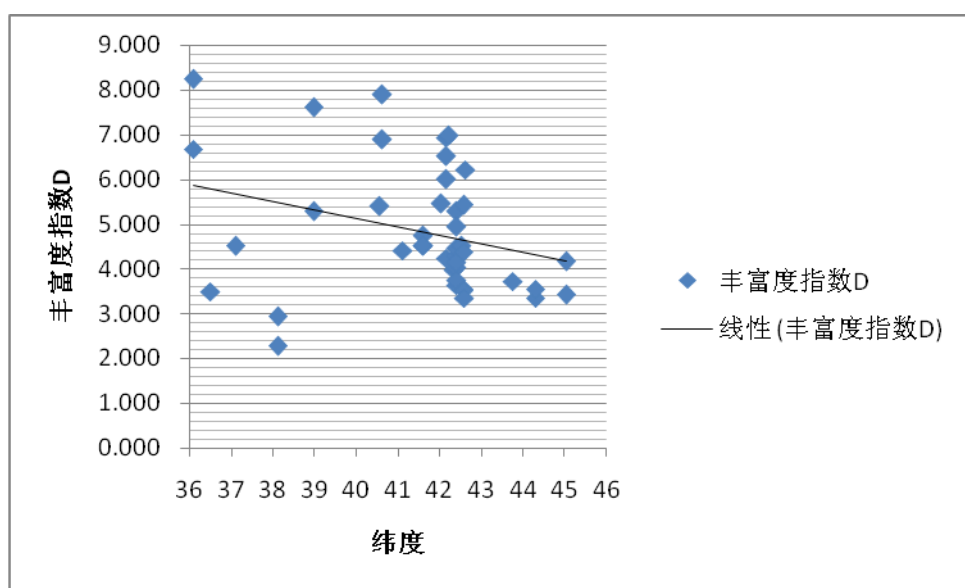


图 4.6 42 个大样方丰富度指数散点图

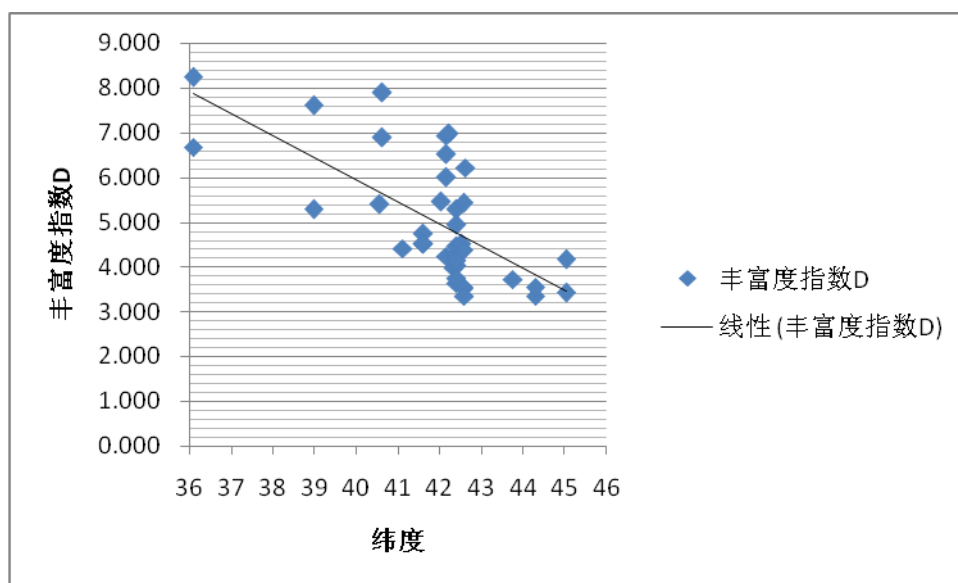


图 4.7 38 个大样方丰富度指数散点图

同样以纬度为横轴做种面积曲线斜率的散点图如下(图 4.8),从图中可以看出,随着纬度升高,种面积曲线斜率基本没有任何变化。考虑前文所述原因,去除掉陕西志丹、清涧和山西临县紫金山三个地点的 4 个样方数据之后,重新做散点图(图 4.9),发现趋势稍有增强,略具随纬度升高种面积曲线斜率降低的趋势,但并不明显,也即是说物种数随面积改变而改变的速率没有明显的地理梯度。各点改变的速率之所以不同的原因,应从生境异质性方面来考虑,而不是地理位置。

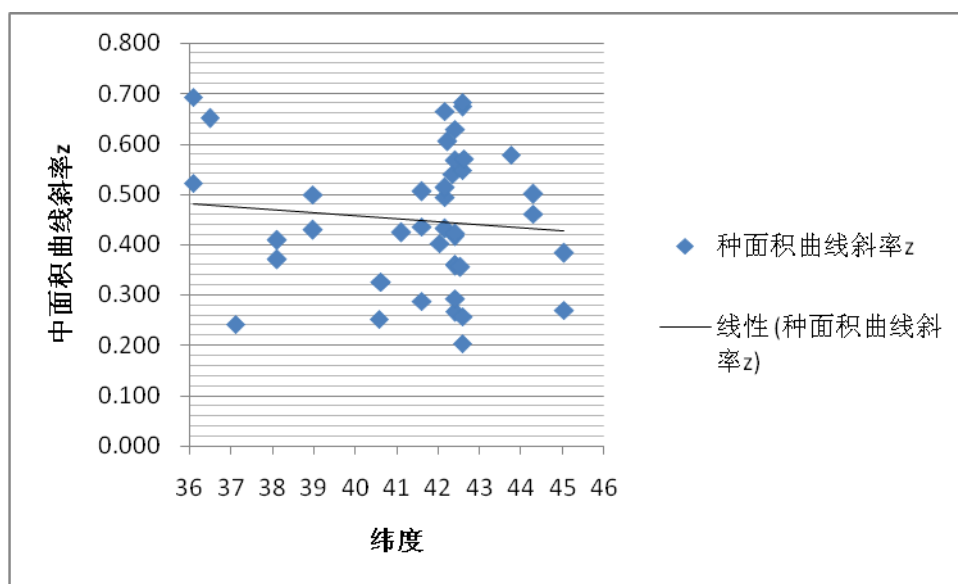


图 4.8 42 个大样方种面积曲线斜率散点图

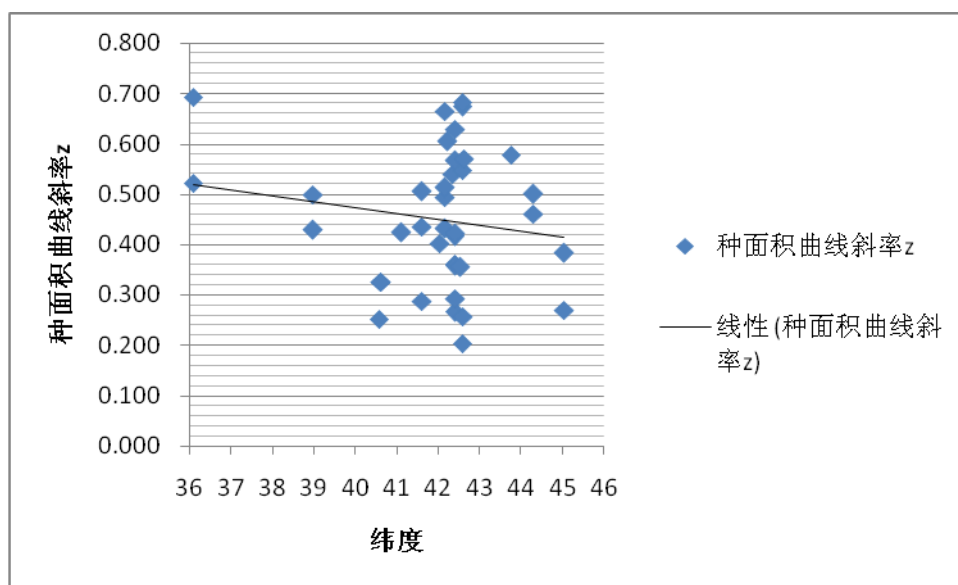


图 4.9 38 个大样方种面积曲线斜率散点图

4.4 气象台站气候资料回归结果

4.4.1 23 个点气候因子数据

根据 81 个气象台站数据和相应的地理位置坐标与海拔数据进行多元回归分析，回归结果和系数如表 4.7：

表 4.7 气候指标的回归分析

因变量	常数项	纬度系数	经度系数	海拔系数	R	样本个数
1 月均温	71.278	-1.531	-0.138	-0.005	0.97	81
2 月均温	84.13	-1.377	-0.271	-0.006	0.975	81
3 月均温	84.898	-1.004	-0.344	-0.006	0.981	81
4 月均温	76.856	-0.623	-0.33	-0.006	0.976	81
5 月均温	71.847	-0.292	-0.345	-0.006	0.959	81
6 月均温	73.743	-0.106	-0.382	-0.006	0.96	81
7 月均温	69.844	0.004	-0.37	-0.006	0.969	81
8 月均温	66.32	-0.123	-0.309	-0.006	0.977	81

9 月均温	65.847	-0.379	-0.263	-0.006	0.975	81
10 月均温	61.716	-0.762	-0.16	-0.006	0.981	81
11 月均温	65.69	-1.204	-0.121	-0.005	0.981	81
12 月均温	65.308	-1.441	-0.096	-0.005	0.97	81
年均温	71.456	-0.736	-0.261	-0.006	0.981	81
年降水量	-2176.582	-54.07	40.899	0.109	0.945	81

注：P 值均小于 0.05

根据回归方程，计算出 23 个地点的气候因子，并根据各取样地点 12 个月份的平均气温计算各取样地点的温暖指数和寒冷指数，将年均温、1 月均温、7 月均温、年降水量、温暖指数（WI）、寒冷指数（CI）结果如表 4.8 所示：

表 4.8 23 个地点的气候因子数据

地点	年均温	1 月均温	7 月均温	年降水量	WI	CI
西吉火石寨	3.18	-10.33	16.74	454.05	43.53	-53.95
志丹麻台林场	7.77	-6.66	21.33	443.73	74.11	-34.90
清涧	9.79	-5.41	23.64	422.39	89.52	-34.36
临县紫金山	5.16	-10.14	19.68	465.32	59.76	-54.44
河曲赵家沟	4.33	-11.58	19.42	442.06	56.39	-64.46
兴和苏木山	0.56	-15.98	16.56	489.79	39.63	-85.15
凉城蛮汗山	2.58	-14.47	18.78	396.80	50.42	-75.78
崇礼狮子沟	1.68	-15.42	17.92	489.68	46.21	-82.32
半坝	0.87	-16.50	17.41	494.88	43.30	-87.86
丰宁大滩	0.89	-16.49	17.42	494.63	43.36	-88.24
多伦	0.72	-16.95	17.48	498.05	43.42	-85.88
围场塞罕坝 1	4.93	-13.51	21.71	434.75	65.51	-67.03
围场塞罕坝 2	1.80	-16.20	18.67	473.28	49.25	-83.71
围场塞罕坝 3	1.69	-16.41	18.65	467.68	49.04	-86.02
围场塞罕坝 4	0.35	-17.57	17.33	495.48	42.41	-92.42
围场塞罕坝 5	1.43	-16.70	18.45	464.87	47.97	-88.05
围场塞罕坝 6	0.02	-17.96	17.10	492.28	41.16	-95.54

围场塞罕坝 7	0.55	-17.57	17.68	474.95	43.97	-93.28
围场塞罕坝 8	0.06	-17.98	17.18	488.07	41.51	-96.21
围场塞罕坝 9	-0.17	-18.19	16.96	494.51	40.39	-97.93
林西宝地	0.16	-18.92	18.08	429.54	45.03	-96.66
巴林左旗石棚沟	2.71	-17.37	21.14	310.09	59.70	-86.54
阿旗罕山林场	0.95	-19.30	19.64	388.61	51.96	3.23

4.4.2 23 个地点近 50 年降水量年际变化

根据气象台站近 50 年来各年降水量和相应的地理位置坐标与海拔高度进行多元回归分析，然后通过回归方程计算 23 个地点近 50 年来各年降水量，并用近 50 年的数据计算每个地点的降水量的离差系数（CV），表示近 50 年来各地点降水的波动状况，结果如图 4.10 所示：

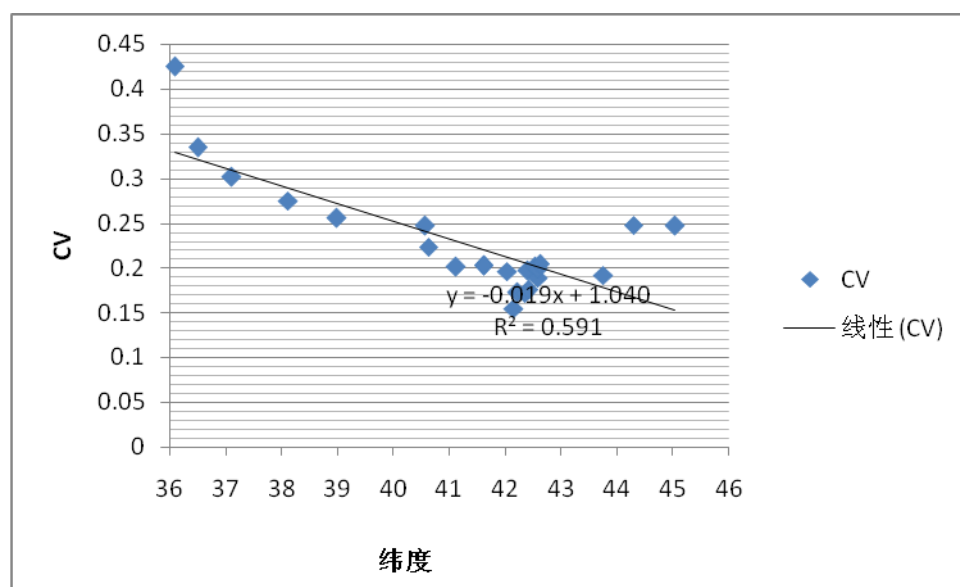


图 4.10 23 个地点近 50 年降水 CV 值散点图

从图中可以看出，23 个地点近 50 年来降水 CV 值具有明显的随纬度变化趋势，也即是说，随着纬度升高，23 个地点的降水波动趋缓。

4.5 多样性影响因子分析

4.5.1 环境因子

根据前文所述原因，去除掉陕西志丹、清涧和山西临县紫金山三个地点的 4 个样方数据

之后，将 20 个地点的气候因子数据对应于 38 个大样方，然后将 38 个大样方的多样性指数和丰富度指数与环境因子（包括经纬度、海拔、年均温、1 月均温、7 月均温、年降水量、温暖指数、寒冷指数、坡度、坡向）进行相关分析，分析结果显示多样性指数和丰富度指数均与经纬度呈显著负相关，与 1 月均温和年均温呈显著正相关，同时多样性指数还与坡度呈显著负相关。表 4.9 为与多样性指数和丰富度指数显著相关的环境因子及相关系数。

表 4.9 与多样性指数和丰富度指数显著相关的环境因子

	多样性指数	丰富度指数	纬度	经度	1 月均温	年均温	坡度
多样性指数	1.00						
丰富度指数	0.90	1.00					
纬度	-0.58**	-0.67**	1.00				
经度	-0.54**	-0.64**	0.95	1.00			
1 月均温	0.66**	0.70**	-0.91	-0.85	1.00		
年均温	0.72**	0.66**	-0.76	-0.71	0.91	1.00	
坡度	-0.45**	-0.31	0.14	0.14	-0.32	-0.50	1.00

**p<0.01

多样性指数和丰富度指数均与经纬度呈显著负相关，说明多样性指数和丰富度指数有随着经纬度增加而减小的趋势，也即是说本文的研究区内，林下草本层多样性有着随经纬度增加而降低的趋势，这个结果同时也印证了前面分析多样性空间格局时的结论，即研究区内，林下草本层多样性具有明显的地理梯度。

多样性指数和丰富度指数均与1月均温和年均温呈显著正相关，说明温度是影响多样性空间格局的一个环境因子，能量假说得到一定验证。

多样性指数与坡度呈也显著负相关，说明多样性指数有随着坡度增大而减小的趋势。进一步做线性回归分析，发现多样性指数与坡度呈显著线性相关（图 4.11），可以说坡度作为生境异质性的一个指标，是一个显著影响多样性空间格局的环境因子。

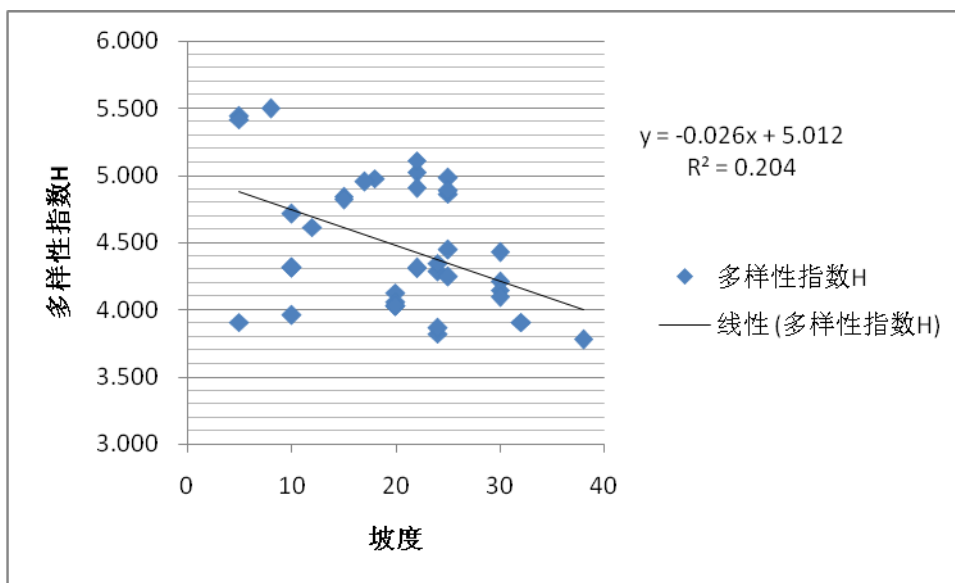


图 4.11 多样性指数与坡度线性回归

4.5.2 近 50 年降水波动影响

基于前文同样的原因，去除掉陕西志丹、清涧和山西临县紫金山三个地点的 4 个样方数据之后，将 20 个地点的近 50 年降水波动（CV 值）对应于 38 个大样方，然后将 38 个大样方的多样性指数和丰富度指数与 CV 值做相关分析，分析结果显示多样性指数与 CV 值没有相关性，但丰富度指数与 CV 值呈显著正相关。

表 4.10 多样性指数和丰富度指数与 CV 值相关分析结果

	多样性指数 H	丰富度指数 D	CV 值
多样性指数 H	1.00		
丰富度指数 D	0.90	1.00	
CV 值	0.26	0.39*	1.00

* $p < 0.05$

前面结果显示丰富度指数和 CV 值均与纬度呈负相关，随着纬度的增加而减小。二者的相关分析结果更进一步证实丰富度指数与 CV 值呈显著正相关，说明丰富度指数随着 CV 值的减小而减小，也即降水波动的幅度也是影响多样性格局的一个因子。

第五章 讨论

5.1 400mm 等雨量线林下草本植物种类多样性空间格局特征

在 4.3 节林下草本植物多样性的空间格局中,结果显示研究区内,多样性指数和丰富度指数有随着纬度增加而降低的趋势,具有一定的纬度梯度格局。在 4.5 节多样性影响因子分析中进一步验证了这个结果,将多样性指数和丰富度指数与经纬度做相关分析,发现它们均显著负相关,表现出随着经纬度的增加而降低的趋势,具有明显的地理梯度。这与通常大范围尺度生物多样性研究的结果相一致(Evans et al,2005),即在大范围尺度上,生物多样性一般随着纬度的增加而降低,其可能的结果是多方面的,水热条件的纬度梯度就是大范围尺度生物多样性空间格局的一个重要影响因子。

本研究中,沿 400mm 等雨量线进行实地调查,分析的结果显示沿着 400mm 等雨量线从南到北,林下草本植物种类多样性有降低的趋势。因为在我国,受到季风气候、地理梯度以及地貌类型等多种因素影响,400mm 等雨量线本就是一条 SW—NE 向的线,从大范围尺度来看就是综合了纬度和经度等地理信息,这个结果进一步验证了沿 400mm 等雨量线,林下草本植物种类多样性具有从西南向东北有着逐渐降低的地理梯度。

5.2 400mm 等雨量线林下草本植物种类多样性空间格局影响因子

通过对多样性指数和丰富度指数与环境因子的相关分析表明,在本研究区内,1 月均温、年均温以及坡度是林下草本植物多样性空间格局的显著影响因子。多样性指数和丰富度指数与 1 月均温和年均温均呈显著正相关,而 1 月均温和年均温同样具有纬度梯度,随着纬度的增加而减小。温度是控制植物生长的重要条件之一,1 月均温更是对多年生草本以及地面芽植物的存活具有显著影响,1 月均温越低,其死亡的几率越大,多样性也受到影响。

相关分析结果多样性指数与坡度呈显著负相关,在通常的研究结果中,坡度是影响多样性格局的一个地形因子,但其解释力并不占主要地位,往往是通过与其他地形因子相结合综合影响光照、热量、土壤水分等直接影响植物生长的因子,从而对多样性格局有一定影响(沈泽昊,2000)。而本研究中,地形因子中,坡度影响显著,推测是因为坡度直接影响土壤水分的含量,在相同土壤类型条件下,坡度越小,土壤水分越多,对于 400mm 等雨量线森林

群落来说,由于处在东亚季风的尾间区,植物受到的干旱胁迫明显,土壤水分的含量对植物生长具有直接影响,从而影响生物多样性。因此在本研究区中,推测坡度是通过影响土壤含水量进而影响多样性空间格局。但由于缺少取样地点土壤成分的分析,不同土壤类型对含水量的影响无法做出定量的分析,以上结论也仅限于推测,留待今后进一步进行。

通过计算取样地点 50 年的降水量,发现随着纬度的增加,50 年降水波动逐渐趋缓,其类似于多样性指数和丰富度指数随纬度增加而变化的趋势,进而将多样性指数和丰富度指数与描述降水快慢的指标(离差系数 CV 值)进行相关分析,发现丰富度指数同 CV 值呈显著正相关。降水波动幅度越大,说明极端生长环境出现的概率越大,可能某一年降水十分丰富,一些原本受水分条件限制的物种能够得以生长;某一年降水比较稀少,植物生长又受到限制。在降水波动幅度大的地区,生境条件变化大,可能使地下种子库萌发,而导致丰富度增加;而降水变化幅度小的地区,群落相对趋于稳定,从而丰富度不及前者。推测降水波动与多样性指数不呈显著相关是因为多样性指数包括了均匀度信息,群落物种分布是否均匀,应从生境异质性来解释,而降水波动变化趋势属于大范围尺度气候变化,只是从宏观上影响生物多样性格局。

5.3 人为活动对多样性的影响

人为活动也会对生物多样性造成影响,樊正球(2001)认为人为轻度干扰即可改变生态系统稳定性,许多生态位特化的物种首先受到威胁,景观破碎对生物多样性的影响更大。在森林草原交错带有些地方,森林砍伐、过度放牧、旅游等等人为干扰活动明显,对脆弱的森林群落来说,景观破碎化严重,森林斑块减少甚至消失,物种多样性受到极大影响,这从野外实际调查也得到部分验证,植物志记载在陕西和山西,沿着 400mm 等雨量线曾有多处地区分布有森林斑块,而实际调查结果却是在很多年之前就已经被人砍了。同时由于人类活动的增加,一些伴人植物入侵,与原生植物竞争,影响原有生态系统,从而也能影响生物多样性。

第六章 结论

本文利用野外植被调查数据、地形数据和气象台站观测数据等资料, 分析了 400mm 等雨量线森林群落草本植物种类多样性格局及影响因子, 证实了热量条件以及降水波动影响多样性格局的两个假说, 得到以下初步结论:

- 1) 400mm 等雨量线森林群落草本植物种类多样性有着沿经纬变化的空间格局, 具有显著的地理梯度, 随着经纬度的增加而减小, 综合考虑为沿着 400mm 等雨量线, 从西南向东北逐减小。
- 2) 400mm 等雨量线森林群落草本植物种类多样性的显著影响因子为 1 月均温、年均温和坡度, 多样性指数和丰富度指数与 1 月均温和年均温呈显著正相关, 多样性指数与坡度呈显著负相关。
- 3) 400mm 等雨量线附近 50 年来降水波动状况对多样性格局有显著影响, 降水波动状况沿 400mm 等雨量线从南到北逐渐趋缓, 表征降水波动幅度大小的离差系数 (CV 值) 与丰富度指数显著正相关。降水波动幅度越大, 物种丰富度越高; 降水波动幅度越小, 物种丰富都越小。

由于研究基础数据和研究手段的限制, 本研究在以下几个方面仍有待进一步深入:

- 1) 由于没有调查地点相应土壤成分以及土壤水分分析, 对物种多样性的环境影响因子考虑不够全面, 而且影响坡度解释多样性格局。
- 2) 由于没有辐射照度实测数据, 未分析光照条件对种类多样性的影响, 但光照条件对 400mm 等雨量线森林群落草本植物种类多样性有影响还有待进一步分析。
- 3) 阴阳坡植物种类的差异是否也影响到森林群落草本植物多样性, 也需要有进一步的调查数据作对比。

参考文献

- Chen HYH, Legare S, Bergeron Y. (2004) Variation of the understory composition and diversity along a gradient of productivity in *Populus tremuloides* stands of northern British Columbia, Canada. *Canadian Journal of Botany*. 82 (9) : 1314-1323.
- Chipman SJ, Johnson EA. (2002) Understory vascular plant species diversity in the mixedwood boreal forest of western Canada. *Ecological Applications*. 12 (2): 588-601.
- Evans, K.L., Gaston, K.J. (2005) Can the evolutionary-rates hypothesis explains species-energy relationships. *Functional Ecology*. 19(6): 899-915.
- Harrington TB, Edwards HB. (1999) Understory vegetation, resource availability, and litterfall responses to pine thinning and woody vegetation control in longleaf pine plantations. *Canadian Journal of Forest Research*. 29 (7): 1055-1064.
- Leniere A, Houle G. (2006) Response of herbaceous plant diversity to reduced structural diversity in maple-dominated (*Acer saccharum* Marsh.) forests managed for sap extraction. *Forest Ecology and Management*. 231 (1-3): 94-104
- Margalef R. (1968). *Perspective in Ecological Theory*. Chicago: University of Chicago Press.
- North M, Oakley B, Fiegenger R, Gray A, Barbour M. (2005) Influence of light and soil moisture on Sierran mixed-conifer understory communities. *Plant Ecology*. 177 (1): 13-24.
- Steege, H. et al. (2006) Continental-scale patterns of canopy tree composition and function across Amazonia. *Nature*, 443: 444-447
- Weiher E. (2003) Species richness along multiple gradients: testing a general multivariate model in oak savannas. *Oikos*. 101 (2): 311-316.
- 白顺江, 陆贵巧, 谷建才, 张锁成, 郑辉, 王雄宾. (2006) 雾灵山物种多样性及景观格局多样性的研究. *河北农业大学学报*. 29(2): 60-64
- 樊正球, 陈鹭真, 李振基. (2001) 人为干扰对生物多样性的影响. *中国生态农业学报*. 9(2): 31-34.
- 李宗善, 唐建维, 郑征, 李庆军, 罗成昆, 刘正安, 李自能, 段文勇, 郭贤明. (2004) 西双版纳热带山地雨林的植物多样性研究. *植物生态学报* 28(6): 833-843
- 刘春迎. (1999) KIRA 指标在中国植被与气候关系研究中的应用. *植物生态学报* 23(2): 125-138
- 刘增力, 郑成洋, 方精云. (2004) 河北小五台山北坡植物物种多样性的垂直梯度变化. *生物多样性*. 12(1): 137-145
- 彭闪江, 黄忠良, 徐国良, 欧阳学军, 张池. (2003) 生境异质性对鼎湖山植物群落多样性的影响. *广西植物*. 23(5): 391-398
- 沈泽昊, 张新时, 金义兴. (2000) 三峡大老岭森林物种多样性的空间格局分析及其地形解释. *植物学报*. 42(6): 620-627
- 沈泽昊, 胡志伟, 赵俊, 王会. (2007) 安徽牯牛降的植物多样性垂直分布特征——兼论山顶效应的影响. *山地学报*. 25(2): 160-168
- 唐志尧, 柯金虎. (2004) 秦岭牛背梁植物物种多样性垂直分布格局. *生物多样性* 12(1): 108-114
- 唐志尧, 方精云, 张玲. (2004) 秦岭太白山木本植物物种多样性的梯度格局及环境解释. *生物多样性* 12(1): 108-114
- 王伯荪, 张炜银, 张军丽. (2001) 海南岛热带山地雨林群落物种多样性的空间格局分析. *热地*

亚热带植物学报9(3):229-234

王庆锁, 王襄平, 罗菊春, 冯宗炜, 李经天, 马玉华, 苏玉华.(1997) 生态交错带与生物多样性.生物多样性5(2):126-131

王庆锁, 冯宗炜, 罗菊春.(2000)河北北部、内蒙古东部森林-草原交错带生物多样性研究.植物生态学报24(2):141-146

王庆锁. (2004) 河北北部内蒙古东部森林草原交错带植被和生物多样性的研究. 北京: 气象出版社.

项华均, 安树青, 王中生, 郑建伟, 冷欣, 卓元年.(2004)热带森林植物多样性及其维持机制.生物多样性12(2):290-300

于顺利, 马克平, 徐存宝, 金淑芳, 宋晓兵, 陈灵芝.(2004).环境梯度下蒙古栎群落的物种多样性特征.生态学报24(12):2932-2939

张荣京, 张永夏, 严岳鸿, 陈红锋, 刑福武.(2005)深圳大鹏半岛常绿季雨林和常绿阔叶林群落物种多样性分析.山地学报23(4):495-501

克里施纳默西(2006) 生物多样性教程.北京:化学工业出版社

张金屯. (2004) 数量生态学. 北京: 科学出版社.

中国科学院内蒙古宁夏综合考察队. (1985) 内蒙古植被. 北京: 科学出版社

附录 1 林下草本植物名录

种名	拉丁名	科	属
阿尔泰狗娃花	<i>Heteropappus</i> Less. <i>altaicus</i> (Willd.) Novopokr.	菊科	狗娃花属
矮紫苞鸢尾	<i>Iris</i> Linn. var. <i>nana</i> Maxim.	鸢尾科	鸢尾属
凹舌兰	<i>Coeloglossum viride</i> (Linn.) Hartm	兰科	凹舌兰属
白花堇菜	<i>Viola</i> Linn. <i>lactiflora</i> Nakai	堇菜科	堇菜属
白芍	<i>Paeonia sterniana</i>	芍药科	芍药属
白头翁	<i>Pulsatilla</i> Adans. <i>chinensis</i> (Bunge) Regel	毛茛科	白头翁属
百金花	<i>Centaurium</i> Hill. var. <i>altaicum</i> (Griseb.) Kitag. et Hara	龙胆科	百金花属
百里香	<i>Thymus mongolicus</i> Ronn.	唇形科	百里香属
败酱	<i>Patrinia scabiosaefolia</i> Fisch. Ex Trev.	败酱科	败酱属
斑叶堇菜	<i>Viola variegata</i>	堇菜科	堇菜属
斑叶兰	<i>Goodyera schlechtendaliana</i> Rchb. F.	兰科	斑叶兰属
瓣蕊唐松草	<i>Thalictrum petaloideum</i>	毛茛科	唐松草属
抱茎苦蕒菜	<i>Ixeris</i> Cass. <i>sonchifolia</i> Hance	菊科	苦蕒菜属
北柴胡	<i>Bupleurum chinense</i>	伞形科	柴胡属
北车前	<i>Plantago media</i> Linn.	车前科	车前属
北京堇菜	<i>Viola</i> Linn. <i>pekinensis</i> (Regel) W. Beck.	堇菜科	堇菜属
北京隐子草	<i>Cleistogenes</i> Keng <i>hancei</i> Keng	禾本科	隐子草属
贝加尔唐松草	<i>Thalictrum baicalense</i>	毛茛科	唐松草属
贝加尔针茅	<i>Stipa Baicalensis</i>	禾本科	针茅属
笔管草	<i>Hippochaete Mildedebile</i> Roxb.	木贼科	木贼属
篦苞风毛菊	<i>Saussurea pectinata</i> Bunge	菊科	风毛菊属
蝙蝠葛	<i>Menispermum</i> Linn. <i>dauricum</i> DC.	防己科	蝙蝠葛属
扁茎黄芪	<i>Astragalus</i> Linn. <i>complanatus</i> R. Br.	豆科	黄芪属
扁蕾	<i>Gentianopsis</i> Ma <i>barbata</i> (Froel.) Ma	龙胆科	扁蕾属
扁蓿豆	<i>Melissitus ruthenica</i>	豆科	草木樨属
并头黄芩	<i>Scutellaria scordifolia</i> Fisch. Ex Schrank	唇形科	黄芩属
苍耳	<i>Xanthium sibiricum</i>	菊科	苍耳属
苍术	<i>Atractylodes</i> DC. <i>lancea</i> (Thunb.) DC.	菊科	苍术属
糙苏	<i>Phlomis</i> Linn. <i>umbrosa</i> Turcz.	唇形科	糙苏属
草本威灵仙	<i>Veronicastrum</i> Heist. ex Farbic. <i>sibiricum</i> (Linn.) Pennell	玄参科	腹水草属
草地风毛菊	<i>Saussurea amara</i>	菊科	风毛菊属
草木樨	<i>Astragalus melilotoides</i>	豆科	黄芪属
草木樨状黄芪	<i>Astragalus</i> Linn. <i>melilotoides</i> Pall.	豆科	黄芪属
草问荆	<i>Equisetum pratense</i>	木贼科	木贼属
草乌头	<i>Aconitum kusnezoffii</i>	毛茛科	乌头属
草原老鹳草	<i>Geranium</i> Linn. <i>pratense</i> Linn.	牛儿苗科	老鹳草属
叉分蓼	<i>Polugonum divaricatum</i>	蓼科 5	蓼属
长瓣铁线莲	<i>Clematis</i> Linn. <i>macropetala</i> Ledeb.	毛茛科	铁线莲属
长梗米蒿	<i>Artemisia</i> Linn. var. <i>longipedunculata</i> Y. R. Ling	菊科	蒿属
长戟叶蓼	<i>Polygonum maackianum</i> Regel	蓼科	蓼属
长毛银莲花	<i>Anemone</i> Linn. <i>narcissiflora</i> Linn. var. <i>crinita</i> (Juz.) Tamura	毛茛科	银莲花属

车前	<i>Plantago asiatica</i> Linn.	车前科	车前属
齿叶紫沙参		桔梗科	沙参属
穿龙薯蓣	<i>Dioscorea</i> Linn. <i>nipponica</i> Makino	薯蓣科	薯蓣属
垂果南芥	<i>Arabis</i> Linn. <i>pendula</i> Linn.	十字花科	南芥属
达乌里黄芪	<i>Astragalus dahuricus</i> (Pall.) DC.	豆科	黄芪属
达乌里苾苳	<i>Cymbaria</i> Linn. <i>dahurica</i> Linn.	玄参科	苾苳属
达乌里羊茅	<i>Festuca dahurica</i> (St.-yves) Krecz. et Bobr.	禾本科	羊茅属
长瓣铁线莲	<i>Clematis macropetala</i> Ledeb.	毛茛科	铁线莲属
大齿山芹	<i>Ostericum</i> Hoffm. <i>grosseserratum</i> (Maxim.) Kitagawa	伞形科	山芹属
大丁草	<i>Leibnitzia</i> Cass. <i>anandria</i> (L.) Nakai	菊科	大丁草属
大羊茅	<i>Festuca gigantea</i> (L.) Vill.	禾本科	羊茅属
大野豌豆	<i>Vicia</i> Linn. <i>gigantea</i> Bunge	豆科	野豌豆属
大叶龙胆	<i>Gentiana macrophylla</i> Pall.	龙胆科	龙胆属
大叶野豌豆	<i>Vicia pseudorobus</i> Fisch. et C. A. Mey.	豆科	野豌豆属
大油芒	<i>Spodiopogon</i> Trin. <i>sibiricus</i> Trin.	禾本科	大油芒属
大针茅	<i>Stipa</i> Linn. <i>grandis</i> P. Smirn.	禾本科	针茅属
大籽蒿	<i>Artemisia sieversiana</i> Ehrhart ex Willd.	菊科	蒿属
等齿委陵菜	<i>Potentilla</i> Linn. <i>simulatrix</i> Wolf	蔷薇科	委陵菜属
地榆	<i>Sanguisorba officinalis</i>	蔷薇科	地榆属
东北堇菜	<i>Viola mandshurica</i>	堇菜科	堇菜属
东北牡蒿	<i>Artemisia</i> Linn. <i>mandshurica</i> (Komar.) Komar.	菊科	蒿属
东方草莓	<i>Fragaria orientalis</i>	蔷薇科	草莓属
东亚唐松草	<i>Thalictrum minus</i> var. <i>hypoleucum</i>	毛茛科	唐松草属
短梗箭头唐松草	<i>Thalictrum</i> Linn. var. <i>brevipes</i> Hara	毛茛科	唐松草属
短毛独活	<i>Heracleum</i> Linn. <i>moellendorffii</i> Hance	伞形科	独活属
短毛裂叶堇菜		堇菜科	堇菜属
短尾铁线莲	<i>Clematis brevicaudata</i> DC.	毛茛科	铁线莲属
多茎野豌豆	<i>Vicia multicaulis</i> Ledeb.	豆科	野豌豆属
多裂蒲公英	<i>Taraxacum dissectum</i> (Ledeb.) Ledeb.	菊科	蒲公英属
多歧沙参	<i>Adenophora</i> Fisch. <i>wawreana</i> Zahlbr.	桔梗科	沙参属
峨参	<i>Anthriscus</i> (Pers.) Hoffm. <i>sylvestris</i> (Linn.) Hoffm.	伞形科	峨参属
二色补血草	<i>Limonium</i> Mill. <i>bicolor</i> (Bunge) Kuntze	白花丹科	补血草属
二叶兜被兰	<i>Neottianthe</i> Schltr. <i>cucullata</i> (Linn.) Schltr.	兰科	兜被兰属
二叶舌唇兰	<i>Platanthera</i> Rich. <i>chlorantha</i> Cust. ex Rchb.	兰科	舌唇兰属
二叶舞鹤草	<i>Maianthemum bifolium</i> (L.) Fr. Schmidt	百合科	舞鹤草属
繁缕	<i>Stellaria</i> Linn. <i>media</i> (Linn.) Cyr.	石竹科	繁缕属
防风	<i>Saposhnikovia divaricata</i>	伞形科	防风属
飞廉	<i>Carduus</i> Linn. <i>nutans</i> Linn.	菊科	飞廉属
费菜	<i>Sedum</i> Linn. <i>aizoon</i> Linn.	景天科	景天属
分枝麻花头	<i>Serratula</i> Linn. <i>cardunculus</i> (Pall.) Schischk.	菊科	麻花头属
风毛菊	<i>Saussurea</i> DC. <i>japonica</i> (Thunb.) DC.	菊科	风毛菊属
拂子茅	<i>Calamagrostis epigeios</i> (Linn.) Roth	禾本科	拂子茅属
福王草	<i>Prenanthes tatarinowii</i> Maxim.	菊科	福王草属
附地菜	<i>Trigonotis</i> Stev. <i>peduncularis</i> (Trev.) Benth. ex Baker et Moore	紫草科	附地菜属

甘菊	<i>Dendranthema lavandulifolium</i> (Fisch. ex Trautv.) Ling et Shih	菊科	菊属
高二裂委陵菜	<i>Potentilla imbricata</i>	蔷薇科	委陵菜属
高山露珠草	<i>Circaea</i> Linn. <i>alpina</i> Linn.	柳叶菜科	露珠草属
高山蓍	<i>Achillea</i> Linn. <i>alpina</i> Linn.	菊科	蓍属
高山紫菀	<i>Aster alpinus</i>	菊科	紫菀属
藁本	<i>Ligusticum</i> Linn. <i>sinense</i> Oliv.	伞形科	藁本属
狗舌草	<i>Senecio</i> Linn. <i>kirilowii</i> Turcz.	菊科	千里光属
狗娃花	<i>Heteropappus hispidus</i>	菊科	狗娃花属
狗尾草	<i>Setaria</i> Beauv. <i>viridis</i> (Linn.) Beauv.	禾本科	狗尾草属
光萼青兰	<i>Dracocephalum</i> Linn. nom. conserv. <i>argunense</i> Fisch. ex Link	唇形科	青兰属
广布野豌豆	<i>Vicia cracca</i>	豆科	黄芪属
鬼针草	<i>Bidens</i> Linn. <i>pilosa</i> Linn.	菊科	鬼针草属
旱麦瓶草	<i>Silene</i>	石竹科	蝇子草属
贺兰山延胡索	<i>Corydalis alaschanica</i> (Maxim.) Peshkova	罂粟科	紫堇属
鹤虱	<i>Lappula myosotis</i>	紫草科	鹤虱属
黑柴胡	<i>Bupleurum smithii</i>	伞形科	柴胡属
红柴胡	<i>Bupleurum</i> Linn. <i>scorzonerifolium</i> Willd.	伞形科	柴胡属
红纹马先蒿	<i>Pedicularis striata</i>	玄参科	马先蒿属
互叶金腰	<i>Chrysosplenium alternifolium</i> var. <i>sibiricum</i>	虎耳草科	金腰属
花旗杆	<i>Dontostemon dentatus</i>	十字花科	花旗杆属
花葱	<i>Polemonium coeruleum</i> Linn.	花荵科	花荵属
华北风毛菊	<i>Saussurea</i> DC. <i>mongolica</i> Franch.	菊科	风毛菊属
华北蓝盆花	<i>Scabiosa</i> Linn. <i>tschiliensis</i> Grun.	川续断科	蓝盆花属
华北耧斗菜	<i>Aquilegia</i> Linn. <i>yabeana</i> Kitag.	毛茛科	耧斗菜属
华北乌头	<i>Aconitum</i> Linn. var. <i>angustius</i> W. T. Wang	毛茛科	乌头属
黄花龙牙	<i>Patrinia scabiosaefolia</i> Fisch	败酱科	败酱属
黄花铁线莲	<i>Clematis</i> Linn. <i>intricata</i> Bunge	毛茛科	铁线莲属
黄精	<i>Polygonatum sibiricum</i> Delar. Ex Redoute	百合科	黄精属
黄毛棘豆	<i>Oxytropis</i> DC. <i>ochrantha</i> Turcz.	豆科	棘豆属
黄囊苔草	<i>Carex korshinskii</i> Kom.	莎草科	苔草属
黄芪	<i>Astragalus membranaceus</i> (Fisch.) Bunge	豆科	黄芪属
黄芩	<i>Scutellaria</i> Linn. <i>baicalensis</i> Georgi	唇形科	黄芩属
灰叶黄芪	<i>Astragalus discolor</i> Bunge ex Maxim.	豆科	黄芪属
火绒草	<i>Leontopodium leontopodioides</i>	菊科	火绒草属
鸡腿堇菜	<i>Viola acuminata</i>	堇菜科	堇菜属
尖齿糙苏	<i>Phlomis dentosa</i> Franch.	唇形科	糙苏属
尖头叶藜	<i>Chenopodium acuminatum</i>	藜科	藜属
节节草	<i>Equisetum ramosissimum</i> Desf.	木贼科	木贼属
金莲花	<i>Trollius chinensis</i> Bunge	毛茛科	金莲花属
堇色早熟禾	<i>Poa ianthina</i> Keng	禾本科	早熟禾属
荆芥	<i>Nepeta cataria</i>	唇形科	荆芥属
景天三七	<i>Sedum aizoon</i>	景天科	景天属
菊叶委陵菜	<i>Potentilla tanacetifolia</i> Willd. ex Schlecht.	蔷薇科	委陵菜属
卷耳	<i>Cerastium arvense</i>	石竹科	卷耳属

绢毛委陵菜	<i>Potentilla sericea</i> Linn.	蔷薇科	委陵菜属
蕨	<i>Pteridium aquilinum</i>	蕨科	蕨属
看麦娘	<i>Alopecurus aequalis</i> Sobol.	禾本科	看麦娘属
苦参	<i>Sophora flavescens</i> Alt.	豆科	槐属
苦苣菜	<i>Ixeris polycephala</i> Cass.	菊科	苦苣菜属
宽叶山蒿	<i>Artemisia stolonifera</i> (Maxim.) Komar.	菊科	蒿属
款冬	<i>Tussilago farfara</i> Linn.	菊科	款冬属
蓝刺头	<i>Echinops sphaerocephalus</i> Linn.	菊科	蓝刺头属
狼毒	<i>Stellera chamaejasme</i>	瑞香科	狼毒属
老鹳草	<i>Geranium wilfordii</i> Maxim.	牻牛儿苗科	老鹳草属
冷蒿	<i>Artemisia frigida</i>	菊科	蒿属
藜芦	<i>Veratrum nigrum</i> Linn.	百合科	藜芦属
辽东蒿	<i>Artemisia verbenacea</i> (Komar.) Kitag.	菊科	蒿属
辽西扁蓿豆	<i>Melissitus liaosiensis</i>	豆科	黄芪属
裂叶蒿	<i>Artemisia tanacetifolia</i>	菊科	蒿属
裂叶堇菜	<i>Viola dissecta</i>	堇菜科	堇菜属
裂叶荆芥	<i>Schizonepeta tenuifolia</i>	唇形科	荆芥属
林地早熟禾	<i>Poa crymophila</i> Keng	禾本科	早熟禾属
林生银莲花	<i>Anemone silvestris</i>	毛茛科	银莲花属
林问荆	<i>Equisetum sylvaticum</i>	木贼科	木贼属
林荫千里光	<i>Senecio nemorensis</i> Linn.	菊科	千里光属
鳞叶龙胆	<i>Gentiana squarrosa</i> Ledeb.	龙胆科	龙胆属
铃兰	<i>Convallaria majalis</i> Linn.	百合科	铃兰属
柳兰	<i>Epilobium angustifolium</i> Linn.	柳叶菜科	柳叶菜属
柳叶沙参	<i>Adenophora coronopifolia</i> Fisch	桔梗科	沙参属
龙江风毛菊	<i>Saussurea amurensis</i> Turcz.	菊科	风毛菊属
龙须菜	<i>Asparagus schoberioides</i> Kunth	百合科	天门冬属
龙牙草	<i>Agrimonia pilosa</i>	蔷薇科	龙牙草属
耧斗菜	<i>Aquilegia viridiflora</i> Pall.	毛茛科	耧斗菜属
鹿蹄草	<i>Pyrola calliantha</i> H. Andr.	鹿蹄草科	鹿蹄草属
轮叶棘豆	<i>Oxytropis chiliophylla</i> Royle	豆科	棘豆属
轮叶沙参	<i>Adenophora tetraphylla</i> (Thunb.) Fisch.	桔梗科	沙参属
麻花头	<i>Serratula centauroides</i>	菊科	麻花头属
马先蒿	<i>Pedicularis reaupinanta</i> L.	玄参科	马先蒿属
猫儿菊	<i>Hypochaeris ciliata</i> (Thunb.) Makino	菊科	猫儿菊属
猫眼草	<i>Euphorbia lunulata</i>	大戟科	大戟属
华北前胡	<i>Peucedanum harry-smithii</i> Fedde ex Wolff	伞形科	前胡属
毛茛	<i>Ranunculus japonicus</i>	毛茛科	毛茛属
毛连菜	<i>Picris hieracioides</i>	菊科	毛连菜属
毛脉山莴苣	<i>Lactuca raddeana</i> Maxim	菊科	莴苣属
毛平车前	<i>Plantago depressa</i> Willd. subsp. <i>turczaninowii</i> (Ganjeschin) N.N. Tsvelev	车前科	车前属
毛蕊老鹳草	<i>Geranium platyanthum</i> Duthie	牻牛儿苗科	老鹳草属
毛细柄黄芪	<i>Astragalus capilipes</i> Fisch. Ex Bge	豆科	黄芪属
莓叶委陵菜	<i>Potentilla fragarioides</i>	蔷薇科	委陵菜属

蒙古马兰	<i>Kalimeris mongolica</i> (Franch.) Kitam.	菊科	马兰属
蒙蒿	<i>Artemisia mongolica</i>	菊科	蒿属
蒙菊	<i>Dendranthema mongolicum</i> (Ling) Tzvel.	菊科	菊属
蒙山莴苣	<i>Lactuca tatarica</i> (L.) C.A.Mey	菊科	莴苣属
棉团铁线莲	<i>Clematis hexapetala</i> Pall.	毛茛科	铁线莲属
牡蒿	<i>Artemisia japonica</i> Thunb.	菊科	蒿属
苜蓿	<i>Medicago lupulina</i> L	豆科	苜蓿属
南牡蒿	<i>Artemisia eriopoda</i>	菊科	蒿属
南玉带	<i>Asparagus oligoclonos</i> Maxim.	百合科	天门冬属
牛蒡	<i>Arctium lappa</i> Linn.	菊科	牛蒡属
牛扁	<i>Aconitum barbatum</i> var. <i>puberulum</i>	毛茛科	乌头属
女娄	<i>Silene aprica</i>	石竹科	蝇子草属
蓬子菜	<i>Galium verum</i>	茜草科	拉拉藤属
披针叶苔草	<i>Carex lanceolata</i>	莎草科	苔草属
匍枝委陵菜	<i>Potentilla flagellaris</i>	蔷薇科	委陵菜属
蒲公英	<i>Taraxacum mongolicum</i>	菊科	蒲公英属
祁州漏芦	<i>Rhaponticum uniflorum</i> (L.) DC	菊科	祁州漏芦属
芥苳	<i>Adenophora tracheloides</i> Maxim.	桔梗科	沙参属
洽草	<i>Koeleria cristata</i> (Linn.) Pers.	禾本科	洽草属
茜草	<i>Rubia cordifolia</i>	茜草科	茜草属
秦艽	<i>Gentiana macrophylla</i> Pall.	龙胆科	龙胆属
青兰	<i>Dracocephalum ruyschiana</i>	唇形科	青兰属
蜻蜓兰	<i>Tulotis fuscescens</i> (L.) Czer.	兰科	蜻蜓兰属
球果堇菜	<i>Viola collina</i> Bess.	堇菜科	堇菜属
全叶马兰	<i>Kalimeris integrifolia</i> Turcz. ex DC.	菊科	马兰属
全缘叶橐吾	<i>Ligularia mongolica</i>	菊科	橐吾属
拳参	<i>Polygonum bistorta</i>	蓼科	蓼属
绒背蓟	<i>Cirsium vlassovianum</i> Fisch. ex DC.	菊科	蓟属
乳白香青	<i>Anaphalis lactea</i> Maxim.	菊科	香青属
乳浆大戟	<i>Euphorbia esula</i> Linn.	大戟科	大戟属
三瓣猪殃殃	<i>G. trifidum</i> L.	茜草科	拉拉藤属
三脉柴胡		伞形科	柴胡属
三脉紫菀	<i>Aster ageratoides</i> Turcz.	菊科	紫菀属
三色沙参		桔梗科	沙参属
沙参	<i>Adenophora stricta</i> Miq.	桔梗科	沙参属
砂韭	<i>Allium bidentatum</i> Fisch. Ex Prokh. Et Ikonnikov-Galitzky	百合科	葱属
山丹	<i>Lilium pumilum</i> DC.	百合科	百合属
山蒿	<i>Artemisia brachyloba</i> Franch.	菊科	蒿属
山尖子	<i>Parasenecio hastatus</i> (Linn.) H. Koyama	菊科	蟹甲草属
山韭	<i>Allium japonicum</i>	百合科	葱属
山黧豆	<i>Lathyrus quinquenervius</i>	豆科	岩黄芪属
山柳菊	<i>Hieracium umbellatum</i> Linn.	菊科	山柳菊属
山马蔺	<i>Iris ruthenica</i> Ker.-Gawl. var. <i>nana</i> Maxim.	鸢尾科	鸢尾属
山牛蒡	<i>Synurus deltoides</i> (Ait.) Nakai	菊科	牛蒡属

山野豌豆	<i>Vicia amoena</i>	豆科	野豌豆属
少花米口袋	<i>Gueldenstaedtia verna</i> (Georgi) Boriss.	豆科	米口袋属
深山堇菜	<i>Viola selkirkii</i> Pursh ex Gold	堇菜科	堇菜属
蹄叶橐吾	<i>Ligularia fischeri</i> (Ledeb.) Turcz	菊科	橐吾属
蓍草	<i>Achillea alpina</i> L.	菊科	蓍草属
石沙参	<i>Adenophora polyantha</i>	桔梗科	沙参属
石生悬钩子	<i>Rubus saxatilis</i>	蔷薇科	悬钩子属
石竹	<i>Dianthus chinensis</i>	石竹科	石竹属
疏毛钩叶委陵菜		蔷薇科	委陵菜属
鼠掌老鹳草	<i>Geranium sibiricum</i>	牻牛儿苗科	老鹳草属
双花黄堇菜	<i>Viola biflora</i>	堇菜科	堇菜属
水金凤	<i>Impatiens noli-tangere</i> Linn.	凤仙花科	凤仙花属
四叶葎	<i>Galium bungei</i> Steud.	茜草科	拉拉藤属
酸模	<i>Rumex acetosa</i> Linn.	蓼科	酸模属
天兰苜蓿	<i>Medicago lupulina</i> Linn.	豆科	苜蓿属
铁杆蒿	<i>Artemisia sacrorum</i>	菊科	蒿属
铁线莲	<i>Clematis florida</i> Thunb.	毛茛科	铁线莲属
兔儿伞	<i>Syneilesis aconitifolia</i> (Bunge) Maxim.	菊科	兔儿伞属
橐吾	<i>Ligularia sibirica</i> (Linn.) Cass.	菊科	橐吾属
椭圆叶花锚	<i>Halenia elliptica</i> D. Don	龙胆科	花锚属
歪头菜	<i>Vicia</i> Linn. <i>unijuga</i> A. Br.	豆科	野豌豆属
委陵菜	<i>Potentilla chinensis</i> Ser.	蔷薇科	委陵菜属
蚊子草	<i>Filipendula palmata</i> (Pall.) Maxim.	蔷薇科	蚊子草属
乌苏里风毛菊	<i>Saussurea ussuriensis</i>	菊科	风毛菊属
乌头	<i>Aconitum formosanum</i> Tamura	毛茛科	乌头属
屋根草	<i>Crepis tectorum</i> Linn.	菊科	还阳参属
无芒隐子草	<i>Cleistogenes songorica</i> (Roshev.) Ohwi	禾本科	隐子草属
五脉山黧豆	<i>Lathyrus quinquenervius</i> (Miq.)Litv.et Kom	豆科	山黧豆属
舞鹤草	<i>Maianthemum bifolium</i> (Linn.) F. W. Schmidt	百合科	舞鹤草属
勿忘草	<i>Myosotis silvatica</i> Ehrh. ex Hoffm.	紫草科	勿忘草属
雾灵沙参	<i>Adenophora wulingshanica</i> Hong	桔梗科	沙参属
锡林沙参		桔梗科	沙参属
细距堇菜	<i>Viola tenuicornis</i> W. Beck.	堇菜科	堇菜属
细叶白头翁	<i>Pulsatilla turczaninovii</i>	毛茛科	白头翁属
细叶藁本	<i>Ligusticum tenuissimum</i> (Nakai) Kitag.	伞形科	藁本属
细叶黄乌头	<i>Aconitum barbatum</i> Pers.	毛茛科	乌头属
细叶菊	<i>Dendranthema maximowiczii</i> (Komar) Tzvel.	菊科	菊属
细叶鸢尾	<i>Iris tenuifolia</i> Pall.	鸢尾科	鸢尾属
细叶远志	<i>Polygala tenuifolia</i> Willd	远志科	远志属
狭叶米口袋	<i>Gueldenstaedtia stenophylla</i> Bunge	豆科	米口袋属
狭叶沙参	<i>Adenophora gmelinii</i> (Spreng.) Fisch.	桔梗科	沙参属
狭叶山野豌豆	<i>Vicia amoena</i> Fisch. ex DC. var. <i>oblongifolia</i> Regel Tent.	豆科	野豌豆属
腺毛委陵菜	<i>Potentilla longifolia</i>	蔷薇科	委陵菜属
香堇菜	<i>Viola odorata</i> Linn.	堇菜科	堇菜属

香青兰	<i>Dracocephalum moldavica</i> Linn.	唇形科	青兰属
香薷	<i>Elsholtzia ciliata</i> (Thunb.) Hyland.	唇形科	香薷属
小车前	<i>Plantago minuta</i> Pall.	车前科	车前属
小红菊	<i>Dendranthema chanelii</i>	菊科	菊属
小花风毛菊	<i>Saussurea parviflora</i> (Poir.) DC.	菊科	风毛菊属
小花火烧兰	<i>Epipactis hellaborine</i> (L.) Crantz	兰科	火烧兰属
小花蜻蜓兰	<i>Tulotis ussuriensis</i> (Reg et Macck) H. Hara	兰科	蜻蜓兰属
小花沙参	<i>Adenophora micrantha</i> Hong	桔梗科	沙参属
小黄花菜	<i>Hemerocallis minor</i> Mill.	百合科	萱草属
小卷耳		石竹科	卷耳属
小藜	<i>Chenopodium serotinum</i> Linn.	藜科	藜属
小玉竹	<i>Polygonatum humile</i> Fisch. Ex Maxim.	百合科	黄精属
楔叶菊	<i>Dendranthema nakdongense</i> (Nakai) Tzvel.	菊科	菊属
缬草	<i>Valeriana officinalis</i> Linn.	败酱科	缬草属
兴安柴胡	<i>Bupleurum sibiricum</i> Vest	伞形科	柴胡属
兴安短柄草	<i>Brachypodium pinnatum</i> (L.) Beauv	禾本科	短柄草属
兴安升麻	<i>Cimicifuga dahurica</i> (Turcz. ex Fischer et C. A. Meyer) Maxim.	毛茛科	升麻属
兴安野青茅	<i>Deyeuxia turczaninowii</i> (Litv.) Y. L. Chang	禾本科	野青茅属
悬钩子	<i>Rubus</i> L.	蔷薇科	悬钩子属
鸦葱	<i>Scorzonera austriaca</i> Willd.	菊科	鸦葱属
亚洲蓍草		菊科	蓍草属
岩败酱	<i>Patrinia rupestris</i> (Pall.) Juss.	败酱科	败酱属
岩青兰	<i>Dracocephalum rupestre</i> Hance	唇形科	青兰属
羊草	<i>Leymus chinensis</i> (Trin.) Tzvel.	禾本科	赖草属
羊茅	<i>Festuca ovina</i> Linn.	禾本科	羊茅属
野艾蒿	<i>Artemisia lavandulaefolia</i>	菊科	蒿属
野草莓	<i>Fragaria vesca</i> Linn.	蔷薇科	草莓数
野火球	<i>Trifolium lupinaster</i> Linn.	豆科	车轴草属
野棉花	<i>Anemone vitifolia</i> Buch.-Ham.	毛茛科	银莲花属
野青茅	<i>Deyeuxia arundinacea</i> (Linn.) Beauv.	禾本科	野青茅属
野瑞香	<i>Diarthron linifolium</i>	瑞香科	瑞香属
野豌豆	<i>Vicia sepium</i> Linn.	豆科	野豌豆属
野亚麻	<i>Linum stelleroides</i> Planch.	亚麻科	亚麻属
页蒿	<i>Carum carvi</i> L.	伞形科	页蒿属
异叶败酱	<i>Patrinia heterophylla</i>	败酱科	败酱属
阴地菫菜	<i>Viola yezoensis</i> Maxim.	堇菜科	堇菜属
银背风毛菊	<i>Saussurea nivea</i>	菊科	风毛菊属
银莲花	<i>Anemone cathayensis</i> Kitag.	毛茛科	银莲花属
隐子草	<i>Cleistogenes</i>	禾本科	隐子草属
硬质早熟禾	<i>Poa sphondylodes</i> Trin.	禾本科	早熟禾属
有斑百合	<i>Lilium concolor</i> Salisb. var. <i>pulchellum</i> (Fisch.) Regel	百合科	百合属
有柄紫沙参		桔梗科	沙参属
鼬瓣花	<i>Galeopsis bifida</i> Boenn.	唇形科	鼬瓣花属
羽裂蓝刺头	<i>Echinops pseudosetifer</i> Kitag.	菊科	蓝刺头属

羽叶风毛菊	<i>Saussurea maximowiczii</i> Herd.	菊科	风毛菊属
玉竹	<i>Polygonatum odoratum</i> (Mill.) Druce	百合科	黄精属
远东茛苳草	<i>Achnatherum extremiorientale</i> (Hara) Keng ex P. C. Kuo	禾本科	茛苳草属
远志	<i>Polygala tenuifolia</i> Willd.	远志科	远志属
杂配藜	<i>Chenopodium hybridum</i>	藜科	藜属
早开堇菜	<i>Viola prioantha</i> Bunge	堇菜科	堇菜属
展毛乌头	<i>Aconitum carmichaeli</i> Debx. var. <i>truppelianum</i> (Ulbr.) W.T.Wang et Hsiao	毛茛科	乌头属
展枝沙参	<i>Adenophora divaricata</i> Franch. et Sav.	桔梗科	沙参属
掌叶多裂委陵菜	<i>Potentilla multifida</i> Linn. var. <i>ornithopoda</i> (Tausch) Wolf	蔷薇科	委陵菜属
掌叶堇菜	<i>Viola dactyloides</i> Roem. et Schult.	堇菜科	堇菜属
针茅	<i>Stipa capillata</i> Linn.	禾本科	针茅属
针苔草	<i>C. onoei</i> Franch. et Sav.	莎草科	苔草属
直穗鹅观草	<i>Roegneria japonensis</i> (Honda) Keng	禾本科	鹅观草属
雉隐天冬	<i>Asparagus schoberioides</i> Kunth	百合科	天门冬属
中华隐子草	<i>Cleistogenes chinensis</i> (Maxim.) Keng	禾本科	隐子草属
钟苞麻花头	<i>Serratula cupuliformis</i> Nakai et Kitag.	菊科	麻花头属
种阜草	<i>Moehringia lateriflora</i> (Linn.) Fenzl	石竹科	种阜草属
皱叶鸦葱	<i>Scorzonera inconspicua</i> Lipsch. ex Pavl.	菊科	鸦葱属
珠芽蓼	<i>Polygonum viviparum</i>	蓼科	蓼属
猪毛菜	<i>Salsola collina</i>	藜科	猪毛菜属
猪殃殃	<i>Rubia aparine</i> var. <i>tenerum</i>	茜草科	拉拉藤属
锥叶柴胡	<i>Bupleurum bicaule</i> Helm	伞形科	柴胡属
紫斑风铃草	<i>Campanula punctata</i>	桔梗科	风铃草属
紫草	<i>Lithospermum erythrorhizon</i> Sieb. et Zucc.	紫草科	紫草属
紫花野菊	<i>Dendranthema zawadskii</i> (Herb.) Tzvel.	菊科	菊属
紫沙参	<i>Adenophora paniculata</i> Nannf	桔梗科	沙参属
紫菀	<i>Aster tataricus</i> Linn. f.	菊科	紫菀属
紫羊茅	<i>Festuca rubra</i> Linn.	禾本科	羊茅属

附录2 林下灌木植物名录

种名	拉丁名	科	属
茶藨子		虎耳草科	茶藨子属
茶条槭	<i>Acer ginnala Maxim</i>	槭树科	槭属
稠李	<i>Padus racemosa (Linn.) Gilib.</i>	蔷薇科	稠李属
葱皮忍冬	<i>Lonicera ferdinandii Franch</i>	忍冬科	忍冬属
大叶小檗	<i>Berberis ferdinandi-coburgii Schneid</i>	小檗科	小檗属
东北鼠李	<i>Rhamnus schneideri Lévl. et Vant. var. manshurica Nakai</i>	鼠李科	鼠李属
冻叶鼠李		鼠李科	鼠李属
二色胡枝子		豆科	胡枝子属
黑果枸杞	<i>Cotoneaster melanocarpus Lodd</i>	蔷薇科	枸杞属
胡枝子	<i>Lespedeza bicolor Turcz.</i>	豆科	胡枝子属
虎榛子	<i>Ostryopsis davidiana Decaisne</i>	桦木科	虎榛子属
花楸	<i>Sorbus pohuashanensis (Hance) Hedl.</i>	蔷薇科	花楸属
华北忍冬	<i>Lonicera tatarinowii Maxim.</i>	忍冬科	忍冬属
花茶藨子	<i>Ribes fargesii Franch.</i>	虎耳草科	茶藨子属
黄花柳	<i>Salix caprea Linn.</i>	杨柳科	柳属
黄花忍冬		忍冬科	忍冬属
灰枸杞	<i>Cotoneaster acutifolius Turcz.</i>	蔷薇科	枸杞属
尖叶胡枝子	<i>Lespedeza hedysaroides (Pall.) Kitag</i>	豆科	胡枝子属
金露梅	<i>Potentilla fruticosa Linn</i>	蔷薇科	委陵菜属
金银木	<i>Lonicera maackii Rupr. Maxim</i>	忍冬科	忍冬属
卷边柳	<i>Salix siuzevii Seemen</i>	杨柳科	柳属
蓝靛果忍冬		忍冬科	忍冬属
毛山楂	<i>Crataegus maximowiczii Schneid.</i>	蔷薇科	山楂属
毛叶水枸杞	<i>Cotoneaster submultiflorus Po</i>	蔷薇科	枸杞属
美蔷薇	<i>Rosa bella Rehd. et Wils.</i>	蔷薇科	蔷薇属
蒙古荚蒾	<i>Viburnum mongolicum (Pall.) Rehd</i>	忍冬科	荚蒾属
蒙古枸杞	<i>Cotoneaster mongolicus Pojark</i>	蔷薇科	枸杞属
拧条锦鸡儿		豆科	锦鸡儿属
牛奶子	<i>Elaeagnus umbellata Thunb</i>	胡颓子科	胡颓子属
平榛	<i>Corylus heterophylla Fisch</i>	榛科	榛属
绒毛绣线菊	<i>Spiraea velutina Franch</i>	蔷薇科	绣线菊

			属
沙棘	<i>Hippophae rhamnoides</i> Linn	胡颓子科	沙棘属
山刺玫	<i>Rosa davurica</i> Pall.	蔷薇科	蔷薇属
山丁子	<i>Malus baccata</i> (Linn.) Borkh	蔷薇科	苹果属
山荆子	<i>Malus baccata</i> (Linn.) Borkh	蔷薇科	苹果属
山杏	<i>Armeniaca sibirica</i> (Linn.) Lam	蔷薇科	杏属
山杨	<i>Populus davidiana</i> Dode	杨柳科	杨属
水栒子	<i>Cotoneaster multiflorus</i> Bge	蔷薇科	栒子属
水杨梅	<i>Geum aleppicum</i> Jacq.	蔷薇科	水杨梅属
小檗	<i>Berberidaceae</i>	小檗科	小檗属
小叶鼠李	<i>Rhamnus parvifolia</i> Bunge	鼠李科	鼠李属
栒子		蔷薇科	栒子属
银露梅	<i>Potentilla glabra</i>	蔷薇科	委陵菜属
照山白	<i>Rhododendron micranthum</i> Turcz	杜鹃花科	杜鹃属
中国黄花柳	<i>Salix sinica</i> (Hao) C. Wang et C. F. Fang	杨柳科	柳属
准噶尔栒子	<i>Cotoneaster soongoricus</i> (Regel et Herd.) Popov	蔷薇科	栒子属

附录3 林下草本植物分布格局

南北均出现	仅出现南部	仅出现北部
阿尔泰狗娃花	白毫花	矮紫苞鸢尾
瓣蕊唐松草	百金花	凹舌兰
北柴胡	百里香	白花堇菜
贝加尔针茅	败酱	白芍
扁蓿豆	抱茎苦苣菜	白头翁
并头黄芩	北京堇菜	斑叶堇菜
苍耳	北京隐子草	斑叶兰
苍术	扁茎黄芪	北车前
草地风毛菊	扁蕾	贝加尔唐松草
草木樨	草木樨状黄芪	笔管草
车前	长瓣铁线莲	篦苞风毛菊
大野豌豆	长梗米蒿	蝙蝠葛
地榆	长戟叶蓼	糙苏
东北堇菜	穿龙薯蓣	草本威灵仙
东亚唐松草	垂果南芥	草问荆
多茎野豌豆	大油芒	草乌头
繁缕	大针茅	草原老鹳草
防风	多裂蒲公英	叉分蓼
风毛菊	多岐沙参	长毛银莲花
拂子茅	二色补血草	齿叶紫沙参
甘菊	费菜	达乌里黄芪
藁本	附地菜	达乌里芯芭
广布野豌豆	高二裂委陵菜	达乌里羊茅
黑柴胡	高山露珠草	大瓣铁线莲
红纹马先蒿	狗舌草	大齿山芹
黄花龙牙	狗尾草	大丁草
黄囊苔草	贺兰山延胡索	大羊茅
黄芪	红柴胡	大叶龙胆
火绒草	互叶金腰	大叶野豌豆
尖齿糙苏	黄花铁线莲	等齿委陵菜
荆芥	黄毛棘豆	东北牡蒿
卷耳	灰叶黄芪	东方草莓
蕨	尖头叶藜	短梗箭头唐松草
辽东蒿	绢毛委陵菜	短毛独活
裂叶蒿	看麦娘	短毛裂叶堇菜
林地早熟禾	苦参	短尾铁线莲
林生银莲花	冷蒿	峨参
龙芽草	辽西扁蓿豆	二叶兜被兰
麻花头	裂叶荆芥	二叶舌唇兰
猫眼草	鳞叶龙胆	二叶舞鹤草
毛连菜	龙江风毛菊	飞廉

莓叶委陵菜	轮叶棘豆	分枝麻花头
苜蓿	毛白花前胡	福王草
南牡蒿	毛平车前	高山蓍草
蓬子菜	毛细柄黄芪	高山紫菀
披针叶苔草	南玉带	狗娃花
蒲公英	绒背蓟	光萼青兰
芥苳	三脉柴胡	鬼针草
茜草	三色沙参	旱麦瓶草
全缘叶橐吾	沙韭	鹤虱
三脉紫菀	山蒿	花旗杆
山韭	山柳菊	花葱
山黧豆	少花米口袋	华北风毛菊
山马蔺	水金凤	华北蓝盆花
深山堇菜	天蓝苜蓿	华北耧斗菜
石沙参	无芒隐子草	华北乌头
鼠掌老鹳草	五脉山黧豆	黄精
双花黄堇菜	细距堇菜	黄芩
铁杆蒿	细叶菊	鸡腿堇菜
歪头菜	细叶远志	节节草
乌苏里风毛菊	狭叶米口袋	金莲花
锡林沙参	狭叶山野豌豆	堇色早熟禾
细叶藁本	香堇菜	景天三七
狭叶沙参	香青兰	菊叶委陵菜
腺毛委陵菜	香薷	苦苣菜
小红菊	小花风毛菊	宽叶山蒿
小花蜻蜓兰	小花火烧兰	款冬
楔叶菊	小花沙参	蓝刺头
野艾蒿	小卷耳	狼毒
野草莓	小藜	老鹳草
野青茅	小玉竹	藜芦
异叶败酱	岩败酱	裂叶堇菜
玉竹	岩青兰	林间荆
远东芨芨草	羊草	林荫千里光
针茅	野棉花	铃兰
直穗鹅观草	野瑞香	柳兰
猪毛蒿	阴地堇菜	柳叶沙参
猪殃殃	有柄紫沙参	龙须菜
紫花野菊	鼬瓣花	耧斗菜
紫菀	远志	鹿蹄草
大籽蒿	早开堇菜	轮叶沙参
野豌豆	掌叶堇菜	马先蒿
	针苔草	猫儿菊
	钟苞麻花头	毛茛
	锥叶柴胡	毛脉山莨菪

毛蕊老鹳草
蒙古马兰
蒙蒿
蒙菊
蒙山莴苣
棉团铁线莲
牡蒿
牛蒡
牛蒡
女娄菜
匍枝委陵菜
祁州漏芦
洽草
秦艽
青兰
蜻蜓兰
球果堇
全叶马兰
拳参
乳白香青
乳浆大戟
三瓣猪殃殃
沙参
山丹
山尖子
山牛蒡
山野豌豆
肾叶橐吾
蓍草
石生悬钩子
石竹
疏毛钩叶委陵菜
四叶葎
酸模
铁线莲
兔儿伞
橐吾
椭圆叶花锚
委陵菜
蚊子草
乌头
屋根草
舞鹤草
勿忘草

雾灵沙参
细叶白头翁
细叶黄头乌
细叶鸢尾
下分叉风毛菊
小车前
小黄花菜
缬草
兴安柴胡
兴安短柄草
兴安升麻
兴安野青茅
悬钩子
鸦葱
亚洲蓍草
羊茅
野火球
野亚麻
页蒿
银背风毛菊
银莲花
硬质早熟禾
有斑百合
羽裂蓝刺头
羽叶风毛菊
杂配藜
展毛乌头
展枝沙参
掌叶多裂委陵菜
雉隐天冬
中华隐子草
种阜草
皱叶鸦葱
珠芽蓼
紫斑风铃草
紫草
紫沙参
紫羊茅



北京大学

本科生毕业论文

森林—草原交错带草本植物分布格局 及其与光照条件的关系

Relationship of Herb Distribution Pattern & Light in the Forest-Steppe Ecotone

姓 名: 杜 泉 滢
学 号: 00313014
院 系: 环境学院
专 业: 生态学
导 师: 刘鸿雁 教授

二零零七年六月

摘要

在森林-草原过渡带, 植被对气候变化非常敏感。由于光照对于温度和水分补偿效应, 草本植物对气候变化的响应可能存在着复杂的格局。

由于没有考虑光照的影响, 传统的植被动态模型中没有考虑这种补偿效应(或称协同作用)。在一些模型中, 仅仅考虑了 C3 和 C4 两种不同的光合途径。如果考虑光照与温度及土壤水分的关系, 森林-草原交错带植被是否对于气候变化敏感? 森林和草原的敏感性是否相同? 回答上述问题对于改进植被动态模型, 进而预测未来气候变化的生态响应具有十分重要的意义。前人的研究注意到了林下草本植物与草原草本植物的不同, 但对于这种差异的原因没有定量的研究。

内蒙古高原东南缘是典型的森林-草原交错带, 本研究重点讨论了该地区的草本植物种类分布格局。从森林到草原, 草本植物的分布随坡度、坡向以及森林覆盖度的变化出现逐渐过渡。光照(地上)和土壤水分条件(地下)都可能影响到植物种类分布的这种变化, 而土壤水分条件又与光照引起的蒸发差异关系密切。为了研究光照对于草本植物种类分布空间差异的综合作用, 我们提出了光照条件对森林草原交错带植被格局的假设模型, 来分析光照, 温度和土壤水分条件的协同作用。

本研究首先建立地形与植被盖度影响下的光照模型, 然后分析了草本植物不同生态类群以及草本植物多样性对光照条件的响应, 证实了光照条件对于森林-草原交错带草本植物种类分布影响的假设, 并且以野外采集数据验证该模型。禾本科、莎草科、C4 植物和一些优势种的重要值以及草本植物多样性指数均与光照条件显著相关。

通过本研究, 森林-草原交错带不同物种的根据其光适应性可以划分为受光照影响显著、受光照影响不显著两类, 其中受光照影响显著的类群中又分为与光照变化正相关和负相关两个类群。模型模拟的结果较好的反映了草本植物的空间分布。研究表明, 虽然水分条件可能对乔木进入阳坡起着决定性作用, 但是光照条件限制了草原草本植物进入林下。光照与温度和土壤水分的协同作用机制维持着森林-草原交错带的植被稳定性。

关键词: 光照类群, 植被动态模型, 草本植物多样性, 协同作用

Abstract

In forest-steppe ecotone, vegetation shows great sensitivity to climate change. A complicated pattern of response of herbaceous plant to climate change might exist, due to the compensatory effect of light on temperature and water.

Without considering the influence of light, conventional vegetation dynamic models did not estimate the compensatory effect (i.e. synergic effect). In some models, only C3 and C4 photosynthetic pathways were considered. If the relationship between light and temperature, light and soil moisture were taken into consideration, will the response of forest-steppe ecotone vegetation to climate change be sensitive? If so, is there any difference between forest sensitivity and steppe sensitivity? The answers to those questions are significant to improving vegetation dynamic models, thus important to predicting future climate change. Former researchers have observed the light-determined herb distribution, but not quantitatively modelled the cause of the difference.

In this study, we mainly discussed the species distribution pattern of southeastern Inner Mongolian Plateau, a typical forest-steppe ecotone. The distribution of herbaceous species gradually shows a transitional trait from forest vegetation to steppe vegetation, following the variation of slope and tree coverage. Light factor (aboveground) and soil moisture (belowground) could both influence this change, while soil moisture is closely related to evaporation initiated by light. To estimate the total effect of light on the spatial variation of plant species distribution, we attempt to establish the light regulation model on vegetation structure at the forest-steppe ecotone, and analyze the relationship of light, temperature, and soil moisture.

We first apply a light distribution model under the control of slope and tree coverage. Secondly, we examine the relationship between light and different ecological traits (taxonomic traits, cotyledons, photosynthetic pathways, and functional groups). Then we establish a light regulation model to simulate the trend of plant species variation with slope and coverage and test it with data collected from field survey. The importance value of Gramineae and Cyperaceae, C4 plants, and some dominant species, as well as species diversity indices all showed significant correlation with light.

Through this research, the light adaptability of various plant species at the forest-steppe ecotone was classified more explicitly, by herbs that are either positively or negatively correlated with light. The result of simulation model well reflected the spatial distribution of herbaceous plants. The research indicated that, though water condition may determine whether arbor species can grow on sunny slopes, the limitation factor of steppe herbs' entering forests is actually light condition. The synergic effect of light, temperature, and soil moisture guarantees the sustaining of vegetation stability at forest-steppe ecotone.

Key Words: light groups, vegetation dynamic model, herb diversity, synergic effect

目录

摘要	ii
Abstract	iii
目录	iv
第一章 前言	1
1. 1 研究背景	1
1. 2 研究进展	2
1.2.1 森林-草原交错带植被格局与影响因子	2
1.2.2 影响森林下层草本植物多样性的因素	3
1.2.3 光照与森林-草原交错带动态变化预测	4
1.2.4 国内相关研究进展	4
1. 3 研究内容及技术路线	6
1.3.1 科学问题及研究内容	6
1.3.2 技术路线	6
第二章 研究区域与研究方法	8
2. 1 研究区概况	8
2.1.1 研究区地理位置	8
2.1.2 研究区气候概况	8
2.1.3 研究区土壤概况	8
2.1.4 研究区水文概况	9
2.1.5 研究区植被概况	9
2.1.6 研究区选择依据	9
2. 2 野外取样	10
2.2.1 样地选择	10
2.2.2 调查方法	12
2. 3 数据分析	12
2.3.1 植物群落调查数据	12
2.3.2 地形数据	14
2.3.3 太阳辐射数据	14
2.3.4 土壤水分和容重数据	15
2.3.5 温度和降水数据	15
2. 4 地形、森林盖度对于辐射的影响	16
2.4.1 坡度、坡向与辐射的关系	16
2.4.2 森林盖度与林下光照的关系	18
第三章 地形格局与草本植物种类分布	22
3. 1 研究区植物物种概况	22
3. 2 不同科的草本植物沿坡向的分布	23
第四章 光照条件对草本植物种类分布和多样性的影响	30
4. 1 林下辐射照度值	30

4. 2 草本植物的生态类群.....	33
4. 3 草本植物种类分布与光照的关系.....	34
4.3.1 优势种分布与光照条件的关系.....	34
1 局地尺度上优势种分布与光照的关系.....	34
2 区域尺度上优势种分布与光照的关系.....	40
4.3.2 C4 植物分布与光照条件的关系.....	40
4.3.3 单子叶植物分布与光照条件的关系.....	41
4.3.4 功能类群植物分布与光照条件的关系.....	43
4. 4 草本植物多样性与光照条件的关系.....	43
4.4.1 α 多样性与光照条件的关系.....	44
4.4.2 β 多样性与光照条件的关系.....	48
4. 5 草本植物的种间联结.....	51
第五章 光照条件对森林-草原交错带草本植物的调控作用.....	56
5. 1 光照对草本植物分布的调控作用.....	56
5. 2 光照与森林-草原交错带的物种多样性.....	57
5. 3 光照与森林-草原交错带的植被动态.....	59
第六章 结论	61
参考文献	62
附录：拉丁名与中文名对照.....	66
致谢	67

第一章 前言

1. 1 研究背景

森林-草原交错带以森林和草原两种植被共存为特色，在世界许多地区均有分布。在落叶阔叶林和温带草原之间的交错带，植被格局以落叶阔叶林和草甸、草原的大型镶嵌体为特征。气候愈湿润，落叶阔叶林占优势，草原呈分散的岛状分布。气候愈干旱，情况就相反，接近草原带，只有岛状森林分布在大片的草原上（沃尔特，1984）。

中国的森林-草原交错带处于欧亚大陆森林草原过渡带的东南边缘，与草原带相连的森林植被类型丰富（吴征镒，1980；侯学煜，1988）。由于处于太平洋季风影响的边缘区域，植被对气候变化敏感，中国的森林-草原交错带是研究中国的全球变化的关键区域。

森林-草原交错带的形成和发展始终是一个动态平衡过程，受地质地貌、气候以及人为干扰的综合影响，其格局、结构乃至生产力在时间和空间上出现明显波动。对其结构、功能和动态特征的研究长期以来一直为科学界所关注（House *et al.*, 2003）。

光照对生态系统的生产力具有决定性作用。光照、土壤水分、温度、动物活动等都可能成为森林和草原局地分异的决定因子。然而一些草原上的种类在森林里也出现了，但不能说明森林会衰退，只是可能因为林窗光照的原因。而在一个具体地点，地形既直接影响辐射分布，又通过辐射分布影响土壤水分，二者均影响到植物的分布，因此，区分不同因子的影响变得更加复杂。

传统的动态植被模型认为光照是不变的，因此剔除了光照的影响，单独分析温度和土壤水分对植被动态的影响。然而在森林与温带草原的过渡带，植被格局更多地表现为森林片段与草原片段共存的森林草原景观，森林片段出现在陡阴坡，而草原片段出现在阳坡。因此有些森林和草原的分异可能并不是温度或降水变化造成，陡阴坡的光照条件有可能是决定性因素。本研究在温带森林-草原过渡带开展，试图通过对森林草本植物和草原草本植物的量化对比，分析光照对森林-草原过渡带植被的控制机制。本文首先提出一个光照控制假说，然后通过野外调查与测量数据来验证这一假说。通过局限于林下的草本植物来指示森林的分布来说明森林和草原的动态。

1. 2 研究进展

森林-草原交错带类型丰富, 欧亚大陆、北美洲、南美洲以及热带非洲都有分布, 但由于其气候背景不同, 植物区系组成和植被特点不同, 在世界不同地区关注的科学问题也不尽相同。本文集中讨论森林光照对森林草本植物和草原草本植物的分异作用。

1.2.1 森林-草原交错带植被格局与影响因子

在热带地区出现的稀树草地, 是在树木分布的干旱极限出现的一种景观, 随着干旱程度的增加, 树木盖度逐渐降低, 表现为一个宽阔的过渡带, 对于这种格局的解释有多种假说。

水分因子对林-草格局的控制是研究最多的, 特别是降水量。Sankaran等(2005)认为在年均降水量(MAP)小于650mm的地点, 木本植物的最大覆盖率随MAP增减而增减, 木本和草本共生系统在水分控制下稳定; 而MAP高于650mm的地点林冠达到郁闭。对南美阿根廷森林-草原交错带进行的分析, 表明针叶林的生长正相关于春季和初夏降水量(Villalba *et al.*, 1997)。

其他气候因素(如温度)也通过控制乔木生长来影响森林-草原交错带的格局。南美阿根廷森林-草原交错带针叶林的生长负相关于生长季节的温度(Villalba *et al.*, 1997)。更多的实验直接测量土壤水分对林-草结构的影响。在萨瓦纳地区光照条件一致的情况下, 土壤水分条件是限制草本植物生长的关键因素。土壤水分时间上的分隔对两种牧草优势种共存起着非常重要的作用, 而土壤水分时间和空间上的分隔对灌-草相互作用影响很大(Anderson *et al.*, 2001; Peters, 2002)。在美国中部干旱地区森林-草原之间的关系表现为对水分的竞争, 温带草原占优势(Pan *et al.*, 2002)。也有一些研究注意到了火与草食动物对于乔木与草本植物相互关系的影响(Daly *et al.*, 2000; Sankaran *et al.*, 2005)。

进而有一些学者探索了光照因子对森林-草原交错带植被格局的影响。Pan 等(2002)对北美哈佛森林三种植被(温带落叶阔叶林、温带针叶林、温带 C3 植物占优势的草原)建立了大尺度的动态模型, 发现落叶阔叶林在美国东部湿润地区占优势, 森林-草原之间的关系表现为对光照的竞争。冠幅影响了植物个体相互间的光照分配(Smith *et al.*, 2001)。

一些研究工作注意到了光照分异引起的森林下层草本植物与草原草本植物在种类、生物量、丰富度、多样性等各方面的差异。Grouzis 等(1997)在非洲北部塞内加尔半干旱地带的研究表明, 森林草本的地上生物量比草原草本多 1.5 到 4 倍, 森林草本的地下生物量约为

草原草本的 3 倍，而根/枝比则是草地较高 (Bandeef *et al.*, 2006)。

1.2.2 影响森林下层草本植物多样性的因素

影响森林下草本层的因素有地形、土壤养分和水分条件、气候因子、直接辐射、乔木冠幅等。林下草本植物依次受光照、土壤水分、杀虫剂、木本凋落物的影响，顺序从大到小排列 (Harrington *et al.*, 1999)。

通过数字高程模型与野外调查的结合发现，在加拿大温带混交林中，坡向、坡度是决定林下物种丰富度、均匀度、多样性的首要因素 (Chipman *et al.*, 2002)。土壤养分条件也是决定林下物种丰富度、均匀度、多样性的重要因素 (Chipman *et al.*, 2002, Chen *et al.*, 2004)。混交针叶林林下草本植物丰富度与影响土壤水分条件的因素关系最大 (North *et al.*, 2005)。在加拿大的温带混交林中，坡向、坡度和表层土壤状况是决定林下物种丰富度、均匀度、多样性的首要因素，其次才是盖度决定的光照。物种多样性和丰富度在越接近坡底部位越大，可能是由于土壤水分和养分的增加 (Chipman *et al.*, 2002)；乔木结构多样性丰富时草本植物多样性丰富 (Leniere *et al.*, 2006)。北美内华达山脉混交针叶林林下草本植物丰富度与直接辐射负相关 (North *et al.*, 2005)。也有学者认为林下植被种类组成与乔木胸高处年龄为 50 年时的树高以及一些气候、土壤变量有关 (Chen *et al.*, 2004)。林下植物丰富度与多样性的增加可能是由于种子库的存在，且在干扰程度和生物量中等的时候丰富度最高 (Weiher, 2003, Leniere *et al.*, 2006)。

对于林下光照的研究最为集中，很多学者认为林下草本层与乔木层的冠幅密切相关。但在不同植被类型中，冠幅对于林下草本的生长作用不尽相同。在亚高山云杉林中，乔木层开阔程度的改变对于林下微环境的影响导致林下草本分布远离随机状态 (Holeksa, 2003)；森林冠幅导致的光照减少是限制入侵物种在乔木层下方分布的主导因子 (Cole *et al.*, 2005)；光照在决定群落演替中草本植物种类的转变起决定作用 (Maundrell *et al.*, 2004)。油松林下禾本科植物种类出现与乔木冠幅呈正相关 (Naumburg *et al.*, 1999)；山杨林乔木层冠幅增加时，林下草本植物生长得到抑制 (Cole *et al.*, 2005)。

那么光照究竟如何影响森林下层草本植被呢？林下单位时间辐射通量密度和光照透过百分比的测量存在几种模型 (Comeau *et al.*, 1998)；有些模型仅仅利用冠幅直径和所处高度来建立不同植物种类的光照模型 (Piboule *et al.*, 2005)。Messier 等 (1998) 在五种树林中距林顶和草本层各 0, 50, 100cm 处的光合光子辐射通量密度的测量，给出了五种乔木冠幅对

于林下光照的削减百分比。林下草本植被的高度与光照透过率正相关，但与森林类型无关；森林上层的光透过率影响林下植被的结构和功能，但对多样性和物种组成影响较小，这说明上层植被对光照的强烈作用，使得林下光照趋于均质（Bartemucci *et al.*, 2006）。Martens 等（2000）建立了草原-森林连续体中树冠盖度与林下光照的关系模型，分别讨论了不同盖度等级、空间格局、乔木高度下，林下光合有效辐射（PAR）的变化，强调了光照对林下草本植物的重要性，但对于光照具体的调控机制目前研究较少。另外，有研究强调了生长季不同阶段的光照对于林下立木更新的影响，发现林下光照在四月份光照最大值的 58%-80% 时种子有正响应，低于这个值时种子无响应而树苗有正响应，而树苗在九月份光照值很低时能一直存活，说明入侵物种在不同生长阶段对光照的反应有所差异（Godefroid *et al.*, 2005）。

对于草本植物的光照类群，目前只是简单地划分为阳性植物、阴性植物、耐阴植物和中性植物，但尚缺少量化，也就是各物种在光照梯度上的优势度分布，对于不同生态类群（如形态分类、光合途径、功能类群、子叶数目）的植物在光照梯度上的分布规律的归纳，尚无统计关系来表达。

1.2.3 光照与森林-草原交错带动态变化预测

在预测未来气候变化的生态响应时，气候因子的间接效应（如森林冠幅、土壤有机物）可能对于现存草原物种组成的差异非常重要，甚至可能成为变化减缓的原因。Lett 等（2003）对美国中部湿地草原的研究指出，在北美高草草原中灌丛稳定性的维持和驱动力是光照，而不是其它资源的增加，而且灌木的移除会增加禾草种类的恢复。那么，在亚洲温带森林-草原交错带，假如去掉森林覆盖的影响，草原是否能完全进入阴坡，特别是遮阴的陡阴坡呢？

Sankey 等（2006）对于美国蒙大拿州物种放牧模式下乔木的树轮分析以及森林的更新分布调查表明十年时间尺度上放牧与森林入侵的线性关系并不明显；Dulamsuren（2005）等通过对蒙古高原肯特山森林-草原过渡带林下草本植物与草原草本植物的对比，认为草原分布在阳坡的格局是自然形成的，也否定了 Hilbig（1995）认为森林-草原交错带中草原分布在阳坡是人为破坏所致的说法，但对限制草原草本植物进入森林的因素没有涉及。

1.2.4 国内相关研究进展

相关的研究工作主要分为森林-草原交错带的植被格局和林下植被与环境因子的关系两个方面。

黄永梅等(2001)利用群落特征和遥感资料划分森林草原过渡带与森林带以及草原带的界线,并对过渡带内部的景观异质性及其形成机制做了进一步的研究。王庆锁(2004)对森林草原交错带的植被类型、分布规律、第一性生产力、环境条件、人为影响进行了系统的总结,对交错带植物多样性进行了比较全面的研究。

在森林-草原交错带环境条件对植被的影响方面有不少研究工作,对农牧交错带植被动态与环境变化的研究得到水分条件是决定植被空间分布格局的主导因素(张军涛,2001;李栋梁,2002;赵哈林,2003)。地形与土壤、光照等直接生境因子对植被格局解释量之和相当。但在不同尺度上,地形特征都是解释能力最强的一组生境变量(沈泽昊,2002)。

森林草本和草原草本的生长和分布,是决定植被空间分布格局以及预测未来森林-草原交错带动态变化的关键因子。半干旱区林下植被的生态位宽度值普遍较小,同时物种间生态位重叠并不普遍,重叠度普遍不大,各种对间对资源的共享趋势不明显,生态位发生分离,显示了林下植被状况差(王正宁等,2005)。在相同林分类型中,随着林分密度的增大,林下植被的种类和数量相应减少,物种丰富度和物种多样性指数也降低,反映出林分内的小环境条件、林木生长状况和林下植被发育水平随林分种类、林分密度变化而变化的特点(刘晨峰等,2004)。森林能够通过改变林下的光照和地表水分而影响了林下植被的生长(张艳华等,1999;王正文等,2001;史军辉等,2005)。某些草本植物林下的分布与光照条件相关显著;盖度与照度之间关系的定量分析能够更清楚地反映林下植物的光适应性,揭示植物的光生态幅特征;光适应性直接影响着林下植物的种间关系,也影响着物种的群落地位和作用(江源等,2001)。有些研究结果表明森林草原带林下草本与草原草本植物分布差异的主要因子是林分的发育阶段,且林分发育阶段的不同超过了森林类型对林下草本植物的影响。在同一发育阶段,由于坡向、坡位、坡度及上层乔木的不同,林下草本植物分布又有差异(徐存宝等,2000)。

另外,在研究光照与坡度、坡向、乔木盖度之间的关系时有些学者注意到了林下光照的异质性问题。在光照空间异质性程度较高、空间变异较复杂的条件下,更新相应呈现出较复杂的空间格局,自相关的变异表现在较小尺度范围。在光照空间异质性程度较低、空间变异复杂性较小的条件下,更新格局的复杂程度明显变小,空间自相关变异表现在较大的尺度上,对更新格局起主要的影响作用,随机变异的影响很小(韩有志等,2004)。

1. 3 研究内容及技术路线

1.3.1 科学问题及研究内容

总体来说,光照、土壤水分、温度、动物活动等都可能都是森林和草原局地分异的决定因子,如果光照是决定因子,草原不可能进入阴坡,特别是光照弱的陡阴坡,也就是说现在的森林分布在陡阴坡是有光照引起的,而并非过去强调的土壤水分差异。如果去掉森林覆盖的影响,草原是否能完全进入阴坡,特别是遮阴的陡阴坡?草本植物的适应性强不一定代表草原能够取代森林,有可能陡阴坡的光照条件是决定性因素。迄今为止,关于光照对草本植物分布控制的具体机理还没有系统的展开研究。

内蒙古高原东南部森林-草原过渡带的植被格局具有典型性,既有森林草原景观,又有疏林草原景观。从森林到草原,草本植物的分布随坡度、坡向以及森林覆盖度的变化出现逐渐过渡。光照(地上)和土壤水分条件(地下)都可能影响到植物种类分布的这种变化,而土壤水分条件又与光照引起的蒸发差异关系密切。本文首先建立坡度、坡向与植被盖度影响下的光照分布模型,对野外调查的植被调查、土壤调查,辐射数据等多种数据进行集成分析,运用地理信息系统工具,分析中国北方典型的森林-草原交错带草本植物种类分布格局的限制因子。本文试图回答以下科学问题:影响草本植物种类分布的因子和机制是什么?森林-草原交错带对未来气候可能发生的变化是否敏感?森林和草原的敏感性是否相同?

本文研究内容包括以下几个方面:

- (1) 概述研究区地形条件对草本植物种类分布的影响;
- (2) 建立研究区地形条件对太阳辐射分布影响的模型;
- (3) 分析研究区乔木(灌木)盖度对林下光照条件的影响;
- (4) 总结不同生态类群的草本植物沿光照梯度的分布规律;
- (5) 建立研究区光照条件对草本植物种类分布影响的模型;
- (6) 分析研究区光照条件对草本植物多样性的影响;
- (7) 讨论限制草本植物分布格局的因素(光照条件、温度和土壤水分)的协同作用;
- (8) 分析森林和草原植被的敏感性差异。

1.3.2 技术路线

本研究技术路线见图1.1。

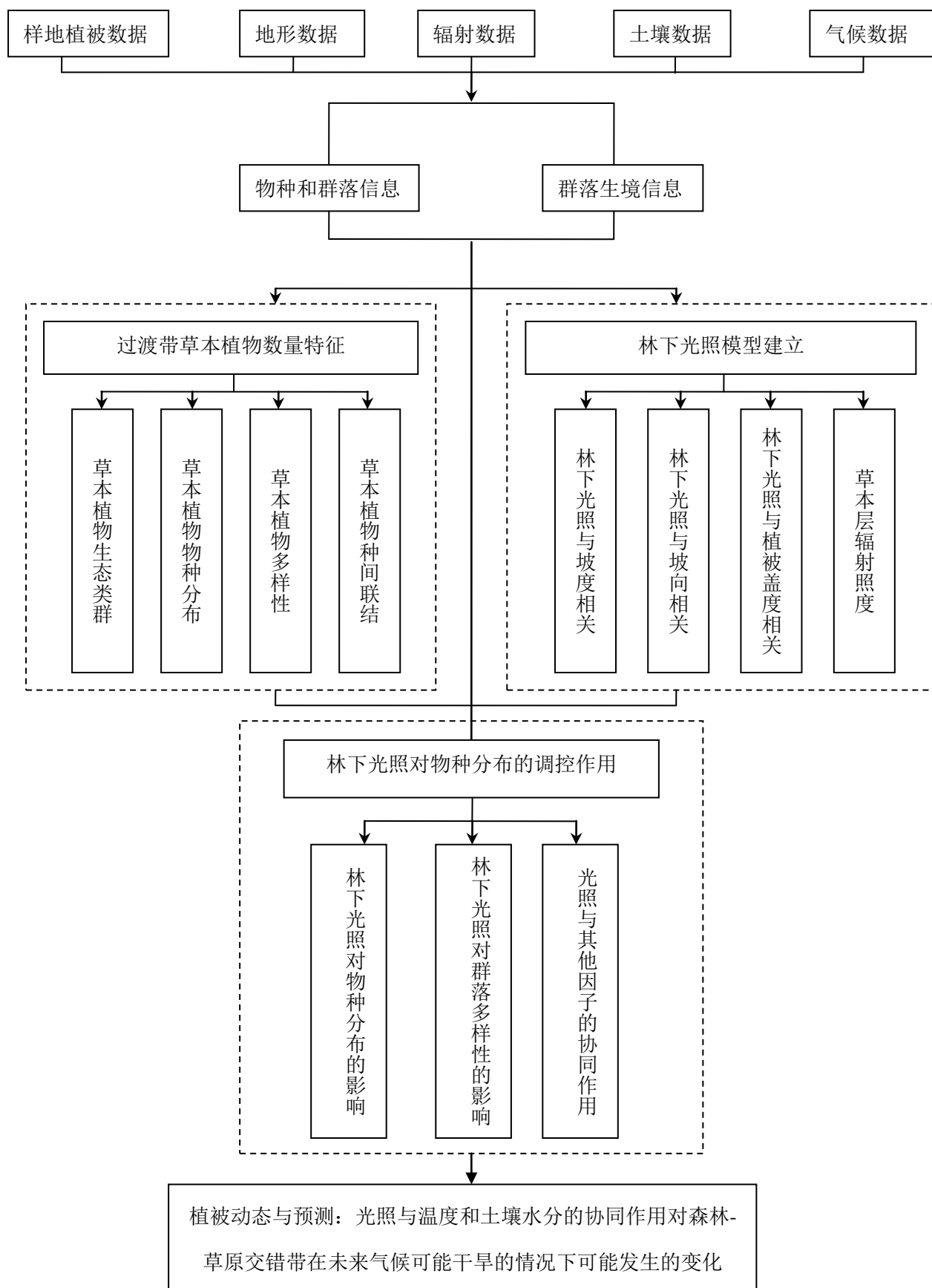


图 1.1 技术路线

第二章 研究区域与研究方法

2. 1 研究区概况

2.1.1 研究区地理位置

本文选择内蒙古高原东南缘森林-草原交错带作为研究区。研究区经纬度范围为 41°06.717'N - 43°42.664' N, E115°21.994' E - 117°15.205' E, 行政区划上包括河北省围场满族蒙古族自治县、崇礼县、张北县, 内蒙古自治区赤峰市克什克腾旗以及锡林郭勒盟。

研究区主体位于内蒙古高原、大兴安岭山地南延部分以及冀北山地交界处。高原面地貌形态多样, 北部为锡林郭勒熔岩台地, 台地南缘有达里诺尔、岗更诺尔等湖泊。西部为浑善达克沙地东缘南北走向的曼达席勒覆沙丘陵。东南和南部为冀北山地, 为中度切割山地, 沟谷海拔高度在500m-700m之间。在坝缘部分, 山地海拔迅速上升到1400m-1700m之间, 最高峰海拔在2000m以上。由此向西、西北进入内蒙古高原, 海拔又缓缓下降(黄永梅等, 2001)。高原的边缘部分俗称“坝上高原”。研究区东北部则为大兴安岭南段山脉及山前丘陵。

2.1.2 研究区气候概况

研究区气候属于温带半湿润季风气候与半干旱大陆性气候的过渡带, 总体上说坝下温度偏高, 坝缘山地和大兴安岭南段山地由于海拔较高而温度偏低, 内蒙古高原内部温度差异较小。年降水量350mm-450mm, 具有明显的东南-西北走向梯度。雨量集中于夏季, 6-8月降水量占全年降水量的60%-70%。水热分配不平衡, 东南(或东)部降水丰富但热量较低; 西北(或西)部热量条件好而降水较少。

2.1.3 研究区土壤概况

研究区土壤类型多样, 由于气候条件的递变性而呈现地域分异。从冀北山地到锡林郭勒熔岩台地, 土壤类型依次为棕壤、灰色森林土、黑钙土、淡黑钙土、暗栗钙土。本区隐域性土壤有风沙土、草甸土、沼泽土和盐渍土(王庆锁, 2004)。浑善达克沙地主要为风沙土。大兴安岭山地一些高海拔的山顶分布着亚高山草甸土。河岸、湖边等低湿地有草甸土、沼泽

土和盐土。

2.1.4 研究区水文概况

研究区河湖众多。闪电河、吐力根河、小滦河、黑风河、獾尾巴河等为滦河的源头和上游支流；萨岭河是辽河上游西拉木伦河的源头。境内河流一般流程短、河槽浅、水量少，多为季节性、间歇性河流。河湖水质较好，但是分布不均，东部和南部河流较密，其他地区有一些内陆湖泊。

2.1.5 研究区植被概况

研究区处于暖温带落叶阔叶林向温带草原过渡的地带，植物区系组成呈明显的过渡性。从冀北山地向内蒙古高原过渡，表现为东亚成分逐渐减少而达乌里-蒙古成分增多（中国科学院内蒙古宁夏综合考察队，1985）。研究区内森林多呈斑块分布于山地阴坡，阳坡多为灌丛或草原，并在低平地和林缘出现草甸。

高原森林草原分布在高原面上，一般丘间平地为羊草（*Leymus chinensis*）草原，缓坡坡顶出现贝加尔针茅（*Stipa baicalensis*）草原片段。陡阴坡上部为岛状分布的森林，向西北方白桦（*Betula platyphylla*）林逐渐被山杨（*Populus davidiana*）林取代。

山地森林草原位于大兴安岭山地南段，植被具有垂直分异，平缓山顶分别为寒生杂类草、禾草草甸和草甸化草原，高海拔山地阴坡有零星兴安落叶松（*Larix gmelinii*）林，中山阴坡以白桦林为主，阳坡为落叶灌丛和线叶菊（*Filifolium sibiricum*）、贝加尔针茅草原。

2.1.6 研究区选择依据

本文选择内蒙古高原东南部森林-草原交错带开展研究，主要依据以下事实：

(1) 森林-草原交错带的草本植物对气候变化的响应可能存在着复杂的格局。研究区是典型的暖温带落叶阔叶林与温带草原的交错地带，植被类型以及植物种类都非常丰富。

(2) 研究区林下草本植物和草原草本植物出现在相同气候条件下，处于 400mm 等降水量线沿线，降水因子对于草本植物分布的影响可以忽略，草本植物分布的限制因子得到了很好的控制，为明确光照条件的调控作用奠定了基础。光照对于温度和土壤水分的补偿效应影响着林下草本和草原草本植物的分布，量化这一效应可以用于改进传统的植被动态模型。

(2) 研究区位于东亚季风气候的尾闾区，是全球变化研究的关键区域（Liu *et al.*, 2002）。

受季风气候的影响, 物种分布格局有独特表现。研究季风气候下森林-草原格局的维持机制有重要意义。

(3) 研究区地形变化明显, 森林分布在陡阴坡, 而草原分布在阳坡。这一格局对于建立坡度、坡向影响下的光照分布模型, 以及地形对植物种类分布的影响都非常适宜。

(4) 研究区基本上呈现了一个完整的过渡带样本, 适用于分析气候、地形、土壤水分与草本植物种类分布的关系。

(5) 当前有多项生态工程在这一地区实施。探究林下草本植物与草原草本植物差异的成因, 对于森林-草原交错带物种组成的合理搭配问题有重要的实践意义。

2. 2 野外取样

野外调查于 2006 年 7 月在研究区内 10 个地点进行, 记录海拔高度、地理位置、坡度、坡向, 乔木种类、数量、高度、冠幅、胸径、基径, 立木更新数量、高度, 灌木种类、数量、高度、冠幅, 以及草本植物种类及相关数据 (见调查方法)。在进行植物群落调查的同时采集相应的土壤样品。

2.2.1 样地选择

样方地点的选择原则是分布在阴坡的天然林以及对应的从坡顶到阳坡的草原, 重点利用天然形成的盖度梯度, 即涵盖森林、灌丛、草原三个植被类型的草本植物种类。因此, 样地设置沿光照条件梯度, 以此剔除温度和降水的差异, 从而单独研究光照的影响。在研究区域内, 主要的天然林群落为白桦 (棘皮桦)、山杨、白桦、油松群落, 本研究涉及白桦林 3 个, 山杨林 3 个, 白桦林 2 个, 油松-白桦混交林 2 个。样地具体情况见表 2.1, 图 2.1。

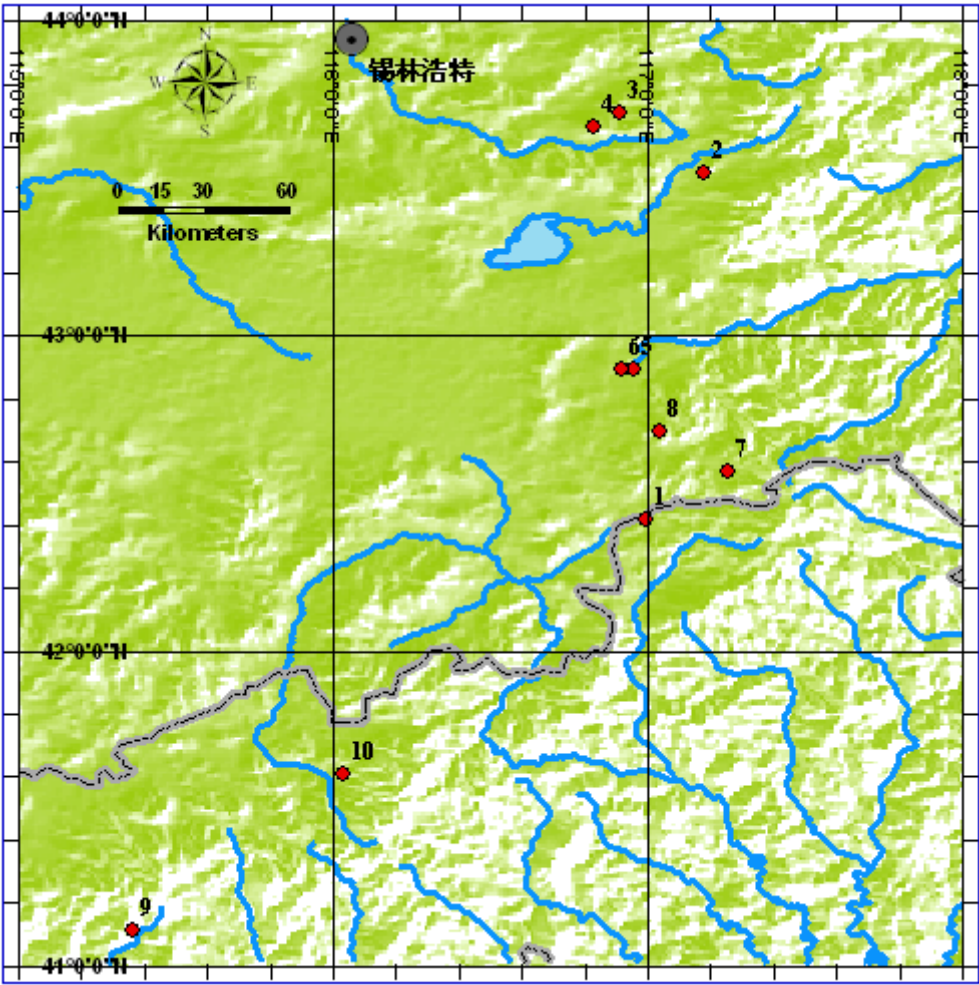


图 2.1 野外植被调查地点分布与高程示意

表 2.1 样地设置及概况

调查地点	编号	调查日期	地理位置	海拔(m)	样线数目	样线长度	群落名称
三道河口	1	060703	42°24.838' N 116°59.715' E	1456	6	50m	油松-白桦
白音敖包	2	060705	43°31.234' N 117°10.528' E		6	50-55m	白桦
扎格斯泰淖尔	3	060707	43°42.664' N 116°54.526' E	1360	6	55m	白桦
扎格斯泰淖尔	4	060707	43°39.783' N 116°49.858' E	1360	6	50m	山杨
源水头	5	060708	42°53.747' N 116°57.342' E		6	55m	油松-白桦
好鲁库	6	060709	42°53.770' N 116°54.963' E	1365	6	52m	山杨
白杆坑	7	060710	42°34.086' N 117°15.205' E	1605	6	25m	白桦
松树井子	8	060710	42°41.842' N 117°02.318' E	1642	4	50m	山杨
狮子沟	9	060722	41°06.717' N 115°21.994' E	1567	4	25m	白桦

半坝村	10	060723	41°36.632' N 116°01.973' E	1612	4	25m	白桦
-----	----	--------	----------------------------	------	---	-----	----

除源水头样线的基线选取垂直于等高线，其余样线的基线均平行于等高线。样线依次穿越阴坡坡底林缘草地、阴坡树林、坡顶草原，到达阳坡草原、灌丛。源水头样地由于林草分佈格局为随坡向转变的逐渐过渡，所以样线仍旧依次穿过沙坡草原、灌木丛、油松林、白桦林等几种植被类型。

2.2.2 调查方法

植物群落调查采用样线法。样线法为一种面积取样技术，在草本植物调查中广泛使用。该方法首先选定一条基线，并以其上的点每隔单位距离（1m）选择一点作为样线起点，然后从每个起点各拉一条样线，每隔单位距离（1m）确定一个取样点，使用全球卫星定位系统（GPS）确定经纬度和海拔高度并记录；分层记录取样点所在位置的草本植物的数据包括植物种名，沿样线所截长度（L），以及植物垂直于样线的最大宽度（M），以备计算各物种重要值和群落指数。然后将每组样线所涉及地段分割成 5m 一段的小样方，本段小样方内的乔木、灌木盖度作为草本植物环境因子，同时估计并记录每段小样方所在面的坡度。各取样地点样线具体数目及长度见表 2.1。

在样线所在地点的阳坡和阴坡分层采集土壤样品，大部分阴坡有重复，小部分阳坡有重复。土壤剖面的挖掘深度从 40cm 到 80cm 不等的剖面，以 10cm 为为一层取样，分别称量湿重后密封。调查结束后回到实验室内，烘干土壤样品并计算土壤含水率，得到土壤水分垂直分布状况。

2. 3 数据分析

2.3.1 植物群落调查数据

- 对于同一样地内的同一物种，首先统计和确定以下各值：
- a. 被样线所截长度的总和（L）；
 - b. 有该种植物的样点数（BN）；
 - c. 植物垂直于样线最大宽度的倒数的总和（ $\Sigma 1/M$ ）。
- 然后按照以下方法计算每个种在该样地内的相对密度、相对盖度（代替相对优势度）和相对频度：

- a. 密度 (D) = $(\Sigma I/M) \times (1/\text{样线总长}) \times 100$;
- b. 相对密度 (RD) = (一个种的密度/所有种的密度之和) $\times 100\%$;
- c. 盖度 (C) = $(L/\text{样线总长}) \times 100$;
- d. 相对盖度 (RC) = (一个种的盖度/所有种的盖度之和) $\times 100\%$;
- e. 频度 (F) = $BN/\text{总样点数}$;
- f. 相对频度 (RF) = (一个种的频度/所有种的频度之和) $\times 100\%$ 。

最后, 计算物种重要值 $IV(\%) = \text{相对密度 (RD)} + \text{相对盖度 (RC)} + \text{相对频度 (RF)}$ 。

在得出每个种在该样地的重要值之后, 又进一步计算物种的分段重要值。具体做法是将每组样线所涉及地段分割成 5m 一段的小样方, 这样小样方处于坡度、坡向的逐渐过渡, 以及乔木灌木盖度的梯度上, 然后利用同样方法计算小样方内出现物种的重要值。

本研究将物种重要值作为光照梯度上的优势度的指标, 然后再对物种进行划分, 归纳草本植物的光照类群, 不同生态类群 (如 C3 与 C4 植物, 单子叶与双子叶植物, 禾本科与豆科植物等) 在光照梯度上的分布的规律性。

本研究中 α 多样性与光照条件的关系选用 Shannon-Wiener 指数作为测度指标 (Magurran, 1988)。具体计算公式如下:

$$H' = -\sum P_i \ln P_i$$

其中 P_i 为样地中某一种的重要值 $IV/100$ 。

β 多样性用来反映不同群落间物种组成上的差别, 不同的群落之间共有物种越少, β 多样性越大。同时, β 多样性还可以表示样方物种沿着环境梯度的替代程度和速率, 也被称为物种周转速率 (species turnover rate)、物种替代速率 (species replacement rate) 和生物变化速率 (rate of biotic change) (Pielou, 1975; Magurran, 1988)。本研究采用以下两种指标对 β 多样性进行测度 (Whittaker, 1972; Magurran, 1988)。

Sørensen 指数:

$$SI = \frac{2c}{a+b}$$

Cody 指数:

$$\beta_c = \frac{g(H) + l(H)}{2} = \frac{a+b-2c}{2}$$

其中, a 和 b 分别为两群落的物种数, c 为两群落的共有种数, $g(H)$ 为沿生境梯度 H 增加的物种数, $l(H)$ 为沿生境梯度 H 失去的物种数。上述指数中, Sørensen 指数反映群落或样方间物种组成的相似性; Cody 指数则反映样方物种组成沿环境梯度的替代速率。

种间联结 (interspecific association) 的研究方法是以物种在样方中出现、不出现为依据, 用 2×2 列联表求出种间的共存概率和关联强度, 指不同物种在空间分布上的相互关联性, 通常是由于群落生境的差异影响了物种的分布而引起的。实际上, 种间联结性是种群间相互作用的结果, 所以, 测定种间联结性对于研究种间的相互作用和群落动态具有重要意义 (张金屯, 2004)。本研究种间联结研究采用 2×2 列联表分析。首先建立 2×2 列联表 (contingency table), 将原始原始植被调查数据矩阵转化为 0、1 形式的二元数据矩阵, 再做出每个种对间的 2×2 列联表, 计算各种对间的 a (种 A 与 B 共同出现)、b (只有种 A 出现)、c (只有种 B 出现)、d (种 A 与 B 均无出现)。首先选取估计值小于 5 时的 χ^2 值检验种间联结的显著性, 有助于修正联结系数因物种的特殊分布现象 (如样地分布频度极小) 造成的偏差。

$$\chi^2 = \frac{N \left(ad - bc - \frac{1}{2} N \right)^2}{(a+b)(c+d)(a+c)(b+d)}$$

然后采用的种间联结系数 (AC) 测定物种亲和性, 并将联结系数值 AC 排列为半矩阵 (semi-matrix) 表达种群联结或相互关系 (彭少麟等, 1999)。

$$\begin{aligned} (ad - bc) / (a + b)(b + d) & \quad ad \geq bc \\ AC = (ad - bc) / (a + b)(a + c) & \quad bc > ad, d \geq a \\ (ad - bc) / (d + b)(d + c) & \quad bc > ad, d < a \end{aligned}$$

2.3.2 地形数据

由于是森林向草原的过渡地带, 该区域内的天然林成块的分布。次生性的天然白桦林常分布于阴坡 (北向), 而草原或草甸则分布在坡顶以及阳坡 (南向)。森林和草地在山坡两边相间分布, 构成该区域内常见的景观, 排除其他环境因子的影响, 为植被与光照、地形因子相互关系的研究提供了方便。实际应用中, 每个样地的坡向均为由南坡经坡顶到北坡, 北坡 ($\beta=180^\circ$), 东 (西) 坡 ($\beta=90^\circ$), 南坡 ($\beta=0^\circ$)。同时估计并记录每段小样方所在面的坡度 α 。同时对于每个样地, 利用全球卫星定位系统 (GPS) 测量经纬度、海拔高度等。

2.3.3 太阳辐射数据

本研究利用中国气象辐射资料台站内蒙古自治区锡林浩特台站自 1990 年 1 月至 2003 年 12 月期间的总辐射月总量数据, 该站点经纬度为 $43^\circ 57' N$, $116^\circ 04' E$, 海拔高度为 989.5m。实际

应用中，因为北方大气透明度比较高，故用总辐射代替直接辐射，使用1990至2003年间7月辐射总量的平均值作为本研究的太阳直接辐射月值。

2.3.4 土壤水分和容重数据

采集土壤样品与植被调查同时进行，使用环刀分层取自新鲜土壤剖面，每份样品 100g 左右，当即称量湿重并记录。回到实验室内将土样装入铝盒，在 105 ℃ 的烘箱内烘 8 小时后，称量干重。分别计算每份样品的土壤容重，以此衡量土壤质地和发育程度，间接反映土壤孔隙度，另外计算出水分含量百分比（有重复时取均值）。

2.3.5 温度和降水数据

气温对于植物的生长、分布至关重要。本研究收集研究区及周边地区15个气象台站的多年平均温度数据（纬度跨度为40°-45°N，经度跨度为113°-119°E）（表2.2，图2.2）。

表 2.2 气象台站信息								
编号	站名	经度	纬度	海拔 (m)	1 月均温 (℃)	7 月均温 (℃)	年降水量 (mm)	数据年份
1	锡林浩特	116.07	43.95	989.5	-18.4	21.3	297.2	1951-1970
2	白音敖包	117.21	43.52	1340.7	-22.7	17.4	390.1	1951-1970
3	林西	118.07	43.43	799	-13.6	21.4	356.8	1951-1970
4	经棚	117.53	43.25	1003.2	-16.4	20.2	362.9	1951-1970
5	那日图	115.8	42.87	1292.5	-18.3	19	317.8	1951-1970
6	乌丹	119.03	42.95	631.9	-12.1	22.8	360.2	1951-1970
7	大局子	117.35	42.58	1510	-19.4	16.1	504	1951-1970
8	正镶白旗	115	42.3	1345.9	-17	19.1	363.7	1951-1970
9	塞罕坝	117.25	42.4	1450	-20.1	17.6	425.9	1959-1994
10	赤峰	118.97	42.27	571.1	-11	23.5	339.8	1951-1970
11	正兰旗	115.98	42.25	1300.1	-17.1	18.9	358.7	1951-1970
12	多伦县	116.47	42.18	1245.4	-16.9	18.8	372.8	1951-1970
13	大仆寺旗	115.27	41.88	1468.9	-16.6	17.8	390.8	1951-1970
14	围场	117.75	41.93	842.3	13.3	20.7	414.3	1961-1970

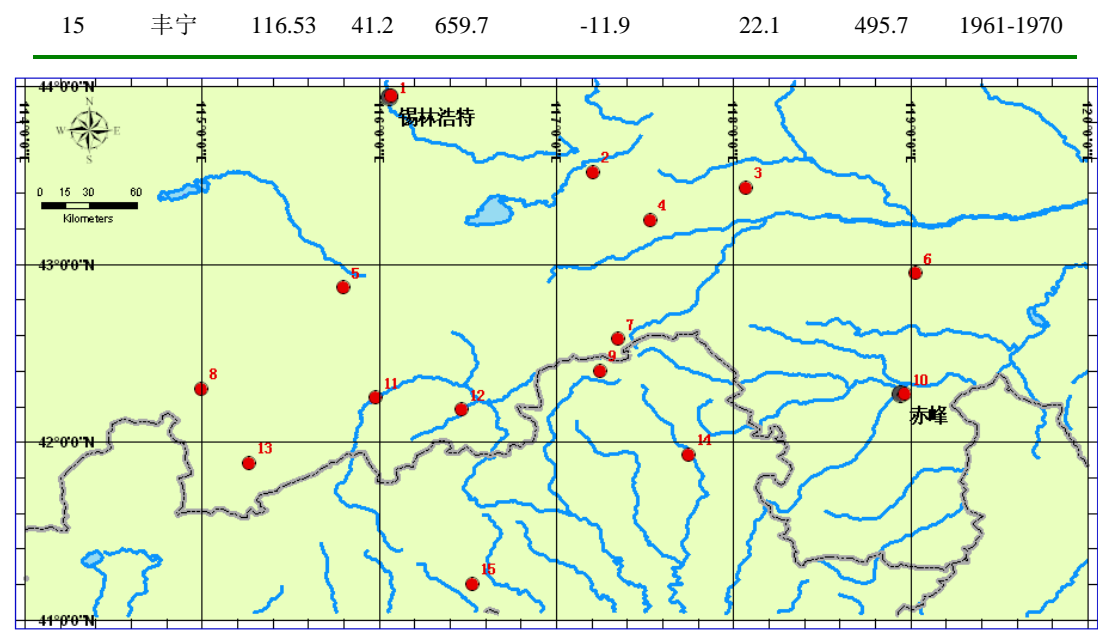


图 2.2 气象台站分布

2. 4 地形、森林盖度对于辐射的影响

2.4.1 坡度、坡向与辐射的关系

太阳直接辐射受到坡向坡度等地形因素的强烈影响,本文利用了研究区内不同坡度和坡向的年太阳直接辐射平均辐射照度。何思源(2006)利用《中国亚热带东部山区坡面太阳能资源和净辐射图集》(翁笃鸣等,1988)所载18°-37°N的数据进行推算,坡向根据气象记录和论文需要利用该纬度范围内北坡($\beta=180^\circ$),东(西)坡($\beta=90^\circ$),南坡($\beta=0^\circ$),坡度 α 从5°-20°的数据,外推到40°。推算出坡面太阳直接辐射换算系数 $K_{\alpha\beta}$ 。利用直接辐射量计算公式和前人计算的其他区域直接辐射量等参数计算了42°N不同坡度和坡向的年太阳直接辐射平均照度,结果显示明显的趋势性(图2.3)。

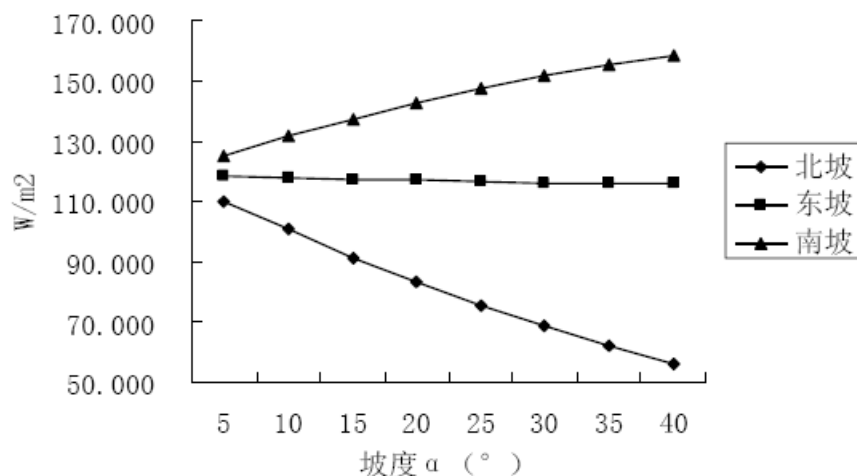


图2.3 42°N不同坡度年太阳直接辐射平均照度（引自何思源，2006）

图2.4显示了，由阴坡到阳坡，太阳直接辐射量逐渐增大，而且坡度越大，坡向带来的辐射差异越大。

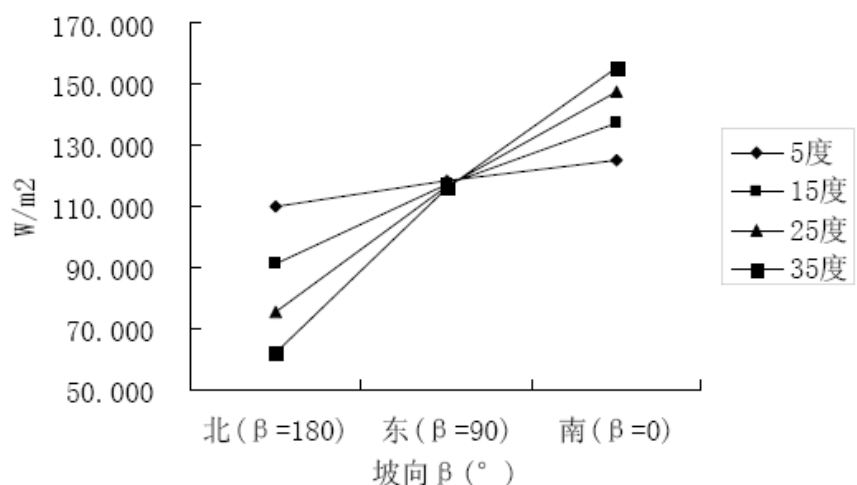


图2.4 42°N不同坡向年太阳直接辐射平均照度（引自何思源，2006）

图2.5显示了不同坡向上各个坡度上太阳直接辐射占水平面太阳直接辐射的比例。很明显的看出，北半球阴坡接受的直接辐射量少于水平面接受的直接辐射量，而阳坡则刚好相反。

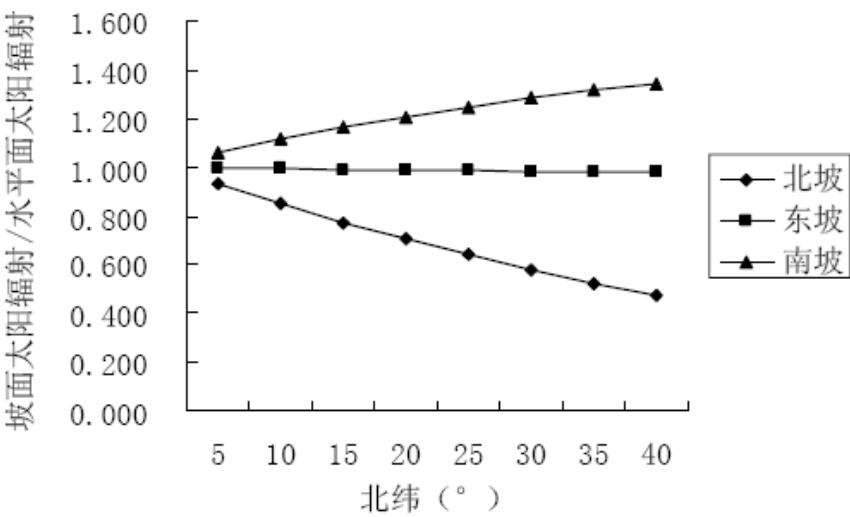


图 2.5 不同纬度坡面太阳辐射占水平面太阳辐射的比例（引自何思源，2006）

在研究区山地内，坡度和坡向造成的直接辐射量差异相当大（表2.3），阴阳坡的直接辐射差异在坡度很小的时候就存在，在坡度增大到25 °以上，阴坡接受的直接辐射量已经不足阳坡的一半，坡度陡峭到40 °时，阴坡接受的直接辐射量仅有阳坡的三分之一强。

表2.3 阴坡占阳坡辐射的比例（引自何思源，2006）

坡度 (°)	5	10	15	20	25	30	35	40
直接辐射比例 (%)	87.8	76.7	66.5	58.5	51.3	45.2	39.9	35.3

2.4.2 森林盖度与林下光照的关系

林下光照环境是决定植被格局和生态系统过程的重要因素,并且可能是植物所利用的所有资源中空间变化最剧烈的因子。林下光照沿植被结构梯度变化,从没有乔木树冠覆盖的草原到几乎完全乔木覆盖的森林。林下光照的空间变化取决于上层乔木的空间格局、高度、冠幅，这在森林-草原连续体中同时发生变化。Martens等（2000）建立了两种样地生长季节的林下光照模型，即系统变化的冠幅、空间格局、高度的人工控制样地，以及三个天然状态下冠幅、空间格局、高度同时变化的自然立地。模型首先计算森林覆盖上部的光合有效辐射（PAR），然后考虑直接辐射被林冠的削减。设计的样地中森林盖度从0-81%，PAR均值随盖度的增加线性减少，空间格局（均一、随机、聚集）不同时PAR均值差别不大（图2.6A）。PAR的方差在聚集格局时最大，均一格局时最小（图2.6B）。

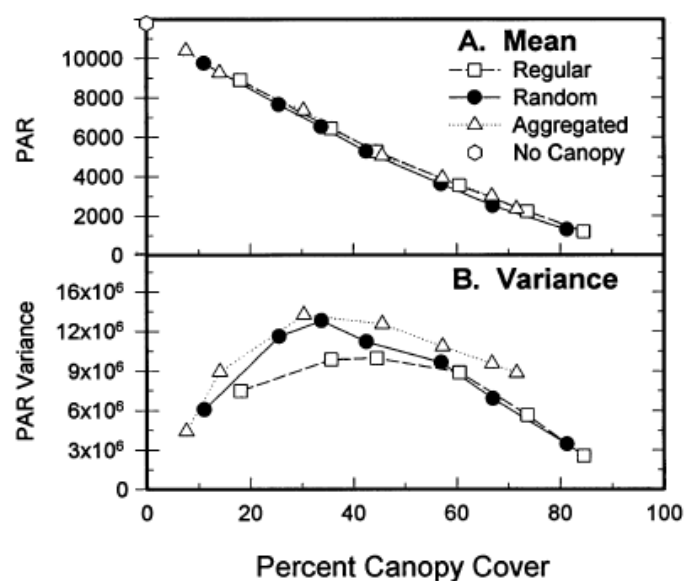


图 2.6 盖度梯度下不同空间格局时 PAR 的变化 (人工样地) (引自 Martens *et al.*, 2000)

PAR 单位: mol m^{-2}

当把林下辐射的总和分为遮荫下和林隙间两部分时, 可以看到这两者的 PAR 均值都是下降的趋势 (图 2.7A), 而三种格局下 PAR 的方差有微小变化 (图 2.7B-D)。

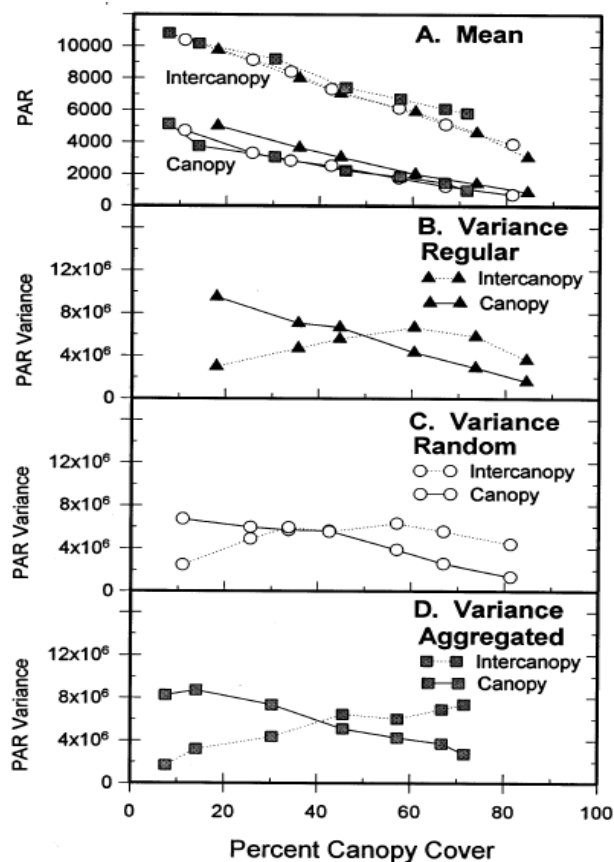


图 2.7 盖度梯度下遮荫下和林隙间 PAR 的变化 (人工样地) (引自 Martens *et al.*, 2000)

PAR 单位: mol m^{-2}

而树冠高度对于林下盖度的影响，树冠位置较低时的 PAR 均值最大，且变化趋势随高度增加而远离线性关系（图 2.8A）。PAR 方差变化在三个高度上均与盖度呈二次曲线关系，在中等盖度时最大，在盖度较高时 PAR 方差对树冠高度变化不敏感（图 2.8B）。

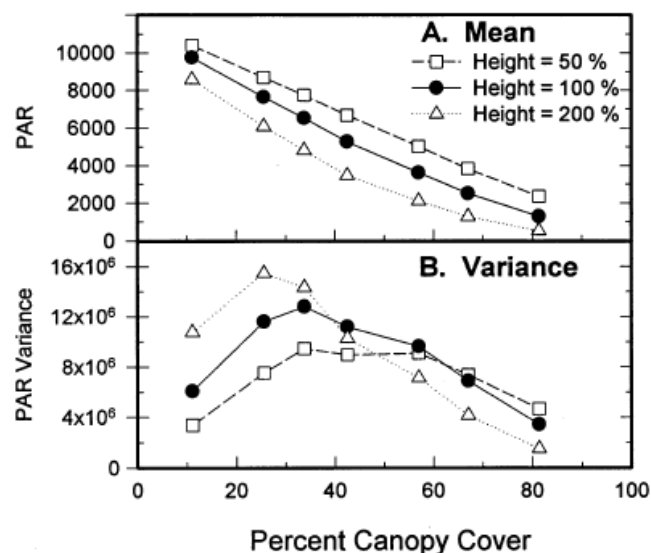


图 2.8 盖度梯度下不同树冠高度 PAR 的变化（人工样地）（引自 Martens *et al.*, 2000）

PAR 单位: mol m^{-2}

不同高度对遮荫下和林隙间的光照分布影响程度不同。对于两种林下位置，林下光照的均值均是矮树最大，盖度高时林隙间 PAR 对于树冠高度更为敏感，而盖度低时遮荫下 PAR 对于树冠高度更为敏感（图 2.9A）。盖度高时，所有高度下的 PAR 方差都是林隙间大于遮荫下的（图 2.9B-D）。在树冠最高的样地，林隙间 PAR 方差始终大于遮荫下（图 2.9D）。

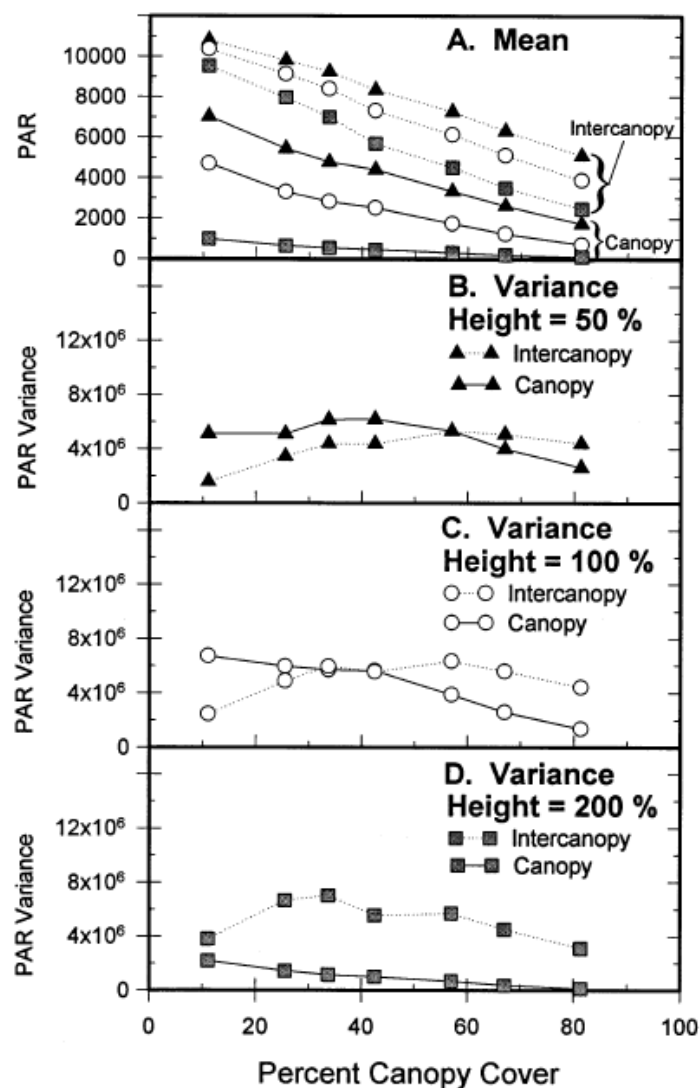


图 2.9 盖度梯度下不同树冠高度林隙间与遮荫下 PAR 的变化(人工样地)(引自 Martens *et al.*, 2000)

PAR 单位: mol m^{-2}

对于三个实际样地的空间结构、海拔高度、实际盖度、树冠高度对光合有效辐射影响的分析,也与人工样地得到的结果一致。综合以上结果,林下的光合有效辐射与乔木盖度的关系如图 2.10 所示,图中虚线表示树冠高度恒定时 PAR 均值和方差的可能趋势,而实线表示森林-草原连续体中盖度和树冠高度同时变化下的 PAR 均值和方差的可能趋势。

综上所述,森林-草原连续体中的林下光照主要取决于乔木层盖度,同时需要用树冠高度和空间格局进行修正。该模型与其他纬度灌木丛的盖度研究结果相吻合,故在本研究中,将乔木盖度与灌木盖度加和,同时作为草本层植物的上层覆盖。

第三章 地形格局与草本植物种类分布

3.1 研究区植物物种概况

研究区植被处于暖温带落叶阔林向温带草原过渡, 森林多呈斑块分布于山地阴坡, 阳坡多为灌丛和草原, 并在低平地和林缘出现草甸。

研究区内植物区系组成复杂, 种类较为丰富, 以菊科、禾本科、蔷薇科、豆科和莎草科为主, 是组成草原、草甸的主要成分, 有的作为优势种和建群种出现, 如贝加尔针茅 (*Stipa baicalensis*)、羊草 (*Leymus chinensis*)、冷蒿 (*Artemisia frigida*)、日阴菅苔草 (*Carex pediformis*) 等 (王庆锁, 2004)。

在本研究的十个样地中共出现草本植物 147 种, 其中菊科 21 种, 禾本科 19 种, 豆科、蔷薇科各 10 种, 百合科、毛茛科各 9 种。

高位芽植物为研究区森林和灌丛的建群种, 本研究涉及有白桦 (*Betula platyphylla*)、山杨 (*Populus davidiana*)、棘皮桦 (*B. dahurica*)、云杉 (*Picea meyeri*)、油松 (*Pinus tabulaeformis*)。林下常见灌木中也有高位芽植物, 本研究涉及有虎榛子 (*Ostryopsis davidiana*)、山刺玫 (*Rosa davidii*)、蒙古荚蒾 (*Viburnum mongolicum*)、金露梅 (*Potentilla fruticosa*)、沙柳 (*Salix psammophila*) 等。

地上芽植物中, 半灌木和小半灌木有达乌里胡枝子 (*Lespedeza dahurica*)、二色胡枝子 (*L. bicolor*)、冷蒿 (*Artemisia frigida*)、百里香 (*Thymus mongolicus*)。草本植物有线叶菊 (*Filifolium sibiricum*)。其余出现在本研究的灌木种类有: 稠李 (*Prunus padus*)、山荆子 (*Malus baccata*)、光叶山楂 (*Crataegus dahurica*)、黑果枸杞 (*Cotoneaster melanocarpus*)、椴斗叶绣线菊 (*Spiraea aquilegifolia*)、楔叶茶藨子 (*Ribes diacanthum*)、沙生桦 (*Betula gmelinii*)、小叶锦鸡儿 (*Caragana microphylla*)、沙地柏 (*Sabina vulgaris*)、细叶小檗 (*Berberis poiretii*)、金银木 (*Lonicera maackii*)、柔毛绣线菊 (*Spiraea pubescens*)、小叶鼠李 (*Rhamnus bungeana*)、美蔷薇 (*Rosa bella*)。

地面芽植物种类较多, 在草甸草原群落起主要作用的有贝加尔针茅 (*Stipa baicalensis*)、糙隐子草 (*Cleistogenes squarosum*)、洽草 (*Koeleria cristata*)、紫羊茅 (*Festuca rubra*)、冰草 (*Agropyron cristatum*)、早熟禾 (*Poa* spp.)、星毛委陵菜 (*Potentilla acaulis*)。高原森林草原分布在高原面上, 一般丘间平地为羊草 (*Leymus chinensis*) 草原, 缓坡坡顶出现贝加尔

针茅 (*Stipa baicalensis*) 草原片断。

莎草科几种苔草在本研究的十个样地中占有非常明显的优势, 包括黄囊苔草 (*Carex korshinskyi*)、披针叶苔草、日阴苔草 (*Carex pediformis*), 均为苔草属多年生草本植物; 禾本科的贝加尔针茅、糙隐子草、拂子茅 (*Calamagrostis epigeios*)、野青茅 (*Deyeuxia arundinacea*) 等, 在研究区的分布也较多, 均为多年生草本植物。另外, 菊科、毛茛科植物在某些群落中也占有优势。

3. 2 不同科的草本植物沿坡向的分布

由于植物的子叶数目和功能类群的划分均涉及不同科的特征, 故本研究首先计算了各个地点所有出现物种所属科的重要值之和, 并且图示各地点的阴阳坡分界线以及森林-草原分界线在样线上的相对位置。图 3.1-3.10 中横坐标显示每个样点的分段小样地, 每个点表示了长为 5m, 宽为样线基线长度 (4m 或 6m) 的小样地内各优势科植物的重要值, 虚线示意山坡纵剖面的坡顶线 (源水头坡度不变而仅坡向改变), 左侧为阳坡 (南坡) 右侧为阴坡 (北坡), 该图示意坡度坡向的实际方位, 以及森林-草原界限的实际位置。纵轴表示各样地所有科的重要值, 总和均为 100 (无量纲的相对优势度)。该图有效地表示了坡向和坡度梯度上主要草本植物科的分布格局。

三道河口的草原与森林分界线恰好为阳坡与阴坡分界线, 阴坡从坡顶至坡底依次分布着油松林与白桦-山杨混交林, 其阴坡中段分布有以虎榛子为主的灌丛带, 坡底乔木所处位置坡度较陡, 接近 40°, 且仍有较密的灌木分布, 以光叶山楂为主。草本植物总体上以莎草科最占优势, 其次为鸢尾科、禾本科和毛茛科。在草原地带, 除了四个主要科以外, 有其他科植物分布, 但均较少; 油松林处在阴坡顶较为平缓的地带, 林下的毛茛科与鸢尾科植物分布较多, 且以鸢尾科的山马薷尤为优势; 灌丛中鸢尾科植物有所减少, 禾本科植物则有所增加, 而莎草科成为最具优势的科。白桦-山杨混交林下植物种类较少, 以莎草科和禾本科最具优势。总体来说, 莎草科与鸢尾科在分布上有一定替代关系, 即鸢尾科占优势时莎草科有所减少, 而禾本科与莎草科的变化趋势较为一致, 且在阴坡禾本科随坡度增大而有所增加 (图 3.1)。

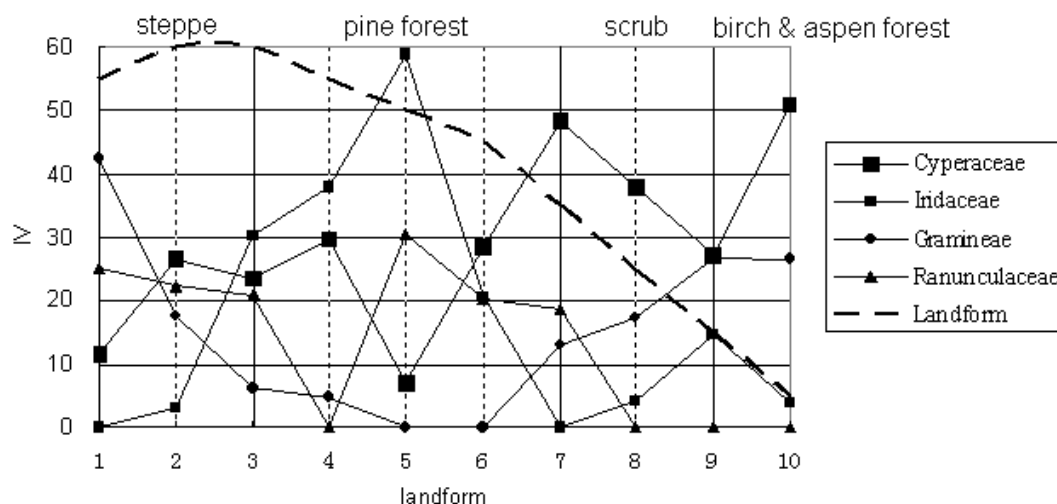


图 3.1 三道河口优势科植物沿地形的分布

白音敖包白桦林分布坡度较为平缓，坡底为大面积延伸的草甸，由于潮湿而有大面积的苔藓分布。白桦林的盖度越接近坡底越为密集。上林缘分布着少量以黑果枸杞为主的灌木，总盖度不超过 10%，下林缘灌木为盖度约 10%的金露梅。草原灌木为耧斗叶绣线菊、金露梅、山刺玫等。禾本科和莎草科植物在草原和白桦林中优势度明显，白桦林中菊科植物分布也较多，而在草甸中，蔷薇科以及其他一些杂类草都有出现，蔷薇科尤为丰富。总体来说，莎草科在白桦林和草甸的分布变化最为明显，而菊科与蔷薇科植物在白桦林与草甸间有一定的替代关系（图 3.2）。

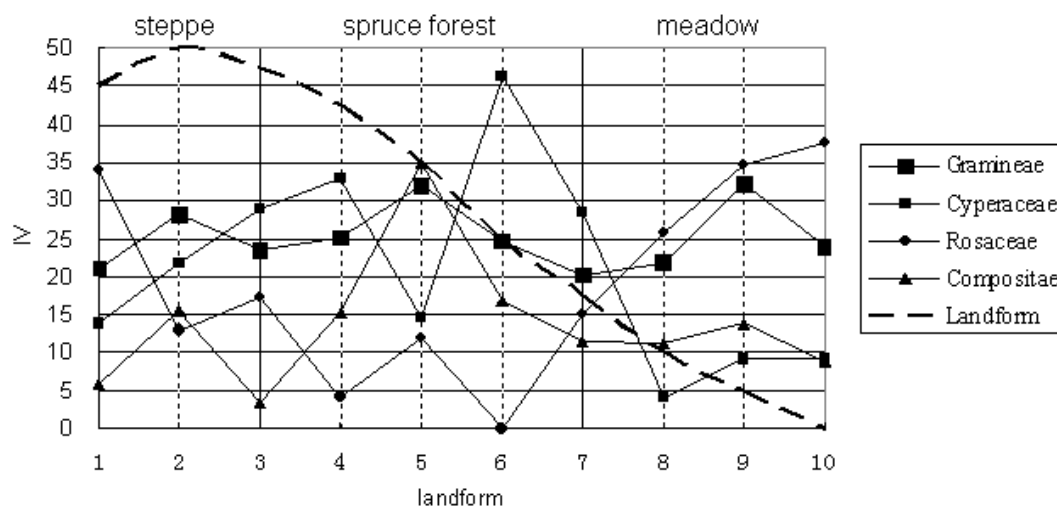


图 3.2 白音敖包优势科植物沿地形的分布

扎格斯泰淖尔白桦林所处阴坡上缓下陡，坡底乔木盖度略低。坡顶灌木有沙柳、山刺玫、楔叶茶藨子，坡底白桦疏林内灌木为沙柳、楔叶茶藨子、沙生桦及小叶锦鸡儿。禾本科、莎

草科、菊科植物在草原的分布，随着接近坡顶的程度而明显增加。另外，莎草科与禾本科在白杆林内部有着相反的变化趋势，莎草科植物增加而禾本科植物减少。总体来说，白杆林中有着更多的草本植物科的分布，菊科自草原至白杆林总体呈下降趋势（图 3.3）。

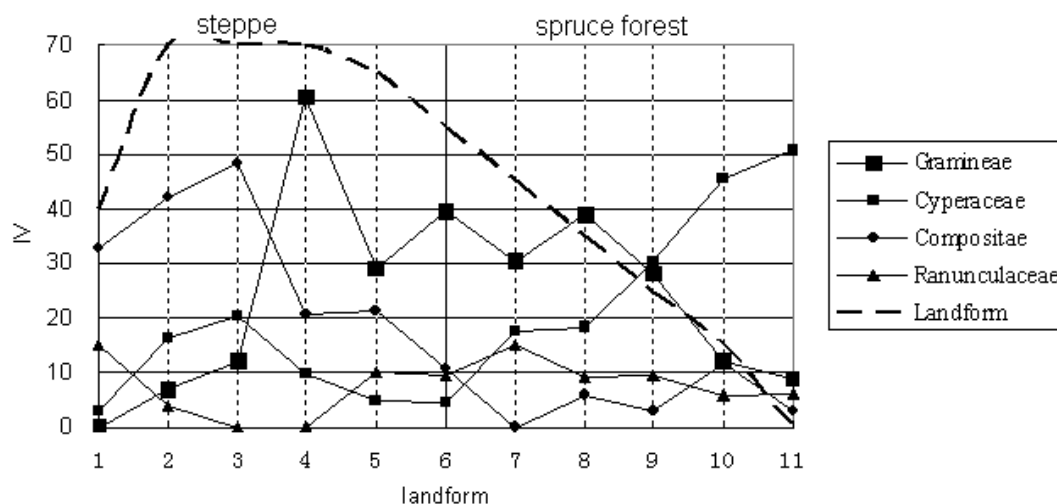


图 3.3 扎格斯泰淖尔白杆林优势科植物沿地形的分布

扎格斯泰淖尔的山杨林分为疏林和密林两个部分，其中密林盖度接近疏林的两倍。疏林灌木以山丁子和稷斗叶绣线菊为主；密林灌木盖度小，以山丁子和金银木为主。阳坡草原中，莎草科、禾本科、毛茛科植物占绝对优势，不过接近坡顶处优势度下降。阴坡接近坡顶处坡度较缓，这三个科的植物分布又有所增加，且以莎草科增加最为迅速。进入密林后，莎草科植物继续明显增加，而禾本科则没有了分布，比较突出的是石竹科和豆科植物分布的增加。总体来说，莎草科植物随着坡度坡向的变化趋势十分明显，且随着乔木盖度增加而始终呈上升趋势（图 3.4）。

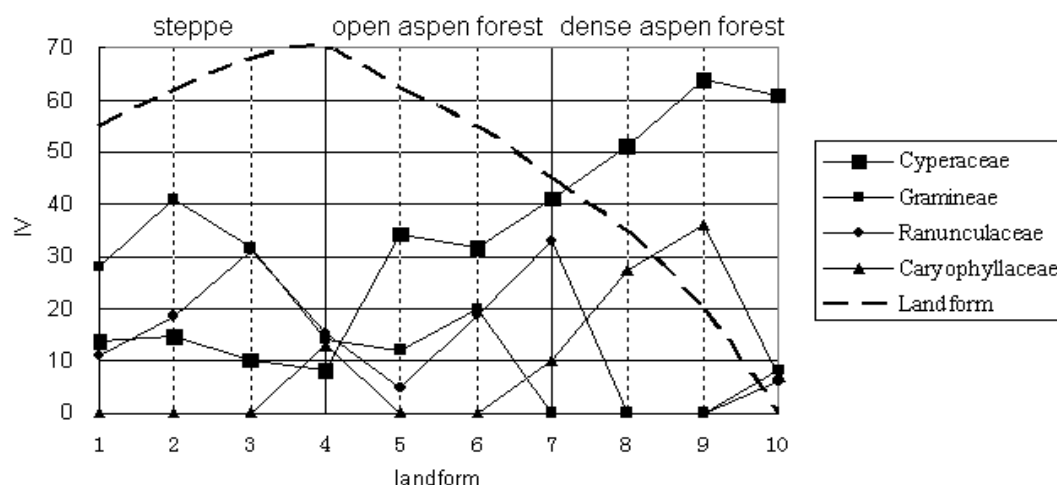


图 3.4 扎格斯泰淖尔山杨林优势科植物沿地形的分布

源水头样线比较特殊，该地点山坡较高且大，而沿垂直等高线方向的林草分界线较为整齐，故选择等高线方向样带开展调查。南坡的沙坡分布物种较少，以菊科和藜科植物为主，进入西南坡灌木丛郁闭度较高，藜科植物有所减少而毛茛科植物增加。西南坡很短而西北坡较长，有少量白桦和油松的分布，莎草科与菊科植物增加明显，而藜科与毛茛科植物均有所减少。油松-白桦混交林下，有大量以虎榛子为主的灌木，还有少量柔毛绣线菊和小叶鼠李。转入北坡的白桦林盖度达到 50%，林下仍有少量灌木分布，草本植物以菊科和莎草科占绝对优势，但两科植物变化趋势不尽相同。总体来说，莎草科植物随着坡向向北变化而增加，毛茛科植物则相反（图 3.5）。

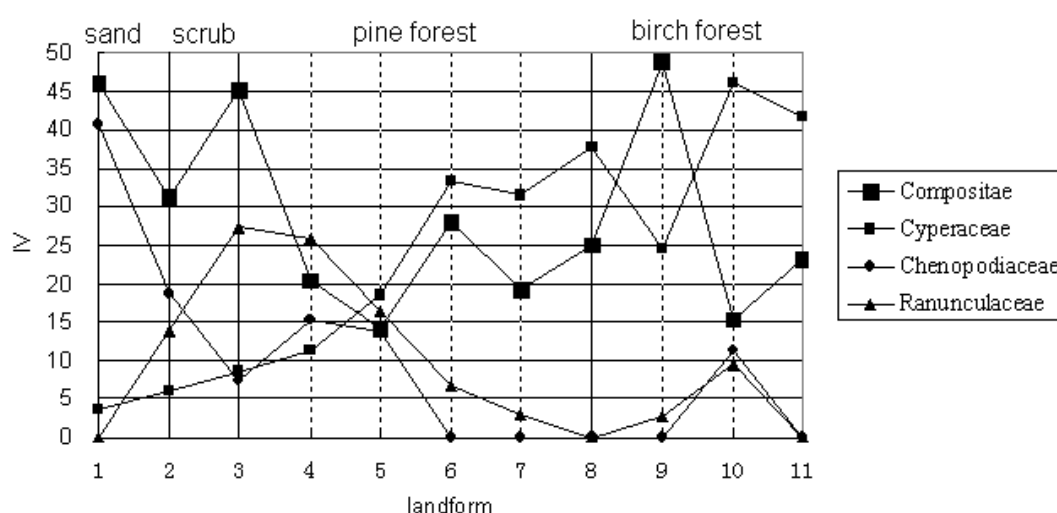


图 3.5 源水头优势科植物沿地形的分布

好鲁库山杨林群落结构相对简单，草原只有禾本科和莎草科植物以及少量的菊科和蔷薇科杂类草。坡顶灌木丛以耧斗叶绣线菊和虎榛子为主，草本植物的禾本科分布有所下降，而莎草科植物先增后减再增。进入盖度为 40%的山杨林，虎榛子占灌木的绝大多数，草本层出现数种其他杂类草，禾本科植物略有增加。总体来说，草本植物以禾本科和莎草科植物为绝大多数，变化趋势比较缓慢（图 3.6）。

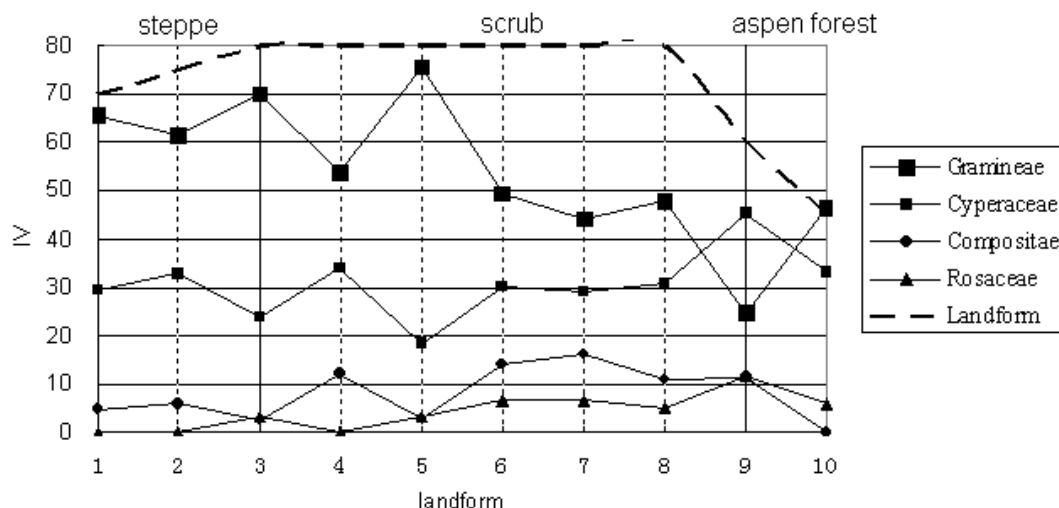


图 3.6 好鲁库优势科植物沿地形的分布

白扞坑整条样线均位于阴坡，草甸、白桦林、草原界限明显，白桦林盖度约为 20%，林下分布少量柔毛绣线菊灌木，盖度 1%。莎草科植物在草甸占据优势，而随着坡位的下降，在进入草原后有明显下降，总体上为禾本科变化较莎草科更为平缓，分布较为均匀，其次还有菊科、蔷薇科的优势分布。总体来说，莎草科进入草原后有明显的减少，其余各科变化不明显（图 3.7）。

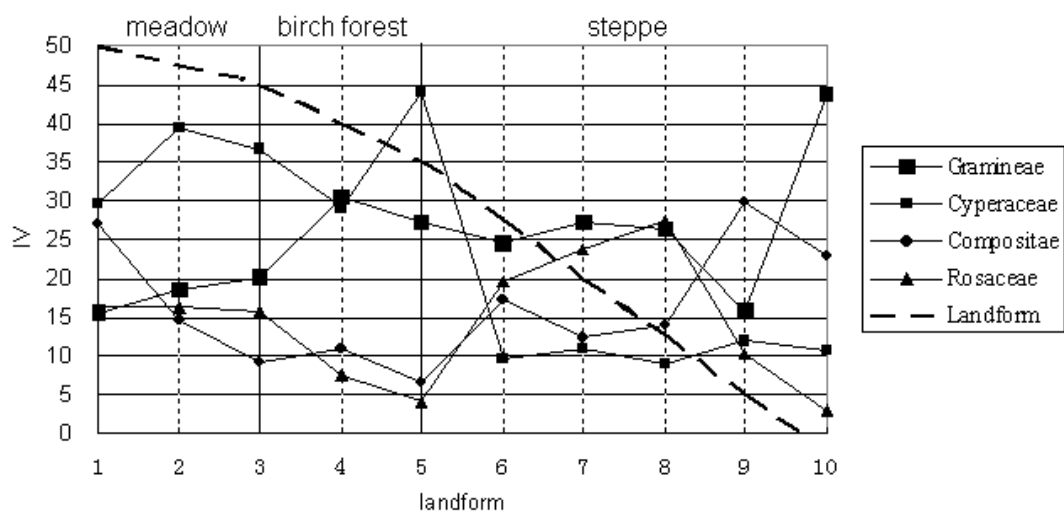


图 3.7 白扞坑优势科植物沿地形的分布

松树井子山杨林中，有 20m 长的平缓坡顶，其上的灌木丛分布以虎榛子为主，盖度达到 50%左右。禾本科和莎草科植物在坡顶有很明显的分布变化，阳坡的草原地带这两个科植物都随接近坡顶距离缩小而减小，过了坡顶以后则有所增加，阴坡山杨林盖度约为 60%，林下随着接近坡底距离减小，其余杂类草植物增加而禾本科与莎草科植物减少。总体来说，

禾本科和莎草科植物在灌丛中分布均少，而在草原和山杨林中有明显的优势分布（图 3.8）。

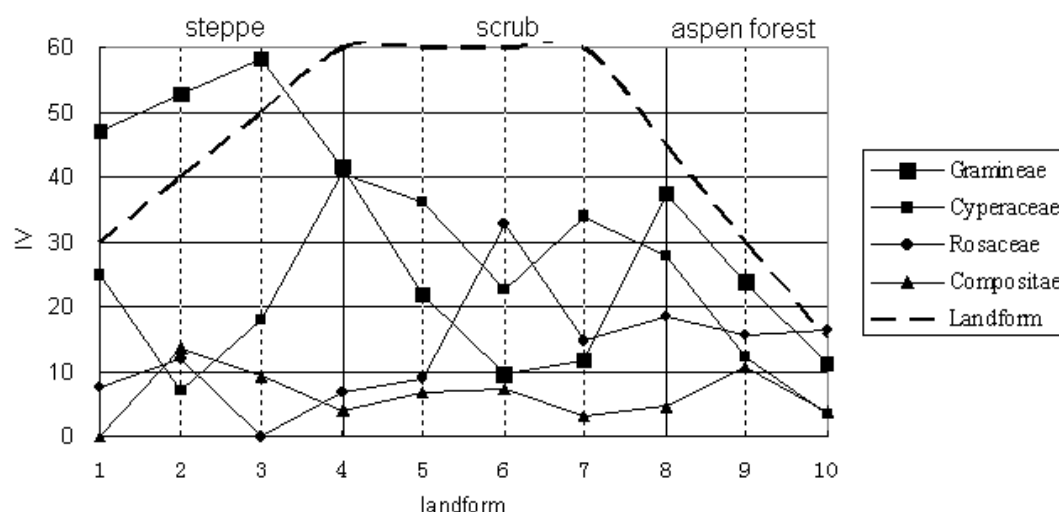


图 3.8 松树井子优势科植物沿地形的分布

狮子沟白桦林盖度达到了 80%，林下灌木以美蔷薇（盖度 50%）和柔毛绣线菊（盖度 30%）为主，林下草本植物生长茂盛，且分层明显。菊科植物随着从草原进入白桦林先减后增再减。毛茛科植物以牛扁为主，分布随着从草原进入白桦林先增后减再增。莎草科植物随着从草原进入白桦林有所增加，特别是在毛茛科植物明显减少的地方，莎草科植物明显增加。总体来说，菊科、毛茛科、莎草科植物占居绝对优势，而菊科和毛茛科植物有明显的替代关系（图 3.9）。

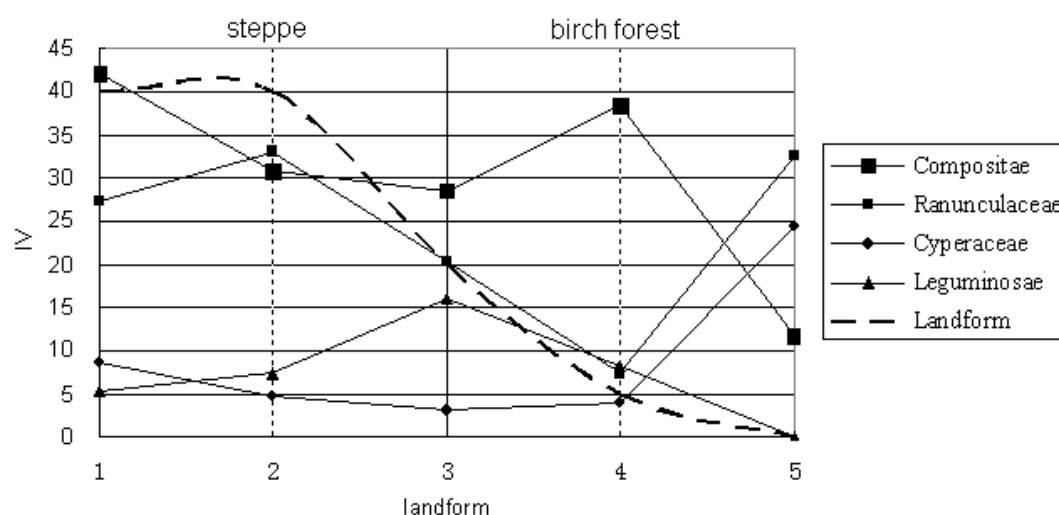


图 3.9 狮子沟优势科植物沿地形的分布

半坝村的白桦林已为棘皮桦林所取代，并且伴有少量落叶松的分布，总盖度达到了 50%，林下灌木为美蔷薇。草本植物层以菊科最为优势，而豆科、莎草科和蔷薇科植物也分布较多，

菊科、豆莎草科存在一致的变化趋势，即先随坡位下降而略又增加，然而进入混交林以后优势度下降，说明其他科植物有所增加。总体来说，菊科、豆科、莎草科、蔷薇科植物占有绝对优势，而进入林下以后优势度均显著减少（图 3.10）。

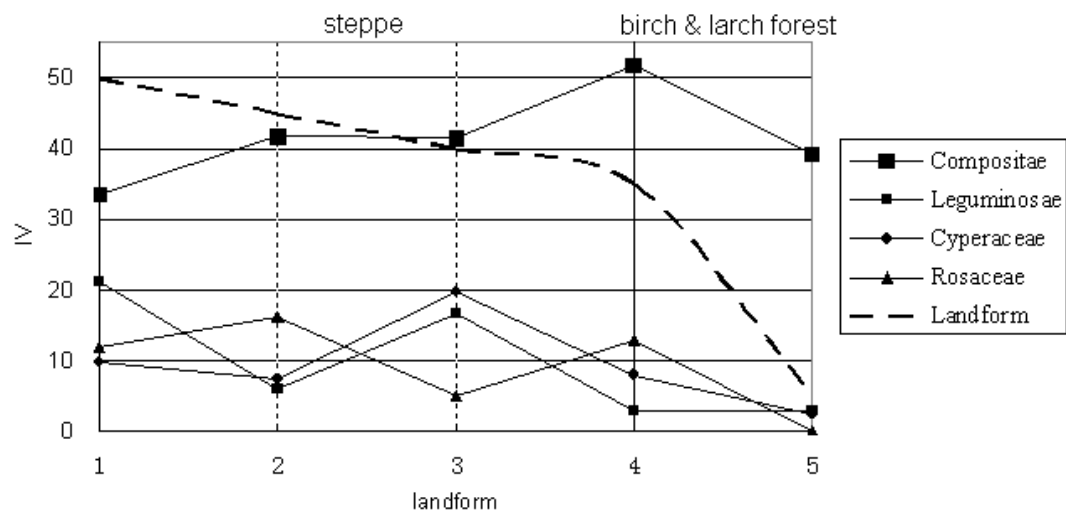


图 3.10 半坝村优势科植物沿地形的分布

第四章 光照条件对草本植物种类分布和多样性的影响

4.1 林下辐射照度值

利用何思源(2006)推算出的研究区坡面太阳直接辐射换算系数 K_{af} , 乘以 1990 至 2003 年间 7 月辐射总量的平均值 ($64669.71\text{MJ}/\text{M}^2$), 得出 42 个不同坡度和坡向乔木层上表面的年太阳直接辐射照度值; 然后利用 Martens 等(2000)建立的林下光照与乔灌木盖度的线性关系, 计算出各坡段草本层上表面的辐射照度值(表 4.1)。

表 4.1 不同坡度和坡向时草本层辐射照度值

	分段(m)	乔灌木盖度 (%)	坡度(°)	坡向	照度系数	林下辐射 (MJ/m^2)
三道河口	0-5	0	5	南	1.06	68549.90
	6-10	0	0	坡顶	1	64669.71
	11-15	40	10	北	0.855	33175.56
	16-20	40	15	北	0.773	29993.81
	21-25	40	20	北	0.706	27394.09
	26-30	40	25	北	0.64	24833.17
	31-35	60	30	北	0.58	15003.37
	36-40	60	35	北	0.524	13554.77
	41-45	125	40	北	0.474	-7663.36
	46-50	125	40	北	0.474	-7663.36
白音敖包	0-4	0	5	南	1.06	68549.90
	5-9	0	0	坡顶	1	64669.71
	10-14	30	5	北	0.931	42145.25
	15-19	35	10	北	0.855	35940.19
	20-24	40	15	北	0.773	29993.81
	25-29	80	20	北	0.706	9131.36
	30-34	30	15	北	0.773	34992.78

	35-39	30	20	北	0.706	31959.77
	40-44	30	20	北	0.706	31959.77
	45-50	30	20	北	0.706	31959.77
扎格斯泰淖尔白桦林	0-4	0	40	南	1.342	86786.76
	5-9	0	0	坡顶	1	64669.71
	10-14	30	0	坡顶	1	45268.80
	15-19	30	0	坡顶	1	45268.80
	20-24	30	15	北	0.773	34992.78
	25-29	65	30	北	0.58	13127.95
	30-34	65	30	北	0.58	13127.95
	35-39	65	30	北	0.58	13127.95
	40-44	65	30	北	0.58	13127.95
	45-49	65	30	北	0.58	13127.95
	50-55	15	40	北	0.474	26055.43
扎格斯泰淖尔山杨林	0-4	0	15	南	1.163	75210.88
	5-9	0	15	南	1.163	75210.88
	10-14	0	15	南	1.163	75210.88
	15-19	82	5	北	0.931	10837.35
	20-24	82	10	北	0.855	9952.67
	25-29	82	10	北	0.855	9952.67
	30-34	95	35	北	0.524	1694.35
	35-39	95	35	北	0.524	1694.35
	40-44	95	35	北	0.524	1694.35
	45-50	95	35	北	0.524	1694.35
源水头	0-4	0	40	南	1.342	86786.76
	5-9	95	40	西南	1.23	3977.19
	10-14	85	40	西北	1.12	10864.51
	15-19	85	40	西北	1.01	9797.46
	20-24	85	40	西北	0.9	8730.41

	25-29	85	40	西北	0.801	7770.07
	30-34	85	40	西北	0.69	6693.32
	35-39	85	40	西北	0.59	5723.27
	40-44	85	40	北	0.474	4598.02
	45-49	85	40	北	0.474	4598.02
	50-55	85	40	北	0.474	4598.02
好鲁库	0-4	0	5	南	1.06	68549.90
	5-9	0	5	南	1.06	68549.90
	10-14	35	5	南	1.06	44557.43
	15-19	35	0	坡顶	1	42035.31
	20-24	35	0	坡顶	1	42035.31
	25-29	35	0	坡顶	1	42035.31
	30-34	35	0	坡顶	1	42035.31
	35-39	35	0	坡顶	1	42035.31
	40-44	0	40	北	0.474	30653.44
	45-52	75	30	北	0.58	9377.11
白扞坑	0-4	0	5	北	0.931	60207.50
	5-9	0	5	北	0.931	60207.50
	10-14	0	10	北	0.855	55292.61
	15-19	21	10	北	0.855	43681.16
	20-24	21	10	北	0.855	43681.16
	25-29	0	25	北	0.64	41388.62
	30-34	0	25	北	0.64	41388.62
	35-39	0	25	北	0.64	41388.62
	40-45	0	25	北	0.64	41388.62
	46-51	0	25	北	0.64	41388.62
松树井子	0-4	0	25	南	1.248	80707.80
	5-9	0	25	南	1.248	80707.80
	10-14	0	25	南	1.248	80707.80

	15-19	50	0	坡顶	1	32334.86
	20-24	50	0	坡顶	1	32334.86
	25-29	50	0	坡顶	1	32334.86
	30-34	50	0	坡顶	1	32334.86
	35-39	60	30	北	0.58	15003.37
	40-44	60	30	北	0.58	15003.37
	45-50	60	30	北	0.58	15003.37
狮子沟	0-5	0	0	坡顶	1	64669.71
	6-10	0	0	坡顶	1	64669.71
	11-15	0	20	北	0.706	45656.82
	16-20	140	15	北	0.773	-19995.88
	21-25	160	10	北	0.855	-33175.56
半坝村	0-4	0	10	北	0.855	55292.61
	5-9	0	10	北	0.855	55292.61
	10-14	45	10	北	0.855	30410.93
	15-19	50	10	北	0.855	27646.30
	20-25	55	30	北	0.58	16878.80

4. 2 草本植物的生态类群

本研究中所有涉及到的草本植物种类名称根据中国植物志中所记载植物形态特征核对。在此基础上,针对各科植物的光合途径,功能类群,子叶数目,研究了各生态类群植物在地形、光照梯度上的分布特征。

根据光合作用的不同中间产物和过程,植物可以分为 C3、C4 和 CAM(景天酸代谢)三种光合类型。与 C3 植物相比,C4 植物光呼吸弱,二氧化碳补偿点低,光饱和点几乎达到全日照,光合作用最适温度高,在强光及其他适合条件下光合速率高。C4 光合作用途径的发现以及对于 C3 和 C4 光合途径的研究在二十世纪七十年代就引起了人们的注意,并在此后越来越受关注。由于 C3 和 C4 植物有着对环境因子的不同需求,所以这两种类型的植物对气候变化、放牧干扰以及营养条件的改变都有着不同的响应。

根据植物分类学上纲的单位将本研究所有出现的物种分为两类，单子叶植物（monocotyledons）和双子叶植物（dicotyledons）。双子叶植物纲的光合、蒸腾速率和水分利用效率均大于单子叶植物（杜菁昀等，2003）。单子叶植物纲又称百合纲，植物多为草本，稀为木本；叶具平行脉或弧形脉；主根不发达，由多数不定根形成须根系，其须根系在形态上具有细根分布均匀等特点，使得其在草原群落中的重要性比在森林群落中大。故本文单独考虑单子叶植物的分布与光照条件的关系。

另外一种划分植物的方法是依据其功能类群（plant functional group）（Tilman *et al.*, 2006），本研究仅涉及草本植物的划分，故可分为禾草类（grass），苔草类（sedge），杂类草（forb），豆科植物（legume）四大类，而不考虑木本植物种类（wood）。

4. 3 草本植物种类分布与光照的关系

4.3.1 优势种分布与光照条件的关系

尺度与格局问题是生态学研究的核心问题（Levin, 1992）。空间尺度是生态学研究不可忽略的一个因素，在不同尺度上的生态格局可能会出现不同的变化。本研究涉及 2 个空间尺度，即一个样点内部局地尺度上物种分布的变化，及所有样点综合考虑时区域尺度上物种分布的变化。

1 局地尺度上优势种分布与光照的关系

在本研究 10 个地点中，出现在一半以上小样地的草本植物被认为是优势种，这些植物种类在不同地点沿林下辐射照度的变化有所不同。通过分析这些优势种在各地点沿光照梯度的变化趋势，可以说明局地尺度光照的变化对于物种分布可能的影响。表 4.2 为林下辐射照度与物种重要值的 Pearson 相关系数。

黄囊苔草是本研究分布最为广泛的植物种类，可以看到其重要值在三道河口、白音敖包、扎格斯泰淖尔白杆林、源水头、松树井子这 5 个地点随着辐射照度的增加而减少；而在扎格斯泰淖尔山杨林、半坝村这 2 个地点重要值随着辐射照度的增加而增加；在剩余 3 个地点分布较少。究其显著性水平，三道河口样地黄囊苔草重要值与辐射照度的 Pearson 相关系数 -0.636，显著性水平 < 0.05 。披针叶苔草的分布也较为广泛，而且在各个分布地点重要值变化

均与光照条件呈负相关，且在扎格斯泰淖尔山杨林显著水平非常好（0.022）。瓣蕊唐松草在白音敖包、扎格斯泰诺尔白扞林、白扞坑 3 个地点重要值均与光照呈显著正相关，相关系数在 0.65-0.71 范围内。糙隐子草在好鲁库与光照条件的关系呈正相关（显著性水平 <0.01 ），其重要值与辐射照度的 Pearson 相关系数为 0.773。在松树井子，拂子茅分布与光照条件的关系呈负相关（显著性水平 <0.05 ），其重要值与辐射照度的 Pearson 相关系数为-0.732；贝加尔针茅分布与光照条件的关系呈正相关（显著性水平 <0.01 ），其重要值与辐射照度的 Pearson 相关系数为-0.900。日阴菅苔草在好鲁库与白扞坑有着一致的变化趋势，其重要值均与林下辐射照度呈显著正相关（显著性水平 <0.05 ），Pearson 相关系数分别为 0.893 和 0.684。其他一些种在不同地点也呈现出随光照变化的一致趋势，如扁蓿豆、羊草、野青茅。只有一个地点占据优势的物种中，扎格斯泰诺尔白扞林中的毛沙芦草重要值与林下辐射照度呈显著正相关（显著性水平 <0.01 ），Pearson 相关系数为 0.838。

表 4.2 优势种重要值与林下辐射照度的 Pearson 相关系数（植物拉丁名见附录）

物种	相关系数	显著性	地点
黄囊苔草	-0.636*	0.048	三道河口
	-0.317	0.373	白音敖包
	-0.541	0.086	扎格斯泰诺尔白扞林
	0.345	0.328	扎格斯泰诺尔山杨林
	-0.086	0.802	源水头
	-0.126	0.729	松树井子
	0.177	0.775	半坝村
披针叶苔草	-0.217	0.547	三道河口
	-0.516	0.104	扎格斯泰诺尔白扞林
	-0.708*	0.022	扎格斯泰诺尔山杨林
	-0.419	0.200	源水头
	-0.579	0.307	狮子沟
瓣蕊唐松草	0.674*	0.033	白音敖包
	0.710*	0.014	扎格斯泰诺尔白扞林
	-0.201	0.554	源水头
	0.656*	0.040	白扞坑

糙隐子草	0.077	0.832	白音敖包
	0.773**	0.009	好鲁库
	0.599	0.067	白扞坑
拂子茅	-0.470	0.145	扎格斯泰诺尔白扞林
	-0.052	0.887	扎格斯泰诺尔山杨林
	-0.732*	0.016	松树井子
铁杆蒿	-0.482	0.134	源水头
	0.508	0.382	狮子沟
	-0.272	0.658	半坝村
紫羊茅	0.171	0.637	白音敖包
	-0.544	0.104	白扞坑
	0.499	0.142	松树井子
贝加尔针茅	0.384	0.274	好鲁库
	0.900**	0.000	松树井子
扁蓿豆	0.347	0.567	狮子沟
	0.563	0.323	半坝村
日阴营苔草	0.893**	0.001	好鲁库
	0.684*	0.029	白扞坑
羊草	-0.156	0.667	好鲁库
	-0.611	0.274	半坝村
野青茅	-0.595	0.070	三道河口
	-0.392	0.262	白音敖包
老芒麦	0.021	0.953	好鲁库
毛沙芦草	0.838**	0.001	扎格斯泰诺尔白扞林
蒙古冰草	0.603	0.065	白音敖包
沙苔	0.472	0.142	扎格斯泰诺尔白扞林
山马蔺	-0.036	0.922	三道河口
无芒雀麦	-0.551	0.079	扎格斯泰诺尔白扞林

注：*显著性水平<0.05；**显著性水平<0.01。

以下分别考虑每个地点上沿光照梯度变化趋势显著的植物种类（图 4.1a-e）。三道河口的黄囊苔草分布随着光照的增强呈显著递减趋势， $R^2=0.4044$ （图 4.1a）。白音敖包的瓣蕊唐松草分布随着光照的增强而呈显著递增趋势， $R^2=0.4545$ （图 4.1b）。扎格斯泰淖尔白杆林的瓣蕊唐松草分布随着光照的增强而呈显著递增趋势， $R^2=0.5038$ （图 4.1c），而毛沙芦草分布随着光照的增强呈显著递减趋势， $R^2=0.7017$ （图 4.1d）。好鲁库的日阴菅苔草分布随着光照的增强而呈显著递增趋势， $R^2=0.7969$ （图 4.1e）。

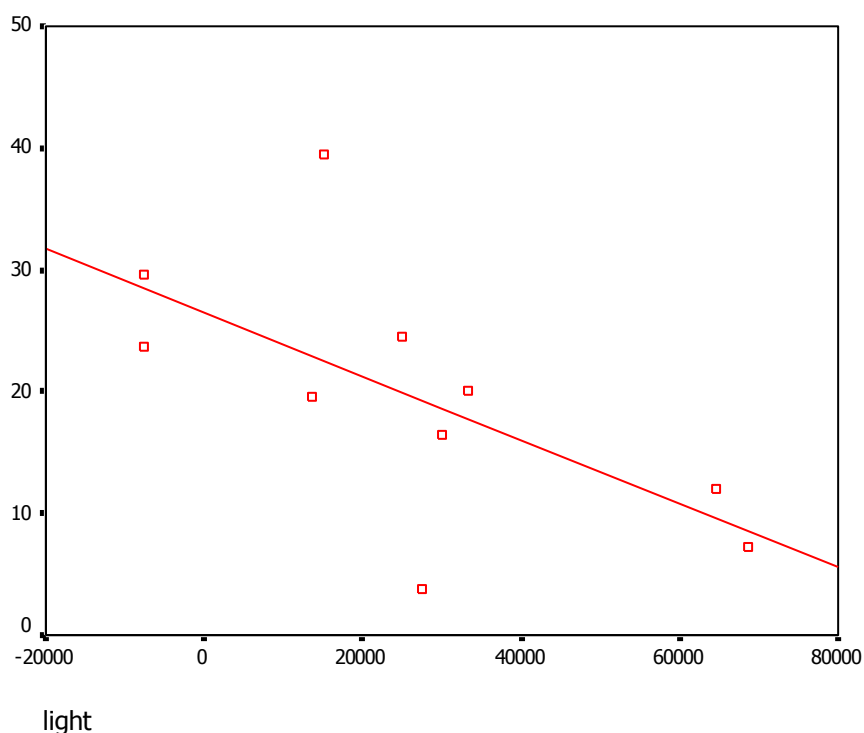


图 4.1a 三道河口黄囊苔草与辐射照度关系(light: MJ/m², IV: %)

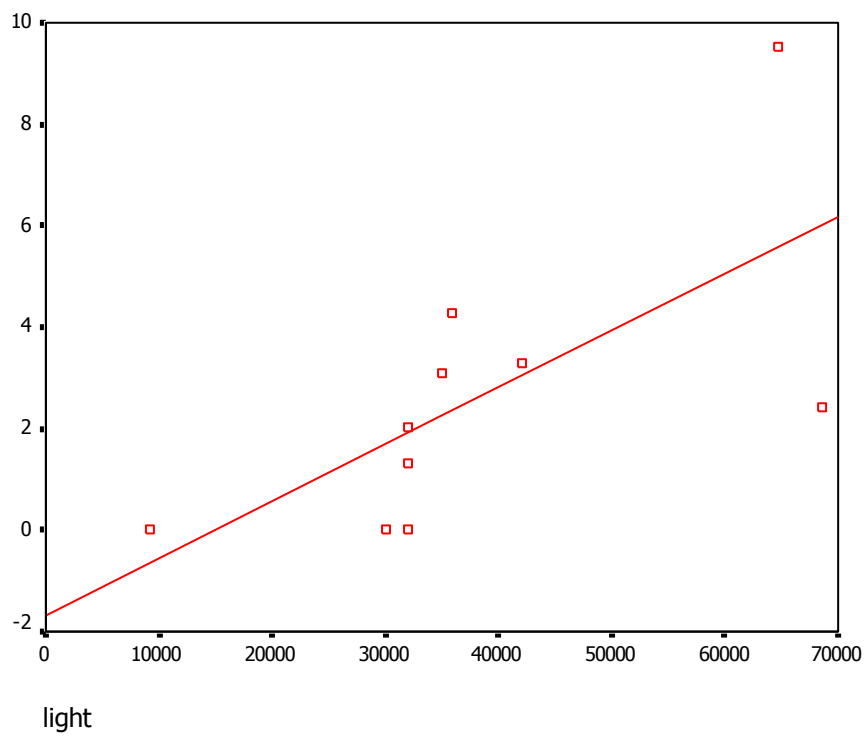


图 4.1b 白音敖包瓣蕊唐松草与辐射照度关系(light: MJ/m², IV: %)

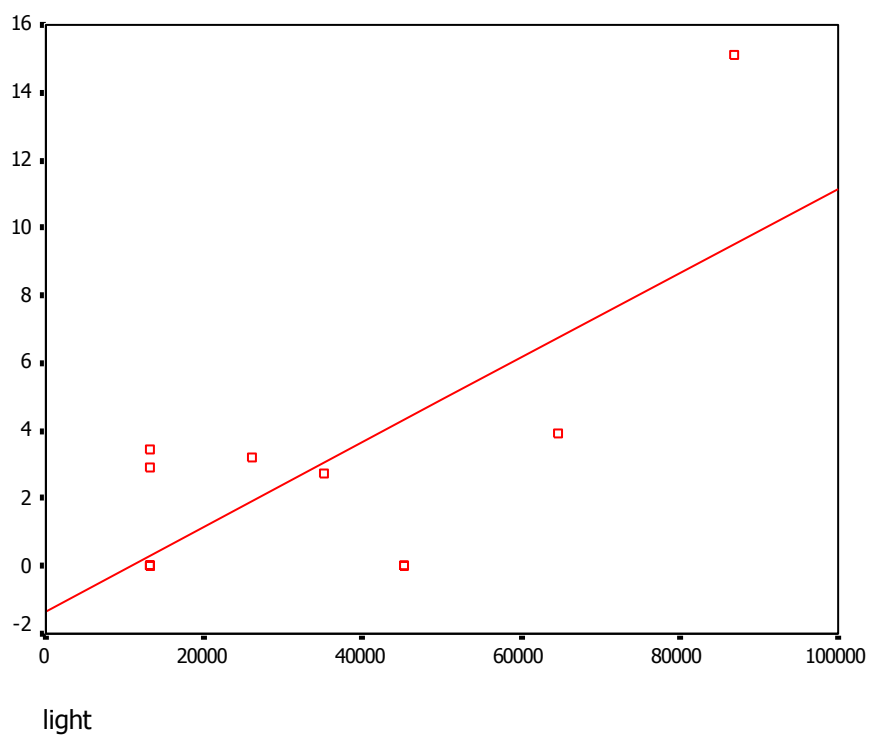


图 4.1c 扎格斯泰淖尔白扞林瓣蕊唐松草与辐射照度关系(light: MJ/m², IV: %)

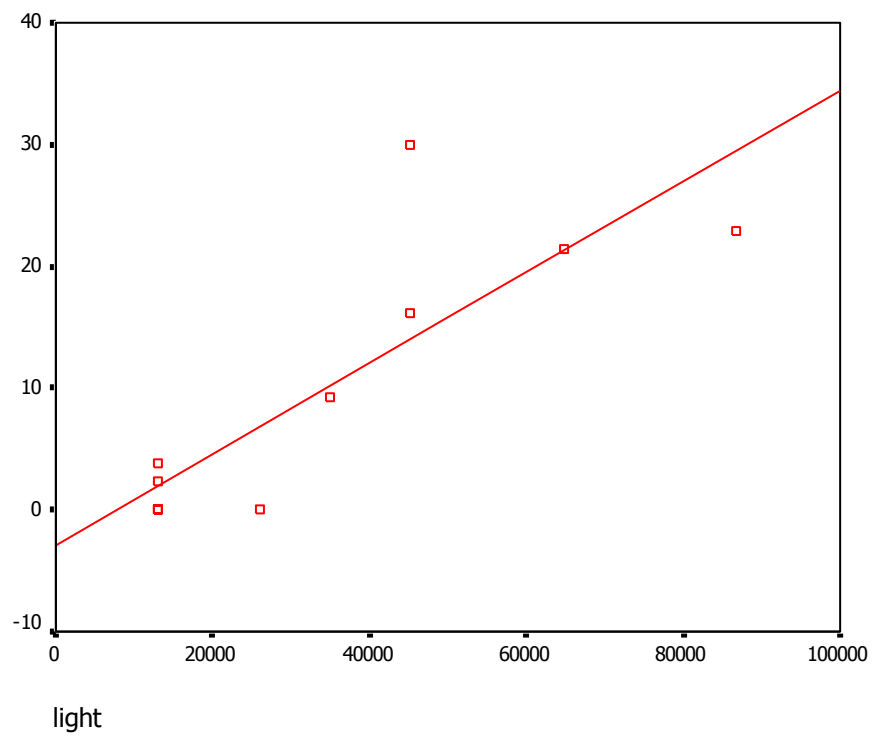


图 4.1d 扎格斯泰淖尔白扞林毛沙芦草与辐射照度关系(light: MJ/m², IV: %)

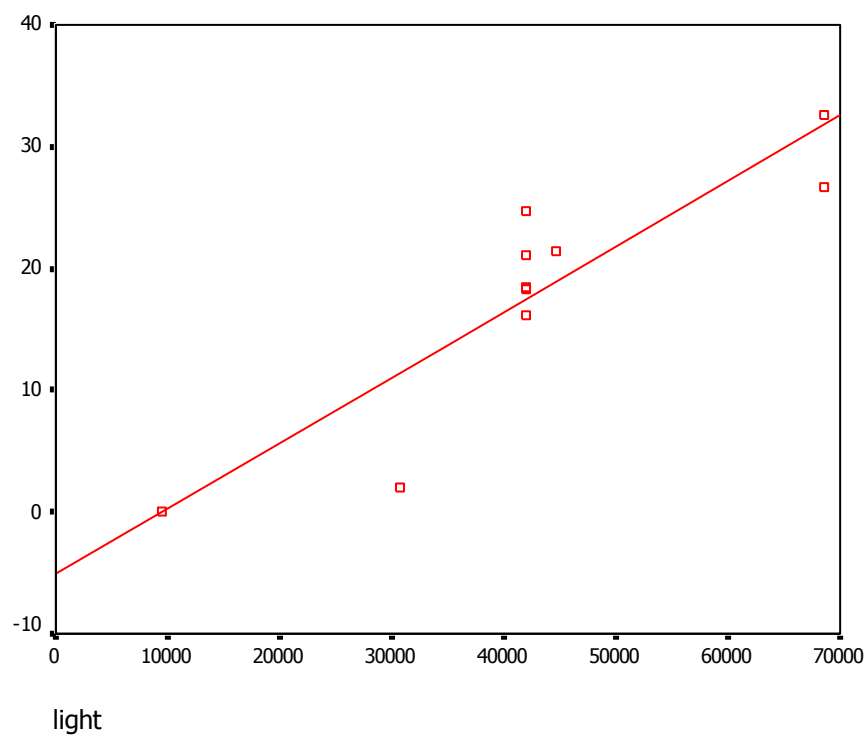


图 4.1e 好鲁库日阴营苔草与辐射照度关系(light: MJ/m², IV: %)

2 区域尺度上优势种分布与光照的关系

本研究涉及的所有样地, 分布的经纬度范围在 $41^{\circ}06.717'N$ - $43^{\circ}42.664'N$, $115^{\circ}21.994'E$ - $117^{\circ}15.205'E$ (图 2.1), 在百公里尺度上, 物种分布的变化及其与光照条件的关系可能与局地尺度有所区别。图 4.3 表示了分布较为广泛的植物种类(出现在一半以上样地的种类)在辐射照度梯度上的变化趋势。

黄囊苔草分布在全部 92 个小样地中的 67 个, 其重要值与辐射照度线性关系相关的显著水平差于对数线性相关的显著性水平, 其重要值对数线性相关的 Pearson 系数为 0.058 (显著性水平 0.639), 对数线性拟和 $R^2=0.0766$ 。瓣蕊唐松草分布在全部 92 个小样地中的 46 个, 其重要值与辐射照度正相关, 但显著性水平较差(Pearson 相关系数 0.063, 显著性水平 0.679), 线性拟和 $R^2=0.0039$ 。披针叶苔草分布在全部 92 个小样地中的 41 个, 其重要值与辐射照度显著负相关 (Pearson 相关系数 -0.426, 显著性水平 0.006), 线性拟和 $R^2=0.1813$ 。其余物种分布数量均少于 40 个小样地。

4.3.2 C4 植物分布与光照条件的关系

根据内蒙古 C4 植物名录(唐海萍等, 2001)和中国 C4 植物名录(殷立娟等, 1997), 研究区内确定为 C4 植物的有 9 种, 分别是禾本科的糙隐子草、老芒麦 (*Elymus sibiricus*), 莎草科的日阴菅苔草 (*Carex pediformis*), 菊科的火绒草 (*Leontopodium leontopodioides*)、线叶菊 (*Filifolium sibiricum*), 藜科的藜 (*Chenopodium album*)、猪毛菜 (*Salsola collina*)、尖头叶藜 (*Chenopodium acuminatum*), 以及景天科的瓦松 (*Orostachys fimbriatus*)。

在这 9 个物种中, 分布超过 10 个小样地的有日阴菅苔草、糙隐子草、老芒麦。日阴菅苔草分布在全部 92 个小样地中的 18 个, 其重要值与林下辐射照度的相关性极微弱 (Pearson 相关系数 0.04), 非常不显著 (0.986)。糙隐子草分布在全部 92 个小样地中的 24 个, 其重要值与林下辐射照度的 Pearson 相关系数为 0.108, 显著性水平 0.614。老芒麦分布在全部 92 个小样地中的 18 个, 其重要值与林下辐射照度的 Pearson 相关系数为 0.259, 显著性水平略好 (0.300)。

当将 C4 植物作为一个整体考虑其与光照条件的关系时, 其重要值之和与林下辐射照度呈显著正相关关系 (Pearson 相关系数 0.389, 显著性水平 0.008), 线性拟和 $R^2=0.1517$ (图 4.3)。

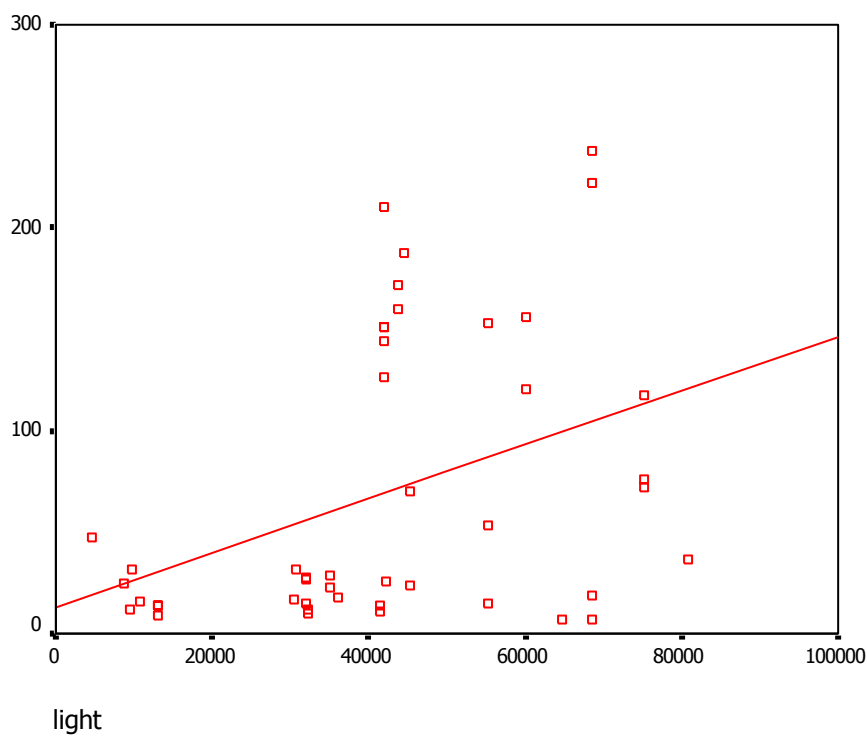


图 4.2 C4 植物与辐射照度的关系(light: MJ/m², IV: %)

4.3.3 单子叶植物分布与光照条件的关系

在本研究中出现的单子叶植物共四科：禾本科、莎草科、百合科、鸢尾科，其余均为双子叶植物（dicotyledons）。

本文首先分别分析了禾本科、莎草科、鸢尾科、百合科的重要值与光照条件的关系进行研究，然后将所有单子叶植物合起来研究其与光照条件的关系（图 4.3）。

禾本科是本研究中分布最优势的科，共出现了 13 属 19 种植物，分布在 92 个小样方的 79 个中，其重要值与林下辐射照度呈显著正相关（显著性水平<0.001），Pearson 相关系数 0.401，且线性拟合效果较好（ $R^2 = 0.1641$ ）（图 4.3a）。

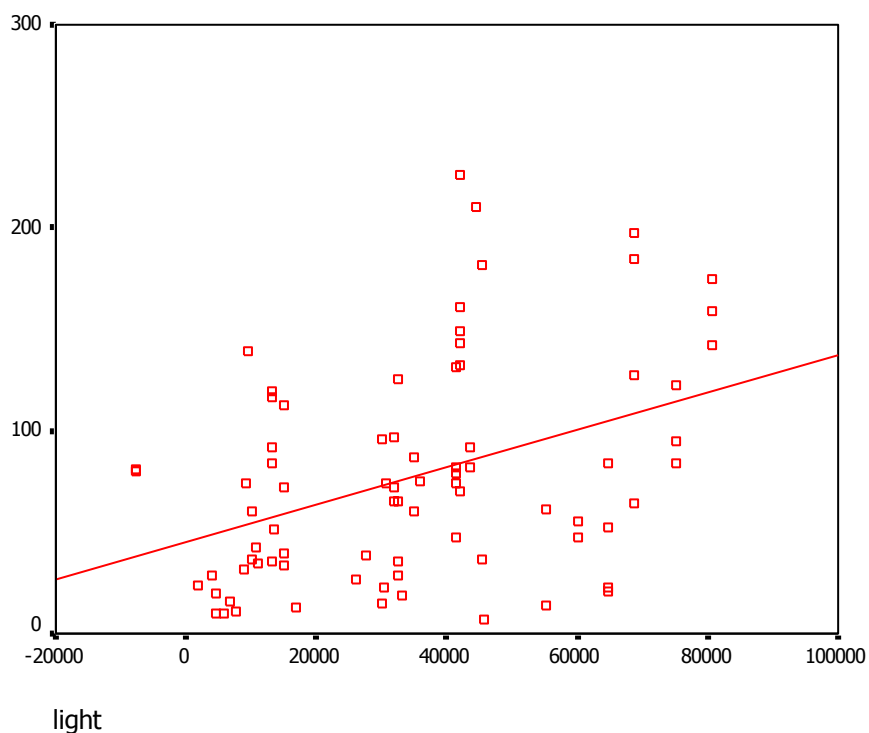


图 4.3a 禾本科植物与辐射照度的关系(light: MJ/m², IV: %)

莎草科是本研究中分布最为广泛的科, 虽然仅出现了 4 种苔草, 但其重要值均占据较大优势, 分布在所有 92 个小样方中, 其重要值与林下辐射照度呈显著负相关 (显著性水平 <0.01), Pearson 相关系数-0.340, 且线性拟合效果较好 ($R^2 = 0.1159$) (图 4.3b)。

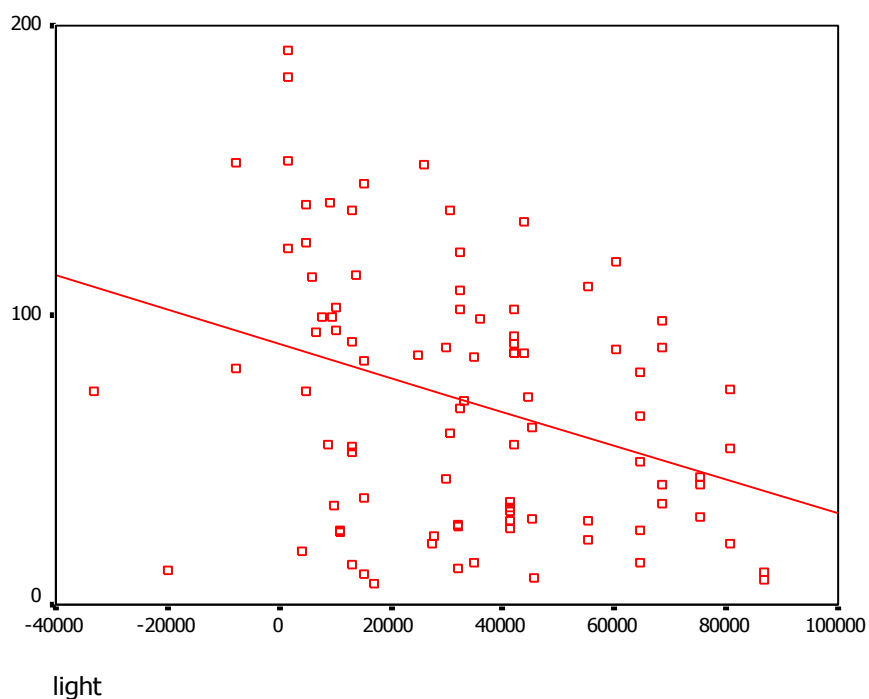


图 4.3b 莎草科植物与辐射照度的关系(light: MJ/m², IV: %)

百合科和鸢尾科沿光照梯度的分布显著性水平较差。百合科分布在 92 个小样方的 22 个中,共 3 属 9 种其重要值与辐射照度呈负相关(Pearson 相关系数-0.209,显著性水平 0.350),鸢尾科分布在 92 个小样方的 18 个中,共 1 属 2 种,其重要值与辐射照度呈负相关(Pearson 相关系数-0.222,显著性水平 0.376)。将两科加和后考虑重要值沿光照梯度的变化,呈负相关关系(Pearson 相关系数-0.177),显著性水平略有提高(0.282)。

当综合考虑所有单子叶植物重要值之和的时候,其沿光照梯度变化十分平缓,仅呈微弱的正相关(Pearson 相关系数 0.062),且显著性水平较差(0.559),这可能是由于禾本科和莎草科占据了单子叶植物的绝大多数,而这两个科与光照的相关性恰好相反,从而抵消。

4.3.4 功能类群植物分布与光照条件的关系

本研究出现的豆科植物 5 属 10 种。豆科是仅次于禾本科和菊科的第三大科,每年豆科植物的固氮量几乎与工业固氮量相等(于振文, 1993),其在自然界的广泛分布和其独特的自生固氮能力决定了其在生态系统中具有举足轻重的地位。禾草类植物在本文中即为禾本科植物,而苔草类植物在本文中即为莎草科植物,且无论在林缘草甸以及阳坡草原,这两类都是最具优势的功能类群。除豆科、禾草类、苔草类以外的其余各种草本植物均属于 forbs。

豆科植物重要值之和与辐射照度呈微弱负相关(Pearson 相关系数-0.024,显著性水平 0.881)。forbs 重要值之和与辐射照度呈微弱负相关(Pearson 相关系数-0.082,显著性水平 0.439)。总体来说,光照条件对豆科和 forbs 两个功能类群的植物影响较小。

禾草类是本研究中分布量最大的功能类群,共出现了 13 属 19 种植物,分布在 92 个小样方的 79 个中,其重要值与林下辐射照度呈显著正相关(显著性水平 <0.01),Pearson 相关系数 0.401,且线性拟和效果较好($R^2 = 0.1641$)(图 4.3a)。

苔草类是本研究中分布最为广泛的功能类群,虽然仅出现了 4 种,但其重要值均占据较大优势,分布在所有 92 个小样方中,其重要值与林下辐射照度呈显著负相关(显著性水平 <0.01),Pearson 相关系数-0.340,且线性拟和效果较好($R^2 = 0.1159$)(图 4.3b)。

4. 4 草本植物多样性与光照条件的关系

以下分析了草本植物多样性在光照梯度上的变化(表 4.3),分别涉及在一个样点的空间范围上物种数量和分布特征的变化,以及在全部研究区的空间范围上物种数量和分布特征的

变化，狮子沟和半坝村由于样方数目不足以反映变化趋势，故不做考虑。

表 4.3 各样点植物多样性与光照条件的关系

地点	Shannon-Wiener		Sørensen		Cody	
	相关系数	显著性	相关系数	显著性	相关系数	显著性
三道河口	0.471	0.17	-0.559	0.118	0.737*	0.024
白音敖包	0.475	0.166	0.252	0.513	0.232	0.548
扎格斯泰淖尔	-0.684*	0.02	0.310	0.383	-0.634*	0.049
扎格斯泰淖尔	0.539	0.108	0.228	0.556	0.141	0.717
源水头	-0.742**	0.009	0.545	0.103	0.313	0.379
好鲁库	-0.690*	0.027	0.811**	0.008	-0.845**	0.004
白扞坑	-0.728*	0.017	0.670*	0.048	-0.713*	0.031
松树井子	-0.601	0.066	-0.033	0.933	-0.215	0.578
所有样方	0.049	0.642	0.223*	0.044	-0.06	0.592

注：*显著性水平<0.05；**显著性水平<0.01。

4.4.1 α 多样性与光照条件的关系

α 多样性指某个群落或生境内部的种的多样性（张金屯，2004），在各小样地内部，光照条件的差异可能会导致 α 多样性的变化。本研究采用 Shannon-Wiener 指数，基于物种重要值，来衡量物种的 α 多样性，首先分析一个样点内各小样地之间的 α 多样性差异(图 4.4a-e，图中 S 表示南坡样地，T 表示坡顶样地，N 表示北坡样地)。考虑到影响草本层光照的因子为坡度、坡向和乔木灌木盖度，当处于同一坡向且坡度不变的情况下，影响草本层光照的因子即为乔木灌木盖度。具体地点的坡度坡向状况在几个连续样地内变化不大。以下分别分析这五个点的 α 多样性变化格局。

在扎格斯泰淖尔白扞林样地，草原的物种多样性明显小于森林的物种多样性。从草原向森林过渡，乔木和灌木层盖度逐渐增加，草本层光照减少。在草原分布区，乔灌层总盖度在 0-30%之间，进入森林分布区之后，乔灌层的总盖度增加到 65%，草本层辐射照度随之从（34992.78W/m²）降低到（13127.95 W/m²）。在南坡和坡顶的草原，草本层光照强，禾草类和苔草类植物占据优势，物种多样性较低，Shannon-Wiener 指数基本在 2 以下；而进入林下，光照强度减弱，较适宜阳性物种和阴性物种的共存，物种多样性也随之增加，Shannon-Wiener

指数大多在 2.5 左右。可以认为，从草原过渡到森林，乔灌层的郁闭度增加使得草本层接收到的光照强度减少，而草本层的物种多样性则随之增加，草本层物种多样性与光照强度成负相关关系。

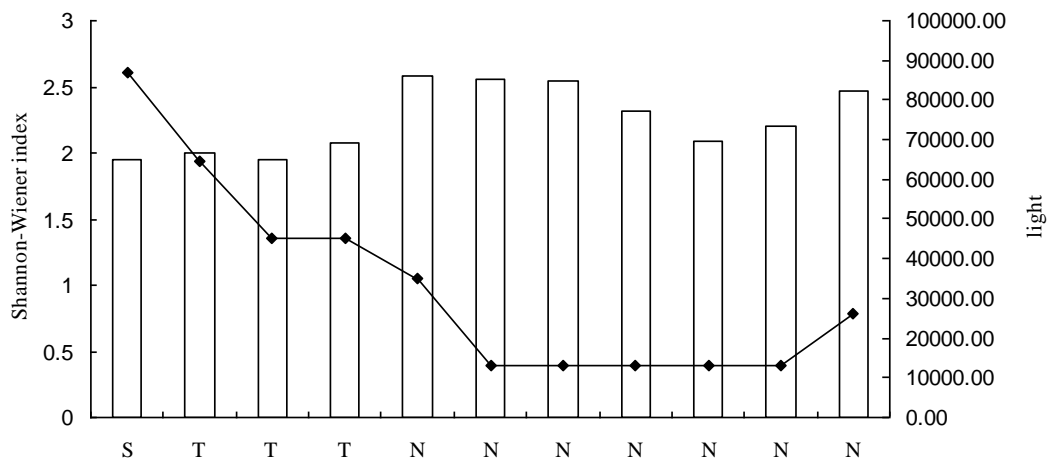


图 4.4a 扎格斯泰淖尔白桦林 α 多样性与光照的关系(light: MJ/m²)

在源水头样地，草原的物种多样性明显小于森林的物种多样性。南坡为无乔木灌木覆盖的沙坡草原，草本层接受全部光照，物种多样性较低，Shannon-Wiener 指数仅为 1.2 左右。转入西南坡为密集的灌丛，盖度陡升至 95%，草本层辐射照度随之从 86786.76W/m² 骤减到 3977.19 W/m²，物种多样性随之增加，Shannon-Wiener 指数达到 2 左右。西北坡出现油松-白桦混交林，加上林下灌木，总盖度在 85%左右，物种多样性在森林内部有所波动，但始终保持在 1.5 以上。可以认为，从草原过渡到森林，乔灌层的郁闭度增加使得草本层接收到的光照强度减少，而草本层的物种多样性则随之增加，草本层物种多样性与光照强度成负相关关系。

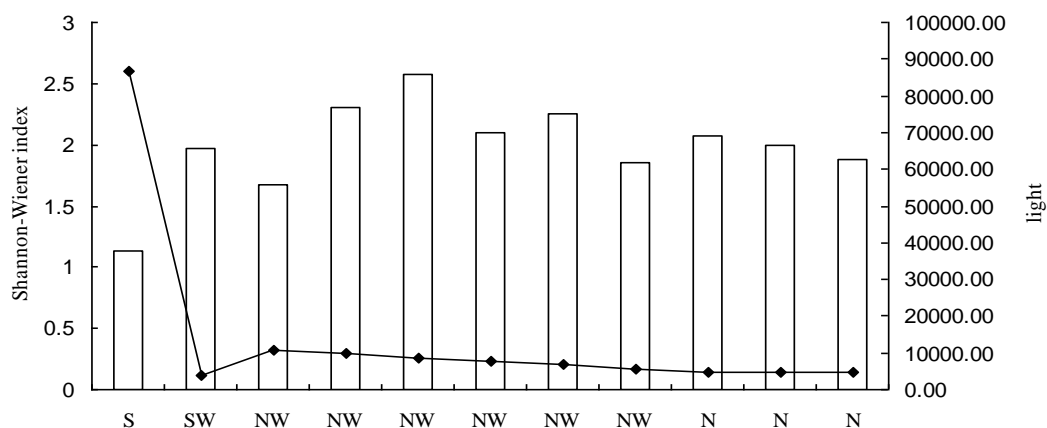


图 4.4b 源水头 α 多样性与光照的关系(light: MJ/m²)

在好鲁库样地，草原物种多样性小于森林的物种多样性。接近南坡坡顶处开始出现盖度为 35% 的灌丛，使得草本层辐射照度从 68549.90 W/m^2 锐减至 44557.43 W/m^2 。坡顶光照始终保持不变，物种多样性有所波动，并且越接近山杨林逐渐增加的趋势越明显，进入北坡山杨林以后，乔木灌木盖度增加到 75%，草本层辐射大幅下降，物种多样性变化趋势无规律，但 Shannon-Wiener 指数始终保持在 2 以上的水平，大于草原的 1.5 左右。可以认为，从草原过渡到森林，乔灌层的郁闭度增加使得草本层接收到的光照强度减少，而草本层的物种多样性则随之增加，草本层物种多样性与光照强度成负相关关系。

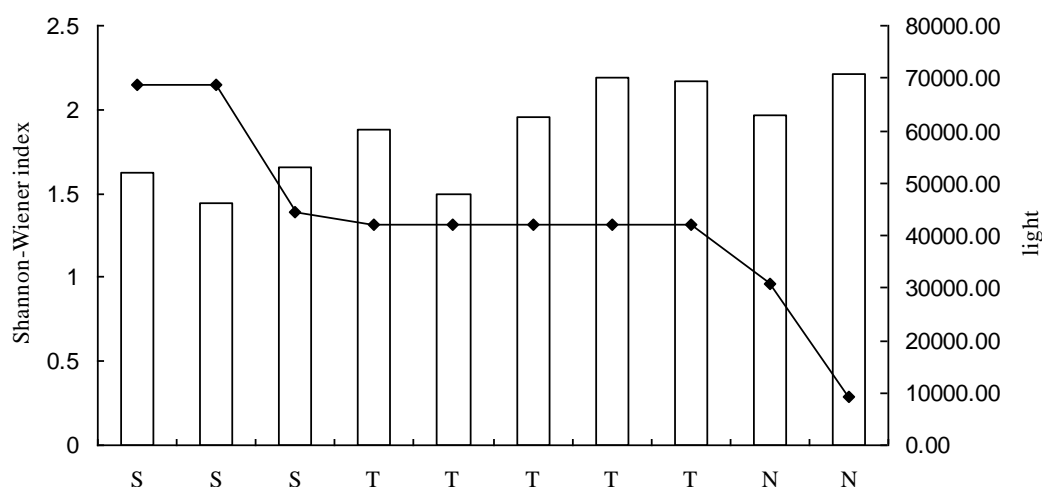


图 4.4c 好鲁库 α 多样性与光照的关系(light: MJ/m^2)

白扞坑整个样地均位于北坡，草甸、白桦林、草原界限明显，白桦林盖度约为 20%，林下分布少量柔毛绣线菊灌木，盖度 1%。坡上段是草甸，随着坡度变化光照逐渐减小，而物种多样性有微弱上升趋势，Shannon-Wiener 指数在 2 左右。进入盖度约为 20% 的白桦林（第 3、4 个样方）内部后，光照减少至 43681.16 W/m^2 ，多样性变化不明显。在坡底草原，虽无乔木灌木覆盖，但由于白桦林坡度较小（ 10° ），而草原坡度较大（ 25° ），光照反而低于白桦林内部（ 41388.62 W/m^2 ），物种多样性增加到一个较高的水平（Shannon-Wiener 指数 2.5 以上）并始终保持。可以认为，从森林过渡到草原，乔灌层的郁闭度减少，使得草本层接收到的光照强度减少，然而，由于郁闭度较小，对于光照的削弱低于坡度对于光照的削弱作用，草本层光照仍然低于有乔木灌木覆盖的森林，物种多样性高于森林，故植被类型对于草本层物种多样性的影响弱于光照强度对于草本层物种多样性的影响，草原分布在光照强度大的地方，其物种多样性低于森林，反之则会高于森林。

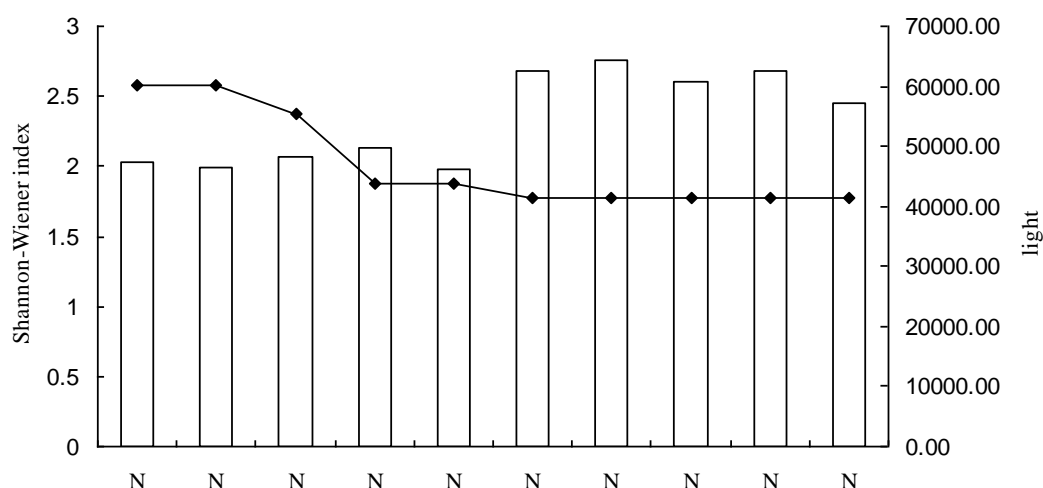


图 4.4d 白扞坑 α 多样性与光照的关系(light: MJ/m²)

在松树井子样地, 草原的物种多样性小于森林的物种多样性。南坡草原无乔木灌木覆盖, 草本植物多样性较低, Shannon-Wiener 指数在 2 以下。进入到坡顶, 灌木盖度约为 50%, 草本层辐射照度从 80707.80 W/m² 下降到 32334.86 W/m², 草本层物种多样性有明显增加, Shannon-Wiener 指数从 1.5 上升至 2.3 以上并保持。北坡为盖度 60% 的山杨林, 草本层光照随着坡向和乔木灌木盖度变化越发降低, 而草本层物种多样性则呈上升趋势, 达到 2.7 左右。可以认为, 从草原地带过渡到森林地带, 乔灌层的郁闭度增加使得草本层接收到的光照强度减少, 而草本层的物种多样性则随之增加, 草本层物种多样性与光照强度成负相关关系。

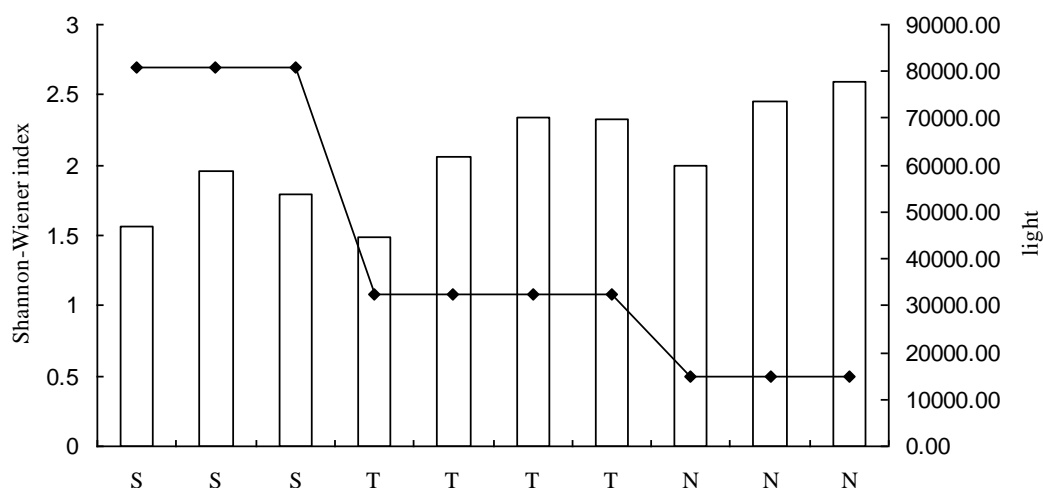


图 4.4e 松树井子 α 多样性与光照的关系(light: MJ/m²)

以上五个样点的 α 多样性与光照条件关系显著, 在显著性水平较好的四个地点, α 多样性均和光照呈显著负相关, 且 Pearson 相关系数在 -0.684 到 -0.742 之间 (表 4.3)。在松树井

子, 这一趋势显著性水平也较好, 为 0.066。可以认为当光照逐渐增强时, α 多样性逐渐减弱。在局地尺度上, 光照是影响物种 α 多样性的一个显著因子。

在此基础上, 各个样点的所有小样地之间的 α 多样性差异与光照条件总体的变化关系 (图 4.5), 反映了研究区区域尺度上的光照对于植物群落 α 多样性的调控作用, 但这一作用并不显著, 反映了空间尺度对于 α 多样性的变化有着显著影响, 即区域尺度与局地尺度上 α 多样性的变化规律有所区别, 局地尺度上光照条件的影响显著, 而区域尺度上则不显著。

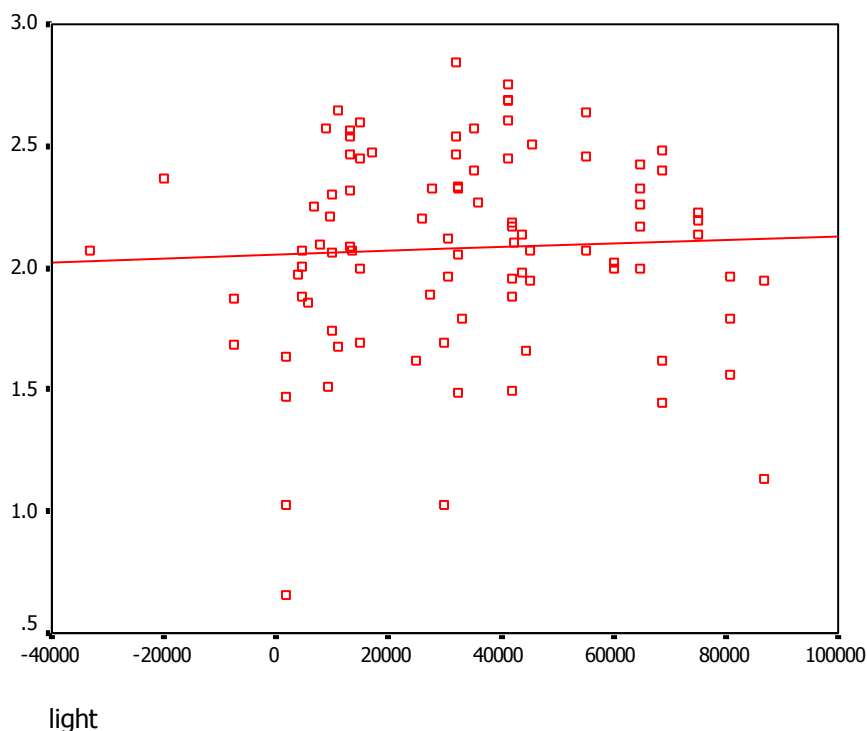


图 4.5 区域尺度上 α 多样性与光照的关系(light: MJ/m²)

4.4.2 β 多样性与光照条件的关系

β 多样性指在一个梯度上从一个生境到另一个生境所发生的种的多样性变化的速率和范围, 是研究群落之间的种多度关系的重要指标 (张金屯, 2004)。在本研究中, 光照条件随坡度、坡向、盖度发生改变, 从而形成各小生境之间连续变化的光照梯度, 适合 β 多样性的研究。本研究采用 Sørensen 指数和 Cody 指数两种指标对 β 多样性进行测度, Sørensen 指数反映群落或样方间物种组成的相似性; Cody 指数则反映样方物种组成沿环境梯度的替代速率。

三道河口、好鲁库、白扞坑三个地点的 Sørensen 指数与 Cody 指数的变化趋势是相反的 (图 4.6a, d, e), 且相关系数的显著性都很好 (表 4.3)。在 β 多样性变化与光照呈显著相关

的所有地点，Sørensen 指数均随着光照的增强而增加，即光照条件好的草原地带相邻群落相似程度高，Cody 指数均随着光照的增强而减少，即光照条件好的草原地带群落间替代速率低（图 4.6a-e）。由于 Sørensen 指数反映的是相邻群落相似的程度，其分子强调两个样地的相似种数目，而 Cody 指数反映的是群落间替代速率，后者分子强调了非相似种数目，所以趋势是反的。表 4.3 同时表明了 Cody 指数是不独立于群落的 α 多样性的，且和 α 多样性变化趋势一致（马克平，1995）。

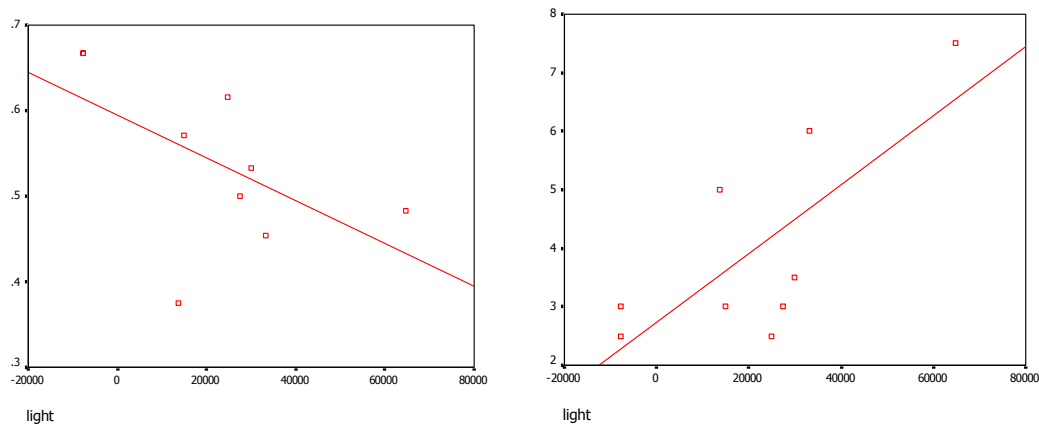


图 4.6a 三道河口 β 多样性与光照的关系(light: MJ/m²)

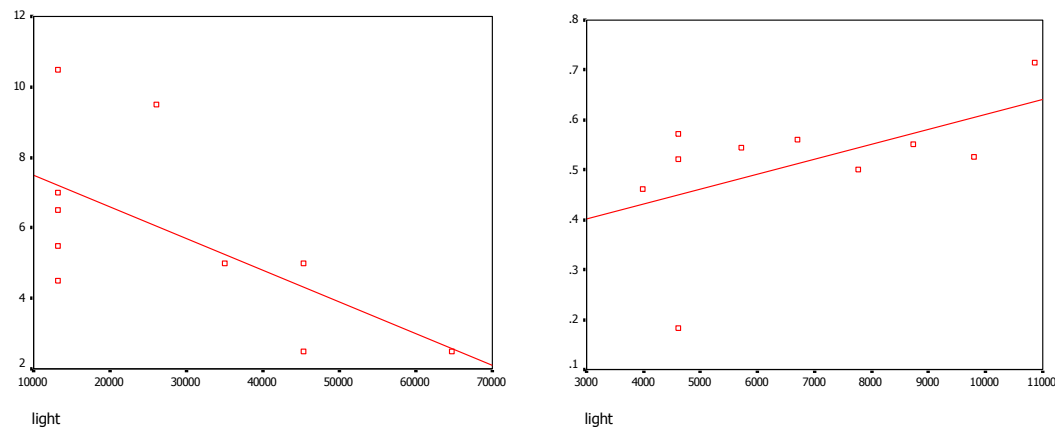


图 4.6b 扎格斯泰淖尔白扞林 β 多样性与光照的关系(light: MJ/m²)

图 4.6c 源水头 β 多样性与光照的关系(light: MJ/m²)

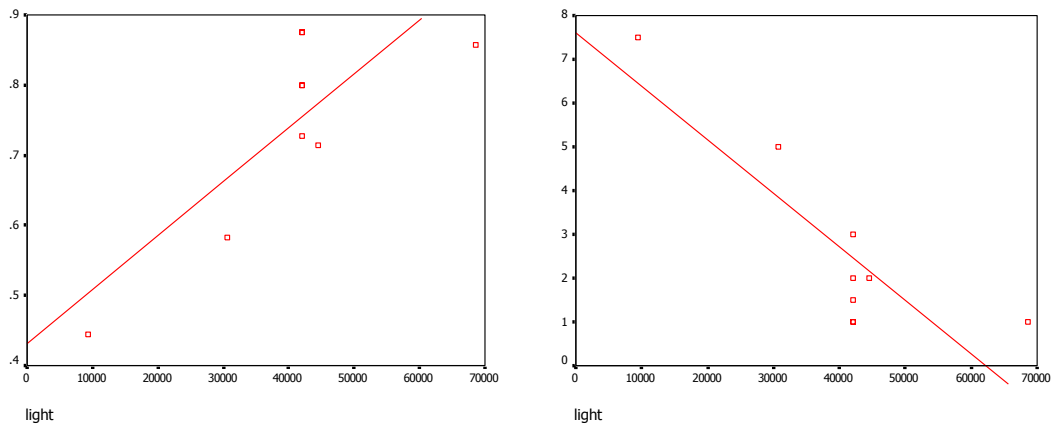


图 4.6d 好鲁库 β 多样性与光照的关系(light: MJ/m²)

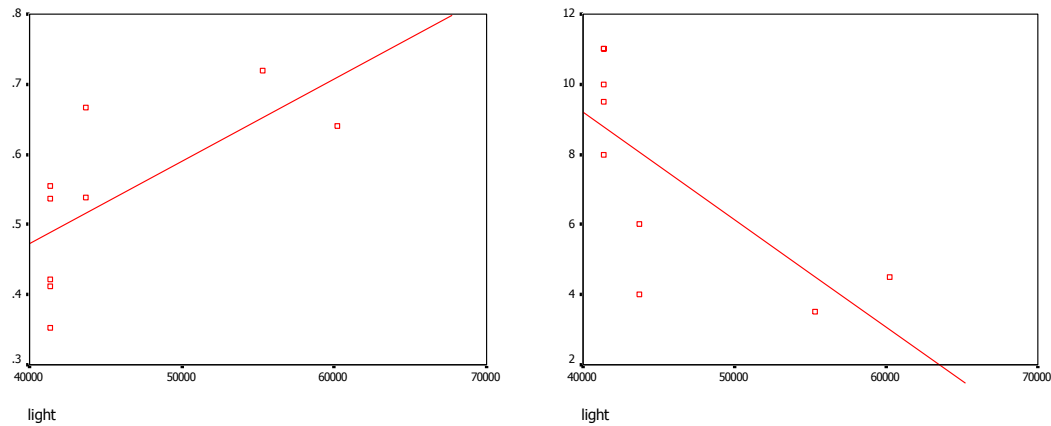


图 4.6e 白杆坑 β 多样性与光照的关系(light: MJ/m²)

在此基础上，各个样点的所有小样地之间的 *Sørensen* 指数与光照条件的变化关系（图 4.7）十分显著（Pearson 相关系数 0.233，显著性水平 0.044， $R^2 = 0.0499$ ），反映了研究区区域尺度上随着光照的增强，植物群落之间的相似性逐渐增加，即草本层辐射照度越强，群落之间种类越趋于相似。这印证了前文的草原群落物种多样性较低的观点。

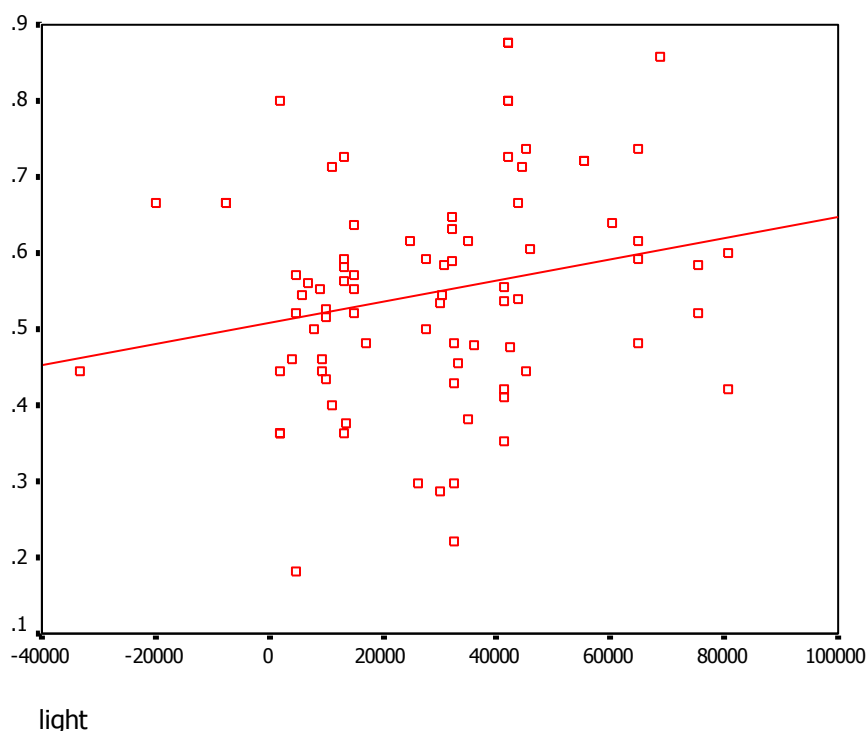


图 4.7 区域尺度上 Sørensen 指数与光照的关系(light: MJ/m²)

4.5 草本植物的种间联结

种间联结性测定是着眼于两个种的个体在样方中共同存在与否来确定的。显著正联结种的分布表现为集群，显著负联结则表现为个体的隔离。集群的生态解释是两种个体的互利或微环境的取向趋同。隔离则是因两种个体的相克或微环境的取向差异大。

本研究总共 92 个样方共记录 147 个植物种。把频度<5%的偶见种剔除后剩 68 个种，得到 92×68 的原始数据矩阵。调查 68 个优势种（表 4.4）在各样方中是否出现；在 2×2 联列表基础上，运用 χ^2 检验检测种间联结性（图 4.9）。当 $\chi^2_{0.05}=3.841$, $\chi^2_{0.01}=6.635$ 。当 $\chi^2<3.841$ 时，说明种间无显著关联（图 4.9）；当 $3.841<\chi^2<6.635$ 时，说明种间关联显著，这样的种对有 201 个（图 4.9 中■与□）；当 $\chi^2>6.635$ 时，说明种间关联极显著，这样的种对有 157 个（图 4.9 中▲与△）。种间关联分 3 种情况：若 $ad>bc$ ，则说明种间存在正关联，2 个物种趋向于同时出现（图 4.9 中■与▲）；若 $ad<bc$ ，则说明种间存在负关联，两物种趋向于互斥（图 4.9 中□与△）；若 $ad=bc$ ，则说明种间无关联性。若种间存在显著关联，则进一步测定其关联程度的大小。测定种间关联程度的指数很多，本文采用联结系数 AC 检测各种对间的联结程度。

表 4.4 图 4.8, 4.9 中 68 种植物的种名与编号（拉丁名见附录）

编号	种名	编号	种名	编号	种名
1	白婆婆纳	24	老芒麦	47	沙苔
2	白芍	25	冷蒿	48	砂韭
3	百里香	26	藜	49	山马蔺
4	瓣蕊唐松草	27	辽西扁蓿豆	50	鼠掌老鹳草
5	北柴胡	28	裂叶蒿	51	铁杆蒿
6	贝加尔唐松草	29	林生银莲花	52	歪头菜
7	贝加尔针茅	30	龙牙草	53	乌苏里风毛菊
8	扁蓿豆	31	麻花头	54	无芒雀麦
9	并头黄芩	32	猫眼草	55	细叶白头翁
10	糙隐子草	33	毛沙芦草	56	细叶鸢尾
11	叉分蓼	34	蒙古冰草	57	腺毛委陵菜
12	车前	35	蒙古虫实	58	小红菊
13	地榆	36	南牡蒿	59	小玉竹
14	东北堇菜	37	牛扁	60	星毛委陵菜
15	拂子茅	38	女娄	61	岩败酱
16	高二裂委陵菜	39	蓬子菜	62	羊草
17	高山紫菀	40	披针叶苔草	63	野青茅
18	黄精	41	匍枝委陵菜	64	硬质早熟禾
19	黄囊苔草	42	洽草	65	杂配藜
20	火绒草	43	茜草	66	直立鹅观草
21	荆芥	44	拳参	67	猪殃殃
22	景天三七	45	日阴菅苔草	68	紫羊茅
23	狼毒	46	沙蒿		

将以上 68 个种中，出现多于 20 个样方（频度>20%）的 11 个种做种间联结星座图（图 4.8）。从图中可以看出，在 20 个有显著关联的种对中，有 9 对显著性水平<0.05 的正联结，其中显著性水平<0.01 的极显著正相关有 6 对；11 对显著性水平<0.05 的负联结，其中显著性水平<0.01 的极显著负相关有 4 对。

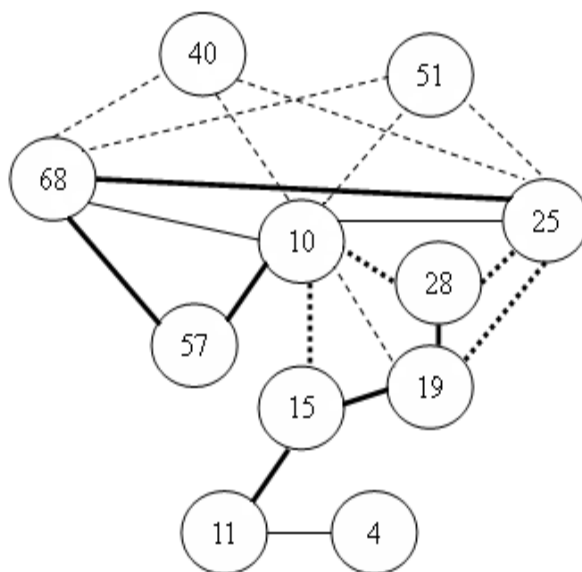


图 4.8 种间关联测定星座图

(细实线正联结 $P < 0.05$; 粗实线正联结 $P < 0.01$; 细虚线负联结 $P < 0.05$, 粗虚线负联结 $P < 0.01$)

进一步采用种间联结系数 AC 测定显著和极显著联结种对的关联程度大小。存在负联结的种对中, 有 5 对极强关联 ($-1.0 \leq AC < -0.9$), 分别是糙隐子草-披针叶苔草、糙隐子草-铁杆蒿、糙隐子草-紫羊茅、冷蒿-披针叶苔草、铁杆蒿-紫羊茅; 有 4 对较强关联 ($-0.9 \leq AC < -0.4$), 分别是糙隐子草-拂子茅、糙隐子草-裂叶蒿、冷蒿-裂叶蒿、冷蒿-铁杆蒿; 有 2 对弱关联 ($-0.4 \leq AC < -0.2$), 分别是糙隐子草-黄囊苔草、黄囊苔草-冷蒿。另外, 关联度低的种对有 3 对 ($-0.2 \leq AC \leq 0.2$), 分别是瓣蕊唐松草-叉分蓼、黄囊苔草-裂叶蒿、披针叶苔草-紫羊茅。存在正联结的种对中, 有 2 对较强关联 ($0.4 \leq AC < 0.9$), 分别是糙隐子草-冷蒿、拂子茅-黄

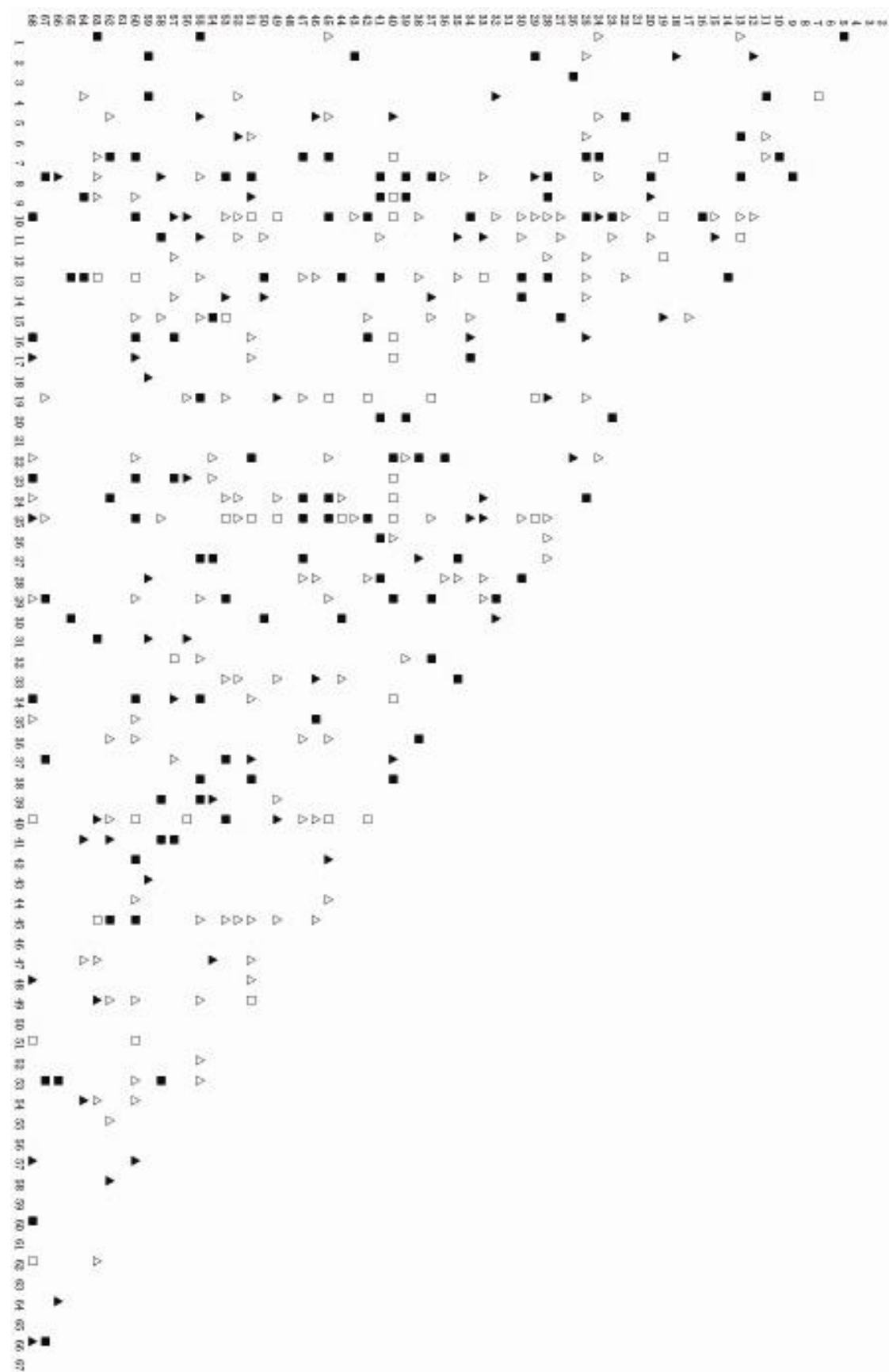


图 4.9 种间关联测定半矩阵图

(■正联结 $P < 0.05$; ▲正联结 $P < 0.01$; □负联结 $P < 0.05$, △ 负联结 $P < 0.01$)

囊苔草；有 4 对弱关联 ($0.2 \leq AC < 0.4$)，分别是叉分蓼-拂子茅、糙隐子草-腺毛委陵菜、冷蒿-紫羊茅、腺毛委陵菜-紫羊茅。

由此可见，与糙隐子草有关联的物种最多，这与 χ^2 检验的结果一致。与糙隐子草呈负关联的有 5 个物种，呈正关联的有 3 个物种。由表 4.2，糙隐子草在大多数情况下与光照条件呈正相关，而与之呈负关联的拂子茅、黄囊苔草、裂叶蒿、披针叶苔草、铁杆蒿则多与光照条件呈负相关。由图 4.8 外推，得到于这些种呈正关联的种还有瓣蕊唐松草和叉分蓼，据此可以得到受光照条件影响显著的物种，并且将 11 物种划分为趋向于出现在强光照条件下和趋向于出现在弱光照条件下两大类群。其余物种，或与光照不显著相关；或出现的频度低于 20%，则种对出现的频度之和必然低于 40%，倾向于呈显著负关联。图 4.9 反映出来所有物种的种间关联的显著性状况，可以认为，所有物种沿光照梯度轴上的分布反映了其出现在林下还是草原的概率，能够指示森林-草原的分布动态。

第五章 光照条件对森林-草原交错带草本植物的调控作用

5.1 光照对草本植物分布的调控作用

本研究中出现草本植物，部分物种以及不同生态类群的响应都有着不同的规律（表 4.2）。

在本研究中出现最多的黄囊苔草属多年生丛生杂草，中旱生植物，广泛分布于内蒙古草原，是草原植物群落中重要的伴生种（陈世苹等，2004），其重要值与光照呈负相关的趋势，表明黄囊苔草在森林下层草本出现时其优势度明显。

日阴营苔草在本研究中与辐射强度呈显著正相关，这与前人研究的结果有一定差异。虽然日阴营苔草性喜阴、喜湿，需要乔木灌木冠层对直射阳光的遮挡，形成其生长的荫蔽环境（王正文等，2001），但是其生长也需要光合作用产物的积累，过分的树冠遮荫也会对日阴营苔草生长产生不利影响。另外，日阴营苔草是 C4 植物，其光饱和点高于 C3 植物，理论上与光照条件的关系也应为正相关。

C4 植物作为一个总体时与辐射照度的正相关十分显著。这是由于 C4 植物固定二氧化碳时水分消耗少，故其水分利用效率高，在干热条件下能够成功生存。本研究中由于草本植物种类数量有限，而内蒙古地区 C4 植物分布较少，所以单个考虑某一 C4 物种时这种趋势并不明显。这既反映了不同尺度上光照对 C4 植物影响的差异性，又反映了所有 C4 植物的分布对光照响应的一致性。

本研究将单子叶植物纲各科分别分析，得到禾本科草本植物和莎草科草本植物各自的分布对于光照条件的响应，同时由于本研究出现的 4 种莎草科均为苔草属植物，故结合植物功能类群这一特征，将这两个科分别划为禾草类和苔草类。在全部样地的所有禾本科植物重要值与区域尺度上的光照梯度呈显著正相关，这表明在研究区影响最占据优势的禾本科植物分布的因子是光照。在全部样地的所有莎草科植物重要值与区域尺度上的光照梯度呈显著负相关，这表明在研究区影响分布最广泛的莎草科植物的分布因子也是光照。这两个科的植物重要值之和占到全部草本植物的 45.62%。光照对于禾本科和莎草科植物的作用很大程度上反映了光照对全部草本植物的影响。然而由于禾本科植物和莎草科植物对于光照的相反响应，当把单子叶植物作为一个整体的时候，其对光照的相应不显著。

土壤的连续蒸发必须有连续供给汽化潜热的能量，而太阳辐射是汽化潜热能量的来源。

其他条件相同时，辐射量大，蒸发量也大。研究区内地形因素造成的坡向和坡度分异明显，这主要影响了气温、地温、湿度和太阳辐射，从而影响土壤水分。

乔木灌木遮阴程度小的条件下，草本层植物既能接受到满足其光合作用所需的最适光照条件，而又同时满足其对阴蔽环境和土壤湿润度的基本需求，所以低覆盖度的森林或灌丛下部的草本植物分布状况，可以看作是草原草本植物和森林草本植物之间的平衡。

光照条件和土壤水分条件在阳坡和阴坡有着相反的变化趋势（表 5.1），在一个具体地点，草本植物对光照条件的敏感性会被土壤水分的作用削弱甚至抵消。然而，有些物种如黄囊苔草、披针叶苔草、日阴菅苔草、瓣蕊唐松草仍然对光照敏感，其分布及优势度与光照变化的关系显著，说明在局地尺度上，光照对于这些物种的控制作用强于土壤水分条件的控制作用。

表 5.1 各坡向上光照与土壤水分状况

	北坡		南坡		坡顶	
	均值	标准差	均值	标准差	均值	标准差
光照	21570.20	19432.5	68861.70	21457.7	47087.64	13039.61
土壤水分	10.92%	11.97%	9.19%	10.90%		

5. 2 光照与森林-草原交错带的物种多样性

群落交错带一般具有一组确定的空间与时间特征，其相互作用多处于两个或两个以上景观成分的边际之间。交错带即代表景观要素间的过渡带，并具有过滤膜的作用，影响能量流动等生态流及生物有机体的循环，因而通常是生物多样性出现较高的场所（Fisher, 1943）。在两个或多个不同性质群落的交错带中，通常表现出强烈的边缘效应（王伯荪等，1986）。生态交错带与生物多样性的关系引起生态学家的关注，主要是由于边缘效应（傅伯杰等，2001）。物种多样性不仅能够表征群落的组成结构，而且也能对环境状况做出指示（郭轶瑞等，2007）

交错带较其周边生境类型具有较高的物种多样性。交错带通常既包括相邻生境群落的多数物种类型，还包括只生长在交错带内部的物种，因此交错带的物种数目及密度一般比相邻群落大。然而交错带与其周边生境是相互影响、相互依赖的有机体，若其周边生境受到破坏，则将影响交错带动植物以及微生物的正常运转，从而导致交错带边缘效应的下降（李瑞等，2006）。不同尺度不同类型的生态交错带均显示出较高的生物多样性（王庆锁等，1997）。交

错带群落多样性的 Shannon-Wiener 指数反映的物种多样性变化表现为演替中后期>演替中期、中前期>演替前期>演替后期，在整个演替进程中为先上升后下降（Rohde, 1992）。

交错带物种多样性高于相邻的群落，是由交错带群落结构的特点和群落所处的地理位置来决定的。交错带不仅具有相邻群落内的物种而且出现了边缘种，造成交错带的群落物种多样性较大。此外，各交错带群落结构多为不稳定状态，群落所处的生境易受外界干扰（高俊峰等，2005）。

混交林的物种多样性比纯林高，主要是由于混交林群落乔木层盖度较低，林内光线居中，较适宜阳性物种和阴性物种的生存，而纯林乔木层盖度较高，林内形成阴性环境，适宜阴性物种生存。因为光的强度影响植物的生存和生长，如果乔木层盖度大，林内光线就比较弱，阳性灌木树种就很难生存，即使存在，也会出现生长缓慢的现象，另一方面，在乔木盖度高的情况下，灌木稀疏，盖度较低。但草本层的光照相对较强，使得草本植物层较为发达，盖度较高，而使整个群落的物种多样性高。由此可见，群落乔木层、灌木层和草本层是相互作用相互影响的（苗莉云等，2005）。

本研究中的各个地点均涉及到一种以上的植被类型交界的情况，可以清晰得到不同植被类型之间的对比。而且由于将限制草本层光照的因子分为坡度、坡向、乔木灌木层盖度三个方面，影响草本层光照的具体因子比较清楚。虽然温带落叶阔叶林-草原交错带的景观为森林出现在阴坡，草原出现在阳坡，但当阴坡下部出现草原的时候，能够明确区分植被类型（由乔木层和灌木层优势种决定）和草本层光照的影响。结果表明，无论植被类型是森林还是草原，草本层实际接受到的光照才是最终决定草本层物种多样性的因子。大多数情况下，草原分布在阳坡，物种多样性低于森林，但在阴坡分布的草原物种多样性反而会高于覆盖度低的森林草本层。这是由于光照受控于除植被类型以外的因子，即地形。在乔木灌木层覆盖度低时，地形因子的作用大于植被类型的作用。

表 5.2 不同坡向上光照、盖度与 α 多样性

	北坡		南坡		坡顶	
	均值	标准差	均值	标准差	均值	标准差
光照	21570.2	19432.5	68861.7	21457.7	47087.64	13039.61
盖度	53.92%	38.82%	27.19%	26.37%	9.29%	20.16%
Shannon-Wiener 指数	2.125	0.441	2.067	0.383	1.894	0.276

本研究开展的纬度范围在 N41° 06.717'- N43° 42.664'内，其中纬度 N41° 上 2 个样点，

N42° 上 5 个样点，N43° 上 3 个样点。随着纬度的升高，多样性有减少的趋势，且多年平均降水量也减少。7 月均温的均值在 N42° 最低，这是由于分布在 N42° 的气象站点平均海拔高于分布在 N41° 的气象站点造成。然而本研究平均海拔为 1496m，高于气象站点海拔，样点实际 7 月均温低于气象站测度，但趋势保持一致，均为自南向北减小。

表 5.3 不同纬度样点 α 多样性与气候均值

纬度(°)	Shannon-Wiener 指数	海拔(m)	7 月均温(°)	年降水量(mm)
41	2.3391	990.30	20.200	433.60
42	2.0164	1168.36	19.475	381.52
43	2.0104	1033.10	20.075	351.75

从森林带到森林-草原交错带，由于环境条件的不同，特别是降水量的逐渐减少，气候由半湿润变为半干旱，森林草本层的物种多样性逐渐下降。纬度造成的气候差异对于物种多样性的影响体现在较大的区域尺度上，而光照对于物种多样性的影响体现在森林-草原交错带的林草分布格局上。在局地尺度上，光照是森林下层草本植物多样性大于草原草本植物多样性的主要决定因子。

5. 3 光照与森林-草原交错带的植被动态

前人根据温度条件和湿度条件对于草本植物生态类群进行了划分。黄永梅等（2001）对研究区草本植物种类空间分布的调查划分，在本研究中出现频度大于 20%的叉分蓼、披针叶苔草、腺毛委陵菜，分属其沿湿度轴和温度轴形成的四种气候组合中的三种不同气候下的生态类群。叉分蓼为出现在暖干气候下沙地种，且出现于整个研究区的各植被类型中；披针叶苔草为出现在暖湿气候下的森林种；腺毛委陵菜为出现在冷干气候下草原种，且仅出现于研究区内的草原带。根据本研究其余优势种与以上三个物种种间联结的强弱，瓣蕊唐松草和拂子茅与叉分蓼正联结，属于同一类；糙隐子草、冷蒿、紫羊茅与披针叶苔草负联结，而与腺毛委陵菜正联结，属于同一类。由此联结关系外推，与披针叶苔草同属一个类群的种类有拂子茅、黄囊苔草、裂叶蒿、铁杆蒿。最终可以将物种划为两个光照类群，其对光照的响应敏感且相反。分布与光照呈显著负关联的种类有瓣蕊唐松草、叉分蓼、披针叶苔草、拂子茅、黄囊苔草、裂叶蒿、铁杆蒿，分布与光照呈显著正关联的种类有腺毛委陵菜、糙隐子草、冷蒿、紫羊茅。此外，其余物种如无芒雀麦为冷湿气候下的亚高山种，日阴苔草为冷干气候下的草原种，但由于其频度小于 20%，种对频度和小于 40%，极易呈现负关联，故不做重

点划分。

由此可见，虽然水分条件可能对乔木进入阳坡起着决定性作用，但是光照条件限制了草原草本植物进入林下。

光照与温度和土壤水分的协同作用决定着森林-草原交错带林草格局，在局地尺度森林盖度低的情况下，草本植物分布受光照的控制不显著，这可能是由于开阔林下草本层性质接近于草原；而在森林内部，特别是乔木与灌木盖度之和超过 50%的林下草本层，物种分布更趋于受光照的控制。

表 5.4 不同盖度水平下光照与物种多样性的关系

	盖度<50%	50%<盖度<100%
样地数目	53	35
光照与多样性相关系数	-0.182	0.338*

注：*显著性水平<0.05。

第六章 结论

本文利用野外植被调查数据、土壤水分数据、地形数据和气象台站观测数据等资料,分析了内蒙古东南缘森林-草原交错带的草本植物种类分布格局及影响因子,证实了光照条件对于森林-草原交错带草本植物种类分布影响的假设,得到以下初步结论:

- (1) 地形和乔木灌木盖度影响下的林下辐射照度很大程度上决定了研究区草本植物种类分布格局。定量分析的结果表明,光照条件与多个优势种重要值之间呈显著线性关系。
- (2) 光照条件对特定的分类和生态类群有着不同程度的影响,禾本科植物、莎草科植物、C4植物的分布与光照关系密切。光照对研究区内的豆科植物影响不显著。
- (3) 光照条件对草本植物群落 α 多样性的影响显著,在局地尺度上,植被类型对草原群落 α 多样性的影响弱于光照条件的影响。而光照条件对 β 多样性在区域尺度上显著,草本植物群落间种类替代速率随林下辐射照度增加而增加。
- (4) 全部草本植物的种间联结表明优势物种种间联结显著,据此将物种划分为趋向于出现在强光照条件下和趋向于出现在弱光照条件下两大类群,趋向于出现在强光照条件下有糙隐子草、腺毛委陵菜、冷蒿和紫羊茅;趋向于出现在弱光照条件下的种类包括拂子茅、黄囊苔草、裂叶蒿、披针叶苔草、铁杆蒿、瓣蕊唐松草和叉分蓼。

由于研究基础和研究手段的局限性,本研究在以下几个方面仍有待继续深入:

- (1) 由于没有辐射照度实测数据,仅仅通过太阳直接辐射推算林下辐射,结果在总值上存在偏差。但趋势是一致的,均与总值成固定比例,暂时不影响分析。
- (2) 土壤水分调查没有配合光照梯度,仅存在阴坡和阳坡的对比。但阴阳坡差别显著,能够大体反映土壤水分与光照协同作用。
- (3) 光照条件对于物种分布的模型仅局限于分布优势的物种,对于其他可能存在的格局欠缺分析。
- (4) 对于森林可能减退后的预测,应该将灌木与乔木单独考虑;假如草原不会进入阴坡,那么灌木的入侵的可能性欠缺定量分析。

参考文献

- Anderson LJ, Brumbaugh MS, Jackson RB. (2001) Water and tree-understory interactions: A natural experiment in a savanna with oak wilt. *Ecology*. 82 (1): 33-49.
- Bandeff JM, Pregitzer KS, Loya WM, Holmes WE, Zak DR. (2006) Overstory community composition and elevated atmospheric CO₂ and O₃ modify understory biomass production and nitrogen acquisition. *Plant and Soil*. 282 (1-2): 251-259.
- Barthemucci P, Messier C, Canham CD. (2006) Overstory influences on light attenuation patterns and understory plant community diversity and composition in southern boreal forests of Quebec. *Canadian Journal of Forest Research*. 36 (9): 2065-2079.
- Chen HYH, Legare S, Bergeron Y. (2004) Variation of the understory composition and diversity along a gradient of productivity in *Populus tremuloides* stands of northern British Columbia, Canada. *Canadian Journal of Botany*. 82 (9) : 1314-1323.
- Chipman SJ, Johnson EA. (2002) Understory vascular plant species diversity in the mixedwood boreal forest of western Canada. *Ecological Applications*. 12 (2): 588-601.
- Cole PG, Weltzin JF. (2005) Light limitation creates patchy distribution of an invasive grass in eastern deciduous forests. *Biological Invasions*. 7 (3): 477-488.
- Comeau PG, Gendron F, Letchford T. (1998) A comparison of several methods for estimating light under a paper birch mixedwood stand. *Canadian Journal of Forest Research*. 28 (12): 1843-1850.
- Daly C, Bachelet D, Lenihan JM, Neilson RP, Parton W, Ojima D. (2000) Dynamic simulation of tree-grass interactions for global change studies. *Ecological Applications*. (2): 449-469 APR 2000.
- Dulamsuren C, Hauck M, Mühlenberg M. (2005) Ground vegetation in the Mongolian taiga forest-steppe ecotone does not offer evidence for the human origin of grasslands. *Applied Vegetation Science*. 8: 149-154.
- Eccles NS, Esler KJ, Couling RM. (1999) Spatial pattern analysis in Namaqualand desert plant communities: Evidence for general positive interactions. *Plant Ecology*. 142: 71-8.
- Fisher RA. (1943) The relation between the number of species and number of individuals in a random sample of an animal population. *Journal of Animal Ecology*. 12: 42-58.
- Godefroid S, Phartyal SS, Weyembergh G, Koedam N. (2005) Ecological factors controlling the abundance of non-native invasive black cherry (*Prunus serotina*) in deciduous forest understory in Belgium. *Forest Ecology and Management*. 210 (1-3): 91-105.
- Grouzis M, Akpo LE. (1997) Influence of tree cover on herbaceous above- and below-ground phytomass in the Sahelian zone of Senegal. *Journal of Arid Environments*. 35 (2): 285-296.
- Harrington TB, Edwards HB. (1999) Understory vegetation, resource availability, and litterfall responses to pine thinning and woody vegetation control in longleaf pine plantations. *Canadian Journal of Forest Research*. 29 (7): 1055-1064.
- Holeksa J. (2003) Relationship between field-layer vegetation and canopy openings in a Carpathian subalpine spruce forest. *Plant Ecology*. 168 (1): 57-67.
- House JJ, Archer S, Breshears DD. (2003) Conundrums in mixed woody-herbaceous plant systems. *Journal of Biogeography*. 30: 1763-1777.
- Jobidon R, Cyr G, Thiffault N. (2004) Plant species diversity and composition along an experimental gradient of northern hardwood abundance in *Picea mariana* plantations. *Forest Ecology and Management*. 198 (1-3): 209-221.

- Jonsson BG, Moen J. (1998) Patterns in species associations in plant communities: The importance of scale. *Journal of Vegetation Science*. 9: 327-33.
- Kovacs-Lang E, Kroel-Dulay G, Kertesz M, Fekete G, Bartha S, Mika J, Dobi-Wantuch I, Redei T, Rajkai K, Hahn I. (2000) Changes in the composition of sand grasslands along a climatic gradient in Hungary and implications for climate change. *Phytocoenologia*. 30 (3-4): 385-407.
- Leniere A, Houle G. (2006) Response of herbaceous plant diversity to reduced structural diversity in maple-dominated (*Acer saccharum* Marsh.) forests managed for sap extraction. *Forest Ecology and Management*. 231 (1-3): 94-104
- Lett MS, Knapp AK. (2003) Consequences of shrub expansion in mesic grassland: Resource alterations and graminoid responses. *Journal of Vegetation Science*. 14 (4): 487-496.
- Levin SA. (1992) The problem of pattern and scale in ecology. *Ecology*. 73(6): 1943-1967.
- Liu HY, Cui HT, Tian YH, Xu LH. (2002) Temporal-Spatial Variances of Holocene Precipitation at the Marginal Area of the East Asian Monsoon Influences from Pollen Evidence. *Acta Botanica Sinica*. 44 (7): 864-871.
- Magurran AE (1988) *Ecological Diversity and Its Measurement*. Princeton University Press, New Jersey.
- Marchand P, Houle G. (2006) Spatial patterns of plant species richness along a forest edge: What are their determinants?. *Forest Ecology and Management*. 223 (1-3): 113-124.
- Martens SN, Breshears DD, Meyer CW (2000) Spatial distributions of understory light along the grassland: forest continuum: effects of cover, height, and spatial pattern of tree canopies. *Ecological Modelling*. 126: 79-93.
- Maundrell C, Hawkins C. (2004) Use of an aspen overstory to control understory herbaceous species, bluejoint grass (*Calamagrostis canadensis*), and Fireweed (*Epilobium angustifolium*). *Northern Journal of Applied Forestry*. 21 (2): 74-79.
- Messier C, Parent S, Bergeron Y. (1998) Effects of overstory and understory vegetation on the understory light environment in mixed boreal forests. *Journal of Vegetation Science*. 9 (4): 511-520.
- Montgomery RA, Chazdon RL. (2001) Forest structure, canopy architecture, and light transmittance in tropical wet forests. *Ecology*. 82 (10): 2707-2718.
- Naumburg E, DeWald LE. (1999) Relationships between *Pinus ponderosa* forest structure, light characteristics, and understory graminoid species presence and abundance. *Forest Ecology and Management*. 124 (2-3): 205-215.
- North M, Oakley B, Fiegenger R, Gray A, Barbour M. (2005) Influence of light and soil moisture on Sierran mixed-conifer understory communities. *Plant Ecology*. 177 (1): 13-24.
- Pan Y, McGuire AD, Melillo JM, Kicklighter DW, Sitch S, Prentice IC. (2002) A biogeochemistry-based dynamic vegetation model and its application along a moisture gradient in the continental United States. *Journal of Vegetation Science*. 13 (3): 369-382.
- Piboule A, Collet C, Frochot H, Dhote JF. (2005) Reconstructing crown shape from stem diameter and tree position to supply light models. I. Algorithms and comparison of light simulations. *Annals of Forest Science*. 62 (7): 645-657.
- Pielou EC (1975) *Ecological Diversity*. John Wiley & Sons Inc.
- Rohde K. (1992) Latitudinal gradients in species diversity: the search for the primary cause. *Oikos*. 65: 514-527.
- Sankaran M, Hanan NP, Scholes RJ, Ratnam J, Augustine DJ, Cade BS, Gignoux J, Higgins ST, Le Roux X, Ludwig F, Ardo J, Banyikwa F, Bronn A, Bucini G, Caylor KK, Coughenour MB, Diouf A, Ekaya W, Feral CJ, February EC, Frost PGH, Hiernaux P, Hrabar H, Metzger KL, Prins HHT, Ringrose S, Sea W, Tews J, Worden J, Zambatis N. (2005) Determinants of wood cover in African savannas. *Nature*. 438: 846-849.

- Sankey TT, Montagne C, Graumlich L, Lawrence R, Nielsen J. (2006) Twentieth century forest-grassland ecotone shift in Montana under differing livestock grazing pressure. *Forest Ecology and Management*. 234 (1-3): 282-292.
- Smith B, IC Prentice, Sykes MT. (2001) Representation of vegetation dynamics in the modelling of terrestrial ecosystems: comparing two contrasting approaches within European climate space. *Global Ecology and Biogeography*. 10 (6): 621-637.
- Sonohat G, Balandier P, Ruchaud F. (2004) Predicting solar radiation transmittance in the understory of even-aged coniferous stands in temperate forests. *Annals of Forest Science*. 61 (7): 629-641.
- Strengbom J, Nasholm T, Ericson L. (2004) Light, not nitrogen, limits growth of the grass *Deschampsia flexuosa* in boreal forests. *Canadian Journal of Botany*. 82 (4): 430-435.
- Tilman D, Reich PB, Knops JMH (2006) Biodiversity and ecosystem stability in a decade-long grassland experiment. *Nature*. 441: 629-632
- Villalba R, Veblen TT. (1997) Spatial and temporal variation in *Austrocedrus* growth along the forest-steppe ecotone in northern Patagonia. *Canadian Journal of Forest Research*. 27 (4): 580-597.
- Weiher E. (2003) Species richness along multiple gradients: testing a general multivariate model in oak savannas. *Oikos*. 101 (2): 311-316.
- Whittaker RH. (1972) Evolution of measurement of species diversity. *Taxon*. 21: 213-251.
- 陈世苹, 白永飞, 韩兴国, 安吉林, 郭富存. (2004) 沿土壤水分梯度黄囊苔草碳同位素组成及其适应策略的变化. *植物生态学报*. 28 (4): 515-522.
- 杜菁昀, 杜占池, 崔晓勇. (2003) 内蒙古典型草原地区常见植物光合、蒸腾速率和水分利用效率的比较研究. *草业科学*. 20 (6): 11-15.
- 高俊峰, 张芸香. (2005) 关帝山次生林区典型森林交错带物种多样性研究. *西北植物学报*. 25 (10): 2017-2023.
- 郭轶瑞, 赵哈林, 赵学勇, 左小安, 云建英. (2007) 科尔沁沙质草地物种多样性与生产力的关系. *干旱区研究*. 24 (2): 198-203.
- 韩有志, 王政权, 谷加存. (2004) 林分光照空间异质性的对水曲柳更新的影响. *植物生态学报*. 28 (4): 468-475.
- 侯学煜. (1988) *中国自然地理 植物地理*(下册). 北京: 科学出版社.
- 黄永梅, 刘鸿雁, 崔海亭. (2001) 内蒙古高原东南缘森林草原过渡带景观的若干特征. *植物生态学报*. 25 (3): 257-264.
- 江源, Meurer M. (2001) 德国南部落叶阔叶林下常见植物的光适应性研究——以德国 Kraichtal 地区落叶阔叶林为例. *植物学报*. 43 (9): 960-966.
- 李栋梁, 吕兰芝. (2002) 中国农牧交错带的气候特征与演变. *中国沙漠*. 22 (5): 483-488.
- 李瑞, 张克斌, 王百田, 杨晓晖, 乔锋, 杨俊杰, 杨莉. (2006) 湿地-干草原生态系统植物物种多样性研究——以宁夏盐池为例. *北京林业大学学报*. 28 (5): 12-17.
- 李新荣, Pabnov BH (1999) 俄罗斯平原针 阔林过度带森林群落组成结构与物种多样性的研究. *生物多样性*. 7 (4): 291-296.
- 刘晨峰, 正宁, 贺康宁, 尹婧, 张卫强, 田晶会. (2004) 黄土高原半干旱区几种人工林的土壤水分、光照变化及其对林分的影响. *西部林业科学*. 33 (3): 34-41.
- 马克平, 刘灿然, 刘玉明. (1995) 生物群落多样性的测度方法(II. β 多样性的测度方法). *生物多样性*. 3 (1): 38-43.
- 苗莉云, 王孝安, 王志高. (2005) 太白红杉群落交错带物种多样性的研究. *广西植物*. 25 (2): 112-116.
- 彭少麟, 周厚诚, 郭少聪等. (1999) 鼎湖山地带性植被种间联结研究. *植物学报*. 41 (11): 1239-1244.
- 沈泽昊. (2002) 山地森林样带植被-环境关系的多尺度研究. *生态学报*. 22 (4): 461-470.
- 史军辉, 黄忠良, 周小勇, 欧阳学军, 李炯, 张池. (2005) 鼎湖山森林群落多样性垂直分布格局的研究. *生*

- 态学杂志. 24 (10): 1143-1146.
- 唐海萍, 刘书润. (2001) 内蒙古地区的 C4 植物名录. *内蒙古大学学报(自然科学版)*. 32 (4): 431-438.
- 王庆锁. (2004) *河北北部内蒙古东部森林草原交错带植被和生物多样性的研究*. 北京: 气象出版社.
- 王正宁, 贺康宁, 张卫强, 刘晨峰, 刘胜. (2005) 半干旱地区植被恢复过程中林下植被生态位特征的研究. *水土保持学报*. 19 (5): 162-165.
- 王正文, 王德利, 臧传来, 杨莲. (2001) 大兴安岭次生林白桦对林下日阴营及其它主要草本植物的影响. *生态学报*. 21 (8): 1301-1307.
- 翁笃鸣. (1986) 中国太阳直接辐射的气候计算及其分布特征. *太阳能学报*. 7 (2): 122-130.
- 沃尔特. (1984) *世界植被*. 北京: 科学出版社.
- 吴征镒(主编). (1980) *中国植被*. 北京: 科学出版社.
- 殷立娟, 李美荣. (1997) 中国 C4 植物的地理分布与生态学研究(I.中国 C4 植物及其与气候环境的关系). *生态学报*. 17 (4): 350-363.
- 于振文. (1993) *作物生理学*. 北京: 农业出版社..
- 张金屯. (2004) *数量生态学*. 北京: 科学出版社.
- 张军涛, 李哲等. (2001) 东北农牧交错区水分条件及其对植被分布的影响. *地理科学*. 21 (4): 297-300.
- 张艳华, 聂绍荃, 王志西. (1999) 林隙对草本植物的影响. *植物研究*. 19 (1): 94-99.
- 赵哈林, 赵学勇, 张铜会等. (2002) 北方农牧交错带的地理界定及其生态问题. *地球科学进展*. 17 (5): 739-747.
- 赵茂盛, Neilson RP, 延晓冬, 董文杰. (2002) 气候变化对中国植被可能影响的模拟. *地理学报*. 57 (1): 28-38.
- 中国科学院内蒙古宁夏综合考察队. (1985) *内蒙古植被*. 北京: 科学出版社

附录：拉丁名与中文名对照

种名	拉丁名	种名	拉丁名
白婆婆纳	<i>Veronica incana</i>	蒙古虫实	<i>Corispermum mongolicum</i>
白芍	<i>Paeonia sterniana</i>	南牡蒿	<i>Artemisia eriopoda</i>
百里香	<i>Thymus mongolicus</i>	牛扁	<i>Aconitum barbatum</i> var. <i>puberulum</i>
瓣蕊唐松草	<i>Thalictrum petaloideum</i>	女娄	<i>Silene aprica</i>
北柴胡	<i>Bupleurum chinense</i>	蓬子菜	<i>Galium verum</i>
贝加尔唐松草	<i>Thalictrum baicalense</i>	披针叶苔草	<i>Carex lanceolata</i>
贝加尔针茅	<i>Stipa Baicalensis</i>	匍枝委陵菜	<i>Potentilla flagellaris</i>
扁蓿豆	<i>Melissitus ruthenica</i>	洽草	<i>Koeleria cristata</i>
并头黄芩	<i>Scutellaria scordifolia</i>	茜草	<i>Rubia cordifolia</i>
糙隐子草	<i>Cleistogenes squarrosa</i>	拳参	<i>Polygonum bistorta</i>
叉分蓼	<i>Polugonum divaricatum</i>	日阴苔草	<i>Carex pediformis</i>
车前	<i>Plantago asiatica</i>	沙蒿	<i>Artemisia desertorum</i>
地榆	<i>Sanguisorba officinalis</i>	沙苔	<i>Carex praeclara</i>
东北堇菜	<i>Viola mandshurica</i>	砂韭	<i>Allium bidentatum</i>
拂子茅	<i>Calamagrostis epigeios</i>	山马蔺	<i>Iris ruthenica</i> var. <i>nana</i>
高二裂委陵菜	<i>Potentilla imbricata</i>	鼠掌老鹳草	<i>Geranium sibiricum</i>
高山紫菀	<i>Aster alpinus</i>	铁杆蒿	<i>Artemisia sacrorum</i>
黄精	<i>Polygonatum sibiricum</i>	歪头菜	<i>Vicia unijuga</i>
黄囊苔草	<i>Carex korshinskii</i>	乌苏里风毛菊	<i>Saussurea ussuriensis</i>
火绒草	<i>Leontopodium leontopodioides</i>	无芒雀麦	<i>Bromus inermis</i>
荆芥	<i>Nepeta cataria</i>	细叶白头翁	<i>Pulsatilla turczaninovii</i>
景天三七	<i>Sedum aizoon</i>	细叶鸢尾	<i>Iris tenuifolia</i>
狼毒	<i>Stellera chamaejasme</i>	腺毛委陵菜	<i>Potentilla longifolia</i>
老芒麦	<i>Elymus sibiricus</i>	小红菊	<i>Dendranthema charetii</i>
冷蒿	<i>Artemisia frigida</i>	小玉竹	<i>Polygonatum humile</i>
藜	<i>Chenopodium album</i>	星毛委陵菜	<i>Potentilla acaulis</i>
辽西扁蓿豆	<i>Melissitus liaosiensis</i>	岩败酱	<i>Patrinia rupestris</i>
裂叶蒿	<i>Artemisia tanacetifolia</i>	羊草	<i>Leymus chinensis</i>
林生银莲花	<i>Anemone silvestris</i>	野青茅	<i>Deyeuxia arundinacea</i>
龙牙草	<i>Agrimonia pilosa</i>	硬质早熟禾	<i>Poa sphondylodes</i>
麻花头	<i>Serratula centauroides</i>	杂配藜	<i>Chenopodium hybridum</i>
猫眼草	<i>Euphorbia lunulata</i>	直立鹅观草	<i>Roegneria japonensis</i>
毛沙芦草	<i>Agropyron mongolicum</i> var. <i>villosum</i>	猪殃殃	<i>Rubia aparine</i> var. <i>tenerum</i>
蒙古冰草	<i>Agropyron mongolicum</i>	紫羊茅	<i>Festuca rubra</i>

致谢

曾以为致谢是论文写作中最轻松的一个环节，然而此刻的不舍使之变得无比沉重。只剩下不到 60 天的时间，我就要离开这个扎根了 22 年的地方，去彼岸追梦。从大一开启宿舍门那一刻起，就注定了这四年大学生活的不平凡。现在毕业论文已接近尾声，时光飞逝，回首这四年，发现自己是如此的幸运，我要真心谢谢身边的每一个人，出现在我生命中的每一天。

不知道到底是我选择了生态还是生态选择了我，但生态系的一切让我确定，这是一个无比正确又充满挑战的选择。我不但从生态系的每一个老师身上感到学术严谨、为人正直的人格魅力，又从家一样的温馨和团结学会积极奋发的生活态度。无论是在专业课授课期间，还是在论文写作期间，我得到的教诲和帮助都使我在选择未来生活的道路时没有迷失自己的方向。刘鸿雁老师平和朴实的学者风范，伴随了我后三年的学习和成长，他敏锐的洞察力和干练的作风，时时在激励我、督促我。未来的五年我仍将坚持生态学的学习和研究，向刘老师学习是我努力的目标。生态系的每一位老师，贺金生老师、方精云老师、郭大立老师、沈泽昊老师、唐志尧老师、崔海亭老师、吉成均老师，都是随时可以求教的对象，他们不知疲倦的指导，使学生感到充实和幸福。何思源师姐、王志恒师兄、任佑师兄为我的论文数据提供了支持，使我更加顺利的完成研究，在此要感谢他们的无私帮助。北大第一届生态本科生，是的，一个八个人共有的自豪称呼，让我对有着这份缘的生态班的每一个人始终充满感激。

37 楼 614 的姐妹们，我们在开始这段旅程的时候从没想到过分别，纵使 we 没分在一个专业，纵使 we 来自不同的家乡，但每当别的宿舍羡慕我们的快乐和关爱时，我都无比骄傲和幸福。你们给我照顾、给我鼓励、给我依靠、给我勇气；我们无话不说、我们一起做梦、我们共同经历苦痛。这一切，该是多么让我怀念！爱心社、阳光志愿者、讲堂志愿者、院慢投垒球队……每一个我曾经洒下过汗水与泪水的地方，都有着 I 信赖的伙伴，都有着 I 放不下的记忆，都有着 I 青春成长的见证，都让我学会如何付出、如何协作、如何爱，让我变得成熟和坚强。在我心中我知道，这是永恒的长跑，好不容易来到这里，明天还要追更多荣耀，无论将来走到哪里，我都会把奉献作为生活永恒的准则，会把真诚作为处事一贯的态度。

As we go on, we remember all the times we had together. As our lives change, come whatever. We will still be friends forever.

我的男朋友李智，遇见你无比幸运，是你让我的梦想变得有力量，是你让我的生活变得有色彩。一起努力的明天，定会充满希望。Last but not least, 我爱我的家人，尤其是父母，他们给我最真挚、最深沉的爱，教会我诚实和善良；感谢他们不计回报的实现我每一个愿望。而现在，女儿即将远行，最大的愿望，就是他们能够平安、健康。



北京大学
www.pku.edu.cn

本科生毕业论文

题目：农牧交错带不同土地利用方式下的土壤风蚀与合理的植被恢复

Soil erosion under different land use types in the
agro-pastural transitional zone and ration
vegetation restoration strategies

姓 名：张 铭 杰

学 号：00313085

院 系：环 境 学 院

专 业：地 理 科 学

导师姓名：刘 鸿 雁 教授

2007 年 6 月

摘 要

我国北方农牧交错带在植被格局上表现为森林草原的交错分布,由于频繁的土地利用变化,植被格局在近 50 年来发生了明显的变化,引起来生态系统服务的相应变化。尽管对这一地区的土壤风蚀有少量的研究,但在土地利用与土壤风蚀,植被和土壤特征与土壤风蚀等方面的研究仍然较少,尤其是将植被覆盖减少土壤风蚀作为一种生态系统服务仍然缺少研究,难以为农牧交错带未来的植被恢复和生态建设提供合理的依据。本文通过不同土地利用方式下土壤风蚀的分析,着重探讨以下科学问题:(1)土地利用与土壤风蚀之间的关系;(2)植被覆盖与土壤风蚀的关系;(3)区域土壤格局与植被建设的途径。

本研究将植被调查与土壤剖面分析结合,根据区域土地利用变化的有关资料,推断土地利用变化与土壤风蚀态之间的关系,为制定切实可行的植被恢复对策提供依据。论文就以下几个方面开展讨论:1. 土壤风蚀的影响因素 2. 土壤风蚀与土壤粗化 3. 土壤风蚀植被恢复对策。

本文的研究结果表明,研究区域内存在强烈的风蚀作用过程。不同土壤类型的侵蚀强度由强到弱为沙质丘陵草原>耕地>退耕还草地>人工林>石质丘陵草原,并且计算出该区域 Cs-137 的背景值,建立了区域土壤风蚀模型并计算出各种不同土地类型的土壤风蚀速率。并且提出了对该区域的保持石质丘陵草原现状态、保护原有人工林等植被恢复建议。

关键词: 农牧交错带 土壤风蚀 CS-137 分析 植被恢复

Abstract

The vegetation of ecotone between cropland and rangeland in northern China is characterized by interweaving of steppe and forest. Due to frequent changes in land-use, the vegetation pattern has changed significantly during the last 50 years, leading to parallel changes of ecosystem service. Despite some researches of soil wind-erosion in this area, the study on land-use and soil erosion, vegetation and soil characteristics, soil wind-erosion are absent. The method of treating decrease of soil erosion by vegetation cover as an ecosystem service is still lack, thus hard to provide evidences for future vegetation restoration and ecological construction in cropland and rangeland ecotone. This study focused on several scientific issues by analyzing soil erosion under various land-use manners: (1) the relationship between land-use and soil erosion; (2) the relationship between vegetation cover and soil erosion; (3) regional soil condition pattern and vegetation restoration pathways.

To find the relationship between the region changing of land using and erosion, and to establish a appropriate coping strategy to vegetation, this research connect vegetation research and analyzing soil section. We argued in the following 3 aspects of this issue: 1. the facts that impact erosion 2. erosion and soil crassitude 3. The approach to recover vegetation

The results indicate: there is strong erosion in the region of interest. While calculating the background of Cs-137 in this region, we set up model of erosion and draw a unitary picture about erosion velocity of different type of soil. The erosion is sandiness grass>tilth>grass>plantation>lithoid grass(from the highest to the lowest). Finally we suggest that to recover the vegetation, this region should be reserved and the original plantation in it should be protected.

Keywords: ecotone between cropland and rangeland erosion

CS-137 analysis plantation

目录

摘 要	i
Abstract	ii
第一章 前言	1
1.1 科学问题	1
1.2 研究进展	1
1.2.1 土地利用变化与生态系统服务功能	1
1.2.2 Cs—137 作为土壤侵蚀的指示的在我国的应用	1
1.3 本文内容框架	2
第二章 研究区域与研究方法	3
2.1 研究区概况	3
2.1.1 农牧交错带概述	3
2.1.2 研究区的自然概况和土地利用变化历史	3
2.1.3 研究区的植被退化与风沙活动	5
2.2 研究方法	6
2.2.1 取样地点概况	6
2.2.2 野外调查方法	6
2.2.3 土壤取样和分析	6
第三章 结果	8
3.1 不同土地利用方式下的 Cs—137 分布	8
3.1.1 不同土地利用方式下分层 Cs—137 含量的均值和方差	8
3.1.2 不同土地利用方式下土壤侵蚀的模式与风蚀速率估算	10
3.2 不同土地利用方式下的土壤粒度分布	12
3.3 森林-草原群落的土壤分异与植被分异	14
3.4 结果分析	15
第四章 讨论	16
4.1 与前人研究结论比较	16
4.2 植被恢复对策	16
4.3 存在的问题和下一步工作:	16
4.3.1 地形条件与土壤风蚀	16
4.3.2 土壤质地与土壤 CS—137 含量的相互影响	16
4.3.3 样地选择与其他土壤类型分析	16
第五章 结论	17
参考文献	18

第一章 前言

1. 1 科学问题

土地利用/土地覆盖研究是当前全球变化研究的核心内容之一。IGBP 和 IHDP 的核心计划 LUCC (Land Use/Cover Change) 主要针对土地利用与土地覆盖的变化引起的全球环境变化开展研究。河北坝上地区地处农牧交错区, 是近 50 年来土地利用变化最为明显的地区之一, 表现为前半段草原的大规模开垦以及后半段的退耕还林还草。

我国北方农牧交错带在植被格局上表现为森林草原的交错分布, 由于频繁的土地利用变化, 植被格局在近 50 年来发生了明显的变化, 引起来生态系统服务的相应变化。尽管对这一地区的土壤风蚀有少量的研究, 但在土地利用与土壤风蚀, 植被和土壤特征与土壤风蚀等方面的研究仍然较少, 尤其是将植被覆盖减少土壤风蚀作为一种生态系统服务仍然缺少研究。本文通过不同土地利用方式下土壤风蚀的分析, 着重探讨以下科学问题: (1) 土地利用与土壤风蚀之间的关系; (2) 植被覆盖与土壤风蚀的关系; (3) 区域土壤格局与植被建设的途径。

1. 2 研究进展

1. 2. 1 土地利用变化与生态系统服务功能

植树造林有助于碳的固存, 但可能会对区域环境带来一些负面影响。植被的种植可以调控地下水的循环和上涌, 但是却会导致地面径流的减少和土壤的盐碱化和酸化。研究表明, 造林地区地表径流会在种植数年内戏剧般地减少; 森林不仅比草地、灌木、农田需要更多的水, 它还会增加营养物质的吸收, 这会使得土壤更贫瘠 (Trading Water for Carbon with Biological Carbon Sequestration. Science, 310(23): 1945-1948) [1]。

随着人口的增加和土地利用方式的改变, 全球范围内土壤的性质正在发生着急剧的变化, 土壤污染、侵蚀、板结、密闭、沙漠化、盐碱化以及营养物质的流失等严重威胁着土壤的安全。而在我国范围内最为严重的问题是土壤的沙化与水土流失, 这主要是由于农业和畜牧业的过度开发造成了这一结果 (Soil and Trouble. Science) [2]。

1. 2. 2 Cs—137 作为土壤侵蚀的指示的在我国的应用

Cs—137 是 20 世纪 50~70 年代原子弹爆炸产生的放射性尘埃, 降落到地表后, 被土壤粘粒和有机物强烈吸附, 基本不被植物吸收和淋溶流失, 半衰期 30.17a, 是研究土壤侵蚀和泥沙沉积的一种良好的示踪源。通过测定不同土壤类型及不同层次的Cs137 含量, 并与背景值相比较, 可以确定土壤侵蚀率, 探讨土壤侵蚀规律。近几十年来, Cs137 法在全球土壤侵蚀研究中取得了显著的成就, 但以往的Cs137 法应用主要集中在水蚀方面, 很少涉及风蚀问题。直到上世纪九十年代才逐渐被用在土壤风蚀的研究领域 (严平 2003) [3]。

Cs137 在我国作为土壤侵蚀的指示已经有多年的研究历史, 近年来更受到广泛重视, 在青藏高原及新疆等干旱、半干旱区有成功的先例。

在我国最早尝试将Cs—137 作为研究土壤风蚀手段的是严平、张信宝等人, 他们首先介绍了Cs—137 方法在传统的研究方法无法提供中等时间尺度, 即近几十年来的风沙过程及其对全球变化的响应的解释能力。并且提出Cs—137 应用在风沙研究中的两个困难: 首先由于地表风蚀、沙粒运动不像水蚀那样具有明显的流域界线, 沙粒在气流中经长距离大范围搬运、沉降, 所以对其 137Cs 的跟踪测定困难较大; 其次由于Cs—137 在土壤中主要被粘粒、

极细沙($< 0.01\text{ mm}$)所吸附,而风成沙的重要成分为 $0.25\sim 0.1\text{mm}$ 的细沙,吸附Cs—137量极微。他们还对Cs137的背景值测量、土壤的风蚀速率和应用Cs—137测定沙丘和灌丛沙堆形成演变、沙尘暴测定、风沙沉积物研究以及治沙效益评价做出了讨论,并且提出了在我国东北、华北、西北及青藏高原地区选取若干典型地区,开展Cs—137背景值调查,进行如风蚀速率、沙丘形成演变等专题研究和建议(严平和张信宝 1998)^[4]。

在随后的工作中,严平等人在青臧高原等地展开了一系列实践性研究活动。他们首先应用Cs—137法研究了土壤风蚀的现代过程,查明青藏高原Cs—137背景值及其分布,根据模型算出了土壤风蚀的平均速率(严平等,2000)^[5]。而后又选择青海共和盆地作为研究区,初步查明了共和盆地Cs—137的区域和剖面分布特征,确定了区域Cs—137背景值,建立了风蚀速率的Cs—137评估模型,估算出土壤风蚀速率,并结合近40年来区域环境变化的背景资料,综合分析现代风蚀过程及其与环境变化的关系(严平等,2000)^[6]。在初步讨论后他们又进一步挖掘数据深入研究,将Cs—137深度分布划分为正常剖面、沉积剖面、侵蚀剖面 and 人为扰动剖面四种类型。以土壤风蚀总量作为输入,风蚀物的输送、沉积和转移作为输出,建立区域蚀积平衡模型(严平和董光荣,2003)^[7]。提出沙丘砂由于遭受反复吹失和沉积,其Cs—137含量逐渐减小,趋于微量的均匀化;而高寒草原的Cs—137含量在区域上也较为均匀,在深度分布上,接近负指数分布曲线保存了相对完好的Cs—137初始沉积剖面,是理想的Cs—137背景值样点(严平等,2003)^[7]。在共和盆地Cs—137背景值的研究中,他们发现其Cs—137剖面满足尖峰分布函数,与公认的理论分布(即负指数分布)相比,呈现出峰值下移和曲线趋平的现象,可能与近几十年来Cs—137的稳定下渗有关(严平等,2003)^[8]。

濮励杰等人在同时期也在新疆地区开展了相应的研究工作,计算出新疆库勒地区荒地、耕地、草地等土地利用类型的土壤侵蚀模数的平均值并探讨了不同土地利用类型与土地退化之间的相关关系及空间特征(濮励杰等,1998)^[9]。

近期在内蒙古等地也有人开展了一定的研究工作。胡云锋等人以内蒙古太仆寺旗为研究区,研究发现不同土地利用类型/土地覆盖等级的Cs—137剖面分布特征差异明显,发现在低覆盖草地和中覆盖草地土壤剖面中,Cs—137活度分布形态为负指数分布;在高覆盖草地土壤剖面中,Cs—137活度分布形态在剖面上部为单峰状,单峰后继续为负指数分布;在耕地剖面中,Cs—137集中在犁底层以上,且均匀分布。对耕地和草地样点分别使用质量平衡模型和剖面分布模型,可以估算得到农耕地、低覆盖草地、中等覆盖草地等3处样点的侵蚀速率分别属于强度侵蚀、中度侵蚀和轻度侵蚀,风力侵蚀强度与地面植被覆盖度呈负相关关系(胡云锋等,2005)^[10]。赵焘等人对采集于滦河源区的土壤进行分析,测定了土壤样品Cs—137的比活度。结果表明,自然栗钙土以及被风蚀土壤剖面中Cs—137比活度随深度呈指数递减式分布,其最大渗透深度可达约30 cm。栗钙土不同粒径土壤颗粒中Cs—137的比活度与粒径关系密切。综合考虑Cs—137在土壤中的分布、土壤有机质含量和质地等因素,可以使其结果将更为准确(赵焘等,2005)^[11]。

1.3 本文内容框架

土地利用的变化必然带来生态系统服务的变化,有关研究表明,河北坝上地区的植被退化与北京地区的沙尘天气关系密切(叶笃正等,2000)^[12]。对于土地利用变化与土壤风蚀之间的关系缺少实测结果,难以为农牧交错带未来的植被恢复和生态建设提供合理的依据。本研究将植被调查与土壤剖面分析结合,根据区域土地利用变化的有关资料,推断土地利用变化与土壤风蚀态之间的关系,为制定切实可行的植被恢复对策提供依据。

第二章 研究区域与研究方法

2.1 研究区概况

2.1.1 农牧交错带概述

中国北方农牧交错带指的是将我国东北、华北农区与天然草地牧区分隔的生态过渡带,即年平均降水量 250 mm~500 mm 的半干旱地区,是我国农业生产条件最为严酷、农业生产力最低的部分,跨越内蒙古、辽宁、河北、山西、陕西、甘肃、宁夏、青海 8 个省(区)(图 1),其中耕地占 26%,草地占 25%,林地占 15%。按地貌组合类型农牧交错带分为三段:即三北交界区(东段)、晋陕甘黄土区(中段)和甘青宁黄土区(西段)。这一地带是我国北方的中、东部农区向西北牧区过渡的自然生态屏障与水源涵养地,北方主要江河大多发源于此。景观表现为自然上的森林草原与灌木草原向荒漠草原过渡,人文上为农区向牧区的过渡,这是气候(季风尾闾区)和地貌(山地丘陵区)双重因素影响的结果,交错带东西带状展布,几乎全带的土地利用都是牧农(林)交错,没有明显的某种用地为主,但是存在着由东南农牧交错向西北牧农交错的过渡(王静爱等,1999)^[13]。

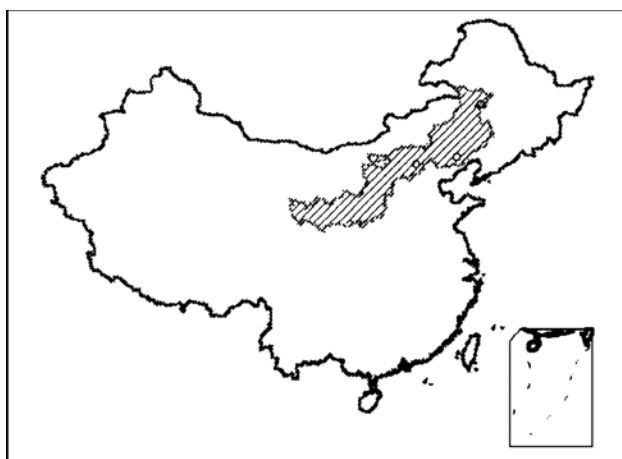


图 2.1 中国北方农牧交错带的位置

2.1.2 研究区的自然概况和土地利用变化历史

2.1.2.1 位置

研究区主体部分为位于内蒙古高原东南部的浑善达克沙地和河北坝上地区,海拔在 1100~1500m 左右。在行政区划上包括河北省张家口地区的张北、康保等县以及承德市的丰宁、围场两县的坝上部分。研究区的地理坐标为 E 112~119 度, N 39~45 度(田育红 2003)^[14]。

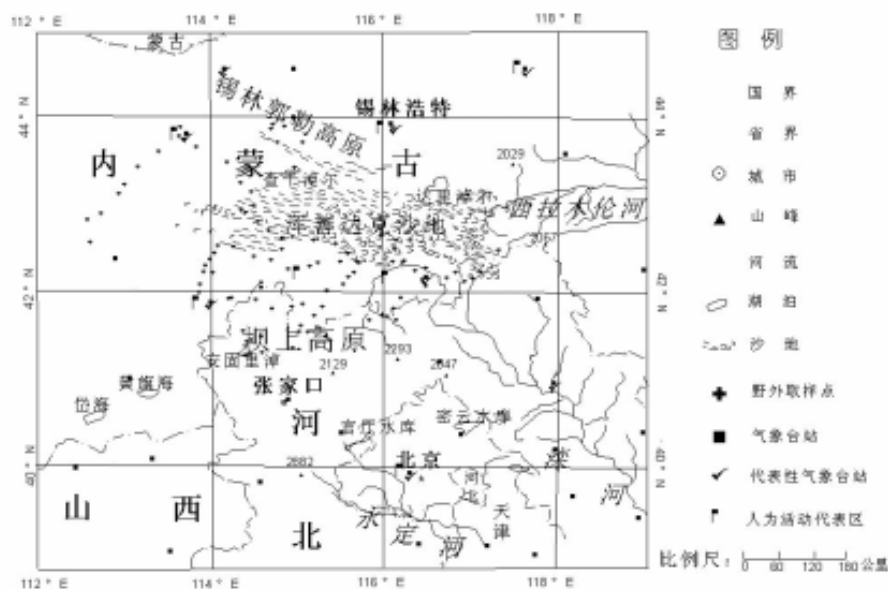


图 2.2 研究区域位置[14]

2.1.2.2 地质地貌

研究区的东南和南部为冀北山地，沟谷海拔在 500~700m 之间，向北和西北方向的内蒙古高原海拔则复又缓缓下降，内蒙古高原的边缘部分与冀北山地交界的部分称为“坝上高原”。在坝缘部分，山地海拔迅速上升到 1400~1700m，最高海拔在 2000m 以上。

研究区地貌类型复杂多样。中部为浑善达克沙地，核心部分为东西向条带状的沙垄，边缘部分为覆沙丘陵。北部为锡林郭勒高原，以波状高平原地貌为代表，有大规模火山活动形成的火山锥和熔岩台地。西北部为苏尼特盆地。南部坝上高原部分以波状高平原为主，有阴山余脉形成的低缓丘陵。在高原面上，有众多湖泊出现，较大的有达里淖尔、查干淖尔和安固里淖尔等（田育红 2003）^[14]。

2.1.2.3 气候

研究区的气候条件为温带大陆性半湿润气候向半干旱气候逐渐过渡。主体部分海拔高，气温低，年降水量在 200~450mm 之间，为季风气候影响的尾闾区（marginal area）。浑善达克沙地与内蒙古其他地区的沙地有所不同，其气候特点是夏季温凉，降水较多，冬季寒冷干燥，热量自东向西递增，风大沙多。研究区中的草原区部分全年 8 级以上的起风时日高达 60~80 天，形成了沙尘暴的动力基础，研究区也被认为是华北等地沙尘天气的重要物源区之一（叶笃正，2000）^[14]。

2.1.2.4 植被和土壤

土壤和植被格局反映了气候条件和地貌特征的空间分异。冀北山地的植被以落叶阔叶林和落叶阔叶灌丛为主，相应的土壤类型为褐土和棕壤。坝上高原东部为草甸草原，土壤为黑钙土。坝上高原西部和锡林郭勒高原则以典型草原植被和栗钙土为主。浑善达克沙地西部为沙地小叶锦鸡儿灌丛草原，东部为榆树疏林草原，土壤为风沙土。在西北部的苏尼特盆地，植被为荒漠化草原，土壤为棕钙土。在高原内部低地处常发育有草甸、盐化草甸与沼泽、盐碱地，相应的土壤类型为草甸土、沼泽土和盐碱土（田育红 2003）^[14]。

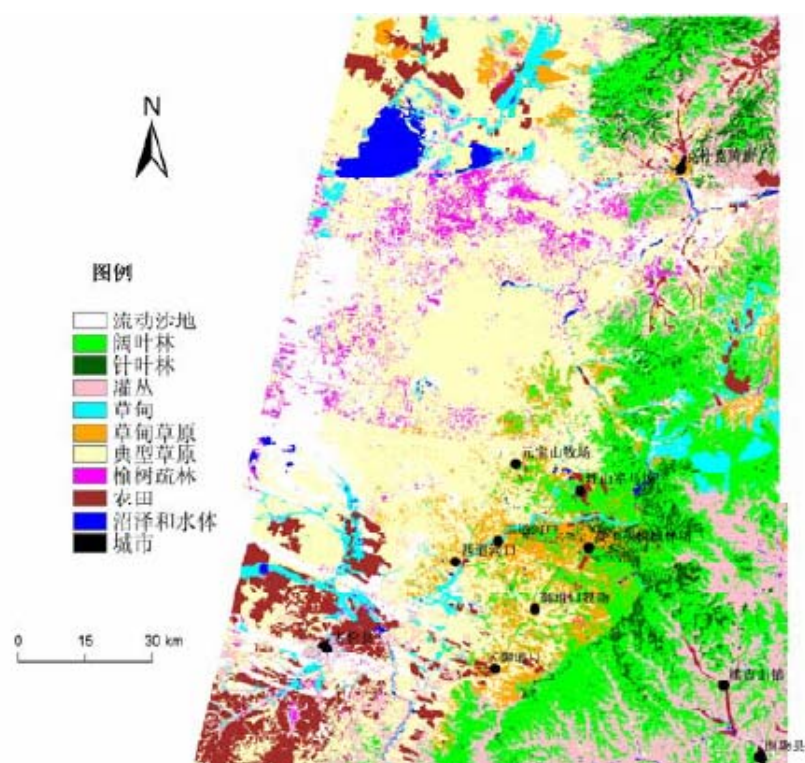


图 2.3 区域植被覆盖情况^[15]

2.1.2.5 研究区人类活动与土地利用

研究区历史上华北、蒙古、东北三大地区经济文化的汇合点，自古以来就是多民族争夺、交流、融合的农牧交错地带，区域开发过程复杂、多变，尤其是十七世纪中叶以来，区域开发速度快、强度大，使这里的生态环境发生了显著的变化。区域的开发和人类活动历史可以分为一下几个阶段：（1）明代以前的农牧交错开发时期，又分为先秦原始开拓阶段、秦西汉初步开发阶段、东汉至五代游牧为主阶段、辽金农业为主开发阶段和元明农牧转换阶段，其特征是数次农牧交错或农牧并存交错分布；（2）清代围场、行宫、晃庄为主全面开发时期，又包括全面开发时期和后期农业缓慢发展与清末围场放垦阶段；（3）民国区域经济曲折发展阶段，民国前期，由于北洋军阀实行移民实边政策，奖励垦辟蒙荒，坝上多伦-沽源一线东南舒缓丘陵草原区又有大量汉人移入开垦，出现了大批农业聚落，蒙族人进一步北移，大部分地区成为半农半牧或农业区（张宝秀，1997）^[16]。

整个研究区的土地利用格局表现为南农北牧，河北坝上地区以及内蒙古多伦县、太仆寺旗、化德县、正蓝旗南部、正镶白旗南部、镶黄旗局部则表现为农牧交错。由南往北，耕地所占的比例逐渐减小。由于地处季风气候尾部区，降水量的波动性明显，这一农牧交错带生态上脆弱，对于人类的干预反应敏感，过度的人为利用已经造成了突出的生态问题（田育红 2003）^[14]。

2.1.3 研究区的植被退化与风沙活动

2.1.3.1 研究区植被退化现状

研究区低湿地草甸、石质丘陵草甸草原和湖滨草甸的植物总平均盖度、多年生植物平均盖度占总盖度的比例都较其它类型偏高，这些类型的植被退化程度相对较轻；撂荒地或退耕

地虽然总盖度比较高,但多年生植物盖度占总草本盖度的比例却非常低(田育红 2003)^[14]。

多年生草本盖度占总盖度比例与植被退化之间则存在着相对较为有规律的关系,即除个别类型外,多年生植物盖度占总盖度的比例较高的类型,其植被退化程度相对较低(田育红 2003)^[14]。

2.1.3.2 风沙活动

根据研究区及周边地区土地利用方式,可以将研究区及周边地区划分为农区、林区、农牧交错区和牧区。在牧区根据植被特点的进一步差异可以划分为草甸草原为主的牧区、典型草原为主的牧区、沙地榆树疏林草原为主的牧区、沙地小叶锦鸡儿灌丛草原为主的牧区和荒漠化草原为主的牧区五个亚区。

50 年来,牧区荒漠化草原亚区沙尘暴的发生近年来有所增加,牧区荒漠化草原亚区在六十年代沙尘暴爆发次数最高,达到 57 次,以后沙尘暴发生的次数逐渐减少,九十年代基本上和五十年代持平。不同区域五十年来沙尘暴的发生次数均呈下降趋势,除个别区域(外,九十年代是沙尘暴爆发次数最少的 10 年(田育红 2003)^[14]。

2.2 研究方法

2.2.1 取样地点概况

样品采集于 2005 年 7 月,取样点选择在内蒙古高原东南缘坝上一围场、坝上一丰宁、坝上一沽源三条样带,主体部分海拔为 1100~1400m。西部为浑善达克沙地,由多条东西走向的沙带组成。东南和南部为冀北山地。气候条件为温带大陆性半湿润气候向半干旱气候逐渐过渡,年降水量在 200~450mm 之间,为季风气候影响的尾闾区(marginal area)。土壤类型多样。从冀北山地向锡林郭勒溶岩台地,土壤类型依此为棕壤,灰色森林土、黑钙土、淡黑钙土、暗栗钙土。在浑善达克沙地主要为风沙土。一些高海拔山顶分布有亚高山草甸土。植物区系组成上有着非常明显的过渡性,从冀北山地向内蒙古高原过渡,表现为东亚成分逐渐减少而达乌里-蒙古成分增多。地表类型包括人工林、沙质丘陵草地、石质丘陵草地、退耕还草地、退耕撂荒地、耕地、黄土、退化草原等。

2.2.2 野外调查方法

采用样方法调查植被覆盖情况,森林群落采用 10 米*10 米的样方,草原群落采用 2 米*2 米的样方进行调查。野外调查中分层记载种类名称、多度、盖度、和高度等信息。对于森林群落分乔木层、灌木层、草本层、枯落物层、立木更新分别进行记载。对于乔木层、每木测量胸径、基径,估测冠幅、树高。对于灌木层和草本层,记载种名、丛数或多度、盖度、高度。对于立木更新,根据高度划分龄级,根据树龄记载不同幼苗和幼树的熟练,定性描述其分布状况。对于枯落物层,记载其组成、覆盖程度和分布等指标。

2.2.3 土壤取样和分析

每个样地挖取一个土壤剖面,深度在 30 厘米以上。用直径 5 厘米的环刀自 30 厘米深处由下至上依此分层取样。每个取样点 6 层土壤样品。

2.2.3.1 Cs137 分析

样品经烘干后,称重、研磨过筛(孔径为 1.0mm, 0.5mm),剔除大颗粒及草根,每个样品挑出 30 克,在核工业北京化工冶金研究院分析测试中心用高纯锗 γ 谱仪进行测试。Cs—137 含量用其 661.6keV γ 射线的全峰面积计算。测试仪器为美国坎培拉公司(ORTEC)生产的高纯锗(Ge)探测器,经前置放大和数字转换后,接 4096 道多道分析仪,采用道边界

法测定。探头的灵敏体积为 100 立方米，对Co60 1.33MeV的 γ 射线能量分辨率为 1.9KeV，峰康比为 50: 1。仪器具有良好的稳定性（道漂小于 1 道/月）和较低的本底（Cs—137 峰面积内本底为 $2.03 \times 10^{-2} \text{Bq}$ ）重复测量相对误差小于 6%。样品测试时间为 300000s。

2.2.3.2 粒度分析

样品经烘干后，称重、研磨过筛（孔径为 1.0mm ， 0.5mm），剔除大颗粒及草根，每个样品挑出 5 克，在北京大学环境学院地表过程分析与模拟教育部重点实验室用激光粒度仪 Mastersizer 2000 纳米粒度仪进行测试。技术参数为 0.02-2000 微米、1000 次/秒扫描速度、高灵敏亚微米区测量性能。

第三章 结果

3. 1 不同土地利用方式下的 Cs—137 分布

3.1.1 不同土地利用方式下分层 Cs—137 含量的均值和方差

表 3.1 各种不同土地类型分层 CS—137 单位含量

样地类型	单位 Bq/kg	0-0.05m	0.05-0.10m	0.10-0.15m	0.15-0.20m	0.20-0.25m	0.25-0.30m
沙质丘陵	均值	0.044	0.076	0.118	0.121	0.112	0.181
	方差	0.000	0.003	0.001	0.001	0.014	0.071
人工林	均值	0.114	0.093	0.085	0.077	0.075	0.055
	方差	0.005	0.002	0.002	0.003	0.003	0.002
耕地	均值	0.101	0.103	0.092	0.080	0.077	0.067
	方差	0.000	0.000	0.000	0.002	0.002	0.002
石质丘陵	均值	0.139	0.105	0.061	0.055	0.047	0.020
	方差	0.008	0.010	0.002	0.002	0.002	0.000
退耕还草地	均值	0.083	0.067	0.074	0.042	0.034	0.035
	方差	0.001	0.002	0.001	0.000	0.000	0.000
区域标准样		0.367	0.146	0.048	0.028	0.015	0.03

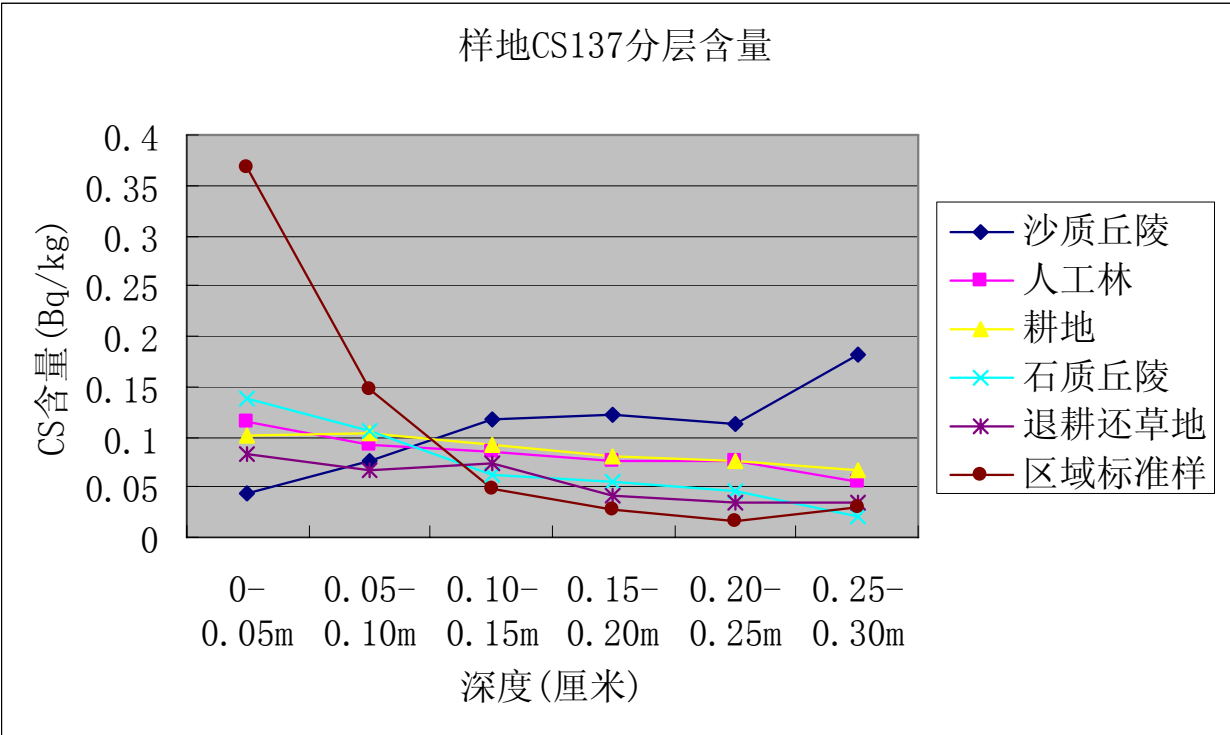


图 3.1 各种不同土地类型分层 CS—137 单位含量

由图 3—1 和表 3—1 可知区域中各种样地表层都存在着严重的侵蚀状况，而直观上来看其侵蚀状况：沙质丘陵草原>退耕还草地>耕地>人工林>石质丘陵草原。而在其下层，沙质丘陵草原出现了明显的堆积形态。

表 3.2 各种不同土地类型分层 Cs—137 单位面积总量含量

单位:							
样地类型	Cs137 Bq/m ²	0-0.05m	0.05-0.10m	0.10-0.15m	0.15-0.20m	0.20-0.25m	0.25-0.30m
沙质丘陵	均值	3.080	5.341	8.261	8.288	7.423	11.799
	方差	0.731	9.291	5.713	3.279	59.780	297.306
人工林	均值	6.281	5.336	4.843	4.146	4.268	3.215
	方差	13.848	4.071	4.026	7.994	7.578	6.783
耕地	均值	5.691	6.262	5.134	4.366	4.396	3.419
	方差	2.283	7.407	0.283	3.487	8.027	5.037
石质丘陵	均值	7.940	5.269	3.024	2.856	2.400	1.075
	方差	27.804	21.409	4.161	7.248	5.073	0.032
退耕还草地	均值	5.225	4.484	5.319	2.579	1.964	1.141
	方差	0.520	1.176	1.113	0.005	0.442	0.044
区域标准样	均值	11.354	5.770	1.966	1.202	0.573	1.237

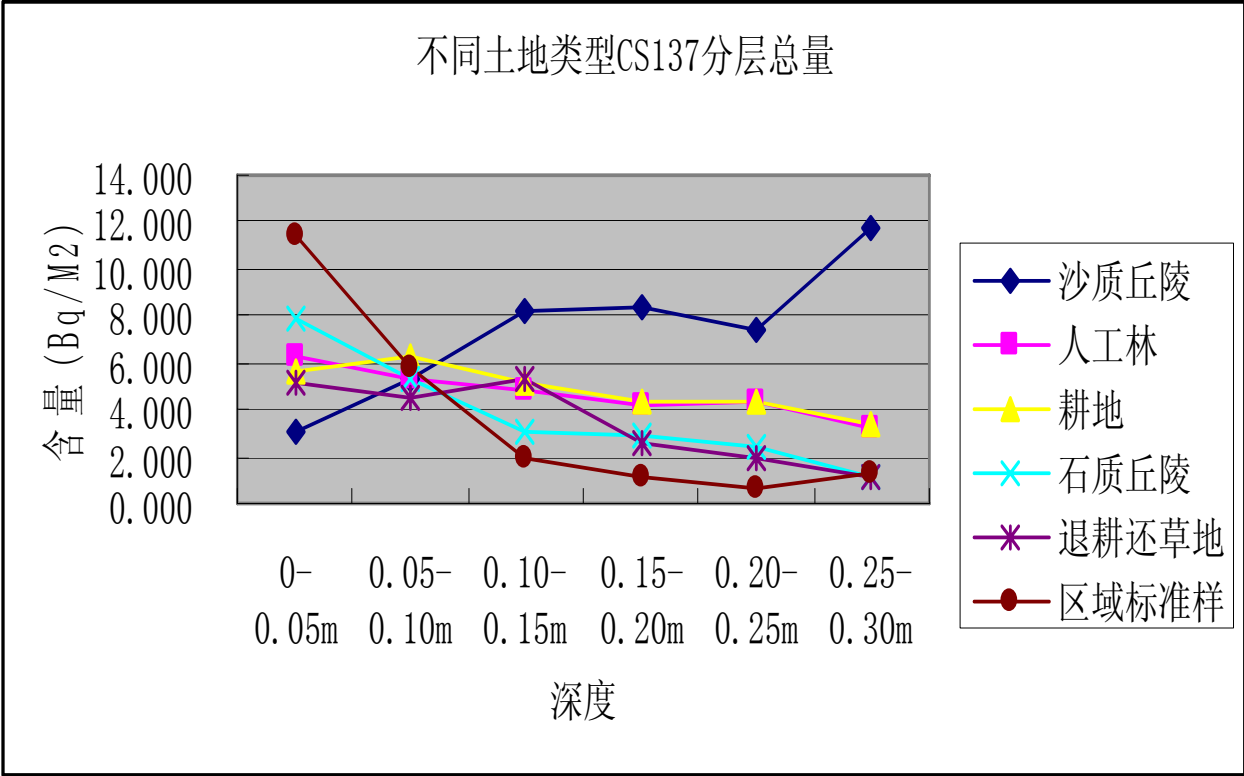


图 3.2 各种不同土地类型分层 Cs—137 单位面积总量含量

由上图可知的结论与用单位含量所得出的结论一致,但是沙质丘陵草原的标准差不正常取值值得怀疑,可能某些样点取值偏离较大。

样点Cs—137 总量采用下列公式计算:
$$CPI = 10^3 \sum_{i=1}^n C_i B d_i D_i$$
 [8] 式中, CPI表示样点的Cs—137 总量 (Bq/ m²), i为采样层序号, n为采样层数, C_i为i采样层的Cs—137 活度 (Bq/kg), B_di为i采样层的土壤容重 (t/ m³), D_i为i采样层的深度 (m)。

表 3.3 各种不同土地类型下 CS—137 活度和 CS—137 单位面积总量

土地类型	样品数	平均CS137 活度	平均CS137 总量
		Bq/kg	Bq/m ²
沙质丘陵	3	0.109	44.192
人工林	3	0.083	28.087
耕地	3	0.087	29.267
石质丘陵	3	0.071	22.563
退耕还草地	3	0.056	20.712
区域背景	1	0.106	22.103

所测样品CS137 活度在 0.017 到 0.488Bq/kg之间，平均值为 0.0726Bq/kg;所测区域CS—137 总量在 10.18 到 44.18 Bq/m²之间，平均值为 27.83 Bq/m². 不同类型土地CS—137 活度单位面积总量的排序为:沙质丘陵草原>耕地>人工林>石质丘陵草原>区域背景>退耕还草地。

而总体上看除退耕还草地外其他各种土地类型都有 CS—137 的富积。与侵蚀情况不符，可能与土壤侵蚀与堆积相互作用有关。

3.1.2 不同土地利用方式下土壤侵蚀的模式与风蚀速率估算

CS—137 背景值是指特定地区保存下来的 CS—137 沉降总量，及未受扰动、非积非蚀条件下的 CS—137 沉积总量。我们所选取的区域标准样符合背景值取样的技术要求。

已有的研究表明，未扰动非耕作土壤剖面中的 CS—137 随深度分布可以归纳为指数型、尖峰型和递减型 3 种类型，相应的分布函数如下：

$$Cs = ae^{-kz} (a > 0, b > 0) \tag{1}$$

$$Cs = a(1 - (k - z/H)^b)(k - z/H)^{b-1} \tag{2}$$

$(a > 0, b > 0, k \leq 1)$

$$Cs = a(1 - z/H)^b (a > 0, b > 0) \tag{3}^{[8]}$$

式中：CS 为某个深度 z（cm）中的 CS-137 活度（Bq/kg）；a、b 和 k 为常数；H 表示剖面中 CS137 的最大探测深度（cm）

在以上 3 个类型中，以指数分布（F1）最为普遍而被多数学者所采纳，被看作核爆炸初期唯一理论化的CS—137 背景值分布函数，其形成机制与物理学上的物质扩散原理有关；尖峰函数（F2）是近年来频繁发现的一种分布形式，其函数型式与指数分布相似，基本符合指数剧减的规律，只是其峰值在 2 到 4cm层位，而不是在地表层位（0 到 1cm），这可能是近几十年来CS—137 在重力作用下长期缓慢扩散、迁移的结果；而递减函数（F3）在背景值剖面中较为罕见，该分布型式有较大的局地性（主要与土质有关），甚至可能与人为扰动有关（图 3.3；严平 2003）^[8]。

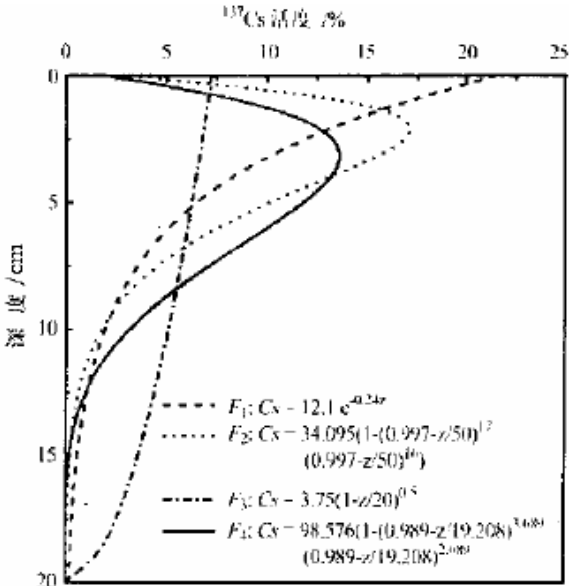


图 3.3 CS-137 活度公式

由于我们取样深度的所限，选取指数递减分布方程式来描述土壤中 CS—137 含量随土壤

深度的增加而变化的情况由式（1）变形可得：

$$C = A_1 \cdot e^{-h/T_1} \quad [11]$$

由区域标准样的值计算可知： $T_1=7.02$ $A_1=0.478$

相关的研究与前文的分析表明区域最大侵蚀深度在可达 30 厘米。本区域降水较少、土壤遭受的淋溶作用微弱，且研究区土壤底土层的土壤质地多为沙质，少有能够吸附并保持Cs—137 的有机胶体或黏粒。所以底层CS137 的比活度较低（赵焱 2005）^[11]。

Owens，Yang 和濮励杰曾分别将 Cs—137 在自然土壤剖面中随深度呈指数递减的分布式引入质量平衡模型，建立了土壤中 Cs—137 背景值估算模型和土壤总流失厚度估算公式即：

$$y = 100 - [R_1(1 - \lambda)^{29} + R_2(1 - \lambda)^{28} + \dots + R_{29}(1 - \lambda)] \cdot (1 - \lambda)^{M-1982} \quad (2)$$

$$C_R = 10\,000 D \int_0^h A_1 \cdot e^{-h/T_1} dh$$

$$= 10\,000 D A_1 \cdot T_1 [1 - e^{-h/T_1}] \quad (3)$$

$$H = - T_1 \cdot \ln(1 - y) \quad (4)^{[11]}$$

式中, y 是某个点Cs—137 总流失百分数; R_t 是第 t 年Cs—137 沉降量占总输入量的百分数; λ 是该地点年平均Cs—137 流失百分比; M 是土壤采样年份 ($M \geq 1982$); C_R 是土壤中Cs—137 的累积量 (Bq/m^2); D 是土壤密度 (g/cm^3); h 是土壤层深度 (cm); H 为总流失的土壤层次厚度 (cm)。

将 $T_1=7.02$, $A_1=0.478$ 代入到方程式（3）中，计算得出研究区土壤中CS—137 的背景值 $C_R=31.33441 Bq/m^2$

将人工林、退耕还草地、耕地、石质丘陵草原的 CS—137 分布形式进行分析，得出其分布方程。

表 3.4 各土地类型参数

	T_1	A_1
沙质丘陵	7.01	0.526
耕地	53.72	0.113
退耕还草地	21.9	0.104
石质丘陵	13.31	0.185
人工林	37	0.122

将上述参数代入方程式（3）中可以计算 CS137 的流失百分数。结果为：

表 3.5 各土地类型 CS 流失百分数

土地类型	Y
沙质丘陵	-0.099
耕地	0.215
退耕还草地	0.487
石质丘陵	0.334
人工林	0.242
标准样	0.000

分别将上述 Y 值代入有关的相关参数代入公式（4），得出各种不同的土地类型土壤累计

流失厚度和近 42 年来（1963 年为 CS137 沉积峰值 2005 年采集样品）土壤风蚀速率分别为：

表 3.6 各土地类型土壤累计流失厚度与平均侵蚀速率

土地类型	H(cm)	V(cm/a)
沙质丘陵	-0.661	-0.016
耕地	13.001	0.310
退耕还草地	14.600	0.348
石质丘陵	5.409	0.129
人工林	10.260	0.244
标准样	0.000	0.000

董治宝等 2000 年的研究表明，在中国半干旱地区土壤风蚀速率一般在 0.04~0.53 cm/a, 我们所得到的研究结果处于此范围之内。

由以上结果我们分析认为该区域各种不同土地类型都处于一定程度的侵蚀状态中，其中退耕还草地的侵蚀最为严重，其侵蚀强度依此为：退耕还草地>耕地>人工林>石质丘陵草原。但是明显应该处于强风蚀状态下的沙质丘陵却显示出了土壤堆积的状态，这应该是需要研究讨论的问题。

3. 2 不同土地利用方式下的土壤粒度分布

将各种土壤类型样点的粒度数据分层加和平均后得到各种不同土壤类型的土壤粒度之间的相互关系。

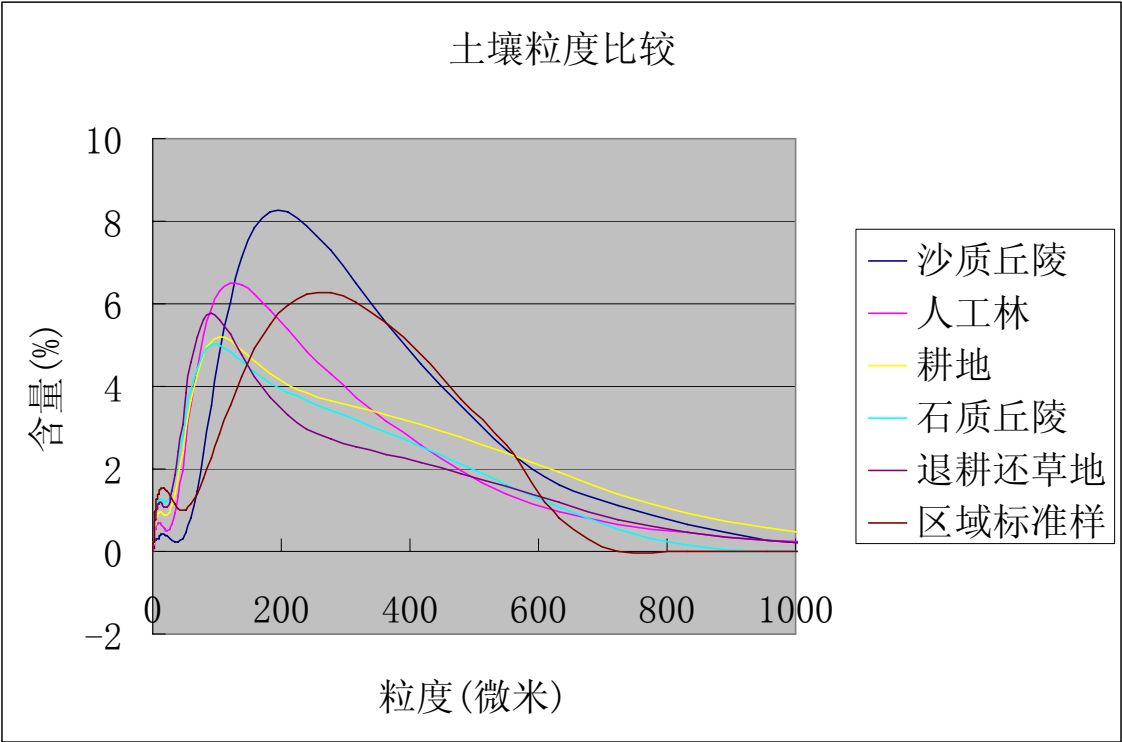


图 3. 3a 各种土地类型样地粒度总体比较

观察图 3. 3a 我们可以了解到石质丘陵草原与耕地的粒度分布形式比较相似，峰尖部分位于较低的粒度范围，而其分布集聚程度并不高；退耕还草地的细粒物质含量最为丰富，而且积聚程度教高，这有可能是长期的风蚀物质积累的结果。人工林的土壤粒度含量相对于耕地、退耕还草地以及石质丘陵草原等颗粒物较粗，分布比较平滑。沙质丘陵的粒度在几种

样地里是最大而且峰值最高的，这是长期风力侵蚀的结果。区域标准样的土壤粒度分布很均匀，接近于正态分布，侵蚀和堆积都不明显。可见该地区沙质丘陵草原长期处于风蚀状态下，而耕地由于人为活动的影响，土壤中细粒物质教多但粒度分布均匀，而很明显的在耕地转化为退耕还草地后土壤有一定的堆积过程。石质丘陵草原可能因为裸露岩石的保护，细粒物质也得到了一定的保留，人工林由于能够防风固沙所以粒度分布较为均匀，但其粒度粗化。

盛学军等人发表的1989年8月到1993年9月在坝上康保县照阳河乡三义村进行的风蚀沙化实验表明，被风蚀扬走的主要是0.05mm以下的细粒物质。叶笃正等人也指出沙尘颗粒集中在0.002-0.063mm之间。陈静生等人通过北京至内蒙古集宁一线21个地点的系统采样，也得出绝大多数地点的降尘以小于0.05mm粒径部分占绝对优势的结论(刘鸿雁等,2003)^[17]。所以我们所选取的粒度以0.05mm为重要的划分标准测量评定。

表 3.4 各种土地类型分层土壤粒度小于 0.05mm 累计含量平均

土地类型	0-5cm	5-10cm	10-15cm	15-20cm	20-25cm	25-30cm
沙质丘陵	4.094	5.240	9.901	9.946	8.159	10.706
人工林	28.957	18.380	16.468	19.780	16.624	17.356
耕地	27.152	29.705	27.920	25.785	23.023	24.395
石质丘陵	40.108	35.491	32.604	31.781	31.409	32.183
退耕还草地	31.648	30.969	31.486	32.974	34.542	34.302
区域标准样	33.375	33.867	32.006	30.985	28.345	24.758

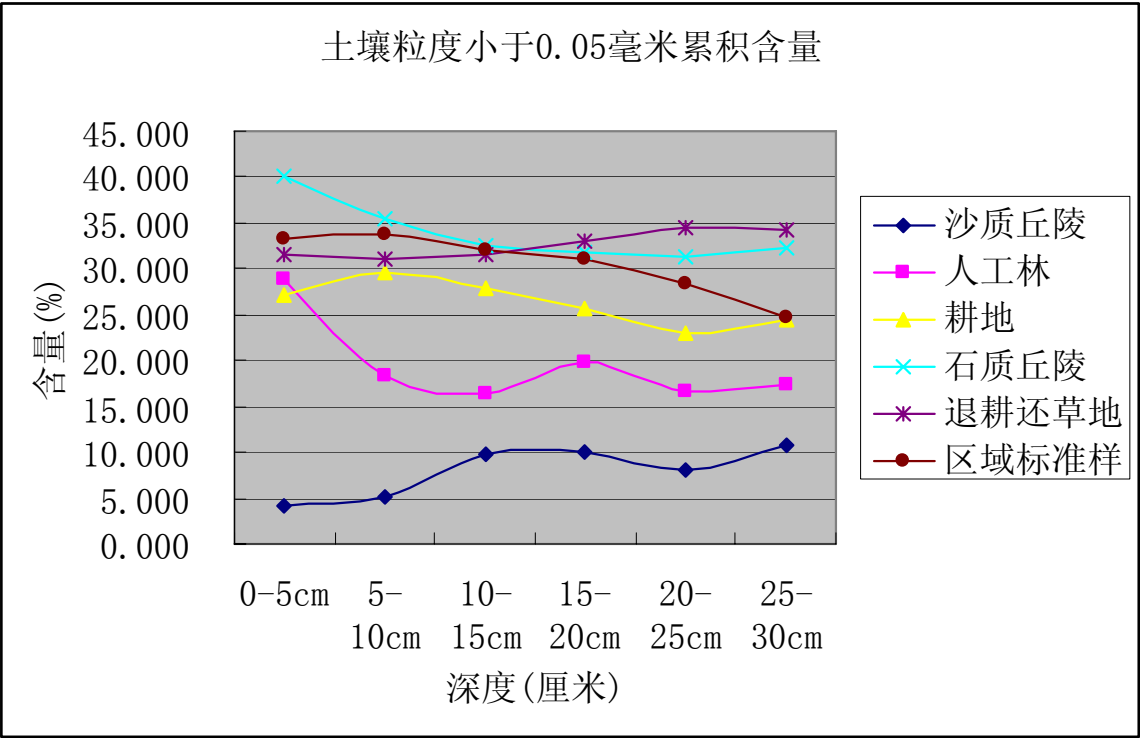
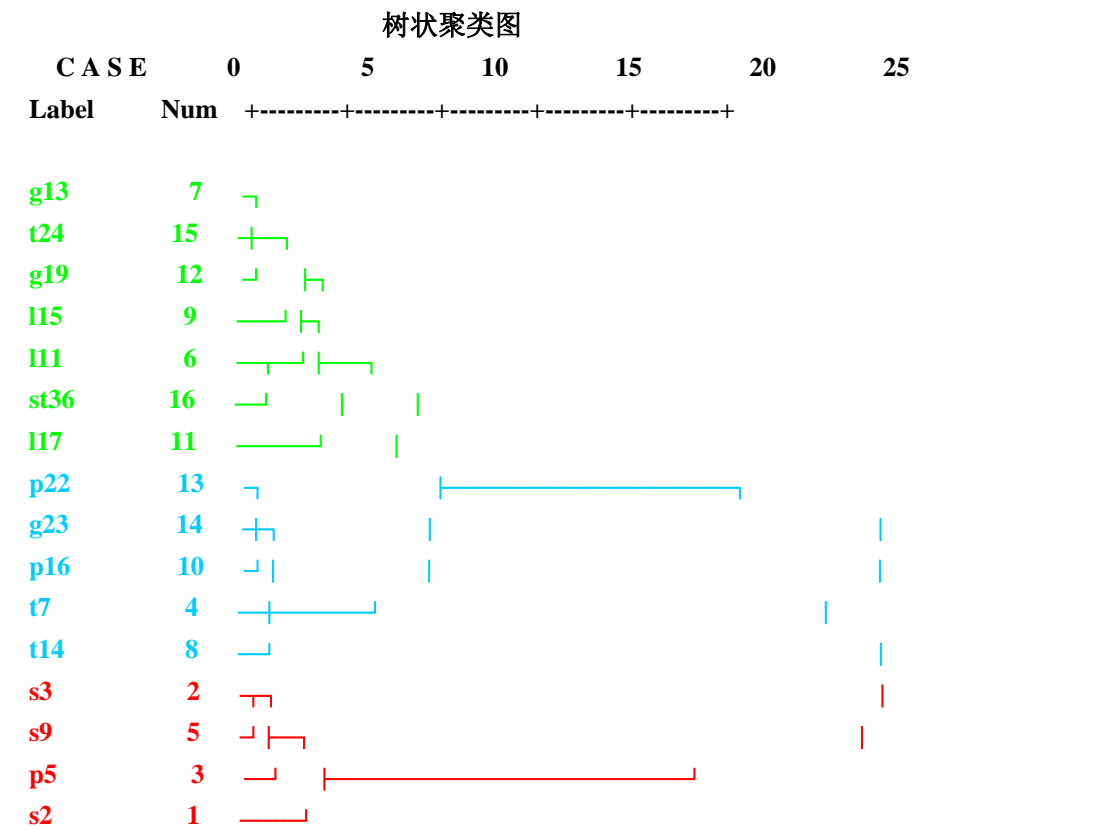


图 3.4 各种土地类型分层土壤粒度小于 0.05mm 累计含量平均

根据图 3.4 我们分析认为沙质丘陵草原毫无疑问地处于强烈的风蚀过程中而人工林表层拥有大量的细粒物质沉积，这应该是人工林防风固沙作用的体现。而其上耕地由于人为影响有少量侵蚀，而且各深度侵蚀较为均匀。退耕还草后土壤的质地得到了一定程度的改善。区域标准样分布均匀无明显的侵蚀和堆积情况。石质丘陵里细粒物质也较多，有可能是风蚀

过后粘土类物质遗留在石质颗粒中的结果。

利用 SPSS，将 16 个样地分别统计各自的分层土壤粒度小于 0.05mm 的土壤累积含量，进行系统聚类法。得到相应的结果。



根据分类树状图我们认为在一定程度上石质丘陵草原和退耕还草地的侵蚀状况较为相似，而耕地和人工林的土壤侵蚀方式有较大的相似性。沙质丘陵草原的情况较为特殊，所以自成一类。尚海林标准样与石质丘陵草原和退耕还草地分为一类应该是由于那两类样地侵蚀程度较低缘故。

3. 3 森林-草原群落的土壤分异与植被分异

研究表明，沙质地表当植被覆盖度小于 60%时即有可能发生风蚀（董治宝 1996）^[18]。将各个样地类型的植被覆盖情况进行研究分析可得表 3—6。（耕地情况人为干扰较大，不作讨论）。

表 3.6 各种土地类型的植被特征

土地类型	项目	草本植物	多年生草本	多年生草本	草本层
		总盖度	植物盖度	盖度所占比例	平均高度 (cm)
人工林	均值	23.333	17.667	0.754	14.904
	方差	233.333	127.583	0.004	13.647
沙质丘陵	均值	45.000	5.750	0.121	13.151
	方差	450.000	15.125	0.001	25.181
石质丘陵	均值	33.333	32.000	0.949	7.456
	方差	408.333	394.750	0.002	27.118
退耕还草地	均值	45.000	30.000	0.667	20.616

由于耕地的人为扰动较大，所以无法从植被状况进行相应的分析，而在退耕还草地中由

于是人工种植的草场,虽然种植了多年生的苜蓿、披碱草等多年生草本植物但其人工干扰也比较强烈。而我们知道在内蒙古地区,风蚀作用多发生在春秋等季,于是多年生草本植物的盖度对土壤侵蚀的影响更为重要。

由表 3.6 我们可以分析得知,虽然在植被总盖度上退耕还草地、沙质丘陵草原>石质丘陵草原>人工林,但是在多年生草本盖度这个指标上石质丘陵草原>退耕还草地>人工林>沙质丘陵草原。而多年草本生草本盖度所占的比例石质丘陵草原>人工林>退耕还草地>沙质丘陵草原。

综合考虑以上几个主要参数我们分析认为:石质丘陵由于土壤表面石质颗粒裸露,能够被风蚀的面积较小,而其在裸土上又有大量的植物特别是多年生植物覆盖,所以其受侵蚀程度应该比较低。而人工林由于其特殊的林地背景,本来就具备一定的防风固沙功能且无法与其他土地类型相比较,但其较高的草本覆盖度和多年生草本生长比例,其受侵蚀程度也相对较少。沙质丘陵虽然草本盖度很高,但是由于其植被多为一年生植物所以无法在风蚀作用强度较高的季节起到防止土壤侵蚀的情况所以风蚀状况最为严重。退耕还草地由于其人为干扰背景所以比较难于判断其土壤情况,但较沙质丘陵应该为轻。

3. 4 结果分析

上文的分析中由 Cs—137 的方法得出了该地区各种不同土地利用类型的风蚀状况,再进而根据其相关的土壤粒度的性质和植被覆盖的情况对各种土地利用类型的风蚀状况给出相应的判断和分析。

根据 CS137 分析方法的结果我们认为该地区的不同土地利用类型的侵蚀状况为:

按 Cs—137 分层含量、总量以及土壤侵蚀速率:

沙质丘陵草原>退耕还草地>耕地>人工林>石质丘陵草原。

根据土壤粒度的分析我们排出的该地区的不同土地利用类型的侵蚀状况为:

(1) 土壤粒度比较:沙质丘陵草原>人工林>耕地>退耕还草地>石质丘陵草原

(2) 土壤粒度累积含量:沙质丘陵草原>人工林>耕地>退耕还草地>石质丘陵草原

而分类研究表明:石质丘陵和退耕还草地的侵蚀状况较为相似,而耕地和人工林的土壤侵蚀方式有较大的相似性。沙质丘陵的情况较为特殊。标准样与石质丘陵等分为一等。

根据植被覆盖的数据我们的分析结论为:

沙质丘陵草原>退耕还草地>人工林、石质丘陵草原。

由上述结论综合分析该地区的土壤风蚀的不同土地类型侵蚀强度的顺序为:

沙质丘陵草原>耕地>退耕还草地>人工林>石质丘陵草原。

其间人工林在土壤粒度中的异常可能是由于其独特的林地背景造成其底层土壤粒度较高。而耕地和退耕还草地的比较一方面由于退耕的还草地本来的自然堆积条件就不太好,受侵蚀比耕地要强,所以侵蚀强度较强,但在退耕还草地中其土壤表面有明显的细粒物质堆积情况。

第四章 讨论

4.1 与前人研究结论比较

田育红等对该区域不同土地类型的侵蚀状况也进行过相关研究。她经过研究认为石质丘陵草原植被处于退化当中，有一定的细颗粒物，沙尘被吹扬的可能性大。耕地也容易被侵蚀。退耕还草地对风蚀有一定的减轻作用。与我们得出的结论基本一致。

4.2 植被恢复对策

由上文的相关研究我们可以知道，在防治沙漠化的过程中无论是退耕还草还是种植人工林都可以较为有效的在一定程度上减缓土壤风蚀的作用。但是在植树种草的区位选择上和所改造的原土地利用类型还是需要科学的验证。首先研究确认在该地区石质丘陵应该是受土壤风蚀影响比人工林和退耕还草地更为轻微，所以不应该在该地区对石质丘陵进行人工植树造林的工作。其次，在的沙地丘陵地区可能并不适宜进行植树种草的防护活动，其原因是由于沙地丘陵的土壤质地条件和水分条件可能并不适宜绿化建设。最后应该认真的保护现有的人工林使之不遭受破坏，因为这些土地利用类型有大量的细颗粒物质的沉降，一旦破坏就有可能成为受风蚀最为严重的沙源，在退耕还草地区也应该更多的选择苜蓿等多年生草本植物作为牧场草种，更好的保护草原防止风蚀。

4.3 存在的问题和下一步工作：

4.3.1 地形条件与土壤风蚀

有关研究成果表明，微地形的改变也会影响土壤风侵蚀，起伏地形如半固定沙丘迎风坡与背风坡、坡顶与坡脚等不同位置之间都会有一定程度的差异。半固定沙丘表面不同部位Cs—137 分布的尖峰所处深度以及峰值大小不同，反映了其表面存在着强度不大的风沙活动。而沙丘中上部为缓慢的风蚀过程，坡脚部分为堆积过程。在双向风作用下，迎风坡中上部风蚀略强于背风坡，坡脚沉积弱于背风坡（张春来 2002）^[19]。而本文的对微地形对土壤风蚀的影响没有进行相应的讨论。

4.3.2 土壤质地与土壤Cs—137 含量的相互影响

不同粒径土壤颗粒中Cs—137 比活度的差异巨大，土壤有机质对Cs—137 也具有较强的吸附能力，从而使土壤颗粒中Cs—137 比活度随土壤有机质含量的增加而有所增加(赵焱 2005)^[11]。而风蚀作用主要集中在粒度 ≤ 0.05 的细颗粒物中，所以土壤本身的性质和土壤风蚀与Cs—137 含量之间有着一定的相关性，而文章没有对土壤性质中机质含量对Cs—137 含量的影响进行讨论，可以在今后改进。

4.3.3 样地选择与其他土壤类型分析

在该区域的标准样分析上与其他地区有所不同，该地区大部分草地草原都经历过一定的风蚀过程，所以选择林地作为标准样地而非天然草原具有一定的可取性，但还需要更多的认证。而在目前的工作中所有的样地都呈现出侵蚀状态，可以在下一阶段采集天然林地，天然草原等样地样品进行分析，也可以结合风沙沉降实验来讨论其风蚀物的输入和输出情况。对沙质丘陵的异常情况和总量的异常也需要再进行进一步试验分析。

第五章 结论

研究区域的CS137 背景值为 31.33441Bq/m^2 ，各种不同的土地类型风蚀强度为沙质丘陵草原>耕地>退耕还草地>人工林>石质丘陵草原，其中耕地的侵蚀速率为 0.310cm/a ，退耕还草地为 0.348cm/a ，人工林为 0.244cm/a ，石质丘陵为 0.129cm/a 。

该地区石质丘陵应该是受土壤风蚀影响最轻的，所以不应该在该地区对石质丘陵进行人工植树造林的工作。在的沙地丘陵地区可能并不适宜进行植树种草的防护活动，其原因这是由于沙地丘陵的土壤质地条件和水分条件可能并不适宜，绿化也应以一年生草本为主改良土壤。保护现有的人工林使之不遭受破坏，因为这些土地利用类型有大量的细颗粒物质的沉降，一旦破坏就有可能成为受风蚀最为严重的沙源。在退耕还草地区也应该更多的选择苜蓿等多年生草本植物作为牧场草种，更好的保护草原防止风蚀。

参考文献

- [1] Robert B. Jackson, 1* Esteban G. Jobbágy, 1, 2Roni Avissar, 3Somnath Baidya Roy, 3 Damian J. Barrett, 4Charles W. Cook, 1Kathleen A. Farley, 1David C. le Maitre, 5 Bruce A. McCarl, 6Brian C. Murray, 7, Trading Water for Carbon with Biological Carbon Sequestration[J], 23 December (2005), Vol 310, science 1944-1947.
- [2] Soil and Trouble, SOURCES: Adapted from Major Land Resource Constraints map created April 2004 by P. Reich and H. Eswaran of USDA/NRCS Soil Survey Division, World Soil Resources, Washington, D.C., from WSR Soil Climate Map and FAO Soil Map of the World, 1995. GLASOD data (L. R. Oldeman et al., 1991) provided by K. Sebastian, IFPRI. Data on compaction in Europe from SOVEUR/ISRIC (2000), science
- [3] 严平¹, 董光荣², 张信宝³, 邹学勇¹, 《青海共和盆地土壤风蚀的¹³⁷Cs法研究(I)—¹³⁷Cs分布特征》[J], 《中国沙漠》, 2003年5月, 第23卷第3期, 268-274.
- [4] 严平, 张信宝, 《¹³⁷Cs法在风沙过程研究中的应用前景》[J], 《中国沙漠》, 1998年6月, 第18卷第2期, 182-186.
- [5] 严平, 董光荣, 张信宝, 张一云, 《¹³⁷Cs法测定青藏高原土壤风蚀的初步结果》[J], 《科学通报》2000年1月, 第45卷第2期, 199-204.
- [6] 严平, 《¹³⁷Cs法在土壤风蚀研究中的应用——以青海共和盆地为例》[J], 《中国沙漠》, 2000年3月, 第20卷第1期, 18.
- [7] 严平¹, 董光荣², 张信宝³, 邹学勇¹, 《青海共和盆地土壤风蚀的¹³⁷Cs法研究(II)—¹³⁷Cs背景值与风蚀速率测定》[J], 《中国沙漠》, 2003年7月, 第23卷第4期, 391-397.
- [8] 严平¹, 董光荣², 《青海共和盆地土壤风蚀的¹³⁷Cs法研究》[J], 《土壤学报》, 2003年7月, 第40卷第4期, 497-502.
- [9] 王宇飞, 濮励杰, 《¹³⁷Cs应用于我国土壤侵蚀研究评述》[J], 《南京大学学报(自然科学)》, 2002年11月, 第38卷第6期, 803-812.
- [10] 胡云锋, 刘纪远, 庄大方, 曹红霞, 闫慧敏, 杨风亭, 《风蚀土壤剖面¹³⁷Cs的分布及侵蚀速率的估算》[J], 《科学通报》, 2005年5月, 第50卷第9期, 933-937.
- [11] 赵烨, 岳建华, 徐翠华, 杜春光, 常艳春, 《¹³⁷Cs示踪技术在滦河源区栗钙土风蚀速率估算中的应用》[J], 《环境科学学报》, 2005年4月, 第25卷第4期, 562-566.
- [12] 叶笃正, 丑纪范, 刘纪远, 张增祥, 王一谋, 周自江, 鞠洪波, 黄笠, 《关于我国华北沙尘天气的成因与治理对策》[J], 《地理学报》, 2000年9月, 第55卷第5期, 513-520.
- [13] 王静爱, 徐霞, 刘培芳, 《中国北方农牧交错带土地利用与人口负荷研究》[J], 《资源科学》, 1999年9月, 第21卷第5期, 19-24.
- [14] 田育红, 《内蒙古东南部》, 硕士论文, 2003.
- [15] 何思源, 《内蒙古东南缘森林—草原交错带植被格局极其环境解释》, 本科论文, 2006.
- [16] 张宝秀, 《内蒙高原东南缘民族变动与经济开发研究》[J], 《北京联合大学学报》, 1997年3月, 第11卷第1期, 1-10.
- [17] 刘鸿雁, 田育红, 丁登, 《内蒙古浑善达克沙地和河北坝上地区不同地表覆盖类型对北京沙尘天气物源的贡献》[J], 《科学通报》, 2003年6月, 第48卷第11期, 1229-1232.
- [18] 董治宝, 陈渭南, 董光荣, 陈广庭, 李振山, 杨佐涛, 《植被对风沙土风蚀作用的影响》[J], 《环境科学学报》, 1996年10月, 第16卷第4期, 437-443.
- [19] 张春来, 董光荣, 邹学勇, 李志刚, 秦芝, 《半固定沙丘表面的¹³⁷Cs沉积特征》[J], 《中国沙漠》, 2002年6月, 第22卷第2期, 154-158.



北京大学

本科生毕业论文

题目:塞罕坝樟子松人工林凋落物类型、土壤深度
和根的径级对分解的影响以及碳氮动态研究

Effects of litter types, soil depth and root
diameters on litter decomposition and its carbon
and nitrogen dynamics

姓 名: 傲 德

学 号: 00826017

院 系: 城市与环境学院

专 业: 生态学

指导教师: 王 巍

二〇一二年六月

摘 要

植物凋落物的分解在地球生物碳循环和生态系统养分循环过程中具有重要作用。本实验研究了中国河北省塞罕坝地区樟子松根和叶凋落物的分解情况,分析了不同因素对樟子松根和叶凋落物分解的影响和碳氮元素含量的变化情况。在原位分解过程中,由于根样品具有较低的 AIF:N, 所以其分解速度较叶凋落物快。同时,根凋落物的分解还受到径级的影响,可以 2mm 和 5mm 为界限将根样品分为三类。在此基础上,发现土壤深度对不同类型的根和叶凋落物的分解过程会产生影响,较高的土壤含水量会促进叶凋落物和粗根的分解。分解过程中不同类型的凋落物的碳含量变化基本相同,均呈下降趋势,而氮含量变化则比较复杂,氮的固化和矿化作用发生在不同的时期。本实验的研究结果从凋落物性质和分解环境等角度解释了影响植物残体分解的机制,并分析了樟子松人工林中营养元素养分循环的过程。

关键词: 分解 根 叶凋落物 根的径级 土壤深度 碳 氮

Abstract

Decomposition of plant litter is key to global carbon cycle and nutrient cycle in ecosystems. We studied the decomposition process of *Pinus sylvestris* var. *mongolica* plantation, the dominant specie in the Saihanba Forestry Center in Hebei Province, northern China; and analyzed the response of litter decomposition to different factors and changing patterns of carbon and nitrogen concentrations. We found: i. Roots, with lower AIF:N, decomposed faster than needle litter; ii. According to the decomposition rate, root samples can be divided into 3 categories by 2mm and 5mm; iii. Higher soil moisture accelerates the decomposition of root and needle litter; and iv. Carbon concentration decreased in the decomposition process, while nitrogen mineralization and immobilization occurred in different stages.

Key words: Decomposition; Roots; Needle litter; Root diameter; Soil depth; Carbon; Nitrogen

目录

第一章	序 言	4
第二章	研究地区与实验设计.....	6
2.1	样地介绍.....	6
2.2	凋落物样品的采集和处理.....	6
2.3	凋落物样品的回收及化学处理.....	6
2.4	数据分析	7
第三章	实验结果.....	8
3.1	凋落物残留量.....	8
3.2	根的径级.....	10
3.3	土壤深度.....	10
3.4	凋落物碳、氮元素的动态变化.....	11
第四章	讨 论	13
4.1	根和叶分解过程对比.....	13
4.2	根的径级对分解过程的影响.....	14
4.3	土壤深度对分解过程的影响.....	15
4.4	凋落物碳、氮元素的动态变化.....	16
结 论	17
致 谢	18
参考文献	19

第一章 序 言

植物凋落物的分解是生态系统的一项基本过程 (Wang *et al.* 2010), 在地球生物碳循环和生态系统养分循环过程中具有重要作用 (Berg *et al.* 1998; Harmon *et al.* 2009; Austin and Ballarín 2010)。大量的 CO₂ 等温室气体通过分解作用释放 (Bontti *et al.* 2009), 这些温室气体在很大程度上会成为改变全球气候的潜在因素 (Berg and McLaugherty, 2008; Cusack *et al.* 2009)。随着温室气体的不断增多, 植物凋落物的分解过程及其受到的多因素的影响也越来越受到关注。这些因素包括分解环境 (Berg *et al.* 1998) 和凋落物物质组成 (Bloomfield *et al.* 1993; Keplin and hüttl, 2001; Prescott *et al.* 2004) 等。

凋落物初始化学元素含量与分解的关系一直是生态系统分解过程研究的重点, 许多研究结果表明, 凋落物初始 N、P、Ca、木质素含量, 以及木质素/N、C/N 等, 会影响凋落物的分解速率, 和营养的循环过程 (McLaugherty and Berg 1987; Ryan *et al.* 1990; Grabovich *et al.* 1995; Gijssman *et al.* 1997; Scott and Binkley 1997)。例如, Prescott *et al.* (2004) 认为, 木质素浓度在分解的第一年会明显影响凋落物分解过程, 而分解 4-5 年后, 因为大多数凋落物的质量损失逐渐相似, 所以凋落物初始的化学物质组成对此时分解的影响变得不再重要。但是也有结果表明, 凋落物分解率和凋落物化学成分组成之间没有显著相关关系 (Castanho, 2008)。然而这些研究主要关注不同物种之间凋落物分解同化学成分之间的关系 (Wang *et al.* 2010; Hobbie *et al.* 2010), 很少同时探究根和叶凋落物在原位分解过程中的差别, 及其初始化学物质组成对分解的影响。

同时, 由于根径 < 2mm 的“细根(fine root)”在生态系统年初级生产力中占据了很大一部分, 并且其周转率可以很好地表征土壤有机质的组成和生态系统的养分循环 (Fornara *et al.* 2009), 在植物根的分解研究中, 大部分学者都采用细根 (Aber *et al.* 1990; Harmon *et al.* 2009; Cusack *et al.* 2009; Wang *et al.* 2010) 作为研究对象, 例如 Ostertag 和 Hobbie (1998) 研究了土壤营养和凋落物组织化学成分对细根和叶凋落物分解的影响, 表明在养分充足的土壤中, 细根的分解速率要比叶凋落物快, 这是因为细根中木质素/N 的值较低。然而, 很少的研究会关注粗根 (coarse root) 的分解, 其中 Majdi (2007) 在对森林枯枝落叶层细根生产量研究的基础之上, 为了观察长期氮添加是否会促进粗根的分解, 选用了挪威云杉的粗根作为样品, 发现因为长期氮添加会促进分解者的活动, 所以能够加速粗根的分解, 这与对细根的影响相似。然而, 目前对粗根和细根的研究相对独立, 没有将二者进行很好的对比, 对不同径级的根在分解过程中的特点也缺乏关注, 很少对比不同径级的根在分解过程中的差别 (Ludovici, 2006)。

此外, 随着土壤深度的改变, 土壤的温度、湿度和质地都会有变化, 植物凋落物的分解作用也许会随着土壤深度的变化而产生差别 (Gill and Burke, 2002)。Hobbie *et al.* (2010) 在对比了不同种植物叶凋落物在地表的分解和细根在地下的分解过程后指出, 地下的分解过程与地表分解过程不一样, 因此二者要分别研究。Bontti *et al.* (2009) 使用了 LIDET (The Long-term Intersite Decomposition Experiment Team) 评估环境变化 (温度、湿度、蒸散量和气候分解指数等) 对分解影响的数据后, 提出温度并不能很好地解释根和叶凋落物分解的变化, 而湿度的差别可以解释部分

原因,对于同一类型的凋落物,土壤相对较高的湿度会加速地下的分解作用。Gill and Burke (2002)把凋落物分解袋埋在了深度为 10cm, 40cm, 70cm 和 100cm 的土壤中,发现凋落物质量损失率从 10cm 到 100cm 是线性递减的,并且不同的物种之间也存在差异。在土壤深度对分解影响的研究中,缺乏对比根和叶凋落物是如何受到土壤深度影响的,和它们在分解期对土壤深度变化的响应机制。

植物凋落物的分解作用是全球碳循环中的关键过程 (Harmon *et al.* 2009),其中植物残体氮等营养元素的矿化作用为土壤提供了重要的无机营养的输入,这些营养元素又可以被其他植物所吸收,这一过程主要受到分解者的控制 (Stefano *et al.* 2010)。分解者的生长具有相对严格的化学元素需求,为了达到平衡的生长条件,碳和其他营养元素的分解作用同时进行 (Sinsabaugh *et al.* 2008)。由于植物凋落物中氮的含量低于分解者的需求,因此在分解初期,分解者会从环境中固持氮元素,直到凋落物中的氮元素含量达到某一临界值后,才会开始净释放氮元素 (Berg and McClaugherty, 2008; Parton *et al.* 2007)。目前,大量研究关注不同物种之间根和叶凋落物分解过程中氮动态的关系,即二者分解速率在不同物种间是否一致 (Cusack *et al.* 2009; Wang *et al.* 2010; Hobbie *et al.* 2010),但是对于同时观测单一物种根和叶凋落物分解过程碳氮动态研究较少。

针对目前的研究进展,本研究关注了我国河北省北端塞罕坝地区樟子松 (*Pinus sylvestris* var. *mongolica* Litv.)人工林根与叶凋落物的分解动态,我们的目的在于: i. 比较根和叶凋落物分解速率存在的差异, ii. 分析不同径级对根凋落物分解率的影响, iii. 比较土壤深度对凋落物分解率的影响, iv. 观测分解过程中根和叶凋落物的碳和氮元素的动态变化。

第二章 研究地区与实验设计

2.1 样地介绍

研究样地设在塞罕坝-北大生态实验站樟子松人工林内,位于中国河北省北端塞罕坝坝上机械林场,经纬度为 42.413°N, 117.241°E。塞罕坝坝上地区地处内蒙古高原南缘,以丘陵为主,海拔 1500-1939 米。气候寒冷,冬长,春秋短,夏季不明显,属寒温带大陆性季风气候。年均气温 -1.4℃,极端最高、最低气温分别为 30.9℃和-43.2℃。年降水量 490mm,蒸发量 1229.9mm。年均无霜期 68 天,积雪时间长达 7 个月。土壤类型以山地棕壤、灰色森林土和风沙土为主。塞罕坝处于森林—草原交错带,植被类型多种多样,包括落叶针叶林、常绿针叶林、针阔混交林、阔叶林、灌丛、草原与草甸和沼泽及水生群落,具有中国最大面积的人工林,樟子松为其优势树种。

2.2 凋落物样品的采集和处理

为了分析不同径级根凋落物分解的过程,将其分为 5 个等级: <0.5mm, 0.5—1mm, 1—2mm, 2—5mm 和 >5mm。在根的采集过程中,选取新鲜的根,因为这样的根样品能够最好的代表即将开始分解的根凋落物(Hobbie *et al.* 2010)。

2010 年 5 月初,在样地内采集林龄为 25 龄的樟子松叶凋落物,和 0-30cm 深度的根系,并将不同样地采集到的样品混匀,进行风干。风干两周后,去除根系上残留的土壤,将叶凋落物记为 L,根样本按照不同径级分别标记为 R1(<0.5mm), R2(0.5—1mm), R3(1—2mm), R4(2—5mm)和 R5(>5mm)。将根剪成 2-3cm 长度,便于装袋、称量。

将所有样品风干至恒重 (Mo *et al.* 2006),称量初始样品的风干重量、烘干重量(65℃烘干 48h),并求出校正系数,用来校正风干的分解样品的烘干重量。分解袋法(Crossley and Hoglund, 1962)用于定期回收分解样品。将分解样品按照不同的类型(即 L、R1、R2、R3、R4 和 R5)放入 20cm*20cm 分解袋内,每一类型设定 4 个重复样本。根据样品采集量的不同,L 分解袋中每袋大约放入 4.500g 叶凋落物风干样品,R1、R2、R3、R4、R5 分解袋中每袋分别放入约 0.700g、0.800g、1.000g、2.200g 和 2.000g 相应的风干样品。2010 年 6 月初分别将其埋入 3 个不同深度的样地土壤中,分别为 0-5cm, 5-10cm 和 10-20cm。为了使样品更好的与土壤接触,将其以 45°倾斜埋入(Ostertag *et al.* 2008)。

2.3 凋落物样品的回收及化学处理

由于坝上地区气候较为寒冷,通常每年 10 月份即开始降雪,而根据年际间冷暖程度不同,第二年的 4、5 月份积雪才能开化,并且分解袋的收取过程只能是在无雪的季节才能完成。所以在埋入分解袋后 70 天(2010 年 8 月)、330 天(2011 年 5 月)、400 天(2011 年 7 月)和 470 天(2011 年 10 月),分别对分解袋进行回收。回收后,用镊子拣出分解的根和叶,除去污染的土

壤和其它杂质，并烘干至恒重(Ostertag *et al.*2008)。

采用重铬酸钾外加热法和凯氏定氮法测定样品的碳和氮含量百分比，采用 Ryan *et al.*(1990)的方法测定生物量组分，用氯仿甲醇溶液处理得到 Extractive（抽提物），然后用浓硫酸处理得到 AS（酸溶性生物量组分）和 AIF（酸不溶组分）的百分比，并用马弗炉烧灰，得到的灰分含量用于进行校正。其中，AS 近似等于纤维素与半纤维素的含量，AIF 近似等于木质素的含量 (Effland,1977)。

此外，采用 EM50 土壤温度水分测定仪连续测定了样地内分解期（2010 年 6-10 月和 2011 年 5 月-10 月）3 个深度的土壤温度和土壤体积含水百分比，并求出土壤生长及平均温度和年平均含水百分比。

2.4 数据分析

基于四次取样后凋落物的残留质量，计算出了凋落物残留质量百分比。同时采用负指数方程 $y=e^{-kt}$ (Silver and Miya, 2001)，计算出了各类凋落物在不同土壤深度的年分解速率 k 。这里， y 是在时间 t （天）时凋落物质量残留率。

同时，为了测定根凋落物的不同径级、根和叶凋落物的不同类型和土壤深度对根和叶凋落物的分别影响，还针对这几种因素分别进行了单因素方差分析和回归分析，以判断其影响的显著性（检验水平均为 $P<0.05$ ）。所有的统计分析在软件 PASW Statistics 18.0 中完成。

第三章 实验结果

3.1 凋落物残留量

在同一深度情况下，不同类型的凋落物残留质量百分比并不相同，同种凋落物在不同的土壤深度的残留量也不相同（图 3.1）。各个深度的植物凋落物在 0-70 天内质量明显减少($P=0.001$ ， $F=15.591$)，但是在之后一直到 470 天时，分解速度明显减慢，甚至基本保持不变，凋落物残留量无显著性差异($P=0.162$ ， $F=1.768$)。

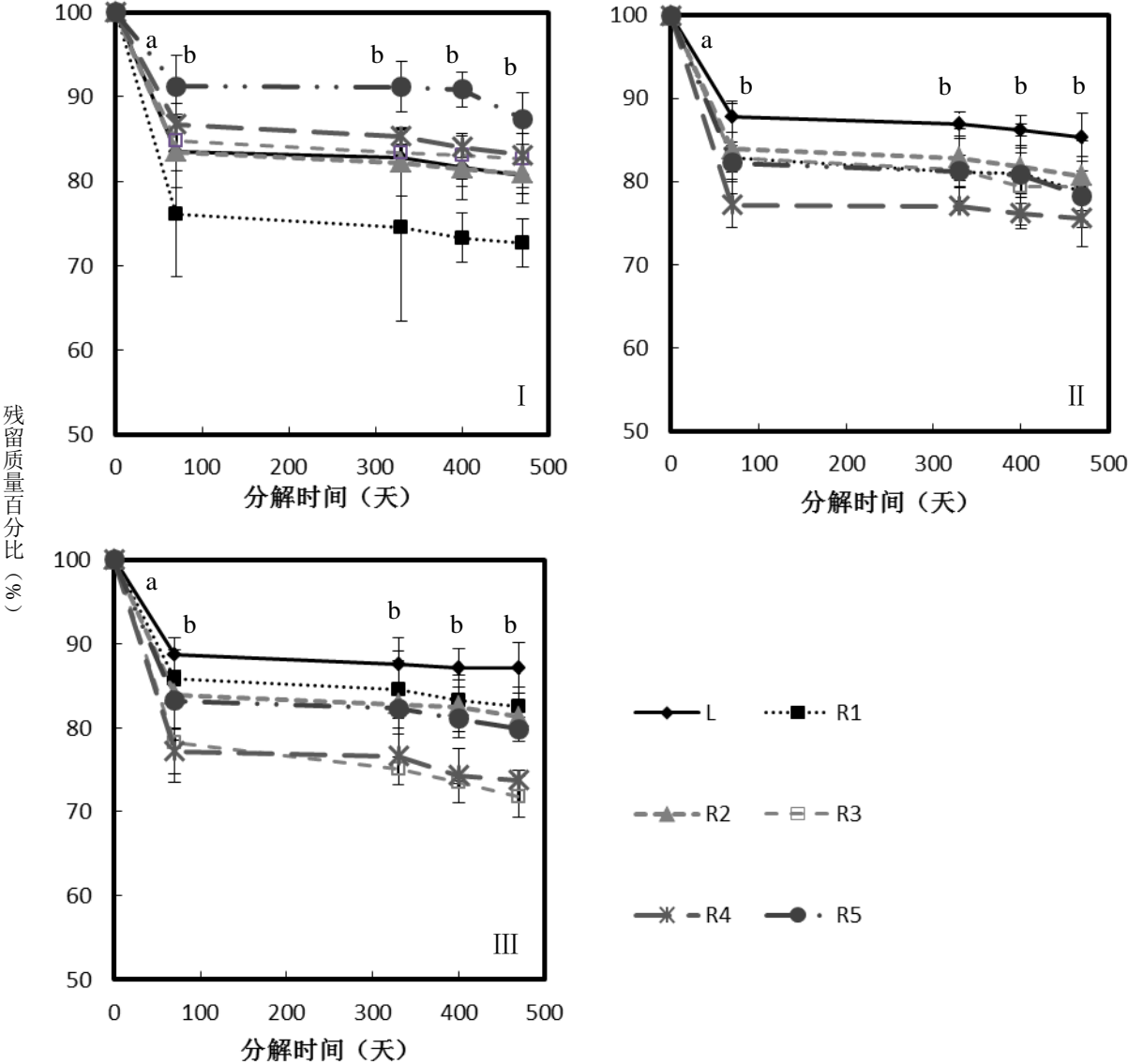


图 3.1 I、II、III分别为土壤深度为 0-5cm、5-10cm 和 10-20cm 条件下不同类型凋落物在每次回收时的残留质量百分比。图中的字母表示每次取样时的残留量百分比是否有显著性差异，相同字母表示没有，不同字母表示有。

在原位分解过程中，至分解的第 470 天，根的平均残留量是 78.18%，叶的平均残留量是 80.69%，高于根的值，并且二者差异显著 ($P=0.035$, $F=5.669$)。在同种样品内做比较，发现根和叶的原位分解速度都较快，即根在地下分解的速度高于地表分解（地表残留量 81.36%，地下残留量 78.18%），但二者差异不显著($P=0.521$, $F=0.435$)；叶在地表分解速度显著高于地下分解（地表残留量 80.69%，地下残留量 86.21%， $P=0.029$, $F=11.007$)。

同时，图 3.1(I)中地表分解过程，根的残留量数据不如地下分解过程(II)(III)集中，比较分散，叶虽然并不是地表分解过程中残留量最小的，但其平均值小于根。在地下分解过程中，根样品的残留量分布比较集中，且均小于叶，可见叶凋落物在地下分解较缓慢。

表 3.1 初始样品元素含量及生物量组分与分解率 k 相关分析

		C(%)	N(%)	P(mg/g)	C:N	N:P
分解率 k	P	0.051	0.092	0.493	0.158	0.063
	R	0.300	-0.260	0.107	0.219	-0.391
		Extractives(%)	AS(%)	AIF(%)	AIF:N	AIF:P
分解率 k	P	0.314	0.249	0.788	0.000**	0.459
	R	0.157	-0.180	0.042	-0.658	-0.116

*.在 0.05 水平上显著相关

**.在 0.01 水平上显著相关

将初始样品元素含量及生物量组分与不同类型凋落物分解率 k 进行相关分析（表 3.1），发现分解率 k 只与 AIF:N 呈显著相关($P=0.000$, $F=10.862$)，与其他指标都无显著性关系，对分解率 k 和 AIF:N 进行回归（图 3.2），二者呈显著负相关。

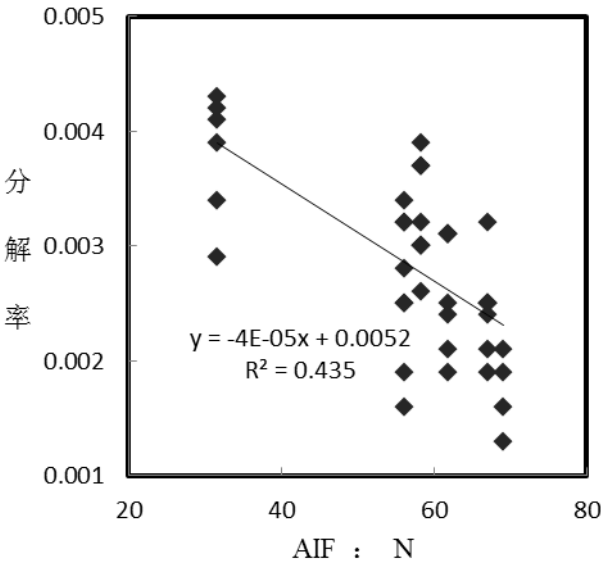


图 3.2 分解率 k 和 AIF:N 之间的关系

3.2 根的径级

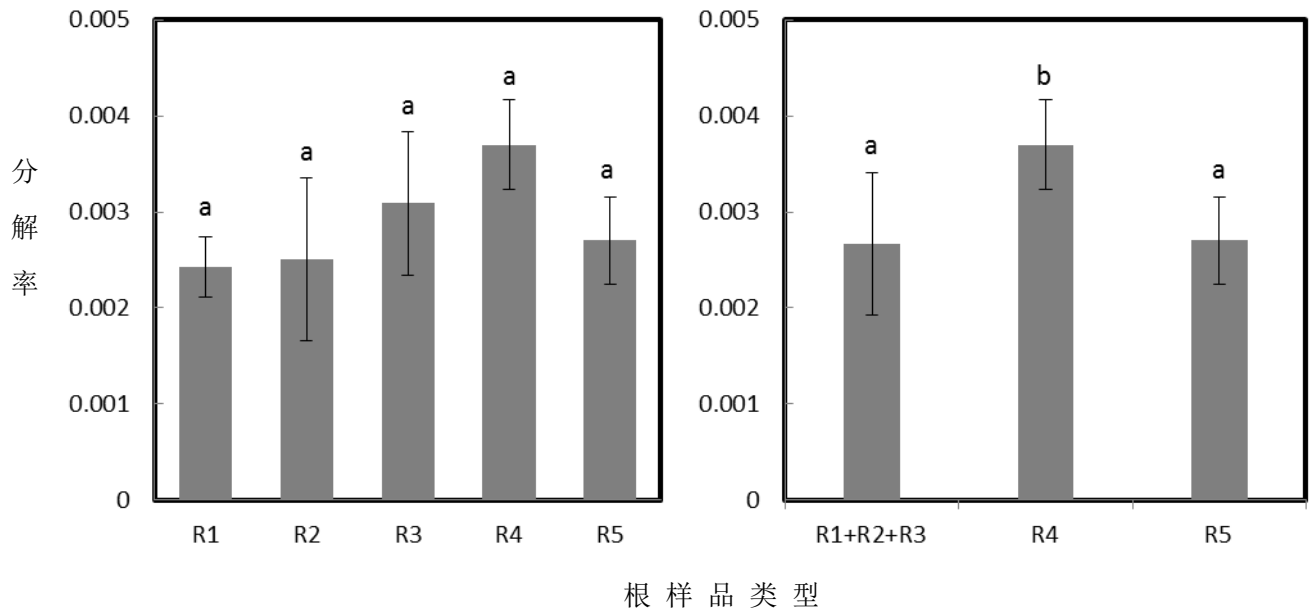


图 3.3 不同根样品的分解率，图 I 表示将根分为 5 类时各类根的分解率，图 II 表示将 R1、R2、R3 合并后三类根样品的分解率，其中字母表示与其他类型根样品分解率比较是否具有显著性差异，相同字母表示没有，不同字母表示有。

将不同径级根的分解率按根的径级(R1, R2, R3, R4, R5)进行单因素方差分析，结果表明，按照上文中将根样品分为 5 类，不同径级的根对其分解率并无显著的影响($F=1.941$, $P=0.117$)。但是，由于在植物根的分解研究中,大部分学者都采用细根(fine root, $<2\text{mm}$)(Aber *et al.*1990; Harmon *et al.*2009; Cusack *et al.*2009; Wang *et al.*2010)作为研究对象，因此将根样品数据进行合并，分为 $<2\text{mm}$ 、 $2-5\text{mm}$ 和 $>5\text{mm}$ 三类，再次进行单因素方差分析，发现按照新的分类方法，根的径级与分解率呈显著性相关($F=3.319$, $P=0.044$)。再将这三类根样品两两对比，进行单因素方差分析，发现 $<2\text{mm}$ 的根与 $2-5\text{mm}$ 的根样品分解率存在显著差异($P=0.041$, $F=6.859$)， $2-5\text{mm}$ 的根与 $>5\text{mm}$ 的根样品存在显著差异($P=0.020$, $F=6.260$)，而 $<2\text{mm}$ 的根样品与 $>5\text{mm}$ 的根样品无显著性差异($P=0.076$, $F=3.310$)。到分解实验结束时的 470 天时， $>5\text{mm}$ 的根样品的平均残留量(81.83%)要高于 $2-5\text{mm}$ 和 $<2\text{mm}$ 的根的平均残留量（二者分别为 77.49%和 78.96%），说明其分解的最慢。

3.3 土壤深度

根据前文研究，R1、R2 和 R3 三类根样品在研究分解时可以进行合并，因此在分析土壤深度及相关物理性质对凋落物分解的影响时，将分解样品分为四类，分别用分解率进行相关性分析。结果表明，土壤深度及相关物理性质对 L、R4 和 R5 三类样品的分解过程都有显著性影响，对于 R1+R2+R3 的分解不存在显著性影响（表 3.3）。

分解期土壤平均温度和平均含水量都与土壤深度显著相关，前者呈负相关，后者呈正相关，

即在所研究的土层深度范围内，土壤温度随深度加大而下降，而土壤含水量呈增加趋势。对于叶凋落物，随着土层的加深，土壤湿度的增大，分解逐渐变缓慢。对于根样品，细根的分解不受土壤深度及温度、湿度的影响，径级>2mm 的两类粗根 R4 和 R5 的分解速度会随着土层的加深变快。前面已经提到，土壤湿度与土壤深度呈正相关，也就是说，粗根分解率的变化趋势与土壤湿度的变化趋势是相一致的，二者呈现显著正相关，而分解率的变化与土壤温度并没有显著关系。

表 3.2 各类凋落物与不同深度土壤性质相关性分析

		土壤深度	土壤年平均温度	土壤年平均含水百分比
分解期土壤平均温度	R	-0.694*	—	—
	P	0.012	—	—
分解期土壤平均含水百分比	R	0.955**	—	—
	P	0.000	—	—
L	R	-0.719**	0.248	-0.789**
	P	0.008	0.137	0.002
R1+R2+R3	R	-0.028	-0.071	-0.064
	P	0.877	0.696	0.724
R4	R	0.718**	-0.125	0.839**
	P	0.009	0.699	0.001
R5	R	0.615*	-0.031	0.751**
	P	0.033	0.923	0.005

*.在 0.05 水平上显著相关

**.在 0.01 水平上显著相关

3.4 凋落物碳、氮元素的动态变化

观察凋落物碳、氮元素动态变化时，采取与上文中同样的方法，将 R1、R2 和 R3 合并，与叶凋落物 L 和 R4、R5 两类根样品进行比较（图 2）。不同样品的碳元素含量百分比在分解过程中主要呈下降趋势，只有径级>5mm 的 R5 在分解期的前 70 天出现上升，而随后呈下降趋势，最终与 R4 碳含量相接近。细根的初始碳含量最低，其在分解过程中也始终呈下降趋势。叶凋落物初始碳含量最高，而下降速度也最快，最终和 R4、R5 碳含量相接近。

各类凋落物中氮含量的变化则差别较大，叶凋落物在分解期前 70 天中，氮含量上升速度很快，经过第 70-330 天的冬季后，氮含量有少许下降，进入第二年的分解期后，氮含量又逐渐上升。R1、R2 和 R3 的细根样品，从分解期开始至第 330 天，氮含量都处于上升趋势至临界值，此后开始下降。径级>2mm 的粗根 R4 和 R5 氮含量变化比较相似，在第一年的分解期，二者都呈下降趋势，第一年的冬季氮含量持续有少许下降，而进入第二年的分解期后，氮含量开始上升，至实验结束还未达到样品初始氮含量，依然处于上升状态。

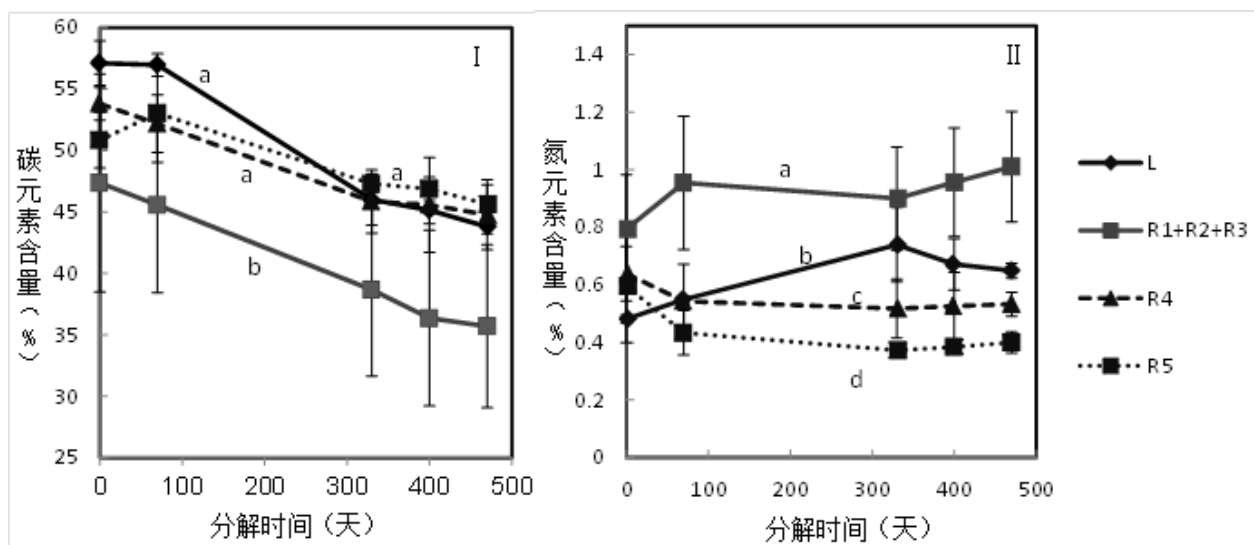


图 3.4 I 为凋落物原位分解时碳元素含量变化，II 为氮元素含量变化。字母表示在全部分解时间内不同凋落物类型之间是否具有显著差异，相同字母表示没有，不同字母表示有。

第四章 讨 论

4.1 根和叶分解过程对比

在比较根和叶的分解过程中,凋落物的化学物质组成的影响一直都是比较复杂的问题(Cusack *et al.*2009),出现过不同的结果和观点。在很多研究中,根比叶凋落物含有更多的木质素和更高的 C:N (Galletti *et al.* 1993; Moretto *et al.* 2001; Moretto and Distel, 2003; Abiven *et al.* 2005), 这会导致同一物种的根分解速率低于叶凋落物(Bloomfield *et al.* 1993; Bryant *et al.*1998; Gorissen and Cotrufo,2000; Kemp *et al.*2003; Majdi 2004)。而在我们这个实验中,根比叶凋落物的残留百分比小,即分解的更快,是因为根样品具有较低的 AIF:N。Ostertag and Hobbie(1999)也提出,根比叶凋落物在营养不十分充分的条件下分解得快,部分原因是根比叶具有更低的 AIF:N(表 4.1)。同时,在早期分解过程中,氮浓度被认为是非常重要的;而在后期分解中,木质素含量被认为是最重要的影响因素(Berg and Matzner,1997)。这也能够解释在本实验中,根凋落物原位分解速度高于叶的现象。分解进入到后期,随着木质素含量对分解作用影响的扩大,根的分解速率很有可能越来越慢,而木质素含量相对较小的叶凋落物的分解速率会变大,逐渐超过根,这是从凋落物样品初始元素含量和生物量组分角度进行的分解过程的预测。

表 4.1 初始样品凋落物元素含量及生物量组分(mean±SD), R 是将 R1 至 R5 合并后,根样品总体的分析结果。

凋落物种类	C(%)	N(%)	P(mg/g)	C:N	N:P
L	57.12±1.81	0.48±0.01	0.19±0.02	118.74±6.59	24.94±1.37
R1	35.31±9.43	1.05±0.12	0.56±0.08	33.32±5.98	18.75±0.67
R2	50.92±2.84	0.77±0.07	0.49±0.03	66.77±8.74	15.66±2.31
R3	52.85±2.21	0.63±0.09	0.40±0.08	85.14±12.02	16.35±4.44
R4	53.80±1.44	0.64±0.10	0.52±0.04	85.76±13.58	12.40±2.62
R5	50.84±2.45	0.60±0.20	0.35±0.06	92.44±29.74	17.06±4.04
R	48.74±5.62	0.74±0.10	0.46±0.05	72.69±9.36	16.04±2.64
凋落物种类	Extractives(%)	AS(%)	AIF(%)	AIF:N	AIF:P
L	18.64±14.26	48.01±15.79	33.35±4.03	69.16±7.17	1723.53±192.21
R1	10.59±4.23	56.28±5.44	33.13±2.98	31.68±1.22	594.41±43.34
R2	7.50±7.37	49.70±4.97	42.81±5.01	56.22±10.07	865.93±83.84
R3	10.78±6.70	47.67±15.01	41.56±12.48	67.14±21.22	1050.62±271.96
R4	12.54±3.83	51.24±5.04	36.23±3.42	58.39±14.57	697.81±66.70
R5	9.71±9.88	56.30±8.99	33.99±1.95	61.93±20.40	999.95±170.23
R	10.22±6.38	52.24±7.49	37.54±4.22	55.07±13.58	841.74±79.44

但是, Hobbie *et al.*(2010)在分析了不同物种地表和地下分解过程后指出,影响根和叶凋落物

分解的元素可能是不同的。例如，较高的半纤维素含量会促进根的分解，较低的木质素含量和较高的 Ca 含量会促进叶凋落物的分解。在本研究中，根样品确实具有较高的 AS（近似看作纤维素和半纤维素的总和）含量，叶凋落物具有较低的木质素含量，但是由于仅针对樟子松一个物种进行了实验，所以还无法对半纤维素和木质素对根和叶分解影响的大小进行比较。

同时，植物凋落物在地上和地下分解过程中可能存在很大的不同，叶凋落物在是否为原位分解条件下表现出的差异很好的证实了这一点。根和叶凋落物在原位分解时的残留量都小于非原位分解，但是在地表和地下两种分解条件下，叶凋落物的分解率存在显著性差异，而根却没有。也就是说，地表和地下的分解环境对于根的分解影响较小，这可能是由于不同径级的根系在所研究土壤深度范围内均有分布，当综合对根样品进行分析时，由于各类型根样品具有均匀的分解位置，并不存在是否为原位分解的差异。然而，叶凋落物在地表的分解要比将其埋在地下时快。Chen *et al.*(2001)认为，植物凋落物化学组成对根和叶分解的影响可能是变化的，因为微生物分解者群落及其活动在不同环境对不同凋落物种类的影响都存在差异。当凋落物处于原位分解状态时，微生物分解者群落能够更有效的对其进行分解，分解者的活动更为旺盛，而处于非原位分解条件时，微生物对凋落物的分解作用受到一定程度的抑制。Ayres *et al.* (2001)进行了叶凋落物移植分解实验(leaf litter transplant experiments)发现，原位优势(home-field advantage)会促进叶凋落物的分解，并认为土壤生物群落与其相关的植物物种有着密切联系，土壤微生物会从长期的进化和短期的生理适应两个方面来加强对植物凋落物分解的专一性。Ayres *et al.*是从位置角度分析了原位优势对分解的影响，从本文的研究结果来看，在叶凋落物的分解过程中土壤深度也具备和位置相似的原位优势。

4.2 根的径级对分解过程的影响

按照之前对根较为细化的分类方法，发现不同径级的根样品之间分解率并没有显著性的差异($F=1.941$, $P=0.117$)，也就是说，较为细化的分类方法无法区分不同径级的根的分解情况。但是受到之前大量研究的启发(Aber *et al.*1990; Harmon *et al.*2009; Cusack *et al.*2009; Fornara *et al.*2009; Wang *et al.*2010)，由于根径 $<2\text{mm}$ 的“细根(fine root)”在生态系统年初级生产力中占据了很大一部分，并且其周转率能够很好地表征土壤有机质的组成和生态系统的养分循环(Fornara *et al.*2009)，便将根径 $<2\text{mm}$ 的样品进行合并分类，单因素方差分析结果表明，其与分解率呈显著性相关($F=3.319$, $P=0.044$)，这也说明同一物种的凋落物在分解过程中，不同径级的根分解存在差异，不能只对细根进行研究，也不能片面的用细根的研究结果代表全部根的分解情况。

同时，图 3.3 表明径级在 2-5mm 的根样品与 $<2\text{mm}$ 和 $>5\text{mm}$ 的根样品的分解率均存在显著差异，而 $<2\text{mm}$ 和 $>5\text{mm}$ 的根之间分解率差异不显著。Ludovici(2006)在对比了根径 $<2\text{mm}$ 和 2-5mm 的根的分解后，指出由于细根有较高的 N、P、Ca 含量，所以对于不同径级的根的研究结果要分开对待，细根的研究结果并不能完全代表所有根样品的分解情况。同时，还有研究认为外生菌根真菌会减慢细根的分解(Langley and Hungate, 2003)，因为外生菌根真菌进入细根后会形成真菌鞘(fungal sheath)，其中富含几丁质，其中含有较高的氮含量，并且不易分解。另一方面，除了元素

含量的差异, 根径本身的粗细程度也会影响到分解情况, 较粗的根会阻碍分解者活动, 从而减缓了分解的速度。

4.3 土壤深度对分解过程的影响

在研究的土壤深度范围 0-20cm 内, 分解期内土壤平均温度随深度的加深显著下降, 而土壤平均含水量显著上升。经过相关分析发现, 径级<2mm 的细根不受土壤深度变化的影响, 而其他样品, 叶凋落物 L 和>2mm 的两类根样品 R4、R5 与土壤深度和土壤平均含水量都呈显著相关, 但是与土壤温度没有显著关系。具体来讲, 土壤深度加深, 土壤湿度增大, 叶凋落物的分解率减小, 而根凋落物的分解率增大。

Bontti *et al.*(2009)在研究了中北美地区草原植被凋落物分解后, 认为温度并不能很好的解释根和叶凋落物分解的变化, 而湿度的差别可以解释部分原因, 对于同一类型的凋落物, 土壤相对较高的湿度会加速地下的分解作用。本研究的结果说明, 较高的湿度会加速 R4 和 R5 的分解速度, 在降水受限的地区, 越靠近地表, 土壤水分越容易蒸散, 同时升高的土壤温度也促进了水分的蒸发作用, 因此降低了土壤含水量, 减慢了粗根的分解。然而, 叶凋落物与粗根的分解情况恰好相反, 是随着土壤深度增加而减慢。这说明, 当叶凋落物在地下分解时, 离开了原位分解环境, 微生物群落组成发生了改变, 这时对叶凋落物分解起决定作用的已不再是土壤的湿度或者温度, 而是分解者的活动。因为土层越深, 分解环境越偏离叶凋落物的原位分解环境, 因此速度越慢。可见, 原位分解环境在叶凋落物分解过程中起到了十分关键的作用。同时, 我们发现径级<2mm 的细根的分解率与土壤深度并没有显著关系, 或者说其分解并没有受到土壤深度的影响, 我认为原因与叶凋落物分解相似, 因为细根主要分布在土壤表层, 当其离开原位分解环境, 放置在深层土壤中分解时, 分解速度将会减慢, 但是由于本实验土壤深度梯度设置的范围较小, 分解率的这种下降趋势并没有能够明显的体现出来。

Wang *et al.*(2010)发现, 对于其研究的四个不同的树的物种, 土壤湿度与它们细根和叶凋落物的分解率均呈正相关, 土壤湿度对细根和叶凋落物的分解有相似的作用, 同时认为土壤湿度是促使细根和叶凋落物具有相似分解过程的主要因素。该研究是将叶凋落物放置在不同湿度的土壤表面观察分解状况, 而本研究是将同种叶凋落物放置在生长环境的不同深度土壤中进行分解, 因此得到了不同的结论。Cusack *et al.*(2009)认为, 由于叶凋落物在地表进行分解, 暴露在空气中, 易受到降水和干旱等自然条件的影响, 而根在土壤中分解, 不易受到外界气候的直接影响, 因此二者的分解过程存在差异。同时, 地上和地下的微生物分解者群落及其活动对根和叶凋落物的化学组成元素的反应也是不同的, 这也会造成二者分解过程的一些变化。本研究中根和叶凋落物对土壤湿度变化的不同响应, 证实了这个观点。近些年也有研究发现, 紫外辐射也会加速半干旱生态系统的分解速度(Parton, 2007), 因为叶凋落物和浅土层的细根在分解过程中会接受到较多的紫外辐射, 这也可能是影响其分解的因素之一, 所以如果将叶凋落物放置在地下, 无法接触到紫外线辐射, 也会减缓分解速率。这些观点都从不同角度解释了在本实验中根和叶凋落物对土壤湿度不同的响应情况。

4.4 凋落物碳、氮元素的动态变化

在整个分解过程中，碳元素含量始终处于下降趋势。由于叶凋落物初始 C/N 值最高(表 4.1)，其碳含量下降速度也最快，这与 Wang *et al.*(2010)的结论一致，叶凋落物较高的初始 C/N 解释了它的碳含量比根样品下降的更快。

Parton(2007)认为，对于叶凋落物，当平均碳氮比降低至 40 以下时，氮元素开始净释放，这被认为是氮开始释放的临界值。由于本研究中取样次数等条件的限制，无法准确计算出樟子松根和叶凋落物氮净释放的临界值，但是依然可以观察到类似现象。本实验中，叶凋落物在原位分解期间，分解期内氮含量均呈现上升趋势，而在冬季分解停滞的阶段内，氮含量有微小下降，在分解期内，叶凋落物碳氮比从 118.61 降低至 68.42，但是始终处于较高的状态，因此一直处于氮固持阶段。而在冬季非分解期，由于在地表受到融雪等因素影响，一小部分可溶性氮经过淋溶作用损失，而进入分解期后，氮固持作用继续进行，导致出现了上文中的变化趋势。径级<2mm 的细根初始碳氮比为 59.62，并且至第 330 天减少到 42.97，在此过程中，氮含量都呈上升趋势，说明微生物对细根的分解十分旺盛，其周转率可以很好地表征土壤有机质的组成和生态系统的养分循环(Fornara *et al.*2009)。但是在此之后，细根凋落物样品碳氮比较低，开始净释放氮元素，含量逐渐下降。与细根相比较，径级>2mm 的粗根的分解过程就不那么活跃了，其氮元素含量从实验开始呈下降趋势，因为粗根分解过程不如细根旺盛，分解者对其氮元素需求并不高，所以在第一年的分解期和冬季粗根氮元素含量减少，但是进入第二年的分解期后，也许由于分解活动继续进行，为了补充冬季由于淋溶等作用损失掉的氮元素，再次出现氮的固持作用，直至分解期结束，氮含量也未能上升至初始值，所以在第二年分解期内，氮的矿化作用始终没有进行。由此，可以预测到在长期分解实验中，粗根的氮含量很可能处于在临界值附近波动的状态。

结 论

本研究可以得到以下结论:

- 1、 在原位分解条件下, 樟子松根比叶凋落物分解的更快, 并且主要受到 $A/F/N$ 的控制;
- 2、 不同径级的根的分解速度不同, 会受到元素含量和径级本身的影响, 并且可以按照 2mm 和 5mm 为界限对根进行分类;
- 3、 土壤深度对樟子松根和叶凋落物的分解有显著影响, 根分解主要受土壤含水量影响, 叶凋落物分解主要受到微生物和气候等条件的影响;
- 4、 在分解过程中, 樟子松各类凋落物样品碳含量均呈下降趋势, 而氮含量变化趋势各不相同, 这受到分解者活动和淋溶作用等影响。

致 谢

本研究及学位论文是在我的导师王娓老师的亲切关怀和悉心指导下完成的。她严肃的科学态度，严谨的治学精神，精益求精的工作作风，深深地感染和激励着我，在此谨向王娓老师致以诚挚的谢意和崇高的敬意。同时，我还要感谢城市与环境学院生态学系的吉成均老师、陈伟乐师兄、陶娜师姐、张馨月师姐、杜志宏师兄、张钰同学，谢谢对我的教导和帮助，让我克服一个个困难和疑惑，直至本文的顺利完成。

参考文献

- Aber JD, Melillo JM, McLaugherty CA (1990) Predicting long-term patterns of mass loss, nitrogen dynamics, and soil organic matter formation from initial fine litter chemistry in temperate forest ecosystems. *Can. J. Bot.* 68:2201-2208
- Abiven S, Recous S, Reyes V, Oliver R (2005) Mineralisation of C and N from root, stem and leaf residues in soil and role of their biochemical quality. *Biology and Fertility of Soils* 42:119-128
- Austin AT and Ballarín CL (2010) Dual role of lignin in plant litter decomposition in terrestrial ecosystems. *PNAS* vol. 107, no. 10, 4618–4622
- Ayres E, Steltzer H, Simmons BL, Simpson RT, Steinweg JM, Wallenstein MD, Mellor N, Parton WJ, Moore JC, Wall DH (2009) Home-field advantage accelerates litter decomposition in forests. *Soil Biology & Biochemistry* 12:1-5
- Berg B, Johansson M, Meentemeyer V and Kratz W. (1998) Decomposition of tree root litter in a climatic transect of coniferous forests in northern Europe: a synthesis. *Scandinavian Journal of Forest Research* 13:402-412
- Berg B, Matzner E (1997) Effect of N deposition on decomposition of plant litter and soil organic matter in forest systems. *Environmental Reviews* 5:1-25
- Berg B, McLaugherty C (2008) Plant litter: decomposition, humus formation, carbon sequestration (second edition)[M]. Springer-Verlag Berlin Heidelberg.
- Bloomfield J, Vogt KA, Vogt DJ (1993) Decay rate and substrate quality of fine roots and foliage of two tropical tree species in the Luquillo Experimental Forest, Puerto Rico. *Plant and Soil* 150:233-245
- Bontti EE, Decant JP, Munson SM, Gathany MA, Przeszlowska A, Haddix ML, Owens S, Burke IC, Parton WJ, Harmon ME (2009) Litter decomposition in grasslands of Central North America (US Great Plains). *Global Change Biology*, 15, 1356–1363
- Bryant DM, Holland EA, Seastedt TR, Walker MD (1998) Analysis of litter decomposition in an alpine tundra. *Can. J. Bot.* 76:1295-1304
- Chen H, Harmon ME, Griffiths RP (2001) Decomposition and nitrogen release from decomposing woody roots in coniferous forests of the Pacific Northwest: a chronosequence approach. *Can. J. For. Res.* 31:246-260
- Crossley DAJ, Hoglund MP (1962) A litterbag method for the study of microarthropods inhabiting leaf litter. *Ecology* 43:571-573
- Cusack DF, Chou WW, Yang WH, Harmon ME, Silver WL and The LIDET TEAM (2009) Controls on long-term root and leaf litter decomposition in neotropical forests. *Global Change Biology* 15, 1339–1355
- Effland MJ (1977) Modified procedure to determine acid insoluble lignin in wood and pulp. *Tech. Assoc. Pulp Pap. Ind.* 60(10): 143-144
- Fornara DA, Tilman D, Hobbie SE (2009) Linkages between plant functional composition, fine root processes and potential soil N mineralization rates. *Journal of Ecology*, 97:48-56
- Galletti GC, Reeves JB, Bloomfield J, Vogt KA, Vogt DJ (1993) Analysis of leaf and fine-root litter from a subtropical montane rain forest by pyrolysis-gas chromatography mass spectrometry. *Journal of Analytical and Applied Pyrolysis* 27:1-14
- Gijsman AJ, Alarcón HF, Thomas RJ (1997) Root decomposition in tropical grasses and legumes, as affected by soil

- texture and season. *Soil Biol Biochem* 29:1443-1450
- Gill RA, Burke IC (2002) Influence of soil depth on the decomposition of *Bouteloua gracilis* roots in the shortgrass steppe. *Plant and Soil*, 241:233-242
- Gorissen A, Cotrufo MF (2000) Decomposition of leaf and root tissue of three perennial grass species grown at two levels of atmospheric CO₂ and N supply. *Plant and Soil* 224:75-84
- Grabovich MY, Dubinina GA, Churikova VV, Churikov SN, Korovina TI (1995) Mechanisms of synthesis and utilization of oxalate inclusions in the colorless sulfur bacterium *Macromonas bipunctata*. *Mikrobiologiya* 64:630-636
- Harmon ME, Silver WL, Fasth B, Chen H, Burke IC, Parton WJ, Hart SC, Curiie WS and LIDET (2009) Long-term patterns of mass loss during the decomposition of leaf and fine root litter: an intersite comparison. *Global Change Biology* 15, 1320–1338
- Hätenschwiler S, Tiunov AV, Scheu S (2005) Biodiversity and litter decomposition in terrestrial ecosystem. *Annu. Rev. Eco. Evol. Syst.* 36:191-218
- Hobbie SE, Oleksyn J, Eissenstat DM, Reich PB (2010) Fine root decomposition rates do not mirror those of leaf litter among temperate tree species. *Oecologia*, 162:505–513.
- Kemp PR, Reynolds GF, Virginia RA, Whitford WG (2003) Decomposition of leaf and root litter of Chihuahuan desert shrubs: Effects of three years of summer drought. *Journal of Arid Environments* 53:21-39
- Keplin B, Hüttel RF (2001) Decomposition of root litter in *Pinus sylvestris* L. and *Pinus nigra* stands on carboniferous substrates in the Lusatian lignite mining district. *Ecological Engineering* 17:285-296
- Langley JA, Hungate BA (2003) Mycorrhizal controls on belowground litter quality. *Ecology* 84:2302-2312
- Ludovici KH, Kress LW (2006) Decomposition and nutrient release from fresh and dried pine roots under two fertilizer regimes. *Can. J. For. Res.* 36: 105-111
- Majdi H (2007) Root and root-lignin degradation in a Norway spruce stand: Effects of long-term nitrogen addition. *Plant Biosystems*, 141:214-221
- McClagherty C, Berg B (1987) Cellulose, lignin, and nitrogen concentrations as rate regulating factors in late stage of forest litter decomposition. *Pedobiologia* 30:101-112
- Mo JM, Brown S, Xue JH, Fang YT, Li ZA (2006) Response of litter decomposition to simulated nitrogen deposition in disturbed, rehabilitated and mature forests in subtropical China. *Plant Soil* 285:135-151
- Moretto AS, Distel RA (2003) Decomposition of and nutrient dynamics in leaf litter and roots of *Poa ligularis* and *Stipa Gyneriodes*. *Journals of Arid Environments* 55:503-514
- Moretto AS, Distel RA, Didone NG (2001) Decomposition and nutrient dynamic of leaf litter and roots from palatable and unpalatable grasses in a semi-arid grassland. *Applied Soil Ecology* 18:31-37
- Ostertag R, Hobbie SE (1999) Early stages of root and leaf decomposition in Hawaiian forests: effects of nutrient availability. *Oecologia*, 121:564–573.
- Ostertag R, Marín-Spiotta E, Silver WL, Schulten J (2008) Litterfall and decomposition in relation to soil carbon pools along a secondary forest chronosequence in Puerto Rico. *Ecosystems* 11:701-714
- Parton B (2007) Effects of ultraviolet radiation on the early stages of litter decomposition in three contrasting grassland ecosystem. *ESA/SER Joint Meeting*.

- Parton W, Silver WL, Burke IC, Grassens L, Harmon ME, Currie WS, King JY, Adair EC, Brandt LA, Hart SC, Fasth B (2007) Global-scale similarities in nitrogen release patterns during long-term decomposition. *Science* 315:361-364
- Prescott CE, Vesterdal L, Preston CM, Simard SW (2004) Influence of initial chemistry on decomposition of foliar litter in contrasting forest types in British Columbia. *Can. J. For. Res.* 34:1714-1729
- Ryan MG, Melillo JM, Ricca A (1990) A comparison of methods for determining proximate carbon fractions of forest litter. *Can. J. For. Res.* 20:166-171
- Scott NA, Binkley D (1997) Foliage litter quality and annual net N mineralization: comparison across North American forest sites. *Oecologia* 111:151-159
- Sinsabaugh RL *et al.* (2008) Stoichiometry of soil enzyme activity at global scale. *Ecology Letters* 11:1252-1264
- Stefano M, John AT, Robert BJ, Amilcare P (2010) Stoichiometric controls on carbon, nitrogen, and phosphorus dynamics in decomposing litter. *Ecological Monographs*, 80(1):89-106
- Wang H, Liu SR, Mo JM (2010) Correlation between leaf litter and fine root decomposition among subtropical tree species. *Plant Soil* 335:289-298

北京大学学位论文原创性声明和使用授权说明

原创性声明

本人郑重声明： 所呈交的学位论文，是本人在导师的指导下，独立进行研究工作所取得的成果。除文中已经注明引用的内容外，本论文不含任何其他个人或集体已经发表或撰写过的作品或成果。对本文的研究做出重要贡献的个人和集体，均已在文中以明确方式标明。本声明的法律结果由本人承担。

论文作者签名： 日期： 年 月 日

学位论文使用授权说明

(必须装订在提交学校图书馆的印刷本)

本人完全了解北京大学关于收集、保存、使用学位论文的规定，即：

- 按照学校要求提交学位论文的印刷本和电子版本；
- 学校有权保留学位论文的印刷本和电子版，并提供目录检索与阅览服务，在校园网上提供服务；
- 学校可以采用影印、缩印、数字化或其它复制手段保存论文；
- 因某种特殊原因需要延迟发布学位论文电子版，授权学校 ☐ 一年 / ☐ 两年 / ☐ 三年以后，在校园网上全文发布。

(保密论文在解密后遵守此规定)

论文作者签名： 导师签名：

日期： 年 月 日

专题研究报告

七星湖和泰丰湖区植被概况

刘鸿雁

一、植物群落类型

1、水生植物群落

七星湖和泰丰湖区水生植物种类包括沉水植物和浮水植物两大类。前者常见的种类有马来眼子菜、两栖蓼、狐尾藻, 后者常见种类有萍蓬草和荇菜。在七星湖水体中主要以浮水植物占优势, 而在泰丰湖水体中主要以沉水植物占优势。

2、沼泽植物群落

沼泽植物群落主要由沼生 (挺水) 植物组成, 包括禾本科和莎草科的种类以及大量的双子叶植物。在水体附近为假鼠妇草沼泽, 主要以禾本科和莎草科植物为主, 常见禾本科种类有假鼠妇草、假稻等。常见的莎草科种类包括灰脉苔草、柄苔草和红穗苔草等。在七星湖水体附近较广泛分布着龙胆科的睡菜和报春花科的黄莲花, 而泰丰湖附近睡菜较少。

3、草甸植物群落

远离岸边出现以灰脉苔草占优势的沼泽化草甸, 形成塔头, 双子叶植物种类丰富, 初步统计共出现 47 种植物, 较常见分布的还有毛茛科的驴蹄草、金莲花、毛茛、低矮华北乌头、

翠雀, 蔷薇科的柳叶绣线菊、蚊子草、地榆, 蓼科的珠芽蓼、毛脉酸模, 豆科的岩黄耆、广布野豌豆、柳叶野豌豆, 玄参科的返顾马先蒿、败酱科的缬草, 伞形科的迷果芹、骨缘当归、辽藁本, 菊科的紫苞风毛菊、裂叶蒿、柳叶蒿、肾叶橐吾, 禾本科的硬质早熟禾。

4. 森林植物群落

在岸边水分条件中等的陡阴坡, 普遍分布着以白桦为主的森林群落, 初步统计的结果表明, 森林中常见的灌木有近 10 种, 包括蔷薇科的山丁子、稠李、土庄绣线菊、刺梅蔷薇和美蔷薇、辽西山植, 忍冬科的金银木。常见草本植物有 56 种, 分布较广的有莎草科的矮紫苞鸢尾、禾本科的野青茅、菊科的小红菊、乌苏里风毛菊, 毛茛科的东亚唐松草、展枝唐松草, 蔷薇科的龙芽草、莓叶委陵菜、菊叶委陵菜、地榆, 豆科的歪头菜、山野豌豆, 景天科的土三七, 蓼科的拳参、珠芽蓼, 芍药科的白芍, 花荵科的花荵, 大戟科的京大戟, 败酱科的缬草、百合科的二叶舞鹤草、藜芦、小玉竹、铃兰等。

5. 草原植物群落

在阳坡和缓阴坡则以草原植被为主, 由于地处林缘, 本区草原植被中双子叶植物种类丰富, 和森林中非常接近。但在草原植物群落中广泛出现耐旱的禾本科贝加尔针茅。初步统计

共出现草本植物 45 种, 较常出现的除禾本科和莎草科的种类外, 还有蔷薇科的高二裂委陵菜、腺毛委陵菜, 豆科的狐尾藻棘豆, 瑞香科的狼毒, 唇形科的荆芥, 茜草科的蓬子菜、伞形科的北柴胡, 百合科的小黄花菜、山丹, 禾本科的无芒雀麦, 鸢尾科的囊苞鸢尾、细叶鸢尾。

二、植被特点

1. 完整的水生生态序列

七星湖、泰丰湖及其周边地区保存了非常完整的水生生态序列。这一序列包括沉水植物、浮水植物、挺水植物、湿生植物、中生植物和旱生植物。这种生态序列只有在森林-草原过渡带才有出现。

2. 独特的高寒河源湿地

由于地处高寒地区, 塞罕坝地区湿地植被的种类组成具有更靠北地区的特点。假鼠妇草沼泽主要分布在东北和内蒙古东部地区, 七星湖周边的假鼠妇草沼泽属于这一类型的分布南缘。

3. 森林、草原、沼泽和水体融为一体

塞罕坝地处森林和草原的交错地带, 地带性的植被包括

暖温带落叶阔叶林和温带草原。而沼泽和水体分布在地势低洼处,与周围的森林和草原植被融为一体,形成非常独特的地理景观。

三、观赏价值

1、重要观赏植物种类

1) 水生植物:萍蓬草(萍蓬草科)、荇菜(龙胆科)

2) 沼生植物:睡菜(龙胆科)、黄莲花(报春花科)

3) 草甸植物:金莲花、驴蹄草、毛茛、低矮华北乌头、翠雀(均为毛茛科植物)

4) 林下草本植物:二叶舞鹤草、藜芦、小玉竹、铃兰(均为百合科植物)、白芍(芍药科)、杓兰(兰科)

5) 草原草本植物:小黄花菜、山丹(均为百合科)、狼毒(瑞香科)、囊苞鸢尾、细叶鸢尾(均为鸢尾科)

2. 重要的观赏植被组合

1) 桦林--草甸--草原组合

2) 水生植被--陆生柳灌丛组合

3) 水生植被-金莲花草甸组合

三道河口林场丘间盆地立地条件初步分析报告

刘鸿雁

2013 年 7 月 6 日，北京大学刘鸿雁教授和 6 名学生在三道河口林场宋场长带领下，对碾盘梁和二龙泉之间丘间盆地的地形、土壤和植被进行了初步调查，试图解读造林成活率低的原因。

一、调查方法

调查人员从盆地底部出发，分布向东南和西北方向横穿盆地，观察地形、土壤和植被的变化，并在盆地底部、西南坡和东北坡做样方各 1 个，描述土壤剖面各 1 个。对所描述的 3 个土壤剖面从地表到剖面底部每 10cm 用环刀取样 1 个，在室内称取湿重后烘干，然后称取干重，然后求得每一层的土壤容重和水分含量。

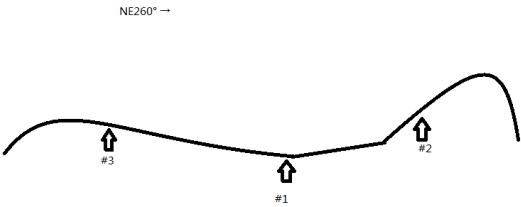


图 1 植物群落样方与土壤剖面所在地形部位

二、初步结果

1. 地形条件

所调查盆地的汇水面积约 5km²，呈长条形，周边均为覆沙丘陵，除坡顶局部低点外，砂层厚度推测普遍超过 1m。

2. 土壤条件

2.1 剖面描述

(1) 盆地底部剖面(#1)

O 层：0-5cm，主要为草的枯叶

A1 层：5-29cm，黑色粘壤土，稍疏松，稍湿润，根系比例 5%，16-29cm 处有砂侵入体

A2 层：29-60cm，黑色粘壤土，稍疏松，稍湿润，可看到明显片状结构

由于底部紧实，未及 C 层

(2) 盆地东北坡剖面(#2)

无明显的土壤分层，表面有少量枯落物，整个土壤剖面为棕黄色砂

(3) 盆地西南坡剖面(#3)

O 层：0-3cm，主要为松针和草的枯叶

A 层：3-50cm，深褐色沙壤土，稍疏松，稍湿润，根系比例 15%

C 层：50cm 以下，黄色砂，疏松，干燥

2.2 剖面容重和水分含量比较

土壤各层容重和水分含量实测结果如表 1 所示，从表 1 可以看出：盆地底部土壤容重

明显低于坡上的两个剖面，而不同层次的土壤水分含量（重量百分比）则普遍为坡上剖面的 3 倍以上。如果换算成体积百分比，盆地底部的水分含量普遍为坡上剖面的 2 倍左右。

表 1 三个剖面土壤容重和水分含量的比较

深度(cm)	土壤容重 (g/cm ³)				土壤含水量 (g/100g)		
	#1	#2	#3		#1	#2	#3
5-10	0.74	1.2	1.1		28.4	5.96	10.8
15-20	0.81	1.3	1.2		29.9	7.21	11.7
25-30	0.74	1.2	1.3		31.2	10.29	10.7
35-40	0.73	1.1	1.3		33.8	12.53	10.3
45-50	0.79				34.3		
55-60	0.75				33.0		

3. 植物群落

3.1 样方描述

(1) 盆地底部样方(#1)

植被类型为沼泽化草甸，草本层总盖度达 95%，4m²样地共记录草本植物 9 种，地榆和蓬子菜为优势种，盖度分别为 60%和 20%。盖度达 5%的种类还有灰脉苔草、石生蝇子草和花苳，其他种类包括箭头唐松草、矮山黧豆、鹅绒委陵菜和缬草。

(2) 盆地东北坡样方(#2)

自然和人工林，乔木层较稀疏。灌木层总盖度 30%，以耧斗叶绣线菊占优势（20%），另有山丁子和细叶小檗。草本层总盖度 95%，以白莲蒿占优势（5%），伴生种有棉团铁线莲、地榆、野罂粟、篇蓄豆、野青茅、硬质早熟禾、蓬子菜、腺毛委陵菜、并头黄芩、小酸模、匍枝委陵菜、瓣蕊唐松草、叉分蓼、大野豌豆和葶苈共 15 种。

(3) 盆地西南坡样方(#3)

为华北落叶松人工林，密度为 20 株/100m²左右。无灌木层。草本层总盖度 30%，以黄囊苔草（60%）、翼茎风毛菊（20%）和羊草（10%）占优势，伴生种有硬质早熟禾、叉分蓼、腺毛委陵菜、白莲蒿、狗舌草、瓣蕊唐松草、蒙蒿、林生银莲花和并头黄芩 9 种。

3.2 群落比较

以上种类可以划分为以下生态类群：

草甸种：地榆、鹅绒委陵菜、缬草、棉团铁线莲、野罂粟、篇蓄豆、石生蝇子草、花苳、蓬子菜、大野豌豆

沼泽种：灰脉苔草、矮山黧豆

草原种：耧斗叶绣线菊、狗舌草、瓣蕊唐松草、并头黄芩、蒙蒿、腺毛委陵菜

森林种：山丁子、细叶小檗、林生银莲花、野青茅、小酸模、匍枝委陵菜

从种类组成可以看出，坡上的植物群落以草原种为主，伴生有森林种，原始植被为天然草原或森林分布边缘的灌丛植被，而盆地底部以草甸种为主，伴生沼泽种。

三、森林成活率低的初步分析

从实地观察来看，成活的人工林明显分布在海拔较高处，沿一条等高线围绕整个盆地。在盆地内部，只有局部高丘上分布有成活的树木。

盆地底部造林难以成活主要是由于沼泽化的环境，以下三个方面说明了这一环境特点：

（1）地形低洼，成为整个盆地的汇水区，覆沙丘陵上的水分下渗快，蒸发小，下渗的水分通过壤中流的形式或者以浅层地下水沿基岩面汇入盆地底部，盆地底部充当了一个小的内陆湖的功能，只不过由于汇水面积小，降水量低，此处没有形成湖泊；

（2）土壤湿度高，A 层下部有明显的片状结构，这些说明土壤的发育是在一个潜育化的环境；

（3）出现一定比例的沼泽种，如灰脉苔草是塞罕坝一带沼泽中的优势种，矮山黧豆也主要在沼泽化草甸中见到，指示这一盆地底部长期处于沼泽化的环境。

盆地底部以下不利条件可能限制了树木的生长：

（1）土壤水分在冬季冻结，使树木根系形成物理损伤。根据调查，这一地区即使在夏季，70cm 以下的土壤经常出现冻结；

（2）与坡地的砂土相比，土壤偏黏重，A 层下部的片状结构限制了植物根系向下生长；

（3）这一地区降水量偏低，在 400mm 以下，较低的空气湿度对幼树的生长不利。而坡上相对良好的根系发育可能在一定程度上补偿了这一局限性。

教学实习报告

塞罕坝野外生态学实习报告

——群落特征与植被退化

00313101 左盼莉

本实习报告基于实习结果系统地分析了植物群落特征与植被退化之间的关系，全文思路清晰，论述准确。特别是从种面积曲线的角度对植被退化进行论述具有新意，是一份非常优秀的实习报告。

一、前言

2005年6月26日至7月4日，在刘鸿雁，郭大力和汪劲武等老师的带领和指导下，我们在塞罕坝地区完成了野外生态学实习。实习主要目的是调查不同生境下的植物群落特征和土壤特征，掌握野外植被调查和土壤调查的基本方法，认识实习地区常见的野生植物，了解植被、土壤与环境要素之间关系的分析方法。

这篇报告将对实习中得到的植物群落和土壤的数据进行归纳和分析，最后将利用本次实习的所得数据，探讨植被的群落特征和物种组成与植被退化的关系。

二、实习方法

1、调查地点

塞罕坝（蒙语之意“美丽的高岭”），位于河北省围场县境内（东经 $116^{\circ}51'$ ~ $117^{\circ}39'$ ，北纬 $42^{\circ}2'$ ~ $42^{\circ}36'$ ），是河北省的重要天然次生林与人工林区，林区总面积6.27万 hm^2 ，森林覆盖率78%，主要树种有落叶松、樟子松、云杉、白桦、山杨等。该地区位于内蒙古高原东南缘，北高南低，主体部分海拔1100~1400m，分为坝上、坝下两部分。坝上是内蒙古高原南缘，海拔1300~1500m，系森林向草原过渡地带，沙丘起伏、地势开阔；坝下是阴山山脉与大兴安岭余脉的交接地带，山高坡陡，沟壑纵横。境内是辽河与滦河两条水系的发源地，河道弯曲、狭窄，并分布较多的洼地、水泡。塞罕坝地区属寒温带大陆性季风气候，冬季漫长低温；夏季短暂干燥多风，光照强烈；昼夜温差大。年均温 $-1^{\circ}C$ ，极端最高温出现在7月，为 $33.4^{\circ}C$ ，极端最低温出现在12月，为 $-43.2^{\circ}C$ 。无霜期短而且不稳定，年均67天。

本次实习以河北塞罕坝机械林场为驻地，选择六条路线，向周围到达河北御道口牧场以及内蒙古克什克腾旗红山军马场和乌兰布统乡，对十二个地点进行了样地调查，包括尚海林白桦林和华北落叶松，蘑菇场白桦林，二道河口白桦林，白杆坑白杆林，大唤起油松林，三道河口油松林，梨树沟蒙古栎林，军马场后站贝加尔针茅草原，蘑菇场贝加尔针茅草原和羊草草原，吐力根河谷低地草甸。

2、植物群落调查方法

对于森林群落，取 $10m \times 10m$ 的大样方，在其中取5个大致分布均匀的 $2m \times 2m$ 的小样方，调查登记每个小样方内的灌木层和草本层（包括每种植物的种名、多度、盖度、叶层和生殖枝的高度、物候相，和它们的总盖度），枯落物层（包括组成，覆盖程度，分布特征，分解程度和分解层/未分解层厚度），以及立木更新（根据高度划分4个龄级：50cm以下，50—100cm，100—150cm，200cm以上；记载每种幼树（幼苗）不同龄级的数量，分布特征，起源和生长状况）。最后记载整个大样方内乔木层的郁闭度以及每木的树种，高度，冠幅，胸径，基径和物候相。

对于草原群落，在样地上均匀选取 4~5 个 $2m \times 2m$ 的样方，依照森林群落中草本层的处理方法进行记录。

3、土壤调查方法

选择有利地形地势挖掘土壤剖面，观测面深度要求 100cm，但一般以可以获得土层基本信息为准，即到达均一母质或基岩。划分土壤层次，记录每层的厚度、名称、界线特点、质地、动植物活动、侵入体和 PH 值。观察采样地点的气候状况，地势地形，基岩/母质，侵蚀排水状况，植被类型和人为干扰。分析以上信息对土壤进行定名并考虑成土过程与环境间的关系。

4、数据分析方法

根据草本层相关数据，计算每个小样方的物种多样性指数，以及每种植物的相对多度和相对盖度，最后得到每个样地的物种多样性指数，以及每种植物的频度，相对频度，相对多度，相对盖度和物种重要值。最后使用 Excel 做出种一面积曲线。相关公式如下：

$$\text{相对多度} = \frac{\text{每种多度}}{\sum \text{每种多度}} \times 100, \quad \text{相对盖度} = \frac{\text{每种盖度}}{\sum \text{每种盖度}} \times 100,$$

$$\text{相对频度} = \frac{\text{每种频度}}{\sum \text{每种频度}} \times 100, \quad \text{物种多样性指数} = -\sum (\text{相对多度} \times \log_2 \text{相对多度}),$$

$$\text{重要值} = \frac{\text{相对密度} + \text{相对频度} + \text{相对优势度}}{300}。$$

。

三、 调查结果

1、样地植被类型和物种组成

1.1 植被类型

根据吴征镒主编的《中国植被》植被分类原则，此次调查的 12 个样地可以划分为 4 个植被型组，5 个植被型，7 个植被亚型，8 个群系组（表 1）。

表 1. 塞罕坝地区实习样地植被分类表

植 被 型 组	植被型	植被亚型	群系组	群系	样地
针叶林	寒 温 性 针 叶 林	寒温性落叶针叶林	落叶松林	华北落叶松林	尚海林
		寒温性常绿针叶林	云杉、冷杉林	白扦林	白扦坑
	温性针叶林	温性常绿针叶林	温性松林	油松林	大唤起，三道河口
阔叶林	落叶阔叶林	山地杨桦林	桦木、桤木林	白桦林	尚海林，蘑菇场，二道河口，
		典型落叶阔叶林	栎林	蒙古栎林	梨树沟
草 原 和 稀 树 草 原	草原	草甸草原	丛生禾草草甸草原	贝加尔针茅草原	军马场后站，蘑菇场
			根茎禾草草甸草原	羊草草原	蘑菇场
草甸	草甸	沼泽化草甸	苔草沼泽化草甸	灰脉苔草草甸	吐力根河谷

1.2 物种组成

白桦林：建群种白桦，与其伴生的树种以林区的先锋树种为主，如棘皮桦和山杨等；灌木层

以柔毛绣线菊为主，尚海林有山丁子和珍珠梅，蘑菇场有美蔷薇；草本层披针叶苔草占优势，尚海林常见物种还有细叶沙参和地榆，蘑菇场有鼠掌老鸛草和歪头菜，二道河口有贝加尔唐松草、蚊子草和山尖子。

白扞林：建群种白扞，伴生有白桦；草本层主要物种为披针叶苔草和硬质早熟禾。

华北落叶松林：优势种为华北落叶松；灌木层为珍珠梅和山尖子；草本层优势种有早熟禾、沙参、地榆、风毛菊和苔草。

油松林：大唤起建群种为油松，伴生种有蒙古栎和大果榆，三道河口乔木层由油松、樟子松和山杨共同组成，还有少量白桦；灌木层为柔毛绣线菊；草本层优势物种为披针叶苔草，大唤起主要物种还有雾灵香花芥、展枝唐松草、铁干蒿和南牡蒿。

蒙古栎林：建群种蒙古栎；灌木层主要为柔毛绣线菊，另有二色胡枝子和虎榛子；草本层主要为披针叶苔草，常见物种有紫羊茅、紫羊茅、白莲蒿、阴地蒿菜、并头黄芩、小红菊和歪头菜。

贝加尔针茅草原：标志种为贝加尔针茅，蘑菇场建群种为日阴营苔草，军马场后站优势种有黄囊苔草、狼毒和地榆。

2、样地的地形地貌、环境条件和人类活动

2.1 地形地势

样地根据坡度可以划分为平缓（ 0° ）、微起伏（ $10^{\circ}-20^{\circ}$ ）和极陡（ $35^{\circ}-40^{\circ}$ ）三组：

第一组——尚海林华北落叶松林（蒙古高原南缘山地坡前平地），蘑菇场羊草草原（蒙古高原小盆地），吐力根河谷草甸（蒙古高原河漫滩）；

第二组——蘑菇场白桦林（蒙古高原缓阴坡中部至顶部/坡度 16° ），蘑菇场贝加尔针茅草原（缓阴坡坡脚/坡度 16° ），尚海白桦林（蒙古高原南缘山地陡阴坡坡脚/坡度 20° ），三道河口油松林（蒙古高原山地阳坡坡脚/坡度 15° ），白扞坑白扞林（蒙古高原山地缓阴坡中部/坡度 10° ）；

第三组——二道河口白桦林（蒙古高原山地陡阴坡坡顶/坡度 38° ），大唤起油松林（冀北山地极陡阳坡坡顶/坡度 40° ），梨树沟蒙古栎林（蒙古高原南缘山地阳坡坡脚/坡度 35° ）。

2.2 气候条件

样地夏季均温 $16\sim 20^{\circ}\text{C}$ ，无霜期 $80\sim 90$ 天，年降水量如图 2 所示。

2.3 土壤状况

样地土壤母质为沙土，结构疏松，以锥形土为主，略显酸性（PH 为 $5.5\sim 6$ ），剖面基本分层为：O 层+砂壤土质 A 层+沙土质 C 层。由于所处小环境的不同，土层发育程度和土壤剖面具体状况有较大差别：吐力根河谷草甸处在河漫滩，受河流侵蚀严重，剖面有大量锈斑；蘑菇场羊草草原植被破坏严重，土壤结构紧密，有机质积累少，全为沙土，有一部分地区也许以前是河流湖波所在地，表层沙土下有色深的砂壤土；二道河口和三道河口有大量坡积物，土层较薄；大唤起油松林坡度很陡，土壤水分储存差，土层干燥，相对于其它森林群落有机物累计少；尚海华北落叶松林地处于平地，郁闭度高，有机质积累多，A 层厚且色深。

2.4 人为影响

尚海林华北落叶松林为人工林，二道河口白桦林也受人工育林影响，蘑菇场羊草草原过度放牧，蘑菇场白桦林和贝加尔针茅草原也受放牧影响，其余样地基本没有人为干扰。

3、样地植物区系成分

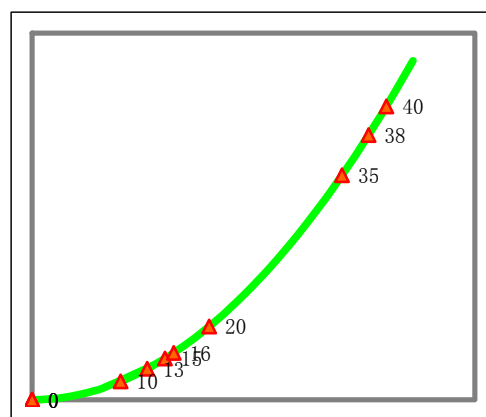


图 1. 样地坡度分布图

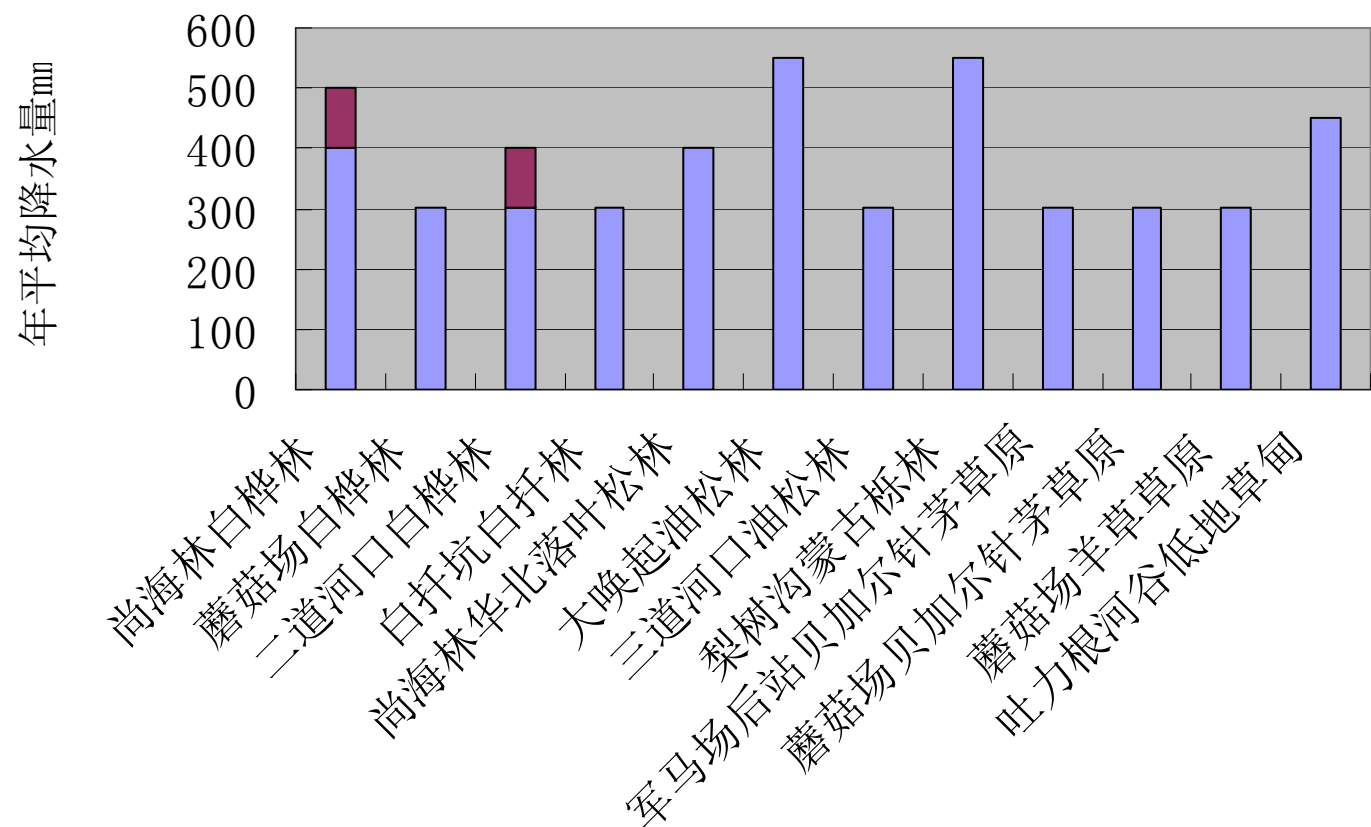


图 2. 样地年降水量分布图

根据样地资料不完全统计，常见植物区系成分主要为北温带成分，其次为旧大陆成分、世界广泛分布成分和温带亚洲成分，有少量属于东亚-北美成分，东亚成分和中国特有成分。表 2 为分布在各地地理成分中的样地内常见属。

表 2. 样地物种的地理区系

北温带成分	杨、柳、桦木、栎、胡颓子、榆、柏、冷杉、落叶松、云杉、松、黄栌、金露梅、绣线菊、蒿、凤毛菊、景天、罂粟、岩黄芪、点地梅、乌头、委陵菜、虎耳草、马先蒿、泽泻、冰草、拂子茅、山蓼、麻黄、柳叶菜、针茅、鸢尾、唐松草、恰草、火绒草、看麦娘
旧大陆成分	沙棘、瑞香、橐吾、小黄菊、荆芥、糙苏、百里香、羊草、隐子草、鸦葱、繁缕、蓝盆花、苜蓿、
世界广布成分	紫菀、龙胆、老鹳草、毛茛、蓼、苔、芦苇、悬钩子、猪毛菜、黄芪
温带亚洲成分	锦鸡儿、线叶菊、米口袋、附地菜、轴藜、大黄、瓦松
东亚-北美成分	胡枝子、珍珠梅
东亚成分	狗娃花、锦带花
中国特有成分	虎榛子

4、植物群落的结构特征

4.1 垂直结构

样地林地植物群落可分为三个层片：乔木层、灌木层和草本层，各层分界明显，没有层间植物。一般而言，三个层片植物相互竞争阳光、水份和养料，会产生制约关系。利用样地调查数据中可利用资料整理成表 3。比较尚海白桦林和尚海华北落叶松林，愈闭度高的林下草本盖度低，灌木层盖度似乎不满足这一规律，但注意到尚海白桦林 20 个小样地中，灌木

层盖度低于 10.5% 的有 15 个样地, 在 10.5~20.5% 之间有 3 个样地, 另有一个 25% 和一个 43%, 所以认为灌木层倾向聚集分布在林窗, 这一部分数据导致了最后结果偏高。而大唤起油松林, 因距尚海林较远, 环境条件有差异, 与前两组没有可比性。

表 3. 样地植物群落垂直结构

样地	尚海白桦林	尚海华北落叶松	大唤起油松
愈闭度	50%	30%	40%
灌木层盖度	11%	8%	6%
草本层盖度	35%	65.7%	38.4%
草本物种多样性指数	4.3	4.1	3.75

4.2 水平结构

比较同一地点不同样地内灌木层, 易知灌木总是丛生生长, 分布不均匀。个样地草本层的种-面积曲线如图 3 所示, 草原群落使用暖色调线条, 森林群落使用冷色调线条。分析得到: (1) 草原群落物种分布比森林群落均匀, 估计 20 m^2 为群落的表现面积, 蘑菇场羊草草原过度放牧, 组成物种少; (2) 森林群落同一样地内草本层物种分布差异较大, 一般 40 m^2 为表现面积, 物种丰富度比草原群落低; (3) 图中明显可见样地四和样地七的种-面积曲线比较特别, 物种丰富度高而且估计表现面积也比较大, 这是因为这两个地方植被处在更替阶段, 同样的证据可以在它们的乔木层组成看到。白扞坑白扞林乔木组成为白扞-白桦, 近年生立木更新以白扞为主, 白桦处于退化状态, 而白扞本应该是残遗树种, 白桦为先锋树种, 所以估计本地经历过白扞-白桦-白扞的演替过程; 二道河口油松林乔木层组成十分复杂, 有樟子松、油松、山杨和白桦, 立木更新中近年生为山杨, 往年生为樟子松和油松。综合乔木的基/胸径得到, 白桦为退化残遗种, 油松和樟子松处在轻度退化阶段, 山杨为先锋树种。

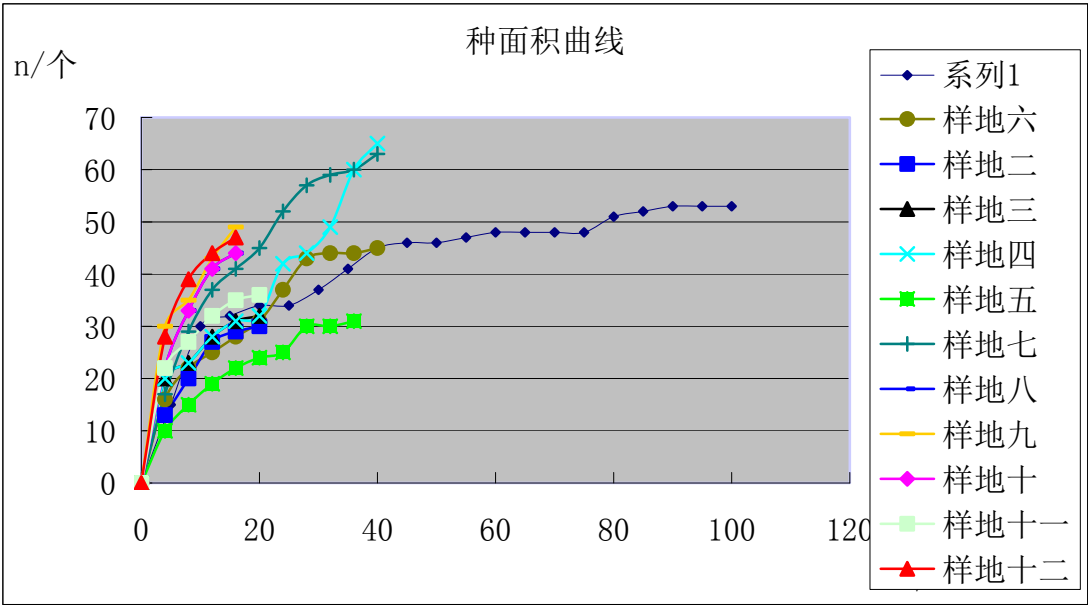


图 3. 12 个样地分别的种-面积曲线。

系列 1: 尚海白桦林; 样地二: 蘑菇场白桦林; 样地三: 二道河口白桦林; 样地四: 白扞坑白扞林; 样地五: 尚海华北落叶松林; 样地六: 大唤起油松林; 样地七: 三道河口油松林; 样地八: 梨树沟蒙古栎林; 样地九: 军马场后站贝加尔针茅草原; 样地十: 蘑菇场贝加尔针茅草原; 样地十一: 蘑菇场羊草草原; 样地十二: 吐力根河谷低地草甸。

四、 讨论

塞罕坝为植被区系交错带，处在森林区域草原区植物区系之间，而且人工林覆盖度高，占到总林地面积的 75%。这使得这一地区成为研究植被退化恢复的有效实验场所。本次实习选择的 12 个样地不完全但具有代表性的反映了塞罕坝地区的植被构成。森林群落中梨树沟蒙古栎林和大唤起油松林代表了低海拔沟谷地区受人为干扰最少的自然植被；尚海华北落叶松林为人工林；白扞坑白扞为残遗种；蘑菇场白桦林是破坏严重的植被；尚海白桦林、二道河口白桦林和三道河口油松林为保育自然植被。草原群落中吐力根河河谷草甸代表了河漫滩草垫，军马场后站贝加尔针茅草原反映了受到保护的草地，蘑菇场贝加尔针茅草原和羊草草原反映了受到破坏的草地。具体讨论如下。

1、草地群落：

表 4. 草地群落基本指数

样地	吐里根河河谷草甸	军马场后站贝加尔针茅草原	蘑菇场羊草草原	蘑菇场贝加尔针茅草原
主体高度 m	0.2~0.4	0.15~0.2	0.06~0.15	0.01~0.1
总盖度	92.5%	87. 5%	41%	35%
物种多样性指数	4.82	4.74	4.29	5.75

从表 4 中可以看出，水分充足土壤肥沃的河谷地区，植被的高度和盖度都很高；军马场后站贝加尔针茅草原是受到保护的割草场，植被长势也是相对很好的；在过度放牧的地区，蘑菇场的两处样地，草场的盖度和高度都明显减少，其中羊草草原处在牧民圈育的草地中，相对于贝加尔针茅草原，植被轻度恢复。但是，草地物种多样性与草场退化程度并没有相关关系。同时，样地主要物种发生很大变化，河谷草甸：灰脉苔草—蚊子草—珠芽蓼—金莲花；军马场后站：黄囊苔草—狼毒—贝加尔针茅—地榆；蘑菇场贝加尔针茅草原：日阴菅苔草—平车前—无芒雀麦—贝加尔针茅—羊草；蘑菇场羊草草原：日阴菅苔草—冷蒿—羊草—平车前。说明在人为破坏严重的地区，羊草、针茅、苔草、恰草、冰草和藜等适口性高的偏中生植物和不耐践踏的丛生禾草种类减少，而猪毛菜、糙隐子草、冷蒿、星毛委陵菜、车前、狼毒和藜芦等耐旱耐践踏植物种类增加。

与比较蘑菇场贝加尔针茅草原，蘑菇场羊草草原退化标志种缺少狼毒和藜芦，而这两个样地所处地点十分相近，考虑到狼毒和藜芦是植株较大容易辨认的非适口性植物，猜测是圈育羊草草原的牧民将其人工清除。

表 5. 草原群落退化标志种的物种组成和总相对盖度

样地	吐里根河河谷草甸	军马场后站贝加尔针茅草原	蘑菇场羊草草原	蘑菇场贝加尔针茅草原
退化标志种	无	狼毒、平车前	糙隐子草、平车前、冷蒿、猪毛蒿、星毛委陵菜	平车前、藜芦、狼毒、车前、糙隐子草
总相对盖度	0	11.42%	17.72%	24.39%

这些样地所在地的土壤都是为在沙性母质上初步发育的雏形土，土壤肥力较差，蓄水能力弱，所以水分和养料的供给对植物生长比较重要。例如在河谷地区，第一水分条件充足，第二没有放牧等人为破坏，土壤有机质积累比较丰富，所以植被发育良好。在放牧地区，土壤有机质供给不足，肥力下降，在风蚀作用下逐渐沙化。但同时，人为影作用影响很大，被保育起来的草地，恢复能力很强。

狼毒在塞罕坝地区是最常见的一种植物，它的根系十分发达，主根膨大可以储藏水分和养料，适宜性好竞争力强，但是植株含有有害化学物质，危害牧业。它的广泛分布虽然可以

防风固沙，但是也是草场退化的一种标志，是需要关注的一个问题。

2、森林群落

塞罕坝森林覆盖率为 78%，其中人工林占总林地面积的 75%，主要乔木有蒙古栎、油松、白桦、白桦、华北落叶松。森林群落草本层相对于草原群落难以考察，首先，森林群落中乔木、灌木和草本层间存在相互制约；其次，乔木层为草本层提供了一个非匀质的环境，例如林下和林窗的光照、水分和土壤养分区别较大。如果将森林群落草本层相关指数（表 6）加以比较，可以得到以下结论：（1）二道河口白桦林取样地处在林窗，所以草本层盖度高；（2）梨树沟蒙古栎林属于原生植被，人为干扰少，群落结构稳定，所以物种多样性高；（3）蘑菇场白桦林植被破坏严重，物种多样性降低；（4）各个森林群落主要草本植物物种相似，如地榆、野青茅、瓣蕊唐松草、披针叶苔草、硬质早熟禾、歪头菜、细叶沙参、小红菊和阴地堇菜，在六个以上样地出现过，而且重要值都相对较大；（5）与草原群落相比，森林群落草本层物种多样性偏低。

表 6. 森林群落草本层相关指数

样地	一	二	三	四	五	六	七	八
总盖度	38.2%	31.9%	15%	35%	75%	65.7%	38.5%	41.8%
物种多样性指数	6.25	4.94	4.87	4.3	4.20	4.1	3.75	3.1

一、梨树沟蒙古栎林；二、三道河口油松林；三、白桦坑白桦林；
四、尚海林白桦林；五、二道河口白桦林；六、尚海华北落叶松林；
七、大唤起油松林；八、蘑菇场白桦林

以上结论说明，讨论森林植被退化的主要参数应该来源于乔木，草本植物物种多样性可以作为补充。例如人工林尚海华北落叶松林，虽然乔木层生长良好，但是草本层物种多样性指数与总盖度不符，部分表现了人工林存在群落结构简单的问题。而且有研究表明，塞罕坝华北落叶松人工林土壤存在持续性的旱化现象（潘湘海,2002），说明现有的群落结构与当地环境不符。

五、 总结

塞罕坝地区植被种类丰富，本次实习的 12 个样地在植被类型，退化程度和地理位置上都具有代表性。通过样地主要参数的对比，本次报告主要讨论了群落组成与植被退化的关系。得出两个重要结论：（1）草原群落退化会引起植被盖度和高度显著变化，物种多样性不能反映群落退化，但群落结构改变很大；（2）森林群落植被退化主要表现在乔木层，群落结构应该用乔木—灌木—草本的综合指数进行评述。

参考资料：

《塞罕坝或北落叶松人工林土壤水翻得研究》，河北林业科技，2002 年 10 月，第 5 期，潘湘海
《塞罕坝植物志》，中国科学技术出版社，1996 年 8 月，黄金祥等主编
《野外生态学——实习指导》，北京大学生态学系，2005 年 6 月，刘鸿雁，郭大力等主编
《中国植被》，科学出版社，1995 年，吴征镒主编

[附录一](#)：植物标本名录

[附录二](#)：植物各科特征

[附录三](#)：土壤记录

后记:

对下届实习生友情提示——实习记录松一分，实习报告苦 N 久。

不同植被类型植物根系对土壤的影响

徐冰 00413017

摘要：在植被与土壤的相互作用中，植物的根系是一个重要的纽带。不同的植被类型中不同的物质组成，使得土壤中的根系具有不同的形态结构、生理特点，导致不同植被类型下的土壤产生了明显的差异。本文通过对坝上地区相间分布的森林、草原植被的研究根据群落调查和土壤调查的结果，提出由于单子叶植物在草原群落中的重要性比在森林群落中大（一个有意思的结论！），而单子叶植物的须根系在形态上又具有细根分布均匀等特点，所以使得草原土壤的质地更细更均一，层次更分明，而森林土壤则具有较厚的腐殖质层。

关键词：植被类型；植物根系；森林土壤；草原土壤；单子叶植物；双子叶植物

植被与土壤之间是相互影响相，互作用的关系。植物的生长活动是土壤形成的关键因素。一定气候条件决定了一定的植被类型，不同类型的植被之下又发育着不同的土壤。特别是在森林和草原这两大类截然不同的植被作用下，森林土壤和草原土壤在很多方面有着明显的差异。

植物体对土壤影响最大的部分就是它的根系。植物的根系是土壤有机质的来源，为土壤微生物的活动提供环境，对土壤的质地、结构、水分状况和营养元素的含量等都有很大的影响^[1]。对于不同类型的植被，其物种组成不同，则其根系的形态结构、生长方式也就不同，对土壤也就会产生不同的作用。

为解释不同植被下土壤的成因，本文选取坝上地区 4 个有代表性的样地（森林、草原植被各 2 个），根据群落调查和土壤调查的直观结果，分析不同植被下土壤的特征差异，及植物根系在这些差异的形成过程中所起的作用。

1. 研究区域概况

坝上地区位于河北省北部，内蒙古高原南缘，是我国半湿润区到半干旱区、华北平原到内蒙古高原、森林植被到草原植被的过渡地带。区域内气候条件多样，植被类型丰富，是生态学研究的关键区域^[2, 3]。由于是森林向草原的过渡地带，该区域内的天然林成块状的分布。次生性的天然白桦林常分布于阴坡，而阳坡则是草原或草甸。森林和草地在山坡两边相间分布，构成该区域内常见的景观，也为植被与各环境因子相互关系的研究提供了方便。

本文选取的 4 块样地分别位于机械林南山和将军泡子附近，两地的具体位置及气候条件见表 1。在同一山丘的阴、阳坡分别取桦林、草原，两种植被，样地编号为：1 号样地，机械林场南山，阴坡桦林；2 号样地，机械林场南山，阳坡草地；3 号样地，将军泡子，阴坡桦林；4 号样地，将军泡子，阳坡草地。

表 1 样地经纬度及气候状况

	经度	纬度	年降水量 (mm)	年均温 (℃)	一月均温 (℃)	7 月均温 (℃)
机械林场	117°15'11"E	42°23'55"N	432	0.71	-17.1	17.0
将军泡子	117°07'29.4"E	42°34'45"N	418.8	0.42	-19.6	17.0

2. 研究方法

2.1 群落调查

用样方法对样地群落进行调查。桦林样地取 $10 \times 10 \text{ m}^2$ 样方，分乔木层、灌木层和草本层调查，其中草本层又在大样方内分取 5 个 $2 \times 2 \text{ m}^2$ 小样方。草原样地取 $2 \times 2 \text{ m}^2$ 样方进行调查，每处有四组重复。

以每个物种相对盖度、相对多度、相对频度求平均的方法，计算各草本物种的重要值；灌木重要值为相对盖度、相对多度和相对高度的平均值。

计算香农-维纳指数，表示物种的多样性^[4]。

2.2 土壤调查

在每个样地内挖掘较完整的土壤剖面，划分土壤层次，记录各层特征。

3. 结果与分析

3.1 森林土壤与草地土壤的异同

根据四个样地土壤调查的结果，分析可知：样地内土壤都由沙质的母质发育而来，淋溶不强烈，多为雏形土，包涵一个较明显的富含有机质的 A 层（腐殖质层）和一个完全由沙子组成的母质层。

森林土壤和草原土壤的不同主要在于以下几点：

- 1) 桦林下的土壤有一个 5cm 左右的枯枝落叶层，草地土壤的枯枝落叶层不明显。
- 2) 森林土壤基岩层以上的总厚度比草原土壤大，其中 A 层的厚度明显大于草原土壤
- 3) 对于母质层以上的 A 层及其他过渡层次，草原土壤比森林土壤的质地更加细腻，团粒结构发育更好。
- 4) 草原土壤的质地、结构更加均一，层次之间的分界比较明显，而森林土壤各层次间则是逐渐过渡的。
- 5) 森林土壤剖面的下部、母质层中常出现深黑色的腐殖质斑块，草原土壤中则没有。

3.2 群落调查结果

在考察群落的物种组成时，考虑到双子叶植物和单子叶植物的根系在形态结构上有明显的不同，他们的根对土壤也会产生不同的影响，因此重点分析双子叶植物和单子叶植物在森林群落和草地群落中所处的地位。

各样地内重要值排在前 20 位的物种的重要值分布情况见图 1—图 4，其中双子叶植物为灰色，单子叶植物为白色。对桦林样地仅表示其草本层的状况。

由图可见，在两个草原样地内，单子叶植物的种数和重要程度都比相应的桦林样地大。表 2 显示了森林和草原群落中单子叶植物和双子叶植物的对比情况，在森林样地中，单子叶与双子叶植物的重要值之比只有 0.1797 和 0.2969，在草原样地，单子叶与双子叶植物的重要值之比则达到了 0.5092 和 0.7247。草原样地中单子叶植物的多样性也有所增加，在 4 号样地，单子叶植物的多样性指数甚至超过了双子叶植物。

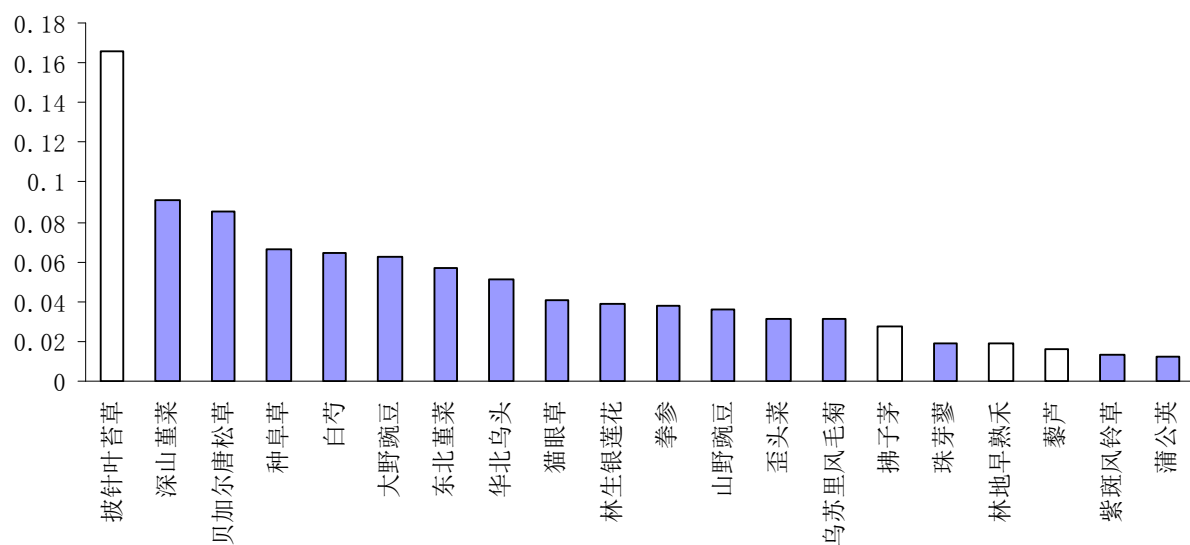


图 1: 1号样地（桦林）各物种重要值分布情况

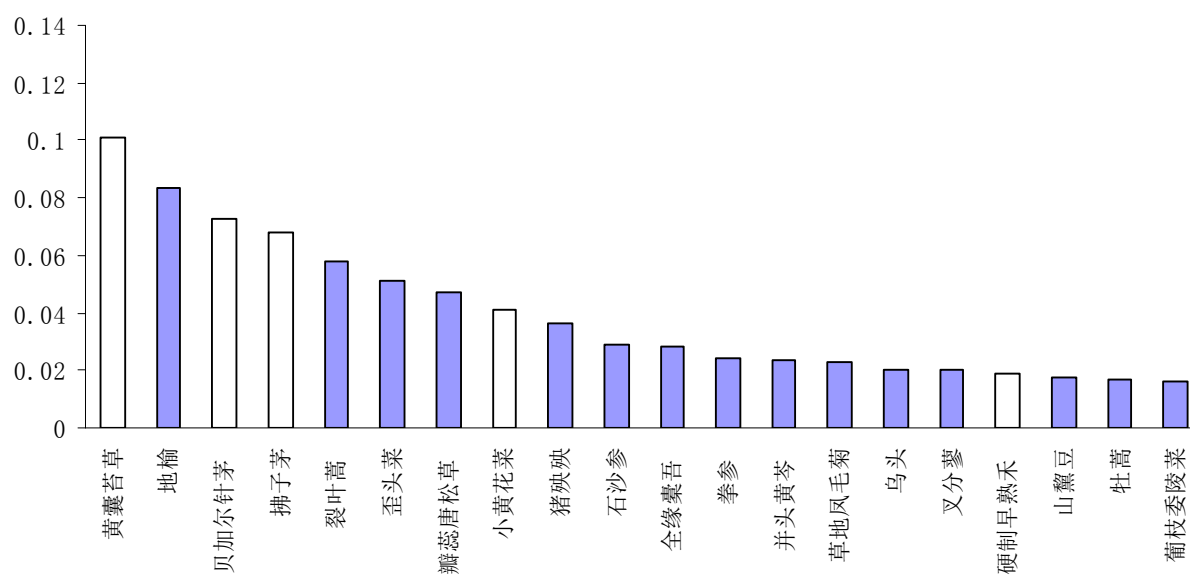


图 2: 2号样地（草地）各物种重要值分布情况

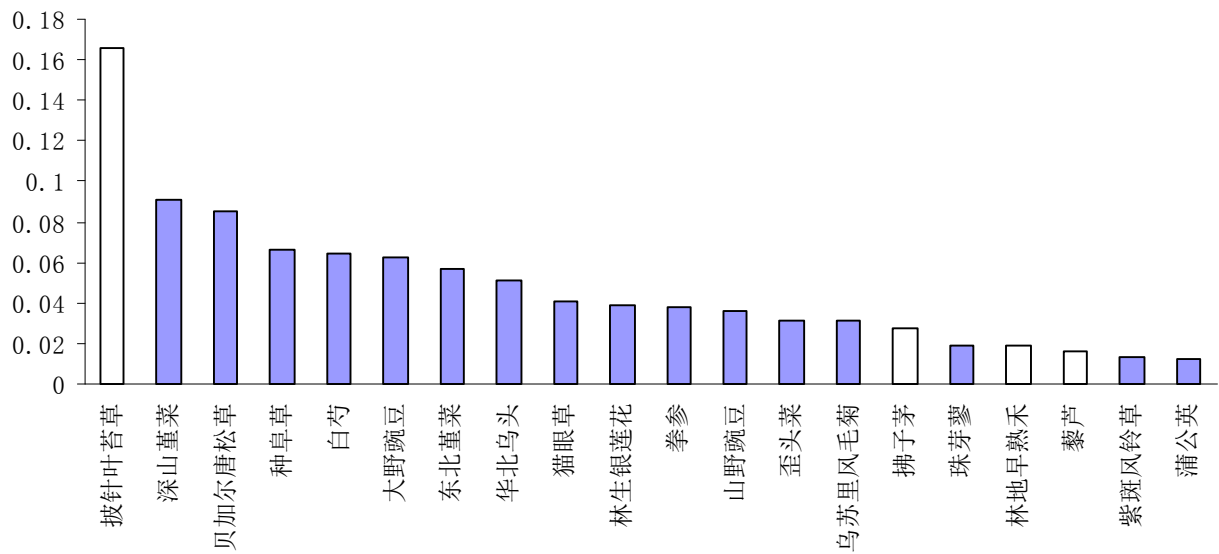


图 3: 3号样地 (桦林) 各物种重要值分布情况

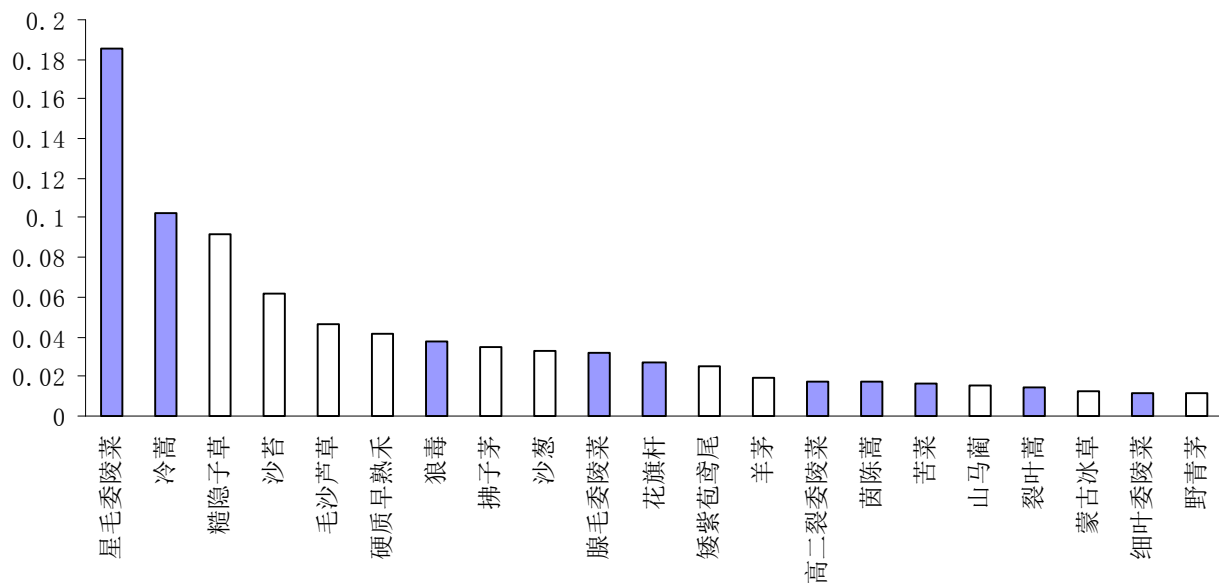


图 4: 4号样地 (草地) 各物种重要值分布情况 (土中蓝色和无色两种图标分别表示什
么??)

表 2: 森林草地群落单子叶植物双子叶植物分布情况对比

			相对多度	相对盖度	相对频度	重要值	多样性指数
森 林	1号样地	双子叶	0.8266	0.8262	0.8902	0.8477	3.2923
		单子叶	0.1734	0.1738	0.1098	0.1523	0.5526
		单子叶/双子叶	0.2097	0.2103	0.1233	0.1797	0.1679
	3号样地	双子叶	0.7812	0.6667	0.8654	0.7711	3.2823

		单子叶	0.2188	0.3333	0.1346	0.2289	0.7033
		单子叶/双子叶	0.2802	0.5000	0.1556	0.2969	0.2143
草地	2号样地	双子叶	0.6359	0.5781	0.7738	0.6626	3.2115
		单子叶	0.3641	0.4219	0.2262	0.3374	1.4645
		单子叶/双子叶	0.5725	0.7299	0.2923	0.5092	0.4560
	4号样地	双子叶	0.5005	0.6389	0.6000	0.5798	2.1610
		单子叶	0.4995	0.3611	0.4000	0.4202	2.1704
		单子叶/双子叶	0.9980	0.5652	0.6667	0.7247	1.0044

由以上分析可知在草原群落中单子叶植物所起的作用比在森林群落中大，所以单子叶植物特殊的根系结构在改良草原土壤时发挥的作用也将比在森林土壤中大（这里不是因果关系！）。

3.3 根系对土壤的影响

3.3.1 根系深度对土壤的影响

表 3：单子叶双子叶植物的根系深度

单子叶		双子叶	
羊草	7.3	扁须豆	14.4
双齿葱	7.7	地榆	11.2
囊包鸢尾	8.5	达乌里黄芪	11.9
贝加尔针茅	7.8	冷蒿	14.3
日阴菅	12.9	星毛委陵菜	10.4
黄囊苔草	11.5	腺毛委陵菜	12.5
黄花菜	10.4	狼毒	35.2
糙隐子草	3.0	瓣蕊唐松草	7.6
恰草	15.5		
冰草	17.6		
平均	10.2	平均	14.7
均方差	4.3	均方差	8.6

（数据来源：周鹏等，2006）

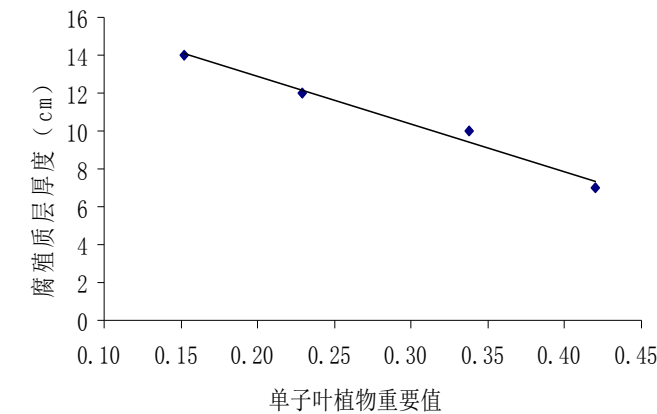


图 5：单子叶植物重要值与土壤腐殖质层厚度的关系

在同样植被下测定的 18 种该地区常见植物根系深度情况如表 3 所示，可见双子叶植物的根系深度平均值略大于单子叶植物，而双子叶植物根深的均方差也比单子叶植物高出了一倍，说明双子叶植物根系的深度差异较大，不同种植物的根系可深可浅，而单子叶植物的根系深度则比较平均。

在土壤发育的过程中，植物的根系是土壤有机质的重要来源，根系的周围是土壤微生物的主要活动场所，所以根系的深度与土壤腐殖质层的厚度有很大的相关性。因此单子叶植物占优势的群落下，土壤的腐殖质层较薄（研究样地中单子叶植物重要值与腐殖质层厚度的关系如图 5 所示），受根系影响的范围边界比较明显；而双子叶植物占优势的群落，土壤的腐殖质层可能较厚，边界不明显。

3.3.2 根系形态结构对土壤的影响

双子叶植物的根是直根系，有一条明显的向下生长的主根，从主根上分出细根，向周围生长；单子

叶植物的根是须根系，有多条须根共同向下生长，从每条须根上都可分出很多细根。这样不同的分级结构使得双子叶植物的根系密度从上到下逐渐递减，而单子叶植物的根系密度在整个根系范围内则是比较均匀的，而且单子叶植物的细根更加丰富。

在土壤发育的过程中，植物的细根对土壤有机质的积累、质地的改良、团粒结构的形成等都发挥着巨大的作用^[5]，所以单子叶植物的根系可以使土壤的质地更加细腻，结构更加疏松，而且单子叶植物根系的这些影响在一定范围内是比较均一的，而双子叶植物根系的生长则会使相应的土壤层次产生逐渐过渡的现象。

这样就从植物根系的角度解释了森林与草原土壤之间为什么会产生上述的几点不同。在草原群落中单子叶植物的种类更加丰富，所起的作用更加重要，而单子叶植物的根系又具有根系深度平均，细根多，根系密度分布均匀等特点，所以就使得与森林土壤相比，草原土壤的质地更细腻、结构更均一、层次也更清晰。

另外在森林土壤中影响着土壤的发育得也不只有草本层的根系。森林植被的地下部分与地上部分一样，也有着分层的现象，乔木灌木的根系可以把生物活动对土壤的改造带入到更深层的土壤中去，成为上下层土壤之间物质循环的通道^[6]，使得森林土壤的结构更加复杂，层次更不分明^[7]。深层土壤中粗大的乔木根系死亡后腐烂，形成埋藏的腐殖质斑块。

4. 结论与讨论

4.1 不同的根系结构导致不同的土壤

森林植被和草原植被的物种组成不同，所以他们的根系分布状况也就有所差异，因此形成了不同的土壤。森林土壤和草原土壤的差异可以从根系的角度去解释：

- 1) 森林植被的根系可以达到很深的层次，林下草本层中双子叶植物所占比例较大，双子叶植物的根系深度比较大，所以森林土壤的深度大，腐殖质层也较厚。
- 2) 草原植被中单子叶植物丰富，而单子叶植物根系中细根多，有利于土壤颗粒的分化、有机质的积累、团粒结构的形成，因此草原土壤的质地更细。
- 3) 单子叶植物的根是须根系，各深度上根密度比较平均，不同物种间根系深度相差不大，所以在单子叶植物相对丰富的草原植被下，土壤的层次更清晰，各层内的质地也更均匀。
- 4) 森林土壤中乔木和灌木的根系可以使有机质在更深层的土壤中积累。

综上所述，植物的根系是沟通植被与土壤的桥梁，在植被与土壤的相作用中发挥着重要的作用。

4.1 其它因素对森林草原土壤相异性的影响

除了植物的根系，还有许多其它的因素也影响着土壤的形成，使得森林和草原的土壤产生了上述的不同。如森林植被产生枯枝落叶积累在土壤表层，草原植被则很少；森林植被能截流大量的降水减缓下渗，减少淋溶等等。本研究中草原样地都处于阳坡，桦林样地都处于阴坡，阴阳坡的差异一方面造就了两种不同的植被，另一方面也会直接影响土壤的性质，比如阴坡上的草地土层薄、土壤质地细也可能是由于阳坡背风，风成的母质本身就比较薄、质地就比较细的缘故，另外阴阳坡不同的水分状况也会对土壤产生较大的影响^[8]。

4.2 根系对土壤的具体影响还有待进一步研究

本研究在野外调查时并不针对根系对土壤的影响这一题目，所以研究过程中还存在很多干扰，如上文所说阴阳坡的影响。如要验证本文中的结论，应选择地形条件、小气候等环境因素完全相同的样地进行试验。

本研究基于野外调查的直观结果，多为定性讨论，缺乏定量研究。如果要更深入地探讨根系对土壤的影响，应具体测量土壤各层次的根密度、孔隙度、有机质含量，营养元素的含量等指标^[7-9]，并深入分析各植物类群根系结构的特点，建立植被—根系—土壤之间关系的完整框架。

参考文献：

- [1] 吴淑杰，韩喜林。土壤结构、水分与植物根系对土壤能量状态的影响。东北林业大学学报，2003，31（3）：24—26。
- [2] 盛学斌，孙建中，刘云霞。坝上地区土地利用与覆被变化对土壤养分的影响。农村生态环境，2002，18（4）：10—14。
- [3] 盛学斌，孙建中，刘云霞。坝上地区古土壤环境变化信息研究。土壤与环境，2000，9（2）：87—90。
- [4] 杨小波，张桃林，吴庆书。海南琼北地区不同植被类型物种多样性与土壤肥力的关系。生态学报，2002，22（3）：190—196。
- [5] 吕春花，郑粉莉。冰草根系生长发育对土壤团聚体形成和稳定性的影响。水土保持研究，2004，11（4）：97—100。
- [6] 李任敏，常建国，吕皎。太行山主要植被类型根系分布及对土壤结构的影响。山西林业科技，1998，3（1）：17—23
- [7] 李勇，张晴雯，李璐。黄土区植物根系对营养元素在土壤剖面中迁移强度的影响。植物营养与肥料学报。2005，11（4）：427—434。
- [8] 杨晓晖，张克斌，侯瑞萍。半干旱沙地封育草场的植被变化及其与土壤因子间的关系。生态学报，2005，25（12）：3212—3219
- [9] 张昌兴，邵安明，黄占斌。不同植被对土壤侵蚀和氮素流失的影响。生态学报，2000，20（6）：1038—1044

林下与草原（草甸）草本植物多样性格局比较分析

2005 级生态学专业 李昂

摘要: 由于所处环境的不同特点, 林下草本植物与草原草本植物不仅在物种组成、水平分布上存在差异, 在多样性格局上也体现出不同。经过计算和分析, 林下草本植物与草原草本植物的 α 多样性不存在显著差异, 而前者的相邻样地间的物种转换率更高。这种多样性格局的不同, 受到生境异质性、生产力、种间竞争、植物分布特性及环境波动等不同因素的影响。

关键词: 物种组成, α 多样性, 物种组成转换率, 生境异质性

全文主题新颖、论证有据、表达准确、逻辑性强。

引文:

在森林-草原交错带的背景下, 森林林下与草原（草甸）共享一个草本植物的“区域种库”, 即拥有潜在的共同的草本物种组成。但由于林下与草原的光照、水分、土壤等非生物因素和种间竞争等生物因素不同, 使得这两种环境下, 草本植物的物种组成具有显著差异。例如, 狼毒是草原的常见种, 在任何一个草原样方都可以调查到, 而在林下却没有分布。此外, 物种的空间分布也各有特点。例如, 玉竹等许多林下草本植物呈集群分布, 而草原草本多呈均匀分布。那么, 物种组成和空间分布的差异是否也意味着多样性格局的不同? 要了解这个问题, 我们需要首先计算各样方的多样性指数, 然后对比林下与草原环境的差异, 通过分析, 从中找出原因, 解释差异。

方法:

1. 组建数据库

我选用了这次野外调查中一组、二组和四组的原始资料, 以保证每个地点有 3 个样方的重复。调查地点涉及尚海林、大光顶、人工落叶松林、未明山、未明山对面山、白杆坑、将军袍子、吐里根河和红山军马场（分别编号为 SHL、DGD、LYS、WMS、WMSD、BQK、JJP、TLGZ、TLGH、HS）, 共 27 个样地。其中森林样地 17 个, 涵盖了白桦林、棘皮桦林、落叶松林、云杉林和蒙古栎林等植被类型; 草原样地 11 个, 涵盖了草原、草甸和湿地等植被类型。

由于森林的最小取样面积较大, 所以森林样地的每个样方资料是五个小样方资料的综合, 这样才能反映出林下草本植物的整体多样性。而每个草原样地只包含一个 2×2 样方。需要说明的是, 这里我们对比的是各取样地点整体的草本物种多样性, 而不是相同面积内的物种丰富度。

根据 α 多样性的测度定义, Shannon-Weiner 指数、Simpson 指数和 Pielou 指数的计算公式中都需要 P_i 作为参数 (P_i 为第 i 种的个体数 N_i 占群落中总个体数 N 的比例, 即 $P_i = N_i / N$)。因此, 我选择了各样方物种的相对密度数据作为运算依据, 而没有采用重要值。

为了便于用数量软件进行统计, 所有的资料被写入同一个 Excel 表格。其中, 纵轴为样地编号, 横轴为物种, 表格内容为在每个样地中各草本物种的相对密度。

2. 数据分析

采用 PC-ORD 作为统计软件, 计算各样地的多样性指数, 并对样地进行分类和排序。在此基础上, 分析两种环境下的多样性格局的差异。

结果:

1. 多样性指数: 结果如图-1:

Summary of 28 plots			N = 177 species							
Num.	Name	Mean	Stand.Dev.	Sum	Minimum	Maximum	S	E	H	D'
1	SHL-1	0.403	1.393	71.410	0.000	10.140	23	0.911	2.857	0.9274
2	SHL-2	0.548	1.657	97.000	0.000	12.600	25	0.943	3.035	0.9430
3	SHL-4	0.564	2.622	99.800	0.000	22.700	26	0.769	2.504	0.8729
4	DGD-11	0.565	1.652	100.030	0.000	10.470	34	0.910	3.210	0.9464
5	DGD-21	0.562	1.460	99.400	0.000	9.200	33	0.949	3.319	0.9564
6	DGD-41	0.561	1.604	99.300	0.000	12.300	30	0.936	3.182	0.9484
7	DGD-12	0.563	1.745	99.670	0.000	12.900	27	0.920	3.033	0.9404
8	DGD-22	0.556	1.678	98.400	0.000	11.400	26	0.942	3.070	0.9432
9	DGD-42	0.566	1.608	100.200	0.000	10.400	28	0.947	3.157	0.9490
10	LYS-1	0.560	1.656	99.100	0.000	9.800	29	0.919	3.094	0.9452
11	LYS-2	0.495	1.456	87.600	0.000	7.800	24	0.953	3.029	0.9457
12	LYS-4	0.439	1.458	77.700	0.000	11.800	29	0.871	2.933	0.9324
13	BQK-1	0.489	1.269	86.640	0.000	8.500	35	0.944	3.356	0.9566
14	BQK-2	0.563	1.511	99.700	0.000	11.600	32	0.943	3.268	0.9539
15	BQK-4	0.561	2.266	99.300	0.000	21.800	24	0.844	2.682	0.9027
16	JJP-1	0.521	1.452	92.200	0.000	11.600	32	0.931	3.227	0.9507
17	JJP-2	0.558	1.501	98.800	0.000	11.200	30	0.955	3.249	0.9538
18	JJP-4	0.566	1.685	100.100	0.000	12.800	35	0.893	3.175	0.9445
19	WMS-1	0.384	1.271	67.920	0.000	11.720	30	0.895	3.043	0.9327
20	WMS-2	0.562	1.638	99.500	0.000	7.800	23	0.968	3.035	0.9466
21	WMS-4	0.563	2.488	99.700	0.000	23.100	23	0.808	2.534	0.8848
22	WMSD	0.562	1.334	99.400	0.000	8.200	40	0.943	3.480	0.9626
23	TLGZ-1	0.563	2.849	99.700	0.000	30.200	17	0.819	2.321	0.8506
24	TLGZ-2	0.568	2.252	100.500	0.000	13.200	13	0.960	2.463	0.9060
25	TLGZ-4	0.567	2.573	100.300	0.000	24.500	15	0.877	2.374	0.8785
26	TLGH-1	0.573	1.397	101.400	0.000	7.700	37	0.947	3.418	0.9609
27	HS-1	0.572	1.414	101.300	0.000	10.300	34	0.961	3.389	0.9600
28	HS-2	0.567	1.666	100.300	0.000	8.400	27	0.933	3.074	0.9458
AVERAGES:		0.540	1.734	95.585	0.000	13.005	27.9	0.914	3.018	0.9336

图-1

其中，标题栏的 S、E、H、D 分别表示物种丰富度、Pielou 均匀度指数、Shannon-Weiner 指数和 Simpson 指数。

以 Shannon-Weiner 指数作为统计数据，对比林下草本与草原草本的多样性，过程及结果如下：

	林下草本	草原草本
平均值	3.067	2.963
方差	0.085	0.149

做假设检验 W (H_0 : 林下草本多样性=草原草本多样性)。其中，T 值为 0.764，小于 1.96（水平为 95%的检验），因此不能否定 H_0 假设。这表明，林下草本与草原草本的 α 多样性不存在显著差异。

2. 样地分类和排序：

聚类分析，将 28 个样地分为 6 组，结果如图-2：

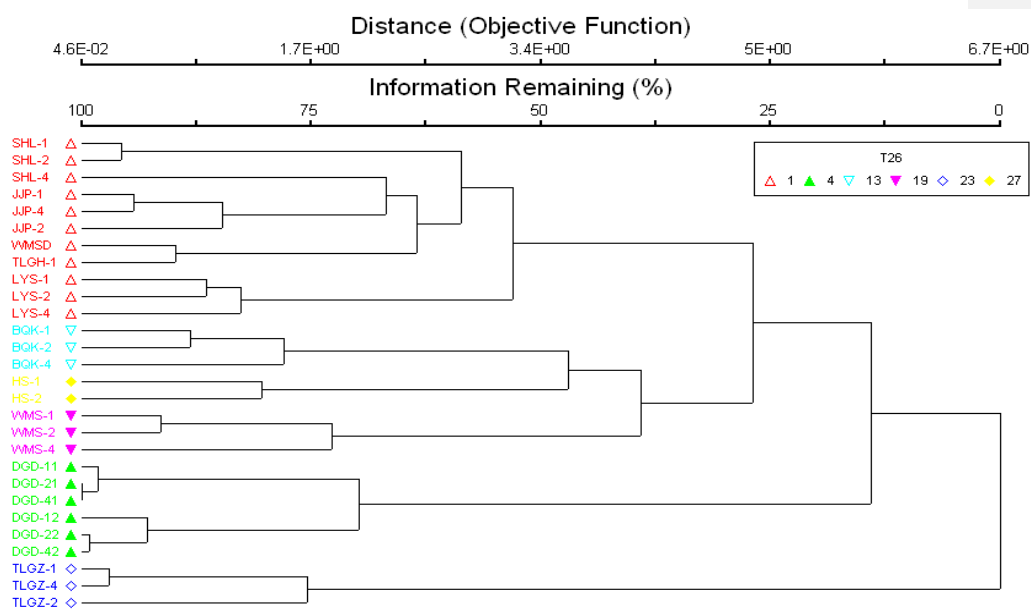


图-2

在分类的基础上，进行 NMS 间接梯度排序，结果如图-3：

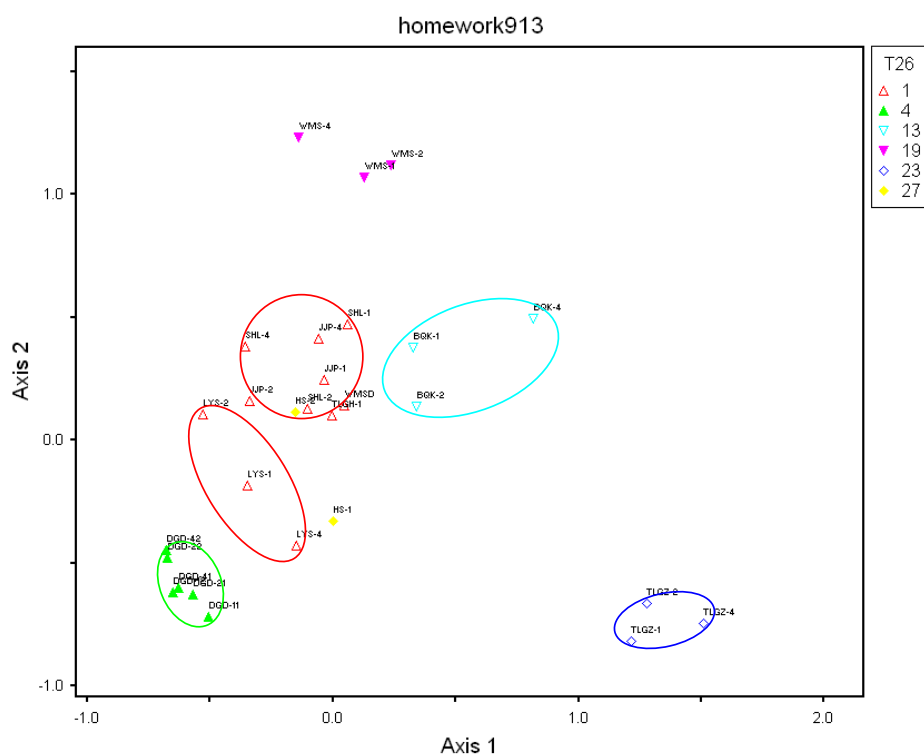


图-3 (绿圈内为大光顶草原样方，蓝圈为吐里根草原样方，淡蓝圈为白杆坑林地样方，两个红圈内分别为人工落叶松林样方和尚海林样方)

可以看出，在排序图上，同一处调查地点的森林样方之间的排序距离较大，而草原样方则比较紧密（红山军马场样方只有 2 个重复，因此距离较大）。这说明，同一地点的各森林样地，物种组成差异较大，而同一地点的各草原样地，物种组成相对一致。

批注 [LHY1]: 这个结果很有意思！

综合分析可以看出，虽然森林林下和草原的草本植物 α 多样性测度没有差异，但森林林下的物种组成更不均匀。在林下同一地点，从一个样地到另一个，物种替代率较高，即具有更高的“ β 多样性”（这里不太确切，但我想表明一种随位置和环境梯度变化，物种组成转换所体现的多样性）。

讨论：

那么，是什么因素导致了这种多样性格局的差异？我认为可以从以下几个方面来寻找解释。

1. 生境异质性

(1) 光照。在草原，光照基本是均质的，在森林则不然。对于林下草本，其所接受的光照除了受到坡度、坡向等地形因素作用外，还受到乔木遮荫的影响。由于森林中的乔木处在动态平衡中，其分布并不均匀，林隙和乔木是镶嵌分布、甚至斑块分布的（如图-4）。因此，林下的光照条件是异质的。

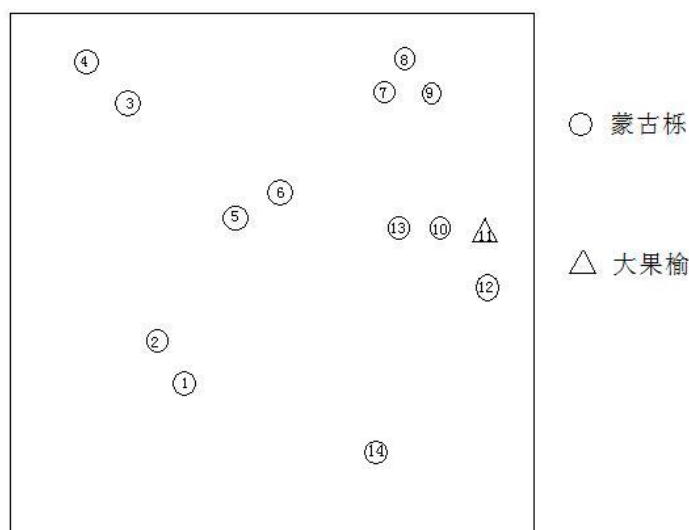


图-4-蒙古栎林乔木分布图

(2) 土壤。林下土壤的异质性也要高于草原。在垂直剖面上，林下土壤具有枯枝落叶层，其分解产生的有机酸，被下渗的降水携带到深层，会加强淋溶和化学风化作用，加剧土壤的垂直分异；而草原土壤的有机质主要由植物死亡分解的根系输入，具有“均腐”的特点，垂直分异不如林下土壤强烈。在水平层面上，林下土壤的异质性更明显。对土壤水分的调查显示（如图-5，6，7，8），同样取 3 个样，在每个深度上，林下土壤的水分含量标准差基本上比草原土壤高。这种土壤的异质性，也使得水分条件具有异质性。

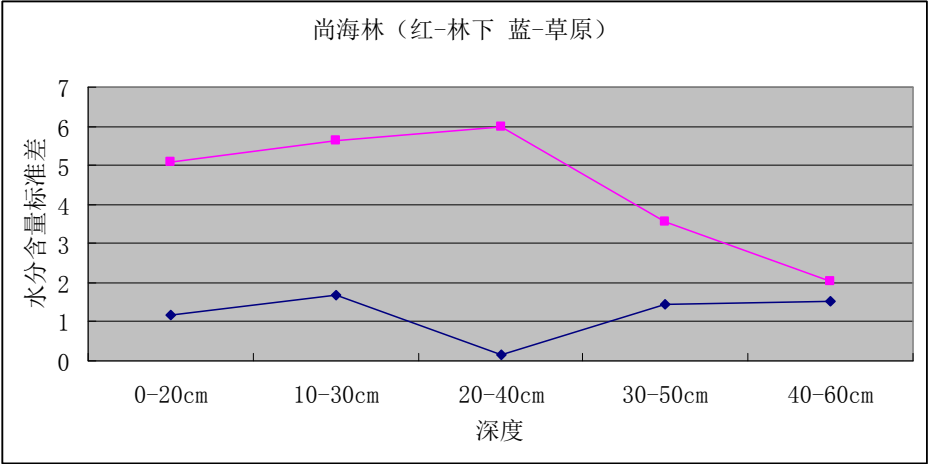


图-5

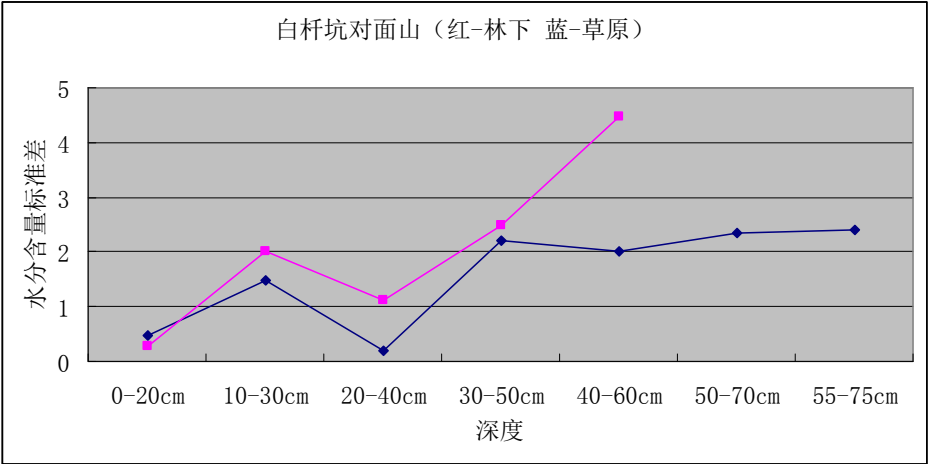


图-6

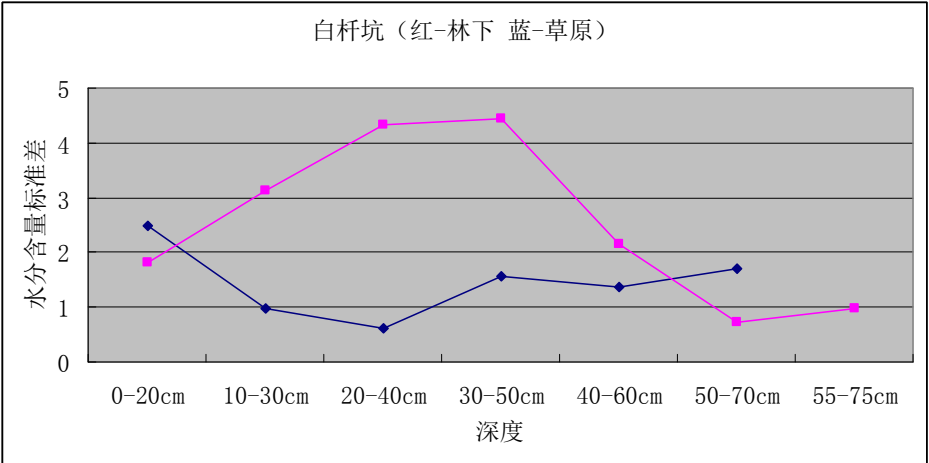


图-7

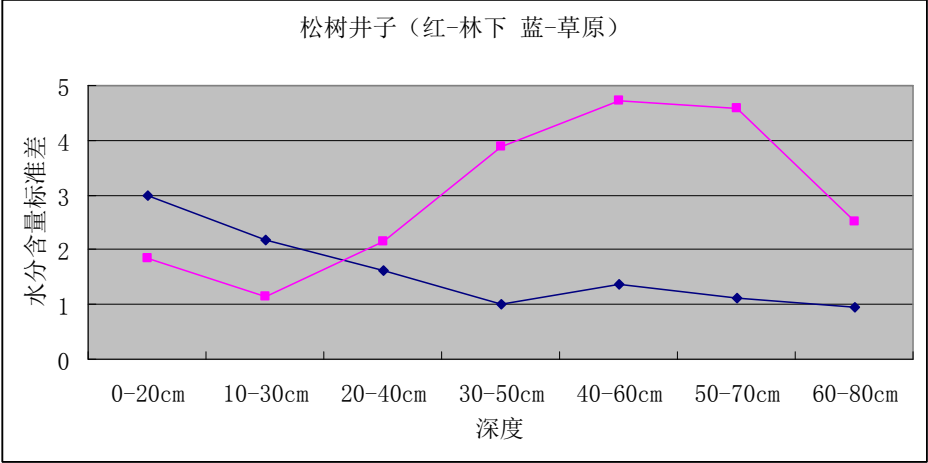


图-8

根据数据分析的结果，生境条件异质性的影响体现在了相邻样地的草本物种替代上，而并没有使 α 多样性的产生差别。那么，又是什么原因平衡了生境异质性的差别对 α 多样性的影响？我推测为后面的几个因素。

2. 生产力和种间竞争

前面提到过，林下草本受到乔木的压制，包括光照的限制和水分的争夺。因此，林下草本的生产力应该低于草原草本（当然，这需要用收割法进行验证）。生产力的低下，很可能限制了林下草本的多样性。而在草原，草本植物占优势，生产力较高。在不受乔木压制的条件下，种间竞争主要表现为草本种类间的竞争，而竞争迫使生态位缩小。高生产力、窄生态位，有利于提升草原草本的多样性。

3. 植物分布特性

光照条件的不同，使得林下草本处在不同的光照生态位上，从而具有不同的分布类型。喜光植物倾向于集群分布在林隙，喜阴植物倾向于集群分布在林荫，而对光照不敏感的草本植物则可能均匀分布，或受到别的因子的影响表现出其他分布。一些植物由于其自身生物学特性，表现出某种分布，如玉竹，其地下茎相连，是一种“克隆植物”，因此呈集群分布。所以，林下草本多呈集群分布，使得其更多表现出一种随位置和环境梯度变化物种组成转换所体现的多样性，而在整体多样性上，并不具有优势。

4. 环境的波动

温带地区草本植物中，地面芽、地下芽和一年生植物占很大比例。草本植物的平均寿命较短，相对于乔木、灌木等木本植物更新很快，这使得草本物种组成可以快速替代。由于草原相对森林是一个开放的系统，所以草原的环境波动更严重，这更加速了物种的替代。快速的替代，会使草原的物种分布更均匀，从而提高 α 多样性（好比一锅沸腾的粥要比凉粥更匀）。

以上的分析，多基于推断，要想彻底弄清这个问题，还需要深入调查，以获得数据支持。对于多样性格局的研究，将有助于我们从另一个角度了解林下和草原这两种不同的环境对草本植物物种组成的影响，从而进一步认识植物与环境的关系。

批注 [LHY2]: 缺结论部分

参考资料:

[1].北京大学环境学院 2007 年夏坝上实习资料总结

[2].Manuel C. Molles Jr. (2002). Ecology-Concepts and Applications,2nd ed. Higher Education Press.

沟谷阴坡林下土壤表层水分梯度的探究

00613017 王旭辉

摘要

阴阳坡分异是一个重要的生态学现象，但阴坡本身的异质性却未引起足够的重视。本文根据实习数据推导阴坡表层土壤水分的分布模式，并尝试用山谷风理论加以初步解释。如果非对称钟型模式得以证实，对于阴阳坡分异现象的研究，多样性研究和土地利用的评估等科学研究和生产活动都有重要的意义。

关键词：

阴坡、土壤水分、异质性

1. 引言(Introduction)

坝上地区属于群落交错带(ecotone)，群落分布受环境因子影响极端敏感，森林和自然草坡交错镶嵌分布。在实习区域，森林群落多分布于阴坡、或沟谷地段，而阳坡和半阳坡多为稀疏灌丛草坡。野外调查发现，该区域郁闭落叶阔叶林多分布在陡阴坡，坡度达到25~39度[1]。

阴阳坡的植被分异是一个非常重要的现象。对于它的研究有助于探求植被分布与环境因子相互做用，并有助于评价和改进土地利用。

国内已经有研究分析阴阳坡植被和土壤水分的差异[8][9][10]。通常在研究这一问题时，在阴坡的采样总是随意的在某一高度随机收集若干样本。然而，我们的野外观测表明，即便是阴坡，土壤水分和林下植被的分布也存在着异质性。忽视这种异质性，将阴坡同质化，有可能导致采样分析不具有代表性，进而导致群落分析和土地利用评估的误差。经验上，许多人认为这种异质性的模式是沟谷阴坡的土壤湿度随高度的上升而下降。然而表层土壤水分的真实分布模式确实是这样吗？

林下植被的分布与表层土壤水分密切相关，是表层土壤水分条件的一个较好的定性指示。本文综合运用本次实习和以往实习采集的草本层群落调查、TDR水分测定和叶面积分析数据来试图描述并分析坝上地区沟谷阴坡表层土壤水分分布模式。

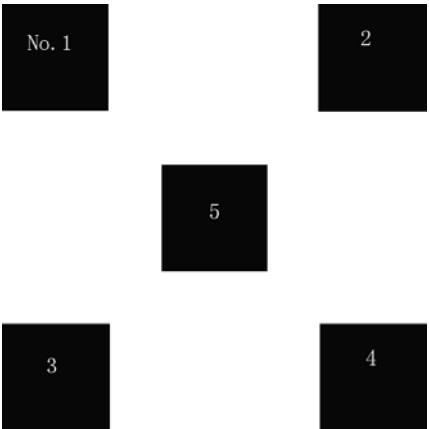
2. 方法(Method)

2.1. 群落调查

群落调查采用快速评估法，具体方法[1]中有详细描述。调查由两组同学分别完成。草本层物种及其高度的描述是准确可信的，盖度数据主观性较强，可能存在一定的误差。本文

仅引用部分沟谷阴坡白桦林下草本层样方调查结果。

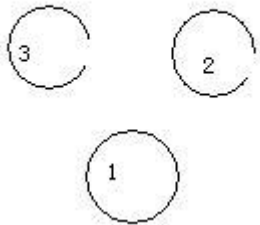
多数情况下，两个小组的样方在坡面的同一或相近高度上。但在二道河口，由于发现沿坡面上升林下草本层发生变化，故两个小组的样方沿坡面相距 60m 左右。下图是每个样地 5 个草本样方的分布模式。



2.2. TDR 土壤水分测定

用 TDR 测试仪在去年所埋设的 PVC 管中测定土壤体积含水量，埋设时将 PVC 管用锤砸至土壤母质层。每个坡面一般有 3-4 根随机放置的 PVC 管，通常集中在 $5\times 5\text{m}$ 的范围以内。

将军泡子 TDR 管埋设模式：



2.3. 叶面积分析

用叶面积分析仪在北京的实验室测定采集得到的华北凤毛菊叶片的面积。由于刘明琦同学在操作时未能测定每片叶子的面积而只测定了每袋叶片的总面积，使得叶面积数据的信息大量丢失，无法进行统计检验给出置信度，只能通过均值猜想其分布模式。

3. 结果(Result)

3.1. 群落调查

以下是二道河口草本层样方的数据对比：

编号:	07——1			
种名	多度	盖度(%)	高度 (cm)	物候相
猪殃殃	sp	1	27	营养期
披针叶苔草	sol	5	21	营养期
乌苏里风毛菊	sol	10	15	营养期
大瓣铁线莲	sol	2	22	营养期
莓叶悬钩子	sol	1	25	营养期
展枝唐松草	sol	2	49/58	花期
歪头菜	sol	1	16/52	花期
种阜草	sol	<1	14/15	花期
毛蕊老鹳草	sol	<1	50/58	花期
金莲花	sol	<1	45/48	花期
地榆	sol	<1	35	营养期
羽节蕨	sol	<1	21	营养期
山野豌豆	sol	<1	28	营养期
广布野豌豆	sol	<1	30	营养期
紫斑风铃草	sol	<1	9	营养期
堇色早熟禾	sol	<1	25	营养期
柳兰	sol	<1	41	营养期

编号:	07——2			
种名	多度	盖度(%)	高度 (cm)	物候相
披针叶苔草	sp	5	18	营养期
乌苏里风毛菊	sp	5	19	营养期
地榆	sp	7	32	营养期
种阜草	sp	3	8/11	花期
羽节蕨	sol	3	19	营养期
山野豌豆	sol	1	36	营养期
猪殃殃	sol	2	27	营养期
展枝唐松草	sol	3	63/70	花期
歪头菜	sol	3	50/55	花期
大瓣铁线莲	sol	2	23/25	果实期
金莲花	sol	<1	22	营养期
野火球	sol	<1	22	营养期
邻生银莲花	sol	<1	24	营养期
裂叶蒿	sol	<1	15	营养期
紫斑风铃草	sol	<1	11	营养期
白缘蒲公英	un	<1	15/38	花期
兔尾儿苗	un	<1	15	营养期

编号:	07——3			
种名	多度	盖度(%)	高度 (cm)	物候相
林地早熟禾	sp	5	38/38	花期

猪殃殃	sol	2	32/33	花期
种阜草	sol	3	14/16	花期
披针叶苔草	sol	2	16	营养期
地榆	sol	1	26	营养期
山野豌豆	sol	1	43	营养期
堇色早熟禾	sol	1	35	营养期
乌苏里风毛菊	sol	1	10	营养期
金莲花	sol	1	20	营养期
大瓣铁线莲	sol	<1	24	营养期
歪头菜	sol	<1	33	营养期
肾叶橐吾	sol	<1	20	营养期
裂叶蒿	sol	<1	20	营养期
银莲花	sol	<1	19	营养期
卷耳	sol	<1	13	营养期

编号:	07——4			
种名	多度	盖度(%)	高度 (cm)	物候相
披针叶苔草	cop3	60	17	营养期
羽节蕨	sp	5	14	营养期
柳兰	sol	3	39	营养期
莓叶悬钩子	sol	1	18	营养期
地榆	sol	<1	17	营养期
猪殃殃	sol	<1	18	营养期
种阜草	sol	<1	10	营养期
大瓣铁线莲	sol	<1	14	营养期
展枝唐松草	sol	<1	58/65	花期
毛蕊老鹳草	sol	<1	23	营养期
山野豌豆	sol	<1	14/17	花期
乌苏里风毛菊	sol	<1	21	营养期
紫斑风铃草	sol	<1	11	营养期
辽藁本	sol	<1	16	营养期
野青茅	un	<1	17	营养期

编号:	07——5			
种名	多度	盖度(%)	高度 (cm)	物候相
披针叶苔草	cop3	50	21	营养期
展枝唐松草	sp	10	39	营养期
糙苏	sol	10	50	营养期
乌苏里风毛菊	sol	1	25	营养期
毛蕊老鹳草	sol	1	37/44	花期
地榆	sol	<1	40	营养期
歪头菜	sol	<1	36	营养期
猪殃殃	sol	<1	28	营养期

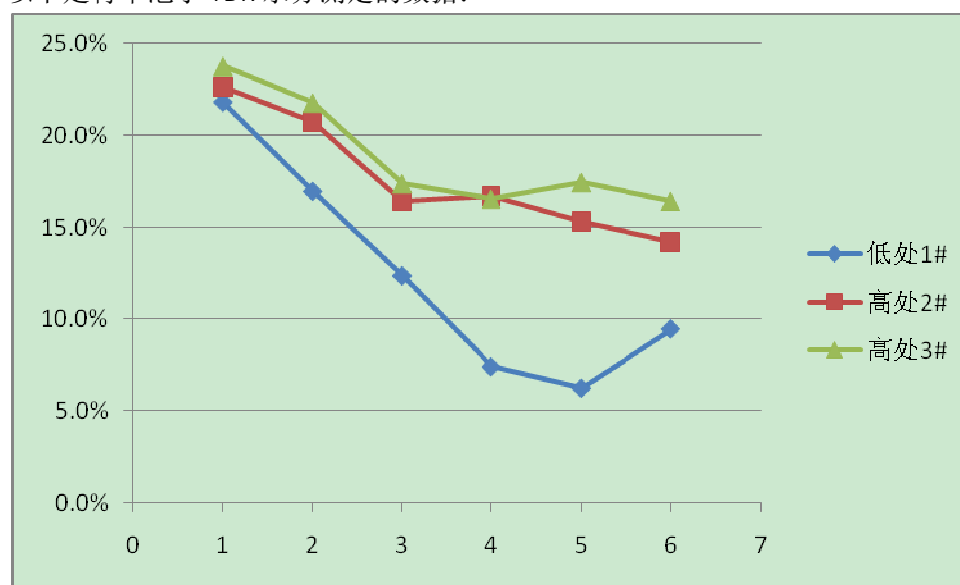
广布野豌豆	sol	<1	36	营养期
山野豌豆	sol	<1	36	营养期
大瓣铁线莲	sol	<1	13	营养期
两齿草	sol	<1	29	营养期
阴地堇菜	sol	<1	30/32	花期
粗根老鹳草	sol	<1	26	营养期
无芒雀麦	sol	<1	36	营养期
矮紫苞鸢尾	sol	<1	24	营养期
紫斑风铃草	sol	<1	11	营养期

在 1 号、2 号和 4 号样方中都发现了喜阴湿的羽节蕨的存在。

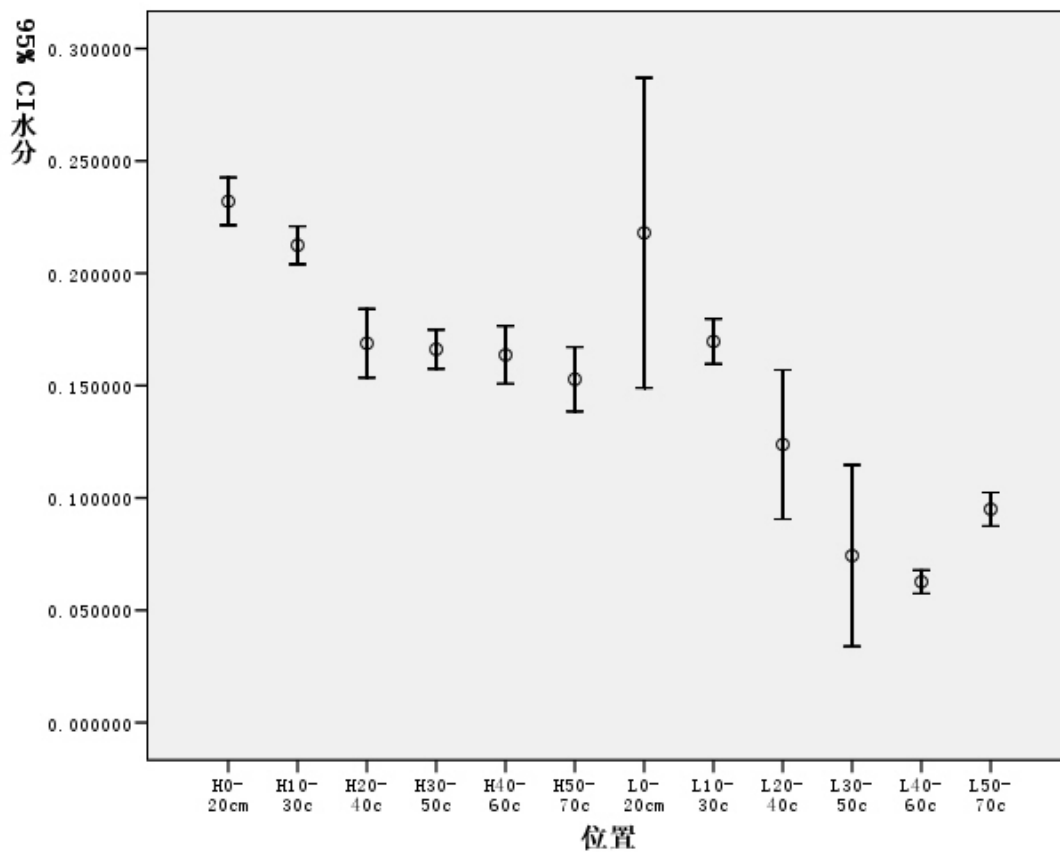
第二组位于坡下部的调查数据尚未整理完成，但笔者查看其原始记录，没有发现蕨类植物的记录。

3.2. TDR 水分测定

以下是将军泡子 TDR 水分测定的数据：

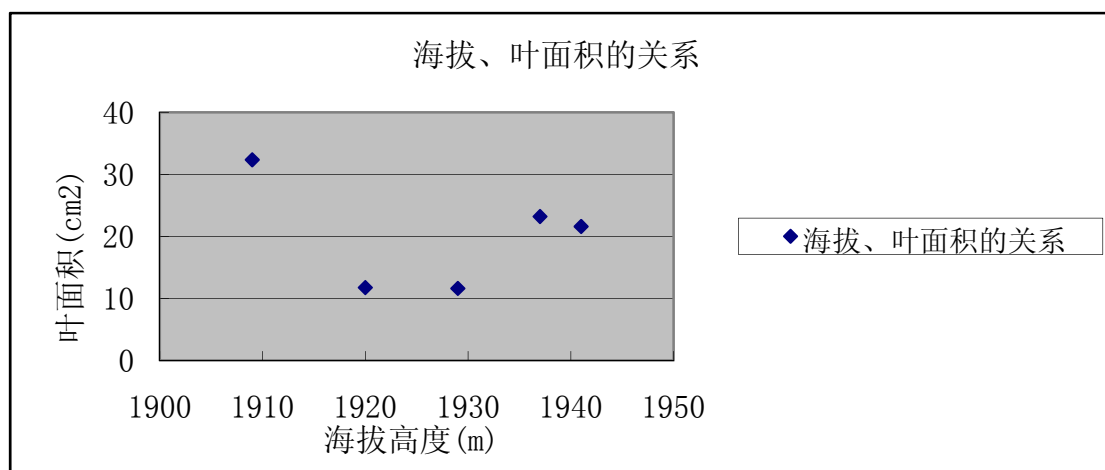


将 2#和 3#管的数据合成为一个 pool 与 1#管数据做方差分析，结果如下，可以看到除最表层土壤以外其它各对应层次均有较显著的差异。

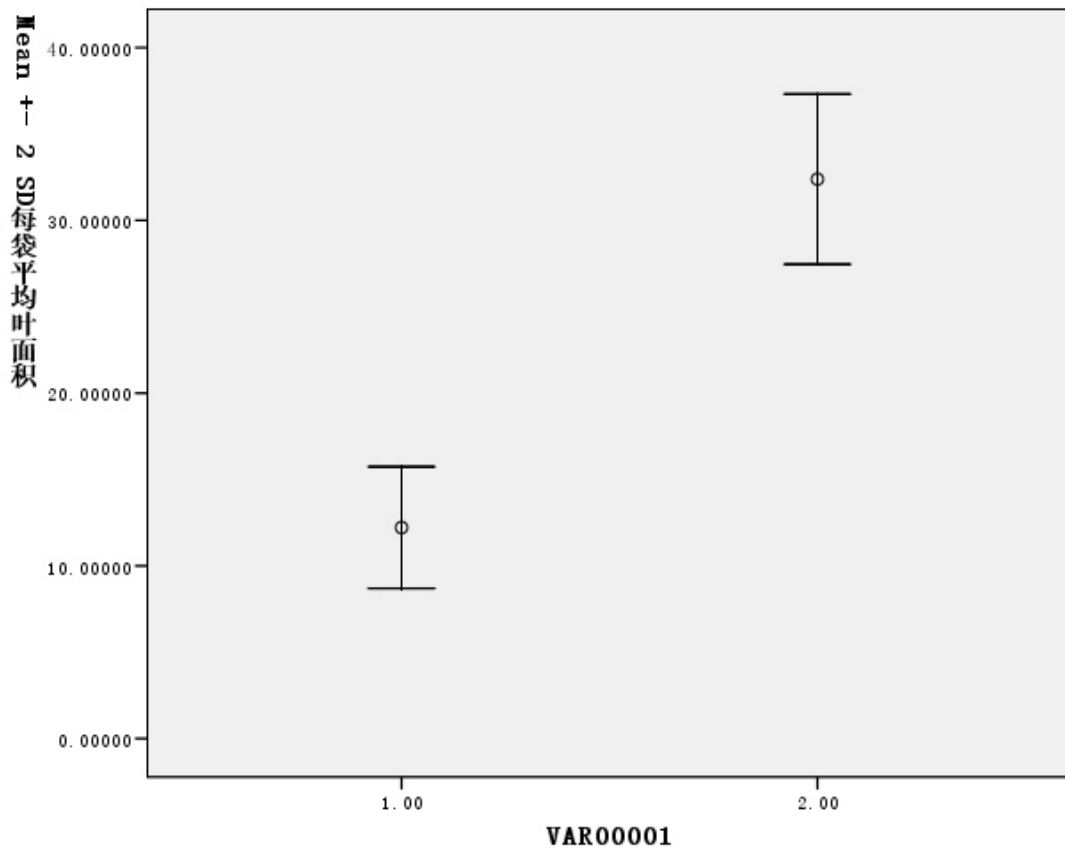


3.3. 叶面积测定

以下是坡高与叶面积的关系：



将林缘与坡肩设定为两个 pool(如下图), 可以看到, 林缘凤毛菊的平均叶面积明显大于坡肩的样本。其中 1 是坡肩叶面积数据集, 2 是林缘数据集。



4. 讨论(Discussion)

蕨类植物在坡中部样方的出现表明坡中部草本植被的生存环境较底部更为湿润。

TDR 测定结果表明坡中部比坡下部水分条件更好，位于阴坡中部的 3 个样点的测定结果的变异（较高的两个样点含水量高于较低的两个样点），这种模式与经验规律相反却与上文所述群落调查的结果相吻合。

华北凤毛菊的采样地点为坡肩草甸和林缘稀疏灌丛，林缘灌丛十分稀疏，光照条件与坡肩相似，然而其叶面积则大于更高位置的样本。有同学认为这是林地的边缘效应，但是这种解释比较牵强，可能将因果关系导致。笔者认为，很可能正是这种水分分布模式决定了树林在坡面的分布范围不可能到达坡顶，在水分含量下降到一定的阈值以后就不能再向上延伸了。

笔者一行曾与清晨前往晾兵台的路上曾观察到阴坡云雾的特殊分布。与通常的假想不同，雾并不是自底向上连续分布，而是仅仅分布在坡中部的上空。由于坡的垂直高度并不大，温度差异并不足以解释这种分布。这可能表明，坡中部的水分条件要好于坡顶和坡底。

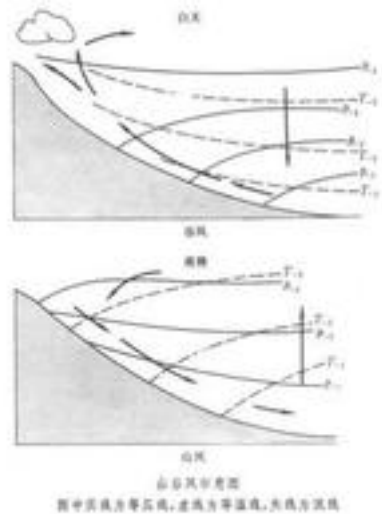
综上，笔者相信沟谷阴坡表层土壤水分的分布可能呈现一种不对称的钟型曲线分布，中间高、两端低。因为坡底通常分布有郁闭的白桦林而坡顶则通常为灌丛或草原。由植被分布不难推知坡底的水分条件要好于坡顶。

这种模式应当如何解释？笔者的文献检索中未见有文章提及这种分布，更没有发现解释这种模式的假说。

表层土壤的水分平衡模式可以概括为： $W1=W0+P-RO-E-Tew$ (刘树华，2004，有修改)，其中 $W1$ 为当前水量， $W0$ 为历史存留水量， P 为降水量， RO 为径流量， E 为土壤蒸发量 Tew

为土壤表层作物蒸腾量。在降水、径流相似的情况下，若假设历史存留水量也相似，则土壤和表层植被的蒸发量可能成为主要原因。

笔者试图用气象学中山谷风的理论来解释这种现象(如图，参见[6])。



夜间坡面的辐射冷却快，温度低，饱和点低。清晨坡底向上运动的湿空气遇冷很快达到饱和，形成了我们观察到的雾。而此时空气相对湿度大于坡底和坡顶。

这种模式抑制和减少了坡中部土壤和草本层植被的蒸发和蒸腾，对于水分的保持具有一定的意义。

但山谷风理论只能解释清晨空气湿度，解释土壤温度的总体状况则显得有些不足 (insufficient)，但通常情况下，空气湿度与土壤湿度具有较好的相关性。有研究表明，与空气的绝对湿度和土壤的绝对湿度相比，空气的相对湿度和土壤水的基质势(matrix potential)与植物的生理生长具有更好的相关性，这也可以为解释这一现象提供一些有益的提示。另一方面，对于植物分布而言究竟是空气湿度还是土壤湿度起决定性作用则还没有定论。沟谷阴坡的特殊性可能导致二者存在分异，从而为分辨空气湿度和土壤湿度对植物的影响提供了一个可能的试验场。

值得注意的是，表层与深层很难界定，本文中笔者倾向于将林下草本植物对土壤水分影响占主导的区域界定为表层，而土壤水分主要受乔木层植物影响的区域以及更深的区域应界定为深层。上文讨论的水分分布模式很可能并不适用于深层土壤。深层土壤的水分平衡如下： $W1=W0+q1-q2-(T_{tot}-T_{ew})$ (刘树华，2004，有修改)，其中 T_{tot} 为植被总蒸腾量。可以看到，这与表层土壤存在显著差别，由于乔木层强大的蒸腾作用和对草本层的遮阴作用，深层土壤的水分分布情况很可能与水分条件的状况相反。

由于数据的收集并不是为研究这个问题所设计，因此本文存在着不少局限性。而由于实习区土层通常较薄，坡顶和坡底的植被类型通常也不同，土壤厚度土壤类型等具有较大的异质性，多变量共变，虽然提供了很多的样本，但也很难加以直接的横向比较。

本次实习为期十天，恰逢湿润年坝上雨季，我们时常在小雨之后进行实习，故这可以解释为什么 TDR 测定时，坡面不同位置 0-20cm 土壤水分为何如此接近。但是，这些植被和土壤水分的分析结果仅能代表雨季的情形，未涉及季节变化和年际变化。而雨季与旱季、湿润年与干旱年之间是否存在模式的变异则有待进一步的研究探讨。

笔者认为，在沟谷阴坡设立一系列的自动微气象和土壤湿度测定装置将有助于进一步观察并解释这一现象。

5. 结论

在坝上地区，沟谷阴坡水分状况和表层土壤含水量并不是随梯度线性变化，而有可能呈现一种中间高两端低的非对称钟型曲线。这种模式表明，在分析阴坡植被或对比阴阳坡的时候，仅仅在一个高度采样分析是不合适的，为了反应这种异质性，应当沿坡面布置若干样点。而这种水分分布模式机理是什么？是否适用于其它地区？则有待于进一步的研究来证实。

6. 参考文献(Reference)

- [1]. 刘鸿雁, 郭大立, 郑成洋, 《野外生态学实习指导》 2008 年 6 月 北京大学生态学系
- [2]. 刘鸿雁 et al 野外生态学教学幻灯片 2008.7
- [3]. 祁兆寰, 王旭辉等 2008 野外生态学实习第一组数据集
- [4]. 李昂等 2007 年野外生态学数据集
- [5]. 刘树华 环境物理学 化学工业出版社 2004
- [6]. 周淑贞等 气象学与气候学 北京 高等教育出版社 1985
- [7]. Reid, I. The influence of slope orientation upon the soil moisture regime and its hydrogeomorphological significance .Journal of Hydrology, 1973, 19 :309-321 .
- [8]. 庄树宏等 昆崙山老杨坟阳坡与阴坡半天然植被植物群落生态学特性的初步研究 植物生态学报 1999, **23** (3) 238~ 249
- [9]. 蒋俊明, 费世民, 王鹏, 雷彻宏, 禾献峰. 干热河谷阴坡和阳坡土壤水分动态研究 四川林业科技 2005(05)
- [10]. 李昆, 陈玉德. 元谋干热河谷人工林地的水分输入与土壤水分研究[J]林业科学研究, 1995,(06) .
- [11]. 余新晓, 张建军, 朱金兆. 黄土地区防护林生态系统土壤水分条件的分析与评价[J]林业科学, 1996,(04) .
- [12]. 王军, 傅伯杰, 蒋小平. 土壤水分异质性的研究综述[J]水土保持研究, 2002,(01) .

大光顶子乌苏里风毛菊叶面积梯度格局分析

00713053 金哲依

本文以大光顶子乌苏里风毛菊叶面积变化的影响因素为主题，全文逻辑清楚，写作规范，结论也有新意，是一篇优秀的实习报告。

摘 要：植物个体大小有随着海拔的升高而减小的趋势，但在塞罕坝大光顶子近坡顶处相对海拔 100 米的生境中，乌苏里风毛菊的叶面积存在差异明显超过了普通海拔梯度所引起的环境因子变化所能解释的范围。通过对沿山坡不同地点乌苏里风毛菊的叶面积和土壤水分测量表明，土壤水分对叶面积梯度格局的形成没有明显贡献，光照很可能是最主要的影响因子。

关键词：叶面积 土壤水分 梯度

前言：

大光顶子（N42° 27.468' 、E117° 32.039' 、海拔 1955 米）为塞罕坝地区的最高峰，坡顶风大，气温低，降水相对林区其他地点较多，其上植被具备高山植被类型的部分特征。对高山植被的长期研究表明，同种植物随着海拔梯度的升高其个体会变小。造成这种现象的主要原因包括温度、水分、风速、光照、土壤养分等。许多 Common Garden 实验都验证了该结论（如 Aston & Bradshaw, 1966, McKay *et al.*, 2001 等）。而在大光顶子的植物群落中，具有明显上述个体大小梯度变化的物种仅有乌苏里风毛菊一种。在实习中发现，从山顶向下不到 150 米的阳坡上聚集分布着乌苏里风毛菊，其叶面积在最底部超过 100cm²，而近坡顶处骤降为 10cm² 左右。在不到 150 米的海拔范围内乌苏里风毛菊的个体大小相差近 10 倍！是什么环境因素导致了大光顶子乌苏里风毛菊的叶面积剧烈变化的梯度格局呢？考虑到数据收集的可行性和有效性，我选取了土壤水分这一指标并探讨了土壤水分对乌苏里风毛菊叶面积梯度格局现状的贡献。

方法与数据：

为探寻乌苏里风毛菊个体大小变化的影响因素，本文以“叶面积”作为其个体大小的指标，这样做的理由是在采集叶片样品时发现，叶片“厚度”不存在差异。

（1）叶面积。以距坡顶 100 米处为相对海拔 0 米，分别在 0 米、25 米、35 米、50 米、70 米、85 米、100 米处，随机摘取 10 片视野内叶面积最大的乌苏里风毛菊叶片。模拟大光顶子近坡顶处地形如图 1 所示。其中相对海拔 0 米处缓地；35 米处为林线，70 米处为树线；

50 米处为单株林下采集的叶子。用 EPSON780 型扫描仪扫描叶片；用 imageJ 软件提取叶面积，并计算数据均值及方差。

(2) 土壤水分。经观察乌苏里凤毛菊的根系主要分布在 0—20cm 处，据此测定 0—20cm 深度的土壤水分。在所有采集叶片的地点挖掘 0—30cm 深的土壤剖面共计 7 个；用环刀在 5—10cm、15—20cm 处各收集一环刀的土壤，共计 14 个样品。称量样品干、湿重，计算土壤含水量。

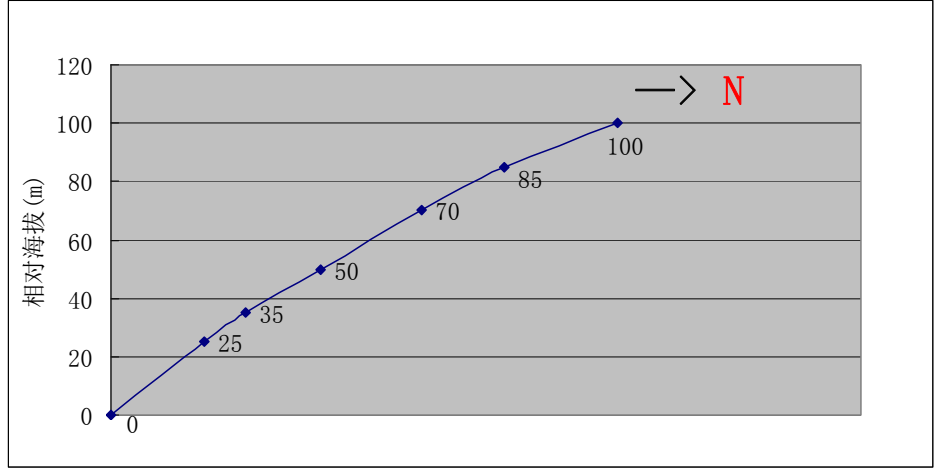


图 1 大光顶子坡顶处地形模拟图

结果:

(1) 叶面积。测量每个采集点的 10 片乌苏里凤毛菊叶片面积，求得均值与方差，所得数据如下表所示：

表一 乌苏里凤毛菊叶面积数据

海拔 (m)	35	60	70	85	85 (单株林下)	105	120	135
Mean (cm ²)	107.74	77.72	58.01	40.41	99.36	36.77	24.71	19.03
SD (cm ²)	15.57	11.28	12.02	4.21	13.23	4.51	2.85	0.83

以相对海拔为 X 轴，叶面积为 Y 轴做图，表示平均叶面积及方差的大小，在 50 米处分别取单株林下与非林下采集的叶面积作图，如图 2—1 及图 2—2 所示：

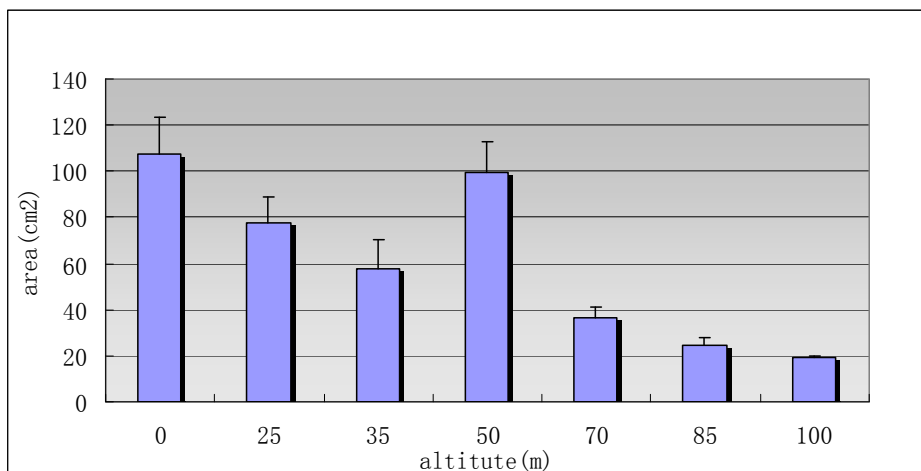


图 2—1 乌苏里凤毛菊叶海拔—叶面积

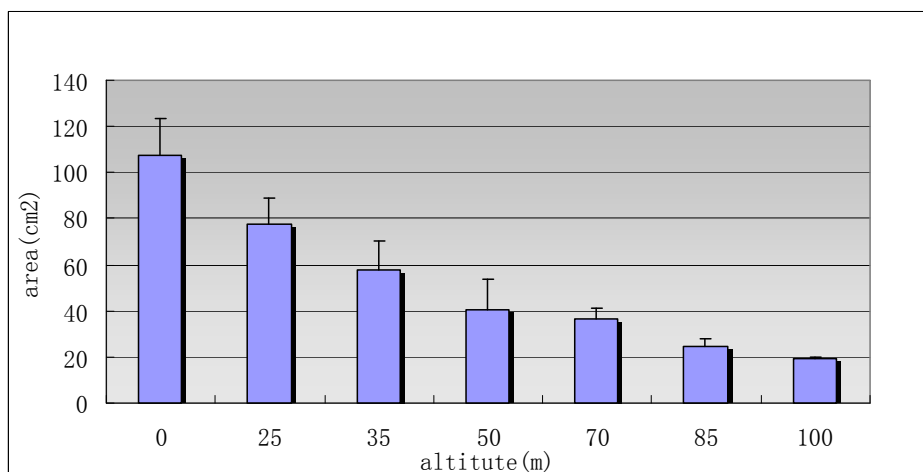


图 2—2 乌苏里凤毛菊叶海拔—叶面积

对比图 2—1 与图 2—2 可以发现，相对海拔 50 米处，单株林下乌苏里凤毛菊叶面积与整体趋势明显不符。以 50 米处单株林下凤毛菊叶面积与非林下凤毛菊叶面积原始数据做 T 假设检验，其中 H_0 : 林下凤毛菊叶面积=非林下凤毛菊叶面积。利用原始数据（林下与非林下分别有 10 个样本点）计算的 T 值为 10.70，远大于 2.5758 ($Z_{0.005}$)，否定 H_0 假设。这表明在显著水平 0.01 下，可以认为林下乌苏里凤毛菊叶面积与非林下乌苏里凤毛菊叶面积存在差异。

利用图 2—2 中数据进行回归分析如图 3 所示：

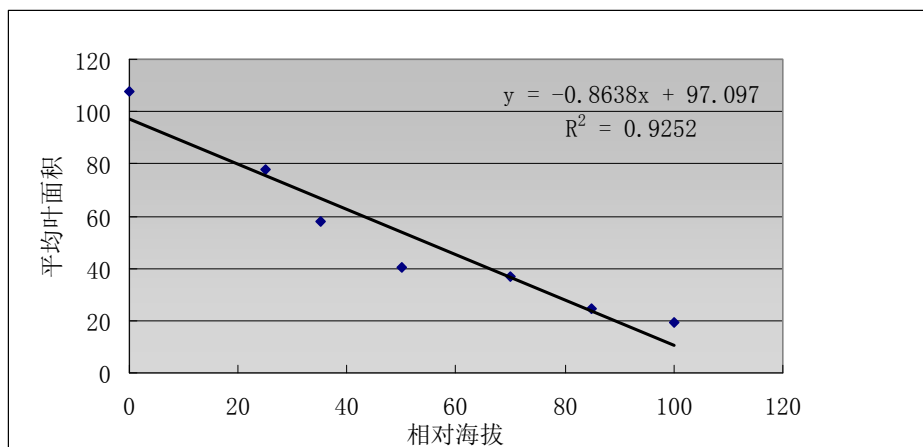


图3 叶面积与相对海拔的回归关系

可以看到,乌苏里凤毛菊叶面积与相对海拔之间存在着较好的相关性。但必须指出的是,相对海拔作为单一指标本身没有太大的意义。相对海拔的变化本质上反映的是光照、风速、土壤水分、土壤养分的变化。

(2) 土壤水分与叶面积。分别以表层土(5—10cm)及浅层土(15—20cm)的相对湿度 P_w 横坐标对海拔作图,分别得到 R^2 为 0.3661 和 0.5394 的正相关关系。这表明土壤水分随海拔梯度升高而便多增加,其中 15~20cm 土壤水分与叶面积的关系如图 4 所示:

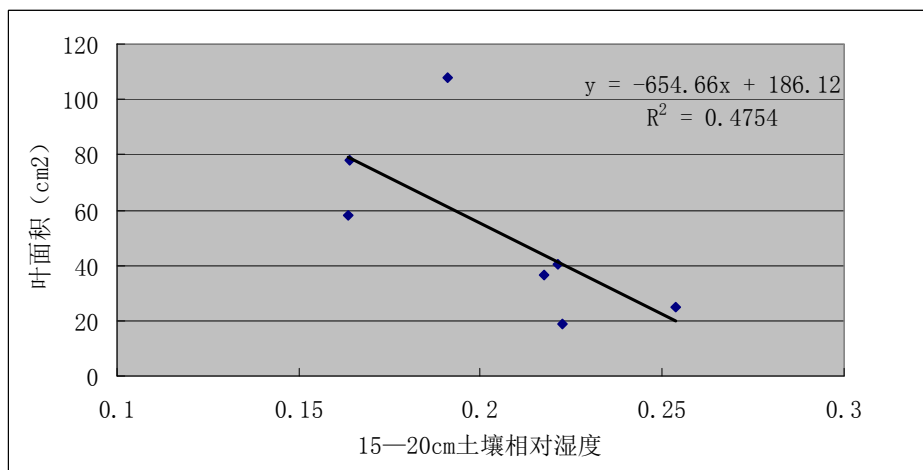


图4 15~20cm 土壤水分—叶面积关系

在上述关系中 R^2 接近 0.5,但考虑到乌苏里凤毛菊多生长于林下、山坡草地、河岸边等较湿润的地点,因此叶面积与土壤水分之间存在着负相关,即水分条件越好叶面积反而越小的结果不能让人接受。合理的解释只能是土壤水分对叶面积梯度格局没有明显的影响力。

综上所述:叶面积梯度与环境梯度,尤其是海拔之间存在着较好的正相关,但海拔实质

批注 [LHY-PKU1]: 也可能根系达到这一深度的植株很少。为什么不用表层土壤湿度

上是对光照、水分、土壤水分、土壤养分的综合反映；土壤水分与海拔之间不存在明显的关联性；土壤水分不是乌苏里凤毛菊叶面积梯度格局形成的主要因素。

讨论：

经过分析我们可以确定土壤水分不是形成乌苏里凤毛菊叶面积梯度格局的主要因素。那么又是什么样的环境梯度在主导着叶面积的差异？

（1）光照。从前面的假设检验可知，林下与非林下叶面积存在明显的差异，而林下与非林下最主要的生境差异为光照。此外，随着海拔升高，光照条件逐渐变好，因此提出“光照是形成叶面积梯度格局的主要因素”这一假说也是很有科学依据的。然而要验证这一假说，就需要测量不同地点的光照强度。又考虑到天气及气候的影响，光强的测定必须长期连续进行。这在目前的工作条件下是几乎不可能实现的。

（2）土壤养分，即土壤碳氮磷含量。土壤中的碳氮磷元素是构建叶面积的重要原材料，碳氮磷含量或与叶面积存在着相关性。但是一方面碳氮磷通常在只在植株体生长的早期起决定作用，分析元素含量应该针对特定时间尺度进行；另一方面，目前根据土壤样品测得的元素含量是生长季之后的土壤碳氮磷，其相对或绝对值的多少不能反映某一地点乌苏里凤毛菊可以获得的营养元素总量。故要探究土壤养分对乌苏里凤毛菊叶面积梯度格局形成的贡献就必须进行控制实验。

（3）地形。地形地貌因素，包括坡度、坡向、风等都会对植株体的生长发育产生影响，而其中风是被讨论最多的环境因子。考虑到在相对海拔 100 米的生境中，近坡顶处风速较林下大得多，故提出“风速导致叶面积梯度格局”的假说也有一定的道理。但要验证这一假说，同样需要长期的观测数据，确定风速、风向等，并以此判定风是否为环境胁迫因子。

（4）温度。以上数据采集于 6 月底 7 月初，正值乌苏里凤毛菊的生长季。但当笔者 9 月份再前往大光顶子调查时发现，此时部分乌苏里凤毛菊开始枯萎，但坡顶与坡底之间乌苏里凤毛菊的叶面积差异有明显减小的趋势。这一现象可以认为坡顶凤毛菊的物候期比坡底晚一些，而造成物候差异的重要原因则为温度。鉴于已有数据中没有延沿坡的土壤温度、大气温度梯度数据，要验证或否定这一假说还有待进一步的实验设计与数据收集。

以上分析较为严谨地论证了土壤水分不是造成大光顶子乌苏里凤毛菊叶面积梯度格局的主导因子，也部分论证了光照对叶面积梯度格局形成的贡献。需要指出的是，限于仪器设备、人力财力状况，目前能够做的分析指标还很少。如有可能，在来年生长季时应该补测光照强度、土壤碳氮磷、土壤温度等数据，通过全面的数据得出可靠的结论。

批注 [LHY-PKU2]: 这一提法很有道理

参考文献:

- [1] 刘鸿雁, 郭大立, 郑成洋, 《野外生态学实习指导》, 2009 年 6 月, 北京大学生态学系
- [2] 贺金生, 普通生态学 I 课程 2009 年课件
- [3] 方精云, 普通生态学 II 课程 2009 年课件
- [4] Manuel C. Molles Jr. (2002). Ecology-Concepts and Applications. 2nd ed. Higher Education Press
- [5] Hans Lambers, F. Stuart Chapin III, Thijs L. Pons. (2008). Plant Physiological Ecology. 2nd ed. Springer Press

针叶林对草本层豆科生物植物种类多样性的影响

00826080

刘果

这是一份主题明确、论述的逻辑性强、写作较为规范的实习报告。不足之处是讨论部分需要加上引文证实某些说法，这样能是你的发现更加令人信服。

摘要：以河北省围场县的白杆林、落叶松林、白桦林和草原共六个样地为研究对象，利用样方法进行植物群落调查，说明针叶林林下草本层多样性较小的原因，以及针叶林对草本层多样性的影响。通过对比得出，在水热条件相当的情况下，针叶林并不会影响生物多样性林下植物物种多样性，而针叶林多要样性较小这一规律产生的原因更多在于针叶林所处地带性植被的特定地区的水热条件。针叶林没有影响多样性的原因可能有二，一是形成自己独有的群落，二是通过抑制促进了多样性。

关键词：针叶林，草本层，生物多样性，抑制作用

批注 [微软用户1]: 抑制什么？

针叶林相比阔叶林或者草原有许多不利于林下植物生长的特点。首先针叶林一般而言终年有叶片存在，减少了林下植物的光照时间，特别是缺少了对于许多植物发育极其重要的早春光照；第二是针叶分解较慢，一方面会在土壤表面堆积遮挡光照抑制植物幼苗发育，另一方面减缓了森林生态系统中的物质循环；第三是针叶在分解后会产生酸性物质，会对植物以及土壤中微生物产生影响。但是，这些抑制作用并不一定会对林下的物种多样性产生影响；物种多样性包含了单位面积物种数以及不同物种之间个体数分配的平均程度，并不仅仅取决于条件是否适宜植物生长。

一般而言，针叶林下的植被比阔叶林而言覆盖面小且物种数少。但是，考虑到针叶林作为一种地带性植被的分布区域纬度比阔叶林的分布区域更高、气候也更加干冷，这一现象产生的原因便可能只是水热条件的地域分布，而非针叶林自身的抑制作用。如果能够在接近的地点作出针叶林和阔叶林的样地对比，就应该能够排除水热差异的干扰，从而分离出针叶林本身抑制作用的影响。同时，针叶林的抑制作用中土壤酸化是个重要因子，而真菌对于酸性较为敏感。豆科植物的根瘤菌为真菌，所以着重分析豆科植物在不同群落中的情况也能为说明针叶林的抑制作用提供线索。

1. 研究方法

研究区域位于河北省围场县，当地降水在 400mm 左右，为林草交错地带，为各种不同植被类型的调查提供了便利。所取的样地分为三个小组，每组两个，一个针叶林一个阔叶林或草原。每组尽量选取海拔、经纬度、坡度、坡向都相近的两个样地，但由于不同群落分布在不同的生境下，这一点难以完全达到。为弥补水热差异的区别，本文着重考察了豆科的生长情况，为针叶林的抑制作用提供说明。三个小组的地理位置如下图所示。

批注 [微软用户2]: 豆科植物能弥补水热差异的区别？

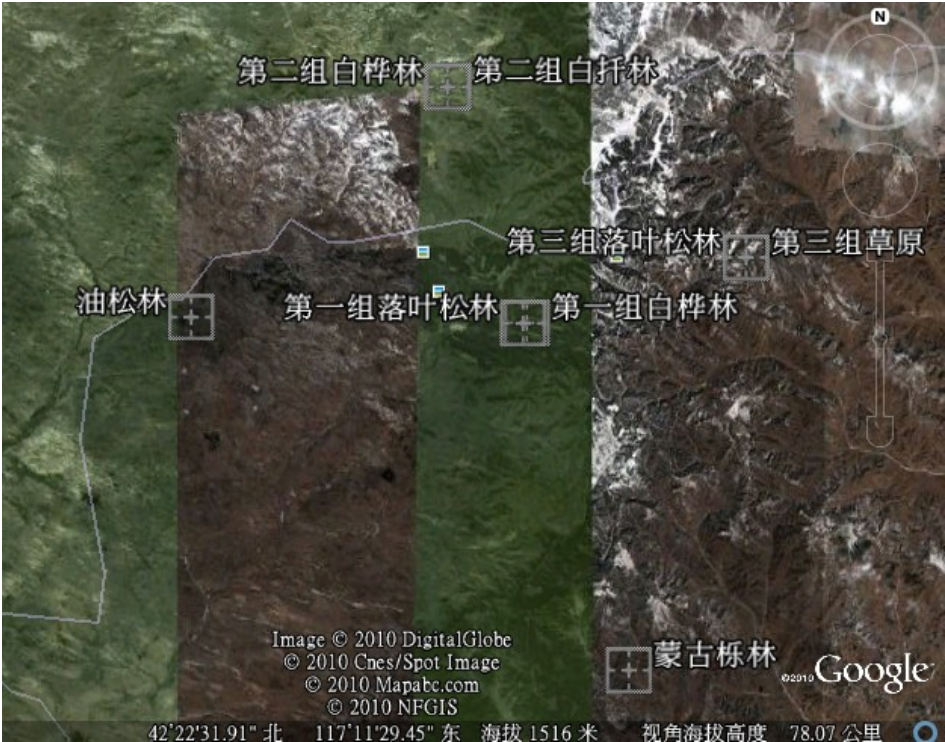


图 1

在草原中，样方以 2 米×2 米为标准；而在森林中，则取 10 米×10 米的大样方，再在其中取 5 个平均分布的 2 米×2 米的小样方，将数据合并为大样方数据。其具体统计方法如下：

10 米×10 米大样方的统计方法：

多度：5 个小样方多度的量化之和。量化标准为 Cop3=100, cop2=75, cop1=50, sp=25, sol=10, un=1。

盖度：为各小样方盖度之平均，未出现该种的小样方记为零。即将各小样方百分比盖度相加除以 5。

株高：各小样方株高之平均。即将各小样方株高相加除以频数。

物候相：各小样方内出现的所有物候相。

2. 结果与分析

三组研究样地的相关参数及其主要统计结果如下表所示。

表 1

	群落	经纬度/°	海拔 /m	坡度 /°	坡 向 /°	α 多 样 性 (Shannon-wiener 指 数) /bit	β 多样性 (Jaccard 指数)
第一	白桦林	42.40995, 117.32155	1630	15	NE310	2.76244	0.19230

批注 [微软用户3]: 缺“表名”

批注 [微软用户4]: 此表中保留 5 位
小数，没有必要

组	落叶松林(人工林)	42.40965, 117.318	1628	0	0	2.56187	
第二组	白桦林	42.57923, 117.24395	1537	11	NE16	1.89763	0.11363
	白桦林	42.57992, 117.24527	1542	32	NE3	3.16035	
第三组	草原	42.4565, 117.53512	1812	0	0	3.02316	0.37209
	落叶松林 (35年人工林)	42.45695, 117.53453	1826	0	0	2.96269	

第一组:

这一组对比的样地位于尚海纪念林林区。两个样地之间海拔相差不大,仅两米;白桦林位于 15° 的西北坡上,而落叶松林位于平地。两个群落之间总盖度差异不大,物种数、 α 多样性皆是白桦林较大,但也不甚明显(白桦林 33 种,落叶松林 29 种)。其共有物种及其在两个群落中的平均株高与相对密度列表如下,下划线者为针叶林中更占优势者:

表 2

物种	白桦林	落叶松林
小红菊	8, 0.061114	25, 0.000411
歪头菜	34, 0.024898	38, 0.020568
瓣蕊唐松草	26, 0.01675	50, 0.010695
地榆	<u>16, 0.01675</u>	<u>28, 0.143974</u>
异叶败酱	16, 0.015844	0.000411
缬草	25, 0.013581	30, 0.010284
硬质早熟禾	<u>30, 0.011317</u>	<u>42, 0.041135</u>
珠芽蓼	40, 0.009054	0.000411
草原老鹳草	<u>10, 0.004527</u>	<u>25, 0.018511</u>
裂叶蒿	<u>25, 0.004527</u>	<u>22, 0.102838</u>

两个样地共有种 10 个,其相似性指数为 0.16981。在白桦林中,披针叶藁草与乌苏里风毛菊占优势,其他在数量上占优势的种依次为鸡腿堇菜、猫眼草、粟草,而这些种在落叶松林中都未出现。而在针叶林中,种阜草占优势,其次为地榆、裂叶蒿、蒙蒿和弯穗鹅观草。白桦林位于西北坡上,水分条件比落叶松林略好;相应地,落叶松林占优势的五个种比白桦林的习性偏干燥。这一点在上表中也有所反映:在白桦林中更占优势的种总体而言比剩下的喜湿。

白桦林中有豆科植物 5 种:山野豌豆、歪头菜、假香野豌豆、野火球和广布野豌豆;而落叶松林中仅有歪头菜一种。显然,针叶林对于豆科生长有所抑制。

第二组:

这一组对比样地位于白桦坑,白桦林与白桦林相互替代分布。在立木更新中,白桦林以白桦为主,而白桦林中以白桦为主。显然,白桦林与白桦林分别会向对方演替。这种在时

间和空间上的交互分布使得这一组成为考察针叶林对林下草本抑制作用的理想对比。所选两个样地相距较近，坡向皆为北偏东；白扦林坡度较大，海拔也比白桦林高五米。

在白扦林的 5 个小样方中有 2 个数据丢失，而白桦林仍有 5 个小样地。样地调查结果显示，尽管白扦林小样方数量较少，但白扦林林下草本种类达到了 33 种，而白桦林林下草本种类仅有 16 种。如果白扦林小样地数据完整的话，两者之间差距无疑会更大。对 α 多样性的计算结果也显示，白扦林样地 α 多样性 (3.16035) 远比白桦林样地 α 多样性 (1.89763) 高。这一组水热、地形条件相似的样地表明，可能针叶林对草本的抑制作用并不会对草本的多样性产生负面影响。

观察两个样地的调查表可知，白桦林下 523 的个体总数中红花鹿蹄草占了 400，而白扦林下个体数在种之间分布较均匀，即使是占优势的白婆婆纳也仅在 630 的总数中占了 85。由于 Shannon-wiener 指数也考虑到了物种之间个体数的平衡，这也是白扦林 Shannon-wiener 指数远大于白桦林的一个重要原因。

批注 [微软用户5]: 如何统计出来的？

表 3

物种	白桦林	白扦林
南牡蒿	3, 0.001083	8, 0.07732
矮紫苞鸢尾	27, 0.022752	27, 0.05799
林地早熟禾	45, 0.065005	50, 0.045103
披针叶藁草	25, 0.189599	20, 0.032216
华北风毛菊	4, 0.001083	20, 0.025773

两个样方共有种仅 5 个，相似性也较低，为 0.11363。在两个林地的共有种中，在白桦林中占优势的林地早熟禾与披针叶藁草比在针叶林中更占优势的南牡蒿、矮紫苞鸢尾与华北风毛菊略喜湿，但差异不甚明显。

白桦林中有歪头菜与广布野豌豆两种豆科植物，而白扦林中有黄花棘豆和辽西篇蓄豆两种。由于针叶林对土壤的酸化需要一定的时间且有一定的滞后性，在这样一个白扦和白桦交互生长的群落里对豆科的抑制便没有体现出来。

第三组：

第三组位于亮兵台草原，一个样地为草原而另一个为 35 年的人工落叶松林。两者均为平地，落叶松林海拔高出 14m。通过这一组样地，可以对比出落叶松林生长后对草原植被的影响。

草原样地的草本层覆盖率大于落叶松林样地，但物种数小于落叶松林。但是，两者样地面积不同；草原样地样方面积为 2 米×2 米，而落叶松林为 10 米×10 米样地内的 5 个 2 米×2 米小样方。如果考虑两者单位面积异质性之不同所带来的对样方面积差异的抵消的话，也许在某种程度上可以相比较；草原样地物种数为 28，而落叶松林样地为 31。计算 α 多样性的 Shannon-wiener 指数可知，草原样地为 3.02316bit 而落叶松样地为 2.96269bit；两者相差极小，在不同的取样方法造成的误差下，可忽略。

表 4

物种	草原	落叶松林
珠芽蓼	45, 0.032808	9, 0.03038
砧草	20, 0.065617	13, 0.093671
兴安蛇床	30, 0.032808	13, 0.126582

繸草	30, 0.032808	17, 0.055696
西伯利亚早熟禾	45, 0.001312	18, 0.017722
歪头菜	50, 0.065617	30, 0.01519
鼠掌老鹳草	10, 0.032808	12, 0.020759
披针叶藁草	25, 0.098425	15, 0.086076
南牡蒿	10, 0.065617	9, 0.113924
毛女娄	15, 0.013123	10, 0.005063
柳兰	25, 0.013123	20, 0.005063
林问荆	35, 0.032808	32, 0.043038
华北风毛菊	35, 0.098425	25, 0.048608
花葱	70, 0.013123	60, 0.005063
地榆	30, 0.065617	24, 0.022785
艾蒿	40, 0.065617	15, 0.005063

由于落叶松林为人工林，两个样方共有种多，共有 16 个，相似性指数 Jaccard 指数也高达 0.37209。在其共有的 16 个种中，总的而言，在落叶松林中占优势的砧草、兴安蛇床、繸草等要比在草原上占优势的鼠掌老鹳草、毛女娄、地榆、艾蒿等更喜湿或耐阴。

在草原样方中，有蒿薹豆、歪头菜和广布野豌豆三种豆科植物；而在落叶松林样方中仅有歪头菜一种豆科植物。这一组落叶松林对豆科植物的抑制作用也较为明显。

3.讨论与结论

从以上结果中可以看出，除了白杉白桦交互生长的第二组以外，一、三组中针叶林对豆科植物的抑制作用表现得较为明显。两组中的针叶林下仅有歪头菜这一种豆科植物出现，且其中歪头菜的相对密度皆小于其对照组。这极有可能是由于针叶分解产生的酸性物质对根瘤菌的抑制作用导致豆科植物失去竞争优势而产生的。对于歪头菜这一物种，有可能它对于根瘤菌依赖较其它豆科植物少。如果推断正确的话，那么针叶林的抑制作用是显而易见的。

但是于此同时，三个组中针叶林林下的物种多样性都没有明显比对照组小；第二组中，甚至白杉林林下物种多样性明显大于白桦林下。当然第二组情况的产生可能更多归因于局地因素，不能说明白杉林林下物种多样性总体而言大于白桦林林下；但是，至少没有发现针叶林的物种多样性有明显的减少。所以，一般而言的针叶林多样性较小可能主要是由于更大尺度的气候因子决定的。

在针叶林抑制作用存在的情况下，它对多样性没有产生影响的原因有多种可能。

首先，针叶林的特殊环境是对大多数植物而言为抑制；但是，这种特殊的生境下也会形成属于自己的群落，其生物多样性并不一定比同等条件的其他群落小。对于这些群落而言，只是不同环境决定的不同群落，与生物多样性并无直接关系。

其次，针叶林环境的抑制作用还可能促进草本层的生物多样性。在水热条件合适的情况下，有时会形成单一或者少数几个种占绝对优势的群落，例如第一组白桦林中披针叶藁草和乌苏里风毛菊占绝对优势，而第二组白桦林中红花鹿蹄草占绝对优势。在气候条件一定的情况下，这些优势种会通过其对相应生态位的占据获得繁殖与营养上的竞争力从而保证其优势地位的延续。然而在针叶林这种对大多数植物而言具有抑制作用的环境中，很难有某几种植物占绝对优势，这也就使得相对空余的生态位可以有更多的物种去填充，从而促进了生物多样性。从样地的数据便可以看出，针叶林的草本层物种的分布更加均匀，即相对密度的方差

批注 [微软用户6]: 能否找到支持这一说法的文献加以引用？

更小。

但是，这两种假设的验证一是需要更大的样本量，二是需要用实验来证明抑制作用在何种尺度下对生物多样性具有促进作用。无论针叶林对物种多样性影响的机制如何。

4. 结论

从以上数据和讨论中可以得出，尽管针叶林的抑制作用存在，但是它对物种多样性并没有产生显著的影响。经验性的对针叶林缺乏多样性的认识经实践检验确实合理，但是可能这一现象产生的原因更多归因于针叶林大多生长在水热条件相对匮乏的地带，而不在于针叶林本身带来的环境。

参考文献：

[1] MANUEL C. MOLLES. Ecology. McGraw-Hill. 2006-10-01

[2] 孙儒泳，李博，诸葛阳，尚玉昌. 普通生态学. 高等教育出版社. 1993-10 第 1 版

带格式的：缩进：首行缩进： 0 厘米

塞罕坝地区白桦林下草本层植物叶级影响因素分析

批注 [L1]: 文章科学问题明确, 思路清楚, 逻辑性强, 写作总体比较规范, 需要注意文献引用的写法

范吾思 1000013239 城市与环境学院 生态系

摘要: 本文通过计算塞罕坝地区五个相似白桦林群落下草本层的两种叶级谱, 并对可能影响草本层叶级的相关环境条件与叶级谱进行了关联性分析, 来探寻在该尺度下白桦林群落草本层叶级谱变化的主要影响因素。得出了在本文的研究尺度上, 相似白桦林群落下草本层的叶级谱主要受到较大尺度上的水热条件影响, 随经纬度体现出由东南向西北叶级递减的规律的结论。

关键词: 塞罕坝 草本层 叶级谱 经纬度

叶级区分叶面积大小, 植物的叶面积受到光照、水分、温度等环境条件的影响; 而一个植物群落的叶级谱则能够在一定程度上反映其所处环境。在所查阅到的资料中, 对植物群落叶级谱的研究多为调查与描述, 却少有关于影响群落叶级谱的主要环境条件的讨论。

在山地环境中, 环境条件不仅受到纬度、海拔等大尺度地形因子的影响, 坡度、坡向等小尺度地形因子也会影响植物生长的环境条件, 受到在实习过程中观察到的现象启发, 在本文, 试图通过对于实习地区五个相似森林群落下草本层的叶级谱的计算, 以及对可能影响草本层叶级的相关环境条件与叶级谱进行关联性分析, 寻找在该尺度下草本层叶级谱的主要影响因素。

1 数据与方法

选取塞罕坝地区五个较为相似的白桦林群落作为研究样本, 之前在野外调查过程中已获得了这五个样地基本群落信息和地理位置信息。

计算各草本层植物叶级^[1]根据植物志给出的叶片形状、大小信息, 运用相近几何图形公式, 粗略估算各样地草本层各植物的平均叶面积, 并按照 Raunkiaer(1934)叶级分类系统逐一进行分级。之后对各样地分别进行统计, 获各个样地的各叶级物种总数分别占该样地总物种数的比例(定义为叶级谱 1); 分别各样地草本层的物种重要值, 再次对各样地分别进行统计后获得各个样地的各叶级物种重要值加和分别占该样地所有物种重要值加和的比例(定

义为叶级谱 2)。

对叶级谱和环境条件进行关联性分析。分别将五个样地按照不同环境条件进行排序，分析在各排序下其两种叶级谱是否表现出明显的变化规律，从而讨论用于排序的环境条件对于叶级谱的变化是否有明显影响。

表 1 样地基本信息

样地编号	群落类型	地理位置	坡度	坡向	纬度	经度
1	白桦林	尚海林	27°	NE320°	42° 24′ 35.68″	117° 19′ 16.31″
2	棘皮桦-白桦林	无名山对侧	11°	NE30°	42° 09′ 17.24″	117° 25′ 34.37″
3	白桦林		16.5°	NE355°	42° 34′ 32.61″	117° 07′ 39.11″
4	白杆-白桦林	克什克腾旗白杆坑	10°	NE30°	42° 34′ 48.81″	117° 14′ 38.43″
5	白桦林	界河	38°	NE51°	42° 25′ 60.52″	117° 18′ 21.93″



图 1 样地位置卫星图

2 结果

2.1 坡向对手叶级谱随坡向的分布影响

由于当地林草交界带的水分特点，所有五个森林样地都位于水分较为充足的北坡，但其朝向与正北方向的夹角大小各异，这一角度影响到光照条件和水分条件，故按照该角度大小对样地进行排序（3-2-4-1-5）。排序之后的叶型谱 1（图 2）和叶型谱 2（图 3）没有表现出

明显的变化趋势。

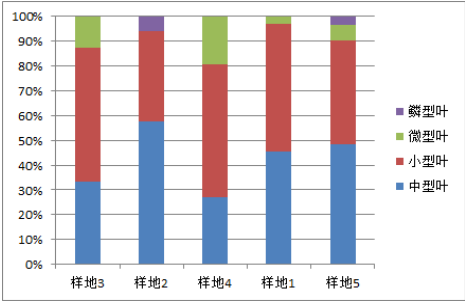


图2 五样地各叶级所占物种数比例
(样地按坡向距正北差值升序排列)

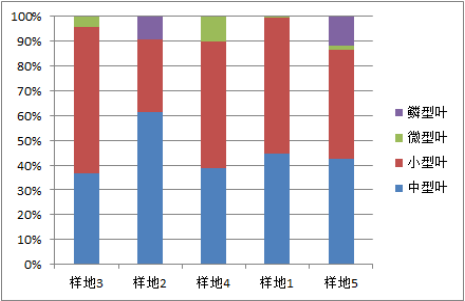


图3 五样地各叶级物种所占物种重要值比例
(样地按坡向距正北差值升序排列)

2.2 叶级谱沿坡度梯度对手叶级谱的分布影响

坡度大小也影响着草本层植物的光照条件和水分条件，按照坡度大小对样地进行排序（4-2-3-1-5），排列后的叶型谱1（图4）和叶型谱2（图5）也没有表现出明显的变化趋势。

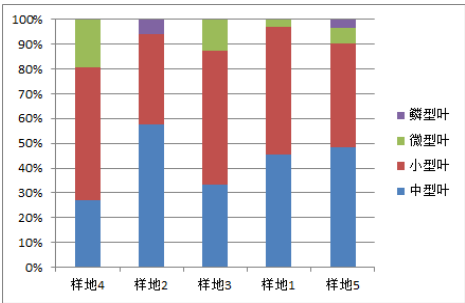


图4 五样地各叶级所占物种数比例
(样地按坡度升序排列)

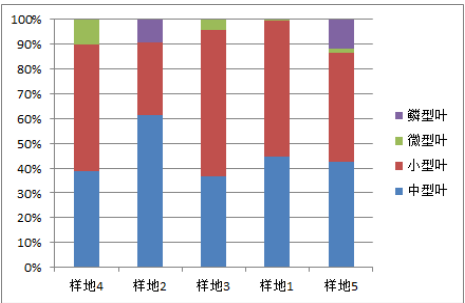


图5 五样地各叶级所占物种重要值比例
(样地按坡度升序排列)

2.3 叶级谱沿纬度的分布对手叶级谱的影响

将五个样地按照纬度由南到北排列（2-1-5-3-4），可明显看出叶级谱1和叶级谱2都有一定的变化规律：由南向北，叶型谱中中型叶所占的比例有下降趋势，而微型叶所占比例有上升趋势。这一点在折线图中体现得更为明显。

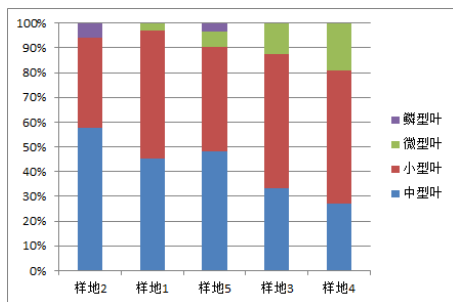


图 6 五样地各叶级所占物种数比例

(样地按纬度从南向北排列)

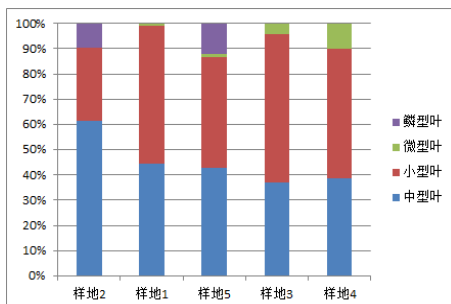


图 7 五样地各叶级所占物种重要值比例

(样地按纬度从南向北排列)

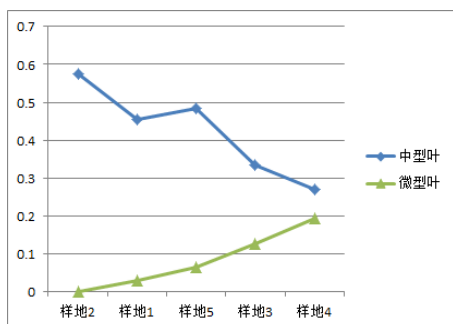


图 8 中型叶和微型叶所占物种数比例在五样

地中变化情况(样地按纬度从南向北排列)

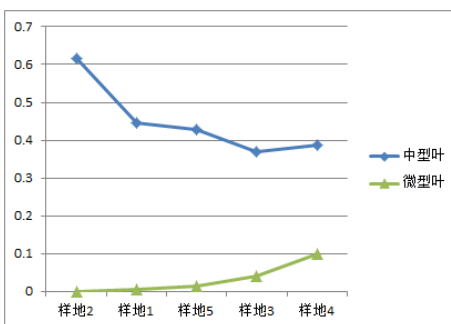


图 9 中型叶和微型叶所占物种重要值比例在五样

地中变化情况(样地按纬度从南向北排列)

2.4 叶级谱沿经度对于叶级谱的分布影响

:将样地按照纬度由西到东排列(3-4-5-1-2),也可看出叶级谱1和叶级谱2都有一定变化规律,由西向东,叶型谱中中型叶所占的比例有所上升趋势,在叶型谱2(图11)中体现更为明显,而微型叶所占比例有所下降趋势。但根据经度排列后得到的叶型谱变化趋势不如按纬度排序所得到的明显。

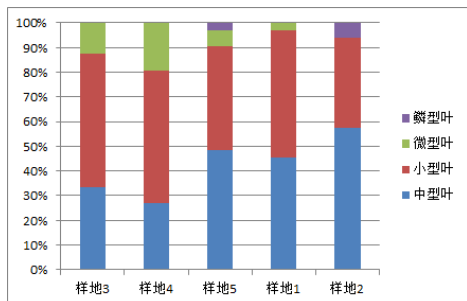


图 10 五样地各叶级所占物种数比例

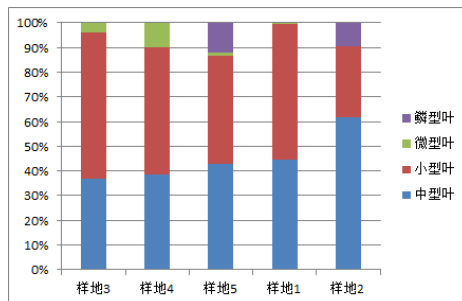


图 11 五样地各叶级所占物种重要值比例

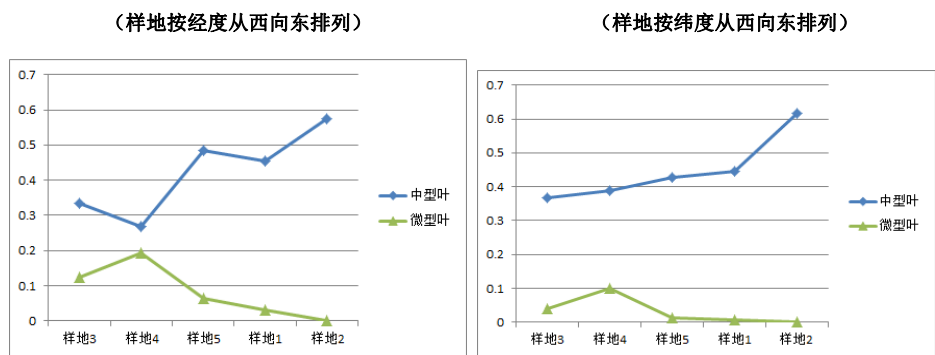


图 12 中型叶和微型叶所占物种数比例在五样地中变化情况（样地按经度从西向东排列）

图 13 中型叶和微型叶所占物种重要值比例在五样地中变化情况（样地按经度从西向东排列）

3 讨论

通过对五个样地按照坡度、坡向、纬度和经度四个条件分别进行的排序，可以发现仅在按照纬度、经度排序的时候五个样地的叶型谱（1、2）表现出了一定的规律性变化，且其变化规律为：由南向北、由东向西，叶型谱（1、2）中的中型叶所占比例有下降趋势，而微型叶所占比例有上升趋势。

这表明在该尺度上，相似白桦林群落草本层的叶级谱的变化主要受到经纬度的影响。鳞型叶在五片样地中变化较大且不规律，但鳞型叶的植物只有草问荆和龙须菜两种，偶然性过大，而除此之外，五片样地的叶级谱的变化规律基本表现为：由南向北、由东向西草本层叶级递减的趋势。

经纬度主要影响水热条件的分布，而从图 14 可看出，样地地区大致有 SE-NW 的温度梯度和水分梯度，由东南向西北，温度降低，水分减少，植物叶片面积减小有减少水分散失的作用，也能减少蒸腾散热，有一定保温作用，这样可以在一定程度上解释叶级谱的变化趋势。而且从五片样地的地理位置来看（图 1），叶级谱变化趋势最明显的的样地排列方式（2-1-5-3-4）也正好大致符合样地从东南向西北的排列。但这一解释需要更多样地的数据以及水分温度数据进行进一步验证。

但是另一方面，纬度增高也会导致光照强度和范围相对减少，草本层位于阴影下的面积增大，这有可能导致植物叶片具有一定阴生特征，叶面积增大。然而这一规律没有在叶级谱随着纬度的变化当中体现出来，很可能是由于在该林草交界带地区水分的影响更为重要，占主导地位。

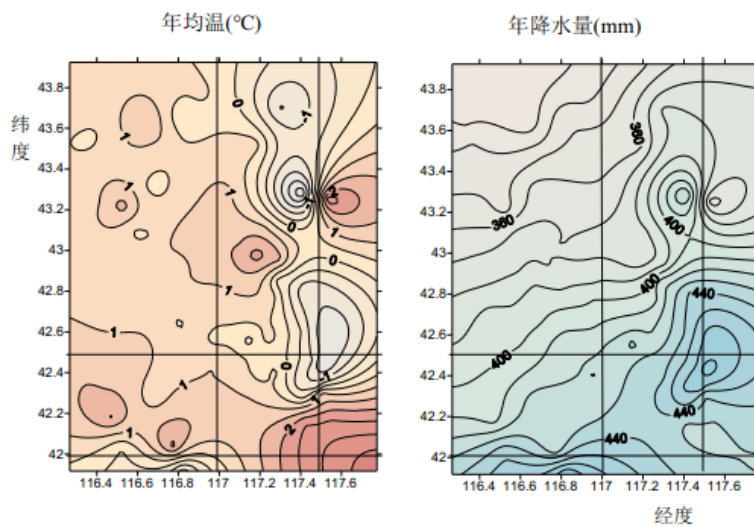


图 14 研究地区主要气候指标的空间分布（刘鸿雁等，2005）

（横线、竖线分别标出样地所跨经纬度范围）

小尺度的地形因素坡向和坡度可以影响光照的强度和范围，理论上对于叶级的大小有一定的影响，但在所研究的五个样地中并没有明显的体现，这说明在所选取的研究尺度上，叶级的影响因素主要为较大尺度的水热条件，而小地形的影响并不显著。但本文由于数据缺失并没有考虑树高和群落密闭度的影响，可能造成一定误差。

4 结论

总结以上的分析结果，本文得到如下几条结论：

- 1、在本文的研究尺度上（纬度跨越约 25° ，经度跨越约 20° ），相似白桦林群落下草本层的叶级谱（1、2）随经纬度有较明显变化趋势。
- 2、由东南向西北，受到大尺度水热条件影响，相似白桦林群落下草本层的叶级谱（1、2）变化体现出叶级递减的趋势。
- 3、其中叶级谱 2（各个样地各叶级物种重要值加和该样地占有物种重要值加和的比例）随经纬度的变化趋势更明显。
- 4、在本文的研究尺度上小尺度地形条件对于叶级谱的影响不显著。

参考文献:

- [1] 祁建, 马克明, 张育新. 北京东灵山不同坡位辽东栎(*Quercus liaotungensis*)叶属性的比较. 生态学报, 2008, 28 (1): 122-128.
- [2] 陈宏伟, 李江, 孟梦, 冯弦, 刘永刚, 周彬. 云南热带山地三种阔叶人工林群落林下植物生活型谱比较. 亚热带植物科学, 2004, 33 (4): 42 -44 .
- [3] 胡家峰, 郭远, 李梦, 谢皓, 陈学珍. 大豆不同叶形叶面积校正系数的研究. 北京农学院学报, 2012, 27 (1): 10-11.
- [4] 楚爱香, 张要战, 蓝玉才, 李艳梅, 许晓利. 多叶羽扇豆最佳叶面积测定方法研究. 陕西农业科学, 2005 (1): 15-17.

批注 [L2]: 注意参考文献的写法, 在文中引文该文献的地方加上标注, 可以是角标的编号, 或者 (作者, 年代)

感想:

这次出野外真真让我爱上了生态学的野外工作, 当一群人在一片荒无人烟的地方齐心协力做同一件事的时候, 那种心灵满足和轻松是在城市里很少能体会到的。

每一位老师同学都给我留下了那以忘怀的回忆, 我一直是喜欢躲在一边看这个世界的人, 很难得在坝上第一次感受到了这么强的归属感。从郭老师和刘老师身上学到和爱上了一些我曾经以为永远不会感兴趣的知识, 从每位同伴那里收获到了欢乐和友谊。

其实很多东西想写, 可是真的面对电脑却不知道如何下笔。不过一句话就够了, 这次野外实习让我发现, 我原来是那么热爱这个生态地科的大集体。

塞罕坝主要群落类型下草本层物种多样性研究

1100013277 城市与环境学院 王凌越

摘要: 该文比较分析了河北塞罕坝森林草原交错带主要群落类型下草本层的物种多样性, 白桦林、沼泽、草甸草原、典型草原的物种组成。计算了各样地的 Simpson 指数和 Shannon—wiener 多样性指数, 并试分析了影响因子和变化趋势。多样性指数 H、均匀度指数 E, 在平均值上有草甸>沼泽>白桦林地>典型草原; 在物种优势度 D 上, 有白桦林>草甸>沼泽>典型草原; 而 Simpson 指数 P, 则有白桦林>草甸>典型草原>沼泽, 且极差较小。不同类型群落之间共有种较少, 而共有优势种则有所重叠, 可作为生境变化指示种加以利用。

河北围场塞罕坝是我国重点保护的一个生态过渡带, 属于典型的森林、草原交错带, 这里的生态环境复杂多样, 是一个特殊的地理区域, 区内有森林、草原和沼泽湿地三大生态景观类型^①。对该区沼泽湿地及其原生性草甸, 各种珍稀动植物资源, 以及典型的森林、草原、草甸、沼泽等自然景观的保护越来越受到生态科学家的重视。过去对该地区植物的研究主要集中在调查植被基本特征、植物区系成分与分类以及过渡性分析等方面, 有关森林—草原生态过渡带的生物多样性研究不多^②。近几年, 王庆锁、黄永梅等对河北北部和内蒙古东部森林草原生态过渡带的生物多样性及景观格局进行过分析^③。植物群落多样性是生物多样性研究的重要组成部分, 因此本文在前人研究的基础上将着重研究该区植物群落多样性, 主要是研究不同林分下的植物多样性, 这也是搞好塞罕坝绿色生态环境建设和有效开发利用森林资源进行生态旅游的重要前提, 同时也为该地区生物多样性的保护与持续利用提供参考和理论依据。

1. 国内研究现状

群落多样性研究是群落生态学研究, 乃至整个生态学研究十分重要的内容。其中群落在组成和结构上表现出的多样性是认识群落的组织水平, 甚至功能状态的基础。也是生物多样性研究中至关重要的方面不同的植物群落在结构和功能上都存在很大的差异, 而具有不同功能作用的物种及其个体相对多度的差异是形成不同群落的基础。因此, 对于群落组织化程度的测度指标即物种多样性的研究具有重要意义。在群落演替过程中的多样性特征是研究群落多样性时空动态规律的重要内容。物种多样性是群落结构和功能复杂性的一种度量, 对群落物种多样性的研究有助于更好地认识群落的组成、结构、功能和动态, 掌握群落演替规律及多样性与群落的演替关系。以往有关植物群落物种多样性的研究较多, 郭正刚、郑元润等对森林植物群落物种多样性进行了研究^④。周志宇等研究了阿拉善荒漠草地恢复演替过程中物种多样性与生产力的变化^⑤。

此外, 植物群落与环境相互间的关系极其密切。一方面环境影响着群落, 另一方面群落也影响着环境, 两者是不可分割的辩证统一体。在对物种多样性进行分析的同时, 研究植物群落物种多样性随环境因子及演替梯度的变化特征是揭示生物多样性与生态因子相互关系的重要方面。因此对植物群落物种多样性进行梯度分析是其研究的一个重要方面。植物群落物种多样性的梯度特征是指在群落组织水平上物种多样性的大小随某一生态因子梯度的有规律性的变化。贺金生等^⑥就纬度、水分、土壤营养成分、海拔、演替等因子对近年来国内外陆地植物群落的研究结果进行了综述, 总结出了一些规律: 如纬度梯度规律, 随着纬度的降低, 群落物种多样性逐渐增大。但不同的群落其变化规律不同, 后来的研究结果并未超出前人总结的这些规律的内容。

2.研究方法

2.1 研究区介绍

塞罕坝位于围场满族蒙古族自治县北部,地处河北省最北端,东西 65.6km,南北 58.6km。地理坐标为:东经 116° 53' ~117. 39', 北纬 42. 02' ~42. 36'。林场处于坝上高原和冀北山地向海河、滦河平原的过渡带,也是北方干旱草原沙地向华北平原过渡的生态脆弱带。地貌上界于两个一级单元即内蒙古熔岩高原和冀北山地之间,主要是高原台地。境内有吐里根河、羊肠河、阴河、依逊河等 4 条河流,是滦河与老哈河上游主要支流的发源地。其地形地貌组合为高原一波状丘陵—漫滩—接坝山地;属寒温带半干旱—半湿润季风气候区。其特点是:冬季漫长,低温寒冷;春季短暂,干燥多风;夏季不明显,光照强烈;无霜期短。昼夜温差大;降水量偏少;风多风大,蒸发量大于降水量;大风、沙暴、干旱、霜冻等灾害性天气比较多。年均气温-1℃,极端最高温 33. 4℃,极端最低温- 43. 2℃;无霜期短,不稳定,年均 67 d,在植物生长季节常有霜冻发生 1 年均日照 2 367. 8h,高于 10℃的年积温 1661. 5℃;年均降水量 452.6 mm,最大年降水量 636.0mm,最小年降水量 258.0mm,年均降水日数 134 d,6—8 月份降水量占年降水量的 67. 6%1 年均蒸发量 1 388 mm,是降水量的 2. 6 倍 1 年均 6 级以上的大风 68 d,最多年份达 119 d(1966 年),最少年份 41 d。土壤由低到高的分布顺序是:棕壤—灰色森林土—黑土。从水平分布讲,本区东部为黑土,中部为灰色森林土,西部为风沙土。目前的塞罕坝植被,森林、灌丛、灌草丛、草原、草甸和沼泽植被并存,既有天然植被。也有人工植被,既有重度受扰的森林植被,也有轻度受扰的灌丛和灌草丛,还有略带原生性质的草原和草甸。

2.2 样地调查方法

植被多样性评价重在实地调查,包括植被群落和物种的历史变迁、现状等方面的调查,一般考虑多样性指数、均匀度和优势度 3 个指标。在实际操作上,多样性调查多采用样方调查。对该地区进行地形、地貌踏查,尽量避开人为干扰。选取具有代表性样带,然后根据研究的目的是在样带上典型取样。

在每一个样方中测定的项目包括:

1)乔木的株数、种数、高度、枝下高、胸径及冠幅;

2)灌木和草本的高度、盖度、多度;

3)生境因子的测定:用 GPS 测定其地理坐标及海拔高度,用罗盘仪测定坡向和坡度,并记录植被状况、土壤类型及林分郁闭度或密度等。

2.3 测度指标

生物多样性指数是把群落结构的某些信息通过公式处理后用综合指数予以表达,是对群落结构的一种简化的反映。生物多样性评价一般由多样性指数 H, 均匀度 E 和优势度 D 三个指标表征。许多生态学家提出了评估物种多样性大小的综合指数,最常用的是夏依指数与辛普森指数,二者皆同时考量物种丰富性及物种均匀性两项指标^①。本文即采用此两种多样性评价方法。其中各指数计算方法为:

多样性指数 H:

$$H=-\sum P_i \ln P_i$$

式中 $P_i=N_i/N$

Pielou 均匀度指数:

$$E=H/H_{\max}$$

式中 H 为实际观察的物种多样性指数，Hmax 为最大的物种多样性指数， $H_{max}=\ln S$ （S 为群落中的总物种数）

Berger-Parker 优势度指数（D）：

$$D= N_{max}/N$$

Simpson 指数 P:

$$P=1-\sum P_i^2$$

通过样方调查获得的数据删选出群落相关的数据（物种，盖度，频度，多度）得到相关物种的重要值的数据。Curtis 重要值计算公式：重要值=相对密度+相对频度+相对盖度

但是由于样方处理相对粗糙，并为获得精确的密度数据，于是采用多度进行粗略的量化。多度采用的是 Drude 的 7 级制表示群落的多度。

量化方法：将多度等级对应于数字级别（即 Soc 对应于 7，Cop3 对应于 6，Cop2 对应于 5，Cop1 对应于 4，Sol 对应于 3，Sp 对应于 2，Un 对应于 1），那么相对多度就是物种多度比上总的物种多度：

$$\text{相对多度}=\text{多度}/\sum \text{多度}$$

于是将重要值的计算公式修改为：

$$\text{重要值}=(\text{相对多度}+\text{相对频度}+\text{相对盖度})/3$$

3.结果与分析

3.1 样地基本情况

本次于塞罕坝林场、红山军马场、吐力根河谷共调查样地 17 个，其中森林群落样地为 10×10m,草甸、草原、典型草原样地面积为 4×4m，平均海拔在 1249~1713m 之间。基本情况见表 1.

表 1 样地基本信息

编号	群落名称	经度	纬度	海拔/m	坡度	坡向
1	白桦林	42° 26.563'N	117° 19.302'E	1549	27°	320°
2	落叶松林	42° 24'34.69"N	117° 19'09.16"E	1612	0	-
3	草甸	42° 1729.20"N	117° 24'04.69"E	1713	3°	0°
4	蒙古栎林	42° 09'32.22"N	117° 25'80.28"E	1327	20°	230°
5	油松林	42° 09'24.80"N	117° 25'21.01"E	1307	40°	260°
8	白桦林	42° 33'24.21"N	117° 07'33.43"E	1520	17°	20°
9	白桦-白杆林	42° 33'24.21"N	117° 07'33.43"E	1532	17°	20°
10	草原	42° 22'48.02"N	116° 38'50.17"E	1313	2°	50°
11	典型草原	42° 16'23.04"N	116° 03'24.58"E	1289	0°	-
12	典型草原	42° 20'01.18"N	116° 22'34.29"E	1249	2°	220°
13	沼泽	42° 27'41.07"N	117° 19'14.81"E	1537	0	30°
14	棘皮桦-白桦林	42° 27'37.58"N	117° 19'16.05"E	1541	25°	0°
15	沼泽	42° 24.801'N	117° 59.717'E	1460	0	-
16	典型草原	42° 24.801'N	117° 59.717'E	1460	35	170°
17	沼泽	42° 24.801'N	117° 59.717'E	1460	5	260°

3.2 草本层植物多样性分析

3.2.1 多样性指数分析

由于蒙古栎林、油松林、落叶松林样本数为 1，无法进行平均、比对处理，故在此只选择白桦林群落为森林群落代表。按白桦林、草甸、典型草原、沼泽分组，分别计算各样地和各组平均多样性指数 H、均匀度指数 E、物种优势度 D、Simpson 指数 P。结果如表 2、表 3。

在 3 个白桦林样地中，草本层 H、E、D、P 差距不大。其中 H 值有样地 8>样地 14>样地 1，在在海拔高度差距不大（极差为 29m）的情况下，通过对比坡度和坡向，发现样地 1、14 坡度相近,且大于样地 8，样地 8、14 坡向相近为阳坡、样地 1 为阴坡。海拔高度主要影响气温，所以在此可以认为，在气温相近的情况下，坡度和坡向是影响林下草本层物种多样性的重要因素，且就样本数据而言，坡向影响效果较大。

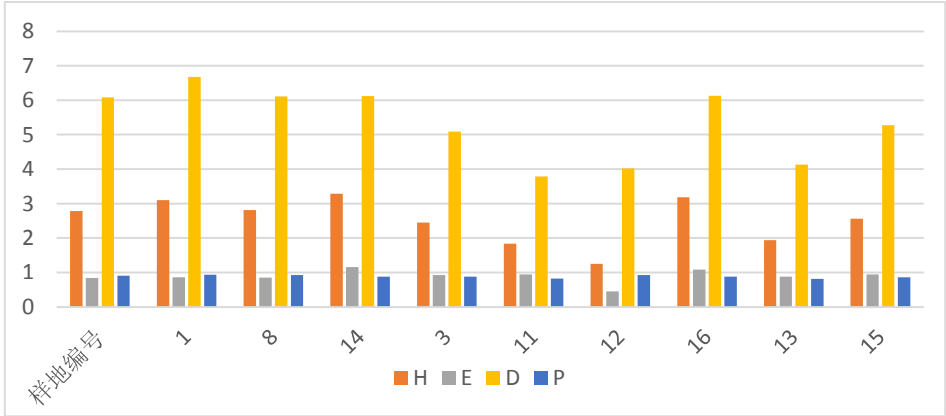
在 3 个典型草原样地中，H 值有样地 11>样地 12>样地 16，且极差相对较大。样地 16H 值最小，其海拔高度比其他 2 样地高 200m 左右，且为阴坡。样地 11、12 的影响因素则主要在于坡向。

在 3 个沼泽样地中，H 值有样地 13>样地 17>样地 15，其中样地 15、17 位置相近，高程相同，只有坡向相反，更进一步说明了坡向对草本层多样性的重要影响。

表 2 各样地草本层植物多样性指数

群落名称	样地编号	H	E	D	P
白桦林	1	2.782898	0.844368	6.078735	0.90607
	8	3.097116	0.864267	6.680635	0.934804
	14	2.812973	0.853493	6.108809	0.92387
草甸	3	3.288949	1.160855	6.122162	0.876994
典型草原	11	2.446256	0.926943	5.085313	0.875398
	12	1.839563	0.945348	3.785473	0.825496
	16	1.250084	0.450872	4.022673	0.92809
沼泽	13	3.181724	1.080587	6.126163	0.87495
	15	1.938108	0.882071	4.135333	0.813805
	17	2.561386	0.945841	5.269436	0.856912

图 1 各样地多样性评测指数



从表 3 的结果来看，草本层物种多样性指数 H、均匀度指数 E，在平均值上有草甸>沼泽>白桦林地>典型草原；在物种优势度 D 上，有白桦林>草甸>沼泽>典型草原；而 Simpson

指数 P，则有白桦林>草甸>典型草原>沼泽，且极差较小。同时，可发现其中 Simpson 指数基本相近。经查阅文献发现，Simpson 多样性指数中稀有物种所起的作用较小，而普遍物种所起的作用较大。这种方法估计出的群落物种多样性需要较多的样本，Routledge(1980)指出如果样本数少于 30 时，会造成过低的估计。

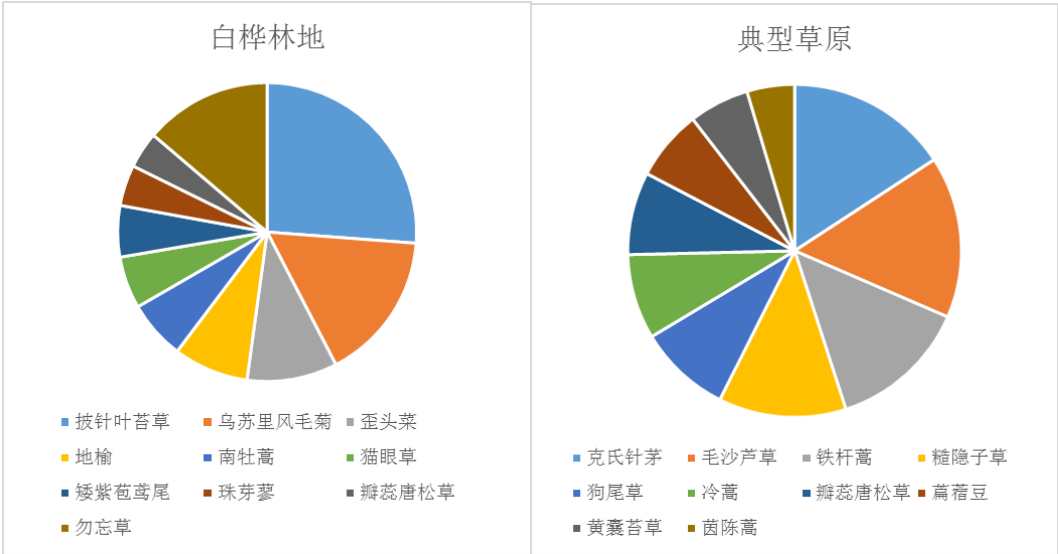
表 3 主要群落类型平均草本层植物多样性指数

群落类型	H	E	D	P
白桦林	2.897662	0.854042	6.289393	0.921581
沼泽	2.560406	0.9695	5.176977	0.848556
典型草原	1.845301	0.774388	4.29782	0.876328
草甸	3.288949	1.160855	6.122162	0.876994

3.2.2 各群落下优势种分析

图 2 显示，白桦林地中最优势种为披针叶苔草、草甸草原为裂叶蒿、典型草原为克氏针茅、沼泽为灰脉苔草。优势种所属科以禾本科、莎草科、菊科、豆科为主，说明了这几种科具有较强的环境适应性。其中，在四个群落均出现且相对占优势的属有蒿属和唐松草属。白桦林地中南牡蒿占优，草甸草原中蒙古蒿、裂叶蒿占优、典型草原中冷蒿、茵陈蒿、铁杆蒿占优、沼泽中草本层有铁杆蒿和蒙古蒿，但不作为优势种出现。白桦林地、草甸草原、典型草原中，瓣蕊唐松草均为优势种，而在沼泽生境中则由箭头唐松草作为替代种出现。

图 2 主要群落下草本层内前 10 优势种及其重要值



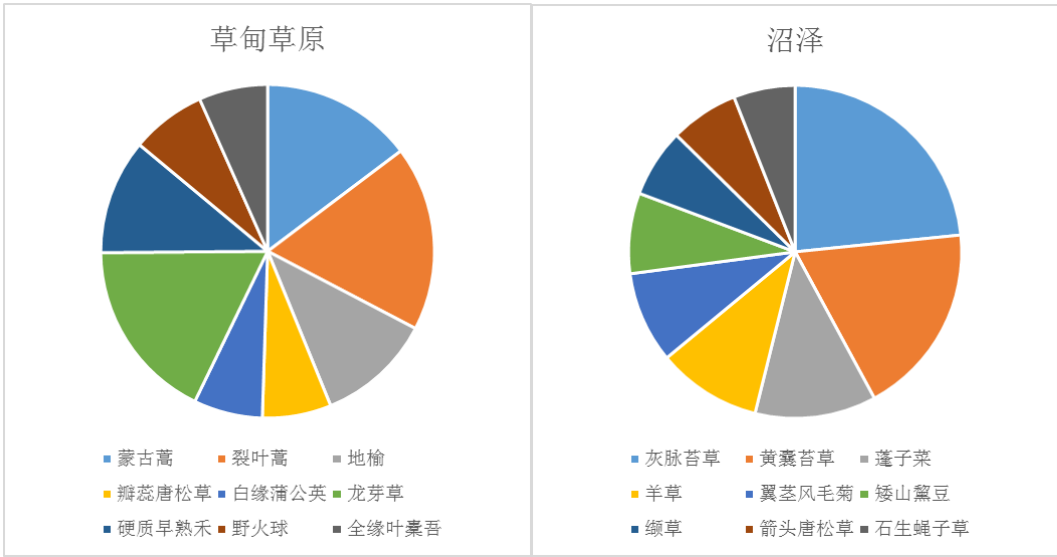


表 4 主要群落下草本层内前 10 优势种及其重要值

群落名称	种名	重要值	群落名称	种名	重要值
白桦林	披针叶苔草	0.192031	典型草原	克氏针茅	0.092343
	乌苏里风毛菊	0.118678		毛沙芦草	0.092081
	歪头菜	0.071657		铁杆蒿	0.079167
	地榆	0.059573		糙隐子草	0.072461
	南牡蒿	0.046652		狗尾草	0.052613
	猫眼草	0.041447		冷蒿	0.048308
	矮紫苞鸢尾	0.040754		瓣蕊唐松草	0.04711
	珠芽蓼	0.032444		篇苳豆	0.040166
	瓣蕊唐松草	0.028911		黄囊苔草	0.034243
	勿忘草	0.100872		茵陈蒿	0.026965
草甸	蒙古蒿	0.123615	沼泽	灰脉苔草	0.115908
	裂叶蒿	0.150623		黄囊苔草	0.0928
	地榆	0.093853		蓬子菜	0.058403
	瓣蕊唐松草	0.056096		羊草	0.050234
	白缘蒲公英	0.056096		翼茎风毛菊	0.044042
	龙芽草	0.148491		矮山黧豆	0.038799
	硬质早熟禾	0.093853		缬草	0.032951
	野火球	0.061071		箭头唐松草	0.032951
	全缘叶橐吾	0.056096		石生蝇子草	0.029647

4.结论与讨论

4.1 结论

经以上分析，可得出的结论有：

1) 在草本层的物种多样性上，参考各样地基本信息，可发现影响因子多样，起重要作用的有坡向、坡度、海拔等。其中，坡向的影响程度最大，在同类型群落中，阳坡的物种多样性明显高于阴坡。以及随坡度增大、海拔增高，物种多样性有下降的趋势；

2) 不同地带植被的群落多样性及生长型结构的变化都表现一定的规律, 无论各群落还是群落内, 都呈现出从森林带到森林草原带、沼泽、草甸草原、典型草原依次降低的趋势, 造成这样的结果可能主要是由于不同的生态系统, 不同的生态梯度, 再加上环境因子的不同程度的变化, 也就造成了物种多样性的区别;

3) 不同群落间共有种不多, 共有的优势属则有蒿属、唐松草属, 说明此二属适应环境能力较强。属内应对不同群落生境而出现的替代分布现象, 也侧面说明该属内植物可作为生境变化指示植物, 从而得到进一步应用。

4.2 分析方法和数据讨论

本次研究所基于的实验数据以及样地资料十分不足, 白桦林、沼泽、典型草原样地选择三处, 草甸草原只有一处, 尤其是重要值的计算上, 显得还不够准确。另外, 对于草原类型的表述以及草原类型的确定上还存在一些待商榷之处。最好是能够在一些标准的草甸草原, 典型草原以及荒漠化草原之中进行研究, 从而确保数据资料的准确性。此外, 本次研究没有包括相关的气象数据和土壤数据, 也未顾及人为影响, 所以还待完善和整理。

关于数据处理方法, 也存在一定问题。Simpson 多样性指数中稀有物种所起的作用较小, 而普遍物种所起的作用较大。这种方法估计出的群落物种多样性需要较多的样本, 此研究中并不敏感。且在调查样地时, 多度、盖度多为目视估测, 必然存在较大误差。

此外, 可以发现实地调查的植物整体上比植物志上的营养枝的高度要偏低。虽然大多都在植物志所取的范围内, 但是仍然明显接近最小值。如果排除了主观的观测问题, 很可能这些草原都处在一个矮化状态, 也许是由于长期的草原气候干旱化^⑧以及沙尘暴^⑨的响应。

参考文献

- ①王庆索;冯宗炜;罗菊春河北北部内蒙古东部森林草原交错带生物多样性的研究[期刊论文]-植物生态学报 2000(02)
- ②高洪文生态交错带(ECOTONE)理论研究进展 1994(01)
- ③王庆锁;王襄平;罗菊春生态交错带与生物多样性[期刊论文]-生物多样性 1997(02)
- ④周志宇阿拉善荒漠草地恢复演替过程中物种多样性与生产力的变化[期刊论文]-草业学报 2003(01)
- ⑤贺金生;陈伟烈陆地植物群落物种多样性的梯度变化特征 1997
- ⑥ .郭正刚白龙江上游地区森林植物群落物种多样性的研究[期刊论文]-植物生态学报 2003(03)
- ⑦ 毛文永 生态环境影响评价概论 北京: 中国环境科学出版社
- ⑧李金花.内蒙古典型草原几种优势植物生态适应对策研究.甘肃农业大学博士学位论文
- ⑨ 于向芝等.内蒙古退化草原 8 种植物叶结构对禁牧的响应.生态学报.2007 年,第 27 卷 4 期